Talanta Vol. 28, pp. 1 to 6
Pergamon Press Ltd 1981. Printed in Great Britain

OIL-MATCHING BY USING A SIMPLE VECTOR MODEL FOR FLUORESCENCE SPECTRA

TIMOTHY J. KILLEEN
Department of Statistics, University of Connecticut, Storrs, CT 06268, U.S.A.

and

DELYLE EASTWOOD and MARTHA SCHULZ HENDRICK
U.S. Coast Guard R&D Center, Avery Point, Groton, CT 06340, U.S.A.

(*Received* 12 *June* 1980. *Accepted* 16 *July* 1980)

Summary—A digitized fluorescence spectrum containing n points may be considered as a vector in n-dimensional space. This concept is used to develop a vector model employing angular distance in n-space as a parameter for comparison of fluorescence spectra of weathered oils. The vector model is applied to the problem of forensic oil-identification, by comparing the spectra of oil-spill samples with the spectra of unweathered and laboratory-weathered oils thought likely suspects. The vector representing the oil-spill spectrum is projected on the hyperplane formed by the spectra of the unweathered and corresponding laboratory-weathered oils to locate the vector which has the smallest angular deviation from the spill vector ("best fit").

Various studies have been made of the use of pattern-recognition techniques for forensic oil-identification.[1,2] The Coast Guard has developed a multi-method package[3] combining various experimental techniques, of various degrees of sophistication, to compare the resulting spectral or chromatographic patterns.

A digitized spectrum may be considered by vector in n-space. Curtis[4] has used this approach to classify oils, by using cluster analysis. In another approach, Brown *et al.*[5] have developed a log-ratio method for comparing pairs of infrared oil spectra considered as vectors. One advantage of the log-ratio method is that the distance is thickness-invariant for infrared spectra and if applied to fluorescence would be independent of the method of normalization. Expressed mathematically, this concept means that two spectra of the same sample theoretically differ only by a multiplicative constant. The vectors $\bar{\mathbf{x}}$ and $A\bar{\mathbf{x}}$ are spectrally identical; therefore, the distance $d(\bar{\mathbf{x}}, A\bar{\mathbf{x}}) = 0$ for all vectors $\bar{\mathbf{x}}$ and scalars A.

In the present paper, a simple vector model using angular distance in n-space as a parameter is considered for comparing oil fluorescence spectra.

The process of comparing the spectra of a spilled oil and its suspected sources is complicated by the spectral changes resulting from the environmental weathering of the spilled oil. Many authors[6–11] have discussed the weathering of oils as a complex process depending on factors such as type of oil, air and water temperatures, photo-oxidation, dispersion of the oil by wave action. The effect of weathering on fluorescence spectra has been shown to be significant within periods ranging from 1 day for light oils to 1 week for heavy oils.[12,13]

In cases of severe weathering of spill samples, artificial weathering[14] of suspected sources has been used in an attempt to improve the degree of match, but with only limited success since the degree of weathering is difficult to approximate in the laboratory.

The present vector model using spectra of laboratory-weathered samples simulates weathered spectra of suspected oil samples which "best match" the spill spectra. It compares the spill spectrum with the space spanned by the spectrum of an unweathered source and the spectrum of its laboratory-weathered counterpart. The vector member of this space which has the smallest angular deviation from the spill vector and is a member of this subspace can easily be located by this process.

The examples given in this paper were taken from room-temperature fluorescence and low-temperature luminescence spectra of oils weathered under known conditions, but a similar approach[15] has since been found useful for infrared spectra as well. When utilized with fluorescence spectra of suspect oils laboratory-weathered under known conditions, this mathematical technique should permit quantitative matching of spill spectra with suspected-source spectra that have been largely corrected for errors due to weathering. The fluorescence methods available have been reviewed by Frank.[16]

THEORY

The method considers a digitized spectrum as an n-dimensional vector, where n is the number of digitized points or peaks on each spectrum. Two fluorescence or infrared spectra (vectors) that differ in

magnitude but not direction in n-space are spectroscopically identical. Such differences are due to variability in instrument performance and sample preparation. Any distance measure which is zero for all such pairs of vectors might be a reasonable choice for use in this problem. The measure chosen is angular distance in n-space.[17] We define the angle between two vectors $\bar{V}$ and $\bar{W}$ to be:

$$\theta_{VW} = \arccos [\bar{V} \cdot \bar{W} / (|\bar{V}| |\bar{W}|)]. \quad (1)$$

Besides the use of angular measurements as distances, the laboratory-weathered sample of the suspect oil is also utilized to decide better whether the suspect matches the spill. The spectrum of a given oil changes continuously as the oil is weathered. That is, the possible spectra of a given weathered oil form a surface in n-space (weathering surface). If the suspect is the actual source of the spill, then its spectrum will be a point on this surface, while the observed spectrum will only be near the surface, owing to random errors. This weathering surface may be approximated by the hyperplane generated by the spectrum of the neat suspect oil and that of its laboratory-weathered counterpart, *i.e.*, by two points on or near the weathering surface. The angle between the spill spectrum vector and the surface appears to be a much better indication of a match or non-match than does some distance measure between the spill and suspect spectra. Figure 1 illustrates these points. We have used $n = 3$ in order to present the idea in its simplest form. The hyperplane generated by $\bar{X}_0$, the unweathered-suspect spectrum, and $\bar{X}_1$, the spectrum of laboratory-weathered specimen of the same oil, is shown with the weathering surface. If $\bar{Y}$, the spill spectrum, is that of another weathered version of $\bar{X}_0$, then it will lie on the weathering surface (curved surface). The projection of $\bar{Y}$ on the hyperplane is $\bar{S}$ and the angular deviation, θ, may be determined.

An additional benefit is realized from consideration of the position of the projection of the spill spectrum in the generated hyperplane, relative to the spectra of a suspect oil. Even though the spill spectrum may be close to the hyperplane, the position of its projection may indicate that the spill is not a weathered version of the suspect oil. This will occur when the projection indicates that weathering has resulted in a vector shift from the neat suspect that is opposite in direction to that for the laboratory-weathered samples. This technique has been extended to be used with more than one laboratory-weathered specimen of a given suspect.

Suppose that the n-dimensional vectors $\bar{X}_0$, $\bar{X}_1$, $\bar{X}_2, \ldots, \bar{X}_k$ are the sequence formed by the digitized spectrum of the neat suspect and by the spectra of k

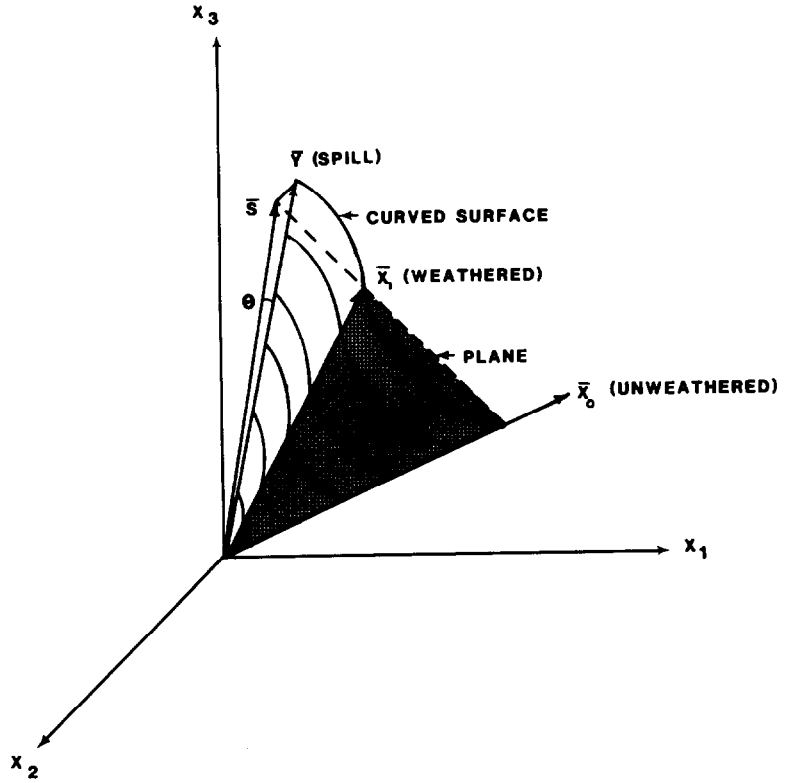


Fig. 1. Three-dimensional representation of the vector method. Fluorescence emission spectra are represented by the vectors $\bar{X}_0$, unweathered oil; $\bar{X}_1$, same oil weathered; and $\bar{Y}$, the spill. $\bar{S}$, the projection of $\bar{Y}$ on the $\bar{X}$, $\bar{Y}$ plane, is the computed simulated match of $\bar{X}$ to $\bar{Y}$. θ is the angle between $\bar{Y}$ and $\bar{S}$ in n-space. The hyperplane is represented by the plane and the weathering surface by the curved surface.

differently laboratory-weathered samples of the same oil. We assume that $\bar{X}_{i+1}$ is more severely weathered than $\bar{X}_i$. Let $\bar{Y}$ denote the digitized spill spectrum, and A denote the space spanned by the vectors $\bar{X}_0$, $\bar{X}_1, \ldots, \bar{X}_k$. Any vector $\bar{S}$ in A is of the form

$$\bar{S} = a_0'\bar{X}_0 + a_1'\bar{X}_1 + a_k'\bar{X}_k \quad (2)$$

where the a's are scalars. $\bar{S}$ may now be rewritten as follows:

$$\bar{S} = a_0\bar{X}_0 + a_1(\bar{X}_1 - \bar{X}_0) + a_2(\bar{X}_2 - \bar{X}_1) + \ldots + a_k(\bar{X}_k - \bar{X}_{k-1}) \quad (3)$$

for spectra weathered no more than $\bar{X}_k$; the previously mentioned weathering surface may be approximated by vectors of the form (2) with the restriction that $a_0 = a_1 = \ldots = a_j = 1$; $0 \leqslant a_{j+1} < 1$; and $a_{j+2} = a_{j+3} = \ldots = a_k = 0$ for some $j = 0, 1, \ldots, k-1$.

The weathering surface may be approximated by a polygonal arc. The remainder of the surface corresponding to heavier weathering than $\bar{X}_k$ may be simply approximated by the vectors of the form shown in equation (3) with $a_i = 1$ for $i < k$ and $a_k \geqslant 1$.

One approach here might be to calculate the angle θ between the spill vector and its projection on the simulate weathering surface described in the previous paragraph, but a mathematically simpler approach has been taken. The spill spectrum vector is projected onto A, the entire subspace generated by $\bar{X}_0$, $\bar{X}_1, \ldots, \bar{X}_k$, and this projection is written in form (3). If the suspect is the true source of the spill, then two things should occur. First, θ should be small and, secondly $a_0, a_1, \ldots, a_k$ should be approximately of the same form as the parameters of the weathering surface.

We now formalize these ideas. We wish to project the vector $\bar{Y}$ onto the hyperplane generated by $\bar{X}_0$, $\bar{X}_1, \ldots, \bar{X}_n$ and locate the $k+1$ a_i'-constants given in (2). Using the method of least squares, we minimize

$$\sum_{i=1}^{n}\left(Y_i - \sum_{j=0}^{k} a_j'X_{ij}\right)^2 \quad (4)$$

where $\bar{X}_j = (X_{1j}, X_{2j}, \ldots, X_{nj})$. Notice that we are minimizing the Euclidean parameters to locate the vector in A which is "closest" to $\bar{Y}$. This same vector also gives the minimum θ. The minimization of (4) is accomplished by solving the $k+1$ linear equations with $k+1$ unknowns.

$$\sum_{i=0}^{k} a_i' \cdot \sum_{j=1}^{n} X_{lj}X_{ij} = \sum_{j=1}^{n} X_{lj}Y_j \quad (5)$$

(for $l = 0, 1, 2, \ldots, k$).

This may be accomplished directly through matrix inversion.[18] Notice that if $a_0', a_1', \ldots, a_k'$ minimize (4), then any constant multiple of these values will be suitable for $\bar{S}$. Letting

$$a_k'' = a_k', \quad a_{k-1}'' = a_{k-1}' - a_k'', \quad a_0'' = a_0' - a_1''$$

and finally

$$a_0 = 1, \quad a_1 = a_1''/a_0'', \ldots, a_k = a_k''/a_0''$$

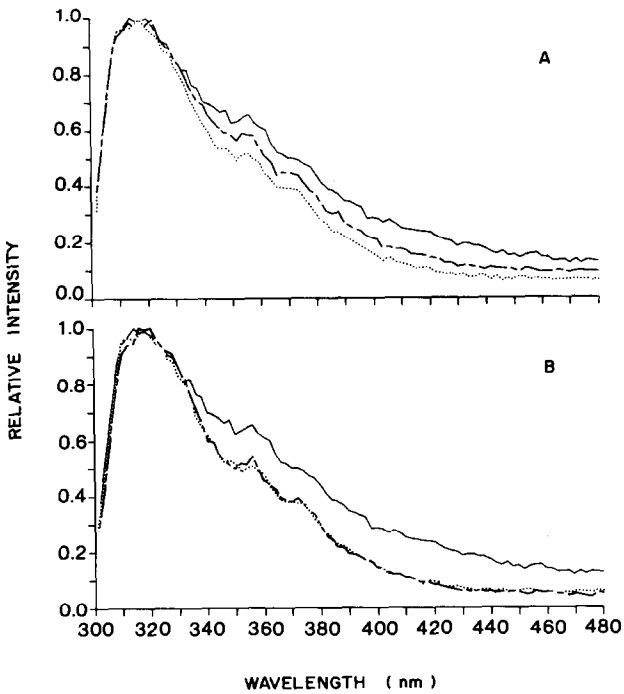


Fig. 2. Vector analysis method applied to fluorescence spectra of a No. 4 fuel oil. Digitized spectra of A: unweathered oil (——), one-day (– – –), and two-day weathered oil (- - - - - - -); B: unweathered oil (——), 4-day weathered oil (- - - - -) and simulated weathered suspect (– — –).

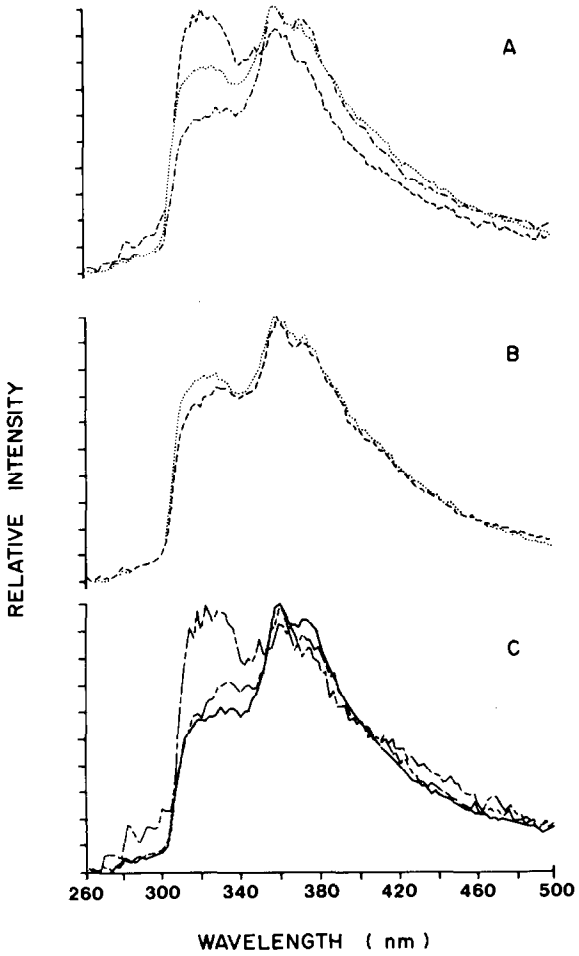


Fig. 3. Vector analysis method applied to fluorescence spectra. A: unweathered No. 4 oil (- - - -) unweathered light crude oil (— — —), and spill (— — —). B: No. 4 oil unweathered (------) and 2-day weathered (— — —). C: The spill (——) compared to the simulated match from the No. 4 oil (— — —) and the light crude oil (— —).

we obtain $\bar{S}$ in the form (3). If $\bar{Y}$ corresponds to a weathered version of the oil giving $\bar{X}_0$, then the a_i should be approximately of the form described in the sentence following equation (3). For weathered oils, $a_1, a_2, \ldots, a_k$ are called weathering constants.

EXPERIMENTAL

The oils used for this study were weathered as follows. For the spectra in Fig. 2, oils were weathered for the Coast Guard in large outdoor tanks containing sea-water, by the Research Institute of the Gulf of Maine (TRIGOM), at an average air temperature of 19.6° and a water temperature of 15.5°. Samples were collected after 1, 2, 3 and 4 days of weathering. For the spectra in Figs. 3 and 4, oils were weathered at the University of Rhode Island either in the laboratory or in outdoor tanks with circulating sea-water at an average air temperature of 21° and a water temperature of 18°. Samples were collected after 2 days and one week of weathering.

All samples were diluted to 20 μg/ml concentration in "Spectroquality" methylcyclohexane (Matheson Coleman and Bell). A Farrand Mark I spectrofluorometer was used, with bandwidths of 10 nm for excitation and 1 nm for emission. The excitation wavelength was 254 nm in all cases. A "Suprasil" Dewar flask containing liquid nitrogen was used with the same instrument for the low-temperature luminescence spectra shown in Fig. 4. All spectra were recorded in digitized form with data points at 2-nm intervals, with a laboratory-constructed microprocessor which was interfaced with a PDP-8 computer.

RESULTS AND DISCUSSION

To illustrate the method, Fig. 2 shows a light No. 4 fuel oil with 1, 2 and 4-day weathered samples, with the 4-day sample representing the spill. The simulated spectrum in Fig. 2B is shown by the projection of the spill vector on the weathering hyperplane to match closely that of the spill, $\theta = 0.031$ rad, whereas for the spill and the unweathered oil, $\theta = 0.192$ rad.

As indicated in Fig. 3, the vector method can also be appled to multiple sources. In Fig. 3A, the spectrum of the spill is compared with unweathered-oil spectra, with no close match apparent. Figure 3B shows the spectra for weathered and unweathered No. 4 oil. Figure 3C indicates that the spectrum for the No. 4 oil that best matches the spill spectrum (which is, in fact, the spectrum for one-week weathered No. 4 fuel oil) is that of the 2-day weathered sample but the best-fit spectrum for the crude oil, generated in the same manner, does not match the spectrum of the spill.

Table 1 lists weathering factors and angles for Figs. 3 and 4. The negative weathering factor for the crude oil suggests that this oil is unrelated to the spill.

Low-temperature luminescence spectra of a light crude oil and a No. 4 fuel oil are shown in Fig. 4. The spectrum of a two-day weathered sample of the crude oil (the spill in this case) is compared with the best fit generated from the spectra of the unweathered and one-week weathered oils. The spectra with the smallest angle between their vectors give the closest visual

Table 1. Angles and weathering factors for spill comparison

Figure	Oil type	Weathering factor, a	θ-values	
			Unweathered oil	Best fit
3	Crude	−0.94	0.267	0.247
3	No. 4	1.86	0.116	0.073
4	No. 4	−0.19	0.145	0.142
4	Crude	0.423	0.056	0.046

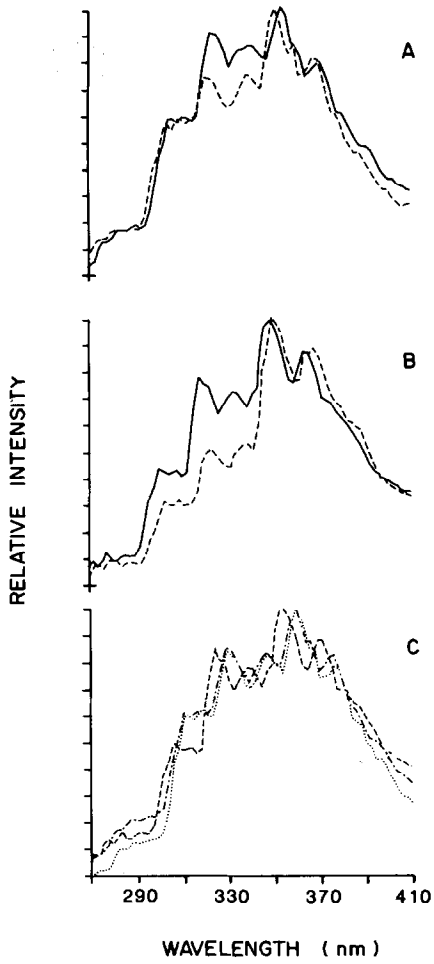


Fig. 4. Vector analysis method applied to low-temperature luminescence spectra (77 K) of light oil. Digitized spectra of A: a light Louisiana crude oil unweathered (——) and weathered for one week (– – –); B: a No. 4 fuel oil, unweathered (——) and weathered for one week (– – –) C: simulated weathered spectra generated from A (— – –) and B (– – –) compared with the spectrum of the spill (– – – –).

match. The weathering factors (Table 1) are less than unity for the match, indicating that the spill is less heavily weathered than the weathered oil.

In Fig. 3, the vector analysis is based on extrapolation of the hyperplane; for Fig. 4, the spill is less weathered than the weathered oil used to generate the hyperplane. These examples were selected because no close matches were apparent by conventional visual comparison.

CONCLUSIONS

The vector analysis method utilizes information in the fluorescence spectra from a suspect oil and at least one laboratory-weathered sample of it for comparison with the spill spectrum in deciding whether or not the spill and the suspect match. It takes into account the observed behaviour of the suspect oil spectrum on weathering and estimates the degree of weathering undergone in the spill. In real-world spills, information about the amount of weathering is often available and may be compared with the estimates of weathering given by the vector method. Such qualitative evidence has been used by scientists in the past but we feel that ours is the first truly quantitative approach to the effects of weathering of oils on their fluorescence spectra.

The vector method has been shown to be a promising mathematical technique for analysis of fluorescence spectra in oil identification. Although the vector method has thus far been tested on only a limited number of oil fluorescence spectra, results are highly encouraging for interpolation or even extrapolation over short weathering periods. It may also have application for analysing mixtures of oils or contaminated oils.

The vector method provides a quantitative basis for comparing fluorescence spectra of weathered oils, of special importance for forensic oil-spill identification.

Acknowledgement—We wish to thank C. W. Brown for providing some of the weathered oil samples.

REFERENCES

1. R. W. Liddell III and P. C. Jurs, *Appl. Spectrosc.*, 1973, **27**, 371.
2. U.S. Coast Guard, University of Connecticut, IEEE, *Proceedings, Workshop on Pattern Recognition Applied to Oil Identification*, Coronado, California, November 1976, IEEE Catalog No. 76 CH 1247-6, published 1977.
3. Chemistry Branch, *Oil Spill Identification System*. U.S. Coast Guard Final Report No. DOT-CG-D-52-77, National Technical Information Service (NTIS) Accession No. ADA044750, June, 1977.
4. M. L. Curtis, *Use of Pattern Recognition for Typing and Identification of Oil Spills*, U.S. Coast Guard Research and Development Center, Avery Point, Groton, CT, Final Report No. DOT-CG-D-38-77, NTIS Accession No. ADA043802, 1977.
5. C. Brown, P. Lynch and M. Ahmadjian, *Data Base Formulation and Application to Real Spills*. In *Proceedings of the Workshop on Pattern Recognition Applied to Oil Identification*, Coronado, California, November 1976 (see reference 2).
6. D. C. Gordon, Jr., D. Keizer, R. Hardstaff and D. G. Aldous, *Environ. Sci. Technol.*, 1976, **10**, 580.
7. W. Harrison, M. A. Winnik, P. T. Y. Kwong and D. Mackay, *ibid.*, 1975, **9**, 231.
8. T. F. Yen, in *Marine Chemistry in the Coastal Environment*, A.C.S. Symposium Series V, 1975, **18**, 231.
9. J. W. Frankenfeld, *Weathering of Oil at Sea*, U.S. Coast Guard Final Report No. DOT-CG-D-7-75, NTIS Accession No. AD787789, 1973.
10. M. Blumer and J. Sass, *Science*, 1972, **176**, 1120.
11. C. A. Parker, H. F. Freegarde and C. G. Hatchard, in *Water Pollution by Oil*, Proc. Seminar Aviemore, *J. Inst. Pet. (London)*, 1971, 237.
12. D. Eastwood, M. S. Hendrick and S. H. Fortier, Pittsburgh Conference on Analytical Chemistry and Applied Spectroscopy, Cleveland, March 1977, Paper No. 395.
13. D. Eastwood, S. H. Fortier and M. S. Hendrick, *Am. Laboratory*, 1978, March, 45.
14. M. Ahmadjian, C. D. Baer, P. F. Lynch and C. W. Brown, *Environ. Sci. Technol.*, 1976, **10**, 777.
15. C. P. Anderson, T. J. Killeen and A. P. Bentz, Pitts-

burgh Conference on Analytical Chemistry and Applied Spectroscopy, Cleaveland, March 1978, Paper No. 397.
16. U. Frank, *Toxicol. Environ. Chem. Rev.*, 1978, **2**, 163.
17. J. Tou and R. Gonzalez, *Pattern Recognition Principles*, p. 87. Addison-Wesley, Reading, Mass., 1974.
18. D. Zelinsky, *A First Course in Linear Algebra*, Academic Press, New York, 1968.

Talanta Vol. 28, pp. 7 to 10
Pergamon Press Ltd 1981. Printed in Great Britain

FLOTATION–PHOTOMETRIC DETERMINATION OF SILICON IN THE FORM OF CHROMOPYRAZOLE II MOLYBDOSILICATE

P. G. KAZ'MIN, E. N. DOROKHOVA and I. P. ALIMARIN
Department of Analytical Chemistry, Moscow State University, Moscow, USSR

(*Received* 2 *May* 1980. *Accepted* 15 *July* 1980)

Summary—The process of concentrating chromopyrazole II α- and β-molybdosilicates by flotation with mixtures of toluene with polar solvents (acetone, ethanol, isoamyl alcohol, cyclohexanol or cyclohexanone) has been studied. It was found that the composition of the complex depends on the acidity of the medium. The complex was isolated from 1.5*M* sulphuric acid. On the basis of elemental analysis the ratio of chromopyrazole II to molybdosilicate was found to be 2:1. Infrared spectroscopy was used to establish that an ion-association complex is formed. The results were used to establish a method for determination of ultratrace levels of silica (2 μg/l.) in high-purity water. The relative standard deviation is 7–11%.

Dyestuffs of the triphenylmethane and rhodamine series are used with success for extractive photometric determination of small amounts of silicon, phosphorus, germanium and arsenic.[1–6] The sensitivity is high, the molar absorptivity generally being about 10^5 $l.mole^{-1}.cm^{-1}$. However, the free dyestuff and dye–molybdate complexes are usually extracted along with the dyestuff–heteropoly acid compound. Various methods are used to eliminate this co-extraction, such as a preliminary selective extraction of the heteropoly acid (with subsequent re-extraction),[2] masking of molybdate ions with oxalic acid,[1] destruction of excess of dyestuff with sodium permanganate,[7] or strong acidification.[8]

Dyestuffs of the antipyrine series, which form intensely coloured compounds with heteropolymolybdates, are promising reagents.[9–12] Antipyrine dyes are analogues of triphenylmethane dyes, differing from them in that one of the phenyl groups is replaced by the antipyrine heterocycle. As a result of this change in structure the dyestuff gains a number of valuable properties, antipyrine dyes being stable in strongly acidic medium and forming more stable compounds with anions because the antipyrine radical is more nucleophilic than the phenyl group.

According to Bondareva and Gaidukova,[13] *bis*(4-dimethylaminophenyl)antipyrylcarbinol (chromopyrazole I) reacts with molybdosilicate to form a complex insoluble in water, chloroform, benzene, *etc.* In our work an analogue of that reagent, *bis*(4-methylbenzylaminophenyl)antipyrylcarbinol (chromopyrazole II) was used. Earlier[14] chromopyrazole II was shown to react with molybdosilicate to form highly coloured insoluble compounds. To increase the sensitivity of silicon determination, the use of an extractive photometric method based on this would be attractive.

It is known that molybdosilicate, the form in which silicon is usually determined, gives two structural isomers, the α- and β-forms. In analytical practice the β-isomer is generally obtained in presence of an excess of molybdate ions. Therefore, the interaction of the dye with molybdate and with both forms of molybdosilicate was examined.

EXPERIMENTAL

Reagents

α-Molybdosilicic acid $H_4SiMo_{12}O_{40}.17H_2O$ was synthesized by the ether extraction method, analysed for silicon and molybdenum and used as a $1.27 \times 10^{-4}M$ solution. Other reagents were 5% ammonium molybdate solution, sodium silicate solution (SiO_2 2.5 μg/ml), 0.04% chromopyrazole II solution, 0.5*M* and 7.5*M* sulphuric acid, 7.5*M* nitric acid, toluene, chloroform, cyclohexanol, cyclohexanone, ethanol, isoamyl alcohol and ether. The reagents and the solvents were of adequate purity. All the solvents were prepared in water distilled twice in quartz apparatus and stored in polyethylene vessels.

Procedure

In the study of the interaction of the β-acid, ammonium molybdate solution (1 ml) was placed in a 50-ml standard flask, 0.5*M* sulphuric acid was added to give pH 1.5–2.0, a calculated amount of standard sodium silicate solution was added with subsequent dilution with water to 35 ml total volume and the mixture was kept for 10–15 min (for complete formation of the β-acid); then a calculated amount of 7.5*M* sulphuric acid solution and 1 ml of 0.04% chromopyrazole II solution were added, and after stirring the mixture was extracted with 10 ml of organic solvent. The complex of the β-acid with chromopyrazole II was concentrated (floated) at the interface in the form of a dark blue-violet film. Then the aqueous phase was separated and the film was dissolved by addition of 10 ml of acetone (ethanol or ether). The absorbance at 590 nm was measured in a 1-cm cuvette. If no film appeared the organic phase was measured photometrically at the same wavelength.

In the study of the interaction of the α-acid with chromopyrazole II, a calculated amount of the α-molybdosilicic acid solution was added to a 50-ml standard flask and diluted with water to 35 ml and then further treated as above.

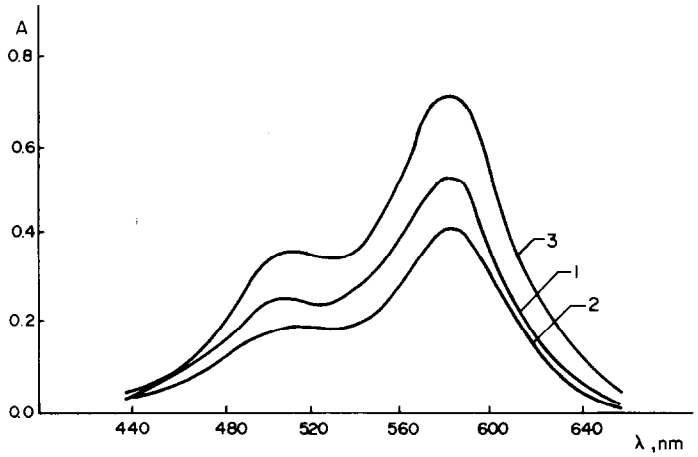


Fig. 1. Absorption spectra of toluene–acetone solutions of the compounds: 1—α-molybdosilicate–chromopyrazole II; 2—molybdate–chromopyrazole II; 3—chromopyrazole II. $C_{\text{chromopyrazole II}} = 2.32 \times 10^{-6}M$, $C_{\alpha\text{-MS}} = 5.07 \times 10^{-6}M$, $C_{\text{Mo}} = 1.74 \times 10^{-6}M$.

For extraction, isoamyl alcohol, cyclohexanone, cyclohexanol, toluene, chloroform, as well as mixtures of cyclohexanol with toluene (1:4, 1:3, 1:1, 3:1, 4:1), cyclohexanone with toluene (1:4, 1:3, 1:1, 3:1, 4:1) and toluene with acetone (1:1) were used.

Determination of silicon

Calibration curve. Ammonium molybdate solution (1 ml) is added to a 200-ml plastic separating funnel* and 1 ml of 0.5*M* sulphuric acid is added to give pH 1.5–2.0 (check with indicator paper). Then standard silicon solution (0.25–4.5 μg of SiO_2) is added and the mixture diluted to 35 ml with doubly distilled water. The mixture is kept for 10–15 min (to form the heteropoly acid completely), then 20 ml of 7.5*M* sulphuric acid and 1 ml of 0.04% dye solution are added, followed by 45 ml of water and 10 ml of acetone–toluene mixture (1:1), and the mixture is shaken for 3 min. A film is formed at the interface. The aqueous phase is separated, and 10 ml of acetone are added to the funnel; the film dissolves rapidly. The toluene–acetone solution is transferred to a 25-ml standard flask and diluted with acetone to the mark. The absorbance at 590 nm is measured against a reagent blank carried through the procedure (the absorbance of the blank measured against water is about 0.18). The final dilution with acetone is not obligatory, because the separation of the aqueous phase is sufficiently complete and the remaining volume of water (about 0.1 ml) can be neglected, but the total volume of the aqueous phase should be kept as constant as possible. The relative standard deviation is 8%. The calibration plot is linear, and described by the equation $y = -0.03 + 0.1918x$ where y is the absorbance and x is the amount of silica present (μg). The method has been used for determination of the silicon content of demineralized and doubly distilled water.

Analysis of samples. Proceed as for the calibration curve, but use an aliquot of sample (containing 0.25–4.5 μg of SiO_2) instead of the standard silicate solution. A correction for the partial extraction of chromopyrazole molybdate should also be made. For evaluation of the correction, 20 ml of 7.5*M* sulphuric acid are diluted with doubly distilled water to about 90 ml, then 1 ml of ammonium molybdate solution is added. In this way no β-molybdosilicic acid is formed from silicon contained in the water. Then the flotation is carried out, and the absorbance of the toluene–acetone solution is recorded as above (the absorbance does not exceed 0.04). After this correction has been applied the silica content is found from the calibration curve.

* Alternatively, a plastic beaker can be used, and the solution transferred to a glass separating funnel after the addition of the 7.5*M* sulphuric acid.

RESULTS AND DISCUSSION

Chromopyrazole II is extracted into chlofororm and cyclohexanone within the acidity range from pH 1.5 to 0.5*M* sulphuric acid.

On extraction with cyclohexanone, the chromopyrazole II–molybdate compound is transferred to the organic phase over the same range of acidity. On extraction with isoamyl alcohol, cyclohexanol, toluene, chloroform and the mixtures of solvents listed above, a film appears at the interface.

Under the same conditions, the compound of chromopyrazole II with α-silicomolybdic acid is extracted with cyclohexanone. When the other solvents and mixtures are used instead, flotation at the interface is observed. Shaking for 3 min is sufficient for total extraction.

This study has shown that for the acidity range investigated there is no solvent which extracts only the chromopyrazole II molybdosilicic acid complex without extracting the dye itself and its compound with molybdate.

The absorption spectra of toluene–acetone solutions of chromopyrazole II ($\lambda_{max} = 580$ nm, $\epsilon = 7.0 \times 10^4$ $l.mole^{-1}.cm^{-1}$), the molybdosilicic acid complex of chromopyrazole II ($\lambda_{max} = 590$ nm, $\epsilon = 1.6 \times 10^5$) and the corresponding molybdate complex ($\lambda_{max} = 590$ nm) are of similar character (Fig. 1). The light-absorption appears to be due to the dye. Both the α- and the β-forms behave similarly.

An attempt to eliminate any influence of the dye and its molybdate by masking the molybdate with oxalic acid and washing the extract with nitric acid was unsuccessful.

When nitric acid is used instead of sulphuric, the dye is extracted into the organic phase over a broad

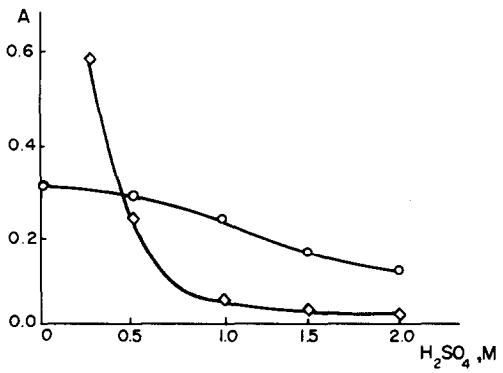


Fig. 2. Dependence of absorbance of toluene–acetone solutions of chromopyrazole II molybdate and chromopyrazole II molybdosilicate on acidity of the medium.

acidity range (from pH 1 to 0.5*M* nitric acid) with all the solvents and their mixtures mentioned above.

The films formed by α-molybdosilicic acid or molybdate are soluble in acetone, ethanol and ether, but the last is inconvenient because of its high volatility. In further work acetone was used.

To increase the sensitivity for silicon, it seemed reasonable to use the flotation phenomenon for concentrating the molybdosilicic acid–chromopyrazole II compound because concentration occurs from practically any volume. The mixture of acetone and toluene was used as the organic phase since it provides the fastest phase separation (10–15 sec).

As shown in Fig. 2, the complex of molybdate with chromopyrazole II is practically not extracted if the acidity exceeds 1.2*M*. The molybdosilicic acid complex, however, undergoes complete flotation over a broad range of acidity (pH 5.50–2*M*) and the dyestuff itself is practically not extracted under these conditions (A_{blank} = 0.03–0.05).

In determination of very small amounts of silicon particular attention should be paid to the blank. During the period required for formation of the β-form at pH 1.5–2.0, a detectable amount of silica passes into solution from the glass (about 3 μg/l., which exceeds the sensitivity of the determination). Once the acidity has been increased, however, dissolution of the glass can be neglected, since formation of the heteropoly acid in 1.5*M* sulphuric acid does not occur. Hence the preparation and storage of the heteropoly acid should be carried out in polyethylene or Teflon vessels, but the final stages can be accomplished in glass vessels.

Compounds of molybdosilicic acid with chromopyrazole II were isolated as solids from the aqueous and organic phases and were analysed for carbon and hydrogen (Table 1). The results show that a compound with molybdosilic acid:chromopyrazole II = 1:2 is formed in 1.5*M* sulphuric acid. On flotation and subsequent dissolution in acetone, the composition remains the same. The ratio of the molar absorptivities of chromopyrazole II and the complex is close to 1:2, which confirms the composition determined. However, the composition of the complex depends on the condition of formation. The methods of equilibrium shift and isomolar series have shown that it is a 1:4 compound that is extracted into the organic phase. This dependence of the composition on the conditions of formation is substantiated by the change in composition with acidity of the medium (Fig. 2). This agrees with the data on the successive protonation of antypyrine dyes with increase in acidity[15] as well as with the data on the composition (1:3) of the complex isolated from 1*M* sulphuric acid.[12]

The infrared spectra of chromopyrazole II and the complexes were recorded (in liquid paraffin and sodium bromide tablets) over the range 400–4000 cm^{-1}. The presence of absorption bands at 930 and 965 cm^{-1} in the spectrum of the molybdosilicic acid complex shows that the heteropolyanion structure is retained in the process of complex formation and that there is no co-ordination of molybdenum to nitrogen. The band at 1540 cm^{-1} (Mo=O stretching vibrations) does not shift to lower frequencies, thus pointing to the absence of any donor–acceptor interaction of the carbonyl group. This is typical of the formation of heteropoly acid complexes with compounds of diantirylpyrylmethane type.[16] The infrared spectrum also demonstrates the absence of hydrogen bonds in the complex, and hence the hydroxyl group is not protonated. The infrared spectroscopy data show that it is an ion-association compound that is formed.

Table 1. Elemental analysis of molybdosilicate–chromopyrazole II complexes isolated from the aqueous (I) and organic phase (II)

	Element	Calculated, % for ML_1	for ML_2	for ML_3	Found, %
I	C	31.58	39.47	45.11	31.6 ± 1.25*
	H	2.76	3.40	3.85	3.1 ± 0.11*
II	C	31.58	39.47	45.11	32.77 32.49
	H	2.76	3.40	3.85	3.24 3.26

* Average values from 6 analyses, calculated by least-squares, are given.

Table 2. The results of silica determination in demineralized and in doubly distilled water

Sample	Volume, *ml*	SiO_2, μg/l.	*n*	*S*, μg/l.	$t_{0.95}S/n$	S_{rel}, %
Water No. 1	70	20	6	1.5	1.6	7
Water No. 2	70	2	5	0.3	0.3	11
Water twice distilled	35	26	6	1.2	1.3	8

The proposed method has the same detection limit as the most sensitive one by Sonnenschein,[17] and can be made lower still by increasing the size of sample, because the completeness of flotation does not depend on the phase-volume ratio, and the concentration can be effected from practically any volume. The cell path-length can also be increased. In this way determination at silica levels below 2 μg/l. becomes possible. Some results for water analysis are given in Table 2.

REFERENCES

1. A. K. Babko and E. M. Ivashkovich, *Zh. Analit. Khim.*, 1972, **27**, 120.
2. A. Golkowska and L. Pszonicki, *Talanta*, 1973, **20**, 749.
3. Yu. F. Shkaravskii and E. M. Ivashkovich, *Ukrain. Khim. Zh.*, 1969, **35**, 961.
4. G. F. Kirkbright, R. Narayaswamy and T. S. West, *Anal. Chem.*, 1971, **43**, 1434.
5. L. I. Ganago and A. N. Prostak, *Dokl. Akad. Nauk Belorus. SSR*, 1969, **13**, 345.
6. A. K. Babko, Z. I. Chalaya and V. F. Mikitchenko, *Zavodsk. Lab.*, 1966, **32**, 270.
7. A. K. Babko, Yu. F. Shkaravskii and V. I. Kulik, *Zh. Analit. Khim.*, 1966, **21**, 196.
8. A. K. Babko, Yu. F. Shkaravskii and A. Golkowska, *Chem. Anal. Warsaw*, 1966, **11**, 1091.
9. V. P. Zhivopiszev, E. G. Bondareva and N. A. Polyakova, *Uchenye Zapiski Permsk. Univ.*, 1973, No. 289, 217.
10. V. A. Istomina, in *Application of Pyrazolone Derivatives in Analytical Chemistry*, p. 127. Perm, Permskii University, 1977.
11. V. P. Zhivopiszev and T. B. Cherepanova, *Zh. Analit. Khim.*, 1977, **32**, 977.
12. E. G. Bondareva and L. V. Portnaya, in *Application of Pyrazolone Derivatives in Analytical Chemistry*, p. 116. Perm, Permskii University, 1977.
13. E. G. Bondareva and N. A. Gaidukova, in *Application of Pyrazolone Derivatives in Analytical Chemistry*, p. 92. Perm, Permskii University, 1977.
14. Z. F. Shakhova, E. N. Dorokhova and E. I. Mironzeva, *Zh. Neorgan. Khim.*, 1968, **13**, 2743.
15. V. P. Zhivopiszev and M. N. Chelnokova, *Zh. Analit. Khim.*, 1963, **18**, 148.
16. V. P. Zhivopiszev and V. A. Istomina, *Uchenye Zapiski Permsk. Univ.*, 1973, No. 289, 232.
17. W. Sonnenschein, *Z. Anal. Chem.*, 1959, **18**, 168.

Talanta Vol. 28, pp. 11 to 18
Pergamon Press Ltd 1981. Printed in Great Britain

LAMINAR DISPERSION IN FLOW-INJECTION ANALYSIS*

JOSEPH T. VANDERSLICE, KENT K. STEWART, A. GREGORY ROSENFELD and DARLA J. HIGGS

Nutrient Composition Laboratory, Nutrition Institute, Human Nutrition Center, Science and Education Administration, United States Department of Agriculture, Beltsville, MD 20705, U.S.A.

(*Received* 6 *May* 1980. *Accepted* 15 *July* 1980)

Summary—Simple expressions are given for the dispersion and the travel times of samples in simple flow-injection analysis systems. The sum of these two quantities is the total residence time of the sample in the system. The expressions are based on numerical solutions of the diffusion–convection equation. Preliminary experiments are in agreement with the derived simple expressions, as are peak curve shapes. Diffusion coefficients can be obtained in a straightforward manner.

Flow-injection analysis (FIA), introduced in 1974,[1–4] is already in widespread use around the globe. The reasons for its success are many;[5] proponents cite its accuracy, reliability, and reproducibility as well as its ease of automation and sample throughput. The absence of air segmentation, as in its counterpart, continuous flow analysis,[6] results in a relatively simple apparatus that can be assembled from already existing and available components and is an ideal system for short sample thoughput times.

It is obvious that guidelines for the design of FIA systems, particularly with respect to sample travel times (initial appearance time at detector), sample dispersion and total residence time, would be invaluable to experimentalists. Such guidelines have been proposed by Růžička and Hansen[7] on the basis of Taylor's solution of the diffusion–convection equation.[8] Useful as these guidelines are, they do not provide analytical expressions based on theory for the appearance times or dispersion in those regions where most experiments are performed.

The theoretical situation is best described by reference to Fig. 1, where a simple diagrammatic representation of the flow of a sample in an FIA system is shown. In an ideal system, a bolus (1a) is injected into the flowing stream; this bolus takes on different shapes as it progresses downstream depending on the parameters of the system. Very early in its progress, the shape is controlled predominantly by convection (1b) but in the later stages by diffusion (1d); in between, both convection and diffusion are significant (1c). Taylor[8,9] supplied solutions for situations (1b) and (1d). However, as will be seen later, the most practical region for FIA systems is that of (1c) where Taylor's solutions, on which previous FIA guidelines depend, are not applicable. Thus, it is not surprising when experiments designed to test the theory often give contradictory results. For example, studies of the dispersion in a typical FIA system give the results shown in Fig. 2.† The volume dispersion‡, $V_{1/2}$, increases rapidly with flow-rate but quickly levels off as the flow-rate is increased above 0.6 ml/min. Such results cannot be explained by Taylor's equations, which predict a steadily increasing dispersion when flow-rate is increased.[7] Incidentally, an interesting view of dispersion is obtained by considering the time dispersion $T_{1/2}$. This is equivalent to volume dispersion ($T_{1/2} = V_{1/2}/q$ where q is the flow-rate) and yields the curve also shown in Fig. 2. From an experimental view, it is often convenient to consider time dispersion rather than volume dispersion; both are directly related to the theoretical results presented in this paper.

Extensive numerical methods for solution of the diffusion–convection equation have been given by Ananthakrishnan *et al.*[10] and Bate *et al.*[11,12] In the present work their numerical methods have been used extensively to obtain results in the regions of interest in FIA. From these results, it is possible to obtain analytical expressions for the initial appearance of a peak at the detector (travel time, t_A) and the total time of observation of the peak (*i.e.*, baseline to baseline, Δt_B). Both t_A and Δt_B can be represented by relatively simple analytical expressions which give their dependence on experimental parameters.

* A preliminary report of this paper was presented by J. T. Vanderslice, K. K. Stewart and A. G. Rosenfeld at the 1980 Pittsburgh Conference on Analytical Chemistry and Applied Spectroscopy, 10–14 March 1980. Abstract Number 090.

† A preliminary report of these data was presented by K. K. Stewart and C. W. Hendrix at the 29th Pittsburgh Conference, 27 February–3 March 1978, Abstract No. 511.

‡ This is a measure of the dispersion of the injected bolus during its pasage through the capillary. If the concentration of the injected species at the observation point is plotted against the volume of fluid pumped through the system, $V_{1/2}$ is the width of the peak at half-height.

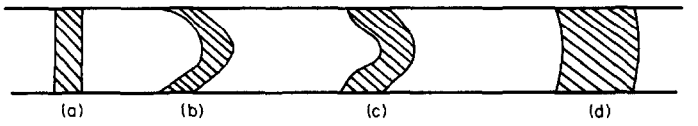


Fig. 1. Shapes of an injected bolus under different conditions: (a) zero time, (b) convection-controlled region, (c) diffusion–convection region, (d) diffusion-controlled. Bolus shapes based on calculations described in this paper.

PREVIOUS NUMERICAL RESULTS

The diffusion–convection equation which controls dispersion in a cylindrical tube is given by:

$$D\left(\frac{\partial^2 C}{\partial x^2}+\frac{\partial^2 C}{\partial r^2}+\frac{1}{r}\frac{\partial C}{\partial r}\right)=\frac{\partial C}{\partial t}+u_0\left(1-\frac{r^2}{a^2}\right)\frac{\partial C}{\partial x} \quad (1)$$

where D is the molecular diffusion coefficient, C is the concentration, x is the distance along the tube, r is the radial distance from the tube axis, a is the radius, t is the time, and u_0 is the maximum velocity at the centre of the tube. This equation is to be solved subject to the boundary conditions

$$\begin{aligned} C(0, x, r) &= 0; \quad x > 0 \\ C(t, 0, r) &= 1; \quad t \geq 0 \\ C(t, \infty, r) &= 0 \\ \frac{\partial C}{\partial r}(t, x, 0) &= \frac{\partial C}{\partial r}(t, x, a) = 0 \end{aligned} \quad (2)$$

These boundary conditions are consistent with the initial conditions shown in Fig. 3a. From the solutions of equation (1), the required solutions for cases where the initial conditions are those of a bolus are

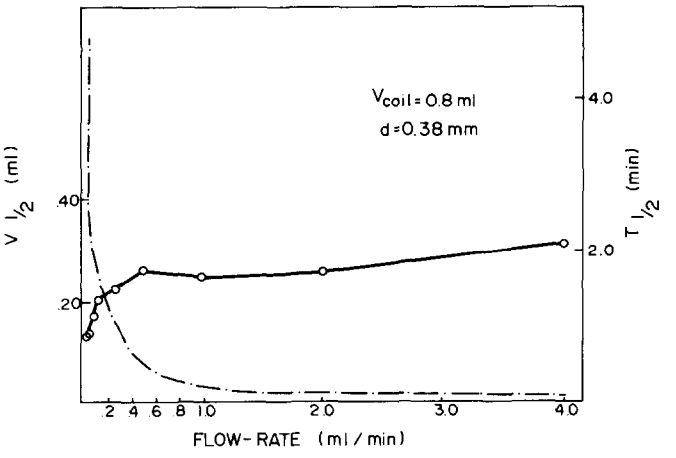


Fig. 2. Measurement of dispersion in an FIA system: volume dispersion $V_{1/2}$ *vs.* flow-rate; time dispersion $T_{1/2}$ *vs.* flow-rate . In this particular case, widths at half-height have been taken as a measure of dispersion. The broken line is the $T_{1/2}$ curve.

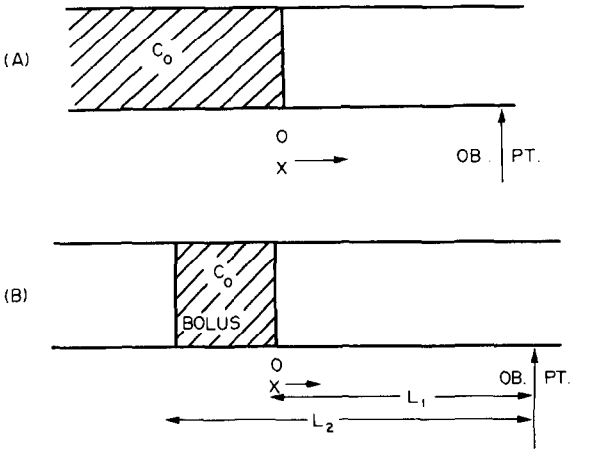


Fig. 3. Upper diagram corresponds to boundary conditions of equation (2); lower to a bolus. L_1 and L_2 are the distances from the leading and trailing edges, respectively, to the detector.

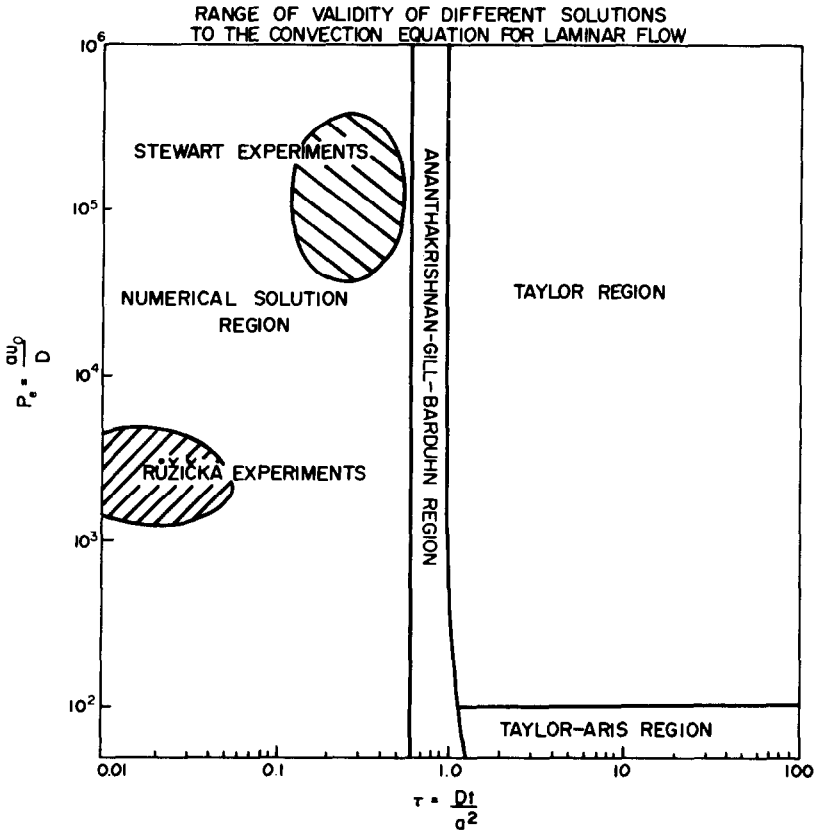


Fig. 4. Valid solutions of the diffusion–convection equation as a function of Peclet Number, P_e, and reduced time, τ. Normal experimental regions for FIA systems are also indicated. The Taylor–Aris region includes the Taylor region while the Ananthakrishnan–Gill–Barduhn region includes all the analytical regions.

simply the differences between the solutions for the leading and trailing edges (Fig. 3b), as shown by Bate *et al.*[12]

Both Ananthakrishnan *et al.* and Bate *et al.* introduced reduced units which make the system of equations dimensionless. Those given by the former have been chosen, and those of interest are

$$P_e = \frac{au_0}{D}; \quad X = \frac{Dx}{a^2u_0}; \quad \tau = \frac{Dt}{a^2} \qquad (3)$$

where P_e is the Peclet number, X is the reduced distance along the tube and τ is the corresponding reduced time. Ananthakrishnan *et al.* have investigated the regions of validity of various analytical solutions of equation (1) as a function of P_e and τ; the graphical summary is shown in Fig. 4. Of critical interest is the fact that the experiments of Stewart and of Růžička have normally been performed in regions where only the numerical solutions of the diffusion–convection equation are valid, as is illustrated in Fig. 4. In regions of experimental interest, *i.e.*, $P_e \geqslant 1000$, $0.002 \leqslant \tau \leqslant 0.8$, axial molecular diffusion effects are relatively small but radial diffusion becomes more important as τ increases; the curve for concentration *vs.* τ finally approximates to an error function curve at $\tau > 0.8$.[11]

NUMERICAL RESULTS AND ANALYTICAL EXPRESSIONS

The intent of this work was to determine whether analytical expressions for the travel times, t_A or τ_A, and the dispersion of a bolus as a function of the parameters of the system could be obtained from the numerical solutions of the diffusion–convection equation in the regions of interest. The baseline to baseline time, Δt_B or $\Delta\tau_B$, was taken as a measure of dispersion.

The method of solution of equation (1) chosen was that given by Ananthakrishnan *et al.*[10] It is a finite difference method wherein an alternating direction implicit procedure is used, which is fully described in their paper. Solutions were generated for the average concentrations as a function of X and τ for the regions from $0.004 \leqslant X \leqslant 1.0$ and for $0.01 \leqslant \tau \leqslant 1.0$.

Solutions for the bolus injection (Fig. 3b) were then obtained from the results by calculating the difference between the solutions for the leading and trailing edges of the bolus[12] as a function of time. In this manner, curves of concentration *vs.* τ_A were generated for a given X_1 and X_2, where $X_1 = DL_1/a^2u_0$ and $X_2 = DL_2/a^2u_0$. Bolus size was varied by making $X_2 > X_1$ by 5, 10, 15, and 20%.

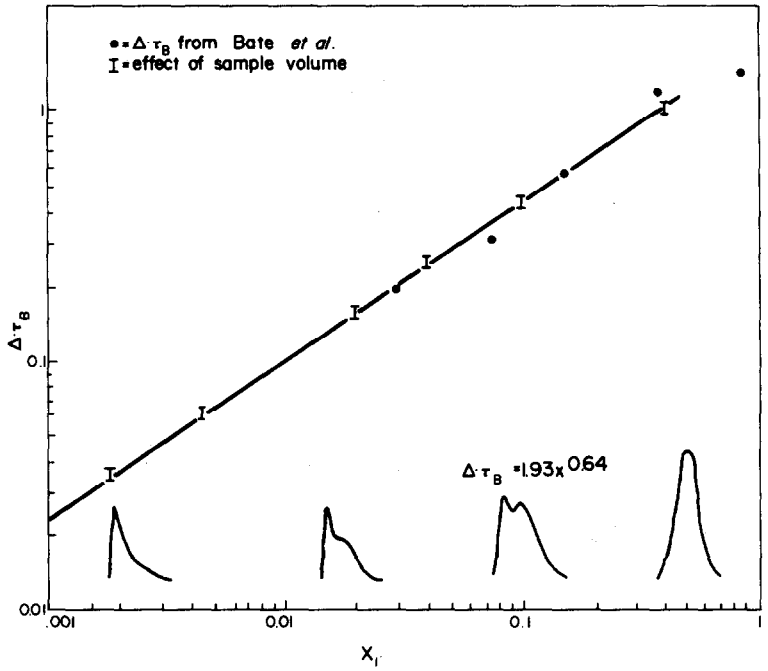


Fig. 5. Baseline to baseline time dispersion *vs.* distance in reduced units. Theoretical curve shapes as a function of X_1 are illustrated. The error bars represent differences due to changes of sample size from 5 to 20% of the total volume of the system. $\Delta\tau_B$ values from Bate *et al.*[11] are also shown together with typical curve shapes for different values of X_1.

The calculations were performed on either the IBM 370 located at the National Institute of Health, Bethesda, MD, USA or on the Zerox Sigma-7 at the Freas-Rooke Computer Center, Bucknell University, Lewisburg, PA, USA. Concentrations as a function of τ, X and P_e from equation (1) were stored on tape, then recalled to obtain the differences required for the solution for the bolus injection. Average concentrations for given values of X_1 and X_2 as a function of τ and P_e were calculated by a five-step numerical formula given by Bickley.[13] An investigation into the convergence and stability conditions for the numerical integration method has been made and will be reported elsewhere.[14]

In the region of interest, $P_e > 1000$, the concentration values were practically independent of P_e, which considerably reduced the labour involved. From the plots of concentrations *vs.* X_1 and X_2, obtained with software supported by the NIH facility, τ_A and $\Delta\tau_B$ were read and tabulated by hand.

Fortunately, the results for τ_A can be summarized in a simple expression. A plot of log τ_A *vs.* log X_1 yields a straight line with no deviations except for the uncertainty of graphical interpretation (estimated to be less than 4%). There is no dependence on sample size and τ_A can be represented by

$$\tau_A = 1.03\, X_1^{1.025}; \quad 0.002 \leqslant X_1 \leqslant 0.8 \qquad (4)$$

It is of interest that τ_A/X_1 $(=u_0 t/L_1)$ is close to unity in the region covered by the calculations. This could only happen if axial diffusion were relatively unimportant.

For the baseline to baseline values, $\Delta\tau_B$, the resulting graph and equation are also simple. Figure 5 is a plot of log $\Delta\tau_B$ *vs.* log X_1 which represents the numerical results for sample sizes from 5 to 20% of the total volume of the system. The variation with sample size is indicated by the vertical bars. The pertinent equation is

$$\Delta\tau_B = 1.93\, X_1^{0.64}; \quad 0.002 \leqslant X_1 \leqslant 0.8 \qquad (5)$$

It is very surprising to find that $\Delta\tau_B$ is relatively insensitive to sample size. Also shown are $\Delta\tau_B$ values extracted from the published curves of Bate *et al.*;[13] the agreement is excellent.

Another point of interest is the shape of the predicted curves as a function of X_1. Even though these are more sensitive to sample size than $\Delta\tau_B$, the general trend is the same, namely, for small X_1, curves resembling those for the convection region are indicated, while at large X_1, curves with normal "Taylor" shapes are seen. In between, the calculations indicate double-peaked curves as shown. These are reasonably similar to the curves calculated by Bate *et al.*[12]

COMPARISON WITH EXPERIMENTAL RESULTS

For comparison with experimental data, it is often easier to convert equations (4) and (5) from reduced units into expressions involving time, lengths, and flow-rate. They become

$$t_A = 109\, a^2 D^{0.025} \left(\frac{L}{q}\right)^{1.025} \qquad (6a)$$

$$\Delta t_B = \frac{35.4\, a^2}{D^{0.36}} \left(\frac{L}{q}\right)^{0.64} \qquad (6b)$$

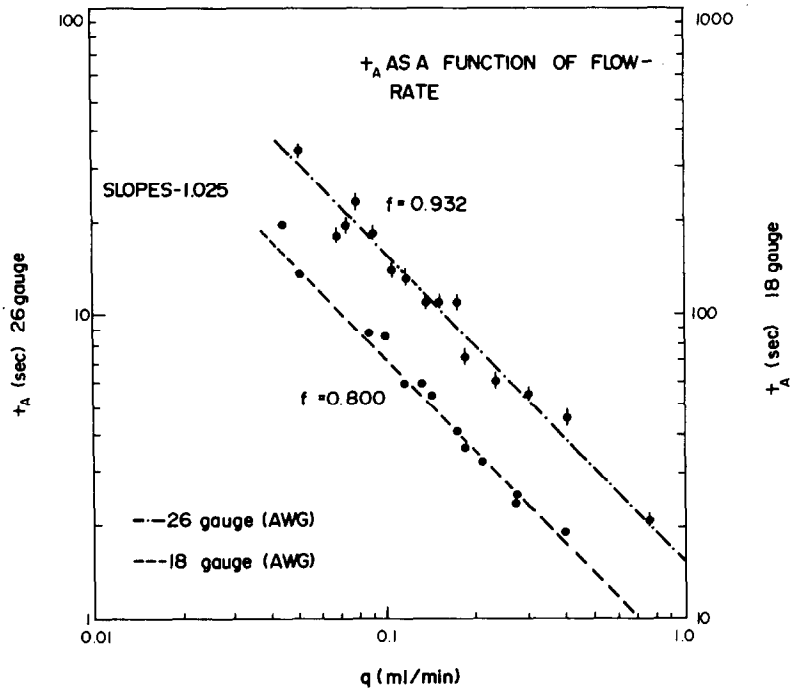


Fig. 6. Theoretical and experimental results for t_A. The slope of -1.025 is the theoretical one. The f factors were obtained from the intercept at $q = 0.1$ with the approximate value of $D = 2.5 \times 10^{-6}$ cm^2/sec.

where the units are as follows: t_A and Δt_B in seconds; L in cm; q in ml/min; D in cm^2/sec.

These expressions do not take into account the dependence of t_A and Δt_B on either concentration or detector sensitivity. As a first approximation, however, it was noted from the theoretical curves that as the initial concentration of the bolus (or sensitivity of the instrument) was varied, Δt_B was proportional to a factor f, and t_A varied in proportion to its reciprocal, $1/f$; f can be expected to vary under experimental conditions from 0.5 to 1.0. Thus the modified equations become

$$t_A = \frac{109\, a^2 D^{0.025}}{f}\left(\frac{L}{q}\right)^{1.025} \qquad (6'a)$$

$$\Delta t_B = \frac{35.4\, a^2 f}{D^{0.36}}\left(\frac{L}{q}\right)^{0.64} \qquad (6'b)$$

Equation (6'a) predicts that, for a given length of tubing, t_A would vary according to $q^{-1.025}$, and equation (6'b) predicts that Δt_B is proportional to $q^{-0.64}$. Thus, log–log plots of t_A and Δt_B *vs.* q should yield straight lines with slopes of -1.025 and -0.64 respectively. Such experiments* have been performed with a simple apparatus constructed from a Harvard syringe pump, an LDC (model CSV) injection valve, AWG 18 or 26 gauge "Teflon" tubing (*i.e.*, 1·07 and 0·46 mm bore respectively), and an Aminco fluoromonitor detector, with a Corning 7-60 excitation and a Wratten 2A emission filter. The flowing stream was water and the sample injected was 2 μl of a 10-μg/ml fluorescein sodium solution. The results, shown in Figs. 6 and 7, indicate agreement with theory within experimental error. Equation (6b) also indicates that the diffusion coefficient can be determined from the intercept if a, L, and f are known. The f factor can be determined from the t_A intercept if a, L and an approximate value of D are known. In fact, this intercept is quite insensitive to changes in D so no more than one iteration is necessary if an incorrect value of D is first chosen. Values for f are shown in Fig. 6. The results for D, shown in Fig. 7, are in remarkably good agreement for the experiments with the different tubings even though the radii are only known to $\pm 10\%$. The average value of 2.48×10^{-6} cm^2/sec can be compared with the value of 3.67×10^{-6} cm^2/sec obtained with an entirely different procedure and under different experimental conditions.[15]

Of the different types of peak shapes shown in Fig. 5, those of particular interest are in the intermediate ranges of X_1 and exhibit double humps. These have rarely been reported in the literature. In fact, it was hard to generate curves of this shape until the reciprocating pump was replaced by a syringe pump. Apparently, the slightest pulsation or turbulence caused by either a reciprocating pump or a mismatched fitting is sufficient to smooth out the double

* Mention of trademark or proprietary product does not constitute a guarantee or warranty of the product by the U.S. Department of Agriculture, and does not imply its approval to the exclusion of other products that may also be suitable.

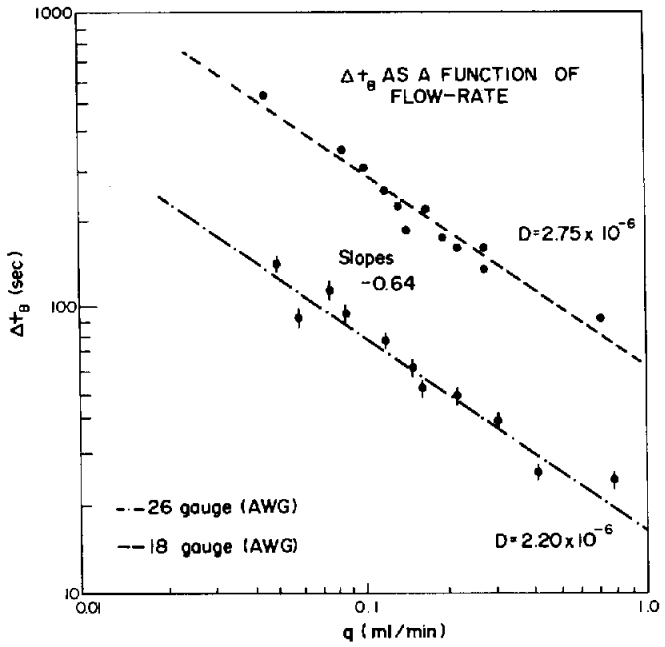


Fig. 7. Theoretical and experimental results for Δt_B. The slope of -0.64 is the theoretical one. Diffusion coefficients were obtained from the intercept at $q = 0.1$.

hump. Typical results with a syringe pump are shown in Figs. 8 and 9. The agreement is considered remarkably good in view of the non-ideality of the system, including the fact that the sample loop and detector cell radii differed from the tubing radii (0·045 and 1 mm respectively), the detector was of finite size, and there were several connectors in the line. In addition, the detector damping was of the order of 2 sec ($\tau = 9 \times 10^{-3}$).

CONCLUSION

The relatively simple equations (6) and (6') obtained for the travel time of a sample after injection and for

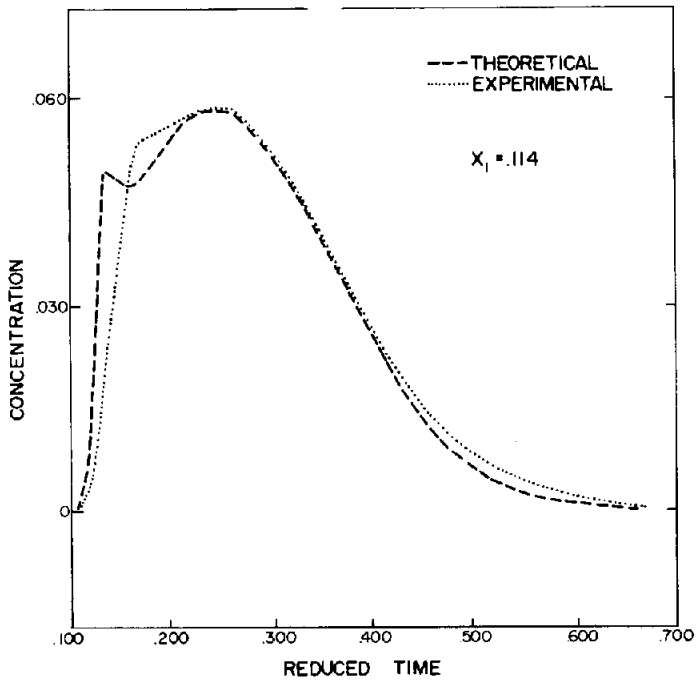


Fig. 8. Experimental vs. theoretical curve shape for $X_1 = 0.114$. Experiments performed in AWG 26 gauge tubing with a length of 30 cm.

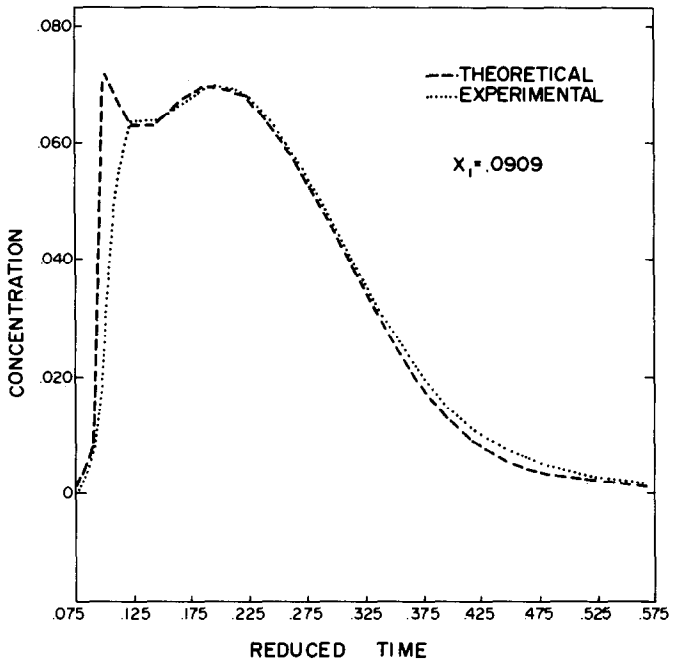


Fig. 9. Experimental *vs.* theoretical curve shape for $X_1 = 0.0909$. Experiments performed in AWG 26 gauge tubing with a length of 30 cm.

the baseline to baseline dispersion in time are obtained from numerical solutions of the laminar flow equation including convection and diffusion in the region of experimental interest for flow-injection analysis. These equations agree with preliminary experiments in FIA systems. Such expressions, together with calculations on curve shape, should be useful to experimentalists who wish to design FIA systems.

The equations are rather explicit in terms of the experimental parameters and yield the following guidelines for simple FIA systems.

(1) The reduced travel time, τ_A, will be approximately equal to the reduced distance, X_1.

(2) The dispersion in time is proportional to the square of the radius and to $(L/q)^{0.64}$.

(3) The larger the diffusion coefficient, the smaller the dispersion.

(4) The volume dispersion (baseline to baseline), $\Delta V_B = q\Delta t_B$, is given by the expression:

$$\Delta V_B = 35.4\, a^2 f (L)^{0.64} \left(\frac{q}{D}\right)^{0.36}$$

(5) The dispersion depends only on the experimentally defined or determined parameters, D, a, L, q and f.

(6) Peak shapes for systems with X_1 greater than 0.3 will be almost symmetrical; for $0.004 \leqslant X_1 \leqslant 0.3$, double-humped peaks should appear. Hence, it is desirable to have a slight amount of pulsation or turbulence in the system if automatic integrators are being used.

(7) When the sample volume is less than 20% of the total volume of the system, there is little effect on the dispersion.

In addition to furnishing guidelines for FIA experiments, the expressions given here, when combined with FIA techniques, offer the possibility of determining diffusion coefficients for molecules of biological interest by a relatively simple method compared to the sophisticated methods now employed.[16] Further work is now in progress to extend this approach to more complicated FIA analyses.

Acknowledgement—This work was supported in part by an Interagency Reimbursable Agreement No. 2Y01-HB60041-05 from the National Heart Lung and Blood Institute, NIH.

REFERENCES

1. J. Růžička and E. H. Hansen, *Anal. Chim. Acta*, 1975, **78**, 17; *Danish Patent Application* No. 4846/84, Sept. 1974; *U.S. Patent* 4,022,575.
2. K. K. Stewart, G. R. Beecher and P. E. Hare, *Fed. Proc.*, 1974, **33**, 1439; *U.S. Patent* 4,013,413.
3. G. R. Beecher, K. K. Stewart and P. E. Hare, 168th Meeting ACS, Div. Agric and Food Chem., Symp. on Chemical and Biological Methods for Protein Quality Determination, Paper No. 22, 1974.
4. K. K. Stewart, G. R. Beecher and P. E. Hare, *Anal. Biochem.*, 1976, **70**, 167.
5. D. Betteridge, *Anal. Chem.*, 1978, **50**, 832A.
6. L. Snyder, J. Levine, R. Stoy and A. Conetta, *ibid.*, 1976, **48**, 942A.
7. J. Růžička and E. H. Hansen, *Anal. Chim. Acta*, 1978, **99**, 37.
8. G. Taylor, *Proc. Roy. Soc. A.*, 1953, **219**, 186.
9. *Idem*, *ibid.*, 1954, **225**, 473.
10. V. Ananthakrishnan, W. N. Gill and A. J. Barduhn, *A. I. Ch. E. J.*, 1965, **11**, 1063.
11. H. Bate, S. Rowlands, J. A. Sirs and H. W. Thomas, *Brit. J. Appl. Phys.* (*J. Phys. D.*), 1969, **2**, 1447.

12. H. Bate, S. Rowlands, and J. A. Sirs, *J. Appl. Physiol.*, 1973, **34**, 866.
13. W. G. Bickley, *Mathematical Gazette*, 1939, **XXIII**, No. 256.
14. J. T. Vanderslice and A. G. Rosenfeld, to be published.
15. K. C. Hodges and V. K. LaMer, *J. Am. Chem. Soc.*, 1948, **70**, 722.
16. H. K. Schackman, in *Methods of Enzymology*, S. P. Colowick and N. O. Kaplan (eds.), 1957, Vol. IV, p. 71.

Talanta Vol. 28, pp. 19 to 23
© Pergamon Press Ltd 1981. Printed in Great Britain
0039-9140/81/0101-0019$02.00/0

DETERMINATION OF TRACES OF CARBON, NITROGEN AND OXYGEN IN MOLYBDENUM AND TUNGSTEN

C. VANDECASTEELE and K. STRIJCKMANS

Institute of Nuclear Sciences, Rijksuniversiteit Gent, Proeftuinstraat 86, B-9000 Gent, Belgium

CH. ENGELMANN

CEN Saclay, B.P. No. 2, F-91190 Gif-sur-Yvette, France

and

H. M. ORTNER

Metallwerk Plansee A.G., A-6600 Reutte, Austria

(*Received* 26 *June* 1980. *Accepted* 14 *July* 1980)

Summary—The determination of carbon and nitrogen in molybdenum and of carbon, nitrogen and oxygen in tungsten, is described. The analytical techniques applied were charged-particle activation (carbon, nitrogen and oxygen), photon activation (carbon and oxygen), combustion (carbon) and vacuum-fusion extraction (nitrogen and oxygen). Chemical methods yielded upper limits in the 2–5 μg/g range. Activation analysis yielded 100 and 8 ng/g for carbon in molybdenum and tungsten respectively, 500 and 74 ng/g for nitrogen in molybdenum and tungsten respectively and 70 ng/g for oxygen in tungsten. The results obtained by charged-particle and photon activation agreed satisfactorily.

In a recent paper,[1] Ortner discussed the influence of traces of carbon, nitrogen and oxygen on the properties of molybdenum and tungsten and the economic importance of the determination of these elements. The work carried out by the working group on non-metals in refractory metals, set up by the Community Bureau of Reference (BCR) and by the refractory metals group of the Chemistry Section of the "Gesellschaft Deutscher Metallhütten und Bergleute" (GDMB) was also summarized. For oxygen in molybdenum different analytical methods agreed satisfactorily and a reference material (BCR No. 23) was certified. For oxygen in tungsten and for carbon and nitrogen in molybdenum and tungsten, it could be concluded only that the concentrations were below 1–10 μg/g and that for chemical methods (fusion-extraction, Kjeldahl method, combustion) several discrepancies occurred. The conclusion was that more development work was required, particularly with highly sensitive activation methods (charged-particle and photon activation). The present paper describes the determination of carbon and nitrogen in molybdenum and tungsten and of oxygen in tungsten by charged particle activation analysis (CPAA) and photon activation analysis (PAA). In each case levels well below 1 μg/g could be determined. Classical methods yielded only upper limits for the concentrations.

Table 1 summarizes the nuclear reactions used and the interfering reactions. The determination of carbon by deuteron activation is free from nuclear interferences if the energy is below 4.9 MeV. The determination of nitrogen and oxygen by proton and helium-3 activation is interfered with by boron, fluorine and sodium.

For the determination of carbon and oxygen by photon activation the maximum photon energy was limited to 25 MeV. Under these conditions the influence of interfering reactions is negligible.

Table 1. Nuclear reactions and nuclear interferences (threshold energies in MeV)

Element	Reaction	Nuclear interference
Carbon	$^{12}C(d,n)\,^{13}N$ (0.3) $^{12}C(\gamma,n)\,^{11}C$ (18.7)	$^{14}N(d,t)\,^{13}N$ (4.9) $^{14}N(\gamma,t)\,^{11}C$ (22.7) $^{16}O(\gamma,\alpha n)\,^{11}C$ (25.9)
Nitrogen	$^{14}N(p,\alpha)\,^{11}C$ (3.1)	$^{11}B(p,n)\,^{11}C$ (3.0)
Oxygen	$^{16}O(^{3}He,p)^{18}F$ (Q > 0) $^{16}O(\gamma,n)\,^{15}O$ (15.7)	$^{19}F(^{3}He,\alpha)\,^{18}F$ (Q > 0) $^{23}Na(^{3}He,2\alpha)\,^{18}F$ (0.4) $^{19}F(\gamma,tn)\,^{15}O$ (27.4) $^{20}Ne(\gamma,\alpha n)\,^{15}O$ (20.4)

Table 2. Irradiation conditions for charged-particle activation

	C		N		O
	Mo	W	Mo	W	W
Particle	d	d	p	p	^{3}He
Energy, *MeV*	5	5	15	15	20
Energy corresponding to the etched depth, *MeV*	2.3–2.7	2.3–2.7	12.5–13.7	13.9–14.1	13.5–14.2
Beam intensity, μA	2	2	1	2	1.5
Irradiation time, *min*	20	20	20	20	20
Beam-intensity monitor foil	Mo, 9.34 mg/cm^2		Cu, 28.16 mg/cm^2		Cu, 28.43 mg/cm^2
Beam-intensity normalization	$^{92}Mo(d,n)^{93m}Tc$		$^{63}Cu(p,n)^{63}Zn$		$^{65}Cu(^{3}He,2n)^{66}Ga$
$t_{1/2}$, *min*	43.0		38.4		560
E_γ, *keV*	390		670		1039

The radionuclides produced are pure β^+-emitters, with half-lives of 2.05 min (^{15}O), 10.0 min (^{13}N), 20.4 min (^{11}C) and 109.7 min (^{18}F).

EXPERIMENTAL

Sample preparation

Molybdenum discs were punched out, at a temperature of about 500°, from sheet material of 1.25 mm thickness, produced by powder metallurgy. The discs were etched with a 4:1 mixture of hydrofluoric and nitric acids, washed with a 1:1 mixture of hydrofluoric and hydrochloric acids and rinsed with water. They were inspected by optical microscopy and found free from cracks. The tungsten samples were prepared similarly. Etching was carried out with a 1:1 mixture of hydrofluoric and nitric acids with subsequent rinsing with water.

Charged-particle activation

Irradiation. Irradiations were carried out with the isochronous cyclotron at Ghent University. Table 2 summarizes the irradiation conditions for the samples. The standards are irradiated for 0.1–2 min at 0.020–0.050 μA beam intensities. The samples and the standards are cylindrical discs 15 mm in diameter and 1–4 mm thick. A thin metal foil is placed in front of the samples and the standards to serve as a beam-intensity monitor.

Chemical etch after irradiation. After irradiation, the samples are chemically etched to remove the activity formed at the surface. For molybdenum the samples are etched in a 4:1 mixture of hydrofluoric (40%) and nitric (14*M*) acids at room temperature, dipped for 20 sec in 12*M* hydrochloric acid, rinsed successively with water and acetone and dried in a hot air stream. This sequence is repeated twice. For tungsten the samples are etched twice in a 1:1 mixture of hydrofluoric (50%) and nitric (14*M*) acids at room temperature, rinsed and dried.

Chemical separation of ^{11}C (determination of nitrogen). The apparatus used was that described by Strijckmans *et al.*[2] The molybdenum and tungsten samples are placed in an alumina combustion tray together with some 0.1-mm copper foil (for Mo), or 1-mm lead foil (for W) (Mo:Cu ratio = 1; W: Pb ratio = 1). A silicon carbide resistance furnace with a maximum working temperature of 1500° is used. The combustion tray is introduced into the furnace under a 0.2 l./min argon flow. The metals are melted for 5 min at 0.1 bar overpressure to avoid reaction with atmospheric oxygen. For 15 min a 0.2 l./min oxygen flow is maintained at an under pressure of *ca.* −0.1 bar, to avoid leakage. The gas flow passes through a condenser, through Schütze reagent (I_2O_5 on silica gel) to oxidize carbon monoxide to carbon dioxide, through two absorption vessels each containing 100 ml of 6*M* nitric acid to trap matrix activity and through two absorption vessels each containing 100 ml of 0.5*M* sodium hydroxide and 1 ml of butanol. The carbon dioxide is trapped in the first sodium hydroxide solution.

Chemical separation of ^{18}F (determination of oxygen). The sample is placed in a nickel crucible containing 10 g of sodium hydroxide, 400 mg of sodium fluoride and 2.5 g of sodium nitrate and heated carefully to dissolve the sample. The melt is cooled and transferred into a beaker. Then 36 ml of water and 30 ml of 14*M* nitric acid (in 3 portions) are added to dissolve the melt. The solution is transferred into a 250-ml distilling flask and 25 ml of 85% phosphoric acid are added. The flask is heated to 130°, and steam introduced, 200 ml of distillate being collected. The pH is adjusted to 5–6 by addition of 14*M* ammonia. Then 10 ml of 1*M* sodium carbonate are added, the mixture is heated to 80°, and 20 ml of 2*M* calcium chloride are added with stirring. The calcium fluoride–calcium carbonate precipitate is filtered off and packed in aluminium foil. The chemical yield is determined by neutron activation[3] and ranges from 59 to 83%.

Measurements. The annihilation radiation is measured with a γ–γ coincidence set-up with two NaI(Tl) detectors in a 180° geometry. The samples (determination of carbon), the calcium fluoride–calcium carbonate precipitate (determination of oxygen) and the standards are placed in a PVC holder, used to centre the samples to ensure complete annihilation. The sodium hydroxide solution, used to trap carbon dioxide (determination of nitrogen) is measured in the

Table 3. Measuring conditions for charged-particle activation analysis (times are given in min)

	C		N		O
	Mo	W	Mo	W	W
Decay time	7–15	11–15	30	30	170–200
Measuring time	4.95	4.95	5	5	29
Period	5	5	6	6	30
Total counting time	50	30–50	60	60	300

absorption vessel and a geometry correction factor is determined to correct for the different detection efficiency for the standard and sample. Repeated measurements of the activity in the samples and the standards are made to obtain the decay curve of the annihilation activity. Table 3 summarizes the measuring conditions. The radiochemical purity is checked by measurements with a Ge(Li) gamma spectrometer. The beam intensity monitors are also measured with this spectrometer.

Analysis of the decay curves. The decay curves were analysed with the CLSQ program.[4] The decay curve for the determination of carbon in molybdenum contained 2 components: ^{13}N and ^{93}Tc ($t_{1/2}$ = 2.73 hr) formed by $^{92}Mo(d,n)^{93}Tc$. The decay curves for carbon in tungsten and those for the determination of nitrogen and oxygen obtained after chemical separation were pure one-component curves. Decay-curve analysis yielded half-lives of 8.5 ± 0.8 min (mean ± standard deviation, 4–6 determinations) and of 10.7 ± 1.8 min for ^{13}N (determination of carbon in molybdenum and tungsten), of 20.3 ± 0.7 min and of 21.0 ± 0.3 min for ^{11}C (determination of nitrogen in molybdenum and tungsten) and of 108.8 ± 15.6 min for ^{18}F (determination of oxygen in tungsten). These values agree satisfactorily with literature data and thus confirm the identity of the radionuclides measured.

Standardization. Graphite, nylon 6 and quartz were used as standards for carbon, nitrogen and oxygen, respectively. The concentrations were calculated as described by Strijckmans *et al.*[2] The "numerical integration method"[5] was applied, using excitation-function data from the literature[6–9] and stopping-power data given by Ziegler *et al.*[10]

Interference of boron with the determination of nitrogen. The $^{14}N(p,\alpha)^{11}C$ reaction is interfered with by the $^{11}B(p,n)^{11}C$ reaction. The boron content was determined by means of the $^{10}B(d,n)^{11}C$ reaction, which is free from nuclear interferences for deuteron energies below 5.9 MeV. Carbon dioxide was separated in the same way as for the determination of nitrogen. Upper limits for boron of 3.7 and 2.2 ng/g were found for molybdenum and tungsten respectively. This corresponds to less than 5.1 and 3.0 ng/g for nitrogen in molybdenum and tungsten.[2]

Choice of the incident energy. The choice of the incident energy is not critical for the determination of nitrogen and oxygen and for carbon in tungsten. It is however very important for the instrumental determination of carbon in molybdenum. Figure 1 gives relative thick-target yields for the $^{92}Mo(d,n)^{93m}Tc$ and $^{100}Mo(d,p)^{101}Mo$ reactions as a function of the energy. These were determined by irradiation of a stack of molybdenum foils with 5-MeV deuterons. For comparison, the thick-target yield for the $^{12}C(d,n)^{13}N$ reaction is also given. The activity produced from molybdenum decreases rapidly with energy. For an incident energy below 3 MeV, the matrix activity is less than 1/500 of that obtained at 5 MeV. An incident energy between 2.3 and 2.7 MeV was chosen.

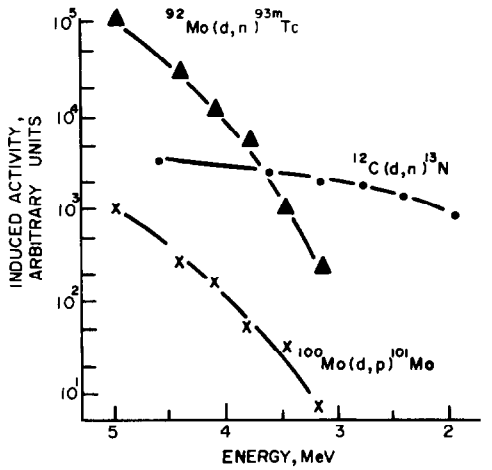


Fig. 1. Relative thick-target yields for the $^{92}Mo(d,n)^{93m}Tc$ (E_γ = 390 keV, $t_{1/2}$ = 43 min) and $^{100}Mo(d,p)^{101}Mo$ (E_γ = 1013 keV, $t_{1/2}$ = 14.6 min) reactions and for the $^{12}C(d,n)^{13}N$ [E_γ = 511 keV (β^+), $t_{1/2}$ = 10.0 min] reaction.

Photon activation

Irradiation and chemical etch. The samples were irradiated with bremsstrahlung photons produced with the linear electron accelerator of the Centre d'Etudes Nucléaires de Saclay. This machine is equipped with a rotating irradiation device connected by a pneumatic transfer system to the laboratory. This device allows irradiation of the samples and the standards under strictly identical conditions, as the standards have the same dimensions as the samples. The irradiation time was 40 and 10 min for the determination of carbon and oxygen, respectively. After the irradiation, the samples are etched in three successive etching baths with the same composition as for charged-particle activation, rinsed and dried.

Chemical separation of ^{11}C (determination of carbon). The chemical separation of ^{11}C is carried out by combustion of the samples (1–2 g) in an oxygen stream (4 l./min) in the presence of 2–4 g of copper oxide and 0.2 g of steel granules (1.2% C). The gases escaping from the reaction mixture are carried by the oxygen stream through (*a*) a furnace containing copper oxide (at 350°) to oxidize carbon monoxide to carbon dioxide, (*b*) a column of Schütze reagent to oxidize the remaining carbon monoxide and (*c*) a trap containing "ascarite" (soda asbestos) to trap the carbon dioxide. The combustion lasts for 3 min and is followed by a 3-min sweep. The apparatus used was identical to that used for the determination of boron, carbon and nitrogen in zirconium by means of deuteron, photon and proton activation respectively.[11,12]

Chemical separation of ^{15}O (determination of oxygen). The chemical separation of ^{15}O is carried out by a reducing fusion in an argon stream (3 l./min). The tungsten samples (3.5 g) are fused in a graphite crucible at 2400° in the presence of nickel (Ni:W ratio = 0.6). The carbon dioxide formed is trapped with "ascarite". The apparatus used is described in detail by Engelmann and Gosset.[13]

Measurements and standardization. The annihilation radiation is measured with two NaI(Tl) detectors in coincidence. Graphite and alumina are used as standards for carbon and oxygen, respectively.

Chemical methods

Carbon analyses were carried out with a LECO CS-144 carbon and sulphur analyser. One-g samples, to which 1.2 g of copper wire was added as accelerator, were burned by high-frequency induction heating at 13.6 MHz. The carbon dioxide evolved was measured by non-dispersive infrared absorption. Mullite crucibles, heated to 1100° for 3 hr and stored in a desiccator, were used.

Nitrogen analyses were carried out with a Balzers Exhalograph EAN-220 nitrogen analyser. Vacuum fusion with a nickel–tin bath (ratio Ni:Sn:sample = 2:1:1) was carried out by resistance heating of a graphite crucible to *ca.* 2300°. Sample weights of 0.5 g were used for molybdenum and 1 g for tungsten.

Oxygen analyses were carried out with a Balzers Exhalograph EAO-201 oxygen analyser, under the same conditions as for the nitrogen analyses. The etching procedure recommended by Quaglia *et al.*[14] was applied before the carbon, nitrogen and oxygen analyses. The molybdenum samples were chemically etched in a 4:1 mixture of hydrofluoric (40%) and nitric (14*M*) acids for 10 sec, washed with hydrochloric acid (12*M*), successively rinsed with water and methanol and dried in a hot air stream (*ca.* 60°).

Table 4. Results (*ng/g*)

	Molybdenum		Tungsten	
	BCR	Plansee	BCR	Plansee
Carbon				
CPAA	72 ± 32* (7)†	97 ± 44 (4)	<15	8.4 ± 2.4 (4)
PAA	130 ± 60 (6)	—	30 ± 30 (6)	—
chemical method	—	⩽3000 (6)	—	⩽3000 (6)
Nitrogen				
CPAA		505 ± 35 (4)	—	74.0 ± 1.2 (4)
chemical method	—	⩽2000 (6)	—	⩽2000 (6)
Oxygen				
CPAA	—	—	66 ± 11 (6)	—
PAA	—	—	74 ± 7 (7)	—
chemical method	—	—	⩽5000 (6)	—

* Standard deviation.
† Number of analyses.

The tungsten samples were chemically etched in a 1:4 mixture of hydrofluoric (40%) and nitric (14*M*) acids for 2 min, successively rinsed with water and methanol and dried. The residual surface content (0.09–0.12 $\mu g/cm^2$ for C, $\leqslant 0.05$ $\mu g/cm^2$ for N and 0.3 ± 0.1 $\mu g/cm^2$ for O) was negligible compared to the blank values from other sources (3–6 μg). Calibration was carried out by gas dosing (CO_2, N_2 or O_2) and analysis of certified reference steels.

RESULTS AND DISCUSSION

Table 4 summarizes the results for molybdenum and tungsten. For each material two series of samples from different production runs, supplied by Metallwerk Plansee A.G., were analysed. One of these was distributed through BCR, the other was obtained directly from Metallwerk Plansee A.G.

Chemical methods yielded upper limits ranging from 2 to 5 $\mu g/g$ for carbon, nitrogen and oxygen. These results are not in contradiction with the relevant activation analysis results (see below) as they were in the case of C in Mo for a GDMB "round-robin" test.[1] This is most likely due to the use of copper as accelerator, whereby pronounced corrosion of the mullite crucible material by the highly acidic MoO_3 melt is reduced by the formation of copper molybdate. The values of $\leqslant 3$ $\mu g/g$ for carbon, $\leqslant 2$ $\mu g/g$ for nitrogen and $\leqslant 5$ $\mu g/g$ for oxygen correspond to the relevant detection limits for the chemical methods as carried out under the conditions described.

The results obtained by charged-particle and photon activation are below 1 $\mu g/g$. The results for oxygen in tungsten are not significantly different at the 90% confidence level. For carbon in molybdenum, photon activation yields significantly higher results, but in view of the low concentrations the difference is acceptable. For carbon in tungsten, both methods indicate very low concentrations, close to the detection limit. At the actual nitrogen concentration found in Mo and W the interference of boron is negligible.

CONCLUSION

The interlaboratory intercomparison between charged-particle activation, photon activation and chemical methods indicates that the first two yield reliable and accurate results for carbon and oxygen in metals even at the 10–100 ng/g level, *i.e.*, for concentrations lower than the detection limit of chemical methods by a factor of 10–1000. To our knowledge this is the first time that a successful interlaboratory and intermethod comparison has been made for such low carbon and oxygen concentrations in metals. From a technical point of view, the oxygen, nitrogen and carbon concentrations found by activation analysis are surprisingly low. It was not thought previously that molybdenum and tungsten with such low concentrations of these elements could be produced by powder metallurgy on an industrial scale, without special precautions. The analysed samples were indeed taken from a normal production of sheet material.

Acknowledgements—Grateful acknowledgement is made to Professor Dr. J. Hoste for the interest shown in this work, to Dr. J. Pauwels (CBNM, Geel, Belgium), for providing some of the samples and to the NFWO and the IIKW for financial support.

REFERENCES

1. H. M. Ortner, *Talanta*, 1979, **26**, 629.
2. K. Strijckmans, C. Vandecasteele and M. Esprit, *Z. Anal. Chem.*, in the press.
3. C. Vandecasteele, F. Adams and J. Hoste, *Anal. Chim. Acta*, 1975, **76**, 27.
4. J. Cumming, in *Applications of Computers to Nuclear and Radiochemistry*, G. O'Kelley (ed.), p. 25. Nucl. Sci. Ser. Rep. NAS-NS 3107, 1963.

5. C. Vandecasteele and K. Strijckmans, *J. Radioanal. Chem.*, 1980, **57**, 121.
6. R. J. Jasczak, R. L. Macklin and J. H. Gibbons, *Phys. Rev.*, 1969, **181**, 1428.
7. K. Wohlleben and E. Schuster, *Radiochim. Acta*, 1967, **8**, 78.
8. W. W. Jacobs, D. Bodansky, D. Chamberlain and D. J. Oberg, *Phys. Rev.*, 1974, **C9**, 2134.
9. C. Vandecasteele, F. Adams and J. Hoste, *Anal. Chim. Acta*, 1974, **71**, 67.
10. J. F. Ziegler, *The Stopping and Ranges of Ions in Matter*, Vol. 3–4, Pergamon, New York, 1977.
11. J. Petit, J. Gosset and Ch. Engelmann, *Mém. Sci. Rev. Métall.*, 1978, **6**, 395.
12. *Idem, J. Radioanal. Chem.*, 1980, **55**, 69.
13. Ch. Engelmann and J. Gosset, *Analysis*, 1978, **6**, 306.
14. L. Quaglia, G. Weber, D. David, J. Van Audenhove and J. Pauwels, *Commission of the European Communities, Eurisotop Rept.* 90, Brussels, 1976.

Talanta Vol. 28, pp. 25 to 30
© Pergamon Press Ltd 1981. Printed in Great Britain
0039-9140/81/0101-0025$02.00/0

THE ANALYSIS OF NICKEL REFINERY SLIMES AND RESIDUES

R. S. YOUNG
Apt. 605, 1178 Beach Drive, Victoria, B.C., Canada

(*Received* 28 *November* 1979. *Revised* 5 *June* 1980. *Accepted* 12 *July* 1980)

Summary—Procedures are outlined for the determination of the 28 elements usually present in the slimes and residues from nickel refineries.

In the refining of nickel, besides the pure metal, an anode slime or sludge is obtained in the electrolytic process and a dry residue from the carbonyl method. Nickel sulphide ores are usually accompanied by small quantities of silver, gold and the platinum metals, which accumulate in the extractive steps and are recovered in the anode slimes and residues. These residues will also contain small amounts of many other substances found in the original ore, and not completely removed from the nickel by the concentrating, smelting, leaching, purification or other metallurgical processes. The varied composition of these slimes and residues, and the frequently high content of precious metals, have made their analysis a lengthy and difficult task. A review of current practices may be useful to many concerned with similar complex metallurgical materials.

The wide range in specific gravity of the constituents of slimes and residues, the frequent presence of metallic phases which are not readily pulverized to pass a 100-mesh sieve, and the monetary value of this material dictate that great care be taken in sample preparation.

Most constituents of slimes and residues can be brought into solution with a conventional combination of acids, followed by fusion of any insoluble residue with carbonate, peroxide or pyrosulphate. It must be remembered that some compounds of the platinum group are nearly insoluble in *aqua regia* and require a peroxide fusion, which is usually done in a zirconium crucible. The volatility of elements such as arsenic, antimony, tin, selenium, tellurium, osmium and ruthenium in certain acids at elevated temperatures must be borne in mind.

Atomic-absorption spectrophotometry (AAS) is used extensively in the analysis of slimes, and Table 1 summarizes the wavelengths, sensitivities and flames used for these determinations. Although the atomization system for these materials in industrial practice is almost always a flame, electrothermal atomization with a graphite rod furnace can be employed.

Aluminium

After removal of the hydrogen sulphide group and precipitation of the "mixed oxide" group with ammonia, electrolysis of the elements of the latter group with a mercury cathode in about 0.3*N* sulphuric acid will leave a solution containing practically only aluminium, which can be determined photometrically with aluminon at 525 nm.[1] In the rare instances when there is enough aluminium for a gravimetric finish to be preferred, traces of titanium, vanadium and zirconium, if present, must be eliminated by a cupferron–chloroform separation.[2]

When aluminium is determined by atomic-absorption, standards and samples should contain about 0.1% potassium or sodium.[3]

Antimony

After distillation of arsenic(III) from hydrochloric acid solution at 108°, antimony can be distilled at 165° and determined photometrically with Rhodamine B at 565 nm,[1,2] or for larger quantities by titration with potassium bromate.[2,4,5]

If antimony is determined by atomic-absorption, the acidity and composition of the standards and unknowns should be roughly similar.[3]

Arsenic

Arsenic(III) can be distilled from hydrochloric acid medium at 108° and determined photometrically by the hydrazine sulphate–ammonium molybdate procedure at 660 or 840 nm.[1,2,6,7] Larger amounts can be titrated with iodine.[2,4,5]

With its resonance line at 193.7 nm, arsenic is obviously not suitable for routine determinations by atomic-absorption. Improved results for this element are given by generation of arsenic hydride by addition of sodium borohydride, and passage of the hydride and hydrogen gas through a flame.

Bismuth

If the hydrogen sulphide group is precipitated and collected, and then treated with a mixture of hydrobromic and sulphuric acids, evaporated to dryness, taken up in dilute hydrochloric acid and treated with sulphur dioxide, bismuth, copper and the platinum metals will be left in solution. Digestion with sodium nitrite at pH 1.5 followed by adjustment to pH 8 with sodium bicarbonate will precipitate bismuth and cop-

Table 1. AAS data for nickel refinery slimes and residues

	Wavelength, *nm*	Sensitivity *μg/ml*	Flame
Aluminium	309.3, 396.2	1	NOA
Antimony	206.8, 217.6, 231.1	1	AA
Arsenic	193.7	poor	All flames absorb strongly
Bismuth	223.1, 306.8	1	AA
Boron	249.7	12	NOA
Calcium	422.7	0.05	AA
Chromium	357.9	0.2	NOA
Cobalt	240.7	0.1	AA
Copper	324.8	0.05	AA
Gold	242.8	0.2	AA
Iridium	208.9	1–8	AA or NOA
Iron	248.3	0.1	AA
Lead	217.0, 283.3	0.2	AA
Magnesium	285.2	0.005	AA
Manganese	279.5	0.03	AA
Nickel	232.0	0.1	AA
Osmium	290.9	1.5	NOA
Palladium	244.8, 247.6, 340.5	2	NOA
Platinum	265.9	10	NOA
Rhodium	343.5	0.5	NOA
Ruthenium	349.9	1	AA
Selenium	196.0	poor	All flames absorb strongly
Silicon	251.6	2	NOA
Silver	328.1	0.05	AA
Tellurium	214.3	0.5	AA
Tin	224.6, 286.3	3–5	NOA
Zinc	213.9	0.01	AA

NOA = Nitrous oxide–acetylene flame.
AA = Air–acetylene flame.

per. Dissolution of the precipitate, followed by treatment with ammonia, after addition of an iron salt, will precipitate bismuth with ferric hydroxide; dissolution of this precipitate in hydrochloric acid and treatment with hydrogen sulphide will isolate bismuth. Final photometric determination by the thiourea method is carried out at 420 nm.[1,2]

When atomic-absorption is employed to determine bismuth, the acidity of standard and test solutions should be roughly similar.[3]

Boron

Boron is often used as a buffering agent in the electrolytic refining of nickel, and small quantities may be found in the anode sludge. It is separated from other elements by volatilization as methyl borate from an acidified solution treated with methanol.[4,5] A photometric measurement using curcumin and measurement at 550 nm is a reliable procedure.[2,8]

Boron can be determined by atomic-absorption, with use of the mean of the lines at 249.7 and 249.8 nm, but the sensitivity is not high.

Calcium

This element, together with magnesium, is usually determined in the filtrate from the aluminium precipitation. Evaporation with nitric acid to remove ammonium salts is followed by dissolution of the residue in a few drops of hydrochloric acid. The determination is completed by addition of a sodium hydroxide–sodium cyanide buffer, Calcon indicator, and titration with standard EDTA solution.[2]

Calcium is readily determined directly by atomic-absorption; addition of lanthanum chloride will overcome the interference of aluminium.[3]

Chromium

In some oxidized nickel ores, the chromium content exceeds that of nickel; small quantities of chromium may therefore be found in the slimes or residues from refining operations. After a hydrogen sulphide separation and treatment of the oxidized filtrate with sodium peroxide, iron and a number of other elements are precipitated, leaving chromium in solution. Final photometric measurement with 1,5-diphenylcarbazide is made at 540 nm.[1,2,9] No element present in nickel refinery slimes or residues will interfere.

Developments in lamp technology in recent years have greatly improved the determination of chromium by atomic-absorption. The addition of 0.1% potassium to standard and test solutions will suppress ionization.[3]

Cobalt

Precipitation of the hydrogen sulphide group, followed by a zinc oxide separation with a reprecipita-

tion, will leave cobalt in the filtrate, where it can be determined gravimetrically with 1-nitroso-2-naphthol[2,4,5] or photometrically with nitroso-R-salt at 520 nm.[1,2,10] If the latter procedure is used, it is preferable to remove nickel first if it is present in more than 25-fold ratio to cobalt. This can be done with dimethylglyoxime, followed by destruction of the organic matter with nitric and sulphuric acids.

Cobalt in slimes and residues can be readily determined by atomic-absorption.

Copper

Copper and a number of other base metals can be separated from the platinum group by digesting the sample with hot sodium nitrite solution at pH 1.5, neutralizing with sodium hydroxide to pH 8, and filtering.[5] Copper and other base metals, with gold, are in the precipitate. Dissolution of this in *aqua regia*, evaporation with hydrochloric acid, and treatment with sulphur dioxide and hydrazine hydrochloride will precipitate selenium, tellurium, silver and gold. Evaporation of the filtrate with hydrobromic–sulphuric acid mixture volatilizes arsenic, antimony and tin. An ammonia separation will remove bismuth and lead along with the hydroxides of iron, aluminium and chromium. Acidification of the filtrate and treatment with hydrogen sulphide will separate copper from nickel and cobalt. The copper is now free from any interference for determination by iodometric titration, electrolysis, or the 2,2′-biquinolyl photometric procedure.[2,4,5,11]

Scarcely any elements interfere in the determination of copper by AAS.[3]

Gold

When base metals are separated from the platinum group by the sodium nitrite method outlined above, gold accompanies them. Treatment with nitric acid dissolves the base metals, leaving gold as a residue.

An alternative is to treat a hydrochloric acid solution of the sample, after removal of silver chloride, with sulphur dioxide and hydrazine hydrochloride to precipitate gold, selenium and tellurium. The latter two can be dissolved in nitric acid, leaving the gold.[2,4,5]

Gold can also be determined by a combination of wet chemistry and fire assay. Heating with sulphuric acid and mercuric sulphate dissolves most base metals, then silver is precipitated as chloride, and the residue containing gold, silver and the platinum metals is transferred to lead foil in a scorifier and carried through the fire assay steps to a gold–silver–platinum metals bead. When the ratio of gold:platinum group:silver is approximately 10:1:33, parting in hot concentrated sulphuric acid dissolves silver, palladium and most of the ruthenium, leaving a residue of gold, platinum, rhodium, iridium and osmium. Dissolution of the residue in *aqua regia* and treatment with sulphur dioxide or oxalic acid in 5% hydrochloric acid will precipitate gold.[2,4,5,12]

Atomic-absorption can be used to determine gold, but the signal from chloride media is considerably suppressed by the presence of iron, nickel and palladium.

Iron

Removal of the hydrogen sulphide group and precipitation of the "mixed oxides" group with ammonia followed by its dissolution will give a solution containing the iron, which can then be reduced and titrated or determined photometrically with 1,10-phenanthroline at 508 nm.[1,2,4,5]

The atomic-absorption signal for iron is remarkably free from chemical interferences, and AAS can be used to determine this element.

Lead

Evaporation of the sample solution with sulphuric acid till fuming, filtration of the residue of lead sulphate, silica, silver chloride, *etc.*, and digestion of this with hot concentrated ammonium acetate solution will dissolve and isolate lead. Evaporation of the lead acetate solution with nitric and sulphuric acids will give a precipitate of lead sulphate.[2] Small amounts of lead can be determined photometrically with dithizone at 520 nm.[1,2]

Lead can easily be determined by AAS with few interferences.

Magnesium

Like calcium, this element is usually determined in the filtrate from the ammonia separation of aluminium, iron, *etc.* The calcium and magnesium are both titrated with EDTA in ammonia–ammonium chloride buffer, with Eriochrome Black T as indicator, and the volume of EDTA needed for the calcium alone is subtracted.

Magnesium has one of the highest sensitivities in AAS determination, and the other constituents of slimes have negligible effect on its absorption signal.

Manganese

After removal of the hydrogen sulphide group, manganese can be precipitated together with aluminium, *etc.* by ammonia if bromine is added first; cobalt, nickel and zinc pass into the filtrate. Dissolution of the precipitate in sulphuric or nitric acid gives a manganese solution free from interferents in the potassium periodate photometric method with measurement at 525 nm.[1,2]

AAS can also be employed for manganese in nickel slimes.[3]

Nickel

For most nickel refinery slimes and residues, the dimethylglyoxime procedure is preferred for determining nickel. Gold and palladium must be removed first by precipitation in the hydrogen sulphide group, whether the nickel is determined gravimetrically or photometrically with dimethylglyoxime at 530 nm.

A few sludges and residues may have a high nickel content, which is best determined by electrolysis in ammoniacal solution. Separation by dimethylglyoxime, evaporation with a mixture of nitric and sulphuric acids to strong fumes of the latter, and addition of a large excess of ammonia will provide a solution ready for the electrolytic determination. For very accurate work, reprecipitation of the nickel dimethylglyoximate is advisable.[2,13–15]

In AAS, nickel is free from interference effects from nearly all foreign ions.

Platinum metals

The frequent occurrence of the platinum metals in nickel sulphide ores makes determination of the platinum group of great importance in the analysis of nickel refinery slimes and residues. A satisfactory procedure for platinum metals in these materials consists of an initial isolation of the platinum group from gold, silver and all base metals, followed by their determination as a combined group in the metallic state. If the individual amounts are required, suitable gravimetric or photometric methods are applied.

Digestion of the sample with *aqua regia*, followed by sintering of any residue with barium peroxide in a porcelain crucible at 800°, addition of hydrochloric acid, removal of barium by sulphuric acid and filtration, will leave the filtrate ready for the sodium nitrite separation of the platinum metals. Addition of sodium carbonate to give pH 8.8, filtration to leave gold and most base metals in the precipitate, addition of hydrochloric acid, and removal of nitrites by addition of formic acid to the boiling solution, is followed by cooling and precipitation of the platinum metals with magnesium. Filtration, ignition at 800°, digestion in 1:9 sulphuric acid, filtration, transfer to an annealing cup placed in a large nickel crucible packed with charcoal, and heating in a muffle will give the total platinum group.

For determination of the individual members, digestion with *aqua regia* and sodium peroxide fusion of any residue will bring all platinum metals into solution. When a slightly acid chloride solution of the platinum metals is distilled with an excess of sodium bromate, only ruthenium and osmium pass over, as the volatile tetroxides. The distillation vapours are first passed through dilute hydrochloric acid to trap the ruthenium tetroxide as ruthenium chloride, and then through alcoholic sodium hydroxide solution to collect the osmium tetroxide as sodium osmate.[12,16] For low ruthenium contents, photometric determination at 675 nm with thiourea in a mixed hydrochloric–sulphuric acid solution is suitable.[17] Higher ruthenium contents are determined by precipitation with sodium bicarbonate and ignition in an atmosphere of hydrogen.[5] Low osmium contents can be determined photometrically at 480 nm with thiourea in hydrochloric acid;[17] higher contents are measured by precipitation with sodium bicarbonate and ignition under hydrogen.

The solution containing platinum, palladium, rhodium and iridium is heated with sodium bromate, and the pH is raised to 8 with sodium bicarbonate to precipitate palladium, rhodium and iridium. Platinum in the filtrate is precipitated with hydrogen sulphide, ignited to the metal, dissolved in *aqua regia*, and precipitated as the metal by formic acid in a hydrochloric acid solution containing sodium acetate.[5] Small amounts of platinum may be determined in hydrochloric acid by the photometric stannous chloride method, with measurement at 403 nm.[17]

The precipitate of palladium, rhodium and iridium is dissolved in hydrochloric acid, and the palladium is precipitated with dimethylglyoxime, filtered off, dried and weighed as the complex.[5] Low contents of palladium may be measured photometrically in 6*M* hydrochloric acid at 470 nm.[17]

The filtrate, containing rhodium and iridium, is evaporated with nitric and sulphuric acids to strong fumes of the latter, cooled, diluted and heated to boiling. Rhodium is precipitated by addition of a solution of titanous chloride, filtered off, dissolved and precipitated again from sulphuric–hydrochloric acid solution with hydrogen sulphide, filtered off and ignited first in air and finally in hydrogen.[5] For very low rhodium content, photometric measurement in 6*M* hydrochloric acid, at 515 nm, can be used.[17]

From the filtrate from the rhodium precipitation with titanous chloride, titanium is removed by cupferron–chloroform extraction. The aqueous layer is evaporated with nitric and sulphuric acids to fumes of the latter, diluted, and adjusted to pH 8 with sodium bicarbonate. Sodium bromate is added, the solution boiled and filtered, and the iridium precipitate ignited in air and finally in hydrogen.[5] Very small amounts of iridium can be measured photometrically (in hydrochloric acid containing a trace of chlorine water) with hydroquinone, at 490 nm.[17]

Determination of the platinum metals by atomic absorption is unfortunately beset with difficulties. Severe depression of the platinum signal occurs in the presence of nearly every element, except gold and zinc, found in nickel sludges. This depression can be minimized by the addition of about 0.5% lanthanum chloride to both test and standard solutions.

Although chemical interferences in the atomic-absorption determination of palladium are fewer than those for other platinum metals, those caused by gold, iridium and rhodium are still severe. The acid concentration (below about 1*M* hydrochloric acid) also affects the signal for palladium. The most sensitive lines, at 247.6 and 244.8 nm, give non-linear responses at concentrations above 50 and 20 μg/ml respectively; the response with the 340.5-nm line is linear up to at least 120 μg/ml.[3]

For atomic-absorption, iridium should be present in the higher oxidation state, usually obtained by the addition of potassium dichromate solution to give a final solution containing about 500 μg of chromium per ml. In both air–acetylene and nitrous oxide–ace-

tylene flames, interference occurs with iron, nickel, palladium, rhodium and zinc.

Osmium can be determined by atomic-absorption, preferably after isolation as the volatile tetroxide.

Ruthenium is subject to many interference effects in atomic-absorption, and is best measured after isolation as the volatile tetroxide.

Rhodium can be determined by atomic-absorption with fewer chemical interferences than most noble metals, but chromium, iridium and nickel produce significant depressions.

Separations of the platinum metals from other elements, and a systematic compilation of separation procedures for each element from every other element, are given in a recent practical handbook.[18]

Selenium

Selenium is nearly always determined in nickel sludges by precipitation with sulphur dioxide from fairly concentrated hydrochloric acid medium. After removal of silver as chloride, and of lead as sulphate, from the solution, passage of sulphur dioxide through a 7–10*M* hydrochloric acid solution of the sample will precipitate selenium and gold. The filtrate can be retained for the tellurium determination, and treatment of the precipitate with nitric acid will dissolve the selenium; gold remains as a residue and can be recovered by filtration. Repetition of evaporation of the filtrate containing selenium and dissolution of the residue with hydrochloric acid, followed by reprecipitation of selenium with sulphur dioxide will yield a pure product for gravimetric determination by collection on a sintered-glass crucible. If the selenium content is very low, it can be determined photometrically with 3,3′-diaminobenzidine at 420 nm.[1,2,19]

At wavelengths shorter than 200 nm all flames absorb strongly; the normal atomic-absorption technique is accordingly not suitable for selenium. Satisfactory results can be obtained by the hydride generation technique mentioned above for arsenic.

Silicon

Although the silicon content of most nickel slimes and residues is low, the gravimetric determination by dehydration with perchloric acid and volatilization of silica with hydrofluoric acid is used in most laboratories, though the photometric molybdenum blue method would be better.[1,2]

Atomic-absorption can also be used.[3,20]

Silver

If a nickel slime or residue contains a fair amount of silver, this can be determined by precipitation as silver chloride, dissolution in ammonia solution and reprecipitation. Very small quantities of silver can be determined with *p*-dimethylaminobenzylidenerhodanine at 495 nm.[1,2]

Small quantities of silver in slimes can also be collected and determined by the combined wet chemistry and fire assay described above for gold. Parting of the bead containing the silver, gold and platinum metals dissolves silver and palladium, and the silver can finally be precipitated as chloride. Palladium has a tendency to be adsorbed by silver chloride, however, and dissolution with ammonia and reprecipitation are advisable.

Atomic-absorption offers a good procedure for silver; the sensitivity is high and interferences are remarkably few.[3,21]

Sulphur

The traditional procedure of oxidation to sulphate and precipitation of barium sulphate from very dilute hydrochloric acid medium, is standard for nickel sludges and residues. The sample is digested with a mixture of potassium bromide and bromine, nitric acid is added, and the solution evaporated to low volume. Hydrochloric acid is added and the solution evaporated to dryness, and silicic acid is dehydrated by repeated moistening with hydrochloric acid and evaporation to dryness each time. Because some platinum metal sulphides are nearly insoluble in *aqua regia*, the residue is fused with sodium peroxide and added to the sample, with further evaporation and dehydration with hydrochloric acid. If the sample contains lead, lead sulphate will be present in the residue. Fusion of the residue with sodium carbonate, dissolution in water, filtration, and addition of this filtrate to the original one will provide a solution containing all the sulphur in the sample, ready for precipitation by barium chloride in about 0.1*M* hydrochloric acid medium. If an appreciable quantity of antimony is present in the slimes, it should be removed by digestion for an hour in warm 2*M* hydrochloric acid with ingot iron filings before adjustment of the acidity and addition of barium chloride.

Tellurium

After the reduction of selenium and gold in concentrated hydrochloric acid by sulphur dioxide, and filtration, dilution to about 1–2*M* acid concentration and the addition of more sulphur dioxide or of hydrazine hydrochloride will precipitate tellurium. Small quantities of tellurium can be determined photometrically, by collection with arsenic after reduction by hypophosphorous acid, complexing with sodium diethyldithiocarbamate in the presence of potassium cyanide, extraction with chloroform and measurement at 415 nm.[1,2]

Atomic-absorption can be used to determine tellurium.[3,22]

Tin

Some nickel refinery sludges and residues contain small quantities of tin, which are usually isolated, after prior distillation of arsenic at 108° and of antimony at 165° from hydrochloric acid medium, by a distillation at 145–160° from a 3:1 mixture of hydrochloric and hydrobromic acids.[2,5] Tin can then be determined by titration with iodine after reduction

with metallic nickel, or more frequently photometrically with dithiol at 530 nm.[2,23] In the dithiol method selenium gives a white turbidity and must first be removed from the distillate with sulphur dioxide.

Atomic-absorption can be employed for tin; except for antimony in large amounts, the elements normally found in nickel slimes do not interfere.[3,24]

Zinc

After dissolution of the sample in *aqua regia*, and sodium peroxide fusion of any residue, the hydrogen sulphide group is precipitated and removed, with reprecipitation if necessary. Adjustment of the filtrate to very low acidity with sulphuric acid, followed by passage of hydrogen sulphide, will precipitate zinc sulphide, which is then dissolved in hydrochloric acid and titrated with potassium ferrocyanide.[2,4,5] For very small quantities of zinc, the photometric dithizone method with measurement at 535 nm is suitable; interferences are eliminated by hydrogen sulphide separation, treatment with ammonia, and addition of potassium cyanide to complex nickel and cobalt before the dithizone extraction.[1,2,25]

Zinc can be readily determined by atomic-absorption; the sensitivity is very high and the interferences are negligible.

REFERENCES

1. E. B. Sandell and H. Onishi, *Photometric Determination of Traces of Metals: General Aspects*, 4th Ed., Wiley, New York, 1978.
2. R. S. Young, *Chemical Analysis in Extractive Metallurgy*, Griffin, London, 1971.
3. K. C. Thompson and R. J. Reynolds, *Atomic Absorption, Fluorescence and Flame Emission Spectroscopy*, 2nd Ed., Griffin, London, 1978.
4. N. H. Furman, ed., *Scott's Standard Methods of Chemical Analysis*, 6th Ed., Vol. 1, Van Nostrand, Princeton, 1962.
5. W. F. Hillebrand, G. E. F. Lundell, H. A. Bright and J. I. Hoffman, *Applied Inorganic Analysis*, 2nd Ed., Wiley, New York, 1953.
6. E. M. Donaldson, *Talanta*, 1977, **24,** 105.
7. W. R. Nall, *Analyst*, 1971, **96,** 398.
8. P. Pakalns, *ibid.*, 1969, **94,** 1130.
9. R. C. Chirnside, H. J. Cluley, R. J. Powell and P. M. C. Proffitt, *ibid.*, 1963, **88,** 851.
10. Methods of Analysis Committee of the Metallurgy (General) Division of B.I.S.R.A., *J. Iron Steel Inst.*, 1954, **176,** Part 1, 63.
11. Methods of Analysis Committee of B.I.S.R.A., *ibid.*, 1956, **182,** 301.
12. F. E. Beamish and J. C. Van Loon, *Analysis of Noble Metals*, Academic Press, New York, 1977.
13. C. L. Lewis, W. L. Ott and N. M. Sine, *The Analysis of Nickel*, Pergamon, Oxford, 1966.
14. C. L. Lewis and W. L. Ott, *Analytical Chemistry of Nickel*, Pergamon, Oxford, 1970.
15. F. A. Lowenheim and R. S. Young, in *Encyclopedia of Industrial Chemical Analysis*, F. D. Snell and L. S. Ettre, eds., Vol. 16, p. 284, Interscience, New York, 1972.
16. W. R. Schoeller and A. R. Powell, *The Analysis of Minerals and Ores of the Rarer Elements*, 3rd Ed., Griffin, London, 1955.
17. S. T. Payne, *Analyst*, 1960, **85,** 698.
18. R. S. Young, *Separation Procedures in Inorganic Analysis*, Griffin, London, 1980.
19. J. Hoste and J. Gillis, *Anal. Chim. Acta*, 1955, **12,** 158.
20. W. J. Price and J. T. H. Roos, *Analyst*, 1968, **93,** 709.
21. P. E. Moloughney, *Talanta*, 1977, **24,** 135.
22. W. D. Cobb, W. W. Foster and T. S. Harrison, *Analyst*, 1976, **101,** 39.
23. Analytical Methods Committee, *ibid.*, 1968, **93, 414.**
24. T. M. Quarrell, R. J. W. Powell and H. J. Cluley, *ibid.*, 1973, **98,** 443.
25. G. Westoo, *ibid.*, 1963, **88,** 287.

Talanta Vol. 28. pp. 31 to 36
© Pergamon Press Ltd 1981. Printed in Great Britain
0039-9140/81/0101-0031$02.00/0

DETERMINATION OF YTTRIUM AND RARE-EARTH ELEMENTS IN ROCKS BY GRAPHITE-FURNACE ATOMIC-ABSORPTION SPECTROMETRY*

J. G. SEN GUPTA
Geological Survey of Canada, Ottawa, Ontario, Canada

(*Received* 20 *May* 1980. *Accepted* 11 *July* 1980)

Summary—With use of synthetic solutions and several international standard reference materials a method has been developed for determining traces of Y, Pr, Nd, Sm, Eu, Gd, Tb, Dy, Ho, Er, Tm, Yb and Lu in rocks by electrothermal atomization in a pyrolytically-coated graphite furnace. Depending on the element, the sensitivity is of the order of 10^{-9}–10^{-12} g at 2500°. To avoid matrix interferences the lanthanides are separated from the common elements by co-precipitation with calcium and iron as carriers. The data for Canadian reference rock SY-2 (syenite), U.S.G.S. reference rocks W-2 (diabase), DNC-1 (diabase) and BIR-1 (basalt), and South African reference rock NIM-18/69 (carbonatite) obtained by graphite-furnace atomization are compared with the values obtained by flame atomic-absorption. The results are in good agreement with literature values.

The good sensitivities for Y, Nd, Sm, Eu, Dy, Ho, Er, Tm and Yb obtained by aspirating ethanolic solutions of their perchlorates into a nitrous oxide–acetylene flame led to the development of an atomic-absorption method for determining these elements in a variety of rocks and minerals.[1,2] However, for traces of Pr, Gd, Tb and Lu, the flame atomic-absorption sensitivities were not adequate for their determination in most rocks. The more sensitive graphite-furnace atomization technique was, therefore, investigated for this purpose.

Sensitivity studies for one or more rare-earth elements by electrothermal atomization have been made by other workers.[3–9] Significant among these is the work of L'vov and Pelieva,[5] who noted that the sensitivities for the rare-earth elements were much higher in a graphite furnace lined with tantalum foil than in an unlined furnace. However, Kuga and Tujii[6] and Grobenski[7] observed an improvement in the sensitivities for the rare-earth elements by a factor of between 2.5 and 10 when a pyrolytically-coated graphite tube was used.

It should be noted here that in the furnace atomization work described above no attempt was made to determine ppm levels of the rare-earth elements in naturally occurring complex materials such as rocks. Data on the rare-earth element contents of rocks is useful in the elucidation of the geochemical histories of the earth and other planetary bodies.[10–12] The purpose of this work was, therefore, to develop suitable procedures for the determination of the rare-earth elements in a variety of rocks by electrothermal atomization.

* Presented at the 27th Canadian Spectroscopy Symposium, Toronto, Ontario, Canada, 6–8 October 1980.

EXPERIMENTAL

Apparatus and operating parameters

An Instrumentation Laboratory (IL) Inc. controlled-temperature furnace (Model 555) equipped with a temperature sensor, atomic-absorption spectrophotometer (Model 151), and a pyrolytic-graphite tube furnace (catalogue no. 44188-01), were used.

The furnace and the temperature sensor were found satisfactory for about 200 determinations after which they required replacement. The sample aliquot was heated in the furnace in an argon (99.999% pure) atmosphere. The time/temperature programme employed for sequential drying, pyrolysing and atomizing the sample is given in Table 1. The atomization peak was recorded on a Perkin–Elmer Model 56 recorder at a chart speed of 60 mm/min. Eppendorf micropipettes with disposable plastic tips were used to inject the sample or the standard solution manually into the furnace.

All other instrumental parameters are given in Table 2.

Calibration curves and sensitivities

For the preparation of calibration curves different aliquots (5, 10, 20 and 25 μl) of the individual rare-earth element solutions (in 0.1*M* nitric acid medium) were atomized in the furnace under the conditions given in Tables 1 and 2 and the absorbances were recorded on the chart. For some elements a furnace memory effect was noticeable. Therefore, between atomization of two samples, blanks were run until the memory effect from the previous sample was negligible. The absorbance peak-heights were used for plotting calibration curves.

The sensitivity values observed for the rare-earth elements are given in Table 3 and compared with those of L'vov and Pelieva.[5] A slightly higher sensitivity is noted in this work with a pyrolytically-coated graphite furnace than that observed by L'vov and Pelieva using a furnace lined with tantalum foil at a similar temperature (2500°).

Reagents

Rare-earth stock solutions. Dissolve an accurately weighed quantity (125 mg) of the oxide of a rare-earth element (99.9–99.999% pure, *e.g.*, Spectrex Ltd.) by heating in dilute nitric acid. In the case of cerium, dissolve cerium dioxide by heating in a solution of nitric acid and hydro-

Table 1. Operating parameters in the determination of rare-earth elements with the IL555 flameless atomizer

Purge gas: Argon	Flow-rate: 15 ft^3/hr					
Operation mode: Auto	Temperature feedback: On					
Auto clean cycle: On	Sample size: 5–25 μl					
Indicated temperature, °C	75	100	500	750	2500	2500
Time setting (× 5 sec):	5	5	3	3	0	1

Table 2. Instrumental parameters in the determination of rare-earth elements by graphite-furnace atomic-absorption spectrometry

Element	Wavelength, *nm*	Light-source (hollow-cathode lamp)	Current, *mA*	Spectral bandpass, *nm*	Furnace temperature, °C
Dy	421.2	Westinghouse	3	0.15	2500
Er	400.8	Westinghouse	6	0.3	2500
Eu	459.4	Westinghouse	4.5	0.15	2500
Gd	368.4	Westinghouse	14	0.15	2700
Ho	410.4	Westinghouse	10	0.15	2500
Lu	336.0	Varian Techtron	17	0.3	2700
Nd	492.5	Westinghouse	10	0.15	2500
Pr	495.1	Cathodeon	12	0.5	2300
Sm	429.7	Westinghouse	6	0.3	2700
Tb	432.7	Cathodeon	11	0.3	2700
Tm	371.8	Westinghouse	19	0.5	2500
Y	410.2	Westinghouse	6	0.3	2500
Yb	398.8	Westinghouse	5	0.3	2500

Table 3. Sensitivity* of rare-earth elements in the determination by graphite-furnace atomic-absorption spectrometry and comparison with other published values

		Sensitivity*	
Element	Furnace temperature, °C	This work (pyrolytically-coated furnace), *g*	L'vov and Pelieva[5] (tantalum-foil lined furnace), *g*
Dy	2500	1.1×10^{-11}	4.0×10^{-11}
	2700	8.8×10^{-12}	
Er	2500	2.3×10^{-11}	6.0×10^{-11}
Eu	2500	4.7×10^{-12}	3.0×10^{-11} (at 2400°)
Gd	2500	2.7×10^{-9}	2.5×10^{-9} (at 2550°)
	2700	4.0×10^{-10}	
Ho	2500	1.2×10^{-11}	6.0×10^{-11}
Lu	2725	2.0×10^{-10}	3.0×10^{-10} (at 2500°)
Nd	2500	1.1×10^{-9}	3.5×10^{-9}
	2550	2.6×10^{-10}	
Pr	2300	3.0×10^{-9}	3.6×10^{-9} (at 2600°)
Sm	2500	2.1×10^{-10}	1.0×10^{-9} (at 2400°)
	2700	7.0×10^{-11}	
Tb	2500	7.0×10^{-10}	4.0×10^{-10} (at 2600°)
Tm	2500	3.0×10^{-12}	2.0×10^{-11} (at 2400°)
Y	2500	1.8×10^{-10}	6.0×10^{-11}
Yb	2500	1.0×10^{-12}	4.0×10^{-12}

* Defined as the weight of the element that gives an absorbance of 0.0044 measured as a peak-height.

Table 4. Interference study with synthetic solutions* of rare-earth elements approximating the compositions of some reference rocks

	Concentrations, *ppm*							
	GA		NIM-G		SY-2		SY-3	
Element	Taken	Found	Taken	Found	Taken	Found	Taken	Found
Y	17	17.5	108	110	120	125	600	625
Pr	7	7	20	22	16	17	125	128
Nd	20	20	71	75	75	76	700	725
Sm	5.2	5.2	18	17.5	17	16.5	108	110
Eu	0.83	0.9	0.4	0.4	2.3	2.3	14	14
Gd	3	3	11	11	11	11	53	57
Tb	0.5	0.6	3	3.3	2.7	2.8	15	16
Dy	2.7	2.6	17	17.5	21	21.5	118	118
Ho	0.5	0.5	5	5.1	7	6.9	22	23
Er	1.5	1.5	13.5	13.8	13	12.5	52	52.5
Tm	0.2	0.2	1.9	1.8	2.5	2.4	10.5	10
Yb	1.4	1.5	12.2	12.2	16	16	55	62
Lu	0.3	0.3	2	2	3	2.9	8	8.3

* Contains Sc, Y, Th and all rare-earth elements plus added iron simulating the concentrate obtained after oxalate and hydroxide separation schemes mentioned in the text.

gen peroxide. Evaporate the solution to dryness (steam-bath), dissolve the residue in 1*M* nitric acid and dilute to 100 ml in a standard flask with the same acid. Store the solution in a tightly stoppered polyethylene bottle. Standardize the stock solution of each rare-earth element by evaporating a 5-ml aliquot to dryness in a 10-ml platinum crucible and igniting to constant weight.

Prepare solutions of 100-ppm concentration of rare-earth elements by mixing an aliquot of the concentrated stock solution with water (final acidity approx. 0.1*M*) and store in polyethylene bottles. Make solutions of lower concentration (0.1–10 ppm) as necessary, by diluting the 100-ppm stock solution with 0.1*M* nitric acid.

Interelement interference studies. For determining the rare-earth elements in rocks by furnace atomization, it is desirable to have these elements free from the bulk of matrix elements. A convenient way to obtain the rare-earth elements as a group from such samples is to volatilize the silicon with hydrofluoric acid, co-precipitate the rare-earths as the oxalates with calcium and then separate from calcium by co-precipitation of the lanthanides with a small amount of added iron. A concentrate prepared in this way contains all the rare-earth elements together with scandium, yttrium, thorium and the added iron. Therefore, for interelement interference studies, synthetic solutions were prepared containing known amounts of the rare-earth elements, together with Sc, Y, Th and Fe at the concentrations expected to be present in a concentrate from 0.5 g of a rock sample. Some typical rare-earth compositions of international standard reference rocks GA (granite), NIM-G (granite), SY-2 (syenite) and SY-3 (syenite)[13] were chosen for this purpose.

The effect of iron on the absorbance of the individual rare-earth element was first studied. It was found that the presence of iron up to the 200-ppm level had no effect on the absorbance of any rare-earth element. The high sensitivities of the rare-earth elements in furnace atomization required dilution of the synthetic solutions to appropriate levels before determination. Suitable concentrations of the original sample for these determinations are given in Note 1 after the procedure below. The results given in Table 4 revealed that interelement effects were negligible.

Recommended procedure

Decompose 1–3 g of the finely crushed rock sample in a 100-ml platinum dish by heating with hydrofluoric, nitric and perchloric acids. After expelling the perchloric acid fumes by heating, cool, and dissolve the residue by warming with a mixture of 10% nitric acid and 5% hydrogen peroxide. Filter, fuse any undissolved residue with potassium pyrosulphate, and after dissolving the fusion product in dilute sulphuric acid, mix with the main solution. Heat to boiling, neutralize with ammonia solution and precipitate the rare-earth elements with methyl oxalate in the presence of calcium equivalent to 0.2 g of CaO as carrier (adding calcium if an insufficient amount is present in the sample).[1] After digestion of the oxalate precipitate on the steam-bath for several hours at pH 3.8–5 (test with a pH-meter), allow to settle overnight and filter off. Wash with 0.1% ammonium oxalate solution, and after destruction of the filter paper with nitric and perchloric acids, dissolve the salts in dilute nitric acid (10%) and hydrogen peroxide (5%) solution. Reprecipitate the oxalates and convert the salts into perchlorates by heating with perchloric acid. Dissolve the salts in dilute nitric acid, add 1g of hydroxylamine hydrochloride and 5 mg of iron, and precipitate the hydroxides with freshly prepared ammonia solution. Add excess of ammonia to maintain the pH above 10 and some filter paper pulp to aid coagulation of the precipitate. Filter and wash with ammonia (5%) and ammonium nitrate (1%) solution. Decompose the paper with nitric and perchloric acids and after dissolving the salts in nitric acid, reprecipitate the hydroxides to remove any residual calcium.

Transfer the filter paper and the precipitate to the original beaker, decompose the paper by boiling under reflux with concentrated nitric acid and 30% hydrogen peroxide. Evaporate to dryness, and if any organic matter remains unattacked, repeat the digestion with nitric acid and hydrogen peroxide, and evaporate to dryness. Dissolve the rare-earth concentrate in 1*M* nitric acid and dilute to 5 or 10 ml in a standard flask with the same acid ("concentrate stock solution A").

Transfer different aliquots of the "concentrate stock solution A" to small standard flasks and make up to volume with water or dilute nitric acid (final acidity approx. 0.1*M*) to give solutions equivalent to 0.1–0.0004 g of the original rock sample per ml. Depending on the sensitivity and concentration of the rare-earth element sought, accurately pipette 5–25 µl of these solutions (see Note 1 below) into the cavity of the graphite tube and operate the furnace and the atomic-absorption spectrophotometer in the automatic modes, using the parameters of Tables 1 and 2. Record the absorbances on chart paper. Use a scale expansion of up to 5×, if necessary. Run blank determi-

Table 5. Determination of yttrium and the rare-earth elements in Canadian reference rock SY-2 and U.S.G.S. reference rocks W-2, DNC-1 and BIR-1 by graphite-furnace and flame atomic-absorption spectrometry

	Concentration, *ppm*							
	SY-2		W-2		DNC-1		BIR-1	
Element	This work	Other values	This work	Other values	This work	Other values	This work	Other values
Ce	153[c]	210?[f]	26[c]	24.4 ± 0.9[d]	15[c]	2.62 ± 0.76[d]	<14	3[e]
				25[e]		10[e]		
Dy	20[b]	21[h]	3.8[a]	3.4 ± 0.6[d]	3.1[a]	2.2 ± 2[d]	2.6[a]	3.5 ± 1.6[d]
		20?[f]	3.8[b]	4[e]	3.0[b]	3[e]	3.0[b]	2[e]
Er	14[b]	13[h]	3.0[a]	—	2.1[a]	—	2.0[a]	—
		12?[f]	3.1[b]		2.3[b]		2.3[b]	
Eu	2.3[b]	2.3[h]	1.3[a]	1.16 ± 0.05[d]	0.6[a]	0.62 ± 0.01[d]	0.6[a]	0.56 ± 0.07[d]
		2.4?[f]	1.2[b]	1[e]	0.6[b]	0.6[e]	0.6[b]	0.5[e]
Gd	23[b]	Range 11–22[g]	12[b]	—	6[b]	<7[e]	5[b]	<7[e]
Ho	5[b]	Range 2.9–7[g]	0.8[a]		0.7[a]	—	0.4[a]	—
			0.8[b]		0.7[b]		0.5[b]	
La	84[c]	85?[f]	15[c]	10.23 ± 0.18[d]	10[c]	3.63 ± 0.17[d]	4[c]	0.74 ± 0.04[d]
				11[e]		3.7[e]		1[e]
Lu	2[b]	3?[f]	0.8[b]	0.52 ± 0.27[d]	0.7[b]	0.41 ± 0.11[d]	0.7[b]	0.2[e]
				0.3[e]		0.3[e]		
Nd	81[b]	75[h]	23[a]	23 ± 4[d]	11[a]	5[e]	4.4[a]	—
	84[c]	71?[f]	24[b]	15[e]	12[b]		4.2[b]	
Pr	17[b]	Range 8–18[g]	12[b]	—	2[b]	—	1[b]	—
Sm	18[b]	17[h]	3[a]	3.1 ± 0.16[d]	2[a]	1.30 ± 0.04[d]	1[a]	0.99 ± 0.03[d]
		15?[f]	3[b]	3[e]	2[b]	2[e]	1[b]	1[e]
Tb	2.9[b]	2?[f]	1[b]	0.93 ± 0.11	0.6[b]	0.44 ± 0.04[d]	0.8[b]	—
Tm	2.5[b]	2.5[h]	0.4[a]	<0.7[e]	0.4[a]	<0.7[e]	0.4[a]	<0.7[e]
		2?[f]	0.5[b]		0.5[b]		0.4[b]	
Y	125[b]	120[h]	24[a]	—	18[a]	—	17[a]	—
	117[c]	130[f]	25[b]		20[b]		17[b]	
			23[c]		18[c]		16[c]	
Yb	15[b]	16[h]	2.1[a]	2.18 ± 0.21[d]	2.1[a]	2.09 ± 0.17[d]	1.8[a]	1.97 ± 0.1[d]
	15[c]	17[f]	2.2[b]	2[e]	2.2[b]	2[e]	1.9[b]	2[e]
			1.7[c]		1.5[c]		1.4[c]	

[a]Flame atomic-absorption value; [b]graphite-furnace atomic-absorption value; [c]arc-emission spectrographic value; [d]van der Sloot and Zonderhuis;[15] [e]Flanagan's approximate value as supplied with the samples; [f]Abbey;[13] [g]Abbey;[14] [h]Sen Gupta.[1]

nations between samples to eliminate the memory effect from the previous sample. In order to draw the calibration curve for a rare-earth element, pipette into the graphite furnace 5, 10, 20 and 25 μl aliquots of a solution of known concentration containing a concentration of iron approximating to that in the unknown sample solution. Record the absorbance peaks on the chart paper. Run blanks between atomizations to eliminate the memory effect. Determine the absorbance peak-heights, draw the calibration curve and evaluate the concentration of the unknown solutions from this curve.

Notes

1. In the determination of rare-earth elements by furnace atomization, use of a concentrate solution equivalent to an original rock sample concentration >0.2 g/ml is not recommended, as interelement interferences resulting in depression of peak-heights may occur. The method works best in dilute solution (rare-earth concentrate present in a solution concentration equivalent to original rock sample concentrations of 0.1 g/ml or less), where interelement effects are nil. Thus suitable original rock concentrations for determining Y, Pr, Nd, Sm, Gd, Tb and Lu are 0.05–0.1 g/ml, although for traces of Pr and Lu in some samples it may be necessary to use a concentration of up to 0.2 g/ml. For Eu, Dy, Ho, Er and Tm, rock sample concentrations of 0.05 g/ml or less (depending on the concentration and sensitivity of the element) are required. For ytterbium, rock sample concentrations of 0.004 g/ml or less are suitable

2. If flame atomic-absorption data are required for comparison (as in this work), then evaporate an aliquot of the "concentrate stock solution A" with perchloric acid to a moist residue, cool, and dissolve the salts in absolute ethanol. Determine Y, Nd, Sm, Eu, Dy, Ho, Er, Tm, Yb (and Pr, Gd, Tb and Lu if present in sufficiently high concentration) in solutions buffered with 1% of lanthanum, by atomic-absorption in a nitrous oxide–acetylene flame, using scale expansion if necessary.[1] If the concentration of lanthanum is high, determine it in the ethanolic perchlorate solution of the concentrate (without spectroscopic buffer added) by atomic-absorption in a nitrous oxide–acetylene flame.

3. In the furnace atomization of cerium and lanthanum, strong negative absorption signals were noticed. These were probably due to emission interference from the graphite furnace at the absorption wavelengths of cerium (520.01 nm) and lanthanum (550.13 nm). Traces of cerium and lanthanum in rocks were, therefore, determined in the concen-

Table 6. Determination of yttrium and the rare-earth elements in South African reference sample NIM-18/69 by graphite-furnace and flame atomic-absorption spectrometry

Constituent	This work	Other values[d]	Average of other values
CeO_2 (%)	0.40[c]	0.48, 0.41, 0.48 0.11*, 0.40, 0.51 0.40, 0.43, 0.50	0.45
Dy_2O_3 (*ppm*)	68[a] 68[b]	42, 40, 66, 60 101, 100, 7*	68
Er_2O_3 (*ppm*)	24[a] 26[b]	10, 19, 1*	15
Eu_2O_3 (*ppm*)	50[a] 56[b]	50, 50, 46, 56 44, 98, 22	52
Gd_2O_3 (*ppm*)	150[a] 154[b]	117, 141, 140 101, 140, 245, 23*	147
Ho_2O_3 (*ppm*)	11.2[a] 11.5[b]	6, 9, 3*	8
La_2O_3 (%)	0.21[a]	0.29, 0.20, 0.25, 0.36 0.30, 0.22, 0.18	0.26
Lu_2O_3 (*ppm*)	4.8[b]	1, 1	1
Nd_2O_3 (%)	0.16[a] 0.16[b] 0.15[c]	0.18, 0.12, 0.17, 0.096, 0.10, 0.15, 0.30, 0.084	0.15
Pr_6O_{11} (*ppm*)	520[a] 580[b]	749, 372, 468, 271, 946, 500, 760, 161	528
Sm_2O_3 (*ppm*)	215[a] 213[b]	280, 161, 238, 301, 50*, 60*, 325, 141	241
Tb_4O_7 (*ppm*)	31[b]	14, 14	14
Tm_2O_3 (*ppm*)	2.9[a] 3.0[b]	5, 2, 2	3
Y_2O_3 (*ppm*)	334[a] 330[b] 328[c]	270, 191, 161 221, 200, 281, 315	234
Yb_2O_3 (*ppm*)	15.7[a] 15.7[b] 15.7[c]	10, 10, 13, 9, 18, 3*	12

[a] Flame atomic-absorption value; [b]graphite-furnace atomic-absorption value; [c] arc-emission spectrographic value; [d]Stock, Steele and Copelowitz;[16] [e] semi-quantitative arc-emission spectrographic value.

* Rejected in calculating the average of other values in the last column.

trates by arc-emission spectrography, following the procedure described in a previous paper.[2]

RESULTS AND DISCUSSION

The graphite-furnace atomic-absorption method was applied to the determination of yttrium and rare-earth elements in a number of standard reference rocks. The results are given in Tables 5 and 6 and compared with the flame atomic-absorption and other values, where available. The agreement between values obtained by different methods and given in Table 5 is satisfactory. In Table 6 the flame and graphite-furnace atomic-absorption values for the rare-earth elements in NIM-18/69 are compared with other values published in a compilation of data by Stock *et al.*[16] After rejection of some very low values from these published data, the averages (column 4 of Table 6) for most rare-earth elements appear to be close to the values obtained in this work. Arc-emission spectrographic values for cerium and lanthanum in the sample solutions used for graphite-furnace atomization are also recorded in Table 5. In the rare-earth concentrate of NIM-18/69, lanthanum was determined by flame atomic-absorption and cerium by arc-emission spectrography (semi-quantitative because of the high concentration). The results are found to be within the range of other reported values.

Acknowledgements—The author expresses his sincere thanks to G. Hall of the Geochemistry Section of GSC for permission to use the instruments for graphite-furnace atomic-absorption work; to R. A. Meeds for providing arc-emission spectrographic data for Y, La, Ce, Nd and Yb on the rare-earth concentrates of the reference rocks supplied; to F. J. Flanagan of the U.S. Geological Survey for permission to publish the atomic-absorption data on the rare-earth elements, obtained in this work for the reference samples W-2, DNC-1 and BIR-1 and to S. Abbey for critical reading of the manuscript.

REFERENCES

1. J. G. Sen Gupta, *Talanta*, 1976, **23**, 343.
2. *Idem*, *Geostandards Newsl.*, 1977, **1**, 149.
3. J. Y. Hwang, C. J. Mokeler and P. A. Ullucci, *Anal. Chem.*, 1972, **44**, 2018.
4. A. Montaser and A. A. Mehrabzadeh, *Anal. Chim. Acta*, 1979, **111**, 297.
5. B. V. L'vov and L. A. Pelieva, *Can. J. Spectrosc.*, 1978, **23**, 1.
6. K. Kuga and K. Tujii, *Bunseki Kagaku*, 1978, **27**, 441.
7. Z. Grobenski, *Z. Anal. Chem.*, 1978, **289**, 337.
8. K. Dittrich, E. John and I. Rohde, *Anal. Chim. Acta*, 1977, **94**, 75.
9. K. Dittrich and K. Borzym, *ibid.*, 1977, **94**, 83.
10. L. A. Haskin, M. A. Haskin, F. A. Frey and T. R. Wildeman, in *Origin and Distribution of the Elements*, L. H. Ahrens (ed.), p. 889. Pergamon, Oxford, 1968.
11. L. A. Haskin, R. O. Allen, P. A. Helmke, T. P. Paster, M. R. Anderson, R. L. Korotev and K. A. Zweifel, in *Proc. Apollo 11 Lunar Sci. Conf., Geochim. Cosmochim. Acta Suppl.*, 1970, **2**, 1213.
12. Y. A. Balashov and P. M. Goryainov, *Geokhimiya*, 1966, No. 3, 312 (in Russian); Eng. Transl. in *Geochem. Int.*, 1966, **3**, 240.
13. S. Abbey, *Geol. Surv. Can. Paper*, 77–34.
14. *Idem*, Canada Centre for Mineral and Energy Technology Report 79-35.
15. H. A. van der Sloot and J. Zonderhuis, *Geostandards Newsl.*, 1979, **3**, 185.
16. H. Stock, T. W. Steele and I. Copelowitz, Nat. Inst. Metall., Repub. S. Afr., Report No. 1807, Johannesburg, 1976.

Talanta Vol. 28, pp. 37 to 41
© Pergamon Press Ltd 1981. Printed in Great Britain
0039-9140/81/0101-0037$02.00/0

AN INSTRUMENTAL METHOD OF SOLUTION PRECONCENTRATION

P. A. MICHALIK and R. STEPHENS
Trace Analysis Research Centre, Department of Chemistry, Dalhousie University, Halifax, Nova Scotia, Canada

(*Received* 28 *May* 1980. *Accepted* 9 *July* 1980)

Summary—Aerosol concentration before atomic-absorption measurement is achieved by use of an electrostatic trapping technique. The effects of various experimental parameters are examined, including those of voltage, trap dimensions, gas flow-rate through the trap and trapping time. It is concluded that the technique offers an inherently clean method of solution preconcentration which is capable of enhancing the signal by an order of magnitude or more.

Various methods are available for preconcentrating samples before chemical analysis. A number of excellent texts have been written which give the appropriate details.[1] All such methods involve some degree of sample handling, with associated risks of contamination, adsorption losses, *etc.* These risks increase as the analyte concentration in the sample falls, which leads to correspondingly increased demands on the skill of the analyst and eventually gives rise to a limiting concentration at which the analysis ceases to be feasible. These problems have been discussed by Chakrabarti *et al.*[2] among others.[3–6]

The present paper examines an attempt to develop a method of instrumental preconcentration suitable for use with a conventional flame atomic-absorption spectrometer. The method is intended to reduce sample handling to near the irreducible minimum, defined in this case by the design of the sample-introduction system used with such spectrometers.

The method adopted is electrostatic dust-precipitation. The aerosol from a conventional pneumatic nebulizer is dried in a heating chamber, desolvated, and collected on a wire electrode which is connected to a high-voltage supply. When sufficient sample has been collected the wire is heated to volatilize the collected material. The flame support-gas (oxidant only) is used to transport the initial aerosol to the wire collector, and later to carry the volatilized material into the flame for atomization and measurement. The first part of the procedure resembles the electrostatic dust-precipitators used on the large scale industrially; the second part is analogous to the furnace–flame combinations which have been described recently.[7]

It is felt that the risks associated with handling very dilute solutions are minimal when pneumatic nebulizers are used. These devices have evolved to the point where it is difficult to conceive of a method which will involve less sample handling, and yet will still serve to introduce a sample solution into a flame. The effectiveness of these devices arises because sample contact-time with the inlet capillary and venturi surfaces is minimal, while droplets which touch the walls of the spray chamber tend to condense out and therefore cease to be important in the analysis. Similar reasoning can be applied to the heating chamber and condenser which are used to effect desolvation (although such units can introduce an added risk of interference effects[8]). Provided that the temperature of the heating chamber is not so high as to induce boiling, and that the diameter of the condenser is not so small as to force gas to bubble through the condensed solvent, wall contamination ceases to be important because any solution affected by it is not used in the analysis. Suitable desolvation systems have been described by a number of workers;[9–15] they include devices capable of handling high concentrations of matrix salts,[9,13–15] which is clearly desirable for any system which is ultimately intended for practical application.

EXPERIMENTAL

The present work is concerned primarily with the development of an efficient aerosol trap, rather than of a complete analytical system. The latter is a more complicated problem, which will be addressed subsequently and in appropriate stages.

Cadmium, lead and zinc were selected for testing the apparatus, because of their ease of volatilization, and the experiments described are confined to examination of the behaviour of these three elements, but there is no reason for supposing that their trapping behaviour is likely to differ from that of other elements.

Apparatus

Figure 1 shows a block diagram of the apparatus. The heating chamber and condenser are similar in design to those described by Veillon and Margoshes.[10] Their insertion causes about a 25% loss of the aerosol delivered by the nebulizer. The flow-splitter was used only to determine the effect of flow-rate on aerosol trapping efficiency; otherwise the entire flow of support gas passed through the aerosol trap.

The trap itself is shown in Fig. 2. The body of the device consists of a length of glass tube carrying a few turns of copper wire on the outside to provide an earth (ground).

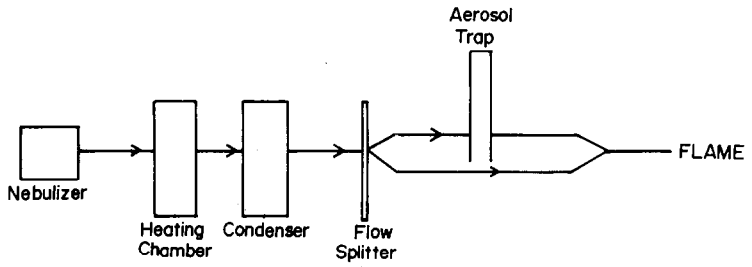


Fig. 1. Block diagram of the apparatus.

In all cases a winding of about one turn per inch was found to be quite sufficient. Unless otherwise stated, the tube was 45 cm long and 2.5 cm in diameter. The ends of the tube were closed with rubber stoppers, each with a 5 cm length of 0.5-mm bore glass tube inserted through its centre. A length of 22-gauge chromel wire (the collector) formed the axis of the system. For trapping a sample the collector wire was connected to a 0–30 kV d.c. supply (Precise Measurements Co., Flemington, N.J.). No difference in behaviour was found for positive or negative polarity of this supply; the experiments described here were all done with a positive collector potential. To volatilize the collected material the chromel wire was disconnected from the high-voltage supply, and connected to a variable transformer to produce the usual electrothermal volatilization. During this heating cycle slight tension was maintained in the wire to counteract its thermal expansion. This arrangement is only applicable for relatively volatile materials, but was extremely convenient for the present investigation because factors such as trap length, outer tube diameter and diameter of the collector electrode could be readily altered. The system therefore permitted the effects of such variables to be established; this information is needed before a trap can be designed which is capable of handling more intractable materials.

To operate the trap, the high-voltage supply was connected and a solution aspirated as usual. Atomic-absorption readings could be taken during this time if required. At the end of the trapping time aspiration was stopped and the collector wire was heated to drive off the sample. This produced an absorption signal as a single pulse (examples are given in Fig. 8 below). No problem was encountered with background absorption, since all the solutions used were made from the pure salts dissolved in demineralized distilled water. Washing by aspirating a few ml of distilled water proved to be adequate for cleaning the unit between readings.

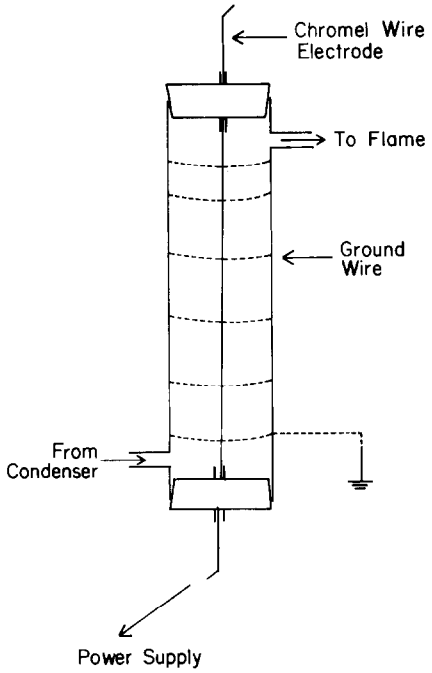


Fig. 2. The aerosol trap.

Mechanism of aerosol collection

The aerosol particles generated by pneumatic nebulization can acquire quite a high electrostatic charge. However, most of this charge appeared to be dissipated in the heating chamber and condenser (some quite spectacular electrical discharges were observed in the former). Thus the collection process appears to operate on electrically neutral particles. This view is confirmed by the observation that the polarity of the high voltage supply can equally well be positive or negative, virtually 100% trapping efficiency being attainable in either case. Therefore the force responsible for aerosol collection is considered to arise from the interaction of the electrostatic field in the trap with the electric dipole which that field induces in each particle. For such a force to cause physical transport of the particle it is necessary for the field to be highly inhomogeneous. The production of such a field is accomplished here by use of a wire electrode of diameter very small in comparison with that of the coaxial earthed winding.

Measurement of trapping efficiency

The trapping efficiency, n, of the device is defined as the fraction of the aerosol mass entering the trap which is actually retained there. Values of n were determined as follows. Calibration curves were plotted for each element by use of the sample introduction system shown in Fig. 1, but with the collector voltage set at zero. The atomic-absorption signal was then measured with the collector voltage set at the required value. The signal was converted into sample concentration by use of the calibration curve. The ratio, r, of this concentration to the corresponding value at zero collector voltage gives the mass fraction of aerosol leaving the trap. Hence $n = (1 - r) \times 100\%$.

RESULTS AND DISCUSSION

Influence of trapping parameters

Figures 3 and 4 show the dependence of n on the length of the trap for collector voltages of 14 and 18 kV, and on collector voltage and solution concentration for a trap length of 45 cm. These results show that trap length and trapping voltage tend to produce complementary effects on n. That is, the higher the voltage used then the smaller the trap can be made, and *vice versa*. In practice a useful upper limit of

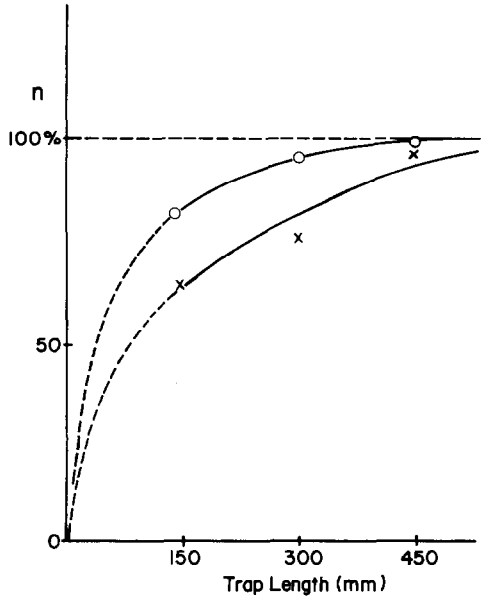


Fig. 3. Effect of trap length on n: O = 18 kV; X = 14 kV. Values shown were measured for Pb at 283.3 nm; similar results are observed for Cd and Zn.

about 18 kV for the voltage was found. At higher voltages flashover became a problem. Therefore, a trap length of 45 cm was used for subsequent work, which gave trapping efficiencies of 90–100% for voltages in the range 14–18 kV.

The effect of solution concentration on n (Fig. 4) shows a similar pattern for each element examined. In each case there is a slight reduction in n as the concentration, and hence the total mass of the particles entering the trap, is increased. The differences in concentration at which n falls below 100% for different elements are presumed to arise from differences in the physical properties, such as density and dielectric constant, of the particles involved. It is also possible that the gas-flow patterns in the particular apparatus used exert some influence. This matter has not yet been investigated in detail. However, the results clearly suggest that no fall-off of n is likely to occur at very low concentrations, where high efficiency is most necessary (this conclusion is also supported by the results in Fig. 7 below).

The effects of support-gas flow-rate and of trap diameter on n are interdependent. Examination of n for various trap diameters and a fixed volumetric gas

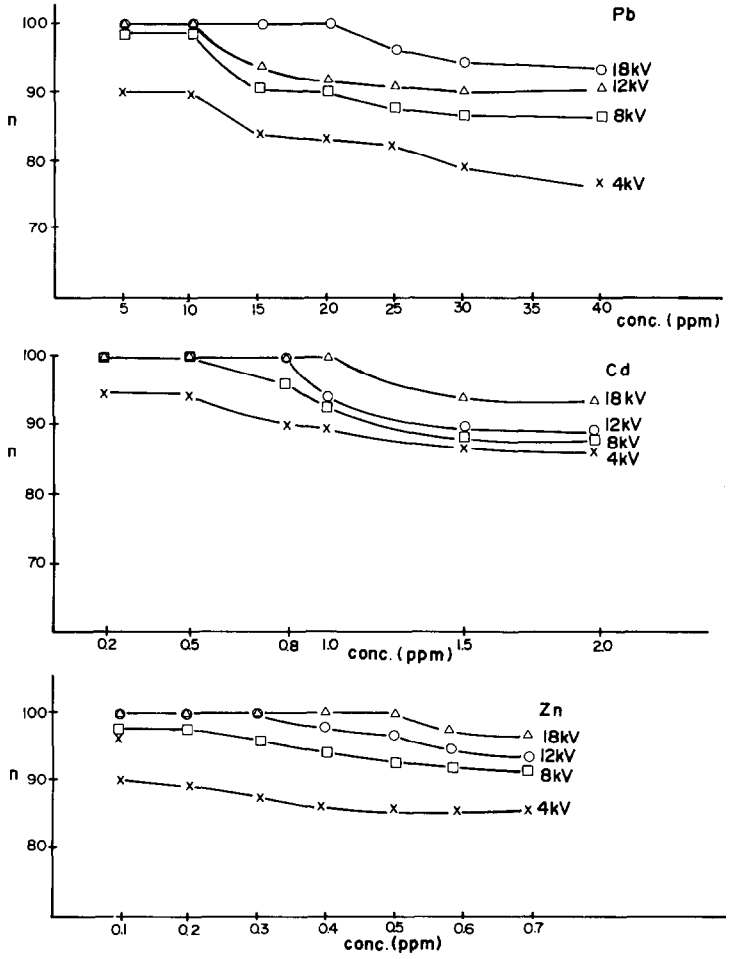


Fig. 4. Effect of solution concentration and collector voltage on n.

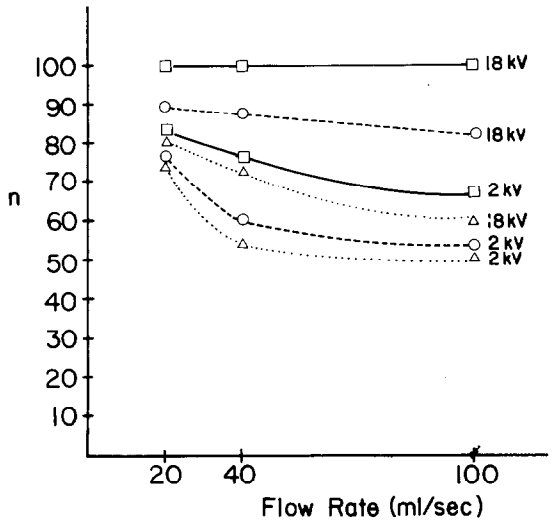


Fig. 5. Effect of flow-rate on n for various trap lengths and collector voltages, measured for 15 ppm Pb. Trap lengths: □ 45 cm; ○ 30 cm; △ 15 cm.

flow-rate showed that no measurable variation occurred. This suggests that any reduction in n due to increased trap diameter is counteracted by a corresponding increase in n due to the decreased linear gas flow-rate through the trap, which leads to an increased residence time for the aerosol particles. The influence of flow-rate alone on n was found by using the flow-splitter (Fig. 1) to control the proportion of the support gas flowing through the trap. Results are shown in Fig. 5. The fall in n with increasing flow-rate is probably a result of the correspondingly reduced residence time of aerosol particles in the trap. In this situation less time is available for particles to cover the distance to the collector from their particular line of flow through the trap. Thus fast-moving particles which enter the trap far from the collector are unable to reach it before they leave the system.

Effect of trapping time

The most important property of the present device for analytical purposes is probably its ability to maintain almost constant trapping efficiency over a period of time. The effect is shown for lead in Fig. 6.

The data show that a slight reduction of trapping efficiency with time occurs at high solution concentrations, presumably because of significant surface coverage of the electrode, and perhaps failure of particles to adhere to areas already covered. At low concentrations, however, it appears to be feasible to extend trapping times almost indefinitely. Times up to 20 min have been used and by no means represent an upper limit.

To illustrate the potential capability of the system, five replicate measurements were made, in each of which 100 ml of a 10-ng/ml lead solution were trapped. The corresponding absorption signals observed at 283.3 nm on volatilizing the trapped samples are shown in Fig. 7. The reproducibility of the system is felt to be adequate (and in any case is probably governed by the volatilization step rather than by the preconcentration process). No difficulty

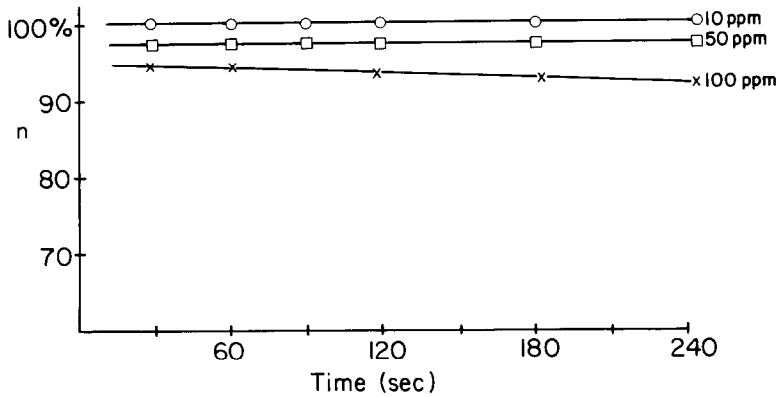


Fig. 6. Effect of trapping time on n. Values measured for Pb at a collector voltage of 18 kV.

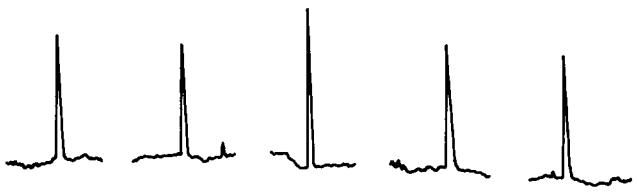


Fig. 7. Repetitive signals, each obtained after trapping 100 ml of a 10-ng/ml solution of Pb. Collector voltage = 18 kV.

was encountered in obtaining the data in Fig. 7 despite the fact that the measurements were made at the end of the experiments described above, by which time the system had been exposed to large volumes of solutions containing high concentrations of all three elements examined; this provides some confirmation that this preconcentration step is inherently clean.

For comparison with the data in Fig. 7, the detection limit of the standard unmodified instrument for lead was found to be about 0.2 ppm at 283.3 nm. Thus it appears clear that the sensitivity can be enhanced by at least an order of magnitude with this system.

CONCLUSIONS

The experiments done show that it is feasible to use electrostatic trapping of aerosol particles as a simple, clean and effective method of sample preconcentration before atomic-absorption measurements. The risks of sample loss or contamination during the process are felt to be minimal because once the sample has left the nebulizer the preconcentration is carried out quite automatically, and effectively in the vapour phase: if any aerosol does touch a potentially contaminating surface it tends to condense and become lost to the analysis. By the time the sample reaches a possible source of contamination (the collector), preconcentration is complete and therefore contamination has ceased to be particularly important.

Encouragingly, no limits have been found for the degree of preconcentration obtainable with the technique. However, it is clear that this is only likely to apply to pure solutions such as were used here; it is almost certain that in practice some limit will be set by the composition of the sample matrix. A further problem that arises is the lack of generality imposed by the use of a heated chromel wire for the volatilization step. Some potential solutions to these problems have been found, and will be discussed in subsequent communications.

Acknowledgement—The authors are indebted to the Natural Sciences and Engineering Research Council, Canada for support of this work.

REFERENCES

1. See, *e.g.*, R. Mavrodineanu and H. Boiteux, *Flame Spectroscopy*, Wiley, New York, 1965; G. F. Kirkbright and M. Sargent, *Atomic Absorption and Fluorescence Spectroscopy*, Academic Press, New York, 1974.
2. K. S. Subramanian, C. L. Chakrabarti and I. S. Maines, *Anal. Chem.*, 1978, **50**, 444.
3. G. C. Eicholz, A. E. Nagel and R. B. Hughes, *ibid.*, 1965, **37**, 863.
4. D. E. Robertson, *Anal. Chim. Acta*, 1968, **42**, 533.
5. R. A. Durst and B. T. Duhart, *Anal. Chem.*, 1970, **42**, 1002.
6. W. G. King, J. M. Rodriguez and C. M. Wai, *ibid.*, 1974, **46**, 771.
7. D. J. Koop, M. D. Silvester and J. C. Van Loon, paper presented at the Pittsburgh Conference on Analytical Chemistry and Applied Spectroscopy, Cleveland, Ohio, March 1978.
8. P. W. J. M. Boumans and F. J. DeBoer, *Spectrochim. Acta*, 1976, **31B**, 355.
9. A. Venghiattis, *Appl. Opt.*, 1968, **7**, 1313.
10. A. Hell, W. F. Ulrich, N. Shifrin and J. Ramírez-Muñoz, *ibid.*, 1968, **7**, 1317.
11. C. Veillon and M. Margoshes, *Spectrochim. Acta*, 1968, **23B**, 553.
12. G. Uny, J. N'Guea Lotton, J. P. Tardiff and J. Spitz, *ibid.*, 1971, **26B**, 151.
13. H. J. Issaq and L. P. Morgenthaler, *Anal. Chem.*, 1975, **47**, 1661.
14. *Idem*, *ibid.*, 1975, **47**, 1668.
15. *Idem*, *ibid.*, 1975, **47**, 1748.

Talanta Vol. 28, pp. 43 to 47
© Pergamon Press Ltd 1981. Printed in Great Britain
0039-9140/81/0101-0043$02.00/0

AEROSOL PRECONCENTRATION ON A LIQUID ELECTRODE

P. A. MICHALIK and R. STEPHENS
Trace Analysis Research Centre, Department of Chemistry, Dalhousie University, Halifax, Nova Scotia, Canada

(*Received* 28 *May* 1980. *Accepted* 9 *July* 1980)

Summary—Electrostatic preconcentration of a dried aerosol is achieved with a water electrode. The system is found to show similar trapping characteristics to those given by wire electrodes, but the subsequent introduction of collected material into a flame atomizer is easier, merely requiring aspiration of the electrode solution after the trapping cycle is complete. The system has been tested for some 40 elements, 5 of which failed to show any response. The failures are attributed to a vapour-phase reaction of the solution aerosol during its passage through the desolvation system, leading to formation of water-insoluble species.

It has been found that the solution aerosol generated by a pneumetic nebulizer can be collected on a wire electrode by application of a suitably high electrostatic potential. The process offers an effective method of sample preconcentration.[1] Two advantages found for the technique are: (*a*) it is inherently clean, since the concentration step is carried out in the vapour phase; (*b*) the degree of preconcentration is extremely high; indeed it is not yet clear which are the limiting factors controlling the minimum concentrations which can be detected with the process. The greatest disadvantage of the original device was its use of a wire collector electrode which was exposed to the support-gas flow, and which required heating in order to vaporize the collected material. The temperatures available with such a system are limited by the melting point of the electrode and/or its resistance to oxidation by the support gas. This restriction limited the applicability of the system to a few elements such as Cd, Pb and Zn, which have salts that can be volatilized at low temperatures. Therefore it is clear that an improved volatilization process is needed before electrostatic preconcentration is likely to be of any real use in analytical spectroscopy. This problem is examined here.

EXPERIMENTAL

It was found that mechanical forces (vibration, gas impingement, or even physical scraping of the surface) failed to remove material from the collector. It is thought this failure was due to the small size of the particles involved, which means that the mechanical forces are small compared to the surface adhesion forces and which permits the particles to be trapped readily within imperfections on the electrode surface. The difficulty was overcome by use of a liquid collector electrode. Distilled water was used throughout this work. Figure 1a shows the design of the trap; Fig. 1b is a block diagram showing how the trap was fitted into the sample-introduction system.

The physical dimensions used for the trap were those found to be optimal when using wire electrodes. That is, it was assumed that the present system would behave in more or less the same way as the original version, provided the radius of curvature of the water electrode was comparable to that of the wire. The experimental results showed this assumption to be justified.

The base of the trap was made of 42 × 12 cm "Plexiglas", with a trough 35 cm long, 2 mm wide and 1.5 mm deep cut in the centre to hold water. The volume of the trough was 1.0 ml. A length of chromel wire was sealed into a hole drilled through the base and into the water trough. This provided electrical contact with the water electrode. The base was surrounded by a canopy made from copper sheet, in the form of a half-cylinder. All sharp corners were filed away inside the canopy. The canopy was earthed at all times. This arrangement provided the necessary non-homogeneous electrostatic field during operation.

The electrode trough was filled with water by means of a hypodermic needle attached to a length of plastic capillary tubing. The needle was inserted through a hole in the canopy, a syringe was attached to the other end of the capillary, and 1 ml of water was injected (Fig. 1). The trapping was done in the same way as with the original system. That is, the water electrode was connected to a high-voltage supply (+15 kV for all the results given here). The sample solution was aspirated through a conventional pneumatic nebulizer, then desolvated, and the dried aerosol was carried to the trap by the support-gas flow.

After trapping, the sample was recovered by disconnecting the high-voltage supply, re-inserting the hypodermic needle into the trough and attaching the plastic capillary to the inlet of the pneumatic nebulizer (Fig. 1). This caused the water in the trough to be drawn through the nebulizer, *i.e.*, the electrode plus concentrated sample became the new sample solution. With the high-voltage turned off there was no further retention of aerosol in the trap, and the concentrated aerosol was carried on into the flame. The resulting signals were observed with the AA5 spectrometer used in the previous work. For reasons of economy, elements which require atomization in a C_2H_2–N_2O flame were trapped by using an air-flow in the support-gas line, and the system was switched over to N_2O only for final measurement.

RESULTS AND DISCUSSION

The signals observed on aspiration of the electrode solution after completion of a trapping cycle were invariably uniform with time. Hence it is considered that the trapped material redissolves on contact with

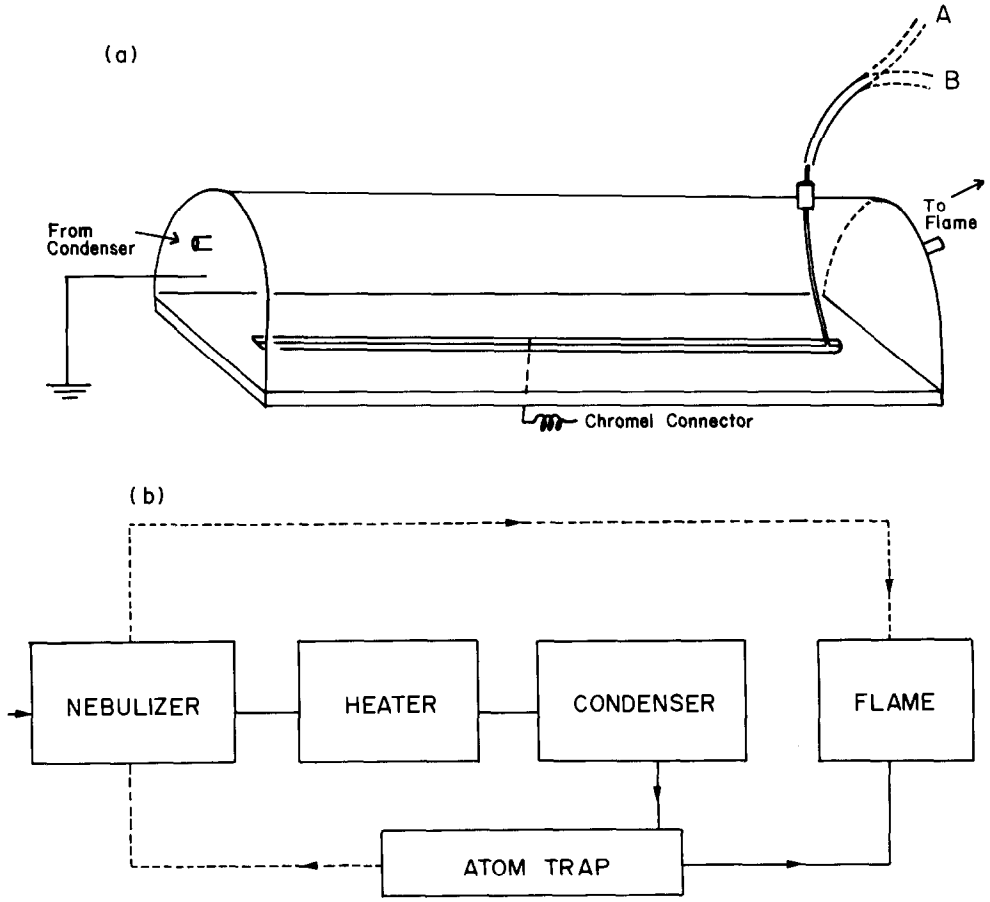


Fig. 1. (a) The trap and inlet/outlet capillary; A, injection; B, aspiration. (b) Block diagram of the sample-introduction system.

the electrode, to give a homogeneous solution. Provided no reaction occurs to change the chemical nature of the aerosol particles during their passage through the desolvation system, this seems to be a reasonable conclusion: of necessity the trapped material is introduced initially in water-soluble form, and the high surface-energy associated with the small size of the particles which reach the electrode is likely to ensure that redissolution is rapid. Apparently sufficient mixing occurs in the electrode solution to ensure the formation of a uniform solution.

The system was tested for memory effects by trapping a 5-ml volume of a 100-ppm solution of Pb^{2+} and aspirating the resulting solution (of approximately 400 ppm concentration) as described above. When the electrode trough was refilled and a blank run, a lead signal corresponding to less than 4 ppm concentration was observed. This is one example of a characteristic which was generally observed, that in general the device is not subject to severe memory effects. Thus simple washing of the electrode trough and sample-introduction system suffices to clean the trap between readings. When only dilute solutions are aspirated this freedom from memory effects is largely inherent, since contamination due to memory effects only influences the preconcentrated solutions; the contamination does not get back to the low-concentration side of the system. If a high concentration of a substance (either the analyte or a matrix element) is aspirated, contamination can be transferred subsequently from the sample-introduction system, for instance by splashing from the walls of the heating chamber, and more careful procedures must be adopted. It is intended to discuss this point more fully at a later date.

The trapping behaviour of the system, that is, the trapping efficiency, the form of the calibration curves, and the behaviour of the system with trapping time, proved to be very similar to that found with the wire collector and will not be discussed in detail. Typical results are shown in Fig. 2, in which a comparison is given between a calibration curve obtained by aspiration of increasing concentrations of Ca^{2+}, in the range 0–9 μg/ml, into an air–acetylene flame with the trap switched off, with that obtained by trapping volumes from 0–9 ml of a 1-μg/ml solution of Ca^{2+}. The results are similar to those obtained previously with the wire collector in that they show no appreciable reduction in performance with increasing volume of sample solution from which material is trapped. The difference in the slopes of the two curves is probably due to the fact that trapping efficiency for the

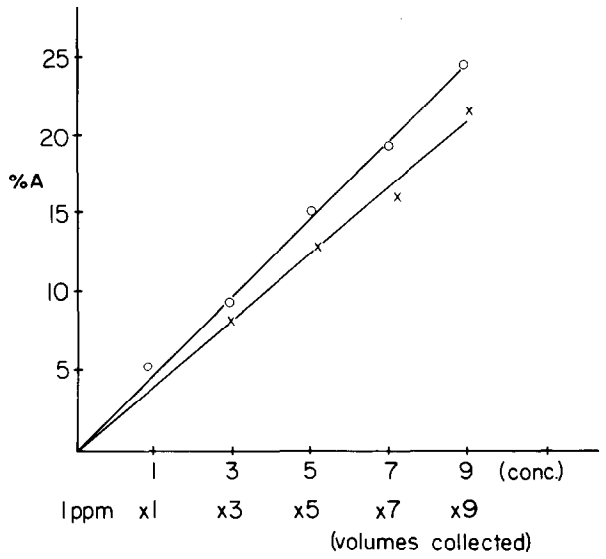


Fig. 2. Calibration curve for calcium; O increasing concentrations of calcium aspirated through the system with zero trapping voltage (μg/ml); × increasing volumes (ml) of a 1-μg/ml solution of calcium which were used for trapping, followed by signal measurement upon re-aspiration.

samples giving the lower curve is not quite 100%. Analogous results have been obtained for the other elements investigated.

Range of applicability of the trap

To assess the scope of the device, trapping and re-aspiration cycles were carried out for some 40 elements. Results are given in Table 1. These results can be summarized in the following observations. First, the device appears either to work completely effectively, trapping and releasing material with virtually 100% efficiency, or else not at all. No intermediate cases have been found. Secondly, trapping appears to occur even when no signal is subsequently observed. This was demonstrated by aspirating a suitably concentrated solution and observing the change in the associated absorption signal as the trapping voltage was increased from zero. In every case the signal fell to a value close to zero as the trapping voltage approached 15 kV. Thus the problem appears to lie in the re-aspiration process. Finally, the elements for which the apparatus failed to work are those which tend to form, irreversibly, highly stable oxides or hydroxides of a potentially polymeric structure.[2] These observations suggest that a possible cause of failure may be the irreversible formation of a water-insoluble solid hydrated oxide within the heating chamber. Although there is no reason why such particles cannot be trapped, if they are unable to redissolve it is likely

Table 1. Elements tested in the trap, and the chemical sources from which solutions of these elements were prepared

Enhancement observed*						Enhancement not observed	
Element	Source	Element	Source	Element	Source	Element	Source
Ag	$AgNO_3$	Ge	GeO_2	Rh	$RhCl_3.3H_2O$	La	$LaCl_3.3H_2O$
Al	$AlCl_3.6H_2O$	Hg	$HgCl_2$	Ru	$RuCl_3.9H_2O$	Nd	$NdCl_3.6H_2O$
B	$Na_2B_4O_7.10H_2O$	K	KNO_3	Sc	$ScCl_3.6H_2O$		
Ba	$Ba(C_2H_3O_2)_2$	Li	$Li_2SO_4.H_2O$	Si	Na_2SiO_3	U	$UO_2(C_2H_3O_2).2H_2O$
Be	$[Be(H_2O)_4]Cl_2$	Mg	Mg/HCl	Sn	$SnCl_2$	Y	$Y(NO_3)_3.6H_2O$
Ca	$CaCl_2$	Mo	Na_2MoO_4	Sr	$SrCl_2$	Zr	$ZrOCl_2.8H_2O$
Co	Co/HCl	Na	NaCl	Ti	$[Ti(H_2O)_6]Cl_3$		
Cr	Cr/HCl	Ni	Ni/HCl	V	V_2O_5/HCl		
Cs	CsCl	Os	$(NH_4)_2OsCl_6$	W	$Na_2WO_4.2H_2O$		
Cu	Cu/HNO_3	Pb	Pb/HNO_3	Zn	ZnO/HCl		
Fe	Fe/HCl	PT	Pt/*aqua regia*				

* In all cases enhancement was tested by selecting a concentration giving an absorption signal in the range of 1–5%, and measuring the absorption with the trap voltage switched off; 1 ml of the solution was then diluted to 10 ml, the entire 10 ml was aspirated and trapped, and the signal from the trapped material was checked for consistency with the original signal. Trapping efficiency was at least 95% for all elements tested.

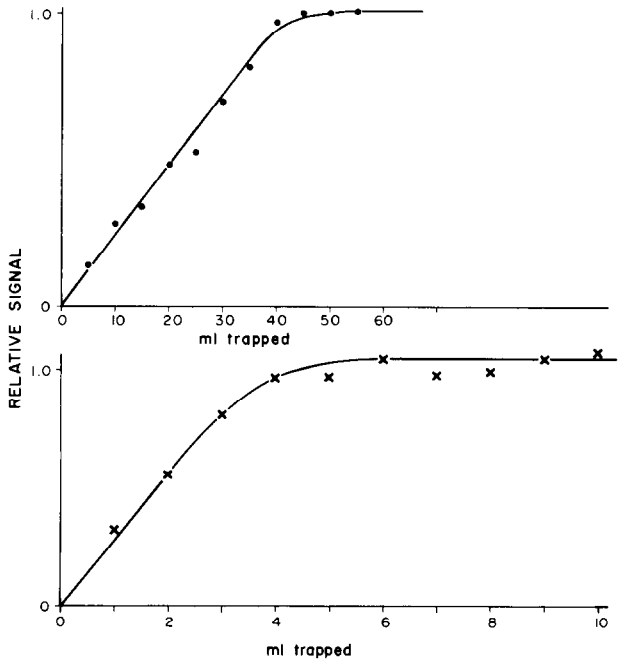


Fig. 3. Response curves for 1-ppm solutions of Pb in 1×10^4 (●) and 1×10^5 (×) ppm NaCl medium.

that they will be subsequently lost owing to the influence of surface tension forces. That is, it is envisaged that when first trapped such particles will float on the water surface, while later they will be left adhering to the sides of the trough during the aspiration step. (In fact, it is possible to detect the presence of non-responding elements in the trough after the aspiration step is complete, but their quantitative recovery has not yet been achieved.)

Influence of sodium chloride

Figure 3 shows the effect of sodium chloride on the trapping behaviour of the system. It is apparent that no serious deviations in the response are encountered, even at high salt concentrations, until the salt level in the electrode solution reaches about 30–40%. This limiting concentration corresponds to a saturated solution of sodium chloride.[3] Thus the breaks in the curves of Fig. 3 are interpreted as marking the solubility limit of the matrix salt in the electrode solution. At higher levels aerosol particles are still found to be trapped, but if they no longer dissolve, and the analyte of interest is retained within the undissolved particles, then the analyte will become lost in a sediment at the bottom of the electrode trough. This represents one limiting factor in the degree of preconcentration which can be expected with the present design of trap.

The behaviour shown in Fig. 3 is encouraging in that it suggests that the system is unlikely to be impractical because of extreme sensitivity towards matrix composition. This is not entirely unexpected, since the trap itself appears to collect any type of aerosol which is presented to it, irrespective of chemical composition, and with close to 100% efficiency. Thus interferences in the system are probably most likely to occur during either nebulization step, or during the subsequent atomization processes. Although interferences of this type are not uncommon they are usually tolerable, since their origins, behaviour and the appropriate correction procedures are in most cases well documented.[4]

Since the apparatus appeared to be performing adequately at this point, it was applied to determination of lead in lake water as an illustration of its practicality. The lake chosen lay within city limits and contained considerable amounts of decaying vegetation and of sodium chloride (due to winter salting of adjacent roads). Thus it was considered that some potentially interfering materials were likely to be present in

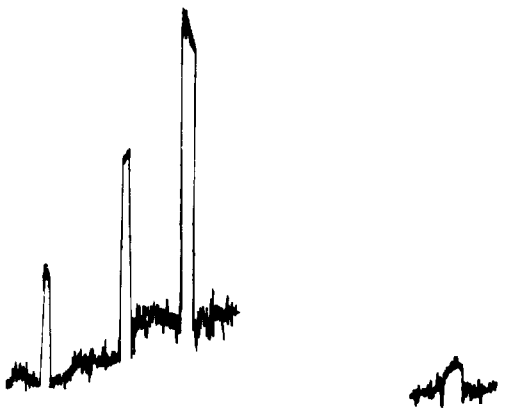


Fig. 4. Signals from left to right are due to the trapping from 50, 100 and 150 ml of lake water, and to a background measurement at 282.0 nm.

the water. Volumes of 50, 100 and 150 ml of untreated water were trapped and measured successively in the manner described. The results (Fig. 4) show that the signals increased in proportion to sample volume, from which it is clear that there is no interference of the type indicated in Fig. 3. The signals correspond to a lead concentration of 0.08 ppm in the original sample. These results were obtained by using the Pb 218.3 nm line, and a 1-sec amplifier time-constant. No particular attempt was made to optimize instrumental parameters such as lamp current, slit-width, nebulization rate, *etc.*, nor was 150 ml close to the maximum sample volume that could have been used. Thus it appears clear that the system is quite capable of measuring Pb concentrations at well below the value found.

CONCLUSIONS

It is found that a water trough will act as an efficient collector electrode during the electrostatic collection of dry aerosol particles. The trapping characteristics of the device appear to be very similar to those reported for wire electrodes: this is not unexpected in view of the physical nature of the trapping process. The liquid electrode has the particular advantage of simplifying the introduction of trapped material into a flame atomizer, and thereby permits the device to be applied to a wide range of elements. It seems likely that the chemical nature of the liquid can be modified to produce some chemical selectivity towards particular species; this possibility has not yet been examined in detail.

The water electrode is thought to operate by dissolving the trapped material to form a homogeneous solution. It appears that the desolvation conditions used are sufficiently mild for the necessity for redissolution not to be a serious handicap. That is, provided material is initially in water-soluble form it is likely to remain so during the desolvation and trapping processes. Exceptions to this have been found, however, such as La, U, Zr. In such cases it is thought that irreversible reaction occurs during desolvation to produce a non-water-soluble aerosol, leading to subsequent inability to transport trapped material into the nebulization system.

The trap will tolerate high sodium chloride concentrations, until the electrode solution becomes saturated. No further concentration of analyte can be obtained beyond this point. Therefore the analyte is considered to be homogeneously distributed within the desolvated aerosol particles. Presumably any other matrix salt will produce analogous effects. Unless it is corrected, this behaviour sets an upper limit to the degree of preconcentration which can be obtained with the present device.

Acknowledgement—The authors are indebted to the Natural Sciences and Engineering Research Council, Canada, for support of this work.

REFERENCES

1. P. A. Michalik and R. Stephens, *Talanta*, 1981, **28**, 37.
2. See *e.g.*, F. A. Cotton and G. Wilkinson, *Advanced Inorganic Chemistry*, Chap. 30, Wiley, New York, 1964.
3. *Handbook of Chemistry and Physics*, 51st Ed., Section B, p. 137, CRC Press, Cleveland, 1971.
4. See, *e.g.*, G. F. Kirkbright and M. Sargent, *Atomic Absorption and Fluorescence Spectroscopy*, Chap. 12, Academic Press, London, 1974.

Talanta Vol. 28. pp. 49 to 53
Pergamon Press Ltd 1981. Printed in Great Britain

1-PHENYL-3-METHYL-4-BENZOYLPYRAZOL-5-ONE AS A GROUP-EXTRACTION REAGENT FOR SPECTROPHOTOMETRIC DETERMINATION OF TRACE ELEMENTS

M. Y. MIRZA and F. I. NWABUE
Department of Chemistry, University of Nigeria, Nsukka, Nigeria

(*Received* 24 *August* 1979. *Revised* 6 *June* 1980. *Accepted* 26 *June* 1980)

Summary—1-Phenyl-3-methyl-4-benzoylpyrazol-5-one has been examined as a regent for detection and solvent extraction of metal ions. The reagent seems to be promising as a group-extraction reagent for the spectrophotometric determination of copper, nickel, cobalt, manganese, zinc, chromium(VI) and molybdenum(VI).

It is known[1,2] that 1-phenyl-3-methyl-4-benzoylpyrazol-5-one (HPMBzP) is a very effective extracting reagent for a number of metals which are extracted with high distribution coefficients at relatively low pH. It has been used for thorium,[3,4] plutonium,[5] copper, gallium, indium, thallium,[6] palladium,[7] iron[3,8] zirconium and niobium.[9,10] The present work was undertaken to study its general applicability for qualitative tests and liquid–liquid extraction. HPMBzP is shown to be a suitable reagent for extractive concentration of nickel, cobalt, manganese, zinc, copper, chromium(VI) and molybdenum(VI) before their spectrophotometric determination,.

EXPERIMENTAL

Reagents

All reagents were of analytical grade and used without further purification unless otherwise mentioned. Stock solutions of the elements were prepared by dissolving appropriate quantities of their salts in 0.1*M* nitric acid. HPMBzP was synthesized by the standard methods,[1,2] and 0.5% ethanolic and 1% chloroform solutions were used for the qualitative and extraction studies respectively.

Standard buffers (potassium chloride/hydrochloric acid, hydrochloric acid/potassium phthalate, sodium hydroxide/potassium phthalate, sodium hydroxide/boric acid) were used to cover the pH range 1–10.

Measurement of distribution ratio

Equal volumes of aqueous and organic phase were shaken mechanically for 5 min at room temperature. The phases were then centrifuged and separated. The distribution ratio was calculated as the ratio of the concentrations in the organic and the aqueous phase. The concentration in the aqueous phase was determined by the methods given below, and that in the organic phase (except for copper) was obtained by stripping with 1*M* hydrochloric acid and using the same methods as for the aqueous phase.

Copper was determined directly in the organic phase by measuring the absorbance at 670 nm against a reagent blank.[6]

Zinc was determined by evaporating an aliquot of the solution to dryness, dissolving the residue, adjusting the pH to 4.0–5.5, adding 2 ml each of 20% sodium thiosulphate solution and 5% potassium cyanide solution, extracting with 0.01% dithizone solution in carbon tetrachloride and measuring the absorbance at 620 nm against a reagent blank.[11]

Cobalt was determined by evaporating an aliquot of solution, taking up in 0.2*M* sodium citrate, adjusting to pH 2.5–5.0, extracting with 0.2% 2-nitroso-1-naphthol solution in chloroform, washing the organic layer with sodium hydroxide and measuring the absorbance at 530 nm against a reagent blank.

Manganese was determined by persulphate oxidation in presence of mercuric sulphate (to mask chloride) and measurement of the absorbance of the permanganate at 525 nm against a reagent blank.

Nickel was determined by neutralizing the solution with ammonia, adding 1% alcoholic solution of dimethylglyoxime, and 6*M* sodium hydroxide and measuring the absorbance at 530 nm against a reagent blank.

Chromium was determined by the diphenylcarbazide method, with measurement of the absorbance at 540 nm.

Molybdenum was determined by extraction of molybdenum(V) thiocyanate with di-isopropyl ether and measurement of the absorbance at 465 nm against a reagent blank.

Qualitative tests

About 5 mg of the metal salt was dissolved in 1 ml of the medium to be tested (buffer solutions of pH 1, 3 and 7 and 2*M* hydrochloric, nitric and sulphuric acids) in a stoppered glass tube. Then 5–10 drops of 0.5% ethanolic solution of HPMBzP were added, and any turbidity or precipitate was extracted with 1 ml of chloroform.

Determination of trace elements

The trace elements (100 μg of each), in salt form, were dissolved in an appropriate buffer solution and the solution extracted twice with an equal volume of 1% HPMBzP solution in chloroform for 5 min each time. From the combined extract, the metals were stripped with 1*M* hydrochloric acid. An aliquot of the extract was used for the spectrophotometric determination of each element.

Determination of trace elements in tropical fruits

Known weights of the peel, core, pulp and seeds of the fruits were ashed at 400–450°. A known weight of the ash was dissolved in dilute hydrochloric acid, and an aliquot of the solution was adjusted to pH 2.0 and extracted twice with an equal volume of 1% chloroform solution of HPMBzP for 5 min each time. The phases were centrifuged

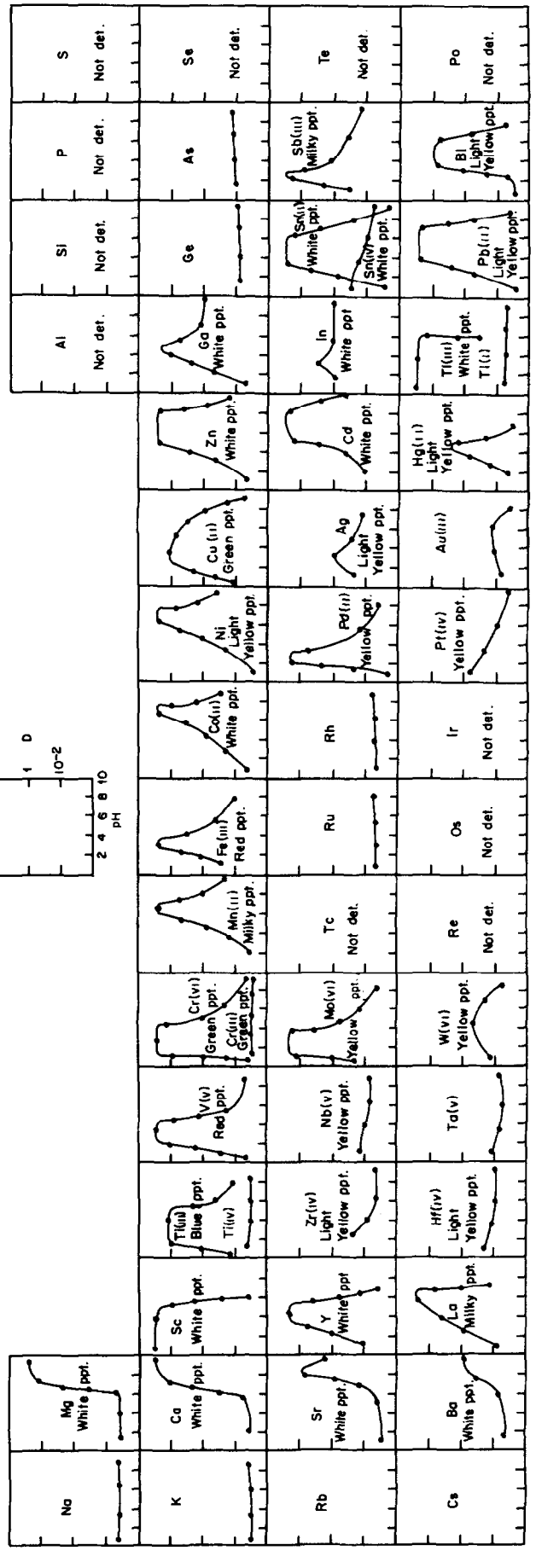


Fig. 1. Effect of pH on the extraction of Group I—V elements with 1% solution of 1-phenyl-3-methyl-4-benzoylpyrazol-5-one in chloroform. (The colour of the precipitate from a qualitative test is indicated below the respective metal; where no colour is given no precipitate was formed.)

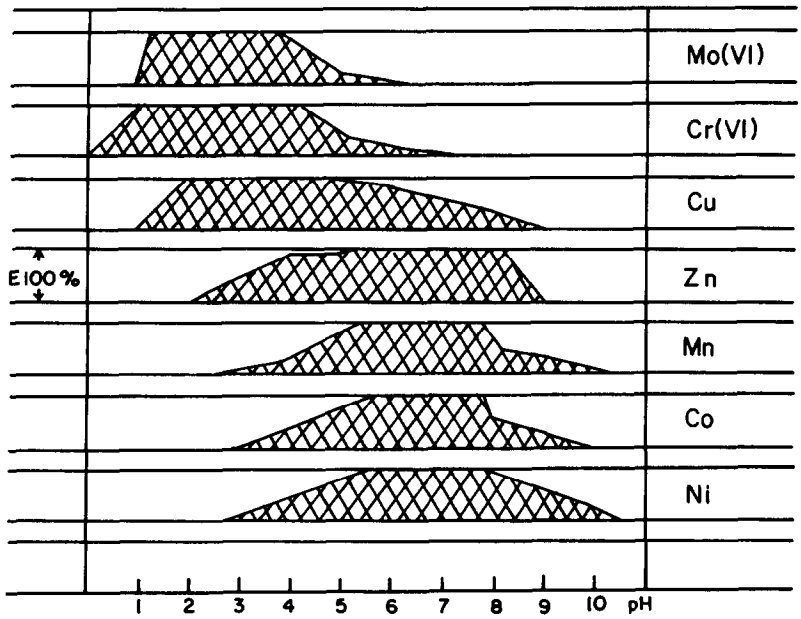


Fig. 2. Range of pH for extraction of nickel, cobalt(II), manganese(II), zinc, copper(II), chromium(VI) and molybdenum(VI) with 1% solution of 1-phenyl-3-methyl-4-benzoylpyrazol-5-one in chloroform.

and separated. Copper was determined directly in the combined organic extracts. Chromium and molybdenum were stripped with 1*M* hydrochloric acid and determined separately.

A second aliquot was adjusted to pH 7.0 with ammonia and buffer and shaken with an equal volume of the HPMBzP solution in chloroform for 5 min. Nickel, cobalt, manganese and zinc were stripped with 1*M* hydrochloric acid and determined individually.

RESULTS AND DISCUSSION

The qualitative tests indicate that most cations react with the reagent in weakly acid and neutral solutions while few form complexes in the presence of 2*M* acids. Magnesium, calcium, strontium, barium, zinc, cadmium, gallium, indium, yttrium, lanthanum, tin(II), antimony(III), manganese(II, VII), aluminium and cobalt form white precipitates, and copper and vanadium(VI) give a green colour or precipitate. Cerium(IV), arsenic (III), tantalum, selenium(VI), and iron(II) form brown colours or precipitates and titanium(III) gives a blue precipitate, Titanium(IV) is hydrolysed at acidities less than 2*M* (except in nitric acid) but gives a yellow precipitate in all acids above 4*M* in concentration. The complexes of lead(II), zirconium, hafnium, bismuth, niobium, molybdenum(VI), tungsten(VI), nickel, palladium(II), platinum(IV) and thorium are yellow or light yellow, and that of uranium(VI) is golden yellow. Vanadium(V) and iron(III) form red precipitates. Sodium, potassium, boron, thallium(II) and rhodium(III), do not give any visible reaction. Tungsten(VI) is hydrolysed only in the presence of acids, but germanium shows hydrolysis in all aqueous media. Most of the complexes are extractable into chloroform and by controlling the acidity of the medium it is possible to use HPMBzP for the separation and determination of several elements.

Figure 1 shows the pH ranges over which the elements are extracted. Rubidium and caesium behave similarly to sodium and potassium. Alkali metals, ruthenium and rhodium are not extracted at all, and zirconium, niobium, hafnium and tantalum are extracted negligibly. The extraction behaviour of selenium, tellurium, rhenium, osmium, iridium, aluminium, silicon, phosphorus, sulphur and polonium was not studied. Alkaline earths are extracted at pH above

Table 1. Analysis of synthetic mixtures

Element	Taken μM	Found μM
Ni	1.70	1.69
		1.66
		1.68
Co	1.70	1.67
		1.67
		1.67
Mn	1.82	1.80
		1.79
		1.78
Zn	1.53	1.52
		1.51
		1.50
Cu	1.57	1.55
		1.55
		1.54
Cr	1.92	1.90
		1.89
		1.89
Mo	1.04	1.02
		1.02
		1.02

Table 2. Mineral composition of various parts of *Annona muricata linn* (Soursop fruit), g/100 g of ash (the ash contents are 0.42, 0.48, 0.29 and 0.35% for the peel, pulp, core and kernel respectively

Element	Peel		Pulp		Core		Kernel	
	With 0.036*M* HPMBzP/$CHCl_3$	With 0.1*M* oxine/$CHCl_3$	With 0.036*M* HPMBz/$CHCl_3$	With 0.1*M* oxine/$CHCl_3$	With 0.036*M* HPMBzP/$CHCl_3$	With 0.1*M* oxine/$CHCl_3$	With 0.036*M* HPMBzP/$CHCl_3$	With 0.1*M* oxine/$CHCl_3$
Copper	4.80	4.95	4.10	4.01	4.50	4.51	5.00	5.30
Zinc	3.80	3.76	7.70	7.00	3.80	3.86	5.50	5.50
Chromium	0.05	—	0.01	—	0.01	—	0.09	—
Molybdenum	Nil	Nil	Nil	Nil	Nil	Nil	Nil	Nil
Cobalt	0.025	0.026	0.061	0.061	0.005	0.004	0.03	0.025
Manganese	0.001	0.003	0.021	0.019	0.001	0.001	0.064	0.066
Nickel	Nil	Nil	Nil	Nil	Nil	Nil	Nil	Nil

Table 3. Mineral composition of various parts of *Chrysophyllum albidum* (Udara fruit), g/100 g of ash (the ash contents are 2.07, 1.03 and 0.81% for the peel, pulp and kernel respectively

Element	Peel		Pulp		Kernel	
	With 0.036*M* HPMBzP/$CHCl_3$	With 0.1*M* oxine/$CHCl_3$	With 0.036*M* HPMBzP/$CHCl_3$	With 0.1*M* oxine/$CHCl_3$	With 0.036*M* HPMBzP/$CHCl_3$	With 0.1*M* oxine/$CHCl_3$
Copper	0.030	0.026	0.011	0.010	0.061	0.060
Zinc	4.60	4.60	7.91	7.70	6.45	6.50
Chromium	Nil	Nil	Nil	Nil	Nil	Nil
Molybdenum	Nil	Nil	Nil	Nil	Nil	Nil
Cobalt	Nil	Nil	Nil	Nil	Nil	Nil
Manganese	0.09	0.091	0.13	0.12	0.10	0.09
Nickel	Nil	Nil	Nil	Nil	Nil	Nil

Table 4. Separation factors of co-extracted metal ions with respect to copper, with 0.036*M* HPMBzP/$CHCl_3$ at pH 2.0

Ion	Concentration m*M*	Separation factor D_{Cu}/D_{metal}
Pd(II)	0.188	0.11
Pt(VI)	0.103	220
Ag(I)	0.185	110
Sb(III)	0.164	0.11
Sn(II)	0.169	61
Ga(III)	0.287	140
Pb(II)	0.097	550

Table 5. Separation factors of the co-extracted metal ions with respect to Cr(VI) and Mo(VI) with 0.036*M* HPMBzP/$CHCl_3$ at pH 2.0

Ion	Concentration m*M*	Separation factor $D_{Cr,Mo}/D_{metal}$
Pd(II)	0.188	16
Pt(IV)	0.103	3.2×10^3
Ag(I)	0.185	1.6×10^3
Sb(III)	0.164	160
Sn(II)	0.169	0.88×10^3
Ga(III)	0.287	2.0×10^3
Pb(II)	0.097	8.0×10^3

7 in the order Mg ~ Ca > Sr > Ba, and tervalent rare earths are extracted at pH 3.8–5.5 in the order Sc > Y > La. Vanadium(V), chromium(VI), manganese(II), iron(III), cobalt(II), nickel, copper(II), zinc, gallium, molybdenum(VI), palladium(II), cadmium, titanium(III), indium, tin(II), antimony(III), thallium(III), lead and bismuth can be quantitatively extracted at appropriate pH values.

Figure 2 shows the pH ranges over which nickel, cobalt, manganese, zinc, copper, chromium and molybdenum are 100% extracted. The first four are quantitatively extracted at pH 5.5–7.8 copper at pH 2.8–4.8 and the last two at pH 1.3–3.8. Copper is only 95% extracted at pH 2.0, but a double extraction at this pH separates Cu, Cr and Mo as a group without co-extraction of several species, *e.g.*, bismuth, cadmium, mercury(II) and tungsten, which are appreciably extracted at pH 3–5. A single extraction at pH 7 is enough for separation of Ni, Co, Mn and Zn as a group. Iron interferes but can be masked with sodium citrate or potassium hydrogen phosphate.

The separation was tested with synthetic mixtures and various fruit samples, and the results are summarized in Tables 1–3.

Table 1 shows the analysis of synthetic mixtures of the two groups of elements, from which it is evident that the method is efficient within the limits of experimental error. Table 2 shows analysis of a fruit sample, *Annona muricata linn.* Copper and zinc are present in high concentrations. Chromium, cobalt and manganese are found only in tracer quantity, and molybdenum and nickel are absent. Table 3 shows the percentages of these elements in *Chrysophyllum albidum.* Zinc is present in large amount, copper and manganese occur in trace quantities and chromium, nickel, molybdenum and cobalt are absent. The results obtained by the 8-hydroxyquinoline method are also shown, and there is good agreement between the results.

Table 6. Separation factors of the co-extracted metal ions with respect to the zinc group elements (Zn, Mn, Co and Ni) with 0.036*M* HPMBzP/$CHCl_3$ at pH 7.0

Ion	Concentration m*M*	Separation factor $D_{Zn,etc.}/D_{metal}$
Ga(III)	0.287	67
Ag(I)	0.185	5.0×10^4
Cd(II)	0.178	1.11
Sn(II)	0.169	25
Sb(III)	0.164	1.1×10^4
Pb(II)	0.097	1.25
Bi(III)	0.096	2.5×10^3

Zirconium, niobium, titanium(IV), sodium, potassium (10 mg of each) and calcium, strontium, barium, scandium, yttrium and lanthanum (1.0 mg of each) do not interfere in the determination of nickel, cobalt, manganese, zinc, copper, chromium and molybdenum each present at the 100 μg/ml level. Lead, vanadium(IV), palladium(II), silver, cadmium, iron(III), gallium, indium, antimony, bismuth, platinum and thallium(III) are co-extracted, but should not interfere if the correct determination methods are used. The separation factors for these metals with respect to the seven trace elements are summarized in Tables 4–6.

Acknowledgement—M.Y.M. is thankful to the Senate Research Grants Committee of the University for the award of a research grant.

REFERENCES

1. B. S. Jensen, *Acta Chem. Scand.* 1959, **13**, 1668.
2. *Idem, ibid.*, 1959, **13**, 1890.
3. Z. K. Karalova and Z. I. Pyzhova, *Zh. Analit. Khim.*, 1968, **23**, 1564.
4. M. Y. Mirza, *Radiochim. Acta*, 1978, **25**, 45.
5. M. K. Chmuova, Pt N. Palei and Yu A. Zolotov, *Zh. Analit. Khim.*, 1966, **23**, 1476.
6. M. Y. Mirza, *Talanta*, 1978, **25**, 685.
7. M. Y. Mirza and R. T. Bailey, *J. Inorg. Nucl. Chem.*, 1979, **41**, 772.
8. M. K. Chmutova and M. E. Kochetkova, *Zh. Analit. Khim.*, 1967, **24**, 216.
9. M. Y. Mirza and F. I. Nwabue, *Radiochim. Acta* (In press).
10. O. Navratil and B. S. Jensen, *J. Radioanal. Chem.* 1970, **5**, 313.
11. E. B. Sandell, *Colorimetric Metal Analysis*, 3rd Ed., Interscience, New York, 1959.

Talanta Vol. 28, pp. 55 to 58
Pergamon Press Ltd 1981. Printed in Great Britain

SHORT COMMUNICATIONS

BENZOHYDROXAMIC ACID AS A REDUCTOMETRIC TITRANT: DETERMINATION OF MANGANESE, CHROMIUM AND VANADIUM IN STEELS

M. K. AHMED* and C. SUBBARAO

Department of Chemistry, Government College of Engineering and Technology, Raipur, 492002, India

(*Received* 12 *October* 1979. *Revised* 27 *February* 1980. *Accepted* 15 *July* 1980)

Summary—A method has been developed for the rapid determination of manganese and chromium by direct stepwise reductometric titration with benzohydroxamic acid, and of vanadium by titration with ascorbic acid (with benzohydroxamic acid as indicator) in the same aliquot. The method is free from the interference of common alloying elements present in steels. Some BCS steel samples have been analysed with good precision and accuracy.

The literature methods[1,2] for the determination of manganese, chromium and vanadium in admixture are laborious, requiring the use of two or more aliquots of sample solutions and selective oxidation of some of these metals several times. Therefore, a method which does not involve these difficulties is desirable.

In recent communications we have reported the use of benzohydroxamic acid as a reductometric titrant, for the determination of manganese[3] and chromium[4] in steels. The present paper deals with the consecutive determination of manganese, chromium and vanadium in the same aliquot and application of the proposed method for the determination of these metals in ores and alloys.

EXPERIMENTAL

Benzohydroxamic acid was prepared and purified by the literature procedure.[5] Its purity was established from its infrared spectrum[6] and m.p. (130°).[7] A standard solution was prepared by dissolving an accurately weighed quantity of the pure benzohydroxamic acid in water and diluting.

Solutions of the various metal ions (10 mg/ml) used in the interference studies were prepared according to West's procedure.[8]

All chemicals used were of analytical-reagent grade.

Procedure

About 0.1 g of sample (accurately weighed) is dissolved in 10 ml of *aqua regia*, by heating. To the cooled solution 5 ml of concentrated sulphuric acid are added and the mixture is heated till dense white fumes appear. Alloys containing a high percentage of the metals to be determined are suitably diluted at this stage, after cooling. The sample solution or an aliquot of it is diluted to 100 ml and 10 ml of 1% silver nitrate solution and 0.5–1.0 g of potassium persulphate are added, followed by 5 ml of concentrated sulphuric acid. The mixture is boiled gently until oxidation of the alloying metal ions to their highest oxidation state is complete and the excess of persulphate is decomposed. The mixture is cooled to room temperature and titrated with the standard solution of benzohydroxamic acid. The first visual end-point, corresponding to the reduction of Mn(VII) to Mn(II) is located when the pink colour disappears completely, leaving a clear slightly yellow solution. This solution is further titrated (5 ml of 1% ferric chloride solution should be added here if the sample solution does not contain ferric ions) with the same benzohydroxamic acid solution till a purple colour is obtained. This second end-point corresponds to the reduction of Cr(VI) to Cr(III). Sufficient potassium fluoride solution is then added to mask the ferric ions. A violet colour is produced when 5 ml of 0.5% benzohydroxamic acid solution are added; the solution is immediately titrated with a standard solution of ascorbic acid till the violet colour completely disappears, leaving a clear sky-blue solution. The volume of ascorbic acid corresponds to the reduction of V(V) to V(IV).

1 ml of 0.1 *M* benzohydroxamic acid
≡ 6.59 mg of manganese

1 ml of 0.1 *M* benzohydroxamic acid
≡ 3.47 mg of chromium

1 ml of 0.1 *N* ascorbic acid
≡ 5.10 mg of vanadium

RESULTS AND DISCUSSION

Potentiometric titrations of permanganate and dichromate, separately, with benzohydroxamic acid in 2–3 *N* sulphuric acid medium, showed that the emf values at the equivalence points were around 950 and 700 mV respectively. As this difference in potentials at the end-point was fairly wide, it was expected that

* *Present address*: Radiochemistry Laboratory, Reactor Research Centre, Kalpakkam-603 102, India.

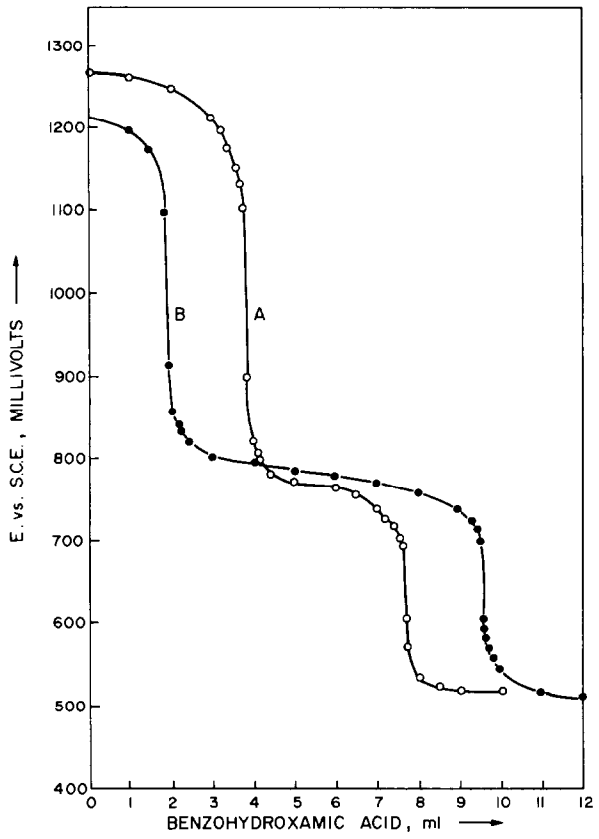


Fig. 1.

Table 1. Determination of permanganate and dichromate in synthetic mixtures

$KMnO_4$, *ml*	$K_2Cr_2O_7$, *ml*	Volume of BHA used Potentiometric* First end-pt	Potentiometric* Second end-pt	Visual First end-pt	Visual Second end-pt
5	10	1.95	9.56	1.95	9.55
10	5	3.86	7.68	3.90	7.70

* Obtained from second-derivative plots.

$KMnO_4 = 4.35 \times 10^{-2}N$; $K_2Cr_2O_7 = 2.86 \times 10^{-2}N$; acidity = $3N$. H_2SO_4; total volume = 100 ml; BHA = $1.86 \times 10^{-2}M$.

Table 2. Determination of manganese, chromium and vanadium in mixtures

Volumes used in the synthetic mixtures, *ml* $KMnO_4$	$K_2Cr_2O_7$	$NaVO_3$	BHA used for Mn, *ml*	BHA used for Cr, *ml*	Ascorbic acid used for V, *ml*	Found, *mg* Mn	Cr	V
1.0	2.0	1.0	0.50	1.18	0.90	0.021 (0.020)	2.59 (2.57)	0.096 (0.096)
3.0	4.0	2.0	1.40	2.34	1.82	0.058 (0.059)	5.13 (5.15)	0.193 (0.192)
5.0	6.0	3.0	2.35	3.52	2.72	0.098 (0.099)	7.72 (7.72)	0.289 (0.288)
2.0	8.0	2.0	0.95	4.70	1.80	0.040 (0.040)	10.30 (10.30)	0.190 (0.192)
5.0	10.0	3.0	2.35	5.88	2.70	0.098 (0.099)	12.89 (12.87)	0.286 (0.288)

* Expected values are given in parentheses.

$KMnO_4$ $1.80 \times 10^{-3}N$; $K_2Cr_2O_7$ $7.43 \times 10^{-2}N$; $NaVO_3$ $1.89 \times 10^{-3}N$; acidity $2.7N$ H_2SO_4; total volume 25 ml; $6.32 \times 10^{-2}M$ BHA; ascorbic acid $1.98 \times 10^{-3}M$.

Table 3. Analysis of standard reference materials

Sample	Mn			Cr		V	
	Taken, *mg*	BHA used, *ml*	Found, %	BHA used, *ml*	Found, %	Ascorbic acid used, *ml*	Found, %
1. BCS 241/1	106.8	0.65	0.30	2.05	5.00	1.35	1.58
Mn = 0.30%	147.9	0.90	0.30	2.85	5.02	1.85	1.56
Cr = 5.03%	132.4	0.80	0.30	2.55	5.02	1.65	1.57
V = 1.57%							
2. BCS 220/1							
Mn = 0.28%	142.8	1.15	0.28	4.10	5.16	2.60	2.10
Cr = 5.13%	139.6	1.15	0.28	4.00	5.15	2.55	2.11
V = 2.09%	117.2	0.95	0.28	3.35	5.14	2.15	2.12
3. BCS 224/1							
Mn = 0.66%	110.6	2.15	0.67	0.65	1.06	0.18	0.19
Cr = 1.06%	152.4	2.95	0.66	0.90	1.06	0.25	0.19
V = 0.19%	129.7	2.50	0.66	0.75	1.04	0.21	0.19

Samples made up to 100 ml after dissolution, and 10-ml aliquots taken for titration. [BHA], sample 1—$7.52 \times 10^{-4}M$ for Mn, $7.52 \times 10^{-3}M$ for Cr; samples 2 and 3—$5.18 \times 10^{-4}M$ for Mn, $5.18 \times 10^{-3}M$ for Cr: [ascorbic acid], sample 1—$2.45 \times 10^{-3}M$; samples 2 and 3—$2.27 \times 10^{-3}M$.

Table 4. Analysis of standard reference materials

	Sample	Taken, *mg*	BHA used, *ml*	Cr found in aliquot, *mg*	Cr, %
1	BCS 211/1	262.6	7.50	1.342	12.8
	(12.8% Cr)	328.2	9.40	1.681	12.8
		234.9	6.70	1.198	12.6
2	BCS 261	260.2	10.05	1.798	17.3
	(17.2% Cr)	216.4	8.35	1.494	17.3
		301.5	11.65	2.083	17.3
3	BCS 235/2	267.9	11.00	1.977	18.5
	(18.6% Cr)	292.4	12.05	2.165	18.5
		199.6	9.20	1.473	18.5
4	BCS 203/3	126.7	10.10	1.806	71.2
	(71.2% Cr)	120.4	9.60	1.717	71.2
		153.1	12.20	2.182	71.2

Samples 1–3, 10-ml aliquot used from 250 ml of solution; sample 4, 5-ml aliquot used from 250 ml of solution. Samples 1, 2, 4, [BHA] $5.16 \times 10^{-3}M$; sample 3, [BHA] $5.18 \times 10^{-3}M$.

Table 5. Analysis of standard reference materials

	Sample	Taken, *mg*	Ascorbic acid used, *ml*	V found in aliquot, *mg*	V, %
1	BCS 203/3	204.3	1.45	0.181	0.09
	(0.09% V)	173.7	1.25	0.156	0.09
		236.3	1.70	0.212	0.09
2	BCS 205/2	101.2	1.85	2.14	52.6
	(52.40% V)	129.9	2.35	2.72	52.3
		145.3	2.65	3.06	52.7

Sample 2, 10-ml aliquot used from 250 ml of solution, [ascorbic acid] $2.27 \times 10^{-2}M$; sample 1 [ascorbic acid] $2.45 \times 10^{-3}M$.

there should be no difficulty in titrating one in the presence of the other. When synthetic mixtures of permanganate and dichromate were titrated potentiometrically with benzohydroxamic acid, two distinct breaks in the titration curve were observed (Fig. 1), indicating that there was no appreciable overlap of the reductions. Titrations to visual end-points yielded the same results (Table 1). Potentiometric titration of sodium vanadate in 4*N* sulphuric acid with benzohydroxamic acid showed that the emf at the equivalence point was also around 700 mV, similar to that in the case of dichromate, but the reaction was very slow. Therefore the vanadium(V) was titrated with standard ascorbic acid solution, with benzohydroxamic acid as indicator.[9] It was observed, during the interference studies, that manganese in quantities of 0.1 mg or less could be accurately determined even in the presence of 10 mg of chromium(VI) and that up to 10 mg of chromium could be satisfactorily determined provided there is not more than 0.3 mg of vanadium(V) present. The results shown in Table 2 clearly show that the proposed method is precise as well as accurate. Some B.C.S. samples have also been analysed by the recommended procedure. The results are recorded in Tables 3–5. Further dilution of the samples may be necessary in order to prevent precipitation of manganese dioxide in the oxidation step. A little experience soon shows when this is necessary. The standard deviations of the titrations ranged from 0.01 to 0.03 ml.

Acknowledgements—The authors are indebted to Professor V. G. Vaidya and Principal R. A. Deshpande of Government College of Engineering and Technology, Raipur, for laboratory facilities. One of the authors (M.K.A.) wishes to thank the Ministry of Education and Social Welfare, Government of India, New Delhi, for awarding a research fellowship under the Research Training Scheme.

REFERENCES

1. R. Lang and F. Kurtz, *Z. Anal. Chem.*, 1931, **86**, 288.
2. R. Lang and E. Faude, *ibid.*, 1937, **108**, 181.
3. M. K. Ahmed and C. Subbarao, *Talanta*, 1978, **25**, 708.
4. *Idem*, *Anal 64*, Annual Convention of Chemists, Waltair, India, 1978.
5. C. R. Hauser and W. B. Renfrow, Jr., *J. Am. Chem. Soc.*, 1937, **59**, 2308; *Organic Synthesis*, 1946, **11**, 67.
6. F. Mathis, *Compt. Rend.*, 1951, **232**, 505.
7. O. Exher and W. Simon, *Collection Czech. Chem. Commun.*, 1965, **30**, 4078.
8. P. W. West, *J. Chem. Educ.*, 1941, **18**, 528.
9. M. K. Ahmed, *Ph.D. Thesis*, Ravishankar University, Raipur, India, 1978.

Talanta Vol. 28, pp. 59 to 61
© Pergamon Press Ltd 1981. Printed in Great Britain
0039-9140/81/0101-0059$02.00/0

p-SULPHOBENZENEAZO-4-(2,3-DIHYDROXY-5-CHLOROPYRIDINE) AS A REAGENT FOR SPECTROPHOTOMETRIC DETERMINATION OF NIOBIUM(V)

YOGENDU SHARMA
Department of Chemistry, Ganjdundwara College, Ganjdundwara, 207242, India

(*Received* 3 *October* 1978. *Revised* 8 *March* 1980. *Accepted* 17 *July* 1980)

Summary—Niobium reacts with *p*-sulphobenzeneazo-4-(2,3-dihydroxy-5-chloropyridine) to form an orange–red ML_2 complex having maximum absorbance at 485 nm in citric acid medium at pH 6.0 ± 0.5. The reaction is slow at room temperature, but complete in 10 min at 60°. The colour is stable for at least 16 hr. The system obeys Beer's law over the concentration range 0.5–8 μg/ml. The molar absorptivity is 5.26×10^3 l.mole^{-1}.cm^{-1}.

In a search for a sensitive and selective reagent for spectrophotometric determination of niobium, some azo compounds have been studied, in particular *p*-sulphobenzeneazo-4-(2,3-dihydroxy-5-chloropyridine). This reagent forms an orange–red complex with niobium in citric acid medium. The citric acid stabilizes the niobium solution against hydrolysis.

EXPERIMENTAL

Reagents

Standard niobium solution (1 mg/ml). Pure niobium pentoxide, (0.1431 g) was fused with 10 g of potassium bisulphate in a silica crucible and after cooling the melt was warmed with 10 ml of 25% citric acid solution. The solution was transferred to a 100-ml standard flask and made up to volume with distilled water, after adjustment of the pH to 4.0 with dilute ammonia solution or sulphuric acid. The solution was standardized with tannin by precipitation and ignition to the oxide.[5]

p-Sulphobenzeneazo-4-(2,3-dihydroxy-5-chloropyridine) solution, 0.25%, in water.

Procedure

Take a portion of sample solution containing 20–200 μg of niobium, add 5 ml of 0.001*M* reagent solution, adjust to pH 6.0 with dilute ammonia solution and make up to 25 ml in a standard flask. Measure the absorbance at 485 nm against a reagent blank prepared similarly and determine the amount of niobium(V) from the calibration curve.

Niobium in steel

Dissolve 100 mg of sample containing 0.5–1.5% niobium in sulphuric acid (1 + 1) and heat to fumes. Cool, add dilute hydrochloric acid, filter off the silica, wash it and ignite it in platinum. Dissolve the impure silica in a few drops of hydrochloric acid and hydrofluoric acid and add it to the original solution. Add 10 ml of *p*-sulphobenzeneazo-4-(2,3-dihydroxy-5-chloropyridine) solution and add 2.5% tannin solution drop by drop with stirring until the precipitation of niobium is complete. Filter off on paper and wash the precipitate with 1% tannin solution. Ignite the precipitate in a silica crucible and fuse the residue with potassium pyrosulphate. Dissolve the cooled cake in 10 ml of 25% citric acid solution and add dilute ammonia solution dropwise to adjust the pH to 6.0. Transfer the solution to a 100-ml standard flask and dilute to volume with distilled water. Take 5 ml of the solution in a 25-ml standard flask, add 10 ml of *p*-sulphobenzene-4-(2,3-dihydroxy-5-chloropyridine) solution, adjust the pH to 6.0 with dilute ammonia solution and dilute to volume with distilled water. After 1 hr measure the absorbance at 485 nm.

RESULTS AND DISCUSSION

Spectral characteristics

The absorption spectrum of the complex at pH 6.0, recorded against the corresponding reagent blank, shows a maximum at 485 nm. The absorbance maximum shifts to shorter wavelengths at lower pH and also decreases (Fig. 1). The maximum absorbance is obtained in the pH range from 5.5 to 6.5.

The molar absorptivity at pH 6 and 485 nm is 5.26×10^3 l.mole^{-1}.cm^{-1} and Beer's law is obeyed over the niobium concentration range 0.5–8 μg/ml. A 5-μg/ml solution gave an average absorbance of 0.450 (standard deviation 0.002, 15 variates).

Effect of temperature and time

Figure 2 shows the colour development curves for heated and unheated solutions. At room temperature (27°), 60 min are needed for full colour development, but only 10 min if the solution is heated at 60–65°. The absorbance remains constant for at least 16 hr.

Interference of foreign ions

The effects were studied by adding the ions to 10-ppm niobium solution, then developing the colour by the usual procedures. Cations were added as nitrates and anions as sodium salts. The tolerance limit was taken as the concentration of ion that did not cause more than ±3% change in the absorbance of a 10-ppm niobium solution.

Thiocyanate, oxalate, tartrate, sulphate, nitrate and phosphate do not interfere; chloride, bromide and

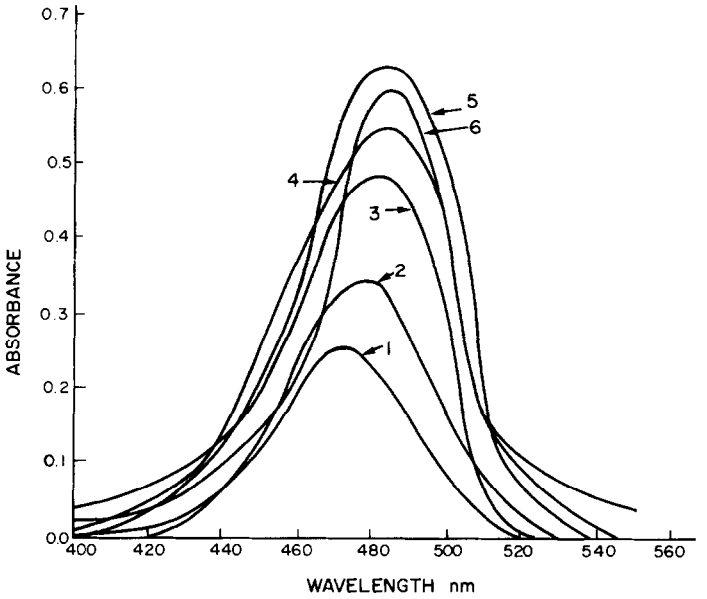


Fig. 1. Absorption spectra of the niobium complex at various pH values. [Nb] $1.0 \times 10^{-5}M$; [SDCP] $1.0 \times 10^{-4}M$; pH: (1) 2; (2) 3; (3) 4; (4) 5; (5) 6; (6) 7.

iodide above 150 ppm interfere. Titanium, tantalum, vanadium(V), tungsten(VI), molybdenum(VI) and uranium(VI) above 175 ppm interfere. Barium, nickel, cobalt(II), aluminium, manganese(II), copper(II), iron(III), chromium(III), bismuth and cadmium up to 200 ppm do not interfere.

Nature of the complex

The method of Vosburgh and Cooper[6] was used to determine the nature of the complex. Equimolar solutions of niobium (M) and the reagent (L) ($1.0 \times 10^{-4}M$) were prepared and mixed to give M:L ratios 1:1, 1:2, 1:3, 1:4, 1:5 in a total volume of 25 ml, at pH 6.0. A blank solution containing all reagents except the ligand was prepared under the same conditions. Absorbance measurements were made from 350 to 550 nm and plotted against wavelength for each M:L ratio. The curves were identical in nature, with maximum absorbance in the region of 485 nm. This suggests the formation of only one complex.

Job's method[7] showed that the complex was ML_2, and this was confirmed by the mole-ratio method.[8,9]

Application

The preliminary separation of niobium with controlled addition of tannin is faster in presence of *p*-sulphobenzeneazo-4-(2,3-dihydroxy-5-chloropyridine) and seems more complete. Cupferron separation may also be used but the present method is less time-consuming. The result for niobium in niobium-stabilized stainless steel is given below. Determination of niobium in synthetic samples gave recoveries of 99%.

Composition of the sample, %				Nb present, %	Nb found,%
Cu	0.08	Mn	0.2	0.80	0.79
Cr	15.4	W	0.05		
Ni	12.03	Si	0.35		
Mo	0.8	C	0.06		
V	0.02				

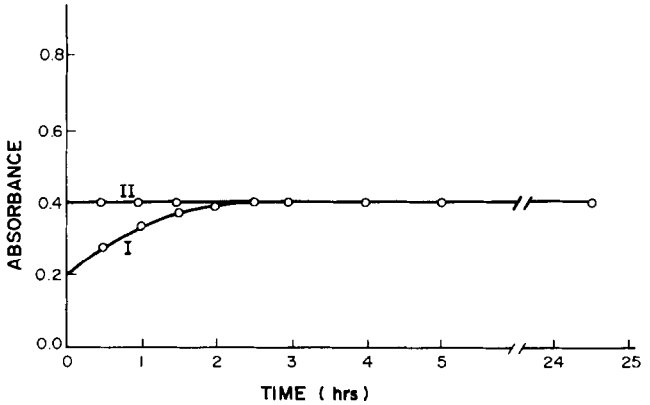


Fig. 2. Effect of heating: I—unheated; II—heated at 60°, [Nb] $1.0 \times 10^{-5}M$; [SDCP] $1 \times 10^{-4}M$.

Acknowledgement—The author is thankful to the University Grants Commission for providing financial assistance.

REFERENCES

1. I. P. Alimarin and H. Hen, *Zh. Analit. Khim.*, 1963, **18**, 182.
2. F. Fairbrother and J. B. Taylor, *J. Chem. Soc.*, 1956, 4946.
3. I. P. Alimarin and I. M. Gibalo, *Zh. Khim. i Khim. Tekhnol.* 1962, **5**, 374.
4. J. L. Kassner, A. Garcia-Porrata and E. L. Grove, *Anal. Chem.*, 1955, **27**, 492.
5. S. Kallmann, in *Treatise on Analytical Chemistry*, I. M. Kolthoff and P. J. Elving, eds., Part II, Vol. 5, p. 238. Interscience, New York, 1964.
6. W. C. Vosburgh and G. R. Cooper, *J. Am. Chem. Soc.*, 1941, **63**, 437.
7. P. Job, *Ann. Chim. (Paris)*, 1928, **9**, 133.
8. A. K. Mukherji and A. K. Dey, *J. Inorg. Nucl. Chem.*, 1956, **6**, 414.
9. *Idem*, *Anal. Chim. Acta*, 1958, **18**, 434.

Talanta Vol. 28, pp. 62 to 64
© Pergamon Press Ltd 1981. Printed in Great Britain
0039-9140/81/0101-0062$02.00/0

LIQUID–LIQUID EXTRACTION OF OSMIUM THIOCYANATE WITH HEXAMETHYLPHOSPHORAMIDE AND DIRECT SPECTROPHOTOMETRIC DETERMINATION IN THE ORGANIC PHASE

BIJOLI KANTI PAL, RAJENDRA PRASAD CHOWDHURY* and B. K. MITRA
Department of Chemistry, Jadavpur University, Calcutta-700032, India

(*Received* 22 *December* 1978. *Revised* 2 *July* 1980. *Accepted* 15 *July* 1980)

Summary—The use of hexamethylphosphoramide (HMPA) in the osmium–thiocyanate system makes the method more sensitive and selective. The blue colour formed by osmium(VIII) with thiocyanate in 1.5*M* hydrochloric acid is intensified in the presence of HMPA and the complex becomes readily extractable into chloroform. The colour system has its absorption maximum at 595 nm and obeys Beer's law over the range 0.5–16 μg of Os per ml. The optimum range is 2–10 μg/ml. The molar absorptivity is 2.09×10^4 l.mole^{-1}.cm^{-1}. The method is simple, sensitive and free from interference from many metal ions, including ruthenium and other platinum metals.

Among the spectrophotometric reagents for osmium we may mention thiocyanate,[1,2] bismuthiol II,[3] thiourea[4] and 1-benzoyl-3-(5-bromo-2-pyridyl)-thiourea.[5] The catalytic methods are the most sensitive,[4] but need rigid control of temperature, acidity, reagents and impurities. The thiocyanate method is sensitive only when diethyl ether is used as extractant. With all other oxygen-containing solvents the sensitivity is poorer, and non-oxygen-containing solvents cannot be used. Interferences from platinum metals is not eliminated in the direct method and the alternative method requires several manipulations.[1] In another thiocyanate method[2] less than 9 ppm Os cannot be determined and Au^{3+}, Rh^{3+}, Ir^{4+}, Pt^{4+}, Fe^{3+} and Cu^{2+} interfere seriously. Bismuthiol II, optimal range 3.0–10.5 ppm and molar absorptivity 1.17×10^4, suffers interference from Cu^{2+}, Cd^{2+}, Pb^{2+}, Pd^{2+}, Sb^{3+} and Bi^{3+}. Thiourea and its derivatives are useful for estimation of Os, but lack sensitivity and cannot be applied to aged solutions.[4]

HMPA has already been used successfully to increase the sensitivity of metal thiocyanate systems,[6–8] and is now applied to Os(VIII).

EXPERIMENTAL

Reagents

Os(VIII) solution was prepared from the tetroxide[9] and standardized iodometrically.[10] Solutions of other platinum metals were prepared from suitable salts (Johnson Matthey) and standardized by accepted methods. All other chemicals were of analytical grade.

The chloroform was distilled before use; HMPA was used as received.

Procedure

In a 50-ml separatory funnel take 10 ml of 3*M* hydrochloric acid, and add a known volume of sample containing 50–250 μg of Os(VIII). Add 2.5 ml of 2% ammonium thiocyanate solution, dilute to 20 ml with water, mix, let stand for 5 min, add 1 ml of HMPA and extract with 20 ml of chloroform. Separate the organic layer, transfer it to a 25-ml standard flask and make up to the mark with chloroform. Let stand for 90 min for complete colour development. Measure the absorbance at 595 nm against a reagent blank in 1-cm glass cells. For low osmium concentrations extract with 10 ml of chloroform and dilute to 15 ml.

RESULTS AND DISCUSSION

Osmium thiocyanate forms a blue complex which is not extractable into chloroform. In the presence of HMPA, however, it becomes readily extractable into chloroform and the intensity of the colour is also enhanced. Presumably a ternary complex is formed with HMPA. It is extractable into both oxygen- and non-oxygen-containing solvents. The absorption maximum is at 595 nm (Fig. 1). The system obeys Beer's law over the range of 0.5–16 μg of Os per ml and the optimum concentration range[11] is 2–10 μg/ml. The molar absorptivity is 2.09×10^4 l.mole^{-1}.cm^{-1}. The photometric error is 2.7%.[12]

Effect of acidity, thiocyanate, HMPA and time

The system shows a maximum colour intensity over the acidity range 1.25–1.75*M* hydrochloric acid, with 2–5 ml of 2% thiocyanate solution in 20 ml of aqueous phase. There is no change in absorbance when the amount of HMPA used is varied between 0.5 and 1.5 ml. Once developed, the colour is stable in the organic phase for about 24 hr.

Effect of interfering ions

The following metal ions do not interfere in determination of 4 ppm of Os in the final solution when present up to the final concentration (ppm) shown in parentheses.

* Present address: Chemical Department, Chloride India Ltd. R and D Centre, Calcutta-700059, India.

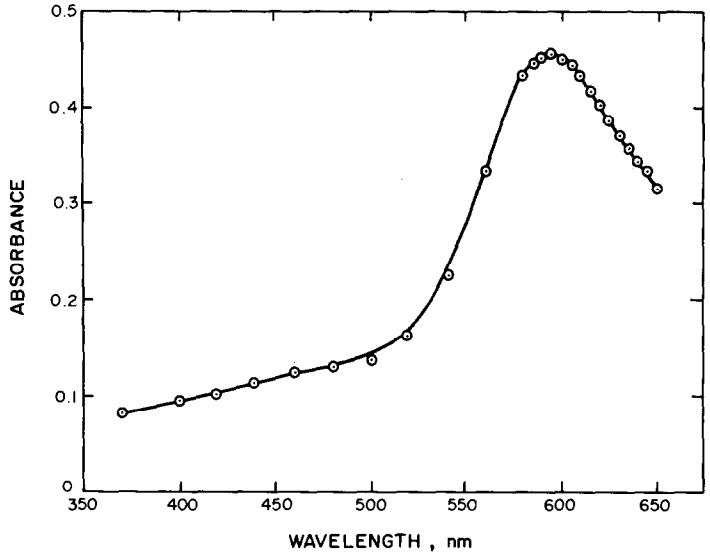


Fig. 1. Absorption spectrum for 4.18 ppm Os.

Pt^{4+} (4), Pd^{2+} (15), Au^{3+} (15), Co^{2+} (30), Cu^{2+} (30), Mo^{6+} (40), U^{6+} (40), V^{5+} (20) and Sb^{3+} (100). The interference of Pt, Pd and Au in higher concentrations (40, 30, 40 ppm respectively) can be eliminated by masking with 100 mg of sodium cyanide. Ti^{4+} and Nb (both 40 ppm) can be masked with 100 mg of ammonium fluoride. Sb^{3+} (more than 100 ppm) gives a low result but this effect can be eliminated by addition of excess of thiocyanate (5 ml of 2% solution) Pb^{2+}, Cr^{3+}, In^{3+}, Se^{4+}, Te^{4+}, Mn^{2+}, Al^{3+} and Bi^{3+} do not interfere. Rh^{3+} and Ru^{3+} remain in the aqueous phase and thus Os can be isolated from Ru^{3+}. Cu^{2+} and Co^{2+} (both 100 ppm) and V^{5+} (100 ppm) can be masked, the first two with 100 mg of EDTA and the last with 100 mg of oxalic acid. Mo^{6+} (100 ppm) can be masked with 100 mg of ammonium fluoride, and Fe^{3+} (100 ppm) with 150 mg of sodium pyrophosphate. Iridium gives a blue colour with thiocyanate and HMPA in 1.5*M* hydrochloric acid, but does not interfere in concentrations below 6 ppm.

Anions such as F^-, PO_4^{3-}, $P_2O_7^{-4}$, SO_4^{2-}, CN^-, EDTA, citrate, oxalate and tartrate do not interfere when present in amounts of several mg. Thiourea interferes seriously.

As a test of the masking method, 100 μg of sodium were determined in the presence of 2500 μg each of Fe(III), Co(II) and Cu(II), with 100 mg of EDTA added to mask Co(II) and Cu(II), followed by 5 ml of 1% ammonium thiocyanate solution, 150 mg of sodium pyrophosphate to mask iron and 100 mg of ammonium fluoride (in solution) as additional masking agent. The mixture was diluted to 20 ml, 1 ml of HMPA was added and the coloured complex was extracted with 20 ml of chloroform, and the determination was completed as already described. In three experiments the amounts found were 95, 102 and 98 μg.

Table 1. Analysis of a synthetic mixture corresponding to syserkite or osmiridium

Present, *ppm*				Os found,
Os	Ir	Ru	Pt	*ppm*
2.0	0.05	0.30	0.10	2.01
4.0	4.0	4.0	1.0	4.01
6.0	6.0	6.0	2.0	6.03

Analysis of osmiridium

Osmiridium can be analysed successfully after decomposition by attack with chlorine and dissolution of the platinum-metal salts in hydrochloric acid.[13] No distillation is required unless the amounts of interfering elements are above the tolerance limit. Results for a synthetic sample of osmiridium are shown in Table 1 and in Table 2 for mixtures of osmium with various platinum metals.

Table 2. Determination of a known concentration of Os in the presence of Pt^{4+} (4), Pd^{2+} (10), Au^{3+} (10), Rh^{3+} (20), Ru^{3+} (20), Cu^{2+} (10), Mo^{6+} (20) and Sb^{3+} (50); the concentration of the diverse ions in ppm is shown in parenthesis

Os taken, *ppm*	4.00	8.00	10.00
Os found, *ppm*	4.02–4.04	8.01–8.03	10.02–10.04
No. of samples	3	3	3

Acknowledgement—The financial help of Jadavpur University through a scholarship to one of us (R.P.C.) is gratefully acknowledged.

REFERENCES

1. J. H. Wiersma and P. F. Lott, *Anal. Chem.*, 1967, **39,** 674.
2. U. Murulikrishna, K. V. Bapaniah, N. S. N. Prasad and P. Kannarao, *Indian J. Chem.*, 1976, **14A,** 291.
3. A. K. Majumdar and S. K. Bhowal, *Anal. Chim. Acta*, 1972, **62,** 223.
4. F. E. Beamish, *The Analytical Chemistry of the Noble Metals*, Pergamon, Oxford, 1966.
5. D. K. Das, M. Majumder and S. C. Shome, *Z. Anal. Chem.*, 1977, **286,** 249.
6. M. Mitra and B. K. Mitra, *Anal. Chim. Acta*, 1977, **94,** 487.
7. *Idem, Talanta*, 1977, **24,** 698.
8. *Idem, ibid.*, 1978, **25,** 597.
9. G. H. Ayres and W. N. Wells, *Anal. Chem.*, 1950, **22,** 317.
10. W. R. Crowell and H. D. Kirschman, *J. Am. Chem. Soc.*, 1929, **51,** 175.
11. A. Ringbom, *Z. Anal. Chem.*, 1938/39, **115,** 332.
12. G. H. Ayres, *Anal. Chem.*, 1949, **21,** 652.
13. A. D. Westland and F. E. Beamish, *ibid.*, 1958, **30,** 414.

Talanta Vol. 28, pp. 65 to 67
© Pergamon Press Ltd 1981. Printed in Great Britain
0039-9140/81/0101-0065$02.00/0

DETERMINATION OF LEAD IN IGNEOUS ROCKS BY DIFFERENTIAL PULSE ANODIC STRIPPING VOLTAMMETRY AT AN HMDE

G. CALDERONI
Istituto di Geochimica dell'Università, 00100 Rome, Italy

(*Received* 7 *April* 1980. *Accepted* 10 *July* 1980)

Summary—A versatile and sensitive voltammetric method has been used for the determination of lead in seven USGS standard rocks and in two CRPG (Centre des Recherches Pétrografiques et Géochimiques, Nancy) standard rocks. The results, showing satisfactory precision and accuracy, are discussed with respect to the sample treatment and the voltammetric method.

Anodic stripping techniques offer a very sensitive method for trace-element analysis and have been applied for the determination of lead in a variety of materials by several workers.[1–11] The present note reports the use of differential pulse anodic stripping voltammetry (dpasv) at a hanging mercury drop electrode (HMDE) for the determination of lead in igneous rocks, with no preliminary extraction. Hydroxylammonium chloride has been selected as supporting electrolyte on account of its reducing power in the acid medium which is needed to avoid precipitation (with its related co-precipitation and sorption phenomena) of several metals as hydroxides, and because these conditions make it possible to achieve a fairly good separation of the peaks of some elements of interest. Hydroxylammonium chloride reduces Cu(II) to Cu(I), so only one peak is found for copper, and Fe(II) in solution is not reduced at the HMDE.

The investigation was concerned first with finding conditions for Cd(II), Pb(II) and Cu(I): conditions and E_p values for the three elements are reported in the caption of Fig. 1. Then attention was devoted to the determination of lead and copper, though the copper determination has not been fully explored. For the lead determination better results were obtained with a 1.25*M* hydroxylammonium chloride solution, and with a plating potential of −0.70 V *vs.* SCE: under these conditions the E_p value for Pb(II) was −0.40 V *vs.* SCE.

EXPERIMENTAL

Reagents

Standard lead solution. Made from Merck RG $Pb(NO_3)_2$ dried at 110°, by dissolving it in doubly distilled water and acidifying with Aristar hydrochloric acid.

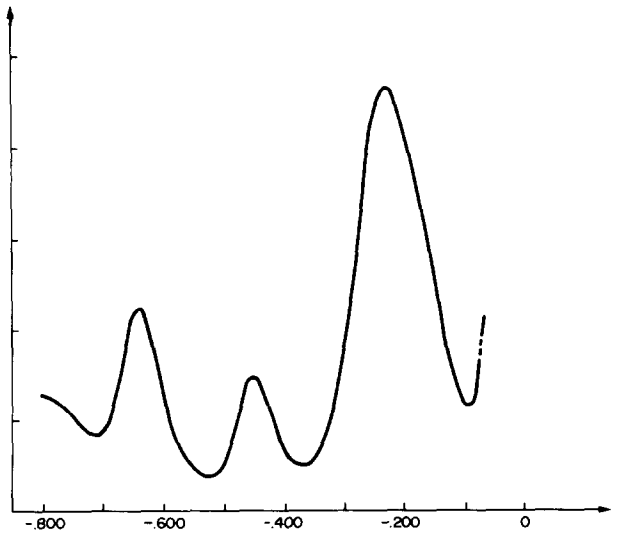


Fig. 1. Dpasv voltammogram showing peaks of Cd(II), Pb(II) and Cu(I) respectively at −0.640, −0.450, −0.225 V *vs.* SCE. HMDE area 0.024 cm^2; cathodic deposition potential −0.850 V; deposition time 3 min; scan-rate 20 mV/sec; pulse height 40 mV; 1.25*M* hydroxylammonium chloride at pH 2.0.

Hydroxylammonium chloride stock solution. Made from twice recrystallized Merck RG material and purified by controlled-potential electrolysis at a mercury-pool cathode at −0.8 V *vs.* SCE.

Merck Suprapur perchloric acid.

Merck RG hydrofluoric acid. Purified by sub-boiling point distillation as described by Lancet and Huey.[12]

Apparatus

All samples were analysed by dpasv at an HMDE, with a 472 WR Amel multipolarograph equipped with a 7040 A *X–Y* Hewlett–Packard recorder. A three-electrode system was employed: a Beckman 39016 electrode and/or a Metrohom E410 electrode as working electrode(s), a platinum electrode as auxiliary and an SCE as reference.

Procedure

Dissolution of the samples follows a procedure similar to that described by Jeffery[13] but the perchloric acid is not totally eliminated. This is in order to avoid both loss of the more volatile components and the formation of insoluble oxides. Thus the final solution is slightly acid and the metal perchlorates dissolve easily in the water added.

Transfer 100–350 mg of sample into a Teflon beaker, add 10 ml of hydrofluoric acid and 2 ml of perchloric acid, and evaporate to incipient dryness on a hot-plate at 200°. Add 2 ml of perchloric acid and evaporate to incipient dryness again, then repeat this step. Dissolve the residue in doubly distilled water and dilute to 50 ml in a standard flask. Pipette a volume of between 1 and 3 ml of this solution into a 25-ml standard flask, and add enough hydroxylammonium chloride stock solution to give a final concentration of 1.25*M* and dilute to volume with doubly distilled water. Transfer 20 ml of this solution into a polarographic cell and deoxygenate for 10 min by passing high-purity nitrogen through the sample. Continue to pass nitrogen over the solution during the electrolysis and stripping steps. Electrolyse at −0.70 V *vs.* SCE for 1–3 min, with magnetic stirring. Record the voltammograms with a sweep-rate of 10 mV/sec and a pulse-amplitude of 40 mV.

RESULTS AND DISCUSSION

To test its applicability and the possibility of interference from other elements present in rocks, the method was used to analyse rock samples ranging from granite through mafic to ultramafic types.

Two samples of each standard were dissolved, and each solution was analysed in triplicate; each measurement was run 4 or 5 times. Instrumental reproducibility, tested up to 10 times in some cases, was always better than 5%. As the peak current was found to vary linearly with the lead concentration the method of standard additions was used for quantitative work, and the measurements were corrected for the dilution caused by each increment added.

Table 1 shows the mean concentration of lead (ppm), the standard deviation (σ) and the relative standard deviation (%) for the standard rocks. As reported by other authors,[8,14] the reproducibility was less satisfactory for dunites and basalts: this fact may indicate some dependence on the type of matrix and a possible lack of homogeneity in the samples. In fact, although the possibility of inhomogeneity of the standards from different stocks has been excluded by Aruscavage and Campbell,[14] Jaffrezic[15] claims that if trace elements are determined in small weights of sample it is possible that the solid subsample taken is not statistically representative of the mean composition of the standard. Diehl[16] has published a photograph showing the inhomogeneity in a standard material. It would certainly be interesting to have more data on which considerations of the statistical distribution of trace-elements in the standards could be based.

Table 1. Results for determination of lead in standard rocks

Standard rock	Lead, *ppm*	$\bar{x} \pm \sigma$, *ppm*	$100\,\sigma/\bar{X}$ %
DTS-1 Dunite	11.74; 10.7; 11.2 11.3; 11.8; 9.0	10.9 ± 1.0	9.1
PCC-1 Peridotite	11.5; 12.0; 11.4 12.6; 12.4; 13.0	12.1 ± 0.6	4.9
W-1 Basalt	6.6; 6.0; 6.7 4.8; 5.2; 6.6	5.9 ± 0.7	11.8
BCR-1 Basalt	17.0; 16.9; 16.5 17.7; 18.4; 16.4	17.1 ± 0.7	4.0
BR Basalt	8.2; 10.0; 9.1 9.7; 9.2; 6.4	8.7 ± 1.3	14.9
AGV-1 Andesite	40.0; 39.3; 36.1 38.7; 35.2; 39.8	38.1 ± 2.0	5.2
GSP-1 Granodiorite	58.1; 58.6; 54.7 57.4; 56.9; 56.8	57.0 ± 1.3	2.2
G-2 Granite	25.0; 24.2; 28.9 26.0; 25.1; 28.3	26.2 ± 1.8	6.8
GH Granite	67.1; 60.5; 66.6 64.5; 67.6; 64.8	65.1 ± 2.6	3.9

Table 2. Lead values for international standard rocks, from the literature, *ppm*

Standard rock	Data from this work	Polarographic data by other authors	Data by flameless atomic absorption[14]	Flanagan's values[17]	Ranges as reported by Wedepohl[18]
DTS-1	10.9 ± 1.0	11.0 ± 4.4[8]	7.6 ± 0.6	14.2	8.3–16
PCC-1	12.1 ± 0.6	9.8 ± 5.9[8]	8.2 ± 0.3	13.3	7.9–13
W-1	5.9 ± 0.7			7.8	6.0 ± 9.4
BCR-1	17.1 ± 0.7		14.1 ± 0.8	17.6	10.9 ± 29.5
BR	8.7 ± 1.3				8–12.5
AGV-1	38.1 ± 2.0	43[7]	36.5 ± 2.1	35.1	33.1–46
GSP-1	57.0 ± 1.3		56.2 ± 1.3	51.3	51.9–67
G-2	26.2 ± 1.8	36[7]	30.2 ± 1	31.2	29.5–30.8
GH	65.1 ± 2.6				15–58

In Table 2 comparison is made between the results of this work and those of other authors. It is worth noting that polarographic results for the analysis of standard rocks are rather scarce, but those results which are available tend to show a fairly good agreement.

Concerning the accuracy we can observe that the results of this paper for DTS-1, PCC-1 and BCR-1 agree with those of Flanagan[17] better than those of Aruscavage and Campbell,[14] but the reverse is true for AGV-1, GSP-1 and G-2. For standards GH and BR only a few results are available for comparison.

Thallium, which has a peak potential very close to that of lead, interferes, as previously pointed out by other authors,[7] and as it has been ascertained in this study testing the analytical procedure proposed by De Capitani *et al.*[8] We found that a given concentration of thallium produces a peak with only one-fifth of the height of a corresponding lead peak for the same concentration. We conclude that interference from thallium is virtually negligible since the thallium concentrations in the USGS standard rocks are very low (maximum 1.3 ppm, according to Flanagan's recommended data).[17]

Acknowledgement—This work was partially supported by CNR (National Research Council of Italy) grant No. 75.00028.05.

REFERENCES

1. J. Dieker and W. E. Van der Linden, *Z. Anal. Chem.*, 1975, **274**, 97.
2. A. A. Cernik, *Proc. Anal. Div. Chem. Soc.*, 1976, **13**, 227.
3. A. H. I. Ben-Bassat, J. M. Blinderman and A. Salomon, *Anal. Chem.*, 1975, **47**, 534.
4. M. J. Pinchin and J. Newham, *Anal. Chim. Acta*, 1977, **90**, 91.
5. V. H. Levin and M. J. Rowell, *Effluent Water Treat. J.*, 1973, **13**, 273.
6. M. Kopanica and V. Stará, *J. Electroanal. Chem.*, 1977, 77, 57.
7. K. A. Khasgiwale, R. Parthasarathy and M. S. Das, *Anal. Chim. Acta*, 1972, **59**, 485.
8. L. De Capitani and A. Maccagni, *Rend. Soc. Ital. Min. Petrol.*, 1978, **34**, 569.
9. G. Piccardi and P. L. Cellini, *Ann. Chim. (Roma)*, 1974, **64**, 1.
10. R. Benvenuti, M. Martini and G. Piccardi, *Rend. Soc. Ital. Min. Petrol.*, 1977, **33**, 799.
11. W. Lund and M. Salberg, *Talanta*, 1975, **22**, 1013.
12. M. S. Lancet and J. M. Huey, *Anal. Chem.*, 1974, **46**, 1360.
13. P. G. Jeffery, *Chemical Methods of Rock Analysis*, p. 156, Pergamon, Oxford, 1970.
14. P. J. Aruscavage and E. Y. Campbell, *Talanta*, 1979, **26**, 1052.
15. H. Jaffrezic, *ibid.*, 1976, **23**, 497.
16. H. Diehl, *Quantitative Analysis*, 1st Ed., p. 310. Oakland Street Press, Ames, Iowa, 1970.
17. F. J. Flanagan, *Geochim. Cosmochim. Acta*, 1973, **33**, 81.
18. K. H. Wedepohl, (ed.), *Handbook of Geochemistry*, Springer, Berlin, 1974.

Talanta Vol. 28, pp. 69 to 71
Pergamon Press Ltd 1981. Printed in Great Britain

ANALYTICAL DATA

SOLUTION STUDIES ON CHELATES OF NICKEL, ZINC AND CADMIUM WITH 2-THIOPICOLINANILIDE

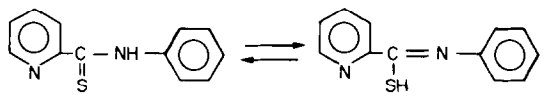
M. MOLINA, C. MELIOS and N. BARELLI
Instituto de Química, UNESP, C.P. 174, Araraquara, 14800, S.P. Brazil

(*Received* 10 *April* 1980. *Accepted* 4 *July* 1980)

Summary—The protonation constants of 2-thiopicolinanilide (TPA) and the stability constants of its complexes with Ni, Zn and Cd have been determined potentiometrically in 50% w/w ethanol–water medium, at 25° and 0.100*M* ionic strength ($LiClO_4$). Co-ordination centres in TPA are suggested.

In recent years several papers have described applications of chelates involving metal ions and thioamides in column and thin-layer chromatography (TLC). The non-polar character and intense colour of many such chelates lend themselves to TLC, and by use of uniform, ultra-thin layers, less than 1-ng amounts of several metals can be separated and identified.[1,2]

The ligand *N*-phenyl-2-thiopicolinamide (2-thiopicolinanilide) (**Ia, Ib**) has very interesting properties as an analytical reagent;[3] solid complexes of this ligand with some transition metal ions have been isolated and characterized,[3] but solution studies have not previously been made. Knowledge of the thermodynamic stability of the metal ion-2-thiopicolinanilide systems is highly desirable for their proper use in analytical work.



Ia Ib

The present investigation deals with equilibrium studies on the binary systems comprising 2-thiopicolinanilide (TPA) and nickel, zinc and cadmium perchlorates, in 50% w/w ethanol—water medium, at 25° and 0.100*M* ionic strength, adjusted with lithium perchlorate.

The following symbols and abbreviations will be used: β_n, stoichiometric overall stability constant of ML_n; C_H, total concentration of dissociable hydrogen ions; C_L, total concentration of TPA; C_L^i, total initial concentration of TPA; C_M, total concentration of *M*(II) perchlorate; C_M^i, total initial concentration of *M*(II) perchlorate; h, concentration of free hydrogen ions; I, ionic strength; K_n, stepwise stability constants of ML_n; [L], molar concentration of free ligand anion: $\bar{n}$, average number of ligands bound to one central group; $ph = -\log h$; S_M, solvent mixture (ethanol–water 50% w/w).

EXPERIMENTAL

Materials and solutions

TPA was synthesized and purified as described earlier.[3] The m.p. of the final product (52.8–53.0°) is in agreement with the literature data.[4] All other chemicals were of analytical purity. All solutions in ethanol–water 50% w/w medium were prepared and standardized just before use.

Apparatus

Grade A glassware was used for all volumetric work. The emf values were read to the nearest 0.1 mV with an Orion model 701 instrument. The investigation was carried out as a number of potentiometric titrations, performed as previously described.[5] Measured values were processed by a Hewlett–Packard model 9810A programmable electronic calculator, with graphical output plotted by a Hewlett–Packard model 9125B incremental plotter.

Methods

Determination of hydrogen-ion concentrations. The emf of the following cell was measured:

⊕ Ag	0.0100*M* $AgClO_4$ 0.0900*M* $LiClO_4$ in S_M	0.100*M* $LiClO_4$ in S_M	Test solution (0.100*M* ClO_4^-) in S_M	Glass electrode ⊖

A Corning 476022 glass electrode and a "Wilhelm" type salt bridge[6] incorporating a silver reference electrode were

Table 1. Summary of emf titration data

C_M^i, mM	C_L^i, mM	ph range	R*	$\bar{n}$ range
		Ni(II)–TPA		
2.00	9.97	3.122–6.545	46	0.46–2.74
		Zn(II)–TPA		
2.00	10.0	3.943–4.502†	8	0.071–0.32
5.00	10.0	3.735–4.209†	16	0.046–0.12
		Cd(II)–TPA		
2.00	10.3	3.943–4.732†	9	0.071–0.37
5.00	10.1	3.752–4.463†	19	0.044–0.18

* R = number of readings.
† Above this ph value precipitation occurs.

Table 2. Stability constants of TPA complexes

Metal ion	log β_1	log β_2	log β_3
Ni(II)	10.06 ± 0.01	18.98 ± 0.02	26.55 ± 0.03
Zn(II)	8.04 ± 0.04	16.1 ± 0.2	24.6 ± 0.5
Cd(II)	8.05 ± 0.04	15.8 ± 0.2	23.4 ± 0.5

used. The ph values for the test solutions were derived from the emf measurements as described elsewhere.[5]

Determination of formation constants. One of the protonation constants, K_1^H (thiol group, **Ib**) was determined by titrating ligand solutions (C_L^i = 5.00–10.0mM), made up to I = 0.100M by adding lithium perchlorate, with lithium hydroxide solution (I = 0.100M, adjusted with lithium perchlorate). The other protonation constant, K_2^H (heterocyclic nitrogen atom) was analogously determined by using perchloric acid as titrant. The K_j^H values were derived[7] from C_L, C_H, K_w and h. The pK_w value (14.15 ± 0.01) was determined—under the experimental conditions for the rest of the work—by a previously described procedure.[5] Complex formation in the metal perchlorate–TPA binary systems was followed at constant C_L/C_M ratios by titrating a solution containing metal perchlorate (C_M^i = 2.00–5.00mM), TPA (C_L^i = 9.97–10.3M) and lithium perchlorate [(0.100–3C_M^i)M] with lithium hydroxide solution (I = 0.100M, adjusted with lithium perchlorate). The concentration variables ($\bar{n}$ and [L]) were calculated[7] from C_M, C_L, C_H, K_j^H and h. The stability constants of the complexes were evaluated as described elsewhere.[8]

RESULTS AND DISCUSSION

TPA is very slightly soluble in water. The reactions of this ligand (HL) with several metal ions, *i.e.*, Ag(I), Hg(I), Hg(II), UO_2(II), Cu(II), Co(II), Pb(II), Ni(II), Cd(II), Zn(II), Mn(II), Fe(II), Fe(III), Al(III), Bi(III), Cr(III) and Sn(IV), in methanolic solutions, have been investigated.[3] Complexes of definite stoichiometry, *i.e.*, CuL_2, CoL_3, NiL_2, CdL_2, ZnL_2 and $HgCl_2(HL)_2$ were isolated. Among the complexes prepared only those involving Cd(II), Ni(II) and Zn(II) are sufficiently soluble in methanol, ethanol or ethanol–water (50% w/w) medium to permit studies on their solution equilibria. In view of this it was judged advisable to initiate solution equilibrium studies with the systems involving Ni(II), Zn(II) and Cd(II). A partly aqueous medium was chosen, as under that condition complex formation can be conveniently followed by ph measurements.[6]

The protonation constants determined are: $\log K_1^H$ = 11.19 ± 0.02 and $\log K_2^H$ = 1.38 ± 0.03. Titration data for the metal ion–TPA systems are summarized in Table 1. The stability constants are given in Table 2.

As shown in Fig. 1, there was good agreement between the computed stability constants and the experimental data [equally good agreement was found for the Zn(II)–TPA system].

It seems very probable that the proton is abstracted from the thiol group in alkaline solution and that

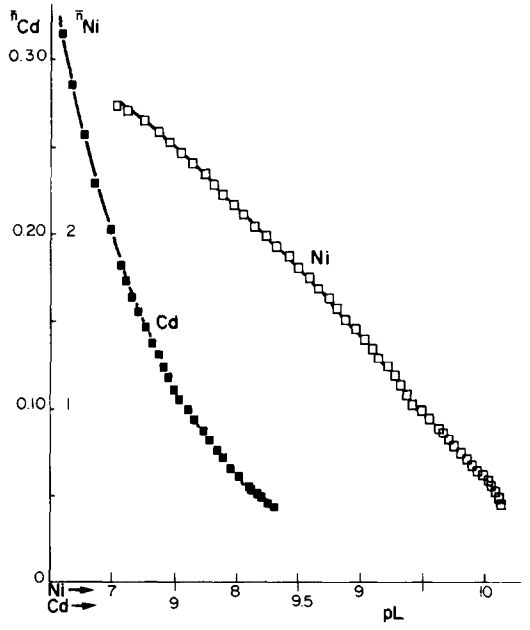


Fig. 1. Formation curves of M(II)–TPA complexes. Squares: experimental values (plotted in part for the Cd system). Full curves: drawn from the corresponding β_n values given in Table 2.

protonation occurs at the heterocyclic nitrogen atom; accordingly, complex formation in solution would proceed through metal-ion co-ordination with the pyridine ring nitrogen atom and the thioamide group sulphur atom. This kind of bonding has also been proposed for the solid complexes.[3,4,9]

There was no major difficulty in studying the Ni(II)–TPA system. Owing to the high solubility of the complex species in the reaction medium, $\bar{n}$ values near 2.8 could be obtained, yielding reliable values for the stability constants. Furthermore this system presents favourable K_n/K_{n+1} ratios; this property often permits the calculation of accurate constants.[10] For the Zn(II) and Cd(II) systems precipitation takes place as early as $\bar{n} = 0.32$ and 0.37, respectively. The formation curves are therefore less accurate. Accordingly, the β_2 and especially the β_3 values for these systems are to be considered only as orders of magnitude for the constants, in spite of the good agreement between the calculated constants and the experimental data. On the other hand, the K_n/K_{n+1} ratios for these two systems are much less favourable than those for the Ni(II) system. It seems worth pointing out that if it is assumed that $\beta_2 = 0$ and/or $\beta_3 = 0$ for both systems, the agreement between the calculated and experimental formation curves is invariably poor.

A comparison of the stability constants obtained in this work shows that for the β_1 values the stability sequence is Ni(II) > Cd(II) ~ Zn(II); when the β_2 and β_3 values are considered the sequence is Ni(II) > Zn(II) > Cd(II). This trend has already been reported for other Zn(II) and Cd(II) complex systems.[11]

REFERENCES

1. W. Lautenschlager, S. Pahlik and G. Tölg, *Z. Anal. Chem.*, 1972, **260**, 203.
2. E. Ludwig, R. Morgenstern and U. Uhlemann, *Anal. Chim. Acta*, 1976, **86**, 157.
3. M. Molina, A. Del'Acqua, C. Melios, F. A. Azevedo and E. Trabuco, *Eclét. Quim.*, 1977, **2**, 87 and references therein.
4. G. V. Glazneva, E. K. Mamaeva and A. P. Zeif, *J. Gen. Chem. USSR*, 1966, **36**, 1503.
5. M. Molina, C. Melios, J. O. Tognolli, L. C. Luchiari and M. Jafelicci Jr., *J. Electroanal. Chem.*, 1979, **105**, 237.
6. G. Faraglia, F. J. C. Rossotti and H. S. Rossotti, *Inorg. Chim. Acta*, 1970, **4**, 488.
7. H. S. Rossotti, *Talanta*, 1974, **21**, 809.
8. M. Molina, C. Melios, A. C. Massabni and T. Takaki, *J. Coord. Chem.*, 1978, **7**, 133.
9. R. W. Kluiber, *Inorg. Chem.*, 1965, **4**, 829.
10. F. J. C. Rossotti and H. Rossotti, *The Determination of Stability Constants*, p. 115. McGraw-Hill, New York, 1961.
11. R. J. Sundberg and R. B. Martin, *Chem. Rev.*, 1974, **74**, 471.

Talanta Vol. 28, pp. 73 to 79
©Pergamon Press Ltd 1981. Printed in Great Britain
0039-9140/81/0201-0073$02.00/0

SUBSTOICHIOMETRIC ISOTOPE DILUTION ANALYSIS FOR TIN WITH SALICYLIDENEAMINO-2-THIOPHENOL COMPLEXATION IN NON-AQUEOUS MEDIUM

APPLICATION TO THE ANALYSIS OF COAL FLY-ASH

HISANORI IMURA and NOBUO SUZUKI*

Department of Chemistry, Faculty of Science, Tohoku University, Sendai 980, Japan

(*Received* 27 *March* 1980. *Revised* 12 *September* 1980. *Accepted* 25 *September* 1980)

Summary—An accurate, precise and selective analytical method for traces of tin by substoichiometric isotope dilution has been developed. The method consists of the extraction of tin(IV) iodide into benzene, the complexation of tin(IV) with a substoichiometric amount of salicylideneamino-2-thiophenol in the benzene phase, and back-extraction of the excess of tin. The substoichiometric separation is reproducible within 0.5–2.4%, and tin can be determined at the microgram level. The method has been applied to the determination of tin in environmental materials, NBS Coal Fly-Ash (SRM 1633) and fly-ash from a coal-fired power plant in Japan.

Traces of tin occur extensively but irregularly in nature. Recently, it has been reported that tin may be one of the essential elements for higher animals.[1] We are interested in the behaviour of this element in the biosphere, together with problems of environmental pollution. The need for a reliable analytical method has long been apparent. In an interlaboratory comparison for trace analysis of environmental samples such as coal, fly-ash, gasoline, and residual fuel oil, the reported values of tin determined by spark-source mass-spectrometry and instrumental neutron-activation analysis varied by more than an order of magnitude. Hence a more thorough investigation of analytical methods for tin is necessary.[2]

Here we give a substoichiometric isotope dilution method for traces of tin. This analytical method has the following advantages:[3,4] (1) the quantitative separation and recovery of the determinand from the matrix are not required, and (2) the only measurements needed are the activities of the substoichiometric extracts. The main source of error is the statistical error in measuring the radioactivity, which can be reduced by using a high enough activity.

A few papers have appeared on the substoichiometric determination of tin by the so-called comparison method.[5–7] In this method, substoichiometric separation of tin after addition of large amounts of tin-carrier to the irradiated samples and standards makes the analytical procedure much easier than the usual substoichiometric isotope dilution method. However, errors due to fluctuation of the neutron flux and to self-shielding of the samples cannot be avoided.

In the present paper, the substoichiometric isotope dilution determination of trace tin with salicylideneamino-2-thiophenol (SATP), has been investigated. It has been reported that reaction of tin(IV) with SATP in aqueous solution does not become appreciable until the mole ratio of SATP to tin(IV) is at least 10-fold.[8] This suggests that quantitative reaction of tin(IV) with SATP in aqueous solution under substoichiometric conditions would not be expected. Accordingly, the reaction has been studied in non-aqueous medium. It is well known that the extraction of tin(IV) from iodide media is highly selective,[9,10] and this extraction system has been adopted for transfer of the tin(IV) into a non-aqueous medium. The substoichiometric separation of tin(IV) takes place in three steps, *viz.* the iodide extraction of tin(IV) into benzene, the substoichiometric complexation with SATP in the benzene phase, and the back-extraction of the excess of tin(IV) from the organic phase. The method has been applied to the determination of tin in environmental samples, National Bureau of Standards coal fly-ash (SRM 1633) and the coal fly-ash obtained from a coal-fired electric power plant in Japan.

* To whom correspondence and requests for reprints should be sent.

EXPERIMENTAL

Reagents

The potassium hydrogen sulphate used as a flux and the hydrofluoric acid were of ultrahigh purity ("Suprapur", E. Merck). The sulphuric acid and hydrochloric acid were also of ultrahigh purity (Wako Pure Chemicals Ltd.). Sodium perchlorate and iodide solutions (both 5*M*) were prepared in redistilled water. The sodium iodide solution was stored in a brown glass bottle. The buffers were prepared from 0.1*M* hydrochloric acid and 0.1*M* sodium acetate for pH <4 and from 0.1*M* acetic acid, 0.1*M* sodium acetate and 0.1*M* sodium hydroxide for the pH region 4–8.

A standard tin(IV) solution (~0.041*M*) was prepared by dissolving the high-purity metal (99.999%) in concentrated sulphuric acid by heating, followed by dilution to give 6*M* acid concentration.

The radioisotope ^{113}Sn was obtained from New England Nuclear (USA), and appropriately diluted with 2.5*M* sulphuric acid. Its specific activity was 19 Ci per g of tin.

Radioactive tin(IV) spike solutions were prepared by adding a few drops of the ^{113}Sn(IV) solution to the standard tin(IV) solution and diluting to volume with 2.5*M* sulphuric acid. The resulting solutions were allowed to stand for over a day before use. The concentrations of the radio-tin(IV) stock solutions used were 4.1×10^{-3}, 4.1×10^{-4} and 4.1×10^{-5}*M*, and the specific activities above *ca.* 0.5 μCi/ml. In practical applications, a 1.03×10^{-5}*M* (1.22 μg/ml) radio-tin(IV) spike solution was prepared and immediately added to the sample solutions containing unknown amounts of tin(IV). Isotopic equilibrium was achieved by keeping at about 90° overnight.

The radioactive tracers of ^{54}Mn, ^{57}Co, ^{57}Ni, ^{67}Cu, ^{74}As, ^{120,122}Sb, and ^{203}Pb used in the interference tests were prepared by photon irradiation with maximum bremsstrahlung energies of 30 and 60 MeV, in the Tohoku University electron linear accelerator. Other tracers, ^{51}Cr, ^{59}Fe, and ^{65}Zn, were purchased from New England Nuclear.

SATP was obtained commercially and its purity (better than 98%) checked by elemental analysis for C, H, N, and S. The 10^{-5}–10^{-3}*M* SATP solutions were prepared in absolute ethanol (99.5%) containing 1% ascorbic acid as stabilizer, and stored in brown flasks. A 10% pyridine solution was made with absolute ethanol. The benzene was purified by the usual methods.

Unless otherwise stated, reagents were of guaranteed reagent grade and used without further purification.

Apparatus

The γ-activity of ^{113}Sn (^{113m}In) was measured with a 50 × 50 mm NaI(Tl) well-type scintillation detector connected to a single-channel analyser.

Procedures

Preparation of sample solutions. A coal fly-ash sample was dried in a desiccator over phosphorus pentoxide to constant weight. About 1 g was weighed into a platinum crucible and 1–2 ml of water, 0.05 ml of concentrated sulphuric acid and 4 ml of hydrofluoric acid were added. The crucible was heated on a hot-plate (at about 80°) for 1–2 hr. Another 0.5 ml of hydrofluoric acid was added, and the solution was evaporated to fumes of sulphuric acid. The residue was then carefully fused with 3–4 g of potassium hydrogen sulphate at 400–600° for 15–30 min. After cooling, the fused mass was heated at 90–95° for 8–11 hr with 5 ml of radio-tin(IV) spike solution (6.10 μg of tin) and about 40 ml of 3.5*M* sulphuric acid to achieve isotopic equilibrium. The solution was then transferred quantitatively into a 100-ml separatory funnel, 6 ml of 5*M* sodium iodide and 20 ml of benzene were added and the funnel was shaken (mechanical shaker) for 1–2 min. The tin(IV) was then stripped with 10 ml of 2.5*M* sulphuric acid, giving complete separation from matrix elements.

Substoichiometric separation of tin(IV). In a 50-ml centrifuge tube fitted with a ground-glass stopper, 10 ml of the sample solution prepared as above [or 10 ml of the radio-tin(IV) spike solution], 8 ml of 5*M* sodium perchlorate and 13 ml of benzene were placed, 2 ml of 5*M* sodium iodide were added and the contents were vigorously shaken for 30 sec. After centrifugation, a 5-ml portion of the benzene phase was pipetted into a 30-ml centrifuge tube fitted with a ground-glass stopper. A substoichiometric amount of SATP in ethanol (1 ml of 2.5×10^{-5}*M* SATP) and 0.1 ml of 10% pyridine solution in ethanol were added, in that order. The contents were moderately mixed after each addition, allowed to stand for 10–30 min, then vigorously shaken for 1 hr with 5 ml of buffer solution (pH 3.8–4.0, and 2.5×10^{-5}*M* in tartrate). After centrifugation, a 3-ml portion of the organic phase was pipetted into a glass test-tube with a fitted cap and allowed to stand for 18 hr to achieve radioactive equilibrium for ^{113}Sn ($t_{\frac{1}{2}}$ 115 d) and ^{113m}In ($t_{\frac{1}{2}}$ 1.66 hr). The γ-activity was measured by scintillation counting. The pH value of the aqueous phase was checked before and after shaking.

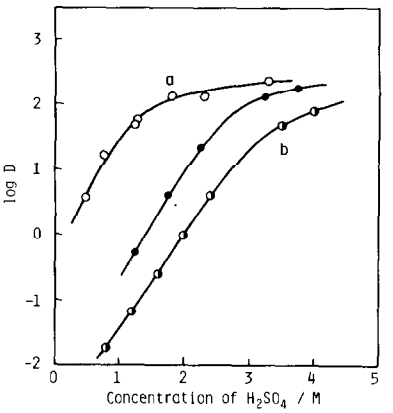


Fig. 1. Extraction of tin(IV) into benzene from 0.5*M* NaI in H_2SO_4, (*a*) with 2*M* $NaClO_4$ present, (*b*) with 0.1*M* HCl present. [Sn(IV)] = 6×10^{-5}*M*, shaking time = 1–2 min.

RESULTS AND DISCUSSION

Iodide extraction of tin(IV)

This is used for transferring the tin(IV) into organic medium to separate it from certain interfering elements and to facilitate the substoichiometric complexation with SATP. The dependence on extraction conditions is shown in Fig. 1. The distribution ratio of tin(IV) is independent of the tin concentration in the range 10^{-6}–10^{-3}*M*. At high acidity, iodine is produced by air-oxidation and is extracted into the benzene, hence the acidity is kept as low as possible. As previously reported,[9] addition of sodium perchlorate significantly enhances the extraction of tin(IV) iodide into benzene, making quantitative extraction possible at lower acidity. As shown in Fig. 1, the distribution ratio of tin(IV) is increased by the presence of sodium perchlorate (at 2.0*M* concentration). In the presence of 0.1*M* hydrochloric acid, however, it decreases by an order of magnitude owing to the formation of chloro-complexes[11] in the aqueous phase, so hydrochloric acid must not be used in the dissolution of samples.

Tin(IV) extracted as the iodide into benzene can be readily stripped with aqueous solutions of various pH values. This is used to separate excess of tin(IV) from the SATP chelate in the procedure.

Formation of tin(IV)–SATP chelate

Any iodine present might interfere in the quantitative reaction of a substoichiometric amount of SATP with tin(IV) in the organic medium, but is taken care of by the ascorbic acid added to the SATP solution as a stabilizer. The results in Fig. 2 show that the sulphuric acid concentration has no influence on the complexation of tin(IV) with a substoichiometric amount of SATP if it does not exceed 3*M*. The effect of higher concentrations of acid may be ascribed to

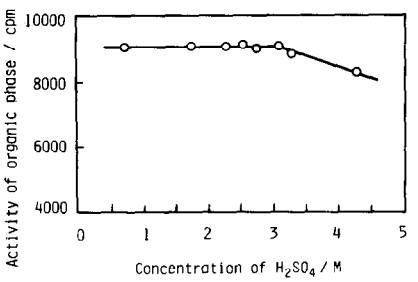


Fig. 2. Effect of the concentration of sulphuric acid in the iodide extraction on the succeeding substoichiometric separation of tin(IV) with SATP. Conditions of the substoichiometric separation: [Sn(IV)] = $4.1 \times 10^{-5}M$, [SATP] = $2.0 \times 10^{-5}M$, [Tart] = $1.0 \times 10^{-4}M$, pH = 3.9, shaking time = 1 hr.

decomposition of SATP by iodine produced in amounts beyond the capacity of the ascorbic acid present.

Addition of pyridine to the non-aqueous medium was found effective in promoting the complexation of tin(IV) with SATP. Table 1 shows the effect of different concentrations of pyridine in the iodide extract containing SATP. The activity of the organic phase is virtually constant with 0.01–0.7% of pyridine present. The stepwise complexation of tin(IV) with SATP in non-aqueous medium in the presence of small amounts of pyridine may be described as follows:

$$SnI_4 + H_2A + 2py \rightleftharpoons SnI_2A \text{ (or } SnI_2A.npy) + 2HI.py \quad (1)$$

$$SnI_2A + H_2A + 2py \rightleftharpoons SnA_2 + 2HI \cdot py \quad (2)$$

where H_2A and py denote SATP and pyridine respectively, the pyridine acting as a base for trapping the hydrogen ions released from the SATP. The apparent decrease in activity with increase in pyridine concentration might be due to solvolysis of the tin complexes.

The rate of formation of the tin(IV)–SATP complex was investigated. The organic extracts containing the iodide, SATP ($2 \times 10^{-4}M$) and pyridine were allowed to stand for 1, 10, 20, 60 and 100 min, and then shaken for 30 min with the buffer solution at pH 3.9.

Table 1. Effect of pyridine on formation of the tin–SATP complex in the benzene phase under substoichiometric conditions*

Concentration of pyridine solution added, %	Activity of organic phase, *cpm*
0	1846
0.5	2213
5	2277
20	2309
40	2304
99	1997

* 5 ml of benzene extract plus 1 ml of SATP solution in ethanol, plus 0.1 ml of the pyridine solution, let stand for 20 min, then shaken with 5 ml of pH-5.7 buffer for 30 min.

The activities of ^{113}Sn in the organic phase were 5979, 5946, 5951, 5981 and 5941 cpm respectively. This result implies that the complex formation in the non-aqueous medium is quite rapid, but it must not therefore be concluded that the 1:2 complex of tin(IV) with SATP is instantaneously and directly formed in the organic medium. In the reaction of tin(IV) with an excess of SATP [$6 \times 10^{-4}M$ SATP and $6 \times 10^{-5}M$ tin(IV)] in the benzene phase after the iodide extraction, a standing time of at least 20 min is required to form the tin(IV)–SATP chelate quantitatively. As will be described later, the shaking of the organic mixture with an appropriate buffer solution seems to play an important role in the formation of the 1:2 chelate under substoichiometric conditions.

Isolation of tin(IV)–SATP chelate

Because a constant amount of tin(IV) must be isolated as the SATP chelate, the washing to remove surplus tin(IV) iodide from the organic phase without affecting the SATP chelate in the organic phase has been investigated. This washing also removes the ethanol present as solvent in the reagent solutions and hence keeps the benzene phase volume constant. It was observed that the tin(IV)–SATP complex in the organic phase was transferred into the aqueous phase during the first few seconds of shaking, the aqueous phase becoming slightly yellow, and then the activity of ^{113}Sn in the organic phase increased on further shaking and soon became constant. These observations may be explained if it is assumed that the 1:1 tin(IV)–SATP complex is formed instantaneously in the non-aqueous medium under substoichiometric conditions, and then the washing with an appropriate buffer strips the tin and SATP and causes formation of the 1:2 tin(IV)–SATP complex, which is finally re-extracted into the organic phase.

The rate of re-extraction as the 1:2 complex depends on the auxiliary complexing agents, if present, in the aqueous phase, and particularly on the pH. The effect of tartrate in the aqueous washing solution was examined for the $4.1 \times 10^{-5}M$ Sn(IV)–$3.0 \times 10^{-5}M$ SATP system. The activities of the organic phase after 30 min of shaking in the presence and absence of $10^{-3}M$ tartrate at pH 5.8 were 2568 and 2225 cpm respectively (this pH was selected in order to make the re-extraction slow enough to be monitored easily: see below). Tartrate may somewhat accelerate the formation of the 1:2 SATP complex by complexing with tin(IV) released from the 1:1 SATP chelate in the aqueous phase. To avoid any unfavourable effect of a high concentration of tartrate, the tartrate concentration is made the same as that of the SATP added.

The effect of pH on the rate of re-extraction of the tin(IV)–SATP chelate from tartrate media was investigated. As shown in Fig. 3, the re-extraction is rapid at pH 2.5–4, but slow at pH > *ca.* 5. These results are consistent with those observed in the direct extraction of tin(IV) with SATP in benzene.[12] The rate of re-

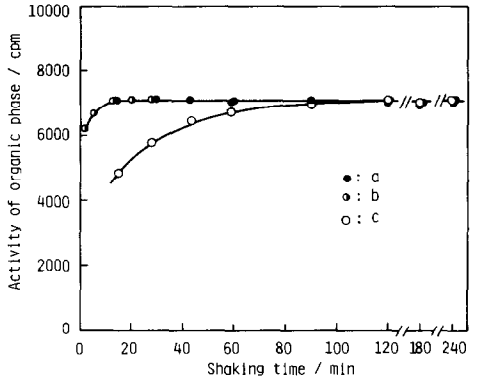


Fig. 3. Dependence of the substoichiometric separation of the Sn(IV)–SATP complex on pH and shaking time. Conditions: [Sn(IV)] = $4.1 \times 10^{-4}M$, [SATP] = $2.0 \times 10^{-4}M$, [Tart] = $1.0 \times 10^{-3}M$. (a) pH = 2.45, (b) pH = 3.94, (c) pH = 5.69.

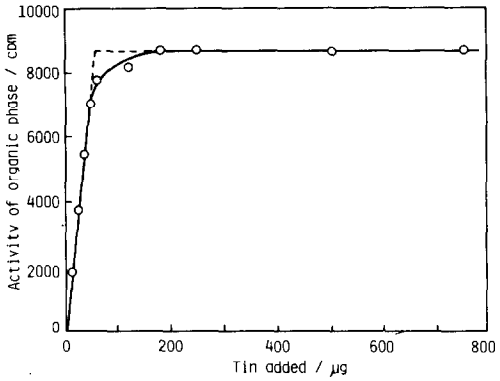


Fig. 5. Reproducibility of the substoichiometric separation of tin(IV) with SATP after the iodide extraction. Conditions: [SATP] = $2.0 \times 10^{-4}M$, [Tart] = $1.0 \times 10^{-3}M$, pH = 3.6–3.9, shaking time = 2 hr.

extraction is high enough at pH 3.9 even with an SATP substoichiometric concentration as low as $2.0 \times 10^{-6}M$, the equilibrium being achieved within 1 hr. The influence of pH on the substoichiometric extraction with $2.0 \times 10^{-4}M$ SATP is clearly seen in Fig. 4. By reaction with a constant but substoichiometric amount of SATP a fixed amount of tin(IV) must remain in the organic phase. Constant activity is observed at pH 2.5–5.3, the relative standard deviation (RSD) of the activity being as low as 0.4%. This plateau pH region, as expected, broadens with increase in the shaking time. Similar results were obtained in the substoichiometric systems with different concentrations of SATP, e.g., with $2.0 \times 10^{-5}M$ SATP a plateau region appeared at pH 2.5–4.5 with shaking for 1.5 hr. When the pH is adjusted to below 2 with $0.1M$ hydrochloric acid, as shown in Fig. 4, extra tin(IV) remains in the organic phase, but not if $0.05M$ sulphuric acid is used instead. This effect may be attributed to the formation of a mixed-ligand

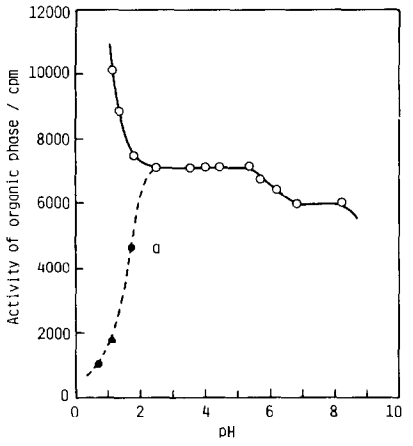


Fig. 4. Dependence of the substoichiometric separation of the Sn(IV)–SATP complex on pH. Conditions: [Sn(IV)] = $4.1 \times 10^{-4}M$, [SATP] = $2.0 \times 10^{-4}M$, [Tart] = $1.0 \times 10^{-3}M$, shaking time = 1 hr. (a) pH adjusted with $0.05M$ sulphuric acid without chloride.

complex of Sn(IV) with chloride and SATP; formation of a corresponding sulphate complex is unlikely on account of the poor complexing ability of the sulphate ion. Such mixed complexes has been found in the extraction of tin(IV) with 8-hydroxyquinoline[13] and *N*-benzoyl-*N*-phenylhydroxylamine[14], namely $SnCl_2(oxine)_2$ and $SnCl_2(BPHA)_2$.

Reproducibility of the substoichiometric separation

The substoichiometric separation was applied to a series of solutions containing different amounts of tin(IV) labelled with ^{113}Sn. As shown in Fig. 5, the radioactivity of the organic phase increases with increase in the amount of labelled tin(IV) until the equivalence point corresponding to a 1:2 ratio of tin(IV) to SATP is reached. At higher tin levels, that is, under substoichiometric conditions, a constant amount of tin(IV) remains in the organic phase, and the reproducibility is very satisfactory. The precision obtained for the substoichiometric separation under various conditions is summarized in Table 2. From these results it is expected that the method can be applied to the determination of as little as a microgram of tin.

Effect of diverse metal ions

The effect of other metal ions on the substoichiometric separation was investigated by adding 0.8–21.0 mg of non-active ion to 10 ml of aqueous solution containing 49 μg of tin(IV). The activities of ^{113}Sn obtained in the presence and absence of the interfering ion were compared. The results are summarized in Table 3, which shows that Fe(III), Cu(II) and V(V) interfere, but several other species do not. The criterion for judging interference to be occurring was an error exceeding 2%. The interference may be ascribed to the decomposition of SATP by the iodine liberated by the oxidation of iodide with these metal ions, and extracted into the organic phase. Fe(III) can be prevented from interfering if it is reduced to Fe(II) with ascorbic acid before the iodide extraction. In general, the interference can be avoided by separating tin(IV)

Table 2. Reproducibility of the substoichiometric separation under various conditions

$2.0 \times 10^{-4}M$ SATP*		$2.0 \times 10^{-5}M$ SATP†		$2.0 \times 10^{-6}M$ SATP‡	
Tin taken, *μg/5 ml*	Activity of organic phase, *cpm*	Tin taken, *μg/5 ml*	Activity of organic phase, *cpm*	Tin taken, *μg/5 ml*	Activity of organic phase, *cpm*
1219	7174	121.9	9202	12.19	10,865
731.6	7181	73.16	9226	7.32	10,682
487.7	7143	48.77	9167	4.88	11,184
365.8	7153	36.58	9083	3.66	11,489
304.8	7085	30.48	9141	3.05	11,082
243.9	7096	24.39	9199	2.44	11,255
243.9	7074	18.29	9224	1.22	11,218
182.9	7048	12.19	9190		
mean $\pm \sigma$ = 7115 $\pm$ 46 cpm		mean $\pm \sigma$ = 9179 $\pm$ 48 cpm		mean $\pm \sigma$ = 11,111 $\pm$ 266 cpm	
RSD = 0.6%		RSD = 0.5%		RSD = 2.4%	

Experimental conditions:
* [Tart] = $10^{-3}M$, pH = 3.9, shaking time = 1 hr.
† [Tart] = $10^{-4}M$, pH = 3.9, shaking time = 1 hr.
‡ [Tart] = $10^{-5}M$, pH = 3.9, shaking time = 1.5 hr.

from the iodine, for example by repeated extractions, that is, tin(IV) is extracted as iodide, stripped with 2–3*M* sulphuric acid, and extracted again as the iodide into benzene, and this is followed by substoichiometric chelate formation with SATP. With this procedure, no interference is observed (*cf.* Table 3). The selectivity of the overall extraction procedure was checked independently as follows: the iodide extraction was performed on an aqueous phase containing the non-active tin(IV) carrier and various radioactive metal ions, and the activity of the organic phase was measured; next, a substoichiometric amount of SATP in ethanol was added to the organic phase, the tin(IV)–SATP chelate was separated, and the activity of the organic phase was measured again. As shown in Table 4, foreign metals other than As(III) and Sb(III) are thoroughly separated from tin(IV) in the iodide extraction, and the contamination by As(III) and Sb(III) is almost completely eliminated by the substoichiometric separation with SATP. Because the iodide extraction is repeated twice (as described above), the analytical procedure has even higher selectivity for the determination of tin(IV).

Determination of tin(IV) in a synthetic mixture

The accuracy and precision of the method were evaluated by determining tin in a synthetic mixture containing a known amount of tin and large amounts of other metals. The results are summarized in Table 5. The reproducibility of the substoichiometric isolation of tin(IV) is seen in the fourth and fifth columns, the RSD values being 0.3%. As the errors in an isotope dilution determination are also dependent on the isotopic dilution ratio, the RSD of 0.6% obtained in these is very satisfactory. The mean value of 16.16 $\pm$ 0.10 μg agrees well with the amount added,

Table 3. Effect of diverse metal ions on the substoichiometric separation of tin(IV) with SATP after the iodide extraction

Other metal ion, *mg*		Interference*, %	Other metal ion, *mg*		Interference,* %
Al(III)	2.7	+0.5	Cu(II)	6.4	−11.1
Ti(IV)	4.8	−1.9	Cu(II)	6.4†	−0.1
V(V)	5.1	−11.9	Zn(II)	6.5	+1.3
V(V)	5.1†	−0.8	Ge(IV)	0.8	−1.4
Cr(III)	5.2	−1.7	As(III)	0.8	−1.3
Mn(II)	5.5	−0.4	Mo(VI)	1.0	+0.5
Fe(III)	5.6	−18.3	Sb(III)	1.2	+1.6
Fe(III)	5.6‡	+0.7	Hg(II)	1.0	−1.7
Co(II)	5.9	+1.6	Pb(II)	21.0	+0.4
Ni(II)	5.9	0	Bi(III)	2.1	−1.2

Experimental conditions: tin taken = 49 μg per 10 ml of aqueous phase, [SATP] = $2.0 \times 10^{-5}M$, [Tart] = $10^{-4}M$, pH = 3.9, shaking time = 1 hr.
* Interference = $100(A_i - A)/A\%$, where A_i and A are the activities of ^{113}Sn separated in the presence and absence of other metal ions respectively.
† The iodide extraction was repeated.
‡ Reduced to Fe(II) by adding 10% ascorbic acid solution.

Table 4. Selectivity of the substoichiometric separation of tin(IV) with SATP after the iodide extraction

Radioactive tracer added, *cpm*		Carrier added, *mg*	Activity of iodide extract, *cpm*	Activity of substoichiometric extract, *cpm*	Decontamination factor†
^{51}Cr	439,813	5.2	0	0	$>10^6$
^{54}Mn	418,827	5.5	0	0	$>10^6$
^{59}Fe	458,005	5.6*	7	7	7×10^4
^{57}Co	942,706	5.9	0	1	$>10^6$
^{57}Ni–^{57}Co	1,636,008	1.4	2	1	$>10^6$
^{67}Cu	2,263,951	6.4*	4	1	$>10^6$
^{65}Zn	480,246	6.5	0	1	$>10^6$
^{74}As	94,172	0.7	4295	30	3×10^3
$^{120,122}Sb$	1,935,160	0.9	78953	68	3×10^4
^{203}Pb	909,408	1.7	30	0	$>10^6$

Experimental conditions; tin taken = 49 μg/10 ml of aqueous phase, [SATP] = $2.0 \times 10^{-5}M$, [Tart] = $10^{-4}M$, pH 3.9, shaking time = 1 hr.

* The amount of tin in the substoichiometric extract was decreased.

† Decontamination factor = $\frac{\text{activity taken}}{\text{activity of substoichiometric extract}}$.

16.25 μg, the deviation being 0.6%. The method is accurate and precise, and can be applied to practical samples.

Determination of tin in coal fly-ash

The coal fly-ash samples were obtained from the NBS and a coal-fired electricity generation plant in Japan. The latter was the finest fraction (*ca.* 80% of it passed through a 300-mesh screen) of the fly-ash treated stepwise with electrostatic precipitators. Table 6 shows the analytical results for the domestic sample together with the analytical conditions. The RSD was 1.8%, confirming that the procedure described is adequate for the determination of tin in fly-ash. A blank analysis performed by the complete procedure showed contamination with tin from reagents and glassware *etc.* was negligible (< 0.01 μg).

Table 5. Determination of tin in a synthetic mixture

Tin taken,* μg	Other metals present,*	*mg*	Active tin in spike (M_s), μg	Activity from spike solution (A_s),† *cpm*	Activity from test sample (A_x), *cpm*	Tin found (M_x),‡ μg
16.25	Al(III)	1.3	16.2_5	21,298, 21,374, 21,402	10,726	16.1_1
	V(V)	2.5				
	Cr(III)	2.6			10,707	16.1_7
	Mn(II)	2.8				
	Fe(III)	2.8			10,663	16.3_0
	Co(II)	2.9				
	Ni(II)	2.9			10,741	16.0_6
	Cu(II)	3.2				
	Zn(II)	3.3				

Mean value ± σ = $16.1_6 \pm 0.1_0$ μg; RSD = 0.6%; deviation from tin taken = −0.6%.

* A 10-ml portion of the synthetic mixture was used for each determination.

† The mean value (±σ), 21,358 (±54) was employed for the calculation.

‡ Calculated from $M_x = M_s\left(\frac{A_s}{A_x} - 1\right)$.

Table 6. Determination of tin in the domestic coal fly-ash

Sample weight, *g*	Amount of $KHSO_4$, *g*	Active tin in spike, μg	Activity from spike solution, *cpm*	Activity from test sample, *cpm*	Tin found, μg	Concentration, μg/g
1.0228*	4.0	6.097	12,434	7223	4.40	4.30
1.0399†	3.5	6.097	32,973	19,090	4.43	4.27
1.0500†	3.0	6.097	32,973	18,719	4.64	4.42

Mean value ± standard deviation = 4.33 ± 0.08 μg/g; RSD = 1.8%.

* Isotopic equilibrium achieved by heating for 8 hr.

† Isotopic equilibrium achieved by heating for 11 hr.

Table 7. Determination of tin in NBS coal fly-ash (SRM 1633)

Sample weight, *g*	Active tin in spike, *μg*	Activity from spike solution, *cpm*	Activity from test sample, *cpm*	Tin found, *μg*	Concentration, *μg/g*
0.9931*	6.097	25,358	12,263	6.51	6.56
			12,183	6.59	6.64
1.0445*	6.097	25,358	13,286	5.54	5.30
			13,575	5.29	5.07
0.9882*	6.097	12,237	6439	5.49	5.56
			6522	5.34	5.41
0.9314*	6.097	8706	4536	5.61	6.02
1.0689†	6.097	12,434	6540	5.50	5.14
			6490	5.58	5.22
0.9488†	6.097	12,434	6346	5.85	6.17
			6378	5.79	6.10
1.1813‡	7.804	35,201	19,347	6.40	5.41

Overall mean value ± standard deviation = 5.7 ± 0.6 μg/g; RSD = 10%.
* Fusion with 3.5 g of flux.
† Fusion with 4.0 g of flux.
‡ Fusion with 3.5 g of flux and radioactive tin.

The results for the NBS SRM 1633 coal fly-ash are summarized in Table 7. To make sure the exchange equilibration between the ^{113}Sn and tin in the sample was complete, in the last experiment in Table 7 the ^{113}Sn spike solution was added before starting the fusion treatment. No significant difference in the tin content was found compared with the ordinary experiments in which the ^{113}Sn spike solution was added after dissolution of the melt in acid. Taking into account the nearly constant analytical results in all the experiments, regardless of different fusion conditions, *viz.* amounts of fusion flux, fusion time, *etc.*, isotopic exchange equilibrium seems to be achieved, except for non-exchangeable tin species, between ^{113}Sn and the tin present after the hydrofluoric acid treatment and potassium hydrogen sulphate fusion followed by the preliminary iodide extraction. The reproducibility of the substoichiometric separation (fourth column) is again very satisfactory (mean RSD 0.8%), but the overall precision of 10% seems rather poor. Because of the high precision for the domestic sample, this result is unexpected. However, it has recently been pointed out that the concentration of elements in coal fly-ash varies remarkably with the particle size.[15] The scatter found for the NBS fly-ash may be ascribable to the sampling statistics or the inhomogeneity of the sample rather than to random errors in the method used.

REFERENCES

1. K. Schwarz, D. B. Milne and E. Vinyard, *Biochem. Biophys. Res. Commun.*, 1970, **40**, 22.
2. D. J. Von Lehmden, R. H. Jungers and R. E. Lee, Jr., *Anal. Chem.*, 1974, **46**, 239.
3. J. Růžička and J. Starý, *Substoichiometry in Radiochemical Analysis*, p. 43. Pergamon, Oxford, 1968.
4. K. Kudo and N. Suzuki, *J. Radioanal. Chem.*, 1975, **26**, 327.
5. I. Obrusník, *Talanta*, 1969, **16**, 563.
6. K. Kudo, H. Iso and T. Shigematsu, *J. Radioanal. Chem.*, 1972, **12**, 451.
7. B. M. Tejam and B. C. Haldar, *Radiochem. Radioanal. Lett.*, 1972, **13**, 25.
8. G. R. E. C. Gregory and P. G. Jeffery, *Analyst*, 1967, **92**, 293.
9. D. D. Gilbert and E. B. Sandell, *Microchem. J.*, 1960, **4**, 491.
10. A. R. Byrne and D. Gorenc, *Anal. Chim. Acta*, 1972, **59**, 81.
11. J. Kragten, *Talanta*, 1975, **22**, 505.
12. H. Imura and N. Suzuki, *Anal. Chim. Acta*, 1980, **118**, 129.
13. A. R. Eberle and M. W. Lerner, *Anal. Chem.*, 1962, **34**, 627.
14. M. Koeva, *Anal. Chim. Acta*, 1979, **104**, 161.
15. J. A. Campbell, J. C. Laul, K. K. Nielson and R. D. Smith, *Anal. Chem.*, 1978, **50**, 1032.

Talanta Vol. 28, pp. 81 to 88
©Pergamon Press Ltd 1981. Printed in Great Britain
0039-9140/81/0201-0081$02.00/0

TITRAGE COULOMETRIQUE DE COMPOSES ACIDES D'INTERET PHARMACEUTIQUE EN MILIEU DIMETHYLSULFOXYDE

M. H. LIVERTOUX et J. BESSIERE

Laboratoire de Chimie et Electrochimie Analytique, Université de Nancy I, CO 140–54037 Nancy Cedex, France

(*Reçu le* 10 *octobre* 1979. *Revisé le* 8 *septembre* 1980. *Accepté le* 17 *septembre* 1980)

Résumé—Le titrage coulométrique des acides conjugués de substances d'intérêt pharmaceutique (dérivés phénothiaziniques N_{10} substitués) est réalisé à moins de 1% près dans le solvant mixte DMSO 90%–eau 10% (en fraction molaire), les concentrations variant de 2 à $5.10^{-3}M$. Le point équivalent est mis en évidence par ampérométrie directe à une électrode de platine poli et en présence de la phénothiazine comme indicateur ampérométrique. La bonne stabilité de l'hydroxyde de tétraéthylammonium dans le solvant permet d'envisager les titrages successifs. Le titrage en série (phénothiazine comme indicateur) de dérivés substitués est réalisé, en présence d'oxygène, avec une précision de 100 ± 1%.

La colorimétrie et la potentiométrie à l'électrode de verre sont les méthodes les plus couramment utilisées pour mettre en évidence la fin de titrage volumétrique ou coulométrique d'un acide,[1–3] mais dans le cas de titrage des solutions colorées ou hétérogènes, les indicateurs acide–base sont inutiles et le fonctionnemennt de l'électrode de verre en milieu aprotique, notamment en milieu basique, n'est pas toujours satisfaisant.

Dans certaines conditions, la détection ampérométrique peut remplacer avantageusement ces techniques.[4,5] Il est possible de suivre le titrage d'un acide de deux manières: (1) l'acide est réductible électrochimiquement par son proton (ampérométrie directe); (2) on utilise un indicateur ampérométrique de fin de réaction. Cette deuxième méthode a un caractère plus général puisqu'elle peut s'appliquer au dosage d'acides non électroactifs.

Les résultats exposés dans ce mémoire concernent le dosage coulométrique avec détection par ces deux méthodes, en milieu diméthylsulfoxyde, d'acides conjugués de substances médicamenteuses et plus particulièrement les chlorhydrates de prométhazine (A), chlorpromazine (B), thioridazine (C), oxomémazine (D), le maléate de lévopromazine (E) et le bisméthanesulfonate de prochlorpromazine (F) (tableau 1).

PARTIE EXPERIMENTALE

Réactifs

La solution Et_4NClO_4 0,1*M* dans le solvant mixte DMSO 90%–eau 10% (solvant S), en fraction molaire, est proposé comme milieu réactionnel. Le DMSO est choisi pour l'étendue de son domaine acid–base,[6,7] même en présence d'eau.[8–13] La quantité d'eau (10% en fraction molaire, soit 2,5% en poids) est nécessaire à la production, in situ, du réactif titrant avec un rendement de 100%.[14–16] Dans ces conditions, le domaine acide–base s'étend sur 25,5 unités de pH.[17] Le caractère basique du solvant S est proche de celui du solvant pur.[18] Le domaine d'électroactivité à l'électrode de platine poli s'étend sur près de 3,5 V. Les limites anodique et cathodique correspondent à l'oxydation et à la réduction de l'eau.[7,19] Le perchlorate de tétraéthylammonium est choisi comme électrolyte support. La réduction de l'eau conduit à la formation d'hydroxydes alcalins peu solubles qui passivent l'électrode de platine poli[14,20] et la rendent inutilisable. Plusieurs auteurs ont noté la dégradation de sels d'ammonium quaternaire en milieu aprotique très basique.[21,22] Les études coulométriques menées dans le solvant S révèlent une stabilité satisfaisante de Et_4NOH. L'eau présente en quantité relativement importante rend le milieu plus acide que le DMSO anhydre[23] et constitue un facteur de stabilité de l'ion hydroxyde.

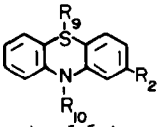
Réactif titrant. L'eau étant plus acide que le DMSO, l'ion hydroxyde est une base forte dans le solvant S. Le choix du réactif titrant dépend essentiellement de la nature de l'acide envisagé: (1) s'il n'est pas électroactif ou s'il l'est uniquement par son proton, les ions HO^- sont produits par réduction de l'eau, (2) s'il est électroactif par d'autres fonctions, le titrage volumétrique est réalisé à l'aide d'une solution aqueuse de Bu_4NOH à 40%. La présence de ce réactif à la concentration 0,01*M* s'accompagne d'une addition d'eau d'environ 0,025*M* qui ne modifie pas sensiblement les propriétés acides du solvant S.

Génération coulométrique des ions hydroxyde. Le titrage coulométrique des acides en milieu DMSO a été abordé par Bos *et al.*[21] Ils envisagent la réduction électrochimique du *m*-crésol à une électrode de platine poli pour titrer des acides de pK_A inférieur à 7,0. Pour des acides plus faibles, ils réduisent le solvant à une électrode de platine platiné et constatent une efficacité en courant de 100%. Il est probable que les ions basiques proviennent de la réduction de l'eau résiduelle plutôt que de celle du DMSO en ion dimsyl.

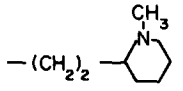
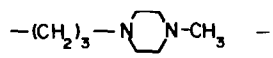
Appareillage

La coulométrie à intensité constante est réalisée dans une cellule électrochimique à compartiments séparés Tacussel équipée de deux électrodes de platine poli de grande surface. Le compartiment anodique contient une solution saturée de Me_4NCl dans le DMSO pur, afin d'éviter la diffusion éventuelle des protons formés par oxydation de l'eau au cours de l'électrolyse. L'intensité (10 mA) est imposée au circuit d'électrolyse à l'aide d'un chronoampérostat Tacussel type CEAM 3D. Le point équivalent est

Tableau 1. Phénothiazines étudiées



formule générale

Composé		R_{10}	R_2	R_9
Prométhazine chlorhydrate	(A)	$-CH_2-CH(CH_3)-N(CH_3)_2$	$-H$	—
Chlorpromazine chlorhydrate	(B)	$-(CH_2)_3-N(CH_3)_2$	$-Cl$	—
Thioridazine chlorhydrate	(C)		$-SCH_3$	—
Oxomémazine chlorhydrate	(D)	$-CH_2-CH(CH_3)-CH_2-N(CH_3)_2$	$-H$	
Lévopromazine maléate	(E)	$-CH_2-CH(CH_3)-N(CH_3)_2$	$-OCH_3$	—
Prochlorpromazine bisméthanesulfonate	(F)		$-Cl$	—

mis en évidence par colorimétrie en présence de bleu de thymol et par ampérométrie directe.

Efficacité en courant. Dans le solvant S, la génération coulométrique des ions HO^- se fait avec un rendement de 100%: 25 μmole de Et_4NOH sont produites à partir du passage d'un courant d'intensité constante puis titrées par une solution molaire d'acide méthanesulfonique, en présence de bleu de thymol. La détermination du point équivalent se fait avec une bonne précision. Elle révèle la bonne stabilité de Et_4N^+ en présence des ions HO^-. Ce résultat est confirmé en dosant l'acide méthanesulfonique par coulométrie en présence du même indicateur (tableau 2).

La présence d'oxygène dissous ne modifie pas le rendement de la coulométrie. En effet la réaction

$$O_2 + 2H_2O + 4e = 4HO^-$$

qui traduit la réduction globale dans le DMSO en présence d'eau,[25] produit le même nombre d'équivalents HO^- par Faraday que la réduction de l'eau.

Courbes voltampérométriques

La connaissance de ces courbes est nécessaire pour préciser la valeur du potentiel à fixer au cours du titrage ampérométrique des acides électroactifs dans le solvant S. Les composés envisagés sont réductibles par leur proton (tableau 3).

Les courbes voltampérométriques sont tracées en utilisant le montage classique à trois électrodes. Le potentiel est imposé et le courant enregistré à l'aide d'un enregistreur Tacussel EPL2 piloté par un tiroir TiPol. L'électrode de travail est une électrode de platine (diamètre 0,8 mm) poli tournante (600 t/mn). Sa surface active est régénérée par polissage mécanique sur pâte d'alumine. L'électrode de référence est la demi-pile proposée par Courtot-Coupez et Le Demezet:[14] $Ag/AgCl_2^-$ $10^{-3}M$/LiCl 0,1M dans le DMSO pur séparée de la solution par un double fritté rempli de la solution Et_4NClO_4, 0,1M dans le solvant S. Son potentiel, déterminé par rapport au système du ferrocène, est égal à $-0{,}665$ V, soit $+0{,}215$ V par rapport à l'e.c.s. aqueuse. L'électrode auxiliaire est une électrode de platine poli.

Le volume de la solution est de 10 ml et les acides sont présents à des concentrations de 2.10^{-3} à $10^{-2}M$. La vitesse de défilement en potentiel est fixée à 150 mV/mn.

La figure 1 montre les vagues cathodiques des solutions d'acide méthanesulfonique et de quelques acides conjugués de substances médicamenteuses. Le bisméthanesulfonate de prochlorpromazine est réductible par ses deux fonctions acide. L'oxygène est également électroactif sur platine poli, mais ne modifie pas le bilan coulométrique. Cependant, sa présence rend délicate la détermination du point équivalent par ampérométrie directe.

Titrage coulométrique des acides conjugués de substances médicamenteuses et détection ampérométrique directe

La tracé des courbes voltampérométriques montre que le point équivalent des réactions de titrage d'acides électroréductibles peut être mis en évidence par ampérométrie directe en imposant à l'électrode de travail un potentiel E_1 de $-1{,}20$ V *vs.* référence, après élimination de l'oxygène dissous par barbotage d'azote.

Le montage expérimental comprend un circuit d'électrolyse (intensité constante 10 mA) et un circuit de mesure du courant cathodique traversant l'électrode indicatrice, portée au potentiel E_1 à l'aide du même enregistreur Tacussel que celui qui permet les tracés voltampérométriques. La détection ampérométrique est couplée à la coulométrie à intensité constante.

Tableau 2. Génération coulométrique de Et_4NOH et titrage coulométrique d'acides forts dans le solvant DMSO 90%–eau 10%–Et_4NClO_4 0,1*M* en présence de bleu de thymol comme indicateur

Composé	Quantité produite ou à titrer, *μmole*	Temps moyen, *sec*	Nombre d'essais	Efficacité en courant,%	Déviation standard, %
Hydroxyde de tétraéthylammonium	25	242,3	9	99,7	0,4
Acide méthanesulfonique	23,1	222,2	10	99,8	0,4
Acide *p*-toluènesulfonique	23,8	230,3	15	99,9	0,4

Titrage ampérométrique des acides conjugués de substances medicamenteuses en présence de phenothiazine

Dans tous les cas, le potentiel est fixé à 0,0 V *vs.* référence (soit −0,225 V *vs.* e.c.s. aqueuse). L'ampérométrie couplée à la réduction coulométrique est réalisée dans les mêmes conditions que précédemment. L'apparition d'un courant au potentiel choisi coïncide avec celle de la coloration jaune de la solution. Les dosages en série sont réalisés en présence de phénothiazine à la concentration $2.10^{-3}M$. Le point équivalent correspond au point d'intersection des tangentes aux deux demi-droites obtenues; chaque dosage est poursuivi jusqu'à génération d'un excès de réactif d'environ 50%. Cette technique de dosage successifs est applicable aux médicaments présentés sous forme galénique (comprimés).

RESULTATS ET DISCUSSION

Détection ampérométrique directe

Il est possible de titrer 25 μmole d'acide conjugué de dérivé phénothiazinique à moins de 1% près. Les dosages successifs sont réalisés: l'addition du composé à doser est effectuée lorsque l'excès de Et_4NOH égale environ 50% de la quantité d'acide à titrer. Les résultats obtenus, rassemblés dans le tableau 4 montrent que la précision est de 100 ± 0,3%.

Le dosage du chlorhydrate de chlorpromazine dans les comprimés est également réalisable.

Après détermination du poids moyen et pulvérisation d'un comprimé, 0,10 g de la poudre obtenue est introduit dans la cellule d'électrolyse. Rapportée à un comprimé, la quantité de chlorpromazine, déterminée par ampérométrie directe est trouvée égale à 100 ± 1 mg. Les résultats obtenus au cours des titrages coulométrique et volumétrique en présence de bleu de thymol (tableau 5) montrent la meilleure précision obtenue par coulométrie-ampérométrie. Les excipients présents ne perturbent ni le rendement de la coulométrie, ni la détection ampérométrique. La suspension obtenue étant colorée, l'ampérométrie semble être une méthode de choix pour la détermination du point équivalent.

Le titrage coulométrique de composés électroactifs à caractère acide (dérivés phénothiaziniques, sels d'alcaloides, acides carboxyliques) est possible en milieu DMSO. Les conditions nécessaires à une efficacité en courant de 100% sont définies. L'hydroxyde de tétraéthylammonium est suffisamment stable pour les besoins analytiques. Les résultats obtenus permettent

Tableau 3. $E_{1/2}$ de quelques acides électroactifs sur platine poli, en milieu DMSO 90%–eau 10%–Et_4NClO_4 0,1*M*

Acides	$pK_{HA}^{H_2O}$	pK_{HA}^{DMSO}	$pK_{HA}^{DMSO-eau*}$	$E_{1/2}$, *V*
méthanesulfonique		fort	fort	−0,34
p-toluènesulfonique		fort	fort	−0,32
ammonium NH_4^+		10,5	9	−0,65
monochloracétique	2,86	8,9		−0,75
propionique	4,87		10,8	−0,96
salicylique	2,97	6,6		−1,05
acétique	4,75	12,6	11,3	−1,15
lactique	3,86			−1,20
valérique	4,82			−1,22
succinique I	4,16	9,5	9,3*	−1,20
succinique II	5,61	16,4	14,0*	non électroactif
phénol	9,99	16,9		non électroactif
Acides conjugués des phénothiazines N_{10} substituées				
(A) Prométhazine. HCl			8,3*	−0,75
(B) Chlorpromazine. HCl	9,3			−0,72
(C) Thioridazine. HCl	9,14			−0,33
(D) Oxomémazine. HCl				−0,77
(E) Lévopromazine. maléate	9,15			−0,82
(F) Prochlorpromazine. $2CH_3SO_3H$ I	3,60			−0,33
II	7,54			−0,88
Thiopropérazine. $2CH_3SO_3H$				−0,50

* Valeurs que nous avons déterminées par potentiométrie à l'électrode à hydrogène dans le DMSO 90%–eau 10%.

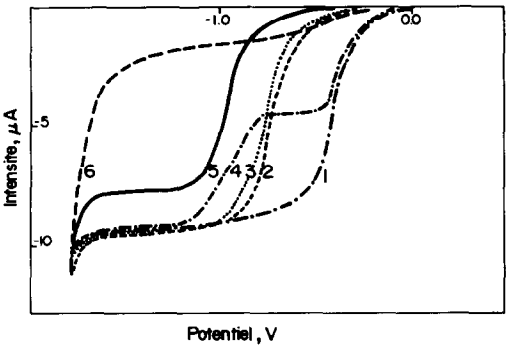


Fig. 1. Courbes voltampérométriques relatives aux dérivés phénothiaziniques (acides conjugués): 1, acide fort; 2, chlorpromazine.HCl; 3, prométhazine.HCl; 4, prochlorpromazine.$2CH_3SO_3H$; 5, thioridazine.HCl; 6, oxygène dissous.

d'envisager la mise au point de techniques automatisées et la détection par osmopile[26] ou par chromatographie.

Cependant, cette technique se limite au titrage et à la détection des acides électroactifs. Si l'on envisage le dosage d'acides plus faibles, non électroactifs, l'emploi d'un indicateur électrochimique de fin de réaction devient nécessaire.

Détection ampérométrique en présence de phénothiazine

Caractère acide de la phénothiazine (PH). Une solution de PH, incolore en milieu neutre et acide, vire au jaune en présence d'ions hydroxyde. Le virage est réversible.

Compte-tenu des propriétés très basiques de l'ion HO^- dans le solvant S, ramené à l'eau, le pH d'une solution molaire est proche de 29. On peut admettre que la fonction –NH– cyclique cède son proton pour donner l'anion P^-, responsable de la coloration jaune.

$$PH + HO^- = P^- + H_2O$$

Le spectre de P^- (figure 2) ne peut être tracé qu'en absence rigoureuse d'oxygène. L'expérience montre que cette espèce est très sensible aux réactions photochimiques et plus particulièrement dans les radiations ultraviolettes, surtout en présence d'oxygène.

Quelques tests qualitatifs effectués en présence d'acides très faibles de pK_A^{DMSO} compris entre 20 et 25

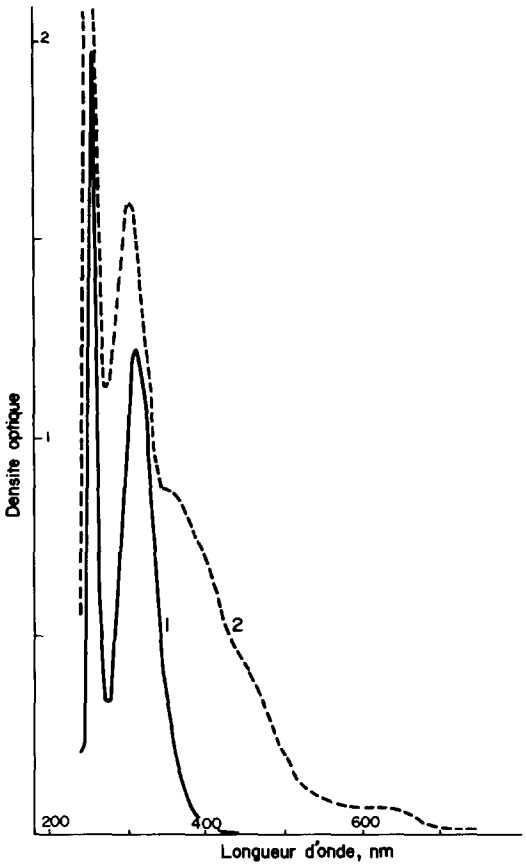


Fig. 2. Spectre de la phénothiazine en milieu DMSO 90%–eau 10%: (1) PH $10^{-4}M$; (2) forme anionique P^-.

(thiourée 20,5; urée 25,1; 2,6 dichloroaniline 25,3) permettent de préciser la zone de virage de cet indicateur unicolore. Les bases utilisées dans l'acétonitrile (acétate $pK_A^{DMSO} = 12{,}6$; la diphénylguanidine $pK_A^{DMSO} = 8{,}6$) sont sans action sur PH. Il en résulte que la phénothiazine se comporte comme un acide faible, proche de la thiourée.

L'électrode à hydrogène étant indicatrice du pH dans le solvant S, il est possible d'évaluer le pK_A^S du couple acide–base PH/P^- par potentiométrie à intensité nulle. Il est égal à 22,5.

La phénothiazine se comporte donc comme un indicateur acide–base unicolore. Le pH d'apparition de la coloration jaune est fonction de sa concen-

Tableau 4. Titrage coulométrique des acides (A), (B), (C), (D), (E) et (F); mise en évidence du point équivalent par ampérométrie directe

Dérivé phénothiazinique étudié	Dosages successifs	Temps moyen, *sec*	Quantités ajoutées, *μmole*	Efficacité en courant, %	Recouvrement, %	Déviation standard,%
A	7	242,0	25	99,7	100,3	0,3
B	10	257,5	27	99,0	100,1	0,4
C	11	241,2	25	100,0	93,0	0,2
D	9	241,4	25	99,9	100,1	0,2
E	6	241,0	25	100,1	99,9	0,2
F	7	241,8	12,5	99,8	100,2	0,3

tration: il sera d'autant plus élevé que l'indicateur sera utilisé en solution plus diluée.

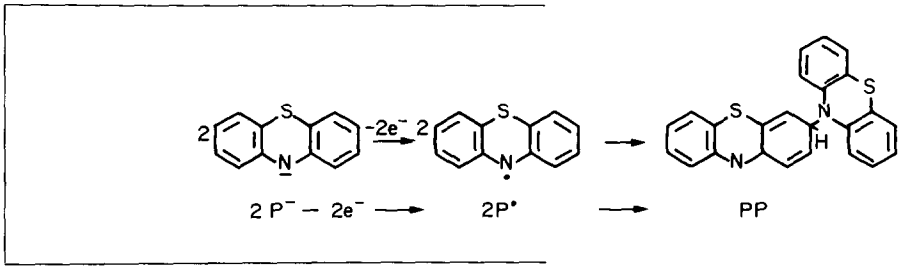
Comportement électrochimique de la phénothiazine dans le solvant S. Les travaux de Billon[27–29] sur la phénothiazine et ses dérivés dans l'acétonitrile ont montré que l'oxydation électrochimique de PH en présence d'un excès d'eau s'effectue selon un processus diélectronique. Une coulométrie à potentiel contrôlé conduit à la formation d'un "produit vert" qui depuis a été identifié comme étant la forme conjuguée PP^+ du biphénothiazinyle 3,10'.

Le tracé voltampérométrique de PH dans le solvant S met en évidence l'oxydation de ce composé en une seule étape diélectronique ($E_{1/2} = +0{,}80$ V). Cette courbe reste inchangée en présence d'acide fort ou faible. Le tracé en voltampérométrie cyclique (figure 3a) d'une solution de PH $5.10^{-3}M$ confirme la mise en jeu de deux électrons: la différence de potentiel entre les deux maxima anodique et cathodique est de 29 mV.

L'addition progressive d'ions hydroxyde à une solution de PH entraîne l'apparition d'une vague anodique décalée de près de 1 V ($E_{1/2} = -0{,}25$ V) par rapport à celle que l'on observe en milieu neutre non tamponné. L'intensité mesurée à $E = 0{,}0$ V croît linéairement avec la concentration de la base ajoutée, jusqu'à une valeur limite correspondant environ à la moitié du courant limite observé au potentiel $E = +1{,}0$ V pour une concentration identique de PH en milieu neutre. Le phénomène est réversible.

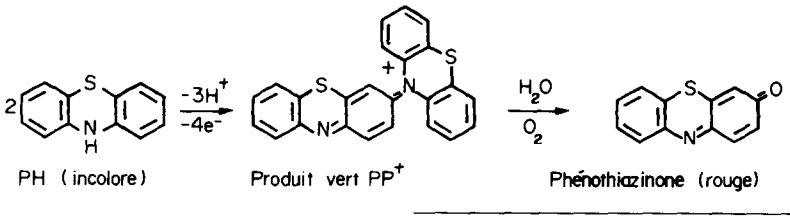
En voltammétrie cyclique, la courbe relative à P^- indique un processus rapide, engageant un seul électron, les maxima anodique et cathodique étant distants de 60 mV (figure 3b).

Compte tenu de ces résultats, il semble logique d'admettre que l'oxydation de P− débute par la formation d'un radical neutre, peu stable, susceptible de se dimériser ensuite pour donner des espèces biphénothiazinyle.



Une électrolyse à potentiel contrôlé ($E = +1{,}0$ V) entraîne la disparition progressive de la vague anodique après la mise en jeu de deux électrons par molécule de PH. La solution incolore passe rapidement au vert, puis au vert sombre et enfin au rouge. La même évolution de coloration a été observée dans le propylèneglycol contenant de l'eau par oxydation chimique en présence d'eau oxygénée et de peroxydase.[30] Le composé rouge a été identifié par ces auteurs comme étant la phénothiazinone. On aurait la suite de réactions:

L'électrolyse d'une solution de PH $2.10^{-3}M$, en présence de Bu_4NOH $4.10^{-3}M$, réalisée à $E = 0{,}0$ V, à l'abri de l'oxygène, entraîne la disparition de la vague précédente après mise en jeu d'un seul électron. La solution obtenue, incolore, n'est plus basique. A $E = +0{,}80$ V, la seconde vague anodique a diminué de moitié. Une vague cathodique apparaît à partir de $-0{,}50$ V. L'addition ultérieure de Bu_4NOH fait réapparaître la coloration jaune et la vague anodique à



Milieu basique. Dans l'acétonitrile, l'utilisation de bases fortes telles que Bu_4NOH est proscrite par suite de la dégradation du solvant. Les données bibliographiques[31–33] s'accordent sur le fait que l'oxydation chimique des phénothiazines en milieu basique conduit à la formation d'un mélange complexe de composés dont on peut isoler deux isomères biphénothiazinyle. Il est probable que la présence d'eau en forte concentration modifie sensiblement le processus d'oxydation.

$-0{,}25$ V. La hauteur est réduite de moitié par rapport à la vague initiale.

Le mécanisme global d'oxydation est complexe et n'a pas été étudié en détail. On peut supposer que en milieu basique, le dimère perd un proton et redonne en partie la phénothiazine et un composé d'oxydation réductible vers $-0{,}50$ V. Cela mérite une investigation plus approfondie qui sort du cadre de cette étude.

Milieu tampon. Il est nécessaire de connaître l'évolution des courbes voltampérométriques relatives à

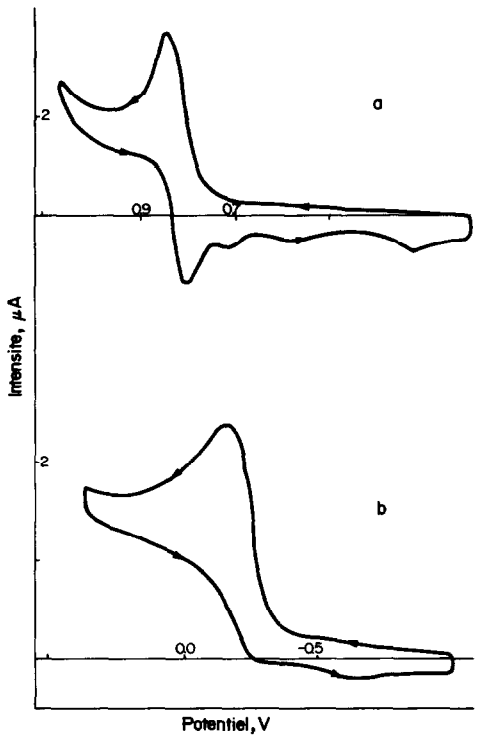


Fig. 3. Voltampérométrie cyclique à une électrode de platine poli (vitesse de balayage en potentiel: 150 mV/sec): (*a*) PH $5.10^{-3}M$; (*b*) même solution en présence de Bu_4NOH $5.10^{-3}M$.

l'oxydation de PH au cours du titrage des acides faibles pour préciser la valeur du potentiel auquel il faut se placer pour déterminer le point équivalent par ampérométrie. Plusieurs cas sont envisagés.

(*a*) Au cours du titrage coulométrique de l'acide acétique ($pK_A^S = 11{,}3$), les ions acétate formés participent au processus d'oxydation de PH: il apparaît une prévague anodique de $E_{1/2} = +0{,}48$ V, dont la hauteur croît avec la concentration en ions acétate. Après le point équivalent, la phénothiazine, sous forme P^-, est oxydable à $-0{,}25$ V. L'addition d'acide fort en excès permet de retrouver la courbe initiale d'oxydation de PH, les ions acétate étant transformés en acide acétique.

(*b*) L'acide succinique, diacide ($pK_{A1}^S = 9{,}3$; $pK_{A2}^S = 14{,}0$) participe successivement par ses deux fonctions au processus d'oxydation de PH (figure 4). La phénothiazine est d'autant plus facilement oxydable que le milieu devient plus basique.

(*c*) Le phénol ($pK_A^{DMSO} = 16{,}9$) et la morphine qui possède un groupement énolique acide dans le solvant

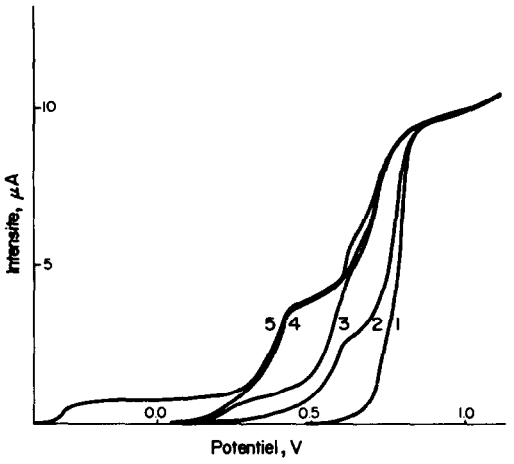


Fig. 4. Evolution des courbes voltampérométriques au cours du titrage des deux fonctions de l'acide succinique par Bu_4NOH, en présence de PH $2.10^{-3}M$.

S, non électroactifs, conduisent à la formation d'une base conjuguée électrooxydable. Mais dans les deux cas, la vague anodique de $E_{1/2} = -0{,}25$ V apparaît après le point équivalent.

(*d*) Le même comportement est observé avec les bases de type B (par exemple la prométhazine).

Si l'on reporte sur un graphique les potentiels de demi-vague relatifs à l'oxydation de PH en présence de bases d'acides faibles du type AH ou BH^+, en fonction du pK_A^{DMSO} des acides correspondants, on observe une variation régulière (figure 5).

Influence de l'oxygène dissous sur les courbes voltampérométriques relatives à la phénothiazine. Une solution de P^- évolue avec le temps en présence d'oxygène et de lumière. Elle vire lentement du jaune au brun avec disparition progressive de la vague anodique de $E_{1/2} = -0{,}25$ V et apparition de deux vagues successives à $+0{,}50$ et $+0{,}80$ V. Il n'y a pas de signal en réduction. L'addition de Bu_4NOH à cette solution colorée fait réapparaître la vague à $-0{,}25$ V.

Ainsi, la phénothiazine reste indicatrice de la présence d'ions HO^- au cours du titrage d'un acide faible réalisé sans dégazage de la solution. L'un des composés apparus possèderait toujours la fonction –NH– cyclique à caractère acide faible. Ce dernier est oxydable à un potentiel proche de celui de P^-, à moins que l'addition des ions HO^- à une "solution évoluée" n'entraîne l'apparition de PH par suite d'une réaction de dismutation.

Sur le plan pratique, on dispose d'un indicateur ampérométrique utilisable directement en présence

Tableau 5. Titrage coulométrique et volumétrique de comprimés de Largactil® (poids moyen 0,404 g; contenu nominal 100 mg)

Essai	Comprimé pulvérisé prise d'essai, *g*	Résultats obtenus, *mg chlorpromazine/cp*	
		coulométrie	volumétrie
1	0,100	100,1	101,8
2	0,100	101,0	102,4

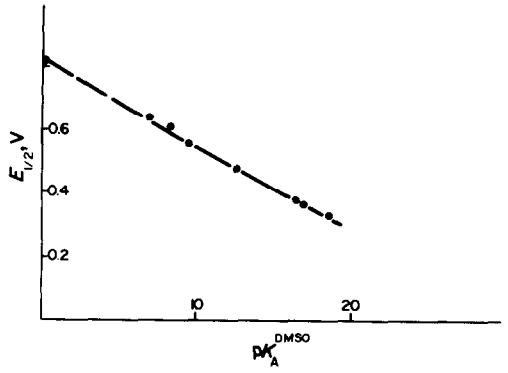


Fig. 5. Courbe représentative des $E_{1/2}$ d'oxydation de la phénothiazine en fonction du pK_A^{DMSO} des acides présents en solution.

d'oxygène. Les opérations de dégazage qui constituent une contrainte lors du titrage d'espèces diluées, ne sont plus indispensables.

Dosages des acides faibles. Les dosages en série d'un grand nombre d'acides faibles (HA ou BH^+) par coulométrie en présence de phénothiazine comme indicateur ampérométrique sont réalisés avec une bonne précision. Dans le tableau 6 sont rassemblés les résultats concernant plus particulièrement les chlorhydrates de dérivés phénothiaziniques N_{10} substitués.

Il est à remarquer que les résultats obtenus au cours du dosage du chlorhydrate de chlorpromazine en présence et en absence d'oxygène sont semblables. La précision est du même ordre de grandeur que lorsque l'on effectue le dosage des mêmes composés par ampérométrie directe.

Le pH d'apparition du courant anodique à potentiel nul dépend de la concentration de l'indicateur; si l'on admet que P^- est électroactif à la concentration $10^{-5}M$ et que la phénothiazine est présente à la concentration $10^{-3}M$, le courant anodique apparaît à

$$pH = 22{,}5 + \log \frac{10^{-5}}{10^{-3}} = 20{,}5.$$

Cette valeur passe à 21,5 si la concentration de l'indicateur diminue d'un facteur 10.

Dans le cas d'un diacide (succinique), on dose indistinctement les deux fonctions carboxyliques alors que par ampérométrie directe, seule la première fonction est titrée. La morphine, non électroactive par sa fonction énolique, est cependant titrable en présence de phénothiazine.

Cette technique ampérométrique semble être bien adaptée au dosage d'espèces fortement colorées. C'est ainsi qu'une solution de Perezone $5.10^{-3}M$, composé présentant un intérêt pharmaceutique, à caractère acide faible et doué d'un fort pouvoir absorbant peut être titré à 1% près par coulométrie en présence de PH comme indicateur ampérométrique.

CONCLUSION

Par ses propriétés acides ($pK_A^S = 22{,}5$), la phénothiazine peut être utilisée comme indicateurs unicolore et ampérométrique au cours du titrage des acides faibles en milieu diméthylsulfoxyde.

La base conjuguée P^- est stable. Son pouvoir réducteur augmente de près de 1 V par rapport à celui de la forme acide PH, mesuré en milieu neutre non tamponné.

La précision des titrages est satisfaisante: 25 μmole est titrée à 1% près. La stabilité de la forme anionique P^- et de l'hydroxyde de tétraéthylammonium permettent les dosages en série. La détection est compatible avec la présence d'oxygène.

Tableau 6. Titrages coulométriques en présence de phénothiazine comme indicateur ampérométrique

Composé étudié	Nombre de dosages	Quantités ajoutées, *µmole*	Temps moyen, *sec*	Courant efficacité, %	Déviation standard, %
(A)	13	25	241,7	99,8	0,2
(B)	11*	27	261,4	100,2*	0,4
	12	27	268,6	100,0	0,9
(C)	12	23	218,6	99,9	0,9

* Série de dosages réalisés en absence d'oxygène; les autres valeurs sont obtenues sans dégazage préalable de la solution.

Tableau 7. Titrage coulométrique de chlorhydrates de dérivés phénothiaziniques et détection ampérométrique

Composé	Quantités ajoutées, *µmole*	Efficacité en courant, %		
		Ampérométrie directe	Présence de phénothiazine sans O_2	avec O_2
Prométhazine chlorhydrate	25	99,2		99,8
Chlorpromazine chlorhydrate	27	99,0	100,2	100,0

Remerciements—Les auteurs remercient vivement les Laboratoires Spécia et Sandoz qui leur ont aimablement procuré les échantillons.

BIBLIOGRAPHIE

1. *Comprehensive Analytical Chemistry*, C. L. Wilson and D. W. Wilson (eds.), Vols. IA and IB, Elsevier, Amsterdam, 1957.
2. J. Kucharsky et L. Safarik, *Titration in Non-aqueous Solvents*, Elsevier, Amsterdam, 1975.
3. I. M. Kolthoff et P. J. Elving, *Treatise on Analytical Chemistry*, Part I, Vol. 11, New York, 1975.
4. G. Charlot, *Chimie Analytique Quantitative*, Vol. 1, Masson, Paris, 1974.
5. J. T. Stock, *Amperometric Titrations*, Interscience, New York, 1965.
6. T. B. Reddy et I. M. Kolthoff, *Inorg. Chem*, 1962, **1**, 189.
7. M. Le Demezet et J. Courtot-Coupez, *Bull. Soc. Chim. France*, 1969, 1033.
8. R. Stewart et J. P. O'Donnell, *J. Am. Chem. Soc.*, 1962, **84**, 493.
9. K. Bowden, A. Buckley et R. Stewart, *ibid.*, 1966, **88**, 947.
10. R. Stewart et J. R. Jones, *ibid.*, 1967, **89**, 5069..
11. K. Bowden et R. Stewart, *Tetrahedron*, 1965, **21**, 261.
12. D. Dolman et R. Stewart, *Canad. J. Chem.*, 1967, **45**, 911.
13. J. C. Hallé, R. Gaboriaud et R. Schaal, *Bull. Soc. Chim. France*, 1969, 1851; 1970, 2047.
14. J. Courtot-Coupez et M. Le Demezet, *ibid.*, 1967, 4744.
15. J. S. Fritz et F. E. Gainer, *Talanta*, 1968, **15**, 939.
16. W. N. Carson et R. Ko, *Anal. Chem.*, 1951, **23**, 1019.
17. M. H. Livertoux, *Thèse 3ème Cycle*, Sciences, Nancy, 1978.
18. J. C. Madec, *Thèse 3ème Cycle*, Brest, 1970.
19. L. Yorner et A. Mentrys, *Annalen*, 1961, **646**, 49.
20. C. Cotman, W. Sheiner, J. Hickly et T. Williams, *Talanta*, 1965, **12**, 17.
21. A. D. Goolsby et D. T. Sawyer, *Anal. Chem.*, 1968, **40**, 83.
22. L. A. Simonson et R. W. Murray, *ibid.*, 1975, **47**, 290.
23. G. A. Harlow, *ibid.*, 1962, **34**, 1482, 1487.
24. M. Bos, S. T. Ijpma et E.A.M.F. Dahmen, *Anal. Chim. Acta*, 1976, **83**, 39.
25. D. T. Sawyer et J. L. Roberts, *J. Electroanal. Chem.*, 1966, **12**, 90.
26. A. Lestienne, *Chim. Anal. (Paris)*, 1962, **44**, 377.
27. J. P. Billon, *Ann. Chim.*, 1962, 183.
28. *Idem*, *Bull. Soc. Chim. France*, 1961, 1923.
29. J. P. Billon, G. Cauquis et J. Combrisson, *J. Chim. Phys.* 1964, **61**, 364.
30. D. J. Cavanaugh, *J. Am. Chem. Soc.*, 1959, **81**, 2507.
31. P. Hanson et O. C. Norman, *J. Chem. Soc., Perkin II*, 1973, 264.
32. G. Cauquis, A. Deronzier, J. L. Lepage et D. Serve, *Bull. Soc. Chim. France*, 1977, 295, 303.
33. Y. Tsujino, *Tetrahedron Lett.*, 1968, 2545; 1969, 763.

Talanta Vol. 28, pp. 89 to 93
Pergamon Press Ltd 1981. Printed in Great Britain

0039-9140/81/0201-0089$02.00/0

NEW ATOMIC-ABSORPTION SPECTROMETRIC, POTENTIOMETRIC AND POLAROGRAPHIC METHODS FOR THE DETERMINATION OF NITRATES*

SAAD S. M. HASSAN

Department of Chemistry, Faculty of Science, Ain Shams University, Cairo, Egypt

(*Received* 10 *April* 1980. *Accepted* 24 *August* 1980)

Summary—New simple, rapid and accurate methods for the determination of organic and inorganic nitrates in the presence of various other ions have been developed. These are based on reduction with cadmium metal and 0.1 *M* hydrochloric acid, in which 4 equivalents of cadmium ions are released per mole of nitrate group, whereby the nitrate–nitrogen is converted into nitrous oxide. Four methods for determining the cadmium were compared: atomic-absorption spectrometry at 228.8 nm, polarography, potentiometric EDTA titration at pH 10 (cadmium ion-selective electrode), and EDTA titration with Eriochrome Black T indicator. Results with an average recovery of 98% (standard deviation 1%) are obtainable and no interferences are caused by high concentrations of many anions and cations.

Methods based on the use of atomic-absorption spectrometry (AAS), ion-selective electrodes or polarography have been suggested for the determination of low concentrations of nitrates in pure solutions. The only AAS procedure found in the literature is based on transformation of the nitrate into the complex $[Cu(I)(neocuproin)_2NO_3]$ by reaction with copper(I) in the presence of neocuproin. The resulting complex is extracted into 4-methylpentan-2-one (isobutyl methyl ketone) and sprayed into an air–acetylene flame for AAS determination of the copper at 324.7 nm.[1] The polarographic procedures involve induced reduction of nitrate by multivalent cations, whereby its reduction wave is shifted to a less negative voltage.[2] Direct potentiometry and potentiometric titration of nitrates, by use of the nitrate ion-selective electrode, have also been described.[3]

However, not only are these methods inapplicable to organic nitrates, but they also suffer from severe interference from chloride, phosphate, sulphate, oxalate and carbonate. These ions affect the stoichiometric extraction of the copper complex in the AAS procedure,[1] tend to prevent complete drop of the current in the polarographic methods,[2] and are only partially sensed by the nitrate electrode.[3] Use of a cation-exchanger in the silver form to remove chloride and precipitation of sulphate with barium before measurement of the nitrate with the nitrate electrode[3] or AAS[4] have been suggested, but these approaches are time-consuming and subject to high errors.

Recently, enzymatic reduction of the nitrate to ammonia, which is then measured potentiometrically with the air-gap electrode, has been described.[5] However, variation in the pH of the test solution, in the concentrations of carbon dioxide or electrolyte on the surface of the electrode-membrane, in the purity of the enzyme, and in the presence of some interfering ions have all been reported[5] to influence the accuracy of the method. Reduction of nitrate with mercury metal and concentrated sulphuric acid, followed by measurement (with the iodide ion-selective electrode) of the mercury(I) ions produced has been described.[6] This procedure can be used in the presence of carbonate and sulphate, but is inapplicable in the presence of high concentrations of chloride and phosphate, owing to partial precipitation of their mercury(I) salts.

Since the determination of organic and inorganic nitrates in the presence of various foreign ions is often required, especially in pharmaceuticals, fertilizers, explosives and industrial effluents, the present investigation was undertaken to develop new methods applicable to the microdetermination of nitrates in the presence of high concentrations of many interfering ions, by use of atomic-absorption spectrometry, polarography, and titrimetry with visual or potentiometric end-point detection.

EXPERIMENTAL

Apparatus

A Unicam SP 1900 atomic-absorption spectrophotometer equipped with digital read-out unit, deuterium lamp (SP 1960) and cadmium hollow-cathode lamp were used under the following conditions: wavelength 228.8 nm, sensitivity setting 287, slit-width setting 104 nm, burner height setting 1 cm, lamp current 4 mA, laminar-flow burner, air flow-rate 4.5 l./min, acetylene flow-rate 1 l./min.

An Orion 901 microprocessor digital millivoltmeter was used to measure potentials between a cadmium ion-selective electrode (Orion 49-48) and a double-junction reference electrode (Orion 90-02) containing 10% potassium nitrate in the outer compartment.

A Radiometer PO4 polarograph was used with a universal U-shaped polarographic cell. The anode compartment

* Based on a paper presented at the XXI Colloquium Spectroscopicum Internationale—8th International Conference on Atomic Spectroscopy, Cambridge, U.K., 1–6 July 1979.

was filled with mercury and saturated potassium chloride solution. The capillary had a drop time of 4.1 sec with a 50-cm head of mercury in open circuit. The mercury flow-rate was 2.07 mg/sec, and the sensitivity was 0.2 μA/mm.

Reagents

Analytical-reagent grade chemicals, and doubly-distilled water were used throughout.

Cadmium metal of purity not less than 99.5% was washed successively with 6*M* hydrochloric acid, water and alcohol, and then dried. Other solutions were 0.005*M* EDTA, 0.1*M* potassium chloride, cadmium chloride in 0.05*M* hydrochloric acid ([Cd] = 0.1 mg/ml), 25% ammonia solution and 0.1*M* hydrochloric acid. A 0.2% mixture of Eriochrome Black T with solid sodium chloride was used as indicator.

The nitrate samples used were of purity not less than 99%, as confirmed by gasometric analysis.[7]

Procedure

Transfer a portion of nitrate sample containing 0.2–2 mg of nitrate-nitrogen to a 100-ml conical flask having a ground-glass neck and a side-arm with gas bubbling tube. Add 10 ml of 0.1*M* hydrochloric acid and attach a water condenser. Heat on a sand-bath while passing carbon dioxide (~50 bubbles/min) through the side-arm. When the solution starts boiling, introduce 50–100 mg of cadmium metal turnings. Continue boiling for 10–15 min under a carbon dioxide atmosphere. Cool the solution and transfer it to a 25-ml standard flask, making up to the mark with doubly-distilled water. Use this test solution for the subsequent measurements. Prepare a blank in exactly the same way.

AAS measurement. Transfer a 1.00-ml aliquot of the test solution to a 100-ml standard flask, add 1 ml of 1% EDTA solution, dilute to the mark with 0.05*M* hydrochloric acid and shake. Aspirate into the air–acetylene flame and measure the absorbance at 228.8 nm. Compare with a calibration graph prepared by treating 0.50–3.00 ml of the 0.1-mg/ml cadmium solution in the same way. 1 mg of Cd ≡ 62.3 μg of nitrate–nitrogen.

Potentiometric and visual titrations. Transfer a 10.0-ml aliquot of the test solution (~0.1–0.7 mg of nitrate-nitrogen) to a 100-ml beaker. Adjust the pH to 10 with aqueous ammonia (~1 ml of 25% solution). Insert the cadmium ion-selective electrode and the double-junction reference electrode, and titrate with 0.005*M* EDTA. Towards the end-point, indicated by rapid potential jumps, add the titrant in 0.02-ml increments. Alternatively, add Eriochrome Black T indicator and titrate with 0.005*M* EDTA till the colour changes from pink to blue. 1 ml of 0.005*M* EDTA ≡ 0.562 mg of Cd ≡ 35.0 μg of nitrate-nitrogen

Polarographic measurement. Transfer 1.00 ml of the reaction solution to a 10-ml standard flask, dilute to the mark with 0.1*M* potassium chloride, mix, and transfer to the polarographic cell. Record the cadmium wave at −0.6 V vs. S.C.E., starting from an applied potential of −0.2 V, and using a sensitivity of 0.2 μA/mm, damping 6, scan speed 8 cm/min and compensation of condenser current 0.2 μA/V. Run a blank under identical conditions. Compare with a calibration graph prepared with 0.2–3 *mM* solutions of standard cadmium chloride in 0.1*M* potassium chloride.

RESULTS AND DISCUSSION

Reaction conditions

The literature on the reduction of nitrates with cadmium metal is concerned with use of basic media,[8–11] which is known to result in nitrite through a 2-electron reduction process according to the equation:

$$NO_3^- + Cd + 2H^+ \rightarrow NO_2^- + Cd^{2+} + H_2O \quad (1)$$

This reaction has been used in the spectrophotometric determination of nitrate by passage of an ammoniacal nitrate solution at pH 8–9 through columns containing precipitated cadmium metal,[9] or coppered[10] or amalgamated[11] cadmium, and determination of the nitrite in the effluent by diazotization and coupling reactions. However, in the present investigation, preliminary attempts were made to determine the nitrates by reaction with pure cadmium metal at pH 9 (ammonia–ammonium chloride buffer) for 30 min, and subsequent AAS measurement of the equivalent amount of cadmium ions released. The results obtained, calculated on the basis of equation (1) were invariably low, probably because of partial precipitation of cadmium hydroxide on the surface of the metal.

Trials were then made to reduce the nitrate with cadmium metal in acidic media. This necessitated a study of the influence of acidity on the dissolution of the metal. The amount of cadmium dissolved in a fixed time by hydrochloric acid of various concentrations, under a carbon dioxide atmosphere, was measured by AAS: 0.01, 0.03, 0.05 and 0.1 mg of cadmium were dissolved in 20 min by refluxing with 0.02, 0.05, 0.1 and 0.2*M* hydrochloric acid, respectively. The reaction of potassium nitrate (*ca.* 1–10 mg) with cadmium metal was then tested by heating with hydrochloric acid of various concentrations under reflux and a flow of carbon dioxide. Four equivalents of cadmium ions per mole of nitrate were reproducibly released by reaction in 0.05–0.1*M* acid (Fig. 1), the results being practically identical for reaction times of 10–20 min (Fig. 2) (relative standard deviation 1–2%). Reaction at room temperature or with hydrochloric acid of concentrations greater than 0.2*M*, or with 0.1*M* acids other than hydrochloric (*e.g.*, sulphuric or acetic) gave inconsistent results fluctuating within the range 3–4 equivalents of cadmium ions per mole of nitrate.

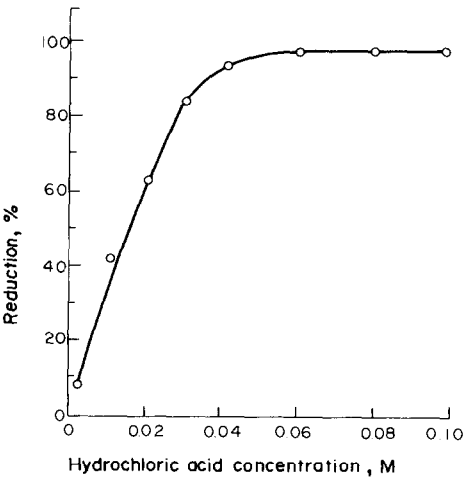


Fig. 1. Effect of hydrochloric acid concentration on the reduction of potassium nitrate by heating with cadmium metal for 15 min.

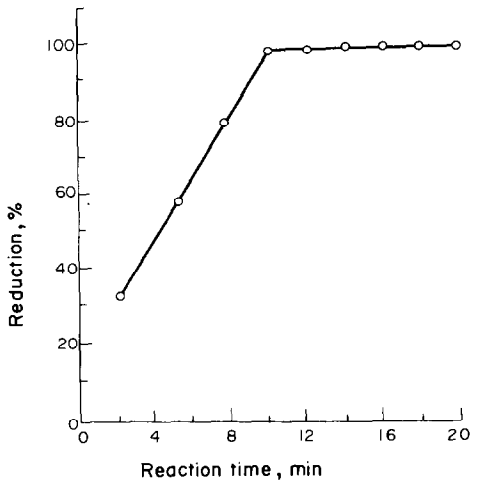


Fig. 2. Effect of time on the reduction of potassium nitrate with cadmium metal by heating with 0.1*M* hydrochloric acid.

Reaction products

In the investigation of the reduction reaction it was observed that nitrite was always absent in the solutions of the reduction products (as indicated by negative response in diazotization and coupling) and that four equivalents of cadmium ions were released per mole of nitrate group reduced.

The gaseous reaction products were swept over "Anhydrone" to absorb water and then into an evacuated 10-cm gas cell (sodium chloride windows) fitted to a Beckman infrared spectrometer (Model IR 20). The infrared spectrum showed strong absorption bands at 1285 cm^{-1} due to $\overset{+}{N} \rightarrow \bar{O}$ stretch, 2224 cm^{-1} due to $N \equiv N$ stretch and combination bands at 3480 and 2788 cm^{-1} due to bending–stretching vibrations, confirming the presence of N_2O.[12]

Further confirmation of the formation of nitrous oxide was obtained by carrying out the reaction in a test-tube with a side-arm attached to the gas-sampling unit of a Beckman gas chromatograph (Model G.C-M). The gaseous products were swept in a stream of helium onto a Porapack Q column maintained at 120°. The thermal-conductivity detector operated at 200 mA gave, in addition to the peak due to water, a peak with a retention time corresponding to that of nitrous oxide (obtained by the dry decomposition of ammonium nitrate) (Fig. 3 A and C). When the reaction was conducted with hydrochloric acid of concentrations greater than 0.5*M*, a third peak was detected, having a retention time corresponding to that of nitric oxide (obtained by the reaction of potassium nitrate with ferrous sulphate in acidic media) (Fig. 3 B and D).

These data indicate that the reaction of nitrate under the prescribed conditions probably proceeds through a 4-electron reduction process:

$$2NO_3^- + 4Cd + 10H^+ \rightarrow N_2O + 4Cd^{2+} + 5H_2O \quad (2)$$

It should be noted that quantitative reduction of nitrate to nitrous oxide has previously only been reported as occurring with some organic reductants.[13–15]

Measurement by AAS

Aliquots of the reaction solution were treated with 1% EDTA solution, and diluted with hydrochloric

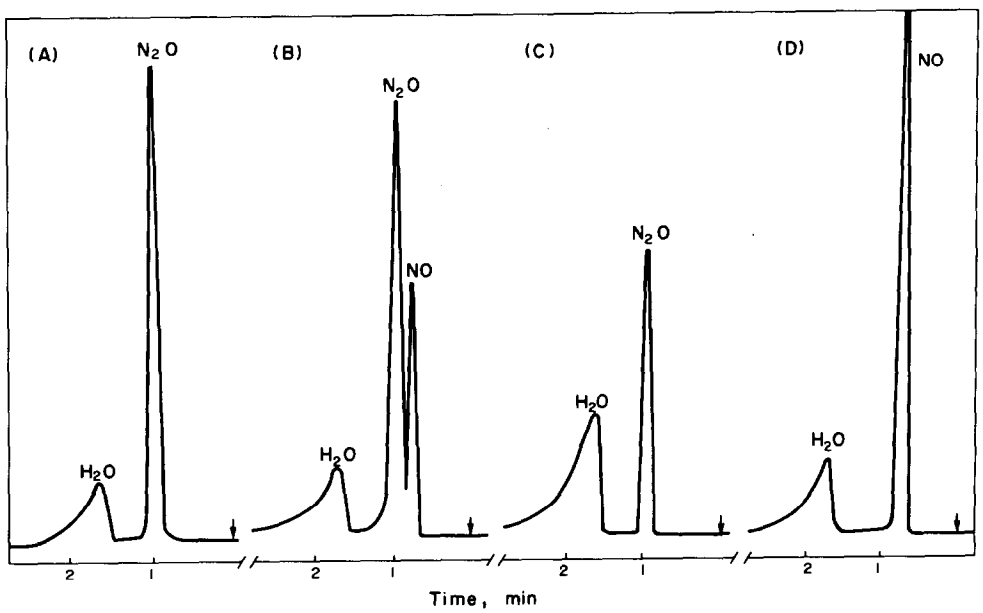


Fig. 3. Chromatograms of nitrous oxide and nitric oxide gases as reduction products of nitrates: (A) gaseous reduction products of potassium nitrate with cadmium metal and 0.1*M* hydrochloric acid; (B) gaseous reduction products of potassium nitrate with cadmium metal and 0.5*M* hydrochloric acid; (C) dry decomposition products of ammonium nitrate; and (D) gaseous reduction products of potassium nitrate with ferrous sulphate and hydrochloric acid.

Table 1. Microdetermination of some nitrates

Sample	Nitrate-nitrogen, %				
		Found			
	Calculated	AAS	Polarography	Cd-ISE	Visually
Sodium nitrate	16.48	16.5	16.1	16.3	16.2
		16.3	16.5	16.4	16.5
		16.4	16.2	16.2	16.4
Potassium nitrate	13.85	13.4	13.5	13.6	13.7
		13.7	13.7	13.5	13.5
		13.5	13.4	13.4	13.6
Calcium nitrate	17.07	16.8	16.9	17.0*	16.8*
		16.6	16.5	16.8*	16.7*
		16.7	16.4	16.9*	16.8*
Barium nitrate	10.72	10.6	10.5	10.5*	10.4*
		10.3	10.1	10.4*	10.6*
		10.5	10.4	10.5*	10.5*

* Based on the consumption of 5 moles of EDTA per mole of calcium or barium nitrate.

acid to bring the final cadmium concentration within the working range (<3 μg/ml). The results obtained with some inorganic nitrates (Table 1) show an average recovery of 97.9% (standard deviation 1.2%). No interferences occur in the presence of up to 100-fold amounts of chloride, sulphate, oxalate, carbonate, phosphate and ammonium ions (Table 2).

Measurement by potentiometric and visual titrations

The cadmium dissolved by the reduction of the nitrates was also measured by potentiometric titration of a separate aliquot with EDTA at pH 10, the solid-state cadmium ion-selective electrode being used. The results obtained with both pure potassium nitrate, and potassium nitrate mixed with up to a 100-fold ratio (to nitrate) of sulphate, chloride, oxalate, carbonate, phosphate and ammonium ions, are equally accurate. The average recovery was 98.5% (standard deviation 0.8%) (Tables 1 and 2). With some metal nitrates, however, the metals are titrated with EDTA along with the cadmium. The reaction products of barium and calcium nitrates were titrated as mixtures of (Ba + 4Cd) and (Ca + 4Cd) per mole of metal nitrate, respectively. Similar results were obtained by titration with EDTA, with Eriochrome Black T as indicator (Table 1).

Measurement by polarography

Cadmium was determined in separate aliquots of the reduction solutions by polarography with potassium chloride as supporting electrolyte. The calibration graph was linear, showing that the system satisfies the Ilkovič equation[16] over the range 0.1–3 m*M* cadmium (≡ 10–200 μg of nitrate-nitrogen). The results obtained for the analysis of some nitrates by this method are also shown in Table 1. The average

Table 2. Microdetermination of potassium nitrate in the presence of some other anions

Compound added	Weight taken, *mg*		Nitrate-nitrogen recovery, %			
	Added salt	Nitrate-nitrogen	AAS	Polarography	Cd-ISE	Visually
NaCl	50	0.24	98.2	98.1	98.8	98.4
	75	0.38	97.5	97.8	98.5	98.3
	100	0.59	97.8	97.3	98.4	98.5
K_2SO_4	50	0.32	98.2	98.4	98.5	98.4
	75	0.43	97.9	98.1	98.2	98.5
	100	0.58	98.4	98.5	98.7	98.6
KH_2PO_4	50	0.18	98.0	98.5	98.2	98.4
	75	0.29	98.9	98.1	98.3	98.6
	100	0.64	98.3	98.4	98.6	98.7
$(COOH)_2$	50	0.28	98.4	98.5	98.4	98.5
	75	0.49	97.7	98.4	98.6	98.2
	100	0.61	98.0	98.2	98.3	98.3
NH_4Cl	50	0.19	97.8	98.3	98.7	97.4
	75	0.24	98.3	98.6	98.5	98.0
	100	0.43	98.0	98.1	98.4	98.3
Na_2CO_3	50	0.20	98.0	97.6	98.5	98.4
	75	0.38	98.4	98.3	98.3	98.2
	100	0.44	97.9	98.1	98.2	98.0

Table 3. Microdetermination of some organic nitrates

Sample	Nitrate-nitrogen, %				
		Found			
	Calculated	AAS	Polarography	Cd-ISE	Visually
Pentaerythritol tetranitrate	17.72	17.5	17.8	17.6	17.6
		17.4	17.6	17.7	17.7
		17.3	17.4	17.4	17.6
Urea nitrate	11.38	11.1	11.4	11.2	11.2
		11.0	11.0	11.1	11.3
		11.2	11.2	11.2	11.3
Guanidine nitrate	11.47	11.1	11.3	11.2	11.4
		11.2	11.5	11.2	11.1
		11.3	11.1	11.4	11.3
Thiamine mononitrate	4.25	4.0	3.9	4.1	4.0
		3.9	4.0	4.0	4.2
		4.1	4.1	4.1	4.3

recovery was 97.8% (standard deviation 1.6%). No interference by various foreign anions could be detected (Table 2). This was also verified by recording the polarograms of 1 m*M* cadmium chloride in 0.1*M* solutions of oxalate, sulphate, chloride, phosphate and ammonium ions, as supporting electrolytes, where the wave-heights and half-wave potentials were all identical.

Determination of organic nitrates

Some organic nitrates investigated were reduced quantitatively by cadmium metal within 10 min with the release of 4 equivalents of cadmium ion per mole of nitrate group. An average recovery of 98.9% (mean standard deviation 1%) were obtained with some organic nitrates in the range of 0.5–50μM (Table 3). Addition of benzoic acid, diphenylacetylene, cinnamic acid, phenol, benzaldehyde, acetophenone, acetamide, acetanilide, benzonitrile, anisole, sulphanilic acid, thioglycollic acid or diphenylsulphide, in up to 100-fold ratio to urea nitrate, did not affect the sensitivity of the method. Nitro and nitroso compounds, however, did interfere.

Advantages and limitations

The proposed method offers the following advantages: (*a*) at least 4 different measurement procedures can be used on the same sample; (*b*) many cations and anions do not interfere; (*c*) accurate and precise results are obtainable, as the reaction involves a favourable conversion factor (1 mg of nitrate-nitrogen ≡ 16 mg of cadmium); (*d*) the reaction is simple and rapid; (*e*) the reagents used are stable and require no special precautions for storage or use.

The AAS procedure is applicable to samples containing foreign cations and anions. Titrations with EDTA are recommended provided heavy metals are absent. The polarographic method can be utilized in the presence of foreign anions, but heavy metal cations with half-wave potentials close to −0.6 V interfere.

REFERENCES

1. Y. Yamamoto, T. Kumamaru, Y. Hayashi and Y. Otani, *Bunseki Kagaku*, 1969, **18,** 359.
2. R. Hamm and C. Withrow, *Anal. Chem.*, 1955, **27,** 1913.
3. J. Veselý, D. Weiss and K. Štulík, *Analysis with Ion-Selective Electrodes*, p. 169. Horwood, Chichester, 1978.
4. G. Hoshikawa and Y. Fudano, *Kagawa Daigaku Nogakuba Gakujutsu Hokoku*, 1976, **27,** 111.
5. C. Kiang, S. Kuan and G. Guilbault, *Anal. Chem.*, 1978, **50,** 1319.
6. S. S. M. Hassan, *Talanta*, 1976, 23, 738.
7. W. Awad and S. S. M. Hassan, *ibid.*, 1969, **16,** 1393.
8. R. Lambert and R. DuBois, *Anal. Chem.*, 1971, **43,** 957.
9. R. Grau and A. Mirna, *Z. Anal. Chem.*, 1957, **158,** 182.
10. A. Henriksen and A. Selmer-Olsen, *Analyst*, 1970, **95,** 514.
11. A. Morris and J. Riley, *Anal. Chim. Acta*, 1971, **43,** 957.
12. S. Pinchas and I. Laulicht, *Infrared Spectra of Labelled Compounds*, p. 218. Academic Press, London, 1971.
13. W. Awad, S. S. M. Hassan and M. Zaki, *Talanta*, 1971, **18,** 219.
14. S. S. M. Hassan, *Mikrochim. Acta*, 1970, 1109.
15. S. S. M. Hassan, *Anal. Chim. Acta*, 1972, **60,** 442.
16. D. Ilkovič, *Collection Czech. Chem. Commun.*, 1934, **6,** 498.

Talanta Vol. 28, pp. 95 to 105
©Pergamon Press Ltd 1981. Printed in Great Britain
0039-9140/81/0201-0095$02.00/0

ETUDE PAR SPECTROSCOPIE RAMAN DE QUELQUES ANOREXIGENES—I

ANOREXIGENES *N*-SUBSTITUES

A. P. GAMOT*, G. VERGOTEN† et G. FLEURY†

Laboratoires de Chimie Générale* et de Physique†, Faculté de Pharmacie, Université de Lille II, rue du Professeur Laguesse, 59045 Lille Cedex, France

(*Reçu le* 18 *janvier* 1980. *Révisé le* 9 *juillet* 1980. *Accepté le* 22 *août* 1980)

Résumé—Les spectres Raman complets de trois anorexigènes ont été enregistrés à l'état polycristallin. Une attribution des raies observées est proposée. Elle montre un certain nombre de similitudes dues essentiellement à la structure phénylalkylaminique de ces composés dont les raies caractéristiques apparaissent à 3060, 1600, 1205, 1157, 1028, 1000, 995, 618 et 460 cm^{-1}. Cependant certaines différences apparaissent sur les spectres, il a été noté en particulier que les raies situées à 3160, 3120 (et l'absence de raie à 3092 cm^{-1}), 1500, 1393 et 802 cm^{-1} sont spécifiques du cyclohexylsulfamate de furfenorex et que les raies situées à 682 et 587 cm^{-1} et 2257 cm^{-1} caractérisent respectivement la chlorhydrate de clobenzorex et le diphénylacétate de fenproporex.

Nous présentons dans ce travail les spectres Raman de trois dérivés d'une famille de composés non phénoliques de structure phénylalkylaminique (du type de l'éphédrine) dans laquelle on trouve:

— d'une part les amines de réveil et d'autres stimulants du système nerveux central,

— d'autre part les anorexigènes qui nous intéressent ici plus particulièrement.

Dans ce premier volet nous présentons et discutons les spectres Raman de trois composés, dérivant de l'amphétamine par différentes substitutions sur l'atome d'azote, et stabilisés sous forme de sels: le cyclohexylsulfamate de furfenorex; le chlorhydrate de clobenzorex; le diphényl acétate de fenproporex (tableau 1).

PARTIE EXPERIMENTALE

Appareillage

Les spectres Raman ont été enregistrés sur un spectromètre Coderg T 800 comprenant un triple monochromateur de 800 mm de distance focale équipé de trois réseaux plans gravés (1800 traits par mm).

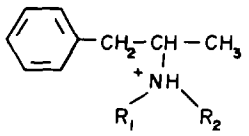
Un laser à argon ionisé (514,5 nm) Spectra Physics modèle 165,03 délivre 600 mW sur l'échantillon. Les principes actifs sont introduits sous forme de poudre polycristalline dans un tube capillaire sans purification supplémentaire.

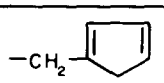
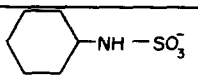
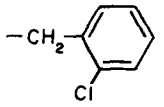
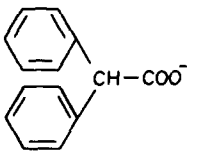
Réactifs

Les principes actifs dont nous avons disposés sont destinés à la fabrication de comprimés ou de gélules. Leur pureté a été contrôlée à l'issue de leur synthèse par des techniques classiques telles que la spectrométrie infra

Tableau 1. Structure des anorexigènes étudiés

Structure générale



	Composé	R_1	R_2	X^-
I	Cyclohexyl sulfamate de furfenorex	$-CH_3$		
II	Chlorhydrate de clobenzorex	$-H$		Cl^-
III	Diphényl acetate de fenproporex	$-H$	$-CH_2-CH_2-CN$	

rouge, la résonance magnétique nucléaire, la chromatographie en phase gazeuse, la potentiométrie en milieu non aqueux, dont le détail sort du cadre de ce travail. Signalons à titre d'exemple que le protocole de contrôle du diphénylacétate de fenproporex fait l'objet d'un projet qui sera bientôt publié dans la Pharmacopée Française.

Methode

Nous donnons à titre indicatif les raies principales du spectre Raman de l'amphétamine base dans le tableau 2. Cette amine est instable et se volatilise légèrement à température ambiante, c'est pourquoi son spectre a été enregistré en figeant la substance en la refroidissant à −80°C.

Les valeurs moyennes en cm^{-1} dans le tableau 2 sont obtenues à partir de deux enregistrements par échantillon.

Les spectres ont été enregistrés à la vitesse de 25 cm^{-1}/mn avec une résolution spectrale de 2 cm^{-1}. Cette vitesse a été choisie de façon à pointer les raies avec la meilleure précison. Elle peut être augmentée lors d'étude de routine pour devenir comparable à celle couramment employée en spectrométrie infra rouge.

Bien que les deux types de spectrométrie IR et Raman soient complémentaires, la spectrométrie Raman présente l'avantage de minimiser les manipulations lors de la préparation de l'échantillon. Il suffit en effet dans la plupart des cas d'introduire quelques milligrammes de produit dans un tube capillaire en verre. D'autre part le spectromètre Raman utilisé permet d'enregistrer en continue le spectre d'un composé de quelques cm^{-1} à 4000 cm^{-1}. Cependant les problèmes parfois rencontrés dans ce type de spectroscopie sont essentiellement dus à la fluorescence extrinsèque de l'échantillon, fluorescence qui peut très souvent être inhibée par irradiation sous le faisceau laser. Parfois certaines molécules ne résistent pas à la puissance du rayonnement et se détruisent au niveau de l'impact du faisceau sur le tube capillaire.

L'enregistrement est alors possible

— soit en diminuant la puissance du laser, l'intensité des raies décroissant proportionnellement,

— soit en n'exposant qu'une surface donnée de l'échantillon pendant un temps très court en utilisant une cellule tournante ou le dispositif d'irradiation laser (D.I.L.) mis au point par notre groupe.

Lors de l'enregistrement des spectres des anorexigènes cités dans ce travail nous n'avons pas rencontré ce type de problème.

RESULTATS ET DISCUSSION

Fréquences caractéristiques dans les spectres Raman

Les substances étudiées présentent en commun la structure phénylalkylaminique. Les différences apparaissent au niveau de la substitution sur l'atome d'azote salifié par différents acides (*cf.* tableau 1). Il est donc logique de penser qu'un certain nombre de raies apparaîtrent sur les spectres à des fréquences voisines. Nous étudierons donc les raies des groupements communs dans un premier temps. Cependant l'intérêt de ce travail réside aussi dans l'étude des raies spécifiques qui permettrent de différencier les trois composés.

Les resultats sont rassemblés dans le tableau 2 où figurent les fréquences observées dans les spectres Raman qui ont servi de base à l'attribution. Nous donnons également les fréquences IR des divers composés.

A titre d'exemple les figures 1 et 2 représentent respectivement les spectres Raman et IR du chlorhydrate de clobenzorex.

La nomenclature adoptée pour les modes de vibration du noyau benzénique est celle de Wilson.[1]

Raies dues aux groupements communs

Cycle benzénique monosubstitué. Pour le cycle phényl monosubstitué 24 vibrations sont essentiellement indépendantes du substituant attaché au noyau, les 6 autres sont sensibles aux substitutions puisque dans ces modes le substituant vibre avec une amplitude appréciable.[2]

Il y a 5 vibrations de valence des CH dont les fréquences tombent dans l'intervalle 3100–3000 cm^{-1}. Goubeau et Kohler indiquent que la fréquence moyenne de la bande Raman dans les monoalkylbenzènes sur les vibrations du CH aromatique est à 3057 cm^{-1}.[3]

Tableau 2.

Cyclohexyl sulfamate de furfenorex (I)				Chlorhydrate de clobenzorex (II)				Diphenyl acetate de fenproporex (III)				
Raman		Infra rouge		Raman		Infra rouge		Raman		Infra rouge		
ν, cm⁻¹	*I*	*ν, cm⁻¹*	*I*	*ν, cm⁻¹*	*I*	*ν, cm⁻¹*	*I*	*ν, cm⁻¹*	*I*	*ν, cm⁻¹*	*I*	Essai d'attribution
3160	mF							3160	ff			3160 bandes caractéristiques de la substitution en 2 sur le noyau furannique
3120	mF											
						3088	ep					3120
										3082	ep	
		3078	ep									
3069	ep			*3073*	ep							
3064	ep											
				3063	F							3057 *ν*(CH) aromatiques
								3061	F			3063
										3059	ep	3061 + les épaulements
3057	F											
						3055	ep					
								3049	ep			
3048	ep											
				3044	f							

Tableau 2—*suite*

Cyclohexyl sulfamate de furfenorex (I)				Chlorhydrate de clobenzorex (II)				Diphenyl acetate de fenproporex (III)				
Raman		Infra rouge		Raman		Infra rouge		Raman		Infra rouge		
ν, cm^{-1}	I	ν, cm^{-1}	I	ν, cm^{-1}	I	ν, cm^{-1}	I	ν, cm^{-1}	I	ν, cm^{-1}	I	Essai d'attribution
				3035	f							
								3033	ep			
						3031	ep					
										3026	f	
				3018	f	3018	ep					
3005	f											
								3002	ff			
				2998	f							
				2983	f	2983	ep					
								2982	ff			
										2972	ep	
2965	F											2965 νCH_3 dégénérée
								2952	f			
2937	F											2937
								2936	ep			2932 ν_{as} CH_2
						2933	F					2931
				2932	mF							
								2931	mF			
		2923	F							2930	ff	
								2907	ff			
2903	ep											
2891	ep											
2884	ep											
				2865	f							
2848	F											
		2836	ep									
						2832	ep					
		2812	ep									
						2792	F					
				2790	ff							
				2759	ff							
		2757	ep							2757	f	
		2710	ep									
						2700	ep					
		2650	ep							2670	f	
		2596	ep									
		2547	ep									
						2532	mF					
		2489	ep							2442	f	
						2440	ep					
						2402	mf					
						2365	ep					
		2356										
								2257	f			2257 Groupement ν (C ≡ N)
										2250	f	
		2066	ep									
		2000	f									
										1965		
		1944	ff									
		1652	ep									
										1622	mf	
		1615	ep									
				1602	F			*1602*	F			1601, 1602, 1602 8a
1601	F											1586, 1584, 1583 8b
		1600	mf			1600	f					(1603 et 1596 amphétamine base)
										1597	ep	
						1595	f					
		1590	ep									
1586	ep											
				1584	ep							
								1583	f			
				1573	F							
						1570	ep					
						1577	mf					
		1544	mf									

Tableau 2—*suite*

Cyclohexyl sulfamate de furfenorex (I)				Chlorhydrate de clobenzorex (II)				Diphenyl acetate de fenproporex (III)					
Raman		Infra rouge		Raman		Infra rouge		Raman		Infra rouge			
ν, cm^{-1}	I	ν, cm^{-1}	I	ν, cm^{-1}	I	ν, cm^{-1}	I	ν, cm^{-1}	I	ν, cm^{-1}	I		Essai d'attribution
		1530	ep							1530	F		
						1508	ff						
1500	F											1500	élongation du cycle furfuryle substitué en 2
						1493	mf			1492	mf		
		1490	mf										
		1482	ep	1482	ff								
						1478	mf						
1461	ep												
		1460	f	1460	f								
						1459	ep						
										1450	mf		
				1447	mF								
		1445	mf										
								1444	ff				
1441	F												
		1440	ep			1439	F						
								1432	ff				
				1430	f								
						1429	ep						
										1424	ep		
						1412	e						
1393	mF											1393	élongation du cycle furannique seul
		1382	mf	1382	f	1382	mf						
								1372	ff				
										1366	F		
		1364	f										
				1355	mF								
						1349	ff						
1348	f											1348	vibration de déformation
												1341	du carbone tertiaire du
		1344	ff									1342	groupement isopropyle
								1342	ff				
				1341	f								
		1332	ff										
1331	f												
										1325	f		
		1314	ff										
				1310	ff							1307	b_{2u} élongation du cycle
												1310	aromatique confondue
1307	ff							*1306*	ff	1306	ep	1306	avec les vibrations de torsion et de balancement —CH
						1304	f						
				1285	mF								
								1284	ff				
										1280	ff		
						1279	f						
1276	ep												
		1275	f										
1266	mF												
								1260	ff				
										1254	ff		
		1253	f										
				1250	ff								
1240	f					1240	ff						
								1236	ff				
										1230	f		
1226	f											1226	vibration de déformation du CH dans le plan
		1223	ep									1209	vibration d'élongation
1209	F											1208	C_6H_5–C
				1208	F								

Tableau 2—*suite*

Cyclohexyl sulfamate de furfenorex (I)				Chlorhydrate de clobenzorex (II)				Diphenyl acetate de fenproporex (III)				Essai d'attribution
Raman		Infra rouge		Raman		Infra rouge		Raman		Infra rouge		
ν, cm^{-1}	I	ν, cm^{-1}	I	ν, cm^{-1}	I	ν, cm^{-1}	I	ν, cm^{-1}	I	ν, cm^{-1}	I	
						1204	ff					1202 ν_{ar-C}
								1202	mF			(1206 amphétamine base)
								1195	ep			
1188	f											
										1187	ff	
				1181	mF							
		1175	ep					1175	mF			
						1174	ff					
				1168	f							
1157	mF							*1157*	mF	1165	ff	1157
				1155	mF							1155 CH déformation dans le
												1157 plan cycle aromatique
1153	ep											no 15
										1148	f	(1157 amphétamine base)
		1145	ep									
						1142	f					
1140	ep											
				1125	f							
		1120	F			1120	f					
										1108	ff	
								1091	ff			
1089	ep											
				1088	mF							
										1083	f	
						1081	mf					
								1077	ff			1076
1076	F											1088 déformation plane de
		1065	ep									1077 CH 18b
1064	ep									1062	f	
				1059	ep							
				1054	mF							
1051	ep					1051	F					
		1050	ep									
						1040	f					
				1037	F					1036	ep	1029 vibration des CH
												1037 aromatiques dans
				1031	ep			*1031*	F			1031 le plan 18a
1029	F											(1030 amphétamine base)
						1025	f					
										1023	f	
		1012	ep									
		1003	ep									
				1002	F							999 respiration trigonale
								1001	F			1002 du cycle b_{1u}
999	F					999	ep					1001 no 12
994	ep											(1000 amphétamine base)
991	ep							*990*	ep			991 déformation des CH
986	ep			*986*	ep							986 cycle aromatique
										982	f	990 vibration no 5
						980	mf					(988 amphétamine base)
		976	ep					970	ff			
		960	ep									
				957	ff							
956	f											
						950	f					
								948	ff			
										942	ff	
929	f											
				927	mF			927	ff			
						920	ff					
		918	ep									
913	f											
								908	ff			
				907	f							
										906	f	

Tableau 2—*suite*

Cyclohexyl sulfamate de furfenorex (I)				Chlorhydrate de clobenzorex (II)				Diphenyl acetate de fenproporex (III)				Essai d'attribution
Raman		Infra rouge		Raman		Infra rouge		Raman		Infra rouge		
ν, cm^{-1}	I	ν, cm^{-1}	I	ν, cm^{-1}	I	ν, cm^{-1}	I	ν, cm^{-1}	I	ν, cm^{-1}	I	
						905	f					
900	f											
				898	f							
						894	ff					
								893	ff			
887	f											
										883	f	
		882	f									
				877	mF							
865	mF											
						862	f					
855	ep											
										851	ff	
								848	f			
				841	mF							
		840	f									
830	F									834	ff	
						831	f					
								821	f			
				820	F							
819	ep											
						815	ep					
813	F											
										810	ff	
								808	ep			
802	F											802 vibration ν_s (C–C) ou respiration du cyclohexane
790	ep							790	f			
										773	ff	
760	f											
				758	ff							
						751	F					
743	f							743	f			
				742	mF							
						737	F					
										735	ep	
730	f									730	mf	
										729	ep	
				727	ff							
						720	ep					
				702	f							
										698	F	
						690	F					
										688	F	682 bande caractéristique du groupement ortho C_6H_4CX (X = Cl)
				682	F							
						672	ep					
648	mF											
								642	f			
										633	mf	
626	mF			*620*	mF							626 Déformation du cycle 620 aromatique non substitué 619 dérive de la vibration no 6b du benzène (615 amphétamine base)
								619	mF			
613	ep											
				612	f							
						610	ff					
		608	F							608	ff	
								607	ep			
605	f											
		593	ep			593	f					
				587	F							
582	f											
										572	ff	

Tableau 2—*suite*

Cyclohexyl sulfamate de furfenorex (I)				Chlorhydrate de clobenzorex (II)				Diphenyl acetate de fenproporex (III)				Essai d'attribution
Raman		Infra rouge		Raman		Infra rouge		Raman		Infra rouge		
ν, cm^{-1}	I	ν, cm^{-1}	I	ν, cm^{-1}	I	ν, cm^{-1}	I	ν, cm^{-1}	I	ν, cm^{-1}	I	
								567	f			
						565	ff					
554	f											554 ν_{as} SO_2
		546	f									535 ν_s SO_2
			f									
535	f					535	ff					
				529	f							
513	f											
						508	f					
				502	f							
										495	f	
		469	ep			468	mf					
467	f			*467*	f							
								465	f			
				457	f	457	ep					
		453	ep									
444	f											
				440	F							
								439	f			
		436	f									
						435	ep					
						421	ep					
411	f											
										397	f	
		391	f									
				387	mF							
						385	f					
								380	f			
						367	ff					
		343	ep									
						339	f					
				336	f							
		325	f									
										324	f	
								322	f			
						312	ff					
301	mF											
						285	ep					
282	ep							282	mF			
										275	f	
273	ep											
				272	ep							
268	mF											
258	ep											
						254	f					
										250	f	
								248	F			
				242	F	242	f					
						223	f					
				222	F							
								192	ep			
								173	mF			
170	f											
				166	F							
120	ep											
				113	ep							
				103	F							vibrations du réseau cristallin
81	ep											
				64	F							
				31	mF							
24	F											
				22	F							
				13	F							

Abréviations: I = intensité; F = fort; mF = moyennement fort; f = faible; ff = très faible; ep = épaulement.

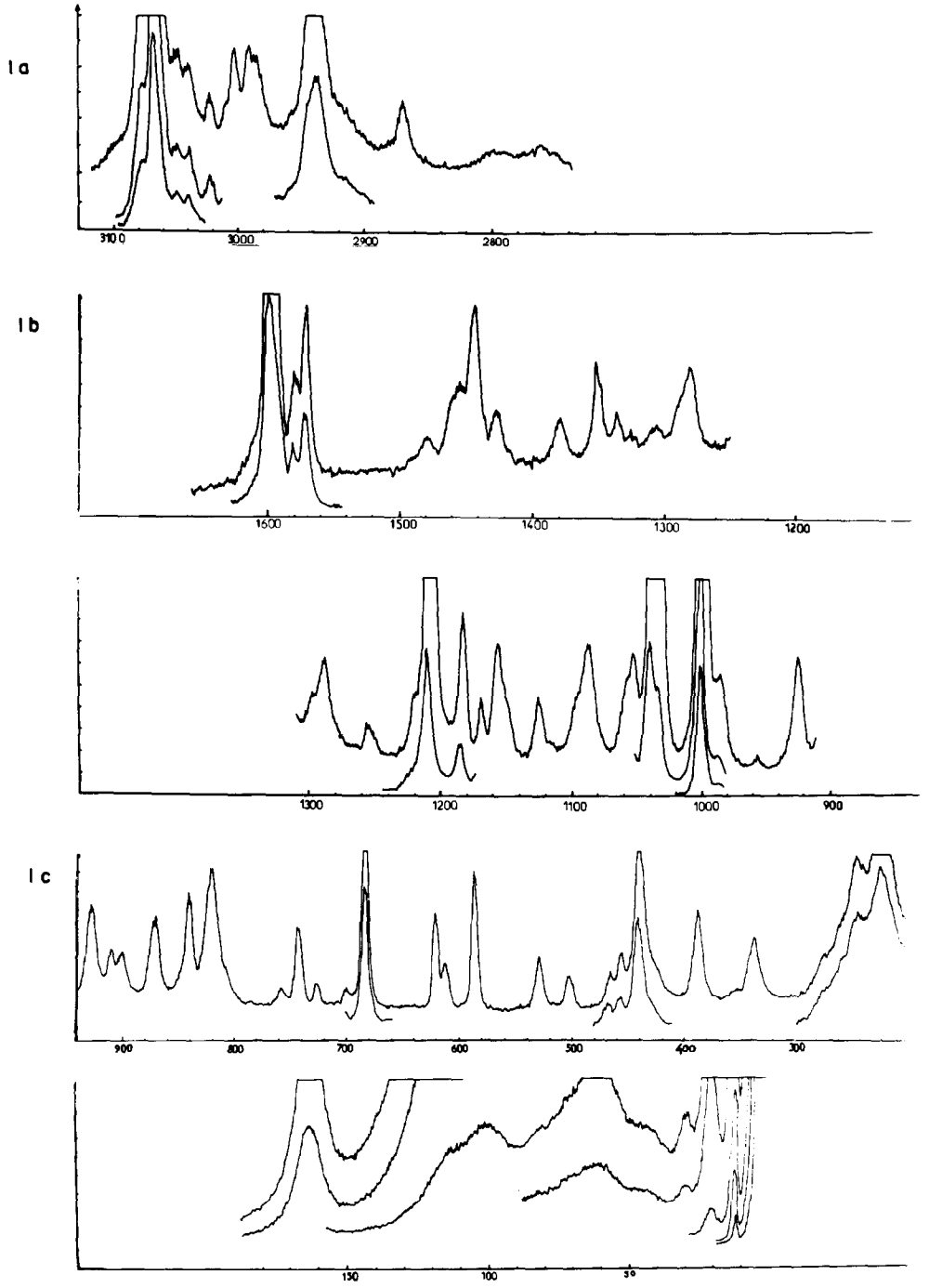


Fig. 1. Spectre Raman du chlorhydrate de clobenzorex: 1a—région spectrale 2700–3100 cm^{-1}; 1b—région spectrale 900–1600 cm^{-1}; 1c—région spectrale 0–950 cm^{-1}.

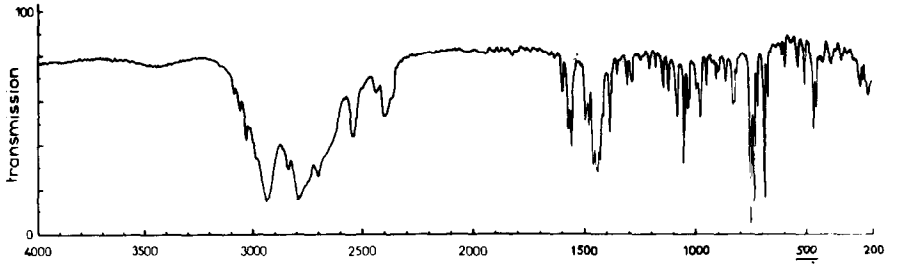


Fig. 2. Spectre IR (200–4000 cm^{-1}) du chlorhydrate de clobenzorex.

Les spectres des composés I, II, III montrent une bande intense située respectivement à 3057, 3063, 3061 cm^{-1} ce qui est en accord avec les auteurs précédents. De part et d'autre de la raie principale apparaissent suivant les cas de 2 ou 3 épaulements.

La raie dégénérée e_{2g} (8a, 8b) correspondant à l'élongation du cycle n'est pas fortement perturbée par la substitution de sorte que les deux fréquences Raman résultantes sont très voisines de celle du benzène (1596 cm^{-1}). Ce couple de vibration indique la présence d'un noyau aromatique mais ne permet pas de distinguer le type de substitution. Sur les spectres les paires de raies correspondant aux vibrations du benzène 8a et 8b apparaissent respectivement à 1601 et 1586 cm^{-1} pour I, 1602 et 1584 cm^{-1} pour II, 1602 et 1583 cm^{-1} pour III. Les raies attribuées à 8a sont beaucoup plus intenses que les raies associées aux modes 8b.

La vibration dégénérée e_{1u} à 1486 cm^{-1} peut aussi éclater en deux bandes (19a, 19b) qui sont très proches de la fréquence primitive cependant ces bandes ont d'une part une très faible intensité en Raman et d'autre part sont souvent masquées par les vibrations de déformation antisymétriques des groupements méthyle attachés au noyau, nous n'avons donc pas remarqué ces bandes sur les spectres Raman.

La vibration b_{2u} (1310 cm^{-1}) d'élongation du cycle n°14 est seulement légèrement décalée par la substitution mais apparaît avec une intensité très faible dans l'intervalle de fréquence couvert par les vibrations de torsion et balancement des méthylènes des substituants alkyle. Sur les spectres la raie de faible intensité située respectivement pour les trois composés à 1307, 1310, 1306 cm^{-1} peut donc difficilement être attribuée seule à la vibration b_{2u}.

La vibration d'élongation symétrique du cycle monosubstitué correspondant (992 cm^{-1}) à la vibration n°1 a_{1g} du benzène est sensible aux substituants et selon Varsanyi[4] doit se trouver dans l'intervalle 1100–1060 cm^{-1} pour les substituants lourds (masse supérieure à 25) et dans l'intervalle 830–620 cm^{-1} pour les substituants légers (masse inférieure à 25). Nous n'avons pas pu sur nos spectres caractériser cette vibration.

Plus intéressante est la vibration correspondante à la déformation du cycle dans le plan ou respiration trigonale du cycle. Elle dérive de la vibration b_{1u} du benzène n°12 (1010 cm^{-1}) et donne lieu, pour les benzènes monosubstitués, à une intense bande Raman située dans l'intervalle 1010–990 cm^{-1}. Cette bande très caractéristique s'est manifestée sur les spectres des composés I, II, III respectivement à 999, 1002, 1001 cm^{-1}.

Pour les benzènes monosubstitués une autre vibration de déformation du cycle dérivée de la vibration du benzène n°6b (606 cm^{-1}) donne lieu à une bande d'intensité moyenne aux environs de 618 cm^{-1}. Les bandes qui apparaissent sur les spectres à 626, 620, 619 cm^{-1} correspondent à cette vibration du benzène.

La fréquence de vibration n°6a des benzènes monosubstitués est assez variable par conséquent il n'a pas été fait de tentative d'attribution.

Des vibrations de déformation des C–H dans le plan (n°3, 9a, 9b, 15, 18a, 18b) c'est celle qui dérive de la 18a qui est la plus utile pour l'identification, elle se traduit par une bande intense en Raman dans l'intervalle 1030–1018 cm^{-1}, de plus elle est caractéristique de la monosubstitution. Elle correspond sur les spectres des composés étudiés aux bandes à 1029, 1037, 1031 cm^{-1}. Bien que la bande située à 1037 cm^{-1} s'écarte sensiblement des autres, il est cependant logique de l'assimiler à bande de même nature du fait de la similitude des trois spectres dans cette zone surtout caractérisée par le voisinage de la vibration b_{1u} n°12 du benzène et par l'intensité forte de ces trois bandes.

La bande issue de la 18b devrait être comprise dans l'intervalle 1082–1065 cm^{-1} mais son intensité très faible aussi en Raman qu'en IR n'a pas permis de la situer.

La vibration e_{2g} dégénérée (n°9a, 9b) à 1178 cm^{-1} est perturbée et donnerait une bande spécifique d'intensité faible en Raman à 1180–1170 cm^{-1} (n°9a) et une bande non spécifique à 410–160 cm^{-1} (n°9b).

Ces bandes faibles n'ont pas été observées sur les spectres. Une bande d'intensité moyenne 1160–1150 cm^{-1} est due à la vibration n°15, elle se manifeste respectivement à 1157 (I et III) et 1155 cm^{-1} (II).

La vibration n°3 (1330–1250 cm^{-1}) est très faible et n'est pas apparue sur les enregistrements de manière significative. De même pour les vibration de déformation du cycle hors du plan: n°4 (700–680 cm^{-1}), n°16a (420–390 cm^{-1}).

Pour les vibrations de déformation des C–H hors du plan du cycle seule la vibration n°5 donne lieu en Raman à une bande suffisamment intense (1000–970 cm^{-1}) qui est caractérisée par un épaulement du côté des basses fréquences sur la bande correspondant à la vibration à 1000 cm^{-1} attribuée à la "respiration" trigonale du cycle. Ces épaulements se trouvent sur les spectres respectivement à 991 (I), 986 (II), 990 (III).

La substitution par un groupement alkyle peut être identifiée par une bande de moyenne ou de forte intensité au voisinage de 1205 cm^{-1}. Les trois composés étudiés présentent cette bande intense à 1209 (I), 1208 (II), 1202 (III) cm^{-1} correspondant certainement à la vibration d'élongation C_6H_5–C.

Groupement isopropyle. La caractérisation du groupement isopropyle est très délicate dans des spectres aussi complexes.

Le groupement isopropyle présente une vibration vers 1350–1330 cm^{-1} qui peut être associé à une vibration de déformation —CH du carbone tertiaire. Cette vibration est rencontrée à 1348 (I), 1341 (II), 1342 cm^{-1} (III). Enfin dans les zones 1175–1165 cm^{-1}, 1150–1140 cm^{-1} correspondant à la déformation de l'isopropyle et 960–950, 920, 835–795 cm^{-1}, 465–430 cm^{-1}, 370–255 cm^{-1} existent des raies correspondant probablement à cette attribution et très

souvent masquée par les vibrations d'autres groupements.

Les vibrations d'élongation —C—H— des alcanes apparaissent dans l'intervalle 3000–2700 cm^{-1}. Ces bandes sont généralement intenses en Raman et ne présentent pas de caractères de spécificité dans l'optique de notre étude. La bande la plus intense [2937 (I), 2932 (II), 2931 cm^{-1} (III)] correspond certainement à la vibration d'élongation antisymétrique CH_2.

La bande observée vers 2965 cm^{-1} est attribuée à la vibration d'élongation dégénérée du groupement méthyle.

L'essai d'attribution de quelques raies correspondant à la structure phénylalkylaminique des composés étudiés montre combien les spectres sont marqués par la présence du cycle benzénique monosubstitué. Nous rappelons les raies caractéristiques les plus importantes:

— bande intense vers 1000 cm^{-1} avec un épaulement près de 995 cm^{-1}
— une bande moyenne ou forte vers 1028 cm^{-1}
— une bande vers 618 cm^{-1}
— une bande moyenne vers 1157 cm^{-1}
— un doublet intense vers 1600 cm^{-1}
— la bande d'élongation des CH aromatiques près de 3060 cm^{-1}
— une bande vers 460 cm^{-1} caractéristiques des alcanes ramifiés
— une bande vers 1205 cm^{-1} correspondant à la vibration d'élongation C_6H_5—C

Le spectre de l'amphétamine base confirme d'une façon logique cette structure phénylalkyaminique puisque l'on retrouve:

— une bande intense à 1000 cm^{-1} avec son épaulement à 988 cm^{-1}
— une bande moyennement forte à 1030 cm^{-1}
— une bande d'intensité moyenne à 615 cm^{-1}
— une bande de faible intensité à 1157 cm^{-1}
— un doublet intense vers 1600 cm^{-1} (1603 et 1596 cm^{-1})
— une série de bandes entre 2700 et 3000 cm^{-1} dont la plus intense se situe à 2906 cm^{-1} (vibration d'élongation des alcanes)
— une bande moyennement forte à 1206 cm^{-1}.

Bien que les attributions précédentes permettent de confirmer la structure d'une partie du squelette de la molécule des trois anorexigènes, la connaissance des fréquences spécifiques à chacun d'entre eux peut être intéressante. C'est pourquoi la partie suivante sera consacrée à l'étude des raies caractéristiques de chacun des composés.

Raies caractéristiques de chaque composé

Cyclohexylsulfamate de furfénorex. La substitution d'un atome d'hydrogène de l'atome d'azote par un groupement furfuryle apporte à ce composé une particularité qui doit permettre de le différencier des autres anorexigènes.

En effet les premiers travaux sur les spectres Raman des noyaux furanniques substitués en 2, 2–5 et 2–3 furent conduits par Matsuno et Han[5] et par Bonino et Manzoni-Anside.[6] Ces auteurs avaient déjà établi que le groupement furfuryle pouvait être aisément distingué des groupements furfurylidène-2 et furoyle-2 sur la base de leur spectre Raman dans la région 1600–1460 cm^{-1}. De plus Sobolev *et al.*[7] dans une étude sur les alkyle furannes, a montré que le spectre dans la région des fréquences d'élongation de la liaison C—H varie suivant le nombre et le type de substituant.

Classiquement un cycle furannique présente trois bandes intenses à 3157, 3122 et 3092 cm^{-1}. Ces bandes sont retrouvées à 3160 et 3120 cm^{-1} dans le cas du cyclohexyl sulfamate de furfénorex avec un changement dans leur intensité relative ce qui est considéré comme une première caractéristique de la substitution en 2 (sur le noyau) à laquelle s'ajoute la disparition de la bande à 3092 cm^{-1}.

Parmi les bandes caractéristiques du cycle d'un groupement 2 furfuryle:

— celle qui apparaît vers 1605–1590 cm^{-1} n'est pas spécifique puisque confondue avec l'une des vibrations e_{2g} du benzène monosubstitué;
— la plus spécifique est la bande de forte intensité qui apparait à 1500 cm^{-1}.

Cette bande n'est pas retrouvé sur les spectres des dérivés (II) et (III), elle pourra donc être choisie préférentiellement pour toute étude de caractérisation. Les deux bandes résultent de l'élongation du cycle furfuryle substitué en 2.

La vibration à 1393 cm^{-1} est spécifique de l'élongation du cycle furannique seul.

Les vibrations de déformation des —CH— "dans le plan" et "hors du plan" sont difficiles à mettre en évidence sur les spectres puisque confondues avec d'autres raies.

Le groupement NH de l'ion cyclohexylsulfamate n'apparait pas comme très significatif. Dans les amines secondaires par exemple la bande NH se situe vers 750–700 cm^{-1} donc difficilement décelable.

La vibration δNH est en général masquée par δCH_2. A l'opposé le groupement cyclohexyle présente une caractéristique importante. La bande située à 802 cm^{-1} réputée pour être la plus significative résulte de la vibration symétrique C—C ou respiration du cycle (forme chaise). Cette bande intense n'apparait pas sur les spectres des autres anorexigènes.

Les autres vibrations de ce cycle ν_{as} CH_2 (2933–2915 cm^{-1}), ν_s CH_2 (2897–2852 cm^{-1}), δ_s CH_2 (1452 cm^{-1}) sont confondues avec d'autres raies sur l'enregistrement.

Enfin les vibrations du groupement SO_2, ν_{as} et ν_s, n'ont pas été détectées, cependant les deux bandes décrites à 555 et 517 cm^{-1} existent sur le spectre à 554 et 535 cm^{-1} et pourraient être attribuées à ces vibrations.

Il n'a pas été trouvé de raies caractéristiques des

sels d'amine tertiaire. Les modes de vibration ν_{C-N^+} (821 cm^{-1}) et $\delta_{C_3-N^+}$ (467 cm^{-1}) correspondent aux bandes observées à 819 et 467 cm^{-1} mais d'intensité trop faible pour pouvoir être utilisés en vue d'une caractérisation de composé.

Chlorhydrate de clobenzorex. Le présence d'un benzénique disubstitué fixé à l'atome d'azote apporte à cette molécule une spécificité se traduisant sur le spectre par une bande intense à 682 cm^{-1} caractéristique de groupe ortho C_6H_4CX (X = Cl). Cette bande est généralement accompagnée d'une deuxième bande intense qui semble être celle située à 587 cm^{-1} et qui n'étant pas retrouvée sur les spectres des deux autres composés est spécifique du chlorhydrate de clobenzorex.

Les sels d'amine secondaire présentent un massif d'absorption intense large et complexe qui s'étend généralement entre 3000 et 2600 cm^{-1} donc peu utilisable pour la caractérisation.

Les raies caractéristiques du chlorhydrate de clobenzorex sont donc situées à 682 et 587 cm^{-1}.

Diphényl acétate de fenproporex. L'élément le plus caractéristique de ce composé est sans doute le groupement $—CH_2—CH_2—CN$ qui présente une vibration à 2257 cm^{-1}.

Région spectrale des basses fréquences (0–250 cm^{-1})

Les spectres Raman de basse fréquence (<250 cm^{-1}) sont très caractéristiques de chaque composé. Les bandes observées sont très intenses en particulier à basse température (−173°). Dans cette région spectrale on s'attend à observer généralement des raies dues aux vibrations de réseau cristallin (cas des échantillons sous forme de poudre polycristalline) en plus de raies intenses dues à des mouvements de torsion (rotation interne) et des mouvements du squelette de la molécule. Néanmoins l'attribution reste très difficile et nécessite l'emploi de techniques variées telles la spectroscopie d'absorption du rayonnement infra rouge lointain, l'étude de la polarisation des raies Raman observées sur un monocristal ainsi que le calcul *a priori* des fréquences de vibration du cristal. Un tel travail sera envisagé ultérieurement sur cette série de composés.

Conclusion

La structure phénylalkylaminique prédominante est confirmée par la position d'un nombre élevé de raies intenses communes aux anorexigènes étudiés et à l'amphétamine base dont ils dérivent. Cependant malgré la complexité des spectres des trois anorexigènes, il a été possible sur la base des données de spectroscopie Raman de caractériser chacun des composés par une ou plusieurs raies spécifiques. Le cyclohexyl sulfamate de furfenorex se distingue par les bandes situées à 3160 et 3120 cm^{-1} et par l'absence de raie à 3092 cm^{-1}. Ces faits sont caractéristiques de la substitution en 2 sur le noyau furannique. Par ailleurs la présence du groupement furfuryle est confirmée par la raie intense à 1500 cm^{-1} et la raie à 1393 cm^{-1} qui dérivent de l'élongation du cycle furannique. La raie intense à 802 cm^{-1}, réputée pour être la plus significative du cyclohexane, résulte de la vibration symétrique C—C ou respiration du cycle. Bien que les deux autres composés soient moins riches en raies spécifiques il est cependant possible de les différencier: le chlorhydrate de clobenzorex présente deux bandes intenses situées à 682 et 587 cm^{-1}, celles-ci traduisent la présence d'un groupe ortho C_6H_4CCl fixé à l'atome d'azote. Enfin le diphénylacétate de fenproporex se distingue par la raie à 2257 cm^{-1} spécifique du groupement $—CH_2—CH_2—CN$.

Remerciements—Cette étude a été effectuée dans le cadre du contrat de récherche avec l'INSERM CRL n°77-1-206. 3 que nous remercions pour le soutien apporté. Nous remercions également les Laboratoires Pharmaceutiques Diamant et Bottu qui nous ont fourni les substances étudiées.

BIBLIOGRAPHIE

1. E. B. Wilson, Jr., *Phys. Rev.*, 1934, **45**, 706.
2. F. R. Dollish, W. G. Fateley et F. F. Bentley, *Characteristic Raman Frequencies of Organic Compounds*, Wiley, New York, 1974.
3. J. Goubeau et E. Kohler, *Chem. Ber.*, 1942, **75**, 65.
4. G. Varsanyi, *Acta. Chim. Acad. Sci. Hung.*, 1966, **50**, 225.
5. K. Matsuno et K. Han, *Bull. Chem. Soc. Japan*, 1934, **9**, 327.
6. G. B. Bonino et R. Manzoni-Anside, *Z. Phys. Chem.*, 1934, **25B**, 327.
7. E. V. Sobolev, V. T. Aleksanyan, R. A. Yarakhanov, I. F. Bel'skii et V. A. Ovodova, *J. Struct. Chem., USSR*, 1963, **4**, 330.

Summary—Raman spectra of a series of three anorexigenic drugs in the polycrystalline state have been recorded. Several spectral similarities have been observed and these are assigned to the basic phenylalkylamine structure of these compounds at the following positions: 3060, 1600, 1205, 1157, 1028, 1000, 995, 618 and 460 cm^{-1}. However, bands specific to each compound characterize the spectra. Furfenorex cyclohexyl sulphamate, for example, displays bands at 3160, 3120, 1500, 1393 and 802 cm^{-1}. The 2-substituted furan ring is characterized by absence of a band at 3092 cm^{-1}. Clobenzorex hydrochloride displays bands at 682 and 587 cm^{-1}, whereas fenproporex diphenylacetate possesses a specific band at 2257 cm^{-1}.

Talanta Vol. 28, pp. 107 to 113
©Pergamon Press Ltd 1981. Printed in Great Britain
0039-9140/81/0201-0107$02.00/0

DIRECT DETERMINATION OF URANYL ION BY NANOSECOND DYE-LASER SPECTROSCOPY

G. A. KENNEY-WALLACE*, J. P. WILSON, J. F. FARRELL
and B. K. GUPTA

Department of Chemistry, University of Toronto, Toronto, Canada

(*Received* 2 *May* 1980. *Accepted* 28 *June* 1980)

Summary—A sensitive and selective technique for the detection and assay of the uranyl ion is described. The technique is based upon the measurement of the luminescence of solutions of uranyl salts excited by pulsed dye-lasers. The effect of the anion, pH and foreign ions on the luminescence behaviour is discussed.

There is considerable current interest in the potential of laser isotope-separation for obtaining enriched uranium. In geophysics, a continuing effort has been directed to the detection and determination of uranium occurring naturally in the form of the uranyl ion, the photochemistry of which has been explored for almost a hundred years. The techniques used in investigating the photochemistry have often been indirect, non-selective and requiring considerable chemical acumen. Despite extensive investigations, many fundamental theoretical and experimental issues are unresolved concerning the spectroscopy and photophysics of the uranyl ion.[1,2]

We report here the first photoselective, direct visible-region excitation of the uranyl ion with a pulsed dye-laser. The laser-induced emission from the UO_2^{2+} species can be detected in the presence of other ultraviolet-absorbing ions through both wavelength and lifetime discrimination. These results are part of a comprehensive study[3,4] of the laser photophysics of the uranyl ion, reported elsewhere.

The fluorimetric techniques initially employed to determine the presence and content of uranium involved the fusion of the uranium compounds with sodium fluoride in platinum crucibles at ~1300 K.[5–7] Although the fusion markedly enhanced the emission on subsequent irradiation, the number of variables involved made the method impractical for routine analysis. Alternative fluorimetric procedures for the determination of uranium were also somewhat complex,[8,9] although it had been shown that the addition of phosphates[10] or phosphoric acid[7] to UO_2^{2+} in aqueous media increased the emission intensity caused by excitation with an ultraviolet lamp.

* Reprint requests.

EXPERIMENTAL

Absorption, excitation and emission spectra were first recorded for a range of uranyl complexes in order to obtain accurate absorption coefficients and to determine the origin and yield of the characteristic green luminescence obtained by excitation with ultraviolet and visible radiation. Emission spectra were obtained with a Perkin-Elmer MP44 fluorescence spectrometer, 2-mm exit slits being used to obtain a spectral resolution of 0.2 nm.

A nanosecond pulsed nitrogen-laser, shown schematically in Fig. 1, was used to excite the uranyl ion complexes at 337 nm, while a nitrogen-laser pumped coumarin-1 or POPOP dye-laser was employed to excite samples at wavelengths of *ca.* 415–450 nm. The lifetime of the laser-

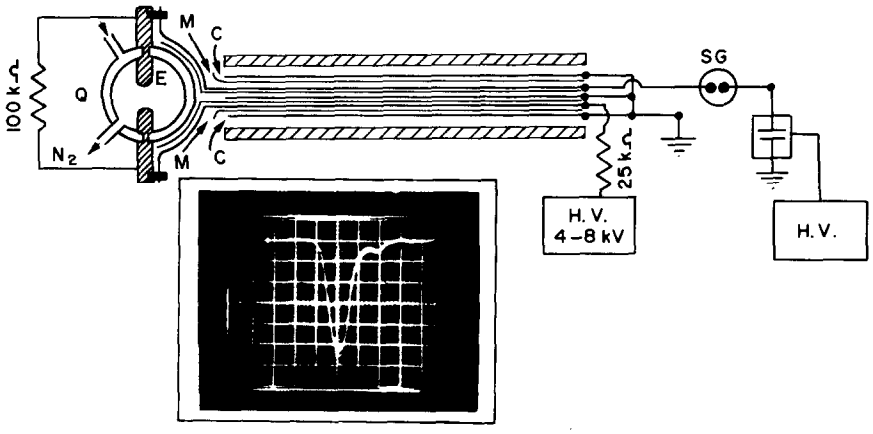


Fig. 1. Schematic diagram of pulsed nitrogen-laser; photograph shows superposition of 22 consecutive laser pulses (fwhm ~10 nsec) on oscilloscope, 10-nsec divisions.

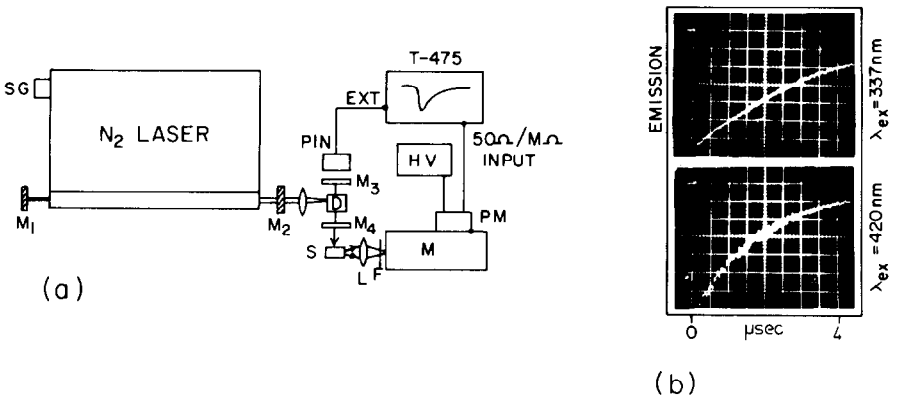


Fig. 2. (a) Schematic diagram of nitrogen-laser pumped dye-laser apparatus; (b) lifetime of laser-induced emission from 0.1*M* aqueous uranyl nitrate: upper trace, λ_{ex} = 337 nm, lower trace λ_{ex} = 420 nm.

induced emission was recorded as a function of the ligand in the uranyl complex, pH, temperature and the presence of a phosphate buffer or alcohol quencher. All uranyl samples were prepared analytically and deoxygenated by passage of nitrogen before use. Lifetime measurements were made as shown schematically in Fig. 2. The output beam from the nitrogen-laser or dye-laser was focused onto the uranyl sample (S) and the emission collected by a lens (L) and focused through a filter (F, $\lambda \geqslant 400$ nm) onto the slit of a 0.25-m monochromator (M). An RCA 1P28 fast photomultiplier (PM) at the exit slit, coupled through either a 50-Ω or a 1-MΩ resistance to a Tektronix 475 (250 MHz) oscilloscope, recorded the time-dependent emission. The oscilloscope was triggered externally by the signal from an HP 4207 PIN diode, positioned behind the back mirror of the dye-laser. With a 50-Ω impedance-matched circuit, the response time of the detection system was $\leqslant$2 nsec.

The nitrogen-laser was based on a travelling wave design[11,12] with a *folded* Blumlein[13] acting as the storage capacitor. In the super-radiant mode, the laser delivered $\leqslant$1 MW in single pulses of 5 nsec duration, while typical operation at 2 Hz, as a resonator with cavity dielectric laser mirrors, led to pulses of 10 nsec duration at powers $\leqslant$200 kW.

The folded Blumlein (Fig. 1) comprised five conductors (C) of 28-gauge, high-grade electrical quality, 3 × 4 ft aluminium sheets, interleaved with 5-mil sheets of Mylar dielectric (M) and sealed to give an effective capacitance of ~0.05 μF. The live plates were attached to the 3-ft aluminium electrodes (E) sealed in the discharge channel, a 1-in. bore 3-ft long quartz tube (Q) with Teflon end-flanges, machined to hold both the end windows and the laser mirrors. Nitrogen flowed counter to the direction of the discharge, the gas pressure being optimized with respect to the electric field gradient across the discharge gap. The travelling-wave discharge was initiated by short-circuiting a live plate to ground with a spark gap (SG), placed across the capacitors and fired through an SCR circuit.

A low-inductance spark gap giving a very fast spark[14] was used, having $\frac{1}{8}$-in. diameter rounded molybdenum electrode pins embedded in a Lucite cylinder and spaced to cause breakdown in the flowing nitrogen when an external 50-kV pulse was applied through an SCR circuit. A thin metal foil about the waist of the Lucite acted as a high-voltage preionizer and ensured discharges that were spatially uniform with minimum time jitter, a fact crucial to the reproducible performance of this laser. The superposition of 22 pulses from this laser is shown in Fig. 1 and illustrates the remarkable degree of pulse-to-pulse reproducibility from the laser when operating under our normal experimental conditions, namely 7 kV charging voltage, nitrogen flowing at 45 mmHg pressure, 16 mm electrode spacing and 2 Hz repetition rate. In fact, the laser can be fired at up to 20 Hz, or even higher frequency, with slight modifications to the SCR circuit, but at the expense of lower peak power, unless significantly higher capacitor voltages are employed.

The dye-laser was transversely pumped by the nitrogen-laser, the beam of which was focused with a spherical lens onto the quartz window of the stainless-steel dye-cell. The dye-cell (D in Fig. 2) was positioned between a 99% reflectivity broad-band laser mirror (M_3, or a holographic grating) and a sapphire output reflector (M_4), with an intracavity spacing of 6 in. Two flow ports linked the cell to the micropump and reservoir, thus permitting dye to flow in order to avoid adverse thermal and photochemical effects. Several kW of power were readily obtained from coumarin-1 in pulses of 10 nsec duration.

RESULTS AND DISCUSSION

Although the photophysical behaviour of aqueous solutions of uranyl nitrate, sulphate and acetate, and zinc acetate, perchlorate and chloride were investigated, only the results for uranyl nitrate will be discussed here, as representative of the analytical potential of this dye-laser technique. Most other chemical studies have been on this particular uranyl compound and so this comparison is appropriate.[15–17] The spectra of most of the other compounds have not previously been published and are described elsewhere.[3,4]

The ultraviolet and visible region absorption spectra of UO_2^{2+} species in aqueous solutions are similar in intensity and profile, but the main peaks of the bands in the visible region exhibit small red shifts with increasing ligand charge. Figure 3 shows the detailed visible absorption spectrum of the UO_2^{2+} ion in nitrate medium. The molar absorptivities for UO_2^{2+} in aqueous uranyl nitrate solution were determined at various laser excitation wavelengths and found to be ϵ_{337} = 14.8, ϵ_{414} = 8.9 and ϵ_{425} = 7.2 $l.mole^{-1}.cm^{-1}$ and are accurate to ±5%. The clear indication of many vibronic peaks in the undulating line shape of the absorption spectrum should be noted.

Figure 4 illustrates the excitation spectrum and the emission spectra obtained following excitation at 337

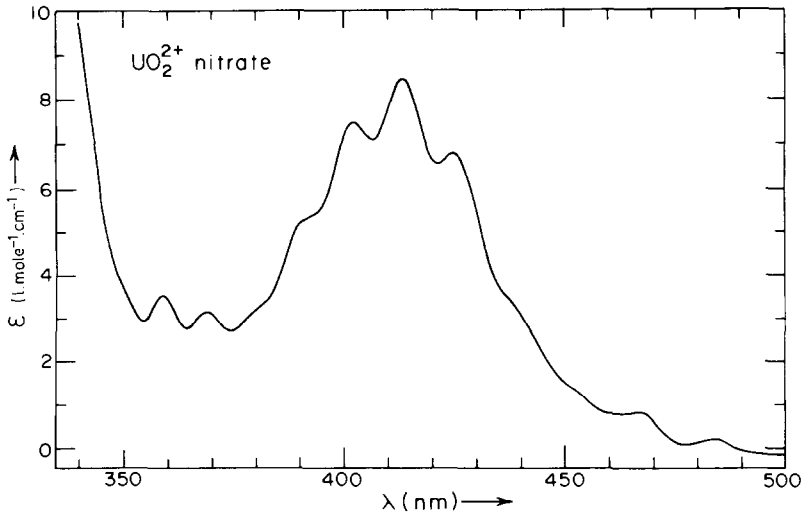


Fig. 3. Visible-region absorption spectrum of uranyl ion. Data from $10^{-2}M$ aqueous uranyl nitrate.

and 414 nm. The peaks in the emission spectra again exhibit slight red shifts with increasing ligand charge. Despite the smaller molar absorptivity, the integrated emission intensity caused by excitation at 414 nm is comparable to that from excitation at 337 nm for this uranyl nitrate sample, clearly indicating that excitation at the longer wavelength yields emission with a higher quantum efficiency. The enhancement in emission caused by the presence of phosphoric or perchloric acid is also illustrated for various ratios of uranyl nitrate to phosphate or perchlorate, in Fig. 5. In all the cases investigated, not only was the emission intensity increased, but a substructure was imposed on the spectrum, reminiscent of that of the solid-state spectra. Figure 5(a) illustrates the influence of $0.76M$ phosphoric acid on the emission from $5 \times 10^{-3}M$ aqueous uranyl nitrate solutions following excitation at 337 nm. A dramatic enhancement is seen, consistent with trends described earlier.[6] The vibronic structure is revealed and the slightly red-shifted emission is enhanced by a factor of over 100, although the absorptivity is increased by a factor of only 2.3.

Figure 5(b) shows the enhanced emission intensity observed from $10^{-2}M$ uranyl nitrate with increasing concentration of perchloric acid, from 1 to $8M$. Unlike phosphate, perchlorate does not complex with the uranyl ion[15–17] and thus it is the influence of the acidity which is under investigation here. Since the molar absorptivity $\epsilon_{337} = 10$ l.mole^{-1}.cm^{-1} remained constant in these acid solutions, the enhancement is due to chemical interactions and is most pronounced in the hydrogen-ion concentration range

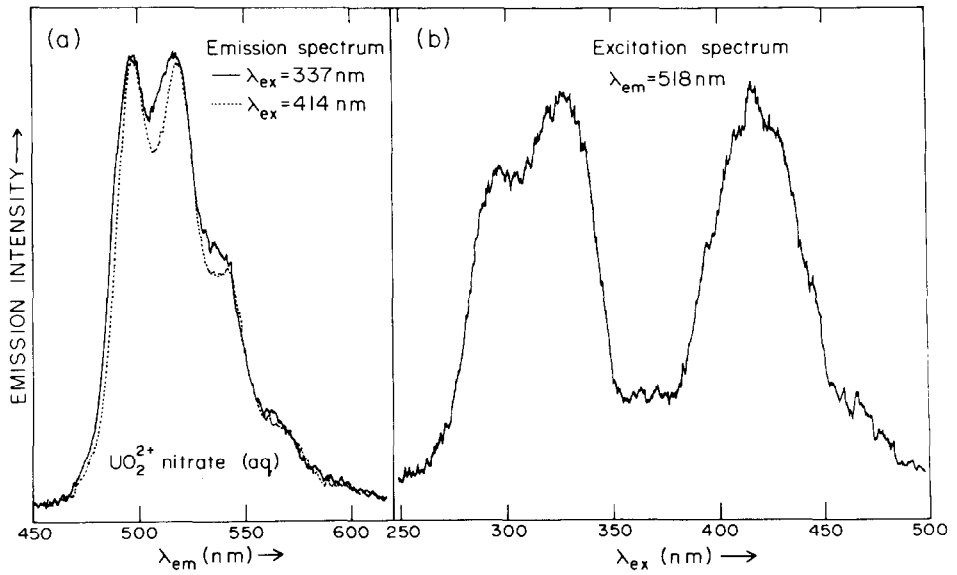


Fig. 4. Emission and excitation spectra of aqueous uranyl nitrate solution excited at 337 and 414 nm.

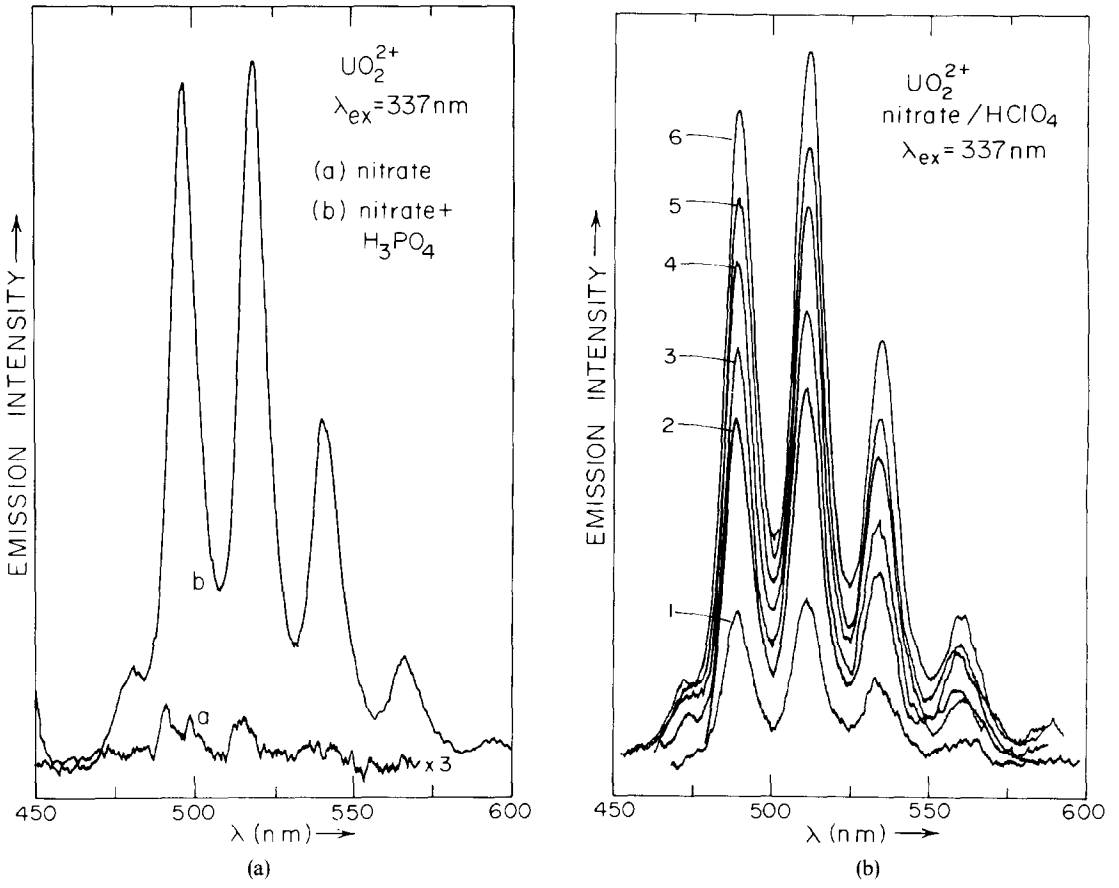


Fig. 5. Enhancement of emission intensity from uranyl nitrate in presence of (a) 0.76*M* phosphoric acid, (b) perchloric acid:spectra numbered 1–5 correspond to concentrations of 1–5*M*, and number 6 to 8*M* $HClO_4$.

1–6*M*, where the emission intensity increases fourfold. Thus the data in Fig. 5 show that substantial and quantitative enhancement of the emission from UO_2^{2+} arises from the presence of excess of phosphate or hydrogen ions, and that there is a small increase in the absorptivity in some cases.

The influence of the pyrophosphate in a series of pyrophosphate buffers adjusted to pH 6 with sodium hydroxide was investigated. Once again the emission intensity was enhanced considerably, and the vibronic structure clearly emerged from the broad envelope that characterizes the normally weak emission from uranyl nitrate solutions. Figure 6(a) shows the influence of increasing proportions of 0.09*M* pyrophosphate buffer on the emission from $10^{-2}M$ uranyl nitrate. The buffer enhances the overall intensity of the emission but the relative intensities and spectral positions of the peaks are not affected. Subsequent studies on the influence of sodium hydroxide showed that it contributed to the emission intensity enhancement factor, although the effect varied from ligand to ligand and appeared most pronounced for uranyl nitrate, where the relative effect of the buffer was 1.5 times that of an equivalent pyrophosphate solution without sodium hydroxide.

The peaks in Fig. 6(a) are separated by 770–890 cm^{-1}, and are slightly broader than, but not too different from those having a typical separation of ~850 cm^{-1} (fwhm ~500 cm^{-1}) in the solid state spectrum of crystalline uranyl nitrate shown in Fig. 6(b). The symmetric stretch in the UO_2^{2+} ion occurs at ~860 cm^{-1}, while the asymmetric stretch and bending modes appear at 930 cm^{-1} and 210 cm^{-1} respectively.[18] The number and positions of the peaks in Fig. 6(a) and (b) are the same, but the relative intensities vary. Similar behaviour was seen for all other uranyl salts in pyrophosphate-buffered, acidic or basic solution and will be discussed elsewhere.[3] The complete photophysical data are presented in Tables 1 and 2.

The radiative lifetime of the laser-induced emission was measured for all the uranyl salts in the various acidic, basic and pyrophosphate-buffered media. Following laser excitation at 337 nm, the relatively long-lived green emission could be readily observed. The lower the temperature, the longer the radiative lifetime. The oscilloscope traces in Fig. 2 show typical emission signals recorded at 514 nm following nanosecond laser excitation (at two different wavelengths) of uranyl nitrate in solution, at 298 K. Figure 7 shows

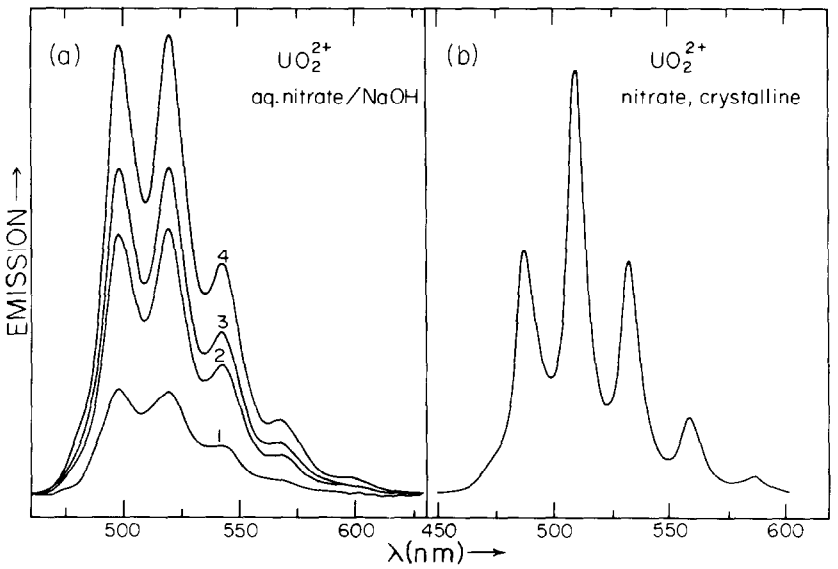


Fig. 6. Comparison of vibronic structure revealed in emission spectra of (a) aqueous uranyl nitrate with increasing proportions of pyrophosphate buffer: (1) aqueous uranyl nitrate, (2) 0.09*M* pyrophosphate buffer: 0.01*M* uranyl nitrate 1:40 v/v, (3) 1:30 v/v, (4) 1:20 v/v; (b) crystalline uranyl nitrate.

Table 1. Principal peaks in uranyl emission spectra

Ligand	Principal emission peaks, *nm*				
NO_3^-(aq)	497	518	543		
NO_3^- + H_3PO_4(aq)	501	521	543	570	
NO_3^-(solid)	488	510	533	559	587
SO_4^{2-}(aq)	491	512	536	560	
SO_4^{2-} + H_3PO_4(aq)	500	521	544	568	
SO_4^{2-}(solid)	495	516	540	567	594
$ZnAc^-$(aq)		515	534		
$ZnAc^-$ + H_3PO_4(aq)	499	521	542	568	
$ZnAc^-$(solid)	482	502	523	547	573
Orthophosphate (solid)	485	502	523	547	573

Table 2. Lifetime (τ) of laser-induced emission from uranyl ion in aqueous solutions

Ligand	τ, *μsec**		
	λ_{ex} = 337 nm	λ_{ex} = 415 nm	λ_{ex} = 450 nm
Nitrate	3.0	2.4	2.9
Nitrate + H_3PO_4	70	89	94
Sulphate	4.8	3.7	4.1
Perchlorate	2.1	1.8	2.2
Zinc acetate	3.3	1.7	2.9
Acetate	2	1.6	2.3

* Data obtained from exponential decay; accurate to ±10% or better.

(top left) the exponential decay of the luminescence from 0.1*M* aqueous uranyl nitrate solution excited at 337 nm and compares it (top right) with the emission recorded from the same sample after dye-laser excitation at 420 nm and (lower left) 450 nm. Note that the radiative lifetimes are the same, 2–3 μsec. No emission could be detected at wavelengths shorter than 460 nm following nitrogen-laser excitation at 337 nm, despite nanosecond time-resolution and a very sensitive photodetector. The lower right trace in Fig. 7 illustrates the similarity of the decay from uranyl sulphate. Thus upon pulsed dye-laser excitation at the wavelengths of the weaker visible-region absorption bands, the excited uranyl samples displayed broad-

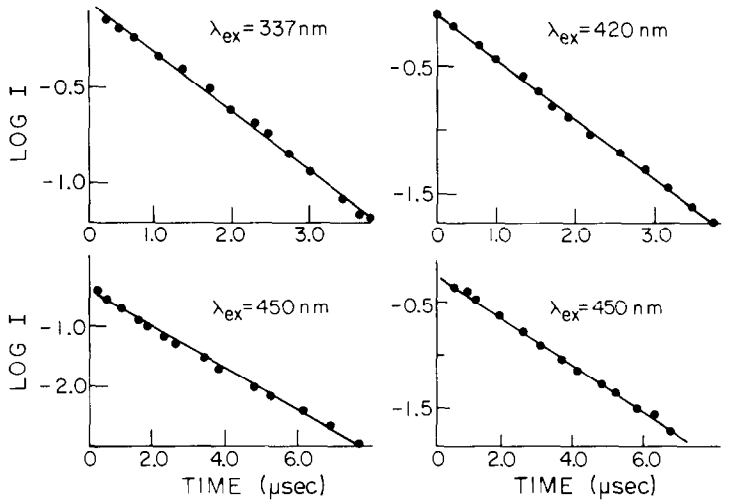


Fig. 7. Exponential decay of laser-induced emission from 0.1*M* uranyl nitrate following nanosecond excitation; λ_{ex}: (a) 337 nm; (b) 420 nm; (c) 450 nm; (d) sulphate solution excited at 450 nm.

band green emission, having the same spectral features and radiative lifetime as those recorded following excitation at 337 nm. The lifetimes for the various uranyl salts ranged from 2 to 4 μsec in aqueous solution, but increased significantly upon addition of phosphoric acid or pyrophosphates. For example, $\tau = 3$ μsec for uranyl nitrate excited at 337 nm increases to $\tau = 70$ μsec in the presence of phosphoric acid. A similar apparent increase in τ to 94 μsec was observed when the same sample was excited at 450 nm. Increase in temperature from 283 K to 323 K decreased the lifetime by a factor of 2.5 for the normal aqueous uranyl nitrate solution. The value of τ was found to be 676 and 249 μsec for uranyl nitrate and sulphate, respectively, in the solid state, consistent with the previously published values of 695 and 265 μsec.[19]

The luminescence intensity, radiative lifetimes and spectral resolution in the emission from the optically excited uranyl ion were all remarkably enhanced in the presence of high concentrations of acid (protons), base (hydroxide ions) and pyrophosphate. These effects are partly due to increases in absorptivity at the excitation wavelengths used, but mostly arise from the formation of chemical complexes, in which the UO_2^{2+} ion acquires a higher probability for *radiative* transitions.

The origin of the visible luminescence of the uranyl ion has been attributed to both fluorescence and phosphorescence.[20,21] In an ion as heavy as UO_2^{2+}, it is arguable whether or not electronic states of pure character exist. The data presented here clearly show that whether excitation occurs in the ultraviolet, the so-called singlet absorption, or in the visible region, triplet absorption, the emission spectrum, lifetime and intensity of optically excited solutions of uranyl nitrate are comparable. No ultraviolet emission could be detected following laser excitation at 337 nm, despite nanosecond time-resolution and very sensitive photodetection. However, the excitation spectrum in Fig. 4 shows that visible emission could arise from this ultraviolet absorption. From these data we conclude that singlet emission, if any indeed occurs, must have less than a hundredth of the intensity of triplet emission and have a lifetime of less than 1 nsec. The green emission characteristic of the uranyl ion originates in a triplet state and decays exponentially (Fig. 7). The small variations found with some complexes could be interpreted as ligand-field effects which influence the competition between radiative and non-radiative pathways back to the ground electronic state. It has been established that the emission following ultraviolet excitation arises from a triplet-like state. Furthermore, this emission can be enhanced in the presence of common chemical species (acid, base) giving interactions which increase the lifetime of the emitting state and reveal the vibronic structure of the complex. These effects are reminiscent of fluorescence enhancement in laser-dyes brought about by imposing rigidity on the flexible molecular framework by internal chemical bonding or by freezing-out rotational motion by use of a highly viscous solvent.

CONCLUSION

The fact that with a pulsed, visible-region dye-laser we can now selectively excite the normally spin-forbidden transition to the excited triplet state in a given vibronic fine structure band of UO_2^{2+} leads immediately to the conclusion that this is a powerful analytical method for UO_2^{2+}. In the presence of other ultraviolet-absorbing species commonly found with this ion, such as metal ions, organic molecules or even the ligand complex itself, UO_2^{2+} cannot be selectively excited by the conventional ultraviolet light sources. If the dye-laser is tuned to a known component of

the triplet visible-region absorption band, the position of which is to some extent matrix-sensitive, the UO_2^{2+} ion alone will be excited and phosphoresce with a lifetime that is also characteristic of its matrix environment. This dye-laser technique should facilitate the determination of the uranyl ion. The photophysical data reported here have yielded new insights into the electronic and molecular complexes of the uranyl ion which will assist in the design of novel laser photoselective chemical separation schemes in aqueous solution. Similar photochemical selectivity has already been recently demonstrated, also for some lanthanide materials.[22,23]

Although relatively high concentrations of uranyl ion were used in these experiments in order to obtain the spectroscopic data, the sensitivity of the technique for low concentrations is excellent, since there are low background contributions from optically excited "impurity" ions. Seldom will the impurities, whether metal ions or complexing ligands, act as "spectral interferences",[8,9] because the excitation source can be tuned into resonance with any of the UO_2^{2+} absorption peaks. Furthermore, the longer lifetimes for UO_2^{2+} in the different complexes shown in Figs. 5 and 6 allow the use of gating techniques and a range of sensitive high-gain photomultipliers with high impedance, to amplify the signals. The triplet-like ground states of these new uranyl complexes display more favourable visible region absorptivities, higher emission intensities and longer radiative lifetimes. These factors not only provide photoselective and quantitative assay of the uranyl ion in aqueous solution, but also permit an increase in the sensitivity by an increase in the laser pulse-intensity.

Acknowledgements—We thank M. R. Corbett for his assistance in measuring the spectral data. This research was partially supported through a Strategic Grant from the Natural Sciences and Engineering Research Council of Canada and the Bickell Foundation.

REFERENCES

1. E. Rabinowitch and R. L. Belford, *Spectroscopy and Photochemistry of Uranyl Compounds*, Pergamon, Oxford, 1964.
2. H. D. Burrows and T. J. Kemp, *Chem. Soc. Rev. (London)*, 1974, **3**, 139.
3. J. P. Wilson, *M. Sc. Thesis*, University of Toronto, 1979.
4. J. P. Wilson and G. A. Kenney-Wallace, *to be published.*
5. H. Le Roux, *Nature*, 1959, **183**, 1180.
6. R. A. Mackay, *Bull. Inst. Mining. Met.*, No. 530, 1951, 129.
7. A. Davydov, T. S. Dobrolyubskaya and A. A. Nemodruk, *Zh. Analit. Khim.*, 1961, **16**, 68.
8. N. R. Andersen and D. M. Hercules, *Anal. Chem.*, 1964, **36**, 2138.
9. G. Alberti and A. Saini, *Anal. Chim. Acta*, 1963, **28**, 536.
10. *Idem, ibid.*, 1963, **28**, 536.
11. J. D. Shipman, *Appl. Phys. Lett.*, 1967, **10**, 3.
12. S. C. Wallace and G. A. Kenney-Wallace, *Int. J. Radiat. Phys. Chem.*, 1975, **7**, 345 and references therein.
13. P. Engelking, *Ph.D. Thesis*, Yale University, 1976.
14. B. K. Gupta, J. Farrell and G. A. Kenney-Wallace, unpublished data (designs available upon request).
15. M. Deschaux and M. Marcantonatos, *Chem. Phys. Lett.*, 1979, **63**, 283; *J. Chem. Soc., Faraday Trans. I*, 1979, **75**, 2273.
16. V. Kazakov, R. G. Bulgakov, Y. E. Nikitin and G. L. Sharipov, *Opt. Spectrosc. (USSR)*, 1976, **41**, 644.
17. M. Moriyasu, Y. Yokoyama and S. Ikeda, *J. Inorg. Nucl. Chem.*, 1977, **39**, 2205.
18. J. LeCompte and R. Freyman, *Bull. Soc. Chim. France*, 1941, **8**, 622.
19. D. D. Pant, D. N. Pande and H. C. Pant, *Indian J. Pure Appl. Phys.*, 1966, **4**, 171.
20. C. K. Jørgensen, *J. Lumin.*, 1979, **18/19**, 63.
21. S. P. McGlynn and J. Smith, *J. Mol. Spectrosc.*, 1961, **6**, 164.
22. T. Donahue, *Opt. Eng.*, 1979, **18**, 181.
23. D. M. Cox, R. B. Hall, J. A. Horseley, G. M. Kramer, P. Rabinowitz and A. Kaldov, *Science*, 1979, **50**, 390.

Talanta Vol. 28, pp. 115 to 118
©Pergamon Press Ltd 1981. Printed in Great Britain
0039-9140/81/0201-0115$02.00/0

SHORT COMMUNICATIONS

ENTHALPIMETRY WITH CATALYTIC REACTIONS—II

DETERMINATION OF THIOUREAS BY THE IODINE–AZIDE REACTION AFTER THIN-LAYER CHROMATOGRAPHIC SEPARATION

NOBUTOSHI KIBA, TOSHIYUKI SUTO* and MOTOHISA FURUSAWA

Department of Chemistry, Faculty of Engineering, Yamanashi University, Kofu-shi, 400, Japan

(*Received* 14 *May* 1980. *Accepted* 22 *August* 1980)

Summary—A enthalpimetric method for the determination of thiourea and its *N*-alkyl derivatives (1,3-dimethyl, 1,3-diethyl and 1,3-di-n-butyl), based on their catalytic effect on the iodine–azide reaction, is described. The thiourea mixtures are separated by thin-layer chromatography, followed by enthalpimetric detection. The error is ± 5% for thioureas in the range 0.05–0.5 μmole.

Thioureas have numerous applications in industrial and agricultural chemistry. The compounds are toxic, goitrogenic and carcinogenic.[1] Simple selective methods for their determination are therefore needed. Many methods, including titrimetric,[2–7] voltammetric,[8,9] colorimetric,[10,11] chromatographic[12,13] and gravimetric,[14] have been reported. The catalytic acceleration of the iodine–azide reaction has been used for the determination of traces of thioureas, with coulometric,[15] spectrophotometric–kinetic,[16] arsenite titration[17–19] and photometric–enthalpimetric[24] procedures for the determination step. The main disadvantage of the method is the lack of selectivity. Therefore, mixtures of thioureas have first to be separated into their components. Karska *et al.*[19] determined ethyl-, phenyl-, diphenyl- and triacetylthiourea after paper chromatographic separation.

In this paper we describe a method for the separation of a mixture of thioureas [thiourea (TU), dimethylthiourea (MTU), diethylthiourea (ETU) and di-n-butylthiourea (BTU)] on silica gel plates with dioxan–benzene–acetic acid (90:80:1) as development solvent, followed by the determination of each thiourea by direct-injection enthalpimetry. The individual spots on the chromatogram are scraped off and the material is suspended in the sodium azide solution. Iodine solution is injected into the suspension. The catalytic reaction takes place instantly and is over within 30 sec. The heat generated by the reaction is monitored with a thermistor probe in a Wheatstone bridge circuit.

* Present address; IATORON Co., Higashi-kanda, Chiyoda-ku, 101.

EXPERIMENTAL

Reagents

All reagents were of analytical reagent grade. A 0.2*M* iodine solution (50.8 g/l.) in 1.0*M* potassium iodide was prepared and standardized by titration with thiosulphate. The sodium azide was checked iodometrically by the method of Feigl *et al.*[20] Solutions were buffered with mixtures (0.1*M*) of potassium hydrogen phthalate and sodium hydroxide (pH 5) or potassium dihydrogen phthalate and sodium hydroxide (pH 6, 7 and 8). TU was recrystallized from 50% aqueous ethanol, MTU from dioxan, and ETU and BTU from 50% aqueous methanol. The purity of the thioureas was checked by the method of Murthy *et al.*[2] Standard solutions of the thioureas were prepared in acetone. The sodium azide solution (0.6*M*) was prepared in the buffer solution (pH 6.0). The Feigl reagent was 0.01*M* iodine-0.5*M* sodium azide solution.[21] The silica gel (Wakogel B-5) was supplied by WAKO chemicals. Osaka. Glass plates, 20 × 20 cm, were coated with a 3-mm thick layer of the gel with a commercial applicator.

Apparatus

The apparatus was similar to that previously described.[22] Experiments were done at 25 ± 0.1° in a thermostat.

Procedure

Portions (5 μl) of each of the standard solutions and of the solution to be analysed were spotted on a silica gel plate with a syringe. After drying, the plate was placed in a developing tank previously saturated with the development solvent. The development solution [dioxan–benzene–acetic acid (90:80:1)] was allowed to ascend to a height of about 12 cm on the plate. The chromatograms were dried in a stream of air and the positions of the spots were located by spraying the chromatograms of the standard solutions with Feigl reagent. The areas on the chromatogram corresponding to the components of the sample mixture were scraped off and suspended in 10 ml of sodium azide solution in the reaction vessel. The cover with its attached thermistor and

stirrer was fitted and the stirrer was started. A 500-μl portion of iodine solution (0.1M) was taken in a syringe which was then placed in position. When thermal equilibrium was reached, as indicated by a steady trace on the thermistor-bridge recorder, the iodine solution was injected rapidly. The height of the temperature pulse (*i.e.*, the temperature change of the solution) was measured. Blank tests were performed to determine the exothermic pulse from the reaction of iodine with azide and the reaction catalysed by impurities in the reagents.

Calibration

Calibration was done with standard solutions for each thiourea, covering the range 50–550 nmole, by pipetting 10 ml of sodium azide solution into the reaction vessel, adding 1–10 μl of thiourea solution, and continuing as described in the procedure.

RESULTS AND DISCUSSION

Separation of mixture of thioureas

Thioureas have been separated by TLC on silica gel, with chloroform–ethyl acetate (10:1) as development solvent,[23] but this solvent system was inapplicable to the separation of our mixtures. Complete separation was accomplished with dioxan–benzene–acetic acid (90:80:1). The R_f values (mean of 5 results) obtained were 0.21, 0.39, 0.59 and 0.69 for TU, MTU, ETU and BTU, respectively. Under these conditions it was possible to separate a mixture containing less than 0.5 μmole of each thiourea in 5 μl of solution, and TU, MTU, ETU and BTU could be detected in 0.1, 0.05, 0.1 and 0.05 μg amounts, respectively. It was possible to separate the thioureas from some other compounds which catalyse the reaction, such as mercaptans, isothiocyanates, thiosulphate and sulphide. For example, the R_f values of butyl mercaptan, ethyl isothiocyanate, sodium thiosulphate and sodium sulphide were 0.95, 1.0, 0.1 and 0.08, respectively.

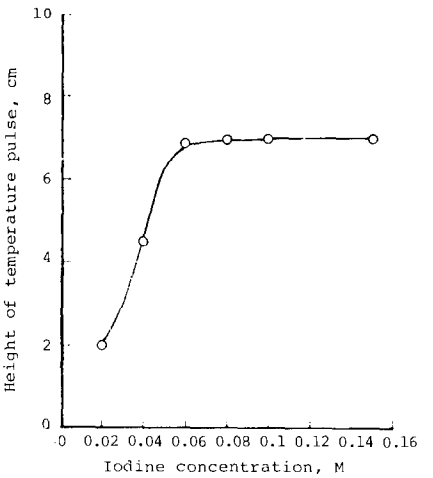


Fig. 2. Effect of iodine concentration on the reaction catalysed by diethylthiourea (10 ml of 0.6M sodium azide–50 μM diethylthiourea, 500 μl of iodine solution, pH 6.0).

Determination of thioureas

The parameters influencing the course of the reaction catalysed by thioureas have been investigated.[15–19] The important parameters are the pH and the concentrations of iodine, azide and thiourea.

Iodine solution was injected into a 0.6M sodium azide–50 μM thiourea solution at various pH values. The rapid catalytic reaction set in as soon as the iodine solution was injected, and was over within 4 min. Figure 1 shows the influence of pH of the solution on the height of the temperature pulse. Coefficients of variation were between 0.6 and 2.6% (5 variates). The extent of the reaction decreased with increasing pH, but the rate of reaction increased. For BTU, the times taken for the reaction to be over were

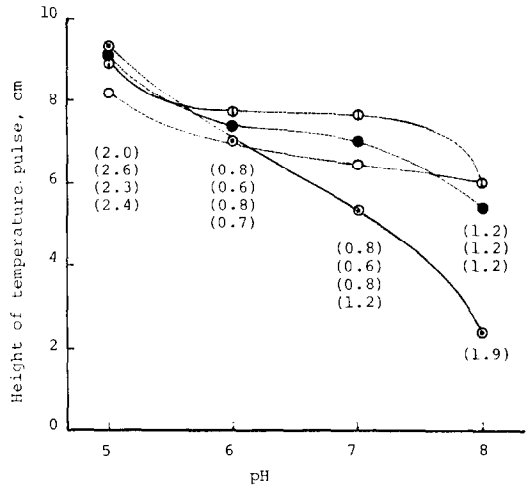


Fig. 1. Effect of pH on the reaction of 10 ml of 0.6M sodium azide–50 μM thiourea solution and 500 μl of 0.1M iodine solution; ⊙——⊙: thiourea; ◐——◐: dimethylthiourea; ○——○: diethylthiourea; ●——●: dibutylthiourea. The figures in brackets under each set of points are the coefficients of variation (%; 5 variates).

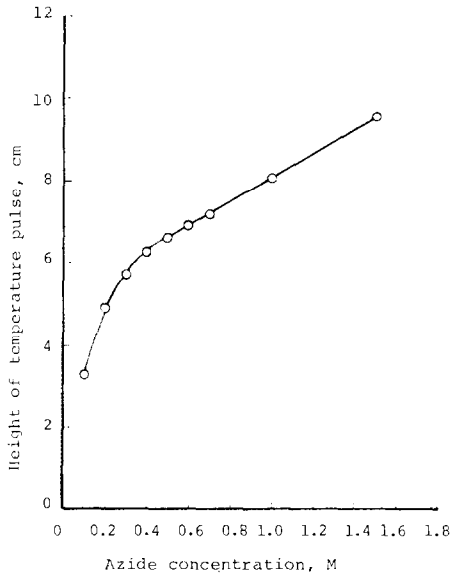


Fig. 3. Effect of azide concentration on the reaction catalysed by diethylthiourea (10 ml of 50 μM diethylthiourea, 500 μl of 0.1M iodine, pH 6.0).

Table 1. Results for thiourea and its *N*-substituted derivatives

	Taken, *nmole*	Found,* *nmole*	Error, %	C.V., %
Thiourea	55	56	+1.8	1.8
	110	112	+1.8	1.7
	220	223	+1.4	1.2
	275	278	+1.1	0.8
	550	558	+1.5	0.7
Dimethylthiourea	48	49	+1.7	1.5
	96	97	+1.1	1.1
	192	193	+0.5	0.8
	240	241	+0.4	0.8
	480	480	±0	0.8
Diethylthiourea	51.5	52.5	+1.7	1.7
	103	105	+1.9	1.3
	206	208	+1.0	0.8
	258	258	±0	0.8
	515	510	+1.0	0.7
Dibutylthiourea	50	49.5	−1.4	1.2
	100	99	−1.0	0.8
	200	199	−1.0	0.8
	251	249	−0.8	0.8
	502	500	−0.4	0.6

* Average of 5 determinations.

3.0, 0.5, 0.5 and 0.3 min at pH 5.0, 6.0, 7.0 and 8.0, respectively. Injection of iodine solution into sodium azide solution containing no thiourea gave exothermic pulses of 0.68, 0.64, 0.51 and 0.34 cm height on the chart for pH 5.0, 6.0, 7.0 and 8.0, respectively. The blank values were subtracted from the total pulse heights. The pH dependence of the reaction decreased in the order TU > BTU > MTU > ETU. These results show that the extent of the reaction is extremely dependent on the pH of the solution and the particular thiourea present. Thus, to obtain reproducible results, careful adjustment of the pH is necessary. The best compromise between sensitivity and reproducibility is given by using a pH of 6.0.

The influence of the concentrations of iodine and sodium azide on the pulse height for ETU are shown in Figs. 2 and 3. The other thioureas gave similar results. The extent of reaction was constant at iodine concentrations above 0.08*M*. With the iodine concentration fixed at 0.1*M*, the influence of the azide concentration was considerable, especially below 0.3*M*. The extent of reaction increased linearly with azide

Table 2. Results for the analysis of the mixtures of the thioureas

Mixture	Taken, *nmole*	Found,* *nmole*	Error, %	C.V., %
Thiourea	510	525	+2.9	3.0
Dimethylthiourea	515	520	+1.0	3.8
Diethylthiourea	497	510	+2.6	3.9
Dibutylthiourea	489	480	−1.8	4.1
Thiourea	51	53	+3.9	4.8
Dimethylthiourea	52	50	−3.8	4.0
Diethylthiourea	50	51	+2.0	5.9
Dibutylthiourea	49	51	+4.1	5.9
Thiourea	520	536	+3.1	3.7
Dimethylthiourea	52	54	+3.8	5.6
Diethylthiourea	50	48	−4.0	4.2
Dibutylthiourea	49	51	+4.1	5.9
Thiourea	102	106	+3.9	4.8
Dimethylthiourea	103	105	+1.9	4.8
Diethylthiourea	102	96	−5.9	5.2
Thiourea	102	106	+3.9	4.7
Diethylthiourea	103	100	−2.9	5.0
Dibutylthiourea	100	97	−3.0	5.2
Dimethylthiourea	103	106	+2.9	4.7
Diethylthiourea	100	100	±0	4.0
Dibutylthiourea	98	96	−2.0	4.2

* Average of 5 determinations.

concentration above 0.4*M*, but this was not advantageous, because of the volatility of hydrozoic acid. At an azide concentration of 1.5*M* (pH 6.0), the height of the pulse for ETU decreased by 6% during the first 20 hr of the life of the reagent. Thus if higher concentrations are used, considerable inconvenience is caused by having to prepare the solution and make calibration curves each day. A sodium azide concentration of 0.6*M* was chosen for convenience and reproducibility, the decrease in the height of the pulse for ETU being less than 2% during the first week of the reagent life if the concentration is below 0.7*M*.

The plots of pulse height against amount of thiourea were linear, the slopes increasing in the order MTU < BTU < ETU < TU.

The results for solutions of known concentrations (Table 1) show that thioureas in the range 50–500 μmole can be determined with relative errors and coefficients of variation of less than 2%.

The results obtained for the analysis of a variety of mixtures are shown in Table 2. Each thiourea in the mixtures was determined with relative error and coefficient of variation of less than 6%.

REFERENCES

1. A. Rosin and M. Bachmilewitz, *Cancer Res.*, 1954, **14,** 494; J. H. Karchmer, *The Analytical Chemistry of Sulfur and Its Compounds*, Part II, p. 668. Wiley, New York, 1972.
2. N. K. Murthy, G. V. Prasad and K. R. Rao, *Talanta*, 1979, **26,** 1049.
3. A. I. Kostromin, I. F. Abdullin and P. K. Agasyan, *Zh. Analit. Khim.*, 1978, 33, 1898.
4. N. Khanna and K. S. Boparai, *Talanta*, 1978, **25,** 591.
5. K. K. Verma, A. Srivastava, J. Ahmed and S. Bose, *ibid.*, 1978, **25,** 469.
6. I. F. Abdullin, A. I. Kostromin and P. K. Agasyan, *Zh. Analit. Khim.*, 1978, **33,** 236.
7. H. L. Kies, *Anal. Chim. Acta*, 1978, **96,** 183.
8. M. R. Smyth and J. G. Osteryoung, Anal. Chem., 1977, **49,** 2310.
9. O. E. Ruvinskii and L. T. Kulaeva, *Zh. Analit. Khim.*, 1977, **32,** 1256.
10. K. Hayashi, Y. Sasaki, S. Tagashira and F. Yanai, *Bunseki Kagaku*, 1977, **26,** 511.
11. B. Mandrou, S. Brun and A. Kinghate, *Ann. Falsif. Expert. Chim.*, 1977, **70,** 223.
12. A. Hashimoto, *Anal. Chem.*, 1979, **51,** 385.
13. B. Mandroll, S. Brun and A. Kinghate, *J. Assoc. Off. Anal. Chem.*, 1977, **60,** 699.
14. A. Cyganski, *Talanta*, 1978, **25,** 52.
15. W. Jedrzejewski and W. Ciesielski, *Chem. Anal. (Warsaw)*, 1978, **23,** 781.
16. J. Richmond, C. Rainey and C. E. Meloan, *Anal. Letters*, 1976, **9,** 105.
17. Z. Kurzawa and M. Zietkiewig, *Chem. Anal. (Warsaw)*, 1974, **19,** 119.
18. Z. Kurzawa and M. Krzymien, *ibid.*, 1968, **13,** 1047.
19. B. Karska and L. Balcerhiewicz, *ibid.*, 1974, **19,** 421.
20. F. Feigl and E. Chargaff, *Z. Anal. Chem.*, 1928. **74,** 376.
21. A. Kjaer and K. Rubinstein, *Acta Chem. Scand.*, 1953, **7,** 528.
22. N. Kiba, M. Nishijima and M. Furusawa, *Talanta*, 1980, **27,** 661.
23. M. B. Devani, C. J. Shishvo and B. K. Dadia, *J. Chromatog.*, 1975, **105,** 186.
24. H. Weisz, W. Meiners and G. Fritz, *Anal. Chim. Acta*, 1979, **107,** 301.

Talanta Vol. 28, pp. 119 to 120
Pergamon Press Ltd 1981. Printed in Great Britain

0039-9140/81/0201-0119$02.00/0

THE USE OF RINSING AND HEATING OF FILTER PAPER IN AN ATTEMPT TO REDUCE PHOSPHORESCENCE BACKGROUND AT ROOM TEMPERATURE*

J. L. WARD, E. LUEYEN-BOWER† and J. D. WINEFORDNER
Department of Chemistry, University of Florida, Gainesville, FL 32611, U.S.A.

(*Received* 7 *April* 1980. *Accepted* 22 *August* 1980)

Summary—Washing or heating the paper is shown generally not to give a significant reduction in the background phosphorescence of filter paper used as a support for room-temperature phosphorimetry.

Advantages of room-temperature phosphorimetry (RTP) over low-temperature phosphorimetry (LTP) are that the procedure is simpler and that cryogenic equipment is not needed, but there is one major limitation, *viz.* that almost all support materials on which significant phosphorescence signals can be induced from analytes also themselves give a broad band of background phosphorescence (at ~400–600 nm) that is often of the same order of intensity as the analyte signals from relatively high analyte concentrations. In the past, support materials for RTP have been chosen rather haphazardly, with relatively little success. The analyte signals obtained with various supports vary over a wide range for a given amount of analyte, but the ratios of analyte signal to blank signal and of signal to noise rarely vary by more than a factor of 2 or 3.[1] The search for better RTP supports cannot be systematized, because the role of the support in the production of the phosphorescence is not known; however, substrates known to be effective can be studied systematically with a view to improving their performance. In the present work, filter paper was the support studied. It is known to induce RTP in a wide variety of samples, is inexpensive and readily available, and is probably the easiest of the useful substrates to work with. Because of the wide variety of papers available (see Table 1 of Reference 1), two were chosen for this work (Schleicher & Schuell 604 and 903 because they gave larger analyte signals and signal-to-noise ratios than the other papers tested).

EXPERIMENTAL

Apparatus

All RTP measurements were made with an Aminco–Bowman spectrophotofluorometer fitted with a 150-W xenon arc lamp, an Aminco–Keirs rotating-can phosphoroscope and a Hamamatsu 1P21 photomultiplier tube. An Aminco ratio photometer supplied high voltage to the photomultiplier in addition to serving as a d.c. amplifier. All line voltages were regulated with a Sorenson 1001 a.c. regulator.

The standard Aminco phosphorescence sample compartment was used with a laboratory-constructed RTP attachment similar to the one described by Paynter *et al.*[2] Six aluminium sample holders, or "fingers", were used to hold ¼-in. diameter filter-paper discs obtained with a standard office paper punch. These discs were placed under the cover plates of the fingers and held in place by two screws.

Once the paper was in the finger, sample and/or heavy-atom solutions were spotted onto it with a "Micropetter" (Scientific Manufacturing Industries), 3 μl being used for the 604 paper and 5 μl for the thicker 903. After spotting, all samples were dried for 10 min under an infrared heat lamp. While still under the heat lamp, the fingers were slipped onto the rod of the RTP attachment and tightened into place by means of a set-screw. The assembly was then immediately transferred to the sample compartment, where it was allowed to cool for 10 min in a flow of dry nitrogen gas. During the cooling, the signals increased over a period of ~9 min, then remained constant for 2–3 min (during which the measurements were made) and then decreased as moisture was collected by the sample support.

Procedures

Washing. The simplest cause of the background phosphorescence might be some impurity adsorbed during manufacture and common to all papers. To examine that possibility, 5½-in. filter-paper discs (Eaton–Dikeman 613) were rinsed with 10 ml of 1*M* sodium hydroxide, 1*M* nitric acid, ethanol, methanol, demineralized water or acetone.[3] Essentially no change was found except that acetone or demineralized water gave about 30–50% reduction in background. Further rinsing experiments were, therefore, performed in two ways. In the first, ¼-in. discs of the filter paper were punched out and soaked for approximately 18 hr in 20 ml of the solvent, then air-dried for examination. In the second, which resembled paper chromatography, 1½ × 3 in. strips of the paper were suspended with their ends dipping into a ½-in. deep layer of solvent in a 250-ml beaker for approximately 18 hr. The paper strips were then air-dried and ¼-in. discs were punched from just above the solvent line.

Several discs were produced for each combination of solvent and rinsing method. Two discs of each type of paper were placed in the sample fingers. One of each was spotted with 1*M* sodium hydroxide/sodium iodide, and the backgrounds of all the discs were measured by the RTP procedure described. Next, each of the discs was spotted with 100-ppm Privine hydrochloride solution and dried

* Research carried out under NIH Grant 5-R01-GM-11372-17

† Present address: Celanese, P.O. Box 1000, Summit, N.J. 07901, U.S.A.

Table 1. Results of soaking and eluting paper substrates with solvents*

Solvent	S & S 604 Plain paper Blank	S & S 604 Plain paper Privine HCl	S & S 604 Treated paper Blank	S & S 604 Treated paper Privine HCl	S & S 903 Plain paper Blank	S & S 903 Plain paper Privine HCl	S & S 903 Treated paper Blank	S & S 903 Treated paper Privine HCl
Acetone†	2	1	2	1	2	1	2	1
Benzene§	1	1	1	1	1	1	1	1
0.1*M* HCl	2	2	2	2	2	2	2	2
0.1*M* H_2SO_4‡	0	0	0	0	0	0	0	0

* 0 = no signal observed; 1 = no change in signal; 2 = signal decreased by a factor of 2; 3 = signal decreased by a factor of 3.

† Also water.

§ Also chloroform, ethanol, hexane, 0.1*M* nitric acid, methanol or methylene chloride.

‡ Also 1*M* sodium hydroxide.

Table 2. Results of heating S & S 604 and S & S 903 at 120°C and 250°C*

Time, *hr*	Plain paper Blank†	Plain paper Privine HCl†	Treated paper Blank	Treated paper Privine HCl
0	1 (1)	1 (3)	1	1
½	1 (1.3)	1 (1.3)	2	2
1	2 (3)	2 (3)	10	10
1½	3 (4)	3 (4)	0	0
2	3 (4)	3 (4)	0	0
2½	3 (0)	3 (0)	0	0

* See table 1 for meaning of symbols.

† Results at 250°C are shown in parentheses; data were taken at 15-min intervals but no trends different from those in the table were evident.

under the infrared lamp, then the phosphorescence was measured. The results are given in Table 1. Because rinsing with water and acetone gave an improvement, several discs were rinsed first with acetone and then with water by the soaking method, but there was no improvement over use of the solvents individually.

Heating. Because washing the filter paper failed to reduce the background significantly, it was thought that the background might be due to a strongly adsorbed impurity. Therefore heating (baking) the paper was considered as a possible means of background reduction.

Discs were punched out, as before, and half of them were treated with 1*M* sodium hydroxide/sodium iodide. All of the discs were placed in an oven at 120°, and test discs were removed at ½-hr intervals. Upon removal from the oven, the discs were placed in the RTP fingers and allowed to cool in the instrument under a nitrogen flush for 10 min, after which, the background phosphorescence measurements were made. Once the background was measured, 100-ppm Privine hydrochloride solution was spotted onto the discs. After 10 min of infrared drying and 10 min of cooling under dry nitrogen, the discs again had their phosphorescence signals measured. The results are shown in Table 2.

No improvement was found in the performance of either the treated or untreated paper, and after ½ hr the treated paper turned visibly brown. After 1½ hr, it was black and had a pasty texture. After 1½ hr, the untreated paper had yellowed and was quite brittle. Repetition at 250° with untreated paper only, with sampling at 15-min intervals, gave similar results (see Table 2). After heating for 2 hr, the discs had begun to char. The phosphorescence signals were halved for papers heated for 45 min, and fell to zero for papers heated for 2¼ hr.

Finally, several discs were successively soaked in each of the solvents (except sulphuric acid and sodium hydroxide solution) shown in Table 1 and were then heated at 120° for ½ hr. Blank and Privine hydrochloride phosphorescence signals were measured for these discs and for a set of untreated discs. An improvement in signal-to-noise ratio by a factor of 2 was given by the combined treatment, which was no better than that obtained by simply rinsing 5½-in. discs with 10 ml of acetone or water. None of the treatments gave the 1–2 orders of magnitude improvement really needed to make RTP more viable as an analytical method.

In a further attempt to find the cause of the background phosphorescence, a handsheet of the raw cellulose material used in making S & S 903 was obtained from Schleicher & Schuell. It exhibited the same background as the 903 paper, and washing and heating it gave the same results as treatment of the finished paper. Purified α-cellulose did not give background phosphorescence signals of the level obtained with the handsheet, nor did it induce RTP from Privine hydrochloride.

DISCUSSION

The cause of the background phosphorescence from paper is still not known and is not easily eliminated. Before progress can be made, the cause of the background must be identified and new papers developed which are free from the species responsible for the background. This is probably most easily done by the paper companies or those with facilities for making their own paper.

REFERENCES

1. E. LueYen-Bower, G. L. Walden, J. L. Ward and J. D. Winefordner, *Talanta*, 1980, **27**, 380.
2. R. A. Paynter, S. L. Wellons and J. D. Winefordner, *Anal. Chem.*, 1974, **46**, 736.
3. E. LueYen-Bower, *Thesis*, University of Florida, 1978.

Talanta Vol. 28, pp. 121 to 122
©Pergamon Press Ltd 1981. Printed in Great Britain
0039-9140/81/0201-0121$02.00/0

DECOMPOSITION OF ORES BY MANGANESE DIOXIDE

ANALYSIS OF COPPER ORES AND CONCENTRATES

S. K. MANDAL, S. B. RAO and B. R. SANT

Regional Research Laboratory, Bhubaneswar 751013, India

(*Received* 11 *June* 1980. *Accepted* 22 *August* 1980)

Summary—Manganese dioxide in presence of sulphuric acid has been used for the decomposition of copper ores and concentrates for determination of copper and iron. The results obtained compare favourably with those obtained by standard methods.

The copper sulphide ores (chalcopyrite, chalcocite, *etc.*) usually contain a considerable amount of iron (mostly as pyrite). In the analysis of such ores, the samples are brought into solution under strong oxidizing conditions, *e.g.*, with perchloric acid[1] or *aqua regia*.[2] Recently[3] we have reported that a mixture of manganese dioxide and sulphuric acid can be used for the decomposition and analysis of chromite. Preliminary experiments showed that under similar conditions sulphide ores of copper could also be decomposed completely with the help of manganese dioxide. The present communication describes the method for the determination of copper and iron in copper ores and concentrates.

EXPERIMENTAL

Reagent

The manganese dioxide is prepared by the method of Selwood *et al.*[4] Add a saturated solution of potassium permanganate slowly to a saturated solution of manganous sulphate in sulphuric acid (1 + 4) at about 60° until no more oxide precipitates. Decant the clear solution and wash the precipitate a few times with water, by decantation. Filter off on a Buchner funnel (Whatman No. 541 filter paper) and wash it free from permanganate and sulphate. Dry at 110–120°. The purity of the oxide is about 99.98%. A commercial product can be used if its iron and copper contents are sufficiently low.

Procedures

Weigh accurately 1 g of the finely ground sample of copper ore or concentrate, previously dried at about 110°, into a 500-ml beaker. Add 3 g of manganese dioxide for copper concentrate or 0.5 g for copper ore and mix thoroughly with a glass rod. Add 50 ml of sulphuric acid (1 + 1) and stir well. Heat the beaker on a hot-plate until white fumes appear. Cool, wash down the sides of the beaker with water and heat the mixture once again until fuming. Add 1–2 g of sodium chloride and heat the solution until all the manganese oxides have dissolved. Heat the solution for some time to expel chlorine. Dilute the solution to about 300 ml and filter through a Whatman No. 40 paper into a 500-ml standard flask. Wash the filter paper thoroughly with water. Make up to the mark and use the solution for the determination of copper and iron.

Copper in concentrate. To a measured fraction of the solution add ammonia solution (1 + 1) dropwise till the pH is 7.5–8. Heat the solution for 1–2 min and filter off at once (Whatman No. 541 paper). Wash the precipitate thoroughly with hot water, dissolve it in hot hydrochloric acid (1 + 1) and reprecipitate with ammonia. Collect the precipitate on a Whatman No. 541 paper and wash it with hot water. Combine the filtrates and washings for the determination of copper. Keep the precipitate for the determination of iron.

To the copper solution add 2 g of ammonium bifluoride, shake well and add 3 g of potassium iodide. Titrate immediately with sodium thiosulphate solution, adding towards the end 3 ml of 1% starch solution and 1–2 g of ammonium thiocyanate.[5]

If the determination is to be completed by electrolysis instead of titrimetry, dissolve the iron precipitate by the addition of sulphuric acid instead of hydrochloric, adjust the acidity of the combined filtrates to that conventionally used for the electrolysis and determine copper by the latter technique.

Copper in ore. To a fraction of the ore solution containing 20–100 μg of copper add 5 ml of 40% ammonium citrate solution, 10 ml of 10% EDTA solution and 2 drops of Cresol Red indicator (0.1% ethanol solution). Add ammonia until the appearance of a red colour (pH about 8.5), dilute to about 70 ml and add 5 ml of freshly prepared 0.1% sodium diethyldithiocarbamate solution. Add 10 ml of chloroform or carbon tetrachloride and shake vigorously for 2 min. Transfer the organic phase quickly

Table 1. Determination of copper and iron in copper ores and concentrates

	Copper, %		Iron, %	
Sample	Present	Found	Present	Found
Ore	3.4	3.3	12.3	12.2
	3.3	3.2	12.3	12.1
	3.2	3.2	12.3	12.4
	0.9	0.9	24.1	24.3
Concentrate	28.1	28.2	28.9	29.0
	23.2	23.1	31.3	31.1
	22.3	22.2	29.9	30.1

Table 2. Effect of manganese(II) on the determination of copper

Spectrophotometric method			Titrimetric method		
Manganese added, *mg*	Copper, *μg*		Manganese added, *mg*	Cooper, *mg*	
	Present	Found		Present	Found
3.1	20.1	20.2	31.0	10.1	9.9
6.2	30.1	30.1	46.5	11.3	11.4
9.3	40.1	39.9	66.0	12.6	12.6
12.4	50.2	50.0	82.5	13.9	13.7
15.5	60.2	60.3	99.0	15.1	15.0

through a dry filter paper into a 25-ml standard flask. Repeat the extraction with 5 ml of the solvent. Make up to the mark with solvent and measure the absorbance against a reagent blank, at 436 nm.[6]

Iron in ores and concentrates. Separate the iron as hydroxide as described above. Dissolve the precipitate in the minimum volume of hot hydrochloric acid (1 + 1). Estimate iron by dichromate titration after the usual stannous chloride–mercuric chloride treatment.[5]

RESULTS AND DISCUSSION

Typical results for the determination of copper and iron in copper ores and concentrates are shown in Table 1. Synthetic solutions containing copper, iron, aluminium and manganese were used for studying the possible interferences in the copper determination. The results in Table 2 show that manganese does not interfere in the spectrophotometric determination of copper with diethyldithiocarbamate. In the titrimetric method it is known that while iron or manganese alone does not interfere, the values for copper are generally high when both are present.[7] The interference due to the combined presence of iron and manganese was overcome by separating iron(III) selectively (along with aluminium) as hydroxide before the copper titration. The results are shown in Table 2.

In the present method manganese dioxide acts as the oxidizing agent and facilitates the quantitative decomposition of copper ore or concentrate. The manganese dioxide reacts with the sulphuric acid to form manganese(IV) sulphate, which is a strong oxidizing agent.[8]

The standard values reported for Cu and Fe were obtained by the conventional method using decomposition with *aqua regia*. The Cu and Fe obtained in the solution were determined titrimetrically or spectrophotometrically. The results in Table 1 show that the values obtained by the present method are comparable with those obtained by the standard procedure.

Further work on the use of manganese dioxide in the decomposition and analysis of other ores is in progress.

Acknowledgements—Grateful thanks are due to Professor P. K. Jena, Director, Regional Research Laboratory, Bhubaneswar, India for his encouragement to carry out the work and permission to publish this paper, and also to the authorities of Hindustan Copper Limited for the samples. The authors also thank the referee for helpful comments.

REFERENCES

1. C. A. Goetz, H. Diehl and C. C. Hach, *Anal. Chem.*, 1949, **21**, 1520.
2. J. P. Mehlig and D. Durst, *Chemist-Analyst*, 1948, **37**, 52.
3. S. K. Mandal, S. B. Rao and B. R. Sant, *Talanta*, 1979, **26**, 135.
4. P. W. Selwood, R. P. Eischens, M. Ellis and K. Wethington, *J. Am. Chem. Soc.*, 1949, **71**, 3039.
5. G. Charlot and D. Bezier, *Quantitative Inorganic Analysis*, Methuen, London, 1957.
6. G. Charlot, *Colorimetric Determination of Elements*, p. 240. Elsevier, Amsterdam, 1964.
7. I. M. Kolthoff and R. Belcher, *Volumetric Analysis*, Vol. III, p. 349. Interscience, New York, 1957.
8. S. K. Mandal and B. R. Sant, *Talanta*, 1976, **23**, 485.

Talanta Vol. 28, pp. 123 to 125
©Pergamon Press Ltd 1981. Printed in Great Britain
0039-9140/81/0201-0123$02.00/0

PRECONCENTRATION OF COBALT(II) IN NATURAL WATERS WITH 1-NITROSO-2-NAPHTHOL SUPPORTED ON SILICA GEL

KIKUO TERADA* and KAZUMITSU NAKAMURA

Department of Chemistry, Faculty of Science, Kanazawa University, Kanazawa 920, Japan

(*Received* 30 *June* 1980. *Accepted* 3 *September* 1980)

Summary—A solid chelating material, 1-nitroso-2-naphthol supported on silica gel, provides a rapid and highly selective mean of preconcentrating cobalt(II) from natural water samples. Cobalt(II) is quantitatively retained on the column of the chelating silica gel at pH >3.0 and flow-rate 1 l./hr. The cobalt is eluted from the column bed with glacial acetic acid or a mixture of acetone and hydrochloric acid (9:1 v/v) and measured by atomic-absorption spectrophotometry. A concentration factor of 100 can be achieved by passing 2.5 litres of sea-water through the column.

The cobalt concentration in open-sea water has been reported to be in the range 0.01–0.046 μg/l.[1] On the other hand, its concentration in stream waters has been found to be 0.037–0.35 μg/l.[1] The extremely low values (≤0.03 μg/l.) necessitate preconcentration to bring the element to a determinable concentration level.

We have already reported the rapid preconcentration of copper, cadmium, lead, and zinc,[2] and mercury[3] with 2-mercaptobenzothiazole supported on silica gel (MBT–SG), and silver, gold and palladium with *p*-dimethylaminobenzilidenerhodanine supported on silica gel (DMABR–SG).[4]

This paper describes a simple and rapid method for preconcentration of cobalt(II) from natural waters by using 1-nitroso-2-napththol supported on silica gel. A similar study using polymer beads soaked with a solution of 1-nitroso-2-naphthol in chlorobenzene has been reported by Ueno *et al.*[5] However, their method required presaturation of the aqueous solution with chlorobenzene before column operation and was somewhat time-consuming (*ca.* 50 hr for 2 litres of the sample).

EXPERIMENTAL

Reagents and apparatus

1-Nitroso-2-naphthol (analytical reagent grade) was recrystallized twice from ligroin. All other reagents used were of analytical reagent grade. Silica gel, chromatographic grade (WAKOGEL C-100), was sieved and the 60–80 mesh fraction was digested in hydrochloric acid (1 + 1) and nitric acid (1 + 2) successively, washed with demineralized water, and dried at 110° for a day. ^{60}Co, as the chloride, was used as radioactive tracer.

A well-type γ-ray scintillation counter, [Kobe Kogyo Co., Model STL; 44.5 × 50.8 mm NaI(Tl) crystal] was used for γ-counting. The column was made in a glass tube (10 mm bore, 140 mm long) with a coarse sintered-glass disc and a stopcock at the bottom.

Procedures

Preparation of the loaded silica gel. About 80 g of the cleaned silica gel was soaked in 150 ml of acetone containing 2.0 g of 1-nitroso-2-naphthol. After standing overnight, the supernatant liquid was removed and the acetone was evaporated at room temperature under reduced pressure. The material was washed with demineralized water until the washings were clear. Finally the greenish–yellow product was dried at 60° under reduced pressure and stored in a dark bottle.

Procedure for batch experiments. The sample solution (10 ml) containing a known amount of cobalt(II) and ^{60}Co was adjusted to the appropriate pH and shaken mechanically with 0.5 g of the chelating silica gel in a 50-ml glass-stoppered centrifuge tube. The supernatant liquid was filtered through a dry filter paper, and an aliquot was submitted to γ-counting.

Procedure for column experiments. The glass column was filled with 3 g of the chelating silica gel to give a bed height of 5 cm. A given volume of aqueous sample (up to 2 litres) containing cobalt(II) spiked with ^{60}Co was adjusted to a suitable pH, and then percolated through the column at a flow-rate of 0.5–16 ml/min under mild suction. The spike contained about 1 mg of inactive cobalt. The column was then washed with 20 ml of demineralized water, the silica gel was transferred to a test-tube and the γ-emission was measured and used to calculate the degree of retention of cobalt.

RESULTS AND DISCUSSION

Characteristics of the chelating silica gel

The amount of chelating reagent on the silica gel was determined spectrophotometrically after its elution from the column bed with acetone, and found to be 20 mg per g of the material. The chelating capacity for cobalt(II) was measured by the column breakthrough method at pH 4.0. A value of 0.03 mmole/g was obtained for both the aqueous solution and the sea-water sample. This was slightly lower than the value calculated by estimating the amount of 1:3 cobalt chelate formed.

* To whom correspondence and requests for reprints should be sent.

Effect of pH on retention of cobalt(II)

The recovery of cobalt(II) from an aqueous solution and from sea-water at various pH values is illustrated in Fig. 1. Cobalt can be quantitatively retained at pH 2.0 from aqueous solution and at pH 3.0 from sea-water. Figure 1 also shows that silica gel alone will retain only 5% of the cobalt present in aqueous solution or sea-water at pH 7. The batch method was used.

Retention of cobalt on the column

In the column operation, it was expected that the retention would be affected by the flow-rate of the water sample. The results in Table 1 show that quantitative sorption of cobalt(II) was attained if the flow-rate was less than 1 l./hr for aqueous solution and sea-water adjusted to pH about 3.5. Although the reagent was tightly bound to the silica gel, a small amount (about 7%) seemed to be desorbed from the column bed during the passage of 2 litres of the water sample. However, since the cobalt chelate, once formed, was very strongly retained on the column and never appeared in the effluent, the dissolution of the reagent had no serious effect on retention of cobalt(II) under the conditions described.

Elution of cobalt

Several reagents were investigated for the elution of cobalt. None of the mineral acids could elute cobalt completely, but as shown in Fig. 2, when 20 ml of glacial acetic acid or 15 ml of a mixed solution of acetone and hydrochloric acid (9:1 v/v) were passed through the column, complete elution of up to 100 μg of cobalt was achieved. The acetic acid eluate is particularly suitable for atomic-absorption spectrophotometry, giving about threefold enhancement of the absorbance observed with aqueous solution. The mixed solvent is also a suitable medium for atomic-absorption spectrophotometry, but the flame is less stable than with acetic acid. In both cases, the reagent

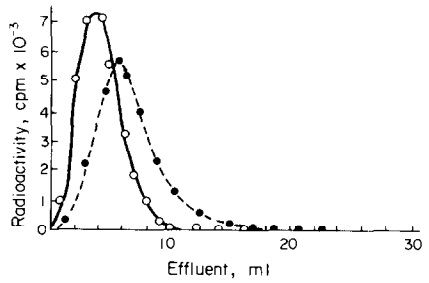


Fig. 2. Elution of cobalt retained on 1-nitroso-2-naphthol-SG; —○— acetone + HCl (9:1 v/v); --●-- acetic acid.

Table 1. Recovery of cobalt(II) by the column method

	Co(II), *ng/ml*	Flow-rate, *ml/min*	Recovery, %
Aqueous solution	0.1	15	98.8
	1*	15	99.0
	20*	16	100.0
	100	16	99.3
Sea-water	0.1*	15	98.0
	1*	15	98.3
	20*	16	99.0
	100	16	98.2

* ^{60}Co was added; 2 litres of sample water were used.

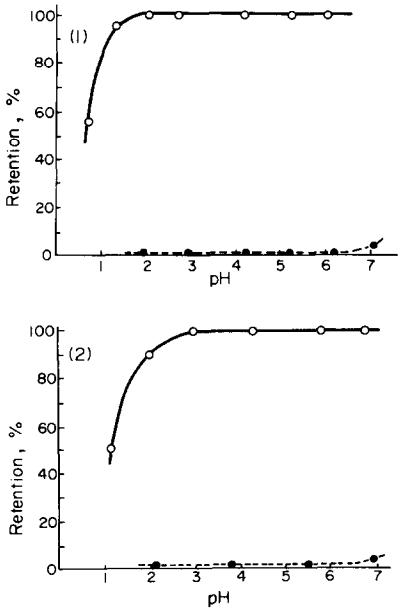


Fig. 1. Effect of pH on retention of cobalt(II) from (1) aqueous solution and (2) sea-water; ○— 1-nitroso-2-naphthol-SG; --●-- untreated silica gel.

Table 2. Effect of metal and other ions on the recovery of 0.1 μg of cobalt(II)*

Ion	Concentration	Recovery of Co, %
Fe^{3+}	10 ng/ml	99.1
	100	98.8
	200	99.5
Cu^{2+}	10 ng/ml	99.7
	100	98.7
	200	99.2
Ni^{2+}	10 ng/ml	99.0
	100	98.2
	200	99.1
UO_2^{2+}	10 ng/ml	99.4
	100	100.0
	200	98.7
EDTA	$10^{-4}M$	99.0
Tartrate	$10^{-4}M$	99.6
Citrate	$10^{-4}M$	100.0
CN^-	$10^{-4}M$	98.5
NH_4^+	$10^{-4}M$	99.8

* 500 ml of sea-water.

Table 3. Recovery of cobalt from water samples with various concentrations of cobalt

	River water (Sai-river)			Sea-water (Tsukumo Bay)		
Co added, *μg*	50	50	50	50	50	50
Sample passed, *ml*	250	1000	2500	250	1000	2500
Co recovered, *μg**	49	48.5	48.3	48.8	48.6	47.8
Recovery, %	98	97	97	98	97	96
Concentration factor	10	40	100	10	40	100

* The values were obtained by atomic-absorption spectrophotometry.

desorbed from the column has no effect on the atomic-absorption measurement.

Effect of various substances on the retention of cobalt

Several metal species that might react with 1-nitroso-2-naphthol, [*viz.* iron(III), copper(II), nickel and uranium(VI)] were examined for their effect on the retention of cobalt(II). The results obtained by the column method are shown in Table 2. At the concentration levels shown, none of the metals interfered with the retention of cobalt at trace levels.

The effect of EDTA, tartrate, citrate, cyanide and ammonium ions was also examined. As shown in Table 2, these species also had no effect on the retention of cobalt. Therefore, this method is considered as highly selective for cobalt in water. It has been assumed that part of the cobalt present in sea-water may exist in the form of cyanocobalamine (vitamin B_{12}) at the level of 0.1–1.0 ng/l.[6] However, this is immaterial in the analysis because the concentration of cobalt in this form should be less than 0.1% of the total cobalt.

Table 3 shows the analytical results for natural stream and sea-waters spiked with a low level of cobalt(II). Sample waters were adjusted to pH 3.5 and passed through the column (5 g of the chelating silica gel) at a flow-rate of 1 l./hr. The water samples were filtered through a 0.45-μm Millipore filter immediately after collection and left to equilibrate with the carrier or tracer spike for 50 days in a precleaned polyethylene container. The loss of ^{60}Co by adsorption on the container wall was about 2% of the initial activity.

Acknowledgements—The authors are grateful to Professor Toshiyasu Kiba for his fruitful discussions. They also wish to thank the Ministry of Education for a Grant-in-Aid.

REFERENCES

1. K. H. Wedepohl, C. W. Correns, D. M. Shaw, K. K. Turekian and J. Zemann (eds.), *Handbook of Geochemistry*, Vol. II/3, Springer-Verlag, New York, 1978.
2. K. Terada, A. Inoue, J. Inamura and T. Kiba, *Bull. Chem. Soc. Japan*, 1977, **50**, 1605.
3. K. Terada, K. Morimoto and T. Kiba, *ibid.*, 1980, **53**, 1605.
4. *Idem*, *Anal. Chim. Acta*, 1980, **116**, 127.
5. M. Kubo, T. Yano, H. Kobayashi and K. Ueno, *Talanta*, 1977, **24**, 519.
6. J. P. Riley, and G. Skirrow (eds.), *Chemical Oceanography*, Vol. 2, Academic Press, New York, 1965.

Talanta Vol. 28, pp. 127 to 130
Pergamon Press Ltd 1981. Printed in Great Britain

0039-9140/81/0201-0127$02.00/0

ANALYTICAL DATA

SPECTROPHOTOMETRIC DETERMINATION OF THE PROTONATION CONSTANTS OF *o*-CRESOLPHTHALEXONE AND THE FORMATION CONSTANTS OF ITS ALKALINE-EARTH-METAL COMPLEXES

F. GAIZER, M. MÁTÉ and J. LÁZÁR*

Department of Chemistry, College of Food Technology, POB 79, Hódmezővásárhely, Hungary

(*Received* 4 *June* 1980. *Accepted* 24 *August* 1980)

Summary—The first three protonation constants of *o*-cresolphthalexone and the two constants of phenolphthalein and *o*-cresolphthalein, and also the formation constants of the Ca^{2+}, Mg^{2+}, Sr^{2+} and Ba^{2+} complexes of *o*-cresolphthalexone (with the compositions MY, MHY and M_2Y) have been evaluated from spectrophotometric data.

o-Cresolphthalexone (*o*-cresolphthalein complexone) was synthesized and proposed as an analytical reagent by Anderegg *et al.*[1,2] Above about pH 8 the colourless compound becomes pink, the colour deepening with increasing pH. Since it forms coloured complexes with alkaline-earth metals and other metal ions, it can be used as a metal-ion reagent. It is most widely used for the spectrophotometric determination of calcium ions,[3–10] since in alkaline medium the concentration-dependence of the colour change induced by calcium ions is linear for 2–10 μg of Ca^{2+} in 10 ml. The only quantitative study of the colour change on interaction with alkaline-earth ions is, to the best of our knowledge, that of Anderegg *et al.*,[1] which was based on potentiometric measurements. The aim of our experiments was to determine spectrophotometrically the formation constants and molar absorptivities of the species formed over a wide range of metal-ion concentrations, and to study the factors influencing the accuracy of the calcium determination. It was also necessary to study the protonation of *o*-cresolphthalexone, phenolphthalein and *o*-cresolphthalein, and determine the individual protonation constants.

In this work the complex equilibria and formation constants are defined as follows (charges are omitted for simplicity).

$$rH^+ + qM + Y \rightleftharpoons H_rM_qY$$

$$\beta = \frac{[H_rM_qY]}{[H^+]^r[M]^q[Y]}.$$

Species not taking part in the reaction *e.g.*, M in the protonation of Y, are omitted.[11]

* Department of Pharmaceutical Chemistry, The Medical University, Szeged, Hungary.

EXPERIMENTAL

Reagents

o-Cresolphthalexone was prepared according to the original description.[1] All other reagents were of analytical grade.

Instruments

A Radiometer pHM-4 pH-meter, along with an RGM 200B glass electrode and a calomel reference electrode, was used to measure pH values. A Unicam SP500 spectrophotometer (1-cm cells) was used for spectrophotometric measurements. All measurements were made at 25 ± 1°.

Procedure

Sodium hydroxide (0.14*M*) and glycine (0.14*M*) solutions were used to adjust the pH of solutions. The concentration of the buffer system in the reaction mixtures after addition of the appropriate dye solution and water was 0.1*M*.

For the preparation of solutions containing *o*-cresolphthalexone, a stock solution of 0.1*M* dye in dimethyl sulphoxide was prepared, and 5.0 ml of this solution were diluted to 1 litre with 0.01*M* sodium acetate. This solution was stable and was used to prepare the reaction mixtures. The equilibria in the reaction mixtures were not influenced by three times this amount of dimethyl sulphoxide.

Calculations

For the calculation of formation constants and molar absorptivities of the individual species from the experimental data pH, T_M, T_Y and A (absorbance), the SPEF3 computer program[11] was used. Values of the unknown parameters were optimized in the program by minimizing the unweighted sum of the squares of the residuals of absorbances. In the calculations, the pH of the reaction mixture was treated as a known quantity.

RESULTS

Absorbances of solutions of *o*-cresolphthalexone at pH values of 10–12.5, and of phenolphthalein and

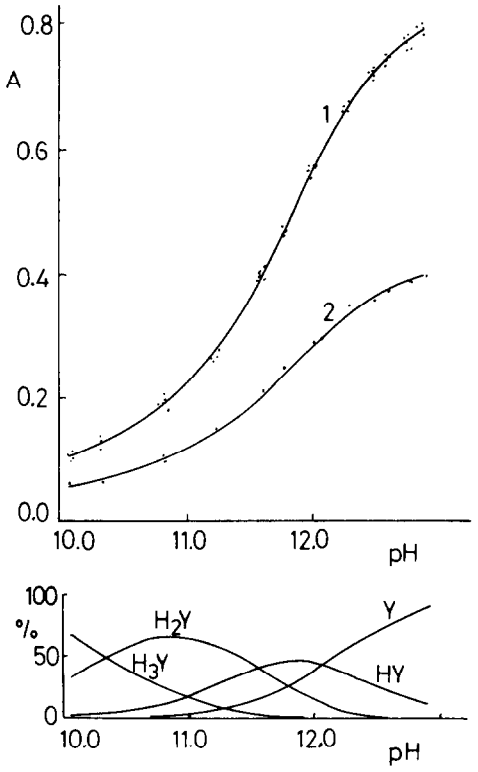


Fig. 1. The absorptivity of solutions of 1: $15 \times 10^{-6}M$ and 2: $7.9 \times 10^{-6}M$ *o*-cresolphthalexone at 596 nm and the distribution of its protonated species as a function of pH. The distribution curves are calculated with the parameters given in Table 1.

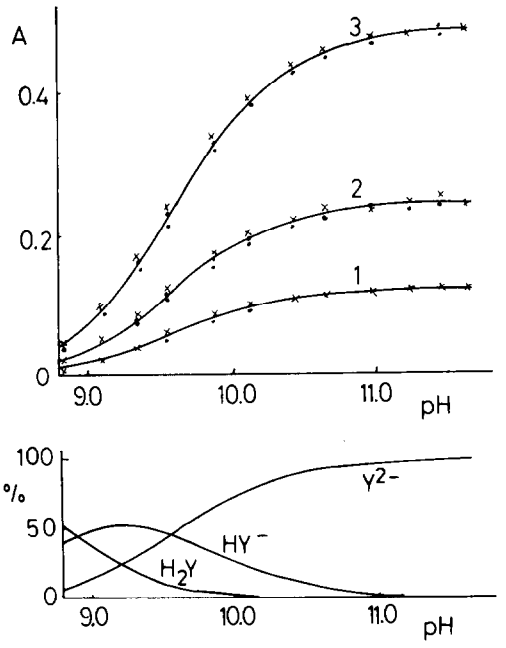


Fig. 2. The absorbance of 1: $3.9 \times 10^{-6}M$, 2: $7.5 \times 10^{-6}M$ and 3: $15 \times 10^{-6}M$ phenolphthalein at 576 nm and the distribution of the protonated species as a function of pH. The distribution curves are calculated with the parameters given in Table 1.

Table 1. Protonation constants and molar absorptivities (ϵ, $l.mole^{-1}.cm^{-1}$) of *o*-cresolphthalexone, phenolphthalein and *o*-cresolphthalein (the probable errors in the parameters are given in brackets)

Group being protonated	*o*-Cresolphthalexone						Phenolphthalein		*o*-Cresolphthalein	
	Anderegg *et al.*			Present work						
	log β	log k	ϵ	log β	log k	ϵ	log k	ϵ	log k	ϵ
			5.54×10^{4}*			5.39×10^{4}*		3.11×10^{4}*		2.75×10^{4}*
			(2.0×10^{3})			(2.0×10^{3})		(1.0×10^{3})		(1.0×10^{3})
			2.64×10^{4}	12.04	12.04	2.88×10^{4}				
$\equiv N$	12.01	12.01	(1.1×10^{3})	(0.07)	(0.07)	(7.5×10^{2})				
			6.68×10^{3}	23.59	11.55	1.15×10^{4}				
$\equiv N$	23.36	11.35	(7.8×10^{2})	(0.12)	(0.05)	(6.0×10^{2})				
				33.97	10.38	4.04×10^{3}	9.54	5.6×10^{2}	9.29	0
ArO^-	31.19	7.83	0	(0.17)	(0.05)	(7.5×10^{2})	(0.04)	(5×10^{2})	(0.03)	(5×10^{2})
							8.90		9.04	
							(0.14)		(0.08)	
ArO^-	38.16	6.97								
$-COO^-$	41.06	2.90								
$-COO^-$	43.28	2.22								
$\delta(A)$†		0.017			0.008			0.0055		0.0036

* Molar absorptivities of deprotonated species. † Estimated absorbance error.

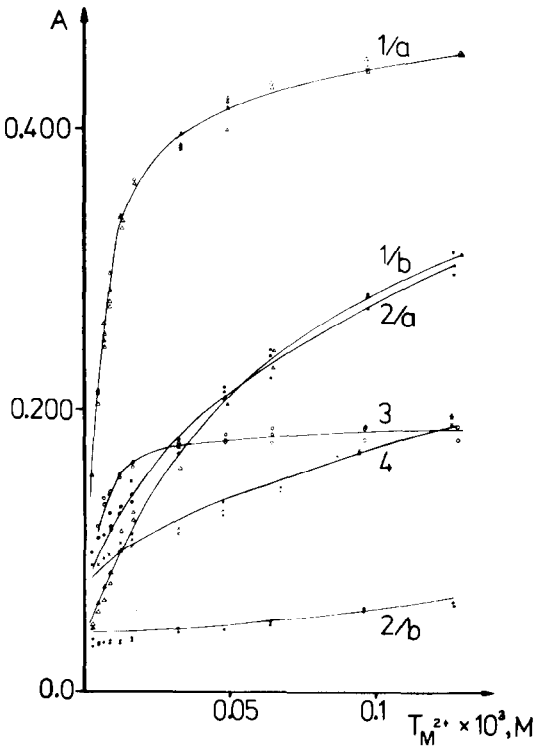


Fig. 3. The absorbance of a solution of $7.9 \times 10^{-6}M$ *o*-cresolphthalexone 1: Ca^{2+}, 2: Sr^{2+}, 3: Mg^{2+} and 4: Ba^{2+} at pH 10.53 and 9.6 (1/b and 2/b). For solutions 1, 2 and 4, λ = 596 nm, and for 3, λ = 594 nm. Curves are calculated with the parameters given in Table 2.

o-cresolphthalein at pH 9–11.6 were measured (Figs 1 and 2). At higher pH values, measured absorbances were unreliable because of decomposition of the dyes. At lower pH values, the dyes are colourless.

The protonation constants given by Anderegg *et al.*[1] indicate that, in the pH range we employed, only the first and second protonations of *o*-cresolphthalexone occur, *i.e.*, protonation of the two nitrogen atoms. Calculation of the optimum values of the molar absorptivities for these complexes by SPEF3 gave very large standard deviations. However, when it was assumed that one of the phenolic oxygen atoms was also protonated under our conditions, optimization of the three protonation constants and four molar absorptivities resulted in standard deviations corresponding to the accuracy of the measurements. The data in Table 1 and the distribution curves in Fig. 1 show that the extent of formation of the species H_3Y is definitely significant. To substantiate the reliability of our protonation constant for the phenolic oxygen, we determined the protonation constants of phenolphthalein and cresolphthalein. Evaluation of the fairly similar experimental data (Fig. 2) resulted in first protonation constants close to the corresponding constant of *o*-cresolphthalexone.

The results of our experiments on the alkaline—earth metal ion—*o*-cresolphthalexone systems are shown in Fig. 3, and the parameters calculated are listed in Table 2. It can be seen that the absorptivity sequence is $Ca^{2+} > Sr^{2+} > Mg^{2+} \sim Ba^{2+}$. In each system, the data can be described well by assuming that the species MY, MHY and M_2Y are present. The curves in Fig. 4 show that all three species are stable, but not to the same extent. With Ca^{2+} and Mg^{2+}, the protonated species predominate, whereas with Sr^{2+} and Ba^{2+}, the non-protonated ones are more abundant. In all four systems, an increase in metal ion concentration favours the formation of the M_2Y species, but not to the same extent. The most stable species are Ca_2Y and Sr_2Y.

DISCUSSION

The program SPEF3,[11] which was written for calculation of formation constants and molar absorptivities from spectrophotometric measurements, proved to be a convenient and reliable method for elucida-

Table 2. Overall formation constants and molar absorptivities ($l.mole^{-1}.cm^{-1}$) of *o*-cresolphthalexone–alkaline earth metal complexes (the probable errors are given in brackets)

Metal ion	Authors	Composition of species, value of parameters H_3MY log β	H_2MY log β	HMY log β	HMY ϵ	MY log β	MY ϵ	M_2Y log β	M_2Y ϵ	δ(A)
Ca^{2+}	Anderegg *et al.*	33.5	26.6	18.9		7.8		12.8	6.7×10^4	
	Present work			19.11 (0.05)	5.04×10^4 (8.0×10^2)	7.91 (0.30)	5.00×10^4 (4.7×10^3)	12.76 (0.08)	6.55×10^4 (1.4×10^3)	0.007
Ba^{2+}	Anderegg *et al.*	32.5	25.6	16.81		6.2		11.4	2.6×10^4	
	Present work			18.17 (0.07)	6.64×10^3 (1.8×10^3)	8.0 (0.08)	1.65×10^4 (8.0×10^2)	11.65 (0.05)	5.45×10^4 (3.2×10^3)	0.005
Mg^{2+}	Anderegg *et al.*	33.4	26.96	19.5		8.9		11.9	8.7×10^4	
	Present work			18.47 (0.05)	4.60×10^4 (1.1×10^3)	8.32 (0.05)	1.34×10^4 (4.7×10^2)	12.05 (0.35)	2.54×10^4 (1.8×10^3)	0.0033
Sr^{2+}	Present work			17.99 (0.05)	5.12×10^3 2.6×10^3	7.75 (0.10)	2.68×10^4 (1.5×10^3)	11.83 (0.04)	6.15×10^4 (2.2×10^3)	0.007

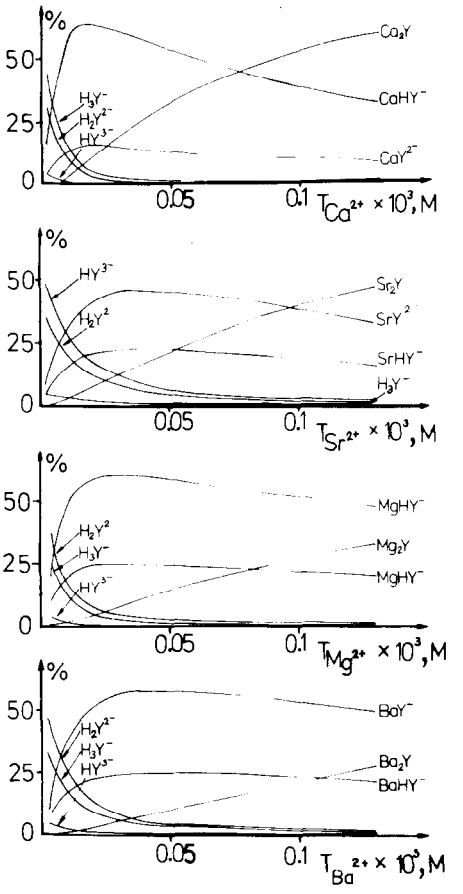


Fig. 4. The distribution of $7.9 \times 10^{-6} M$ *o*-cresolphthalexone among its complexes at pH 10.53. The curves are calculated with the parameters given in Table 2.

tion of these fairly complicated systems. This would have been very difficult by the other methods available. In principle, the least-squares treatment of such systems ought to result in reliable parameters, but uncertainties arise because a particular calculated absorbance can be obtained with a series of pairs of values for the formation constant and the molar absorptivity, the number of these depending on the accuracy, the amount of change in the absorbance readings and the concentration range of the measurements. On the other hand, when two or more complexes are formed in the same region, or when there is extensive overlapping of the formation ranges, the experimental data may be evaluable on the basis of fewer species than are actually present in the system, so complexes formed in small amount can very easily be overlooked. In the systems studied we did not observe such uncertainties, although optimization of three formation constants and four molar absorptivities was necessary.

The protonation and overall formation constants obtained are generally in good agreement with those found by Anderegg *et al.*[1] The only exception is the third protonation constant of *o*-cresolphthalexone which is assigned a very small value by Anderegg *et al.* Our calculations suggest that our error for this parameter is not larger than that for the other parameters, and the corresponding constants of phenolphthalein and *o*-cresolphthalein are also fairly large, so there is nothing to indicate that our constant is unreliable. The formation constants of the strontium complexes have not previously been determined by other authors.

Figure 4 shows that in the spectrophotometric determination of calcium ions with *o*-cresolphthalexone at pH 10.5, the species mainly responsible for the colour change in CaHY. Although CaY is also formed, in smaller amount, it does not affect the determination, since the absorptivities of the two species are practically identical. Our equilibrium calculations show the optimum pH for Ca^{2+} determinations to be ~ 10.5. As regards the factors influencing the accuracy of the analytical method (stability of solution, colour development, effect of oxygen, etc.), our experiments led to conclusions similar to those of Sarkar and Chauhan.[5] In contrast with several other proposed procedures, the method we used did not give appreciable differences between the absorbances of duplicate solutions. Water was used as reference solution, and the experimental technique was standard.

REFERENCES

1. G. Anderegg, H. Flaschka, R. Sallman and G. Schwarzenbach, *Helv. Chim. Acta*, 1954, **37**, 113.
2. G. Schwarzenbach, *Analyst*, 1955, **80**, 713.
3. F. H. Pollard and J. V. Martin, *ibid.*, 1956, **81**, 348.
4. R. Cameroni and A. Albasini, *Atti. Soc. Nat. Mat. Modena*, 1964, **95**, 25.
5. B. C. R. Sarkar and U. P. S. Chauhan, *Anal. Biochem.*, 1967, **20**, 155.
6. K. H. Kim, *Korean J. Pathol.*, 1971, **5**, 19.
7. M. Boross and L. Szilágyi, *Kisérl. Orvostud.*, 1974, **26**, 96.
8. W. S. Stavropoulos, B. J. Thiegs and R. F. Mack, *U.S. Pat.* 3,938,954; *Chem. Abstr.*, 1976, **84**, 132321z.
9. L. G. Morin, *Am. J. Clin. Pathol.*, 1974, **61**, 114.
10. D. Durchassaing, O. G. Ekindjian and G. Leluan, *Anal. Biol. Clin. (Paris)*, 1977, **35**, 133.
11. F. Gaizer and M. Máté, *Acta Chim. Hung. Acad. Sci.*, 1980, **103**, 355.

Talanta Vol. 28, pp. 131 to 133
©Pergamon Press Ltd 1981. Printed in Great Britain
0039-9140/81/0201-0131$02.00/0

ANALYTICAL PROPERTIES OF THE BIS(4-PHENYL-3-THIOSEMICARBAZONE) OF 1,3-CYCLOHEXANEDIONE AND ITS 2-METHYL AND 5,5'-DIMETHYL DERIVATIVES

J. RODRIGUEZ, A. GARCIA DE TORRES and J. M. CANO-PAVON

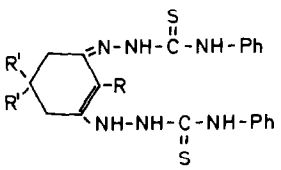
Department of Analytical Chemistry, Faculty of Chemistry, University of Seville, Seville-4, Spain

(*Received* 2 *May* 1980. *Accepted* 25 *August* 1980)

Summary—The analytical properties of the title compounds have been investigated. The 5,5'-dimethyl derivative is the most selective of the three.

Thiosemicarbazones have been widely used for spectrophotometric determination of metal ions and their analytical applications have been reviewed.[1] In recent years, some phenylthiosemicarbazones have been studied as reagents[2–9] because their reactions are more sensitive and their complexes more easily extracted than those of the corresponding thiosemicarbazones. However, compounds with the bis(phenylthiosemicarbazone) grouping have received little attention. The bis(4-phenyl-3-thiosemicarbazone) of biacetyl has been used as reagent for the spectrophotometric determination of copper[10] and zinc[11] and bis(phenylthiosemicarbazones) derived from glyoxal and related compounds have been investigated;[12,13] the corresponding derivatives of β-diketones have been not studied, however.

In this paper, the analytical properties of the bis(4-phenyl-3-thiosemicarbazone) derivatives of 1,3-cyclohexanedione (**I**), 2-methyl-1,3-cyclohexanedione (**II**) and 5,5'-dimethyl-1,3-cyclohexanedione (**III**) are described for the first time. 1,3-Cyclohexadione bis(thiosemicarbazone) has been studied with promising results,[14] and some 1:1 chelates have been isolated.[15]



I.- R=R'=H

II.- R=-CH_3, R'=H

III.- R=H, R'=-CH_3

EXPERIMENTAL

Reagents

Reagents **I**, **II** and **III** were used as 0.1 and 0.2% solutions in dimethylformamide in the chelation study.

Preparation of the compounds

A solution of 1.0–1.2 g of the corresponding β-diketone in 15–20 ml of ethanol was mixed with 2.0 g of 4-phenyl-3-thiosemicarbazide dissolved in 75 ml of hot ethanol, refluxed for 1 hr, then cooled to room temperature. The yellow crystals that separated were collected, and washed with hot ethanol (yield: 50–70%). The melting points were 216–218° for **I**, 214–216° for **II** and 189–191° for **III**. Analysis gave the following results, **I**: 58.5% C, 5.6% H, 20.7% N, 15.3% S; $C_{20}H_{22}N_6S_2$ requires 58.53% C, 5.35% H, 20.48% N, 15.63% S. **II**: 59.3% C, 5.6% H, 19.8% N, 14.7% S; $C_{21}H_{24}N_6S_2$ requires 59.40% C, 5.66% H, 19.80% N, 15.09% S. **III**: 59.7% C, 5.9% H, 19.2% N and 15.5% S; $C_{22}H_{26}N_6S_2$ requires 60.23% C, 5.97% H, 19.16% N, 14.64% S. The results for **III** are not as satisfactory as those for **I** and **II**, especially the figures for C and S.

Chelation studies

The pH range over which complexation occurred, as indicated by colour formation, was determined for each combination of metal ion and test compound. Absorption spectra in the visible range were recorded for solutions buffered to give more complete complexes formation.

RESULTS AND DISCUSSION

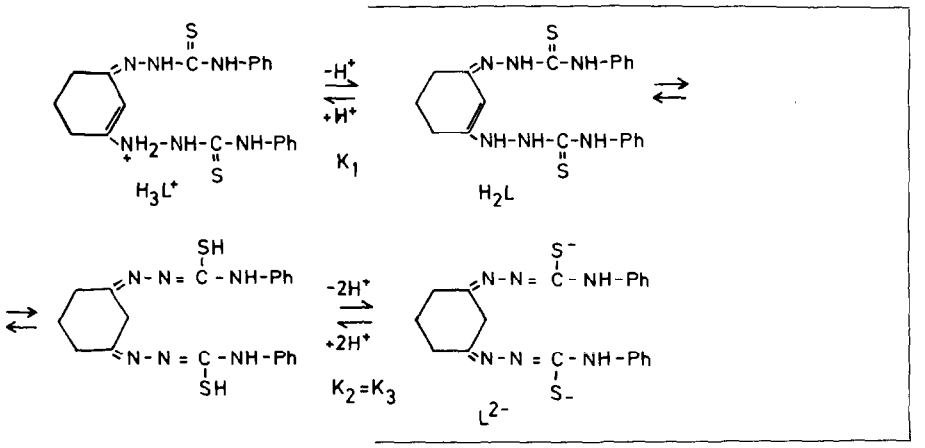
Some of the physico-chemical properties of the ligands are summarized in Table 1. The ultraviolet absorption spectra show bathochromic shifts with increasing pH. The dissociation constants were calculated from the relation of absorbance to pH, by the Stenstrom and Goldsmith[16] and Sommer[17] methods. The pK values shown in Table 1 are the arithmetic means of the values obtained from measurements at three different wavelengths.

The protonated reagents show only two dissociation steps. These were studied by taking the NMR spectra of the reagent solutions, at different pH values, in a 1:1 mixture of dimethylsulphoxide d_6 and deuterium oxide; the pH was adjusted with dilute deuterated sodium hydroxide solution in deuterium oxide. The first dissociation seems probably due to the loss of the proton of the quaternary ammonium group; the second dissociation step is due to the loss of the proton of the –SH group in both phenylthiosemicarbazone groups. The pK values, however, are different from those of other *vic*-bisthiosemicarbazones and *vic*-bisphenylthiosemicarbazones studied previously; this fact may be attributed to the influence of the CH_2 group. Since the molecules are symmetrical and the dissociable protons of the two thiosemicarbazide groups are far apart, the dissociation constants for these two groups would be expected to be

Table 1. Physicochemical properties of the ligands

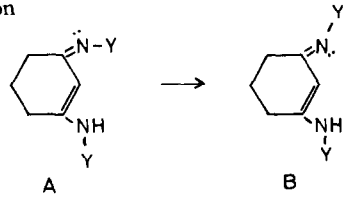
Property	Ligand I	II	III
Solubility in ethanol, *g/l.*	0.060	0.028	0.033
Solubility in dimethylformamide, *g/l.*	>34.8	>74.5	>29.4
Solubility in chloroform, *g/l.*	0.38	0.093	0.036
Solubility in methyl isobutyl ketone, *g/l.*	0.360	0.250	0.130
Solubility in amyl alcohol, *g/l.*	0.140	0.039	0.036
C=N frequency (stretch) cm^{-1}	1650m	1625m	1600s
C=S frequency (stretch) cm^{-1}	1170s	1180s	1180s
$-CH_2-$ protons (NMR), *ppm*	3.0–3.4	1.7–2.0	3.0–3.4
–NH– protons (NMR), *ppm*	1.0–1.9	3.1–3.3	9.0–9.8
	5.7–5.9	9.2–9.7	3.1–3.3
	9.2–9.6		
Aromatic and ethylenic protons (NMR), *ppm*	6.8–7.6	6.8–7.8	6.8–7.6
$-CH_3$ protons (NMR), *ppm*	—	1.7–2.0	0.9–1.1
pK_1	4.12	3.52	3.85
$pK_2 = pK_3$	7.70	7.40	7.85

very similar and not distinguishable by spectrophotometry. According to the NMR spectra the dissociation scheme is as follows:



However, in the compounds II and III, in accord with the NMR spectra of the neutral species it seems probable that two other resonance forms with two double bonds must be taken into account; in the first form, the double bonds are at C_3-C_4 and C_6-C_1, and in the second form at C_2-C_3 and C_6-C_1.

Solutions of **I** and **III** become more reactive in storage, the absorptivity of the chelates being greater when the reagents are at least a day or two old. However, the NMR and ultraviolet spectra and the optical activity do not change for at least a week. This is suggested as due to a prototropic equilibrium in solution, with the methylene proton at C_2 participating in modification of the configuration of the imine double bond, so that an *anti* stereoisomer B is formed, which is more suitable than the *syn* form (A) for coordination



In compound **II**, however, this modification does not occur, owing to steric hindrance by the methyl group.

Reactions of metal ions with these reagents were tested at different pH values. The most sensitive reactions were those of Co(II), Fe(II) and (III), Bi, Ni, Cd, Zn and U(VI), at pH > 6. The photometric data are summarized in Table 2.

The results compiled in Tables 1 and 2 provide a basis for judging the potential analytical utility of the compounds as chromogenic reagents. Compound **I** shows the most promise as a sensitive reagent for uranium(VI) and compound **III** for iron(II), nickel, cobalt, bismuth and cadmium; unfortunately both lack selectivity, the species mentioned all giving mutual interference, presumably because of their high affinity for sulphur atoms.

Compound **II** is more selective, and its copper (II) complex is formed in very acid medium, so that the determination of copper may be feasible in the presence of foreign ions. From this point of view compound **II** may be an interesting analytical reagent.

In general, the properties of bisthiosemicarbazones and bisphenylthiosemicarbazones of β-diketones are quite different from those of the corresponding α-diketone compounds. This is an excellent example of

Table 2. Photometric properties of complexes

Ligand	Metal ion	λ, *nm*	Optimum pH	ϵ, $l.mole^{-1}.cm^{-1}$
I	U(VI)	640	6–8	1.8×10^4
I	Zn(II)	570	6–8	2.3×10^4
I	Pb(II)	550	6–8	1.9×10^4
I	Co(II)	455	4–6	1.3×10^4
II	Cu(II)	480	<2	3.5×10^3
II	Co(II)	485	4–6	8.8×10^3
II	Hg(II)	450	4–6	5.5×10^4
III	Fe(II)	475	6–8	2.6×10^4
III	Fe(III)	485	6–8	1.7×10^4
III	Ni(II)	470	6–8	2.5×10^4
III	Bi(III)	470	6–8	3.9×10^4
III	Co(II)	470	6–8	2.2×10^4
III	Cd(II)	590	6–8	7.9×10^3

how increased separation between co-ordinating groups can appreciably modify sensitivity and selectivity.

REFERENCES

1. R. B. Singh, B. S. Garg and R. P. Singh, *Talanta*, 1978, **25**, 619.
2. J. M. Cano-Pavón and F. Pino, *Anal. Lett.*, 1974, **7**, 159.
3. J. M. Cano-Pavón, J. C. Jimenez Sanchez and F. Pino, *Anal. Chim. Acta*, 1975, **75**, 335.
4. J. L. Gómez Ariza, J. M. Cano-Pavón and F. Pino, *Talanta*, 1976, **23**, 440.
5. J. L. Gómez Ariza and J. M. Cano-Pavón, *Anal. Lett.*, 1976, **9**, 677.
6. M. T. Martinez Aguilar, J. M. Cano-Pavón and F. Pino, *Anal. Chim. Acta*, 1977, **90**, 335.
7. M. T. Martinez Aguilar and J. M. Cano-Pavón, *Mikrochim. Acta*, 1977 **II**, 631.
8. M. T. Martinez Aguilar and J. M. Cano-Pavón, *Anal. Lett.* 1978, **11**, 373.
9. R. S. Patel, K. J. Shah, Y. N. Bhatt and K. K. Patel, *Chem. Era*, 1976, **12**, 104.
10. A. G. Asuero and J. M. Cano-Pavón, *Analyst*, 1978, **103**, 140.
11. *Idem*, *Mikrochem. J.*, 1978, **23**, 142.
12. V. Niederschulte and K. Ballschmiter, *Z. Anal. Chem.*, 1972, **261**, 191.
13. K. Ballschmiter, *ibid.*, 1973, **263**, 203.
14. J. J. Berzas Nevado, J. A. Muñoz Leyva and M. Román Ceba, *Talanta*, 1976, **23**, 257.
15. J. J. Berzas Nevado, *Thesis*, University of Extremadura, Badajoz, Spain, 1977.
16. W. Stenstrom and N. Goldsmith, *J. Phys. Chem.*, 1926, **30**, 1683.
17. L. Sommer, *Folia Fac. Sci. Nat. Univ. Purkynianae, Brno*, 1964, **5**, 1.

Talanta Vol. 28, pp. 134 to 136
Pergamon Press Ltd 1981. Printed in Great Britain

0039-9140/81/0201-0134$02.00/0

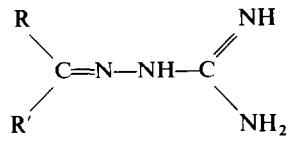
ANALYTICAL PROPERTIES OF PYRIDINE-2-ALDEHYDE GUANYLHYDRAZONE

M. ROMAN CEBA, J. J. BERZAS NEVADO and A. ESPINOSA MANSILLA
Department of Analytical Chemistry, University of Extremadura, Badajoz, Spain

(*Received* 25 *April* 1980. *Accepted* 14 *July* 1980)

Summary—The modified synthesis and analytical properties of pyridine-2-aldehyde guanylhydrazone are described for the first time. The solubility, spectral characteristics, pK values and reactions with 40 inorganic species are reported.

Schiff's bases are interesting as analytical reagents. Oximes, hydrazones and thiosemicarbazones have been the most widely studied, but guanylhydrazones have not previously been studied as analytical reagents. Guanylhydrazones were first synthesized by Thiele and Dralle.[1] Their importance is due to their pharmacological properties. Their general structure is

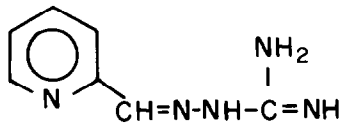


where R and R′ are H or any organic radical.

Guanylhydrazones have a similar structure to thiosemicarbazones. The great affinity of sulphur for coordination of metal ions poses a serious hindrance in the use of thiosemicabazones as analytical reagents, since it makes selective methods difficult to establish. The replacement of the sulphur atom of the thiosemicarbazones by the imine group of the guanylhydrazones can increase the selectivity.

The reactivity of Schiff's bases is also dependent, however, on the structural characteristics of the aldehyde or ketone which is condensed with the amine. Pyridine-2-aldehyde has been used extensively.

In this paper the modified synthesis, properties and analytical possiblities of pyridine-2-aldehyde guanylhydrazone (PAG) are described for the first time.



The reagent was synthesized as the dihydrochloride in 1965 by Farbwerke Hoechst and has been tested as a pharmacological agent.[2]

EXPERIMENTAL

Reagents

All solvents and reagents should be of analytical-reagent grade.

Synthesis of PAG. The synthesis of pyridine-2-aldehyde guanylhydrazone dihydrochloride is described in the literature,[2] but we have used the nitrate instead of the dihydrochloride, which simplifies the synthesis and gives a much better yield.

A solution of 3.679 g of aminoguanidine nitrate in 20 ml of water was added to 2.970 g of pyridine-2-aldehyde in 20 ml of ethanol and the mixture was refluxed for 2 hr. Yellow crystals separated (after the solution has been cooled to 2–5°), and when recrystallized from aqueous ethanol (50%) and dried over sulphuric acid had m.p. 182–183°. Elemental analysis gave C 37.3%, H 4.4%, N 36.8%, $C_7H_9N_5 . HNO_3$ requires C 37.2%, H 4.4%, N 37.1%.

Solubility

The solubility of PAG in several solvents at room temperature was determined by Wittemberger's method.[3] PAG is very soluble in dimethylformamide (406 g/l.), methanol (55 g/l.), water (42 g/l.) and ethanol (14 g/l.) and sparingly soluble in cyclohexane, methyl isobutyl ketone, chloroform, carbon tetrachloride and isoamyl alcohol.

Stability

Dilute aqueous solutions of PAG ($2.2 \times 10^{-5} M$) are reasonably stable and $4.4 \times 10^{-3} M$ solutions are stable for longer than a week. Acid and basic PAG solutions are also very stable.

Spectral characteristics

The infrared spectrum was obtained (KBr discs), and the bands were assigned (cm^{-1}) to the stretching vibrations of —NH— (3380, 3310 and 3140), C=N (1680), the "guanido" group NH—C(=NH)—NH_2 (1630 and 1600) and the C=C pyridine group (1580 and 1420).

The NMR spectrum was obtained in D_2O with DSS as internal reference. The peaks (δ, ppm) were assigned: 7.45 m and 8.50 dm (protons 5 and 6, pyridine ring), 7.70–8.00 m (protons 3 and 4, pyridine ring), and 7.87 s (proton —CH= group). The coupling constant measured were (Hz): $J_{3,5}$ 1.5; $J_{4,5}$ 7.3 and $J_{5,6}$ 4.2.

The NMR spectrum was also obtained in DMSO d_6 with TMS as internal reference. The peaks (δ, ppm) were assigned: 8.33 d (proton 3, pyridine ring), 7.86 m (proton 4, pyridine ring), 7.48 m (proton 5, pyridine ring), 8.67 d (proton 6, pyridine ring), 8.25 s (proton —CH= group) and 8.05 (protons, amine groups). The coupling constants measured were (Hz): $J_{3,4}$, 8.0; $J_{3,5}$, 1 and $J_{5,6}$, 5.0.

The ultraviolet absorption spectra for the reagent in water, ethanol and methanol media showed similar maxima between 285 and 290 nm. Bathochromic shifts were produced on changing from water to dimethylformamide as solvent (from 285 to 335 nm).

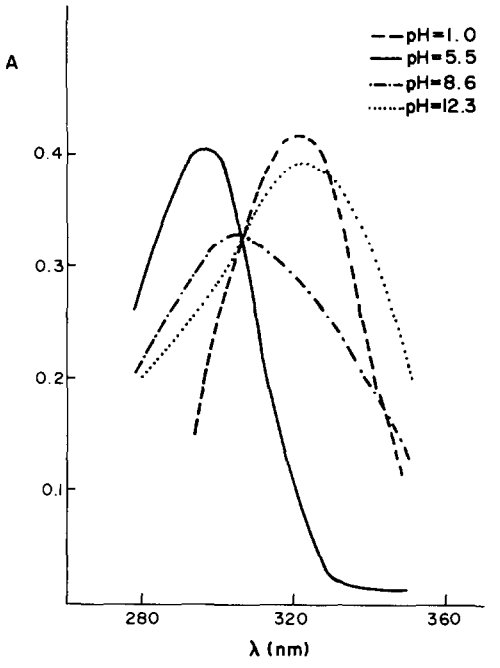


Fig. 1. Absorption spectra of $2.21 \times 10^{-5} M$ PAG in water at different pH-values.

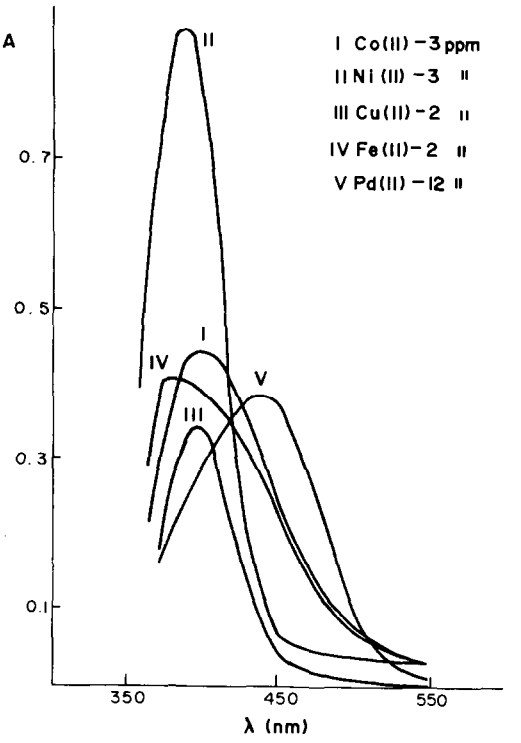


Fig. 2. Absorption spectra of solutions of compounds formed in sodium hydroxide medium.

Ultraviolet absorption spectra at various pH values are shown in Fig. 1. Bathochromic shifts were produced in acid and alkaline media.

The ionization constants of $2.2 \times 10^{-5} M$ aqueous PAG solutions were determined by Phillips and Merritt's method[4] at ionic strength 0.1, temperature 20°, and different pH values 0.5 to 12.8. The average results obtained were: $pK_1 = 3.25 \pm 0.05$ and $pK_2 = 8.4 \pm 0.3$. The pK values were also measured potentiometrically on a $1.25 \times 10^{-2} M$ PAG solution, ionic strength 0.1, temperature 20°: $pK_1 = 3.28$ and $pK_2 = 8.05$.

To determine the ionic species of PAG that take part in the acid–base equilibria, ion-exchange and electrophoretic studies were made. In either acidic or basic medium, PAG is retained on a strong acid cation-exchanger in sodium form.

Electrophoresis shows that in both acid and basic medium, PAG shifts towards the cathode, which indicates that PAG is cationic even in basic medium ($pH > pK_2$).

Qualitative tests

The reaction of PAG with 40 inorganic cations, up to concentrations of 1 g/l., at various pH values, was investigated. PAG reacts with Co(II), Ni(II), Fe(II), Cu(II) and Pd(II), giving a yellow colour. Fe(II) also forms a very unstable violet colour. The absorption spectra of the complexes formed by the reagent with Co(II), Ni(II), Fe(II), Cu(II) and Pd(II) at the most favourable pH were recorded at 350–700 nm against reagent blanks. Maximum absorption occurs between 375 and 440 nm (Fig. 2). The most important results are summarized in Table 1. The other species tested were Ag(I), Pb(II), Pt(IV), Bi(III), Fe(III), Al(III), Cr(III), Cr(VI), Zn(II), Cd(II), Ti(IV), Mn(II), U(VI), Ce(IV), W(VI), La(III), Th(IV), Hg(II), As(III), Te(IV), Ca(II), Ba(II), Sr(II), Hg(I), Mo(VI), Au(III), Mg(II), Y(III), In(III), As(V), Ge(IV), V(V), Sb(III), Li(I), Rh(III).

Table 1. Characteristics of pyridine-2-aldehyde guanylhydrazone compounds

Ion	Medium	λ, nm	pD*	ϵ, $l.mole^{-1}.cm^{-1}$	Colour
Co(II)	NH_3/NH_4^+	390	6.9	9.9×10^3	Yellow
	NaOH		6.9		Yellow
Ni(II)	NaOH	375	5.3	16.6×10^3	Yellow
Cu(II)	$AcOH/AcO^-$		5.5		Blue-green
	NaOH	380	6.3	13.0×10^3	Yellow
Pd(II)	$AcOH/AcO^-$	440	6.3	3.4×10^3	Yellow
	NH_3/NH_4^+		6.3		Yellow
Fe(II)	NH_3/NH_4^+	380	4.6	11.8×10^3	Yellow
	NaOH		4.6		Yellow

* pD = logarithm of reciprocal of detection limit concentration.

Various organic solvents were tested as extractants for the PAG–metal complexes. Only complexes of the following ions are extracted: Cu(II) into carbon tetrachloride, Ni(II) into methyl isobutyl ketone (both in the presence of sodium perchlorate) and Fe(II) into isoamyl alcohol (giving a strong red colour in basic medium).

RESULTS AND DISCUSSION

Pyridine-2-aldehyde guanylhydrazone is easily obtained by condensation between the aldehyde and aminoguanidine nitrate.

The bathochromic shifts in acid and alkaline media indicate that in solution at least three different forms of PAG can be present. The bathochromic shift in acid medium may be due to protonation of the nitrogen atom in the pyridine ring, since it is very similar to that of pyridine and its derivatives.[5]

According to the ion-exchange and electrophoretic studies we propose the following protonation steps:

$$H_3L^{3+} \underset{\longleftarrow}{\overset{K_1}{\longrightarrow}} H_2L^{2+} \underset{\longleftarrow}{\overset{K_2}{\longrightarrow}} HL^{+}$$

PAG is more selective as a reagent than pyridine-2-aldehyde thiosemicarbazone,[6] because of replacement of the sulphur atom by the =NH group.

A fundamental advantage of PAG is its high solubility in water, which permits its use in aqueous media. It can be used as a specific reagent for identification of Co(II) and Ni(II) in group 3B (Co, Ni, Mn and Zn) in classical qualitative analysis.

(*a*) Identification of Ni(II): the yellow colour given with PAG in basic medium is extracted with MIBK and is clear evidence of Ni(II).

(*b*) Identification of Co(II): A yellow colour with PAG in NH_4Cl/NH_3 medium is positive evidence of Co(II).

The stability, solubility in water, absence of absorption in the visible region, and the sensitive reactions with Pd(II), Cu(II), Ni(II), Co(II) and Fe(II), indicate that PAG should be useful for spectrophotometric determination of these ions.

REFERENCES

1. J. Thiele and E. Dralle, *Annalen*, 1898, **302**, 278.
2. Farbwerke Hoechst AG, *Neth. Patent Appl.*, 6410378, C 07 d (a 16K).
3. W. Wittenberger, *Chemische Laboratoriumstechnik*, 4th Ed., p. 101. Springer, Vienna, 1950.
4. J. P. Phillips and L. L. Merritt, *J. Am. Chem. Soc.*, 1943, **70**, 410.
5. H. C. Brown and D. H. McDaniel, *ibid.*, 1955, **77**, 3752.
6. J. M. Cano Pavón, *Ch.D. Thesis*, Seville, 1971.

Talanta Vol. 28, pp. 137 to 143
© Pergamon Press Ltd 1981. Printed in Great Britain
0039-9140/81/030137-07$02.00/0

POTENTIOMETRIC STUDIES ON THE COMPLEX FORMATION BETWEEN METHYLMERCURY(II) AND SOME KETO- AND AMINO-CARBOXYLIC ACIDS

MOHAMMAD JAWAID* and FOLKE INGMAN

Department of Analytical Chemistry, The Royal Institute of Technology, 100 44 Stockholm 70, Sweden

(*Received* 2 *October* 1980. *Accepted* 9 *October* 1980)

Summary—The protonation of pyruvic and laevulinic acid, L-serine, L-cysteine, L-methionine and L-asparagine, and their complex formation with methylmercury(II) ions, have been studied by a potentiometric method, in 1.0*M* sodium nitrate medium at 25°. The protonation and equilibrium constants were evaluated by using the computer program LETAGROP–ETITR. The limitations of the experimental method are explained. The participation of different functional groups of the ligands in binding methylmercury(II) and the biological significance of the complex formation are discussed.

The deleterious effects of organomercurials on man and the environment are now well documented[1–5] and the use of these compounds as fungicides and in seed-dressing, *etc.* has been banned in many countries. Several studies[6–10] have shown that both inorganic and metallic mercury can be methylated in the presence of certain bacteria found in sea sediments. Moreover, it has also been shown that it is methylmercury species which are easily absorbed and accumulated by living organisms and thus pose potential danger to the health of man and animals.

A study of the solution chemistry of organomercurials, their complex formation with the ligands present in natural and biological systems, and the stability and specificity of the complexes so formed, can provide useful information about the nature and magnitude of binding between the organomercurials and such ligands, which, in turn, can be used to evaluate the methods of removing these undesirable substances from biological systems employing chelation therapy.[11]

Various techniques have been used for studying the solution chemistry of organomercurials. Simpson[12] employed solvent extraction and polarography to investigate interaction between methylmercury(II) and organic ligands such as cysteine, glutathione and histidine. Solvent extraction was also used by Niitsu *et al.*[13] to study the distribution of R–Hg(II) (R = methyl, ethyl or propyl) in the two-phase system 1.0*M* (H,Na) (Cl)/benzene in presence of cysteine. Rabenstein and co-workers[14–18] made use of NMR to study the hydrolysis of methylmercury(II) and its complex formation with some selected amines, aminocarboxylic acids, glutathione, methionine, cysteine and DL-penicillamine. Hojo *et al.*[19] studied the complexes of methylmercury and phenylmercury with DL-penicillamine and some other sulphur-containing ligands by infrared spectrometry, PMR and potentiometry. X-Ray, infrared and Raman spectroscopy[20–22] have also been used by some workers to investigate the structure of organomercurial complexes with some sulphur-containing ligands.

The work described here is a part of our systematic studies on methylmercury(II) and its complex formation with ligands that are present in natural and biological systems. In previous publications we have reported the results on the hydrolysis of methylmercury(II),[23,24] its complexes with the ligands found in natural waters[23,25,26] and some simple carboxylic and aminocarboxylic acids[24] and with EDTA.[27] The present paper describes the results on the complex formation between methylmercury(II) and some simple keto-acids, namely pyruvic and laevulinic acid, and the representative aminocarboxylic acids L-serine, L-cysteine, L-methionine and L-asparagine. These acids have been chosen because they contain some model functional groups such as carboxylate, amino, thio-ether and sulph-hydryl, which can provide potential co-ordination sites for binding metals to proteins, peptides, *etc.*

The method employed is based on potentiometric titrations covering a wide concentration range of the components, and the computer analysis of the collected data by the program LETAGROP–ETITR.[28] The protolytic equilibria of these acids were also studied under similar conditions (ionic medium, temperature, *etc.*) and the protonation constants thus evaluated were used in the subsequent calculations.

EXPERIMENTAL

Reagents

Sodium pyruvate and laevulinic acid (analytical grade) and L-serine, L-cysteine, L-methionine and L-asparagine

* Present address: National Institute of Environmental Medicine, 104 01 Stockholm, Sweden.

(Merck biopure grade) were assayed by potentiometric titrations.[29] Carbon dioxide-free sodium hydroxide[30] was standardized against hydrochloric acid by the Gran method. Methylmercury hydroxide (Ventron Alfa, Denmark) was assayed as described previously.[24] Sodium nitrate (p.a., Merck) was recrystallized once before use. All the solutions were prepared in freshly boiled doubly distilled water.

Potentiometric titrations

The titrations were performed in a 200-ml (Metrohm EA 880) glass vessel with a lid having five inlets for burette, electrodes, degassing tubes, *etc.* The cell used can be written as

Reference half-cell	v ml of 1.0M Na(OH,NO_3) V_0 ml of 1.0M (H,MeHg,Na) (L,NO_3)	Glass electrode

where v is the volume of the titrant added and V_0 the initial volume of the solution in the titration vessel. MeHg and L represent methylmercury(II) and fully deprotonated ligand, respectively.

The electrodes used were combined glass and silver/silver chloride electrodes (Ingold, micro-design). The emf was read to 0.1 V with a digital voltmeter. The temperature was kept at 25 ± 0.05° with an oil-bath.

$[H^+]$ was calculated from the equation

$$E = E'_0 + 59.156 \log[H^+] + j[H^+] \quad (1)$$

The practical details and meaning of the symbols have already been given.[24]

CALCULATION METHODS

We assume that the components H, MeHg and L react to form a complex of composition $(H)_l(MeHg)_m(L)_n$. The equilibrium constant, β_{lmn} of the reaction is given by the expression

$$\beta_{lmn} = [(H)_l(MeHg)_m(L)_n][H]^{-l}[MeHg]^{-m}[L]^{-n} \quad (2)$$

The charges are omitted for convenience.

The mass-balance equations are

$$C_H = [H] + \Sigma l\beta_{lmn}[H]^l[MeHg]^m[L]^n = C_{HCalc} \quad (3)$$

$$C_{MeHg} = [MeHg] + \Sigma m\beta_{lmn}[H]^l[MeHg]^m[L]^n \quad (4)$$

$$C_L = [L] + \Sigma n\beta_{lmn}[H]^l[MeHg]^m[L]^n \quad (5)$$

where C stands for the total analytical concentration and the square brackets for the equilibrium concentration of the components/complexes. If there is more than one ligand in the solution, the model can be extended accordingly, by inclusion of further mass-balance equations.

For potentiometric titrations, the following relationship is valid for the proton excess.

$$C_H = (C^*_H \cdot V_0 - C^*_{OH} \cdot v)/(V_0 + v) = C_{Hexp} \quad (6)$$

where

C^*_H = the initial concentration of the ionized and potentially ionizable hydrogen

C^*_{OH} = the molar concentration of sodium hydroxide in the titrant

V_0 = the initial volume of the solution in the titration vessel

v = the volume of titrant added

To illustrate the computer calculations, we shall hereafter use C_{Hcalc} and C_{Hexp} for C_H in equations (3) and (6), respectively.

The program LETAGROP–ETITR, when supplied with an initial estimate of β_{lmn}, and the known quantities C_{MeHg}, C_L [equations (4) and (5), respectively] and [H] (hereafter called h) from equation (1), can calculate, for each experimental point, the values of C_{Hcalc} from equation (3) and minimize the error-square sum

$$U = \sum_1^{Np} (C_{Hcalc} - C_{Hexp})^2 \quad (7)$$

where Np is the number of experimental points available and C_{Hexp} is calculated from equation (6) by the procedure BDTV in the program.

The program is used to test a series of probable chemical models describing various complexes that may be formed in a solution of known composition. The chemical model which gives the minimum error-square sum, explains the data satisfactorily within the limits of experimental error, and is most plausible from co-ordination chemistry considerations, is accepted as the "best" model.

RESULTS AND DISCUSSION

Some experimental data for the titration of L-serine, L-cysteine, L-methionine and L-asparagine, in presence of the same amount of methylmercury(II) are plotted in Fig. 1, as $Z = (H - h)/C_{MeHg}$ as a function of pH. For almost similar solution composition, the Z-curves of the biprotic acids L-serine and L-methionine are nearly superimposable over the whole pH range, whereas that for L-asparagine deviates slightly from the other two at higher pH. This probably indicates that the methylmercury(II) complex of L-asparagine is less stable than those of the other two amino-acids. For L-cysteine the formation curve is similar in shape but lies well above the other three, because L-cysteine was considered a triprotic acid for calculating the analytical proton excess.

The results of the computer calculations are summarized in Table 1, which includes the equilibrium constants for the formation of various complexes of methylmercury(II) with these ligands as well as the protonation constants of the acids in the same ionic medium. The chemical models given in the table were accepted as the "best" in each case for the present

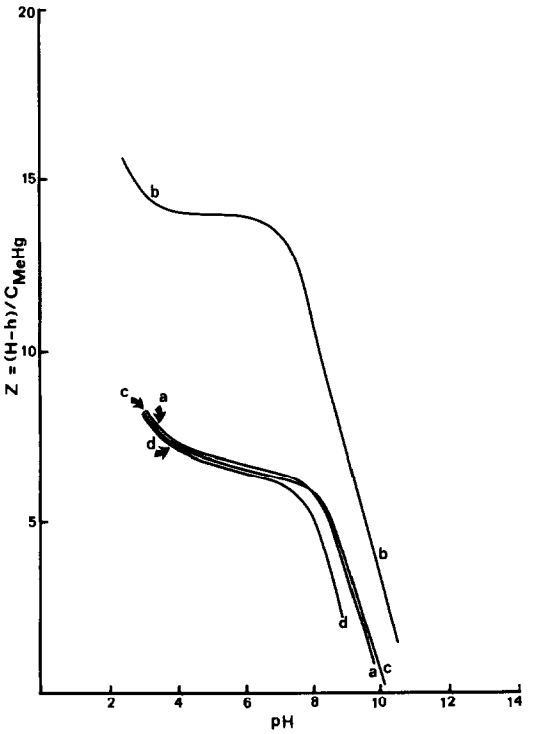


Fig. 1. Titration of $2.50 \times 10^{-2}M$ solution of (a) L-serine, (b) L-cysteine, (c) L-methionine and (d) L-asparagine, in presence of $3.32 \times 10^{-3}M$ methylmercury(II) solution, shown as $Z = (H - h)/C_{MeHg}$ as a function of pH. Note that L-cysteine is taken as a triprotic acid for calculating the analytical proton excess. $H = C_{H\,exp}$

experimental conditions. All the other models tried gave a rather high error-square sum and systematic deviations. In the calculations, the formation of hydrolysed methylmercury species was taken into account, by use of the equilibrium constants reported earlier.[24]

The potentiometric titration method used in this work implies the titration of a weak acid with a strong base. If metal ions that form complexes with the ligand are present in the solution the ligand will appear to be a conditionally stronger acid than if it were present alone. This strengthening effect is used to evaluate the complexation between the metal ions and the ligand. However, when the complexation is very strong, as in the case of cysteine, the acid will appear conditionally strong, that is, completely dissociated, and still stronger complexation will not affect the titration curve further. Thus, there is a limit to the strength of complexes that can be evaluated by this method.

For the MeHg(II)–cysteine system, the limiting value for $\log \beta_{011}$ is 9–10. The analysis of the experimental data obtained by titrating a solution of methylmercury(II) in presence of cysteine alone will therefore always yield this limiting value, and *although the fit to the model will be very good the results so obtained will be entirely erroneous.*

One way to increase the range is to introduce a second ligand into the system, that can compete for the metal ions. We have used iodide as an appropriate auxiliary complexing agent because it is an aprotic ligand that forms a fairly strong 1:1 complex with methylmercury(II).[31] The results obtained by analysing the experimental data from titration of a solution of methylmercury(II) in presence of cysteine and an excess of iodide are also given in Table 1.

The situation can be clarified by using the concept of conditional constants and side-reaction coefficients.[32] Let the main reaction characterizing the titration of a weak acid HA with strong base (omitting charges) be

$$HL \rightarrow H + L (+OH \rightarrow L + H_2O); \quad K_a = \frac{[H][L]}{[HL]}$$

If the metal ion M is now introduced, forming complexes with L, the following side-reaction will occur:

$$L + M \rightarrow ML \qquad K_{ML} = \frac{[ML]}{[M][L]}$$

The side-reaction coefficient is given by

$$\frac{[L']}{[L]} = \alpha_{L(M)} = \frac{[L] + [ML]}{[L]} = 1 + [M]K_{ML} \geq 1$$

The conditional constant for the main reaction is

$$K_a' = \frac{[H][L']}{[HL]} = \frac{[H][L]\alpha_{L(M)}}{[HL]} = K_a\alpha_{L(M)}$$

Since $K_a' > K_a$, the main reaction will proceed further to the right upon the introduction of M, and the acid will consequently be conditionally stronger. As the value of $\alpha_{L(M)}$ is increased, the titration curve approaches that for the titration of a strong acid and a further increase of $\alpha_{L(M)}$ will have no effect on the titration curve. In other words, the value of K_a' for HL can never be greater than C_{HL}, the total concentration of HL.

Example. Titration of a $0.01M$ solution of acid HL having $pK_a = 8$. The pH at the half-neutralization point will be ~8. For a titration of a $0.01M$ solution of a strong acid (*e.g.*, $pK_a = -5$) the corresponding pH is ~2.3. Since K_a' can never become greater than C_{HL} the limiting value of $\alpha_{L(M)}$ is in this case $C_{HL}/K_a = 10^{-2}/10^{-8} = 10^6$, corresponding to $K_{ML} \sim 10^9$, assuming $[M] \sim 10^{-3}M$. Further increase of $\alpha_{L(M)}$ will have no more influence on the titration curve.

The introduction of an aprotic ligand such as iodide will lower the free concentration of M with a consequent reduction of $\alpha_{L(M)}$ as a result:

$$M + I \rightarrow MI; \qquad K_{MI} = \frac{[MI]}{[M][I]}$$

$$\alpha_{M(I)} = \frac{[M']}{[M]} = \frac{[M] + [MI]}{[M]} = 1 + [I]K_{MI} \geq 1$$

$$\alpha_{L(M)} = 1 + [M]K_{ML}' = 1 + \frac{[M']}{\alpha_{M(I)}} K_{ML}$$

Table 1. The equilibrium constants log β_{lmn} for the formation of $(H)_l(MeHg)_m(L)_n$ species in 1.0*M* (Na,H) (NO_3,L) ionic medium at 25 ± 0.05°, which minimize the error-square sum, $U = \sum_{1}^{Np}(C_{H\,calc} - C_{H\,exp})^2$; the limits given [$\log\beta \pm 3\delta(\beta)$] correspond approximately to ±3 standard deviations

Acid/ligand	pH range	C_{MeHg}, $10^{-3}M$	C_L, $10^{-2}M$	Complexes assumed l,	m,	n	$\log\beta \pm 3\delta(\beta)$	U_{min}	δ(H)	Np
Pyruvic acid	2.0–5.5	0	0–2.50	1,	0,	1	2.12 ± 0.01	0.710	0.113	57
CH_3COCOO^-	1.8–4.1	0–4.97	0–1.25	0,	1,	1	2.31 ± 0.08	0.569	0.094	66
Laevulinic acid	3.1–6.0	0	0–2.50	1,	0,	1	4.34 ± 0.01	0.612	0.097	66
$CH_3CH_2COCOO^-$	3.3–5.4	0–3.32	0–3.75	0,	1,	1	2.51 ± 0.04	0.175	0.051	69
L-Serine	2.7–9.6	0	0–3.75	1,	0,	1	8.97 ± 0.01	0.260	0.060	75
$HOCH_2CH(NH_2)COO^-$				2,	0,	1	11.16 ± 0.01			
	3.0–9.5	0–4.97	0–2.50	0,	1,	1	6.93 ± 0.06	0.476	0.097	52
L-Cysteine	2.1–10.7	0	0–2.60	1,	0,	1	10.15 ± 0.01	0.845	0.083	125
$^-SCH_2CH(NH_2)COO^-$				2,	0,	1	18.27 ± 0.01			
				3,	0,	1	20.17 ± 0.01			
	3.1–10.2	0–3.32	0–3.75	0,	1,	1 (a)	(9.72 ± 0.13)	1.379	0.108	120
				1,	1,	1 (a)	(18.06 ± 0.12)			
	2.9–11.1	0–2.21	0–0.17	0,	1,	1 (b)	15.70 ± 0.12	0.290	0.123	19
				1,	1,	1 (b)	24.96 ± 0.08			
L-Methionine	2.0–10.0	0	0–2.50	1,	0,	1	9.04 ± 0.01	0.292	0.068	65
$H_3CSCH_2CH_2CH(NH_2)COO^-$				2,	0,	1	11.22 ± 0.01			
	3.1–10.2	0–3.32	0–2.50	0,	1,	1	7.17 ± 0.17	0.855	0.150	40
L-Asparagine	2.2–9.4	0	0–2.50	1,	0,	1	8.69 ± 0.01	0.555	0.081	86
$H_2NCOCH_2CH(NH_2)COO^-$				2,	0,	1	10.84 ± 0.01			
	2.6–8.9	0–4.98	0–2.50	0,	1,	1	6.32 ± 0.06	0.541	0.084	77

$\delta(H) = (U_{min}/Np)^{1/2}$.

(a) Obtained without the use of iodide as an auxiliary complexing agent. The values are erroneous, as shown in the discussion, and should be regarded only as an example of how good the fit to the model can be.

(b) Obtained by using iodide (0.05–0.1*M*) as auxiliary complexing agent, and log $K(MeHg^+ + I^- \rightleftharpoons MeHgI) = 8.6$.[31]

The same *total* concentration of M will now produce a lower value of $\alpha_{L(M)}$.

Table 2 summarizes the results for the complex formation between methylmercury(II) and some carboxylic and aminocarboxylic acids reported by various workers. Most of the results, obtained by different methods, are comparable; the small differences in some cases can be attributed to the different ionic media and the temperatures. However, in the case of L-cysteine the differences are more significant. One reason is that different experimental methods were used and some workers were not aware of the limitations of their chosen method. The greatest differences can be seen between some results obtained by potentiometric titration using the glass electrode,[19] and results obtained by liquid/liquid distribution experiments.[12,13] The difference is about 8 logarithmic units. This agrees fairly well with what can be predicted from the discussion above on potentiometric titration of cysteine. This is evident from Table 1, where the values found by the present authors, both with and without iodide as an auxiliary complexing agent, are listed.

Attention also needs to be paid to the significance of the acid dissociation constants of cysteine. If no complexation occurs, the sulph-hydryl proton will dissociate slightly before the proton on the amino-group. Once the sulph-hydryl proton has dissociated, the amino-group proton will be more strongly retained, giving rise to the *macroscopic* protonation constants listed in Table 1. Since, however, the bond between sulphur and mercury is particularly strong, complexation of cysteine with methylmercury(II) will block the sulph-hydryl group and evaluation of an acid–base titration of the complex will yield a value for the *microscopic* protonation constant of the amino-group. This protonation has been studied by Rabenstein and by Hojo and co-workers, by NMR methods.

It is known that an approximate relationship exists between the first dissociation constants of a series of acids and the stability constants of their 1:1 complexes with a given metal. Such a relationship can be used to estimate the stability constants of the metal complexes of closely related substances if their pK_a values and one K_{ML} value are known. Figure 2 demonstrates such a relationship for the methylmercury(II) complexes of some simple carboxylic, keto- and amino-carboxylic acids, with a correlation coefficient of 0.99 if L-cysteine and hydroxide are excluded. The greater deviation in the case of these last two can be attributed to the fact that they are not closely related to the others and the complexation takes place in a different manner; in the case of cysteine it is the deprotonated sulph-hydryl group which binds methylmercury most strongly.

In Fig. 3, the equilibrium distribution of various species in the methylmercury(II)–cysteine–iodide system are shown as functions of pH. The calculations, done with the computer program HALTAFALL,[33]

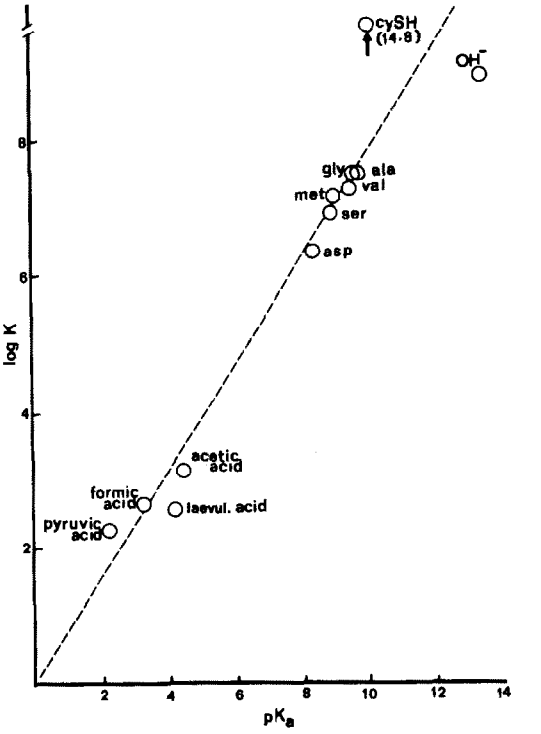


Fig. 2. Relationship between the first dissociation constant of the acids and the stability constant of their 1:1 complexes with methylmercury(II). Some data were taken from ref. 24. $pK_w = 13.61$ in $1.0M$ $NaNO_3$ ionic medium.

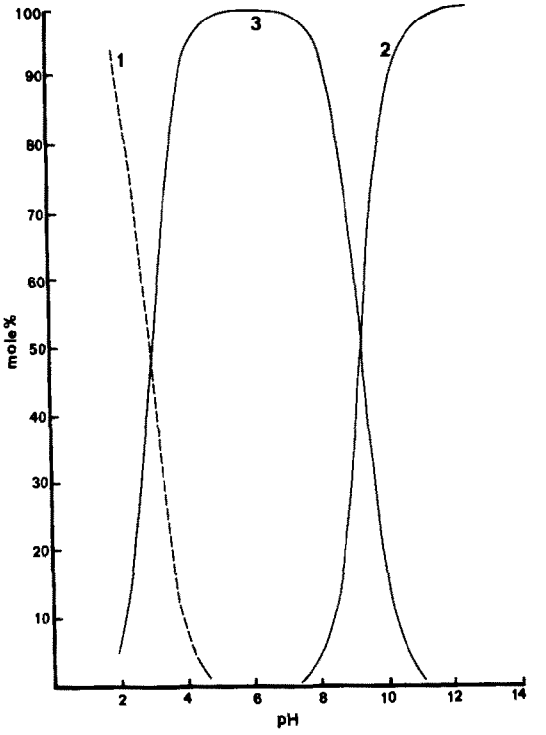


Fig. 3. The equilibrium distribution of the species in the methylmercury(II)–cysteine–iodide system as a function of pH. Curve 1 is for MeHgI, 2 for $MeHgL^-$ and 3 for MeHgLH. $C_{MeHg} = 1.00 \times 10^{-3}M$, $C_L = 1.00 \times 10^{-2}M$, $C_I = 0.1M$.

Table 2. The equilibrium constants, log K, for the formation of methylmercury(II) complexes with some carboxylic, keto- and amino-carboxylic acids in different systems

Acid/ligand	Equilibrium reactions	log K[a]	Ionic medium	Method	Ref.
Formic acid	$MeHg^+ + L^- \rightleftharpoons MeHgL$	2.67	0.4*M*?	NMR	15
		2.68 ± 0.01	1.0*M* $NaNO_3$	GE	24
Acetic acid	$MeHg^+ + L^- \rightleftharpoons MeHgL$	3.6	undefined	POL	12
		3.18	0.4*M*?	NMR	15
		3.20 ± 0.04	1.0*M* $NaNO_3$	GE	24
Pyruvic acid	$MeHg^+ + L^- \rightleftharpoons MeHgL$	2.31 ± 0.08	1.0*M* $NaNO_3$	GE	This work
Laevulinic acid	$MeHg^+ + L^- \rightleftharpoons MeHgL$	2.51 ± 0.04	1.0*M* $NaNO_3$	GE	This work
Glycine	$MeHg^+ + L^- \rightleftharpoons MeHgL$	7.88 ± 0.05	0.4*M*?	NMR	16
		6.07	undefined	NMR/GE	19
		7.52 ± 0.05	1.0*M* $NaNO_3$	GE	24
α-Alanine	$MeHg^+ + L^- \rightleftharpoons MeHgL$	7.52 ± 0.05	1.0*M* $NaNO_3$	GE	24
β-Alanine	$MeHg^+ + L^- \rightleftharpoons MeHgL$	7.56 ± 0.07	0.4*M*?	NMR	16
dl-Valine	$MeHg^+ + L^- \rightleftharpoons MeHgL$	7.41 ± 0.01	0.4*M*?	NMR	16
		7.27 ± 0.06	1.0*M* $NaNO_3$	GE	24
L-Serine	$MeHg^+ + L^- \rightleftharpoons MeHgL$	6.93 ± 0.06	1.0*M* $NaNO_3$	GE	This work
L-Cysteine[b]	$MeHg^+ + LH^- \rightleftharpoons MeHgLH$	15.7	0.1*M*?	DISTR	12
		15.16[c]	1.0*M* (Na,H)Cl	DISTR	13
		7.19[d]	undefined	PMR/GE	19
		14.81 ± 0.12[e]	1.0*M* $NaNO_3$	GE	This work
	$MeHg^+ + HLH \rightleftharpoons MeHgLH + H^+$	7.1	0.1*M*?	DISTR	12
		7.04[f]	1.0*M* (Na,H)Cl	DISTR	13
		6.69 ± 0.12	1.0*M* $NaNO_3$	GE	This work
	$MeHg^+ + L^{2-} \rightleftharpoons MeHgL^-$	15.70 ± 0.12	1.0*M* $NaNO_3$	GE	This work
	$MeHg^+ + H^+ + L^{2-} \rightleftharpoons MeHgLH$	24.96 ± 0.08	1.0*M* $NaNO_3$	GE	This work
	$MeHgL^- + H^+ \rightleftharpoons MeHgLH$	9.05	0.4*M*?	NMR	17
		8.92	undefined	PMR/GE	19
		9.25 ± 0.14	1.0*M* $NaNO_3$	GE	This work
	$MeHgCl + HLH \rightleftharpoons MeHgLH + H^+ + Cl^-$	1.71	1.0*M* (Na,H)Cl	DISTR	13
L-Methionine	$MeHg^+ + L^- \rightleftharpoons MeHgL$	7.40 ± 0.01	0.4*M*?	NMR	18
		7.17 ± 0.16	1.0*M* $NaNO_3$	GE	This work
L-Asparagine	$MeHg^+ + L^- \rightleftharpoons MeHgL$	6.32 ± 0.06	1.0*M* $NaNO_3$	GE	This work

(a) Temperature 25° if not otherwise specified.
(b) $HLH_2^+ = HSCH_2CH(NH_3^+)COOH$; $HLH = HSCH_2CH(NH_3^+)COO^-$; $HL^- = HSCH_2CH(NH_2)COO^-$ $LH^- = {}^-SCH_2CH(NH_3^+)COO^-$ and $L^{2-} = {}^-SCH_2CH(NH_2)COO^-$
(c) Calculated value assuming ($MeHg^+ + Cl^- \rightleftharpoons MeHgCl$), log K = 5.33,[26] and pK of the cysteine thiol group (pK_{SH}) = 8.12.
(d) At 22°.
(e) Calculated value.
(f) Calculated with the equilibrium constants given in (c) above.

are based on the equilibrium constants given in Table 1.

The results show that of the potential co-ordination sites available in amino-acids, the deprotonated sulph-hydryl group can bind methylmercury(II) most strongly. The complexation, however, depends predominantly on the pH of the solution, owing to protonation of the ligand and hydrolysis of methylmercury(II). In neutral solution the following order of binding power is most likely to prevail:

sulph-hydryl > amine > hydroxide > carboxylate

Only the 1:1 complexes are formed in presence of an excess of the ligand, because methylmercury(II) has very little Lewis acidity after co-ordinating with a sulph-hydryl or amino-group. However, with an excess of methylmercury(II), L-cysteine may also form a 2:1 complex, (log β = 12.40),[19] the second methylmercury ion being co-ordinated to the amino-group. The formation of such a species was considered to be very unlikely under the experimental conditions used in the present studies and was not of interest because in biological systems the ligand is always present in excess.

Since cysteine residues are the integral component of many sulphur-containing proteins, the present results support the conclusion that the sulph-hydryl group is the main target in metal poisoning, because after co-ordinating with methylmercury it can disrupt the enzyme structure and consequently impede its normal catalytic functions.

REFERENCES

1. T. Takeuchi, *Minamata Disease. A Study of Toxic Systems by Organic Mercury*, Univ. of Kumamato, 1966.
2. K. Irukayama, *Adv. Water Pollut. Res.*, 1967, **3,** 153.
3. *FAO Fisheries Rept.*, No. 99, Rome, 1971.
4. K. Borg, H. Wanntorp, K. Erne and E. Hanko, *J. Appl. Ecol.*, 1971, **3,** 171.
5. J. M. Wood, *Adv. Environ. Sci. Technol.*, 1971, **2,** 39.
6. J. M. Wood, F. S. Kennedy and C. G. Rosen, *Nature*, 1968, **220,** 173.
7. S. Jensen and R. Jernelöv, *ibid.*, 1969, **223,** 753.
8. J. S. Thayer, *J. Chem. Educ.*, 1971, **48,** 807.
9. W. Muller, *Vom Wasser*, 1972, **39,** 257.
10. M. Imura, E. Sukegawa, S. K. Pan, K. Kagao, J. Y. Lim, T. Kwan and T. Ukita, *Science*, 1971, **172,** 1248.
11. M. M. Jones and T. H. Pratt, *J. Chem. Educ.*, 1976, **53,** 342.
12. R. B. Simpson, *J. Am. Chem. Soc.*, 1961, **83,** 4711.
13. M. Niitsu, T. Manri and N. Iritani, *Bull. Chem. Soc. Japan*, 1978, **51,** 2165.
14. D. L. Rabenstein, C. A. Evans, M. C. Tourangeau and M. J. Fairhurst, *Anal. Chem.*, 1975, **47,** 338.
15. S. Libich and D. L. Rabenstein, *ibid.*, 1973, **45,** 118.
16. D. L. Rabenstein, R. Ozubko, S. Libich, C. A. Evans, M. T. Fairhurst and C. Suvanprakorn, *J. Coord. Chem.*, 1974, **3,** 263.
17. D. L. Rabenstein and M. T. Fairhurst, *J. Am. Chem. Soc.*, 1975, **97,** 2086.
18. M. T. Fairhurst and D. L. Rabenstein, *Inorg. Chem.*, 1975, **6,** 1413.
19. Y. Hojo, Y. Sugiura and H. Tanaka, *J. Inorg. Nucl. Chem.*, 1976, **38,** 641.
20. Y. S. Wong, P. C. Chieh and A. J. Carty, *Can. J. Chem.* 1973, **51,** 2597.
21. N. J. Taylor, Y. S. Wong, P. C. Chieh and A. J. Carty, *J. Chem. Soc., Dalton Trans.*, 1975, 438.
22. A. J. Carty and R. Kishimoto, *Aust. J. Chem.*, 1977, **30,** 669.
23. O. Budevsky, F. Ingman and D. H. Liem, *Acta Chem. Scand.*, 1973, **27,** 1277.
24. M. Jawaid, F. Ingman and D. H. Liem, *ibid.*, 1978, **32,** 333.
25. F. Ingman and D. H. Liem, *ibid.*, 1974, **28,** 947.
26. M. Jawaid, F. Ingman, D. H. Liem and T. Wallin, *ibid.*, 1978, **32,** 7.
27. M. Jawaid, *Talanta*, 1978, **25,** 215.
28. P. Brauner, L. G. Sillén and R. Whiteker, *Arkiv Kemi*, 1969, **31,** 365.
29. L. Pehrsson, F. Ingman and A. Johansson, *Talanta*, 1976, **23,** 769.
30. *Some Laboratory Methods in Current Use at the Department of Inorganic Chemistry*, The Royal Institute of Technology, Stockholm, Sweden (available on request).
31. M. Schellenberg and G. Schwarzenbach, *Helv. Chim. Acta*, 1965, **48,** 28.
32. A. Ringbom, *Complexation in Analytical Chemistry*, Wiley/Interscience, New York, 1963.
33. N. Ingri, W. Kakolowicz, L. G. Sillén and B. Warnqvist, *Talanta*, 1967, **14,** 1261.

Talanta Vol. 28. pp. 145 to 148
© Pergamon Press Ltd 1981. Printed in Great Britain
0039-9140/81/030145-04$02.00/0

ROOM-TEMPERATURE PHOSPHORESCENCE AND FLUORESCENCE OF NITROGEN HETEROCYCLICS ADSORBED ON SILICA GEL CHROMATOPLATES

ROBERT J. HURTUBISE

Chemistry Department, University of Wyoming, Laramie, Wyoming 82071, U.S.A.

(*Received* 11 *July* 1980. *Accepted* 9 *October* 1980)

Summary—The room-temperature phosphorescence of benzo[*f*]quinoline and phenanthridine has been enhanced considerably by spotting HBr–ethanol solutions of the compounds onto silica gel chromatoplates. Acridine showed no room-temperature phosphorescence but gave very strong fluorescence on silica gel chromatoplates. The analytical aspects are discussed, and some evidence is provided for the interactions of the compounds with the substrate.

Lloyd and Miller[1] commented on the earliest known report of room-temperature phosphorescence (RTP). Yen-Bower *et al.*[2] have discussed the present status and future of room-temperature phosphorimetry. Several investigators have shown the usefulness of RTP as an analytical technique.[3–11] Some workers have given partial explanations for the interactions between adsorbate and sorbent which are necessary to give RTP from compounds adsorbed on solid surfaces.[12–17]

In the present work hydrobromic acid was found to enhance the RTP of benzo[*f*] quinoline (B[*f*]Q) and phenanthridine more than hydrochloric acid did. Acridine gave no RTP under any of the conditions investigated, but yielded a very intense fluorescence when adsorbed on silica gel chromatoplates. Hydriodic acid had been found previously not to induce RTP from B[*f*]Q,[17] so was not investigated in this work.

EXPERIMENTAL

Apparatus

All RTP and fluorescence data were obtained with a Farrand MK-2 spectrofluorometer fitted with a phosphorescence rotary chopper and a thin-layer chromatogram scanner. Interchangeable metal slits giving band-widths of 5 or 10 nm were used at the entrance and exit positions of both the excitation and emission monochromators. For RTP measurements, a slit program of 5 nm, 5 nm (entrance) and 5 nm, 5 nm (exit) or 5 nm, 5 nm (entrance) and 10 nm, 10 nm (exit) was used. In addition, the largest slit provided by the manufacturer was used in the optical head just below the chromatoplate. For solid-surface fluorescence measurements 2.5-nm band-width slits were used, with a medium-size slit in the optical head. For solution-fluorescence measurements the 2.5-nm slits were used.

Reagents

Ethanol was purified by distillation. B[*f*]Q, phenanthridine, acridine were recrystallized. Indole and carbazole were >99% pure reagents (Aldrich Chemical Co., Milwaukee, Wisconsin). EM Laboratories plastic-backed TLC chromatoplates and Macherey, Nagel & Co. plastic-backed TLC plates and CEL 300 AC-30 (acetylated cellulose) TLC chromatoplates were used.

Procedures

Solutions were prepared in neutral or acidic ethanol and were sufficiently concentrated for only 1 μl of each solution to be needed. Experimental details of the spotting technique were given earlier.[9] The chromatoplates were dried for 15 min at 110° then cooled to room temperature, and the luminescence signals were measured with the Farrand MK-2.

RESULTS AND DISCUSSION

RTP of B[f]Q

Previously it was reported that RTP was observed from B[*f*]Q adsorbed on silica gel chromatoplates from ethanolic hydrochloric or hydrobromic acid solutions.[17] Figure 1 compares the relative RTP signals

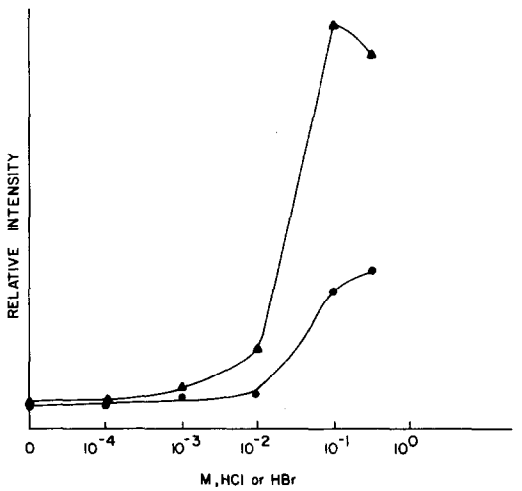


Fig. 1. The RTP of 100 ng of B[*f*]Q *vs.* HCl (●) and HBr (▲) concentration in ethanol.

from 100 ng of B[*f*]Q adsorbed on silica gel from solutions with different acid concentrations. It is seen that the hydrobromic acid system yielded substantially greater RTP signals than the hydrochloric acid system. Earlier work[9] showed that the hydrochloric acid curve levelled off at acid concentrations $>0.5M$. It was reported earlier that some commercial silica gel chromatoplates contain a salt of polyacrylic acid as a binder, and it was necessary to use these chromatoplates to induce RTP.[17] When the chromatoplate is treated with acid, the polyacrylate is partially or completely converted into polyacrylic acid. It was postulated that carboxyl groups of the polyacrylic acid formed hydrogen bonds with the π-ring system of $B[f]QH^+$ and that the $-NH^+$ entity formed a hydrogen bond with a carbonyl oxygen atom of polyacrylic acid. This bonding holds the compound rigidly and allows strong RTP to be detected.[17] The additional enhancement in RTP observed with hydrobromic acid in this work is probably due to the external heavy-atom effect. The hydrobromic acid appears to serve a dual purpose, indicated by the following reaction. (It is assumed that the polyacrylate is the sodium salt).

$$—COONa + HBr \rightarrow —COOH + NaBr$$

The carboxyl groups should anchor B[*f*]Q, and bromide ions from the sodium bromide should cause an increase in the rate of intersystem crossing, resulting in greater phosphorescence yield than that from the corresponding hydrochloric acid system. Bromide ions from the hydrobromic acid might also participate in the heavy-atom effect, but the chromatoplates were heated at 110° for about 15 min, so a large fraction of any excess of acid was volatilized. Figure 1 shows that hydrobromic acid concentrations greater than $0.1M$ cause a decrease in RTP. This could be due to a quenching effect by acid not removed from the chromatoplate, but this aspect was not investigated further. There is no corresponding decrease for the hydrochloric acid system.

A striking aspect of Fig. 1 is the relatively large jump in RTP in both systems, especially the hydrobromic acid one. The curves look somewhat like titration curves. However, the 100 ng of B[*f*]Q used is 5.6×10^{-4} μmole so the B[*f*]Q should have been completely protonated at acid concentrations lower than that of the sharp rise in the curves. For example, with both curves the mid-point of the sharp rise occurs at about $0.05M$ acid or 0.05 μmole of acid spotted onto the chromatoplate. Previously, infrared data had shown that the binder (the polyacrylate salt) in the chromatoplate was converted into the acid form upon acid treatment.[17] Saunders[18] commented that if hydrochloric acid is added to aqueous solutions of polyacrylic acid, there is a decrease in viscosity because the ionization of the polyacrylic acid is reduced and the polymer chains become more tightly coiled. If sodium hydroxide is added, many of the carboxyl groups become ionized, mutual repulsion forces the polymer chains to uncoil, and the extended chains result in a higher solution viscosity. A contributing factor in the strong RTP observed under acidic conditions may therefore be that molecules of B[*f*]Q are entrapped by the tightly coiled polymer chains. This aspect needs further investigation.

Table 1. Comparison of RTP signals of 100 ng B[*f*]Q spotted from ethanol and ethanolic HCl, HBr, and NaBr solutions onto an EM silica gel chromatoplate

Solution	Relative intensity*
Ethanol	1.0
HCl ($0.1M$)	4.0
HBr ($0.1M$)	16
NaBr ($0.1M$)	2.6

* Mean for duplicate spots; chromatoplates dried twice at 110°C for 15 min.

Table 1 compares the RTP intensities for B[*f*]Q adsorbed from ethanol and from ethanolic hydrochloric acid, hydrobromic acid and sodium bromide solutions. The results show that sodium bromide enhances the RTP of B[*f*]Q but certainly not as much as hydrobromic acid, indicating that acidic conditions contribute substantially to strong RTP.

The linear range for phosphorescence from B[*f*]Q in the $0.1M$ ethanolic hydrobromic acid system was approximately 0–50 ng. The coefficient of correlation was 0.997. The limit of detection was calculated as 8 ng, taken as that for a sample signal equal to twice the background signal. Earlier a linear range of 0–125 ng and a limit of detection of 3 ng were reported for the hydrochloric acid system.[9] The earlier data were obtained with a modified spectrodensitometer. The data obtained in this work were obtained with a commercially available spectrophotofluorometer and a TLC scanning attachment. It seems that the modified spectrodensitometer yields lower limits of detection, but this aspect would have to be checked by further varying the experimental conditions.

RTP of other compounds

The RTP of 100 ng of phenanthridine on an EM chromatoplate was enhanced by a factor of 1.8 when the sample solution was prepared in ethanolic $0.1M$ hydrobromic acid instead of the corresponding hydrochloric acid medium, but the phenanthridine signal from the hydrobromic acid system was smaller by a factor of 2.3 than that of 100 ng of B[*f*]Q in the same medium. The limit of detection of phenanthridine in this system was calculated to be 16 ng. Previously the limit of detection in the ethanolic $0.1M$ hydrochloric acid system was reported as 6 ng (again with the modified spectrodensitometer).[9]

Carbazole, indole, and acridine yielded no RTP when adsorbed onto EM silica chromatoplates from ethanol, or the ethanolic $0.1M$ acid media, but acridine gave strong fluorescence when adsorbed from

Table 2. Excitation and emission wavelengths for acridine adsorbed on silica gel and 30% acetylated cellulose chromatoplates from neutral and 0.1*M* acid ethanolic solutions

Chromatoplate	λ_{ex}, *nm*	λ_{em}, *nm*
EM silica gel (neutral)	353	452, 472
EM silica gel (acidic)	354	452, 474
Silica gel-G (neutral)	354	452, 473
Silica gel-G (acidic)	352	452, 473
30% acetylated cellulose (neutral)	356	454, 469
30% acetylated cellulose (acidic)	357	452, 467

these solutions. Some of these aspects will be discussed in the next section.

Fluorescence of acridine

Fluorescence excitation and emission spectra were obtained from acridine adsorbed on silica gel, aluminium oxide, and 30% acetylated cellulose chromatoplates from ethanol and ethanolic 0.1*M* hydrochloric acid. Table 2 gives the major excitation and emission wavelengths for acridine adsorbed on silica gel and 30% acetylated cellulose. For both brands of silica and the 30% acetylated cellulose chromatoplates, the excitation and emission wavelengths are essentially the same. This suggests that the same form of acridine is adsorbed on these surfaces from either neutral or acidic solution. The excitation and emission spectra of acridine adsorbed on an aluminium oxide chromatoplate were ill-defined because of fluorescent impurities in the aluminium oxide. Table 3 shows the excitation and emission wavelengths for acridine in neutral and acidic ethanol solutions. Comparison with the emission wavelengths in Table 2 suggests that protonated acridine is responsible for the fluorescence from the chromatoplates. Lloyd[19] discussed the fluorescence of acridine in a silica-gel microcolumn detector for use in high-performance liquid chromatography. He indicated that when acridine dissolved in 1,2-dichloromethane was excited as it passed through the column, it was protonated in the excited state by silica gel and the protonated acridine emitted fluorescence. The data in Table 2 suggest that the protonated form of acridine is emitting fluorescence from both silica gel and acetylated cellulose (the emission wavelengths are similar for both the neutral and acidic systems). In this work, the chromatoplate

Table 3. Excitation and emission wavelengths for acridine in neutral and acidic ethanol

Solvent	λ_{ex}, *nm*	λ_{em}, *nm*
Ethanol (neutral)	271, 319, 394	400, 416, 440
Ethanol (acidic)	271, 329, 379, 401, 420	458, 476

Table 4. Comparison of fluorescence signals from 100 ng of acridine spotted from acid–ethanol solutions onto an EM silica gel chromatoplate

[HCl], *M*	Relative intensity
0	1.0
0.02	1.6
0.06	1.7
0.10	1.9
0.20	1.6

was dried and then the emission data were obtained; thus it appears that silica gel and 30% acetylated cellulose can protonate acridine in the "dry" state. In Lloyd's system, the silica gel was "wet" with 1,2-dichloromethane. From comparison of the excitation wavelength for a given sample in Table 2 with the excitation wavelengths in Table 3, no conclusion can be drawn about the protonation of acridine in the excited state, because of the many excitation wavelengths for the solution system. Mataga *et al.*[20] have shown that acridine and other nitrogen heterocycles are more basic in the excited singlet state; thus this condition should favour protonation of acridine by silica gel and 30% acetylated cellulose.

Mataga and Tsuno[21] have shown that the fluorescence of acridine increases with increased acid concentration. The concentration of hydrochloric acid was varied to obtain a measure of the change in fluorescence intensity of acridine with acid content. Table 4 shows the results obtained for acridine adsorbed on silica gel; no large changes in the fluorescence intensity were observed. The solid-surface fluorescence excitation and emission spectra were obtained for all the samples in Table 4 and only slight changes in the shapes of peak maxima of the spectra were observed. These results suggest that a large fraction of the acridine adsorbed from a neutral ethanol solution was protonated by the silica gel. The increase in fluorescence with increase in acid concentration up to 0.10*M* implies that silica gel does not completely protonate the acridine adsorbed from neutral ethanol solution. However, changes caused in the silica gel by the acid could account for partial increase in the fluorescence yield. For example, Deanin[22] discussed the Si–O–Si bond and its lability in acid medium. It seems that excess of acid would attack siloxane groups to produce additional silanol groups. Also, Ford and Hurtubise[17] showed the importance of the EM chromatoplate binder, polyacrylic acid or its salt, in the RTP of B[*f*]Q. Their infrared results indicated the binder was present as a salt and at a level of about 5% by weight. As discussed earlier, addition of acid to a chromatoplate containing the binder converted carboxylate groups into carboxyl groups. The formation of silanol groups and carboxyl groups could possibly alter the environment so that the fluorescence of acridine would be enhanced. Acridine was present on the chromatoplate in 5.6×10^{-4} μmole amount. For

a 0.02*M* hydrochloric acid medium, 0.02 μmole of acid was spotted onto the chromatoplate, so excess acid was present in the solution and on the chromatoplate. The formation of a chloride salt on the chromatoplate by the reaction of hydrochloric acid with the polyacrylate should be considered, *e.g.* sodium chloride from sodium polyacrylate. Possibly the decrease in fluorescence with 0.20*M* hydrochloric acid, shown in Table 4, is related to the amount of chloride salt on the chromatoplate. Experiments with variation of acid concentration were not done with silica gel G or 30% acetylated cellulose.

ANALYTICAL CONSIDERATIONS

Using hydrobromic acid to enhance the RTP of B[*f*]Q and phenanthridine has the advantage of lowering the detection limits. Other pyridine-type heterocyclics should show a similar effect and this aspect is being investigated. The background signal from the chromatoplates was not considered a serious problem and good RTP detection limits were obtained. However, if the background signal were substantially decreased a considerable improvement in the detection limits would be achieved. Lowering of substrate background was discussed recently by Yen-Bower *et al.*[2]

The experimental procedure for obtaining both fluorescence and RTP in this work was very simple. For example, 1 μl of solution was spotted onto the chromatoplate, the chromatoplate was dried for 15 min, and the signals were then measured with a commercial spectrophotometer with a TLC scanning attachment. The fact that commercial equipment can be readily used is important because solid-surface luminescence analysis is easily available to analysts. The reproducibility was good. The samples were run in duplicate and no large variations were noted. Similar results were found earlier[9] with a different instrument.

The fact that no RTP was obtained for acridine is not a serious disadvantage. Intense fluorescence signals were obtained for this compound and thus acridine can be determined by solid-surface fluorescence. Ford and Hurtubise[23] developed a separation method for B[*f*]Q and phenanthridine in shale oil and identified the two components by obtaining both solid-surface fluorescence and RTP for each constituent. The results obtained in this work and the work just mentioned indicate that both solid-surface fluorescence and phosphorescence should be considered for analytical development work. If a compound does not yield RTP, it should be tested for fluorescence and *vice versa*. If a compound yields both RTP and fluorescence, then the information can be very useful in characterization and identification work because of the additional information obtained. Also, the additional information may help in minimizing luminescence impurities by choosing the technique that gives the smaller interfering signal.

Acknowledgement—This work was partially supported by the Department of Energy (Office of Basic Energy Sciences) under contract No. DE-AC02-80ER10624.

REFERENCES

1. J. B. F. Lloyd and J. N. Miller, *Talanta*, 1979, **26**, 180.
2. E. L. Yen-Bower, J. L. Ward, G. Walden and J. D. Winefordner, *ibid.*, 1980, **27**, 380.
3. E. M. Schulman and C. Walling, *J. Phys. Chem.*, 1973, **77**, 902.
4. R. A. Paynter, S. L. Wellons and J. D. Winefordner, *Anal. Chem.*, 1974, **46**, 736.
5. P. G. Seybold and W. White, *ibid.*, 1975, **47**, 1199.
6. T. Vo-Dinh, G. L. Walden and J. D. Winefordner, *ibid.*, 1977, **49**, 1126.
7. I. M. Jakovljevic, *ibid.*, 1977, **49**, 2048.
8. R. M. A. von Wandruszka and R. J. Hurtubise, *ibid.*, 1976, **48**, 1784.
9. C. D. Ford and R. J. Hurtubise, *ibid.*, 1979, **51**, 659.
10. E. L. Yen-Bower and J. D. Winefordner, *Appl. Spectrosc.*, 1979, **33**, 9.
11. L. J. C. Love, M. Skrilec and J. G. Habarta, *Anal. Chem.*, 1980, **52**, 754.
12. R. M. A. von Wandruszka and R. J. Hurtubise, *ibid.*, 1977, **49**, 2164.
13. E. M. Schulman and R. T. Parker, *J. Phys. Chem.*, 1977, **81**, 1932.
14. C. D. Ford and R. J. Hurtubise, *Anal. Chem.*, 1978, **50**, 610.
15. E. L. Yen-Bower and J. D. Winefordner, *Anal. Chim. Acta*, 1978, **102**, 1.
16. G. J. Niday and P. G. Seybold, *Anal. Chem.*, 1978, **50**, 1577.
17. C. D. Ford and R. J. Hurtubise, *ibid.*, 1980, **52**, 656.
18. K. J. Saunders, *Organic Polymer Chemistry*, pp. 121–122. Chapman & Hall, London, 1973.
19. J. B. F. Lloyd, *Analyst*, 1975, **100**, 529.
20. N. Mataga, Y. Kaifu and M. Koizumi, *Bull. Chem. Soc. Japan*, 1956, **29**, 373.
21. N. Mataga and S. Tsuno, *ibid.*, 1957, **30**, 368.
22. R. D. Deanin, *Polymer Structure, Properties and Applications*, p. 40. Cahners Books, Boston, 1974.
23. C. D. Ford and R. J. Hurtubise, *Anal. Lett.*, 1980, **13(A6)**, 485.

Talanta Vol. 28, pp. 149 to 155
Pergamon Press Ltd 1981. Printed in Great Britain

0039-9140/81/030149-07$02.00/0

PHOTOMETRIC COMPLEX-FORMATION TITRATION OF SUBMICROMOLAR AMOUNTS OF ZIRCONIUM

J. KRAGTEN

Natuurkundig Laboratorium, Universiteit van Amsterdam, Valckenierstraat 65, 1018 XE Amsterdam, The Netherlands

and

A. PARCZEWSKI

Department of Analytical Chemistry, Jagiellonian University, Krakow, Poland

(*Received* 2 *October* 1980. *Accepted* 7 *October* 1980)

Summary—Even in strongly acidic solution Zr(IV) forms polynuclear hydroxide complexes. In these compounds tetrameric units play a dominant role. When the Zr atoms in these units are interconnected through double OH-bridges (olated bonds) quantitative formation of Zr–EDTA is possible at room temperature. When the double OH-bridges are replaced by single oxygen-atom bridges (oxolated bonds) the units are less reactive. The oxolated tetramers are still capable of reacting quantitatively with EDTA if heated to about 100°; higher oxolated polymers are not. When these higher polymers are formed during the initial adjustment of conditions for a titration, large errors will be observed. By suitable treatment of the solutions oxolation can be restricted sufficiently to permit titrations with an error of less than 1%. Semi-Xylenol Orange has been found to be a suitable indicator for direct titrations; back-titrations are performed with Bi^{3+}, with PAR as indicator.

Zirconium ions can form several polynuclear hydroxide complexes, even in strongly acidic medium. The complexes exhibit a variety of chemical properties. Some are inert; others remain reactive with indicators, EDTA, sulphate, oxalate and other ions. In some cases the reaction products are non-stoichiometric. This behaviour is the reason why unreliable results may easily arise in determination of zirconium by spectrophotometry and complexometry, techniques which generally offer good possibilities for accurate determinations of small amounts of metals.

The literature gives the impression that when good reproducibility is achieved, this is related in some way to specific treatment of the zirconium solutions. The simplest supposition would be that the treatment led to the predominance or possibly even the quantitative formation of mononuclear reaction products.

Faced with the need to determine μg amounts of zirconium in the presence of 1000 times as much silver with an error of less than about 0.5% we decided to investigate systematically which treatments might lead to accurate results in complexometry at the micromolar level. Recently published new views on the hydrolytic behaviour of zirconium have been used to explore suitable ways to form mononuclear Zr–EDTA complexes quantitatively. It will be shown that both direct titration and back-titration of zirconium are possible with an error less than 1% and a relative standard deviation of 0.5%.

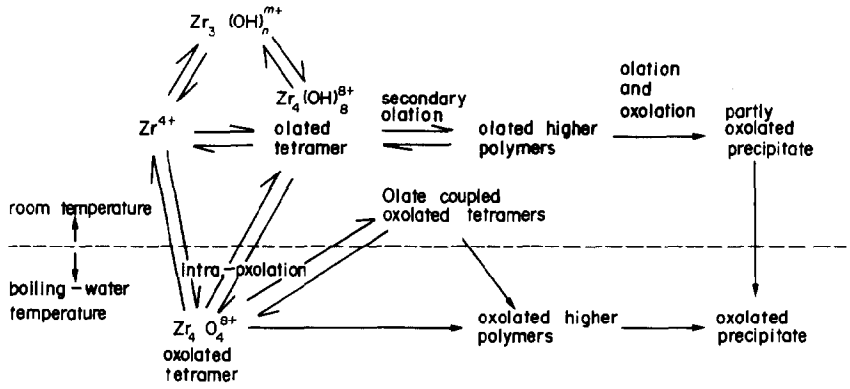
Hydrolytic behaviour of zirconium

Zirconium ions are rather small and have a strong tendency to hydrolyse. Therefore the aqueous chemistry of zirconium is mostly confined to strongly acidic solutions. Until recently it was assumed that both in solids and in aqueous solutions Zr(IV) was present as the zirconyl ion, ZrO^{2+}. Nowadays a tetrameric structure in which four zirconium ions are linked through double olate bridges (Fig. 1), are regarded as the fundamental ionic structural unit. This tetrameric unit reacts rapidly at room temperature with EDTA and indicators, in which case the olate bridges are broken down and mononuclear compounds are formed.[1–4] In strongly acidic medium the olated tetramer is in equilibrium with Zr^{4+} ions.

At higher pH these reactions are obscured by hydrolytic formation of nearly inert hydroxides. The hydrolytic behaviour can be represented schematically as shown in Scheme 1. The right-hand side of this scheme is given in a simplified form. The occurrence of the different compounds depends upon the acidity, zirconium concentration and temperature. To give insight into the practical implications, different experimental situations will be elucidated below.

When moderately acidic concentrated zirconium solution is allowed to stand, two processes will take place.[1] The first is that the tetrameric units form octamers and higher homologues by further secondary olation. In these enlarged olated polymers the bonds between the tetrameric units are of nearly the same strength as those within the tetramers. This secondary olation process proceeds at room temperature and is reversible.

The second process is the oxolation of the bonds within and between the tetrameric units (oxygen



Scheme 1.

bridges are formed between the zirconium ions). It leads to new tetrameric units such as those shown in Fig. 2. These units are more compact and have much stronger internal bonds. The oxolation is slow at room temperature, but proceeds rapidly at elevated temperatures.

Both the olated and the oxolated tetramers have been isolated as nitrates with maintenance of their distinct properties.[4] The two zirconyl nitrates are white crystalline substances, indistinguishable both in outward appearance and in elemental analysis. We have a hydroxide nitrate $Zr_4(OH)_8.(NO_3)_8.4H_2O$ and an oxide nitrate $Zr_4O_4.(NO_3)_8.8H_2O$; a unique "zirconyl" ion ZrO^{2+} does not exist.[4] The commercially available nitrate (and presumably also the chloride) will contain a mixture of both tetrameric forms.

Oxolated tetramers need heating and a strongly acidic medium to achieve equilibrium with Zr^{4+} ions. In moderately acidic solution and at low zirconium concentrations intra-oxolation is reversible at boiling-water temperatures with EDTA present in excess. Oxolated higher polymers, especially those occurring at higher zirconium concentrations, are more resistant. In these compounds the intertetrameric bonds are extensively oxolated. They are not split up by EDTA, but form precipitates of non-stoichiometric composition. If the analytical concentration of zirconium is below $10^{-3}M$, these higher polymers can be broken up into Zr^{4+} ions (quantitatively) at 100° in 5 min after acidification to $2M$ hydrochloric, nitric or perchloric acid concentrations.[5] (The system is then outside the region of polycomplexation, Fig. 3.[6])

In aqueous solution zirconium can be present in the Zr^{4+} form, but Zr^{4+} ions will predominate only at low concentrations and in strongly acidic medium ($<10^{-5}M$ Zr at $1M[H^+]$, or $<10^{-3}M$ Zr at $2M[H^+]$, see Fig. 3).

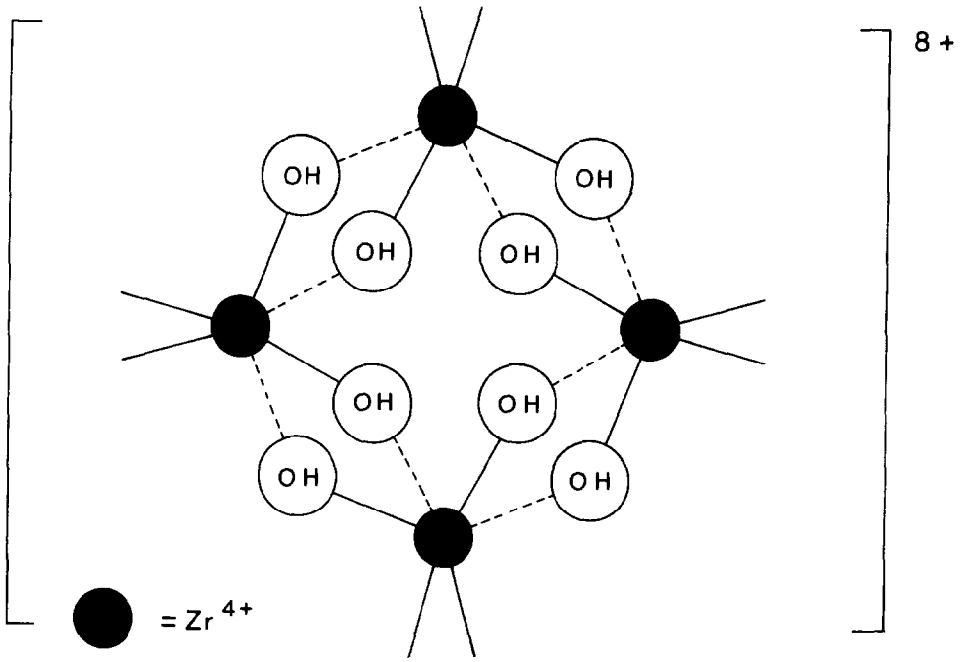


Fig. 1. The olated tetramer.

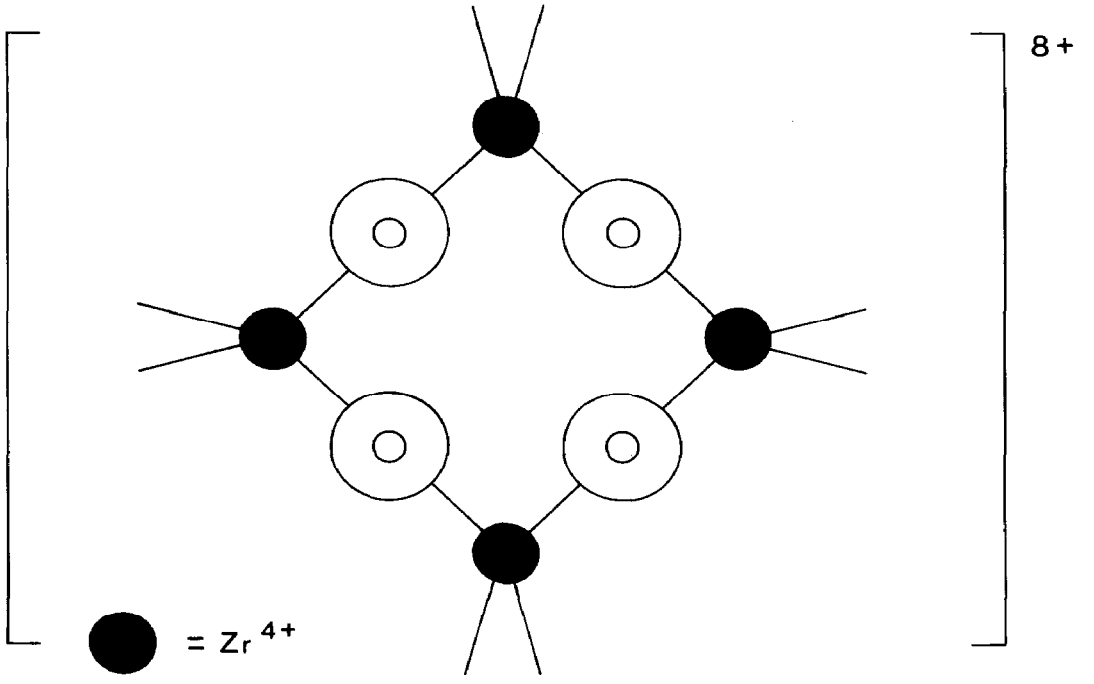


Fig. 2. The oxolated tetramer.

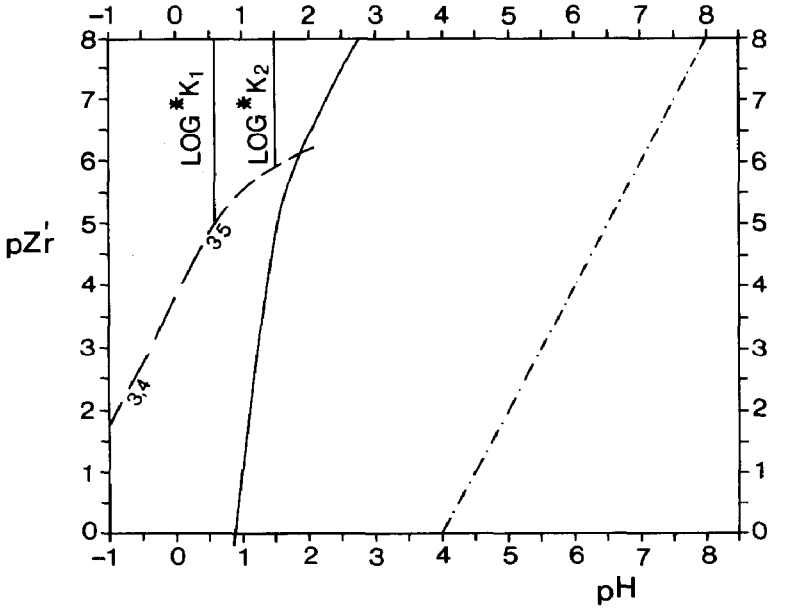


Fig. 3. The solid line surrounds the region of freshly precipitated hydrous zirconium (hydr)oxide. The dashed line marks the region where more than 1% of the total amount of zirconium in solution is present in some polynuclear hydroxide form. The main components formed under the different borderline conditions are indicated near the borderline sections. The vertical lines bound the predominance areas of mononuclear hydroxides. The dot–dash line indicates the borderline of precipitation when EDTA is present in 0.0001*M* excess. The data used for the plot are estimated for ionic strength 2, perchloric acid medium and room temperature:

$\log {}^*\beta_1 = -0.6$
$\log {}^*\beta_2 = -2.1$
$\log {}^*\beta_3 = -6.5$
$\log {}^*\beta_4 = -11.2$
$\log {}^*\beta_5 = -17$

$\log {}^*\beta_{43} = 5.1$
$\log {}^*\beta_{53} = 5.5$
$\log {}^*\beta_{84} = 8.0$

$\log {}^*K_{s0} = -0.4$

$\log K_{Zr\text{EDTA}} = 29.0$

$\log K_{HZr\text{EDTA}} = 20.7$

At the $10^{-2}M$ level Zr^{4+} ions are hydrolysed even in strongly acidic medium (Fig. 3). Besides $Zr_4(OH)_8^{8+}$, $Zr_3(OH)_4^{8+}$ and $Zr_3(OH)_5^{7+}$ have been proposed to explain the hydrolytic phenomena observed at room temperature.[7,8] Baes and Mesmer[8] considered the possible entities and critically reviewed the hydrolysis constants. Using these constants, Kragten[6] found that if only 1% of the zirconium is present as a polycomplex, the predominating species is either $Zr_3(OH)_4^{8+}$ or $Zr_3(OH)_5^{7+}$ (Fig. 3). When the polycomplex fraction is higher the tetramer $Zr_4(OH)_8^{8+}$ will predominate. The trimeric compounds can be regarded as intermediates in the formation of the ring-shaped tetramer. It is obvious that the scheme describing the hydrolytic properties of zirconium holds so long as anions other than hydroxide do not interact with the hydrolysis products. It is certain that chloride, nitrate and perchlorate ($I = 2$) do not influence the degree of polymerization.[9]

Olated higher polymers will coagulate to form a hydrous oxide precipitate at $pc_H > 1$.[5,8] This precipitate is by no means in equilibrium with the solution. An aging process, consisting mainly of oxolation and dehydration, will begin immediately after precipitation. On acidification at room temperature this precipitate dissociates only partly into the desired active forms Zr^{4+} and $Zr_4(OH)_8^{8+}$. In general, heating for some minutes at boiling-water temperature in a medium of $5M$ acid (hydrochloric, nitric or perchloric) is necessary to break up the oxolated bonds quantitatively and to make zirconium fully accessible again for analytical purposes.[5] If a precipitate has been heated to dryness, the oxolation will be so strong that only concentrated hydrofluoric acid will be able to redissolve the residue quantitatively in a form suitable for analysis. (If perchloric acid is used for the dissolution instead of hydrofluoric, oxolated polymers precipitating with EDTA will be formed.)

It should be noted that the information above has been gathered from investigations using extraction with Pyrocatechol Violet,[1,2] conductimetry,[2,4] co-precipitation,[2] X-ray analysis,[3] infrared spectroscopy,[3] thermogravimetry,[3] densitometry,[4] rheology,[4] refractometry,[4] ion-exchange chromatography,[4] acidimetry,[7] dialysis[9] and light-scattering.[10]

In general the olated and oxolated polymers differ in their behaviour towards anions. Without losing its structure, the oxolated tetramer $(Zr_4O_4)^{8+}$, for instance, can form salts with the general composition $(Zr_4O_4)X_8$ with $X = Cl^-, NO_3^-, ClO_4^-$. On dissolution of the salt half the anions will split off, leaving a complex $(Zr_4O_4X_4)^{4+}$, in which the other anions remain (weakly) bound.[5] The olated tetramer does not react with these anions at moderate concentrations.

Sulphate can take over the bridge function of the hydroxide ions in the olated tetramer,[1,5] reinforcing its branches and consequently decreasing its reactivity. Such a substitution has not been observed in the oxolated compounds; obviously the Zr–O–Zr bridge is too strong for it.

Sulphate reacts with the oxolated compounds to form a precipitate. This has also been observed with phosphate, citrate, tartrate, oxalate, and as we already know, EDTA.[2,5]

Fluoride forms very strong complexes with zirconium and can break up both types of tetramer. Because of the high side-reaction coefficient, fluoride has to be removed quantitatively before zirconium can be titrated.

The complexometry of zirconium

The reaction of zirconium with EDTA has been investigated at different pH-values.[5] Under defined conditions Bobtelsky and Rafailoff[11] observed successive end-points when zirconium was titrated with EDTA or *vice versa*. Considering these experimental conditions in the light of the previous section it can be concluded that olated chain-like polymers predominated and that the stoichiometric ratios at the end-points were related to the chain-lengths of the zirconium polycomplexes.

In other cases where obviously oxolated long-chain polymers predominated, non-stoichiometric precipitates were formed.

In strong acid medium Zr^{4+} ions and EDTA ($=H_4Y$) form soluble 1:1 complexes, as has been established by potentiometry,[12–14] ion-exchange and adsorption studies,[15–19] and proton magnetic resonance methods.[20] The existence of ZrY, ZrHY and Zr(OH)Y has been reported. (Even stability constants have been estimated[21–24].) There is evidence that at high concentrations a dimer Zr_2Y_2 is formed,[25,26] and the existence of a mixed dinuclear compound ($NdZrY_2$) also seems very likely.[25,27] However, at normal concentrations and certainly at the low level we are using, their influence can be neglected.

The conditional stability constant of ZrY can be calculated only fairly roughly from the thermodynamic stability constants[21–24] and the hydrolysis constants of monomeric Zr–OH species.[8] Nevertheless the estimated[6] $\log K' \simeq 11$ for $[H^+] = 0.1M$ is sufficiently large to allow titrations at very low concentrations.[28,29] Taking into account the titration condition $\log(C_{Zr}K'_{ZrEDTA}) > 3.5$ for an error of $<1\%$, and making allowance for the indicator side-reaction, a titration at a zirconium concentration of even $10^{-6}M$ should be possible. Theoretically, back-titrations should also be possible.[30] It has been found experimentally that even a $5 \times 10^{-7}M$ concentration can be titrated.)

There remains the question whether practical conditions can be arranged so that Zr and EDTA will react quantitatively in 1:1 ratio. In the past, several procedures for direct titrations and back-titrations of mmole amounts of Zr have been proposed.[5] Most procedures suffer from a lack of accuracy as a result of interference by large oxolated polymers. Kotrlý *et al.*[31] showed that in the range $3–15 \times 10^{-6}M$ zirconium can be titrated at pc_H 0.5 with high accuracy. Their zirconium stock solutions were, in fact, free

from oxolated higher polymers, since their experimental titration conditions corresponded to a point outside the polycomplex region in Fig. 3 and oxolated polymers were not present and could not interfere.

From their experience with dilute solutions and the phenomenon that EDTA is able to break up both the olated and the oxolated tetramers present at higher concentrations, it was concluded that in principle it might be possible to titrate zirconium accurately at higher concentrations and pc_H 1. Experimentally it has been confirmed that with photometric end-point detection both direct titration and back-titration of zirconium in the range 10^{-4}–$10^{-5}M$ can be performed conveniently at pc_H 1. The experimental conditions correspond to a point inside the polycomplex region of Fig. 3, and consequently olated polymers and presumably oxolated tetramers will be present during the initial stages. The crucial point is that the generation of oxolated higher polymers must be avoided during the preparation of the titration solution. This is possible at concentrations below $10^{-3}M$ in the way given in the next section. At higher concentrations ($10^{-2}M$) less accurate results are obtained. It seems likely that under these conditions (pc_H 1) oxolated higher polymers are irreversibly formed in the titration system.

EXPERIMENTAL

Indicator selection

Most triphenylmethane metallochromic indicators form 2:2 compounds with metal ions having high charge and co-ordination number. When M_2I_2 compounds are present systematic deviations may be expected when photometric end-point detection by extrapolation is used, if the concentrations are low and the wavelength selected is at the absorbance maximum of M_2I_2.[29,32]

Theoretically the systematic deviations will be inversely related to the strength of the M_2I_2 complex. Systematic deviations of up to -10% could be demonstrated for thorium titrations with Xylenol Orange (XO) as indicator at the pH at which the Th–XO complex is just formed.[29,32]

XO has been tested for its usefulness in zirconium titrations. From the shape of the titration curve and the systematic deviation found on extrapolation ($\sim -6\%$) it can be concluded that zirconium and XO form an M_2I_2 complex. A typical example is given in Fig. 4 for an acidity of $0.1M$ $[H^+]$. Theoretically the systematic deviation decreases at higher pH because of the increase in the conditional stability constant of M_2I_2, but in practice this is not possible because of the effect of hydrolysis of zirconium. Kotrlý selected a wavelength of 530 nm, a value presumably near the wavelength of the isosbestic point of Zr(XO) and $Zr_2(XO)_2$, instead of 575 nm where $Zr_2(XO)_2$ has its maximum absorbance. From our experience with zirconium and earlier investigations with thorium and bismuth, the wavelength needs empirical selection for each individual titration if high accuracy is wanted, because the experimental conditions vary too widely for the same wavelength to be used successfully. In general, indicators forming M_2I_2 complexes are therefore less suitable.

Semi-Xylenol Orange (SXO) is a triphenylmethane dye with only one iminodiacetic acid group; it does not form 2:2 complexes. We have not established whether zirconium and SXO form predominantly a 1:1 complex or a 1:2 complex at pc_H 1, but this is unimportant because theoretically 1:n complexation does not lead to systematic deviations.[29] Accurate end-points have been found experimentally (Fig. 4). It can be seen that zirconium and SXO (both at the $10^{-5}M$ level) form a complex even at pc_H 0. Titrations can be performed at $pc_H > 0.4$. The reaction of Zr–SXO with EDTA proceeds slowly at room temperature. Heating to 90° is necessary to make the titration practicable.

Some azo dyes were also tested but turned out to be unsuitable; the pc_H of the titration had to be so high that complete exclusion of oxolation was impossible (see note on reaction with PAR).

For the back-titration, bismuth is used with PAR as indicator. This combination allows a titration at a pc_H as low as 1.5. In principle thorium, with SXO, can also be used for the back-titration, but has the disadvantage that a higher pc_H (2) is needed, which leads more easily to manipulative errors, with a consequently lower accuracy (as Zr–EDTA dissociates at pH > 5–6, neutralization with base has to be performed without overshooting; this is more difficult at higher final pH values; see also results and discussion).

Apparatus

The photometric titrations were performed in a Zeiss PMQ II spectrophotometer with a titration assembly for

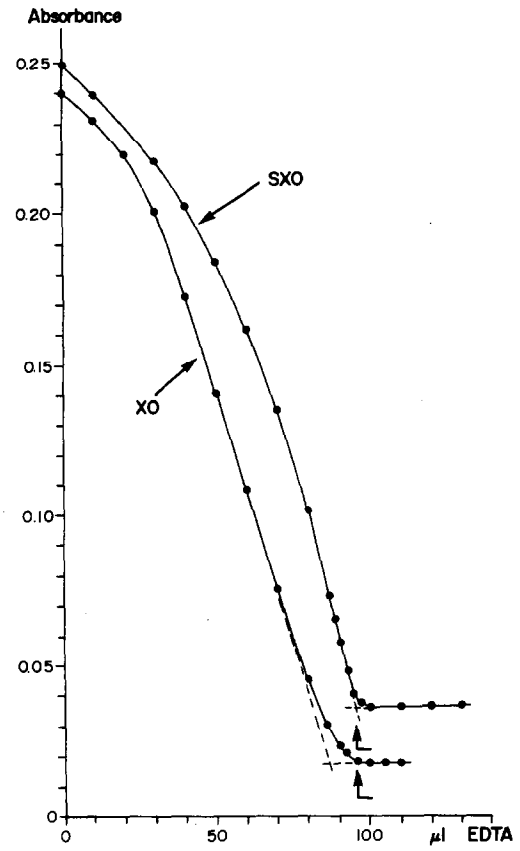


Fig. 4. Curves of the photometric titration of 44.4 µg of Zr in perchloric acid medium at pc_H 1 and 90°, with $0.005M$ EDTA. The curves were obtained with SXO and XO as indicator (present in excess) at wavelengths 530 and 575 nm respectively. With SXO there is no significant systematic deviation. The arrows indicate the equivalence points. The end-point found on extrapolation shows a large systematic deviation in the case of Xylenol Orange.

10- and 20-ml cells (2-cm path-length) complete with heating facility and an air-driven magnetic stirrer. The titrant solutions were added with a Metrohm E457 microburette. The tips of the 0.5-ml syringes were bent upwards in order to prevent gravitational diffusional losses when they were immersed in the fluid.

The water was purified by sub-boiling demineralized water in quartz distillation apparatus.[33]

The pH-equipment was calibrated in concentration units.

Reagents

All solutions were prepared from analytical-reagent grade chemicals and sub-boiled water.[33]

Ethylenediaminetetra-acetic acid disodium salt solution, 5×10^{-3}M. Standardized against "Specpure" copper with purified 1-(2-thiazolylazo)-2-resorcinol (TAR) as indicator. It was found that the blanks were less than 0.1% and that the mean value had a relative standard deviation of 0.15%.

Indicator solutions: XO and SXO 5% in water, PAR 5% in alcohol. Commercial XO was used, SXO was prepared similarly to XO,[34] but with a deficit of iminodiacetic acid. Both indicators were purified by extraction. Commercial PAR was used without purification.

Zirconium solution A, 2×10^{-3}M. A 50-mg amount of zirconium metal (99.9% pure) was dissolved in 0.5 ml of concentrated hydrofluoric acid in a 50-ml Teflon beaker (vigorous reaction in the cold). To this solution 0.5 ml of concentrated nitric acid and 0.5 ml of perchloric acid were added. The solution was heated to expel hydrogen fluoride and continued until white fumes of perchloric acid appeared. If it was feared that solid material would separate and dry up, some drops of concentrated nitric or perchloric acid were added. After cooling to room temperature the material was transferred to a 250-ml standard flask with 1*M* perchloric or nitric acid and made up to the mark with this acid.

Properly made stock solutions were found to be stable for at least a month.

Zirconium solution B, 10^{-4}M. This solution was prepared from solution *A* by dilution with 0.1*M* nitric or perchloric acid. Solution *B* was found to be stable for at least a week if kept at room temperature. Possible changes in the hydrolytic state had no measurable influence on the titre.

Bismuth solution, 0.005M. Bismuth nitrate dissolved in dilute nitric acid (pc_H 0.5).

Procedure for direct titrations

Transfer 5 ml of solution *B*, containing 40–50 μg of zirconium, to a titration cell. Dilute with 0.1*M* perchloric or nitric acid to 20 ml. Heat the solution on a hot-plate to about 90°, put it in the heated titration assembly of the spectrophotometer and keep the temperature at 90°. Add 20 μl of the SXO solution and titrate with EDTA at a wavelength of 530 nm. Find the end-point by graphical extrapolation.

Procedure for back-titrations

Transfer 5 ml of zirconium solution *B*, containing 40–50 μg of zirconium, to a titration cell. Add an appropriate amount of EDTA and stir for 2 min. Add dilute nitric acid (pH 1.5) and adjust the pH of the final solution to 1.5 by dropwise addition of dilute ammonia solution (1 + 5). Add 20 μl of the alcoholic PAR solution and titrate photometrically with bismuth at a wavelength of 530 nm. Find the end-point by graphical extrapolation.

RESULTS AND DISCUSSION

Some results are given in Table 1. Oxolation produced by heating at pc_H 1 does not interfere in the direct titration. Both SXO and EDTA can break down the oxolated products if the titration is performed at 90°.

The use of alkaline solutions for pH-adjustment of the solutions for a direct titration should be avoided. Local excesses of base can cause disintegration of the Zr–SXO complex and the formation of a zirconium hydroxide precipitate which, once formed, will not redissolve completely; negative systematic deviations will then be found. The pH adjustment should be done by dilution with a properly selected dilute acid with which the titration-cell can be filled up.

It is not necessary to acidify the EDTA titrant solution. The small additions of titrant do not lead to systematic deviations.

In the case of back-titrations it is not necessary to heat the solution after the addition of EDTA in excess. The olated tetramer will have reacted in 2 min at pc_H 1.0. For the back-titrations the pc_H has to be adjusted to 1.5. If sodium hydroxide is used for that purpose, negative errors will be obtained as Zr–EDTA will be locally converted into a $Zr(OH)_4.nH_2O$ precipitate. The precipitation region of Zr–EDTA in the pZr′–pH diagram starts at pH ~ 6 (Fig. 3) and is deeply penetrated. Nevertheless

Table 1. Direct titration (*A*) and back-titration (B) determination of 44.4 μg of zirconium

Method	Sample	Medium	Zr found, μg	Number of samples	σ_{rel}, %	Syst. error, %
A	Zr	$HClO_4$, pc_H 1.0	44.2	4	0.7	not significant
	Zr + Ag (50 mg)†	$HClO_4$, pc_H 1.0	44.4	4	1.1	not significant
	Zr	$HClO_4$, pc_H 1.0	44.1	12*	0.2	0.7
	Zr	HNO_3, pc_H 1.0	44.2	4	0.2_5	0.5
B	Zr	HNO_3, pc_H 1.5	44.5	4	0.4_5	not significant
	Zr + Ag (50 mg)§	HNO_3, pc_H 1.5	44.5	6	0.8	not significant
	Zr + Ag (50 mg)†	HNO_3, pc_H 1.5	44.1	4	0.7	not significant

* Three series of 4 portions, taken at pc_H 0.9, 1.0 and 1.1, did not differ significantly and have been combined.
† Treatment as for real samples (evaporation not to dryness).
§ Stock solutions of Zr and Ag were mixed without further treatment.

the systematic errors seldom exceed 5‰, indicating that the precipitation proceeds rather slowly. The use of dilute ammonia, which causes less penetration of the precipitation region because of buffer action, turns out to be allowable (for theory of manipulation errors see refs. 8 and 35). Significant deviations were not observed when dilute ammonia was added drop by drop with vigorous stirring.

Fluoride and sulphate interfere and have to be expelled by heating with concentrated perchloric acid if they are introduced in the dissolution of alloys.

Up to 10 times more concentrated zirconium solutions can be titrated with the same accuracy.

The analysis has been applied to Zr–Ag samples. The samples were dissolved in 1 ml of nitric acid to which a few drops of hydrofluoric acid had been added. After dissolution about 1 ml of perchloric acid was added and the solution was evaporated almost to dryness in order to remove hydrogen fluoride; this treatment was repeated. Then the solution was diluted with 1*M* nitric acid. The procedure was then the same as for zirconium alone, as described in the experimental section. Silver in amounts up to about 1000 times that of zirconium does not interfere. In the case of the Ag–Zr samples it turned out that significant deviations appeared if during the dissolution and evaporation some of the solids dried out. This effect can be attributed to oxolation of the zirconium polymers. This can be reversed by heating with 5*M* perchloric acid, but this has the disadvantage of introducing a blank because of the comparatively large amount of acid necessary.

In conclusion it can be said that zirconium can be titrated successfully if the formation of oxolated higher polymers or precipitation of hydroxide is prevented during adjustment of the pH. Heating and localized high pH, especially in combination, have to be avoided.

Note. The reaction with PAR (pyridylazoresorcinol) shows a peculiar kinetic phenomenon which is worth reporting. If PAR and oxolate-free zirconium solutions (both $10^{-4}M$) are mixed at pc_H 1, the yellow colour changes slightly. If the unbuffered solution is then neutralized rapidly to pH 3–3.5, the solution will remain at this pH for about 10 sec, then the pH jumps to ~8 and the solution turns purple-red. The phenomenon can be reversed by acidification to pc_H 1, and the sequence of events can be repeated many times. It is assumed that PAR reacts with the tetramer as the pH is raised, and prevents precipitation, and that the pH-jump is caused by a release of hydroxide ions from the olate tetramer $[Zr_4(OH)_8^{84}]$.

Acknowledgement—We are indebted to Mrs. L. G. Decnop-Weever for putting purified Semi-Xylenol Orange at our disposal and for critically reading the manuscript.

REFERENCES

1. G. A. Yagodin, A. M. Chekmarev and V. G. Kazak, *Zh. Neorgan. Khim.*, 1970, **15**, 1284; (*Russ. J. Inorg. Chem.*, 1970, **15**, 659).
2. G. A. Yagodin, V. G. Kazak and V. V. Tarasov, *ibid.*, 1972, **17**, 2399; (1972, **17**, 1252).
3. G. A. Yagodin, E. G. Teterin and V. G. Kazak, *ibid.*, 1972, **17**, 3026; (1972, **17**, 1591).
4. G. A. Yagodin and V. G. Kazak, *ibid.*, 1973, **18**, 107; (1973, **18**, 53).
5. S. V. Elinson and K. I. Petrov, *Analytical Chemistry of Zirconium and Hafnium*, pp. 20–37. Ann Arbor–Humphrey Science Publishers, London, 1969.
6. J. Kragten, *Atlas of Metal–Ligand Equilibria in Aqueous Solution*, p. 767. Horwood, Chichester, 1978.
7. A. J. Zielen and R. E. Connick, *J. Am. Chem. Soc.*, 1956, **78**, 5785.
8. C. F. Baes, Jr. and R. E. Mesmer, *The Hydrolysis of Cations*, pp. 152–158. Wiley, New York, 1976.
9. A. K. Babko and G. I. Gridchina, *Zh. Neorgan. Khim.*, 1961, **6**, 1326.
10. Y. Shiokawa, A. Sato and S. Suzuki, *Bull. Chem. Soc. Japan*, 1976, **49**, 2456.
11. M. Bobtelsky and R. Rafailoff, *Anal. Chim. Acta*, 1957, **17**, 308.
12. L. O. Morgan and N. L. Justus, *J. Am. Chem. Soc.*, 1956, **78**, 38.
13. B. J. Intorre and A. E. Martell, *ibid.*, 1960, **82**, 358.
14. *Idem, Inorg. Chem.*, 1964, **3**, 81.
15. A. N. Ermakov, I. N. Marov and T. A. Evtikova, *Zh. Neorgan. Khim.*, 1966, **11**, 1155.
16. L. I. Tikhonova, *Zh. Strukt. Khim.*, 1967, **12**, 939.
17. M. Kyrš and R. Caletka, *Talanta*, 1963, **10**, 1115.
18. R. Caletka, M. Kyrš and J. Rais, *J. Inorg. Nucl. Chem.*, 1964, **26**, 1443.
19. J. Prášilová and J. Havlíček, *ibid.*, 1970, **32**, 953.
20. Y. O. Aochi and D. T. Sawyer, *Inorg. Chem.*, 1966, **5**, 2085.
21. V. G. Sochevanov and G. A. Volkova, *Zh. Neorgan. Khim.*, 1969, **14**, 118; (*Russ. J. Inorg. Chem.*, 1969, **14**, 61).
22. L. G. Sillén and A. E. Martell, *Stability Constants*, 2nd Ed., Special Publ. No. 17, The Chemical Society, London, 1964.
23. *Idem, ibid.*, Supplement No. 1, Special, Publ. No. 25, 1972.
24. R. M. Smith and A. E. Martell, *Critical Stability Constants*, Plenum Press, New York, 1974.
25. T. V. Ternovaya, V. P. Shelest, N. A. Kostromina and Ts. B. Konunova, *Zh. Neorgan. Khim.*, 1975, **20**, 3221; (*Russ. J. Inorg. Chem.*, 1975, **20**, 1979).
26. *Idem, ibid.*, 1977, **22**, 3050.
27. *Idem, ibid.*, 1979, **24**, 666.
28. J. Kragten, *Talanta*, 1971, **18**, 311.
29. *Idem, Mikrochim. Acta*, 1971, 821.
30. *Idem, Talanta*, 1973, **20**, 937.
31. S. Kotrlý, V. Staffa and M. Zimáková, *Sb. Ved. Praci, Vys. Skola Chem. Technol. Pardubice*, 1970/II-23, 37.
32. J. Kragten, *Z. Anal. Chem.*, 1973, **264**, 356.
33. E. C. Kühner, R. Alvarez, P. J. Paulsen and T. J. Murphy, *Anal. Chem.*, 1972, **44**, 2050.
34. D. C. Olson and D. W. Margerum, *ibid.*, 1962, **34**, 1299.
35. J. Kragten, *Talanta*, 1977, **24**, 483.

Talanta Vol. 28, pp. 157 to 160
© Pergamon Press Ltd 1981. Printed in Great Britain
0039-9140/81/030157-04$02.00/0

EXTRACTION OF TIN BY THE USE OF POLYURETHANE FOAM

V. S. K. Lo and A. Chow

Department of Chemistry, University of Manitoba, Winnipeg, Manitoba, Canada

(*Received* 9 *July* 1980. *Accepted* 6 *October* 1980)

Summary—Three types of polyurethane foam were tested for the extraction of tin by static and flow systems. The amount of tin extracted varied with the type of foam, acid strength, and chloride and metal-ion concentrations. Quantitative extraction and recovery could be achieved. Open-cell polyurethane foam sponge is thought to act as a "solid solvent-extractant" for tin from aqueous solution. Distribution coefficients up to 5.6×10^3 were obtained and the capacity of the foam was up to 8% tin by weight.

Flexible polyurethane foam has been used as an absorbent for a number of substances since 1970 when Bowen[1] first reported its use. Many other studies of the extraction and separation of various inorganic and organic species from aqueous solution have been reviewed by Braun[2,3] and by Moody.[4]

Although tin has a relatively low order of toxicity, it is still considered to be a pollutant and may be of concern as industrial uses increase. Tin can be extracted from aqueous solution by diethyl ether[5] or di-isopropyl ether[6] and has also been separated from other metals by ion-exchange,[7] paper chromatography,[8] gas chromatography[9] and electrochromatography.[10] This paper reports the extraction and recovery of tin from aqueous solution by use of polyurethane foam.

EXPERIMENTAL

Materials

Three types of polyurethane foam were studied; a polyester polyurethane (DiSPo plugs) obtained from Canlab (Winnipeg, Canada), an acid-resistant polyether polyurethane obtained from Union Carbide, and normal polyether polyurethane cut from commercial sheets of open-cell foam.

A radioactive tracer solution of tin(IV) chloride was prepared by bubbling chlorine into a solution of $^{119m}SnCl_2$ in 4*M* hydrochloric acid (NEN Canada Ltd) for 2 hr. All other chemicals were reagent-grade and the water used was doubly distilled and demineralized.

Tin(II) solution was freshly prepared from tin(II) chloride in 3*M* hydrochloric acid, on the day of use. A 1000 ppm stock solution of tin(IV) was prepared by dissolving tin metal powder in 12*M* hydrochloric acid, making up to volume with 1.2*M* hydrochloric acid, and letting stand for several weeks (it was then used over a period of a year). Before dilution for use in test samples, the solution was tested with mercuric chloride to establish the absence of tin(II). The tin solutions were standardized by iodimetric titration.[11]

Procedure

Pyrex tubes (2 cm outer diameter and 25 cm long) fitted with Teflon stopcocks were used for making the columns. The foam (diameter $\geq$ 2.1 cm) was placed at the bottom of the column and a low vacuum was applied to the solution-filled column to remove any trapped air from the foam. The solution was then allowed to flow through the foam at a rate of 0.07–0.11 $ml.min^{-1}.cm^{-2}$.

Some static experiments were performed by placing some foam in a beaker with the desired amount of solution and using the base of a measuring cylinder to compress the foam periodically. Alternatively, a single automatic squeezer consisting of an eccentric motor-driven cam pushing a glass plunger up and down in a glass cell (2.5-cm stroke, 30 strokes/min) was used, or a large multiple automatic squeezer consisting of an eccentric cam (91 cm long, 14 cm diameter), turned by a heavy-duty motor, which depressed and released as many as 10 glass plungers (5-cm stroke, 24 strokes/min) in a thermostatically controlled air-bath at 22.0 $\pm$ 0.5°.

Sample solutions were analysed with a Model 306 Perkin–Elmer atomic-absorption spectrometer, under the standard conditions listed in the Perkin–Elmer handbook,[12] or by a radioactive tracer technique using a Baird Atomic Model 530 gamma spectrometer with a 2-in, well-type NaI(Tl) detector. Aliquots of the tin(IV) tracer solution ($^{119m}SnCl_4$) were mixed thoroughly with the samples to yield a counting rate of at least 10 times the background. A 15-ml aliquot was taken from each sample and counted in 20-mm diameter test-tubes which fitted exactly into the well of the counter. The activity of all samples was determined by counting for five successive 100-sec intervals and correcting for the background.

The following equations were used:

$$\% \text{ Extraction} = \frac{\text{concentration before extraction—concentration after extraction}}{\text{concentration before extraction}} \times 100$$

$$\text{Distribution coefficient} = \frac{\text{concentration of metal on foam}}{\text{concentration of metal in final solution}}$$

In the second equation both concentrations were expressed in w/w terms.

The recovery of tin was determined by counting the stripping solution (0.1*M*, 0.1*M* hydrochloric acid, sodium hydroxide, water or acetone). The activities were corrected for matrix effects by using standards prepared in the same media. The degree of stripping from the foam was first calculated and then the overall recovery.

Alternatively, the foam could be counted directly after being dried by squeezing between paper towels.

RESULTS AND DISCUSSION

Polyester polyurethane (DiSPo)

Some preliminary static and flow experiments using the polyester polyurethane foam indicated maximum extraction of both tin(II) and tin(IV) from ~6*M* hydrochloric acid. Although nearly complete extraction of tin(IV) could be achieved with a slow flow-rate of 0.1 ml/min, the distribution coefficient was found to be only 120 ± 8 for 6*M* hydrochloric acid and 732 ± 23 for 10*M* lithium chloride medium after 45 min when the static system was used. Because this foam had poor stability in acid and began to disintegrate after 45 min in 6*M* hydrochloric acid, no further studies were considered practical.

Acid-resistant foam

The extraction of tin(IV) by acid-resistant foam from hydrochloric acid media was determined by using atomic-absorption spectrometry, while the extraction from hydrobromic acid was examined by the tracer technique. The curve of degree of extraction against hydrochloric acid concentration shows a maximum of 33% at 4*M* acidity while that for the hydrobromic acid system shows a maximum of 60% at 7*M* acidity. Increasing concentrations of lithium chloride enhance the extraction of tin(IV) by the acid-resistant foam. When the squeezing time for the extraction of tin(IV) from 0.2*M* hydrochloric acid and 10*M* lithium chloride was increased, the percentage extracted rose rapidly during the first 2 hr and reached a plateau of 95 ± 2% after 6 hr at which it was considered that equilibrium had been reached. The distribution coefficient was 2280 ± 50 which is considerably higher than that obtained with polyester foams.

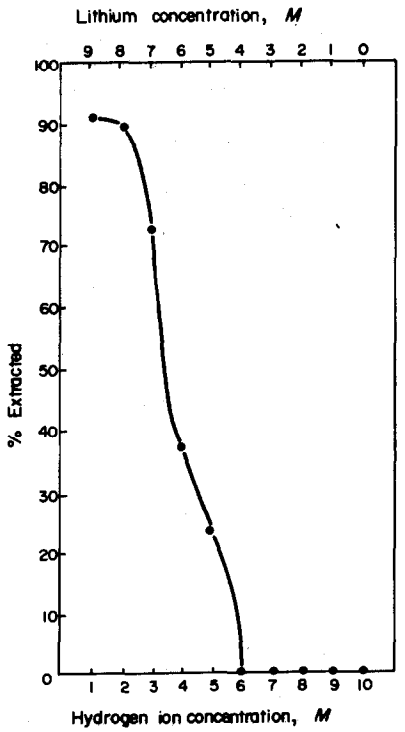


Fig. 1. Effect of hydrochloric acid and lithium chloride concentration on the extraction of tin(IV) by acid-resistant foam. Tin(IV) concentration 100 ppm; volume 150 ml; squeezing time 6 hr.

Figure 1 shows the effect of hydrochloric acid and lithium chloride concentrations on the extraction of tin(IV) by acid-resistant foam. The chloride concentration was kept at 10*M* and the hydrogen-ion concentration was increased.

At high hydrogen-ion concentration the extraction decreases drastically, perhaps because of formation of a species which is not extractable. However, it was observed that the foam swelled in 10*M* hydrochloric acid, to about 2½ times its original size, which suggests that the lower extraction may be due to some alteration in the structure of the foam.

The capacity of acid-resistant foam was determined with tin(IV) concentrations from 200 to 1000 ppm. The degree of extraction decreased but the amount of tin extracted per gram of foam was about the same for the three highest tin(IV) concentrations. The average of these three highest results gave a capacity of 62 ± 8 mg/g of foam or 6% by weight of tin. This is considered higher than that which could be due to surface adsorption, since the surface area of the foam was shown to be 0.081 m^2/g by the B.E.T. method using krypton.[13] If $SnCl_4$ was the extractable species, one molecule would occupy a surface area of 7.98×10^{-19} m^2. The 6% by weight of tin would need an area of 111 m^2/g of foam if the extractable species was present only on the surface of the foam. Therefore, the extraction process must involve absorption in addition to adsorption.

Tin(IV) could be recovered from the foam by the use of water, 0.1*M* hydrochloric acid or 0.1*M* sodium hydroxide. Only 40–50% of the tin(IV) was recovered with water or 0.1*M* sodium hydroxide, but 95 ± 3% could be recovered with 0.1*M* hydrochloric acid.

Regular polyurethane foam

The extraction of tin(IV) from various concentrations of hydrochloric acid was investigated by the tracer technique. This indicated maximum extraction from 3*M* hydrochloric acid with a distribution coefficient of 141 ± 9 and minimal extraction at hydrochloric acid concentrations below 1*M*.

The effect of hydrofluoric, hydrobromic and hydriodic acids on the extraction of tin(IV) by regular polyurethane foam was also examined. The tin tracer was added to 3*M* solutions of the acids and the foams were squeezed for 2 hr. At an acid concentration of 3*M*, tin(IV) was 0% extracted from hydrofluoric acid, 32% from hydrochloric acid, 18% from hydrobromic acid and 32% from hydriodic acid. The extraction of tin(IV) with diethyl ether[14,15] is 17% from 6*M* hydro-

Table 1. Effect of metal halides on the extraction of tin(IV) by regular polyurethane foam*

Metal halide	Sn extracted, %
LiCl	14 ± 2
NaCl	25 ± 2
KCl	34 ± 2
LiBr	33 ± 2
NaBr	38 ± 2
KBr	40 ± 4
LiI	28 ± 2
NaI	37 ± 2
KI	39 ± 4

* Volume of solution, 50 ml; squeezing time, 2 hr; tin(IV) concentration, tracer only; concentration of metal halide, 3*M*.

chloric acid and 85% from 4*M* hydrobromic acid. Tin is extracted to a greater extent from hydrobromic acid than from hydrochloric acid but at an acid concentration of 3*M* it is extracted more efficiently from hydrochloric acid. The size of the anion does not seem to have a consistent effect on the extraction process.

Table 1 shows the effects of solutions of metal halides (3*M*) on the extraction of tin(IV) by regular polyurethane foam. The tin(IV) tracer was extracted to an extent of 1% from 1*M* sodium fluoride, and 15% from 1*M* sodium chloride. As the size of the cation increases, the extent of extraction increases and this is also the case when the size of the anion is increased from chloride to bromide. The extent of extraction of the tracer from bromide and iodide solution was identical.

The extraction of 100 ppm of tin(IV) from 3*M* hydrochloric acid in the presence of 100 and 1000 ppm of Bi(III), Cu(II), Fe(II), Fe(III), Sb(III), Sb(V) and Zn(II) chlorides was studied. Only iron(III) at 1000 ppm interfered. This could be due to iron(III) competing with tin(IV) for the sites available on the foam. Thus, the extraction of iron(III) by the foam would lower its capacity for tin(IV).

Figure 2 shows the effect of lithium chloride concentration on the extraction of tin(IV) by regular polyurethane foam. The curve shows a gradual increase in extraction as the concentration of lithium chloride increases, so it appears that the extraction of tin(IV) is chloride-dependent. The distribution coefficient was calculated to be 5630 ± 120. With 50 ml of solution, it was found that up to 98 ± 2% of the tin(IV) could be extracted from 10*M* lithium chloride and 0.12*M* hydrochloric acid with 6 hr of squeezing.

The capacity of regular polyurethane foam for tin(IV) is 81 ± 9 mg/g. Tin(IV) could be recovered from the foam to the extent of 95 ± 3% by squeezing it for 6 hr in 50 ml of 0.1*M* hydrochloric acid. Acetone was found to recover 98.7 ± 0.5% of the tin(IV). Improved precision was achieved by counting the

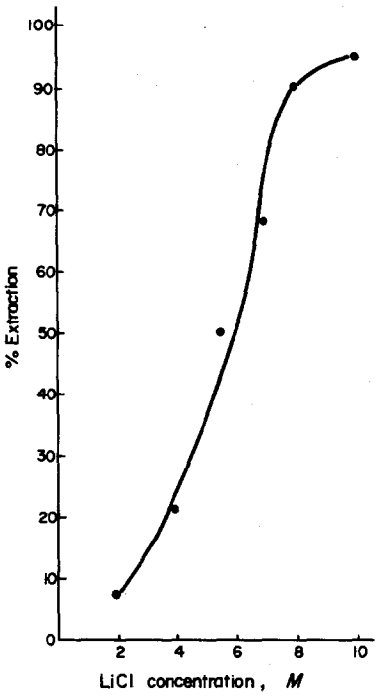


Fig. 2. Effect of lithium chloride concentration on the extraction of tin(IV) by regular polyurethane foam. Tin(IV) concentration 100 ppm; volume 150 ml; squeezing time 24 hr.

foam itself for unrecovered radioactivity, rather than counting the recovery solvent.

Table 2 gives a summary of the distribution coefficients for the three types of foam studied. The results showed that regular polyurethane foam is 2.5 times better than acid-resistant foam and 7.5 times better than DiSPo plugs. The hydrochloric acid–lithium chloride system was better than the hydrochloric acid system, perhaps because of more complete formation of the extractable species or because of the effect of the hydrogen ion.

It is thought that $HSnCl_5$ could be one of the more extractable species in the Sn(IV)–foam system. The following equations involve the formation of a series of species, each of which would have a different extractability.

$$Sn^{4+} + Cl^- \rightleftharpoons SnCl^{3+}$$

$$SnCl^{3+} + Cl^- \rightleftharpoons SnCl_2^{2+}$$

$$SnCl_2^{2+} + Cl^- \rightleftharpoons SnCl_3^{+}$$

$$SnCl_3^{+} + Cl^- \rightleftharpoons SnCl_4$$

$$SnCl_4 + Cl^- \rightleftharpoons SnCl_5^-$$

$$SnCl_5^- + H^+ \rightleftharpoons HSnCl_5(\text{aqueous})$$

$$HSnCl_5(\text{aqueous}) \rightleftharpoons HSnCl_5(\text{foam})$$

The species $HSnCl_5$ would distribute itself between the aqueous phase and the foam. The extractability of such species by the foam would depend on the hydro-

Table 2. Distribution coefficients of tin(IV)

Foam type	Distribution coefficient	
	HCl system	HCl–LiCl system
DiSPo plugs	120 ± 8	732 ± 23
Acid-resistant foam	129 ± 7	2280 ± 48
Regular polyurethane foam	141 ± 9	5630 ± 119

HCl system	DiSPo plugs	Acid-resistant foam	Regular polyurethane foam
Tin(IV) concentration, *ppm*	100	100	Tracer
Volume of solution, *ml*	20	150	150
Squeezing time, *hr*	3/4	1	2
HCl concentration, *M*	6	4	3

HCl–LiCl system	DiSPo plugs	Acid-resistant foam	Regular polyurethane foam
Tin(IV) concentration, *ppm*	100	100	100
Volume of solution, *ml*	150	50	150
Squeezing time, *hr*	24	6	24
HCl concentration, *M*	0.12	0.12	0.12
LiCl concentration, *M*	10	10	10

gen-ion, metal-ion and chloride concentrations. When the hydrogen-ion concentration is high, species such as H_2SnCl_6 may be formed and less readily extracted. Thus quantitative extraction would require the optimal combination of the hydrogen-ion, metal-ion and chloride concentrations.

An alternative explanation for the extraction process could involve the protonation of ether sites in the polymer and requires the presence of hydrogen, tin and chloride ions. The mechanism of the extraction of tin by polyurethane foam may be more complicated than this but more studies on the physical nature of the foam and the identification of the complex species involved are required.

This work suggests that the use of polyurethane foam is more effective than the conventional diethyl ether system. Polyurethane foam seems to act as the equivalent of a free ether or ester in solution and yet offers the advantages of a relatively inert support for various complexing agents such as tri-n-butyl phosphate,[16] dimethylglyoxime[17] and dithizone.[18] The foams can be adopted for field use since they are easy to carry, light, reusable and relatively inexpensive.

Acknowledgement—This work was supported by the National Research Council of Canada.

REFERENCES

1. H. J. M. Bowen, *J. Chem. Soc.*, 1970, 1082.
2. T. Braun and A. B. Farag, *Talanta*, 1975, **22**, 699.
3. *Idem, Anal. Chim. Acta*, 1978, **99**, 1.
4. G. J. Moody and J. D. R. Thomas, *Analyst*, 1979, **104**, 1.
5. H. M. Irving and F. J. C. Rossotti, *ibid.*, 1972, **77**, 801.
6. F. C. Edwards and A. F. Voigt, *Anal. Chem.* 1949, **21**, 1204.
7. R. Klement and A. Kuhn, *Z. Anal. Chem*, 1956, **152**, 146.
8. S. Harasawa, *Nippon Kagaku Zasshi*, 1951, **72**, 423.
9. R. A. Keller and H. Freiser, in *Gas Chromatography*, R. P. W. Scott (ed.), p. 307. Butterworths, London, 1960.
10. A. K. Majumdar and B. R. Singh, *Anal. Chim. Acta*, 1958, **18**, 220.
11. R. B. Fischer and D. G. Peters, *Quantitative Chemical Analysis*, Saunders, Toronto, 1968.
12. *Analytical Methods for Atomic Absorption Spectrometry*, Perkin–Elmer, Norwalk, Connecticut, 1973.
13. P. J. Dawson, personal communication.
14. F. Mylius and C. Hiittner, *Ber. Dt. Chem. Ges.*, 1911, **44**, 1315.
15. R. Bock, H. Kusche and E. Bock, *Z. Anal. Chem.*, 1953. **138**, 167.
16. T. Braun and A. B. Farag, *Talanta*, 1972, **19**, 828.
17. D. W. Lee and M. Halmann, *Anal. Chem.*, 1976, **48**, 14, 2214.
18. T. Braun and A. B. Farag, *Anal. Chim. Acta*, 1974, **69**, 85.

Talanta Vol. 28, pp. 161 to 167
© Pergamon Press Ltd 1981. Printed in Great Britain
0039-9140/81/030161-07$02.00/0

AQUAMETRIC SUBMICRO DETERMINATION OF WATER CONTENT OF BIOPOLYMER PREPARATIONS AND ITS APPLICATION IN DERIVING HYDRATION ISOTHERMS

F. B. SHERMAN and YU. I. KHURGIN

N. D. Zilinsky Institute of Organic Chemistry, U.S.S.R. Academy of Sciences, 47 Leninsky Prospect, Moscow, 117334, U.S.S.R.

(*Received* 20 *June* 1980. *Accepted* 3 *October* 1980)

Summary—A rapid aquametric submicro method is proposed for determining 10–100 μg of bound water in 20–600 μg amounts of biopolymers. This method has been applied in deriving isotherms of water-vapour adsorption by biopolymer preparations (proteins, *t*RNA), in a dynamic mode requiring only 5 mg of the substance. The BET equation was used to determine the effective capacity (h) of a monolayer in the course of sorption ($\bar{h}$) and desorption ($\tilde{h}$), corresponding to accessible primary hydration sites on the biopolymer molecule surface. As has been established for proteins with known spatial structure, ω-amide groups of Asn and Gln residues and ion-pair forming groups do not participate in the formation of the BET-monolayer during sorption. Such an interpretation of the isotherms underlies the estimation of the number of surface and screened polar groups in the molecules of biopolymers with a spatial structure not yet established from amino-acid analysis and hydration isotherms. The maximum hydration (H_s) of globular proteins is much less pronounced than that of *t*RNA, which can be explained by an irregular arrangement of sterically separated primary hydration sites which do not form a matrix for distribution and ordering of water at great distances. The deficiency of sorption sites because of sterically inaccessible groups is a trait common to biopolymers in general. Therefore, hydration isotherms may characterize certain aspects of the macromolecular structure, such as compactness, degree of screening of the polar groups, regularity of arrangement of the primary hydration sites, and so on.

The presence of bound water in lyophilized preparations of proteins and other biopolymers calls for introduction of correction factors in preparing their solutions. That is why determination of the water content in biopolymer preparations is a matter of practical interest to experimenters.

The capacity for tight binding (adsorption) of water is an extremely important property of biopolymers. The importance of the role of bound water is beyond any reasonable doubt. An essential fact in interpretation of the molecular behaviour is that it is precisely in an aqueous medium that a unique spatial structure of functionally active biopolymers is formed, which can persist under conditions of relatively intensive dehydration.[1,2] A typical example is the possibility of an enzymatic reaction in a lyophilized mixture of α-chymotrypsin and a substrate.[3] This process occurring in the solid phase in the absence of liquid water necessitates a certain amount of adsorbed water.[4] Also, analysis of biopolymer hydration isotherms, *i.e.*, the relationship between the degree of hydration of the preparation and the water-vapour pressure above it, is a widely used method for studying proteins.

Normally, the water content of solid biopolymer preparations is determined gravimetrically[5,6] or by methods involving the Fischer reagent.[7–9] An important factor determining the accuracy of water-content measurements in deriving hydration isotherms is the time it takes for equilibrium to be established between the biopolymer and water vapour. Gravimetric analysis is the traditional technique but requires a relatively large amount of the preparation as well as much time because of the slowness of equilibration.

We have developed a procedure for determining the water content of biopolymer preparations by use of the Fischer reagent under dynamic conditions, *i.e.*, in a flow of humidified inert carrier gas.[7] Analysis under dynamic conditions is advantageous in that the equilibration time and consumption of biopolymer are greatly reduced. Hydration isotherms of some globular proteins have been derived by this method.[10,11] It is now becoming more and more important to examine the hydration of protein and other biopolymer preparations which are difficult to obtain in sufficient amounts. With this in view we have developed a submicro technique for water-content determination in less than 1 mg of biopolymer. This method has made it possible to obtain hydration isotherms with not more than 5 mg of the biopolymer. This paper deals with the submicro technique and more particularly with the conditions under which hydration and dehydration isotherms are derived.

EXPERIMENTAL

Apparatus

The device for obtaining the hydration isotherms is shown in Fig. 1. The necessary relative vapour pressure (P/P_S) in the range 0.1–0.95 is attained by passing an inert gas (nitrogen) through a saturator containing water or appropriate sulphuric acid solutions (or saturated salt solutions) at various temperatures. The temperature of the saturator and absorption tube is controlled to within $\pm 0.15°$ with a thermostat. The water-content of the carrier gas at constant flow-velocity is measured with an automatic piezoelectric sorptive moisture meter or an absolute method based on weighing, at definite time intervals, a Pregl tube filled with "Anhydrone" or phosphorus pentoxide.

It has been established that the carrier gas reaches constant humidity in the system after 30–60 min, so the Pregl tube is attached (Fig. 1) about an hour after the device is switched on, then some 10 min later is detached, weighed on a microbalance in the usual way[12] and re-attached to the adsorption tube. Exactly 30 min later the Pregl tube apparatus is removed, weighed again, re-attached for another 30 min and weighed. The difference between the pairs of weighings is used to determine the water content in the nitrogen passed during the given time interval:

$$W = S/U\tau$$

where W is the absolute water content (g/l.) of the carrier gas, S is the difference (mg) between two successive weighings, U is the flow-rate (ml/min) of the carrier gas, τ is the exposure time (min). The values of W are then converted into mmHg and the corresponding values of P/P_S are found, P being the absolute water-vapour pressure of the carrier gas and P_S the saturated water-vapour pressure at the temperature of the adsorption tube. The values of P and P/P_S obtained in this way differed from the literature data (for saturated aqueous salt solutions under steady-state conditions) by not more than 4%.

The equipment is assembled as follows (Fig. 1). The saturator (2) is dried, and filled with the saturating solution through a funnel until the saturator coil is fully immersed, the ground-glass joint remaining dry. The saturator is connected to the absorption tube (1), with the joint kept dry. This joint, which has no water jacket, is carefully insulated with asbestos and lagged to prevent condensation of water vapour from the carrier gas. Moisture is also removed from the inner surface of the adapter (5) in desorption experiments (*i.e.*, with decreasing values of P/P_S). This reduces the time necessary to attain a steady-state value of P/P_S. The carrier gas is brought to the desired temperature in the coil accommodated inside the water jacket of the adsorption tube, then, heated to 25°, into the working part of the tube.

The carrier gas (nitrogen) flow-rate is controlled by a fine-control valve and checked by means of a calibrated flowmeter. The device is designed to operate at a carrier-gas velocity of 4–50 ± 0.5 ml/min, a temperature of 5–90°, and in the range of P/P_S values from 0.02 to 0.95.

Sampling

The error of a single weighing on a microbalance normally does not exceed 2 μg, so the relative error in weighing a 0.2–0.6 mg sample is in the neighbourhood of 1%. The biopolymer samples are placed in special nickel-plated metal microboats. The biopolymer preparation is first thoroughly ground in an agate mortar and the amount weighed is evenly spread over the bottom of the boat. The boats are smaller than those previously described,[10,11] the dimensions being 8 × 4 × 3 mm. The size has been reduced so that the consumption of Karl Fischer reagent in the blank test (titration of the empty boat) is a very small fraction of that in the titration of the sample. All weighing operations must be performed with special care to avoid penetration of dust, the boats and samples being transported in a closed container. The weighed samples are placed in the adsorption tube and the amount of water adsorbed by the biopolymer is determined by Karl Fischer titration after the boat with sample has been transferred from the adsorption tube into the titration cell (Fig. 2).

Determination of microgram amounts of water with Karl Fischer reagent

The dual all-glass apparatus for Karl Fischer titration and storage of the reagent (Fig. 2), together with the ancillary equipment (titration flasks with sealed-in platinum

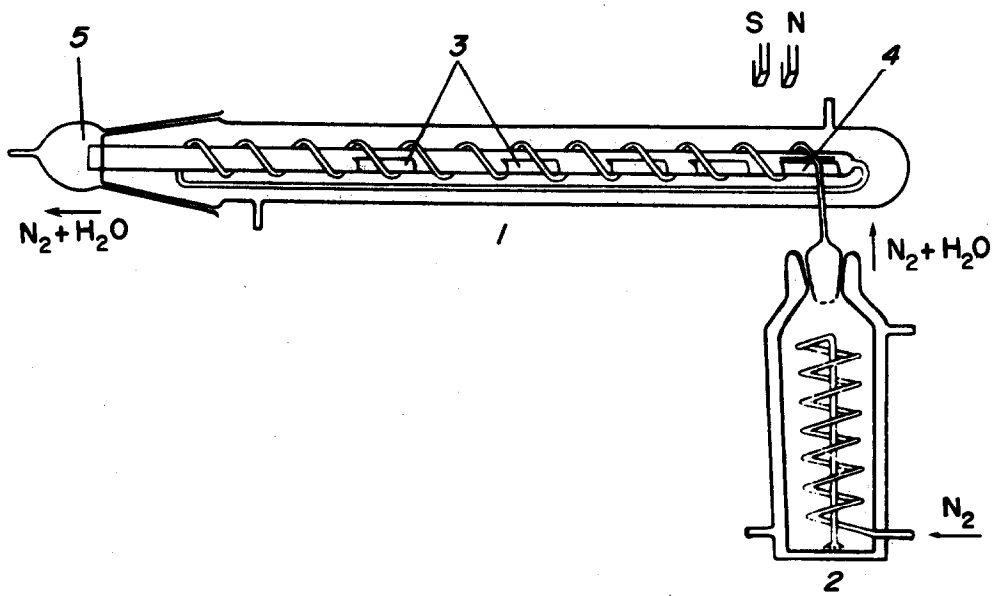


Fig. 1. Apparatus for determining the water-vapour adsorption isotherms of solid biopolymer preparations under dynamic conditions: 1—adsorption tube with water jacket and coil; 2—saturator; 3—boats with samples; 4—iron bar; 5—detachable adapter for connecting the moisture meter sensor or the Pregl tube.

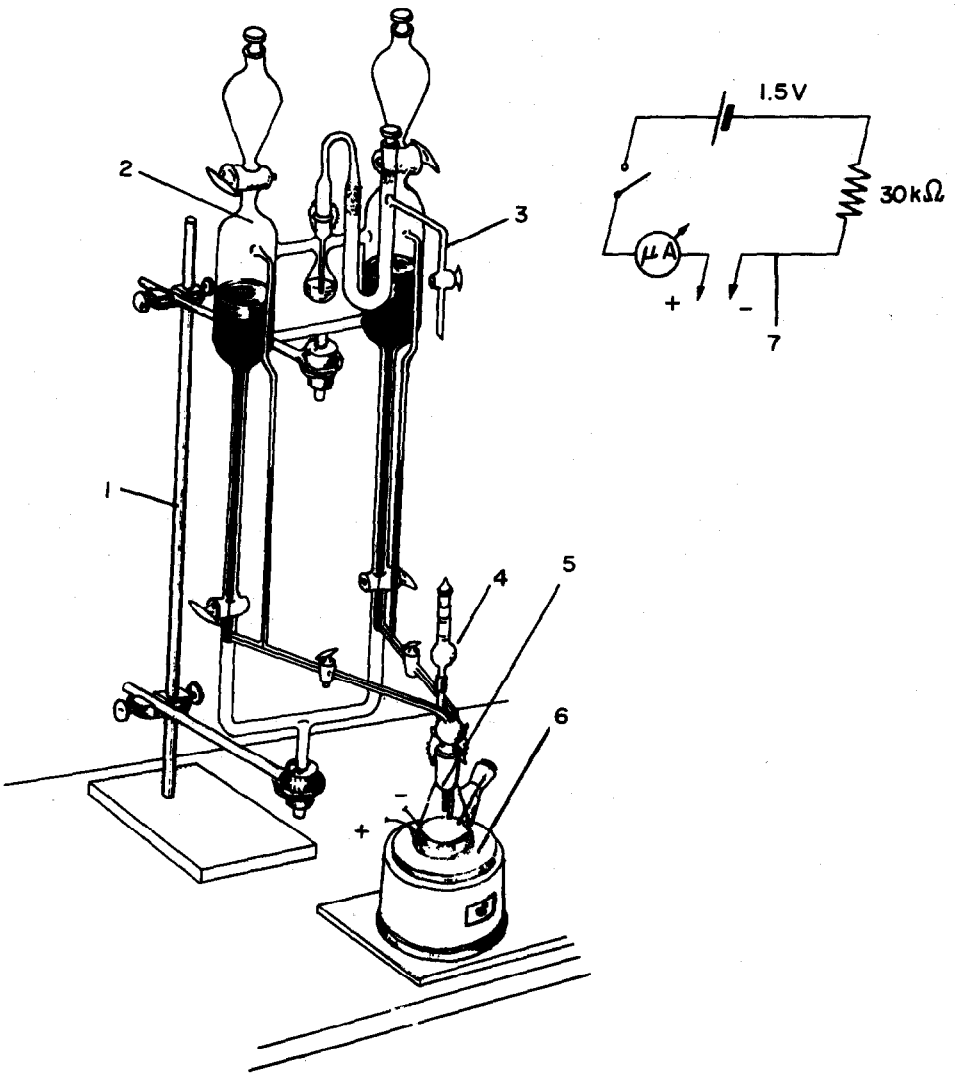


Fig. 2. Apparatus for electrometric titration of water with the Karl Fischer reagent: 1—stand; 2—unit with two microburettes (2 and 5 ml) and two vessels for storage of the Fischer reagent; 3 and 4—guard tubes; 5—titration flask; 6—magnetic stirrer; the circuit of the electrometric unit is shown on the right.

electrodes, the electrometric end-point detection system, means of protecting the reagent against atmospheric moisture, *etc.*) has been described elsewhere.[12]

Preparation of Karl Fischer reagent

Two reagents are prepared, with water equivalents (WE) of 0.8–1.2 and 0.03–0.06 mg/ml. The first of these reagents is prepared by the usual method[12,13] and standardized with weighed amounts of doubly distilled water (2–4 mg) or sodium acetate trihydrate (4–8 mg). It is sufficient to standardize it once a week since the WE decreases by not more than 0.02 mg/ml over this period. The reproducibility of the WE is 0.003–0.005 mg/ml or better.

Preparation of the reagent with a WE of 0.03–0.06 mg/ml is rather difficult:[13] at low WE values, a decrease or increase in the iodine concentration is not followed by any perceptible change in the colour of the solution. Therefore, to prepare such a highly diluted reagent the following procedure is used: a flask with a long narrow neck is filled with 150 ml of the Fischer reagent with a WE of 0.8–1.2 mg/ml, then an aqueous solution of methanol (3:1) is added dropwise until the reagent is completely discoloured. After that, 2–5 ml of a standard Fischer reagent with a WE of 3–4 mg/ml are added to the mixture, and the solution turns reddish brown. The prepared reagent is allowed to stand for 1–2 hr and then rapidly transferred into the right-hand vessel of the titration unit (Fig. 2), fitted with a 2-ml microburette. The WE of the reagent is adjusted with the aid of weighed amounts (0.8–1.5 mg) of sodium acetate trihydrate or by a check titration of benzene containing a known amount (0.03–0.05%) of water. The WE must be checked daily, immediately before use, because it decreases by 0.005–0.01 mg/ml in the course of a week. The requisite reproducibility of the WE and relative stability of the highly diluted Fischer reagent can be achieved only if the titration cell is additionally protected against atmospheric moisture, the sensitivity of electrometric detection of the end-point is enhanced, and the reversible redox pair I_2/I^- is stabilized by the presence of an excess of iodine.

Titration procedure

The titration cell is coupled to the titration unit and 0.5–1 ml of solvent is introduced together with the magnetic stirrer bar (Fig. 2) through the side-arm. To simplify the

titration procedure a single-unit device can be used, with a 2-ml burette (graduated to 0.005 ml).[12] In that case, methanol is taken in a dark-glass phial, dehydrated with a strong Fischer reagent, and used as the solvent for the sample. Air is removed from the flask by passage of dry nitrogen for 20–30 sec. The nitrogen is dried by passage through successive columns of silica gel (doped with cobalt chloride as indicator), "Anhydrone", and phosphorus pentoxide on pumice, ground quartz or asbestos.

The diluted Fischer reagent must be handled with special care, so before titration, the burette and the attached flask are together partially inserted into a polyethylene bag, and a tube is introduced into the latter for supplying dry nitrogen at a rate of 15–25 ml/min, then the bag is closed. The constant flow of dry nitrogen during the titration ensures reliable protection of the solvent in the flask against atmospheric moisture. The solvent in the flask is dehydrated, first with concentrated, then with diluted reagent, until the end-point is attained (*i.e.*, appearance of iodine traces), detected biamperometrically.[14]

Before the sample is introduced, it should be checked that dehydration of the solvent is complete and that the equivalence point has been determined correctly. To this end, the so-called "equivalence point time" (τ_{et})[12] is measured. It is the time interval during which the pointer of the microammeter is at rest at i_{max} (with the stirrer off), and must be 5–15 sec. At a greater or lesser value of τ_{et} the solution will be under- or overtitrated respectively. After the preliminary titration (which is not taken into account in the calculations) is complete, a weighed amount of the biopolymer is introduced through the side-arm, the reagent is brought to the necessary level in the burette, and the titration is continued until τ_{et} is attained. The WE of the diluted reagent and the blank for the empty boat at each preset value of P/P_S are determined under the same conditions and the same solvent as for titration of the sample. To compensate for possible systematic determination errors, the sample and blank titrations must be performed within a predetermined time interval (10–15 sec).

To determine the water content in the starting air-dry biopolymer the sample is taken in a Teflon cup (12 mm deep, diameter 5 mm) fitted with a ground-in stopper, or in one of the nickel-plated boats. To provide reliable titration results, the sample must be emulsified as much as possible, which requires a suitable solvent. For most proteins the best solvent other than water is dimethyl sulphoxide.[15] However, it should be borne in mind that in a Fischer reagent medium (solution of sulphur dioxide, iodine, iodide and methyl sulphate in pyridine and methanol[12]), irrespective of the solvent used, irreversible denaturation of biopolymers probably takes place, which allows the determination of their water of hydration,[7] including the tightly bound water (in the interior of a globular protein) the presence of which has been established by X-ray analysis.[16–18]

The hydration (H) of the biopolymer is calculated for each value of P/P_S from the formula

$$H = 100a\,\mathrm{WE}/1.8s$$

where H is the amount of water bound to the biopolymer, in mmole/g; a is the volume of Fischer reagent used in the sample titration, minus the blank, in ml; S is the mass of the absolutely dry starting sample weighed out, calculated with due account for the sample humidity during weighing, in mg.

Hydration isotherms

The static and dynamic measurements differ considerably. When a McBain sorption balance or the gravimetric exsiccator method is used, the adsorption takes place in an enclosed volume with gradually varying P/P_S and the experiment normally starts after careful removal of water from the surface of the preparation at a residual water-vapour pressure of less than 10^{-5} mmHg. Under dynamic conditions, on the contrary, it is more convenient to conduct the experiment at atmospheric pressure in a flow of inert carrier-gas.[10,11]

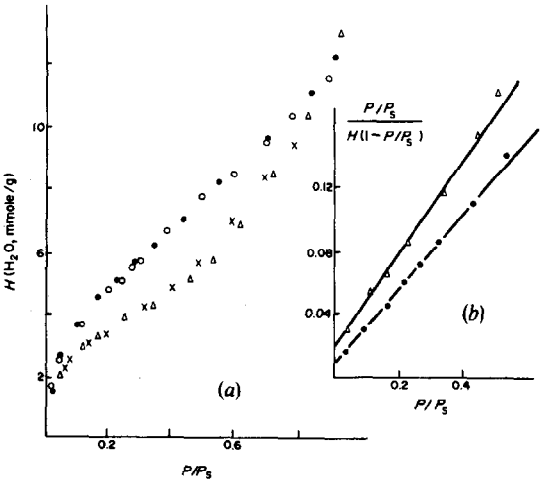


Fig. 3. (*a*) Isotherms of sorption and desorption of water vapour by a preparation of chymotrypsinogen A, derived under dynamic conditions with microgram samples (● sorption; △ desorption) and milligram samples (○ sorption; × desorption). (*b*) Same data in the co-ordinates of the BET equation (microgram samples).

In our method, the apparatus is set up, a glass-encapsulated iron bar is positioned at the inlet end of the adsorption tube (Fig. 1), followed by quartz boats 80 mm long, each accommodating five nickel-plated microboats containing weighed amounts (0.2–0.6 mg) of the sample to be analysed (Fig. 1).

The measurement of the water-vapour adsorption starts with determination of the maximum hydration (H_S) of the preparation after preliminary hydration of all the protein samples at a "maximum" value of $P/P_S \geqslant 0.92$. Under

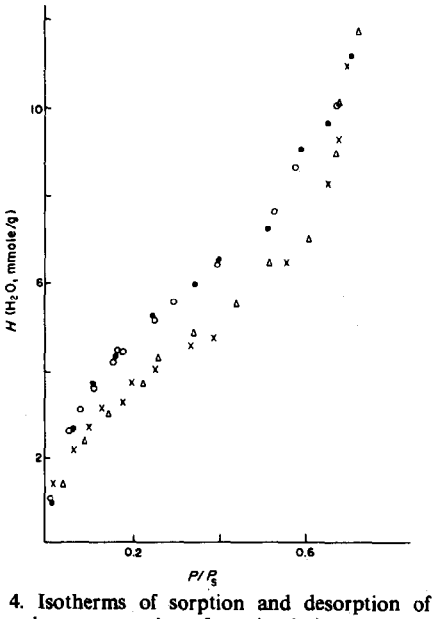


Fig. 4. Isotherms of sorption and desorption of water vapour by a preparation of pepsin, derived under dynamic conditions with microgram samples (● sorption; △ desorption) and milligram samples (○ sorption; × desorption).

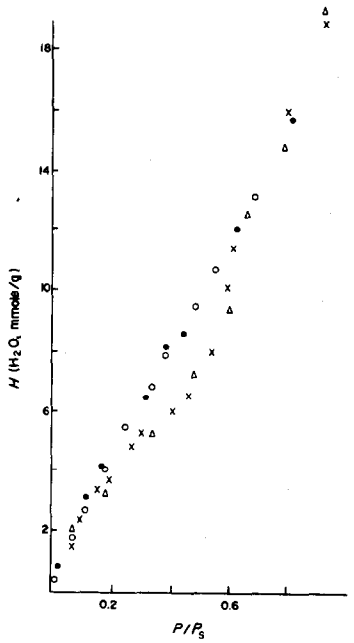


Fig. 5. Isotherms of sorption and desorption of water vapour by a preparation of *t*RNA isolated from yeast, derived under dynamic conditions with microgram samples (● sorption; △ desorption) and milligram (○ sorption; × desorption).

dynamic conditions this value does not exceed 0.95. The desorption process is conducted with P/P_S being decreased in increments of at least 0.1 and at each stage, after adsorption equilibrium has been established, a quartz boat is carefully withdrawn with the aid of the magnet (Fig. 1), and the desired microboat is removed from it with forceps and transferred into the titration cell (Fig. 2), where the amount of water bound to the biopolymer is determined. In the same way, at each given value of P/P_S, the empty microboat is titrated (blank test), and a correction applied in the calculations as already explained. To obtain the minimum value of $P/P_S \simeq 0.01$ attainable with the apparatus, the value of H_{min} is determined, then the steps above are repeated but with P/P_S increasing to H_{max} in increments of 0.1. As a result, a sorption isotherm is derived (Figs. 3–5).

The measurements are normally made at 25°, with the carrier gas flow-rate being 8 ± 0.5 ml/min. The time taken to complete a full cycle of adsorption by 2 or 3 biopolymer preparations does not exceed 10 days. The reproducibility of the isotherms, that is determination of the values of H over the entire range of P/P_S values, is ±5% or better (Table 1).

Preparations used

In the experiments use was made of salt-free preparations of chymotrypsinogen A produced by "Reanal" (Hungary) (Fig. 3) and pepsin (Fig. 4), as well as a preparation of total *t*RNA isolated from baker's yeast[19] (Fig. 5).

RESULTS AND DISCUSSION

It was the principal aim of our studies to develop a sensitive and rapid method for quantitative determination of bound water in very small amounts (0.2–0.6 mg) of biopolymers. This problem is steadily gaining in importance because most newly discovered proteins, nucleic acids, polysaccharides and other substances of biological importance cannot be isolated in amounts sufficient for detailed investigation by "classical" methods. With regard to studies of the interaction between biopolymers and water, this problem becomes particularly acute since the weighing methods normally recommended for determining hydration require large amounts of the substance (to attain the desired accuracy) and much time (for steady-state hydration to be attained). The dynamic submicro technique proposed in this paper offers a solution to both problems.

Derivation of isotherms suitable for interpretation requires at least five values of the degree of hydration at different P/P_S ratios in the course of sorption and desorption. In addition, some of the preparation is consumed in determining the initial water content and the purity (ultimate analysis for C, H, N, initial

Table 1. Adsorption (H, mmole of H_2O/g) of water vapour by "dry" preparations of chymotrypsinogen, pepsin, and *t*RNA at 25°: dynamic conditions; 0.2–0.6 mg of sample

Chymotrypsinogen A				Pepsin				*t*RNA			
Sorption		Desorption		Sorption		Desorption		Sorption		Desorption	
P/P_S	H	P/P_S	H	P/P_S	H	P/P_S	H	P/P_S	H	P/P_S	H
0.035	2.01	0	1.59	0.035	1.28	0	0.83	0.650	2.15	0	0.75
0.100	2.80	0.030	2.56	0.080	2.29	0.060	2.75	0.170	3.35	0.110	3.10
0.165	3.25	0.90	3.51	0.135	3.05	0.100	3.78	0.331	5.25	0.160	4.12
0.245	3.75	0.160	4.40	0.205	3.72	0.155	4.40	0.432	7.10	0.320	6.40
0.335	4.20	0.215	5.00	0.280	4.29	0.235	5.39	0.300	6.45	0.440	8.55
0.455	5.04	0.270	5.45	0.335	4.65	0.340	6.00	0.375	6.28	0.250	5.80
0.530	5.65	0.340	6.03	0.425	5.45	0.400	6.60	0.430	7.45	0.290	7.14
0.455	5.04	0.270	5.45	0.335	4.65	0.340	6.00	0.375	6.28	0.250	5.80
0.530	5.65	0.340	6.03	0.425	5.45	0.400	6.60	0.430	7.45	0.290	7.14
0.620	6.80	0.445	6.92	0.515	6.47	0.505	7.25	0.525	8.83	0.375	8.83
0.725	8.35	0.550	8.00	0.602	7.03	0.580	8.95	0.590	10.19	0.455	10.50
0.830	10.23	0.700	9.50	0.675	8.09	0.645	9.65	0.630	12.21	0.510	11.66
0.935	12.80	0.840	10.95	0.715	11.72	—	—	0.680	15.02	0.545	12.41
—	—	0.910	12.10	—	—	—	—	0.705	17.38	0.610	14.31
								—		0.665	15.89

Table 2. Reproducibility of measurements of H values at different values of P/P_S under dynamic conditions for deriving isotherms of water vapour adsorption by "dry" preparations of chymotrypsinogen at 25°, with microgram samples

Sample, *mg*	P/P_S	H, *mmole/g*	S_r, %	Process
0.5–0.6	0.165	3.31	4.3	sorption
0.5–0.6	0.160	4.38	4.1	desorption
0.3–0.5	0.335	4.25	3.2	sorption
0.2–0.4	0.445	6.88	2.5	desorption
0.2	0.945	12.75	2.2	sorption
0.2	0.840	10.94	1.8	desorption

H—average of 6 determinations.
S_r—relative standard deviation of the mean.

water and ash content). Hence, for economy of material, the weights of sample used in the isotherm studies should be in the range 0.2–0.6 mg and will contain 0.01–0.1 mg of bound water when P/P_S ranges from 0.1 to 0.95. Such small amounts of water, particularly at $P/P_S < 0.3$, can be determined only with the aid of a highly diluted Fischer reagent (WE < 0.1 mg/ml), which calls for special handling procedures avoiding contact with atmospheric moisture (see the experimental section).

Dynamic hydration experiments cut down the time it takes to achieve a steady-state amount of water bound to the preparation. The kinetics of hydration and dehydration of protein preparations with water vapour have been dealt with at length[10] in discussion of determining the water content in 3–6-mg samples by Karl Fischer method. In these experiments, steady-state hydration was established in not more than 3 hr even in the case of the slowest process (dehydration of highly dried and hydration of highly humid preparations). Comparison of the kinetic curves of hydration and dehydration of chymotrypsinogen, derived in this work and in earlier experiments[10] has shown that reducing the sample size by a factor of 5–10 does not produce any tangible effect on either the time needed to establish steady-state hydration or the trend of the kinetic curves. This is indicative of the high sensitivity and reproducibility of titration of the biopolymer-bound water with the Fischer reagent. In the case of the 0.2–0.6-mg samples, the relative standard deviation of the mean result (S_r) increases slightly with decreasing values of P/P_S, *i.e.*, with decreasing amounts of bound water, irrespective of the direction of the process (sorption or desorption), but does not exceed 4.3% (Table 2).

The advantage of the dynamic method become manifest when hydration isotherms of biopolymers, that is relationships between the amount of bound water on the biopolymer preparation and the relative water-vapour pressure (P/P_S) above it, are derived (Figs. 3–5). The hydration isotherms of globular proteins provide information on the interaction between water and the biopolymer surface. The hydration isotherms are quantitatively described in terms of various adsorption equations.[1] The most widely used method is the polymolecular adsorption equation of Brunauer, Emmet and Teller (BET equation),[20] which permits discrimination, in the "hydration shell" of the biopolymer, of the fraction h including the water molecules more tightly bound to the surface (effective monolayer according to BET). As was shown earlier,[21] the BET equation adequately describes the initial portion ($P/P_S < 0.5$) of both sorption and desorption isotherms (Figs. 3–5). We have shown that in the case of globular proteins with a known spatial structure there is a sufficiently rigorous agreement between the values of h and the number of surface polar amino-acid residues (n_Σ).[2,10,11,21] The difference in the values of $\vec{h}$ from the sorption isotherm and $\overleftarrow{h}$ from the desorption isotherms (Table 3) also permits discrimination, in the effective monolayer, of the hydration sites binding water in a relatively weaker manner.[2,10,11,21] The data obtained permit prediction of the degree of screening of the polar groups in the inner part of a globular protein.[11]

The considerations above have prompted us to compare, for three different biopolymers, the parameters of the BET equation from the sorption ($\vec{h}$) and desorption ($\overleftarrow{h}$) isotherms derived by different modifications of the dynamic method described here. For the preparation of chymotrypsinogen A, the values of h obtained gravimetrically under static conditions (on a McBain balance) are also given.[21] As can be inferred from the tabulated data (Table 3), the way in which the adsorption equilibrium is established at the same water-vapour pressures may affect

Table 3. Hydration parameters of chymotrypsinogen, pepsin and *t*RNA, obtained under dynamic conditions, mole of H_2O/mole of biopolymer

Biopolymer	N_Σ	$\vec{h}$		$\overleftarrow{h}$	
		Submicroanalysis	Microanalysis	Submicroanalysis	Microanalysis
Chymotrypsinogen	126 (101)	81	75	107	97
Pepsin	166	121	114	163	155
*t*RNA*	219	119	109	150	158

N_Σ—number of primary hydration sites corresponding to the biopolymer composition; given in brackets for chymotrypsinogen is the number of surface primary hydration sites (n_Σ).
* A molecular weight of 216×10^4 (76 nucleotides) is accepted for an individual *t*RNA molecule.[22]

the degree of hydration of the biopolymer, but, in this case the values of h according to BET are independent of the method by which the isotherms are derived.

The determination of the values of h by rectifying the hydration isotherms in the co-ordinates of the BET equation involves an error of about $\pm 5\%$. The observed discrepancies between the results of processing the isotherms derived by different methods (Table 3) range from 6 to 10%, which is less than twice the error of calculating these parameters. However, there is a tendency to overstate the values of $\vec{h}$ and $\bar{h}$ when the dynamic submicroanalysis technique is used (with the exception of the value of $\bar{h}$ for a preparation of total *t*RNA). The submicro version of the aquametric method naturally introduces an additional error into determination of the hydration of the preparations and into the derivative values of $\vec{h}$ and $\bar{h}$, owing to the lower accuracy of weighing the samples and to the use of a highly diluted Fischer reagent. Nevertheless, the submicro analysis technique developed by us permits determination of the presence of 0.01–0.1-mg amounts of water in submilligram (0.2–0.6 mg) samples of biopolymer preparations, which is normally very difficult to achieve in investigating biopolymers. It makes it possible to obtain the effective monolayer values according to BET ($\vec{h}$ and $\bar{h}$) with only 5–10 mg of the preparation, which substantially extends the range of biopolymers for which hydration isotherms can be derived and, consequently, provides information on maximum hydration (H_S) and distribution of polar amino-acid residues between the surface and the inner part of the biopolymer molecule.

Acknowledgements—The authors would like to thank A. A. Baev and T. V. Venkstern for their valuable advice and for a sample of total *t*RNA from baker's yeast, and L. M. Ginodman for a sample of pepsin.

REFERENCES

1. I. D. Kuntz and W. Kauzmann, *Advan. Protein Chem.*, 1974, **28**, 239.
2. Yu. I. Khurgin, *Zh. Vses. Khim. Obshch.*, 1976, **6**, 684.
3. Yu. I. Khurgin, N. V. Medvedeva and V. Ya. Roslyakov, *Biofizika*, 1977, **22**, 1010.
4. V. Ya. Roslyakov and Yu. I. Khurgin, *ibid.*, 1972, **37**, 493.
5. J. Mitchell and D. M. Smith, *Aquametry*, 2nd Ed., Vol. 1, Wiley, New York, 1977.
6. A. Pande, *Handbook of Moisture Determination and Control*, Vols. 1–4, Dekker, New York, 1974–1975.
7. F. B. Sherman, U. Tusupkaliev, V. A. Klimova and Yu. I. Khurgin, *Izv. Akad. Nauk SSSR, Ser. Khim.*, 1973, 1401.
8. P. B. Rao and W. P. Bryan, *J. Mol. Biol.*, 1975, **97**, 119.
9. *Idem*, *Biopolymers*, 1978, **17**, 1957.
10. V. A. Klimova, U. Tusupkaliev, F. B. Sherman, Yu. I. Khurgin and A. D. Klyachko-Gurvich, *Izv. Akad. Nauk SSSR, Ser. Khim.*, 1973, 2111.
11. Yu. I. Khurgin, F. B. Sherman and U. Tusupkaliev, *Biokhimiya*, 1977, **42**, 490.
12. V. A. Klimova, in *Basic Methods of Microanalysis of Organic Compounds*, p. 180. "Khimiya", Moscow, 1975.
13. A. M. Lvov, V. A. Klimova and L. I. Semenova, *Zh. Analit. Khim.*, 1968, **23**, 1192.
14. T. H. Beasly, H. W. Ziegler Sr., R. L. Charles and P. King, *Anal. Chem.*, 1972, **44**, 1833.
15. Yu. I. Khurgin, V. Ya. Roslyakov, Yu. M. Azizov and Ye. D. Kaverzneva, *Izv. Akad. Nauk SSSR, Ser. Khim.*, 1968, 2840.
16. J. J. Birktoft and D. M. Blow, *J. Mol. Biol.*, 1972, **68**, 187.
17. T. Imoto, L. N. Johnson, A. C. T. North, D. C. Philips and J. A. Rupley, in *The Enzymes*, Vol. 7, Boyer P. D. (ed.), pp. 655–868. Academic Press, New York, 1972.
18. F. A. Quiocho and W. N. Lipsomb, *Advan. Protein Chem.*, 1971, **25**, 1.
19. S. N. Isaenko and V. D. Akselrod, *Biokhimiya*, 1971, **36**, 956.
20. S. Brunauer, P. H. Emmet and E. Teller, *J. Am. Chem. Soc.*, 1938, **60**, 309.
21. Yu. I. Khurgin, V. Ya. Roslyakov, A. L. Klyachko-Gurvich and T. R. Brueva, *Biokhimiya*, 1972, **37**, 485.
22. A. A. Baev and T. V. Venkstern, *Mol. Biol.* 1977, **11**.

Talanta Vol. 28, pp. 169 to 172
Pergamon Press Ltd 1981. Printed in Great Britain

0039-9140/81/030169-04$02.00/0

ATOMIC-ABSORPTION SPECTROCHEMICAL ANALYSIS FOR ULTRATRACE ELEMENTS IN GEOLOGICAL MATERIALS BY HYDRIDE-FORMING TECHNIQUES: SELENIUM

G. PAOLO SIGHINOLFI and CARLO GORGONI
Istituto di Mineralogia, Università di Modena, Italy

(*Received* 16 *July* 1980. *Accepted* 3 *October* 1980)

Summary—A method based on hydride generation for the AAS determination of selenium at nanogram levels in geological materials is described. The sample is decomposed by *aqua regia* attack in a sealed Teflon bomb. After treatment with hydrochloric acid, selenium is converted into hydrogen selenide by reaction with sodium borohydride and determined by AAS. Matrix interference effects have been investigated, but though they are rarely significant, the standard-additions method is recommended. The absolute sensitivity of the method is about 2.0 ng of Se (in 10 ml of solution). Detection limits of about 5–10 ng in a 1.0-g sample have been achieved with the use of "Suprapure" reagents. The selenium content of some USGS, CRPG and ANRT reference samples is reported.

A number of studies have shown that the metal-hydride vapour procedures are among the most promising advances in analysis for ultratrace elements by atomic-absorption spectrophotometry (AAS).[1–10] These techniques may be applied in the determination of Hg, Se, Te, As, *etc.*, which can be obtained in the gaseous phase as a hydride or metal (Hg) vapour by chemical reduction. The major advantages of these techniques are that they are relatively simple and rapid, and characterized by very high analytical sensitivity. It is known, however, that the hydride generation process is frequently affected by severe interelemental interference effects, so this technique can usually be applied successfully only to the determination of a few elements in relatively simple media such as natural waters or biological solutions. In the case of more complex chemical matrices, such as geological materials, only mercury is currently determined by the vapour-forming technique. We propose to test the analytical capabilities of hydride-forming techniques for other ultratrace elements in geological materials. Here a method for the determination of selenium is described and analytical data relative to some geological reference samples are reported.

GENERAL ANALYTICAL COMMENTS

The analytical procedure used is based on the generation of a volatile selenium compound (hydrogen selenide) from an ionic selenium solution by reduction with sodium borohydride as described in the literature. In the case of analysis of geological materials, some aspects (sample dissolution, optimization of analytical sensitivity and control of matrix interelemental effects) need investigation in detail.

Sample decomposition

The following factors were considered in choosing the sample dissolution procedure: (*a*) selenium is a highly volatile element which may easily be lost during sample attack, even at moderate temperature; (*b*) selenium has a marked calcophilic character which leads to its virtual absence in non-sulphide mineral phases;[11] (*c*) the severity of the known interelemental interferences suggests that the selenium should be separated from matrix elements.

Considerations (*b*) and (*c*) led to the choice of a partial sample dissolution (by *aqua regia*) that is strongly selective for sulphide phases. Loss by volatilization was prevented by the use of a sealed Teflon bomb similar to the one described by Bernas.[12] Repeated attack on the same sample has shown (Fig. 1) that small volumes of *aqua regia* (2 ml for up to 1 g of silicate rock) are sufficient for the complete dissolution of the selenium contents of common rock samples. The use of small amounts of reagents derives from the need to minimize blank values and control the interference of nitrate. The attack on the selenium-bearing phases when a sealed Teflon bomb is used at a relatively high temperature (160°) is very rapid: all the selenium is dissolved in about 60 min (Fig. 1). The controlled *aqua regia* atmosphere during the attack and the subsequent addition of concentrated hydrochloric acid should ensure the complete conversion of selenium into selenite, as required for optimal hydride generation.

Optimization of analytical sensitivity

Selenium is an ultratrace element in most geological materials, frequently occurring at below the 100 ng/g level.[11] For this reason the optimization of sensi-

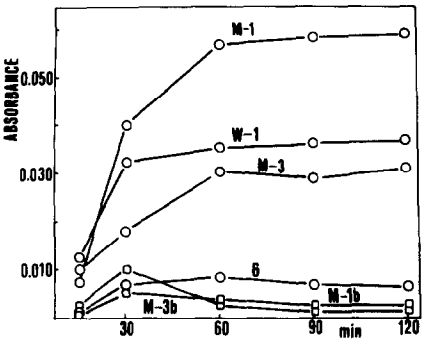


Fig. 1. Selenium recovered after *aqua regia* attack in the Teflon bomb. W-1: USGS reference sample; M-1, M-3: basaltic rock; G: granitic rock; M-1b, M-3b: second attack cycle on the M-1 and M-3 samples.

tivity and efficiency is critical. Previous studies suggest that a number of parameters affect metal vapour or hydride generation and the efficiency of the absorption phenomena. It has been shown[13] that selenium must be present as selenite to give optimal hydride generation. Hydrochloric acid is usually used as reducing agent.[14] The effects of parameters such as acid concentration and cell temperature have already been investigated.[15] Here the effects of the pressure of the charring gas and of the volume of the reacting solution are studied. The absorption signal increases with decreasing argon or nitrogen pressure (Fig. 2). Thus a low (about 1.2 bar) gas pressure should be used. The absorption signal tends to increase with decreasing volume of reaction solution (Fig. 2), as is also the case for mercury.[10] At the same time, however, the reproducibility of the signal becomes poorer, so very small volumes cannot be used. A 10-ml volume seems to be the best compromise.

Control of interelemental interference effects

The determination of metals by hydride-forming techniques may be affected by serious matrix interference effects.[16–19] It has been shown that the most severe interferences arise from any element or compound affecting the reduction to the hydride form. A number of elements may interfere in selenium hydride generation, but the most serious interferences arise from nitrate and from transition metals (Ni, Cu, Co, *etc.*) and noble metals (Au, Pt, Pd, *etc.*), these last usually present as trace or ultratrace elements in geological materials. The inhibitory effect of nitrate can easily be avoided by evaporation of the reagent (*aqua regia*) after the attack in the Teflon bomb. However, a series of experiments on solutions of geological materials and on aqueous selenium solutions suggested that the formation of selenium hydride from about 4*M* chloride solution is unaffected by the presence of nitrate at concentrations up to about 2*M*. For this reason, as the nitric acid concentration in the analytical solution is only about 0.3*M*, its removal seems unnecessary; moreover, omission of the evaporation step also avoids any possible loss of volatile selenium compounds during this stage.

As regards the interference effects of metals, the compositional complexity of geological materials makes the investigation of the interference of single elements unrealistic. The sum of interferences by the silicate or non-silicate matrices may be estimated by analysing with the standard-additions method geological materials of widely varying composition (acid, mafic, ultramafic rocks, sulphides, *etc.*). Most of the standard-additions calibration plots obtained are practically parallel to the standard calibration plot (Fig. 3) and this indicates that in most cases interelemental interferences are absent or negligible.

In other cases, such as for the nickel-rich (about 0.1%) P-1 ultramafic rock, the standard-additions calibration plot shows that matrix interferences are present. The plot for aqueous selenium solutions containing gold confirms the interfering effect of the noble metals. This means that in the analysis of geological materials only the interferences by specific elements (Ni, Cu, Au, Pt, *etc.*), which are very occasionally present in discrete amounts in common rocks,

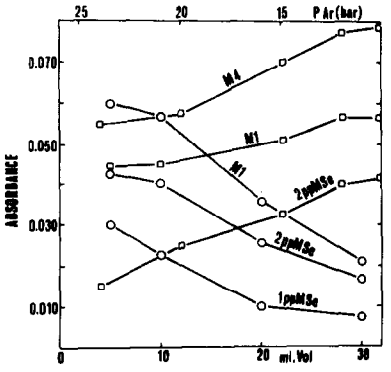


Fig. 2. Effects of the calibration volume (○: P_{Ar} = 1.2 bar) and of the gas pressure (□: calibration volume = 10 ml) on the absorbance reading. M-1, M-4: basaltic rock [ppM (parts per milliard = ng/ml].

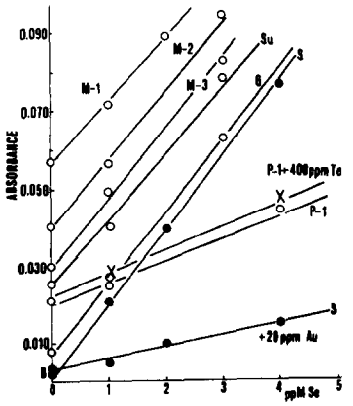


Fig. 3. Study of matrix interferences on Se determination by standard-additions calibration plots. S: standard calibration plot; M-1, M-2, M-3: basaltic rock; G: granitic rock; P: ultramafic rock (pyroxenite); Su: pyrites; B: blank.

need be considered. The use of masking agents is in some cases effective in removing interference in hydride generation.[20] For example, the use of tellurium(IV) has been found useful in the determination of selenium,[21] because the Te^{2-} formed by borohydride reduction will form very stable tellurides with some interfering ions.[22] Nevertheless, the addition of tellurium(IV) was found ineffective in removing or reducing matrix interference in analysis of the sample P-1 (the interference being attributed to the presence of nickel) (Fig. 3). For these reasons we recommend the use of the standard-additions procedure for the analysis of geological materials of unknown composition, since it should eliminate the effect of strongly interfering elements such as Ni, Cu, noble metals *etc.*

EXPERIMENTAL

Apparatus

A Perkin–Elmer Model 603 atomic-absorption spectrophotometer, Model 56 recorder, electrodeless discharge selenium lamp, and MHS-10 Mercury/Hydride System were used, under the following conditions.

Spectrophotometer

Wavelength 196.0 nm
Spectral band-width 0.7 nm

MHS-10 module

Cell heating	Air/C_2H_2
Reductant	3% $NaBH_4$ + 1% NaOH solution
Charring gas	Ar (1.2 bar)
Calibration vol.	10 ml

Reagents and standards

Certified standard selenium solution (1000 μg/ml) was obtained commercially. A 0.1-μg/ml Se solution was prepared daily by diluting the concentrated standard with demineralized water. "Suprapure" hydrochloric and nitric acids were used.

Procedure

Weigh 0.1–1.0 g of powdered sample into a 60-ml Teflon vessel (for design see Bernas[12]), add 2 ml of *aqua regia* and stir the mixture to wet the sample. Place the Teflon vessel in the bomb and seal tightly. Heat the bomb at 160° for 90 min. After cooling, add 10 ml of concentrated hydrochloric acid, filter and transfer the filtrate to a 25-ml standard flask. Place three equal fractions (from 1 to 8 ml, depending on the Se content of the sample) of this solution in the reaction tubes and dilute them to the 10-ml mark with 2*M* hydrochloric acid. With a micropipette add known amounts of the 0.1-μg/ml Se solution to two aliquots and from the three absorption readings plot the standard-addition graph. Calculate the Se content in the sample from

$$\text{Se} = \frac{-25\,[\text{Se}]}{vw}\ \text{ng/g}$$

where v is the volume (ml) of the fraction used for preparing each standard-additions solution, w is the weight (g) of the sample, and [Se] is the intercept on the x-axis of the plot of absorption signal against weight (ng) of selenium added to the standard-additions solution ([Se] should be zero or negative).

RESULTS

Sensitivity and reproducibility

The absolute sensitivity of the method depends on the degree of contamination from reagents and handling. With the use of "Suprapure" chemical reagents in the amounts recommended, the blank signal is very low (Fig. 3). Ten ml of 0.2-ng/ml Se solution (2 ng of Se absolute) gave an absorption reading about twice that of the blank. Thus, 2 ng of selenium represents the detection limit. This corresponds to determination limits of around 5–10 ng/g in the sample when the standard-additions procedure is used. This is adequate for determination of selenium in most geological materials. Instrumental precision was checked by means of a series of replicate readings on selenium solutions at different concentrations. Very good reproducibility (2–3% coefficient of variation) was found over the whole concentration range 0.2–5.0 ng/ml.

Geological reference samples

Selenium has been determined in some USGS, CRPG and ANRT geological reference samples. The

Table 1. Selenium in geological reference samples (*ng/g*)

Sample	Se found	Literature data						
		Ref. 23	Ref. 24	Ref. 25	Ref. 26	Ref. 27	Ref. 28	Ref. 29
W-1	104, 114	130	110		124	100		
BCR-1	80, 84	100	103	110	124		118	79
GSP-1	72, 80	<400	59				88	
PCC-1	32, 42	<180	22				31	
AGV-1	<11	<140	8					
G-2	<16	<700	5		102			
DTS-1	<16	<300	4					
BR	35							
UB-N	125, 136							
DT-N	<15							
GH	<14							
JG-1	<15							
Syenite-1	11, 17							
Sulphide	27, 32 × 10^3							
M-1 (alkalic basalt)	178†							

† Average of 10 determinations; coefficient of variation 9%.

results are reported in Table 1. The limited availability of some samples, such as G-2, GH, AGV-1, which are very poor in Se, permits only estimates of the upper concentration limits. For most of the samples sufficiently high in selenium (*e.g.*, W-1, BCR-1, GSP-1, *etc.*) there is relatively good agreement between our data and the literature data. Duplicate analysis on most of the reference samples and replicate determinations (10) on the non-reference sample M-1 (basaltic rock) indicate an acceptable reproducibility of the bulk analysis. An error of less than 10% may be considered satisfactory. Data on the Sulphide reference material suggest that the method is particularly suitable for microanalysis (about 1 mg of sample) of natural selenium-rich materials such as sulphide ores and meteoritic materials.

Acknowledgement—This work was carried out with financial support of the Consiglio Nazionale delle Ricerche, Roma.

REFERENCES

1. W. R. Hatch and W. L. Ott, *Anal. Chem.*, 1968, **40**, 2085.
2. G. Lindstedt, *Analyst*, 1970, **95**, 264.
3. E. J. Knudson and G. D. Christian, *Anal. Lett.*, 1973, **6**, 1039.
4. J. Tofaletti and J. Savory, *Anal. Chem.*, 1975, **47**, 2091.
5. P. N. Vijan and G. R. Wood, *Talanta*, 1976, **23**, 89.
6. G. M. Hieftje, T. R. Copeland and D. R. de Olivares, *Anal. Chem.*, 1976, **48**, 142R.
7. D. D. Siemer, P. Koteel and V. Jariwala, *ibid.*, 1976, **48**, 836.
8. G. M. Hieftje and T. R. Copeland, *ibid.*, 1978, **50**, 300R.
9. D. D. Siemer and P. Koteel, *ibid.*, 1977, **49**, 1096.
10. G. P. Sighinolfi and C. Gorgoni, *Geostandards Newsletter*, in the press.
11. F. Leutwein, *Handbook of Geochemistry*, Chap. 34, *Selenium*, Springer, Berlin, 1971.
12. B. Bernas, *Anal. Chem.*, 1968, **40**, 1682.
13. M. Landsford, E. M. McPherson and M. J. Fishman, *At. Abs. Newsl.*, 1974, **13**, 103.
14. K. C. Thompson and D. R. Thomerson, *Analyst*, 1974, **99**, 595.
15. E. Jackwerth, P. G. Willmer, R. Höhn and H. Berndt, *At. Abs. Newsl.*, 1979, **18**, 66.
16. A. E. Smith, *Analyst*, 1975, **100**, 300.
17. F. D. Pierce and H. R. Brown, *Anal. Chem.*, 1976, **48**, 693.
18. *Idem*, *ibid.*, 1977, **49**, 1417.
19. H. D. Fleming and R. G. Ide, *Anal. Chim. Acta*, 1976, **83**, 67.
20. G. F. Kirkbright and M. Taddia, *ibid.*, 1978, **100**, 145.
21. *Idem.*, *At. Abs. Newsl.*, 1979, **19**, 68.
22. L. G. Sillén and A. E. Martell, *Stability Constants*, p. 151. Spec. Publ. No. 17, The Chemical Society, London, 1964.
23. F. J. Flanagan, *Geochim. Cosmochim. Acta*, 1973, **37**, 1189.
24. A. O. Brunfelt and E. Steinnes, *ibid.*, 1967, **31**, 283.
25. L. A. Haskin, R. O. Allen, P. A. Helmke, T. P. Paster, M. R. Anderson, R. L. Korotev and K. A. Zfeifel, *ibid.*, Suppl. I, 1970, **2**, 1213.
26. E. P. Mignonsin and I. Roelandts, *Chem. Geol.*, 1975, **16**, 137.
27. R. A. Nadkarni and B. C. Haldar, *Radioanal. Lett.*, 1971, **7**, 303.
28. M. M. Schnepfe and F. J. Flanagan, *Chem. Geol.*, 1973, **12**, 77.
29. J. W. Morgan, R. Ganapathy, H. Higuchi and U. Krähenbühl, *Geochim. Cosmochim. Acta*, 1976, **40**, 861.

Talanta Vol. 28, pp. 173 to 176
© Pergamon Press Ltd 1981. Printed in Great Britain
0039-9140/81/030173-04$02.00/0

DETERMINATION OF SULPHIDE, POLYSULPHIDE, THIOCARBONATES AND SULPHUR BY EXTRACTION WITH TRIBUTYLTIN HYDROXIDE, AND OF THIOSULPHATE BY HYDROGENATION

MIECZYSŁAW WROŃSKI

Department of Chemical Technology, University of Łódź, Łódź, Poland

(*Received* 1 *April* 1980. *Revised* 10 *September* 1980. *Accepted* 3 *October* 1980)

Summary—The methods presented involve the separation of sulphur compounds by means of a hexane solution of tributyltin hydroxide (TBT), followed by titration with *o*-hydroxymercuribenzoic acid in the presence of dithizone as indicator. Free sulphide is selectively extracted from strongly alkaline solution, whereas the polysulphides and thiocarbonates are extracted at pH 9–10. The polysulphide and thiocarbonate extracts decompose to form TBT–sulphide, sulphur and carbon disulphide. Treatment with sulphite, stannate(II), copper, vinyl cyanide and ethylenediamine, and hydrogenation with zinc and hydrobromic acid have been applied in the course of the analysis. The sulphur is determined by its attack on copper to form copper(I) sulphide which is subsequently dissolved in aqueous potassium cyanide solution and the sulphide separated by extraction.

Investigation of the absorption of carbon disulphide from air and gases by aqueous polysulphides according to the reaction,

$$S_n^{2-} + CS_2 = CS_4^{2-} + (n-2)S$$

requires simple and rapid analytical methods. As the reaction

$$S^{2-} + CS_2 = CS_3^{2-}$$

may also occur, and the solution contains various organic compounds and a large excess of thiosulphate, the analysis is rather complicated and the methods available for estimation of polysulphide and thiosulphate[2–6] are not of direct use. Some attempts have been made to use amperometric titration[7,8] but only the application of extraction with tributyltin (TBT) and titration with *o*-hydroxymercuribenzoic acid (HMB) has provided a practical solution to the problem.

In this paper the term "polysulphide sulphur" means the dissolved sulphur $(n-1)\,[S_n^{2-}]$, "free sulphide" means the monosulphide $[S^{2-}]$, "total sulphides" $[S_n^{2-}]$, and "total-sulphides sulphur" $n[S_n^{2-}]$. A distinction is made between average sulphur number, n, and corrected average sulphur number, x, as given by the equations $[S_n^{2-}] = [S^{2-}] + [S_x^{2-}]$ and $[S^{2-}] + x[S_x^{2-}] = n[S_n^{2-}]$. The corrected sulphur number is the average sulphur number with monosulphide excluded. If $[S^{2-}] = 0$, $x = n$. It has been found that free sulphide can be selectively extracted from a strongly alkaline solution containing polysulphide and thiocarbonates. Sulphide added to a solution of polysulphide, *e.g.*, tetrasulphide, can be recovered quantitatively in a few minutes, indicating that the transfer of sulphur from S_4^{2-} to S^{2-} is slow at room temperature and may be followed analytically. Treatment with sulphite converts 1 mole of polysulphide into 1 mole of monosulphide, and treatment with stannate(II) converts one mole of polysulphide into x moles of monosulphide.

$$S_x^{2-} + (x-1)\,SO_3^{2-} = S^{2-} + (x-1)\,S_2O_3^{2-}$$

$$S_x^{2-} + (x-1)SnO_2^{2-} + 2(x-1)OH^- = xS^{2-} + (x-1)SnO_3^{2-} + (x-1)H_2O$$

Sulphur dissolved in organic solvents can be determined as described in the literature,[2] by reaction with copper to form copper(I) sulphide and decomposition of this with hydrochloric acid to yield hydrogen sulphide. The modified method suggested in this paper involves dissolution of the copper(I) sulphide in potassium cyanide solution, followed by TBT-extraction and HMB-titration of the sulphide. The procedure is also applicable to determination of total-sulphides sulphur in TBT extracts, the reaction being:

$$Bu_3Sn\text{–}S_x\text{–}SnBu_3 + 2(x-1)Cu = Bu_3Sn\text{–}S\text{–}SnBu_3 + (x-1)Cu_2S$$

and in the presence of air:

$$Bu_3Sn\text{–}S\text{–}SnBu_3 + 2Cu + \tfrac{1}{2}O_2 = Bu_3SnOSnBu_3 + Cu_2S$$

Polysulphides and thiocarbonates can be extracted with TBT in hexane at pH 9–10, but the extract decomposes to form bis(tributyltin) sulphide, sulphur and carbon disulphide. Carbon disulphide does not react with copper but sulphur and bis(tributyltin) sulphide do to form copper(I) sulphide. Treatment of the sample with sodium sulphite followed by extraction

will produce an extract containing bis(tributyltin) sulphide and carbon disulphide, the first of which can be titrated with HMB after removal of carbon disulphide by volatilization, and in another aliquot both compounds can be titrated after addition of ethylenediamine. A second approach involves the separation of carbon disulphide by distillation and its independent determination.

In order to complete the analysis the thiosulphate has still to be determined. If the iodometric method cannot be applied on account of the presence of iodine-consuming organic compounds, then hydrogenation with zinc and hydrobromic acid to form hydrogen sulphide, followed by absorption and titration with HMB, is the most convenient method.

EXPERIMENTAL

Reagents

TBT hydroxide solution in hexane 0.05*M*). Shake 20 g of tributyltin chloride, 100 ml of hexane and 100 ml of 2*M* sodium hydroxide, remove the aqueous layer, filter the hexane layer and dilute with hexane to 1 litre.

Solutions of HMB for titration in organic solvents. To 16 g of *o*-hydroxymercuribenzoic anhydride dissolved in a mixture of 20 g of diethanolamine and 50 ml of water, add 200 ml of ethanol, set aside for some hours, and filter. Standardize the solution with diphenylthiourea[1] and dilute to 0.005*M* with ethanol-water (3:1 w/v) containing 1% w/v diethanolamine. Dilute this solution to 0.0002*M* with ethanol–water (9:1 v/v) containing 1% diethanolamine. Keep the stock solution in a refrigerator. The same procedure can be used for preparation of aqueous HMB solutions by using water instead of the ethanol.

Tin(II) chloride solution, 5%. Freshly prepared, with some hydrochloric acid added.

Potassium cyanide solution. Dissolve 1 g of potassium cyanide, 2.5 g of potassium hydroxide and 1 g of disodium EDTA dihydrate in 100 ml of water.

Polysulphide solutions. Prepared by melting crystalline sodium sulphide with sulphur, dissolving the melt in 0.1*M* sodium hydroxide and filtering. The stock solutions (~0.5*M*) were diluted as required, analysed by procedures 2, 7 and 8, and used within 1 hr of dilution.

Sodium trithiocarbonate solution. Obtained by shaking 0.5*M* sodium sulphide containing 1% of sodium sulphite, with excess of carbon disulphide, for 24 hr in a nitrogen atmosphere, removal of carbon disulphide by extraction with benzene, and removal of unreacted sulphide by extraction with TBT in hexane, from 1*M* sodium hydroxide medium.

Sodium perthiocarbonate solution. Obtained by shaking carbon disulphide with sodium disulphide in 0.1*M* sodium hydroxide for a few minutes, and extraction with benzene.

Procedures

General remarks. The extraction is carried out by shaking 5–25 ml of aqueous sample for 1 min with 2–5 ml of 0.05*M* TBT in hexane. Sulphide in trace quantities can be extracted from 500 ml of sample. Two ml of the extract are used for titration, with 0.2–0.5 ml of 2*M* potassium hydroxide and ethanol and butanol added to give a homogeneous solution; dithizone is used as indicator. For titration with $2 \times 10^{-4}M$ HMB, the titrand is 2 ml of extract, 1 ml of ethanol, 1 ml of butanol, 0.2 ml of 2*M* potassium hydroxide and just enough dithizone to give a full colour change on addition of 0.1 ml of $2 \times 10^{-4}M$ HMB.

1. *Selective determination of free sulphide.* Extract the free sulphide from 1*M* sodium or potassium hydroxide, wash the extract 2 or 3 times with 3 ml of 2*M* potassium hydroxide and titrate with HMB.

2. *Determination of total sulphides.* Add 0.2–1 g of sodium sulphite to the alkaline sample, set aside for 10 min or heat for 2 min on a water-bath until the yellow colour disappears, add 2–5 ml of 2*M* potassium hydroxide and either titrate directly with HMB, if thiocarbonates are absent, or carry out the extraction, wash the extract 2 or 3 times with 3 ml of 0.2*M* potassium hydroxide and titrate the extract with HMB, if thiocarbonates are present.

3. *Determination of total-sulphide sulphur and 1/4 of the perthiocarbonate sulphur.* Add to the sample a solution prepared by mixing 0.2–0.4 ml of 5% tin(II) chloride solution and 3 ml of 2*M* potassium hydroxide, wait 1 min, carry out the extraction, wash the extract 2 or 3 times with 0.2*M* potassium hydroxide and titrate with HMB. Note: a high concentration of thiosulphate will produce a positive error. Trithiocarbonate and sulphite do not interfere.

4. *Determination of either elemental sulphur in organic solvents or total-sulphide sulphur and 1/4 of the perthiocarbonate sulphur.* Roll 2 g of 40-mesh copper gauze into a spiral of 2 cm length, place it in a 16-mm diameter test-tube and rinse it successively with dilute nitric acid, water, dilute potassium cyanide solution, water and ethanol. Add 1 ml of ethanol and 2 ml of the sample, heat to boiling and set aside for 10 min. Remove the liquid, rinse the copper gauze 3 times with methanol and add 3 ml of the potassium cyanide solution, shake for 2 min and transfer the solution into a 25-ml separating-funnel. Shake the gauze with another 3 ml of potassium cyanide solution and rinse the copper with three or four 2-ml portions of water, combining all the liquid in the separating-funnels. Carry out the extraction with 2 ml of TBT in hexane, wash the extract with two 3-ml portions of 2*M* potassium hydroxide, transfer the extract to the titration vessel, rinse the funnel with 5 ml of ethanol, add 0.5 ml of 2*M* potassium hydroxide and 1 ml of butanol and titrate with $5 \times 10^{-3}M$ HMB. Note: in analysis of sulphides a part of the TBT–sulphide may not react with copper and will then remain in the organic solvent; therefore after the treatment with copper transfer the sample and the methanol washings into a titration vessel, add 1 ml of 2*M* potassium hydroxide and 1 ml of butanol and titrate with HMB. Add the volume of HMB used, if any, to the result previously obtained.

5. *Determination of total sulphides and thiocarbonates.* Add about 1 g of sodium sulphite to the sample, set aside for 10 min, add sodium bicarbonate in excess and carry out the extraction with 5 ml of TBT in hexane and apply the following procedures.

(*a*) Evaporate 2 ml of the extract on a water-bath, add 2 ml of ethanol, 2 ml of butanol, 0.5 ml of 2*M* potassium hydroxide and titrate with $5 \times 10^{-3}M$ HMB.

(*b*) To another 2 ml of the extract add 4 ml of 25% w/v solution of ethylenediamine in butanol, heat for 2 min on the water-bath, add 2 ml of 2*M* potassium hydroxide and titrate with $5 \times 10^{-3}M$ HMB.

Note: the TBT–sulphide and carbon disulphide present in the extract can be separated by distillation and determined independently; to do this place 2 ml of the extract and 2 ml of methanol in a vessel 20 mm in diameter and 70 mm long, connected to an inverted U-tube, the other arm of which dips into 4 ml of 25% ethylenediamine solution in butanol, contained in a test-tube, where the vapours obtained on heating are condensed; place the vessel in hot water to vaporize first the hexane and carbon disulphide and then the methanol; dissolve the residue in the vessel with ethanol and titrate with HMB to obtain the sulphide content; titration of the distillate will correspond to carbon disulphide from the thiocarbonates.

6. *Determination of thiosulphate by hydrogenation.* Place 1–2 ml of the sample (containing 0.025–0.1 mmole of thiosulphate) in a test-tube 16 mm in diameter and 130 mm long, make acidic to Methyl Orange, remove any hydrogen

sulphide and carbon disulphide by passage of a stream of air, add 3–4 ml of 40% w/w hydrobromic acid and 2–4 g of zinc in about 1-g granules, close rapidly with a rubber stopper provided with a fermentation lock containing 2 ml of 2*M* potassium hydroxide and set aside for 20 min. Transfer the contents of the fermentation lock to the titration vessel quantitatively, rinsing the lock several times with water, and titrate with 0.05*M* HMB, using dithizone as indicator. The zinc should be tested to see whether hydrogen sulphide is evolved from it. Trithionate and tetrathionate are also reduced to hydrogen sulphide but elemental sulphur is not.

7. *Determination of thiosulphate and polysulphide sulphur (thiocarbonates absent).* Add to 5–20 ml of sample 1 ml of saturated sodium sulphite solution, heat on a water-bath for 2–5 min, add 0.5 ml of vinyl cyanide and continue heating for another 5 min. Cool, add 10% w/w sulphuric acid in excess and titrate with 0.02–0.2*N* iodine, using starch as indicator. Note: sulphide and sulphite react with vinyl cyanide to form $S(CH_2CH_2CN)_2$ and $HO_3SCH_2CH_2CN$ respectively, which are not oxidizable by iodine in acid solution.[6] As thiosulphate does not react with vinyl cyanide the consumption of iodine will correspond to the thiosulphate originally present and the thiosulphate produced by reaction of polysulphide and sulphite.

8. *Determination of consumption of iodine in acid solution.* Add an aliquot of sample to an iodine solution containing an excess of sulphuric acid and back-titrate the unused iodine with thiosulphate.

CALCULATIONS

Let us express the numbers of moles of HMB consumed per litre of sample as N_r, where r is the number of the procedure used (procedures 1–6). As 1 mole of sulphide consumes 2 moles of HMB, it follows that

$$0.5N_1 = [S^{2-}]$$

$$0.5N_2 = [S^{2-}] + [S_x^{2-}] = [S_n^{2-}]$$

$$0.5N_3 = 0.5N_4 = [S^{2-}] + x[S_x^{2-}] + [CS_4^{2-}]$$

$$0.5N_{5a} = [S^{2-}] + [S_x^{2-}] + [CS_3^{2-}] + [CS_4^{2-}]$$

$$0.5N_{5b} = [S^{2-}] + [S_x^{2-}] + 2[CS_3^{2-}] + 2[CS_4^{2-}]$$

$$0.25N_6 = [S_2O_3^{2-}]$$

The concentrations of the sulphur compounds are expressed as molarities. One mole of carbon disulphide consumes two moles of HMB after the reaction with ethylenediamine.[9] Expressing the consumption of iodine in equivalents per litre of sample in procedures 7 and 8 by N_7 and N_8 we can write:

$$N_7 = (n-1)[S_n^{2-}] + [S_2O_3^{2-}]$$
$$N_8 = 2[S_n^{2-}] + [S_2O_3^{2-}]$$

If thiocarbonates are present:

$$N_8 = 2[S_n^{2-}] + 2[CS_3^{2-}] + 2[CS_4^{2-}] + [S_2O_3^{2-}]$$

Consequently we may calculate the results as follows.

1. Unknown: n and $[S_n^{2-}]$; procedures 2 and 3 or 2 and 4.

$$[S_n^{2-}] = 0.5N_2; \quad n = \frac{N_3}{N_2} = \frac{N_4}{N_2}$$

2. Unknown: x, $[S^{2-}]$ and $[S_x^{2-}]$; procedures 1, 2 and 3 or 1, 2 and 4.

$$[S^{2-}] = 0.5N_1; [S_x^{2-}] = 0.5N_2 - 0.5N_1;$$

$$x = \frac{N_3 - N_1}{N_2 - N_1} = \frac{N_4 - N_1}{N_2 - N_1}$$

3. Unknown: $[S_n^{2-}]$, n and $[S_2O_3^{2-}]$; procedures 2, 7 and 8.

$$[S_n^{2-}] = 0.5N_2; \quad [S_2O_3^{2-}] = N_8 - N_2;$$

$$n = \frac{2N_7 - 2N_8 + 3N_2}{N_2}$$

Note: in analyses 1, 2 and 3 thiocarbonates are absent.

4. Unknown: $[CS_4^{2-}]$, $[S_n^{2-}]$, n and $[S_2O_3^{2-}]$; procedures 2, 3, 5a and 6.

$$[S_n^{2-}] = 0.5N_2; \quad [CS_4^{2-}] = 0.5N_{5a} - 0.5N_2;$$
$$[S_2O_3^{2-}] = 0.25N_6;$$

$$n = \frac{N_3 - N_{5a} + N_2}{N_2}$$

Note: trithiocarbonate absent.

5. Unknown: $[S^{2-}]$, $[CS_3^{2-}]$, $[CS_4^{2-}]$ and $[S_2O_3^{2-}]$; procedures 1, 3, 5a and 6.

$$[CS_4^{2-}] = 0.5N_3 - 0.5N_1; [CS_3^{2-}]$$
$$= 0.5N_{5a} - 0.5N_3;$$
$$[S_2O_3^{2-}] = 0.25N_6$$

RESULTS AND DISCUSSION

It may be concluded from the results in Tables 1 and 2 that the TBT extraction is very useful for the determination of sulphide in water at the ng/ml level and that the free sulphide can be selectively determined in the presence of cyanide, thiocarbonates and polysulphide. The procedure may be recommended for kinetic investigation of sulphur transfer from polysulphide to monosulphide ions. Table 3 indicates that the sulphur in copper(I) sulphide can be determined by dissolution of the sample in potassium cyanide and TBT extraction. The method is also applicable to determination of elemental sulphur in organic solvents as well as sulphur in compounds convertible into copper(I) sulphide. The results given in Table 4 involve the analysis of samples prepared from sulphur and sodium hydroxide. It follows from the sulphur

Table 1. Determination of sulphide in 500 ml of water containing 3 g of potassium hydroxide, by extraction with 3 ml of 0.05*M* TBT in hexane and titration of 2 ml of the extract with $2 \times 10^{-4}M$ HMB

Sulphide as hydrogen sulphide, μg/500 ml		
Taken	Found	Average
5.2	5.6, 4.9, 5.1, 5.5	5.2
10.5	10.4, 9.9, 10.9, 10.5	10.4

Table 2. Determination of sulphide by procedure 1

Sulphide as hydrogen sulphide, *mg/20 ml*		
Taken	Found	Also present
0.323	0.319, 0.321, 0.327	—
0.323	0.322, 0.325, 0.328	0.005*M* KCN
—	0.025, 0.022	0.005*M* Na_2CS_4
0.323	0.335, 0.340	0.005*M* Na_2CS_4
—	0.021, 0.025	0.003*M* Na_2CS_3
0.323	0.343, 0.345	0.003*M* Na_2CS_3
—	0.044, 0.042	0.005*M* Na_2S_4
0.323	0.361, 0.368	0.005*M* Na_2S_4

Table 3. Determination of elemental sulphur dissolved in hexane, by procedure 4

Sulphur, *mg*		
Taken	Found	Average recovery, %
0.714	0.700, 0.710, 0.708, 0.711, 0.709	99.1
1.428	1.428, 1.425, 1.415, 1.420, 1.428	99.6
0.357	0.354, 0.357, 0.354, 0.351, 0.350	98.9

balance that the sulphur number obtained by combined procedures 2, 7 and 8 may be regarded as reliable. Determination of sulphur number by procedures 2, 7 and 8 gave a mean value of 4.09, consistent with the values 4.23, 4.10, 3.88, 4.01 obtained with procedures 2 and 3, and the values 4.05, 4.14, 4.09, 4.03 obtained with procedures 2 and 4. The determination of total carbon disulphide by procedure 5 gave 1.91 ± 0.07 mg found by difference and 1.87 ± 0.03 mg found by distillation, the amount taken being 1.88 mg. The determination of thiosulphate by procedure 7 gave 6.43 ± 0.03 mg (6.40 mg taken) and 12.9 ± 0.2 mg (12.8 mg taken).

Table 4. Determination of thiosulphate and polysulphide by combined procedures 2, 7 and 8

Sulphur taken, *mg*	Found, *mmole* $S_2O_3^{2-}$	S_n^{2-}	*n*	Sulphur found, *mg*
69.0	0.50	0.54	2.07	67.8
101.7	0.65	0.87	2.15	101.5
315.0	1.56	2.64	2.54	314.4
79.7	0.47	0.64	2.38	78.6
107.7	0.71	0.81	2.46	108.9

Samples prepared by dissolving a known amount of sulphur in 1–3 ml of 20% sodium hydroxide solution at 100°; sulphur found is calculated from sulphur balance as 64 × (mmole of $S_2O_3^{2-}$) + 32*n* × (mmole of S_n^{2-}) = mg of S.

REFERENCES

1. M. Wroński, *Talanta*, 1977, **24**, 347.
2. A. V. Hanley and F. W. Czech and W. N. Tuller, in *The Analytical Chemistry of Sulfur and its Compounds*, Part I, I. H. Karchmer (ed.) Wiley-Interscience, New York, 1970.
3. A. J. Danielsen, K. Johnsen and P. Landmark, *Norsk Skogind.*, 1969, **23**, 378.
4. J. Papp, *Cellulose Chem. Technol.*, 1971, **5**, 147.
5. J. Sanae, S. Hiromu, H. Takeo and T. Toshio, *Talanta*, 1972, **19**, 1650.
6. M. Wroński, *Acta Chim. Acad. Sci. Hung.*, 1961, **28**, 303.
7. *Idem, J. Polymer Sci.*, 1956, **19**, 213.
8. *Idem, Faserforsch. Textiltechn.*, 1956, **7**, 372.
9. *Idem, Chem. Anal. (Warsaw)*, 1961, **6**, 865.

Talanta Vol. 28, pp. 177 to 181
© Pergamon Press Ltd 1981. Printed in Great Britain
0039-9140/81/030177-05$02.00/0

ELECTROTHERMAL ATOMIZATION OF CALCIUM AND STRONTIUM IN A MOLYBDENUM MICRO-TUBE

MASAMI SUZUKI* and KIYOHISA OHTA

Department of Chemistry, Faculty of Engineering,
Mie University, Kamihama-cho, Tsu, Mie-ken 514, Japan

(*Received* 24 *April* 1980. *Revised* 28 *May* 1980. *Accepted* 29 *September* 1980)

Summary—The excitation and ionization of calcium and strontium in a molybdenum micro-tube atomizer and their use in atomic-absorption spectrometry are described. Increasing hydrogen flow led to complex calcium atomization profiles for absorption measurements, but decreasing hydrogen flow resulted in higher atomic emission. Ionization of calcium and its suppression by potassium were also observed. Strontium was measured effectively by atomic absorption because of the higher sensitivity. Increasing hydrogen flow resulted in a lower atomization temperature and higher absorption for strontium, while decreasing hydrogen flow resulted in higher atomic emission. No interference from 100-fold amounts of magnesium, calcium and sodium was found for atomization of strontium, but 100-fold amounts of aluminium shifted the peak temperature for strontium though with no variation of appearance temperature and peak absorption. A small shift in peak temperature was observed for strontium in the presence of 100-fold amounts of phosphate.

Although the use of electrothermal atomization in atomic-absorption spectrometry is now widespread little work has been published on electrothermal atomization of calcium and strontium. Cragin *et al.*[1] have determined calcium at below the 5 μg/l. level in glacial snow samples with a graphite atomizer and Berggren *et al.*[2] have used a carbon-rod atomizer for the determination of calcium in biological materials. A graphite atomizer has also been used to measure strontium in blood serum[3] and soil.[4] Approximately, 20 pg of calcium and 5 pg of strontium can be determined in the graphite tube furnace. The excitation potentials of the resonance lines for alkaline earth elements are relatively low. This fact allows sensitive measurements of these elements to be made by flame emission spectrometry. The ionization potentials are also relatively low.

Recently, atomic emission obtained with an electrically heated carbon furnace has been used for determination of some elements and the potential of this technique as an analytical tool has been recognized.[5] Significant improvements in detection limits are obtained for alkali metals, compared to those obtained by carbon-furnace atomic-absorption spectrometry. Ionization has been shown to occur when carbon furnaces are used.[6]

However, the formation of stable carbides in carbon atomizers results in the release of alkaline-earth elements in the atomic form being slow. Attempts have been made to prevent carbide formation by lining the graphite tube with tantalum foil.[7] Metal atomizers reduce the possibility of formation of carbides and metal atomizers appear to be attractive for atomization of alkaline-earth metals. The metal microtube atomizer needs only a short heating period to provide an environment with a uniform temperature throughout the atomizer. The maximum atom cloud concentration is reached in an extremely short period of time, in contrast to conventional carbon atomizers.

This paper describes measurements of the excitation and ionization of calcium and strontium taking place in molybdenum micro-tube atomizers[8] and the resultant effects on atomic-absorption measurements. Atomic emission from a molybdenum micro-tube atomizer is also discussed as a possible analytical technique.

EXPERIMENTAL

Apparatus

All absorption and emission measurements were made with a Nippon Jarrell-Ash 0.5-m Ebert-type monochromator coupled to an R106 photomultiplier tube (Hamamatsu TV Co.) and a fast-response amplifier.[9] The output signal from the amplifier was monitored on a Memoriscope (Iwatsu MS-5021) with a time constant of 1 μsec.

A molybdenum micro-tube (15 mm long and 2 mm bore) was used as the atomizer. It was made from molybdenum sheet (0.05 mm thick). The micro-tube was mounted on two copper supports so that there was no localized variation in tube temperature. The micro-tube atomizer was enclosed in a Pyrex chamber (300 ml volume) which had two silica end-windows to allow transmission of the light-beam. The chamber was purged with argon and hydrogen.

Two light apertures (0.5 mm diameter) were positioned in front of the monochromator entrance slit so that the light-beam from the hollow-cathode lamp passed through the centre of the micro-tube and through the apertures.

* To whom correspondence and requests for reprints should be addressed.

The apertures reduced the micro-tube emission to a negligible extent.

The atomizer surface temperature was measured with a photodiode (Hamamatsu TV Co., S641). The signal from the photodiode was calibrated with an optical pyrometer. The signal from the photodiode and the absorption or emission signal were recorded simultaneously by using the two beams of the Memoriscope.

A calcium hollow-cathode lamp (Hamamatsu TV Co.) was used for absorption measurements of atoms at 422.67 nm and a strontium hollow-cathode lamp (Hamamatsu TV Co.) for absorption measurements of atoms at 460.73 nm and ions at 407.77 nm. Atomic emission measurements were also made at 422.67 nm and 460.73 nm for calcium and strontium, respectively. Ionic emission for calcium was measured at 393.37 nm.

All sample solutions were injected with a glass micropipette (1 μl) into the micro-tube through a 0.3-mm hole, drilled at the mid-point of the tube.

Reagents

Stock solutions (1 mg/ml) of calcium and strontium were prepared by dissolving their carbonates in hydrochloric acid and diluting with demineralized water. Dilute solutions were prepared immediately before use. Demineralized water gave no signal for alkaline-earth elements. All reagents were of analytical reagent grade and checked for calcium or strontium as impurities.

Procedure

Samples of 1 μl of the element of interest were injected into the micro-tube and dried at 100° for 30 sec. Samples were then atomized by heating to a final temperature of 2300°. The measurements of atomic emission for strontium and ionic emission for calcium and strontium were achieved by increasing the sensitivity of the vertical deflection system of the Memoriscope. Operation of the photomultiplier at increased gain was necessary for measurements of the ionic absorption of calcium and strontium.

RESULTS AND DISCUSSION

Electrothermal atomization of calcium

The addition of hydrogen to argon as the purge gas in the absorption chamber has a favourable effect on the electrothermal atomization of some elements with metal micro-tube atomizers.[10] Hydrogen also serves to protect the atomizer from oxidation by traces of oxygen in the argon. Therefore, the dependence of atomic absorption and emission profiles on hydrogen flow-rate was examined for calcium. The results are shown in Figs. 1 and 2. Atomic absorption and emission profiles were traced with different vertical deflection scales on the Memoriscope at the same photomultiplier voltage. Complex absorption profiles were seen on addition of hydrogen to the argon. Increasing hydrogen flow resulted in reduction of the atomic emission. In pure argon no atomic emission was observed, although a higher background still remained. The reason for this observation is not clear. Figure 3 shows the variation of atomic-emission signals with increasing amounts of calcium. This result suggests the possibility of the determination of calcium by atomic emission in a molybdenum micro-tube atomizer. However, improvements in atomizer design will be necessary for greater sensitivity of atomic emission. Accurate measurements of atomic absorption were difficult to make without contribu-

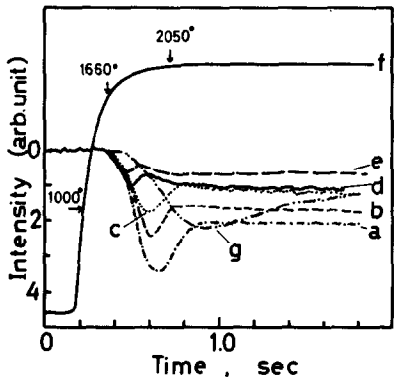


Fig. 2. Memoriscope traces showing effect of flow-rate of hydrogen on atomic emission of calcium (100 pg): *a*, Ar 480 ml/min and H_2 20 ml/min; *b*, Ar 400 ml/min and H_2 100 ml/min; *c*, Ar 300 ml/min and H_2 200 ml/min; *d*, Ar 100 ml/min and H_2 400 ml/min; *e*, H_2 500 ml/min; *f*, temperature increase; *g*, background at Ar = 500 ml/min. Photomultiplier voltage 770 V; vertical scale of Memoriscope 0.5 V/div.

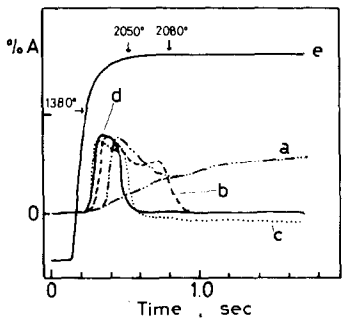


Fig. 1. Memoriscope traces showing effect of flow-rate of hydrogen on atomic absorption of calcium (100 pg): *a*, Ar 500 ml/min; *b*, Ar 480 ml/min and H_2 20 ml/min; *c*, Ar 100 ml/min and H_2 400 ml/min; *d*, H_2 500 ml/min; *e*, temperature increase. Photomultiplier voltage 770 V; vertical scale of Memoriscope 1 V/div.

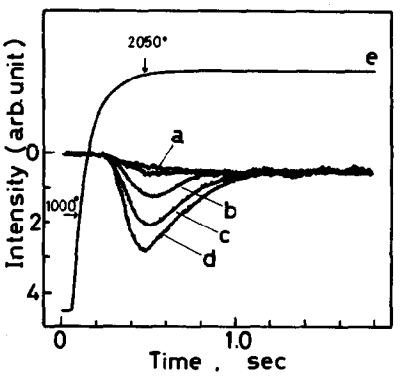


Fig. 3. Memoriscope traces for atomic emission of different amounts of calcium: *a*, 0.1 pg; *b*, 1 pg; *c*, 10 pg; *d*, 50 pg; *e*, temperature increase. Gas flow-rates, Ar 480 ml/min and H_2 20 ml/min.

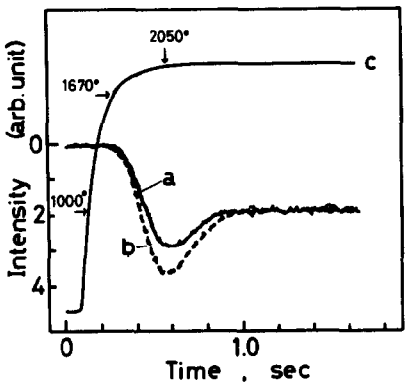


Fig. 4. Memoriscope traces for ionic emission of calcium (100 pg): *a*, no potassium; *b*, 500 ng of potassium added; *c*, temperature increase. Gas flow-rates, Ar 480 ml/min and H_2 20 ml/min.

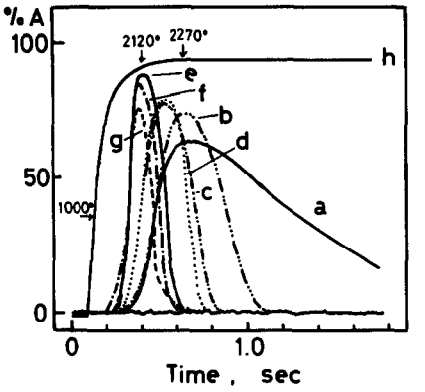


Fig. 5. Memoriscope traces showing effect of flow-rate of hydrogen on atomic absorption of strontium (50 pg): *a*, Ar 500 ml/min; *b*, Ar 480 ml/min and H_2 20 ml/min; *c*, 450 ml/min and H_2 50 ml/min; *d*, Ar 400 ml/min and H_2 100 ml/min; *e*, Ar 300 ml/min and H_2 200 ml/min; *f*, Ar 100 ml/min and H_2 400 ml/min; *g*, H_2 500 ml/min; *h*, temperature increase. Photomultiplier voltage 730 V; vertical scale of Memoriscope 0.5 V/div.

tions from atomic emission when the present detection system was used, because an unmodulated light source was employed for fast tracing of the atomization signals on the Memoriscope.

Calcium has an ionization potential of 6.11 eV and measurements of the emission of ionized species could be made. Figure 4 shows the profiles recorded during the atomization stage for calcium ionic emission. In flame spectrometry ionization is often suppressed by use of elements with a low ionization potential. The suppression of the calcium ionic emission (during the micro-tube atomization) by the addition of potassium (ionization potential 4.339 eV) to the calcium solution is analogous to that used in flame spectrometry. No molecular emission was observed for calcium.

Detection limits were calculated from peak heights in the atomization profiles and defined as that concentration giving an absorption or emission signal:background ratio of 2. In metal micro-tube atomization the detection limit is restricted by the small sample volume (1 μl). Therefore the detection limits are given in absolute terms (pg). A detection limit of 12 pg was obtained under the optimized conditions for the atomic emission of calcium. The detection limit was difficult to calculate from the peak height for atomic absorption because of the complex absorption profiles.

Electrothermal atomization of strontium

Figures 5 and 6 show the Memoriscope traces during the electrothermal atomization of strontium. These demonstrate the effect of hydrogen flow-rate on the atomic absorption and emission of strontium. The atomic absorption profiles were traced with the emission signals attenuated by reducing the sensitivity for the vertical deflection of the Memoriscope by a factor of about 5. The emission signals were negligible for the strontium concentrations tested. The atomic-absorption profiles are characterized by sharper and narrower curves, showing higher peak absorption with increasing hydrogen flow. The increased reducing nature of the gas phase may be responsible for the improvement in the atomization characteristics. No background was observed in the atomic-absorption measurements.

Higher atomic emission for strontium was observed at flow-rates of hydrogen lower than those used for calcium. The profiles for both atomic absorption and emission in pure argon were more rounded, with the decay from the maximum having lower slope. Maximum emission signals were shown at the same temperature at which atomic-absorption signals were a maximum. Ottaway and Shaw[5] have shown that emission maxima in graphite-furnace atomic emission spectrometry occur later in time than do the absorption maxima, since atomization takes place at a lower temperature than that which is optimum for excitation. Alder *et al.*[11] found a similar phenomenon for aluminium and suggested that this was a result of

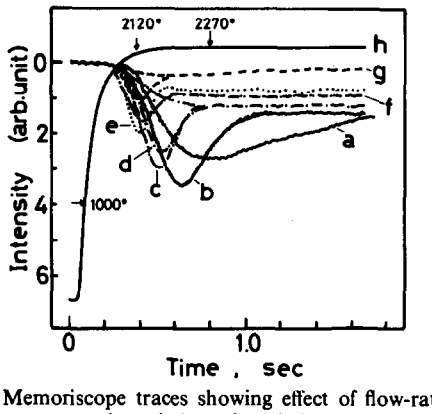


Fig. 6. Memoriscope traces showing effect of flow-rate of hydrogen on atomic emission of strontium (50 pg): *a*, Ar 500 ml/min; *b*, Ar 480 ml/min and H_2 20 ml/min; *c*, Ar 450 ml/min and H_2 50 ml/min; *d*, 400 ml/min and H_2 100 ml/min; *e*, Ar 300 ml/min and H_2 200 ml/min; *f*, Ar 100 ml/min and H_2 400 ml/min; *g*, H_2 500 ml/min; *h*, temperature increase. Photomultiplier voltage 30 V; vertical scale of Memoriscope 0.1 V/div.

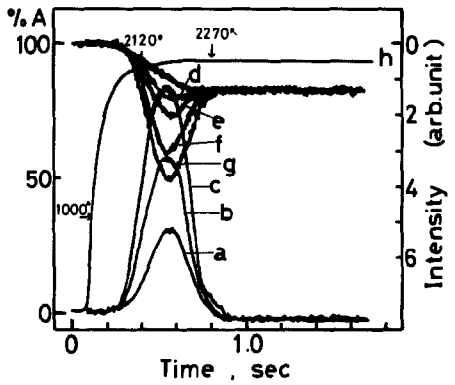


Fig. 7. Memoriscope traces for atomic absorption and emission of different amounts of strontium: *a* and *d*, 10 pg; *b* and *e*, 25 pg; *c* and *f*, 50 pg; *g*, 100 pg. *a–c* for absorption and *d–g* for emission. Detection conditions as for Fig. 5 for absorption and Fig. 6 for emission. Gas flow-rates, Ar 450 ml/min and H_2 50 ml/min.

atoms being formed in the ground state at a temperature below that at which significant emission occurs. The results for molybdenum micro-tube atomizers differed from those for carbon atomizers. This is presumably due to the fast uniform heating of micro-tube atomizers compared with that of carbon atomizers. No molecular emission was observed for strontium. The atomic absorption and emission signals obtained with increasing amounts of strontium are presented in Fig. 7.

Strontium has a lower ionization potential (5.692 eV) and therefore it seems possible that some degree of ionization might occur during the atomization process. Figure 8 shows the Memoriscope traces for strontium ionic absorption at different hydrogen flow-rates. Measurements were made at an increased photomultiplier voltage so as to observe the ionic absorption profiles with the Memoriscope. Higher absorption was shown at lower hydrogen flow-rates, but weak absorption was observed in pure argon. Changes in hydrogen flow-rate have different effects on absorption and emission and this phenomenon requires further investigation. The suppression of ionization with potassium was also observed for the ionic absorption and emission of strontium. Lower ionic absorption and emission have little effect on measurements of atomic absorption for strontium.

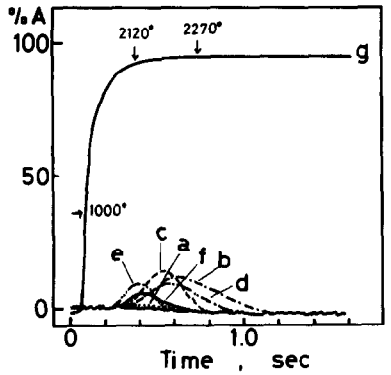


Fig. 8. Memoriscope traces showing effect of flow-rate of hydrogen on ionic absorption of strontium (50 pg): *a*, Ar 500 ml/min; *b*, Ar 480 ml/min and H_2 20 ml/min; *c*, Ar 450 ml/min and H_2 50 ml/min; *d*, Ar 400 ml/min and H_2 100 ml/min; *e*, Ar 300 ml/min and H_2 200 ml/min; *f*, Ar 100 ml/min and H_2 400 ml/min, and H_2 500 ml/min; *g*, temperature increase. Photomultiplier voltage 780 V; vertical scale of Memoriscope 0.5 V/div.

Absolute detection limits of 1.1 and 5 pg were obtained under the optimized conditions for atomic absorption and emission of strontium, respectively. The coefficient of variation was 2.6% (11 determinations) for atomic absorption of 50 pg of strontium. The poor detection limit for atomic emission resulted from the higher noise level compared with that for atomic absorption. The atomic-absorption mode is recommended for the measurement of strontium because of its higher sensitivity and lower noise levels in absorption profiles.

Aluminium, calcium, magnesium and phosphate are some of the most important interfering substances in atomization of strontium in an air–acetylene flame. The effects of 100-fold amounts of aluminium, magnesium, calcium, sodium and phosphate on electrothermal atomization of 50 pg of strontium were tested. The metals tested were added as their chlorides (and phosphate as the sodium salt). All the samples were checked for background effects and reagent blanks. Aluminium shifted the peak temperature (the temperature at which maximum absorption is observed) for strontium, although the appearance temperature and peak height remained the same (Fig. 9). Phosphate also gave a small shift in the peak temperature. No interferences from calcium, sodium and magnesium were observed. Almost identical effects were shown on the measurements of atomic emission of strontium, although a small depressant effect was observed for calcium.

Sample analysis

Some samples were analysed for strontium and the

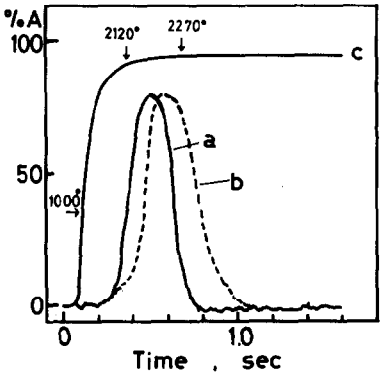


Fig. 9. Memoriscope traces showing effect of aluminium on strontium absorption: *a*, 50 pg of Sr; *b*, 50 pg of Sr and 5 ng of Al; *c*, temperature increase. Gas flow-rates, Ar 450 ml/min and H_2 50 ml/min.

Table 1. Determination of strontium in some samples

Sample	Strontium, μg/ml		Recovery, %
	Added	Found§	
Milk*	—	0.53	
	0.10	0.64	102
	0.20	0.76	104
Tap water†	—	0.021	
	0.006	0.028	104
Sea-water	—	6.0	
	2.5	8.7	102

* 100-fold dilution.
† 500-fold dilution.
§ Mean of three determinations.

results are listed in Table 1. Dilution was required, because of the high sensitivity of strontium atomic absorption. Samples were diluted 100- and 500-fold with demineralized water for milk and tap water respectively. Samples were spiked with strontium and the recovery found to be almost quantitative. Alkaline-earth elements are readily subject to contamination, so care must be taken in handling samples.

CONCLUSIONS

Atomic emission and ionization were observed in the electrothermal atomization of calcium and strontium with a molybdenum micro-tube. Atomic absorption of strontium could be measured without interference from these phenomena, but complex absorption profiles and pronounced atomic emission made it difficult to measure calcium accurately. The application of atomic emission in a molybdenum micro-tube appears to be worthy of further study for the determination of alkaline-earth metals.

Acknowledgement—This work was supported in part by a Grant-in-Aid for Special Project Research from the Ministry of Education, Science and Culture, Japan.

REFERENCES

1. J. H. Cragin and M. M. Meuron, *At. Absorpt. Newsl.*, 1973, **12**, 37.
2. P. O. Berggren, O. Berglund and B. Hellman, *Anal. Biochem.*, 1978, **84**, 393.
3. F. Bek, J. Janowskova and B. Moldam, *At. Absorpt. Newsl.*, 1974, **13**, 47.
4. E. S. Gladney, L. E. Wangen and R. D. Aguilar, *Anal. Lett.*, 1977, **10**, 1083.
5. J. M. Ottaway and F. Shaw, *Analyst*, 1975, **100**, 438.
6. *Idem, ibid.*, 1976, **101**, 582.
7. B. Weltz, *Atomic Absorption Spectroscopy*, p. 137. Verlag Chemie, Weinheim, 1976.
8. K. Ohta and M. Suzuki, *Talanta*, 1976, **23**, 560.
9. *Idem, ibid.*, 1979, **26**, 207.
10. *Idem, Anal. Chim. Acta*, 1979, **104**, 293.
11. J. F. Alder, A. J. Samuel and R. D. Snook, *Spectrochim. Acta*, 1976, **31B**, 509.

Talanta Vol. 28, pp. 183 to 186
© Pergamon Press Ltd 1981. Printed in Great Britain
0039-9140/81/030183-04$02.00/0

SHORT COMMUNICATIONS

AUTOPROTOLYSIS CONSTANTS BY COULOMETRIC TITRATION

STANISŁAW GŁAB and ADAM HULANICKI
Department of Chemistry, University of Warsaw, Poland

(*Received* 23 *January* 1980. *Revised* 12 *August* 1980. *Accepted* 3 *October* 1980)

Summary—A procedure is described for the evaluation of autoprotolysis constants in which a strong acid is titrated with coulometrically generated strong base. A two-compartment cell is used, and the acid may be added as such to the solvent under study, or generated *in situ* in the cell. When a silver auxiliary electrode can be used, as with solutions containing bromide ion, a single-compartment cell may be used, which seems to give more accurate results because it avoids the errors caused by diffusion of solution through the diaphragm. The results for the constants obtained for ethylene glycol, for methanol and for water are in reasonable agreement with values in the literature.

The application of non-aqueous and mixed solvents in physicochemical and analytical investigations requires a knowledge of the autoprotolysis constants, which give information directly relevant to the extent of the acidity scale. A variety of procedures has been used for the evaluation of autoprotolysis constants, mainly based on potentiometric titrations.[1,2] Reliable results require high-precision work, and therefore such parameters as concentrations of the solutions, and the presence of acidic and basic impurities, must be accurately evaluated. It might be expected that both a simplification and an improvement of the procedure would be obtainable by using coulometric titrations.

In general, the coulometric generation of acids or bases requires a cell with separate anode and cathode compartments so as to prevent reaction between the electrolysis products, but the presence of the diaphragm increases the total resistance of the cell, which in the case of non-aqueous solutions is quite high even without the diaphragm. The use of a more porous diaphragm decreases the resistance but increases the risk of diffusion of the solutions through the diaphragm.

The autoprotolysis constant may be calculated from potentials measured during the course of a titration of a strong acid, which may be added as a solution of appropriate concentration in the solvent of interest, or generated coulometrically at the anode. The acid is then titrated with a coulometrically generated base. The e.m.f. measured in the indicator circuit with an electrode sensitive to solvated protons is given by the equation:

$$E_a = E_a^0 + 59.16 \log [SH_2^+] \qquad (1)$$

where E_a^0 represents the standard potential for the indicator electrode in the acidic range at 25°, and $[SH_2^+]$ is the actual concentration of the proton, expressed by means of the equation

$$[SH_2^+] = \frac{Q_{EP} - Q}{FV} \qquad (2)$$

where Q_{EP} is the charge consumed up to the end-point of titration of the acid, Q is the charge up to a given point of the titration curve, at which the measured potential is E_a, V is the volume of the solution, and F is the Faraday constant.

Similarly, after the end-point of the titration, when the cathodically generated base is in excess, the potential of the electrode is given by

$$E_b = E_b^0 - 59.16 \log[S^-] \qquad (3)$$

where E_b^0 is the standard potential for the basic range, and the concentration of the excess of base is given by

$$[S^-] = \frac{Q - Q_{EP}}{FV} \qquad (4)$$

The concentration autoprotolysis constant, $K_s^c = [SH_2^+][S^-]$, is calculated as

$$pK_s^c = \frac{E_a^0 - E_b^0}{59.16} \qquad (5)$$

The values of the two standard potentials E_a^0 and E_b^0 should be calculated for a number of points on the titration curve: their constancy over the whole range indicates the absence of systematic errors.

The usual procedure for the determination of an autoprotolysis constant requires preparation of solutions of the acid and the base in the solvent investigated. For at least one of these solutions the exact concentration must be determined independently. In the coulometric procedure described, with coulometric generation of the base, only one solution con-

taining the acid and the conducting electrolyte has to be prepared, and its concentration is determined from the coulometric alkalimetric titration curve, assuming 100% current efficiency for generation of the base.

A modification of the coulometric procedure is based on coulometric generation of the acid in the given solvent. This needs only the preparation of a single solution of the conducting electrolyte in which the acid is initially generated (anodically), and then, after reversal of the polarity, the base. The concentration of acid is evaluated from the number of coulombs consumed in the acid generation, while the amount of base is calculated from the charge consumed from polarity reversal to the equivalence point of the recorded potentiometric titration curve. This allows immediate comparison of the current efficiencies of the two processes in the solvent investigated. Equality of the current efficiencies for the two processes indicates that both processes are probably occurring with 100% efficiency.

This procedure also offers the possibility of using completely anhydrous perchloric acid solutions, generated in perchlorate media, which is otherwise complicated if the solution has to be prepared from concentrated aqueous perchloric acid.

Coulometric acid–base titrations can be done without having separate anode and cathode compartments if a silver anode is used, on which the electrode process in the presence of halide ions occurs with the formation of sparingly soluble products.[3] In aqueous and in some non-aqueous solutions containing moderate halide concentrations the solubility of the silver as halide complexes is low enough not to cause an appreciable error, and the precipitate formed remains firmly bound on the electrode. Nevertheless, it must always be checked that the silver error[4] does remain at a low level.

The advantages of this method may not be generally applicable, however, because in some solvents the halide ions behave as weak bases reacting with the solvated protons to give slightly dissociated acids which interfere in the determination of the autoprotolysis constants. Another type of interference occurs when undesired side-reactions occur, such as formation of slightly soluble lyate salts in the vicinity of the cathode.

For confirmation that the coulometric procedures described here do give accurate results, the autoprotolysis constants of some known systems, including ethylene glycol, methanol, water and their mixtures were measured.

EXPERIMENTAL

Reagents

Water. Twice distilled from quartz apparatus.

Methanol. Analytical grade, containing approx. 0.15% water, as determined by Karl Fischer titration.[5]

Ethylene glycol. Dried with anhydrous sodium sulphate and distilled at 7.5 mmHg pressure.

Sodium perchlorate, sodium bromide, perchloric acid (72%). Analytical grade.

Apparatus

Radelkis, coulometric analyser OH-404, Beckman 4500 pH-meter with glass indicator electrode, and a silver–silver bromide electrode, or a bromide ion-selective electrode (50% AgBr–50% Ag_2S), as reference electrode. In the generating circuit a platinum gauze working electrode with a surface area of about 40 cm^2, and a silver counter-electrode of about 30 cm^2 surface area were used.

All measurements were carried out at 25° in solutions deaerated and protected with argon gas, and stirred with a magnetic stirrer.

Procedures

Measurements with a single-compartment coulometric cell. The coulometric cell was equipped with the platinum cathode and silver anode and the indicator system consisted of a glass electrode and a bromide ion-selective reference electrode. The electrolyte solution was 150 ml of 0.05*M* sodium bromide and approximately 0.004*M* perchloric acid. Base was generated by passing a constant current of 5 mA.

Measurements with a two-compartment coulometric cell. The anode and cathode compartments were separated by two porosity-4 sintered-glass diaphragms, with the intervening space filled with a 3% sodium perchlorate in agar solution. Both electrodes in the generating circuit were of platinum, and the surface area of the working electrode was about 5 cm^2. A glass electrode was used as indicator electrode, coupled with a bromide ion-selective electrode as reference, placed either directly in the solution or separated by a sintered-glass diaphragm. The electrolyte solution was 50 ml of 0.05*M* sodium perchlorate and 0.05*M* sodium bromide in the appropriate solvent. Perchloric acid was

Table 1. Determination of the autoprotolysis constant of ethylene glycol in the two-compartment cell

Charge, *mC*	*E*, *mV*	E_a^0, *mV*	E_b^0, *mV*
3002	270.0	410.0	
4003	268.8	410.0	
5004	267.9	410.5	
6000	266.5	410.5	
7002	265.0	410.5	
8020	263.5	410.6	
9003	261.9	410.5	
10011	260.0	410.0	
11011	258.1	410.5	
12001	255.9	410.4	
13002	253.5	410.3	
14002	250.9	410.3	
28001	−287.0		−468.1
29003	−292.4		−468.2
30005	−296.8		−467.9
31001	−300.8		−468.0
32003	−304.2		−468.1
33006	−307.2		−468.1
Average		410.4	−468.1

$pK_s^c = 14.85$; $pK_s = 15.57$

The acid in a 50-ml cell was generated by passage of 24000 mC, and then titrated with electrogenerated base: current 5 mA; equivalence point for base generation corresponds to Q_{PE} = 23800 mC; electrolyte: 0.05*M* sodium bromide and 0.05*M* sodium perchlorate.

Table 2. Determination of the autoprotolysis constant of ethylene glycol in the single-compartment cell

Charge, *mC*	*E*, *mV*	E_a^0, *mV*	E_b^0, *mV*
1001.5	413.3	590.2	
2200.0	411.4	590.5	
3001.6	409.7	590.3	
4002.2	407.5	590.2	
5303.1	404.1	589.7	
6001.9	402.3	589.8	
7002.0	399.4	589.7	
8000.9	396.3	589.5	
9000.0	392.6	589.5	
10002.2	388.5	589.5	
11100.2	383.1	590.1	
12004.0	377.6	590.1	
19000.1	−91.9		−308.2
20001.4	−99.4		−308.7
21001.2	−105.1		−308.9
22000.3	−109.5		−308.7
23002.0	−113.2		−308.6
24002.4	−116.8		−308.9
25003.5	−119.9		−309.0
Average		589.9	−308.7
$pK_s^c = 15.19$		$pK_s = 15.65$	

The acid, in 150 ml of 0.05*M* sodium bromide in ethylene glycol, was titrated with cathodically generated base: current 5 mA; Q_{PE} = 15700 mC.

added to give a concentration of 0.004*M* and the base was generated by passing a constant current of 5 mA.

RESULTS AND DISCUSSION

Autoprotolysis constants were determined for ethylene glycol, methanol and water. The detailed records for procedures in both types of cells are given in Tables 1 and 2. The concentration constants pK_s^c were recalculated to obtain the thermodynamic values

$$pK_s = pK_s^c - 2\log f_\pm \qquad (6)$$

by using the known ionic strength and the Debye–Hückel equation

$$-\log f_\pm = \frac{Az^2\sqrt{I}}{1 + Ba\sqrt{I}} \qquad (7)$$

where $A = 1.825 \times 10^6\ (\epsilon T)^{-3/2}$, $B = 50.29\ (\epsilon T)^{-1/2}$ and $a = 5$.[8] The temperature for all measurements was 298 K and the values taken for the dielectric constants ϵ were 37.7 for ethylene glycol and 32.6 for methanol.[7]

The values obtained are in good agreement with those in the literature. The pK_s values obtained for ethylene glycol and methanol in the cell with separate working and auxiliary electrode compartments are slightly smaller than those obtained with the single-compartment cell. This suggests that a small error is introduced by diffusion of water through the diaphragm.

Similar reasons are probably responsible for a small difference of about 200 mC, *i.e.* 0.8%, between the charge consumed in the generation of acid and of base. Previous studies have shown that in ethylene glycol the efficiencies of generation for acid and for base do not differ by more than 0.1%.[6] Therefore the diffusion of acid through the membrane seems a better explanation for the discrepancy, though the presence of some basic impurities in the solvent could cause the same effect.

In the course of base generation at the cathode in methanol a slight deposit was seen at the electrode, but this is reckoned to cause only a minor error. Slightly better results were obtained when the silver/silver bromide reference electrode was separated by an electrolyte bridge or when a bromide ion-selective electrode was used. The reduction of silver from the bromide complex was also not observed when another reference electrode was used. This effect may be more harmful when other solvents with stronger solvating properties for silver are investigated.

Table 3. Autoprotolysis constants determined for some solvents at 25°

Solvent	pK_s Calculated	Literature	Ref.	Procedure	Reference electrode
Ethylene glycol	15.65	15.72	1	A	Ag/AgBr
	15.57			B	Ag/AgBr
Methanol	16.69	16.7	7	A	Ag/AgBr
	16.48			B*	Ag/AgBr
	16.48			C*	Ag/AgBr
	16.50			C	Br-selective
Water	13.98	14.0	8	A	Ag/AgBr
	14.01			B	Ag/AgBr
	13.92			C	Ag/AgBr

A. One-compartment cell. Electrolyte: 0.05*M* NaBr.

B. Two-compartment cell. Acid anodically generated. Electrolyte: 0.05*M* $NaClO_4$ and 0.05*M* NaBr.

C. Two-compartment cell. Electrolyte: 0.004*M* $HClO_4$, 0.05*M* $NaClO_4$ and 0.05*M* NaBr.

* Reference electrode separated from the solution by sintered-glass diaphragm.

The results obtained for the autoprotolysis constant under various conditions are collected in Table 3. They indicate that the proposed methods give good results, but that special attention must be paid in cases when diffusion of solutions through the diaphragms can take place.

REFERENCES

1. P. Zikolov, A. Astrug and O. Budevsky, *Talanta*, 1975, **22**, 511.
2. M. Galus, S. Głab, G. Grekulak and A. Hulanicki, *ibid.*, 1979, **26**, 169.
3. J. J. Lingane, *Anal. Chim. Acta*, 1954, **11**, 283.
4. E. Bishop and M. Riley, *Analyst*, 1973, **98**, 315.
5. W. Pawłowski and W. Jedral, *Chem. Anal. Warsaw*, 1980, **25**, 151.
6. S. Głab and A. Hulanicki, in *Coulometric Analysis*, ed. E. Pungor. Proceedings of Conference at Matrafured, 1978. Akadémiai Kiadó, Budapest, 1979, p. 221.
7. G. Charlot and B. Trémillon, *Les réactions chimiques dans les solvants et les sels fondus*, Gauthier-Villars, Paris, 1963.
8. R. A. Robinson and R. H. Stokes, *Electrolyte Solutions*, 2nd Ed., p. 230. Butterworths, London, 1968.

Talanta Vol. 28, pp. 187 to 188
© Pergamon Press Ltd 1981. Printed in Great Britain
0039-9140/81/030187-02$02.00/0

NMR ASSAY OF EPHEDRINE HYDROCHLORIDE IN TABLETS

M. M. A. HASSAN, M. UPPAL ZUBAIR and J. S. MOSSA

Departments of Pharmaceutical Chemistry and Pharmacognosy, College of Pharmacy, Riyad University, Riyad, Saudi Arabia

(*Received* 25 *April* 1980. *Revised* 8 *September* 1980. *Accepted* 25 *September* 1980)

Summary—A rapid NMR method is described for the determination of ephedrine hydrochloride. The relative standard deviations are 1.5% and 1.2% for the pure drug and tablets respectively. The results for synthetic mixtures and tablets are comparable to those obtained by the B.P. 1973 method. In addition, the NMR spectrum furnishes a specific means of identification of ephedrine.

Ephedrine hydrochloride (I) [(−)-2-methylamino-1-phenylpropan-1-ol, HCl] is obtained from certain species of Ephedra,[1] namely, *Ephedra Sinica* Stapf, *Ephedra equisetina* Bunge and *Ephedra distachya* (Fam. Ephedraceae) and by synthesis.[2] It is mainly used medicinally as a sympathomimetic in the treatment of asthma and in hay fever.[1] Several methods have been reported for its determination. A gravimetric method is based on precipitation with hexabromotelluric acid[3] and the B.P.[4] gives a titration method for tablets and a non-aqueous titration technique for the assay of pure ephedrine hydrochloride. Other methods used include titrimetric,[5–9] conductimetric,[10–12] potentiometric,[13,14] colorimetric,[15–20] and spectrophotometric[21] procedures. Separational methods are based on paper, thin-layer,[22–24] gas–liquid[25–29] and high-pressure liquid[29] chromatography. Gas-liquid chromatography, mass spectrometry,[30] and ion-exchange resins have been employed for the separation and estimation of ephedrine.[31,32]

Some of these methods are fairly specific but tend to be lengthy and expensive. Because the dose of ephedrine hydrochloride is relatively high (30 mg) and its NMR spectrum has a characteristic resonance pattern, NMR spectroscopy has been investigated as a means of analysing for the drug.

EXPERIMENTAL

A Varian T-60A 60-MHz NMR spectrometer was used, with acetamide as internal standard. All chemical shifts were referred to sodium 3-(trimethylsilyl)propionate.

Analysis of tablets

Weigh and finely powder not less than 20 tablets. Weigh accurately a portion of the powder equivalent to about 150 mg of I, into a glass-stoppered centrifuge tube. Add 4 ml of distilled water containing an accurately weighed amount of acetamide (20–40 mg). Stopper and shake for 3 min and then centrifuge. Transfer about 0.5 ml of the clear supernatant solution into a precision NMR spectrometer and obtain the spectrum, adjusting the spin-rate to eliminate the spin side-bands as much as possible. Integrate the peaks of interest (the three-proton secondary methyl doublet of I at 1.16 ppm and the three proton singlet of acetamide at 2 ppm) at least three times and take the means.

The amount of I is calculated by simple proportion:

$$\text{I} = \frac{\text{ephedrine . HCl integral}}{\text{acetamide integral}} \times 3.72 \times \text{weight of acetamide}$$

where 3.72 is the ratio of the molecular weights of ephedrine hydrochloride and acetamide.

RESULTS AND DISCUSSION

The NMR spectrum of ephedrine hydrochloride in D_2O displays the chemical shifts of which are listed in Table 1. The secondary methyl proton doublet centred at 1.16 ppm, the *N*-methyl proton singlet at 2.83 ppm and the aromatic-proton singlet at 7.43 ppm can be used for the determination. For this work the doublet at 1.16 ppm was chosen. Acetamide[33] is used as internal standard, on the basis of its methyl three-proton singlet at 2 ppm, which is sufficiently separated from the 1.16-ppm doublet of I and the solvent signal at 4.73 ppm to allow satisfactory determination. Since water readily dissolves both I and acetamide, and its two-proton singlet of water at 4.73 ppm does not interfere with the upfield protons of these compounds, it is used as the solvent. Use of the expensive deuterium oxide is unnecessary.

A series of mixtures of I (20–150 mg) with about a third of its weight of acetamide was prepared and analysed. The recovery ranged from 96.8 to 102.2%, mean 99.3%, standard deviation 1.5%. For quantitative NMR it is best to take the test substance and the

Table 1. Chemical shifts of ephedrine hydrochloride in D_2O

Group	Chemical shift, δ
a–CH–CH_3	1.16 (d)
b–N–CH_3	2.83 (s)
c–CH–CH_3	3.53 (m)
d–CH–OH	5.20 (d)
e–C_6H_5	7.43 (s)

(s) = singlet, (d) = doublet, (m) = multiplet.

Table 2. Determination of ephedrine hydrochloride in standard mixtures by NMR

Mixture	Acetamide internal standard added, *mg*	Ephedrine.HCl		
		Added, *mg*	Found, *mg*	Recovery, %
1	7.6	22.1	22.05	99.8
2	17.0	48.6	48.47	99.7
3	21.9	54.1	52.35	96.8
4	28.6	74.1	75.74	102.2
5	32.2	79.2	78.30	98.9
6	29.8	99.7	99.16	99.5
7	33.4	125.3	124.21	99.1
8	40.3	148.8	146.89	98.7
			Average	99.3
			Std. devn.	±1.5

internal standard in the ratio of their molecular weights, provided the same numbers of protons are involved for both. In this case a 3:1 ratio of ephedrine to acetamide is suitable.

When this method was applied to commercial tablets of **I**, the results obtained for a nominal 150 mg of **I** were 150.5 mg (standard deviation 1.6 mg) by the NMR method, and 150.7 mg (s.d. 2.0 mg) by the B.P. (1973) method (8 replicates in both cases). There was no evidence of interference from the excipients present.

The method is rapid, accurate and specific. Moreover, major impurities in the sample may be identified and determined.

Acknowledgement—The authors are thankful to Mr. Khalid N. K. Lodhi of the Central Laboratory, College of Pharmacy, Riyad University for running the NMR spectra.

REFERENCES

1. G. E. Trease and W. C. Evans, *Pharmacognosy*, 11th Ed., pp. 56–57, Bailliere Tindall, London, 1978.
2. R. H. F. Manske and T. B. Johnson, *J. Am. Chem. Soc.*, 1929, **51**, 580, 1906.
3. Q. Tuyen and I. Grecu, *Rev. Chim. (Bucharest)*, 1977, **28**, 585.
4. *British Pharmacopoeia*, pp. 181–185, Her Majesty's Stationery Office, London, 1973.
5. L. G. Chattan and M. Pernarowski, *Drug Standards*, 1954, **22**, 1.
6. M. Kusznieruk and T. Warmuzinska, *Anal. Abstr.*, 1967, **14**, 7096.
7. O. Hans-Hartung, D. Rossbach and G. Rohde, *Dtsch. Apoth.-Ztg.*, 1977, **117**, 418.
8. E. Zoltai and E. Posgay, *Acta Pharm. Hung.*, 1977, **47**, 217.
9. J. Katsy, *ibid.*, 1974, **44**, 217.
10. Z. P. Yakusheva and E. T. Tkachuk, *Sb. Stat. Aspirantov Soiskatel, Min. Vyssh. Sred. Spets. Obrazov. KazSSR, Khim. Khim. Tekhnol.*, 1965, No. 3–4, 89, *Referat. Zh. Khim.*, 19GD, 1966, (20), Abstract No. 20G 248.
11. K. Fukamachi, R. Nakagawa, M. Morimoto and N. Ishibashi, *Bunseki Kagaku*, 1975, **24**, 428.
12. J. Jarzebinski and P. Suchocki, *Farm. Pol.*, 1977, **33**, 151.
13. K. I. Evstratova and A. A. Kochegina, *Farmatsiya (Moscow)*, 1976, **25** (6), 25.
14. P. Chakarova and O. J. Budevski, *Electroanal. Chem.*, 1976, **73**, 369.
15. M. Kusznieruk and T. Warmuzinski, *Farm. Pol.*, 1966, **22**, 515.
16. D. Brzezinska and J. Pliszcznska, *ibid.*, 1966, **22**, 439.
17. D. Brzesinka and L. Maciaszek, *ibid.*, 1965, **21**, 353.
18. D. W. Robertson, F. Matsui and W. N. French, *Can. J. Pharm. Sci.*, 1972, **7**, 47.
19. R. Dynakowski, D. Bzezinska-Drygienie and A. Bastosiak, *Farm. Pol.*, 1971, **27**, 327.
20. A. Zolein and M. Gracza, *Acta Pharm. Hung.*, 1975, **45**, 101.
21. C. C. Charles, *J. Assoc. Off. Anal. Chemists*, 1975, **58**, 852.
22. R. Rasplandy, *Compt. Rend.*, 1954, **238**, 2527.
23. A. Brantner, J. Vamos and M. Gracza, *Gyogyszereszet*, 1976, **20**, 369.
24. T. Burat, *Turk. Hij. Tecr. Biyol. Derg.*, 1977, **37**, 199.
25. H. Tetsuyasu, K. Satoshi and N. Michinori, *Bunseki Kagaku*, 1965, **14**, 586.
26. H. J. Wesselman and W. L. Koch, *J. Pharm. Sci.*, 1968, **57**, 845.
27. G. P. Welling, K. P. Lee, J. A. Patel, J. E. Walker and J. G. Wagner, *J. Pharm. Sci.*, 1971, **60**, 1629.
28. U. Shigeo, H. Kazuo and K. Shozi, *Eisei Kagaku*, 1976, **22**, 275.
29. J. Troschuetz-Merzhaeuser and E. F. Rolder, *Z. Anal. Chem.*, 1977, **285**, 377.
30. I. Hiroshi and M. Asao, *Chem. Pharm. Bull.*, 1977, **25**, 1215.
31. L. Saunders, P. H. Elworthy and R. Fleming, *J. Pharm. Pharmacol.*, 1954, **6**, 32.
32. J. Jarzebinski, *Acta Pol. Pharm.*, 1976, **33**, 493.
33. M. M. A. Hassan and El-Sayed A. Aboutabl, *Spectrosc. Lett.*, 1979, **12**, 351.

Talanta Vol. 28, pp. 189 to 191
© Pergamon Press Ltd 1981. Printed in Great Britain
0039-9140/81/030189-03$02.00/0

SENSITIVE SPECTROPHOTOMETRIC DETERMINATION OF NICKEL(II) WITH 2-(5-BROMO-2-PYRIDYLAZO)-5-DIETHYLAMINOPHENOL

WEI FU-SHENG, QU PEI-HUA, SHEN NAI-KUI and YIN FANG

Department of Chemistry, China Science and Technology University, Hefei, China

(*Received* 30 *August* 1980. *Accepted* 1 *October* 1980)

Summary—A simple, selective and highly sensitive procedure for spectrophotometric determination of nickel has been developed. At pH 5.5, nickel reacts with 2-(5-bromo-2-pyridylazo)-5-diethylaminophenol in water–ethanol medium to form a red-violet complex which has two absorption maxima, at 520 and 560 nm. The molar absorptivity at 560 nm is 1.26×10^5 l.mole^{-1}.cm^{-1}. Beer's law is obeyed for 0–15 μg of nickel. Nickel in aluminium alloys and electroplating waste-water has been determined by this method.

In China, 2-(5-bromo-2-pyridylazo)-5-diethylaminophenol (5-Br-PADAP) has attracted much attention as a spectrophotometric reagent, because of its high sensitivity and good selectivity. Recently it was used to determine Cu(II),[1,2] Mn(II),[3] Nb,[4] Sb(III),[5,6] U(VI),[7–9] V(V)[10] and Zn,[11] with satisfactory results. A brief review of analytical applications of this reagent has been given by Wei *et al.*[12]

5-Br-PADAP forms a red-violet complex with nickel, but its utility as a chromogenic reagent for this metal has not been investigated. This paper describes its use for the spectrophotometric determination of nickel in aluminium alloys and nickel electroplating waste-water.

EXPERIMENTAL

Reagents

Nickel solution. Dissolve 0.1000 g of pure nickel metal in 10 ml of nitric acid (1 + 1). Dilute to give the 10-μg/ml working standard.

5-Br-PADAP ethanolic solution, 0.02%.

Sodium acetate buffer (pH 5.5). Dissolve 200 g of sodium acetate ($NaC_2H_3O_2 \cdot 3H_2O$) in water, add 9 ml of glacial acetic acid and dilute to 1000 ml.

Procedure

Transfer a sample containing not more than 15 μg of nickel into a 25-ml standard flask. Add, with swirling, 1 ml of acetate buffer (pH 5.5), 10 ml of ethanol and 2 ml of 5-Br-PADAP solution. Dilute to volume with water and mix well. Measure the absorbance at 560 nm in a 1-cm cell against a reagent blank after 30 min. Prepare a calibration curve for the range 0–15 μg of nickel.

RESULTS AND DISCUSSION

Absorption spectra

The absorption spectra of 5-Br-PADAP and its nickel complex at pH 5.5 in 50% ethanolic medium are shown in Fig. 1. The absorption maximum of the reagent is at 445 nm, and the nickel complex exhibits two maxima at 520 and 560 nm. The absorbance of the reagent is insignificant at 560 nm. All absorbance measurements are therefore made at this wavelength.

Effect of variables

A pH study of the complexation of 5-Br-PADAP with nickel shows that the coloured complex has constant absorbance in the pH range 5–10. In order to decrease the effect of foreign ions, pH 5.5 is preferred. The absorbance values at pH 5.5 of a water–ethanol (1:1) solution containing 10 μg of nickel and increasing amounts of 5-Br-PADAP show that maximum absorbance is reached when the reagent:metal molar ratio lies between 4:1 and 10:1. Temperature has an effect on the time required for full colour development of the complex. At 15°, the solution should be kept for 30 min for complete colour development; the colour intensity remains virtually constant for 24 hr.

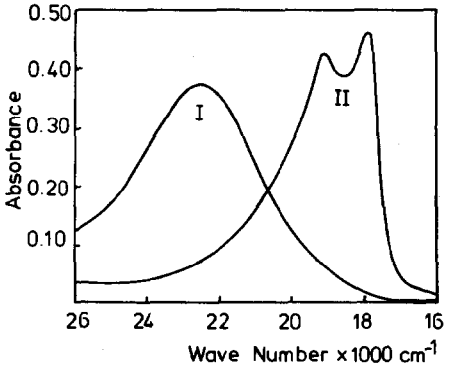


Fig. 1. Absorption spectra of 5-Br-PADAP and its nickel complex (pH 5.5; 1-cm cell). I—5-Br-PADAP $8.0 \times 10^{-6}M$ II—Ni-5-Br-PADAP, $4.0 \times 10^{-6}M$.

Table 1. Determination of nickel in aluminium alloys and waste-water

Sample	Ni found, %	
	Present method	Dimethylglyoxime method
Aluminium alloy 1	1.93, 1.96, 1.96	1.96
Aluminium alloy 2	0.120, 0.115, 0.123	0.116
Aluminium alloy 3	0.506, 0.513, 0.506	0.506
Aluminium alloy 4	1.02, 1.00, 1.04	1.04
Waste-water 1	8.3, 8.0 × 10^{-6}	8.1 × 10^{-6}
Waste-water 2	3.62, 3.70 × 10^{-6}	3.64 × 10^{-6}

Table 2. Sensitivities of methods for the spectrophotometric determination of nickel

Method	λ, nm	ϵ, $10^4\ l.mole^{-1}.cm^{-1}$	Reference
Dimethylglyoxime	445	1.5	15
α-Furil dioxime	435	2.0	16
4-(2-Pyridylazo) resorcinol	494	7.3	17
1-(2-Pyridylazo)-2-naphthol	570	5.0	18
2-(2-Thiazolylazo)-5-dimethylaminophenol	575	4.6	19
1-(2-Thiazolylazo)-2-naphthol	592	3.8	20
4-(2-Pyridylazo)thymol	610	2.1	21
4-[(2-Methylanabazine)-α'-azo]-*p*-cresol	590	2.5	22
2-(5-Bromo-2-pyridylazo)-*p*-cresol	610	3.84 ± 0.16	23
2-(5-Bromo-2-pyridylazo)-5-dimethylaminophenol	558	12.8	24
5-Br-PADAP	560	12.6	Present method

Effect of foreign ions

The effect of foreign ions on determination of 10 μg of nickel was examined. The following ions [when present in the amounts (in mg) shown in brackets] do not interfere: K^+(10), Na^+(2), NH_4^+(10), Be^{2+}(1), Mg^{2+}(5), Ca^{2+}(5), Sr^{2+}(5), F^-(40), Cl^-(5), Br^-(1), I^-(1), NO_3^-(5), SO_4^{2-}(5), CH_3COO^-(20), $P_2O_7^{4-}$(25), PO_3^-(100), $S_2O_3^{2-}$(10), SiO_3^{2-}(10), ClO_4^-(10), $B_4O_7^{2-}$(10), Ba^{2+}(0.1), Al^{3+}(0.2), Pb^{2+}(0.1), Cd^{2+}(0.1), Mn^{2+}(0.1), Y^{3+}(0.1), As^{3+}(0.5), PO_4^{3-}(0.5), Zn^{2+}(0.05), Hg^{2+}(0.04), Cr^{3+}(0.05), La^{3+}(0.05), Au^{3+}(0.02), Sb^{3+}(0.02), Mo(VI)(0.02) and Ag^+(0.01). Cu^{2+}(0.4), Fe^{3+}(0.05), Al^{3+}(2) and Zr^{4+}(0.05) can be masked by the addition of thiosulphate, metaphosphate and fluoride. Co^{2+}(0.01) interferes.

Composition of the complex

The composition of the complex was determined by the continuous-variation method[13] and the mole-ratio method.[14] Both methods indicate the formation of a 1:2 complex.

Samples analysed

The method can be applied to the determination of nickel in aluminium alloys and nickel electroplating waste-water. The results of analysis in comparison with the dimethylglyoxime method[15] are given in Table 1, indicating that the procedure is satisfactory.

Comparison with other reagents

5-Br-PADAP is one of the most sensitive reagents for nickel and compares favourably with other nickel reagents. The method is simple and rapid, works over a wide range of pH values and is fairly free from interferences. There is no need for extraction and the complex formed is stable for a long time. The sensitivities of the various methods are compared in Table 2.

REFERENCES

1. Z. D. Hu, F. K. Gao and J. S. Kuo, *Fenxi Huaxue*, 1978, **6**, 446.
2. N. F. Ye, F. S. Wei and Yin Fang, *J. Univ. Sci. Technol. China*, 1980, **10**, 78.

3. F. S. Wei, P. H. Qu and Y. R. Zhu, *Fenxi Huaxue*, in the press.
4. Y. R. Zhu, F. S. Wei, P. H. Qu and N. K. Shen, *Acta Chim Sinica*, in the press.
5. J. Y. Gao and Z. D. Wu, *Fenxi Huaxue*, 1978, **6**, 165.
6. Y. R. Zhu, F. S. Wei and N. K. Shen, *Huanjin Kexue Chongkan*, in the press.
7. D. A. Johnson and T. M. Florence, *Talanta*, 1975, **22**, 253.
8. *Idem*, *Anal. Chim. Acta*, 1971, **53**, 73.
9. P. Y. Kong and G. G. Zhong, *Acta Sci. Nat. Univ. Sunyatseni*, 1980, **1**, 68.
10. Z. D. Hu and J. Y. Gao, *Huaxue Tongbao*, 1979, No. 3, 44.
11. F. S. Wei and Y. R. Zhu, *J. Univ. Sci. Technol. China*, 1979, **9**, 41.
12. F. S. Wei, Y. R. Zhu and N. K. Shen, *Huaxue Shiji*, 1980, 52 (Chinese).
13. P. Job, *Ann. Chim. (Paris)*, 1928, **9**, 113.
14. J. H. Yoe and A. L. Jones, *Ind. Eng. Chem., Anal. Ed.*, 1944, **16**, 111.
15. Z. Marczenko, *Spectrophotometric Determination of Elements*, pp. 370–373. Horwood, Chichester, 1976.
16. *Idem*, *op. cit*, pp. 373–374.
17. S. Shibata, *2-Pyridylazo Compounds in Analytical Chemistry*, p. 131, in *Chelates in Analytical Chemistry*, Vol. 4, H. Flaschka and J. A. Barnard, Jr. (eds.), Dekker, New York, 1972.
18. *Idem*, *op. cit.*, p. 42.
19. K. Kasiura and Z. Sytniewska, *Chem. Anal. (Warsaw)*, 1968, **13**, 177.
20. K. Kasiura, *ibid.*, 1969, **14**, 375.
21. T. M. Mirzakasimov, K. Z. Rakhmatullaev and Sh. T. Talipov, *Uzb. Khim. Zh.*, 1968, **29**, 12.
22. E. L. Krukovskaya and Sh. T. Talipov, *Izv. Akad. Nauk Kaz. SSR, Ser. Khim.*, 1973, **23**, 10.
23. L. S. Krysina, T. N. Zholondkovskaya and V. M. Khomemko, *Dokl. Tskha*, 1975, No. 208, 239; *Chem. Abstr.*, 1976, **84**, 98445m.
24. S. Shibata, M. Furukawa and K. Toei, *Anal. Chim. Acta*, 1973, **66**, 397.

Talanta Vol. 28, pp. 192 to 194
© Pergamon Press Ltd 1981. Printed in Great Britain
0039-9140/81/030192-03$02.00/0

ELECTROCHEMICAL STUDY OF THE OXIDATION OF TIN(II) AT GLASSY CARBON ELECTRODES

P. KIEKENS, H. VERPLAETSE and E. TEMMERMAN

Laboratory of Analytical Chemistry, Ghent University, J. Plateaustraat, 22, 9000 Ghent, Belgium

(*Received* 10 *June* 1980. *Accepted* 25 *September* 1980)

Summary—The voltammetric characteristics of the Sn(IV)/Sn(II) system have been studied at a glassy carbon rotating disk electrode in 4*M* hydrochloric acid. Anodic oxidation of Sn(II) produces a single well-defined wave, which has been examined in the temperature range 20–50°, and shows distinct irreversibility. The kinetic parameters of the oxidation reaction have been calculated. Kinetic features of the reduction of Sn(IV) to Sn(II) were not evaluated because the reduction proceeds directly to tin metal.

Only a few workers have reported on the kinetic parameters of the oxidation of Sn(II) at solid electrodes.[1–5] It is proposed by Lerner and Austin,[1] Vetter,[2] and Ateya and Austin[5] that the oxidation of Sn(II) proceeds by two consecutive one-electron transfer steps at platinum and graphite electrodes in concentrated hydrochloric acid. The first electron transfer would be rate-determining at large overpotentials and the second at low ones. It is also assumed that the concentration of the intermediate Sn(III) is very small and constant (steady state), causing no mass-transfer polarization.

According to Bishop and Hitchcock,[3] this redox pair is characterized by a slow charge-transfer in bromide plus perchloric or hydrobromic acid media, with a single two-electron transfer step, or two consecutive one-electron steps. However a definite conclusion cannot be reached.

From their studies with gold and mercury electrodes in 6*M* hydrochloric acid, Kadish and Stamp[4] concluded that the Sn(IV)/Sn(II) system is quite complex and that chemical reactions, competitive with the electron-transfer steps, should be considered.

In this study the kinetics of the anodic oxidation of Sn(II) have been investigated at a glassy carbon rotating disk electrode in 4*M* hydrochloric acid.

EXPERIMENTAL

Reagents

Experiments were carried out in 4*M* hydrochloric acid to suppress hydrolysis. Solutions were prepared from analytical grade reagents and water freshly generated by a Milli-Q system (Millipore Inc.) and deaerated with nitrogen containing less than 1 ppm of oxygen.

Stock solutions of Sn(II) were prepared by dissolving $SnCl_2.5H_2O$ (Merck) in warm concentrated hydrochloric acid and standardized by titration with ceric sulphate. Because Sn(II) is very sensitive to air-oxidation, all solutions were carefully deaerated with high-purity nitrogen before Sn(II) was added. Deaeration was also continued between successive voltammetric runs and a nitrogen atmosphere was maintained above the test solutions. Sn(II) stock solutions were renewed when any significant oxidation was detected. Sn(IV) solutions were prepared by quantitative oxidation of Sn(II) with hydrogen peroxide, followed by boiling to destroy the excess of peroxide.

Instrumentation

The electrolysis cell was a Teflon vessel (about 150 ml capacity) equipped with a glassy carbon rotating disk electrode (Tokai Electrode Mfg. Co., Tokyo, geometric surface area 0.194 cm^2), a platinum auxiliary electrode (10 cm^2) and a saturated calomel electrode (SCE) to which all potentials are referred, unless otherwise specified. The reference electrode was separated from the cell by a salt-bridge, with a capillary junction placed within 2 mm of the edge of the disk electrode, which was centrally placed in the vessel. The salt-bridge was filled with concentrated hydrochloric acid and the connection to the SCE was made by a U-tube containing saturated potassium chloride solution. The cell, salt-bridge and reference electrode system were placed in a water-bath, the temperature of which was controlled by a thermostat to 0.1°.

The electrode was rotated by a Brion-Leroux motor (BIROTAX type I) and the speed was strictly controlled with a servo control unit (Tacussel Asservitex). The rotation rate was measured with a proximity probe (Philips PR 9373) and frequency meter (Philips PM 6601).

Potential control was maintained by means of a Tacussel sweep generator GSATP and bipotentiostat BI-PAD. Curves were registered with a Hewlett-Packard X–YY′ recorder, model HY 7046 A. Viscosities were determined with an Ostwald viscometer. A Paar Precision Density Meter type DMA02D was employed for density measurements.

Electrode pretreatment

The glassy carbon working electrode was polished by standard metallographic techniques. Final polishing to a mirror-like surface was performed with 0.05-μm alumina on Buehler microcloth. The electrode was rinsed with water and activated by cycling the potential between 1.2 and −1.0 V *vs.* SCE (evolving oxygen and hydrogen for cleaning) for 10 min at a scan-rate of 0.030 V/sec in 1*M* hydrochloric acid. The electrode was then held successively at −0.5 and 0.0 V *vs.* SCE for 5 min to remove any oxide film possibly formed and metallic impurities that might have been deposited at −0.5 V. During this pretreatment nitrogen was passed through the solution. Finally the electrodes were transferred into the previously deaerated test solution containing Sn(II) and/or Sn(IV).

Procedure

Generally the current–potential curves were recorded from 0.0 V as initial potential, first in the anodic direction up to 1.2 V and then returning to −0.4 V before going back to zero potential. Only curves from scans in the anodic direction, on a reduced surface, were taken into account. The scan rate was 0.005 V/sec.

RESULTS AND DISCUSSION

Voltammetric experiments

Current–voltage curves for the oxidation of Sn(II) in 4*M* hydrochloric acid were recorded as a function of rotation speed, Sn(II) concentration and temperature between 20 and 50°. The reduction of Sn(IV) gave a single wave, not completely separated from the hydrogen reduction wave. Well-defined tin oxidation peaks always appeared during the subsequent anodic scan when a significant cathodic reduction current was observed previously. A somewhat better defined Sn(IV) reduction wave appeared when 9*M* hydrochloric acid medium was used, although still without a distinct limiting current plateau. It is known[6] that only with a very large chloride concentration will a well-developed doublet wave be produced.

Figure 1 depicts current–voltages curves for the oxidation of 7.0m*M* Sn(II) at 20° in 4*M* hydrochloric acid. The currents at the foot of the curves were rather irreproducible, and depended on whether the curves were recorded with increasing or decreasing potential.

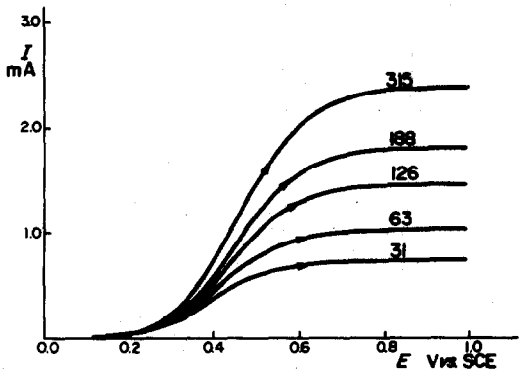


Fig. 1. Current–voltage curves for oxidation of 7.0m*M* Sn(II) in 4*M* HCl, on a glassy carbon rotating disk electrode at 20°C. Each curve is labelled with the rotation speed (rad/sec).

Convective-diffusion controlled oxidation of Sn(II)

It was found that the limiting currents were proportional to the square root of the rotation speed, with zero intercept for all concentrations and temperatures. From this it is clear that the Levich equation[7] for a convective-diffusion limited process was obeyed. Figure 2 illustrates the dependence of the limiting current, I_L, on $\omega^{1/2}$ for 3.5m*M* Sn(II) at various temperatures.

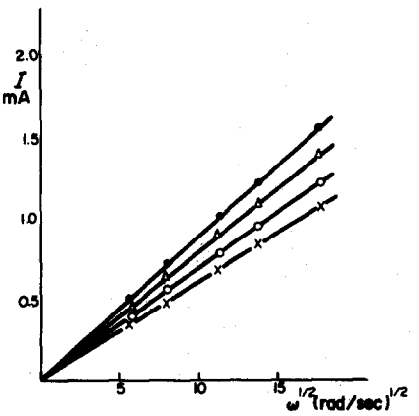


Fig. 2. Dependence of limiting currents on $\omega^{1/2}$ for various temperatures: (×) 20, (○) 30, (△) 40 and (●) 50°C; [Sn(II)] = 3.5m*M*.

From the increase in the limiting currents with temperature. Arrhenius plots were constructed, from which the experimental activation energy related to the diffusion process[8] was found to be 9.5 ± 1 kJ/mole, a value in the usual range. According to Milner[9] the temperature coefficient of the diffusion coefficient is generally about 2–3% per °C. The experimental results were in agreement with this figure. At 50°, the I_L values were 45–50% larger than at 25°.

Table 1 assembles the temperature-dependence of the diffusion coefficient, density and kinematic viscosity for 7.0m*M* Sn(II). From these data the radius of the reducing species was calculated to be 0.23 ± 0.05 nm, from the Einstein–Stokes relation,[10] with an Einstein–Stokes ratio, $D\eta/T$, almost constant over the range 20–45°.

Evaluation of kinetic parameters

When $\log I/(I_L - I)$ was plotted *vs.* potential, which is the Tafel plot corrected for mass-transport effects, straight lines were obtained for currents from $0.1I_L$ to $0.95I_L$. From the gradients we determined an anodic transfer coefficient, β, of 0.35 ± 0.02, which was independent of temperature and rotation rate. This is a rather low value and is reflected in the anodic curves in which a high overpotential is necessary before the potential-independent plateau is reached. The value of the transfer coefficient suggests the first electron-

Table 1. Physical characteristics of 7.0m*M* Sn(II) in 4*M* HCl at different temperatures

Temperature, °C	Density, g/cm^3	Kinematic viscosity, cm^2/sec	Diffusion coefficient of Sn(II), cm^2/sec
20	1.107	0.012660	7.0×10^{-6}
25	1.105	0.011551	7.3×10^{-6}
30	1.103	0.010550	7.9×10^{-6}
35	1.100	0.009966	8.6×10^{-6}
40	1.098	0.009381	9.3×10^{-6}
45	1.096	0.008940	10.0×10^{-6}

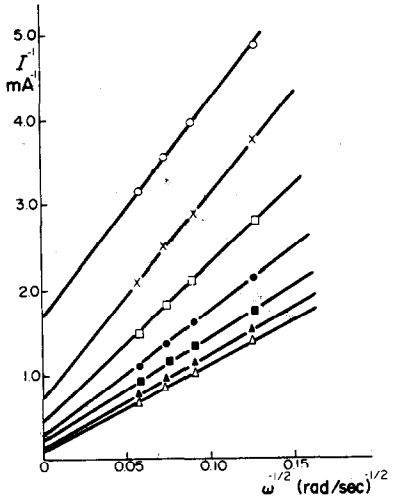


Fig. 3. Dependence of I^{-1} on $\omega^{-1/2}$ for 7.0mM Sn(II) on glassy carbon at 20°C. (○) 0.330; (×) 0.360; (□) 0.390; (●) 0.420; (■) 0.450; (▲) 0.480; (△) 0.510 V *vs.* SCE.

transfer to be rate-determining[11] in that potential range. Analogous values of β were given by Bishop and Hitchcock[3] while Ateya and Austin[5] found β to be 0.41.

To calculate the rate of the process, the reciprocals of the currents preceding the limiting plateau were plotted against $\omega^{-1/2}$. The linear relationships obtained are shown in Fig. 3 and are also characteristic of a first-order process.

Extrapolation to infinite rotation speed allowed us to evaluate the rate constants. This technique was first used by Frumkin and Tedoradze[12] and by Jahn and Vielstich.[13] As the Sn(IV)/Sn(II) oxidation–reduction potential evaluated by Huey and Tartar[14] depended on the acidity and the couple was found to behave irreversibly, rate constants were evaluated at $E = 0.0$ V *vs.* SHE (standard hydrogen electrode), which is close to the standard potential. This gives an apparent rate constant, k^0_{SHE}, of 2.0×10^{-7} cm.sec at 20°. It is concluded that this redox system is distinctly irreversible. This is also confirmed by the dependence of the half-wave potentials on the rotation speed;[15] they become more anodic at higher rates of rotation. They also shift to more negative potentials at higher temperatures.

To determine the apparent energy of activation, E_a, rate constants at different temperatures were evaluated and plotted against the reciprocal of the absolute temperature (T). The potential of the reference electrode was corrected for the temperature change according to the values tabulated by Ives and Janz.[16] From the linear plots and the relation

$$E_a = -2.3R\left[\frac{\partial \log k^0_{SHE}}{\partial(1/T)}\right]_E$$

the energy of activation was found to be 40.5 ± 5 kJ/mole on glassy carbon which has weak anisotropic properties.[17]

REFERENCES

1. H. Lerner and L. G. Austin, *J. Electrochem. Soc.*, 1965, **112**, 636.
2. K. J. Vetter, *Electrochemical Kinetics*, pp. 152, 481. Academic Press, New York, 1967.
3. E. Bishop and P. H. Hitchcock, *Analyst*, 1973, **98**, 635.
4. K. M. Kadish and J. Stamp, *Anal. Lett.*, 1973, **6**, 909.
5. B. G. Ateya and L. G. Austin, *J. Electroanal. Chem.*, 1974, **51**, 85.
6. J. J. Lingane, *J. Am. Chem. Soc.*, 1945, **67**, 919.
7. V. G. Levich, *Physicochemical Hydrodynamics*, p. 69. Prentice Hall, Englewood Cliffs, N. J., 1962.
8. D. Möller and K.-H. Heckner, *J. Electroanal. Chem.*, 1972, **36**, 277.
9. G. W. C. Milner, *The Principles and Applications of Polarography and other Electroanalytical Processes*, p. 45. Longmans, London, 1957.
10. J. O'M. Bockris and A. K. N. Reddy, *Modern Electrochemistry*, Vol. 1, p. 380. Plenum Press, London, 1970.
11. J. Albery, *Electrode Kinetics*, p. 132. Clarendon Press, Oxford, 1975.
12. A. N. Frumkin and G. A. Tedoradze, *Z. Elektrochem.*, 1958, **62**, 251.
13. D. Jahn and W. Vielstich, *J. Electrochem. Soc.*, 1962, **109**, 849.
14. C. S. Huey and H. V. Tartar, *J. Am. Chem. Soc.*, 1934, **56**, 2585.
15. J. Koryta, J. Dvořak and V. Boháčková, *Electrochemistry*, p. 269. Methuen, London, 1970.
16. D. J. G. Ives and G. J. Janz, *Reference Electrodes, Theory and Practice*, p. 161. Academic Press, New York, 1961.
17. H. E. Zittel and F. J. Miller, *Anal. Chem.*, 1965, **37**, 200.

Talanta Vol. 28, pp. 195 to 197
© Pergamon Press Ltd 1981. Printed in Great Britain
0039-9140/81/030195-03$02.00/0

SOLVENT EXTRACTION STUDIES ON THE MIXED LIGAND COMPLEXES OF LANTHANIDES WITH ANTIPYRINE AND PERCHLORATE

M. V. KRISHNA MURTHY and D. SATYANARAYANA*
Department of Chemistry, Andhra University, Waltair, India

(*Received* 3 *July* 1980. *Accepted* 7 *September* 1980)

Summary—Lanthanide ions are found to form colourless mixed-ligand complexes with antipyrine in presence of perchlorate at pH 4.0, and these are quantitatively extractable into nitrobenzene. The composition of the extracted species is shown to be metal:antipyrine:perchlorate = 1:6:3. The variation of the extraction constants with atomic number of the lanthanides is attributed to the "tetrad effect".

Antipyrine (apy) is known to form complexes with several elements.[1] Several solid compounds formed by antipyrine with rare-earth (Ln) salts have been characterized and reported,[2–6] including the iodides $[Ln(apy)_6I_3]$[5] and perchlorates $[La(apy)_6(ClO_4)_3]$,[6] but the extraction of these complexes has not so far been reported. We present here our investigations on the solvent extraction of the perchlorates.

EXPERIMENTAL

Reagents

Stock lanthanide solutions were prepared by dissolving appropriate amounts of the pure oxides in perchloric acid, and were standardized by EDTA titration.[7]

Antipyrine was recrystallized from benzene. A 1*M* solution in demineralized water was prepared and standardized iodometrically.[8]

Doubly distilled nitrobenzene was used throughout. Other reagents used were of analytical grade. All experiments were done at room temperature (28 ± 1°).

Extraction procedure

To 5.00 ml of a solution containing about 4.5 ppm of lanthanide, 1.0 ml of 1*M* antipyrine, 1.0 ml of 3*M* sodium perchlorate and 5.0 ml of demineralized water were added, the pH was adjusted to 4.0 with dilute perchloric acid and sodium hydroxide solution, and the volume was made up to 15.0 ml. The mixture was transferred into a separatory funnel and shaken with 15.0 ml of nitrobenzene for 1 min, and allowed to stand for separation of the two phases.

The amount of lanthanide in the separated aqueous phase was determined with 4-(2-pyridylazo)-resorcinol.[9] The amount of lanthanide in the organic phase was determined by the same method after stripping with two portions of 0.1*M* perchloric acid.

RESULTS AND DISCUSSION

Preliminary experiments indicated that nitrobenzene was the best among the solvents tested, the others being diethyl ether, benzene, chloroform, carbon tetrachloride, isoamyl alcohol, isobutyl methyl ketone and 1,2-dichloroethane. Of the anions studied (chloride, nitrate, acetate and perchlorate), perchlorate was found to give the best recovery. The optimum shaking time was found to be 1 min.

Optimum parameters

The effect of pH was studied over the range 2.0–8.0, and the optimum was found to be 3.2–6.0 (Table 1).

Table 1 also shows the minimum amounts of antipyrine and perchlorate required for quantitative extraction of the lanthanides into nitrobenzene at pH 4.0, and the recovery.

The recovery was determined with various concentrations of the lanthanides under the optimum conditions. The average recoveries shown in Table 1 indicate that the extraction is essentially quantitative in all the systems.

The partition coefficient of antipyrine between nitrobenzene and water at pH 4.0 was determined, the antipyrine being measured in both the phases by an iodometric method.[8] The value obtained ($P = 3.2$) was in good agreement with that reported by others.[10]

Composition of the extracted species

Slope analysis was used for determining the composition of the extracted species. Plots of log D *vs.* log [reagent] showed that the ratios of lanthanide to antipyrine and to perchlorate were 1:6 and 1:3 respectively, giving the overall composition of the extracted species as $Ln(apy)_6(ClO_4)_3$. This was confirmed at two metal ion concentrations and two pH values for all the lanthanides.

Extraction equilibrium constant, K_E

The formation and extraction of the colourless lanthanide-antipyrine-perchlorate complexes can be represented as

$$M^{3+}_{aq} + 6apy_{aq} + 3ClO^-_{4\,aq} \rightleftharpoons [M(apy)_6(ClO_4)_3]_{aq} \rightleftharpoons [M(apy)_6(ClO_4)_3]_{org}$$

* To whom correspondence and requests for reprints should be sent.

Table 1. Optimum conditions and extraction equilibrium constants of lanthanide-antipyrine-perchlorate complexes; ionic strength 0.20 ± 0.01; temperature 28 ± 1°C

M^{3+}	pH	[Antipyrine] [M]	[Perchlorate] [M]	Average recovery, %	log K_E
La	3.3–6.5	2500	3800	99.6	14.01
Ce	3.4–6.0	2500	3800	99.3	14.10
Pr	3.3–6.0	2500	3800	99.7	14.38
Nd	3.2–6.0	3200	3800	99.4	13.94
Sm	3.2–6.0	3200	3000	99.5	14.07
Eu	3.3–6.4	3200	3000	99.6	14.61
Gd	3.2–6.4	3500	3000	99.7	15.02
Tb	3.2–6.5	3500	2000	99.6	15.80
Dy	3.2–6.0	3800	2000	99.3	15.56
Ho	3.3–6.0	3800	2000	99.4	15.39
Er	3.3–6.0	3800	2000	99.7	15.50
Tm	3.2–6.0	3800	2000	99.6	16.08
Yb	3.2–6.0	3800	2000	99.4	16.03
Lu	3.3–6.0	3800	2000	99.5	15.79

The extraction equilibrium constant, K_E can be written as

$$K_E = \frac{[M(apy)_6(ClO_4)_3]_{org}}{[M^{3+}]_{aq}[apy]^6_{aq}[ClO_4^-]^3_{aq}} \quad (1)$$

and the distribution ratio as

$$D = \frac{[M(apy)_6(ClO_4)_3]_{org}}{\sum[M_i]_{aq}} \quad (2)$$

where $\Sigma[M_i]_{aq}$ is the sum of the concentrations of the lanthanide species in the aqueous phase. At the concentrations and pH values used, these species will be the aquo-ions and hydroxo-complexes, and to a first approximation their concentration sum can be written simply as $[M^{3+}]_{aq}$, as in equation (1). Taking logarithms after substituting the value of D in equation (1) and rearranging the terms gives

$$\log D = \log K_E + 6 \log [apy]_{aq} + 3 \log [ClO_4^-]_{aq} \quad (3)$$

where the equilibrium concentrations $[apy]_{aq}$ and $[ClO_4^-]_{aq}$ are calculated from the mass-balance equations:

$$[apy]_{total} = [apy]_{aq} + [apy]_{org} + 6[M(apy)_6(ClO_4)_3]_{org} \quad (4)$$

$$[ClO_4^-]_{total} = [ClO_4^-]_{aq} + 3[M(apy)_6(ClO_4)_3]_{org} \quad (5)$$

Equation (4) can be simplified and rearranged to give

$$[apy]_{aq} = \frac{[apy]_{total} - 6[M(apy)_6(ClO_4)_3]_{org}}{1 + P} \quad (6)$$

The slopes of the plots of $\log D$ *vs.* $\log [apy]_{aq}$ and $\log [ClO_4^-]_{aq}$ should thus give straight lines of slope 6 and 3 respectively and the intercepts can be used for computation of the K_E values (given in Table 1).

The variation of K_E with atomic number of the lanthanide is shown in Fig. 1. It can be seen that in addition to the expected (but small) discontinuity at Gd^{3+} which can be attributed to the half-filled shell effect,[11] there are dips between Nd^{3+} and Sm^{3+} and between Ho^{3+} and Er^{3+}, which are presumably due to the "tetrad effect",[12] which has been attributed either to minor variation in nephelauxetic ratio[13] or to the dependence of the coefficients of the Racah interelectronic repulsion parameters E^1 and E^3 on the quantum numbers L and S for the electronic ground state of the M^{3+} ions.[14]

Mechanism

Antipyrine is a good neutral donor ligand which co-ordinates to the lanthanide ion through the carbonyl oxygen atom. Assuming a co-ordination number of 6 for the lanthanides, the extraction can be explained in terms of formation of an ion-association complex $[Ln(apy)_6^{3+}](ClO_4^-)_3$. This is supported by the conductance studies on these complexes prepared in solid state, which showed that they are predominantly 1:3 type electrolytes.[6]

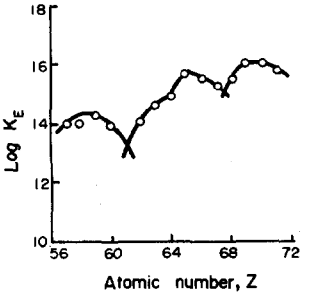


Fig. 1. Variation of K_E with atomic number.

Interferences

The interference of various ions was studied. Common anions such as chloride, nitrate, acetate, sulphate, thiosulphate, thiocyanate, fluoride, phosphate, pyrophosphate, citrate, tartrate and oxalate show no interference even at 1000-fold ratio to lanthanide, but chelating agents such as EDTA, HEDTA, DCTA and DTPA interfere seriously by forming complexes with the lanthanides.

Be, Mo(VI), Ca, Mg, Al, Co(II), Ni and Zn in 100-fold amounts relative to the lanthanide do not interfere with the extraction. Cd is tolerable up to 50-fold ratio to lanthanide. However Fe(III), Cu(II), V(V), U(VI) and Th interfere by forming extractable complexes, even at 5–10-fold ratio to lanthanide. The interference of these metals can be eliminated by prior extraction with sodium diethyldithiocarbamate into chloroform–acetone (5:2) at pH 3.0 and discarding the organic phase.[15]

Acknowledgements—The authors are thankful to Apache chemicals (U.S.A.) and E. Merck (Germany) for providing rare-earth oxides as gifts. One of them (M. V. K.) is thankful to the Council of Scientific and Industrial Research, New Delhi for the award of a Fellowship.

REFERENCES

1. V. K. Akimov and A. I. Busev, *Zh. Analit. Khim.*, 1971, **26**, 134.
2. E. W. Dorfurt and O. Schliephake, *Z. Anorg. Allgém. Chem.*, 1928, **170**, 129.
3. J. K. Marsh, *J. Chem. Soc.*, 1951, 1337.
4. S. S. K. Murthy and S. Sounderarajan, *J. Less-Common Metals*, 1967, **13**, 619.
5. M. Gerloch and D. J. Mackey, *J. Chem. Soc. A*, 1970, 3030, 3040; 1971, 2605, 2612; 1971, 3372; *J. Chem. Soc. Dalton. Trans.*, 1972, 37, 42; 1972, 410, 415.
6. V. N. K. Murthy and S. Sounderarajan, *Proc. Indian Acad. Sci.*, 1967, **A65**, 148.
7. I. M. Kolthoff and P. J. Elving (eds.), *Treatise on Analytical Chemistry*, Part II, Vol. 8, p. 57. Interscience, New York, 1963.
8. I. M. Kolthoff and R. Belcher, *Volumetric Analysis*, Vol. III, p. 403. Interscience, New York, 1957.
9. M. V. K. Murthy and D. Satyanarayana, *Mikrochim. Acta*, 1980, **I**, 97.
10. V. P. R. Rao, V. V. Sarma and A. S. R. K. Murthy, *Proc. Indian Acad. Sci.*, 1976, **A84**, 150.
11. E. Hesford, E. E. Jackson and H. A. C. McKay, *J. Inorg. Nucl. Chem.*, 1959, **9**, 279.
12. D. F. Peppard, C. A. A. Bloomquist, E. P. Horwitz, S. Lewey and G. W. Mason, *ibid.*, 1970, **32**, 339.
13. L. J. Nugent, *ibid.*, 1970, **32**, 3485.
14. S. Siekierski, *ibid.*, 1970, **32**, 519.
15. R. A. Chalmers and D. M. Dick, *Anal. Chim. Acta*, 1964, **31**, 520.

Talanta Vol. 28, pp. 199 to 200
© Pergamon Press Ltd 1981. Printed in Great Britain
0039-9140/81/030199-02$02.00/0

ANALYTICAL DATA

POTENTIOMETRIC DETERMINATION OF STABILITY CONSTANTS OF CYANOACETATO COMPLEXES OF COBALT(II), NICKEL(II), COPPER(II), ZINC(II), CADMIUM(II) AND LEAD(II)

T. MATUSINOVIĆ and I. FILIPOVIĆ

Laboratory of Inorganic Chemistry, Faculty of Technology, University of Zagreb, POB 179, 41000 Zagreb, Croatia, Yugoslavia

(*Received* 11 *June* 1980. *Accepted* 31 *August* 1980)

Summary—Stability constants of cyanoacetato complexes of cobalt(II), nickel(II), copper(II), zinc(II), cadmium(II) and lead(II) were determined potentiometrically at 25.0 ± 0.1° and ionic strength 2*M* (sodium perchlorate). The stability constants were evaluated by a weighted least-squares method.

The determination of the composition and stability of metal-ion cyanoacetato complexes is part of a series of investigations in our laboratory, intended to yield some insight into the factors affecting the stability of monocarboxylato complexes.

EXPERIMENTAL

Potentiometric measurements were made with a Metrohm EA 109 glass electrode and E436 potentiograph, with volume reproducibility of ±0.01 ml and potential reproducibility ±0.2 mV. Solutions were purged with purified nitrogen for 15 min before the measurements. Titrations took 30 min; nitrogen was passed over the surface of the solution, which was stirred magnetically. All determinations were made at 25.0 ± 0.1°, and at ionic strength 2*M* (sodium perchlorate).

Each system was studied at two metal-ion concentrations, both of these at two monocarboxylic acid-to-salt ratios of 2:1 and 1:1. Concentrations of Cu(II) were 30 and 60m*M*, and of Co(II), Ni(II), Zn(II), Cd(II) and Pb(II), 50 and 100m*M*. The total ligand concentration was up to 0.4*M*.

Cobalt(II), nickel(II) and cadmium(II) perchlorates were prepared from perchloric acid and the corresponding carbonates, the copper(II), zinc(II) and lead(II) salts from the corresponding oxide and perchloric acid. All were recrystallized three times. Metal-ion concentrations in the stock solutions were determined by complexometric potentiometric titration with a mercury indicator electrode.[1]

Table 1. Stability constants of cyanoacetate complexes; $T = 25.0°$; $I = 2M$ ($NaClO_4$)

Metal ion	log K_1	log β_2
Co(II)	0.39 ± 0.02	
Ni(II)	0.44 ± 0.02	
Zn(II)	0.50 ± 0.02	
Cd(II)	0.70 ± 0.02	0.84 ± 0.02
Cu(II)	0.93 ± 0.02	1.29 ± 0.02
Pb(II)	1.14 ± 0.02	1.68 ± 0.04

$pK_A = 2.48$ (our value).

RESULTS AND DISCUSSION

A PDP-8/E minicomputer was programmed to calculate the average number, $\bar{n}$, of ligands bound to the central metal ion, the free-ligand concentrations, [L], and values of the function

$$F_0([L]) = 1 + \sum_{i=1}^{N} \beta_i [L]^i.$$

A weighted least-squares procedure[2] was then used to evaluate the stability constants.

The results are given in Table 1. There was no evidence of the formation of polynuclear and/or hydroxo complexes.

The stability-constant values found show that the stabilities of the systems follow the order:

$$Co(II) < Ni(II) < Cu(II) > Zn(II), Cd(II) < Pb(II)$$

These cyanoacetate complexes are very weak, in accordance with the low basicity of the ligand ($pK_A = 2.48$), so their stability is governed mainly by the ligand basicity. The only stability constants given in the literature for cyanoacetate complexes refer to those of copper(II). They are the unpublished values (log $K_1 = 0.87$ and log $\beta_2 = 1.00$) of Rossotti and Carson,[3] determined at temperature of 25° at $I = 3M$ (sodium perchlorate). These values are in good agreement with ours.

Acknowledgement—The authors are indebted to the Scientific Research Council of Croatia for financial support.

REFERENCES

1. G. Schwarzenbach, *Die Kompleksometrische Titration*, F. Enke, Stuttgart, 1960.

2. I. Piljac, B. Grabarić and I. Filipović, *J. Electroanal. Chem.*, 1973, **42**, 433.
3. L. G. Sillén and A. E. Martell (eds.), *Stability Constants of Metal–Ion Complexes*, The Chemical Society, London, 1964; Supplement No. 1, The Chemical Society, London, 1971.

Talanta, Vol. 28, pp. 201 to 206, 1981
Printed in Great Britain

0039-9140/81/040201-06$02.00/0
Pergamon Press Ltd

A REVIEW OF RECENT USES OF PHOSPHORIMETRY FOR ORGANIC ANALYSIS*

J. L. WARD, G. L. WALDEN and J. D. WINEFORDNER†
Department of Chemistry, University of Florida, Gainesville, FL 32611, U.S.A.

(*Received* 1 *October* 1980. *Accepted* 24 *October* 1980)

Phosphorimetry involves the measurement of radiation emitted by organic molecules excited by radiational means. In 1944, Lewis and Kasha[1] identified the phenomenon of phosphorescence as the result of a radiative transition from an excited triplet state to the ground state. In 1957, Kiers, Britt and Wentworth[2] evaluated a number of analytical uses of phosphorescence. They described the potential for obtaining selectivity in phosphorimetry by spectral resolution of the excitation and emission radiation and alluded to time resolution.

In 1958, Freed and Salmre[3] described the construction of a phosphorimeter used for analytical determinations of several drugs. Later (1962), Parker and Hatchard modified a spectrofluorimeter for measurement of phosphorescence spectra. A year later, Latz and Winefordner[5] described a spectrophosphorimeter and its use in determination of aspirin in blood serum. Since that time, much of the work in the field of phosphorimetry has been carried out by Winefordner's research group, but a number of researchers have recently become involved in room-temperature phosphorimetry.

This review will be devoted to the use of low-temperature phosphorimetry, room-temperature phosphorimetry, pulsed-source/gated-detector/time-resolved phosphorimetry and several specialized phosphorimetric techniques for the quantitative measurement of low concentrations of organic molecules. We will primarily be concerned with advances since the 1975 reviews of phosphorimetry by Aaron and Winefordner[6] and by O'Donnell and Winefordner.[7] A more thorough review of the fundamental aspects of phosphorimetry and instrumentation, will be found in the books by Parker,[8] Schulman,[9] Wehry,[10] Guilbault,[11] and Zander.[12]

Because excited molecules tend to remain in the first excited triplet state (T_1) for some characteristic lifetime (ranging from msec to sec), non-radiative energy loss (quenching) occurs. As a result, in order to observe phosphorescence, it is essential to minimize non-radiative de-excitation processes of T_1 such as collisions with solute or solvent molecules. The conventional approach has been to minimize collisions by freezing the sample to 77 K in liquid nitrogen to give a rigid frozen matrix. This technique has been given the name low-temperature phosphorescence, LTP. More recently, a convenient means of observing phosphorescence at room temperature, RTP, has been developed. In this technique, a solution of the molecular species is placed on a solid substrate, such as filter paper, and dried. The adsorbed molecules are held rigidly on the substrate, and for many species intense phosphorescence is observed.

LOW-TEMPERATURE PHOSPHORESCENCE (LTP)

In the past, most of the analytical studies using phosphorimetry have been carried out at 77 K; however, very little has been done in the field of LTP since the 1975 reviews.[13–16] In spite of the sensitivity of LTP for many biologically and environmentally important molecules and the selectivity arising from time resolution in addition to spectral resolution, LTP has failed to catch on as a popular method for routine analysis. This lack of popularity can, perhaps, be attributed to two major inconveniences, both of which are related to the necessity for very low temperatures.

First, in order to achieve a low temperature, some cryogenic equipment is necessary. Since liquid nitrogen is the typical coolant, this equipment usually involves a storage dewar flask for the liquid, as well as the quartz dewar flask into which the samples are inserted. In order to avoid absorption of excitation radiation and interference resulting from emission by the dewar flask, it is necessary that at least the optical portions of the sample dewar flask be constructed of expensive high-grade optical quartz. In addition to the expense of the liquid nitrogen and the equipment for handling it, some hazard exists whenever liquid nitrogen is transferred.

An alternative to the use of liquid nitrogen is the use of closed-cycle cryogenic refrigerators. There are, however, disadvantages in their use as well. The initial investment is very high. In addition, the low capacity and long cool-down periods of such equipment do not lend themselves well to the number of repetitive measurements required for the routine analysis of many samples.

* Work supported by NIH GM-11373-17.
† To whom reprint requests and correspondence should be sent.

Table 1. Comparison of limits of detection for several organic species by conventional colorimetry, fluorimetry and phosphorimetry[6]

Compound	Detection limit, *ng/ml*		
	Colorimetry	Fluorimetry	Phosphorimetry
Vitamin K_3	2000	400	70
6-Methylmercaptopurine	—	10	0.6
LSD-25	50	6	8
Psilocin	—	100	6
Ibogaine HCl	—	7	10

Secondly, there is great inconvenience involved in actually introducing the sample into the system. Typically, a long quartz capillary cell is gradually lowered into the quartz dewar flask within the instrument. The rate of cooling of the sample cell causes variation in the resulting sample matrix, *i.e.*, the cooled matrix can be a clear glass, a cracked glass or a snow. Analytical measurements of clear glasses are quite reproducible if the sample cell can be reproducibly positioned in the instrument. Once the capillary comes into contact with the liquid nitrogen the sample cools very rapidly, resulting in cracked glasses or snows for most solvents, unless the capillary is allowed to cool gradually over the liquid nitrogen before contact. This results in very tedious, time-consuming procedures. Although most commercial phosphorimeters use immersion cooling of the sample, a more ideal cooling system is based upon conduction cooling of a short capillary-sample cell in a copper-block cooled by liquid nitrogen. Two such devices have recently been described.[17,18] Use of these new devices has reduced sample turn-over time to about one sample/min (a 3–5-fold reduction in time). In addition, there has been a reduction in the amount of liquid nitrogen handling required, and the expense is reduced as a result of the elimination of optical-grade quartz dewar flasks.

The major past advantages of conventional low-temperature phosphorimetry have been: (*i*) low detection limits; (*ii*) wide-range linear analytical calibration curves; (*iii*) great selectivity of measurement. Conventional phosphorimeters consist of a xenon-arc source, excitation monochromator, immersion-cooled cell with phosphoroscope, emission monochromator, photomultiplier detector, and electronic measurement system. Because detection limits depend upon the limiting signal-to-noise ratio ($S/N = 3$) and because the signal-to-noise ratio is usually dependent upon the phosphorescence flicker of the solvent background, detection limits are determined primarily by the impurities in the solvents used, rather than by the source intensity, because increasing the source intensity increases the signal and the noise by the same factor, resulting in no improvement in S/N. With good solvents (purified by means of distillation, extraction, *etc.*), it is possible to detect various organic molecules in sub-nanogram amounts and at concentrations below 1 μg/ml (see Tables 1 and 2). Because

Table 2. Comparison of minimum detectable amounts for several organic molecules by fluorimetry and phosphorimetry[6]

Compound	Limit of detection, *ng*	
	Fluorimetry	Phosphorimetry
Tyrosine	1000	0.4
Epinephrine	0.5	4
Dopamine	10	3
LSD-25	6	0.2
Psilocin	100	0.1
Adenine	100	0.4

the phosphorescence signal is linearly related to concentration from the detection limit to concentrations where self-absorption or self-quenching occurs (self-absorption of phosphorescence by analyte species is not very important because of the red shift of phosphorescence; self-quenching involves non-radiative de-excitation by collisions of excited and ground-state analyte species). Therefore linear analytical calibration curves covering as much as a 10^4–10^6-fold change in analyte concentration result. The greater selectivity of phosphorimetry is rather obvious because more compounds absorb than fluoresce and more fluoresce than phosphoresce. This is both a blessing and a burden. If the analyte phosphoresces intensely in its native state, then obviously phosphorimetry is a potentially useful technique. If the analyte does not phosphoresce with sufficient intensity for analytical use, then either phosphorimetry cannot be used or the molecule or its environment must be modified to allow analysis. Modification of the environment can be by means of "heavy-atom solvents" containing heavy ions, such as I^- (in NaI) or Ag^+ (in $AgNO_3$). The molecule can be modified by a chemical reaction to produce a more strongly phosphorescent species. It should be mentioned that the addition of "heavy-atom solvents" results (in many cases) in both an increase in phosphorescence intensities *and also* in a decrease in phosphorescence lifetime; it is possible that this decrease can result in a low measured signal if the phosphoroscope chopping rate is too low.

Finally, the precision of phosphorimetry measurements is typically 10% relative standard deviation. With care in cell-positioning and cleanliness, 1–2% RSD is possible, but difficult to achieve.

Table 3. Detection limits of several typical compounds by RTP[50]

Compound	Limit of detection, *ng*	
	1*M* NaOH	1*M* NaOH + 1*M* NaI
Adenine	7	4
p-Aminobenzoic acid	0.5	0.06
Anturane	—	5
Apresoline	8	3
Cocaine	76	51
Esidrex	50	127
Guanine	260	23
6-Methylmercaptopurine	0.1	0.2
Priscoline HCl	—	50
Privine HCl	0.1	0.9
Procaine HCl	2	0.9
Ritaline HCl	10	2
Salicylic acid	3	0.7
Thiopropazate 2HCl	19	7
Trasentine HCl	—	4
Tryptophan	6	0.2
Vinblastine sulphate	6	—
Vioform	—	92

ROOM-TEMPERATURE PHOSPHORESCENCE (RTP)

It has recently been pointed out[19] that the earliest observations of phosphorescence from organic molecules at room temperature were made by Millson in 1944.[20] He observed long-lived photoluminescence from cotton fibres. News of these first observations was not widely known until 1954.[21] In 1958, Brown observed phosphorescence from paper chromatograms irradiated with ultraviolet light.[22] In 1967, Roth reported the observation of RTP from a large number of organic compounds.[23] Several years later, Schulman and Walling rediscovered the technique and showed that it had some possible analytical uses.[24,25] Since then, RTP has received considerable attention.[26–63] As yet, the ideal substrate (some material which will hold the analyte species in a matrix sufficiently rigid to minimize second-order quenching processes without introducing a phosphorescence background of its own) has not been found.[59] Of all the substrates so far tried, filter paper seems to be the most promising because it has been observed to induce phosphorescence from a great number of compounds; however, filter paper also gives rise to a broad-band background (from about 400 to about 600 nm) which often interferes with quantitative measurements. Attempts to remove or reduce the background have been unsuccessful.[60]

RTP of organic molecules on a number of substrates beside filter paper has been studied, including silica gel,[63] alumina, asbestos and glass fibres,[24,25] sodium acetate,[30] sucrose and starch,[36] and aqueous micellar solutions.[57,61] RTP has also been observed from stretched polymer films.[64]

In addition, RTP has been observed for non-ionic compounds and polyaromatic hydrocarbons,[38] as well as for ionic compounds. Mechanistically, it is believed that the compounds are held tightly to the solid support, resulting in a decrease in the non-radiative decay of the excited triplet state.

The influence of heavy-atom solvents on RTP has been studied by several workers.[28,29,33,37,38,40,42,43,54,65–68] The heavy-atom effect, by means of increased spin–orbital coupling between the excited singlet and the triplet states and between the triplet and the ground singlet states results in an increase in phosphorescence intensity, a decrease in the fluorescence intensity, and a decrease in the phosphorescence lifetime.[69] The heavy-atom effect is most striking amongst the non-ionic organic compounds where phosphorescence appears only if the heavy atom is present.[38,43] In Table 3, RTP detection limits for several organic molecules are listed. In Table 4, the influence of several heavy atoms on the phosphorescence intensities of several organic molecules is given.

Generally, as would be expected, the phosphorescence lifetimes of species measured by RTP are less than the lifetimes of the same species measured by LTP.[24,25,38,40,41] Similar results have been found for compounds imbedded in polymer blocks.[70]

A comparison of detection limits for several organic compounds measured by RTP and LTP is given in

Table 4. Summary of effects of several heavy atoms upon RTP of several polynuclear aromatic hydrocarbons[43]

Compound	I_{Pb}/I_{Tl}*	I_{Hg}/I_{Tl}*	I_{Ag}/I_{Tl}*
Chrysene	0.07	0.01	0.3
Corone	0.05	0.05	0.4
1,2,5,6-Dibenzanthracene	0.05	0.01	0.3
Pyrene	0.07	0.01	0.2

* I_M/I_{Tl} = ratio of phosphorescence signal with heavy atom Pb, Hg, or Ag to phosphorescence signal with Tl. All solutions were of the same concentration and the solvent was 10/90 v/v ethanol/water.

Table 5. Comparison of detection limits of several organic molecules measured by RTP and LTP[41]

Compound	Limit of detection, ng RTP	LTP
1-Ethyl-1,4-dihydro-7-methyl-4-oxo-1,8-naphthyridine-3-carboxylic acid	0.2 (250)*	0.01 (830)*
1-Ethyl-1,4-dihydro-4-oxo-1,8-naphthyridine-3,7-dicarboxylic acid	0.4 (320)	0.01 (490)
7-(Acetylamino)-1-ethyl-1,4-dihydro-4-oxo-1,8-naphthyridine-3-carboxylic acid	0.4 (430)	0.1 (1630)
1-Ethyl-1,4-dihydro-7-hydroxy-4-oxo-1,8-naphthyridine-3-carboxylic acid	0.1 (490)	0.02 (1850)
7-Methyl-1,8-naphthyridine-4-ol	0.02 (310)	0.02 (1550)

* Values in parentheses are phosphorescence lifetimes (msec).

Table 5. In all cases, LTP gives lower detection limits than RTP. Despite its poorer sensitivity, RTP is still potentially useful as a routine analytical method because (*i*) no cryogenic equipment, which is expensive and rather complex to use, is needed; (*ii*) no time-consuming degassing of the solvent is needed; (*iii*) the entire procedure can be readily automated;[32,45] (*iv*) chromatographic separations can be done on the substrate before the analysis. Finally, it should be stressed that in one case, the determination of *p*-aminobenzoic acid in tablets by RTP was more sensitive than the USP XVIII method.[30]

PULSED-SOURCE/GATED-DETECTOR PHOSPHORIMETRY

Pulsed-source time-resolved phosphorimetry is a useful means of measuring mixtures of fast-decaying phosphors. Fisher and Winefordner[71] first showed the experimental usefulness of this approach following the theoretical prediction by O'Haver and Winefordner.[72] The basic approach is to pulse a light-source repetitively and to delay the repetitive measurement of the signal for a time t_d. By this approach, the signal from rapidly decaying species (*e.g.*, fluorescent species), source-light scatter, or fast phosphors, decays to a very small fraction of its initial value, whereas that from slowly decaying species is much less affected. As a result, the phosphorescence signals of certain decayers are enhanced relative to those from other decayers.

Fisher and Winefordner[71] and later O'Donnell, Harbaugh and Winefordner[73–75] all used a xenon flash-tube source (repetitively pulsed xenon flash-tubes) in place of the continuous operated xenon-arc source and phosphoroscope, and either a boxcar averager (to gain temporal information at one value of t_d) or a signal averager (to gain temporal information at many t_d values, *i.e.*, an entire phosphorescence decay curve). More recently, Boutilier and Winefordner[66,67] have replaced the pulsed-source excitation monochromator with either a pulsed N_2-laser (producing mainly the 337.1-nm line) or a flash-tube-pumped dye-laser (variable output with frequency doubler; from ~220 to 800 nm). The reason for using a laser is *not* primarily because of the much greater peak powers (the detection limit is independent of source intensity, as discussed in a previous section), *but rather* because of the clean temporal characteristics of the laser pulses and the opportunity to perform time-resolution to enhance the sensitivity and selectivity of the measurement.

When a pulsed-source/time-resolved phosphorimeter is used, modification of the sample environment by the heavy-atom effect is quite useful. In Table 6, variations of phosphorescence lifetimes of several organic molecules in several solvent environments are listed. In Table 7, a comparison of phosphorimetric detection limits for several organic molecules excited by either the pulsed N_2-laser (337.1 nm) and/or the doubled-frequency flash-tube-pumped dye-laser (270 nm) are given.

SYNCHRONOUS, DERIVATIVE, AND PHASE-RESOLVED PHOSPHORIMETRY

Synchronous phosphorimetry has been proposed as a means of increasing the selectivity of phosphorimetry by Vo-Dinh *et al.*[44,76] In this technique (also applicable to fluorimetry), the excitation and emission monochromators of a conventional phosphorimeter are set with a wavelength separation of $\Delta\lambda = \lambda_{em} - \lambda_{ex}$ = constant, and then both monochromators are scanned at the same rate. In this method, a phosphorescence peak occurs only when the excitation wavelength, λ_{ex}, and the emission wavelength, λ_{em}, respectively, correspond simultaneously to wavelengths at which excitation and phosphorescence

Table 6. Phosphorescence lifetimes of several organic molecules at 77 K[67]

Compound	Lifetime, *sec** E/W*	KI/E/W*	$AgNO_3$/E/W*
Morphine	0.03	0.04	0.002
Codeine	0.02	0.01	0.002
Phenobarbital	2.9	2 (0.002)†	—
Cocaine	2	0.09 (0.0002)†	—
STP (DOM)	3	0.7 (0.044)†	—
Butazolidin	0.07	0.02	0.004
Vinblastine sulphate	6	1 (0.1)†	0.001
Phenylcyclidine (PCP)	5	0.05 (0.002)†	—

* Solvents: E/W = 10/90 v/v ethanol/water; KI/E/W = 0.75*M* KI in 10/90 v/v ethanol/water; $AgNO_3$/E/W = 0.1*M* $AgNO_3$ in 10/90 v/v ethanol water.
† Lifetime of short-lived component is given in brackets.

Table 7. Comparison of limits of detection for several organic molecules by laser*-excited time-resolved phosphorimetry[67]

Compound	Limits of detection, μg/ml* E/W†	KI/E/W†	$AgNO_3$/E/W†	M/W§
Morphine	1	4	1	—
Codeine	0.2	0.9	0.2	—
Phenobarbital	0.007	0.01	—	—
STP (DOM)	0.008	0.04	—	0.01
Butazolidin	0.04	0.2	0.2	—
Vinblastine	0.03	0.07	0.006	—
Benzophenone	0.9 (0.2)	2 (0.4)	0.6 (0.1)	—
Quinine	2 (13)	0.4 (9)	0.2 (3)	—
Phenanthrene	5 (9)	4 (14)	2 (0.3)	—
Carbazole	0.5	0.3	0.04	—
Phenylcyclidine (PCP)	0.09	0.04 (0.3)	—	0.03

* All values with N_2-laser source (337.1 nm excitation) except those in brackets which are with flash-tube-pumped dye-laser source (270-nm excitation).

† See Table 6 for solvent compositions.

§ Values for conventional (xenon-arc source) phosphorimetry: solvent 10/90 v/v methanol/water.

emission occur. For example, if λ_{ex} corresponds to an excitation peak but no phosphorescence occurs for ($\lambda_{em} = \lambda_{ex} + \Delta\lambda$), then no phosphorescence signal results. This technique leads to sharper phosphorescence peaks. It can also be used to cut out the phosphorescence of an interferent if the wavelength separation, $\Delta\lambda$, selected for the analyte is significantly different from that for the interferent.

Vo-Dinh *et al.*[44,76] have used synchronous phosphorimetry to differentiate isomeric polynuclear aromatic compounds in a Synthoil sample by using room-temperature phosphorimetry as well as room-temperature fluorimetry. By RTP, a mixture of 17 ng of pyrene, 10 ng of phenanthrene and 26 ng of acridene was differentiated and analysed.

Second-derivative phosphorescence was used by VoDinh and Gammage[49] for room-temperature phosphorimetry. By means of taking the second derivative (electronic differentiation) of the standard phosphorescence emission spectrum, overlap between phosphorescence bands could be reduced and the phosphorescence background interference decreased. Detection limits by RTP for several polynuclear aromatic hydrocarbons were in the ng range (0.7 ng for pyrene, 34 ng for naphthalene and 5 ng for phenanthrene).

Phase-resolved phosphorimetry was proposed by Mousa and Winefordner[77] as a method complementary to time-resolved phosphorimetry. This method is based upon the use of a modulated variable-frequency source and a phase-sensitive lock-in amplifier (the other instrumental components are the same as in conventional phosphorimetry); a phosphoroscope is not needed. Because of the different phase and amplitude relationships of the luminescent species in a mixture, it is possible to "phase in" one component and "phase out" another component. Lue Yen and Winefordner[78] have shown more recently that this technique does not have the superior noise-rejection capability of time-resolved phosphorimetry, and so this method has and will probably continue to find little use other than for the measurement of phosphorescence lifetimes from the phase-angle relationship.

CONCLUSIONS AND FUTURE DEVELOPMENTS

The most exciting studies to be done in the next few years will certainly involve: (*i*) use of pulsed lasers with gated detection for time-resolved phosphorimetric analysis of real mixtures; (*ii*) development of conduction cooling as a routine analytical device for phosphorimetry; (*iii*) use of TV detectors for presentation of a greater amount of structural information; (*iv*) use of room-temperature phosphorimetry in routine clinical studies; (*v*) use of alternative excitation sources, such as X-ray generators;[79] (*vi*) use of selective solvents, such as the matrices described by Shpolskii *et al.*[80] and Persanov,[81] to "narrow" the spectral transitions.

REFERENCES

1. G. N. Lewis and M. J. Kasha, *J. Am. Chem. Soc.*, 1944, **66**, 2100.
2. R. J. Kiers, R. D. Britt and W. E. Wentworth, *Anal. Chem.*, 1957, **29**, 202.
3. S. Freed and W. Salmre, *Science*, 1958, **128**, 1341.
4. C. A. Parker and C. G. Hatchard, *Analyst*, 1962, **87**, 664.
5. J. D. Winefordner and H. W. Latz, *Anal. Chem.*, 1963, **35**, 1517.
6. J. J. Aaron and J. D. Winefordner, *Talanta*, 1975, **22**, 707.
7. C. M. O'Donnell and J. D. Winefordner, *Clin. Chem.*, 1975, **21**, 285.
8. C. A. Parker, *Photoluminescence of Solutions*, Elsevier, New York, 1968.
9. E. G. Schulman, *Fluorescence and Phosphorescence Spectroscopy: Physicochemical Principles and Practice*, Pergamon Press, New York, 1977.
10. E. L. Wehry, *Modern Fluorescence Spectroscopy*, Vols.. 1 and 2, Plenum Press, New York, 1976.

11. G. G. Guilbault, *Practical Fluorescence, Theory, Methods, and Techniques*, Dekker, New York, 1973.
12. M. Zander, *Phosphorimetry, the Application of Phosphorescence to the Analysis of Organic Compounds*, Academic Press, New York, 1968.
13. L. A. Gifford, J. N. Miller, D. L. Phillips, D. T. Burns and J. W. Bridges, *Anal. Chem.*, 1975, **47**, 1699.
14. N. Strojny and J. A. F. de Suilva, *J. Chromatog. Sci.*, 1975, **13**, 583.
15. J. A. F. de Silva, N. Strojny and K. Stika, *Anal. Chem.*, 1976, **48**, 144.
16. A. W. H. Mau and M. Puza, *Photochem. Photobiol.*, 1977, **25**, 601.
17. J. L. Ward, R. P. Bateh and J. D. Winefordner, *Appl. Spectrosc.*, 1980, **34**, 15.
18. J. L. Ward, R. P. Bateh, G. L. Walden and J. D. Winefordner, *ibid.*, 1980, **34**, 348.
19. J. B. F. Lloyd and J. N. Miller, *Talanta*, 1980, **26**, 180.
20. H. E. Millson, *The Phosphorescence of Textile Fibers and Other Substances*, Calco Tech. Bull, 753, American Cyanamid Co., 1944 (quoted in Refs. 1 and 3).
21. H. R. Mauersberger, in *Matthew's Textile Fibers*, 6th Ed., H. R. Mauersberger, ed., p. 38. Wiley, New York, 1954.
22. D. J. Brown, *J. Chem. Soc.*, 1958, 1974 (quoted in Ref. 1).
23. M. Roth, *J. Chromatog.*, 1967, **30**, 276.
24. E. M. Schulman and C. Walling, *Science*, 1972, **178**, 53.
25. *Idem, J. Phys. Chem.*, 1973, **77**, 902.
26. R. A. Paynter, S. L. Wellons and J. D. Winefordner, *Anal. Chem.*, 1974, **46**, 736.
27. S. L. Wellons, R. A. Paynter and J. D. Winefordner, *Spectrochim. Acta*, 1974, **30A**, 2133.
28. P. G. Seybold and W. White, *Anal. Chem.*, 1975, **47**, 1199.
29. T. Vo-Dinh, E. Lue Yen and J. D. Winefordner, *ibid.*, 1976, **48**, 1186.
30. R. M. A. von Wandruszka and R. J. Hurtubise, *ibid.*, 1976, **48**, 1784.
31. J. L. McHale and P. G. Seybold, *J. Chem. Educ.*, 1976, **53**, 654.
32. T. Vo-Dinh, G. L. Walden and J. D. Winefordner, *Anal. Chem.*, 1977, **49**, 1126.
33. I. M. Jakovljevic, *ibid.*, 1977, **49**, 2048.
34. R. M. A. von Wandruszka and R. J. Hurtubise, *Anal. Chem.*, 1977, **49**, 2164.
35. *Idem, Anal. Chim. Acta*, 1977, **93**, 331.
36. E. M. Schulman and R. T. Parker, *J. Phys. Chem.*, 1977, **81**, 1932.
37. W. White and P. G. Seybold, *ibid.*, 1977, **81**, 2035.
38. T. Vo-Dinh, E. Lue Yen-Bower and J. D. Winefordner, *Talanta*, 1977, **24**, 146.
39. C. D. Ford and R. J. Hurtubise, *Anal. Chem.*, 1978, **50**, 610.
40. G. J. Niday and P. G. Seybold, *ibid.*, 1978, **50**, 1577.
41. C. G. de Lima and E. M. de M. Nicola, *ibid.*, 1978, **50**, 1658.
42. E. Lue Yen Bower and J. D. Winefordner, *Anal. Chim. Acta*, 1978, **101**, 319.
43. *Idem, ibid.*, 1978, **102**, 1.
44. T. Vo-Dinh and R. B. Gammage, *Anal. Chem.*, 1978, **50**, 2054.
45. E. Lue Yen Bower and J. D. Winefordner, *Appl. Spectrosc.*, 1979, **33**, 9.
46. G. L. Walden and J. D. Winefordner, *ibid.*, 1979, **33**, 166.
47. J. J. Aaron and J. D. Winefordner, *J. Agric. Food Chem.*, 1979, **27**, 1233.
48. *Idem, Analusis*, 1979, **7**, 168.
49. T. Vo-Dinh and R. B. Gammage, *Anal. Chim. Acta*, 1979, **107**, 261.
50. E. Lue Yen Bower, *Ph.D. Thesis*, University of Florida, Gainesville, 1978.
51. M. L. Meyers, R. Zellmer, R. K. Sorrell and P. G. Seybold, *J. Luminesc.*, 1979, **20**, 215.
52. C. D. Ford and R. J. Hurtubise, *Anal. Chem.*, 1979, **51**, 659.
53. M. L. Meyers and P. G. Seybold, *ibid.*, 1979, **51**, 1609.
54. T. Vo-Dinh and J. R. Hooyman, *ibid.*, 1979, **51**, 1915.
55. R. T. Parker, R. S. Freelander, E. M. Schulman and R. B. Dunlap, *ibid.*, 1979, **51**, 1921.
56. C. D. Ford and R. J. Hurtubise, *ibid.*, 1980, **52**, 656.
57. L. J. C. Love, M. Skalec and J. G. Habarta, *ibid.*, 1980, **52**, 754.
58. J. B. F. Lloyd, *Analyst*, 1978, **103**, 775.
59. E. Lue Yen-Bower, J. L. Ward, G. Walden and J. D. Winefordner, *Talanta*, 1980, **27**, 380.
60. J. L. Ward, E. Lue Yen-Bower and J. D. Winefordner, *ibid.*, 1981, **28**, 119–120.
61. K. Kalyanasundaram, F. Grieser and J. K. Thomas, *Chem. Phys. Lett.*, 1978, **51**, 50.
62. J. N. Miller, D. L. Phillipps, D. T. Burns and J. W. Bridges, *Anal. Chem.*, 1978, **50**, 613.
63. C. D. Ford and R. J. Hurtubise, *ibid.*, 1980, **52**, 656.
64. J. J. Dekkers, G. Ph. Hoornweg, K. J. Terpstra, C. Maclean and N. H. Velthorst, *Chem. Phys.*, 1978, **34**, 253.
65. J. Najbar, J. B. Birks and T. D. S. Hamilton, *ibid.*, 1977, **23**, 281.
66. G. D. Boutilier and J. D. Winefordner, *Anal. Chem.*, 1979, **51**, 1384.
67. *Idem, ibid.*, 1979, **51**, 1391.
68. M. L. Meyers and P. G. Seybold, *ibid.*, 1979, **51**, 1609.
69. S. P. McGlynn, T. Azami, and M. Kinoshita, *Molecular Spectroscopy of the Triplet State*, Prentice-Hall, Englewood Cliffs, N.J., 1969.
70. P. F. Jones and S. Siegel, *J. Chem. Phys.*, 1969, **50**, 1134.
71. R. P. Fisher and J. D. Winefordner, *Anal. Chem.*, 1972, **44**, 948.
72. T. C. O'Haver and J. D. Winefordner, *ibid.*, 1966, **38**, 1258.
73. C. M. O'Donnell, K. F. Harbaugh, R. P. Fisher and J. D. Winefordner, *ibid.*, 1973, **45**, 609.
74. K. F. Harbaugh, C. M. O'Donnell and J. D. Winefordner, *ibid.*, 1973, **45**, 381.
75. *Idem, ibid.*, 1974, **46**, 1206.
76. T. Vo-Dinh, R. B. Gammage, A. R. Hawthorne and J. H. Thorngate, *Env. Science Tech.*, 1978, **12**, 1297.
77. J. J. Mousa and J. D. Winefordner, *Anal. Chem.*, 1974, **46**, 1195.
78. E. Lue Yen and J. D. Winefordner, *ibid.*, 1977, **49**, 1262.
79. A. P. de Silva., G. J. Oestreich and V. A. Fassel, *ibid.*, 1976, **48**, 915.
80. E. V. Shpolskii, A. A. Ll'ind and L. A. Klimova, *Dokl. Akad. Nauk SSR*, 1952, **87**, 935.
81. R. I. Persanov, *Russ. J. Anal. Chem.*, 1962, **17**, 503.

Talanta, Vol. 28, pp. 207 to 214, 1981
Printed in Great Britain. All rights reserved

0039-9140/81/040207-08$02.00/0
Copyright © 1981 Pergamon Press Ltd

SELECTIVE AND QUANTITATIVE SEPARATION OF ZINC AND LEAD FROM OTHER ELEMENTS BY CATION-EXCHANGE CHROMATOGRAPHY IN HYDROHALIC ACID–ACETONE SOLUTIONS

A. H. VICTOR and F. W. E. STRELOW

National Chemical Research Laboratory, P.O. Box 395, Pretoria
0001, Republic of South Africa

(*Received* 3 *September* 1980. *Accepted* 7 *November* 1980)

Summary—Zinc and lead can be separated from Cd, Bi(III), In and V(V) by eluting these elements with 0.2*M* hydrochloric acid in 60% acetone from a column of AG50W-X8 cation-exchange resin, zinc and lead being retained. Mercury(II), Tl (III), As(III), Au(III), Sn(IV), Mo(VI), W(VI) and the platinum metals have not been investigated quantitatively, but from their distribution coefficients, should also be eluted. Vanadium(V), Mo(VI) and W(VI) require the presence of hydrogen peroxide. Zinc and lead can be eluted with 0.5*M* hydrochloric acid in 60% acetone or 0.5*M* hydrobromic acid in 65% acetone and determined by AAS; the alkali and alkaline-earth metal ions, Mn(II), Co, Ni, Cu(II), Fe(III), Al, Ga, Cr(III), Ti(IV), Zr, Hf, Th, Sc, Y, La and the lanthanides are retained on the column, except for a small fraction of copper eluted with zinc and lead. Separations are sharp and quantitative. The method has successfully been applied to determination of zinc and lead in three silicate rocks and a sediment.

Although relatively few elements interfere in the atomic-absorption determination of zinc and lead,[1] the large variations found in the published results for direct atomic-absorption determination of zinc and lead in standard rocks[2–6] indicate that there is interference from some other elements or viscosity problems due to high salt concentrations. It was therefore decided to develop a general and selective method for separation of zinc and lead from matrix elements so that accurate results could be obtained for their content in complex materials to be used as standards.

The method most generally used for separation of zinc from other elements is anion-exchange in hydrochloric acid medium; Zn, Cd, Hg(II), Bi(III), Au(III) and most of the platinum metals are strongly retained and can be separated from many other metals such as Mn(II), Co, Ni, Cu(II), Al, Fe(III), Ga, Ti(IV), V(V), the alkali and alkaline earth metals and lanthanides, which can all be eluted with ~0.5*M* hydrochloric acid.[7] Unfortunately, lead is not very strongly retained, its sorption being maximal from ~1.5*M* hydrochloric acid ($K_d \sim 25$). Hence relatively large amounts of lead cannot be effectively separated from large amounts of iron(III) without the use of inconveniently large columns. Anion-exchange chromatography in hydrochloric acid therefore does not seem to be the ideal approach for the simultaneous separation of zinc and lead from other elements.

Strongly acid cation-exchange resins have the advantage of a higher capacity and generally better exchange kinetics, but will not give selective separation of zinc and lead from most other elements, in aqueous mineral acid media, some of the separation factors being too small. However, the selectivity increases dramatically when water-miscible organic solvents are present. Hydrochloric acid–acetone has been used by Fritz *et al.* for the quantitative separation of mg amounts of Bi(III), Cd, Zn, Fe(III), Cu(II), Co and Mn(II) from each other,[8] as well as small amounts of Cu(II), Ni, Co and Mn(II) from large amounts of Cd, Fe(III) and Zn.[9] The separation of lead, however, was not included in these studies. Forced-flow cation-exchange chromatography in hydrochloric acid–isopropyl alcohol and/or hydrochloric acid–acetone media has also been employed for the separation of zinc, lead and transition elements from each other,[10,11] as well as the separation of Bi(III), Cd, In and Zn,[12] but no quantitative results have been given. Further, only trace amounts of the elements were tested. Strelow *et al.* have developed a selective method for the separation of indium from zinc, lead, gallium and many other elements in hydrohalic acid–acetone medium.[13] They have also shown qualitatively that zinc can be separated from many other elements in hydrochloric acid–acetone[14] or hydrobromic acid acid–acetone media,[15] and that zinc and lead can be separated from each other and from elements in the latter medium.[15]

The systematic studies of cation-exchange distribution coefficients of 54 cations in aqueous acetone containing hydrochloric acid[14] or hydrobromic acid[15] indicated that it should be possible to separate zinc and lead selectively from all other elements. When a complex mixture is sorbed from ~0.2*M* hydrochloric acid in 60% acetone, followed by elution with the same medium, Cd, Hg(II), In, Tl(III), Bi(III), As(III), Sn(IV), V(V), Mo(VI), W(VI) and the platinum metals should pass through a column of AG50W-X8 resin,

while zinc, lead and many other elements should be retained. Zinc and lead could then be eluted with either 0.5*M* hydrochloric acid in 60% acetone or 0.5*M* hydrobromic acid in 65% acetone while the alkali and alkaline earth metals, Mn(II), Co, Ni, Cu(II), Fe(III), Al, Ga, Cr(III), Ti(IV), Zr. Hf, Th, Sc, Y, La and the lanthanides should remain on the column. The neighbouring elements in the elution would be indium ahead of zinc and lead, and lithium behind them. The quantitative separation of zinc and lead from indium, lithium and typical other elements was therefore investigated and the results used in designing the separation and determination of zinc and lead in the standard rock W-1 and three secondary reference samples.

EXPERIMENTAL

Reagents, solutions and apparatus

Analytical reagent-grade chemicals were used throughout. Stock 10-mg/ml solutions of zinc and lead in 0.5*M* nitric acid were prepared from 99.9% pure zinc metal and lead nitrate and standardized with EDTA. Water was distilled and passed through an Elgastat demineralizer.

The resin used was AG50W-X8 strongly acid sulphonated polystyrene cation-exchanger (Bio-Rad Laboratories, Richmond, California) of 200–400 mesh particle size. Borosilicate glass tubes of 20 mm bore and 40 cm length, fitted with a porosity-2 sintered-glass plate and a tap at the bottom and a B19 joint at the top, were used for the columns.

A Varian-Techtron AA5 spectrometer was used for atomic-absorption measurements.

Elution curves

A column containing 60 ml (20 g dry weight) of AG50-X8 resin was prepared and equilibrated by passage of about 100 ml of 0.2*M* hydrochloric acid in 60% acetone. The resin column was about 19 cm in length and 2 cm in diameter. A solution of 100 ml of 0.2*M* hydrochloric acid in 60% acetone containing 1 mmole each of cadmium and zinc was passed through the column, and the column was washed with 0.2*M* hydrochloric acid in 60% acetone at a flow-rate of 2.5 ± 0.3 ml/min until zinc appeared in the eluate (*ca.* 800 ml). The eluate was collected automatically in 25-ml fractions. After removal of the acid and acetone by evaporation, the residues from the fractions were diluted and analysed. A similar technique was used for investigation of other mixtures, and of the effect of use of hydrobromic acid—acetone mixture.

Quantitative separations

Standard solutions of the chlorides or nitrates of zinc and lead and one or two other elements were measured out in triplicate and each was evaporated to dryness, its residue then being dissolved in 20 ml of 1*M* hydrochloric acid and diluted with water and acetone to about 100 ml to give a medium of 0.2*M* hydrochloric acid in 60% acetone. Each solution was passed through a column of 60 ml (20 g dry weight) of AG50W-X8 resin (200–400 mesh) previously equilibrated with 0.2*M* hydrochloric acid in 60% acetone and rinsed in with three portions of the same reagent. Weakly sorbed species were eluted with the same acid—acetone mixture (250 ml for cadmium and bismuth, 400 ml for indium). Vanadium(V) was eluted with 250 ml of 0.01*M* nitric acid containing 0.15% hydrogen peroxide.

Zinc and small amounts of lead were eluted with 200 ml of 0.5*M* hydrochloric acid in 60% acetone; 200 ml of 0.5*M* hydrobromic acid in 65% acetone were used for the elution of mg amounts of lead. Elements still retained after the elution of zinc and lead were eluted with hydrochloric acid [250 ml of 1*M* acid for lithium; 250 ml of 3*M* acid for copper(II), iron(III) and gallium].

Eluates containing acetone were diluted with ~100 ml of water to minimize formation of condensation products of acetone during evaporation. Excess of acid and acetone was removed by evaporation and residual organic matter was oxidized by heating with nitric and perchloric acids. The elements were then determined by suitable methods (Table 1). Atomic-absorption measurements were made as

Table 1. Analytical methods used

Element	Method
Zn, Pb	Complexometric titration with EDTA at pH 5.5 with Xylenol Orange as indicator. Small amounts by atomic-absorption spectrometry.
Cd	Complexometric titration with EDTA in slight excess of ammonia, Methylthymol Blue as indicator.
Cu(II), In	Complexometric titration with excess of EDTA and back-titration with $ZnSO_4$ at pH 5.5, Xylenol Orange as indicator. Small amounts by atomic-absorption spectrometry.
Bi(III)	Complexometric titration with EDTA in 0.1*M* HNO_3, Xylenol Orange as indicator.
Fe(III), Ga	Complexometric titration with excess of DCTA and back-titration with $ZnSO_4$ at pH 5.5, Xylenol Orange as indicator. Small amounts of Fe(III) by atomic-absorption spectrometry.
Li	Atomic-absorption spectrometry.
V(V)	Oxidation to V(V) with $HClO_4$ and titration with Fe(II), barium diphenylaminesulphonate as indicator.

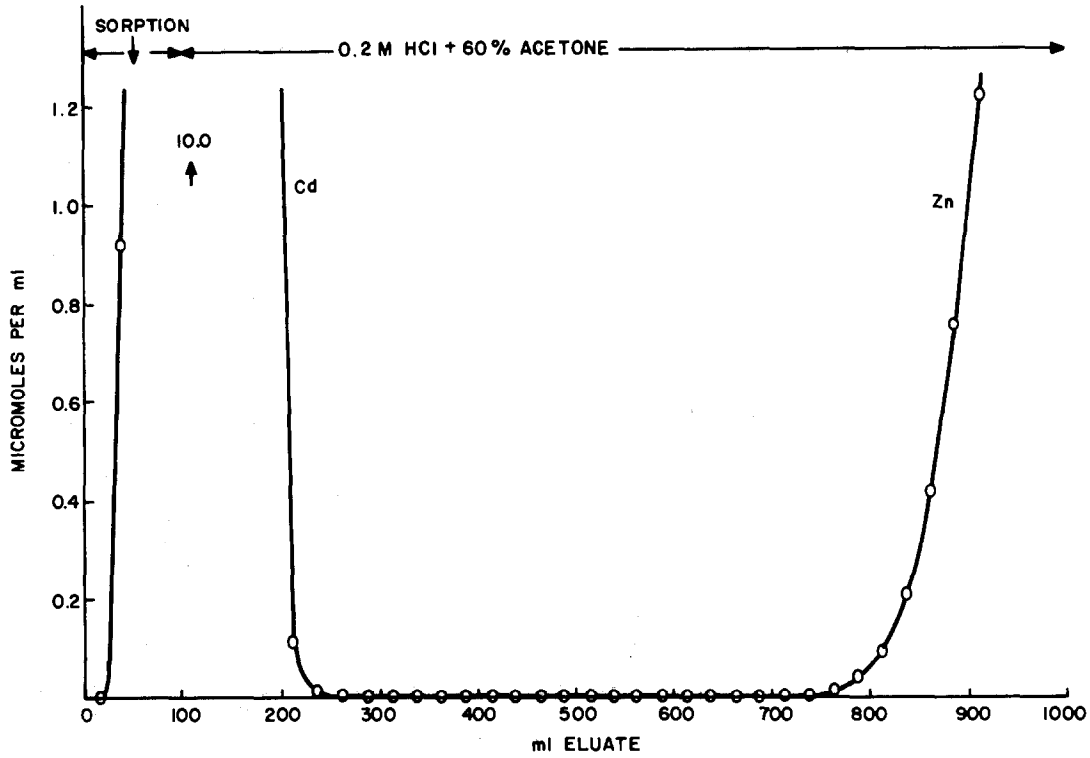


Fig. 1. Elution curve for 1 mmole each of Cd and Zn. Column of 60 ml (19 × 2.0 cm) of AG50W-X8 resin, 200–400 mesh. Flow-rate 2.5 ± 0.3 ml/min. Eluent 0.2*M* HCl–60% acetone.

soon as possible after dilution of the samples to appropriate volume with 0.1*M* nitric acid.

Separation and determination of zinc and lead in silicate rocks and sediments

About 1 g of finely ground sample was weighed out and dissolved by heating with a mixture of 10 ml each of perchloric, hydrochloric and hydrofluoric acids in a 100-ml Teflon beaker as previously described.[16] The solution was evaporated until about 1 ml remained, then the salts were dissolved in about 100 ml of water. The insoluble residue was filtered off, washed and ignited, then decomposed by heating with a mixture of 1 ml each of perchloric and hydrofluoric acids and 5 ml of 20% orthophosphoric acid in a 30-ml platinum crucible until a clear viscous mass of polyphosphoric acid remained.[17,18] The cooled product was dissolved in 20 ml of 0.5*M* hydrochloric acid containing a few drops of 30% hydrogen peroxide and the solution boiled in a covered beaker for 5 min to depolymerize the phosphoric acid, and then cooled. Next, 30 ml of acetone and a few drops of hydrogen peroxide were added and the solution (about 50 ml, consisting of 0.2*M* hydrochloric acid in 60% acetone) was passed through a 60-ml (20-g dry weight) column of AG50W-X8 resin, previously equilibrated with 0.2*M* hydrochloric acid in 60% acetone, containing 0.1% hydrogen peroxide. The sorption solution was allowed to drain to the top of the column, the beaker was rinsed with 5-ml portions of the equilibration solution and the column was washed by passage of 40 ml of the same solution and drained until the liquid reached the top of the resin. The original solution filtrate, which had meanwhile been evaporated to fumes of perchloric acid and then diluted to 100 ml with equilibration mixture, was then passed through the column. The column was washed with 150 ml of the equilibration solution and the eluate discarded. Finally zinc and lead were eluted with 200 ml of 0.5*M* hydrochloric acid in 60% acetone, containing 0.1% hydrogen peroxide.

The eluate containing zinc and lead was evaporated as previously described and in the case of the three silicates the residue was dissolved in 2 ml of 0.5*M* nitric acid and diluted to 10 ml with water. Half the solution was used for atomic-absorption determination of zinc after appropriate dilution with 0.1*M* nitric acid and lead was determined in the rest. In the case of the sediment, however, the eluate was diluted to 1 litre.

RESULTS AND DISCUSSION

Cadmium (Fig. 1) and bismuth(III) can be eluted and separated ahead of zinc and lead by elution with 250 ml of 0.2*M* hydrochloric acid in 60% acetone, from a column of 60 ml of AG50W-X8 resin (200–400 mesh), but 400 ml of the same eluent are required for the quantitative elution of indium, even for 1-mg quantities (Fig. 2). Under these conditions zinc and lead are still fairly strongly retained and the first trace of zinc appears in the eluate only after passage of 600 ml of 0.2*M* hydrochloric acid in 60% acetone (Fig. 1). Because vanadium(V) showed considerable tailing during elution with 0.2*M* hydrochloric acid in 60% acetone containing 0.1% of hydrogen peroxide, in spite of a distribution coefficient[14] of 5.5, 0.01*M* nitric acid containing 0.15% hydrogen peroxide[19] was used for the fast and quantitative elution of vanadium(V) before the other elements. Although Hg(II), As(III), Au(III), Sn(IV), Mo(VI), W(VI) and the

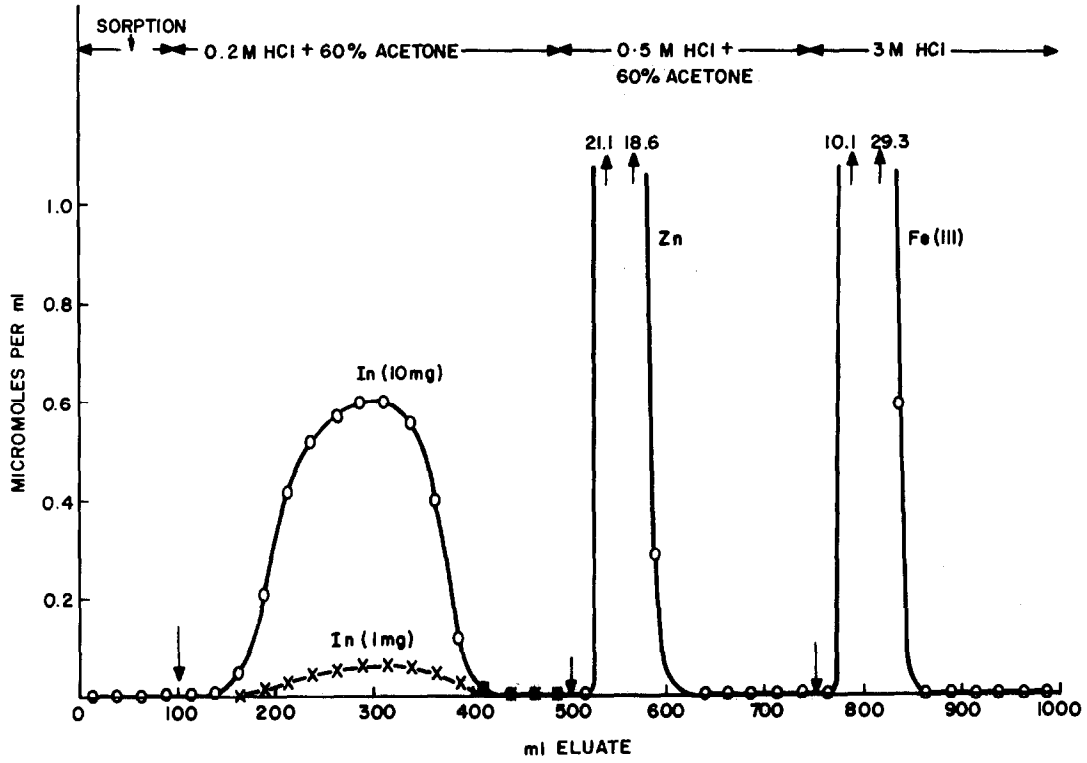


Fig. 2. Elution curve for 10 mg (and 1 mg) of In and 1 mmole each of Zn and Fe(III). Column size and flow-rate as for Fig. 1.

platinum metals have not been investigated quantitatively, they should also be eluted and separated ahead of zinc and lead with 0.2*M* hydrochloric acid in 60% acetone, according to their known distribution coefficients and elution behaviour.

After the elution of Cd, Bi(III), In, V(V), *etc.*, zinc and lead can then be eluted with 200 ml of either 0.5*M* hydrochloric acid in 60% acetone or 0.5*M* hydrobromic acid in 65% acetone (Figs. 3 and 4). In hydrochloric acid medium zinc is eluted somewhat ahead of lead and *vice versa* in hydrobromic acid medium. Separations of zinc and lead from other elements are sharp and quantitative as can be seen from the results in Table 2. When large quantities of lead are to be separated, the hydrobromic acid system is preferable to the hydrochloric acid system. Atomic-absorption studies have shown that zinc and lead can be determined without mutual interference in solutions of 0.1*M* nitric acid containing both elements in ratios ranging from 1000:1 to 1:1000, if an air–acetylene flame is used, with the 213.9 and 217.0 nm lines for zinc and lead respectively. When large quantities of both zinc and lead are to be separated from other elements by the proposed elution scheme and atomic-absorption spectrometry is unattractive for the final determination, zinc and lead can be separated from each other by anion-exchange chromatography in hydrobromic acid–nitric acid medium.[20]

After the elution of zinc and lead, the more strongly retained alkali and alkaline earth metals, Mn(II), Co, Ni, Cu(II), Fe(III), Al, Ga, Cr(III) and Ti(IV) can be eluted with 3*M* hydrochloric acid. When Ba, Zr, Hf, Y, Sc, La or lanthanides are present, 4 or 5*M* hydrochloric acid is required for their elution. Of the group of elements which remain on the column after the elution of zinc and lead, lithium is the least strongly retained. By use of a 60-ml column of AG50W-X8 resin, 5 mg of lithium can effectively be separated from zinc and lead, but this amount is considered to be close to the tolerance limit. The other elements may be present in much larger amounts. The results in Table 2 indicate that the recovery of about 50 mg of copper(II) is not quite quantitative (99.6%). About 180 μg of copper were found in the zinc–lead eluate, indicating that a small fraction of the copper was eluted with 0.5*M* hydrochloric acid in 60% acetone in spite of an overall distribution coefficient[14] of 92. However, the presence of small amounts of copper has no influence on the atomic-absorption determination of zinc and lead in 0.1*M* nitric acid medium.

The proposed method provides an excellent means for the accurate determination of zinc and lead and is applicable to rocks, sediments or any other material containing these elements, and the values and standard deviations obtained for the three rocks and a sediment (Tables 3 and 4) indicate that the method should be useful for standardization purposes. The values obtained for diabase W-1 are in reasonable agreement with the published recommended values, although somewhat higher. In the case of the three

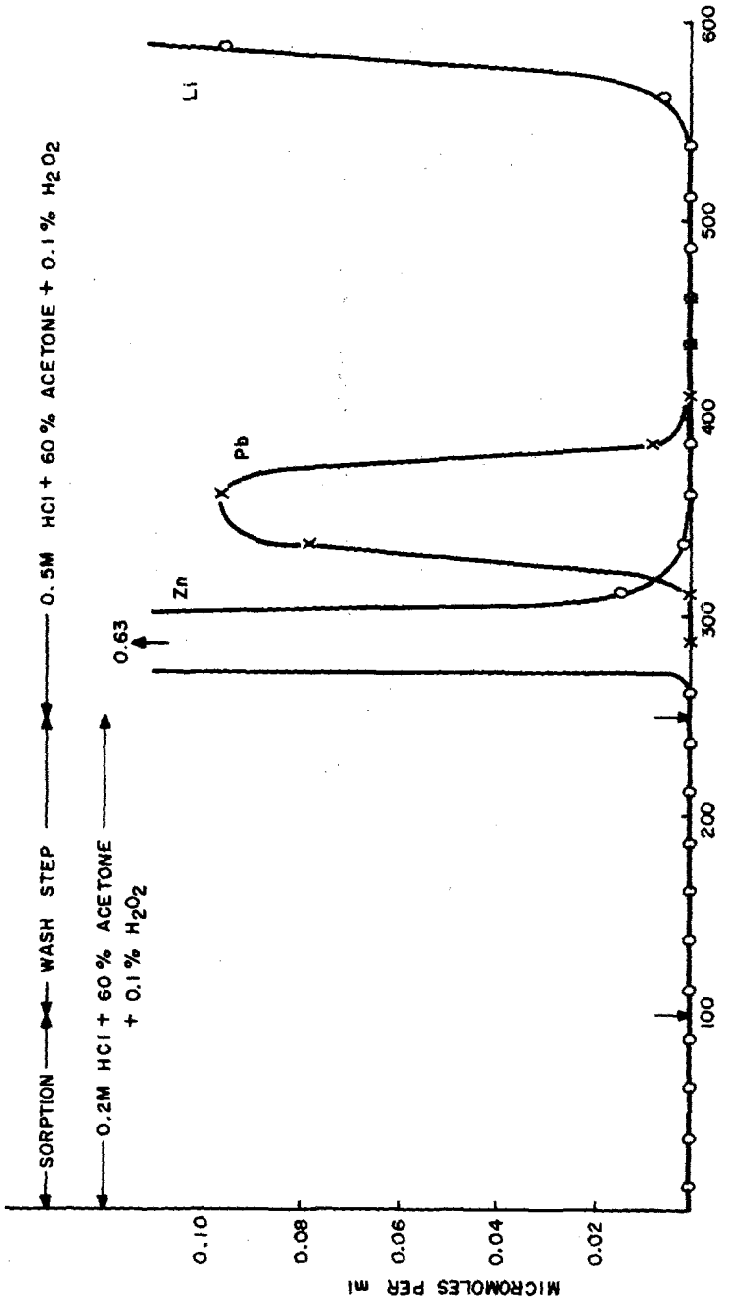


Fig. 3. Elution curve for 1 g of NIM-D spiked with 1 mg each of Zn, Pb and Li. Column size and flow-rate as for Fig. 1. Eluent 0.5*M* HCl–60% acetone.

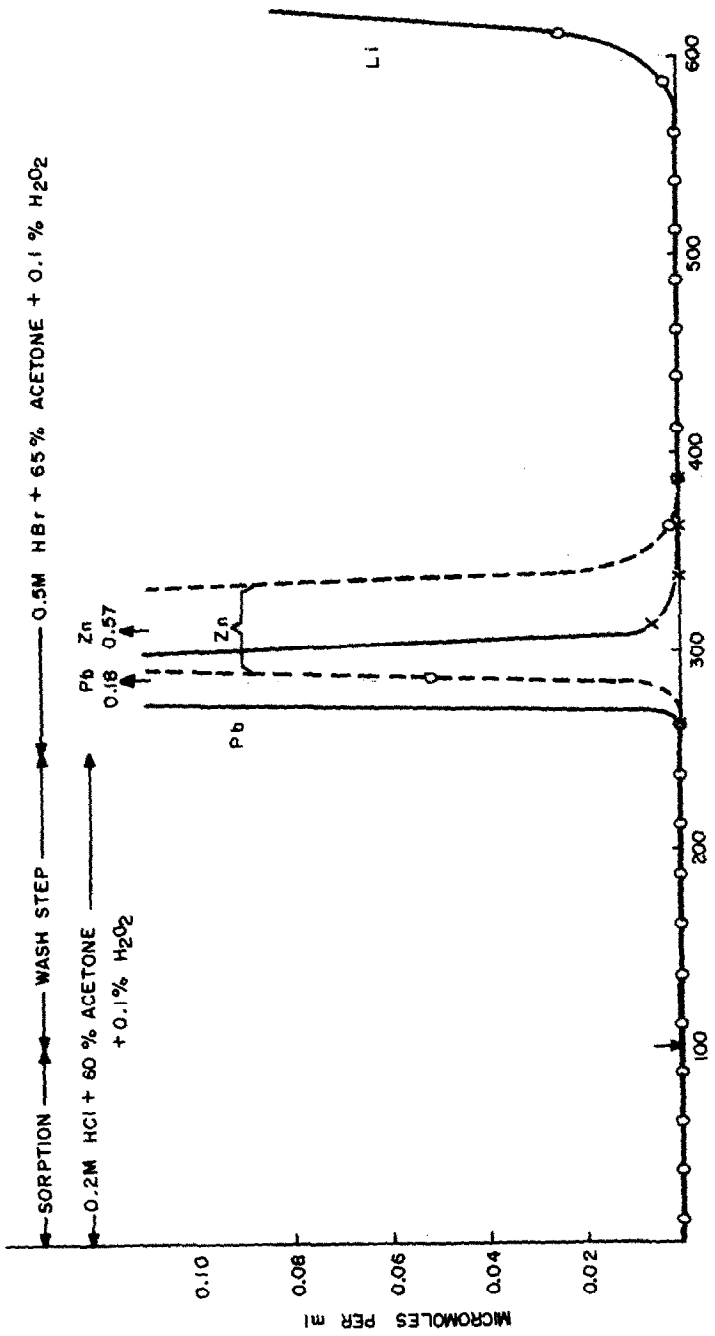


Fig. 4. Same conditions as for Fig. 3. Eluent 0.5*M* HBr–65% acetone.

Table 2. Results of quantitative separations of synthetic mixtures

Taken, *mg*		Foung,* *mg*	Taken, *mg*		Found,* *mg*
Zn	0.1000	0.1001 ± 0.0001	Cd	51.25	51.25 ± 0.02
Pb	0.1000	0.1001 ± 0.0001	Zn	0.1000	0.1001 ± 0.0001
Fe(III)	101.46	101.47 ± 0.05	Pb	0.1000	0.1001 ± 0.0002
			Cu	51.36	51.17 ± 0.02
Zn	49.96	49.96 ± 0.01			
Fe(III)	50.73	50.73 ± 0.01	Bi	51.52	51.52 ± 0.02
			Zn	0.1000	0.1000 ± 0.0002
Zn	99.92	99.93 ± 0.02	Pb	0.1000	0.1000 ± 0.0002
Fe(III)	0.1000	0.1001 ± 0.0003	Li	5.04	5.04 ± 0.01
Pb†	19.89	19.89 ± 0.01	V(V)	20.05	20.05 ± 0.01
Fe(III)	101.46	101.47 ± 0.04	Zn	0.0500	0.0500 ± 0.0002
			Pb	0.1000	0.1000 ± 0.0002
Pb†	19.89	19.89 ± 0.01			
Fe(III)	0.1000	0.1002 ± 0.0003	In	11.51	11.51 ± 0.01
			Zn	49.96	49.96 ± 0.02
			Ga	70.72	70.71 ± 0.03

* Means of triplicate determinations with calculated standard deviations. AAS results are means of 25–35 readings. EDTA titrations are precise to 0.1% or better.

† Pb eluted with 200 ml of 0.5*M* HBr in 65% acetone; in all other cases Pb and Zn eluted with 200 ml of 0.5*M* HCl in 60% acetone.

Table 3. Results for the determination of Zn in rocks

Sample	Zn found, *ppm*	Average value, *ppm*	Recommended or approximate value, *ppm*
Diabase W-1	92.3, 92.0 92.1, 92.2	92.2 ± 0.1	86*
Kimberlite S-7	72.3, 72.4 72.7, 72.7	72.5 ± 0.2	60†
Dolerite S-18	96.0, 96.1 95.6, 95.4	95.8 ± 0.3	77†
Sediment S-14	0.649, 0.648% 0.648, 0.648%	0.648 ± 0.001%	—

* Ref. 21.
† Ref. 22.

Table 4. Results for the determination of Pb in rocks

Sample	Pb found, *ppm*	Average value, *ppm*	Recommended or approximate value, *ppm*
Diabase W-1	9.74, 9.75 9.90. 9.59	9.75 ± 0.13	7.8*
Kimberlite S-7	23.5, 23.5 23.3, 23.3	23.4 ± 0.1	10†
Dolerite S-18	26.6, 26.7 26.6, 26.5	26.6 ± 0.1	—
Sediment S-14	1.459, 1.460% 1.460, 1.462%	1.460 ± 0.001%	—

* Ref. 21.
† Ref. 22.

secondary reference samples of the National Institute for Metallurgy, South Africa, no recommended values are yet available and there are only approximate zinc values for the dolerite and kimberlite and an approximate lead value for the latter. The newly obtained zinc and lead values for these three samples should therefore be quite useful.

REFERENCES

1. S. J. Royal and R. C. Mallett, *Handbook of the Interference Effects Encountered in Atomic Absorption Spectrophotometry at the National Institute for Metallurgy, S. Afr. Inst. Metallurgy*, Project No. 05776, 1978.
2. M. Fleischer, *Geochim. Cosmochim. Acta*, 1969, **33**, 65.
3. F. J. Flanagan, *ibid.*, 1969, **33**, 81.
4. N. M. Sine, W. O. Taylor, G. R. Webber and C. L. Lewis, *ibid.*, 1969, **33**, 121.
5. M. Roubalt, H. De La Roche and K. Govindaraju, *Sci. Terre*, 1970, **15**, 351.
6. T. W. Steele, A. Wilson, R. Goudvis, P. J. Ellis and A. J. Radford, *Geostand. Newsl.*, 1978, **2**, 71.
7. K. A. Kraus and F. Nelson, *Proc. Intern. Conf., Peaceful Uses Atomic Energy, Geneva*, 1956, **7**, 113.
8. J. S. Fritz and T. A. Rettig, *Anal. Chem.*, 1962, **34**, 1562.
9. J. S. Fritz and J. E. Abbink, *ibid.*, 1965, **37**, 1274.
10. K. Kawazu and J. S. Fritz, *J. Chromatog.*, 1973, **77**, 397.
11. K. Kawazu, *ibid.*, 1977, **137**, 381.
12. K. Kawazu and H. Kaiyama, *ibid.*, 1978, **151**, 339.
13. F. W. E. Strelow, C. H. S. W. Weinert and T. N. Van der Walt, *Talanta*, 1974, **21**, 1183.
14. F. W. E. Strelow, A. H. Victor, C. R. Van Zyl and C. Eloff, *Anal. Chem.*, 1971, **43**, 870.
15. F. W. E. Strelow, M. D. Hanekom, A. H. Victor and C. Eloff, *Anal. Chim. Acta*, 1975, **76**, 377.
16. F. W. E. Strelow, C. J. Liebenberg and A. H. Victor, *Anal. Chem.*, 1974, **46**, 1409.
17. F. W. E. Strelow, C. J. Lienberg and F. von S. Toerien, *Anal. Chim. Acta*, 1969, **47**, 251.
18. F. von S. Toerien, *D.Sc. Thesis*, University of Pretoria, October 1969.
19. F. W. E. Strelow and A. H. Victor, *J. S. African Chem. Inst.*, 1975, **28**, 272.
20. F. W. E. Strelow, *Anal. Chem.*, 1978, **50**, 1359.
21. F. J. Flanagan, *Geochim. Cosmochim. Acta*, 1973, **37**, 1189.
22. T. W. Steele, Personal communication.

Talanta, Vol. 28, pp. 215 to 220, 1981
Printed in Great Britain

0039-9140/81/040215-06$02.00/0
Pergamon Press Ltd

SOME APPLICATIONS OF LIGAND-EXCHANGE—I. RECOVERY OF PHENOLIC COMPOUNDS FROM WATER

B. M. PETRONIO, A. LAGANÁ and M. V. RUSSO
Istituto di Chimica Analitica dell Università, Rome, Italy

(*Received* 7 *August* 1980. *Accepted* 31 *October* 1980)

Summary—The properties of a chelating ion-exchanger in the iron(III) form in contact with an aqueous solution containing phenolic compounds have been studied. The phenols retained are completely displaced by elution with an ethanolic sodium hydroxide solution.

Phenols are among the most common water pollutants and this class is included in the list of priority pollutants.[1] The concentrations of these compounds in natural water vary to some degree because of their degradability, but in river[2] and other[3] water samples they are present at the μg/l. level, generally 75 μg/l. or less. It has long been known that pentachlorophenol is toxic;[4] various researchers have found substantial amounts of this compound in the environment, and Buhler *et al.*[5] have confirmed its presence in municipal sewage and river water. It is well known that chlorinated phenols can arise from the sterilization of drinking water by chlorination.[6]

These compounds and phenol itself contribute an unpleasant medicinal odour and taste to drinking water even at low concentration. Moreover, many substituted phenols have been found to be harmful to fish; *o*-chlorophenol at levels less than 1.0 μg/l. has caused fish tainting and the organoleptic qualities of certain fish have been altered by 2,4-dichlorophenol at the 1.0 μg/l. level.[7]

A suitable method is therefore needed for low-level determination of phenols and for their identification.

The standard methods for determination of phenols in water are based on their reaction with 4-aminoantipyrine[8] or related compounds[9] and spectrophotometric measurement of the products, but these are used for determining total phenols. Moreover, this method does not respond equally to all phenols, some *p*-substituted phenols are not determined and the result for total phenols may be significantly erroneous.

Some of these problems are overcome by the chromatographic methods, which involve preconcentration of trace quantities of phenols on solid sorbents and their release with an extracting agent. Active carbon,[10] ion-exchange resins such as Amberlite XAD-2, XAD-4 or XAD-7[11–14] or polymers[15,16] are used as sorbents. Desorption is carried out with methanol–diethyl ether mixture[17] or acetone–water mixture[11] or by a stripping method.[16] Alternatively, acetate esters can be formed by direct addition of acetic anhydride to the dilute aqueous phenolic solution. These esters are extracted with methylene chloride and determined by gas chromatography.[18] The phenolic compounds are not often directly extracted; although the extraction can be enhanced by acidification of the water sample, recovery is never quantitative.

The method reported in this paper is based on "ligand-exchange chromatography" (LEC).[20] In this procedure a cation-exchange resin in the Fe(III) form acts as a solid sorbent, removing phenols quantitatively from the liquid phase by formation of complexes with metal bound to the resin, even with very dilute solutions. Subsequent competitive displacement of the organic ligands co-ordinated to the metal ion permits recovery of the phenols.

A limited series of experiments with cation-exchange resin in the transition-metal form (copper, nickel, iron) was performed by Webster *et al.*[21] to investigate the use of the resins as adsorbents of ligands from non-aqueous solutions: alkylphenols and salicylic acid were sorbed from mineral oil. Cation-exchange resins in the Fe(III) form have been used in ligand-exchange chromatography by Fujimura *et al.*[22–24] to separate organic isomers such as the hydroxybenzoic acids (*o*-, *m*- and *p*-isomers) or nitrosonaphthols but recoveries of phenols from water by LEC have not, to our knowledge, been reported in the literature.

EXPERIMENTAL

Reagents

The following phenols from the EPA list of priority pollutants[1] were studied: **I** = 2-chlorophenol, **II** = 2-nitrophenol, **III** = phenol, **IV** = 2,4-dimethylphenol, **V** = 2,4-dichlorophenol, **VI** = 2,4,6-trichlorophenol, **VII** = 4-chloro-3-hydroxytoluene, **VIII** = 4,6-dinitro-2-hydroxytoluene, **IX** = 2,4-dinitrophenol, **X** = pentachlorophenol, **XI** = 4-nitrophenol.

Standard solutions of these (50 mg/ml) were prepared by weighing the pure substances and dissolving them in acetone. Portions of these solutions were then diluted with distilled water to give the test samples.

All chemicals were analytical grade.

Work carried out on a grant from the National Council of Research (Italy).

Chelex resin [Fe(III) form]

An exchanger of the polystyrene–iminodiacetic acid type (Chelex 100, Bio-Rad) was used. A 7-g amount of the resin (100–200 mesh) in the sodium form was converted into the Fe(III) form with ferric chloride solution by vigorous mechanical shaking for 12 hr to reach equilibrium. The resin was then placed in a glass tube (12 mm bore) ready for chromatographic use, and washed with distilled water until the effluent was free from Fe(III). The packed resin column was 8 cm long.

Analytical procedure

Retention of phenolic compounds from water. The test samples (1 litre) obtained from dilution of the standard solution in distilled water at different pH values or in river water and containing 100 μg of each compound per litre were passed through the chromatographic column at specified flow-rates. The eluate and an equal volume of test sample were each extracted with three 20-ml volumes of methylene chloride after acidification to pH 2. The extract was dried with granular anhydrous sodium sulphate and after addition of an internal standard was concentrated in a rotary evaporator to a volume of approximately 0.3 ml and analysed by gas chromatography.

The phenols retained on the exchanger were displaced by passing through the column 300 ml of a 5:1 v/v mixture of 1*M* sodium hydroxide and ethanol. After acidification the solution was extracted with three 10-ml portions of methylene chloride and the extract was dried, concentrated and analysed after addition of the internal standard, as already described. Each experiment was repeated three times.

The conditions for the gas chromatography were as follows.

Column: glass capillary, 14 m coated with 12% FFAP, detection by flame-ionization detector.
Carrier gas: hydrogen at a flow-rate of 0.5 ml/sec.
Injector temperature: 300°.
Volume injected: 5 μl.
Column temperature: programmed from 100 to 200° at 1.25°/min.
Final isothermal chromatography: temperature 200°; hydrogen flow-rate 1.05 ml/sec.

RESULTS AND DISCUSSION

To determine the best operating conditions, the effects of flow-rate and pH were examined (Tables 1 and 2). The recovery increases with decrease in flow-rate and a value of 2 ml/min was selected as a compromise between good recovery and economy in time.

Preliminary tests showed that the phenols were not retained on the exchanger not treated with the iron(III) solution, except for 4-chloro-3-hydroxytoluene and partially 2,4-dimethylphenol and 2,4-dichlorophenol (Table 3). It is evident that the recovery of the phenols from water, except for 4-chloro-3-hydroxytoluene, is a chromatographic process that involves the iron(III) bound to the stationary phase, presumably by formation of iron(III)–phenol complexes. The complex formation is indicated in some instances by the appearance of a coloured band in the resin. For the 2,4-dimethylphenol and 2,4-dichlorophenol a simultaneous sorption process cannot be excluded. In any case it is known that most aromatic compounds are adsorbed on ion-exchange resins by van der Waals interactions between the solute and the resin matrix.

Since it is reasonable to assume that the iron(III) is bound in much the same way as copper(II) to Dowex A-1 to form the structure[25]

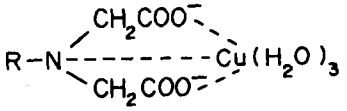


Table 1. Effect of flow-rate on recovery (%) of phenolic compounds (100 ng/ml of each) from distilled water

Flow-rate, ml/min	Phenol I	II	III	IV	V	VI	VII	VIII	IX	X	XI
1	78	94	44	93	100	100	100	100	100	100	100
2	66	78	30	73	100	100	100	100	100	100	100
3	41	70	28	60	100	100	100	180	75	100	100

Table 2. Effect of pH on recovery (%) of phenolic compounds from distilled water; flow-rate 2 ml/min

pH	Phenol I	II	III	IV	V	VI	VII	VIII	IX	X	XI
3	86	93	42	93	100	100	100	100	100	100	100
6	66	78	30	73	100	100	100	100	100	100	100
9	63	72	28	74	100	91	91	100	100	100	100
12	10	30	11	18	26	24	26	80	40	45	10

Table 3. Recovery (%) of phenolic compounds from distilled water with Chelex resin in different forms; flow-rate 2 ml/min, pH = 6

Resin form	Phenol I	II	III	IV	V	VI	VII	VIII	IX	X	XI
Na^+	0	8	2	40	42	0	90	0	0	0	0
Fe^{3+}	66	78	30	73	100	100	100	100	100	100	100
$FeOH^{2+}$	13	24	17	71	30	17	92	19	32	17	20

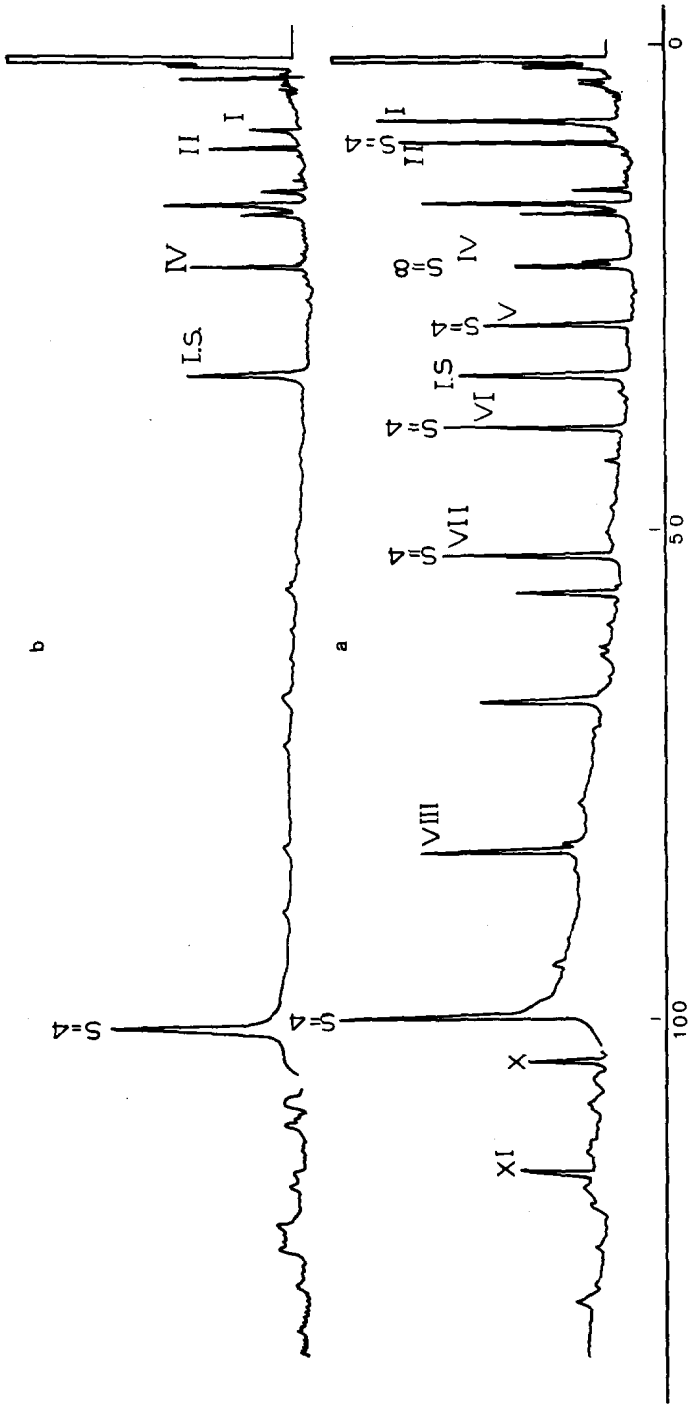


Fig. 1. Chromatogram of river water with standards added. (a) Before passage through the iron(III)–Chelex resin (*length* 8 *cm*); (b) after passage through the iron(III)–Chelex resin. *Sensitivity* (S) = 2 except where otherwise stated.

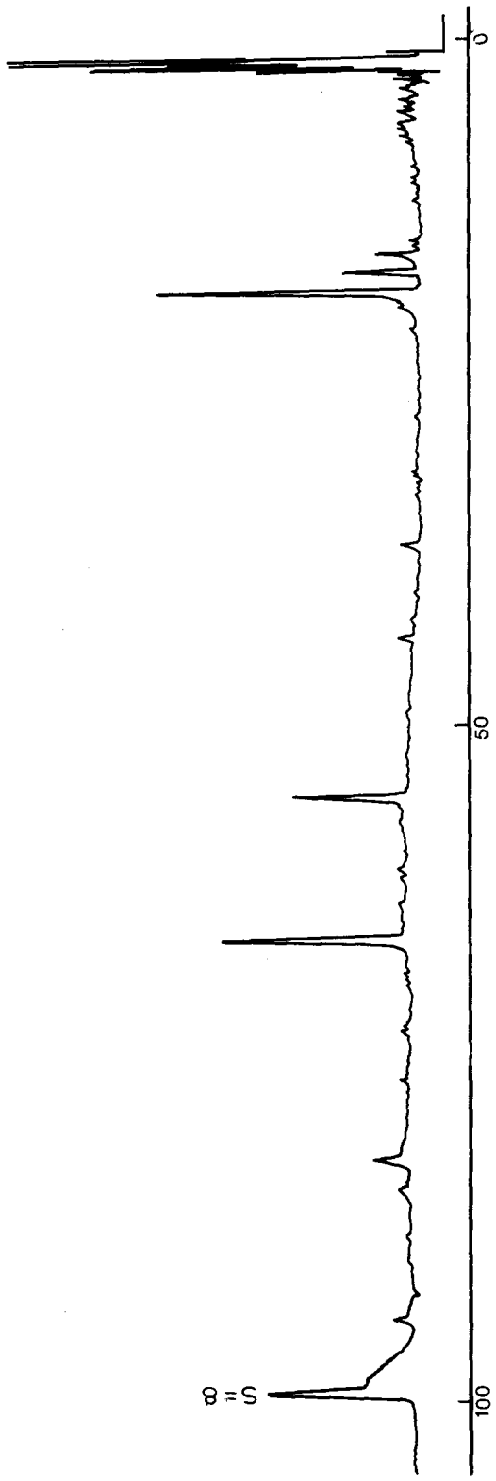


Fig. 2. Chromatogram of river water. Sensitivity (S) = 2 except where otherwise stated.

the addition of phenols presumably causes a displacement of water molecules from the co-ordination sphere of the metal ion. This idea can be formulated in terms of the following equilibria for the reaction in water:[26]

$$ROH + [Fe(H_2O)_6]^{3+} \rightleftharpoons H_2O + [Fe(H_2O)_5(ROH)]^{3+}$$

$$[Fe(H_2O)_5(ROH)]^{3+} + H_2O \rightleftharpoons H_3O^+ + [Fe(H_2O)_5(RO)]^{2+}$$

where the iron forms a 1:1 complex with the monohydric phenol ROH.[27]

The pH effect varies from compound to compound but the recovery is best at pH < 3. If a litre of the basic solution (pH 12), is divided into two equal portions and these are passed in succession through the same chromatographic column, the behaviour observed is interesting. The column retains 60–70% of the phenols present in the first 500 ml of solution, but a very much lower proportion of these in the second. Moreover, because the concentration of phenols IV, V, VI and VII in the effluent from passage of the second portion of solution is greater than that in the influent, we can assume that these phenols, retained by the column during the passage of the first 500 ml, are partially eluted when the second portion passes through. When the experiment is repeated with an acid solution, in the first portion only phenol is present in the effluent, whereas small quantities of compounds I, II and IV appear in the second fraction. This difference in behaviour may be ascribed to the presence of hydroxide ions but not to the volume of water passed through (as it would in the case of frontal chromatography). The difference in recovery at different pH values can be attributed to competition between the hydroxide ions, present in large excess, and the phenols; some water molecules co-ordinated to the ferric ions in the resin phase would be displaced by hydroxide ions from the aqueous solution. This is demonstrated by the fact that when a basic solution (pH 9) is passed through the chromatographic column in the iron(III) form the pH of the effluent rapidly falls to 4.5, and is restored to that of the influent only when a large quantity of water has been passed through.

When an aqueous solution of the phenols is passed through the column (metal form, saturated with hydroxide ions), the results listed in Table 3 are obtained and the pH of the effluent is moderately basic. There is evidently a partial displacement of the hydroxide ions co-ordinated to the metal ion and the organic ligand is itself co-ordinatively bound to the exchanger. In this case the low recovery of the phenols from water is probably due to the different co-ordinating power between iron(III) and phenol and between iron(III) and hydroxide ion. Therefore we have used the hydroxide affinity for recovery of the phenolic compounds from the iron(III)–Chelex resin. When 100 ml of 1*M* sodium hydroxide are passed through the column the phenols retained are totally displaced (except for pentachlorophenol, for which recovery is very low). Elution with 300 ml of ethanolic sodium hydroxide removes all the phenols. To check the efficiency of the method, 0.1 ppm of each phenol was added to a river-water sample, which was then adjusted to pH 3 with hydrochloric acid, passed through the column and eluted with ethanolic alkali, and the recoveries were determined.

The recoveries were 78% for 2-chlorophenol and 2-nitrophenol, 70% for the 2,4-dimethylphenol and 100% for the others. Figure 1 shows the chromatograms obtained. The relatively low recovery of compounds I, II and IV from river water is due to the interference of other substances present (Fig. 2); the COD, BOD and MBAS (Methylene Blue anionic surfactant) values were 190, 30 and 0.15 mg/l. Since compounds I, II and IV are not strongly retained on the iron(III)–Chelex resin (Table 2), the presence of more easily retained substances in the water sample can diminish the quantity of compounds I, II and IV retained. It is possible to overcome this drawback by increasing the length of the column or using two columns in series: 100% recovery was obtained with a column packed with 14 g of resin (length 15 cm). Moreover, as can be seen from Fig. 1, in the chromatogram of river water with added standards, the peaks for 2,4-dinitrophenol and phenol were absent, suggesting that these compounds had reacted with substances present in the river water, in agreement with their reactivity. This view is supported by the fact that these compounds were not lost to the analysis in similar tests when the solution was made with distilled water.

It should be remarked that in a chromatogram of the eluate (ethanolic alkali) there was no trace of the peaks of some compounds that were originally present in the river water but not in the effluent after passage through the chromatographic column; they were presumably retained on the column by a sorption process.

Conclusion

Phenolic compounds may be recovered from water by use of a chelating resin in the iron(III) form, but the sample solutions must be acidified to avoid competition between hydroxide ions and phenols for co-ordination to the iron(III).

The chelating resin in the metal form is superior to the solid sorbents generally employed, on account of its affinity for ligands. Since the co-ordinating power differs for the various iron–phenol complexes, it is possible to separate the phenols by using a solution containing a competing ligand, such as hydroxide ion, at different concentrations, but this requires further investigation.

REFERENCES

1. *Sampling and Analysis Procedures for Screening of Industrial Effluents for Priority Pollutants*, U.S. Environmental Protection Agency, Environmental Moni-

toring and Support Laboratory, Cincinnati, Ohio, 1977.
2. H. Kunte and J. Slemrova, *Z. Wasser Abwasser Forsch.*, 1975, **8**, 176; *Chem. Abstr.*, 1976, **85**, 112577.
3. S. Goren-Strul, H. F. W. Kleijn and A. E. Mostaert, *Anal. Chim. Acta*, 1966, **34**, 322.
4. J. R. Plimmer, *Environ. Health Persp.*, 1973, **3**, 41.
5. D. R. Buhler, M. E. Rasmussen and H. S. Nakaue, *Environ. Sci. Technol.*, 1973, **7**, 929.
6. M. Deinzer, F. Schaumburg and E. Klein, *Environ. Health Persp.*, 1978, **24**, 209.
7. *Water Quality Criteria Blue Book 1972*, Environmental Studies Board, National Academy of Science and Engineering, Washington, D.C., 1974.
8. R. L. Whitlock, S. Siggia and J. E. Smola, *Anal. Chem.*, 1972, **44**, 532.
9. *Standard Methods for Examination of Water and Waste Water*, 13th Ed., American Public Health Association, New York, 1971.
10. R. J. Martin and K. S. Al-Bahrani, *Water Res.*, 1977, **11**, 991.
11. C. D. Chriswell, R. C. Chang and J. S. Fritz, *Anal. Chem.*, 1975, **47**, 1325.
12. J. Zerbe, *Chem. Anal. (Warsaw)*, 1979, **24**, 85; *Anal. Abstr.*, 1979, 4H43.
13. P. van Rossum and R. G. Webb, *J. Chromatog.*, 1978, **150**, 381.
14. W. H. Glaze, J. E. Henderson, J. E. Bell and V. A. Wheeler, *J. Chromatog. Sci.*, 1973, **11**, 580.
15. S. F. Stephan and J. F. Smith, *Water Res.*, 1977, **11**, 339.
16. Z. Vozňáková and M. Popl, *J. Chromatog. Sci.*, 1979, **17**, 682.
17. E. Břízová, M. Popl and J. Čoupek, *J. Chromatog.*, 1977, **139**, 15.
18. R. T. Coutts, E. E. Hargesheimer and F. M. Pasutto, *ibid.*, 1979, **179**, 291.
19. J. P. Miure and M. W. Dietrich, *J. Chromatog. Sci.*, 1973, **11**, 559.
20. F. Helfferich, *Nature*, 1961, **189**, 1001.
21. P. V. Webster, J. N. Wilson and M. C. Franks, *Anal. Chim. Acta*, 1967, **38**, 193.
22. K. Fujimura, M. Matsubara and W. Funasaka *J. Chromatog.*, 1971, **59**, 383.
23. W. Funasaka, T. Hanai, K. Fujimura and T. Ando, *ibid.*, 1973, **78**, 424.
24. K. Fujimura, T. Koyama, T. Tanigawa and W. Funasaka, *ibid.*, 1973, **85**, 101.
25. H. Loewenschuss and G. Schmuckler, *Talanta*, 1964, **11**, 1399.
26. S. Soloway and S. H. Wilen, *Anal. Chem.*, 1952, **24**, 979.
27. H. Broumand and J. H. Smith, *J. Am. Chem. Soc.*, 1952, **74**, 1013.

Talanta, Vol. 28, pp. 221 to 224, 1981
Printed in Great Britain. All rights reserved

0039-9140/81/040221-04$02.00/0
Copyright © 1981 Pergamon Press Ltd

DETERMINATION OF SULPHATE CONTENT OF ANIONIC SURFACTANTS: SODIUM DI-2-ETHYLHEXYL SULPHOSUCCINATE

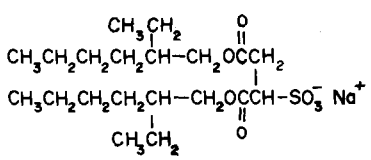
S. M. F. TAVERNIER* and R. GIJBELS

Department of Chemistry, University of Antwerp (U.I.A.), Universiteitsplein 1, B-2610 Wilrijk, Belgium

(*Received* 9 *October* 1980. *Accepted* 30 *October* 1980)

Summary—A simple nephelometric method for the determination of sulphates in the anionic surfactant Aerosol-OT is described. The method is based on the formation and stabilization of a barium sulphate dispersion in a water–alcohol mixture and measurement of the turbidity at 650 nm. Beer's law is followed for sodium sulphate concentrations in Aerosol-OT ranging from 0 to 7000 μg/g. The lower determination limit is about 100–200 μg/g and the reproducibility about 5% for typical commercial Aerosol-OT samples. The method can also be used for other anionic surfactants by adjusting the water–ethanol ratio of the solvent.

Sodium di-2-ethylhexyl sulphosuccinate (Aerosol-OT) is an important anionic surfactant used for practical purposes in non-aqueous as well as aqueous solutions. The structural formula of Aerosol-OT is shown below. The considerable solubilizing power of this surfactant for water and for aqueous salt solutions in non-aqueous solvents has been the subject of numerous studies (*e.g.*, References 1 and 2). Recently it has been shown that the differences in solubilizing behaviour of Aerosol-OT reported by various authors are due to the presence of different amounts of inorganic impurities.[1] Addition or removal of small quantities of inorganic salts can dramatically affect the solubilizing power, with attendant repercussions for practical applications.



Inorganic contaminants are introduced during the synthesis of the surfactant.[3] Di-2-ethylhexyl fumarate is treated with a slight excess of sodium hydrogen sulphite, which usually contains sodium sulphate as impurity. After the reaction mixture has been dried the inorganic salts are removed by dissolving the crude product in benzene, and filtering off the precipitate. The rather strong solubilizing power of Aerosol-OT, however, hinders complete elimination of all inorganic salts, in this case, sodium sulphate and sodium sulphite. In order to predict the solubilizing properties of the surfactant a determination of both impurities is necessary. Whereas the sulphite content can be obtained by using standard procedures, no direct method exists for sulphate determination in anionic surfactants. From the solubilizing behaviour of commercially available Aerosol-OT, Kunieda *et al.*[1] estimated that it contains approximately 0.6% w/w sodium sulphate.

The standard methods for sulphate determination fail in the presence of large amounts of Aerosol-OT. Gravimetric determination is not possible, owing to the low solubility of Aerosol-OT in water, and its tendency to flocculate in the presence of added electrolyte, as a result of which the barium sulphate precipitate is contaminated by flocculated surfactant when excess of barium chloride is added. Similarly, nephelometric determination by means of a barium sulphate dispersion in water is not feasible. Mineralization of Aerosol-OT offers no solution, since the matrix will itself yield large amounts of sodium sulphate.

The solubility of Aerosol-OT can be increased by using an alcohol–water mixture as the solvent; the composition of this mixture should be such that Aerosol-OT is not flocculated in the presence of added electrolyte, and that all the barium chloride added is still soluble.

Since it is tedious to remove all the adsorbed surfactant, the gravimetric method is not attractive, and a nephelometric determination is preferable. As will be shown later, the presence of appreciable amounts of sodium sulphite may increase the turbidity, since barium sulphite has itself a limited solubility in the alcohol–water mixture. Hence, even if the sulphite content of the Aerosol-OT is not of immediate interest it should be determined in order to assess its effect on the sulphate determination.

The method proposed can also be used for other anionic surfactants. It may, however, be necessary to adjust the alcohol–water ratio, as other surfactants show other flocculation tendencies.

* Aspirant of the Belgian "Nationaal Fonds voor Wetenschappelijk Onderzoek".

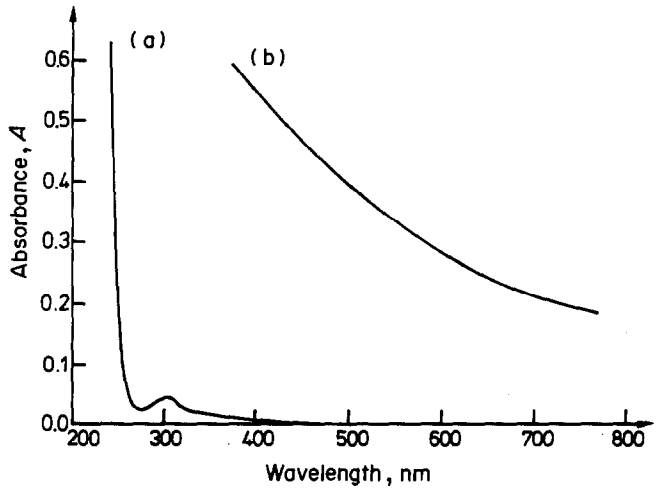


Fig. 1. Absorbance of a blank (a) and a sample (b) as a function of wavelength: measured with a double-beam spectrophotometer against a reference solution consisting of 20 ml of EtOH, 9 ml of H_2O, 2 ml of 2.5% $BaCl_2$ solution, 1 ml of 4*M* HCl.

EXPERIMENTAL

Reagents

All chemicals used were of analytical-reagent grade, except for Na_2SO_3 (Merck–reinst), and Aerosol-OT (Fluka–purum).

Aqueous sodium sulphate solution, sulphate concentration ~500 μg/ml. Prepared from the anhydrous salt and standardized gravimetrically.[4]

*Aqueous sodium sulphite solution, ~15 m*M. This solution should be freshly prepared. The following procedure is used to remove traces of sulphate present. Dissolve about 300 mg of anhydrous sodium sulphite in 200 ml of doubly distilled water. Add 1 ml of 2.5% barium chloride solution and 1.5 ml of concentrated hydrochloric acid. Filter through a paper or crucible with suitable pore size. To a test portion of the filtrate add barium chloride solution. If a precipitate is formed, repeat the procedure. Neutralize the final solution to pH 7 with sodium hydroxide solution and store it in a stoppered flask. Standardize by adding iodine and acetic acid, and back-titrating with sodium thiosulphate solution, using starch as indicator.[5]

*Aqueous barium chloride solution, 0.1*M. Filtered before use.

Aqueous sodium chloride solution, 0.75%.

*Aqueous sodium thiosulphate solution, 0.1*M. Standardized in the usual way.

Wij's solution: Iodine (0.2*N*) prepared as in Ref. (6).

Azeotropic ethanol–water mixture. Obtained by distillation, b.p. 78.5°, it is referred to as ethanol in the text.

Stabilizing solution. Prepared from Aerosol-OT after removal of inorganic salts by precipitation in alcoholic medium: dissolve 25 g of Aerosol-OT in 500 ml of ethanol, cool to −40°, and after 24 hr filter off the precipitate on a fine filter. This solution has to be freshly prepared, and is best stored at low temperature (below 0°).

Hydrochloric acid, 4M.

Procedure for sulphate determination

Take 18 ml of ethanol in an Erlenmeyer flask, add 1 g of the Aerosol-OT sample and dilute to 20 ml with ethanol. Add 1 ml of 4*M* hydrochloric acid with stirring, then 9 ml of doubly distilled water and mix thoroughly. Add 2 ml of barium chloride solution while stirring gently, let stand for 15 min, then measure the absorbance at 650 nm against a blank, identical to the sample but containing an additional 2 ml of doubly distilled water instead of the barium chloride solution. Before the measurement shake the solution gently to homogenize it. Take care to avoid the formation of air bubbles.

Prepare a calibration graph by taking 20-ml portions of the stabilizing solution and proceed as described above, but instead of the 9 ml of water, add increasing amounts of the standard sulphate solution together with the necessary amounts of water to give a total added volume of 9 ml.

Procedure for sulphite determination

A slight variation of an existing procedure is used.[7] Dissolve 10 g of Aerosol-OT in 50 ml of carbon tetrachloride and add 10 ml of Wij's solution. Prepare a blank by adding exactly the same amount of Wij's solution to 50 ml of carbon tetrachloride. Let both solutions stand for 30 min. Back-titrate the excess of iodine with the 0.1*M* sodium thiosulphate, using starch solution as indicator, with vigorous stirring.

RESULTS AND DISCUSSION

Sulphate determination in Aerosol-OT

The absorbance of the blank and of a test-mixture measured against the same reference solution is shown in Fig. 1, as a function of the wavelength. As seen from Fig. 1 the sensitivity decreases with increasing wavelength. The absorbance is very stable when 1 g of Aerosol-OT is present, as this stabilizes the precipitate and identical readings are obtained even after 12 hr. Smaller amounts of Aerosol-OT result in less stability. For commercial samples, 1 g of Aerosol-OT corresponds to rather large amounts of sodium sulphate. For that reason it is more convenient to use a lower sensitivity (*i.e.*, to measure at longer wavelength) in order for Beer's law to be obeyed within the concentration range of interest for commercial Aerosol-OT. At 650 nm Beer's law is followed over the sodium sulphate concentration range 0–6580 μg/g in Aerosol-OT. The correlation coefficient (*r*) was found to be 0.9974 for ten samples (*N*) within the concentration range mentioned and the relation of the

Table 1. Composition of samples used to check the possible flocculation of Aerosol-OT on addition of electrolytes (SS = stabilizing solution; AOT = Aerosol-OT sample 1)

SS 20 ml—HCl (4*M*) 1 ml—H_2O 9 ml—$BaCl_2$ (2.5%) 2 ml
SS 20 ml—HCl (4*M*) 1 ml—H_2O 9 ml—H_2O 2 ml
SS 20 ml—HCl (4*M*) 1 ml—H_2O 9 ml—NaCl (0.75%) 2 ml
AOT 1 g *ad* EtOH 20 ml—HCl (4*M*) 1 ml—H_2O 9 ml—H_2O 2 ml
AOT 1 g *ad* EtOH 20 ml—HCl (4*M*) 1ml—H_2O 9 ml—NaCl (0.75%) 2 ml

absorbance (A) to the sodium sulphate content concentration was

$$A = 0.007_4 + 7.45_5 \times 10^{-5} \times C_{Na_2SO_4}$$

where C is in μg of sodium sulphate per g of Aerosol-OT.

The effect of a number of variables was investigated. The addition of hydrochloric acid is necessary to prevent the formation of precipitates of barium carbonate and sulphite. The amount of barium chloride added is sufficient for sodium sulphate contents up to *ca.* 3% w/w in Aerosol-OT. Addition of more barium chloride is not recommended, as it may promote the flocculation of Aerosol-OT, and it has itself a limited solubility in the ethanol–water mixture.

Small variations of temperature up to 35° do not affect the absorbance. Heating over a long period at higher temperature (*e.g.*, 79° for 30 min) reduces the absorbance (in this case by 25%).

The effect of the presence of other inorganic salts was verified by adding increasing amounts of sodium sulphite solution and sodium chloride solution instead of water (9 ml total for water and electrolyte solution). Addition of sodium chloride up to 2.5% (w/w in Aerosol-OT) did not affect the results. Sodium sulphite concentrations below 1% (w/w in Aerosol-OT) did not interfere; higher concentrations gave an increase in the turbidity. All samples investigated contained less than 0.1% of sodium sulphite.

A check was made on the possible flocculation of Aerosol-OT upon addition of barium chloride or other electrolytes. No difference in absorbance could be observed between the solutions listed in Table 1. This indicates (1) that no flocculation of Aerosol-OT occurs in the ethanol–water mixture on addition of small amounts of electrolyte; (2) that the purified Aerosol-OT (stabilizing solution) does not contain a measurable quantity of sulphate; (3) that it does not matter which of the solutions is taken as the reference blank for determining the absorbance, but the fourth solution in Table 1 is recommended as it allows correction for possible interferents in the sample being investigated.

It is recommended that all reagents and solutions are filtered before use, to avoid the presence of interfering dust particles.

Precision of sulphate determination

The precision was estimated by preparing six sets of solutions, each set containing seven identical samples. The first two sets contained a known added amount of sodium sulphate. The next two sets were prepared from a commercially available Aerosol-OT sample (sample no. 1), and the last two from another commercial Aerosol-OT (sample no. 2). The absorbance was measured three times in each determination. The results are given in Table 2. Inspection of this table reveals that sulphate can be determined with fair precision (*ca.* 5%) in typical commercial Aerosol-OT samples. The error is of the same order of magnitude. The sixth set was also investigated with standard addition of known amounts of sodium sulphate to sample no. 2. The measured absorbance *vs.* added concentration (in μg of sodium sulphate per g of Aerosol-OT) yielded a straight line ($r = 0.9938$, $N = 4$, $A = 0.238_2 + 7.71 \times 10^{-5} C_{Na_2SO_4}$). The slope corresponds fairly well with that of the calibration graph. The concentration found agrees, within experimental error, with the concentration found by the direct method.

Determination of sulphite and sulphate in commercial Aerosol-OT samples

Sodium sulphite and sulphate were determined in Aerosol-OT samples of different grades, supplied by different companies:

Sample 1: AEROSOL-OT 100%, Ets. R. De Jonghe pvba, Ghent
Sample 2: AEROSOL-OT, technical grade (same supplier)
Sample 3: COMPLIMIX 100 (purified Aerosol-OT) Cyanamid Co., Rotterdam
Sample 4: AEROSOL-OT, USP XV, Merck, Darmstadt
Sample 5: AEROSOL-OT, Fluka a.g., Buchs
Sample 6: sample 5, purified according to Eicke.[8]

The sulphite content was determined first, by the procedure described above. Calibration with known amounts of sodium sulphite yielded a straight line ($r = 0.995$, $N = 5$, ml of $Na_2S_2O_3$ solution consumed $= 0.1613 + 0.307 \times$ ml of Na_2SO_3 solution added). The theoretical slope was 0.3168. The results for determination of sulphite in different samples are given in Table 3. The errors indicated are those estimated for the burette readings. From Table 3 it is found that the sulphite content is far too low ($\ll 1\%$ w/w) to interfere with the sulphate determination.

The results for the sulphate determination are also given in Table 3. It is seen that the sulphate content of

Table 2. Determination of Na_2SO_4 in artificial mixtures and in commercial samples

Na_2SO_4 added, μg/g	Na_2SO_4 found, μg/g	Standard deviation ($N = 7$) μg/g	Relative %
4387	4200	±210	5.0
2924	3010	±120	4.0
Sample 1	3730	±140	3.7
Sample 1	3570	±190	5.3
Sample 2	3310	±170	5.1
Sample 2*	3090	—	—

* By standard-addition method.

these commercial samples is quite variable. Differences may even occur between different lots purchased from the same supplier. The estimate of the sulphate content given by Kunieda *et al.*[1] (0.6% w/w Na_2SO_4) is in fair agreement with the sulphate content found in the commercial samples investigated (*ca.* 0.3–0.5% w/w).

The average sulphite content of commercial Aerosol-OT samples is usually quite low, less than 0.1% w/w. The differences in solubilizing power described in the literature appear to be mainly due to the presence of variable amounts of sodium sulphate in the commercial Aerosol-OT samples, from less than 0.01 up to 0.5% w/w. The purification method described by Eicke[8] seems to be effective in eliminating the inorganic impurities, reducing the total salt content from *ca.* 0.50 to 0.02% w/w.

Table 3. Sodium sulphite and sodium sulphate content in six commercial samples

No.	Na_2SO_4, μg/g	Std. devn., μg/g	Na_2SO_3, μg/g	Std. devn., μg/g	$Na_2SO_4 + Na_2SO_3$, μg/g
1	3650	140	50	60*	3700
2	3200	170	90	60*	3290
3	≤100	200*	100	60*	~200
4	2200	200	740	60*	2940
5	4650	220	90	60*	4740
6	≤100	200*	100	60*	~200

* Estimated.

Acknowledgements—One of the authors (S.T.) wishes to thank the Belgian "Nationaal Fonds voor Wetenschappelijk Onderzoek" for granting a scholarship. The director of ERGOS laboratory, R. Goovaerts, is gratefully thanked for his suggestions and stimulating discussions.

REFERENCES

1. H. Kunieda and K. Shinoda, *J. Coll. Interf. Sci.*, 1979, **70**, 577.
2. A. Kitahara, *Adv. Coll. Interf. Sci.*, 1980, **12**, 109.
3. E. Müller (ed.), Houben-Weyl, *Methoden der Organischen Chemie*, Vol. IX, p. 383. Thieme Verlag, Stuttgart, 1967.
4. ASTM, *Manual on Industrial Water and Industrial Waste Water*, p. 246. ASTM, Philadelphia, 1960.
5. J. Rodier, *L'analyse chimique et physico-chimique de l'eau*, p. 167. Dunod, Paris, 1971.
6. R. Weast (ed.), *Handbook of Chemistry and Physics*, p. D-122. The Chemical Rubber Company, Cleveland, 1977.
7. G. Eeckhout, *Analytische Chemie*, p. 273. Snoeck-Ducaju, Ghent, 1947.
8. H. F. Eicke, *J. Coll. Interf. Sci.*, 1979, **68**, 440.

Talanta, Vol. 28, pp. 225 to 231, 1981
Printed in Great Britain. All rights reserved

0039-9140/81/040225-07$02.00/0
Copyright © 1981 Pergamon Press Ltd

APPLICATION OF AN INTENSIFIED DIODE ARRAY SYSTEM TO DIAGNOSIS OF MATRIX EFFECTS AND THE RAPID SEQUENTIAL DETERMINATION OF THIAMINE AND RIBOFLAVIN WITH FLUORESCENCE DETECTION

MARY ANDRIEU RYAN* and J. D. INGLE, JR.†
Department of Chemistry, Oregon State University, Corvallis, Oregon 97331, U.S.A.

(*Received* 11 *September* 1980. *Accepted* 24 *October* 1980)

Summary—The unique capabilities of a multiple wavelength spectrofluorometer based on an intensified diode array detector are used for diagnosis of matrix effects and for rapid sequential determination of two analytes. This system is used to investigate problems due to background fluorescence, blank reactions, and scattering for the determination of thiamine in cereal and urine samples by a fluorometric kinetic procedure. A novel determination of thiamine and riboflavin in vitamin pills is based on monitoring the native fluorescence of riboflavin over one wavelength region, and the rate of formation of fluorescent thiochrome from thiamine over another wavelength region, after a computer-controlled change in the pH of the reaction mixture.

Recent improvements in rapid-scanning multichannel detectors have allowed their application to even low light-level fluorescence measurements. The increased sensitivity has been obtained through the use of a microchannel plate electron-multiplier in the intensified diode array (IDA)[1] and through one or more intensification stages in the silicon-intensified target (SIT) or intensified SIT vidicon (ISIT).[2] The application of these detectors to fluorescence measurements has been reviewed.[3,4]

The applications of the IDA to measurement of steady-state fluorescence signals with a commercial system[5] and with the system used in this paper,[6] or a prototype,[7] have been reported. Sub-μg/l. detection limits for quinine sulphate are easily obtained. Shot-noise in blank signals rather than noise in the dark signal is the limiting noise-source for low-background fluorescence samples.[6,7] Kinetic fluorescence measurements have also been made with these detectors.[5-8] The IDA system has been used in the reaction-rate method for thiamine. In this reaction thiamine is slowly oxidized by Hg(II) at pH 12 to fluorescent thiochrome. The rate of increase in fluorescence due to the formation of thiochrome is directly proportional to the thiamine concentration from the detection limit of $2 \times 10^{-8} M$ to $1 \times 10^{-4} M$ when a photomultiplier tube (PMT) detector and a 16-sec measurement period are used.[9] With the IDA, the detection limits were about double those obtained with the PMT. The new larger aperture diode array should provide even better results.[10]

Despite the fact that these detectors have been shown to have sufficient speed and sensitivity for kinetic fluorescence measurements, the applicability and power of these detectors in analysis have not been fully exploited. This paper presents some unique applications of the IDA detector made possible by the hardware–software system developed in our laboratory. The IDA system is shown to be very useful in the examination of unfamiliar matrices before application of the kinetic method for thiamine. The multichannel capabilities of the IDA system provide information inaccessible with a conventional scanning monochromator; for example, spectra from urine samples having rapidly changing fluorescence. The ability to obtain, store, manipulate and display numerous spectra rapidly is very convenient in the examination of extracts from cereal samples. Observing more than one wavelength simultaneously provides the information on several species that is needed for detecting matrix effects or for simultaneous determinations. The capabilities of the IDA system have been used for a unique determination of thiamine and riboflavin. Both analytes may be determined in rapid succession in the same run under the optimum conditions for each. This compares favourably with previous adaptations of the standard methods for the determination of both vitamins in the same sample, which either involved compromise conditions[11] or determined the vitamins in separate runs after the same sample preparation.[12]

EXPERIMENTAL

The components of the IDA system are described in detail elsewhere but, in brief, are composed of the IDA detector (Tracor Northern TN-1223-2I) and in-house timing, signal-processing, digitization and logic circuitry for

* Present address: Tektronix, Inc., P.O. Box 500, Beaverton, OR 97077, U.S.A.
† To whom correspondence and requests for reprints should be addressed.

the computer interface with the PDP 11/20 minicomputer.[6] Data were output on a Tektronix T-4002 graphics terminal, a Tektronix 4601 hard-copy unit, and a teletype. Software was developed which controlled the timing of the experiments, acquired, displayed and manipulated spectra, performed calculations and output data. Interactive BASIC and assembly language routines were used. Flow-charts and program listings are too lengthy to be represented here but have been discussed in detail elsewhere[6] and may be obtained from the authors. The IDA detector and its *f*/3 polychromator were substituted for the PMT and emission monochromator on the spectrofluorometer as previously described.[5]

The spectrofluorometer[13] uses a standard 1-cm fluorescence sample cell and has provision for injection of the last reagent to initiate the reaction with a TTL logic-controlled precision liquid dispenser. For the rapid sequential determination of thiamine and riboflavin to be described, a special version of the IDA system software was developed and connections were made between the computer and the automatic precision liquid dispenser to dispense 0.5 ml of pH-12 0.4*M* dipotassium hydrogen phosphate buffer at the appropriate point in the analysis. An excitation wavelength of 366 nm, an excitation monochromator spectral bandpass of 17 nm, and an IDA intensifier setting of 4 were used for all measurements unless stated otherwise. The detection limit is defined as the concentration yielding an analytical signal or rate equal to twice the standard deviation of the blank signal or rate, respectively.

The cereal samples were prepared by a method similar to the standard procedure[14] for thiamine determination. Briefly, 1.4 g of dry (but not dried) crushed cereal sample in a 50-ml Erlenmeyer flask is heated with 15 ml of 0.1*M* hydrochloric acid at below boiling point on a hot-plate for 30 min. The cooled mixture is centrifuged for 10 min at about 120 rpm. The supernatant liquid is saved and the solid recentrifuged with 5 ml of 0.1*M* hydrochloric acid. The supernatant liquids are combined and made up to 25 ml with 0.1*M* hydrochloric acid. Before analysis this solution is filtered through a 1.2-μm Millipore filter and diluted by a factor of 20 with 0.01*M* hydrochloric acid.

The urine samples were collected in black Teflon bottles and frozen. At the time of analysis, the thawed samples were filtered through a 1.2-μm Millipore filter to remove any precipitate. Dilutions were made with 0.01*M* hydrochloric acid.

The multivitamin–mineral tablets were prepared for analysis by a method similar to the standard method[14] for riboflavin. Thiamine is extracted at the same time. The ground tablet and 150 ml of 0.1*M* hydrochloric acid in a 250-ml Erlenmeyer flask are heated for 30 min, at below the boiling point, on a hot-plate. The cooled solution is filtered through Whatman No. 1 paper and diluted to 500 ml with 0.1*M* hydrochloric acid. The resulting solution is then filtered through a 0.45-μm Millipore filter and further diluted by a factor of 100 with 0.01*M* hydrochloric acid.

The kinetic method for determination of thiamine and its application to the analysis of vitamin pills are described in detail elsewhere[9] and the same kinetic method is applied to cereal and urine samples in this paper. The reaction mixture consists of 1 ml of sample solution, 1 ml of $2.5 \times 10^{-3}M$ Hg(II), and 1 ml of pH-12.2 0.2*M* phosphate buffer which is injected to initiate the reaction. The blank for thiamine determination is the same except that 1 ml of 0.01*M* hydrochloric acid is substituted for the mercury solution since thiochrome will not form in the absence of Hg(II). The blank measurement is not needed for kinetic determination of thiamine in vitamin pills or cereal as there is no blank rate, but is used to determine the standard deviations of the blank for calculation of detection limits.

For the sequential analysis of thiamine and riboflavin in vitamin pills, the same basic kinetic procedure for thiamine is used except that the reaction mixture consists of 0.5 ml of sample solution, 1 ml of $2.5 \times 10^{-3}M$ Hg(II), 1 ml of 0.01*M* hydrochloric acid, and 0.5 ml of pH-12.2 0.4*M* phosphate buffer. The blank for the thiamine determination involves substitution of 1 ml of 0.01*M* hydrochloric acid for the mercury solution. For riboflavin determinations, the reaction mixture is the same as above for thiamine, except that measurements are made before addition of the phosphate buffer. The blank for the riboflavin analysis is the same as the blank for the standard method.[14] First, 20 mg of sodium dithionite are added with mixing to 2 ml of sample solution. Then 0.5 ml of this solution and 2 ml of 0.01*M* hydrochloric acid are added to the sample cell and the fluorescence is measured as soon as possible, because the solution eventually becomes cloudy. The dithionite reduces riboflavin to a non-fluorescent product. This provides an internal blank, for which it is assumed that the only fluorescent species affected is riboflavin. The Hg(II) solution is not added to the riboflavin blank because is is reduced to mercury by dithionite.

For comparison purposes, riboflavin was determined separately by the standard AOAC method.[14] The method used for the comparison is identical to the procedure outlined above except that 1.0 ml of 0.01*M* hydrochloric acid is substituted for the mercury solution required for the thiochrome reaction.

Standard additions were used for all final determinations. For the determination of thiamine in cereal and urine, a standard thiamine solution was added before final dilution. In the simultaneous determination of thiamine and riboflavin in vitamin pills, 1.0 ml of a standard thiamine or riboflavin solution was substituted for 1.0 ml of 0.01*M* hydrochloric acid in the reaction mixture.

RESULTS AND DISCUSSION

The IDA system was used to investigate urine and cereal extract sample matrices to determine the applicability of the kinetic method for thiamine to these types of samples. The IDA system allowed spectra to be obtained in a fraction of the time required with a scanning monochromator. The ability to plot multiple spectra on the graphics terminal made comparisons rapid and sure. The IDA system aided in the selection of analytical wavelengths and bandpasses by rapidly determining the extent of spectral overlap of the emission of two fluorescent compounds in a solution. The CROSSHAIR option in the program was used to obtain wavelength, channel number, and signal magnitude (*i.e.*, fluorescence intensity) of points in the spectra displayed on the graphics terminal.

Determination of thiamine in cereal

Figure 1 shows the spectra of the extract from breakfast cereal to be analysed for thiamine. It should be noted that the spectra presented here are uncorrected fluorescence spectra and are hand tracings of hard-copy output. In the process of reproduction a slight smoothing or distortion of the response of individual diodes may have occurred. However, care was taken to represent faithfully the spectral information of interest here. The greater fluorescence at approximately 520 nm in the pH-2 solution (Fig. 1, spectrum B) can be attributed to riboflavin. This was determined from studies of riboflavin standards with the

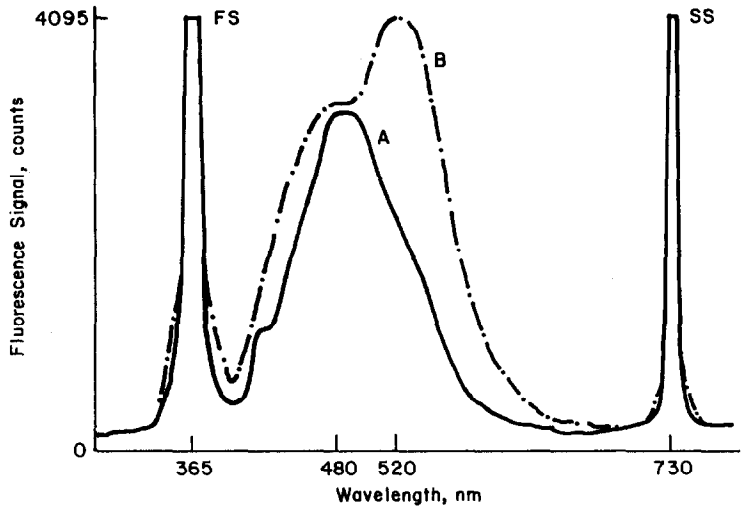


Fig. 1. Fluorescence emission spectra of cereal extract at (A) pH 12, (B) pH 2: 1-sec integration; SS is second order scatter peak, FS is first order scatter peak.

IDA. The uncorrected emission maximum for riboflavin is at 520 nm and the emission at pH 12 for riboflavin is only 20% as great as it is at pH 2 and not distinct in spectrum A. The change in fluorescence with pH at 520 nm is the same as that for riboflavin, and the cereal was specified to contain riboflavin.

The spectrum also shows significant background fluorescence at 480 nm. In the kinetic method for thiamine, thiamine is oxidized to thiochrome which fluoresces with emission at 445 nm. The background fluorescence peak is sufficiently wide to overlap strongly with the thiochrome emission and there would be little advantage in using a shorter wavelength for the thiochrome measurement. The peaks at 365 and 730 nm are the first and second order scatter peaks, respectively. These peaks are flat-topped because the diode array is saturated at these channels. The magnitude of even the second order scatter peak, labelled SS, indicates that scattering of excitation radiation may be a problem with this type of sample. From standard solutions made with doubly distilled water even the first order peak does not give saturation with a 1-sec integration time. The scattering results in an increased background signal at all wavelengths; this signal is about 2% of the second order scatter peak signal. The steady-state signal resulting from scattered light would not be measured in a kinetic method but the noise contribution would raise the detection limit and decrease the precision of the analysis. The presence of noise in the scattered light in

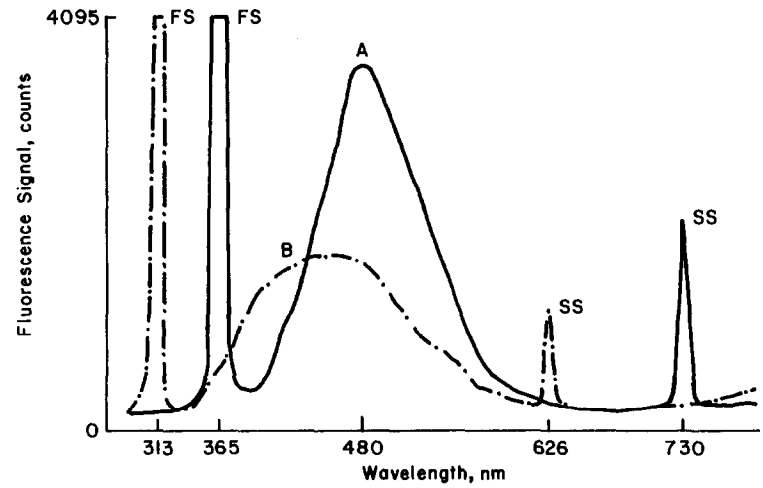


Fig. 2. Fluorescence emission spectra of cereal extract at pH 12 at two excitation wavelengths. (A) λ_{ex} = 365 nm, λ_{em} = 480 nm, (B) λ_{ex} = 313 nm, λ_{em} = 440 nm, 1-sec integration, FS is first order scatter, SS is second order scatter peak.

the analytical wavelength region and of noise in the background fluorescence sets the detection limit at about $2 \times 10^{-7}M$ thiamine in this matrix when the PMT is used.

Figure 2 shows spectra of the same extract at two different excitation wavelengths. Since the emission maximum changes with excitation wavelength, these spectra indicate, as does Fig. 1, that more than one fluorophore is present in the solution.

Thus by using the IDA to examine this matrix it can be rapidly established that there is significant background fluorescence and scattering, and that the background fluorescence is caused by riboflavin and at least one other component. Fluorescence maxima are also determined. Multiple spectra are displayed and compared on the graphics terminal without wavelength uncertainty due to mechanical positioning.

The IDA was replaced by a PMT as the detector and Kellog's "Most" breakfast cereal was analysed by the kinetic method for thiamine. The absorbance at the excitation wavelength of the cereal extract at the dilution and pH used for the determination was 0.15 and caused a 17% decrease in the expected thiochrome fluorescence signal, owing to a significant prefilter absorption effect. Other experiments confirmed that quenching (reduction in the thiochrome quantum efficiency) was insignificant and that post-filter absorption effects (absorption at the emission wavelengths) were minor. Therefore a standard addition procedure was used with both the kinetic thiamine method and the standard equilibrium-based AOAC thiochrome method for thiamine.[14] The standard method is the one previously used to test the accuracy of the kinetic method for the determination of thiamine in vitamin pills.[9]

Five samples from the same box of cereal were analysed and the kinetic method indicated a thiamine concentration of 52 μg/g of cereal, while the standard method indicated 50 μg/g, a 4% difference. The cereal box indicates the thiamine concentration should be 35 μg/g. The relative standard deviation (RSD) of the kinetic method was about 10% because of working near the detection limit in order to reduce the prefilter effect. The detection limit for thiamine in this matrix was $1.6 \times 10^{-7}M$ which is equivalent to a detection limit of 19 μg/g in the dry cereal. The detection limit for thiamine in the cereal matrix is about an order of magnitude higher than in demineralized distilled water because the background signal and noise are about 50 and 7 times larger, respectively, in the cereal extract. Although this sample contains both thiamine and riboflavin, the sequential analysis discussed below would be applicable to this type of sample if the diothionite reduced only the riboflavin, so that a proper blank measurement could be made.

Determination of thiamine in urine

Figure 3 shows spectra obtained during the spontaneous background reaction which occurs when urine which has been frozen, filtered and diluted by a factor of 5 is adjusted to pH 12. The background fluorescence is so great that an integration time as short as 50 msec is sufficient to obtain a signal approaching saturation. The difference between spectra A and C is shown in Fig. 4. The increase in fluorescence takes place at approximately 450 nm. The spectra in Figs 3 and 4 and the information they provide could not be obtained with the scanning monochromator and PMT commonly used with this fluorometer because the increase in the fluorescence at 450 nm is so rapid that the peak at 465 nm would have been distorted.

When the oxidant in the kinetic method for thiamine, Hg(II), is added to the urine sample and the pH is raised to 12.2 by the addition of the buffer, the

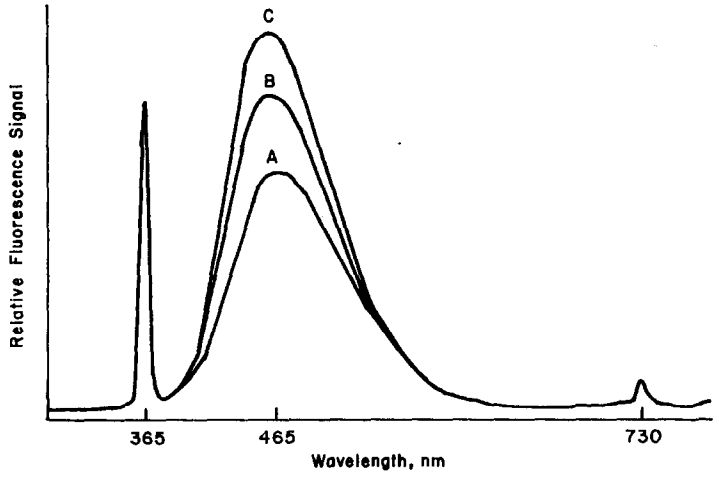


Fig. 3. Fluorescence spectra obtained during blank reaction of diluted urine sample: 0.05-sec integration, $\lambda_{em} = 465$ nm (A) $t = 0$ sec, (B) $t = 30$ sec, (C) $t = 90$ sec. The solution in the fluorometer cell contained 1 ml of diluted urine sample, 1 ml of H_2O, 1 ml of pH 12.2 phosphate buffer.

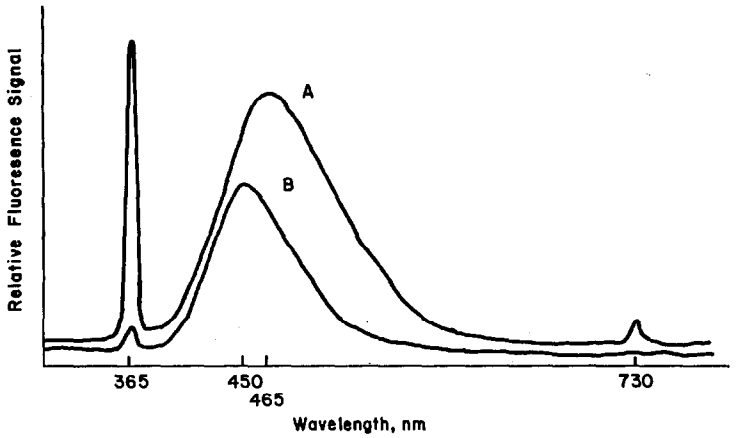


Fig. 4. Fluorescence difference spectrum from blank reaction in diluted urine sample. (A) Fluorescence at time $t = 0$ sec, $\lambda_{em} = 465$ nm, same as A in Fig. 3; (B) the difference between spectra C and A in Fig. 3, $\lambda_{em} = 450$ nm; 0.05-sec integration, pH 12.

background signal at all wavelengths increases dramatically because of scattering, and also increases with time. By use of the IDA system, it was found that the rate of the background reaction was lower when the oxidant was present. This could not easily be found with the PMT system because the increased signal due to scattering would be measured as an apparent fluorescence signal. However, the IDA system could be used to observe the increased signal due to scattering, in a spectral region where is no change in fluorescence, and to correct the total 450-nm signal for scattering.

Further studies confirmed that the kinetic thiamine method is not suitable for urine samples. The primary problem is that the increase in fluorescence due to the blank reaction and scattering is in the same spectral region and on the same time scale as the analytical reaction. The substance forming in the blank reaction has an emission maximum at 450 nm compared to 445 nm for thiochrome. Several compounds commonly found in urine, such as nicotinic acid, nicotinamide methochloride, salicylates, quinine, and atabrine, fluoresce in this general region and have been reported to interfere with the standard procedure for thiamine.[16]

A number of additional problems are presented by the urine matrix. First the blank reaction is not very reproducible, having an RSD of about 30%. Secondly, the native fluorescence of urine is relatively high in the region of thiochrome fluorescence. Urine diluted 20-fold and without Hg(II) added has a background signal about 80 times that from distilled water. In this matrix, the detection limit for thiamine with the kinetic method is about $1 \times 10^{-7} M$ which is in the range reported for thiamine in urine after a 20-fold dilution.[17] Thirdly, the oxidant is participating in the blank reaction, which means that it would not be possible to make a proper blank measurement to correct the total rate for the blank reaction. In addition, the effective oxidant concentration in the thiamine reaction is reduced owing to the interaction of Hg(II) with other species in the sample. This would cause a slower thiamine reaction rate and make a standard-additions procedure necessary.

All these problems make it obvious that separations (solvent extraction, ion-exchange)[17] are necessary before the kinetic method can produce acceptable results with these samples. However, the most time-consuming steps of the standard method[14] are the separation steps, and using these procedures in conjunction with the kinetic method would remove the most significant advantage of the kinetic method, leaving the standard method as the method of choice for this type of sample.

Rapid sequential determination of thiamine and riboflavin

The multichannel capabilities of the IDA system have also been utilized for the sequential determination of thiamine and riboflavin in vitamin pills. In this analysis the riboflavin concentration is determined from its steady-state fluorescence, as it is in the standard method,[14] and the thiamine concentration is determined with the kinetic method.[9] The steps are as follows. (1) The analyst introduces the sample or standard solution and the Hg(II) solution into the sample cell as described in the experimental section. At pH 2 the thiamine is sufficiently stable not to be oxidized by Hg(II) and the fluorescence quantum efficiency of riboflavin is much greater than at very high pH. The Hg(II) does not affect the riboflavin fluorescence signal. (2) The analyst signals the computer program to begin the analytical measurements, by depressing a key on the computer terminal. (3) The program initiates a scan and acquires a spectrum of the riboflavin in the sample over a 2-sec integration period (spectrum A in Fig. 5). (4) A signal is then sent by the computer to activate an automatic precision liquid dispenser which injects 0.5 ml of pH-12.2 buffer into the sample cell. At pH 12.2, the fluorescence of ribo-

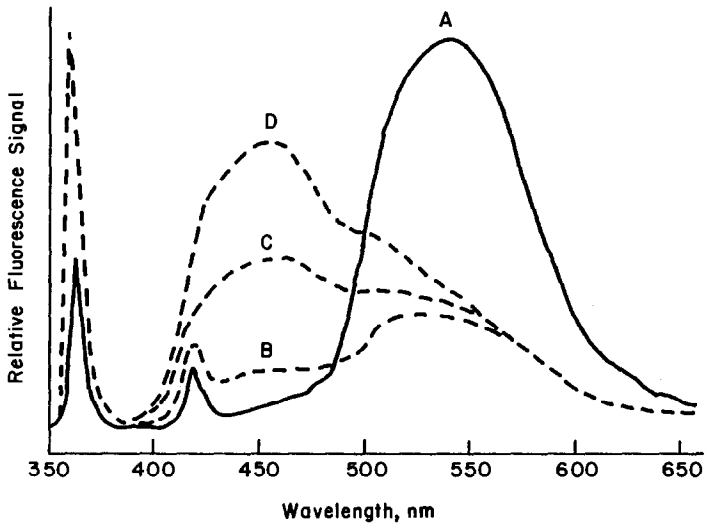


Fig. 5. Spectra obtained during simultaneous determination of thiamine and riboflavin. (A) $t = 0$ sec, riboflavin at pH 2; (B) $t = 16$ sec, thiochrome at pH 12; (C) $t = 40$ sec, thiochrome at pH 12; (D) $t = 80$ sec, thiochrome at pH 12: 2 sec total integration time (4 summed 0.5-sec integrations) for each spectrum.

flavin is only about a fifth of that at pH 2, and thiamine begins to react to form fluorescent thiochrome. (5) After a timed delay of 14 sec, which includes time for complete mixing of the sample and buffer, another spectrum is obtained with a 2-sec integration time (B in Fig. 5), which shows the decreased riboflavin fluorescence and the formation of thiochrome. (6) Subsequent spectra (C and D in Fig. 5) at controlled time intervals show the further increase in thiochrome fluorescence. (7) after the requested number of spectra have been obtained, the rate of the thiochrome reaction is calculated, *i.e.*, the difference between spectra B and C over the range 444–456 nm (sum of signals from 10 diodes centred at the peak of thiochrome fluorescence). The net riboflavin signal in the 533–545 nm region (sum of signals from 10 diodes centred at the peak of riboflavin fluorescence) is obtained by subtracting a spectrum of a blank previously stored from spectrum A.

Points which were considered in the development of this method included potential interference between the two analytes and the type of samples to which the method is applicable. For the riboflavin determination, the steady-state fluorescence of riboflavin is being measured and compounds which absorb significantly at the excitation or emission wavelengths could interfere. Thiamine does not absorb at wavelengths longer than about 310 nm and thiochrome has not yet formed when the riboflavin signal is measured. This is in contrast to an earlier simultaneous analysis for these vitamins in which compromise conditions were used. In that case the presence of thiochrome affected the signal measured for riboflavin and a special nonlinear calibration grid was required.[11]

Samples to which this analysis could be applied would have the two analytes in approximately the same concentration or thiamine in excess. Previous studies of the thiamine kinetic method[9] showed that when the riboflavin concentration is up to five times that of the thiamine the effect on the mean thiamine rate at the $1 \times 10^{-6} M$ thiamine level was less than one standard deviation of the mean rate, and the detection limit was poorer by a factor of three compared to measurements made with pure solutions of thiamine. When riboflavin is about ten times more concentrated than the thiamine, the slow decomposition of riboflavin at high pH under ultraviolet irradiation will produce a small negative rate equivalent to 3% of the rate measured for the thiochrome reaction of $1 \times 10^{-6} M$ thiamine.

Multivitamin–mineral tablets are a suitable sample for the sequential analysis because they usually contain thiamine and riboflavin at approximately the same concentration levels. The previous interference study for thiamine[9] showed that the level of potential interferents in this type of sample could be tolerated by the kinetic method. In addition the interference study showed that there were no other significant fluorophores in the solution under the reaction conditions. Vitamin A is fluorescent but it decomposes readily to a non-fluorescent compound during sample preparation.

The sequential analysis scheme was applied to three Bi-Mart multivitamin–mineral tablets. It has previously been demonstrated[9] that the kinetic thiamine procedure used in this work gives accurate results for the determination of thiamine in vitamin pills. The automated sequential procedure indicated that the vitamin pills contained 2.3 mg of thiamine, compared to the nominal value of 2.5 mg. Other studies[9] of the

thiamine part of the determination were carried out on synthetic vitamin–mineral preparations identical in composition to commercial preparations but containing known amounts of thiamine and other components. The amounts of thiamine found agreed to within 10% with the amount taken and the amount found by the standard U.S.P. thiamine method. The sequential procedure indicated that the vitamin pills contained 10.2 mg of riboflavin ($3.98 \times 10^{-7} M$ in solution) compared to 10.4 mg determined by the standard procedure. The nominal value is 10 mg. The detection limits for thiamine and riboflavin under the conditions used were $6 \times 10^{-8} M$ and $7 \times 10^{-10} M$, respectively, in this matrix.

A significant advantage of this sequential analysis is that the time needed is only about a third of that for separate determination by standard methods. Another advantage is that the riboflavin can be determined under the conditions optimum for that analyte but in the same run as the thiamine.

Acknowledgements—Acknowledgement is made to the NSF (Grant No. CHE-76-16711 and CHE-79-21293) for partial support of this research, and one of us (M. A. R.) gratefully acknowledges an NSF graduate fellowship and an American Chemical Society, Division of Analytical Chemistry Summer Fellowship sponsored by General Motors Research Laboratory. Presented in part at the 1979 Pittsburgh Conference, Cleveland, Ohio and the 1980 Pittsburgh Conference, Atlantic City, New Jersey.

REFERENCES

1. L. Perko, J. Haas and D. Osten, *Proc. Soc. Photo-Opt. Instrum. Eng*, 1977, **116**, 56.
2. Y. Talmi, *Anal. Chem.*, 1975, **47**, 700A.
3. J. D. Ingle, Jr. and M. A. Ryan, in *Modern Fluorescence Spectroscopy*, Vol. III, E. L. Wehry (ed.), Plenum Press, New York, 1981.
4. Y. Talmi, D. C. Baker and J. R. Jadamec, *Anal. Chem.*, 1978, **50**, 936A.
5. M. A. Ryan, R. J. Miller and J. D. Ingle, Jr., *ibid.*, 1978, **50**, 1772.
6. M. A. Ryan, *Ph. D. Thesis*, Oregon State University, 1980.
7. M. A. Ryan and J. D. Ingle, Jr., Paper 512 presented at the Pittsburgh Conference on Analytical Chemistry and Applied Spectroscopy, March 1979, Cleveland, OH.
8. E. Kohen, C. Kohen and J. M. Salmon, *Microchim. Acta*, 1976, **II**, 195.
9. M. A. Ryan and J. D. Ingle, Jr., *Anal. Chem.*, 1980, **52**, 2177.
10. R. W. Simpson, *Rev. Sci. Instrum.*, 1979, **50**, 730.
11. W. E. Ohnesorge and L. B. Rogers, *Anal. Chem.*, 1956, **28**, 1017.
12. J. K. Edijala, *Analyst*, 1979, **104**, 637.
13. R. L. Wilson and J. D. Ingle, Jr., *Anal. Chem.*, 1977, **49**, 1060.
14. *Official Methods of Analysis of the Association of Official Analytical Chemists*, W. Horowitz (ed), pp. 771–775. AOAC, Washington, D.C., 1970.
15. *United States Pharmacopeia*, 19th Ed., pp. 629, 911. United States Pharmacopeial Convention, Inc., Rockville, MD, 1975.
16. R. J. Henry, *Clinical Chemistry: Principles and Techniques*, p. 721. Harper and Row, New York, 1964.
17. R. L. Roser, A. H. Andrist and W. H. Harrington, *J. Chromatog.*, 1978, **146**, 43.

Talanta, Vol. 28, pp. 233 to 236, 1981
Printed in Great Britain. All rights reserved

0039-9140/81/040233-04$02.00/0
Copyright © 1981 Pergamon Press Ltd

ETUDE ELECTROCHIMIQUE DES SELS DE NITRYLE EN MILIEU APROTONIQUE

JEAN-CLAUDE FISCHER, ABDELHATEF BOUGHRIET et MICHEL WARTEL

Université des Sciences et Techniques de Lille, Laboratoire de Chimie Minérale I, BAT C8, 59655 Villeneuve d'Ascq Cedex, France

(*Reçu le* 3 *juillet* 1980. *Accepté le* 23 *octobre* 1980)

Résumé—L'étude de la réduction de sels de nitryle, sur électrode de platine poli, a été réalisée dans le sulfolane. L'ion NO_2^+ est réduit selon le schéma simple: $2NO_2^+ + 2e^- \rightleftharpoons 2NO_2 \rightleftharpoons N_2O_4$. Le transfert de charge est suivi d'une réaction rapide de dimérisation favorisée par le nombre donneur élevé du sulfolane. L'ion nitryle est beaucoup plus oxydant que l'ion nitrosyle dans le sulfolane, alors que dans le nitrométhane et l'acétonitrile ces deux oxydants sont de force voisine. Cette propriété nous a permis d'expliquer le rôle de l'eau résiduelle lors de la réduction des ions NO_2^+.

Ce travail a été entrepris afin de mieux connaître le comportement électrochimique de composés pouvant entrer dans la constitution de générateurs électriques à haute énergie.

Ainsi, après l'étude de la dissociation ionique de sels de nitrosyle (N_2O_4, NOCl) en milieu dipolaire aprotonique,[1] nous nous sommes intéressés aux dérivés oxygénés de l'azote plus oxydants: les sels de nitryle. En effet, si N_2O_4 a déjà été proposé comme dépolarisant dans une pile à semi combustible[2] il est logique de penser que l'ion NO_2^+, plus électrophile que NO^+, doit permettre de réaliser des piles plus performantes.

L'étude électrochimique des sels de nitryle a déjà été réalisée, à température proche de l'ambiante, dans les solvants non aqueux: nitrométhane[3,4] et acétonitrile.[5] Pour notre part, nous avons préféré utiliser le sulfolane comme milieu réactionnel pour les raisons suivantes:

—les sels de nitryle ont une solubilité trop faible dans le nitrométhane (la solubilité de NO_2ClO_4 est inférieure[6] à 0,08*M*);

—l'acétonitrile n'est pas suffisamment inerte[6] vis-à-vis de NO_2^+;

—le sulfolane, enfin, a été très utilisé pour l'étude du mécanisme de la nitration[6] à partir des sels de nitryle.

PARTIE EXPERIMENTALE

Le sulfolane est purifié selon la méthode déjà décrite.[7] Le perchlorate de tétraéthylammonium est séché à 60° sous pression réduite.

Le perchlorate de nitryle est préparé dans le nitrométhane par addition d'un excès de N_2O_5 à une solution de $HClO_4$, H_2O. Le solide recueilli après filtration est lavé par du tétrachlorure de carbone. Le produit obtenu contient selon les échantillons de 5 à 8% de $NOClO_4$.

N_2O_5 est préparé par déshydratation de l'acide nitrique en phase vapeur au moyen de l'anhydride phosphorique.[8] Le produit obtenu est sublimé sous un courant d'oxygène ozonisé.

Le tétrafluoroborate de nitryle est un produit Merck. Il contient aussi $NOBF_4$ que nous avons caractérisé par spectroscopie Raman.

Les courbes intensité–potentiel en régime stationnaire ont été tracées à 30 ± 0,1° à l'aide d'un ensemble voltampérométrique Tacussel. La vitesse de l'électrode indicatrice de platine (diamètre 0,8 mm) est de 10 tours/sec. La vitesse de balayage des potentiels est de 5 mV/sec.

La voltammétrie cyclique a été réalisée à l'aide de la même électrode. L'électrode de référence a déjà été décrite.[1]

Toutes les manipulations sont effectuées en boîte à gants. Le potentiel de demi-vague du système ferrocène–ferricinium est pris comme origine de l'échelle de potentiel.

Le dosage de l'eau est effectué par la méthode Karl Fischer (réactif généré par coulométrie) après avoir tracé le domaine d'électroactivité du solvant.

RÉSULTATS ET DISCUSSIONS

L'étude dans le sulfolane des courbes intensité–potentiel sur électrode de platine poli, a été réalisée à 30° en milieu perchlorate de tétraéthylammonium 0,1*M*.

La figure 1 représente le faisceau de courbes $i = f(E)$ obtenu lors de la réduction de l'ion NO_2^+. Le sel utilisé en premier lieu a été le perchlorate de nitryle. Toutes les courbes ont été enregistrées dans le sens de balayage de potentiel cathodique–anodique. Les courbes obtenues dans ces conditions sont reproductibles et bien définies.

L'eau résiduelle, dont la présence est inévitable, joue un rôle important surtout dans le cas où les espèces actives sont peu concentrées. Afin de minimiser l'effet parasite de l'eau, nous avons été amenés à n'utiliser que des échantillons de solvant contenant moins de 10^{-3} mole d'eau par litre. Néanmoins, la présence de l'eau résiduelle reste en partie responsable de l'évolution des courbes obtenues, lorsque l'on fait varier la concentration en sel de nitryle. En effet, le perchlorate de nitryle étant très facilement hydrolysable, comme l'a d'ailleurs signalé Olah, lors de ses études sur les réactions de nitration,[6] seuls les produits d'hydrolyse, les acides perchlorique et nitrique,

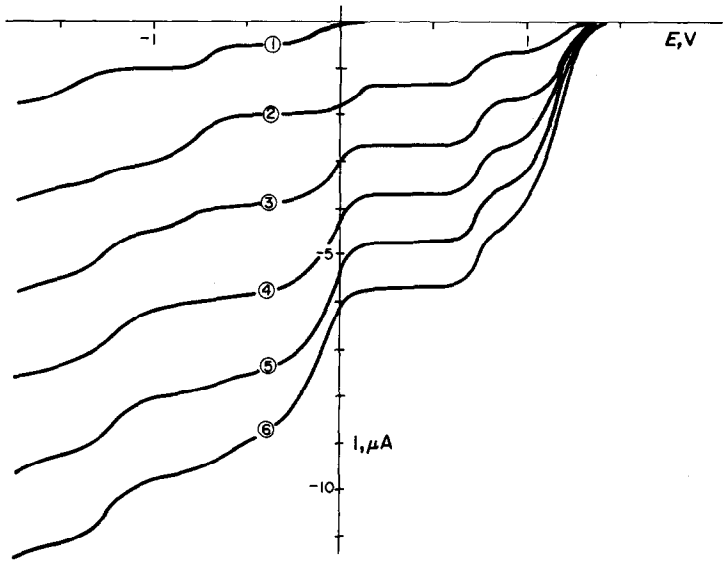


Fig. 1. Faisceau de courbes $i = f(E)$ relatives à la réduction de NO_2ClO_4 à différentes concentrations exprimées en mole/l. ① $6{,}1 \cdot 10^{-4}$; ② $2{,}12 \cdot 10^{-3}$; ③ $3{,}80 \cdot 10^{-3}$; ④ $5{,}58 \cdot 10^{-3}$; ⑤ $7{,}17 \cdot 10^{-3}$; ⑥ $8{,}75 \cdot 10^{-3}$.

apparaissent sur la courbe 1 (Fig. 1). Les vagues cathodiques obtenues lors de cet essai correspondent respectivement à la réduction des protons des acides perchlorique et nitrique. La vague dont le potentiel de demi-vague est le plus négatif est due à la réduction de l'oxygène résiduel.

Lorsque la concentration en NO_2^+ augmente (courbe 2) et devient supérieure à celle de l'eau, l'allure de la courbe est notablement modifiée. Nous observons alors cinq vagues cathodiques dont les potentiels de demi-vague ont respectivement pour valeur 1,18; 0,74; 0,05 – 0,80 et −1,23 V par rapport au potentiel de demi-vague du système ferrocène–ferricinium.

La première vague a été attribuée à la réduction:

$$2NO_2^+ + HClO_4 + 2e^- \rightleftharpoons NO^+ + ClO_4^- + HNO_3 \quad (I)$$

le transfert de charge étant suivi de la réaction chimique entre l'acide perchlorique et le produit de réduction de NO_2^+. Une étude plus détaillée de cette première vague, pour des concentrations en NO_2^+ plus élevées, est décrite plus loin.

Les vagues suivantes sont identiques à celles que l'on obtient en étudiant un mélange synthétique de $NOClO_4$, N_2O_4 et HNO_3. Si la deuxième vague peut être attribuée sans ambiguité à la réduction de NO^+ provenant de la réaction (I) mais également de l'impureté ($NOClO_4$) contenue dans l'échantillon de perchlorate de nitryle, l'interprétation des autres vagues est plus délicate. Nous pensons néanmoins que la réduction de N_2O_4 en présence d'acide nitrique que l'on peut écrire:

$$N_2O_4 + 2HNO_3 + 2e^- \rightleftharpoons 2HNO_2 + 2NO_3^- \quad (II)$$

est responsable de la troisième vague cathodique, N_2O_4 provenant de l'oxydation de NO par l'oxygène résiduel. La réaction (II) a déjà été proposée par Serve[3] lors de l'étude du mécanisme de réduction de N_2O_4 dans le nitrométhane. Les deux dernières vagues correspondent alors à la réduction des protons de l'acide nitrique en excès et de l'acide nitreux formé:

$$HNO_3 + e^- \rightleftharpoons \tfrac{1}{2}H_2 + NO_3^- \quad (III)$$

et

$$HNO_2 + e^- \rightleftharpoons \tfrac{1}{2}H_2 + NO_2^- \quad (IV)$$

Pour des concentrations plus élevées en sel de nitryle, le transfert de charge, lors de la réduction de NO_2^+, n'est plus suivi de la réaction chimique citée plus haut, l'acide perchlorique ayant été entièrement consommé par la réaction (I). Nous pensons que la réduction directe de NO_2^+ s'effectue selon:

$$2NO_2^+ + 2e^- \rightleftharpoons 2NO_2 \rightleftharpoons N_2O_4 \quad (V)$$

le dimère étant stabilisé[9] par le pouvoir donneur d'électrons relativement élevé du sulfolane.[10] Cette réduction seule est alors responsable de l'accroissement du palier de diffusion relatif à la première vague cathodique. L'augmentation de la concentration de N_2O_4, ainsi produit à l'électrode, a pour conséquence d'augmenter les hauteurs des vagues correspondant aux réactions (II) et (IV) et de diminuer celle correspondant à la réaction (III) par consommation de l'acide nitrique. Cette interprétation est confirmée par l'allure:

—de la courbe 4 où la vague attribuée à la réduction de l'acide nitrique a disparu, HNO_3 ayant été totalement consommé lors de la réduction de N_2O_4;

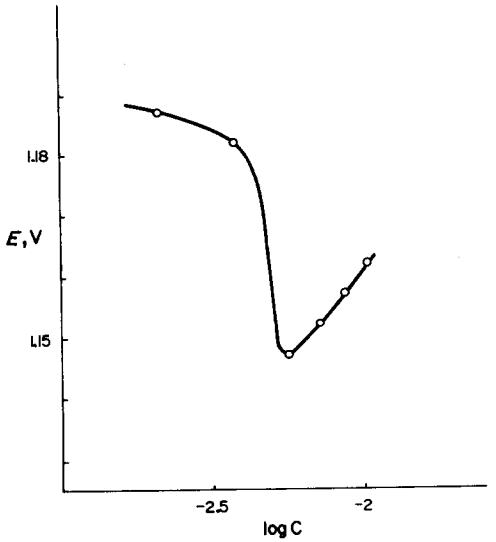


Fig. 2. Evolution du potentiel de demi-vague de réduction de NO_2^+ en fonction du logarithme de la concentration.

—des courbes 5 et 6 où la vague de réduction de l'acide nitreux n'augmente plus, la concentration de N_2O_4 étant supérieure à celle de l'acide nitrique.

Sur la courbe 6, la vague correspondant à la réduction de N_2O_4 est moins bien définie, l'équilibre

$$N_2O_4 + e^- \rightleftharpoons NO + NO_3^- \qquad (VI)$$

venant se superposer à l'equilibre (II).

La vague due à la réduction de NO^+, relativement importante aux faibles concentrations en NO_2^+ [formation de NO^+ essentiellement due à la réaction (I)] n'augmente que très faiblement par la suite, en raison de la présence de perchlorate de nitrosyle dans le perchlorate de nitryle.

Le but de ce travail étant l'étude des propriétés oxydantes des sels de nitryle, nous nous sommes plus particulièrement intéressés à la première vague cathodique. La hauteur du palier de diffusion est proportionnelle à la racine carrée de la vitesse de rotation de l'électrode, ce qui montre que le phénomène est contrôlé par la diffusion. Si l'on porte le courant limite de diffusion en fonction de la concentration en sel de nitryle ajouté, l'intersection de la droite obtenue avec l'axe des abscisses permet de retrouver la teneur en eau initiale du solvant, c'est-a-dire la concentration en acides perchlorique et nitrique formés. La teneur en eau trouvée ($8 \cdot 10^{-4}$ mole/l.) montre bien que la réaction (V) ne peut donc être observée seule, la réaction (I) intervenant quasi-simultanément. Cette hypothèse est confirmée par l'étude de l'évolution du potentiel de demi-vague en fonction de la concentration (Fig. 2). En effet, l'allure de la courbe ne peut s'expliquer que par l'intervention des deux couples oxydo-réducteurs (I) et (V), ce dernier, correspondant à la réaction électrochimique de potentiel de demi-vague plus faible, ne devenant prépondérant qu'aux fortes concentrations en NO_2^+. Le potentiel de demi-vague varie alors quasi-linéairement avec la concentration, en accord avec une dimérisation rapide de NO_2. La formation de N_2O_4 lors de la réduction des sels de nitryle nous a été également suggérée par:

—la coulométrie à potentiel contrôlé;
—l'étude de la transformée logarithmique;
—la voltammétrie cyclique.

En effet, la coulométrie á potentiel contrôlé (0,925 V) où le nombre d'électrons échangés par mole de NO_2^+ est voisin de l'unité (en tenant compte de l'hydrolyse), donne une solution incolore, donc de concentration en NO_2 négligeable. Si l'on fait abstraction de la première vague cathodique, la courbe intensité–potentiel en régime stationnaire, obtenue après électrolyse, n'est pas modifiée, ce qui laisse supposer que la dimérisation de NO_2 est rapide. De plus, si l'on étudie la transformée logarithmique

$$E = f\left[\log \frac{(i_{NO_2^+} - i)^2}{-i}\right]$$

de la première vague cathodique de la courbe 6 de la figure 1, on obtient une droite, alors qu'aucune relation linéaire n'est obtenue si l'on suppose une cinétique de dimérisation très lente.[11] Remarquons toutefois que la pente de la droite (voisine de 100 mV/unité de log) obtenue dans le premier cas est très supérieure à la valeur théorique (30 mV/unité de log), c'est á dire que le transfert électronique n'est pas rapide, mais pas non plus suffisamment lent pour être considéré comme irréversible. Ce résultat est corroboré par une étude par voltammétrie cyclique (Fig. 3). Ainsi, un balayage de potentiel effectué entre 0,94 et 1,94 V fait apparaître un pic anodique et un pic cathodique comparables à ceux que l'on obtient lors de l'étude dans les mêmes conditions d'une solution de N_2O_4. Cependant le pic cathodique observé lors de l'étude des sels de nitryle est plus important en raison de la réaction (I) irréversible. Le pic anodique n'apparaît que lorsque la concentration en NO_2^+ est supérieure à trois fois au moins la teneur en eau initiale du solvant, ce que notre schéma proposé laissait prévoir.

L'étude mathématique plus approfondie des courbes voltammétriques n'a pu être effectuée en raison de l'interférence des réactions dues aux produits d'hydrolyse.

Les courbes voltammétriques tracées à partir de solutions de tétrafluoroborate de nitryle sont similaires, le sel commercial utilisé contient également une quantité non négligeable de tétrafluoroborate de nitrosyle, ce dernier ayant été caractérisé par spectroscopie Raman.

CONCLUSION

Si l'on fait abstraction des vagues apportées soit par l'eau résiduelle, soit par NO^+, la réduction des sels de nitryle s'effectue selon le schéma simple:

$$2NO_2^+ + 2e^- \rightleftharpoons N_2O_4$$

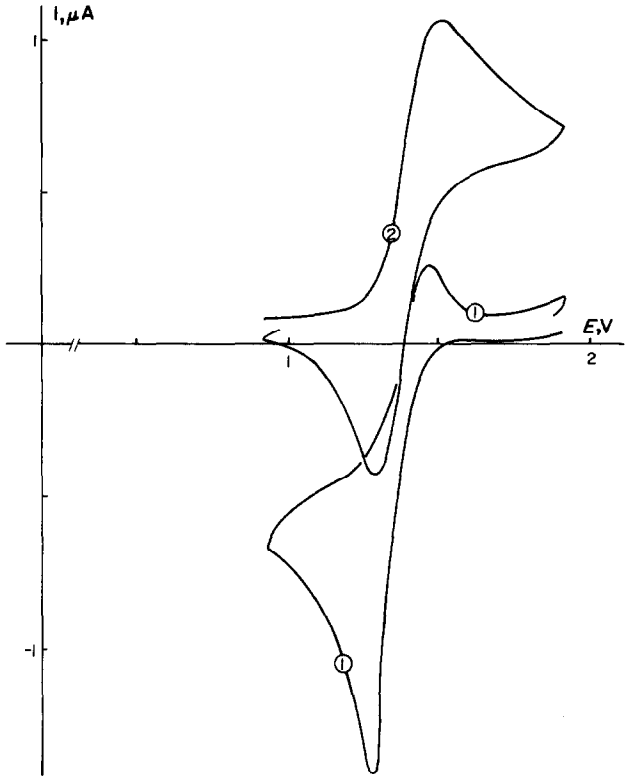


Fig. 3. Voltammétrie cyclique ① $[NO_2ClO_4] = 7{,}17 \cdot 10^{-3} M$; ② $[N_2O_4] = 5{,}76 \cdot 10^{-3} M$. La vitesse de balayage est 20 mV/sec.

puis, à un potentiel beaucoup plus faible:

$$N_2O_4 + e^- \rightleftharpoons NO + NO_3^-$$

Ce mécanisme est à rapprocher de ceux proposés dans l'acétonitrile[5] et le nitrométhane.[3,4] Cependant, le caractére oxydant de NO_2^+ vis-à-vis de NO^+ est nettement plus marqué dans le sulfolane. En effet, l'écart entre les potentiels de demi-vague relatifs aux réductions des entités NO_2^+ et NO^+ n'est que de 20 à 50 mV dans le nitrométhane et l'acétonitrile alors qu'il est supérieur à 300 mV dans notre solvant pour des concentrations voisines. Cette différenciation notable des pouvoirs oxydants des sels de nitryle et de nitrosyle, nous a permis de bien mettre en évidence le rôle joué par l'eau résiduelle. Nos résultats sont en accord avec le mécanisme E.C.E. proposé par Serve[3] quant à la réduction de NO_2^+ dans le nitrométhane, en présence d'acide perchlorique (les réactions de réduction de NO_2^+ et de NO^+ formé par action de l'acide perchlorique sur N_2O_4, n'étant pas séparées dans ce solvant).

Le sulfolane se révèle être un solvant de choix pour la mise en évidence du caractère oxydant des sels de nitryle. Nous avons d'ailleurs utilisé cette propriété pour réaliser des piles NO_2^+–métal alcalin. La force électromotrice obtenue dans le cas du lithium est de 4,8 V.

LITTERATURE

1. M. Wartel, A. Boughriet et J.-C. Fischer, *Anal. Chim. Acta*, 1979, **110**, 211.
2. C. R. Schlaikjer, *Brevet Etats-Unis d'Amérique*, No. 236532, 1972.
3. D. Serve, *Thèse*, Grenoble AO 7174, 1972.
4. G. Cauquis et D. Serve, C.R. Acad. Sc. Paris, 1968, **267C** 460.
5. G. Bontempelli, G. A. Mazzochim et F. Magno, *J. Electroanal. Chem.*, 1974, **55**, 91.
6. G. A. Olah et S. J. Kuhn, *Friedel-Crafts and Related Reactions*, Vol. III, Part 2, Interscience, New York, 1964.
7. P. Pierens, Y. Auger, J-C. Fischer et M. Wartel, *Can. J. Chem.*, 1975, **53**, 2989.
8. J. Heubel, *Compt. Rend.*, 1961, **252C**, 3268.
9. T. F. Redmond et B. B. Wayland, *J. Phys. Chem.*, 1968, **72**, 1626.
10. V. Gutmann, *Chem. Tech.*, 1977, 255.
11. R. Bonnaterre et G. Cauquis, *J. Electroanal. Chem.* 1971, **32**, 199.

Summary—The electrochemical reduction of NO_2ClO_4 solutions at a platinum electrode in sulpholane has been studied. The results suggest the following scheme for the reduction of NO_2^+: $2NO_2^+ + 2e^- \rightleftharpoons 2NO_2 \rightleftharpoons N_2O_4$. A fast dimerization of nitrogen dioxide, which is favoured by the high donor number of sulpholane, follows the charge-transfer step. The NO_2^+ ion is much more oxidative than the NO^+ ion in sulpholane, whereas the oxidizing power of the two species is nearly the same in nitromethane or acetonitrile solution. This result can be used to explain the role of water present at trace level.

Talanta, Vol. 28, pp. 237 to 240, 1981
Printed in Great Britain. All rights reserved

0039-9140/81/040237-04$02.00/0
Copyright © 1981 Pergamon Press Ltd

STABILITY CONSTANTS OF CHLORO-COMPLEXES OF CADMIUM(II) IN SEA-WATER MEDIUM

MARIA DE LURDES S. SIMOES, MARIA CÂNDIDA T. A. VAZ and J. J. R. FRAÚSTO DA SILVA
Centro de Química Estrutural, Complexo Interdisciplinar, Lisboa, Portugal

(*Received* 22 *April* 1980. *Accepted* 21 *October* 1980)

Summary—Potentiometry with ion-selective electrodes and anodic stripping voltammetry were used to measure the stability constants for cadmium chloro-complexes at 20 ± 0.1° in synthetic sea-water and at an ionic strength of 0.700 ($NaClO_4$ + NaCl). The values of β_{ML} and β_{ML_2} obtained by the two methods are in good agreement.

In a study of the interactions of very low concentrations of metal ions with the inorganic macroconstituents of the ocean and with organic pollutant ligands, the need arose for a consistent set of stability constants of various cadmium complexes. A survey of the literature[1–4] showed that the available data were inhomogeneous and incomplete, so we have determined the stability constants of the chloro-complexes of cadmium(II) in an artificial medium similar to Guincho near-shore sea-water (Cascais, Portugal).

THEORY

The stability constants were determined by potentiometry with cadmium and chloride ion-selective electrodes and by anodic-stripping voltammetry (ASV). In the potentiometric method simulated sea-water was titrated with a solution of cadmium nitrate in the same medium. The free Cd^{2+} and free Cl^- values were used for calculating the stability constants from

$$\frac{C_{Cd} - [Cd^{2+}]}{[Cd^{2+}][Cl^-]} = \beta_1 + \beta_2[Cl^-] \qquad (1)$$

where C_{Cd} is the total concentration of cadmium species and β_1 and β_2 are the overall stability constants of the complexes $CdCl^+$ and $CdCl_2$ in the medium.

In the ASV procedure, the ionic strength and cadmium concentration were kept constant and the chloride concentration varied, with C_{Cl} always $> C_{Cd}$ (otherwise, even a reversible wave becomes distorted and may split into two or more parts).[5] There is a cathodic shift in the stripping potential with increase in ligand concentration, because the rate of labile-complex formation is greater than the rate of oxidation of metal from the amalgam. This can be checked by cyclic voltammetry, by comparing the shifts of the reduction and oxidation peaks (which correspond to the deposition and stripping steps of ASV).[6]

Since the peak potential is related to the half-wave potential by the expression

$$E_p = E_{\frac{1}{4}} + \frac{1.1\,RT}{nF} \qquad (2)$$

Lingane's method[7] can be used to determine the desired stability constants in a reversible process:

$$\Delta E_{\frac{1}{4}} = (E_{\frac{1}{4}})_S - (E_{\frac{1}{4}})_C = \frac{RT}{nF} \ln \frac{D_C^{\frac{1}{4}} \beta_j C_X^j}{D_S^{\frac{1}{4}}} \qquad (3)$$

The subscripts S and C refer to the simple and complexed species respectively and β_j is the overall stability constant of the jth complex. This method can be used when only one species is formed in solution over a range of ligand concentrations, and it has been stated[8] that if the stability constants of the various complexes differ by more than a factor of 10, the plot of $\Delta E_{\frac{1}{4}}$ *vs.* log C_X is not linear, but consists of several almost linear segments which can be interpreted individually, each corresponding to a different value of j. However, the appearance of an apparently segmented curve has been attributed by others[9] to use of insufficient data or of incorrect conditions. According to the same authors,[9] when only two detectable species exist in solution (which means that their formation constants are substantially larger than all the others), the ligand number calculated from the slope of the least squares line for all the points lies between the coordination numbers of the two dominant species, and if it is close to an integer may be mistakenly assumed to indicate the presence of only one complex. When the dominant successive formation constants differ by less than a factor of 50 the ligand number calculated from the slope is not an integer within experimental error. It should, however, be noted that experimental errors may remove the curvature from this function, but do not change the slope.[9]

In both cases the DeFord and Hume method has been stated to be preferable to Lingane's.[9] In our case a small amount of curvature was found in the function $\Delta E_{\frac{1}{4}}$ *vs.* log C_X, and we treated the results by

both the Lingane equation and the DeFord and Hume method.[10]

We also used the critical apparent potential,[3,11] (E_p^*), that has the same significance as $E_{\frac{1}{4}}$ for calculations. The E_p^* values can be determined from a series of voltamperograms at different chloride concentrations, by varying the deposition potentials (E_d) and plotting i_p *vs.* E_d.[3,11] It is assumed that the amount of the species deposited will vary with E_d, so the peak currents will be αi_L, where α is a measure of the metal deposited ($\alpha < 1$) and i_L is the limiting current.

The anodic-stripping method is limited because the ligand must be present in excess, but has the advantage of greater sensitivity and lower detection limit, which allows the use of concentrations closer to those of natural waters. Since in the potentiometric methods we can better reproduce the sea-water medium, the two methods can be considered to be complementary, and it is of interest to compare the results from both.

EXPERIMENTAL

Reagents

All reagents were of analytical grade. Sodium perchlorate and chloride were dissolved in distilled and demineralized water ($K \leqslant 0.1\ \mu S$). It was found by ASV that the cadmium(II) content of these solutions was negligible.

The required amounts of the cadmium nitrate were dissolved in distilled and demineralized water and the solutions standardized by EDTA titration[12] or atomic absorption.

The simulated sea-water was $2.7 \times 10^{-2} M$ in magnesium sulphate, $1.4 \times 10^{-2} M$ in calcium chloride, $1.2 \times 10^{-2} M$ in potassium chloride, $0.43 M$ in sodium chloride, $2.1 \times 10^{-2} M$ in magnesium chloride and buffered to pH 7.9 with borate buffer ($5 \times 10^{-3} M$ boric acid/$5 \times 10^{-4} M$ sodium hydroxide).

Instruments

Potential measurements were made to 0.2 mV on a Coleman model 38A pH-meter with an Orion cadmium electrode and Phillips chloride electrode, both *vs.* a Corning saturated calomel electrode (SCE). The titrant was added from Eppendorf micropipettes to the stirred solution. The SCE was separated from the titration vessel by a bridge filled with saturated sodium nitrate solution to prevent formation of potassium perchlorate and to minimize changes in junction potential.

Voltammetric measurements were made with a Bruker model E-100 polarograph. A Metrohm E-410 hanging mercury drop electrode was used as working electrode with a Metrohm SCE as reference and a platinum wire as counter-electrode. The SCE was separated from the sample solution by the same type of bridge as in the potentiometry. The salt bridge was emptied daily and cleaned by standing overnight in Merck "suprapur" nitric acid (1 + 1). Pure nitrogen was used for deaeration after passage through a tower filled with supporting electrolyte, to saturate it with the vapour. During measurements nitrogen was passed over the surface of the solution.

In both techniques the cells were water-jacketed and kept at 20 ± 0.1°.

The instrumental settings were: d.c. mode; current 0.100 μA full scale; voltage scan 5 mV/sec; deposition potential −800 mV, changed to about −550 mV in the pseudo-polarogram method.[3] The SCE always had its filling hole exposed, so that contact with the solution was maintained and contamination of the filling solution avoided; no disturbances in ASV such as instrument overload, peak shifts, irregular behaviour or oscillation in the stripping curve[13] were then observed.

As the cell may adsorb metal ions or release them at other times, it was always kept filled with pure $6M$ nitric acid for some hours, then rinsed with water before the runs.

Procedure

For potentiometric determinations, we titrated 50 ml of simulated sea-water with $0.5M$ cadmium nitrate solution in the same medium. The emf values measured were converted into pCd and pCl values by means of calibration graphs (obtained with 5×10^{-5}–$10^{-3} M$ cadmium nitrate and 0.2–$0.6M$ sodium chloride solutions respectively, at the same ionic strength, adjusted with sodium perchlorate). The mean ionic strength calculated for all the titration points was 0.60 (±3%). The electrode potentials are given by the Nernst expressions $E = K + S\log[Cd^{2+}]$ and $E = K' - S'\log[Cl^-]$, where S and S' are the slopes and K and K' the intercepts. The slopes found were close to the theoretical values. Regular polishing of the cadmium electrode surface is necessary for proper functioning.

In the ASV determinations the pseudo-polarograms were recorded for 25-ml portions of each solution, $2.0 \times 10^{-7} M$ in cadmium, with chloride concentration varying between 7×10^{-4} and $0.700M$ and all at the same ionic strength (0.700). The solutions were deaerated with stirring (30 min), then a series of anodic-stripping experiments was performed in the solution, each at a different plating potential.[3] Plating lasted for 150 sec at E_d (between −800 and −550 mV) and stirring was stopped 15 sec before plating, after which the solution was allowed to become quiescent. During the last 4 sec of plating time the potential was switched to the rest potential (always −800 mV, where Cd is not oxidized), to define the baseline of the peak, then the anodic run was recorded.[4] From three of these voltamperograms an average value for E_p was calculated for each ligand concentration.

RESULTS AND DISCUSSION

The total cadmium concentration in unpolluted sea-water is about 10^{-9}–$10^{-10} M$ and a value of $10^{-7} M$ is typical of pronounced pollution.[14] For this reason, we chose a concentration of $2 \times 10^{-7} M$ for the ASV measurements. Lower values are still measurable, but contamination problems become more serious. For potentiometry we had to use higher cadmium concentrations because the detection limit was poorer. The temperature of 20° was chosen because it is suitable for our subsequent studies on speciation with biological models.

In both methods the system behaves as thermodynamically reversible, so the Nernst equation is followed. The results obtained by the two methods were compared to check their consistency, especially because the stability constants are so small, which may be the source of the discordant results obtained by different authors.

For the potentiometry we used a simulated sea-water similar to Guincho near-shore water and the cadmium sulphate complexes were ignored,[14] since calculations based on the literature values[2] (log $\beta_1 = 1.08$, log $\beta_2 = 2.0$ at 25° and $I = 0.5$) give an

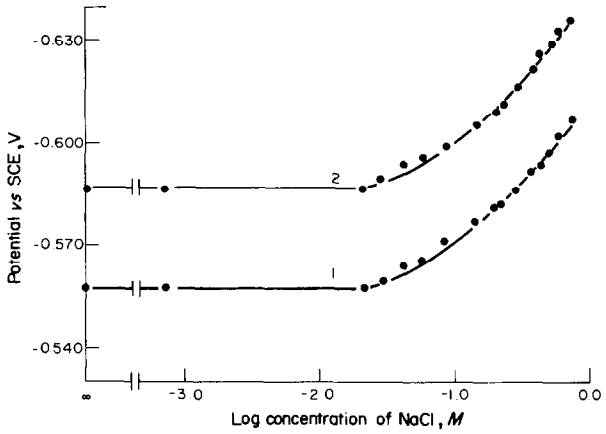


Fig. 1. Peak potential (1, E_p) and critical apparent potential (2, E_p^*) as a function of chloride ion concentration for a total cadmium concentration of $2.0 \times 10^{-7}M$ and at constant ionic strength $0.700M$ ($NaCl + NaClO_4$).

abundance of 1–2% for the first complex and 0.3–0.5% for the second.

Since the free cadmium and free chloride concentrations were determined independently in the potentiometry, the formation of calcium and magnesium chloro-complexes does not affect the calculation of the constants. Our simulated sea-water does not contain bicarbonate, but the extent of formation of cadmium–carbonate complexes is small for the same reason as for the sulphate complexes.

The potentiometric results lead to the conclusion that, for total cadmium concentrations of 4.8×10^{-2}–$9.3 \times 10^{-2}M$ (free cadmium ion concentrations of 2.3×10^{-3}–$6.5 \times 10^{-3}M$) and chloride concentrations of 0.36–0.43M, two chloro-complexes of cadmium, with $\beta_1 = 3 \pm 1$ and $\beta_2 = 100 \pm 7$ (Table 1) are formed.

These values do not agree with the literature values. Most of the latter refer to different experimental conditions, but even those reported[2] for 25° and $I = 0.5M$ are $\beta_1 = 22$ and $\beta_2 = 50$.

Branica *et al.*,[3] using a similar medium of ionic strength of 0.700 ($NaClO_4$ + NaCl), a cadmium concentration of $5 \times 10^{-9}M$ and pH 8, concluded from an ASV study that only the $CdCl^+$ complex is present, with $\beta_1 = 33$. Brown[4] used a cadmium concentration of $4.4 \times 10^{-5}M$, ionic strength of 0.10, pH 5.00 and chloride concentration 0.050–0.1M, and reported formation of $CdCl^+$ ($n = 1.1 \pm 0.1$) with log $\beta_1 = 3.2 \pm 0.2$ which is quite different from the Branica result.

As our potentiometric results did not agree with the results of these authors, the same system was also studied by ASV.

Branica *et al.*[3] showed that E_p^* is independent on the concentration of cadmium in the range 5×10^{-9}–$10^{-4}M$ in $0.700M$ sodium chloride, which means that the same set of complexes should be formed for metal concentrations within these limits. Even if there is a small amount of cadmium adsorption onto trace solid particles or the vessel, our results should not be affected. The results obtained for the functions E_p *vs.* log C_X and E_p^* *vs.* log C_X are shown in Fig. 1. As expected, the curves are similar. The least-squares straight line for the points on curve 2 has the equation $E_p^* = (-32 \pm 3)\log C_X - 638 \pm 2$, which corresponds to a mean ligand number $\bar{n} = 1.1$ and $\beta_1 = 56$.

Both curves can be interpreted as consisting of segments. For curve 2 the the first segment ($[Cl^-] = 0.2$–$0.7M$) gives the equation $E_p^* = (-50 \pm 1)\log C_X - 646 \pm 6$, which corresponds to $\bar{n} = 1.75$ and $\beta_2 = 114$. The second gives $E_p^* = (-19 \pm 5)\log C_X - 622 \pm C_X - 622 \pm C_X - 622 \pm C_X - 622 \pm C_X - 622 \pm 6$ for $[Cl^-] = 0.012 - 0.15M$, from which we can calculate $\bar{n} = 0.6$, $\beta_1 = 16$, but if the segment is extended from $[Cl^-] = 0.012M$ to $[Cl^-] = 0.1M$ the values are $E_p^* = (-27 \pm 3)\log C_X - 633 \pm 4$, $n = 0.9$, $\beta_1 = 38$.

Curve 1 gives similar expressions with slightly higher errors, because the imprecision in E_p is about ± 4 mV and in E_p^* only ± 1 mV, as a result of instrumental errors.

The least-squares treatment of all the experimental points leads to the conclusion that only the $CdCl^+$ species seems to exist, with $\beta_1 = 56$, but the segmentation treatment leads to postulation of the existence of $CdCl^+$ and $CdCl_2$, with stability constants of about 15–40 for the first and 114 for the second.

The function $\Delta E_{\frac{1}{2}}$ *vs.* log C_X is slightly curved, which may be interpreted as implying existence of two complexes with stability constants differing by more than one order of magnitude,[8] and the DeFord and Hume method is preferred.[9] If only $CdCl^+$ and $CdCl_2$ exist in the solution the DeFord and Hume equation[10] $F_1(X)$ is equal to $\beta_1 + \beta_2$ [X] and a plot of $F_1(X)$ *vs.* [X] for values of E_p and E_p^* gives straight lines. In fact both plots are linear with correlation coefficients of 0.996 and 0.998, respectively. The literature[2] refers to complexes of higher co-ordination numbers: $CdCl_3^-$ with log $\beta_3 = 1.5 \pm 0.2$ and $CdCl_4^{2-}$ with log $\beta_4 = 1.7$ for $t = 25°$ and ionic strength 1.0 and 0.0

Table 1

Method	Temperature, °C	Ionic strength	log β_1	log β_2	$[Cd^{2+}]$, %	$[CdCl^+]$, %	$[CdCl_2]$, %
Potentiometry	20.0 ± 0.1	0.600	0.5 ± 0.1	2.00 ± 0.03	3.5	5.4	91.1
Anodic-stripping voltammetry, E_p values	20.0 ± 0.1	0.700	0.8 ± 0.1	1.97 ± 0.03	3.5	10.7	85.8
Anodic-stripping voltammetry, E_p^* values	20.0 ± 0.1	0.700	0.78 ± 0.06	2.00 ± 0.01	3.3	10.1	86.6

respectively. However, these species were not detected in our experiments, probably because, if they exist, their concentration is too small to affect the calculation of the stability constants of the main species.

The equations for the functions F_1 (X) *vs.* [X] are $F_1(X) = (100 \pm 3)[X] + 6 \pm 1$ for E_p^* values and $F_1(X) = (94 \pm 5)[X] + 6 \pm 2$ for E_p. Hence there is good agreement between the potentiometric and voltammetric values for the stability constants of the cadmium chloro-complexes in sea-water medium. The values of β_1 differ a little but reasonably so in view of the small concentration of $CdCl^+$ and the rather different media and concentration levels for the two methods.

In Table 1 we summarize the results, together with the calculated concentrations of the different species in Guincho near-shore sea-water, where organic carbon is minimal and the total chloride concentration is 0.512*M*.

It seems reasonable to state that both species, $CdCl^+$ and $CdCl_2$, are present in sea-water, the second being dominant. This conclusion differs from those drawn by other authors, but this is because of differences in handling the data. The least-squares treatment for one or two sets of points is an oversimplification which may lead to wrong results, and the DeFord and Hume method should be used.

REFERENCES

1. L. G. Sillén and A. E. Martell, *Stability Constants of Metal-Ion Complexes*, 2nd Ed. and Suppl. No. 1, The Chemical Society, London 1964, 1971.
2. R. M. Smith and A. E. Martell, *Critical Stability Constants*, Vol. 4, Plenum Press, New York, 1976.
3. M. Branica, D. M. Novak and S. Bubić, *Croat. Chem. Acta*, 1977, **49**, 539.
4. S. D. Brown, *Ph.D. Thesis*, University of Washington, 1978.
5. D. R. Crow, *Polarography of Metal Complexes*, p. 72. Academic Press, New York, 1969.
6. R. D. Guy and C. L. Chakrabarti, *Proc. Intern. Conf. Heavy Metals in the Environment*, 1975, 275.
7. J. J. Lingane, *Chem. Rev.*, 1941, **29**, 1.
8. R. Cernatescu, I. Popescu, A. Cracium, M. Bostan and N. Iorga, *Stud. Cercetari Stiint. Inst. Chim. Iasi*, 1958, **9**, 1.
9. L. N. Klatt and R. L. Rouseff, *Anal. Chem.*, 1970, **42**, 1234.
10. D. D. DeFord and D. N. Hume, *J. Am. Chem. Soc.*, 1951, **73**, 5321.
11. A. Zirino and S. P. Kounaves, *Anal. Chem.*, 1977, **49**, 56.
12. H. A. Flaschka, *EDTA Titrations*, 2nd Ed., Pergamon Press, Oxford, 1967.
13. Princeton Applied Research, Analytical Instrument Division, *Technical Note* 109A, 1974.
14. B. Raspor, P. Valenta, H. W. Nürnberg and M. Branica, *The Science of the Total Environment*, 1978, **9**, 87.

Talanta, Vol. 28, pp. 241 to 249, 1981
Printed in Great Britain. All rights reserved

0039-9140/81/040241-09$02.00/0
Copyright © 1981 Pergamon Press Ltd

LOGARITHMIC DIAGRAMS AS AN AID IN COMPLEXOMETRIC TITRATIONS WHERE 1:2 OR 2:1 AS WELL AS 1:1 METAL–LIGAND COMPLEXES ARE REGARDED AS PRINCIPAL SPECIES

STEN JOHANSSON
Department of Analytical Chemistry, Royal Institute of Technology, S-100 44 Stockholm 70, Sweden

(*Received* 10 *July* 1980. *Accepted* 25 *August* 1980)

Summary—Logarithmic diagrams have earlier been used for theoretical treatment of complexometric titrations where only the 1:1 complex is formed in the main reaction between a metal ion M and a ligand L. This approach has now been extended to include titrations where 1:2 and 2:1 complexes are also formed. Four different types of diagram can be drawn. These diagrams can be used to determine pM (or pL) at the equivalence point, the titration ratio at different pM (or pL) values and the titration error. One of these diagrams is easy to construct and use. The method also has the advantage that it can directly indicate whether the titration is best performed with 1:1 or 2:1 (1:2) stoichiometry. Two typical examples, namely the titration of a manganese solution with triethylenetetraminehexa-acetic acid and of a copper solution with pyridine-2,6-dicarboxylic acid, are discussed. The two titrations proceed with the formation of the complexes Mn_2L (2:1) and CuL_2 (1:2) respectively, in addition to the 1:1 complex in each instance.

Johansson and Wänninen[1] have shown that logarithmic diagrams are a convenient means of surveying the conditions for a complexometric titration. Johansson[2] has given an exposition of the use of logarithmic diagrams and Gran-plots to construct titration curves and to determine the equivalence point in potentiometric complexometric titrations.

Their approach was, however, limited to only those titrations involving the formation of a 1:1 complex between the metal and the titrating ligand; that is, complexes of the type ML, MH_nL and $M(OH)_nL$. The formation of acid or basic complexes was taken into consideration by making use of the appropriate side-reaction coefficients (α-coefficients) in accordance with Ringbom's concept.[3] This is, of course, the most important type of complexometric titration. However, instances involving the formation of complexes of the type M_2L or ML_2 together with acid or basic variants that affect the shape of the titration curve are not uncommon.

Wänninen[4] has shown how a titration producing ML is affected by the formation of M_2L. He has considered the formation of ML as the main reaction and that of the 2:1 complex as a side-reaction. Harju and Ringbom[5] have treated the opposite problem, where the formation of M_2L is considered as the main reaction and the effect of the formation of the 1:1 complex on the main reaction is calculated by means of an α-coefficient. This coefficient, however, changes during the course of the titration, which implies that the conditional constant also changes. If the problem is confined to evaluation of the conditions at the equivalence point or in its vicinity, it is simplified so that [M] and the titration error can easily be calculated. If titration curves are to be constructed, however, this procedure (employing an α-coefficient that varies during the titration) is not satisfactory. This problem has been dealt with by Freese *et al.* in two papers,[6,7] in which they derived formulae for calculating the titration curves when ML and ML_2 or ML and M_2L are formed.

The present work is also limited to these two instances where either ML and ML_2 or ML and M_2L are formed, since all three types of complexes are only rarely formed in the course of one and the same titration.

Calculations according to the formulae given by Freese *et al.* are rather cumbersome. If only a general outline of the titration curve and the possibilities of the titration method is desired, the logarithmic diagrams can prove to be a less time-consuming alternative since it is easily decided whether the titration shall be terminated at the first or second equivalence point. Such diagrams are easy to construct since they consist for the most part of straight lines. A prerequisite is that the equilibria are such that the relationship between the different species is determined by a single variable, called the master variable. If we assume that A is titrated with B (A and B can be either M or L), four different types of logarithmic diagrams can be distinguished:

(1a) AB_2 is formed; pA master variable;
(1b) AB_2 is formed; pB master variable;
(2a) A_2B is formed; pA master variable;
(2b) A_2B is formed; pB master variable.

In all four instances the complex AB is also formed. Formation of acid and basic complexes is taken into

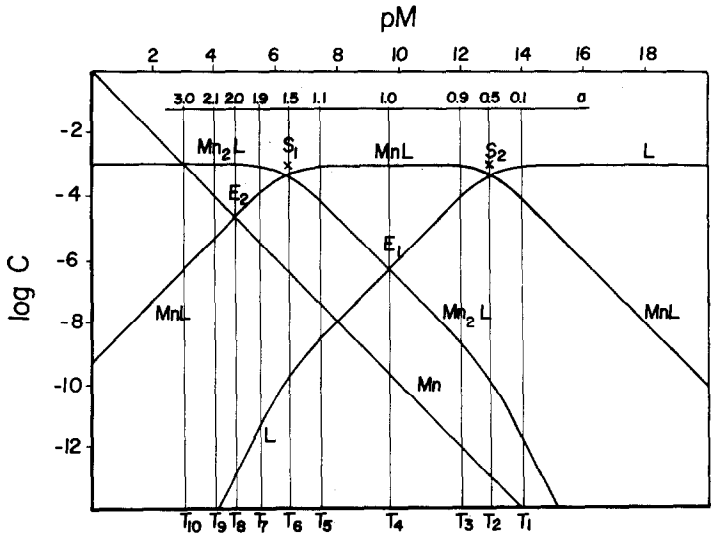


Fig. 1. Logarithmic diagram for the titration of TTHA (H_6L) with manganese at pH = 9.0. The total concentration of TTHA is 0.001*M* and pMn is used as master variable. A scale for the titration ratio *a* is introduced in the diagram.

consideration by converting the equilibrium constants for the main reactions into conditional constants. This of course presumes a constant pH value. In order to illustrate the possibilities offered by the logarithmic diagrams two examples will be treated in detail.

EXAMPLE I. M_2L AND ML ARE FORMED

An example of this type of titration has been discussed in detail by Harju and Ringbom,[5] namely that of a manganese solution with triethylenetetraminehexa-acetic acid (TTHA = H_6L). To simplify the theoretical treatment they have assumed that the titration is done in reverse, *i.e.*, L is titrated with Mn(II). The first equivalence point is reached when MnL is formed and the second when Mn_2L is formed. A titration of type 2 according to the classification above is thus treated as a titration of type 1. They made use of the following constants: $\log K_{MnL}^{Mn,L} = 14.5$; $\log K_{MnHL}^{H,MnL} = 8.74$; $\log K_{MnH_2L}^{H,MnHL} = 3.45$; $\log K_{Mn_2L}^{Mn,MnL} = 6.54$ (concentration constants, $\mu = 0.1$; 25°). The titration was to be performed at pH 9.0 and the total concentration, C_L, of TTHA was 0.001*M*.

At pH 9.0 $\alpha_{Mn(OH)}$ is negligible and $\log\alpha_{L(H)} = 1.74$. From this value together with the constants above the following conditional constants are calculated:

$$Mn + L' = MnL'; \log K_{MnL'}^{Mn,L'} = 12.95 \quad (1)$$

$$Mn + MnL' = Mn_2L; \log K_{Mn_2L}^{Mn,MnL'} = 6.35 \quad (2)$$

In calculating these conditional constants, both reactions are considered as main reactions. Formation of other complexes is accounted for in the α-coefficients.

In the following, all stability constants and concentrations may be regarded as conditional. However, the prime signs will be omitted except where they are required for clarifying the presentation. As only a general view of the titration is usually required, dilution effects can generally be ignored, but if the dilution is considerable the diagram should reflect the conditions at points of particular interest, usually the equivalence point(s).

Construction of the diagram

A general view of the titration is easily obtained with the aid of a logarithmic diagram. Either pMn (Fig. 1) or pL (Fig. 4) can be chosen as the master variable. The simplest diagram is obtained when pMn is chosen, which gives a diagram of type 1b.

pM as master variable, L is titrated with M. In the logarithmic diagram lines are drawn that indicate how the logarithms of the concentrations of different species vary with pMn. Therefore, expressions must be derived that show how [L], [MnL] and [Mn_2L] are related to [Mn]. The following expressions are obtained:

$$[L] = \frac{C_L}{1 + [Mn]K_{MnL} + [Mn]^2K_{MnL}K_{Mn_2L}} \quad (3)$$

$$[MnL] = \frac{[Mn]K_{MnL}C_L}{1 + [Mn]K_{MnL} + [Mn]^2K_{MnL}K_{Mn_2L}} \quad (4)$$

$$[Mn_2L] = \frac{[Mn]^2K_{MnL}K_{Mn_2L}C_L}{1 + [Mn]K_{MnL} + [Mn]^2K_{MnL}K_{Mn_2L}} \quad (5)$$

where C_L is the total concentration of TTHA, and K_{MnL} and K_{Mn_2L} are the conditional constants as defined by equations (1) and (2) respectively.

Conversion of equation (3) into logarithmic form gives

$$\log [L] = \log C_L - \log (1 + [Mn]K_{MnL} + [Mn]^2K_{MnL}\,K_{Mn_2L})$$

which in this instance gives

$$\log [L] = -3.0 - \log (1 + [Mn]10^{12.95} + [Mn]^2 10^{19.30})$$

The expression in parenthesis will be dominated by different terms as [Mn] is varied.

1. The first term dominates when $[Mn] < 10^{-12.95}$ which gives log [L] = −3.0, a horizontal line in the logarithmic diagram.

2. The second term dominates when $10^{-12.95} < [Mn] < 10^{-6.35}$ which gives log [L] = −3.0 − log ($[Mn]10^{12.95}$) = pMn − 15.95. This is an equation for a straight line with slope + 1 in the diagram.

3. The third term dominates when $[Mn] > 10^{-6.35}$, which gives log [L] = 2 pMn − 22.30. This is an equation for a straight line with slope + 2.

The graph representing log [L] in the diagram accordingly consists of three linear parts. Around the points of intersection (pMn = 12.95; log [L] = −3.0) and (pMn = 6.35; log [L] = −9.60) the graph is rounded off. When pMn is 12.95 then log [L] = −3.3 and when pMn = 6.35, log [L] = −9.90. With the aid of this information, a graph can be drawn as shown in Fig. 1.

In a similar way the following expression can be derived from equation (4):

$$\log [MnL] = \log [Mn] + 12.95 - 3.0 - \log (1 + [Mn]10^{12.95} + [Mn]^2 10^{19.30}).$$

1. When the first term in parenthesis dominates, then log [MnL] = − pMn + 9.95 which is an equation for a straight line with slope − 1.

2. When the second term dominates, then log [MnL] = − 3.0.

3. When the third term dominates, then log [MnL] = pMn − 9.35, which is an equation for a straight line with slope + 1.

As in the preceding instance, the graph representing log [MnL] in the diagram consists of three linear parts and is rounded off near the points of intersection (pMn = 12.95; log [MnL] = −3.0) and (pMn = 6.35; log [MnL] = −3.0) and as before, the real intersection points lie 0.3 units under the intersection points of the straight lines.

For Mn_2L, the following is obtained from equation (5): log $[Mn_2L,] = 16.30 - \log (1 + [Mn]10^{12.95} + [Mn]^2 10^{19.30})$. This equation, in the same manner as before, yields

1. log $[Mn_2L] = -2$ pMn + 16.30
2. log $[Mn_2L] = -$pMn − 3.35
3. log $[Mn_2L] = -3.0$

These three equations give rise to the graph which is marked as Mn_2L in Fig. 1.

From the example above the following general rules for drawing a logarithmic diagram can be formulated. These rules are valid when L is titrated with M, forming ML and M_2L.

1. Draw the co-ordinate axes: pM from 0 to, say, 20 and log C from 0 to, say, −14.

2. Draw a straight line with slope −1 from the origin. This line shows how log [M] varies with pM.

3. Mark out the two system points (log K_{M_2L}; log C_L) and (log K_{ML}; log C_L). These are marked as S_1 and S_2 in Fig. 1.

4. With the aid of these system points, plot the linear parts of the graphs which represent log [L], log [ML] and log $[M_2L]$. Combine the linear branches of the graphs representing the same species so that the intersection points of the graphs lie 0.3 units under the intersection points of the prolonged straight lines.

5. Mark the graphs with the appropriate symbols.

The principle of this technique is essentially the same as that used in the construction of logarithmic diagrams for acid–base equilibria, discussed in detail by Sillén.[8]

Use of the diagram

Titration curve. A vertical line moved from right to left in the diagram represents the change in conditions as the titration proceeds. Accordingly, lines can be drawn representing the titration ratio $a = C_M/C_L$, (where C_M and C_L are the total concentrations of metal and ligand respectively), *i.e.*,

$$a = \frac{[M] + [ML] + 2[M_2L]}{[L] + [ML] + [M_2L]}$$

at various stages in the titration. Ten such lines, T_1–T_{10}, are drawn in Fig. 1. For line T_1, [Mn] and $[Mn_2L]$ can be neglected compared with other species, and [MnL] is 1/10 of C_L, since the distance between the MnL- and L-lines is 1.0 logarithmic unit. This gives

$$a = \frac{[MnL]}{C_L} = 0.1; \quad \text{pMn} = 14.0$$

In the same way a and pMn are calculated for the other lines:

Line	a	pMn
T_2	0.5	12.95
T_3	0.9	12.00
T_4	1.0	9.65 first equivalence point, E_1
T_5	1.1	7.40
T_6	1.5	6.35
T_7	1.9	5.40
T_8	2.0	4.68 second equivalence point, E_2
T_9	2.1	4.00
T_{10}	3.0	3.00

(It is not necessary actually to draw these lines. As shown in the figure they can be included in the diagram as an a scale. This scale is not uniform, and each value of a has to be deduced from the logarithmic diagram according to the equation defining a.)

With the aid of these values, a titration curve can be drawn which is similar to the curve obtained when a diprotic acid is titrated with a strong base. The curve is shown in Fig. 2.

Titration error. The logarithmic diagrams also offer a possibility to evaluate how accurately a certain titration can be performed. This problem has been

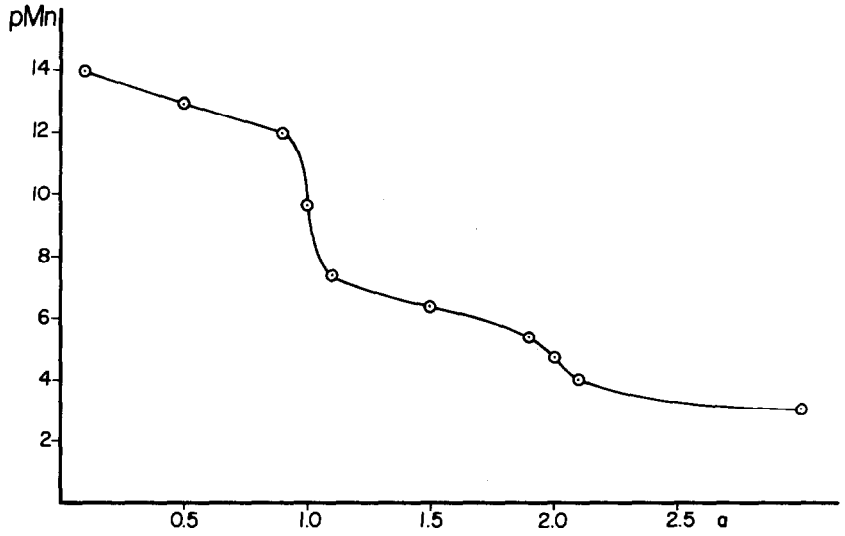


Fig. 2. Theoretical titration curve for the potentiometric titration of 0.001M TTHA with manganese. The curve is constructed from the logarithmic diagram in Fig. 1.

dealt with by Johansson and Wänninen.[1] (As for acid–base titrations, see Sillén[8] and Wänninen.[9]) If more than one principal complex is formed, the conditions become rather complicated and it will be convenient to choose a somewhat different formulation of the titration error.

If the titration is terminated when $a = a_1$ instead of $a = 1$, the relative error is $(a_1 - 1)/1$. Likewise, if the titration is terminated when $a = a_2$ instead of $a = 2$, the relative error will be $(a_2 - 2)/2$. The magnitude of the error is determined by the difference between pM at the end-point and at the equivalence point. If pM is determined potentiometrically, the difference, ΔpM, will be rather small, *e.g.*, between −0.1 and +0.1 pM units. When an indicator is used, the uncertainty becomes greater and ΔpM is usually in the range from ±0.3 to ±0.5 pM units if the end-point is observed visually. If there is no indicator available that changes colour at the equivalence point, a systematic error is also introduced. With the aid of logarithmic diagrams and the method given below, a relative titration error which includes both the systematic and random errors can be calculated.

In their example Harju and Ringbom used Methylthymol Blue as the indicator. It changes colour at pMn = 7.0,[3] *i.e.*, the end-point lies between the first and the second equivalence points. The relative titration error (R.T.E.) at the first equivalence point E_1 can be calculated as follows:

$$\text{R.T.E.} = \frac{a-1}{1} = \frac{[\text{Mn}] + [\text{MnL}] + 2[\text{Mn}_2\text{L}]}{[\text{L}] + [\text{MnL}] + [\text{Mn}_2\text{L}]} - 1$$

$$= \frac{[\text{Mn}] - [\text{L}] + [\text{Mn}_2\text{L}]}{[\text{L}] + [\text{MnL}] + [\text{Mn}_2\text{L}]}$$

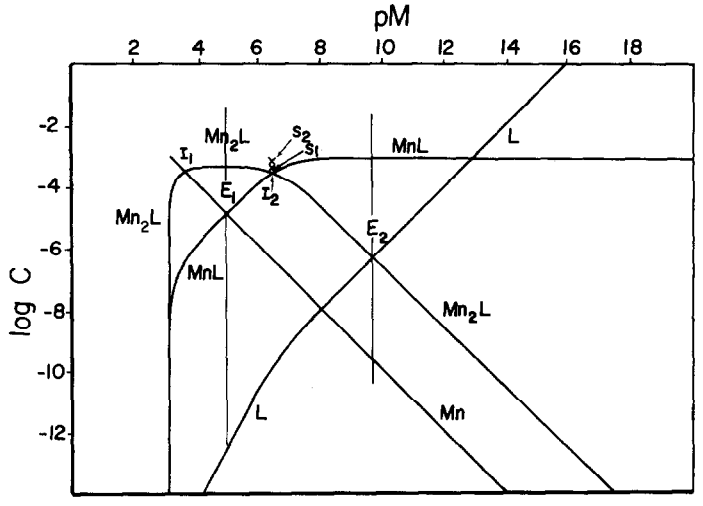


Fig. 3. Logarithmic diagram for the titration of manganese with TTHA(H_6L) at pH = 9.0. The total concentration of manganese is 0.001M and pMn is used as master variable.

When the titration is terminated at pMn = 7.0, from Fig. 1 the value

$$\text{R.T.E.} = \frac{10^{-7.0} - 10^{-9.0} + 10^{-3.75}}{10^{-3}} \approx 10^{-0.75}$$

$$= +18\%$$

is obtained.

In order to minimize the error it is necessary to titrate to the first perceptible colour change, which is traditionally assumed to correspond to 10% of the indicator having changed colour. At this point pMn = 8.0 and if the calculations are done with ΔpMn = $\pm$0.5, the titration will be terminated at a pMn value between 7.5 and 8.5. At pMn = 7.5 the following expression is obtained

$$\text{R.T.E.} = \frac{10^{-7.5} - 10^{-8.5} + 10^{-4.20}}{10^{-3}} = +6.5\%$$

and at pMn = 8.5

$$\text{R.T.E.} = \frac{10^{-8.5} - 10^{-7.5} + 10^{-5.15}}{10^{-3}} = +0.7\%$$

The relative titration error range from +0.7 to +6.5% thus includes both the systematic and random errors, when the solution is titrated to the first appearance of a change in colour.

The relative titration error at the second equivalence point E_2 will be

$$\text{R.T.E.} = \frac{a-2}{2} = \frac{[\text{Mn}] - [\text{MnL}] - 2[\text{L}]}{2 \times 10^{-3}}$$

In this instance, the titration must be continued until the colour change appears complete, *i.e.*, when 90% of the indicator has changed colour. Here pMn = 6.0 and if we assume as before that ΔpMn = $\pm$0.5, the titration will be terminated at pMn between 5.5 and 6.5.

At pMn = 5.5

$$\text{R.T.E.} = \frac{10^{-5.5} - 10^{-3.70} - 2 \times 10^{-12.5}}{2 \times 10^{-3}} = -10\%$$

and at pMn = 6.5

$$\text{R.T.E.} = \frac{10^{-6.5} - 10^{-3.25} - 2 \times 10^{-9.5}}{2 \times 10^{-3}} = -28\%$$

Other types of diagram

pM as master variable, M titrated with L. If the titration described above is performed in the normal way, that is Mn is titrated with L, the logarithmic diagram will be somewhat modified, Fig. 3. This is a diagram of type 2a. In this instance the total concentration of Mn is 0.001*M* and consequently the concentration of Mn_2L can never be higher than $5 \times 10^{-4}M$ or $10^{-3.3}M$. Hence three system points are obtained: S_1(6.35; −3.3), S_2 (6.35; −3.0) and S_3 (12.95; −3.0). The first system point, S_1, is used instead of S_2 when Mn_2L is the dominant species. The points of intersection I_1 and I_2 lie 0.5 logarithmic units (log 3) below the line log C = −3.0. The concentration of manganese is $10^{-3}M$ from the beginning, so the Mn-line starts at pMn = 3.0. At vertical line E_1, [MnL] and [Mn] are equal and [L] can be neglected. The titration ratio will then be

$$a = \frac{[\text{L}] + [\text{MnL}] + [\text{Mn}_2\text{L}]}{[\text{Mn}] + [\text{MnL}] + 2[\text{Mn}_2\text{L}]} = \frac{1}{2}$$

and E_1 is thus the first equivalence point, where

$$\text{pMn} = \frac{6.35 + 3.30}{2} = 4.82$$

At this point pMn will not be exactly the same as at the second equivalence point in the titration done in the opposite direction (the pMn is then 4.68). The difference is due to the fact that in the latter case $[Mn_2L]$ is 0.001*M*. Accordingly the relative error will also not have quite the same value.

At the second equivalence point the titration is continued until the colour change is complete. This gives the same error range as that for the reverse titration, but with opposite sign, *i.e.*, an R.T.E. range from −6.5 to −0.7%.

pL as master variable. If pL is chosen instead of pMn as the master variable, we get the diagrams which are shown in Figs. 4 and 5. The first of those depicts the equilibria for titrating L with Mn, and the other illustrates the titration of Mn with L.

The system points used for constructing the diagram in Fig. 4 have the co-ordinates

S_1: [(12.95 − 6.35 + 3.0) = 9.60; −3.0]

S_2; [(12.95 + 6.35 − 3.0) = 16.30; −3.0]

At pL greater than 9.60 the slope of the Mn-line is $+\frac{1}{2}$ and that of the MnL-line is $-\frac{1}{2}$. Vertical lines E_1 and E_2 represent the conditions at the first and second equivalence points respectively.

The diagram in Fig. 5 is similar to that in Fig. 4, but the concentration of Mn_2L in this instance is only half as high, *i.e.*, $10^{-3.30}M$. Hence this diagram has four system points: S_1 (9.60; −3.0), S_2 (9.60; −3.15), S_3 (16.30; −3.15) and S_4 (16.30; −3.0).

Comparison between the different logarithmic diagrams

The titration of Mn with L and *vice versa* (where L is TTHA) has been discussed above. This is a typical example of a reaction in which both ML and M_2L are formed.

The diagram shown in Fig. 1 is the easiest to construct. It is very similar to that for the titration of a diprotic acid with a strong base. The disadvantage of this type of diagram is that it is valid for the titration of L with M, whereas normally M is titrated with L. But if it is only desired to determine the pM value at the equivalence point and estimate the titration error, such a diagram is still a good help. It should be kept in mind that the maximum concentration of M_2L is

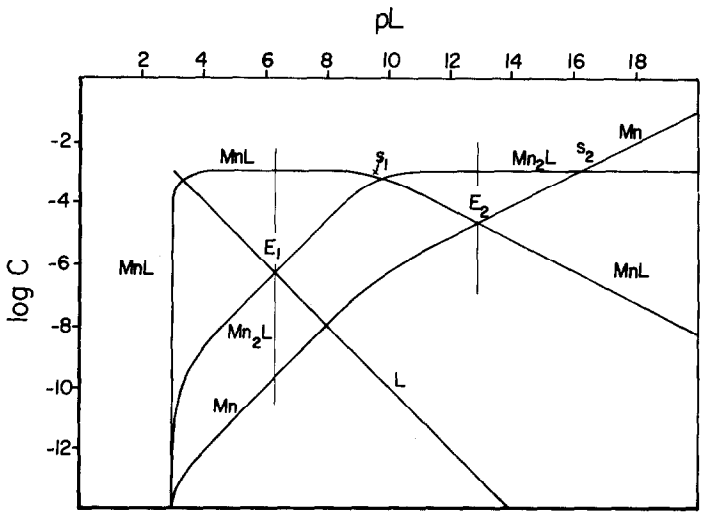


Fig. 4. Logarithmic diagram for the titration of TTHA (H_6L) with manganese at pH = 9.0. The total concentration of TTHA is 0.001*M* and pL is used as master variable.

only half of the total concentration of M. This means that the pM at the first equivalence point becomes 0.15 logarithmic unit lower than that for titration of L with M.

EXAMPLE II. ML_2 AND ML ARE FORMED

Freese *et al.*[6] have treated this problem theoretically and have compared their theoretical values with those obtained from a photometric titration without an indicator.

Here the same example is considered, namely the titration of a copper solution with pyridine-2,6-dicarboxylic acid, but now it is treated with the aid of logarithmic diagrams. A 0.001*M* Cu(II) solution is titrated with pyridine-2,6-dicarboxylic acid (H_2L) at pH = 5.5. At this pH, the conditional constants are

$$Cu + L = CuL; \log K_{CuL} = 8.08$$

$$CuL + L = CuL_2; \log K_{CuL_2} = 7.32$$

It is necessary to calculate pCu and the relative titration errors at the two equivalence points, and to construct an approximate titration curve, *i.e.*, plot $[CuL_2]$ against the titration ratio *a*.

In this instance also, a diagram of type 1*b* is the simplest to construct, *i.e.*, a logarithmic diagram in which pL is used as the master variable, for titration of Cu with L. The diagram is shown in Fig. 6 and the system points are (7.32; −3.0) and (8.08; −3.0). Guidelines with slopes of +1 and −1 are drawn from both system points and a horizontal guideline is drawn through the points. Further guidelines with slopes of

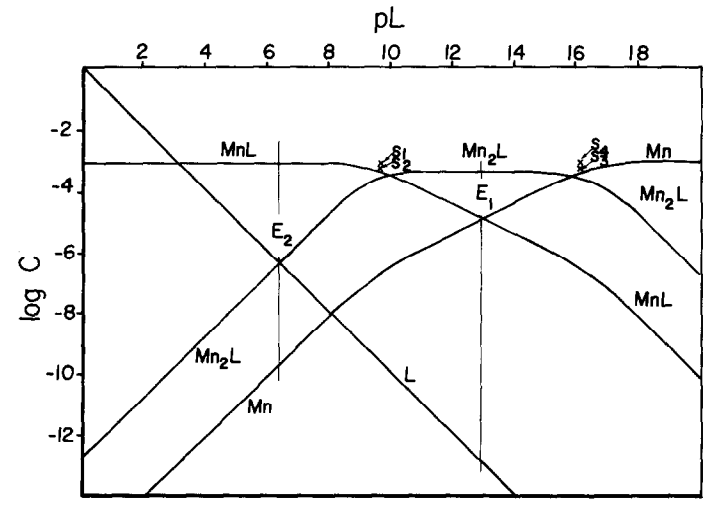


Fig. 5. Logarithmic diagram for the titration of manganese with TTHA (H_6L) at pH = 9.0. The total concentration of manganese is 0.001*M* and pL is used as master variable.

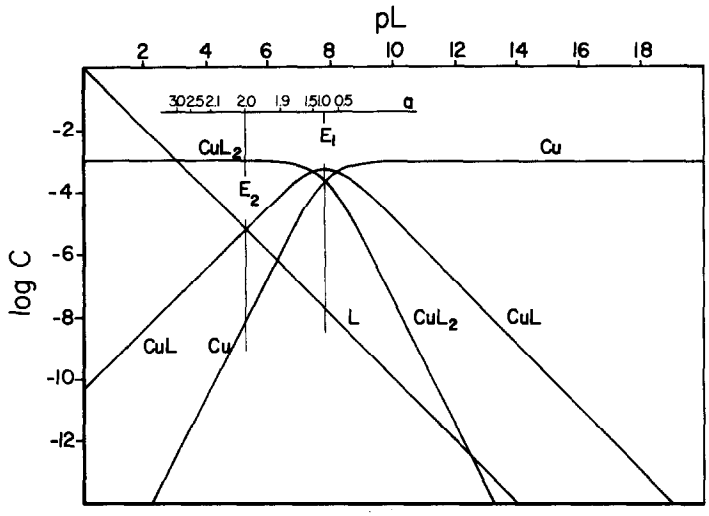


Fig. 6. Logarithmic diagram for the titration of copper with pyridine-2,6-dicarboxylic acid (H_2L) at pH = 5.5. The total concentration of copper is 0.001 M and pL is used as master variable.

+2 and −2 are drawn from a point half-way between the system points. The main parts of the lines are connected with short curves as before: The Cu- and CuL-lines intersect 0.3 logarithmic unit under system point (8.08; −3.0), the CuL_2- and CuL-lines intersect 0.3 logarithmic unit under system point (7.32; −3.0). The Cu-line passes 0.3 logarithmic unit below the intersection of the Cu-guidelines with slopes +1 [drawn from system point (8.08; −3.0)] and +2. In the same way the CuL_2-line passes 0.3 logarithmic unit below the intersection of the CuL_2-guidelines having slopes −1 [drawn from system point (7.32; −3.0)] and −2 (cf. Fig. 1 and paragraph 4 in the section dealing with the general rules for drawing a logarithmic diagram). It is noteworthy that the concentration of CuL will never be as high as $10^{-3}M$.

Vertical lines E_1 and E_2 in the diagram represent the conditions at the equivalence points. At E_1, [Cu] and [CuL_2] are equal and [L] can be neglected; that is, the titration ratio a is given by

$$a = \frac{[CuL] + 2[CuL_2]}{[Cu] + [CuL] + [CuL_2]} = 1$$

At E_2, [CuL] and [L] are equal and [Cu] can be neglected, so

$$a = \frac{[L] + [CuL] + 2[CuL_2]}{[CuL] + [CuL_2]} = 2$$

and

$$pL = \frac{3.00 + 7.32}{2} \sim 5.2$$

At the first equivalence point, pCu is approximately 3.6 whereas at the second equivalence point it is 8.1. In the titration of a 0.001M Cu(II) solution, pCu changes from 3.0 at the start to 3.6 at the first equivalence point but to 8.1 at the second equivalence point. The change in pCu at the second equivalence point is accordingly about 5 logarithmic units, whereas that at the first equivalence point is hardly observable. A titration curve with some points taken from the logarithmic diagram is shown in Fig. 7.

The relative titration error in titrating to the first equivalence point becomes large. In titrating to the second equivalence point the relative titration error will be

$$\text{R.T.E.} = \frac{a - 2}{2} = \frac{[L] - [CuL]}{2 \times 10^{-3}}$$

At this stage the slope of the Cu-line in Fig. 6 is +2. This means that if [Cu] is changed by +0.6 logarithmic unit, [L] changes by −0.3 and [CuL] by +0.3 logarithmic unit. At the equivalence point

$$[L] = [CuL] = 10^{-5.2}.$$

Assuming $\Delta pCu = \pm 0.6$ the relative titration error will be

$$\text{R.T.E.} = \pm\frac{10^{-4.9} - 10^{-5.5}}{2 \times 10^{-3}} = \pm 0.5\%$$

From the logarithmic diagram it is evident that [CuL] at the second equivalence point is less than 1% of [CuL_2]. The concentration of Cu is much lower still. All three species are coloured, but in spite of this, if a proper wavelength is chosen for the photometric titration, the interference from Cu and CuL can be minimized. If a wavelength at which only CuL_2 absorbs light can be chosen, the graph of A (A = absorbance) against the titration ratio a will be a straight line from the origin to a maximum when $a = 2$, and then A will remain constant, since the dilution is not taken into consideration.

This is valid only if the formation of CuL is not taken into account. In the present instance this can-

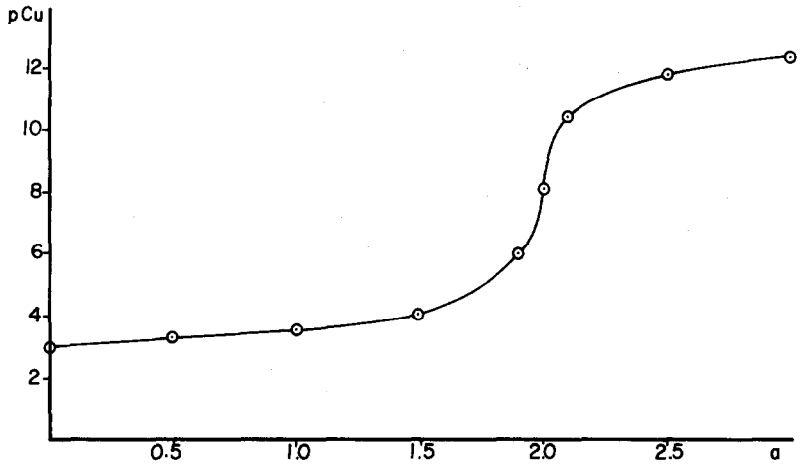


Fig. 7. Theoretical titration curve for the potentiometric titration of 0.001*M* copper with pyridine-2,6-dicarboxylic acid. The curve is constructed from the logarithmic diagram in Fig. 6.

not be allowed. From the logarithmic diagram it is easy to obtain values of the concentration of CuL_2 relative to C_{Cu}. It is only necessary to measure the vertical distance between the line log $C = -3.0$ and the CuL_2-line. For instance if the distance is 1 logarithmic unit, the relative concentration (*i.e.*, $[CuL_2]/C_{Cu}$) will be 0.1. Corresponding values of the titration ratio a and the relative concentrations are (0.0; 0.00), (0.5; 0.08), (1.0; 0.24), (1.5; 0.57), (1.9; 0.91), (2.0; 1.00) and (2.5; 1.00). The curve shown in Fig. 8 is in good agreement with that given by Freese *et al.* for the titration monitored at 1100 nm. In the photometric titration Cu and CuL have a slight absorption at this wavelength and the initial absorbance values are somewhat higher.

In this example, a direct spectrophotometric determination will probably give somewhat better results than the photometric titration. As the logarithmic diagram shows, the concentration of CuL at 50% excess of L (*i.e.*, $a = 3$), is less than 10^{-4} $[CuL_2]$ and [Cu] is much lower still. These two species do not interfere in the determination and L does not absorb at 1100 nm.

DISCUSSION

In analytical work there may be motives for devoting a rather large effort to the *evaluation* of the result. It may for example be necessary to use a computer in order to obtain dependable results quickly. When *designing* analytical methods, however, the analyst wants to review the possibilities of the method in a fast simple way. His aims are then to estimate the relative error of the method and perhaps to check which parameters will affect the result. He may also wish to get an idea of the shape of a titration curve. The combined use of logarithmic diagrams and conditional constants appears to offer a very good solution to these problems. The logarithmic diagrams are particularly useful for solving problems in titrimetric analysis and liquid–liquid extraction separations. In order to make the best possible use of the logarithmic diagrams it is necessary to know beforehand what type of diagram to choose and how to draw it. Of the different types of diagram discussed in this paper, type 1b has proved to be the easiest to draw and interpret. For the analytical chemist who is

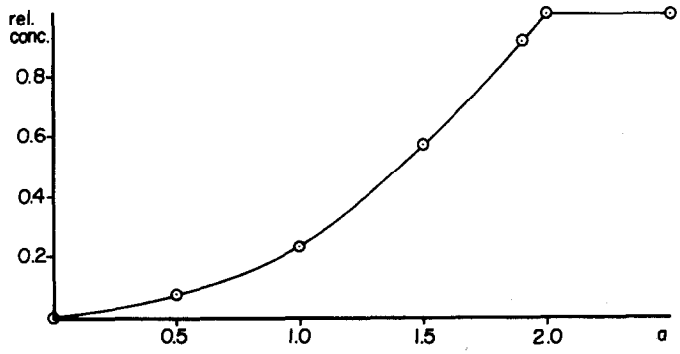


Fig. 8. Theoretical titration curve for the photometric titration of 0.001*M* copper with pyridine-2,6-dicarboxylic acid (H_2L) at 1100 nm, assuming that only CuL_2 absorbs light. The curve is constructed from the logarithmic diagram in Fig. 6.

familiar with the use of logarithmic diagrams it is a matter of just a couple of minutes to collect the data necessary to give him an idea of the possibilities of a method.

Acknowledgements—I am indebted to Professors Axel Johansson and Folke Ingman for valuable discussions and comments on the manuscript.

REFERENCES

1. A. Johansson and E. Wänninen, in I. M. Kolthoff and P. J. Elving (eds.), *Treatise on Analytical Chemistry*, Part I, Vol. 11, Chap. 117. Interscience, New York, 1975.
2. A. Johansson, *Talanta*, 1973, **20**, 89.
3. A. Ringbom, *Complexation in Analytical Chemistry*, Wiley-Interscience, New York, 1963.
4. E. Wänninen, *Acta Acad. Aboensis, Math. Phys.*, 1960, **21**, 17.
5. L. Harju and A. Ringbom, *Anal. Chim. Acta*, 1970, **49**, 205.
6. F. Freese, G. den Boef and G. J. van Rossum, 1972, **58**, 429.
7. *Idem, ibid.*, 1972, **61**, 67.
8. L. G. Sillén, in I. M. Kolthoff and P. J. Elving *ibid.* (eds.), *Treatise on Analytical Chemistry*, Part I, Vol. 1, Chap. 8. Interscience, New York, 1959.
9. E. Wänninen, *Talanta*, 1980, **27**, 29.

Talanta, Vol. 28, pp. 251 to 254, 1981
Printed in Great Britain. All rights reserved

0039-9140/81/040251-04$02.00/0
Copyright © 1981 Pergamon Press Ltd

SHORT COMMUNICATIONS

OBSERVATIONS ON A DROPPING-MERCURY ELECTROCHEMICAL DETECTOR FOR FLOW-INJECTION ANALYSIS AND HPLC

SAMUEL J. LYLE and M. IDRIS SALEH
The Chemical Laboratories, The University of Kent at Canterbury, Kent, England

(*Received* 4 *August* 1980. *Accepted* 22 *October* 1980)

Summary—An electrochemical detector cell having a dropping-mercury working electrode and an Ag/AgCl reference electrode is examined with reference to applications in flow-injection analysis and high-performance liquid chromatography. The working electrode, fed by a horizontal capillary, is capable of delivering mercury at fast dropping rates which can be varied by a control device in the cell. Examples of application to inorganic and organic electroreducible species are considered and advantages and limitations relative to other electrochemical detector devices are discussed.

Electrochemical reactions are capable of providing a sensitive means of detection and determination of electroactive species in a flowing liquid system. A convenient mode of operation is that in which the indicating electrode is held at a fixed potential and the current is measured. Under appropriate working conditions the current is proportional to the bulk concentration of electroactive species in the cell; such devices are frequently known as amperometric detectors. Cells containing indicating electrodes made from silver,[1,2] carbon,[3,4] platinum[5] or mercury[6–8] have been described. Of these, the last mentioned, offers the possibility of a constantly renewable electrode surface in the form of a flowing or dropping-mercury electrode (dme). In the work described here a dme incorporated in a cell based on that designed by Michel and Zatka[6] is examined in a flow-injection system and as a detector in high-performance liquid chromatography (HPLC). Advantages and limitations relative to other electrochemical detector devices are discussed.

EXPERIMENTAL

Reagents

All chemicals used were of reagent grade. The zinc acetate, cadmium acetate, and copper (II) chloride were dissolved in water to give approximately 0.1*M* solutions of each. Lead acetate was dissolved in water acidified with nitric acid to pH 4.5 to give a 0.01*M* lead solution. Mercuric oxide was dissolved in the minimum quantity of concentrated nitric acid and diluted with water to give a 0.1*M* solution. These solutions were standardized by EDTA titration and diluted with 0.1*M* potassium chloride for flow-injection study or with mobile phase for HPLC, as required. Nitrobenzene and *p*-nitrophenol were each dissolved in Britton–Robinson buffer/methanol mixture (1:1 v/v) of apparent pH 4.5, to give 0.01*M* solutions.

Instrumentation and operating conditions

The cell incorporated a horizontal glass capillary delivering mercury drops. The drop-rate was controlled by the static mercury head and by a glass rod on the same axis as the capillary.[6] The control end of the rod "confronted" the mercury drops and its distance from the capillary orifice, which was flush with the channel wall, determined the drop-rate. (The drop-rate used is $\geqslant$ 1 drop/sec, compared to about 0.25 drop/sec in ordinary voltammetry.) The cell body was made from a "Perspex" cylinder of diameter 5 cm and depth 6 cm. The inlet and outlet channels were drilled to have just under $\frac{1}{16}$-in. bore and threaded to accommodate $\frac{1}{16}$-in. outer diameter stainless-steel tube with Swagelok fittings. In the present work the outer diameter of the capillary was 1.5 mm and the bore was 0.06 mm. The mercury and the test liquid were channelled off separately at a T-junction below the reference electrode, the mercury passing into the vertical arm of a U-tube and the test-liquid to waste (at a right angle to the U-tube) at the top of the mercury reservoir created by the U-tube. The reference electrode was Ag/AgCl in 0.1*M* potassium chloride in contact with the test liquid through a sintered polyethylene plug. Otherwise the layout and geometry of the detector were the same as in Fig. 1 of ref. 6. A General Purpose Polarograph (Cambridge Instrument Co. Ltd.) was used as the source of adjustable constant potential at the working electrode. The detector output was connected to a potential/time chart-recorder.

The flow-injection system was controlled by a peristaltic pump (Technicon AutoAnalyser pump, Mark I) with pump tubing of different diameters to give a range of flow-rates. Samples were introduced into the flowing stream from a syringe through a septum. The effective tube-diameter into the detector was 1.5 mm.

The chromatograph for HPLC consisted of a pneumatic pump (Haskel model 28030) attached to interchangeable stainless-steel columns through a pressure-fluctuation damping system made from 100 cm of $\frac{1}{16}$-in. coiled stainless-steel tube and 30 cm of $\frac{1}{4}$-in. diameter stainless-steel tube filled with glass beads 150–200 μm in diameter. The samples were introduced through a valve injector (Specac 30.100) having interchangeable sample loops.

A Pye-Unicam LC3 ultraviolet detector was used for comparison with the electrochemical detector.

Octadecylsilane chemically bonded to silica gel (Partisil-10 ODS) was used in the separation of *p*-nitrophenol and nitrobenzene. A cation-exchange column (Ionex SA 15) was used in the chromatography of copper and zinc. Both columns were stainless steel, 10 cm long and 5 mm bore, and packed in the laboratory.

The carrier for metal ions in the flow-injection system was 0.1*M* potassium chloride. The mobile phase in the chromatographic separation of copper and zinc was an aqueous solution (pH 4.0) 0.1*M* in sodium tartrate, 0.04*M* in tartaric acid and 0.04*M* in sodium chloride. In the study of *p*-nitrophenol and nitrobenzene, the carrier was Britton–Robinson buffer/methanol (1:1 v/v) of apparent pH 4.5. Before use all solutions were purged of oxygen with nitrogen gas.

RESULTS AND DISCUSSION

Figure 1 gives current/potential curves for various metal ions in 0.1*M* potassium chloride, used as a carrier liquid in the flow-injection system. Zinc(II) is reduced only at potentials more negative than about −1.0 V relative to the reference electrode, so response from it can be eliminated by working at less negative potentials, at which Cu(II), Cd(II), Hg(II), or Pb(II) would be electroactive. This selectivity is illustrated in Fig. 2 for copper and zinc partially separated by ion-exchange chromatography and it can be just as readily demonstrated for flow-injection systems. Inspection of Fig. 1 will indicate other examples of selective detection of constituents of mixtures of these metal ions. Such detector selectivity would be of more value in flow-injection analysis than in chromatography.

Current/potential curves for *p*-nitrophenol and nitrobenzene are given in Fig. 3. A large polarographic-type maximum was obtained with *p*-nitrophenol. The width of the maximum is probably partly determined by the forced flow of the liquid past the electrode. The use of a surfactant as maximum suppressor in the chromatography detection system is probably not feasible because of interference with column performance. On the other hand, incorporation of such a suppressor in a flow-injection system would not necessarily lead to difficulties. For chromatographic detection the working electrode was held at −1.7 V to avoid the gross effects of this maximum; recorded elution peaks were symmetrical and tailing was not in evidence. The dme detector gave detection limits of 41 ng for *p*-nitrophenol and 37 ng for nitrobenzene, compared to 14 and 12 ng respectively when the ultraviolet detector was used at 254 nm (the detection limit was taken to be the minimum amount of electroactive component giving a peak of height twice that of the mean background noise level). Linearity of dme detector response extended up to at least 25-μg and 20-μg amounts of *p*-nitrophenol and nitrobenzene respectively. In the detection of metal ions the sensitivity was lower and the upper concentration limits of the linearity of response limited the working ranges. For copper and zinc under operating conditions of −1.5 V, the detection limits were 0.3 μg and 1.6 μg respectively and the upper limits for linearity of response were around 16 μg for either metal ion at flow-rates of 6 ml/min. With the experimental arrangement described, the detector functions in the presence of a carrier electrolyte as in voltammetry, and the recorder response will be linearly related to the detector current only as long as the resistance between the electrodes remains constant. Consequently effective change of electrolyte concentration brought about by increasing the reducible metal ion concentration causes departure from linearity, as observed. This problem is not expected to occur to the same extent with neutral electroactive species such as nitrobenzene, diluted as described here. The mercury drop-rate was 1 drop/sec in these tests. Other experimental tests revealed that the drop-rate affects the magnitude of the detector response. The detector signal was found to decrease with increasing drop-rate above about 1.4 drops/sec in tests with nitrobenzene

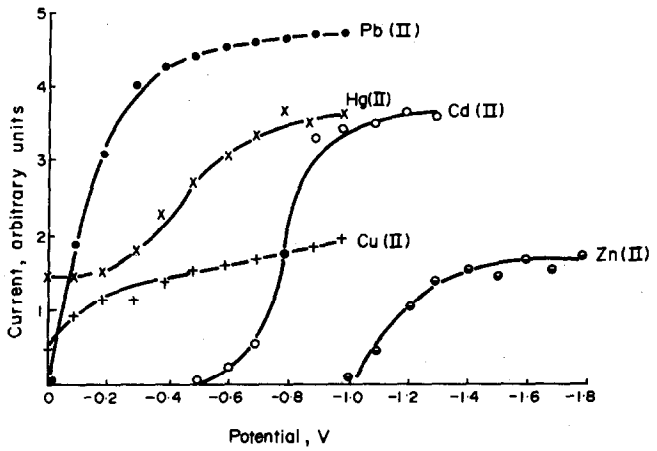


Fig. 1. Current/potential curves for metal ions undergoing electroreduction at the dme detector operating at 1 drop/sec in the flow-injection system. At each potential 10 μl of 0.01*M* metal-ion solution were injected into 0.1*M* KCl flowing at 1.33 ml/min.

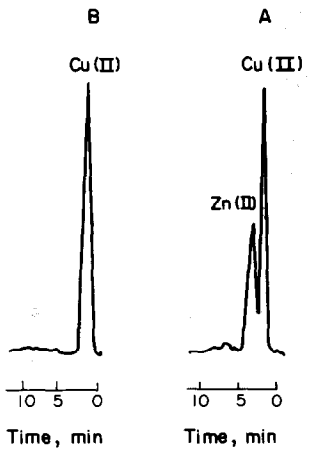


Fig. 2. Chromatograms of Cu(II) and Zn(II) partially separated on an Ionex SA 15 column and detected at different applied potentials at the dme (drop-rate, 1 drop/sec); A, −1.5 V and B, −0.5 V. The eluent flow rate was 6.0 ml/min and each injection (50 μl) contained 9.8 μg of Zn(II) and 9.5 μg of Cu(II).

in the methanolic Britton–Robinson buffer solvent system, but was independent of drop rate in the range 1–1.4 drop/sec (1 drop/sec was the lowest rate tested).

For comparison with the dme detector, some experiments were performed with a detector built to the design published by Blaedel and Yim.[5] This incorporates a platinum working electrode and an Ag/AgCl reference electrode in 0.1*M* potassium chloride. Both detectors gave good reproducibility in the flow-injection system. With cadmium as test ion the coefficients of variation for 10 repetitive injections were 4.1% and 3.6% for the dme and platinum sensors respectively. About half of the error arises from variation in the volume dispensed from the syringe. However, after some use the platinum electrode response decreases owing to surface contamination. Although the response is restored after cleaning, this is a considerable drawback for both flow-injection and chromatographic detection purposes. At present, when a solid working electrode is used, this problem is probably best overcome by the wall-jet mode of operation.[9]

Many of the basic properties of the dme cell described here have been examined by Michel and

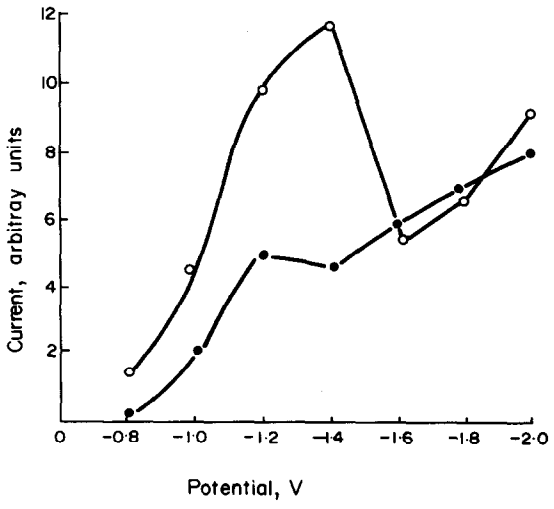


Fig. 3. Current/potential curves for the reduction of nitrobenzene (●) and *p*-nitrophenol (○) at the dme operated at 1 drop/sec in the flow-injection system: 10 μl of a 0.01*M* solution of each was injected into the Britton–Robinson buffer/methanol stream, flow-rate, 2.0 ml/min, at the selected potentials.

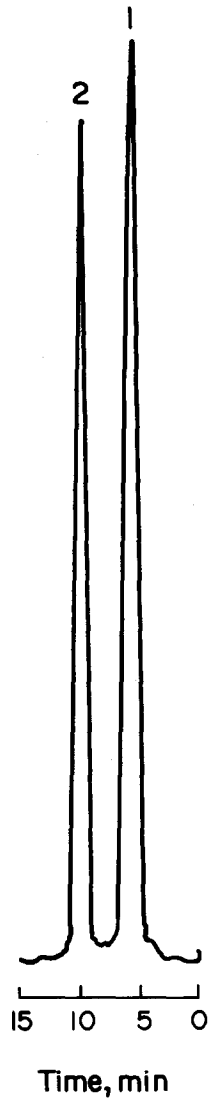


Fig. 4. Chromatographic separation of *p*-nitrophenol (1) and nitrobenzene (2), with use of the dme detector operated at 1 drop/sec. The column was packed with Partisil-10 ODS (10 μm diameter) and the sample solution was 30 μl of *p*-nitrophenol (20.9 μg) and nitrobenzene (18.5 μg), in, and eluted with, Britton–Robinson buffer/methanol at a flow-rate of 1 ml/min. The applied potential was −1.7 V.

Zatka[6] and by Frei *et al.*[7,8] who introduced a third electrode into the system to compensate for change in potential drop from the working to the reference electrode. Thus they examined dependence of response on flow-rate, mercury pressure and drop-time and eluent composition; time-constants as a function of flow-rate and corresponding response volumes were also measured. Overall detector-signal size decreases with increasing flow-rate in a manner which is only partly predictable at present.[10] The active cell volume has been estimated[6] to be <1 μl and this leads to the expectation of very good detector resolution. The constantly renewable electrode surface and the large hydrogen-ion overvoltage are obvious further advantages. High electrical noise levels due to growth and decay of mercury drops are a disadvantage. The large cathodic range for electroreduction processes, complementing the anodic range of glassy carbon, gives a detector with selective capability in flow-injection analysis and useful applications in HPLC. However, the need for a supporting electrolyte effectively confines applications to reversed-phase and ion-exchange chromatography.

REFERENCES

1. J. E. Girard, *Anal. Chem.*, 1979, **51**, 836.
2. B. Pihlar, L. Kosta and B. Hristovski, *Talanta*, 1979, **26**, 805.
3. J. W. Dieker, W. E. van der Linden and H. Poppe, *ibid.*, 1979, **26**, 511.
4. D. G. Swartzfager, *Anal. Chem.*, 1976, **48**, 2189.
5. W. J. Blaedel and Z. Yim, *ibid.*, 1978, **50**, 1722.
6. L. Michel and A. Zatka, *Anal. Chim. Acta*, 1979, **105**, 109.
7. H. B. Hanekamp, W. H. Voogt, P. Bos and R. W. Frei, *Anal. Lett.*, 1979, **A12**, 175.
8. H. B. Hanekamp, P. Bos, U. A. Th. Brinkman and R. W. Frei, *Z. Anal. Chem.*, 1979, **297**, 404.
9. B. Fleet and C. J. Little, *J. Chromatog. Sci.*, 1974, **12**, 747.
10. S. J. Lyle and M. I. Saleh, *Proc. Anal. Div. Roy. Soc. Chem.* in the press.

Talanta, Vol. 28, pp. 255 to 256, 1981
Printed in Great Britain

0039-9140/81/040255-02$02.00/0
Pergamon Press Ltd

PRECONCENTRATION OF CYANIDE FROM WATER BY EXTRACTION WITH TRIBUTYLTIN HYDROXIDE

MIECZYSŁAW WROŃSKI
Department of Chemical Technology, University of Łódź, Poland

(*Received* 30 *June* 1980. *Revised* 15 *August* 1980. *Accepted* 12 *September* 1980)

Summary—Samples of water (500 ml) are extracted with 25 ml of 0.25*M* tributyltin hydroxide in trichloroethylene, which is then stripped with 2*M* sodium hydroxide, the organic reagent being used for a further extraction of the water sample; this cycle is carried out four times. The combined sodium hydroxide extracts are then titrated with silver nitrate solution, with *p*-dimethylbenzylidenerhodanine as indicator. Mean recoveries are around 99%, and the limit of determination is 4 μg/l. Thiocyanate, sulphide, methanethiol and complex cyanides do not interfere.

The high toxicity of free cyanide ions for animals and humans, together with the widespread industrial applications of cyanide, creates a need for a sensitive and selective method capable of determining free cyanide at the 0.01 mg/l. level in the presence of cyanide complexes and other anions, including sulphide and thiocyanate. Titrimetric procedures[1–4] are selective but not sufficiently sensitive, and the popular benzidine–pyridine method of Aldridge[5] lacks selectivity. The standard methods for the separation of cyanide, involving distillation, are in many respects not satisfactory,[6] and the various contributions made towards solving the problem of the determination of cyanide in waters[7–11] do not seem to have overcome all the difficulties.

This paper describes a new approach to the separation problem, based on the observation that tributyltin hydroxide reacts with cyanide to form the corresponding organotin salt, which can be extracted into organic solvents, of which trichloroethylene is the most suitable:

$$(C_4H_9)_3SnOH + CN^- \rightleftharpoons (C_4H_9)_3SnCN + OH^-$$

An increase in hydroxide ion concentration will shift the equilibrium to the left and cyanide will be displaced from the organic phase. The optimum pH for the extraction of cyanide is in the range 7–10, but the selectivity is best at pH 9.5–10, enabling cyanide to be separated from thiocyanate and other anions which may interfere in the final estimation.

EXPERIMENTAL

Reagent

Tributyltin (0.25M) in trichloroethylene (TBT solution). Dissolve 8 ml of tributyltin chloride in 92 ml of trichloroethylene, and shake with 50 ml of 2*M* sodium hydroxide. Separate the organic phase, filter it and keep it for the cyanide separations.

Procedure

To a 500-ml water sample in a suitably large separating funnel add 10 g of ammonium sulphate, 4 g of sodium carbonate, and 1 g of EDTA (disodium salt). When these salts have dissolved, add 25 ml of the TBT solution and shake the funnel about 100 times in 40–60 sec. Transfer the extract to a small funnel and strip the cyanide from it by shaking with 3.5 ml of 2*M* sodium hydroxide for 30 sec. Return the solvent to the large funnel and shake it with the sample as before, and run the alkali into a titration flask. Apply this sequence four times, collecting the four sodium hydroxide extracts in the titration flask. Add 2 g of boric acid to the flask, then 0.2 ml of 0.02% solution of *p*-dimethylaminobenzylidenerhodanine in propan-zol, and titrate with 0.0002–0.01*M* silver nitrate solution until the colour changes from yellow to red. Use a blank containing silver nitrate and indicator for end-point comparison.

RESULTS

When double extractions and strippings were carried out at different pH values, the recoveries were as follows: pH 7.5–9.5, 96%; pH 10, 90%; pH 11, 38%; pH 12, 2%.

The stripping of cyanide from the organic phase with 2*M* sodium hydroxide is not quantitative. At pH 7.5–9.5 the overall transfer of cyanide from the sample to 2*M* sodium hydroxide is 70% for a single extraction–stripping cycle, and 80% for a single extraction with double stripping. That is why the four-stage extraction system is used.

Sulphide and methanethiol are also extracted into the organic phase, but are not stripped by the sodium hydroxide, so do not interfere. To separate larger amounts of sulphide and methanethiol, the sample is made 0.1*M* in sodium hydroxide and extracted with TBT solution in carbon tetrachloride. The extract is discarded, the aqueous phase adjusted to pH 9.5 by addition of sulphuric acid, and the cyanide extracted as above.

The cyanide can also be determined by the standard photometric procedures, as thiocyanate is

Table 1. Determination of free cyanide in 500 ml of water by extraction with tributyltin hydroxide

Cyanide Taken, μg	Found, μg	Recovery, %
4096	4030, 4000, 4020, 4050	98.3
4056*	4045, 4020	99.4
115	113, 116, 115, 110, 114	99
114*	110, 112	97
23	22.3, 23.2, 23.0, 23.1, 22.7	99
4.9	5.0, 4.3, 4.3, 5.1, 4.2	94

* The sample contained 1.5 mg of hydrogen sulphide, which was removed by preliminary extraction at pH 3 with 10 ml of 0.025*M* TBT in carbon tetrachloride.

co-extracted only to the extent of 0.1%, and complex cyanides not at all if the pH is above 7.5.

The results in Table 1 suggest that the procedure is reliable over a wide range of cyanide concentrations, with recoveries of around 99%. Levels of 0.01 mg/l. can be determined within ±20% error, which is just satisfactory for water pollution control purposes. The limit of determination is therefore put at 4 μg/l.

REFERENCES

1. J. A. Ryan and G. W. Culshaw, *Analyst*, 1944, **69**, 370.
2. M. Wroński, *Chem. Anal., Warsaw*, 1960, **5**, 293.
3. R. M. Dagnal, M. T. El-Ghamry and T. S. West, *Talanta*, 1960, **13**, 1667.
4. T. Mukoyama, *Bunseki Kagatu*, 1956, **5**, 12.
5. W. N. Aldridge, *Analyst*, 1945, **70**, 475.
6. *Water Cyanides No. 1: Study No. 29*, Analytical Reference Service U.S. Department of Health, Education and Welfare, Cincinnati, Ohio, 1967.
7. H. A. C. Montgomery, D. K. Gardiner and J. G. G. Gregory, *Analyst*, 1969, **94**, 284.
8. P. J. Barton, C. A. Hemmer and D. C. Kennedy, *J. Water Pollut. Control Fed.*, 1978, **50**, 234.
9. P. Borato, P. F. Rossi and F. Percivale, *Rass. Chim.*, 1978, **30**, 97.
10. T. J. Rohm and R. Davidson, *Anal. Lett.*, 1978, **11**, 1023.
11. G. Nota and C. Improta, *Water Res.*, 1979, **13**, 177.

Talanta, Vol. 28, pp. 257 to 258, 1981
Printed in Great Britain

0039-9140/81/040257-02$02.00/0
Pergamon Press Ltd

A NEW AND RAPID TITRATION OF ANTIMONY(III) WITH POTASSIUM DICHROMATE, WITH IRON(II) AS INDUCTOR

K. SRIRAMAM, B. S. R. SARMA, A. R. K. VARA PRASAD and P. RAVINDRANATH
Department of Chemistry, Nagarjuna University, Nagarjunanagar, 522 510 (A.P) S. India

(*Received* 3 *September* 1980. *Accepted* 22 *October* 1980)

Summary—The optimum conditions for the titration of antimony(III) with dichromate, and diphenylaminesulphonic acid as indicator, have been established. No iodine catalyst is used; the analytical reaction is based on an induced reaction with iron(II) as inductor. The titration can be done as easily as an iron(II) titration and the end-point is equally sharp. Titrations are possible with 0.01*N* solutions.

Potassium dichromate has the advantage of being a primary standard, but under normal conditions its reaction with antimony(III) appears to be too slow to permit a direct titration. Knop[1] proposed a method in which the oxidation was allowed to proceed for 2–3 hr, but the end-point is not sharp and the method is therefore unattractive.[2] Recently a titration procedure that uses diphenylamine as indicator and iodine as catalyst has been reported.[3] However, it suffers from the following drawbacks: (*i*) the working acidity is critical and limited to 2.5*M* sulphuric acid, (*ii*) the end-point has to be approached dropwise because of the slowness of the indicator–antimony(III) reaction, (*iii*) the end-point colour is not clear and (*iv*) it is inapplicable to dilute solutions (0.01*N*). Less desirable oxidizing titrants for antimony(III) are permanganate, iodate and bromate; the difficulties encountered with them have been well documented.[4] Titration with cerium(IV) sulphate, with diphenylamine or one of its derivatives as indicator, also has a slow indicator reaction, despite the use of an iodine catalyst.[5]

We now propose a new and rapid titrimetric method for the determination of antimony(III) with potassium dichromate as titrant and diphenylaminesulphonic acid as indicator. An iodine catalyst is not required.

EXPERIMENTAL

Reagents

Antimony(III) solution, 0.025*M*. Prepared by dissolving the required amount of antimony(III) chloride in 3*M* hydrochloric acid, and standardized against potassium bromate as described by Vogel.[6] More dilute solutions were prepared by dilution with 3*M* hydrochloric acid.

Iron(II) sulphate solution, 0.05*M*. Prepared by dissolving ammonium ferrous sulphate in 0.5*M* sulphuric acid.

Indicator solution. A 0.1% solution of barium diphenylaminesulphonate in water. All other reagents used were of analytical-reagent grade.

Procedure

A 5–8-ml portion of antimony(III) solution (containing 1.5–24 mg of antimony) is taken in a 100-ml conical flask along with 5 ml of an iron(II) solution of such concentration that the mole ratio of iron(II) to antimony(III) is >1:1. Enough 5*M* sulphuric acid is added for the acidity to be 0.5–1.5*M* near the end-point, then the mixture is diluted to 50 ml with water. Two ml of 85% phosphoric acid and 0.2 ml of indicator solution are added. The mixture is then titrated with 0.05 or 0.01*N* potassium dichromate. The colour change at the end-point is from green to violet and is quite sharp. A separate 5-ml portion of the iron(II) solution is titrated in a similar manner (but without antimony present). The difference between the two titration volumes corresponds to the antimony(III).

Hydrochloric acid may be used instead of sulphuric, but then the working acidity can be only 0.5*M*. The titration can also be done in 0.5–1.0*M* sulphuric acid without the addition of phosphoric acid because of the relatively high transition potential (0.84 V) of the indicator (in agreement with a report by Kolthoff and Sarver[7]).

The minimum concentration of chloride for a successful titration is 0.3*M*. Chloride concentrations >0.5*M* in the titrand seem to result in an unfavourable induction factor and the reaction of antimony(III) is not complete before the iron(II) is completely oxidized. However, the addition of another portion of iron(II) at this stage will allow the titration to be completed successfully.

The need for a second portion indicated by the intermittent appearance of an intense light violet colour during the titration (usually at ~0.2–0.5 ml short of the end-point) that disappears in a few sec (the true end-point colour is intense and lasts for more than 15 min). The addition of iron(II) in two portions is recommended for two reasons. The addition of all the iron(II) at the start is not always successful, especially at high acid and chloride concentrations. Also, if the second addition is not necessary, reagent can be saved. With the following modified procedure, titrations can be done in 2*M* sulphuric acid and 1*M* chloride (near the end of the titration); however, if some or all of the chloride derives from hydrochloric acid, the total mineral-acid concentration should not exceed 4*N*.

*Modified procedure for solutions containing more than 0.5*M *chloride in the titration mixture*

A solution containing 1.5–24 mg of antimony(III) is taken in a conical flask. Iron(II) solution (0.05*M* or 0.01*M*) is taken in burette I and the initial reading is noted. About 5 ml are added at first (it is not necessary to read the burette at this stage). Enough 5*M* sulphuric acid is added to give an acidity of 0.5–2*M* near the end-point. The mixture is diluted to 50 ml and 2 ml of 85% phosphoric acid and 0.2 ml of indicator solution are added, then the mixture is titrated with dichromate from burette II, until a

violet colour is just perceptible in the solution. Then about 2.5 ml more iron(II) solution are added from burette I, and the titration with dichromate is continued. The colour change at the end-point is from green to violet and is as sharp as in the unmodified procedure. Both burettes are read, and the "blank" titration is done on the volume of iron(II) solution used in the test run. The difference between the two titration volumes again corresponds to the antimony(III).

From the results of eight determinations the mean relative error and coefficient of variation were found to be 0.2% and 0.1$_4$% respectively.

Interferences

Amounts of 58 mg of cobalt, 100 mg of nickel, 150 mg of zinc, 300 mg of lead (most of it present in precipitated form during the titration) and 26 mg of bismuth do not interfere in the determination. Copper, manganese and arsenic(III) interfere even when present in small quantities.

Differential titration of iron(II) and antimony(III)

Rao *et al.*[5] found that iron(II) alone can be determined in a mixture by titration with cerium(IV) sulphate, with diphenylaminesulphonic acid as indicator. By combination of the procedure just described with that of Rao *et al.*, iron(II) and antimony(III) can be determined differentially. In the titration with dichromate, it may be necessary to add a known amount of iron(II) in order to adjust the iron(II):antimony(III) ratio to the optimum value.

RESULTS AND DISCUSSION

The reaction of diphenylaminesulphonic acid with dichromate is known to be slow in the absence of a trace of iron(II)[7] and/or iron(III) phosphate complex.[8] The direct titration of antimony(III) with dichromate is, however, not possible even after the addition of excess of iron(III) and phosphoric acid to the titrand. Evidently the reduction of oxidized indicator by antimony(III) is also slow. The procedure now proposed does not work when the mole ratio of iron(II) to antimony(III) is less than 1:1 but higher proportions of iron(II) do not disturb the titration. Under the optimum conditions, the titration can be done as easily as an iron(II) titration. The end-point is very sharp and the colours are clear. The titration can be done in either sulphuric or hydrochloric acid media, and the working ranges of acidity are 0.5–2.0*M* and 0.5–1.5*M* respectively. Titrations with 0.01*N* solutions are very accurate and no indicator correction need be applied, because the iron(II) blank titration automatically compensates for it. Although the titration of a mixture of iron(II) and antimony(III) with dichromate gives a total value, the titration with cerium(IV) and the same indicator, but without iodine catalyst, gives only the iron(II) value;[5] a differential procedure is thus possible when the two are present together.

These observations indicate that the reaction of antimony(III) with dichromate is a coupled reaction which proceeds through an induction mechanism such as:

$$Fe(II) + Cr(VI) \rightleftharpoons Fe(III) + Cr(V) \quad (1)$$

$$Cr(V) + Sb(III) \rightarrow Cr(III) + Sb(V) \quad (2)$$

Reaction step (1) is fast[9] and it is plausible that reaction step (2) is also fast, because the complementary two-electron transfer reaction provides an easier route, the chloride present in the antimony(III) solution probably facilitating such an exchange.[10] The reaction of oxidized indicator with iron(II) is also fast; the presence of iron(II) throughout the course of titration thus eliminates the effect of slowness of the indicator–antimony(III) reaction.

The successful action of the indicator in titrations with ceric sulphate[5] and dichromate with or without a catalyst, is puzzling, in view of the reported oxidation of diphenylaminesulphonic acid by antimony(V) to give the violet colour in hydrochloric acid medium; the details of the Russian work[11] are not, however, available to us. The prerequisite of their photometric determination is that antimony should be present as antimony(III) in the solutions to be analysed. It is converted into $SbCl_6^-$ by oxidation with sodium nitrite in the presence of 6*M* hydrochloric acid, the excess of nitrite being removed with urea. It seems likely that one of the reaction products from nitrite is the cause of the colour reaction with diphenylaminesulphonic acid. It is probable that $SbCl_6^-$ is involved in the reaction in such a manner that the antimony undergoes no net change in oxidation state but participates in the stoichiometry of the colour reaction (*e.g.*, antimony(V) can act as a Lewis acid). In a separate experiment we have observed no colour formation on mixing antimony(V) and indicator solutions under the experimental conditions used for the titration.

Acknowledgement—One of us (A.R.K.V.P.) gratefully acknowledges the financial assistance given by CSIR, New Delhi (India) as a Research Fellowship.

REFERENCES

1. J. Knop, *Z. Anal. Chem.*, 1923, **63**, 96.
2. I. M. Kolthoff and R. Belcher, *Volumetric Analysis*, Vol. III, p. 196. Interscience, New York, 1957.
3. N. F. Mody, K. K. Desai and B. N. Oza, *J. Inst. Chem. (Calcutta)*, 1976, **48**, 125.
4. I. M. Kolthoff and R. Belcher, *op. cit.*, pp. 73, 457 and 513.
5. G. G. Rao, S. G. Viswanath and M. Gandikota, *Anal. Chim. Acta*, 1975, **79**, 273.
6. A. I. Vogel, *Text Book of Quantitative Inorganic Analysis*, 4th Ed., p. 386. Longmans, London, 1973.
7. L. A. Sarver and I. M. Kolthoff, *J. Am. Chem. Soc.*, 1931, **53**, 2902.
8. E. Brennecke, in *Newer Methods of Chemical Analysis*, W. Böttger (ed.), trans. R. E. Oesper, p. 159. Van Nostrand, New York, 1938.
9. J. H. Espenson and E. L. King, *J. Am. Chem. Soc.*, 1963, **85**, 3328.
10. A. G. Sykes, *Advan. Inorg. Chem. Radiochem.*, 1967, **10**, 182.
11. L. Naruskevicius, R. Kazlanskas and J. Skadanskas, *Zavodsk. Lab.*, 1972, **38**, 1435; *Chem. Abstr.*, 1973, **78**, 92136.

Talanta, Vol. 28, pp. 259 to 261, 1981
Printed in Great Britain. All rights reserved

0039-9140/81/040259-03$02.00/0
Copyright © 1981 Pergamon Press Ltd

ESTIMATION OF XYLENES WITH CHLORAMINE-T

S. M. MAYANNA and K. V. UMA*

Department of Chemistry, Central College, Bangalore University, Bangalore 560 001, India

(*Received* 26 *February* 1980. *Revised* 16 *September* 1980. *Accepted* 7 *November* 1980)

Summary—The reaction between xylenes and chloramine-T has been found to proceed quantitatively over a wide range of experimental conditions. A back-titration procedure in which xylenes are reacted with excess of chloramine-T in 1*M* perchloric acid–0.03*M* sodium chloride medium has been developed. Inorganic ions other than chloride do not interfere. The method can be used for estimating xylenes in the presence of some other petrochemicals.

Chloramine-T can act as an oxidizing agent[1] or a chlorinating agent.[2] The oxidative properties of chloramine-T have been used for assaying several organic and inorganic compounds,[3,4] but little analytical use has been made of the chlorination properties. Xylenes are widely used in industry and can readily be chlorinated. The kinetics of chlorination of aromatic hydrocarbons by antimony chloride,[5] hypochlorous acid[6] and alkyl hypochlorites[7] have been studied. Xylenes are usually estimated by spectroscopic[8] and gas chromatographic[9] techniques, but a chemical method would be useful. In this communication a titrimetric estimation of xylenes with chloramine-T is described.

EXPERIMENTAL

Reagents

Chloramine-T was purified by the method of Morris *et al.*[10] An approximately 0.1*N* solution was prepared and standardized iodometrically. Xylenes were distilled before use. Aqueous solutions of the xylenes (0.25 mg/ml) were prepared in triply distilled water or standard buffer solutions.[11]

* Department of Chemistry, Maharani's Science College for Women, Bangalore.

Preliminary studies

A direct titration of xylene at room temperature (25–28°) with chloramine-T (CAT) with a visual or potentiometric end-point was found impracticable, because the chlorination, though rapid, was not instantaneous, so a back-titration procedure was developed.

In preliminary experiments with CAT, 1 ml of xylene solution (1.33 mmole) was added to a known and excessive volume of CAT solution (6.66 mmole) in an iodine-flask. The reaction mixture was set aside, with occasional shaking, then the excess of CAT was determined by back-titration. The experimental conditions (time *etc.*) were systematically varied. A typical set of results for the degree of chlorination of *p*-xylene (pX), *m*-xylene (mX) and *o*-xylene (oX) in different media is given in Table 1. It is seen that chlorination is slow at all pH values. The degree of chlorination was slightly better in acidic solution than in alkaline medium. Among the mineral acids only hydrochloric acid favoured chlorination. Chlorination was non-stoichiometric and not reproducible in various media other than acidic solution containing chloride ions. It is known[12] that CAT itself decomposes in concentrated acidic chloride solution. Therefore, in the present estimation perchloric acid containing chloride was employed. The rate of chlorination increased gradually with increase of the concentration of chloride but the increase became rapid at chloride concentrations $\geqslant 0.02M$. At constant chloride concentration, the rate of chlorination increased with increase of acid concentration. The time-dependence of the degree of chlorination

Table 1. Degree of chlorination of xylenes with chloramine-T

Medium	[CAT]† / [pX]	[CAT]† / [mX]	[CAT]† / [oX]	Medium	[CAT]† / [pX]	[CAT]† / [mX]	[CAR]† / [oX]
pH 1	0.60	0.59	0.59	0.1*M* CH_3COOH	0.24	0.21	0.22
pH 2	0.35	0.34	0.35	0.1*M* $HClO_4$	0.26	0.23	0.24
pH 3	0.16	0.12	0.14	0.1*M* $HClO_4$*	0.53	0.47	0.50
pH 4	0.13	0.08	0.10	0.2*M* $HClO_4$*	0.74	0.60	0.61
pH 5	0.09	0.06	0.07	0.4*M* $HClO_4$*	0.79	0.73	0.75
pH 6	0.06	0.05	0.06	0.6*M* $HClO_4$*	0.84	0.74	0.81
pH 7	0.05	0.04	0.05	0.8*M* $HClO_4$*	0.88	0.80	0.82
pH 8	0.04	0.03	0.03	1.0*M* $HClO_4$*	0.94	0.89	0.92
0.1*M* NaOH	0.00	0.00	0.00	1.0*M* $HClO_4$§	0.82	0.75	0.78
0.1*M* HCl	0.65	0.62	0.62	1.0*M* $HClO_4$‡	1.00	0.95	0.98
0.1*N* H_2SO_4	0.21	0.19	0.19	1.0*M* $HClO_4$‖	1.00	1.00	1.00

Xylene taken 1.33 mmole; CAT taken 6.66 mmole; time 30 min.
† CAT reacted (mmole): xylene taken (mmole).
§ 0.005*M* NaCl.
* 0.01*M* NaCl.
‡ 0.02*M* NaCl.
‖ 0.03*M* NaCl.

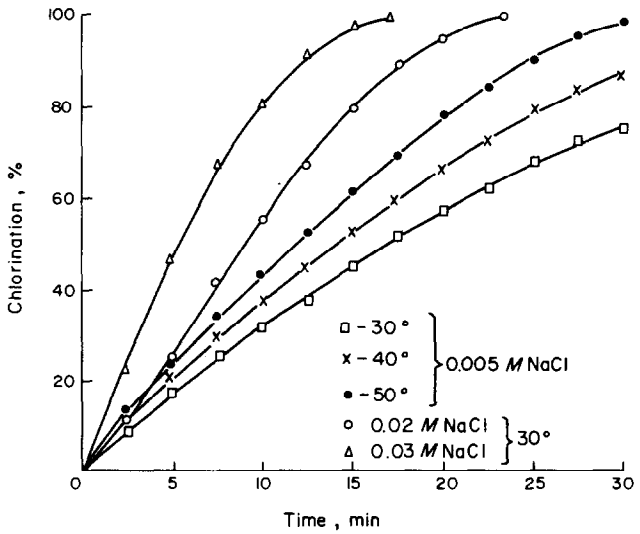


Fig. 1. Rate of chlorination of *p*-xylene under different experimental conditions. $[HClO_4] = 1M$; $[CAT] = 0.02N$.

(fraction of xylene chlorinated) under different experimental conditions is given in Fig. 1. It is clear from the figure that temperature has a considerable effect on the rate of chlorination.

Recommended procedure

Prepare an aqueous solution of the xylenes. Add a portion of known volume containing 0.1–2 mmole to 100 ml of 0.02*N* CAT. Add enough perchloric acid and sodium chloride solution (of known concentration) to give a concentration of 1*N* perchloric acid and 0.03*N* sodium chloride. Set aside for about 30 min at laboratory temperature (~25°) with occasional shaking. Rinse down with 20 ml of distilled water, add 25 ml of 2*N* sulphuric acid and 20 ml of 10% potassium iodide solution and titrate with 0.02*N* sodium thiosulphate. Run a blank titration with the same volume of CAT under identical conditions. The amount (*x* mg) of xylene is given by

$$x = 53y(V_1 - V_2)$$

where *y* is the molarity of the thiosulphate solution, V_1 the blank titration and V_2 the test sample titration.

RESULTS AND DISCUSSION

Some typical results are given in Table 2. The maximum error is about 1%. Table 3 gives results for analyses for xylene in the presence of some petrochemicals. The reaction stoichiometry is 1:1:

$$C_6H_4(CH_3)_2 + RNClNa + HCl \rightarrow C_6H_3Cl(CH_3)_2 + RNH_2 + NaCl$$

where

$$R = CH_3C_6H_4SO_2.$$

The presence of chlorinated xylene (ring substituted) in the reaction products was detected by spot-tests.[13] *p*-Toluenesulphonamide was identified by chromotographic analysis.[14] The detailed investigation of the systems brought out the following facts.

(*i*) Foreign ions such as Na^+, K^+, Zn^{2+}, Ba^{2+}, NO_3^-, PO_4^{3-}, ClO_4^- and SO_4^{2-} (up to ionic strength 0.2) have no influence on the rate of chlorination. Sulphate at higher concentration has an inhibitory effect.

(*ii*) Chloride has a significant effect on the rate of chlorination.

Table 2. Estimation of xylenes with chloramine-T

p-Xylene, *mg*		*m*-Xylene, *mg*		*o*-Xylene, *mg*	
Taken	Found	Taken	Found	Taken	Found
0.51	0.52	0.53	0.52	0.55	0.56
1.03	1.03	1.06	1.05	1.10	1.12
2.06	2.07	2.12	2.10	2.20	2.21
4.12	4.15	4.24	4.23	4.40	4.43
7.74	7.74	7.96	8.01	8.80	8.86
10.32	10.36	10.67	10.70	11.00	11.08
13.41	13.42	13.80	13.68	13.20	13.25
16.51	16.58	16.98	17.10	17.60	17.63
20.64	20.53	21.23	21.20	22.00	22.04
24.76	24.77	25.48	25.55	26.40	26.40

$[HClO_4] = 1M$; $[NaCl] = 0.03M$; temperature 30°C; time = 30 min.

Table 3. Estimation of 10.0 mg of *p*-xylene in presence of some petrochemicals

Petrochemical,* (~5 *mg*)	*p*-Xylene found, *mg*
Benzene	10.01
Toluene	9.00
Naphthalene	9.20
Cyclohexane	9.85
Octane	9.92
Pentane	10.10
Hexane	10.08

* In alcohol solution.
$[HClO_4] = 1M$; $[NaCl] = 0.03M$; $[CAT] = 0.02N$; time = 30 min.

(*iii*) The stoichiometry is unaffected by the reversal of the order of addition of CAT and xylene.

(*iv*) Toluene and naphthalene interfere slightly.

In acidic solution CAT gives several species[14–17] such as $RNCl_2$, RNHCl, H_2OCl^+, HOCl and Cl_2 which may chlorinate the organic substrates. The kinetics of chlorination of xylene in acidic solution are under detailed investigation, which may throw light on the mechanism.

Acknowledgements—The authors are grateful to Professor G. K. Narayana Reddy, Head, Department of Chemistry, Central College, Bangalore University, Bangalore, for providing laboratory facilities. One of the authors (K.V.U.) wishes to express grateful thanks to the Director of Collegiate Education, Government of Karnataka for kind encouragement.

REFERENCES

1. J. Coull, H. B. Hope and B. Gouguall, *J. Am. Chem. Soc.*, 1935, **57**, 1489.
2. F. G. Soper and G. F. Smith, *J. Chem. Soc.*, 1926, 1582.
3. A. Berka, J. Vulterin and J. Zýka, *Newer Redox Titrants*, p. 37. Pergamon Press, New York, 1965.
4. E. Bishop and V. F. Jennings, *Talanta*, 1958, **1**, 197.
5. R. Corriu and C. Caste, *Tetrahedron*, 1969, **25**, 4949.
6. P. B. D. de la Mare and L. Main, *J. Chem. Soc. B*, 1971, 90.
7. V. L. Heasley, G. E. Heasley, D. M. Ingle, P. D. Devis and T. L. Rold, *J. Org. Chem.*, 1973, **38**, 2549.
8. J. Jokal and J. Knizek, *Acta Chim. Acad. Sci. Hung.*, 1962, **33**, 17.
9. J. Romovacek and N. Novotny, *Brennstoff, Chem.*, 1961, **42**, 161.
10. J. C. Morris, J. A. Salazan and M. A. Wineman, *J. Am. Chem. Soc.*, 1948, **70**, 2036.
11. A. Findlay, *Practical Physical Chemistry*, p. 268. Longmans, London, 1954.
12. A. George, *M.Sc. Dissertation*, Bangalore University, India, 1978.
13. F. Feigl, E. Jungreis and V. Lipetz, *Anal. Chem.*, 1964, **36**, 885.
14. D. S. Mahadevappa and N. M. Madegowda, *Talanta*, 1975, **22**, 771.
15. D. R. Pryde and F. G. Soper, *J. Chem. Soc.*, 1931, 1510.
16. T. Higuchi, K. Ikeda and A. Hussain, *J. Chem. Soc., B*, 1967, 546.
17. K. V. Uma and S. M. Mayanna, *Bull. Chem. Soc., Japan*, 1978, **51**, 1047.

Talanta, Vol. 28, pp. 262 to 264, 1981
Printed in Great Britain

0039-9140/81/040262-03$02.00/0
Pergamon Press Ltd

DETERMINATION OF THIOCARBAMYL SULPHENAMIDES, THIURAM DISULPHIDES AND DIBENZOTHIAZYL DISULPHIDE BY AMPEROMETRIC TITRATION

DIPAK K. BASU, BASUDAM ADHIKARI, DHANANJAY PAL and AJIT K. CHAUDHURI

Department of Macromolecules, Indian Association for the Cultivation of Science, Calcutta-700032, India

(*Received* 30 *September* 1980. *Accepted* 3 *November* 1980)

Summary—An amperometric method for the determination of thiocarbamyl sulphenamides has been developed, based on the cleavage of the S–N bond by hydriodic acid. The method can also be applied for the cleavage of the S–S bond in thiuram disulphides and dibenzothiazyl disulphide, and thus provides a useful means for the estimation of these compounds as well.

Benzothiazole sulphenamides are well-known for their delayed-action curing of rubber and yielding vulcanizates with superior physical properties. The ultra-accelerators, thiuram di- and mono-sulphides, on the other hand, are characterized by rapid cure and production of vulcanizates of improved thermal and oxidative stability. Use of thiocarbamyl sulphenamides as accelerators in the vulcanization of rubber has received much attention recently since they combine both processing safety and rapid cure with improved vulcanizate properties. However, no attempt seems to have been made to develop analytical methods for these accelerators. Here we describe a simple titrimetric method for the estimation of thiocarbamyl sulphenamides, depending on the cleavage of the S–N bond by hydriodic acid. The latter can also cleave the S–S bond of the thiuram disulphides and dibenzothiazyl disulphide, and on this basis these disulphides can also be determined.

EXPERIMENTAL

Apparatus

The apparatus[1] used for the amperometric titration was described in the previous communication.[2]

Reagents

The accelerators *N*,*N*-diethylthiocarbamyl-*N'*-cyclohexyl sulphenamide (DETCS), m.p. 64.5°; *N*-cyclopentamethylene thiocarbamyl-*N'*-cyclopentamethylene sulphenamide (CPTCS), m.p. 101°; *N*-oxydiethylene thiocarbamyl-*N'*-oxydiethylene sulphenamide (OTOS), m.p. 136°; tetraethylthiuram disulphide (TETD), m.p. 70°; dicyclopentamethylenethiuram disulphide (CPTD), m.p. 130°, and *N*-cyclohexyl-2-benzothiazole sulphenamide (CBS), m.p. 100°, were prepared[3–5] and purified in the usual way with some necessary modifications. Recrystallized 2-mercaptobenzothiazole (MBT), m.p. 178° and dibenzothiazyl disulphide (MBTS), m.p. 179°, were used. All other reagents used were of analytical-reagent grade.

Procedure

Estimation of DETCS at 0°. One ml of 0.01*M* methanolic DETCS solution was taken in a 100-ml flat-bottomed vessel fitted with a B50 stopper, 2.5 g of potassium iodide were added, followed by 1 ml of water and enough methanol (3 ml) to give a clear solution. One ml of 1*M* hydrochloric acid was then added and the mixture allowed to stand in an ice-bath for about 5 min in the dark; 45 ml of water were then added to the mixture and the iodine liberated was titrated amperometrically with 0.01*M* sodium thiosulphate. There was practically no blank value.

$$2 \text{ moles of DETCS} \equiv 1 \text{ mole of } I_2$$

Estimation of DETCS at room temperature. The reaction was done under the conditions above but at room temperature. In this case use of a higher proportion of hydrochloric acid did not affect the result, and under these conditions

$$1 \text{ mole of DETCS} \equiv 1 \text{ mole of } I_2$$

The same procedure was used for the estimation of the other thiocarbamyl sulphenamides CPTCS and OTOS, and also the thiuram disulphides TETD and CPTD.

$$1 \text{ mole of thiuram disulphide} \equiv 1 \text{ mole of } I_2$$

Estimation of MBTS. In this case the sample is dissolved in chloroform instead of methanol, and the reaction medium was diluted with 40 ml of ethanol to keep in solution the MBT formed.

HPLC of TETD formed from DETCS at 0°. In a pear-shaped flask in an ice-bath, 1 ml of 0.01*M* DETCS in methanol was placed, followed by 2 ml of acetonitrile, 2 g of potassium iodide, 5 ml of water and 1 ml of 1*M* hydrochloric acid. After the mixture had stood for 5 min in the dark, thiosulphate solution was added to consume the iodine liberated. The contents of the flask were made ammoniacal and evaporated under vacuum. The residue obtained was extracted with chloroform, which was then removed under vacuum. Finally the residue was dissolved in acetonitrile–water mixture (70:30) and injected into a Waters μC_{18} column, with CBS as internal standard. Comparison of the chromatogram of this test solution with that of a standard solution containing the same amount of CBS and the amount of TETD calculated to be formed from 1 ml of 0.01*M* DETCS clearly indicated that the formation of TETD was quantitative.

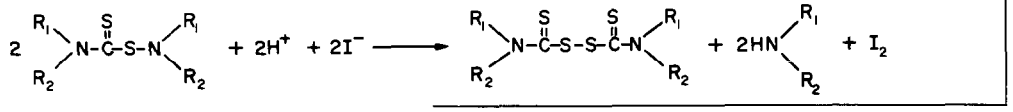
HPLC of MBT formed from MBTS. One ml of 0.01*M* MBTS in chloroform, 7 ml of ethanol, 2 g of potassium iodide and 1 ml of 1*M* hydrochloric acid were added in that order to a pear-shaped flask, which was then kept in the dark at room temperature for 5 min. The rest of the procedure was the same as that just described but with the

calculated amount of MBT instead of TETD in preparation of the standard solution.

RESULTS AND DISCUSSION

The analytical method reported earlier[2] for the estimation of benzothiazole sulphenamides, was based on the action of hydriodic acid (potassium iodide and hydrochloric acid) on the sulphenamides and by amperometric titration of the liberated iodine with thiosulphate. As was pointed out, to obtain accurate and reproducible results proper adjustment of the ratio of hydrochloric acid to sulphenamide concentration is essential for the sulphenamide to be quantitatively converted into MBTS, and further reaction of the MBTS with the acid iodide mixture to be negligible. The reaction temperature has also to be maintained at 0°

However, when this procedure was applied to thiocarbamyl sulphenamides it was found that the reactant concentrations have to be varied somewhat and a higher proportion of hydrochloric acid used, or erratic results are obtained. Strict control of the reactant concentrations and the temperature is also essential to get satisfactory results. By analogy with the benzothiazole sulphenamides, the reaction occurring with the thiocarbamyl sulphenamides may be described as



The formation of tetraethylthiuram disulphide from DETCS has been confirmed by isolating it from the reaction products and subjecting it to infrared and HPLC analysis, the results being compared with those for an authentic sample of TETD.

However, if the DETCS reaction is done at room temperature, the reaction becomes faster and more facile, and no thiuram disulphide can be isolated. Presumably the intermediate thiuram disulphide also reacts with hydriodic acid under these conditions with further liberation of iodine.

We have confirmed that this further reaction at room temperature is quantitative. Thus it is more advantageous to do the reaction at room temperature and determine the total iodine liberated, strict adjustment of the acidity no longer being essential. The analytical results for three thiocarbamyl sulphenamides, DETCS, CPTCS and OTOS, are reported in Table 1. It is seen that the nature of the substituents on the carbamate and sulphenamide nitrogen atoms does not affect the speed of the reaction, which is complete within 5 min. The results are correct to within ±1%.

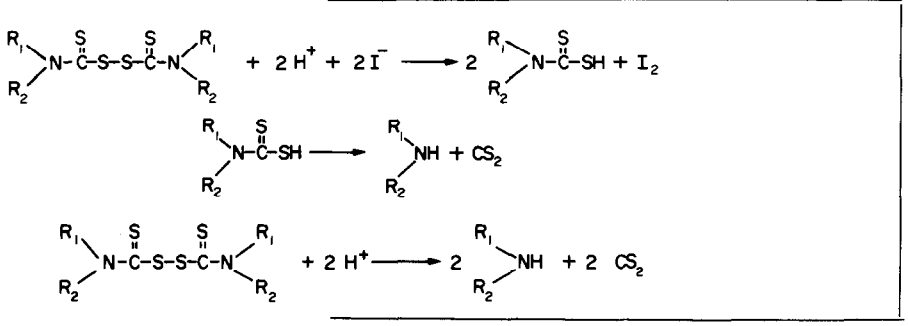
Table 1. Estimation of thiocarbamyl sulphenamides, thiuram disulphides and dibenzothiazyl disulphide

Accelerator	Taken, *mg*	Found, *mg*
DETCS	2.46	2.46 2.48 2.46*
CPTCS	2.44	2.44 2.46 2.44
OTOS	2.48	2.48 2.46 2.46
TETD	2.96	2.96 2.96 2.93
CPTD	3.20	3.20 3.23 3.23
MBTS	3.32	3.35 3.32 3.29

*Reaction at 0°C.

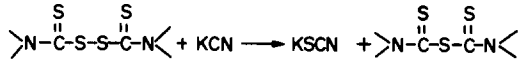
It is evident that thiuram disulphides can be estimated by the same procedure.

Methods for estimation of thiuram disulphides usually involve decomposition with mineral acids and determination of the amount of carbon disulphide or the corresponding amine formed.



Callan and Strafford[6] used mineral acid in the presence of magnesium filings and estimated the carbon disulphide formed, by converting it into xanthate. Stevenson[7] pointed out the shortcomings of earlier methods and recommended the use of mixed mineral acids along with zinc sulphate solution. Ravindranath

and Patel[8] estimated the carbon disulphide produced, by oxidation with acidified chloramine-T. Brock and Louth[9] determined thiuramsulphides by identification of their decomposition products. Alternatives are to react the thiuram disulphide with potassium cyanide and determine the thiocyanate formed, by amperometric[10] or conductometric titration[11] with silver nitrate.



All these methods are cumbersome and time-consuming, involving a number of operations. Our method is simple and rapid (complete within 10 min), and gives reproducible results with good precision (±1%). It can also be applied for the estimation of MBTS, which, as reported earlier,[2] is also decomposed by hydriodic acid at room temperature to yield MBT.

That MBT is formed has been confirmed by comparison of the infrared spectrum of the product with that of an authentic sample. The yield has been shown to be quantitative by HPLC. The reaction is complete within 5 min. Results for the estimation of TETD, CPTD and MBTS are also included in Table 1.

REFERENCES

1. I. M. Kolthoff and W. E. Harris, *Ind. Eng. Chem., Anal. Ed.*, 1946, **18**, 161.
2. D. K. Basu, B. Adhikari, D. Pal and A. K. Chaudhuri, Talanta, 1980, **27**, 671.
3. G. E. P. Smith, Jr., G. Alliger, E. L. Carr and K. C. Young, *J. Org. Chem.*, 1949, **14**, 935.
4. A. D. Cummings and H. E. Simmons, *Ind. Eng. Chem.*, 1928, **20**, 1173.
5. E. L. Carr, G. E. P. Smith, Jr. and G. Alliger, *J. Org. Chem.*, 1949, **14**, 921.
6. T. Callan and N. J. Strafford, *J. Soc. Chem. Ind.*, 1924, **43**, 1T.
7. A. Stevenson, *J. Sci. Food Agric.*, 1964, **15**, 509.
8. K. Ravindranath and C. C. Patel, *Analyst*, 1968, **93**, 342.
9. M. J. Brock and G. D. Louth, *Anal. Chem.*, 1955, **27**, 1575.
10. P. K. Chatterjee, D. Banerjee and A. K. Sircar, *J. Sci. Ind. Res. (India)*, 1960, **19B**, 118.
11. W. Scheele and C. Gensch, *Kautschuk Gummi*, 1954, **7**, WT 122.

Talanta, Vol. 28, pp. 265 to 267, 1981
Printed in Great Britain

0039-9140/81/040265-03$02.00/0
Pergamon Press Ltd

THE QUANTITATIVE DETERMINATION OF HYDRATED CALCIUM SULPHATES IN CEMENT BY USE OF SELF-GENERATING ATMOSPHERE THERMOGRAVIMETRY

T. B. SMALLWOOD* and C. D. WALL

Blue Circle Industries Ltd., Research Division, London Road, Greenhithe, Kent, England

(*Received* 3 *September* 1980, *Accepted* 28 *October* 1980)

Summary—A method is described for the quantitative determination of hydrated calcium sulphates in cement by use of self-generating atmosphere thermogravimetry. The method is rapid and precise and can be applied (with a suitably modified sample container) with most thermogravimetric equipment.

The major component of Portland cement is a clinker manufactured by sintering a mixture of calcareous material (chalk or limestone) and an argillaceous material (clay or shale) at a temperature around 1450°. This clinker, if mixed with water, "flash sets" to give an unworkable product. In order to control the set, calcium sulphate, usually in the form of naturally occurring gypsum ($CaSO_4.2H_2O$) is ground with the clinker to form cement. This gypsum may contain variable quantities of naturally occurring anhydrite (β-anhydrite).

During the milling process, part of the kinetic energy of the grinding media is dissipated as heat, causing some dehydration of the gypsum to occur, resulting in a mixture of gypsum, its hemihydrate ($CaSO_4.\frac{1}{2}H_2O$) and anhydrite ($CaSO_4$). The quantities of the various calcium sulphates present in a cement have a significant effect on its hydration mechanism and are thus of considerable interest in determining manufacturing conditions and in the study of the hydrating cement system.

Wet chemical methods[1] for determining gypsum and its hemihydrate are unsuitable for cements. Infrared spectroscopy will differentiate gypsum, its hemihydrate and β-anhydrite qualitatively but its quantitative capabilities are limited. Thermogravimetry (TG) with a shallow crucible as sample container and a heating rate of 4°/min fails to resolve the consecutive weight losses. Slower heating rates permit partial resolution of the weight losses, but the method then becomes very time-consuming.

The quasi-isothermal TG technique,[2] in which the temperature programme is halted at the onset of each weight loss, requires a high level of expertise and close supervision of the equipment in order to achieve reproducible results, and as such is unsuitable as a routine method.

An alternative approach is to use the technique of self-generating atmospheres (SGA)[3] in which a gas evolved from one reaction is constrained within the sample environment in order to delay the start of a second reaction.

EXPERIMENTAL

Instrumentation

A Stanton–Redcroft thermobalance (model TR-1) was used throughout. The instrumental conditions employed were:

Sensitivity	100 mg FSD
Atmosphere	Static air
Heating rate	4°/min
Sample weight	5 g
Chart speed	6 in./hr

Procedure

A Pyrex glass container was constructed (Fig. 1). Its ground-glass stopper produces a gas-tight seal, while a

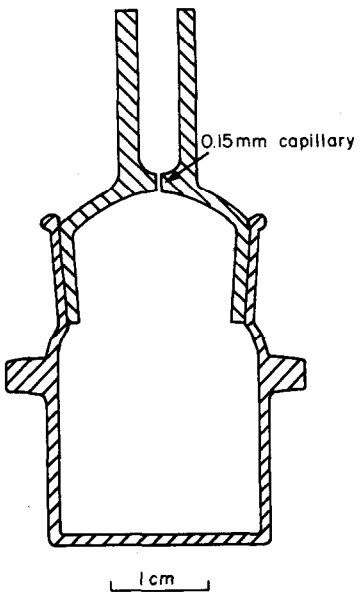


Fig. 1. Self-generating atmosphere sample-holder for thermogravimetry.

* To whom correspondence and requests for reprints should be addressed.

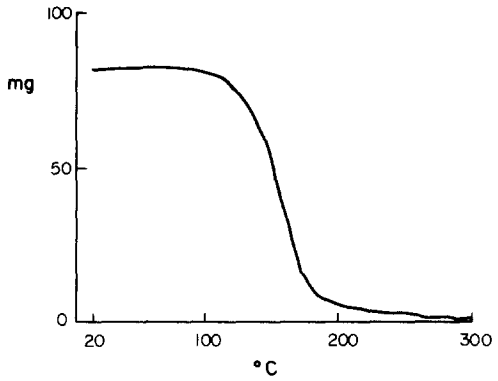


Fig. 2. TG curve for a cement heated in an open sample container.

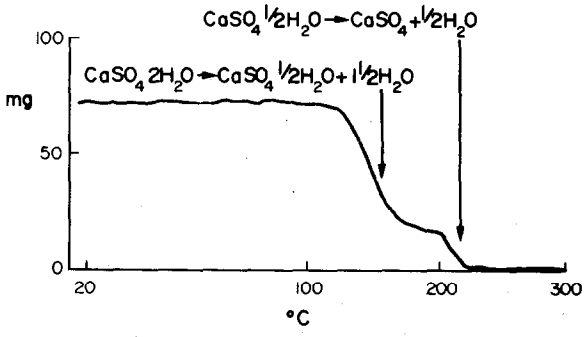


Fig. 3. TG curve for a cement heated in an SGA sample container.

0.15-mm diameter capillary opening in the stopper permits slow loss of water vapour. Three glass studs fused to the side of the container enable it to sit on the ringed support rod of the thermobalance.

The cross-sectional area of the capillary, the sample weight and the heating rate are important parameters in achieving good resolution. In view of the instrumentation available it was decided to use as standard conditions a sample weight of 5 g, a heating rate of 4°/min, and to adjust the dimensions of the capillary accordingly.

The first cell produced had a capillary 0.35 mm in diameter and gave poor resolution. The available cross-sectional area was progressively reduced by inserting stainless-steel wires of successively increased diameter. Resolution improved with decreasing cross-sectional area of the opening down to 0.01767 mm^2 (equivalent to a capillary 0.15 mm in diameter). Further reduction of the cross-sectional area resulted in loss of resolution. A buoyancy-correction curve was prepared by means of replicate analysis of 5 g of calcined alumina.

By extrapolation to locate the onset of each discrete weight loss, and correction for buoyancy effects, the quantity of gypsum and its hemihydrate present can be determined. Additionally, if the sulphate contents of the original clinker and finished cement are known, it is possible to calculate the total anhydrite ($\gamma + \beta$).

RESULTS AND DISCUSSION

Only a single weight loss is observed on a TG curve for gypsum heated in a normal open sample container, Fig. 2.

The dehydration of gypsum to γ-anhydrite is a two-stage process:[4]

$$CaSO_4.2H_2O \rightarrow CaSO_4.\tfrac{1}{2}H_2O + 1\tfrac{1}{2}H_2O$$

$$CaSO_4.\tfrac{1}{2}H_2O \rightarrow CaSO_4 + \tfrac{1}{2}H_2O$$

The two stages are clearly observable when an SGA sample container is used (Fig. 3).

A correction for the buoyancy effect is applied to each weight loss, by means of the buoyancy curve measured for the thermobalance employed.

The calculation from the weight losses depends on whether both gypsum and its hemihydrate are present.

(*a*) *Gypsum only.* A two-stage weight loss will be observed, the first being three times the second.

$$\text{Gypsum} = \frac{\text{Total weight loss} \times 100 \times 4.78}{\text{Sample weight}}\%$$

(*b*) *Gypsum and hemihydrate present.* A two-stage weight loss will be observed, the first less than three times the second.

$$\text{Gypsum} = \frac{\text{First stage weight loss} \times 100 \times 6.37}{\text{Sample weight}}\%$$

$$\text{Hemihydrate} = \frac{(\text{Total weight loss} - \tfrac{4}{3} \times \text{first stage weight loss}) \times 100 \times 16.1}{\text{Sample weight}}\%$$

(*c*) *Hemihydrate only* Only one weight loss is observed.

$$\text{Hemihydrate} = \frac{\text{Weight loss} \times 100 \times 16.1}{\text{Sample weight}}\%$$

The procedure described takes approximately 1½ hr to perform and requires no more skill than the conventional TG method. The method gives adequate precision, as demonstrated by the data in Table 1, which were collected by analysing the same cement ten times, over a period of several days.

Results obtained from the analysis of ten different ordinary Portland cement samples are given in Table 2 and demonstrate the range of values typically encountered.

Table 1. Reproducibility of the TG–SGA analysis of an unhydrated cement

	H_2O ex-gypsum	H_2O ex-hemihydrate
Mean, %	0.291	0.142
Standard deviation, %	0.0104	0.0075
Coefficient of variation, %	3.6	5.2

Table 2. Analysis of Portland cement samples

Sample	Gypsum, %	Hemihydrate, %
1	2.9	Not detected
2	2.8	0.6
3	1.8	1.9
4	1.1	1.3
5	0.7	1.3
6	0.3	1.9
7	0.4	0.3
8	Not detected	0.6
9	Not detected	1.6
10	Not detected	4.0

The method can be used for similar differential weight loss measurements at higher temperature (*e.g.*, for analysis of dolomite) if the sample-holder is made from fused quartz.

REFERENCES

1. *Analysis of Calcareous Materials*, SCI Monograph No. 18, Soc. Chem. Ind., London, 1964.
2. C. J. Keattch, *J. Appl. Chem.*, 1967, **17**, 27.
3. P. D. Garn, *Thermoanalytical Methods of Investigation*, Academic Press, London, 1965.
4. H. G. Adie, *Can. J. Chem.*, 1964, **42**, 792.

Talanta, Vol. 28, pp. 268 to 270, 1981
Printed in Great Britain. All rights reserved

0039-9140/81/040268-03$02.00/0
Copyright © 1981 Pergamon Press Ltd

SEPARATION BEHAVIOUR OF NITROXYLENE ISOMERS ON POLYOLS AND POLYETHERS IN GAS–LIQUID CHROMATOGRAPHY

AOI ONO

Chemical Laboratory, Takada Branch, Faculty of Education Niigata University, Nishishiro-cho, Joetsu-shi, 943 Japan

(*Received* 16 *September* 1980. *Accepted* 24 *October* 1980)

Summary—Of the six nitroxylene isomers, 2,4- and 2,3-nitroxylene are the most difficult to separate by GLC, but they have been effectively separated on various acidic polyols as stationary phases. Although polyethylene glycol could not generally separate the 2,4- and 2,3-nitroxylene isomers, polyethylene glycol 20*M* could, and polypropylene glycol could separate all the six isomers effectively.

Although Kreicberga *et al.*[1] and Novrocik *et al.*[2] have reported the separation of 3- and 4-nitro-*o*-xylene (2,3- and 3,4-dimethylnitrobenzene) by gas–liquid chromatography (GLC), there have been few systematic studies on the separation of all the dimethylnitrobenzene isomers.

Nitrofluorenes, nitro-9-fluorenones,[3,4] sugars and mixed phases of two kinds of sugars[4] have been reported to be effective liquid phases for the separation of nitroxylenes.

This paper reports the results obtained with polyols, acidic polyols and polyethers as stationary phases. It has been found that polyoxy acids and polypropylene glycols give effective separations.

EXPERIMENTAL

Liquid phases

DL-Glyceric acid (DL-GLA), tartronic acid (TAA), L-malic acid (L-MAL), DL-malic acid (DL-MAL), L-tartaric acid (L-TAR), meso-tartaric acid (m-TAR), meso-erythritol (m-ERO), diglycerol (DIL), pentaerythritol (PEL), L-ascorbic acid (L-ASC), and mucic acid (MUA) of guaranteed reagent grade, and polyethylene glycol 400 (PEG 400), 600 (PEG 600), 1000 (PEG 1000), 1540 (PEG 1540), 2000 (PEG 2000), 4000 (PEG 4000), 6000 (PEG 6000), 20M (PEG 20M), polypropylene glycol 424 (PPG 424), 1024 (PPG 1024), 2000 (PPG 2000) and tetraethylene glycol (TEG) of extra reagent grade were obtained from the Nakarai Chemical Co. (Kyoto, Japan) and used after further purification.

Samples

2,6-Dimethylnitrobenzene (2,6-DMNB), 2,5-dimethylnitrobenzene (2,5-DMNB), 2,4-dimethylnitrobenzene (2,4-DMNB), 2,3-dimethylnitrobenzene (2,3-DMNB), 3,5-dimethylnitrobenzene (3,5-DMNB) and 3,4-dimethylnitrobenzene (3,4-DMNB) of guaranteed reagent grade, were obtained from Tokyo Kasei Kogyo (Tokyo, Japan) and used after purification. Purity was checked by GLC analysis, and by running infrared and NMR spectra.

Apparatus and chromatographic procedure

A Shimadzu Model GC-5A gas chromatograph equipped with a flame-ionization detector was used. The separation column was a 2.25 m × 3 mm stainless-steel U-tube packed with Sil-O-Cel C_{22} firebrick (60–80 mesh) support coated with 20% (w/w) of liquid phase. The column and injector temperatures were 140° and 270° respectively. Nitrogen was used as carrier gas at 25 ml/min.

The acid-washed Sil-O-Cel C_{22} firebrick, 60–80 mesh, (Johns-Manville, Denver, Colo., U.S.A.) was coated with the liquid phase, then heated in an electric oven at the column temperature for 10 hr to remove solvent, and was finally kept under a stream of nitrogen for 6 hr. at a temperature *ca.* 10° higher than the column temperature used.

RESULTS AND DISCUSSION

In previous papers,[3,4] nitrofluorenes, nitro-9-fluorenones and sugar alcohols were reported to be effective liquid phases for the separation of DMNB isomers.

Experience with these stationary phases suggested that it might be worth investigating polyols for separating the nitroxylenes. Polyols were found to be effective for the separation of the dimethylphenol isomers (xylenol isomers)[3,4] as were acidic vicinal polyols, and it was concluded that strong hydrogen-bonding of the acidic proton of the vicinal polyol with the dimethylphenol isomers is responsible for the separation of the 2,4- and 2,5-dimethylphenol isomers.[5]

It was therefore expected that hydrogen-bonding between polyols (sugars and sugar alcohols) and DMNB isomers would assist in the separation of these isomers. This expectation formed the starting point for further investigation of the behaviour of the different isomers on various stationary phases.

As Tables 1 and 2 show, DL-GLA, TAA, DL-MAL, L-TAR, m-TAR and L-ASC effectively separated all the six DMNB isomers, but L-MAL and MUA could not separate 2,3-DMNB from 2,4-DMNB.

Separation of 2,4- and 2,3-DMNB presents the greatest difficulty. In the separation of dimethylphenol isomers, the 2,4- and 2,5-dimethylphenol isomers, the most difficult pair to separate, were resolved on acidic polyols which give strong hydrogen-bonding with the two isomers, and these liquid phases were

Table 1. Relative retention* of dimethylnitrobenzene isomers on polyols

Liquid phase	Relative retention*					
	2,6-	2,5-	2,3-	2,4-	3,5-	3,4-
DL-GLA	1.00	1.68	1.82	2.05	2.41	3.36
TAA	1.00	1.64	1.92	2.00	2.21	3.01
L-MAL	1.00	2.54	2.77	2.77	4.54	4.54
DL-MAL	1.00	1.44	1.59	1.89	2.21	2.29
L-TAR	1.00	1.60	1.80	2.07	2.50	3.43
m-TAR	1.00	1.66	1.85	2.14	2.52	3.38
MUA	1.00	1.76	2.00	2.00	2.47	3.35
m-ERT	1.00	1.59	1.82	2.00	2.27	3.36
PET	1.00	1.61	1.85	2.07	2.31	3.16
DIL	1.00	1.78	2.25	2.25	2.25	3.56
L-ASC	1.00	1.68	1.91	2.14	2.59	3.45

* Relative to 2,6-dimethylnitrobenzene and based on adjusted retention time. The column headings give the positions of the methyl groups.

Table 2. Separation factors* of dimethylnitrobenzene isomers on polyols

Liquid phase	Separation factor				
	2,5-/2,6-	2,3-/2,5-	2,4-/2,3-	3,5-/2,4-	3,4-/3,5-
DL-GLA	1.68	1.09	1.13	1.18	1.39
TAA	1.64	1.17	1.04	1.11	1.36
L-MAL	2.54	1.09	1.00	1.64	1.00
DL-MAL	1.44	1.10	1.19	1.17	1.04
L-TAR	1.60	1.13	1.15	1.21	1.37
m-TAR	1.66	1.11	1.16	1.18	1.34
MUA	1.76	1.14	1.00	1.24	1.36
m-ERT	1.59	1.14	1.10	1.14	1.48
PET	1.61	1.15	1.12	1.12	1.37
DIL	1.78	1.26	1.00	1.00	1.58
L-ASC	1.68	1.14	1.12	1.21	1.33

* Ratio of adjusted retention times of two adjacent peaks.[6]

Table 3. Relative retention of dimethylnitrobenzene isomers on polyethers

Liquid phase	Relative retention*					
	2,6-	2,5-	2,3-	2,4-	3,5-	3,4-
PEG 400	1.00	1.50	1.78	1.78	2.00	2.71
PEG 600	1.00	1.60	1.87	1.87	2.07	2.73
PEG 1000	1.00	1.56	1.81	1.81	2.06	2.69
PEG 2000	1.00	1.53	1.79	1.79	2.00	2.58
PEG 1540	1.00	1.62	1.92	1.92	2.15	3.00
PEG 4000	1.00	1.57	1.79	1.79	2.14	2.86
PEG 6000	1.00	1.53	1.67	1.67	2.07	2.73
PEG 20M	1.00	1.69	2.00	2.14	2.14	3.17
PPG 424	1.00	1.45	1.59	1.77	1.95	2.73
PPG 1024	1.00	1.45	1.68	1.82	1.91	2.68
PPG 2000	1.00	1.42	1.54	1.71	1.92	2.75
PEG 1540(a)	1.00	1.72	1.88	2.12	2.28	3.72
PEG 1540(b)	1.00	1.56	1.61	1.83	2.67	3.06
TEG	1.00	1.62	1.82	1.82	2.15	2.85

* See footnote to Table 1.

Table 4. Separation factors* of dimethylnitrobenzene isomers on polyols

Liquid phase	Separation factor				
	2,5-/2,6-	2,3-/2,5-	2,4-/2,3-	3,5-/2,4-	3,4-/3,5-
PEG 400	1.50	1.19	1.00	1.12	1.36
PEG 600	1.60	1.17	1.00	1.11	1.32
PEG 1000	1.56	1.16	1.00	1.14	1.31
PEG 2000	1.53	1.17	1.00	1.12	1.29
PEG 1540	1.62	1.19	1.00	1.12	1.40
PEG 4000	1.57	1.14	1.00	1.20	1.34
PEG 6000	1.53	1.09	1.00	1.24	1.32
PEG 20M	1.69	1.18	1.07	1.00	1.48
PPG 424	1.45	1.10	1.11	1.10	1.40
PPG 1024	1.45	1.16	1.08	1.05	1.40
PPG 2000	1.42	1.08	1.11	1.12	1.43
PEG 1540(a)	1.72	1.09	1.13	1.08	1.63
PEG 1540(b)	1.56	1.03	1.14	1.46	1.15
TEG	1.62	1.12	1.00	1.18	1.33

* See footnote to Table 1.

also effective for the separation of DMNB isomers. MUA and L-MAL are vicinal acidic polyols and though they would be expected to show strong hydrogen-bonding with the isomers they cannot separate them.

m-ERT and PET separated all the isomers: m-ERT is a vicinal tetrol and PET is a radial (quaternary) polyol, three hydroxy groups of which are vicinal. It can be concluded that vicinal triols or radial tetrols are effective stationary phases. However, DIL, which is a tetrol with two separate pairs of vicinal hydroxy groups, could not separate the 2,4- and 2,3-DMNB isomers.

Separations of the six isomers were obtained on hexoses and sugar alcohols,[4] and though some hexitols could separate the isomers, others, such as sorbitol and dulcitol, could not. It can be concluded that the carbonyl group of the hexoses and also the configuration of the hexitols, play a role in effecting these separations.

Acidic triols (DL-GLA, TAA and DL-MAL) were effective for the separation, probably on account of their carbonyl group and active hydrogen atom.

As Tables 3 and 4 show, the PEGs, except PEG 20M, could not separate 2,4- and 2,3-DMNB, and PEG 20M *could* do this, it could not separate 2,4- and though 3,5-DMNB. All the isomers except for 2,4- and 2,3-DMNB were also resolved on a variety of common liquid phases, both polar and non-polar such as polyethers, esters and polyesters Apiezon-L, paraffin, dioctyl phthalate, polyethylene glycol adipate *etc.*[3] However, the liquid phases effective for separating all the isomers, seem to be quite specific, with special features.

It is remarkable that PEG 20M separates 2,4- and 2,3-DMNB but not 2,4- and 3,5-DMNB: the reason is not clear. Further, PPG 424, PPG 1024 and PPG

2000 separated all the isomers, from which it may be concluded that the methyl groups along the chain play some role in the separation process. It is interesting to note that a different batch of PEG 1540 could resolve all the isomers, although the original batch of PEG 1540 could not. PEG 1540(a) and PEG 1540(b) were from the second batch of PEG 1540: the sample PEG 1540(a) was conditioned at 160° and the sample PEG 1540(b) at 150° and they showed different separation efficiencies in the separation of 2,4- and 3,5-DMNB. The PEGs showed different separation behaviour according to the molecular weight distribution.

The inability of certain other phases to resolve 2,4- and 2,3-DMNB showed that diols or tetrols with no vicinal hydroxide groups are ineffective for these separations.

REFERENCES

1. D. Kreicberga, S. Valtera and O. Neilands, *Latv. PSR Zinat. Akad. Vestis., Kim. Ser.*, 1970, 170.
2. J. Novrocik, K. Komarek and J. Poskocil, *J. Chromatog.*, 1976, **124**, 73.
3. A. Ono, *ibid.*, 1979, **180**, 170.
4. A. Ono and Y. Masuda, *ibid.*, 1980, **197**, 25.
5. A. Ono, *Chromatographia*, in the press.
6. L. S. Ettre, *J. Chromatog.*, 1979, **165**, 235.

Talanta, Vol. 28, pp. 271 to 273, 1981
Printed in Great Britain

0039-9140/81/040271-03$02.00/0

DETERMINATION OF MERCURY BY ATOMIC-ABSORPTION SPECTROPHOTOMETRY

Zs. WITTMANN

Hungarian Oil and Gas Research Institute, József Attila u. 34, H-8200 Veszprém, Hungary

(*Received* 13 *May* 1980. *Accepted* 21 *October* 1980)

Summary—A flameless atomic-absorption system has been developed for the determination of low concentrations of mercury in gaseous, solid and liquid samples of organic and inorganic materials.

Various approaches to analysis for mercury are presented in the literature,[1] including flameless atomic-absorption methods.[2] A typical approach for determining mercury in solution is that of Hatch and Ott,[3] in which the mercury ions are reduced to the element with tin(II) chloride and swept into the atomic-absorption cell with air. Vaughn and McCarthy[4] separated mercury from interfering substances present in soils, rocks and gases by passing the sample vapours over gold foil; the mercury could be released by heating at 500°. Their modified method has been used to determine mercury in geological samples, soil and rock,[4–10], coal,[11,12] hair and fish,[13,14] water,[15,16] gases and air.[17–21]

It is desirable to have a mercury collection system which is simple and selective, and capable of determining mercury in both organic and inorganic materials in solid, liquid or gaseous form. This paper describes an apparatus which meets these requirements.

EXPERIMENTAL

Apparatus

The apparatus developed in our laboratory is shown in Fig. 1. The sample (10–1000 mg) is placed in a quartz boat. Solid or liquid samples are heated in an electric furnace, decomposition products being transported by a carrier-gas over the gold wire used to trap the mercury by amalgamation, and then being vented to atmosphere. The mercury trapped is then vapourized by heating the gold with an electric furnace and the mercury vapour carried through the absorption cell by a flow of air; as a result, the mercury atomic-absorption signal at 253.7 nm increases sharply to a maximum and quickly returns to zero.

Gas samples are simply passed over the gold wire, and the mercury is vapourized and measured as already described.

Very low concentrations of mercury in liquid samples are determined after a preliminary concentration step by reduction and collection of the released mercury on gold wire.

The reduction cell is a three-necked vessel, two of the necks for inlet and outlet of the carrier gas, and the third for addition of the sample *etc.*

RESULTS AND DISCUSSION

A number of parameters which affect the determination of mercury with this system were investigated.

The sample is burned in a stream of carrier gas at a temperature high enough to liberate mercury quantitatively. The temperature must be at least 650° because the most stable mercury compound, mercury(II) fluoride, decomposes at 645°.[11] A temperature of 1000–1200° should be sufficient for any kind of sample. In the case of solid samples, fine particle size is necessary for good results to be obtained for soils, ores and organic materials. Wimberley[11] found that samples ground to pass through an 80-mesh sieve gave good results. According to O'Gorman *et al.*[12] 200-mesh material is advantageous for determination of mercury in coals. Our own work indicates that 80–100-mesh material gives good results. For the mercury trap about 1 g of 100-μm diameter pure gold

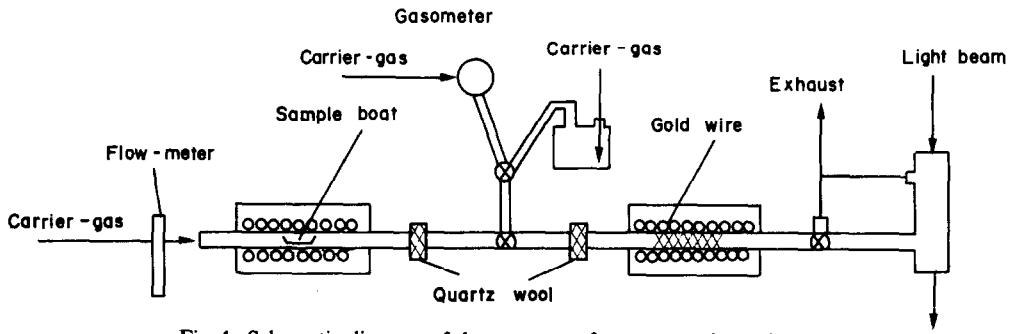


Fig. 1. Schematic diagram of the apparatus for mercury determination.

Table 1. Mercury recovered after amalgamation on gold wire at different temperatures (carrier-gas air at 100 l./hr)

Temperature, °C	Hg added, ng	Hg recovered, ng
25	50	48
107	50	51
154	50	50
172	50	51
196	50	50
210	50	47
251	50	43
300	50	9

wire is used in a 5-mm bore quartz tube. The thickness of the wire is not very critical, because the sorption takes place on the surface.

In the case of samples containing organic matter, interference can be caused by incompletely burned organic matter condensing on the gold and burning off when the gold is heated, producing smoke along with mercury in the absorption cell. According to O'Gorman *et al.*[12] and Weissberg,[6] a double gold trap solves this problem. Our study (Table 1) confirms Weissberg's observation[6] that heating the gold trap to a temperature as high as 170° during the mercury collection does not result in loss of mercury but does reduce the condensation of organic matter on the gold surface. Using a single gold trap at 170° gives good results for determination of mercury in organic matter.

After amalgamation the mercury is released by heating to 600–700° with an electric furnace for 1 min. This temperature range proved to be the most advantageous.

The sensitivity can be increased by reducing the rate of air flow (Fig. 2). We use air as carrier-gas at a flow-rate of 100 l./hr, but other gases (nitrogen, helium, argon or oxygen), may also be used.

In the reduction method, the mercury vapour can

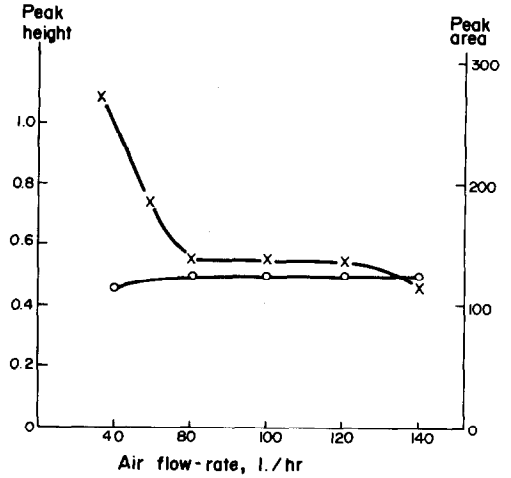


Fig. 2. Effect of air flow-rate on the determination of mercury (50 ng). O Peak height; × peak area.

be collected from a stream of air by amalgamation with gold. Liquid samples containing mercury at very low concentrations (<5 ng/ml) can be dealt with in this way, with as much as 500 ml of sample.

Olafsson[15] used tin(II) chloride acidified with nitric acid, but found that a greatly reduced carrier-gas flow-rate was necessary for reproducible results to be obtained, because at fast flow-rates droplets of water were carried over to the mercury collector.

No water droplets arise in our apparatus and any traces of moisture are evaporated from the gold trap by heating it at 170°, and carried out of the system by the carrier-gas. We use solid reductants such as Devarda's alloy or iron powder (about 1 g for 500 ml of sample); 30-min reduction time with an air-flow of 100 l./hr will give recovery of mercury at the 200–300 ng/l. level.

Calibration

A calibration curve is prepared by thermal decomposition of known amounts of mercury(II) chlor-

Table 2. Recovery experiments

Sample	Hg content of sample, ng	Hg added, ng	Hg total recovered, ng
Soil	—	25	23
		10	11
Rock	—	25	25
		10	9
Plant	—	25	28
		10	12
Coal	—	25	22
		10	8
Beer	5	25	29
	5	10	13
Tap water	8	25	37
	8	10	18
Air		ng/l.	ng/l.
		10	12
		50	45
		80	77

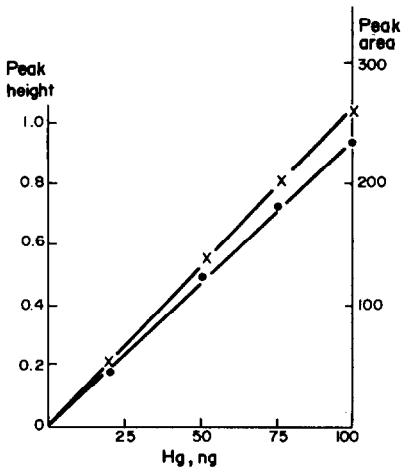


Fig. 3. Mercury calibration curves obtained by peak-area (×) and peak-height (●) measurements (arbitrary units).

ide (Fig. 3). Both peak areas and peak heights give linear calibration plots.

Recovery experiments on various types of sample gave the results shown in Table 2. Known amounts of mercury(II) solution were added to the solid samples, which were then allowed to stand for 2–3 hr, so that most of the water evaporated. The liquid samples were spiked with known amounts of mercury(II) solution and then analysed in the usual way.

In the case of gas samples, a known volume of air was passed through a heated glass tube containing mercury(II) solution of known concentration and then into a plastic balloon. The contents of the balloon were passed through the gold trap.

The time required for the analysis of one sample is normally 4–5 min, but liquid samples with very low mercury concentrations (<5 ng/ml) require about 35 min.

The relative standard deviation calculated for ten replicate measurements at the 50-ng level in solid, liquid and gas samples was 10%.

REFERENCES

1. S. Chilov, *Talanta*, 1975, **22**, 205.
2. A. M. Ure, *Anal. Chim. Acta*, 1975, **76**, 1.
3. W. R. Hatch and W. L. Ott, *Anal. Chem.*, 1968, **40**, 2085.
4. W. W. Vaughn and J. M. McCarthy, *U.S. Geol. Survey Prof. Paper*, 501-D, D 123, 1964.
5. L. M. Azzaria, *Can. Dep. Energy, Mines Resour., Geol. Surv. Can.* 1967, Paper 65–54, 13.
6. B. G. Weissberg, *Econ. Geol.* 1971, **66**, 1042.
7. A. B. Carel, *Anal. Chim. Acta*, 1975, **78**, 479.
8. K. Kato, A. Ando and T. Kishimato, *Bunseki Kagaku*, 1972, **21**, 1057.
9. H. G. Henry, K. R. Stever, W. L. Barry and H. H. Heady, *Appl. Spectrosc.* 1972, **26**, 288.
10. O. I. Joensuu, *Appl. Spectrosc.*, 1971, **25**, 526.
11. J. W. Winberley, *Anal. Chim. Acta*, 1975, **76**, 337.
12. J. V. O'Gorman, N. H. Suhr and P. L. Walker, *Appl. Spectrosc.*, 1972, **26**, 44.
13. D. H. Anderson, J. H. Evans, J. J. Murphy and W. W. White, *Anal. Chem.* 1971, **43**, 1511.
14. W. A. Willford, R. J. Messelberg and H. L. Bergman, *J. Assoc. Off. Anal. Chemists*, 1973, **56**, 1008.
15. J. Olafsson, *Anal. Chim. Acta* 1974, **68**, 207.
16. M. J. Fishman, *Anal. Chem.*, 1970, **42**, 1961.
17. J. Sculman and G. Widmark, *Intern. J. Environ. Anal. Chem.*, 1972, **2**, 29.
18. S. J. Long, D. R. Scott and R. J. Thompson, *Anal. Chem.*, 1973, **45**, 2227.
19. S. H. Williston, *Geophys. Res.*, 1968, **73**, 7051.
20. T. J. Kneip, R. S. Ajemian, J. Driscoll, F. I. Grunder, L. Kornreich, J. W. Loveland, J. L. Mogers and R. J. Thompson, *Health Lab. Sci.* 1974, **11**, 342.
21. *Idem, ibid.*, 1975, **12**, 158.

Talanta, Vol. 28, pp. 274 to 276, 1981
Printed in Great Britain. All rights reserved

0039-9140/81/040274-03$02.00/0
Copyright © 1981 Pergamon Press Ltd

PREPARATION AND PROPERTIES OF A NEW CHELATING RESIN CONTAINING 1-NITROSO-2-NAPHTHOL AS THE FUNCTIONAL GROUP

J. P. GHOSH and H. R. DAS
Department of Chemistry, Presidency College, Calcutta-700073, India

(*Received* 3 *July* 1980. *Accepted* 25 *August* 1980)

Summary—A macroreticular polystyrene-based chelating ion-exchanger containing 1-nitroso-2-naphthol as the functional group has been synthesized. The exchange-capacity of the resin for a number of metal ions such as copper(II), iron(III), cobalt(II), nickel(II), palladium(II) and uranium(VI) as a function of pH has been determined. The sorption and elution characteristics for palladium(II) and uranium(VI) have been thoroughly examined with a view to utilizing the resin for separation and concentration of uranium and palladium. Uranium(VI) has been separated from a mixture of ten other metal ions by sorption on the chelating resin and selective elution with 0.5*M* sodium carbonate. Palladium(II) has been separated from various metal ions by selective sorption on the resin in 1*M* hydrochloric acid medium.

1-Nitroso-2-naphthol was one of the first organic analytical reagents and forms chelate complexes with a number of metal ions in addition to cobalt, such as copper(II), iron(III), nickel(II), palladium(II), uranium(VI).[2–4] Its incorporation in a resin matrix should be of interest in connection with concentration and separation of traces of heavy metal ions.[5]

The synthesis and metal-sorption characteristics of a macroreticular polystyrene-based resin containing 1-nitroso-2-naphthol as functional group are described in this paper.

EXPERIMENTAL

Synthesis of the resin

The starting material was a 30–60 mesh macroreticular polystyrene–divinylbenzene copolymer containing 8% divinylbenzene (Bird & Co., India). The polystyrene resin was nitrated and reduced to the amino-compound, then this product was diazotized according to the procedure described by Davies *et al.*[6] The diazotized product was rapidly filtered off, washed with cold distilled water until free from acid and then coupled at 0–5° with a solution of 1-nitroso-2-naphthol in 5% aqueous sodium hydroxide solution (3.5 g of 1-nitroso-2-naphthol for 5 g of the starting resin), over a period of 7 days. The resin was then filtered off and thoroughly washed with distilled water until free from alkali. It was then extracted in a Soxhlet extractor with alcohol for 3 days. Finally, it was washed with dilute hydrochloric acid, then with demineralized water until free from acid. The resin was air-dried and sieved, the particles of 30–60 mesh being used.

Resin characterization

Water regain. Dry resin was immersed in demineralized water for 48 hr, then filtered off by suction, weighed, dried at 80° for 48 hr and reweighed.

Estimation of nitrogen and amino-groups. The nitrogen content of fully dried samples of the nitrated polystyrene, aminopolystyrene and the chelating resin made from it was determined by the Dumas method. The amino content of the aminopolystyrene was determined by non-aqueous titrimetry. A known weight of the fully dried amino-compound was heated with an excess of a standardized solution of perchloric acid in glacial acetic acid at 100° for 72 hr. After filtration, the excess of perchloric acid was back-titrated with a standard solution of sodium acetate in glacial acetic acid, with Crystal Violet as indicator.[7]

Exchange-capacity determination. For determining the exchange-capacity of the resin, six metal ions, namely copper(II), iron(III), cobalt(II), nickel(II), palladium(II) and uranium(VI) were chosen. Capacities were determined in the pH range 1.0–7.0, the appropriate pH being maintained with buffers prepared with 0.2*M* hydrochloric acid and 0.2*M* sodium acetate. The air-dried resin (0.2 g) was equilibrated with the buffer, and enough metal ion solution adjusted to the same pH was added to give a 0.1*M* concentration of the metal ion in the solution. After shaking for 24 hr the mixture was filtered, and the resin was thoroughly washed with the buffer until free from the metal ion. The sorbed metal ion was then completely eluted with a suitable reagent [0.5*M* sodium carbonate for uranium(VI); for palladium(II) concentrated hydrochloric acid followed by a dilute acidic solution of thiourea; for the other metal ions, 3*M* hydrochloric acid]. The eluted metal ions, except uranium, were determined by atomic-absorption spectrometry. The uranium was determined spectrophotometrically with oxine.[8]

Studies with resin-blanks. To confirm that the nitroso group in the resin is involved in chelate formation with the metal ions, an azo resin was synthesized by coupling diazotized aminopolystyrene with 2-naphthol and the exchange-capacity of this azo-resin, particularly for uranium(VI), was examined at different pH values for comparison.

Equilibration rate. Equilibration rates with copper(II), palladium(II) and uranium(VI) were studied for the resin.[9] The time required for 50% uptake of copper(II), palladium(II) and uranium(VI) was determined at pH 5.6, 0.5 and 5.9 respectively.

Column operations

A glass column, 40 cm long, 8 mm bore, was used. Air-dried resin (5 g) was immersed in demineralized water and allowed to swell for 24 hr. The column was then packed with the fully swollen beads, the bed volume being about 12 ml. The bed was thoroughly washed with 1*M* hydrochloric acid, then with demineralized water until free from acid.

The sorption and recovery characteristics for palladium(II) and uranium(VI) in the presence of various metal

ions were thoroughly studied. A small amount of a mixture of the test metal ion and foreign metal ion was allowed to flow through the resin column. Sorbed palladium(II) was eluted completely with about 10 bed-volumes of concentrated hydrochloric acid followed by about 3 bed-volumes of $10^{-3}M$ thiourea in dilute hydrochloric acid (pH 3.0). Sorbed uranium(VI) was eluted with 10 bed-volumes of 0.5*M* sodium carbonate. The eluted metal ion was then estimated as already described.

Separation procedures

For the separation of palladium(II) from a mixture with ten other metal ions, namely copper(II), zinc(II), chromium(III), manganese(II), iron(III), cobalt(II), nickel(II), cadmium(II), mercury(II) and aluminium(III), the sample was made 1*M* in hydrochloric acid. The resin column was equilibrated with 1*M* hydrochloric acid, the sample was allowed to flow through it at 1.5 ml/min, the column was thoroughly washed with 1*M* hydrochloric acid, and the sorbed palladium(II) was eluted as just described, at a flow-rate of 1.5 ml/min.

Uranium(VI), added as uranyl nitrate, was separated from a mixture containing ten other metal ions by two different procedures. In the first the pH of the sample was adjusted to around 2.0 with hydrochloric acid and sodium acetate. The resin column was equilibrated with pH-2 buffer. The sample was run through the column at 1 ml/min, then the column was washed thoroughly with pH-2 buffer, and the sorbed uranium was eluted with 10 bed-volumes of 0.5*M* sodium carbonate at a flow-rate of 1 ml/min. The sorbed copper(II), iron(III) and traces of zinc(II) were then eluted with 3*M* hydrochloric acid. In the second method, the same technique was used but the pH was maintained at 5.9.

RESULTS AND DISCUSSION

It is somewhat surprising that 1-nitroso-2-naphthol, being such a familiar analytical reagent, has not so far been incorporated in a resin matrix. This may be because theoretical considerations suggest that 1-nitroso-2-naphthol should show little tendency to be coupled with a diazo-compound or other species generally used to synthesize chelating resins, because the active position in the 2-naphthol is already blocked with the nitroso group. However, in the course of our investigations it has been found that in the aminated polystyrene there are a considerable number of unconverted nitro groups. Now the nitro groups, being electron-withdrawing, make the diazo-cation (ArN_2^+) a very strong electrophile, which can couple with the ligand (1-nitroso-2-naphthol), most probably at the somewhat electron-enriched 6-position.

A characteristic feature of the infrared spectrum of the chelating resin is the presence of distinct bands at 1350, 1410 and 1510 cm^{-1}, corresponding to the nitroso group, a band at 1600 cm^{-1} due to the tautomeric oxime group, and a band at 3150 cm^{-1} due to the O–H stretching frequency of the phenol group.

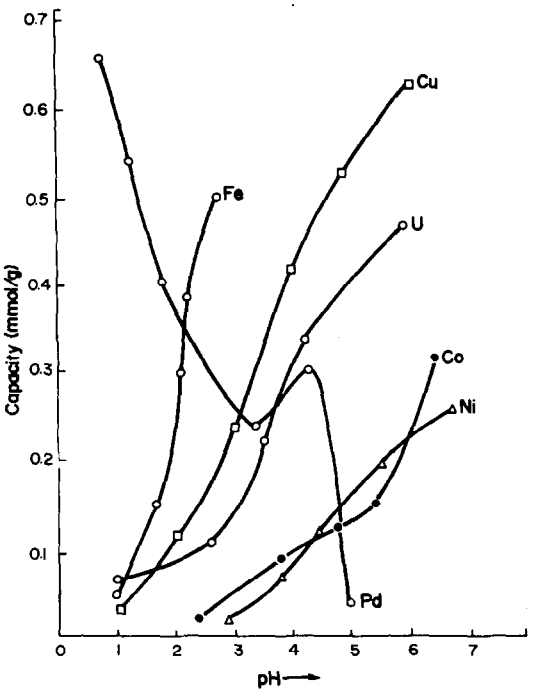


Fig. 1. Total exchange-capacity of the 1-nitroso-2-naphthol resin for different metal ions as a function of pH.

The nitrated and aminated polystyrene were found to contain 10.6 and 12.2% nitrogen respectively, but the aminated product contained only 5.0% of amino-nitrogen (from the estimation of amino groups). These results indicate that in the aminated product, 7.2% nitrogen is present as unconverted nitro groups.

The nitrogen content of the chelating resin was found to be 7.3%, which shows that there is 54% conversion of the amino groups. Calculations based on these data show that there should be about 0.94 mmole of ligand-nitrogen, 0.43 mmole of unchanged amino-nitrogen and 1.97 mmole of unchanged nitro-nitrogen per g of the dry chelating resin. The maximal exchange-capacity of the resin for palladium(II) was found to be 0.67 mmole/g (Fig. 1). If the resin–metal complexes are 1:1 complexes (which is most likely) the maximal exchange-capacity should be 0.94 mmole/g. Steric factors are probably responsible for

Table 1. Separation of Pd(II) from Cr(III), Mn(II), Fe(III), Co(II), Ni(II), Cu(II), Zn(II), Cd(II), Hg(II), Al(III) (separation medium 1*M* HCl)

Taken		
Pd(II), *mg*	Foreign metal ion (each), *mg*	Pd(II) found after elution, *mg*
4.80	20.0	4.70
1.20	20.0	1.20
0.25	10.0	0.24
0.10	10.0	0.098
0.05	10.0	0.048

Table 2. Separation of U(VI) from Cr(III), Mn(II), Fe(III), Co(II), Ni(II), Cu(II), Zn(II), Cd(II), Hg(II), Al(III)

U(VI) taken, *mg*	Foreign metal ion taken (each), *mg*	Sorption pH	U(VI) found after elution, *mg*
1.00	20.0	2.0	1.00
0.50	10.0		0.48
0.10	10.0		0.10
5.00	5.0	5.9	4.98
1.00	1.0		1.00
0.50	5.0		0.50
0.10	5.0		0.10

the maximal practical exchange-capacities being lower than the theoretical values.

Equilibration studies with copper(II) and palladium(II) show that the times required by the resin for 50% uptake are 45 and 50 min respectively. For uranium(VI), the time is about 2 hr. Hence the resin is suitable for column operations if the flow-rate is low. The water-regain of the resin (0.53 g/g) is satisfactory.

The recoveries of 1.2 mg of palladium(II) or 2.0 mg of uranium(VI) from mixtures with 20 or 5 mg respectively of the individual metal ions already listed were 97.5–100% and 99.5–101% respectively. Hence attempts were made to separate palladium(II) and uranium(VI) from mixtures of these metal ions.

Separation of palladium(II) was based on the observation that in 1*M* hydrochloric acid medium, appreciable amounts of palladium were sorbed on the resin-column whereas all the other metal ions except minute traces of copper(II) were not sorbed at all. Results are shown in Table 1. If 2*M* hydrochloric acid is used as the sorption medium the contamination with copper(II) is completely eliminated, but the resin-capacity for palladium(II) is almost halved. More than 98% of the sorbed palladium(II) can be desorbed with concentrated hydrochloric acid, but for eluting the last traces of palladium(II) a dilute solution of thiourea (at pH 3) has to be used.

Selective elution was used for separation of uranium(VI) from various other metal ions. Results are presented in Table 2. At pH 2.0 only uranium(VI), copper(II), iron(III) and traces of zinc(II) are sorbed on the resin, the other metal ions passing through. At pH 5.9 most of the metal ions are sorbed on the resin. In both cases the uranium(VI) is selectively eluted with 0.5*M* sodium carbonate. At pH 2.0, the uranium-capacity of the resin is low, so large amounts of uranium cannot be sorbed on the resin, whereas at pH 5.9 the uranium-capacity is fairly high, so large amounts of uranium can be sorbed. However, at pH 5.9 appreciable amounts of most other metal ions are also sorbed, thus reducing the effective capacity for uranium(VI). Hence if small amounts of uranium(VI) are to be separated from large amounts of the other metal ions, separation at the lower pH would be preferable. On the other hand, if large amounts of uranium(VI) are to be separated from small amounts of the other metal ions, separation at the higher pH would be better.

The exchange-capacity of the blank resin containing 2-naphthol was practically zero for uranium(VI) even at pH 5.9.

CONCLUSION

The 1-nitroso-2-naphthol chelating ion-exchange resin has been found to be stable in acid and alkaline solutions. The resin is useful for the separation of palladium(II) and uranium(VI) from various metal ions, and may be utilized for concentration of traces of palladium(II) and uranium(VI), particularly for the estimation of uranium in sea water. The stability of the chelating functional group in the resin is quite good, the exchange-capacity of the resin remaining more or less the same after quite a number of working cycles.

Acknowledgements—We are thankful to M/s Bird & Co. (India) for supplying us with the polystyrene resin and to Mr. B. Dasgupta of the Geology Department, Presidency College, for his technical assistance. One of us (J.P.G.) thanks the University Grants Commission, New Delhi, for a fellowship under the Faculty Improvement Programme for college teachers.

REFERENCES

1. M. Ilinsky and G. V. Knorre, *Ber.*, 1885, **18,** 699.
2. E. Cogan, *Anal. Chem.*, 1960, **32,** 973.
3. I. T. Takahashi and R. J. Robinson, *ibid.*, 1960, **32,** 1350.
4. F. D. Snell and C. T. Snell, *Colorimetric Methods of Analysis*, Vol. IIA, p. 290. Van Nostrand, Princeton, 1959.
5. A. Sugii and N. Ogawa, *Talanta*, 1979, **26,** 970.
6. R. V. Davies, J. Kennedy, E. S. Lane and J. L. Willans, *J. Appl. Chem.*, 1959, **9,** 368.
7. G. E. Ficken and E. S. Lane, *Anal. Chim. Acta*, 1957, **16,** 207.
8. A. I. Vogel, *A Textbook of Quantitative Inorganic Analysis*, 4th Ed., p. 163. Longmans, London, 1978.
9. H. Eccles and F. Vernon, *Anal. Chim. Acta*, 1973, **66,** 231.

Talanta, Vol. 28, pp. 277 to 280, 1981
Printed in Great Britain. All rights reserved

0039-9140/81/040277-04$02.00/0
Copyright © 1981 Pergamon Press Ltd

ANALYTICAL DATA

COMPLEX FORMATION EQUILIBRIA BETWEEN 1-HYDROXY-7-SULPHO-2-NAPHTHOIC OR 1-HYDROXY-4,7-DISULPHO-2-NAPHTHOIC ACID AND IRON(III) IN 0.1*M* $NaClO_4$ MEDIUM

LAURI H. J. LAJUNEN*, EERO AITTA and SEPPO PARHI
Department of Chemistry, University of Oulu, Linnanmaa, SF-90570 Oulu 57, Finland

(*Received* 23 *June* 1980, *Accepted* 3 *September* 1980)

Summary—The equilibria for formation of iron(III) complexes with 1-hydroxy-7-sulpho-2-naphthoic and 1-hydroxy-4,7-disulpho-2-naphthoic acids in aqueous 0.1*M* sodium perchlorate medium at 25° have been studied by spectrophotometric and potentiometric methods. The data are well described in terms of a series of stepwise complexes, $FeL_r^{(3-rn)+}$ in both systems (L^{n-} denotes the unprotonated ligand anion).

In this paper we continue our studies on the iron(III) complexes with aromatic *o*-hydroxycarboxylic acids, in a search for suitable reagents for spectrophotometric determination of iron. We have already reported the formation of three mononuclear iron complexes with one salicylic-type ligand, 1-hydroxy-4-sulpho-2-naphthoic acid.[1] Here we report on the 1-hydroxy-7-sulpho-2-naphthoic and 1-hydroxy-4,7-disulpho-2-naphthoic acid systems.

EXPERIMENTAL

Reagents

1-Hydroxy-7-sulpho-2-naphthoic acid was prepared by dissolving 1-hydroxy-4,7-disulpho-2-naphthoic acid in sulphuric acid dihydrate at 130–135°, and heating for 15 min at 145–150°.[2]

1-Hydroxy-4,7-disulpho-2-naphthoic acid was prepared from 1-hydroxy-2-naphthoic acid by sulphonation with an ice-cold mixture of 4 parts of 20% fuming sulphuric acid and 3 parts of 96% sulphuric acid.[3,4]

The acids were converted into their sodium salts with sodium chloride, and the crude products were recrystallized several times from hot water. The purities of the compounds were tested by potentiometric neutralization titrations and ^1H and ^{13}C NMR spectrometry.

The iron(III) perchlorate stock solution was prepared by dissolving iron powder in perchloric acid and standardized by potentiometric titration with 0.1*M* sodium hydroxide, after passage through a cation-exchanger. The concentrations of the ligand and free strong acid in the reaction mixtures were determined by potentiometric neutralization titrations, with equivalence points determined by Gran's method.[5]

Apparatus

A Radiometer DTS 633 digital titration system was used, consisting of an ABU 13 autoburette, a PHM 64 pH-meter and a TTT 61 digital titrator, together with an equal-increment accessory constructed in this laboratory.[6] The free hydrogen-ion concentration $[H^+]$ was determined with a glass and calomel electrode (0.01*M* NaCl, 0.09*M* $NaClO_4$) system calibrated before each experiment by measuring the emf (E_R) when the titration vessel contained a solution with a known free hydrogen-ion concentration, $[H^+]_R$. The unknown hydrogen-ion concentration, $[H^+]$, was then calculated from the equation:

$$-59.16 \log[H^+]/[H^+]_R = (E_R - E_j') - (E - E_j'') \quad (1)$$

where E_j' and E_j'' are the liquid junction potentials, calculated from

$$E_j' = 52.5\,[H^+]_R \text{ and } E_j'' = 52.5\,[H^+].$$

A Pye Unicam SP 8–100 spectrophotometer equipped with a 10-mm autocell and a superimpose accessory was used for the absorbance measurements.

Procedures

The protonation constants of 1-hydroxy-4,7-disulpho-2-naphthoic acid were determined potentiometrically by keeping the total concentration of ligand, C_L, constant and varying the total hydrogen-ion concentration, C_H, by addition of sodium hydroxide. Seven series of measurements were made, with C_L varied between 0.002 and 0.03*M*, and $-\log[H^+]$ between 2 and 11, about 200 data points being obtained.

The stability constants of the iron(III) complexes were evaluated from 12 separate emf titrations, in which the mixtures with known initial concentrations of iron(III) (C_M), ligand and protons were titrated with sodium hydroxide solution. In these measurements C_M, C_L and C_H were varied between 0.001 and 0.025*M*, $C_L:C_M$ was varied between 2 and 25.

In the spectrophotometric work, absorbance readings were taken in the wavelength region 450–750 nm, where the ligands show little or no absorption. Altogether 24 test solutions were prepared for the two iron(III)–ligand systems, with C_M and C_L, varied between 0.0001 and 0.001*M*, and $-\log[H^+]$ between 0.6 and 6.5.

*Reprint requests.

Table 1. The values of the protonation constants of 1-hydroxy-4-sulpho-2-naphthoic (1), 1-hydroxy-7-sulpho-2-naphthoic (2) and 1-hydroxy-4,7-disulpho-2-naphthoic (3) acids determined potentiometrically at $I = 0.1$ ($NaClO_4$) and 25°C; the errors given are three times the standard deviations; $K_n = K(H_{n-1}L + H = H_nL)$

Acid	$\log K_1$	$\log K_2$	$\log \beta_{0,2,1}$	Refs.
(1)	11.65	2.50	14.15	13
(2)	12.37	2.73	15.10	2
(3)	11.119 ± 0.006	2.208 ± 0.005	13.33	This work

Table 2. The values of the stability constants determined spectrophotometrically at $I = 0.1$ ($NaClO_4$) and 25°C, the wavelengths of maximum absorption, λ_{max}, and corresponding molar absorption coefficients, ϵ_{max}, for the iron(III) complexes of 1-hydroxy-4-sulpho-2-naphthoic (1), 1-hydroxy-7-sulpho-2-naphthoic (2) and 1-hydroxy-4,7-disulpho-2-naphthoic (3) acids; the errors given are three times the standard deviations

Ligand	Species	$\log \beta$	λ_{max}, nm	ϵ_{max}, $l.mole^{-1}.cm^{-1}$	Refs.
(1)	FeL	14.037 ± 0.009	580	1570 ± 20	1
	FeL_2^{3-}	25.012 ± 0.024	530	2840 ± 40	
	FeL_3^{6-}	32.35 ± 0.06	495	3290 ± 50	
(2)	FeL	15.853 ± 0.016	600	1470 ± 30	This work
	FeL_2^{3-}	27.433 ± 0.039	535	1820 ± 40	
	FeL_3^{6-}	34.11 − 0.09	470	2960 ± 130	
(3)	FeL^-	14.686 ± 0.024	565	1630 ± 50	This work
	FeL_2^{5-}	24.74 ± 0.06	520	2970 ± 150	

Calculations

The equilibrium constants were calculated as overall stability constants, $\beta_{q,p,r}$, with the program SCOGS[7,8] for the potentiometric data and the program SQUAD[9] for the absorbance data:

$$\beta_{q,p,r} = K(qFe^{3+} + pH^+ + rL^{n-} = Fe_qH_pL_r^{(3q-rn)+}) \quad (3)$$

Because the protonation of 1-hydroxy-4,7-disulpho-2-naphthoic acid has been previously examined only in 0.5*M* sodium perchlorate medium, it was necessary to determine the protonation constants in 0.1*M* sodium perchlorate medium. Table 1 shows the protonation-constant values used in the calculations of the stability constants.

The hydrolysis of iron(III) was taken into account by using the constants $\log \beta_{1,-1,0} = -3.05$, $\log \beta_{1,-2,0} = -3.26$ and $\log \beta_{2,-2,0} = -2.91$.[10]

RESULTS AND DISCUSSION

The calculations were begun with the assumption that only the series of stepwise complexes $FeL_r^{(3-rn)+}$ is formed. The next stage was to consider protonated, hydrolysed and polynuclear complex species. The inclusion of such complex compounds was unsuccessful, and hence all the data were interpreted in terms of the mononuclear complexes, to obtain the stability constant values given in Tables 2 and 3. Hydrolytic reactions interfered with the measurements at pH above about 5 in the case of the iron(III)–1-hydroxy-4,7-disulpho-2-naphthoic acid system even when a large excess of ligand was present, so we were unable to determine β_3 for this system. The 1:1 complexes form at such high acidity (*e.g.*, the FeL^- complex of 1-hydroxy-4,7-disulpho-2-naphthoic acid begins to form at pH <0.5) that the potentiometric method could not be used to determine the stability constants of these complexes. The $\log \beta_1$ values determined spectrophotometrically were used as non-variable constants in computations with the potentiometric data. Table 2 also shows the stability constants of the iron(III) complexes of 1-hydroxy-4-sulpho-2-naphthoic acid evaluated earlier by the spectrophotometric method.

The equilibria are similar to those of 1-hydroxy-4-sulpho-2-naphthoic and 5-sulphosalicyclic acids, as could be predicted.[1,12] There was no evidence of water-soluble protonated, hydrolysed or polynuclear complex compounds.

The stability of the 1-hydroxy-7-sulpho-2-naphthoic acid complexes is higher than that of the 1-hydroxy-4-sulpho-2-naphthoic acid complexes, in agreement with the overall basicity of the ligand anions

Table 3. Values of the stability constants of the iron(III) complexes of 1-hydroxy-7-sulpho-2-naphthoic (1) and 1-hydroxy-4,7-disulpho-2-naphthoic (2) acids determined potentiometrically at $I = 0.1$ ($NaClO_4$) and 25°C; the errors given are three times the standard deviations

Ligand	$\log \beta_1$	$\log \beta_2$	$\log \beta_3$
(1)	15.853 (fixed)	26.811 ± 0.014	34.049 ± 0.020
(2)	14.686 (fixed)	24.40 ± 0.04	

Table 4. Stepwise stability constants and log (k_n/k_{n+1}) values for different metal complexes of 1-hydroxy-4-sulpho-2-naphthoic (1), 1-hydroxy-7-sulpho-2-naphthoic (2) and 1-hydroxy-4,7-disulpho-2-naphthoic (3) acids at $I = 0.1$ ($NaClO_4$) and 25°C; $k_n = K(ML_{n-1} + L = ML_n)$.

Ligand	M	Method	log k_1	log k_2	log k_3	log (k_1/k_2)	log (k_2/k_3)	Refs.
(1)	Fe^{3+}	sp	14.04	10.97	7.34	3.07	3.63	1
	Be^{2+}	gl	11.19	8.87		2.32		13
	Cu^{2+}	gl	9.84	6.67		3.17		13
(2)	Fe^{3+}	sp	15.85	11.58	6.68	4.27	4.90	This work
	Be^{2+}	gl	11.85	8.66		3.19		2
	Cu^{2+}	gl	10.21	6.41		3.80		2
(3)	Fe^{3+}	sp	14.69	10.05		4.64		This work

sp = Spectrophotometric method.
gl = Potentiometric method.

(Table 1). The stability of the first Fe(III) complex of 1-hydroxy-4,7-disulpho-2-naphthoic acid is greater than that of the corresponding 1-hydroxy-4-sulpho-2-naphthoic acid complex, whereas the stability order of the bis-complexes is the reverse. This is due to the electrostatic interaction between different species in the course of the complex formation as well as the steric factors caused by the sulphonato group: the electrostatic attraction between the Fe(III) cation and L^{4-} anion of 1-hydroxy-4,7-disulpho-2-naphthoic acid is greater than that between the Fe(III) cation and L^{3-} anion of 1-hydroxy-4-sulpho-2-naphthoic acid. The 1:1 iron(III) chelate of the monosulphonic acid is uncharged, whereas that of the disulphonic acid is negatively charged, making addition of the second ligand more difficult in the latter case. Table 4 lists the log (k_n/k_{n+1}) values for the various equilibrium systems. In general, these values are high, mainly because of electrostatic repulsion between the negatively charged oxygen atoms in the hydroxyl, carboxyl and sulphonato groups of the ligands. The steric hindrance caused by by the sulphonato group must also be taken into consideration; it is greater for a sulphonato group at C-7 that at C-4.

The sulphonated *o*-hydroxynaphthoic acid chelates of iron(III) are significantly more stable than those of other metal ions studied previously in this laboratory.[2–4,6,13,14] For example, the stability of the 1:1 1-hydroxy-4-sulpho-2-naphthoic acid complexes decreases in the order (log β_1 in parentheses) Fe(III) (14.04) > Al(III) (12.64) > UO_2(VI) (11.20) ~ Be(II) (11.19) > Cu(II) (9.84) > Eu(III) (8.69).

Figure 1 shows the distribution of the iron(III) species in the 1-hydroxy-7-sulpho-2-naphthoic and 1-hydroxy-4,7-disulpho-2-naphthoic acid systems in the $-\log [L]$ region studied.

Figure 2 shows the absorption spectra for the $FeL_r^{(3-rn)+}$ chelates of 1-hydroxy-7-sulpho-2-naphthoic and 1-hydroxy-4,7-disulpho-2-naphthoic acids, calculated with the program SQUAD. The corresponding spectra for the 1-hydroxy-4-sulpho-2-naphthoic acid chelates were presented earlier.[1] It can be seen from Table 2 and Fig. 2 that λ_{max} decreases with the number of ligand anions co-ordinated in each case, which means that the ligand fields increase with increasing number of ligands in the complexes. It can also be seen that the ϵ_{max} values increase with the number of co-ordinated ligand anions.

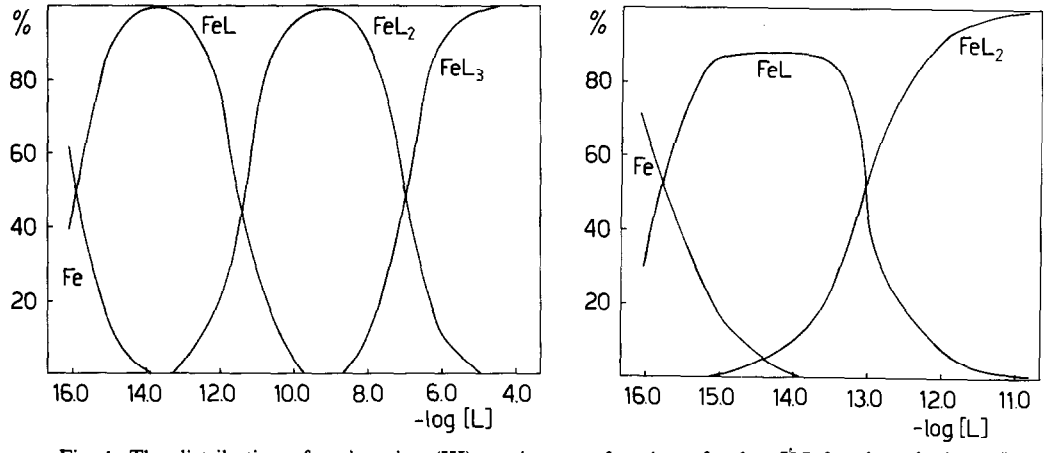


Fig. 1. The distribution of various iron(III) species as a function of $-\log [L]$ for the 1-hydroxy-7-sulpho-2-naphthoic acid (left) and 1-hydroxy-4,7-disulpho-2-naphthoic acid (right) systems at $I = 0.1$ ($NaClO_4$) and 25°C.

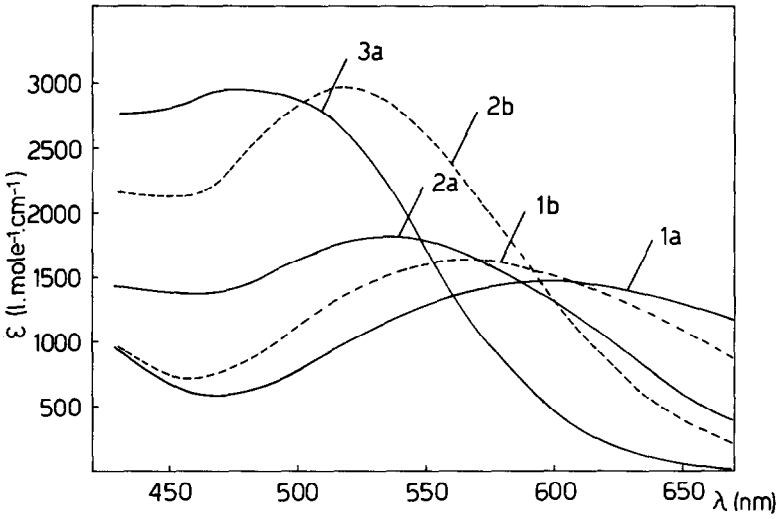


Fig. 2. The absorption spectra of the FeL (1a), FeL_2^{3-} (2a) and FeL_3^{6-} (3a) complexes of 1-hydroxy-7-sulpho-2-naphthoic acid, and FeL^- (1b) and FeL_2^{5-} (2b) complexes of 1-hydroxy-4,7-disulpho-2-naphthoic acid in aqueous solution.

According to our investigations, at least the 4- and 7-sulpho derivatives of 1-hydroxy-2-naphthoic acid seem to be valuable reagents for iron, and their use in a spectrophotometric method for determining iron in polymetallic ores will be published later.

REFERENCES

1. L. H. J. Lajunen, S. Parhi and H. Ruotsalainen, *Finn. Chem. Lett.*, 1979, 227.
2. L. H. J. Lajunen and T. Hiljanen, *Acta Univ. Oul. A* 105 (1980).
3. L. H. J. Lajunen and M. Tikanmäki, *Finn. Chem. Lett.*, 1978, 96.
4. K. Räisänen and L. H. J. Lajunen, *Org. Magn. Res.*, 1978, **11**, 12.
5. G. Gran, *Analyst*, 1952, **77**, 661.
6. L. H. J. Lajunen, J. Eloranta and A. Kukkohovi, *Finn. Chem. Lett.*, 1979, 11.
7. I. G. Sayce, *Talanta*, 1968, **15**, 1397; 1971, **18**, 653.
8. I. G. Sayce and V. S. Sharma, *ibid.*, 1972, **19**, 831.
9. D. J. Leggett and W. A. E. McBryde, *Anal. Chem.*, 1975, **47**, 1065.
10. L. G. Sillén and A. E. Martell, *Stability Constants of Metal-Ion Complexes*, Suppl. 1, Spec. Publ. 25, Chemical Society, London, 1971.
11. A. Agren, *Acta Chem. Scand.* 1954, **8**, 1059.
12. W. A. E. McBryde, J. L. Rohr, J. S. Pencier and J. A. Page, *Can. J. Chem.*, 1970, **48**, 2574.
13. L. H. J. Lajunen, *Finn. Chem. Lett.*, 1978, 129.
14. L. H. J. Lajunen and R. Anttila, Unpublished results.

Talanta, Vol. 28, pp. 281 to 286. 1981
Printed in Great Britain. All rights reserved

0039-9140/81/050281-06502.00/0
Copyright © 1981 Pergamon Press Ltd

APPLICATION OF PHASE-TITRATIONS FOR ESTIMATION OF ADULTERATION OF GASOLINE AND HIGH-SPEED DIESEL WITH KEROSENE

S. K. SURI*, K. PRASAD and J. C. AHLUWALIA
Chemistry Department, Indian Institute of Technology, New Delhi-16, India

and

D. W. ROGERS
Chemistry Department, Long Island University, Brooklyn, NY 11201, U.S.A.

(*Received* 16 *July* 1980. *Revised* 6 *November* 1980. *Accepted* 11 *December* 1980)

Summary—A simple, cheap and quick routine method based on phase-titration has been developed for the estimation of adulteration of gasoline and high-speed diesel with kerosene. Since no instrumentation is required, the method can be used as a field method for analysis at filling stations. Adulteration of gasoline with kerosene can be determined to ±1%, and of diesel with kerosene to ±2%. Even non-technical personnel with a few days' training can analyse fuel samples by this method.

In India, gasoline and high-speed diesel are sold at a taxation rate much higher than that of kerosene. Also, high-speed diesel, because of its extensive use in transport and agriculture, is always in short supply. Analysis of a large number of gasoline and high-speed diesel samples collected from several gasoline stations for the purpose of quality control has revealed that the dealers generally adulterate these two petroleum fractions with kerosene. The adulteration of gasoline with kerosene results in increased knock, engine wear and possibly more serious consequences.[1]

Various physical and chemical properties are utilized in quality-control tests for petroleum fuels; these tests include gas chromatographic analysis, measurement of relative density, boiling point, flash point *etc.* These tests are time-consuming and require a well equipped laboratory, and a large number of analysts if more than a few samples are to be analysed for adulteration every day.

During our investigations on applications of liquid–liquid equilibria, we have developed a simple, cheap, quick and accurate routine method for the quantitative analysis of mixtures of kerosene with gasoline or high-speed diesel, that is suitable for adulteration tests.

The phase-separation method was first proposed by Bogin[2] for the analysis of binary mixtures. The theoretical aspects were worked out by Rogers *et al.*[3] for the binary and pseudo-binary mixtures and by Suri[4–7] for ternary mixtures.

Gasoline, high-speed diesel and kerosene are complex mixtures of hydrocarbons distilling over particular temperature ranges.[8] In view of the regular gradation in the properties of hydrocarbons, each distillation fraction from crude petroleum can be regarded as a single hydrocarbon with an effective molecular weight dependent on the distillation temperature range. Analysis of binary mixtures of kerosene with gasoline or high-speed diesel is therefore similar to analysis of a binary hydrocarbon mixture. The hydrocarbons exhibit such closely similar solubility behaviour that simple solubility tests cannot be used to differentiate them. However, addition of a third consolute component can increase the miscibility of two mutually immiscible or partially miscible components to an extent dependent on various factors, including the nature and amount of the consolute component added. A number of such additives, *e.g.*, methanol, ethanol, acetone, can be used to homogenize the almost immiscible mixture of water and a hydrocarbon. We prefer acetone because of its low cost, ready availability, ease of purification, and the possibility of recycling it, as it is non-azeotropic with water.

The effect of a consolute component on the mutual miscibilities of a hydrocarbon with water is given by the binodal curve of the resultant ternary system. Preliminary experiments showed that though the mutual miscibilities of various hydrocarbons in water are of the same order of magnitude, the addition of acetone yields fairly distinct solubility curves. The significant differences between these solubility curves can be used to develop procedures based on liquid–liquid equilibrium for the analysis of binary mixtures of hydrocarbons or of different petroleum fractions.

Three sets of binary mixtures of acetone with gasoline, kerosene and high-speed diesel, of varied composition, were prepared and titrated with water to the turbidimetric end-point. The titration value was plotted as a function of composition and the results

* To whom all correspondence may be addressed.

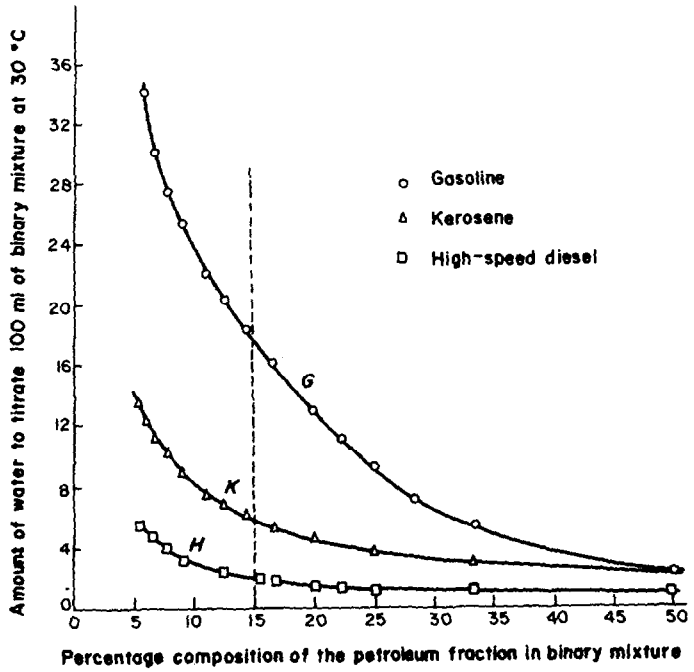


Fig. 1. Titration values for binary mixtures at 30 ± 0.1°.

obtained are shown in Fig. 1. If a ternary mixture (*e.g.*, gasoline, kerosene and acetone) is titrated with water, the titration value, which is a function of the composition of the ternary mixture, will fall in the area between the calibration curves *G* and *K* of Fig. 1. Since only the three components are present at the start of the titration, the titration value is a function of the concentration of only two of them, and hence the locus of the titration value required to produce a turbidimetric end-point, as a function of the composition of the ternary mixture being titrated, is a three-dimensional surface of the type shown in Fig. 2. In

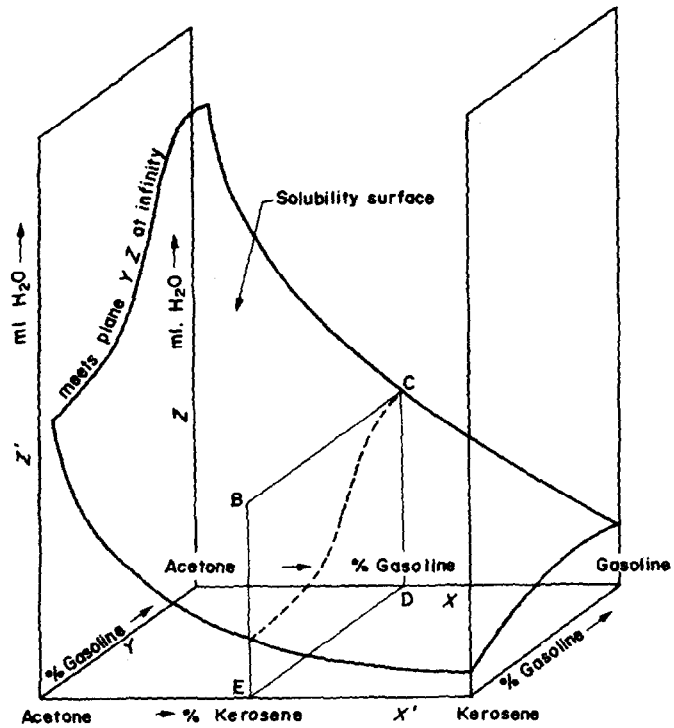


Fig. 2. The solubility surface for the gasoline–kerosene–acetone–water system.

Table 1. Specifications of the petroleum fractions used in the present study

Property	Gasoline	Kerosene	High-speed diesel
Boiling point, °C			
10% recovery	70	200	—
50% recovery	125	—	—
90% recovery	180	—	366
Final boiling point	215	300	—
Flash point, °C	−40	35	38
Density, ρ^{25}, g/cm^3	0.730	0.787	0.829
Refractive index, n_D^{25}	1.4145	1.4395	1.4637

this figure, since the solubility surface should meet the pure acetone line at infinity, only a part of the solubility surface is shown. The edges of the solubility surface on the planes xz and $x'z'$ correspond to the titration values for the binary mixtures of gasoline + acetone and kerosene + acetone (curves G and K of Fig. 1) respectively. For a fixed proportion of the consolute component acetone, the titration value (which is then a function of the relative amounts of gasoline and kerosene in the ternary mixture) is given by the line obtained by the intersection of the solubility surface with a plane $BCDE$ perpendicular to the plane xy and parallel to the plane yz, and corresponding to the specified concentration of acetone in the ternary mixture. This line can be used as the calibration curve for the analysis of binary mixtures of gasoline and kerosene.

A particular concentration of acetone in the solution can be represented by the appropriate plane parallel to BCDE in Fig. 2 or by a vertical line in Fig. 1. The intersections of the vertical line with curves K and G in Fig. 1 give the upper and lower limits of the titration values on the corresponding calibration curve in Fig. 2 and corresponding to 0 and 100% gasoline respectively. The greater the separation between the curves K and G in Fig. 1, the greater will be the slope of the calibration curve and hence the greater the accuracy of determination. Curves K and G (also curve H) in Fig. 1 tend to converge as they approach 0% acetone. Hence the concentration of acetone used in the analysis should be high rather than low.

Mixtures of kerosene and high-speed diesel can be analysed similarly.

EXPERIMENTAL

Materials

Guaranteed-reagent grade acetone was dried over anhydrous potassium carbonate and distilled before use.[9] Distilled water was used as titrant. Samples of gasoline, kerosene and high-speed diesel were supplied by Indian Oil Corporation Ltd., Delhi and conformed to the specifications in Table 1.

Procedure

Transfer a known volume of sample solution to a 125-ml conical flask, add a magnetic stirrer follower, and fit a two-hole stopper, through one hole of which passes the tip of a 5-ml microburette. Place a sheet of thermal insulating material between stirrer and flask to prevent heating of the solution by the stirrer motor, and place the entire assembly inside an air thermostat which can be kept at a temperature constant to ±0.1°. When the sample has reached the required temperature, titrate with water to a turbidimetric end-point: such end-points are quite sharp and can be found to within 1 or 2 drops of water. Typical titrations take from 2 to 5 min each. Care should be taken to keep evaporation losses to a minimum.[10]

DISCUSSION

Optimum volume ratio for consolute component

The optimum volume ratio of acetone to fuel sample can be found, with reservations, from Fig. 1. Although the curves are more widely separated for mixtures with more acetone, the end-points are not as clear as when there is less acetone present, so a compromise is made. The optimum lies in the range 75–85% v/v acetone. The precision also tends to be better when larger samples are taken.

The calibration curve for the analysis of kerosene–gasoline mixtures is given by the broken line in the plane BCDE in Fig. 2. This curve was constructed by titrating 100-ml portions of ternary mixtures containing the same proportion of acetone but varying proportions of gasoline and kerosene. The results are plotted in a more conventional manner in Fig. 3, and also in Fig. 4 for the diesel–kerosene system. Only the right-hand half is normally needed and can be defined as precisely as desired, by increasing the number of calibration points.

It can be seen from Figs. 3 and 4 that a mixture containing 20% of hydrocarbon gives better discrimination over a wider range of composition than will mixtures containing higher hydrocarbon contents, particularly for the range 0–30% kerosene which is of interest for determining the adulteration of gasoline or high-speed diesel with kerosene. The hump shown in Fig. 3 is due to the complexity of the quaternary phase diagram, and makes it difficult to select the optimum consolute concentration for good precision at low adulteration levels.

Effect of temperature

Temperature influences the calibration curves because it has a significant effect on the phase equi-

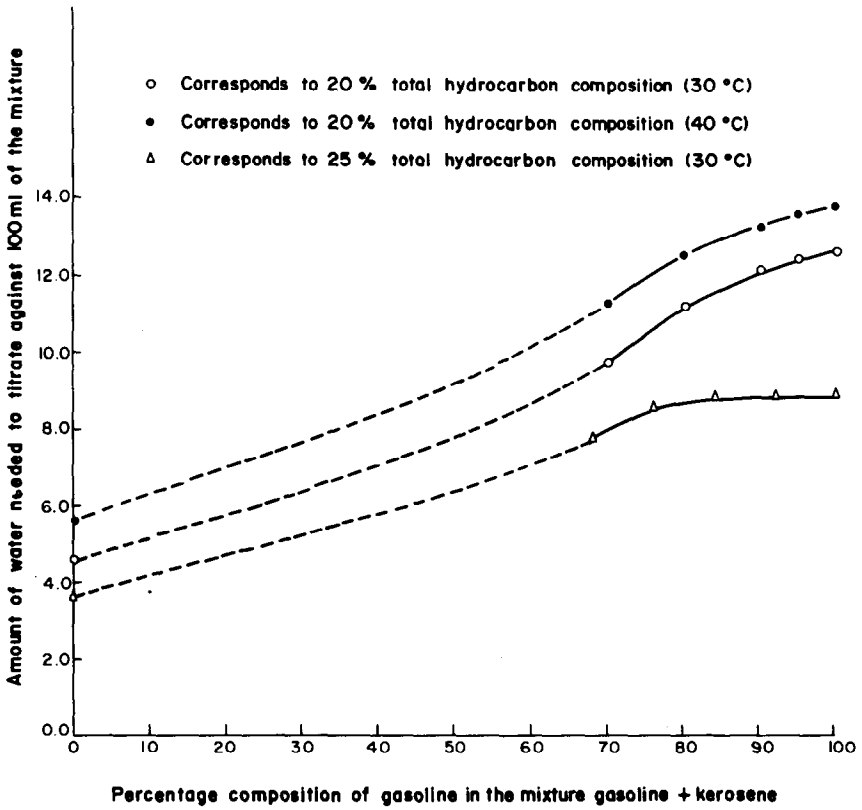


Fig. 3. Calibration curves at 30 ± 0.1° and 40 ± 0.1° for kerosene–gasoline mixtures.

libria. The calibration curves for the two systems investigated were obtained at 30 ± 0.1° and 40 ± 0.1° and are shown in Figs. 3 and 4. The curves in a set are more or less parallel. A 10° increase in temperature changes the titration value by ~ 10–15%. If the temperature is controlled to ±0.1° during an experiment, the contribution of this factor to uncertainty in the titration value is about 0.15%, which is negligible in comparison with the end-point error.

Effect of weathering of fuel sample on the titration sample

Calibration curves obtained for a fuel sample kept over a period of about 8 months in the laboratory, with the room temperature varying between 15 and 35°, could be reproduced to within 0.5%. "Weathering" therefore has a negligible effect on the calibration curves and hence also on the results of analysis.

The effect of dissolved salts on the titration

Preliminary experiments with water containing various known concentrations of calcium showed that the precipitation of salt from water samples containing up to ~ 1000 ppm of calcium does not interfere with detection of the turbidimetric end-point.

Up to 0.5% of organic impurities such as other hydrocarbons, methanol, acetals, does not affect the results significantly, but water present as an impurity in the acetone used is a serious source of error: 0.1% of water in the acetone may introduce an uncertainty of up to 0.7% in the analysis. Water in the acetone is the most difficult impurity to remove, but the concentration can be brought down to around 0.1% very

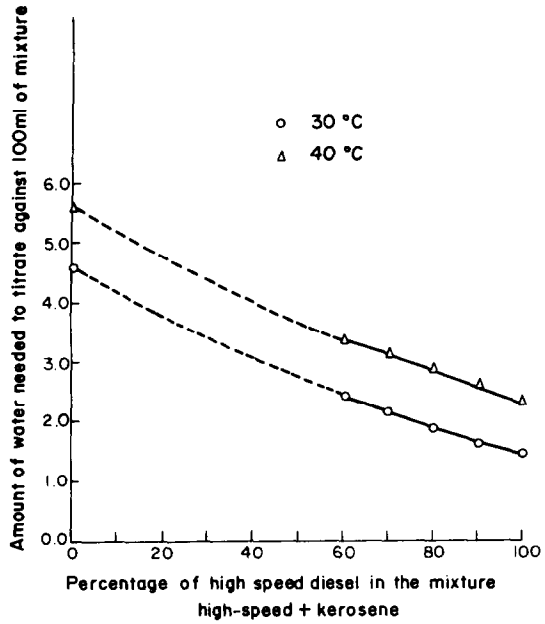


Fig. 4. Calibration curves at 30 ± 0.1° and 40 ± 0.1° for kerosene–high-speed diesel mixtures.

conveniently by drying with salts such as calcium sulphate ("drierite"), potassium carbonate *etc.*[9] and this is recommended for the routine dehydration of the acetone.

When the same batch of acetone is used both for the calibration and the analyses, the errors arising from impurities cancel out.

Source of the crude petroleum

It is well established that the composition of crude petroleum and hence of each distillation fraction varies with the boiling range and source of the crude. It is therefore likely that the characteristics which influence the acetone–petroleum fraction–water ternary phase diagram, such as average molecular weight, aromatic content *etc.*, will be different for crudes obtained from different sources. The calibration curves for binary mixtures of distillation fractions of crude petroleum obtained from different sources are therefore expected to be different. Binary mixtures of different grades of gasoline and kerosene will also be expected to yield different calibration curves.

We have not yet studied the influence of the source of the crude on the calibration curve, but we do not expect the error arising from these factors to exceed ~2–3% if a calibration curve for a particular petroleum fraction from one source is used for petroleum fractions obtained from a different source.

Application in the field

The procedure can be used as a field method to estimate the adulteration of samples of gasoline or high-speed diesel with kerosene. In addition to burettes and pipettes, the items needed are a precision thermometer, dry acetone, and standard calibration curves obtained in the laboratory at various temperatures, preferably at 5° intervals, to allow interpolation to the actual temperature of analysis. Alternatively, the calibration curves can be obtained in the field.

The compositions of some synthetic mixtures of known composition analysed in the field (on various days and at various temperatures) are recorded in Table 2. It is observed that the absolute error for determination of kerosene in gasoline is up to about 1.5%. The absolute error for determination of kerosene in high-speed diesel is rather higher, up to 3.5%. The accuracy and precision of the laboratory method are shown in Table 3. The lowest adulteration levels that can be detected reliably are ~4% of kerosene in high-speed diesel and ~1.5% in gasoline, but these limits can be lowered by titrating larger samples.

Table 2. Comparison of results for synthetic mixtures (field method)

Kerosene, %		
Present	Found	Temperature of analysis, °C
	Kerosene + gasoline	
3.9	5.2	37
13.8	14.6	32
16.8	17.2	32
18.0	16.5	35
	Kerosene + high-speed diesel	
4.6	6.8	37
12.0	14.1	37
17.8	19.9	37
25.9	26.4	32
30.4	33.9	35

Table 3. Results and standard deviations for fuel samples adulterated with 10% kerosene

Sample	Kerosene found, %	Number of determinations
Gasoline	9.8 ± 0.3	6
High-speed diesel	9.7 ± 0.5	8

Comparison with other methods

Gas chromatography can be used to estimate as little as 0.5% of kerosene in gasoline fairly accurately,[12] but for the determination of kerosene in high-speed diesel, where both fuels are high-boiling fractions, the precisions of the gas-chromatographic method and the proposed procedure are about the same.

The densities of kerosene and gasoline or high-speed diesel differ by ~0.05 g/cm^3 and 1% adulteration corresponds to a difference of ~5×10^{-4} g/cm^3 in densities. Further, the temperature coefficient of density for gasoline[11] is ~8.2×10^{-4} g.cm^{-3}.deg^{-1}. If density is to be used to determine the degree of adulteration, laboratory facilities would be required to attain the same performance as our field method.

Advantages

The method is comparable or, in certain respects, even superior to other physical methods of analysis such as measurement of specific gravity or refractive index. The phase-titration technique is far simpler and requires only ordinary laboratory equipment.

It is rapid, taking only 2–5 min per sample, so a large number of samples can be analysed in a day by one operator. Little expertise is required. A non-technical quality-control inspector can use the method in the field with the aid of predetermined calibration curves.

The method is cheap and requires only about 100 ml of acetone (which can be recycled if required) per sample. No indicator solutions are needed, and tap-water can be used as the titrant. Sample-size has no effect on the detection of the end-point.

Acknowledgements—The authors thank the Department of Science and Technology, Government of India, for financial support for this work. They also wish to express their gratitude to the Indian Oil Corporation, New Delhi, for the generous gift of fuel samples.

REFERENCES

1. E. M. Goodger, *Hydrocarbon Fuels, Production, Properties and Performance of Liquids and Gases*, Macmillan, London, 1975.
2. C. D. Bogin, *Ind. Eng. Chem.*, 1924, **16**, 38.
3. D. W. Rogers, D. L. Thompson and I. D. Chawla, *Talanta*, 1966, **13**, 1389.
4. S. K. Suri, A. P. Rao and V. Ramakrishna, *Indian J. Chem.*, 1966, **4**, 194.
5. S. K. Suri, *Talanta*, 1970, **17**, 577.
6. *Idem, ibid.*, 1972, **19**, 804.
7. *Idem, ibid.*, 1974, **21**, 604.
8. A. L. Waddams, *Chemicals from Petroleum*, 3rd Ed., Murray, London, 1973.
9. J. A. Riddick and W. B. Bunger (eds.) *Techniques of Organic Chemistry*, Vol. II, *Organic Solvents*, Wiley-Interscience, New York, 1970.
10. D. A. Dunnery and G. R. Atwood, *Talanta*, 1968, **15**, 855.
11. H. M. Spiers (ed.) *Technical Data on Fuel*, pp. 269–70, British National Committee World Power Conference, London, 1962.
12. N. C. Saha, Indian Oil Corporation Research Centre, Faridabad, India, personal communication.

Talanta. Vol. 28, pp. 287 to 293, 1981
Printed in Great Britain. All rights reserved

0039-9140/81/050287-07$02.00/0
Copyright © 1981 Pergamon Press Ltd

TITRATION OF VANADIUM(IV) WITH CERIUM(IV) SULPHATE, WITH FERROIN AS INDICATOR, IN AQUEOUS ACETONE AS FACILE REACTION MEDIUM

AN ANALYTICAL AND MECHANISTIC STUDY

K. SRIRAMAM, B. S. R. SARMA, B. SYAMA SUNDAR and N. RAMABRAHMA SASTRY
Department of Chemistry, Nagarjuna University, Nagarjuna Nagar, 522 510 (A.P.) India

(*Received* 16 *September* 1980. *Accepted* 2 *December* 1980)

Summary—A new procedure for the titration of vanadium(IV) with cerium(IV) sulphate, with ferroin as indicator, in aqueous acetone medium is reported. A differential determination of iron(II) and vanadium(IV) is also possible. A probable mechanism for the fast ferriin–vanadium(IV) reaction in acetone medium is given.

Earlier workers[1,2] recommended that the potentiometric titration of vanadium(IV) with cerium(IV) sulphate should be done at elevated temperature. It is generally believed that the reaction is too sluggish at room temperature.

Rao and Dikshitulu[3,4] used phosphoric acid as catalyst for both potentiometric and visual end-point titrations. They remark that the catalyst speeds up the primary reaction as well as the oxidized indicator–vanadium(IV) reaction. Other catalysts used in the indicator methods are acetic acid[5] and hexacyanoferrate(III).[6]

Rechnitz and Rao[7] made a kinetic study to identify the cause of sluggishness in the titration and choose the optimum conditions for use of acetic acid as the catalyst. Their study pertained to the experimental conditions near the potentiometric titration end-point. The second-order rate constant of the primary reaction in 1*M* sulphuric acid was found to be 1350 ± 100 l.mole^{-1}.sec^{-1}, so they regarded the reaction as fast. The apparent sluggishness was attributed to slow potential equilibration of the V(V)/V(IV) system at the platinum electrode. The spectrophotometric titration was rapid and accurate. No explanation was offered for the favourable action of acetic acid on the ferriin–vanadium(IV) reaction although the rate constants were determined.

We also find that the uncatalysed reaction is fast enough for potentiometric or spectrophotometric titration (with 0.1*N* solutions and small titration volumes), but this is probably because there is usually a 2–3 min interval between titrant addition and measurement. With indicators, however, the titrant is added almost continuously and the indicator undergoes simultaneous competitive reactions with the main reactants.

It is then more meaningful to speak of the relative rates of the primary and indicator reactions rather than of the absolute speed of the main reaction. For example, the oxidation of ferroin by cerium(IV) is more rapid ($K = 1.6 \times 10^5$ l.mole^{-1}.sec^{-1} at 25° in 1*M* sulphuric acid) than the oxidation of vanadium(IV). Therefore, at each addition of oxidant the ferroin colour disappears quickly but returns slowly, showing the slowness of the ferriin–vanadium(IV) reaction. Phosphoric acid, acetic acid or hexacyanoferrate(III) will catalyse the latter reaction enough to make the titration practicable. The effect of these catalysts on the vanadium(IV)–cerium(IV) reaction is irrelevant, provided it does not make the primary reaction slower than the indicator reactions, or accelerate the indicator reduction and retard the indicator oxidation (*cf.* Sriramam and Gopala Rao).[5] The question of retardation was not considered by Rechnitz and Rao.[7] It should be noted that the rates of the competitive reactions depend on the concentrations of the reactants. For example, in the titrations with catalyst present the intermittent colour change is usually observed towards the close of the titration, when the vanadium(IV) concentration is low, but never in the initial stages of the titrations.

Titrations with phosphoric acid as catalyst suffer from the formation of cerium(IV) phosphate, which sticks to the sides of the titration vessel. Although the titrations in acetic acid medium are sharp and accurate there is a limitation to the amount of mineral acid that can also be present.

Hexacyanoferrate(III) cannot be used if the acidity is higher than 0.5*N*, and if iron(II) is present cannot be added until all the iron(II) has been oxidized (to avoid the formation of Prussian blue), so prior knowledge of the iron(II) content would be necessary.

We have now observed that if acetone is added in quantity to the titration mixture, vanadium(IV) can be titrated with cerium(IV) in 0.5–2.5*N* sulphuric acid, with ferroin as indicator, at room temperature. Mixtures of iron(II) and vanadium(IV) can be analysed by means of two titrations under different conditions.

Table 1. Determination of vanadium

Vanadium(IV), *mg* Taken	Found	Relative error, %
23.89	23.87	0.1
21.50	21.57	0.4
19.05	19.10	0.3
12.43	12.46	0.3
4.727	4.73	0.1
4.410	4.41	0.0
3.729	3.74	0.3
2.384	2.38	0.2

EXPERIMENTAL

Reagents

Vanadium(IV) sulphate solution (0.1*M*) and cerium(IV) sulphate solution (0.1*M*), both in 1*N* sulphuric acid, prepared and standardized as described earlier.[3] Ferroin solution, 0.01*M*.

All other chemicals used were of analytical-reagent grade.

Apparatus

A quinhydrone electrode (1*M* sulphuric acid), bright platinum electrodes, and an inverted U-tube fitted with porous porcelain discs at the ends and filled with 1*M* sulphuric acid to serve as a salt bridge were used in the potentiometric investigation.

Procedure

A volume of 5–10 ml of vanadium(IV) containing 2.5–25 mg of vanadium was treated with enough 5*M* sulphuric acid to give an overall final acidity of 0.5–2.5*N*, water to make up to 30 ml, and 15–25 ml of acetone followed by 1 drop of ferroin, and then titrated with 0.05*N* cerium(IV) sulphate at the usual speed until near the end-point, a 10-sec delay then being allowed between additions. In titrations with 0.01*N* reagents, a 30-sec delay was allowed between the later additions. At the end-point the colour changed from red to light yellow and was very sharp and permanent. A white precipitate appeared during the titration, but did not affect the results. An indicator correction of 0.06 ml of 0.01*N* cerium(IV) should be applied for each drop of indicator. Some typical results are given in Table 1.

Interferences

Amounts of 55 mg of iron(III), 9 mg of chromium(III), 230 mg of cerium(III), 84 mg of vanadium(V), 200 mg of nickel, 10 mg of manganese(II), 160 mg of copper(II), 300 mg of zinc(II), 12 mg of cobalt(II) and 440 mg of chloride were found not to interfere in the titration.

Differential titration of iron(II) and vanadium(IV)

By combination of the procedure just described with that of Walden *et al.*,[8] iron(II) and vanadium(IV) were determined differentially. One aliquot was titrated with cerium(IV) sulphate in 10–12*N* sulphuric acid to give the iron(II) content. Another aliquot was titrated as described above and gave the total of iron(II) and vanadium(IV). Typical results are given in Table 2.

Effect of acetone

The influence of the acetone concentration on the speed of the indicator oxidation and reduction reactions was studied and the results are recorded in Table 3. They show that while the indicator oxidation is somewhat retarded by acetone, the indicator reduction is accelerated. However, no intermittent colour change is observed during a titration, because, in contrast to blank experiments, the ferroin is never fully oxidized, so there is less ferriin to be reduced by vanadium(IV). At the end-point the bulk of the ferroin colour usually disappears within 5 sec of addition of the last drop, although the complete colour change takes longer.

Table 2. Determination of vanadium(IV) and iron(II) in mixtures

Taken, *mg*		Found, *mg*		Relative error, %	
Fe(II)	V(IV)	Fe(II)	V(IV)	Fe(II)	V(IV)
12.85	11.72	12.82	11.67	0.2	0.4
9.49	21.65	9.47	21.57	0.3	0.4
4.122	4.564	4.13	4.57	0.1	0.1
2.692	2.893	2.70	2.89	0.4	0.0

Table 3. Influence of acetone concentration on indicator oxidation and reduction in 1*N* H_2SO_4 (0.05 ml of 0.01*M* ferroin is treated with enough 5*M* sulphuric acid and acetone and diluted to 50 ml with water)

Acetone, % *v/v*	Time taken for bulk of colour change, *sec* Discharge*	Reappearance†
0	Almost instantaneous	Very slow
10	4	60
20	8	20
30	16	15
40	20	9
50	45	4

* On the addition of 0.06 ml of 0.01*M* cerium(IV) sulphate.

† On the addition of 0.05 ml of 0.05*M* vanadium(IV) to the oxidized indicator solution.

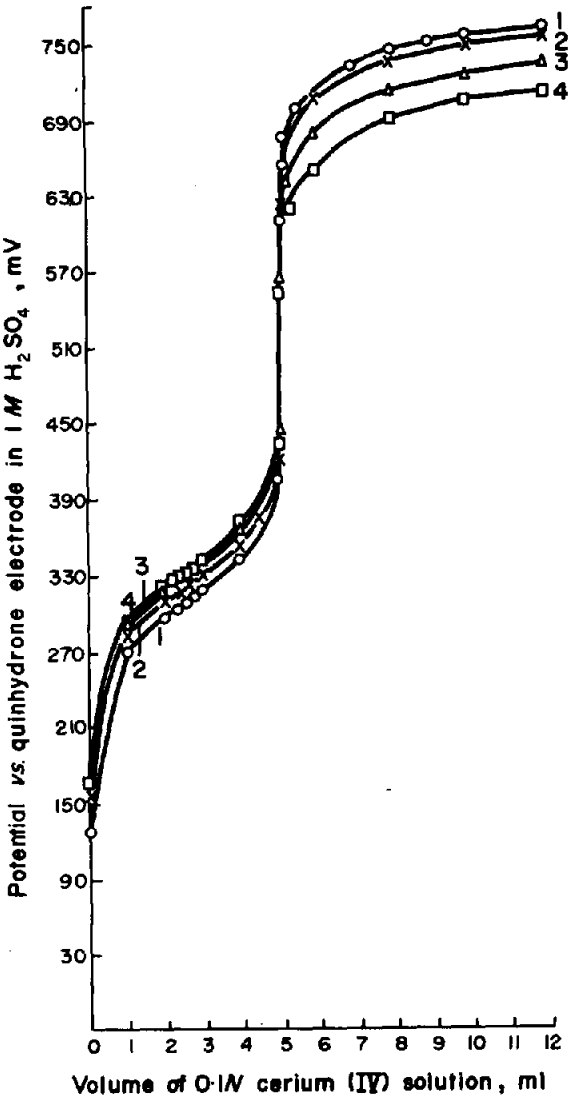


Fig. 1. Potentiometric titration with 0.1*M* cerium(IV) sulphate at 29°C: 5.0 ml of ~0.1*M* vanadium(IV) + 4 ml of 10*N* H_2SO_4 + *x* ml of acetone + water to make 45 ml. Curve 1: O——O (*x* = 0), Curve 2: ×——× (*x* = 5), Curve 3: △——△ (*x* = 15), Curve 4: □——□ (*x* = 25).

Potentiometric investigation

Vanadium(IV) sulphate solution and cerium(IV) sulphate solution (0.1*M*) in 0.5*M* sulphuric acid were prepared from the salts to avoid formation of a precipitate during the titration.

Vanadium(IV) solution (5 ml) and the required amounts of 5*M* sulphuric acid and acetone were mixed and diluted to 45 ml with water, then titrated potentiometrically with a bright platinum electrode (ignited beforehand) and a quinhydrone electrode in 1*M* sulphuric acid (E'_0 = 0.696 V *vs.* NHE).[9] A 2-min delay after each addition was allowed before potential measurement. The quinhydrone electrode potential was checked by using it in a titration of iron(II) with cerium(IV) in 1*M* sulphuric acid. The results are given in Table 4 and represented graphically in Fig. 1.

The values found for the formal potentials of the V(V)/V(IV) and Ce(IV)/Ce(III) systems in 0.5*M* sulphuric acid were in good agreement with those reported earlier.[9,10]

Spectrophotometric investigation

The absorption spectra of vanadium(IV) and vanadium(V) in 0.5*M* sulphuric acid with and without acetone [50% (v/v)] present were recorded against reagent blanks and are shown in Fig. 2. Acetone had a small hyperchromic effect on the vanadium(IV) spectrum and a small hypsochromic effect on the vanadium(V) spectrum.

The absorption spectra of ferroin in 0.5*M* sulphuric acid without and with acetone [50% (v/v)] present were nearly identical. The absorption spectrum of ferriin in 0.5*M* sulphuric acid was also recorded (Fig. 3), but that in the presence of acetone could not be obtained because of the rapid dissociation of ferriin in the presence of acetone. The kinetics of dissociation of ferriin in 0.5*M* sulphuric acid in the presence and absence of acetone were followed spectrophotometrically at 590 nm and the results are shown in Fig. 4.

Finally the absorption spectra of a mixture of ferroin and vanadium(IV) in 0.5*M* sulphuric acid without and with acetone [50% (v/v)] present were recorded, to evaluate any mutual effects [Fig. 5].

DISCUSSION

The blank experiments (Table 3) show that acetone retards the indicator oxidation but accelerates the indicator reduction. The titration can be done at the usual speed until near the end-point, where the drops should be added at 5–10 sec intervals. The colour change is sharp and reversible but reverse titrations are not possible, because cerium(IV) oxidizes acetone.[11] However, the cerium(IV)–acetone reaction does not affect the direct titration because the vanadium(IV)–cerium(IV) reaction is much faster, and the vanadium(V)–acetone reaction is very slow. The titration conditions are, in fact, comparable to those used in the titration of iodide with cerium(IV) in presence of large amounts of acetone.[12]

When acetone is present in a potentiometric titration there is a considerable drift in potential with time after the end-point, presumably because of the acetone–cerium(IV) reaction. The formal redox potential of the V(V)/V(IV) system is raised by the presence of acetone (Table 4).

There is an insinuation[13] that in analytical papers there is often no regard paid to the properties of vanadium species present in solution. The absorption spectra of vanadium(V) and vanadium(IV) solutions have therefore been studied in an attempt to identify the species involved and correlate them with the potential data. The interpretation of the electronic spectra is not simple because of the strong $O(p\pi) \rightarrow V(d\pi)$ charge-transfer bands; most attempts to assign and interpret the bands have been largely qualitative or empirical.[14] The bands in VO_2^+ are most simply visualized as charge-transfer transitions since vanadium(V) has no *d*-electrons and hence no *d*–*d* transitions. However, VO^{2+} shows both crystal field and charge-transfer bands as vanadium(IV) has a $3d^1$ configuration. There are two important crystal-field transitions giving bands in the visible region. The longer wavelength band is the more intense, as it is

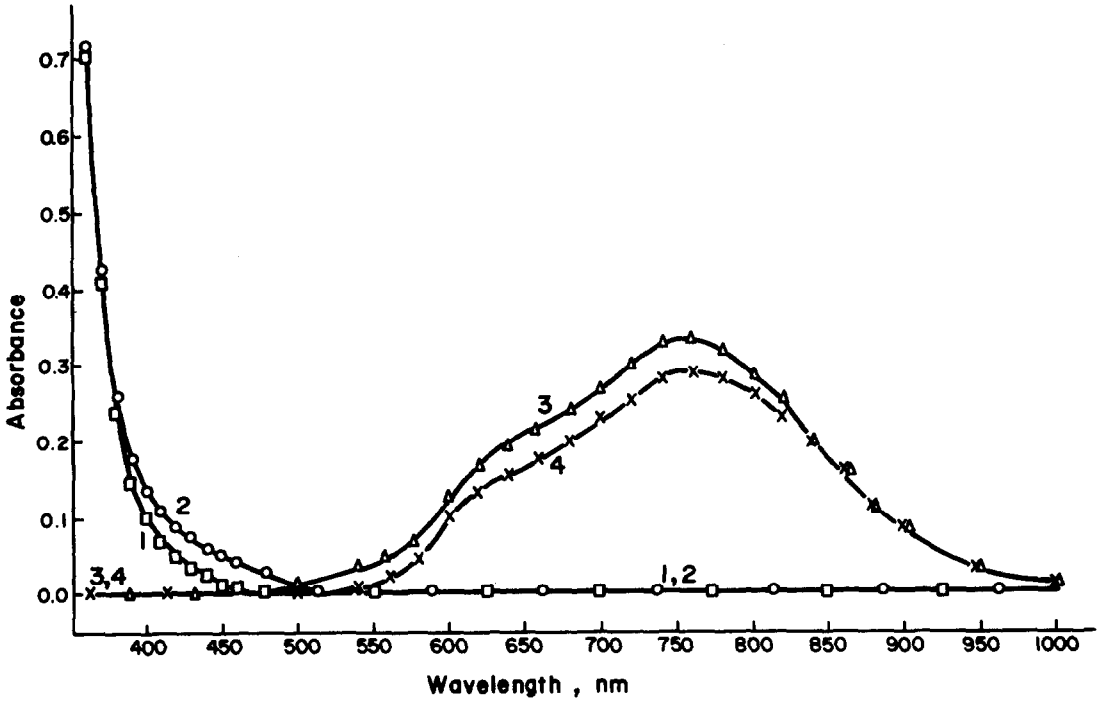


Fig. 2. Absorption spectra of vanadium. Curve 1: □——□ $1 \times 10^{-2}M$ vanadium(V) in $1N$ H_2SO_4 containing 50% v/v acetone. Curve 2: ○——○ $1 \times 10^{-2}M$ vanadium(V) in $1N$ H_2SO_4. Curve 3: △——△ $2 \times 10^{-2}M$ vanadium(IV) in $1N$ H_2SO_4, containing 50% v/v acetone. Curve 4: ×——× $2 \times 10^{-2}M$ vanadium(IV) in $1N$ H_2SO_4.

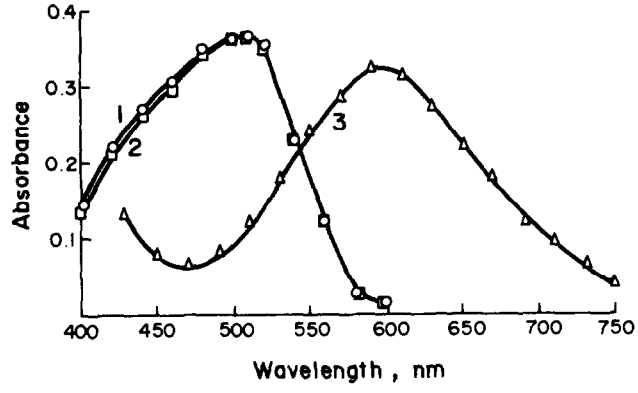


Fig. 3. Absorption spectra of indicator forms. Curve 1: ○——○ $\sim 4 \times 10^{-5}M$ ferroin in $1N$ H_2SO_4. Curve 2:.□——□ $\sim 4 \times 10^{-5}M$ ferroin in $1N$ H_2SO_4, containing 50% v/v acetone. Curve 3: △——△ $\sim 4 \times 10^{-4}M$ ferriin in $1N$ H_2SO_4.

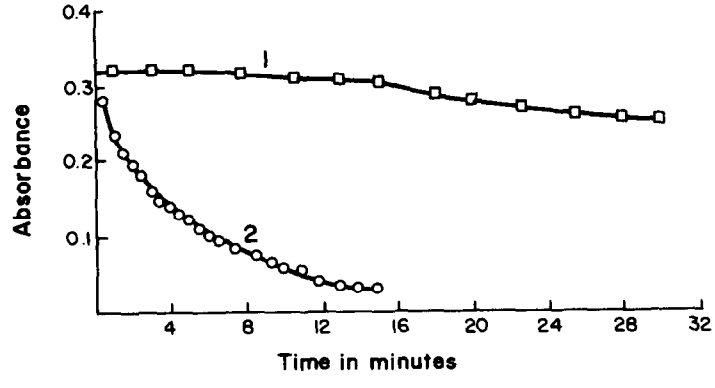


Fig. 4. Kinetics of dissociation of ferriin at 28°C. Curve 1: □——□ $4 \times 10^{-4}M$ ferriin in $1N$ H_2SO_4. Curve 2: ○——○ $4 \times 10^{-4}M$ ferriin in $1N$ H_2SO_4, containing 50% v/v acetone.

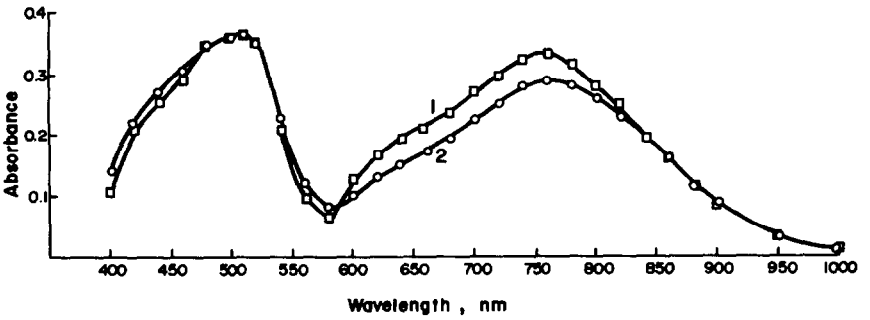


Fig. 5. Absorption spectra of vanadium(IV) + ferroin. Curve 1: □——□ $2 \times 10^{-2}M$ vanadium(IV) + $4 \times 10^{-5}M$ ferroin in $1N$ H_2SO_4 containing 50% v/v acetone, Curve 2: ○——○ $2 \times 10^{-2}M$ vanadium(IV) + $4 \times 10^{-5}M$ ferroin in $1N$ H_2SO_4.

Table 4. Results of potentiometric investigation ($0.5M$ sulphuric acid medium)

Acetone, % v/v	Potential jump per 0.05 ml of $0.1M$ cerium(IV), mV	Conditional potential vs. NHE, V	
		V(V)/V(IV)	Ce(IV)/Ce(III)
0	175	1.005	1.45
10	157	1.016	—
30	100	1.023	—
50*	95	1.032	—

* Transition potential of ferroin indicator under these titration conditions is found to be 1.15–1.16 V *vs.* NHE.

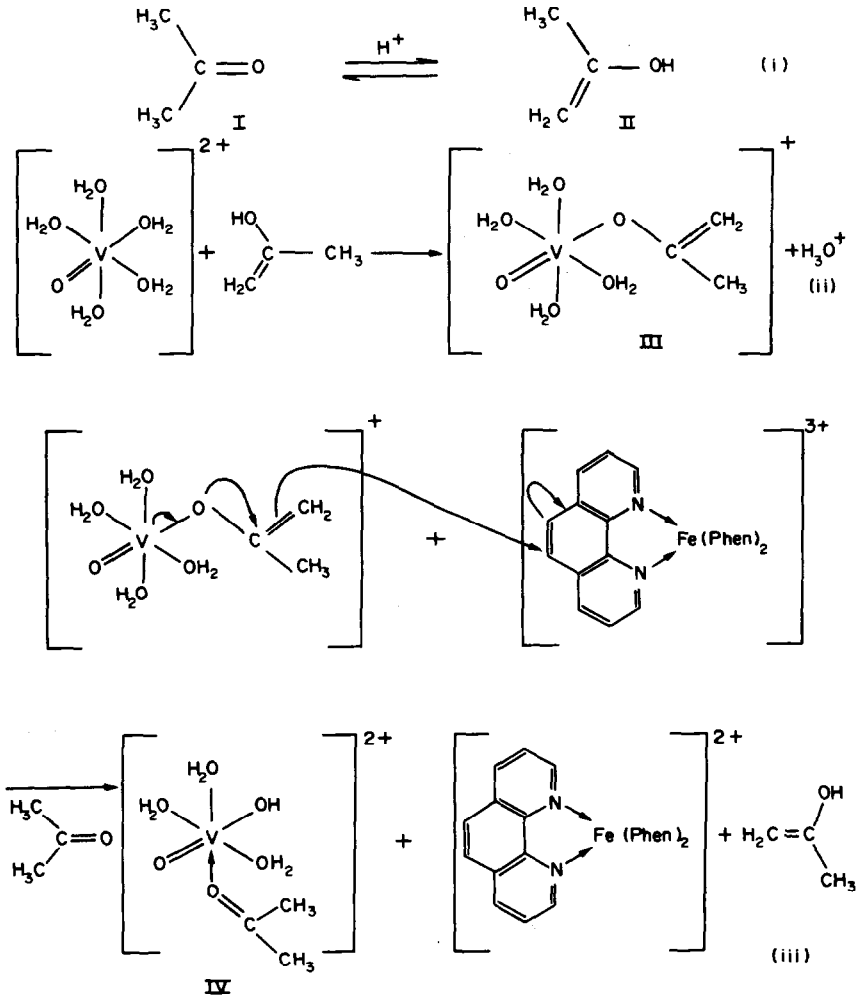
orbitally allowed, while the other is allowed vibronically[15] and appears as a weak shoulder on the short wavelength side of the first band. The charge-transfer band in the ultraviolet region hides the third crystal-field band.[13]

However, the spectra of both species are sensitive to solvents.[13] The effect due to orientation of solvent molecules in the second co-ordination sphere is not as important as the effect due to the addition of a solvent molecule in a position *trans* to the V–O bond, where it can influence the electron density on the metal and affect the acceptor properties of the metal towards the oxygen atom. Addition of acetone to the blue aquo-ion $VO(H_2O)_5^{2+}$ is found to cause only a small hyperchromic shift under our experimental conditions (Fig. 2). On the basis of the "average environment"[16] for mixed ligands, the weighted average, when a weak-field ligand such as acetone substitutes for another weak-field ligand (water), will not change much, so any band shift will only be small. The change in band intensity may be understood if the acetone ligand is present as the deprotonated enol form (see scheme below), which will decrease the electron density on the metal in the enolate complex (structure **III**) because the electronegativity of carbon is increased by presence of the carbon–carbon double bond.[17]

Changes in the electric dipole-moment of the ground and excited states because of the different electron distribution are expected to cause changes in the integrated band intensities.[18] There is evidence[19] for enolization of acetone [equilibrium (i)].

Vanadium(V) is present as $VO_2(H_2O)_3^+$ in sufficiently acidic aqueous solutions. No absorption maximum is observed in the wavelength regions studied, but there is generally a small hypsochromic effect at around 450 nm, in acetone medium (Fig. 2). If the intensity of the charge-transfer band again changes because of a change in the electron density on the metal, an opposite effect in the acceptor properties of metal towards the oxygen atom in the V=O bond may explain the change. The keto form of the ligand is probably preferred here, with co-ordination through the carbonyl oxygen atom (structure **IV**), with delocalization of the $p\pi$ electrons into the metal orbital, though this is only partial because the V–carbonyl oxygen bond distance is larger. Waters[19] also favours the idea of co-ordination through the carbonyl oxygen atom to the metal ion, as the kinetics of oxidation of ketones by vanadium(V) in acid medium indicates. The spectral evidence thus points to the interaction of vanadium(IV) and (V) with acetone to some extent or other. The relative changes in bonding energies of the two vanadium species cannot be deduced, however, and so cannot be correlated with oxidation potential of the system. If a high V=O bond energy is the determining factor in the energies of the two complexes, a decrease in the π-bond character of vanadium(V) species should decrease it, while an increase in the π-bond energy of vanadium(IV) species should increase it, the π-bond effect arising from the interaction with acetone. The resulting increase in the conditional potential of the V(V)/V(IV) system reflects the same effect.

Similar studies were made with ferroin but there was apparently no spectral evidence of acetone interaction with the complex. There was also no mutual effect of ferroin and vanadium(IV) in acetone medium (Fig. 5). The higher transition potential (1.15–1.16 V) of ferroin in this titration [*cf.* 1.10 V in the iron(II)–cerium(IV) titration in $1M$ sulphuric acid at the indicator concentration used][20] is therefore all the more difficult to explain. However, dissociation of both the ferroin and ferriin complexes is more rapid in



the presence of acetone, that of ferriin being much the faster, which was why the spectrum of ferriin in acetone medium could not be recorded quantitatively.

The ferriin–vanadium(IV) reaction may be faster for thermodynamic or kinetic reasons. There is only a small difference (~ 30 mV) in the potentials of the two systems in acetone medium (Table 4). This may not be an important factor as the reaction is thermodynamically feasible anyway. The influence of acetone on the indicator oxidation and reduction reactions is somewhat similar to that of acetic acid. It is therefore reasonable to assume that the same mechanism applies for both, as there is structural similarity in the active group. A kinetic study on the lines used by Rechnitz and Rao[7] was not undertaken because (*a*) it was thought that no additional useful information would be obtained, and (*b*) the instability of some of the reaction species when acetone is present would make observation and interpretation difficult and unreliable.

It is believed that the reaction scheme proposed explains adequately the fast electron-transfer in the vanadium(IV)–ferriin reaction.

Step (i) is enolization of the ketone, which is known to be acid-catalysed.[19] Ester formation of the enol with vanadium(IV) is the reaction in step (ii). As the mechanism of electron-transfer with the substitution-inert complex, ferriin, is likely to be outer sphere, the double bonds in the two complexes facilitate easy electron movement. The reaction in step (iii) may be compared with the oxidation mechanism of cyclohexanone by ferriin[21] where the double bonds in both structures form the basis of the double bridge for electron-tunnelling.[22]

However, structure IV may not be the final form. We tried to prepare this compound by reacting vanadium(IV) sulphate with 50% v/v acetone–1*M* sulphuric acid mixture, and obtained a crystalline solid [most probably unreacted vanadium(IV) sulphate], a (gel-like) semi-solid and a liquid (containing only a small amount of vanadium). We separated the semi-solid and dried it over concentrated sulphuric acid in a desiccator. It changed into a crystalline solid after about 48 hr. We compared the infrared spectrum of this solid with that of vanadium(IV) sulphate.

Although it was difficult to assign the frequencies with any definiteness, the V=O stretching frequency ($\sim 980\ cm^{-1}$) seemed not to be very much affected in the acetone complex. However, there was a new strong absorbance peak at $1090\ cm^{-1}$, which may be due to the enol form of the acetone.[23] The peak due to the carbonyl group, at about $1720\ cm^{-1}$, is entirely absent in the spectrum of the acetone complex, so the enolic analogue of structure **IV** may be the product actually formed.

Acknowledgement—Financial assistance to one of us (NRS) from the Council of Scientific and Industrial Research, New Delhi, India is gratefully acknowledged.

REFERENCES

1. N. H. Furman, *J. Am. Chem. Soc.*, 1928, **50**, 1675.
2. H. H. Willard and P. Young, *Ind. Eng. Chem.*, 1928, **20**, 972.
3. G. Gopala Rao and L. S. A. Dikshitulu, *Talanta*, 1962, **9**, 857.
4. *Idem*, *ibid.*, 1962, **9**, 289.
5. K. Sriramam and G. G. Rao, *ibid.*, 1966, **13**, 1468.
6. N. V. Rao and V. V. S. E. Dutt, *Anal. Chim. Acta*, 1970, **51**, 553.
7. G. A. Rechnitz and G. N. Rao, *Anal. Chem.*, 1967, **39**, 1192.
8. G. H. Walden, Jr., L. P. Hammett and S. M. Edmonds, *J. Am. Chem. Soc.*, 1934, **56**, 350.
9. D. N. Hume and I. M. Kolthoff, *ibid.*, 1934, **65**, 1895.
10. W. M. Latimer, *Oxidation Potentials*, 2nd Ed., Prentice-Hall, New York, 1952.
11. J. Shorter, *J. Chem. Soc.*, 1962, 1868.
12. D. Lewis, *Ind. Eng. Chem., Anal. Ed.*, 1936, **8**, 199.
13. J. Selbin, *Chem. Rev.*, 1965, **65**, 153.
14. F. A. Cotton and G. Wilkinson, *Advanced Inorganic Chemistry*, p. 816. Wiley Eastern Pvt. Ltd., New Delhi, 1969.
15. C. J. Ballhausen and H. B. Gray, *Inorg. Chem.*, 1962, **1**, 111.
16. B. N. Figgis, *Introduction to Ligand Fields*, p. 236. Wiley-Interscience, New York, 1966.
17. C. A. Coulson, *Valence*, pp. 142, 218. ELBS and Oxford University Press, Oxford, 1974.
18. R. S. Drago, *Physical Methods in Inorganic Chemistry*, p. 148. Affiliated East West Press Pvt. Ltd., 1968.
19. W. A. Waters, *Mechanism of Oxidations of Organic Compounds*, pp. 91, 98. Methuen, London, 1965.
20. K. Sriramam, *Talanta*, 1976, **23**, 864.
21. J. S. Littler and I. G. Sayce, *J. Chem. Soc.*, 1964, 2545.
22. C. S. G. Phillips and R. J. P. Williams, *Inorganic Chemistry*, Vol. II, pp. 446–448. Oxford University Press, Oxford, 1966.
23. J. B. Lambert, H. B. Shurvell, L. Verbit, R. G. Cooks and G. H. Stout, *Organic Structural Analysis*, p. 240, Macmillan, London, 1976.

Talanta. Vol. 28. pp. 295 to 300. 1981
Printed in Great Britain. All rights reserved

0039-9140/81/050295-06$02.00/0
Copyright © 1981 Pergamon Press Ltd

FUNDAMENTAL INVESTIGATION OF THERMAL PROPERTIES OF RARE-EARTH β-DIKETONATES

TAITIRO FUJINAGA, TOORU KUWAMOTO, KENJI SUGIURA and SHIGEKAZU ICHIKI
Department of Chemistry, Faculty of Science, Kyoto University, Kyoto 606, Japan

(*Received* 24 *April* 1980. *Revised* 18 *November* 1980. *Accepted* 27 *November* 1980)

Summary—The thermal properties of the rare-earth chelates of Htfa (trifluoroacetylacetone) and Hhfa (hexafluoroacetylacetone) have been investigated. Thermogravimetric curves were obtained by heating samples in the injection chamber of a gas chromatograph, both in an atmosphere of helium, and of helium containing ligand vapour. None of the chelates was completely vaporized in a helium atmosphere at temperatures up to about 240°, but the tfa chelate of Lu and all the hfa chelates were completely vaporized in the atmosphere of helium containing ligand vapour. The vapour pressures and heats of vaporization of these chelates were also measured.

Many of the metal β-diketone chelates possess abnormally high vapour pressure and high thermal stability. These characteristics of these chelates have attracted special interest in the field of separation by gas chromatography.

For example, many investigators have examined the volatilization of numerous β-diketonates.[1–10] Baskin *et al.*[11] elucidated the mechanism of a thermal dissociation reaction by differential thermal analysis. Von Hoene *et al.*[12] and Rudolph *et al.*[13] identified thermally dissociated products by mass spectrography. Charles *et al.*[1] determined the thermal stability by measuring the vapour pressure of the chelates as a function of increasing temperature. Vapour pressures and heats of vaporization or sublimation of various metal β-diketone chelates have been measured by many workers. Berg *et al.*[14, 15] made a detailed study of the vapour pressures of a series of metal β-diketonate chelates, and discussed the effect of the substituent group or the steric structure of the chelates on the volatility. Sievers *et al.*[16] and Swain *et al.*[17] measured the vapour pressures of a series of lanthanide chelates of dipivaloylmethane and heptafluorodimethyloctanedione and noted that the vapour pressure of the chelate increases with the atomic number of the lanthanide. Swain *et al.* also measured vapour pressures of quadrivalent actinide chelates.[18]

Although the metal β-diketonates have a relatively high vapour pressure and thermal stability, thermal decomposition inevitably occurs at high temperature, which reduces the usefulness of the gas chromatography of these metal chelates. To overcome this we have developed a new method which we call "gas chromatography with ligand vapour as carrier additive (LVGC)", and have succeeded in eluting the chelates completely.[19–25] However, the thermal behaviour of the chelates in an atmosphere containing ligand vapour was not clear.

This paper describes the investigation of the thermal behaviour of the rare-earth β-diketone chelates in an atmosphere containing ligand vapour and in a helium atmosphere.

EXPERIMENTAL

Preparation and identification of β-diketonates

Rare-earth 1,1,1-trifluoropentane-2,4-dione (Htfa) chelates and 1,1,1,5,5,5-hexafluoropentane-2,4-dione (Hhfa) chelates were synthesized as follows.

The rare-earth oxide (other than cerium) was dissolved in 1*N* hydrochloric acid, and then 1*N* ammonia solution was added to precipitate the rare-earth hydroxide. The precipitate was washed with distilled water by decantation several times until the supernatant liquid was neutral, and was then filtered off. A small excess of chelating agent (Htfa, Hhfa) was added to the precipitate, and the mixture was gently heated on a water-bath. The chelate was dissolved in isopropyl ether, and the insoluble material filtered off. The solvent was then evaporated. The crude chelate, in which a monohydroxo *bis*-ligand complex might be present, was air-dried and dissolved in water-free acetone. An equimolar amount of the chelating agent was added to this solution, and the mixture was refluxed for about 1 hr. Then the acetone was evaporated off, and the chelate washed with hexane to remove excess of chelating agent. The product was recrystallized from benzene if necessary. For synthesis of the cerium chelate, cerium(III) chloride was dissolved in distilled water, and a small amount of hydroxylamine hydrochloride solution was added to prevent oxidation of cerium(III) hydroxide to cerium(IV) hydroxide. Then ammonia solution was added to precipitate the cerium(III) hydroxide, and the rest of the procedure was the same as that for the other chelates.

The elemental analyses and melting points of these chelates are shown in Table 1. From the elemental analysis, it is estimated that these chelates contain about two molecules of water of crystallization, and that discrepancies between the melting points reported here and those found by others are probably the result of different products being obtained.

Apparatus

A Shimadzu model GC-6A gas chromatograph equipped with a ligand vapour generator (Fig. 1) was used. This generator was manufactured by the authors for the purpose of adding a definite amount of ligand vapour to the carrier gas.[19–25] The ligand concentration in the carrier

Table 1. Elemental analysis and melting points of various chelates

Chelate	H % Found	H % Calcd.	C % Found	C % Calcd.	Ln % Found	Ln % Calcd.	Atomic ratio C:Ln	Molecular formula used for calculation	m.p., °C Found	m.p., °C Literature	Remarks
Eu-tfa	2.4_3	2.49	27.4	27.84	23.2	23.48	14.9	$Eu(tfa)_3.2H_2O$	117–120	144–146[26], 132–134[27]	Air-dried
Sm-tfa	2.6_3	2.50	27.7	27.91	23.4	23.29	14.8	$Sm(tfa)_3.2H_2O$	123–125	147–149[26]	Air-dried
Nd-tfa	2.5_2	2.52	28.6	28.17	22.5	22.55	15.3	$Nd(tfa)_3.2H_2O$	133–135	147–149,[26] 133–134[27]	Dried at 60°, 15 min in a stream of helium
Pr-tfa	2.6_6	2.53	28.4	28.32	21.9	22.15	15.3	$Pr(tfa)_3.2H_2O$	158–160	136–138,[26] 133–134[27]	Dried at 70°, 15 min in a stream of helium
Ce-tfa	2.3_8	(2.81)	26.0	(26.06)	23.4	(23.39)	13.0	Mixed chelates*	(118–120)	—	Air-dried
Ce-tfa	1.5_2	(2.65)	24.5	(24.52)	27.0	(27.02)	10.6	Mixed chelates**	(178–181)	—	Dried at 120°, 60 min in a stream of of helium
La-tfa	2.6_4	(3.27)	23.6	(23.68)	23.4	(23.51)	11.7	Mixed chelates†	(120–122)	—	Air-dried
La-tfa	1.6_1	(2.93)	23.5	(23.49)	26.4	(26.39)	10.3	Mixed chelates††	(135–138)	—	Dried at 120°, 60 min in a stream of helium
Eu-hfa	1.0_0	0.87	22.6	22.27	19.1	18.78	14.9	$Eu(hfa)_3.2H_2O$	122–125	176–177[26]	Air-dried
Sm-hfa	1.0_3	0.87	22.4	22.31	19.1	18.62	14.7	$Sm(hfa)_3.2H_2O$	113–117	144–145,[26] 125[27]	Air-dried
Nd-hfa	1.1_3	0.88	22.4	22.48	18.3	18.00	14.7	$Nd(hfa)_3.2H_2O$	127–130	141–142,[26] 117[27]	Air-dried
Pr-hfa	1.1_4	0.88	22.8	22.57	17.8	17.66	15.1	$Pr(hfa)_3.2H_2O$	126–129	148–151[26]	Dried at 100°, 30 min in a stream of helium
Ce-hfa	1.0_6	0.88	22.4	22.60	17.7	17.57	14.7	$Ce(hfa)_3.2H_2O$	99–101	125–126[26]	Air-dried
La-hfa	1.1_5	0.89	23.1	22.63	17.2	17.45	15.6	$La(hfa)_3.2H_2O$	128–131	143–146,[26] 120–125[27]	Dried at 100°, 30 min in a stream of helium

* $Ce(OH)(tfa)_2 + Ce(tfa)_3 + H_2O$ (2:3:15). **(2.0:0.27:4.9).
† $La(OH)(tfa)_2 + La(tfa)_3 + H_2O$ (2:1:14). ††(2.0:0.13:6.7).

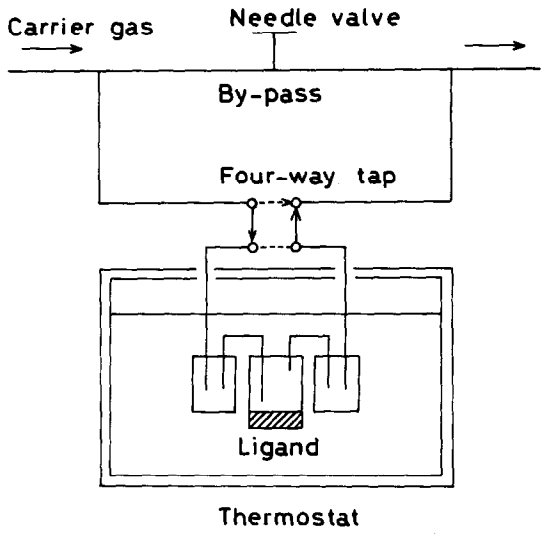


Fig. 1. Ligand vapour generator.

gas was about 1.0% v/v, and was mainly controlled by the temperature of the thermostat. When the vapour of Hhfa was added, the needle-valve was also used to control the ligand concentration, because the vapour pressure of Hhfa is too high at room temperature.

Sample tube

A Pyrex sample tube (88 mm × 3.5 mm bore, 0.5 mm wall thickness) was used. A definite amount of a chelate was put into it and quartz wool was stuffed into both ends. The tube containing the chelate was inserted into the injection chamber (5 mm bore) of the gas chromatograph as shown in Fig. 2.

RESULTS AND DISCUSSION

Thermogravimetric curves

The injection chamber of the gas chromatograph was used instead of a thermobalance to obtain thermogravimetric curves. The method was as follows.

A precisely weighed sample tube containing a chelate (10.0 mg) was inserted into the injection chamber, which was preheated to a preselected temperature, and the entrance was tightly closed with a silicone stopper. Carrier gas (pure helium or helium containing ligand vapour) was passed through the tube. The tube was kept at the chosen temperature for 15 min. Then the tube was taken out, and both ends of the tube were immediately sealed with Teflon caps, in a flow of carrier gas. After cooling, the sample tube was weighed. The temperature of the injection chamber was raised in 30° increments, and the operation described above was repeated at each temperature. The dependence of the weight loss of the sample on temperature was thus observed.

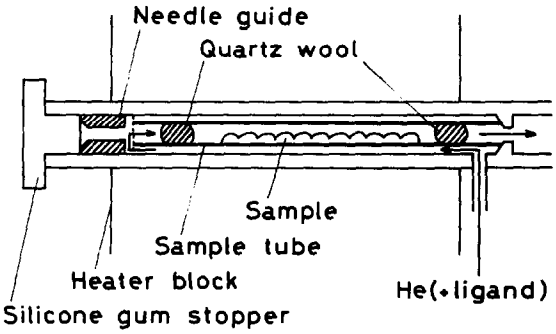


Fig. 2. Sample chamber.

The temperature equilibrium of the sample tube at different temperatures was examined as follows. A mercury thermometer was inserted instead of the sample tube into the injection chamber, and the rate of temperature rise of the thermometer was measured. From the result, it was estimated that the sample tube reaches constant temperature within 1–2 min at temperatures in the range 120–240°. However, in the procedure, the sample tube was heated at each temperature for 15 min in order to obtain values that were as accurate as possible.

Intrinsically in this method, some thermal decomposition of the chelates owing to contact with air cannot be avoided when the sample tube is taken out of the injection chamber, but its amount of decomposition is negligible because the time when the chelates are in contact with air is very short. In practice, when comparing this method with the usual thermobalance method, there was found to be no basic difference between the two.

Thermograms of the chelates

The thermogravimetric curves were obtained in an atmosphere of pure helium and in an atmosphere of helium containing ligand vapour, by the method described above.

The tfa chelates. The thermogravimetric curves of the tfa chelates of Lu, Eu, Sm, Nd, Pr, Ce and La in the helium carrier gas and in the helium gas containing ligand vapour are shown in Fig. 3. In the helium carrier gas, the water of crystallization of $Lu(tfa)_3$ was liberated slowly at a temperature below 60°. The weight of the sample was approximately constant throughout the temperature range 60–130°, but the chelate was found to vaporize at 150° with some thermal dissociation. The residue at 240° was about 50% of the sample. In the carrier gas containing ligand vapour, the weight decreased slowly with increase of temperature up to 160°, then rapidly above 160°. Finally there was little residue (1–2%) at 240°. From this fact, it was deduced that the additive ligand in the carrier gas recombined with the thermally decomposed chelate.

Similar effects were observed for the Eu, Sm, Nd, Pr, Ce and La tfa chelates, but these chelates were not completely vaporized at 240° even in the carrier gas containing ligand vapour.

The hfa chelates. It is already known that the hfa chelates are thermally more stable and more volatile than the tfa chelates. The thermogravimetric curves of the hfa chelates of Lu, Eu, Sm, Nd, Pr, Ce and La are shown in Fig. 4. In this figure, the 7 curves in the presence of ligand vapour are not well defined near

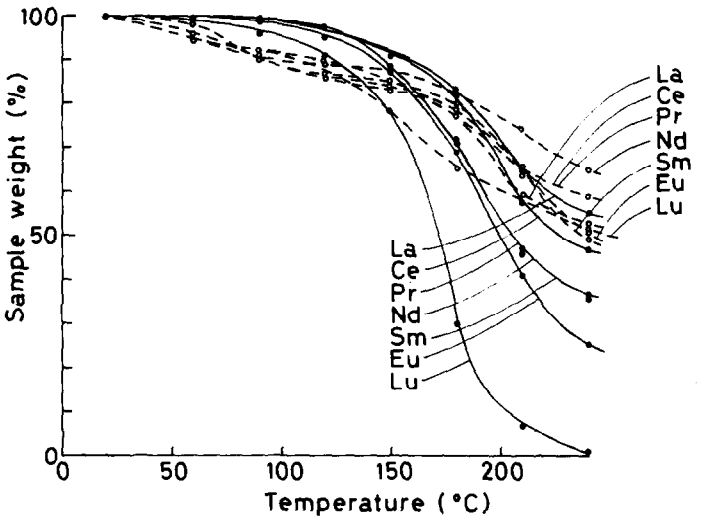


Fig. 3. Thermogravimetric curves of tfa chelates of Lu, Eu, Sm, Nd, Pr, Ce and La. --O--, in pure helium gas; ——●——, in helium gas containing ligand vapour. Flow-rate: 30 ml/min.

the abscissa, so these parts are expressed by dotted lines. In the helium carrier gas, the water of crystallization of $Lu(hfa)_3$ was liberated slowly from the chelate as the temperature increased, and the chelate was vaporized rapidly at a temperature above 90°, but was partially dissociated at a temperature above 200°. The residue was about 10% of the sample. From this result, it was deduced that the $Lu(hfa)_3$ chelate is more volatile than the $Lu(tfa)_3$ chelate, but is not vaporized completely in an atmosphere of helium gas. However, in the carrier gas containing ligand vapour, it was found that the weight of $Lu(hfa)_3$ was not changed at a temperature below 100° and the melting point was lowered to 90° from 105° in the atmosphere of helium gas, and the compound was completely vaporized at a temperature near 130°. From this fact, it was confirmed that the thermal dissociation of $Lu(hfa)_3$ was suppressed by the presence of additive ligand in the helium carrier gas.

For the $Sm(hfa)_3$ chelate, it was found that in the helium carrier gas, the water of crystallization of the chelate was liberated slowly in the temperature range 60–100°, and the weight of the chelate was not changed in the temperature range 100–120°. Vaporization of the chelate commenced at 120°, and proceeded as the temperature was increased. The residue (at >200°) was about 20% of the sample. However, in the carrier gas containing ligand vapour, the $Sm(hfa)_3$ chelate was vaporized completely at a temperature of nearly 150°.

The behaviour of the Eu, Nd, Pr, Ce and La hfa chelates was similar to that of the $Sm(hfa)_3$ chelate. In

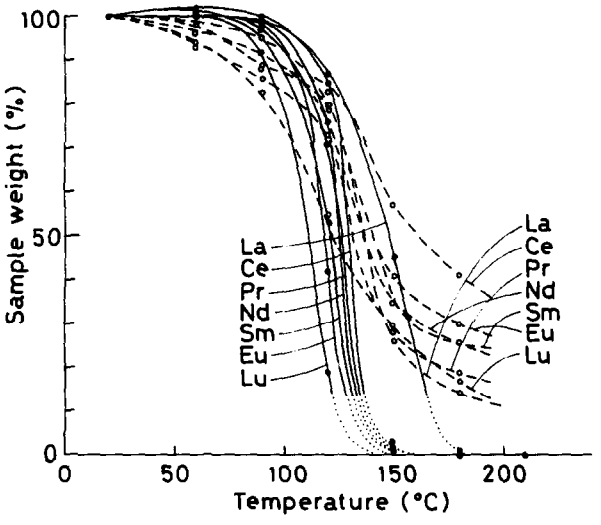


Fig. 4. Thermogravimetric curves of hfa chelates of Lu, Eu, Sm, Nd, Pr, Ce and La. Symbols and flow-rate are as in Fig. 3.

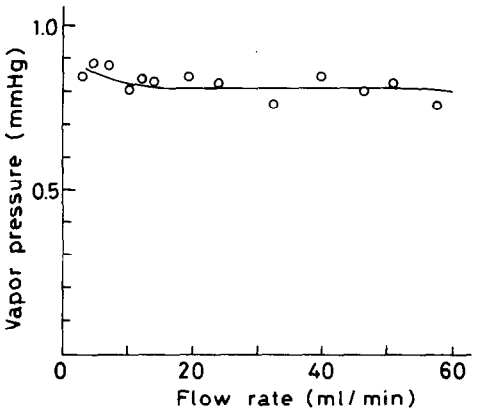


Fig. 5. Relation between flow-rate and vapour pressure. Sample: $Be(tfa)_2$ chelate. Temperature: 85°.

addition, the order of the volatility of these chelates in an atmosphere of helium and ligand vapour was in the reverse order of the atomic number.

Measurement of vapour pressure of metal chelates

It is possible to calculate the vapour pressure of a chelate from the weight loss (amount vaporized) per unit time and the flow-rate of the carrier gas. The equation to be used in the calculation is

$$P = 18{,}700 \frac{X}{MF}$$

where

P = vapour pressure of the chelate (mmHg)
X = rate of weight loss (mg/min)
M = molecular weight of the chelate
F = flow-rate of the carrier gas measured at 27° (ml/min).

The vapour pressure of the $Be(tfa)_2$ chelate was measured as an example, and it was confirmed that the amount of chelate vaporized in unit volume of the carrier gas was constant even if the flow-rate of the carrier gas was changed over the range 15–50 ml/min (Fig. 5). Therefore, it was estimated that the carrier gas was saturated with chelate vapour at a temperature of 85°. It was necessary to preheat the sample in the injection chamber for a while in order to remove the effect of the water of crystallization before the measurement of the vapour pressure.

This method was compared with the conventional method in order to confirm its reliability. The result is shown in Fig. 6. The solid line shows the vapour pressure *vs.* temperature curve of the $Be(tfa)_2$ chelate measured by our method. The slope of the line changes at a temperature of 112°, which shows the melting point of the chelate. The dashed line shows the curve measured with an isoteniscope by Berg *et al.*[15] It was considered that the disagreement of these curves was dependent on the change of vapour pressure caused by the elimination of the water of crystallization of the $Be(tfa)_2$ chelate, and Berg's vapour-pressure values were measured as the sum of the vapour pressure of the water of crystallization and that of the $Be(tfa)_2$ chelate itself.

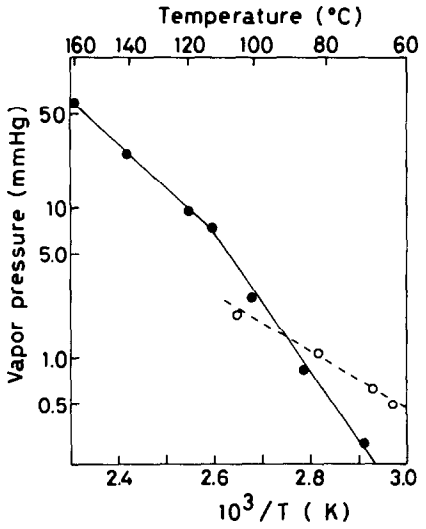


Fig. 6. Vapour pressure *vs.* temperature curves for $Be(tfa)_2$ chelate. ——, authors' method; – – –, isoteniscope method.

Vapour pressure and heat of vaporization of rare-earth chelates

The heat of vaporization of metal chelates can be calculated from the slope of Clausius–Clapeyron

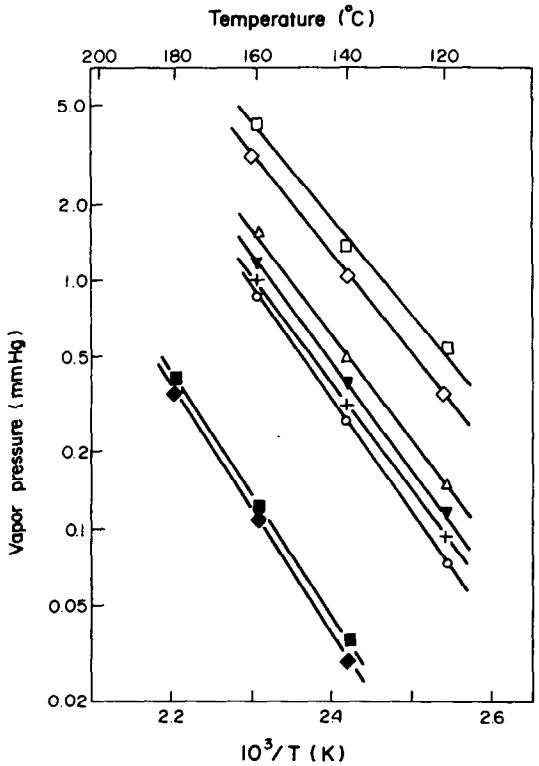


Fig. 7. Vapour pressure *vs.* temperature curves for rare-earth chelates in helium gas containing ligand vapour. □, $Eu(hfa)_3$; ◇, $Sm(hfa)_3$; △, $Nd(hfa)_3$; ▼, $Pr(hfa)_3$; ×, $Ce(hfa)_3$; ○, $La(hfa)_3$; ■, $Eu(tfa)_3$; ◆, $Sm(tfa)_3$.

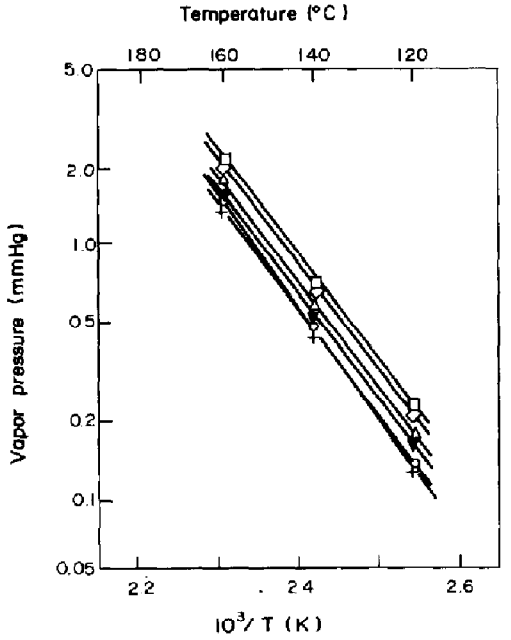


Fig. 8. Vapour pressure *vs.* temperature curves for rare-earth chelates in pure helium gas. Symbols are as in Fig. 7.

plots, as shown by the equation

$$\ln P = -\frac{\Delta H}{RT} + \frac{\Delta S}{R}.$$

It was found from Figs 7 and 8 that the vapour pressure of the chelate increased with decrease in ionic radius of the central rare-earth ion (except for the La hfa chelate in a helium atmosphere), and that the vapour pressure of the hfa chelate was higher than that of the tfa chelate, as already known. A similar relation between the retention times and ionic radii is also known in gas chromatography. From these facts, it is concluded that if the ligand is the same, the order of elution of the chelates in gas chromatography is strongly dependent on the vapour pressures of the chelates.

ΔH_{vap} values calculated from the slopes are shown in Table 2. The ΔH_{vap} value in the carrier gas containing ligand vapour was somewhat smaller than that in the helium carrier gas for each chelate, and the value of ΔH_{vap} tended to decrease with decrease in the ionic radius of the central rare-earth ion. In this experiment, the vapour pressures of the Eu, Sm, Nd, Pr, Ce and La tfa chelates in the helium carrier gas and the Nd, Pr, Ce and La tfa chelates in the carrier gas containing ligand vapour could not be measured correctly, because these chelates were thermally decomposed under the measurement conditions.

Table 2. Heats of vaporization of various chelates

Chelate	ΔH_{vap}, kcal/mol. in Helium containing ligand vapour	ΔH_{vap}, kcal/mol. in Pure helium
$Eu(hfa)_3$	18.1 ± 0.3	19.5 ± 0.3
$Sm(hfa)_3$	18.3 ± 0.2	19.6 ± 0.3
$Nd(hfa)_3$	19.5 ± 0.2	19.6 ± 0.2
$Pr(hfa)_3$	19.8 ± 0.2	19.8 ± 0.2
$Ce(hfa)_3$	19.8 ± 0.2	19.9 ± 0.2
$La(hfa)_3$	21.1 ± 0.2	20.9 ± 0.3
$Eu(tfa)_3$	22.6 ± 0.2	—
$Sm(tfa)_3$	23.3 ± 0.2	—

As a result of this work, the thermal characteristics of these rare-earth chelates in the carrier gas containing ligand vapour have been made clear, and the fundamental data for ensuring complete elution in their gas chromatography have been obtained.

REFERENCES

1. R. G. Charles and M. A. Pawlikowski, *J. Phys. Chem.*, 1958, **62**, 440.
2. W. W. Wendlandt, J. L. Bear and G. R. Horton, *ibid.*, 1960, **64**, 1289.
3. R. G. Charles and A. Perroto, *J. Inorg. Nucl. Chem.*, 1964, **26**, 373.
4. C. S. Springer, D. W. Meek and R. E. Sievers, *Inorg. Chem.*, 1967, **6**, 1105.
5. R. E. Sievers, J. W. Connolly and W. D. Ross, *J. Gas Chromatog.*, 1967, **5**, 241.
6. K. J. Eisentraut and R. E. Sievers, *J. Inorg. Nucl. Chem.*, 1967, **29**, 1931.
7. T. Shigematsu, M. Matsui and K. Utsunomiya, *Bull. Chem. Soc. Japan*, 1969, **42**, 1278.
8. A. Kito, Y. Miyake, H. Kobayashi and K. Ueno, *Bunseki Kagaku*, 1971, **20**, 1363.
9. K. Utsunomiya, *Anal. Chim. Acta*, 1972, **59**, 147.
10. C. A. Burgett and J. S. Fritz, *Talanta*, 1973, **20**, 363.
11. Y. Baskin and N. S. Krishna Prasad, *J. Inorg. Nucl. Chem.*, 1963, **25**, 1011.
12. J. von Hoene, R. G. Charles and W. M. Hickam, *J. Phys. Chem.*, 1958, **62**, 1098.
13. G. Rudolph and M. C. Henry, *Inorg. Chem.*, 1964, **3**, 1317.
14. E. W. Berg and J. T. Truemper, *J. Phys. Chem.*, 1960, **64**, 487.
15. *Idem, Anal. Chim. Acta*, 1965, **32**, 245.
16. J. E. Sicre, J. T. Dubois, K. J. Eisentraut and R. E. Sievers, *J. Am. Chem. Soc.*, 1969, **91**, 3476.
17. H. A. Swain, Jr and D. G. Karraker, *J. Inorg. Nucl. Chem.*, 1971, **33**, 2851.
18. *Idem, Inorg. Chem.*, 1970, **9**, 1766.
19. T. Fujinaga, T. Kuwamoto and S. Murai, *Talanta*, 1974, **18**, 429.
20. *Idem, Anal. Chim. Acta*, 1974, **71**, 141.
21. *Idem, Mem. Fac. Sci., Kyoto Univ.*, 1974, **34**, 301.
22. T. Fujinaga, T. Kuwamoto, S. Murai and K. Sugiura, *ibid.*, 1974, **34**, 309.
23. T. Fujinaga, T. Kuwamoto, S. Murai, K. Yamada and K. Sugiura, *ibid.*, 1974, **34**, 321.
24. T. Fujinaga, T. Kuwamoto and K. Kimoto, *Talanta*, 1976, **23**, 753.
25. *Idem, IARC Reports, Kyoto Univ.*, 1976, **2**, No. 2, 15.
26. E. W. Berg and J. J. Chiang Acosta, *Anal. Chim. Acta*, 1968, **49**, 101.
27. R. W. Moshier and R. E. Sievers, *Gas Chromatography of Metal Chelates*, Pergamon, Oxford, 1965.

Talanta, Vol. 28, pp. 301 to 311, 1981
Printed in Great Britain. All rights reserved

0039-9140/81/050301-11$02.00/0
Copyright © 1981 Pergamon Press Ltd

EFFECTS OF SOME COMPLEX-FORMING LIGANDS ON THE POTENTIAL OF ANTIMONY pH-SENSORS

STANISLAW GLAB*, GUNNAR EDWALL†, PER-ARNE JÖNGREN† and FOLKE INGMAN‡

Departments of Applied Physics† and Analytical Chemistry‡, The Royal Institute of Technology, S-100 44 Stockholm 70, Sweden

(*Received* 13 *October* 1980. *Accepted* 10 *November* 1980)

Summary—The *E vs.* pH relationship for oriented monocrystalline antimony electrodes was studied in various ionic media, containing no buffer or one of several common buffer substances, and the stability of the electrode potential with time was investigated. Several makes of commercially available polycrystalline antimony electrodes were also studied. The results indicate that tris(hydroxymethyl)aminomethane may be used for calibration of antimony electrodes, but most other commonly used buffer substances, *e.g.*, orthophosphate, yield erroneous results. Monocrystalline antimony electrodes are preferable to polycrystalline ones, especially when measurements are made in unstirred solutions. The long-term stability of monocrystalline electrodes is superior to that of polycrystalline ones.

Antimony–antimony(III) oxide electrodes have for more than 50 years been used to determine pH. Their principal advantages are that they are sturdy and easy to miniaturize, and have low impedance. Therefore, antimony electrodes should be well suited for use in many special situations, *e.g.*, when pH is to be determined in a very restricted volume of solution. At present, antimony electrodes are arousing much interest as indicator electrodes for *in vivo* measurements of pH in biological systems, since they offer an attractive alternative to the fragile high-impedance miniaturized glass electrodes which are also used for this purpose.

The major drawbacks of the commonly used polycrystalline antimony electrodes are poor stability, resolution and repeatability, and sensitivity to complex-forming ligands present in the sample solution. A substantial improvement in the first three of these may be obtained by using oriented monocrystalline antimony electrodes instead of polycrystalline ones.[1] The effects of complex formation will of course be the same, irrespective of the physical structure of the electrodes.

The mechanism of the antimony–antimony(III) oxide electrode is not fully understood despite many investigations during its five decades of use as a pH-sensor. Because most of the pH-buffers used for calibrating glass or antimony electrodes contain complex-forming ligands, ignoring the possibility of complex formation easily leads—and has often led in the past—to misinterpretation of the behaviour of the antimony electrode.

The aim of the present work was to study the effects of different ligands on the electrode response, in order to find an ionic medium and a buffer system with as small an effect as possible on the electrode potential. Such a system could then form a reference solution for further studies of the effects of other buffer systems on the electrode response.

BACKGROUND

During the past 15 years several authors have published work on antimony electrodes, including Bishop[2–5] who, with various co-workers, studied factors affecting the response. Among the factors investigated was the influence of oxygen on zero-current and polarized antimony electrodes.

Various authors have studied the influence of carbonate and of phosphate on the potential of antimony electrodes. One of the early contributions was made by Gysinck[6], who observed a kink in the calibration curves between pH 7.12 and 8.17. In this pH region, phosphate buffers were used for calibration and the effect observed has been named the "Gysinck effect". Other workers, such as Karlmark and Sohtell[7] have reported results that suggest that bicarbonate can affect the Sb potential.

A very good account of the early work was given by Quehenberger[8] who summarized the partly contradictory results of previous workers and discussed them in the light of his own results. The review will not be repeated here; the reader is referred to Quehenberger's paper for details.

Since Quehenberger's work was published, Caflish *et al.*[9] have reported work on the manufacture and utilization of antimony electrodes. Their observation that antimony electrode potentials changed when nitrogen was passed through the solution was suggested to be the result of small amounts of rare gases in the nitrogen. A much more likely explanation is that the oxygen concentration in the solutions decreased. This would be in accordance with the findings of both the earlier and more recent research.[10]

* On leave from the Department of Chemistry, Warsaw University, Warsaw, Poland.

Dolinsky and Šimaček[11] described a procedure for linearizing the response for the pH range 1.68–9, by applying correction factors to adjust for the Gysinck effect at pH above 7.1 and for another effect that they observed at low values of pH. Similar effects have been reported by previous workers, *e.g.*, Ives,[12] and are likely to arise from the use of a complex-forming buffer substance during the calibration procedure in acidic solution.

Polycrystalline antimony electrodes were used in all these studies.

It is clear that considerable confusion still exists as to the proper procedures for calibration and use of antimony electrodes as pH-sensors. In all previous work, buffers were used for calibration of the pH-scale. We decided to use a technique independent of buffers for the calibration of the scale, and to use oriented monocrystalline antimony electrodes.[13] Thus it would be possible to study the response of antimony electrodes in solutions of different ionic media containing no buffer, and then expand the study by adding pH buffers. This would make it possible to see the effects of the buffer substances directly.

We also decided to compare the stability of the potential with time for monocrystalline electrodes and some commercially available polycrystalline antimony electrodes, and investigate the effect of stirring.

EXPERIMENTAL

Although a pH-electrode actually responds to variations in hydrogen-ion activity, it is possible to calibrate it in terms of concentration, provided that the activity coefficients can be kept constant, *e.g.*, by doing the experiments at constant ionic strength. The glass electrode has been studied very thoroughly and shown to give a modified Nernstian response to variations in hydrogen-ion concentration in widely varying media[14] (pH $\leq$ 10), the equation being

$$E = E^{0\prime} + j(\mathrm{H}^+) + \frac{RT}{nF} \ln [\mathrm{H}^+] \qquad (1)$$

where $E^{0\prime}$ is a constant which may vary slightly from one experiment to another, $j(\mathrm{H}^+)$ is a term accounting for the pH-dependent part of the activity coefficients and the liquid-junction potential, and $(RT/nF)\ln [\mathrm{H}^+]$ is the concentration term.

The variations in $E^{0\prime}$ make it necessary to calibrate the electrodes in the solution to be used for the measurement. This can conveniently be done by a so-called "E^0-titration", in which a known amount of strong acid is titrated with strong base, an E-value being measured after each addition of base. The results are used to calculate values of $E^{0\prime}$, j and the concentration of strong base.[15]

It is important to realize that when the experiments are done in this way, the exact concentration of acid titrated in the $E^{0\prime}$-titration forms the basis for subsequent calculations and measurements. Normally, it is much easier to prepare a pure standard solution of acid than to prepare a pure standard solution of a strong base. The base used must not contain carbonate or any other weak acid–base system as an impurity.

It is also important to realize that, although $E^{0\prime}$ and j for the glass electrode may attain somewhat different values in different ionic media even at the same ionic strength, the values of the hydrogen-ion concentration calculated from equation (1) will be the same for all media, since the E-values measured in the different media will vary accordingly. The correct hydrogen-ion *concentrations* can thus be calculated from the glass electrode measurements.

We used this technique to make comparative measurements with a glass electrode and an antimony electrode in different ionic media. The negative logarithm of the hydrogen-ion *concentration* of the solution—denoted by ph in this paper—after each addition of titrant was calculated from the glass electrode potential. The antimony electrode potentials were then related to the calculated ph values (N.B. not the measured pH, which refers to the hydrogen-ion *activity*).

After the E^0-titration, the direction of the titration can be reversed and the solution back-titrated with acid of known concentration, or a suitable buffer substance can be added and the solution titrated further with acid or base. In this way, it is possible to check the behaviour of the electrodes during subsequent titration cycles.

All experiments were done at 25° and constant ionic strength of 0.16 except when the effect of varying the ionic strength (between 0.05 and 0.5) was being studied and when perchlorate and nitrate media were compared, when the ionic strength was 0.5. The salt of the acid used in the titration was employed as the ionic medium (*e.g.*, in nitrate medium, nitric acid was used as the titrant).

Apparatus

The titration unit for measuring potentials of antimony electrodes at various ph-values consisted of a combination glass/silver–silver chloride electrode (HA-401 M5, Ingold, Switzerland), a varactor electrometer amplifier capable of scanning six antimony electrodes and one glass electrode,[16] and a tape punch (Facit, Sweden). The stability of the potential of the antimony electrodes was studied by using similar equipment but with a chart-recorder (8235/05, Philips, The Netherlands) in place of the tape punch.

Polycrystalline electrodes made by three different manufacturers (P301 Radiometer, Denmark; IN 9063, Ingold, Switzerland and Sb3, Tacussel, France), two of each, were used for comparison with the monocrystalline antimony electrodes. The monocrystalline electrodes (of 99.99% pure Sb) were made at this institute as described by Edwall.[1]

Reagent-grade chemicals were used throughout.

Procedure

Normally, 100 ml of a solution containing the buffer system to be studied and neutral salt to give the desired ionic strength were titrated with acid to ph 6.2 or to ph 2. The solution was then titrated with base to ph 8.5 or to ph 10, respectively. The cycle was then repeated with acid and base. Six antimony electrodes, one glass electrode and a silver–silver chloride reference electrode containing 3*M* potassium chloride solution in the salt bridge* were used simultaneously and the potential differences were read in sequence by the measuring system. Eight readings were recorded for each electrode before switching to the next one. The total time for the measuring sequence was 90 sec for all channels. Then, another addition of titrant was made and the measuring sequence was started after an equilibration period of 30 sec. The potential differences were recorded and later processed by a standard statistical covariance computer program. Generally, the number of points obtained in a titration was around 80.

Before a titration was started, air was bubbled through the test solution for 10 min, then the air was shut off and the solution was stirred with a magnetic stirrer.

To compare the stability of the commercial polycrystalline antimony electrodes and the monocrystalline elec-

* In perchlorate solution the reference electrode was in a "Wilhelm" bridge[17], containing 0.01*M* $AgClO_4$, 0.49*M* $NaClO_4$/0.50*M* $NaClO_4$.

trodes, the potentials of six electrodes against a common silver–silver chloride reference electrode, containing 3*M* potassium chloride solution, in a solution of hydrochloric acid saturated with respect to antimony ions, were sequentially recorded. The solutions were saturated with respect to SbOCl precipitate in excess and filtered after equilibration. The recording was continued over a period of about 150 hr. Stirring was employed during a brief period of the experiment.

RESULTS

The result of the titration in pure sodium nitrate medium (with no buffer added) is shown in Fig. 1. (Monocrystalline electrodes were used for these titrations.) The interpolated potential value at ph 7.4 was -369.2 ± 0.9 mV for six electrodes. The slope of the *E vs.* ph line was -53.8 mV/ph unit if all the experimental points were included. The points in the ph range 2–4.3 gave -54.6 mV/ph unit and the points in the range 8.5–9.7 gave -52.9 mV/ph unit for the slope.

Figure 2 shows the behaviour of monocrystalline antimony electrodes in sodium nitrate medium in the presence of 0.020*M* TRIS [tris(hydroxymethyl)aminomethane]. The ionic strength was 0.16. The measured potential values at ph 7.4 were -370.4 ± 0.8 mV against an Ag/AgCl reference electrode. The slope of the *E vs.* ph line was in this case -53.9 mV/ph unit for all the experimental points, and -54.1 mV/ph

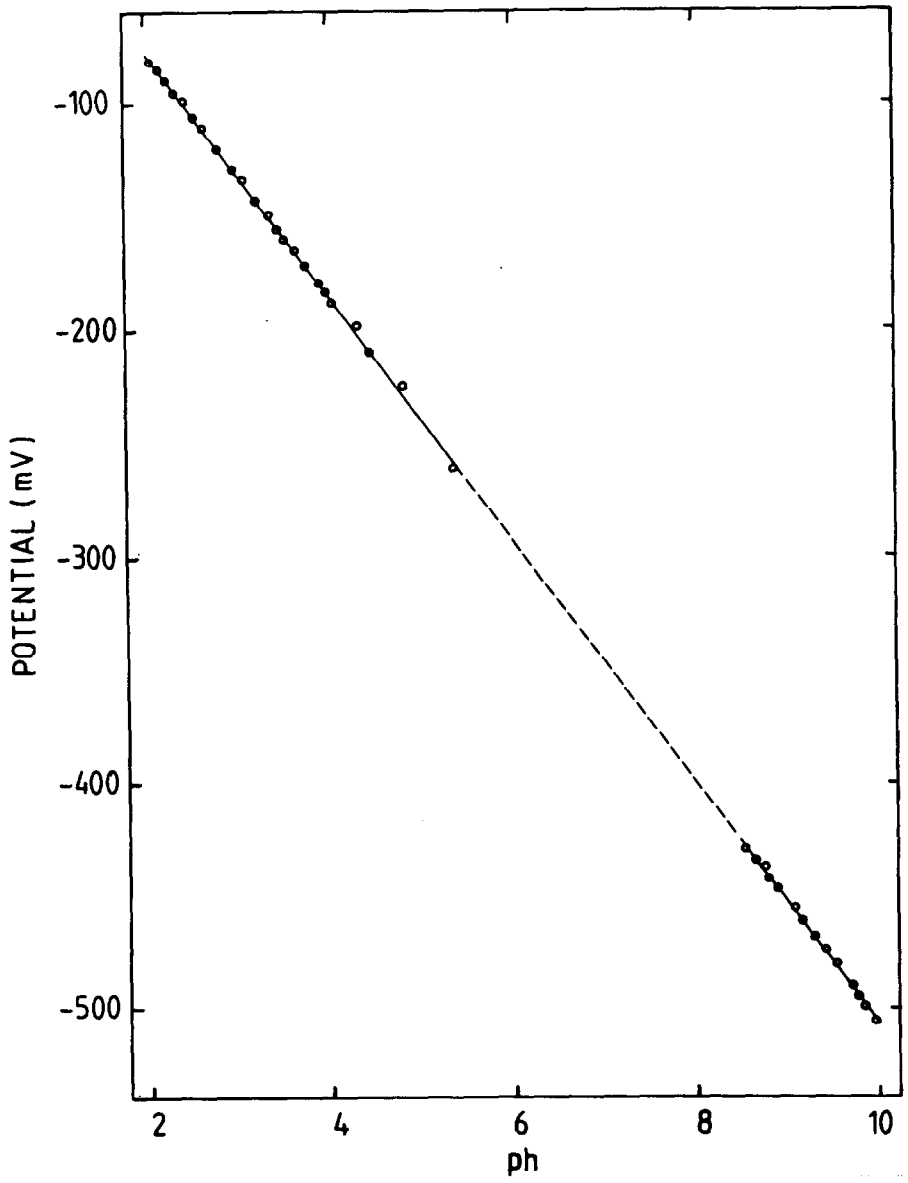


Fig. 1. Titration of a solution of 0.16*M* sodium nitrate with nitric acid and sodium hydroxide (containing sodium nitrate to keep the ionic strength at 0.16) at 25°. There are 76 data points. Monocrystalline electrodes were used for measuring the potentials.

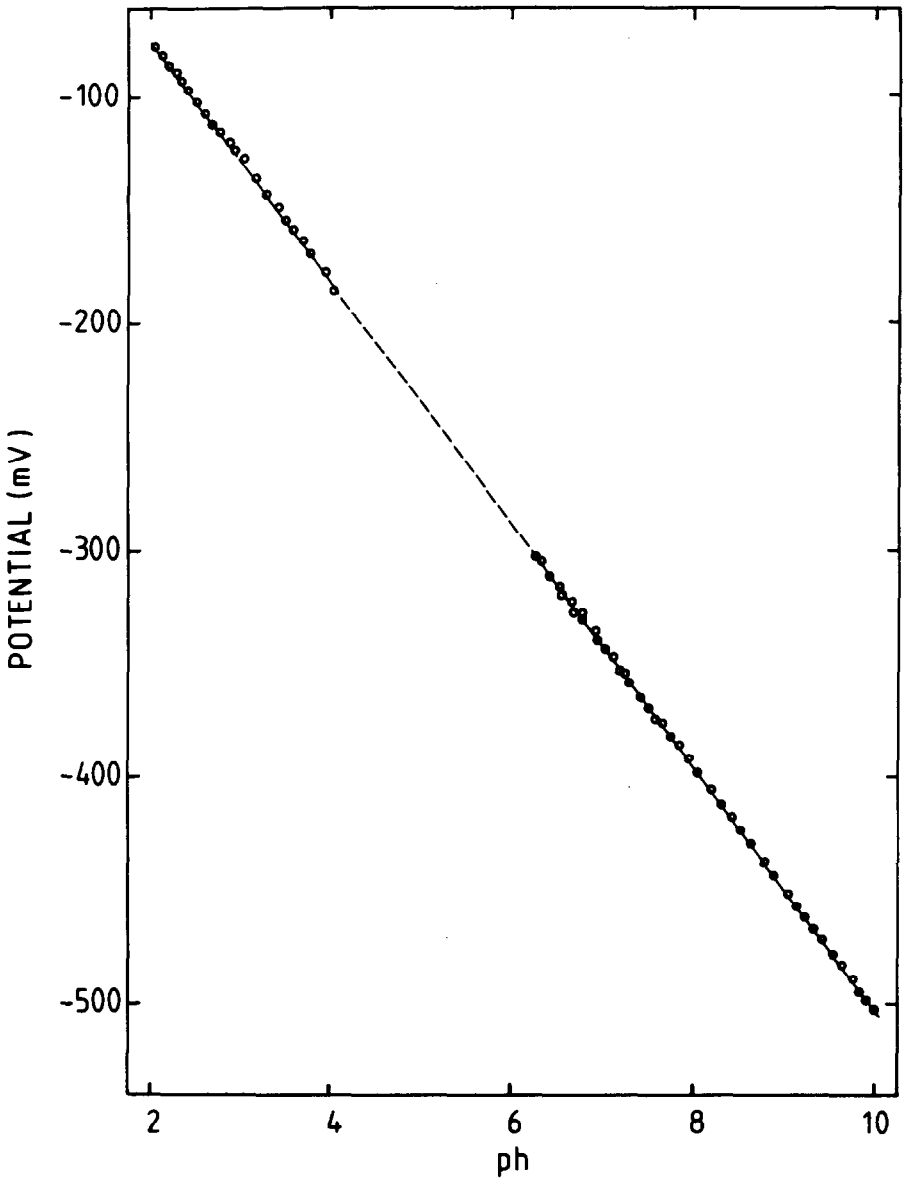


Fig. 2. Titration of 0.02*M* TRIS/0.14*M* sodium nitrate. There are 81 data points.

unit for the points in the ph range 2–4.3. The points in the alkaline range 8.5–9.7 gave −53.9 mV/ph unit.

Table 1 lists the results of the measurements on new and old monocrystalline antimony electrodes in nitrate and chloride and mixed nitrate–chloride media, all containing TRIS. It is seen that the effect of increasing age of the electrode is greater in chloride medium than in nitrate. In both cases the potentials change towards more positive values as the electrodes age, and the potentials of the older electrodes become more positive with increasing chloride concentration.

Figure 3 shows the results of a comparison between the potentials of a monocrystalline antimony electrode in sodium nitrate and sodium perchlorate media at ionic strength 0.5 in presence of TRIS. The higher ionic strength used in these experiments was chosen in order to enable us to study any differences in the complex-forming properties of the two ligands with antimony. The values of the potential changed by less than 2 mV when the medium was changed.

Table 2 lists the results of our measurements with monocrystalline antimony electrodes in sodium nitrate solutions of various concentrations. The solutions also contained TRIS.

Figure 4 shows the potentials of the antimony electrode *vs.* a silver/silver chloride electrode as a function of the concentration of TRIS at constant ionic strength (0.16). Six monocrystalline antimony electrodes were used.

Similar experiments were done with orthophos-

Table 1. Values of the potential ($E_{7.4}$, mV) at ph 7.4 and the slope (S, mV/ph) of the E *vs.* ph line for the ph-range 6.4–8.5 in solutions containing 0.02M TRIS and $NaNO_3$ or NaCl. "New" monocrystalline electrodes (used for about 40 hr) were used in the experiments with an asterisk. The "old" electrodes had been used for about 140 hr

Composition of the solution	Number of experimental points	Antimony electrodee												Standard deviation, mV
		No. 1		No. 2		No. 3		No. 4		No. 5		No. 6		
		$E_{7.4}$	S	$E_{7.4}$	S	$E_{7.4}$	S	$E_{7.4}$	S	$E_{7.4}$	S	$E_{7.4}$	S	
0.16M NaCl*	78	−372.7	−52.1	−374.1	−51.9	−374.0	−52.1	−373.2	−52.0	−372.8	−52.1	−373.2	−51.9	0.78
0.16M NaNO$_3$*	77	−372.1	−51.3	−373.6	−51.5	−372.8	−51.5	−372.2	−51.5	−372.1	−51.9	−372.6	−51.7	0.70
0.16M NaCl	81	−366.1	−53.5	−365.1	−52.9	−365.4	−53.1	−362.8	−53.0	−363.6	−53.4	−366.1	−53.2	1.20
0.16M $NaNO_3$	78	−370.1	−52.1	−370.3	−53.0	−369.1	−52.8	−366.4	−52.4	−368.2	−52.7	−368.0	−52.9	1.00
0.12M NaCl + 0.04M $NaNO_3$	81	−366.7	−52.8	−369.9	−52.4	−366.9	−52.2	−367.1	−53.3	−363.4	−52.3	−367.2	−54.4	0.35
0.08M NaCl + 0.08M $NaNO_3$	75	−368.0	−55.5	−368.3	−54.5	−367.9	−54.4	−368.2	−55.2	−367.1	−55.5	−368.4	−55.1	0.77
0.04M NaCl + 0.12M $NaNO_3$	74	−368.8	−52.4	−372.1	−52.4	−363.3	−52.6	−370.0	−52.8	−364.1	−53.0	−367.8	−52.9	0.75

Table 2. Values of the potential ($E_{7.4}$, mV) at ph 7.4 and the slope (S, mV/ph) of the E *vs.* ph line for the ph range 6.4–8.5 in solutions containing 0.02M TRIS and different concentrations of sodium nitrate. Monocrystalline electrodes were employed. E^0 values refer to the glass–silver/silver chloride electrode couple

Concentration of $NaNO_3$, M	Number of experimental points	Antimony electrode												Standard deviation, mV	E^0, mV
		No. 1		No. 2		No. 3		No. 4		No. 5		No. 6			
		$E_{7.4}$	S	$E_{7.4}$	S	$E_{7.4}$	S	$E_{7.4}$	S	$E_{7.4}$	S	$E_{7.4}$	S		
0.05	62	−372.0	−52.0	−373.1	−51.9	−372.8	−51.8	−371.8	−51.8	−372.0	−52.1	−372.5	−51.5	0.36	401.01
0.10	80	−371.0	−52.0	−372.8	−52.4	−372.7	−52.3	−371.8	−52.0	−371.4	−52.5	−372.0	−52.1	0.92	401.14
0.16	81	−371.3	−52.0	−372.4	−51.9	−372.3	−52.0	−371.2	−52.0	−371.2	−52.1	−371.6	−52.3	0.63	401.16
0.50	80	−364.2	−52.5	−364.2	−53.5	−363.8	−53.2	−362.2	−53.4	−363.4	−53.7	−364.2	−52.8	1.10	407.71

Table 3. Values, of the potential ($E_{7.4}$, mV) at ph 7.4 and the slope (S, mV/ph) of the E *vs.* ph line for the ph range 6.4–8.5 in TRIS solutions. Polycrystalline electrodes were employed

Concentration of solution	Number of experimental points	Ingold 1		Ingold 2		Tacussel 1		Tacussel 2		Radiometer 1		Radiometer 2		Standard deviation mV
		$E_{7.4}$	S	$E_{7.4}$	S	$E_{7.4}$	S	$E_{7.4}$	S	$E_{7.4}$	S	$E_{7.4}$	S	
0.16M NaCl	81	−370.2	−53.0	−372.6	−53.0	−362.9	−52.7	−362.8	−53.7	−363.4	−52.7	−364.1	−53.0	1.26
0.16M $NaNO_3$	81	−370.6	−52.5	−372.3	−52.8	−366.9	−52.5	−368.0	−52.8	−367.5	−52.7	−367.3	−52.4	0.56

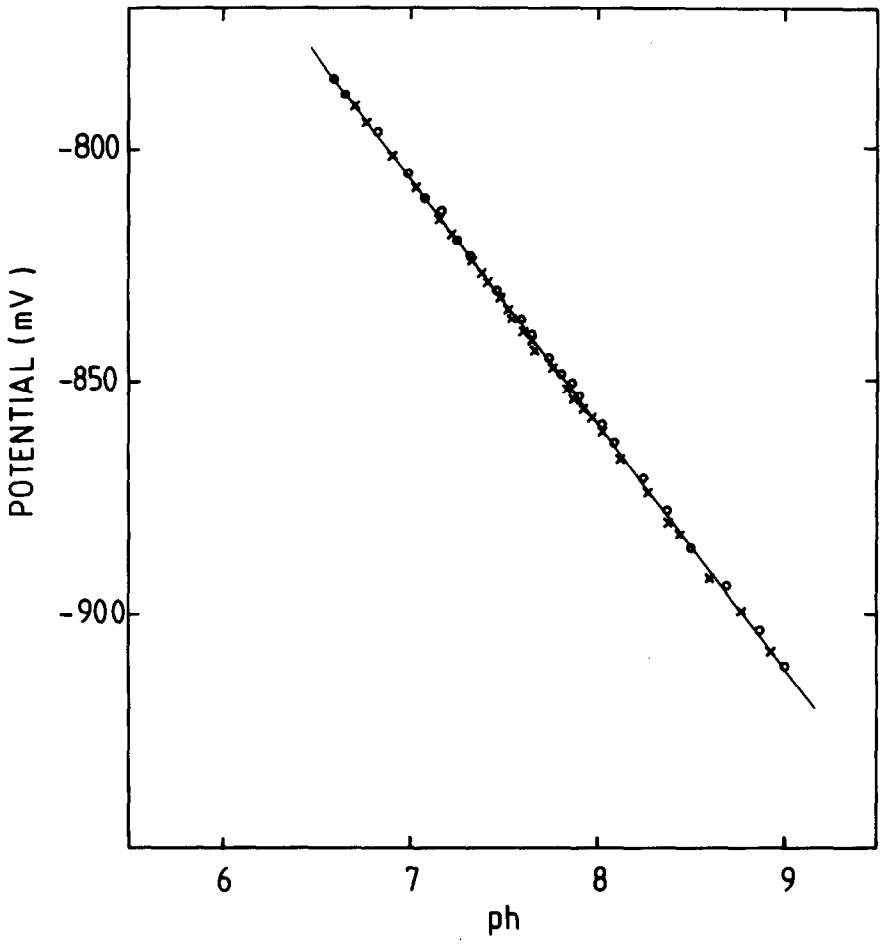


Fig. 3. Titration of a solution of 0.02*M* TRIS/0.5*M* sodium nitrate (points denoted by ×) or 0.5*M* sodium perchlorate (points denoted by O) with nitric acid and sodium hydroxide solution (containing sodium nitrate or perchlorate to give the same ionic strength). There are 81 points on each curve.

phate instead of TRIS at the ph-values 5.90, 6.50, 7.40 and 7.80. In this case significant slopes were obtained for the first two ph-values and were −3.90 and −2.73 mV/decade. For the last two ph-values non-significant slopes (−1.07 and 0.24 mV/decade) were obtained.

Figure 5 shows the *E vs.* ph plots for titrations in sodium nitrate medium (ionic strength 0.16) containing different ligands that are likely to form complexes with antimony, namely orthophosphate, tartrate, citrate, oxalate and EDTA. Acetate was also tested and gave results very similar to phosphate. It can be seen that all these ligands affect the response of the antimony electrode in at least some part of the ph-range. In most cases the effects are greatest at ph between about 4 and 7. All curves except the one for EDTA coincide with the solid line valid for TRIS above ph ~8. Orthophosphate and acetate coincide with the TRIS line below ph ~3.

When the electrodes were used to monitor titrations of TRIS in nitrate medium after the phosphate titrations, the first titration sometimes yielded slightly different *E* values from those expected but the results of subsequent titrations were as expected.

Preliminary titrations on blood plasma indicate that plasma phosphate does not greatly affect the antimony electrode potential, perhaps because the calcium present in the plasma is sufficient to bind the phosphate.

Comparison of the oriented monocrystalline electrodes with some different makes of polycrystalline electrodes gave the results shown in Table 3. Two each of the electrodes made by Ingold, Radiometer and Tacussel were tested together with a glass electrode and a reference electrode in 0.16*M* sodium chloride or sodium nitrate in the presence of TRIS. In general, the Gysinck effect was more pronounced for the polycrystalline electrodes than for the monocrystalline electrodes. The aging phenomenon—resulting in a drift of $E_{7.4}$ towards more positive values—was greater for the polycrystalline electrodes. Differences in quality could also be observed—the $E_{7.4}$-values were more negative for the better elec-

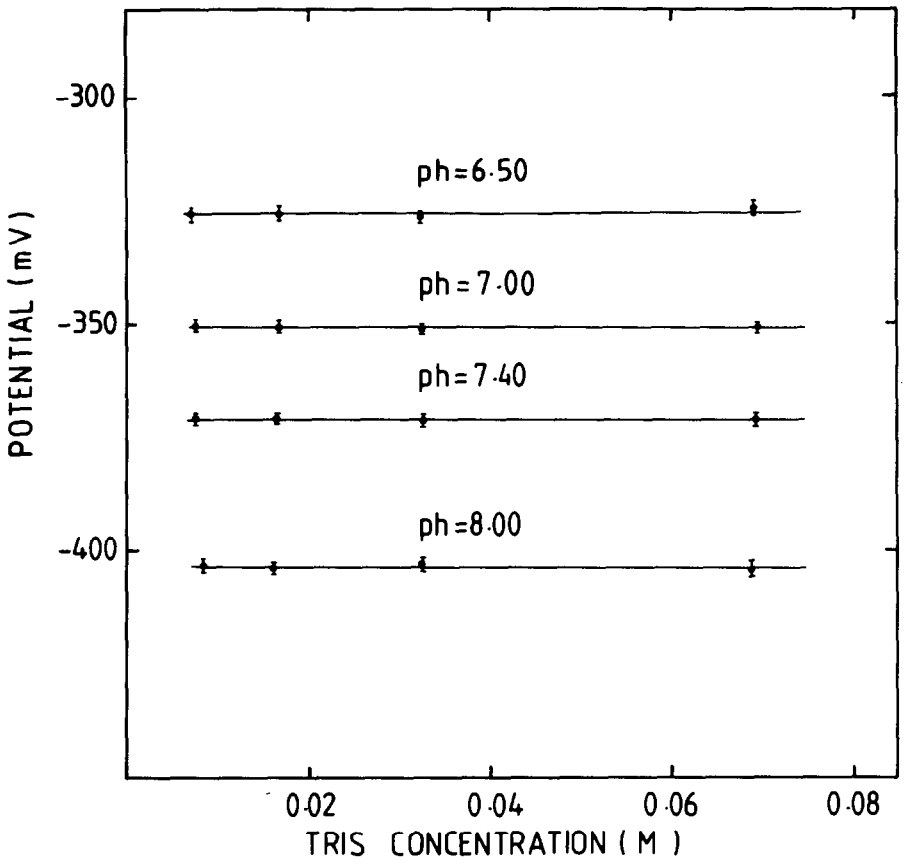


Fig. 4. Mean E-values for six monocrystalline antimony electrodes as a function of the TRIS concentration at different values of ph. Statistically significant slopes were obtained for ph 6.5, 7.00, 7.40 and 8.00; they were -1.20, -1.05, -1.48 and -1.86 mV/decade, respectively. The standard deviations of the potential (~ 0.8 mV) are shown as vertical bars.

trodes, which were also more stable with time, and had potentials similar to the monocrystalline electrodes. (The reader is referred to the first two lines of Table 1 for comparison with the monocrystalline electrodes.)

The results of a study of the stability of the electrode potentials with time are presented in Figs. 6 and 7. Most of the measurements were made in unstirred solution. Stirring was started after 6 hr and run for 2 hr with the monocrystalline electrodes, and started after 3.5 hr and run for 3 hr with the polycrystalline electrodes. All the monocrystalline electrodes behaved similarly and the drift was less than 2–3 mV over the entire duration of the test, which was 122 hr. The effect of stirring on the potential was less than 0.5 mV. The polycrystalline electrodes show much greater drift of potential with time. The study lasted for 146 hr. All the electrodes showed an initial drift of about 10–20 mV during the first 3 hr. The effect of stirring was also much greater than for the monocrystalline electrodes.

DISCUSSION

The difference between the slopes in the acidic and alkaline range of the E *vs.* ph lines observed for the monocrystalline electrodes in pure nitrate medium could not be detected in solutions containing TRIS. We do not know the reason for this effect. Without TRIS, the buffer capacity of the system is of course very low. Some glass electrodes are known to change their E^0 value at about pH 6–9 when the solution is titrated from acidic to alkaline[18] and this may be responsible for the observed effect. One possible reason for the change is said to be a change in the gel layer on the glass membrane.

Close comparison of Fig. 1 with Fig. 2 shows that a small change in potential of 1–2 mV occurs when TRIS is added to the nitrate solution. This effect could be due to weak complexation of antimony in solution, or to a reaction on the electrode surface, but it is so small as to be negligible in medical and biological pH measurements. The measurements were made by consecutive titrations with the same electrodes.

The effect of substituting 0.5M sodium nitrate for 0.5M sodium perchlorate, TRIS being used as buffer substance, was less than 2 mV. From this, it may be concluded that both ionic media form about equally strong (or weak) complexes with antimony. The vari-

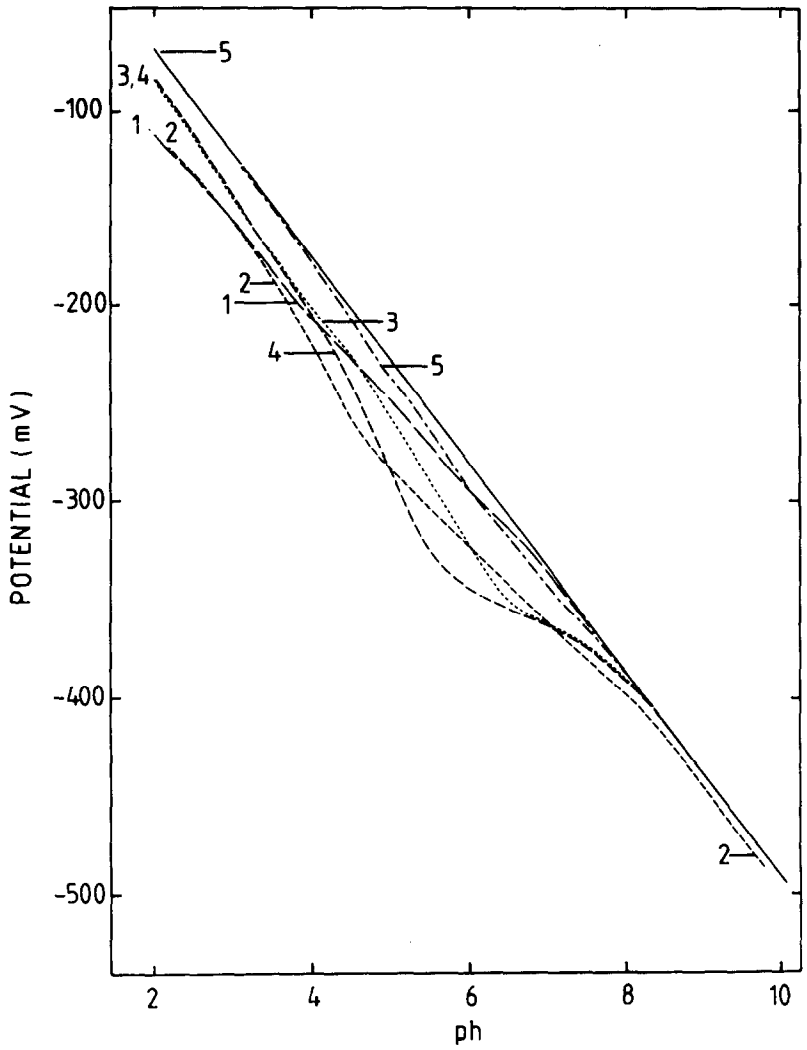


Fig. 5. The effect of various complex-forming ligands on the response of monocrystalline antimony electrodes. The solutions were 0.02*M* in ligand and 0.14*M* in sodium nitrate and were titrated with nitric acid and sodium hydroxide [ionic strength 0.16 ($NaNO_3$)]. The solid line is for TRIS (80 points). The other curves are: 1: oxalate; 2: EDTA; 3: citrate; 4: tartrate; 5: orthophosphate (25 points were used in constructing each curve).

ation of the potential with increasing ionic strength (increasing sodium nitrate concentration, Table 2) is also small, which suggests that the complexes of antimony with nitrate and perchlorate ions are weak. With increasing sodium nitrate concentration, the potentials are shifted slightly towards more positive values. The somewhat greater difference between the values obtained for $c_{NaNO_3} = 0.16M$ and $c_{NaNO_3} = 0.50M$ is probably due to a change in potential of the reference electrode. This is also seen in the E^0 value of the glass electrode–reference electrode couple which is given in the column at the extreme right in Table 2.

No appreciable effect could be observed when chloride was substituted for nitrate in stirred solutions containing TRIS. However, when phosphate was used as buffer substance instead of TRIS, a great effect on the measured antimony electrode potentials was noted. This effect has been reported earlier by Green and Giebisch.[19] The *E*-values at ph ~ 2 are the same in solutions containing either of these buffer substances. At ph ~ 9–10, the same *E*-values are again measured and the slopes of the curves are approximately equal. The kink in the curve recorded with phosphate present is also obvious at ph ~ 6.7–7.7. The slope of the curve is appreciably higher for the phosphate-containing solution up to ph ~ 6.7 than for the TRIS solution. In contrast to Green and Giebisch's results, our measurements show very little dependence of the Sb-potential on the phosphate concentration. Green and Giebisch used 0.15*M* sodium chloride medium and observed a definite shift of the potential towards more negative values as the phos-

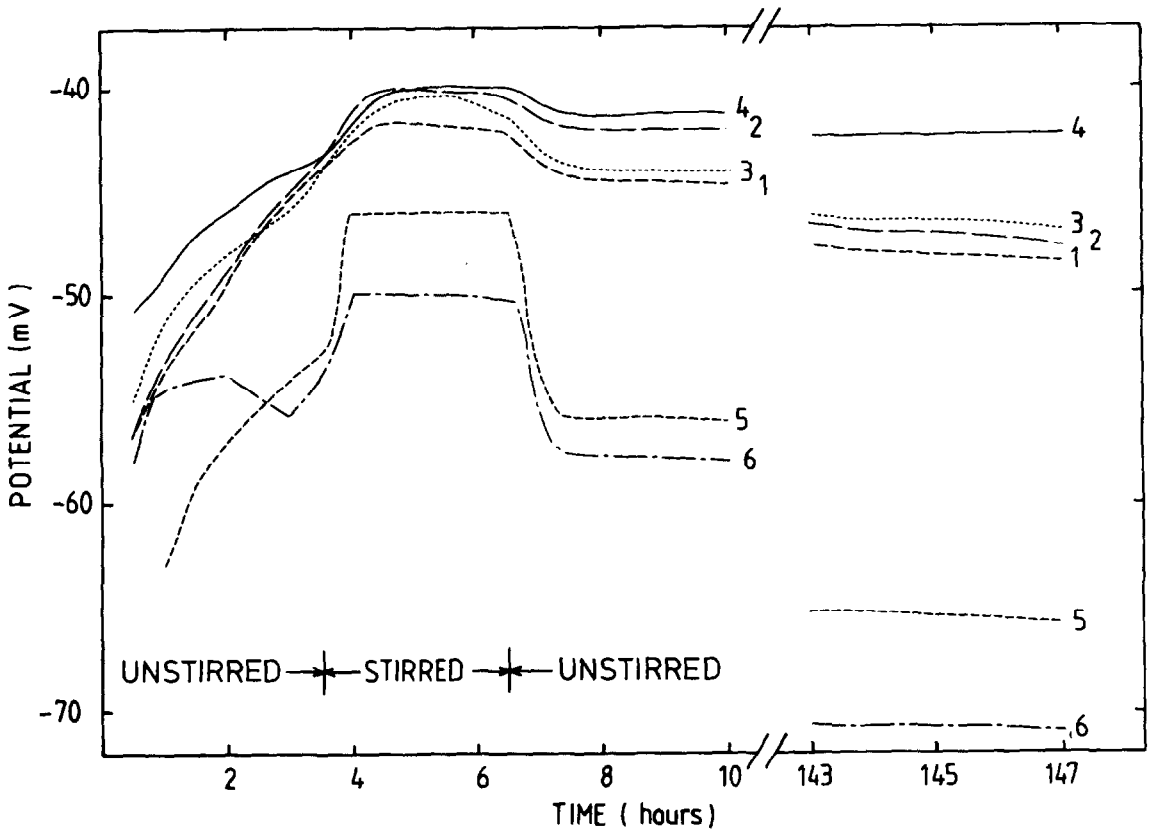


Fig. 6. The stability of the polycrystalline antimony electrodes as a function of time. The measuring solution was made by saturating distilled water with SbOCl and adding sodium hydroxide to give a ph of 1.7. The electrodes were: 1 and 2: Ingold; 3 and 4: Radiometer; 5 and 6: Tacussel.

phate concentration was increased. Their pH-range was ~5–7.4. We were not able to reproduce Green and Giebisch's results for sodium chloride as ionic medium.

The effects of phosphate on the potential *vs.* ph curve may be connected with complexation of antimony by phosphate. Other ligands known to form soluble complexes with antimony(III) are tartrate, citrate, oxalate and EDTA. These ligands too have a great effect on the *E vs.* ph curves of the monocrystalline antimony electrode. At ph 2 the effect is greatest with EDTA and oxalate. The complexation constants for antimony with EDTA determined by Bhat *et al.*[20] suggest that antimony is complexed even at low pH-values. The effects seen in Fig. 5 could thus be due to complexation of antimony by EDTA. Similarly, oxalate is known to form protonated complexes with several metal ions and it is not unlikely that this may occur with antimony. Moreover, the first dissociation constant of oxalic acid is $10^{-1.1}$, which implies that the major oxalic acid species at ph 2 is $HOOC \cdot COO^-$.

Citric and tartaric acids are weaker than oxalic acid, and form weaker complexes with metal ions than does EDTA. Thus, complexation with these ligands should result in less pronounced effects on the *E vs.* pH curve of the antimony electrode at ph 2.

The curves for orthophosphate and acetate coincide with the curve for TRIS in the acidic range at ph 2. Most known phosphate complexes with metal ions are formed with the HPO_4^{2-} ion and are not very strong, so any effects should be observed at higher ph-values. This is in agreement with our experimental results. Acetate also forms rather weak complexes with metal ions.

In the alkaline ph-range all curves except the EDTA curve again coincide with the TRIS line. This could mean that no complex can compete with hydrolysis of antimony in this ph-range. The exception is again EDTA, which has been suggested to form mixed complexes with antimony and one or two hydroxide ions,[20,21] although other explanations have been put forward.[22]

We did some preliminary experiments on the bicarbonate system, and found no marked effect of bicarbonate ions on the measured antimony potential. Quehenberger's suggestion[8] that Karlmark and Sohtell's "bicarbonate effect"[7] could in fact be a phosphate effect is therefore supported by our results.

The study on the stability of the potential of the

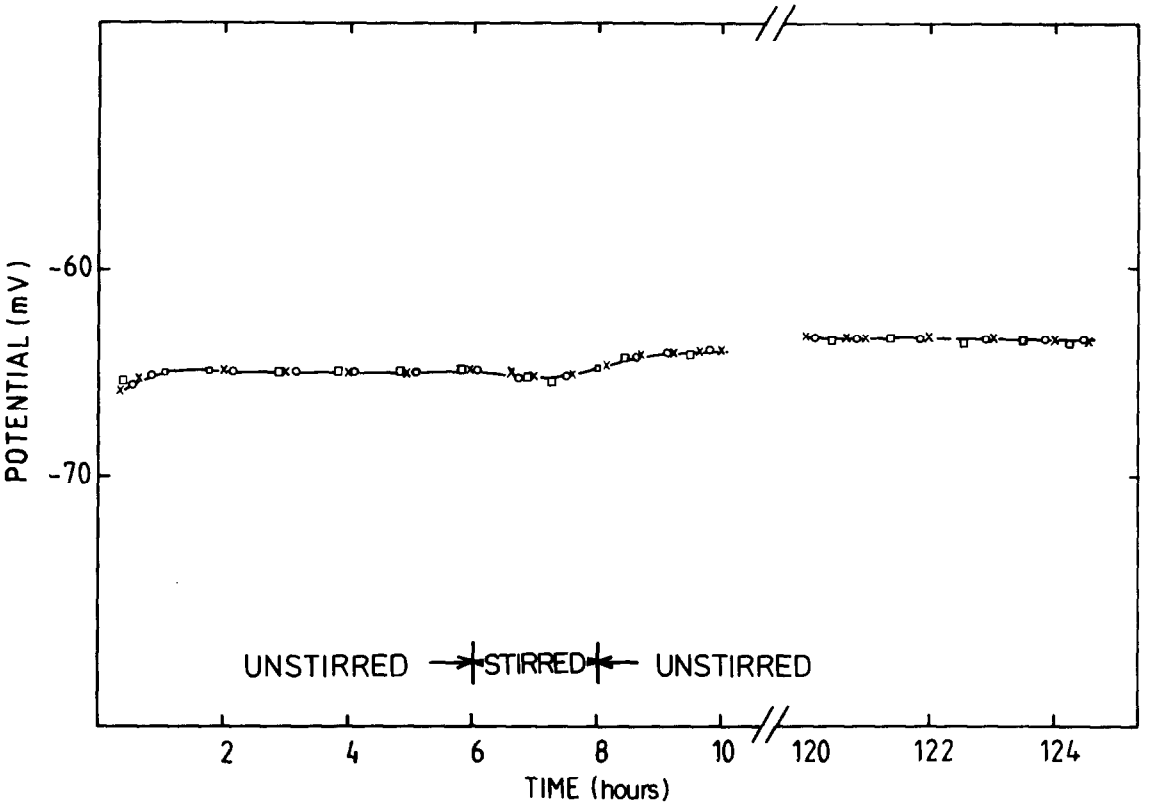


Fig. 7. The stability of three monocrystalline antimony electrodes as a function of time. In this case sodium hydroxide was added to a saturated SbOCl solution to give ph 1.9.

antimony electrodes with time shows that in unstirred solution the monocrystalline electrodes are much better than the polycrystalline ones. Pitting corrosion is more likely to take place on the polycrystalline electrode surface than on the oriented monocrystalline surface and this may be a reason for the better long-term stability of the latter type. In our experiments, the same monocrystalline electrodes were used for a total of about 400 hr in sodium nitrate medium, most of the time in the presence of TRIS but also in the presence of phosphate. At the end of this period the *E*-values were about 4 mV more positive than when the electrodes were used for the first time.

Marked differences could be observed between the different makes of polycrystalline antimony electrodes. The Ingold electrodes were generally the best, having potentials similar to the monocrystalline electrode and showing the least drift in unstirred solution. The other types showed great individual variations in potential, strong dependence on the stirring conditions and greater drift of the potential with time. Different crystal structures in the different electrodes are probably responsible for these effects.

At present, work is in progress that aims at clarifying some of the electrode processes by using cyclic voltammetry and high-frequency impedance measurements. We are also trying to develop a procedure for calibrating antimony electrodes for use in pH-measurements in plasma and other biological fluids.

CONCLUSIONS

The conclusions that can be drawn from our results are as follows.

1. Sodium nitrate and sodium perchlorate ionic media appear to have no influence on the response of antimony electrodes. Chloride seems to be more corrosive and should be avoided if possible. If not, new monocrystalline antimony electrodes should be used.

2. TRIS is a suitable buffer for standardizing antimony electrodes. Phosphate, citrate, tartrate and oxalate buffers should not be used.

3. Polycrystalline antimony electrodes should not be used for measurements in unstirred solution, but monocrystalline electrodes yield acceptable results. In stirred solutions, polycrystalline electrodes are satisfactory, but monocrystalline ones are better.

Acknowledgements—The authors wish to express their gratitude to Mrs Karin Lindgren, Mr Arnold Olofsson and Mr Rune Persson for skilled technical assistance, to the National Swedish Board for Technical Development for financial support, and to Mrs Karin Mattson, who has skilfully prepared the manuscript.

REFERENCES

1. G. Edwall, *Electrochim. Acta*, 1979, **24**, 595, 605, 613.
2. E. Bishop and G. D. Short, *Talanta*, 1964, **11**, 393.
3. G. D. Short and E. Bishop, *Anal. Chem.*, 1965, **37**, 962.
4. E. Bishop and T. J. N. Webber, *Analyst*, 1973, **98**, 697.
5. E. Bishop and M. Riley, *ibid.*, 1973, **98**, 307.
6. Th. Gysinck, *Arch. Suikerind.*, 1932,711; *Chem. Abstr.*, 1933, **27**, 2325.
7. B. Karlmark and M. Sohtell, *Anal. Biochem.*, 1973, **53**, 1.
8. P. Quehenberger, *Pflügers Arch.*, 1977, **368**, 141.
9. C. R. Caflish, L. R. Pucacco and N. W. Carter, *Kidney Int.* 1978, **14**, 126.
10. P.-A. Jöngren and G. Edwall, *Electrochim. Acta*, 1980, **25**, 1585.
11. A. Dolinsky and I. Šimaček, *Cesk. Gastroenterol. Vyziva*, 1978, **32**, 21.
12. D. J. G. Ives, in *Reference Electrodes*, D. J. G. Ives and G. J. Janz (eds.), p. 322. Academic Press, New York, 1961.
13. G. Edwall, *Med. Biol. Eng.*, 1978, **16**, 661.
14. A. Johansson and S. Johansson, *Analyst*, 1978, **103**, 305.
15. L. Persson, F. Ingman and A. Johansson, *Talanta*, 1976, **23**, 76.
16. G. Edwall, *Rev. Sci. Instrum.*, 1977, **48**, 1545.
17. W. Forsling, S. Hietanen and L. G. Sillén, *Acta Chem. Scand.*, 1952, **6**, 901.
18. L. Ciavatta, *Ark. Kemi*, 1963, **20**, 417.
19. R. Green and G. Giebisch, in *Ion Selective Microelectrodes* H. J. Berman and N. C. Herbert (eds.), p. 63. Plenum Press, New York, 1974.
20. T. R. Bhat and R. K. Iyer, *Z. Anorg. Allgem. Chem.* 1965, **335**, 331.
21. U. Y. Ozer and R. F. Boguchi, *J. Inorg. Nucl. Chem.*, 1971, **33**, 4143.
22. G. Anderegg and S. Malik, *Helv. Chim. Acta*, 1970, **53**, 564, 577.

Talanta. Vol. 28. pp. 313 to 317. 1981
Printed in Great Britain. All rights reserved

0039-9140/81/050313-05$02.00/0
Copyright © 1981 Pergamon Press Ltd

ELECTROCHEMICAL BEHAVIOUR OF SOME NEUROLEPTICS: HALOPERIDOL AND ITS DERIVATIVES

J.-C. VIRE,* M. FISCHER and G. J. PATRIARCHE
Institute of Pharmacy, Brussels Free University, Campus Plaine 205/6, B-1050 Brussels, Belgium
and
G. D. CHRISTIAN
Department of Chemistry, University of Washington, Seattle, WA 98195, U.S.A.

(*Received* 23 *September* 1980. *Accepted* 10 *November* 1980)

Summary—The electrochemical characteristics of Haloperidol and related compounds, representative neuroleptics of the butyrophenone family, have been investigated as a function of pH and concentration by direct-current, alternating-current and differential-pulse polarography and cyclic voltammetry at a hanging mercury drop electrode. A single cathodic wave representing an irreversible two-electron reduction is obtained, and its half-wave potential differs from that characteristic of aromatic ketone reduction. Adsorption processes disturb the wave behaviour and an adsorption prewave is observed at high concentrations. Quantitative measurements were successful in the concentration range 1×10^{-4}–$1 \times 10^{-6}M$ (0.4 mg/l.), the lower concentration representing the detection limit by differential-pulse polarography.

Very few electrochemical studies have been made on the important neuroleptics of the butyrophenone family. Classical polarographic quantitative determinations have been employed for the determination of these compounds in admixture in pharmaceutical preparations.[1–3]

We report here the elucidation of the electrochemical behaviour of Haloperidol and related butyrophenone derivatives at the dropping mercury electrode, and define the most suitable parameters and solution conditions for analytical measurements.

EXPERIMENTAL

Instrumentation

Polarographic studies [direct current (d.c.), alternating current (a.c.) and differential pulse (d.p.)] were carried out with a Tacussel type P.R.G. 34 polarograph and a saturated calomel reference electrode (SCE). The operating parameters were as follows:

d.c.: voltage scan: 5 mV/sec; drop time: 1.1 sec
a.c.: voltage scan: 5 mV/sec; drop time: 1.1 sec; superimposed sinusoidal amplitude: 10 mV; frequency: 90 Hz.
d.p.: voltage scan: 2 mV/sec; drop time: 2 sec; pulse amplitude: 40 mV; pulse delay: 1.90 sec; pulse duration: 40 msec.

Cyclic voltammetry measurements at scan-rates of 1 V/sec or greater were made with a Tacussel triangular-wave signal generator, type G.S.T.P., coupled with a U.A.P. 4 unit and a Telequipment D.M. 64 oscilloscope. For voltage scans at 500 mV/sec or less, a Tacussel type P.R.T. 10-0.5 potentiostat was used together with a signal generator constructed in our own laboratory. Current–voltage curves were recorded on a Hewlett-Packard 7035 *X–Y* recorder.

Controlled-potential coulometric measurements were accomplished with a P.A.R. model 173 potentiostat and model 179 coulometer. A P.A.R. model 377-1 mercury electrode coulometric cell with a synchronous stirring motor was used.

A salt bridge with porous Vycor (Corning) separators isolated the auxiliary electrode from the sample solution, keeping diffusion very low, but offering little resistance to current.

Another salt bridge isolated the reference electrode from the sample solution. The mercury pool area was 12.5 cm^2.

Quantitative polarographic measurements were made with a P.A.R. model 174 A polarograph with a P.A.R. type SMDE 303 working electrode and a silver–silver chloride reference electrode. This electrode arrangement allowed measurements to be made by the d.c. sampling technique for determinations at low concentrations, in which a large portion of the capacitative current is eliminated by making measurements with a static (non-growing) mercury drop. Polarograms were recorded with a Houston RE 0074 *X–Y* recorder.

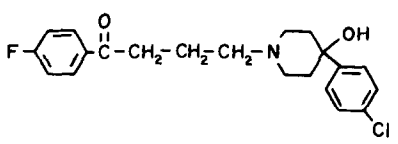
The experimental error was about 0.2%.

Reagents

Buffers were prepared from sodium dihydrogen phosphate (Merck 6345), sodium acetate (Merck 6268) or sodium tetraborate (Merck 6308), all at 0.033*M*. The pH was adjusted with the aid of a pH-meter by adding hydrochloric acid or potassium hydroxide solution.

The Haloperidol (Janssen Pharmaceutica, Patent Nos. ZR 1625 and B 8601) was used without further purification. Solutions were prepared immediately before the experiments were performed.

The compound is 4-[4′-(*p*-chlorophenyl)-4′-hydroxy-1-piperidinyl]-1-(*p*-fluorophenyl)-1-butanone:



* To whom correspondence should be sent.

RESULTS AND DISCUSSION

Choice of solvent

Butyrophenones are soluble in acidic aqueous media, but an organic solvent must be added to give adequate solubility in neutral or basic solution, *i.e.*, a mixed solvent system must be employed. We have investigated several solvent systems, and find that a 20% propylene carbonate–30% methanol–50% water mixture is an excellent compromise for good solubility and minimal adsorption effects. Propylene carbonate is a very good solvent for butyrophenones, but the presence of methanol is required to improve the miscibility of this solvent with water. The propylene carbonate results in a small negative shift (30 mV) in the observed half-wave potentials, possibly because of introduction of a junction potential at the reference electrode (a three-electrode cell was employed to minimize the *iR* drop). Propylene carbonate is unfortunately subject to degradation in alkaline media and cannot be used at pH > 9. Therefore, dimethylformamide (DMF) was used in place of the propylene carbonate–methanol mixture for solutions of pH > 9; a 40% DMF–60% water mixture was employed. DMF was not used in neutral or acidic solutions because it promotes distortion of the butyrophenone wave.

Effect of pH

Polarograms for Haloperidol were obtained over the pH range 1–13. A well-defined cathodic wave is exhibited in d.c. (Fig. 1) polarography and the limiting current is independent of pH up to pH 10. At pH > 10, the wave becomes distorted and smaller. Controlled-potential coulometric measurements in alkaline media (pH 9) indicate a two-electron change. The half-wave potential increases linearly with increasing pH, with a slope of 51 mV/pH unit, except for a small inflection between pH 8.6 and 10 (Fig. 2).

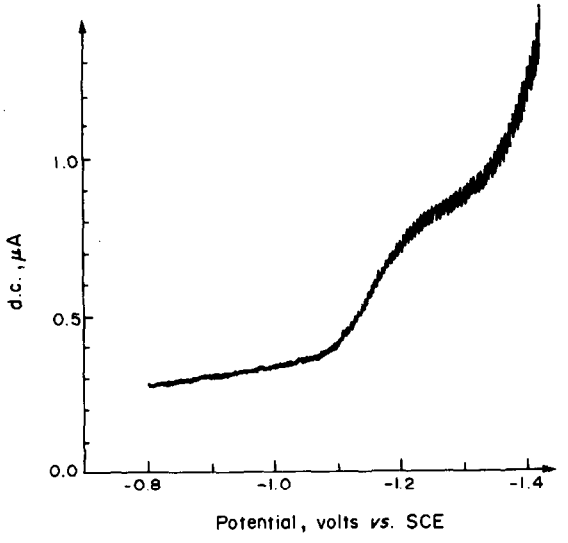


Fig. 1. The d.c. polarographic wave of 2.5 × $10^{-4}M$ Haloperidol at pH 3.

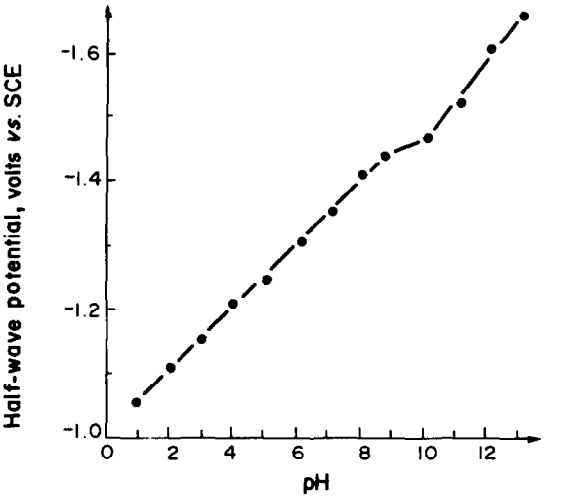


Fig. 2. Dependence of d.c. polarographic half-wave potential of 2.5 × $10^{-4}M$ Haloperidol on pH.

This dependence suggests the consumption of two protons per Haloperidol molecule in the reduction.

It is well known that the carbonyl group in ketones is reduced in the protonated form, resulting in formation of a radical which can dimerize in acidic medium.[4–8] Alternatively, a reversible wave corresponding to the first electron transfer is followed by a second wave due to reduction of the free radical to the alcohol. This is the case of benzophenone.[9] In the present case, in acidic medium the wave is irreversible (see below), and the two-electron transfer is simultaneous.[10] This peculiar mechanism with Haloperidol cannot be attributed to the aliphatic chain. It is known that the presence of an aliphatic radical does not affect the half-wave potential of the first reduction wave[5,11] nor does substitution on the aliphatic group.[5] However, it is known that the nature of the organic solvent and its relative concentration can sometimes cause the wave which corresponds to the radical formation to shift to more negative potentials, causing a merging with the following radical reduction wave.[5] This appears to be the case in the present work, *i.e.*, a single two-electron wave appears. In addition, a wave would normally not appear in acidic medium, but does so in this case in the presence of the organic solvent. At high concentrations (*e.g.*, $10^{-3}M$) an adsorption prewave appears at about 150 mV before the main reduction wave.

Electrochemical properties

Cyclic voltammetry demonstrates the total irreversibility of this system at scan-rates from 10 mV/sec to 100 V/sec (Fig. 3). Adsorption is also indicated by the hysteresis of the curve on the reverse scan. Also, repeated scans on the same drop result in a gradual elimination of the wave. The single wave observed in the d.c. polarography is reflected in a single reduction peak in the d.p. polarography (Fig. 4). The a.c. polarography also suggests the occurrence of significant

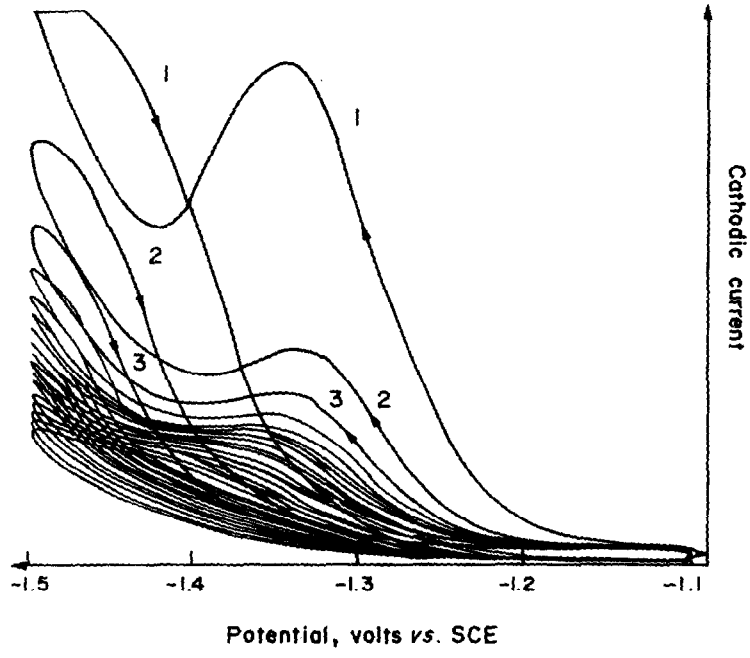


Fig. 3. Cyclic voltammograms of $2.5 \times 10^{-4}M$ Haloperidol at pH 6. Each curve represents successive scans on a single drop. Scan-rate 300 mV/sec.

adsorption. When acid media are used, a flat peak appears only when the phase is changed progressively from 90 ; the adsorption decreases at higher pH values, and the peak-height increases in magnitude as the pH is increased.

The d.c. polarographic wave exhibits a temperature coefficient of 10%/deg at pH 10, too large to correspond to simple diffusion control. It is possible that the current is limited by the rate of a chemical reaction at the electrode, such as a reaction corresponding to protonation of the carbonyl group. Such a process has been demonstrated for the reduction of acetophenone by Frumkin *et al.*[12]

Effect of concentration

The reduction of the carbonyl group of Haloperidol can be used for quantitative analysis. The limiting or peak current is proportional to the concentration of the depolarizer over a tenfold concentration range [1×10^{-4}–$1 \times 10^{-5}M$ (d.c. or sampling polarography) or 1×10^{-5}–$1 \times 10^{-6}M$ (d.p. polarography)]. Although the limiting current plateau covers a range of only 100 mV before the electrolyte discharge in d.c. polarography at pH 5, this is adequate for quantitative measurements. The following correlation coefficients are obtained between measured current and concentration: for 10^{-4}–$10^{-5}M$: d.c. ($r = 0.996$); sampling ($r = 0.999$); d.p. ($r = 0.996$) (Fig. 4). For lower concentrations (10^{-5}–$10^{-6}M$), $r = 0.994$ (d.p.). The lowest concentration represents detection of 0.4 mg/l., or 1 μg of Haloperidol in the cell. In alkaline medium, the limiting or peak current diminishes, perhaps because of deprotonation of the carbonyl group.

Other derivatives

Four butyrophenones of the Haloperidol family were studied and are listed in Table 1. The group substituted at the end of the butyl chain modifies only

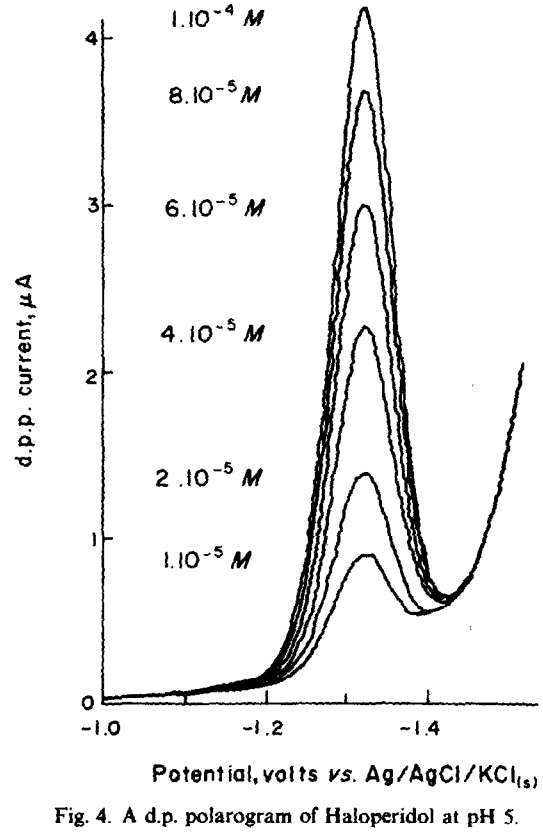
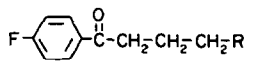
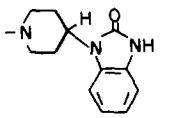
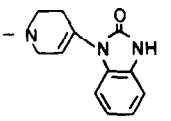
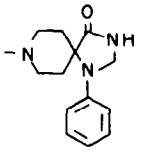
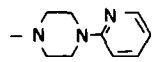


Fig. 4. A d.p. polarogram of Haloperidol at pH 5.

Table 1. Other butyrophenone compounds studied

General formula 

Compound	R
Benperidol	
Droperidol	
Spiperone	
Azaperone	

slightly the electrochemical behaviour of the molecule. The half-wave potential for each derivative as a function of pH is very similar to that of Haloperidol. Hence, it is not possible to differentiate the compounds in admixture. The reduction in all cases remains a two-electron step, as determined by coulometry. However, adsorption phenomena are more pronounced in the case of Benperidol and Droperidol than in the case of the other compounds.

Figure 5 shows two d.p. polarographic peaks for Benperidol at high concentration ($10^{-3}M$), similar to those observed for Haloperidol. The first is an adsorption peak, the second a diffusion-controlled peak. Cyclic voltammetry (Fig. 6) shows that the first

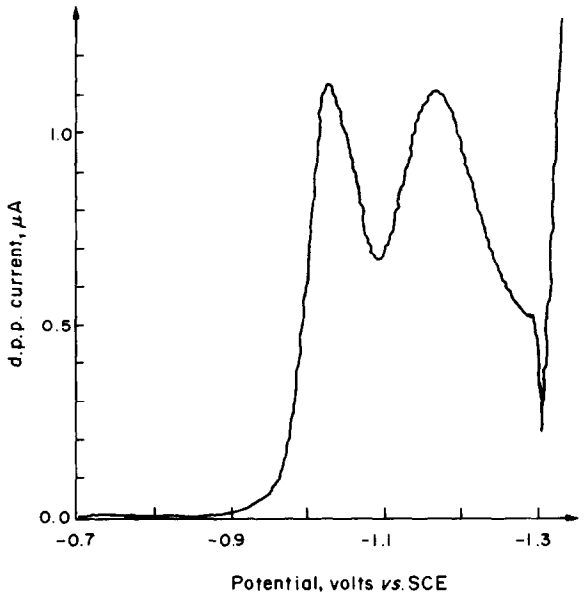


Fig. 5. A d.p. polarogram of $1 \times 10^{-3}M$ Benperidol at pH 1.

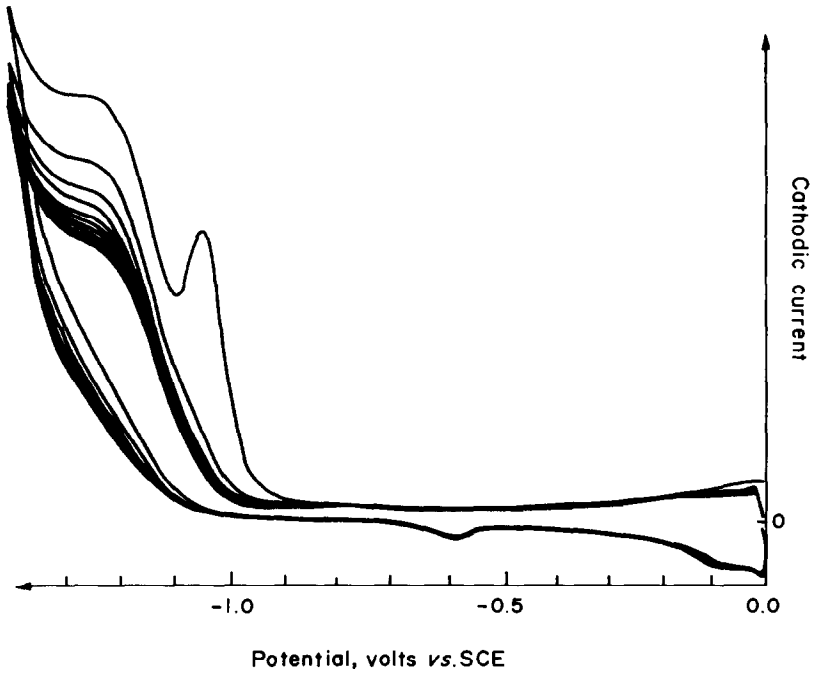


Fig. 6. Cyclic voltammograms of $1 \times 10^{-3}M$ Benperidol at pH 1. Successive scans on the same drop. Scan-rate 300 mV/sec.

peak disappears after the first scan and that the reduction is irreversible. All four compounds can be quantitatively determined. The concentration ranges and correlation coefficients are similar to those reported for Haloperidol.

Conclusions

Results obtained in the studies of Haloperidol and its derivatives indicate that the reduction mechanism for these butyrophenones is different in acidic medium from that for other aromatic ketones. The two-electron transfer is simultaneous. No radical formation is apparent. A judicious choice of solvents is needed to minimize adsorption phenomena. Quantitative measurements are possible over the range 10^{-4}–$10^{-6}M$.

Acknowledgements—We express our appreciation to Janssen Pharmaceutica (Beerse, Belgium) who kindly provided pure samples of the butyrophenone compounds. This research was partially supported by the Fonds National de la Recherche Scientifique (F.N.R.S. Belgium) (G.J.P.) and the National Institutes of Health (GM 22311-05) (G.D.C.).

REFERENCES

1. J. Volke, L. Wasilewska and A. Ryvolova-Kejharova, *Pharmazie*, 1971, **26**, 399.
2. A. Mikolajek, A. Krzyzanowska and J. Fidelus, *Z. Anal. Chem.*, 1974, **272**, 39.
3. Janssen Pharmaceutica, personal communication.
4. S. Patay, *The Chemistry of the Carbonyl Group*, Interscience, London, 1966.
5. G. W. C. Milner, *The Principles and Applications of Polarography and other Electroanalytical Processes*, Chapter 22. Longmans, London, 1957.
6. P. Zuman, *Substituent Effects in Organic Polarography*, Plenum Press, New York, 1967.
7. *Idem, Collection Czech. Chem. Commun.*, 1968, **33**, 2548.
8. M. Dejardin, G. J. Patriarche, C. L. Lapiere and P. Zuman, *J. Electroanal. Chem.*, in the press.
9. R. Pointeau and J. Bonastre, *Elements de Polarographie*, Masson, Paris, 1970.
10. G. J. Patriarche, M. Chateau-Gosselin, J. L. Vandenbalck and P. Zuman, in *Electroanalytical Chemistry*, A. J. Bard (ed.), Vol. XI, p. 141. Dekker, New York, 1979.
11. I. M. Kolthoff and J. J. Lingane, *Polarography*, Vol. II, Chapter 39. Interscience, New York, 1952.
12. A. N. Frumkin and A. B. Ershler, *Progress in Electrochemistry of Organic Compounds*, Vol. I, Plenum Press, London, 1971.

Talanta, Vol. 28, pp. 319 to 322, 1981
Printed in Great Britain. All rights reserved

0039-9140/81/050319-04$02.00/0
Copyright © 1981 Pergamon Press Ltd

SHORT COMMUNICATIONS

ROTATING-DISC ELECTRODE DETERMINATION OF NITROGEN DIOXIDE CONCENTRATED IN *N,N*-DIMETHYLFORMAMIDE

NORIKO SHINOZUKA and SHIGEO HAYANO

Institute of Industrial Science, The University of Tokyo, 22-1, Roppongi 7 Chome, Minato-ku, Tokyo 106, Japan

(*Received* 13 *August* 1980. *Revised* 20 *October* 1980. *Accepted* 19 *November* 1980)

Summary—Nitrogen dioxide at ppm levels in air is concentrated in *N,N*-dimethylformamide and determined by voltammetry at a rotating-disc electrode. The oxidation currents for nitrite are measured under the same conditions as the nitrogen dioxide reduction and are used as standards. The results are in good accordance with the values calculated from the absorption measurements.

In an earlier paper[1] we reported studies on the absorption of nitrogen dioxide, at ppm levels in air, by *N,N*-dimethylformamide (DMF) and dimethylsulphoxide (DMSO). The nitrogen dioxide thus concentrated in DMF was determined directly by an electrochemical method which is now described in this paper.

The electrochemical reactions of nitrogen dioxide and nitrite ion in acetonitrile and DMSO have been investigated by Arvia and co-workers.[2,3] They reported that in DMSO nitrite is oxidized to dinitrogen tetroxide which then reacts with the solvent. They also showed that in acetonitrile oxidation of nitrite yields dinitrogen trioxide and nitrate. Bontempelli and co-workers[4] have studied the anodic behaviour of nitrite in acetonitrile and conclude that nitrite undergoes three consecutive oxidation steps with the formation of NO and NO_3^-, of N_2O_4 and of NO_2^+, respectively. They have suggested[5] that NO and NO_3^- are formed during reduction of N_2O_4. Recently, Bruno *et al.*[6] observed that NO_2 in DMSO gives a differential pulse polarogram with three peaks in the cathodic potential range while NO gives only two peaks in the same potential range.

The results and interpretations just quoted are not necessarily in agreement, which makes it difficult to establish the true electrochemical reactions of nitrite and nitrogen dioxide.

We have employed a rotating ring-disc electrode system to study the electrochemical reactions of NO_2 in DMF, because it has a relatively high sensitivity, allows both reduction and oxidation reactions to be observed, and provides information about the electrode processes. The oxidation current of NO_2^- at the rotating disc electrode has been used to determine the NO_2 concentration in DMF. The results obtained are better than those reported for our previous study of the absorption of NO_2 in DMF.

EXPERIMENTAL

DMF was distilled after dehydration over activated alumina. Tetraethylammonium perchlorate specially prepared for polarography by Nakarai Chemicals Co. was used as a supporting electrolyte without further purification. Other chemicals used were of guaranteed reagent grade. All gases were obtained from Kokan Chemicals Co. The concentration of NO_2 in mixtures with nitrogen was determined by the chemiluminescent method.

A rotating ring–disc electrode system (Nikko Keisoku Co.) with a glassy carbon disc and a platinum ring-disc electrode was used. The counter-electrode was a platinum wire. An Ag–AgCl electrode was used as reference. The electrode system is shown in Fig. 1.

The procedure for absorption of NO_2 in DMF was the same as previously described.[1] The solutions to be measured electrochemically were deaerated by passage of

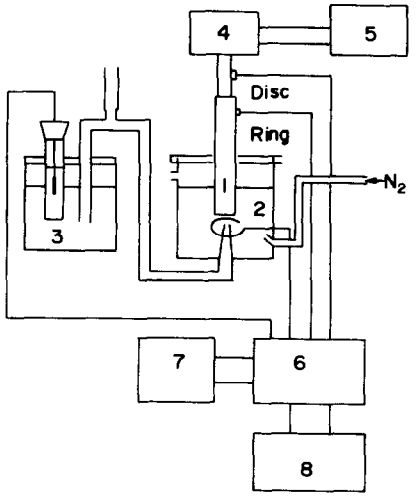


Fig. 1. Electrode system. (1) Ring–disc electrode; (2) Pt counter-electrode; (3) Ag–AgCl reference electrode; (4) motor; (5) speed-controller; (6) dual potentiostat; (7) potential-sweep generator; (8) X–Y recorder.

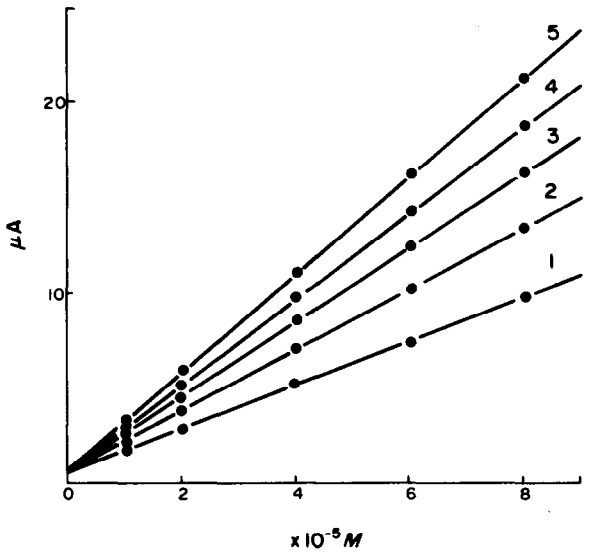


Fig. 2. Dependence of the limiting current on the nitrite ion concentration. Rotation speed: (1) 500, (2) 1000, (3) 1500, (4) 2000, (5) 2500 rpm. Glassy carbon disc electrode: radius = 0.25 cm.

nitrogen through them. During the measurement nitrogen was passed over the solution. The electrode surface was polished with alumina just before each measurement. A PAR Model-170 Electrochemical System (Princeton Applied Research) was employed for polarography. All determinations and absorption experiments were done at 25°.

RESULTS AND DISCUSSION

Electrochemical behaviour of nitrite and nitrogen dioxide in DMF

The voltammograms of sodium nitrite dissolved in DMF show an oxidation wave at $E_{1/2} = 0.58$ V (*vs.* Ag–AgCl) in the potential range between -1.0 and $+1.2$ V. A reduction wave is observed at about $E_{1/2} = -0.70$ V when a solution of NO_2 absorbed in DMF is electrolysed in the same potential range.

The oxidation currents of nitrite at the rotating glassy-carbon disc-electrode depend linearly on the square root of the rotation speed and on the concentration (Fig. 2), though the straight lines do not pass through the origin; large residual currents seem to be responsible for this. The reduction currents for NO_2 absorbed in DMF also show a linear dependence on the square root of the rotation speed and on the NO_2 bubbling time. A ring–disc voltammogram for nitrite is shown in Fig. 3. The disc and ring currents are measured against the disc potential, which is raised from 0 to 1.2 V to bring about oxidation, while the ring potential is maintained at -1.0 V, the potential at which NO_2 is completely reduced. The ring currents (reduction) increase in proportion to the oxidation currents for the nitrite at the disc electrode. A ring–disc voltammogram for NO_2 is shown in Fig. 4. The concentration of the NO_2 was calculated on the basis of 90% absorption efficiency. In the figure the disc potential is scanned in the negative direction, while the ring potential is held at $+1.0$ V. The oxidation currents increase in proportion to the reduction currents of NO_2. When the ring potential is changed from 0.4 to 1.0 V at 0.1 V intervals and the disc potential is changed each time from 0 to -1.0 V, the ring current increases with the ring potential; this corresponds to oxidation of the nitrite.

A diffusion-controlled current is obtained when the d.c. polarogram is recorded for reduction of NO_2 dissolved in DMF. The diffusion coefficients calculated

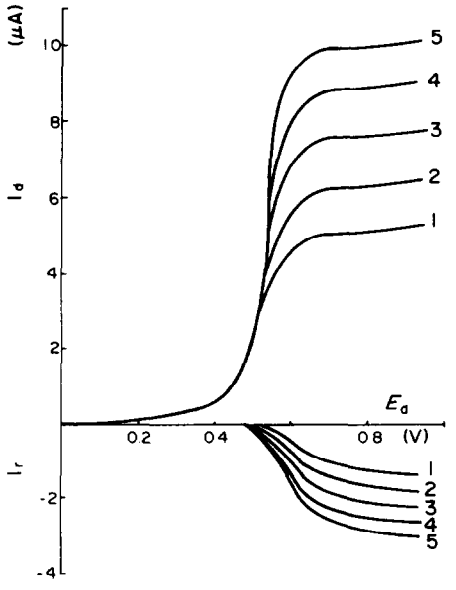


Fig. 3. Ring–disc voltammogram for nitrite on glassy-carbon disc-electrode and platinum ring-electrode NO_2^- $2 \times 10^{-4}M$; ring potential -1.0 V; rotation speed: (1) 500, (2) 1000, (3) 1500, (4) 2000, (5) 2500 rpm.

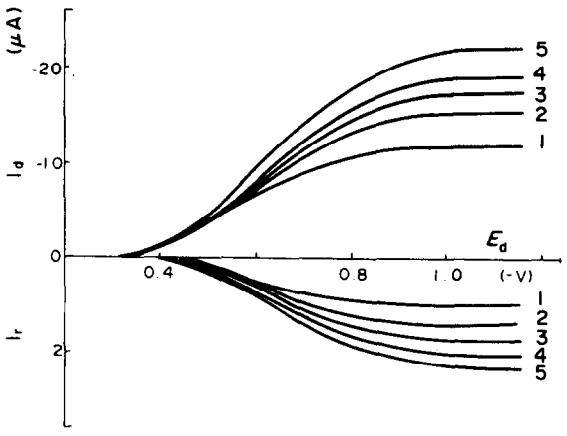


Fig. 4. Ring–disc voltammogram of NO_2 at platinum electrodes. Rotation speed: (1) 500, (2) 1000, (3) 1500, (4) 2000, (5) 2500 rpm. Ring potential +1.0 V, NO_2 $5.1 \times 10^{-5} M$.

from the Ilkovič equation, assuming the number of electrons transferred (n) to be unity, are $2–3 \times 10^{-5}$ cm^2/sec. Based on the same assumption the diffusion coefficients calculated from the Levich equation[7] are around 3×10^{-5} cm^2/sec. If $n = 0.5$ or 2, the diffusion coefficient will be about three times or one third of the value for $n = 1$, respectively.

These results indicate that nitrite is oxidized to nitrogen dioxide at about +0.6 V and that nitrogen dioxide is then reduced to nitrite at about −0.7 V. As no oxidation currents are observed when a solution of NO_2 absorbed in DMF is electrolysed first in the anodic region (0–1.0 V), it would seem that the absorbed NO_2 does not change to NO_2^- in the solution.

The question of why the collection efficiencies (the ratio of ring current to disc current) are smaller than those calculated for the geometry of the electrode, is now under investigation in relation to a more detailed study of the electrode process.

Use of nitrite calibration in determination of NO_2 absorbed in DMF

According to the Levich equation, the rotating-disc current is proportional to $D^{2/3}$, D being the diffusion coefficient of an electroactive species. If the diffusion coefficients of NO_2 and NO_2^- are assumed to be the same, which may be accepted in some cases, the concentration of NO_2 can be calculated from a calibration curve for NO_2^-.

NO_2 solutions prepared by bubbling a nitrogen and NO_2 mixture into DMF are measured in terms of reduction currents and concentrations are determined by means of the calibration curves shown in Fig. 2. The values thus obtained are compared in Table 1 with those calculated from the flow-rate and the bubbling time, and good agreement is found. Good reproducibility is also obtained. The absorption efficiencies, which are the ratios of the observed concentrations to those calculated for complete absorption, are higher by 2–3% than those measured by the Saltzmann method.[1] The difference may be attributed to the difference in diffusion coefficients of NO_2 and NO_2^- in the electrochemical method.

In the measurement of the NO_2 reduction current, care must be taken to obtain reproducible results. The electrode should be placed deep enough in the sample solution to avoid the influence of the nitrogen flowing over the solution surface. Oxygen interferes in the reduction of nitrogen dioxide so much that it must be eliminated as completely as possible. Glassy carbon electrodes show better reproducibility than platinum electrodes.

Influence of sulphur dioxide

Sulphur dioxide presents the most serious interference in this determination of nitrogen dioxide. In one experiment, an SO_2–nitrogen mixture (17.6 ppm SO_2) was bubbled into DMF in the same way as for NO_2 absorption: the SO_2 absorption efficiency in DMF was not determined accurately, but seems to be about

Table 1. Determination of NO_2 absorbed in DMF

Bubbling time, *min*	Concentration calculated, *M*	Concentration determined, *M*	Absorption efficiency, %
30	5.6×10^{-5}	5.3×10^{-5}	95
		5.2×10^{-5}	93
		5.3×10^{-5}	94
45	8.4×10^{-5}	8.1×10^{-5}	96
		8.1×10^{-5}	96
		8.0×10^{-5}	95
60	11.2×10^{-5}	10.4×10^{-5}	93
		10.4×10^{-5}	92
		10.7×10^{-5}	95

NO_2: 9.16 ppm in nitrogen.

35% for a bubbling rate of 300 ml/min and 50 ml of DMF. Garber and Wilson[8] have studied the determination of SO_2 in DMSO and obtained 100% absorption efficiency for ambient air levels of SO_2. DMF seems to be a much poorer solvent than DMSO for SO_2.

The $E_{1/2}$ for the reduction of SO_2 is -0.74 V; separation of the NO_2 reduction current from that for SO_2 in the rotating disc voltammogram is difficult when both gases are absorbed together.

Conclusion

Nitrogen dioxide concentrated from air by bubbling through DMF can be determined at a rotating-disc electrode with a calibration curve based on a nitrite oxidation-current calibration curve; SO_2 interferes and must be eliminated.

Acknowledgement—We wish to thank Y. Nakazato and Y. Yaoita for their experimental work.

REFERENCES

1. N. Shinozuka, M. Karayama and S. Hayano, *Talanta*, 1979, **26**, 55.
2. J. A. Wargon and A. J. Arvia, *Electrochim. Acta*, 1972, **17**, 649.
3. C. E. Castellano, A. J. Calandra and A. J. Arvia, *ibid.*, 1974, **19**, 701.
4. G. Bontempelli, G-A. Mazzocchin, F. Magno and R. Seeber, *J. Electroanal. Chem.*, 1974, **55**, 101.
5. G. Bontempelli, G-A. Mazzocchin and F. Magno, *ibid.*, 1974, **55**, 91.
6. P. Bruno, M. Caselli, M. De Monica and A. Di Fano, *Talanta*, 1979, **26**, 1011.
7. V. G. Levich, *Physicochemical Hydrodynamics*, p. 60. Prentice-Hall, Englewood Cliffs, N.J., 1962.
8. R. W. Garber and C. E. Wilson, *Anal. Chem.*, 1972, **44**, 1357.

Talanta, Vol. 28, pp. 323 to 326, 1981
Printed in Great Britain. All rights reserved

0039-9140/81/050323-04$02.00/0
Copyright © 1981 Pergamon Press Ltd

THE REACTIONS OF PENTACYANOFERRATE(II) IONS

SPECTROPHOTOMETRIC STUDY, DETECTION AND DETERMINATION OF *N*-HETEROCYCLIC ALDOXIMES

NICOLETTA BURGER and VINKA KARAS-GAŠPAREC
Department of Chemistry and Biochemistry, Faculty of Medicine, University of Zagreb, 41000 Zagreb, Šalata 3, Yugoslavia

(*Received* 26 *May* 1980. *Revised October* 1980. *Accepted* 10 *November* 1980)

Summary—The interactions of pyridine-4-aldoxime and pyridinium-4-aldoxime chloride with ammine- and nitrosyl-pentacyanoferrate(II) have been studied. The compounds react to form coloured water-soluble oximatopentacyanoferrate(II) complexes, which have been investigated spectrophotometrically. The reactions have been made the basis of spot-tests for these oximes and for their spectrophotometric determination.

As an extension of earlier observations on the colour reaction between nitrosobenzene and potassium ferrocyanide after ultraviolet irradiation or catalytic decomposition [one of the decomposition products is the aquopentacyanoferrate(II)][1] it was found several years ago in this laboratory that aquo, ammine or nitrosyl substituted pentacyanoferrate(II) can react with various aliphatic and heterocyclic oximes to produce coloured water-soluble compounds.[2–4] The reactions probably take place through a common intermediate, the aquopentacyanoferrate(II) ion, which forms in aqueous solutions of the ammine-[5–7] and alkaline solutions of the nitrosyl-pentacyanoferrate(II).[8] Dissociation of the water molecule yields 5-co-ordinate pentacyanoferrate(II)[9,10] which reacts with the oxime as the new entering ligand. Since the nature of the reaction product depends very much on the chemical nature of the oxime and the reaction conditions, most of the investigations have concerned the structure and mechanism of formation of the substituted pentacyanoferrates. However, because many oximes, especially pyridiniumaldoximes, are antidotes for organophosphorus compounds,[11,12] knowledge of these reactions may also have some practical importance.

In the present work the reactions of amminepentacyanoferrate(II) and nitrosylpentacyanoferrate(II) (abbreviated here as AmP and NP) with pyridine-4-aldoxime (Py4A) and its hydrochloride (P4A) were studied, and applied for the detection and determination of small quantities of the oximes. The reactions with *N*-methylpyridinium-4-aldoxime iodide (PAM-4) have been reported previously,[2–4] but the spot-test with AmP is mentioned here, along with some comparative information.

EXPERIMENTAL

Reagents

All reagents used were of analytical-reagent grade. Redistilled water was used throughout. Britton–Robinson buffers[13] of pH 6.98 and 7.90 were prepared by mixing 100 ml of phosphoric, boric and acetic acid mixture (all 0.04*M*) with 52.5 and 60.0 ml of 0.20*M* sodium hydroxide respectively.

Solutions of $Na_3[Fe(CN)_5NH_3]\cdot 3H_2O$ were prepared by dissolving the "Touzart-Matignon" reagent in water 10–15 min before use. The $Na_2[Fe(CN)_5NO]\cdot 2H_2O$ was a "Kemika" reagent. Its aqueous solution remains stable for several days if kept in the dark.

The oximes were "Fluka" reagents. Their aqueous solutions remain stable for days.

Constant ionic strengths of 0.05 and 0.1 were obtained by addition of sodium chloride solutions of appropriate concentrations.

Procedures

A. To 2 ml of Britton–Robinson buffer of pH 6.98 add 1 ml of oxime solution (containing 10–70 μg of Py4A or 10–100 μg of P4A) and 2 ml of $10^{-3}M$ AmP solution. Mix well, and measure the absorbance at 435 nm (Py4A) or 440 nm (P4A) against a reagent blank after about 1 hr.

B. To 2 ml of 0.06*M* sodium hydroxide add 2 ml of $10^{-3}M$ NP, mix well and after 10 min add 1 ml of a solution containing the above-mentioned quantities of the oximes. Mix, and measure the absorbance at 420 nm against a reagent blank after about 1 hr.

Find the amount of the oxime by reference to a calibration curve or a calibration equation.

Spot-tests

A. To 1 drop (0.05 ml) of Britton–Robinson buffer of pH 6.98 (or pH 7.90 in the case of PAM-4) add 1 drop of the test solution and 1 drop of $10^{-3}M$ AmP. Compare the colour with that of a reagent blank.

B. To 1 drop of $10^{-3}M$ NP add 1 drop of 0.06*M* sodium hydroxide, mix and let stand for 10 min. Add 1 drop of the test solution and compare the colour with that of a reagent blank.

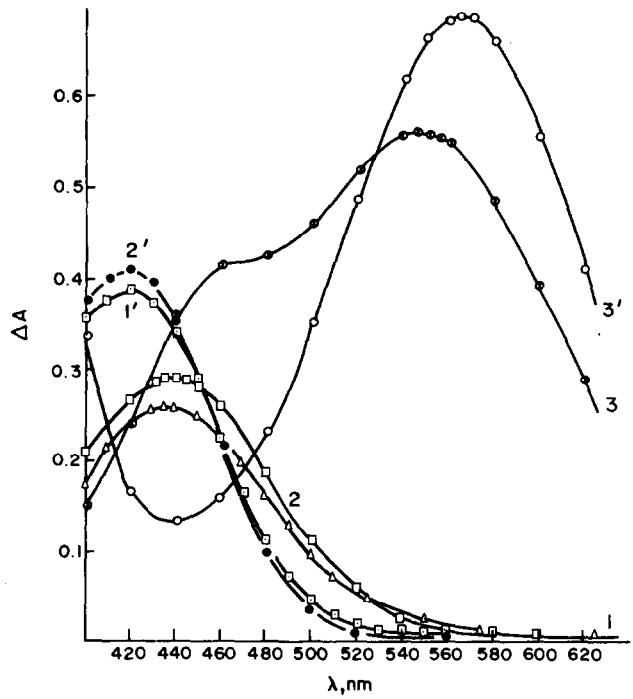


Fig. 1. Absorption spectra of the complexes at 22 C. 1—[Py4A] = [AmP] = $8 \times 10^{-5}M$; 2—[P4A] = [AmP] = $8 \times 10^{-5}M$; 3—[PAM-4] = [AmP] = $5 \times 10^{-4}M$; 1'—[Py4A] = [NP] = $1 \times 10^{-4}M$; 2'—[P4A] = [NP] = $1 \times 10^{-4}M$; 3'—[PAM-4] = [NP] = $1 \times 10^{-3}M$.

Isolation and characterization of the reaction product of Py4A and AmP

A solution of 0.0611 g of Py4A in 1.5 ml of ethanol was mixed with a solution of 0.0326 g of AmP in 2 ml of water, and the dark orange mixture was evaporated to dryness *in vacuo*. The solid was transferred onto Schleicher & Schüll white-band filter paper and was washed with about 30 ml of ethanol until the washings no longer contained oxime (as shown by evaporation). The rust-brown powder was dried and washed again with 15 ml of ethanol. The yellow-orange product was dried in the dark, first in air, then in a desiccator over anhydrous calcium chloride or sodium hydroxide and finally in a vacuum desiccator over phosphorus pentoxide.

Qualitative analysis showed that the compound contains sodium. Iron was determined complexometrically as Fe^{3+} after the destruction of the compound with *aqua regia* and C, H, N were found by elemental analysis: found: C 27.7%; H 3.3%; N 20.8%; Fe 11.4%: this corresponds to a hexahydrate, $C_{11}H_{18}N_7O_7FeNa_3$, which requires C 27.24%; H 3.74%; N 20.22%; Fe 11.52%. The yellow aqueous solution of the isolated complex turns pale on addition of

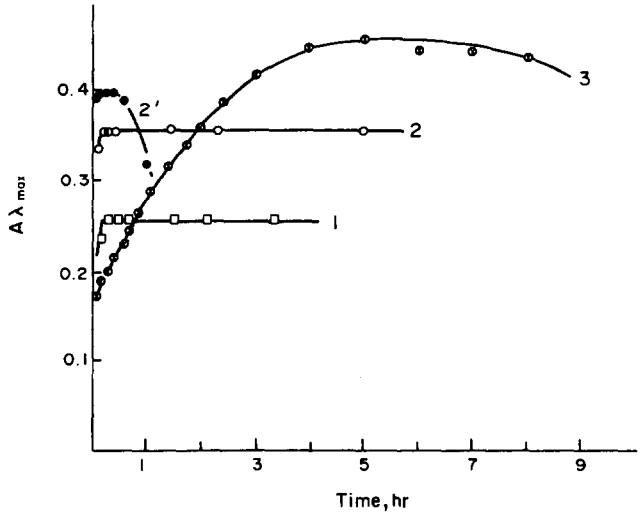


Fig. 2. Variation of the absorbance as a function of time, at 22°C. 1—[Py4A] = [AmP] = $8 \times 10^{-5}M$; 2—[P4A] = [AmP] = $1 \times 10^{-4}M$; absorbances measured against reagent blanks. 2'—[P4A] = [AmP] = $1 \times 10^{-4}M$; 3—[PAM-4] = [AmP] = $1 \times 10^{-4}M$; absorbances measured against water.

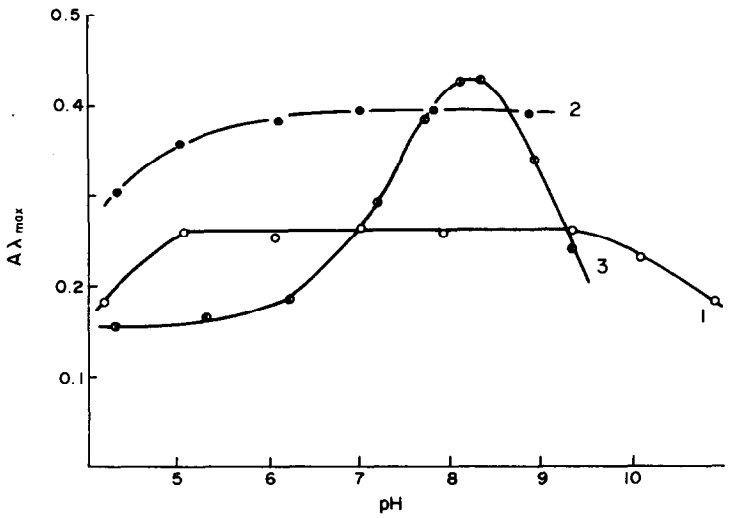


Fig. 3. Effect of pH on the AmPF complex formation at 22°C. 1—[Py4A] = [AmP] = $8 \times 10^{-5} M$; Absorbances measured against appropriate blanks. 2—[P4A] = [AmP] = $1 \times 10^{-4} M$; 3—[PAM-4] = [AmP] = $4 \times 10^{-4} M$.

hydrogen peroxide, but does not change on addition of ascorbic acid, which indicates that the iron is present in oxidation state (II).

RESULTS AND DISCUSSION

Reactions with AmP

The oximes examined react with AmP to form coloured complexes, the absorption spectra of which are shown in Fig. 1.

Py4A and P4A behave very similarly. Their yellow complexes with AmP form quite quickly and are stable enough to permit the measurements required (Fig. 2). From the figure it is obvious that in the case of P4A it is more convenient to measure the absorbance against the reagent blank than against water. (This is because the reagent decomposes faster than the complex and there is spectral overlap between the absorption peaks of the two.)

The reactions are generally independent of the pH of the medium (Fig. 3) but the ionic strength has a slight influence on the complex formation. The spectra do not vary with pH except for a hypsochromic shift of λ_{max} by a few nm at pH $\geqslant$ 12. PAM-4 reacts more slowly (Fig. 2) and the pH has a very significant effect (Fig. 3).

The composition of the complexes was determined by the method of continuous variations[14,15] and by the slope-ratio method,[16] and found to be 1:1 for Py4A and P4A. The instability constants were calculated from the Job plots and by the methods of Harvey and Manning[17] and of Buděšínský[18] (Table 1).

The complexes are very photosensitive; on exposure to light the solutions rapidly decompose and turn pale.

Reactions with NP

The complexes form only in very alkaline medium (pH > 11), Fig. 4. The Py4A and P4A complexes both have maximum absorption at 420 nm (Fig. 1), and that of PAM-4 is at 565 nm. PAM-4 again reacts much more slowly. The compositions and instability constants of the first two complexes are similar to

Table 1. Spectral characteristics, optimum conditions of formation, composition, and instability constants of the AmP (I = 0.05) and NP (I = 0.1) complexes (22°C)

Complex	λ_{max}, *nm*	pH	Reaction time, *min*	Composition	Instability constants, pK			ϵ, $l.mole^{-1}.cm^{-1}$
					Job plot[14,15]	Harvey and Manning[17]	Buděšínský[18]	
Py4A–AmP	435	5–9*	15	1:1	5.28 ± 0.15	5.28 ± 0.12	5.40	4.40×10^3
Py4A–NP	420	~12	60		5.24 ± 0.11	5.30	5.13	4.54×10^3
P4A–AmP	440	5–9*	15	1:1	5.41 ± 0.06	5.43 ± 0.17	5.47	4.58×10^3
P4A–NP	420	~12	60		5.28	5.34	5.36	5.28×10^3
PAM-4–AmP	540–555	8	360					
PAM-4–NP	565	~12	360					

* Optimum pH = 7.

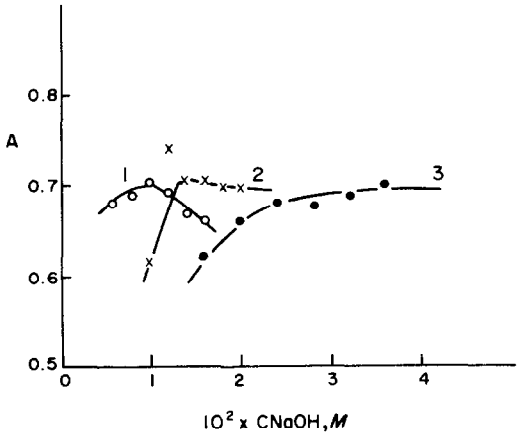


Fig. 4. Dependence of the reaction with NP on NaOH concentration. 1—[Py4A] = [NP] = $2 \times 10^{-4}M$; 2—[P4A] = [NP] = $2 \times 10^{-4}M$; 3—[PAM-4] = [NP] = $1 \times 10^{-3}M$; absorbances measured against water; $I = 0.1$; temperature 22°C.

those for the AmP complexes and are shown in Table 1.

Applications

The reactions were applied to determination and detection of small quantities of Py4A and P4A. It is necessary to use at least a 4–5-fold excess of NP and AmP but too large an excess (over 10-fold) must be avoided. Beer's law is obeyed over the ranges (μg in 5 ml of reaction mixture) 6–70 (Py4A–AmP); 7–100 (P4A–AmP); 6–60 (Py4A–NP); 7–100 (P4A–NP).

The spot-tests give a yellow colour with the oximes and permit the detection of about 0.4 μg of Py4A and P4A, and 5 μg of PAM-4. Any species forming precipitates or complexes with pentacyanoferrate(II) under the conditions used will interfere. Thus Cu^{2+}, Hg^{2+}, Au^{3+}, some pyridine derivatives,[19,20] and alkyl and aryl hydrazines and hydroxylamines[21] will interfere.

REFERENCES

1. S. Ašperger, *Trans. Faraday Soc.*, 1952, **48**, 617.
2. V. Karas-Gašparec and K. Weber, *Z. Phys. Chem. (Leipzig)*, 1968, **237**, 235.
3. V. Hankonyi, V. Ondrušek, V. Karas-Gašparec and Z. Binenfeld, *ibid.*, 1972, **251**, 280.
4. V. Hankonyi, N. Burger and V. Karas-Gašparec, *ibid.*, 1975, **256**, 87.
5. A. D. James, R. S. Murray and W. C. E. Higginson, *J. Chem. Soc. Dalton Trans.*, 1974, 1273.
6. H. E. Toma and J. Malin, *Inorg. Chem.*, 1973, **12**, 2084.
7. Z. Bradić, M. Pribanić and S. Ašperger, *J. Chem. Soc. Dalton*, 1975, 353.
8. J. H. Swinehart and P. A. Rock, *Inorg. Chem.*, 1966, **5**, 573.
9. H. E. Toma and J. M. Malin, *ibid.*, 1974, **13**, 1772.
10. *Idem, ibid.*, 1973, **12**, 1039.
11. N. Engelhard and W. D. Erdmann, *Arzneim. Forsch.*, 1964, **14**, 870.
12. W. A. Groff and R. I. Ellin, *Clin. Chem.*, 1969, **15**, 72.
13. H. M. Rauen, *Biochemisches Taschenbuch*, pp. 651, 654. Springer, Berlin, 1965.
14. P. Job, *Ann. Chim. (Paris)*, 1928, **9**, 113.
15. W. C. Vosburgh and G. R. Cooper, *J. Am. Chem. Soc.*, 1941, **63**, 437.
16. J. H. Yoe and A. L. Jones, *Ind. Eng. Chem., Anal. Ed.*, 1944, **16**, 111.
17. A. E. Harvey and D. L. Manning, *J. Am. Chem. Soc.*, 1950, **72**, 4488.
18. B. W. Budějínský, *Z. Anal. Chem.*, 1972, **258**, 186.
19. V. Hankonyi, V. Ondrušek and V. Karas-Gašparec, *Acta Pharm. Jugosl.*, 1972, **22**, 7.
20. T. A. Larue, *Anal. Chim. Acta*, 1968, **40**, 473.
21. F. Feigl, *Spot Tests in Organic Analysis*, 7th Ed., Elsevier, Amsterdam, 1966.

Talanta, Vol. 28, pp. 327 to 328, 1981
Printed in Great Britain

0039-9140/81/050327-02$02.00/0
Pergamon Press Ltd

SELECTIVE COMPLEXOMETRIC DETERMINATION OF PALLADIUM, WITH THIOUREA AS MASKING AGENT

K. N. RAOOT and SARALA RAOOT
Defence Metallurgical Research Laboratory, Kanchanbagh, Hyderabad-500258, India

(*Received* 24 *September* 1980. *Accepted* 10 *November* 1980)

Summary—A method is proposed for selective complexometric determination of palladium, thiourea being used as masking agent. An excess of EDTA is added and the surplus EDTA is back-titrated at pH 5–5.5 with lead nitrate, with Xylenol Orange as indicator. Thiourea is then added to decompose the palladium–EDTA complex and the liberated EDTA is again back-titrated with lead nitrate. The interference of various cations has been studied.

Complexometric methods[1–6] for palladium, involving both direct titration and back-titrations, generally deal with its determination in pure solution or in the presence of platinum-group metals which do not react with EDTA. With increasing use of alloys of palladium with copper and nickel as electrical contacts and of those with rare earths as magnetic materials, it was felt desirable to evolve simple complexometric procedures for the determination of palladium in presence of metal ions forming strong chelates with EDTA. This could only be achieved by finding selective masking agents for palladium. Finding suitable reagents for this purpose had been one of our interests for the past few years and we have suggested dimethylglyoxime,[7] 1,2,3-benzotriazole[8] and 1,10-phenanthroline[9] in our earlier papers.

Here we describe the use of thiourea for selective decomposition of the palladium–EDTA complex at pH 5–5.5 at room temperature. The liberated EDTA is then titrated against standard lead nitrate solution, with Xylenol Orange as indicator. A large number of metal ions, including copper, do not interfere.

EXPERIMENTAL

Reagents

Palladium chloride solution. Prepared by dissolving 1.0 g of the salt (Johnson–Matthey) in the minimum amount of hydrochloric acid, making up to 1 litre and standardizing.

EDTA solution, 0.01*M*.

Lead nitrate solution, 0.01*M*.

Xylenol Orange indicator. A 0.1% aqueous solution.

Thiourea. A 1% aqueous solution.

Solutions of various metal ions (concentration 1 mg/ml) were prepared from the analytical grade salts. All other chemicals were of analytical-reagent grade.

Determination of palladium in presence of other cations

To a solution containing 4–40 mg of palladium and varying amounts of foreign metal ions, add excess of 0.01*M* EDTA and dilute to 100 ml with distilled water. Adjust to pH 4–5 by dropwise addition of dilute sodium hydroxide solution and finally to 5–5.5 with sodium acetate–acetic acid buffer. Add a few drops of Xylenol Orange indicator and back-titrate the excess of EDTA with 0.01*M* lead nitrate to the sharp colour change from yellow to red. Add 2–20 ml of 1% thiourea solution (4 mg of reagent for each mg of palladium), shake, and titrate the liberated EDTA with 0.01*M* lead nitrate to the same end-point as in the first titration.

Table 1. Determination of palladium in presence of foreign metal ions

Ion, *mg*		Palladium, *mg* Taken	Found
Cu^{2+}	6.00	11.50	11.48
	12.00	11.50	11.54
	28.00	4.03	4.05
Zn^{2+}	20.00	17.25	17.29
	10.00	5.75	5.79
Ni^{2+}	20.00	5.75	5.75
	10.00	17.25	17.18
Pb^{2+}	25.00	5.75	5.72
	12.50	11.50	11.48
Cd^{2+}	15.00	11.50	11.48
	5.00	40.25	40.23
Co^{2+}	20.00	17.25	17.30
	10.00	28.75	28.82
Mn^{2+}	5.00	8.63	8.67
	5.00	17.25	17.35
Bi^{3+}	5.00	17.25	17.29
	15.00	8.63	8.62
Fe^{3+}	20.00	5.75	5.77
	5.00	17.25	17.25
Al^{3+}	25.00	11.50	11.48
	5.00	40.25	40.33
Y^{3+}	18.00	5.75	5.72
	6.00	17.25	17.18
La^{3+}	24.00	11.50	11.44
	6.00	23.00	23.04
Ce^{3+}	25.00	4.03	4.02
	5.00	17.25	17.25
Gd^{3+}	24.00	11.50	11.48
	6.00	34.50	34.40
Sm^{3+}	20.00	8.63	8.62
	4.00	40.25	40.10
Ti^{4+}	10.00	4.03	4.05
	15.00	5.75	5.79
Zr^{4+}	15.00	4.03	3.99
	10.00	8.63	8.62

Table 2. Determination of palladium in synthetic solutions and solid alloy samples

Alloy*	Palladium, *mg* Taken	Found‡
40% Cu–Pd	24.00	23.95
		24.00§
43% Cu–Pd†	22.80	22.88
		22.78§
39% Sm–Pd†	24.40	24.37
		24.40§
64% Sm–Pd†	18.00	18.00
		17.98§
40% Ni–Pd	24.00	23.95
		24.00§
35% Co–Pd	26.00	25.98
		25.98§

* Simulated samples unless otherwise indicated.
† Solid sample.
‡ Mean of 2 estimations.
§ By ascorbic acid gravimetric method.

Application to alloys

Dissolve 0.1–0.2 g of sample in the minimum amount of *aqua regia* and dilute to 100 ml in a standard flask. Transfer a suitable aliquot to a 250-ml conical flask, add excess of 0.01*M* EDTA and dilute to 100 ml with distilled water. Adjust the pH to 5–5.5 and complete the determination as described above.

RESULTS AND DISCUSSION

The decomposition of the palladium–EDTA complex with thiourea is quantitative at pH 5–5.5 even at a temperature as low as 8°. Many cations can be tolerated (Table 1). Since the reagent has been employed earlier for masking of copper[10,11] and mercury,[12] their effects on the present titration were studied. At pH 5–5.5, addition of 1 g of thiourea releases only the equivalent of 0.1 ml of 0.01*M* EDTA from the copper–EDTA complex in 10 min, and only 6 times as much in 30 min. Since the second titration is done immediately after addition of the thiourea, the error from this source should be negligible. However, an error of 1.5–2% was observed in determination of the lowest amount of palladium (4 mg). The interference of copper can be obviated by adding the minimum excess of thiourea and preferably conducting the titration at 8–10°. Mercury, however, interferes seriously and so does tin(IV). Manganese, owing to the low stability of its EDTA complex under the conditions employed, causes difficulty in the end-point detection, particularly when more than 5 mg of it is present.

Table 2 presents the results of the analysis of synthetic solutions and alloy samples. It is seen from this table that the results obtained by the present method are in good agreement with those obtained by the gravimetric method using ascorbic acid.[13]

Of our earlier reagents, dimethylglyoxime and benzotriazole are associated with precipitate formation, which makes the handling of more than 15 mg of palladium difficult. They also require heating of the solution to 60° for complete release of EDTA. Although 1,10-phenanthroline yields a soluble complex in the cold with up to 18 mg of palladium, various cations interfere and hence the reagent has limited application. The present masking agent has overcome almost all the limitations of the earlier reagents, forming a soluble complex with comparatively large quantities of palladium, releasing the EDTA instantaneously at room temperature or even at lower temperatures, and not reacting with a large number of other metal–EDTA complexes under the conditions used.

Acknowledgements—Grateful thanks are due to Dr V. S. Arunachalam, Director, DMLR, for permission to communicate this paper. Thanks are also due to Dr D. P. Lahiri and Dr P. Subramaniam for their keen interest in this work.

REFERENCES

1. W. M. McNevin and O. Kriege, *Anal. Chem.*, 1955, **27**, 535.
2. J. Kinnunen and B. Merikanto, *Chemist-Analyst*, 1955, **44**, 11.
3. V. Suk and M. Malát, *ibid.*, 1956, **45**, 30.
4. J. Kinnunen and B. Merikanto, *ibid.*, 1958, **47**, 11.
5. . Khalifa and M. M. Khater, *Z. Anal. Chem.* 1962, **191**, 339.
6. I. M. Yurist and Z. V. Tynkova, *Zavodsk. Lab.*, 1962, **28**, 798.
7. K. N. Raoot and S. Raoot, *Indian J. Chem.* 1974, **12A**, 1007.
. K. N. Raoot, S. Raoot and V. G. Vaidya, *ibid.*, 1979, **18A**, 90.
9. S. Raoot and K. N. Raoot, *Indian J. Tech.*, in the press.
10. R. Přibil and V. Veselý, *Talanta*, 1961, **8**, 743.
11. O. B. Budevsky and L. Simova, *ibid.*, 1962, **9**, 769.
12. R. P. Singh, *ibid.*, 1969, **16**, 1447.
13. R. Ripan and G. Pop, *Rev. Rom. Chim.* 1967, **12**, 13.

Talanta, Vol. 28, pp. 329 to 331, 1981
Printed in Great Britain. All rights reserved

0039-9140/81/050329-03$02.00/0
Copyright © 1981 Pergamon Press Ltd

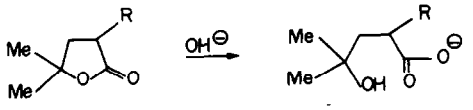
STUDY OF HYDROLYSIS OF AMIDO-SUBSTITUTED γ-BUTYROLACTONES BY pH-STAT TITRATION AND ULTRAVIOLET SPECTROSCOPIC ANALYSES

DAVID M. RACKHAM*, JIBAN K. CHAKRABARTI and GEOFFREY L. O. DAVIES
Lilly Research Centre Limited, Erl Wood Manor, Windlesham, Surrey, England

(*Received* 10 *October* 1980. *Accepted* 20 *November* 1980)

Summary—pH-Stat titration and ultraviolet absorption spectroscopy have been used to study the rates of ring-opening in a series of γ-butyrolactones and their analogues. The half-lives for the lactones can be related to Hammett inductive and steric parameters.

The hydrolysis of γ-lactones and other esters occurs readily under basic (or strongly acidic) conditions and that of simple derivatives has been extensively studied by kinetic procedures.[1]



Two common methods of determining the rate of hydrolysis include spectrophotometry[2] and titration of the liberated hydroxy-acid to constant pH (pH-stat titration[3]). We have used a combination of these to investigate the rate constant for the opening of the lactone ring in a series of α-amino and α-amido substituted γ-butyrolactones[4] and to determine the rate of ring-opening in two lactam derivatives. The γ-butyrolactones have been evaluated in terms of strychnine antagonism to determine whether they can mimic the effects of the benzodiazepine group of drugs in this respect.[4] The neurotransmitters γ-aminobutyric acid and glycine have been implicated in explanations of certain pharmacological responses of the benzodiazepines. For this reason it was of interest to study the rate of ring opening of the lactones (to give α-amino-γ-hydroxybutyric acids) to see whether stability was related to biological activity. However, no correlation was found, as will be reported elsewhere.[4] The present paper presents the analytical aspects of the work.

EXPERIMENTAL

Ultraviolet absorption spectra were recorded on a Pye Unicam SP 800 spectrophotometer, the samples being dissolved in 0.1*M* Teorell and Stenhagen buffer.

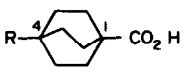
The titrations were done in 25% w/w methanol in water medium in a temperature-controlled cell fitted with a glass/calomel electrode system and a nitrogen bubbler, together with a calibrated syringe for addition of 0.1*M* sodium hydroxide. The butyrolactone under study was introduced into the solvent mixture (at pH 10.0). As the pH of the solution fell with generation of the hydroxy-acid, a relay caused the syringe and an associated transducer to add more titrant to restore the initial pH. The signal from the transducer was fed to a chart-recorder, thus giving a continuous plot of titrant consumed, as a function of time. A diagram of this apparatus has been given elsewhere.[5]

All measurements were carried out at 37° and at a constant ionic strength of 0.1*M* maintained with potassium chloride.

RESULTS AND DISCUSSION

Using the pH-stat apparatus described above, we have measured the pseudo-first-order rate-constants for the lactone ring-opening in 13 substituted γ-butyrolactones at pH 10.0 and 37°. Table 1 gives the half-lives for this hydrolytic reaction together with the inductive and steric substituent constants available in the literature.

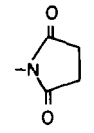
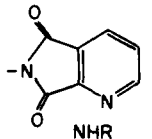
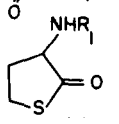
Several workers have divided the Hammett-type substituent constants[9] into inductive (σ_I[6,7] or F[8]) and resonance (σ_R or R) contributions. Positive values of σ_I or F denote electron withdrawal from a reaction site by an inductive mechanism. Table 1 shows that such substituents (compounds 3–10, 12, 13) are associated with a decrease in the half-life of the lactone with increasing ease of nucleophilic attack at the ring carbonyl group. A decrease in $t_{1/2}$ is also seen when an electron-withdrawing chlorine atom is substituted in the benzamide ring (*cf.* compounds 6 and 5) but the effect is much attenuated by distance (five bonds). Several workers have shown that inductive effects are clearly transmitted through this number of bonds. Indeed the σ_I scale was established by using the single-bond framework of 4-substituted bicyclo-[2.2.2]octane-1-carboxylic acids.



Thus changing R from H to NO_2 causes an increase in acidity by a factor of ten,[10] and the rate of

* To whom correspondence and requests for reprints should be addressed.

Table 1. Half-lives for the hydrolysis of γ-butyrolactones at pH 10.0 and 37°

Compound	Substituent R	Half-life, min	σ_I^{6-8}	F^{*8}	Molar refractivity*[8]
1	NH_2	98.7	0.00	0.0	1.03
2	$NHCH_2Ph$	209	−0.09	−0.08	30.0
3	$NHCOCH_3$	36.4	0.29	0.32	11.2
4	NHCO(1-adamantyl)	65.5			40.6†
5	NHCOPh	47.5	0.20	0.30	30.3
6	NHCOPh(2-Chloro)	45.5			
7	NHCOCH=CHPh	20.0		0.22	40.2‡
8	NHCO(2-pyridyl)	27.3			
9	$NHCONH_2$	14.8	0.27	0.24	9.81
10	NHCONHPh	64.5	0.25		35.3
11	H¶	100			
12		17.8 (87)§			
13		0.2 (36.5)§			
14		356	0.00		1.03
	(R_1 = H)				
15	As for 14 (R_1 = $COCF_3$)	45.8	0.45		11.2

*Values for σ, F and molar refractivity are quoted for the group attached to NH, *i.e.*, H for NH_2, CH_2Ph for $NHCH_2Ph$, *etc.*

†For 1-adamantyl without CO.

‡For group −CH = CHCOPh.

¶Derivative without the *gem*-dimethyl group.

§Half-life for succinimide or maleimide ring-opening.

alkaline hydrolysis of the bicyclo-octane-1-carbethoxy esters increases by a factor of 20 when R changes from H to CN.[11]

In contrast, $t_{1/2}$ is increased by the electron-releasing property (negative σ_I and F) and the steric size of the benzyl group in compound 2 (as measured by the molar refractivity parameter[8]).

This increase is also clearly seen in changing from the small (methyl, compound 3) to the large (1-adamantyl, compound 4) alkylamido derivatives. In addition, although the compounds 9 and 10 have almost identical σ_I parameters, the large difference in their steric sizes (as indicated by the molar refractivity) is reflected in the shorter half-life of the smaller molecule.

Two thia analogues of the butyrolactones were also studied by pH-stat titration. The thialactone compound 14 hydrolysed very much more slowly[12] than the lactone compound 11 and this can be related to the lower electronegativity of the sulphur atom (S = 2.5, O = 3.5 on the Pauling scale). As in the lactone series, the introduction of an electron-withdrawing substituent (compound 15) decreases $t_{1/2}$ for the thialactone.

By use of ultraviolet absorption spectroscopy, it was possible to follow the loss of the chromophore for the succinimide and maleimide rings of compounds 12 and 13 and to calculate the rate of imido ring-opening. The initial breakdown of the lactone ring in compounds 12 and 13 did not significantly affect this chromophore. In both cases, the imide ring opened much more slowly than the lactone. The bracketed values in Table 1 give the half-lives for this process.

These results should be of assistance in future work on these compounds.

REFERENCES

1. A. A. Frost and R. G. Pearson, *Kinetics and Mechanism*, 2nd Ed., p. 327. Wiley, New York, 1961.
2. E. Brochmann-Hansen, P. Schmid and J. D. Benaman, *J. Pharm. Sci.*, 1965, **54**, 783.
3. C. W. Chong, L. W. Dittert, H. B. Kostenbauder and J. V. Swintosky, *ibid.*, 1967, **56**, 1647.
4. J. K. Chakrabarti, C. H. Cashin and S. Sutton, to be published.
5. A. F. Cockerill, G. L. O. Davies and D. M. Rackham, *J. Chem. Soc. Perkin II*, 1974, 723.

6. M. Charton, *J. Org. Chem.*, 1964, **29**, 1222.
7. R. W. Taft, E. Price, I. R. Fox, I. C. Lewis, K. K. Andersen and G. T. Davis, *J. Am. Chem. Soc.*, 1963, **85**, 3146.
8. C. Hansch and A. Leo, *Substituent Constants for Correlation Analysis in Chemistry and Biology*, Wiley, New York, 1979.
9. N. B. Chapman and J. Shorter (eds.), *Advances in Linear Free Energy Relationships*, Plenum Press, London, 1972.
10. D. H. Holtz and L. M. Stock, *J. Am. Chem. Soc.*, 1964, **86**, 5188.
11. J. D. Roberts and W. T. Moreland, *ibid.*, 1953, **75**, 2167.
12. C. M. Stevens and D. S. Tarbell, *J. Org. Chem.*, 1956, **19**, 1996.

Talanta, Vol. 28, pp. 332 to 333, 1981
Printed in Great Britain. All rights reserved

0039-9140/81/050332-02$02.00/0
Copyright © 1981 Pergamon Press Ltd

DETERMINATION OF ASCORBIC ACID WITH FERRICYANIDE

N. RUKMINI, V. S. N. P. KAVITHA and K. DEVENDRA VIJAYA
Department of Chemistry, Andhra University, Waltair 530003, India

(*Received* 27 *May* 1980. *Revised* 11 *September* 1980. *Accepted* 18 *November* 1980)

Summary—Ascorbic acid can be determined by titration with potassium ferricyanide in sulphuric, phosphoric or hydrochloric acid media. Twelve indicators, including ferroin and some triphenylmethane and thiazine dyes, have been found suitable. The method has been successfully applied to assay of commercial products for vitamin C. Several organic substances likely to be associated with ascorbic acid in preparations and plant tissues do not interfere.

Potassium ferricyanide is available in high purity and can easily be recrystallized from water.[1] It has a high equivalent weight and can be used as a primary standard after repeated recrystallization and drying at 100°. Its aqueous solutions are very stable when prepared and preserved properly. It has been used for titration of ascorbic acid in approximately neutral medium,[2–5] and also in 4*M* sulphuric acid with barium diphenylamine sulphonate (BDS) as indicator,[6] but it was observed that though BDS is rapidly oxidized by ferricyanide, the oxidized form is not readily reduced by ascorbic acid. In our experience, however, the end-point is not very satisfactory, so we have examined the use of other indicators. We have already reported that the redox potential of ferricyanide is increased remarkably at high acidity and that ferroin can be used as the indicator.[7] Further work has revealed that some triphenylmethane dyes and thiazine derivatives are also suitable indicators under these conditions and can be used in the titration of ascorbic acid with ferricyanide. Thiazine dyes are normally used as indicators in titrations of strong reductants, the unstable leuco dye being oxidized to the blue or bluish green form at the end-point, but the further oxidation of the blue dye to its pink product is seldom utilized.[8,9] The proposed method has been applied successfully for the assay of vitamin C preparations.

EXPERIMENTAL

Reagents

*Potassium ferricyanide, 0.1*M. Prepared by dissolving an accurately weighed amount of analytical-grade reagent which has been recrystallized from water and dried at 100°.

*Ascorbic acid, 0.05*M. Prepared from analytical-reagent grade material, stabilized with EDTA and formic acid and standardized with iodate.[10]

Indicators. Ferroin (0.025*M*), 0.1% solutions of Erioglaucine (C.I.671), Eriogreen (C.I.735), Setaglaucine (C.I.658) and Xylenecyanol FF (C.I.715) and 0.05% solutions of Methylene Blue (C.I.52015), Toluidine Blue (C.I.52040), New Methylene Blue (C.I. 52030), Methylene Green, Azure A, Azure B and Azure C, prepared in demineralized water.

Analytical-reagent grade chemicals were used whenever possible.

Procedure

Take enough sulphuric acid (10*M*) or concentrated hydrochloric or phosphoric acid to give the desired acidity (Table 1) at the end-point. Dilute with distilled water if necessary and cool. Add the ascorbic acid solution and one drop of ferroin or 0.2 ml of triphenylmethane dye solution or 0.1 ml of thiazine dye solution, and titrate with ferricyanide solution to the sharp colour change at the end-point.

For analysis of commercial preparations (vitamin C tablets, injection solutions and syrups) make a solution of the sample in demineralized water such that the ascorbic acid concentration is 3–5 mg/ml, and filter if the solution is very turbid. Acidify and titrate as above.

RESULTS AND DISCUSSION

From preliminary experiments we found that ferricyanide oxidizes ferroin in 5–10*M* sulphuric acid, 7–10*M* hydrochloric acid or 9–13*M* phosphoric acid and the triphenylmethane dyes in 5–10*M* sulphuric acid or 9–13*M* phosphoric acid. The dyes can also be oxidized in hydrochloric acid media but the colour change is too poor to be useful. However, narrower acidity ranges are necessary for the determination of ascorbic acid (Table 1). If the acidity is too high, premature end-points are obtained because the reduction of the oxidized form of the indicator by ascorbic acid is slow. If the acidity is too low, neither the indicator nor the ascorbic acid is oxidized. In hydrochloric acid medium only ferroin functions satisfactorily as the indicator.

All the indicators give sharp colour changes. With 0.1*N* solutions an inert atmosphere is not needed, but with more dilute solutions (<0.025*N*) it is necessary

Table 1. Conditions for the determination of ascorbic acid with ferricyanide in various acid media

Indicator	H_2SO_4, *M*	HCl, *M*	H_3PO_4, *M*
Ferroin	5–7.5	7.5–10	9–11
Erioglaucine	6.5–8	—	12–13
Eriogreen	7–8	—	12–13
Setoglaucine	7–8	—	12–13
Xylene Cyanol FF	6.5–8	—	12–13
Thiazine dyes	7–9	—	12–13

for titrations in sulphuric and hydrochloric acid media but not in phosphoric acid media.

Tables 2 and 3 show some results for pure ascorbic acid solutions and some commercial preparations, and comparative results by the BP method.[11]

Interferences

Strong oxidants and reductants interfere. Coloured ions such as copper(II), nickel and cobalt(II) interfere. Cerium(III), arsenic(III), hydroxylamine hydrochloride and hydrazine sulphate do not interfere, but antimony(III), iron and manganese(II) do. Vanadium(IV) gives results that are only 0.5–1% too high in phosphoric acid media, but are very high in the other media. An advantage of the method is that organic compounds such as oxalic, tartaric, citric and malic acids, or glucose, fructose and sucrose, which are likely to be present with ascorbic acid in commercial preparations and plant tissues, do not interfere. The non-interference of oxalic acid is particularly important, as it can be used as a potential extractant[12] for ascorbic acid from fruit juices and multivitamin preparations.

Acknowledgements—One of us (V.S.N.P.K.) thanks the Council of Scientific and Industrial Research (India) for the award of a research fellowship.

REFERENCES

1. I. M. Kolthoff, R. Belcher, V. A. Stenger and G. Matsuyama, *Volumetric Analysis*, Vol. III, pp. 236, 645. Interscience, New York, 1957.
2. K. Hubicka, *Ann. Univ. Mariae Curie-Sklodowska, Lublin–Polonia, Sect. AA*, 1957, **10**, 35.
3. J. A. C. van Pinxteren and E. Verloop, *Pharm. Weekblad*, 1958, **23**, 203, 982.
4. L. Erdey and G. Svehla, *Z. Anal. Chem.*, 1956, **150**, 407.
5. B. R. Sant, *Chemist-Analyst*, 1958, **47**, 65.
6. G. S. Sastry and G. G. Rao, *Talanta*, 1972, **19**, 212.
7. N. Rukmini, V. S. N. P. Kavitha and K. R. Rao, *ibid.*, 1979, **26**, 579.
8. N. Rukmini and V. S. N. P. Kavitha, *Acta Cinecia Indica*, 1979, **5**, 44.
9. U. Muralikrishna, *Ind. J. Chem.*, 1972, **10**, 559.
10. R. Erdey and E. Bodor, *Z. Anal. Chem.*, 1952, **136**, 109: *Magy. Kem. Foly.* 1952, **58**, 295.
11. *British Pharmacepoeia*, p. 36. HMSO, London, 1973.
12. J. D. Ponting, *Ind. Eng. Chem., Anal. Ed.* 1943, **15**, 389.

Table 2. Determination of ascorbic acid with ferricyanide

Indicator	Acid	Range determined, *mg*	Error range, %
Ferroin	H_2SO_4	13.24–88.24	0.1–0.4
	HCl	13.24–88.24	0.2–0.4
	H_3PO_4	13.24–88.24	0.2–0.4
Triphenylmethane dyes	H_2SO_4	13.24–88.24	0.2–0.4
	H_3PO_4	13.24–48.53	0.2–0.4
Thiazine dyes	H_2SO_4	13.24–88.24	0.2–0.4
	H_3PO_4	13.24–48.53	0.2–0.5

Table 3. Assay of commercial vitamin C preparations: amount (*g*) present in 5 tablets or 30 ml of syrup or 5 ampoules of injection solution

Sample	BP method[8]	Ferricyanide method		
		Ferroin	Erioglaucine	Methylene Blue
Tablets				
	2.52	2.52	2.51	2.52
	2.48	2.49	2.48	2.48
Ampoules				
	2.50	2.50	2.50	2.50
	2.52	2.52	2.52	2.52
Syrups				
	3.62	3.62	3.64	3.64
	3.78	3.78	3.75	3.76

Talanta, Vol. 28, pp. 334 to 336, 1981
Printed in Great Britain. All rights reserved

0039-9140/81/050334-03$02.00/0
Copyright © 1981 Pergamon Press Ltd

BASIC INVESTIGATIONS ON BACKGROUND PROBLEMS IN THE PLATINUM-LOOP METHOD IN COMPARISON TO GRAPHITE-FURNACE AND FLAME ATOMIC-ABSORPTION SPECTROPHOTOMETRY

S. GÜCER* and H. BERNDT

Institut für Spektrochemie und angewandte Spektroskopie, Postfach 778, D-4600 Dortund 1, Federal Republic of Germany

(*Received* 19 *September* 1980. *Accepted* 12 *November* 1980)

Summary—The platinum-loop method of flame-AAS/AES gives lower detection limits for volatile elements than conventional working modes of flame-AAS/AES. The background problems of the method are compared with those of the other AAS-techniques (flame- and furnace-AAS). In this initial study, the background spectra of two alkali-metal halides (NaCl, NaI) are investigated. It is found that for NaCl the intensity of the molecular background absorption is about 400 times greater in the furnace method than with the loop technique. In the short wavelength region of the spectrum (<220 nm) Raleigh scattering is negligible in the loop method, compared with furnace-AAS.

In the platinum-loop method of flame-AAS/AES (atomic-absorption spectrometry/atomic-emission spectrometry), the substance to be determined is introduced into the flame by means of a platinum-wire loop. Special equipment had been developed,[1] which for volatile elements gives detection limits that are generally lower by two orders of magnitude than those obtained in the conventional working modes (continuous aspiration).[2]

A number of publications[3–6] have described the various background problems encountered during application of the classical AAS methods (flame and graphite-furnace methods), and have been mentioned in the various monographs on AAS,[7–11] and the platinum-loop method may be expected to pose similar problems. Although this method is a variant of flame-AAS it shows some similarities to the cuvette technique. Both the furnace and loop techniques are pulse methods in which the substance to be determined is vaporized directly in the optical absorption zone. Both techniques allow the choice of a temperature programme for sample pretreatment before the atomization step is started.

The present investigation is an initial study of the background problems encountered in the loop method, and a comparison with those of the flame and furnace methods.

Alkali-metal halides were chosen as the model substances, because they are often the main inorganic components in organic matrices and can cause considerable interference in trace determinations.

The "non-atomic absorption" caused by the alkali-metal halides has two main causes. First, there is light-scattering, primary Raleigh scattering, which occurs in both the furnace and the flame methods; the scattering increases in proportion to the square of the volume of the particle concerned and inversely with respect to the fourth power of the wavelength used. Secondly, the alkali-metal halides absorb part of the hollow-cathode radiation by molecular absorption, which can be described by the Lambert–Beer law.

In AAS-analysis these effects combine to give the background signal, which is qualitatively very similar for both the flame and cuvette techniques. However, their individual contributions at a given total absorbance can differ by several orders of magnitude, depending on the amount of alkali-metal halide.[12]

The Raleigh scattering and molecular absorption can in principle be compensated for with the aid of a deuterium-lamp background-corrector. Most currently available AA-spectrometers fitted with background-correction can give an absorbance compensation of approximately 1. In practical terms, this means that a high alkali-metal salt content will strongly interfere in a direct trace determination and make it impracticable. Although the graphite-furnace technique has high detection power, the background signals are rather high, whereas in flame-AAS there is less background interference, but the method is frequently not sensitive enough. Hence with both methods chemical separation and preconcentration are required for the determination of trace concentrations.

EXPERIMENTAL

The background spectra of sodium chloride and iodide solutions were investigated with the aid of the loop method, the sample solution being initially evaporated to dryness by electrical heating outside the flame, and then introduced into the flame by electromechanical transport.[1] The spectrum was resolved with a McPherson monochromator (focal length 1 m, 2400-grooves/mm grating, entrance slit-width 100 μm, exit slit-width 100 μm) and recorded photoelectrically. The sample volume was 40 μl and the concentration selected so that the amount of substance on the loop was 2000 μg of sodium chloride (34 μmole) or 300 μg of sodium iodide (2 μmole). The background absorption in a Beckman graphite-furnace was

* Present address: EGE-University, Chemical Faculty, Izmir, Turkey.

measured for the same absolute amounts of sodium iodide and for 10 μg of sodium chloride.

RESULTS AND DISCUSSION

Figure 1 shows the background spectra from sodium chloride, measured by the loop and furnace techniques. As expected, both methods showed maximal molecular absorption in the same wavelength region, but there is a significant difference in the wavelength region 200–220 nm. In normal flame-AAS and in furnace-AAS, the background absorption in this region increases, probably because of Raleigh scattering. With the loop technique, however, the background absorption in this region decreases to below the limit of detection. We can explain this difference in behaviour by considering the vaporization processes when the loop method is used. Individual particles are vaporized from the heated wire into the flame and it is assumed that only atomic or molecular particles are emitted from the wire surface, and that these particles are too small to cause an increase of the background by Raleigh scattering, whereas the non-atomic absorption in the short-wave region when the furnace and normal flame techniques are used is mainly caused by light-scattering.

In the case of sodium iodide (Fig. 2), it is more difficult to make a definite statement about light-scattering and molecular absorption as contributing factors to the background, because sodium iodide has a molecular absorption band at wavelength shorter than 200 nm. However, the absorption is very small and because of the vaporization mechanism in the loop technique, it seems probable that only molecular absorption takes place, with very little chance of light-scattering. The higher background in the furnace technique can be attributed to light-scattering from sodium iodide particles in the cooler zones of the furnace (see below). Figure 1 shows that in the region of the absorption maximum about 400 times as much sodium chloride is needed in the loop technique to produce the same background absorption as that given with the graphite-furnace technique. This is because the particles emitted from the wire surface immediately reach the flame temperature and are therefore almost completely dissociated within the measuring zone, whereas in the furnace technique recombination to molecules can occur in the cooler zone after vaporization, so that within the measuring zone there is a higher molecular concentration and hence greater absorption.

In the case of sodium iodide this ratio of absolute amounts needed to give the same absorbance is much smaller (about 15 at ~325 nm). The difference in behaviour may be explained in terms of the dissociation energies (NaCl 3.58 eV; NaI 3.26 eV). The less stable sodium iodide will be more extensively dissociated than sodium chloride at the same furnace temperature. This is substantiated by the fact that the furnace-method background is very much greater for sodium chloride (Fig. 1) than sodium iodide (Fig. 2). It must be remembered, however, that the curves shown are

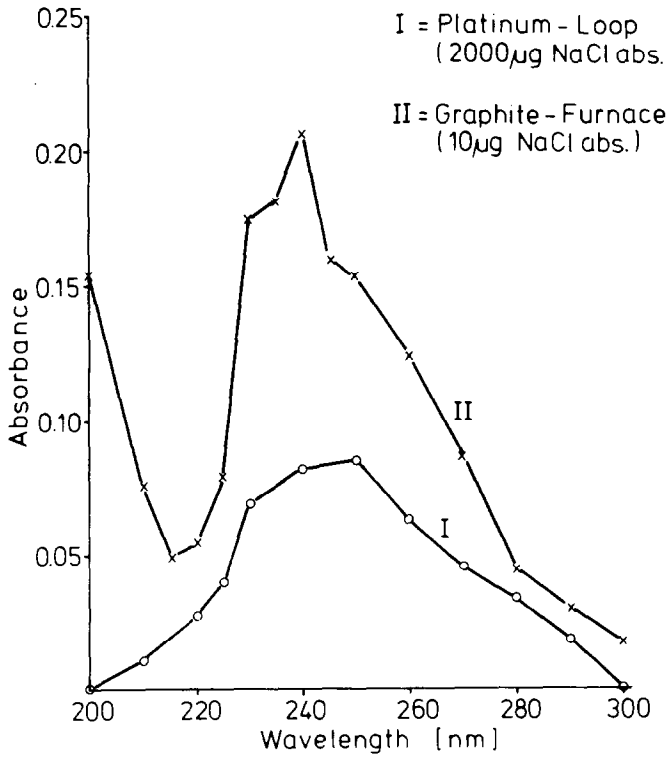


Fig. 1. Background spectra for sodium chloride in platinum-loop (I) and graphite-furnace (II) AAS.

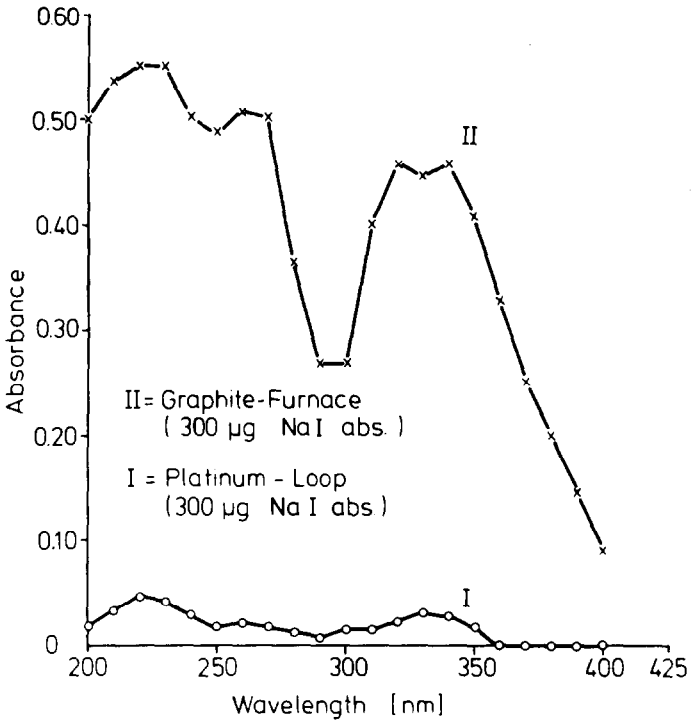


Fig. 2. Background spectra for sodium iodide in platinum-loop (I) and graphite-furnace (II) AAS.

only qualitative indications of the behaviour, and the quantitative results vary according to the furnace used and the temperature programme selected.

On account of this difference in behaviour, the detection limits attainable with the loop method can be lower by a factor of 15–500 than those obtained by conventional flame-AAS. The considerably smaller background in the short-wave region is most probably due to the virtual absence of Raleigh scattering and is one of the major factors contributing to the decidedly greater power of detection; other factors such as the use of a short-slit burner, rapid vaporization, elimination of nebulization, *etc.*, were described in the preceding paper.[1]

Acknowledgements—The co-operation between the Institut für Spektrochemie und angewandte Spektroskopie, Dortmund, FRG and the EGE-University, Izmir, Turkey, is supported by NATO Research Grant No. 1949. The work for this paper was carried out with the financial assistance of the Bundesministerium für Forschung und Technologie and the Ministerium für Wissenschaft und Forschung des Landes Nordrhein-Westfalen. We would also like to thank Dr. H. Massmann, ISAS, for some interesting discussions on the paper.

REFERENCES

1. H. Berndt and J. Messerschmidt, *Spectrochim. Acta*, 1979, **34B**, 241.
2. *Idem*, unpublished work.
3. S. R. Koirtyohann and E. E. Picket, *Anal. Chem.*, 1966, **38**, 585.
4. B. R. Culver and T. Surles, *ibid.*, 1975, **47**, 920.
5. M. J. Adams, G. F. Kirkbright and P. Rienvatana, *At. Absorb. Newsl.* 1975, **14**, 105.
6. H. Massmann, Z. El Gohary and S. Gücer, *Spectrochim. Acta*, 1976, **31B**, 399.
7. G. F. Kirkbright and M. Sargent, *Atomic Absorption and Fluorescence Spectroscopy*, p. 514. Academic Press, London, 1974.
8. W. J. Price, *Spectrochemical Analysis by Atomic Absorption*, p. 183, Heyden, London, 1979.
9. B. Welz, *Atomic Absorption Spectroscopy*, p. 109, Verlag Chemie, Weinheim/Bergstr., 1976.
10. J. C. Van Loon, *Analytical Atomic Absorption Spectroscopy*, p. 44, Academic Press, New York, 1980.
11. J. A. Dean and T. C. Rains, *Flame Emission and Atomic Absorption Spectrometry*, Vol. 1, p. 267, Dekker, New York, 1969.

Talanta, Vol. 28, pp. 337 to 339, 1981
Printed in Great Britain. All rights reserved

0039-9140/81/050337-03$02.00/0
Copyright © 1981 Pergamon Press Ltd

KINETIC STUDIES OF ION-EXCHANGE OF COBALT(II) AND NICKEL(II) ON A RESIN LOADED WITH 5-SULPHO-8-QUINOLINOL

H. AKAIWA, H. KAWAMOTO and K. OGURA

Department of Chemistry, Faculty of Technology, Gunma University, Kiryu-shi, Gunma 376, Japan

(*Received* 2 *September* 1980. *Accepted* 16 *October* 1980)

Summary—The mechanism of ion-exchange of cobalt(II) and nickel(II) on a resin loaded with 5-sulpho-8-quinolinol has been studied, and the chelate-forming reaction in the resin matrix shown to be rate-determining. The observed rate seems to be related to the rate of water-exchange with the metal ion in the aqueous phase, suggesting that complexation in the resin matrix may proceed according to the Eigen mechanism.

The use of resins loaded with a chelating agent was first exploited[1] as a tool for selective preconcentration of trace metals before instrumental analysis.It has successfully been applied to the neutron-activation determination of trace metals in natural water samples[2,3] and the substoichiometric separation of zinc.[4] The rate of ion-exchange was found to be rather small compared with that on ordinary cation-exchange resins. This has led us to undertake the kinetic studies described below.

Early kinetic studies of ion-exchange were summarized by Helfferich, who identified three separate stages: film-diffusion, particle-diffusion and chemical reaction at the fixed ionic groups.[5] Turse and Rieman concluded that the rate-determining step of the ion-exchange reaction for several bivalent metals on Dowex A-1 was chemical reaction.[6] However, later workers could not verify this conclusion.[7,8] Recently, Matsuzuru and Wadachi reported that the rate-determining steps for sorption of cobalt(II) and cerium(III) on Dowex A-1 were particle-diffusion and chemical reaction, respectively.[9] The differences in the conclusions concerning the rate-determining step show that kinetic studies of the ion-exchange process are difficult. On the other hand, since the capacity of the resin studied in the present work can be changed easily, the resin should be well suited for kinetic studies.

EXPERIMENTAL

Reagents and apparatus

Stock solutions of cobalt(II) and nickel(II) (each 100 μg/ml) were prepared by dissolving weighed amounts of cobalt nitrate and nickel sulphate in water. The resin was prepared by adsorbing 5-sulpho-8-quinolinol on an anion-exchange resin, Diaion SA 100 (Cl-form, 100–200 mesh) in 0.1*M* ammonia solution. The adsorption of 5-sulpho-8-quinolinol on the resin was shown to be quantitative by spectrophotometric studies and the ion-exchange capacity of the resin for the reagent was found to be nearly equal to that for chloride ion.[10] All chemicals used in this work were of guaranteed grade. Metal ions remaining in eluates were determined with a Hitachi 170-30 atomic-absorption spectrophotometer.

Procedure

A 500-mg portion of the loaded resin was placed in a standard flask. Acetate buffer solution and a known amount of metal-ion solution were added and the mixture was diluted to 100 ml with water and stirred magnetically for a prescribed period. The metal-ion content and the pH of the supernatant solution were measured. The concentration of acetate buffer was kept below 0.01*M* throughout.

RESULTS AND DISCUSSION

The rate of ion-exchange was shown to depend on the concentration of 5-sulpho-8-quinolinol in the anion-exchange resin, indicating that film-diffusion is not the operative ion-exchange mechanism. In the case of the limited bath method, the kinetic equation for ion-exchange controlled by particle-diffusion was derived by Kressman and Kitchener,[11] and later applied to examination of the ion-exchange process.[9] The experimental data obtained from the present work were examined by use of this equation, and it was concluded that the rate-determining step was not particle-diffusion, but might be chemical reaction.

Assuming that the ion-exchange reaction is first-order with respect to metal-ion concentration, the following equation can be obtained:

$$-\frac{d[M]}{dt} = k_{obs}[M] \qquad (1)$$

where [M] and k_{obs} represent the concentration of a bivalent metal ion in the solution phase and an apparent rate constant, respectively. Integration of equation (1) gives:

$$\ln \frac{[M]_{t_1}}{[M]_{t_2}} = k_{obs}(t_2 - t_1) \qquad (2)$$

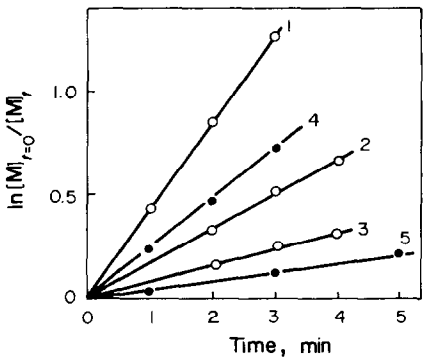


Fig. 1. Effect of agitation time on the sorption of metal ions. Temperature 20°. Cobalt(II) (—○—): $[HQ]_{tot}$ 3.86 mmole/g of resin; 1, pH 5.25; 2, pH 4.13; 3, pH 3.91. Nickel(II) (—●—): $[HQ]_{tot}$: 0.33 mmole/g of resin; 4, pH 4.98; 5, pH 4.10.

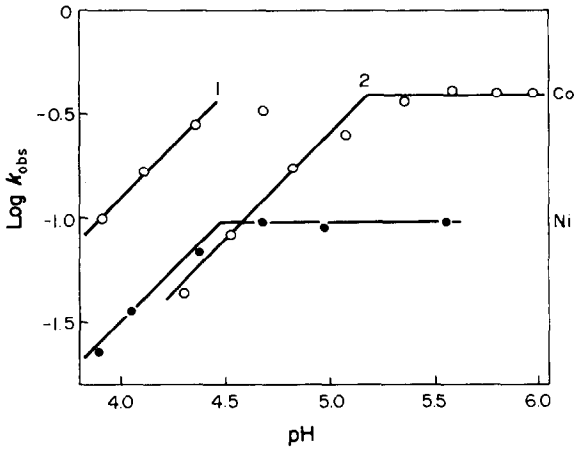


Fig. 2. Effect of pH on the sorption rate of metal ions. Temperature 20°. Cobalt(II) (—○—); $[HQ]_{tot}$: 1, 3.86 mmole/g of resin, 2, 0.27 mmole/g of resin. Nickel(II) (—●—); $[HQ]_{tot}$: 0.27 mmole/g of resin.

where $[M]_{t_1}$ and $[M]_{t_2}$ are the concentrations at times t_1 and t_2. Equation (1) corresponds to that adopted by Matsuzuru and Wadachi.[9] According to equation (2), a plot of $\ln [M]_{t_1}/[M]_{t_2}$ against $(t_2 - t_1)$ should be a straight line having a slope of k_{obs}. In fact, each plot of our results is a straight line, as can be seen in Fig. 1. The ion-exchange reactions were therefore first-order with respect to the metal-ion concentration.

Increasing the 5-sulpho-8-quinolinol concentration in the resin was found to increase the k_{obs} value, suggesting that the rate-determining step is the complexation process in the resin. The slopes of log–log plots were unity, showing that the reaction is first-order with respect to reagent concentration. The effect of pH on ion-exchange rate is shown in Fig. 2. Above a certain pH the reaction is zero-order with respect to the hydrogen-ion concentration, but at lower pH is first-order with respect to hydroxide-ion concentration.

These results can be explained by the reaction

$$M_r + HQ_r \xrightarrow{k_+^0} MQ_r + H_r \qquad (3)$$

where M, HQ and k_+^0 are the bivalent metal ion, 5-sulpho-8-quinolinol and the rate constant, respectively, the subscript r denotes the resin phase and charges are omitted for simplicity. The kinetic equation based on reaction (3) can be written as:

$$\text{rate} = k_+^0 [M]_r[HQ]_r \qquad (4)$$

It is assumed that diffusion of metal and hydrogen ions between the solution and the resin phase is rapid and that equilibrium is established immediately. The Donnan theory is then applicable and gives the following equations:

$$\frac{[M]_r}{[M]} = \frac{\gamma_M a_x^2}{\gamma_{M_r} a_{x_r}^2} = K_M^* \qquad (5)$$

$$\frac{[H]_r}{[H]} = \frac{\gamma_H a_x}{\gamma_{H_r} a_{x_r}} = K_H^* \qquad (6)$$

where γ denotes an activity coefficient and a_x is the activity of the co-ion x. It is assumed that K_M^* and K_H^* are constant, because the ionic strength and the concentration of the co-ion x are constant under the present experimental conditions. In the pH-range studied, the chelating agent can exist in the resin as both H_2Q and HQ and mass-balance gives the equation

$$[HQ]_{tot} = [HQ]_r + [H_2Q]_r = [HQ]_r\left(1 + \frac{[H]_r}{K_a^0}\right) \qquad (7)$$

where $[HQ]_{tot}$ and K_a^0 represent the total concentration of 5-sulpho-8-quinolinol and the acid dissociation constant of this reagent in the resin, respectively.

Combining equations (4)–(7) gives

$$k_{obs} = \frac{k_+^0 K_a^0 K_M^* [HQ]_{tot}}{K_a^0 + K_H^*[H]} \qquad (8)$$

and a plot of log k_{obs} *vs.* log $[HQ]_{tot}$ should give a straight line having a slope of unity and this was found to be the case. The pH-dependence of k_{obs} can be explained by equation (8). At high enough pH, equation (8) approximated to

$$k_{obs} = k_+^0 K_M^* [HQ]_{tot} \qquad (9)$$

showing that the reaction is zero-order with respect to hydrogen-ion concentration, in agreement with the results given in Fig. 2. At low pH:

$$k_{obs} = \frac{k_+^0 K_a^0 K_M^* [HQ]_{tot}}{K_H^*[H]} \qquad (10)$$

indicating that the reaction is first-order with respect to hydroxide-ion concentration, in agreement with the results shown in Fig. 2.

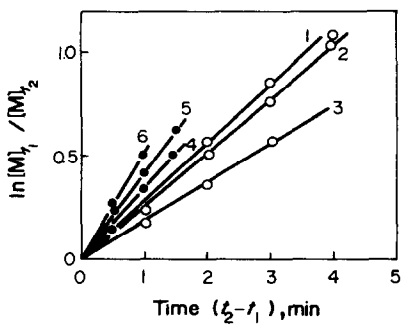


Fig. 3. Effect of agitation time on the sorption rate. pH 5.70; $[HQ]_{tot}$ 0.27 mmole/g of resin; temperature 20°; —○— $t_1 = 0$; —●— $t_1 = 0.5$ min; 1, Mn(II); 2, Co(II); 3, Ni(II); 4, Cu(II); 5, Zn(II); 6, Cd(II).

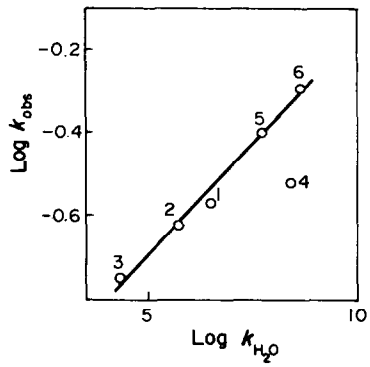


Fig. 4. Relationship between ion-exchange rate and water-exchange rate (k_{H_2O}, sec^{-1})·[14] 1, Mn(II); 2, Co(II); 3, Ni(II); 4, Cu(II); 5, Zn(II); 6, Cd(II).

Kinetic studies on the complexation of nickel with 5-sulpho-8-quinolinol in aqueous medium were conducted by Johnson and Wilkins.[12] According to their results, the protonated form H_2O is inactive toward nickel and complexation in weakly acidic solution proceeds according to

$$Ni^2 + HQ \rightarrow NiQ^+ + H^+ \qquad (11)$$

The initial step was considered to be rate-determining and controlled by the water-exchange process. Reaction (11) corresponds to equation (3), so complexation in the resin may also be controlled by the water-exchange process. If so, the rate of ion-exchange should be related to the water-exchange rate for the corresponding metal ion. Examples given in Fig. 3 show that equation (3) is also applicable to the cases of some other bivalent metal ions. The slope of each plot given in Fig. 3 is equal to the corresponding value of k_{obs}, which can be correlated with the water-exchange rate, k_{H_2O}, suggesting that complexation in the resin may proceed according to the Eigen[14] mechanism (Fig. 4). The exception is copper(II), which is explained by considering the mechanism of the formation of copper oxinate in the aqueous phase, where ring closure and not water-exchange is rate-determining.[13]

REFERENCES

1. H. Akaiwa, H. Kawamoto, N. Nakata and Y. Ozeki, *Chem. Lett.*, 1975, 1049.
2. H. Akaiwa, H. Kawamoto and N. Nakata, *J. Radioanal. Chem.* 1977, **36**, 59.
3. H. Akaiwa, H. Kawamoto, K. Ogura and K. Tanaka, *Radioisotopes*, 1979, **28**, 291.
4. H. Akaiwa, H. Kawamoto and K. Ogura, *Talanta*, 1977, **24**, 394.
5. F. Helfferich, *Ion Exchange*, p. 252. McGraw-Hill, New York, 1962.
6. R. Turse and W. Rieman III, *J. Phys. Chem.*, 1961, **65**, 1821.
7. A. Schwarz, J. A. Marinsky and K. S. Spiegler, *ibid.*, 1964, **68**, 918.
8. A. Varon and W. Rieman III, *ibid.*, 1964, **68**, 2716.
9. H. Matsuzuru and Y. Wadachi, *Nippon Kagaku Kaishi*, 1973, 643.
10. H. Akaiwa, H. Kawamoto, K. Ogura and S. Kogure, *Radioisotopes*, 1979, **28**, 681.
11. T. R. E. Kressman and J. A. Kitchener, *Discuss. Faraday Soc.*, 1949, **4**, 90.
12. W. A. Johnson and R. G. Wilkins, *Inorg. Chem.*, 1970, **9**, 1917.
13. K. Kustin, R. F. Pasternack and E. M. Weinstock, *J. Am. Chem. Soc.*, 1966, **88**, 4610.
14. M. Eigen, *Ber. Bunsenges. Phys. Chem.*, 1963, **67**, 753.

Talanta. Vol. 28. pp. 341 to 344. 1981
Printed in Great Britain. All rights reserved

0039-9140/81/050341-04$02.00/0
Copyright © 1981 Pergamon Press Ltd

ANALYTICAL DATA

THERMOMETRIC TITRATION OF β-ARYL-α-MERCAPTOPROPENOIC ACIDS AND DETERMINATION OF THE STOICHIOMETRY OF THEIR METAL COMPLEXES

A. IZQUIERDO and J. CARRASCO

Department of Analytical Chemistry, Faculty of Chemistry, University of Barcelona, Spain

(*Received* 2 *September* 1980. *Accepted* 10 *December* 1980)

Summary—Automatic thermometric titration was applied to some β-aryl-α-mercaptopropenoic acids and the stoichiometry of their complexes with several metal ions was investigated. The heats of neutralization of the mercapto-acids with sodium hydroxide and the heats of their reaction with metal ions were calculated.

The β-aryl-α-mercaptopropenoic acids are a group of compounds that we are studying as analytical reagents,[1,2] some of their reactions with metal ions having analytical possibilities owing to their sensitivity.

This paper deals with the influence of methoxyl substituents on the acidity of the mercapto and carboxylic groups, the test compounds being the 3-(2-methoxyphenyl) (**I**), 3-(4-methoxyphenyl) (**II**), 3-(2,3-dimethoxyphenyl) (**III**), and 3-(3,4,5-trimethoxyphenyl) (**IV**) 2-mercaptopropenoic acids, which have been titrated thermometrically with sodium hydroxide in aqueous alcohol media; the heats of neutralization of both acidic groups have been calculated. The method has also been used to find the stoichiometry and heats of formation of the precipitates or complexes given by these mercapto-acids with certain metal ions.

EXPERIMENTAL

Reagents

The mercapto-acids were synthesized by condensation of rhodanine with the appropriate aldehyde, followed by alkaline hydrolysis,[3] and purified by crystallization from benzene.[4–11] All other reagents were analytical grade.

Apparatus

The temperature was measured with a fast-response thermistor and Wheatstone bridge system using the electrical circuit proposed by Lumbiarres *et al.*[12] The thermistor resistance was found by the Lumbiarres method[12] to be 11.95 kΩ at 20°, the temperature used throughout.

The bridge parameters were calculated to give a linear response to temperature changes in the interval used, and to be compatible with a chart-recorder of 1 MΩ input impedance.

The titration assembly (Fig. 1), consisted of a 50-ml polystyrene vessel 5 cm in diameter surrounded by a 4-cm thick layer of expanded polystyrene for heat insulation. The thermistor, the burette tip and the heater (R_c) were fixed to the lid, and the solution was stirred by a paddle rotating at 500 rpm. The titrant was delivered at constant rate by a 2.5-ml automatic burette, Radiometer model ABU 12.

Procedure

The sample was placed in the titration cell, diluted to 40 ml, and adjusted to ionic strength 0.1 with potassium nitrate. After temperature equilibration, the base-line was recorded for 10 min before the titration was started. Titrant was added at 0.142 ml/min until well past the end-point (to give the heat of dilution of the system) and recording was stopped some minutes later (to give the cooling rate). Figure 2 shows a typical titration curve. The end-point was given by the intersection of the dilution line and the reaction-period line. The temperature increase was determined according to Barthel's method.[13]

Determination of the enthalpy of reaction

The enthalpy of reaction can be found from the temperature change by determination of the enthalpimetric constant of the cell,[14–17] or by use of electrical heating or by means of a calibration curve for a reaction of known enthalpy change.

The calibration-curve method was used in this work, the reaction being neutralization of sodium hydroxide with hydrochloric acid ($\Delta H = -13.35$ kcal/mole at 25°).[18] From Barthel's equation[18]

$$\Delta H_R = -[13.35 + 0.07\,(25.0 - t)] \text{ kcal/mole}$$

where t is the mean temperature (°C) of the solution, the quantities of heat produced in neutralization of various amounts of alkali are calculated and plotted against temperature. The calibration curve obtained had the equation $y = 0.0004 + 1.0170x$ with a correlation coefficient of 0.999. By means of the calibration curve, the enthalpy of any reaction can be calculated by titration of an exactly weighed quantity under the same conditions of volume, ionic strength, stirring-rate and titrant addition as for the calibration experiments.

RESULTS AND DISCUSSION

Heat of neutralization of NaOH with HCl in aqueous alcohol

Because the test compounds are not very soluble in water, solutions in 50% v/v aqueous ethanol had to be

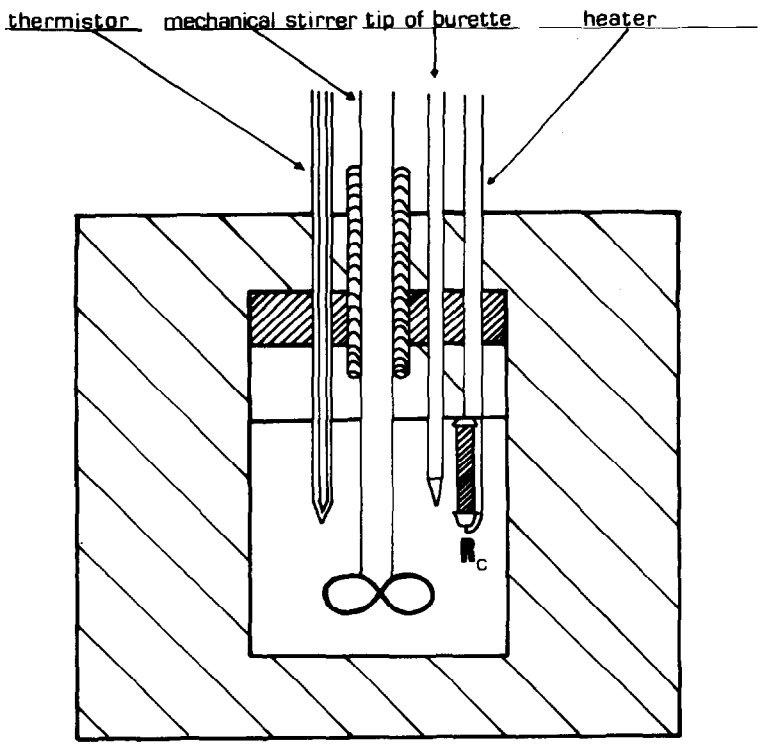


Fig. 1. Adiabatic titration unit.

used, and accordingly the enthalpy of neutralization of sodium hydroxide with hydrochloric acid had to be determined in the same medium. The electrical calibration method was used, with the circuit[12] shown in Fig. 3.

The steady power source (S.P.S.) was regulated between 1.5 and 11.5 V with a maximum output current of 600 mA. The ballast resistor R_{ex} and heating resistance R_c were both 9.8 and R_c was varnished for protection against the reagents and to avoid electrical losses. The standard resistor R_p (9.303 Ω at 19°) was made of constantan wire coiled on bakelite and immersed in a glycerine bath to dissipate heat easily. The digital voltmeter (DiVi) was a Sinclair Multi-

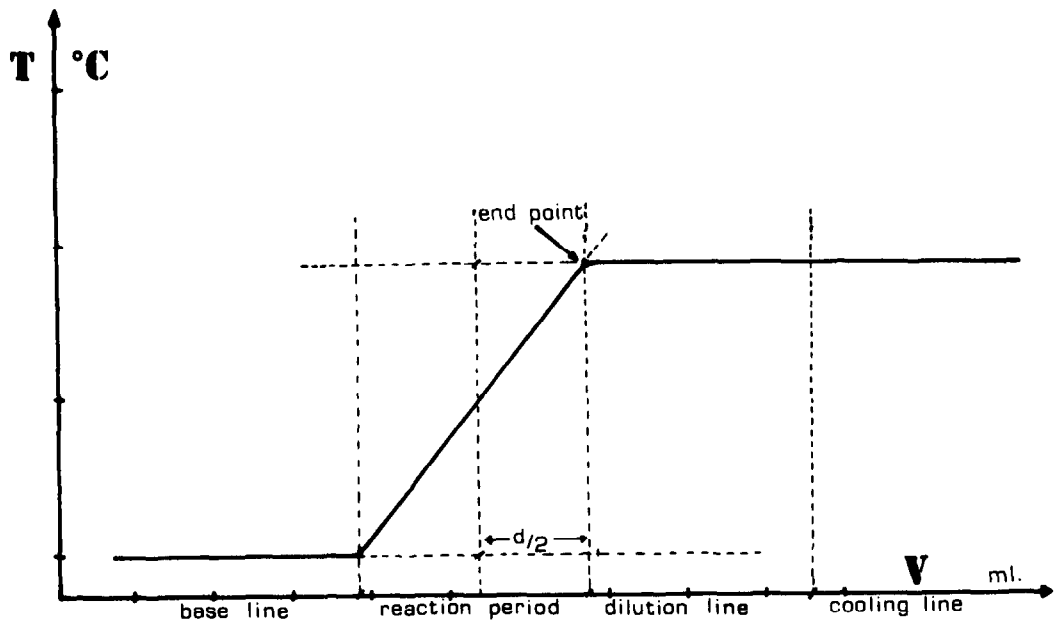


Fig. 2. Typical thermometric-titration curve.

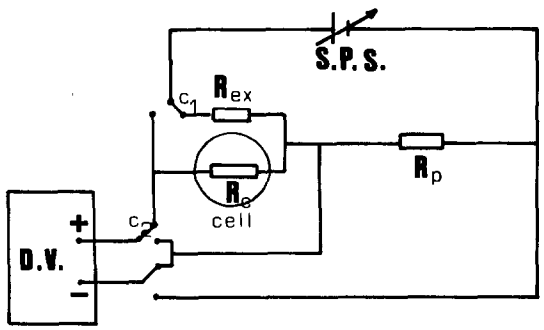


Fig. 3. Schematic calibration circuit.

meter model PDM-35. Switch c_1 switches on the heating resistance in the cell and c_2 connects either R_c or R_p to the voltmeter.

The slope method was used to determine the enthalpy of reaction. The slopes for the standard reaction titration and the electrical titration were measured. According to Tyson *et al.*,[18]

$$\Delta H = -\frac{E_c E_p}{4.185\, R_p F N} \times \frac{S_1}{S_2}$$

where E_c and E_p are the voltage drops across the standard resistor and the calibration heater, S_1 and S_2 are the slopes of the chemical and electrical titrations respectively, F is the rate of titrant addition (ml/sec), and N is the normality of the titrant.

Application of this method to the NaOH/HCl neutralization reaction in aqueous media gave $\Delta H = -13.77$ kcal/mole at 19°, in agreement with the value given by Barthel.[18] The same value was obtained for the same reaction in aqueous ethanol (50% v/v).

With this value and the calibration curve constructed from it, the values of ΔH for reaction of sodium chloride and potassium bromide with silver nitrate in aqueous ethanol (50% v/v) were calculated, and agreed with the values $\Delta H_{AgCl} = -15.67 \pm 0.19$ and $\Delta H_{AgBr} = 19.94 \pm 0.05$ kcal/mole for aqueous medium at 19°, given in the literature.[20–23]

Titration of β-aryl-α-mercaptopropenoic acids

The mercapto-acids in aqueous ethanol (50% v/v) medium were titrated with 0.5 or 1*M* sodium hydroxide in the same solvent. The titration curves corresponded to successive neutralization of the carboxylic and thiol groups (p*K* values 3-3.5 and 8–8.5 respectively[24]).

Table 1 gives the heats of neutralization of both acidic groups for each of the four mercapto-acids studied, measured by means of the calibration curve and of electrical calibration.

Stoichiometry of some compounds formed by metal ions and β-aryl-α-mercaptopropenoic acids

Thermometric titration was used to determine the composition and heats of formation of the precipitates given by the mercapto-acids studied, with Ag^+, Pb^{2+}, Cd^{2+}, Cu^{2+} and Hg^{2+}, and the complex formed with Ni^{2+}.

A 0.01*M* solution of the mercapto-acid in aqueous ethanol (50% v/v) was titrated with a 1*M* solution of the cation in the same medium but if the metal salt was insoluble under these conditions (Cu^{2+} and Hg^{2+}) the mercapto-acid was dissolved in water containing the stoichiometric quantity of sodium hydroxide required and titrated with an aqueous solution of the metal ion.

Table 1.

Acid	Method	No. of detns.	ΔH, *kcal/mole* –COOH	Std. devn.	–SH	Std. devn.
3-(2-Methoxyphenyl)-2-C.C.	6	−11.2	0_9	−6.4	0.2_7	
mercaptopropenoic	C.E	4	−11.4	0.2_7	−6.5	0.1_9
3-(4-Methoxyphenyl)-2-	C.C.	6	−11.4	0.1_4	−6.4	0.1_3
mercaptopropenoic	C.E.	4	−11.4	0.1_5	−6.4	0.1_6
3-(2,3-Dimethoxyphenyl)-2-	C.C.	6	−11.6	0.1_8	−6.6	0.1_7
mercaptopropenoic	C.E.	4	−11.7	0.1_1	−6.8	0.0_2
3-(3,4,5-Trimethoxyphenyl)-2-	C.C.	6	−11.5	0.1_1	−6.2	0.0_6
mercaptopropenoic	C.E.	4	−11.7	0.2_3	−6.4	0.1_8

C.C. Calibration curve.
C.E. Electrical calibration.

Table 2.

Cation	Stoichiometry Reagent:cation	No. of detns.	ΔH, *kcal/mole*	Std. devn., *kcal/mole*
Ag^+	1:1	8	−26.2	0.1_2
Pb^{2+}	1:1	4	−9.4	0.1_4
Cd^{2+}	2:1	4	−22.3	0.1_0
Cu^{2+}	2:1	8	−31.1	0.1_9
Hg^{2+}	2:1	4	−37.2	0.2_0
Ni^{2+}	2:1	5	−10.3	0.1_7

The composition of the precipitates agreed with the elemental analysis of the product, and the soluble complex formed had the same stoichiometry as that found spectrophotometrically by the continuous-variations,[25,26] molar ratio[27] and slope methods.[28]

REFERENCES

1. A. Izquierdo and J. Calmet, *Quim. Anal.*, 1974, **28**, 148.
2. A. Izquierdo and M. Giné, *An. Quim.*, 1978, **74**, 53.
3. P. L. Julian and B. M. Sturgis, *J. Am. Chem. Soc.*, 1935, **57**, 1126.
4. S. Sugasawa and H. Sigehara, *Ber. Dtsch. Chem. Ges.*, 1941, **74b**, 459.
5. C. Ravazzone and R. Valero, *Ann. Chim. (Rome)*, 1962, **52**, 305.
6. C. Granacher, M. Mero, A. Ofner, A. Kloppenstein and E. Schatter, *Helv. Chim. Acta*, 1923, **6**, 458.
7. R. Gaudry and R. A. McIvor, *Can. J. Chem.*, 1951, **29**, 427.
8. T. Ito, T. Ishii and M. Nishio, *Agr. Biol. Chem. (Tokyo)*, 1965, **29**, 728.
9. J. A. Barltrop, *J. Chem. Soc.*, 1946, 958.
10. M. Gerard, *Ann. Chim. (Paris)*, 1941, **16**, 326.
11. E. Campaigne and W. E. Krighbaum, *J. Org. Chem.*, 1961, **26**, 1326.
12. J. Lumbiarres, C. Mongay and V. Cerdá, *Analusis*, 1980, **8**, 62.
13. J. Barthel, *Thermometric Titrations*, p. 27. Wiley, New York, 1975.
14. M. P. Ben-Yair and J. Jordan, *Abstracts of Papers, XII Congr. Intern. de Chimie Pure Appliquée*, New York, September 1951, **42**, 43.
15. E. Popper, L. Roman and P. Marcu, *Talanta*, 1964, **11**, 515.
16. *Idem, ibid.*, 1965, **12**, 249.
17. *Idem, ibid.*, 1967, **14**, 1163.
18. J. Barthel, F. Becker and N. G. Schmahl, *Z. Phys. Chem. (Frankfurt)*, 1961, **29**, 58.
19. C. B. Tyson, Jr., W. H. McCurdy, Jr. and C. E. Bricker, *Anal. Chem.*, 1961, **32**, 1640.
20. G. J. Ewing and C. J. Marzac, *ibid.*, 1966, **38**, 1575.
21. J. Barthel, N. G. Schmahl and L. Lenz, *Z. Anal. Chem.*, 1968, **233**, 328.
22. K. F. Jahr, G. Wiese and G. Schuchart, *Z. Phys. Chem. (Frankfurt)*, 1968, **61**, 73.
23. M. J. Sienko and R. A. Plane, *Physikalische Anorganische Chemie*, Hirzel, Stuttgart, 1965.
24. A. Izquierdo and J. Carrasco, unpublished work.
25. P. Job, *Ann. Chim. (Paris)*, 1928, **9**, 113.
26. *Idem, ibid.*, 1936, **6**, 97.
27. J. H. Yoe and L. Jones, *Ind. Eng. Chem., Anal. Ed.*, 1944, **16**, 97.
28. A. E. Harvey and D. L. Manning, *J. Am. Chem. Soc.*, 1950, **72**, 4488.

Talanta. Vol. 28, pp. 345 to 347. 1981
Printed in Great Britain. All rights reserved

0039-9140/81/050345-03$02.00/0
Copyright © 1981 Pergamon Press Ltd

ANNOTATIONS

THE TIRON RADICAL AS INDICATOR SUBSTANCE IN CATALYTIC DETERMINATION OF TRACE METALS

M. OTTO, J. STACH, R. KIRMSE and G. WERNER

Department of Chemistry, Karl-Marx-University Leipzig, 7010 Leipzig, Liebigstrasse 18, GDR

(*Received* 5 *September* 1980. *Accepted* 11 *December* 1980)

Summary—The tiron–hydrogen peroxide reaction used for catalytic determination of trace metals is studied with respect to the indicator substance—the oxidation product of tiron absorbing at 440 nm. Contrary to assumptions in the literature, it is shown by electrochemical techniques, EPR spectroscopy and visible spectrophotometry that the indicator substance is not the *o*-quinone derivative of tiron (λ_{max} = 372 nm) but the tiron semiquinone radical with a *g*-value of g_o = 2.0049 and molar absorptivity = (3.5 ± 0.5) × 10^3 l.mole^{-1}.cm^{-1} at 440 nm.

Catalytic methods for determination of trace metals, based on the tiron–hydrogen peroxide reaction, have been proposed by various authors.[1–5] For determination of cobalt, Bognár *et al.*[1,2] monitored the catalytic reaction at a wavelength of 440 nm, and described the oxidation product as the *o*-quinone derivative. This oxidation product, however, was not detected by Kucharkowsky,[4] who used a wavelength of 336 nm to monitor a daughter product of the primary oxidation product. On the other hand, the primary oxidation product was also identified as the *o*-quinone derivative in a kinetic study of the manganese-catalysed tiron–hydrogen peroxide reaction (ϵ_{440} = 2.1 × 10^3 l.mole^{-1}.cm^{-1}),[6] and again in the catalytic determination of nickel with this indicator reaction.[5] Furthermore, during investigations of the tiron–hydrogen peroxide reaction in catalytic three-component analysis for Co, Mn and Ni, we were able to adjust the reaction conditions in such a way that the oxidation product absorbing at 440 nm could be used as the indicator substance for cobalt.[7]

From mechanistic studies of the catalytic reaction it became evident, however, that the indicator substance cannot be the proposed *o*-quinone derivative[2,5,6]

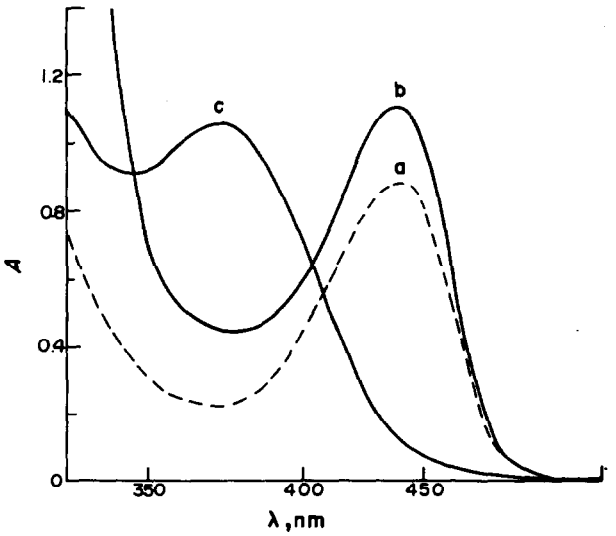


Fig. 1. Absorption spectra of tiron oxidized in alkaline medium by the catalytic reaction (*a*), anodically at glassy-carbon (*b*), and electrochemically in acidic medium (*c*). (*a*) 5 × 10^{-4}*M* tiron; 5 × 10^{-4}*M* H_2O_2; pH 10.2 (borate buffer); 10^{-7}*M* Co^{2+}; 1-cm cell; 2-min reaction; (*b*) 0.3*M* tiron; pH 10.0 (borate buffer); electrolysis time 55 min; 0.1-cm cell; (*c*) 1.2 × 10^{-2}*M* tiron; 1*M* $HClO_4$; electrolysis for 4 min at 1.2 V.

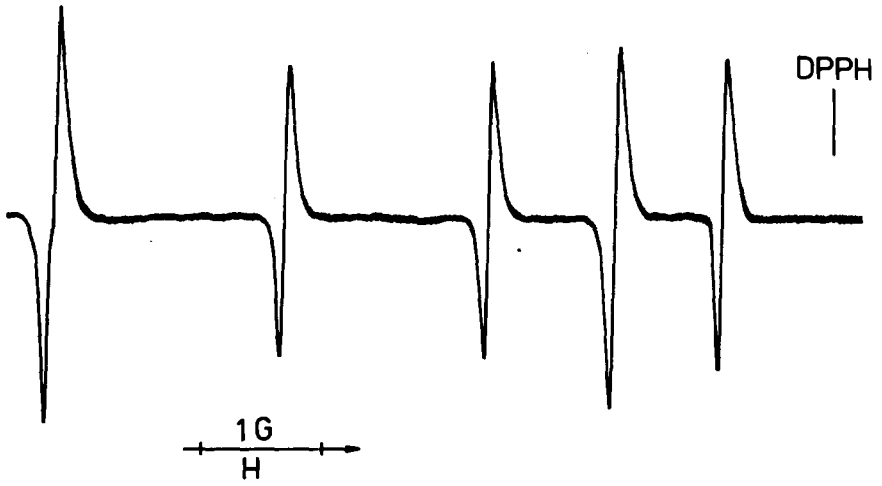


Fig. 2. EPR-spectrum of the radicals obtained by anodic oxidation of tiron. At 22°; for other conditions see Fig. 1*b*.

because the longest-wavelength absorption band of *o*-benzoquinone occurs at 370 nm.[8] For that reason, in the present study the primary oxidation product of tiron was characterized in more detail by spectroscopic and electrochemical techniques, and the tiron radical was shown to be the real indicator substance in all these catalytic determinations.[2,5–7]

EXPERIMENTAL

Reagents

Analytical-reagent grade chemicals and doubly distilled water were used throughout. Tiron (1,2-dihydroxybenzene-3,5-disulphonic acid, disodium salt) obtained from Riedel de Haen was used without further purification.

Apparatus and procedures

Electrochemical measurements were made at 22° with a Beckmann Electroscan 30 by use of a conventional three-electrode cell with a glassy-carbon working electrode (VEB Elektrokohle Lichtenberg, GDR) and a saturated calomel electrode (SCE). For controlled-potential electrolysis an H-cell was used, with platinum-foil working and auxiliary electrodes, separated by a glass frit. Absorption spectra were recorded on a Zeiss Specord spectrophotometer, and the EPR-spectra were measured with a Varian E-112 ESR spectrometer.

RESULTS AND DISCUSION

The cobalt-catalysed oxidation of tiron with an equimolar hydrogen peroxide solution in alkaline medium produces a strong absorption at 440 nm [Fig. 1(*a*)]. From the literature it was assumed that this absorption band should arise from a semiquinone radical, since these radicals absorb in the range 400–450 nm.[9] However, the tiron radical could not be detected in the reaction mixture by EPR, possibly because its concentration was too low. For that reason the reactant concentrations were increased to $1.5 \times 10^{-2}M$ tiron, $1.94 \times 10^{-2}M$ hydrogen peroxide and $10^{-5}M$ Co(II), which yielded a concentration of product high enough to be detected by EPR. A sufficiently high concentration of oxidation product could be obtained more easily by anodic oxidation of tiron at a potential of 1.2 V on platinum [Fig. 1(*b*)], a technique which was used for further characterization of the radical because hydrogen peroxide and the catalyst were absent, and undesirable side-reactions were avoided. An EPR-spectrum of the anodically oxidized tiron solution is shown in Fig. 2. The spectrum consists of six partially overlapping signals which belong to two different radicals. The line quartet with an intensity of 1:1:1:1 results from the interaction of the unpaired electron with the two non-equivalent ring protons of the tiron radical. The coupling constants derived from the spectrum are $a_{H(4)} = 3.61$ G and $a_{H(6)} = 1.93$ G ($g_o = 2.0049$). The second radical shows only a doublet splitting, with a coupling constant of $a_H = 4.54$ G ($g_o = 2.0052$). The

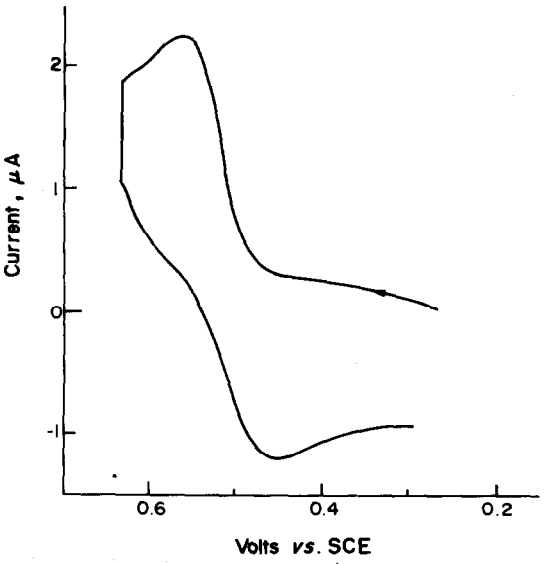
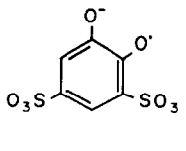
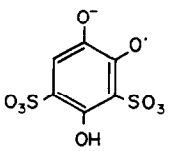


Fig. 3. Cyclicvoltammogram of $5 \times 10^{-5}M$ tiron solution at pH 2.5 (Britton–Robinson buffer). Scan-rate 0.02 V/sec.

assignment of the EPR signals to the two radicals is made possible by examining the effect of pH. At pH <9 only the line quartet is observed, whereas in strongly alkaline medium (pH >11) the doublet splitting is dominant. This finding correlates with small differences in the visible absorption spectra of the tiron radical: changing the pH from 8 to 13 shifts the absorption maximum from 440 to 426 nm as well as increasing the absorbance slightly. According to Stone and Waters[10] the primary radical is the semiquinone of tiron (**I**) with two doublets in the EPR-spectrum, and the secondary radical (**II**) has a doublet

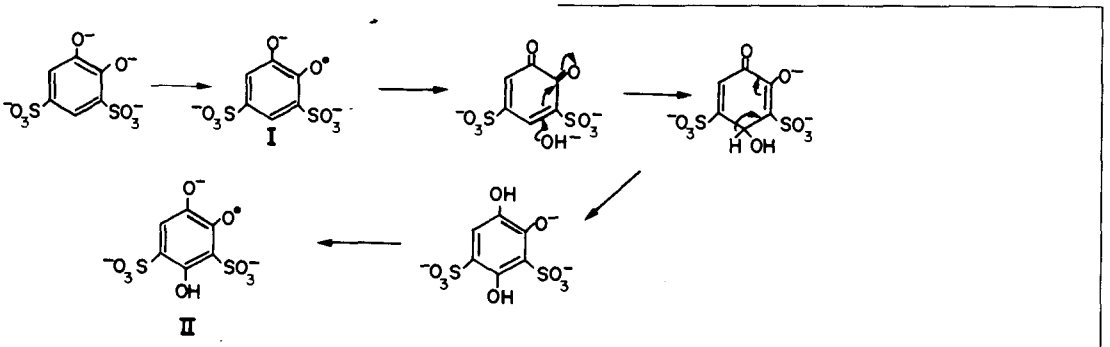


I



II

EPR-splitting, and is formed according to the reaction sequence



Because these catalytic reactions are carried out in the pH range 9–11,[1–5] both forms of radical contribute to the indicator substance. The absorption maximum at 440 nm can be assigned to **I**, and that at 426 nm to **II**.

Although the spectroscopic data show the tiron radical to be the real indicator substance, we have also investigated the suggested indicator substance *o*-benzoquinone-3,5-disulphonic acid. The oxidation of tiron to the *o*-quinone derivative can be observed in acidic media[11] because there is no further reaction to give the radical obtained in alkaline solution. A cyclic voltammogram of the quasi-reversible tiron–*o*-quinone system in acidic solution is given in Fig. 3. Controlled-potential electrolysis of tiron at 1.2 V in 1*M* perchloric acid produced a compound with an absorption band with $\lambda_{max} = 372$ nm [Fig. 1(*c*)], which is to be expected for derivatives of *o*-benzoquinone.[8]

Alkalization of that solution to pH 9 again produced the tiron radical, with the same absorption characteristics as in Fig. 1(*b*). This pH-changing technique could be used to estimate the molar absorptivity of the semiquinone from the ratio of absorbances of the *o*-quinone derivative at 372 nm and the semiquinone at 440 nm, with a value of 1.5×10^3 $l.mole^{-1}.cm^{-1}$ for the molar absorptivity of the *o*-quinone derivative.[12] On the assumption that all of the quinone reacts with excess of tiron in alkaline medium to give the semiquinone (**I**), a molar absorptivity of $(3.2 \pm 0.3) \times 10^3$ $l.mole^{-1}.cm^{-1}$ was calculated, comparable to the values for other semiquinones, determined by combined spectroscopic and pulse radiolysis studies.[9] The molar absorptivity of the secondary radical (**II**) was determined by alkalization of the acidic solution of the quinone to pH >11 and found to be $(3.5 \pm 0.5) \times 10^3$ $l.mole^{-1}.cm^{-1}$. Care was needed because further reactions of the radical take place, caused by light and dissolved oxygen.

The difference between these molar absorptivities and that obtained by Tiginyanu[6] is probably due to the latter having determined the value from kinetic curves of the manganese-catalysed reaction, where it cannot be supposed that only one oxidation product is formed.

REFERENCES

1. J. Bognár, *Mikrochim. Acta*, 1961, 901.
2. J. Bognár and O. Jellinek, *Acta Chim. Acad. Sci. Hung.*, 1961, **29**, 21.
3. R. Kucharkowsky and H. Döge, *Z. Anal. Chem.*, 1968, **238**, 241.
4. R. Kucharkowsky, *Dissertation*, Dresden 1971.
5. I. F. Dolmanova, G. A. Zolotova, T. P. Kabanova and V. M. Peshkova, *Vest. Mosk. Univ.*, 1968, **6**, 96.
6. Ya. D. Tiginyanu, *Koord. Khim.*, 1976, **2**, 809.
7. M. Otto and G. Werner, publication in preparation.
8. *UV-Atlas organischer Verbindungen*, Verlag Chemie, Weinheim, 1971.
9. P. S. Rao and E. Hayon, *J. Phys. Chem.*, 1973, 77, 2274.
10. T. J. Stone and W. A. Waters, *J. Chem. Soc.*, 1965, 1488.
11. E. Mentasti and E. Pelizzetti, *Transition Met. Chem.*, 1976, **1**, 281.
12. E. Mentasti, E. Pelizzetti, E. Pramauro and G. Giraudo, *Inorg. Chim. Acta*, 1975, **12**, 61.

Talanta, Vol. 28, pp. 349 to 352, 1981
Printed in Great Britain

0039-9140/81/060349-04$02.00/0
Pergamon Press Ltd

CONDUCTOMETRIC TITRATION OF NITRATE BY FORMATION OF THE SILVER–1,10-PHENANTHROLINE–NITRATE TERNARY COMPLEX

ICHIRO HAYASHIDA, MITSUHIKO TAGA and HITOSHI YOSHIDA

Department of Chemistry, Faculty of Science, Hokkaido University, Nishi-8, Kita-10, Sapporo-shi, Hokkaido, Japan

(*Received* 9 *July* 1980. *Revised* 16 *December* 1980. *Accepted* 7 *January* 1981)

Summary—Nitrate forms an insoluble ternary complex, $Ag(phen)_2NO_3$, with silver in the presence of 1,10-phenanthroline (phen). A simple and direct conductometric titration of nitrate, based on the formation of this ternary complex, has been investigated. The sample solution is adjusted to pH 4.3 with acetate buffer and titrated with 0.1*M* $Ag(phen)_2^+$ complex solution in 40% ethanol–water mixture. The relative error is less than 0.5% and relative standard deviation less than 0.4%. The effect of ammonium ion and urea has also been studied. The method has been successfully applied to determination of nitrate-nitrogen in fertilizer.

Many titrimetric methods have been reported for the determination of nitrate, most of them being indirect methods based on reduction with iron(II), titanium (III), tin(II), *etc.*[1] These methods have been applied to the determination of nitrate-nitrogen in fertilizer, but involve rather complicated procedures and strict control of conditions. Furthermore, they cannot be applied directly to samples containing ammonia-nitrogen or urea.

However, it is well known that nitrate forms precipitates with a few organic or organometallic compounds such as nitron,[1] diphenylthallium(III)[2,3] and dicyclohexylthallium(III)[4] ions, and amperometric[5] or potentiometric[6] titrations of nitrate have been based on these reactions, although these, too, have their difficulties.

Several anions form insoluble ternary complexes with silver in the presence of 1,10-phenanthroline (phen), and we have recently proposed the conductometric titration of perchlorate by formation of $Ag(phen)_2ClO_4$ and pointed out that conductometric titration with $Ag(phen)_2^+$ can be applied for determination of several anions.[7] Nitrate also forms an insoluble ternary complex $Ag(phen)_2NO_3$ with this reagent, and in the present work we exploit this for a facile and direct determination of nitrate, especially in fertilizers.

EXPERIMENTAL

Apparatus

A TOA Electronics Ltd. digital conductimeter model CM-15A was used for measuring the conductance and a Riken Denshi Co. Ltd. X–Y recorder model D-51P for recording the titration curve obtained with a Mettler titration system model DV-11.

Reagents

$Ag(phen)_2^+$ complex solution, 0.1M in 40% ethanol–water. Prepared by dissolving 17 g of silver acetate and twice the equivalent molar quantity of 1,10-phenanthroline monohydrate in 400 ml of ethanol and diluting to 1 litre with distilled demineralized water, and standardized as follows. An aliquot is transferred into a 100-ml beaker, treated with ammonia solution until colourless, diluted to *ca.* 100 ml and titrated conductimetrically with sodium sulphide solution prepared and standardized by Kirsten and Carsten's method.[8] The complex solution is standardized every two weeks (though no significant change in the concentration during this period has been observed).

Standard nitrate solution 0.02*M*. Prepared from analytical-reagent grade potassium nitrate dried to constant weight at 110° (1.6218 g dissolved with distilled demineralized water and diluted to 1 litre).

Nitron solution, 10% w/v in 5% v/v acetic acid. All other chemicals were of analytical-reagent grade.

Titration procedure

Transfer the sample solution containing between 10 and 30 mg of nitrate into a 100-ml beaker. Adjust the pH to 4.3 with 2 ml of 3*M* acetate buffer and dilute to *ca.* 100 ml with distilled demineralized water. [When heavy-metal ions are present in the sample solution, dilute to *ca.* 75 ml with distilled demineralized water, and titrate conductometrically with 0.2*M* phen solution (in 40% ethanol–water) to mask them.] Titrate with 0.1*M* $Ag(phen)_2^+$ at the rate of 0.20 ml/min or less and record the change of conductance.

RESULTS AND DISCUSSION

Titration curve

Figure 1 shows a typical conductometric titration curve for nitrate. Three inflection points, P, Q and R, were obtained on the titration curve. The positions of the points P and Q shifted to the left with increasing nitrate concentration. It was presumed that these inflection points are associated with either an induction period or supersaturation of the solution with

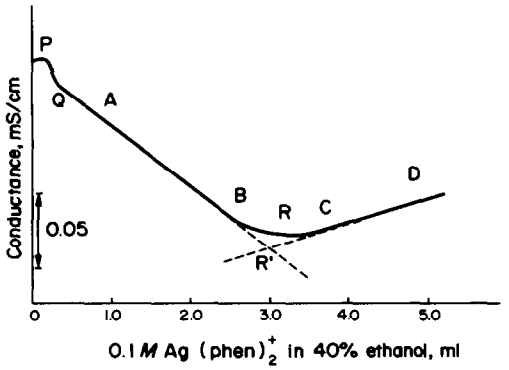


Fig. 1. Typical conductometric titration curve of nitrate ion. NO_3^- 19.89 mg; 2 ml of 3*M* acetate buffer solution, pH 4.3; total volume 100 ml; titration speed 0.20 ml/min.

ternary complex. The end-point (R') was located easily, at the intersection of lines AB and CD, and shows that the molar ratio of nitrate to silver ion is 1.0. It can be presumed that the induction or supersaturation persists only as far as point P, and disappears between points P and Q. Nitrate (conductivity 71.4 S.cm^2) in the sample solution is replaced by acetate (conductivity 40.9 S.cm^2) from the titrant in the stage between Q and R. The increase in conductance after R is due to the increase in concentration of both the $Ag(phen)_2^+$ complex and acetate as the counter-ion for this complex.

Composition of ternary complex

The molar ratio of phen to silver in the ternary complex was examined by a spectrophotometric method based on absorbance of the $Fe(phen)_3^{2+}$ complex. A series of solutions was prepared as follows: take a constant amount of silver ion in a standard flask, adjust to pH 4.3, add various amounts of phen from 0.0 to 3.0 in molar ratio to the silver, add a small excess of nitrate relative to silver, dilute to the mark, filter through a 0.22-μm membrane filter and develop the colour with iron(II) solution. Measure the absorbance at 510 nm. The break-point on the graph of the results shows the molar ratio of phen to silver is 2.0. From this result and the molar ratio of nitrate to silver at the end-point in Fig. 1, it may be concluded that the composition of this ternary complex is Ag^+:phen:NO_3^- = 1:2:1. This composition agrees with the reported formula.[9,10]

Effect of pH and concentration of phen in the titrant

It is not easy to prepare a titrant in which the molar ratio of phen to silver is exactly 2.00. To examine the influence of excess of phen in the titrant, titrants containing a small excess of phen were prepared and the relationship between optimum pH and molar ratio of phen to silver was investigated. The results are given in Fig. 2 and Table 1. They obviously show that the maximum pH-range for determination of nitrate decreases with increasing concentration of phen in the titrant. However, at pH 4.3 a 2.12 molar ratio of phen to silver causes no interference.

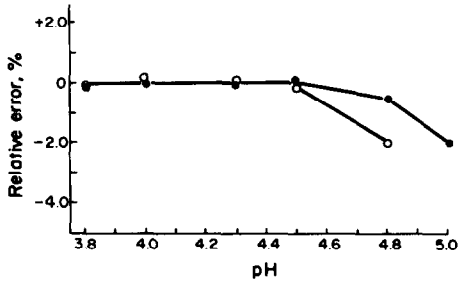


Fig. 2. Effect of pH. Other conditions as for Fig. 1. Molar ratio of phen/Ag^+: —●— 2.01; —○— 2.06.

Effect of various solvents

Ethanol, methanol or acetone as solvent for the titrant caused no significant difference in the titration curve, but the ethanol concentration must be less than 50%, or curvature appears in the region AB on the titration curve. When a solvent concentration of less than 30% is used, the solubility of the reagents is poor. For these reasons, a 40% concentration of ethanol is used (Table 1).

Effect of buffer concentration and total volume

When citrate, oxalate or tartrate buffer is used, there is a large positive error owing to formation of insoluble precipitates with the titrant. Therefore, acetate buffer is used. The addition of 0.5–2.5 ml of 3*M* acetate buffer has no effect on the determination. With increasing total volume an increasingly negative error arises, but the titration is satisfactory when the total volume is between 75 and 125 ml.

Effect of titration speed

As the method is based on precipitation, the results are affected by titration speed. A positive error arises with increasing titration speed, but the relative error is <0.5% when titrant is added at 0.20 ml/min or less.

Effect of diverse ions

A titration curve in the presence of zinc, as an example of heavy metal ions, is shown in Fig. 3 (curve 1). Two inflection points are observed. The curve up

Table 1. Effects of molar ratio, phen/Ag^+, and concentration of ethanol (nitrate ion taken: 19.89 mg)

[phen]/[Ag^+]	Ethanol, (%)	Nitrate found, *mg*	Error, %
2.01	40	19.90	+0.1
2.06	40	19.91	+0.1
2.12	40	19.85	−0.2
2.31	40	19.67	−1.1
2.50	40	19.51	−1.9
2.01	20	19.91	+0.1
2.02	30	19.87	−0.1
2.01	50	19.88	−0.1

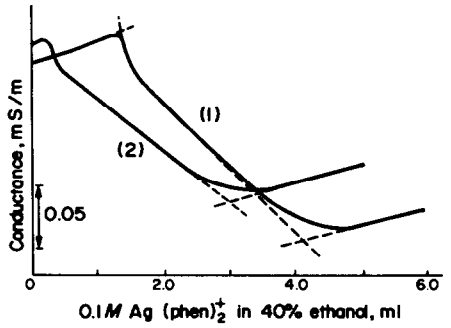


Fig. 3. Titration curves for nitrate in the presence of (1) 0.3 mmole of zinc; (2) 0.3 mmole of zinc and slight excess of masking agent. Other conditions as for Fig. 1.

to the first inflection point corresponds mainly to formation of the $Zn(phen)_3^{2+}$ complex, and the second to formation of the nitrate ternary complex. There was a large negative error, mainly due to the ligand substitution reaction between the zinc and silver.

To remove the effect, the metal ions were masked by addition of the necessary amount of phen, in advance. As a large excess of phen will itself cause error, the amount to be added for masking was found by conductometric titration with 0.2*M* phen (in 40% ethanol–water) at pH 4.3 as described previously.[11] The titration curve for nitrate in the presence of the amount of phen estimated in this way is also shown in Fig. 3 (curve 2). It is thus possible to determine nitrate without interference by metal ions. There is fair tolerance since excess of phen up to 0.8 mmole and of ethanol up to 3% in the final solution is permissible (Fig. 4).

On the other hand, as many other anions besides nitrate react with $Ag(phen)_2^+$, errors arose when these were present in the sample solution.

The effect of diverse ions on the determination of nitrate was investigated in detail. The results are summarized in Table 2. The centre column indicates the permitted limit for diverse ions to give a relative error of <0.5% in determination of 19.89 mg of nitrate. Cadmium, cobalt (II) and zinc in equimolar ratio to nitrate and nickel in up to half this ratio do not interfere. A 5-fold molar ratio of ammonium ion and 2-fold ratio of urea to nitrate also will not interfere. Nitrite is tolerated only at 0.1 molar ratio to nitrate. Perchlorate, iodide, thiocyanate and thiosulphate interfere at any concentration, and the tolerance for bromide and cyanide is very low (Table 2).

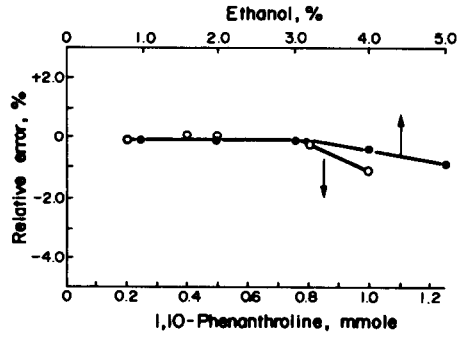


Fig. 4. Effect of amounts of 1,10-phenanthroline and ethanol. NO_3^- 19.89 mg; 2 ml of 3*M* acetate buffer, pH 4.3; total volume 100 ml; titration speed 0.20 ml/min. —○— phen, —●— ethanol.

Determination of nitrate

Nitrate (9.95–29.85 mg) was titrated with $Ag(phen)_2^+$ in 40% ethanol–water solution according to the rec-

Table 2. Effect of diverse species (nitrate taken: 19.89 mg)

Species (X)	Added as	[X]/ [nitrate]	Nitrate found, *mg*	Error (%)
none	—	—	19.94	+0.3
Ca^{2+}	acetate	1.0	19.82	−0.4
Mn^{2+}*	acetate	2.0	19.80	−0.5
Cu^{2+}*	acetate	0.25	19.80	−0.5
Co^{2+}*	acetate	1.0	19.84	−0.3
Cd^{2+}*	acetate	1.0	19.82	−0.4
Ni^{2+}*	acetate	0.5	19.85	−0.2
Zn^{2+}*	acetate	1.0	19.87	−0.1
NH_4^+	acetate	5.0	19.90	+0.1
F^-	sodium salt	1.5	19.93	+0.2
Cl^-	sodium salt	0.15	19.97	+0.4
Br^-	potassium salt	0.01	20.00	+0.5
CN^-	potassium salt	0.02	19.94	+0.3
NO_2^-	sodium salt	0.1	19.90	+0.1
SO_4^{2-}	sodium salt	0.3	19.94	+0.3
urea		2.0	19.97	+0.4

* 0.2*M* phen (in 40% ethanol–water) added.

Table 3. Determination of nitrate

Taken, *mg*	Found,* *mg*	Error*, %	Relative std. devn., %
9.95	9.96	+0.1	0.3
14.92	14.86	−0.4	0.4
19.89	19.92	+0.2	0.2
24.86	24.88	+0.1	0.3
29.85	29.99	+0.5	0.3

* Mean of 5 determinations.

Table 4. Determination of nitrate-nitrogen in commercial fertilizer sample (Shosan Ammonia)

	Nitrate-nitrogen, %*	
	Proposed method	Nitron method
	17.26	17.23
	17.10	17.17
	17.22	17.20
	17.19	—
	17.09	—
Mean	17.17	17.20
Rel. std. devn.	0.4%	0.2%

* The value certified by the manufacturer is 17.2%.

ommended procedure. Analytical results are given in Table 3. The relative standard deviation was $<0.4\%$ and relative error $<0.5\%$.

This method was applied to determination of nitrate-nitrogen in a commercial fertilizer, "Shosan-ammonia". The sample was analysed by the proposed method and the nitron method.[1] The results shown in Table 4 agreed satisfactorily and with the data reported by the manufacturer.

REFERENCES

1. A. J. Clear and M. Roth, in *Treatise on Analytical Chemistry*, Part II, Vol. 5, I. M. Kolthoff and P. J. Elving, eds., pp. 271, 273. Interscience, New York, 1961.
2. E. Krause and A. von Grosse, *Chem. Ber.*, 1925, **58**, 272.
3. J. S. DiGregorio and M. D. Morris, *Anal. Lett.*, 1968, **1**, 811.
4. H. Hartmann and G. Bäthge, *Angew. Chem.*, 1953, **65**, 107.
5. J. S. DiGregorio and M. D. Morris, *Anal. Chem.*, 1970, **42**, 94.
6. A. Hulanicki and M. Maj, *Talanta*, 1975, **22**, 767.
7. I. Hayashida, H. Yoshida, M. Taga and S. Hikime, *Bunseki Kagaku*, 1980, **29**, 304.
8. W. Kirsten and C. Carstens, *Anal. Chim. Acta*, 1951, **5**, 272.
9. P. Pfeiffer and W. Christeleit, *Z. Anorg. Allgem. Chem.*, 1938, **239**, 133.
10. J. R. Hall, M. R. Litzow and R. A. Plowman, *Aust. J. Chem.*, 1966, **19**, 197.
11. H. Yoshida, I. Hayashida, M. Taga and S. Hikime, *Bunseki Kagaku*, 1977, **26**, 461.

Talanta. Vol. 28. pp. 353 to 358. 1981
Printed in Great Britain. All rights reserved

0039-9140/81/060353-06$02.00/0
Copyright © 1981 Pergamon Press Ltd

ELECTROTHERMAL ATOMIC-ABSORPTION DETERMINATION OF BARIUM IN BRINES AND CAUSTIC SODA SOLUTIONS

FADHIL JASIM and MAHMOOD M. BARBOOTI
Department of Chemistry, College of Science, University of Baghdad, Baghdad, Iraq

(*Received* 24 *April* 1980. *Revised* 24 *November* 1980. *Accepted* 5 *January* 1981)

Summary—A method is described for the determination of barium at trace levels (0.2–2.5 ng) in the presence of a large amount of sodium chloride or sodium hydroxide (up to 750,000-fold) by electrothermal atomic-absorption spectrophotometry. The method involves making the sample solutions 1*M* with respect to nitric acid and directly injecting 5-μl aliquots into a pyrolytic-graphite furnace. Sodium chloride can be completely removed during the ashing stage of the heating cycle, without chemical pretreatment. On the basis of experimental results obtained, an explanation for the negative deviation of the calibration graphs noticed in ETA-AA is given, with nickel and barium atomization data as examples. Factors affecting the atomization peak shape and sensitivity for barium are also discussed.

The occurrence of barium in some industrial matrices affects the quality and performance of processing. In the viscose rayon industry, barium is among the trace elements that cause incrustations in the spinnerette holes, and result in the threads coming out of these holes being comparatively weak because of irregular cross-section. Preliminary scanning electron microscopy and X-ray microanalysis of the spinnerettes have shown[1] that the incrustations are due to corrosion. Barium, together with other trace elements such as Zn, Si, K, Ca, and Fe, may catalyse the decomposition of the gold–platinum alloy of the spinnerette, forming incrustations and irregular edges around the perifery of each hole. The viscose is contaminated with barium through the caustic soda used for the dissolution of the pulp. The caustic soda is usually prepared electrolytically from brine. Barium carbonate suspension is added during purification of the sodium chloride, and traces of barium find their way to the final stages. The electrolysis may concentrate barium in the caustic soda produced, since barium present in the brine may be reduced and amalgamate with mercury of the cathode. Thus the barium content increases.

One of the methods available for barium determination is atomic-absorption spectrophotometry (AAS). The flame atomization technique has shortcomings, among which are the spectral and chemical interferences from the matrix materials, and the limited detectability.[2] In the analysis of brines the nitrous oxide–acetylene flame can be used for the barium concentration range 2–10 μg/ml.[3] Barium determination by the graphite-furnace method has two drawbacks: carbide formation from contact of the metal with the graphite surface at high temperatures,[4–6] and early degradation of the graphite tubes.[5] However, the determination is not influenced by mineral acids[7] and is improved when argon is used as purge-gas instead of nitrogen.[8,9] Moreover, the modifications of graphite furnaces, including pyrolytic graphite coating,[10] tantalum lining[11] and metal carbide coating[12] of the graphite tubes are useful in barium determination.[5,9] Barium has been determined in sea-water (which is characterized by the relatively high salt concentration) with use of automatic background correction with a tungsten iodide lamp as a continuum source.[13,14] The chromium line at 541.6 nm has been used for detection of the background signal due to graphite volatilization.[9] Szydlowski and Vianzon[15] reported some effects of the sodium chloride matrix when electrothermal atomization was used for the AAS determination of barium. They claimed that there is an optimum concentration of sodium chloride, which gives improved sensitivity.

Attention has recently been drawn to the graphite furnace atomic-emission spectrometric determination of barium in calcium carbonate,[16] potable waters and sediments,[17] with a detection limit of 0.8 ng/ml[17] and a determination limit of 0.036 μg/ml, for sample volumes of 50 μl.[16]

The present paper describes studies on the determination of subnanogram quantities of barium directly in concentrated sodium chloride and sodium hydroxide solutions by AAS with electrothermal atomization.

EXPERIMENTAL

Apparatus

A Varian–Techtron AA-5 atomic-absorption spectrophotometer equipped with a CRA 63 carbon-rod atomizer was used. Pyrolytic graphite tubes (Ringsdorff high-purity

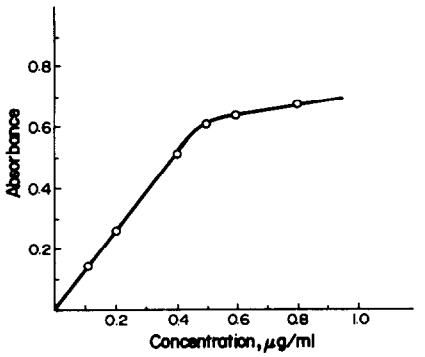


Fig. 1. Calibration graph for barium with 5-μl aliquots.

graphite grade R.W.I.) were used. The spectrophotometer was connected with a Varian 9176 chart-recorder. The photomultiplier tube used was an R955 (Hamamatsu, Japan) which is characterized by a wide range of spectral response. A masking plate with a 3-mm diameter circular aperture was positioned immediately after the tube furnace to block out light other than that passing through the furnace. The radiation source was a Varian–Techtron barium hollow cathode lamp. A slit-height device supplied by the manufacturer was fitted to the slit-mechanism drum of the monochromator and set at 3 mm. The spectrophotometer was normally operated with the least damping and no scale expansion. The instrumental settings were as follows.

AA-5

Wavelength, *nm*	553.6
Spectral bandpass, *nm*	0.4
Lamp current, *mA*	15
Argon flow-rate, *l./min*	4.5
Cooling water flow-rate, *l./min*	0.5
Sample size, *μl*	5
Recorder chart-speed, *cm/min*	5
Recorder f.s.d., *mV*	10

CRA-63

	Dry	Ash	Atomize
Time, *sec*	30	25	4.0
Voltage, *V*	3.5	8.5	9.0

Reagents

All reagents were of analytical grade. Demineralized distilled water was used for preparation of solutions, dilution, and final rinsing of glassware. A barium stock solution (1000 μg/ml) was prepared in 1% hydrochloric acid, and diluted to 50 μg/ml (weekly) and 5.0 μg/ml (daily) to make the calibration standard solutions. The standards were made 1*M* in nitric acid.

Sampling

Raw salt was sampled according to Vogel.[18] Brines, caustic soda solutions, and demineralized water samples were collected in different batches during processing, over a period of four months.

Preparation of samples for analysis

Brines. Samples, 5 or 10 ml, were placed in 50-ml standard flasks together with 3 ml of concentrated nitric acid and with or without an appropriate volume of standard barium solution for direct and standard-addition measurements, then diluted to the mark with demineralized water.

Caustic soda. Samples ranging from 1 to 3 ml were placed in 50-ml standard flasks with enough nitric acid to give a final acid concentration of 1*M*, and further treated as for brine samples.

Raw salts. The powdered salt samples were kept at 90° for at least two days before analysis. Accurately weighed samples of about 4–5 g were dissolved in demineralized water heated to 70° and filtered into 50-ml standard flasks. A 3-ml portion of concentrated nitric acid was added to each flask and the solutions were finally diluted to volume with demineralized water.

Synthetic samples. Standard barium solutions containing a maximum of 8% of sodium chloride were prepared for use in studies of the effects of the sodium chloride matrix on barium.

RESULTS AND DISCUSSION

Calibration graph

The calibration graph is shown in Fig. 1. It is linear up to a barium concentration of 0.5 μg/ml, which corresponds to an absolute amount of 2.5 ng of barium. Repetition of the analysis of an individual standard shows that for concentrations above 0.6 μg/ml the absorbance signals alternate in magnitude, the first, third, fifth *etc.* being lower than the second, fourth, sixth *etc.*, but the values within the two groups agree (Fig. 2). When a tube-cleaning run is performed between each pair of replicate standardization runs, the replicate signals become equal. A similar effect was observed for nickel, when this was used as a model element in attempts to find an explanation for

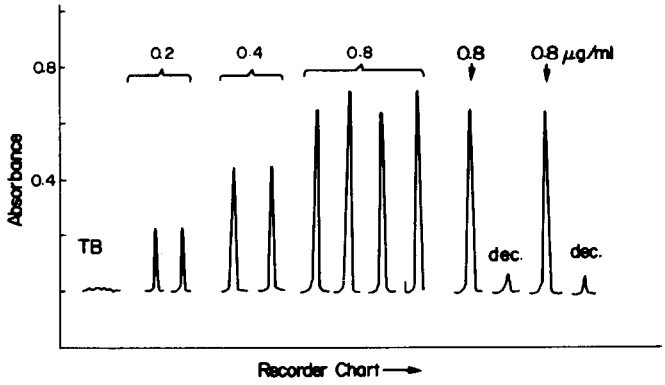


Fig. 2. Replicate runs for various concentrations of barium. TB refers to tube blank runs, and dec. refers to decontamination runs.

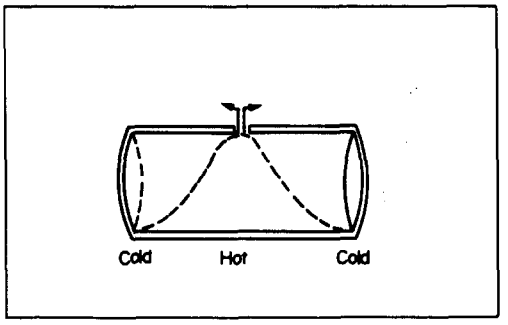


Fig. 3. Longitudinal section of the tube furnace.

this behaviour. The pronounced curvature at higher concentrations may be at least tentatively accounted for as follows.

In electrothermal atomization the carbon monoxide partial pressure in the carbon tube may rise to 0.1 atm,[19] and other gases remaining from the preceding ash stage may contribute to the total pressure. The longitudinal distribution of heat in the tube furnace shows a temperature gradient[20] and hence a density gradient from the middle of the tube towards the ends (Fig. 3). This means that there may be a gradient in the distribution of the gases inside the tube. The combination of the various gradients could result in incomplete escape of atomized analyte from the tube at higher analyte concentrations, resulting in a memory effect, and an apparently higher concentration if the same sample is immediately run again. Support for this view is given by the fact that the signals obtained during a tube-cleaning firing are close to the differences between the signals from successive firings of the same sample (Fig. 2), and also to the deviation from the extrapolation of the linear part of the calibration graph (Fig. 4). Attribution of this deviation to the response time of the recording system[21] is not sufficient to explain these experimental findings. In flame AAS, the problem of calibration graph curvature has been attributed to spectral interferences, and attempts have been made to expand the linear range by using better monochromators and applying instrumental scale expansion,[22] but these considerations do not apply in this case.

Shape of the AA peak

In principle the shape of the peak is a function of atomization rate, amount of analyte, and time of atom formation, in addition to other factors related to the physical properties of the analyte. We therefore examined various atomization conditions (voltage/time combinations). The appearance time of the barium peak is dependent on the heating programme used; the higher the voltage the shorter the appearance time. All the appearance times obtained for the various heating programmes correspond to a temperature of 2000 ± 20 K (Fig. 5). The boiling point of barium[23] is 1913 K and the vapour pressure of monatomic barium attains values above 300 mmHg at temperatures above 1900 K.[24] The temperatures were evaluated by referring to temperature–time profiles similar to those reported by Maessen and Posma.[19] Thus the atomization of barium proceeds by the sequence

$$BaO \xrightarrow[\text{heat}]{\text{graphite}} Ba_{(s)} \xrightarrow{\text{heat}} Ba_{(l)} \xrightarrow{\text{heat}} Ba_{(g)}. \quad (1)$$

Atomization efficiency

The efficiency of atomization with the various heating programmes has been estimated by applying the formula:[25]

$$\text{efficiency} = N_{peak}/N_0 = \frac{2\tau_2^2}{\tau_1^2}(\tau_1/\tau_2 - 1 + e^{-\tau_1/\tau_2}) \quad (2)$$

where N_{peak} is the number of atoms present at the peak maximum, N_0 = the total number of atoms in the sample, τ_1 = time of atom formation, τ_2 = residence time of atoms.

A typical atomization peak is illustrated in Fig. 6, where the parameters listed above are indicated. These parameters have been calculated for the various heating programmes and the results are listed in Table 1 together with the peak-heights and peak-areas related to them. It is clear that the peak-area is independent of the heating programme as it represents the whole effect, whereas clear differences can be observed between the peak-heights obtained under different heating conditions. These results are in agreement with those reported for certain metals.[25] However, some authors[25,26] have paid no attention to the statistical weight of a transition when dealing with the theoretical evaluation of AA peaks. L'vov[27] tackled the problem of calculating the atom population at the peak maximum with a more fundamental approach, taking the statistical weights of the transition into account. Others[25,26] considered that the atom population at the peak maximum approaches the total number of atoms in the sample as the heat-

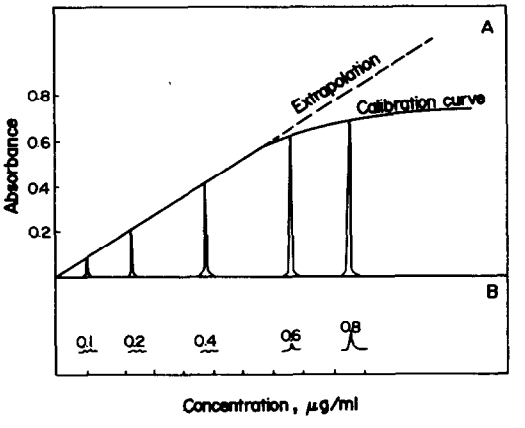


Fig. 4. Relation between residual signal and deviation from linearity.

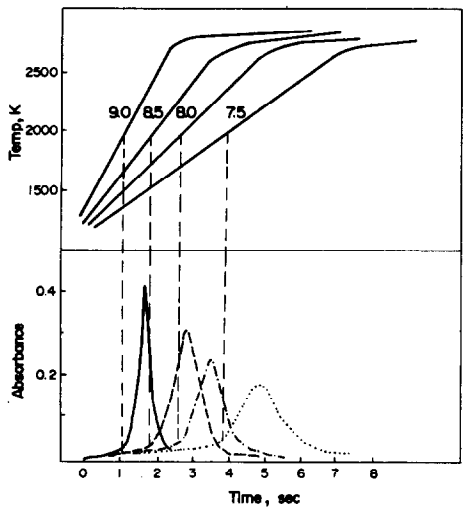


Fig. 5. Relation between the appearance time (lower part) with the atomization voltage (upper part).

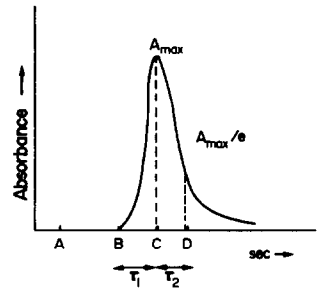


Fig. 6. Typical atomization peak. A, start of atomization step; A–B, appearance time; B–C, atom formation time; C–D, residence time.

ing rate is increased. It must be emphasized here that the atom population at the peak maximum does increase as the atomization rate increases, but for all allowed transition lines the increase is determined by the statistical weights of the transitions.

Effect of analyte concentration on the peak shape

It has been reported[28] that the analyte concentration has a large effect on the shape of the AA peak for copper atomized with a Varian-Techtron CRA-63 furnace. The appearance temperature decreases as the amount of metal atomized increases, though the position of the peak maximum is independent of the concentration. The authors[28] ascribed this observation to the thermodynamic equilibrium of the atomization process. Barium is atomized by a mechanism similar to that for copper, so a similar concentration effect might be expected. This is found not to be the case, however, as Fig. 7 shows.

Analysis of synthetic samples

For optimizing the heating conditions for the drying, ashing and atomization steps, synthetic solutions containing various concentrations of barium in 4–10% sodium chloride solution were used.

Fast heating in the drying stage results in sputtering of the salt particles in the tube and causes partial loss of the analyte.Therefore the drying temperature of the sodium chloride solutions must be lower than that for aqueous solutions in general, and the drying time longer. For sodium chloride solutions Frech and Cedergren[29] used sample sizes much smaller than the capacity of the tube furnace, to overcome sputtering problems. In the present work the drying voltages and times are those for 5-μl samples.

In the determination of barium, no loss of the analyte is expected to occur during removal of the sodium chloride matrix, because the appearance temperature of barium is very much higher than the temperature used for evaporation of the salt. A longer ashing time is necessary for complete removal of the matrix in our samples than that used for sea-water samples,[14] because the salt concentration is higher, but the results for atomization of barium in sodium chloride solutions of up to 8% concentration indicate practically 100% recovery of the barium.

In trial experiments where the ashing was incomplete, a sharp, fast and non-reproducible peak at the beginning of the atomization stage was recorded in addition to the barium peak. Careful and complete ashing resulted in the disappearance of this unwanted peak, which arose from the sodium chloride remaining after incomplete ashing. It is easy to distinguish between this non-AA peak and the barium peak because the furnace needs some time to reach the appearance temperature for barium, and this means that the two peaks are well separated. However, some

Table 1. Peak-heights, peak-areas and atomization efficiency for 0.2 μg of Ba per ml, with various heating programmes

Atomization voltage, *V*	Peak-height,* *abs. units*	Peak-area, *arbitrary units*	Appearance time, *sec*	τ_1, *sec*	τ_2, *sec*	N_{peak}/N_0†	Appearance temperature, *K*
7.5	0.17	264	1.72	2.76	1.80	0.637	1980
8.0	0.23	253	1.45	1.74	1.44	0.694	1990
8.5	0.28	260	1.12	1.37	1.2	0.707	2015
9.0	0.41	273	0.85	0.94	0.85	0.713	2010

* Corrected for background.
† See the text for comment on this parameter.

Table 2. Barium concentration (μg/ml) in rayon plant samples

Sample	Ba found Direct	Std. addn.	Recovery of added Ba, %	Remarks
1	0.64	0.68	93	30–31% brine
2	0.43	0.43	100	prepared for
3	0.73	0.72	98	electrolysis
4	8.40	8.32	99.2	50% NaOH solution
5	7.40	7.65	103.3	freshly prepared
6	0.42	0.40	95	28% spent brine
7	0.32	0.33	103	coming out of
8	0.46	0.47	102	the cell
9	n.d.	n.d.	99	Plant demineralized
10	n.d.	n.d.	100	water
11	n.d.	n.d.	99	Raw salt used in
12	n.d.	n.d.	97	preparation
13	n.d.	n.d.	98	of the brine

n.d. = not detectable.

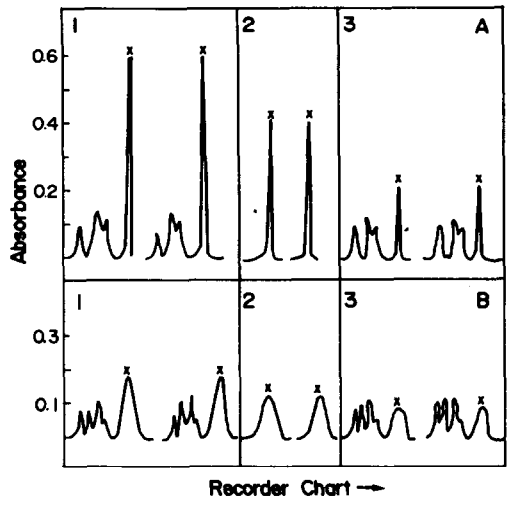


Fig. 8. Results of standard additions using step atomization (A), and ramp atomization (B). 1, 5-fold diluted brine + 1.0 ng of Ba; 2, 1.0 ng of Ba; 3, 5-fold diluted brine. Atomization peaks are marked with a cross (×).

barium is lost by co-evaporation in the fast removal of sodium chloride at the beginning of the atomization stage, and this leads to poorer reproducibility for barium.

Ramp atomization was also used for the analysis of the sodium chloride solutions, but without ashing. Figure 8 shows a comparison of the ramp and step atomization modes. Complete resolution of the non-AA and barium peaks is obtainable with ramp atomization but the barium peak is broader and lower than that obtained by step atomization. Sharper and higher peaks can be obtained at higher ramp rates, but the resolution of the peaks and hence the reproducibility becomes worse.

Effect of the matrix on the performance of the tube

It is worth reporting that the working life of the tube furnace is surprisingly shorter when sodium-rich solutions are analysed. In their study of the effects of a calcium carbonate matrix on barium determination, Thompson and Godden[8] attributed the shortening of the graphite rod life to a reaction between calcium and carbon. Alkali metals have the ability to form intercalation compounds with graphite.[30] This phenomenon may be the reason for the easy deterioration of our graphite tube during analysis of sodium-rich samples.

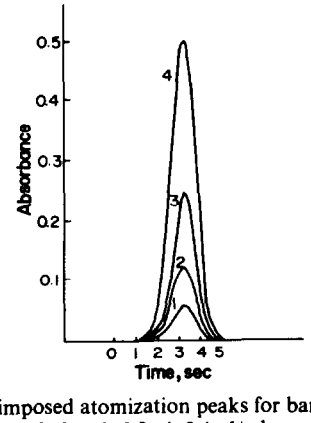


Fig. 7. Superimposed atomization peaks for barium 1, 1.05; 2, 0.1; 3, 0.2; 4, 0.4 μl/ml.

Applications

The method has been applied to the direct determination of barium in samples (Table 2) taken at the Rayon State Company, Al-Hindiya, Babylon, Iraq, in the period from September to the end of December 1979.

The barium concentration was first roughly estimated so that the samples could be diluted accordingly. All samples were analysed the day after sampling. From each sample four solutions were prepared; two for direct reading against calibration standards, and the other two for the standard addition method with different additions of the standard. Sample signals were always bracketed by standards to deal with the gradual changes in tube performance. The results are listed in Table 2.

CONCLUSION

Electrothermal AAS can be considered as one of the most sensitive methods for determination of barium in sodium chloride and sodium hydroxide solutions. Sample preparation involves only acidification with nitric acid before analysis. The barium concentration for 1% absorption is 0.002 μg/ml for aqueous solutions and 0.0025 μg/ml for sodium-rich samples, with 5-μl injections. The detection limit is 0.0027 μg/ml. The relative standard deviations at the 0.1 and 0.2 μg/ml levels are 4.8 and 4.5% respectively.

REFERENCES

1. *Swedish Forest Product Research Laboratory*, 1978, 5859–Billeruds AB.
2. W. A. Magill and G. Svehla, *Z. Anal. Chem.* 1974, **268**, 180.
3. G. E. Fletchers and G. A. Collins, *U.S. Bur. Mines Rept. Invest.*, 1974, RI-7861.
4. G. D. Renshaw, *At. Absorp. Newsl.*, 1973, **12**, 158.
5. H. J. Sherfiniski, *ibid.*, 1975, **14**, 26.
6. R. Cioni, A. Mazzucotelli and C. Ottonelle, *Anal. Chim. Acta*, 1976, **82**, 415.
7. J. F. Alder and D. A. Hickman, *At. Absorp. Newsl.*, 1977, **16**, 110.
8. K. C. Thompson and R. G. Godden, *Analyst*, 1975, **100**, 198.
9. P. Lagas, *Anal. Chim. Acta*, 1978, **98**, 261.
10. R. E. Sturgeon and C. L. Chakrabarti, *Anal. Chem.*, 1977, **49**, 90.
11. G. D. Renshaw, C. A. Pounds and E. I. Pearson, *At. Absorp. Newsl.*, 1973, **12**, 55.
12. V. J. Zatka, *Anal. Chem.*, 1978, **50**, 538.
13. R. D. Beaty and M. M. Cooksey, *At. Absorp. Newsl.*, 1978, **17**, 53.
14. M. S. Epstein and A. T. Zander, *Anal. Chem.*, 1979, **51**, 915.
15. F. J. Szylowski and F. R. Vianzon, *Anal. Lett.*, 1978, **11B**, 161.
16. R. C. Hutton, J. M. Ottaway, T. C. Rains and M. S. Epstein, *Analyst*, 1977, **102**, 429.
17. L. Ebdon, R. C. Hutton and J. M. Ottaway, *Anal. Chim. Acta*, 1978, **96**, 63.
18. A. I. Vogel, *Quantitative Inorganic Analysis*, 3rd Ed., pp. 187, 188. Longman, London, 1972.
19. F. J. M. J. Maessen and F. D. Posma, *Anal. Chem.*, 1974, **46**, 1439.
20. R. E. Sturgeon and C. L. Chakrabarti, *Prog. Anal. At. Spectrosc.*, 1978, **1**, 126.
21. F. J. Langmyhr, *Analyst*, 1979, **104**, 993.
22. L. De Galan and G. F. Samaey, *Spectrochim. Acta*, 1969, **24B**, 679.
23. R. C. Weast, *Handbook of Chemistry and Physics*, Ed., CRC, Ohio, 1974.
24. J. Bohdansky and H. E. J. Schins, *J. Inorg. Nucl. Chem.*, 1968, **30**, 2331.
25. R. E. Sturgeon, C. L. Chakrabarti, I. S. Maine, and P. C. Bertels, *Anal. Chem.*, 1975, **47**, 1240.
26. W. M. G. T. van den Broek and L. De Galan, *ibid.*, 1977, **49**, 2176.
27. B. V. L'vov, *Atomic Absorption Spectrochemical Analysis*, Hilger, London, 1970.
28. E. J. Czobik and J. P. Matousek, *Talanta*, 1977, **24**, 573.
29. W. Frech and A. Cedergren, *Anal. Chim. Acta*, 1977, **88**, 57.
30. A. K. Holliday, G. Hughes and S. M. Walker, in *Comprehensive Inorganic Chemistry*, A. F. Trotman-Dickinson, ed., Vol. 1, pp. 1271–6. Pergamon Press, Oxford, 1973.

Talanta, Vol. 28, pp. 359 to 364, 1981
Printed in Great Britain. All rights reserved

0039-9140/81/060359-06$02.00/0
Copyright © 1981 Pergamon Press Ltd

ELECTROTHERMAL ATOMIC-ABSORPTION SPECTROPHOTOMETRIC DETERMINATION OF MOLYBDENUM

MAHMOOD M. BARBOOTI* and FADHIL JASIM
Department of Chemistry, College of Science, University of Baghdad, Baghdad, Iraq

(*Received* 12 *September* 1980. *Accepted* 5 *January* 1981)

Summary—The sensitivity for determining Mo by ETA–AA is dependent on the heating programme employed when the peak-height method is used, but not when the peak area is used for evaluation of the AA signals. The linear range is greater at lower heating rate. Molybdenum can be directly determined in up to 8% NaCl solution without chemical pretreatment or background correction by making use of the high ashing temperature allowed, at which the matrix NaCl can be totally removed. The minimum recovery is 94.5%. Amounts of alkaline earth metals greater than 4000 times the amount of Mo give scatter signals, but these are time-resolved from the Mo signal. Any small effect on the peak height or area can be compensated for by background correction. The interference of tungsten is significant even at low concentrations (2–5 μg/ml) owing to the formation of stable compounds. Mo is determined in brines and acid digests of phosphate rocks after preconcentration and separation with the APDC–MIBK system, by ETA–AA of the organic extracts with or without mineralization.

In the earliest reports on the determination of molybdenum by atomic-absorption spectrophotometry (AAS), the fuel-rich air–acetylene flame was used for atomization.[1, 2] The method has been applied recently for determining down to 0.001% of Mo in ores, irons and steels after a separation–concentration step.[3] The use of the nitrous oxide–acetylene flame is useful to overcome some of the interferences encountered when other flames are used for AAS determination of molybdenum.[4] Several authors[5–7] have reported on these interference effects and means of overcoming them, but their results differ. Sutcliffe[8] criticized the use of aluminium for suppression of interference from many metals and mineral acids and stated that it enhances the AA signal of molybdenum from the N_2O–C_2H_2 flame. The electrothermal atomization (ETA) methods were first applied in the AAS of molybdenum by Bodrov and Nikolaev.[9] Many authors have since reported on various aspects of the use of ETA for molybdenum, especially the graphite-furnace method.[10–15] The method is often preceded by separation steps[11, 13, 16] although the element can be determined directly in very complex solutions such as synthetic sea-water without separation or even background correction.[15] Wilson[17] has reported that when a furnace coated with pyrolytic graphite is used, the sensitivity of the AAS method decreases gradually with age of the tube. This suggests gradual destruction of the tube coating by the repeated exposure to high temperature, resulting in increased porosity of the graphite surface.[18] In a recent report Studnicki[19] has concluded that acids at concentrations lower than 1% strongly influence the molybdenum signal and that calcium strongly decreases it, an effect which can be suppressed by some additives.

In the literature cited there is no comprehensive study of the ETA of molybdenum, covering the atomization conditions, the interferences of common elements and the direct application of organic solutions. It is the aim of the present work to supply such information. The method is applied for the determination of molybdenum in brines and phosphate rocks after solvent extraction.

EXPERIMENTAL

Apparatus

A Varian–Techtron AA-5 atomic-absorption spectrophotometer equipped with a CRA-63 carbon rod atomizer (tube version), a deuterium arc continuum source and a model 9176 strip-chart recorder was used. The spectrophotometer was fitted with a Hamamatsu R 955 photomultiplier tube. A slit-height device supplied by the manufacturer was fitted to the slit-mechanism drum and set at 3 mm. In all experiments a lamp current of 7 mA, and a spectral band-pass of 0.4 nm were used. No scale expansion or damping was used. The 313.3-nm line from a Varian-Techtron molybdenum hollow cathode lamp was employed.

Drying and ashing conditions were varied according to the nature of the solution injected. Unless otherwise stated, the atomization voltage was 9 V, applied for 5–6 sec. For aqueous solutions 5-μl aliquots were injected with an Excalibor Autopette micropipette, and an SGE 10-μl syringe was used for the injection of organic solutions.

Reagents

All reagents were of analytical grade. A BDH 1-mg/ml standard AAS molybdenum solution was used as stock solution, and diluted to 40 μg/ml (weekly) and further to 4 μg/ml as required. The solutions analysed were made 0.2*M* in nitric acid.

* To whom correspondence should be addressed.

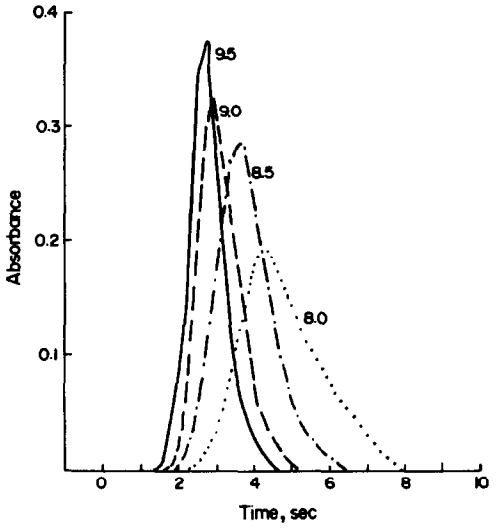


Fig. 1. The AA signals for 1 ng of Mo at different atomization voltage settings: 1, 9.5; 2, 9.0; 3, 8.5; 4, 8.0 V.

Procedure

The phosphate rock samples were decomposed by treating a 0.5-g powdered sample (accurately weighed) in a platinum crucible with 15 ml of a 1:1:10 v/v mixture of nitric, perchloric and hydrofluoric acids, and heated on a sand-bath at ~65° to complete dryness. The residue was taken with 10 ml of 1:1 HCl, boiled, making sure of complete dissolution, and filtered into a 100-ml calibrated flask.

Solvent extraction with the APDC/MIBK (ammonium pyrrolidinedithiocarbamate/methyl isobutyl ketone) system was then applied as recommended by Watson.[20] The organic extracts were analysed in two ways. The first involved mineralization by gentle evaporation of the organic solvent, boiling with nitric acid and evaporation to dryness, followed by leaching with 6*M* hydrochloric acid and final dilution with water. The second was by direct injection of the organic extract into the tube furnace. Brine samples were similarly extracted and analysed. Known amounts of molybdenum were added to the unknown samples to check the efficiency of the extraction. The calibration standard solutions were prepared in a similar manner to the samples.

RESULTS AND DISCUSSION

Characteristics of the absorption signals

The effect of the voltage setting during the atomization stage is shown in Fig. 1. It is clear that with increasing voltage the AA peak for molybdenum becomes sharper and higher but has the same integrated absorbance (Table 1). This suggests that for better sensitivity by the peak-height method, higher atomization voltages must be used. Sturgeon *et al.*[21] were not able to study the effect of atomization voltage on determination of molybdenum, for instrumental reasons, and assumed the behaviour would be similar to that found for tin and aluminium, a conclusion which differs from our findings. For tin and aluminium the increase in the atomic residence time, τ_2 (defined as the time required for the signal to decrease from its maximum A_{max} to A_{max}/e), with decreasing voltage, is not large enough to compensate for the decrease in the peak absorbance, resulting in decrease in the peak area.

With increasing atomization voltage the ratio τ_1/τ_2 (τ_1 is the atomization time, measured as the time elapsed between the signal appearing and A_{max} being reached) increases correspondingly. The atomization efficiency, which is the ratio of the number of atoms at the absorbance maximum to the total number of atoms in the injected solution, decreases with increasing atomization voltage. It is clear from Table 1 that both τ_1 and τ_2 decrease with increasing heating rate. The decrease in τ_1 is expected because the rate of atomization (production and introduction of neutral atoms into the analysis volume) increases as the temperature of the heating surface increases. The decrease in the residence time, τ_2, suggests an increasing rate of loss of atomic vapour. Both convection and diffusion are responsible for this increase in the rate of loss. The role of diffusion in the temperature-dependence of τ_2 was shown by L'vov.[22] The rate of convection increases with temperature as a result of the temperature gradient from the centre of the tube to the ends becoming steeper at higher heating voltages.

The mass of molybdenum atomized has no effect on the mechanism of atom formation, since the ratio τ_1/τ_2 is independent of the mass of molybdenum analysed (Table 2). For moderately volatile elements, *e.g.*, copper, these times are relatively constant regardless of the mass of the analyte atomized.[21] Table 2 indicates that with increasing amount of molybdenum in the tube, τ_1 and τ_2 both increase correspondingly, keeping their ratio constant.

Effect of the purge gas

The sensitivity is about 25% higher with argon than with nitrogen as purge gas, but the detection limit and

Table 1. The effects of the atomization voltage on the characteristics of the transient absorbance signals of 1.0 ng of Mo

Voltage, *V*	Peak absorbance	Peak area, *arbitrary units*	τ_1, *sec*	τ_2, *sec*	Appearance time, *sec*	τ_1/τ_2	Atomization efficiency*
8.0	0.192	883	1.46	1.86	1.98	0.78	0.78
8.5	0.280	890	1.32	1.08	1.69	1.22	0.69
9.0	0.330	880	1.20	0.84	1.50	1.43	0.66
9.5	0.375	886	0.94	0.60	1.32	1.57	0.63

* Atomization efficiency = N_{max}/N_0 where N_{max} is the number of atoms at the peak maximum and N_0 is the total number of atoms in the sample atomized.

Table 2. The effect of the mass of Mo on the characteristics of the transient absorbance signals*

Mo, *ng* τ_1/τ_2	τ_1 *sec*	τ_2 *sec*	τ_1/τ_2
0.5	1.38	0.96	1.43
1.0	1.68	1.18	1.42
2.0	1.80	1.23	1.46
4.0	1.98	1.32	1.50

* All signals produced under the same atomization conditions.

precision remain the same. The use of nitrogen is therefore quite adequate. The dependence of the absorbance on the flow-rate of the purge gas is shown in Fig. 2. The low absorbance at flow-rates lower than 4.0 l./min may be attributed to incomplete removal of the gases from the atomization surface, which is an important factor in determining the rate of atom formation.[22] The atoms formed then need to pass through this layer of foreign gas, and relaxation is likely to occur in the atom-formation process. As the rate of flow increases (4–5.2 l./min) a steady increase of the absorbance is observed, followed by a sharp decrease in absorbance at flow-rates above 5.2 l./min, caused mainly by the cooling effect of the faster gas-flow. The optimum range of flow-rates is 4–5 l./min, in which a change of 0.1 l./min alters the signal by $<2\%$.

Calibration

Sturgeon *et al.*[21] recommended peak integration for

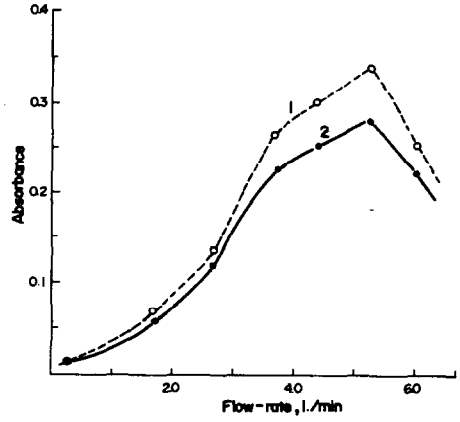


Fig. 2. Effect of the flow-rate of the purge-gas on the absorbance of 1 ng of Mo: 1, argon; 2, nitrogen.

constructing the working curves for molybdenum and vanadium. In our study, two atomization heating programmes were used and both peak height and peak area recorded (Fig. 3). The linear range is the same whether peak height or peak area is used, but is greater at the lower atomization voltage. The peak-area method is more advantageous, however, because it gives the same sensitivity whatever the atomization temperature. The highest sensitivity is given by the peak-height method at the higher atomization voltage (Table 3).

Molybdenum in sodium chloride matrix

The determination of molybdenum and other elements in sea-water and brines is important, so one of

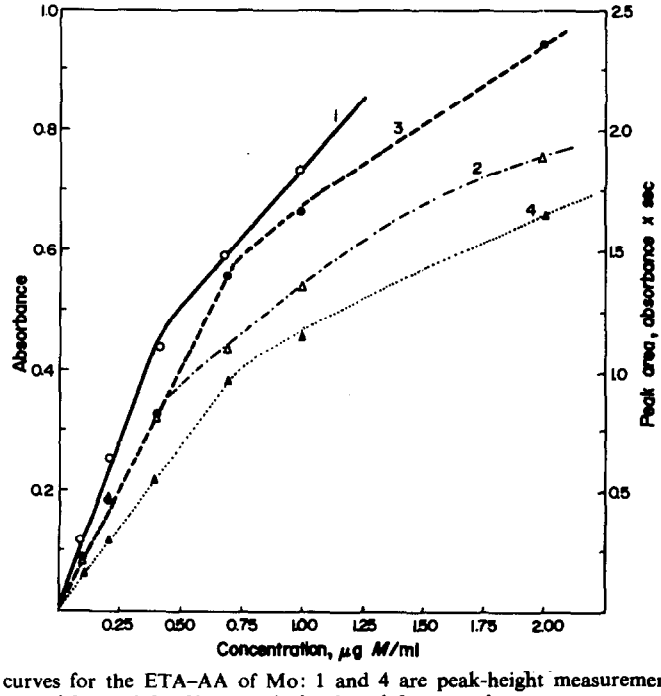


Fig. 3. Working curves for the ETA–AA of Mo: 1 and 4 are peak-height measurements recorded at atomization voltages of 9.0 and 8.5 V respectively; 2 and 3 are peak-area measurements recorded at atomization voltages of 9.0 and 8.5 V respectively.

Table 3. Analytical results for the ETA–AA of Mo

Parameter	Peak height method Atomization voltage 9.0 V	8.5 V	Peak-area method*
Reciprocal sensitivity, *pg*	13.5	27.0	11.0†
Detection limit ($S/N = 2$), *pg*	29.2	31.0	30.5
Relative std. devn., % (10 readings)	2.9	3.1	3.1
Upper linear-range boundary, *ng*	2.0	3.5	Same as for the peak-height method

* For atomization at either 8.5 or 9 V.
† The amount of Mo which gives an area of 0.0044 sec × absorbance.

the aims of this work was to study the ETA of molybdenum in brines containing 2–8% sodium chloride. Brines from the Rayon Plant, Babylon, Iraq, were used as test samples. The relatively high ashing temperature allowed in the ETA of molybdenum makes it possible to volatilize sodium chloride completely during the ashing stage without loss of the analyte. Nakahara and Chakrabarti[15] reported that when sodium chloride solutions were ashed at temperatures lower than 1100°, the molybdenum signal was higher than that from pure solutions. However, our experiments show that ashing temperatures below 1100° result in incomplete removal of sodium chloride in this stage, and that a sharp but non-reproducible peak appears immediately at the start of the atomization stage, before the AA peak for molybdenum. Figure 4 shows that the NaCl and Mo peaks are completely time-resolved and that there is no overlap of the background and analyte signals as there is elsewhere stated[15] to be. Manual checking of the absorption signals with use of a deuterium continuum source has proved that at the optimum ashing voltage there is complete removal of the sodium chloride matrix, with none left at the atomization stage. The molybdenum AA signal appears only when the atomizer temperature reaches 2130°, at which no sodium chloride is expected to be present. Accordingly, molybdenum has been determined at levels ≥ 0.05 μg/ml in brines of up to 8% sodium chloride concentration, without background correction.

Interference of Mg, Ca, Sr and Ba

The effect of some constituents of synthetic seawater on the AA of molybdenum at the 2.5-mg level has been reported;[15] it was stated that ashing temperatures of ~1000° and ~1100° are effective for the complete removal of $MgCl_2$ and $CaCl_2$ respectively. In our study the AA of molybdenum at the 0.5 ng level in the presence of 4000 times as much Mg, Ca and Sr (added as the chlorides) was measured. Ashing temperatures as high as 1400° were not enough to destroy the matrix, a reproducible small sharp peak still showing up at the beginning of the atomization stage. The molybdenum signal is well time-resolved from this sharp peak but the peak heights are increased by 0, 6 and 3% by Mg, Ca and Sr respectively, and the peak areas by 4, 10 and 5% respectively (Fig. 5). It is clear from the figure that with automatic background correction complete compensation can be obtained for the scatter signal due to these elements and the incandescent graphite. Barium at levels up to 500 times that of the molybdenum has no effect, and does not give the sharp scatter peak given by the other alkaline earth elements. This is mainly due to the high volatilization temperature of barium and its oxo-compounds which are the usual products of such high-temperature treatment.

Effects of Al, V and W

The presence of 100 ng of aluminium increases the absorbance of 0.5 ng of molybdenum by 0.052, this increase being entirely a background signal due to the aluminium.

Vanadium in up to 200-fold w/w ratio to molybdenum shows no significant effect on the AA signal.

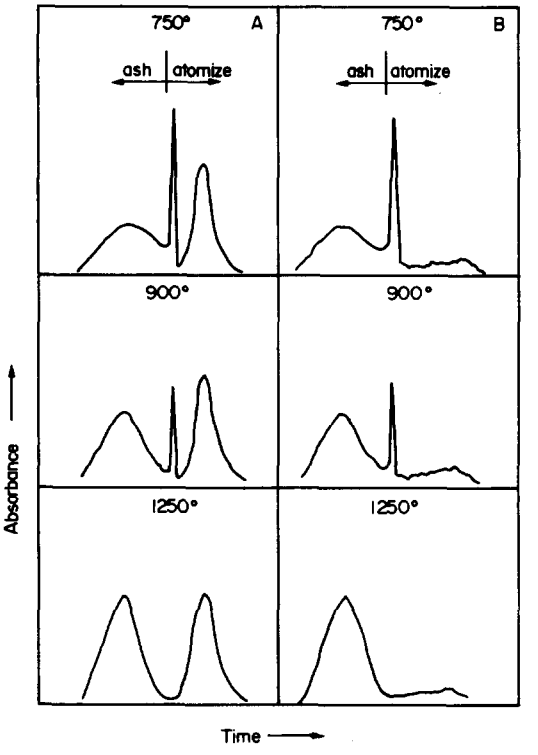


Fig. 4. The effect of the ashing temperature on the absorption signal of 1 ng of Mo + 0.3 mg of NaCl.

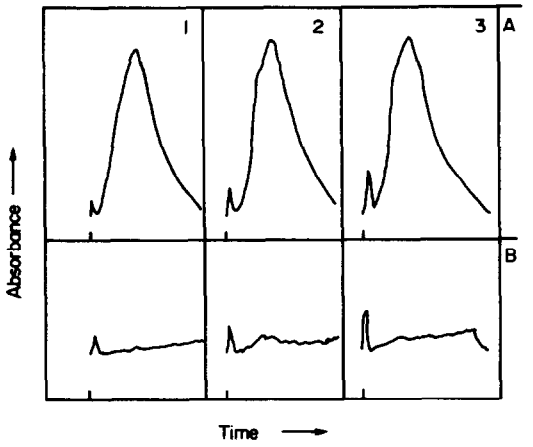


Fig. 5. A, Total absorption signals of 0.5 ng of Mo in the presence of 2 μg of Mg, 1; Ca, 2; and Sr, 3. B, Background absorption signals.

Tungsten, however, causes severe interference. Levels up to 10 ng of tungsten have no direct effect, but owing to incomplete vaporization under the heating conditions available, the tungsten accumulates during repeated runs and memory effects are noticed. Generally, with increasing concentration of tungsten the atomizer tube becomes contaminated, which hinders the atomization of molybdenum. This may be due to the formation of highly stable species likely to occur in the Mo–W–C system.[23]

Effect of mineral acids

The effects of increasing concentrations (0–5*M*) of mineral acids on the ETA/AA signal of 1.0 ng of molybdenum are given in Fig. 6. With all the acid solutions analysed, to destroy the strong acid matrix it was necessary to raise the ashing temperature to 1000° instead of the 750° usually used for the aqueous solutions. No significant effect was observed for nitric acid over the whole range of concentrations tested. Hydrochloric acid increasingly suppresses the signal as the concentration is increased to 1*M*, but at higher concentrations the signal remains constant. The suppression is at most 10%. Similar observations have been reported for these two acids in the flame AAS of molybdenum. The signal is significantly suppressed by increasing the phosphoric acid concentration above 0.1*M*. The effect of the acid on the ETA/AA of highly volatile elements, *e.g.*, Cd, Zn, or Pb is to raise the atomization temperature because of the formation of stable pyrophosphates which need higher temperatures for decomposition.[24] In the flame, phosphoric acid has been found to cause serious suppression of the AA signal of molybdenum and this was attributed to the change in viscosity of the solution (as was the similar effect of sulphuric acid).[8] Severe suppression is observed with sulphuric acid even at low concentration (0.05*M*) a behaviour which may be attributed to the co-volatilization of some molecular molybdenum species (probably MoO_3) along with the volatile decomposition products of sulphate.

Effect of MIBK

The size of the sample injected into the tube furnace has been found to be important for obtaining better sensitivity. Injection of 1, 2, 4, and 8 μl of the MIBK extract of a 0.4-μg/ml molybdenum solution gave absorbances of 0.083, 0.17, 0.28 and 0.39 respectively. These values show deviation from linearity with increasing volume. The low viscosity of MIBK causes the injected liquid to seep along the tube furnace rather than survive as a droplet in the central part of the tube. The distribution of the sample along the tube causes atomization at different rates because the temperature at the ends is lower than that at the centre of the tube. Furthermore, part of the injected liquid often runs out of the ends of the tube [but reproducible readings can still be obtained even with the larger samples (8 μl)]. A sample volume of 2 μl of the organic solution is therefore suggested as optimum.

However, multiple injection, *e.g.*, 4 μl injected and dried followed by another 4 μl and application of the

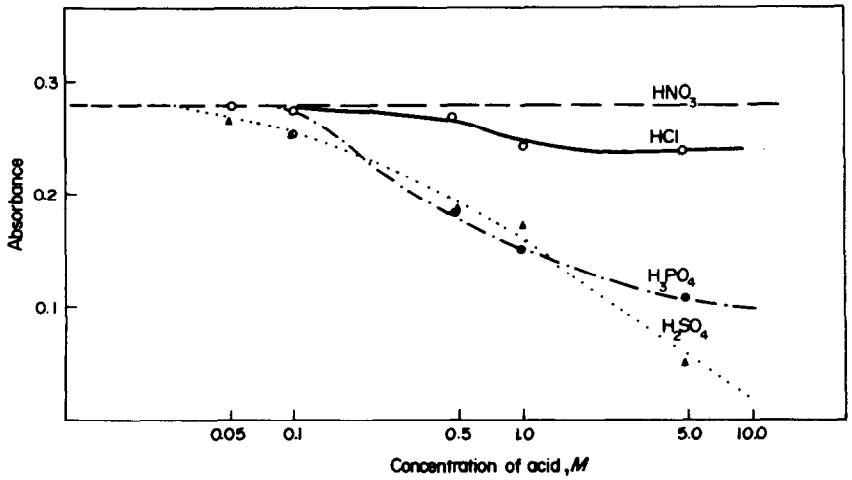


Fig. 6. Effect of mineral acids on the AA signal of 1 ng of Mo.

Table 4. Results of the solvent extraction–ETA/AA of selected samples*

No.	Description	Mo concentration, μg/ml		Mo content, μg/g
		Mineralized extract	Organic extract	
1.	Standard phosphate rock PH1†	0.148	0.151	12.2
2.	Sample 1 + Mo, 0.3 μg/ml	0.435	0.455	12.5
3.	Umm Alradhuma phosphorite	0.061	0.063	6.04
4.	Sample 3 + Mo, 0.2 μg/ml	0.25	0.27	6.71
5.	Core phosphate	0.201	0.218	17.4
6.	Fine-grain phosphorite	0.129	0.133	10.7
7.	Brine No. 1	0.150	0.185	0.037
8.	Sample 7 + Mo, 0.2 μg/ml	0.354	0.380	0.036
9.	Spent brine	0.037	0.041	0.008
10.	Raw salt§	0.103	0.105	0.130
11.	Sample 10 + Mo, 0.2 μg/ml	0.300	0.306	0.131

* All figures are compared with 0.4-μg/ml Mo extracted in the same manner, with reproducibility of ±3.4%.
† The recommended Mo value is 12.5 μg/g.
§ Taken as an 8% aqueous solution.

heating steps, gives an absorbance that though reproducible is lower than that from a single 8-μl injection. This may be attributed to the fact that before the ashing and atomization steps the residue from the multiple injection will exist as multiple layers rather than the thin layer from a single injection. The effect of the heating surface, the graphite, will be lower on the upper layers, resulting in a lower rate of atomization and hence lower peak absorbance.

The tube furnace lasts for a larger number of firings with organic solutions than with aqueous solutions. Because of the pronounced suppression of the AA signal by phosphoric and hydrochloric acids it was necessary to separate the molybdenum from the acid digest of the phosphate rocks. The APDC/MIBK system was used, which gave a 2–3-fold concentration in the final organic extracts. The brine samples were also extracted to preconcentrate the molybdenum because its concentration in the fivefold diluted brines (5–6% sodium chloride) was too low for direct injection. The results are given in Table 4. The recovery is better when the organic extracts are directly injected into the atomizer than when they are mineralized, because there is less risk of loss of the analyte and interference by the acids is avoided.

CONCLUSION

Whereas it has previously been reported[19] that molybdenum cannot be determined in the presence of 500–1000 ppm of sodium chloride, it is now found that up to 8% sodium chloride concentration has no effect on the recovery of molybdenum.

The effect of the alkaline-earth salts has been reinvestigated because of the rather ambiguous results[19] reported, and it has been found that their effect is due to scatter signals of the salts.

The effects reported[19] for the mineral acids indicated that it would be difficult to analyse an acid digest of a biological or geochemical sample. However, it is shown in the present study that these acids generally have a limiting concentration below which the interference becomes insignificant.

REFERENCES

1. D. J. David, *Analyst*, 1961, **86**, 730.
2. R. A. Mostyn and A. F. Cunningham, *Anal. Chem.*, 1966, **38**, 121.
3. E. Donaldson, *Talanta*, 1980, **27**, 79.
4. G. F. Kirkbright, A. M. Smith and T. S. West, *Analyst*, 1966, **91**, 700.
5. C. L. McIsaac, *Engng. Min. J.*, 1969, **170**, 155.
6. J. C. Van Loon, *At. Absorp. Newsl.*, 1972, **11**, No. 3.
7. T. V. Ramakrishna, P. W. West and J. W. Robinson, *Anal. Chim. Acta*, 1969, **44**, 437.
8. P. Sutcliffe, *Analyst*, 1976, **101**, 949.
9. N. V. Bodrov and G. I. Nikolaev, *Zh. Analit. Khim.*, 1969, **24**, 1314.
10. H. M. Donega and T. E. Burgess, *Anal. Chem.*, 1970, **42**, 1521.
11. R. A. A. Muzzarelli and R. Rocchetti, *Anal. Chim. Acta*, 1973, **64**, 371.
12. V. B. Schweizer, *At. Absorp. Newsl.*, 1975, **14**, 137.
13. D. R. Dreesen, E. S. Gladney, J. W. Owens, B. L. Perkins, C. Wienke and L. E. Wangen, *Environ. Sci. Technol.*, 1977, **11**, 1017.
14. J. Sneddon, J. M. Ottaway and W. B. Rowston, *Analyst*, 1978, **103**, 776.
15. T. Nakahara and C. L. Chakrabarti, *Anal. Chim. Acta*, 1979, **104**, 99.
16. E. A. Statseva, N. M. Popova, I. G. Yudelevich, N. G. Vanifatova and Y. A. Zolotov, *Z. Anal. Chem.*, 1980, **300**, 28.
17. D. O. Wilson, *Commun. Soil Sci. Plant Anal.*, 1979, **10**, 1319.
18. R. E. Sturgeon and C. L. Chakrabarti, *Anal. Chem.*, 1977, **49**, 90.
19. M. Studnicki, *ibid.*, 1979, **51**, 1336.
20. C. A. Watson, *Ammonium Pyrrolidinedithiocarbamate*, Monograph 74, Hopkin and Williams, England, 1971.
21. R. E. Sturgeon, C. L. Chakrabarti, I. S. Mains and P. C. Bertles, *Anal. Chem.*, 1975, **47**, 1240.
22. B. V. L'Vov, *Atomic Absorption Spectrochemical Analysis*, Hilger, London, 1970.
23. G. J. Throop, P. Rogl and E. Rudy, *High Temp. High Press.*, 1978, **10**, 553.
24. E. J. Czobik and J. P. Matousek, *Talanta*, 1977, **24**, 573.

Talanta. Vol. 28. pp. 365 to 368. 1981
Printed in Great Britain

0039-9140/81/060365-04$02.00/0
Pergamon Press Ltd

THE DETERMINATION OF LEAD IN MOSSES BY MEANS OF ITS CATALYTIC EFFECT ON THE PERSULPHATE OXIDATION OF PYROGALLOL RED

R. G. ANDERSON and B. C. BROWN*

Department of Physical Sciences, The Polytechnic, Wolverhampton, England

(*Received* 15 *October* 1980. *Accepted* 5 *January* 1981)

Summary—Lead is determined in aqueous solution in the concentration range 0.002–10 μg/ml by its catalytic effect on the oxidation of Pyrogallol Red at pH 8.5. The method has been applied to the determination of lead in mosses by means of a wet ashing procedure using nitric and perchloric acids and separation from interfering ions by extraction as the dithizone complex into chloroform, and back-extraction.

Over the last decade, the determination of lead in plant material has become of major importance because of increased awareness of the detrimental role of lead in the environment. Consequently, numerous methods have recently been developed for the determination of lead in plant material at low concentrations. Techniques on which these are based include atomic-absorption, either with flame[1,2] or electrothermal atomization,[3–5] polarography[6] and optical emission and X-ray fluorescence.[7,8] Most of these methods require fairly sophisticated instrumentation, however. We wish to describe a procedure based on the catalytic effect of lead on the oxidation of Pyrogallol Red by persulphate.[9,10] The advantages of the method are that analyses are possible in the sub-μg/ml range with instrumentation no more sophisticated than a simple colorimeter.

EXPERIMENTAL

Apparatus

All spectroscopic measurements were made on a Pye Unicam SP800 recording spectrophotometer operated at constant wavelength, with 4-cm cells unless otherwise specified.

A Foxall Colorimeter, with 1-cm cells, was used for the colorimetric measurements.

Atomic-absorption measurements were made with a Varian–Techtron AA6 Spectrometer operated at 283.3 nm, with an air–acetylene flame. A scale-expansion factor of 20 was used.

A Hilger and Watts Large Quartz Spectrograph was used for qualitative analysis of a dry-ashed sample of moss in connection with the interference studies.

All glassware was treated by rinsing successively with nitric acid (1 + 1), demineralized water, 10% Decon 90 solution and demineralized water, and then treated with 'Repelcote' (Hopkin and Williams). It was then kept solely for use in this work.

Reagents

All reagents were of analytical grade and used without further purification. Stock solutions were prepared in demineralized water, and included lead nitrate (lead concentration 1000 μg/ml, further diluted as required), 0.02*M* sodium tetraborate, 0.08*M* boric acid, 0.10*M* potassium persulphate, Pyrogallol Red ($2.5—40 \times 10^{-5}M$, in ethanol–water, 1:9).

All the stock solutions were stable for long periods, except the last two, which were prepared daily.

Mineralization of the moss samples

The moss was oven-dried for 4 days at 100° and then samples (0.01 or 0.1 g) were weighed into 50-ml Kjeldahl flasks. Nitric acid (1 ml) plus a few drops of perchloric acid was added to each. The mixtures were cautiously heated for about 10 min until the initial reaction had subsided and then strongly heated to complete the oxidation. The residue was diluted to 5 ml with dilute nitric acid.

Separation of the lead from interfering ions[11]

To the mineralized solution 7.5 ml of an ammonia–cyanide–sulphite mixture (0.15 g of anhydrous sodium sulphite dissolved in 35 ml of concentrated ammonia solution and 3.0 ml of 10% potassium cyanide solution diluted to 100 ml) were added and the pH was adjusted to 9.5 with hydrochloric acid. This solution was shaken gently for 10 min with 25 ml of 0.0015% solution of purified[12] dithizone in chloroform. The organic layer was separated and the lead was stripped with 10 ml of nitric acid (pH 2–3) and the resulting aqueous phase diluted to 20 ml with water.

Kinetic measurements

For all kinetic measurements the appropriate amounts of Pyrogallol Red, sodium tetraborate and boric acid stock solutions were mixed and diluted to 50 ml (solution A). A second solution (solution B) was prepared from the appropriate lead solution (standard or extract from sample) and potassium persulphate stock solution. Solutions A and B were mixed, a portion was immediately placed in the spectrophotometer or colorimeter cell and its absorbance at 530 nm monitored as a function of time. A plot of the difference between initial absorbance and absorbance after 200, 300 or 600 sec against final lead concentrations in the standard solutions was prepared and used to determine the lead concentrations in the extracts from the ashed moss samples.

* Present address: New College, King Street, Wellington, Telford, Shropshire.

Table 1. Absorbance decrease (in 600 sec) at 530 nm due to oxidation of $3 \times 10^{-5}M$ Pyrogallol Red as a function of oxidant and buffer concentration

$[K_2S_2O_8]$, $10^{-4}M$	ΔA	
	Buffer 1	Buffer 2
2	0.062	0.049
4	0.122	0.099
8	0.257	0.201

Buffer 1: 10 ml of boric acid solution/5 ml of borax solution.

Buffer 2: 20 ml of boric acid solution/10 ml of borax solution.

RESULTS AND DISCUSSION

Choice of dye

The dyes originally studied by Yasinskene and Kalesnikaite were 3,4-dihydroxyazobenzene[10] and Pyrocatechol Violet[9] as well as Pyrogallol Red[10] and stilbazo.[10] However, we wished to study dyes that were readily available commercially and therefore selected Pyrogallol Red and stilbazo for further study. Preliminary studies, however, showed that the lead-catalysed Pyrogallol Red system was the more sensitive by a factor of about five. Since stilbazo offered no particular advantages, Pyrogallol Red was selected for further study.

Optimum conditions for the catalytic oxidation

Initial studies showed that the order of addition of reagents is critical. Obviously, the dye and oxidant must not come together before timing of the reaction starts. Nor must the lead be mixed with the buffer, or precipitation will occur.[10] Hence the two-solution system was developed.

In establishing the optimum conditions and in particular in seeking to reduce the limit of detection, we found that the rate of the uncatalysed reaction had to be low enough for accurate measurements to be made on the catalysed reaction. We found that the rate of the uncatalysed reaction varies linearly with potassium persulphate concentration and is not insignificant as reported previously[10] (Table 1). The rate of the catalysed reaction has also been found to depend linearly on oxidant concentration.[10] We also found that the uncatalysed reaction rate decreased with increasing buffer concentration, possibly owing to formation of a complex between the dye and borate, stabilizing the dye against oxidation (Table 1).

Varying the dye concentration enabled us to vary the optimum lead concentration range that could be determined, but for each dye concentration the optimum buffer and oxidant concentrations had to be re-established. The optimum conditions are summarized in Table 2.

Calibration curves were obtained in two ways.

(1) The decrease in absorbance of the mixture of solutions A and B, measured at the absorption maximum of Pyrogallol Red (530 nm) precisely 200 or 300 sec after mixing was plotted against lead concentration in the same solution. Figure 1 shows a typical calibration curve. Although the curves are non-linear they can be accurately drawn and are suitable for analytical measurements.

(2) A plot of pA (where A is the absorbance of the mixed solution at 530 nm) against lead concentration in the final solution is linear up to a lead concentration of at least 5 μg/ml. A plot of reciprocal of absorbance against lead concentration over the range 0.01–2.0 μg/ml is reasonably linear, but a comparison of correlation coefficients showed the pA plot to give the better fit.

However, for analytical purposes we preferred to use the non-linear plots, since these enabled us to fit the line most closely to the observed data, without having to make any assumptions concerning the nature of the relation.

The total range covers a 5000-fold change in lead concentration, or a 50-fold change for any one set of conditions. The limit of detection is found to be 0.002 μg/ml in the final solution and is fixed by the ability to differentiate between the signals from the catalysed and uncatalysed reactions. The upper limit of determination is fixed by the absorbance of Pyrogallol Red. These ranges and limits of detection compare favourably with those quoted by Dolmanova *et al.*[13] of 0.03–0.2 μg/ml for the method in which lead binds an inhibitor (bipyridyl) in the iron(III)-catalysed oxidation of *p*-phenetidine.

An attempt was made to improve the limit of detection by washing all reagent solutions with a 1% solution of dithizone in chloroform to remove any trace heavy metals. However, this resulted in a higher limit of detection and no improvement in accuracy, possibly because of traces of dithizone remaining in the aqueous layer. Temperature control also failed to improve precision or accuracy.

Interferences

These were studied under the most sensitive conditions for lead. Table 3 shows the decrease in absorb-

Table 2. Experimental conditions for the kinetic determination of lead

Lead concentration range, μg/ml	Upper	10	2.0	0.1
	Lower	0.2	0.01	0.002
Boric acid stock solution, *ml*		5	5	5
Sodium tetraborate stock solution, *ml*		5	5	5
Potassium persulphate stock solution, *ml*		8	8	16
Pyrogallol Red stock solution, *ml*		15	15	15
Concentration of Pyrogallol Red stock solution, *M*		4×10^{-4}	10^{-4}	2.5×10^{-5}
Time between mixing and measurement, *sec*		300	300	200
Cell path-length, *cm*		1	4	4

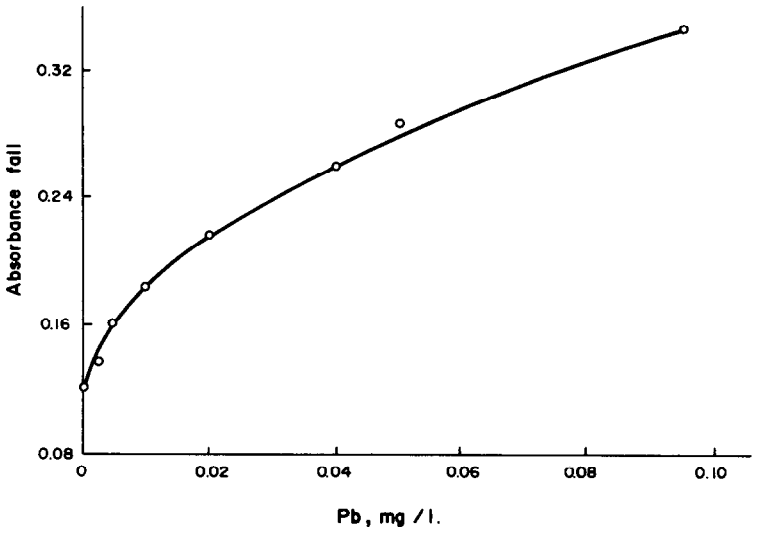


Fig. 1. Calibration graph for 0.002–0.100 mg of lead per litre.

ance in 100 sec for no added metal, for 10^{-8} and $10^{-7}M$ lead and for other metals found by spectrographic analysis to be present in the dry-ashed plant material. Numerous ions are observed to cause increase in the absorbance change, indicating the need for a preliminary separation of lead. Extraction by dithizone into chloroform[11] was chosen for this separation.

Determination of lead in plant material

The plant material selected for study was moss (*Hypnum cupressiforme*), collected from the bark of an oak tree at Carno, Caersws, Powys.[14] This sample was chosen because the lead content is known to be low, and the analysis of these mosses by atomic absorption has been studied,[14] and provides a comparison of values.

Table 3. Absorbance decrease in 100 sec with various compounds added (other conditions as in column 4 of Table 2)

Compound	Concentration, *M*	ΔA
—	—	0.060
$Pb(NO_3)_2$	10^{-8}	0.068
$Pb(NO_3)_2$	10^{-7}	0.108
$Mg(NO_3)_2$	10^{-5}	0.140
$Mg(NO_3)_2$	10^{-6}	0.078
$MnSO_4$	10^{-6}	0.118
$KAl(SO_4)_2$	10^{-5}	0.048
$KAl(SO_4)_2$	10^{-6}	0.052
$Ca(NO_3)_2$	10^{-5}	0.072
$Ca(NO_3)_2$	10^{-6}	0.060
$TiCl_4$	10^{-6}	0.062
$Cr(NO_3)_3$	10^{-6}	0.068
$CuSO_4$	10^{-6}	0.064
$NH_4Fe(SO_4)_2$	10^{-6}	0.050
$(NH_4)_6Mo_7O_{24}$	10^{-6}	0.061
$SnCl_2$	10^{-6}	0.057
$HClO_4$	5	0.122

The moss samples were analysed in three ways.

(1) *With a recording spectrophotometer.* The weight of dried sample taken for analysis was 0.01 g. The solution obtained from it was analysed kinetically for lead with the conditions for the concentration range 0.002–0.1 μg/ml. (For the results quoted in Table 4, a larger sample was taken and an aliquot of solution equivalent to a 0.01-g sample was diluted to 20 ml for the kinetic measurement, and the remaining solution used for the atomic-absorption analysis.)

(2) *With a manual colorimeter.* The sample taken for ashing was 0.18 g. The conditions were those for the concentration range 0.2–10 μg/ml lead, the final extract of lead being in 10 ml of solution. The decrease in absorbance was measured over 600 seconds. The lead range was less than that obtained in method (1), being only 0.1–0.6 μg/ml.

(3) *By atomic absorption.* The procedure for the ashing and extraction was the same except that the sample size was 0.1 g and the back-extract was analysed conventionally by atomic absorption.

Results of the analyses are shown in Table 4. Samples T were representative of the whole moss.

Table 4. Results for the analysis of dried moss samples for lead (μg/g)

Sample	Kinetic method	Atomic absorption
T1	40	37
T2	50	55
T3	50*	
G1	40	26
G2	32	24
B1	24	19
B2	30	31

* Result obtained colorimetrically, all other kinetic results being obtained spectrophotometrically.

Samples G and B represent samples of green and brown sections of the moss and illustrate the ability of the method to be applied to small sections of plant material.

The pooled standard deviation for the spectrophotometrically determined kinetic results is 5.8 μg/g ($\nu = 3$), but this value reflects heterogeneities in the sample as well as uncertainties in the analytical procedure. The error of the kinetic measurements is estimated as ±6 μg/g, most of this arising in the measurement of the decrease in absorbance (estimated as 5–15% relative depending on the lead concentration). Yasinskene and Kalesnikaite[10] also quote an error of "not greater than 15%". The errors associated with the atomic-absorption data were also estimated at about 15%, from the relative standard deviation of a single determination (3–8 readings per determination).

Comparison of the kinetic results with those obtained by atomic absorption showed that, at the 95% confidence level, the correlation between the results is significant ($r = 0.866$) while the apparent bias towards high values for the kinetic method is insignificant ($t = 1.46$). The correlation between the two methods would have been better were it not for samples G, which gave a higher result kinetically than by atomic absorption. However, in the light of the statistical tests as a whole, we would not wish to attempt to draw any conclusions from this observation.

CONCLUSIONS

We have demonstrated that the kinetic method of Yasinskene and Kalesnikaite[9,10] may be applied to the determination of lead in plant material at trace levels. The precision and accuracy are comparable to those of conventional atomic absorption but the sample size can be reduced by a factor of 10. Although the limit of detection (0.002 μg/ml) is higher than that quoted for graphite-furnace atomic-absorption (2 pg,[15] which is equivalent to 0.02 μg/ml for a 100-μl sample), we were able to obtain results on moss sample solutions with lead concentrations in the range 0.01–0.02 μg/ml, which compares well with a limit of detection of 0.035 mg/ml quoted recently for a carbon-rod atomic-absorption procedure for plant material.[4] Moreover, we were able to achieve this with a simple spectrophotometer. The main disadvantage of the method, that it involves a preliminary solvent extraction separation, is shared by many more sophisticated instrumental methods.[1,3–6]

REFERENCES

1. Y. Yano and N. Odaka, *Bunseki Kagaku*, 1978, **27**, T25.
2. M. D. K. Abo-Rady, *Z. Anal. Chem.*, 1979, **296**, 380.
3. R. W. Dabeka, *Anal. Chem.*, 1979, **51**, 902.
4. A. M. Ure, M. P. Hernandez-Artiga and M. C. Mitchell, *Anal. Chim. Acta*, 1978, **96**, 37.
5. W. Oelschlager and W. Lautenschlaegen, *Z. Anal. Chem.*, 1977, **287**, 28.
6. M. Kapel and M. E. Komaitis, *Analyst*, 1979, **104**, 124.
7. J. S. C. McKee, M. L. H. Wise, J. R. Holt and A. Meredith, *J. Radioanal. Chem.*, 1976, **31**, 461.
8. R. D. Irons, E. A. Schenk and R. D. Giauque, *Clin. Chem.*, 1976, **22**, 2018.
9. E. I. Yasinskene and S. Z. Kalesnikaite, *Zh. Analit. Khim.*, 1968, **23**, 1169.
10. *Idem, ibid.*, 1970, **25**, 87.
11. A. I. Vogel, *A Textbook of Quantitative Inorganic Analysis*, 3rd Ed., p. 900. Longmans, London, 1961.
12. *Standard Methods of Chemical Analysis*, F. J. Welcher (ed.), 6th Ed., Vol. IIA, p. 194. Van Nostrand, Princeton, 1963.
13. I. F. Dolmanova, G. A. Zolotova and T. N. Mazko, *Zh. Analit. Khim.*, 1977, **32**, 1025.
14. I. C. Trueman, Personal communication.
15. C. W. Fuller, *Electrothermal Atomisation for Atomic Absorption Spectrometry*, p. 73. Chemical Society, London, 1977.

Talanta, Vol. 28, pp. 369 to 376. 1981
Printed in Great Britain. All rights reserved

0039-9140/81/060369-08$02.00/0
Copyright © 1981 Pergamon Press Ltd

HYDRODYNAMIC MODULATION VOLTAMMETRY

JOSEPH WANG
Department of Chemistry, New Mexico State University, Las Cruces, NM 88003, U.S.A.

(*Received* 3 *November* 1980. *Accepted* 31 *December* 1980)

Summary—Highly efficient background-correction techniques applicable to voltammetric methods of trace analysis can be developed by modulating the convection rate of the solution at a solid electrode surface. The theoretical aspects, advantages, disadvantages, and analytical applications of the various batch and flow approaches to hydrodynamic modulation voltammetry are discussed, together with trends in future developments.

The ever-widening clinical, environmental or technological significance attached to the presence of minute concentrations of many substances in a variety of complex materials has led to continued efforts to enhance the sensitivity of analytical methods used for their determination. Electroanalytical techniques provide the sensitivity necessary in a variety of situations, and for many practical problems offer the most promising methodology.

The development of advanced polarographic techniques (*e.g.*, differential-pulse and square-wave polarography) has increased the sensitivity of dropping mercury electrode (DME) techniques to the submicromolar concentration level. Though the DME has an excellent cathodic range, its anodic range is limited by anodic dissolution as mercury ions at about +0.4 V *vs.* the standard calomel electrode (SCE). This means that many important substances (*e.g.*, drugs, coenzymes) cannot be determined with the DME, but can be electrochemically oxidized at various solid electrodes (*e.g.*, carbon, gold or platinum). With the increasing need for trace analysis for many organic compounds and biochemicals, it has become necessary to develop sensitive and reliable solid-electrode techniques.

One of the great disadvantages of using solid electrodes for analysis at trace and ultratrace levels is that changes in potential at solid surfaces are accompanied by changes in the surface chemistry as well as by traditional double-layer charging. These surface processes may involve a change in the oxidation state of a surface functional group, as in the case of carbon electrodes,[1] or the formation of various oxides and/or adsorbed hydrogen films, as in the case of some metallic surfaces (*e.g.*, platinum or gold[2]). The charge required to bring about these surface reactions results in the flow of a substantial current, which often obscures the small analytical currents characterizing the particular species at the trace level. Equation (1) summarizes the various components of the total current (i_{tot}) observed at solid convective electrodes:

$$i_{tot} = i_{cn} + i_{ncn} + i_{sur} + i_{ch} \quad (1)$$

where i_{cn} is the mass-transport component, which is related to the convective transport of electroactive material in solution; i_{ncn} is the non-convective component, which is related to electrolysis of the solvent or supporting electrolyte; the component i_{sur} is due to the various surface-controlled processes (discussed above), and i_{ch} is the double-layer charging current (compared to the DME, the solid electrode shows a charging current associated only with changing potential since the electrode area is constant); i_{sur} and i_{ch} are transients and are independent of mass-transport.

Solid-electrode linear-scan voltammetry performs optimally at the millimolar concentration level. At lower levels the effect of surface-controlled processes is increased, resulting in irreproducible current–potential data. Potential-pulse techniques, which successfully enhance the sensitivity with a DME (detection limit $\sim 1 \times 10^{-8} M$ for differential-pulse polarography) are not efficient when used with solid electrodes. This is due to the large transient background currents (i_{sur} and i_{ch}) associated with the abrupt changes in potential. The short sampling times (~ 50 msec) used by various commercial pulse polarographs were designed to discriminate against the rapidly decaying charging current; however, they do not discriminate against the transient surface reactions, which can take many minutes to settle down. Because of these increased background currents, attempts to use various potential-pulse techniques at solid electrodes have resulted in only slight improvements in detection limit as compared to linear-scan voltammetry.[3,4]

Background currents may be minimized by avoiding potential-scanning techniques. In steady-state voltammetry (SSV),[5] various constant potentials are applied, for a sufficiently long time (10–30 min) at each potential to allow the transient currents to decay before the steady-state current is read. With transient currents eliminated, the steady-state background currents are very low, permitting measurements to be made on species at micromolar concentrations. A serious drawback of SSV is the long time (a few

hours) required to obtain a current–potential curve. Another way to avoid scanning the potential and to obtain reproducible current–potential data for trace analysis with solid electrodes is to use the several electrodes each at a different potential in the same cell.[6] The serious problems associated with this approach are the need for sophisticated electronics and the cumbersome cell design.

A real breakthrough in the analytical exploitation of solid electrodes appears to be the introduction of sensitive solid-electrode techniques based upon hydrodynamic modulation voltammetry (HMV). HMV retains the high sensitivity of SSV while significantly reducing the time required to collect the data. After about 20 years during which hydrodynamic voltammetry at solid electrodes owed its analytical importance to its role in other techniques (*e.g.*, amperometric titrations, stripping analysis), in the last few years it has become recognized as an analytical technique in its own right. The various HMV techniques, their theories and applications, are the subject of the present review.

The concept of hydrodynamic modulation voltammetry

A successful measurement procedure depends on isolation of the signal of interest. In electroanalytical measurements it is the electrolysis of the electroactive species in the solution that is of analytical interest. With forced-convection solid electrodes the principal effort is therefore directed towards isolation of i_{cn}, which can be used as a measure of concentration:[7]

$$i_{cn} = nFACT \tag{2}$$

where n is the number of electrons transferred per molecule, F is the Faraday constant, A is the electrode surface area, and C is the bulk concentration of the electroactive species. T is the mass-transfer coefficient, which is proportional to the flux of electroactive material at the electrode surface: it has the following general forms for rotating and for flow-through electrodes respectively:

$$T = K\omega^{\alpha} \tag{3}$$

$$T = K'V^{\alpha'} \tag{4}$$

where ω is the rotation speed, V the solution flow-rate, and K,K', α and α' are constants characterizing the hydrodynamic pattern and cell geometry.

A practical and effective way of isolating i_{cn} from the various background components [equation (1)] is to pulse the solution hydrodynamically (*e.g.*, by varying the speed of a rotating electrode, or of the flow-rate of the solution through a stationary electrode). The hydrodynamic pulsing [between two convection rates, high (H) and low (L)] produces a pulsation only in i_{cn}, which may easily be measured:

$$\begin{aligned}\Delta i_{tot} &= (nFACT_H + i_{ncn} + i_{sur} + i_{ch}) - \\ &\quad (nFACT_L + i_{ncn} + i_{sur} + i_{ch}) \\ &= nFAC\,(T_H - T_L)\end{aligned} \tag{5}$$

By combining equation (3) or (4) with (5) the fluctuations in the measured current (Δi_{tot}) associated with changes in rotation speed or flow-rate are obtained:

$$\Delta i_{tot} = nFKAC\,(\omega_H^{\alpha} - \omega_L^{\alpha}) \tag{6}$$

$$\Delta i_{tot} = nFK'AC\,(V_H^{\alpha'} - V_L^{\alpha'}) \tag{7}$$

Δi_{tot} is essentially independent of currents associated with double-layer charging, adsorptive processes, reorganization of surface groups and solvent decomposition. Background pulsed currents (dependent on mass-transport) are usually orders of magnitude lower than the background-current contributions to i_{tot} measured in conventional voltammetric methods, and the sensitivity is consequently much higher (detection limits at the 10^{-9}–$10^{-8}M$ levels).

Figure 1 illustrates the principle of HMV; it shows hypothetical solid-electrode voltamperograms for a blank solution (curve a), and for the same solution after the addition of two electro-oxidizable species (A, B) at low concentration, for two different convective rates [low (curve b) and high (curve c)]. Periodic pulsing of the convective rate (between low and high) would result in the well-defined Δi–E curve (d), which is free from background interferences.

APPROACHES TO HMV

Batch analysis

Miller and Bruckenstein and co-workers have examined several aspects of the hydrodynamically

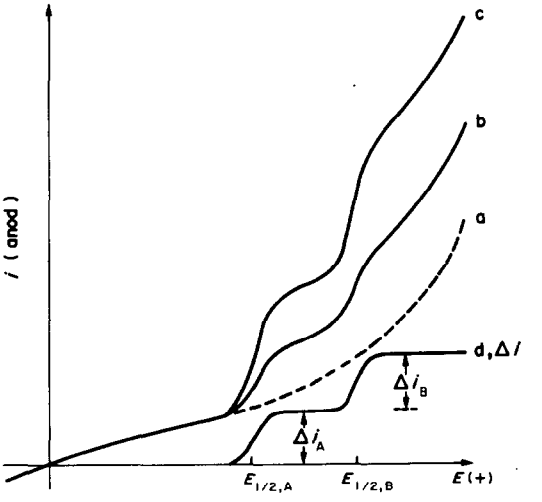


Fig. 1. Hydrodynamic (a, b, c) and hydrodynamic modulation (d) voltamperograms. (a) Current–potential curve for the blank solution. (b, c) Current–potential curves for the same solution following addition of two hypothetical oxidizable substances (A and B), for two convective rates, low and high, respectively. (d) Hydrodynamic modulation voltamperogram for the same solution, obtained by periodic pulsing of the convective rate between low and high values [because there is minimal interference from mass-transport dependent background processes arising from electroactive impurities, similar background current–potential curves (shown in (a)) are obtained at the two convective rates].

modulated rotating disk electrode.[8,9] The rotating disk electrode (RDE) is well known for its very efficient and well-defined mass-transport behaviour. According to Levich[10] the mass-transport limiting current at the RDE is given by:

$$i_{cn} = 0.62\,nFAD^{2/3}\omega^{1/2}\nu^{-1/6}C \qquad (8)$$

where D is the diffusion coefficient and ν the kinematic viscosity.

The technique of hydrodynamic modulation at the rotating disk electrode (HMRDE) involves sinusoidal modulation of the speed of rotation of an RDE about a fixed central value ($\omega_0^{1/2}$) with peak-to-peak amplitude $\Delta\omega^{1/2}$, such that

$$\omega^{1/2} = \omega_0^{1/2} + \Delta\omega^{1/2}\sin(\sigma t) \qquad (9)$$

where σ is the modulation frequency and t is the time. $\Delta\omega$ is always smaller than ω_0, and is usually about 1% of ω_0. For example, if $\omega_0^{1/2} = 60$ rpm$^{1/2}$ and $\Delta\omega^{1/2} = 6$ rpm$^{1/2}$, then the speed of rotation varies between 3564 and 3636 rpm. The usable modulation frequency (usually 3–6 Hz) is dependent on the inertia and response of the motor–electrode system. At these low frequencies, and for small amplitude modulations ($\Delta\omega^{1/2}/\omega^{1/2} \leq 0.1$) the time-dependent current is derived directly from Levich's equation [equation (8)]:

$$i(t) = 0.62\,nFAD^{2/3}\nu^{-1/6}C[\omega_0^{1/2} + \Delta\omega^{1/2}\sin(\sigma t)] \qquad (10)$$

and the peak-to-peak response is given by

$$\Delta i = i_{\omega_0}(\Delta\omega/\omega_0)^{1/2} \qquad (11)$$

This sinusoidal component (which is usually much smaller than the steady-state analytical current) is recovered from the total current by filtering and passing through a lock-in amplifier or full-wave rectifier.[11]

HMRDE has been found to yield excellent Δi–E data at the submicromolar concentration level, even in the presence of interference from surface processes and solvent-electrolysis reactions. The selectivity of HMRDE for mass-transport processes has been illustrated for various electrode materials (silver, platinum, graphite, gold and amalgamated gold) and a variety of electroactive species [nitrobenzene, quinhydrone, sulphide, Hg(II), Tl(I) and Fe(II)–Fe(III)].[11] As an example, RDE and HMRDE voltamperograms for $2.0 \times 10^{-7}M$ Tl(I) in $0.01M$ perchloric acid are shown in Fig. 2. While there is no detectable difference between the background and the Tl(I) reduction current in the RDE curve, a well-defined Δi–E curve is obtained in the HMRDE mode. Similar measurements on nitrobenzene at an amalgamated gold disk electrode have indicated a detection limit of about $2 \times 10^{-9}M$, based on the signal-to-noise ratio of the system. This indicates that forced-convection electrodes coated with mercury and operating in the HMV mode offer advantages for reductions (as do the uncoated electrodes for oxidations) even when compared with the DME operated in the potential-pulse

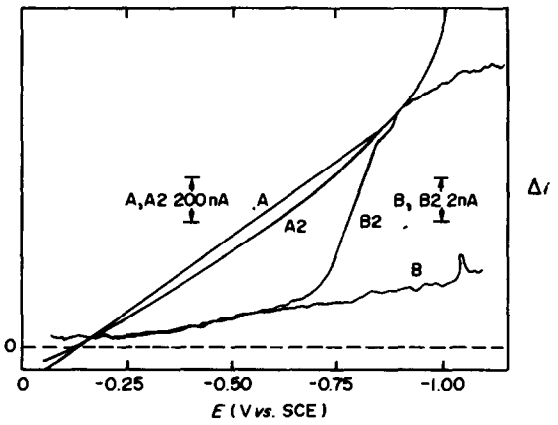


Fig. 2. Controlled-potential cathodic scans of Tl(I), with an amalgamated gold disk "electrode". All A traces are RDE curves, all B traces are HMRDE curves. (A,B) $0.01M$ $HClO_4$; (A2, B2) $2.0 \times 10^{-7}M$ Tl^+ in $0.01M$ $HClO_4$. Current sensitivities indicated by markers, zero current for all curves is the dashed line. For all curves, $\omega_0^{1/2} = 60$ rpm$^{1/2}$. B, $\Delta\omega^{1/2} = 6$ rpm$^{1/2}$. $\sigma/2\pi = 3$ Hz, averaging time-constant is 3 sec, and scan-rate is 2 mV/sec (reproduced by permission of the American Chemical Society).

mode. This is because the mass-transport is more efficient and because there are fewer double-layer complications (since the surface area remains constant). Similar modulated RDE responses can be obtained with small sample volumes in a cell with a capacity of 1 ml,[12] which is of particular interest to clinical chemists.

Miller and Bruckenstein and co-workers have published the results of detailed theoretical and experimental studies of the HMRDE. They found that the concentration profile adjusted slowly to a sudden change in the speed of rotation ($\Delta\omega$) of an RDE, held at a potential giving a limiting current, compared to the rapid adjustment of the fluid velocity.[13] These hydrodynamic relaxation phenomena limit the maximum rate of scan and modulation frequency that will yield results which can be interpreted by steady-state theory (Levich equation). A study of these relaxation phenomena as a function of the modulation frequency has permitted the determination of diffusion coefficients. The theory of the HMRDE has been improved recently by Tokuda and Bruckenstein[14] for higher modulation frequencies, for which the instantaneous limiting current cannot be predicted adequately by the Levich equation. Though the mathematical model becomes more complicated for higher modulation frequencies, there are experimental advantages, such as shortened analysis time and simpler signal processing.

The theory of the sinusoidally modulated disk electrode has been extended to cover situations of mixed kinetic and convective-diffusion control.[15] This theory has been both proposed and verified for the cases where both the reactant and product remained in solution and where one of them is a solid. Relationships between modulated current, steady-state cur-

rent, potential, concentration, and kinetic and transport parameters have been derived for these situations. These current–potential relationships have been compared with those of the conventional RDE. While for a reversible electrode reaction the normalized HMRDE and RDE current–potential plots are superposable, this is not the case for the completely irreversible process where convective transport affects both the wave shape and the half-wave potential. This theory has led to the measurement of kinetic parameters such as rate constants for quasi-reversible electron-transfer reactions. HMRDE kinetic studies are especially useful when surface and mass-transport processes occur simultaneously with the electron-transfer process. This theory was tested by Kanzaki and Bruckenstein[16] for irreversible reactions and the Δi–E curves were shown to be more sensitive to kinetic effects than the conventional i–E curves. Detailed discussion of these kinetic models is beyond the scope of this review.

In addition to the sinusoidally modulated RDE, various other control approaches have been used, with ω being scanned linearly with respect to t, t^2 and $\exp(kt)$.[9] These approaches were aimed at recording Levich plots (i_l *vs.* $\omega^{1/2}$) automatically and at measuring surface concentrations of kinetically active species. Such automatically recorded Levich plots are especially advantageous (compared to the manual point-by-point measurements) when the electrode surface is changing rapidly with time, owing to adsorption or electrodeposition, and a fast scan is required.

Pulsed-rotation voltammetry (PRV) is a special case employing a hydrodynamically modulated disk electrode. This approach involves changing the applied potential and measuring the difference (Δi_{tot}) between the currents at two selected rotation speeds. Compared to use of the sinusoidally-modulated RDE this approach results in minimum attenuation of the steady-state analytical response since low and high rotation speeds (*e.g.*, 300 and 1500 rpm) are usually selected for the two current measurements. Blaedel and Engstrom have evaluated the analytical potential of this approach, using a glassy-carbon RDE.[17] Good signal-to-noise ratios were obtained for a 10nM solution of ferricyanide in phosphate buffer.

Figure 3 shows a comparison of the background current–potential curves for a phosphate buffer, obtained in the conventional-scanning, SSV and PRV modes. The pulsed-rotation mode shows an extremely low background (around 1 nA except at extreme potentials), indicating good correction for currents due to surface processes and solvent electrolysis. PRV has been applied for electrochemical kinetic studies of the Fe(II)–Fe(III) system, diazepam, riboflavin and flavin coenzymes and the NAD^+–NADH system.[18–20] Heterogeneous rate constants, the standard potentials and the transfer coefficients were all measured at micromolar concentration levels. In contrast to the curves recorded by scanning voltammetry and SSV, undistorted, well-defined Δi–E curves can be

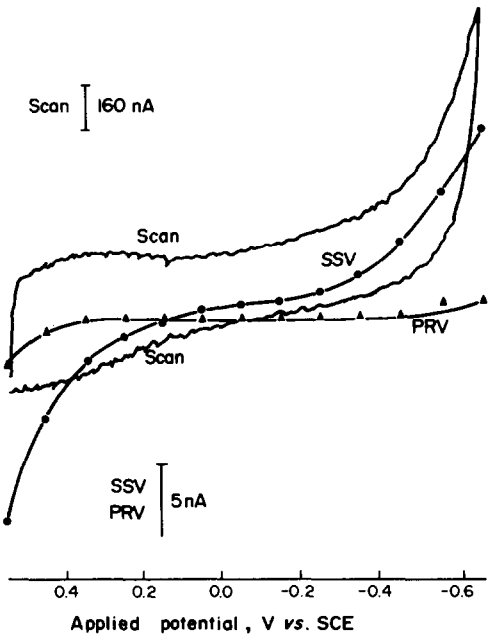


Fig. 3. Comparison of background current–potential curves for 0.1M phosphate buffer (pH 7.5), by scanning, SSV and PRV techniques.[17] Rotating glassy-carbon disk electrode. Rotation speeds, 500 rpm for "Scan" and SSV, 500 and 1500 rpm for PRV. Pulsing frequency, 15 sec (reproduced by permission of the American Chemical Society).

recorded at this concentration level with PRV, even in the vicinity of the limits set by the useful potential range of the system (*e.g.*, reduction of NAD^+ or diazepam at extreme potentials, up to -1.6 V *vs.* Ag/AgCl). PRV is particularly useful for the electrochemical determination of many biochemicals and drugs which have low solubilities in water. The technique has been placed under automated control by a desk-top programmable calculator.[21] Such a system provides increased data-collection and more precise control of the experiment, at very reasonable cost. PRV has recently been coupled with use of a rotating porous-carbon disk electrode.[22] The compensation of the high background current that accompanies the high analytical current makes it possible to determine ferrocyanide and NADH at submicromolar concentrations.

Continuous-flow systems

One of the most important advantages of electrochemistry is the ease with which it can be adapted for monitoring flowing streams. Electroanalytical flow-detectors are being increasingly applied to the monitoring of chromatographic column effluents, for environmental and industrial warning systems, and in high-speed clinical analysers. Although early work in this field involved the DME, solid electrodes have been extensively studied and successfully applied in

recent years. The possibility of using either the anodic or the cathodic potential range, the simple (low-volume) cells and low noise-levels all add to the attractiveness of flow-through solid electrodes.

The electroanalytical monitoring of very low concentrations is limited by the signal-to-background ratio of the detector. Even hydrodynamic amperometry at a *fixed* potential lacks the sensitivity required for trace and ultratrace analysis. Moreover, many chromatographic experiments involve monitoring at extreme potentials where the background is often far greater than the chromatographic peak heights. The use of d.c. offset compensation of the background is not always possible, owing to changes in its level (flow-rate variation, change in solvent composition, *etc.*). Operation at different applied potentials is reported to produce up to a tenfold change in the detectability of d.c. amperometric measurements, because of the differences in the magnitude of the background current.[23] In addition to making constant-potential amperometric measurements it is important to obtain current–potential data for low concentrations of analyte in a flowing solution, since such data allow the use of flow sensors to monitor several species in a single sample without the use of a chromatographic column. Obtaining such data is also very useful in chromatographic detection where hydrodynamic voltamperograms of specific chromatographic fractions can provide important information for identification of compounds as they are eluted.

For all these purposes a sensitive measurement technique designed to discriminate against the background current must be used. Potential-pulse techniques do not offer enhanced sensitivity when employed with solid-electrode flow-cells.[23,24] A sensitive flow-detector based on hydrodynamic modulation was suggested by Blaedel and Boyer in 1971.[25] They demonstrated that the stopped-flow technique provided improved sensitivity for tubular electrodes when the difference between the steady-state currents at zero and at high flow-rates was measured. Figure 4 shows current–time tracings for a blank solution and a sample solution, with annotations to define the various current components associated with the stopped-flow procedure. Of principal interest is the analytical current, defined as the difference between the measured on–off currents for the sample and the blank, and taken as proportional to the sought-for concentration of electroactive species [equation (7), with $V_L' = 0$]. The main advantages of this procedure are its inherent sensitivity (since the zero-flow current is equal to zero, all the steady-state analytical signal is exploited for the determination) and the simplicity of operation (turning a stopcock on and off). The sensitivity achieved by the stopped-flow procedure has been further increased by employing a large surface area flow-through electrode consisting of a porous plug of reticulated vitreous carbon (RVC).[26] Combining the large analytical current of the RVC with the

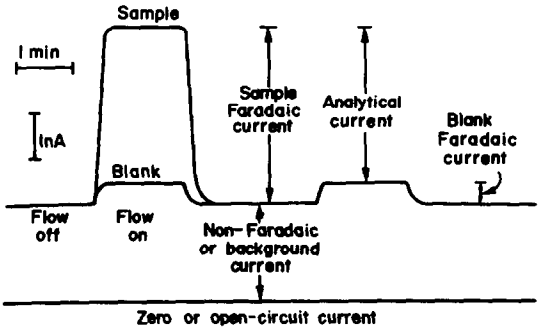


Fig. 4. Definitions of the currents measured by the stopped-flow technique.[25] (Reproduced by permission of the American Chemical Society).

efficient discrimination against the accompanying high background current allows a limit of detection of around 1 n*M* to be achieved for ferrocyanide. The main drawback of the stopped-flow procedure is its long cycling time (about a minute) because of the slow relaxation of the diffusion boundary layer when the flow is stopped.

The pulsed-flow technique of Blaedel and Iverson,[27] in which the flow-rate of a solution passing through a tubular electrode is switched between two values, allows measurements to be made at the micromolar concentration level (with high signal-to-noise ratio), with cycling times of about 15 sec. Since a very low flow-rate is used to provide the lower current state, minimum attenuation of the steady-state analytical signal is obtained [equation (7)]. However, the response time of this approach has precluded its use as a detection system for liquid chromatography or flow-injection analysis, where rapid response is required. Blaedel's group at the University of Wisconsin has been pursuing ways of developing a rapid pulsed-flow technique for these important applications. By reduction of the distance through which the diffusion boundary layers have to relax when the flow is changed, a rapid pulsed-flow procedure (about 1 Hz) can be obtained.[28,29] Various thin-channel electrodes (*e.g.*, a thin tubular electrode, or a thin-layer cell) have been used for this purpose. At higher pulse rates, the difference current is attenuated, approaching zero at very fast modulation. The natural pulsation of a reciprocating piston pump has been exploited to provide the rapid modulation mode. Rapid fixed-potential measurements as well as linear-scan (200 mV/min) hydrodynamic voltammetry have been reported. This procedure was coupled with flow-injection analysis for analysis of micromolar dopamine solutions at a rate of 120 samples per hour.

A flow-cell with an RDE has permitted the development of a new hydrodynamic modulation approach, based upon stopping the rotation of the electrode, while maintaining a constant low flow-rate.[30] The current difference resulting from such a hydrodynamically pulsed mode is given by:

$$\Delta i = nFAC(K\omega^z - K'V^{z'}) \qquad (12)$$

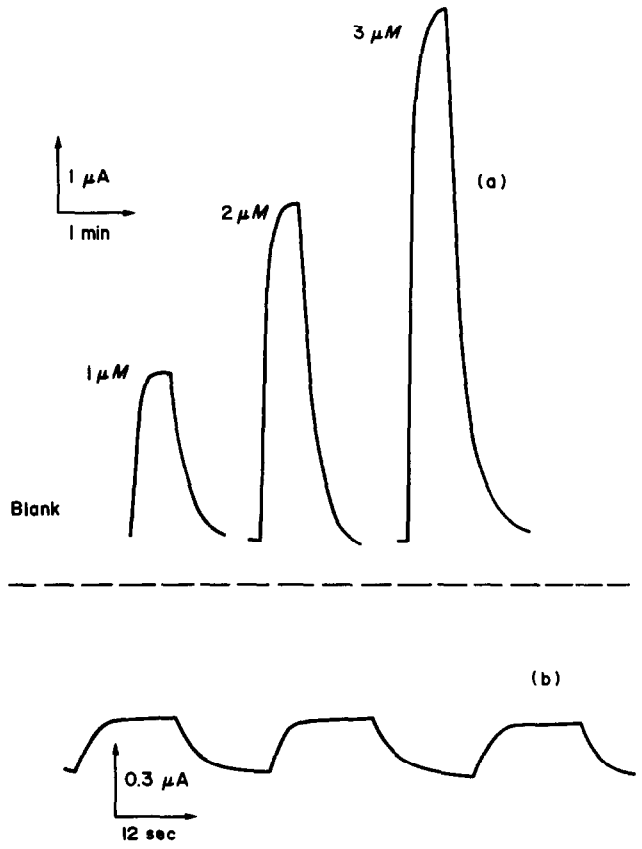


Fig. 5. Pulsed-rotation response for 1, 2 and 3 μM ascorbic acid (a) and 0.5 μM dopamine (b).[31] Rotation pulsed between 0 and 1250 rpm. Constant flow-rate of 2.25 ml/min (a) and 1 ml/min (b). Supporting electrolyte, 0.1M phosphate buffer (a), and 0.1M citric acid and 0.025M KH_2PO_4 (b). RVC disk thickness 1.8 mm (a) and 8.4 mm (b). Applied potential, +0.75 V (reproduced by permission of the American Chemical Society).

Special features of this approach are its high sensitivity (due to the efficient mass-transport of the RDE), the simplicity of operation, and the use of a constant flow-rate. Modulation rates ranging from 0.1 to 1 Hz are reported as well as well-defined current–potential curves for micromolar ascorbic acid solutions. When pulsing between two rotational speeds is applied (instead of stopped-rotation) the resulting current difference is further attenuated, becoming virtually independent of flow-rate. Blaedel and Wang advocated combining the stopped-rotation approach with a flow-through rotating porous disk electrode,[31] which resulted in a further increase in sensitivity, owing to the large electrode surface area. Figure 5 illustrates typical stopped-rotation responses for the oxidation of ascorbic acid and dopamine at micro- and submicromolar levels obtained with a rotated porous flow-through electrode. The high sensitivity, low noise-level, and precision of the response are apparent from these tracings.

Table 1 summarizes the characteristics and applications of the various HMV approaches discussed in this paper.

FUTURE DIRECTIONS

Each of the HMV approaches mentioned can provide useful analytical data for many electroactive species which give essentially useless signals in conventional scanning voltammetry at solid electrodes. Many analytical problems which could never have been attacked by conventional voltage-scanning techniques can be handled by HMV.

Almost all the publications on HMV techniques have appeared within the last decade. These techniques have not yet been fully explored and many innovations may be expected in the near future, resulting in significant improvements in sensitivity, selectivity and speed, and in simplified operation. There are so many possible ways of enhancing convective transport, of coupling various convection modes, and of incorporating new electrode configurations which may be used for these purposes. For example, new approaches based on a rapidly moving barrier (located very close to the electrode surface), and on the wall-jet electrode,[33] may result in a very sensitive and rapid response. Other variations which

Table 1. Characteristics of various HMV methods

Method	Equation for current difference	Species measured	Detection limit, M	Ref.	Comments
Sinusoidally modulated RDE	$\Delta i = i_{\omega_0}(\Delta\omega/\omega_0)^{1/2}$	Tl(I), Fe(II)/Fe(III), Hg(II), sulphide, nitrobenzene, quinhydrone	2×10^{-9}	8–16	Rapid modulation (3–6 Hz), Δi much smaller than i_{ω_0}
PRV, batch	$\Delta i = 0.62nFAD^{2/3}\upsilon^{-1/6}C(\omega_H^{1/2} - \omega_L^{1/2})$	Fe(II)/Fe(III), NAD^+/NADH, diazepam, riboflavin and flavin coenzymes	10^{-8}	18–22, 32	$\omega_H \gg \omega_L$ resulting in large Δi
Stopped-flow, tubular electrode	$\Delta i = 5.43nFAD^{2/3}X^{2/3}CV^{1/3}$	Fe(III)	10^{-8}	25	Simple operation (on/off switching of stopcock). X = electrode length
Stopped-flow, porous plug electrode	$\Delta i = nFCVR$	Fe(II)	10^{-9}	26	R = degree of conversion, long cycling time
Pulsed-flow, tubular electrode	$\Delta i = 5.43nFAD^{2/3}X^{2/3}C(V_H^{1/3} - V_L^{1/3})$	Fe(II)/Fe(III), dopamine	10^{-8}	27–29	Rapid modulation (1 Hz) provided by a reciprocating pump
Stopped-rotation, flow-through RDE	$\Delta i = nFAC(K\omega^z - K'V^{z'})$	Ascorbic acid, Fe(II), NADH	4×10^{-8}	30	Simple operation; use of constant flow-rate
Stopped-rotation, flow-through rotated porous disk electrode	$\Delta i = nFAC(T_1 - T_2)$	Ascorbic acid, dopamine	5×10^{-9}	31	$T_1 = f(\omega,V)$ $T_2 = f(V)$
Stopped-rotation, under continuous stirring	$\Delta i = nFAC(K\omega^z - K''m^{z''})$			34	Large current amplitude and operation; m = stirring rate

may offer better performance include derivative pulsed-convection, pulsed-potential coupled with pulsed-convection, and hydrodynamically modulated membrane-covered or chemically modified electrodes.[34] Flow-detectors, operating in the HMV mode, can be expected to find wider application in liquid chromatography. This would result in enhanced sensitivity (down to the subnanogram level) and an expanded "potential window" of the detector (allowing detection of many important species having extreme redox potentials, such as phenols), and would be very useful in the case of programmed gradient elution, where the change in the composition of the mobile phase results in changes in the background current. Much still to be done on the theoretical side, *e.g.*, the relaxation of the diffusion boundary layer, and the microstructure of the concentration profile when the convection rate is changed, must be investigated in greater detail for different electrode geometries. Further pursuit of these theoretical aspects will surely lead to the design of even more advanced approaches.

While considerable progress is being made in the development and application of various HMV approaches, the technique has not yet achieved general acceptance. One of the main reasons is that while "home-made" instruments are being used successfully, commercial instrumentation of this type is not available. Experience has shown that, instrumental methods became widely used only when a reliable instrument can be purchased. Therefore, the most significant changes are likely to result from the introduction of commercial microcomputer-controlled HMV equipment. The introduction of such instruments would accelerate the application of HMV for many important analytical problems. For many environmental, industrial and clinical problems (*e.g.*, *in-vivo* monitoring of clinical variables, quality control of many drugs, analysis of dissolved oxygen, *in-situ* monitoring of organic pollutants, *etc.*) HMV may provide the key for establishing a new analytical methodology.

REFERENCES

1. R. E. Panzer and P. J. Elving, *J. Electrochem. Soc.*, 1972, **119**, 864.
2. S. Gilman in *Electroanalytical Chemistry*, Vol. 2, Bard, A. J., ed., p. 111. Dekker, New York, 1967.
3. P. Söderhjelm, *J. Electroanal. Chem.*, 1976, **71**, 109.
4. J. W. Dieker, W. E. van der linden and H. Poppe, *Talanta*, 1978, **25**, 151.
5. W. J. Blaedel and R. A. Jenkins, *Anal. Chem.*, 1974, **46**, 1952.
6. W. R. Matson, W. M. Mogayzel, Jr., R. Vitukevich and E. W. Zink, Pittsburgh Conference, Atlantic City, 1980, Paper 103.
7. J. Jordan and R. A. Javick, *Electrochim. Acta*, 1962, **6**, 23.
8. B. Miller and S. Bruckenstein, *J. Electrochem. Soc.*, 1970, **117**, 1032.
9. B. Miller, M. I. Bellavance and S. Bruckenstein, *Anal. Chem.*, 1972, **44**, 1983.
10. V. G. Levich, *Physicochemical Hydrodynamics*, p. 60. Prentice-Hall, Englewood Cliffs, NJ, 1962.
11. B. Miller and S. Bruckenstein, *Anal. Chem.*, 1974, **46**, 2026.
12. *Idem, ibid.*, 1974, **46**, 2033.
13. K. Tokuda, S. Bruckenstein and B. Miller, *J. Electrochem. Soc.*, 1975, **122**, 1316.
14. K. Tokuda and S. Bruckenstein, *ibid.*, 1979, **126**, 431.
15. B. Miller and S. Bruckenstein, *ibid.*, 1974, **121**, 1558.
16. Y. Kanzaki and S. Bruckenstein, *ibid.*, 1979, **126**, 437.
17. W. J. Blaedel and R. C. Engstrom, *Anal. Chem.*, 1978, **50**, 476.
18. W. J. Blaedel and Y. Hahn, *Arch. Pharm. Res. (Korea)*, 1979, **2**, 111.
19. W. J. Blaedel and R. C. Engstrom, *Proc. 7th Technicon Intern. Congress*, New York, 1976, p. 63.
20. W. J. Blaedel and Y. Hahn, *Anal. Chem.*, submitted for publication.
21. R. C. Engstrom and W. J. Blaedel, *J. Chem. Biomed. Environ. Instrum.*, 1979, **9**, 61.
22. W. J. Blaedel and J. Wang, *Anal. Chem.*, 1980, **52**, 76.
23. W. Lund, M. Hannisdal and T. Greibrokk, *J. Chromatog.*, 1979, **173**, 249.
24. D. G. Swartzfager, *Anal. Chem.*, 1976, **48**, 2189.
25. W. J. Blaedel and S. L. Boyer, *ibid.*, 1971, **43**, 1538.
26. W. J. Blaedel and J. Wang, *ibid.*, 1979, **51**, 799.
27. W. J. Blaedel and D. Iverson, *ibid.*, 1979, **49**, 1563.
28. W. J. Blaedel and Z. Yim, *ibid.*, 1980, **52**, 564.
29. W. J. Blaedel and J. Wang, *ibid.*, 1981, **53**, 78.
30. *Idem, Anal. Chim. Acta*, 1980, **116**, 315.
31. *Idem, Anal. Chem.*, 1980, **52**, 1697.
32. W. J. Blaedel and G. A. Mabbot, *ibid.*, 1978, **50**, 933.
33. J. Yamada and H. Matsuda, *J. Electroanal. Chem.*, 1973, **44**, 189.
34. J. Wang, work in progress.

Talanta. Vol. 28, pp. 377 to 381. 1981
Printed in Great Britain

0039-9140/81/060377-05$02.00/0
Pergamon Press Ltd

DETERMINATION OF NOVOCAINE IN PHARMACEUTICAL PREPARATIONS WITH NOVOCAINE$^+$-SELECTIVE MEMBRANE ELECTRODES

D. NEGOIU*, M. S. IONESCU and V. V. COŞOFREŢ
Institute of Chemical and Pharmaceutical Research, 74351 Sos. Vitan 112, Bucharest, Romania

(*Received* 20 *October* 1980. *Accepted* 31 *December* 1980)

Summary—Liquid-membrane ion-selective electrodes made with the ion-association complexes of novocaine with tetraphenylborate or dipicrylamine are proposed for use in the determination of novocaine by direct potentiometry or by potentiometric titration with sodium tetraphenylborate. The titration method is preferred, and the mean relative error for 4–12 mg of novocaine hydrochloride is 0.5%.

The control of drug quality is a branch of analytical chemistry that has a wide impact on public health, so the development of reliable, quick and accurate methods for determination of the active ingredient is welcomed.

In recent years, ion-selective membrane electrodes have been used more and more in drug-quality control, but no pharmacopoeia has yet introduced their use for assays, though this will probably be done in the next few years.

An important advantage of ion-selective membrane electrodes is that they can, in principle, be designed for any ionic species, even for organic ions with complicated structures and high molecular weight.[1–7]

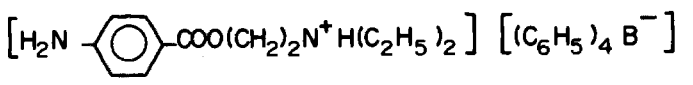
Novocaine (neocaine, procaine, ethocaine, syncaine, kerocaine, *etc.*—2-diethylaminoethyl *p*-aminobenzoate hydrochloride—is a short-acting local anaesthetic. It is less toxic than cocaine, but because of its poor penetration of intact mucous membranes is useless for surface application.

A rapid specific method applicable to the determination of novocaine in the presence of the basic organic or inorganic species often accompanying it in pharmaceutical preparations is needed because most of the available methods are susceptible to environmental reaction conditions and suffer from lack of specificity, sensitivity and stoichiometry.

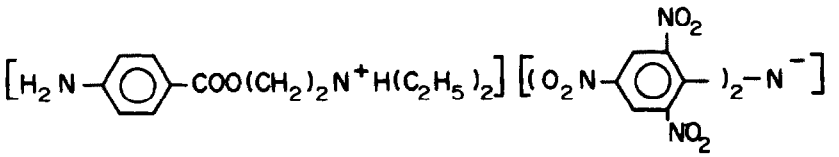
Most pharmacopoeias[8–10] recommend determination of the pure substance by diazotization of the primary amino-group by titration with 0.1*N* sodium nitrite. Determination of the active ingredient in pharmaceutical preparations requires a preliminary extraction followed by ultraviolet spectrophotometry or densitometry, but the method is tedious and rather inaccurate.

We describe here a simple, rapid and accurate method for the determination of novocaine in some pharmaceutical preparations, based on the use of a novocaine-selective membrane electrode. Construction of other novocaine-sensitive electrodes has been described in the literature.[11,12] An Hg^{2+} or Ag^+-selective membrane electrode has also been used for evaluating the purity of this drug.[13,14]

Our novocaine-selective membrane electrodes are based on liquid membranes consisting of the ion-association complexes I and II.



I Membrane for electrode A



II Membrane for electrode B

* National Institute of Chemistry, 77208 Spl. Independenţei 202, Bucharest, Romania.

EXPERIMENTAL

Apparatus

Direct potentiometric measurements were made at room temperature in mechanically stirred solutions, with a digital pH/mV-meter (Pracitronic) and the novocaine-selective electrode and a saturated calomel electrode (SCE) (type K401, Radiometer). The SCE was connected to the sample solution by a saturated sodium nitrate bridge. The pH measurements were made with a G 202 C glass electrode (Radiometer) and an SCE. The potentiometric titration curves were recorded with an automatic outfit composed of a TTT2 titrator, ABU12 autoburette and SBR2c titrigraph recorder (Radiometer), with an SCE and the two novocaine-selective electrodes. An Ag^+/S^{2-}-crystal membrane electrode (Model 94–16, Orion) was used for argentimetric titration of the sodium tetraphenylborate solution (0.01*M*) for standardization purposes.

Reagents

All reagents used were of analytical-reagent grade.

Sodium tetraphenylborate solution, 0.01*M*. Dissolve 0.85 g of sodium tetraphenylborate in the minimum of distilled water, filter, and dilute to 500 ml with distilled water. Standardize by potentiometric titration with 0.01*M* silver nitrate (with a silver-selective electrode and SCE).

Preparation of the liquid membranes

(*a*) *Novocaine–tetraphenylborate.* Mix 10 ml of 0.01*M* novocaine hydrochloride solution with 20 ml of sodium tetraphenylborate solution. Filter off the precipitate on a porosity-4 sintered-glass crucible, wash with distilled water and dry at 100° for 1 hr. Dissolve the precipitate in 25 ml of nitrobenzene. Dry the solution by passage through filter paper and anhydrous sodium sulphate, then dilute to 100 ml with nitrobenzene. This is the liquid membrane ($10^{-3}M$) for electrode A.

(*b*) *Novocaine-dipicrylaminate.* To obtain the liquid membrane for electrode B, mix 10 ml of 0.01*M* novocaine hydrochloride in a separating funnel with 10 ml of 0.01*M* dipicrylamine (dissolved in dilute sodium carbonate solution by heating). The novocaine–dipicrylaminate ion-association complex is precipitated. Add 25 ml of nitrobenzene and shake the two phases for 15 min. Separate the phases and dry the organic layer by passage through filter paper and anhydrous sodium sulphate. Transfer to a 100-ml flask and dilute to volume with nitrobenzene.

Nitrobenzene is a suitable solvent for liquid membranes, because of its high partition coefficient, and its high dielectric constant which gives high conductance to the membrane. Also, it is of low volatility, which is reflected in the maintainance of a constant concentration of the membrane and consequently of the conditional standard potentials, E'_0.

Construction of the novocaine-selective membrane electrodes

The construction of the electrodes has been described previously[15,16] and consists of impregnating the support material (a graphite rod 15 mm long and 6.5 mm in diameter, made water-repellent) with the electrode material dissolved in nitrobenzene. The internal reference electrode is eliminated by using a stainless steel wire introduced into the graphite rod. The electrodes are stored in the relevant liquid membrane solutions and are washed with distilled water between measurements.

Recommended procedures

Direct potentiometry. Prepare 10^{-2}, 10^{-3} and $10^{-4}M$ standards (I = 0.1, $NaNO_3$, pH 5.0) by serial dilution of 0.1*M* novocaine hydrochloride. Place the novocaine and reference electrodes in the stirred standard solutions in the order 10^{-3}, 10^{-4}, $10^{-2}M$. Plot E against log concentration. Determine the unknown concentration from the calibration curve.

Potentiometric titration. Place the electrodes in the sample solution (30–40 ml, concentration *ca.* $10^{-3}M$, pH 5.0), then titrate with 0.01*M* sodium tetraphenylborate. The end-point corresponds to the maximum slope on the E *vs.* volume titration curve. (1 ml of 0.01*M* tetraphenylborate is equivalent to 2.73 mg of novocaine hydrochloride).

Injectable aqueous solutions (Gerovital and Aslavital). Transfer the contents of an ampoule with distilled water into a 25-ml standard flask and dilute to volume. Take 3.0 ml of this solution in a 50-ml beaker, add 20 ml of distilled water and adjust the pH to 5.0 with hydrochloric acid and/or sodium hydroxide solution. Titrate potentiometrically with 0.01*M* tetraphenylborate as above. The weight of novocaine hydrochloride in the ampoule is $V \times f \times 25 \times 273/3$ mg where V is the volume of sodium tetraphenylborate solution used and f is the molarity of the titrant.

Tablets (Gerovital H_3 and Aslavital). Weigh (W mg) and finely powder 20 tablets. Transfer about a quarter (accurately weighed, w mg) to a 100-ml beaker, extract with 25 ml of distilled water, filter into a 200-ml standard flask and dilute to volume with distilled water. Take 5.0 ml from this solution in a 50-ml beaker, add 20 ml of distilled water, adjust to pH 5.0 and titrate potentiometrically as above. The average weight of novocaine hydrochloride per tablet = $V \times f \times 546 \times W/w$ mg.

RESULTS AND DISCUSSION

The electrode function

The emf measurements were made with the electrochemical cell:

novocaine-selective membrane electrode (A or B)	novocaine.HCl (C), I = 0.1 ($NaNO_3$), (pH 5.0)	satd. $NaNO_3$ solution	SCE (I)

where C is the novocaine concentration, ranging from 10^{-1} to $10^{-6}M$. The emf is given by:

$$E_{I(A)} = E'_{0(A)} + 0.047 \log[\text{novocaine}^+] \text{ (for electrode A)} \quad (1)$$

and

$$E_{I(B)} = E'_{0(B)} + 0.048 \log[\text{novocaine}^+] \text{ (for electrode B)} \quad (2)$$

where the E'_0 values are the conditional standard potentials for electrodes A and B, under the conditions of use of cell (I). The measurements were carried out at constant ionic strength (I = 0.1, $NaNO_3$) and junction potentials were kept constant.

Figure 1 shows the electrode functions for the two electrodes. The responses are linear over the range 10^{-5}–$10^{-1}M$ with sub-Nernstian slopes (47 mV/decade for electrode A and 48 mV/decade for electrode B). The slopes of the curved parts are only about 25 mV/decade for 10^{-5}–$10^{-6}M$ solutions.

Extrapolating to p[novocaine] = 0 gives 273 mV for $E'_{0(A)}$ and 292 mV for $E'_{0(B)}$ (both values *vs.* SCE).

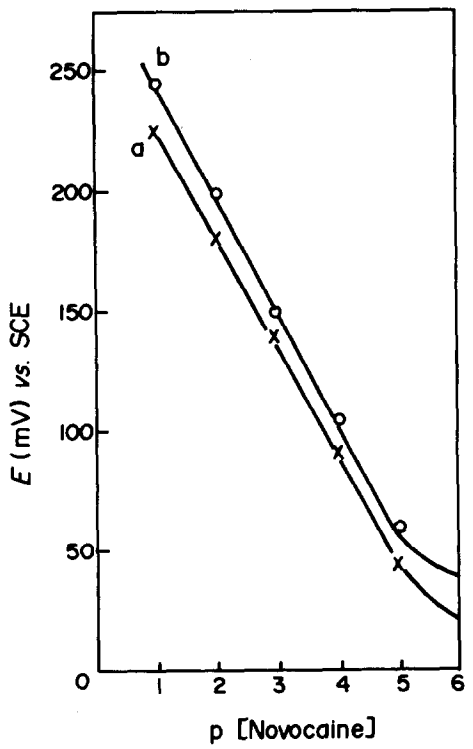


Fig. 1. The electrode functions of the novocaine-selective membrane electrodes: (*a*) electrode A; (*b*) electrode B (I = 0.1, $NaNO_3$; pH 5.0).

Selectivity

Novocaine very often has to be determined in preparations in which it is mixed with organic and inorganic substances. These substances constitute a serious problem in the various existing methods of analysis and have to be adequately removed before the novocaine determination. The effect of some of these substances on the responses of our electrodes was estimated by measuring the selectivity coefficients, $K_{nov.,j}$, by the method of Srinivasan and Rechnitz[17] and the equation:

$$\log K_{nov.,j} = \frac{E_{II} - E_{I(A\text{ or }B)}}{S} + \log [\text{novocaine}^+] - \log [\text{interferent}^{z+}]^{1/z} \qquad (3)$$

where $E_{I(A\text{ or }B)}$ is the emf of cell (I) for $C_{novocaine} = 0.01M$, E_{II} is the emf of an electrochemical cell of type (II) and S is the electrode slope.

novocaine-selective membrane electrode (A or B)	interferent^{z+} ($C = 0.01M$) $I = 0.1$ ($NaNO_3$) (pH 5.0)	satd. $NaNO_3$ solution	SCE (II)

The results obtained with commonly met concomitants (Table 1) indicate that only atropine, codeine and pyramidone are likely to cause interference. The data in Table 1 show that the $K_{nov.,j}$ values are similar for both electrodes.

Table 1. Selectivity coefficients for the novocaine-selective membrane electrodes ($C_{Novocaine} = C_{Interferent}{}^{z+} = 0.01M$; pH = 5.0; I = 0.1 ($NaNO_3$))

Substances tested	Selectivity coefficient, log $K_{nov.,j}$ Electrode A	Electrode B
Leucine	5.04	4.54
Ephedrine	1.70	2.04
Benzoic acid	4.53	4.27
Nicotinic acid	4.32	3.75
Triethanolamine	3.15	2.79
Piperazine	4.06	3.56
Pyramidone	1.17	1.00
Codeine	1.25	1.13
Caffeine	2.91	2.70
Atropine	0.51	0.78
Urea	4.51	4.15
Sodium nitrate ($I = 0.01M$)	5.72	4.48
Disodium phosphate	5.55	3.70
Potassium nitrate	3.89	3.92
Potassium sulphate	3.68	3.56

Influence of pH

The effect of pH on the potentials of the electrodes was examined by measuring the emf of the cell in novocaine hydrochloride solutions in which the pH was varied by adding appropriate amounts of hydrochloric acid and/or sodium hydroxide solution. At pH values between 2 and 6, no significant change in the membrane potential was observed (for the two electrodes and for different concentrations of novocaine hydrochloride). At pH values higher than 6–6.5, the novocaine base in the aqueous test solutions precipitates, so the emf values are shifted towards more negative values (Fig. 2).

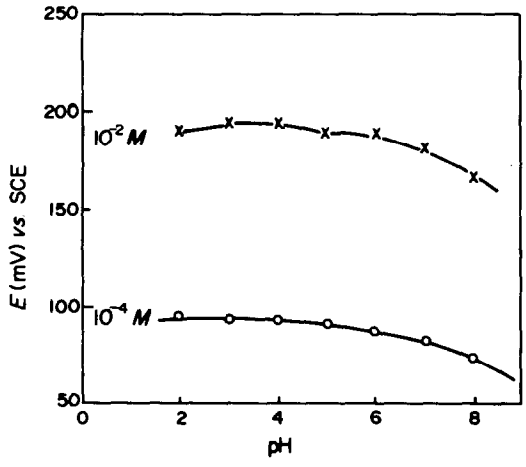


Fig. 2. Influence of pH on the response of electrode A for different novocaine hydrochloride concentrations.

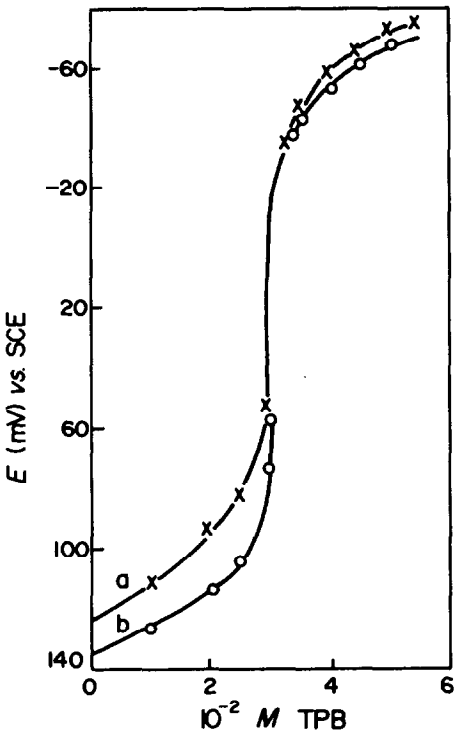


Fig. 3. Potentiometric titration of 30 ml of $10^{-3}M$ novocaine hydrochloride with $0.01M$ tetraphenylborate at pH 5.0: (*a*) electrode A; (*b*) electrode B.

Response time

The electrode response times were measured for novocaine hydrochloride solutions of different concentrations. For both electrodes the response times were about 3 min in the 10^{-6} and $10^{-5}M$ solutions, and about 30 sec in $10^{-4}M$ solutions. In more concentrated solutions the response times were of the order of a few seconds.

ANALYTICAL APPLICATIONS

Both electrodes can be used in the potentiometric determination of novocaine both by direct potentiometry and by potentiometric titration. We found titration to be advantageous, especially in the case of determination of novocaine in complex pharmaceutical preparations, because it is difficult to keep the constant ionic strength required for direct measurements. The most suitable titration reagent was found to be sodium tetraphenylborate ($0.01M$ aqueous solution or more dilute) which is stable for periods of up to a month.

Figure 3 shows the potentiometric titration curves of $10^{-3}M$ novocaine hydrochloride (pH 5.0, adjusted with hydrochloric acid and/or sodium hydroxide solution) obtained with the two electrodes. The obvious jumps of potential in both cases allow accurate evaluation of the equivalence volumes.

In the determination of the active principle in the pharmaceutical preparations such as Gerovital and Aslavital (ampoules or tablets, composition given in Tables 2 and 3) both electrodes had almost similar behaviour. None of the additional ingredients affected the results of the determinations. In all cases, reproducibility was good. The mean relative error for 4–12 mg of novocaine hydrochloride does not exceed ±0.5%.

Table 2. Determination of novocaine hydrochloride in aqueous injectable solutions with a novocaine-selective membrane electrode*

Pharmaceutical product	Composition	Ampoule	Nominal amount,† *mg*	Found, *mg*	Found, *mg/ampoule*
Gero H_3	1 ampoule (5 ml) contains 100 mg of novocaine.HCl; 6 mg of benzoic acid; 5 mg of potassium metabisulphite; 1 mg of disodium hydrogen phosphate; distilled water to 5 ml	I	4	3.92	98.0
			8	7.97	99.7
			12	11.92	99.4
			12	11.97	99.5
		II	8	7.78	97.3
			12	11.84	98.7
		III	12	11.79	98.3
Aslavital	1 ampoule (5 ml) contains 100 mg of novocaine.HCl; 64 mg of glutamic acid; 6 mg of benzoic acid; 24 mg of potassium hydroxide; 5 mg of potassium metabisulphite; 0.5 mg of disodium hydrogen phosphate; distilled water to 5 ml	I	12	11.99	99.9
			12	12.07	100.6
		II	12	12.26	102.8
			12	12.38	103.3
			12	12.40	103.4
			12	12.35	103.1
			12	12.35	103.1
		III	12	11.79	98.3
			12	11.82	98.5
		IV	12	11.94	99.5
			12	11.94	99.5

* Electrode A was used.

† Assuming ampoule conforms exactly to specification.

Table 3. Determination of novocaine hydrochloride in tablets with a novocaine†-selective membrane electrode*

Pharmaceutical product	Composition (per tablet)	Nominal amount taken,† *mg*	Found, *mg*	Found, *mg/tablet*
Gerovital H_3		5.0	5.02	100.3
	100 mg of novocaine.HCl;	5.0	5.02	100.3
	6 mg of benzoic acid;	7.5	7.45	99.2
	5 mg of potassium metabisulphite;	7.5	7.49	99.9
	0.5 mg disodium hydrogen phosphate;	7.5	7.49	99.9
	excipiens q.s.	10.0	10.00	100.0
Aslavital				
	100 mg of novocaine.HCl;	5.0	4.92	98.4
	6 mg of benzoic acid;	5.0	4.95	99.0
	5 mg of potassium metabisulphite;	7.5	7.40	98.6
	0.5 mg of disodium hydrogen phosphate;	7.5	7.42	99.0
	30 mg of vitamin B_6;	7.5	7.37	98.3
	200 mg of meso-inositol;	10.0	9.87	98.7
	excipiens q.s.			

* Electrode A was used.
† Assuming tablets conform exactly to specification.

REFERENCES

1. M. Ionescu and V. V. Coşofreţ, *Rev. Chim. (Bucharest)*, 1980, **31**, 1005.
2. *Idem, ibid.*, 1980, **31**, 1088.
3. G. E. Baiulescu and V. V. Coşofreţ, *Applications of Ion-Selective Membrane Electrodes in Organic Analysis*, Horwood, Chichester, 1977.
4. W. Selig, *Ion-Selective Electrodes in Organic Elemental and Functional Group Analysis*, Lawrence Livermore Laboratory, UCRL-52393, 1977 and 1978.
5. V. V. Coşofreţ, *Ion Selective Electrode Rev.*, 1980, **2** (No. 4).
6. R. P. Buck, *Anal. Chem.*, 1978, **50**, 17R.
7. G. H. Fricke, *ibid.*, 1980, **52**, 259R.
8. *British Pharmacopoeia*, Vol. I, p. 367. Her Majesty's Stationary Office, London, 1980.
9. *U.S. Pharmacopeia*, 1975, XIX, p. 409.
10. *Rom. Pharmacopeia*, 1976, IX, p. 569.
11. E. Hopîrtean and F. Cörmos, *Stud. Univ. Babeş-Bolyai, Ser. Chem.*, 1977, **22**, 35.
12. C. Luca, C. Baloescu, G. Semenescu, T. Tolea and E. Semenescu, *Rev. Chim. (Bucharest)*, 1979, **30**, 72.
13. V. V. Coşofreţ, P. G. Zugrăvescu and G. E. Baiulescu, *Talanta*, 1977, **24**, 461.
14. V. V. Coşofreţ, *Rev. Roum. Chim.*, 1978, **23**, 1489.
15. G. E. Baiulescu, V. V. Coşofreţ and C. Christescu, *Rev. Chim., (Bucharest)*, 1975, **26**, 429.
16. M. Ionescu, St. Cilianu, A. A. Bunaciu and V. V. Coşofreţ, *Talanta*, in the press.
17. K. Srinivasan and G. A. Rechnitz, *Anal. Chem.*, 1969, **41**, 1203.

Talanta, Vol. 28, pp. 383 to 387, 1981
Printed in Great Britain

0039-9140/81/060383-05$02.00/0
Pergamon Press Ltd

DETERMINATION OF SULPHA-DRUGS WITH ION-SELECTIVE MEMBRANE ELECTRODES

M. IONESCU, S. CILIANU, A. A. BUNACIU and V. V. COŞOFREŢ

Institute of Chemical and Pharmaceutical Research Bucharest, 74351-Sos. Vitan 112, Bucharest-3, Romania

(*Received* 4 *August* 1980. *Accepted* 26 *December* 1980)

Summary—A liquid-membrane mercury(II)-sensitive electrode is used for determination of various sulpha drugs by addition of excess of mercuric nitrate and potentiometric back-titration of the surplus mercury(II) with EDTA. The performance of the electrode is compared with that of an Ag_2S crystal-membrane electrode. Attempts to prepare a sulphamethoxazole-sensitive electrode failed.

The appearance and large-scale development of ion-selective membrane electrodes have produced spectacular achievements in the last few years. Theoretically, it should be feasible to construct such electrodes for any ionic species. However, in practice there are a number of difficulties, depending on the nature of the ion for which the electrode should be selective. For organic ions, the difficulties encountered in obtaining anion-selective electrodes are much greater, proof being the fact that until now none of the many manufacturing companies has yet perfected such a type of sensor. On the other hand much research is done on determination of organic compounds with either membrane electrodes selective for an inorganic ion, or with new types of membrane electrodes with selectivity for the organic ion.[1–4]

For the determination of sulpha-drugs, the only ion-selective membrane electrode method published so far was developed by Hazemoto *et al.*[5] and uses an electrode sensitive to sulphamerazine and sulphisomidine, two sulphonamides with antibacterial effects. These electrodes were based on a nitrobenzene solution of the ion-association complex of the iron(II)–bathophenanthroline chelate and the sulpha-drug. The electrodes have a limited linear response range (10^{-1}–$10^{-3}M$), and the response is influenced by the presence of certain organic substances frequently found in pharmaceutical preparations.

Other new methods of determination, especially chromatographic ones, have recently been developed but their speed and accuracy sometimes do not give full satisfaction.[6–11]

In this paper we probe a simple and more rapid and accurate method for the determination of some sulpha-drugs, based on the well-known ability of these compounds to form highly insoluble mercury(II) compounds:[12,13]

$$2R\text{–}SO_2\text{–}NH\text{–}R' + Hg^{2+} \rightarrow (R\text{–}SO_2\text{–}N(R')\text{–})_2Hg + 2H^+$$

For the quantitative determination, an Hg^{2+}-selective electrode of our own construction and a commercial silver sulphide crystal electrode were used.

Recently, Hg^{2+}-selective liquid membrane electrodes have been based on mercury(II) chelates dissolved in suitable organic solvents.[14–18] The one used in this work uses the chelate of Hg^{2+} with 1-(2′,3′,5′-tri-*O*-benzoyl-β-D-ribofuranosyl)-4-thioxo-5-benzylthio-6-azauracil, dissolved in chloroform, as the membrane. The reagent, denoted by HR (a weak organic acid) was recently obtained and characterized by Cristescu.[19]

EXPERIMENTAL

Apparatus and reagents

The emf values were measured at room temperature in stirred solutions, with an MV-87 digital pH/mV-meter (Prăcitronic, East Germany). The potentiometric titration curves were recorded with an automated outfit composed of a Radiometer TTT2 titrator, ABU 12 autoburette and SBR 2c recorder. A saturated calomel electrode (K401, Radiometer) was used as reference electrode. The direct potentiometric measurements were carried out in stirred solutions, with an Ag^+/S^{2-} selective membrane electrode (Orion, Model 94-16) and a sulphamethoxazole liquid-membrane electrode of our own construction. The pH measurements were made with a glass–calomel electrode pair (types G202C and K401, Radiometer, respectively). The absorption spectra of HR and its Hg(II) chelate were obtained with a PMQ-3 spectrophotometer (West Germany).

All reagents used were of analytical grade, except HR, which was obtained and purified as it described earlier.[19]

Preparation of the liquid membranes

Hg^{2+}-selective electrode. To make the liquid membrane, 10 ml of $10^{-2}M$ mercuric nitrate at pH 6.0 (adjusted with hexamine) were shaken in a separating funnel for 5 min with 10 ml of chloroform containing 0.0695 g of HR, then

the phases were separated and the organic layer was dried by passage through anhydrous sodium sulphate, transferred to a 100-ml standard flask and diluted to volume with chloroform. The concentration of the chelate in this solution was $5 \times 10^{-4}M$.

Sulphamethoxazole-sensitive electrode. To obtain the liquid membrane, 20 ml of $10^{-3}M$ sulphamethoxazole at pH 9.0 (adjusted with sodium hydroxide) were shaken in a separating funnel for 30 min with 20 ml of $10^{-3}M$ benzalkonium chloride in nitrobenzene. The phases were separated and the nitrobenzene layer was dried by passage through anhydrous sodium sulphate, transferred to a 100-ml standard flask and diluted to volume with nitrobenzene. The concentration of the ion-association complex in this solution was $2 \times 10^{-4}M$.

Construction of the electrodes

The construction of the electrodes has been described previously[20,21] and consists of impregnating the support material (a graphite rod 15 mm long, 6.5 mm diameter, made water-repellent) with Hg(II)–HR solution in chloroform or sulphamethoxazole–benzalkonium solution in nitrobenzene, respectively. The internal reference electrodes are eliminated by using a stainless-steel wire introduced into a graphite rod. The electrodes are stored in the appropriate organic phase and are washed with distilled water between measurements.

Procedure

The weighed sample (*ca.* 10 mg) is dissolved in about 5 ml of methanol in a 100-ml beaker, and 5 ml of $10^{-2}M$ mercuric nitrate are added. After the precipitation, 10 ml of distilled water are added and the pH is adjusted to 6.0 with hexamine. The pair of electrodes (Hg^{2+} or Ag^{+}/S^{2-} selective working electrode and SCE reference) are introduced into the solution, which is then titrated with $10^{-2}M$ EDTA, with stirring. The electrode potential E is recorded as a function of the titrant volume V and the graph of E *vs.* V is plotted. The end-point corresponds to the maximum slope on the titration curve.

RESULTS AND DISCUSSION

Hg^{2+}-selective electrode

The electrode function, E–pHg^{2+}. The emf measurements were made with the electrochemical cell:

$$\text{Hg}^{2+}\text{-selective membrane electrode} \;\Big|\; \text{Hg}^{2+}\,(C_{\text{Hg}^{2+}}),\ \mu = 0.5M\,(\text{KNO}_3) \;\Big|\; \begin{matrix}\text{satd.}\\ \text{KNO}_3\\ \text{soln.}\end{matrix} \;\Big|\; \text{SCE} \qquad \text{(I)}$$

where $C_{Hg^{2+}}$ is the Hg^{2+} concentration, ranging from 10^{-1} to $10^{-5}M$. The emf of the cell (I) is given by:

$$E_{\text{I}} = E_0' + 0.0285 \log[\text{Hg}^{2+}]$$

where E_0' represents the conditional standard potential of the electrode under the conditions of use. The measurements were made at constant ionic strength ($\mu = 0.5M$, KNO_3) and the junction potential was kept constant.

The linear response range of the electrode is 10^{-1}–$10^{-4}M$ Hg^{2+} with a slope of 28.5 mV/decade, and E_0' is 513 mV *vs.* SCE, a value approaching that of the Hg^{2+}-selective membrane electrodes constructed previously.[15–18] The inability to obtain a better detection limit with this electrode is probably due to the adsorption of Hg^{2+} ions at the end of the electrolyte bridge and on the surface of the glass vessel.

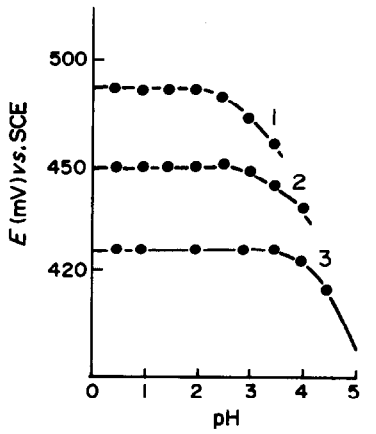


Fig. 1. The effect of pH on response of the Hg^{2+}-selective membrane electrode. 1—$Hg(NO_3)_2$, $10^{-1}M$; 2—$Hg(NO_3)_2$, $10^{-2}M$; 3—$Hg(NO_3)_2$ $10^{-3}M$.

Influence of pH. In Fig. 1 we show the effect of pH on the response of the liquid-state Hg^{2+}-selective membrane electrode at different mercuric nitrate concentrations. The pH range in which the potential remains constant is relatively narrow because of the hydrolysis of mercury(II).

The direct potential measurements for calibration of the electrode were done at pH 1.5 (adjusted with nitric acid).

Response time. The dynamic response is a most important factor in direct potentiometric determinations

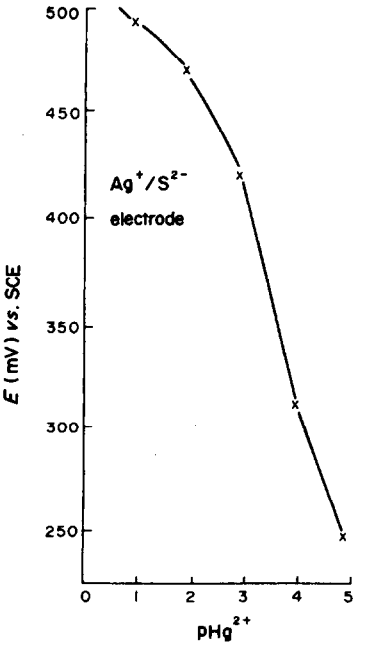


Fig. 2. The response of the Ag^{+}/S^{2-}-crystal membrane electrode, Orion Model 94-16, to different concentrations of Hg^{2+}.

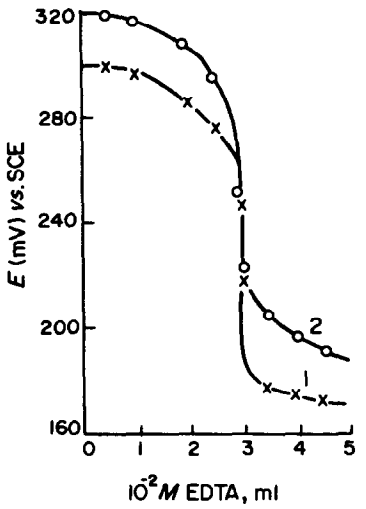


Fig. 3. The potentiometric titration of 30 ml of $10^{-3}M$ $Hg(NO_3)_2$ (pH 6.0) with $10^{-2}M$ EDTA. 1—Ag^+/S^{2-}-selective electrode; 2—Hg^{2+}-selective electrode.

or potentiometric titrations. The response characteristics of the electrode were evaluated by introducing it into mercuric nitrate solutions of different concentrations but identical acidity (pH 1.5) and noting the emf values as a function of time. The response time of the electrode in dilute solutions ($pHg^{2+} = 4$ and 5) is less than 4 min, and in concentrated solutions is only a few seconds.

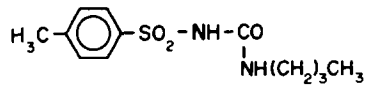
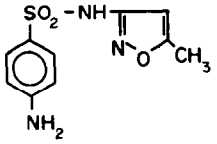
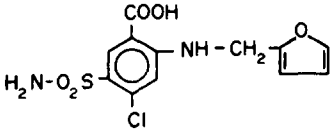
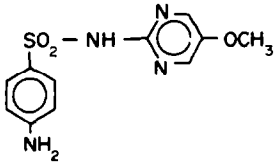
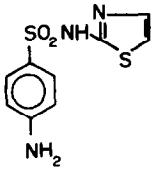
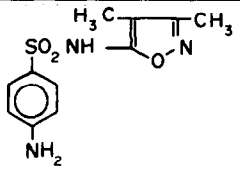
Selectivity. The selectivity coefficients $K_{Hg^{2+},M^{z+}}$, were calculated by the method of Srinivasan and Rechnitz,[22] from the relation:

$$\log K_{Hg^{2+},M^{z+}} = \frac{E_{II} - E_I}{28.5} + \log [Hg^{2+}] - \log [M^{z+}]^{2/z}$$

where E_I is the emf of cell (I) for $C_{Hg^{2+}} = 0.01M$, and E_{II} is the emf of an electrochemical cell of the type:

Hg^{2+}-selective membrane electrode	$M^{z+}(C_{M^{z+}} = 10^{-2}M)$, $\mu = 0.5M\,(KNO_3)$	satd. KNO_3 soln.	SCE (II)

Table 1. Sulpha-drugs determined with membrane-electrodes

Sulpha-drug	Formula	Category
Tolbutamide		Antidiabetic
Sulphamethoxazole		Bacteriostatic
Furosemide		Diuretic
Sulphamethoxydiazine		Bacteriostatic
Sulphathiazole		Used for staphylococcal infections
Sulphafurazole		Bacteriostatic

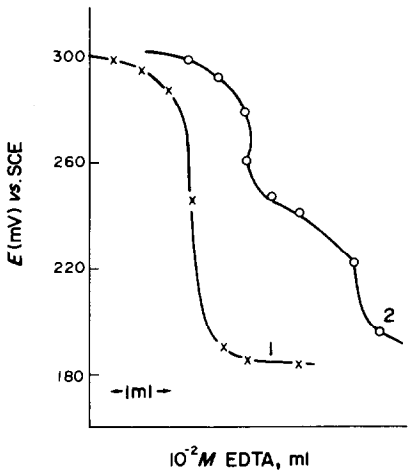


Fig. 4. The potentiometric titration of sulpha-drugs with the Ag^+/S^{2-}-selective electrode. 1—4 ml of $10^{-2}M$ tolbutamide + 4 ml of $10^{-2}M$ $Hg(NO_3)_2$ + 20 ml of distilled water (pH 6.0); 2—4 ml of $10^{-2}M$ sulphamethoxidiazine + 4 ml of $10^{-2}M$ $Hg(NO_3)_2$ + 20 ml of distilled water (pH 6.0) (curve 2 is displaced for clarity).

where M^{z+} represents any of the main metal cations that form more or less stable compounds with HR. In all cases the nitrates were used, at pH 1.5. Of all the cations tested (Pb^{2+}, Co^{2+}, Al^{3+}, Bi^{3+}, Cd^{2+}, Ni^{2+}, Zn^{2+}, Cu^{2+} and Ag^+) only Ag^+ interferes.

Sulphamethoxazole-sensitive electrode

Our efforts to obtain an electrode selective for sulphamethoxazole for use in sulpha drug determinations by direct potentiometry, were without success: the electrode function was linear over only a narrow range of activities and non-reproducible, and the response slope was only 33 mV/decade. The emf measurements were made at pH 9.0.

Ag^+/S^{2-}-crystal membrane electrode

This electrode is considered one of the most reliable of all those available, and is frequently used in titrimetric determinations in which Hg(II) is used as titrant.[23–25] Some experiments made by Potman and Dahmen[24] in order to elucidate the mechanism of the interaction of Hg^{2+} ions with the Ag_2S electrode led to the conclusion that this electrode has a linear response to Hg^{2+} with a slope of 60 mV/decade, corresponding to the following ion-exchange process taking place on the surface of the Ag_2S crystal membrane:

$$Hg^{2+} + Ag_2S_{crystal} \rightarrow [AgHgS]^+_{crystal} + Ag^+$$

Our results are not in agreement with Potman and Dahmen's data with regard to the linear response of the electrode to Hg^{2+}. The electrode slope obtained by us was about 110 mV/decade (Fig. 2), the response time of the electrode to Hg^{2+} was longer (*ca.* 7 min for $10^{-5}M$, *ca.* 5 min for the range 10^{-3}–$10^{-4}M$ and a few seconds for the range 10^{-2}–$10^{-1.5}M$), and the electrode function was non-reproducible. The mechanism of this electrode in potentiometric titrations with Hg^{2+} remains unknown, although it gives good results.

Applications to sulpha-drug determination

The good behaviour of the two electrodes (Hg^{2+}-selective and Ag^+/S^{2-} crystal membrane) in potentiometric titrations is well demonstrated in Fig. 3, which presents the curves for potentiometric titration of Hg(II) with EDTA at pH 6.0 (hexamine buffer). There is a large potential jump at the equivalence point in both cases, and a maximum error of 0.6%. Similar curves were obtained for titrations with nitrilotriacetic acid.

Any of the sulpha-drugs examined (Table 1) could be directly titrated with mercury(II), with end-point detection by either electrode, but the addition of an excess of Hg^{2+} for complete precipitation of the sulpha drug and the back-titration of the surplus with EDTA or NTA led to more satisfactory results.

Figure 4 shows the two types of curves obtained for the back-titration. Curve 1 is for determination of tolbutamide [only one potential jump, which corresponds to the end-point for the excess of Hg(II)], and curve 2 is for determination of sulphamethoxydiazine, where the first potential jump corresponds to the end-point for the excess of Hg(II), and the second, less evident and smaller, corresponds to completion of the dissolution of the Hg(II)–sulpha drug precipitate by EDTA or NTA.

We determined tolbutamide in amounts ranging between 4 and 12 mg with an absolute error which did not exceed 1.5%. Seven replicate determinations of sulphamethoxazole in the range 10^{-2}–$10^{-3}M$ gave an average recovery of 99.2% and mean relative standard deviation of 0.4%.

Other drugs successfully titrated included furosamide, sulphamethoxydiazine, sulphathiazole and sulphafurazole.

REFERENCES

1. G. E. Baiulescu and V. V. Coşofreţ, *Applications of Ion-Selective Membrane Electrodes in Organic Analysis*, Horwood, Chichester, 1977.
2. W. Selig, *Ion Selective Electrodes in Organic Elemental and Functional Group Analysis. A Review*, Lawrence Livermore Laboratory, Rept. UCRL-52393, 1977.
3. W. Selig, *Ion Selective Electrodes in Organic Elemental and Functional Group Analysis. A Review*, Lawrence Livermore Laboratory, Rept. UCRL-52393, 1977.
4. J. Koryta, *Anal. Chim. Acta*, 1979, **111**, 1.
5. N. Hazemoto, N. Kamo and Y. Kobatake, *J. Pharm. Sci.*, 1976, **65**, 435.
6. A. Bye and G. J. Land, *J. Chromatog.*, 1977, **139**, 181.
7. P. H. Cobb and G. T. Hill, *ibid.*, 1976, **123**, 444.
8. J. Crommen, *J. Pharm. Belg.*, 1977, **32**, 128.
9. L. J. Dombrowski, R. S. Brown and E. L. Pratt, *J. Pharm., Sci.*, 1977, **66**, 1413.
10. N. Nose, S. Kobayashi, A. Hirose and A. Watanabe, *J. Chromatog.*, 1976, **123**, 167.
11. N. M. Treff, V. M. S. Ramanujam and F. G. Cantelli, *Talanta*, 1977, **24**, 188.

12. Z. Blagojevic and P. Bradic, *Arhiv. Farm* (*Beograd*), 1960, **4**, 193.
13. I. Popa and A. Voicu, *Farmacia* (*Bucharest*), 1962, **7**, 399.
14. J. Růžička and J. C. Tjell, *Anal. Chim. Acta*, 1970, **51**, 1.
15. V. V. Coşofreţ, *Rev. Chim.* (*Bucharest*), 1976, **27**, 240.
16. G. E. Baiulescu and V. V. Coşofreţ, *Talanta*, 1976, **23**, 677.
17. V. V. Coşofreţ, P. G. Zugrăvescu and G. E. Baiulescu, *ibid.*, 1977, **24**, 461.
18. G. E. Baiulescu, V. V. Coşofreţ and M. Blasnic, in *Ion Selective Electrodes*, E. Pungor (ed.), p. 207, Akadémiai Kiadó, Budapest, 1978.
19. C. Cristescu, *Monatsh. Chem.*, 1977, **108**, 1455.
20. V. V. Coşofreţ, *Doctoral Thesis*, Polytechnic Institute of Bucharest, Bucharest, 1975.
21. G. E. Baiulescu, V. V. Coşofreţ and C. Cristescu, *Rev. Chim.* (*Bucharest*), 1975, **26**, 429.
22. K. Srinivasan and G. A. Rechnitz, *Anal. Chem.*, 1969, **41**, 1203.
23. J. L. Swartz and T. S. Light, *Orion Newsl.*, 1970, **2**, (Nos. 7/8), 36; 1970, **2**, (Nos. 9/10), 41.
24. W. Potman and E. A. M. F. Dahmen, *Mikrochim. Acta*, 1972, 303.
25. M. S. Ionescu, V. V. Coşofreţ, T. Panaitescu and M. Costescu, *Anal. Lett.*, 1980, **13**, 715.

Talanta. Vol. 28, pp. 389 to 393, 1981
Printed in Great Britain. All rights reserved

0039-9140/81/060389-05$02.00/0
Copyright © 1981 Pergamon Press Ltd

CONTINUOUS SPECTROPHOTOMETRIC DETERMINATION OF COPPER, NICKEL AND ZINC IN COPPER-BASE ALLOYS BY FLOW-INJECTION ANALYSIS

ROKURO KURODA* and TADASHI MOCHIZUKI

Laboratory for Analytical Chemistry, Faculty of Engineering, University of Chiba, Yayoi-cho, Chiba, Japan

(*Received* 12 *November* 1980. *Accepted* 24 *December* 1980)

Summary—Flow-injection methods have been developed for the determination of copper, nickel and zinc in copper-base alloys, including several types of brasses, deoxidized copper, beryllium copper and German silver. The system for copper and nickel involves the measurement of the absorbance of the copper(II) and nickel(II) aquo-complexes at 805 and 410 nm, respectively, after simple dissolution of the sample in a nitric acid–phosphoric acid mixture. The system needs no further reagents and the sample solutions can be analysed at rates of up to 280 /hr for copper (or nickel in German silver) without any carry-over. The system for zinc consists of automatic dilution of the injected sample with a thiosulphate–acetate buffer solution and the subsequent measurement of the absorbance of the zinc–Xylenol Orange complex at 568 nm. This system permits analysis rates of up to 90/hr for zinc solutions, with no carry-over. The procedures have been applied to standard copper-base alloys. The results agreed satisfactorily with the certified values. The precision ranges are 0.2–0.7% for copper and nickel and 0.5–0.8% for zinc.

Since its introduction by Růžička and Hansen and by Stewart in 1975, flow-injection analysis has found wide application, especially in agricultural, environmental, clinical and pharmaceutical analyses. Recent progress has been reviewed in several articles.[1–4] Despite its great potential for automatic analysis of alloys, flow-injection analysis has been little applied in this area.[5] We have attempted to develop rapid procedures for the determination of copper, nickel and zinc in a variety of copper-base alloys by means of spectrophotometric flow-injection analysis. A simple flow system allows the rapid determination of copper (60–99.9%) and nickel (in German silver only) by direct measurement of the absorbance of their aquo-complexes. Spectrophotometric detection with Xylenol Orange (XO) permits the rapid determination of zinc, with minimum consumption of reagents because of the small sample size.

EXPERIMENTAL

Reagents

Standard solutions. Standard copper solution was prepared by dissolving 1 g of pure copper metal in 20 ml of 7*M* nitric acid and diluting exactly to 100 ml with distilled water [Cu(II) 10 mg/ml]. Standard nickel solution was prepared by dissolving 12 g of nickel nitrate in 1.4*M* nitric acid and diluting to 100 ml with the same acid [Ni(II) 25 mg/ml] and standardized complexiometrically. Standard zinc solution was prepared by dissolving 0.2 g of pure zinc metal in 20 ml of 7*M* nitric acid and diluting exactly to 100 ml with distilled water [Zn(II) 2 mg/ml].

Masking agent–buffer solution. Ten g of sodium thiosulphate dissolved in 1*M* acetic acid–1*M* sodium acetate buffer solution (pH 5.9) and diluted to 1 litre with the buffer.

Xylenol Orange solution. A 0.012% aqueous solution.

Apparatus

The systems for the determination of copper, nickel and zinc are shown in Fig. 1. The systems were assembled from 1.0-mm Teflon tubing except for a back-pressure coil (0.5 mm), valve and connectors. An SJ-1211H peristaltic pump (Atto, Japan) was operated with Tygon pump tubing (1/8 or 1/16 in. bore) to obtain the desired flow-rates. A sample-injection valve (Nihon Seimitsu NV-508-6M) made of Teflon with a Teflon sample loop (bore 1.0 mm) was used for sampling. A Shimazu Model UV-180 spectrophotometer equipped with a Nihon Seimitsu NS-FC-210 flow-through cell (volume 31.4 μl, light-path 10 mm) was used, coupled with a Shimazu Chromatopac C-R1A data-processer to record the peaks and simultaneously calculate the peak heights or areas.

Sample dissolution

Determination of copper and zinc. A sample weighing about 60 mg is dissolved in a mixture of 2 ml of 0.01*M* phosphoric acid and 10 ml of 7*M* nitric acid and diluted exactly to 50 ml with distilled water. A further tenfold dilution is made for the determination of zinc.

Determination of nickel. A 1.0-g of German silver is taken and treated as for copper determination.

Flow-injection analysis

Copper and nickel. Carrier solution C (1.4*M* nitric acid) is pumped into the analytical line at a flow-rate of 8.0 ml/min with a peristaltic pump [Fig. 1(a)]. The sample solution (318 μl in our apparatus) is introduced into the carrier stream by a six-way loop-valve injector V and the

* To whom correspondence and requests for reprints should be sent.

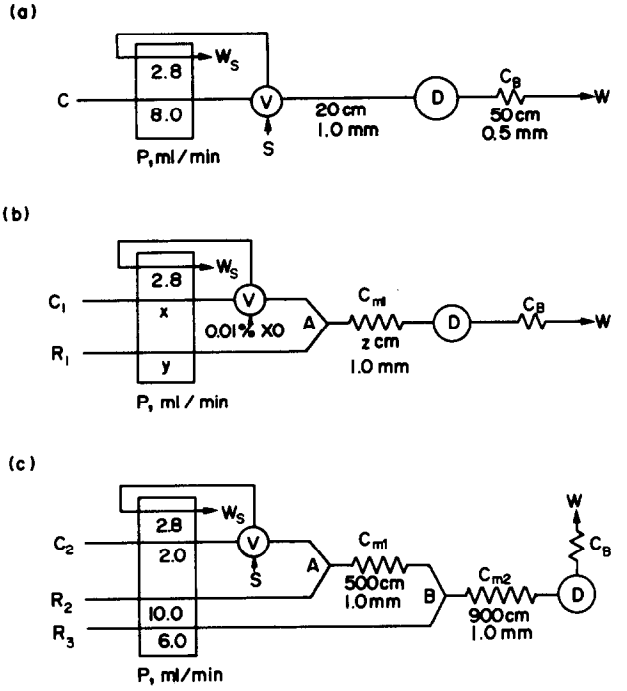


Fig. 1. Flow diagrams. (a) System for determination of copper and nickel. C: carrier (1.4*M* HNO_3); V: sample-injection valve; S: sample; P: peristaltic pump; D: spectrophotometer; C_B: back-pressure coil; W: waste; W_S: sample waste. (b) Automatic sample-dilution system. C_1: carrier (distilled water); R_1: reagent (distilled water). (c) System for the determination of zinc. C_2: carrier (0.14*M* HNO_3); R_2: masking agent–buffer solution (1% $Na_2S_2O_3$–acetate buffer, pH 5.9); R_3: colorimetric reagent (0.012% Xylenol Orange solution); A, B: confluence points; C_{ml}, C_{m2}: mixing coils. The numerals under the tubes or coils refer to their lengths in cm and their internal diameters in mm.

absorbance of the aquo-complex is monitored in the flow-through cell D at 805 nm for copper(II) and 410 nm for nickel(II), respectively, against the carrier solution as reference. A narrow coil C_B (50 cm long) is attached to the exit of the flow-through cell, as a back-pressure coil.

Zinc. Carrier solution C_2 (0.14*M* nitric acid) is pumped into the analytical line at a flow-rate of 2.0 ml/min and the sample solution S (148 µl) is introduced into the carrier solution by the injection valve V [Fig. 1(c)]. The sample slug meets the masking agent–buffer solution R_2 at the point A. In the mixing coil C_{ml} the sample is diluted, copper(II) and lead(II) being masked at the same time. The mixture and the colorimetric reagent flow R_3 (0.012% Xylenol Orange solution) merge at the point B. The colour reaction proceeds in the mixing coil C_{m2}, and the absorbance of the chelate is measured at 568 nm against the waste solution containing no sample constituents.

For calibration, similarly treated standard solutions are injected into the line between the sample runs. The area or the height of the absorbance peak can be used for the calibration.

RESULTS AND DISCUSSION

For rapid continuous spectrophotometric analysis of the alloys for the major components the preparation of the sample solution should be as simple as possible, and the same solution should be suitable for both the copper and the zinc determination. For this purpose a mixture of nitric and phosphoric acids is satisfactory, yielding no precipitation of hydrated

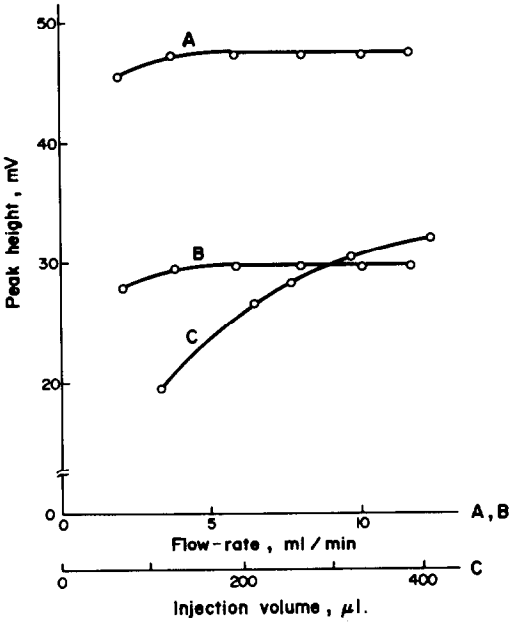


Fig. 2. Effects of flow-rate and injection volume on peak height—aquo-complex method. Sample concentration: A: Cu(II), 3 mg/ml; B: Cu(II), 2 mg/ml. Sample injection volume: 318 µl for A and B. C: Cu(II), 2 mg/ml. Flow-rate of carrier kept constant at 8.0 ml/min.

stannic oxide and providing effective masking of iron with phosphate. Copper(II) aquo-complexes exhibit an absorption maximum at 800–810 nm, with molar absorptivity 12.9 $l.mole^{-1}.cm^{-1}$. Such a low sensitivity is well suited to the determination of copper in copper-base alloys[6]. The absorbance is not affected by variation in the nitric acid concentration. The nickel(II) aquo-complexes also absorb at 805 nm to some extent, causing a 7% positive error when present at the same w/v concentration as the copper(II).

The nickel(II) has an absorption maximum at 393 nm, but the nitrous acid produced in the dissolution process interferes at this wavelength so the absorbance is measured at 410 nm, at which the molar absorptivity is 3.8 $l.mole^{-1}.cm^{-1}$, providing a basis for the determination of nickel in German silver.

Xylenol Orange reacts with zinc to form a coloured complex,[7] which exhibits an absorption maximum at 568 nm. The chelate is best formed at pH 5.7–5.8. Copper(II) and lead(II) interfere, but they are effectively masked with thiosulphate. However, nickel(II) still interferes seriously, and the method cannot be applied to nickel alloys unless a suitable masking agent can be found.

Optimization of flow system

The effects of flow-rate and injection volume on the peak height are shown in Fig. 2 for the determination of copper. Flow-rates greater than 5.0 ml/min give a constant absorbance peak-height for an injection

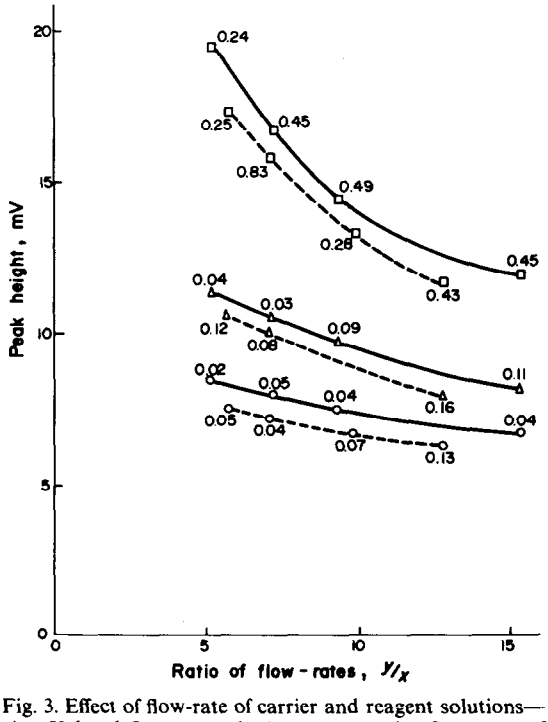


Fig. 3. Effect of flow-rate of carrier and reagent solutions—zinc–Xylenol Orange method. x, y: respective flow-rates of carrier and reagent solutions; mixing coil length, z: 100 cm (□), 300 cm (△), 500 cm (○); total flow-rate: 12.0 ml/min (——), 8.0 ml/min (– – –). The numerals at each point indicate the standard deviation.

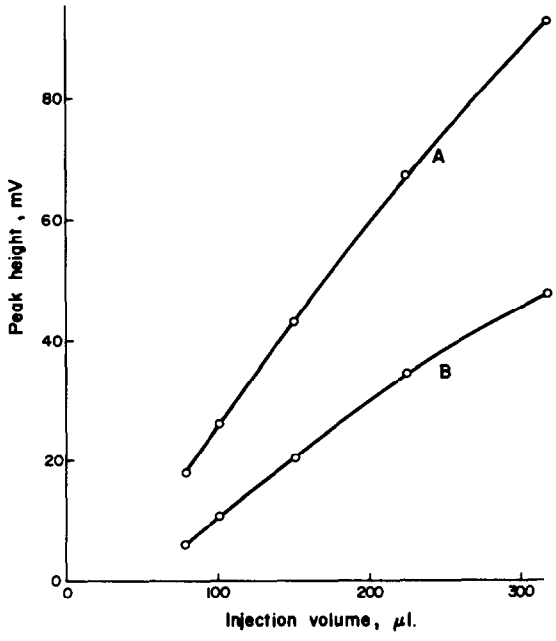


Fig. 4. Effect of injection volume—zinc–Xylenol Orange method. Sample concentration: A: Zn(II) 40 µg/ml; B: Zn(II) 20 µg/ml.

volume of 318 µl. The injection volume has a significant effect, yielding increased peak height and reproducibility with increasing injection volume. However, increasing the injection volume widens the sample zones and lowers the sampling rate, so that 318 µl is taken as a compromise. This allows analysis of 280 copper solutions per hour, without any carry-over. The optimum conditions for nickel are the same as those for copper.

The Xylenol Orange method is too sensitive to be applied directly to the analysis for zinc. To simplify the sample dilution we decided to dilute the sample within the flow system with a combined masking agent–buffer solution, as illustrated in Fig. 1(b). To examine the effectiveness of this dilution system, the 0.01% Xylenol Orange solution (78 µl) was introduced by the sample-injection valve V into the analytical line, where the total flow rate ($x + y$) was kept constant at either 8.0 or 12.0 ml/min and the ratio of flow-rates y/x (y is the flow-rate of the diluent) and the length of coil C_{m1} were varied over the ranges 5–15 and 100–500 cm, respectively. The results are illustrated in Fig. 3. Increasing either the coil length or the dilution ratio lowered the peak height but improved the reproducibility. The 12-ml/min total flow-rate gives better precision than the 8 ml/min rate. On the basis of these observations we decided to set C_{m1} = 500 cm, x = 2.0 ml/min and y = 10.0 ml/min and incorporated this flow-dilution system into the total flow system as indicated in Fig. 1(c). A long mixing coil C_{m2} (900 cm) is necessary to obtain a stable base-line. The flow-rate of the Xylenol Orange solution R_3 was varied over the range 2.0–10.0 ml/min with a sample-injection volume of 78 µl (zinc

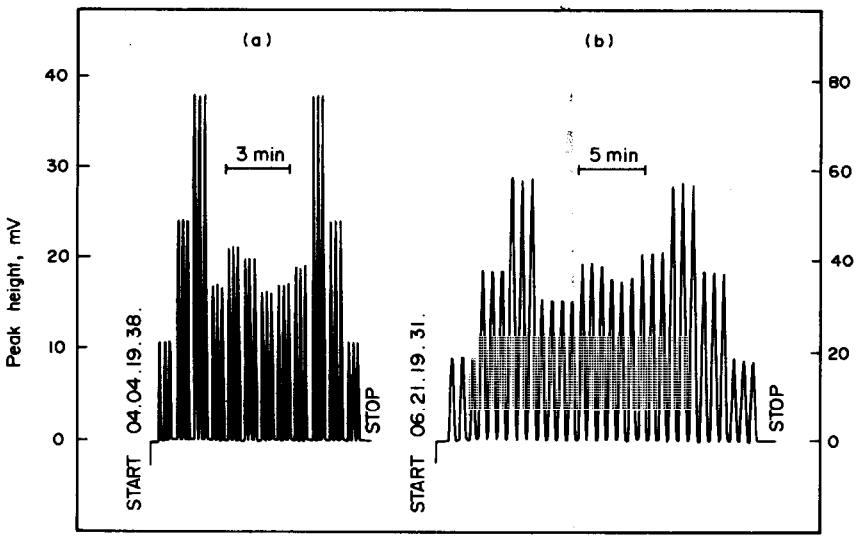


Fig. 5. Determination of copper and zinc in copper-base alloys. (a) Runs for copper. Sampling rate 280/hr with the flow diagram shown in Fig. 1(a). From left to right is shown a series of aqueous copper standards (0.8, 1.6 and 2.4 mg/ml), followed by six copper-base alloys and additional calibration runs. Each standard or sample is analysed in triplicate. (b) Runs for zinc. Sampling rate 90/hr with flow diagram shown in Fig. 1(c). From left to right is shown a set of zinc standards (26, 45 and 64 μg/ml) and four copper-base alloys, followed by another calibration run. Each is analysed in triplicate.

concentration 20 or 40 μg/ml), and the optimum was found to be 6 ml/min; lower rates made the base-line unstable and higher rates broadened the peaks. The sample-injection volume also has a significant effect on the peak height, which increases sharply with increasing injection volume, as illustrated in Fig. 4. Larger injection volumes increase the sensitivity and precision, but limit the speed of analysis owing to broadening of the peaks. We chose an injection volume of 148 μl, which gives no carry-over. This allows analyses of 90 sample solutions for zinc per hour.

Determination of copper, nickel and zinc in standard reference samples of copper-base alloys

Routine runs for the determination of copper and zinc in the copper-base alloys tested are illustrated in Fig. 5, together with those for a series of aqueous copper and zinc standards. The results are given in Table 1. The copper content of the alloys tested ranges from 60 to almost 100% (deoxidized copper) and can be determined with relative standard deviation (rsd) of 0.2–0.7%. Zinc is determined over the range 30–40% with an rsd of 0.5–0.8%. Agreement of the results with the certified values for copper and zinc is satisfactory. Only German silver was analysed for nickel, and again the result and certified value agree satisfactorily.

From the practical point of view, the rate-determining step in the alloy analysis is not the flow-injection system, but the other steps including sample weighing, dissolution and dilution to standard definite volume.

The precision of the flow-injection analyses described here is rather good, owing to the simple flow-systems developed, but the specifications for copper-base alloys often have comparatively narrow toler-

Table 1. Determination of copper, nickel and zinc in standard samples of copper-base alloys by flow-injection analysis

Sample†	Cu, %		Ni, %		Zn, %	
	Found*	Certified	Found*	Certified	Found*	Certified
Brass[a], class 1	70.5_6(0.5)	70.61	—		29.3_5(0.8)	29.36
Brass[b], class 3	60.3_2(0.3)	60.62	—		39.3_0(0.6)	39.35
Naval brass[c], class 1	62.6_0(0.7)	62.16	—		36.8_7(0.5)	36.82
Leaded brass[d], class 2	59.6_8(0.2)	59.63	—		39.2_0(0.5)	39.12
Phosphorus-deoxidized copper[e]	99.8_5(0.6)	99.94	—		—	
Beryllium copper[f]	97.6_6(0.5)	97.71	—		—	
German silver[g]	—		18.3_1(0.4)	18.21	—	

*Values in parentheses are the relative standard deviations.

† Provided by Japan Brass Makers' Association.

Other constituents (%) [a] Pb 0.00_9, Fe 0.01_5. [b] Pb 0.01_3, Fe 0.01_3. [c] Pb 0.0066_4, Sn 1.00_2, Fe 0.010_1. [d] Pb 1.21_1, Sn 0.00_9, Fe 0.02_4. [e] P 0.019_2. [f] Si 0.055_5, Fe 0.034_3, Co 0.26_8, Be 1.89_4. [g] Pb 0.002_9, Mn 0.26_8, Fe 0.014_8, Co 0.0048, Cu 55.11_1, Zn 26.39_3.

ance limits, *e.g.* 3–4% for copper in brasses and 4–6% for copper in German silvers. The precision should be high enough to ensure maximum economy in the production of alloys containing high-cost constituents such as copper and especially nickel. If a precision of 0.1% is desired, comparable to that of standard volumetric methods, replicate analysis and averaging are recommended. Ten consecutive runs on the same sample will result in an improvement in the precision by a factor of 3, *i.e.*, to 0.07–0.23% for copper and 0.17–0.27% for zinc. The high sampling rate of the flow-injection system compensates for the need for replication, and the overall analysis rate is about 28 samples per hour for copper or nickel and 9 per hour for zinc, which is in line with most industrial laboratory requirements.

REFERENCES

1. J. Růžička and E. H. Hansen, *Anal. Chim. Acta*, 1978, **99**, 37.
2. D. Betteridge, *Anal. Chem.*, 1978, **50**, 832A.
3. J. Růžička and E. H. Hansen, *NBS Spec. Publ.*, No. 519, 1979, p. 501.
4. *Idem*, *Anal. Chim. Acta*, 1980, **114**, 19.
5. R. Kuroda, T. Mochizuki and K. Oguma, *Bunseki Kagaku*, 1980, **29**, T73.
6. M. Namiki and J. Kimura, *ibid.*, 1978, **27**, T39.
7. K. Študlar and I. Janoušek, *Talanta*, 1961, **8**, 203.

Talanta, Vol. 28, pp. 395 to 396. 1981
Printed in Great Britain

0039-9140/81/060395-02$02.00/0
Pergamon Press Ltd

SHORT COMMUNICATIONS

PEACEFUL PYROLYSIS—A NOVEL METHOD FOR THE DECOMPOSITION OF METAL–PERCHLORATE COMPLEXES OF ORGANIC LIGANDS

M. R. GOPALAKRISHNAN NAIR, M. J. KURIAN and C. P. PRABHAKARAN*
Department of Chemistry, University of Kerala, Trivandrum 695001, Kerala, India

(*Received* 24 *October* 1980. *Accepted* 6 *January* 1981)

Summary—Perchlorate complexes of vanadium(IV), iron(III), dysprosium, yttrium, copper(II) and nickel with the organic ligands dimethyl sulphoxide, antipyrine, 4-aminoantipyrine, 4-(2-hydroxynaphthyl)-azoantipyrine, and 4-(2,4-dihydroxyphenyl)azoantipyrine have been prepared and analysed for their metal content after decomposition by a non-explosive pyrolytic technique, *viz.* heating with ammonium chloride. The results obtained agree with those obtained by the standard methods. This pyrolytic technique is found to be very convenient, rapid and accurate.

Metals such as titanium, vanadium, chromium, iron and the rare earths are usually estimated in their complexes with organic ligands by simple pyrolysis of the complexes to the metal oxide. This method is not acceptable in the case of the perchlorate complexes of these metals with organic ligands since most of them explode violently on heating, as expected for perchlorates in combination with elements such as carbon and hydrogen. Therefore "wet" methods are used for the decomposition of such perchlorate complexes. These methods are time-consuming and involve a number of steps; the degree of skill needed in such processes is so high that accuracy is not always attained. We report here a relatively simple method, "peaceful pyrolysis"—thermal decomposition without explosion—of the metal perchlorate complexes to the respective metal oxides. Perchlorate complexes of metals which do not give definite oxides can also be subjected to this technique, the residue obtained being dissolved in a suitable mineral acid and analysed for the metal. We present the results of our investigations of a few metal perchlorate complexes, some of which have already been described elsewhere, and others which were prepared for the first time.

EXPERIMENTAL

The following twelve perchlorate complexes were subjected to peaceful pyrolysis.

Dimethyl sulphoxide (DMSO) complexes of iron(III) and vanadium(IV) perchlorates.[1,2]

Antipyrine (AP) complexes of iron(III) and vanadium-(IV) perchlorates.[3]

4-Aminoantipyrine (AAP) complexes of dysprosium and yttrium perchlorates.[4]

4-(2-Hydroxynaphthyl)azoantipyrine (NAAP) complexes of vanadium(IV), copper(II) and nickel perchlorates.[5]

4-(2,4-Dihydroxyphenyl)azoantipyrine (RAAP) complexes of vanadium(IV), copper(II) and nickel perchlorates.[5]

Reagents

Analytical-reagent grade (BDH) ammonium chloride was resublimed before use. Dysprosium and yttrium perchlorates were prepared from the oxides and perchloric acid. Vanadium(IV) perchlorate was prepared according to Cotton and Francis.[2] Copper(II), nickel and iron(III) perchlorates were obtained from the carbonates and perchloric acid. The antipyrine, 4-aminoantipyrine and DMSO used were reagent-grade (BDH). 4-(2-Hydroxynaphthyl)azoantipyrine and 4-(2,4-dihydroxyphenyl)azoantipyrine were prepared by diazotization of 4-aminoantipyrine and coupling of the diazo product with 2-naphthol and resublimed resorcinol respectively as given in the literature.[6,7]

Preparation of the complexes

The DMSO, AP and AAP complexes were prepared according to the literature.[4] The NAAP and RAAP complexes were prepared by the following general method.

The vanadium(IV) perchlorate complexes were prepared by adding just over 0.005 mole of the salt in solution in the minimum quantity water to 0.005 mole of the ligand dissolved in methanol and refluxing for 3–4 hr to complete the reaction. The copper and nickel(II) perchlorate complexes were prepared similarly in acetone medium. In some cases the complexes precipitated and in others they were obtained by reduction of the volume. The complexes were filtered off, washed several times with water, allowed to dry in air, washed with benzene, and dried over phosphorus pentoxide under vacuum.

General method for peaceful pyrolysis

About 0.1–0.2 g of finely powdered complex is weighed accurately into a weighed silica crucible. About five times its weight of finely powdered resublimed ammonium chlor-

* Author to whom all correspondence should be addressed.

Table 1. Analysis of perchlorate complexes metals by peaceful pyrolysis

No.	Complex	Theory	Metal % By pyrolysis	By standard methods	Literature value
1	$Fe(DMSO)_6(ClO_4)_3DMSO$	6.20	6.23	6.23	6.21
2	$Fe(AP)_6(ClO_4)_3$	3.76	3.75	3.73	3.79
3	$Dy(AAP)_6(ClO_4)_3$	9.73	9.75	9.77	9.67
4	$Y(AAP)_6(ClO_4)$	5.54	5.61	5.62	5.75
5	$(VO)(DMSO)_5(ClO_4)_2$	3.98	3.90	3.90	3.89
6	$(VO)(AP)_4(ClO_4)_2$	2.50	2.50	2.50	2.49
7	$(VO)_2(NAAP)_3ClO_4$	7.81	7.92	7.92	—
8	$(VO)_2(RAAP)_3ClO_4$	8.48	8.55	8.55	—
9	$Cu(NAAP)ClO_4$	12.19	11.88	11.87	—
10	$Cu(RAAP)ClO_4$	13.07	12.87	12.82	—
11	$Ni(NAAP)_2(ClO_4)_2$	6.04	6.06	5.97	—
12	$Ni(RAAP)_2(ClO_4)_2$	7.30	7.38	7.28	—

ide is added (10–15 times for DMSO complexes) and mixed intimately with it by repeated gentle shaking of the crucible. The crucible is covered with a lid and heated gently until fuming ceases. The contents are then ignited, in presence of air, to constant weight, yielding the metal oxide. In the case of V_2O_5 a correction is applied and carried out.[8]

Metal estimation by standard methods

For comparison, the metal contents of all the complexes were determined by the standard methods. Weighed quantities of the complexes were decomposed by digestion with concentrated sulphuric acid. The solutions obtained were diluted and used for the estimation of the respective metals. Vanadium was precipitated as the cupferron complex, ignited to V_2O_5 and weighed. Iron was determined as Fe_2O_3 after precipitation as hydroxide. Dysprosium and yttrium were precipitated as their oxalates, ignited and weighed as the oxides.[9] Copper was determined by iodometry and nickel as dimethylglyoximate.

RESULTS AND DISCUSSION

The metals in the first eight complexes were estimated as their oxides by the peaceful pyrolysis method. The results were compared (Table 1) with the metal values obtained by standard methods described in the literature, which involve a number of steps. The values obtained by the peaceful pyrolysis method are closer to the theoretical values.

The metals in the last four complexes were determined after the peaceful pyrolysis by dissolving the oxides in acid, and using well-known methods for the analysis. The results obtained are in good agreement with those obtained by the acid decomposition of the complexes and subsequent determination of the metals by the standard methods, but the thermal decomposition method is faster.

WARNING. The method has been tested only for the compounds listed, and although it is *thought* to be safe for complexes which can be decomposed safely by acid decomposition, it is **strongly recommended** that before its application to other compounds on the scale given in the procedure it should be tested with a **small** sample with stringent safety precautions in case of explosion.

Acknowledgement—One of the authors (M.J.K.) is thankful to C.S.I.R. India for the award of a Junior Research Fellowship.

REFERENCES

1. Sathyanarayana and C. C. Patel, *Indian J. Chem.*, 1967, **5**, 360.
2. F. A. Cotton and R. Francis, *J. Am. Chem. Soc.*, 1960, **83**, 2986.
3. A. Ravi, J. Gopalakrishnan and C. C. Patel, *Indian J. Chem.*, 1967, **5**, 356.
4. J. Chacko, C. P. Prabakaran and C. G. R. Nair, *ibid.*, 1975, **13**, 411.
5. M. R. G. Nair and C. P. Prabhakaran, Unpublished work.
6. Sh.T. Talipov, R.Kh. Dzhiyanbaeva and N. G. Smaglyuk, *Mzb. Khim. Zh.*, 1970, **14**, No. 3, 6.
7. A. I. Vogel, *Text-Book of Practical Organic Chemistry*, 3rd Ed., E.L.B.S., 1973.
8. A. I. Vogel, *Text Book of Quantitative Inorganic Analysis*, 3rd Ed., Longmans, London, 1964.
9. I. M. Kolthoff and P. J. Elving (eds.), *Treatise on Analytical Chemistry*, Part II, Vol. 8, Interscience, New York, 1963.

Talanta. Vol. 28, pp. 397 to 398, 1981
Printed in Great Britain

0039-9140/81/060397-02$02.00/0
Pergamon Press Ltd

TITRIMETRIC DETERMINATION OF CERTAIN MERCAPTANS WITH MERCURIC CHLORIDE

K. K. TIWARI and R. M. VERMA

Department of Chemistry, University of Jabalpur, Jabalpur 482001, India

(*Received* 30 *September* 1980. *Accepted* 26 *December* 1980)

Summary—A procedure is described for the semimicro determination of certain mercaptans, by means of their reaction with mercuric chloride. The acid liberated during the reaction is titrated with standard alkali after addition of sufficient potassium iodide to convert the surplus mercuric chloride into a stable soluble complex. The procedure has been applied to determine 0.12–1 mmole of these compounds; the results are accurate to within 0.5%.

The high chemical reactivity of the mercapto group gives rise to a number of chemical reactions which can be used for its determination, these being mainly the oxidation to disulphide[1–13] or the formation of a metal mercaptide.[14–24] The oxidative methods can suffer from over-oxidation[6,11–13] or slow reaction,[25] and interference from some other sulphur-containing groups. The copper mercaptide methods[14–17] are regarded by Siggia[26] as less accurate than the iodine method. Iodometric determination of excess of copper[18] can suffer from partial oxidation of the mercaptide by the iodine liberated.[14]

Mercaptans react with mercuric chloride to liberate hydrochloric acid:

$$RSH + HgCl_2 = RSHgCl + HCl$$

and Sampey and Reid[25] titrate the acid, using Methyl Orange or Methyl Red as indicator; they observe that the results are always low because with both the end-point pH is too low, but has to be used to avoid interference by the formation of mercuric hydroxide. Ratkovics and Szepesvary[27] used Bromocresol Green as the indicator and showed that the error was ±2%. The difficulty caused by mercuric hydroxide is circumvented in the present work by adding an excess of potassium iodide before titrating the liberated acid. The iodide forms a highly stable soluble complex with the surplus mercury(II), and phenolphthalein can then be used as the indicator.

EXPERIMENTAL

Reagents

Sodium hydroxide solution, 0.1*M*. Standardized with oxalic acid and diluted to 0.05 and 0.02M as required.

Table 1. Determination of mercaptans with mercuric chloride

Compound	Found, *mg**	Comparison method, *mg*	Average deviation, %	Relative standard deviation, %
1-Thioglycerol	108.3	108.0[a]	0.3	0.3
	13.56	13.50	0.5	0.5
2-Mercaptoethanol	78.2	78.0[a]	0.3	0.3
	9.80	9.75	0.5	0.4
2-Mercaptopropionic acid†	106.1	106.0[b]	0.1	0.1
	13.30	13.25	0.4	0.4
Thioglycollic acid†	92.1	92.0[c]	0.1	0.1
	11.55	11.50	0.4	0.4
2-Mercaptosuccinic acid†	75.1	75.0[b]	0.1	0.2
	15.06	15.00	0.4	0.3
1-Propanethiol	76.1	76.0[c]	0.1	0.3
	9.54	9.50	0.5	0.6
2-Propanethiol	76.2	76.00[c]	0.3	0.3
	9.54	9.50	0.5	0.4
1-Dodecanethiol	202.2	202.0[c]	0.1	0.2
	25.37	25.25	0.5	0.6

* Average of 6 determinations.
† Carboxyl group also taken into consideration in calculations.
[a] Tetrathionate method.
[b] Hexacyanoferrate method.
[c] Iodine method.

Mercuric chloride, saturated solution in water.

Mercaptan solutions. Standardized by different procedures, as shown in Table 1. Dodecyl mercaptan was dissolved in acetone, and both propyl mercaptans were dissolved in 3:1 v/v water–acetone mixture.

Procedure

To the aqueous sample solution containing 0.12–1 mmole of mercaptan, add about 5 ml of saturated mercuric chloride solution. Swirl the solution for 1 min. Add 1–2 g of potassium iodide and shake until the red precipitate first formed disappears. Some insoluble mercaptides will also dissolve at this stage. Add 4–5 drops of 1% phenolphthalein solution and titrate with standard sodium hydroxide solution.

In the case of dodecyl mercaptan, add about 20 ml of water after the mercaptide formation, because in pure acetone medium the colour change of phenolphthalein is not sharp.

RESULTS AND DISCUSSION

The method has been applied to various simple mercaptans and to some containing hydroxy and carboxyl groups as well, and the results presented in Table 1 show that quantities as little as 0.125 meq of these mercaptans can be determined with an average deviation of 0.1–0.5%

Unlike the oxidimetric procedures, the method does not require strict reaction conditions. However, mercaptans containing the amino-group, such as cysteine or 2-mercaptoethylamine hydrochloride, cannot be determined by this method because of the basic nature of the amino-group. Carbon tetrachloride, carbohydrates, sulphur and disulphides do not interfere, but acidic salts and compounds with an amino-group or of basic nature interfere. Alcohols do not interfere if present in small amount but larger quantities cause overconsumption of alkali. The red mercuric iodide precipitate does not appear, and the solution becomes yellow (a yellow turbidity appears in the case of insoluble mercaptides) and the colour interferes with detection of the end-point.

Acknowledgement—The authors are thankful to University Grants Commission, New Delhi, for financial assistance to one of them (K.K.T.).

REFERENCES

1. J. W. Kimball, R. L. Kramer and E. E. Reid, *J. Am. Chem. Soc.*, 1921, **43**, 1199.
2. J. A. R. Cooper and G. S. Maingot, *Anal. Chem.*, 1955, **27**, 1479.
3. J. MacLeod, *J. Gen. Physiol.*, 1951, **34**, 705.
4. D. S. Mahadevappa and N. M. H. Gowda, *Talanta*, 1975, **22**, 771.
5. K. K. Verma, J. Ahmed and S. Bose, *Z. Anal. Chem.*, 1976, **128**, 278.
6. L. Hellerman, F. P. Chinard and P. A. Ramsdell, *J. Am. Chem. Soc.*, 1941, **63**, 2551.
7. K. K. Verma and S. Bose, *Anal. Chim. Acta*, 1973, **65**, 236.
8. A. E. Mirsky, *J. Gen. Physiol.*, 1941, **24**, 725.
9. A. Shrivastava and S. Bose, *J. Indian Chem. Soc.*, 1974, **51**, 736.
10. A. Shrivastava, *Talanta*, 1979, **26**, 917.
11. J. P. Danhey, *Int. J. Sulphur Chem.*, 1971, **C6**, 159.
12. J. P. Danhey and M. Y. Oester, *J. Org. Chem.*, 1967, **32**, 1491.
13. I. M. Kolthoff and W. E. Harris, *Anal. Chem.*, 1949, **21**, 963.
14. E. W. Ellis, *ibid.*, 1951, **23**, 1777.
15. G. R. Bond, *Ind. Eng. Chem., Anal. Ed.*, 1933, **5**, 257.
16. S. B. Sant and B. R. Sant, *Anal. Chem.*, 1959, **31**, 1879.
17. E. Turk and E. E. Reid, *Ind. Eng. Chem., Anal. Ed.*, 1945, **17**, 713.
18. H. Roth, *Mikrochim. Acta*, 1958, 769.
19. R. K. Kunkel, J. E. Buckley and G. Gorin, *Anal. Chem.*, 1959, **31**, 1098.
20. P. Borgstrom and E. E. Reid, *Ind. Eng. Chem., Anal. Ed.*, 1929, **1**, 186.
21. J. S. Fritz and T. A. Palmer, *Anal. Chem.*, 1961, **33**, 98.
22. M. Wroński, *Analyst*, 1964, **89**, 800.
23. C. A. Brown, *Anal. Chem.*, 1967, **39**, 1882.
24. D. C. Greeg, P. E. Boufford and R. Borton, *ibid.*, 1961, **33**, 269.
25. J. R. Sampey and E. E. Reid, *J. Am. Chem. Soc.*, 1932, **54**, 3404.
26. S. Siggia and I. G. Hanna, *Quantitative Organic Analysis Via Functional Groups*, p. 723. Wiley-Interscience, New York, 1979.
27. F. Ratkovics and P. Szepesvary, *Magy. Kem. Folyoirat*, 1958, **64**, 472.

Talanta, Vol. 28, pp. 399 to 401, 1981
Printed in Great Britain

0039-9140 81 060399-03$02.00 0
Pergamon Press Ltd

A RAPID SPECTROPHOTOMETRIC METHOD FOR DETERMINATION OF ZINC IN MILK

O. S. CHAUHAN, B. S. GARG, R. P. SINGH
Department of Chemistry, University of Delhi, Delhi 110007, India

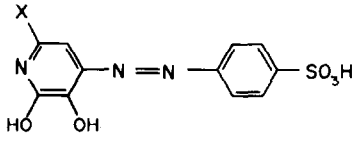
and

ISHWAR SINGH
Department of Chemistry, M.D. University, Rohtak-124001, India

(*Received* 29 *August* 1979. *Revised* 27 *November* 1980. *Accepted* 5 *January* 1981)

Summary—1-(2',3'-Dihydroxypyridyl-4'-azo)benzene-4-sulphonic acid and the corresponding 5'-chloro-substituted acid are proposed as sensitive reagents for zinc. Cyanide masking and selective demasking of zinc can be used to deal with the interference of many metal ions, cadmium can be masked with semithiocarbazide, and thiosulphate can be used for masking Hg(II), Pd(II) and Os(VIII). The molar absorptivities are about 1.3×10^5 l.mole^{-1}.cm^{-1}. The method has been used for determinating zinc in milk.

Zinc is essential for growth of micro-organisms, plants and animals, but its essentiality for human beings was recognized only recently. It is now evident that not only nutritional but also conditioned zinc deficiency may cause complications in many diseases. It plays an important role in the metabolism of proteins and nucleic acids and is apparently essential for synthesis of DNA and ribosomal RNA.[1] A number of papers have been published giving values for zinc in individual foodstuffs and in diets, but little attention has been paid to zinc in various kinds of milk. The present communication introduces two new water-soluble heterocyclic azo-dyes, 1-(2',3'-dihydroxypyridyl-4'-azo)benzene-4-sulphonic acid (DHP-4S, I) and 1-(5'-chloro-2'3'-dihydroxypyridyl-4'-azo)benzene-4-sulphonic acid (CPD-4S, II) as spectrophotometric reagents for zinc.



I, DHP-4S, X=H
II, CPD-4S, X=Cl

The sensitivities of the reagents for zinc are superior to those of the well known heterocyclic azo-dye reagents [molar absorptivities (l.mole^{-1}.cm^{-1}): zinc–PAN,[2] 5.8×10^4 at 550 nm; zinc–PAR,[3] 6.34×10^4 at 495 nm; zinc–PAC,[4] 2.8×10^4 at 580 nm; zinc–CPD-4S, 1.25×10^5 at 550 nm; zinc–DHP-4S, 1.32×10^5 at 540 nm]. The proposed method has been made selective for the determination of zinc by use of the differential demasking technique of Platte and Marcy[5] and a modified method proposed by Watkins *et al.*[6]

EXPERIMENTAL

Solutions

Stock solutions. Standard zinc solution was prepared by dissolving appropriate amounts of analytical-reagent grade zinc oxide in perchloric acid and standardized complexometrically with EDTA. CPD-4S and DHP-4S were synthesized[7] by coupling diazotized *p*-sulphanilic acid with 5-chloro-2,3-dihydroxypyridine and 2,3-dihydroxypyridine respectively, at ~0°. The product was kept overnight in a freezer, filtered off and dried. The purity was checked by TLC, and $1 \times 10^{-3}M$ solutions were prepared by dissolving 0·330 and 0·295 g respectively in doubly distilled water and making up to 1 litre.

A 1% chloral hydrate solution was prepared for demasking zinc from its cyanide complex.

A 5% ascorbic acid solution was prepared and kept in amber glass bottles; it was discarded after two days.

Fresh samples of cow, goat, buffalo and camel milk were procured from Bawana village, Delhi. Other samples were collected from government supply milk booths and milkmen in the university area.

All other reagents used were of analytical grade.

Procedure for zinc

To a suitable aliquot (in a 10-ml standard flask) containing 1–5 μg of zinc per ml, add sufficient I or II (Table 1) followed by 2.5–4 ml of 0.02*M* sodium hydroxide. Dilute to volume and measure the absorbance at λ_{max} against a reagent blank. Prepare a calibration curve similarly.

RESULTS AND DISCUSSION

Addition of aqueous CPD-4S or DHP-4S solution to a zinc solution gives a water-soluble magenta complex at pH above 10. The solubility of the reagents and their zinc complexes in water at any pH gives an advantage over PAR and PAN.[8] However, coloured complexes are also formed with Cd(II), Hg(II), Fe(II), Co(II), Ni(II), Cu(II), Pd(II) and Os(VIII) at room temperature. The interference of

Table 1. Physico-chemical and analytical characteristics of the complexes

Characteristic	Zinc–CPD-4S complex	Zinc–DHP-4S complex
λ_{max}, *nm*	550	540
pH range (0.02*M* NaOH, *ml per 10 ml*)	1.5–4.0	2.5–5.0
Moles of reagent required per mole of metal ion for complete complexation	20	25
Beer's law validity range, *ppm*	0–0.58	0–0.55
Optimum concentration range, *ppm*	0.09–0.50	0.10–0.48
Composition (M:L) determined by Job's method	1:2	1:2

Hg(II), Pd(II) and Os(VIII) can be removed by masking with thiosulphate, and Cd(II) can be masked with 0.5% semithiocarbazide solution. Interference by other transition metals can be dealt with by the methods given by Platte and Marcy[5] and Watkins *et al.*[6] Preliminary investigations showed that ascorbic acid or chloral hydrate did not affect the zinc–CPD-4S or zinc–DHP-4S complex. Hence 2% potassium cyanide solution is added to form the cyanide complexes of the interfering metals and zinc, and the zinc complex is then preferentially destroyed by excess of 1% chloral hydrate solution in presence of 5% ascorbic acid (a few drops), leaving the other stable cyanide complexes in solution. The zinc ions thus released are determined spectrophotometrically with CPD-4S or DHP-4S. The role of ascorbic acid[6] is to reduce Cu(II) or Fe(III), if any, to Cu(I) or Fe(II), the cyanide complexes of which are more stable towards chloral hydrate. Other base metals either do not form complexes with **I** or **II**, or else form very weak complexes or those which decompose on standing or boiling.

Various physico-chemical characteristics of the complexes are summarized in Table 1.

Effect of foreign ions

In the analysis of a 0.33-μg/ml zinc solution with CPD-4S or DHP-4S, the ions F^-, Cl^-, Br^-, I^-, NO_2^-, NO_3^-, SCN^-, $S_2O_3^{2-}$, SO_3^{2-}, SO_4^{2-}, $S_2O_8^{2-}$, oxalate, thiourea, citrate, tartrate, semithiocarbazide (STC), diethyldithiocarbamate (DTC), borate, phosphate, Al(III), In(III), Sn(II), Sb(III), La(III), Ti(IV), Cr(III), Mn(II), Fe(III), UO_2^{2+}, Mo(VI), W(VI), Zr(IV), Hf(IV), Th(IV), alkaline-earth and platinum-metals [except Os(VIII) and Pd(II)] do not interfere at room temperature when present in up to at least 100-fold w/w ratio to zinc. When masking agents are used the maximum limits for other ions (in ppm) which do not cause a deviation of more than 2% in the absorbance are: Cd(II) (10, masked with 0.5% STC); Hg(II), Os(VIII) and Pd(II) (20, masked with $S_2O_3^{2-}$ or thiourea); Pb(II) (25, masked with 0.5% STC); Cu(II), Co(II), Ni(II) and Fe(II) (10, masked as CN^- complexes in presence of chloral hydrate).

Determination of zinc in milk samples

Dry-ashing[9] is used in determining the zinc contents of milk. Add 25.0 ml of milk dropwise to a heated crucible to evaporate without frothing. After the moisture has been removed, heat strongly to 450–500°. Cool and add 1.0 ml of concentrated nitric acid. Evaporate to dryness and ignite again at 450–500° for ~1 hr. Utmost care should be taken to avoid loss by sputtering. Dissolve the resulting white ash in the minimum of dilute nitric acid and make up the volume to 25.0 ml in a standard flask. Pipette 1 or 2 ml of the solution, mask the interfering metals as indicated below and determine zinc by the procedure just given.

Recovery of zinc from milk samples

The standard milk samples were spiked by adding 1.60 and 3.25 μg of zinc and the total zinc was determined with both reagents. Table 2 reports the recovery data obtained with DHP-4S and confirms the precision of the method. It was noted that the zinc

Table 2. Results and recovery data for zinc, in various milk samples, with DHP-4S as reagent

Milk sample	No. of analyses	Zn(II) found*, μg/10 ml range	Zn(II) found*, μg/10 ml average	Zn(II) added μg/10 ml A	Zn(II) added μg/10 ml B	Zn(II) recovery, % A	Zn(II) recovery, % B
Cow	8	3.65–4.00	3.80	1.60	3.25	96	102.0
Buffalo	8	2.90–3.25	3.10	1.60	3.25	95	99
Goat	5	3.80–4.10	3.95	1.60	3.25	103	97
Camel	3	2.50–2.80	2.60	1.60	3.25	102	91
Govt. supply:							
Mother Dairy	10	3.85–4.20	4.05	1.60	3.25	97	104
Delhi Milk Scheme	8	3.65–4.00	3.85	1.60	3.25	96	98

* In milk sample.

content of various milk samples collected from milk booths or of milk kept overnight in galvanized utensils was higher than that of fresh samples. This may be attributed to contamination with zinc during pasteurization, *etc.*

Acknowledgement—One of the authors (O.S.C.) is thankful to the University Grants Commission, New Delhi, for the award of a Teacher Fellowship.

REFERENCES

1. F. Fernandez-Madrid, A. S. Prashad and D. Oberleas, *J. Lab. Clin. Med.*, 1973, **82**, 951.
2. W. Burger and H. Elvers, *Z. Anal. Chem.*, 1959, **171**, 225.
3. M. Hniličková and L. Sommer, *Collection Czech. Chem. Commun.*, 1961, **26**, 2189.
4. G. Nakagawa and H. Wada, *Nippon Kagaku Zasshi*, 1962, **83**, 1098.
5. J. A. Platte and V. M. Marcy, *Anal. Chem.*, 1959, **31**, 1226.
6. R. Watkins, L. M. Weiner and B. Zak, *Microchem. J.*, 1971, **16**, 14.
7. J. P. Gupta, *Ph.D. Thesis*, University of Delhi, 1977.
8. S. Shibata, in *Chelates in Analytical Chemistry*. H. A. Flaschka and A. J. Barnard, Jr. (eds.), Vol. 4, Dekker, New York, 1972.
9. A. A. Schilt and P. J. Taylor, *Anal. Chem.*, 1970, **42**, 220.

Talanta, Vol. 28, pp. 402 to 404, 1981
Printed in Great Britain. All rights reserved

0039-9140/81/060402-03502.00/0
Copyright © 1981 Pergamon Press Ltd

GAS CHROMATOGRAPHIC DETERMINATION OF DIMETHYLARSINIC ACID IN AQUEOUS SAMPLES

SYOZO FUKUI, TERUHISA HIRAYAMA, MOTOSHI NOHARA and YOSHIHIKO SAKAGAMI
Kyoto College of Pharmacy, Yamashinaku, Kyoto, Japan

(*Received* 11 *August* 1980. *Revised* 10 *December* 1980. *Accepted* 23 *December* 1980)

Summary—Procedures are described for the determination of dimethylarsinic acid in aqueous samples by gas chromatography of iododimethylarsine. Dimethylarsinic acid is converted into iododimethylarsine rapidly and quantitatively by treatment with hypophosphorous acid and potassium iodide, the resulting iododimethylarsine is extracted with toluene and determined with a gas chromatograph equipped with an electron-capture detector. The detection limit is 0.005 ppm as As. Recoveries from urine are over 95%. Other arsenicals do not give any response in the chromatography. The method has been applied to the determination of dimethylarsinic acid in urine and in water extracts of sea-weeds.

Dimethylarsinic acid (DMAA) has been recognized as a major intermediate in metabolism of arsenicals in the body and environmental micro-organisms, and has been found as a ubiquitous arsenical in urine and the environment.[1–4]

Most methods for determination of DMAA are based on its reduction to dimethylarsine and subsequent electric-discharge emission spectroscopy or atomic-absorption spectrometry, coupled with isolation of dimethylarsine from other arsenic hydrides.[5–10]

Some gas chromatographic methods based on the conversion of DMAA into volatile compounds such as diethyldithiocarbamate[11] or bromodimethylarsine[12] have been reported.

A method involving the conversion of DMAA into iododimethylarsine (IDA) with hydriodic acid, followed by determination with electron-capture gas chromatography has also been reported.[13] Because of the high sensitivity and selectivity of this method, a modification, mainly of the procedure for reduction and iodination of DMAA, has been attempted. It is based on the rapid and quantitative conversion of DMAA into IDA by treatment with hypophosphorous acid and potassium iodide; it also contributes toward stabilization of the resulting IDA, and simplification of the procedure.

EXPERIMENTAL

Apparatus

A Shimadzu model 3BE gas chromatograph equipped with a ^{63}Ni electron-capture detector and a 3 mm × 2 m glass column containing 10% SE-30 on 60–80 mesh Chromosorb AWA were used. The column was conditioned by preliminary introduction of IDA solution (prepared by treating stock DMAA solution by the procedure described below) to saturate IDA-adsorbing sites in the column. The oven and detector temperatures were both 80°, the carrier gas was nitrogen and its flow-rate 60 ml/min. The sensitivity was set so that 0.1 ng of As (as IDA) gave 30–40% full-scale deflection. A Hitachi model M-80 GC-MS was used to confirm that IDA was formed.

Reagents

Hypophosphorous acid (Wako Pure Chemicals Co.) was 50% w/v, certified grade. DMAA (Wako Pure Chemicals Co.) was recrystallized from aqueous ethanol. IDA was prepared by the procedure described by Soderquist *et al.*[13] Monomethylarsonic acid was obtained from Ventron Corp.

Toluene was distilled, and checked for purity by gas chromatography. Other chemicals were reagent grade. DMAA stock solution (100 ppm of As), prepared in distilled water, was reasonably stable for one week. Working solutions of 0.01–0.1 ppm (of As) were prepared by fresh dilution of the stock solution.

Procedure

Take 5 ml of aqueous sample in a glass-stoppered test-tube, add 5 ml of hypophosphorous acid and 5 g of potassium iodide, and shake the mixture until the potassium iodide has dissolved. Add 5 ml of toluene and shake again for 2 min, then allow to stand for several minutes. Introduce 1 μl of the upper toluene layer into the gas chromatograph by microsyringe. If a thick emulsion occurs, centrifuge the mixture at 3000 rpm. Handle reagent blanks and the working solutions similarly.

RESULTS AND DISCUSSION

The procedure using hypophosphorous acid and potassium iodide achieves rapid and quantitative conversion of DMAA into IDA even in presence of water, so the prior evaporation of the sample to dryness (as in the procedure by Soderquist *et al.*[13]) can be eliminated. Figure 1 shows that the optimum quantities of reagents are 5 ml of hypophosphorous acid and 5 g of potassium iodide.

Typical gas chromatograms obtained by this method are shown in Fig. 2. The retention time of the peak in Fig. 2 closely agrees with that of synthetic IDA. The identity of the product was confirmed by GC–mass spectrometry, which gave *m/e* values of 232 [$(CH_3)_2AsI$], 217 [CH_3AsI], 202 [AsI], 127 [I], 105 [$(CH_3)_2As$] and 90 [CH_3As], as shown in Fig. 3.

The need for rapid sample work-up and gas chromatography on account of the hydrolytic instability of IDA

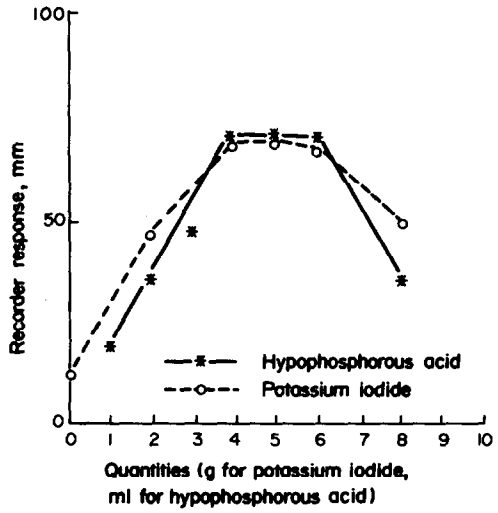


Fig. 1. Influence of quantities of hypophosphorous acid and potassium iodide on the conversion of DMAA into IDA.

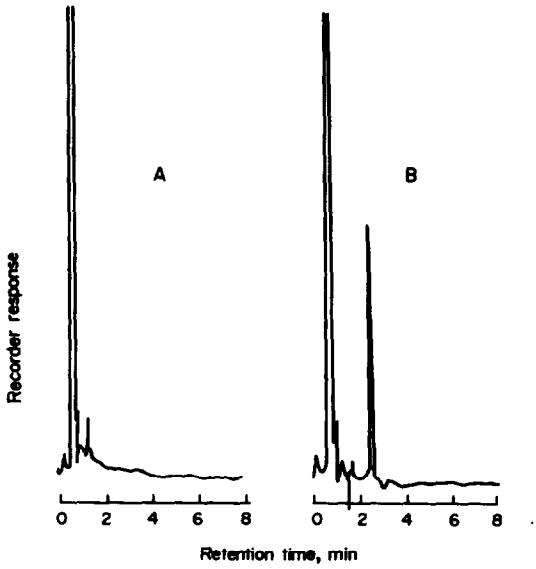


Fig. 2. Gas chromatograms of: (A) blank, (B) 0.02 ppm DMAA working standard.

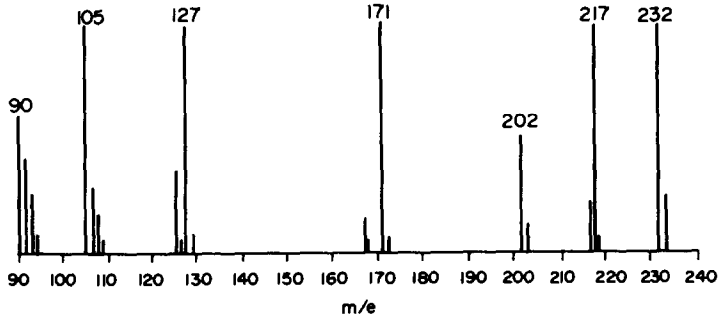


Fig. 3. Mass spectrogram of IDA obtained from DMAA solution (10^5 ppm as As).

was noted by Soderquist *et al.*[13] However, in the present method the IDA is fairly stable in the toluene layer, even when this is in contact with the aqueous reaction mixture, the detector response to IDA in the toluene layer remaining constant for 12 hr. These results suggest that any hydrolytic degradation of the IDA is counteracted by resynthesis. A calibration graph of peak-height *vs.* amount of DMAA was linear up to 0.1 ng (as As). Assuming a 1-μl injection volume, the lower limit of detection is 0.005 ppm.

Monomethylarsonic acid and inorganic arsenate or arsenite did not yield any products giving a gas chromatographic response.

Di-iodomethylarsine and tri-iodoarsine are probably formed from monomethylarsonic acid and arsenate or

Table 1. Recovery tests of DMAA from urine

DMAA added, $\mu g/ml$ (of As)	DMAA found,* $\mu g/ml$ (of As)	Recovery,* %
0	0.030	
0.020	0.049 (0047–0.050)	95 (85–100)
0.040	0.068 (0.066–0.071)	95 (90–103)
0.060	0.091 (0.087–0.094)	102 (95–107)
0.080	0.111 (0.108–0.113)	101 (98–104)
0.100	0.130 (0.128–0.139)	100 (98–109)

* Averages of five runs, ranges in parentheses.

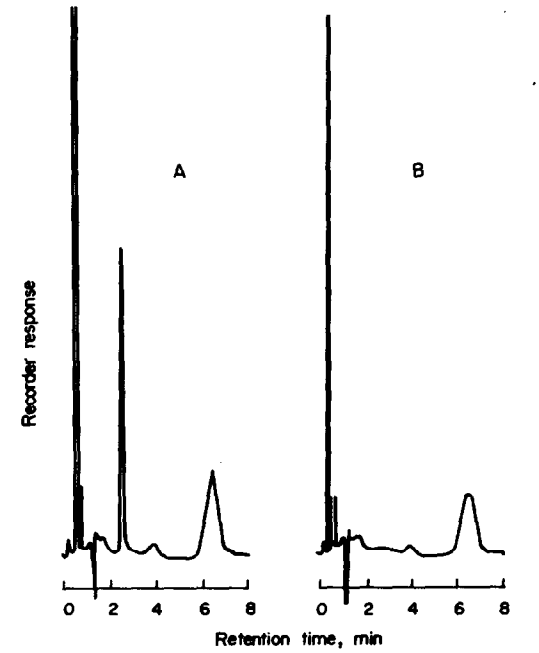


Fig. 4. Gas chromatograms of: (A) urine sample, (B) toluene layer washed with water.

arsenite respectively, but because of their high boiling points (128°/16 mm,[14] and 403°,[15] respectively; the b.p. of IDA[16] is 154°), are not likely to be eluted. The results of recovery tests for DMAA in urine are shown in Table 1. Typical gas chromatograms for DMAA in urine are shown in Fig. 4. The target peak shown in Fig. 4 (A) completely disappeared when the upper toluene layer was shaken with water for 40 min, indicating that the peak results from a single hydrolysable substance.

Acknowledgement—The work was supported by a grant for Environmental Preservation Research from the Environmental Agency.

REFERENCES

1. J. M. Wood, *Science*, 1974, **189**, 1049.
2. E. A. Woolson, *Environmental Health Perspectives*, 1977, **19**, 73.
3. W. P. Rideley, L. D. Dizikes, A. Cheh and J. M. Wood, *ibid.*, 1977, **19**, 43.
4. R. S. Braman and C. C. Foreback, *Science*, 1973, **182**, 1247.
5. R. S. Braman, L. L. Justen and C. C. Foreback, *Anal. Chem.*, 1970, **42**, 1480.
6. F. E. Lichte and R. K. Skogerboe, *ibid.*, 1977, **44**, 180.
7. R. S. Braman, L. L. Justen and C. C. Foreback, *ibid.*, 1972, **44**, 2195.
8. R. S. Braman, D. L. Johnson, C. C. Foreback, J. M. Ammons and J. L. Bricker, *ibid.*, 1977, **49**, 621.
9. E. A. Crecelius, *ibid.*, 1978, **50**, 826.
10. C. Feldman, *ibid.*, 1979, **51**, 664.
11. E. H. Daughtrey Jr., A. M. Fitchett and P. Mushak, *Anal. Chim. Acta*, 1975, **79**, 199.
12. B. J. Gudzinowicz and H. F. Martin, *Anal. Chem.*, 1962, **34**, 648.
13. C. J. Soderquist, D. G. Crosby and J. B. Bowers, *ibid.*, 1974, **46**, 155.
14. R. D. Feltham, *J. Organometal. Chem.*, 1967, **7**, 285.
15. I. T. Millar, H. Heaney, D. M. Heinekey and W. C. Fernelius, *Inorganic Syntheses*, 1960, **VI**, 113.
16. J. Bailar Jr., *ibid.*, 1939, **I**, 103.

Talanta, Vol. 28, pp. 405 to 407, 1981
Printed in Great Britain. All rights reserved

0039-9140/81/060405-03$02.00/0
Copyright © 1981 Pergamon Press Ltd

THE SEPARATION AND DETERMINATION OF FATTY ACIDS BY ISOTOPIC DILUTION AND RADIOGAS–LIQUID CHROMATOGRAPHY

D. A. BEARDSLEY
School of Health and Applied Sciences (Chemistry Section), Leeds Polytechnic, Leeds, England

(*Received* 3 *November* 1980. *Accepted* 23 *December* 1980)

Summary—A number of static phases have been evaluated for the GLC separation of fatty acids. Of those investigated, only AT 1200 was capable of resolving the isomeric forms of the acids. A radiogas–liquid chromatographic method incorporating isotopic dilution analysis has been developed for the determination of n-butyric acid. The proposed method has been applied to the determination of the acid in hydrolysed butter fat and milk chocolate extracts.

Gas–liquid chromatography has been applied to food analysis for about 30 years. The work up to 1974 has been reviewed by Dickes and Nicholas[1] and the more recent applications are the subject of a Talanta Review.[2] Radiogas–liquid chromatography has been reviewed by James,[3] Karmen,[4] and Scott.[5] In principle it can be used to identify and determine radioactive components in any mixture which can be separated by gas–liquid chromatography. Volatile fatty acids can be determined by the Reichert, Polenske and Kirschner process;[6] this method, however, requires a relatively large sample weight and is time-consuming. The hydroxamic acid index method[7] has the advantage of using a smaller sample weight, but is empirical. The use of GLC for the determination of fatty acids is well documented. Its application to the determination of propionic acid in food has been reviewed by Walker and Green,[8] and Phillips and Sanders[9] have described a method for the determination of butyrate esters in fats, by hydrolysis to butyric acid and use of valeric acid as an internal standard.

This paper describes a radiogas–liquid chromatographic procedure involving radioactive isotopic dilution analysis for the determination of fatty acids. The sample solution in suitable form is mixed with a ^{14}C-labelled fatty acid of known original specific activity, and subjected to GLC separation. The resulting specific activity of the fatty acid is determined by splitting the effluent gas from the column into two streams, one of which is fed to a flame-ionization detector (FID) and the other, after passage over heated copper(II) oxide, to a gas-flow proportional counter. The weight of fatty acid in the sample is calculated by using the equation for direct isotopic dilution analysis:

$$y = y_s\left(\frac{S_1}{S_2} - 1\right)$$

where y = weight of fatty acid in the sample aliquot, y_s = weight of ^{14}C-labelled fatty acid added, S_1 = specific activity of the labelled fatty acid before isotopic dilution and S_2 = specific activity of the labelled fatty acid after isotopic dilution.

The method has the advantage that quantitative separation of the desired acid is not essential. It is only necessary to determine the specific activity of a pure sample of the fatty acid with adequate precision. A constant splitting-ratio and a linear mass response of the FID over the mass range are, however, essential.

EXPERIMENTAL

Apparatus

The radio-GLC system consists of a Pye series 104 chromatograph with flow-controller units and twin injection heaters. The column is coupled to a flow-splitter assembly giving a nominal 1:1 split. One effluent stream is fed to an FID detector, the signal from which is integrated electronically with a Vidar 6300 digital integrator and recorded on a two-channel recorder. The other effluent stream passes through a quartz tube packed with copper(II) oxide and heated to 700° and then through magnesium perchlorate for removal of water. The carbon dioxide thus obtained is passed into a Panax radiogas detector system incorporating a gas-flow proportional counter (EHT 1480V), with cosmic-guard (EHT 850V), and anti-coincidence gate circuit for measurement of the $^{14}CO_2$. The signal is fed to the recorder and integrated with a scalar coupled through the ratemeter. The carrier-gas is an argon–carbon dioxide mixture (95:5), at a flow-rate of 40 ml/min.

The proportional-counter efficiency, given by

$$\text{efficiency} = \frac{100 \times C \times F}{A \times V}\,\%$$

where C = number of counts, F = carrier-gas flow-rate (ml/min), A = activity applied (dpm) and V = counter volume (ml) is claimed to be 94.5% for carbon-14. The system is fully described by Simpson.[10]

Reagents

^{14}C-labelled n-butyric acid solution. An ampoule of sodium butyrate (250 μCi, 59 mCi/mmole, Radiochemical Centre, Amersham) was opened, 1 ml of 1% phosphoric acid was pipetted into it and the contents were washed out into a 5-ml standard flask with distilled water, mixed with 1 ml of 2500-μg/ml non-active n-butyric acid solution and diluted to volume with distilled water. The concentration was determined by reverse isotopic dilution analysis.

Propionic, n-butyric, isobutyric, n-valeric, isovaleric and hexanoic acid solution (500 μg/ml). Prepared by dissolving 1 g (accurately weighed) of the acid in water and diluting to 100 ml with distilled water, and further dilution of 5 ml to 100 ml with distilled water.

Selection of the column

Various columns were tested for isothermal separation of the six fatty acids. A 5-ft column of 5% "free fatty acid phase" on Chromosorb G (AW–DCMS) operated at 145° at a flow-rate of 40 ml/min after overnight conditioning at 180° gave severe tailing of the peaks and very poor resolution of the acids.

The results for 10% Carbowax 20M–TPA on Chromosorb W (AW–DCMS) (column A, 5 ft, flow-rate 40 ml/min, temperature 110°, conditioned overnight at 200° with flow), Chromosorb 101 (80–100 mesh) (columns B and C, flow-rate 40 ml/min, conditioned overnight at 250° with flow), and 10% AT 1200 + 1% H_3PO_4 on Chromosorb W(AW) (80–100 mesh) (column D, 5 ft, flow-rate 40 ml/min, temperature 110°, conditioned overnight at 175° with flow) are given in Table 1.

Column A did not fully resolve the acid pairs propionic/isobutyric and n-butyric/isovaleric. Lowering the temperature to 90° permitted resolution of the latter pair. The 5-ft column B gave incomplete resolution when the two iso-acids were present. Increasing the length to 9 ft (column C), and the temperature to 180° gave complete resolution but relatively long retention times. At higher temperatures resolution of the acids was not complete. It has been claimed that the use of a 5% "free fatty acid phase" coating on Chromosorb 101 improves the resolution of the lower fatty acids, but we observed no improvement in resolution with either a 5-ft or a 9-ft column.

All the Chromosorb 101 columns suffered gradual degradation with repetitive injection of aqueous solutions of the acids and this was enhanced in the presence of phosphoric acid, which was used to liberate the acids from the saponified samples. The columns darkened near the injection port and erratic baselines were obtained.

Column D, with the packing marketed by Alltech Associates Inc., proved to be the ideal phase for the resolution of the acids (Table 1), but the chromatographs showed an additional peak at a retention time of about 75 min. The area of this peak was directly related to the volume of aqueous phase injected. It was found that if the column was prepared without phosphoric acid present in the packing, the extra peak did not appear. Prolonged exposure of AT 1200 to water and 1% phosphoric acid at 140° in a sealed tube followed by subsequent injection of the liquid phase onto a column of 10% AT 1200 (free from phosphoric acid) indicated that the peak was associated with a reaction of AT 1200 with phosphoric acid. Details of the nature of the static phase could not be elicited from the manufacturers so this aspect was not pursued. For further work a column of 10% AT 1200 alone on Chromosorb W (AW–DCMS) was used. It was further found that after a prolonged exposure to samples containing phosphoric acid degradation of the column occurred and the extra peak reappeared in the chromatograms.

Table 1. Retention times (*min*) for fatty acids

Acid	Column A	B (5 ft, 140°)	C (9 ft, 180°)	D
Propionic	2.8	2.9	9.0	3.3
Isobutyric	3.0	3.2	11.0	5.4
n-Butyric	4.0	4.4	14.0	7.4
Isovaleric	4.8	4.9	17.0	9.5
n-Valeric	6.8	6.4	22.0	13.7
Hexanoic	10.4	9.7	36.0	18.3

Development of the method for determination of n-butyric acid

For the determination the essential requirement is precise measurement of y_s, S_1, and S_2. S_1 and S_2 are independent of the mass isolated, so the reproducibility of the sample injection volume is not important.

It is essential, however, that the splitting ratio for the carrier-gas should remain constant during the analysis. No variation was observed over an 8-hr period of continuous operation. Variation from day to day might occur because of slight differences in gas pressure when setting up the GLC equipment. It is concluded that no significant error should result for a batch of analyses done within a period of continuous operation of the equipment. The accuracy and precision of determination of the specific activity were tested by repeated injection of ^{14}C-labelled n-butyric acid solution (Table 2).

The linearity of the FID was established by injection of aqueous n-butyric acid samples over the concentration range 10–500 μg/ml. A straight-line relationship was found (correlation coefficient = 0.99).

As a test of the procedure the method was applied to the determination of n-butyric acid in the products from hydrolysis of a milk chocolate extract and pure butter fat. The results were then compared with those obtained with valeric acid as internal standard (Phillips and Sanders method[9]).

Analytical procedure

An accurately weighed 0.1-g portion of the rendered fat sample was introduced into a 50-ml conical flask and 3 ml of 0.5*M* ethanolic potassium hydroxide were added. The flask was covered with a watch-glass and heated on a steam-bath for 15 min, then the watch-glass was removed and the ethanol evaporated. The flask was allowed to cool, and 3 ml of distilled water were added. When a clear solution had been obtained, 3 ml of 0.5% phosphoric acid were added to precipitate the insoluble fatty acids. The

Table 2. Reproducibility of the determination of the specific activity of ^{14}C-labelled n-butyric acid

Number of counts: Proportional counter	Electronic integrator	Specific activity (*S*)
15486	39557	0.40_1
16024	41121	0.39_6
16850	41421	0.40_6
15770	40208	0.39_2
15951	40160	0.39_7
15789	41821	0.39_8
15950	41970	0.38_0
16680	42288	0.39_4
16900	43490	0.38_9
15480	38660	0.40_0
15112	38174	0.39_6
14401	35912	0.40_1

$n = 12$; $S = 0.39_5$; std. devn. = 0.007; C of V = 1.8%.

Table 3. Analyses of samples

Sample	Sample weight g	Internal standard method R_1	n_1	CV_1, %	R_2	n_2	CV_2, %	C_4, %	Isotopic dilution method S_1	n_1	CV_1, %	S_2	n_2	CV_2, %	C_4, %
Butter fat	0.1418	0.93_0*	13	3.1	0.90_0*	10	2.2	3.6_4	0.41_4†	7	2.3	0.21_3	7	2.1	3.6_3
		0.87_2§	19	2.8	0.84_6§	19	3.7	3.6_3							
Milk chocolate extract	0.1511	0.24_7*	8	2.3	0.84_8*	8	1.8	0.96	0.44_8†	10	1.6	0.35_7	10	1.9	0.92

* Electronic integration.
† Standard 545 μg/ml.
§ Triangulation.

solution was then filtered through a moistened 7-cm Whatman No. 1 filter paper into a 10-ml standard flask. The precipitate was washed with water and the solution made up to volume with distilled water.

For the internal standard method, the standard solution was made by mixing 5 ml of 500-μg/ml n-butyric acid solution with 1 ml of 2500-μg/ml valeric acid solution; 5 ml of sample extract were mixed with 1 ml of 2500-μg/ml valeric acid solution.

For the isotopic dilution method, 1 ml of standard ^{14}C-labelled n-butyric acid solution was mixed with 1 ml of sample extract. All the pipetting was done with a Finnpipette (precision 1%) and 1-μl samples were injected into the GLC column.

Calculation of results

In the internal standard method the n-butyric acid content (% C_4) was calculated from

$$\% C_4 = \frac{0.5 R_1}{R_2 W}$$

where R_1 = peak-area ratio for the sample; R_2 = peak-area ratio for the standard; W = sample weight (g).

For the isotopic dilution method the equation already given was used.

RESULTS AND DISCUSSION

The results of the analyses are given in Table 3. The method was tested for concentrations lower by a factor of 10, with a 50-μg/ml n-butyric acid solution and the ^{14}C standard diluted by a factor of ten. The mean, based on 10 results, was found to be 50.5 μg/ml with a standard deviation of 0.5 μg/ml.

The reproducibilities of the specific activity measurements and of the linearity of response of the FID over the concentration range 10–500 μg/ml meet the criteria for precise determination of the n-butyric acid by the proposed method. The analytical results together with the statistical analysis given in Table 3 indicate that the method compares very favourably with the internal standard method. In both methods a reproducible injection volume is not essential. Problems associated with variation in response factors do not arise. The proposed method can be applied to any fatty acid provided it is sufficiently volatile and can be obtained in a suitable radio-labelled form.

The investigation showed that only one static phase, AT 1200, was capable of good resolution of all six acids, though FFAP and Chromosorb 101 were suitable for the unbranched acids.

A method has been described,[10] for determination of acid derivatives by use of both ^3H and ^{14}C labelling to quantify the degree of derivative formation. It is hoped to develop a substoichiometric method for such samples to avoid determination of the mass involved.

Acknowledgement—Many thanks are due to D. Little for invaluable technical assistance given during this research work.

REFERENCES

1. G. J. Dickes and P. V. Nicholas, *Gas Chromatography in Food Analysis*, Butterworths, London, 1976.
2. G. J. Dickes, *Talanta*, 1979, **26**, 1965.
3. A. T. James, *New Biochemical Separations*, A. T. James and L. J. Morris (eds.), Van Nostrand, London, 1964.
4. A. Karmen, *J. Assoc. Off. Agric. Chem.*, 1964, **47**, 15.
5. P. G. W. Scott, *Process Biochem.*, 1967, 16.
6. *Methods of Analysis of Oils and Fats*, BS 684: 1958, British Standards Institute, London, 1958.
7. R. Bassette and M. Keeney, *J. Assoc. Off. Agric. Chem.*, 1956, **39**, 469.
8. G. H. Walker and M. S. Green, *J. Assoc. Publ. Anal.*, 1965, **3**, 87.
9. A. R. Phillips and B. J. Sanders, *ibid.*, 1968, **6**, 89.
10. C. Bishop, R. F. Glascock, E. M. Newell and V. A. Welch, *J. Lipid Res.*, 1971, **12**, 777.

Talanta. Vol. 28, pp. 408 to 410. 1981
Printed in Great Britain. All rights reserved

0039-9140/81/060408-03$02.00/0
Copyright © 1981 Pergamon Press Ltd

KINETIC DETERMINATION OF PHENOLS BY A FIXED-TIME METHOD

L. R. SHERMAN*, V. L. TRUST and H. HOANG
Department of Chemistry, The University of Akron, Akron, Ohio 44325, U.S.A.

(*Received* 7 *August* 1980. *Accepted* 2 *December* 1980)

Summary—The fixed-time kinetic method is used for the determination of 15 phenols in methanol and acetic acid by measurement of the yellow products from the oxidation of the phenols with sodium metaperiodate. An increase in acid and metaperiodate concentrations enhances the rate of reaction, whereas the use of 2-propanol as the solvent decreases it.

Phenols are determined directly by means of their absorption at wavelengths near 275 nm, their amino-antipyrene derivatives,[1] or their oxidation with nitric acid and iodate.[2]

The fixed-time method of kinetic analysis is based on the equation $\chi = KaCt$ where χ is the parameter measured, K is the analytical rate constant, a is an experimental constant, C is the concentration of the analyte, and t is the predetermined time at which χ is measured.[3] Since a stoichiometric reaction is not necessary, this method can be used to analyse materials which give reaction products that are unknown or variable. As with any kinetic method, it is most desirable to make measurements during the early portion of the reaction when the concentration of the measured species is changing rapidly but little concentration change has occurred for the other reagents.

At elevated temperatures (30–100°) phenolic materials are rapidly oxidized by periodate to quinols and quinones, which possess a broad absorption band with λ_{max} near 340 nm.[4–6] The absorbance of this band can be used as the measurement parameter in a kinetic method for determination of phenols.

EXPERIMENTAL

Instrumentation and reagents

A Bausch and Lomb Spectronic 20 spectrophotometer was used to monitor the reaction, at 462 nm. At this wavelength some of the oxidation products produce a shoulder on the absorption band. Glacial acetic acid (Fischer Reagent ACS), methanol (Fisher Certified ACS), 2-propanol (Fisher Certified ACS), and sodium metaperiodate (Fisher Certified ACS) were used as received. The melting point of each of the other reagents was checked against the published[7] value(s). If a reagent was discoloured or had a melting-point discrepancy, a fresh bottle of reagent of adequate standard was procured.

Procedure

Stock solutions (approximately 2 mg/ml) of the test reagents were prepared in methanol; in the rare case that the material was insoluble in methanol, *e.g.*, starch, the stock solution was prepared in demineralized water. Calibration curves were prepared by placing 0, 1, 2, 3, 4, and 5 ml of stock solution in 10-ml volumetric flasks, adding 2 ml of glacial acetic acid and 1 ml of sodium metaperiodate solution (~43 mg/ml), and diluting to volume with demineralized water. The samples were thoroughly mixed and placed in a constant-temperature bath at 50 ± 1° for a predetermined time. The samples were then cooled to room temperature and the absorbance immediately determined at 462 nm, against the zero-concentration standard as a blank. Table 1 gives the exact conditions for each reagent. The test samples were treated in the same way.

RESULTS AND DISCUSSION

The results of this study are summarized in Table 1. Higher temperatures decrease the digestion time, especially for those materials requiring more than 30 min, but the correlation coefficient (linearity of response, absorbance *vs.* concentration) is much poorer at higher temperatures. The lack of linearity for higher temperatures is probably due to inability to quench the reaction rapidly enough or to greater variation in the products.

The oxidation of phenols by periodates is first-order with respect to phenol and to oxidizing agent, and second-order overall.[8–10] An increase in periodate concentration increases the velocity of the *p*-bromophenol reaction linearly, but non-linearity occurs with many other phenols. Because an excess of periodate is essential, yet excessive quantities favour over-oxidation,[11] a concentration of approximately 20 times that of the analyte is used. The same periodate concentration must be used for standards and samples. The analytical range is dependent on the periodate concentration; the minimum determinable is the level at which statistically meaningful data can be obtained, the maximum level is that at which non-linearity occurs.

An increase in acetic acid concentration enhances the reaction rate (Fig. 1), a result which is consistent with previous studies.[8,11] However, high acidity produces reactions with polyhydroxy materials which are

* Author to whom correspondence and reprint requests should be sent.

Table 1. Materials and conditions used

Compound	Time, *min*	Slope, *Ka*	Correlation coefficient	Concentration range, *ppm*
Phenol	120	0.058	0.95	80–900
o-Cresol	15	0.322	0.99	60–700
m-Cresol	30	0.172	0.99	75–1000
Catechol	2	2.39	0.98	20–500
Resorcinol	5 at 25°C	1.43	0.97	30–500
Phloroglucinol	30	0.827	0.99	50–600
p-Chlorophenol	120	0.0702	0.96	50–950
p-Bromophenol	30	0.435	0.99	50–800
2,4-Dichlorophenol	120	0.392	0.99	50–1000
4-Chloro-3-methylphenol	30	0.063	0.97	80–800
2-Phenylphenol	30	0.177	0.99	50–1000
4-Phenylphenol	30	0.314	0.98	50–1100
p-Tert.butylphenol	30	0.220	0.98	50–1000
p-Tert.amylphenol	30	0.276	0.98	50–1000
m-Aminophenol	15	0.291	1.00	60–700
p-Benzoquinone	30	NR	NA	NA
Camphoric acid	30	NR	NA	NA
Salicylic acid	60	NR	NA	NA
p-Nitrophenol	30	NR	NA	NA
Hexamethylenetetramine	60	NR	NA	NA
Starch	60	NR	NA	NA
Quinhydrone	15	Not linear	>0.2	NA

NR = no reaction; NA = not applicable.

too fast to measure and also enhances the formation of interfering products. Other acids (phosphoric, hydrochloric, sulphuric) give a variety of strongly coloured products, and poor results.

Ethanol, ethylene glycol, 2-propanol (IPA), glycerine and acetone were also tried as solvents instead of methanol. Ethanol, glycerine, and ethylene glycol were successful for use with 2-phenylphenol and 4-tert.butylphenol. The velocity of the reaction was lower in acetone with these two phenols and for a 20-min digestion the correlation coefficient was less than 0.8. When IPA was used as solvent, an increase in acetic acid concentration decreased the reaction rate for *p*-bromophenol. However, this is believed to be a solvent effect,[10,13] because increasing the IPA: methanol ratio when both solvents were present decreased the reaction rate (Fig. 2). Since H_5IO_6 is probably the oxidizing species in acid media,[4] the inhibition of the rate by IPA is probably due to a shift in equilibrium from H_5IO_6 to IO_4^-, as expressed in the equations below, because IPA competes with the periodate for the water molecules.

$$H_5IO_6 \rightleftharpoons H^+ + H_4IO_6^-$$

$$H_4IO_6^- \rightleftharpoons IO_4^- + 2H_2O$$

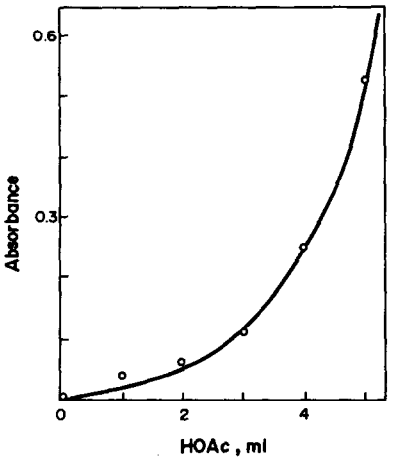


Fig. 1. Effect of acetic acid concentration on the reaction rate: 5.88 mg of 4-phenylphenol, 3 ml of methanol, 1 ml of $NaIO_4$ solution (43 mg/ml), *x* ml of acetic acid (8*M*), diluted to 10 ml with water, digested for 30 min at 50°.

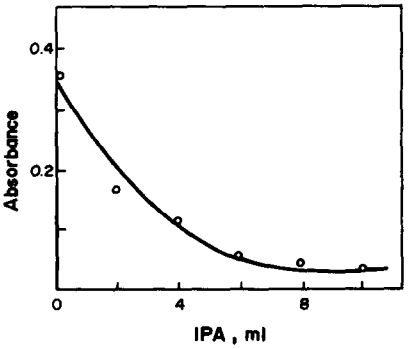


Fig. 2. Effect of 2-propanol on the reaction rate: 10.12 mg of 4-phenylphenol, 3 ml of $NaIO_4$ solution (43 mg/ml), 5 ml of methanol, 5 ml of glacial acetic acid, *x* ml of IPA, diluted to 25 ml with water, digested for 30 min at 50°.

The only material tested which yielded a change in absorbance that could not be analysed by the fixed-time method was quinhydrone. No linear relationship was obtained, probably because of the large number of reaction products.

Attempts to analyse multicomponent systems by using several fixed times were unsuccessful. The large number of products probably caused the difficulty. It is possible that multicomponent systems might be analysed by the fixed-concentration method or the tangent method, but these require a spectrophotometer with a temperature-controlled cell compartment.

The average precision (agreement between results obtained by different operators for the same sample) is $\pm$ 4.5% at 250 ppm of phenol.

Interferences

Highly coloured material, the absorbance of which cannot be corrected for by means of a blank, will interfere. *p*-Nitrophenol, which has been previously reported as an interfering material,[2] also interferes. However, if a known quantity of *p*-nitrophenol is added to the standards, a curve can be prepared which compensates for the *p*-nitrophenol present in the sample. Quinhydrone strongly interferes and no correction can be made for it. The non-reacting materials listed in Table 1 do not interfere at the 1000-ppm level in the phenol solutions.

Acknowledgement—This research was supported by The University of Akron Faculty Research Grant No. RG595.

REFERENCES

1. *ASTM* D-1783-70.
2. M. M. Beg, Q. S. Usmani and I. C. Shukla, *Analyst*, 1977, **102**, 306.
3. K. B. Yatsimirskii, *Kinetic Methods of Analysis*, pp. 43–45. Pergamon Press, London, 1966.
4. P. S. Radhakrishnamuri, S. C. Pati and V. Sriramulu, *Indian J. Chem.*, 1976, **14A**, 955.
5. E. Adler, G. Anderson and E. Edman, *Acta Chem. Scand.*, 1975, **B29**, 909.
6. H. H. Willard and A. L. Wooten, *Anal. Chem.*, 1950, **22**, 423.
7. *Handbook of Chemistry and Physics*, 47th Ed., R. C. Weast, ed., Chemical Rubber Co., Cleveland, 1966.
8. E. T. Kaiser and S. W. Widman, *J. Am. Chem. Soc.*, 1966, **88**, 5820.
9. E. Mentasti, E. Pelizzetti and C. Baiocchi, *J. Chem. Soc., Dalton Trans.*, 1977, 132.
10. L. R. Sherman and C. S. Ford, *J. Elisha Mitchell Sci. Soc.*, 1972, **88**, 191.
11. G. Dryhurst, *Periodate Oxidation of Diols and other Functional Groups*, p. 119. Pergamon Press, London, 1970.
12. D. N. Sharma and Y. K. Gupta, *Indian J. Chem.*, 1975, **13**, 56.
13. R. D. Guthrie, *Chem. Ind. (London)*, 1960, 56.

Talanta, Vol. 28, pp. 411 to 414, 1981
Printed in Great Britain. All rights reserved

0039-9140/81/060411-04$02.00/0
Copyright © 1981 Pergamon Press Ltd

PRELIMINARY COMMUNICATION

SILANIZATION OF STAINLESS-STEEL FRITS FOR USE IN TRACE METAL ANALYSIS BY HIGH PERFORMANCE LIQUID CHROMATOGRAPHY

Young-Tzung Shih and Peter W. Carr*

Department of Chemistry, University of Minnesota,
Minneapolis, Minnesota 55455 USA

(Received 3 April 1981. Accepted 6 April 1981)

Summary- A simple method has been developed to minimize the interferences related to the metal parts of an analytical system used for trace metal analysis by HPLC. This is accomplished by blocking the exposed metal surfaces with an organosilane. The effect of the silanized stainless steel frits has been demonstrated by injecting diethyldithiocarbamate into columns with and without high metal surface area components. The coating of the silane is quite stable for routine use.

Dithiocarbamates are valuable reagents for the separation and photometric determination of heavy metals.[1,2] Schwedt[3] in his comprehensive review has demonstrated that reversed-phase HPLC can be used to separate diethyldithiocarbamate metal chelates. Recently, Häring and Ballschmiter[4] pointed out that glass or Teflon components should be used where possible in the analytical system in order to avoid ligand exchange, memory effects, and contamination phenomena. Behner and Hubbard[5] also found interferences from the stainless steel column used with an amperometric detector.

In this laboratory, we are using dithiocarbamates for trace metal analysis by reversed phase HPLC and have observed severe interferences from the metal components in the system. The principal source of the interference has been identified as the stainless-steel (s.s.) frits in the end-fittings of the columns. We have eliminated the problem by silanizing the s.s. frits with an organosilane. This effectively allows the use of conventional HPLC s.s. columns for the determination of trace metals.

Experimental

Liquid chromatography

The liquid chromatograph is comprised of the following components: an Altex 110A pump, a Rheodyne 7120 injector with a 20-µl sample loop and an LDC UV 254 nm absorbance detector.

The analytical columns used here were Supelco RP-8 columns and Water RCM-100 C_{18} columns. We have found it convenient to use two pre-columns placed in series prior to the injector. The first was a 25 cm x 4.6 mm s.s. column packed with 60-200 mesh silica gel and the other a 10 cm x 4.6 mm s.s. column packed with diamine modified 60-200 mesh silica gel[6] which removes heavy metal from the buffered mobile phase.

The HPLC system was flushed with 100-150 ml of 1.0mM Na_2EDTA in 70/30 methanol/H_2O at pH 7.0 (1.0mM sodium phosphate buffer) before daily use. The mobile phase was 70/30 methanol/H_2O containing 1.0mM TRIS (Research Organic, Inc.) buffer at pH 8.25. All pH values reported here were those of the aqueous solution prior to the addition of methanol. The flow

* To whom requests for reprints should be sent.

rate was fixed at 2 ml/min. The Ni(II) bis-diethyldithiocarbamate, $Ni(Et_2dtc)_2$, and Fe(III) tris-diethyldithiocarbamate, $Fe(Et_2dtc)_3$, were prepared by adding $Ni(NO_3)_2$ or $Fe(NO_3)_3$ and sodium diethyldithiocarbamate (Fisher Scientific Co.) to the mobile phase and were then stored in brown sample vials.

All reagents were recrystallized before use. Ethyltrimethoxysilane was obtained from Petrarch System, Inc. (Levittown, PA, USA) and was used as received. Water was purified by use of a Continental deionized water system and then by passing through an XAD-2 (Mallinckrodt) column. The methanol (MCB Co.) and the purified water were filtered through a Millipore filter (type HA, 0.45μm) before use.

Silanization procedure

Ethyltrimethoxysilane (0.5 ml) was dissolved in 5 ml of undried toluene in a vial. The two s.s. frits were placed in the solution and a vacuum applied via an aspirator to the vial for about 1 minute. Vacuum impregnation was repeated 10 times. The solvent was slowly but completely evaporated at 90°C in an oil bath. The frits were "baked" under atmospheric pressure at 115°C for 3-4 days. The silane used and the procedure employed were chosen to insure the polymerization of the silane and a stable coating. The silanized frits were washed by putting them into a blank column and pumping through 100% methanol at 2 ml/min for one hour before use.

Results and Discussion

In trace metal analysis, with dithiocarbamate type ligands, contact between the metal chelates and the metal parts of the analytical system should be minimized. The extent of the substitution reaction between the metal parts and the metal complexes is dependent upon the stability of complexes. In general, the order of formation constant of different metal diethyldithiocarbamates is $Hg^{++} > Ag^{+} > Cu^{++} > Ni^{++} > Co^{++} > Bi^{+++} > Pb^{++} > Cd^{++} > Fe^{+++} > Sn^{++} > Zn^{++}$.[1] We believe that the metal exchange reaction can explain the fact that the limits of detection for Hg^{++}, Ni^{++}, Cu^{++} and Co^{++} diethyldithiocarbamates are very much better than those for Pb^{++}, Zn^{++}, Cd^{++}, Bi^{+++} diethyldithiocarbamates,[7] because the second group of complexes are readily replaced by nickel from the stainless steel surface.

The reaction between the stainless steel and the ligand will also cause some deviation from qualitative and/or quantitative results. Fig. 1a shows the results of injecting the sodium salt of diethyldithiocarbamate. The extra peaks are identified as the $Ni(Et_2dtc)_2$ and $Fe(Et_2dtc)_3$ complexes. The peak height ratio of these extra peaks to the free ligand peak is different at different sample concentrations (Fig. 1b). This indicates that these

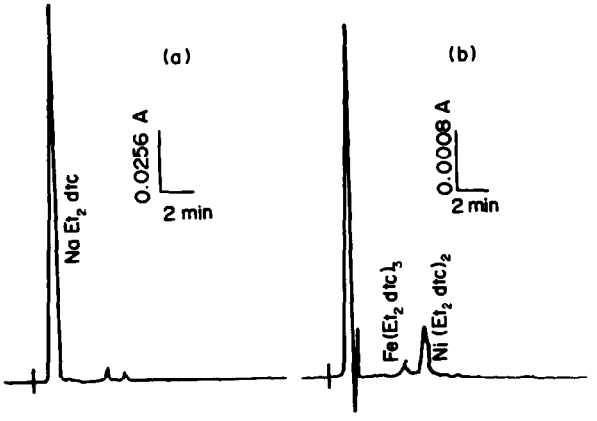


Fig. 1. Chromatogram of Et_2dtc^- using a Supelco C_8 column with unsilanized s.s. frits. Sample concentrations were (a) $1x10^{-4}$M (b) $1x10^{-6}$M.

species were not present as a contaminant in the sample. We believe that the diamine pre-column would remove all detectable metal from the buffered eluent. The source of these extra peaks was further explored by varying the solvents and buffers, and by using a syringe with a glass plunger. Results from these tests still show the same extra peaks and demonstrate the most likely source of contamination is from the metal parts in the analytical system. This was proved (Fig. 2) by examining the behavior of free ligand, Et_2dtc^- in a Waters RCM-100 column whose walls are polyethylene and whose end fittings are very thin metal spreader plates at each end of the column bed. The metal components have extremely low surface area relative to those in a conventional column.

Heizmann[8] used a glass column to reduce the contact between the metal chelates and the metal parts of the analytical system but found an s.s. column had a much better separation efficiency. Henderson et al.[9] used a glass-lined column to prevent the decomposition of metal complexes and found that adverse column interactions were still present to some extent

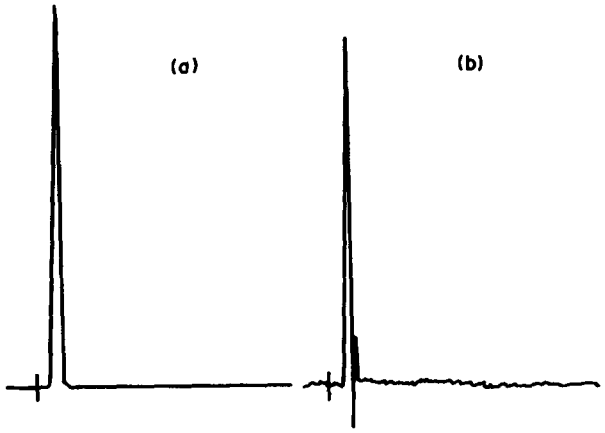


Fig. 2. Chromatogram of Et_2dtc^- using an RCM-100 column. See Fig. 1 for sample concentrations.

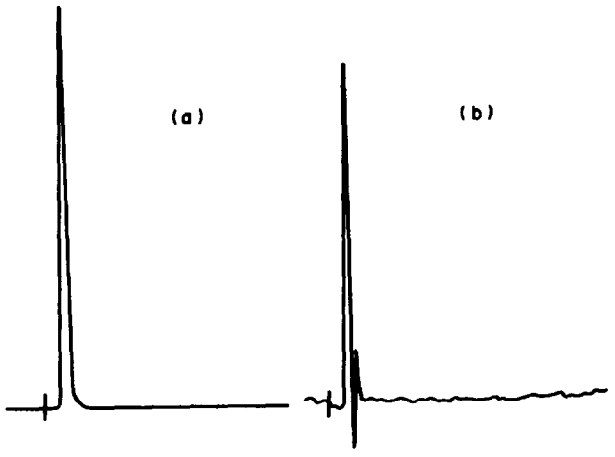


Fig. 3. Chromatogram of Et_2dtc^- using a Supelco C_8 column with silanized s.s. frits. See Fig. 1 for sample concentrations.

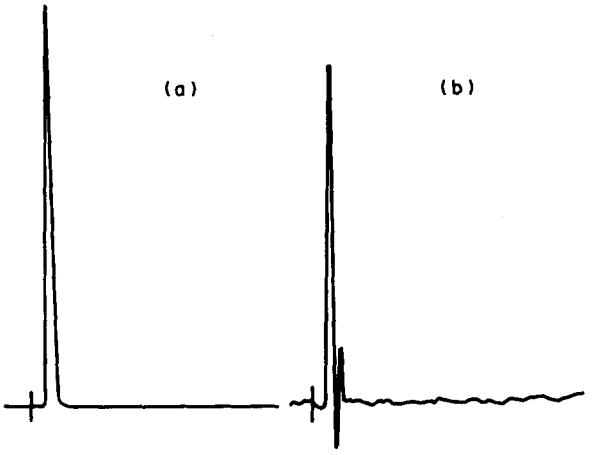


Fig. 4. Chromatogram of Et_2dtc^- using a Supelco C_8 column with silanized s.s. frits after flushing with 20 l. of mobile phase. See Fig. 1 for sample concentrations.

It is our experience that the performance of a column with Teflon frits is not as good as a column with regular s.s. frits. It is obvious that the s.s. frits have a much larger surface area than does s.s. tubing. We circumvented the problem by blocking the exposed metal surface of the s.s. frits with an organosilane (Fig. 3). After flushing with 20 liters of mobile phase through the silanized frits, the chromatographic results were obtained as in Fig. 4. It is evident that the silanized process can minimize the interference due to metal parts of any analytical system for trace metal analysis.

Acknowledgements

The authors wish to thank Mark Watson for his helpful advice on silanization procedure. This work was supported by a grant from the National Institutes of Occupational Safety and Health.

References

1. G.D. Thorn and R.A. Ludwig, *The Dithiocarbamates and Related Compounds*, Elsevier Publishing Company, New York, 1962.
2. E.S. Sandell and H.Onishi, *Photometric Determination of Traces of Metals*, 4th Ed., pp. 512-532, Wiley-Interscience, New York, 1978.
3. G. Schwedt, *Chromatographia*, 1979, 12, 289.
4. N. Häring and K. Ballschmiter, *Talanta*, 1980, 27, 873.
5. E.D. Behner and R.W. Hubbard, *Clin. Chem.*, 1979, 25, 1512.
6. D.E. Leyden, *X-ray Fluorescence Analysis of Environmental Samples*, p. 145, T.G. Dzubay (ed.), Ann Arbor Science Publications, Inc., 1977.
7. M. Moriyasn and Y. Hashimoto, *Anal. Lett.*, 1978, A 11 , 593.
8. P. Heizmann and K. Ballschmiter, *J. Chromatog.*, 1977, 137, 153.
9. D.E. Henderson, R. Chaffee and F.P. Novak, *J. Chromatog. Sci.*, 1981, 19, 79.

Talanta, Vol. 28, pp. 415 to 417. 1981
Printed in Great Britain.

0039-9140/81/060415-03$02.00/0
Pergamon Press Ltd

LETTERS TO THE EDITOR

TEMPERATURE EFFECTS IN THE DETERMINATION OF IODIDE WITH IODATE

Sir,

In the course of some recent research it was necessary to analyse accurately a sample of boron tri-iodide. This was done by hydrolysing the sample in water and determining the boric and hydriodic acids produced. The hydriodic acid was determined by the Andrews method,[1] which is described in many textbooks[2-7] as a reliable way of determining iodide and several other reducing agents. In our work, however, the method gave irreproducible results for iodide. At first it was thought that boron species were interfering but subsequent experiments showed that this was not the case. The method was further investigated with standard solutions of dried analytical-reagent grade potassium iodide (100.02% purity) of different concentrations. The results for some of these solutions were again irreproducible and the object of this letter is to draw attention to this problem of poor precision.

The 0 - 5° titrations were repeated instead of the 18 - 22° of the Vogel method.[2]

Table 1 shows the effect of temperature on the spread of the results and Table 2 shows the effect of temperature on precision for all the iodide concentrations examined. In this work the precision was considered to be poor if the standard deviation of a set of titration volumes was significantly greater than the accepted value of 0.04 ml for a routine titrimetric method,[8] although for high-precision titrimetry a standard deviation of 0.02 ml would be expected.[9] Thus the standard deviations of 0.2 and 0.57 ml for the 2.0 and 20.0 g/l solutions at 18 - 22° indicated poor precision, whereas for the titrations 0 - 5° the precision was improved to 0.04 ml for all concentrations.

Table 1. The effect of temperature on the titration results for 18-g/l. potassium iodide solution

Temp., °C	Volume of KIO_3 (0.025M) required, ml						Standard deviation ml
18 - 22	21.62	21.70	21.56	21.80	21.60	21.60	0.09
0 - 5	21.70	21.60	21.65	21.68	21.69	21.61	0.04

The end-points for the titrations at 18 - 22° remained stable for periods varying from a few minutes to several hours, the latter if the solutions were kept at below room temperature after the end-point was reached. Titrating at 0 - 5° gave end-points that were consistently stable for more than 2 hours, even after standing at room temperature. The reason for the improvement obtained by titration at low temperature is not understood at present but is not due to prevention of volatilization of iodine, since precise results (standard deviation 0.04 ml) were obtained at 18 - 22° with analytical-reagent grade acid and iodide concentrations of 2.0 and 8.0 g/l. The laboratory-grade acid seemingly contained an impurity which interfered with the iodide - iodate reaction, and the kinetics of the interfering reaction were affected by temperature to the extent that at 0 - 5° its rate was negligible. It should be noted that the seemingly high values for the recovery (Table 2) are in agreement with Andrews' original findings.

Table 2. The effect of temperature on the precision

Temperature, °C	[KI], g/l.	No. of titrations, n	Standard deviation, s, ml	Mean recovery, %	95% Confidence interval ($ts/\sqrt{n}$) %
18 - 22	2.0	7	0.2	102.6	±3.2
	8.0	5	0.07	100.0	±0.36
	20.0	7	0.57	101.5	±2.2
0 - 5	2.0	6	0.04	98.9	±0.7
	8.0	12	0.04	100.4	±0.3
	20.0	6	0.04	100.1	±0.2

Tests have shown that if the impurities listed as possibly present in the laboratory-grade acid are added to the analytical-grade acid there is no change in the performance of the method, so presumably there may be an unlisted impurity in the laboratory-grade acid that is removed in manufacture of the analytical-grade acid.

We recommend that only analytical-grade acid be used for this titration, and that as an insurance policy the test solution should be cooled to 5° in an ice bath, and an ice-cube (made from distilled water) added to it, before titration.

We wish to thank Dr. J.F. Tyson for valuable comments and advice, and the SRC for a maintenance grant to R.E.S.

Department of Chemistry,
Loughborough University of Technology,
Loughborough, Leicestershire, U.K.

A.G. Briggs
R.E. Simmons

18 February 1981

REFERENCES

1. L.W. Andrews, J. Am. Chem. Soc., 1903, 25, 756.
2. A.I. Vogel, A Textbook of Quantitative Inorganic Analysis, 3rd Ed., p. 375. Longmans, London, 1961.
3. H.A. Laitinen and W.E. Harris, Chemical Analysis, 2nd Ed., p. 426. McGraw-Hill, London, 1975.
4. R. Belcher and A.J. Nutten, Quantitative Inorganic Analysis, 3rd Ed., p. 253. Butterworths, London, 1970.
5. I.M. Kolthoff and R. Belcher, Volumetric Analysis, Vol. III, p. 449. Interscience, New York, 1957.
6. G.S. Jamieson, Volumetric Iodate Methods, Chemical Catalog Co., New York, 1926.
7. J.H. Thompson, in Comprehensive Analytical Chemistry, C.L. Wilson and D.W. Wilson (eds.), Vol. 1B, p. 274. Elsevier, Amsterdam, 1960.
8. F.W. Fifield and D. Kealey, Principles and Practice of Analytical Chemistry, p. 24. International Textbook Co., London, 1975.
9. C. Woodward and H.N. Redman, High Precision Titrimetry, Society for Analytical Chemistry, London, 1973.

Talanta, Vol. 28, p. 418, 1981
Printed in Great Britain

0039-9140/81/060418-01$02.00/0
Pergamon Press Ltd

IODAMINE-B AS AN OXIDIMETRIC TITRANT IN AQUEOUS MEDIUM

Sir,

We have found that iodamine-B can be substituted for iodamine-T in the procedures described by Pillai and Indrasenan[1] and will give results of comparable precision and accuracy. We were unable to prepare the pure sodium salt, but the pure potassium salt can be prepared by the method of Roberts.[2] Aqueous solutions of the reagent are unstable unless made alkaline; they are then stable for about a month. We recommend preparation in 0.1M potassium hydroxide medium. The conditional potential is +0.50 V at 30° and pH 10.

Department of Post-graduate Studies and Research in Chemistry,
Manasagangotri, Mysore-570006, India

Rangaswamy
H.S. Yathirajan

31 March 1981

REFERENCES

1. C.P. Krishna Pillai and P. Indrasenan, Talanta, 1980, 27, 751.
2. E. Roberts, J. Chem. Soc., 1923, 123, 849.

Talanta, Vol. 28, pp. 419 to 424, 1981
Printed in Great Britain. All rights reserved

0039-9140/81/070419-06$02.00/0
Copyright © 1981 Pergamon Press Ltd

SPECTROPHOTOMETRIC STUDY ON THE REACTIONS OF IRON(II) AND IRON(III) WITH BROMOPYROGALLOL RED AND HEXADECYLTRIMETHYLAMMONIUM BROMIDE

HE XI-WEN* and DONALD P. POE

Department of Chemistry, University of Minnesota, Duluth, MN 55812, U.S.A.

(*Received* 4 *December* 1980. *Accepted* 21 *January* 1981)

Summary—Bromopyrogallol Red (BPR) combines with iron(III) in the presence of hexadecyltrimethylammonium bromide (CTMAB) to form an intensely blue complex having a molar absorptivity of 5.20×10^4 l.mole^{-1}.cm^{-1} at 635 nm. The complex contains three molecules of BPR co-ordinated to an iron(III) ion, and two molecules of CTMAB associated with each BPR molecule, giving the overall formula $(CTMAB)_6(BPR)_3Fe(III)$. Iron(II) also reacts with BPR and CTMAB in the presence of dissolved oxygen to form the iron(III) complex. No oxidizing or reducing agents are required for the determination of total iron in mixtures of iron(III) and iron(II), and Beer's law is followed from 0.05 to 0.5 ppm iron (1.00-cm cells). Of nine metal ions tested at the 1-ppm level, only manganese(II) and vanadium(V) interfere. Copper(II), cobalt(II), zinc, lead, nickel, aluminium and chromium(III) produce little or no interference when present at 100 ppm concentration.

In a series of investigations Bromopyrogallol Red has been studied as a chromophoric reagent for uranium,[1,2] silver,[3,4] niobium,[5] lanthanum,[6] scandium,[7] germanium,[8] and thorium.[9] Also, Bromopyrogallol Red and quaternary ammonium salts form mixed-ligand complexes with aluminium,[10] zirconium,[11] molybdenum,[12] and tungsten.[13] We also note that a highly sensitive method for the spectrophotometric determination of iron by use of similar reagents has been recently reported.[14] It is based on the extraction of an iron–Pyrogallol Red–zephiramine complex into chloroform. In this paper we present a spectrophotometric method for the determination of iron, based on the sensitive colour reaction of iron(II) and iron(III) with Bromopyrogallol Red (BPR) and hexadecyltrimethylammonium bromide, also referred to as cetyltrimethylammonium bromide (CTMAB). The reagents react with aqueous solutions of iron(III) to form a stable blue complex. The same complex is formed with iron(II) in the presence of dissolved oxygen. Conditions for colour development, the structural formula and composition of the complex, and the influence of other ions are reported. The proposed method is very sensitive and selective for iron, and it was found that the Fe–BPR–CTMAB complex could be used in the spectrophotometric determination of iron.

EXPERIMENTAL

Reagents

Iron(II) solution, 1.00 × 10^{-3}M. Prepared by dissolving $FeSO_4.7H_2O$ (99.9% pure by titration with standard permanganate) in deaerated 1*M* sulphuric acid. The permanganate solution was standardized against electrolytic iron by the Jones reductor method.

Iron(III) solution, 1.00 × 10^{-3}M. Prepared by dissolving 1.4313 g of $Fe_2(SO_4)_3 \cdot 3.22H_2O$ in 250 ml of 1*M* sulphuric acid. The composition of the ferric sulphate was determined by reduction and titration with standard permanganate.

Bromopyrogallol Red solution, 1.00 × 10^{-4}M. Prepared by dissolving 0.02791 g of BPR (Eastman Kodak in 500 ml of 50% v/v aqueous ethanol. This solution was standardized with silver by the continuous variations method.[3]

CTMAB solution, 5.00 × 10^{-3}M. Prepared by dissolving 0.9113 g of CTMAB powder (Sigma Chemical Co.) in 500 ml of water. The purity of the reagent was assessed by the supplier by NMR, infrared, m.p. (232–238°) thin-layer chromatography (one spot observed), and titration with perchloric acid (98% minimum assay).

Solutions of interfering ions were prepared from the metal salts. All other reagents were analytical reagent grade. Water was distilled and demineralized.

Apparatus

Absorption measurements and spectra were obtained with a Beckman spectrophotometer, model Acta II, in conjunction with a Sargeant SRL recorder, and 1.00-cm borosilicate glass cells. A Corning research pH meter, model 112, was calibrated against NBS buffers for pH measurements.

Procedure for determination of iron

Place an aliquot containing not more than 16 μg of iron in a 25-ml standard flask. Add 10.0 ml of BPR solution (to yield $4.0 \times 10^{-5}M$ total concentration) and 1.0 ml of CTMAB solution (to yield $2 \times 10^{-4}M$ total concentration). Adjust the pH to 3.5–5.5 with 0.2*N* sodium hydroxide, and dilute to the mark with distilled water. After 30 min measure the absorbance at 635 nm against a reagent blank.

RESULTS AND DISCUSSION

Absorption spectra

A series of solutions containing a constant amount of iron(II) or iron(III) was prepared at pH 3.7. The absorption spectra measured against the correspond-

* On leave from Department of Chemistry, Nan-Kai University, Tianjin, The People's Republic of China.

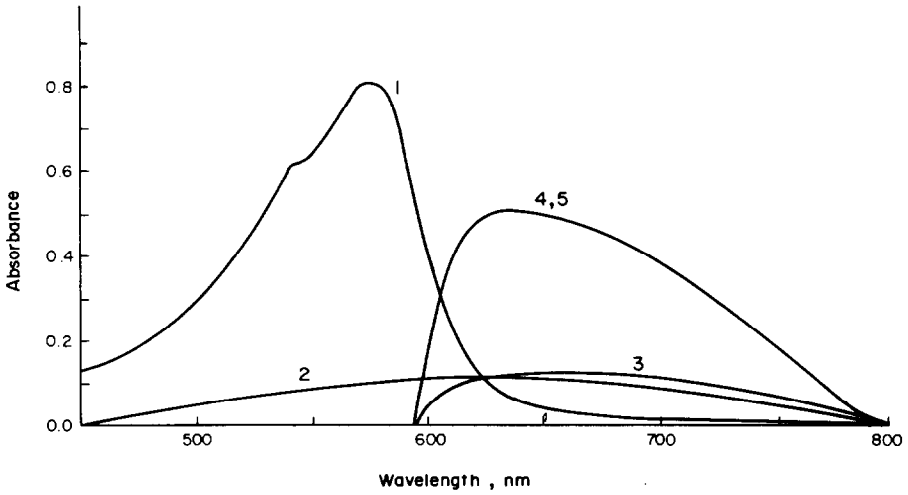


Fig. 1. Absorption spectra of BPR derivatives. [Fe] = $1.00 \times 10^{-5}M$, [BPR] = $3.3 \times 10^{-5}M$, [CTMAB] = $2.0 \times 10^{-4}M$, pH = 3.7, 1.00-cm cells. Curve 1, BPR + CTMAB *vs.* water; 2, iron(II) + BPR *vs.* BPR; 3, iron(III) + BPR *vs.* BPR; 4, iron(II) + BPR + CTMAB *vs.* BPR + CTMAB; 5, iron(III) + BPR + CTMAB *vs.* BPR + CTMAB.

ing reagent blanks are shown in Fig. 1. Solutions containing only CTMAB and either iron(II) or iron(III) are colourless. Both iron(II) and iron(III) react with BPR to form a purple complex, but when BPR, CTMAB and either iron(II) or iron(III) are mixed, a blue complex is formed with maximum absorption at 635 nm. The absorptivity is also increased about fourfold in the presence of CTMAB. Judging from the absorption spectra, iron(II) and iron(III) appear to give identical complexes with BPR and CTMAB. It will be shown later than both form the iron(III) complex.

Effect of pH

The effect of pH on the absorbance of the complex at 635 nm is shown in Fig. 2. The absorbance is maximal and nearly constant at pH 3.5–5.5. This optimum pH range is wide enough for pH-adjustment not to be critical.

Effect of temperature and time

The absorbance is unaffected by temperature over the range from 20 to 50°. Hence, normal variations in laboratory temperature will have no effect. At room

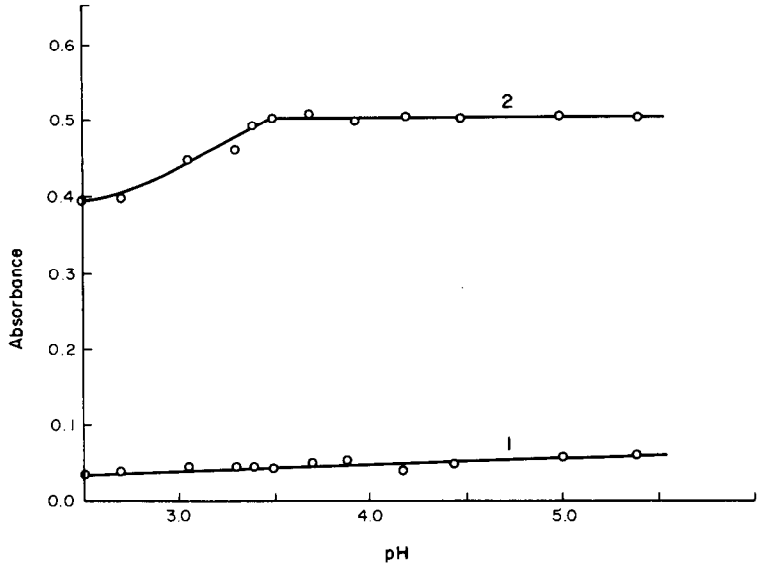


Fig. 2. Effect of pH on absorbance of Fe–BPR–CTMAB complex. [Fe] = $1.00 \times 10^{-5}M$, [BPR] = $4.0 \times 10^{-5}M$, [CTMAB] = $2.0 \times 10^{-4}M$, 1.00-cm cells, wavelength = 635 nm. Curve 1, BPR + CTMAB *vs.* water; 2, iron(II) + BPR + CTMAB *vs.* BPR + CTMAB.

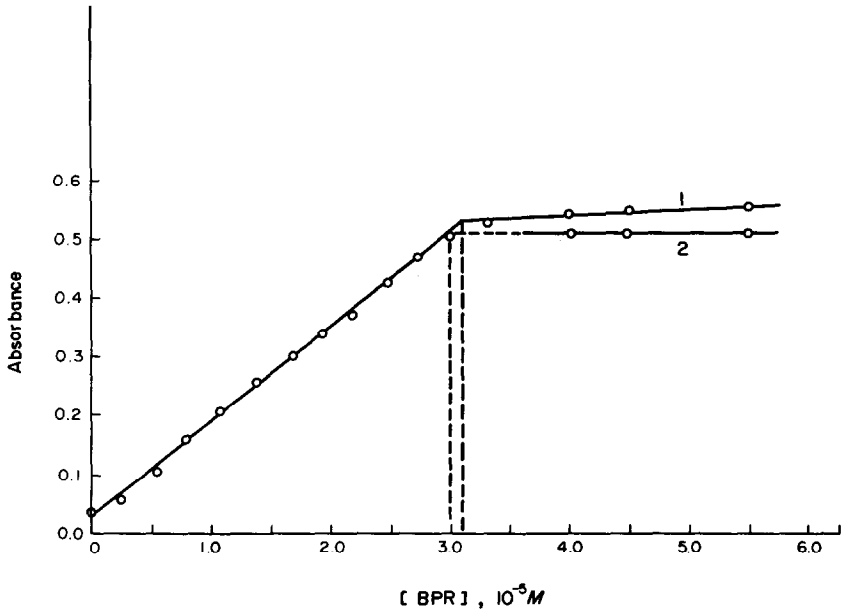


Fig. 3. Mole-ratio study of Fe–BPR–CTMAB system; effect of BPR concentration. [Fe] = $1.00 \times 10^{-5}M$, [CTMAB] = $2.0 \times 10^{-4}M$, pH = 3.7, wavelength = 635 nm, 1.00-cm cells. Reference solution is water in curve 1, reagents in curve 2.

temperature the colour intensity increases during the first 20 min, and remains constant for at least 2 days.

Composition of the complex

The mole-ratio method[15] was used to determine the ratio of BPR to iron. Figure 3 shows that maximum colour intensity is obtained at a molar ratio of iron(II) to BPR of 1:3. It appears that no additional complex formation occurs beyond this point.

The effect of CTMAB concentration is shown in Fig. 4. The concentration ratio of iron(II) to BPR was maintained constant at 1:4. The molar ratio of iron to CTMAB in the complex is apparently 1:6, although this value is somewhat uncertain owing to the limitations of the experiment. Also, no change in absorbance occurs at much higher concentrations of CTMAB, but a slight decrease does occur when [CTMAB] = $10^{-3}M$.

The combining ratios of Fe–BPR–CTMAB under various conditions were determined from a triangular diagram.[16,17] Solutions were prepared so that the total concentration of Fe + BPR + CTMAB was

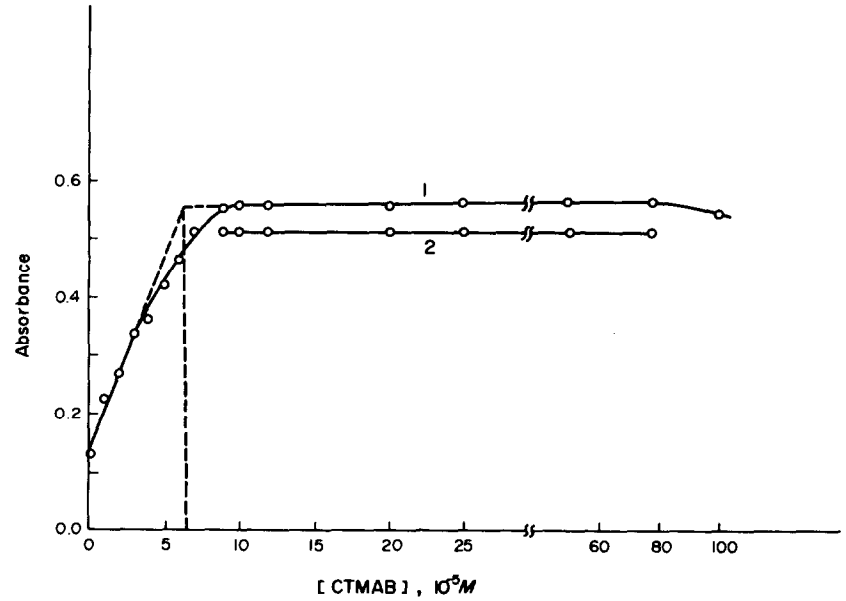


Fig. 4. Mole ratio study of Fe–BPR–CTMAB system; effect of CTMAB concentration. [BPR] = $4.0 \times 10^{-5}M$. Other conditions same as in Fig. 3.

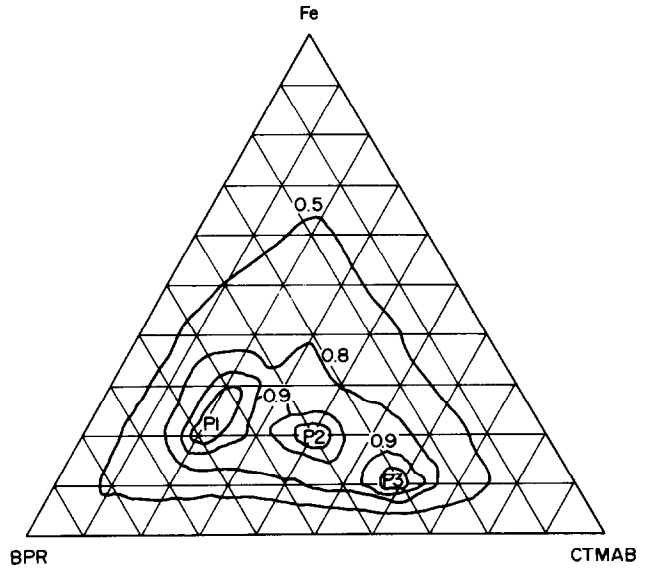


Fig. 5. Triangular absorbance diagram of Fe–BPR–CTMAB system. Total concentration of Fe + BPR + CTMAB = $2.0 \times 10^{-4}M$, pH = 3.7, wavelength = 635 nm, 1.00-cm cells.

$2.0 \times 10^{-4}M$, the pH was adjusted to 3.7, and the absorbance was measured at 635 nm. The results are shown in Fig. 5. This figure shows P_1, P_2 and P_3 as the maximum absorbance points in the triangular diagram. The corresponding combining ratios of Fe:BPR:CTMAB are 1:3:1, 1:2:2 and 1:3:6, respectively. When an excess of reagents is used, only a single complex is formed, in which the ratio of Fe:BPR:CTMAB is 1:3:6. This conclusion is supported by the molar-ratio studies reported above (Figs. 3 and 4).

Oxidation state of iron in the complex

As we stated earlier, the absorption spectrum of the Fe–BPR–CTMAB complex is the same whether iron is added as iron(II) or iron(III). Addition of hydroxylamine hydrochloride or ascorbic acid (100 mg/25 ml) causes the blue colour to fade slowly, but bubbling with air will regenerate it. If iron(II) is added to a deaerated solution of BPR and CTMAB almost no colour is produced, but when air is bubbled through the solution, the deep blue complex is formed. We therefore conclude that the blue complex contains iron in the +3 oxidation state. Thus the iron(III) derivative is formed regardless of whether iron(II) or iron(III) is added, provided sufficient dissolved oxygen is present and no reducing agents are present.

Additional evidence for an oxidation state of +3 comes from a study of the reactions of iron(II) and iron(III) with BPR in the absence of CTMAB at pH 3.7. The continuous-variations method[18] showed (Fig. 6) that iron(III) forms a 1:3 complex with BPR, whereas iron(II) forms a 1:2 complex, which implies that the iron in the 1:3:6 Fe–BPR–CTMAB complex is in the +3 oxidation state.

Structure and charge of the Fe–BPR–CTMAB complex

Although the results above clearly demonstrate that the combining ratio is 1:3:6, the actual composition may be some multiple of this. If we express the formation of the complex as:

$$m\text{Fe} + n\text{BPR} + p\text{CTMAB} = \text{Fe}_m(\text{BPR})_n(\text{CTMAB})_p$$

then the formation constant is:

$$K = \frac{[\text{Fe}_m(\text{BPR})_n(\text{CTMAB})_p]}{[\text{Fe}]^m[\text{BPR}]^n[\text{CTMAB}]^p} \quad (1)$$

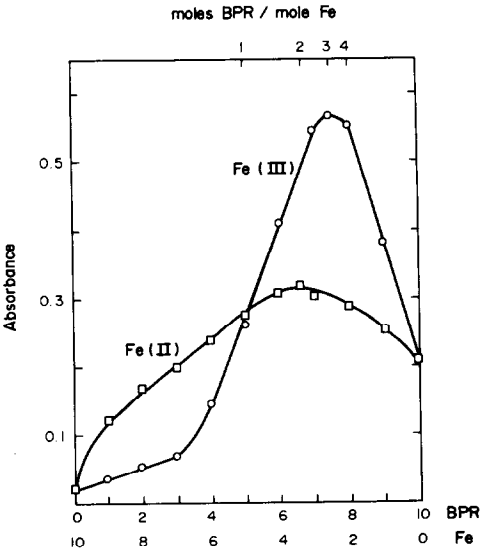


Fig. 6. Continuous-variations study of Fe–BPR systems. Total concentration of Fe + BPR = $2.0 \times 10^{-4}M$, pH = 4.0, wavelength = 635 nm, 1.00-cm cells.

The concentration of the complex is related to the absorbance by:

$$[Fe_m(BPR)_n(CTMAB)_p] = \frac{A}{\epsilon l} \quad (2)$$

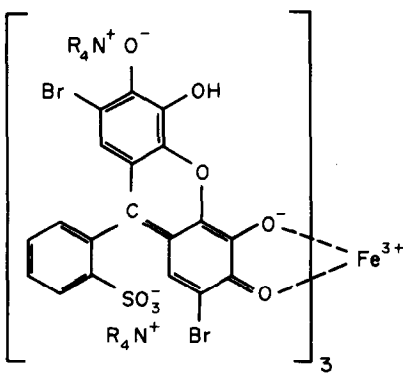
where ϵ = molar absorptivity and l = cell path-length. By substituting (2) into (1) and simplifying, we obtain:

$$\log A = m\log[Fe] + n\log[BPR] + p\log[CTMAB] + \log K\epsilon l \quad (3)$$

It is possible to determine m, n or p by maintaining the pH and all concentrations constant except for that of the corresponding component.[19–22] Variation of [Fe] at constant excess [BPR] and [CTMAB] gave a linear plot of slope $m = 0.9$ for log A *vs.* log [Fe]. Because the combining ratio of Fe:BPR:CTMAB is known to be 1:3:6, we conclude that the true formula of the complex is expressed by $m = 1$, $n = 3$, $p = 6$.

The charge on the complex was inferred from its interactions with ion-exchange resins. When the blue complex was passed through a column of Amberlite IR-120 (a sulphonic acid type cation-exchange resin) the eluate was a deep purple solution, identical to the $(BPR)_3Fe(III)$ complex. The surface-active agent CTMAB was apparently absorbed by the resin. When the blue complex was passed through a column of Amberlite IRA-400 strong base anion-exchange resin, the eluate contained the original blue complex, with no retention on the resin. These results suggest that the complex is neutral. This conclusion is supported by the observation that when all three reagents are mixed in combining ratio for the blue complex, a blue precipitate readily forms.

According to the evidence presented above, we assign the following structure to the blue complex:



Adherence to Beer's law

A plot of absorbance at 635 nm *vs.* concentration of iron in presence of excess of BPR and CTMAB at pH 3.7 does not pass through the origin but is linear from 1.4 to 14 μg of Fe per 25 ml. The molar absorptivity is 5.20×10^4 l.mole^{-1}.cm^{-1} at 635 nm.

Table 1. Effects of other ions on the determination of Fe(III) or Fe(II). Iron taken: 12.0 μg/25 ml

Ions	Concentration of ion added, *ppm*	Iron found, μg
Cu(II)	1	12.0
	100	12.3
Co(II)	1	12.0
	100	12.0
Zn(II)	1	12.0
	100	11.4
Pb(II)	1	12.0
	100	11.6
Ni(II)	1	12.0
	100	12.3
Al(III)	1	12.0
	100	11.4
Cr(III)	1	12.0
	100	12.1
Mn(II)	1	10.9
V(V)	1	12.6

Table 2. Determination of total iron (12.0 μg taken)

Iron added, μg		Iron found, μg
Fe(III)	Fe(II)	
1.0	11.0	12.3
1.7	10.3	12.0
3.4	8.6	12.0
5.1	6.9	12.3
6.9	5.1	12.2
8.6	3.4	11.7
10.3	1.7	12.0
11.0	1.0	12.3

Interferences

The effects of many ions on the determination of Fe were studied under the conditions used in the proposed procedure. The results are summarized in Table 1. Of the ions tested, only Mn(II) and V(V) produced significant errors at the 1 ppm level. Most other ions had almost no effect even when present at 100 ppm.

Determination of total iron

The proposed method is well-suited for the determination of total iron because the addition of an oxidizing or reducing agent is not required. To substantiate this, a series of solutions was prepared containing iron(II) and iron(III), (total iron concentration constant). The total iron found by this method was always within 3% of the correct value, as shown in Table 2.

REFERENCES

1. M. Šucmanová-Vondrová, J. Havel and L. Sommer, *Collection Czech. Chem. Commun.*, 1977, **42**, 1812.
2. V. F. Lukyanov and E. P. Duderova, *Zh. Analit. Khim.*, 1961, **16**, 60.
3. R. M. Dagnall and T. S. West, *Talanta*, 1961, **8**, 711.
4. T. S. West, *Analyst*, 1962, **87**, 630.
5. E. A. Shteiman, Z. G. Dobrynina and E. A. Mordovskaya, *Zavodsk. Lab.*, 1964, **30**, 1200.

6. V. Suk, *Collection Czech. Chem. Commun.*, 1966, **31**, 367.
7. T. Schimizu, *Talanta*, 1967, **14**, 473.
8. G. Popa and I. Paralescu, *ibid.*, 1968, **15**, 272.
9. V. D. Vasilenko, M. V. Shanyce and V. I. Bolbas, *Zh. Analit. Khim.*, 1967, **22**, 1818.
10. A. S. Arkhangelskaya and L. A. Molot, Paper deposited at VINITI, No. 1734, 25 June 1974.
11. M. Deguchi, Y. Omura and M. Yashiki, *J. Pharm. Soc. Japan*, 1973, **93**, 825.
12. M. Deguchi, M. Iizuka and M. Yashiki, *Bunseki Kagaku*, 1974, **23**, 760.
13. M. Deguchi and T. Mamiya, *ibid.*, 1976, **25**, 60.
14. T. Korenaga, S. Motomizu and K. Toei, *Anal. Chim. Acta*, 1979, **104**, 369.
15. J. H. Yoe and A. L. Jones, *Ind. Eng. Chem., Anal. Ed.* 1944, **16**, 111.
16. A. B. Calder, *Photometric Methods of Analysis*, p. 261. Elsevier, New York, 1969.
17. A. K. Babko, *Physiochemical Analysis of Complex Compounds in a Solution*, AN USSR, Kiev, 1955.
18. P. Job, *Ann. Chim. Paris*, 1928, **9**, 113.
19. H. Bent and C. French, *J. Am. Chem. Soc.*, 1941, **63**, 569.
20. C. Lewis and D. A. Skoog, *ibid.*, 1962, **84**, 1101.
21. Shi Huiming and He Xi-Wen, *Acta Sci. Nat. Univ. Nankaisis*, 1965, **6**, 11.
22. Shi Huiming and He Xi-Wen, *Fenxi Huaxue*, 1979, 7, 228.

Talanta, Vol. 28, pp. 425 to 430. 1981
Printed in Great Britain. All rights reserved

0039-9140/81/070425-06$02.00/0
Copyright © 1981 Pergamon Press Ltd

ION-PAIR EXTRACTION AND FLUORIMETRIC DETERMINATION OF POTASSIUM WITH 18-CROWN-6 AND EOSIN

A. SANZ-MEDEL*, D. BLANCO GOMIS and J. R. GARCIA ALVAREZ
Departamento de Química Analítica, Facultad de Ciencias, Universidad de Oviedo, Oviedo, Spain

(*Received* 20 *October* 1980. *Accepted* 21 *January* 1981)

Summary—A highly sensitive and selective fluorimetric determination of potassium is proposed, based on solvent extraction of the ion-pair formed between a large anion and the cationic complex of K^+ with a crown ether. Sensitivity is achieved by selection of a highly fluorescent counter-ion of the fluorescein group (eosin). A linear working range from 0.01 to 1 ppm of potassium is obtained, which gives a higher sensitivity than any similar method for potassium determination. The relative standard deviation is 4–5%. Selectivity is achieved by matching the radius of the cavity of the 18-crown-6 to the ionic radius of potassium. The system used is exceptionally selective for extraction of potassium in the presence of alkali or alkaline-earth metal cations. The proposed method has been successfully applied to the determination of potassium in blood serum.

Although flame photometry and atomic absorption are widely used, there is still a need for practical molecular spectrophotometric methods for potassium or sodium determination. A recent approach to this problem is the use of macrocyclic compounds with cavities of the right size to accommodate alkali metal cations.[1] In particular, crown ethers are used. The product is usually not coloured or fluorescent. However, a direct colorimetric or fluorimetric determination of the cation is possible by solvent extraction of the ion-pair formed by the crown ether complex and an organic anion which is either highly coloured (spectrophotometry) or highly fluorescent (fluorimetry). Such a colorimetric potassium determination has been reported[2] and we propose here a fluorimetric method which provides improved sensitivity.

Selectivity for potassium can be achieved by matching the radius of the cavity of the crown ether to the ionic radius of K^+, and improved by judicious choice of the solvent extraction system, in terms of the nature and charge of the counter-ion[3,4] and the solvating properties and dielectric constant of the organic solvent.[2,5,6] The stability constants for the crown ether–alkali metal complexes[2,7] and the extraction data[8] indicate that 18-crown-6 (1,4,7,10,13,16-hexaoxacyclo-octadecane) is the most suitable for selective complexation of potassium and it was therefore employed in the present work. It will be referred to as L.

Sensitivity is achieved by using fluorimetry in conjunction with a counter-ion possessing high fluorescence quantum efficiency, *e.g.*, fluorescein and its derivatives. Fluorimetric assays for potassium include the use of chelates with 8-hydroxyquinoline or zinc uranyl acetate,[9] but has neither adequate sensitivity or selectivity. A fluorimetric determination of potassium by solvent extraction of the ion-pair of dibenzo-18-crown-6-K^+ with anilinonaphthalene sulphonate has also been reported.[10]

In the present work, a detailed investigation of the extraction of the 18-crown-6-K^+ complex with different fluorescent counter-ions and organic solvents has led to the establishment of a new and very useful fluorimetric determination. The method has been successfully applied to the determination of potassium in serum.

EXPERIMENTAL

Preliminary investigations

Various acidic fluorescent dyes of the fluorescein group, including fluorescein, dichlorofluorescein, tetrabromofluorescein (eosin), tetraiodofluorescein (erythrosin) and tetrachlorotetrabromofluorescein (Rose Bengal Extra) were studied as counter-ions for the 18-crown-6-K^+ complex. A fixed amount of potassium (20.0 μg), was treated with a fixed 6-fold molar excess of L and 2 ml of a 0.1% aqueous solution of the dye being tested and the ion-pair complex was extracted into dichloromethane (equal volumes of aqueous and organic phases were used); the excitation and emission spectra of the organic layer were recorded. The pH was varied between 2 and 9 according to the acidity constant of the dye used.

The results showed that only erythrosin and eosin gave analytically useful fluorescence signals in comparison with the corresponding blanks without potassium. Photochemical decomposition was observed for erythrosin, but use of eosin produced stable and reproducible fluorescence intensity measurements. Therefore eosin was chosen as the counter-ion.

Benzene, bromobenzene, 1,2-dichloroethane, chloroform, carbon tetrachloride and dichloromethane were tested as solvents for the extraction of the eosin complex. The fluorescence intensities, corrected for the corresponding blank,

* To whom correspondence and requests for reprints should be addressed.

for 20.0 μg of potassium were in the order dichloromethane > 1,2-dichloroethane > chloroform > carbon tetrachloride. No fluorescence was observed when benzene or bromobenzene was used.

Apparatus

Fluorescence measurements were made with a double-monochromator spectrofluorimeter (Aminco SPF-125S) equipped with a 150-W xenon arc lamp and a 1-P-21 photomultiplier; 2-mm slits (22-nm spectral bandpass) were used on both monochromators to obtain the maximum sensitivity compatible with good definition of the maxima. Fused quartz cells (1 × 1 × 5 cm) were used throughout. Any variation in the output intensity of the xenon arc source was checked after each set of measurements by measuring the fluorescence intensity of a standard 1-ppm solution of quinine bisulphate in 0.1*N* sulphuric acid.

Reagents

All reagents were of analytical grade and redistilled and demineralized water was used.

18-Crown-6 solution, 0.1M. Prepared from the Merck reagent.

Potassium chloride stock solution, 1.907 g/l. (K^+ = 1000 ppm). Working standard solutions were freshly prepared by dilution of the stock solution.

Eosin solution, 0.1%. The disodium salt (0.1 g) was dissolved in 100 ml of redistilled water and the solution was passed through a Dowex 50 W-X8 resin column, previously saturated with lithium carbonate solution.

Buffer solution (pH 6.0). Lithium carbonate (7.39 g) and trichloroacetic acid (27.4 g) dissolved in redistilled and demineralized water (the CO_2 evolved being allowed to escape at room temperature) and then diluted to 1 litre.

Dilute acetic acid, 0.1% v/v.

Dichloromethane. Merck Uvasol grade for fluorimetry.

General procedure

Pipette standard potassium solution (from 0.05 to 5 μg of potassium) into a series of 50-ml separating funnels. To each funnel add 0.5 ml of 18-crown-6 solution, 2.5 ml of eosin solution, 0.1 ml of 0.1% acetic acid and 0.5 ml of buffer solution, and dilute to 5 ml with redistilled and demineralized water (final pH 5.9 ± 0.1). After mixing, add 5 ml of dichloromethane (previously equilibrated with the aqueous phase mixture with no potassium present) and extract the complex by mechanical shaking for 5 min. Separate the phases and measure the fluorescence intensity I_F of the organic phase at 563 nm (excitation wavelength 322 nm).

Run a reagent blank in the same way and subtract its fluorescence from that of the sample. The plot of the corrected fluorescence against amount of potassium should be a straight line passing through the origin.

Procedure for serum potassium determination

Into a screw-capped 10-ml centrifuge tube pipette 0.1 ml of serum sample, followed by 4.9 ml of 1.5% aqueous trichloroacetic acid solution. Mix well and heat for 5 min in a thermostatic bath at 80° to accelerate protein precipitation, then centrifuge the mixture for 5 min. Transfer 0.1 ml of the supernatant liquid into a separating funnel, raise the pH to about 6 (by adding 0.1 ml of 0.5% aqueous lithium carbonate solution) and continue as described for the general procedure.

RESULTS AND DISCUSSION

Excitation and fluorescence spectra

Figure 1 shows the excitation and emission spectra of the blank and the complex extracted into dichloromethane from an aqueous medium of pH 5.9. These spectra are uncorrected for variations in the emission characteristics of the lamp and the response characteristics of the photomultiplier. The green fluorescence of the extracted ion-pair exhibits two main excitation maxima: one at 322 nm and a more intense one at 545 nm. The emission maximum appears at 563 nm, irrespective of which of the two excitation wavelengths is used.

The blank spectra are similar but slightly shifted to shorter wavelengths. The high blank values obtained for excitation at 545 nm forced us to choose the less sensitive 322 nm excitation wavelength, with which the sample/blank signal ratio was optimal.

The lithium salt of eosin was used instead of the sodium salt because it gives a lower blank.

Effect of pH

As expected, the extraction pH critically influences the fluorescence intensity obtained (Fig. 2). The extraction process is pH-controlled because eosin is a weak diprotic acid, H_2A, and the pH must be high enough to produce the singly-charged eosinate anion (HA^-) and permit extraction of the KL^+–HA^- complex, but not so high that doubly-charged eosinate anions (A^{2-}) are formed, which would hinder the extraction. As shown in Fig. 2 maximum fluorescence is obtained if the extraction is done at pH 5.9 ± 0.1.

Reagent concentrations

Variation of the crown ether concentration, with 4.0 ppm of potassium and a sixfold molar excess of cosin and the optimum pH, gives constant maximum fluorescence intensity at [L] ≥ 0.03*M* (Fig. 3,a). For extraction of less than 1 ppm of potassium by the general procedure a crown ether concentration of 0.01*M* gives maximum I_F, the blank signal being considerably less than with 0.03*M* crown ether reagent. Therefore a final 18-crown-6 concentration of 0.01*M* was selected.

Variation of the eosin concentration with [L] fixed at 0.03*M* and with 4.0 ppm of potassium (Fig. 3,b) shows that the fluorescence intensity becomes constant at a total eosin concentration ≥ $5 \times 10^{-4}M$. For reproducible extraction, excess of counter-ion is essential (2.5 ml of 0.1% eosin solution diluted to 5 ml will give an eosin concentration of $7 \times 10^{-4}M$).

No significant effect of increasing ionic strength (from 0.1 to 0.7 ml of buffer solution) was noted.

Rate of extraction and stability of the extract

A plot of corrected I_F *vs.* shaking time shows that a constant reproducible value is reached after 60 sec of shaking. The order of addition of the reagents is unimportant.

The temperature of the solutions was 20 ± 5° and no significant variation of I_F with temperature was noted in this range.

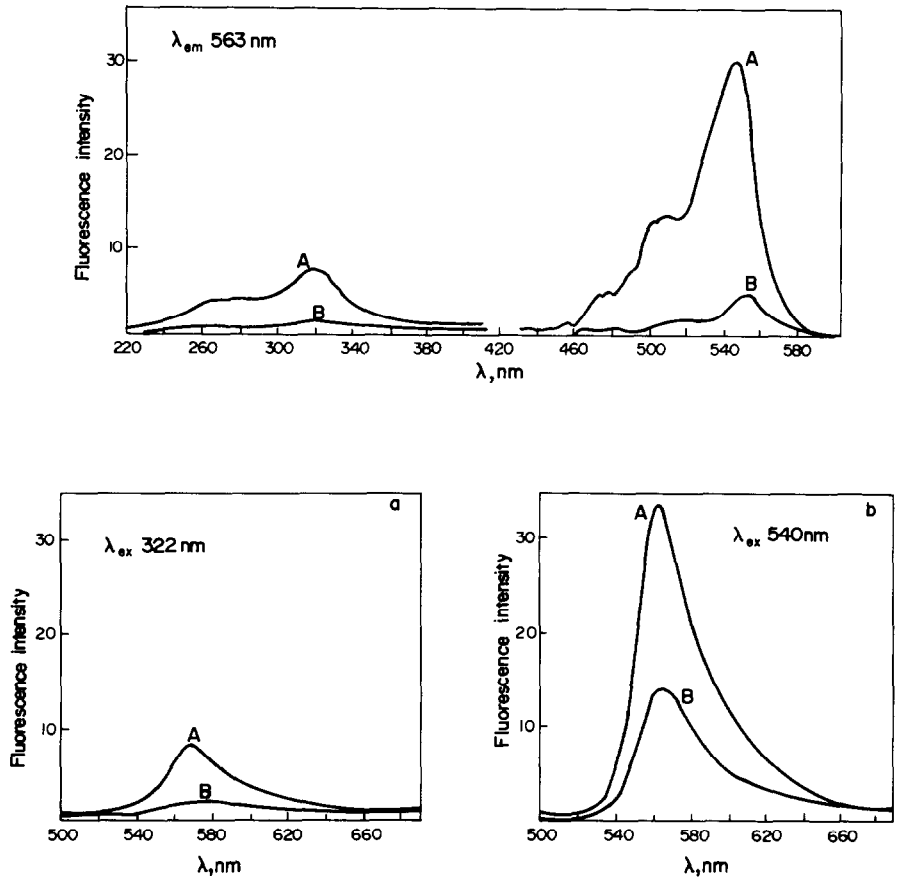


Fig. 1. Excitation and emission spectra of blank (B) and ion-association potassium complex (A). Above—excitation spectra; below—emission spectra.

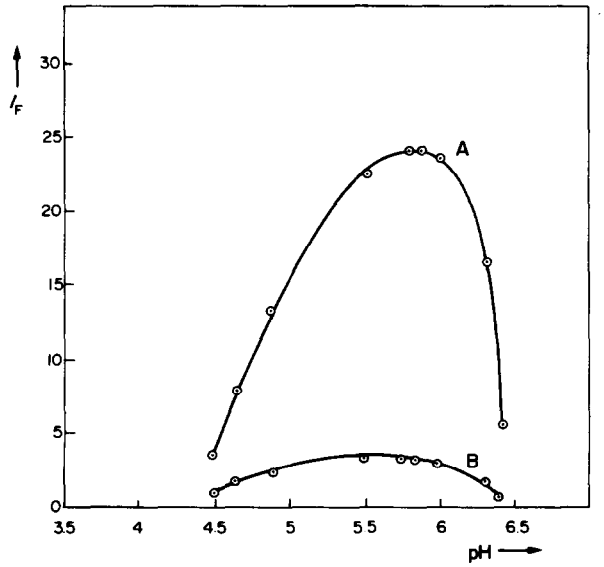


Fig. 2. Variation of fluorescence intensity with pH. (A) Ion-association potassium complex; (B) reagent blank.

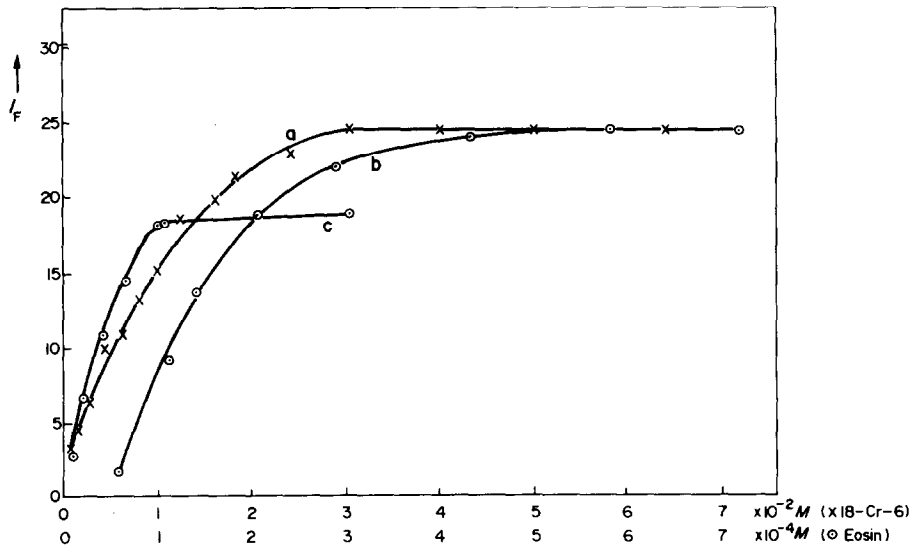


Fig. 3. Influence of 18-crown-6 and eosin concentrations on fluorescence intensity. (*a*) K^+ 4 ppm, eosin $7 \times 10^{-4}M$, 18-crown-6 varied; (*b*) K^+ 4 ppm, 18-crown-6 $0.03M$, eosin varied; (*c*) K^+ 1 ppm, eosin $7 \times 10^{-4}M$, 18-crown-6 varied.

Precision

The recommended procedure was applied to the repetitive determination of 1.5 μg of potassium over several days. Ten determinations produced a relative standard deviation of 4.9%.

Effect of foreign ions

The effect of common alkali and alkaline-earth metal ions on the determination of 1.5 μg of potassium by the recommended procedure was investigated. Lead, iron and aluminium were also tested. Except for lithium, 150 μg of foreign ion were initially used and the effect was subsequently reinvestigated at lower levels for those cations which were found to interfere. An ion was considered to interfere when it changed the fluorescence intensity for 1.5 μg of potassium by more than twice the relative standard deviation (*i.e.*, by more than ± 10%).

The results are shown in Table 1. It can be seen that for alkali-metal cations the degree of interference is in the order $NH_4^+ > Cs^+ > Na^+ \gg Li^+$, as might be expected from the values of the stability constants of the corresponding LM^+ complexes in the aqueous phase. [2,7,11,12] The selectivity for potassium is better than that reported by Kenyu *et al.*[10] In fact, NH_4^+ is the only serious interference, but this is readily overcome by making the sample solution alkaline with lithium hydroxide and boiling (lithium can be tolerated in relatively high concentrations).

The effect of alkaline-earth metal cations (except for calcium and magnesium which form weak complexes with L) is smaller than expected, considering that the stability constants reported[12] for LSr^{2+} (log K_f = 2.72) and LBa^{2+} (log K_f = 3.87) are greater than that of 'K^+' (log K_f = 1.9). This indicates that the extractability of the ion-pair complexes is the decisive factor. This is also illustrated by the fact that interference by the alkaline-earth metals decreases in the order Sr > Ba > Ca > Mg even though the LBa^{2+} complex is more stable than the LSr^{2+} complex, a result in agreement with Takeda and Kato's findings for picrate as counter-ion.[13]

In brief, our results support Takeda and Kato's conclusion[13] that the ratio of the size of the metal ion to that of the crown ether cavity (this ratio is related to K_f) is not always the dominant factor in the extractability, and the association constant for the complex extracted may be decisive

($K_{assn} = [LM^A_{n_{org}}]/[LM^{n+}][A^-]^n$; A = counter-ion)

may be decisive.

The most serious interference is from lead, as predictable from the stability constant of the LPb^{2+} complex and its high extractability as an ion-association complex.[13] According to the results of Kenyu *et al.*[10] dibenzo-18-crown-6-K^+ is considerably less affected by lead interference. The tervalent cations Al^{3+} and Fe^{3+} do not interfere.

Figure 4, where the relation between I_F (for 1.5 μg of the metal ion) and ionic diameter is plotted, well illustrates the excellent selectivity for potassium relative to other alkali and alkaline-earth metal cations.

Stoichiometry of the extracted complex

There have been numerous studies of the stoichiometry and structure of the complexes of 18-crown-6, dicyclohexyl-18-crown-6 and dibenzo-18-crown-6 with potassium, and of their ion-association complexes with counter-ions such as halides, thiocyanate, nitrophenolates,[14,15] anilinonaphthalene sulpho-

Table 1. Effect of foreign ions (M) on the determination of 1.5 μg of potassium

Cation	M:K (molar ratio)	Apparent recovery, % 18-Crown-6/eosin method*	Dibenzo-18-crown-6/anilinoaphthalene sulphonate method†
Li^+	2000	112	
	1000	100	
	100		110
	10		103
Na^+	200	135	
	100	106	
	10		140
	1		106
Cs^+	10	135	
	5	116	
	1		190
NH_4^+	10	155	
	2	135	
	1	100	120
Mg^{2+}	200	122	
	100	103	100
Ca^{2+}	100	125	100
	50	106	
Sr^{2+}	10		170
	5	150	
	2	118	
	1	102	110
Ba^{2+}	20	160	
	10		130
	5	110	
	1		101
Pb^{2+}	100		110
	0.2	175	
	0.1	132	
Fe^{3+}	100	100	
Al^{3+}	100	100	

* Present work; † Kenyu *et al.*[10]

Table 2. Potassium determination in blood serum

Sample	Flame photometry, *ppm*	Proposed method, *ppm*
1	160	150
2	172	175
3	172	170
4	224	225
5	144	143
6	208	200
7	136	130
8	128	125
9	160	155
10	152	148

nate,[10] *etc.* The stoichiometry of such ion-association complexes is invariably of the type LK^+-A^-. The same 1:1:1 stoichiometry was found in our work, by the extended Job method[16] and fluorescence measurements, so the species extracted must have singly deprotonated eosin (HA^-) as the counter-ion.

Potassium determination in blood serum

The method was tested by applying it to the determination of potassium in serum. The results agreed well with those obtained by flame photometry, as shown in Table 2.

Although 0.1 ml of serum was used, the sensitivity of the method is so high that the necessary sample volume can easily be reduced to 5–10 μl of serum. This ability to analyse very small samples is of importance in some practical problems, *e.g.*, analysis of blood from babies, and can make this the method of choice instead of the flame photometry techniques which require greater volumes of serum.

Acknowledgement—Acknowledgement is made to the National Institute of Silicosis of Oviedo for the grant of the Aminco SPF-125S spectrofluorimeter for this research.

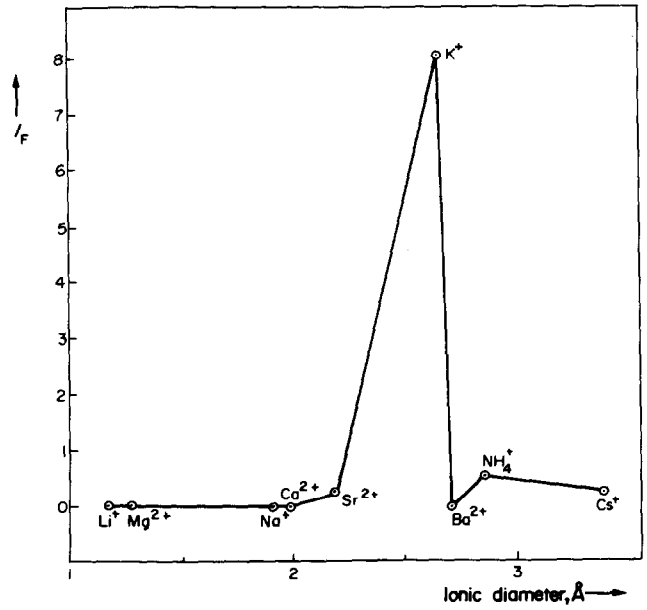


Fig. 4. Relation between fluorescence intensity and ionic diameter of alkali and alkaline-earth metal cations.

REFERENCES

1. I. M. Kolthoff, *Anal. Chem.*, 1979, **51**, 1R.
2. H. Sumiyoshi, K. Nakahara and K. Ueno, *Talanta*, 1977, **24**, 763.
3. Y. Marcus and L. E. Asher, *J. Phys. Chem.*, 1978, **82**, 1246.
4. M. Jawaid and F. Ingman, *Talanta*, 1978, **25**, 91.
5. M. Jimenez Reyes, A. G. Maddock, G. Duplatre and J. J. Scheleiffer, *J. Inorg. Nucl. Chem.*, 1979, **41**, 1365.
6. K. H. Wong, G. Konizer and J. Smid, *J. Am. Chem. Soc.*, 1970, **11**, 92.
7. J. D. Lamb, R. M. Izatt, C. S. Swain and J. Christensen, *ibid.*, 1980, **16**, 102.
8. T. Iwachido, A. Sadakane and K. Tôei, *Bull Chem. Soc. Japan*, 1978, **51**, 629.
9. G. G. Guilbault, *Practical Fluorescence*, p. 249. Dekker, New York, 1973.
10. K. Kenyu, S. Katsuhiko and I. Nobuhiko, *Bunseki Kagaku*, 1978, **27**, 291.
11. H. K. Frensdorff, *J. Am. Chem. Soc.*, 1971, **93**, 600.
12. R. M. Izatt, R. E. Terry, B. L. Haymore, L. D. Hansen, N. K. Dalley, A. G. Avondet and J. J. Christensen, *ibid.*, 1976, **98**, 7620.
13. Y. Takeda and H. Kato, *Bull. Chem. Soc. Japan*, 1979, **52**, 1027.
14. R. M. Izatt, *Synthetic Multidentate Macrocyclic Compounds*, p. 216. Academic Press, New York, 1978.
15. R. M. Izatt and J. J. Christensen, *Progress in Macrocyclic Chemistry*, Vol. 1, p. 120. Wiley, New York, 1979.
16. H. Irving and T. B. Pierce, *J. Chem. Soc.*, 1959, 2565.

Talanta, Vol. 28, pp. 431 to 435, 1981
Printed in Great Britain. All rights reserved

0039-9140/81/070431-05$02.00/0
Copyright © 1981 Pergamon Press Ltd

CATALYTIC INFLUENCE OF Cl^-, Br^-, I^- AND SCN^- ON THE CYCLIC VOLTAMMETRIC BEHAVIOUR OF Sb(III)

H. VERPLAETSE, P. KIEKENS, E. TEMMERMAN and F. VERBEEK

Laboratory of Analytical Chemistry, State University Ghent, J. Plateaustraat 22, 9000 Ghent, Belgium

(*Received* 26 *November* 1980, *Accepted* 21 *January* 1981)

Summary—The electrocatalysis of the reduction of Sb(III) ions at a mercury electrode by Cl^-, Br^-, I^- and SCN^- ions and its dependence on the hydrogen-ion concentration has been studied in 4*M* (H, Na)ClO_4 solutions by cyclic voltammetry. The electrocatalytic capacity increases considerably in the order $Cl^- < SCN^- < Br^- < I^-$ and a ligand-bridging mechanism is probably involved. Increasing the acidity at constant bridging-ligand concentration enhances the reaction rate. This can be explained by assuming that the influence of the hydrogen-ion concentration on the bridged activated complex is the same as on the Sb(III) complexes present in the bulk of the solution. From an analytical point of view it is important that the reduction of Sb(III) ions at a mercury electrode proceeds reversibly in the presence of Cl^-, Br^-, I^- or SCN^- ions.

In aqueous solutions of oxyacids Sb(III) ions are irreversibly reduced at a mercury electrode. The reduction rate increases when comparatively small amounts of halide ions are present.[1,2]

In a previous communication[3] we reported on the polarographic and cyclic voltammetric behaviour of Sb(III) in 4*M* H(Cl, ClO_4) with $C_{Cl^-} \geq 0.1M$. The reduction proceeds reversibly and is accompanied by significant reactant adsorption, which was studied in detail by chronocoulometry.

It was thought worthwhile to investigate the electrocatalytic effect and its dependence on the concentration of hydrogen ions in solution in the presence of Cl^-, Br^-, I^- and SCN^- ions. Use was made of cyclic voltammetry, which provides an efficient criterion for reversibility through the measurement of the separation of the anodic and cathodic peak potentials.

EXPERIMENTAL

Cyclic voltammetric measurements were carried out with the apparatus described earlier.[4] The working electrode was a sitting mercury drop electrode (Beckman 39016) with a volume of 2 μl. The other electrodes and cell were also described previously.[3] Stock solutions of Sb(III) were prepared by dissolving analytical grade Sb_2O_3 in the appropriate supporting electrolyte. The water used was freshly generated by a Milli-Q system (Millipore Inc.).

Br^-, I^- and SCN^- ions were added to the various 4*M* (H, Na)ClO_4 solutions, as their sodium salts. For Cl^- ions to bring about a substantial acceleration of the reaction rate considerably larger amounts are necessary than for the other anions. In order to keep the hydrogen-ion concentration in the solution constant, Cl^- ions were added to the 4*M* (H, Na)ClO_4 solutions under study as 4*M* (H, Na)Cl with the same relative cation composition. In a preliminary experiment sodium chloride was added instead of hydrochloric acid to find whether there would be any change in the electrocatalytic effect, but no significant influence was found.

Because of the proximity of the Sb(III)/Sb(Hg) waves and the onset of the oxidation curve of mercury, which shifts towards more negative potentials in the presence of the added ions, certain precautions had to be taken. When mercury is oxidized in the presence of Br^- or I^- ions, at the starting potential of the cyclic voltammetric curve, Hg_2Br_2 and Hg_2I_2 are formed and accumulate at the electrode surface. When they are reduced during the subsequent scan an excess of anions is present at the electrode surface ($Hg_2X_2 + 2e \rightleftharpoons 2Hg + 2X^-$), which would affect the results. Therefore the initial potentials of the voltammetric curves were made as negative as possible and applied to the cell just before the start of the potential sweep. Between the recordings and during the renewal of the sitting mercury drop, the working electrode was disconnected from the voltammetric circuit.

RESULTS

Cyclic voltammetric curves of Sb(III) were recorded in 4*M* (H, Na)ClO_4 solutions at a constant scan-rate of 0.1 V/sec in the presence of varying amounts of Cl^-, Br^-, I^- and SCN^- ions. The cathodic (E_p^c) and anodic (E_p^a) peak potentials were evaluated as a function of the concentration of these anions in the cell solution.

For a reversible system at 25° the peak separation, $E_p^c - E_p^a = \Delta E_p$, has a minimal value of $58/n \approx 20$ mV for a 3-electron reaction. This value becomes larger with decreasing reaction rate. The halide or SCN^- concentration for which reversible behaviour was attained was used as a quantitative criterion for the electrocatalytic capacity of the anion.

Results are given in Figs. 1–3, in which the observed peak separations are plotted as a function of the logarithm of the halide concentration. When the concentration of electrocatalytic anion increases, ΔE_p decreases as expected. At the lower anion concentrations the curves are linear or have at least a linear

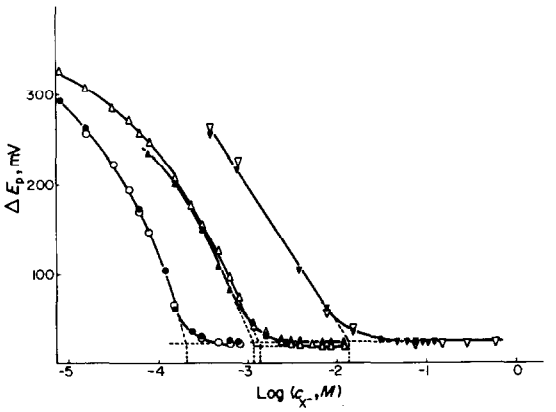


Fig. 1. Dependence of the cyclic voltammetric peak separation in 4*M* $HClO_4$ on the logarithm of c_{X^-}, the added concentration of electrocatalytic anion. X^- = Cl^-: 0.1m*M* (▽) and 1m*M* (▼) Sb(III); X^- = Br^-: 0.1m*M* (○) and 0.5m*M* (●) Sb(III); X^- = SCN^-: 0.1m*M* (△) and 1m*M* (▲) Sb(III).

section which can be extrapolated. The intersection point with the line drawn through the ΔE_p points obtained at larger anion concentrations was used as a quantitative measure for the electrocatalytic capacity. These points are summarized in Table 1.

Because of the interference of the reduction of Hg_2I_2 no reliable quantitative results could be obtained for solutions containing I^- ions. Qualitatively, however, I^- ions proved to be more electrocatalytically active than Br^- ions.

In solutions containing comparatively large concentrations of Cl^- and Br^- ions a sharp second cathodic peak was superposed on the normal peak and prevented the measurement of E_p^c. When the Sb(III) concentration was higher, smaller amounts of Br^- ions were necessary to give rise to this second peak. In solutions containing Br^- ions the Sb(III) concentration was therefore kept below 0.5m*M*, which allowed the use of Br^- ion concentrations up to 0.8m*M* in 4*M* perchloric acid. The interfering peak also occurred in the presence of Cl^- ions when the

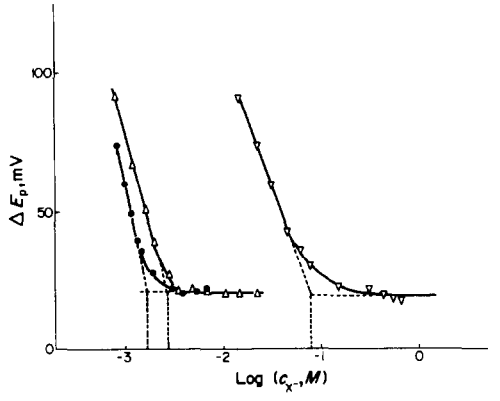


Fig. 2. Dependence of the cyclic voltammetric peak separation in 0.5*M* $HClO_4$ + 3.5*M* $NaClO_4$ on the logarithm of c_{X^-}, the added concentration of electrocatalytic anion. $c_{Sb(III)}$ = 0.1 m*M*; X^- = Cl^- (▽); Br^- (●) and SCN^- (△).

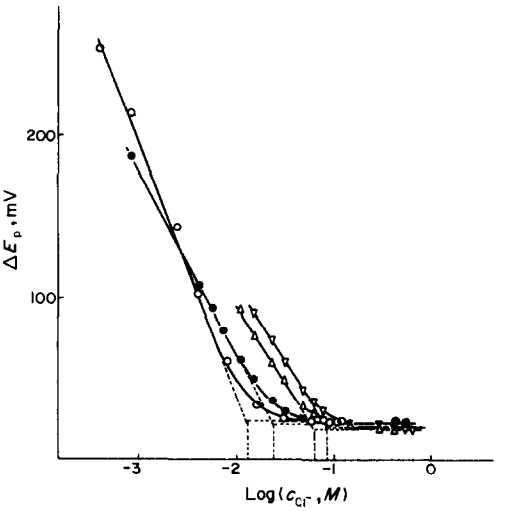


Fig. 3. Dependence of the cyclic voltammetric peak separation on the logarithm of the concentration of Cl^- ions added to 4*M* $HClO_4$, 1m*M* Sb(III) (○); 2*M* $HClO_4$ + 2*M* $NaClO_4$, 0.5m*M* Sb(III) (●); 1*M* $HClO_4$ + 3*M* $NaClO_4$, 0.1m*M* Sb(III) (△); and 0.5*M* $HClO_4$ + 3.5*M* $NaClO_4$, 0.1m*M* Sb(III) (▽).

concentration of acid was 1*M* or less, which could be prevented by the use of sufficiently low Sb(III) concentrations (0.1m*M*).

It follows from Figs. 1 and 2 and Table 1 that the electrocatalytic capacity increases considerably in the order Cl^- < SCN^- < Br^- and is almost independent of the Sb(III) concentration. With increasing halide concentration in the "reversible" (Figs. 1–3) range, E_p^c shifted towards more negative potentials for Cl^- ions, but remained constant for Br^- and SCN^- ions. For Cl^- this can be explained by increased complexation of Sb(III). The concentrations of Br^- and SCN^- ions are too low compared to the concentration of Sb(III) for complex-formation effects to be detectable in this way.

The influence of the hydrogen-ion concentrations was investigated in more detail in chloride-containing electrolytes and is shown in Fig. 3 and the second column of Table 1. It is clear that with decreasing acidity a larger amount of chloride needs to be present in order to cause reversible behaviour. The relevant data in Figs. 1 and 2 and Table 1 show that the same is true for Br^- and SCN^- ions. However the effect of the acidity on the electrocatalytic capacity of SCN^- ions is smaller than for Cl^- and Br^- ions.

Finally it should be mentioned that at the lowest concentrations of catalytic anions a double cathodic peak appeared, especially at lower hydrogen-ion concentrations. A small pre-peak occurred at more positive potentials than the main peak. With increasing concentration of catalytic anion the pre-peak grew at the expense of the original main peak. Eventually only the pre-peak remained, and became the reversible peak, when the halide concentration was further increased. In Figs. 1–3 ΔE_p values are given only for anion concentrations for which the peak at more

Table 1. Summary of intersection points in Figs. 1–3

Electrolyte composition	$[Cl^-]$,*M*	$[Br^-]$,*M*	$[SCN^-]$,*M*
4*M* $HClO_4$	1.3×10^{-2}	2.2×10^{-4}	1.2×10^{-3}
2*M* $HClO_4$ + 2*M* $NaClO_4$	2.6×10^{-2}	—	—
1*M* $HClO_4$ + 3*M* $NaClO_4$	6.5×10^{-2}	—	—
0.5*M* $HClO_4$ + 3.5*M* $NaClO_4$	8.2×10^{-2}	1.7×10^{-3}	2.7×10^{-3}

positive potentials was larger than the original main peak.

DISCUSSION

Electrocatalysis by anions has been attributed to several phenomena[5,6] such as double-layer effects, the formation of complexes in the bulk of the solution or in the double layer, and ligand bridging.

That electrocatalysis is due to double-layer effects is, however, very improbable, since the observed accelerations of the reaction rate are too high.[6,7] This will be especially valid in supporting electrolytes of high ionic strength, since double-layer effects decrease with increasing ionic strength of the solution.

A Br^- ion concentration of about 0.22m*M* is sufficient to make the reduction of 1m*M* Sb(III) reversible but allows only a small fraction of the Sb(III) present to be complexed. Furthermore the concentration of catalytic anion necessary to cause reversible behaviour does not depend on the bulk concentration of Sb(III). These considerations are not compatible with bulk-complexation effects as the cause for the observed electrocatalysis.

Surface-complexation effects between Sb(III) and adsorbed anions are not probable either, *e.g.*, because the electrocatalytic capacity of SCN^- ions is considerably higher than that of Cl^- ions, unlike the amounts specifically adsorbed,[8] and also the stabilities of their complexes with Sb(III) are not expected to differ widely. As far as we know, stability constants for the complexes of Sb(III) with SCN^-, Br^- and I^- ions have not been published. The fact that F^- ions are not electrocatalytically active,[1,9] although they form much stronger complexes than Cl^- ions with Sb(III)[1] makes it improbable that electrocatalysis would be caused solely by complexation effects.

The absence of electrocatalysis with F^- ions, which are not specifically adsorbed at the electrode, while I^- and Br^- ions enhance the reduction rate even when only very small amounts are present, offers evidence that a ligand-bridging mechanism is involved. This is further substantiated by the fact that the electrocatalytic capacity, unlike the expected tendency for complexing Sb(III),[10] drastically increases in the order $Cl^- < Br^- < I^-$, in which the specific adsorption also increases.[11] This mechanism, in which adsorbed anions are directly involved in the electron-transfer between metal ion and electrode can be represented as

$$Sb^{3+} + pX^-_{ads} \longrightarrow SbX^{(3-p)+}_{p,ads} \xrightarrow{3e} Sb(Hg) + pX^-_{ads} \quad (1)$$

in which possible complexation and/or solvation of reactant and reaction product have been omitted for clarity.

Indirectly the validity of the anion-bridging theory is also substantiated by the fact that the acceleration of the reduction is paralleled by a corresponding speeding up of the oxidation reaction, which involves the oxidation of antimony amalgam. In the latter case both double-layer and complexation effects in solution have to be excluded because the amalgam will not be influenced by the composition of the supporting electrolyte and there is no double-layer at the amalgam side of the electrode–solution interface.

Expressing the reduction rate at constant potential in terms of a rate constant and the activities of bridging anion and metal ion at the electrode surface, we can write

$$v = k_{X^-} a^p_{X^-,ads} a_{Sb^{3+}} \quad (2)$$

where k_{X^-} is a constant which may depend on the kind of bridging anion.

According to Table 1, with decreasing hydrogen-ion concentration larger concentrations of the bridging anions have to be present in order to provoke the same electrocatalytic effect. In the positive-potential region of interest, the substitution of H^+ by Na^+ ions in the various 4*M* (H, Na)ClO_4 solutions will have only a negligible influence on the composition of the double-layer and the origin of the pH-dependence of the electrocatalytic effect should in the first instance be looked for in the state in which the Sb(III) is present in solution.

According to Jander and Hartmann,[12] in perchloric acid medium Sb(III) is present as $Sb(H_2O)^{3+}_x$ and SbO^+ [or $Sb(OH)^+_2$], the transition between the two forms being fast. The bridging could be hindered, then, if it requires an Sb–O bond to be broken.

In this respect it is interesting to note that in the case of Bi(III), the voltammetric behaviour of which is quite similar to that of Sb(III), only the hydrated ion gives rise to electrocatalysis.[13] This could be proved because the equilibrium between both species present in perchloric acid medium, $Bi(H_2O)^{3+}_x$ and $BiOH^{2+}$, is established only very slowly. As a result the reduction of Bi(III), in contrast to the behaviour of Sb(III), remains pH-dependent even after it has been made reversible by the addition of a sufficient amount of bridging anion.

Accordingly, if it is assumed that only hydrated Sb(III) would be involved in the electrocatalysed reduction reaction, the complete reaction can be

written as

$$Sb(OH)_2^+ \rightleftharpoons Sb_{aq}^{3+} \xrightarrow{pX_{ads}^-} SbX_{p,ads}^{(3-p)+} \xrightarrow{3e} Sb(Hg) + pX_{ads}^- \quad (3)$$

where a possible additional complexation of the Sb(III) species has been omitted for clarity.

Equation (2) then has to be modified, and when it is assumed that the first reaction on the left-hand side of equation (3) is in equilibrium, it can be written as

$$v = k' a_{X^-,ads}^{p} a_{H^+}^{2} \cdot a_{Sb(OH)_2^+} \quad (4)$$

where

$$k' = k_{X^-} \cdot K \quad \text{and} \quad K = a_{Sb_{aq}^{3+}} / a_{Sb(OH)_2^+} a_{H^+}^2.$$

The experimental results are in qualitative agreement with equation (4), as at higher pH a larger surface activity of adsorbed anions will be necessary to keep the reduction rate constant. A more quantitative treatment of the results was not possible because of the lack of activity data, and because of potential effects resulting from the fact that the presence of the various bridging ligands affects the peak potentials in a different way when the pH is changed. For example, on passing from 4*M* perchloric acid to 0.5*M* perchloric acid + 3.5*M* sodium perchlorate (Table 1) 6.3 times as much Cl^- or 7.7 times as much Br^- has to be added to make the reduction reversible. However, when the hydrogen-ion concentration is decreased the reduction wave of Sb(III) shifts to a more negative potential in presence of Br^- ions than in presence of Cl^- ions and the corresponding smaller specific adsorption of Br^- ions has to be compensated by a larger bulk Br^- ion concentration.

When the same comparison is made for SCN^- ions, only 2.3 times as much SCN^- is needed in 0.5*M* perchloric acid + 3.5*M* sodium perchlorate (Table 1). The fact that HSCN is a less strong acid is not involved, because it is still largely dissociated ($\geq 96\%$) in 4 and 0.5*M* acid solutions.[14] The large divergence from the behaviour in Cl^- and Br^--containing electrolytes can hardly be explained by activity and/or potential effects in the sense described before. Therefore the explanation of the influence of the acidity of the solution on the electrocatalytic effect by the assumption that only the hydrated ion is prone to electrocatalysis seems to be incorrect.

Generally it was found that when the bridging-ligand concentration was low (*e.g.*, $c_{Cl^-} \leq 0.1M$) the reduction takes place at more positive potentials with increasing hydrogen-ion concentration. For large chloride concentrations (*e.g.*, $c_{Cl^-} \geq 1M$) a shift in the negative direction was observed. Similar observations were made by Pantani and Desideri[15] and Biernat *et al.*[16,17] This also manifests itself in the dependence of the stability constants of Sb(III)–halide complexes on the acidity.[15,16] These effects can be explained in the following way. When the concentration of bridging anion is low, Sb(III)–anion complexes with low coordination number prevail and $SbCl_x(OH)_y^{3-x-y}$ compounds are formed. With increasing hydrogen-ion concentration this complexation with hydroxide ions is repressed. On the other hand, when the anion concentration is large, the Sb(III)–anion complexes are mainly negatively charged because of the high coordination,[3] and $H_ySbCl_x^{3+y-x}$ species are formed, The experiments of Pantani and Desideri[15] indicate that protonation with 1–3 hydrogen ions occurs, corresponding to the presence of $HSbCl_4$, H_2SbCl_5 and H_3SbCl_6 in solution. With increasing hydrogen-ion concentration this protonation is enhanced. It is clear that the complexation of Sb(III) is not simple and that mixed complexes are common.

Reconsidering the effect of acidity on the electrocatalysis, it is obvious it may be assumed that the influence of hydrogen-ion concentration on the complexation in solution will also hold for the bridged activated complex. The stability of this complex then will decrease with decreasing acidity, in agreement with the experimental results. In equation (2) the acidity then directly affects the constant k_{X^-}, which is correlated to the stability of the bridged activated complex.

The fact that the electrocatalytic effect of SCN^- ions is less dependent on hydrogen-ion concentration should be accompanied then by a similar dependence of the complexation of Sb(III) with SCN^- ions in solution. Unfortunately this could not be verified because no data about the complexation of Sb(III) by SCN^- ions and its dependence on pH are available.

Additional evidence in support of the hypothesis put forward can be found in the electrocatalytic effect of the bridging anions upon the reverse reaction, which involves the oxidation of antimony amalgam, and its dependence on hydrogen-ion concentration. It was found that the anodic reaction rate at constant concentration of bridging anion also decreases with decreasing acidity. When an antimony atom is oxidized and leaves the mercury electrode it will be stabilized by the specifically adsorbed anions and a bridged complex will be formed. This complex will then be influenced by the hydrogen-ion concentration in the same way as for the reduction. An intermediate can be imagined in which antimony orbitals overlap with those of the adsorbed ion as well as with those of the electrode. Indeed, such a situation is also likely to occur in the case of the cathodic reduction, rather than the hypothesis that the rate-enhancement is due to the electron-conducting property of the bridging ion, which was suggested by Heyrovský.[18]

The oxidation reaction can then be written as

$$Sb(Hg) + pX_{ads}^- \xrightarrow{3e} SbX_{p,ads}^{(3-p)+} \longrightarrow Sb_{aq}^{3+} + pX_{ads}^- \quad (5)$$

in which possible additional complexation and/or solvation steps have been omitted.

The reaction rate can be expressed as

$$v = k'_{X^-} a^{\beta}_{X^-,ads} a_{Sb(Hg)} \quad (6)$$

Equations (2) and (6) reflect the gradual increase of the reduction and oxidation rate at constant potential with the surface activity and thus the bulk concentration of the bridging anion.

Analytical significance

In polarographic and voltammetric analysis a sufficiently fast electron-transfer rate is desirable. In classical d.c. polarography irreversibility causes the shape and half-wave potential of the wave to change, but the limiting current remains the same, so from an analytical point of view the influence of reversibility is minor. When techniques such as linear sweep voltammetry, a.c. polarography or differential pulse polarography are used, however, the peaks are sharper and peak-currents higher for a reversible electrochemical reaction. This improves both the sensitivity of the determination and the resolution of the peaks. Hence it is important that the reduction of Sb(III) at a mercury electrode is reversible in presence of Cl^-, Br^-, I^- or SCN^- ions.

Acknowledgement—The authors wish to thank the N.F.W.O. for financial support.

REFERENCES

1. A. M. Bond, *J. Electrochem. Soc.*, 1970, **117**, 1145.
2. A. A. Moussa, M. M. Abou-Romia and H. A. Ghaly, *Electrochim. Acta*, 1974, **19**, 957.
3. H. Verplaetse, P. Kiekens, E. Temmerman and F. Verbeek, *J. Electroanal. Chem.*, accepted for publication.
4. *Idem, ibid.*, 1980, **115**, 235.
5. A. M. Bond, *Electrochim. Acta*, 1972, **17**, 769.
6. R. de Levie, *J. Electrochem. Soc.*, 1971, **118**, 185C.
7. L. R. Taylor, B. A. Parkinson and D. C. Johnson, *Electrochim. Acta*, 1975, **20**, 1005.
8. H. Wroblowa, Z. Kovac and J. O'M. Bockris, *Trans. Faraday Soc.*, 1965, **61**, 1523.
9. P. W. West, J. Dean and E. J. Breda, *Collection Czech. Chem. Commun.*, 1948, **13**, 1.
10. F. A. Cotton and G. Wilkinson, *Advanced Inorganic Chemistry*, 3rd Ed., Wiley, New York, 1972.
11. P. Delahay, *Double Layer and Electrode Kinetics*, Interscience, New York, 1966.
12. G. Jander and H. J. Hartmann, *Z. Anorg. Allg. Chem.*, 1965, **339**, 239, 256.
13. S. Lipscey, *Thesis*, Rutgers University, New Jersey, 1972.
14. D. D. Perrin, *Dissociation Constants of Inorganic Acids and Bases in Aqueous Solution*, IUPAC, Butterworths, London, 1969.
15. F. Pantani and P. G. Desideri, *Gazz. Chim. Ital.*, 1959, **89**, 1360.
16. J. Biernat, B. Ziegler, M. Zrałko and P. Kondziela, *J. Electroanal. Chem.*, 1975, **63**, 444.
17. P. Kondziela and J. Biernat, *Rocz. Chem.*, 1975, **49**, 1489.
18. J. Heyrovský, *Disc. Faraday Soc.*, 1947, **1**, 212.

Talanta, Vol. 28, pp. 437 to 440, 1981
Printed in Great Britain. All rights reserved

0039-9140/81/070437-04$02.00/0
Copyright © 1981 Pergamon Press Ltd

X-RAY FLUORESCENCE DETERMINATION OF COBALT ON POLYURETHANE FOAM

A. CHOW, G. T. YAMASHITA and R. F. HAMON
Department of Chemistry, University of Manitoba, Winnipeg, Manitoba, Canada

(*Received* 31 *December* 1980. *Accepted* 21 *January* 1981)

Summary—Although the extraction and preconcentration of several species by polyurethane foam have been reported, very few methods have included a direct determination of the component on the polymer. Cobalt thiocyanate is highly extractable by polyether polyurethane from solutions of 3*M* NH_4Cl and 1*M* NH_4SCN. After extraction of the cobalt the foam discs can be analysed by X-ray fluorescence, which gives a linear response for samples treated identically. Cobalt at levels as low as 0.05 ppm can be quantitatively extracted and cobalt determined in the presence of several other metal ions.

The extraction and preconcentration of various metals from aqueous solution by polyurethane foam has received considerable investigation[1,2] over the past few years because of the high extraction, large capacity and low flow-resistance. This method requires careful control of the solution composition to ensure efficient extraction and some degree of component separation. Several authors have used polyurethane foam as a preconcentration or separation method before recovery for analysis by atomic-absorption spectrometry or radiochemical analysis. Others have determined only the extraction capability of the foam, by determination of the metal concentration in the solution before and after extraction.

The extraction of cobalt thiocyanate by polyurethane foam has been reported by Braun *et al.*,[3–5] Hamon[6,7] and Maloney *et al.*[8] This method has a high distribution coefficient and is a fairly rapid process which may be applied for a variety of metals.

The direct determination of the extracted component in the polyurethane foam has seldom been reported. Radioiodine has been extracted from aqueous solution[9–11] and from milk[12] into polyurethane foam holding a hydrophobic immobilizing phase containing iodine. These foams were analysed directly for iodine-131 by gamma spectrometry.

Schiller and Cook[13] investigated the extraction of ionized, colloidal and very finely precipitated gold with polyurethane foam. Although most of the results were based on measurements of gold-198 tracer left in solution, neutron-activation analysis of the gold-containing foam was used for a few samples. This required either a 4- or 12-day cooling period and although a very sensitive trace technique, did not give fully consistent results. Tanaka *et al.*[14] extracted an alkylbenzenesulphonate–Crystal Violet complex into polyurethane foam and estimated the concentration by direct visual comparison with a series of standards, or by spectrophotometry after recovery with methanol. Open-cell polyurethane foam loaded with various organic reagents has been used to detect metal ions directly by the colour formed.[15] With this technique, a direct comparison could be made with extracted standards, or, with a foam column system, the length of the coloured region could be related to the original solution concentration. The determinations of zinc and lead with dithizone, copper with rubeanic acid, and cobalt thiocyanate with Amberlite LA-1 were reported.

Although neutron-activation analysis can generally be used for the direct determination of many elements isolated on polyurethane foam, the difficulties involved in standard preparation and in handling radioactive materials, plus the restricted availability of irradiation facilities, limit the general application of such a method. X-Ray fluorescence (XRF) equipment also has a wide range of application and is more commonly available to the analyst. The sensitivity of the particular analysis depends on the X-ray equipment available and the element sought. This paper describes the direct XRF determination of cobalt on polyurethane foam, after its extraction from thiocyanate solution.

EXPERIMENTAL

Apparatus

A Perkin–Elmer model 306 atomic-absorption spectrometer with a cobalt hollow-cathode lamp (Cathodeon Ltd.) was used to determine the cobalt extraction for the majority of the samples. The wavelength was set at 240 nm with a slit-width setting of 4 (band-pass 0.7 nm). Nickel, iron, copper, lead and zinc lamps were used as required.

A Baird-Atomic model 530 gamma-spectrometer was used to measure the activity of ^{60}Co solutions.

Direct X-ray analysis of the foam samples was performed with a New England Nuclear NER-496 X-ray fluorescence exciter system coupled to a Tennelec TC909 power supply. A Nuclear Semiconductor 512 amplifier, usually set at coarse gain 1, provided an increased signal for display on a Tracor Northern TN-1705 pulse height analyser. The NER-496 XRF exciter system used a 0.5-Ci ^{241}Am source distributed in a shielded annulus placed around the Si(Li) detector. Normally, each foam disc was placed on a 6.1 × 10^{-4}-cm thick Mylar film 2 cm above

the beryllium window of the detector. One series of foams was analysed on an Applied Research Laboratories multichannel X-ray quantometer, with a tungsten X-ray tube.

Polyurethane foams of the polyether type, 0.48 and 0.64 cm thick, were obtained from local commercial sources. The foams were squeezed in cylindrical flasks with Pyrex plungers closely fitted through the flask covers. Chromatography columns (25 mm outer diameter) with sintered-glass discs and plastic stopcocks were used for flow-through extractions.

Reagents

A standard 1000-ppm cobalt solution was prepared by dissolving 1.002 g of the metal (99.8% pure) in a little 6*M* hydrochloric acid, made up to 1 litre of solution containing 1% v/v of the acid, and diluted for use in standards and extraction solutions. Solutions of 5*M* ammonium chloride and 5*M* ammonium thiocyanate were prepared in water. All chemicals were of analytical reagent grade, except as noted, and the water used was distilled and demineralized.

Procedure

The polyurethane foams were soaked in 1% hydrochloric acid for 15 hr with occasional squeezing, dried between clean paper towels, and then extracted in a Soxhlet with acetone for 6 hr. The foams were then squeezed and air-dried and cut into circular discs by hand, with sharpened tubular bits.

Initially, clean foam discs (approx. 3.5 cm in diameter) were placed in the cylindrical flasks with solutions containing ammonium thiocyanate and final cobalt concentrations of 1–5 μg/ml. The preliminary studies showed that although the cobalt was not effectively extracted and thus did not provide a significantly sensitive method by XRF determination, the method was at least feasible.

Previous work by Hamon[6,7] has shown that high ionic strength improves the extraction of the cobalt-thiocyanate complex. Solutions containing 30 ml of 5*M* ammonium chloride, 10 ml of 5*M* ammonium thiocyanate, and appropriate volumes of 100-ppm cobalt solution, were diluted with water to 50 ml to give final cobalt concentrations of 0–5 μg/ml in 3*M* ammonium chloride/1*M* ammonium thiocyanate. Smaller foam discs (about 1.8 and 2.3 cm in diameter) were squeezed continuously in these solutions for 30 min. After squeezing, the extracted samples and similar standards were analysed for cobalt concentration by atomic-absorption spectrometry. After the foams had been dried in air, each disc was centred on Mylar film held about 2 cm over the detector for X-ray analysis. The spectra were accumulated for 100 sec and the peak height was integrated over the region from 6.6×10^3 to 7.4×10^3 eV. Each sample was integrated eight times (four times on each side), the values were averaged, and the average blank was subtracted to give the final count. The integrated counts obtained from each side of the foams showed a difference of less than 3%.

A foam disc containing 250 μg of cobalt was placed at various heights, 1.8–2.5 cm, above the detector but there was no significant variation in the results.

The effect of volume was studied with solutions of 50, 75, 100 and 150 ml containing 0.5 ml of 100-ppm cobalt solution with 20 ml of a radioactive ^{60}Co solution in 3*M* ammonium chloride/1*M* ammonium thiocyanate. Aliquots of 15 ml of each sample were counted to determine the initial ^{60}Co levels and then returned to their respective solutions, with a foam disc weighing 44 ± 3 mg. After 10 min of continual squeezing the foams were removed to prevent continued extraction and 15-ml aliquots of solution were measured again for their activity. The aliquots and foams were then returned to their solutions for another 10 min of extraction and the procedure was repeated for a total extraction time of 30 min in the case of the 50- and 75-ml solutions and of 60 min for the 100- and 150-ml volumes. All activities were corrected for background.

Table 1. Effect of time on extraction

Time, min	Extraction %			
	50 ml*	75 ml*	100 ml*	150 ml*
10	97.8	91.7	74.3	61.2
20	99.7	98.7	83.8	72.1
30	99.7	99.0	93.3	86.0
40			96.0	91.3
50			96.9	93.6
60			97.1	94.3

* Volume of 1.0-ppm cobalt solution in 3*M* NH_4Cl/1*M* NH_4SCN, extracted with 44 ± 3 mg of polyurethane foam.

It is evident from Table 1 that cobalt is more readily extracted from smaller volumes, since after 20 min of squeezing, 99% was extracted from the 50- and 75-ml solutions while only 97% or less was extracted after 60 min from the larger volumes. To obtain quantitative extraction with these or greater volumes of solution would require more time or larger weights of foam.

To determine the effective concentration range of this technique a series of solutions consisting of 50 ml of 3*M* ammonium chloride/1*M* ammonium thiocyanate containing 2.5–100 μg of cobalt and some ^{60}Co tracer were extracted for 30 min with foam discs approximately 2.3 cm in diameter (weighing 44 ± 3 mg). The data showed that for this entire concentration range, 30 min of squeezing was sufficient time to yield 99.5 ± 0.2% extraction.

Solutions with cobalt concentrations of 0.25–2.5 μg/ml but without radioactive tracer were similarly extracted. The atomic-absorption measurements showed a high degree of cobalt extraction for all the samples studied, and although the sensitivity of this determination at low concentrations was poor, the previous study with ^{60}Co had indicated a very high extraction. The calibration graph of the XRF data *vs.* cobalt concentration was linear, the equation being cps = 5.69 × initial Co concentration (μg/ml) + 0.75.

Six foam discs 2.8 cm in diameter and 0.48 cm thick were squeezed in 50-ml solutions containing 0–5 μg/ml cobalt and 3*M* in ammonium chloride and 1*M* in ammonium thiocyanate. A second experiment used foams of 0.64 cm thickness, while all other conditions remained constant. Both series showed high extraction of cobalt, as evaluated by atomic-absorption spectrometry, and produced linear calibration curves for X-ray activity *vs.* cobalt concentration, as shown in Fig. 1.

A set of five foam discs was prepared from 1–5 μg/ml cobalt solutions. Each of the discs from these solutions was counted separately by XRF for 100 sec. To observe the effect of foam thickness, the disc from the 5-μg/ml solution was placed on top of each of the other foams in turn and the pair analysed by XRF. The X-ray data in Table 2(*a*) from both of these trials showed a linear variation with initial concentration, with a slight enhancement relative to the sum of the counts expected for the paired foams. This suggests that the geometry was not ideal and that thicker foams could be used somewhat more effectively for preconcentration and determination of the cobalt. Foam discs were used to extract cobalt from each of four similar solutions containing 5 μg mL. As well as being counted separately on both sides, the foams were stacked in combinations of two, three and four and counted. The data in Table 2(*b*) show an increasing deviation from the expected values as the number of stacked foam discs was increased, because of the decrease in efficiency of the counting geometry.

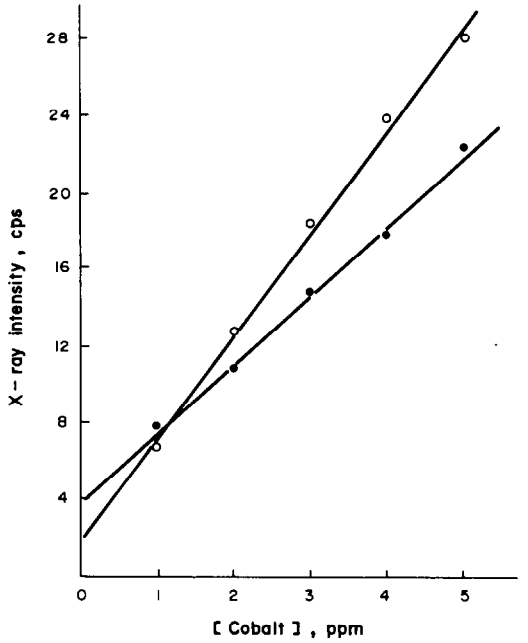


Fig. 1. (●) 0.48-cm thick foams weighing 33.0 ± 0.8 mg; (○) 0.64-cm thick foams weighing 44.4 ± 0.9 mg, 50 ml of cobalt solution in 3*M* NH_4Cl/1*M* NH_4SCN, extracted for 30 min.

Copper, iron, lead, zinc and nickel at the 1-μg/ml level were tested for interference in the analysis of 50-ml of 1-μg/ml cobalt solutions which were 3*M* in ammonium chloride and 1*M* in ammonium thiocyanate. Blanks containing 1 μg/ml of the potential interferents but no cobalt were also tested. The ammonium chloride used here was a technical grade and therefore its solution was premixed with ammonium thiocyanate solution (to give 3:1 molar ratio) and passed through a column of polyurethane foam plugs in order to remove any excess of iron or zinc, as thiocyanate complexes. All extractions were done for 30 min with continuous squeezing. The X-ray fluorescence analysis was run with a coarse gain setting of 2 to spread the spectra for easier study, with integration between 6.7×10^3 and 7.4×10^3 eV for cobalt, 6.2×10^3 and 7.4×10^3 eV for iron, 7.4×10^3 and 7.8×10^3 eV for nickel, 8.0×10^3 and 8.4×10^3 eV for copper, and 8.4×10^3 and 9.0×10^3 eV for zinc. No lead peaks were observed at these settings. The extraction of cobalt and each interferent was determined by atomic-absorption spectrometry. All samples examined showed 100% extraction of cobalt, with the extraction of the interferent elements ranging from 0% for nickel to 90% for iron. The determination of cobalt was unaffected by the presence of any of these metals.

X-Ray fluorescence was also used in the secondary emission mode. The ^{241}Am γ-source was inverted to cause monochromatic X-rays to be emitted by the pure target metal and these X-rays were used to cause X-ray fluorescence of the sample. The targets used were molybdenum, tin, and dysprosium. Each target produced significantly lower X-ray counts for the cobalt samples of foam and a lower signal-to-background ratio than did direct irradiation of samples of foam.

In addition to analysis with the energy-dispersive NER-496 exciter system, the 0.25–2.5 μg/ml samples were run on an Applied Research Laboratories X-ray quantometer unit with a wavelength-dispersive function, to obtain higher sensitivity. The tube current was set at 27.3 mA and the tube voltage was 37.5 kV. Each foam sample was placed in a specially designed holder made from a 5 × 5 cm square of 1.5-mm thick plastic with a 2.3 cm (diameter) hole drilled in its centre. The hole was covered with Mylar film, which prevented any direct contact between the samples and the X-ray tube window. The air was evacuated from the sample chamber before readings were taken. The maximum scale reading (100 mV) was set for the foam from a 2.5-μg/ml solution and all measurements were made in units of mV/50 sec. The results showed a linear relationship between cobalt concentration and X-ray measurements. The sensitivity was increased about 10 fold, as indicated by a signal-to-noise ratio of 2.2 for this system as compared to 0.2 for the XRF exciter system, both at the 0.25-ppm cobalt level.

Passive extractions with a flow-through system could also be done by using chromatography columns with sintered-glass discs and foams of the same diameter as the column. With 0.64-cm thick foams having an average weight of 44 ± 3 mg, 50-ml aliquots of 3*M* ammonium chloride/1*M* ammonium thiocyanate solutions with cobalt concentrations from 0.25 to 2.0 μg/ml were run through the foam twice at a flow-rate of approximately 1 ml/min. The extraction of cobalt was quantitative, as determined by atomic-absorption measurements, and the foams were quite suitable for XRF analysis.

DISCUSSION

The direct determination of cobalt thiocyanate on polyurethane foam by X-ray fluorescence has been found to be both quantitative and qualitative. Results show linear calibration over the cobalt concentration range from 0.25 to 2.5 ppm. The lowest concentration studied, 0.05 ppm, gave 99% extraction over a 30-min period, which suggests that cobalt at even lower concentrations could be extracted provided that larger volumes of solution, thicker foams and longer extraction times were used. Use of an X-ray quantometer gave higher sensitivity, and direct analysis at the ng/ml level should be possible.

Table 2. Effect of various foam combinations

	Original cobalt concentration, *ppm*	X-Ray fluorescence, *cps*	
		Expected	Found
(*a*)	1.0	—	6.8
	2.0	—	13.7
	3.0	—	19.8
	4.0	—	27.0
	5.0	—	32.0
	5.0 + 1.0*	38.8	44.0
	5.0 + 2.0	45.7	52.3
	5.0 + 3.0	51.8	58.3
	5.0 + 4.0	59.0	65.3
(*b*)	5.0	—	25.4
	5.0	—	26.1
	5.0	—	26.9
	5.0	—	26.6
	5.0 + 5.0	51.5	46.5
	5.0 + 5.0 + 5.0	78.4	56.1
	5.0 + 5.0 + 5.0 + 5.0	105.0	62.4

Samples: 50 ml in 3*M* NH_4Cl/1*M* NH_4SCN.
Extraction time: 30 min.
Foam size: 44 ± 3 mg.
* Lower concentration foam placed closest to detector.

Nickel, lead, iron, zinc, and copper do not interfere with the cobalt determination since their complexes are either unstable or not extracted onto the foam, as in the case of nickel and lead, or they can be electronically separated according to their XRF energies, as seen with iron, zinc and copper. The electronic separation shows that this technique can be extended to other metal thiocyanates. The capacity of the foam is a limiting factor, however, since deviations in completeness of extraction and linearity of response occur when the total amount of thiocyanate complexes extracted (including interfering thiocyanates as well as cobalt thiocyanates) exceeds the capacity of the foam.

Several other metal complexes are known to be extractable by polyurethane foam and should also prove useful for direct determinations on the foam. Overall, the XRF method may be applied to a wide variety of elements preconcentrated by polyurethane foam, without need for a recovery procedure, and with few (if any) interferences.

Acknowledgement—This work was financially supported by the Natural Sciences and Engineering Research Council of Canada.

REFERENCES

1. T. Braun and A. B. Farag, *Anal. Chim. Acta*, 1978, **99**, 1.
2. G. J. Moody and J. D. R. Thomas, *Analyst*, 1979, **104**, 1.
3. T. Braun, A. B. Farag and M. P. Maloney, *Anal. Chim. Acta*, 1977, **93**, 191.
4. T. Braun and A. B. Farag, *ibid.*, 1978, **98**, 133.
5. T. Braun and M. N. Abbas, *ibid.*, 1980, **119**, 113.
6. R. F. Hamon, *Ph.D. Thesis*, University of Manitoba, 1981.
7. R. F. Hamon and A. Chow, *Abstracts 60th CIC Conference*, Montreal, Canada, 1977.
8. M. P. Maloney, G. J. Moody and J. D. R. Thomas, *Proc. Chem. Soc. Anal. Div.*, 1977, **14**, 244.
9. S. Palagyi and T. Braun, *J. Radioanal. Chem.*, 1979, **51**, 267.
10. S. Palagyi and E. Bila, *Radiochem. Radioanal. Lett.*, 1978, **32**, 87.
11. T. Braun and S. Palagyi, *Anal. Chem.*, 1979, **51**, 1697.
12. S. Palagyi and R. Markusova, *Radiochem. Radioanal. Lett.*, 1978, **32**, 103.
13. P. Schiller and G. B. Cook, *Anal. Chim. Acta*, 1971, **54**, 364.
14. T. Tanaka, K. Hiiro and A. Kawahara, *Bunseki Kagaku*, 1973, **22**, 523; *Chem. Abstr.* 1973, **79**, 87234.
15. T. Braun and A. B. Farag, *Anal. Chim. Acta*, 1974, **73**, 301.

Talanta. Vol. 28. pp. 441 to 446. 1981
Printed in Great Britain. All rights reserved

0039-9140/81/070441-06$02.00/0
Copyright © 1981 Pergamon Press Ltd

EXTRACTION AND PRECONCENTRATION OF COPPER FROM WATER, SOILS, LUBRICATING OILS AND PLANT MATERIALS AND ITS SUBSEQUENT DETERMINATION BY ATOMIC-ABSORPTION SPECTROPHOTOMETRY*

M. EJAZ†

Department of Applied Science, College of Engineering, King Abdul Aziz University, P.O. Box 1540, Jeddah, Saudi Arabia

SHAMUS-ZUHA, WASIM DIL, ANIS AKHTAR and SHAMIM A. CHAUDHRI

Pakistan Institute of Nuclear Science and Technology, Nilore, Rawalpindi, Pakistan

(*Received* 18 *February* 1980. *Revised* 9 *January* 1981. *Accepted* 19 *January* 1981)

Summary—The extraction and preconcentration of the cupric thiocyanate complex with 4-(5-nonyl)pyridine in benzene is possible from neutral or up to 2*M* HCl, 0.5*M* HNO_3 or 0.25*M* H_2SO_4 solutions. The method has considerable advantages over previously recommended extraction procedures because of selectivity, completeness of extraction in a single operation, short contact period, minimum amount of complexing agents needed and wide tolerance to various solution parameters. The complex formed from as little as 1 μg of copper can be extracted quantitatively into 1 ml of the organic phase from 500 ml of natural water. An extraction method is described which in combination with AAS can be used to determine copper in water, soils, fresh and used lubricating oils and plant-ash solutions down to the ng/ml or ng/g level.

Atomic-absorption spectrophotometry has been widely used for the determination of copper in water,[1,2] lubricating oils,[3] biological materials,[4,5] metals and alloys[6,7] *etc.* Several common liquid anion-exchangers, chelating agents and carboxylic acids used for separation of copper have been dealt with in many papers (references 8, 9 and references cited therein) of both fundamental and practical interest. In many cases the co-extraction of other elements and the narrow tolerance limits are a problem. The present work is concerned with the use of 4-(5-nonyl)-pyridine as an extractant for copper from aqueous thiocyanate solutions before its determination by atomic-absorption spectrophotometry. The extraction of copper from aqueous solutions containing thiocyanate ions has already been reported.[5,10,11] The present system offers the advantage of high efficiency in a single-step extraction from neutral or acidic solutions in the presence of only 0.1*M* potassium thiocyanate, and does not require the use of salting-out agents. The results show that the reagent has considerable potential for the preconcentration of toxic metal ions from neutral solutions and is also useful in the analytical processes that use acid decomposition of soil and ore materials.

* Dedicated to Professor Dr. Mohammed Mohammed Omar Jamjoom.

† To whom correspondence and requests for reprints should be sent.

EXPERIMENTAL

Reagents and instrumentation

All chemicals were analytical reagent grade. 4-(5-Nonyl)-pyridine (NPy) was obtained from K & K Laboratories, Plainview, N.Y. Distilled water was demineralized in a mixed-bed ion-exchange column and then distilled again after addition of alkali and permanganate. A standard solution of copper was prepared from analytical grade cupric chloride, and suitably diluted for the AAS calibration.

A Carl-Zeiss FMD-3 atomic-absorption spectrophotometer equipped with a Perkin–Elmer HGA-74-heated graphite atomizer unit, a Servogor S RE 541 recorder and a deuterium lamp for background compensation were used, with a copper hollow-cathode lamp. ^{64}Cu tracer was obtained by irradiation of cupric chloride in a thermal column in the research reactor PARR-1 of the Pakistan Institute of Nuclear Science and Technology.

Extraction procedure

Organic and aqueous solutions of the desired composition were shaken together for 5 min. Precise control of the equilibration time is not required because the extraction can be completed in a few seconds. We selected a time of 5 min because we had previously investigated[12,13] some other systems under these conditions. The equilibrium studies were carried out at 23 ± 3°. The phases were separated and centrifuged, and the activity of 500 μl of each phase was counted. The equipment for the radiochemical assay was described previously.[12] To study the effect of the phase volume ratio, 1 ml of organic phase was used for various volumes (50–500 ml) of aqueous solution which had previously been saturated with the pure organic phase.

Procedure for dissolution of lubricating oils

A 1-g sample was taken in a 50-ml conical flask which was placed on a hot-plate, the surface temperature of

which was raised from 150° to 400° in 30–60 min and was kept at this temperature until a charred mass was left in the flask. The flask was then removed and cooled. Next 5 ml of a 1:1 v/v mixture of nitric and perchloric acids were added and the mixture was heated on the hot-plate with its surface temperature raised from 150° to 200° in 30–60 min and then kept at 200° until the solution became clear. The solution was then cooled and suitably treated to give 0.1*M* nitric acid/0.1*M* potassium thiocyanate medium.

Decomposition procedure for leaves

Allan's method[7] was used, 0.5–2 g of oven-dried (70°) plant material being mixed with 3 ml of 72% perchloric acid and 17 ml of concentrated nitric acid, left overnight to prevent foaming in the heating, then heated slowly until the solution became colourless. The volume was then reduced to 2 ml and 10 ml of water were added and the mixture was brought to the boil. After cooling, the solution was filtered and made 0.1*M* in both potassium thiocyanate and nitric acid for solvent extraction.

Water samples

Water samples were made 0.1*M* in both nitric acid and potassium thiocyanate, and then extracted with 0.1*M* NPy in benzene.

Procedure for opening-out of soil

The nitric acid/hydrogen peroxide method[14] was employed for opening-out the IAEA intercomparison soil No. 5. The sample was oven-dried at 105–110° and a 0.1-g portion was slurried with 0.5 ml of water to minimize splash and facilitate rapid reaction with the acid; 5 ml of conc. nitric acid were added to the slurry and the mixture was heated at 100° for 2 hr, then cooled for 15 min. Then 3 ml of 30% hydrogen peroxide were added dropwise to the mixture, and heating was continued for another hour with intermittent gentle swirling.

RESULTS AND DISCUSSION

Initially, attempts were made to extract copper(II) as chloride, sulphate or nitrate from the corresponding aqueous mineral acid solutions but in no instance was extraction observed. Figure 1 shows the dependence of the partition coefficient on the equilibrium concentration of hydrochloric, nitric or sulphuric acid when extraction is made from 0.02*M* potassium thiocyanate medium. Higher extraction of copper is obtained, for a given acidity, in the presence of thiocyanate because the latter leads to the formation of larger and less hydrated complexes. Maximum extraction is obtained only at relatively low acid concentrations (up to 0.1*M*) and the distribution coefficients for copper decrease with increasing acid concentration. This can be explained as due to the formation of relatively less extractable metal complexes or to a decrease in the concentration of the extracting agent as a result of competitive extraction of the acids. In the case of hydrochloric acid, the extraction decreases with increase in acid concentration up to 1*M* and then levels off. In nitric acid media there is an abrupt fall in the extraction of the metal at around 0.2*M* acid concentration, similarly to the corresponding zinc system,[13] and this can be interpreted as due to competition of the acid for the NPy. In the sulphuric acid system, the degree of extraction decreases as the bisulphate/sulphate ratio increases in the aqueous phase. Figure 1 shows that from aqueous solutions of thiocyanate in the mineral acids, the extraction of the metal is fairly good and decreases in the order $HCl > HNO_3 > H_2SO_4$.

The dependence of the distribution coefficient on thiocyanate concentration was studied for constant copper ($<10^{-6}M$) and extractant (0.1*M*) concentration, and varied thiocyanate concentration. The results are shown in Fig. 2. In most of the curves the slope of the linear parts below 0.1*M* thiocyanate concentration is close to 2. Separate investigations have shown that copper is extracted, with fairly high *D* values from simple aqueous 0.1*M* potassium thiocyanate. It is, therefore, indicated that the extraction is independent of the nature of the anions of the supporting acids, and the extraction system may be represented as:

$$Cu^{2+}_{aq} + 2SCN^{-}_{aq} + n NPy_{org} \rightleftharpoons [Cu(NPy)_n(SCN)_2]_{org}$$

and the concentration equilibrium constant is

$$K = \frac{[Cu(NPy)_n(SCN)_2]_{org}}{[Cu^{2+}]_{aq}[NPy]^n_{org}[SCN^-]^2_{aq}}.$$

As

$$D = \frac{[Cu(NPy)_n(SCN)_2]_{org}}{[Cu^{2+}]_{aq}},$$

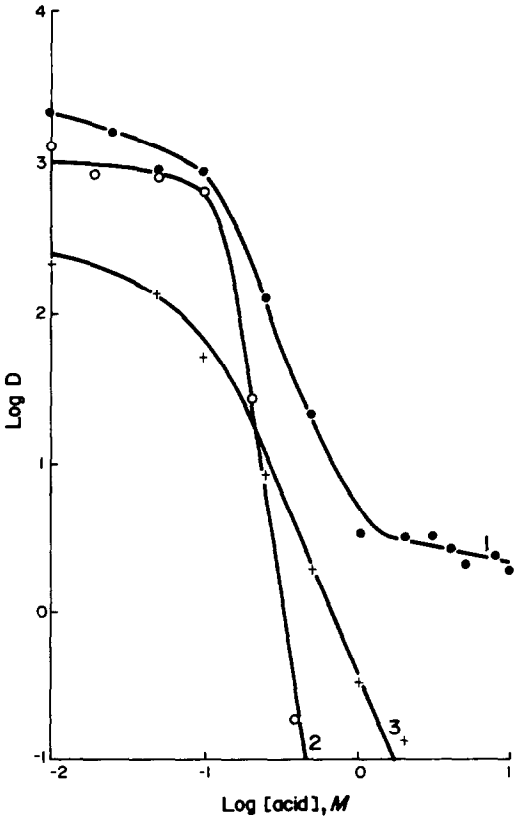


Fig. 1. The distribution of Cu(II) between aqueous mineral acid solutions 0.02*M* in potassium thiocyanate, and 0.1*M* NPy in benzene. (1) HCl, (2) HNO_3, (3) H_2SO_4.

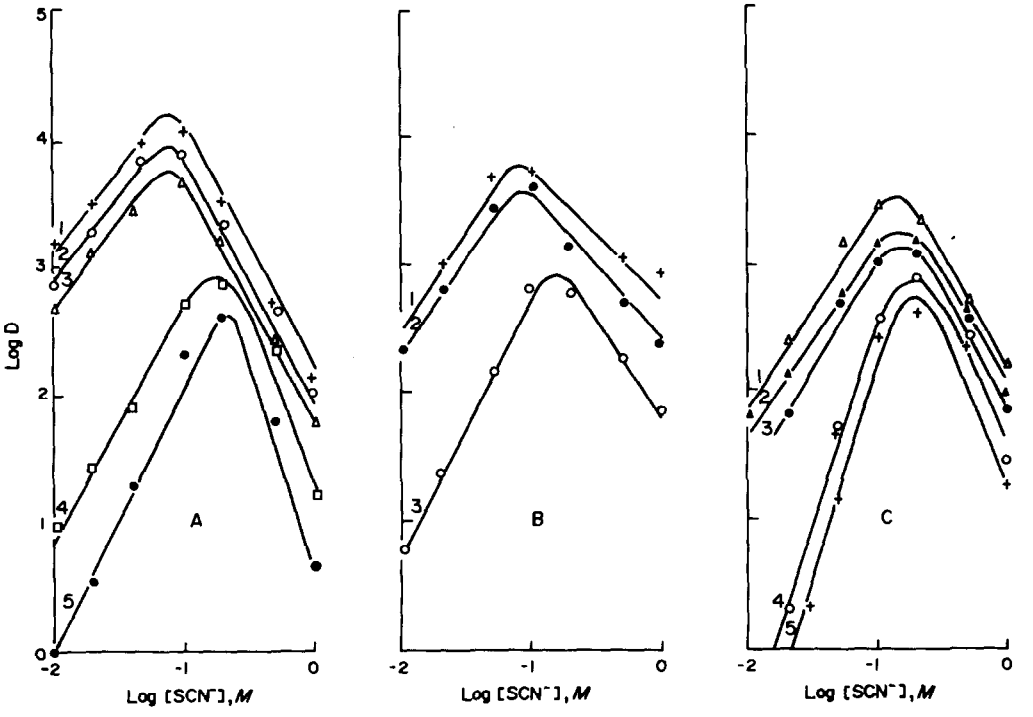


Fig. 2. Variation of the distribution coefficient of Cu(II) between constant acidity aqueous solutions of varied thiocyanate ion concentration, and 0.1*M* NPy in benzene. (A) [HCl]: (1) 0.005*M*, (2) 0.05*M*, (3) 0.1*M*, (4) 0.5*M*, (5) 3.0*M*. (B) [HNO_3]: (1) 0.01*M*, (2) 0.1*M*, (3) 0.25*M*. (C) [H_2SO_4]: (1) 0.01*M*, (2) 0.05*M*, (3) 0.1*M*, (4) 0.5*M*, (5) 1.0*M*.

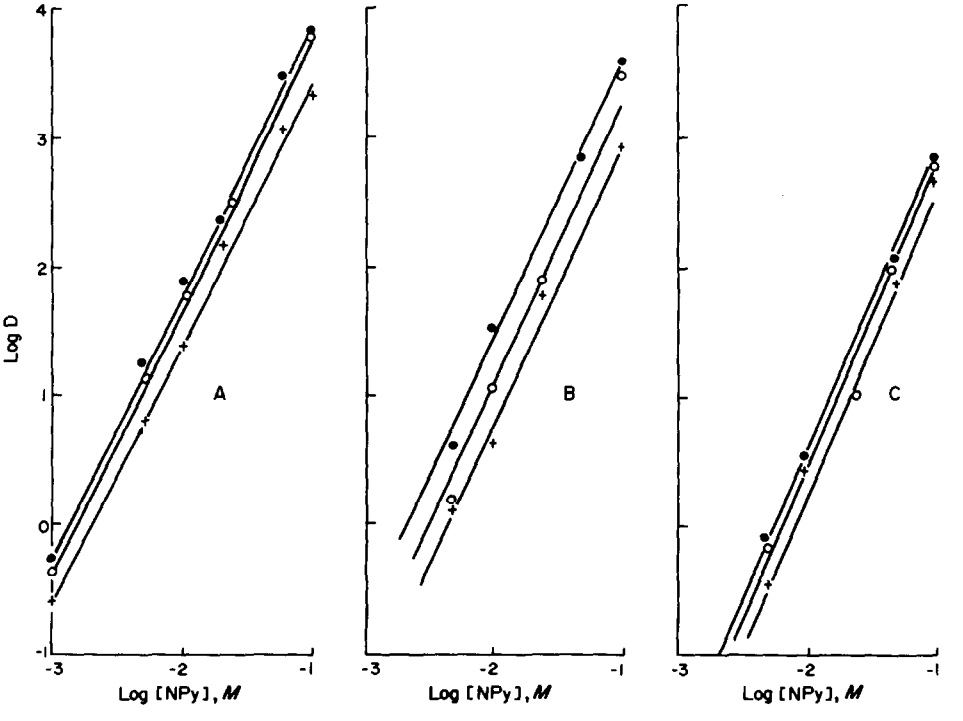


Fig. 3. Dependence of the distribution coefficient of Cu(II) on the concentration of NPy for constant acidity aqueous solutions which were 0.1*M* with respect to thiocyanate. (A): (1) 0.01*M* HCl, (2) 0.01*M* HNO_3, (3) 0.01*M* H_2SO_4. (B): (1) 0.1*M* HCl, (2) 0.1*M* HNO_3, (3) 0.1*M* H_2SO_4. (C): (1) 1.0*M* HCl, (2) 0.25*M* HNO_3, (3) 0.5*M* H_2SO_4.

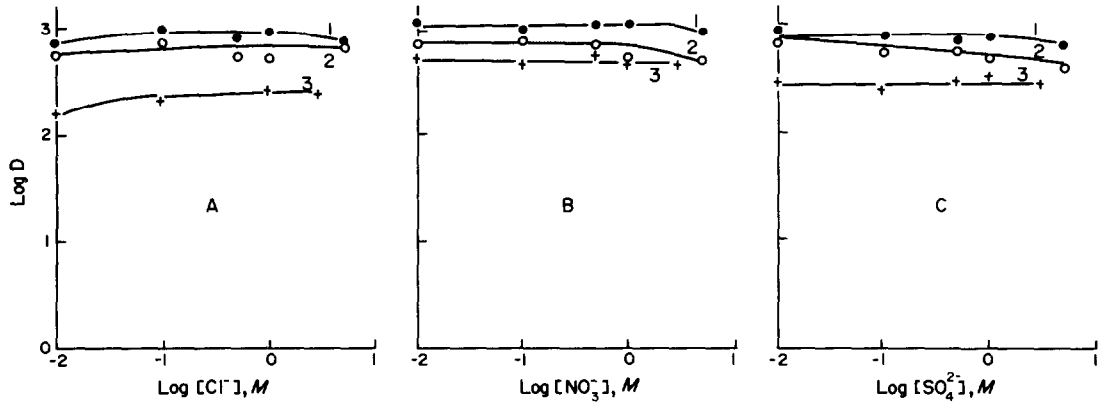


Fig. 4. The effect of chloride, nitrate and sulphate concentrations on the distribution coefficient of Cu(II) for the corresponding mineral acid solutions which were 0.1*M* with respect to thiocyanate, and 0.1*M* NPy in benzene. (A): (1) 0.01*M* HCl, (2) 0.1*M* HCl, (3) 1.0*M* HCl. (B): (1) 0.01*M* HNO_3, (2) 0.1*M* HNO_3, (3) 0.25*M* HNO_3. (C): (1) 0.01*M* H_2SO_4, (2) 0.05*M* H_2SO_4, (3) 0.1*M* H_2SO_4.

at constant thiocyanate concentration

$$\log D = \log K' + n\log[\mathrm{NPy}]_{org}$$

where $K' = K[SCN^-]^2_{aq}$. Therefore, n can be deduced from a log–log plot (Fig. 3) of D against [NPy], and is about 2. Hence the extracted species is presumably $Cu(NPy)_2(SCN)_2$.

To ascertain whether the extraction procedure is applicable to high concentrations of copper, loading studies were made with water and mineral acid solutions (0.01–0.1*M*) for constant thiocyanate and NPy concentrations (both 0.1*M*) and varying copper concentrations, and it was found that under the optimal conditions, copper can be extracted under a variety of conditions to give a maximum concentration of around 3 g/l in the organic phase, which suggests the formation of disolvates.

The data so far reported in this paper deal with partition studies with equal volumes of the phases. Since copper is one of the toxic elements for which a preconcentration is needed before its determination as an inorganic pollutant in water, we examined the extraction under optimal conditions with different organic to aqueous phase-volume ratios. It was found that even 1:500 organic:aqueous ratio did not have a significant effect on the extraction efficiency, which is rather exceptional. This could be attributed to the soft base nature of the substituted pyridine

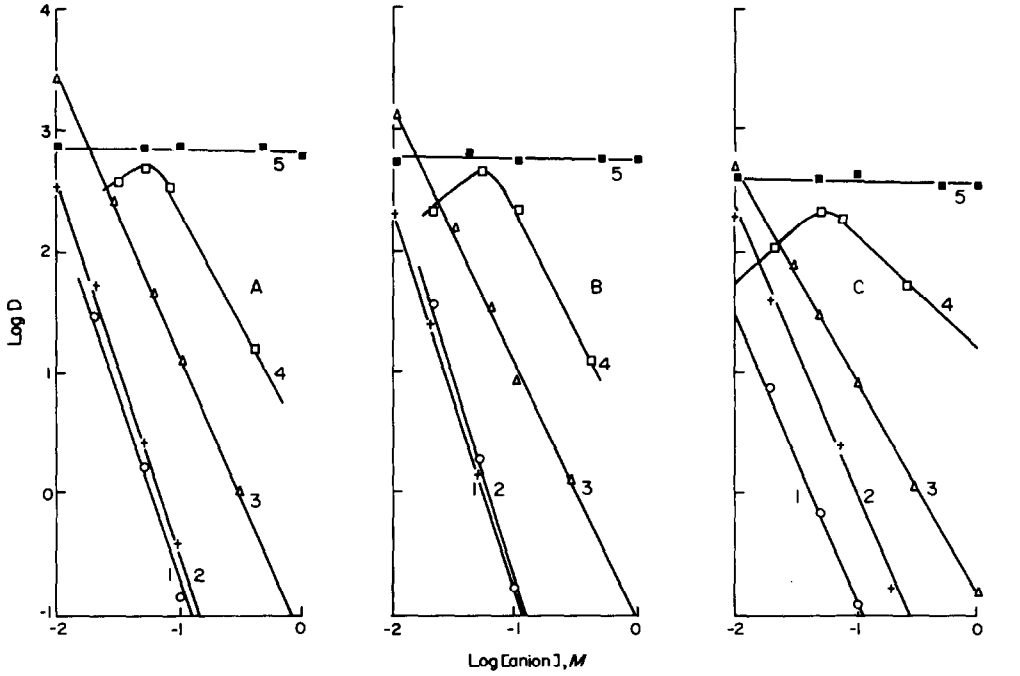


Fig. 5. The effect of the addition of various anions on the distribution coefficient of Cu(II) between 0.01*M* aqueous mineral acid solutions 0.1*M* potassium thiocyanate, and 0.1*M* NPy in benzene. (A) HCl, (B) HNO_3, (C) H_2SO_4, (1) thiosulphate, (2) oxalate, (3) citrate, (4) acetate, (5) ascorbate.

Table 1. Distribution coefficients and separation factors of different metal ions with respect to Cu(II) in 0.1*M* NPy/benzene–mineral acid (0.1*M* with respect to potassium thiocyanate) extraction systems

Ion	Concentration, *M*	Distribution coefficients			Separation factors		
		0.01*M* HCl	0.01*M* HNO_3	0.01*M* H_2SO_4	0.01*M* HCl	0.01*M* HNO_3	0.01*M* H_2SO_4
Tc(VII)	C.F*	3.8	3.3	4.5	1.8×10^3	1.6×10^3	4.4×10^2
Mo(VI)	10^{-5}	7.3	1.4	2.5	9.3×10^2	3.8×10^3	8.0×10^2
Cr(VI)	C.F*	0.03	0.06	0.01	2.3×10^5	8.0×10^4	2.0×10^5
Mo(V)	10^{-5}	1.9	0.91	7.5	3.5×10^3	5.0×10^3	2.6×10^2
Hf(IV)	10^{-7}	0.06	0.05	0.15	1.1	1.1×10^5	1.3×10^4
Nb(V)	10^{-5}	0.00	0.00	0.00	$\sim 10^6$	$\sim 10^5$	$\sim 10^5$
Zr(IV)	10^{-5}	0.11	0.08	0.14	6.1×10^4	6.7×10^4	1.4×10^4
La(III)	10^{-7}	0.01	0.04	0.03	6.8×10^5	1.3×10^5	6.6×10^4
Nd(III)	10^{-7}	0.12	0.01	0.07	5.7×10^4	5.3×10^5	2.8×10^4
Y(III)	10^{-8}	0.00	0.00	0.00	$\sim 10^6$	$\sim 10^7$	$\sim 10^6$
Fe(III)	10^{-4}	120	52	58	57	102	42
Au(III)	10^{-6}	0.81	1.50	6.25	8.3×10^3	3.6×10^3	3.2×10^2
Cr(III)	C.F	0.00	0.00	0.0	$\sim 10^6$	$\sim 10^5$	$\sim 10^5$
As(III)	10^{-5}	0.00	0.00	0.00	$\sim 10^5$	$\sim 10^6$	$\sim 10^5$
Hg(II)	10^{-7}	2050	550	860	3.3	9.6	2.3
Zn(II)	10^{-8}	780	1400	1760	873	3.8	1.2
Sr(II)	10^{-8}	0.00	0.05	0.11	$\sim 10^6$	1.1×10^5	1.8×10^4
U(VI)	10^{-3}	5.9	5	12	1.2×10^3	1.1×10^3	1.7×10^2
Co(II)	10^{-7}	520	1000	150	13.5	5	15
Cs(I)	10^{-8}	0.00	0.00	0.00	10^5	10^6	10^6
Ag(I)	10^{-8}	6	73	60	1.1×103	72	20

* C.F = Carrier-free.

($pK_{BH^+} \sim 5.9$), which forms strong neutral solvates with copper and other metal ions (which are classified as soft acids and are capable of donating *d* or *p* electrons with the formation of π-bonds).

The results in Fig. 4 show that in chloride, nitrate, and sulphate media the extraction is not affected when salts of the acid are added to the corresponding aqueous mineral acid solutions containing thiocyanate at 0.1*M* concentration.

The extraction of copper from 0.01*M* mineral acids which were 0.1*M* in thiocyanate and contained various other anions was also investigated (Fig. 5). In all the three mineral acid systems, there is a regular decrease in the extraction of copper with increasing concentration of thiosulphate, oxalate or citrate ions in the aqueous phase. In the case of acetate, the partition of copper increases with acetate concentration up to 0.1*M* and then decreases at relatively high acetate concentrations. The distribution coefficient, however, remains more or less constant in the case of ascorbate. The results show that thiosulphate, oxalate and citrate can be used for the back-extraction of copper.

Several metals were tested for extraction with 0.1*M* NPy in benzene from 0.01*M* hydrochloric, nitric and sulphuric acid solutions containing the optimal concentration of thiocyanate, by a method similar to that for copper. Table 1 displays the distribution coefficients for the toxic and associated base metals and the results show that NPy is an excellent reagent for the separation of toxic metals as a group from most of the associated base metals. Separate studies indicated that the distribution coefficients of the elements are not

Table 2. Determination of Cu in different sets of distilled and tap water samples by AAS after preconcentration by a factor of 10 by solvent extraction in 0.1*M* NPy in benzene (values in ng/ml)

	I	II	III	IV
Distilled water	8.2	7.8	6.0	6.5
	8.5	7.8	5.2	7.2
	8.2	7.2	5.5	6.8
	8.5	7.2	4.5	7.5
	9.2	7.5	4.5	6.2
	8.8 ± 0.5	7.5 ± 0.3	5.1 ± 0.6	6.8 ± 0.5
Tap water	10.0	8.2	8.2	12.0
	10.0	9.0	8.0	9.0
	18.0	9.2	8.0	10.0
	9.8	9.5	8.0	8.5
	10.0	—	—	—
	12.0 ± 3.1	9.1 ± 0.6	8.1 ± 0.1	9.5 ± 1.6

Table 3. AAS determination of Cu in fresh and used aircraft lubricating oils and in spinach samples from different sources, after extraction with 0.1*M* NPy in benzene (values in μg/g)

Fresh oil	Used oil	Spinach 1	Spinach 2
1.48	2.94	14.5	17.6
1.60	2.94	16.5	19.7
1.48	3.43	14.5	21.2
1.48	2.94	18.5	21.0
1.48	3.18	16.5	19.5
1.48	3.01	14.5	16.4
1.60	3.06	18.5	
1.60		18.5	
1.48		18.5	
		14.5	
1.52 ± 0.06	3.07 ± 0.18	16.5 ± 1.9	19.2 ± 1.9

very much influenced when the concentration of the supporting acids is increased from 0.01 to 0.1*M* in the 0.1*M* potassium thiocyanate medium.

Atomic-absorption measurements

Copper was extracted into the NPy/benzene phase from aqueous solutions. A sample size of 20 μl was selected for injection into the graphite tube. The heating programme for the copper determination was

Stage 1	Stage 2	Stage 3	Stage 4
150°C	900°C	2550°C	2650°C
1 min	1 min	10 sec	10 sec

All determinations were done with background compensation. The results for determination of copper in different tap and distilled water samples, based on a preconcentration factor of 10, are summarized in Table 2. The detection limits of the method can be considerably improved by preconcentration, *e.g.*, in the case of water samples ng/ml levels of copper have been determined by equilibrating 10 ml of aqueous phase with 1 ml of organic phase. In practice a preconcentration factor of 100 is possible. Copper determinations in fresh and used aircraft lubricating oils, two spinach-leaf samples from different sources, and IAEA intercomparison soil No. 5 have been done to check the application of the method to various matrices. The results are reported in Table 3. In the case of the soil sample the IAEA reported value[15] is 77.1 ± 4.7 μg/g (dry weight) and our value is 74.4 ± 5.6 μg/g.

REFERENCES

1. D. A. Segar and J. G. Gonzales, *Anal. Chim. Acta*, 1972, **58**, 7.
2. J. P. Riley and D. Taylor, *ibid.*, 1968, **40**, 479.
3. J. F. Alder and T. S. West, *ibid.*, 1972, **58**, 331.
4. R. K. Roschuik, *J. Dairy Sci.*, 1972, **55**, 750.
5. C. J. Pickford and G. Rossi, *At. Absorption Newsl.*, 1975, **14**, 78.
6. B. G. Stephens and H. L. Felkel, Jr., *Anal. Chem.*, 1975, **47**, 1676.
7. J. E. Allan, *Spectrochim. Acta*, 1961, **17**, 467.
8. J. H. Culp, R. L. Windham and R. D. Whealy, *Anal. Chem.*, 1971, **43**, 1321, and references therein.
9. A. Bartecki and W. Apostoluk, *J. Inorg. Nucl. Chem.*, 1978, **40**, 109 and references therein.
10. D. A. Tinsley and A. Iddon, *Talanta*, 1974, **21**, 633.
11. M. Yanagasawa, H. Kihara, M. Suzuki and T. Yaneuchi, *ibid.*, 1970, **17**, 888.
12. M. A. Qureshi, M. Farid, A. Aziz and M. Ejaz, *Sepn. Sci. Techn.*, 1978, **13**, 843.
13. M. Iqbal, M. A. Qureshi and M. Ejaz, *Talanta*, 1978, **25**, 371.
14. K. V. Krishnamurty, E. Shpirt and M. M. Reddy, *At. Absorption Newsl.*, 1976, **15**, 68.
15. IAEA/RI/46, Jan. 1978, Table 61.

Talanta. Vol. 28, pp. 447 to 450. 1981
Printed in Great Britain

0039-9140/81/070447-04$02.00/0
Pergamon Press Ltd

DOSAGE PAR SPECTROGRAPHIE D'EMISSION, DE TRACES D'OXYGENE A L'AIDE D'UNE SOURCE A IMPULSION

C. TRICHÉ, G. PITET et M. R. DORIGNAC

Laboratoire de Chimie Analytique, Faculté des Sciences Pharmaceutiques, 31 Allée J. Guesde, 31400 Toulouse, France

(*Reçu le* 3 *juillet* 1980. *Revisé le* 22 *octobre* 1980. *Accepté le* 15 *janvier* 1981)

Résumé—Une source à impulsion de puissance suffisamment élevée est proposée pour obtenir le spectre d'étincelle de l'oxygène, à la pression atmosphérique et dans la région visible et ultra-violette du spectre. Un circuit d'allumage, de construction simple, permet d'amorcer la décharge et d'effectuer un dosage jusqu'à 100 ppm en atmosphère d'argon. Pour améliorer la limite de sensibilité il faut d'une part, faire intervenir un transfert d'énergie à partir d'atomes métastables d'un élément et d'autre part, éviter la formation d'un fond continu dû aux transitions libre–lié. L'emploi d'une atmosphère d'hélium permet ainsi d'améliorer la limite de sensibilité jusqu'à 20 ppm.

Dans des travaux antérieurs[1–3] nous avons montré par la technique des fils explosés qu'il est possible de réaliser des sources d'excitation dont les températures sont suffisamment élevées pour exciter dans les conditions opératoires les plus classiques, non seulement les spectres des éléments métalliques mais aussi ceux des non-métaux les plus électronégatifs dont les halogènes.

Des études fondamentales de ces sources[3,4] nous ont permis d'aborder des problèmes plus appliqués comme celui des dosages des métalloïdes à l'état de traces dans les produits pharmaceutiques.[1,2]

Un autre problème analytique assez fréquent est posé par la détermination de l'oxygène dans les molécules et les ions minéraux: sa solution implique le recours à certaines méthodes assez sophistiquées pour l'analyste telles que le spectromètre de masse ou l'analyseur ionique.

La détermination spectrographique de l'oxygène revet les difficultés communes à presque tous les métalloïdes: volatilité des états moléculaires précurseurs de l'excitation ou de l'ionisation élémentaire, potentiels d'excitation et d'ionisation particulièrement élevés, transitions électroniques impliquant des niveaux d'énergie tels que les radiations les plus sensibles sont émises dans un domaine de longueur d'onde inférieur à 2000 Å, nécessitant par conséquent des installations sous vide.

Une autre difficulté provient de la présence de l'oxygène dans l'atmosphère qui impose de travailler, tout au moins au niveau de la source d'excitation, dans un milieu ambiant qui peut être soit un gaz rare comme l'hélium ou l'argon soit un gaz diatomique (azote).

Enfin l'augmentation de la sensibilité implique une multiplication des décharges et impose aussi bien par sécurité que par commodité un dispositif d'amorçage automatisé extérieur à la décharge.

Nous avons cherché la solution dans une source d'excitation beaucoup plus puissante que celles utilisées habituellement en analyse spectrographique; des auteurs comme Levintov[5] soulignent qu'il est nécessaire de disposer d'une énergie cent fois supérieure à celle mise en oeuvre pour obtenir le spectre des métaux si on désire exciter les métalloïdes.

Il existe plusieurs procédés d'analyse par spectrographie d'émission, mettant en jeu une quantité importante d'énergie: à l'aide d'un arc à courant continu à haute intensité[6,7] Fassel,[8] Runge et Bryan,[9] puis Vilnat *et al.*[10,11] dosent l'oxygène à partir de 100 ppm dans les métaux en atmosphère de gaz rare avec un arc d'intensité 20 A. Avec un arc d'intensité plus élevée (48 A) Plotniskii et Rudoï[12,13] dosent l'oxygène entre 500 et 15.000 ppm dans le carbure de titane en atmosphère d'argon sous une pression de 600 mmHg tandis que Sventitskii et Taganova[14] dosent l'oxygène dans le titane avec un arc de 20 A sous 120 V. Kravchenko et Kurochkin[15] dosent l'oxygène dans le carbure de silicium entre 1000 et 70.000 ppm en opérant en atmosphère d'argon.

A l'aide de la haute fréquence[16,17] Barabanschikova *et al.*[18] déterminent 10^{-5} p/v d'oxygène dans le néon sous une pression de 10 mmHg.

L'étincelle glissante sous vide permet à Vodar[19] et ses collaborateurs[20] de doser 10 ppm d'azote et 50 ppm d'oxygène dans des métaux.

Levintov et Sventitskii (pour la bibliographie voir ref. 4) à l'aide d'une étincelle sous basse pression d'hélium dosent l'oxygène dans les métaux jusqu'à 50 ppm. Il semble que Pfeilsticker[21] ait été le premier à proposer l'emploi d'une source basse tension pour effectuer le dosage des métalloïdes (0,4–2 mF, 0,5 μH, 220–300 V) sous pression réduite (2–20 mmHg). Cette source fut adoptée par de nombreux auteurs soviétiques pour la détermination des métalloïdes dans les métaux.[22,23]

A l'aide d'une multisource (400 V, 2 mF, 50 μH, durée de l'exposition 20 sec) Hirokawa[24] dose l'oxygène dans les aciers à partir de 200 ppm en atmosphère d'hélium à la pression de 500 mmHg. S'interessant au même problème Falkova[25] utilise de préférence une atmosphère d'hydrogène sous 270 mmHg.

Shubina *et al.*[26] ont montré qu'une décharge basse tension excite les raies d'arc du triplet rouge de l'oxygène se trouvant dans une matrice métallique (acier) alors qu'à concentration égale dans l'azote environnant, ils n'observaient pas de raies. Par la suite, Cartlidge et Sale[27] également avec une source basse tension (250 V) et de capacité élevée (8 mF) observent les mêmes raies du triplet rouge de l'oxygène, la matrice étant en cuivre et l'atmosphère environnante étant constituée d'azote à la pression atmosphérique. Ils utilisent un système à trois électrodes, c'est-à-dire qu'ils amorcent la décharge à l'aide d'une étincelle auxiliaire superposée à une haute fréquence. La courbe d'étalonnage est comprise entre 0,01 et 0,16%.

PARTIE EXPERIMENTALE

Description de nos conditions opérationnelles

Source d'énergie. Nous utilisons une source à impulsion de capacité 0,25 mF et de tension 2,5 kV. La quantité d'énergie emmagasinée est assez importante (0,78 kJ) et elle peut être libérée en un temps très court (200 μsec), la décharge observée à l'aide d'un oscillographe cathodique étant amortie. La puissance de la décharge permet alors d'obtenir une température suffisamment élevée pour que l'émission des raies de l'oxygène soit intense dans la région visible du spectre.[3]

Cellule d'excitation en atmosphère controlée (Fig. 1). La cellule permettant de travailler en atmosphère contrôlée est constituée d'un cylindre de verre (diamètre int. 8 cm) de 5 mm d'épaisseur comportant un disque de quartz afin de permettre au rayonnement ultra-violet d'atteindre la fente d'entrée du spectrographe. Aux extrêmités du cylindre sont deux disques de bakélite percés d'orifices afin de permettre le passage des électrodes. Sur le cylindre sont prévus deux embouts afin de faire circuler un courant gazeux à la pression choisie.

Dispositif d'amorçage. Nous utilisons un système à trois électrodes décrit Fig. 2. La décharge entre les électrodes 1 et 2 de la source à impulsion est amorcée par une électrode starter 3. Cette électrode est soumise à un train d'impulsions électriques de haute tension fournies par le secondaire d'une bobine d'induction de voiture automobile (12 V). Les impulsions délivrées au primaire, très brèves et de fréquence 100 Hz, sont produites à partir du secteur 220 V par un circuit d'allumage diac-triac (D-T), comandé par un bouton pressoir P.

Mode opératoire et résultats obtenus

La poudre à étudier est composée d'un mélange homogène de poudre MgO + MgF_2 et de poudre de charbon (70 mg d'échantillon + 35 mg de poudre de charbon RW 0 Ringsdorff) préalablement séché. Cet ensemble est comprimé 10 sec sous 100 atm. et nous obtenons un cylindre de 4 mm de hauteur et 3 mm de diamètre. Ces comprimés sont disposés dans le cratère cylindrique

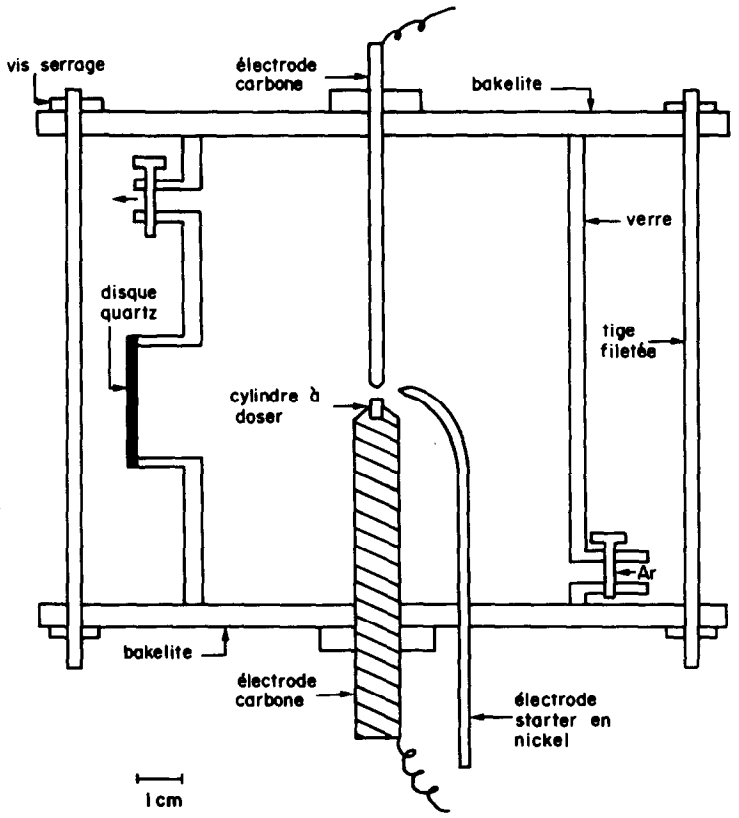


Fig. 1. Cellule d'excitation à atmosphère contrôlée.

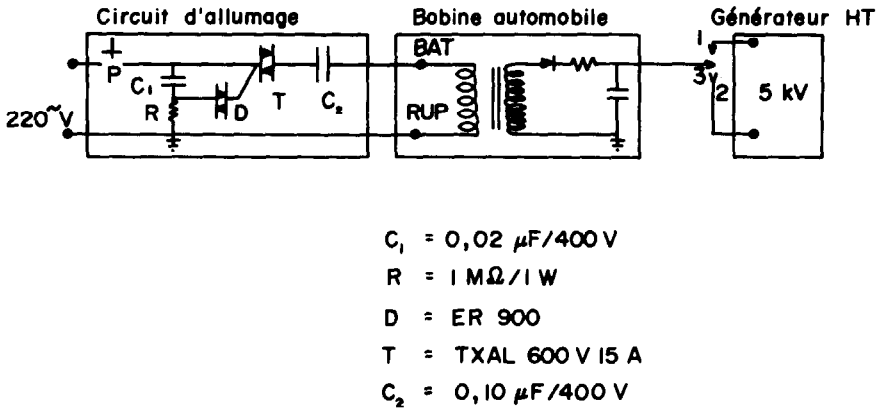


Fig. 2. Schéma du circuit d'amorçage.

(diamètre 3,1 mm, profondeur 3 mm) de l'électrode inférieure en carbone. La contre-électrode est également en carbone et est disposée de telle façon que l'espace inter-électrode soit de 2,5 mm. Le principe des comprimés permet d'avoir une meilleure reproductibilité des résultats, l'échantillon n'étant plus soufflé lors de la décharge.

Nous effectuons les décharges dans une atmosphère d'argon et d'après les mesures de température des différentes régions du plasma[3] nous choisissons de projeter la zone centrale sur la fente d'entrée du spectrographe. Les spectres sont pris à l'aide d'un spectrographe Hilger sur film TRI X (sensibilité 400 ASA).

L'échantillon contenant des traces d'oxygène sous forme de MgO est préparé selon les indications données plus haut et disposé à l'anode. Le spectre obtenu après une dizaine de décharges présente les raies caractéristiques des éléments de la poudre et de l'argon.

A la différence des autres auteurs, nous obtenons peu de raies d'arc de l'oxygène, mais nous observons un certain nombre de raies d'étincelle.

Pour effectuer un dosage d'oxygène nous faisons varier la proportion de MgO dans le mélange et nous utilisons le couple de raies 3749,49 Å (O II) et 3786,40 Å (Ar II). Une dizaine de décharges suffisent pour obtenir un point de la courbe d'étalonnage qui est une droite. La limite de sensibilité est de 0,01%. Ces résultats concernent le fluorure de magnésium, la limite de sensibilité est fonction habituellement de la nature de la matrice et en général elle est la moins bonne en présence d'un métal alcalin. Dans ce cas en effet la température du plasma se trouve abaissée, le potentiel d'excitation particulièrement faible pour les métaux alcalins entrainant donc un abaissement de la température[30] et de la puissance disponible pour l'excitation des autres atomes présents.[2] Plus loin nous montrerons que d'autres facteurs peuvent encore intervenir dans la modification de la sensibilité, ne serait ce que la variation de contraste entre la raie d'analyse et le fond continu.

Nous avons défini la justesse et la précision de la méthode au moyen d'échantilllons de référence que nous avons réalisés avec le maximum de rigueur pour définir à la fois leur homogénéité et leur concentration. A partir de ces teneurs que nous considerons comme référence, les résultats obtenus sur 5 prises d'essai d'un même échantillon, en utilisant la courbe expérimentale d'étalonnage, ne s'écartent jamais de plus de 8% de la concentration théorique.

INTERPRÉTATION DES RÉSULTATS

L'existence du fond continu, modifie considérablement le contraste de la raie et nous oblige à prendre en considération ses variations d'intensité en fonction de la nature et de la pression du gaz dans lequel on produit la décharge.

D'après nos observations, l'intensité du fond continu est directement proportionnelle à la pression entre 160 et 700 mmHg. De même, l'intensité des raies de l'argon et de l'oxygène ionisés une fois (Ar II et O II) croissent proportionnellement à la pression en accord avec la relation d'Einstein–Boltzmann:

$$I = N/Qhvg Ae^{-E/kT}$$

où Q = fonction de partition, g = poids statistique du niveau d'énergie, h = constante de Planck, v = fréquence de la raie, A = probabilité de transition, E = potentiel d'ionisation, T = température du plasma, k = constante de Boltzmann.

L'intensité I de la raie est fonction de la densité N des atomes rayonnants; nous admettons en accord avec un concept généralisé en spectrographie, que N est lui-même proportionnel à la pression du gaz environnant.

Comme la température du plasma augmente en même temps que la pression, l'accroissement de l'intensité des raies[28] est justifié tant que l'intensité maximale de celles-ci n'est pas atteinte.

Pour une pression déterminée, l'intensité du fond continu décroit quand on passe de l'argon à l'azote puis à l'hélium. Les éléments à potentiel d'ionisation élevé tels que l'hélium s'ionisent en effet très difficilement et, par suite, le phénomène de recombinaison électron–ion devient pratiquement négligeable. Par contre, les éléments à potentiel d'ionisation moins élevé, comme l'argon s'ionisent plus facilement et le fond continu dû aux transitions libre–lié devient relativement plus intense.[32]

Si nous considérons maintenant l'intensité des raies d'analyse, l'argon donne déjà de bons résultats mais son remplacement par l'hélium s'accompagne d'une nette amélioration de la sensibilité, la limite de détection passant de 100 à 20 ppm.

L'ionisation ou l'excitation de l'oxygène en atmosphère d'hélium peut être attribuée aux chocs de deuxième espèce selon le processus suivant (transfert

Penning):

$$He_m + O \rightarrow He + O^+ + e$$

Ricard et Lefebvre[29] étudiant la décharge H.F. dans un tube de quartz contenant de l'hélium à la pression atmosphérique, obtiennent le spectre de ce gaz et celui de ses impuretés. Parmi celles-ci, ils notent la présence des raies d'oxygène et proposent le mécanisme suivant:

$$He^+ + O_2 \rightarrow He + O^+ + O$$

pour expliquer une émission renforcée de la raie O I à 7773 Å. Ils estiment cependant que les transferts d'excitation font surtout intervenir des états métastables de l'hélium.

Dans notre dispositif expérimental décrit ci-dessus, nous n'observons aucune raie appartenant à l'hélium ionisé: en conséquence, si des ions He^+ sont présents dans le plasma, nous admettons qu'ils sont en quantité insuffisante pour influencer nettement le spectre de l'oxygène. D'autre part, nous ne pouvons pas attribuer l'ionisation de l'oxygène en atmosphère d'argon à des chocs de deuxième espèce puisque l'énergie du niveau métastable du gaz environnant est plus faible que le potentiel d'ionisation de l'oxygène. En conséquence, nous attribuons l'ionisation de l'oxygène observée sur nos clichés à des chocs électroniques.

Eléments	P.I., *eV*	Energie des niveaux métastables du gaz environnant, *eV*
He	24,48	19,73
Ar	15,69	11,51
O	13,51	4,1
N	14,49	3,5

Conclusions

A l'aide d'une source à impulsion basse tension mais de capacité relativement élevée il est possible d'obtenir les raies de l'atome ionisé d'oxygène. Cette source de puissance élevée permet également d'effectuer des dosages en atmosphère d'argon dans un domaine de concentration compris entre 100 et 2000 ppm; nous avons montré que cela est interessant dans le domaine de la chimie minérale mais en outre les problèmes de dosage de l'oxygène dans les métaux que des industriels nous ont posé dans le passé nous permettent de penser que les métallurgistes peuvent aussi être interessés.[31] Toutefois il ne faudra pas perdre de vue que l'effet de matrice jouant un rôle important, de nouveaux étalonnages s'imposeront. En cristallogénie, on peut rencontrer des composés légèrement non stoechiométriques et dont certains sites sont partiellement occupés par des atomes d'oxygène. Dans certains cas, pour effectuer le dosage, une atmosphère d'argon est suffisante, mais la sensibilité sera améliorée si l'on peut d'une part, faire intervenir un transfert d'énergie à partir d'atomes métastables d'un élément et d'autre part, éviter le phénomène de recombinaison électron–ion générateur de fond continu. L'hélium parait être un des éléments les mieux appropriés, la limite de détection atteignant alors 20 ppm dans certains cas.

LITTERATURE

1. O. Fitte-Hygounenc, *Thèse*, Toulouse, 1972.
2. G. Pitet, O. Hygounenc et C. Triché, *Analusis*, 1973, **2**, 601.
3. C. Triché et G. Heshmat-Chaaban, *Spectrochim. Acta*, 1974, **29B**, 121.
4. C. Triché, *Thèse*, Toulouse, 1971.
5. I. Levintov, *Zh. Tekh. Fiz.*, 1947, **17**, 795.
6. S. A. Borovik, *Dokl. Akad. Nauk. USSR*, 1949, **63**, 315.
7. G. Contamin *Comm. Energie At. Rappt.*, CEA-R-2826, 1965.
8. V. A. Fassel et R. W. Tabeling, *Spectrochim. Acta*, 1956, **8**, 201.
9. E. F. Runge et F. R. Bryan, *Appl. Spectrosc.*, 1956, **10**, 68.
10. J. Vilnat, J. Desbras-Guédon, Al el Dine Abdellatif, *Compt. Rend.*, 1963, **257**, 3582.
11. J. Vilnat, *Thèse*, Paris, 1964.
12. V. M. Plotniskii, *Zavodsk. Lab.*, 1970, **36**, 1068.
13. V. M. Plotniskii et A. N. Rudoï, *ibid.*, 1971, **11**, 1324.
14. N. S. Sventitskii et K. I. Taganova, *Bull. Acad. Sci. USSR*, 1955, 1110.
15. L. E. Kravchenko et V. P. Kurochkin, *Zh. Analit. Khim.*, 1972, **27**, 398.
16. A. Gatterer, *Mikrochim. Acta*, 1952, **36**, 796.
17. G. Pitet, J. Farre, C. Azaïs et P. Josserand, *Compt. Rend.*, 1967, **264B**, 371.
18. N. N. Barabanschikova, N. N. Dykhno et O. O. Talakin, *Zavodsk. Lab.*, 1969, **35**, 1347.
19. B. Vodar, *Rapt. 16° Congrès GAMS*, 1953, 17.
20. R. Berneron et J. P. Moreau, *C. Inf. Tech. Cent. Doc. Sider.*, 1978, **35**, 2249.
21. K. Pfeilsticker, *Spectrochim. Acta*, 1940, **1**, 424; *Z. Metallkunde*, 1941, **7**, 267; *Mikrochim. Acta*, 1955, 358.
22. I. S. Marshak, *Usp. Fiz. Nauk USSR*, 1960, **71**, 631; 1962, **5**, 478.
23. K. P. Andreeva et G. P. Startsev, *Metody Issled. Opred. Gazov. Met.*, 1973, 88.
24. K. Hirokawa, *Spectrochim. Acta*, 1971, **26B**, 463.
25. O. B. Falkova, *Bull. Acad. Sci. USSR*, 1955, **19**, 137.
26. S. B. Shubina, A. B. Shaevich, S. I. Kilina, S. I. Melnikov et L. A. Bazonova, *Zavodsk. Lab.*, 1962, **28**, 942.
27. D. Cartlidge et G. Sale, *Spectrochim. Acta*, 1972, **27B**, 421.
28. G. Heshmat-Chaaban, *Thèse*, Toulouse, 1975.
29. A. Ricard et J. Lefebvre, *Analusis*, 1978, **6**, 299.
30. P. W. J. M. Boumans, *Theory of Spectrochemical Excitation*, Hilger and Watts, London, 1966.
31. G. Abravanel, *Thèse*, Toulouse, 1966.
32. I. Kenawy, Dissertation, Buchum, 1980.

Summary—A pulsed source of sufficiently high power is proposed to obtain the spark spectrum of oxygen under atmospheric pressure and within both the visible and ultraviolet range of the spectrum. A simply made ignition circuit starts the discharge and allows determination of 100 ppm of oxygen in an argon atmosphere. To improve the limit of sensitivity, it is necessary on the one hand to have a transfer of energy from metastable atoms of one element, and on the other hand to avoid the formation of a continuum as a result of transitions between the free and bound states. The use of a helium atmosphere thus allows the improvement of the limit of sensitivity to 20 ppm.

Talanta. Vol. 28. pp. 451 to 454. 1981
Printed in Great Britain. All rights reserved

0039-9140/81/070451-04$02.00/0
Copyright © 1981 Pergamon Press Ltd

COMPLEXES DE DERIVES ALLOXANNIQUES—I

COMPLEXES DU FER(II) AVEC L'ACIDE VIOLURIQUE ET L'ACIDE THIO-2 VIOLURIQUE

NASEEM DELANNOY, JEAN-MARIE DEGORRE, ALBERT DELANNOY et JACQUES NICOLE
Laboratoire de Chimie Analytique, Ecole Nationale Supérieure de Chimie de Lille, B.P. 40, 59650 Villeneuve d'Ascq, France

JEAN HENNION*
Groupe d'Etudes Appliquées, U.E.R. de Chimie, Université des Sciences et Techniques de Lille, 59655 Villeneuve d'Ascq, France

(*Reçu le 9 mai* 1980. *Revisé le 6 octobre* 1980. *Accepté le 15 janvier* 1981)

Résumé—L'étude de la complexation du fer(II) par l'acide violurique d'une part, et par l'acide thio-2 violurique d'autre part, est réalisée par conductimétrie, potentiométrie et spectrophotométrie dans le visible à 25° en milieu aqueux. La formation d'un complexe triviolurate ferreux $[Fe(C_4H_2N_3O_4)_3]^-$ et d'un complexe trithioviolurate ferreux $[Fe(C_4H_2N_3O_3S)_3]^-$ est mise en évidence. Ils absorbent tous deux fortement, le premier à 605 nm et le second à 615 nm. La détermination de la constante de stabilité des complexes est faite à force ionique 0,5*M* par potentiométrie et spectrophotométrie. Les deux techniques donnent des valeurs très proches l'une de l'autre: $4{,}0 \pm 0{,}3 \cdot 10^8$ et $8{,}3 \pm 0{,}7 \cdot 10^8$ pour le triviolurate et $1{,}1 \pm 0{,}5 \cdot 10^9$ et $1{,}45 \pm 0{,}7 \cdot 10^9$ pour le trithioviolurate.

Outre ses applications biologiques, l'acide violurique ($C_4H_3N_3O_4$: oxime-5 alloxanne) a une utilisation importante en chimie analytique dans la détermination des métaux. Il est employé comme révélateur en chromatographie sur papier,[1–4] réactif de précipitation,[5] mais c'est en colorimétrie qu'il est le plus fréquemment utilisé.[6–10]

Les premières études de l'action de l'acide violurique sur des ions fer(II) ne mentionnent que la formation de sels.[11,12] Dans ses travaux sur le dosage colorimétrique du fer, Cerny[13] note la formation d'un complexe diviolurate ferreux. Quant à Leermakers et Hoffman[14] et Faus *et al.*,[15] ils mettent en évidence la présence du complexe triviolurate, qui est confirmée par l'étude structurale par spectrométrie réalisée par Raston et White.[16]

Comme le précédent, l'acide thio-2 violurique ($C_4H_3N_3O_3S$: thio-2 oxime-5 alloxanne) est utilisé principalement en chimie analytique dans la détermination des métaux par gravimétrie[17] et colorimétrie.[18–20] La formation d'un complexe coloré fer(II)–acide thio-2 violurique dans le dosage du fer a été signalé par Singh[21] et la réaction de complexation a été étudiée par Toropova *et al.*,[22] qui ont mis en évidence le tétrathioviolurate ferreux.

Les résultats peu nombreux et parfois contradictoires des travaux antérieurs nous ont incités à reprendre l'étude de la complexation des ions ferreux par ces deux acides en milieu aqueux par conductimétrie, potentiométrie et spectrophotométrie.

* L'auteur à qui on doit adresser la correspondance.

PARTIE EXPERIMENTALE

Réactifs

Toutes les solutions sont préparées avec de l'eau distillée, déminéralisée et bouillie. L'acide violurique (produit Fluka de qualité purum) est recristallisé plusieurs fois dans le méthanol et séché sous vide; la pureté du produit final est supérieure à 99,9%. Les solutions sont dosées par potentiométrie avec la soude. Le sel monosodique de l'acide violurique est préparé en solution aqueuse par action de la soude sur l'acide, le rapport soude/acide étant légèrement inférieur au rapport théorique pour éviter la formation du sel disodique. L'addition d'éthanol à la solution entraîne la précipitation de cristaux roses qui sont lavés à l'alcool et séchés sous vide. Les solutions sont dosées par échange d'ions. Le cation est échangé sur Amberlite IR 120 (H), l'éluat étant dosé par la soude. L'anion est échangé sur Amberlite IRA 400 (Cl) et l'éluat dosé par argentimétrie.

L'acide thio-2 violurique est préparé par nitrosation de l'acide thio-2 barbiturique (Merck, pour analyse). A température ordinaire et sous agitation constante, le mélange nitrite de sodium–acide chlorhydrique (en léger excès) est ajouté goutte à goutte à une solution d'acide thio-2 barbiturique très concentrée. Après refroidissement de la solution, il se dépose un solide jaune citron qui est lavé plusieurs fois à l'eau froide, puis à l'alcool et séché sous vide; la pureté du produit final est supérieure à 99,8%. Les solutions d'acide, dosées par la soude, sont peu stables et ne peuvent être stockées plus d'une journée, même à l'abri de la lumière sous atmosphère inerte.

Le thioviolurate monopotassique est préparé par action du nitrite de potassium sur l'acide thiobarbiturique vers 60° en milieu aqueux et précipité par addition d'alcool sous forme de cristaux bleu-verts. Les solutions sont dosées de la même façon que celles du violurate monosodique.

Les solutions de soude sont préparées exemptes de carbonate et stockées sous atmosphère inerte.

Les autres réactifs sont des produits pour analyse Merck et utilisés sans purification.

Appareillage

Le conductimètre W.B.R. à générateur de 1000 Hz et amplificateur logarithmique est couplé à une cellule de mesure de constante 0,98 cm^{-1}.

Les mesures de pH sont effectuées avec un potentiomètre Radiometer du type pHm 52, une électrode de verre et une électrode au calomel saturé. La chaîne potentiométrique est étalonnée à 25° et à force ionique 0,5*M* ($NaNO_3$).

Les cuves spectrophotométriques (Hellma spectrosil) utilisées avec un spectrophotomère Jouan DF 170 à double faisceau ont un trajet optique de 2 mm.

Mode opératoire

Les études conductimétriques et potentiométriques sont réalisées dans un vase de titrage maintenu à 25 ± 0,1° avec un volume initial de solution de 100 ml. L'interaction des ions ferreux et de l'acide violurique ou du violurate monosodique et de l'acide thioviolurique ou du thioviolurate monopotassique est suivie par conductimétrie. Dans le premier cas, la concentration des solutions est de $1{,}5 \cdot 10^{-3}M$, dans le second, elle est de $3 \cdot 10^{-4}M$.

La neutralisation par la soude de divers mélanges acide–sulfate ferreux est étudiée par potentiométrie. La concentration en acide violurique est maintenue constante et égale à $5{,}15 \cdot 10^{-3}M$; elle est de $1{,}2 \cdot 10^{-3}M$ pour l'acide thioviolurique. La concentration en ions Fe^{2+} est telle que l'on a les rapports Fe^{2+}/acide égaux à 1/3, 1/6 et 1/12. Chaque mélange est à force ionique 0,5*M* ($NaNO_3$). La solution de soude est 0,1*M* et se trouve à la même force ionique que les mélanges.

Trois méthodes expérimentales sont employées en spectrophotométrie. (1) La méthode des variations continues, avec une concentration totale (ions Fe^{2+} + acide) de $1{,}25 \cdot 10^{-3}M$ pour l'acide violurique et de $1{,}2 \cdot 10^{-3}M$ pour l'acide thioviolurique. (2) La méthode des variations successives avec une concentration initiale en acide violurique de $2{,}45 \cdot 10^{-3}M$ ou en sulfate ferreux de $8{,}2 \cdot 10^{-4}M$ et de $3{,}1 \cdot 10^{-3}M$ en acide thioviolurique ou $4 \cdot 10^{-4}M$ en sulfate ferreux. (3) Une méthode de dilution[23] avec une concentration initiale en acide violurique de $2{,}45 \cdot 10^{-3}M$ et en ions ferreux de $8{,}2 \cdot 10^{-4}M$ et des facteurs de dilution égaux à 1,5; 2; 3 et 4. Pour l'acide thioviolurique, les facteurs de dilution sont les mêmes et la concentration initiale en acide est de $1{,}85 \cdot 10^{-3}M$ et $6{,}2 \cdot 10^{-4}M$ en sulfate ferreux.

Dans chacune des méthodes le pH est maintenu à 4,58 avec un tampon acétate de sodium–acide perchlorique et à force ionique 0,5*M* ($NaClO_4$). L'anion ClO_4^- est choisi de préférence à NO_3^- en raison de son manque d'absorption dans le proche ultraviolet, ce qui évite une incidence possible sur les mesures d'absorbance. Pour l'acide violurique, les mesures d'absorbance sont effectuées à 590, 605 et 620 nm, et à 600, 615 et 630 nm pour l'acide thio-2 violurique.

RESULTATS ET DISCUSSION

Complexation par l'acide violurique

La coloration de la solution en bleu foncé caractérise l'interaction des ions ferreux et de l'acide violurique ou de son sel monosodique. Quel que soit le sens d'addition des réactifs, les graphes obtenus en conductimétrie sont similaires; il existe un point singulier et un seul pour le rapport molaire complexant/métal égal à 3 (Fig. 1). Au cours de la réaction, la conductance de la solution croît constamment, et la croissance est plus accentuée lorsque le complexant est sous sa forme acide. Ceci prouve la libération de protons lors de la réaction de complexation dont l'équation est du type:

$$3H_nA + M^{2+} \rightleftharpoons |M(H_{n-j}A)_3|^{(3j-2)-} + 3jH^+ \quad (1)$$

La réaction peut donc facilement être étudiée par potentiométrie.

Les courbes de neutralisation par la soude des divers mélanges acide–sulfate ferreux sont semblables; elles ne possèdent qu'une seule équivalence pour le rapport base/acide égal à 1. C'est donc la forme biprotonée de l'acide violurique qui est complexante suivant la réaction:

$$3C_4H_3N_3O_4 + Fe^{2+} \rightleftharpoons Fe(C_4H_2N_3O_4)_3^- + 3H^+ \quad (2)$$

La stabilité du complexe triviolurate formé est caractérisée par la valeur de la constante β_3 telle que:

$$\beta_3 = \frac{[Fe(C_4H_2N_3O_4)_3^-]}{[Fe^{2+}][C_4H_2N_3O_4^-]^3} \quad (3)$$

En utilisant la conservation de masse des différentes espèces en solution et la neutralité électrique, en introduisant la fonction de formation de Bjerrum, $\bar{n}$, nous obtenons la relation:

$$\log \frac{\bar{n}}{3 - \bar{n}} = 3 \log[C_4H_2N_3O_4^-] + \log \beta_3 \quad (4)$$

Cette équation est résolue graphiquement en portant $\log[\bar{n}/(3 - \bar{n})]$ en fonction de $\log[C_4H_2N_3O_4^-]$. Dans le calcul de $\bar{n}$ et $[C_4H_2N_3O_4^-]$ interviennent la constante de première acidité de l'acide violurique k_1^M et la constante d'acidité de la deuxième fonction de l'acide sulfurique, car dans le bilan électrique de la solution, il faut tenir compte des ions SO_4^{2-}. Pour k_1^M nous retenons la valeur $5{,}7 \cdot 10^{-5}$ déterminée lors d'un travail précédent;[24] pour l'acide sulfurique la littérature[25] donne la valeur $3{,}98 \cdot 10^{-2}$.

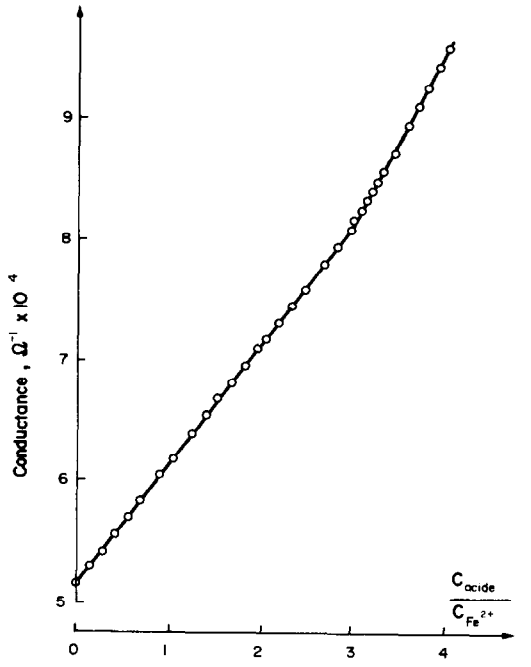


Fig. 1. Variation de la conductance lors de l'addition d'acide violurique à une solution de sulfate ferreux à concentration initiale $1{,}5 \cdot 10^{-3}M$.

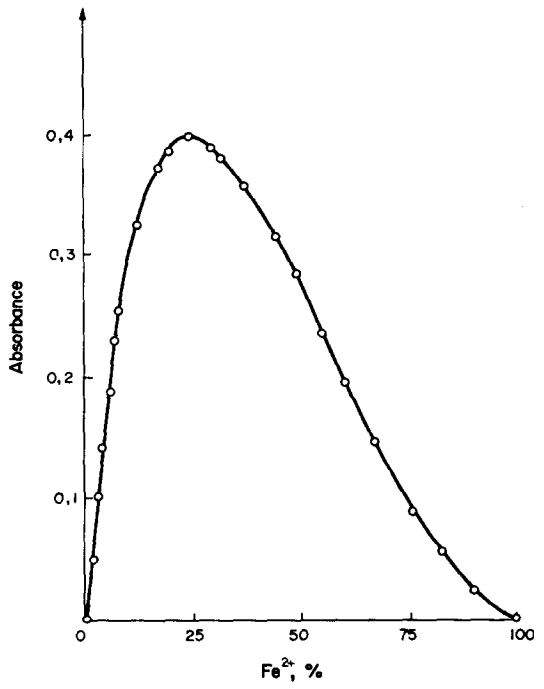


Fig. 2. Spectrophotométrie; méthode des variations continues. Concentration totale (Fe^{2+} + acide violurique) $1{,}25 \cdot 10^{-3} M$. Longueur d'onde 605 nm.

Appliquée à chaque courbe de neutralisation, la relation (4) donne une droite unique de pente 3 et dont l'ordonnée à l'origine est 8,61. La valeur de la pente confirme bien le rapport complexant/métal déterminé précédemment, et de la valeur 8,61 nous pouvons déduire la constante de stabilité du complexe qui est égale à $\beta_3 = 4{,}0 \pm 0{,}5 \cdot 10^8$.

Le triviolurate ferreux a un spectre d'absorption dans le visible caractérisé par une importante bande située entre 500 et 700 nm dont le sommet se trouve à 605 nm. L'absorbance du complexe est maximale dans la zone de pH comprise entre 4 et 5; à pH = 4,58 et à longueur d'onde 605 nm, l'absorptivité du complexe est égale à $6{,}95 \pm 0{,}05 \cdot 10^3$ l·mole^{-1}·cm^{-1}.

La méthode des variations continues n'est employée que qualitativement, car dans le cas de complexes de rapport supérieur à 2, cette méthode graphique donne une valeur beaucoup trop imprécise de la constante de stabilité. Les courbes obtenues ont un maximum situé vers 25% en Fe^{2+} et une tangente horizontale à 100% en Fe^{2+} (Fig. 2). Ces résultats confirment les hypothèses émises sur la formule stoechiométrique du complexe et prouvent qu'il est mononucléaire.

Les courbes de variations successives présentent un seul point singulier pour le rapport Fe^{2+}/acide égal à 1/3 (Fig. 3). Le traitement mathématique de ces courbes[26] conduit à une valeur de la constante de stabilité égale à $2{,}5 \pm 0{,}5 \cdot 10^8$.

La méthode de dilution,[23] mise au point au laboratoire permet la détermination de la constante de stabilité d'un complexe par comparaison de l'absorbance de deux solutions contenant le complexe à deux concentrations différentes. Si C représente la concentration théorique en complexe (réaction de complexation totale) de la solution la plus concentrée, p le rapport de dilution de deux solutions ($p > 1$) et r le rapport des deux absorbances, dans notre cas, nous avons:

$$\beta_3 = \frac{\left(r^{3/4} - \frac{r}{p}\right)(r^{3/4} - 1)}{27\,C^3\left(\frac{r}{p} - 1\right)^4}. \qquad (5)$$

Avec les cinq solutions que nous avons préparées, nous obtenons donc 10 valeurs de la constante β_3, dont la moyenne est égale à $2{,}8 \pm 0{,}3 \cdot 10^8$.

Dans le cas de la spectrophotométrie, nous avons considéré dans le calcul de β_3 que la quantité d'acide violurique qui n'a pas réagi, se trouve sous la forme $C_4H_2N_3O_4^-$; il faut donc faire intervenir le facteur $(1 + \{H^+\}/k_1^M)^3$ dans lequel $\{H^+\}$ représente l'activité des protons déduite du pH, k_1^M étant la constante de première acidité considérée précédemment. La valeur de la constante de stabilité déterminée par spectrophotométrie devient donc égale à $8{,}3 \pm 0{,}7 \cdot 10^8$.

Complexation par l'acide thio-2 violurique

Les résultats sont très semblables à ceux obtenus pour l'acide violurique. La conductimétrie donne une formule stoéchiométrique à 3 complexants par métal. Les courbes de neutralisation présentent aussi une

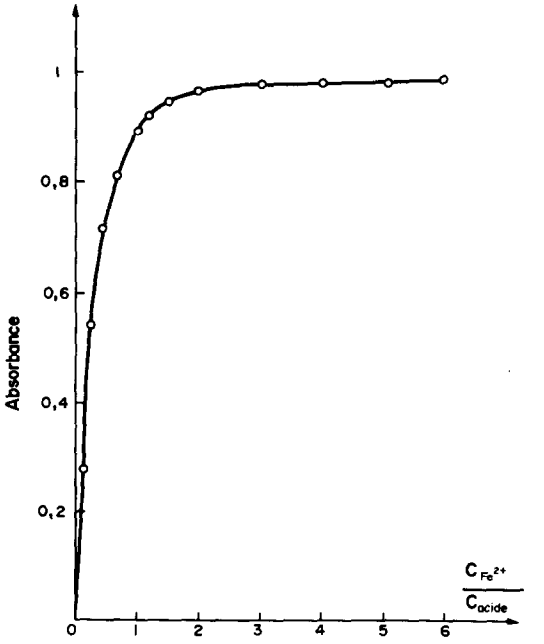


Fig. 3. Spectrophotométrie; méthode des variations successives. Concentration initiale en acide violurique $2{,}45 \cdot 10^{-3} M$. Longueur d'onde 605 nm.

seule équivalence pour le rapport base/acide égal à 1 et la réaction de complexation s'écrit:

$$3C_4H_3N_3O_3S + Fe^{2+} \rightleftharpoons Fe(C_4H_2N_3O_3S)_3^- + 3H^+ \quad (6)$$

La constante de stabilité du complexe trithioviolurate:

$$\beta'_3 = \frac{[Fe(C_4H_2N_3O_3S)_3^-]}{[Fe^{2+}][C_4H_2N_3O_3S^-]^3} \quad (7)$$

peut être calculée par la relation:

$$\log \frac{\bar{n}}{3-\bar{n}} = 3 \log[C_4H_2N_3O_3S^-] + \log \beta'_3. \quad (8)$$

La valeur de la constante de première acidité de l'acide thio-2 violurique retenue pour le calcul de β'_3 est $1{,}62 \cdot 10^{-4}$.[27] La résolution graphique de la relation (8) conduit à une droite de pente 3 et d'ordonnée à l'origine 9,04, ce qui donne $\beta'_3 = 1{,}1 \pm 0{,}5 \cdot 10^9$.

Le spectre d'absorption dans le visible du complexe trithioviolurate ferreux se caractérise par une bande entre 500 et 700 nm et le maximum d'absorption est situé à 615 nm. A cette longueur d'onde et à pH = 4,58, l'absorptivité est de $3{,}76 \pm 0{,}05 \cdot 10^3$ l.mole^{-1}.cm^{-1}.

Les courbes obtenues par la méthode des variations continues ont un maximum pour 25% en Fe^{2+} et une tangente horizontale à 100% en Fe^{2+}. Le traitement mathématique des courbes de variations successives donne pour β'_3 la valeur $6{,}5 \pm 0{,}5 \cdot 10^8$. La valeur moyenne obtenue par la méthode de dilution est égale à $7{,}4 \pm 0{,}9 \cdot 10^8$. La valeur corrigée retenue est $\beta'_3 = 1{,}45 \pm 0{,}7 \cdot 10^8$.

Dans la détermination des constantes de stabilité β_3 et β'_3, nous n'avons pas tenu compte de l'hydrolyse des ions Fe^{2+} qui génère l'espèce $Fe(OH)^+$, puisque dans le domaine de pH où a lieu la réaction de complexation, il y a moins de 1‰ de la concentration en ions ferreux libres qui soit hydrolysé.

Les trois techniques expérimentales que nous avons utilisées donnent, pour chaque complexe, des résultats concordants pour la formule stoechiométrique qui confirment les résultats antérieurs les plus récents. La corrélation entre les valeurs numériques des constantes de stabilité est également très satisfaisante. La seule valeur bibliographique de constante de stabilité est celle du complexe violurique déterminée par Faus *et al.*[15] à 25° et à force ionique 0,2*M* par spectrophotométrie; elle est très proche de nos valeurs puisqu'elle est égale à $6 \cdot 10^8$.

La comparaison entre les résultats de la complexation par l'acide violurique et l'acide thio-2 violurique du fer(II) montre que l'action de ces deux complexants est très voisine. Les complexes ont même coloration et même formule stoéchiométrique et leur stabilité est très comparable. La substitution de l'oxygène en position 2 par un soufre dans l'acide violurique ne semble avoir pour effet que de renforcer légèrement la stabilité du complexe. Cette constatation est confirmée par le fait que les acidités de l'acide thio-2 violurique sont plus fortes que celles de l'acide violurique.[24,27]

LITTERATURE

1. H. Erlenmeyer, H. V. Hahn et E. Sorkin, *Helv. Chim. Acta*, 1951, **34**, 1419.
2. W. Bock-Werthmann, *Z. Anal. Chem.* 1963, **198**, 403.
3. E. C. B. Ammann et V. H. Lynch, *Anal. Biochem.*, 1964, **7**, 387.
4. J. Beltan-Martinez et J. Faus-Paya, *J. Chromatog.*, 1975, **103**, 392.
5. J. W. L. van Litgen et H. van Velthuyzen, *Mikrochim. Acta*, 1964, 759.
6. M. Ziegler, *Z. Anal. Chem.*, 1958, **164**, 387.
7. S. Valladas-Dubois et J. Lemerle, *Compt. Rend.*, 1965, **260**, 145; **261**, 972.
8. F. Popea et A. C. Biancu, *Rev. Roum. Chim.*, 1970, **15**, 1319.
9. L. V. Ershova, *Zavodsk. Lab.*, 1972, **38**, 905.
10. K. Matsusaki, *Yamaguchi Daigaku Kogakubu Kenky Hokoku*, 1978, **28**, 249.
11. A. Hantsch, *Ber.*, 1909, **42**, 986.
12. W. K[illegible], E. Erfle, E. V. Roll et K. Schiller, *Z. Physiol. Chem.*, 1926, **155**, 157.
13. P. Černý, *Chem. Listy*, 1957, **51**, 735.
14. P. A. Leermakers et W. H. Hoffman, *J. Am. Chem. Soc.*, 1958, **80**, 5663.
15. J. Faus, J. Moratal et J. Beltran, *Rev. Acad. Cienc. Exactas, Fis-Quim. Nat. Zaragoya*, 1977, **32**, 67.
16. C. L. Raston et A. H. White, *J. Chem. Soc., Dalton Trans.*, 1976, 1915.
17. R. S. Chawla, Y. Dutt et R. P. Singh, *Talanta*, 1969, **16**, 119.
18. R. S. Chawla et R. P. Singh, *Mikrochim. Acta*, 1970, **332**, 496.
19. L. V. Ershova, V. M. Ivanov et A. I. Busev, *Zh. Analit. Khim.*, 1974, **29**, 1367.
20. R. S. Chawla et R. P. Singh, *J. Indian Chem. Soc.*, 1975, **52**, 169.
21. R. P. Singh, J.9*ibid.*, 1960, **37**, 442.
22. V. E. Toropova, O. Yu. Timofeeva et Z. P. Evteeva, *Zh. Analit. Khim.*, 1971, **26**, 1545.
23. J. Hennion, *Thèse*, Lille, 1974.
24. N. Delannoy, A. Delannoy, J. Hennion et J. Nicole, *Compt. Rend.*, 1978, **287C**, 527.
25. L. G. Sillén et A. E. Martell, *Stability Constants of Metal-Ion Complexes*, 2nd Ed., The Chemical Society, London, 1964.
26. K. Momoki, J. Sekino, H. Sato et N. Yamaguchi, *Anal. Chem.*, 1969, **41**, 1286.
27. J. M. Degorre, A. Delannoy, J. Hennion et J. Nicole, *Bull. Soc. Chim. France*, 1979, 471.

Summary—The complexes of iron(II) with violuric acid and 2-thioviolurie acid have been studied by conductimetry, potentiometry, and spectrophotometry at 25° in aqueous medium. The formation of triviolurate $[Fe(C_4H_2N_3O_4)_3^-]$ and trithioviolurate $[Fe(C_4H_2N_3O_3S)_3^-]$ compounds with iron(II) is confirmed, and their maximum absorptions are at 605 nm and 615 nm respectively. The stability constants of these complexes were determined at ionic strength 0.5*M* by potentiometry and spectrophotometry. These two methods gave nearly the same results: $(4.0 \pm 0.3) \times 10^8$ and $(8.3 \pm 0.7) \times 10^8$ for the violurate complex and $(1.1 \pm 0.5) \times 10^9$ and $(1.45 \pm 0.7) \times 10^9$ for the thioviolurate complex.

Talanta, Vol. 28, pp. 455 to 459, 1981
Printed in Great Britain. All rights reserved

0039-9140/81/070455-05$02.00/0
Copyright © 1981 Pergamon Press Ltd

INFLUENCE OF SOME MATRIX ELEMENTS ON ATOMIZATION OF COBALT IN GRAPHITE-FURNACE ATOMIC-ABSORPTION SPECTROMETRY

A. HULANICKI, R. KARWOWSKA and J. SOWINSKI
Department of Chemistry, University of Warsaw, Warsaw, Poland

(*Received* 28 *October* 1980. *Accepted* 9 *January* 1981)

Summary—The influence of some chlorine, sulphur and phosphorus compounds on cobalt atomization in a graphite cuvette has been investigated. On the basis of atomization curves and estimated atomization energies the mechanisms of several processes have been proposed. Excess of chlorine is responsible for losses of cobalt as chloride and also for formation of a compound with graphite which causes atomization to occur at a temperature 300 K higher than that in the absence of graphite. In presence of sulphur, the atomization goes through sulphide formation but a reaction with graphite is also suspected. The presence of phosphorus significantly increases the rate of atomization, which enhances the peak height for cobalt. The mechanism probably involves dissociation of phosphate salts.

Only a few papers have dealt with investigation of interferences in electrothermal atomization of cobalt in atomic-absorption spectroscopy. Campbell and Ottaway[1] have proposed an atomization mechanism based on reduction by the carbon of the graphite cuvette:

$$CoO_{(s)} + C_{(s)} \rightarrow Co_{(g)} + CO_{(g)}$$

The free energy change for this reaction becomes negative at 1770 K, which is in good agreement with the temperature of appearance of cobalt atoms in the atomizer (1720 K). Aggett and Sprott[2] have observed atomization of cobalt to occur at 1570 K in a graphite furnace, compared with 1770 K in a tantalum boat, indicating reduction of the oxide by the graphite. Sturgeon *et al.*[3] found similar behaviour for cobalt chloride and nitrate, which supports the view that in both cases oxide reduction precedes the vaporization (ΔH = 406 kJ/mole) and dimer dissociation (ΔH = 184 kJ/mole). The experimentally evaluated atomization energy values were in good agreement with those theoretically estimated.

Matrix components often cause interference in practical analytical procedures. Simmons[4] found that iron decreased the cobalt signal, and that manganese enhanced it. Cruz and Van Loon[5] noted a negative error when cobalt was determined in the presence of 1% of calcium carbonate or magnesium nitrate, but similar concentrations of alkali-metal or aluminium nitrate did not interfere. Julshamm[6] found that the perchloric acid used for mineralization of biological material caused *ca.* 20% error in the cobalt result when present in 1*M* concentration. To overcome matrix effects Hudnik *et al.*[7] separated cobalt with iron dithiocarbamate as collector, while Batley and Matousek[8] used electrochemical separation on a mercury-film graphite electrode. Volland *et al.*[9] stated that besides other factors, the graphite surface, gas impurities or acid contamination influence the results of cobalt determination.

The purpose of this paper is to investigate the effect of some common matrix components on the atomization of cobalt.

EXPERIMENTAL

Apparatus

Perkin–Elmer 300A atomic-absorption spectrophotometer, with HGA-72 graphite cuvette and Hitachi–Perkin–Elmer 159 recorder. Cathodeon hollow-cathode lamp. Eppendorf micropipettes, Unipan 304 peristaltic pump.

Reagents

Solutions of cobalt sulphate, nitrate and chloride (concentration 1.00 mg/ml) were prepared from the hydrated salts in approx. 0.01*M* solution of the corresponding acid. The solution of cobalt phosphate (20 μg/ml) was prepared by appropriate dilution of a saturated aqueous solution.

The diethyldithiocarbamate (DDTC) cobalt complex was obtained by extraction from aqueous solution into methyl isobutyl ketone (MIBK) or carbon tetrachloride.

Measurements

Absorbance measurements were made at 240.7 nm, with a 0.2-nm band-pass. The hollow-cathode lamp current was 12 mA. Non-specific absorbance was measured either under identical conditions with solutions not containing cobalt, or the non-absorbing 239.3-nm cobalt line was used. Argon was used as sheath-gas at a flow-rate of 1.5 l./min.

For absorbance measurements, a 10-μl sample was evaporated for 15 sec at 370 K, ashed for 30 sec at 1420 K and atomized for 10 sec at 2930 K, the heating rate being 900 K/sec. For recording atomization curves the temperature was increased in the atomization step at an average heating rate of 90 K/sec from 1420 K to 2930 K.

For estimating the atomization energy, the drying and ashing steps were as indicated above, then the cuvette was cooled to room temperature, heated first to 570 K, and then to 2930 K at a heating rate of 21 K/sec. In these measurements the temperature was monitored with a photo-sensitive diode. This procedure was similar to that

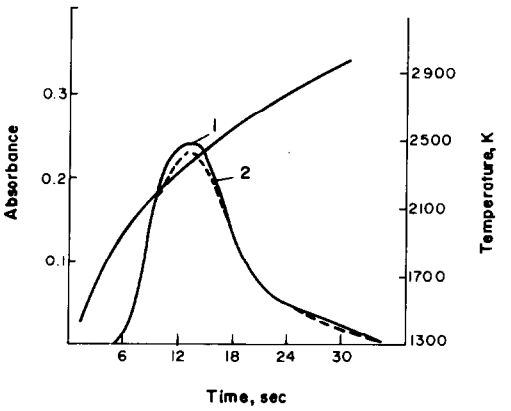


Fig. 1. Atomization curves for 16 ng of cobalt, atomization rate 90 K/sec. Curve 1—$CoCl_2$ in 0.1*M* HCl; curve 2—$Co(NO_3)_2$ in 0.1*M* HNO_3.

used by Rowston and Ottaway.[10] Atomization energies determined in various cuvettes under comparable conditions indicated that the error in the results did not exceed 50 kJ/mole.

RESULTS AND DISCUSSION

The effect of chlorine

The atomization curves for 20 ng of Co present as chloride or nitrate in the corresponding 0.1*M* acid (Fig. 1) are similar, as was earlier pointed out by Sturgeon *et al.*,[3] which suggests a similar atomization mechanism in both cases. The estimated atomization energy (420 kJ/mole) is in good agreement with the literature value for vaporization of cobalt at 298 K.[3] When a nitrate solution of cobalt at higher concentrations is atomized, the atomization curve shows the presence of two dominating processes. In the range 1620–1740 K the calculated atomization energy is 560 kJ/mole, but in the range 1740–1790 K the energy decreases to a level close to that observed for chloride, *i.e.* 430 kJ/mole. Until now there has been no reasonable explanation of the first process, which precedes the cobalt vaporization. Because the atomization curves in hydrochloric acid medium are easily reproducible they will be considered as standard curves in the course of this investigation.

The excess of chlorine in these samples has practically no effect on the atomization processes, because most probably it is removed as hydrogen chloride in the presence of the hydrogen originating from decomposition of water.[12]

The influence of chlorine is much more significant when a non-aqueous solvent such as carbon tetrachloride is used. In this case, in our experiments the cobalt was present as the diethyldithiocarbamate chelate, but the effect of the chelating agent is insignificant, as can seen from Fig. 2, showing the result when methyl isobutyl ketone was used as the solvent. The effect of carbon tetrachloride on cobalt atomization is similar to that observed for iron[13] and is represented by an approx. 300 K increase in the temperature for maximum atomization, compared to the standard curve for cobalt.

The presence of carbon tetrachloride influences not only the atomization processes but also the decomposition step. While for aqueous or MIBK solutions the decomposition proceeds at 1420 K, for organic samples in carbon tetrachloride at this temperature a significant decrease in the peak-height is observed (Fig. 2, curve 3) because of the loss of cobalt as the volatile chloride, the boiling point of which is 1326 K. This confirms that when the decomposition temperature is above the boiling point of the more volatile species, most of the cobalt is removed from the cuvette before the atomization step. The temperature actually needed for removal of the cobalt chloride is somewhat higher than the boiling point because of uneven temperature distribution in the cuvette.

The removal of cobalt chloride, which causes a decrease in the integrated absorbance signal for cobalt atoms, is at least partially connected with the diffusion of cobalt chloride into the graphite structure, which becomes more easily penetrated after treatment with chlorine.[14] As a result, the small peak of cobalt appears at higher temperature than in the case of aqueous solutions or organic solvents that are not chloro-compounds. When cobalt in carbon tetrachloride medium is atomized from a tantalum boat without direct contact with graphite, the carbon tetrachloride evaporates very early and does not influence the atomization of the cobalt. Also, if carbon tetrachloride vapour is added (0.2% v/v) to the sheath gas, it has no influence on the atomization temperature, though it decreases the atomic absorbance of cobalt by about 60% because of the gas-phase reaction between cobalt and chlorine. The direct quantitative evaluation of the contribution of these reactions is not possible, because they strongly depend on the quality of the surface of the graphite cuvette. With a new

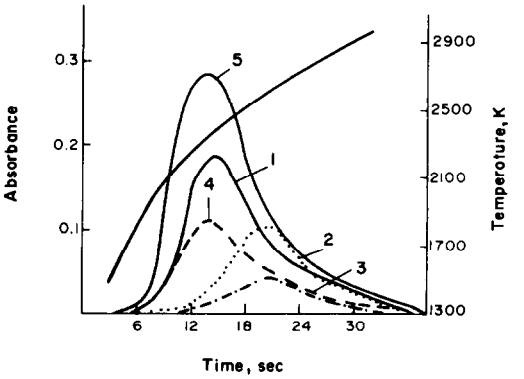


Fig. 2. Atomization curves for 20 ng of cobalt. Curve 1—Co–DDTC in MIBK, thermal decomposition at 1420 K, 30 sec; curve 2—Co–DDTC in CCl_4, thermal decomposition at 1070 K, 30 sec; curve 3—Co–DDTC in CCl_4, thermal decomposition at 1420 K, 30 sec; curve 4—$CoCl_2$ in 0.1*M* HCl, sheath gas containing 0.2% v/v CCl_4; curve 5—$CoCl_2$ in 0.1*M* HCl.

cuvette that has not previously been heated, the interaction of carbon tetrachloride with the graphite is seriously restricted, but increases with greater porosity of the material.

The unfavourable excess of chlorine in the atomizer, which may result in losses of atomic cobalt vapour, can be removed by addition of water to the cuvette. At temperatures above 920 K the free energy change of the reaction

$$H_2O + C = H_2 + CO$$

becomes negative, and chlorine may be removed in the form of hydrogen chloride.[12] When addition of the sample of Co–DDTC in carbon tetrachloride is followed by addition of microgram amounts of water, the peak height for cobalt increases significantly. In the absence of water the absorbance recorded for 20 ng of cobalt was 0.02 (for temperature increased at 90 K/sec). With addition of 5 and 50 μl of water the absorbances were 0.10 and 0.21, respectively. It may be postulated that water does not influence the stability of the water–graphite compound, because no double peak, which is found in the case of iron,[13] is observed.

Hydrocarbons act similarly to water, decomposing to give hydrogen. When the organic cobalt sample (10 ng) in carbon tetrachloride was treated with 10% of n-hexane, the absorbance increased from 0.03 to 0.32. When a 1:9 v/v mixture of carbon tetrachloride and n-hexane was used as solvent, the absorbance increased to 0.52. In these experiments the sample was pyrolysed for 30 sec at 1420 K, and the rate of temperature increase for the atomization step was 900 K/sec.

Effect of sulphur

The atomization curve for 20 ng of cobalt as sulphate in 0.1*M* sulphuric acid differs in shape and magnitude from those obtained under the standard conditions ($CoCl_2$ in 0.1*M* hydrochloric acid). The maximum temperature is 50 K lower, and the peak absorbance increases by 10% for rapid atomization (900 K/sec) or by 20% for slow atomization (90 K/sec), showing the influence of kinetic parameters (Table 1).

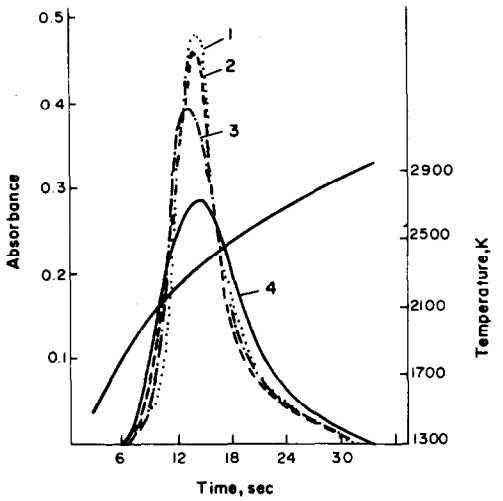


Fig. 3. Atomization curves for 20 ng of cobalt. Curve 1—$CoCl_2$ in 0.1*M* HCl, cuvette impregnated with 20 μl of CS_2; curve 2—$CoCl_2$ in 0.1*M* HCl, with addition of elemental sulphur; curve 3—$CoSO_4$ in 0.1*M* H_2SO_4; curve 4—$CoCl_2$ in 0.1*M* HCl.

Similar change in the shape of the atomization curve is observed when a cobalt chloride sample in a graphite cuvette is treated with either carbon disulphide or elemental sulphur (Fig. 3). The peak absorbance increases significantly, especially with slow atomization (Table 1), though the reproducibility is then poor. The effect of carbon disulphide is independent of whether it is added before or after the cobalt sample, so long as the cuvette is not heated above 2570 K, which indicates that at this temperature sulphur is completely removed from the cuvette.

These effects are connected with the interaction of the analyte and sulphur with graphite and were not observed when the sample was atomized from the tantalum boat. Formation of graphite compounds in the presence of excess of sulphur was noted by Croft.[15] In our experiments, small amounts of sulphur, as was shown by the atomization of Co–DDTC

Table 1. Peak-heights and integrated absorbances of cobalt atomized under various conditions; average values (in relative units) of 3–5 measurements

Solution added to cuvette	HCl, 0.1*M*	HNO_3, 0.1*M*	H_2SO_4, 0.1*M*	HCl 0.1*M* + CS_2	HCl 0.1*M* + S	H_3PO_4 0.1*M*
10 ng of Co 900 K/sec Peak height	80.5	78	90	100	98	89
20 ng of Co 90 K/sec						
Peak height*	73	72	101	116	103	117
Integrated absorbance	107	104	106	107	102	104

* Peak heights for 90-K/sec atomization rate are poorly reproducible.

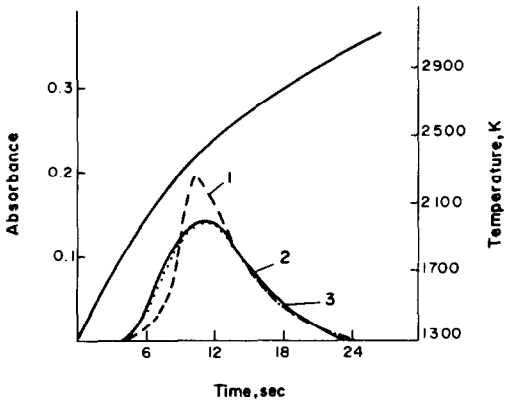


Fig. 4. Atomization curves for 10 ng of cobalt. Curve 1—$CoCl_2$ in 0.1*M* H_3PO_4; curve 2—$CoCl_2$ in 2% Na_2HPO_4 solution; curve 3—$CoCl_3$ in 0.1*M* HCl.

in MIBK solution, were without effect and atomization proceeded as it did under standard conditions.

The atomization energy evaluated in the absence of excess of sulphur was 440 kJ/mole, in good agreement with the heat of vaporization of cobalt (Table 2). When the cuvette was impregnated with carbon disulphide the atomization energy in the temperature range 1610–1700 K was 570 kJ/mole. This corresponds approximately to the heat of vaporization of cobalt (428 kJ/mole) minus the heat of formation of cobalt sulphide ($\Delta H_f = -84.5$ kJ/mole).

The presence of sulphuric acid alone also complicates the atomization of cobalt, as this acid forms stable compounds with graphite.[16] This influences the atomization mechanism for cobalt. In the range 1660–1700 K the atomization energy of cobalt then becomes 700 kJ/mole. This is not readily explained, since for the temperature range 1700–1800 K the evaluated energy of 540 kJ/mole is approximately equal to that found in the presence of carbon disulphide.

Effect of phosphorus

In the presence of phosphoric acid the peak absorbance of cobalt increases relative to that for hydrochloric acid solutions (Table 1). The atomization curves are much sharper and their height is over 50% greater if the slow atomization rate is used. Such behaviour was observed not only for phosphoric acid but also for solutions containing diammonium hydrogen phosphate, which decomposes thermally to phosphoric acid. In contrast, disodium hydrogen phosphate has no effect, probably because of its higher thermal stability.

The cobalt absorption was also enhanced when dilute solutions of cobalt phosphate were atomized, which indicates that in contrast to the case with chlorine and sulphur, even the stoichiometric amount of phosphorus is sufficient for appearance of the effect. This is certainly a kinetic effect because the presence of phosphorus is practically without influence on the integrated absorbance for cobalt.

The effect of phosphorus on determination of zinc, cadmium and lead has been reported by Czobik and Matousek,[17] and Dittrich *et al.*[18] indicate that the formation of thermally stable zinc or cadmium phosphates results in their sudden evaporation at higher temperature, with enhancement of the atomic-absorption peak-height.

The atomization energy determined for a sample of 5 μg of Co as $CoCl_2$ in 0.1*M* phosphoric acid is 710 kJ/mole. This is significantly higher than that found for atomization through the evaporation of cobalt atoms, but is close to the value obtained in presence of sulphur. The magnitude of this energy also excludes any mechanism involving dissociation of cobalt phosphides, for which the heats of formation are significantly smaller.

CONCLUSIONS

The characteristics of the atomization curves and the values of the atomization energies (Table 2) for cobalt in the graphite cuvette indicate the possibility of elucidating the probable mechanism of atomization under various conditions.

The simple mechanism involving metal evaporation as the rate-determining process was observed in the case of hydrochloric acid solutions and for

Table 2. Atomization energies measured with graphite cuvette

Composition of samples	Appearance temp., *K*	Temperature range, *K*	Measured atomization energy, *kJ/mole*	Literature value, *kJ/mole*
$CoCl_2$/0.1*M* HCl	1440	1500–1650	420	428*
$Co(NO_3)_2$/0.1*M* HNO_3	1560	1620–1740	560	?
		1740–1790	430	428*
$CoCl_2$/0.1*M* H_3PO_4	1460	1690–1770	710	?
$CoSO_4$/0.1*M* H_2SO_4	1550	1640–1700	700	?
		1700–1800	540	428 + 84.5†
Co–DDTC/MIBK	1480	1540–1620	440	428
$CoCl_2/H_2O$, cuvette impregnated with CS_2	1540	1610–1700	570	428 + 84.5†

* Ref. 3: heat of vaporization of $Co_{(s)}$ at 298 K.
† Ref. 11: heat of formation of $CoS_{(s)}$ at 298 K.

Co–DDTC dissolved in methyl isobutylketone. Such a process is accompanied by another which precedes it at lower temperatures, when a large (5 μg) sample in nitric acid medium is atomized. The nature of this second process is still unresolved, and the effect disappears when small amounts of cobalt (10–20 ng) are atomized. The influence of the sample mass may be connected with the poorer contact between sample and cuvette as has been mentioned in the literature.[3,19]

A more complicated reaction probably occurs when some of the components, such as chlorine or sulphur, react with the graphite cuvette. In the case of chlorine an active graphite compound is presumably formed and is responsible for a shift of the maximum of the atomization curve towards higher temperatures. The best way to eliminate such phenomena, when they interfere in the analytical procedure, is to generate gaseous hydrogen from water or hydrocarbons to remove chlorine as hydrogen chloride.

Atomization of cobalt in presence of excess of sulphur compounds most probably proceeds through sulphide formation, as suggested by the energies concerned. In the reducing atmosphere this occurs even when the sample contains only sulphuric acid, which on the one hand is responsible for sulphide formation, and on the other, through its reaction with graphite, significantly influences the mechanism of cobalt atomization. Removal of sulphur from the graphite cuvette needs temperatures up to 2300 K, but the position of the peak maximum is not significantly influenced by sulphur compounds. It seems probable that the unexplained energy value of ~700 kJ/mole at 1600–1700 K is connected with a more complicated mechanism.

In presence of phosphoric acid a similar energy value has been estimated, which cannot easily be related to probable reaction mechanism. It is possible that the enhancing effect of phosphorus is predominantly kinetic in character, as mentioned by other authors.[17]

REFERENCES

1. W. C. Campbell and J. M. Ottaway, *Talanta*, 1974, **21**, 837.
2. J. Aggett and A. J. Sprott, *Anal. Chim. Acta*, 1974, **72**, 49.
3. R. E. Sturgeon, C. L. Chakrabarti and C. H. Langford, *Anal. Chem.*, 1976, **48**, 1792.
4. W. J. Simmons, *ibid.*, 1975, **47**, 2015.
5. L. B. Cruz and J. C. Van Loon, *Anal. Chim. Acta*, 1974, **72**, 231.
6. K. Julshamm, *Atom. Absorp. Newsl.* 1977, **16**, 149.
7. V. Hudnik, S. Gomišček and B. Gorenc, *Anal. Chim. Acta*, 1978, **98**, 382.
8. G. E. Batley and J. P. Matousek, *Anal. Chem.* 1977, **49**, 2031.
9. G. Volland, G. Kölblin, P. Tschöpel and R. Tölg, *Z. Anal. Chem.*, 1977, **284**, 1.
10. W. B. Rowston and J. M. Ottaway, *Analyst*, 1979, **104**, 645.
11. *Gmelins Handbuch der Anorganischen Chemie, System No. 58, Kobalt*, Teil A, p. 614. Verlag Chemie, Weinheim, 1961.
12. W. Frech and A. Cedergren, *Anal. Chim. Acta*, 1976, **82**, 93.
13. R. Karwowska, E. Bulska and A. Hulanicki, *Talanta*, 1980, **27**, 397.
14. J. J. Pitts and L. L. Lyon, *Proc. Conf. Carbon 5th, Univ. Park, Penna*, 1961, **1**, 132.
15. R. C. Croft, *Austr. J. Chem.*, 1956 **9**, 184.
16. A. R. Ubbelhode and R. A. Levis, *Graphite and its Crystal Compounds*, Oxford, 1960.
17. E. J. Czobik and J. P. Matousek, *Talanta*, 1977, **24**, 573.
18. K. Dittrich, W. Mothes and P. Weber, *Spectrochim. Acta*, 1978, **33B**, 325.
19. O. Vyskočilová, V. Sychra, D. Kolihová and P. Püschel, *Anal. Chim. Acta*, 1979, **105**, 271.

Talanta, Vol. 28, pp. 461 to 467, 1981
Printed in Great Britain

0039-9140/81/070461-07$02.00/0
Pergamon Press Ltd

DETERMINATION OF ALUMINIUM IN IRON, STEEL AND FERROUS AND NON-FERROUS ALLOYS BY ATOMIC-ABSORPTION SPECTROPHOTOMETRY AFTER A MERCURY-CATHODE SEPARATION AND EXTRACTION OF THE ALUMINIUM–ACETYLACETONE COMPLEX

ELSIE M. DONALDSON

Mineral Sciences Laboratories, Canada Centre for Mineral and Energy Technology, Department of Energy, Mines and Resources, Ottawa, Canada

(*Received* 10 *December* 1980. *Accepted* 7 *January* 1981)

Summary—A method for determining 0.0005% or more of total aluminium in high- and low-alloy steels, iron and ferrovanadium is described. Iron, chromium and other matrix elements are separated from aluminium by electrolysis with a mercury cathode and aluminium is separated from tungsten, titanium, vanadium and phosphate by chloroform extraction of its acetylacetone complex at pH 6.5 from an ammonium acetate–hydrogen peroxide medium. The extract is evaporated to dryness and organic material is destroyed with nitric and perchloric acids. Aluminium is determined by atomic-absorption spectrophotometry in a nitrous oxide–acetylene flame, at 309.3 nm, in a 5% v/v perchloric acid medium containing 1000 μg of sodium per ml. Acid-soluble and acid-insoluble aluminium can also be determined. The method is also applicable to copper- and nickel-base alloys. Results obtained by this method are compared with those obtained spectrophotometrically with Pyrocatechol Violet, after the separations described above followed by the separation of the residual co-extracted iron and copper by a combined ammonium pyrrolidinedithiocarbamate–cupferron–chloroform extraction from 10% v/v hydrochloric acid medium.

A reasonably simple and reliable flame atomic-absorption spectrophotometric (AAS) method for the determination of ~0.0005–0.05% of total aluminium in both low- and high-alloy steels was required for use in routine work in the CANMET chemical laboratory. Because of the low sensitivity of AAS for aluminium and because iron interferes in the determination in a nitrous oxide–acetylene flame,[1–3] most previous investigators[4–6] agree that a separation from iron and a concentration step are required for the accurate determination of ≤0.01% of aluminium by conventional AAS.

Several recent AAS methods for determining both acid-soluble and acid-insoluble aluminium in mild steels involve the preliminary separation of the bulk of the iron from aluminium by extraction of the chloro-complex into isobutyl acetate from a strongly acidic hydrochloric acid medium.[4,5] This is followed by the evaporation of the aqueous phase to small volume[5] or to dryness[4] before the ultimate AAS determination of aluminium. In these methods, considerable iron remains in the solution after the extraction step. Furthermore, they are not applicable to high-alloy steels containing tungsten or a large amount of chromium, copper, nickel or manganese. Another AAS method for determining total aluminium in both high-alloy and mild steels is based on methyl isobutyl ketone extraction of the iron(III) chloro-complex and the subsequent separation of aluminium from the bulk of the alloying constituents mentioned above, by extracting it as the acetylacetone complex from a weakly acidic medium with pure acetylacetone.[6] After concentration of the extract by evaporation, aluminium is determined by spraying the solution into the flame. In this method, an inordinately large volume of acetylacetone is used for the extraction of aluminium, and the residual iron and many other elements are co-extracted under the conditions employed. About ten years ago, the author developed a spectrophotometric method, based on complex formation with Pyrocatechol Violet, for the determination of small amounts of aluminium in iron, steel and other materials.[7] This method also involves the separation of aluminium by extraction of its acetylacetone complex, after the preliminary separation of iron, chromium, nickel, molybdenum and various other elements by electrolysis with a mercury cathode. However, the selectivity of the acetylacetone extraction step was increased by extracting the aluminium complex into chloroform from 0.05*M* acetylacetone medium in the presence of hydrogen peroxide as a complexing agent for molybdenum, tungsten, titanium and vanadium. The residual co-extracted iron and small amounts of other co-extracted elements

Crown Copyrights Reserved.

were subsequently separated from aluminium by a combined ammonium pyrrolidinedithiocarbamate–cupferron–chloroform extraction from a 10% hydrochloric acid medium, after stripping of the complex from the chloroform phase into concentrated hydrochloric acid. Because the mercury-cathode separation in conjunction with the acetylacetone extraction–pre-concentration step described in this method produces a solution that is essentially free of matrix elements except for a small amount of iron, it was considered that an AAS finish could readily be applied after the extraction step.

This paper describes the successful determination of total aluminium or both acid-soluble and acid-insoluble aluminium in mild and high-alloy steels and in ferrovanadium. Total aluminium can also be determined in copper- and nickel-base alloys. After a preliminary mercury-cathode separation of matrix elements from a 2–3% v/v perchloric or sulphuric acid medium, aluminium is separated from the remaining elements, except residual iron or copper, by chloroform extraction of its acetylacetone complex at pH 6.5 from a 0.1*M* acetylacetone–ammonium acetate–hydrogen peroxide medium. The extract is evaporated to dryness and the residue is treated with nitric and perchloric acids. Results obtained by this method are compared with those obtained previously by the spectrophotometric Pyrocatechol Violet method.[7]

EXPERIMENTAL

Apparatus

A Varian–Techtron model AA6 spectrophotometer, equipped with a 6-cm laminar-flow nitrous oxide–acetylene burner and an aluminium hollow-cathode lamp, was used under the following conditions (Note 1).
Wavelength: 309.3 nm
Lamp current: 10 mA
Spectral band-pass: 0.20 nm
Height of light-path above burner: 9 mm
Acetylene flowmeter reading: 6.75 (~4.5 l./min)
Nitrous oxide flowmeter reading: 6 (~8.5 l./min)
Flame: non-luminous, ~1.5–2 cm "red feather"
Aspiration rate: 2 ml/min

Reagents

Standard aluminium solution. 1000 μg/ml. Dissolve 1.000 g of high-purity aluminium metal and about 5 mg of high-purity iron metal (Note 2) by heating gently in a covered 400-ml beaker with 20 ml of concentrated hydrochloric acid. Cool and dilute to 1 litre with water. Prepare a 100-μg/ml solution by diluting 20 ml of this stock solution to 200 ml with water. Prepare the diluted solution fresh as required.

Acetylacetone, 20% solution. Dilute 20 ml of acetylacetone and 30 ml of ethyl alcohol to 100 ml with water. This solution is stable for at least one week.

Sodium 10 mg/ml solution. Dissolve 12.7 g of sodium chloride in water and dilute to 500 ml.

Perchloric acid, 50% v/v.

Sulphuric acid, 1% v/v.

Hydrogen peroxide, 30%.

Ammonium acetate solution, 50%.

Procedures

Calibration solutions. Add 10 ml each of 50% perchloric acid and 10-mg/ml sodium solution to each of nine 100-ml standard flasks; then, from a burette, add to the first eight flasks 1, 2, 3, 5, 10, 15, 20 and 25 ml respectively, of the 100-μg/ml standard aluminium solution. The last flask contains the zero calibration solution. Dilute each solution to volume with water (Note 3).

Iron, steel and nickel–chromium alloys. Transfer 0.1–1 g of sample (Note 4) containing not more than 2 mg of aluminium to a 400-ml beaker, then cover the beaker and add 15 ml of concentrated hydrochloric acid and 5 ml of concentrated nitric acid. Heat until the sample has dissolved, then add 20 ml of concentrated perchloric acid (Note 5) and evaporate the solution to fumes of perchloric acid. Remove the cover and carefully evaporate the solution to 5–7 ml. Cool, add ~50 ml of water and heat to dissolve the salts. Add about a quarter of a Whatman filter pulp tablet, macerate it with a stirring rod, then filter the solution (Whatman No. 40 paper) into a 400-ml beaker and transfer the residue quantitatively to the filter paper. Wash the paper and the residue three times with water, then three times with 1% sulphuric acid to ensure the complete removal of perchloric acid. Evaporate the filtrate to about 75 ml (Note 6). Carry a blank through the whole procedure.

Transfer the paper containing the residue to a 30-ml platinum crucible, burn off the paper at a low temperature and ignite at 600–700°. Cool the crucible and add 1 ml each of 50% sulphuric acid and concentrated nitric and hydrofluoric acids. Heat gently to dissolve the residue, then evaporate the solution to dryness. Fuse the residue with 2 g of fused sodium hydrogen sulphate (Note 7), then cool the crucible and transfer it to a 250-ml beaker containing ~50 ml of water. Cover the beaker and heat gently to dissolve the melt. Remove the crucible after washing it thoroughly with water (Note 8), then add the solution to the initial filtrate.

Transfer the solution to a mercury-cathode cell, dilute to ~200 ml with water and electrolyse for 75 min at ~10 A. Filter the electrolyte (Whatman No. 541 paper) into the 400-ml beaker that initially contained the solution. Wash the cathode cell and the paper thoroughly with water, then discard the paper. Add 5 ml of concentrated hydrochloric acid and 3 ml of 50% sulphuric acid and evaporate the solution until 1.5–2 ml of sulphuric acid remain (Note 9). Cool the beaker, add 50 ml of water, heat gently until the solution is clear (Note 10), then cool it to room temperature.

In succession, add 2 ml of 30% hydrogen peroxide, 5 ml of 20% acetylacetone solution and 10 ml of 50% ammonium acetate solution to the solution, then, using a pH-meter, adjust the pH of the solution to 6.5 ± 0.1 with concentrated ammonia solution. Transfer the solution to a 125-ml separatory funnel, add 10 ml of chloroform, stopper and shake for 2 min. Allow several min for the layers to separate, then drain the chloroform phase into a 100-ml beaker. Extract the aqueous phase twice more by shaking it for 1 min each time with 5 ml of chloroform, then wash it by shaking it for ~30 sec with 5 ml of chloroform. Add 5 drops of concentrated hydrochloric acid to the combined extracts and evaporate to dryness in a hot water-bath. Add 1 ml of 50% perchloric acid and 2 ml of concentrated nitric acid, then cover the beaker and heat on a hot plate until fumes of perchloric acid are evolved (Note 11). Cool the solution to room temperature and add ~3 ml of water. Transfer the blank solution to a 10-ml standard flask containing 1 ml of 10-mg/ml sodium solution and dilute to volume with water. Depending on the expected aluminium content, transfer the sample solution to a standard flask of appropriate size (10–100 ml) and add sufficient 10-mg/ml sodium solution for 1 ml to be present for each 10 ml of final solution. If necessary, add sufficient 50% perchloric acid for 1 ml to be present for each 10 ml of final solution in excess of 10 ml (Note 12), and dilute the solution to volume with water.

Measure the absorbances at 309.3 nm when the resulting

solutions are aspirated into a strongly reducing nitrous oxide–acetylene flame (Note 13). Calculate the aluminium contents (in mg) from the sample and blank absorbances and those obtained concurrently for calibration solutions that bracket the sample and blank concentrations. Correct the result obtained for the sample solution by subtracting that obtained for the blank solution.

Ferrovanadium. Decompose 0.1–0.5 g of sample containing up to 2 mg of aluminium as described above, using 20 ml of 50% sulphuric acid instead of concentrated perchloric acid. Heat the solution until the evolution of oxides of nitrogen ceases, then remove the cover and evaporate to 5–7 ml. Cool, add 50 ml of water, heat to dissolve the salts, then proceed with the filtration of the solution (Note 14), the treatment of the residue, the mercury-cathode separation (Note 15), the extraction (Note 16) and the subsequent determination of aluminium as described above.

Copper-base and nickel–copper alloys. Transfer 0.1–1 g of sample containing up to 2 mg of aluminium to a 400-ml beaker (Note 17), then cover the beaker and add 5 ml each of water and concentrated nitric acid and 20 ml of 50% sulphuric acid. Heat the solution until the evolution of oxides of nitrogen ceases, then remove the cover and evaporate to 5–7 ml. Cool, add 50 ml of water and, if necessary, heat to dissolve the salts. Transfer the solution to an electrolytic cell, dilute to 200 ml with water and proceed with the mercury-cathode separation (Note 15), the extraction and the subsequent determination of aluminium, as described above.

Notes

1. A strongly reducing, non-luminous nitrous oxide–acetylene flame is required to obtain the highest sensitivity for aluminium. The height at which the beam from the hollow-cathode lamp passes through the flame is also extremely important.[1,3] Consequently, after all other instrumental parameters have been set, the acetylene and nitrous oxide flow-rates should be adjusted to give the maximum absorbance when a solution containing aluminium is aspirated into the flame.

2. Iron hastens the dissolution of the aluminium metal.

3. The calibration solutions should be prepared fresh every week.

4. More than 1 g of sample is not recommended because too much iron may remain in the solution after the mercury-cathode separation. The residual iron is co-extracted and, if a large amount is present, may result in an explosive reaction when the final solution is evaporated to fumes of perchloric acid. Too much iron can also cause a slight positive error in the aluminium result.

5. For iron and steel of low chromium content and high titanium, vanadium, molybdenum or tungsten content, add 20 ml of 50% sulphuric acid instead of perchloric acid and proceed as described for ferrovanadium.

6. If the acid-soluble aluminium content of the sample is required, proceed with the mercury-cathode separation, the extraction and the subsequent determination of aluminium as described.

7. One gram of a mixture consisting of 75% by weight of sodium carbonate and 25% by weight of fused boric acid can also be used for fusion of the insoluble material.[4] However, the melt should be dissolved in water containing ~2 ml of 50% sulphuric acid.

8. If the acid-insoluble aluminium content of the sample is required, it can be determined in the resulting solution. In this case, omit the mercury-cathode separation, add the volumes of hydrogen peroxide, acetylacetone and ammonium acetate solutions recommended in the subsequent part of the procedure, and proceed with the pH-adjustment, the extraction and the determination of aluminium as described. The total amount of aluminium present in the sample can then be determined by adding that found in the acid-insoluble material to that found in the filtrate (Note 6).

The separate determination of acid-insoluble aluminium is recommended if an appreciable amount of tungsten trioxide is present in the acid-insoluble material. In this case, add 5 ml of 30% hydrogen peroxide and the recommended volumes of acetylacetone and ammonium acetate solutions to the solution obtained after dissolving the melt, then add sufficient concentrated ammonia solution to dissolve the tungsten trioxide. Acidify the solution with 50% sulphuric acid, adjust the pH to 6.5 ± 0.1 and proceed with the extraction and subsequent determination of aluminium.

9. This step volatilizes any mercury left in the solution. Sulphuric acid solutions of aluminium should not be evaporated to dryness. This results in the formation of an anhydrous aluminium sulphate that is virtually insoluble in water or in dilute acid and causes a low result for aluminium.[8]

10. If the extraction cannot be completed the same day, allow the solution to stand overnight at this point.

11. The solution should not be allowed to evaporate to dryness. If the atomic-absorption determination cannot be completed the same day, allow the solution to stand overnight at this point. The final aluminium solution is not always stable on prolonged standing.

12. Additional 50% perchloric acid is not required if the final volume of the solution is to be 10 ml, because 1 ml is added to the residue remaining after the removal of chloroform. For final sample solution volumes of 25, 50 or 100 ml, add 1.5, 4 or 9 ml, respectively.

13. Between 5- and 10-fold scale expansion is recommended for the determination of aluminium.

14. It is not necessary to wash the paper and residue with 1% sulphuric acid as described in the procedure for iron and steel.

15. It is not necessary to add 3 ml of 50% sulphuric acid after the mercury-cathode separation.

16. More than 2 ml of 30% hydrogen peroxide—as recommended in the procedure for iron and steel—will be required for samples of high vanadium content. Approximately 1 ml is required to complex 30 mg of vanadium. Five millilitres should be added for a 0.5-g sample of ferrovanadium containing about 30% of vanadium. The solution should be yellow—not green—after the pH-adjustment.

17. If the sample contains silicon, use a 400-ml Teflon beaker and add 1 or 2 ml of concentrated hydrofluoric acid during the decomposition step.

RESULTS

Atomic-absorption finish after separation of aluminium by extraction of its acetylacetone complex

Tests showed that, after the separation of aluminium by extraction of its acetylacetone complex into chloroform at pH 6.5 as described earlier,[7] aluminium can readily be determined by AAS in a nitrous oxide–acetylene flame after evaporation of the extract and a small amount of concentrated hydrochloric acid to dryness and destruction of the organic material in the residue with nitric and perchloric acids as described in the proposed method. At least 0.5 ml of concentrated perchloric acid is required for this decomposition step. Consequently, a perchloric acid concentration of 5% by volume was chosen for the sample and calibration solutions because a final sample solution volume of at least 10 ml is necessary for the determination of small amounts of aluminium. To

suppress the ionization of aluminium, 1000 μg of sodium (as the chloride) per ml was also added to the sample and calibration solutions.[9]

Effect of diverse ions

The electrolyte obtained after the separation of iron, chromium and other matrix elements from a dilute perchloric or sulphuric acid solution of an iron or steel sample by electrolysis with a mercury-cathode would contain the titanium, zirconium, vanadium and phosphorus (as phosphate) present in the sample, some of the manganese and tungsten and small amounts of residual iron, chromium, molybdenum and possibly nickel, cobalt and copper. It was shown previously[7] that tungsten, niobium and tantalum can be kept in solution, and that molybdenum, titanium and vanadium can be prevented from co-extracting as acetylacetone complexes, by complexing them with hydrogen peroxide during the extraction of the aluminium–acetylacetone complex into chloroform at pH 6.5 from a 0.05*M* acetylacetone medium. Under these conditions, only iron(III), copper(II) and beryllium are completely co-extracted. Cobalt(II), lead and chromium(III), which is produced in an acid medium containing hydrogen peroxide, are very slightly co-extracted, and more than about 8 mg of phosphate causes a low result for aluminium because of the formation of aluminium phosphate. Tests, in which aluminium was extracted from a 0.1*M* acetylacetone medium to increase the range of the proposed method, showed that up to at least 10 mg of iron(III) or 5 mg of copper(II) will not interfere in the extraction of up to at least 2 mg of aluminium. Furthermore, these quantities of iron and copper will not cause significant error in the aluminium result when the final solution is diluted to 10 ml. A larger amount of iron can cause a slight positive error (~ 3% at the 100-μg level) in the result. However, analysis of the final sample solutions derived from 1-g samples of iron and steel showed that usually less than 5 mg of iron will remain in the electrolyte after the mercury-cathode separation.

Up to at least 10 mg of cobalt(II), lead, nickel and chromium(III), 20 mg of manganese(II) and phosphate, and 5 mg of niobium and tantalum can be present during the extraction step without interfering in the extraction or subsequent determination of aluminium. In the presence of 2 ml of 30% w/v hydrogen peroxide, up to at least 60 mg of vanadium(V) and 20 mg of molybdenum(VI), tungsten(VI) and titanium(IV) will not interfere in the extraction of aluminium. Interference from up to at least 150 mg of vanadium can be avoided by adding 5 ml of 30% hydrogen peroxide before the pH-adjustment. Any insoluble tungsten trioxide present at this stage can be dissolved by adding concentrated ammonia solution. Subsequently, the solution should be acidified with dilute sulphuric acid followed by the adjustment of the pH to 6.5 ± 0.1 with concentrated ammonia solution.

The effect of beryllium on the determination of aluminium by AAS was not investigated because it is not usually present in iron and steel. Although it was found previously[7] that small amounts of zirconium can interfere in the extraction of aluminium by causing emulsification in the chloroform phase, up to at least 0.5 mg will not interfere in the proposed method.

Applications

To test the reliability of the proposed method, it was applied to the analysis of National Bureau of Standards (NBS) and British Chemical Standards (BCS) certified reference iron, steel and ferrovanadium samples and to a stainless steel to which known amounts of aluminium were added. It was also applied to NBS copper- and nickel-base alloys. The results of these analyses, which are the means of four or five AAS measurements, are given in Table 1. All the results shown are for individual samples. The results obtained previously for some of these reference materials by the spectrophotometric Pyrocatechol Violet method[7] are also given in Table 1.

Precision

The precision at about the 0.0005 and the 0.002% levels of aluminium was tested by analysing one series of five samples of a BCS high-silicon steel for both acid-soluble and acid-insoluble aluminium. A second series of five samples was analysed for total aluminium. Although this reference material has not been certified for aluminium, results for acid-soluble, acid-insoluble and total aluminium have been reported by previous investigators.[4,5,10] The results of these tests, which are the means of four or five AAS measurements on each sample solution, are given in Table 2.

DISCUSSION

Table 1 shows that the results obtained for the NBS and BCS iron, steel, ferrovanadium and non-ferrous alloys are in good agreement with the certified values and, where applicable, with the results obtained previously by the Pyrocatechol Violet method.[7] The results obtained for the stainless-steel sample to which known amounts of aluminium were added, agree with the total calculated amount present.

Table 2 shows that the relative standard deviation for acid-soluble aluminium at the 0.0004% level—and consequently also for total aluminium—is relatively high. This is partly due to the magnitude of the reagent blank, which is given below. At the 0.002% level, the precision of the results for acid-insoluble aluminium, for total aluminium determined by adding acid-insoluble and acid-soluble aluminium and for total aluminium determined in one step is comparable with that obtained by Shaw and Ottaway[10] by flameless AAS and with that obtained by Jenkins and Jones[5] and other investigators using conventional

Table 1. Determination of aluminium in NBS and BCS iron, steel and ferrous and non-ferrous alloys

Sample	Nominal composition, %	Certified value and range, % *Al*	Al found, % Spectrophotometric Pyrocatechol Violet method	Al found, % Atomic-absorption spectrophotometry
NBS-14e Basic open-hearth steel	0.4 Mn, 0.2 Si	0.059*	0.060	0.062
NBS-19g Acid open-hearth steel	0.6 Mn, 0.2 Si, 0.4 Cr, 0.03 Ti, 0.03 Nb	0.030	0.027, 0.028	0.028 (0.028†)
NBS-55c Open-hearth iron		0.003*	0.0012, 0.0009	0.0016, 0.0011
NBS-55e Open-hearth iron		0.002 (0.001–0.003)	—	0.0008, 0.0006 (0.0011, 0.0007†)
NBS-61 Ferrovanadium	31.2 V, 1.2 C, 3.6 Mn, 7.8 Si, 1.3 Ni, 0.7 Mo, 0.2 Ti, 0.2 P	0.02 (0.01–0.03)	0.022	0.021, 0.021
NBS-100A Manganese steel	0.4 C, 1.7 Mn, 0.2 Si	0.040 (0.039–0.042)	—	0.037, 0.037 (0.037†)
NBS-101F 18 Chromium–10 nickel steel	10.0 Ni, 18.5 Cr, 0.9 Si, 0.3 V (0.0007 Al)‡	0.0057§	—	0.0056
		0.0107§	—	0.011_0
		0.0207§	—	0.021_5
NBS-106B Chromium–molybdenum–aluminium steel	0.5 Mn, 0.3 Si, 1.2 Cr, 0.2 Mo	1.07 (1.06–1.09)	1.08_1	
NBS-125 High silicon steel	0.1 Mn, 5.0 Si	0.261 (0.25–0.270)	0.263	0.266
NBS-170A Basic open-hearth steel	0.3 Mn, 0.3 Ti, 0.04 Zr	0.046 (0.036–0.058)	0.046	0.049, 0.048
BCS-326 Mild steel	0.3 Mn	0.005 (0.003–0.007)	0.0031, 0.0034	—
BCS-327 Mild steel	0.2 Mn, 0.1 V	0.020 (0.016–0.023)	0.017	0.019
BCS-328 Mild steel	0.4 Mn, 0.2 V	0.048 (0.045–0.053)	0.048	0.050
BCS-329 Mild steel	0.1 Mn, 0.1 V	0.058 (0.052–0.062)	0.059	0.059
NBS-62B Manganese bronze	57.4 Cu, 38.0 Zn, 1.3 Mn, 1.0 Sn	0.97 (0.94–0.98)	0.975	0.956, 0.943
NBS-158 Silicon bronze	90.9 Cu, 2.7 Si, 1.3 Mn, 1.0 Sn	0.54 (0.53–0.56)	0.539	0.536
NBS-162A Nickel–copper alloy	63.9 Ni, 30.6 Cu, 1.6 Mn, 0.9 Si	0.50 (0.49–0.50)	0.503	0.500
NBS-169 Electrical-heating alloy	77.2 Ni, 20.3 Cr, 1.4 Si, 0.04 Zr	0.095 (0.087–0.105)	—	0.095
NBS-349 Heat-resisting alloy	57.2 Ni, 19.5 Cr, 4.0 Mo, 3.1 Ti, 0.3 Si, 0.4 Mn, 14.0 Co, 0.08 Zr	1.23*	—	1.22_3
NBS-C1100 Cartridge brass	67.4 Cu, 32.2 Zn	0.008	0.0075	0.0079
NBS-C1101 Cartridge brass B	69.5 Cu, 30.3 Zn	0.0006	—	0.0002, 0.0002, 0.0002

* NBS provisional result.

† Results in brackets obtained after fusing the insoluble material with sodium carbonate and fused boric acid as described in Note 7.

‡ Mean of 2 results, viz., 0.0006_5 and 0.0006_9%, by the atomic-absorption method.

§ Value includes aluminium present ‡ and that added to a 1-g sample.

Table 2. Determination of acid-soluble, acid-insoluble and total aluminium in a high-silicon steel

Sample	Al found by proposed method, %				Al found by other methods, *			
	Acid-soluble	Acid-insoluble	Soluble + insoluble	Total	Acid-soluble	Acid-insoluble	Soluble + insoluble	Total
BCS-317 High-silicon steel	0.00050	0.0018	0.0023	0.0022	0.00036 (10%)†	0.0022 (10%)†	0.0026	—
	0.00048	0.0020	0.0025	0.0021	0.00033‡	0.0019‡	0.0022	0.0022‡
	0.00043	0.0016	0.0020	0.0022	0.00040§	0.0018§	0.0022	—
	0.00044	0.0014	0.0018	0.0020	0.00043 (14%)¶	0.0016 (12%)¶	0.0020 (10%)	—
	0.00025	0.0017	0.0020	0.0020				
Mean	0.00042	0.0017	0.0021	0.0021				
Standard deviation	0.00010	0.00022	0.00028	0.00010				
Relative standard deviation (RSD), %	24	13	13	5				

* Results in each horizontal row were obtained by the same investigators.
† Mean of 12 results obtained by Jenkins and Jones[5] by conventional AAS during reproducibility tests (RSD in brackets).
‡ Mean of 3 results obtained by Cobb *et al.*[4] by conventional AAS.
§ Mean of 5 results obtained by Shaw and Ottaway[10] by flameless AAS.
¶ Mean of 10 results obtained by Shaw and Ottaway[10] during reproducibility tests (RSD in brackets).

AAS.[4,6] The precision of the results obtained for total aluminium determined in one step is better than that obtained when acid-soluble and acid-insoluble aluminium are determined separately and added. However, this is expected from statistical considerations and because of the fewer manipulations required. Table 2 also shows that the results obtained for acid-soluble, acid-insoluble and total aluminium by the proposed method are in excellent agreement with those obtained by previous investigators.

Although sodium hydrogen sulphate is recommended for fusion of the acid-insoluble material in methods for determining total aluminium in iron, steel and various other materials,[11,12] Cobb *et al.*[4] found that the use of this flux produced variable and low results for aluminium in several BCS mild steel samples. Consequently, they recommended a mixture of sodium carbonate and boric acid. The particular reference materials used in their tests were not immediately available. However, the results obtained for acid-insoluble and total aluminium in the BCS high-silicon steel by the proposed method (Table 2) show that sodium hydrogen sulphate is a suitable reagent for fusion purposes. This is also indicated in Table 1. The results obtained for NBS samples 19g, 55e and 100A by the proposed method involving the use of sodium hydrogen sulphate for fusion of the acid-insoluble material are in excellent agreement with those obtained (shown in brackets) when a mixture of sodium carbonate and fused boric acid was used for fusion purposes.

The proposed method has some definite advantages over the recent AAS method[6] mentioned earlier, which is also applicable to high-alloy steels, and which involves a preliminary separation of iron by methyl isobutyl ketone extraction of the chloro-complex. In this method, the sample, including the acid-insoluble material, is decomposed in a Teflon-lined (85-ml capacity cup) pressure bomb. Aluminium is ultimately separated from the bulk of the alloying constituents such as chromium and nickel by a double extraction of its acetylacetone complex into 50 ml of pure acetylacetone which, because of its low density, requires the use of two separatory funnels. The combined acetylacetone extracts are then concentrated to ~7 ml by evaporation in an oil-bath at 150–160° and aluminium is determined by spraying the extract into the flame. This requires the use of calibration solutions prepared in a similar manner by extracting known amounts of aluminium into pure acetylacetone. Part of the manganese, lead, cobalt and nickel present in the sample, much of the niobium, titanium and vanadium, most of the copper, tin and zirconium, and all of the iron(III) remaining after the methyl isobutyl ketone extraction step will be co-extracted with the aluminium. In the proposed method for iron and steel, 1 ml of acetylacetone is used and the aluminium complex is extracted into chloroform which, because of its high density, is convenient to use when multiple extractions are required.

The extract is easily evaporated to dryness in the presence of a small amount of concentrated hydrochloric acid, and aluminium is ultimately determined in an aqueous medium which facilitates the preparation of calibration solutions. After a mercury-cathode separation, and in the presence of hydrogen peroxide as a complexing agent, essentially only the residual iron and a small amount of chromium(III) are co-extracted with the aluminium. As stated previously, at the 1-g level, usually less than 5 mg of iron(III) will remain in the electrolyte. Although the pressure-bomb decomposition step described in the Headridge and Sowerbutts method[6] would be advantageous for the determination of total aluminium, this was not pursued in this work because of the low capacity (25 ml) of the Teflon cup in the available commercial acid-digestion bombs. Attempts to evaporate the solution obtained after dissolving 1 g of steel with *aqua regia* to low volume in a 25-ml Teflon cup resulted in considerable loss of sample by spray.

The proposed method also has some advantages over the previous AAS methods involving the preliminary separation of iron by isobutyl acetate extraction of the chloro-complex.[4,5] In these methods, ~50–150 mg of iron remain in the aqueous phase after the extraction. This requires the addition of iron to the calibration solutions to eliminate error. In the proposed method, so little iron remains in the electrolyte after the mercury cathode separation that the addition of iron to the calibration solutions is not necessary.

The results shown in Table 1 for the copper-base alloys were obtained after ultimately separating aluminium by acetylacetone extraction. However, tests showed that at the 1-g copper level, less than 0.5 mg remains in the electrolyte after the mercury-cathode separation. Consequently, the extraction step would not usually be necessary for copper-base alloys, and probably not for most nickel-base alloys, unless appreciable titanium, tungsten or vanadium is present. However, the mercury-cathode separation should be carried out in a perchloric acid medium instead of a sulphuric acid medium and the electrolyte should be evaporated to ~0.5 ml if the final solution for the AAS determination is to be 10 ml.

The proposed method is suitable for iron and steel containing as little as 0.0005% of aluminium and for copper- and nickel-base alloys containing ~0.0002% or more. However, the accuracy that can be obtained at these levels depends on the magnitude of the respective reagent blanks. In this work, the blank varied from ~12 to 20 μg of aluminium during the determination of total aluminium in iron and steel. Approximately two-thirds of the aluminium present in this blank resulted from the sodium hydrogen sulphate used for fusion of the acid-insoluble material. The blanks obtained after fusion with sodium carbonate and fused boric acid were of the same magnitude. Those obtained during the analysis of the non-ferrous materials varied from ~5 to 8 μg of aluminium.

REFERENCES

1. M. D. Amos and P. E. Thomas, *Anal. Chim. Acta*, 1965, **32**, 139.
2. P. König, K.-H. Schmitz and E. Thiemann, *Z. Anal. Chem.*, 1969, **244**, 232.
3. J. Y. Marks and G. G. Welcher, *Anal. Chem.*, 1970, **42**, 1033.
4. W. D. Cobb, W. W. Foster and T. S. Harrison, *Lab. Pract.*, 1975, **24**, 143.
5. R. H. Jenkins and C. P. Jones, *Proc. Soc. Anal. Chem.*, 1972, **9**, 266.
6. J. B. Headridge and A. Sowerbutts, *Analyst*, 1973, **98**, 57.
7. E. M. Donaldson, *Talanta*, 1971, **18**, 905.
8. I. M. Kolthoff and P. J. Elving, *Treatise on Analytical Chemistry*, Part II, Vol. 4, p. 377. Interscience, New York, 1966.
9. W. Slavin, *Atomic Absorption Spectroscopy*, p. 79. Interscience, New York, 1968.
10. F. Shaw and J. M. Ottaway, *Analyst*, 1975, **100**, 217.
11. *Annual Book of ASTM Standards, Chemical Analysis of Metals; Sampling and Analysis of Metal Bearing Ores*, Part 12, pp. 549, 653, 655, 692. American Society for Testing and Materials, Philadelphia, 1979.
12. Z. Šulcek, P. Povondra and J. Doležal, *CRC Crit. Rev. Anal. Chem.*, 1977, **6**, 255.

Talanta, Vol. 28, pp. 469 to 472, 1981
Printed in Great Britain. All rights reserved

0039-9140/81/070469-04$02.00/0
Copyright © 1981 Pergamon Press Ltd

SHORT COMMUNICATIONS

AN INDIRECT METHOD FOR DETERMINING PHOSPHORUS IN ALUMINIUM ALLOYS BY ATOMIC-ABSORPTION SPECTROMETRY*

J. L. BERNAL, M^a. J. del NOZAL, L. DEBAN and A. J. ALLER

Department of Analytical Chemistry, Faculty of Science, Prado de la Magdalena, Valladolid, Spain

(*Received* 28 *January* 1980. *Revised* 28 *October* 1980. *Accepted* 23 *December* 1980)

Summary—An indirect method is described for the determination of phosphorus in aluminium alloys. Ammonium molybdate is added to a solution of the aluminium alloy and the molybdophosphoric acid formed is selectively extracted into n-butyl acetate. The twelve molybdenum atoms associated with each phosphate ion are determined by direct atomic-absorption spectrometry with the n-butyl acetate phase in a nitrous oxide–acetylene flame, with measurement at 313.2 nm. The most suitable conditions have been established and the effect of other ions has been studied.

Most methods for the determination of phosphate are based on the formation of heteropoly acids.[1] The sensitivity and selectivity of these methods are enhanced, if the complex is extracted into a suitable organic solvent[2–6] before measurement. Such methods have been used in atomic-absorption spectrophotometry[7] in place of direct flame atomic spectrometric methods,[8] the phosphorus content being determined indirectly by formation and extraction of phosphomolybdic acid and determination of the molybdenum in the organic phase by atomic absorption.[9–12] An alternative[13,14] is to decompose the heteropolymolybdate in the separated extract and to strip the molybdenum into an aqueous phase for subsequent determination. The selectivity of the extraction, and the factors which affect it (principally the pH) have been widely investigated.

Despite the difficulties related to the use of organic solvents in atomic-absorption work, many applications have been made of this method for determination of phosphorus, *e.g.*, in biochemical,[17–21] agricultural,[22] metallurgical,[14,23–25] water[10,26–28] and rock[14] analysis.

This paper describes a method for the determination of phosphorus in aluminium-based alloys by indirect atomic-absorption, taking into account the possible interference of other ions.

EXPERIMENTAL

A double-beam Pye–Unicam SP-1900 atomic-absorption spectrometer was used in conjunction with a Unicam molybdenum hollow-cathode lamp. The instrument conditions used throughout were: slit-width 0.15 mm; wavelength 313.2 nm; lamp current 7 mA; a 10-cm burner was used with the air–acetylene flame and a 5-cm burner with the nitrous oxide–acetylene flame, both burners having a 0.7-mm wide slot.

Reagents

Ammonium molybdate solution. Dissolve 10.69 g of ammonium molybdate tetrahydrate, $(NH_4)_6Mo_7O_{24}.4H_2O$, in distilled water and dilute to 1 litre.

Standard phosphorus solution. Dissolve 0.1098 g of potassium dihydrogen phosphate, KH_2PO_4, in distilled water and dilute to 1 litre.

Wash solution. Nitric acid diluted 1:1 with distilled water.

Use analytical-reagent grade chemicals and store all solutions in polyethylene bottles to avoid contamination with silicon.

Procedure

Dissolve the sample [large enough to give a final phosphorus concentration of 0.1–1 μg/ml, but not less than 0.5 g (to avoid problems of inhomogeneity)] in 25 ml (more if necessary) of a 10:10:1 v/v mixture of nitric acid (1 + 1), hydrochloric acid (1 + 1) and hydrogen peroxide (30%) by heating in a covered Teflon flask. For phosphorus contents >0.01%, make this solution up to a suitable standard volume (*e.g.*, 50 ml) and use a suitable aliquot for the subsequent analysis. Dilute this solution to about 50 ml with demineralized water, add 5 ml of ammonium molybdate solution and swirl the mixture for 3 min. Adjust to pH 1, transfer to a 100-ml glass separating funnel, then shake with 20 ml of n-butyl acetate for 1 min. Discard the aqueous phase and wash the organic phase with three 10-ml portions of wash solution. Spray the organic phase directly into the flame and determine the molybdenum content. Use the organic solvent for determining the blank.

RESULTS AND DISCUSSION

Extraction of phosphomolybdic acid

The extraction of molybdic acid into various solvents was investigated by shaking vigorously 20 ml of

* Taken in part from the Ph.D. work of A. J. Aller.

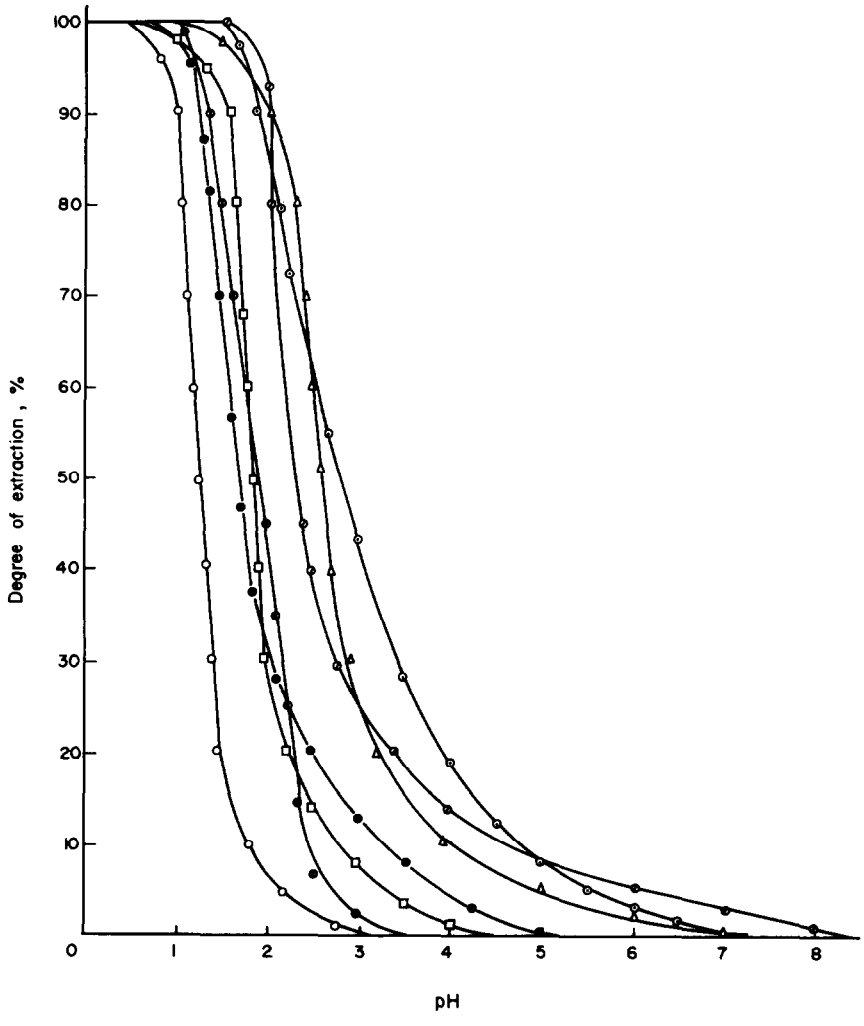


Fig. 1. Relationship between degree of extraction and pH for the organic solvents used. —○— Diethyl ether; —●—● Acetophenone; —□— MIBK; —⊗—⊗— b-butyl acetate; —◐— n-butanol; —⊙—⊙— n-amyl alcohol; —△— isoamyl alcohol.

solvent with the aqueous molybdate solution (at various pH values) for 1 min and measuring the amount of molybdate in the organic phase. The same solvents were tested as extractants for phosphomolybdic acid, the solvent being added to a 0.5-ppm phosphorus solution obtained by mixing 10 ml of ammonium molydate reagent with potassium of dihydrogen phosphate solution and adjusted to the desired pH with buffer. Preliminary experiments showed that shaking for 1 min was sufficient. The results are shown in Fig. 1, where it can be seen that the amount extracted increases as the pH decreases and becomes quantitative over the pH range 0.4–1.6, depending on the solvent. For further work the pH was adjusted to 1 for convenience.

From the results it was deduced that under the conditions used the best solvent is n-butyl acetate, because it is the most highly selective and gives virtually 100% extraction in a single step. It is recommended that before aspiration into the flame the organic phase is washed to remove any molybdate reagent mechanically carried over from the aqueous phase.

Calibration graph and optimum concentration ranges

When the recommended procedure is used, the calibration graph for the determination of phosphorus is linear over the range 0.01–1 ppm of phosphorus in the original aqueous solution.

Precision

A series of absorbance values was obtained by replicate (tenfold) analysis of 25 ml of aluminium alloy solution containing 0.8 ppm of phosphorus. The average absorbance was 0.48 and the relative standard deviation was 1.2% with the air–acetylene flame and 0.8% for the nitrous oxide–acetylene flame.

Table 1. Concentrations (ppm) of Si, As, W and Ge which do not interfere in the phosphorus determination (0.5 ppm in aqueous solution) when different organic solvents are used

Solvent	Si	As	W	Ge
n-Butyl acetate	4000	3000	4000	4000
MIBK	10	20	800	20
Acetophenone	200	300	200	200
Diethyl ether	2000	300	3000	2000
n-Amyl alcohol	100	60	300	80
Isoamyl alcohol	60	50	400	40
n-Butanol	30	20	60	50

Detection limits and sensitivity

With a nitrous oxide–acetylene flame the detection limit is nearly 0.01 ppm of phosphorus in the aqueous solution, and the sensitivity (concentration for 1% absorption) is of the order of 0.02 ppm. The practical concentration range is 0.08–1 ppm.

The determination in the air–acetylene flame has a practical range of 0.1–1 ppm. The detection limit of aqueous phosphorus solutions can be lowered to 0.03 ppm and the sensitivity is 0.05 ppm (for 1% absorption).

Effect of foreign ions

The effect of a number of ions on the determination of 0.5 ppm of phosphorus by the recommended procedure has been investigated. An ion was considered not to interfere if it produced less than 5% change in the absorbances. No interference was observed from 5000 ppm of the following ions when tested individually: Bi^{3+}, Ca^{2+}, Cd^{2+}, Ce^{3+}, Cr^{3+}, Cu^{2+}, Fe^{3+}, Hg^{2+}, Mg^{2+}, La^{3+}, Mn^{2+}, Nb^{5+}, Pb^{2+}, Ni^{2+}, Sb^{3+}, Se^{4+}, Te^{4+}, Ti^{4+}, V^{5+}, Zn^{2+}, Zr^{4+}, F^-, Cl^- and NO_3^-.

To study the effect of silicon, arsenic, tungsten and germanium, different quantities of these elements were added to samples of 1 g of high-purity aluminium alloy and the degree of extraction under various conditions was investigated. As seen from Table 1, none of these elements (over an appreciable range of concentration) interfered with the determination of phosphorus if n-butyl acetate was used as extractant. The use of other solvents increases the interference by these elements.

Application of the method to metallurgical samples

The accuracy of the method was assessed by the determination of P in B.C.S. and other aluminium alloys. Table 2 shows the results, which confirm the validity and suitability of the proposed method.

REFERENCES

1. *Analiticheskaya Khimia Fosfora*, Nauka, Moscow, 1974.
2. A. Syty and J. A. Dean, *Appl. Optics*, 1968, **7**, 1331.
3. J. Paul and W. F. R. Pover, *Anal. Chim. Acta*, 1960, **22**, 185.
4. J. Paul, *Mikrochim. Acta*, 1965, 830.
5. *Idem, ibid.*, 1965, 836.
6. *Idem, Anal. Chim. Acta*, 1966, **35**, 200.
7. M. S. Cresser, *Solvent Extraction in Flame Spectroscopic Analysis*, Butterworths, London, 1978.
8. D. C. Manning and S. Slavin, *Atom. Abs. Newsl.*, 1969, **8**, 132.
9. G. F. Kirkbright, A. M. Smith and T. S. West, *Analyst*, 1967, **92**, 411.
10. W. S. Zaugg and R. J. Knox, *Anal. Chem.*, 1966, **38**, 1759.
11. T. Kumamaru, Y. Otani and Y. Yamamoto, *Bull. Chem. Soc. Japan*, 1967, **40**, 429.
12. T. V. Ramakrishna, J. W. Robinson and P. W. West, *Anal. Chim. Acta*, 1969, **45**, 43.
13. T. R. Hurford and D. F. Boltz, *Anal. Chem.*, 1968, **40**, 379.
14. C. Riddle and A. Turek, *Anal. Chim. Acta*, 1977, **92**, 49.
15. L. A. Trudell and D. F. Boltz, *Mikrochim. Acta*, 1970, 1220.
16. S. J. Simon and D. F. Boltz, *Anal. Chem.* 1975, **47**, 1758.
17. W. S. Zaugg and R. J. Knox, *Anal. Biochem.*, 1967, **20**, 282.
18. G. Linden, S. Turk and B. Tarodo de la Fuente, *Chim. Anal. Paris*, 1971, **53**, 244.
19. G. Devoto., *Boll. Soc. Ital. Biol. Speriment.*, 1968, **44**, 424.
20. J. A. Parsons, B. Dawson, E. Callahan and J. T. Potts, Jr., *Biochem. J.*, 1970, **119**, 791.
21. Y. Kidani, H. Takemura and H. Koike, *Bunseki Kagaku*, 1974, **23**, 212.

Table 2. Determination of phosphorus in aluminium alloys*

Sample	Designation	P found, % air–C_2H_2	P found, % N_2O–C_2H_2	Certified P content, %
Aluminium alloy	BCS 181	0.0012	0.0010	0.0012
II Si–Al	BCS 182/1	0.0009	0.0008	0.0009
Devarda's alloy	BDH	0.0119	0.0115	0.0116
Aluminium alloy	L-2520	0.0827	0.0820	0.0825
Aluminium alloy	L-2521	0.0763	0.0760	0.0760
Aluminium alloy	L-2530	0.0801	0.0791	0.0796
Aluminium alloy	L-2550	0.0912	0.0911	0.0910
Aluminium alloy	L-2560	0.0560	0.0563	0.0561
Aluminium alloy	L-2561	0.0360	0.0358	0.0355
Aluminium alloy	L-2571	0.0165	0.0163	0.0160

* Courtesy of E.N.D.A.S.A.

22. T. G. Carreno and F. D. Macias, *Anal Edafol. Agrobiol.* 1971, **30,** 501.
23. Y. Inokuma and J. Endo, *Tetsu to Hagane*, 1977, **63,** 1026.
24. I. G. Yudelevich, L. M. Buyanova, N. F. Bakhturova and T. M. Korda., *Zh. Analyt. Khim.*, 1977, **32,** 28.
25. A. M. Baialordo and A. Gomez-Coedo, *Rev. Metal.*, 1973, **9,** 35.
26. V. Rozenblum, *Anal. Lett.* 1975, **8,** 549.
27. A. Sapek and B. Sapek, *SCAN*, 1976, **7,** 10.
28. M. J. Fishman and D. E. Erdman, *Anal. Chem.*, 1977, **49,** 139R.

Talanta, Vol. 28, pp. 473 to 476, 1981
Printed in Great Britain

0039-9140/81/070473-04$02.00/0
Pergamon Press Ltd

DIFFERENTIAL-PULSE ANODIC VOLTAMMETRIC DETERMINATION OF PHOSPHATE, SILICATE, ARSENATE AND GERMANATE AS β-HETEROPOLYMOLYBDATES AT A STATIONARY GLASSY-CARBON ELECTRODE

A. G. FOGG and N. K. BSEBSU
Chemistry Department, Loughborough University of Technology, Loughborough, Leicestershire, U.K.

and

B. J. BIRCH
Unilever Research, Port Sunlight, Merseyside, U.K.

(*Received* 6 *November* 1980. *Accepted* 1 *December* 1980)

Summary—Anodic voltammetry at a stationary glassy-carbon electrode has beeen applied to the determination of phosphate (in the presence of silicate), silicate (in the presence of phosphate), arsenate and germanate as β-heteropolymolybdates stabilized with acetone, with the solution conditions of existing colorimetric procedures.

12-Molybdophosphate gives an anodic wave at a stationary glassy-carbon electrode, and this wave has been made the basis of a method of determining orthophosphate.[1] Thus voltammetry can serve as an alternative finish to spectrophotometry for the determination of phosphate: this method may be of advantage in terms of sensitivity and convenience in automatic analysis using flow systems.

The voltammetric finish should be applicable to a range of heteropoly acid procedures for silicate, arsenate and germanate as well as for phosphate. The present communication describes its application to the determination of these ions under the solution conditions developed by Chalmers and Sinclair[2,3] for the stabilization of β-heteropolymolybdates with acetone to prevent their conversion into the corresponding α-heteropolymolybdates. Their direct procedures for the spectrophotometric determination of arsenate and germanate[2] have been adapted but in the case of phosphate and silicate the procedures adapted were those for selective determination in mixtures, by use of masking procedures.[3] To determine silicate, β-12-molybdophosphate is destroyed by the addition of mannitol (excess of molybdate being simultaneously masked), and in the determination of phosphate, β-12-molybdophosphate is formed in the presence of tartaric acid under conditions in which β-12-molybdosilicate is not formed.

EXPERIMENTAL

Differential-pulse voltammograms were obtained with a PAR 174 polarographic analyser (Princeton Applied Research) with three-electrode operation (glassy-carbon working electrode, platinum counter-electrode and calomel reference electrode). A sweep-rate of 5 mV/sec, a pulse height of 50 mV and a pulse frequency of 0.5 sec were used. A strictly timed sequence was used in obtaining the voltammograms. The clean, dry glassy-carbon electrode was placed in the solution to be analysed for 10 sec on open circuit before the circuit was closed at 0 V. Scanning was commenced after a further 20 sec, when the electrode signal had settled.

The glassy-carbon electrode was cleaned between scans by washing in 1*M* sodium hydroxide, and then water, with the aid of non-abrasive tissues as in our previous phosphate procedure.[1] This did not seem to be absolutely essential, however, with the present partly non-aqueous solution conditions, and this cleaning step could possibly be omitted.

The solution conditions developed by Chalmers and Sinclair[2,3] were found to be directly applicable in the voltammetric procedures. The procedures given below are essentially those of Chalmers and Sinclair[2,3] except for the voltammetric finish. The original papers should be consulted for further details as to how the solution conditions for the formation and stabilization of β-heteromolybdates were optimized.

Reagents

Standard phosphate solution, approx. 0.28 mg of PO_4^{3-} *per ml.* Dissolve about 0.4 g, accurately weighed, of potassium dihydrogen phosphate in water and dilute to 1 litre in a standard flask.

Standard arsenate solution, As approx. 0.24 mg/ml. Weigh accurately about 2 g of disodium hydrogen arsenate heptahydrate, dissolve it in water and dilute to 1 litre.

Standard silica solution, approx. 0.05 mg of SiO_2 *per ml.* Weigh accurately about 0.05 g of quartz into a nickel crucible and fuse it with about 2 g of sodium carbonate. Cool the melt, dissolve in water, dilute to 1 litre and store in polythene.

Standard germanium solution, Ge approx. 0.22 mg/ml. Dissolve about 0.16 g, accurately weighed, of germanium dioxide in dilute ammonium solution (silica-free), neutralize with dilute sulphuric acid and dilute to 500 ml.

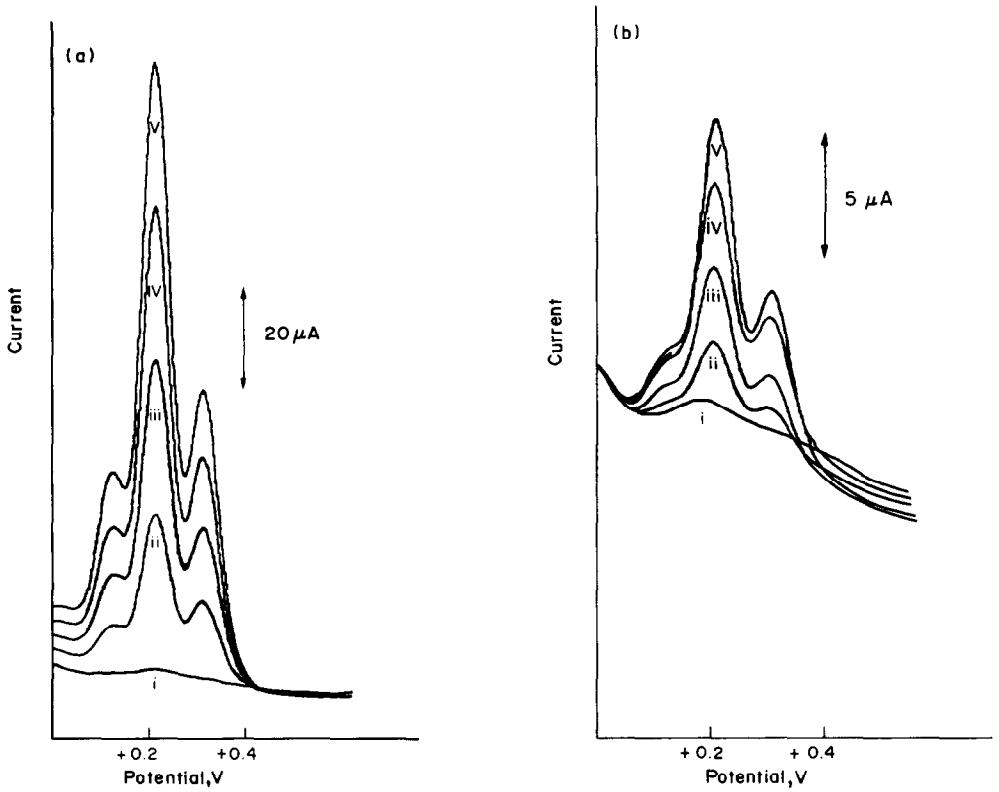


Fig. 1. Voltammograms of β-12-molybdophosphate. Equivalent orthophosphate concentrations: (a) (i) 0, (ii) 1, (iii) 2, (iv) 3 and (v) $4 \times 10^{-4} M$; (b) (i) 0, (ii) 1, (iii) 2, (iv) 3 and (v) $4 \times 10^{-5} M$.

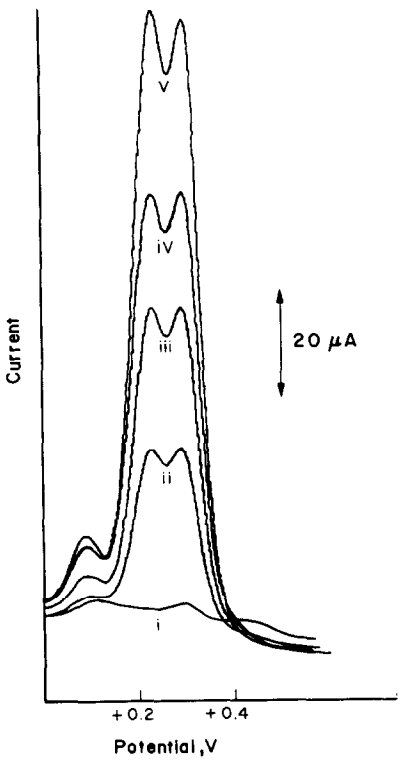


Fig. 2. Voltammograms of β-12-molybdosilicate. Equivalent silicate concentrations: (i) 0, (ii) 1, (iii) 2, (iv) 3 and (v) $4 \times 10^{-4} M$.

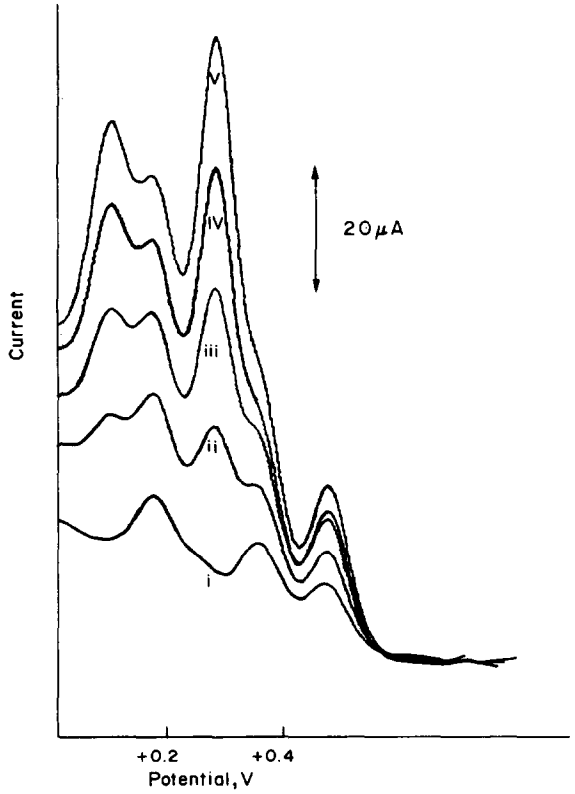


Fig. 3. Voltammograms of β-12-molybdoarsenate. Equivalent arsenate concentrations: (i) 0, (ii) 1, (iii) 2, (iv) 3 and (v) $4 \times 10^{-4} M$.

Ammonium molybdate solution, 8% w/v. Prepare and store in polythene.

Ammonium molybdate/sulphuric acid solution. Dissolve 40 g of ammonium paramolybdate tetrahydrate in 500 ml of water in a polythene beaker, and add 500 ml of 1*M* sulphuric acid. Mix, and store in polythene.

Sodium molybdate/tartaric acid/hydrochloric acid solution. Dissolve 15 g of sodium molybdate dihydrate and 12 g of tartaric acid in water, add 45 ml of concentrated hydrochloric acid and dilute to 500 ml. A brown colour develops in the reagent solution after a few days: discard it three days after preparation.

Procedure for phosphate

Place 26 ml of acetone and 10 ml of sodium molybdate/tartaric acid/hydrochloric acid solution in a 50-ml standard flask, add the sample solution containing 0.05–1.5 mg of phosphate, dilute at once to the mark and mix. During the next 30 min transfer the solution to the voltammetric cell and obtain a differential-pulse voltammogram between 0 and +0.5 V.

Procedure for silicate

Place 10 ml of the ammonium molybdate/sulphuric acid solution and 5 ml of acetone in a 50-ml standard flask. Add the sample solution containing 0.15–1 mg of silica. Rinse down the inside of the neck of the flask, mix the solution and let it stand for 15 min. Add 10 ml of 10% mannitol solution, dilute to the mark, and mix. After 15 min transfer the solution to the voltammetric cell and obtain a differential-pulse voltammogram between 0 and +0.5 V.

Procedure for arsenic

Pipette an aliquot of sample solution containing 0.4–1.5 mg of arsenic(V) into a 50-ml standard flask. Add 7 ml of 4*M* sulphuric acid, 7 ml of 8% ammonium molybdate solution and 16 ml of acetone, dilute to the mark with water and mix. After 30 min transfer the solution to the voltammetric cell and obtain a differential-pulse voltammogram between 0 and +0.6 V.

Procedure for germanium

In a 50-ml standard flask place 6 ml of ammonium molybdate solution, 10 ml of acetone, and 3 ml of 1*M* sulphuric acid. Add an aliquot of sample solution containing 0.4–1.5 mg of germanium, dilute to the mark with water, mix and allow to stand for 5 min. During the next 20 min transfer the solution to the voltammetric cell and obtain a differential-pulse voltammogram between 0 and +0.5 V.

RESULTS AND DISCUSSION

Typical differential-pulse voltammograms obtained to produce calibration graphs for the determination of phosphate, silicate, arsenate and germanate by the recommended procedures are shown in Figs. 1–4. The calibration graphs are slightly curved, proportionately smaller signals being obtained at higher concentrations, but reproducibility is good, typical coefficients of variation (10 determinations) being <3%. In the procedures for the determination of phosphate and silicate at least a 10-fold molar ratio of the other anion can be tolerated. Under the solution conditions of our previous procedure for phosphate,[1] continuous adsorption of 12-molybdophosphate occurred at the glassy-carbon electrode, resulting in higher signals. Thus the size of the differential-pulse current depended on the length of time the glassy-carbon

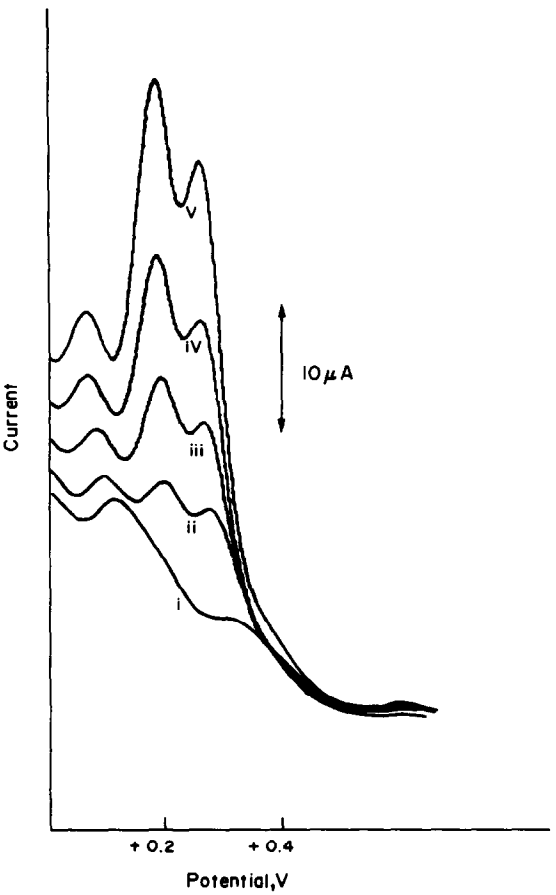


Fig. 4. Voltammograms of β-12-molybdogermanate. Equivalent germanate concentrations: (i) 0, (ii) 1, (iii) 2, (iv) 3 and (v) $4 \times 10^{-4} M$.

electrode had been in contact with the measured solution before the voltammogram was run. This was not the case here under the partially non-aqueous conditions; nevertheless it is convenient to standardize with the minimum times needed to allow the electrode and the polarographic signal to stabilize before the scan.

The voltammograms obtained are clearly characteristic of the individual heteropoly acids but at this stage no attempt has been made to correlate the voltammograms with the structures of the heteropoly acids.

Positive-going and negative-going linear sweep and cyclic voltammetric experiments have been carried out on the phosphate and silicate systems. These indicate that the peaks obtained in the positive-going scans used in the present procedures arise from the reoxidation of material reduced earlier in the scans, as is also the case with the aqueous phosphate system.[1]

The intention of this paper is to illustrate the possibility of using anodic voltammetry at a stationary glassy-carbon electrode to determine phosphate, silicate, arsenate and germanate as heteropoly acids,

rather than to recommend the voltammetric procedures given in place of the analogous spectrophotometric ones. Indeed the procedure is more complicated and would be less suitable for straightforward analyses. The use of the voltammetric method may, however, have advantages in some applications involving coloured or turbid solutions. Further studies are being made of applications both with static and hydrodynamic systems.

REFERENCES

1. A. G. Fogg and N. K. Bsebsu, *Analyst*, in the press.
2. R. A. Chalmers and A. G. Sinclair, *Anal. Chim. Acta*, 1965, **33**, 384.
3. *Idem*, *ibid.*, 1966, **34**, 412.

Talanta, Vol. 28, pp. 477 to 480, 1981
Printed in Great Britain

0039-9140/81/070477-04$02.00/0
Pergamon Press Ltd

SPECTROPHOTOMETRIC DETERMINATIONS OF ISONIAZID WITH METOL AND VANADATE, FERRICYANIDE OR IRON(III)

P. SIRAJ, R. RAMA KRISHNA, S. S. N. MURTY, B. S. REDDY and C. S. PRAKASA SASTRY

Department of Chemistry, Andhra University, Waltair 530003, India

(*Received* 9 *November* 1979. *Revised* 1 *June* 1980. *Accepted* 30 *November* 1980)

Summary—Three spectrophotometric methods for the assay of isoniazid with metol and vanadate, iron(III) or ferricyanide have been developed. The common excipients in pharmaceutical preparations do not interfere. The recovery and precision are similar to those of the official B.P. method.

The identification and determination of isoniazid (isonicotinic acid hydrazide) have recently been reviewed.[1] The spectrophotometric methods include the use of oxidants such as vanadate,[2–14] iron(III),[15] and ferricyanide.[16–19] Other reactions include the formation of the copper complex,[20] and the nickel-catalysed formation of a hydroxamic acid which is then complexed with iron(III).[21] Organic reagents used include chlorodinitrobenzene,[22] ethchlorvynol,[23] 2,3-dichloro-1,4-napthoquinone,[24] *p*-nitrobenzoyl chloride,[25] 4-nitrobenzaldehyde[26] and pyridoxal.[26] We have recently reported a spectrophotometric method for assay of primary arylamines with metol and dichromate but have found that it is not suitable for isoniazid in low concentrations. However, use of vanadate, ferricyanide or iron(III) in place of dichromate gives satisfactory results.

EXPERIMENTAL

Reagents

Metol solutions (0.1, 0.2 and 0.45%) were always freshly prepared. The oxidants were 0.015*M* ammonium vanadate, 0.033*M* iron(III) ammonium sulphate in 0.07*M* sulphuric acid and 0.02*M* potassium ferricyanide. Pure isoniazid (Fluka) was dissolved in doubly distilled water and the solution was standardized by the B.P. method[28] and diluted as required. It was stored in the dark. Potassium hydrogen phthalate–hydrochloric acid buffers[29] (pH 2.2 and 3.3) were prepared.

Procedures

Vanadate method. To 1–5 ml of solution containing 50–500 μg of isoniazid, add 15 ml of buffer (pH 2.2), 2 ml of 0.2% metol solution and 3 ml of 0.015*M* ammonium vanadate and dilute to 25 ml in a standard flask with water. Measure the absorbance of the green solution at 605 nm between 4 and 6 min later against a reagent blank. Prepare a calibration curve similarly.

Ferricyanide method. To 1–5 ml of solution containing 30–226 μg of isoniazid add 15 ml of buffer (pH 3.3), 2 ml of 0.45% metol solution and 3 ml of 0.02*M* ferricyanide, dilute to 25 ml in a standard flask and measure the absorbance of the green solution at 610 nm between 35 and 55 min later against a reagent blank. Prepare the calibration curve similarly.

Iron(III) method. To 1–5 ml of solution containing 40–160 μg of isoniazid add 2 ml of 0.1% metol solution and 3 ml of 0.033*M* iron(III), dilute to 25 ml in a standard flask and measure the absorbance of the grey solution at 410 nm between 45 and 75 min later against a reagent blank. Prepare the calibration curve similarly.

Analysis of pharmaceutical preparations. Powder and weigh 20 tablets. Weigh a quantity of the powder equivalent to 0.4 g of isoniazid and dissolve it in 100 ml of water, filter through a porosity-4 sintered-glass crucible and dilute the filtrate to 250 ml. Dilute this solution as necessary and determine the isoniazid content by one of the three procedures.

RESULTS AND DISCUSSION

Effect of pH

The optimum pH range for complete colour development is 1.9–2.4 for the vanadate and iron(III) systems, and 3.1–3.5 for the ferricyanide system. The sulphuric acid in the iron(III) reagent is sufficient to give the required pH, but buffer is added to the other two.

Amounts of oxidant and metol

It is found that 2.7–3.4 ml of 0.015*M* vanadate and 3.6–5.2 mg of metol, or 2.8–3.3 ml of 0.02*M* ferricyanide and 8.4–9.9 mg of metol, or 2.6–3.5 ml of 0.033*M* iron(III) and 1.6–2.8 mg of metol in a total volume of 25 ml are essential for complete colour development.

The spectral characteristics of the three systems are shown in Table 1. The precision and accuracy were found by analysis of samples (10 variates) containing known amounts of isoniazid. The results are summarized in Table 2. The results obtained by the proposed methods and the B.P. method for isoniazid tablets are compared in Table 3. The coloured product is not extractable into nitrobenzene, n-butanol, ethyl acetate, isobutyl methyl ketone, chloroform or 1,2-dichloroethane. Phenolic substances such as resorcinol, hydroquinone, pyrogallol, phloroglucinol, picric acid and paracetamol do not produce a similar colour when used in place of the metol, nor does *p*-benzoquinone.

Table 1. Optical characteristics

Reagent	Beer's law limits, $\mu g/25$ ml	Molar absorptivity, $l.mole^{-1}.cm^{-1}$
Metol–vanadate	50–500	4.4×10^3
Metol–ferricyanide	30–225	4.76×10^3
Metol–iron(III)	40–160	7.18×10^3

Table 2. Precision and accuracy

Method	Isoniazid, mg		Relative standard deviation, %
	Taken	Found	
Metol–vanadate	0.412	0.410	0.1
Metol–ferricyanide	0.206	0.207	0.3
Metol–iron(III)	0.103	0.104	0.7
B.P. method	38.0	38.3	1.5

Each result is an average of 10 separate analysis.

Table 3. Assay of isoniazid in tablets

Sample	Nominal content, mg	Found, mg			
		Vanadate method	Ferricyanide method	Iron(III) method	B.P. method
1	50	47.9	47.8	48.1	48.4
2	100	97.6	97.8	98.2	98.6

Each result is an average of three determinations.

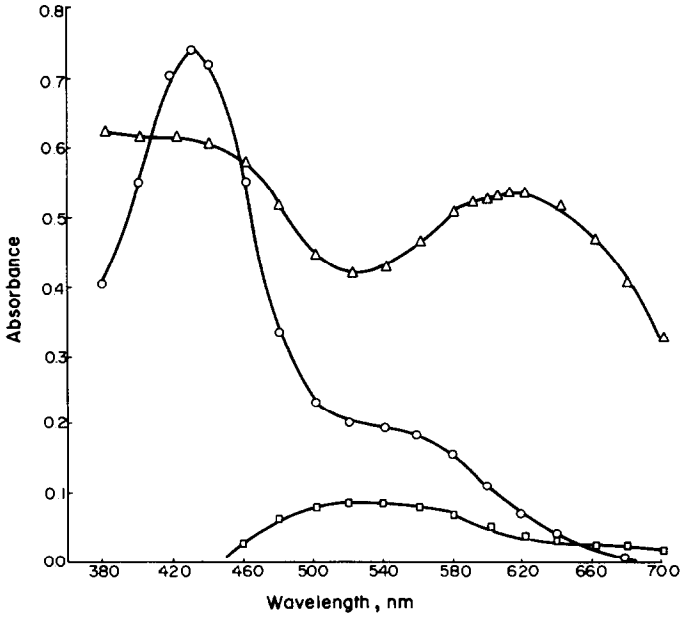


Fig. 1. Absorption spectra of the INH–metol–vanadium(V) system. ○ INH/vanadium *vs.* vanadium; □ metol/vanadium *vs.* vanadium; ◇ INH/metol/vanadium *vs.* metol/vanadium. Metol $4.65 \times 10^{-4}M$; vanadium(V) $18 \times 10^{-4}M$; INH $12.04 \times 10^{-5}M$.

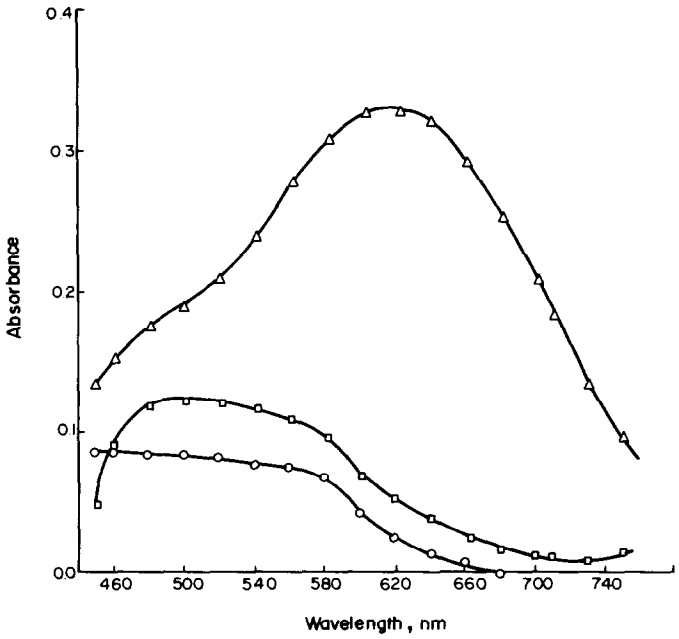


Fig. 2. Absorption spectra of the INH–metol–ferricyanide system. ○ INH/ferricyanide *vs.* ferricyanide; □ metol/ferricyanide *vs.* ferricyanide; ◇ INH/metol/ferricyanide *vs.* metol/ferricyanide. Metol $10.45 \times 10^{-4}M$; ferricyanide $24 \times 10^{-4}M$; INH $6.02 \times 10^{-5}M$.

It has been shown that with either metol or isoniazid alone, none of the oxidants gives any colour other than its own (except for the vanadate–isoniazid system which is yellow with λ_{max} 430 nm), whereas with both present a characteristic colour develops in each case. The absorption spectra are presented in Figs. 1–3. The absorption maximum shifts towards longer wavelengths after addition of metol to the 1:1 vanadate–isoniazid or the 1:1 ferricyanide–isoniazid complex whereas the shift is to shorter wavelengths for iron(III).

Tests with metol, isoniazid and the reduced forms of the three oxidants showed that no complexes were formed with the reductants. As the presence of all

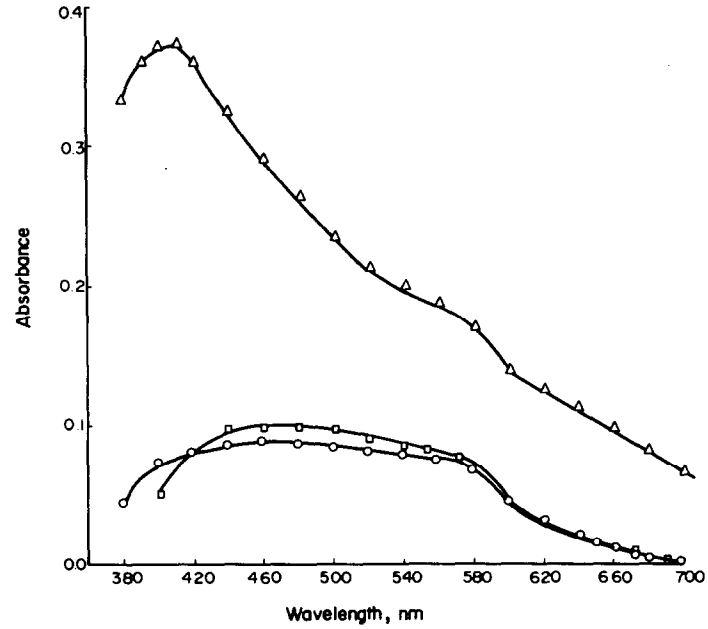


Fig. 3. Absorption spectra of INH–metol–iron(III) system. ○ INH/iron *vs.* iron; □ metol/iron *vs.* iron; ◇ INH/metol/iron *vs.* metol/iron. Metol $2.93 \times 10^{-4}M$; iron(III) $40 \times 10^{-4}M$; INH $4.52 \times 10^{-5}M$.

three components (metol, oxidant and isoniazid) is found to be essential for the development of the characteristic colour, we believe that a ternary intermediate, involving a metol–oxidant–isoniazid complex, is formed. This intermediate may be similar in nature to that reported earlier as occurring in the oxidation of metol with hydrogen peroxide in the presence of copper(II).[30] The stability of the coloured species for a limited period in each case may be due to slow decomposition of the ternary intermediate to oxidation products of metol and isoniazid.

Interferences

In the determination of 400 μg of isoniazid, up to 8 mg of glucose, lactose, starch, talc, magnesium stearate, calcium phosphate, sodium chloride and isonicotinic acid will not interfere; nor will up to 4 mg of streptomycin, ethambutal and hydrazine or 1.5 mg of *p*-aminosalicylic acid. The interference of 2 mg of bisulphite can be avoided by adding the requisite quantity of acetone.

Acknowledgements—We are grateful to the authorities of Andhra University, Waltair, and CSIR, New Delhi, for the award of research fellowships to two of us (R.R.K. and P.S.).

REFERENCES

1. G. A. Brewer, *Anal. Profiles Drug Subst.*, 1977, **6**, 183.
2. A. Alessandro, *G. Med. Mil.*, 1954, **104**, 195; *Chem. Abstr.*, 1954, **48**, 13790*d*.
3. P. V. Rao, G. B. B. Rao and P. S. Murti, *Mikrochim. Acta*, 1974, 979.
4. M. T. Marrosa, *Rev. Port. Farm.*, 1969, **19**, 206; *Chem. Abstr.*, 1971, **74**, 15757*d*.
5. J. Deltombe and R. Stainier, *J. Pharm. Belg.*, 1962, **17**, 239; *Chem. Abstr.*, 1964, **61**, 5461*a*.
6. O. Wollenberg, *Klin. Wochschr.*, 1952, **30**, 906; *Chem. Abstr.*, 1953, **47**, 2087*i*.
7. H. Kellner and H. Südhof, *Klin. Wochschr.*, 1953, **31**, 287; *Chem. Abstr.*, 1953, **47**, 7014*g*.
8. R. W. Roberts and K. W. Deuschle, *Am. Rev. Respirat. Diseases*, 1959, **80**, 904; *Chem. Abstr.*, 1961, **55**, 10551*d*.
9. E. Paunescu, *Acad. Rep. Populare Romine, Inst. Biochim. Studii Cercetari Biochim.*, 1961, **4**, 117; *Chem. Abstr.*, 1962, **56**, 56, 16081*a*.
10. E. Paunescu and M. Buzescu, *Rumanian Med. Rev.*, 1961, **5**, 38; *Chem. Abstr.*, 1962, **57**, 10502*g*.
11. G. A. Smirnov and T. I. Kozulitsyna, *Lab. Delo*, 1964, **10**, 48; *Chem. Abstr.*, 1964, **60**, 11039*f*.
12. N. Maier and V. Moisescu, *Beitr. Klin. Tuberk.*, 1964, **128**, 213; *Chem. Abstr.*, 1964, **61**, 8773*a*.
13. D. Peukert, *Arzneimittel-Forsch.*, 1957, **7**, 304; *Chem. Abstr.*, 1957, **51**, 13047*b*.
14. W. Wareska, *Polski Tygod. Lekar.*, 1953, **8**, 1736; *Chem. Abstr.*, 1955, **48**, 14082*c*.
15. H. L. Avanza, *Jornada Med. Buenos Aires*, 1955, **9**, 673; *Chem. Abstr.*, 1956, **50**, 7003*f*.
16. M. B. Jacobs, *Science*, 1953, **118**, 142.
17. P. Castal, G. Carli, G. Gras and P. Cambon, *Trav. Soc. Pharm. Montpellier*, 1955, **15**, 27; *Chem. Abstr.*, 1958, **49**, 14080*e*.
18. M. B. Jacobs, *J. Am. Pharm. Assoc.*, 1953, **42**, 346.
19. P. Blanc, P. Bertrand and L. Liandier, *Lyon Pharm. Spec.*, 1956, **161**, 4; *Chem. Abstr.*, 1959, **53**, 22185*c*.
20. S. Zommer and T. Lipiec, *Acta Polon. Pharm.*, 1963, **20**, 229; *Chem. Abstr.*, 1965, **62**, 1517*g*.
21. J. W. Munson and K. A. Connors, *J. Pharm. Sci.*, 1972, **61**, 211.
22. M. Movrin, M. Jaksevac and M. Medic-Saric, *Sci. Phar.*, 1978, **46**, 126; *Chem. Abstr.*, 1978, **89**, 186126*m*.
23. M. Rizk, M. I. Walash and N. I. A. Rabou, *Arch. Pharm. Chem., Sci. Ed.*, 1978, **6**, 26; *Chem. Abstr.*, 1978, **89**, 80270*p*.
24. M. B. Devani, C. J. Shishoo, M. A. Patel and D. D. Bhalara, *J. Pharm. Sci.*, 1978, **67**, 661.
25. V. V. Petrenko and L. P. Tarasyuk, *Farm. Zh. (Kiev)*, 1977, **1**, 63; *Chem. Abstr.*, 1977, **86**, 177367*b*.
26. P. R. Shah and R. R. Raje, *J. Pharm. Sci.*, 1977, **66**, 291.
27. R. R. Krishna and C. S. P. Sastry, *Talanta*, 1979, **26**, 861.
28. *British Pharmacopoeia*, p. 256, HMSO, London, 1973.
29. Yu. Lurie, *Handbook of Analytical Chemistry*, p. 255, Mir, Moscow, 1975.
30. K. Eckschlager, I. Horsák and J. Vepřek-Šiška, *Collection Czech. Chem. Commun.*, 1974, **39**, 2353.

Talanta, Vol. 28, pp. 481 to 483, 1981
Printed in Great Britain. All rights reserved

0039-9140/81/070481-03$02.00/0
Copyright © 1981 Pergamon Press Ltd

KINETIC METHOD FOR MICRODETERMINATION OF THE INSECTICIDE PHOSALONE

G. PETROV and D. BACHVAROVA*

Department of Chemistry, University of Sofia, Sofia, Bulgaria

(*Received* 4 *March* 1980. *Revised* 29 *October* 1980. *Accepted* 9 *January* 1981)

Summary—The alkaline hydrolysis of the insecticide *S*-([6-chloro-2-oxo-3(2H)-benzoxazolyl]methyl)-*O,O*-diethylphosphorodithioate (phosalone) results in *O,O*-diethylphosphorothioate and 6-chloro-3-mercaptomethylbenzoxazolone. Phosalone and its hydrolysis products act as activators in the copper(II) catalysis oxidation of hydroquinone by hydrogen peroxide in feebly alkaline medium. The activating effect is due to formation of complexes with the reduced form of the catalyst. The kinetics of the catalysed oxidation reaction in the presence of these activators have been investigated spectrophotometrically and a kinetic method for determination of submicroamounts of the activators has been developed.

S-([6-Chloro-2-oxo-3(2H)-benzoxazolyl]methyl)-*O,O*-diethylphosphorodithioate (phosalone) is used as an insecticide with a wide scope of action. It can be detected and determined by chemical,[1] chromatographic,[2–9] spectrophotometric[10–13] and biological[14] methods. The spectrophotometric methods are based on the complexation of phosalone or of its hydrolysis product *O,O*-diethylphosphorodithioic acid with transition metal ions such as Ag(I), Cu(I), Cu(II), Ni(II) and Pd(II).

The aim of the present work was to develop a kinetic method for determination of phosalone and its hydrolysis products. The copper-catalysed oxidation of hydroquinone with hydrogen peroxide was chosen as a model reaction. It has been established that phosalone and its hydrolysis products form complexes with Cu(I), and that these are effective activators of the catalytic reaction.[11]

EXPERIMENTAL

Phosalone was purified by repeated recrystallization from ethanol/water solution. It was hydrolysed by heating 2.0 g of it with 50 ml of 5% sodium hydroxide solution for 45 min at 75°. The solution was then cooled, and neutralized with dilute hydrochloric acid, and the precipitate filtered off. The filtrate was extracted repeatedly with benzene and ether, then the combined extract was dried with anhydrous sodium sulphate, concentrated and cooled. The precipitate was collected, and the combined products were recrystallized from ethanol: 1.1 g (99.9% yield) of 6-chloro-3-mercaptomethylbenzoxazolone (m.p. 85–87°C) was obtained. Its identity was confirmed from the infrared spectrum [peaks at 1480 and 1610 cm^{-1} (condensed benzene ring), 1790 cm^{-1} (carbonyl group) and 2600 cm^{-1} (thiol group)] and the nitrogen content (6.29%; $C_8H_6O_2SCIN$ requires 6.49%).

Reagents

*Hydroquinone solution, 0.055*M.

*Hydrogen peroxide solution, 1.6*M.

Borate buffer (pH 7.8). Prepared from 800 ml of 0.2*M* boric acid and 200 ml of 0.025*M* sodium tetraborate.

Copper sulphate solutions, 5.00×10^{-3}, 5.00×10^{-4} and $5 \times 10^{-5}M$.

Phosalone and 6-chloro-3-mercaptomethylbenzoxazolone solutions, 5.00×10^{-3}, 5.00×10^{-4}, 5.00×10^{-5}, 5.00×10^{-6} and $5.00 \times 10^{-7}M$ in methanol (phosalone) and in water (the hydrolysis product).

All reagents used were of analytical-reagent grade and the solutions were prepared with doubly distilled solvents. All solutions were brought to 25° before use.

Photometric kinetic determination of phosalone and its hydrolysis product

In a dry 10-ml standard flask take 0.5 ml of hydroquinone solution, 1.00 ml of hydrogen peroxide solution, 100 ml of copper sulphate solution and 1.00 ml of activator solution (phosalone or its hydrolysis product), dilute to the mark with buffer solution and mix. Monitor the absorbance (*A*) at 420 nm in a 4- or 5-cm cell for 10 min. From the slopes of plots of *A* *vs.* time for different activator concentrations, a calibration curve of tan α *vs.* activator concentration can be plotted.

Determination of phosalone residues in apples

Finely macerate the sample, and extract a 50-g portion with 100 ml of acetone. Filter the extract, distil off the acetone under reduced pressure, and extract the aqueous residue with three 20-ml portions of chloroform. Dry the extract with anhydrous sodium sulphate, and evaporate the solvent under reduced pressure. Dissolve the residue in 5 ml of benzene and pass the solution through a column (6 mm diameter) of 2.2 g of a 10:4:1 florisil–celite–activated carbon mixture and eluate the phosalone with 15 ml of benzene. Remove the benzene from the eluate under reduced pressure, hydrolyse the residue by the method described and dissolve the product in methanol; use this solution for the photometric (kinetic) determination. The lower limit of determination is 0.005 μg/ml in the solution used in the determination.

DISCUSSION

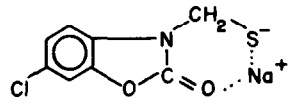
According to the literature,[8,11] the alkaline hydrolysis of phosalone leads to *O,O*-diethylphosphorodithioate. Our experiments, however, under similar conditions led to *O,O*-diethyl phosphorothioate and 6-chloro-3-mercaptomethylbenzoxazolone, which was isolated and proved. The possibility of stabilization of

* Present address: Institute of Organic Chemistry, Academy of Science, Sofia, Bulgaria.

Table 1. Calibration graphs tan $\alpha = aC_a + b$, where C_a = activator concentration, at $5 \times 10^{-4}M$ concentration of the catalyst, Cu(II)

Activator	a	b
Phosalone	1.72 ± 0.11	0.02 ± 0.0003
6-Chloro-3-mercaptomethylbenzoxazolone	9.52 ± 0.40	0.05 ± 0.001
Diethylthiophosphorothioate and 6-chloro-3-mercaptomethyl benzoxazolone	13.73 ± 0.28	0.07 ± 0.005

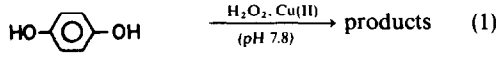
the latter by chelation in alkaline medium is one of the factors favouring cleavage of the P–S bond in the alkaline hydrolysis of phosalone.



Pyridine was used by Dolmanova and Peshkova[15] as activator in the determination of Cu(II) by its catalysis of the oxidation of hydroquinone with hydrogen peroxide, and the reaction mechanism was established by Sharma *et al.*[16–18] The activation of homogeneous catalytic reactions has been described in detail.[19] It is considered that the activators (histidine, ethylenediamine, *etc.*) form complexes with the catalyst Cu(II) and its reduced form Cu(I), and this favours the radical reaction mechanism. The rate-limiting step is the reduction of the Cu(II) complex, which can be accelerated by activator-ligands which form stable tetrahedral Cu(I) complexes.

We have established that phosalone and its hydrolysis products are suitable activators in this reaction. On the basis of the reaction kinetics we have obtained in all cases a linear calibration graph of tan α *vs.* concentration of phosalone or its hydrolysis products (Table 1).

The determination of the activator is based on the validity of the equations:



$$\frac{dx}{d\tau} = k_1 C_a^y C_s C_{Cu} + k_2 C_a C_s + k_3 C_s \quad (2)$$

$$A = KC_a^y \quad (3)$$

where C_{Cu} = concentration of Cu(II), C_s = concentration of hydroquinone, C_a = concentration of activator, A = absorbance, k_1, k_2, k_3 and K = constants.

Comparison of the kinetic data for various activators [pyridine (Py), phosalone (Ph), 6-chloro-3-mercaptomethylbenzoxazolone (B) and an equimolar mixture of (B) and *O,O*-diethylphosphorothioic acid (TPh)] under identical conditions shows that the activation efficiency increases as follows:

	no activator	Ph	Py	B	TPh + B
relative rate of the catalytic reaction	0.8	1.0	1.2	2.0	3.0

The significantly greater activating effect of the combined phosalone hydrolysis products can be explained by their participation as unidentate ligands in the formation of a stable complex with Cu(I), probably through their sulphur donor-atoms. The activation by phosalone has been attributed to several sources. Phosalone is said to act to some extent as a catalyst of the reaction, most likely through formation of perphosphate by its alkaline hydrolysis.[20,21] Two other competitive reactions are possible, however: hydrolysis of phosalone catalysed by Cu(II) according to the push-pull mechanism,[22,23] and oxidation of phosalone and of the hydrolysis products to the respective oxygen analogues. The sulphur ligands form more stable complexes than their oxygen analogues with Cu(I).[24] Thus it can be expected that the oxygen analogues of phosalone and its hydrolysis products will play a less significant role in the activation step. It is difficult to evaluate from the available data the specific participation of each of these reactions, but the low activating effect of phosalone shows that its oxidation proceeds to a considerable extent.

The catalytic method developed for quantitative determination of phosalone and its hydrolysis products has a sensitivity of 0.005 ppm referred to the concentration in the determination solution and can be successfully used for serial analysis of samples of these substances.

REFERENCES

1. T. Mirhaitov and L. T. Ikramov, *Sud. Med. Ekspertiza*, 1970, **13**, 29.
2. P. J. Bunyan, *Analyst*, 1964, **89**, 615.
3. A. Ahrem and A. Kuznetzova, *Thin-Layer Chromatography* (*Russian*), Izd.. Nauka, Moscow, 1965.
4. K. Müller, *Z. Anal. Chem.*, 1963, **215**, 253.
5. T. Mirhaitov and L. Ikramov, *Pharmazia*, 1973, **22** (No. 6), 64.
6. E. Kosmatii, B. Tverskaya, F. Polonskaya, *Pesticide Analysis Methods* (Russian), N. Melnikov, ed., Izd. Nauka, Moscow, 1972.
7. W. O. Grauer and J. N. Seiber, *Bull. Environ. Contam. Toxicol.*, 1971, **6**, 183.
8. M. Lefar, A. Guardigli, W. Chow and P. Martinski, *J. Agr. Food Chem.*, 1971, **19**, 742.
9. *Analytical Methods for Pesticides and Plant Growth Regulators*, G. Zweig, ed., Academic Press, New York, 1973. Col. VII, p. 385.
10. M. M. Laurent, *Soc. Usin. Chim. Rhone-Poulenc, Paris*, 1963, **7**, 1.
11. G. Vilezhanina and R. Kalmikova, *Problems of Analytical Chemistry* (Russian), Izd. AN USSR, Moscow, 1972.

12. K. F. Novikova and F. R. Meltser, *Zh. Analit. Khim.*, 1971, **26**, 1651.
13. K. F. Novikova and T. A. Varlamova, *Methods for Determination of Pesticides in Water* (Russian), Vol. 1, p. 98. IChSZR., Kiev, 1973.
14. R. L. Metcalf and R. March, *J. Biol. Chem.*, 1953, **177**, 524.
15. I. Dolmanova and V. Peshkova, *Zh. Analit. Khim.*, 1964, **19**, 297.
16. V. S. Sharma, J. Schubert, E. R. White and L. S. Bergelson, *J. Am. Chem. Soc.*, 1968, **90**, 4476.
17. V. S. Sharma and J. Schubert, *ibid.*, 1969, **91**, 6291; *Inorg. Chem.*, 1971, **10**, 251.
18. V. S. Sharma, J. Schubert, H. B. Brooks and F. Sicilio, *J. Am. Chem. Soc.*, 1970, **92**, 822.
19. P. R. Bontchev, *Talanta*, 1972, **19**, 675.
20. B. Gehauf, J. Epstein, G. B. Wilson, B. Witten, S. Sass, V. E. Bauer and W. H. C. Rueggeberg, *Anal. Chem.*, 1957, **29**, 278.
21. L. Larsson, *Acta Chem. Scand.*, 1958, **12**, 273.
22. R. C. Courtney, R. L. Gustafson, S. J. Westerback, H. Hyytiainen, S. C. Chabarek, Jr. and A. E. Martell, *J. Am. Chem. Soc.*, 1957, **79**, 3030.
23. A. E. Martell, *Advan. Catalysis*, 1957, **9**, 319.
24. K. Burger, *Organic Reagents in Metal Analysis*, Akadémiai Kiadó, Budapest, 1973.

Talanta, Vol. 28, pp. 485 to 486. 1981
Printed in Great Britain

0039-9140/81/070485-02$02.00/0
Pergamon Press Ltd

ANNOTATION

DETECTION OF AROMATIC NITRO COMPOUNDS BY MEANS OF THEIR π-COMPLEXES WITH *N,N*-DIETHYLANILINE

KRISHNA K. VERMA and SUNIL K. DUBEY

Department of Chemistry, University of Jabalpur, Jabalpur 482001, India

(*Received* 6 *March* 1980. *Revised* 8 *January* 1981. *Accepted* 26 *January* 1981)

Summary—The π-complexes of nitro-aromatics are found to be more intensely coloured in the solid state than in solution. Thus nitro compounds, on spraying with *N,N*-diethylaniline on paper or thin-layer plates, yield yellow, red, brown or violet colours when the solvent is evaporated. The detection limit is 1–5 μg. Several donor groups do not vitiate the test when present as substituents.

Feigl *et al.*[1] detected nitro compounds by fusing them with diphenylamine or tetrabase. The colour fades when the melt is cooled but reappears on heating. This test is applicable to mono-, di- and polynitro compounds. The development of colour is due to the formation of a charge-transfer complex.[2,3] 1,4-Quinones interfere with the test. Hydrazines and amines have been detected with nitro compounds in this way.[4]

Sharma and Tiwari[5] detected and determined some aromatic nitrocompounds as their charge-transfer complexes with *N,N*-diethylaniline in chloroform, the detection limit being stated as 40–150 μg. The authors did not recommend this method for compounds also containing donor groups, but we think this recommendation referred only to the determination method and not to the spot test. As an extension of their work,[5] a modified test for the selective and sensitive detection of a number of nitro-aromatics by means of their π-complexes with *N,N*-diethylaniline is described. These complexes appear to be more intensely coloured in the solid state than in solution. Thus, aromatic nitro compounds, on mixing with *N,N*-diethylaniline, produce yellow, orange, red, brown or violet colours when the solvent is evaporated. Several donor groups, when present on the nitro-aromatics, do not vitiate the test. The limit of identification is 1–5 μg.

EXPERIMENTAL

Reagents

A 10% solution of *N,N*-diethylaniline in carbon tetrachloride was used. All nitro compounds were high-purity chemicals. Silica gel G plates (0.2 mm) and Whatman No. 1 chromatography paper were used.

Procedure

Spot 1–2 μl of the test solution in acetone onto paper or a thin-layer plate with a microlitre syringe and allow the solvent to evaporate. Spray with *N,N*-diethylaniline and let the solvent evaporate. Development of a yellow, orange, red, brown or violet colour indicates a positive test.

For the spot-test, put one drop each of the test solution and the reagent on a thin-layer plate. Place a second drop of the reagent at the centre of the dried and developed spot and allow the solvent to spread and evaporate. A sharp and intensely coloured ring results.

When the sample is coloured, place two drops of the test solution separately on a thin-layer plate and compare them after one has been treated with the reagent as above.

RESULTS

The test gives positive tests for the following aromatic nitro compounds, with the colours and detection limits (μg) shown in parentheses.

1,3-Dinitrobenzene (reddish-brown, 1), nitrobenzene (orange, 1), 4-nitrotoluene (yellow, 3), 3-nitrobenzoic acid (yellow-brown, 4), 3-nitrophenol (yellow, 4), 1-nitronaphthalene (yellow, 3), 3,5-dinitrobenzoic acid (red, 1), 1-chloro-2,4,6-trinitrobenzene (red, 1), 4-nitrobenzaldehyde (orange-red, 2), 1,3,5-trinitrobenzene (red, 1), 5-nitrosalicylic acid (yellow, 4), 2,4-dinitrotoluene (orange, 2), 4-nitrobenzylchloride (yellow, 5), 2-chloro-5-nitrobenzaldehyde (orange, 3), 1-chloro-2,4-dinitrobenzene (yellow, 4), 3-nitroiodobenzene (yellow, 5), 4-nitrobenzoic acid (yellow, 4), 4-nitrophenol (yellow, 4), 4,4′-dinitrobiphenyl (red, 1), 2,4-dinitrophenol (red-brown, 1), 4-chloro-3,5-dinitrobenzonitrile (violet, 1), 4-amino-3-nitropyridine (yellow, 5), 1,5-difluoro-3,4-dinitrobenzene (red, 1), 2,4,6-trinitrobenzaldehyde (brown, 1), 1,3,5-trinitrobenzene (red, 1), 2,4,7-trinitro-9-fluorenone (red, 1), 1,3-dinitronaphthalene (reddish brown, 1), 2,4-dinitroanisole (orange, 3), 2-nitro-1,4-dichlorobenzene (red, 1) and 4-nitrobenzamide (orange, 3).

The π-complexes of picric acid, nitroanilines, 4- and 2,4-dinitrophenylhydrazines are masked by the intense colours of the parent compounds. 2,3,5,6-Tetrachloro-1,4-benzoquinone gives a typical blue colour not yielded by any nitro-aromatic. Other compounds

with electronegative substituents, *e.g.*, 1,4-dibromo- or dichloro- and 1,3,5-tribromobenzene do not produce any colour.

REFERENCES

1. F. Feigl and V. Anger, *Spot-Tests in Organic Analysis*, p. 295. Elsevier, Amsterdam, 1975.
2. L. N. Ferguson, *The Modern Structural Theory of Organic Chemistry*, p. 104. Prentice-Hall, New Delhi, 1966.
3. C. N. R. Rao, *Ultra-Violet and Visible Spectroscopy*, p. 171. Butterworths, London, 1975.
4. H. E. Malone, *Talanta*, 1975, **22**, 97.
5. J. P. Sharma and R. D. Tiwari, *Mikrochim. Acta*, 1974, 323.

Talanta. Vol. 28. pp. 487 to 502. 1981
Printed in Great Britain. All rights reserved

0039-9140/81/070487-16$02.00/0
Copyright © 1981 Pergamon Press Ltd

INTRODUCTION TO MICROPROCESSORS

GARY HORLICK
Department of Chemistry, University of Alberta, Edmonton, Alberta, Canada

(*Received* 18 *July* 1980. *Accepted* 6 *December* 1980)

The nature of scientific and electronic instrumentation is currently undergoing revolutionary changes as a result of the development of microprocessors. These remarkable devices have allowed the development of a new class of "intelligent" instruments having capabilities greater than previously thought possible. To utilize these capabilities to the full, scientists must have a basic understanding of microprocessors and the nature of microprocessor-based systems. One-sentence definitions of complex devices are, perhaps, dangerous, but very simply, a microprocessor is an electronic device that can rapidly process binary-coded data under stored program control. Indeed, this definition fits almost any electronic digital computer. What, in part, sets microprocessors apart from more traditional digital computers is simplicity (relatively few parts) and remarkably low cost combined with a high level of capability.

A simple microprocessor system consists of a central processing unit (CPU), and memory and input/output (I/O) subsystems. These basic units are interconnected by a system of communication lines called buses. A typical configuration is shown in Fig. 1 and this complete system is called a microcomputer. The term microprocessor is normally reserved for the central processing unit.

The buses are a very important part of the architecture of microcomputers. Buses are simply a set of lines (wires) with common functionality. Most systems are interconnected by three buses, a data bus, an address bus, and a control bus. Binary-coded data are transferred throughout the system on the data bus. Most current microprocessors are 8-bit devices, that is they normally perform their programmed operations on 8-bit binary words (often called bytes) in parallel. Thus the typical data bus is 8 bits wide. The data bus is also a bidirectional bus. This simply means that data can be transferred, although not simultaneously, in both directions on the bus, *i.e.*, both to and from the CPU and memory or an I/O device.

The address bus is used to address, *i.e.* identify uniquely, a memory location or an I/O device. It is a unidirectional bus (*i.e.*, only the CPU can send out address information) and in most systems based on 8-bit CPUs it is 16 bits wide. Thus up to 65,536 memory locations and/or input/output devices can be accessed. The control bus structure varies widely from system to system and is discussed in detail by Codding in a companion article.[1]

In the next sections these subsystems of a microcomputer system will be outlined in more detail with specific reference to and comparison of 8080, 8085 and 6502 microprocessors. These CPUs represent some of the most common units in use today.

THE CENTRAL PROCESSING UNIT

Basic architecture

The heart of a microcomputer is the central processing unit. The functional units of the CPU include an accumulator, an arithmetic logic unit (ALU), an instruction decoder, a register array, a timing and control unit, and I/O. A block diagram of an arrangement based on the architecture of the 8080 is shown in Fig. 2. It is this total system, integrated onto a single integrated circuit, that is commonly called a microprocessor.

The accumulator is the central register of the CPU and most, if not all, data manipulations and transfers involve the accumulator. For the CPUs under consideration it is an 8-bit register. Closely associated with the accumulator is the arithmetic logic unit (ALU). It too is an 8-bit unit and all arithmetic (addition and subtraction) and logic operations (OR, AND, EXCLUSIVE-OR) are carried out in the ALU. Another register (not shown in the block diagram) closely associated with the CPU and the ALU is the flag register. The flag register is, in reality, a set of flip-flops that contain status and housekeeping information about the current data-manipulations taking place in the accumulator. Common flags include CARRY which is set if an arithmetic operation generates a carry-out of the most significant bit, ZERO which is set if the contents of the accumulator are zero and SIGN which is used to indicate whether the number is positive or negative.

An important block in the CPU is the register array. This unit typically contains a small amount of what might be called scratch-pad memory (*i.e.* temporary storage area) and two important operational registers, the program counter and the stack pointer. The program counter (PC) points to the location in the memory where the next instruction to be executed resides. It is a 16-bit register in both the 8080/85 and 6502 CPUs. The stack pointer is a register that contains the address of the next entry to be placed on the stack. The stack is an area of memory which is set aside in which data and/or addresses are stored and

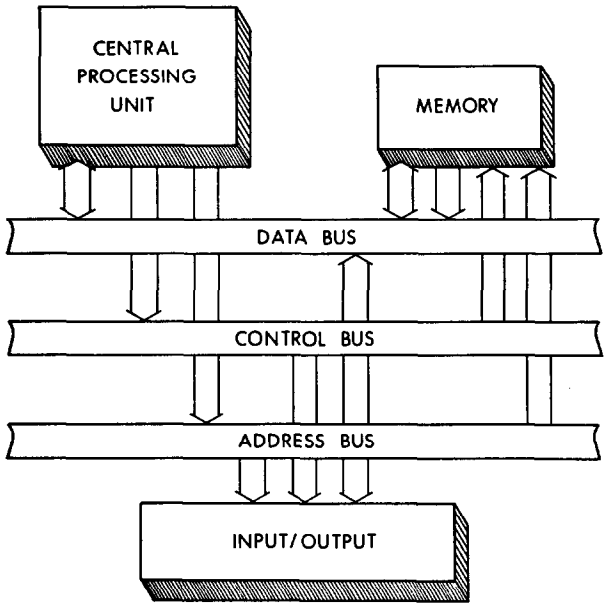


Fig. 1. Block diagram of a microcomputer.

retrieved on a last-in, first-out basis. The stack pointer is 16 bits wide in the 8080/85 systems but only 8 bits in the 6502 systems. In the 8080/85 systems six 8-bit registers are available for "scratch-pad memory" in the register array. For several operations these are grouped as three 16-bit register pairs. Only two 8-bit registers are available on the 6502 in addition to the accumulator. The central register structures of the CPUs are summarized in Fig. 3.

Some software considerations

The true power of computing systems lies, in the concept of sequential execution of stored programs, under programmed control. The instruction decoder is the hardware unit that interprets the instructions. The instruction decoder and timing and control blocks act together to sequence the system during execution of software commands. The instruction sets of most microprocessors may be broken down into

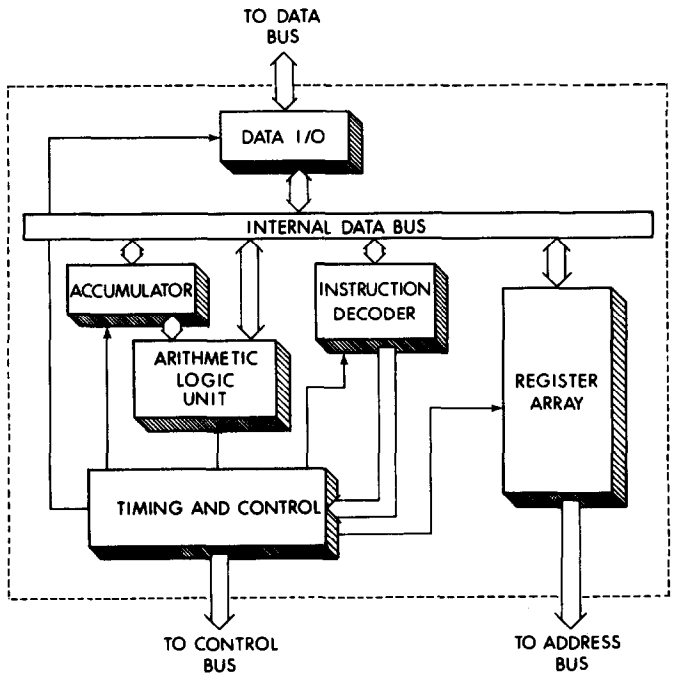


Fig. 2. Block diagram of a microprocessor.

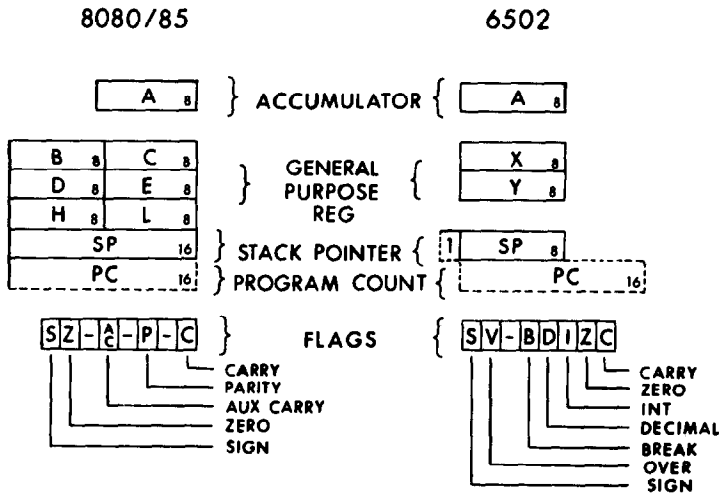


Fig. 3. Central register structures of the 8080/85 and 6502 CPUs.

five basic groups and these are listed and summarized in Table 1. A detailed description of instruction sets will not be attempted here, but it is important to appreciate that an instruction may consist of one, two or three bytes. It is also particularly useful to classify instructions on the basis of the manner in which addressing is accomplished. Addressing refers to accessing a particular memory location, register or input/output device so that data may be read into or out of that location or that another instruction can be read out of a location. The 8080/85 and 6502 systems differ considerably in some aspects of their addressing capability.

Four basic addressing modes are used in 8080/85 systems. In the *implied mode* a one-byte instruction contains both an operation code (op code) and address information. For example, if two bits are used for the op code and three bits each for source and destination codes, four different instructions may be arranged, to transfer data between 8 different source and destination locations. Such a format is used for register–register moves in the 8080/85s. *Immediate mode* instructions consist of two or three bytes. The first byte contains the operation code and any necessary address information and the second byte (and in some instructions the third byte) contains the data to be operated on. *Absolute mode* instructions consist of three bytes, the first being the op code and the next two bytes the 16-bit address in the order low byte, high byte. Finally the 8080/85 systems make extensive use of *register indirect addressing* which is a single-byte instruction with the address information assumed to be in a register pair in the register array. Register pair HL is frequently used in this manner. These instruction formats and addressing modes are summarized in Fig. 4.

TABLE I. Types of instructions

(1) DATA TRANSFER—move data between registers or between memory and registers.
(2) ARITHMETIC—add, subtract, increment or decrement data in registers or memory.
(3) LOGICAL—AND, OR, XOR, compare, rotate or complement data in registers or memory.
(4) BRANCHING—conditional and unconditional jump (branch, subroutine calls and returns).
(5) STACK, I/O, MACHINE CONTROL—I/O instructions (8080/85 only), stack operations, and internal flag operations.

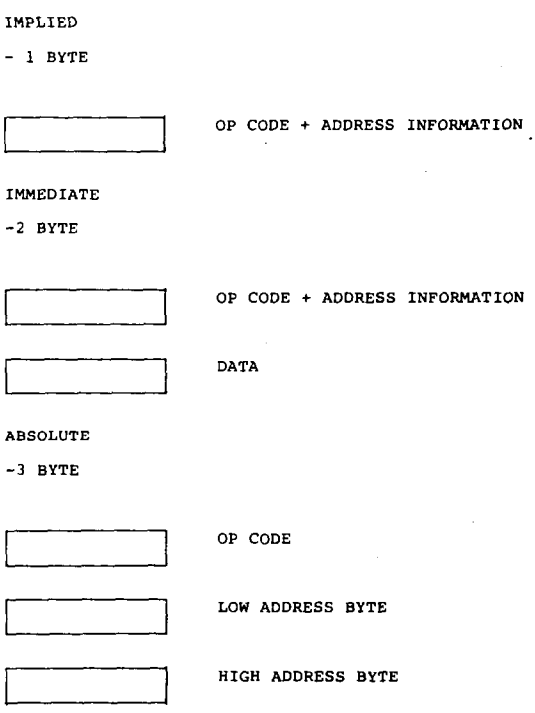


Fig. 4. Instruction formats of 8080/85 CPUs.

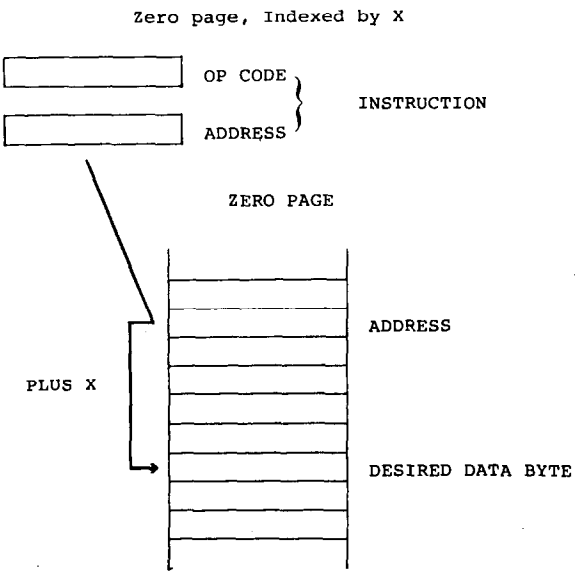


Fig. 5. Indexed addressing with 6502 CPUs.

Six basic types of addressing modes are used in the 6502 systems. The implied, immediate and absolute modes are all used in a format generally similar to that of the 8080/85 systems although the immediate mode is restricted to a two-byte format. The absolute mode has the additional feature that the 16-bit address can be indexed by one of the central registers, either register X or Y. In addition, a variation of absolute addressing is available known as *zero page addressing*, a two-byte absolute mode instruction in which the high address byte is assumed to be zero. This provides a simple format for addressing the first 256 bytes of memory. This zero page mode can also be used in the indexed mode as illustrated schematically in Fig. 5. *Relative addressing* is used for the BRANCHING group of instructions in the 6502 systems. These are two-byte instructions, the first byte being the op code and the second byte an offset that is added to the program counter to generate the desired address. In other words, relative addressing is indexed program counter addressing. Finally two somewhat more complex addressing modes are available on the 6502 systems, *indexed indirect* and *indirect indexed*. These modes are illustrated in Fig. 6. The indexed indirect mode is very useful in accessing single data points from a variety of addresses. In a sense, in comparison to 8080 type systems, a whole page of H and L registers is available. The indirect indexed mode, in contrast, is primarily used to access arrays of data stored in consecutive memory locations.

It is clear from this brief discussion of the format of instructions that instruction execution time must vary from instruction to instruction. For example, the processor cycle of the 8080 can be broken down into three subunits; states, machine cycles and an instruction cycle. These are illustrated in Fig. 7. The period of a state is related to the basic clock rate of the

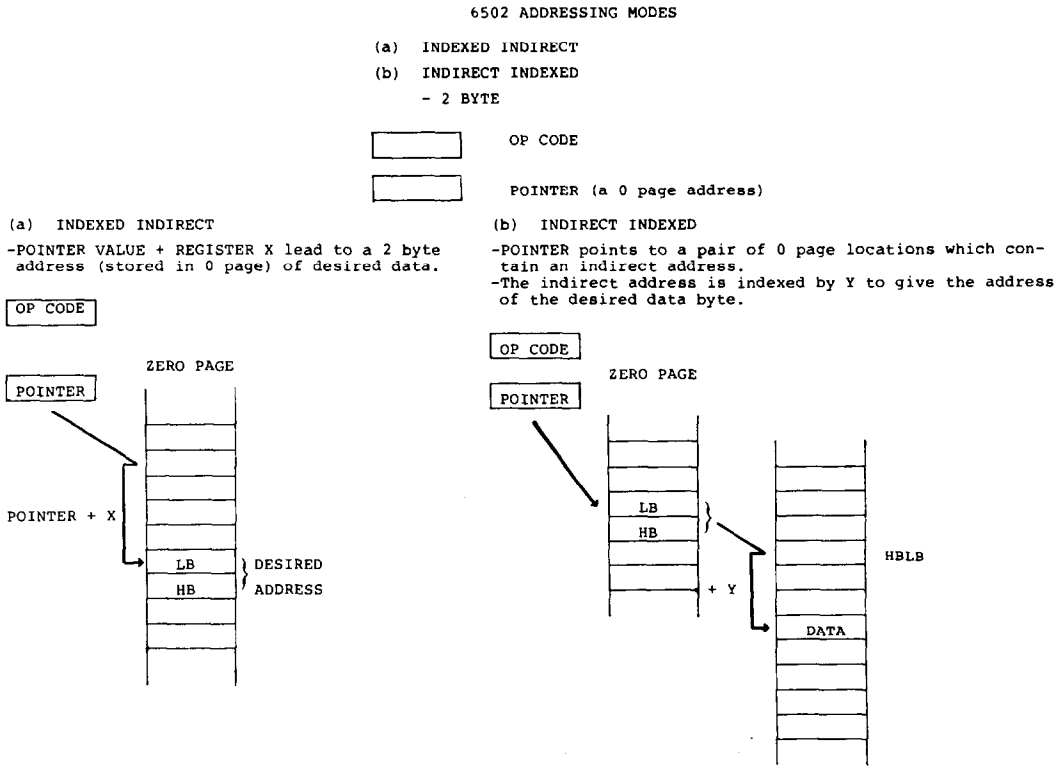


Fig. 6. Indexed indirect and indirect indexed addressing with 6502 CPUs.

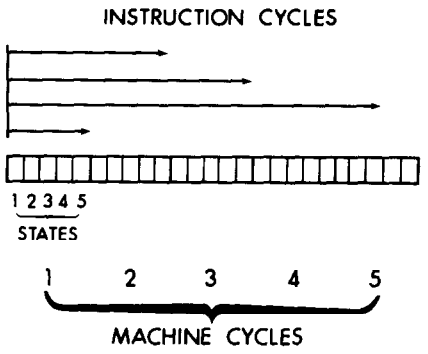


Fig. 7. The 8080 processor cycle.

processor and is 0.5 μsec in a 2-MHz 8080 system. Five states comprise a machine cycle and up to five machine cycles may be necessary to execute some instructions. Because of the complexity of instruction cycles care must be exercised in comparing the speed of one microprocessor with that of another or with that of a minicomputer, as simple comparison on only the basis of clock rate may be quite misleading.

Complete details on CPU timing and software can be obtained from manufacturers' literature and books listed in the literature appendix. Only some of the basic aspects of the hardware and software architecture of microprocessors have been outlined in this section. The next sections will cover more specifically the 8080, 8085 and 6502 systems, primarily from the hardware point of view.

8080 SYSTEMS

The 8080 CPU unit and buses

The basic features of the 8080 CPU are summarized in Table 2. Many CPUs require some immediate support chips in order to function correctly and effectively. Three chips make up the basic 8080 CPU as illustrated in Fig. 8. In addition to the 8080, a clock generator driver and a system controller and bus driver are required. As noted in Table 2 the data and control lines are multiplexed. Multiplexing is frequently used in microprocessor CPUs. For the 8080, at the CPU level, data and control information are time multiplexed onto the same pins coming out of

TABLE 2. 8080 CPU features

1. 8-Bit arithmetic logic unit
2. 8-Bit accumulator
3. Registers (on chip RWM)
   —six 8-bit registers
4. Address (16), data (8) and control buses
5. Data and control buses multiplexed
6. Power requirements +5 V, −5 V, +12 V
7. 3-Chip CPU
   —8080 CPU
   —8224 clock generator
   —8228 system controller

the CPU. During the first part of a machine cycle, control information is put on the "data" lines, after which, data is put on these same lines. The function of the 8228 is to demultiplex this information and form the independent data and control buses. The 8228 system controller and bus driver consists of two basic subunits as shown schematically in Fig. 9. A data latch is used to latch and hold the control information that appears on the 8080 CPU data lines at the beginning of a machine cycle. This held information is used to set up the control bus. Data information is then sent to and from the data bus *via* a tri-state 8-bit parallel bidirectional bus driver. The tri-state nature of both these subunits is critical to the architecture and individuality of the buses.

A non-inverting tri-state gate is illustrated in Fig. 10. In the enabled mode it simply acts as a logic-level buffer amplifier but in the disabled mode it goes into a high output-impedance state, *i.e.*, it acts as though switched out of the output line. It is this capability of tri-state gates that is crucial for maintaining the integrity of microprocessor buses. Two devices connected to a 4-bit bus are shown in Fig. 11. In a structured bus system only one device at a time can have control of a bus. Thus, if Device 1 is enabled, Device 2 must be disabled so that only one device at a time is imposing logic information on the bus.

The devices illustrated in Fig. 11 can only put information on the bus. Many devices must be able to both "read and write" information off and onto buses. The basic architecture of a simple 4-bit bidirectional bus system is shown in Fig. 12. The $\overline{CS}$ line acts as a

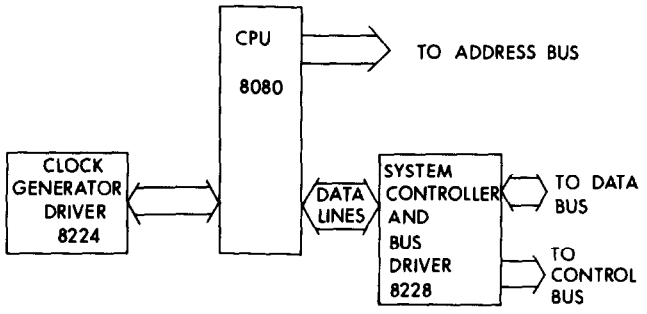


Fig. 8. Block diagram of the 3-chip 8080 CPU configuration.

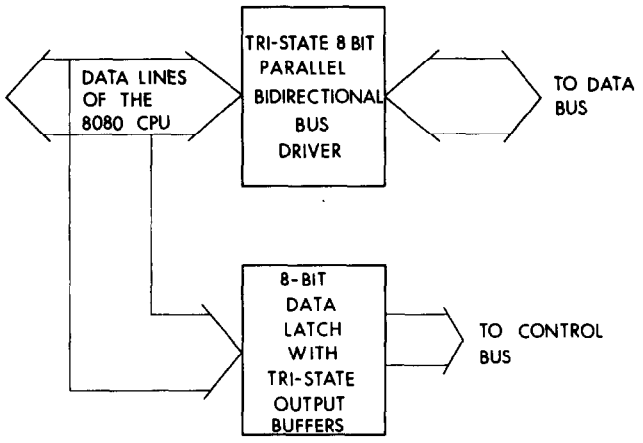


Fig. 9. Block diagram of the 8228 system controller and bus driver.

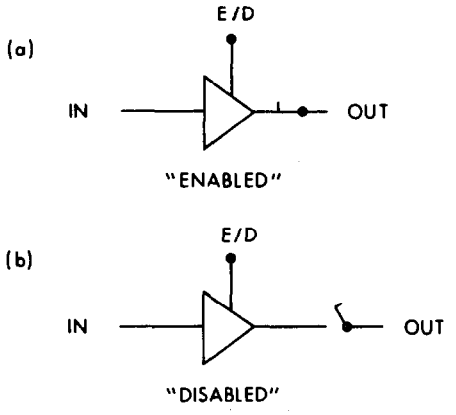


Fig. 10. The tri-state gate (E/D = enable/disable).

device selection line and the $\overline{\text{DIEN}}$ line controls data direction. Thus buses provide the communication network of the microcomputers and tri-state gate architecture allows proper information flow.

Memory

After the CPU, the memory is the next most important unit in a microprocessor system (see Fig. 1). The memory serves many functions, including program storage, data storage, stack allocation and look-up table storage. In microprocessor systems two basic types of memory are used, read/write memory (RWM) and read only memory (ROM). Although both types of memory are random access memories (RAM) in that any stored word can be accessed in any order, the term RAM is used interchangeably with RWM. Read/write memory is completely general purpose memory. It can be further subdivided into static and dynamic types. The contents of static memory remain stable as long as the power supply remains on, but dynamic memory requires frequent (msec time-scale) refresh cycles in order to maintain the contents. The content of RWM is lost whenever the system is turned off.

Read only memory (ROM) is permanent memory (*i.e.* independent of whether the power supply is on or off) used primarily for storage of frequently used programs. The contents of ROM cannot be altered after manufacture. Various types of ROM programmable by the user are available that can be erased and reprogrammed. Such erasable programmable read

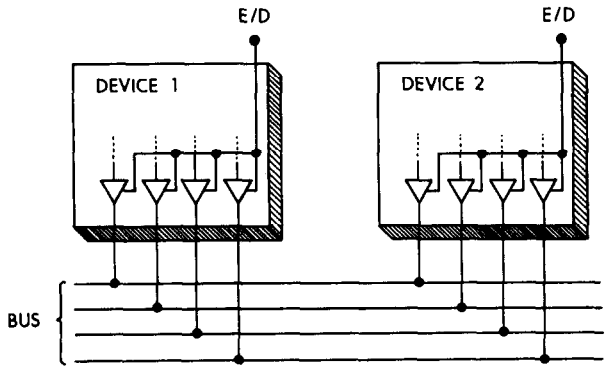


Fig. 11. Tri-state output devices attached to a bus.

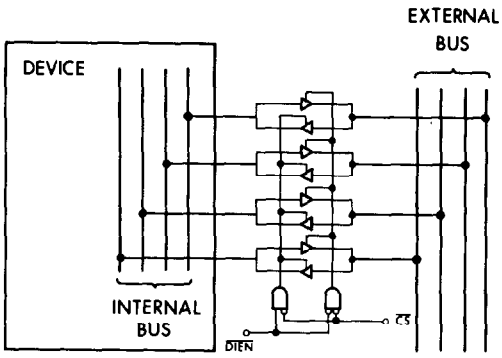


Fig. 12. A bidirectional bus.

only memory (EPROM) is often used during system development in place of ROM.

The architecture of a simple memory is shown in Fig. 13. Several important aspects of microprocessor memories and terminology are illustrated in this figure. Memory architecture is highly dependent on the basic memory chip utilized. In this case 2111s are used, which are organized in a 4-bit 256-word arrangement. Two of these chips are required to construct one block of 8-bit memory (see Fig. 13). The first 8 bits of the address bus can be used to access uniquely each of the 256 8-bit words. Additional memory can be built up in 256 blocks. Up to 8 blocks can be addressed by using the next three bits of the address bus and a 3-line to 8-line decoder to generate the block-select signals.

In addition to the term "block" the terms "page" and "field" are often used. These three terms tend to be used interchangeably but they do not necessarily mean the same thing. The term page refers to a 256-word section of memory, *i.e.*, the amount of memory addressable by an 8-bit word. Thus for the memory illustrated in Fig. 13, page and block size are identical. However, had the memory shown in Fig. 13 been built with 2114 chips (4-bit by 1024-word arrangement) a block would have been 1024 words in size. Thus block size depends on memory chip architecture. More details on addressing memory are provided in the article by Codding.[1]

Support chips

Some of the most exciting and important developments in microprocessor systems are occurring in the area of support chips. Very sophisticated and "intelligent" programmable support chips are now available that can significantly aid overall system design and development. A list of some of the more common 8080 support chips is presented in Table 3. In order to illustrate the power of these support chips, the 8255 programmable peripheral interface and the 8253 programmable interval timer will be briefly discussed.

A block diagram of the 8255 is shown in Fig. 14. It consists of three 8-bit input/output ports, A, B and C, one of which (port C) can be subdivided into two 4-bit ports. It can be programmed under software control to operate in a remarkable number of different configurations. The 8255 has three basic input/output modes: mode 0—basic I/O, mode 1—strobed I/O and mode 2—bidirectional bus. In mode 0 the device is programmed as two 8-bit and two 4-bit ports, any port can be input or output, outputs are

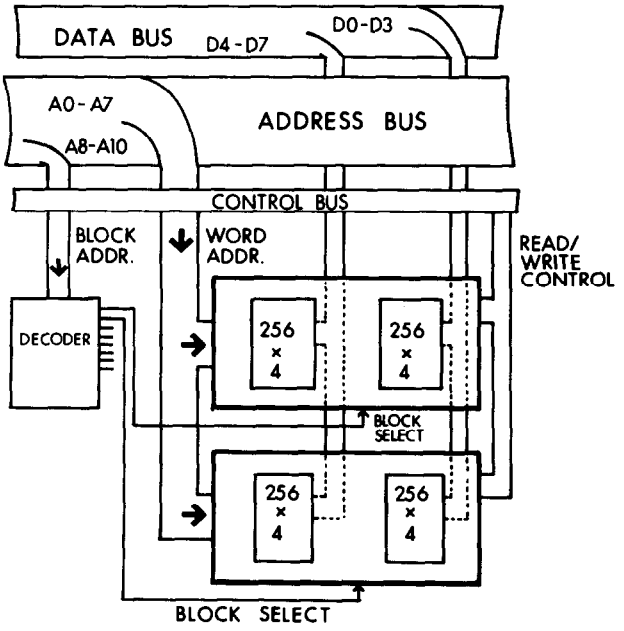


Fig. 13. Typical memory interface.

TABLE 3. 8080 Support chips

	General Purpose
8251	Communication interface —USART
8253	Interval timer —three 16-bit counters
8255	Peripheral interface —three 8-bit I/O ports
8257	DMA controller
8259	Interrupt controller —8 vectored priority interrupts
	Dedicated Function
8271	Floppy disk controller
8275	CRT controller
8279	Keyboard/display interface

latched, inputs are not latched and a total of 16 configurations is possible for mode 0. These are all illustrated in Fig. 15. In mode 1 the device is programmed as two 8-bit I/O ports each with a 4-bit control port. The 8-bit ports can be either input or output and both inputs and outputs are latched. The 4-bit port is used for control and status of the 8-bit port. The mode 1 configuration is shown schematically in Fig. 16. In mode 2 one port, port A, is programmed as a full bidirectional bus port with 5 bits of port C used for control and status. Both inputs and outputs are latched. This mode is shown schematically in Fig. 17. Note that modes can be mixed in that port B can be used in mode 0 while port A is used in mode 2. Clearly the 8255 is a powerful and versatile chip for general purpose interfacing. A very simple example is shown in Fig. 18.

The 8253 programmable interval timer is another powerful general purpose support chip. A block diagram of the 8253 is shown in Fig. 19. It contains three 16-bit presettable down-counters (BCD or binary) programmable in six modes. The modes are listed and shown schematically in Fig. 20. In mode 0, N clock pulses after a software input of the N value a $0 \rightarrow 1$ transition occurs at the output. The clock signal is connected to the counter from an external source. In mode 1, an N value is again made the input by means of software but counting of the clock does not begin until a hardware trigger-signal is received at the gate input. The device in this mode is a software programmable "one shot" or monostable multivibrator. Modes 2 and 3 are both divide-by-N counter modes and modes 4 and 5 provide software and hardware triggered strobes. As each 8253 contain three such counters, numerous timing, sequencing and counting operations can be carried out with this device.

Many other powerful operations can be implemented by the support chips listed in Table 3. This brief discussion of only two of the chips (the 8255 and 8253) should indicate to the reader the power and versatility that is generally designed into programmable support chips.

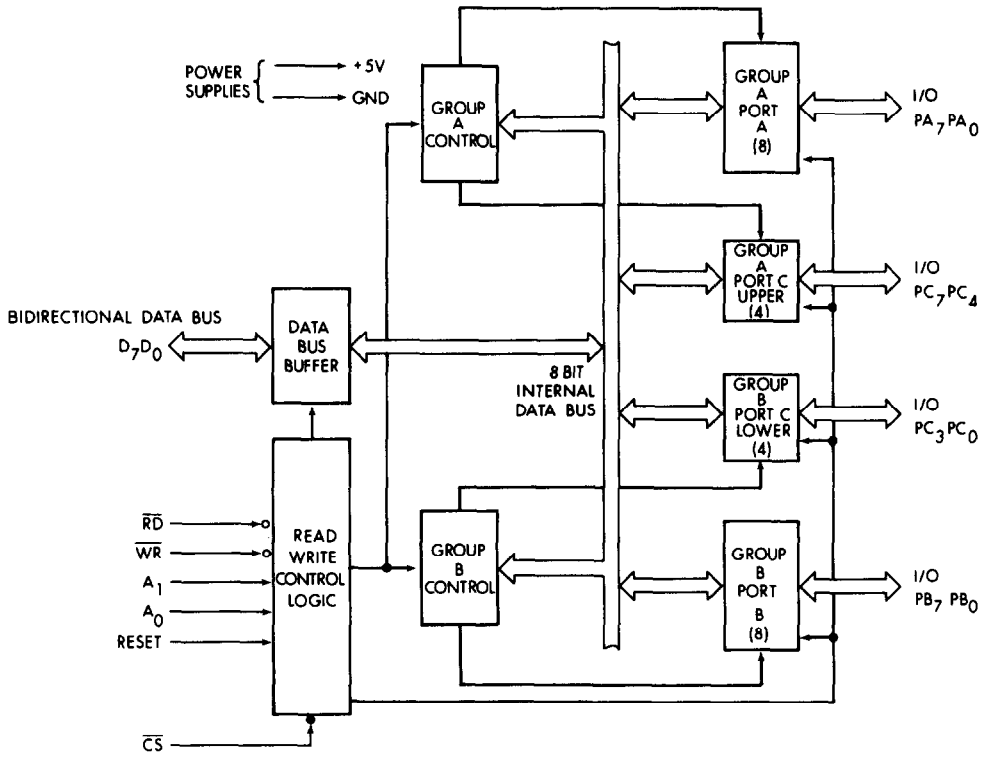


Fig. 14. Block diagram of the 8255 programmable peripheral interface.

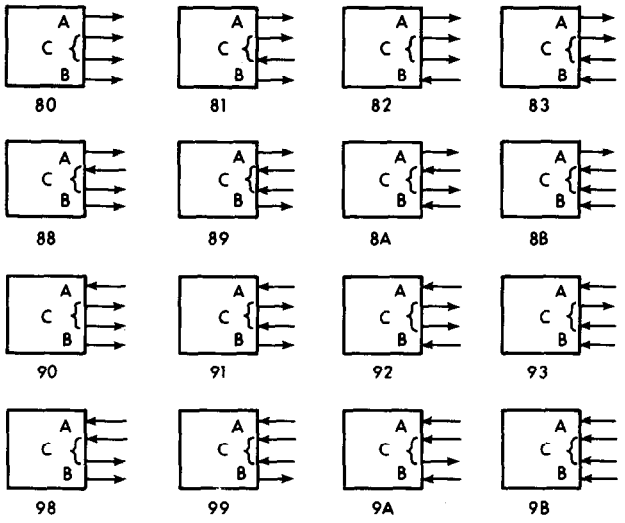


Fig. 15. Mode 0 configurations of the 8255.

8085 SYSTEMS

The basic features of the 8085 CPU are summarized in Table 4. This CPU is similar to the 8080 although some important differences exist. Comparison of Tables 2 and 4 shows that the 8085 differs from the 8080 in that it is the address and data buses that are multiplexed. The 8085 also has several additional features, including vectored interrupts, a serial I/O port, no need for the clock generator and system controller support chips, and requires only a 5-V power supply.

Some special peripheral components for the 8085 are available that allow a complete microprocessor system to be built with a small number of chips. These special components include the 8155 RAM, I/O and timer, which contains 256 words of 8-bit RAM, two 8-bit and one 6-bit I/O ports, and one 14-bit interval timer; the 8355 ROM and I/O which contains 2 kbyte of ROM and two 8-bit I/O ports; and the 8755, an EPROM version of the 8355. Thus we see a trend towards multifunction support chips with a chip like the 8155 combining memory, I/O ports

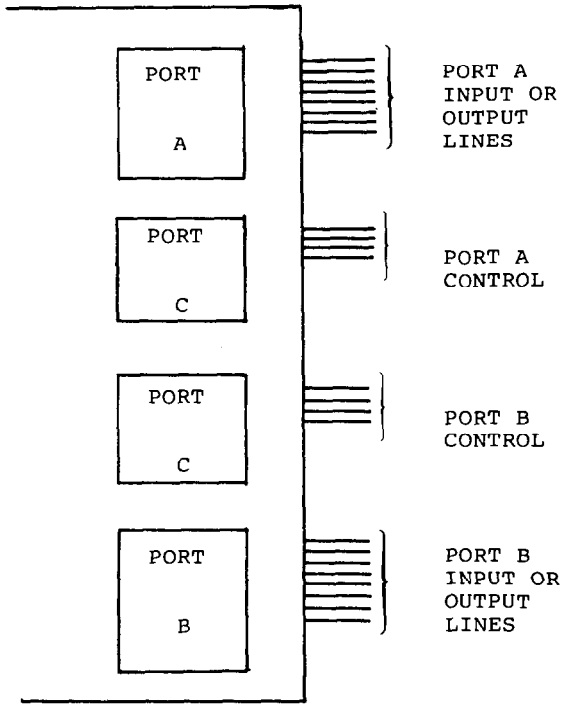


Fig. 16. 8255 mode 1 schematic diagram.

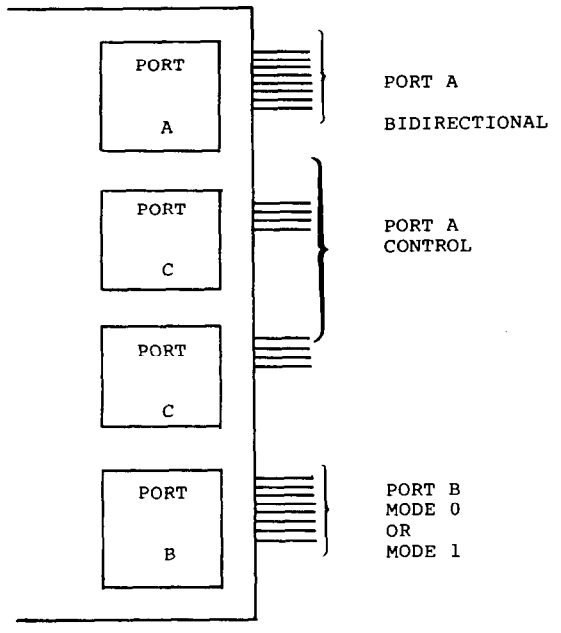


Fig. 17. 8255 mode 2 schematic diagram.

TABLE 4. 8085 CPU features

1. 8-Bit arithmetic logic unit
2. 8-Bit accumulator
3. Registers (on chip RWM)
   —six 8-bit registers
4. Address (16), data (8) and control buses
5. Address and data buses multiplexed
6. Vectored interrupts
7. Serial I/O port (TTY interface)
8. On-chip clock generator
9. On-chip system controller
10. Power requirements +5 V

and interval timer capability. The simplest 8085 system can be built with just these three chips, as shown in Fig. 21. Although these 8085 special peripheral components facilitate construction of simple systems all 8080 family support devices discussed in the previous section can be readily interfaced to the 8085 CPU.

6502 SYSTEMS

The basic features of the 6502 CPU are summarized in Table 5. As indicated earlier, the 6502 has

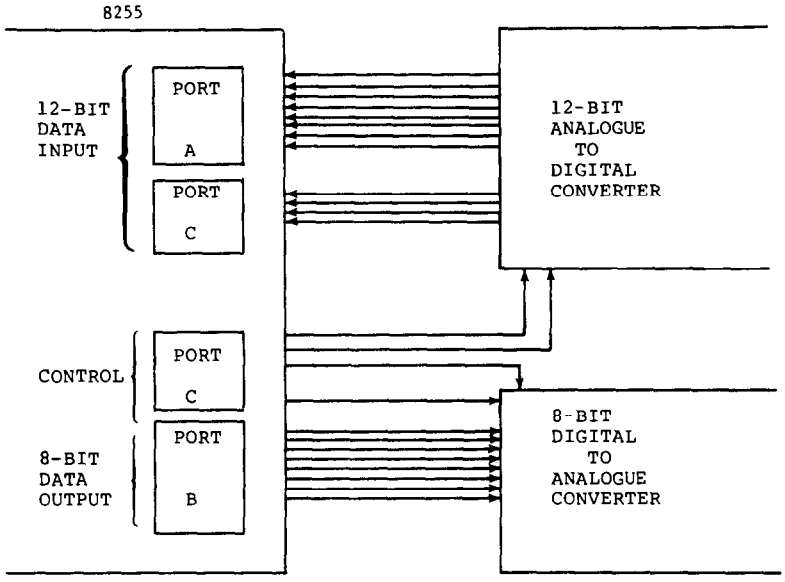


Fig. 18. 8255 data I/O example.

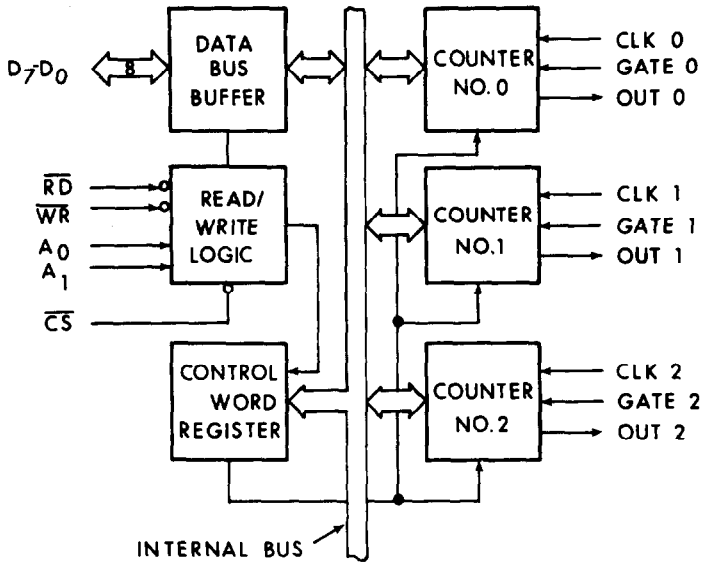


Fig. 19. Block diagram of the 8253 programmable interval timer.

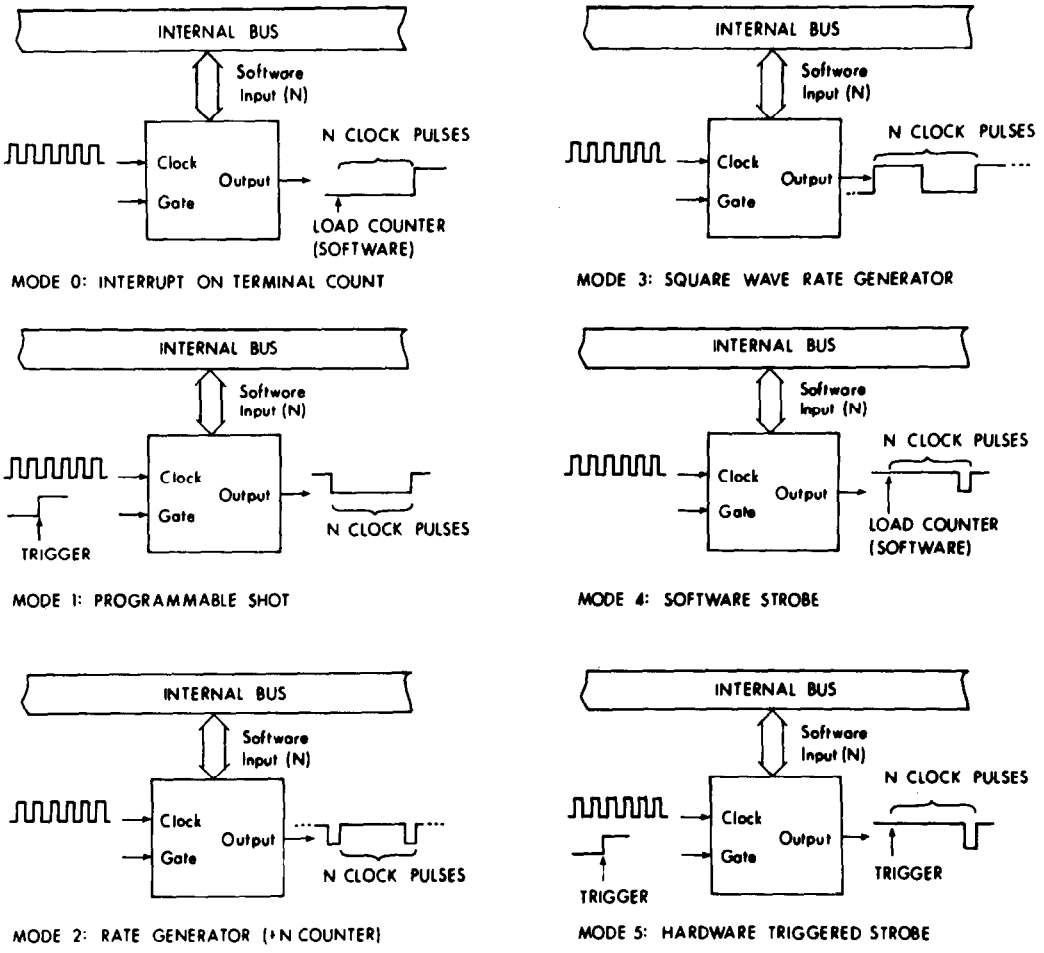


Fig. 20. Schematic of 8253 modes.

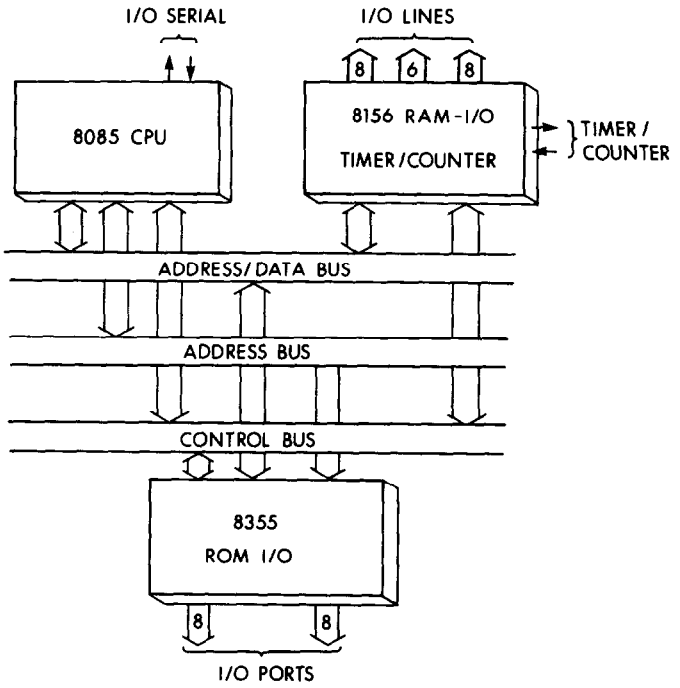


Fig. 21. 8085 system 3-chip microcomputer.

TABLE 5. 6502 CPU features

1. 8-Bit arithmetic logic unit
2. 8-Bit accumulator
3. Registers (or chip RWM)
   --two 8-bit registers
4. Address (16), data (8) and control buses
5. On-chip clock generator
6. Power requirements +5 V

considerable architectural differences from the 8080/85 systems, particularly in terms of central register capability. Several support chips are available for 6502 systems and these are listed in Table 6. Note that most are multifunction chips analogous to the 8085 support chips. The 6520 peripheral interface adapter is the basic digital I/O chip of the 6502 family and is analogous, in a way, to the 8255 discussed earlier. It contains two 8-bit I/O ports and two control ports and is shown schematically in Fig. 22. An important feature of the 6520 ports and, in general, of all 6502 familyI/O ports, is that all lines are fully independently programmable. For example, the lines of port A may be set individually as either input or output lines. In contrast, on the 8255 *all* lines of port A had to be either input or output (mode 0). This is a powerful feature of the ports of the 6502 family.

The 6522 versatile interface adapter is a particularly useful multifunction interface chip. It contains two 8-bit I/O ports and two control ports, analogously to the 6520, but in addition has an 8-bit shift register, a 16-bit counter and a 16-bit timer counter. A schematic diagram of the 6522 is shown in Fig. 23.

SUMMARY AND A LOOK FORWARD

Clearly in one article it is impossible to discuss all microprocessors that are currently available. The reader is referred to the literature appendix for sources of information on all types of microprocessor systems. The comprehensive "*An Introduction to Microcomputers*" (Vols. 2 and 3) (see Appendix I, section II B) is particularly useful. However, the systems outlined here (8080, 8085 and 6502) together with similar chips (Z80 and 6800) do represent the vast majority of 8-bit CPU systems currently in use.

TABLE 6. 6502 Support chips

General Purpose

6520 Peripheral interface adapter
- —two 8-bit I/O ports

6522 Versatile interface adapter
- —two 8-bit I/O ports
- —two 16-bit interval timer/counters

6532 RAM, I/O, interval timer device
- —128 RWM
- —two 8-bit I/O ports
- —one 8-bit interval timer + scaler

ROM

6530 ROM, RAM, I/O, Interval timer device
- —1-kbyte ROM
- —64 RWM
- —two 8-bit I/O ports
- —one 8-bit interval timer + scaler

6531 ROM, RAM, I/O, counter
- —2-kbyte ROM
- —128 RAM
- —15-line (two-port) digital I/O
- —16-bit counter
- —8-bit serial data channel

Dedicated Function

6511 Asynchronous communication interface adapter

6541 Keyboard/display controller

6545 CRT controller

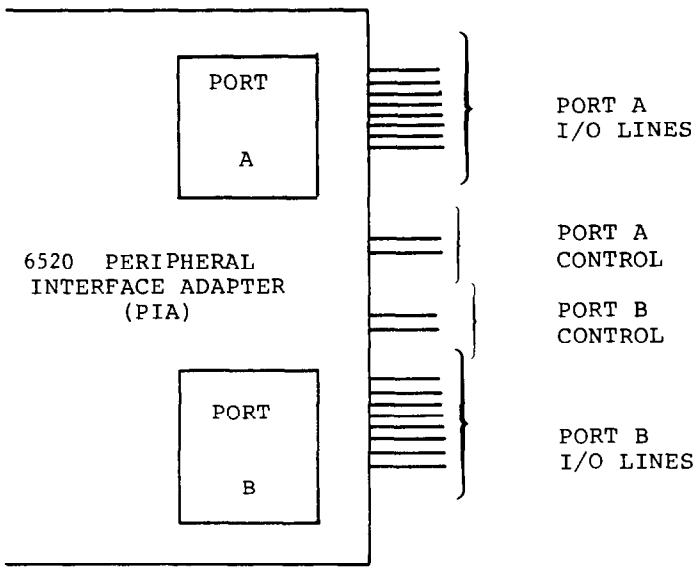


Fig. 22. Schematic diagram of the 6520 peripheral interface adapter.

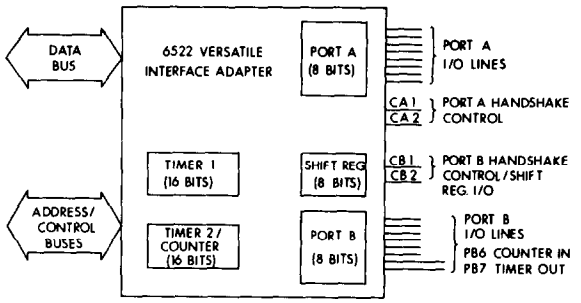


Fig. 23. Schematic diagram of the 6522 versatile interface adapter.

TABLE 7. Summary of single-board microcomputer features

Hardware Features of the SDK-80

1. 8080A CPU
2. 1-kbyte 8111 RWM
3. 4-kbyte 2708 EPROM
4. 8251 Programmable communication interface —serial I/O (*i.e.*, TTY)
5. 8255 Programmable peripheral interface —48 digital I/O lines
6. Breadboard area

Hardware Features of the SDK-85

1. 8085 CPU
2. 0.5-kbyte RWM (8155)
3. 4-kbyte ROM/EPROM (8355/8755)
4. 14-Bit timer/counter (8155)
5. 76 digital I/O lines (8155/8355)
6. Keyboard/display (8279)
7. Serial I/O port for TTY (8085)
8. Breadboard area

Hardware Features of the KIM-1

1. 6502 CPU
2. 1-kbyte RWM (6102)
3. 128-word RWM (6530)
4. 2-kbyte ROM (6530)
5. 15 digital I/O lines (6530)
6. Interval timer (6530)
7. TTY interface
8. Audio tape (cassette) interface
9. Keyboard/display

Without question, the best follow-up is purchase of a microprocessor system and subsequent work with it. In the author's laboratory initial exposure to microprocessors was provided through utilization of simple single-board systems such as the Intel SDK-80 and SDK-85, and the KIM-1.[2,3] The basic hardware features of these boards are summarized in Table 7. Although these systems have their place in simple low-cost data acquisition and control applications it might now be best to start out with a single-board system like the Rockwell AIM-65. The AIM-65 is a 6502-based single-board microprocessor and its features are summarized in Table 8. For its size, it is a very powerful beginning system with excellent hardware and software features, including a full keyboard, resident high-level language and on-board hardcopy. Current price for a complete system is about U.S. $600. Beyond the single-board systems, the hobby/consumer/small-business computer products may be considered. Popular systems includ the PET (Commodore Business Machines), Apple (Apple Computer, Inc.) and the TRS-80 (Radio Shack) which can be coupled with peripherals such as disks and printers to give relatively high-level computing systems.

TABLE 8. AIM-65 features

1. 6502 CPU
2. 4-kbyte RWM
3. 8-kbyte ROM monitor
   4-kbyte ROM assembler
   8-kbyte ROM BASIC (Microsoft)
4. 6522 Versatile interface adapter (VIA)
   —16 I/O lines
   —4 handshake lines
   —2 timer/counters
   —1 serial shift register
5. 20-column thermal printer
6. Full keyboard
7. 20-column display
8. Cassette interfaces (2)
9. TTY interface
10. Expansion connector

TABLE 9. 8748 Single-chip microcomputer

1. Accumulator
2. Arithmetic logic unit
3. Instruction decoder
4. Register array
5. Timing and control
6. Data I/O
7. User RAM
8. Timer/event counter
9. Peripheral interface ports
10. 1-kbyte resident EPROM

A class of CPUs that was not discussed in this presentation comprises the so-called single-chip microcomputers such as the Intel 8048 family. The features of the 8748 are summarized in Table 9. It is called a single-chip microcomputer because one integrated circuit contains all the necessary functions of a full microcomputer, *i.e.*, a CPU, RAM and ROM memory, I/O ports and a timer/counter. This system and ones like it (Motorola's 6801) are designed primarily for very dedicated high-volume applications and the small single-unit user will normally find their capabilities too limited and their low-volume utilization not cost-effective when compared to the CPUs and systems discussed earlier.

Another interesting class of CPUs beginning to appear combines both digital and analogue capability. Examples are the Intel 8022 and the unique Intel 2920. The analogue components of these chips consist primarily of analogue multiplexers, sample-and-hold amplifiers and digital-to-analogue converters. In particular, the Intel 2920 contains a 4-channel input analogue multiplexer and sample-and-hold amplifier, a comparator, an 8-bit digital-to-analogue converter, 8 output analogue channels, a 192 × 24 bit EPROM, a 40 × 25 bit RAM and a 28-bit ALU. This chip is designed for real-time signal processing and, as with the single-chip microcomputers, it will probably be used primarily in dedicated high-volume applications. However, the reader should keep in mind the capabilities of these chips, as future developments are sure to result in more generalized chips being developed.

What about the future? The clear trend is toward the development of full 16-bit microprocessors. Among the more prominent systems are the 8086 from Intel, the 68000 from Motorola, the Z8000 from Zilog and the 9900 from Texas Instruments. It is beyond the scope of this presentation to discuss these systems in any detail. Important general trends with most of these systems are incorporation of a large number of central registers into the CPU, 16-bit hardware multiply–divide commands, some 32-bit operations, very large (20–24 bit) address buses allowing the direct addressing in some CPUs of several megabytes of memory, and powerful indirect and indexed addressing modes. While manufacturers tend to claim that "the future is now" in that these CPUs are available, most require rather powerful and sophisticated support chips in order for effective systems to be developed, and most of these are only just about to become available. These include high-level support chips for I/O control, floating-point arithmetic and memory management. Also it is interesting to note that as an intermediate step some manufacturers have developed CPUs that have a 16-bit internal architecture but are 8-bit devices externally. Examples are the 8088 from Intel and the 6809 from Motorola. Thus, while the 16-bit systems are coming, the development systems are currently somewhat costly and complex. Without question the 8-bit systems will remain very useful for many years to come and there should be no hesitation in acquiring and utilizing such systems for laboratory data-acquisition and control.

REFERENCES

1. E. G. Codding, *Talanta*, 1981, **28**, 503.
2. E. D. Salin, M. W. Blades and G. Horlick, *ibid.*, 1981, **28**, 519.
3. M. W. Blades and G. Horlick, *ibid.*, 1981, **28**, 527.

APPENDIX I

LITERATURE AND DATA SOURCES

I. *Partial list of periodicals*

Note. Many of these can be found in hobby computer stores.

Byte. Byte Publications, Inc., 70 Main St., Peterborough, NH, USA, 03458. Monthly.

Electronic Design. Hayden Publishing Co., Inc., 50 Essex St., Rochelle Park, NH, 07662.

Electronics. McGraw-Hill, Inc., 1221 Avenue of the Americas, New York, NY, 10020. Bi-weekly.

Interface Age. McPheters, Wolfe & Jones, 6515 Sunset Blvd., Suite 202, Hollywood, CA, 90028. Monthly.

Kilobaud. Kilobaud Magazine, Peterborough, NH, 03458. Monthly.

Personal Computer World. Sportscene Publishers (PCW) Ltd., 14 Rathbone Place, London, W1P 10E.

Computing Today. Modmags Ltd., 145 Charing Cross Road, London WC2H 0EE.

II. *Book list—manuals*

A. Scelbi Software Manuals. Scelbi Computer Consulting Inc., 1322 Rear Boston Post Rd., Milford, CT, 06460.

1. Machine Language Programming for the 8080
2. 8080 Monitor Routines
3. An 8080 Assembler Program
4. An 8080 Editor Program
5. Scelbi's '6800' Software Gourmet Guide and Cookbook
6. Scelbi's '8080' Software Gourmet Guide and Cookbook

B.

A. Osborne, McGraw-Hill, 630 Bancroft Way, Dept. E18, Berkeley, CA, 94710.

1. An introduction to Microcomputers, Vol. 2—Some Real Products (extensive data on all CPU's)
2. An introduction to Microcomputers, Vol. 3—Some Real Support Devices (extensive data on all microprocessor support devices)

C.

Intel Literature. Intel Corporation/Literature Department, 3065 Bowers Ave., Santa Clara, CA, 95051.

1. MCS-80 Users Manual
—good technical manual for 8080 family chips
2. MCS-85 Users Manual
—8085 family system
3. MCS-86 Users Manual
—8086 family system
4. 8080/8085 Assembly Language Programming Manual
5. Memory Design Handbook
6. Microcomputer Systems Handbook
7. MCS-48 Users Manual
8. UPI-41 Users Manual

D. Sources of information and data sheets on 6500 series microprocessors and support chips.

MOS Technology Inc.
950 Rittenhouse Rd.
Norristown, PA 19401

Rockwell International
Microelectronics Devices
P.O. Box 3669
Anaheim, CA 92803

Synertek
P.O. Box 552
Santa Clara, CA 95052

III. *Articles*

Microcomputers—a comparative evaluation, M. Firebaugh, L. Johnson and W. Stone, *The Physics Teacher*, 1978, 459 (A very good though slightly dated article comparing a number of small computer systems. Very readable).

Summaries of architectures and instruction codes for 8080A/8085, 6800, Z80, CDP 1802, 6100 and TMS 9900. *Electronic Design*, 1978, **11**, 208.

How to choose a microprocessor. L. Frenzel, *Byte*, 1978, July, 124. (A good low-level discussion of the various CPUs. Emphasizes the importance of software).

1978 Index to software. *Interface Age*, 1978, November, 50. (An extensive list of available software and manufacturers for small computers. Also numerous literature references.)

Recent applications of digital computers in analytical chemistry. D. D. Perrin, *Talanta*, 1977, **24**, 339. (Good overview with an emphasis on software and applications.)

FORTH's forte is tighter programming. S. M. Hicks, *Electronics*, 114 1979, March 15.

APL makes splash in small computers. J. G. Posa, *Electronics*, 1978, Dec. 21, 68.

Mating the IEEE-488 bus to micros. *Electronic Design*, 1978, **24**, Nov. 22.

Microprocessor special issue and data manual. *Electronic Design*, 1979, **27**, 24.

A brief summary of 16 bit systems. *Electronics*, 1980, **53**, No. 11, 89.

A discussion of the 8087 floating point mathematics subsystem. *Electronics*, 1980, **53**, No. 11, 114.

A data acquisition and control system based on the new Commodore PET microcomputer. T. M. Jedju, *Rev. Sci. Instr.*, 1979, **50**, 1077.

Microprocessor-controlled system for automatic acquisition of polentiometric data and their non-linear least-squares fit in equilibrium studies. H. Gampp, M. Maeder, A. D. Zuberbühler and T. A. Kaden, *Talanta*, 1980, **27**, 513

A microcomputer-based system for the processing of spark source mass spectrometry photoplates. A. Pilate and F. Adams, *Anal. Chim. Acta*, 1980, **122**, 57.

Staircase voltammetry and pulse polarography with a microcomputer controlled polarograph. P. Barret, L. J. Davidowski and T. R. Copeland, *Anal. Chim. Acta*, 1978, **122**, 67.

A microprocessor control system for automated multiple flow injection analysis. K. K. Stewart, J. F. Brown and B. M. Golden, *Anal. Chim. Acta*, 1980, **114**, 119.

Adaptation of the 8253 timer as a programmable real time clock for minicomputer applications. J. C. Lennox, *Anal. Chem.*, 1980, **52**, 585.

Laboratory microcomputer system for the development of microcomputer-controlled analytical instrumentation, E. B. Buchanan Jr. and M. L. Buchanan, *Talanta*, 1980, **27**, 947.

A microcomputer-controlled square-wave polarograph, E. B. Buchanan Jr. and W. J. Sheleski, *Talanta*, 1980, **27**, 955.

Microcomputer interfacing—the 80 family microprocessors. Field, P. E., *Am. Lab.*, 1980, **12**, No. 6, 83. One of a long-term continuing series of short articles on all aspects of microprocessors.

Laboratory data-acquisition capabilities of microcomputers, E. D. Salin, M. W. Blades and G. Horlick, *Talanta*, 1981, **28**, 519.

Microprocessor-controlled integrating read-out systems for photomultiplier tubes. M. W. Blades and G. Horlick, *Talanta*, 1981, **28**, 527.

Interfacing, addressing and accessing peripherals with microprocessors. E. G. Codding, *Talanta*, 1981, **28**, 503.

Construction of a microcomputer-based reaction rate ratemaker, M. A. Ryan and J. D. Ingle, Jr., *Talanta*, 1981, **28**, 539.

Microprocessor-controlled system for automatic acquisition of kinetic data of gas uptake under constant pressure, H. Gampp, *Talanta*, 1981, **28**, 535.

Use of added random noise to improve bit-resolution in digital signal averaging, R. M. Belchamber and G. Horlick, *Talanta*, 1981, **28**, 547.

Data-logging system based on the Intel 8748 single-chip microprocessor, R. M. Belchamber and G. Horlick, *Talanta*, 1981, **28**, 543.

The impact of microprocessors on analytical instrumentation, D. Betteridge and T. B. Goad, *Analyst*, 1981, **106**, 257.

VI. Recent Books

The 8080/8085 Microprocessor Book, Wiley-Interscience, New York, N.Y., 1980. Compilation of Intel literature.

R. C. Camp, T. A. Smay and C. J. Triska, *Microprocessor Systems Engineering*, Matrix Publishers, Inc., 30 NW 23rd Place, Portland, Oregon 97210, 1979. Good book on 6502 and AIM-65 systems.

APPENDIX II

SELECTED CHIP NUMBER INDEX

I. *6500 Series CPU's and Support Chips*
—MOS Technology
—Rockwell International
—Synertek
6502 Single chip 8-bit microprocessor
6520 Peripheral interface adapter (PIA)
6522 Versatile interface adapter (VIA)
6530 1-kbyte ROM, 64 RAM, I/O, Timer (RRIOT)
6531 2-kbyte ROM, 128 RAM, I/O, Counter (RRIOC)
6532 128 RAM, I/O, Timer (RIOT)
6545 CRT controller
6551 Asynchronous communication interface adapter

II. *Intel CPU Group*
8080 Single chip 8-bit microprocessor
8085 Single chip 8-bit microprocessor —2nd generation "8080"
8086 Single chip 16-bit microprocessor
8048 Single chip 8-bit microcomputer complete with I/O ports, clock, timer and 1-kbyte ROM
8748 EPROM version of 8048
8224 Clock generator and driver
8228 System controller and bus driver
8284 Clock generator and driver (8086)
8288 Bus controller for 8086

III. *Intel Peripheral and Support Chips*
8205 High-speed 1 out of 8 binary decoder
8212 8-bit input/output port
8214 Priority interrupt control
8216 4-bit parallel bi-directional bus driver
8251 Communication interface
8253 Interval timer
8255 Peripheral interface
8257 DMA controller
8259 Interrupt controller
8271 Floppy disk controller
8275 CRT controller
8279 Keyboard/display interface
8282/8283 8-bit input/output port
8286/8287 8-bit parallel bi-directional bus driver
8291 GPIB talker/listener
8292 GPIB controller
8294 Data encryption unit
8295 Dot matrix printer controller
MCS-85 Series support chips (8085)
8155 256 ROM, I/O ports and timer
8355 2-kbyte ROM and I/O ports
8755 2-kbyte EPROM and I/O ports

IV. *Memory*
RAM
2111(8111) 1024 bit RAM
2114 1024 × 4 bit RAM
EPROM
2708 1 kbyte × 8 EPROM
2716 2 kbyte × 8 EPROM
2732 4 kbyte × 8 EPROM

V. *Some other chips*
9511 Arithmetic processor, Advanced Micro Devices
6800 8-bit CPU from Motorola
68000 16-bit CPU from Motorola
Z80 8-bit CPU from Zilog
Z8000 16-bit CPU from Zilog
9900 16-bit CPU from Texas Instruments

Talanta. Vol. 28. pp. 503 to 518. 1981
Printed in Great Britain. All rights reserved

0039-9140/81/070503-16$02.00/0
Copyright © 1981 Pergamon Press Ltd

ADDRESSING, ACCESSING AND INTERFACING PERIPHERAL DEVICES TO MICROPROCESSORS

EDWARD G. CODDING
Department of Chemistry, University of Calgary, Calgary, Alberta, Canada

(*Received* 22 *January* 1980. *Accepted* 16 *May* 1980)

Summary—To utilize the full potential of microprocessors, particularly the small and inexpensive single board systems, for dedicated data acquisition and instrumental system-control functions, it is imperative that researchers have an appreciation of the concepts for addressing, accessing and interfacing peripheral devices to microprocessor systems. These concepts are presented for the Intel 8080, 8085 and Mostek 6502 microprocessors with specific examples for the SDK 80 (8080), SDK 85 (8085) and KIM-1 (6502) single-board microprocessor systems. Features of the control bus architecture are discussed with regard to the movement of data to or from peripheral devices and memory. Utilization of control bus signals and addresses generated from the user program to address and access memory and peripheral devices are discussed and illustrated. The ability of these three microprocessors to handle and service interrupt requests from peripheral devices is discussed. The concepts for interfacing input and output peripheral devices, such as analogue-to-digital and digital-to-analogue converters, to these microprocessors are discussed and illustrated. Software programs suitable for use as subroutines, for input and output of data with these devices are presented and discussed.

Recent developments in the capabilities and sophistication of microprocessors and microprocessor peripherals has led to an enormous proliferation of these devices in the field of scientific instrumentation. Several commercial instrument manufacturers have introduced products (atomic-absorption spectrophotometers, ion-meters, spectrophotometers, *etc.*) which have microcomputers as an integral part of the instrumental control and/or data acquisition and display electronics. Further, many researchers have recognized, and are taking advantage of, the unique capabilities of microprocessors to develop small microcomputer systems which are dedicated to performing the operational or control functions of a specific experimental system. Numerous examples of typical applications have appeared in the recent literature.[1–8] The availability of powerful, versatile and inexpensive microprocessor kits, such as the Intel[9] SDK-80 or SDK-85 and Mostek[10] KIM, which are based on the Intel 8080, 8085 and Mostek 6502 microprocessors respectively, and the associated development of equally versatile peripheral support devices will certainly enhance the development of dedicated measurement/control systems.

However, for the researcher who is unfamiliar with microprocessor architecture or the fundamentals of interfacing, addressing, and accessing peripheral devices associated with microprocessors, the task of designing dedicated microprocessor systems may seem insurmountable. Horlick[11] has presented a general discussion of microprocessor architecture, including related support devices. The purpose here is to present some fundamental considerations of interfacing peripheral devices to microprocessor systems and the establishment of device addresses which allow the microprocessor to access the peripheral devices.

MICROPROCESSOR BUS STRUCTURE

As discussed by Horlick,[11] the central processing unit (CPU) of a microprocessor communicates with its associated peripheral devices (here a peripheral device can be taken as memory or any input/output device) through, in general, three system buses. A bus is simply a number of parallel connections between the microprocessor and a peripheral device, through which information is transferred. The architecture of bus structures varies between manufacturers but may be represented schematically as shown in Fig. 1.

The three system buses are named after the type of signals which they carry, as the address, data/instruction and control buses. The address bus will normally be 16 bits wide (have 16 parallel connections) and carry the 16-bit binary encoded address (A0–A15) of the memory location or device which the microprocessor expects to access. This bus is typically unidirectional, *i.e.*, the information flow is from the microprocessor to the device. The data bus is typically 8 bits wide (D0–D7) and carries data or program instructions to or from a memory location or peripheral device. The data bus is bidirectional since data may be transferred from the microprocessor to a device and *vice versa*. Thus the address bus provides an address which may be decoded to select one of the various peripheral devices associated with the microprocessor while the data bus provides for the transfer of data (or instructions) between the CPU and the peripheral device.

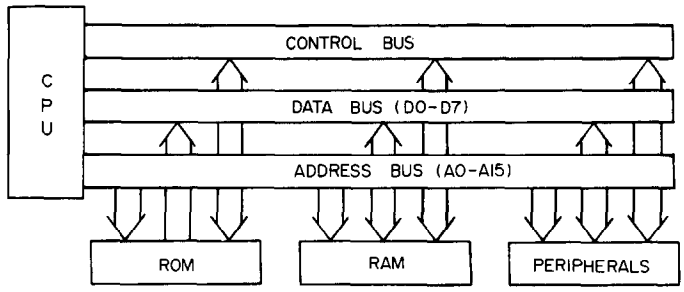


Fig. 1. Block diagram of a microprocessor and associated system buses.

The role of the control bus is to control the bidirectional data bus and to synchronize the movement of data between the CPU and memory or peripheral devices. These functions are realized by means of control signals which are generated by the CPU during the execution of an instruction. The control signals, which appear on the control bus, convey information regarding the status of the CPU and any operation which the CPU is undertaking, *i.e.*, writing or reading data into or out of a memory location or peripheral device. Specifically which memory location or device is involved ("accessed") must be determined by decoding the 16-bit address present on the address bus while the data are moved by the data bus. Thus, an understanding of the control bus function is imperative as it provides the researcher with the means to access peripheral devices which have been interfaced to the microprocessor. Here consideration will be given to the Intel 8080, 8085 and Mostek 6502.

Intel 8080 control bus

The Intel 8080 control bus signals[12] are listed in Table 1. These signals can be divided into three groups: those related to data movement to or from the microprocessor, those related to interrupt requests from peripheral devices and those (RESET, $\overline{\text{READY}}$ and HOLD) which may be externally employed to control processor operation. The first two groups are extensively utilized in interfacing and accessing peripheral devices. The first group; memory read ($\overline{\text{MEMR}}$), memory write ($\overline{\text{MEMW}}$), input read ($\overline{\text{I/OR}}$) and output write ($\overline{\text{I/OW}}$) signals signify that the microprocessor is expecting to perform a read or write operation from a memory location or peripheral input/output device, respectively. These control signals are designated as active when low.[13] They are normally held in a "logic high" state, signified as "logic 1", and reset to a "logic low" state, signified as "logic 0", to indicate that a particular operation is to occur. Thus, the mnemonic $\overline{\text{MEMR}}$ should be read as "memory read when low", the bar signifying "active when low". The function of these signals can be illustrated as follows. Consider that the 8080 CPU is executing an instruction which involves data being read from memory, such as a MOV A,M instruction. The CPU places the 16-bit address of the memory location on the address bus and then generates a $\overline{\text{MEMR}}$ control signal. This signifies that a read operation is to occur from the address currently on the address bus. The $\overline{\text{MEMR}}$ is also utilized to "enable" (*i.e.*, make available for use) the memory location, thus synchronizing the placing of data on the data bus with the read operation of the CPU.

The second group; interrupt (INT) and interrupt acknowledge ($\overline{\text{INTA}}$) signify that a peripheral device is requesting the microprocessor to cease its current processing and to service the device instead, and that the microprocessor has acknowledged the interrupt request from the device. Thus, peripheral devices have a mechanism for directing the microprocessor to interrupt its current processing and interact with the device. This interaction could simply be the input or

Table 1. Intel 8080 control bus signals

$\overline{\text{MEMR}}$	a read from memory operation
$\overline{\text{MEMW}}$	a write into memory operation
$\overline{\text{I/OR}}$	a read from IO device operation
$\overline{\text{I/OW}}$	a write into IO device operation
$\overline{\text{INT}}$	interrupt request
$\overline{\text{INTA}}$	interrupt acknowledge
$\overline{\text{RESET}}$	initialize microprocessor
$\overline{\text{READY}}$	device or memory not ready
HOLD	hold request, microprocessor activates tristate gates in its bus circuitry, disconnecting itself from its buses
HLDA	hold acknowledge

Table 2. Intel 8085 control bus signals

$\overline{RD}$	a read operation occurring
$\overline{WR}$	a read operation occurring
IO/$\overline{M}$	operation referencing IO device (active high) or memory (active low).
ALE	address latch enable
INTR	interrupt request
$\overline{INTA}$	interrupt acknowledge
RST 5.5, RST 6.5, RST 7.5, TRAP	hardware restart inputs; result in direct calls to addresses 003CH, 0034H, 002CH and 0024H, respectively.

In addition: $\overline{RESET}$, $\overline{READY}$, $\overline{HOLD}$, HLDA as for the Intel 8080.

output of new data, or could be much more sophisticated. The implementation of interrupts for the 8080, 8085 and 6502 will be discussed below.

Intel 8085 control bus

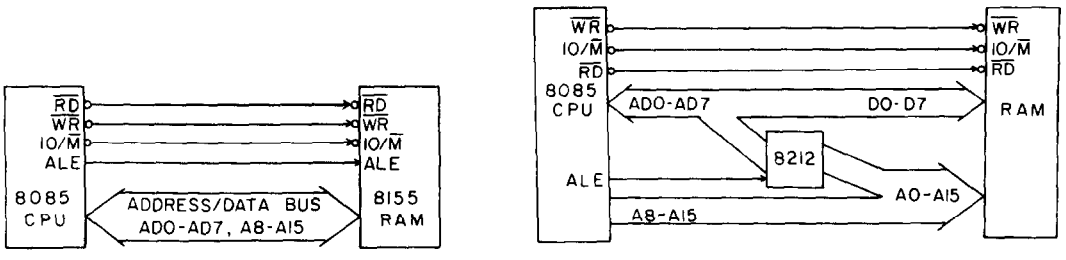
The Intel 8085[14] is an advanced version of the 8080 and as such has a somewhat simplified control bus structure. The 8085 control signals are given in Table 2. As in the 8080 case, these signals can be divided into three groups having effectively the same functions as the 8080 control signals. The first group will be considered in detail here and the second group will be discussed below. The first group consists of the control signals $\overline{WR}$ and $\overline{RD}$ which are "active low" signals indicating whether a write or read operation, respectively, is to occur. In conjunction with these two an IO/$\overline{M}$ signal is generated to indicate whether the read/write operation refers to a peripheral device (IO/$\overline{M}$ active high) or a memory location (IO/$\overline{M}$ active low). Thus, the combination of $\overline{WR}$ or $\overline{RD}$ and IO/$\overline{M}$ control signals provides information regarding the type of operation to occur and the type of device (memory or peripheral) being referenced, as well as synchronizing the data transfer in a manner analogous to the 8080. Specifically which peripheral device, or memory location, is being referenced must be determined from the address present on the address bus.

The address and data bus architecture of the 8085 differs from the 8080 in that the 8085 uses a time-multiplexed address and data bus and thus has a combined bus which is only 16 bits wide. During the execution of an instruction which involves data transfer, the appropriate device address appears first on the address bus (A0–A15) followed by the data on the low-order byte (8 bits) of the address bus (A0–A7).[14] It is, therefore, necessary to save the low order address byte by "latching" it before the appearance of data on the bus. The 8085 family peripheral devices (including memory) contain internal latches for this purpose. The 8085 generates a control signal, the "address latch enable" or ALE, which enables these latches when address information is present on the bus. A block diagram of this system is shown in Fig. 2a. When the 8085 is used with 8080 family devices, the user must provide the address latch to demultiplex the address/data bus. This can be accomplished with a device such as the Intel 8212 8-bit data latch as shown schematically in Fig. 2b. In this case the ALE latches the low-order address byte into the 8212 latch which demultiplexes the address/data bus.

The Intel 8080 and 8085 are unique in that they generate control signals which are specifically intended for use with input/output peripheral devices. These are the $\overline{I/OW}$ and $\overline{I/OR}$ for the 8080 and IO/$\overline{M}$ active high for the 8085. The availability of these control signals provides additional versatility in accessing peripheral devices as will be discussed below.

Mostek 6502 control bus

The Mostek 6502 microprocessor does not generate control signals which explicitly signify that the data transfer is to or from a peripheral device rather than a



(a) (b)

Fig. 2. Intel 8085 interconnections to (a) family random access memory and (b) non-family random access memory.

Table 3. Mostek 6502 control bus signals

SYNC	instruction being fetched from memory
R/$\overline{W}$	read operation (active high) or write operation (active low) is occurring.
$\overline{NMI}$, $\overline{IRQ}$	vector interrupt requests to addresses FFFAH and FFFEH, respectively
$\overline{RESET}$	initialize the microprocessor
$\overline{READY}$	device or memory not ready.

memory location. The 6502 control signals are given in Table 3. A single control signal, R/$\overline{W}$, is utilized to signify the execution of a read (R/$\overline{W}$ active high) or write (R/$\overline{W}$ active low) operation. Since the 6502 does not generate control signals specifically related to memory or peripheral devices, the source or destination of the read/write operation must be determined from the 16-bit address present on the address bus.

ADDRESSING MEMORY AND PERIPHERAL DEVICES

The 8080, 8085 and 6502 microprocessors utilize a 16-bit address bus resulting in 65,536 unique addresses numbered from 0 to 65,535, or from 0000H to FFFFH (the postfix H will be used[13] to identify hexadecimal* notation to base 16; F signifies 15) which may be assigned as addresses for memory locations or peripheral devices. When used in conjunction with the control bus signals, the 16-bit address allows the microprocessor to address and access any individual memory location or peripheral device.

As described above, the Intel 8080 and 8085 microprocessors generate control signals (see Tables 1 and 2) which are specifically intended to facilitate data transfers to or from peripheral devices. This technique of accessing peripheral devices is termed *isolated IO* since addresses for peripheral devices are assigned effectively in parallel to memory addresses and hence do not encroach on the addresses utilized for memory space. The 8080/8085 instruction sets contain two instructions, IN and OUT, for implementing isolated IO data transfers. The IN instruction results in the transfer of one data byte (8 bits) from a 1-byte address to the microprocessor accumulator. When this instruction is executed, the 8-bit address is placed on the address bit (A0–A7), an $\overline{I/OR}$ (8080) or IO/$\overline{M}$ and $\overline{RD}$ (8085) control signal is generated to signify a read operation from a peripheral device, and data are then transferred to the microprocessor accumulator from the device. Similarly, the OUT instruction transfers one datum byte from the microprocessor accumulator to a 1-byte address and generates control bus signals to indicate that a write operation to a peripheral

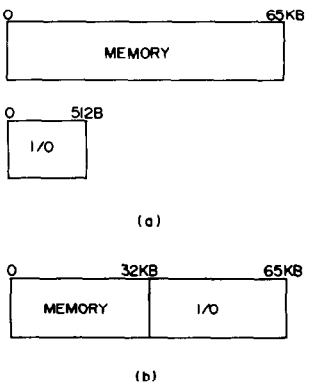
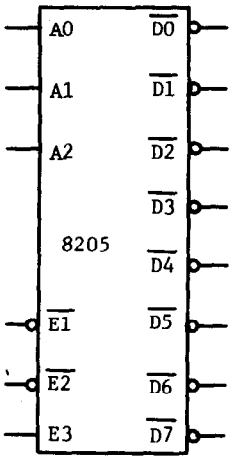


Fig. 3. (a) Isolated IO memory allocation, (b) memory mapped IO memory allocation; KB = kbyte (1000 bytes).

device is under way. Thus, the transfer of data to or from peripheral output or input devices may be easily accomplished with two instructions. Since these instructions use an 8-bit address, only 256 different input or output peripheral devices may be accessed. However, this is certainly sufficient for any practical laboratory application. Memory allocation for isolated IO addressing, illustrated in Fig. 3a, ensures that 65 kbyte are available for memory while an additional 512 addresses, which are effectively parallel to the memory addresses, are available for peripheral devices.

The particular device which the microprocessor is attempting to access must be determined by decoding the 1-byte address associated with IN/OUT instructions to generate a "device select" control signal ($\overline{DS}$) for the desired device. The device address appears on the low-order byte (A0–A7) of the address bus when the instruction is executed. The decoding operation can be conveniently carried out by utilizing a binary decoder such as the Intel 8205 1-out-of-8 decoder which is shown in Fig. 4. As shown in the 8205 logic table, this device uniquely decodes three input address bits (A0–A2) to select one of the eight decoded outputs ($\overline{D0}$–$\overline{D7}$). Note that the selected output is reset to logic 0 while the other outputs remain at logic 1. Further, the 8205 may only be enabled by the correct combination of logic levels of the enable inputs, $\overline{E1}$, $\overline{E2}$ and E3. The 8205 will be active only when $\overline{E1}$ and $\overline{E2}$ are logic 0 and E3 is logic 1. Thus, when using the IN/OUT instructions in conjunction with two decoders it is possible to select individually eight input and eight output devices by utilizing only the first three address bits A0–A2. The bus connections are shown in Fig. 5. Figures 5a and 5b show the bus connections when the 8080 microprocessor is used. In Fig. 5a the 8205, which is selecting input devices, will be enabled when $\overline{I/OR}$ is logic 0 and $\overline{I/OW}$ is logic 1 as will be the case when an IN instruction is being executed. Similarly, in Fig. 5b, the 8205 selecting output devices will be enabled when $\overline{I/OW}$ is logic 0 and $\overline{I/OR}$ is logic 1 as when an OUT instruction is executed. The addresses of the eight devices will be

* Editorial note. "Hexadecimal" is etymologically incorrect, since it mixes Greek and Latin roots, and 'sexadecimal" would perhaps be a more correct form.



LOGIC SYMBOL

PIN NAMES

A0—A2	Address Inputs
$\overline{E1}$–E3	Enable Inputs
D0—D7	Decoded Outputs

LOGIC TABLE

Address			Enable			Decoded Outputs							
A0	A1	A2	$\overline{E1}$	$\overline{E2}$	E3	0	1	2	3	4	5	6	7
L	L	L	L	L	H	L	H	H	H	H	H	H	H
H	L	L	L	L	H	H	L	H	H	H	H	H	H
L	H	L	L	L	H	H	H	L	H	H	H	H	H
H	H	L	L	L	H	H	H	H	L	H	H	H	H
L	L	H	L	L	H	H	H	H	H	L	H	H	H
H	L	H	L	L	H	H	H	H	H	H	L	H	H
L	H	H	L	L	H	H	H	H	H	H	H	L	H
H	H	H	L	L	H	H	H	H	H	H	H	H	L
X	X	X	L	L	L	H	H	H	H	H	H	H	H
X	X	X	H	L	L	H	H	H	H	H	H	H	H
X	X	X	L	H	L	H	H	H	H	H	H	H	H
X	X	X	L	H	L	H	H	H	H	H	H	H	H
X	X	X	H	L	H	H	H	H	H	H	H	H	H
X	X	X	L	H	H	H	H	H	H	H	H	H	H
X	X	X	H	H	H	H	H	H	H	H	H	H	H

Fig. 4. Logic symbol and logic table for the Intel 8205 1-out-of-8 decoder.

00H–07H and can be the same for both input and output devices since the $\overline{I/OW}$ and $\overline{I/OR}$ control bus signals are being used to enable the appropriate decoder.

Figures 5c and 5d show the bus connections when the 8085 microprocessor is used. In Figure 5c the 8205, which is selecting input devices, will be enabled when $\overline{RD}$ is logic 0 and IO/$\overline{M}$ is logic 1, as will be the case when an IN instruction is being executed. In Fig. 5d the 8205 is selecting output devices and will be enabled when $\overline{WR}$ is logic 0 and IO/$\overline{M}$ is logic 1 as would be the case when an OUT instruction is being

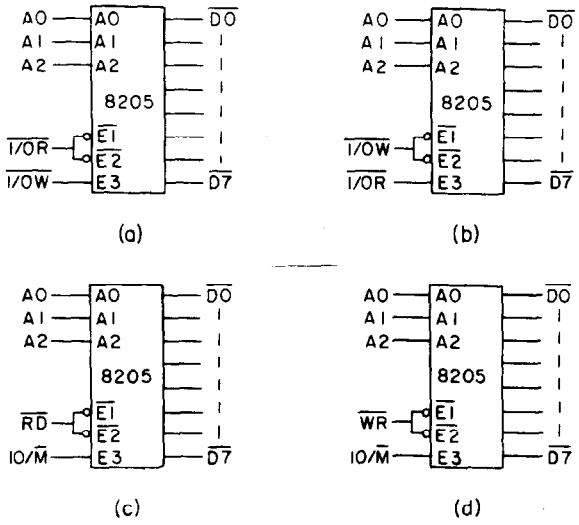


Fig. 5. Effecting isolated IO addressing with the Intel 8205 decoder with the 8080 for (a) input, (b) output and 8085 for (c) input and (d) output devices.

Table 4. Some memory referencing instructions available for memory mapped IO

MOV	r,M	address contents to register
MOV	M,r	register contents to address
MVI	M	immediate move to address
LDA	M	address contents to accumulator
STA	M	accumulator contents to address
LHLD	M	address contents to HL register
SHLD	M	HL register contents to address
ADD	M	add address contents to accumulator
SUB	M	subtract address contents from accumulator
	Logic operations, *i.e.* AND, XRA, ORA, CMP	

executed. The addresses assigned to the peripheral devices could be the same as described for the 8080. Thus, addressing and accessing a small number of peripheral devices. eight input and eight output, becomes quite straightforward by use of isolated IO.

However, the isolated IO technique is quite restrictive in terms of programming versatility, since all data transfers, both input and output, must occur through the microprocessor accumulator and utilize only two instructions. A great advantage in programming versatility can be realized by employing a peripheral-device addressing technique known as *memory mapped IO*. In this mode a portion of the 65 kbyte of memory addresses is assigned to be addresses for peripheral devices, which allows these devices to be accessed as if they were memory locations. A convenient allocation of memory space would be to retain the address space 0000H–7FFFH for memory and assign the upper 32 kbyte, 8000H–FFFFH, as peripheral device addresses. Thus, if the most significant address bit, A15, were logic 1 the address would be referencing a peripheral device and if A15 were logic 0 memory would be referenced. The memory allocation is illustrated in Fig. 3b.

The advantage of this addressing mode is that it allows any of the memory referencing instructions, such as those in Table 4, to be used in transferring data to or from peripheral devices, thus providing considerable programming versatility.

If only a few peripheral devices are to be accessed, four input and four output devices for example, address bit A15 may be used directly to enable the 8205 binary decoder as shown in Fig. 6. Since $\overline{E1}$ and $\overline{E2}$ are grounded (logic 0) the 8205 will be enabled whenever E3 (A15) is logic 1. The addresses of the eight decoded outputs, device selects for peripheral devices, are in the range 8000H–8007H. In addition, since control bus signals are not being used to enable the binary decoder, both input and output devices can be accessed from the same decoder, each device having a unique address. For example, four input devices could be addressed 8000H–8003H and four output devices addressed 8004H–8007H, or any combination of these. The advantage of memory mapped IO addressing is that it allows the use of any memory referencing instruction to transfer data to or from the peripheral devices. In addition, it is possible to perform logic and arithmetic operations directly on data from input devices. It should further be noted that data transfers are not limited to accumulator operations and that 8080/8085 instructions such as LHLD or SHLD which can accomplish the transfer of two data bytes to or from two successive addresses will result in a programming advantage as well. Further, there may be a speed advantage as many of these instructions can be executed more rapidly than the IN/OUT instructions.

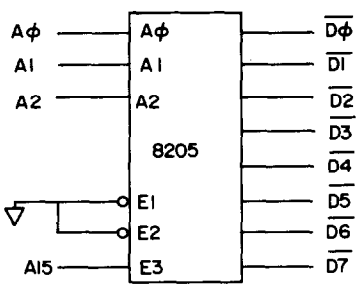
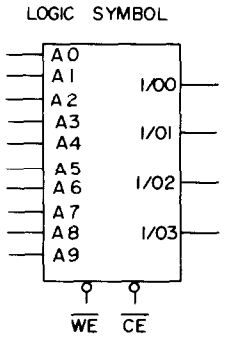


Fig. 6. Effecting memory mapped IO addressing with the Intel 8205 decoder.

The Mostek 6502 microprocessor instruction set does not contain instructions which are explicitly intended for isolated IO applications nor does the microprocessor generate control signals for this purpose. Instead, the 6502 employs the memory mapped IO technique described above and utilizes memory referencing instructions to effect data transfers.

Memory addressing and accessing

It was noted above that a 16-bit address bus allows the generation of 65,536 unique addresses which may be assigned to memory or peripheral devices. It is generally convenient, for addressing purposes, to subdivide this memory space into smaller segments called blocks or fields. The size of a block (the number of address locations) is conveniently taken to be the number of memory locations contained in the particular random access memory (RAM) chips being employed. For illustration, consider the Intel 2114 RAM chip[9] which is organized as 4 bits wide with



PIN NAMES

I/00 —I/03	DATA INPUT /OUT PUT
$\overline{WE}$	WRITE ENABLE
$\overline{CE}$	CHIP ENABLE
A0 —A9	ADDRESS INPUTS

Fig. 7. Logic symbol and pin names for the Intel 2114-bit × 1024-word random access memory.

1024 memory locations. The 2114 is shown schematically in Fig. 7. Two 2114 RAMs may be connected in parallel, as shown in Fig. 8, to yield an 8 bit × 1 kbyte memory block which would require 10 address bits, A0–A9, for internal addressing. The first 4 bits of data, I/00–I/03 are stored in one 2114 and the second 4 bits, I/04–I/07, are stored in the other. The 2114 also requires two control signals for operation; a chip enable, $\overline{CE}$, which enables the 2114 for a read or write operation, and a write enable, $\overline{WE}$, which enables the chip to be written into. $\overline{WE}$ will be active high for a read operation. The microprocessor's memory could be enlarged by placing several 1-kbyte memory blocks in series. An 8-kbyte memory could be made by placing eight such blocks in series. Address bits A0–A9 are required by each memory block for internal address selection and would be connected in parallel to each block. Address bits A10, A11 and A12 could then be utilized to select one of the eight memory blocks. This function could be easily realized by using a binary decoder such as the Intel 8205 which was described above. Use of address bits A10–A12 and control bus signals, in conjunction with an Intel 8205, to generate chip enable, $\overline{CE}$, signals is illustrated in Fig. 9 for the 8080, 8085 and 6502 microprocessors. Figure 9a illustrates the configuration for use with the 8080. The control bus signals $\overline{MEMW}$ and $\overline{MEMR}$ are ANDed together to generate the 8205 $\overline{E}1$ and $\overline{E}2$ enable inputs. When either $\overline{MEMW}$ or $\overline{MEMR}$ is active low, signifying a memory write or read, the AND gate output will be low as required for $\overline{E}1$ and $\overline{E}2$ to enable the 8205. E3 is permanently high. The address bits A10–A12 are decoded to select the appropriate output, and hence memory block. The memory block (address range) being accessed is also tabulated along with the A10–A12 address bits. In the case of the 8085, shown in Fig. 9b, the IO/$\overline{M}$ control signal, which is active low during a memory referencing operation, provides the $\overline{E}1$ and $\overline{E}2$ enable signal directly. Again, E3 can be held permanently high. Address bits A10–A12 are decoded to select the appropriate output which becomes the $\overline{CE}$ for the desired memory block. The corresponding circuit for a 6502 is shown in Fig. 9c. The 6502 control bus generates only the R/$\overline{W}$ signal which signifies a read or write operation and as such is not useful as an 8205 enabling control signal. However, the remaining address bits, A13–A15, can be used to enable the 8205 as shown in Fig. 9c. Here, the 8205 will be enabled only when A13, A14 and A15 are logic 0. Whenever one of these address bits is logic 1, implying that some other device is being accessed, this 8205 will not be enabled.

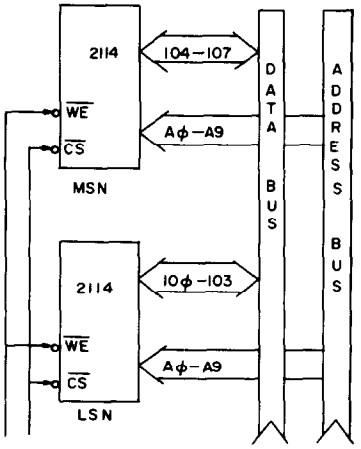


Fig. 8. Interconnection of two 2114 random access memory chips to obtain an 8-bit × 1024-word memory block.

The generation of memory $\overline{WE}$ and $\overline{CE}$ signals utilizing the Intel 8085 control signals is illustrated in Fig. 10.

INTERRUPTS

In the earlier discussion regarding the nature of the control bus signals generated by the 8080, 8085 and 6502 microprocessors, it was noted that these, indeed most, microprocessors carry a mechanism by which a peripheral device may request the microprocessor to provide a service to it. The generic term applied to this mechanism is *interrupt*. The interrupt function provides a means for peripheral devices to request the microprocessor to suspend its current operation and execute a service program to satisfy the needs of the peripheral device. This service could be to read data from the device, supply new data to the device, or perhaps perform some control function. As with the control bus structure, interrupt capability varies greatly between products.

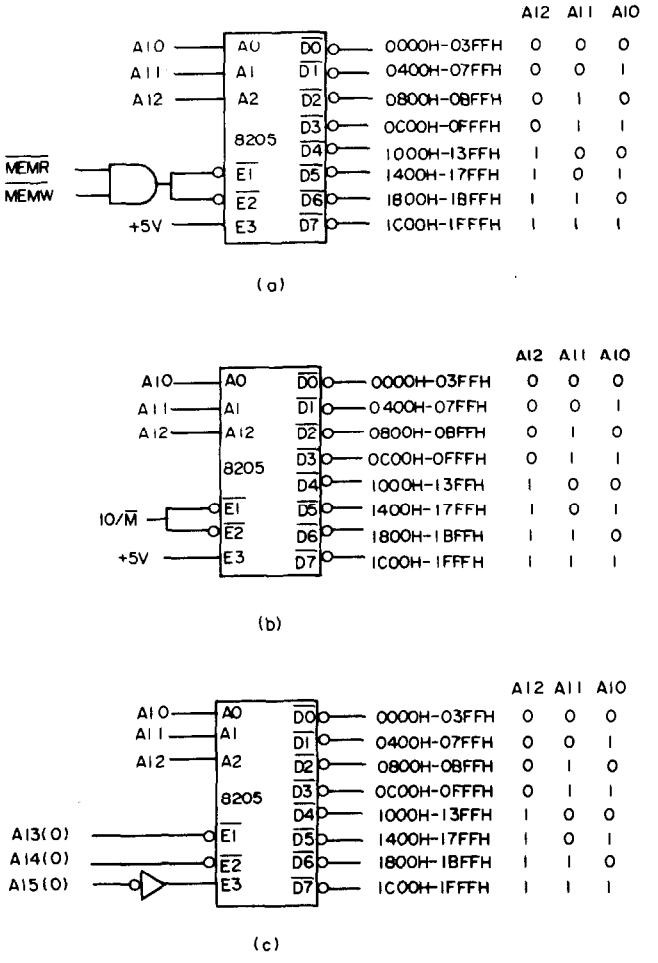


Fig. 9. Utilizing an Intel 8205 decoder and the microprocessor control signals and address bus to access up to 8 kB of random access memory with the (a) Intel 8080, (b) Intel 8085 and (c) Mostek 6502.

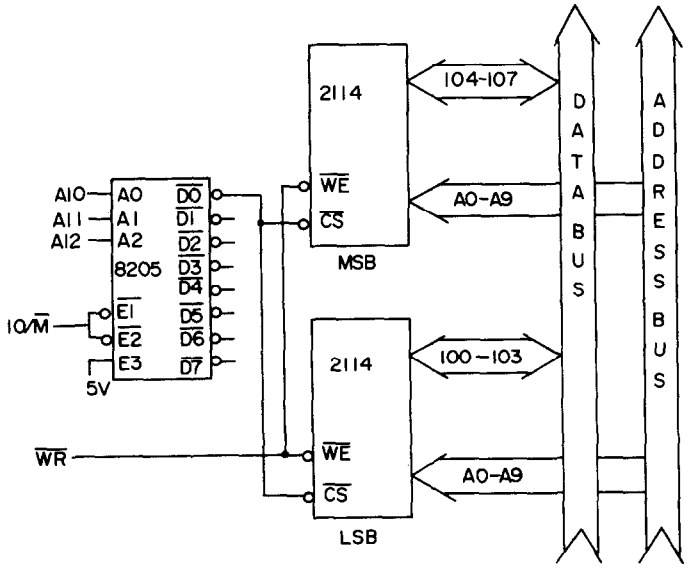


Fig. 10. Accessing a 1-kB block of 2114 random access memory addressed in the range 0000H-03FFH with the Intel 8085 microprocessor and 8205 decoder.

The 8080 interrupt function

The Intel 8080 has only one level of interrupt control, *i.e.*, the microprocessor has only a single interrupt request input. This interrupt function may be enabled or disabled under program control, and to prevent multiple requests is automatically disabled following an interrupt request. When a peripheral device requires service from the microprocessor it may initiate the interrupt by raising the interrupt request control input (INT) to an active high level. At the completion of the current instruction the microprocessor recognizes the interrupt request, ceases normal program execution, acknowledges the interrupt by putting out an $\overline{\text{INTA}}$ signal and enters a special "instruction fetch" cycle in which the microprocessor expects the peripheral device to provide the next instruction to be executed. This instruction must lead to the service routine for the peripheral device and must be either a subroutine CALL instruction or one of the eight special restart instructions, RST 0–RST 7, contained in the 8080 instruction set. If the instruction is a CALL statement, the microprocessor also expects the peripheral device to provide the 16-bit starting address for the service routine. The 8080 then transfers program control to the service routine in the same manner as going to a subroutine. Upon completion of the service routine, one of the return-from-subroutine instructions, such as RET, will return the program control to the normal sequence, which will continue as if the interrupt had not occurred.

If the instruction supplied by the peripheral device is one of the eight special restart instructions, RST 0–RST 7, the microprocessor initiates an immediate subroutine CALL to one of eight fixed addresses; 0000H, 0008H, 0010H, 0018H, 0020H, 0028H, 0030H or 0038H. Note that each of these addresses is the start of an 8-byte segment which might typically contain a jump instruction, JMP, followed by the 16-bit starting address of a peripheral device service routine. Since, as in the previous case, the restart instructions are effectively subroutine call instructions, program control can be returned to the normal sequence by a return-from-subroutine instruction such as RET.

Regardless of whether a call or a restart instruction is given, utilizing the 8080 interrupt feature is not straightforward. Either the peripheral device must be intelligent enough to provide the proper instruction and address to the 8080 upon receiving the $\overline{\text{INTA}}$, or the researcher must hardwire the appropriate instruction and address onto the data bus and provide for it to be accessed when the $\overline{\text{INTA}}$ and $\overline{\text{MEMR}}$ control signals are received. An alternative approach would be to employ an Intel 8259 Programmable Interrupt Controller. This is an intelligent peripheral controller which may be programmed, under software control, to contain the appropriate instructions (CALL or RST N; where N = 0–7) and addresses, which would then be provided to the microprocessor. It also has the capability to manage interrupt requests from up to eight peripheral devices. The 8259 interrupt controller thus relieves the researcher of the task of generating appropriate instructions and addresses from hardwired circuits.

The 8085 interrupt function

The Intel 8085 interrupt structure is more sophisticated than that of the 8080 and as a result more convenient to use. The 8085 supports five levels of interrupt, *i.e.*, it has five interrupt control lines; INTR, RST 5.5, RST 6.5, RST 7.5 and TRAP as given in Table 2. The first four of these interrupts are maskable while the last, TRAP, is not. The term maskable means that they may be individually enabled or disabled under program control. The TRAP interrupt cannot be disabled. An interrupt request input is automatically disabled by the microprocessor after the request has been recognized, to prevent multiple interrupt requests on a single input. However, the other interrupt requests are not automatically disabled, allowing multiple interrupts on different interrupt request inputs.

The 8085 interrupt request INTR functions in precisely the same manner as the 8080 INT interrupt request discussed above. However, the remaining 8085 interrupt requests are functionally quite different and are referred to as *vectored interrupts*. An interrupt request to one of these inputs results, upon completion of the current instruction, in the execution of a direct subroutine CALL instruction to fixed addresses *without* further interaction between the 8085 and peripheral device. These fixed addresses are 0024, 002CH, 0034H and 003CH for the TRAP, RST 5.5, RST 6.5 and RST 7.5 interrupt requests, respectively. These addresses would then typically contain a jump instruction, JMP, followed by the 16-bit starting address of the appropriate service routine for the peripheral device initiating the interrupt request. As in the 8080 case, upon completion of the service routine, program control can be returned to the normal program sequence by the execution of a return-from-subroutine instruction, such as RET.

An additional feature of the 8085 interrupts is that they have been assigned priorities in the order TRAP > RST 7.5 > RST 6.5 > RST 5.5 > INTR. An interrupt request of higher priority, *e.g.*, RST 7.5, may interrupt the service routine of a lower priority interrupt request, *e.g.*, RST 6.5. However, a lower priority interrupt request may not interrupt a higher priority interrupt request. This priority structure allows the researcher to ensure that a peripheral device which is generating critical data receives prompt and uninterrupted service from the microprocessor by assigning that device to a high-priority interrupt request input.

The 6205 Interrupt Function

The Mostek 6502 interrupt structure supports two levels of interrupts, *i.e.*, two interrupt request inputs, $\overline{\text{NMI}}$ and $\overline{\text{IRQ}}$. The $\overline{\text{IRQ}}$ interrupt request is maskable under software control while the $\overline{\text{NMI}}$ is not.

The $\overline{\text{NMI}}$ and $\overline{\text{IRQ}}$ are vectored interrupts with addresses of FFFA–FFFBH and FFFE–FFFFH, respectively. Upon completion of the current instruction the 6502 microprocessor will recognize an interrupt request and initiate a jump-to-subroutine instruction, JSR (the 6502 does not support subroutine CALL instructions). The microprocessor expects to find the 16-bit starting address of the interrupt request service routine stored at the appropriate vector address as given above. Upon completion of the service routine, program control can be returned to the normal program sequence with a return-from-subroutine instruction, RTS.

As with the 8085, the 6502 interrupts have been assigned priorities, $\overline{\text{NMI}} > \overline{\text{IRQ}}$. Thus, an $\overline{\text{NMI}}$ interrupt request may interrupt the service routine for an $\overline{\text{IRQ}}$ request, but the reverse is not allowed.

INTERFACING PERIPHERAL DEVICES

Attempts to interface peripheral devices directly to the microprocessor bus are often unsuccessful because of incompatibilities between the device and the system bus. While occasional problems arise from electrical incompatibilities (*e.g.*, incompatible voltage levels) the more common problems involve the data-transfer rate and synchronization of data transfers between the microprocessor and peripheral device. Devices such as digital-to-analogue converters (DACs) typically have analogue output settling times of 5–50 μsec which are long compared to the rates at which microprocessors are capable of data output. Further, the response time of some display devices, such as servo recorders, is quite long (in the msec range) and hence the microprocessor data-transfer rate must be reduced. Input devices, such as analogue-to-digital converters (ADCs), also present problems in that the microprocessor may not be ready to accept the input data at the time the device presents them to the data bus and the input data must be held until the microprocessor is ready to accept them. Thus, it is often desirable to interface a device indirectly to the system buses by means of some intermediate component which ensures that electrical and data-rate compatability can be achieved.

Particularly useful devices in this regard are the Intel 8255 Programmable Peripheral Interface and the Mostek 6530 Versatile Interface Adaptor which have been presented previously[10–12] and will not be discussed in detail here. It is only necessary to note that the 8255 contains 24 parallel digital I/O pins which are grouped into two 8-bit and two 4-bit ports. These ports may be software programmed into a variety of input/output configurations, thus facilitating the movement of digital data to or from the microprocessor. The 8255 also incorporates a degree of on-chip address decoding and hence can be conveniently addressed in either the isolated IO or memory mapped IO modes. Similarly, the 6530 contains 16 parallel digital I/O pins which are grouped into two 8-bit ports. The 6530 also contains on-chip address decoding and hence may be accessed and programmed directly under software control.

In cases where the output device is incapable of operating at the high data-transfer rates typical of microprocessors it will be necessary to latch, or hold, the data in an intermediate device normally called a buffer, until the output device has had ample time to respond to the new data. The Intel 8212 8-bit buffer[11,12] serves as an excellent data buffer between system buses and input or output devices. The 8212 consists of an 8-bit data latch with tristate output buffers, control and device selection logic, as well as internal logic which generates an interrupt request signal each time new data are latched into the buffer. This interrupt request can be used either directly or as a flag to notify peripheral devices that new data are present. If the 8212 is being used as a buffer between the system data bus and an output device, such as a DAC, data are latched into the buffer by decoding the appropriate device address as previously discussed. The latched data will be retained until the 8212 is either cleared or a new data word is latched. Thus, the output device can be provided ample time to respond to a data word before output of a new word.

Difficulty arises when attempts are made to interface input peripheral devices, such as ADCs, to the system bus. The difficulty stems from the characteristic of TTL (transistor–transistor logic) devices that when the device output is logic 0 the device output terminal presents a low impedance to ground. If several TTL devices are connected in common and one of the device outputs is logic 0, the outputs of the remaining devices are effectively connected to ground and the state of their logic levels will be lost. To avoid this situation all input devices must be connected to the data bus through a tristate buffer.[11,13] The outputs of the Intel 8212 are tristate buffered and hence it may be utilized to interface input devices to the data bus. Generally, devices such as the 8255 and 6530 digital IO ports provide a more flexible, easily addressed and accessed solution to this problem. The interfacing examples illustrated below will employ these devices.

Among the more common operations are the acquisition of digitized data, representing an analogue signal, from an analogue-to-digital converter (ADC) and the consequent display of the acquired data either on a video terminal, such as an oscilloscope, or a strip-chart recorder utilizing a digital-to-analogue converter (DAC). The following examples will illustrate the application of 8255 and 6530 digital data I/O ports and simple software programs to the movement of digital data to and from the microprocessor.

Digital data acquisition

Typical data-word lengths employed for analogue-to-digital conversions in the laboratory are 10 or 12 bits (resolutions of 0.1% and 0.02%, respectively). For

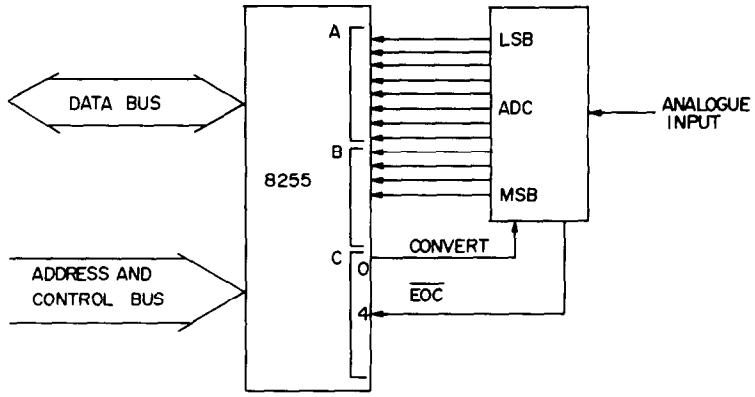


Fig. 11. A 12-bit ADC interface to an Intel 8080/8085 utilizing the 8255 Programmable Peripheral Interface.

illustration, consider that 12-bit data are being acquired. Since the microprocessor and peripheral devices being considered here employ 8-bit data buses, two read operations will be required to transfer 12 bits from the peripheral device to the microprocessor. Actually, the procedure being outlined here will accommodate 9–16-bit data. The scheme is to acquire a given number of data points from an analogue-to-digital converter and store the points sequentially in the microcomputer's memory.

Analogue-to-digital converters require a START CONVERT pulse to initiate the quantization of the analogue signal value.[15] The START CONVERT pulse can be generated either by external circuity or by the microprocessor under program control. Assume the latter case here. The analogue-to-digital converter will put out an END OF CONVERSION ($\overline{EOC}$) pulse to indicate its status. Typically, the $\overline{EOC}$ would normally be logic low and would go logic high during the conversion operation, returning to logic low at the completion of the conversion. Thus, the $\overline{EOC}$ signal may be tested by the microprocessor to determine when new data are available.

Figure 11 shows, in block diagram form, a 12-bit ADC interfaced to an INTEL 8080 microprocessor through the INTEL 8255 Programmable Peripheral Interface (PPI). Recall that this device has three programmable 8-bit IO ports. In this example, ports A and B are programmed as input ports for the 12-bit ADC value and port C is used for the control signals. Port C bit C0 is used for output of the ADC START CONVERT pulse and bit C4 is used for input of the $\overline{EOC}$ status signal from the ADC. A program which could be used as a subroutine for input and storage of 12-bit data points is given in Table 5. The addresses used in conjunction with the IN and OUT instructions are explicit for the 8255 on an INTEL SDK-80 single board microcomputer. The program initiates data conversion by output of a pulse on port C bit 0. Bit 4 of port C is then checked to determine when conversion is complete, *i.e.*, when the $\overline{EOC}$ has returned to logic 0. Upon completion, the first 8 bits of the datum point are input from port A and stored in memory, followed by the next 4 bits from port B. The point counter (register B) is decremented and if more points are to be acquired the program jumps to CLOCK to initiate the acquisition of another datum point. This process is repeated until 100 values have been acquired, upon which the subroutine returns to the calling program.

Figure 12 illustrates a similar circuit for interfacing a 12-bit ADC to a MOSTEK 6502 microprocessor through the 6530 Versatile Interface Adaptor (VIA). Recall that this device contains two programmable 8-bit IO ports.[10,11] In this example port A is programmed for input of the first 8 bits of the ADC value, and bits 0–3 of port B are programmed for input of the next 4 bits of the ADC value. In addition, bit 6 of port B is programmed as an output pin for the ADC START CONVERT pulse and bit 7 as input pin for the ADC $\overline{EOC}$ status signal. A program which could be employed as a subroutine for input and storage of data is given in Table 6. The addresses employed in conjunction with the VIA are explicit for the MOSTEK KIM-1 single board microprocessor. This program is conceptually identical to that presented in the example for the SDK-80. A START CONVERT pulse is output from bit 6 of port B. Port B, which also has the upper 4 bits of the datum point on bits 0–3, is made the input and bit 7 is checked to determine whether $\overline{EOC}$ is low (conversion done). If so, the accumulator is restored and the upper 4 bits of the data are stored in memory. Port A is then input to obtain the first 8 bits and these are stored in a subsequent memory location. The point counter, register X, is decremented and if more points are required the program jumps to PULSE and repeats the process. When a sufficient number of points have been acquired the subroutine returns to the calling program.

Thus, input of digital data from an ADC may be easily accomplished by utilizing peripheral devices

Table 5. Example of program for input of 12-bit digital data by utilizing the Intel 8255 Programmable Peripheral Interface

INPUT:	1000	21	LXI	H,1200	starting address for data storage
	1001	00			
	1002	12			
	1003	3E	MVI	A,9A	program 8255 for ports A–B input
	1004	9A			
	1005	D3	OUT	F7	C0–C3 output, C4–C7 input
	1006	D7			
	1007	06	MVI	B,64	point counter, 100 values
	1008	64			
CLOCK:	1009	3E	MVI	A,01	output a pulse on C0 to be START CONVERT
	100A	01			
	100B	D3	OUT	F6	pulse to ADC
	100C	F6			
	100D	AF	XRA	A	clear accumulator
	100E	D3	OUT	F6	C0 back to zero
	100F	F6			
CHECK:	1010	DB	IN	F6	input port C, check bit 4. If logic high
	1011	F6			ADC not done,
	1012	A7	ANA	A	
	1013	C2	JNZ	CHECK	repeat until bit 4 logic low
	1014	10			
	1015	10			
READ:	1016	DB	IN	F4	input port A, first 8 bits of data
	1017	F4			
	1018	77	MOV	M,A	store in memory,
	1019	2C	INR	L	increment address
	101A	DB	IN	F5	input port B, next 4 bits of data
	101B	F5			
	101C	77	MOV	M,A	store in memory,
	101D	2C	INR	L	increment address,
	101E	05	DCR	B	decrement point counter;
	101F	C2	JNZ	CLOCK	if not zero, get another point
	1020	09			
	1021	10			
	1022	C9	RET		done, return from subroutine

such as the 8255 PPI or 6530 VIA to interface the ADC to the microprocessor. Further, the software programs to effect the data acquisition are both straightforward and short, as illustrated in Tables 5 and 6.

Output of data in analogue form

After acquiring the appropriate number of data points it is often most convenient to display the data, for visual inspection, in an analogue format, on an oscilloscope or strip-chart recorder, for example. The conversion of digital data into an analogue format is accomplished with a digital-to-analogue converter (DAC).[13] The output of digital data to a DAC may be easily accomplished by utilizing the peripheral devices previously discussed, the PPI and VIA.

Figure 13 shows, in block diagram form, an 8-bit DAC interfaced to an 8080 microprocessor through an 8255 PPI. Since output signals of the 8255 are latched, *i.e.*, data remain valid until changed, the data-word may simply be made the output to the 8255 and

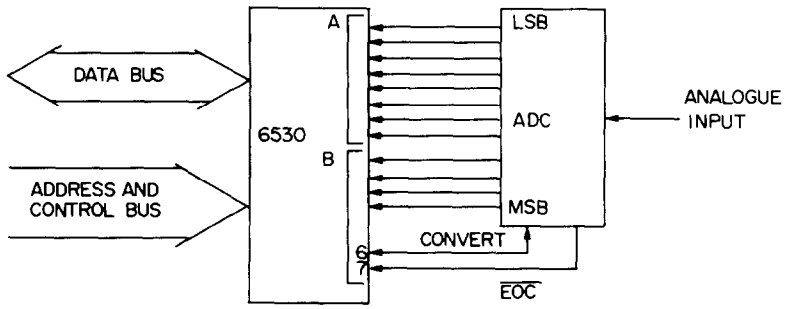


Fig. 12. A 12-bit ADC interface to a MOSTEK 6502 utilizing the 6530 Versatile Interface Adaptor.

Table 6. Example of program for input of 12-bit digital data by utilizing the Mostek 6530 Versatile Interface Adaptor

INPUT:	0100	A2	LDX	C8	reg X point counter and zero page address
	0101	C8			
	0102	A9	LDA	00	program port A for all bits input. Port A least
	0103	00			
	0104	8D	STA	1701	significant 8 bits
	0105	01			
	0106	17			
	0107	A9	LDA	40	program port B for B6 output, all others input.
	0108	40			
	0109	8D	STA	1703	port B, B0–B3 most significant 4 bits
	010A	03			
	010B	17			
PULSE:	010C	A9	LDA	40	output 1 to B6 port B
	010D	40			
	010E	8D	STA	1702	
	010F	02			
	0110	17			
	0111	A9	LDA	00	output 0 to B6 port B. generates a pulse for ADC
	0112	00			
	0113	8D	STA	1702	START CONVERT
	0114	02			
	0115	17			
EOC:	0116	AD	LDA	1702	get port B input
	0117	02			
	0118	17			
	0119	2A	ROL		rotate MSB left to carry. If
	011A	B0	BCS	FA	0, ADC has finished conversion.
	011B	FA			If not go to EOC
	011C	6A	ROR		rotate right, restore accumulator
	011D	29	AND	0F	mask upper 4 bits to 0
	011E	0F			
	011F	95	STA	00,X	store on zero page indexed by reg X
	0120	00			
	0121	CA	DEX		decrement reg X
	0122	AD	LDA	1700	get port A, least significant 8 bits
	0123	00			
	0124	17			
	0125	95	STA	00,X	store on zero page indexed by reg X
	0126	00			
	0127	CA	DEX		decrement reg X
	0128	D0	BNE	E2	reg X = 0? If not, get another point. Go to PULSE
	0129	E2			
	012A	60	RTS		yes, done. Return from subroutine.

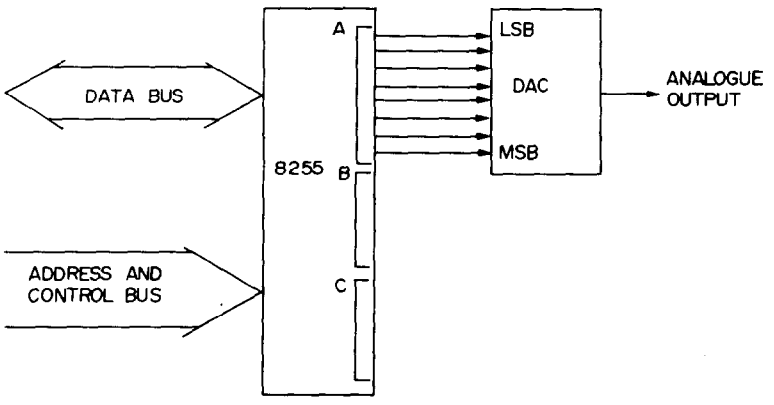


Fig. 13. An 8-bit DAC interface to an Intel 8080/8085 utilizing the 8255 Programmable Peripheral Interface.

Table 7. Example of program to output 8-bit digital data to a DAC by utilizing the Intel 8255 Programmable Peripheral Interface

OUTPUT:	1000	21	LXI	H,1200	starting address for data to be output
	1001	00			
	1002	12			
	1003	3E	MVI	A,80	program 8255 for port A output
	1004	80			
	1005	D3	OUT	F7	
	1006	F7			
NEXT:	1007	7E	MOV	A,M	move first data point to
	1008	D3	OUT	F4	accumulator and output to the 8255
	1009	F4			
	100A	2C	INR	L	increment data address
	100B	7D	MOV	A,L	and compare to 64H.
	100C	FE	CPI	A,64	If not equal, more points to output, get the next point
	100D	64			
	100E	C2	JNZ	NEXT	
	100F	07			
	1010	10			
	1011	C9	RET		all points output, return to calling program

hence on to the DAC. Since only 8-bit data words are the output, the DAC has been interfaced to port A, which has been programmed as an output port. A program which could be employed as a subroutine for output of digital data to the DAC is shown in Table 7. This program gives outputs of 100 8-bit data values, which are stored in memory starting at address 1200H, to the 8255 port A. Following the output of each data point the address is incremented and the value compared with the value at the address corresponding to the last point. If they are identical, the subroutine returns to the calling program; if they are not, the program fetches the next value and uses it as output. The process is repeated until all the data points have been dealt with.

Figure 14 illustrates a similar interface for the MOSTEK 6502 through the 6530 VIA. Again, since only 8-bit data form the output, the DAC has been interfaced to port A, all pins of which have been programmed to function as outputs. The 6530 output pins are also latched so that data remain valid until changed under program control. A program which may be used as a subroutine for output of data to the DAC is shown in Table 8. Conceptually this program is identical to that given in Table 7. The program gives outputs of 100 8-bit data values, which are stored in memory, starting at 00H on page zero. Following the output of each value the address, register X, is incremented and the value compared with the final value, 64H. If they are equal, all the data points have been used and the subroutine returns to the calling program. If not, the program fetches the next value for output, repeating the process until all the values have been output.

Thus output of digital data in an analogue format for display or control purposes can be easily achieved by utilizing peripheral interface devices such as the 8255 or 6530 digital IO ports. Further, the software programs required for the data transfer, as illustrated in Tables 7 and 8, are straightforward and brief. However, it should be noted that the program examples presented for output of data to a DAC will result in output of the data as rapidly as the microprocessor is capable of cycling through the program, which would be about 10 μsec per point. While such high transfer rates are desirable with video displays, such as an

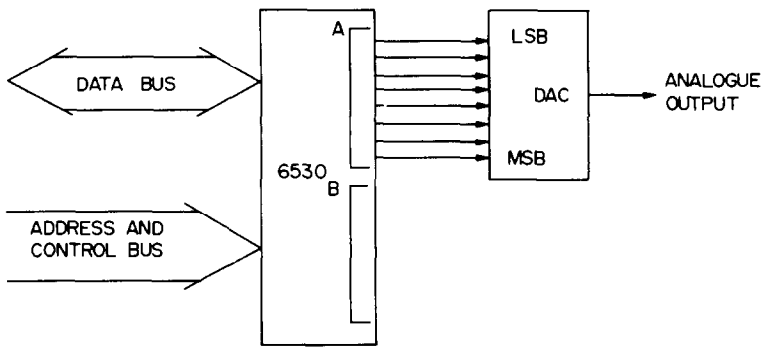


Fig. 14. An 8-bit DAC interface to a MOSTEK 6502 utilizing the 6530 Versatile Interface Adaptor.

Table 8. Example of program for output of 8-bit digital data to a DAC by utilizing the Mostek 6530 Versatile Interface Adapter

OUTPUT:	0100	A9	LDA	FF	program all pins of 6530
	0101	FF			port A as output
	0102	8D	STA	1701	address for 6530 control port
	0103	01			
	0104	17			
	0105	A2	LDX	00	starting address for data on page zero
	0106	00			
	0107	A0	LDY	64	point counter, 100 values
	0108	64			
	0109	84	STY	FF	store the point counter
	010A	FF			
NEXT:	010B	B5	LDA	00,X	get data from zero page indexed by reg X
	010C	00			
	010D	8D	STA	1700	output data to 6530 port A
	010E	00			
	010F	17			
	0110	E8	INX		increment data address
	0111	E4	CPX	FF	compare with final address
	0112	FF			
	0113	D0	BNE	F6	if not equal, go to NEXT and get next value
	0114	F6			
	0115	60	RTS		if equal, return to calling program

oscilloscope, to ensure a flicker-free display, they are much too fast when compared with the typical response time of Y–t or X–Y recorders, which might be of the order of 100 msec. Thus, when plotting data it will be necessary to reduce the data output rate by, for example, introducing a software delay loop in the output program. Such delay loop may operate simply by loading a register with a value and then decrementing the register and checking to determine whether the value has gone to zero, before output of the next data point. Thus, by selecting an appropriate value to count down, delay times compatible with the output-device response-time can be obtained.

Acknowledgements—Financial support from the University of Calgary and the Natural Sciences and Engineering Research Council of Canada is gratefully acknowledged.

GLOSSARY

Accumulator: Register in the CPU which is the centre for most arithmetic and logical operations.
Active high: Level "1" is used to activate or enable.
Active low: Level "0" is used to activate or enable.
ADC: Analogue to digital converter.
Address: A digital number used to access an individual memory location, peripheral chip, or I/O device.
Binary: The base 2 number system; its digits are called bits.
Bit: Binary digit.
Buffer: A temporary storage area for a device.
Bus: A set of parallel wires used to transfer address, data or control information between devices. Only one of the devices can put information on a particular bus at any one time. Any number of devices can simultaneously read information off the bus.
Byte: Eight bits.
CPU: Central processing unit. Often used to refer to a microprocessor.
DAC: Digital to analogue converter.
Disable: To disallow.
DMA: Direct memory access. A technique which allows data to be put into or removed from memory without the use of the CPU; DMA is often used when very high data-transfer rates are required.
Enable: To allow.
EPROM: Erasable PROM: the PROM can be programmed by the user and then erased by the user, usually with ultraviolet light.
Flags: Flip-flops in the CPU which are set as the result of certain operations; their state can be tested by some instructions which will be executed according to the state of the flag.
Handshake: A communication system between CPU and device whereby an operational command is sent by the CPU only on request from the device.
HEX: Hexadecimal.
Hexadecimal: The base 16 number system which uses the digits 0–9 and the letters A–F as the basic numerals.
Initialize: To set the various registers, counter and address to their starting values when the computer is turned on at the beginning of a computer routine, or at prescribed points in the routine.
Interrupt: The process by which an external device demands service from the CPU.
I/O: Input/output.
Latch: A simple, strobed, digital storage device. Typically used for temporary storage of logic information.
Latching: The action of strobing a latch to effect the storage of logic information.
Machine language: The coding used directly by a CPU as an instruction set.

Memory:	Holds program instructions or data and must be addressed location by location in order to access stored information.
Memory mapping:	The use of a unique memory address to enable I/O data transfer to or from a port which is selected by that address.
Microcomputer:	A computer with a microprocessor.
Microprocessor:	A device that executes instructions.
Port:	The portion of a computer through which an interface to a device is made.
Program counter:	A register which the CPU uses to point to the next instruction in memory to be executed (PC).
PROM:	Programmable read only memory. This is ROM which can be programmed once by the user. Then it becomes ROM.
Register:	A single or multiple byte scratchpad memory normally residing in the CPU.
R/W memory:	Memory which can be read or written into, sometimes called RAM.
RAM:	Random access memory. See R/W memory.
ROM:	Read only memory. See also PROM and EPROM. This is memory which has a program or data permanently burned in. The computer may read ROM but may not alter it.
Stack:	A variable area of memory in which data and/or addresses are stored and retrieved by a last-in-first-out process.
Stack pointer:	An internal register of most CPUs, containing the address of the most recent stack entry.
Strobe:	A digital pulse which effects some action at a specific point in time, such as the asynchronous transfer of digital information.
Word:	A given number of bits used by a CPU. Common word sizes are 8 and 16 bits for small computer systems.

REFERENCES

1. P. D. Gaarenstroom, J. C. English, S. P. Perone and J. W. Bixler, *Anal. Chem.*, 1978, **50**, 811.
2. D. S. Leggett, *ibid.*, 1978, **50**, 718.
3. H. E. Eaton and J. D. Stuart, *ibid.*, 1978, **50**, 587.
4. R. E. Dessy, *ibid.*, 1977, **49**, 1100A.
5. J. A. Perry, M. F. Bryant and H. V. Malmstadt, *ibid.*, 1977, **49**, 1702.
6. S. R. Crouch, D. N. Baxter, E. H. Pals and E. R. Johnson, *ibid.*, 1978, **50**, 291A.
7. T. E. Edmonds, *Anal. Chim. Acta*, 1979, **108**, 155.
8. H. Freiser and C. R. Martin, *Anal. Chem.*, 1979, **51**, 803.
9. Intel Corporation, 3065 Bowers Avenue, Santa Clara, CA 95051, U.S.A.
10. MOS Technology Inc., 950 Rittenhouse Rd., Norristown, PA 19401, U.S.A.
11. G. Horlick, *Talanta*, 1980, **28**, 487.
12. *Intel 8080 Microcomputer User's Manual*, Intel Corporation, 3065 Bowers Avenue, Santa Clara, CA 95051, U.S.A.
13. H. V. Malmstadt, C. G. Enke and S. R. Crouch, *Electronic Measurements for Scientists*, Benjamin, New York, 1974.
14. *Intel 8085 Microcomputer User's Manual*, Intel Corporation, 3065 Bowers Avenue, Santa Clara, CA 95051, U.S.A.
15. *Analog-Digital Conversion Handbook*, Analog Devices, Norwood, Mass. 02062, 1972.

Talanta, Vol. 28, pp. 519 to 525, 1981
Printed in Great Britain. All rights reserved

0039-9140/81/070519-07$02.00/0
Copyright © 1981 Pergamon Press Ltd

LABORATORY DATA-ACQUISITION CAPABILITIES OF MICROCOMPUTERS*

ERIC D. SALIN, M. W. BLADES and GARY HORLICK
Department of Chemistry, University of Alberta, Edmonton, Alberta, Canada

(*Received* 18 *July* 1980. *Accepted* 7 *December* 1980)

Summary—Some microcomputers have been evaluated in terms of their features and capabilities for basic laboratory data-acquisition tasks. The systems studied include the SDK-80 (8080), SDK-85 (8085), and KIM-1 (6502) single-board microcomputers, and the PET consumer/hobby-market microcomputer. Data-acquisition software benchmarks were tested on all the systems, and inexpensive analogue-to-digital and digital-to-analogue hardware subsystems were developed for the PET. The acquisition rates for 10-bit data under machine-language control range from 15 to 25 kHz, but under high-level (BASIC) language-control drop to about 100 Hz.

It is becoming increasingly popular and effective to utilize microprocessors and microcomputers in the laboratory environment for data acquisition and control.[1–7] However, a bewildering array of microprocessors and microprocessor systems is currently available and many researchers are faced with the question of which system will be best for their needs. In an effort both to educate ourselves and also to aid others we have carried out an evaluation of some single-board microprocessor systems and one consumer/hobby market microcomputer in terms of their features and capability for basic laboratory data-acquisition tasks.

Single-board microcomputers

The simplest microprocessor systems are the so-called single-board microcomputers. The basic functional units of a single-board microcomputer are shown in block diagram form in Fig. 1. A single-board microcomputer consists of a microprocessor-based central processing unit (CPU), memory, which is normally a combination of read–write memory (RWM), often called random access memory (RAM), and read only memory (ROM), and input/output subsystems. These subunits are interconnected with a bus system consisting of address, data and control buses. Three popular single-board microcomputers are the SDK-80 (8080 CPU), the SDK-85 (8085 CPU)[8] and the KIM-1 (6502 CPU).[9] The hardware features of each are summarized in Table 1. The hardware features can be augmented by system expansion. Both the SDK-80 and SDK-85 have breadboard areas where a small amount of additional hardware can be located, e.g., more memory I/O ports, ADCs, DACs. The KIM-1 lacks such on-board expansion but can be expanded by using commercially available boards.[10,11]

As supplied, the boards can only be programmed at the machine-language level. To run the microcomputer and aid in machine-language programming all boards come with a system monitor in ROM. The features of the monitors are summarized in Table 2. The monitors are written as a group of subroutines. These subroutines can be accessed by user-written programs which can significantly aid program development by supplying simple number-conversions, and memory and I/O access routines. In all three systems the monitor is available in this way. As with hardware, these simple software capabilities can be augmented with floating-point packages, machine-language assemblers or high-level languages if so desired.

Data acquisition benchmarks

Benchmarks, *i.e.*, specific software/hardware tasks, are a popular way of comparing computing systems.

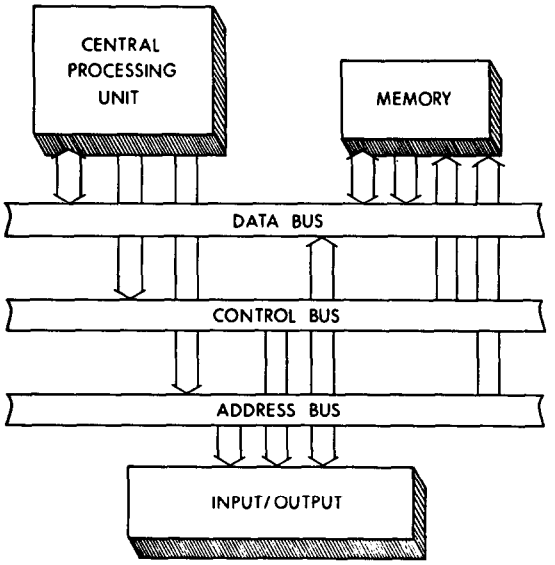


Fig. 1. Block diagram of a microcomputer.

* Presented in part at the Pittsburgh Conference, Cleveland, Ohio, 1979.

Table 1. Single-board summary

	SDK-80	SDK-85	KIM-1
CPU	8080	8085	6502
Clock, *MHz*	2	3	1
RWM, *kbyte*	1	0.5	1.1
ROM/EPROM, *kbyte*	4	4	2 (ROM)
Monitor size, *kbyte*	1	2	2
Digital I/O lines	48	76	15
Timer/counter	No	14-bit	8-bit + scaler
Serial I/O (TTY)	yes	yes	yes
Keypad/HEX display	no	yes	yes
Cassette interface	no	no	yes
Breadboard area	yes	yes	no
Delivered as	kit	kit	assembled
Power, *V*	+5, +12, −10	+5, −10	+5, +12

However, most benchmarks are designed to test only the basic computation speed of the microcomputer CPU. Such benchmarks may not be the most meaningful in terms of laboratory data-acquisition tasks, which normally involve operations such as digital I/O to and from DACs and ADCs. Two basic types of data-acquisition benchmarks have been developed and tested in order to compare the three single-board microcomputers mentioned above. Both benchmarks involved data-acquisition by the microcomputer system from a 10-bit analogue-to-digital converter interfaced to standard input/output ports available on the board. Ten-bit words were used because they are the shortest commonly employed for analogue-to-digital conversion in the laboratory.

These microcomputers and their associated digital I/O ports can handle only 8 bits at a time. Thus two "read" operations were required for data acquisition and the benchmarks were actually valid for 9–16 bits of digital input. After acquisition, the first benchmark integrated (sums) $2^{16} - 1$ (65,535) successive conversions. The summation was carried out in four 8-bit registers (SDK-80, SDK-85) or memory locations (KIM-1) providing 32-bit resolution. The second benchmark sequentially stored the acquired 10-bit numbers in memory (two memory locations per data point) as would be done in acquiring a complete waveform or signal. In both cases the microcomputer had to send a "START CONVERT" pulse to the ADC and then "wait" for the "END OF CONVERT" pulse before acquisition and integration or storage of the data point. However, it was assumed that the ADC was infinitely fast and hence that there was no delay between the arrival of the START CONVERT pulse and the generation of the END OF CONVERT pulse.

Table 2. Monitor functions

A. General (SDK-80, SDK-85, KIM-1)
1. Machine-language programming and editing
2. List/examine memory locations
3. Initiate program execution
4. Communication with TTY

B. SDK-85, KIM-1
1. Keypad/display interaction
2. Paper tape I/O (TTY)

C. KIM-1
1. Cassette I/O

Block diagrams of the integration benchmark for each system are shown in Fig. 2. These block diagrams are not meant to show hardware/software flow in detail but are presented only to give a feeling for the hardware features utilized and some of the differences between the single-board microcomputers tested. For the SDK-80 (Fig. 2a) an 8255 programmable peripheral interface was used as the I/O port (see Horlick[12] for a summary of microcomputer hardware). This chip has three programmable 8-bit I/O ports. Ports A and B were used for the 10-bit ADC value and port C was used for the control signals. The 8080 CPU contains sufficient general purpose registers (six) to allow the 32-bit integration to be performed in the CPU. With the SDK-85 (Fig. 2b) system the ports provided on the 8155 chip were used for the data acquisition. This chip is one of the 8085 special peripheral components combining RAM (256 word) I/O (two 8-bit and one 6-bit I/O ports) and a 14-bit interval timer. As with the 8080, integration was done in the CPU registers. With the KIM-1 system (Fig. 2c) the ports are part of the 6530, which combines 1 kbyte of ROM, 64 words of RAM, two 8-bit I/O ports and one 8-bit interval timer and scaler in one chip. The 6502 CPU has only two general-purpose registers over and above the accumulator, so the integration was done in four sequential memory locations. Block diagrams of the storage benchmark are not presented, as they are very similar to those for the integration benchmark except that the acquired data points are stored sequentially in memory rather than summed. Annotated listings of the programs are available on request. They range in size from 30 to 70 bytes, depending on the CPU and the task.

The benchmark rates are summarized in Table 3. The SDK-85 "wins", but really all the systems are quite comparable, there being no drastic difference between the rates. Also the CPU clock rates must be

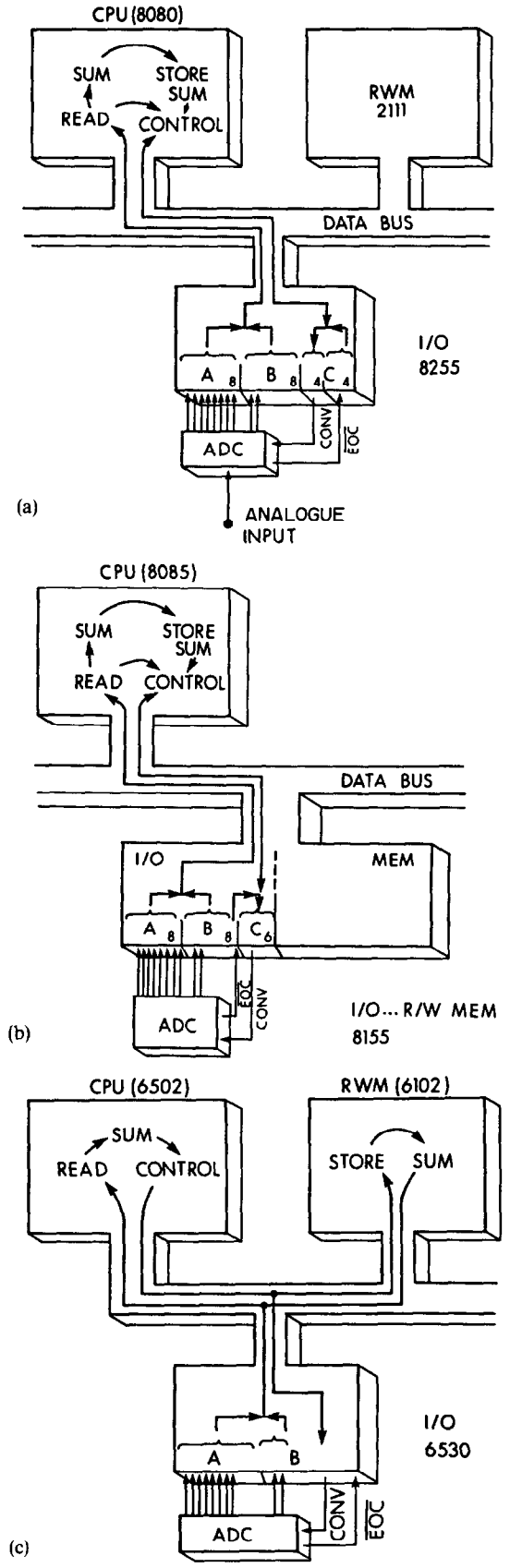


Fig. 2. Block diagrams of integration benchmarks (a) SDK-80, (b) SDK-85, (c) KIM-1.

Table 3. Benchmark rates (*kHz*)

	SDK-80	SDK-85	KIM-1
Integration	15	22	14
Storage	15	25	16

kept in mind, the SDK-80 being 2 MHz, the SDK-85 3 MHz, and the KIM-1 1 MHz. In this sense the KIM-1 does quite well considering it has the slowest clock rate. Faster CPUs are available for all systems and benchmark rates would improve accordingly if they were used.

In addition we wanted to compare the systems on as equal a footing as possible, so we did not implement direct memory access (DMA) for which there is a specific 8080 series support chip. This could improve the rate of data-transfer to memory by as much as an order of magnitude.

Thus the main conclusion is that with these simple single-board microcomputers 9–16-bit data can be acquired at rates ranging from 15 to 25 kHz. It does not matter much which CPU is used, and it is rather the overall features of the complete system, *i.e.*, number of I/O lines, cassette interface, EPROM space, that will be the factors determining the choice of system.

Consumer/hobby-market microcomputers—the PET

Some of the most active developments in computing systems and hardware today are taking place in the so-called hobby market. Products are now becoming available, that, although aimed at the consumer market, offer the scientist significant capability for laboratory data-acquisition and processing at costs often less than a tenth of that of hardware available from the traditional sources of scientific computers. In fact, if the trends and developments continue, the so-called consumer/hobby market may soon, by sheer volume and attendant improvements in cost/performance ratio, become the dominant source of computing systems for many laboratory data-acquisition and processing needs.

One of the most prominent "home/hobby" computers is the Commodore PET.[13,14] The basic features of this computer are summarized in Table 4.

Table 4. PET features

1. 6502 CPU
2. 8-kbyte RWM
3. 14-kbyte ROM
   —8-kbyte BASIC, OS, MONITOR
4. CRT display
   —40 characters × 25 lines
5. Keyboard
6. Cassette (two)
7. 8-bit digital I/O port (6522)
8. IEEE 488 instrument interface
9. Expansion port
   —6502 address, data and control buses
   —memory expansion select lines

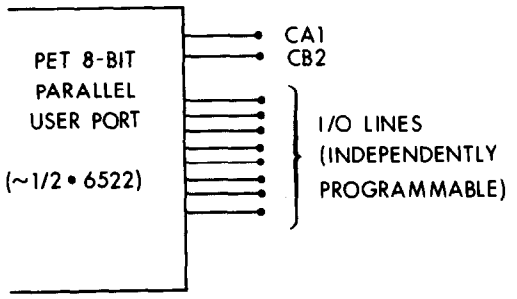


Fig. 3. Block diagram of PET parallel 8-bit port.

Integrated into a compact package is a keyboard, CRT graphics screen, cassette storage and a 6502-based processor complete with BASIC software in ROM. In addition the PET is reasonably well set up with hardware input/output (I/O) capability. It has an IEEE 488 bus port, an 8-bit digital I/O port and direct connector access to the 6502 address and data buses.

To a first approximation the computerization of an experiment involves two steps, data input/output and data processing. The data input/output step requires analogue and digital I/O hardware along with both high-level and machine-language control of these I/O subsystems. Direct high-level language control of I/O hardware provides easy access to these subsystems, while machine-language control is necessary for sophisticated software control. Once data are acquired, processing is generally, in terms of man hours, most efficiently carried out with a high-level language. With minimal expansion, the I/O hardware and software features of the PET provide it with excellent capability for data I/O and processing as outlined above.

For most laboratory applications analogue I/O (DAC and ADC subsystems) and additional digital I/O must be added to the PET. We have developed some simple and inexpensive DAC and ADC subsystems for the PET and have also characterized the I/O data rates for these systems under both high-level language (BASIC) and machine-language control. In addition the digital I/O has been expanded beyond that available at the 8-bit I/O port.

Parallel 8-bit port of the PET

A block diagram of the parallel 8-bit port that is provided on the PET is shown in Fig. 3. This port is part of a 6522 versatile interface adapter chip which is one of the 6500 family of programmable peripheral chips.[12] A block diagram of the complete 6522 chip is shown in Fig. 4. This chip contains two 8-bit digital I/O ports with all lines independently programmable, handshake control lines, an 8-bit shift register, a 16-bit timer and a 16-bit timer/counter. It is important to note that somewhat less than half of the features of the 6522 are available at the PET 8-bit port. The lines available include the port A I/O lines and the CA1 and CB2 control lines. All other features of the 6522 are used internally by the PET.

This port is very easy to access and control with BASIC commands. As can be seen in Table 5 our results indicate that the maximum data-rate for this port under BASIC control is about 100 Hz.

Faster rates can be expected under machine-language control. A simple benchmark program that was used to test the machine language output rate is shown in Table 6. The port was set up in BASIC and then by using the SYS command we jumped to a simple machine-language program that continuously cycled a series of 256 8-bit data points out of the port, as might be done in "refreshing" an oscilloscope for data display. Under machine-language control the output data-rate was 154 kHz, a considerable improvement over BASIC control.

We have used this port, in conjunction with a digital-to-analogue converter to provide an analogue output channel from the PET for strip-chart recorder or oscilloscope display of waveforms. We used a National DAC-08[15] digital-to-analogue converter and it was directly wired to the port pins. Thus with very

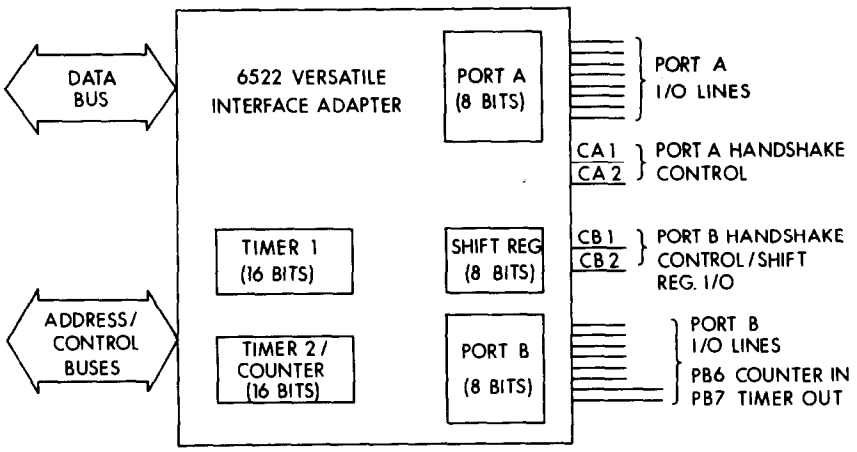


Fig. 4. Block diagram of the 6522 versatile interface adapter.

Table 5. BASIC benchmarks for PET 8-bit parallel user port

A. BASIC POKE TEST

```
10 POKE 59459,255      Set up port for output
20 POKE 59471,255      Set all bits high
30 POKE 59471,0        Set all bits low
40 GOTO 20             Do it again
```

11 Hz (9 msec/POKE)

B. BASIC 8 bit output from data array

```
40 POKE 59459,255      Set port for output
50 FOR J = 1 TO 255
60 POKE 59471, A(J)    Output array data
80 NEXT
```

86 Hz (12 msec/point)

C. BASIC STORAGE 8-BIT DATA

```
10 POKE 58459,0        Set port for input
15 DIM A(255)
20 FOR J = 1 TO 255
30 A(J) = PEEK (59471) Get and store data
40 NEXT
```

91 Hz (11 msec/point)

Table 6. PET machine language program for rapid output (8-bit data, 256 points)

```
POKE 59459,255: Set up port for output
SYS (700)
START:  LDA DATA,X    Get data
        STA DRA       Output data
        INX           Increment pointer
        JMP START     Go again
```

Length: 10 bytes
Data output rate: 154 kHz (6.5 μsec/point)

simple software such as that shown in Tables 5 and 6 and a $5.00 chip an analogue output channel can easily be added to the PET.

Ten-bit ADC subsystem for the PET

Analogue-to-digital conversion and logging of converted points is one of the most common laboratory data-acquisition tasks. In the vast majority of cases the required ADC resolution is greater than 8 bits. A 10-bit ADC (Analogue Devices 571) has been interfaced to the PET through the 8-bit port by use of a simple multiplexer. The 571 is a complete 10-bit successive approximation ADC contained in a single 18-pin integration counter package costing about $50.00. The conversion time is specified at 25 μsec. A block diagram of the interface is shown in Fig. 5 and a detailed schematic of the tri-state gate multiplexer is shown in Fig. 6. The use of tri-state gates results in a very simple multiplexer design. The data-acquisition program is shown in Table 7. The 10-bit conversion is brought in and stored away 5 bits at a time with a machine-language segment. The input data-rate for the 10-bit number is 14 kHz (77 μsec/point). After acquisition of the desired data array, the 10-bit numbers are assembled from the two 5-bit segments and printed out by use of BASIC. In this application the importance of being able to switch easily between machine-language and BASIC programming is illustrated. For high speed, data acquisition is done in machine language but for ease of numerical manipulation we quickly switch to BASIC.

Digital I/O expansion of the PET

In order to incorporate DAC, ADC and digital I/O capability on the PET the number of available I/O lines must be expanded. This is relatively easy to do

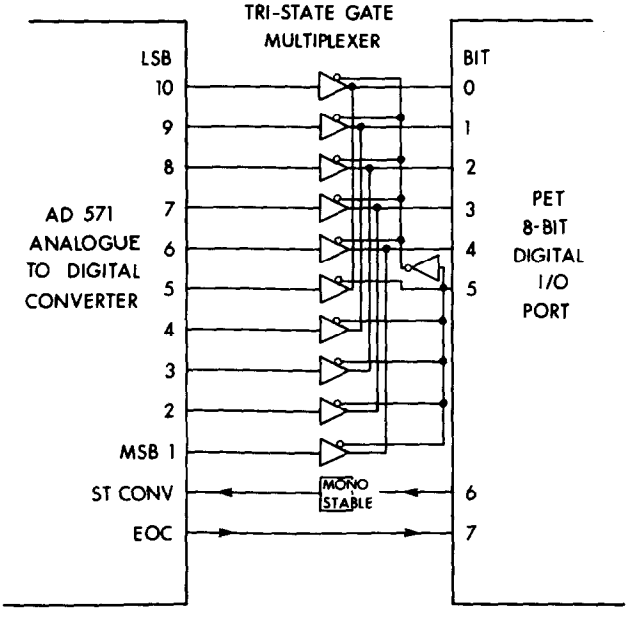


Fig. 5. Block diagram of the analogue-to-digital converter interface.

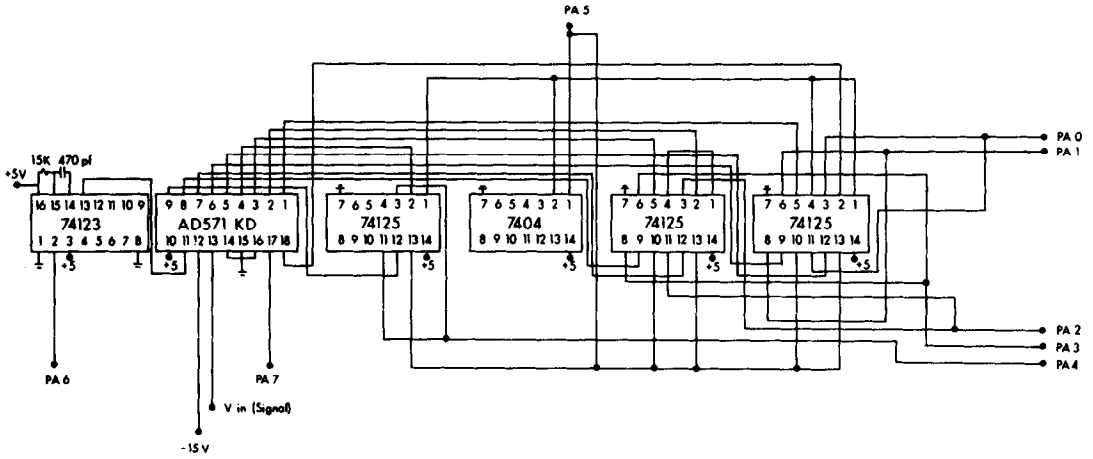


Fig. 6. Schematic of the tri-state gate multiplexer. (74123, monostable; AD571 KD, analogue-to-digital converter; 74125, Quad tri-state gates; 7404, HEX inverter).

by using the PET expansion port. This port contains the 6502 address, data and control buses along with memory-expansion select lines. A block diagram of the connection of the 6520 peripheral interface adapter to this port is shown in Fig. 7. No interface circuits between this port and the 6520 chip were necessary, simply direct connection of the appropriate pins. The 6520 is a simplified version of the 6522 as it contains only the two 8-bit ports and control lines. With this simple addition ($7.00) the PET now has 24 digital I/O lines. The machine-language data I/O rates of the 6520 interfaced to the PET as shown in Fig. 7 were comparable to those of the PET 8-bit port.

Conclusions

The PET is only one of many inexpensive computers available as a result of the consumer/hobby market that has recently developed,[16,17] and new systems are appearing almost monthly. Indeed, enhanced larger memory versions of the PET (16 and 32 kbyte) are now available. In addition, one very powerful but

Table 7. PET ADC-multiplexer program

```
 5 INPUT N
10    SYS  (6160)
      LDA  #60      SET BITS 5 AND 6 AS OUTPUTS
      STA  DDRA
      LDY  #N       LOAD THE NUMBER OF POINTS
      LDX  #00      SET X AS POINTER TO BOTTOM OF
                    PAGE
      LDA  #20      START A/D CONVERSION, SEND PULSE
      STA  DRA
      LDA  DRA      GET PORT A DATA FOR SIGN CHECK
                      BIT 7
      BMI  A        FOR END OF CONVERT, EOC
      AND  #1F      CLEAN OFF BITS 7, 6 AND 5
      STA  0019,X   STORE LOWER 5 BITS
      LDA  #00      CHANGE TRISTATE TO READ HIGH
                      5 BITS
      STA  DRA
      LDA  DRA      GET UPPER 5 BITS
      AND  #1F      CLEAN OFF BITS 7, 6 AND 5
      STA  001A,X   STORE UPPER 5 BITS
      INX           MOVE POINTER
      LDA  #60      PREPARE FOR NEW A/D CONVERSION
      STA  DRA
      DEY           DECREMENT THE COUNTER
      BNE  START    GO AGAIN IF NOT DONE
      RTS           RETURN TO BASIC
20    FOR J = 1 TO N
25    X = PEEK (6400 + J) + 32*PEEK(6656 + J)
30    PRINT x
40    NEXT
50    STOP
```

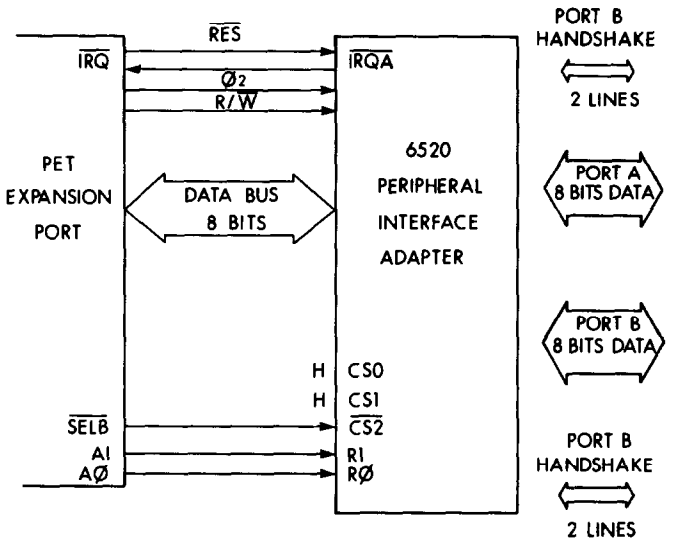


Fig. 7. Interface connections for the 6520 and the PET expansion port.

simple system is the AIM-65.[11,18–20] The AIM-65 is a 6502-based single-board microcomputer complete with a full keyboard; 20-character display; 20-column printer (thermal dot matrix); 4-kbyte RAM; 8-kbyte ROM; a 6522 versatile interface adapter (VIA) containing two 8-bit I/O ports with handshake, 8-bit shift register, two 16-bit counters, TTY interface; audio cassette interface; ROM assembler; and 8-kbyte BASIC (MICROSOFT) in ROM. The power and convenience of this very inexpensive system ($500) are quite remarkable. It is particularly useful to have an on-board high-level language. Also we have tested our benchmarks on the AIM-65 and rates are comparable to the KIM-1 system and the PET.

Finally, the key concluding point is that with simple hardware interfaces such as those illustrated in this presentation, these simple microcomputers can become quite powerful laboratory-oriented computer systems for remarkably little cost.

Acknowledgements—Financial support by the University of Alberta and the Natural Sciences and Engineering Research Council of Canada is gratefully acknowledged.

REFERENCES

1. T. E. Edmonds, *Anal. Chim. Acta*, 1979, **108**, 155.
2. D. I. Leggett, *Anal. Chem.*, 1978, **50**, 718.
3. C. R. Martin and H. Freiser, *ibid.*, 1979, **51**, 803.
4. N. Busch, P. Freyer and H. Szameit, *ibid.*, 1978, **50**, 2166.
5. A. H. B. Wu and H. V. Malmstadt, *ibid.*, 1978, **50**, 2090.
6. H. E. Eaton and J. D. Stuart, *ibid.*, 1978, **50**, 587.
7. F. Morley, I. K. O'Neill, M. A. Pringuer and P. B. Stockwell, *ibid.*, 1979, **51**, 579.
8. Intel Corp., 3065 Bowers Ave., Santa Clara, CA 95051.
9. MOS Technology Inc., 950 Rittenhouse Rd., Norristown, PA 19401.
10. JADE Computer Products, 4901 W. Rosecrans Ave., Dept. B, Hawthorne, CA 90250.
11. Seawell Marketing Inc., 315B N. W. 85th, Seattle, WA 98117.
12. G. Horlick, *Talanta*, 1981, **28**, 487.
13. *Byte*, 1977, **2**, No. 10, 50.
14. Commodore Business Machines, Inc., 901 California Ave., Palo, Alto, CA 94304.
15. H. V. Malmstadt, C. G. Enke and S. R. Crouch, *Experiments in Digital and Analog Electronics*, p. 201. E-L Instruments Inc., Derby, Connecticut, 1977.
16. *Interface Age*, 1979, **4**, No. 13, 130.
17. *Ibid.*, 1979, **4**, No. 8, 50,
18. Rockwell International, Microelectronics Devices, P.O. Box 3669, Anaheim, CA 92803.
19. T. Fox, *Interface Age*, 1980, **5**, No. 11, 74.
20. R. C. Camp, T. A. Smay and C. J. Triska, *Microprocessor Systems Engineering*, Matrix Publishers, 30 NW 23rd Place, Portland, OR 97210.

Talanta, Vol. 28, pp. 527 to 534, 1981
Printed in Great Britain. All rights reserved

0039-9140/81/070527-08$02.00/0
Copyright © 1981 Pergamon Press Ltd

MICROPROCESSOR-CONTROLLED INTEGRATING READ-OUT SYSTEMS FOR PHOTOMULTIPLIER TUBES*

M. W. BLADES and GARY HORLICK
Department of Chemistry, University of Alberta, Edmonton, Alberta, Canada

(*Received* 18 *July* 1980. *Accepted* 6 *December* 1980)

Summary—Two types of wide dynamic range integrating read-out systems for photomultiplier tubes have been developed. One system is based on a voltage-to-frequency converter-counter system and the second is based on summing a large number of analogue-to-digital converter values. Both systems operate under microprocessor control. The microprocessor controls and sequences the acquisition of replicate integrated measurements and software is provided for calculation of background-corrected values, standard deviations for up to 32 replicate values and signal-to-noise ratios. Development and implementation of this software capability in a small system is greatly facilitated by use of a hardware floating-point package. All program software is stored in erasable programmable read-only memory. This system has been particularly useful for the acquisition of data from a single-channel inductively-coupled plasma atomic-emission spectrometer.

The photomultiplier (PM) tube is the most widely used detector for spectrochemical measurements in the ultraviolet and visible spectral regions. Although many diverse experimental arrangements exist, a rather large number of the applications have very similar basic measurement requirements. In our own laboratory we had a need for a general-purpose wide dynamic range integrating read-out system. One of the main applications for this system was the acquisition of basic signal-to-noise ratio data for spectrochemical sources such as the inductively coupled plasma. For this application a background-subtraction capability was required so that a blank (*i.e.*, plasma spectral background) and/or photomultiplier tube dark-current signal could be automatically subtracted from an analyte emission reading. In addition, to facilitate the signal-to-noise ratio studies, automatic acquisition of replicate integrated measurements was required along with subsequent calculation of standard deviations and signal-to-noise ratios. Finally it was desirable to have all data logged in a systematic fashion to a hard-copy read-out device.

These basic requirements essentially dictated the development of a microprocessor-based read-out system. In fact we developed two types of wide dynamic range integrating read-out systems, both of which operate under microprocessor control. In both systems the output current signal from the PM tube is first converted into a voltage with an operational amplifier. In the first measurement system (Fig. 1) this voltage is then converted into a frequency by a wide dynamic range (6 orders of magnitude) voltage-to-frequency converter. The voltage-to-frequency (v-to-f) converter is interfaced to an 8080-based single-board microcomputer, the Intel SDK-80. The key subsystem in this interface is the Intel 8253 programmable interval timer chip. Utilizing two of these chips in conjunction with the SDK-80 microcomputer gives, in a sense, a very flexible software programmable frequency meter for the measurement of the v-to-f converter output. In the second system (Fig. 1) a monolithic 10-bit successive approximation ADC is interfaced to the SDK-80. Capability for integrating measurement over a wide dynamic range is achieved by summing a large number of conversions.

In both systems the microprocessor controls the acquisition of replicate integrated measurements and software is included for background subtraction, and the calculation of standard deviations of the replicate values and signal-to-noise ratios. Development of this software capability in a small system was greatly facilitated by use of the Advanced Micro Devices AM9511 Arithmetic Processing Unit. This chip (24-pin package) is capable of performing fixed-point single and double precision (16- or 32-bit) arithmetic and floating-point single precision (24-bit mantissa, 7-bit exponent) arithmetic. Functions performed include addition, subtraction, multiplication, division, trigonometric and inverse trigonometric functions, square roots, logarithms and exponentials. The use of this chip greatly expedited overall software development and shortened execution time, compared to software floating-point packages. Both systems are described in detail.

EXPERIMENTAL

Components common to both measurement systems are the operational amplifier (OA) and the SDK-80 single-board microcomputer. The OA is the Analog Devices

*Presented, in part, at the Pittsburgh Conference, Cleveland, Ohio, 1979.

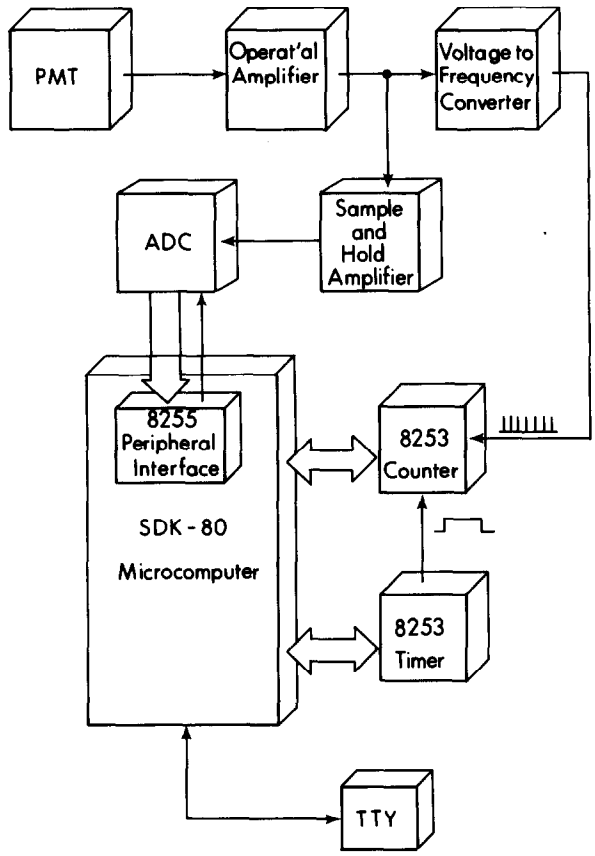


Fig. 1. Block diagram of the v-to-f converter and analogue-to-digital converter based measurement systems.

Model 52K, a low-noise, low-drift, precision FET amplifier. It is operated with a 10-MΩ feedback resistor in parallel with a 450-pf capacitor. Thus the output voltage is 1 V for an input current of 10^{-7} A from the PM tube.

The heart of both measurement systems is the Intel SDK-80 single-board microcomputer. The basic hardware features of this board include an 8080 A central processing unit, 1 kbyte of read/write memory (8111s), 4 kbyte of 2708 erasable programmable read-only memory (EPROM), an 8251 programmable communication interface used for serial I/O to the teletype, and two 8255 programmable peripheral interface chips providing 48 digital I/O lines. In addition a small but very useful breadboard area is provided. All additional circuitry for both applications was placed in this breadboard area (see Fig. 2), except for the voltage-to-frequency converter and operational amplifier, which were located near the PM tube.

System based on the voltage-to-frequency converter

The voltage-to-frequency converter used was the Analog Devices Model 460 k, a high-accuracy unit with a six-decade (1–10^6 Hz) dynamic range.

The key subsystem of this measurement system is the Intel 8253 programmable interval timer. A block diagram of this 24-pin integrated circuit is shown in Fig. 3. It consists of three independent 16-bit presettable down-counters (band-width from d.c. to 2 MHz), read/write logic, a control-word register and a data-bus buffer. The read/write logic controls the overall device operation such as loading and reading of the various counters as well as loading of the control word register. The counters can be software programmed to act as either binary or BCD counters and each counter can be independently programmed to operate in any of six different modes. The basic operation of each mode is illustrated schematically in Fig. 4.

Mode 0 is a software-triggered interrupt in which an interrupt signal, a rising edge at the output terminal, is generated N clock pulses after software-loading of N on the counter. In Mode 1 (programmable one-shot or monostable) an external trigger (rising edge) applied to the gate input generates a zero-level pulse at the output. The duration of the pulse is N clock pulses where N is again a software-loaded value. Modes 2 and 3 are both divide-by-N counter modes. In Mode 2 the output is a zero-level pulse 1 clock pulse in duration every Nth clock pulse, while in Mode 3 the output is a symmetrical divided-by-N waveform. Mode 4 provides a software-triggered strobe, a zero-level pulse of 1 clock period duration that occurs N clock pulses after a software loading of the counter. Mode 5 (hardware-triggered strobe) provides a similar operation but requires an external trigger, a rising edge at the gate input. The discussion above and Fig. 4 provide only a brief and basic description of the operation and capabilities of the 8253. For complete details Intel's literature should be consulted.

The complete schematic for connection of the 8253s to the SDK-80 is shown in Fig. 5. One 8253 functions as the counter for the measurement of the voltage-to-frequency converter output and the other generates the counter time base (integration time) for the first 8253. Simplified diagrams of the integration timer and counter are shown in Fig. 6.

The integration time is derived from the 2.048-MHz clock of the microprocessor. Counter 0 on the timer 8253 is operated in Mode 2 (binary) (divide-by-N counter) by loading HEX 3C into the control register. This counter is

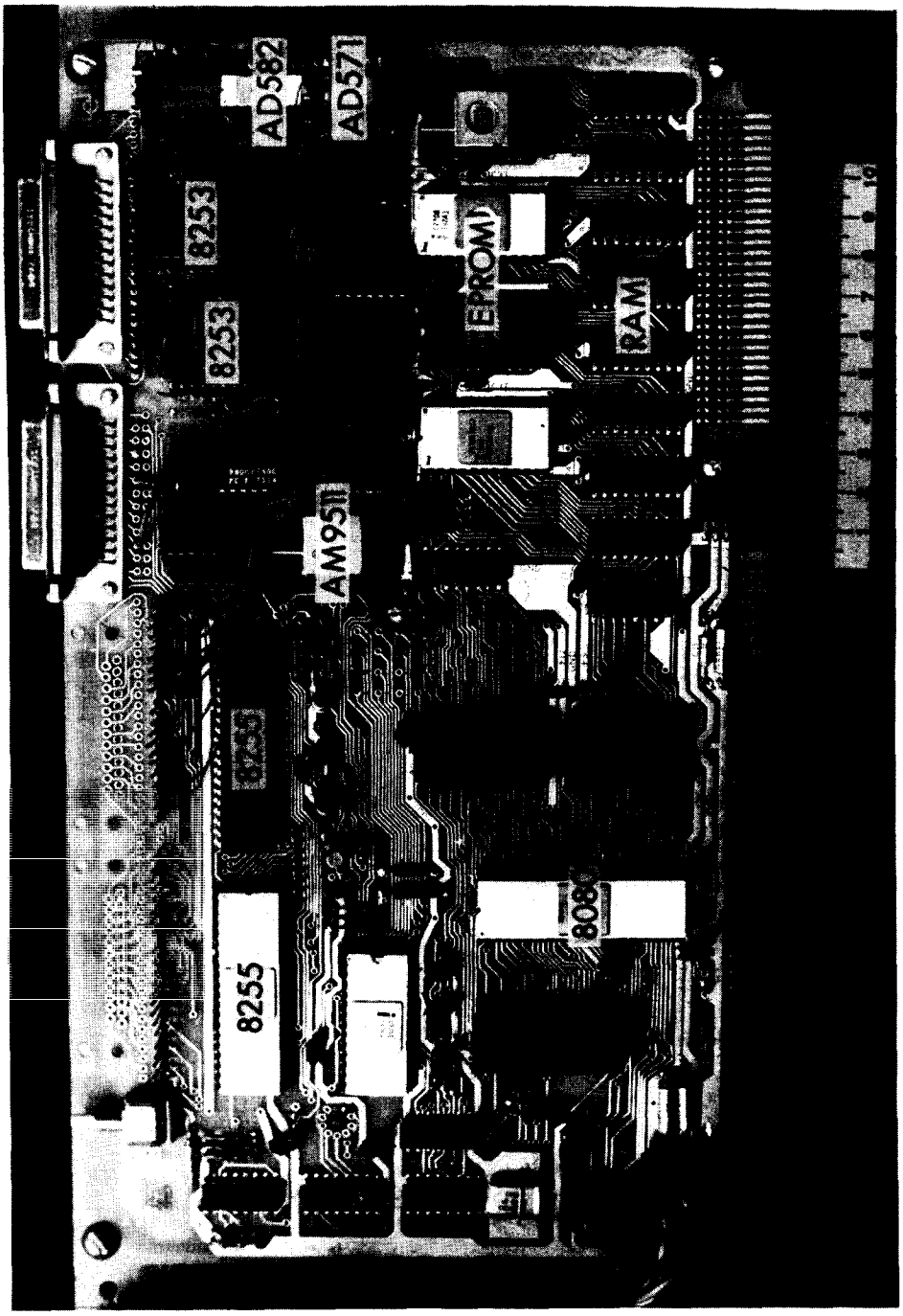


Fig. 2. Photograph of SDK-80 microcomputer board with additional circuitry. The 8080 is the CPU, the 8255s are Programmable Peripheral Interface Chips, the AM9511 is an Arithmetic Processing Unit, the 8253s are programmable counter/timer chips, the AD582 is a sample-and-hold amplifier, and the AD571 is a 10-bit analogue-to-digital converter. The scale is in cm.

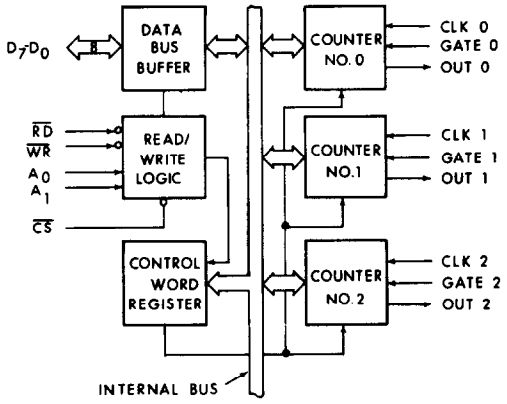


Fig. 3. Block diagram of the 8253 programmable interval timer.

then preset to HEX 5004 which divides the 2.048-MHz clock signal down to 100 Hz which is available at the output pin of counter 0. This 100-Hz signal is connected to the clock input of the second counter. Counter 1 (the second counter) on the same integration counter (IC) is programmed to operate in Mode 5 (BCD) (hardware-triggered strobe) by loading the control register with HEX BB, and is preset with a BCD number input from the teletype. For example, presetting this counter with 0100 results in a 1-sec integration time. Thus integration times from 0.01 to 99.99 sec in 0.01-sec intervals can be set by TTY input.

The other 8253 is used to count the pulses produced by the voltage-to-frequency converter for the integration time generated by the timer 8253. In order to obtain the desired resolution, two counters on this second chip are cascaded, providing 32-bit resolution. Both 16-bit counters are set to operate in Mode 2 (binary) by loading the control register with HEX BC and 7C. The counters are preset with HEX FF for full count.

An 8255 programmable peripheral interface chip that is a standard feature of the SDK-80 board is used to aid sequencing of the measurement. A measurement is initiated by outputting a logic 0 followed by a logic 1 at one bit of port B. This sets the flip-flop (Q = 1) which enables the gates of both the timer and counter 8253s. Note that both 8253s have NAND gates on the cascade line from output to the succeeding input of each IC. This is necessary because we found that the 8253s do not count the first pulse which is used to set up the counter. For this reason a charge-delay monostable multivibrator is used to set up the counters at the start of the measurement. The charge-delay monostable is triggered by the falling edge at $\overline{Q}$ of the flip-flop.

When the timer 8253 reaches its full count its output undergoes a $1 \rightarrow 0$ transition which toggles the flip-flop

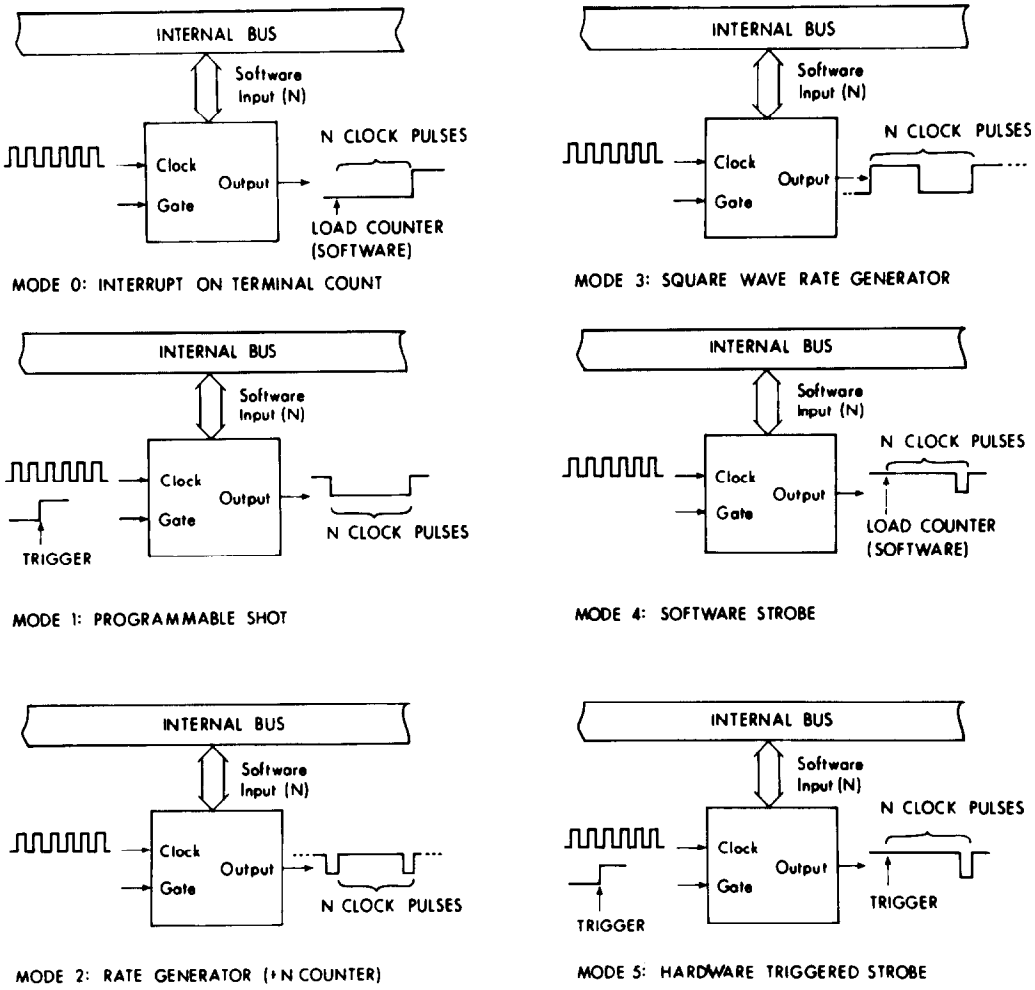


Fig. 4. Schematic representations of the 8253 modes.

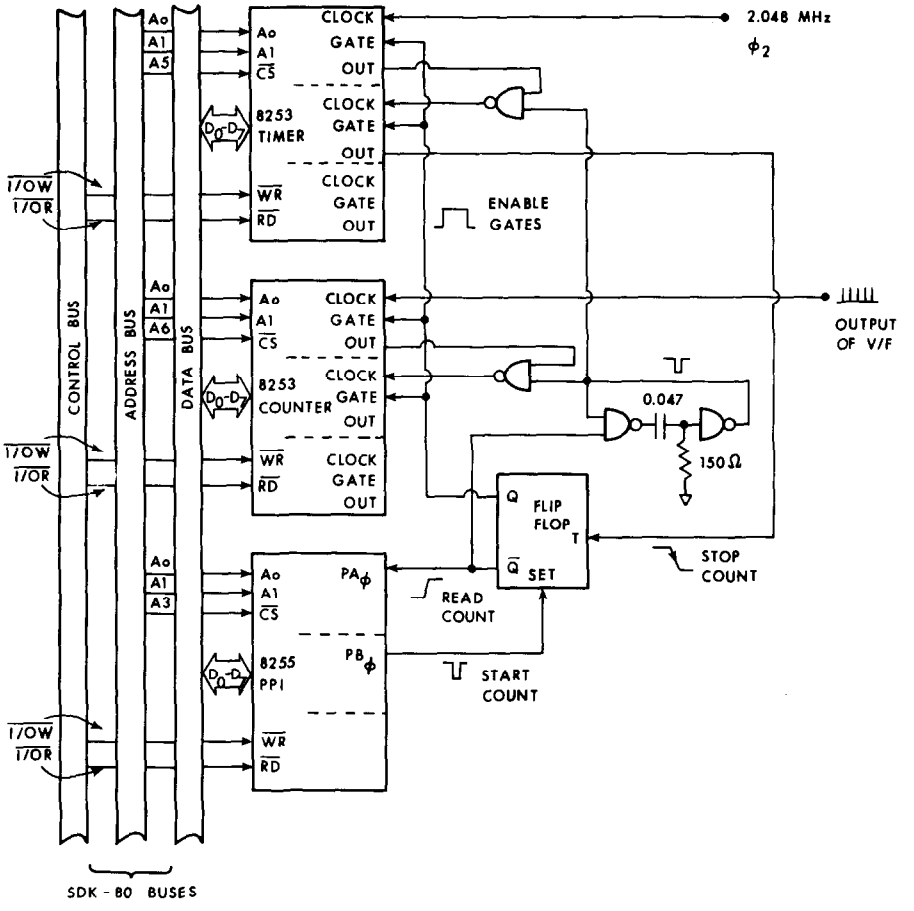


Fig. 5. Circuit diagram of the complete programmable frequency meter as interfaced to the SDK-80.

setting Q to "0", thus disabling all gates and terminating the count measurement. During counting, the status of the flip-flop is continuously monitored by inputting $\overline{Q}$ of the flip-flop to bit 0 of port A on the 8255. When counting is completed ($\overline{Q}$ = "1") the microcomputer enters a routine that reads the binary numbers in the counter 8253 and stores them in memory.

System based on the successive-approximation ADC

The complete schematic of this system is shown in Fig. 7. An Analog Devices AD571 was chosen as the ADC. It is a 10-bit unit with a specified conversion time of 25 μsec. The ADC was front-ended with an Analog Devices AD582 sample-and-hold amplifier. The sample-and-hold amplifier-ADC subsystem was interfaced to the SDK-80 through the

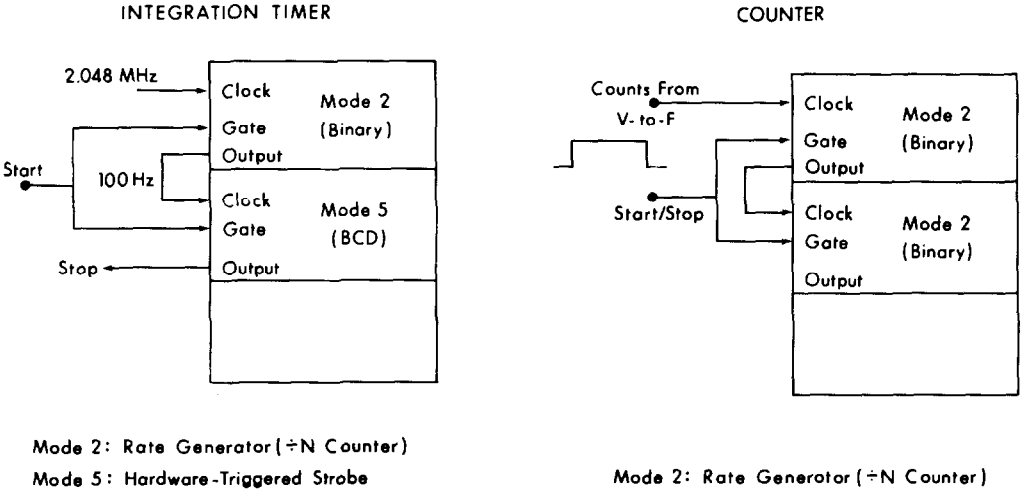


Fig. 6. Simplified block diagrams of the integration timer and the counter.

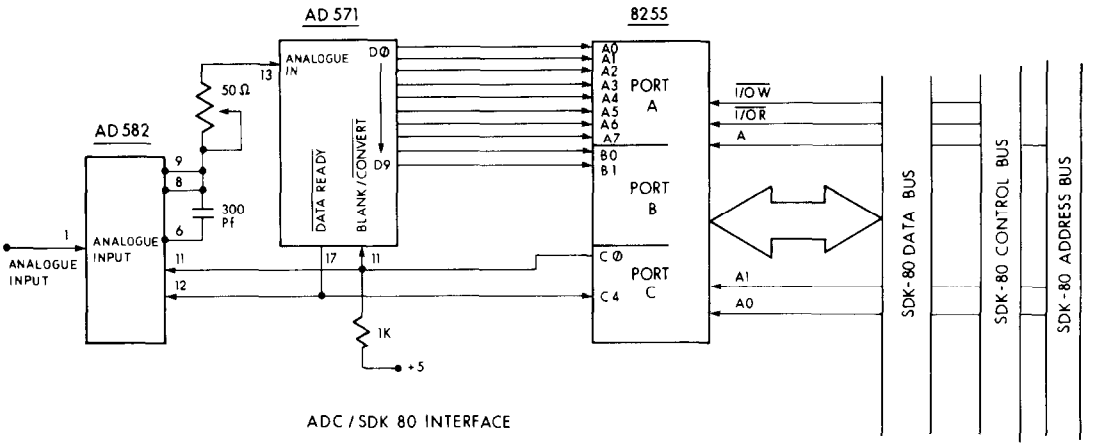


Fig. 7. Circuit diagram of the analogue-to-digital converter based system as interfaced to the SDK-80.

8255 programmable peripheral interface chip. Acquisition of a data point is initiated by a pulse from pin C0 of port C, and upon receipt of the $\overline{\text{DATA READY}}$ signal the converted 10-bit value is read into the microprocessor by use of ports A and B of the 8255. Integration is achieved by summing a large number of converted values. For example a 1-sec integration is achieved by summing 10,923 conversions. Even though we are using a 10-bit converter the integrated value has a resolution of about 16–17 bits as a result of the summation (signal averaging) step.[2]

Software development

The key to the versatility and power of a microprocessor-based system is software control. The SDK-80 single-board microcomputer has room for 1 kbyte of read/write memory (RAM) and 4 kbyte of ROM (*i.e.*, four 2708 EPROMs). One EPROM contains the standard 1-kbyte MONITOR provided with the SDK-80 kit. The MONITOR provides software to communicate with a TTY, enter and edit user programs, examine, list or change memory locations, and initiate execution of programs with breakpoint capability. In addition to providing general system control, several MONITOR routines are called and utilized by other programs developed for this application. Utility programs were required for reading and writing paper tapes on the TTY. Unfortunately Intel did not provide these programs in the SDK-80 MONITOR. Paper tape input/output programs were obtained from the Intel user library.[3]

In order to do more arithmetic on a microprocessor than the simplest binary additions and subtractions, a set of so-called floating-point routines is required. We initially adapted a floating-point package from Findley[4] for use in our system. However it soon became too wasteful of both time and memory-space to set up a complete floating-point package on a microprocessor system as small as this, for anything beyond routines for floating-point normalization, addition, subtraction, multiplication, division and TTY output.

Full floating-point capability is now provided on our system by using the Advanced Micro Devices AM9511 Arithmetic Processing Unit. This chip is essentially a complete hardware floating-point package. The AM9511 contains an internal stack onto which operands are loaded from the 8080 CPU over the system data bus. The appropriate execution command is sent to the AM9511 and the result of the operation is left on the stack. A command summary for the AM9511 is shown in Table 1 and the schematic for the hardware interface to the SDK-80 is shown in Fig. 8. It is difficult to overemphasize the extent to which the use of this chip has expedited overall software development for this system.

Table 1. AM9511 command summary

1. *FIXED POINT*... 16 or 32 BIT	
ADD	MULTIPLY
SUBTRACT	DIVIDE
2. *FLOATING POINT*... 25 BIT MANTISSA, 7 BIT EXPONENT	
ADD	MULTIPLY
SUBTRACT	DIVIDE
SQUARE ROOT	SIN
COS	TAN
ASIN	ACOS
ATAN	LOG
LN	EXP
X TO POWER Y	
3. *DATA MANIPULATION*	
FLOATING POINT TO FIXED POINT (16 and 32 BIT)	
FIXED POINT TO FLOATING POINT (16 and 32 BIT)	
CHANGE SIGN	
READ/LOAD STACK	

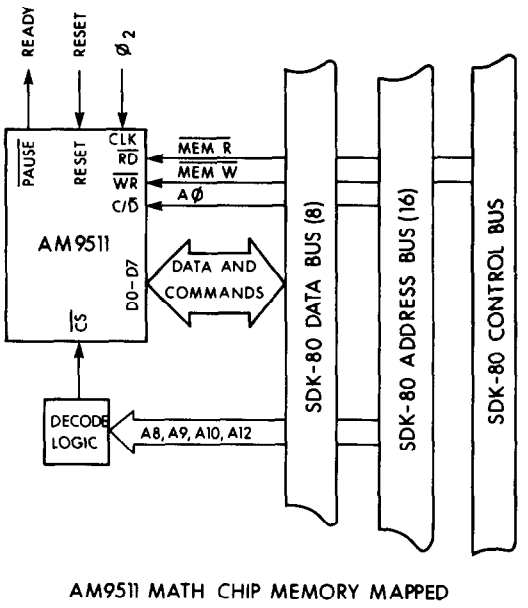


Fig. 8. Interface circuit for the AM9511 to the SDK-80.

All programs were placed in EPROM (2708s). The 2708s were programmed by using the Intel PROMPT-80 system. Program development and assembly were carried out with a cross-assembler running on a PDP-11 minicomputer in our laboratory.

RESULTS AND DISCUSSION

The TTY output for a typical run (v-to-f system) for the measurement of an analyte emission signal from an ICP source is illustrated in Fig. 9. The operator types in the desired integration time (1.00 sec) and number of replicate measurements ($16 \equiv 10_{16}$). Note that the number of repeats must be designated in HEX. This is a typical concession that often has to be made in dealing with a minimum-configuration microprocessor system such as the single-board SDK-80. In our case it simply was not worth the programming time and in particular the programming space to include a conversion routine. The integration time could be input in decimal format because the second counter on the timer 8253 was being operated in a BCD mode. Finally the operator indicates whether this is a background or sample (analyte) run and types a sample identification code. The measurements are then carried out, in this case 16 consecutive 1-sec integrations, the measurements are summed and averaged, the background is subtracted, the standard deviation and signal-to-noise ratio are calculated, and all data are logged to the TTY. The background subtracted is that measured in a previously acquired so-designated run, and would represent, for example, the output signal for a blank solution.

The TTY dialogue for the ADC-based integrating system is essentially identical except that the integration time is chosen by indicating the number of ADC conversions to be summed. A 1-sec integration is equivalent to 10,923 conversions. Judged from the signal-to-noise ratios (the reciprocal of the relative standard deviation when $n = 32$) for several analyte signals, the performance of the v-to-f and ADC based systems as integrating measurement systems was essentially identical, *i.e.*, equivalent signal-to-noise ratios were obtained for the same signal and integration times for both systems. However, practical differences do exist between these two systems with respect to factors such as cost, set-up time and expansion to multichannel measurements.

While costs are admittedly hard to pin down these days, the ADC with its attendant sample-and-hold amplifier was a little more expensive than the v-to-f converter and 8253 counter/timer chips, but not very much. In terms of set-up time (*i.e.*, interfacing to the SDK-80) the ADC-based system was simpler, as it was done by using the standard on-board chips, while with the v-to-f system, the 8253-based programmable frequency meter had to be developed and interfaced. With respect to expansion to simultaneous multichannel measurements (*i.e.*, for a direct-reading spectrometer using several photomultiplier tubes) the v-to-f system is, perhaps, more effective. A proposed approach is illustrated in Fig. 10. Each channel requires an operational amplifier, a v-to-f converter and a 32-bit counter (*i.e.*, 2/3 of an 8253). A single microprocessor could easily control the complete system, as once the counters are set up for the measurement they need not be read until the integration is complete. No software intervention is necessary during integration and in general software requirements for such a system would be minimal. Of course, multichannel ADC systems could also be set up and in fact

```
INT TIM?  0100
# REPTS?  10
BACK(B)/SAMP(S)?  S
ID?  1

+0.2526000E+04
+0.2543000E+04
+0.2530000E+04
+0.2534000E+04
+0.2536000E+04
+0.2534000E+04
+0.2539000E+04
+0.2549000E+04
+0.2534000E+04
+0.2535000E+04
+0.2539000E+04
+0.2538000E+04
+0.2545000E+04
+0.2534000E+04
+0.2537000E+04
+0.2551000E+04

SUM:   +0.4060400E+05
AVE:   +0.2537750E+04
BSB:   +0.2461750E+04
STD:   +0.6587867E+01
S/N:   +0.3736793E+03
```

Fig. 9. Typical TTY dialogue and output for a run with the v-to-f converter based measurement system.

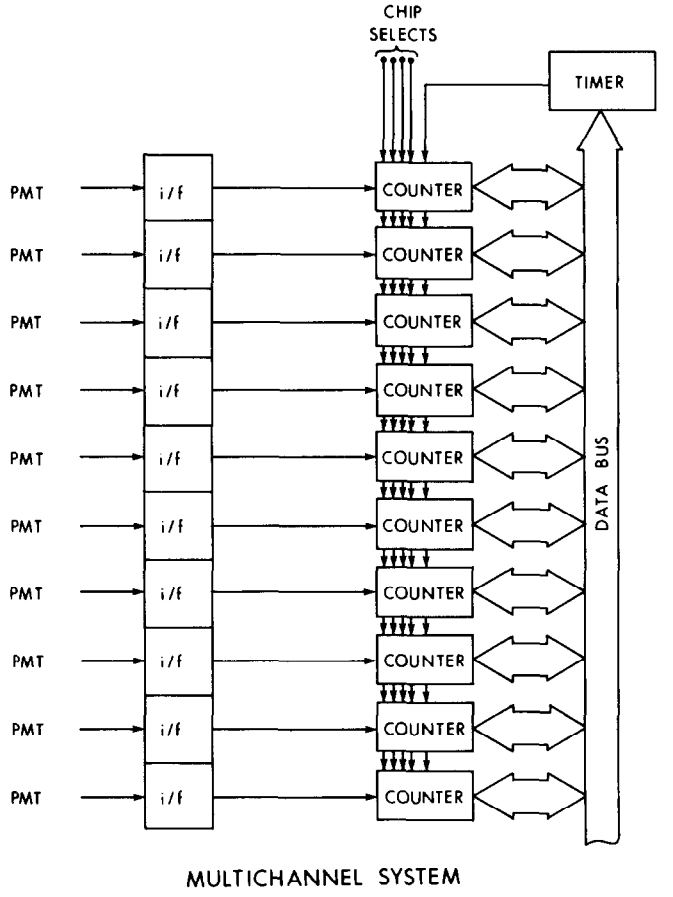


Fig. 10. Proposed approach for a multichannel measurement system based on the v-to-f converter and counter integration system.

the read-out system for one current direct-reading spectrometer[5] is based on analogue integration at each channel with subsequent multiplexing to a single ADC. In particular, the software needed for this system is more complex than that proposed in Fig. 10, in part because of the dynamic range limitations associated with analogue integration. However, our goal here is not to pick a "best" system, but simply to indicate that the v-to-f based system, when developed with software programmable counters, can potentially provide a powerful microprocessor-controlled multichannel integrating read-out system for PM tubes.

CONCLUSIONS

Single-board microprocessor systems, such as the one used in this application, can easily provide the basis for intelligent data acquisition and processing systems. The system described here is applicable to a wide variety of spectrochemical measurements involving photomultiplier tubes. Versatility is built in as a result of the capability of programmable chips such as the 8253 counter/timer chip and, in particular, because of software control of the system by EPROM-based routines. Indeed, the complete single-board microprocessor system can easily be dedicated to an entirely new task simply by inserting an appropriate EPROM.

In our laboratory this system has been used for acquisition of data from a single-channel inductively-coupled plasma atomic-emission spectrometer. It has been particularly useful for signal-to-noise ratio measurements and studies, where it has relieved the tedium of collecting, calculating and logging the large amounts of statistical data.

Acknowledgements—Financial support by the University of Alberta and the Natural Sciences and Engineering Research Council of Canada is gratefully acknowledged.

REFERENCES

1. *8080 Microcomputer Peripherals User's Manual*, Intel Corp., 3065 Bowers Ave., Santa Clara, CA 95051, U.S.A.
2. H. V. Malmstadt, C. G. Enke, S. R. Crouch and G. Horlick, *Optimization of Electronic Measurements*, p. 124. Benjamin, Menlo Park, California, 1974.
3. Intel Corp., *User's Library*, 3065 Bowers Ave., Santa Clara, CA 95051, U.S.A.
4. R. Findley, *Scelbi '8080' Software Gourmet Guide and Cook Book*, Scelbi Computer Consulting, Inc., 1322 Rear-Boston Post Road, Milford, CT 06460, U.S.A.
5. A. F. Ward, *Am. Lab.*, 1978, **10**, No. 11, 79.

Talanta, Vol. 28, pp. 535 to 538, 1981
Printed in Great Britain. All rights reserved

0039-9140/81/070535-04$02.00/0
Copyright © 1981 Pergamon Press Ltd

A MICROCOMPUTER-CONTROLLED SYSTEM FOR AUTOMATIC ACQUISITION OF KINETIC DATA OF GAS UPTAKE AT CONSTANT PRESSURE

HARALD GAMPP
Institute of Inorganic Chemistry, University of Basel, CH-4056 Basel, Switzerland

(*Received* 14 *October* 1980. *Accepted* 12 *November* 1980)

Summary—A microcomputer-controlled apparatus for measuring the kinetics of gas uptake in a chemical reaction at constant pressure and temperature is described. The slight pressure decrease caused by consumption of the gas is transformed into an electrical signal. A microprocessor stores the time at which the signal occurs and activates a motor-driven burette to restore the original pressure. At the end of the experiment, the data are recorded on magnetic tape by a cassette recorder and can be transferred from the tape to a desk computer for plotting or further mathematical treatment. The performance of the apparatus is illustrated by the example of the catalytic oxidation of benzoin in dimethyl sulphoxide.

In many investigations of catalytic systems, the kinetics of gas absorption are measured at constant pressure and temperature.[1] This is usually done with a gas burette, where constant pressure is maintained in a thermostatically controlled reaction vessel by means of a levelling bulb, and the volume of the gas consumed is read visually.[2] In many biological and biochemical studies, a Warburg apparatus working at constant volume is used.[3,4] Because of the need for constant attention by the operator, these techniques are rather tedious and not suitable for prolonged runs. An automatic apparatus not only frees the operator from taking individual readings but also allows more precise measurements to be made in the case of fast reactions.

In recent years several automatic systems have been described,[5–7] in which the data are obtained as analogue signals and are displayed on a millivolt recorder. However such systems may not work at constant pressure,[5] or may be suitable only for micro amounts of gas,[6] or be rather complicated to construct.[7] In addition, the data still have to be digitized manually for further treatment.

The present paper describes a fully automatic gas volumeter that is simple to construct and can be assembled from readily available laboratory equipment with little extra work. (In fact, the most expensive parts of the system, the microprocessor and the motor-driven burette, are the same as already used in our titrating system.[8]) About 1 mmole of gas can be taken up, thus allowing isolation of the products by conventional methods or by chromatography after the kinetic measurement.

The apparatus is based on a Zilog Z80 microprocessor chip, which maintains the system at constant pressure by means of a motor-driven burette, reads the data and stores them on magnetic tape. For further use the data can be transferred to a desk computer (*e.g.*, an HP 9835 or APPLE II).

As a chemical application, we studied the oxidation of benzoin in dimethyl sulphoxide (dmso), catalysed by autoxidized copper(I).[9]

EXPERIMENTAL

Apparatus

The apparatus (Fig. 1) consists of a controlled-temperature reaction vessel, a 20-ml motor-driven burette (Metrohm E 415) capable of adding volume increments of

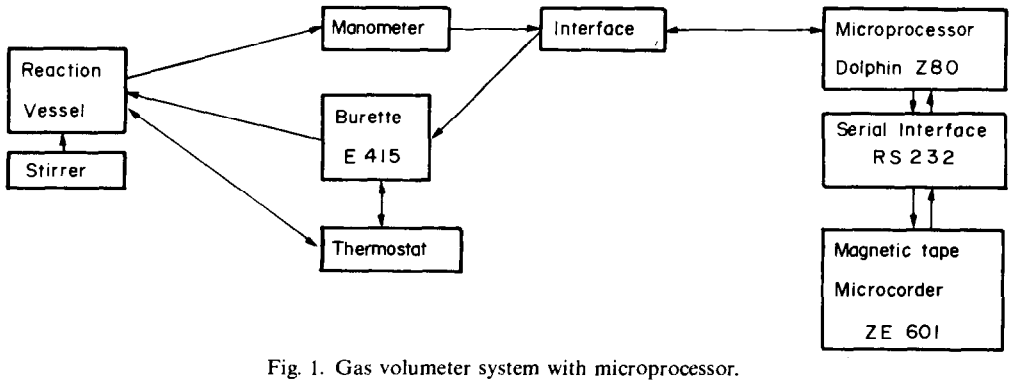


Fig. 1. Gas volumeter system with microprocessor.

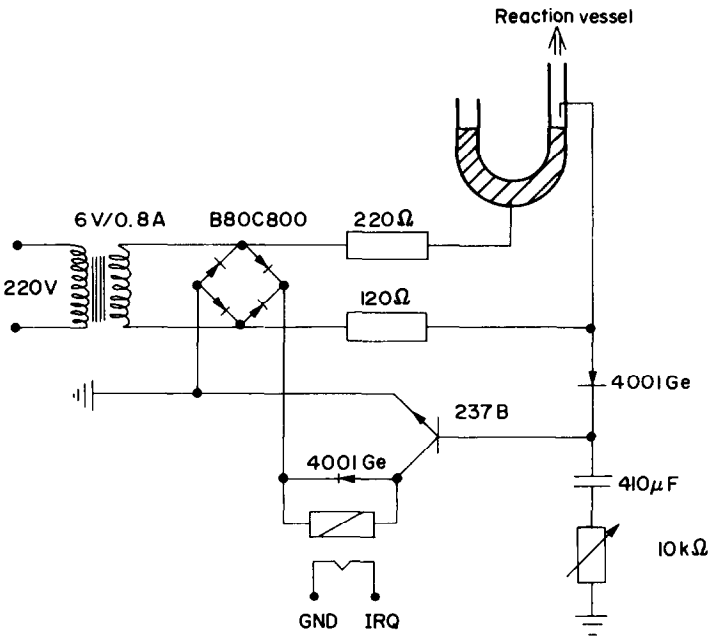


Fig. 2. Pressure-control unit. Interface for generating an interrupt in case of pressure decrease in the reaction vessel.

0.1 ml, a magnetic stirrer, a thermostat, a pressure-control unit (Fig. 2), a Dolphin microcomputer system (Z80 microprocessor, 0.5 kbyte ROM, 1.5 kbyte RAM, 2 kbyte EPROM, 8 lines parallel input/output) with serial interface (Stoppani Ltd.) and a magnetic tape recorder (Zinniker ZE 601) with FSK modem 1200-baud data transfer and an input-output compatible with an RS 232.

The reaction vessel is immersed in a thermostatic bath and equipped with the magnetic stirrer. The burette and the pressure control are kept at constant temperature and connected with flexible tubing, which is also kept at constant temperature, to the reaction vessel. As gas is consumed, the pressure in the system decreases and the circuit between the two Pt–Ir contacts is closed by displacement of the aqueous sodium sulphate solution in the U-tube (Fig. 2). In order to avoid electrolysis, only a small alternating current of 18 mA flows through the solution; it has therefore to be transformed by the a.c. switching amplifier into a signal that can be detected by the microprocessor as an interrupt. The use of an aqueous solution instead of mercury in the U-tube manometer has the advantage of higher sensitivity because of the faster response. The motor-driven burette is used to restore the original pressure by diminishing the gas volume in the system by increments of 0.1 ml. The $6 output of the microprocessor is interfaced through an optoelectronically decoupled amplifier of Darlington type to the switch of the burette motor (Fig. 3).

Reagents

The benzoin used (Fluka, purum) was recrystallized from hot ethanol, $Cu(CH_3CN)_4BF_4$ was synthesized,[10] and the dmso (Merck, uvasol) was freshly distilled over calcium hydride under reduced pressure in a nitrogen atmosphere.

Operation

In the catalytic experiments, the reaction vessel was a round-bottomed flask with a dropping funnel and a magnetic stirrer. Under a stream of oxygen, a solution of the substrate was placed in the flask and a solution of the catalyst was put in the dropping funnel, then the apparatus was closed. After thermal equilibrium was reached, which took about 15 min, atmospheric pressure was restored in the system with the aid of a syringe. The reaction was started by mixing the two solutions, by opening the stopcock between funnel and flask. At the same time the microprocessor program, which had been loaded from magnetic tape, was started by reading in the experiment number. Thereafter the measurement proceeded automatically.

*Program**

The software was written in CALM Z80 assembled by hand in machine language, stored on magnetic tape and read into RAM before the start of the experiment. The program (Fig. 4), 150 bytes long, consists of a main program, for generation and display of the reaction time (in

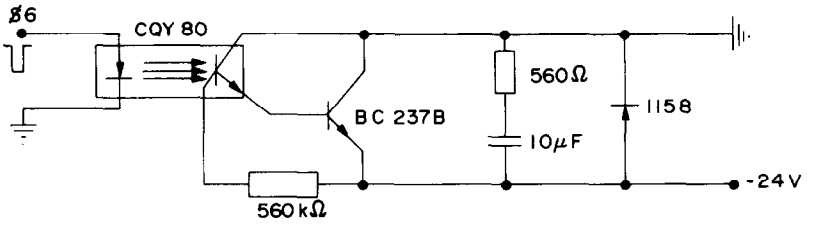


Fig. 3. Interface for burette-motor activation.

* Programs are available on request.

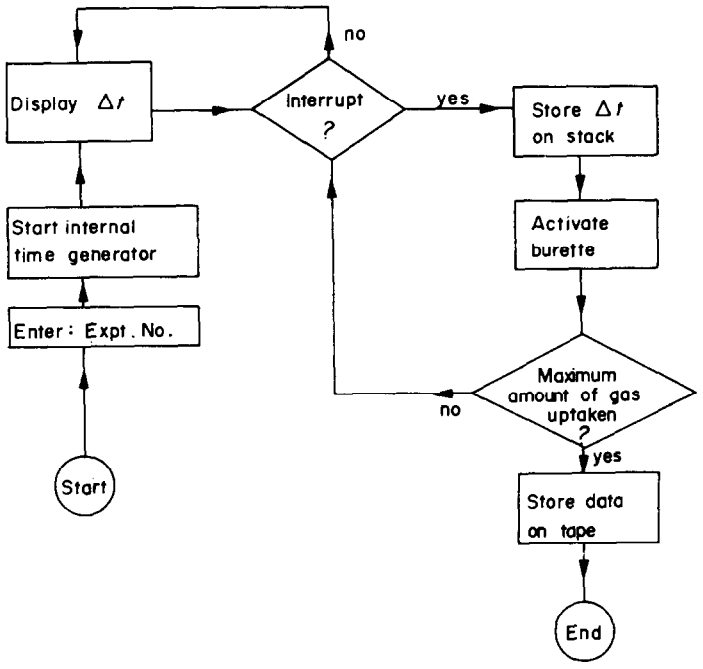


Fig. 4. Data-acquisition program flow-chart for kinetic measurements.

tenths of minutes), and of a subroutine for storage of the data and activation of the burette.

In addition, monitor subroutines stored in EPROM are used, which process the data between the tape recorder and the memory of the microprocessor.

Once the program has been started by reading in the experiment number from the keyboard, the time-counter is initialized and the program enters the time-generating loop. As soon as an interrupt from the pressure-control unit is detected, the program branches to the interrupt subroutine, where it stores the actual time in the RAM and switches on the burette motor by giving a signal on the $6 output of the microprocessor. Each addition of 0.1 ml takes 0.9 sec, determined by the motor. Next, the program tests whether the whole content of the burette has already been added, and if this is not yet the case returns to the main loop. After all the data are collected, they are transferred from the RAM to the magnetic tape. If the reaction has ended before all the 20 ml of gas have been consumed, the data can be stored on tape by operating a switch on the keyboard of the microprocessor.

The data can be read from the recorder by any computer with an RS 232 interface. A BASIC program has been written for an HP 9835 desk computer, which reads the data and creates a data file on the HP tape. The experimental points in the file are then plotted with an appropriate program.

RESULTS AND DISCUSSION

The accuracy and sensitivity of the apparatus depend on its gas-tightness, on the inertia of the pressure control, on the constancy of temperature, and on the dead volume of the system (30 ml for burette and tubing plus the volume of the reaction vessel). As the differences in pressure between the atmosphere and the system will be small, there is no problem in keeping the apparatus gas-tight. Apart from the U-tube of the manometer, the temperature of the whole system can be kept within $\pm 0.1°$ or better when working at room temperature. The use of a salt solution instead of mercury in the U-tube gives a higher sensitivity. Depending on the dead volume, amounts of gas as small as 0.05 ml can be detected (see Table 1, last entry). The accuracy as a function of the total gas volume was tested by removing 5 ml of gas with a gas-tight syringe from reaction vessels of 5, 100 and 200 ml capacity, respectively. For each dead volume, the amount of gas added by the burette was determined 10 times, and the mean values and their standard deviations are given in Table 1. In all cases

Table 1. Accuracy and sensitivity of the apparatus as a function of the total gas volume (10 replicates)

Total gas volume, *ml*	Volume of gas removed with syringe, *ml*	Mean volume of gas added by burette, *ml*	Standard deviation of the mean, *ml*	Sensitivity,* *ml*
35	5.0	4.97	0.048	0.05
130	5.0	4.99	0.074	0.08
230	5.0	4.99	0.099	0.12

* The minimum decrease in gas volume that can be detected by the pressure-control unit.

the mean values are very close to the theoretical value and their standard deviation is about the same as the experimentally determined sensitivity. Hence, the accuracy of the results obtainable with our apparatus is limited by the burette, which can only add volume increments of 0.1 ml. A gas consumption of 20 ml can thus be resolved into 200 steps, so the maximum error from this source should be 0.5%. A better resolution can be obtained with a smaller burette and smaller reaction vessel.

Chemical example

In our investigation of the oxidation of benzoin to benzil, catalysed by autoxidized copper(I) in dmso,[9] we obtained a large number of kinetic data with the apparatus described. For example, 10 ml of 0.0054*M* $Cu(CH_3CN)_4BF_4$ in dmso were stirred under oxygen for a time t_{ox}. Then 10 ml of 0.08*M* benzoin in dmso were added. The curves obtained (Fig. 5) show that with the autoxidized copper(I), there was a nearly linear uptake of oxygen with time, after the induction period. The maximum rate of gas consumption, v_{max}, which can be related to the concentration of the active catalyst,[11] decreases with increasing age of the autoxidized solutions. The mathematical analysis of the dependence of v_{max} on t_{ox} suggests that a copper species which can no longer be regenerated as a catalyst under the conditions of Fig. 5 is formed according to a second-order rate law.[9]

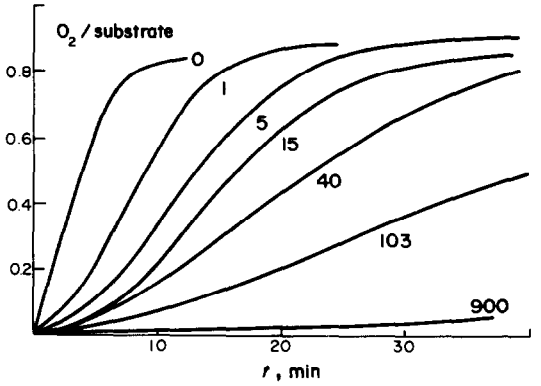


Fig. 5. Oxidation of benzoin, catalysed by autoxidized Cu(I) in dmso. Molar ratio of O_2 consumed to initial substrate, *vs.* time. The age of the catalyst (in minutes) is given in the figure.

CONCLUSIONS

The apparatus can be used to measure the kinetics of gas uptake at rates up to 6.5 ml/min. A total volume of 20 ml of gas can be taken up, with resolution to 0.5%. The apparatus is simple to construct and consists mainly of readily available laboratory equipment. Its operation is simple and, apart from mixing the reactants, fully automatic. The system is flexible and can easily be expanded to operate under pressures other than atmospheric or to measure the uptake of volumes from 5 to 50 ml. The data can be stored on magnetic tape, and read from the recorder by any computer with an RS 232 interface, or transferred directly to the desk computer through the RS 232 interface, but the tape-recording allows several sets of data to be processed in a single batch. Any microprocessor or microcomputer capable of interrupt handling can be used to control the system and acquire the data. The pressure transducer system is only one of the many available, but it was found best for our purposes. Light-activated switches are readily available and could be used equally, and a computer-triggered valve could be used to start the reaction.

Acknowledgements—The author thanks Mr. R. Kissner for design and construction of the interfaces, and the Swiss National Science Foundation (grant No. 2.924–0.77) and the Stiftung der Portlandcementfabrik Laufen for financial support. He also thanks the referee for some interesting and useful suggestions for further development of the equipment.

REFERENCES

1. H. Gampp and A. D. Zuberbühler, in *Metal Ions in Biological Systems*, H. Sigel (ed.), Vol. XII, Dekker, New York, 1981.
2. A. I. Vogel, *Quantitative Inorganic Analysis*, 3rd Ed., p. 1054 ff. Longmans, London, 1966.
3. W. W. Umbreit, R. H. Burris and J. F. Stauffer, *Manometric Techniques*, Burgens, Minneapolis, 1957.
4. O. Warburg and G. Krippahl, *Ann.*, 1957, **604**, 94.
5. J. W. Timberlake and J. C. Martin, *Rev. Sci. Instr.*, 1973, **44**, 151.
6. D. D. Davis and K. L. Stephenson, *J. Chem. Educ.*, 1977, **54**, 394.
7. C. D. Thompson and N. Hackerman, *Rev. Sci. Instr.*, 1973, **44**, 1029.
8. H. Gampp, M. Maeder, A. D. Zuberbühler and Th. A. Kaden, *Talanta*, 1980, **27**, 513.
9. H. Gampp and A. D. Zuberbühler, in preparation.
10. *German Patent* No. 1230025, 1966; *Chem. Abstr.*, 1967, **19**, 488.
11. H. Gampp and A. D. Zuberbühler, *J. Mol. Cat.*, 1980, **7**, 81.

Talanta. Vol. 28, pp. 539 to 542. 1981
Printed in Great Britain. All rights reserved

0039-9140/81/070539-04$02.00/0
Copyright © 1981 Pergamon Press Ltd

CONSTRUCTION OF A MICROCOMPUTER-BASED REACTION-RATE RATEMETER

MARY ANDRIEU RYAN* and J. D. INGLE, JR.†

Department of Chemistry, Oregon State University, Corvallis, Oregon 97331, U.S.A.

(*Received* 11 *September* 1980. *Accepted* 24 *October* 1980)

Summary—The design and construction of a ratemeter based on a KIM-1 single-board microcomputer are discussed. The reaction monitor signal is digitized with a voltage–frequency converter and the resulting data points are stored in computer memory. Through software, the reaction-rate is calculated by the fixed-time computation method. A unique software–hardware combination is used for conversion from binary to binary-coded decimal format so that the results are printed in decimal notation. The characteristics of the ratemeter are compared with those of earlier ratemeters.

Modern instrumentation for reaction-rate measurements normally includes a ratemeter or circuitry to calculate and display the initial rate of a reaction, which is then related to the analyte concentration. This method is more advantageous than extracting the rate information from recorder or oscilloscope tracings because it is more rapid and convenient (*i.e.*, it reduces data-reduction time and provides instant feedback) and can also be more precise and accurate.

The fixed-time computation method is often used, in which the change in the reaction monitor signal over a fixed measurement time is calculated. This is usually done by integration of the reaction monitor signal over the whole measurement time.[1–4] By subtraction of the integral over the first half of the measurement time from the integral over the second half, a value is obtained which under suitable experimental conditions is proportional to the reaction-rate and the analyte concentration.[1–4] This fixed-time integration method was first implemented with analogue circuits using operational amplifiers[1] and later with entirely digital circuitry.[3,4] The digital-circuit calculation involved converting the analogue monitor signal into a train of pulses with a voltage–frequency converter (V/F) and directing these pulses into cascaded up–down counters. The up/down counting was used to achieve the integration and subtraction operations and the final digital result was output to a printer. Hard-wired timing circuitry was used in conjunction with switches for selection of delay and measurement times.

Another fixed-time digital integration system was devised[5] in which a minicomputer controlled the timing and functions of the external digital ratemeter and the rate information was output to a teletype. Here the timing functions could easily be changed since they were controlled by software.

Once a computer is incorporated in the kinetic-measurement system, several functions become available, including control of external hardware to monitor or control the experiment, storage of data, calculation of reaction rates, sophistication of data reduction, output of data in various formats, interaction with the operator, logical decisions on performing these functions, *etc.* Some researchers[2,6,7] have totally dispensed with any type of external ratemeter and digitized and stored the basic reaction-rate data in computer memory. Through software, the fixed-time or any other method of rate-computation (*e.g.*, least squares) can be used for calculating the rate.

With the development of inexpensive single-board microcomputers, a ratemeter designed around a dedicated microcomputer becomes economically attractive. This paper describes a ratemeter based on a KIM-1 microcomputer (MOS Technology, Inc., Norristown, PA). This KIM (keyboard interface monitor) ratemeter is more powerful and flexible than earlier such ratemeters.[1,3,4] In addition, data obtained during a reaction are stored to allow further calculations to be performed after the reaction. Since the functions of the KIM ratemeter are controlled by software, they may be easily modified. This ratemater is ideal for situations where low-level signals need to be measured precisely. It was designed to be used in fluorescence kinetic methods where the fluorescence signal increases with time. Although some commercial instruments for kinetic measurements use built-in microprocessors for rate calculations, the KIM ratemeter can be used to convert at little expense kinetic instrumentation not already using a microcomputer for rate calculations.

INSTRUMENTATION AND SOFTWARE

The features and operation of the KIM-1 are documented in detail.[8] The features pertinent to this application are (1) 1024 bytes (1 kbyte) of static random-access memory (RAM), (2) 14 input–output (I/O) lines that are

* Present address: Tektronix, Inc., P.O. Box 500, Beaverton, OR 97077, U.S.A.

† To whom correspondence and requests for reprints should be addressed.

bidirectional and individually programmable, (3) a cassette-tape interface for program and/or data storage or input, (4) a 20-mA current loop–teletype (TTY) interface, (5) an interval timer, (6) a 2-kbyte ROM (read-only memory) operating system which is the monitor in the KIM, (7) a six-digit seven-segment LED (light-emitting diode) display and (8) a 23-key hexadecimal (base-16) keypad.

With a single-board microcomputer such as the KIM, certain restrictions must be taken into account. These are the limited memory (1 kbyte) and limited number of I/O lines (14). Also, the computations must be kept simple to conserve memory and to minimize software development time. Of course these restrictions can be lifted (at additional expense) by adding extra memory boards, I/O boards, and software.

It was also desired to use the existing BCD (binary-coded decimal) printer in our laboratory rather than a teletype or a serial input printer which could be directly connected through the KIM–TTY interface. The printer requires that all lines (36 for the 9 BCD digits used here) be held at the proper signal level throughout the printing period (about 0.34 sec). Thus the use of this type of printer requires conversion of output data into BCD format and additional hardware for simultaneous output of 36 bits of information. The final design was based on working within these constraints and designing the system with minimal external hardware to simplify construction, and minimal software to retain a reasonable amount of the limited memory for data storage.

A block diagram of the KIM ratemeter is shown in Fig. 1 and a simplified flow diagram of the data-collection program is given in Fig. 2. Detailed schematics and flow diagrams as well as program listings (all in 6502 assembly language) are available from the authors on request. The circuitry external to the KIM is mounted on one printed-circuit (PC) board. The KIM and the additional PC board are powered by a supply which provides +12 V (0.5 A), ±15 V (0.5 A) and + 5 V (3 A).

The KIM ratemeter consists of four basic parts: digitization and input circuitry, the KIM with control and calculation software, printer-interface circuitry, and the printer. The input signal is digitized by using a V/F and counting or integrating the resultant pulses for a software-controlled integration period. The KIM interval timer is used to provide the basic timing interval. The longest possible convenient time interval of 0.25 sec was used for all work, but shorter times can be selected. The two binary counters along with the KIM act as the counter circuit. The printer interface and BCD conversion circuitry consists of 9 cascaded decade BCD counters. The KIM calculates a rate or voltage magnitude represented as a binary number. The BCD conversion is done by outputting a number of pulses equivalent to the binary result into the BCD counters through 3 I/O lines. The BCD counters hold the final result until the KIM sends a pulse by one I/O line to trigger the printer. One more I/O line is used to clear the BCD counters before the next conversion, and two more I/O lines, used previously for the input circuitry, are also used to provide a TTL (transistor-transistor logic) pulse to trigger an automatic injector.

The operation of the KIM ratemeter is as follows. The program is loaded from a tape cassette. Variables are input through the keypad and examined on the LED display. Four variables must initially be input: (1) the delay time (*i.e.*, number of 0.25-sec periods before data are taken), (2) the total integration time per data point (number of 0.25-sec integration periods during which the data are added together into one data word), (3) the type of calculation to be performed (rate and/or signal magnitude), and (4) the number of data points per calculation. Once the variables are entered, the operator starts the program by entering a specific address with the keypad and pushing GO. The program then causes a 30-μsec pulse to be output, which activates an automatic precision liquid-dispenser. The dispenser injects the last reagent, which initiates the reaction. A computer-controlled delay period allows time for mixing of the reactants and for any induction period of the reaction. After the delay period the pulse train from the V/F is gated to the two binary counters and the timing for that data point is begun. The overflow of the two binary counters (*i.e.*, the pulse train from the V/F divided by 256) is counted directly by the KIM and stored

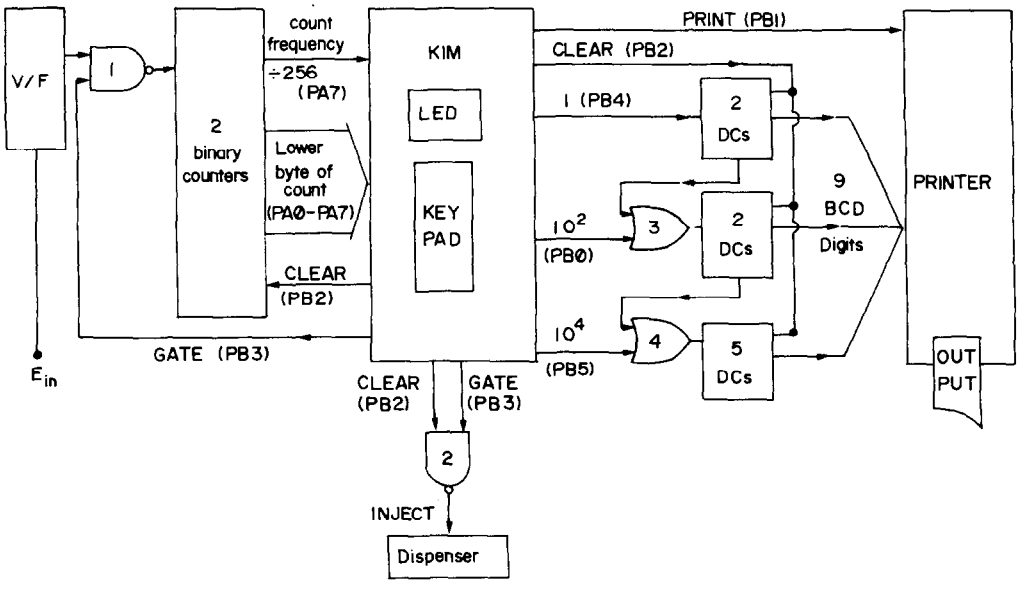


Fig. 1. Block diagram of KIM ratemeter. V/F = Teledyne Philbrick model 7405; binary counters = DM7493A; gates 1 and 2 = DM7403 Quad 2-input NAND gate; gates 3 and 4 = DM7432 Quad 2-input OR gate; DC = DM7490 decade counter; printer = Newport Model 810. Not shown: V/F output buffered by DM74126 tri-state buffer; PB2 I/O line buffered by DM7407 hex buffer; PA0–PA7 are bits 0–7 and PB0–PB5 are bits 0–5 of the A and B I/O ports of the KIM.

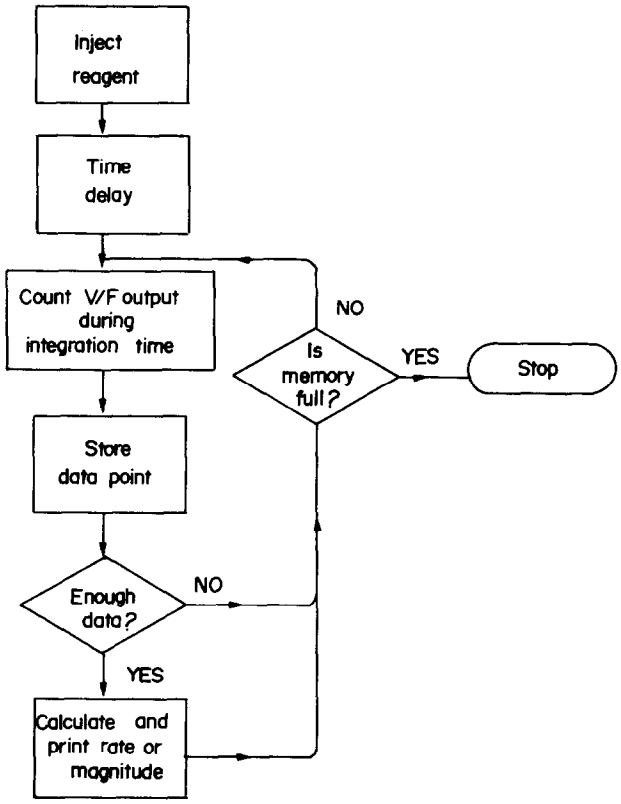


Fig. 2. Simplified flow diagram of KIM ratemeter data-collection program.

in the upper byte of the data point. At the end of the integration time the 8 bits from the two binary counters are transferred and stored in the lower byte of the 16-bit data point. This process of obtaining and storing data points is repeated until the requested number of data points have been accumulated, at which point the specified calculation is made, the BCD counters are cleared, the binary to BCD conversion is made, and a 90-msec pulse is sent to activate the printer. After a 0.34-sec delay for printing, the process of data collection, calculation, and printing will be repeated until the memory allotted for data storage (102 2-byte data points) is full or the operator overrides the program by pushing the ST (stop) key. Rate and/or magnitude calculations are performed and printed during the reaction only if the requested number of data points per calculation is less than 102.

Rates are obtained by subtracting the sum of the data points in the first half of the measurement period from the sum of the data points in the last half of the measurement period. This is identical to the rate calculation process in a hardware digital ratemeter previously reported.[3] Signal magnitudes are calculated by summing the requested number of data points. Since each data point is 2 bytes (double precision), the rate and magnitude calculations are performed in triple precision (3 bytes).

After the memory is full or the operator has halted the run, the collected data are still in memory. By input of new variables through the keypad, rates and/or magnitudes, with different delay or total measurement times from those chosen before the kinetic run, can be calculated and printed in the same manner and by use of the same subroutines as the calculations described earlier.

The V/F type of ADC (anologue to digital converter) was chosen over other types of ADC (*e.g.*, successive approximation) because, when conversion speed is not critical, it provides the highest resolution, the largest dynamic range, and excellent linearity, at the lowest cost. The V/F used has an output of 100 kHz/V up to 10 V, with less than 0.02% non-linearity. With a 1-sec integration time it has a resolution of 10 μV and a dynamic range of 10^6.

The KIM could be used to count the V/F pulses directly (with an additional "monostable" to stretch the pulse width) but the maximum frequency would be limited to about 20 kHz owing to the length of the software counting loop which detects level changes, and thus would curtail input voltage to 0.2 V as well as limit the dynamic range. Since the KIM is used to count the overflow from two external cascaded 4-bit binary counters, frequencies up to 5 MHz and the full dynamic range of the V/F may be used. Doing this increases the amount of software slightly and also the number of I/O lines required. More software is needed to transfer the 8 bits of information in the binary counters to computer memory. Eight I/O lines are required to transfer these data (one of these I/O lines is also used for the overflow) and two more I/O lines to clear and gate the counters.

The software and hardware for BCD conversion were chosen for speed to reduce the dead-time (*i.e.*, the time during which no data are taken). If one I/O line was directed into the input of the first of 9 cascaded decade counters, it would take over 2 min to count by ones from 0 to 2^{24} (16,777,215 in decimal notation). To reduce the conversion time, one pulse is output first for each 10^4 unit, then each 10^2 unit, and finally each 10^0 unit in the 3-byte data word. Note that the I/O line for the 10^4 count is linked by an OR gate with the output from the fourth decade counter (DC) and the I/O line for the 10^2 count with the output of the second DC. This conversion is done in software by subtracting 60,000 from the most significant (MS) byte of the 3-byte data word if it is non-zero, and

outputting 6 pulses to the fifth DC. This is repeated until the MS byte becomes zero. Next 200 is subtracted from the second byte if it is non-zero and 2 pulses are output to the third DC. This is repeated until the second byte becomes zero. Finally a number of pulses equal to the value in the lowest byte is output to the first DC. This BCD conversion routine takes about 90 msec and the rate calculation typically takes less than 10 msec, so the printing time of 340 msec limits the dead-time. Without BCD conversion, printing and calculation, the dead-time between data points is about 64 μsec.

Since each data point is composed of two bytes in the computer memory, the largest decimal number corresponding to a data point is 65535. Since the V/F outputs 100 kHz/V, signal levels up to 655 mV can be accommodated when each data point represents 1.0 sec, or up to 2.62 V when each data point is 0.25 sec. An error message is printed if a data point overflows two bytes or if the rate calculated is negative. The integration time could be reduced (*e.g.*, by changing the number in two locations) to 0.065 sec, with one integration per data point, to use the full 10-V range of the V/F. The 0.25-sec integration time normally used is more than sufficient for fluorescence rate measurements.

The 102 2-byte data points stored may represent integration times from 0.25 to 64 sec. Thus total times of 25.5–6528 sec may be represented by the 102 stored data points. All data are stored in page zero, whereas the program occupies most of the three remaining 256-byte pages of the RAM.

RESULTS AND DISCUSSION

The ratemeter was tested in terms of linearity, accuracy, and precision with respect to signal level, rate, and integration time, as previously described for a hardwired ratemeter.[4] Excellent accuracy and linearity were obtained and were comparable to those obtained previously[4] as expected since the V/F and basic rate-computation technique were the same as previously used. Typical standard deviations of steady-state signals from a reference voltage source (Heath model EU-80A) were about 1 count (10 μV) for integration times of 1–16 sec.

One of the significant advantages of the KIM ratemeter over the hardware ratemeter[4] is its ability to store the data points obtained during a reaction. This is valuable in two ways. First it allows recalculations to be performed on the same data but with different integration times or delay periods, and signal magnitudes and/or rates to be determined without repetition of the experiment. Secondly, it gives a significantly shorter dead-time between data points than do hardwired ratemeters,[1,3,4] since the data over a large part of the reaction curve can be obtained without printing and later the rate over short reaction periods can be calculated. With a hardwired ratemeter[4] or even a minicomputer-controlled ratemeter with external up–down counters,[5] the rate can only be calculated over the preselected measurement time and no data can be obtained during printing (typically 0.3 sec). Thus the KIM ratemeter is more suitable for fast rate-measurements such as with stopped-flow apparatus.

CONCLUSIONS

The KIM ratemeter is a useful addition to kinetic instrumentation. At $170 the KIM-1 microcomputer is inexpensive enough to be dedicated to this application. It is convenient to use, is small, and has low power requirements. The KIM ratemeter performs precise and accurate rate and/or magnitude calculations. It has significant advantages over hardware ratemeters because of its speed, flexibility, and data-storage capability. The design of the circuitry allows input of current or voltage to the V/F, or the input of an external pulse train from another source (*e.g.*, photon counting) to the counting circuit.

The KIM can be easily upgraded with a motherboard and more memory to allow a higher level language to be used for more sophisticated calculations, other types of rate calculation (*e.g.*, variable time, least squares), and interaction with an operator. Other more recent 6502-based single-board microcomputers such as the AIM (Rockwell International Corporation, Anaheim, CA) and SYM (Synertek Systems Corporation, Santa Clara, CA) could also be used to enhance its capabilities since they include an 8-kbyte BASIC interpreter and 4 kbytes of RAM on board. The circuits and assembly-language subroutines of the KIM ratemeter would still be valuable for data collection and output on the printer.

Acknowledgements—Acknowledgement is made to the NSF (grants CHE-76-16711 and CHE-79-21293) for partial support of this reasearch, and one of us (M.A.R.) gratefully acknowledges an NSF graduate fellowship and an American Chemical Society, Division of Analytical Chemistry Summer Fellowship sponsored by General Motors Research Laboratory.

REFERENCES

1. E. M. Cordos, S. R. Crouch and H. V. Malmstadt, *Anal. Chem.*, 1968, **40**, 1812.
2. H. V. Malmstadt, C. J. Delaney and E. A. Cordos, *ibid.*, 1972, **44**, No. 12, 79A.
3. J. D. Ingle, Jr. and S. R. Crouch, *ibid.*, 1970, **42**, 1055.
4. R. L. Wilson and J. D. Ingle, Jr., *Anal. Chim. Acta*, 1976, **83**, 203.
5. E. S. Iracki and H. V. Malmstadt, *Anal. Chem.*, 1973, **45**, 1766.
6. G. E. James and H. L. Pardue, *ibid.*, 1969, **41**, 16.
7. B. G. Willis, J. A. Bittikofer, H. L. Pardue and D. W. Margerum, *ibid.*, 1970, **42**, 736.
8. *KIM-1 Microcomputer Module*, Publications 6500-15B, 6500-10A, 6500-50A, MOS Technology, 950 Rittenhouse Rd., Norristown, PA, U.S.A., 1976.

Talanta, Vol. 28, pp. 543 to 546, 1981
Pergamon Press Ltd. Printed in Great Britain

0039-9140/81/070543-04$02.00/0

DATA-LOGGING SYSTEM BASED ON THE INTEL 8748 SINGLE-CHIP MICROPROCESSOR

R. M. BELCHAMBER and GARY HORLICK

Department of Chemistry, University of Alberta, Edmonton, Alberta, Canada

(*Received* 5 *December* 1980. *Accepted* 8 *January* 1981)

Summary—A simple microprocessor-based data-acquisition system is presented that is capable of acquiring replicate integrated signal values and logging them to a serial data terminal.

One of the most common data-logging tasks in the laboratory is the acquisition of repeated measurements of an averaged or integrated signal. A versatile way to integrate a signal is through the summation of a large number of rapidly acquired digitized signal values.[1] For example, if a measurement system is capable of acquiring digitized signal values at a rate of 1000 conversions per second, it is simply necessary to sum 10, 100, 1000, or 10,000 conversions to obtain precise signal integration periods ranging from 10 msec to 10 sec. A simple microprocessor-based system has been developed in our laboratory to acquire integrated signal values in this fashion.

The microprocessor chosen for this application was the Intel 8748. This is a so-called single-chip microcomputer in that it contains, in *one* integrated circuit, all the main functional units of a complete computer,[2] *i.e.*, a central processing unit (CPU), input/output (I/O) ports, a timer/event counter, random access memory (RAM) and read only memory (ROM). The specific features of the 8748 are summarized in Table 1 and a block diagram of the chip is shown in Fig. 1.

The 8748 is one chip in the "8048" family of single-component 8-bit microcomputers.[3] A summary of the "8048" family of microcomputers is presented in Table 2. The 8748 is the development chip for the 8048. The difference between the two chips is that the 8748 has erasable programmable read only memory (EPROM) while the 8048 is strictly ROM-based, *i.e.*, it must be factory-programmed. In general, the 8048 family was developed for high-volume control applications and once a user has developed a set program using the 8748 or the 8035 or 8039 with off-chip RAM or EPROM, factory mask-programmed 8048s or 8049s can be manufactured. Within this family the 8022 (see Table 2) seems almost ideal for laboratory data-acquisition as it contains an on-chip analogue-to-digital converter (ADC). However, this chip is again ROM-based, limiting its usefulness to users of it in quantity. Thus, the 8748 is the only single-chip microcomputer in this family that can be effectively utilized by users of one or a few chips. However, as outlined in Table 1, it has excellent features and capabilities that should allow the development of a very compact intelligent data-acquisition system with a minimal number of integrated circuits.

Table 1. Summary of 8748 features

1. Full 8-bit central processing unit
2. Data memory (RAM)—64 words × 8 bits
3. Program memory (EPROM)—1024 × 8 bits
4. Input/output ports
   (*a*) Ports 1 and 2
   —each 8 bits wide
   —all pins independantly programmable as either input or output
   —outputs latched
   —inputs not latched
   (*b*) Bus port
   —8-bit bidirectional port
   —all pins either input or output
   —outputs latched
   —inputs not latched
5. Input lines
   —3 input lines T0, T1 *and* testable with the conditional jump instruction and INT an interrupt
6. Timer/counter
   —8-bit binary presettable counter

The Intel Prompt 48 unit was used for system development, program debugging and EPROM programming. It should be noted that the 8048 family has its own language that is not compatible with 8080/85s.

A schematic diagram of the data-acquisition system is shown in Fig. 2. It consists of a sample-and-hold amplifier, an analogue-to-digital converter and the 8748 microprocessor. The teletype interface for the 8748 is shown in Fig. 3. These circuits were breadboarded with a Model ADD-8000 analogue–digital designer available from E & L Instruments. This unit provides SK-10 breadboard cards for circuit construction which fit into a mainframe containing power supplies, logic-level switches and indicators, a voltage reference source and a function generator.

The sample-and-hold amplifier (AD582) and the analogue-to-digital converter (AD571) were obtained from Analog Devices. The sample-and-hold amplifier has a combined aperture and settling time (to 0.01%) of about 0.6 μsec and an acquisition time of about 6 μsec. The AD571 is a 10-bit successive approximation ADC with a conversion time of 25 μsec. Only the

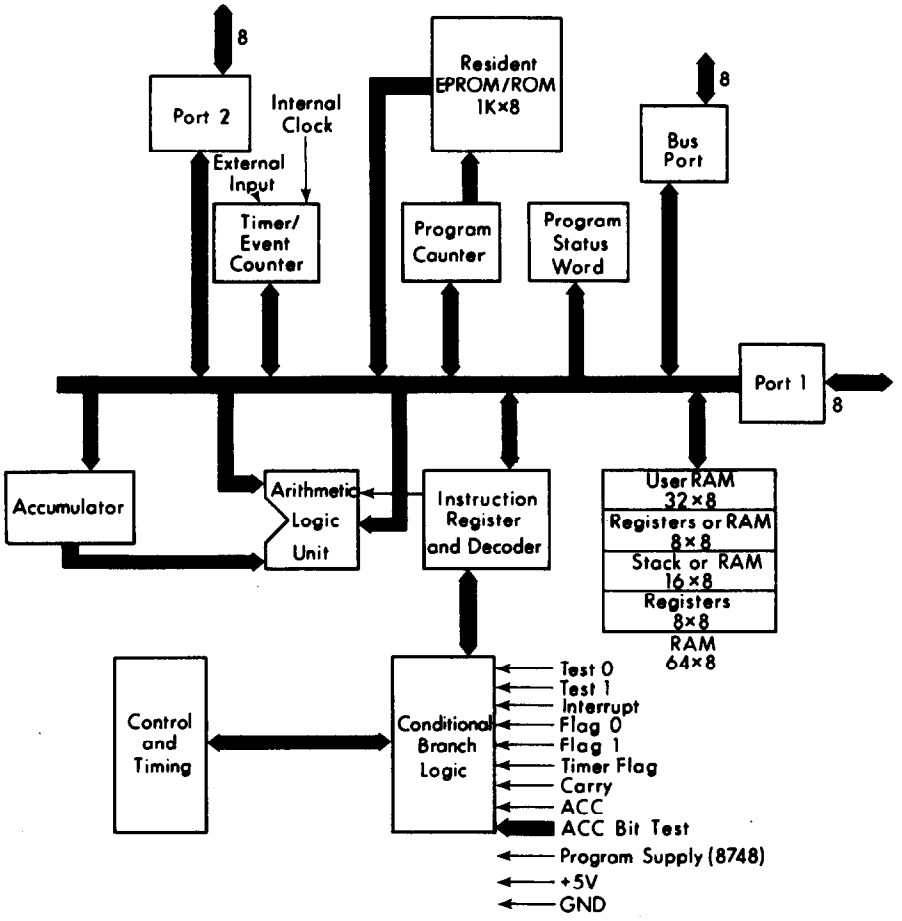


Fig. 1. Block diagram of 8748.

eight most significant bits are used in this application. This significantly simplified both the hardware aspects of data acquisition and the software complexity, which was particularly important as programming space was at a premium. An 8-bit conversion provides adequate resolution when a large number of conversions are summed to provide an integrated signal value. This point is discussed and illustrated in a companion paper.[4] The dynamic range of the ADC was set at 0–10 V, resulting in a quantization limit of 39 mV. The eight digital lines from the ADC were interfaced to the 8748 through Port 1.

Table 2. "8048" Family of single-component 8-bit microcomputers

8048—1-kbyte ROM, 64-byte RAM, 27 I/O lines, 8-bit timer/counter, full CPU
8748—EPROM version of 8048
8035—8048 without on-chip ROM
8049—2-kbyte ROM, 128-byte RAM, version of 8048
8039—8049 without on-chip ROM
8021—1-kbyte ROM, 64-byte RAM, 21 I/O lines, 8-bit timer/counter, full CPU
8022—2-kbyte ROM, 64-byte RAM, 28 I/O lines, on-chip 8-bit ADC with sample-and-hold and two multiplexed input channels.

The sample-and-hold amplifier and the analogue-to-digital converter were interconnected as recommended in literature supplied by Analog Devices.[5] A conversion is initiated by a positive pulse generated at bit 5 of Port 2. This puts the sample-and-hold amplifier in the hold mode and triggers the ADC. The amplifier is held in the hold mode by the $\overline{DR}$ (NOT data ready) line of the ADC, which remains high during conversion. The return of the $\overline{DR}$ to the low state at the end of conversion is sensed at the T0 input line of the 8748 and the 8-bit value is read into the 8748. At the same time the sample-and-hold amplifier returns to the track mode.

Inside the 8748 the new 8-bit value is added to the sum of the previous conversions. The addition is carried out in triple precision (24 bits). This allows a maximum of 65,536 full-scale 8-bit ADC conversions to be accumulated. After the addition, the program checks to see whether the requested number of conversions have been summed, and if not, initiates another conversion. The number of conversions to be summed in order to achieve the desired signal-integration period is hardware-set at pins of Port 2 which are read at the start of the data-acquisition program. Application of a positive 1 logic level at the appropriate pin selects 1, 10, 100, 1000, 10000 or 65,536

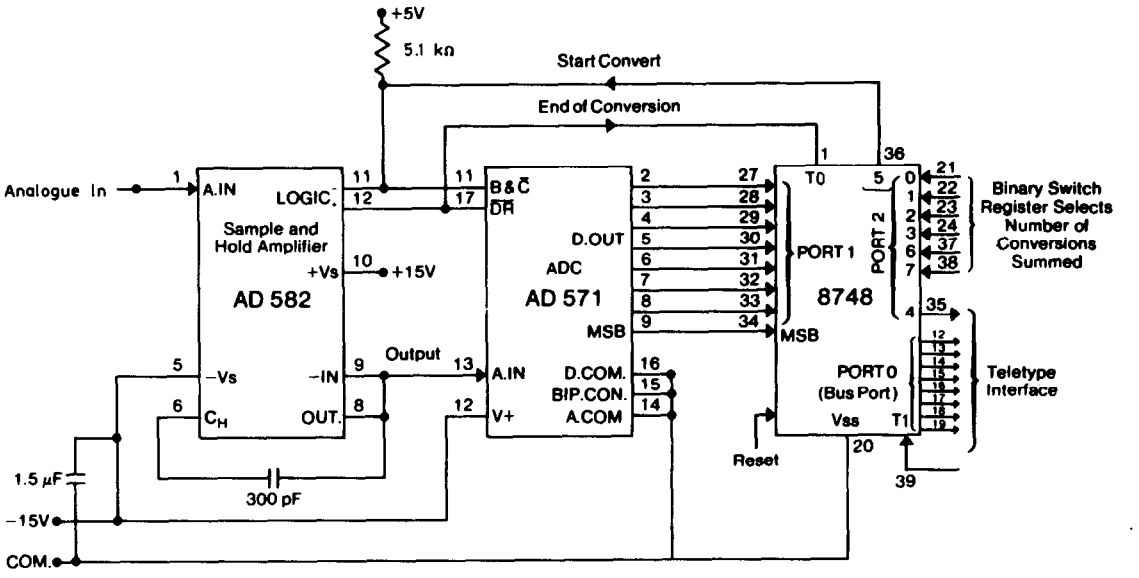


Fig. 2. Schematic diagram of the data-acquisition system.

conversions to be summed. When the selected number of conversions have been summed the 24-bit binary sum is converted into an 8-digit BCD number and output to the teletype. The basic data-rate for conversion is 4.4 kHz, thus a summation of 65,536 conversion represents an integration period of about 15 sec. The acquisition of replicate integrated measurements was also programmed into the software. For our applications 32 replicate integrated measurements were automatically sequenced and logged to the teletype. This allowed the reliable calculation of statistical quantities of the measured values, such as standard deviation and signal-to-noise ratios. Unfortunately, this simple 8748 system was not large enough to do such calculations directly.

The 8748 was interfaced to the teletype by means of an universal asynchronous receiver transmitter (UART)[6] through the bus port, Port 0 (Fig. 3). The output routine converts the BCD digits into 7-bit ASCII code which the UART then transmits serially to the teletype. The transmission of a character is initiated by application of a positive pulse to the data strobe input of the UART from bit 4 of Port 2 on the 8748. The UART must be externally clocked at a rate appropriate for the device to which data are being sent. Teletypes operate at 110 baud (110 bits/sec). The clock frequency, provided by the function generator on the ADD-8000 breadboard system, was set at 1760 Hz. This is the correct input frequency in order to allow the UART to transmit data at 110 baud. When

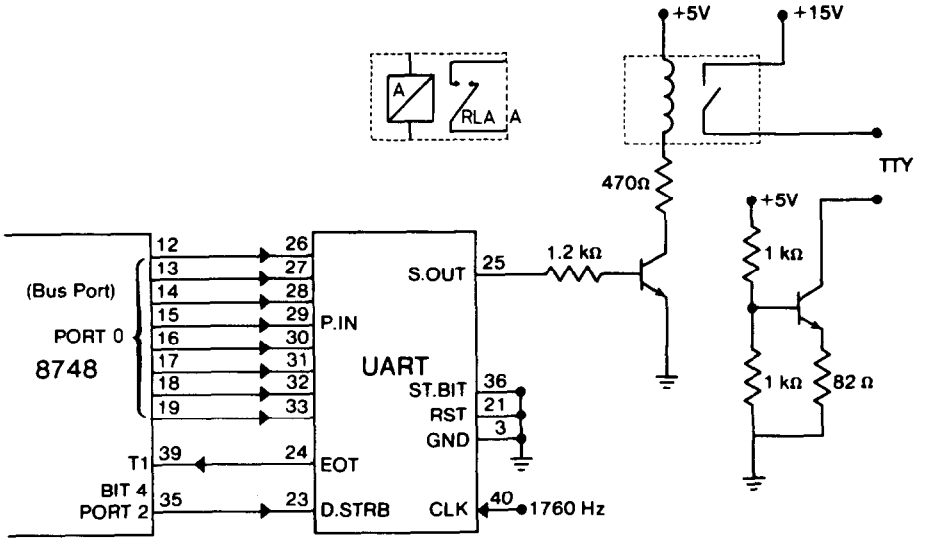


Fig. 3. Schematic diagram of the 8748-teletype interface. The inset in dashed lines is a relay and is shown in both American and European symbols.

transmission of a single character is complete, the end of transmission (EOT) line of the UART is sensed at the T1 input line of the 8748 and the next character is output. The rest of the circuitry in Fig. 3 provides the 20-mA current loop used to interface the UART to the teletype.[6]

In this application the teletype was used as a passive printer and information could not be transmitted to the 8748 from it. One practical reason was the fact that the unexpanded 8748 did not contain sufficient programming space to accommodate the necessary programs. On the other hand, this was also in keeping with our basic philosophy of keeping the system small. We did not want a system that required inputs from an expensive device such as a teletype in order to function. That is also why, in fact, a simple switch register was used to select the integration period.

In conclusion, the 8748 single-chip microcomputer can be used to develop simple intelligent data-logging systems. The system discussed and illustrated here consists of only four integrated circuits, the sample-and-hold amplifier, the analogue-to-digital converter, the 8748 and the UART. It is capable of acquiring digitized signal values with a resolution of 8 bits at rates up to 4.4 kHz. Preselected numbers of conversions can be summed to obtain integrated signal measurements. Summation is carried out in triple precision (24 bits) and up to 32 replicate measurements can be sequentially acquired and logged, in BCD format, to a serial terminal such as a teletype. The measurement capability of this system is discussed and illustrated in some detail in a companion paper.[4]

It must be pointed out, however, that without the ADD-8000, a timer chip and power-supply chips would also be required, and that the need for a support system such as the Intel Prompt 48 for development may prove too expensive unless other uses can be found for it.

REFERENCES

1. M. W. Blades and G. Horlick, *Talanta*, 1981, **28**, 527.
2. G. Horlick, *ibid.*, 1981, **28**, 487.
3. *MCS-48 Microcomputer Users Manual*, Intel Corporation, 3065 Bowers Ave., Santa Clara, CA 95051.
4. R. M. Belchamber and G. Horlick, *Talanta*, 1981, **28**, 547.
5. Analog Devices, Route 1, Industrial Park, P.O. Box 280, Norwood, Mass 02062. AD571 Product Information.
6. D. G. Larsen and P. R. Rony, *Bugbook IIA, Using the Universal Asynchronous Receiver/Transmitter*, E & L Instruments, Inc., Derby, Conn. 06418, 1975.

Talanta, Vol. 28, pp. 547 to 549, 1981
Pergamon Press Ltd. Printed in Great Britain

0039-9140/81/070547-03$02.00/0

SHORT COMMUNICATION

USE OF ADDED RANDOM NOISE TO IMPROVE BIT-RESOLUTION IN DIGITAL SIGNAL AVERAGING

R. M. BELCHAMBER and GARY HORLICK
Department of Chemistry, University of Alberta, Edmonton, Alberta, Canada

(*Received* 5 *December* 1980. *Accepted* 8 *January* 1981)

Summary—A simple equation is presented that can be used to predict the improvement in bit-resolution that can be obtained by digital signal averaging in the presence of added random noise.

Digital signal averaging is one of the most common instrumental methods used today to improve the signal-to-noise ratio of a measurement. It is important to keep in mind that for digital signal averaging to be effective a certain amount of noise *must* be present in the signal. In the absence of noise an averaged signal will be distorted by quantization effects which result from the finite bit-resolution of the analogue-to-digital converter (ADC) associated with the digital signal averager and no amount of averaging can remove these effects or improve measurement precision or accuracy. If a relatively small amount of random noise is present in the signal (standard deviation of the noise equal to about one half of the quantization level, *i.e.*, the least significant bit, of the ADC) then the net effect of quantization is to increase the variance of the signal by $q^2/12$ where q is the magnitude of the quantization level.[1–3] Thus, if quantization effects are severe (*i.e.*, the original signal is noise-free relative to the bit resolution of the ADC) it will be advantageous to *add* random noise to the signal before averaging the digitized values.[4–6] In this communication a simple practical equation is presented that can be used to estimate the effective bit-resolution that can be achieved by signal averaging in the presence of added random noise.

As mentioned above, with sufficient noise in a signal the effect of quantization, under signal averaging, is to increase the variance of the signal by $q^2/12$. Thus the total signal variance (V_T) may be expressed as:

$$V_T = \frac{q^2}{12} + (qf)^2 \qquad (1)$$

where q is the magnitude of the quantization level and $(qf)^2$ is the variance of the noise added to the signal, expressed in units of the quantization level. Thus, if the standard deviation (or root-mean-square value) of the added random noise is twice the magnitude of the quantization level, f would be 2. Signal averaging in the presence of random noise improves the signal-to-noise ratio [defined as (signal/standard deviation)] in proportion to the square root of the number of signal repetitions averaged ($N^{1/2}$), thus the final signal-to-noise ratio $(SNR)_F$ may be expressed as:

$$(SNR)_F = \frac{S}{q\left(\frac{1}{12} + f^2\right)^{1/2}} \cdot N^{1/2} \qquad (2)$$

where S is the magnitude of the signal. It is instructive to express equation (2) in terms of effective bit-resolution $(BR)_{eff}$ of the final signal-to-noise ratio, *i.e.*, $\log_2[(SNR)_F]$:

$$(BR)_{eff} = \log_2\left(\frac{S}{q}\right) - \tfrac{1}{2}\log_2\left(\frac{1}{12} + f^2\right) + \tfrac{1}{2}\log_2 N \qquad (3)$$

The first term of equation (3) represents the bit-resolution of a single measurement. It is important to emphasize that this is *not* equal to the bit-resolution of the ADC but is proportional to the ratio of the relative magnitude of the signal to the quantization level of the ADC. The full bit-resolution of an ADC is utilized only when the signal fills the dynamic range of the ADC. The second term represents the loss in bit-resolution due to quantizing effects and the level of added noise. The third term represents the build-up of bit-resolution that results from signal averaging when the least significant bit of the ADC is randomized.

A simple microprocessor-controlled data-logger[7] was used to obtain data to test equation (3). This system (based on the Intel 8748) contained an 8-bit successive approximation ADC with a dynamic range of 0–10 V and a quantization level of 39 mV. The ADC was front-ended with a sample-and-hold amplifier. Eight-bit conversions could be acquired at a rate

Table 1. Bit resolution of ADC measurements

f	Conversions summed	Effective precision of ADC, *bits* Experimental	Equation (3)
0.5	1	7.6	6.8
	10	8.5	8.5
	100	9.9	10.1
	1000	12.1	11.8
	10000	13.8	13.4
	65536	14.4	14.8
1.0	1	6.1	5.9
	10	7.6	7.6
	100	9.1	9.2
	1000	11.1	10.9
	10000	12.5	12.6
	65536	13.6	13.9
2.0	1	4.5	5.0
	10	6.7	6.7
	100	8.6	8.3
	1000	10.1	10.0
	10000	11.5	11.6
	65536	12.7	13.0

of 4.4 kHz and up to 65,536 successive conversions could be summed. The sum was accumulated with triple precision (*i.e.*, 24 bits). Finally, 32 repeat measurements of the summed conversions were automatically acquired and logged to a teletype by this system. Complete details are provided elsewhere.[7]

Input d.c.-level analogue test signals were generated with a 16-bit digital-to-analogue converter (Data Systems DAC-169). By use of this DAC, voltage levels over the range 0–10 V could be generated that were variable in steps as small as 0.153 mV. This DAC was used to provide a stable test signal to which various levels of random noise were added. A General Radio 1390B random-noise generator was used as the noise source. The DAC and noise signals were summed together with an operational amplifier.

Test signals were generated consisting of a 5-V d.c. level upon which was superimposed 20-mV, 40-mV and 80-mV rms random noise (5 Hz–20 kHz bandwidth). These noise levels correspond to $f = 0.5$, 1 and 2. The data logger outlined above was used to acquire 32 repeat measurements of one ADC conversion and 32 repeat measurements of 10, 100, 1000, 10,000 and 65,536 summed ADC conversions. On the basis of the 32 repeat measurements the standard deviation (σ) of the acquired signal in each case could be calculated and the signal-to-noise ratio ($\overline{S}/\sigma$) evaluated. The resulting values, expressed in terms of bit-resolution [$\log_2(\overline{S}/\sigma)$], are presented in Table 1 along with those calculated from equation (3). The agreement is quite good. Thus, if the measurement system is amenable to signal averaging, the effective bit-resolution of an ADC can be significantly improved if averaging is carried out in the presence of sufficient random noise. Equation (3) is useful in estimating the benefit to be gained.

This improvement in bit-resolution is further illustrated in Fig. 1. The DAC was again used to provide a test signal, but this time the output of the DAC was set at 2.500 V and then increased by 2.5-mV increments to 2.550 V. The data logger was used to measure 1000 summed conversions at each incremental value, with and without added random noise (20-mV rms $\equiv f = 0.5$). Without added random noise, the 8-bit ADC of the data logger can clearly only resolve signal changes of at least 39-mV (*i.e.*, the value of the least significant bit) even if digitized values are summed. From Table 1, with 20-mV rms added random noise and 1000 summed conversions, the effective bit-resolution should improve to about 12 bits, making the least significant bit equivalent to about 2.5 mV. It can be seen in Fig. 1 that 12-bit resolution is achieved because 2.5-mV incremental changes in DAC output are accurately measured

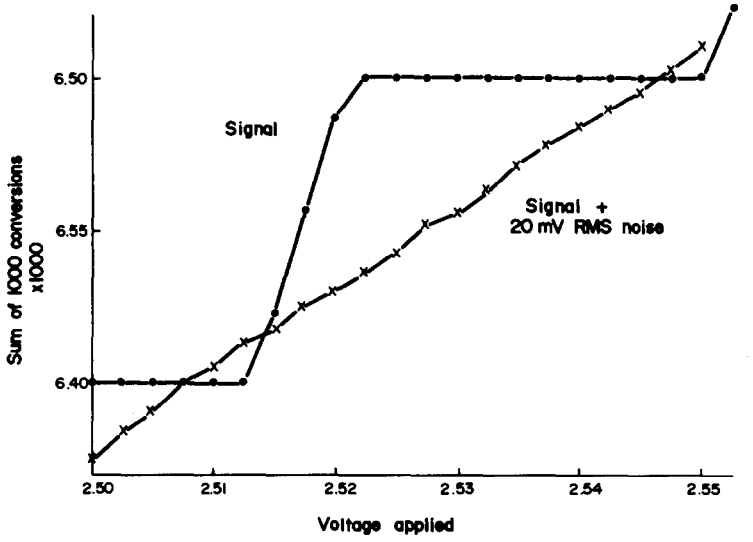


Fig. 1. Bit-resolution improvement of 8-bit ADC to 12 bits by signal averaging with added random noise (see text for discussion).

when averaging is carried out in the presence of this level of added random noise.

The examples presented in this paper have focused on 8-bit ADCs because this is the most convenient word length to manipulate in and interface to 8-bit microprocessors. In addition, some manufacturers have developed microprocessors with self-contained 8-bit ADCs and DACs. Examples are the Intel 8022 and 2920. With the considerations discussed here, these systems need not be thought of as limited to 8-bit precision or resolution when used for data acquisition. All considerations presented are, of course, equally applicable to higher resolution conversions. In fact the incremental cost in moving from a 12-bit converter to say a 16-bit converter is quite high. Thus, if data-acquisition time allows, signal averaging can be used to achieve the desired higher bit-resolution. Finally, the considerations presented in this paper lead to some interesting conclusions about lower resolution converters. If the signal is noisy enough it should be possible to relax the bit-resolution specification for the ADC used. In fact with very noisy signals it is possible to relax the specification all the way to a *one*-bit converter, *i.e.*, a comparator or threshold detector. This measurement approach has recently been discussed in the literature[8] and such one-bit converters have been successfully utilized to facilitate the digital data-acquisition of repetitive noisy signals at very high sampling rates.[9]

REFERENCES

1. B. Widrow, *Trans. Am. Inst. Elec. Eng.*, 1961, **77**, 555.
2. P. C. Kelly and G. Horlick, *Anal. Chem.*, 1973, **45**, 518.
3. L. M. Schwartz, *ibid.*, 1980, **52**, 1141.
4. I. Coleman, *J. Opt. Soc. Am.*, 1966, **56**, No. 8, IV.
5. J. Butterworth, P. E. MacLaughlin and B. C. Moss, *J. Sci. Instrum.*, 1967, **44**, 1029.
6. G. Horlick, *Anal. Chem.*, 1975, **47**, 352.
7. R. Belchamber and G. Horlick, *Talanta*, 1981, **28**, 543.
8. Z. L. Kovacs, *IEEE Trans. Instrum. Meas.* 1979, **IM-28**, 152.
9. T. G. Schmalz and W. H. Flygare, in *Laser and Coherence Spectroscopy*, J. I. Steinfeld (ed.), p. 136. Plenum Press, New York, 1978.

Talanta. Vol. 28. pp. 551 to 556. 1981
Printed in Great Britain. All rights reserved

0039-9140/81/080551-06$02.00/0
Copyright © 1981 Pergamon Press Ltd

SELECTIVE METAL SORPTION ON CROSS-LINKED POLY(VINYLPYRIDINE) RESINS

ATSUSHI SUGII, NAOTAKE OGAWA, YUKIKAZU IINUMA and HISASHI YAMAMURA
Faculty of Pharmaceutical Sciences, Kumamoto University, Kumamoto 862, Japan

(*Received* 29 *April* 1980. *Revised* 3 *February* 1981. *Accepted* 15 *February* 1981)

Summary—The sorption behaviour of several metal ions on five kinds of poly(4- or 2-vinylpyridine) resins, cross-linked with divinylbenzene, and with different surface properties, are examined. All the resins proposed sorb some metal ions effectively in a similar manner by anion-exchange, while the sorption of metal ions by complex formation with the pyridine moiety is strongly affected by the surface properties of the resins. A macroreticular poly(4-vinylpyridine) resin shows high affinity for copper and nickel ions in acetate buffer. Sodium chloride and/or methanol added to the working solutions influence the sorption capacities for metal ions. This resin was applied to the separation of copper/cobalt and nickel/cobalt and the concentration of copper from sea-water by a column operation.

A number of chelating ion-exchange resins have been prepared for the separation and/or enrichment of metal ions. Attempts to use poly(vinylpyridine) resins, in which the pyridine moiety takes part in complex formation, for the separation of metal ions have been made by several investigators. Wolf *et al.*[1] prepared some amphoteric resins by emulsion copolymerization of 4-vinylpyridine, acrylonitrile (or acrylic acid) and divinylbenzene, and explored their ion-exchange behaviour toward certain metal ions. Another type of amphoteric resin containing the pyridine group and used for the separation of platinum from palladium was reported by Popov *et al.*[2] The complex-forming properties of resins based on copolymers of *N*-[β-(5-vinyl-2-pyridyl)ethyl]amine and *N*,*N*′-bis[β-(5-vinyl-2-pyridyl)ethyl]-substituted diamine have been studied with respect to copper, cobalt and nickel ions.[3] The selective sorption and desorption of silver with poly(vinylpyridine) resins were reported by Saldadze *et al.*[4] Nishide and Tsuchida[5] also reported selective sorption of metal ions on cross-linked poly(4-vinylpyridine) resins prepared with a metal ion as template. However, no detailed report has been found on the relation between the surface properties of poly(vinylpyridine) resins and the sorption of metal ions.

This paper describes the sorption behaviour of several metal ions on five kinds of cross-linked poly(vinylpyridine) resins with various surface properties. The effect of the surface properties of the resins on metal sorption is discussed on the basis of ion-exchange and complex formation. In addition, the separation of cobalt/copper and cobalt/nickel and the concentration of copper from sea-water by using a macroreticular poly(4-vinylpyridine) resin are described.

EXPERIMENTAL

Materials and reagents

Macroreticular (MR) type poly(4-vinylpyridine) (4VP) and poly(2-vinylpyridine) (2VP) resins cross-linked with divinylbenzene were prepared by the method previously reported[6] and purified by washing successively with 1*M* hydrochloric acid, water, 1*M* sodium hydroxide, water and methanol. After drying under vacuum, the resins were screened to 35–60 mesh. Gel-type 4VP resin was prepared by the method described for MR resins, except for the diluent, and purified in the same way as the MR resins.

The radioisotopes ^{59}Fe, ^{60}Co, ^{63}Ni, ^{65}Zn, ^{109}Cd and ^{203}Hg (as chloride or nitrate) supplied by the New England Nuclear Corp. and the Radiochemical Centre Amersham were used as tracers. All other reagents used in this study were reagent grade.

Apparatus

The radioactivity of the tracers, with the exception of ^{63}Ni, was measured with a sodium iodide crystal detector (Aloka Co., Ltd., models TDC-5U and NDW-351). In the case of ^{63}Ni, a liquid scintillation counter (Aloka Co., Ltd., LSC-502) was used for the β-counting. Manganese(II), copper(II), palladium(II), tin(IV) and gold(III) were determined by complexometric titration or with a Shimadzu AA-610S atomic-absorption spectrophotometer.

Sorption of metal ions by batch operation

Unless otherwise stated, the test solutions were shaken with 100 mg of each resin for 24 hr, and the other experimental conditions were the same as described in a previous paper.[7] For the adjustment of pH, an acetate buffer (1*M*) and hydrochloric acid were used in the pH ranges of 3–7 and 1–2, respectively.

Separation of cobalt and copper

One gram of 4VP-T(20) was packed into a glass tube (0.5 × 20 cm) and conditioned with 30 bed-volumes of 1*M* acetate buffer (pH 4.0). After conditioning, 1 ml of a mixed solution of cobalt(II) and copper(II) spiked with the radioisotope (^{60}Co) was poured onto the upper surface of the column and then 50 ml of the acetate buffer were allowed to pass through the column at a flow-rate of

0.4–0.6 ml/min. Copper retained on the column was eluted with 1*M* hydrochloric acid.

Separation of cobalt and nickel

Two grams of 4VP-T(20) were slurried with 1*M* acetate buffer (pH 4.0) containing 5% of sodium chloride and poured into the glass tube. After the column had been washed with the buffer, 50 ml of a mixed solution of cobalt(II) and nickel(II) (pH 4.0), spiked with the radioisotopes, were passed through the column at a flow-rate of 0.6–0.8 ml/min, and the column was washed with 100 ml of the buffer to remove cobalt completely, then nickel retained on the column was eluted with 1*M* hydrochloric acid.

Concentration of copper from sea-water

The surface coastal sea-water was taken at Misumi, Kumamoto-ken and filtered through 0.45-μm membrane filters. The sea-water samples were passed through 4VP-T(20) columns (2 g, 1 × 5 cm). Copper retained on the column was eluted with 50 ml of 2*M* hydrochloric acid containing 3% of sodium chloride, at a flow-rate of 5 ml/min and the concentrations of copper were determined.

RESULTS AND DISCUSSION

Analytical data and the surface properties of the 4VP and 2VP resins used in this study are listed in Table 1, in which T and I are abbreviations for toluene and iso-octane, which were used as diluents in the copolymerization process. Among the resins listed, 4VP-G is a gel-type and the others are MR-type resins. The nitrogen contents of the resins are proportional to the amounts of vinylpyridine monomers used, and the base capacities determined are in good agreement with the calculated values based on the nitrogen contents. 4VP-I(20) is in the form of opaque beads, but its specific surface area is very small and the surface structure may be close to that of a gel bead. The surface area increases with increasing degree of cross-linking in a similar manner to the polystyrene resins.[8] The apparent pK_a values of the typical MR resins are determined from their titration curves,[9] and the values for 4VP-T(20) and 2VP-I(20) are 4.2 and 3.3, respectively.

Poly(vinylpyridine) resins would be expected to show anion-exchange behaviour toward certain anions. On the other hand, it is necessary to take into consideration sorption by the formation of complexes with metal ions. As a preliminary experiment, the sorption behaviour of metal ions such as mercury(II), cadmium(II) and zinc(II) on the resins with 20% cross-linkage were examined. These ions are sorbed on each resin in a similar manner in the presence of chloride ion (below pH 2), and the order of sorption is mercury > cadmium > zinc, which corresponds to that of the stability constants of the chloro-complexes.[10] However, a rather different mode of sorption is found in the pH region 3–7, where the contribution of another sorption mechanism which is not conventional ion-exchange is expected.

The sorption on the resins from 0.1*M* hydrochloric acid containing various concentrations of mercury, cadmium and zinc ions is shown in Fig. 1. These resins, though having different surface properties and configurations, show the same sorption pattern over a wide range of metal concentrations. In the case of mercury, its maximum capacity, 6.0 mmole/g, is nearly equal to the base capacity. This suggests that $HgCl_3^-$ is involved in mercury sorption on the resins under the experimental conditions. However, cadmium and zinc ions show only low affinity even at the higher concentrations.

The effect of concentration of sodium chloride on the sorption of the metal ions from 0.1*M* hydrochloric acid is shown in Fig. 2. It is of interest that the extent of sorption of mercury decreases with increase in the concentration of sodium chloride, whilst in the case of cadmium and zinc, a different sorption behaviour is observed. A relationship exists between the chemical species of the metal ions and the chloride ion concentrations, as calculated from their stability constants, and is shown in Fig. 3. It is clear that most of the

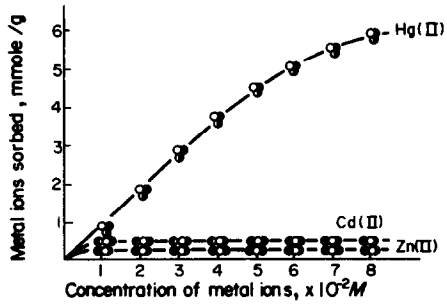


Fig. 1. Sorption of mercury(II), cadmium(II) and zinc(II) from various concentrations of metal ions in 0.1*M* hydrochloric acid. —○—: 4VP-T(20); —●—: 4VP-G(20); —◐—: 2VP-I(20).

Table 1. Properties of poly(vinylpyridine) resins

Resin*	Nitrogen content, %	Base capacity, *meq/g*		Specific surface area, m^2/g	Pore volume, cm^3/g	Pore diameter, *nm*
		Calcd.	Found			
4VP-T(10)	10.79	7.71	7.45	7.8	0.024	12.3
4VP-T(20)	8.51	6.08	6.00	55.0	0.085	6.2
4VP-I(20)	8.38	5.98	6.07	≪1	0.024	—
4VP-G(20)	8.49	6.06	5.73	0	0	0
2VP-I(20)	8.40	6.00	6.05	12.4	0.035	11.3

* Parentheses indicate degree of cross-linking (%).

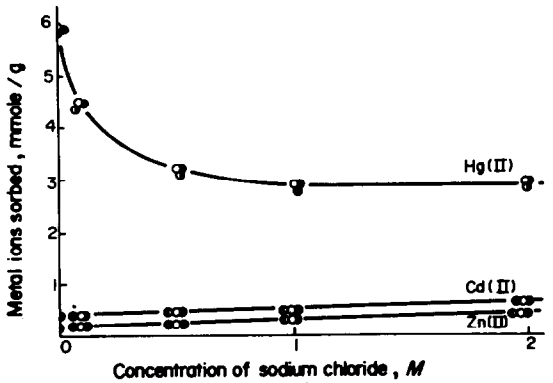


Fig. 2. Sorption of mercury(II), cadmium (II) and zinc(II) in 0.1*M* hydrochloric acid containing various concentrations of sodium chloride. Symbols are the same as those described in Fig. 1.

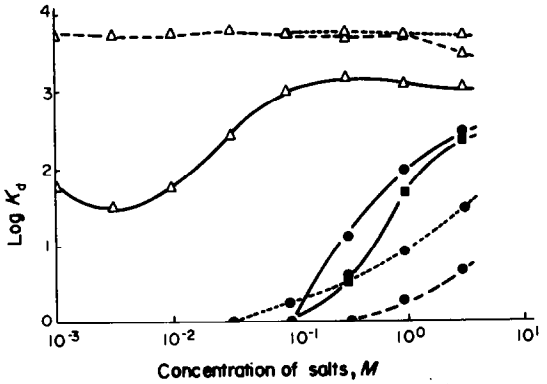


Fig. 4. Sorption of metal ions on 4VP-T(20) from 0.1*M* perchloric acid in the presence of neutral salts. Concentration of metal ions: $1 \times 10^{-4}M$. ■: zinc(II); ●: cadmium(II); △: mercury(II); ——: sodium chloride; – – –: sodium nitrate; -----: sodium perchlorate.

mercury exists as the anionic chloro-complex, $HgCl_4^{2-}$, at higher concentrations of chloride. This agrees with the decrease in the sorption of mercury in the presence of sodium chloride shown in Fig. 2. For sodium chloride concentrations above 1*M* the mercury capacity decreases to half the maximum capacity, and the ratio of ligand to metal corresponds to 2:1. In the case of cadmium and zinc, the increase of sorption at higher concentrations of sodium chloride can be accounted for the formation of their anionic chloro-complexes.

Sorption of copper, zinc, cadmium and mercury on 4VP-T(20) from 0.1*M* perchloric acid containing neutral salts has been examined, and the results are shown in Fig. 4. Copper is not sorbed at all. Mercury shows a high distribution coefficient exception when sodium chloride is present, when the extent of sorption is reduced appreciably. Zinc is sorbed only from solutions containing higher concentrations of sodium chloride. The amount of cadmium or zinc sorbed increases with increasing concentration of sodium chloride. An increase in the distribution coefficient for cadmium is also observed when nitrate or perchlorate is present. So far, the mechanism of the sorption of mercury and cadmium from perchloric acid solutions has not been identified. Direct sorption of the cations may be considered.

In Fig. 5, the distribution coefficients of 10 metal ions in hydrochloric acid medium are shown. These results are similar to those for Dowex-1 × 10, a strongly basic anion-exchange resin with a quarternary ammonium salt as the functional group.[11] The extent of metal sorption is correlated with the formation constants of the anionic chloro-complexes.

The sorption of cobalt, nickel, copper, zinc, cadmium and mercury ions, which form complexes with pyridine, on the five resins in acetate buffer (1*M*, pH 3–7) was then studied. 4VP-G(20), 4VP-I(20) and 2VP-I(20) show low affinity for these metal ions, except mercury. 4VP-T(10) and 4VP-T(20), however,

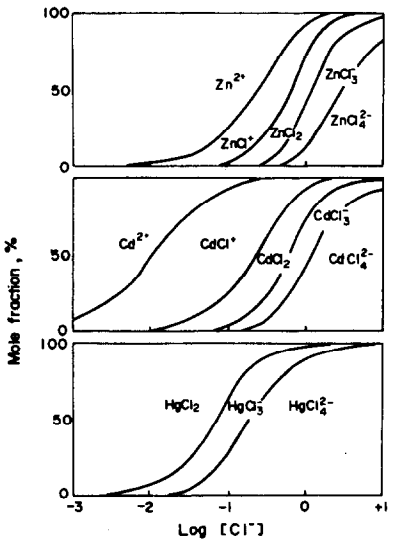


Fig. 3. Relationship between distribution of metal chloro-complexes and concentrations of chloride ions.

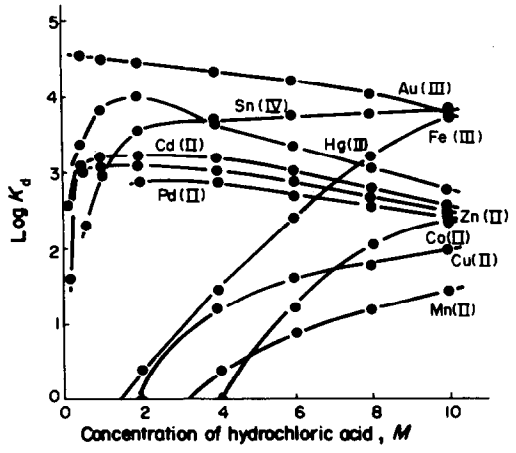


Fig. 5. Distribution coefficients (K_d) of metal ions on 4VP-T(20) in hydrochloric acid. Concentration of metal ions: $5 \times 10^{-3}M$.

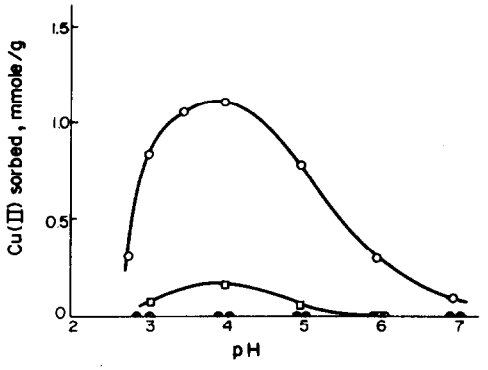


Fig. 6. Sorption of copper(II) on various kinds of resins. Concentration of metal ion: $5 \times 10^{-2}M$. —○—: 4VP-T(20); —●—: 4VP-G(20); —□—: 4VP-I(20); —◐—: 2VP-I(20).

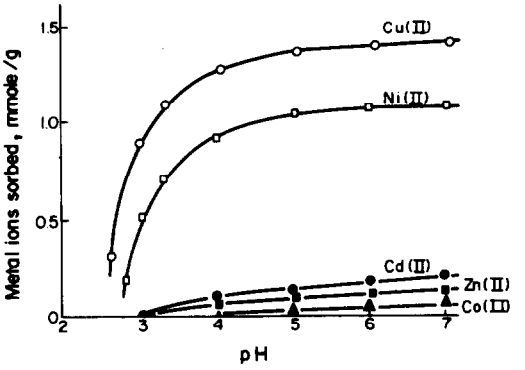


Fig. 8. Sorption of metal ions on 4VP-T(20) in the presence of 10% methanol. Concentration of metal ions: $5 \times 10^{-2}M$.

sorb all these metal and show high affinity for copper and nickel. Mercury is completely sorbed on the resins. The sorption behaviour of copper on the resins is shown in Fig. 6. Although the 20% cross-linked resins have nearly equal base capacity and the same or similar chemical composition, it is of interest that they differ in metal sorption behaviour. This may be explained on the basis of differences in their surface properties, namely 4VP-G has no macroporosity, 4VP-I is also similar to the gel resins, and 2VP-I has porosity but the nitrogen atom in the pyridine moiety is adjacent to the polymer chain.

A typical pH-profile of the sorption of metal ions on 4VP-T(20) is shown in Fig. 7. The 4VP-T resins may have suitable surface properties and configuration for metal complex formation. Maximum sorption of the metal ions is observed at pH 4.0 in aqueous solution and the amounts of sorption decrease with increasing pH. This is explained by assuming that the 4VP-T resins become less hydrophilic above pH 5. In fact, the resins floated to the surface of the working solutions at pH above 5. In order to increase the hydrophilic behaviour of the resins, we used a methanolic medium for the metal sorption study, and the result with 4VP-T(20) is shown in Fig. 8. The decrease in capacity at pH above 5 is no longer observed if 10% of methanol is present. In addition, the capacities are higher. In the case of 4VP-T(10), the sorption capacities increase in proportion to the pyridine content in the polymer unit. Under the experimental conditions, the order of sorption is mercury > copper > nickel > cadmium > zinc > cobalt.

Figure 9 shows the sorption of copper in the presence of sodium chloride and nitrate at pH 6.0. It has been reported that in the case of metal sorption by complex formation the extent of sorption of metals is not decreased by the presence of a neutral salt, but it is decreased in the case of ion-exchange.[12] The copper capacity is found to be independent of the concentration of sodium nitrate, which suggests that 4VP-T sorbs copper not by ion-exchange but by complexation. However, the sorption capacity for copper increased with increasing sodium chloride concentration, which suggests that chloride contributes to the complex formation. The molar ratio of nitrogen to copper in the resin is 3:1 in the presence of sodium chloride, but 4:1 in its absence. Therefore, displacement of ligand by chloride must be considered. The colour of the resin-sorbed copper is green in the pres-

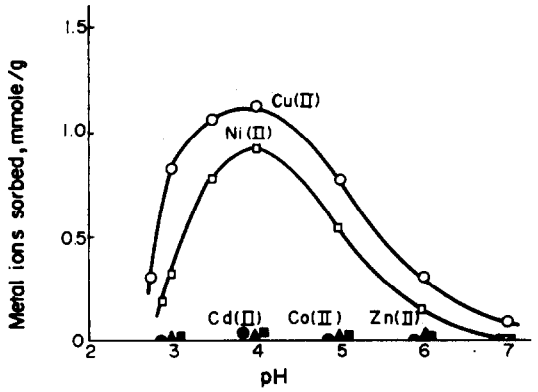


Fig. 7. Sorption of metal ions on 4VP-T(20) from aqueous solution. Concentration of metal ions: $5 \times 10^{-2}M$.

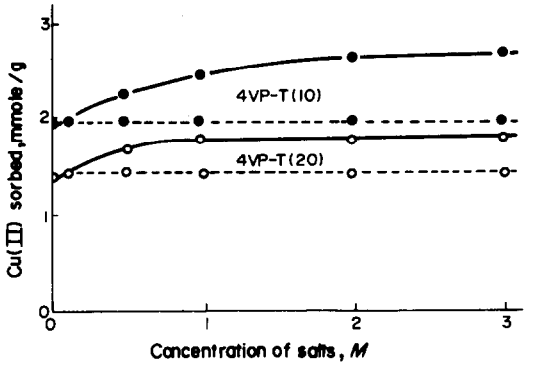


Fig. 9. Effect of sodium chloride (——) and sodium nitrate (---) on sorption of copper(II) with 4VP-T(10) and 4VP-T(20) at pH 6 in the presence of 10% methanol. Concentration of copper(II): $5 \times 10^{-2}M$.

ence of chloride, but blue in its absence. Similar behaviour is observed in the sorption of nickel, and sodium bromide also increases the capacity for copper and nickel.

4VP-T(20) has been applied to the separation of cobalt/copper and cobalt/nickel systems by column operation. Although these metal ions are separable from each other by using the difference in their anion-exchange behaviour shown in Fig. 5, another separation method based on complex formation by the resin was applied here. The times for 50% uptake of copper and nickel from $1 \times 10^{-2} M$ cupric and nickel nitrate solutions at pH 4 were found to be 3 and 5 min, respectively. The time for copper is shorter than that for the copper-selective oxime resin reported previously,[7] and it suggests that the new resin is suitable for column operation. Cobalt is separable from copper and nickel because it is not retained on the column at pH 4, and both retained metals can be eluted with $1M$ hydrochloric acid. The separation data are listed in Table 2.

Finally, concentration of copper from sea-water was examined. The effect of flow-rate on metal sorption from a sea-water sample spiked with copper is shown in Table 3. Copper is well sorbed from sea-water adjusted to pH 4 with acetate buffer, and this can be used for its determination in sea-water. The results are shown in Table 4 with the recovery data,

Table 2. Separation of cobalt(II)/copper(II) and cobalt(II)/nickel(II) from their mixed solutions

Metal	Added, μg	Recovered, μg	Recovery, %
Co	590.0	601.0	101.8
Cu	63.5	62.7	98.7
Co	590.0	584.0	99.0
Cu	635.0	635.0	100.0
Co	295.0	288.5	97.8
Cu	63.5	62.7	98.7
Co	590.0	593.0	100.5
Ni	59.0	58.4	99.0
Co	590.0	592.0	100.3
Ni	590.0	580.0	98.3

Table 3. Effect of flow-rate on sorption of copper in sea-water spiked with copper

Flow-rate, ml/min	Copper sorbed, μg	
	Sample A	Sample B
1	50	50
3	49	50
5	49	50
10	48	50
20	48	49
25	48	49

Sample A (200 ml): sea-water spiked with 50 μg of copper(II).

Sample B (202 ml): sample A plus 2 ml of $1M$ acetate buffer (pH 4.0).

Table 4. Determination of copper in sea-water

Copper added, μg	Found (mean values)*, μg
0	2.4
4	6.3
8	10.1

Sample: 5 litres of sea-water containing 50 ml of $1M$ acetate buffer (pH 4.0).

Flow-rate: 5 ml/min.

* Five determinations were made and the values were corrected for copper in the buffer.

and the concentration found (0.4–0.5 μg/l) agrees well with the values obtained by using Dowex A-1.

Conclusions

Poly(vinylpyridine) resins sorb metal ions by two mechanisms: by conventional ion-exchange and by complexation. The surface properties of the resins affect the complex formation but not the ion-exchange. Appropriate porosity and suitable configuration of the functional groups on the resin matrices are necessary for formation of stable metal complexes. In addition, various substances, such as sodium chloride and methanol, when added to the working solutions strongly influence the metal sorption capacities. Poly(vinylpyridine) resins are expected to be more stable than conventional anion-exchange resins prepared from chloromethylated polystyrene resin and amines, because the chemically stable pyridine moiety is the only functional group in the resins. Among the resins tested, the MR type 4VP-T series is the most interesting and could be applied to the separation and concentration of metal ions.

Acknowledgements—The authors thank Miss M. Kashima for technical assistance. Thanks are also due to the members of the Central Research Laboratory, Sumitomo Chemical Co., Osaka, Japan, for measurements of the surface properties of the resins.

REFERENCES

1. F. Wolf, R. Hauptmann and D. Warnecke, *Z. Anal. Chem.*, 1968, **238**, 432.
2. A. N. Popov, Yu. S. Kononov and M. K. Makarov, *Izv. Sib. Otd. Akad. Nauk SSSR, Ser. Khim. Nauk*, 1966, 50; *Chem. Abstr.*, 1967, **67**, 39764k.
3. E. S. Barketov, V. D. Kopylova, V. B. Kargman, M. I. Druzin and K. M. Saldadze, *Zh. Analit. Khim.*, 1970, **25**, 440; *Chem. Abstr.*, 1970, **73**, 26189a.
4. K. M. Saldadze, V. B. Kargman, V. D. Kopylova and T. P. Larina, *Zh. Analit. Khim.*, 1972, **27**, 246; *Chem. Abstr.*, 1972, **77**, 25264s.
5. H. Nishide and E. Tsuchida, *Makromol. Chem.*, 1976, **177**, 2295.
6. A. Sugii and K. Harada, *J. Chromatog.*, 1979, **178**, 71.
7. A. Sugii, N. Ogawa and H. Hashizume, *Talanta*, 1979, **26**, 189.
8. A. Sugii, N. Ogawa and H. Imamura, *ibid.*, 1979, **26**, 941.

9. F. Helfferich, *Ion Exchange*, p. 84. McGraw-Hill, New York, 1962.
10. W. Walkowiak, D. Bhattacharyya and R. B. Grieves, *Anal. Chem.*, 1976, **48**, 975.
11. K. A. Kraus and F. Nelson, *Proc. Intern. Conf. Peaceful Uses Atomic Energy, Geneva*, 1956, **7**, 113.
12. E. M. Moyers and J. S. Fritz, *Anal. Chem.*, 1977, **49**, 418.

Talanta. Vol. 28. pp. 557 to 560. 1981
Printed in Great Britain. All rights reserved

0039-9140/81/080557-04$02.00/0
Copyright © 1981 Pergamon Press Ltd

COLUMN EXTRACTION CHROMATOGRAPHY OF NON-VOLATILE PLATINUM METALS

S. PRZESZLAKOWSKI and A. FLIEGER

Department of Inorganic and Analytical Chemistry, Medical School, 20-081 Lublin, Poland

(*Received* 21 *November* 1980. *Revised* 13 *January* 1981. *Accepted* 8 *February* 1981)

Summary—Mixtures of Pd(II)–Pt(IV)–Ir(IV) and of Rh(IV)–Pd(II)–Pt(IV)–Ir(IV) have been separated by column chromatography on silica treated with a tri-n-octylammonium salt, by three-step elution with mixtures of hydrochloric acid (2.25*M*) and nitric acid (3, 4 and 5*M*). The optimal conditions for separation were identified from preliminary paper-chromatographic data and the results of column experiments for the individual metals. Single bands for each non-volatile platinum metal were found for the proposed chromatographic system and satisfactory recoveries of single metals from mixtures were obtained. The simple method proposed requires only one column for the separation, which can be repeated at least three times on the same column. The separation needs about 2 hr elution time.

The separation of the platinum metals is one of the most difficult problems in analytical chemistry and although many ion-exchange methods for this purpose have been described,[1–4] the difficulties in complete elution of iridium, platinum and rhodium (due to the tendency to formation of mixed-ligand complexes, polynuclear complexes and to redox reactions) limits the use of ion-exchange methods in analytical practice. For instance, the separation of iridium and platinum requires the presence of both metals in definite oxidation states, which is often secured by the addition of reducing agents.[6–11] However, the separation of iridium(III) and rhodium(III) is difficult because both metals are eluted together from anion-exchange resins, in the first portions of eluate.

Column extraction chromatography,[12] which sometimes has advantages in comparison with chromatography on solid ion-exchange resins has been applied only occasionally for the separation of noble metals. Akaza *et al.*[13] separated the mixture Au–Pt–Pd with the system tributyl phosphate–hydrochloric acid. Earlier Cerrai and Testa[14] separated the same mixture of metals by use of cellulose treated with tri-n-octylphosphine oxide and three-step elution with hydrochloric acid (for palladium and platinum) and nitric acid (for gold). The mixture Au–Pt–Pd–Ir–Rh was succesfully separated by Pohlandt and Steele[15] by extraction chromatography on silica treated with tributyl phosphate but their procedure is complicated and requires the use of three columns and two different eluents—sulphuric acid and hydrochloric acid—which markedly lengthens the analysis time. Our earlier paper-chromatographic results obtained for the system tri-n-octylamine–hydrochloric and nitric acid mixture,[16] suggested the possibility of separation of non-volatile noble metals by column extraction chromatography, which was confirmed by the single example of a rhodium–palladium–platinum mixture. Because it was found that iridium(IV) forms only a single spot in this chromatographic system (the presence of nitric acid in the eluent prevents its reduction), more detailed investigations on the separation of the mixture of non-volatile noble metals by column extraction chromatography were undertaken and are described in the present paper, special attention being paid to the platinum–iridium separation.

EXPERIMENTAL

Materials

Pure tri-n-octylamine (Serva) was additionally purified by vacuum distillation, the fraction boiling at 190–200°/5–10 mmHg being collected.

Silica gel, 0.05–0.2 mm (Merck), was purified by repeated treatment with 3*M* hydrochloric acid (until it gave no colour reaction with ammonium thiocyanate), washed several times with distilled water (until there was negligible reaction with silver nitrate) and dried at 105°. It was then fractionated by Köhn's method,[17] the 0.06–0.1 mm fraction being collected.

The following noble metal compounds, of analytical grade, were used: H_2PtCl_6, 30% solution (State Mint, Warsaw) and $PdCl_2$ (POCh, Poland). The iridium sponge (Johnson-Matthey) was of "Specpure" grade, and the $RhCl_3$aq. (Fluka) and platinum–rhodium alloy (State Mint, Warsaw) were of pure grade.

All other reagents were of analytical grade.

Solutions of noble metals

Standard iridium(IV) solution was prepared by fusing 0.176 g of iridium sponge with 0.8 g of sodium peroxide, dissolving the residue in distilled water, adding 120 ml of concentrated hydrochloric acid, heating the solution to boiling and diluting with distilled water to 200 ml. This solution was diluted to the desired concentration with 10*M* hydrochloric acid. Solutions of platinum, palladium and rhodium were prepared by dissolving the appropriate salt in 10*M* hydrochloric acid. The platinum content was determined gravimetrically,[18] and the rhodium cerimetrically.[19] The platinum–rhodium alloy was dissolved in the manner described previously.[16]

Procedure

Glass columns (10 × 300 mm) were used, packed with the purified silica gel (0.06–0.1 mm) as the support for the stationary phase. Tri-n-octylamine (TOA) was converted

into salt form by shaking a 0.35 or 0.1*M* solution of it in chloroform with an equal volume of a mixture of hydrochloric and nitric acids ($c_{HCl} = 2.25M$; $c_{HNO_3} = 3M$). After separation of the phases, the organic phase was filtered through a cellulose filter and 50 ml of it were mixed with 40 g of silica gel. The diluent was then evaporated with a vacuum evaporator on a water-bath. The coated support remained a white powder containing 0.042 g (0.052 ml) or 0.13 g (0.16 ml) of substituted ammonium salt per gram, depending on the concentration of TOA salt in the solution used for impregnation of the silica gel. The dried sorbent (10 g or 7.5 g) was then slurried with 50 ml of the first eluent, poured into the column and covered with a Whatman No. 4 cellulose filter. The column lengths were 190 mm (10 g of silica) or 150 mm (7.5 g of silica), the organic phase volumes 1.6 ml (when 0.35*M* TOA was used for impregnation) or 0.52 ml (0.1*M* TOA) for 190 mm columns, and the hold-up volumes 8.25 ml or 6.5 ml (determined from the retention volumes of nickel, which is not retained), depending on the column length. After the column had been washed with 8 ml of the first eluent, 1 ml of an individual metal ion solution or of a synthetic mixture was introduced into it. Elution under hydrostatic pressure (head 250 mm) was used for the separation, 1.5-ml fractions being collected by a fraction collector equipped with a drop-counter. The whole elution for the separation of the mixture Rh–Pd–Pt–Ir needed 135 min at a mean flow-rate of 0.5 ml/min. The flow-rates in other experiments were 0.41–0.56 ml/min, depending on the column length and nitric acid concentration in the eluent.

The metals were determined in each fraction: palladium and platinum with a single-beam Pye–Unicam SP 192 atomic-absorption spectrometer, rhodium and iridium spectrophotometrically at 500 nm (Rh) and 415 nm (Ir); the calibration graphs were based on rhodium(III) or iridium(IV) solutions in the mixture of acids used as the eluent. In one experiment (repeated three times) platinum in the total eluate was also determined colorimetrically with tin(II) chloride,[20] after removal of nitric acid by evaporation with concentrated hydrochloric acid (over a 3 hr heating period).

Paper chromatography experiments were performed as described previously.[16]

RESULTS AND DISCUSSION

The experimental data obtained by the use of laminar techniques in extraction chromatography are often utilized in planning the separation of metal-ion mixtures by column chromatography.[21] Although the paper chromatography results for noble metals obtained with the system liquid anion-exchanger/mixture of hydrochloric and nitric acid had been described earlier,[16,22] some additional experiments on paper strips impregnated with a 0.35*M* solution of tri-n-octylammonium salt were carried out, mainly for the pair Pt(IV)–Ir(IV), in order to compare the results with the data obtained by use of the column technique. All experiments (paper and column chromatography) were always performed at constant concentration of hydrochloric acid (2.25*M*) in the eluent.

The experimental results for palladium, platinum and iridium are given in Fig. 1 in the form of the separation factors for the pairs Pt–Pd and Ir–Pt (paper chromatography) or ratio of retention volumes of iridium and platinum (column chromatography) plotted against nitric acid concentration in the eluent. The results indicate that although the selectivity of separation of iridium and platinum is somewhat greater in paper chromatography, both curves are parallel and the selectivity of separation decreases with increase of the nitric acid concentration in the eluent; on the other hand, the separation factors for the pair Pt–Pd decrease more rapidly with increasing nitric acid concentration.

The retention volumes of palladium, platinum and iridium, calculated from paper chromatographic data and determined in column experiments, are collected in Tables 1 and 2. Although the calculated retention volumes were always higher than those determined by column chromatography, especially at higher loadings of silica with liquid anion-exchanger, the ratio of $V_{R_{exp.}}/V_{R_{calc.}}$ was always constant and independent of the metal ion and the composition of the eluent used. Therefore, the retention volumes can be calculated by the modification of an equation given by Ghersini and Cerrai:[21]

$$\frac{V_R}{V_m a} - 1 = \frac{A_m V_s}{A_s V_m}\left(\frac{1}{R_F} - 1\right) = K\left(\frac{1}{R_F} - 1\right)$$

where a denotes the experimental value of $V_{R_{exp.}}/V_{R_{calc.}}$, which changes with the extractant concentration in the impregnating solution. The differences between calculated and experimental retention volumes are probably partially due to changes in the concentration of hydrochloric and nitric acid at the eluent front in paper chromatography (known also from other chromatographic systems[23]) and the use of different supports, which can bind part of the extractant with different strength, but the main cause seems to be the removal of part of the extractant from the support by the eluent. Because it was found that the elution curves and retention volumes changed only

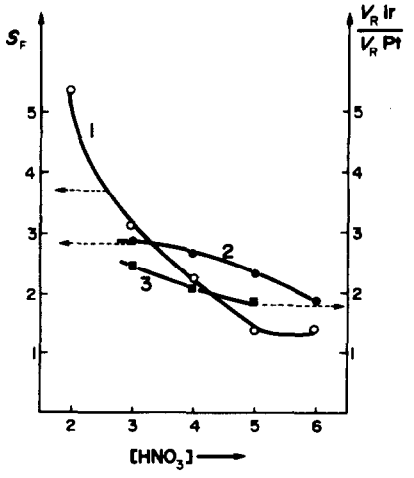


Fig. 1. Separation factors for Pt and Pd (curve 1) and Ir(IV) and Pt (curve 2) calculated from paper chromatography data and the ratio of retention volumes of iridium and platinum (column chromatography—curve 3) plotted against nitric acid concentration in the eluent. Paper or silica gel treated with 0.35*M* TOA salt in chloroform; concentration of HCl in the eluent constant (2.25*M*).

Table 1. Comparison of experimental retention volumes for palladium(II), platinum(IV) and iridium(IV) with those calculated from independent paper chromatography experiments (silica or paper treated with 0.35*M* solution of tri-n-octylammonium salt in chloroform; concentration of hydrochloric acid in the acid eluent constant at 2.25*M*)

Metal	Concentration of HNO_3 in eluent, *M*	Paper chromatography		Column chromatography	
		R_F	$V_{R_{calc.}}$, *ml*	$V_{R_{exp.}}$, *ml*	$\frac{V_{R_{exp.}}}{V_{R_{calc.}}}$
Pd	2	0.30	85.4	30.0	0.35
Pd	3	0.40	57.0	22.5	0.39
Pt	3	0.20	138.0	43.5	0.32
Pt	4	0.38	60.8	22.5	0.37
Pt	5	0.50	40.0	17.0	0.42
Ir	3	0.08	301.0	107.0	0.36
	4	0.14	153.0	46.0	0.30
	5	0.30	73.0	30.5	0.42
				mean	0.366

Table 2. Comparison of experimental retention volumes for iridium (IV) with those calculated from independent paper chromatography experiments (silica or paper treated with 0.1*M* solution of tri-n-octylammonium salt in chloroform; concentration of hydrochloric acid in the eluent mixture constant at 2.25*M*)

Concentration of nitric acid in eluent, *M*	Paper chromatography		Column chromatography	
	R_F	$V_{R_{calc.}}$, *ml*	$V_{R_{exp.}}$, *ml*	$\frac{V_{R_{exp.}}}{V_{R_{calc.}}}$
4	0.38	32.3	21.0	0.72
5	0.51	22.4	18.0	0.80

insignificantly when three successive elutions of platinum (eluent: 2.25*M* HCl + 4*M*HNO_3) were performed on the same column, it seems that excess of extractant is removed from the silica during preparation of the column and its washing with the eluent, and this leads to a decrease in the real volume of the stationary phase in the column. Thus the explanation of the differences between the calculated and experimental retention volumes requires a more detailed investigation. Nevertheless, from a practical viewpoint high loadings of the support with extractant are preferable for the separation of larger quantities of platinum metals and therefore in further column experiments the silica gel was always treated with a 0.35*M* solution of the tri-n-octylammonium salt in chloroform.

Table 3. The determination of palladium, platinum and iridium after the separation of synthetic mixtures by column chromatography

	Added, *μg*	Found, *μg*	Error, %
Pd(II)	525	515*	−1.9
	1550	1548	−0.36
	1100	1166	+6.0
Pt(IV)	850	810	−4.7
	1050	1029	−2.0
	1800	1802*	+1.0
Ir(IV)	176	174	−1.1
	88	86*	−2.2

* Mean value from 3 successive determinations.

Although a low concentration of nitric acid in the eluent is preferable for the separation of palladium from platinum and of platinum from iridium, the retention volumes are then high and the elution curves are distinctly more diffuse in comparison with

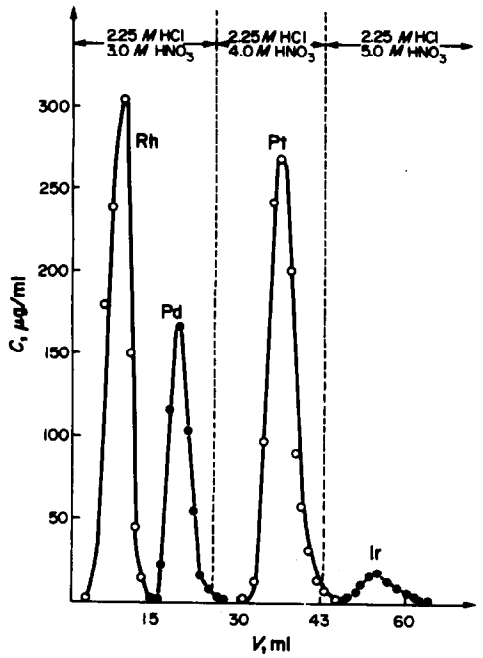


Fig. 2. Separation of Rh (950 *μg*), Pd (525 *μg*), Pt (1050 *μg*) and Ir(IV) (88 *μg*). Column length 150 mm; mean flow-rate 0.5 ml/min.

Table 4. The determination of rhodium, palladium, platinum and iridium after the separation of a synthetic mixture by column chromatography

	Added, μg	Found, μg	Error, %
Rh(III)	950	965	+1.6
Pd(II)	525	522	−0.6
Pt(IV)	1050	1032	−1.8
Ir(IV)	88	87	−1.1

those obtained at higher concentration of nitric acid. Therefore the choice of nitric acid concentration used for the elution of individual metals should be a compromise, taking into account both the separation factors as well as the retention volumes. Although very sharp elution curves were obtained for iridium with low amounts of the stationary phase (when the silica gel was treated with 0.1*M* TOA salt solution in chloroform), the retention volumes were then too low to permit the separation of iridium from other platinum metals—see Table 2.

On the basis of several column chromatographic separations of Pd–Pt–Ir mixtures it was found that the following concentrations of nitric acid in the eluent (the concentration of hydrochloric acid in the eluent being kept constant at 2.25*M*) are optimal for individual metals: 3*M* for palladium, 4*M* for platinum and 5*M* for iridium. Table 3 reports the results of the determination of the separated metals in the individual fractions. It was found that at least three successive separations of Pd–Pt–Ir(IV) can be performed on the same column, if it is washed beforehand with the first eluent used for the separation.

An example of separation of a mixture containing all the non-volatile platinum metals by a three-step elution procedure is given in Fig. 2 and Table 4. The proposed procedure was applied to the determination of platinum and rhodium in a platinum–rhodium alloy (containing approximately 10% Rh), which was found to contain 90.2% Pt and 12.5% Rh.

In our opinion, the proposed simple and relatively rapid separation method can be utilized not only for analytical purposes but also for the isolation of individual high-purity non-volatile platinum metals from their mixtures and for the separation of platinum metals from gold, which is very strongly retained by the stationary phase used and cannot be eluted even by mixtures of concentrated hydrochloric and nitric acid.

Acknowledgements—This work was supported by the Institute of Chemistry of the Maria Curie-Skłodowska University in Lublin (Grant No. MR.I.14.Ia.1). Thanks are due to Professor Dr Edward Soczewiński for helpful discussion and for his interest in this work.

REFERENCES

1. F. E. Beamish, *The Analytical Chemistry of the Noble Metals*, Pergamon Press, Oxford, 1966.
2. F. E. Beamish and J. C. Van Loon, *Recent Advances in the Analytical Chemistry of the Noble Metals*, Pergamon Press, Oxford, 1972.
3. V. Sýkora and F. Dubský, *Sb. Vys. Školy Chem.-Technol. v Praze, Anal. Chem.* 1974, **H10**, 113.
4. G. I. Ginzburg, N. A. Yezerskaya, I. V. Prokofeeva, N. F. Fedorenko, V. I. Shlenskaya and N. K. Belskii, *Analiticheskaya khimiya platinovikh metallov*, Nauka, Moscow, 1972.
5. E. Blasius and U. Wachtel, *Z. Anal. Chem.*, 1954, **142**, 341.
6. S. S. Berman and W. A. E. McBryde, *Can. J. Chem.*, 1958, **36**, 835.
7. E. Blasius and D. Rexin, *Z. Anal. Chem.*, 1961, **179**, 105.
8. A. A. Korobkin, *Izv. Vyssh. Ucheb. Zavedenii, Tsvetnaya Met.*, 1960, **3**, 99; *Chem. Abstr.*, 1961, **55**, 12219.
9. Yu. S. Kononov, A. N. Popov and M. K. Makarov, *Izv. Sib. Otd. AN SSSR, Ser. Khim. Nauk*, 1969, 150.
10. J. Chwastowska, R. Dybczyński and H. Maleszewska, *Chem. Anal. (Warsaw)*, 1971, **16**, 891.
11. K. Brajter and K. Słonawska, *ibid.*, 1979, **24**, 273.
12. T. Braun and G. Ghersini, (eds.), *Extraction Chromatography*, Elsevier, Amsterdam, 1975.
13. I. Akaza, T. Kiba and T. Kiba, *Bull. Chem. Soc. Japan*, 1970, **43**, 2063.
14. E. Cerrai and T. Testa, *Energia Nucl. (Milan)*, 1961, **8**, 510.
15. C. Pohlandt and T. W. Steele, *Talanta*, 1972, **19**, 839.
16. S. Przeszlakowski and A. Flieger, *ibid.*, 1979, **26**, 1125.
17. M. Köhn, *Landwirtschaftliche Jahrbücher*, 1928, **67**, 4; J. Gliński, M. Malicki, R. Turski and M. Misztal, *Przewodnik do ćwiczeń gleboznawstwa*, Z. Wyższa Szkoła Rolnicza, Lublin, 1972.
18. A. P. Blackmoore, M. A. Marks, R. P. Barefoot and F. E. Beamish, *Anal. Chem.*, 1952, **24**, 11.
19. O. C. Saxena, *Microchem. J.*, 1968, **13**, 1930.
20. Z. Marczenko, *Spektrofotometryczne oznaczanie pierwiastków*, p. 499. PWN, Warsaw, 1979. *Spectrophotometric Determination of Elements*, p. 433. Horwood, Chichester, 1976.
21. G. Ghersini and E. Cerrai, in T. Braun and G. Ghersini, (eds.), *Extraction Chromatography*, p. 366. Elsevier, Amsterdam, 1975.
22. S. Przeszlakowski and A. Flieger, *Chromatographia*, 1978, **11**, 647.
23. E. Cerrai and G. Ghersini, in J. C. Giddings and R. A. Keller, (eds.), *Advances in Chromatography*, Vol. 9, p. 3. Dekker, New York, 1970.

Talanta. Vol. 28. pp. 561 to 564. 1981
Printed in Great Britain. All rights reserved

0039-9140/81/080561-04$02.00/0
Copyright © 1981 Pergamon Press Ltd

FLOTATION–SPECTROPHOTOMETRIC METHOD FOR DETERMINING PALLADIUM BY MEANS OF THE ION-ASSOCIATION COMPLEX OF PENTABROMOPALLADATE(II) WITH RHODAMINE 6G

Z. MARCZENKO and M. JAROSZ

Department of Analytical Chemistry, Technical University, Warsaw, Poland

(*Received* 4 *August* 1980. *Revised* 9 *October* 1980. *Accepted* 7 *February* 1981)

Summary—The conditions for the formation of a suitable coloured palladium ion-association complex with a basic dye have been examined, and a spectrophotometric method developed for the determination of palladium with bromide and Rhodamine 6G (R6G). Benzene is used for flotation and dimethylformamide for dissolution of the ion-association complex. The molar absorptivity is 3.0×10^5 l. mole^{-1}.cm^{-1} at 530 nm. Beer's law is obeyed up to a palladium concentration of 0.3 μg/ml. The composition of the complex is $[R6G^+]_3[PdBr_5^{3-}]$. Platinum interferes severely but other platinum metals interfere to a lesser degree. The method has been applied to the determination of traces of palladium in metallic platinum after a preliminary separation with nickel dimethylglyoximate as collector.

Interest is growing in sensitive spectrophotometric methods based on ion-association complexes of anionic metal complexes and basic dyes.[1,2] The most frequently used anions are halide and pseudohalide complexes, but anionic complexes formed with chelating organic reagents (*e.g.*, oxine and its derivatives, some carboxylic acids) can also be used.

Simple ion-association complexes with basic dyes (*i.e.*, reactant ratio 1:1) are generally soluble in non-polar organic solvents and form the basis of extraction–spectrophotometric methods. A less numerous group of complexes comprises compounds of more complex structure which are insoluble in organic solvents, but during shaking with them precipitate at the phase boundary or adhere to the walls of the vessel. This group of ion-association complexes with basic dyes is the basis of flotation–spectrophotometric methods. The sparingly soluble compound, separated from the aqueous and organic phases, is dissolved in a suitable polar solvent, and the absorbance of the solution is then measured.

The purpose of the present work was to find a suitable colour system (anionic complex + basic dye) for a sensitive flotation–spectrophotometric method for determination of palladium.

There are some literature data on the extraction of the azide–palladium–Methylene Blue system[3] and the thiocyanate–palladium–Crystal Violet system.[4] Flotation–spectrophotometric methods for the determination of platinum and rhodium have already been developed in our laboratory.[5,6]

EXPERIMENTAL

Apparatus and reagents

Absorption spectra were measured with a Specord spectrophotometer, and absorbances with a VSU 2-P spectrophotometer with 1-cm cells.

Standard palladium solution (1 mg/ml) was prepared by dissolving a suitable amount of palladium(II) chloride in water containing 10 ml of concentrated hydrochloric acid and diluting to volume with water in a 500-ml standard flask, and standardized gravimetrically with dimethylglyoxime. Working solutions were obtained by suitable dilution of the stock solution.

Rhodamine 6G (R6G) solution ($1 \times 10^{-3}M$) was prepared from a commercial preparation (BDH) purified by precipitation from ethanolic solution with 5-fold amount of diethyl ether.

Procedure

Place the test solution, containing not more than 8 μg of palladium, in a separatory funnel. Add 8 ml of 10% potassium bromide solution and 2.5 ml of Rhodamine 6G solution. Adjust the pH to about 2.5 with 0.1*M* hydrochloric acid and dilute to 25 ml with water, mixing after adding each reagent. Shake the solution with 10 ml of benzene for 45 sec. Remove the aqueous phase and wash the benzene phase and the separated complex with three 10-ml portions of water (shaking time 30 sec). Carefully decant both phases and dissolve the precipitate in dimethylformamide. Transfer the solution to a 25-ml standard flask, dilute to the mark with the solvent and measure the absorbance at 530 nm against a reagent blank.

Determination in platinum

Dissolve the platinum sample (~50 mg) in 4 ml of *aqua regia* and evaporate the solution to dryness on a boiling water bath. Add 2 ml of concentrated hydrochloric acid and evaporate to dryness. Dissolve the residue in 5 ml of hot 1.5*M* hydrochloric acid. Allow the solution to cool and add 2 mg of nickel (nickel chloride solution), dilute to about 50 ml with water, add 1 ml of 1% sodium dimethylglyoximate solution and 10 ml 20% sodium acetate solution and mix. After 30 min filter off the precipitate and mineralize it with 3 ml of concentrated hydrochloric acid and 2 ml of concentrated nitric acid. Evaporate to dryness (on a water-bath) and dissolve the residue in 5 ml of 1.5*M* hydrochloric acid. Precipitate nickel and palladium, mineralize

and dissolve as above. Adjust the pH to about 2.5 with dilute ammonia solution and determine palladium as described.

RESULTS AND DISCUSSION

Choice of coloured system

Preliminary studies were devoted to finding the best ion-association system. A wide acidity range was covered, from pH 4.5 (acetate buffer) to 1*M* hydrochloric acid. The amount of palladium used was 10 μg per 25 ml of final aqueous solution. The concentration of the dye was $1 \times 10^{-4}M$. The aqueous solutions were shaken with 10 ml of benzene or chloroform.

The following basic dyes were examined: Rhodamine B and Rhodamine 6G (xanthene dyes), Crystal Violet (triphenylmethane dye), Methylene Blue (thiazine dye), Meldola Blue and Capri Blue (oxazine dyes), and Bindschedler's Green (indamine dye). Palladium was converted into anionic halide and pseudohalide (Cl^-, Br^-, I^-, SCN^-, N_3^-) complexes; 4-(2-pyridylazo)-resorcinol (PAR) and 4-(2-thiazolylazo)-resorcinol (TAR) complexes were also used.

The azide–palladium–Methylene Blue and palladium–TAR–Crystal Violet or –Rhodamine B ion-association complexes are non-quantitatively extracted by chloroform.

Quantitative flotation was observed in two systems: palladium–bromide–Rhodamine 6G (benzene) and palladium–thiocyanate–Methylene Blue (benzene). Partial separation of palladium by flotation was observed in the systems with iodide–Methylene Blue (chloroform), thiocyanate–Methylene Blue (chloroform), thiocyanate–Crystal Violet (benzene), azide–Crystal Violet (benzene), iodide–Capri Blue (chloroform), thiocyanate–Capri Blue (chloroform or benzene), PAR–Rhodamine B (or Crystal Violet) (benzene).

In the further work the system palladium–bromide–Rhodamine 6G was investigated in detail.

Flotation of the complex

The effect of the initial acidity of the aqueous phase

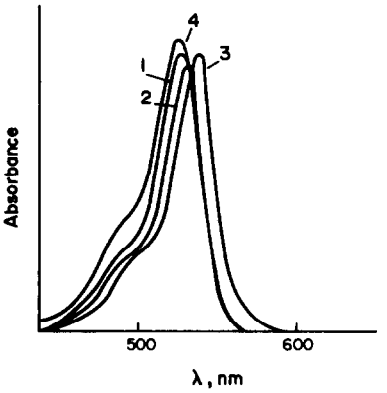


Fig. 2. Absorption spectra of solutions of the ion-association complex in: 1—methanol or acetone, 2—ethanol, 3—dimethylformamide. Curve 4—aqueous solution of Rhodamine 6G. The concentration of Rhodamine 6G is the same in each solution.

on the absorbance of the final solution in dimethylformamide was examined. The flotation compound is formed quantitatively when the pH of the aqueous solution is in the range 1.5–3.5 (Fig. 1). The pH of the test solution can be adjusted to 2.5 without use of a buffer.

For quantitative flotation at least a 30-fold molar excess of Rhodamine 6G is necessary. A large excess of bromide is also needed, maximum absorbance being obtained with a bromide concentration $\geqslant 0.2M$.

Time and temperature have no effect on the formation and flotation of the complex. The palladium bromide complex forms rapidly and the same results are obtained whether the flotation is done at once or after 20 min. Heating up to 90° in the absence of the basic dye has no effect on the final results.

The solvents tested for the flotation were benzene, toluene, carbon tetrachloride, chloroform and di-isopropyl ether. Flotation takes place only with benzene and carbon tetrachloride. Benzene was chosen for further use because separation of the product is easier when the organic solvent is lighter than water.

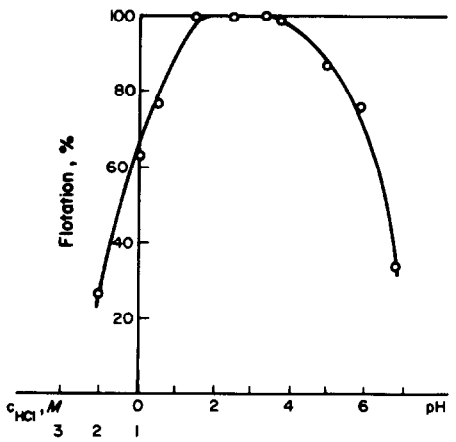


Fig. 1. Dependence of degree of separation on acidity of aqueous solution.

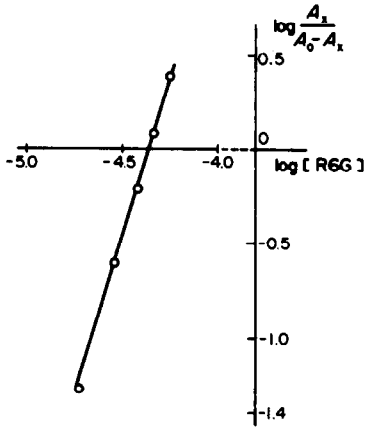


Fig. 3. Determination of the mole ratio Pd:R6G and the stability constant by the Bent and French method.

The volume ratio of the liquid phases has no effect on the final results. The minimum shaking time is about 30 sec but shaking times longer than 60 sec result in higher blank values. After separation of the aqueous phase the excess of free dye must be removed from the ion-association complex by washing: the benzene phase and the precipitate are shaken with three portions of water.

Various water-miscible polar solvents were tried for dissolution of the complex: methanol, ethanol, acetone and dimethylformamide (DMF). The absorption spectra of solutions of the complex in these solvents and of an aqueous solution of Rhodamine 6G are shown in Fig. 2. The differences in λ_{max} are small and the absorption spectrum of a Rhodamine 6G solution in DMF is identical with that of the complex in this solvent. Dimethylformamide, which dissolves the separated compound the most rapidly, was chosen for further use. Under the chosen conditions the precipitate is practically free from the ion-association complex of the dye with bromide. The blank is low, about 0.05.

Composition of the complex

The palladium added is quantitatively recovered in the compound separated by flotation. The mole ratio of bromide to palladium in this compound was established as 5:1 by use of the radioisotope ^{82}Br, individual results being 4.9, 5.2, 4.4, 5.0, 5.3, 4.6. The ratio found by a preparative method was slightly lower (individual results: 4.8, 4.6, 4.1, 4.8, 4.6, 4.3, 4.7). Bromide may have been lost during the lengthy procedure. The separated and washed product was dissolved in a mixture of water and dimethylformamide, and palladium was separated by precipitation with dimethylglyoxime with nickel as collector. The Rhodamine 6G cations were separated on a cation-exchange column of Amberlite IRC-50, and the bromide was determined by an amplified spectrophotometric method[7] (oxidation to bromate with hypochlorite, removal of excess of oxidant, conversion of bromate into bromine with potassium bromide, decolorization of Methyl Orange).

The molar ratio of palladium to Rhodamine 6G in the compound was established by comparison of the absorbance of dimethylformamide solutions of known amounts of the compound (molar absorptivity, ϵ, 3.0×10^5 l.mole^{-1}.cm^{-1} at 530 nm) and of Rhodamine 6G (ϵ 9.7×10^4 at 530 nm) and found to be 1:3. This was confirmed (Fig. 3) by the Bent and French method.[8] The compound is therefore $[R6G^+]_3[PdBr_5^{3-}]$.

For the reaction:

$$3R6G^+ + PdBr_5^{3-} \rightleftharpoons [R6G^+]_3[PdBr_5^{3-}]$$

the equilibrium constant is given by the equation:

$$K = \frac{\{[R6G^+]_3[PdBr_5^{3-}]\}}{[R6G^+]^3[PdBr_5^{3-}]}$$

hence

$$\log K = \log D - 3 \log [R6G^+]$$

where:

$$\log D = \log \frac{A_x}{A_0 - A_x} = \log \frac{\{[R6G^+][PdBr_5^{3-}]\}}{[PdBr_5^{3-}]}$$

(A_x = absorbance for given R6G concentration, A_0 = maximum absorbance). The values of the equilibrium constants calculated for 5 different concentrations of R6G give $K = (1.27 \pm 0.37) \times 10^{13}$ at a probability level of 90% (Fig. 3).

Characteristics of the method

The calibration graph obtained under optimum conditions obeys Beer's law up to a palladium concentration of 0.3 μg/ml.

The precision and accuracy were determined at three palladium levels (Table 1).

The effect of the other platinum metals was examined. Because of the inertness of the redox equilibria of these metals the solution was kept at 70° for 30 min before the Rhodamine 6G was added. To prevent formation of free bromine small amounts of phenol were added. In 10-fold ratio to palladium, ruthenium and osmium do not interfere but rhodium and iridium give rise to positive errors of about 10 and 30%, respectively. Platinum interferes in any amount.

Mercury and molybdenum give positive errors of about 35% when present in 5-fold ratio to palladium and a 10-fold ratio of cadmium gives 40% error. Gold, bismuth and manganese (10-fold ratios) give about 10% error. Indium and thallium(III) do not interfere at the 100-fold ratio level but gallium gives 20% error. Zn, Ni, Co, Fe(III), Sn(IV) and Sb(III) have no effect even at 1000-fold ratio to palladium.

Chloride and sulphate do not interfere even at 2*M* concentration. Nitrate interferes at the 0.05*M* level but perchlorate interferes even at $5 \times 10^{-4}M$ concentration.

Table 1. Precision of the results (7 determinations) for palladium

Palladium, μg		Standard deviation μg	Relative standard deviation, %	Confidence limits (probability level 0.95)
added	found			
1.00	1.01	0.08	7.5	1.01 ± 0.07
4.00	3.99	0.17	4.1	3.99 ± 0.15
8.00	7.93	0.21	2.6	7.93 ± 0.19

Table 2. Determination of Pd in high-purity platinum (sample weights 50 mg; 5 determinations)

Palladium found	Standard deviation	Confidence limits (probability level 0.95)
4.60 μg	0.21 μg	4.60 ± 0.26 μg
9.2×10^{-3}%	3.0×10^{-4}%	$(9.2 \pm 0.8) \times 10^{-3}$%

The selectivity of the method is thus rather poor, but the sensitivity is higher than that of other methods.

The method has been applied to determination of palladium in high-purity platinum. A preliminary separation is essential. Extraction of palladium dimethylglyoximate with chloroform proved ineffective because of co-extraction of about 1.5% of the platinum. Even after repeated separation (after evaporation of solvent and mineralization) the extract still contained about 10 μg of platinum. Good separation was obtained by double precipitation of palladium with dimethylglyoxime, with nickel as collector.[9] Table 2 gives some data on the precision and accuracy. In a separate analysis of palladium-free platinum spiked with 4 μg of palladium the recovery was 90–100% (five determinations).

REFERENCES

1. Z. Marczenko, *C.R.C. Crit. Rev. Anal. Chem.*, 1981, **10.**
2. Z. Marczenko, *Mikrochim. Acta*, 1977 **II,** 651.
3. R. Kuroda, N. Yoshikuni and Y. Kamimura, *Anal. Chim. Acta*, 1972, **60,** 71.
4. Z. M. Khvatkova and V. V. Golovina, *Zh. Analit. Khim.*, 1979, **34,** 2035.
5. Z. Marczenko and J. Maruszak, *Chem. Anal. (Warsaw)*, 1979, 24, 341.
6. Z. Marczenko and E. Kowalczyk, *Anal. Chim. Acta*, 1979, **108,** 261.
7. H. A. Laitinen and K. W. Boyer, *Anal. Chem.*, 1972, **44,** 920.
8. H. Bent and C. French, *J. Am. Chem. Soc.*, 1941, 63, 568.
9. Z. Marczenko, *Spectrophotometric Determination of Elements*, p. 412. Horwood, Chichester 1976.

Talanta, Vol. 28, pp. 565 to 573, 1981
Printed in Great Britain. All rights reserved

0039-9140/81/080565-09$02.00/0
Copyright © 1981 Pergamon Press Ltd

A DESK-COMPUTER PROGRAM FOR CALCULATION OF THE PARAMETERS OF ACID–BASE TITRATION CURVES AND PROTONATION OR METAL-COMPLEX STABILITY CONSTANTS FROM POTENTIOMETRIC DATA

F. GAIZER and A. PUSKÁS

Department of Chemistry, College of Food Technology, Hódmezövásárhely, POB 79 and Gy. Juhász Teacher's Training College, Szeged, Hungary

(*Received* 24 *September* 1980. *Accepted* 29 *January* 1981)

Summary—The program MINIPOT is designed to run on a desk-computer with 16-kbyte of memory. It can calculate the optimum values of the parameters of a blank acid–base titration in any solvent, and the protonation/deprotonation or overall stability constants of a maximum of four species with compositions H_qL_p or M_qL_p from potential, titrant volume and analytical concentration data. The program, written in BASIC, is based on the least-squares principle and is capable of simultaneous refinement of a maximum of four parameters.

The technical development (in memory, speed, *etc.*) of desk-computers and their more frequent availability in chemical laboratories has created a demand for desk-computer programs capable of solving chemical problems which previously required large computers. In recent years we have developed a number of programs, based on the least-squares principle, which solve problems in the field of complex equilibria, and have successfully used these for the evaluation of spectrophotometric,[1–4] potentiometric[5,6] and solubility[1] measurements. We have now succeeded in simplifying these programs in such a way that they will run successfully on desk-computers in a reasonably short time, while yielding practically the same information as the larger computer programs. The program MINIPOT, presented here, is based on the previously published program PH-POT[6] and is written in BASIC for a WANG 2200 desk-computer with 16-kbyte of memory.

THE PROGRAM

MINIPOT permits calculation of the parameter values that describe experimental data obtained potentiometrically with an electrode sensitive to hydrogen ions or metal ions. $\Sigma(\Delta E)^2$ is the sum that is minimized, for the experimental points can then be treated with the same (unit) weight.[7] The program can refine simultaneously a maximum of four parameters by a procedure based on the Gauss method.[2,3] For faster and more reliable convergence, it has been made possible to calculate the value of a scalar, multiplication of the correction vector by which yields better parameter values.[8] In addition, we have built a small section into the program for searching for parameter values.

MINIPOT can solve two types of problem.

1. From the potential (E), volume of base added (v_{OH}) and total concentration (T_H, T_{OH}) data for a blank acid–base titration curve in any solvent, it can calculate the optimum values of the parameters of equation (1):

$$E = E^\circ + g\log[H^+] - j_H[H^+] - j_{OH}K_s/[H^+] \quad (1)$$

where E° is the standard potential (in mV) of the measuring electrode, g is 59.16/z (at 25°), j_H and j_{OH} are constants to take into account the diffusion potentials, and K_s is the ionic product of the solvent. In this problem T_{OH}, the concentration of the titrant solution, has also been made a refinable parameter.

2. It can calculate the optimum values of the overall formation constants of a maximum of four species defined as follows:

$$qB + pA \rightleftharpoons B_qA_p; \quad \beta_{qp} = [B_qA_p]/[B]^q[A]^p \quad (2)$$

B can denote a proton or a metal ion. In the former case the protonation ($+q$) or deprotonation ($-q$) constants of species A, and in the latter case the overall stability constants of metal complexes B_qA_p, are calculated.

CONSTRUCTION AND USE OF THE PROGRAM

MINIPOT consists of a main program and three subroutines. The main program can be divided into three parts. (1) Input and preparation of data for the subsequent calculation (up to line 250). (2) Search procedure for the parameter values (lines 280–390). The search is carried out by changing one of the parameters stepwise between fixed input limits or by amounts depending on the parameter value. The value resulting in the smallest standard deviation is retained. (3) Refinement of the parameters for which the serial numbers are read into the array S1 (lines

400–820). In all cases, only one refinement or search cycle is done. The subroutine EQUSOLV generates values for E_{calc} from the set of parameters given by the main program and feeds them into the array E1. The subroutine has the same algorithm as that in the program PH-POT.[6] The subroutine PRINT prints out the initial and calculated data. The subroutine LIGOPT recalculates the concentration of total base in the reaction mixtures with the modified T_{OH} value.

Variables

F: the task to be executed. F = 0 results in parameter refinement, and F = 1 or 2 in parameter search within limits either given or dependent on the value of the parameter (see line 330).
F1: number of parameters to be refined.
F2: F2 = 1 leads to optimization of the correction vector, otherwise F2 = 0.
J1, J2 and J3: j_H, j_{OH} and K_s (used when W = 2).
K: serial number of the first experimental point to be included.
L: starting iteration value for the free ligand concentration.
N: step between serial numbers of experimental points to be included.
N1, N2 and N3: numbers of experimental points, parameters and complexes.
N4: if N4 = 1, the percentage of T_M, and if N4 = 2, the percentage of T_L in the individual complexes is calculated and printed.
M1, M2 and M3: T_M or T_H, T_{OH} and T_L in the solution.
M4, M5 and M6: T_M or T_H, T_{OH} and T_L in the titrant.
P1–P4: numbers of ligands in individual complexes.
Q1–Q4: numbers of protons or metal ions in individual complexes.
R: if R = 0, there is no print-out: otherwise 1, 2 or 3. It may be reset at several points in the program.
T1: set at +1 if no starting values for the roots of the mass balance equations are available; otherwise −1.
T3, T4 and T5: starting value, step and upper limit for parameter-value search.
T6: serial number of the parameter for which a value is to be sought.
T7: number of steps to be executed after a minimum in the standard deviation is reached in the search for a parameter value (1 is enough).
V: serial number of the last experimental point to be included.
V0: volume of solution (titrand).
V1: where to go after executing the current task (see lines 380 and 820).
W: if W = 1, a blank acid–base titration curve is evaluated, if W = 2, overall stability constants are calculated.

Arrays

A: free ligand concentrations
B: free hydrogen-ion or metal-ion concentrations
E: measured potentials
P: the parameters. If W = 1, P(1)–P(6) are log K_s, log j_H, log j_{OH}, log T_{OH}, E° and g. If W = 2, they are log β_1–β_4, E° and g.
S1: serial number(s) of the parameter(s) to be refined.
T: increments of parameters for the numerical differentiation.
V1: volume of titrant added.

Some remarks on the use of the program

1. When the overall stability constants of metal complexes are to be calculated (W = 2), J1 and J2 must be made zero, and a very small number (*e.g.*, 10^{-30}) must be assigned to J3 to make J3/B^2 negligibly small.

2. In line 130 the logarithms of the starting values for the roots of mass balance equations must be input with −1 for T1; alternatively, if no starting values are available, the inputs are zero, with +1 for T1.

3. If the number of complexes is less than 4, the value zero must be given to the unused variables q and p.

4. The following values are suggested for the increments of the parameters: for log K_s, log j_H and log j_{OH}, 0.03–0.06; for g, 0.05–0.2; and for log β, 0.03–0.1.

5. The program always executes only one refinement cycle or search, then jumps to the label given by the variable V1.

DISCUSSION

Our experience with MINIPOT has been very favourable: its convergence is reliable, even if four parameters are refined simultaneously, and, when the correction vector is also optimized, divergence cannot occur. The running time of the programme is also fairly favourable. It is mainly determined by the time taken for solution of mass balance equations, a few seconds for each experimental point if good starting values are available for the roots. All the other matrix operations take about 10 sec for each parameter to be refined. The only appreciable restriction on the program is the 16-kbyte capacity of the computer, which allows calculation with only 40–50 experimental points.

In constructing the program we tried to make it easily adaptable to other equilibrium problems. Therefore, some parts are written in such a way that they can be used either as they are or with only small changes. For example, the procedure for refinement of the parameters can be used for any problem, if the experimental points have equal weights. If weighting is necessary, a weighting matrix must be built in. For the refinement procedure to be used, all that must be written is a special subroutine (EQUSOLV here) to generate the E_{calc} values for the given problem and feed them into the array E1. The treatment of the parameters by their serial numbers also makes for general applicability; it has the advantage that the number of parameters to be refined is not restricted, and allows the refinement of parameters chosen on chemical or experimental grounds.

With the exception of E° and g, the refinement is carried out with the logarithms of the parameters. In this way the elements of the G matrix[6] are of nearly the same magnitude, which simplifies the problem mathematically.

We have developed similar programs for evaluation of spectrophotometric measurements and calculation of the molar absorptivities and overall stability constants of the complexes formed. These programs can be used for complexes M_qL_p with the data A *vs.* T_L and/or T_M, for complexes $H_rM_qL_p$ with the data A *vs.*

T_M and pH and for mixed ligand complexes MA_nB_{N-n} [$N = 2$–4; $n = 1$-($N - 1$)] with the data A *vs.* T_{MA_N} and/or T_{MB_N}, where A is absorbance.

APPENDIX—TWO NUMERICAL EXAMPLES

Problem 1 (W = 1)

A strong acid (10.0 ml; 0.05*M*) was titrated potentiometrically with 0.093626*M* strong base in a 1:1 propylene glycol–water mixture. Forty experimental points (titrant volume and glass electrode potential values) were taken (N1 = 40). The values of the following six parameters (N2 = 6) are to be found: log K_s, log j_H, log j_{OH}, log T_{OH}, $E°$ and g.

From the middle part of the titration curve a value of about −60 mV can be calculated for $E°$. The ionic product of water can be taken as the starting value for K_s, 59.15 mV for g, and the analytically determined value for T_{OH}. Small numbers can initially be assigned to j_H and j_{OH}. First, log K_s and $E°$ must be calculated from the middle part of the titration curve (only points 14–33 are used).

Input:

Line 60: 1, 40, 6, 1, 10.0, 0.05, 0, 0, 0, 0.093626, 0,
Line 120:
0.4, −144.9, 0.6, −146.1, 0.8, −146.7,
1.0, −148.2, 1.2, −148.7, 1.4, −153.2,
1.6, −153.8, 1.8, −154.3, 2.0, −157.5,
2.2, −158.5, 2.4, −161.0, 2.6, −161.5,
2.8, −166.4, 3.0, −167.2, 3.2, −169.3,
3.4, −170.1, 3.6, −174.1, 3.8, −179.9,
4.0, −183.2, 4.2, −189.2, 4.4, −192.8,
4.6, −199.6, 5.0, −224.9, 5.1, −232.8,
5.2, −245.9, 5.3, −271.2, 5.8, −715.6,
5.9, −722.6, 6.0, −728.2, 6.2, −739.3,
6.4, −745.8, 6.6, −750.5, 6.8, −754.2,
7.0, −756.8, 7.2, −760.3, 7.8, −766.8,
8.0, −769.0, 8.4, −772.1, 8.8, −775.0
9.2, −778.0,
Line 210:
−14, 0.1, 1, 0.03, 1, 0.03, −1.0286, 0.02, −60, 0.1, 59.16, 0.1,
Line 230:
14, 33, 1,

Task:

Search for log K_s (T6 = 1) with (T4 =) 0.1 step (F = 1) between limits (T3 =) −14.2 and (T5 =) −12. After reaching a minimum value for U, execute two further steps (T7 = 2), and then back for new task (V1 = 4).

Input:

Line 260: 1,1,
Line 290: −14.2, 0.1, −12, 1, 1, 2, 4,

Output:

Optimum values: log K_s = −13.7; U = 237.7.

Task:

Search for $E°$ (T6 = 5) with (T4 =) 2 mV step (F = 1) between limits (T3 =) −70 and (T5 =) −50 mV. One step after U_{min} (T7 = 1), and back for new task (V1 = 4).

Input:

Line 260: 1, 3,
Line 290: −70, 2, −50, 5, 1, 1, 4.

Output:

Optimum values: $E°$ = −62; U = 192.3.

Task:

Search for better $E°$ with step and limits determined by its actual value (F = 2). With T3 = 1.05 and T5 = 0.95, the limits will be −65.1 and −58.9, and with T4 = −0.003, the step will be 0.186. (Note that since $E°$ is negative, a negative value must be assigned to T4 to obtain a positive value for step.) Back for new task (V1 = 4).

Input:

Line 260: 2, 1,
Line 290: 1.05, −0.003, 0.95, 5, 1, 1, 4,

Output:

Optimum values: $E°$ = −62.68; U = 184.

Task:

Refinement (F = 0) of log K_s [S1(1) = 1] and $E°$ [S1(2) = 5], *i.e.*, of two parameters (F1 = 2) with the calculation of the correction scalar (F2 = 1). New refinement follows (V1 = 5).

Input:

Line 260: 0, 3,
Line 410: 2, 1, 5, 3,
Line 430: 1, 5,

Output:

Optimum values: log K_s = −13,713, $E°$ = −62.46; U = 181.5.

Task:

The same refinement again, but subsequently the remaining experimental points are included in the calculations (V1 = 3).

Input:

Line 410: 2, 1, 3, 3,
Line 430: 1, 5,

Output:

Optimum values: log K_s = −13.712, $E°$ = −62.46; U = 181.4.

Input:

Line 230: 1, 40, 1,

Task:

Search for log j_H (T6 = 2) with (T4 =) 0.2 step (F = 1) between limits (T3 =) 1.0 and (T5 =) 5.0. One step after U_{min} (T7 = 1), and back for new task (V1 = 4).

Input:

Line 260: 1, 1,
Line 290: 1.0, 0.2, 5.0, 2, 1, 1, 4,

Output:

Optimum values: log j_H = 1.4; U = 374.6.

Task:

The same as the previous one, but the search will be made for log j_{OH} (T6 = 3).

Input:

Line 260: 1, 1,
Line 290: 1.0, 0.2, 5.0, 3, 1, 1, 4,

Output:

Optimum values: log j_{OH} = 2.6; U = 194.3.

Task:

Refinement (F = 0) of the four parameters (F1 = 4) log K_s, log j_H, log j_{OH} and $E°$ (the elements of S1 will be 1, 2, 3 and 5), and calculation of the correction scalar (F2 = 1). New refinement follows (V1 = 5).

Input:

Line 260: 0, 1,
Line 410: 4, 1, 5, 3,
Line 430: 1, 2, 3, 5,

Output:

Optimum values: log K_s = −13.659, log j_H = 1.523, log j_{OH} = 2.779, E° = −62.42; U = 157.5.

Task:

The same as the previous one, but without optimizing the scalar calculation (F2 = 0). Back for new task (V1 = 4).

Input:

Line 410: 4, 0, 4, 3,
Line 430: 1, 2, 3, 5,

Output:

The same values as the former ones.

Task:

Search for log T_{OH} (T6 = 4) with (T4 =) 0.004 step (F1 = 1) between limits (T3 =) −1.032 and (T5 =) −1.0. One step after U_{min}, and back for new task (V1 = 4).

Input:
Line 260: 1, 1,
Line 290: −1.032, 0.004, −1.0, 4, 1, 1, 4,

Output:

Optimum values: log T_{OH} = −1.0288; U = 150.6.

Task:

Refinement (F = 0) with optimizing of scalar calculation (F2 = 1) of the four parameters (F1 = 4) log K_s, log j_H, log j_{OH} and E° (S1: 1, 2, 3 and 5), and end of calculation (V1 = 6).

Input:

Line 260: 0, 1,
Line 410: 4, 1, 6, 3,
Line 430: 1, 2, 3, 5,

Output:

Optimum values: log K_s = −13.66 ± 0.02, log j_H = 1.47 ± 0.38, log j_{OH} = 2.78 ± 0.07, E° = −62.54 ± 0.7; U = 150.34, σ = 2.07 mV.

Problem 2 (W = 2)

A 1.5951 × $10^{-3}M$ polypeptide solution was prepared by dissolution in 0.05*M* strong acid, and 10.0 ml were titrated with 0.09358*M* strong base.

The 17 experimental points used for calculation come from the middle part of the titration curve. In this region four dominant complexes (H_qL_p) are formed, with (q, p) = (2, 1), (1, 1), (−1, 1) and (−2, 1).

Approximate values for free hydrogen-ion and ligand (peptide) concentrations of the individual experimental points are not given (all the elements of arrays B and A are zero, and +1 is assigned to T1). As a starting value for the free peptide concentration ([L]), 0.0005 is given. The values of K_s, j_H, j_{OH}, E° and g are those for the input blank curve (problem 1).

Input:

Line 60: 2,
Line 70: 17, 6, 4, 2, 3, 10.0, 0.05, 0, 0.0015951, 0, 0.09358, 0, 0.0005, 29.5, 616.5, 2.1878E-14,

Line 130:

5.1, −313.0, 0, 0, 5.15, −330.0, 0, 0,
5.2, −345.3, 0, 0, 5.25, −370.0, 0, 0,
5.3, −402.0, 0, 0, 5.35, −484.0, 0, 0,
5.4, −550.0, 0, 0, 5.45, −577.0, 0, 0,
5.5, −612.0, 0, 0, 5.55, −635.0, 0, 0,
5.6, −653.0, 0, 0, 5.65, −664.0, 0, 0,
5.7, −672.4, 0, 0, 5.75, −681.0, 0, 0,
5.8, −689.7, 0, 0, 5.85, −696.0, 0, 0,
5.9, −701.2, 0, 0,

Line 190: 2, 1, 1, 1, −1, 1, −2, 1,
Line 210: 7, 0.04, 3, 0.03, −11, 0.04, −21, 0.05, −62.54, 0.1, 59.16, 0.1,
Line 230: 1, 17, 1, 1,

Task:

Search for the approximate log β values with (T4 =) 0.5 step (F = 1) for each, between the limits 7–12, 3–8, −11−−5 and −21−−15 in order of input. One step after U_{min}. Back for new task in all cases (V1 = 4).

Input:

Line 260: 1, 3,
Line 290: 7, 0.5, 12, 1, 1, 1, 4,
Line 260: 1, 3,
Line 290: 3, 0.5, 8, 2, 1, 1, 4,
Line 260: 1, 3,
Line 290: −11, 0.5, −5, 3, 1, 1, 4,
Line 260: 1, 3,
Line 290: −21, 0.5, −15, 4, 1, 1, 4,

Output:

Optimum log β values: 9.5, 5.0, −8.5 and −18.5; U = 780.

Task:

Refinement (F = 0) of the four log β values (F1 = 4, S1: 1, 2, 3 and 4) with optimization of scalar calculation (F2 = 1). Back for new refinement (V1 = 5).

Input:

Line 260: 0, 1,
Line 410: 4, 1, 5, 3,
Line 430: 1, 2, 3, 4,

Output:

Optimum log β values: 9.29, 5.17, −8.47 and −18.7; U = 319.

Task:

Repetition of the previous refinement, no optimizing scalar calculation (F2 = 0), and end of calculation (V1 = 6).

Input:
Line 410: 4, 0, 6, 3,
Line 430: 1, 2, 3, 4,

Output:

Final values: log β_2 = 9.25 ± 0.09, log β_1 = 5.14 ± 0.07, log β_{-1} = −8.47 ± 0.05 and log β_2 = −18.73 ± 0.09; U = 318.8, σ = 5.5 mV.

REFERENCES

1. F. Gaizer, P. Buxbaum, E. Papp-Molnár and K. Burger, *J. Inorg. Nucl. Chem.*, 1974, **36**, 849.
2. F. Gaizer, *Magy. Kém. Foly.* 1977, **83**, 250.
3. F. Gaizer and M. Máté, *Acta Chim. Acad. Sci. Hung.*, 1980, **103**, 355.
4. F. Gaizer, M. Máté and J. Lázár, *Talanta*, 1981, **28**, 127.
5. F. Gaizer and I. Szalay, *Magy. Kém. Foly.* 1972, **78**, 488.
6. F. Gaizer, *Acta Chim. Acad. Sci. Hung.*, 1980, **103**, 397.
7. *Idem*, *Coord. Chem. Rev.*, 1979, **27**, 195.
8. W. E. Wentworth, *J. Chem. Educ.*, 1965, **42**, 96.

```
10 REM PROGRAMME MINIPOT
20 DIM L(40),M(40),N(40),E(40),P(6),T(6),A(50),B(50),E1(40)
30 DIM C(4,4),C5(4,4),D(40),G(4,40),S1(4),G1(4),G2(4),F(40)
40 DIM C1(40),C2(40),C3(40),C4(40),V1(40)
50 Z=LOG(10):Z1=1/Z:E5=1000
60 READ W:IF W>1 THEN 70:READ N1,N2,R,V0,M1,M2,M3,M4,M5,M6:GOTO 120
70 READ N1,N2,N3,N4,R,V0,M1,M2,M3,M4,M5,M6,L,J1,J2,J3
80 REM *N1,N2,N3* NO. OF MEASD. POINTS, PARAMS, COMPLEXES
90 REM *N4* PERCENT FOR T-M (=1) OR T-L (=2); *R* PRINT; *V0* VOL. OF TITRAND
100 REM *M1,...,M6* T-H/M, T-OH, T-L IN TITRAND, THEN THOSE IN TITRAND
110 REM *L* START VAL. FOR FREE LIGAND; *J1,J2,J3* LOG(J-H, J-OH, K-S)
120 FOR I=1 TO N1:IF W>1 THEN 130:READ V1(I),E(I):GOTO 150
130 READ V1(I),E(I),B(I),A(I):B(I)=EXP(Z*B(I)):A(I)=EXP(Z*A(I))
140 REM *V1* VOL. OF TITRANT; *E* MEASD. EMF; *B,A* LOG START VALUE
        FOR FREE METAL/H AND LIGAND;
150 X1=V0+V1(I):M(I)=(V0*M1+V1(I)*M4)/X1:N(I)=(V0*M2+V1(I)*M5)/X1
160 IF W=1 THEN 170:L(I)=(V0*M3+V1(I)*M6)/X1
170 IF R=0 THEN 180:PRINTUSING 1340,I;M(I)*E5;N(I)*E5;L(I)*E5;E(I);V1(I)
180 NEXT I:PRINT :PRINT
190 IF W=1 THEN 210:READ Q1,P1,Q2,P2,Q3,P3,Q4,P4
200 REM *Q1,P1,...,Q4,P4* STOICH. COEFFS. OF SPECIES
210 FOR I=1 TO N2:READ P(I),T(I):NEXT I
220 REM *P,T* PARAMETER AND INCREMENT. SEQUENCE, IF W=1, THEN LOG(K-S,
        J-H, J-OH, T-OH), E-0, G; IF W=2, THEN LOG(BETA-1,...,4),E-0, G
230 INPUT K,V,N:IF W=1 THEN 260:INPUT T1
240 REM *K,V,N* FIRST, LAST, EXP. POINT AND STEP;
250 REM *T1* IF THERE ARE ROOTS =-1, OTHERWISE =+1
260 INPUT F,R:GOSUB 830:GOSUB 1280:U1=U:IF F=0 THEN 410
270 REM *F* THE TASK TO BE EXECUTED; *R* PRINT
280 REM *** SEARCH PROCEDURE FOR PARAMETER VALUE ***
290 INPUT T3,T4,T5,T6,R,T7,V1:IF F=1 THEN 340
300 REM *T3,T4,T5* START, STEP, UPPER LIMIT OF PARAM. SEARCH;
310 REM *T6* SER. NO. OF PARAM. TO BE SEARCHED FOR;
320 REM *R* PRINT; *T7* STEPS AFTER MINIMUM; *V1* CONTROL
```

```
330 T3=P(T6)*T3:T4=P(T6)*T4:T5=P(T6)*T5
340 P(T6)=T3:GOSUB 1470:GOSUB 830:GOSUB 1280:T8=H:T9=P(T6):GOTO 370
350 GOSUB 1470:GOSUB 830:GOSUB 1280:IF H>T8 THEN 360:T8=H:T9=P(T6):GOTO 370
360 T7=T7-1:IF T7=0 THEN 380
370 P(T6)=P(T6)+T4:IF P(T6)<=T5 THEN 350
380 P(T6)=T9:PRINTUSING 390,T6,T9:GOSUB 1470:ON V1 GOTO 60,190,230,260,410:END

390 %THE OPTIMUM VALUE OF PARAMETER NO. #### IS =-########.######
400 REM *** REFINEMENT PROCEDURE FOR PARAMETER VALUES ***
410 INPUT F1,F2,V1,R:MAT C=ZER(F1,F1):MAT C5=ZER(F1,F1)
420 REM *F1* NO. OF PARAM(S). TO BE REFINED; *F2* IF =1, THEN CORR. VECTOR
      OPT., OTHERWISE =0; *V1* CONTROL; *R* PRINT
430 MAT INPUT S1(F1):PRINT "PARAMETERS TO BE REFINED:":MAT PRINT S1;
440 REM *S1* SER. NO. OF PARAM(S). TO BE REFINED
450 REM *** ERROR VECTOR, D ***
460 FOR I=K TO V STEP N:D(I)=E(I)-E1(I):F(I)=E1(I):NEXT I
470 REM *** G MATRIX ***
480 FOR K1=1 TO F1:J=S1(K1):P(J)=P(J)+T(J):T6=J:GOSUB 1470:GOSUB 830
490 FOR I=K TO V STEP N:G(K1,I)=(E1(I)-F(I))/T(J):NEXT I
500 P(J)=P(J)-T(J):GOSUB 1470:NEXT K1
510 REM *** C MATRIX ***
520 FOR K1=1 TO F1:FOR K2=1 TO F1:C(K1,K2)=0:FOR I=K TO V STEP N
530 C(K1,K2)=C(K1,K2)+G(K1,I)*G(K2,I):NEXT I
540 C(K2,K1)=C(K1,K2):NEXT K2:NEXT K1
550 REM *** INVERSION OF MATRIX C INTO C5 ***
560 FOR I=1 TO F1:FOR K1=1 TO F1:C5(I,K1),C5(K1,I)=0:NEXT K1:C5(I,I)=1
570 NEXT I:C5(F1,F1)=1:FOR K1=1 TO F1:V3=C(K1,K1):FOR I=1 TO F1
580 C(K1,I)=C(K1,I)/V3:C5(K1,I)=C5(K1,I)/V3:NEXT I:FOR L=1 TO F1
590 IF L-K1=0 THEN 610:V3=C(L,K1):FOR I=1 TO F1
600 C(L,I)=C(L,I)-V3*C(K1,I):C5(L,I)=C5(L,I)-V3*C5(K1,I):NEXT I
610 NEXT L:NEXT K1
620 REM *** MULTIPL. OF ERROR VECT AND G-TRANSP. ***
630 FOR I=1 TO F1:S=0:FOR J=1 TO V:S=S+G(I,J)*D(J):NEXT J:G1(I)=S:NEXT I
640 REM *** CORRECTION VECTOR, G2 ***
650 FOR I=1 TO F1:S=0:FOR J=1 TO F1
660 S=S+C5(I,J)*G1(J):NEXT J:G2(I)=S:NEXT I:A6,I6=1
```

```
670 IF F2=0 THEN 690:PRINT "U1=",U1
680 K6=R:R=0:I6=0:K7=1:A6=.5:GOTO 700
690 PRINT "REFINED PARAMETERS:":PRINT
700 FOR K1=1 TO F1:J=S1(K1):P(J)=P(J)+G2(K1)*A6:NEXT K1
710 GOSUB 1470:GOSUB 830
720 IF I6>0 THEN 800:IF K7=0 THEN 740:U2=U:PRINT "U2=",U2
730 K7=0:GOTO 700
740 U3=U:PRINT "U3=",U3:R=K6:U4=U1-2*U2+U3:IF U4>0 THEN 770
750 A6=1:IF U3<U1 THEN 760:A6=0
760 PRINT "CONCAVE ALFA, IS MADE EQUAL WITH",A6:GOTO 780
770 U4=(U1-U3)/(4*U4):A6=.5+U4:PRINT "ALFA=",A6
780 A6=1-A6:I6=1:IF ABS(A6)<3 THEN 790:A6=2
790 A6=-A6:GOTO 690
800 GOSUB 1280:U1=U:FOR I=1 TO F1:J=S1(I):U7=SQR(ABS(C5(I,I)))*H
810 PRINT "ERROR OF PARAMETER OF NO. ";J;":";U7:NEXT I
820 ON V1 GOTO 60,190,230,260,410:END
830 REM EQUSOLV
840 IF R=0 THEN 850:PRINTUSING 1400,P(1);P(2);P(3);P(4);P(5);P(6):PRINT
850 E1=EXP(Z*P(1)):E2=EXP(Z*P(2)):E3=EXP(Z*P(3)):U,S2=0
860 IF W=1 THEN 870:C2,C3,C4=0:A=L:T1=T1-1:E4=EXP(Z*P(4))
870 FOR I=K TO V STEP N:B1=M(I)-N(I)
880 IF W>1 THEN 910:B=.5*(ABS(B1)+SQR(B1^2+4*E1))
890 IF B1>=0 THEN 900:B=E1/B
900 C1(I)=E2*B:C2(I)=E3*E1/B:E1(I)=P(5)+P(6)*Z1*LOG(B)-C1(I)-C2(I):GOTO 1090
910 B=EXP(Z*(E(I)-P(5))/P(6)):A1=L(I):B1=M(I)-N(I)
920 A2=A1*.0011:B2=ABS(B1*.0011):T2,S1=0:IF T1>=0 THEN 930:A=A(I):B=B(I)
930 T2=T2+1:IF T2>8 THEN 1100
940 C1=E1*A^P1*B^Q1:A3=A+C1*P1:B3=B+C1*Q1-J3/B
950 D1=1+C1*P1^2/A:D2=1+C1*Q1^2/B+J3/B^2:D3=C1*P1*Q1
960 ON N3 GOTO 1030,1010,990,970
970 C4=E4*A^P4*B^Q4:A3=A3+C4*P4:B3=B3+C4*Q4
980 D1=D1+C4*P4^2/A:D2=D2+C4*Q4^2/B:D3=D3+C4*P4*Q4
990 C3=E3*A^P3*B^Q3:A3=A3+C3*P3:B3=B3+C3*Q3
1000 D1=D1+C3*P3^2/A:D2=D2+C3*Q3^2/B:D3=D3+C3*P3*Q3
1010 C2=E2*A^P2*B^Q2:A3=A3+C2*P2:B3=B3+C2*Q2
1020 D1=D1+C2*P2^2/A:D2=D2+C2*Q2^2/B:D3=D3+C2*P2*Q2
```

```
1030 Y1=A3-A1:Y2=B3-B1:D4=D3/A:D3=D3/B:D5=D1*D2-D3*D4:IF D5=0 THEN 1100
1040 A=A+(D3*Y2-D2*Y1)/D5:B=B+(D4*Y1-D1*Y2)/D5
1050 IF ABS(Y1)>A2 THEN 930:IF ABS(Y2)>B2 THEN 930
1060 IF A<0 THEN 1100:IF A>A1 THEN 1100:IF B<0 THEN 1100
1070 A(I)=A:B(I)=B:C1(I)=C1:C2(I)=C2:C3(I)=C3:C4(I)=C4
1080 E1(I)=P(5)+P(6)*Z1*LOG(B)-J1*B-J2*J3/B
1090 D(I)=E(I)-E1(I):S2=S2+1:U=U+D(I)^2:GOTO 1270
1100 A=L:B=EXP(Z*(E(I)-P(5))/P(6)):IF T1>=0 THEN 1110:A=A(I):B=B(I)
1110 G1=2:D5=B
1120 G2=2:D6=A
1130 C1=E1*A^P1*B^Q1:A3=A+C1*P1:B3=B+C1*Q1-J3/B
1140 ON N3 GOTO 1180,1170,1160,1150
1150 C4=E4*A^P4*B^Q4:A3=A3+C4*P4:B3=B3+C4*Q4
1160 C3=E3*A^P3*B^Q3:A3=A3+C3*P3:B3=B3+C3*Q3
1170 C2=E2*A^P2*B^Q2:A3=A3+C2*P2:B3=B3+C2*Q2
1180 IF ABS(A1-A3)<A2 THEN 1210:IF A1-A3<0 THEN 1200
1190 D6=G2*D6:A=A+D6:GOTO 1130
1200 G2= 5:D6=G2*D6:A=A-D6:GOTO 1130
1210 IF B1>0 THEN 1220:B4=B3-B1:GOTO 1230
1220 B4=B1-B3
1230 B5=ABS(B4):IF B2>B5 THEN 1070:IF B1<0 THEN 1260:IF B4<0 THEN 1250
1240 D5=G1*D5:B=B+D5:GOTO 1120
1250 G1=.5:D5=G1*D5:B=B-D5:GOTO 1120
1260 IF B4<0 THEN 1240:GOTO 1250
1270 NEXT I:RETURN
1280 REM PRINT
1290 IF R<=1 THEN 1420:FOR I=K TO V STEP N:IF W>1 THEN 1330
1300 PRINTUSING 1350,I,V1(I),M(I)*E5,N(I)*E5,E(I),E1(I),D(I),C1(I),C2(I)
1310 GOTO 1410
1320 IF R<=1 THEN 1410
1330 PRINTUSING 1340,I,V1(I),M(I)*E5,N(I)*E5,L(I)*E5,E(I),E1(I),D(I)
1340 %#####-###.##-###.####-###.#### -###.####-#####.##-#####.##-#####.##
1350 %#####-###.##-###.####-###.####-#####.##-#####.##-#####.##-####.##-####.##
1360 IF R<=2 THEN 1410:IF N4>1 THEN 1370:X6=100/M(I):GOTO 1380
1370 X6=100/L(I)
1380 PRINTUSING 1390,C1(I)*X6,C2(I)*X6,C3(I)*X6,C4(I)*X6,100*B(I)/M(I),
```

```
    A(I)*100/L(I)
1390 %-################. ##-#####. ##-#####. ##-#####. ##-#####. ##-#####. ##
1400 %-##############. ####-###. ####-###. ####-###. ####-#####. ##-#####. ##
1410 NEXT I
1420 PRINTUSING 1430,":";U
1430 %SQUARE OF RESIDUALS#  #.####^^^^
1440 H=SQR(U/(S2-F1-1)):PRINT :PRINTUSING 1450,":";H
1450 %STANDARD DEVIATION #  #.####^^^^
1460 PRINT HEX(0A0A0A):RETURN
1470 REM LIGOPT:IF W=2 THEN 1490:IF T6<>4 THEN 1490:E4=EXP(Z*P(4))
1480 FOR I=1 TO N1:N(I)=(V0*M2+V1(I)*E4)/(V0+V1(I)):NEXT I
1490 RETURN
```

Talanta. Vol. 28. pp. 575 to 583. 1981
Printed in Great Britain. All rights reserved

0039-9140/81/080575-09$02.00/0
Copyright © 1981 Pergamon Press Ltd

AN ARBITRARY CORRECTION FUNCTION FOR CO_2 EVOLUTION IN ACID–BASE TITRATIONS AND ITS USE IN MULTIPARAMETRIC REFINEMENT OF DATA

MICHEL WOZNIAK and GUY NOWOGROCKI
Ecole Nationale Supérieure de Chimie de Lille, Université de Lille I,
BP 40, 59650 Villeneuve d'Ascq, France

(*Received* 19 *November* 1980, *Accepted* 27 *January* 1981)

Summary—A great number of acid–base titrations are performed under an inert gas flow: in the procedure, a variable amount of CO_2—from carbonated reactants—is carried away and thus prevents strict application of mass-balance equations. A function for the CO_2 evolution is proposed and introduced into the general expression for the volume of titrant. Use of this expression in multiparametric refinement yields, besides the usual values (concentrations, acidity constants...), a parameter characteristic of this departure of CO_2. Furthermore, a modified weighting factor is introduced to take into account the departure from equilibrium caused by the slow CO_2 evolution. The validity of these functions was successfully tested on three typical examples: neutralization of strong acid by sodium carbonate, of sodium carbonate by strong acid, and of a mixture of hydrochloric acid, 4-nitrophenol and phenol by carbonated potassium hydroxide.

Numerous analytical results and values of acidity constants are obtained from potentiometric titrations. Appreciable improvements in the interpretation of experimental data have been brought about by using multiparametric refinement.[1–8] However, the results can be somewhat affected by the presence of carbon dioxide and its ionized forms in solution.

If a closed system is used,[9] the influence of carbonate ions can be taken into account by a mathematically rigorous treatment of the data. Unfortunately, this mode of operation suffers from the serious practical drawback that the equilibration is rather slow. Conversely, in classical neutralizations under a flow of inert gas, an apparent stabilization of the potential is attained rather rapidly, but as some CO_2 is given off, the mass-balance equations are not satisfied and only approximate treatments can be considered. Addition of barium chloride to the reactants to precipitate barium carbonate can reduce the carbonate interference, but may introduce other errors by interaction of barium with analyte.

In a previous paper,[7] we proposed using a discontinuity in the total concentration of added carbonate. Although improving the precision of the results, this was still not quite completely satisfactory: the treatment was not general enough, some high correlations between effects of various parameters occurred and the introduction of a discontinuity in the least-squares calculation gave high standard deviations because of the non-randomness of the residuals.

We propose here to utilize a semi-empirical function to correct for the evolution of CO_2 from the solution. The choice of the equations was founded on interpretation of titration curves involving carbonate: nitric acid neutralized by sodium carbonate, sodium carbonate neutralized by nitric acid, and a mixture (hydrochloric acid, 4-nitrophenol and phenol) titrated with carbonated potassium hydroxide.

EXPERIMENTAL

Instrumentation and titration procedure

The automated titration system described previously[8] was used: it consisted of a Radiometer PHM 64 potentiometer, a Tacussel EBX 1 automatic burette and a Hewlett–Packard 9825A calculator.

The sample solution was placed in a jacketed cell kept at 25.00 ± 0.05°. The electrodes used were either a Schott type N65 pH combined electrode or a Schott type N glass electrode and an Ingold type 303 reference calomel electrode. A stream of purified and presaturated nitrogen was bubbled through the solution or flowed over the solution. Magnetic stirring was used.

The calculator controlled the stepwise additions of titrant by means of a micrometric syringe (2.5 ml) adapted to the automatic burette.[10] After each addition, the potential E was monitored by the calculator until the potential change $\Delta E/\Delta t$ was less than a certain maximum value (0.1 or 0.05 mV/min) or when a preset maximum time was attained (2, 4, 8 or 16 min). For each experimental point, the values of volume of titrant, potential E and potential drift $\Delta E/\Delta t$ were stored on magnetic tape. That is the currently used procedure in the titration studies: as carbon dioxide is constantly carried away by the nitrogen stream,

the carbonate equilibria are slowly displaced and some potential values are indeed taken in a non-equilibrium state (or if the carbonate concentration is low, in a state of false equilibrium).

Reagents

The solutions of sodium carbonate (2.21×10^{-2} and $7.06 \times 10^{-4}M$) were made by weighing out appropriate amounts of analytical-grade sodium carbonate (Carlo Erba, primary standard); solutions of nitric acid (2.00×10^{-4} and $0.100M$) were prepared by dilution of standardized nitric acid. These solutions, except for the $0.100M$ nitric acid, were also $0.100M$ in potassium nitrate (Merck, *pro anal.*).

The mixture of acids was obtained from standardized $1.00M$ hydrochloric acid and by weighing out 4-nitrophenol (Merck) and phenol (Carlo-Erba, RPE-ACS). The ionic strength was adjusted to 1.00 by adding potassium chloride (Merck, *pro anal.*). To emphasize the phenomena due to presence of carbonate, the $1.00M$ potassium hydroxide (Prolabo) used as titrant was deliberately carbonated by addition of potassium carbonate (Carlo-Erba) to give a final carbonate concentration close to $3 \times 10^{-2}M$.

All these solutions were prepared from distilled CO_2-free water.

Preliminary determinations

The purity and acidity constants of the components of the mixture were obtained, at 25°, in $1M$ potassium chloride medium, from the curves for neutralization of the pure compounds by "carbonate-free" potassium hydroxide; the values computed are: $\log \beta = 6.922$ ($3\sigma = 0.006$) for 4-nitrophenol and $\log \beta = 9.715$ ($3\sigma = 0.01$) for phenol.

The overall acidity constants of carbonic acid were determined by titration of $5 \times 10^{-3}M$ hydrochloric acid in a closed system, in $1M$ potassium chloride medium, with $1M$ potassium hydroxide in $0.204M$ potassium carbonate. The volumes of the solution and of the gaseous phase were 200 and 30 ml respectively.[9] The multiparametric refinement led to the values $\log \beta_1 = 9.59$ ($3\sigma = 0.02$) and $\log \beta_2 = 15.57$ ($3\sigma = 0.04$), the liquid–gas equilibrium constant being fixed at $K_p = 3.98 \times 10^{-2}$ mole.l^{-1}.atm^{-1}, as determined previously.[9] The carbonated potassium hydroxide used in this work was analysed under the same experimental conditions (closed system). The potassium ion concentration and the total carbonate concentration were found to be $H_x^0 = -1.063M$ and $C_x^0 = 3.68 \times 10^{-2}M$ respectively. It must be pointed out that, even with a small gas volume, the duration of a titration in a closed system is rather lengthy: in the pH-range where reabsorption of CO_2 can occur, the stabilization time exceeds 10 min for each experimental point.

THEORETICAL

The curves for titration of a strong acid with sodium carbonate (Fig. 1) or of sodium carbonate with a strong acid (Fig. 2) lie between the theoretical curves that can be computed on the hypothesis of perfect conservation of CO_2 in solution (Fig. 1f and Fig. 2f) or on the hypothesis of total liberation according to $CO_3^{2-} + H_2O \rightarrow CO_2 + 2\,OH^-$ (Fig. 1g and Fig. 2g). Obviously, no existing method can produce such curves.

We have tested many empirical functions to take into account the progressive evolution of CO_2: we present here the most satisfactory, which gives the true value of the carbonate concentration and acceptable values for the acidity constants of carbonic acid in the computations.

Calculated volume of titrant

The refinement is based on adjustment between the observed and calculated volumes of reagent for each experimental point. The mathematical expression for the calculated volume v_n is derived from the electroneutrality equation, which for titrations of sodium carbonate with nitric acid, or *vice versa*, is:

$$v_0 H_i^0 + (v_0 + v_n)(2[CO_3^{2-}] + [HCO_3^-] + [OH^-]) = -v_n H_x^0 + (v_0 + v_n)\ [H^+] \quad (1)$$

in which subscripts i and x refer to an initial species and an added species respectively. Thus H_i^0 or H_x^0 are the total concentrations of strong acid when positive, and the total concentrations of Na^+ when negative; v_0 is the initial volume of the solution.

If C_i^0 and C_x^0 are the initial and added concentrations of carbonate (*i.e.*, the total concentrations irrespective of the actual species present), we should theoretically have, for the first volume v_1 added

$$(v_0 + v_1)([H_2CO_3] + [HCO_3^-] + [CO_3^{2-}]) = v_0 C_i^0 + v_1 C_x^0$$

As some CO_2 is carried away by the gaseous flow, the proportion which leaves the solution will be evaluated by means of an empirical function G_n. The total amount of carbonate remaining in the solution is then:

$$(v_0 C_i^0 + v_1 C_x^0)(1 - G_1)$$

and consequently

$$(v_0 + v_1)(2[CO_3^{2-}] + [HCO_3^-]) = (v_0 C_i^0 + v_1 C_x^0)(1 - G_1)(2 - \bar{n}_H)$$

where $\bar{n}_H$ is the average number of bound protons [$\bar{n}_H = (2\beta_2[H^+]^2 + \beta_1[H^+])/(\beta_2[H^+]^2 + \beta_1[H^+] + 1)$], β_1 and β_2 being the overall stability constants of HCO_3^- and H_2CO_3.

For the second addition of titrant, this equation becomes

$$(v_0 + v_2)(2[CO_3^{2-}] + [HCO_3^-]) = \{(v_0 C_i^0 + v_1 C_x^0)(1 - G_1) + (v_2 - v_1)C_x^0\}(1 - G_2)(2 - \bar{n}_H)$$

and so on until the nth increment

$$(v_0 + v_n)(2[CO_3^{2-}] + [HCO_3^-]) = [\ldots\{(v_0 C_i^0 + v_1 C_x^0)(1 - G_1) + (v_2 - v_1)C_x^0\}(1 - G_2)\ldots + (v_n - v_{n-1})C_x^0](1 - G_n)(2 - \bar{n}_H)$$

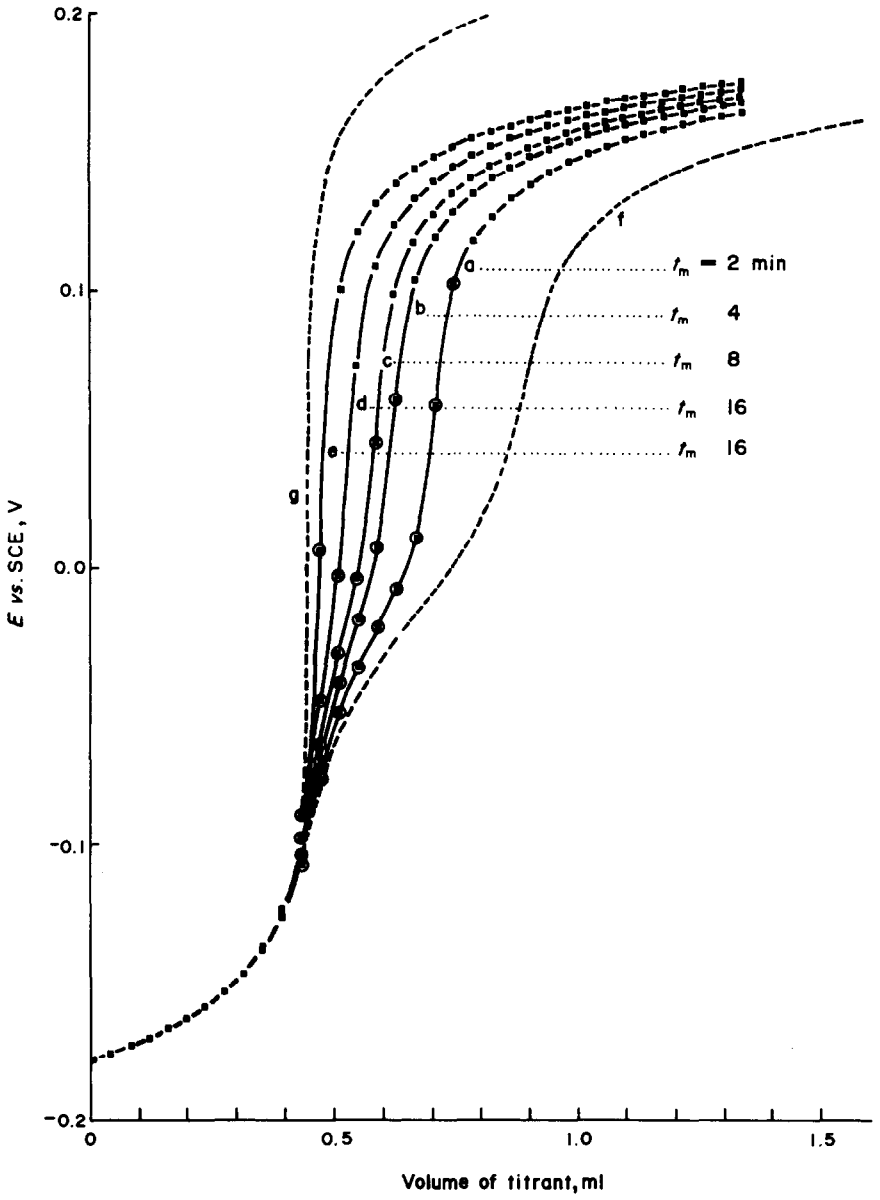


Fig. 1. Titration curves (a, b, c, d, e) of 100 ml $2 \times 10^{-4}M$ of nitric acid with $0.0221M$ sodium carbonate, under nitrogen, corresponding to different maximum waiting times t_m (25.0°, $0.1M$ KNO_3). a, b, c, d, nitrogen flowing over the solution; e, nitrogen bubbling in the solution. ⊙ non-equilibrium state ($\Delta E/\Delta t > 0.1$ mV/min). f, calculated curve, assuming the conservation of CO_2 in solution; g, calculated curve, assuming the quantitative evolution of CO_2.

By combination with equation (1), we finally obtain for the calculated volume at point n

$$v_{nc} = v_0 \frac{H_i^0 + \left\{C_i^0 \prod^{n}(1 - G_n) - \frac{F_n}{v_0} C_x^0(1 - G_n)\right\}(2 - \bar{n}_H) - [H^+] + \frac{K_w}{[H^+]}}{-H_x^0 - C_x^0(1 - G_n)(2 - \bar{n}_H) + [H^+] - \frac{K_w}{[H^+]}} \qquad (2)$$

with

$$F_n = F_{n-1} + G_{n-1}(v_{n-1} - F_{n-1})$$

and

$$F_0 = G_0 = 0.$$

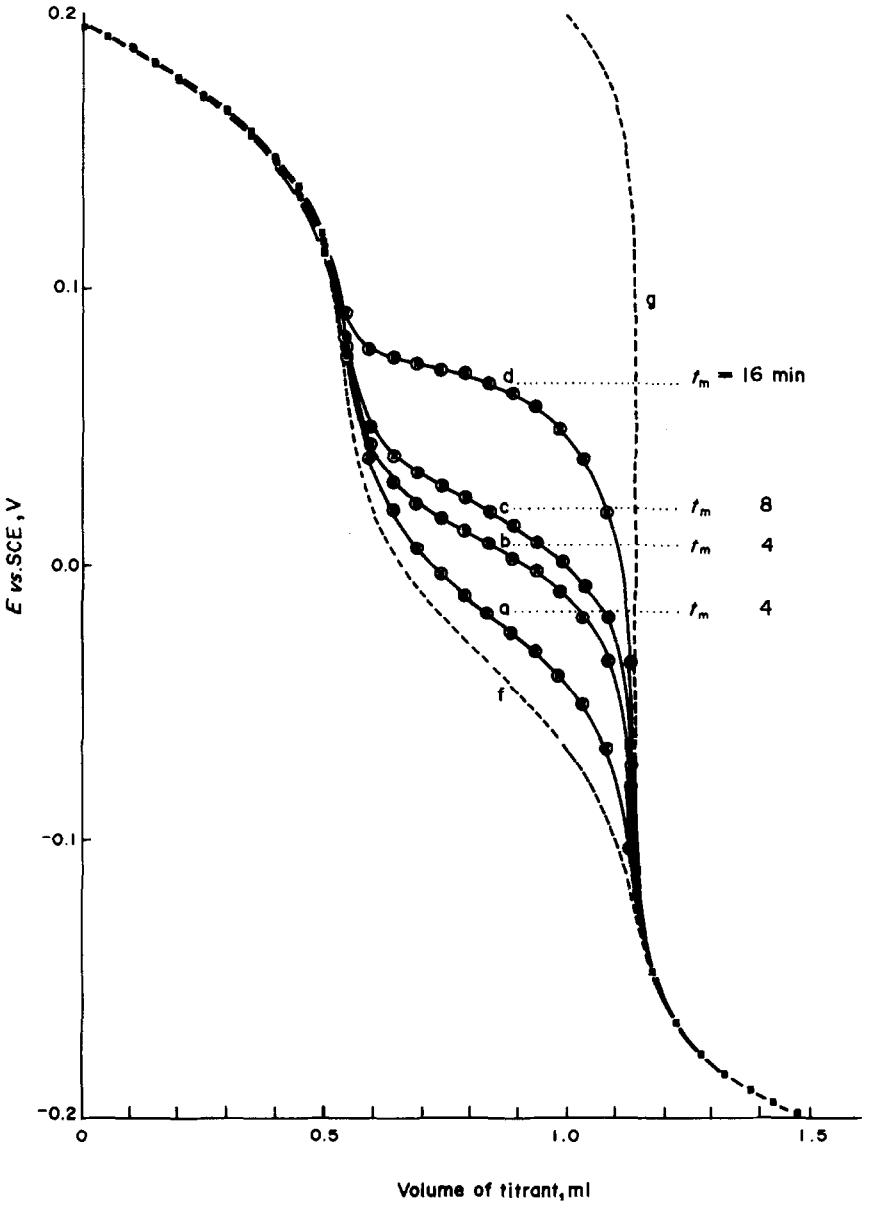


Fig. 2. Titration curves (a,b,c,d) of 80 ml of $7.06 \times 10^{-4}M$ sodium carbonate with $0.1M$ nitric acid, under nitrogen, corresponding to different maximum waiting times t_m (25.0°, $0.1M$ KNO_3). a, nitrogen flowing over the solution; b, c, d, nitrogen bubbling in the solution; symbols as in Fig. 1.

The preceding demonstration can be applied to neutralizations of protolyte mixtures and leads to the general expression

$$v_{nc} = v_0 \frac{H_i^0 + \sum_{d=1}^{D} C_d^0(N_d - \bar{n}_{Hd}) + \left\{C_i^0 \prod^{n}(1 - G_n) - \frac{F_n}{v_0} C_x^0(1 - G_n)\right\}(2 - \bar{n}_H) - [H^+] + \frac{K_w}{[H^+]}}{-H_x^0 - \sum_{b=1}^{B} C_b^0(N_b - \bar{n}_{Hb}) - C_x^0(1 - G_n)(2 - \bar{n}_H) + [H^+] - \frac{K_w}{[H^+]}} \quad (3)$$

where D and B are the numbers of protolytes in the starting solution and the titrant respectively, N_d and N_b being the corresponding numbers of bound protons.[4]

The form given to the function G_n must reflect the physical observations: obviously, in acidic medium, departure of CO_2 is nearly quantitative and G_n must be close to unity. In less acidic solution the evolution takes place at a far reduced rate and G_n

must decrease accordingly. We have tested functions of the form

$$G_n = \frac{\alpha\beta_2[H^+]^2 + \gamma\beta_1[H^+] + \delta}{\alpha\beta_2[H^+]^2 + \beta_1[H^+] + 1} \quad (4)$$

The parameters α, γ and δ are related to departure of CO_2 from its different forms in solution and will be adjusted in the refinement.

Data processing

The unknown parameters are refined by a least-squares method which minimizes the function

$$\sum^{N} W_n(v_n - v_{nc})^2$$

which was described in our previous papers.[4,5,7,8] The weighting term W_n was introduced to take into account the experimental errors in measurement of volume and potential and was given the form:

$$\frac{1}{W_n} = \sigma_{0v}^2 + \sigma_{0E}^2\left(\frac{\partial v_{nc}}{\partial E_n}\right)^2$$

where σ_{0v}^2 and σ_{0E}^2 are the variances of v and E, estimated from the resolution of the burette and the voltmeter.

In the present case, it is logical to place but limited trust in the experimental points where departure of CO_2 causes a potential drift and the weighting factor must decrease when $\partial E_n/\partial t$ is high, so a new form of W_n is used.

$$\frac{1}{W_n} = \sigma_{0v}^2 + \sigma_{0E}^2\left(\frac{\partial v_{nc}}{\partial E_n}\right)^2 + k_0^2\left(\frac{\partial v_{nc}}{\partial E_n}\right)^2\left(\frac{\partial E_n}{\partial t}\right)^2 \quad (5)$$

The last term introduces the time as a variable and can be taken as an evaluation of the deviation from equilibrium; $k_0(\partial E_n/\partial t)$ represents the error due to potential drift which must be added to the instrumental uncertainty σ_{0E} and which can be caused by various phenomena (CO_2 evolution, diffusion potential relaxation, glass electrode equilibration . . .).

In the classical experiments, for which the potential drift is not recorded, it can be noted that the equilibria are chiefly disturbed in the pH range where HCO_3^- is the predominant species, but not at its maximum concentration, and that $|\partial E_n/\partial t|$ increases with $|\partial E_n/\partial v_{nc}|$. We have found that the expression

$$\left(\frac{\partial E_n}{\partial t}\right) = \left[k\sigma_{0E}\left(\frac{\partial E_n}{\partial v_{nc}}\right)\frac{\beta_1[H^+]}{\beta_2[H^+]^2 + \beta_1[H^+] + a}\right]^2$$

gives figures very close to the experimental values, the positive constant a being introduced to shift the maximum drift to lower pH values. The weighting factor then takes the form

$$\frac{1}{W_n} = \sigma_{0v}^2 + \sigma_{0E}^2\left[\left(\frac{\partial v_{nc}}{\partial E_n}\right)^2 + k_1^2\left(\frac{\beta_1[H^+]}{\beta_2[H^+]^2 + \beta_1[H^+] + a}\right)^2\right] \quad (6)$$

With $a = 500$, expression (6) reproduces fairly well the weighting factors computed from the experimental drift, as can be seen in Fig. 3, at least in our experimental conditions.

The value of k_1 was chosen so as to obtain a weighted standard deviation s

$$s^2 = \sum^{N} W_n(v_n - v_{nc})^2/(N - P),$$

where P is the number of adjusted parameters in the refinements, in the range of unity. In the titration of a mixture of acids, it was found that a value of 10 for k_1 gave coherent results.

For the experiments involving only carbonate as weak protolyte, several particular programs were written, permitting examination of various hypotheses on the CO_2-departure function G_n. For the titration of the mixture of protolytes, the multiparametric refinement program MUPROT[7,8] was used to process the experimental data, after modifications according to equations (3) and (4).

All the programs were written in HPL language, akin to BASIC, for the 9825 Hewlett–Packard calculator (with 16 kbyte of user-accessible memory). The programs are available from the authors on request.

RESULTS AND DISCUSSION

Neutralization of strong acid with sodium carbonate

Figure 1 shows the titration curves obtained for various experimental conditions. Stable potentials were reached fairly rapidly in acidic medium (liberation of CO_2 is practically immediate) or in basic medium (CO_2 evolution negligible).

The refinement program was based on equation (2) for the calculated volume of reagent with H_i^0 (>0) strong acid concentration and C_x^0 total concentration of carbonate, including the CO_2 absorbed from the atmosphere ΔC_x^0. H_x^0 is the concentration of Na^+ known from the weight of sodium carbonate: $H_x^0 = -2(C_x^0 - \Delta C_x^0)$. C_i^0, the concentration of CO_2 in the acid solution at the start, was taken to be zero.

The refined parameters were α, γ, δ [expression (4)], β_1, β_2, C_x^0, ΔC_x^0 and E_0 (standard potential of the electrode chain). The results of two typical adjustments are listed in Table 1; β_1 and β_2 are common to all the curves, the other parameters were computed for each individual curve. For clarity, only the mean values of γ, δ, C_x^0 and E_0 are reported (all these calculated values being within the confidence ranges, taken as 3σ). The standard deviations of the volume s_v ($\sigma_{0E} = k_0 = 0$), more representative than the weighted standard deviation, were also evaluated: with regard to the experimental conditions they were quite acceptable. Although introducing parameters γ and δ improves the interpretation of the experimental data, it can be seen that use of the simplified G_n function with $\gamma = \delta = 0$ leads to satisfactory results for the concentrations as well as for the acidity constants. This is well verified in the second example.

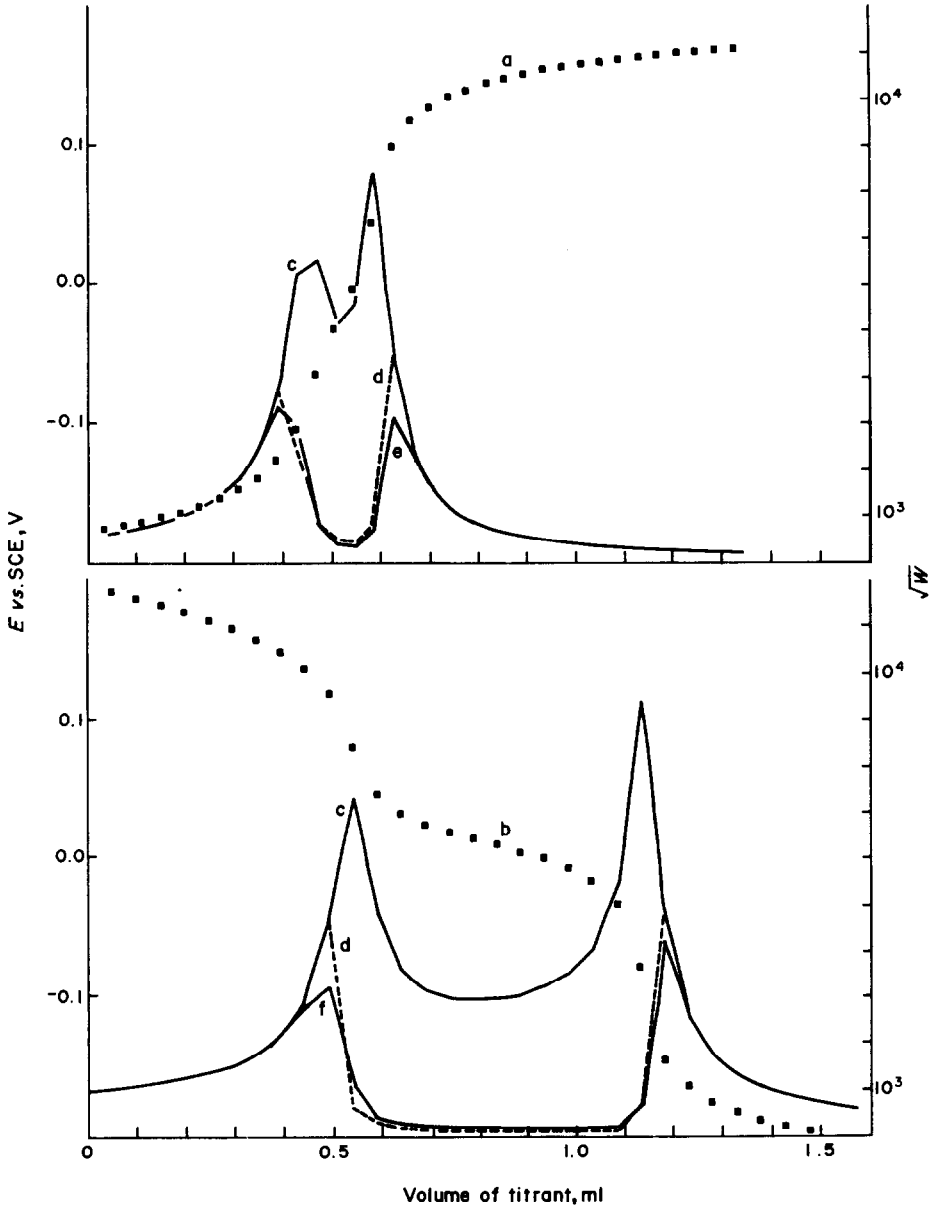


Fig. 3. Plots of $\sqrt{W_n} = f(v)$, calculated from equation (5) or (6) with $\sigma_{oV} = \sigma_{oE} = 10^{-4}$ and for different titrations (a = curve c, Fig. 1, and b = curve b, Fig. 2). c, equation (5), $k_0 = 0$. d, equation (5), $k_0 = 1$. e, equation (6), $k_1 = 50$, $a = 500$. f, equation (6), $k_1 = 100$, $a = 500$.

Neutralization of sodium carbonate with nitric acid

The curves shown in Fig. 2 exhibit the expected decreases in potential, highly distorted by the departure of CO_2. In the range of coexistence of HCO_3^- and H_2CO_3, the potential drifts were coupled with higher $\partial v_{mc}/\partial E_n$ values than those in the previous experiments, so the weighting factors were consequently very small (Fig. 3).

The data were treated by the same procedures: here H_x^0 is the concentration of strong acid, C_i^0, ΔC_i^0 and H_i^0 are respectively the initial concentration of carbonate, the concentration of absorbed CO_2 and the sodium ion concentration: $H_i^0 = -2(C_i^0 - \Delta C_i^0)$.

The results (Table 2) are quite satisfactory even though the confidence ranges are rather high, chiefly for β_2 and α: this is caused by the very small weighting terms used for those experimental points where these parameters have greater influence.

From these two examples, it appears that a single function for the CO_2 evolution can be applied as well for initial carbonate as for added carbonate: with this function, it is possible to obtain very coherent results for the carbonate concentrations in spite of the evi-

Table 1. Results of the titrations of nitric acid (v_0 = 100 ml, $H_i^0 = 2 \times 10^{-4} M$) with sodium carbonate (C_x^0), temperature 25°, 0.1M KNO_3; 35 data points per curve

Parameters	Expected values	Refined values[a] (3σ)	Refined values[a] (3σ)
α titration a[b]		$2.7(0.8) \times 10^{-3}$	$1.6(2.6) \times 10^{-4}$
α titration b		$5.0(1.5) \times 10^{-3}$	$1.7(0.4) \times 10^{-3}$
α titration c		$7.0(2.1) \times 10^{-3}$	$3.2(0.6) \times 10^{-3}$
α titration d		$1.4(0.5) \times 10^{-2}$	$1.0(0.2) \times 10^{-2}$
α titration e		$5.6(2.3) \times 10^{-2}$	$8.4(1.4) \times 10^{-2}$
$\bar{\gamma}$			0.035(0.007)
$\bar{\delta}$			−0.015(0.003)
$\bar{C}_x^0 \times 10^2$	2.21	$2.22_8(0.03)$	2.229(0.008)
$\bar{E}_0$		$6.71_3(0.01)$	6.711(0.004)
$\log \beta_1$	9.76[c]	9.59(0.02)	9.28(0.05)
$\log \beta_2$	15.86[c]	15.60(0.14)	15.34(0.06)
s[d]		7.6	2.2
s_v[e]		6×10^{-3} ml	2.7×10^{-3}ml

a fixed parameters $K_w = 1.33 \times 10^{-14}$; electrode response slope = 1/0.05916.
b see Fig. 1 for the experimental conditions.
c reference 9.
d W_n calculated from expression (5) with $\sigma_{0v} = \sigma_{0E} = 10^{-4}$; $k_0 = 1$.
e W_n calculated from expression (5) with $\sigma_{0v} = 1$; $\sigma_{0E} = k_0 = 0$.

dent disparity of the experimental curves. The simplified form of G_n

$$G_n = \frac{\alpha\beta_2[H^+]^2}{\alpha\beta_2[H^+]^2 + \beta_1[H^+] + 1}$$

is quite sufficient to interpret the data sensibly and is maybe more realistic as it supposes liberation of CO_2 to occur essentially through its H_2CO_3 form.

Neutralization of acid mixture by carbonated potassium hydroxide

The simplified function G_n has been applied to treatment of this last example. Obviously, use of such a function will be more satisfactory when the carbonate concentration is low, as in the usual case of slightly carbonated alkali. This is illustrated here for the titration of a synthetic mixture of strong acid (75.5 mole%), 4-nitrophenol (13.8 mole%) and phenol (10.7 mole%) with deliberately carbonated potassium hydroxide. These compounds were chosen because of their acidity constants, close to those of carbonic acid. Figure 4 shows the actual neutralization curve of the mixture and the curve calculated on the hypothesis of perfect conservation of CO_2: evidently, the carrying away of CO_2 in the gas flow causes displacement of the equivalence points.

To perform the refinement, it is necessary to know precisely the characteristics of the titrating solution, *i.e.*, the total concentration of alkali-metal ion H_x^0 and the actual carbonate concentration C_x^0. These values ($H_x^0 = -1.063M$ and $C_x^0 = 3.68 \times 10^{-2} M$) were obtained from a titration in a closed system in which the carbonate is conserved *i.e.*, $\alpha = 0$. A second neutralization performed under a gas flow led to $\alpha = 3.0 \times 10^{-4}$ ($3\sigma = 5 \times 10^{-5}$), the actual carbonate concentration being fixed in the refinement. This α value can be supposed constant in all the subsequent neutralizations if the operating conditions are kept identical (titrant increments, maximum waiting

Table 2. Results of the titrations of sodium carbonate (v_0 = 80 ml, concentration C_i^0) with nitric acid ($H_x^0 = 0.1M$), temperature 25.0°, 0.1M KNO_3, 35 data points per curve

Parameters	Expected values	Refined values[a] (3σ)	Refined values[a] (3σ)
α titration a[b]		$5.8(4.7) \times 10^{-2}$	$8.2(2.4) \times 10^{-2}$
α titration b		$4.6(1.5) \times 10^{-1}$	$5.7(0.9) \times 10^{-1}$
α titration c		$8.2(2.5) \times 10^{-1}$	1.0(0.1)
α titration d		4.4(1.1)	6.6(0.8)
$\bar{\gamma}$			0.013(0.009)
$\bar{\delta}$			−0.08(0.1)
$\bar{C}_i^0 \times 10^4$	7.06	7.11(0.04)	7.09(0.01)
$\Delta\bar{C}_i^0 \times 10^4$		0.4(0.1)	1.0(0.3)
$\bar{E}_0$		$6.74_1(0.02)$	6.731(0.007)
$\log \beta_1$	9.76[c]	9.76(0.04)	9.93(0.10)
$\log \beta_2$	15.86[c]	16.06(0.11)	16.10(0.06)
s[d]		10.5	3.1
s_v[e]		9.1×10^{-3} ml	3.3×10^{-3} ml

a,c,d,e see Table 1.
b see Fig. 2 for the experimental conditions.

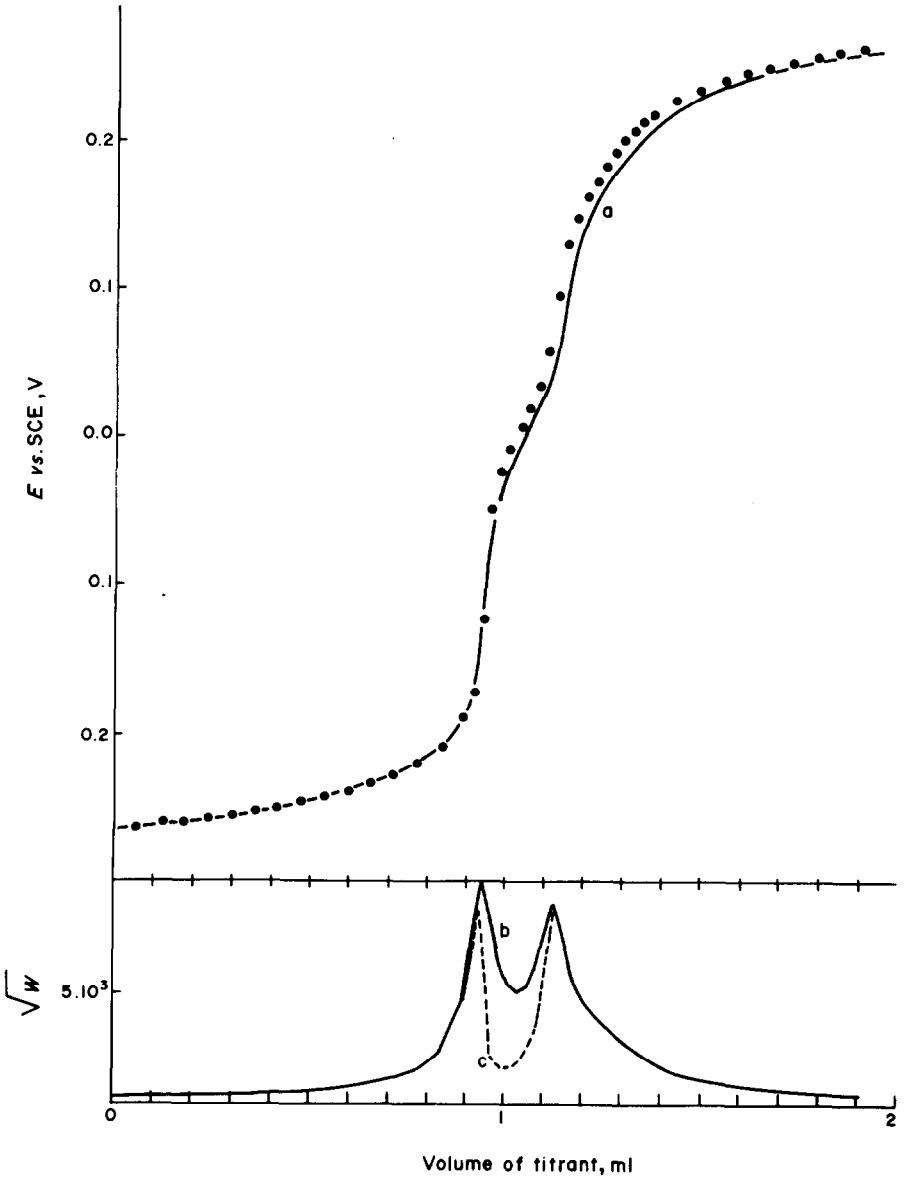


Fig. 4. Titration curve for a mixture of hydrochloric acid, 4-nitrophenol and phenol with carbonated potassium hydroxide, under nitrogen, maximum waiting time 4 min, maximum voltage drift allowed 0.05 mV/min (25.0°, 1*M* KCl). ● experimental points. a, calculated curve, supposing CO_2 conserved in solution. b, $\sqrt{W_n} = f(v)$, equation (6), $\sigma_{ov} = \sigma_{oE} = 10^{-4}$, $k_1 = 0$. c, $\sqrt{W_n} = f(v)$, equation (6), $\sigma_{ov} = \sigma_{oE} = 10^{-4}$, $k_1 = 10$.

time, gaseous flow). These preliminary determinations are necessary because of the impracticability of refining all the parameters in a single experiment: because of the large number of unknowns, the standard deviations become too large and some correlations appear between variables (chiefly between α and C_x^0).

The data for titration of the mixture can then be refined according to different schemes:

(a) if the carbonate concentration is supposed exactly known, we can refine the coefficient α which characterizes the CO_2 behaviour;

(b) conversely, the α coefficient can be maintained constant and the carbonate concentration C_x^0 refined: this is maybe more realistic as the hydroxide solution can absorb atmospheric CO_2 and its concentration slowly changes in course of time.

The results obtained on the basis of these two hypotheses are reported in Table 3. The values are concordant and agree well with the expected concentrations (relative errors $< 1\%$). The computed acidity constants are very close to the values obtained in closed system. The standard deviations are, not surprisingly, rather high: the number of parameters refined is large and the correlation coefficients are im-

Table 3. Results of the titration of a mixture of hydrochloric acid (H_i^0), 4-nitrophenol (C_1^0, β_{11}) and phenol (C_2^0, β_{12}) with carbonated potassium hydroxide ($H_x^0 = -1.063M$, C_x^0) $v_0 = 200$ ml, temperature 25.0°, 1M KCl, maximum waiting time = 4 min, maximum voltage drift allowed 0.05 mV/min, number of data points 45

Parameters	Expected values	Assumption: CO_2 evolution Refined values (3σ)		Assumption: CO_2 conservation Refined values (3σ)	
H_i^0, $10^{-3}M$	5.00	4.999(0.002)	4.999(0.002)	4.999(0.002)	4.995(0.005)
C_1^0, $10^{-4}M$	9.11	9.15(0.4)	9.10(0.2)	9.39(0.2)	7.89(0.09)
$\log \beta_{11}$	6.922	6.924(0.019)	6.925(0.019)	6.924(0.019)	7.035(0.029)
C_2^0, $10^{-4}M$	7.09	7.07(0.7)	6.96(0.2)	7.68(0.3)	5.67(0.3)
$\log \beta_{12}$	9.715	9.700(0.013)	9.698(0.015)	9.706(0.014)	9.753(0.059)
C_x^0, $10^{-2}M$	3.68	3.2(1.8)	3.68	0.8(0.5)	3.68
$\alpha \times 10^4$	3.0	3.0	3.9(4.1)	0	0
$-\log K_w$		13.749(0.03)	13.753(0.006)	13.728(0.006)	13.757(0.012)
E_0		6.783(0.002)	6.783(0.002)	6.783(0.002)	6.785(0.005)
s^a		1.03	1.03	1.03	3.44

Fixed parameter: electrode response slope = 1/0.05916.
Carbonic acid: $\log \beta_1 = 9.59$; $\log \beta_2 = 15.57$.
a W_n calculated from expression (6) with $\sigma_{0v} = \sigma_{0E} = 10^{-4}$; $k_1 = 10$.

portant because of the proximity of the various acidity constants.

For the sake of comparison, the refinement procedures were performed again, with the same weighting scheme, but with $\alpha = 0$, as if the CO_2 remained in solution (Table 3, columns 3 and 4). The acidity constants are only slightly modified but the concentrations of the weak acids are grossly erroneous: 3% and 8% error if the carbonate concentration is refined, 13% and 20% error if that concentration is supposed known from a previous titration!

These results show unambiguously that a refinement process must take into account *all* the causes of systematic error; that is to say, in the present case, the carbonate concentration and a representation (even empirical) of the departure of carbon dioxide from the solution. In spite of its simplicity, it is evident that the function proposed here leads to values very close to those expected. It is to be noted that, under certain conditions, a low value of the weighted mean deviation (Table 3, column 3) is not representative of a good refinement: this criterion can be misleading as to the validity of the mathematical process.

CONCLUSIONS

The carbon dioxide evolution function we propose here leads to a general expression for the calculated reagent volume, which reflects rather accurately the real phenomena and permits the obtention of quite correct results when used in multiparametric refinement. The parameters of the function are dependent on the operating mode and especially on the rate of addition of the titrant, the flow-rate of the gas stream, and the maximum time allowed between addition of titrant and reading of potential. This time must, however, be sufficient for stabilization of the electrode response in the pH range where CO_2 liberation does not interfere.

Another important point of the refinement is the choice of a weighting function, which must lessen the importance of data points taken in a non-equilibrium state of the system.

Obviously, these expressions can easily be included in a program for microcomputers and thus are likely to increase the reliability of automatic potentiometric titrators when a stream of gas is flowed over the solution.

Finally, it must be noted that these expressions are necessary only when the compounds analysed have acidity constants in the same range as carbonic acid ($5 \lesssim pH \lesssim 10.5$). We have checked that outside this range, the carbonate concentration could be taken as constant without notable alteration in the results of multiparametric refinements.

REFERENCES

1. F. Ingman, A. Johansson, S. Johansson and R. Karlsson, *Anal. Chim. Acta*, 1973, **64**, 113.
2. D. M. Barry and L. Meites, *ibid.*, 1974, **68**, 435.
3. D. M. Barry, L. Meites and B. H. Campbell, *ibid.*, 1974, **69**, 143.
4. G. Nowogrocki, J. Canonne and M. Wozniak, *Bull. Soc. Chim. France*, 1976, 5.
5. *Idem, ibid.*, 1976, 1369.
6. D. Murtlow and L. Meites, *Anal. Chim. Acta*, 1977, **92**, 285.
7. M. Wozniak and G. Nowogrocki, *Talanta*, 1978, **25**, 633.
8. G. Nowogrocki, J. Canonne and M. Wozniak, *Anal. Chim. Acta (Computer Techniques and Optimization)*, 1979, **112**, 185.
9. M. Wozniak and G. Nowogrocki, *Talanta*, 1979, **26**, 581.
10. G. Nowogrocki, J. Canonne and M. Wozniak, *Bull. Soc. Chim. France*, 1978, I-371.

Talanta. Vol. 28. pp. 585 to 589. 1981
Printed in Great Britain

0039-9140/81/080585-05$02.00/0
Pergamon Press Ltd

DETERMINATION OF TELLURIUM IN COPPER, LEAD AND SELENIUM BY ATOMIC-ABSORPTION SPECTROMETRY AFTER EXTRACTION OF THE TRIOCTYLMETHYLAMMONIUM–TELLURIUM BROMIDE COMPLEX

IWAO TSUKAHARA* and TOSHIMI YAMAMOTO

The Furukawa Electric Co. Ltd., Central Research Laboratory, 2-9-15, Futaba, Shinagawa-ku, Tokyo, Japan

(*Received* 7 *October* 1980. *Accepted* 26 *January* 1981)

Summary—A simple, rapid and sensitive combined solvent extraction and atomic-absorption spectrometric method has been developed for the determination of tellurium in copper, lead, selenium and blister copper. Tellurium is extracted as the trioctylmethylammonium–tellurium(IV) bromide complex into butyl acetate and determined by flame atomic-absorption spectrometry of the extract. As little as 1 μg of tellurium in a sample can be determined. The extraction of tellurium from hydrobromic acid solution with trioctylamine has also been investigated.

The determination of tellurium in copper, lead and selenium is of importance in their metallurgical evaluation. Tellurium around the 1 ppm level in these materials has usually been determined by spectrophotometry with diethyldithiocarbamate.[1,2] However, the methods are tedious and time-consuming, because they involve complicated procedures for prior separation of tellurium from interfering elements or matrices; in addition, the tellurium diethyldithiocarbamate complex is unstable to light. It is, therefore, desirable to develop a simple, rapid and sensitive method for the determination of trace quantities of tellurium in these materials.

Atomic-absorption spectrometry provides a sensitive method for the determination of trace quantities of tellurium, usually in combination with a prior separation or concentration technique. Reichel and Bleakley,[3] Bédard and Kerbyson,[4] and Britske and Sedykh[5] have determined tellurium in copper by flame atomic-absorption spectrometry (AAS), hydride evolution AAS, and graphite-furnace AAS, respectively; these methods are somewhat tedious as they involve preseparation of tellurium by co-precipitation with lanthanum hydroxide[3,4] or with elemental arsenic.[5] The solvent extraction technique, combined with AAS, provides a simple and rapid method for the determination of tellurium. Beaty[6] and Jedrzejewska[7] have successfully used isobutyl methyl ketone extraction of tellurium from hydrochloric acid solution followed by an atomic-absorption finish, for the determination of traces of tellurium in selenium[6] and copper.[7]

The extraction behaviour of tellurium with high molecular weight amines in various media, *i.e.*, with dodecyl(trialkylmethyl)amine (Amberlite LA-1),[8] trioctylamine[9] or tribenzylamine[10] from hydrochloric acid,[8–10] hydrobromic acid,[9] hydriodic acid[9] or sodium iodide–perchloric acid[9] solution, has been investigated and these reagents have been shown to be good extractants for tellurium(IV). It was considered that extraction of tellurium with a high molecular weight amine or quaternary ammonium salt could be used in conjunction with AAS for its determination at the trace level in the materials mentioned. In the present work, the use of AAS after extraction of tellurium(IV) with trioctylamine (TOA) and trioctylmethylammonium bromide (TOMABr) from hydrobromic acid medium has been investigated and applied to the determination of trace quantities of tellurium in copper, lead and selenium.

EXPERIMENTAL

Apparatus

A Hitachi model 208 atomic-absorption spectrophotometer with a three-slot 100-mm long burner, a Hamamatsu TV model L233-52NQ tellurium hollow-cathode lamp and a Hitachi model 056 recorder were used with the following operating conditions: wavelength 214.3 nm; slit-widths 0.18 mm (entrance) and 0.18 mm (exit); burner-height position 2; lamp current 4 mA; air flow-rate 14 l./min; acetylene flow-rate 2 l./min.

Reagents

TOA solution. Dilute 10 ml of TOA to 200 ml with butyl acetate.

TOMABr solution. Dilute 10 ml of trioctylmethylammonium chloride (Capriquat) to 200 ml with butyl acetate. Transfer this solution to a separatory funnel and shake with two 200-ml portions of 3*M* hydrobromic acid for 5 min each time (discard the aqueous layers).

* To whom correspondence and requests for reprints should be addressed.

Wash solution. Mix 550 ml of water, 120 ml of concentrated hydrobromic acid (sp.gr. 1.47) and 330 ml of sulphuric acid (1 + 1).

Standard tellurium solution. Dissolve 0.500 g of tellurium metal in 10 ml of concentrated nitric acid. Add 40 ml of sulphuric acid (1 + 1) and evaporate the solution to fumes of sulphur trioxide to expel nitric acid. Make up to 500 ml with water and dilute to the desired concentration immediately before use.

Procedure for investigation of extraction conditions and interferences

Transfer a portion of standard tellurium solution (20 μg of Te) to a 200-ml separatory funnel. Add 45.0 ml (for TOA extraction) or 30.0 ml (for TOMABr extraction) of 5*M* hydrobromic acid and dilute to 150 ml with water. Extract tellurium by shaking vigorously with 10.0 ml of the TOA or TOMABr solution for 5 min. Discard the aqueous layer. Transfer the organic layer to a 10-ml graduated test-tube, and make up the volume, which decreases to some extent during the extraction, to 10 ml by adding butyl acetate. Spray into the flame and measure the atomic-absorption signal, correcting the value by subtracting the reagent blank.

Procedures for the analysis of samples

Copper and selenium. Decompose 5 g (for copper) or 0.5–5 g (for selenium) of sample with 35 ml of nitric acid (1 + 1) and 50 ml of sulphuric acid (1 + 1) (for copper) or with 30 ml of concentrated nitric acid and 50 ml of sulphuric acid (1 + 1) (for selenium); heat gently to assist decomposition. Evaporate the solution to fumes of sulphur trioxide. Add 100 ml of water and heat gently to dissolve the salts. Transfer the solution to a 200-ml separatory funnel, add 30.0 ml of 5*M* hydrobromic acid and dilute to 150 ml with water. Shake vigorously with 10.0 ml of the TOMABr solution for 5 min. Discard the aqueous layer. Wash the organic layer by shaking with 50 ml of the wash solution for 30 sec. Discard the aqueous layer. Treat the organic layer as described in the investigational procedure and measure the atomic-absorption signal.

Lead. Decompose 0.5–5 g of sample with 30 ml of nitric acid (1 + 2); heat gently to assist decomposition. Add 50 ml of sulphuric acid (1 + 1) and evaporate to fumes of sulphur trioxide. Add 20 ml of water, transfer the solution and lead sulphate precipitate to a 100-ml standard flask, and dilute to the mark with water, and allow the precipitate to settle. Transfer a 50.0-ml aliquot of the supernatant solution to a 200-ml separatory funnel and dilute to about 100 ml with water. Add 30.0 ml of 5*M* hydrobromic acid and make up to 150 ml with water. Complete the determination as for copper and selenium samples.

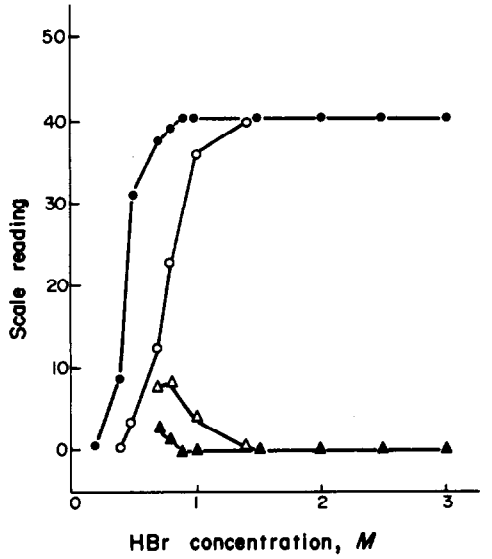


Fig. 1. Effect of hydrobromic acid concentration. Tellurium taken 20 μg; TOA or TOMABr concentration in the solvent 5% v/v. ○, △ TOA; ●, ▲ TOMABr. ○, ● first extraction; △, ▲ second extraction.

Blister copper. Decompose 5 g of sample with 35 ml of nitric acid (1 + 1) and 50 ml of sulphuric acid (1 + 1); heat gently to assist decomposition. Evaporate the solution to fumes of sulphur trioxide. Add 100 ml of water and heat gently to dissolve the salts. Transfer the solution to a 200-ml standard flask and dilute to the mark with water. Transfer an aliquot (containing less than 30 μg of Te) of the solution to a 200-ml separatory funnel, add 30.0 ml of 5*M* hydrobromic acid and dilute to 150 ml with water. Complete the determination as for copper and selenium samples.

Calibration. Transfer portions (containing up to 30 μg of Te) of standard tellurium solution to 200-ml separatory funnels. To each solution and a blank (water), add 10 ml of sulphuric acid (1 + 1) and 30.0 ml of 5*M* hydrobromic acid, and dilute to 150 ml with water. Treat these solutions as for samples and plot a curve of the atomic-absorption signal against amount of tellurium.

RESULTS AND DISCUSSION

Extraction conditions

The optimal conditions for the extraction of tellurium with TOA and TOMABr from hydrobromic acid solution were investigated by using the procedure described above, with variation of one parameter at a time.

The concentration of hydrobromic acid in the aqueous phase was varied from 0.2 to 3.0*M*; two successive extractions with two 10-ml portions of the TOA or TOMABr solution were made to determine the extraction efficiency of tellurium. The largest atomic-absorption signal for the first extraction was obtained in the hydrobromic acid concentration ranges 1.5–3.0*M* with TOA and 0.9–3.0*M* with TOMABr. No signal was observed for the second extraction in these ranges (Fig. 1). No difference between the signals for the TOA and TOMABr systems was observed at the respective optimal hydrobromic acid concentrations. The aspiration rate of the organic layer into the flame was also measured; the aspiration efficiency was independent of the hydrobromic acid concentration used. These results show that tellurium is completely extracted by the first extraction with TOA from 1.5–3.0*M* hydrobromic acid and with TOMABr from 0.9–3.0*M* hydrobromic acid. The hydrobromic acid concentration of 1.5*M* with TOA, above which tellurium is quantitatively extracted, is somewhat different from the concentration of 1.0*M* reported by Suzuki *et al.*[9] for use with 5% v/v TOA in xylene.

The concentrations of TOA and TOMABr in the solvent were varied from 0.2 to 10% v/v. For each TOA or TOMABr concentration, two successive extractions with 10-ml portions of the solvent (and a measurement of the aspiration efficiency) were made

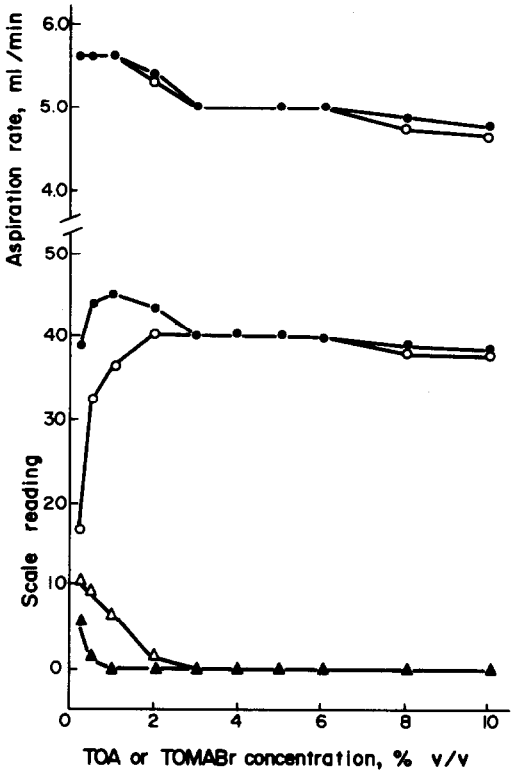


Fig. 2. Effects of TOA and TOMABr concentrations in the solvent. Tellurium taken 20 μg; hydrobromic acid concentration 1.5*M* in TOA system and 1.0*M* in TOMABr system. Symbols as for Fig. 1.

(Fig. 2). The results of the second extraction indicate that tellurium is quantitatively extracted with TOA concentrations above 3% and with TOMABr concentrations above 1%. The atomic-absorption signals for the first extraction, however, decreased gradually with increasing TOA and TOMABr concentrations in the ranges 6–10% TOA and 1–10% TOMABr, though the extraction of tellurium was complete. At these concentrations the aspiration rate also decreased, probably because of an increase in the solvent viscosity, with increasing TOA and TOMABr concentrations, but signal-to-aspiration rate ratios were almost constant (Fig. 2); this indicates that the decrease in signal is due to lowering of the aspiration efficiency.

The volume of the solvent decreased to some extent in the extraction because of dissolution of some of the butyl acetate in the aqueous phase. The extent of decrease depended on the acid and salt concentrations in the aqueous phase, so signals of different magnitudes occurred for different acid and salt concentrations and the same amount of tellurium. This undesirable effect was eliminated by the adjustment of the volume of the organic layer to 10 ml by addition of butyl acetate.

The absorption signals were independent of shaking time from 1 to 10 min.

Effects of other acids

The effects of sulphuric, hydrochloric, nitric and perchloric acids on the extraction of tellurium were investigated (Table 1). Sulphuric and hydrochloric acids up to at least 4*M* had no effect in both the TOA and TOMABr systems. Nitric acid above 0.05*M* in the TOA system and above 0.2*M* in the TOMABr system, and perchloric acid above 0.01*M* in both systems lowered the extraction of tellurium.

Effects of various elements

On the basis of the results above, the TOMABr–HBr system was adopted. The effects of various ions

Table 1. Effects of other acids on the extraction of tellurium

Acid	Concentration *M*	Extraction system* and scale reading TOA–HBr	TOMABr–HBr
No addition		40.0	40.0
H_2SO_4	1.0	39.9	40.0
	2.0	40.1	40.1
	3.0	40.7	39.9
	4.0	40.5	40.0
HCl	1.0	40.1	40.0
	2.0	40.1	40.1
	3.0	39.9	40.0
	4.0	39.4	40.0
HNO_3	0.05	40.1	40.1
	0.10	38.6	40.0
	0.20	36.5	40.0
	0.50	5.2	39.0
	1.0		38.1
	2.0		34.5
$HClO_4$	0.01	39.7	39.8
	0.05	38.6	11.7
	0.10	28.9	4.0
	0.20	24.3	2.3
	0.50	17.9	

* Tellurium taken 20 μg; HBr concentration 1.5*M* in TOA system and 1.0*M* in TOMABr system; TOA or TOMABr concentration in the solvent 5% v/v.

Table 2. Analytical results for various samples

Sample	Sample taken, *g*	Te added, *μg*	Total Te found, *μg*	Te content of sample, *ppm*	Average, *ppm*
Copper metal	5.00	0	1.9	0.4	
(tough pitch)	5.00	0	1.9	0.4	0.3
	5.00	10*	11.5	0.3	
	5.00	10*	11.5	0.3	
Copper metal	5.00	0	1.1	0.2	
(V.M.C.)	5.00	0	1.3	0.3	0.2
	5.00	10*	11.2	0.2	
	5.00	10*	11.2	0.2	
Lead metal	5.00	0	<2	<0.4	
	5.00	0	<2	<0.4	<0.4
	5.00	10*	10.6	<0.4	
	5.00	10*	11.4	<0.4	
Lead metal	2.00	0	9.4	4.7	
	2.00	0	10.4	5.2	5.1
	2.00	10*	20.1	5.0	
	2.00	10*	20.6	5.3	
Lead metal	0.50	0	31.2	62	
	0.50	0	33.0	66	64
	0.50	20*	51.4	63	
	0.50	20*	52.0	64	
Selenium metal	5.00	0	7.0	1.4	
	5.00	0	7.5	1.5	1.5
	5.00	10*	16.9	1.4	
	5.00	10*	17.6	1.5	
Selenium metal	2.50	0	13.4	5.4	
	2.50	0	14.0	5.6	5.5
	2.50	10*	23.6	5.4	
	2.50	10*	24.0	5.6	
Selenium metal	0.50	0	12.0	24	
	0.50	0	12.3	25	25
	0.50	10*	22.5	25	
	0.50	10*	22.5	25	
Blister copper	5.00	0	18.2	3.6	
	5.00	0	20.2	4.0	3.9
	5.00	20*	40.4	4.1	
	5.00	20*	38.4	3.7	
Blister copper	5.00	0	59.0	12	
	5.00	0	60.0	12	11
	5.00	50*	103	11	
	5.00	50*	104	11	
Blister copper	5.00	0	930	0.019%	
	5.00	0	940	0.019	0.019%
	5.00	1000*	1950	0.019	
	5.00	1000*	1950	0.019	

* Tellurium, in the form of aliquots of standard tellurium solution, was added to the solid samples before decomposition.

on the extraction and determination of tellurium by this system were then examined.

There was no interference from 5 mg of Al, Be, Ce(III), Ce(IV), Co(II), Cr(III), Hg(II), In, Mg, Mo(VI), Ti(IV), V(V), Zr; 30 mg of Ca, Mn(II); 100 mg of As(III), As(V), Fe(III), Sb(III), Sb(V); 3 g of Ni; 5 g of Se(IV).

Up to 2 mg of Ag, 20 mg of Au(III), 5 mg of Cd, 60 mg of Pd(II), 2 mg of Pt(IV), 50 mg of Sn(IV), 1 mg of Tl(I) and 3 mg of Tl(III) did not interfere, but larger amounts caused negative errors.

Copper above 4 g, bismuth above 30 mg, and zinc above 10 mg caused negative errors; those from 5 g of copper, 50 mg of bismuth and 500 mg of zinc could be eliminated by washing the organic layer with 50 ml of the wash solution (1*M* hydrobromic–3*M* sulphuric acid) for 30 sec. Lead above 50 mg caused a negative error; that from 100 mg of lead could be eliminated by washing the organic layer with 50 ml of 1*M* hydrobromic acid for 30 sec.

Applications

Tellurium in copper, lead, selenium and blister copper was determined by the proposed method (Table 2). The amounts of tellurium added to samples before decomposition were recovered quantitatively. As little as 1 μg of tellurium in a sample or in an aliquot of the sample solution could be determined.

The proposed method is simple, rapid and sensitive.

REFERENCES

1. C. L. Luke, *Anal. Chem.*, 1959, **31**, 572.
2. H. Bode, *Z. Anal. Chem.*, 1955, **144**, 90.
3. W. Reichel and B. G. Bleakley, *Anal. Chem.*, 1974, **46**, 59.
4. M. Bédard and J. D. Kerbyson, *Can. J. Spectrosc.*, 1976, **21**, 64.
5. M. E. Britske and E. M. Sedykh, *Zh. Analit. Khim.*, 1978, **33**, 321; *Anal. Abstr.*, 1978, **35**, 4B136.
6. R. D. Beaty, *Anal. Chem.*, 1973, **45**, 234.
7. H. Jedrzejewska, *Chem. Anal. (Warsaw)*, 1973, **18**, 117; *Anal. Abstr.*, 1973, **25**, 2967.
8. G. Nakagawa, *Nippon Kagaku Zasshi*, 1960, **81**, 446.
9. T. Suzuki, T. Sotobayashi and S. Koyama, *Bunseki Kagaku*, 1974, **23**, 999.
10. G. Nakagawa, *Nippon Kagaku Zasshi*, 1960, **81**, 1258.

Talanta, Vol. 28, pp. 591 to 597, 1981
Printed in Great Britain. All rights reserved

0039-9140/81/080591-07$02.00/0
Copyright © 1981 Pergamon Press Ltd

KINETICS AND MECHANISM OF MERCURY(II)-CATALYSED REPLACEMENT OF CYANIDE IN HEXACYANOFERRATE(II) BY *p*-NITROSODIPHENYLAMINE

MADHU PHULL and P. C. NIGAM*

Department of Chemistry, Indian Institute of Technology, Kanpur-208016, U.P., India

(*Received* 12 *August* 1980. *Revised* 27 *October* 1980. *Accepted* 5 *January* 1981)

Summary—The mercury(II)-catalysed replacement of cyanide in hexacyanoferrate(II) by *p*-nitrosodiphenylamine (*p*-NDA) in aqueous solution has been investigated spectrophotometrically by measuring the change in absorbance of the green complex ion, $[Fe(CN)_5.p\text{-NDA}]^{3-}$, at 640 nm. Activation parameters of the catalysed and uncatalysed reactions have been calculated. The effects of the dielectric constant and water content of the medium on reaction rates are used to explain the formation of a polar activated complex and suggest an I_d mechanism for the catalysed reaction. The varying catalytic activity of Hg(II) as a function of concentration has been discussed.

The thermal decomposition of hexacyanoferrate(II) is a slow reversible process [equation (1)]. The pentacyanoaquo complex produced has been reported[1] to react with aromatic nitroso compounds, giving intensely coloured products. Mercury, silver, gold and palladium, which readily form cyanide complexes, are known to catalyse these reactions.[2–4] Mercury is a pollutant that has been engaging our attention and we have been looking for a kinetic method for determination of mercury in trace amounts. The search resulted in investigation of the kinetics and mechanism of the mercury-catalysed reaction between hexacyanoferrate(II) and *p*-nitrosodiphenylamine (*p*-NDA), which gives a bright green complex (λ_{max} 640 nm) presumably with pentacyanoaquoferrate(II). The absorbance of this complex obeys the Lambert–Beer law at low concentrations.

The uncatalysed reaction takes about 24 hr to attain maximum absorbance, and the green complex then decomposes, especially in presence of the ethanol needed to dissolve *p*-nitrosodiphenylamine, which is sparingly soluble in water.

The stoichiometry of the complex has been established as 1:1 by the mole-ratio[5] and slope-ratio[6] methods. From previous knowledge of a similar reaction with nitrosobenzene,[7] the reaction is believed to take place in the following steps:

$$Fe(CN)_6^{4-} + H_2O \underset{k_{-1}}{\overset{k_1}{\rightleftharpoons}} [Fe(CN)_5.H_2O]^{3-} + CN^- \text{ (slow)} \quad (1)$$

$$[Fe(CN)_5.H_2O]^{3-} + p\text{-NDA} \longrightarrow [Fe(CN)_5.p\text{-NDA}]^{3-} + H_2O \quad (2)$$

$$CN^- + H_2O \longrightarrow HCN + OH^- \quad (3)$$

Mercury is known[7] to catalyse the decomposition of hexacyanoferrate(II) in the following manner:

$$Hg^{2+} + Fe(CN)_6^{4-} \xrightarrow{H_2O} [Fe(CN)_5.H_2O]^{3-} + HgCN^+ \quad (4)$$

$$HgCN^+ + H^+ \longrightarrow Hg^{2+} + HCN \quad (5)$$

In basic solution the catalyst is not regenerated. Because of hydrolysis the catalytic action is expected to be reduced, as is found from pH-dependence studies. The aquopentacyanoferrate(II) reacts with nitroso compounds to produce coloured products which may be utilized for following these reactions spectrophotometrically (in our case the green compound, λ_{max} 640 nm, was used).

EXPERIMENTAL

Reagents

Doubly distilled water was used to prepare all solutions.

Potassium hexacyanoferrate(II) stock solution was prepared, and kept in dark amber-coloured bottles to prevent photodecomposition, and appropriately diluted immediately before use. Dilute solution of mercury(II) chloride was prepared daily to prevent loss by adsorption on glass. *p*-Nitrosodiphenylamine is only slightly soluble in water. A stock solution was prepared in alcohol and then diluted with water to an alcohol content of 10%. This solution is stable for months.

Citrate and acetate buffers were found to give some turbidity with *p*-nitrosodiphenylamine, so potassium hydrogen phthalate/sodium hydroxide buffer of pH 4.8 was used to bring the initial pH of the reactant solutions to 5.0–5.2. Potassium nitrate was used to maintain the ionic strength at 0.1.

Procedure

The reaction rate was determined by measuring the change in absorbance of the product at 640 nm.

* Author to whom correspondence and reprint requests should be sent.

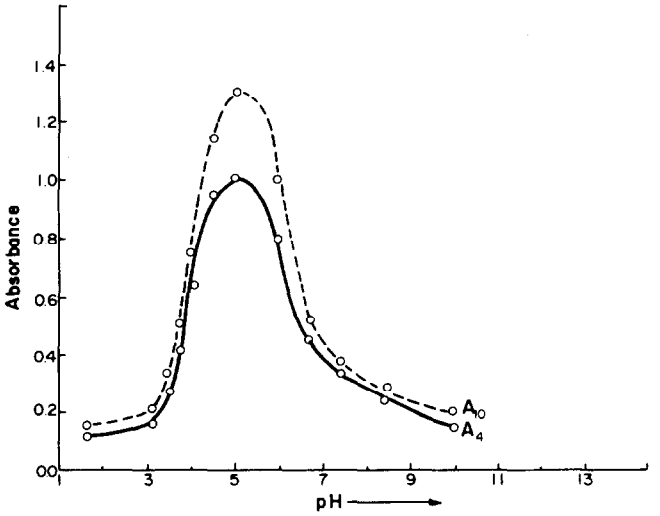


Fig. 1. Effect of pH on Hg^{2+}-catalysed substitution of CN^- in hexacyanoferrate(II) by *p*-NDA at 30°C; $[Fe(CN)_6^{4-}] = 9.6 \times 10^{-4}M$; [*p*-NDA] = $9.6 \times 10^{-4}M$ (in 50% alcohol); $[HgCl_2] = 1.2 \times 10^{-5}M$.

Mercury(II) chloride and potassium hexacyanoferrate(II) do not interfere and *p*-NDA absorbs to only a small extent, for which a correction was applied.

All solutions were placed in a thermostat for 30 min, then appropriate quantities were mixed in the sequence *p*-NDA, buffer and mercury(II) chloride. Hexacyanoferrate(II) was injected to start the reaction. The solution was shaken and immediately transferred to a 1-cm cell in a temperature-controlled cell-compartment. Initial-rate plots were used to find the dependence on [*p*-NDA] and $[Fe(CN)_6^{4-}]$, and the fixed-time procedure to find the dependence on pH and $[Hg^{2+}]$. The alcohol content for all kinetic runs was kept fixed at 10%. The rate decreases with increase in alcohol concentration.

Hydrochloric acid was used for studying the effect of pH. Use of perchloric acid resulted in faster oxidation of the hexacyanoferrate(II) to form Berlin blue.

The complexation of mercury(II) with *p*-NDA was also checked. A very small change in absorbance at λ_{max} of *p*-NDA was seen, but the complexation was very slow and could be ignored. To avoid any interference the mercury(II) chloride and *p*-NDA were mixed just before the run.

RESULTS

Effect of pH

Figure 1 shows the effect of pH on the absorbance measured 4 min (A_4) and 10 min (A_{10}) after mixing. The rate is maximal at pH 5–5.2. The decrease in rate at higher pH may be due to shortage of the protons needed to regenerate the catalytic species, and/or to decrease in concentration of Hg^{2+} as a result of hydrolytic precipitation as the hydroxide. The rate is reduced at low pH values because of protonation of $Fe(CN)_6^{4-}$. The distribution of the protonated products as a function of pH has been calculated from the protonation constants[8,9] by the computer program SCOGS[10] and is shown in Fig. 2. At pH about 5, $Fe(CN)_6^{4-}$ and $HFe(CN)_6^{3-}$ predominate. The rate may also be reduced at lower pH because of protonation of the *p*-NDA.

Effect of reagent concentrations

With the optimum pH fixed at 5.0–5.2, $[Fe(CN)_6^{4-}] = 0.01M$ and $[Hg^{2+}] = 7.6 \times 10^{-6}M$, the concentration of *p*-NDA was varied from 1.12×10^{-4} to $5 \times 10^{-4}M$. Higher concentration of *p*-NDA was not possible because of limited solubility in the reaction medium. At lower concentrations the reaction scarcely occurred. A plot of initial rate *vs.* [*p*-NDA] was linear up to [*p*-NDA] = $4.15 \times 10^{-4}M$ (Fig. 3).

The concentration of $Fe(CN)_6^{4-}$ was varied between 4×10^{-4} and $5.3 \times 10^{-3}M$, with [*p*-NDA] = $4.76 \times 10^{-4}M$ and other conditions as before. A plot of log (initial rate) *vs.* log $[Fe(CN)_6^{4-}]$ gave a slope of 0.8 up to $\sim 10^{-3}M$ $Fe(CN)_6^{4-}$ and 0.3 at higher concentrations but did not tend towards zero (Fig. 4). Independent experiments showed that the forward rate is inversely proportional to $[CN^-]$ at high CN^- concentration.

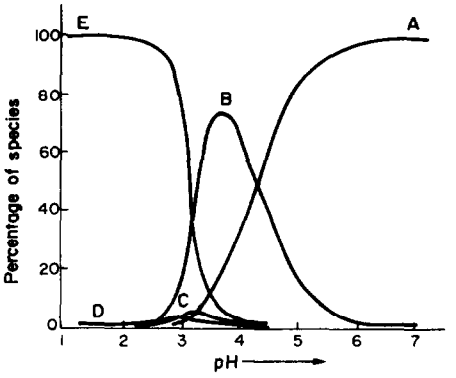


Fig. 2. Species distribution of $Fe(CN)_6^{4-}$ as a function of pH. $[Fe(CN)_6^{4-}] = 5 \times 10^{-3}M$; A = $Fe(CN)_6^{4-}$; B = $HFe(CN)_6^{3-}$; C = $H_2Fe(CN)_6^{2-}$; D = $H_3Fe(CN)_6^-$; E = $H_4Fe(CN)_6$.

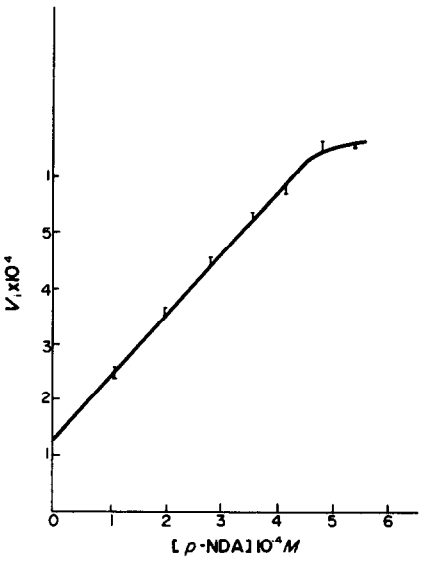


Fig. 3. Effect of *p*-NDA concentration on initial reaction rate at 25.0 ± 0.1°C; pH = 5.0–5.2; I = 0.15.

The effect of $[Hg^{2+}]$ was examined with [*p*-NDA] = $4.0 \times 10^{-4}M$ and $[Fe(CN)_6^{4-}] = 4.0 \times 10^{-4}M$, pH 5.2 and temperature of 25°. Figure 5 shows the plot of A_2 *vs.* $[Hg^{2+}]$ (A_2 is the absorbance after 2 min). The catalytic activity of $HgCl_2$ increases until the Hg^{2+} and $Fe(CN)_4^{2-}$ concentrations are equal and then steeply declines. Similar behaviour was confirmed for higher concentrations of $Fe(CN)_6^{4-}$. The intercept obtained by extrapolation of the initial linear portion of the curve gives the rate of the uncatalysed reaction. The decline in rate at higher mercury concentration may be due to formation of a binary adduct $[Fe(CN)_6^{4-}.HgCl_2]$, which would decrease the forward rate of reaction (1). The existence of a similar complex between $Fe(CN)_6^{4-}$ and $Hg(CN)_2$ has been postulated by Beck *et al.*[11]

Effect of temperature

The uncatalysed and catalysed reactions were studied at 20–40°. Higher temperatures were not tried for fear of decomposition of the green complex. Plots of log (initial rate) *vs.* $1/T$ gave straight lines from which the activation parameters were calculated. These are listed in Table 1. E_a for the uncatalysed reaction is 19.1 kcal/mole. This value, though approximate because initial rates were used instead of rate constants, is comparable to the values obtained by previous workers.[12] This value appears to relate to the rate-determining step, the dissociation of hexacyanoferrate(II) to pentacyanoferrate(II). The activation energy for the catalysed reaction is 16.3 kcal/mole, about 3 kcal/mole lower, which is a significant decrease considering that the concentration of mercury catalyst is as low as $4 \times 10^{-7}M$ in the reaction mixture.

Effect of ionic strength

A negative salt effect was found when the ionic strength (I) was varied from 0.1 to 0.9, with potassium nitrate, the reactant concentrations

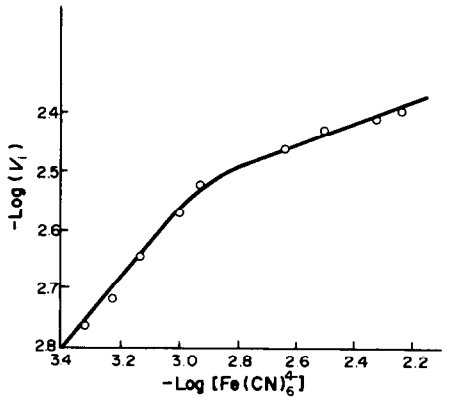


Fig. 4. Dependence of the initial reaction rate on concentration of $Fe(CN)_6^{4-}$ at 25.0 ± 0.1°C; pH = 5.0–5.2; I = 0.1.

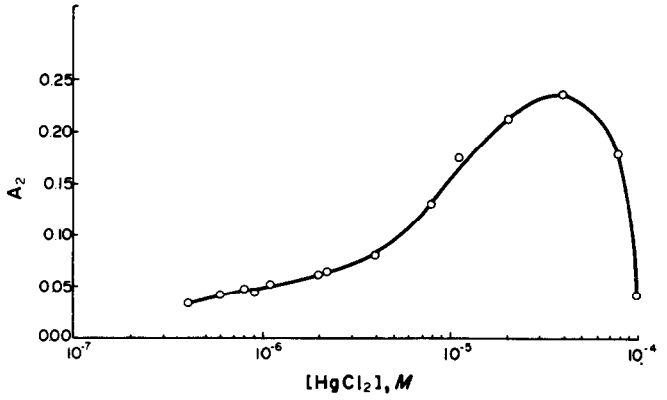


Fig. 5. Dependence of the rate of substitution of CN^- in hexacyanoferrate(II) by *p*-DNA on $[HgCl_2]$ at 25.0 ± 0.1°C; pH = 5.0–5.2; $[Fe(CN_6^{4-}] = 4 \times 10^{-4}M$; [*p*-NDA] = $4 \times 10^{-4}M$; I = 0.1.

Table 1. Activation parameters for the uncatalysed and catalysed substitution of CN^- in hexacyanoferrate(II)

Uncatalysed	Catalysed
E_a = 19.1 kcal/mole	E_a = 16.2 kcal/mole
$\Delta H^{\ddagger 0}$ = 18.5 kcal/mole	$\Delta H^{\ddagger 0}$ = 15.7 kcal/mole
$\Delta S^{\ddagger 0}$ = −13 cal.mole^{-1}.deg^{-1}	$\Delta S^{\ddagger 0}$ = −21 cal.mole^{-1}.deg^{-1}

being $[Fe(CN)_6^{4-}] = 5 \times 10^{-3}M$, [*p*-NDA] = $2.5 \times 10^{-4}M$ and $[HgCl_2] = 3.2 \times 10^{-6}M$. The first two concentrations are not rate-limiting. A plot of log (initial rate) *vs.* I does not give the slope that would be expected if the reaction between $Fe(CN)_6^{4-}$ and Hg^{2+} involved ionic species.[13] The catalytic effect of mercury appears to be due to ion-pair formation between $Fe(CN)_6^{4-}$ and Hg^{2+} (or $HgCl^+$).[14] If potassium chloride is used for ionic strength control the rate is found to decrease considerably, probably because of formation of $HgCl_2$ $HgCl_3^-$ and $HgCl_4^{2-}$.

Effect of dielectric constant of the medium

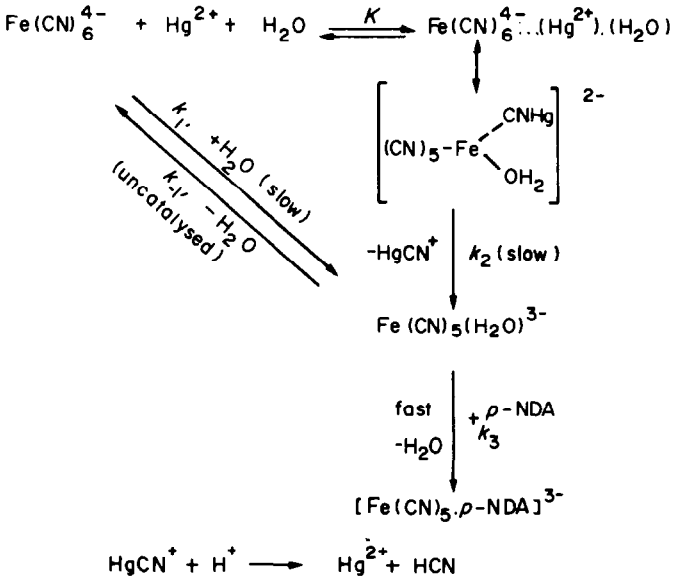
This effect was investigated to gain insight into the nature of the activated complex. The dielectric constant of the medium was changed by varying the alcohol content. A plot of log (initial rate) *vs.* $(D-1)/(2D+1)$ was linear (the values of D were those for a temperature of 30°). This shows that the activated complex is more polar than the reactants[15] and the products of the rate-determining step are ions—a fact which is relevant to understanding of the mechanism. Also the life of the ion-pairs is enhanced by decreasing the dielectric constant, causing lowering of the rate.

Effect of water concentration

The foregoing results point to the existence of either a D or an I_d mechanism for the reaction. The distinction between them is often difficult to make. The water concentration in the medium was altered by addition of various amounts of alcohol. The rate decreased as the water content decreased (Fig. 6). A similar effect was observed in the replacement of 3-cyanopyridine by pyridine in $[Fe(CN)_5^{3-}.(PyCN)]$.[16] The results are interpreted in terms of an I_d mechanism involving an $[Fe(CN)_5(H_2O)HgCN]^{2-}$ reaction intermediate. If a D mechanism was followed the effect of change in water concentration on the rate would be negligible.

DISCUSSION

The influence of the concentrations of $Fe(CN)_6^{4-}$, *p*-NDA and Hg^{2+}, and the other observations reported above lead us to propose the following mechanistic scheme.



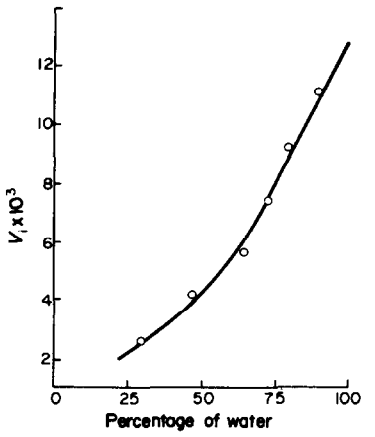


Fig. 6. Dependence of initial rate on water concentration in the substitution of CN^- in $Fe(CN)_6^{4-}$ by *p*-NDA at 30 ± 0.1°C.

If we consider the uncatalysed reaction, the rate of formation of the complex is given by

$$\frac{d[Fe(CN)_5^{3-}\cdot p\text{-NDA}]}{dt} = k_3[Fe(CN)_5H_2O^{3-}] \times [p\text{-NDA}] \quad (6)$$

Substitution of the steady-state concentration of $Fe(CN)_5H_2O^{3-}$ in equation (6) gives

$$\text{rate} = \frac{k_3k_1[Fe(CN)_6^{4-}][p\text{-NDA}]}{k_{-1}[CN^-] + k_3[p\text{-NDA}]} \quad (7)$$

At lower concentrations of *p*-NDA, *i.e.*, when $k_{-1}[CN^-] \gg k_3[p\text{-NDA}]$, equation (7) reduces to an expression predicting first-order dependence on [*p*-NDA]. However, for higher concentrations of *p*-NDA, *i.e.*, when the first term in the denominator can be ignored, the expression reduces to a form showing independence of *p*-NDA concentration. This has been found to be the case (Fig. 3). Since part of the reaction goes by the uncatalysed path this observation is not unexpected. The observed inverse dependence on cyanide concentration at high $[CN^-]$ is also explained by equation (7).

The catalytic activity of Hg^{2+} at low concentration can also be explained by the proposed mechanistic scheme if the rate-determining step is assumed to be decomposition of the activated complex. The overall reaction (both uncatalysed and catalysed) in presence of amounts of *p*-NDA that are non rate-limiting can now be written as

$$\text{rate} = \frac{d[Fe(CN)_5^{3-}\cdot p\text{-NDA}]}{dt} = k_1[Fe(CN)_6^{4-}] + \frac{k_2K[Fe(CN)_6^{4-}][Hg^{2+}][H_2O]}{1 + K[Fe(CN)_6^{4-}]} \quad (8)$$

Table 2. Comparison of calculated and experimental rates (10^{-4} *mole*.l^{-1}.sec^{-1}) at $[Fe(CN)_6^{4-}] = 5.0 \times 10^{-3}M$, $[p\text{-NDA}] = 5.0 \times 10^{-4}M$, pH = 5.0, $I = 0.1$ (KNO_3), temperature = 25 ± 0.1°, (based on $k_1 = 2.0 \times 10^{-2}$ sec^{-1}, $k_2 = 17.5$ sec^{-1} and $K = 2.62 \times 10^2$

$[Hg^{2+}]$, $10^{-7}M$	Calculated rate	Experimental rate
4.0	3.27	3.13
5.0	3.75	3.68
6.0	4.31	4.27
8.0	5.40	5.38
10.0	6.49	6.20

where K = equilibrium constant for binding of Hg^{2+} and water to $Fe(CN)_6^{4-}$. Equilibrium is supposed to lie to the right and the value of K to be >1. When $[Fe(CN)_6^{4-}]$ is small and $K[Fe(CN)_6^{4-}] \ll 1$, and as $[H_2O]$ is large in aqueous media, the observed rate constant is

$$k = k_1 + k_2'K[Hg^{2+}] \quad (9)$$

but for higher concentrations of $Fe(CN)_6^{4-}$, *i.e.*, when $K[Fe(CN)_6^{4-}] \gg 1$,

$$\text{rate} = k_1[Fe(CN)_6^{4-}] + k_2'[Hg^{2+}] \quad (10)$$

where

$$k_2' = k_2[H_2O]$$

The second term in equation (8) also explains the levelling off of the rate at higher $[Fe(CN)_6^{4-}]$ and the variable order of dependence on $[Fe(CN)_6^{4-}]$ in presence of small concentrations of mercury.

It is possible to evaluate the constants k_1, k_2 and K; k_1 can be obtained from the intercept and k_2 from the slope of a plot of equation (10). These values can be inserted in equation (9). to obtain the equilibrium constant K. The values of the constants at $I = 0.1$, temperature 25° and pH = 5.0–5.2 are:

$$k_1 = (2.0 \pm 0.1) \times 10^{-2}\ sec^{-1}$$

$$k_2 = 17.5\ sec^{-1},\ \log K = 2.42 \pm 0.02$$

Although this value of k_2 was obtained with high $[Fe(CN)_6^{4-}]$ it can be shown to be also valid for lower concentrations. We can obtain k_2 from a plot of rate *vs.* $[Fe(CN)_6^{4-}]$ according to the equation

$$\text{rate} = \{k_1 + k_2K[Hg^{2+}][H_2O]\}[Fe(CN)_6^{4-}]$$

by substituting for k_1, K and $[Hg^{2+}]$ in the value of the slope. The agreement between the two values of k_2 is fairly good (17.5 and 15.9 sec^{-1}).

Finally, the values of k_1, k_2 and K can be inserted in equation (8) along with concentration terms to calculate the rates under specified conditions and these can be compared with experimental values. This comparison is provided in Table 2. The agreement between calculated and observed rates is seen to be quite good. It is interesting that the value of K obtained in this work is similar to the value determined by Beck[21] for the complex $[Fe(CN)_6^{4-}.Hg(CN)_2]$ ($\log K = 2.38 \pm 0.01$).

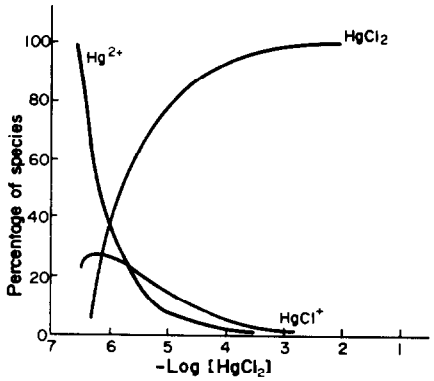


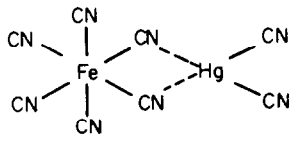
Fig. 7. Species distribution of $HgCl_2$ as a function of its concentration.

The effect of $[Hg^{2+}]$ on the rate at higher concentrations (Fig. 5) calls for detailed consideration. The rapid increase of rate at $[Hg^{2+}] > 4 \times 10^{-6}M$ may be explained as follows. The Hg–Cl bond in $HgCl_2$ has 28% ionic character[17] and the following equilibria exist:

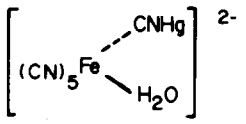
$$Hg^{2+} + Cl^- \overset{K_1}{\rightleftharpoons} HgCl^+$$

$$HgCl^+ + Cl^- \overset{K_2}{\rightleftharpoons} HgCl_2$$

Values of K_1 and K_2 for the conditions of our experiments are not available, but the values[18] $\log K_1 = 6.62$ and $\log K_2 = 6.36$ at $I = 0.5M$ ($NaClO_4$) and $[H^+] = 0.1M$ have been used to calculate the distribution of the various species in aqueous $HgCl_2$ solution (Fig. 7). It can be seen that at $[HgCl_2] > 10^{-6}M$, the $HgCl^+$ concentration is considerable and at still higher concentration $HgCl_2$ predominates. It is not unreasonable to suppose that $HgCl^+$ can also form an ion-pair with $Fe(CN)_6^{4-}$ (*cf.* $\log K_{HgCNCl} = 10.52$;[19] $\log K_{HgCN} = 17$)[20] but the adduct formed is looser than that with Hg^{2+} (probably because of smaller polarizing power). This adduct decomposes faster than that with Hg^{2+} and hence the rate is enhanced. With $[Hg^{2+}] > 4 \times 10^{-5}M$ (at $[Fe(CN)_6^{4-}] = 4 \times 10^{-5}M$) the rate falls rapidly. It appears that this happens because of formation of a 1:1 or higher complex between $Fe(CN)_6^{4-}$ and $HgCl_2$. This complexation removes the catalytic species, *viz.* Hg^{2+} and $HgCl^+$ from the field, and causes a sharp decline in rate (Fig. 5). This assumption is in line with earlier work of Beck[21] who demonstrated the formation of complexes such as $[Fe(CN)_6^{4-}.Hg(CN)_2]$ and $[Fe(CN)_6^{4-}.2Hg(CN)_2]$. This type of compound is found to be formed when $Fe(CN)_6^{4-}$ is added to $Hg(CN)_2$. However, another compound $Hg_2Fe(CN)_6$ is formed when $Hg(NO_3)_2$ is added to $Fe(CN)_6^{4-}$ solution.[22] According to Beck[21] the first complex may be represented as



Thus our postulate about the role of Hg^{2+} in the proposed mechanism appears to be justified. After the initial attachment of Hg^{2+}, the ion-pair rapidly isomerizes to form



which reacts rapidly with *p*-NDA through loss of the water. This conclusion is also supported by the effect of the dielectric constant on the rate, which shows that the activated complex is more polar than the reactants.

The effects of varying the water concentration by adding alcohol shows that water is involved in the activated complex. This favours an I_d mechanism rather than a *D* mechanism, *i.e.*, the formation of a 7-co-ordinated activated complex as an intermediate, not a 5-co-ordinated one. The decrease in entropy of activation for the catalysed reaction (Table 1) further strengthens this supposition. Also the order of activation energy for the catalysed and uncatalysed reaction is indicative of metal–ligand rupture between Fe and CN.

Acknowledgements—One of the authors (Mrs. M. Phull) is thankful to the University Grants Commission, Government of India, for award of a fellowship under its F.I.P. Scheme. The second author (PCN) is grateful to the Department of Science and Technology, G.O.I. for a research grant.

REFERENCES

1. O. Baudisch, *Ber.*, 1929, **62**, 2706.
2. S. Asperger and I. Murati, *Anal. Chem.*, 1954, **23**, 513.
3. K. B. Yatsimirskii and M. N. Orlova, *Zh. Neorgan. Khim.*, 1959, **4**, 741.
4. J. Das and K. Datta, *J. Indian Chem. Soc.*, 1974, **51**, 553.
5. P. Job, *Ann. Chim. (Paris)*, 1928, **9**, 113.
6. H. H. Willard, L. L. Merritt, Jr. and J. A. Dean, *Instrumental Methods of Analysis*, 4th Ed., p. 121. Litton, New York, 1977.
7. S. Asperger and D. Pavlovic, *J. Chem. Soc.*, 1955, 1449.
8. W. A. Eaton, P. George and G. I. Hanaria, *J. Phys. Chem.*, 1967, **71**, 2016.
9. B. V. Nekrasov and G. V. Zotov, *J. Appl. Chem. USSR*, 1941, **14**, 264.
10. D. D. Perrin and I. G. Sayce, *Talanta*, 1967, **14**, 833.
11. M. T. Beck and E. C. Porzsolt, *J. Coord. Chem.*, 1971, **1**, 57.
12. S. Asperger and I. Murati, *J. Chem. Soc.*, 1953, 1041.

13. C. H. Rochester, *Progress in Reaction Kinetics*, 1971, **6**, 145.
14. S. Asperger, A. Zimic, D. Curtila, D. Pavlovic, I. Murati and W. Reynold, *J. Chem. Soc.*, 1973, 1284.
15. J. G. Kirkwood, *J. Chem. Phys.* 1934, **2**, 351.
16. T. R. Sullivan, D. R. Stranks, J. Burgess and R. I. Haines, *J. Chem. Soc.* (*Dalton*), 1977, 1460.
17. G. Allen and E. Warhurst, *Trans. Faraday Soc.*, 1958, **54**, 1786.
18. L. D. Hansen, R. M. Izatt and J. J. Christensen, *Inorg. Chem.*, 1963, **2**, 1243.
19. V. I. Belevantsev and B. I. Peshchevitskii, *Koord. Khim.*, 1979, **5**, 27.
20. J. J. Christensen, R. M. Izatt and D. Eatough, *Inorg. Chem.*, 1965, **4**, 1278.
21. M. T. Beck, *Fourteen—a magic number of coordination chemistry*. Presented at XX-ICCC, Calcutta.
22. A. Bellomo, *Talanta*, 1975, **22**, 197.

Talanta, Vol. 28, pp. 599 to 600, 1981
Printed in Great Britain

0039-9140/81/080599-02$02.00/0
Pergamon Press Ltd

SHORT COMMUNICATIONS

BARIUM OXALATE AS A SELECTIVE SOLID REAGENT FOR THE ABSORPTION OF SULPHUR TRIOXIDE

R. BELCHER and S. J. MORRIS*

Department of Chemistry, University of Birmingham, P.O. Box 363, Birmingham, U.K.

(*Received* 7 *January* 1981. *Accepted* 3 *March* 1981)

Summary—Barium and calcium oxalate monohydrates have been shown to be more suitable absorbents for sulphur trioxide than either anhydrous or hydrated oxalic acid. All four compounds are selective absorbents for the trioxide and do not absorb sulphur dioxide. Similarly all are effective absorbents for sulphuric acid aerosol, although the calcium salt may be decarboxylated under these conditions. Lead oxalate and formate may be suitable for the absorption of SO_3 and H_2S, and SO_3, H_2S and SO_2 respectively.

Oxalic acid has been used previously to absorb sulphur trioxide; carbon monoxide and carbon dioxide are formed and can be determined either with an infrared analyser[1] or by gas chromatography.[2,3]

$$(COOH)_2 + SO_3 \rightarrow H_2SO_4 + CO + CO_2$$

It has the drawback that eventually it becomes semi-liquid and the gas flow is impeded. Reagents which yield solid products should be superior; hence barium and calcium oxalate monohydrates were examined. Both were superior to the hydrous and anhydrous forms of oxalic acid. Molecular emission cavity analysis (MECA)[4] showed that all the absorbents retained sulphur after the passage of sulphur trioxide and none was found to absorb sulphur dioxide.

EXPERIMENTAL

An SO_3-enriched stream of nitrogen was produced by bubbling dry nitrogen through a 25% w/v solution of sulphur trioxide in concentrated sulphuric acid. The concentration of sulphur trioxide could be increased by warming the solution. Any sulphuric acid aerosol produced was removed by passing the gas through a mixture of phosphorus pentoxide and pumice. The gas mixture was passed through an absorption tube of 3.5 mm bore, containing a 5-cm length of a slightly compressed packing of the absorbent concerned. The effluent gas was then passed through a bubbler containing water; any sulphur trioxide remaining gave a characteristic mistiness caused by the formation of sulphuric acid aerosol.[5]

Barium and calcium oxalate monohydrates were freshly prepared as very fine particles (<250 μm).[6] Oxalic acid (anhydrous and the hydrate) and pumice were ground and then sieved to give various ranges of particle size (<175, 175–250, 250–425 and 425–850 μm). The barium and calcium salts could be mounted on pumice by stirring equal weights of the salt and sieved pumice with a small amount of acetone and then allowing the acetone to evaporate before drying at 60°. The absorption tube was packed with absorbent and the flow-rate of the gas mixture through the tube was varied in the range 30–275 ml/min. The first appearance of misty fumes in the bubbler indicated unreacted sulphur trioxide.

RESULTS AND DISCUSSION

The efficiency of absorption of all the absorbents was shown to be improved by reduction of particle size; thus the mounting of the barium and calcium salts on pumice was not advantageous. The most convenient particle size is 175–250 μm, as this provides high efficiency of absorption and unrestricted gas flow-rates.

Table 1 shows the maximal flow-rate of gas through the absorption tube if mist is not to appear in the bubbler. The figures in brackets indicate the approximate flow-rate of gas to give the same linear flow-velocity through an absorption tube of 1 cm bore.

Addition of small amounts of all four compounds to a 25% w/v solution of sulphur trioxide in concentrated sulphuric acid at room temperature gave immediate effervescence. The evolved gases burnt in air with a blue flame, characteristic of carbon monoxide. However, only the calcium salt gave any observable

Table 1.

Absorbent (175–250 μm)	Maximal flow-rate, *ml/min*
Oxalic acid dihydrate	35 (275)
Oxalic acid anhydrous	50 (400)
Barium oxalate monohydrate	225 (1800)
Calcium oxalate monohydrate	275 (2250)

* Present address: Department of Chemistry, University College, Swansea, Wales.

effervescence when added to concentrated sulphuric acid alone at room temperature and this rapidly subsided. Oxalic acid dihydrate gives effervescence only on warming.[7]

When the SO_3-enriched nitrogen was bubbled through water before passage through the absorption tube, it was found that the gas flow-rates could be increased slightly above the values quoted in the table and still give complete absorption. The absorbents were thus efficient for the removal of sulphuric acid aerosol in all cases.

It was clear that the anhydrous form of the acid was rather better than the hydrated form, but both became more efficient after some use. This may be due to the greater ease of absorption of sulphur trioxide by the sulphuric acid initially formed. Consequently the acid absorption tube should be mounted vertically with introduction of the gas mixture at the top to reduce possible loss. The metal salts do not suffer from this disadvantage although formation of pyrosulphate could give negative errors. When the used absorbents were examined by MECA, it was found that absorption of sulphur trioxide had occurred in all cases. Passage of sulphur dioxide diluted with nitrogen, under similar conditions, gave no trace of retained sulphur. Similar experiments with hydrogen sulphide showed no retention of sulphur by the barium and calcium salts, but unexpectedly a sulphur flame was obtained for both anhydrous and hydrated oxalic acid. The reaction of sulphur trioxide with barium or calcium oxalate is presumably:

$$M(COO)_2 + SO_3 \rightarrow MSO_4 + CO + CO_2$$

Carbon dioxide and monoxide were detected, but quantitative measurements were not made. The absorbents may be used to determine sulphur trioxide in the presence of sulphur dioxide by measurement of the carbon monoxide and dioxide produced, or they may be used, especially with low levels of sulphur trioxide, to determine total sulphur trioxide over a period of time by analysis of the absorbent itself for sulphate by, for example, MECA.

A few experiments with lead formate showed it to be as efficient as the barium and calcium oxalate monohydrates for absorption of sulphur trioxide, and it also absorbs sulphur dioxide. Thus it might serve as a suitable reagent for the simultaneous absorption of hydrogen sulphide, sulphur trioxide and sulphur dioxide. Lead oxalate might absorb only the first two gases, but these possibilities were not examined.

$$Pb(HCOO)_2 + SO_3 \rightarrow PbSO_4 + H_2O + 2CO$$

Acknowledgement—One of us (S.J.M.) thanks the Science Research Council for a studentship.

REFERENCES

1. R. L. Bond, W. J. Mullin and F. J. Pinchin, *Chem. Ind. London*, 1963, 1902.
2. R. Bent, W. R. Ladner and W. J. Mullin, *ibid.*, 1967, 461.
3. I. G. Dobrochiver, N. Y. Zuzykina, L. N. Shishkin and B. V. Osipov, *Zavodsk. Lab.*, 1972, **38**, 659; *Chem. Abstr.* 1973, **78**, 37580.
4. R. Belcher, S. L. Bogdanski and A. Townshend, *Anal. Chim. Acta*, 1973, **67**, 1.
5. S. J. Morris, *M.Sc. Thesis*, Birmingham University, 1979, and references therein.
6. R. Belcher and A. J. Nutten, *Quantitative Inorganic Analysis*, 3rd Ed., Butterworths, London, 1970.
7. F. G. Mann and B. C. Saunders, *Practical Organic Chemistry*, 4th Ed., Longmans, London, 1960.

Talanta. Vol. 28. pp. 601 to 602. 1981
Printed in Great Britain. All rights reserved

0039-9140/81/080601-02$02.00/0
Copyright © 1981 Pergamon Press Ltd

IMPROVED METHOD FOR TITRIMETRIC DETERMINATION OF SULPHIDE BY THE IODINE–AZIDE REACTION

NOBUTOSHI KIBA and MOTOHISA FURUSAWA
Department of Chemistry, Faculty of Engineering, Yamanashi University, Kofu-shi, 400, Japan

(*Received* 9 *April* 1980. *Revised* 12 *November* 1980. *Accepted* 25 *January* 1981)

Summary—A sensitive procedure for the determination of sulphide is described. The method depends on the extent to which the iodine–azide reaction has been catalysed by sulphide, and this is measured by titration of the amount of iodine consumed in a fixed time period.

The determination of traces of sulphide in aqueous solution is frequently needed as the final step after reduction of various matrices in analyses for total sulphur. Sulphide has been determined by titrimetry,[1–3] coulometry[4,5] and photometry.[1,6–9] Babko *et al.*[3] proposed a titrimetric method for the determination of sulphide by use of the iodine–azide reaction. Sodium hydroxide solution (0.1*M*) is often used for absorbing hydrogen sulphide. In the present work, the use of ammoniacal zinc sulphate solution for the absorption was investigated. The optimal conditions for the determination of sulphide in this solution by the catalytic reaction are discussed.

EXPERIMENTAL

Reagents

The sodium azide[10] and hydrazine sulphate[11] were checked iodimetrically. A 0.1*M* stock solution of iodine in 0.5*M* potassium iodide was prepared and standardized by titration with thiosulphate. The absorption solution was prepared by mixing a solution of 5 g of zinc sulphate heptahydrate in 500 ml of water with 300 ml of a solution containing 6 g of sodium hydroxide and 70 g of ammonium sulphate, and diluting to 1 litre with water. A stock sulphide solution ($1 \times 10^{-3}M$) was prepared by about 0.24 g of sodium sulphide nonahydrate in 1 litre of absorption solution and standardized iodimetrically immediately before use. All chemicals used were of analytical grade.

Procedure

Hydrogen sulphide was absorbed in 10 ml of absorption solution, 1.60 g of sodium azide were added and then the solution was neutralized to pH 7.2 with 0.2*M* hydrochloric acid (pH checked by pH-meter). The solution was transferred to a 25 ml standard flask and made up to volume with absorption solution adjusted to pH 7.2. A 20-ml portion was pipetted into a flask fitted with a stopper and 10 ml of standard iodine solution were added. The mixture was kept at 25° in a thermostat for 15 min with occasional shaking. The excess of iodine was titrated with standard hydrazine sulphate solution in the presence of starch as indicator. Since the reaction of iodine and hydrazine sulphate proceeds quantitatively only between pH 7.0 and 7.4,[12] solid sodium bicarbonate was added whenever necessary. Blank tests were performed to determine the blanks from the reagents themselves and from the walls of the apparatus.

Calibration

Calibration was done with sulphide solutions prepared by absorbing a gas mixture containing hydrogen sulphide. The hydrogen sulphide was evolved by acidification of standard sulphide solutions (20 ml) as in the method reported by Cresser,[13] removed with a stream of nitrogen at a flow-rate of 100 ml/min and absorbed in 10 ml of absorption solution in an absorption bottle.[14] Calibration curves were prepared for two sulphide ranges (10^{-4}–10^{-6} and 10^{-5}–$10^{-7}M$) with two sets of standard solutions (0.02*M* iodine–0.01*M* hydrazine sulphate and 0.005*M* iodine–0.0025*M* hydrazine sulphate, respectively).

RESULTS AND DISCUSSION

The results obtained for sodium sulphide, zinc sulphide and cadmium sulphide appear in Table 1. The sodium sulphide solutions (20 ml) were acidified with 2 ml of 6*M* hydrochloric acid and the hydrogen sulphide was swept into the absorber by maintaining the flow of nitrogen at 100 ml/min for 5 min. Zinc sulphide and cadmium sulphide were suspended in water. The evolution and absorption of hydrogen sulphide were carried out as already described. The results show that sulphides in the range 5×10^{-9}–1×10^{-6} mole can be determined with relative errors and coefficients of variation of 6% or less.

Optimization of conditions

pH of the solution. The iodine consumption decreases linearly with an increase of pH over the range 6.5–7.5. The measurements under acidic conditions were not advantageous because of the vaporization of hydrogen sulphide during the pH-adjustment and the 15-min incubation. Further, the titration with hydrazine can be successfully performed only between pH 7.0 and 7.4.[12] A pH value of 7.2 was chosen.

Table 1. Determination of sulphides

	Amount of sulphide, 10^{-8} mole		Coefficient of variation, %	Error, %
	Added	Found	($n = 5$)	
Na_2S	0.54	0.57	5.8	5.6
	0.90	0.86	5.8	4.4
	1.80	1.71	5.3	5.0
	5.40	5.56	4.4	3.0
	50.4	51.4	3.6	2.0
	100.8	101.8	2.3	1.0
ZnS	1.56	1.48	5.8	5.1
	7.80	7.42	5.7	4.9
	15.6	15.1	4.5	3.2
	78.0	75.7	3.8	2.9
CdS	1.06	1.01	5.5	4.7
	5.30	5.04	4.9	4.9
	10.6	10.2	4.1	3.8
	53.0	51.4	3.7	3.0
	106.8	1.3.6	3.8	3.0

Conditions: sodium azide 1.60 g/25 ml, reaction time 15 min, reaction temperature 25°C, pH 7.2.

Azide concentration. The iodine consumption increased linearly with increase of azide concentration from 0.5 to 1.5*M*. At higher concentrations the results were subject to serious error because of the evolution of hydrazoic acid gas. An azide concentration of 0.985*M* (1.60 g/25 ml) was chosen for accuracy.

Iodide concentration. An increase in iodide concentration caused a decrease of iodine consumption. However, for accurate work, enough iodide had to be present to prevent the volatilization of iodine from the standard iodine solutions and from the reaction mixture during the incubation period. For this reason, a 0.1*M* stock solution of iodine in 0.5*M* potassium iodide was chosen.

Reaction temperature. The temperature was varied from 20 to 35°. The extent of reaction was greater at higher temperature than at low. At temperatures of 20–25° the reactions were terminated after 10 min. At temperatures of 30–35°, the reactions were allowed to run for 25 min. A reaction temperature of 25° and reaction time of 15 min were chosen.

Possible interferences from arsine and methyl mercaptan, two gases which can be generated by reductive decomposition techniques, were investigated. Arsine up to 10^{-3} mole did not interfere, though the absorption solution turned faintly yellow. Methyl mercaptan gave positive errors, since the extent of the catalysis was the same as that of sulphide under the conditions used.

REFERENCES

1. A. Watson, E. Grallath, G. Kaiser and G. Tölg, *Anal. Chim. Acta*, 1978, **100**, 413.
2. P. Y. Serre and H. Bozon, *Analysis*, 1977, **5**, 304.
3. A. K. Babko and A. S. Segeda, *Zh. Analit. Khim.*, 1968, **23**, 727.
4. K. Gijsbers, L. Bastings and R. van de Leest, *Analyst*, 1974, **99**, 376.
5. M. C. van Grondelle, F. van de Craats and J. D. van der Laarse, *Anal. Chim. Acta*, 1977, **92**, 267.
6. R. R. Moest, *Anal. Chem.*, 1975, **47**, 1204.
7. W. J. Kirsten, *Mikrochim. Acta*, 1978 **II**, 403.
8. L. S. Tsebrii, V. Z. Orlova, L. A. Belyantseva and E. I. Vail, *Zavodsk. Lab.*, 1979, **45**, 499.
9. J. F. Alder and K. Kargosha, *Anal. Chim. Acta*, 1979, **107**, 231.
10. F. Feigl and E. Chargaff, *Z. Anal. Chem.*, 1928, **20**, 376.
11. R. A. Penneman and I. F. Audrieth, *Anal. Chem.*, 1948, **20**, 1058.
12. H. E. Malone, *The Determination of Hydrazine-Hydrazide Groups*, p. 43. Pergamon Press, Oxford, 1970.
13. M. S. Cresser, *Lab. Pract.*, 1978, 639.
14. *Japan Industrial Standard*, JIS R 3503.

Talanta, Vol. 28, pp. 603 to 606, 1981
Printed in Great Britain. All rights reserved

0039-9140/81/080603-04$02.00/0
Copyright © 1981 Pergamon Press Ltd

SPECTROPHOTOMETRIC DETERMINATION OF IRON WITH 1-HYDROXY-4-SULPHO-2-NAPHTHOIC ACID

LAURI H. J. LAJUNEN* and EERO AITTA
Department of Chemistry, University of Oulu, Linnanmaa, SF-90570 Oulu 57, Finland

(*Received* 23 *June* 1980. *Revised* 15 *December* 1980. *Accepted* 13 *January* 1981)

Summary—1-Hydroxy-4-sulpho-2-naphthoic acid (H_3L) is proposed as a spectrophotometric reagent for determination of iron. It gives a red-brown chelate, FeL_3^{6-}, with λ_{max} 500–520 nm at pH 8 ($\epsilon = 3.3 \times 10^3$ l. mole^{-1}. cm^{-1}). In this wavelength region the reagent has no absorption. Most common cations and oxo-anions do not interfere. In the determination of iron in polymetallic iron ores and aluminium alloys the relative error and relative standard deviation of the method were found to be better than 1 and 0.5%, respectively. 1-Hydroxy-4-sulpho-2-naphthoic acid seems to be a more sensitive and accurate reagent for iron than 5-sulphosalicylic acid, and the number of interfering ions is smaller than in the 1,10-phenanthroline or thiocyanate methods.

Iron(III) forms stable complexes with salicylic acid and its derivatives, and 5-sulphosalicylic acid has been used for its spectrophotometric determination.[1] We have already studied the formation, composition and stability of the iron(III) complexes of three ligands analogous to sulphosalicylic acid, namely 1-hydroxy-4-sulpho-2-naphthoic, 1-hydroxy-7-sulpho-2-naphthoic and 1-hydroxy-4,7-disulpho-2-naphthoic acids, in a search for reagents for spectrophotometric determination of iron.[2,3]

Here we report on the use of 1-hydroxy-4-sulpho-2-naphthoic acid and its application to analysis of polymetallic iron ores and an aluminium alloy.

EXPERIMENTAL

Reagents

The preparation and purification of 1-hydroxy-4-sulpho-2-naphthoic and 1-hydroxy-7-sulpho-2-naphthoic acid monosodium salts have been reported elsewhere.[2–4]

Stock solutions of iron(III) were prepared and standardized as already described.[3]

Apparatus

A Pye Unicam SP 8-100 spectrophotometer equipped with a 10-mm autocell and a "superimpose" accessory was used.

Determination of iron with 1-hydroxy-4-sulpho-2-naphthoic acid

Add 50 ml of 1% 1-hydroxy-4-sulpho-2-naphthoic acid solution to 10 ml of solution containing up to 0.15 mg of iron. Adjust the pH to 8 with ammonia/ammonium chloride buffer and dilute to 100 ml. Similarly make 3 or 4 standard iron solutions containing 0.005–0.15 mg of iron. As the reagent has no absorbance at wavelengths longer than 450 nm, water can be used as the reference. Measure the absorbance of the test and standard solutions at 520 nm, and deduce the amount of iron in the sample solution from the calibration curve. If the analysis solution contains large amounts of Mn, Co or Pb, these elements must be removed before the determination.

* To whom correspondence and requests for reprints should be addressed.

RESULTS AND DISCUSSION

Complex-formation equilibria

Both the spectrophotometric and the potentiometric (pH-titration) measurements clearly revealed the stepwise formation of mononuclear complexes FeL, FeL_2^{3-} and FeL_3^{6-} at $I = 0.1$ ($NaClO_4$) and 25°, the logarithms of the overall stability constants being 14.04, 25.01 and 32.4 respectively,[2] analogously to the iron(III)–5-sulphosalicylic acid system.[1]

The absorption maxima of the complexes occur at 580 nm (FeL), 530 nm (FeL_2^{3-}) and 495 nm (FeL_3^{6-}), the molar absorptivities being 1.57×10^3, 2.84×10^3 and 3.29×10^3 l. mole^{-1}. cm^{-1} respectively.[2] The 1:3 chelate is suitable for spectrophotometric determination of iron(III).

Effect of pH and time

Figure 1 shows that the tris-chelates of iron(III) with 1-hydroxy-4-sulpho-2-naphthoic (**I**) and 1-hydroxy-7-sulpho-2-naphthoic (**II**) acids are both formed at pH ~ 8. Above ~8.5 the absorbance of the FeL_3^{6-} chelate of **I** remains almost constant, whereas that of the corresponding chelate of **II** begins to decrease because of hydrolysis reactions. In both systems pH 8 seems optimal.

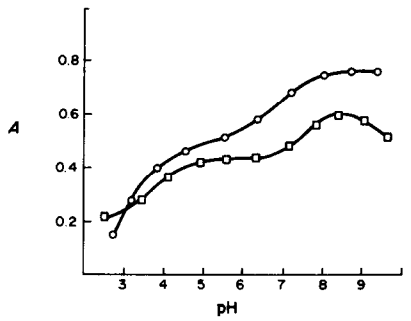


Fig. 1. The pH–absorbance plots for iron(III)–1-hydroxy-4-sulpho-2-naphthoic acid (○) and iron(III)–1-hydroxy-7-sulpho-2-naphthoic acid (□) systems at $I = 0.1$ ($NaClO_4$) and 25°C. $C_{Fe} = 0.0002M$ and $C_L : C_{Fe} \approx 20$.

Both chelates are formed immediately after mixing of the reagents, but the absorbance for the chelate with **I** remains constant for at least 24 hr, whereas that for the chelate with **II** begins to decrease immediately after formation of the complex (Fig. 2). It was found that keeping the test solution in the dark before the absorbance measurement had no effect on the stability of either complex.

Calibration curves

Beer's law was found to be obeyed when the concentration ratio of ligand to metal ion was >20 for **I** and >30 for **II**, and the mean linear regression coefficients (five replicates, with five iron concentrations) were 0.99 and 0.97, respectively.

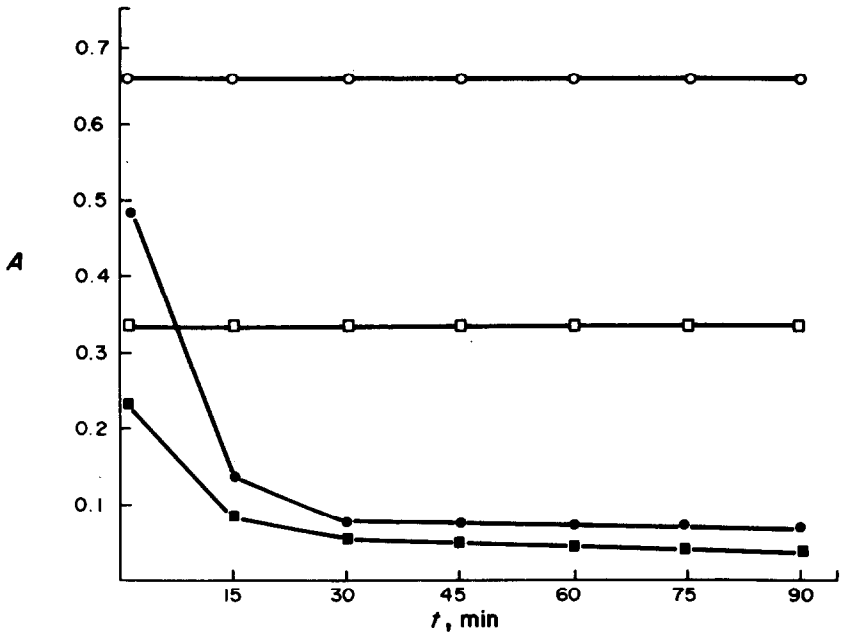


Fig. 2. Effect of time on the absorbances of the FeL_3^{6-} chelates of 1-hydroxy-4-sulpho-2-naphthoic acid [$C_L = 0.005M$; $C_{Fe} = 0.0002M$ (○) and $C_{Fe} = 0.0001M$ (□)] and 1-hydroxy-7-sulpho-2-naphthoic acid [$C_L = 0.005M$; $C_{Fe} = 0.0002M$ (●) and $C_{Fe} = 0.0001M$ (■)] at 500 nm and pH 8.

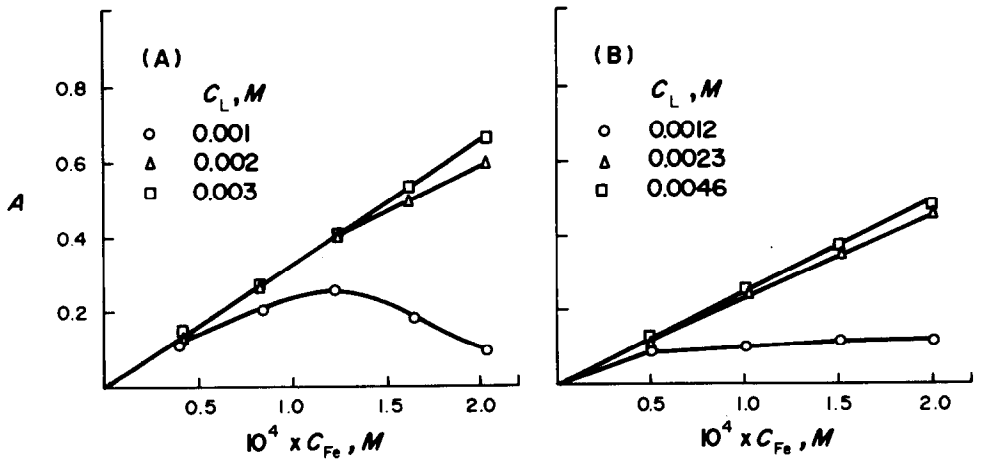


Fig. 3. Calibration curves for the iron(III)–1-hydroxy-4-sulpho-2-naphthoic acid (A) and iron(III)–1-hydroxy-7-sulpho-2-naphthoic acid (B) systems at pH 8 with variable amounts of the reagents.

Table 1. The absorbances (at 500 and 520 nm) for solutions containing Fe^{3+} ($C_{Fe} = 1.0 \times 10^{-4}M$) and 1-hydroxy-4-sulpho-2-naphthoic acid ($C_L = 6.5 \times 10^{-3}M$) with different amounts of Co^{2+}, Mn^{2+}, Pb^{2+} or VO^{2+} ions

M^{n+}	C_M, M	Absorbance 500 nm	Absorbance 520 nm
		0.425	0.372
Co^{2+}	2.5×10^{-5}	0.428	0.372
	3.8×10^{-5}	0.431	0.374
	5.0×10^{-5}	0.434	0.385
Pb^{2+}	1.5×10^{-5}	0.427	0.372
	3.0×10^{-5}	0.432	0.379
Mn^{2+}	0.4×10^{-5}	0.427	0.372
	1.0×10^{-5}	0.430	0.376
VO^{2+}	1.0×10^{-4}	0.427	0.373
	1.5×10^{-4}	0.429	0.376

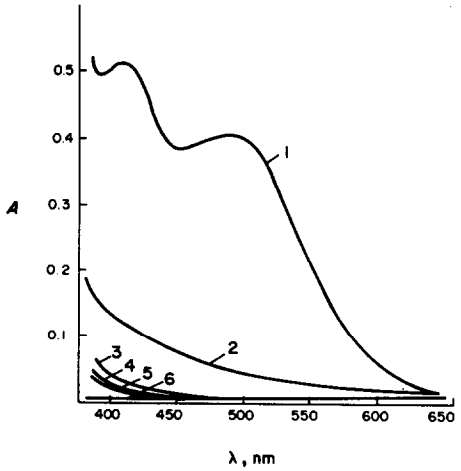


Fig. 4. Absorption spectra of aqueous solutions containing 1-hydroxy-4-sulpho-2-naphthoic acid ($C_L = 0.0065M$) and metal ions indicated ($C_M = 0.0001M$) at pH 8. 1, Fe^{3+}; 2, Mn^{2+}; 3, Cr^{3+}; 4, VO^{2+}; 5, reagent alone and with Zn^{2+}, Cd^{2+}, Al^{3+}, Ni^{2+} or Cu^{2+}; 6, base-line (pure water).

Interferences

Only common cations and anions were examined, especially those which interfere in the earlier spectrophotometric methods for iron. Figure 3 shows the absorption spectra for $0.0065M$ 1-hydroxy-4-sulpho-2-naphthoic acid at pH 8 in the presence of various metal ions. Most of the metal ions studied produce no absorption with 1-hydroxy-4-sulpho-2-naphthoic acid at wavelengths longer than 450 nm, and thus do not interfere. Al^{3+}, Zn^{2+}, Cd^{2+}, Ni^{2+}, Ag^{+}, Hg^{2+}, VO_3^-, CrO_4^{2-}, WO_4^{2-}, MoO_4^{2-} and PO_4^{3-} do not interfere when present in up to 100-fold molar ratio to iron, but the best wavelength for determination of iron is 520 nm instead of 500 nm. The interference by Cr^{3+} can be avoided by oxidation of Cr^{3+} to CrO_4^{2-}. Cu^{2+} does not interfere if the absorbance measurements are made immediately. Mn^{2+}, Pb^{2+}, Co^{2+} and VO^{2+} interfere with the determination when their concentrations in the test solution exceed 4, 15, 25 and 100%, respectively, of that of the iron (Table 1).

Test of the method

The method was tested on three iron sulphide ores and an aluminium alloy, ten separate determinations being made in each case. For comparison, one of the samples was analysed spectrophotometrically with 1-hydroxy-7-sulpho-2-naphthoic and 5-sulphosalicylic acids. As can be seen from Table 2, the results obtained with 1-hydroxy-4-sulpho-2-naphthoic acid are better than those obtained with the other two spectrophotometric reagents. 1-Hydroxy-7-sulpho-2-naphthoic acid gave the poorest performance and proved useless for the purpose.

Table 2. Determination of iron (10 replicates). Abbreviations: 142HSN = 1-hydroxy-4-sulpho-2-naphthoic acid, 172HSN = 1-hydroxy-7-sulpho-2-naphthoic acid and 5SSA = 5-sulphosalicylic acid

	Composition of the samples (Certificate values reported by the manufacturers, %)	Method	Iron found, % Range	Iron found, % Mean	Relative error, %	Standard deviation, %
(a)	Fe(57.76), MgO(5.12), CaO(2.59), Cu(0.04), Mn(0.14), Cr(0.09), Al_2O_3(1.10), SiO_2(9.00), S(0.89)	142HSN	57.2–57.5	57.4	−0.1	0.2
		172HSN	51.6–52.9	52.2	−9.6	0.7
		5SSA	53.7–54.9	54.2	−6.2	0.7
(b)	Fe(0.93, Al(81.08), Cu(4.66), Zn(4.06), Si(5.24), Ni(0.18), Mn(0.38), Mg(0.35), Pb(2.21), Sn(0.90)	142HSN	0.93_3–0.94_2	0.937	+0.8	0.3
(c)	Fe(32.20), Zn(30.70), Cu(0.37), Ni(0.18), Co(0.28), S(35.0)	142HSN	32.1–32.5	32.3	+0.3	0.3
(d)	Fe(33.10), Cu(26.20), Zn(1.36), Ni(0.06), Co(0.18), S(34.80)	142HSN	32.8–33.3	33.1	0.0	0.5

(a) Dr. Hoepfner's Analysensubstanzen: Eisenerz XXVI, Nr. 998, (b) Dr. Hoepfner's Analysen-substanzen: Aluminium-Legierung VII, Nr. 998, (c) Outokumpu Oy: ZnR, No. 8, (d) Outokumpu Oy: CuR, No. 4.

Conclusions

Of the sulphonated 1-hydroxy-2-naphthoic acids, only the 4-sulphonic acid is useful for spectrophotometric determination of iron. Its advantages are (*a*) the iron chelate has a broad absorption band at 450–600 nm, so single-beam filter instruments can be used; (*b*) the chelate is stable at pH 8; (*c*) the method is more sensitive and accurate than that with 5-sulphosalicylic acid; (*d*) synthesis of the reagent is simple; (*e*) Al^{3+}, Zn^{2+}, Cd^{2+}, Ni^{2+}, Cu^{2+}, Ag^{+}, Hg^{2+}, VO_3^-, CrO_4^{2-}, WO_4^{2-}, MoO_4^{2-} and PO_4^{3-} do not interfere in 100-fold ratio to Fe^{3+}, though Mn^{2+}, Co^{2+}, Pb^{2+} and VO^{2+} cannot be tolerated in more than trace amounts. In contrast, Ag^{+}, Hg^{2+}, MoO_4^{2-}, Ni^{2+} and WO_4^{2-} interfere with the 1,10-phenanthroline method, and Ag^{+}, Cu^{2+} and MoO_4^{2-} with the thiocyanate method.[4]

However, there are drawbacks: (*a*) the solubility of the reagent in aqueous media is poor; (*b*) the concentration of the reagent must be more than 20 times that of the iron; (*c*) metal cations other than alkali-metal ions consume the reagent by complexation, so the total concentration of iron(III) and these cations must be lower than about 0.002*M* in the solutions to be analysed.

Acknowledgement—A grant awarded by the Tauno Tönning Foundation is gratefully acknowledged.

REFERENCES

1. L. G. Sillén and A. E. Martell, *Stability Constants of Metal-Ion Complexes*, The Chemical Society, Spec. Publ. 25, London, 1971.
2. L. H. J. Lajunen, S. Parhi and H. Ruotsalainen, *Finn. Chem. Lett.*, 1979, 227.
3. L. H. J. Lajunen, E. Aitta and S. Parhi, *Talanta*, 1981, **28**, 227.
4. L. Meites (ed.), *Handbook of Analytical Chemistry*, McGraw-Hill, New York, 1963.

Talanta. Vol. 28. pp. 607 to 609. 1981
Printed in Great Britain. All rights reserved

0039-9140/81/080607-03$02.00/0
Copyright © 1981 Pergamon Press Ltd

A SIMPLE METHOD FOR THE DETERMINATION OF BENZO[*a*]PYRENE AND BENZO[*k*]FLUORANTHENE IN A MIXTURE

A. M. MOHAN RAO, R. RAJAGOPALAN and K. G. VOHRA
Division of Radiological Protection, Bhabha Atomic Research Centre, Bombay–400 085, India

(*Received* 19 *March* 1980. *Revised* 5 *February* 1981. *Accepted* 18 *February* 1981)

Summary—Atmospheric particulate matter is routinely analysed for the concentration of the carcinogen benzo[*a*]pyrene (BaP). Benzo[*k*]fluoranthene (BkF) has identical spectral characteristics and interferes in the fluorimetric estimation. A simple method for the determination of BaP in the presence of BkF is described. Based on quenching of the fluorescence of BaP by the addition of small amounts of nitromethane, the method can be used for accurate estimation for wide concentration ratios of BaP to BkF ranging from 0.1 to 10.0.

The measurement of polycyclic aromatic hydrocarbons is routinely conducted for air pollution studies. The most widely used procedure consists of separation of the particulate extract by thin-layer chromatography and spectrofluorimetric estimation. Among the various polycyclic aromatic hydrocarbons the commonly occurring compounds are benzo[*a*]pyrene, benzo[*k*]fluoranthene, benzo[*e*]pyrene and perylene (this group was designated the benzopyrene fraction by earlier workers). All these compounds are separable by thin-layer chromatography. Benzo[*a*]pyrene is highly carcinogenic, benzo[*e*]pyrene is defined as weakly carcinogenic and the other two are non-carcinogenic. Recent studies have shown that the nitro-derivatives of perylene are mutagenic.[1] Thus it is important that the determination of each of these is accurate and free from interference by the others. The widely differing R_f values on TLC plates should ensure good separation but in practice it is often difficult to make it complete. The excitation and emission spectra of benzo[*a*]pyrene (BaP) and benzo[*k*]fluoranthene (BkF) are almost identical (Figs. 1 and 2). Thus, it is difficult to ascertain the extent of mutual interference of BkF and BaP in their determination in the TLC-separated fractions of environmental samples. A simple technique for estimating both BaP and BkF in a solution is described below. This method has been checked by measuring standard mixtures of these two compounds.

EXPERIMENTAL

The TLC-separated sample to be analysed for BaP or BkF is dissolved in 4 ml of spectrochemical grade toluene. The emission intensity at 414 nm is measured with the excitation wavelength set at 388 nm. The sample is then transferred into a stoppered test-tube, 0.2 ml of nitromethane is added and the solution is mixed. The emission intensity is measured again. This reading corresponds to the intensity due to BkF. The calibration curve for BkF in toluene (or the toluene–nitromethane mixture) is linear and hence the amount of BkF in the sample can be estimated. Once the amount of BkF is estimated it is easy to estimate the amount of BaP from the total emission intensity of the toluene solution.

The measured fluorescence intensities for different concentrations of BaP and BkF in toluene are shown in Table 1. The measurements are for three different concentration ratios (0.1, 1.0 and 10.0) of BaP and BkF. The effect of addition of nitromethane on the emission intensities is also shown in Table 1. Addition of 0.2 ml of nitromethane to toluene containing BaP reduced the emission intensity to about 5% of its initial value for BaP concentrations between 0.05 and 0.5 μg/ml whereas the emission intensity due to BkF was reduced only to 75% of its initial value. Thus by the addition of 5% of nitromethane it is possible to quench practically all the fluorescence of BaP and observe essentially the fluorescence due to BkF in the mixture. This method has been used to determine the interference due to BkF in TLC-separated fractions to be analysed for BaP.

DISCUSSION

A similar method was proposed by Sawicki *et al.*[2] for estimating compounds containing the fluoranthene structure, in the presence of other non-fluoranthene hydrocarbons. According to them, compounds such as anthracene, phenanthrene, pyrene, benzo[*a*]anthracene, benzo[*a*]pyrene and perylene are non-fluorescent in nitromethane solution but hydrocarbons containing the fluoranthene structure fluoresce. The quenching of the fluorescence of non-fluoranthene hydrocarbons by the addition of nitromethane is attributed to the formation of a non-fluorescent π-complex in the excited state of these compounds. Nitropropane and tetranitromethane also act as quenchers, the latter being the most effective. In the method proposed by us it is possible to measure both

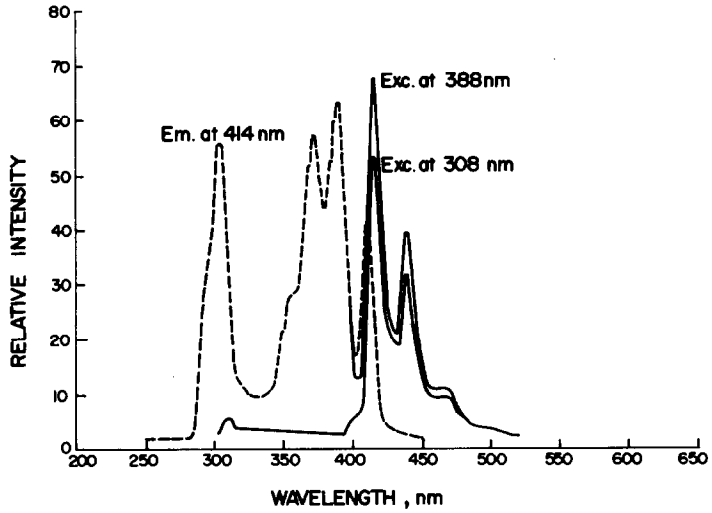


Fig. 1. Excitation and emission spectra for benzo[*a*]pyrene in toluene.

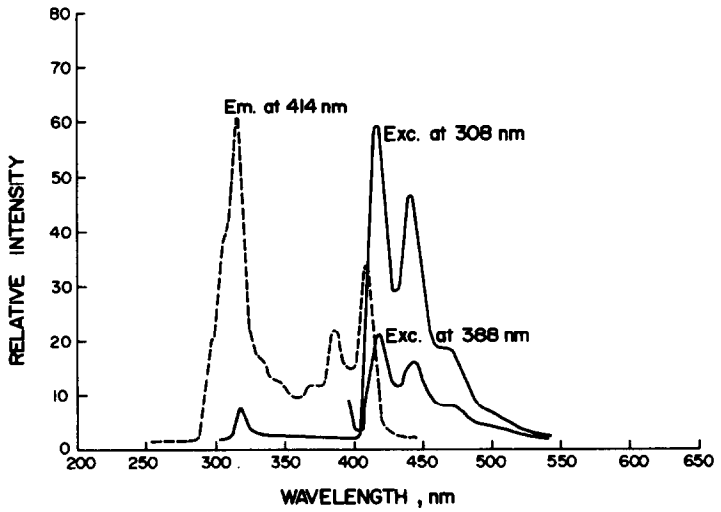


Fig. 2. Excitation and emission spectra for benzo[*k*]fluoranthene in toluene.

BaP and BkF in the same sample. Nitromethane is an explosive and toxic chemical but in our method only very small quantities are needed.

In another method for estimating BaP and BkF in a mixture, Dubois and Monkman[3] propose using the difference in the ratios of the emission intensities for BaP and BkF at excitation wavelengths of 308 and 385 nm. According to them, when BkF and BaP are both excited at 308 nm the response of BkF is 25 times that of BaP, so that when excitation at 308 nm is used the observed intensity can be ascribed to BkF with an error of only +4% when the amounts of BaP

Table 1. Fluorescence intensities of benzo[*a*]pyrene and benzo[*k*]fluoranthene in toluene (4 ml)

Volume of nitromethane, μl	Fluorescence intensities (arbitrary units)						
	0.2 μg BaP	2.0 μg BaP	0.2 μg BkF	2.0 μg BkF	0.2 + 0.2 μg BaP + BkF	0.2 + 2.0 μg BaP + BkF	2.0 + 0.2 μg BaP + BkF
0	0.121	1.20	0.099	0.99	0.216	1.095	1.23
50	0.027	0.27	0.095	0.95	0.124	1.045	0.365
100	0.013	0.147	0.084	0.87	0.100	0.855	0.225
150	0.007	0.096	0.078	0.81	0.087	0.825	0.170
200	0.005	0.066	0.072	0.75	0.081	0.765	0.135

and BkF in the sample are equal. However, the error rapidly increases with BaP/BkF ratio, and a fair amount of computation is needed.

There are two possibilities for application of the quenching technique. In the first, the BaP and BkF spots are eluted and the solutions are combined, and the emission is measured before and after addition of nitromethane; the values obtained can be used to calculate the amounts of both species, by means of simultaneous equations and values of the specific fluorescences (intensity per μg) of the two species measured in absence and presence of nitromethane. In the second, the simultaneous equation method can be applied to the two spots individually and the amounts of each species summed, or (if the resulting error can be tolerated) the major species in each spot can be determined and the contaminant ignored. This last method is easy to use and gives direct concentration data. The method is applicable to a wide range of concentration ratios of BaP to BkF, from 0.1 to 10.0. However, the amount of BaP or BkF in the sample to be estimated should be below 0.5 μg/ml so that the response is linear. Larger amounts of nitromethane are needed to quench larger amounts of BaP in the mixture and hence it is desirable to dilute the sample so that the BaP fluorescence is practically completely quenched by the addition of 0.2 ml of nitromethane.

REFERENCES

1. J. N. Pitts, Jr., K. A. Van Cauwenberghe, D. Grasjean, J. P. Schmid, D. R. Fitz, W. L. Belser, Jr., G. B. Knudson and P. M. Hynds, *Science*, 1978, **202**, 515.
2. E. Sawicki, T. W. Stanley and W. C. Elbert, *Talanta*, 1964, **11**, 1433.
3. L. Dubios and J. L. Monkman, *Intern. J. Air Wat. Poll.*, 1965, **9**, 131.
4. A. M. M. Rao and K. G. Vohra, *Atmos. Environ.*, 1975, **9**, 403.

Talanta, Vol. 28, pp. 610 to 612, 1981
Printed in Great Britain. All rights reserved

0039-9140/81/080610-03$02.00/0
Copyright © 1981 Pergamon Press Ltd

TRACE ELEMENT DETERMINATION IN ENVIRONMENTAL POLLUTION: A KINETIC METHOD FOR MERCURY ESTIMATION

MADHU PHULL, H. C. BAJAJ and P. C. NIGAM*
Department of Chemistry, Indian Institute of Technology, Kanpur-208016, India

(*Received* 12 *August* 1980. *Revised* 27 *October* 1980. *Accepted* 22 *January* 1981)

Summary—A method is developed for the estimation of mercury in trace concentrations by measuring spectrophotometrically its catalytic effect on the rate of substitution of *p*-nitrosodiphenylamine into hexacyanoferrate(II). Under the specified conditions the detection limit is found to be $2.0 \times 10^{-8}M$, relative standard deviation 1.4%. The effect of other ions is discussed.

Mercury can be estimated in very low concentrations by extraction of its dithizone or dinaphthylthiocarbazone complex, or by atomic absorption.[2,3] Catalysed substitution of nitrosobenzene,[4] α,α′-bipyridyl[5] or 1, 10-phenanthroline[6] into hexacyanoferrate(II) has been used for trace determination of Hg, Ag and Au. Nitrosobenzene gives the highest sensitivity, but its solution decomposes on keeping. In this paper we describe a sensitive kinetic method for estimation of mercury(II) by use of *p*-nitrosodiphenylamine (*p*-NDA) as incoming ligand in this substitution reaction.

EXPERIMENTAL

Reagents

Stock solutions of $5.0 \times 10^{-3}M$ *p*-NDA in alcohol, $10^{-2}M$ mercury(II) chloride, $0.2M$ potassium hydrogen phthalate, $0.1M$ sodium hydroxide and $0.1M$ potassium hexacyanoferrate(II) are prepared, the last being stored in a dark amber-coloured bottle. The mercury and hexacyanoferrate(II) solutions are freshly diluted as required. A phthalate–sodium hydroxide buffer and potassium nitrate are used to maintain pH and ionic strength respectively.

Procedure

All solutions are brought to the same temperature by immersion in a thermostat at $25 \pm 0.1°$ for 30 min. A 0.5-ml portion of $5.0 \times 10^{-3}M$ *p*-NDA and 3.5 ml of buffer are mixed immediately before the run, to avoid any interaction between them. As there is a perceptible though very small interaction between *p*-NDA and Hg(II), 0.5 ml of mercury sample solution is also added immediately before the run, then 0.5 ml of hexacyanoferrate(II) solution is added (by syringe) to initiate the reaction. The solution is transferred to a 1-cm cell in a temperature-controlled cell-compartment kept at $25° \pm 0.1°$ by circulation of water from the thermostatic bath, and the absorbance at 640 nm is measured after 15 min.

* To whom correspondence and requests for reprints should be addressed.

RESULTS AND DISCUSSION

A plot of A_{15} (*i.e.*, the absorbance 15 min after mixing of the reagents) *vs.* $[Hg^{2+}]$ when hexacyanoferrate(II) is present in excess and *p*-NDA in non-rate-limiting excess is linear. The expression relating A_{15} at 25° to $[Hg^{2+}]$ between 1×10^{-7} and $1 \times 10^{-6}M$ is given in equation (1). The relationship at higher $[Hg^{2+}]$ is more complicated.[7]

$$A_{15} = 0.103 \times 10^{6}[Hg^{2+}] + 0.103 \qquad (1)$$

The absorbances after shorter or longer reaction times also give linear relationships but the chosen time of 15 min gives a sufficient and convenient absorbance.

The rate expression[7] for this reaction in presence of a non-rate-limiting excess of *p*-NDA and a relatively large excess of ferrocyanide is

$$\frac{d[Fe(CN)_5^{3-}.p\text{-NDA}]}{dt} = k_1[Fe(CN)_6^{4-}] + k_2'[Hg^{2+}] \qquad (2)$$

where the first term corresponds to the uncatalysed reaction and the constant k_2' is made up of the rate-constant for slow decomposition of the activated complex formed between Hg^{2+}, $Fe(CN)_6^{4-}$ and H_2O and some other concentration terms. This expression predicts the linear relationship between rate and concentration of mercury. It must be borne in mind, however, that for good results the ratio of the rate for the catalysed reaction to that of the uncatalysed reaction must be high. So $[Fe(CN)_6^{4-}]$ should be high enough for equation (2) to apply but not too high to make the rate of the uncatalysed path significant.

An instantaneous and not insignificant change in absorbance is observed immediately after the reac-

Table 1. Error in the proposed kinetic method for mercury estimation $[Fe(CN)_6^{4-}] = 5.0 \times 10^{-3}M$; [p-NDA] = $5.0 \times 10^{-4}M$; pH = 5.0; $\mu = 0.1M$; temp. = 25 ± 0.1°C)

$[Hg^{2+}]$ added, $10^{-7}M$	$[Hg^{2+}]$ found*, $10^{-7}M$	Relative standard deviation, %
1.0	0.97	4.3
2.0	2.03	2.3
3.0	3.00	1.6
4.0	4.20	1.9
5.0	4.81	1.0
6.0	6.02	0.8
7.0	7.02	0.5
8.0	8.02	0.6
9.0	8.99	0.5
10.0	9.97	0.3

* Average of at least three runs.

tants are mixed, followed by a slow absorbance change. The first change is due to reaction between $Fe(CN)_5 \cdot H_2O^{3-}$ [already present in the reaction medium due to thermal and photodecomposition of $Fe(CN)_6^{4-}$] and p-NDA. Thus it is advisable always to prepare a fresh solution of $K_4Fe(CN)_6$ by dilution from the stock solution in order to minimize this background reaction.

Application of the Arrhenius equation to the rate constants of the catalysed and uncatalysed reactions gives the expression

$$\frac{k_c}{k_u} = a' \exp\left[\frac{E_u - E_c}{RT}\right]$$

where a' is the quotient of the pre-exponential factors for the catalysed and uncatalysed reactions and E_c and E_u are the respective activation energies (E_c = 16.2 kcal and E_u = 19.1 kcal). The k_c/k_u ratio decreases only slightly with rise in temperature and so 25° is a suitable temperature. The relative decrease in the k_c/k_u ratio is about −1.5% per degree. Therefore, while any convenient temperature may be chosen for a complete set of runs (provided it is kept constant), if a precision thermostatic bath is not available, it is possible to work at room temperature without appreciable sacrifice of accuracy.

The detection limit (X_d) was calculated according to the method of Tanaka,[8] from the expression:

$$X_d = \overline{X}_{b1} + t\sqrt{2}\,S_{b1}$$

where $\overline{X}_{b1}$ is the average and S_{b1} the standard deviation of the blank values; S_{b1} is taken as k_nR, k_n being the factor for obtaining S from the range R of n results. Tanaka advises taking t as 3. The detection limit calculated for the method under the specified conditions corresponds to a $2 \times 10^{-8}M$ concentration of Hg^{2+}. Improvement can be achieved by increasing the time interval to 30 min or more but this would increase the total analysis time correspondingly. The relative standard deviations for triplicate determinations range from 0.3% for $10^{-6}M$ mercury(II) to 4.3% for $10^{-7}M$ (Table 1).

The effects of various interfering and non-interfering ions and their tolerance limits are given in Table 2. Interference by Cd^{2+}, Ni^{2+}, Cu^{2+} (at low mercury concentration) can be explained as being due

Table 2. Effect of various ions ($[Fe(CN)_6^{4-}] = 5.0 \times 10^{-3}M$; [p-NDA] = $2.5 \times 10^{-4}M$; $\mu = 0.1M$; pH = 5–5.2; temp. = 25 ± 0.1 C; $[HgCl_2] = 8.0 \times 10^{-7}M$)

Ion	Concentration, M	$[Hg^{2+}]$ found* $10^{-7}M$	Relative standard deviation, %
Pb^{2+}	2.0×10^{-5}	8.0	0.6
Ni^{2+}	2.0×10^{-5}	7.5	0.5
	1.0×10^{-5}	7.7	0.6
Cu^{2+}	8.0×10^{-6}	8.0	0.6
Cd^{2+}	2.0×10^{-5}	7.6	0.6
	1.0×10^{-5}	8.0	0.6
Zn^{2+}	2.0×10^{-5}	8.0	0.6
Ag^{+}	2.0×10^{-5}	8.3	0.5
	1.0×10^{-5}	8.1	0.4
PO_4^{3-}	2.0×10^{-5}	7.8	0.6
	1.0×10^{-5}	8.0	0.6
I^-	2.0×10^{-5}	8.0	0.6
CN^-	4.8×10^{-5}	4.3	0.8
	2.4×10^{-6}	7.5	0.5
	9.8×10^{-7}	8.0	0.6
$S_2O_3^{2-}$	2.0×10^{-6}	7.7	0.6
	1.0×10^{-6}	8.0	0.6
Oxalic acid	2.0×10^{-5}	8.0	0.6
EDTA	2.0×10^{-5}	6.5	0.5
AsO_2^-	8.0×10^{-6}	8.1	0.6
Bi^{3+}	8.0×10^{-6}	8.0	0.6
Sn^{2+}	1.0×10^{-5}	7.8	0.6
SO_4^{2-}	4.0×10^{-5}	7.9	0.6
Br^-	2.0×10^{-5}	7.7	0.6

* Average of at least three runs.

to their salt formation with $Fe(CN)_6^{4-}$. Ag^+ catalyses the reaction but to a lesser extent. Thiosulphate, EDTA, CN^- *etc.* complex with Hg^{2+} and thus mask its catalytic activity.

We have therefore established that Hg^{2+} can be determined at trace levels (1×10^{-7}–$1 \times 10^{-6}M$) by a kinetic method in presence of a number of metal ions present in 10–50-fold concentration ratio to mercury. The method is proposed for trace determination of mercury in the environment.

Acknowledgements—One of the authors (Mrs. M. Phull) is grateful to the University Grants Commission, and a second (H.C.B) to the Council of Scientific and Industrial Research, for award of their respective fellowships. The third author (P.C.N) is grateful to the Department of Science and Technology, for a research grant.

REFERENCES

1. Analytical Methods Committee, *Analyst*, 1965, **90**, 515.
2. B. Delaughter, *At. Absorp. Newsl.*, 1970, **9**, 49.
3. G. U. Kalb, *ibid.*, 1970, **9**, 84.
4. S. Asperger and I. Murati, *Anal. Chem.*, 1954, **26**, 513.
5. K. B. Yatsimirskii and M. N. Orlova, *Zh. Neorgan. Khim.*, 1959, **4**, 741.
6. J. Das and K. Datta, *J. Indian Chem. Soc.*, 1974, **51**, 553.
7. M. Phull and P. C. Nigam, *Talanta*, 1981, **28**, 591.
8. N. Tanaka, *Kyoto fu Esci Kugai Kenkyosho Nempo*, 1977, **22**, 121; *Chem. Abstr.*, 1979, **90**, 114401.

Talanta, Vol. 28, pp. 613 to 615, 1981
Printed in Great Britain. All rights reserved

0039-9140/81/080613-03$02.00/0
Copyright © 1981 Pergamon Press Ltd

AN APPLICATION OF SILANED GLASS BEADS TO THE PRECONCENTRATION AND SPECTROPHOTOMETRIC DETERMINATION OF TRACES OF PHOSPHORUS WITH MOLYBDATE

SHIGERU TAGUCHI and KATSUMI GOTO
Department of Chemistry, Faculty of Science, Toyama University, Toyama, Japan 930

and

HIROTO WATANABE
Department of Applied Chemistry, Muroran Institute of Technology, Muroran, Japan 050

(*Received* 25 *November* 1980, *Accepted* 21 *January* 1981)

Summary—Silaned glass beads are applied to the preconcentration and spectrophotometric determination of phosphorus as the phosphomolybdenum blue complex. Traces of phosphorus in water are collected as a phosphomolybdenum blue complex on a column of the beads. The phosphomolybdenum blue is eluted with *N*,*N*-dimethylformamide and the absorbance of the eluate continuously monitored at 700 nm. The height of the very sharp peak obtained is proportional to the amount of phosphorus present and 0.1–0.5 μg of phosphorus in a 10-ml sample can be determined reproducibly. Interference from arsenate is eliminated by addition of a reducing agent. High concentrations of silica cause a small positive error. This method is applicable to the analysis of river water and sea-water samples.

The molybdenum blue method is the most widely used for determining small amounts of phosphorus. It has been modified by several authors to achieve more rapid colour development,[1–4] and higher selectivity[5–7] and sensitivity.[8,9] Solvent extraction with hexanol[9] or isobutanol[8,9] is a useful means of concentrating traces of the phosphomolybdenum blue complex. However, only a 10-fold concentration can be achieved by this method and the sensitivity is not always adequate for analysis of natural water samples. We have already proposed an adsorption–elution and spectrophotometric method for trace analysis,[10] in which cobalt was adsorbed as its 2-(2-pyridylazo)-5-diethylaminophenol complex on silaned glass beads, and eluted with a small volume of ethanol–hydrochloric acid mixture, the absorbance of the eluate being measured at 575 nm. A 50–500-fold concentration can be achieved with this method. A similar technique was used for preconcentration in the ICP–AES analysis of sea-water samples.[11]

Preliminary experiments showed that the molybdenum blue complex can also be adsorbed on silaned glass beads, and eluted with a small volume of *N*,*N*-dimethylformamide (DMF). This communication describes a highly sensitive spectrophotometric determination of phosphorus involving preconcentration in this way. Very high sensitivity is attained by continuously monitoring the absorbance of the eluate.

EXPERIMENTAL

Reagents

Mixed reagent. The reagent for the determination of phosphorus is prepared as described by Murphy and Riley;[3] 4.8 g of ammonium paramolybdate tetrahydrate and 0.1 g of potassium antimonyl tartrate are dissolved in 500 ml of 4*N* sulphuric acid.

Reducing agent. Prepared fresh daily as described by Schouwenburg and Walinga,[5] and modified by Johnson;[6] 20 ml of 3.5*N* sulphuric acid, 40 ml of 14% sodium metabisulphite solution and 40 ml of 1.4% sodium thiosulphate solution are mixed.

Standard phosphorus solution. Prepared by dissolving potassium dihydrogen phosphate in water.

Adsorbent. Prepared as reported previously.[10]

Apparatus

Monitor. Absorbance measurements were made with a Kyowa Seimistu KLC-2290 spectrophotometer furnished with an 8 μl flow-cell and connected to a recorder.

Column preparation. The column, in a tube 5 mm in diameter and 150 mm in length, was prepared by adding a slurry of the beads in ethanol until the height of the bed was 140 mm. It was washed with water to remove the ethanol.

Procedure

Take a sample solution containing less than 0.5 μg of phosphorus, add 1 ml of mixed reagent and make up to 10 ml with phosphorus-free water. Samples larger than 10 ml (up to 50 ml) can be handled if 1 ml of mixed reagent is added per 10 ml of sample, and further dilution is then

unnecessary. Add about 10 mg of ascorbic acid. After 10 min, pass the solution through the column, using a pump. Then, pump *N,N*-dimethylformamide through the column at a rate of 1 ml/min while monitoring the absorbance at 700 nm, using a micro flow-cell.

RESULTS AND DISCUSSION

Optimum conditions

The conditions for the colour development of the phosphorus complex and the masking of arsenic were similar to those reported by earlier workers.[5,6,9] The amounts of the mixed reagent and the reducing agent were varied with sample volume. A 10 min reaction time is sufficient for complete colour development of the complex.

Eluent and elution curves

Several organic solvents were tested for elution of the adsorbed complex. Figure 1 shows typical elution curves. A is the reagent blank for elution with DMF. The negative signal may be caused by the difference between the indexes of refraction of water and DMF. B is the elution curve in the presence of phosphorus. First negative and then sharp positive signals are recorded. The positive signal is caused by the elution of the complex.

The peak height, defined as the difference between the minimum absorbance of the blank and the maximum absorbance of the complex, is proportional to the amount of phosphorus. In DMF, the complex shows absorption maximum at 700 nm. Varying the eluent flow-rate from 0.3 to 1.3 ml/min does not affect the determination. Methanol and ethanol do not easily elute the complex. Acetone causes non-reproducible results.

Determination of phosphorus

Table 1 shows the determination of phosphorus present in various concentrations and in various sample volumes. Phosphorus at the μg/l. level can be determined reproducibly. A 10-ml sample volume is sufficient for determination of 0.1 μg of phosphorus. The small sample volume is of great advantage when a sample solution has to be treated with perchloric acid to decompose organic phosphorus compounds.

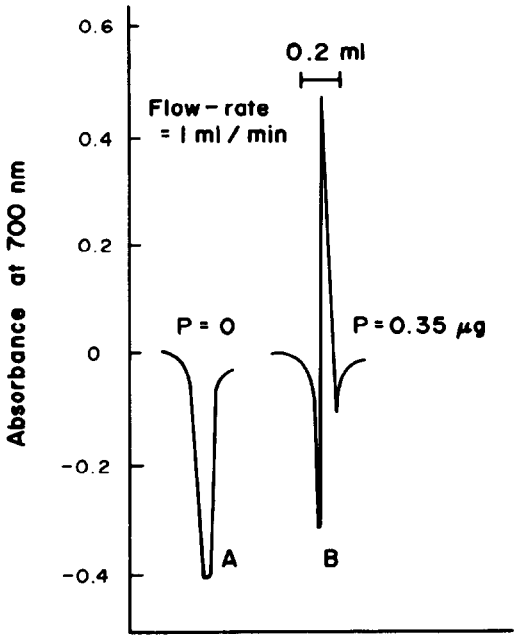


Fig. 1. Elution curves: A, reagent blank; B, phosphomolybdenum complex: (eluent *N,N*-dimethylformamide).

At lower concentrations a larger sample size may give more precise results.

Effect of diverse ions

It is known that high concentrations of foreign species other than silicon, arsenic and germanium do not interfere with the determination of phosphorus as phosphomolybdenum blue. In common natural water samples, germanium is not likely to be present at such a high concentration as to interfere. Arsenate, like phosphate, forms a complex with molybdate, which becomes blue on reduction and interferes with the determination. Schouwenburg and Walinga[5] eliminated the interference by reducing arsenic(V) to arsenic(III) with a mixture of sodium metabisulphite and sodium thiosulphate.

Table 2 shows the effect of arsenic on the determination of phosphorus in the absence and presence of the reducing agent. One ml of reducing agent is sufficient to eliminate the interference from 0.05 μg of

Table 1. Effect of phosphorus concentration and sample volume on the determination

P concn., μg/l.	Volume, ml	P taken, μg	No. of detns.	Abs. (mean)	C.V*., %
4.12	20	0.082	5	0.186	5.3
	50	0.206	5	0.505	2.6
8.24	25	0.206	5	0.510	2.4
10.3	10	0.103	5	0.250	2.7
	20	0.206	7	0.505	2.4
51.5	10	0.515	5	1.30	2.5

* Coefficient of variation.

Table 2. Effect of arsenic(V) on the determination of phosphorus in the absence and presence of the reducing agent

As(V) concn., μg/l.	P found concn., μg/l.	P recovery, %
0	5.15	—
1.0*	5.36	104
2.0*	5.67	110
5.0*	6.44	123
5.0†	5.25	102
10.0†	5.46	106

* In the absence of the reducing agent.
† In the presence of 1 ml of the reducing agent.

arsenic(V) in the determination of 0.05 μg of phosphorus. The addition of the reducing agent makes the slope of the calibration curve slightly lower.

Table 3 shows the effect of silica on the determination. High concentrations of silica cause a slightly positive error. Fortunately, in common natural waters, the silica concentrations are usually less than 50 mg/l., which is too small to cause interference. However, the extent of silica interference depends upon the reaction time. For example, a silica concentration of 50 mg/l. causes more than 10% positive error in determination of phosphorus at the 10-μg/l. level, if the solution is set aside for 60 min before passage through the column.

Analyses of river water and sea-water samples

Table 4 shows the results obtained by the "standard addition" method for some natural waters. Before the colour development, the samples were filtered through a 0.45 μm Millipore filter and treated with perchloric acid to decompose organic phosphorus compounds. In both cases, satisfactory results were obtained.

Table 3. Effect of silica on the determination of phosphorus

P concn. μg/l.	SiO_2 concn., mg/l.	P found, μg/l.	Recovery, %
5.15*	50	6.03	117
10.3†	20	10.4	101
	30	10.5	102
	50	10.7	104
	100	11.0	107
51.5†	50	54.1	105
	100	55.6	108

* Volume is 20 ml.
† Volume is 10 ml.
Reaction time is 10 min.

Table 4. Analyses of river water and sea-water samples, and recovery tests

P added, μg	P found, μg	P recovery, μg	P recovery, %
River water			
none	0.07	—	—
0.05	0.12	0.05	100
0.10	0.17	0.10	100
0.20	0.27	0.20	100
Sea-water			
none	0.12	—	—
0.15	0.26	0.14	93
0.20	0.31	0.19	95
0.30	0.42	0.30	100

Sample volume is 10 ml.

CONCLUSION

As will be seen in Fig. 1, the molybdenum blue complex is concentrated in a very small volume (approx. 0.2 ml) of the eluate. A very high sensitivity is thus obtained by continuously monitoring the absorbance of the eluate. The success of the method may be due in part to the choice of adsorbent. Since adsorption–desorption phenomena occur only on the alkylsilane groups attached to the surface of glass beads, and since our glass beads have no inner surfaces,[10] it is expected that the adsorption–desorption equilibria will be quickly attained, giving rise to a very sharp elution peak.

Acknowledgement—This work was partially supported by a grant from the Ministry of Education of Japan.

REFERENCES

1. M. Jean, *Anal. Chim. Acta*, 1956, **14**, 172.
2. *Idem*, *ibid.*, 1962, **31**, 24.
3. J. Murphy and J. P. Riley, *Anal. Chim. Acta*, 1962, **27**, 31.
4. J. E. Going and S. J. Eisenreich, *ibid.*, 1974, **70**, 95.
5. J. C. van Schouwenburg and I. Walinga, *ibid.*, 1967, **37**, 271.
6. D. L. Johnson, *Environmental Sci. Technol.*, 1971, **5**, 411.
7. E. Kitazume, N. Shibata and N. Hashimoto, *Anal. Chim. Acta*, 1977, **91**, 375.
8. C. H. Kueck and D. F. Boltz, *ibid.*, 1956, **28**, 1168.
9. H. L. Goltman, *Methods for Chemical Analysis of Fresh Waters*, p. 69. Blackwell, Oxford, 1969.
10. S. Taguchi and K. Goto, *Talanta*, 1980, **27**, 817.
11. H. Watanabe, K. Goto, S. Taguchi, J. W. McLaren, S. S. Berman and D. S. Russell, *Anal. Chem.*, submitted for publication.

Talanta, Vol. 28, pp. 616 to 618, 1981
Printed in Great Britain. All rights reserved

0039-9140/81/080616-03$02.00/0
Copyright © 1981 Pergamon Press Ltd

AN APPLICATION OF BIS[2-(5-CHLORO-2-PYRIDYLAZO)-5-DIETHYLAMINOPHENOLATO]COBALT(III) CHLORIDE TO THE EXTRACTION AND SPECTROPHOTOMETRIC DETERMINATION OF SULPHONATED AND SULPHATED SURFACTANTS

SHIGERU TAGUCHI, ISSEI KASAHARA, YŌICHI FUKUSHIMA and KATSUMI GOTO

Department of Chemistry, Faculty of Science, Toyama University, Toyama 930, Japan

(*Received* 18 *July* 1980. *Revised* 7 *October* 1980. *Accepted* 21 *October* 1980)

Summary—Bis[2-(5-chloro-2-pyridylazo)-5-diethylaminophenolato]cobalt(III) is proposed for the extraction and spectrophotometric determination of sulphated and sulphonated surfactants. The complex and the surfactants form ion-pairs which are extracted into benzene from 0.1*M* hydrochloric acid. The absorbance of the benzene phase is measured at 560 nm against a reagent blank. Less than 25 μg of sodium di-(2-ethylhexyl) sulphosuccinate in 50–200 ml of sample solution is determined reproducibly by the proposed method. When applied to river water samples, the proposed method gives results which agree very well with those obtained by the standard Methylene Blue method. However, the proposed method is simpler and more sensitive than the Methylene Blue method.

Numerous methods have been proposed for the spectrophotometric determination of sulphonated and sulphated surfactants.[1–8] The Methylene Blue (MB) method is the one most widely used,[1] but it has distinct disadvantages. First, Methylene Blue is not stable in aqueous solution and the decomposition products must be eliminated before use by extraction with chloroform. Secondly, because of the low extractability of Methylene Blue–surfactant ion-pairs, a double extraction is necessary.

We have already proposed a method in which bis[2 - (2 - pyridylazo) - 5 - diethylaminophenolato] - cobalt(III) (Co–PADAP) is used in place of Methylene Blue.[8,9] This method is simpler and more sensitive than the MB method, and a single extraction suffices. It was found, however, that the Co–PADAP method gave lower values than the MB method when applied to river water samples.[9]

In developing a method based on ion-pair extraction, there are two important experimental factors to be considered. One is the choice of solvent for the extraction: it is well known that the dielectric constant of the solvent is one of the most important parameters affecting extractability, particularly of ion-pair species.[10,11] When the solvent has a high dielectric constant other ions, for example those added to adjust the pH of the solution, may be co-extracted and interfere with the determination. On the other hand, when the solvent has a low dielectric constant, the extraction of the ion to be determined may be incomplete. In the development of the Co–PADAP method, many solvents were tested to find one which would extract smaller surfactant anions and give results similar to those obtained by the MB method. Unfortunately, no solvent was really satisfactory.

The other important factor is the choice of reagent. The size of an ion is also an important parameter affecting ion-pair extraction.[10,11] Larger counter-ions should be used to extract smaller ions. If a larger cation than that of the Co–PADAP complex were to be used for the extraction, smaller molecular weight surfactants might also be extracted. In this communication, bis[2-(5-chloro-2-pyridylazo)-5-diethylaminophenolato]cobalt(III), Co–5Cl-PADAP, is proposed for the extraction and spectrophotometric determination of sulphonated and sulphated surfactants. The MB and Co–PADAP methods are compared with the new method.

EXPERIMENTAL

Reagents

The Co–5Cl-PADAP was synthesized in almost the same way as Co–PADAP[8] except that 5-chloro-aminopyridine was used in place of aminopyridine. It was used as a 0.05% aqueous solution of its chloride. Sodium di-(2-ethylhexyl) sulphosuccinate (SSS) (Kanto Chemicals Co. Inc., purity 96.5%) was used as a model surfactant. Other surfactants were obtained from Tokyo Kasei Co., Inc.

Procedure

Take 50–200 ml of sample solution containing less than 25 μg (as equivalent SSS) of surfactants, in a beaker. Adjust the pH to 1 with hydrochloric acid. Transfer the solution to a separatory funnel and add 2 ml of the Co–5Cl-PADAP solution and 5 ml of benzene. Shake for 1 min, and allow the layers to separate. Transfer the benzene layer into a cell and measure the absorbance at 560 nm against a

reagent blank. Calculate the surfactant concentration from the calibration curve constructed with SSS.

RESULTS AND DISCUSSION

Solvent for extraction

Many solvents were tested for the extraction of the surfactants from 0.1*M* hydrochloric acid medium in a similar way to that employed in the studies on Co–PADAP.[8]

With solvents of higher dielectric constant, such as nitrobenzene, MIBK, 1,2-dichloroethane, chlorobenzene, 1,1,2-trichloroethane and chloroform, fairly high absorbances were obtained even in the absence of the surfactants. In these cases, Co–5Cl-PADAP may be extracted as $[Co(5Cl\text{-}PADAP)_2]^+Cl^-$. The solvents of lower dielectric constant, such as carbon tetrachloride and cyclohexane, do not extract the reagent even in the presence of the surfactants.

Among the solvents tested, only benzene gave satisfactory results. With this solvent, no Co–5Cl-PADAP is extracted as the chloride, while its ion-pairs with surfactant anions are completely extracted. Xylene and toluene, although having dielectric constants similar to that of benzene, do not completely extract the surfactants in a single extraction.

Other conditions

Addition of 2 ml of 0.05% Co–5Cl-PADAP is sufficient for complete extraction of 25 μg of SSS from 200 ml of sample solution. A shaking time of 30 sec is sufficient for complete extraction. Changing the sample size in the range 50–200 ml has little effect on the recovery. The molar absorptivity of the extracted species is about 5.9×10^4 l.mole^{-1}.cm^{-1}.

Effect of diverse ions

Table 1 shows the effect of diverse ions on the determination of SSS. High concentrations of almost all other ions do not interfere with the determination. Only perchlorate and iodide cause slightly negative errors at high concentrations. In the presence of these ions, a part of the reagent is precipitated as flocs at the interface between the phases. However, these interfering ions are not likely to be present in normal samples at such a high concentration as to interfere.

Table 1. Effect of diverse ions on the determination of SSS

Ion	Concn., *M* (*ppm*)	Absorbance	Error, %
—	—	0.340	—
F^-	0.1 (19,000)	0.346	+1.8
Cl^-	0.2 (7200)	0.349	+2.6
Br^-	0.1 (8000)	0.323	−5.0
	0.01 (800)	0.330	−2.0
I^-	10^{-4} (13)	0.329	−3.2
	10^{-5} (1.3)	0.331	−2.6
HCO_3^-	0.1 (6100)	0.345	+1.5
NO_3^-	0.01 (440)	0.346	+1.8
ClO_4^-	10^{-5} (1)	0.316	−4.6
	10^{-6} (0.1)	0.338	−2.4
SO_4^{2-}	0.1 (9600)	0.346	+1.8
PO_4^{3-}	0.1 (9500)	0.336	−1.2
K^+	0.1 (3900)	0.336	−1.2
Na^+	0.1 (2300)	0.335	−1.4
Ca^{2+}	0.1 (4000)	0.350	+2.9
Mg^{2+}	0.1 (2430)	0.348	+2.3
Fe^{3+}	5×10^{-4} (28)	0.333	−2.2
Laurate	10^{-5} (2.2)	0.345	+1.5

Sample 50 ml, SSS taken 0.267 ppm.

Comparisons between the MB, Co–PADAP and Co–5Cl-PADAP methods

Extracted species. Figure 1 shows the results of recovery tests on a series of homologous surfactants of various chain-lengths (C_6–C_{18} alkyl sulphonates) obtained by the three methods. The range of chain-

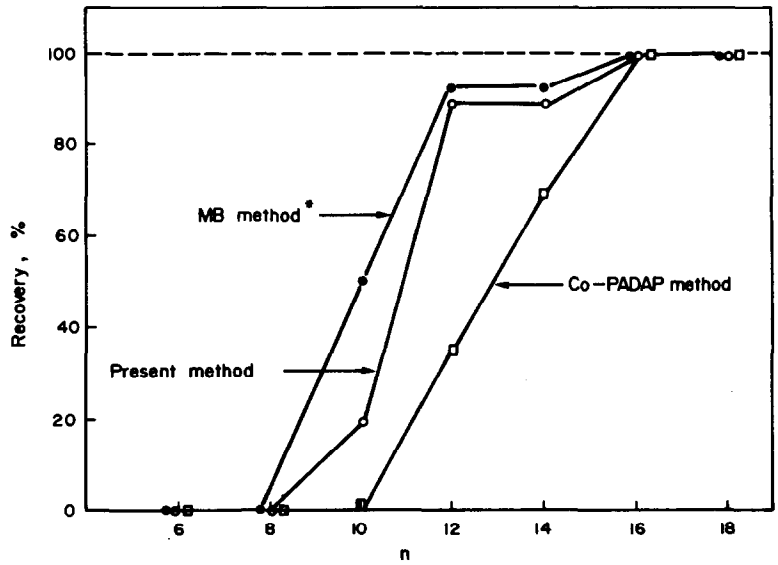


Fig. 1. Effect of chain-length (n) of sulphonated surfactant on the recovery. *MB method; Abbott's procedure, double extraction.

Table 2. Precision and sensitivity*

	Method		
	MB	Co–PADAP	Co–5Cl-PADAP
Absorption maximum, *nm*	650	550	560
Mean of absorbance	0.084	0.484	0.518
Standard deviation	0.0081	0.0082	0.0093
Relative std. devn., %	9.8	1.7	1.8

* Obtained from 10 determinations with 50 ml of 0.4 ppm SSS solution (1-cm cells).

Table 3. Comparison between the results obtained by the three methods

Sample		Surfactant found, *ppm* of SSS	
River water	MB*	Co-PADAP	Co–5Cl-PADAP
A	0.36	0.27	0.37
B	0.23	0.16	0.21
C	0.58	0.42	0.54
D	0.03	0.021	0.037

* MB method; Abbott's procedure, sample size 50 ml; 1-cm cells.

lengths of the surfactants which can be determined extends to shorter chains with the MB and the present methods, whereas shorter chain-length surfactants are not determined by the Co-PADAP method. Thus, with water samples containing shorter chain-length surfactants, which might occur in natural water samples as degradation products of common commercial surfactants, the Co–PADAP method always gives lower results than the MB method and the present method. It is expected that the results obtained by the present method should agree with those obtained by the MB method.

Stability of the reagents and the absorbance of the reagent blank. Methylene Blue decomposes in aqueous solution fairly rapidly. On the other hand, Co–PADAP is stable in 0.8*M* hydrochloric acid and Co–5Cl-PADAP is stable even in 2.5*M* hydrochloric acid. The absorbance of the reagent blank with the MB method is greater than 0.01, while that for Co–PADAP and present methods is negligible.

Extraction procedure. In the MB method, the decomposition products of Methylene Blue must be eliminated before use, by extraction with chloroform. A double extraction is necessary for complete extraction of the surfactants. In the Co–PADAP and the present method, no pre-extraction procedure is necessary and a single extraction is sufficient for complete separation.

Precision and sensitivity. Table 2 shows the standard deviations and relative standard deviations obtained by the three methods for ten water samples containing 20 μg of SSS in 50 ml. It is clear that the present method is the most sensitive of the three. Its precision is satisfactory.

Analyses of river water samples. Table 3 shows a comparison of analyses of river water samples by the three methods. In each case, the Co–PADAP method gave somewhat lower results than the other two. As described above, the lower molecular weight surfactants may not be determined by the Co–PADAP method. On the other hand, satisfactory agreement is obtained between results obtained by the MB method and the present method. The Methylene Blue Active Substance (MBAS) values obtained by earlier workers can be compared directly with the results obtained by the present method.

REFERENCES

1. J. Cross, *Anionic Surfactants–Chemical Analysis*, p. 193. Dekker, New York, 1977.
2. K. Oba, K. Miura, H. Sekiguchi, R. Yagi and A. Mori, *Water Research*, 1976, **10**, 149.
3. M. Uchiyama, *ibid.*, 1977, **11**, 205.
4. K. Tōei, H. Tomita, S. Motomizu and J. Tetsumoto, *Bunseki Kagaku*, 1978, **27**, 138.
5. St. Janava and R. Borissova-Pangarova, *Talanta*, 1978, **25**, 279.
6. J. Kawase, A. Nakae and M. Yamanaka, *Anal. Chem.*, 1979, **51**, 1640.
7. K. Higuchi, S. Monya, H. Shimoishi, H. Miyata and K. Tōei, *Bunseki Kagaku*, 1980, **29**, 180.
8. S. Taguchi and K. Goto, *Talanta*, 1980, **27**, 289.
9. S. Taguchi, K. Miyajima, I. Kasahara and K. Goto, *Kogyo Yosui (Industrial Water)*, 1980, No. 260, 10.
10. Y. Yamamoto, *Bunseki Kagaku*, 1972, **21**, 418.
11. S. Motomizu, T. Iwachido and K. Tōei, *Bunseki*, 1980, 234.

Talanta. Vol. 28, pp. 619 to 621. 1981
Printed in Great Britain. All rights reserved

0039-9140/81/080619-03$02.00/0
Copyright © 1981 Pergamon Press Ltd

ESCA INVESTIGATION OF THE SURFACE OF MIXED PRECIPITATES

KICHINOSUKE HIROKAWA, YUETSU DANZAKI and MASAOKI OKU
The Research Institute for Iron, Steel and Other Metals, Tohoku University, Sendai, Japan

(*Received* 15 *September* 1980. *Accepted* 15 *January* 1981)

Summary—Quantitative ESCA has been used for studying the surface of mixed precipitates. When the precipitation is complete and homogeneous, as with titanium and zirconium hydroxides, almost complete correlation is found between the atomic ratio of the elements in the precipitate and that estimated by the Hirokawa–Ebel method, but not for incomplete mixed precipitation, as with copper and silver hydroxides. When precipitated copper and silver are reduced to the metals with iron or zinc, the surface is enriched in copper.

The use of ESCA for studying precipitation phenomena has been reported.[1] The surface of mixed precipitates has now been examined by ESCA, the model substances being copper–nickel, titanium–zirconium and copper–silver hydroxides, and the product of metal reduction of the copper–silver precipitate. It is shown that ESCA is useful for examining surface enrichment effects.

EXPERIMENTAL

An AEI-ES 200 electron spectrometer with $AlK_{\alpha 1,2}$ (1486.6 eV) radiation was used as described earlier.[1–5] Quantitative ESCA calculations were done by the Hirokawa–Ebel method (HE method),[3–6] which does not use reference samples, but physical and experimental parameters. Spectral line pairs observed were Ti $2p_{3/2}$/Zr $3d_{3/2,5/2}$ for titanium–zirconium hydroxides, Ni $2p_{3/2}$/Cu $2p_{3/2}$ for nickel–copper hydroxides, and Ag $3d_{5/2}$/Cu $2p_{3/2}$ for silver–copper hydroxides and the reduced metals. Samples and reagents used include copper–nickel alloys, hydrofluoric–nitric acid solution of titanium and zirconium, nitric acid solution of copper and silver, sodium hydroxide, iron powder (100-mesh) and granular zinc.

RESULTS AND DISCUSSION

Hydroxide precipitation

As an example of a quantitative, homogeneous and stable mixed precipitate, the titanium–zirconium hydroxide precipitate was selected. Iron or magnesium was used as an auxiliary precipitant. Samples were prepared as follows.

A hydrofluoric–nitric acid solution of 30–45 mg of titanium–zirconium mixture was heated to fumes with 8 ml of 9*M* sulphuric acid in a platinum dish; 30–45 mg of magnesium or iron were also added to the solution before fuming, when an auxiliary precipitant was used. The salts were dissolved in 30 ml of water and the solution was poured into 32 ml of 6*M* sodium hydroxide, diluted to about 100 ml with water and boiled for about 5 min. The precipitate was filtered off, washed with water, dried in air and subjected to ESCA measurement.

A correlation of about 1:1 is obtained between the atomic ratio of titanium to zirconium in the mixed precipitate and that estimated by the HE method for the surface distribution, as shown in Fig. 1. This indicates that the total error from the sample preparation, measurement, matrix effects and the calculation method was within ±20%. A similar result was obtained for the precipitate of copper and nickel hydroxides produced in the presence of bromine, as also shown in Fig. 1.

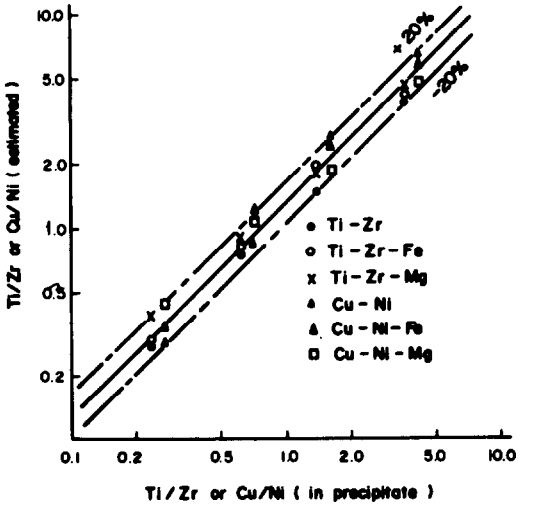


Fig. 1. Atomic ratios of Ti to Zr and of Cu to Ni in mixed precipitates *vs.* surface ratios estimated by ESCA.

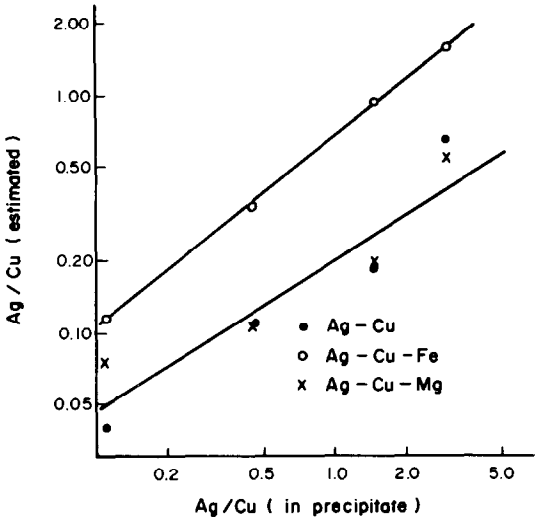


Fig. 2. Correlation between atomic ratio of Ag to Cu in mixed precipitate (pH 12) and that estimated by ESCA.

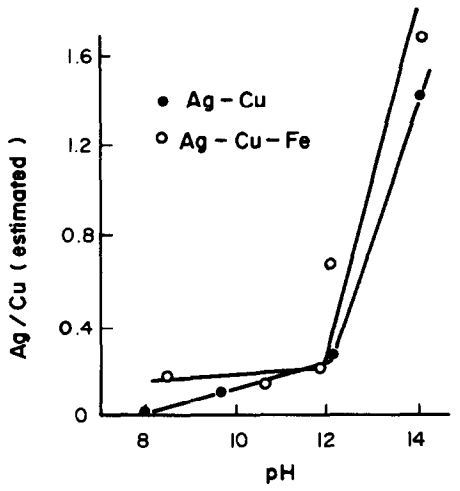


Fig. 3. Effect of pH on atomic ratio of Ag to Cu on the surface of precipitates, estimated by ESCA.

The copper–silver hydroxide mixture was studied as an example of incomplete joint precipitation. Samples were prepared by dissolving 10 mg of copper–silver alloys of various compositions in 5 ml of 8.5*M* nitric acid and diluting to about 50 ml with water; when an auxiliary precipitant was to be used, 10 mg of magnesium or iron were added before dissolution of the sample. The pH of the solution was adjusted to 12 with 6*M* sodium hydroxide. The solution was diluted to about 100 ml, and boiled for about 5 min. The precipitate was filtered off, washed with water, dried in air and subjected to ESCA measurement. The correlation between the atomic ratio of silver to copper in the precipitate and that estimated by the HE method for the surface distribution on the precipitate is given in Fig. 2. Figure 3 shows the influence of pH on the atomic ratio estimated by the HE method. In this case the precipitate was formed from a solution containing 10 mg of silver and 20 mg of copper (atomic ratio of Ag to Cu 0.3), and the pH was confirmed before the filtration. The effect of addition of 30 mg of iron as auxiliary precipitant was also examined. The results showed that joint precipitation was incomplete, and that copper was enriched on the surface of the precipitate. Auxiliary precipitants did not have much effect.

Reduced copper–silver precipitate

Copper and silver were selected for studying the effect of reducing a mixed precipitate to the metals, because their ions are easily reduced. One gram of electrolytic iron powder was added to about 100 ml of 1*N* sulphuric acid containing 20 mg of copper and 10 mg of silver (atomic ratio of Ag to Cu 0.3) at room temperature. The product was filtered off, washed with water, dried under vacuum (about 10^{-3} mmHg) and subjected to ESCA measurement. The effect of

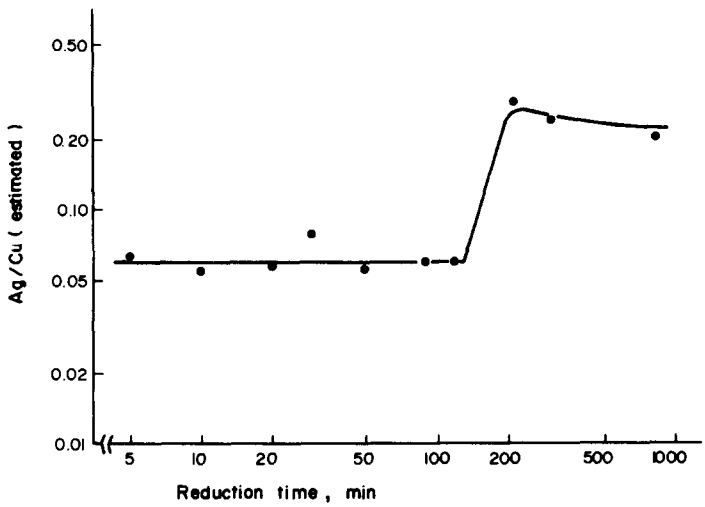


Fig. 4. Effect of reduction time on atomic ratio of Ag to Cu on the surface of the precipitate, estimated by ESCA.

reduction time on the atomic ratio of silver to copper estimated by the HE method is shown in Fig. 4. When the iron was not completely disssolved, the atomic ratio of silver to copper on the precipitate surface was about 0.06, and when the iron had almost all dissolved it was about 0.3. When reduction was performed by heating and the precipitate was filtered off immediately after all the iron had dissolved, a ratio of 0.3 was again obtained. However, when these reduction products were analysed by atomic-absorption, the atomic ratio of silver to copper in the bulk precipitates was about 0.3 whether the iron had completely dissolved or not.

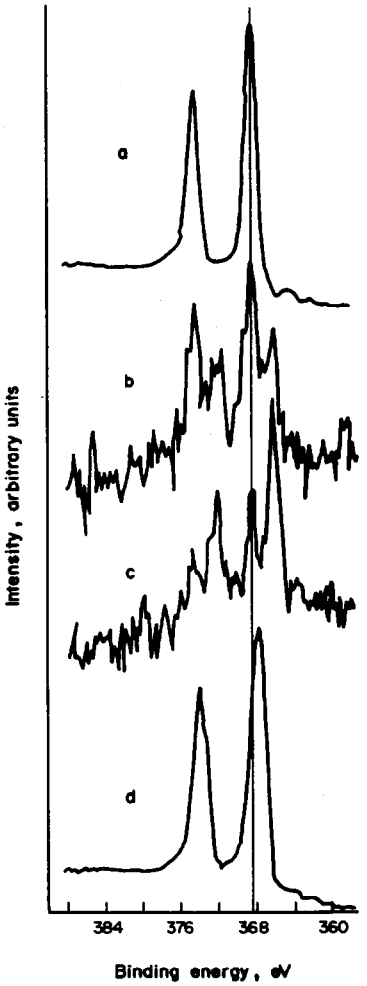


Fig. 5. Ag 3*d* spectra for some mixed precipitates. Ag reduced by granular Zn from 100 ml of 1*N* sulphuric acid containing Ag and 20 mg of Cu; (*a*) Ag 100 mg, (*b*) Ag 0.3 mg, (*c*) Ag 0.1 mg, (*d*) precipitate from 100 ml of pH-12 solution containing 25 mg of Ag and 5 mg of Cu.

The results indicate that copper is enriched on the surface of the precipitate while the iron is dissolving according to the equilibrium $Cu^{2+} + Fe \rightleftharpoons Cu + Fe^{2+}$. After all the iron has dissolved, part of copper on the surface of the precipitate is dissolved because of aerial oxidation. The presence of 0.9–2.4 mg of dissolved copper (about 10% of the total copper) in the filtrate after the reduction was found by atomic-absorption analysis. Similar results were obtained when a sulphuric acid solution of 20 mg of copper and 0.1–100 mg of silver was reduced by heating with 1 g of granular zinc (which dissolved completely). It seems that the surface phenomena are influenced by the reductant used and the reduction procedure. To obtain a more homogeneous and complete mixed precipitate by metal reduction, it is recommended to heat with finely divided metal powder, and to filter off immediately or in the presence of reductant after the reduction procedure.

In the silver spectrum of the product from reduction of a dilute silver solution with zinc (*e.g.*, 20 mg of copper and 0.1–0.3 mg of silver) a well-resolved peak at 2.4 eV lower binding energy than that for the metal peak was often found, as shown in Fig. 5. For the reduction product from treating with zinc 100 ml of 1*M* perchloric acid containing 20 mg of copper and 0.1 mg of silver, a peak at 1.2 eV lower binding energy than that for the metal peak has also been found. Only the peak for silver metal has been found in the spectrum of the reduction product from dilute silver solution containing no copper. It has been confirmed experimentally that the new peak is not due to silver oxides.[7] The ESCA spectrum of silver hydroxide, which is difficult to prepare, has not been observed. However, the difference between the inner subshell binding energy of silver oxide and that of the sulphate is not very large,[8] and it can be assumed that the surface of the reduction product may be silver covered by a thin layer of the hydroxide or sulphate, or a silver compound similar to the hydroxide.

REFERENCES

1. K. Hirokawa and M. Oku, *Talanta*, 1980, **27**, 741.
2. K. Hirokawa, F. Honda and M. Oku, *Z. Anal. Chem.*, 1977, **286**, 41.
3. K. Hirokawa and M. Oku, *Talanta*, 1979, **26**, 855.
4. *Idem*, *Z. Anal. Chem.*, 1977, **285**, 192.
5. K. Hirokawa, T. Sato and M. Oku, *ibid.*, 1979, **297**, 393.
6. M. F. Ebel, *Surf. Inter. Anal.*, 1979, **1**, 58.
7. G. Schon, *Acta Chem. Scand.*, 1973, **27**, 2623.
8. S. W. Gaarestroom and N. Winograd, *J. Chem. Phys.*, 1977, **67**, 3500.

Talanta, Vol. 28, pp. 623 to 625, 1981
Printed in Great Britain

0039-9140/81/080623-03$02.00/0
Pergamon Press Ltd

ANNOTATION

CORRELATION BETWEEN THE HARD AND SOFT CHARACTER AND THE VISIBLE ABSORPTION SPECTRA OF XYLENOL ORANGE AND METHYLTHYMOL BLUE COMPLEXES WITH BIVALENT METAL IONS

SADAAKI MURAKAMI and TAKASHI YOSHINO

Department of Chemical Technology, Faculty of Engineering, Yamaguchi University, Tokiwadai, Ube 755, Japan

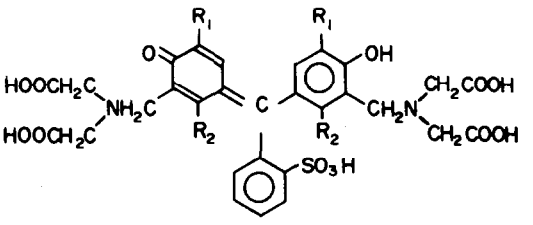
(*Received* 13 *August* 1980. *Accepted* 22 *January* 1981)

Summary—The changes in the spectra of Xylenol Orange and Methylthymol Blue complexes with several bivalent metal ions have been investigated in terms of the chemical bonding between the phenolic oxygen atom and the metal ion, and the hard and soft character of the donor and acceptor. The value of this approach to indicator action is discussed.

The colour change of an indicator as a result of metal-complex formation, as well as the stability of the complex, is one of the most important factors in its analytical application: the greater the colour change on complexation, the more useful the indicator. In general, the visible-region absorption spectra of the metal complexes of the indicators have no well-defined relation with the stabilities of the complexes. This may be because the stabilities result from the total interactions of the metal ion and all the donor atoms involved, whilst the changes of the spectra on complexation result mainly from the chemical bond between the metal ion and the donor atom conjugated with the chromophoric group. It has been found that the visible absorption spectra of metal complexes of Semi-Glycinecresol Red (SGCR),[1] Semi-Xylenol Orange (SXO)[2] and Semi-Methylthymol Blue (SMTB)[2] have an interesting relation with the hard and soft character[3] of the metal ions, and their utility as indicators has been discussed on the basis of this relation.

In the present work, the changes in the visible-region absorption spectra of Xylenol Orange (XO) and Methylthymol Blue (MTB) on complexation with several bivalent metal ions have been investigated along the lines used in the previous studies.[1,2] The metal ions studied are Co(II), Ni(II), Cu(II), Zn(II), Pb(II) and Cd(II), and the spectral data are those determined previously.[4–6]

In weakly acidic media (pH *ca.* 4–6), both XO and MTB exist as the acid species, H_iL^{i-6} (i = 3–6), and form the complex species, MHL^{3-}, with accompanying colour change from yellow to violet or blue (the proton of MHL^{3-} is attached to the nitrogen atom of the unco-ordinated iminodiacetate group). In more acidic media (pH < *ca.* 4), these ligands form the complex, MH_2L^{2-}, but without appreciable colour change because the phenolic oxygen atom does not co-ordinate to the metal ions. In alkaline media, on the other hand, they exist as species for which i = 2–0 and form the complex, ML^{4-}, with either no accompanying colour change or a change from violet or blue to red or reddish violet. With regard to the phenolic group, it is undissociated in the acid species (i = 3–6), but dissociated in the species with i = 2–0. Each type of these species has its absorption maximum at almost the same wavelength (λ_{max}, nm, of H_iL^{i-6}: XO 434–439, MTB 435 for i = 3–6; XO 578–582, MTB 607–617 for i = 2–0), because the dissociation of protons other than the phenolic one does not cause appreciable colour change. Accordingly, the wavelength shift, $\Delta\lambda_{max}$, on complexation is taken as a



	R_1	R_2
XO	CH_3	H
MTB	$CH(CH_3)_2$	CH_3

measure of the change in the spectrum when the complexes ML^{4-} and MHL^{3-} are formed by the ligand species, L^{6-} and H_4L^{2-}, in alkaline and weakly acidic media, respectively.

$$\Delta\lambda_{max}(1) = \lambda_{max}(ML) - \lambda_{max}(L)$$

$$\Delta\lambda_{max}(2) = \lambda_{max}(MHL) - \lambda_{max}(H_4L)$$

The values of $\Delta\lambda_{max}(1)$ and $\Delta\lambda_{max}(2)$ are plotted in Figs. 1 and 2 against the quantity, E_n^*, introduced by Klopman[7] to evaluate the hardness and softness of metal ions in aqueous solution. The absolute values of both $\Delta\lambda_{max}(1)$ and $\Delta\lambda_{max}(2)$ show their maximum or minimum at E_n^* *ca.* -1.5 eV for XO and *ca.* -1 eV for MTB. $\Delta\lambda_{max}(1)$ is negative, *i.e.*, there is a hypsochromic shift, whereas $\Delta\lambda_{max}(2)$ shows a bathochromic shift. $\Delta\lambda_{max}(1)$ is caused by co-ordination of the phenolic oxygen atom to the metal ion, while $\Delta\lambda_{max}(2)$ is due to replacement of the phenolic hydrogen atom with metal ion. The stronger the interaction between the phenolic oxygen atom and the metal, the greater the hypsochromic shift in the spectrum of the complex: the larger change of the colour in alkaline media, compared to that in weakly acidic media, is a result of the spectrum of the complex becoming nearer to that of the protonated free ligand, with regard to the phenolic oxygen atom. The same effect acts in opposite directions in $\Delta\lambda_{max}(1)$ and $\Delta\lambda_{max}(2)$, so the discussion will be confined to $\Delta\lambda_{max}(1)$.

The visible-region absorption spectra of sulphonpthalein indicators are attributable to an electronic $\pi - \pi^*$ transition characteristic of the sulphonphthalein nucleus. The spectrophotometric, potentiometric, electroanalytical and ESR studies[1,2,4–6,8,9] suggest that the spectral change on complexation results mainly from the interaction between the phenolic oxygen atom and the metal ion. Some effect of the iminodiacetic acid residue on the colour change is expected. However, this may be slight, taking into account the fact that the colour change is very small when proton-dissociation or co-ordination takes place in groups other than the phenolic group. Accordingly, the argument on $\Delta\lambda_{max}$ will be centred on the phenolic oxygen atom, although there is still some doubt whether it can be completely isolated from the hard and soft character of the iminodiacetic acid residue and the effect, on the benzene ring, of the metal ion acting through that residue.

The correlation of $\Delta\lambda_{max}(1)$ with E_n^* may be explained in terms of the hard and soft acid and base (HSAB) theory.[3] The higher E_n^*, the harder the acceptor, which then tends to form complexes with the harder donors by ionic interaction: the lower E_n^*, the softer the acceptor, which then prefers the soft donors and covalent interaction; the coupling would otherwise have lower interaction.[7] We cannot evaluate the extent of the ionic and covalent bondings between the phenolic oxygen atom and the metal ion. However, from the behaviour of $\Delta\lambda_{max}(1)$ as a function of E_n^*, it can be deduced that the hypsochromic shift in λ_{max} of XO and MTB species, L^{6-}, in complexation to form ML^{4-} arises from (*i*) the localization of the π-electron density on the phenolic oxygen atom by the inductive effect of the positive charge on the metal ion, and (*ii*) the electron transfer from the π-electron system into the covalent bonding orbital between the phenolic oxygen atom and the metal ion.[1,2] The first of these interactions will be strengthened with increase in hardness and the second with increase in softness. Thus the phenolic oxygen atom has maximum affinity for the metal ions of E_n^* around -1.5 eV for XO and -1 eV for MTB as a result of the maximum stabilization energy being due to the total perturbation energy of the ionic and covalent interactions.[7]

As seen in the plots in Fig. 1, MTB shows large values of $-\Delta\lambda_{max}(1)$ over a wide range of E_n^*, but XO shows a small value over a narrow range. This may be one of the reasons why MTB is useful over a wide pH range from the acidic to the alkaline side, whereas XO is, in general, applicable only in acidic media (complexometric or spectrophotometric determination of the metal ions other than alkaline earth metals with MTB in alkaline media needs some auxiliary chelating agent to avoid the hydrolysis of metal ions).[10,11]

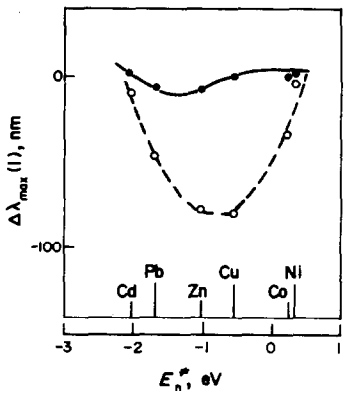


Fig. 1. Plots of $\Delta\lambda_{max}(1)$ *vs.* E_n^*.
●: XO and ○: MTB.
$\lambda_{max}(L)$: XO 582 and MTB 617 nm.

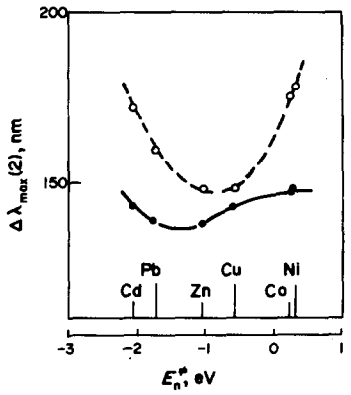


Fig. 2. Plots of $\Delta\lambda_{max}(2)$ *vs.* E_n^*.
●: XO and ○: MTB.
$\lambda_{max}(H_4L)$: XO 434 and MTB 435 nm.

The same behaviour was found in $\Delta\lambda_{max}$ for SMTB and SXO which are by-products in the synthesis of MTB and XO respectively and have the same sulphonphthalein nucleus. The same explanation may be applied for MTB and XO as for SMTB and SXO:[2] the MTB sulphonphthalein nucleus is enhanced in its π-electron density by the more electron-donating substituents, two isopropyl and two methyl groups as seen in the formula (XO has only two methyl groups), resulting in more flexibility of MTB for both electron localization on the phenolic oxygen atom and for electron transfer into the covalent bonding orbital.

CONCLUSION

The HSAB theory is widely applied in considering the stabilities of metal complexes; for unidentate or simple ligands in particular, this theory is very powerful in explaining the specific behaviour of their complexes.[12] Even for multidentate ligands such as EDTA and similar compounds, it can be partly applied by separating the thermodynamic quantities accompanying complex formation into the electrostatic and non-electrostatic contributions.[13,14] Thus it is reasonable to extend this theory to the spectral changes on complexation of indicators, and the colour changes for XO and MTB have been examined qualitatively, centring the argument on the chemical bonding between the phenolic oxygen atom and the metal ion. However, there are always difficulties in attempting to interpret specific changes, *e.g.*, $\Delta\lambda_{max}$, in terms of parameters which present some averaging of the complex balance of electronic interactions in a complex molecule. A fuller study than that attempted here is required and the argument must be made much tighter.

REFERENCES

1. T. Yoshino, S. Murakami, K. Arita and K. Ishizu, *Talanta*, 1979, **26**, 479.
2. S. Murakami, *J. Inorg. Nucl. Chem.*, 1981, **43**, 335.
3. R. G. Pearson, *J. Am. Chem. Soc.*, 1963, **85**, 3533.
4. T. Yoshino, H. Imada, S. Murakami and M. Kagawa, *Talanta*, 1974, **21**, 211.
5. S. Murakami, K. Ogura and T. Yoshino, *Bull. Chem. Soc. Japan*, 1980, **53**, 2228.
6. M. Murakami, T. Yoshino and S. Harasawa, *Talanta*, 1967, **14**, 1293.
7. G. Klopman, *J. Am. Chem. Soc.*, 1968, **90**, 223.
8. T. Yoshino, S. Murakami and M. Kagawa, *Talanta*, 1974, **21**, 199.
9. K. Ogura, K. Seno, S. Murakami and T. Yoshino, *J. Inorg. Nucl. Chem.*, 1980, **42**, 1165.
10. M. Otomo, *Bunseki Kagaku*, 1972, **21**, 436.
11. J. Körbl and R. Přibil, *Collection Czech. Chem. Commun.*, 1958, **23**, 873.
12. G. H. Nancollas, *Coord. Chem. Rev.*, 1970, **5**, 379.
13. G. Degischer and G. H. Nancollas, *J. Chem. Soc. (A)*, 1970, 1125.
14. S. Murakami and T. Yoshino, *J. Inorg. Nucl. Chem.*, in the press.

Talanta. Vol. 28. pp. 627 to 628. 1981
Pergamon Press Ltd. Printed in Great Britain

LETTER TO THE EDITOR

REDOX TITRATIONS USING CHLORBROMAMINE-T AS A NEW OXIDANT IN NON-AQUEOUS MEDIA

SIR,

We wish to report the use of N-chloro-N-bromo-p-toluenesulphonamide (Chlorbromamine-T) as an oxidimetric titrant in non-aqueous media. It combines the properties of its predecessors, dichloramine-T[1,2] and dibromamine-T.[3]

We prepared it from p-toluenesulphonamide by Paterson's method.[4] p-Toluenesulphonamide (17.1 g) was dissolved in 500 ml of water containing 4 g of sodium hydroxide. The solution was cooled to below 5° and liquid bromine (8 g) was added drop by drop with constant stirring. When the bromine had been taken up completely, a solution of sodium hydroxide (4 g) in 20 ml of water was added and the solution was cooled to below 5°. Then gaseous chlorine was passed through the solution, which was kept at below 5°, until it became neutral. The lemon yellow precipitate product was filtered off, washed with water and dried over phosphorus pentoxide in the absence of light. The melting point was 73°. Analysis gave N 4.8%, S 11.0%, Cl 12.9%, Cl + Br 40.2%; $CH_3C_6H_4SO_2NClBr$ requires N 4.9%, S 11.3%, Cl 12.5%, Cl + Br 40.6%.

The solubility in glacial acetic acid is 67.3 g/l. at 30°. A 0.1N (0.025M) solution is fairly stable when kept in an amber bottle. It can be standardized iodometrically, as suggested for dichloramine-T.[1] The half-cell is

$$RNClBr + 2H^+ + 4e^- \rightleftharpoons RNH_2 + Cl^- + Br^-$$

and the conditional redox potential in glacial acetic acid is +1.37 V at 30°.

Arsenic(III), antimony(III), iron(II), thallium(I), ascorbic acid, hydrazine, phenylhydrazine, semicarbazide, hydroquinone, ferrocyanide, aniline, phenol, oxine and anthranilic acid can be titrated potentiometrically; Quinoline Yellow or p-ethoxychrysoidine can be used as indicator for titration of the first nine of these. Thiosulphate, thiourea, thiocyanate, Reinecke's salt, cobalt and zinc tetrathiocyanatomercurates, thiosemicarbazide and its complexes with zinc, cadmium and mercury(II), dithiocarbamate and its complexes with copper(II) and zinc, and xanthate and its complexes with copper(I) and zinc(II) can be determined by back-titration. The maximum error is 0.5%.

Chlorbromamine-T has some advantages over its predecessors. For instance, auxiliary agents are not needed in potentiometric titration of hydrazine whereas dichloramine-T requires perchloric acid[2] and dibromamine-T requires hydrochloric acid.[3] For the titrations with visual indication of the end-point potassium bromide is not needed, whereas it is with

dichloramine-T. In the back-titration procedures the oxidation times are shorter than those with dichloramine-T or dibromamine-T.

Department of Chemistry,
University of Kerala,
Trivandrum-695001, India

K.D. MAHILAMONY
P. INDRASENAN

23 April 1981

REFERENCES

1. T.J. Jacob and C.G.R. Nair, Talanta, 1972, 19, 347.
2. V.R. Nair and C.G.R. Nair, ibid., 1973, 20, 696.
3. C.G.R. Nair and P. Indrasenan, ibid., 1976, 23, 239.
4. L.O. Paterson, U.S. Patent 3,147,259, (1 Sept. 1964); Chem. Abstr., 1964, 61, 13325d.

Talanta, Vol. 28, pp. 629 to 635, 1981
Printed in Great Britain. All rights reserved

0039-9140/81/090629-07$02.00/0
Copyright © 1981 Pergamon Press Ltd

SOME FUNDAMENTAL CONSIDERATIONS ON ANALYTICAL HIGH-FREQUENCY PLASMAS

P. F. E. VAN MONTFORT* and J. AGTERDENBOS

Analytisch Chemisch Laboratorium der Rijksuniversiteit Utrecht, Croesestraat 77a, 3522 AD Utrecht, Netherlands

(*Received* 3 *September* 1980. *Revised* 8 *December* 1980. *Accepted* 13 *March* 1981)

Summary—Several possible models for plasmas, and their fundamental background, are discussed. The recent literature on investigations of fundamental plasma models and plasma parameters is reviewed.

A plasma can be defined as a gas or vapour in a partially ionized state, and thus is composed of atoms, molecules, ions and free electrons.[1] Some of the atoms, ions and molecules of the plasma will be in the excited state.

PLASMA MODELS

Thermal equilibrium (T.E.)

The simplest model for a plasma is that of thermal equilibrium. It is governed by the principle of microreversibility, which means that every energy-transfer process is exactly balanced by the reverse process.[2] For instance, the number of transitions per unit of time from a level p to a level q, by absorption of radiation, is exactly the same as the number of transitions per unit of time from level q to level p, with emission of radiation. The same holds for radiationless transitions between levels p and q, caused by collisions.

When a plasma is in T.E. all microscopic states can be calculated from the temperature, which is the only variable. Thus we can deduce the following.

(*a*) The number of particles dN with velocity between v and $v + dv$ is given by Maxwell's law:

$$dN = 4\pi N v^2 \left(\frac{M}{2\pi kT}\right)^{3/2} \exp\left[-\frac{Mv^2}{2kT}\right] dv \qquad (1)$$

where M is the atomic weight of the particles considered, N the number of those particles, and k Boltzmann's constant.

(*b*) The number of particles (N_p) in a certain level p is calculated from

$$\frac{N_p}{N} = \frac{g_p}{Z(t)} e^{-E_p/kT} \qquad (2)$$

where

$$Z(t) = \sum_j g_p e^{-E_p/kT},$$

$Z(T)$ being the partition function, g_p the statistical weight and E_p the energy of level p. Theoretically there is an infinite number of levels with finite, hardly differing energies before the ionization limit is reached. However, in practice $Z(T)$ does not become infinite, because the electric field due to neighbouring particles reduces the ionization limit so that the number of energy levels becomes finite.

(*c*) The degree of ionization is given by the Saha equation, which gives in principle the relation between the ionization equilibrium constant $K_i(T)$, the ionization energy E_i and the temperature T:

$$K_i(T) = \frac{(2\pi m)^{2/3}(kT)^{5/2}}{h^3} \frac{2Z_i}{Z_a} e^{-E_i/kT} \qquad (3)$$

where Z_i and Z_a are the partition functions for the ionic and atomic states respectively.

(*d*) The emission intensity of a spectral line for the transition from level q to level p can be calculated from Einstein's formula:

$$I_{q\to p} = \frac{N_0}{Z} \frac{2\pi\epsilon^2 h g_q f}{\epsilon_0 m \lambda^3} e^{-E_{q\to p}/kT} \qquad (4)$$

where N_0 is the number of particles in the ground state, f is the oscillator strength, g_q is the statistical weight and E_q the energy of level q, ϵ_0 the dielectric constant and λ the wavelength.

Local thermal equilibrium (L.T.E)

Perfect thermal equilibrium never exists in laboratory plasmas, for two reasons. First, in a laboratory plasma, there is a clear temperature gradient, because the centre is at a temperature of, *e.g.*, 4000 K, whereas a few mm or cm outside the centre of the plasma the temperature is room temperature. Therefore the plasma could be considered to be built up of volume elements at different temperatures,[1,2] each volume element being in thermal equilibrium.

Secondly, as a consequence of the small dimensions of the plasma, a large part of the emitted radiation escapes without being reabsorbed. This causes a relative overpopulation of the ground state, because the emission process is not balanced by self-absorption. The extent of the deviation from Boltzmann's law thus caused is determined by the ratio of radiative

* Present address: T.N.O., Centraal Instituut voor Voedingsonderzoek, Utrechtseweg 48, Zeist, Netherlands.

and collisional de-excitation processes. For sufficiently high particle concentrations (for which de-excitation is mainly collisional) the laws for thermal equilibrium still hold in good approximation.

Partial local thermal equilibrium: the thermal limit

For some elements the radiative transition probability increases and the impact cross-section for collisions with electrons decreases for levels with low quantum numbers (*i.e.*, near the ground state).[3] With low electron densities, the radiative de-excitations—which cause a further depopulation of the excited states—are so predominant for levels p with principal quantum numbers below a certain level, the "thermal limit", that these levels can no longer be considered to be in L.T.E. For levels q with principal quantum numbers above the thermal limit, the relations for L.T.E. still hold. Under these conditions a plasma can be considered to be in partial local thermal equilibrium (P.L.T.E.). In some of the following sections, methods are described for quantifying, for analytical plasmas, the degree of deviation from (P.L.)T.E.; these methods are only tentative, however.

The corona model

At very low electron concentrations (n_e), two energy-transfer processes, not described above, take place to an increasing extent. They are:

(1) spontaneous emission of radiation;
(2) radiative recombination of particles.[4]

For electron concentrations below $10^{11}/cm^3$ and plasma temperatures above 10^4 K, the so-called corona model can be formulated. Three-particle recombination:

$$P_{z+1,p} + e + e \rightarrow P_{z,q} + e \qquad (5)$$

(z is the charge of the particle P, and p and q are the energy levels) plays only a minor role in this model because of the low electron concentration. Much more important is radiative recombination:

$$P_{z+1,p} + e \rightarrow P_{z,q} + h\nu_{continuum} \qquad (6)$$

The rate of this process is proportional to the electron concentration. The ionization equilibrium is therefore a balance between radiative recombination (6) and ionization by collisions of electrons with the atoms ($P_{z,p} + e \rightarrow P_{z+1,q} + 2e$).

The ions are mainly in the ground state because their average excitation energy is larger than the energy of the electrons. The population of the excited levels is determined by a balance between the rate of collisional excitation from the ground state and the rate of spontaneous radiative decay.[5] So far, plasmas conforming to the corona model have not been applied in analytical chemistry.

Radiative ionization recombination (R.I.R.) model[6]

The R.I.R. model, applied to a low-pressure hydrogen radiofrequency plasma, postulates two groups of electrons, *i.e.*, one group with a relatively high density and low energy and the second group with a relatively low density and high energy. The total energy distribution of the electrons becomes the sum of two Maxwell distributions.

In the case of a hydrogen plasma, the high kinetic-energy electrons (e) cause ionization according to:

$$H + e \rightarrow H^+ + e + e \qquad (7)$$

For levels with principal quantum numbers below the thermal limit, recombination (and hence population of the excited atomic levels) is due to the low kinetic-energy electrons (e) according to:

$$H_p^+ + e \rightarrow H_q + h\nu_{continuum} \qquad (8)$$

followed by:

$$H_q \rightarrow H_p + h\nu_{q \rightarrow p} \qquad (9)$$

For levels with principal quantum numbers above the thermal limit the atoms are in thermal equilibrium with the ionization level, so the occupation of these levels is ruled by the reverse of reaction (7). For hydrogen ($z = 1$) the expression for the thermal limit given by Griem[5] becomes

$$n_{th} = 126 n_e^{-2/17} \left(\frac{kt_e}{V_i}\right)^{1/17} \exp\left[\frac{4V_i}{17 n_{th}^3 kt_e}\right] \qquad (10)$$

where V_i is the ionization energy for hydrogen, k is Boltzmann's constant and n_e and t_e are the concentration and temperature of the low-energy electrons. Brassem *et al.*[7] give the same expression but with a printer's error in the index to n_e.

RECENT PRACTICAL INVESTIGATIONS ON THE PLASMA MODELS

Several types of modern analytical plasmas can be distinguished. The radiofrequency plasma, which can be capacitively or inductively coupled, the plasma jet, which is a modified arc, and the microwave-induced plasma (M.I.P.) which is fed by a microwave field of 2450 MHz.

The M.I.P. with working pressure 0.1–0.5 mmHg

Brassem *et al.*[7] calculated, for a 0.2-mmHg argon or helium M.I.P. to which 1% of hydrogen has been added, the H_α and H_β emission intensities according to the L.T.E. and R.I.R. models. To do this they had to calculate $[H_q]$ (the concentration of hydrogen atoms in the qth level), from which the emission intensities can easily be found from $I_{qp} = A_{qp} h\nu_{qp} [H_q]$ (where A_{qp} is the transition probability). For levels below the thermal limit, three possible R.I.R. reactions are assumed:

$$H_q + e \underset{k_q^d}{\overset{k_q^i}{\rightleftarrows}} H^+ + e + e \qquad (11)$$

where e is a high-energy electron and e is a low-energy electron, k_q^i is the rate constant for the ioniz-

ation process, and k_q^d is the rate constant for the reverse process,

$$H^+ + e \xrightarrow{k_q^s} H_q + h\nu_{\text{continuum}} \qquad (12)$$

where k_q^s is the rate-constant for this two-body combination, and

$$H_q \xrightarrow{A_{qp}} H_p + h\nu_{qp} \qquad (13)$$

where A_{qp} is the transition probability. The reaction-rate constants can be calculated according to Schlüter's expression.[8] From these constants $[H^+]$ can be calculated, assuming that a steady state ($d[H^+]/dt = 0$) exists. After substitution for $[H^+]$ in the reactions above, $[H_q]$ and hence I_{qp} can be found. In order to calculate Schlüter's reaction-rate constants, however, the four parameters N_e, T_e, n_e and T_e have to be known, where n and T are the population density and temperature, respectively, for the species indicated by subscript. T_e and n_e can be directly measured with the double-probe system and N_e and T_e have to be estimated. The experimentally measured H_α and H_β line intensities were higher by a factor of 10^8 than the values calculated from the thermal models with an assumed electron temperature of about 4000 K, and about higher by a factor of 10^2 than the intensities calculated according to the R.I.R. model described above.

The conclusion can be drawn that the thermal model does not hold for this plasma and that the R.I.R. model gives considerable improvement. It is noticed here that the deviation from linearity between the H concentration and the H_α and H_β emission intensities is more important than suggested by Brassem *et al.*[7] Hence the value of the above-mentioned factors is questionable.

The M.I.P. with working pressure 1–25 mmHg

Busch and Vickers[9] studied an argon and a helium M.I.P. (3–25 mmHg) and measured, *inter alia*, the following parameters. The electron temperature was measured with the double-probe system;[10,11] the spectroscopic temperature was determined by measuring the ratios of several line intensities; the electron density was determined by measuring positive currents ($[e^-] = [\text{ions}]$) and finally the concentration of metastable argon atoms $[Ar^m]$ was determined by atomic absorption. A very large discrepancy was found between the spectroscopic and electronic temperatures of the argon M.I.P. (4200 K and 33,000 K respectively).

The following explanation of this discrepancy was proposed. The double-probe method gives the electron temperature of only the high kinetic-energy electrons, but the electron density measured was the sum for the low and high kinetic-energy electrons. The excited levels from the ionization limit down to the thermal limit are predominantly collisionally populated (by recombination) when the electron density is low. This results in a Boltzmann partition corresponding to a temperature of about 4500 K. The bound electrons are in equilibrium with the electrons of low kinetic energy (and at high density) and the high kinetic-energy electrons play no part in the recombination process.

It was also found that the measured electron temperature increased with the ionization potential of the noble gas, because the plasma can only exist if sufficient ions are produced to balance the loss by recombination, *etc.* If the plasma gas has a high ionization potential, high kinetic-energy electrons, *i.e.*, a high electron temperature will be required to maintain the plasma. Metastable argon atoms (Ar^m) were also found to play a part in the ionization process:

$$Ar^m + X \rightarrow Ar + X^+ + e \qquad (14)$$

where X is an atom with a lower ionization potential than the excitation potential of the metastable argon.

An increase of the line intensities with increased applied microwave-power, W, was explained as due to the increase of the electron pressure with increasing W. Because of the electroneutrality law, the number of positive ions will also increase, so the possibility for radiative recombination increases.

When metal atoms (*e.g.*, mercury) were added to the plasma, the atomic lines of the metal were emitted with high intensity. It was found that the intensity of the mercury lines in the argon plasma was greater than in the helium plasma. This is in agreement with the fact that $n_e(\text{Ar}) > n_e(\text{He})$ (n_e is the sum of the low and high kinetic-energy electrons).

Avni and Winefordner[12] performed double-probe measurements on pure argon, helium and nitrogen M.I.P.s, for a number of plasma parameters: the electric field (E), electron (j_e) and ion (j_i) current densities, electron density (n_e), electron temperature (T_e), electron conductivity (σ_e), ion density (n_i), electron mean free path λ_e, electron (μ_e) and ion (μ_i) mobilities, and ion-diffusion coefficient (D_i). These parameters could be either directly measured or calculated. The gas temperature of the plasma was determined by the line-reversal method directly from the intensities of the spectroscopic lines. The authors criticised Busch and Vickers for calculating the spectroscopic temperature from argon lines with levels far above the ground-state level. According to Avni and Winefordner a considerable part of the process of population of these levels takes place non-thermally *e.g.* by $Ar^+ + e \rightarrow Ar^*$. The closer the energy level of the line involved to the ground-state level, the greater is the probability of thermal population. The mean electron density ($\bar{n}_e$) was not taken equal to the ion density—which can be easily measured—but was calculated from

$$\bar{n}_e = -\frac{2\rho}{e\mu_e r E^2} \cdot \frac{dT}{dr} \qquad (15)$$

where e is the charge on the electron, ρ the thermal conductivity, and r the distance from the axis of the cylindrical plasma. In this way a discrepancy was found between n_i and n_e ($n_i > n_e$); this would apparently result in a net space charge and thus in an electrical field. At low plasma pressures (<4 mmHg) a very strong increase in the electron temperature was found when a few micrograms of metal were added. This was explained by the fact that the bombardment of the metal atoms by argon ions releases electrons of high kinetic energy. The gas temperatures measured according to the line-reversal method were in agreement with the gas temperatures found by Busch and Vickers, and about one order of magnitude lower than the electron temperature, indicating non-L.T.E. behaviour.

Avni and Winefordner further found an increase in the electron temperature with applied microwave power, in contradiction of the work of Busch and Vickers. However, when comparing different authors' results it should be realized that the power values read on microwave generator meters may often be in error, as was shown by Jütte and Agterdenbos.[13] Also in contradistinction to Busch and Vickers, Avni and Winfordner found an increase in the electron concentration with the working pressure, but no increase of the ion concentration, the latter being explained by a decrease of the net (positive) electrical field.

Finally[12] the mean electron density $\bar{n}_e$ in the argon plasma was calculated from the Elenbaas–Heller energy-balance equation for steady-state plasma conditions:

$$\operatorname{div}(\rho \operatorname{grad} T) + j_e E = 0 \tag{16}$$

No agreement was found between the value of $\bar{n}_e$ calculated from equation (16) and the $\bar{n}_e$ value from the double-probe measurements. This indicates that a steady state is not reached in the argon plasma. Kawaguchi *et al.*[14] studied a low-pressure helium M.I.P. into which metals (Me) were vaporized from a filament. From the analytical curves obtained from these metals when potassium chloride or other salts were added the authors gave a working hypothesis for the plasma mechanism which differed from the usual R.I.R. model as follows. In addition to the usual R.I.R. reactions:

$$\mathrm{Me} + \mathrm{e} \rightarrow \mathrm{Me}^+ + \mathrm{e} + \mathrm{e} \tag{17}$$

$$\mathrm{Me}^+ + \mathrm{e} \rightarrow \mathrm{Me}^* + \mathrm{h}\nu_{\mathrm{cont}} \tag{18}$$

$$\mathrm{Ar}^m + \mathrm{Me} \rightarrow \mathrm{Ar} + \mathrm{Me}^+ + \mathrm{e} \tag{19}$$

they now also proposed:

$$\mathrm{MeCl} + \mathrm{e} \rightarrow \mathrm{Me}^+ + \mathrm{Cl} + \mathrm{e} + \mathrm{e} \tag{20}$$

and

$$\mathrm{He}^m + \mathrm{MeCl} \rightarrow \mathrm{He} + \mathrm{Me}^+ + \mathrm{Cl} + \mathrm{e} \tag{21}$$

The new (highly energy-consuming) reactions proposed are possible because of the very high (5×10^4 K) electron temperature of the plasma (the energy of He^m is much higher than that of Ar^m).

The sealed M.I.P.—the electrodeless discharge lamp (EDL)

Cooke *et al.*[15] and Jansen *et al.*[16] have investigated the spectral line profiles in a closed M.I.P. (an EDL) at 2–15 mmHg argon pressure, with a few μg or mg of a volatile element, but have not considered the fundamental mechanism of the plasma. Browner and Winefordner[17] investigated EDLs with external heating of the quartz walls of the lamps. It was found that the spectral emission intensity was proportional to $n_g n'_e$ (n_g = density of the radiating atoms in the ground state, n'_e = density of electrons with electron energies greater than the energy of the upper level of the transitions). Plots were made of the radial output $B_s\lambda^3/gf$ (B_s is the corrected radiance, g the statistical weight of the upper level and f the emission oscillator strength), *vs.* upper energy level of the electronic transition. From these plots it appeared that the mean electron energy was below 3 eV.

The M.I.P. at atmospheric pressure

Beenakker[18] used a specially designed microwave cavity to create a helium plasma at atmospheric pressure. An important part in the excitation mechanism of this plasma is supposed to be played by the reactions of metastable atoms. Four types of reaction are suggested:

$$\mathrm{A}^m + \mathrm{X} \rightarrow \mathrm{A} + \mathrm{X}^+ + \mathrm{e} \tag{22}$$

$$\mathrm{A}^m + \mathrm{X}^+ \rightarrow \mathrm{A} + \mathrm{X}^{2+*} + \mathrm{e} \tag{23}$$

$$\mathrm{A}^m + \mathrm{X} \rightarrow \mathrm{A} + \mathrm{X}^* \tag{24}$$

$$\mathrm{A}^m + \mathrm{X}^+ \rightarrow \mathrm{A} + \mathrm{X}^{+*} \tag{25}$$

(A^m is a metastable atom of the support gas A, and X is the analyte). Of course it is necessary that $E(\mathrm{A}^m) > E_x^{\mathrm{ion}}$ for the ionization and $E(\mathrm{A}^m) \simeq E_x^{\mathrm{exc}}$ for the excitation.

The low kinetic-energy electrons are especially effective for the recombination:

$$\mathrm{e} + \mathrm{A} + \mathrm{X}^+ \rightarrow \mathrm{A} + \mathrm{X}^* \tag{26}$$

The high kinetic-energy electrons sustain the plasma:

$$e + \mathrm{A} \rightarrow \mathrm{A}^+ + 2\mathrm{e} \tag{27}$$

or can give direct excitation such as

$$e + \mathrm{X} \rightarrow \mathrm{X}^* + \mathrm{e} \tag{28}$$

$$e + \mathrm{X}^+ \rightarrow \mathrm{X}^{+*} + \mathrm{e} \tag{29}$$

Ions can also be involved in the excitation process:

$$\mathrm{A}^+ + \mathrm{X} \rightarrow \mathrm{A} + \mathrm{X}^{+*} \tag{30}$$

Some characteristics of this atmospheric helium M.I.P. are:

(1) line spectra of all elements present are found (*e.g.*, chlorine: Cl^+ lines);

(2) the same analysis lines occur at reduced pressure and at atmospheric pressure;

(3) only the ion lines of S, P, Cl, Br and I with excitation energies in a limited range (12.3–15.9 eV) are found;

(4) no ion lines for C, N, O and F are found (excitation energies >20 eV).

Considering the energies of the He_2^m metastable species (13.3–15.9 eV) Beenakker supposes that the principal excitation mechanism for ion-line emission is

$$He_2^m + X^+ \rightarrow X^{+*} + 2He \qquad (31)$$

For the argon M.I.P. only the ion lines of C, P, S, and I are found, probably because the excitation energy of the ions is greater than the excitation energy of Ar^m. Of course recombination of X^+ with low-energy electrons can be expected, resulting in atom-line emission.

Other considerations on M.I.P.s and I.C.P.s

Greenfield *et al.*[19,20] measured different temperatures of an I.C.P., *viz.* kinetic gas temperature, electron temperature and excitation temperature. With increasing differences between the values of these temperatures an increased deviation from L.T.E. occurs. In plasmas with very high gas temperatures high continuum radiation I_r is found because

$$I_r = Kn_e^2/T^{\frac{1}{2}} \qquad (32)$$

and n_e increases strongly with the temperature.

Aldous *et al.*[21] found that for a metal introduced into an argon M.I.P. the metal signal increased with applied microwave power. They explained this as due to an increase in the plasma dimensions and not an increase of plasma temperature and electron pressure. Eckert[22] studied a closed rf-I.C.P. and calculated the plasma temperature from the intensity of two lines (1 and 2) according to:

$$T = \frac{e(V_2 - V_1)/k}{\ln \dfrac{\lambda_2 g_1 A_1}{\lambda_1 g_2 A_2} + \ln \dfrac{I_2}{I_1}} \qquad (33)$$

where A = transition probability, V = excitation potential, e = electronic charge, and g is the usual statistical factor. From this formula it was found that the temperature in the plasma ranged from 6450 to 8740 K. It is remarked here that Eckert's assumption of L.T.E. in this case seems doubtful. Eckert[23] also calculated the radial temperature distribution in a closed atmospheric-pressure argon rf-I.C.P. with an rf power of 530 W and 25 MHz, using the Elenbaas–Heller energy-balance equation which in its general form is

$$\sigma E^2 = \nabla(\kappa \nabla T) = 0 \qquad (34)$$

where σ = electrical conductivity, κ = thermal conductivity and E = electrical field. The assumptions were made that the plasma is symmetric and in L.T.E., that radiation losses and flow circulation effects can be neglected, and that the entire rf power dissipated in the plasma volume is lost by static heat conduction to the walls. From the calculations it appears that the temperature distribution in the plasma is not quite homogeneous. A hot spot (6000 K) is present in the plasma and in the region of the wall the temperature decreases to 1000 K. Haarsma *et al.*[24] gave a critical review of the preparation and use of an electrodeless discharge lamp (EDL) but did not mention the fundamental aspects: they stated, however, that a plasma will be extinguished if the concentration of quenchers (*e.g.*, H_2O, O_2 and N_2) reaches a critical value. Kirkbright and Ward[25] calculated the number of particles to be expected in the viewing zone of an I.C.P., and thence the intensity to be expected for the analysis lines (they assumed L.T.E. to exist). They also discussed the background continuum radiation in the plasma. Three kinds of background radiation were considered: bremsstrahlung, cyclotron radiation and real blackbody radiation. Experimentally it appeared that the background radiation of an I.C.P. with $T = 8250$ K (T_{kin}) mainly consists of bremsstrahlung (W_B). The following expression was found to hold:

$$W_B = \frac{32\pi}{3}\left(\frac{2\pi kT}{3m^3}\right)^{1/2}\left(\frac{e^2}{4\pi\epsilon_0 c}\right)^3 \frac{N_e N_i Z^2 \mu}{h} G_{ff}(T) \qquad (35)$$

where μ = refractive index of the plasma (≈ 1), $G_{ff}(T)$ = the Gaunt factor (≈ 1), N_e and N_i = electron and ion densities, Z = atomic number. For a plasma with a core volume of 8 cm^3, T = 9000 K and $N_e = 2 \times 10^{15}/cm^3$, it can be calculated from the formula that W_B reaches the considerable value of *ca.* 175 W.

Henriksen *et al.*[26] gave a theoretical calculation of the electromagnetic fields involved in cylindrical electrodeless discharges (I.C.P.s). No conclusions about a discharge mechanism classification were given.

Novak *et al.*[27] have considered the effect of pulsed rf-excited metal EDLs on the radiant output, but drew no mechanistic conclusions.

Eckert[28] has given a theoretical treatment of the analytical properties of a sealed rf-argon-I.C.P. into which metals are introduced. The plasma was considered to be cylindrical and in L.T.E. With the temperature field of the plasma, as calculated before,[22] the spatial distributions of trace element atoms and ions and the specific line intensity emitted from these particles were calculated. The number of metal atoms (Me) in a volume element was calculated from the ratio n(Me)/n(Ar) and the gas laws. The density of electrons, atoms and ions as a function of temperature was calculated by solving the combination of (1) the Saha equation, (2) the charge-balance equation for the plasma and (3) the mass-balance equation. From Einstein's formula [equation (4)] the emission coefficients and thence the specific and total power emitted by the Me lines in the plasma were calculated for magnesium. It appeared that the emission coefficient of the Me ion-line increased monotonically with temperature, whereas the emission coefficient of an atomic

line passed through a maximum in the particular temperature range where the transition from metal-dominated to gas-dominated ionization occurred. The temperatures associated with this maximum were called "norm temperatures". It was noticeable that in certain cases the power emitted per particle could be even higher (8.4×10^{-15} W) than the shot-noise level ($\sim 10^{-15}$ W) of a photoelectric detector. From the data obtained, analytical curves and detection limits could easily be calculated. Finally, it should be mentioned that no wall effects, *i.e.*, absorption or release of analyte elements, were considered.

Barnes *et al.*[29] have calculated temperature and velocity profiles for a nitrogen I.C.P., but drew no conclusions about the mechanism.

Recent considerations on the I.C.P.

The role of metastable helium and argon species in the excitation of atoms in an M.I.P. was described above. For an I.C.P. a similar excitation process had been suggested earlier by Mermet.[30] The problem has been investigated in more detail by Boumans and de Boer.[31]

The reactions suggested as occurring in an argon I.C.P. are:

$$Ar^m + X \rightarrow Ar + X^+ + e \tag{36}$$

$$Ar^m + X \rightarrow Ar + X^{+*} + e \tag{37}$$

When L.T.E. is assumed, the intensity ratio of ion and atom lines (I_i/I_a) can be calculated as follows.

$$\left(\frac{I_i}{I_a}\right)_{LTE} = \frac{4.83 \times 10^{15}}{n_e}\left(\frac{g_q A_{qp}}{\lambda_{qp}}\right)_i \times \left(\frac{\lambda_{qp}}{g_p A_{qp}}\right)_a T^{3/2}\, 10^{-5040(V_{ion}+V_{qi}-V_{qa})/T} \tag{38}$$

where g_p and V_q (eV) are the statistical weight and excitation energy of the upper level of the transition $q \rightarrow p$, A_{qp} (sec^{-1}) and λ_{qp} (Å) are the corresponding transition probability and wavelength, and i and a refer to ions and atoms respectively. It is then possible to calculate $(I_i/I_a)_{LTE}$ and to formulate the ratio of the experimental and L.T.E. intensity ratios as the deviation from L.T.E. With $n_e = 10^{16}/cm^3$ and $T_{kin} = 5850$ K the deviation reaches a value of 10–10^3.

The following reaction is therefore supposed to take place

$$Ar^m + e \rightarrow Ar^+ + 2e \tag{39}$$

This means that Ar^m also acts as an "ionizant", so n_e reaches a higher value than that calculated by assuming L.T.E. This is in agreement with the overpopulation of the excited levels. Furthermore it appeared that the introduction of an easily ionizable element M in the plasma caused only a small change in n_e and in the concentration of Ar^m. This can again be explained in terms of metastable species as follows. The system strongly acts as a buffer according to:

$$M + Ar^m \rightarrow M^+ + Ar + e \tag{40}$$

and

$$M + e \rightarrow M^+ + 2e \tag{41}$$

giving

$$Ar^m + e \rightleftharpoons Ar^+ + 2e \tag{42}$$

The loss of metastable species through reaction (40) (and thereby increase in n_e) is compensated by recombination of the liberated electrons with Ar^+ to form new metastable species [reaction (42)]. The points mentioned above can be considered as a working hypothesis for explanation of the following facts: (*i*) the electron density is much higher than that calculated for L.T.E., (*ii*) n_e and the concentration of Ar^m are only slightly influenced by easily ionizable matrices, (*iii*) the ratio of the intensity of the ion lines to the intensity of the atom lines is much higher than that calculated for L.T.E. [because of reaction (39)].

Kornblum and De Galan[32] have discussed the theoretical aspects of temperature measurement in plasmas (especially the I.C.P.). They have also given some theoretical criteria for classifying the excitation mechanisms in different plasmas. The criterion applied for the presence of T.E. in a d.c. arc was:

$$\frac{T_e - T_{kin}}{T_e} = \frac{M}{m_e}\frac{\lambda_e E}{3kT_e} \ll 1 \tag{43}$$

(λ_e = free path of the electron, m_e = mass of the electron and M = mass of the atom involved). Substituting the values determined for λ and E yields for an ICP $T_e - T_{kin} = 800$ K (T_e being 6500 K). This difference does not preclude T.E. The experimentally observed differences are much larger (4000 K), so this criterion is obviously not directly applicable to the I.C.P.

The criterion for L.T.E., taken from Griem,[33] was

$$n_e \geqslant 3.0\sqrt{T_e}(\Delta E)^3 \tag{44}$$

where ΔE is the energy-level difference (cm^{-1}) for the line involved. This inequality holds if collisional deactivation exceeds radiative deactivation by an order of magnitude. The energy difference ΔE is decisive here. For instance, the excitation energy of the argon lines used, with respect to the ground state, was 124×10^3 cm^{-1} (1 eV = 8.7×10^3 cm^{-1}), which would require a value of $n_e \geqslant 5 \times 10^{17}/cm^3$ in equation (44). This is much higher than was actually observed in the I.C.P. However, the energy difference between the upper argon levels was only 8×10^3 cm^{-1}, corresponding to an electron density of only $1.3 \times 10^{14}/cm^3$, which is even lower then actually measured. It was concluded that the transitions between the upper argon levels are likely to be in L.T.E. It is obvious that the criteria mentioned above do not show clearly the extent of T.E. to be expected in an I.C.P.

Walters *et al.*[34] reported measurements of excitation, ionization, electron temperatures and positive ion concentrations in a 144-MHz argon or neon I.C.P. In this plasma, the electron temperature T_e, measured with Johnson and Malter's probe system,[10]

was again found to be much greater then the excitation temperature (T_e) calculated according to:

$$T_{ex} = \frac{5040(\epsilon_1 - \epsilon_2)}{\log\left(\frac{gA_1}{gA_2}\right) - \log\left(\frac{\lambda_1}{\lambda_2}\right) - \log\left(\frac{E_1}{E_2}\right)} \quad (45)$$

where ϵ = energy of an upper state level, A = Einstein's coefficient of spontaneous emission, λ = wavelength of the line involved and E = integrated spectral radiance.

Also, the ionization temperature, calculated according to Saha, was found to be much lower than T_e. Both facts indicate a serious deviation from L.T.E. for such an I.C.P. When a small amount of a metal (Tl) was added to the plasma, a significant increase in T_e and the positive ion concentration was found; obviously the metal acts as a releasing agent. Finally it should be mentioned that there is a perfect analogy between the results of this work and the Busch and Vickers investigations[9] on the M.I.P.

REFERENCES

1. E. L. Grove, *Analytical Emission Spectroscopy*, Part II, p. 110. Dekker, New York, 1972.
2. *Idem, op. cit.*, p. 308.
3. J. Cooper, *Rept. Prog. Phys.*, 1966, **23**, 35.
4. F. Cabannes and J. Chappelle, *Reactions Under Plasma Conditions*, Vol. I, p. 367. Wiley–Interscience, New York.
5. H. R. Griem, *Plasma Spectroscopy*, p. 160. McGraw-Hill, New York, 1964.
6. H. Schlüter, *Z. Naturforschung*, 1961, **16A**, 972.
7. P. Brassem, F. J. M. J. Maessen and L. de Galan, *Spectrochim. Acta*, 1978, **33B**, 753.
8. H. Schlüter, *Z. Naturforschung*, 1963, **18A**, 439.
9. K. W. Busch and T. J. Vickers, *Spectrochim. Acta*, 1973, **28B**, 85.
10. E. O. Johnson and L. Malter, *Phys. Rev.*, 1949, **76**, 1411.
11. *Idem, ibid.*, 1950, **80**, 58.
12. R. Avni and J. D. Winefordner, *Spectrochim. Acta*, 1975, **30B**, 281.
13. B. A. H. G. Jütte and J. Agterdenbos, *ibid.*, 1979, **34B**, 133.
14. H. Kawaguchi, I. Atsuwa and B. L. Vallee, *Anal. Chem.*, 1977, **49**, 266.
15. D. O. Cooke, R. M. Dagnall and T. S. West, *Talanta*, 1972, **19**, 1309.
16. B. J. Jansen, Tj. Hollander and L. P. L. Franken, *Spectrochim. Acta*, 1974, **29B**, 37.
17. R. F. Browner and J. D. Winefordner, *ibid.*, 1973, **28B**, 263.
18. C. I. M. Beenakker, *ibid.*, 1977, **32B**, 173.
19. S. Greenfield, H. McD. McGeachin and P. B. Smith, *Talanta*, 1975, **22**, 1.
20. *Idem, ibid.*, 1975, **22**, 553.
21. K. M. Aldous, R. M. Dagnall, B. L. Sharp and T. S. West, *Anal. Chim. Acta*, 1971, **54**, 233.
22. H. U. Eckert, *Aerospace Rept.*, No. ATR-77 (9471)-2, 1977.
23. *Idem, J. Appl. Physics*, 1977, **48**, 1467.
24. J. P. S. Haarsma, G. J. de Jong and J. Agterdenbos, *Spectrochim. Acta*, 1974, **29B**, 1.
25. G. F. Kirkbright and A. F. Ward, *Talanta*, 1974, **21**, 1145.
26. B. B. Henriksen, D. R. Keefer and M. H. Clarkson, *J. Appl. Physics*, 1971, **42**, 5460.
27. J. W. Novak and R. F. Browner, *Anal. Chem.*, 1978, **50**, 407.
28. H. U. Eckert, *Spectrochim. Acta*, 1978, **33B**, 591.
29. R. M. Barnes and S. Nikdel, *J. Appl. Physics*, 1976, **47**, 3929.
30. J. M. Mermet, *Compt. Rend.* 1975, **281B**, 273.
31. P. W. J. M. Boumans and F. J. de Boer, *Spectrochim. Acta*, 1977, **32B**, 365.
32. G. R. Kornblum and L. de Galan, *ibid.*, 1977, **32B**, 71.
33. H. R. Griem, *Plasma Spectroscopy*, p. 151. McGraw-Hill, New York, 1964.
34. P. E. Walters, T. L. Chester and J. D. Winefordner, *Appl. Spectrosc.*, 1977, **31**, 1.

Talanta, Vol. 28, pp. 637 to 646, 1981
Printed in Great Britain. All rights reserved

0039-9140/81/090637-10$02.00/0
Copyright © 1981 Pergamon Press Ltd

THE DETERMINATION OF SELENIUM BY ATOMIC-ABSORPTION SPECTROMETRY: A REVIEW

M. VERLINDEN*, H. DEELSTRA and E. ADRIAENSSENS†

University of Antwerpen (U.I.A.), Department of Pharmaceutical Sciences, Universiteitsplein, 1, B-2610 Wilrijk, Belgium

(*Received* 22 *December* 1980. *Accepted* 11 *March* 1981)

Summary—A comprehensive review is given of the determination of selenium by the various atomic-absorption spectrometry methods that have been developed, covering the use of various flame and electrothermal ionization methods, hydride techniques, preconcentration and separation, and giving an appraisal of the results.

The development of atomic-absorption spectrometry (AAS) since 1960 has brought about a real revolution in the field of trace analysis.[1] This relatively simple, fast, sensitive and reasonably precise technique has to a large extent replaced analytical methods such as colorimetry and fluorimetry which could sometimes be rather time-consuming. AAS still remains attractive to analysts in spite of the availability of potentially more sensitive techniques such as neutron-activation analysis or spark-source mass spectrometry. Moreover, these techniques require expensive equipment and are not readily available to most analytical laboratories.

Traces of selenium can be determined by fluorimetry[2,3] but the method is cumbersome, slow and subject to many interferences, which led to attempts to determine selenium by flame AAS, but the first attempts were not very successful, and offered no improvement over other techniques. As a result of persistent, research however, determination of selenium by AAS can now easily sustain comparison with other methods.

This paper outlines the evolution of determination of selenium by AAS to give a better understanding of its capabilities and to illustrate the work of investigators from all parts of the world.

DETERMINATION BY CONVENTIONAL FLAME AAS

Allan[4] was the first to describe the determination of selenium by AAS. He used a hollow-cathode lamp (HCL) and the less sensitive 204-nm line. For aqueous standards and an air-acetylene flame a 5-ppm selenium solution gave 1% absorption. Sprague *et al.*[5] used the more sensitive selenium resonance line at 196.1 nm, and obtained 1% absorption for a 1-ppm standard. They were also the first to apply flame AAS for the determination of selenium in a real sample (a copper alloy).

Rann and Hambly[6] and Allan[7] described two major difficulties limiting the successful use of flame AAS for determination of selenium. First the stability and intensity of the hollow-cathode lamp are poor and the life span is short. Secondly the main selenium resonance line is in the far ultraviolet region of the spectrum, where a very high proportion of the radiation is absorbed by air and flame gases. Rann and Hambly[6] and Dagnall *et al.*[8,9] described the construction and use of microwave-excited electrodeless discharge lamps (EDLs) for selenium which give higher intensity, better stability and longer life than the hollow-cathode lamps. However, the construction of these EDLs remained problematic[10,11] and it was not until 1973 that they became commercially available.[12–14]

Allan[7] had found that a hydrogen–air flame absorbed 50% of the incident radiation at 196.1 nm and an air–acetylene flame absorbed 70%. Dagnall[8] used a nitrogen–hydrogen–(entrained air) flame with a three-slot burner and was able to reduce absorption by the flame to 20%. However, because of the low temperature of this flame (300–500°) thermal breakdown of selenium compounds might be incomplete and interferences from ions and molecules would be likely to occur. Kahn and Schallis[15] used an argon–hydrogen–(entrained air) flame with a premix burner and a three-slot burner head. The background absorption from this flame at 196.1 nm was only 13%, but the argon–hydrogen flame appeared to be much more subject to matrix effects than the air–acetylene flame. They also tried to improve their results by adding oxygen to the flame but this caused a radical decrease in the absorption by selenium standards. Chakrabarti[16] compared the sensitivities obtained at different wavelengths with air–acetylene and air–hydrogen

* Research Assistant of the National Fund for Scientific Research (Belgium).

† Metallurgie Hoboken-Overpelt NV.

flames and determined optimum experimental conditions. He studied the effect of interfering cations and anions at 1000-fold ratio to selenium in an air–acetylene flame. Kirkbright *et al.*[17] used nitrogen sheathing of an air–acetylene flame to reduce the background radiation. The background absorption (at 196.1 nm) was also reduced, from 70 to 28%, and the detection limit lowered by a factor of three from 3.6 to 1.2 μg/ml. Interferences were the same as with a conventional air-acetylene flame, however. Kirkbright and Ranson[18] introduced a nitrogen-separated fuel-rich nitrous oxide–acetylene flame which still further lowered the background absorption. The increased temperature of this flame and its reducing properties permitted atomization of refractory oxides and gave considerable freedom from chemical interferences, although a loss of sensitivity was observed.

Several workers investigated interferences that are encountered in the cooler flames such as nitrogen–hydrogen or argon–hydrogen flames. Nakahara *et al.*[19] studied the effects of 28 cations and 4 commonly used acids on the determination of selenium by AAS with an air–hydrogen flame, and later[20] claimed that interferences in the argon–hydrogen flame could be minimized by adding excess of tin (as stannous chloride). Others, however, found this method not entirely successful.[21]

Severne and Brooks[22,23] dealt with interferences by separating selenium from the matrix by co-precipitation with arsenic and dissolving the precipitate in nitric acid before atomizing it in the nitrogen–hydrogen flame. Reichel and Bleakley[24] separated traces of selenium from a copper matrix by co-precipitation with lanthanum hydroxide. Mulford[25] used ammonium pyrrolidinedithiocarbamate (APDC) and solvent extraction into a solvent such as methyl isbutyl ketone (MIBK) to separate and concentrate selenium and aspirated the extract directly into the flame. Chakrabarti[16] used sodium diethyldithiocarbamate (DDTC) to form $Se(DDTC)_4$ and extracted it into MIBK. This extraction improved the sensitivity by a factor of 1.5 for an air–hydrogen flame and 2.4 for an air–acetylene flame. Chambers and McClellan[26] evaluated several complexing agents and organic solvents; the organic phase was stripped with aqueous cyanide solution and the aqueous solution was atomized in an air–acetylene or nitrogen–(entrained air)–hydrogen flame.

Watling[27] described the use of a slotted quartz tube in conjunction with different flames for the determination of selenium, antimony, arsenic and mercury. The use of this tube resulted in much enhanced absorbances for selenium in an air–acetylene flame. No interferences were observed and the precision was considerably better than for the ordinary flame.

Khalighie *et al.*[28] used a water-cooled silica tube placed at the tip of the primary reaction zone of an air–acetylene flame to trap the analyte compounds formed in the lower part of the flame. These compounds were released and atomized by increasing the temperature of the tube. The atomic absorption in a zone near the surface was measured. Several atomization mechanisms were postulated.[29]

Another interesting atomic-absorption method was developed by Lau and Lott.[30] As in the fluorimetric methods, selenium was reacted with 2,3-diaminonaphthalene (DAN) to give the piazselenol, which was then reacted with an excess of aqueous palladium(II) chloride after extraction into chloroform. The resulting $Pd(DANSe)_2Cl_2$ complex was then nebulized in an air–acetylene flame and the palladium absorption signal measured.

Table 1 gives a survey of the sensitivities and detection limits obtained for selenium with several flame AAS systems. Applications of flame AAS worth mentioning are the determination of traces of selenium in stainless steel,[31] organometallic compounds in rubber-manufacturing processes,[32] and in animal feed premix.[21]

BOAT OR WIRE IN FLAME SYSTEMS

AAS detection limits can be improved by methods which eliminate the nebulizer (which has $< 10\%$ efficiency as a means of transporting sample into the flame), such as the tantalum-boat sampling system,[33,34] or by use of electrothermal atomization. Only volatile elements such as As, Pb, Cd, Te, Se can be determined with the boat system, because of the relatively low temperature attainable. At wavelengths shorter than 200 nm, introduction of the boat into the flame causes pronounced effects and the use of deuterium-lamp background-compensation is mandatory in this region. For selenium, absolute detection limits of 10 ng (in 1 ml of sample) have been obtained, but the precision is poor.[34] Golembeski[35] has used the tech-

Table 1.

Flame	Sensitivity, *ppm/1% absorption*	Detection limit, *ppm*	References
Air–acetylene	0.5–3	0.2–3	5,6,8,12,13,15,18,21
Air–hydrogen	0.4–1	1	16
Argon–hydrogen/ nitrogen–hydrogen	0.15–1.1	0.05–1.15	8,15,21–23
Nitrous oxide–acetylene	1.5–6.5	1.8–2.5	12,18

nique for the determination of selenium in rocks, and extended detection down to 0.06 ppm with good precision.

Delves has modified the sampling-boat system[36] but the absolute detection limits for selenium were poorer: 100 ng (in 100 μl).[37] Using the selenium line at 206.3 nm, Clark *et al.*[38] obtained a detection limit of 22 ng (5 μl), the detection limit being taken as a signal equal to the noise.

A technique somewhat similar to the Delves-cup technique was described by Lund *et al.*[39] They preconcentrated the analyte of interest by electrolytic deposition on a platinum wire, which they then placed in an air–acetylene flame for atomization. To improve the sensitivity a quartz tube was placed above the filament, with a central hole facing it. Alkali and alkaline-earth metal salts, which usually cause severe background absorption in flame AAS, were thus not only removed before atomization but also acted as supporting electrolytes in the preconcentration step. The standard-additions method proved mandatory for calibration. The detection limit for selenium was superior to that obtained with the Delves-cup technique: 5 ng/ml with a 2-min electrolysis. The main disadvantages of these non-nebulizer techniques are the very small number of elements for which they can successfully be used and the poor precision for elements with resonance lines at wavelengths shorter than 200 nm.

ELECTROTHERMAL ATOMIZATION

L'vov described the graphite-furnace technique as early as 1959.[40,41] It was modified later by Massmann.[42,43] Even before instruments for graphite-furnace AAS became commercially available, around 1970, several workers had been applying the new technique for the determination of selenium. Matoušek[44] found a detection limit of 72 pg in 2 μl. As Ediger[45] pointed out, some matrix–analyte combinations present problems owing to the extreme volatility of the analyte, as is the case of selenium. The analyte may then be partly or completely lost during the ashing of the matrix. He therefore introduced the principle of matrix modification, by adding nickel to a sample in which volatile elements were to be determined. The nickel–selenium compound, probably nickel selenide, was thermally stable up to 1200°. This effect was not unique to nickel; addition of copper was also reported to allow the use of higher charring temperatures. Henn used molybdenum.[46,47] He noted that much higher charring temperatures (up to 1400°) could be used without loss of selenium and explained this behaviour by postulating the formation of a heteropolymolybdate anion containing a selenium atom in its centre. Szydlowski, however, found the use of molybdenum to yield poorer sensitivity than the use of either nickel or copper.[48] Saeed *et al.*[49] studied the effect of copper, iron and silver on the thermal stability of radioactive selenium present either in inorganic form or a metabolized form in rat whole blood. These authors found copper and iron to be incapable of stabilizing either form of selenium, whereas silver and nickel were satisfactory.

Most of the applications of graphite-furnace AAS dealt with below are concerned with water analysis,[46,47,50–55] metallurgical samples,[56–61] foods[48,62–65] or body fluids.[49,66,67]

Baird *et al.*[50,51] used carbon-rod atomization to determine traces of selenium in waste waters. They used a nitric acid–perchloric acid digestion to oxidize organic material. The presence of concentrated nitric acid was necessary to suppress the intensity of the background perchloric acid peak, and prevent depression of the selenium peak. At 1-g/l. concentrations, alkali-metal halides caused significant background absorption.

Henn[46,47] noted severe enhancement or depressant effects on the signal from 50-μg/ml selenium samples, by 26 out of 31 cations studied at the 10-μg/ml level. Errors ranged from 61% depression by tin to 278% enhancement by vanadium. Nickel and molybdenum enhanced the signal by 85 and 243% respectively. Further increase of the interferent metal concentration to 100 μg/ml or more caused very severe background absorption, exceeding the compensating capabilities of a deuterium lamp background-corrector. Cationic interferences were eliminated by removal of the ions by ion-exchange. Remaining interferences from anions were dealt with by adding molybdenum to the solution. The molybdenum not only reduced matrix interferences but also extended the charring temperature range to 1400°.

Martin *et al.*[54] devised a destruction procedure for use in the determination of selenium in water, waste water, sediment and sludge by electrothermal AAS, using a nitric acid–hydrogen peroxide digestion and adding nickel nitrate to both samples and standards. They found that many suppressive effects of metals and anions could be partly compensated for by the presence of nickel at a concentration of 1%. Nevertheless the standard-additions method often remained mandatory, even for environmental water samples.[54]

Welcher *et al.*[56] tried to optimize electrothermal AAS for the rapid determination of selenium and other volatile metals in high-temperature alloys. They found, like other workers, that the total acid concentration should be limited to 10% v/v to minimize background effects. For several alloys the matrix interferences were severe and led the authors to recommend matrix-matching of standards and samples. Marks *et al.*[60] introduced solid alloy samples into the furnace and induced atomization without a pre-atomization heating cycle. Selenium was determined in chromium metal by Hamner *et al.*[59] and in copper by Mullen,[58] who separated selenium from the copper matrix by co-precipitation with ferric hydroxide, collected the precipitate on a filter paper disc, and analysed portions of the disc by furnace AAS. Ohta and Suzuki[57] constructed a molybdenum micro-tube

atomizer for the determination of selenium in metallurgical samples. Extraction of Se from the sample with 3,3'-diaminobenzidine proved to yield a more accurate determination.

Meyer *et al.*[61] determined traces of selenium in copper, copper alloys, silver, gold, lead and bismuth after heating at approximately 1100° in a stream of oxygen, the SeO_2 formed being trapped in a cooled receiver, dissolved in nitric acid and determined by furnace AAS.

In the field of food analysis, and analysis of biological samples in general, Ihnat has performed extensive and critical studies on the use of carbon-furnace atomization[62–64] for the determination of selenium. Samples were digested with a nitric acid–perchloric acid–sulphuric acid mixture. The influence of several acids was studied and it was concluded that the presence of traces of perchloric acid in sulphuric acid resulted in poor absorbance signals. Nitric and perchloric acids were superior matrices and their optimum concentrations were established to be 0.5 and 1*M* respectively (in the presence of nickel). Recovery experiments indicated that sample matrices could seriously interfere with the selenium signal.

These interferences were obviated by isolating selenium from the matrix by reduction and precipitation with ascorbic acid. The filter and precipitate were digested and nickel was added before by graphite-furnace AAS for selenium. The addition of nickel greatly improved the recovery and precision.

Shum *et al.*[65] used graphite-furnace AAS for the determination of selenium in fish and food products. Szydlowski[48] optimized a graphite-furnace AAS method for the analysis of complex carbohydrate matrices. He used a nitric acid–perchloric acid digestion and relied on solvent extraction to minimize interference. The selenium was reacted with 2,3-DAN under standardized conditions, and the piazselenol was extracted into decahydronaphthalene. Copper was added to ensure the complete breakdown of the chelating agent during atomization and the prevention of volatilization of the analyte. A similar extraction technique has been applied by Nève and Hanocq[67] for the determination of selenium in human plasma and erythrocytes. After digestion, the Se(IV) is reacted with 4-chloro-1,2-diaminobenzene, which is soluble in toluene. Ishizaki[66] used dithizone to chelate selenium and extracted the complex into carbon tetrachloride. Blood and other biological samples were first decomposed by oxygen-flask combustion. Interfering cations were removed by passing the digest through a column of cation-exchange resin. Kamada *et al.*[55] studied the extraction behaviour of Se(IV) and Se(VI) with DDTC, APDC and dithizone. They concluded that DDTC extraction at pH 3.5–4.5 into chloroform is best for the selective separation of Se(IV) and Se(VI).

Saeed *et al.*[49] determined selenium in serum without destruction of the organic matrix. They transferred small aliquots of serum directly into the graphite-furnace tube, added nickel and atomized electrothermally. They noted that the method was unsuitable for the determination of selenium in whole blood, because of the serious spectral interferences that arose from the large amounts of iron present.

THE VOLATILE HYDRIDE TECHNIQUE

Hatch and Ott[68] described a "vapour generation" technique for the determination of mercury in solution by AAS. It employed a reduction procedure with stannous sulphate. The mercury vapour was removed from the solution with a stream of air introduced into a quartz-windowed atomization cell. Holak used a similar technique for the determination of arsenic,[69] based on the generation of arsine, which had been established for years as an official method for separating arsenic from a solution.[70] Holak trapped the volatile arsine in a tube cooled with liquid nitrogen, desorbed it and swept it into the air–acetylene flame of an AA spectrometer. This technique was then used to determine selenium,[71] the hydride being atomized in an argon–hydrogen–(entrained air) flame. The technique offered several potential advantages. All the selenium present was converted into the hydride and introduced at once into the atomization device. Moreover it was hoped that chemical interferences could be minimized by this separation of the analyte from the sample matrix. Numerous papers have since dealt with the hydride-evolution technique, with applications to the determination of selenium in natural waters.[53,72–80] environmental samples,[81,82] blood,[83] urine,[82] foods,[62,84–88] animal feed and forage samples,[89–91] metallurgical samples,[92–94] glass[96] and petroleum.[97]

Methodology

Arsenic(V) and selenium(VI) are first reduced to arsenic(III) and selenium(IV) by letting potassium iodide and stannous chloride react with the acidified sample, then zinc metal is added and hydrogen, arsine and hydrogen selenide are evolved. The hydrides are swept from the solution by an inert gas stream. The potassium iodide and stannous chloride solutions have been used with different concentrations.[62,71,73–75,80,97–103] Yamamoto[99] and Church and Robison[101] omitted the potassium iodide and were able to generate hydrogen selenide equally well. The stannous chloride appreciably accelerates the reduction process, however.[99] Fiorino *et al.*[84] stated that the addition of sodium iodide might even prevent the generation of H_2Se and this was confirmed by observations by Yamamoto *et al.*[104] and by Clinton.[83] Walker *et al.*[97] demonstrated that the catalytic effect of tin(II) on the Zn/HCl reduction was only required for weakly acidic media. They observed loss of selenium if acidic solutions with stannous chloride present were left standing for a certain time before the Zn/HCl reduction. They suspected that elemental selenium was formed and agglomerated, thus deplet-

ing the selenite in solution.[97] Yamamoto and Kumamaru[104] noticed that the presence of more than 0.04% stannous chloride impoverished the sensitivity by 30% and also gave poorer reproducibility. They therefore decided to use the Zn/HCl system as sole reductant. Granular zinc,[71,99,101] zinc tablets,[104] and zinc dust or slurry[62,73,80,97,100,103] have been used. Several workers have found the sensitivity to depend upon the reaction time between the addition of zinc to the acidified sample and flushing of the hydride vapours from the generator flask into the atomization cell. Goulden and Brooksbank[74] tried aluminum powder instead of zinc, and found reaction times of a few minutes necessary for complete reduction. However, others have pointed out that waiting too long to release the hydrides from the generator flask may cause a decrease in sensitivity, because of partial dissolution of the hydride in the liquid phase.[100,101] Besides the Zn/HCl reduction system other reducing agents such as $TiCl_3$/Mg/HCl have been used.[105]

Schmidt and Royer[72] were the first to report the generation of hydrides by reduction with sodium borohydride. Sodium borohydride was found to be superior to zinc with regard to reduction yields and contamination of the blank. Ever since, it has been the reductant of choice.

It has often been used as pellets[53,72,82,88,89,92,94,104–108] but McDaniel *et al.*[81] found that pellets were only 40–60% as efficient as borohydride solutions; they attributed this to the very fast and localized generation of hydrogen when pellets are dropped into an acidic solution. Attempting to automate the determination of arsenic by arsine generation, Vijan and Wood[91] were the first to use solutions of sodium borohydride instead of pellets. Soon after, Thompson and Thomerson[109] used a 1% solution of sodium borohydride for the generation of hydrogen selenide. The concentrations used have varied widely, ranging from 0.5 to 8%.[76–79,80–82,84,86,90,91,93,95,96,104,109–124] Sodium borohydride solutions need to be stabilized by alkalization, but the concentration of alkali should not be too high lest the solution viscosity becomes so high that homogeneous dispersion of the hydrogen bubbles is no longer certain, which would be reflected in poor precision. Concentrations of 1–2% sodium hydroxide stabilize the solutions satisfactorily.[85,117] Comparative studies of the different reduction systems have been made.[81,104] Yamamoto and Kumamaru concluded that both the Zn/HCl and the sodium borohydride systems yielded equally good sensitivity and precision.[104] Using radiotracers, McDaniel *et al.*[81] investigated the reduction efficiency of several hydride-generation methods and found the Zn/HCl systems very inefficient, 88% of the selenium present remaining unreacted. Sodium borohydride yielded higher recoveries, although conversion into the hydride and transfer to the atomizer were not quantitative in most systems. The efficiency of hydride generation is strongly dependent on the use of optimized chemical and physical parameters, but these are mainly determined by the design of the apparatus.[85,86,110] Most workers have simply optimized their own particular system, whether laboratory-made or commercially available.[85,91,117] Hydrochloric acid (0.4–6*M*) has usually been the acid of choice, although sulphuric acid is equally suitable.[62,85,116,117] Many workers have recognized that increasing the analyte solution volume has an adverse effect on peak absorbance measurements.[92,93,100,110,117] The selenium must also be present in the quadrivalent form, and any selenate must be quantitatively converted into selenite.[74,75,78,83,91–93,109,118] Cutter[78] discussed several ways of doing this and found heating the solution in a boiling water-bath, at a hydrochloric acid concentration of 4*M*, to be the only suitable method. This has also been stated by other authors.[75,118]

Instrumentation

Reaction chambers have included large test-tubes, Erlenmeyer flasks, wash-bottles or pear-shaped flasks. The hydride evolved has been transferred in two principal ways: either the hydride is conveyed directly into the atomization cell as it is generated, or some form of storage is used before the transfer to the atomizer. In the former case the system acts as a continuous-flow system; in the latter case all of the hydride formed is introduced in a burst into the atomizer, and a "transient" sharp signal is observed. Goulden and Brooksbank called this a "batch operation".[74]

Most of the early procedures included some form of collection of the generated hydride. The hydride was collected in a rubber balloon,[71–73,93,98,102,106] a collapsible plastic bag or a pressurized chamber,[99,104,105] or it was simply stored in the head-space of the generator.[100,101]

After the introduction of sodium borohydride as the reductant, continuous-flow systems became popular, because the reduction reactions proceeded much faster. In some cases the excess of hydrogen generated served as a propellant for the transfer of the hydride to the atomization cell, but in most cases inert gas streams were used to carry the hydride to the cell.[74,85,90,91,100,101] Moreover, flushing the system with an inert gas in order to remove air had proved necessary. Yamamoto[99] demonstrated that purging the air from the generation/atomization system was necessary in order for precise results to be obtained. From the literature it is apparent that gas-flow adjustments during the sweeping phase are critical in most open-ended atomization systems.[76,109,125] In most cases argon has been used as carrier gas although nitrogen is cheaper and gives comparable results; helium has also been used.[78,101] Many authors have stressed the importance of keeping the dead volume between the generation solution and the atomization cell as small as possible in order to obtain a highly concentrated atom cloud in the atomization cell.[85,110]

The design of most apparatus has undergone modifications to facilitate the addition of reagents, decrease the duration of an analysis and diminish errors due to

numerous manipulations in the course of the analysis. Automated designs have been described.[74,76,91,111]

In recent years several authors have demonstrated the importance of taking into account the kinetics of the reduction of different elements to their covalent hydrides. They propose collection procedures for hydrides that are slowly evolved, while hydrides that are formed very rapidly or that are unstable should be transferred directly for atomization. Chapman and Dale[112] introduced a versatile gas-handling system that is inserted between the generator flask and the atomization cell, and that leaves the operator with the choice of collecting the hydride (advised for selenium or arsenic) or using the direct transfer mode. Most investigators, however, have preferred cold-trap procedures in which the hydride is stripped from the solution, dried and collected in a liquid-nitrogen trap.[78,81,108,110,126] After a minute the cold trap is removed from the liquid nitrogen and warmed, and the hydride is vaporized and transferred at once into the atomizer. Because the boiling point of hydrogen is lower than that of nitrogen, such methods remove the excess of hydrogen generated, so the hydride is much less diluted when introduced into the atomization cell and better sensitivities should be obtained.[110] As pointed out by Siemer[110] these procedures eliminate reduction and stripping kinetics as possible sources of variation in the overall performance of the method. Cold-trap methods always include a drying step because any moisture would condense and clog the trap tube, and impair the revolatilization of the hydride.[81]

Atomizers

The first applications of hydride generation usually involved atomization in an argon–hydrogen–(entrained air) flame. The excess of hydrogen generated along with the hydride often perturbed the flame, changing its composition and thus also causing a change in the absorption of the flame. Though use of the deuterium background-corrector was found to reduce the blank signals,[98] in almost every other study with this flame background correction was judged unnecessary.[85] The relatively cool and non-absorbing argon–hydrogen–(entrained air) flame from a Boling triple-slot burner has been used by many investigators,[53,62,71–73,77,82,86,92,94,97–100,102,103,105–108,111,119–121] as have nitrogen–hydrogen–(entrained air)[75,83,84,88,89,93,118] and even helium–hydrogen–(entrained air) flames.[78,101] In some cases the diffusion flame has been confined by a tube.[74,78,80,90,91,110,127] Church and Robison[101] noted that the use of helium instead of argon as carrier gas reduced flame noise and increased the sensitivity two-fold. Ihnat[85] pointed out that the flow-rates of the flame gases need adjustment according to the kind of reduction system used. Zn/HCl reduction requires high argon flow-rates to dilute the excess of hydrogen generated by the reduction. Flames used in conjunction with the sodium borohydride system were easier to balance; the lower flow-rates resulted in a 30% enhancement of the sensitivity in comparison with a "stiff" flame. Fiorino,[84] Corbin[77] and Ihnat[85] used shielded flames in order to minimize drafts from the ambient air, thus improving flame stability and suppressing baseline noise. Background absorption in the flame often necessitated the use of a deuterium corrector and influenced the signal to noise ratio unfavourably.

Dědina and Rubeška[127] have studied the atomization mechanism of hydrogen selenide in a tube-confined fuel-rich hydrogen–oxygen diffusion flame. They found that atomization was not achieved by thermal decomposition, but was due to free radicals generated in the flame. They showed that selenium atoms were lost from the flame mainly by reactions on the quartz surface of the tube. On the basis of both theoretical and experimental data they also studied the relation between the amount of hydride present and the absorption signal. Chu *et al.*[128] were the first to describe the use of an electrically heated silica tube for the thermal decomposition of arsine in an argon atmosphere. This method is twice as sensitive as decomposition in an argon–hydrogen–(entrained air) flame because of the longer residence time of the atom cloud in the optical path and the much reduced noise levels.

Schmidt and Royer[72] noted that use of a quartz furnace tube heated by an argon–hydrogen–(entrained air) flame from a single-slot burner significantly eliminated noise. Thompson and Thomerson[109] used a stoichiometric air–acetylene flame to heat a 17 cm long open-ended silica tube. The hydrides were introduced through a side-arm in the centre of the tube. The excess of hydrogen was prevented from igniting at the ends of the tube by a transverse stream of nitrogen. This type of cooling system has also been used by others.[125] In other cases, as in some commercially available instruments, quartz windows have been fitted to the quartz tube, so that a closed circuit is obtained. Some authors have remarked, however, that as they are part of the optical system, these windows need to be extremely clean in order to allow maximal transmission of light in the far ultraviolet region of the spectrum.[109,129] A slight loss in sensitivity when quartz windows are used has been reported.[74,91,109] Nakashima[79] used nitrogen–hydrogen–(entrained air) flame to heat his quartz tube. Vijan and Wood[91] tried to improve the sensitivity by increasing the length of an electrically heated silica tube in which an (entrained air)–hydrogen flame was burning. Contrary to expectation at 10-cm quartz tube generated signals that were 25% higher than those from a 16- or 28-cm tube. Goulden and Brooksbank[74] also used an electrically heated quartz furnace, in which an argon–hydrogen–(entrained air) flame was burning, but Siemer *et al.*[90,110] did not use electrical heating. Electrically heated silica tubes without flames have been increasingly adopted.[76,95,112–114,119,122–124,129,130] Tempera-

tures between 850 and 950° have proved suitable for the thermal decomposition of hydrogen selenide.[76,117,125,130]

Several authors have observed deterioration of the inner surface of the quartz tube,[112,117,123,125,131] which impoverishes the sensitivity and precision. Some workers have overcome this by inserting small silica tubes within the original tube so that a new surface is exposed to the hydrides and exchange or "renewal" of the surface is made feasible.[112,123] All these hydride-generation procedures used hydrochloric acid to provide the acidic medium for the evolution of hydrogen. Verlinden[131] noticed that using hydrochloric acid could shorten the life of a quartz tube to as little as 24 hr of continuous use. She proposed the use of sulphuric acid instead, thus prolonging the life of the tube by at least a factor of 20 and considerably decreasing the day-to-day variability.

Knudson and Christian[108] used a graphite (carbon) furnace for combustion of the hydrides, and atomization of H_2Se in a heated carbon furnace has been used by others.[53,81] Fricke *et al.*[126] have used hydride generation in conjunction with detection by plasma emission spectrometry. Thompson[113] passed the hydride into an argon–hydrogen–(entrained air) flame and used atomic-fluorescence for the detection.

Sensitivity, detection limit, precision

Because of the wide range of hydride generators and atomizers and the resulting differences in optimized parameters, it is difficult to compare published data with regard to analytical performance of the hydride-generation technique. Moreover, there is much confusion about definition of the term detection limit, so users of the data should always check the definition applied.

Ihnat and Miller[86] have reported an extensive collaborative study undertaken to evaluate the overall performance of the method, regardless of the type of generator that was used. They investigated the precision of the various stages, the overall reproducibility and the interlaboratory precision of the method. They concluded that the method showed little bias but was unacceptable with regard to precision. Their results showed the existence of laboratory-dependent systematic errors. Raptis *et al.*[124] have also demonstrated that the hydride-evolution method may be afflicted with systematic errors, which do not depend on the method of sample preparation but are assumed to be caused by interferences from concomitant ions in the digest. They advise the use of the method of standard additions and the development of separation techniques to further isolate selenium from the matrix.

The sensitivity and the detection limit seem to be less dependent on the nature of the reduction system used[104] than the kind of atomization system. The sensitivity obtained by hydride evolution and combustion of the hydride in an electrically heated quartz tube is similar to that obtained by the graphite-furnace solution technique (~ 1 μg/l.) whereas the determination of the hydride with an argon–hydrogen–(entrained air) flame is only a third as sensitive.[119] Owing to the large sample volumes that can be used in the hydride methods, compared to a graphite-furnace solution technique, the relative detection limits for the former can be reduced to the pg/ml range. As the maximum sample volume is mainly determined by the design of the generator, absolute detection limits, may reflect the analytical capabilities of a given design better than do the relative detection limits and usually range from 0.5 to 60 ng. The detection limit for real samples instead of standard solutions is higher and generally ranges from 25 to 80 ng.[62,86] Siemer[110] showed that cold-traps do not necessarily improve absolute detection limits, because poor efficiency of the hydride transfer to the atomizer is a factor often overlooked. However, if efficient hydride transfer is guaranteed, a twofold improvement in sensitivity is obtained, mainly owing to the separation of the huge volume of hydrogen generated during the reduction reaction, thus minimizing dilution of the hydride.[110] Preconcentration methods for water samples have extended the method to the pg/ml range.[79,80]

The precision of the determination step depends on the concentration level of the analyte and on the generation and atomization systems used. Reported values usually range between 1 and 5% relative standard deviation. The overall relative standard deviation can be considerably greater however.[86]

Interferences

Almost all papers on hydride-generation AAS deal to some extent with possible interferences. Smith[107] made the first systematic study on the influence of 1 mg of each of 48 cations on the determination of 2 μg of selenium. Sodium borohydride was used as the reductant, with an argon–hydrogen–(entrained air) flame. Yamamoto and Kumamaru[104] compared the effect of diverse ions with both the zinc and the sodium borohydride reduction systems and found the degree of interference of given ions to depend on the nature of the reductant used, some ions giving more interference in the borohydride system than in the Zn/HCl system and *vice versa*. Smith[107] found that Fe^{3+}, Co^{2+}, Cd^{2+}, and Pb^{2+} suppress the selenium signal moderately whereas Ag^+, Cu^{2+}, Ni^{2+}, Hg^{2+}, Sn^{2+}, $Cr_2O_7^{2-}$, I^-, MnO_4^- and NO_3^- can interfere strongly. Pierce and Brown compared the interference of several anions and cations in the method using borohydride reduction and combustion in an electrically heated quartz furnace[114] and in the argon–hydrogen flame.[119] The quartz tube system was less subject to interferences.

In almost every paper that has included observations on the influence of acids the strongly suppressing effect of nitric acid and sulphuric acid has been recognized. These effects are more pronounced in closed-furnace systems than in systems that use an open-ended tube.[117] Meyer *et al.*[123] investigated a number of cross-interferences, using a commercially

available hydride-generation system coupled with a closed electrically heated quartz cell. Suppression of the selenium signal generally seemed to depend on the absolute concentration of interferent rather than on the concentration ratio between selenium and the interfering ion. The influence of the acidity and the volume of the sample was fully investigated. The condition of the inner surface of the quartz tube proved to be important.[123] Verlinden and Deelstra[129] studied the effects of other hydride-forming elements on the determination of selenium. Tin and bismuth interfered severely, mercury, antimony, and germanium were considered to be moderately interfering, whereas arsenic and tellurium interfered only at high concentration levels. Most of the interferences in the hydride AAS methods occur during the reduction step and can be explained by the formation of very insoluble selenides or by preferential reduction of metals present in the matrix. If these metals are reduced to their elemental state they can cause depression of the selenium signal by co-precipitating selenite or decomposing the hydride or impairing its evolution.[107,122,123,129]

Several authors have tried to overcome interferences by applying masking agents or by separating selenium from the matrix. Meyer *et al.*[123] noticed that increasing the acidity of the hydride-generation solution reduced interferences from copper and silver ions. Increasing the volume of the evolution medium led to reduction of the suppressive effect of nickel and cobalt but not that of silver or arsenic(III). Kirkbright has described the use of thiosemicarbazide and 1,10-phenanthroline to minimize the suppressive effects of copper on arsine generation and to obviate those of nickel, palladium and platinum, but in the case of selenium these masking agents were found to be ineffective.[120,121] However, he was able to restrict these interferences by forming compounds more stable than the selenides. Thus addition of controlled amounts of tellurium(IV) led to the formation of stable copper, palladium or platinum telluride rather than the corresponding selenide. The addition of ethylenediaminetetra-acetic acid counteracts the effects of nickel and cobalt, but is only partially effective for copper, cadmium or lead.[122] Robért has demonstrated that precipitation of selenium with lanthanum is incomplete when metals sulphide concentrates are analysed. He therefore recommended fusing the sample with sodium peroxide, leaching the melt with water and filtering off copper and nickel.[125]

Use of the method of standard additions is essential in many cases.[123,124,130,132]

CONCLUSION

Comparative studies[53,62,110,119] as well as this survey of the literature have shown that in the past decade AAS has been established as an adequate method for the determination of selenium in the sub-ng/ml range. The best absolute sensitivity and detection limit are obtained with the graphite-furnace technique, the median values being 50 and 100 pg respectively. The hydride-generation technique allows the use of large sample volumes and therefore offers the most favourable relative sensitivity and detection limit: 0.8 and 0.25 ng/ml respectively.[63]

Interferences during the atomization step are severe in the graphite-furnace technique and make the use of background-correction mandatory, and may even then still be severe. Interference during atomization rarely occurs in the hydride-evolution method, but interferences during the reduction step, especially by copper, nickel and the noble metals, are common. Interferences are the principal limitation of both methods and for some samples the sensitivity and accuracy can be considerably impaired. With both methods it is possible to determine nanogram quantities of selenium. The hydrogen selenide AAS methods offer the convenience and the rapidity required for routine analysis.

Acknowledgement—Marleen Verlinden wishes to express her thanks to the National Fund for Scientific Research (Belgium), whose grant supported this work.

REFERENCES

1. A. Walsh, *Spectrochim. Acta*, 1955, **7**, 108.
2. J. H. Watkinson, *Anal. Chem.*, 1966, **38**, 92.
3. C. A. Parker and L. G. Harvey, *Analyst*, 1962, **87**, 558.
4. J. E. Allan, *Spectrochim. Acta*, 1962, **18**, 259.
5. S. Sprague, D. C. Manning and W. Slavin, *At. Abs. Newsl.*, 1964, **20**, 27.
6. C. S. Rann and A. N. Hambly, *Anal. Chim. Acta*, 1965, **32**, 346.
7. J. E. Allan, *4th Australian Spectroscopy Conference*, August 1964.
8. R. M. Dagnall, K. C. Thompson and T. S. West, *At. Abs. Newsl.*, 1967, **6**, 117.
9. *Idem, Talanta*, 1967, **14**, 551.
10. R. M. Dagnall and M. D. Silvester, *Anal. Chem.*, 1971, **44**, 204.
11. D. O. Cook, R. M. Dagnall and T. S. West, *Anal. Chim. Acta*, 1971, **56**, 17.
12. W. B. Barnett, *At. Abs. Newsl.*, 1973, **12**, 142.
13. W. B. Barnett, J. W. Vollmer and S. M. Denuzzo, *ibid.*, 1976, **15**, 33.
14. G. E. Bentley and M. L. Parsons, *Anal. Chem.*, 1977, **49**, 551.
15. H. L. Kahn and J. E. Schallis, *At. Abs. Newsl.*, 1968, **7**, 5.
16. C. L. Chakrabarti, *Anal. Chim. Acta*, 1968, **42**, 379.
17. G. F. Kirkbright, M. Sargent and T. S. West, *At. Abs. Newsl.*, 1969, **8**, 34.
18. G. F. Kirkbright and L. Ranson, *Anal. Chem.*, 1971, **43**, 1238.
19. T. Nakahara, M. Munemori and S. Musha, *Anal. Chim. Acta*, 1970, **50**, 51.
20. T. Nakahara, H. Nishino, M. Munemori and S. Musha, *Bull. Chem. Soc. Japan*, 1973, **46**, 1706.
21. S. Ng, M. Munroe and W. McSharry, *J. Assoc. Off. Anal. Chemists*, 1974, **57**, 1260.
22. B. C. Severne and R. R. Brooks, *Anal. Chim. Acta*, 1972, **58**, 216.
23. *Idem, Talanta*, 1972, **19**, 1467.
24. W. Reichel and B. G. Bleakley, *Anal. Chem.*, 1974, **46**, 59.
25. C. E. Mulford, *At. Abs. Newsl.*, 1966, **5**, 88.

26. J. C. Chambers and B. E. McClellan, *Anal. Chem.*, 1976, **48**, 2061.
27. R. J. Watling, *Anal. Chim. Acta*, 1977, **94**, 181.
28. J. Khalighie, A. M. Ure and T. S. West, *ibid.*, 1979, **107**, 191.
29. *Idem, ibid.*, 1980, **117**, 257.
30. H. K. Y. Lau and P. F. Lott, *Talanta*, 1971, **18**, 303.
31. E. A. Peterson, *At. Abs. Newsl.*, 1970, **9**, 129.
32. G. R. Supp and I. Gibbs, *ibid.*, 1974, **13**, 71.
33. H. L. Kahn, G. E. Peterson and J. E. Schallis, *ibid.*, 1968, **7**, 35.
34. H. L. Kahn, *ibid.*, 1968, **7**, 40.
35. T. Golembeski, *Talanta*, 1975, **22**, 547.
36. H. T. Delves, *Analyst*, 1970, **95**, 431.
37. J. D. Kerber and F. J. Fernandez, *At. Abs. Newsl.*, 1971, **10**, 78.
38. D. Clark, R. M. Dagnall and T. S. West, *Anal. Chim. Acta*, 1972, **60**, 219.
39. W. Lund, Y. Thomassen and P. Døvle, *ibid.*, 1977, **93**, 53.
40. B. V. L'vov, *Inzhener.-Fiz. Zh., Akad. Nauk Belorus. SSR*, 1959, **2**, 44.
41. *Idem, Spectrochim. Acta*, 1961, **17**, 761.
42. H. Massmann, *Z. Anal. Chem.*, 1967, **225**, 203.
43. *Idem, Spectrochim. Acta*, 1968, **23B**, 215.
44. J. P. Matoušek, *Am. Lab.*, 1971, **3**, June, 45.
45. R. D. Ediger, *At. Abs. Newsl.*, 1975, **14**, 127.
46. E. L. Henn, *Anal. Chem.*, 1975, **47**, 428.
47. *Idem*, A.S.T.M. STP 618, 1977, 54.
48. F. J. Szydlowski, *At. Abs. Newsl.*, 1977, **16**, 60.
49. K. Saeed, Y. Thomassen and F. J. Langmyhr, *Anal. Chim. Acta*, 1979, **110**, 285.
50. R. B. Baird, S. Pourian and S. M. Gabrielian, *Anal. Chem.*, 1972, **44**, 1887.
51. R. B. Baird and S. M. Gabrielian, *Appl. Spectrosc.*, 1974, **28**, 273.
52. J. C. Guillaumin, *At. Abs. Newsl.*, 1974, **13**, 135.
53. B. B. Mesman and T. C. Thomas, *Anal. Lett.*, 1975, **8**, 449.
54. T. D. Martin, J. F. Kopp and R. D. Ediger, *At. Abs. Newsl.*, 1975, **14**, 109.
55. T. Kamada, T. Shiraishi and Y. Yamamoto, *Talanta*, 1978, **25**, 15.
56. G. G. Welcher, O. H. Kriege and J. Y. Marks, *Anal. Chem.*, 1974, **46**, 1227.
57. K. Ohta and M. Suzuki, *Anal. Chim. Acta*, 1975, **77**, 288.
58. J. D. Mullen, *Talanta*, 1976, **23**, 846.
59. R. M. Hamner, D. L. Lechak and P. Greenberg, *At. Abs. Newsl.*, 1976, **15**, 122.
60. J. Y. Marks, G. G. Welcher and R. J. Spellman, *Appl. Spectrosc.*, 1977, **31**, 9.
61. A. Meyer, Ch. Hofer and G. Tölg, *Z. Anal. Chem.*, 1978, **290**, 292.
62. M. Ihnat, *J. Assoc. Off. Anal. Chemists*, 1976, **59**, 911.
63. M. Ihnat and R. J. Westerby, *Anal. Lett.*, 1974, **7**, 257.
64. M. Ihnat, *Anal. Chim. Acta*, 1976, **82**, 293.
65. G. T. Shum, H. P. Freeman and J. F. Uthe, *J. Assoc. Off. Anal. Chemists*, 1977, **60**, 1010.
66. M. Ishizaki, *Talanta*, 1978, **25**, 167.
67. J. Nève and M. Hanocq, *Anal. Chim. Acta*, 1977, **93**, 85.
68. W. R. Hatch and W. L. Ott, *Anal. Chem.*, 1968, **40**, 2085.
69. W. Holak, *Anal. Chem.*, 1969, **41**, 1712.
70. *Official Methods of Analysis*, 11th Ed., Association of Official Analytical Chemists, Washington D.C., 1970.
71. F. J. Fernandez and D. C. Manning, *At. Abs. Newsl.*, 1971, **10**, 86.
72. F. J. Schmidt and J. L. Royer, *Anal. Lett.*, 1973, **6**, 17.
73. J. S. Caldwell, R. J. Lishka and E. F. McFarren, *J. Am. Water Works Assoc.*, 1973, **5**, 731.
74. P. D. Goulden and P. Brooksbank, *Anal. Chem.*, 1974, **46**, 1431.
75. M. Lansford, E. M. McPherson and M. J. Fishman, *At Abs. Newsl.*, 1974, **13**, 103.
76. F. D. Pierce, T. C. Lamoreaux, H. R. Brown and R. S. Fraser, *Appl. Spectrosc.*, 1976, **30**, 38.
77. D. R. Corbin and W. M. Barnard, *At. Abs. Newsl.*, 1976, **15**, 116.
78. G. A. Cutter, *Anal. Chim. Acta*, 1978, **98**, 59.
79. S. Nakashima, *Anal. Chem.*, 1979, **51**, 654.
80. R. J. Watling, *Spectrochim. Acta*, 1980, **35B**, 451.
81. M. McDaniel, A. D. Shendrikar, K. D. Reiszner and P. W. West, *Anal. Chem.*, 1976, **48**, 2240.
82. T. J. Kneip, *Health Lab. Sci.*, 1977, **14**, 53.
83. O. E. Clinton, *Analyst*, 1977, **102**, 187.
84. J. A. Fiorino, J. W. Jones and S. G. Capar, *Anal. Chem.*, 1976, **48**, 120.
85. M. Ihnat and H. J. Miller, *J. Assoc. Off. Anal. Chemists*, 1977, **60**, 813.
86. *Idem, ibid.*, 1977, **60**, 1414.
87. K. Kolar and A. Widell, *Mitt. Gebiete Lebensm. Hyg.*, 1977, **68**, 259.
88. J. Flanjak, *J. Assoc. Off. Anal. Chemists*, 1978, **61**, 1299.
89. S. Ng and W. McSharry, *ibid.*, 1975, **58**, 987.
90. D. D. Siemer and L. Hagemann, *Anal. Lett.*, 1975, **8**, 323.
91. P. N. Vijan and G. R. Wood, *Talanta*, 1976, **23**, 89.
92. H. D. Fleming and R. G. Ide, *Anal. Chim. Acta*, 1976, **83**, 67.
93. R. V. D. Robért, *Natl. Inst. Metall. Republ. S. Afr., Rept.* 1838, 1976.
94. M. Bedard and J. D. Kerbyson, *Can. J. Spectrosc.*, 1976, **21**, 64.
95. L. P. Greenland and E. Y. Campbell, *J. Res. U.S. Geol. Survey*, 1977, **5**, 403.
96. R. Hermann, *At. Abs. Newsl.*, 1977, **16**, 44.
97. H. H. Walker, J. H. Runnels and R. Merryfield, *Anal. Chem.*, 1976, **48**, 2056.
98. D. C. Manning, *At. Abs. Newsl.*, 1971, **10**, 123.
99. Y. Yamamoto, T. Kumamaru, Y. Hayashi and M. Kanke, *Anal. Lett.*, 1972, **5**, 717.
100. J. Y. Hwang, P. A. Ullucci, C. J. Mokeler and S. B. Smith, *Am. Lab.*, 1973, **5**, March, 43.
101. M. R. Church and W. H. Robison, *Intern. J. Environ. Anal. Chem.*, 1974, **3**, 323.
102. H. C. Freeman and J. F. Uthe, *At. Abs. Newsl.*, 1974, **13**, 75.
103. A. M. de Kersabiec, B. Giraud and J. Nicolas, *Compt. Rend.*, 1976, **282D**, 2025.
104. Y. Yamamoto and T. Kumamaru, *Z. Anal. Chem.*, 1976, **281**, 353.
105. E. N. Pollock and S. J. West, *At. Abs. Newsl.*, 1973, **12**, 6.
106. F. J. Fernandez, *ibid.*, 1973, **12**, 93.
107. A. E. Smith, *Analyst*, 1975, **100**, 300.
108. E. J. Knudson and G. D. Christian, *Anal. Lett.*, 1973, **6**, 1039.
109. K. C. Thompson and D. R. Thomerson, *Analyst*, 1974, **99**, 595.
110. D. D. Siemer and P. Koteel, *Anal. Chem.*, 1977, **49**, 1096.
111. F. J. Schmidt, J. L. Royer and S. M. Muir, *Anal. Lett.*, 1975, **8**, 123.
112. J. F. Chapman and L. S. Dale, *Anal. Chim. Acta*, 1979, **111**, 137.
113. K. C. Thompson, *Analyst*, 1975, **100**, 307.
114. F. D. Pierce and H. R. Brown, *Anal. Chem.*, 1976, **48**, 693.
115. R. D. Wauchope, *At. Abs. Newsl.*, 1976, **15**, 64.
116. W. Lautenschlager, J. Maassen and W. Oelschlager, *Landwirtsch. Forsch.*, 1976, **29**, 59.
117. M. Verlinden, J. Baart and H. Deelstra, *Talanta*, 1980, **27**, 633.

118. K. G. Brodie, *Intern. Lab.*, 1977, March, 65.
119. F. D. Pierce and H. R. Brown, *Anal. Chem.*, 1977, **49**, 1417.
120. G. F. Kirkbright and M. Taddia, *Anal. Chim. Acta*, 1978, **100**, 145.
121. *Idem*, *At. Abs. Newsl.*, 1979, **18**, 68.
122. G. Mausbach, *GIT Fachz. Lab.*, 1979, **23**, 898.
123. A. Meyer, Ch. Hofer, G. Tölg, S. Raptis and G. Knapp, *Z. Anal. Chem.*, 1979, **296**, 337.
124. S. Raptis, G. Knapp, A. Meyer and G. Tölg, *ibid.*, 1980, **300**, 18.
125. R. Robért and G. Balaes, *Natl. Inst. Metall. Republ. S. Afr., Rept.* 2023, 1979.
126. F. N. Fricke, W. D. Robbins and J. A. Caruso, *J. Assoc. Off. Anal. Chemists*, 1978, **61**, 1118.
127. J. Dědina and I. Rubeška, *Spectrochim. Acta*, 1980, **35B**, 119.
128. R. C. Chu, G. P. Barron and P. Baumgarner, *Anal. Chem.*, 1978, **44**, 1476.
129. M. Verlinden and H. Deelstra, *Z. Anal. Chem.*, 1979, **296**, 253.
130. J. R. S. Broughton and C. W. Fuller, *Proc. Anal. Div. Chem. Soc.*, 1977, **14**, 112.
131. M. Verlinden, to be published.
132. M. Verlinden, *Ph.D. Dissertation*, University of Antwerpen, 1981, in preparation.

Talanta, Vol. 28, pp. 647 to 652, 1981
Printed in Great Britain. All rights reserved

0039-9140/81/090647-06$02.00/0
Copyright © 1981 Pergamon Press Ltd

COMBINED ASSAY AND DETERMINATION OF BIOACTIVITY OF POLYENE ANTIBIOTICS BY FLOW NEPHELOMETRY

ANTHONY E. BEEZER and BABUR Z. CHOWDHRY*

Department of Chemistry, Chelsea College, University of London, Manresa Road, London SW3 6LX, England

(*Received* 27 *November* 1980. *Accepted* 9 *March* 1981)

Summary—The application of a simple and inexpensive method, flow nephelometry, to the assay and measurement of relative bioactivity of polyene antibiotics is reported. The responding organism was *Saccharomyces cerevisiae* NCYC 239 in the mid-exponential phase of growth. The relative bioactivity of the polyene antibiotics is shown to be in the order lucensomycin > nystatin > candicidin > amphotericin B > pimaracin. The method is suitable for automation.

Polyene antibiotics have been used for many years as pharmacological agents in human and veterinary medicine.[1,2] Such antibiotics are also widely used in biochemical studies of the structure and metabolism of eucaryotic cells.[3]

A number of diverse analytical methods have been proposed for the quantitative, qualitative and bipotency analysis of the polyene antibiotics.[4] In particular, microbiological methods[5] and (increasingly during the last decade) physicochemical methods[6] have been reported for the assay of these antimicrobial agents. However, the only methods reported for combined quantitative and biopotency assay of polyene antibiotics have been classical microbiological methods[7] and flow microcalorimetry techniques using viable micro-organisms.[8–11] Both these types of method suffer from certain drawbacks. The most widely used classical microbiological method is the agar plate diffusion assay. In this method the diameters of zones of microbial-growth inhibition induced by standards and unknown samples of drugs are directly related to the logarithms of the drug concentrations. However, the zone diameters are affected by many physical and environmental factors.[12] These include the relative biological activities of standard and sample, composition of the medium, size and age of the inoculum, and chemical composition and rate of diffusion of the drugs (both standards and samples), particularly if the raw drug material is heterogeneous in composition. Any comparison made between the biopotency of different polyene antibiotics by classical microbiological techniques is also questionable because the assay methods reported have been conducted under diverse experimental conditions in different laboratories.[13]

Although the reported flow microcalorimetry methods for quantitative and biopotency analysis of polyene antibiotic raw materials[8–10] and derivatives[11] show advantages, such as decreased time of assay (< 1 hr), increased sensitivity and better reproducibility compared to both classical microbiological and other physicochemical methods, they also suffer from certain disadvantages. Flow microcalorimetry instrumentation is also expensive and is not commonly used in routine analytical laboratories.[14]

We have found that by use of standardized experimental conditions and a simple, inexpensive technique, flow nephelometry, polyene antibiotics can be bioassayed quantitatively and their relative biopotency measured. An essential feature of this work is the use of standardized inocula stored in liquid nitrogen,[15] which allows strict comparability between experiments. The responsive organism used in the assays is *Saccharomyces cerevisiae* NCYC 239.

EXPERIMENTAL

Nephelometer

Flow nephelometry readings were obtained by using a Vitatron modular photometer system (type 940.320.MSE; Fig. 1) employing a tungsten light-source, a 546-nm filter and a clear glass cuvette with opaque base (1 × 1 cm). The signal from the flow nephelometer was displayed on a digital read-out system and flow nephelometry curves were recorded on an MSE potentiometric recorder.

Organism, growth and storage

Saccharomyces cerevisiae NCYC 239 was obtained from the National Collection of Yeast Cultures (Food Research Institute, Colney Lane, Norwich). This yeast was selected because its non-aggregating characteristics were appropriate for flow nephelometry. The yeast was maintained on yeast–beef agar slopes made from "Lab Lemco" powder, 1.5 g/l., yeast extract, 3.0 g/l., mycological peptone, 6.0 g/l., glucose, 1.0 g/l. and agar No. 3, 12.5 g/l. Inoculated slopes were incubated at 37° for 24 hr and then at 25° for 24 hr.

Yeast suspensions were prepared in a modification of antibiotic medium No. 3 (Oxoid) containing, in sterilized

* Present address: Sterling Chemistry Laboratory, Yale University, 225 Prospect Street, New Haven, Connecticut 06520, U.S.A.

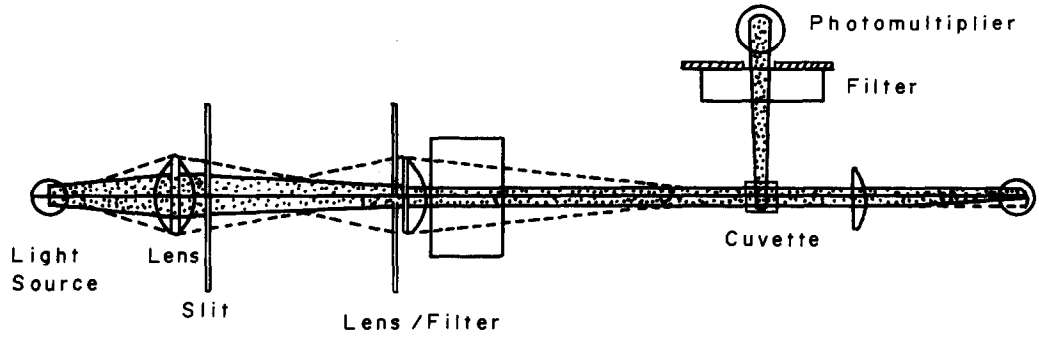


Fig. 1

glass-distilled water, "Lab Lemco" powder, 1.5 g/l., yeast extract, 1.5 g/l., mycological peptone, 5.0 g/l., NaCl, 20.0 g/l., glucose, 11.0 g/l., K_2HPO_4, 1.32 g/l., KH_2PO_4, 3.68 g/l., and adjusted pH 6.0.

Yeast suspensions of *Saccharomyces cerevisae* NCYC 239 were prepared as follows. Sterilized medium (100 ml) was inoculated from a slope and incubated for 24 hr at 30° on a reciprocating shaker (90 cycles/min); 5 ml of this culture were transferred into fresh medium (100 ml) and shaken for 16 hr. Ten flasks were then inoculated (10.0 ml each) from the second culture flask and incubated for 8 hr. The resultant growth was centrifuged, washed and resuspended in a minimal volume of saline (0.9% w/v, about 10.0 ml) and inoculated aseptically into 10 l. of sterile medium [sterility was achieved by use of ethylene oxide (50.0 ml) which was added to the medium and the temperature held for 5 hr at 30° then for 18 hr at 60°, followed by a further 2 hr at 30°] contained in a microfermenter (New Brunswick MF-14). This culture was then incubated at 30°, with stirring at 200 rpm, an air flow of 1500 ml/min and input pressure of 0.3 bar. The fermenter contents were stirred with a magnetic stirrer. After the incubation period (12 hr), at which point the yeast cells were in the early stationary phase, the cells were removed from the medium by centrifugation (MSE High Speed 18, equipped with a continuous-flow rotor; rotor velocity 7000 rpm, throughput rate approximately 400 ml/min). The cells were resuspended in sterile saline and subjected to three washings (MSE 18 bench centrifuge, 4000 rpm for 10 min). The final yeast cream was resuspended in about 250 ml of saline.

Yeast cell numbers and respiratory activity were determined by flow microcalorimetry experiments involving examination of power output *vs.* time curves, as described by Beezer *et al.*[15] and the counting procedure of Ketterer.[16] The yeast cells, in ampoules containing 2.0-ml portions of the cell suspension (equivalent to approximately 10^7 cells/ml), were then frozen in liquid nitrogen as described previously.[15]

Antibiotics

Nystatin and amphotericin B (Squibb and Sons, Ltd, Merseyside, U.K.); pimaracin (natamycin) (C-Gist Brocades, NV, Holland); candicidin (Pharmax, Crayford, U.K.) and lucensomycin (etruscomycin) (Farmitalia, Milan, Italy) were used. All antibiotics were stored, as recommended, under nitrogen at −20° until required, and subjected to ultraviolet spectroscopic investigation (Perkin–Elmer 145 double-beam spectrophotometer) on receipt. Their ultraviolet spectroscopic properties were in accord with the literature values.[6] The polyene antibiotics are heterogeneous mixtures of closely related compounds.[4,6] The materials used in this study were used as received from the manufacturers, *i.e.*, without further purification. These are also the materials used in pharmaceutical preparations. Stock solutions of the antibiotics were prepared in 0.3% dimethylformamide/phthalate buffer (potassium hydrogen phthalate 0.20*M* and sodium hydroxide 0.04*M*), pH 6.0, and stored in the dark before use. Fresh solutions of antibiotics were used for each set of experiments.

Fermenter

Yeasts were grown to the mid-exponential phase of growth in a thick glass fermenter vessel (5.4 cm internal diameter × 8.8 cm depth) of approximately 200 ml capacity. The vessel was sealed with a neoprene ring under a threaded head-plate which contained six ports. These ports were for inlet and outlet tubes to and from the flow nephelometer cuvette, thermometer, antibiotic addition and gas supply. The gas exhaust was fitted with a reflux condenser. The fermenter was placed on a magnetic stirring unit in an annular vessel which allowed circulation of thermostatically controlled water (30 ± 0.2°). Homogeneous cell-suspension was achieved by using a Teflon-coated magnetic stirring bar. The fermenter vessel was sterilized by autoclaving.

Flow nephelometry measurements

For a typical flow nephelometry incubation, 150.0 ml of sterilized growth medium (of the composition given above) were placed in the fermenter vessel and anaerobic conditions were obtained by flushing the growth medium with oxygen-free nitrogen for about 15 min before inoculation and then keeping an atmosphere of nitrogen above the medium. This growth medium was passed through the flow nephelometry cuvette by means of an LKB Perpex 10200 peristaltic pump at a flow-rate of 52.0 ml/min. In order to inoculate the growth medium the following timetable was strictly followed. An ampoule of yeast, stored in liquid nitrogen and containing 10^7 cells/ml was thawed at 40° for 3 min; 2 min after completion of the thawing, the growth medium was inoculated with 1.0 ml of the thawed yeast suspension by means of an automatic Gilson pipette. After 1 min the contents of the fermenter vessel were pumped into the flow nephelometer cuvette (through Teflon tubing of 1.0 mm bore) and then returned to the growth vessel after the "baseline" medium had run to waste.

When the cells in the fermenter vessel had reached the mid-exponential phase of growth (after incubation for 10 hr in the fermenter vessel) solutions of antibiotics dissolved in 0.3% dimethylformamide/phthalate buffer (pH 6.0) were added to the fermenter vessel in 1.0-ml portions from an automatic pipette, so that the final antibiotic concentration was 10^{-6}–$10^{-5}M$. The addition of 1.0 ml of 0.3% dimethylformamide/phthalate buffer (pH 6.0) to the fermenter vessel at the mid-phase of exponential growth of yeast cells served as a control experiment. After each experiment the flow nephelometer cuvette and Teflon tubing were thoroughly cleaned by pumping 0.1*M* sodium hydroxide through the system, followed by sterilized demineralized water.

All experiments were conducted with the same batch of liquid-nitrogen stored inocula and polyene antibiotics. The

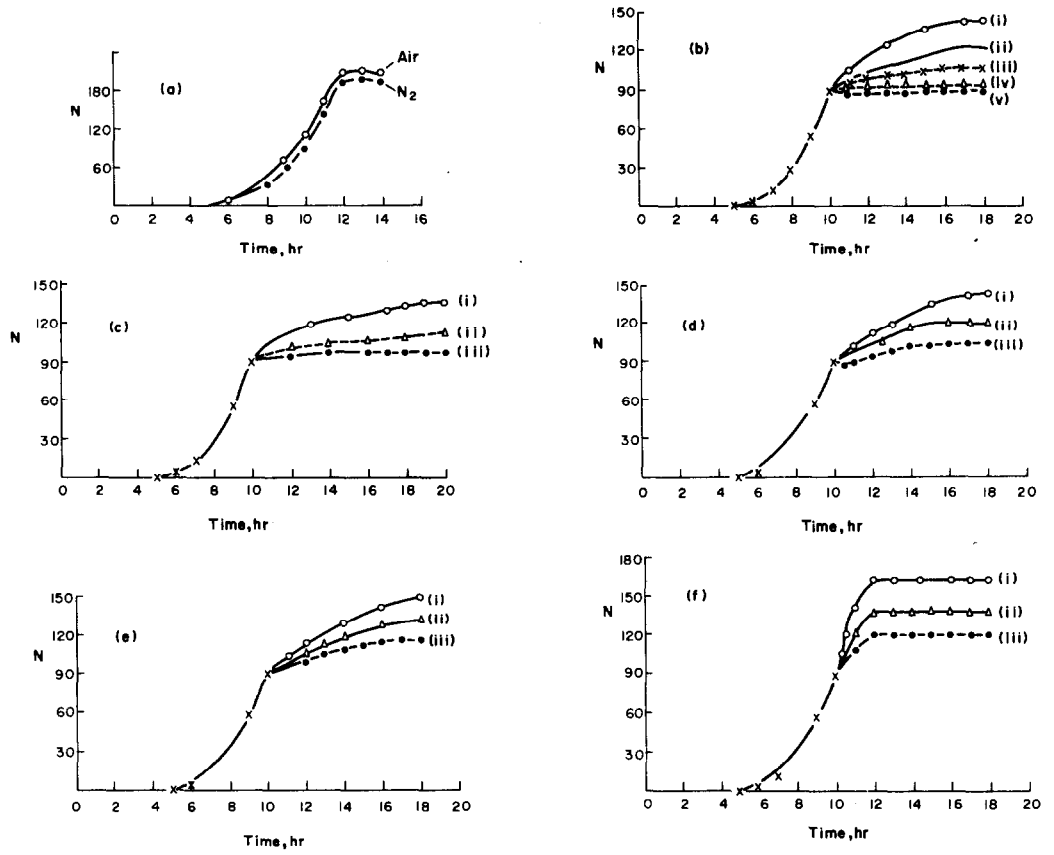


Fig. 2. Flow nephelometry readings (N) for (a) yeast cells alone, and yeast cells in the presence of (b) lucensomycin, (c) nystatin, (d) candicidin, (e) amphotericin B and (f) pimaracin. The antibiotics were present at concentrations of (i) 1×10^{-6} *M* (ii) 5×10^{-6} *M* (iii) 1×10^{-5} *M* except for lucensomycin where the concentrations were (i) 1×10^{-6} *M* (ii) 1.25×10^{-6} *M* (iii) 2.5×10^{-6} *M* (iv) 5×10^{-6} *M* (v) 1×10^{-5} *M*. Initial cell concentrations of 1×10^{7}/150 ml of growth medium. The inoculation takes place at the time indicated by the branching of the curves.

flow nephelometry curves shown above for each antibiotic concentration represent the mean of five determinations. Experiments with yeast cells which had not undergone a freezing procedure gave flow nephelometric curves identical to those for yeast cells which had been frozen, except for a slightly longer, 20 min, lag phase period. All experiments were conducted in a room maintained at 25°.

The nephelometer reading was plotted against antibiotic concentration to give a calibration curve.

RESULTS

Flow nephelometry of yeast cells

Mid-stationary-phase yeast cells added to the growth medium in the absence of antibiotics (Fig. 2a) show a lag phase (A) indicated by a low nephelometer reading. This is followed by exponential growth (B) resulting in an exponential change in the nephelometer readings. When the cells reach the stationary phase (C) the flow nephelometer readings become constant.

The flow nephelometry curve shown in Fig. 2a was not altered if 0.3% dimethylformamide/phthalate buffer was added to yeast cells in the mid-exponential phase.

Addition of drugs to mid-exponential phase cells

The addition of polyene antibiotics to yeast cells at the mid-phase of exponential growth results in flow nephelometry curves (Figs. 2b–2f) which vary according to the nature and concentration of the antibiotics used. The means and standard deviations for flow nephelometry readings of antibiotic-treated incubations are given in Table 1. Plots of the final level of instrument response *vs.* concentration of antibiotic in the fermenter vessel (Fig. 3) give a linear dose–response relationship for the 10^{-6}–10^{-5}*M* range for all the antibiotics tested, except lucensomycin. The information in Fig. 3 can be used for quantitative analysis and bioactivity analysis of the polyene antibiotics tested.

The flow nephelometry curves show that inoculation with the antibiotic rapidly decreases the rate of cell growth (and/or increase in cell size). At certain antibiotic concentrations yeast-growth continues but not at the rate achieved in the absence of antibiotics. The processes which contribute to the shape of the yeast cell–antibiotic flow nephelometry curves are complex and ill understood. Nevertheless the kinetics of the cell–antibiotic interactions are faithfully

Table 1. Typical results for flow nephelometry bioassay of lucensomycin (the other antibiotics studied give similar behaviour)

Time, min \ Concentration, μM	Mean nephelometer reading (±s.d.)				
	1	1.25	2.5	5	10
11	106 ± 3	101 ± 1	95 ± 1	92 ± 1	87 ± 1
12		105 ± 2	97 ± 2	92 ± 1	87 ± 2
13	125 ± 1	109 ± 3	99 ± 1	92 ± 1	88 ± 3
14		111 ± 1	102 ± 1	92 ± 2	87 ± 2
15	138 ± 1	113 ± 2	104 ± 3	92 ± 2	88 ± 3
16		118 ± 2	106 ± 2	92 ± 2	87 ± 2
17	141 ± 2	122 ± 2	106 ± 2	92 ± 2	87 ± 2
18	143 ± 2	122 ± 1	106 ± 2	92 ± 2	

recorded by the flow nephelometer. Because the instrument gives a continuous record of the effect of polyene antibiotics on yeast cells (as do microcalorimetric assays),[8–11] interesting analytical data can be obtained.

DISCUSSION

In flow nephelometry the light scattered by suspended particles, in this case yeast cells, is viewed at right angles to the collimated beam. The scattered-light intensity at a given scattering angle is dependent on the concentration, size and shape of the particles, the wavelength of the incident light and the ratio of the refractive indices of the yeast cells and their surrounding medium.[17] In this instance the technique was used primarily to investigate the possibility of quantitative and bioactivity assay of polyene antibiotics.

The dose–response relationship (instrument response *vs.* concentration) holds over the concentration range 10^{-6}–$10^{-5}M$ for all the antibiotics tested, except for lucensomycin. For this antibiotic there are apparently two linear dose–response relationships: for 1×10^{-6}–$5 \times 10^{-6}M$ and 5×10^{-6}–$1 \times 10^{-5}M$. These findings parallel those obtained by flow microcalorimetry,[9] and it was suggested then that the existence of these two ranges revealed differences in modes of action. For all the polyenes tested, the use of flow

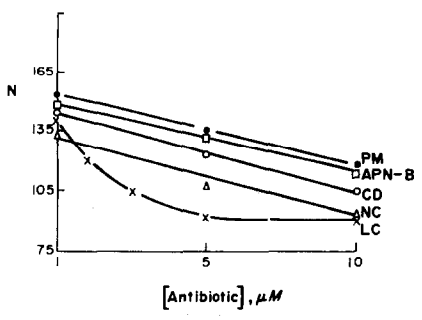


Fig. 3. Dose–response curves for polyene antibiotics by flow nephelometry (PM = pimaracin, APN-B = amphotericin B, CD = candicidin, NC = nystatin and LC = lucensomycin).

nephelometry appears to offer a useful alternative to current[6] bioassay techniques. It possesses the additional advantage that, being a flow system, it is capable of automation. Moreover, since measurements require to be made only over a short time interval (20 min or so) in the otherwise lengthy experiments (~10 hr), the samples can be put into a "train" and examined sequentially. Thus, in practice, some saving in time can result from use of this technique.

Although no detailed explanation can be given to explain the change in flow nephelometer readings for yeast cells in the presence of polyene antibiotics, investigations using this technique could be a valuable aid in exploring the mechanism of action of polyene antibiotics. The change in readings could be due to (*i*) death of micro-organisms (this may be dependent on the age of the cells) (*ii*) shrinkage in overall size of all cells, or (*iii*) combination of (*i*) and (*ii*). Some insight into the mechanism of action and hence the changes in flow nephelometry readings may be obtained by studies of cell viability and size in the presence and absence of polyene antibiotics. Cell size could be determined by using Coulter-counter techniques,[18] which unfortunately were not available to us during the course of this study. However, Brotherton,[18] in determining MIC values and ED_{50} values for some antifungal agents by using a Coulter-counter technique showed that though the cells increased in size they decreased in number, but he gave no indication of the accuracy of the method used, and the method appears not to be suitable for routine bioassay. It should be noted, however, that Venables and Russell,[19] using absorbance measurements, observed a reduction of *ca.* 26% in mean cell size following incubation of cells with nystatin at concentrations comparable to those used in the present study. However, they solubilized their nystatin in dimethylformamide/water mixtures, which may have made the nature of the interaction of the antibiotic with the yeast cells different from that in our study, in which dimethylformamide/phthalate buffer was employed for solubilization of antibiotics. Furthermore, their experiments were conducted in the absence of substrate and over a 90-min time period, compared to the

Table 2. Comparison of bioactivity ranking orders

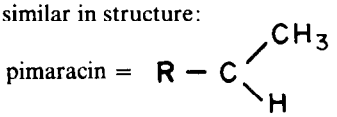
Drug	MIC, μg/ml	Bioactivity ranking order of polyene antibiotics: Flow nephelometry* (equimolar solutions)	Flow microcalorimetry* (equimolar solutions)	"Antiyeast activity"[20]	General order of membrane activity
Nystatin	0.8–3.1	4	4	2	3
Amphotericin B	0.09–0.5	2	2	1	1
Candicidin	0.03	3	3	—	—
Pimaracin	0.9–15.0	1	1	3	2
Lucensomycin	—	5	5	—	2

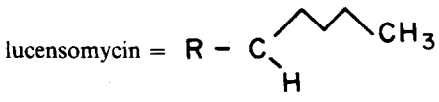
* Experiments conducted in growth media.

several hours of incubation with antibiotics in the present study.

Since the final levels of the flow nephelometry curves represent the final concentration, shape and size of yeast cells in the presence of polyene antibiotics, they can be taken as a measure of the relative biopotency (bioactivity) of these agents (Fig. 3). The relative order of bioactivity of polyene antibiotics obtained in the present study, together with the order obtained by classical microbiological techniques, model membrane studies, diverse "antiyeast experiments"[20] and flow microcalorimetry methods published previously, are shown in Table 2. The relative orders of bioactivity obtained by flow nephelometry and flow microcalorimetry are the same. They differ, however, from other more classically derived orders. Reservations concerning the use of MIC values for bioactivity assay of antibiotics by classical microbiological methods have been expressed by Greenwood.[21] Furthermore the orders of polyene antibiotic bioactivity obtained by studies of model membrane systems and antiyeast activity of polyene antibiotics reflect, perhaps, "the toxicity of the polyene antibiotics rather than their precise mode of antimicrobial activity". Apart from flow microcalorimetry studies and the present flow nephelometry studies no other reports exist of the comparison of the relative bioactivity of polyene antibiotics by use of a wide variety of antibiotics, defined experimental conditions and standardized inocula.

It is also interesting to note the differences shown by lucensomycin and pimaracin in terms of the final flow nephelometer readings at each concentration of the antibiotics used. The two antibiotics are very similar in structure:





However, the flow nephelometry curves show substantial differences in the interaction of these two antibiotics with yeast cells, perhaps confirming that lucensomycin and pimaracin have significantly different modes of action[22] within the concentration ranges studied here. Pimaracin is the only antibiotic which does not cause such an abrupt change in flow nephelometer readings for yeast cells as do the other polyene antibiotics. This may be a further indication of the differences in mode of action between this antibiotic and other polyene antibiotics.

In conclusion, flow nephelometry can be used as a simple, inexpensive, technique for simultaneous quantitative and bioactivity analysis of polyene antibiotics. It is, being a flow system, capable of automation. Information concerning the overall interaction of polyene antibiotics with yeast cells can also be obtained. Further analysis of such information may aid in devising better methods of polyene antibiotic analysis as well as in obtaining data on the mode of action of these antimicrobial agents.

REFERENCES

1. Y. Takahashi and K. Kuroda, *J. Antibiot. (Tokyo) Suppl. II*, 1950, A1.
2. R. Y. Cartwright, *J. Antimicrob. Chemother.*, 1975, **1**, 141.
3. S. McLaughlin and M. Eisenberg, *Ann. Rev. Biophys. Bioeng.*, 1975, **4**, 335.
4. A. H. Thomas, *Analyst*, 1976, **101**, 321.
5. T. B. Platt, J. D. Levin, J. Gentle and M. A. Leitz, in *Analytical Microbiology*, F. Kavanagh (ed.), Vol. 2, p. 147. Academic Press, New York, 1972.
6. B. Z. Chowdhry, *M.Sc. Thesis*, London University, 1975.
7. W. Mechlinski, in *CRC Handbook of Microbiology*, A. I. Laskin and H. Lechevalier (eds.), Vol. 4, pp. 93–107. Chemical Rubber Co., Cleveland, 1973.
8. A. E. Beezer, R. D. Newell and H. J. V. Tyrrell, *Anal. Chem.*, 1977, **49**, 34.
9. A. E. Beezer, B. Z. Chowdhry, R. D. Newell and H. J. V. Tyrrell, *ibid.*, 1977, **49**, 1781.
10. A. E. Beezer and B. Z. Chowdhry, *Experientia*, submitted for publication.
11. *Idem, Talanta*, 1980, **27**, 1.
12. P. Sharma, *Ph.D. Thesis*, London University, 1980.
13. J. W. Lightbown, M. Koqut and K. Uemura, *Bull. Wld. Hlth. Org.*, 1963, **29**, 87.
14. N. Langerman and R. L. Biltonen, in *Methods of Enzymology*, C. Hirs and S. Timasheff (eds.), Vol. 61. Academic Press, New York, 1979.
15. A. E. Beezer, R. D. Newell and H. J. V. Tyrrell, *J. Appl. Bacteriol.*, 1976, **41**, 197.
16. H. Ketterer, *Brauwissenschaft*, 1956, **14**, 59.

17. F. P. Hochgesang, in *Treatise on Analytical Chemistry*, I. M. Kolthoff and P. J. Elving (eds.), Part I, Vol. 5. Wiley–Interscience, New York, 1964.
18. J. Brotherton, *Mykosen*, 1976, **19**, 361.
19. P. Venables and A. D. Russell, *Microbios*, 1972, **6**, 239.
20. J. M. T. Hamilton-Miller, *Adv. Appl. Microbiol.*, 1974, **17**, 109.
21. D. Greenwood, *J. Antimicrob. Chemother.*, 1976, **2**, 312.
22. B. De Kruyff and R. A. Demel, *Biochem. Biophys. Acta*, 1974, **339**, 57.

Talanta. Vol. 28, pp. 653 to 663, 1981
Printed in Great Britain. All rights reserved

0039-9140/81/090653-11$02.00/0
Copyright © 1981 Pergamon Press Ltd

INVESTIGATION AND ANALYTICAL APPLICATION OF THE SULPHIDE–HYPOBROMITE CHEMILUMINESCENCE REACTION

J. TECKENTRUP and D. KLOCKOW*
Universität Dortmund, Abteilung Chemie, Postfach 50 05 00, D-4600 Dortmund 50, FRG

(*Received* 30 *January* 1981. *Accepted* 3 *March* 1981)

Summary—The results of an investigation of the sensitized and non-sensitized chemiluminescence reaction between sulphide and hypobromite in alkaline solution are presented. The reaction can be used for the determination of traces of sulphide at concentrations above $5 \times 10^{-8} M$. For this purpose a special flow system is employed which includes coulometric generation of reagent, and photon-counting. The flow system can also be combined with a special microdistillation apparatus, making it possible to analyse impregnated filters such as are used for the collection of hydrogen sulphide from ambient air.

Chemiluminescence reactions are becoming increasingly important for analytical purposes. This is demonstrated by a number of review articles, which deal with chemiluminescence reactions in liquid[1,2] or gaseous[1,3] media, and their analytical applications.

A few years ago we reported observations of chemiluminescence phenomena accompanying the reaction between sulphide and hypohalite in aqueous solution and proposed applying this system to the determination of traces of sulphide.[4] In the meantime, Burguera and Townshend have found that light is also emitted during the oxidation of sulphide by hydrogen peroxide in the presence of catalysts such as osmium tetroxide or peroxidase.[5,6]

In the following we present the results of our further investigations of the sulphide–hypobromite system and describe the application of this reaction to the determination of small amounts of sulphide. For this purpose a special flow system has been used in combination with coulometric generation of the reagent. We have demonstrated that the technique can be employed for the analysis of impregnated filters such as are utilized for the collection of traces of hydrogen sulphide in ambient air. The proposed separation of the hydrogen sulphide by microdistillation in an inert carrier gas can be combined directly with the flow system.

EXPERIMENTAL

Determination of sulphide in aqueous solution

Flow system. This consists of a peristaltic pump, the coulometric cell and the flow-cell, all interconnected by PVC tubes of 0.7 mm bore (Fig. 1). The pump (Ismatec mp-ge) is equipped with three silicone-rubber tubes of 1 mm bore for the transport of reagents and analyte (channels a, b, c), and with one tube of 3 mm bore for the waste (d). The coulometric cell (Fig. 2), in which bromine is produced by anodic oxidation of bromide, consists of two polyethylene T-joints connected to each other by a silicone-rubber tube. The electrodes are lengths of platinum wire, 1 mm in diameter. The solution of electrolytically generated bromine is mixed with the buffer or a buffered sensitizer solution in a third T-joint (see Fig. 2). The premixed reagent is delivered directly into the flow-cell.

The modular flow-cell (Fig. 3), with an inner volume of 190 μl, is similar to the cell described by Stieg and Nieman.[7] Its inner diameter of 9 mm is the same as that of the cathode of the photomultiplier. The PVC supply lines are simply inserted into the corresponding holes drilled in the PTFE base of the device (see Fig. 3). The premixed reagent and the sample are brought together in the cell. It has proved advantageous to mix the reactants by intensive mechanical stirring with a glass rod inserted into the cell through the central hole.

In order to prevent the solution from leaking out of the stirrer support, the solution is pumped out of the cell to waste at a rate (*ca.* 20 ml/min) more than double that at which the reactants enter it (channels a, b and c: 3 × 2.7 ml/min). The difference in pumping rate is compensated for by air coming into the cell through the stirrer support.

The flow-cell with stirrer and stirrer motor, the coulometric cell and the photomultiplier together with its shield, are mounted in a light-tight photon-counting chamber made from aluminium tube (Fig. 4). The windows of the flow-cell and the photomultiplier are fixed directly face to face in order to minimize light loss. The supply lines are tied in a bundle and passed into the chamber through a black Tygon® tube. The entire photon-counting chamber is cooled by tap water to a working temperature of *ca.* 15°.

Coulometer. The constant-current power supply used for bromine generation was homemade. The current can be adjusted to values between 1 and 1000 μA at voltages up to 27 V.

Photon-counting system. An EMI photomultiplier, type 9862 B/350, is used: its dark-counting rate is about 40 cps at 15° and at 2100 V applied from the stabilized power supply (Ortec 456 H). The pulses at the anode are processed in a pulse counter (Ortec 5 C 1 with pulse-height analyser 5 C 14) and the signals read from an 8-digit display. An internal digital-to-analogue converter allows the count-rates to be registered on a chart recorder. For most purposes the measurements are made from the traces on

* Reprint requests.

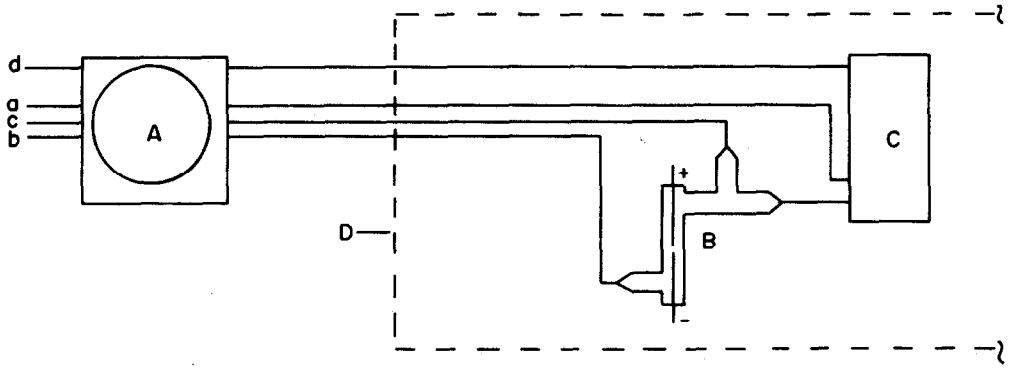


Fig. 1. Flow system, schematic view. A: peristaltic pump; B: coulometric cell; C: flow-cell; D: photon-counting chamber; a, b, c, d: channels for analyte (a), KBr solution (b), buffer (sensitizer) solution (c), and waste (d).

the chart recorder rather than as count-rates from the digital display.

Reagents and solutions. All chemicals used were reagent grade (Merck) unless otherwise specified. Demineralized distilled water was always used for preparing the solutions.

The carbonate buffer stock solution (pH 10.0), is made by dissolving 35.8 g of $Na_2CO_3 \cdot 10H_2O$ and 10.5 g of $NaHCO_3$ (*i.e.*, 0.125 mole of each) in water and diluting to 2.5 l. The stock solution is diluted as required.

The sulphide stock solution, 0.01 *M*, is made by dissolving 0.6 g of $Na_2s \cdot 10H_2O$ in water, adding 200 μl of 1*M* sodium hydroxide, and diluting to 250 ml, and is standardized daily, *e.g.* by potentiometric titration with silver nitrate. The sulphide working solutions are prepared by diluting the stock solution with $10^{-3}M$ sodium hydroxide or $10^{-2}M$ carbonate buffer. Multiple dilution steps should be avoided. The standard flasks used for the dilutions have to be coated with black paint (for protection of the solutions from light) and should be employed only for preparing these sulphide solutions.

The electrolyte solution is $10^{-2}M$ potassium bromide, and the sensitizer reagent consists of 48 mg (*ca.* 1.5×10^{-4} mole) of Azur B (Merck No. 9210) and 30 ml of carbonate buffer stock solution diluted to 3 l. in a polyethylene bottle and kept in diffuse daylight for 3 days, then transferred into a brown glass flask and stored under an inert atmosphere (nitrogen or argon).

Procedure. In order to achieve a good mechanical and thermal stability the instruments are allowed to run for 30 min before the first measurement is made. The following solutions are pumped through the flow system.

Channel a: $10^{-2}M$ buffer or $10^{-3}M$ sodium hydroxide (blank), according to the sample solutions to be analysed.
Channel b: $10^{-2}M$ potassium bromide.
Channel c: sensitizer reagent (permanently kept under inert atmosphere) or $10^{-3}M$ carbonate buffer solution.

The instruments should have the following settings:
Peristaltic pump: feed rate 2.73 ml/min per channel (potentiometer setting 4).
Constant-current source for coulometric bromine production: 8.4 μA ($\equiv 10^{-6}M$ bromine in electrolyte pumped at 2.73 ml/min) for the sensitized reaction in the range between 10^{-7} and $10^{-6}M$ sulphide; 42 μA ($\equiv 5 \times 10^{-6}M$ bromine) for the sensitized reaction in

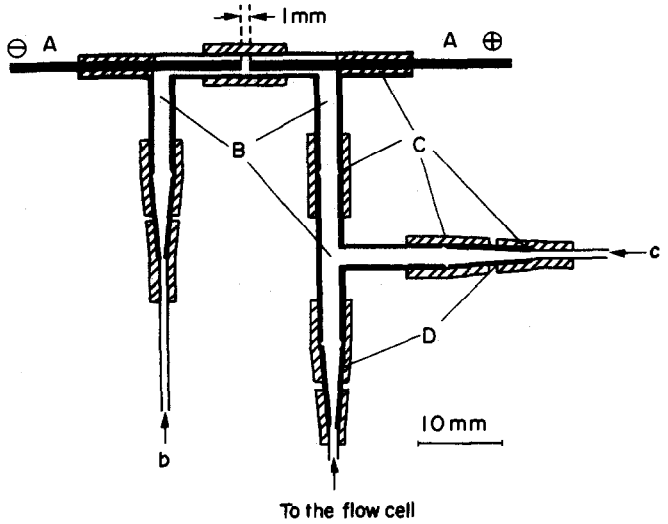


Fig. 2. Coulometric cell. A: platinum electrodes, 1 mm diameter; B: polyethylene T-joints; C: silicone-rubber tubing; D: polyethylene taper joints; b, c: supply lines for KBr solution (b), and buffer (sensitizer) solution (c).

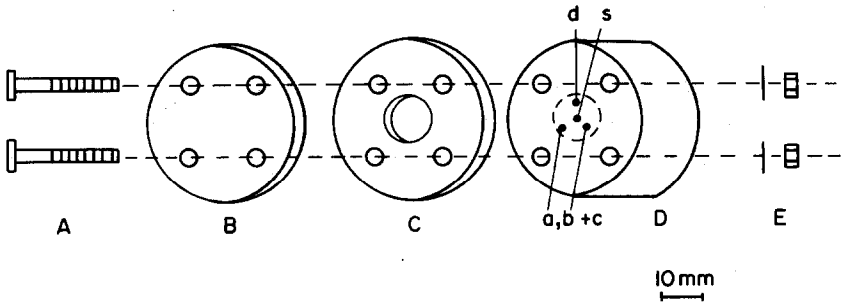


Fig. 3. Flow-cell, exploded view. A: Screws, about 35 mm long; B: window, polyacrylate; C: volume-forming disc, PTFE, with a central hole of 9 mm diameter; D: PTFE base; E: nuts; a, b + c, d, s: holes for the supply of analyte (a) and premixed reagent (b + c), for removal of waste (d), and for the stirrer (s).

the standard range; 420 μA ($\equiv 5 \times 10^{-5} M$ bromine) for the non-sensitized reaction. By comparison with a freshly prepared bromine solution it was shown experimentally that the coulometric efficiency was practically 100% in agreement with results obtained by other authors.[8,9]

Photon-counting system: high-voltage power supply 2100 V (EMI 9862); preamplifier gain ×35; lower threshold 0.05 V; window 0.5 V; counting time 1 sec (10 scc), auto repeat.

After the run-in period, the signals produced by the buffered samples and standards are measured. This is done either by transporting the solutions continuously to the flow-cell in channel a or by injecting them into a constant buffer flow in channel a. For this purpose any suitable injection valve can be employed. The one developed and used in our laboratory will be described elsewhere. The evaluation is made by means of the recorded signal heights, either graphically, or numerically by using second-order linear regression.

Separation of sulphide from impregnated filters

Distillation apparatus. The distillation equipment is employed for the reductive separation of H_2S from filters impregnated with silver nitrate and then loaded with silver sulphide. It is made of a four-way glass valve (a, Fig. 5), the first inlet of which forms a gas-absorption tube (b) of 2 ml volume, and the second is connected to a 10-ml still (c). The still consists of two parts, each fitted with a ground-glass flange and held together by a PVC screw connection. The carrier-gas is supplied by a three-way valve (g), which serves as a delivery valve for the reagent solution as well.

The distillation apparatus is integrated into the chemiluminescence flow system as shown in Fig. 6. The carrier-gas (nitrogen or argon) is passed through a needle valve (B) and a flowmeter (C) to the three-way valve (g). The reduction solution (see below) can be injected into the gas flow by means of a dispenser (D). A reservoir (G) contains the buffer solution used for sample transport. During H_2S separation this solution can be pumped through the connections 3 and 4 of the four-way valve (a, Fig. 5) and through the injection valve (F) into the flow-cell. The inner diameters of the inlet pipes 1, 3 and 4 of the four-way valve (a, Fig. 5) are reduced to about 0.7 mm by insertion of suitable silicone-rubber tubes. This diminished cross-section prevents the receptor solution (see below) in tube (b) from flushing back into the still (c) and keeps the dead volume in the flow system small.

Reagents and solutions. The reduction reagent is made by dissolving 225 g (1 mole) of $SnCl_2 \cdot 10H_2O$ in a mixture of 1 litre of concentrated hydrochloric acid (36–38% w HCl) and 1 litre of water. This reagent has to be kept at room temperature for three days until all sulphur contamination is completely reduced, then it is purged thoroughly with nitrogen or argon. The acid content of the solution is checked titrimetrically and corrected to 5.9M by addition of water or of hydrochloric acid. Acid concentrations greater than 5.9M lead to an unwanted escape of acid during the distillation and hence to neutralization of the absorption solution.

The absorption solution is $10^{-3} M$ carbonate buffer, and the cleaning solution is made by diluting 2 ml of a sulphur-free liquid detergent concentrate, *e.g.*, MC 1000 (Medico Chemie, Düsseldorf) with 98 ml of water.

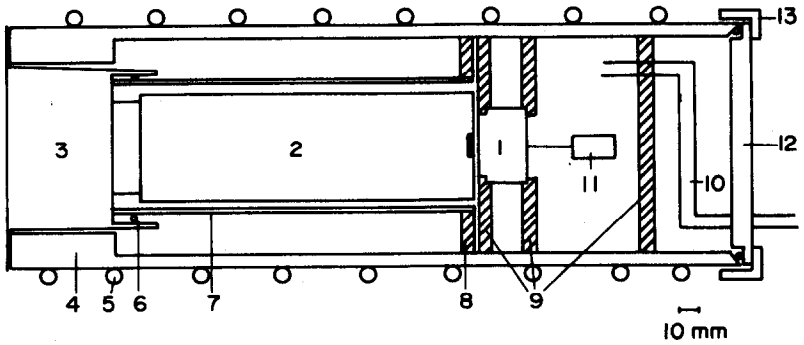


Fig. 4. Photon-counting chamber. 1: flow-cell; 2: photomultiplier; 3: photomultiplier socket; 4: aluminium housing; 5: copper coil for cooling water; 6: O-ring; 7: electromagnetic shield, MU metal; 8: PVC support; 9: PVC supports for the flow system; 10: Tygon® tube carrying the supply lines; 11: stirrer motor; 12: cap; 13: cap nut.

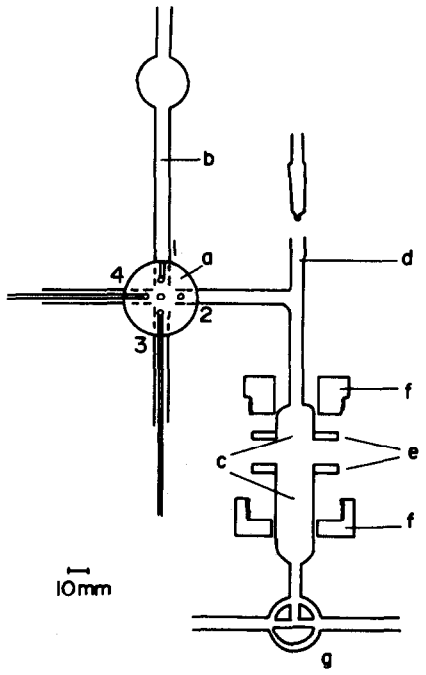


Fig. 5. Distillation apparatus, borosilicate glass. a: four-way valve with inlcts 1, 2, 3 and 4; b: gas-absorption tube; c: two-piece still with ground flanges e; d: tube for feeding the still with a liquid sample, fitted with a ground-glass stopper (NS 7.5); f: screw connection; g: three-way valve.

The impregnation solution[10] is made by dissolving 5.6 g of silver nitrate in water and diluting to 100 ml with addition of 1 ml of 1*M* nitric acid and 10 ml of glycerol.

Precleaning and impregnation of filters and preparation of filter samples. Whatman GF/F glass-fibre filters, diameter 37 mm, are treated with the reduction reagent for 48 hr, with occasional stirring. The liquid is then purged with nitrogen or argon, and the filters are washed with first 1*M* hydrochloric acid and then 1*M* nitric acid in order to remove tin(II) and chloride respectively. Finally the filters are rinsed with water until the rinsings are neutral. The cleaned filters are dried over silica gel in a desiccator and stored there until used. The operations are carried out under a protective atmosphere obtained by passing nitrogen or argon through the washing solutions and through the desiccator. Immediately before preparation of the filter samples the filters are impregnated with the silver nitrate solution. A micropipette is used to transfer 200 μl of this solution onto the centre of a filter, so that only a small outer ring remains unwetted. Onto the still wet filter 5–50 μl of a freshly prepared $10^{-4}M$ sulphide solution are pipetted. In order to avoid contamination from the laboratory atmosphere this loading has also to be performed under a protective atmosphere. The filters can be stored in a desiccator under nitrogen or argon for at least a week without significant changes in sulphide content.

Procedure. When not in use, part (c) of the distillation apparatus (Figs. 5 and 6) is kept filled with 1*M* hydrochloric acid. Before a new series of measurements is started, a thorough cleansing and preconditioning according to the following scheme is necessary. The hydrochloric acid is replaced with cleaning solution and the apparatus is left to stand overnight. Then valve (a) (Figs. 5 and 6) is switched to position X (Fig. 6) and the absorption tube (b) is filled with the absorption solution.

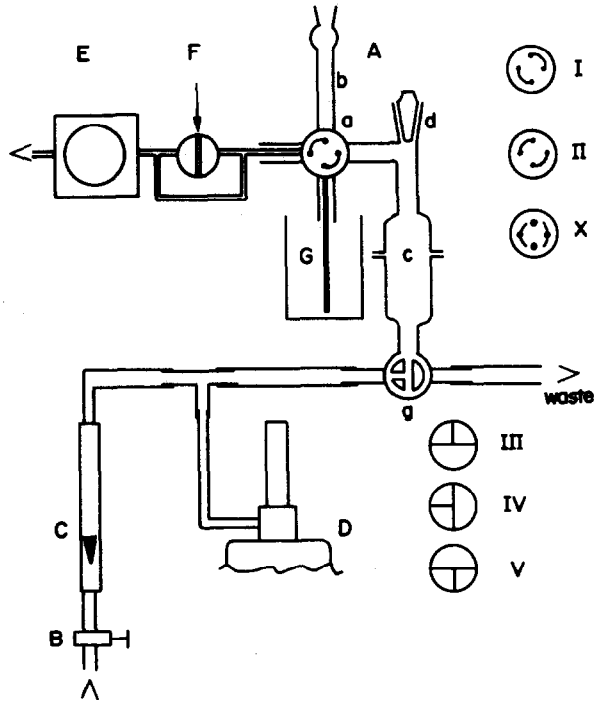


Fig. 6. Integration of the distillation apparatus, A, into the chemiluminescence flow system, schematic view. B: needle-valve; C: flowmeter; D: dispenser; E: peristaltic pump; F: injection valve[25] for feeding the system with sulphide standard solutions; G: buffer reservoir; I, II, X: positions of the four-way valve a; III, IV, V: positions of the three-way valve g; other terms as in Fig. 5.

The still (c) is drained by the three-way valve (g) and rinsed with water. The valve is cleaned and greased and the still is filled again with 1*M* hydrochloric acid. The absorption solution is then sucked out of tube (b) completely, and the four-way valve (a) is disassembled and thoroughly cleaned with diluted hydrochloric acid and water. This valve must not be greased at all. One of the bore holes of the valve has to be carefully dried. It should be specially marked and used only for carrier-gas feed. After the four-way valve has been reassembled, the still (c) is drained (about 30 min after filling).

With a flow of 50 ml/min of argon or nitrogen passing through the distillation apparatus [valve (g) in position IV], the still (c) is opened at the flanges and valve (a) is switched to position I. By this means the analyser flow system is rinsed with the buffer solution contained in the reservoir (G). An impregnated filter, loaded with sulphide, is cut into three strips of about equal size. The strips are put into the still, which is then closed again with the screw connection. One ml of the absorption solution is pipetted into the absorption tube (b), then the generation of H_2S is started by pumping 7 ml of the reduction reagent into the carrier-gas flow by means of the dispenser (D), thus transferring the solution into the still (c). The H_2S formed is transported by the carrier gas to the absorption tube (b), the gas flow preventing the absorption solution from flushing back into the system.

After a reaction time of 12 min the four-way valve (a) is switched to position II. By this means the carrier gas bubbles through the reservoir (G), and the absorption solution is passed into the analyser flow system. The empty absorption tube is rinsed with *ca.* 0.5 ml of absorption solution. The still (c) is then drained by switching valve (g) to position III. The lower part of the still is removed, the filter strips are taken out and the valves switched to their initial positions I and IV, respectively. After reassembly of the still the distillation apparatus is ready for a new sample.

When the apparatus is out of operation the still (c) is filled completely with cleaning solution (if out of use overnight) or with 1*M* hydrochloric acid (if out of use for a longer period). In these cases the two valves are in the positions X and V, respectively.

RESULTS AND DISCUSSION

The non-sensitized reaction between sulphide and hypohalite

Without a catalyst, luminescence could be observed only with hypohalites as oxidants. For our investigation hypobromite was chosen, because it can easily be produced coulometrically and because the light intensities achieved are higher by a factor of 20 than those obtained with hypoiodite. Hypochlorite yields only slightly higher emission intensities than does hypobromite.

The dependence of the luminescence intensity on the hypobromite concentration is very complicated (Fig. 7). For each sulphide concentration a maximum is exhibited, the position of which is shifted towards higher hypobromite concentrations with increasing sulphide concentration. For $10^{-6}M$ sulphide solutions the maximum occurs with 200–300% excess of oxidant; with $10^{-5}M$ sulphide solutions a 500% excess leads to the highest emission intensity. The maxima can be explained by postulating either a non-luminescent competing reaction, or quenching by the hypobromite. Similar behaviour has been found for hypoiodite and hypochlorite.

The chemiluminescence of the reaction may be observed at pH values from 6 to >12 (Fig. 8). This

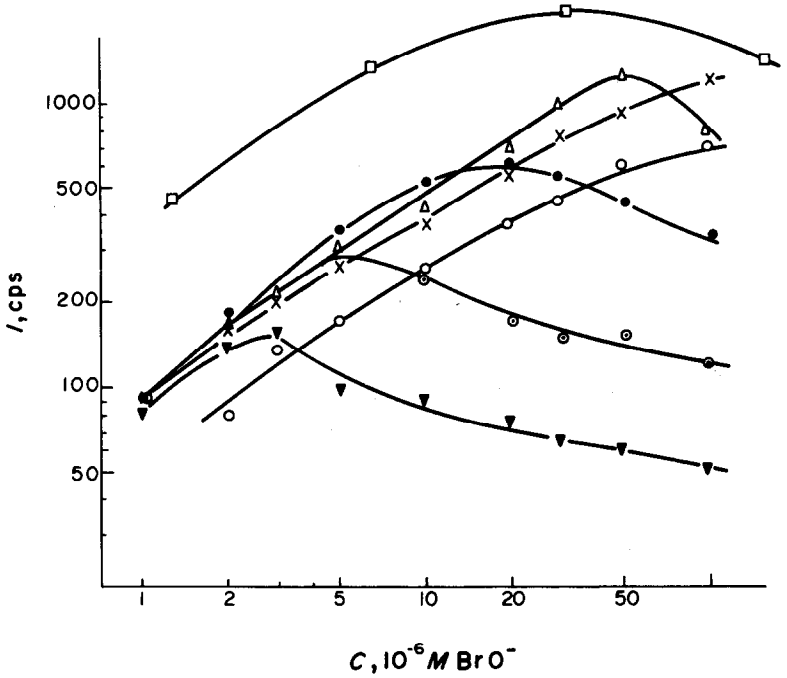


Fig. 7. Chemiluminescence intensity as a function of the hypobromite concentration at different sulphide concentrations. Measurements without sensitizer. Sulphide concentrations: $10^{-6}M$ (▼), $2 \times 10^{-6}M$ (⊙), $5 \times 10^{-6}M$ (●), $10^{-5}M$ (△), $2 \times 10^{-5}M$ (×), $10^{-4}M$ (○). The corresponding curve for hypochlorite as an oxidant (□) was obtained with a $10^{-5}M$ sulphide solution.

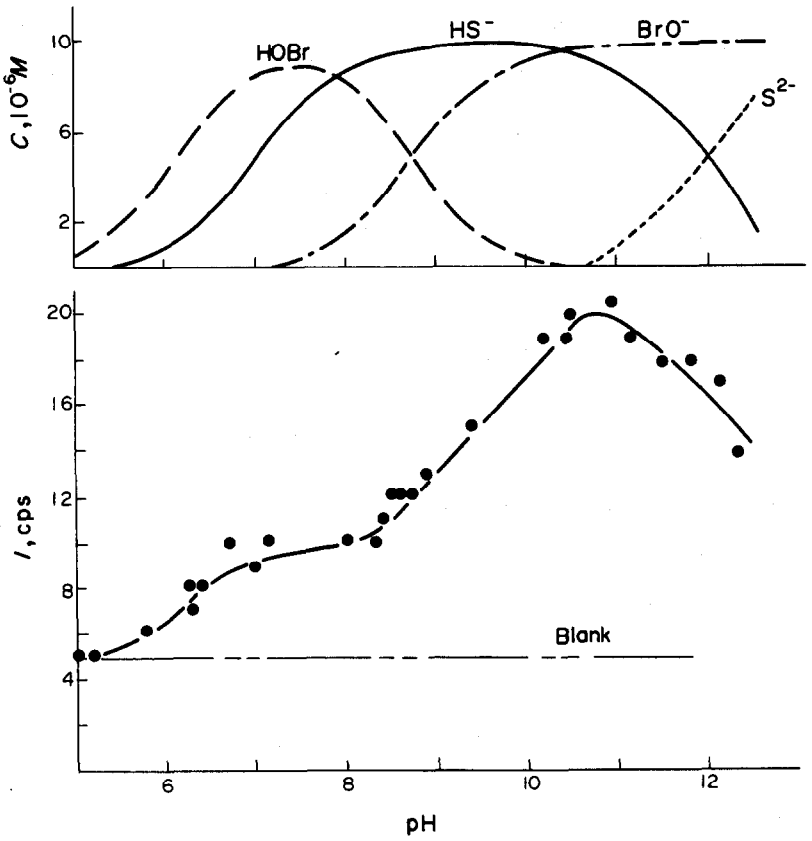


Fig. 8. Lower part: chemiluminescence intensity as a function of pH. Measurements without sensitizer. Channel a: $10^{-5}M$ sulphide in $10^{-4}M$ NaOH; channel b: $10^{-5}M$ hypobromite in $10^{-2}M$ KBr; channel c: $10^{-3}M$ borate or phosphate buffer; pH measured at the waste channel d. Upper part: ranges of existence of HS^- (——), S^{2-} (· · · · ·), HOBr (– – –), and BrO^- (– · –), calculated[26,27] for concentrations of $10^{-5}M$ sulphide and $10^{-5}M$ hypobromite in $10^{-2}M$ KBr.

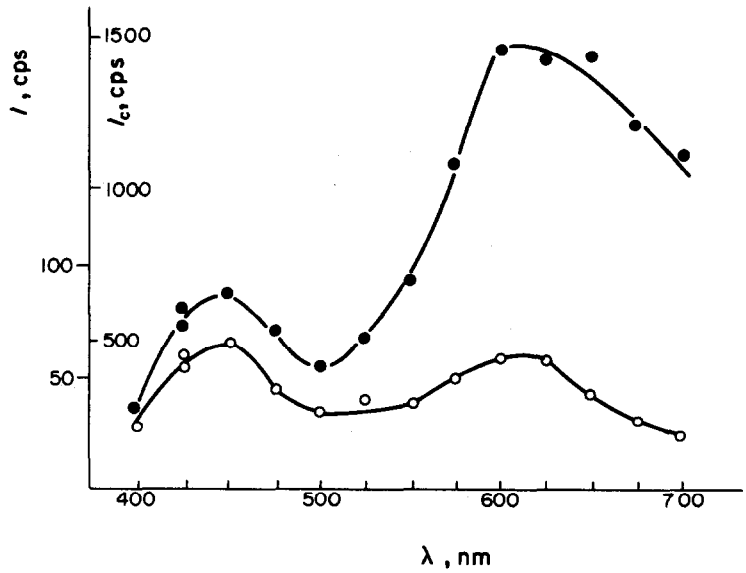


Fig. 9. Emission spectrum for the non-sensitized chemiluminescence reaction between sulphide ($10^{-5}M$ in $10^{-3}M$ NaOH) and hypobromite ($5 \times 10^{-5}M$ in $10^{-2}M$ KBr). Measurements made by inserting interference filters between flowcell and photomultiplier. Filters (type Al, bandwidth 20 nm) obtained from Jenaer Glaswerk Schott u. Gen., Mainz, Germany. O——O: Uncorrected spectrum (intensities I) ●——●: spectrum corrected with respect to transmission of filters and spectral response of the photomultiplier (intensities I_c).

corresponds to the range of existence of the hydrosulphide anion (see Fig. 8, upper part). The distinct increase in the emission intensity at pH above 8 fits remarkably well with the concentration curve of the hypobromite anion (see Fig. 8). A maximum in luminescence intensity is achieved at pH 11. Above this pH the concentration of the sulphide ion increases, whereas the concentration of hydrosulphide decreases. In slightly acidic solutions no light emission can be observed. This phenomenon may be due to the formation of either hydrogen sulphide or hypobromous acid or both (see Fig. 8).

The oxidation of sulphide by halogens leads to different reaction products depending on the pH and the halogen used.[11] In reaction mixtures with low oxidation potential colloidal sulphur is the final product, whereas in strongly oxidizing media mainly sulphate is formed. The oxidation potentials of the halogens and their oxyacids are a complicated function of pH and well-defined stoichiometric reactions can often only be achieved at the ends of the oxidation potential range. In the reaction with iodine in neutral medium elemental sulphur is produced quantitatively, whereas chlorine in a neutral or alkaline medium leads to a complete oxidation of sulphide to sulphate.[11] Under the reaction conditions chosen for the determination of sulphide by chemiluminescence (bromine as oxidant at pH 9.5–11) the formation of a complex mixture of sulphur compounds is to be expected.

The spectrum of the light emitted in the reaction between hypobromite and sulphide shows two maxima, at about 450 nm and 620 nm (Fig. 9). The position of the shorter-wavelength maximum corresponds to the results obtained by Burguera and Townshend[5] who found maximum emission at 440 nm for the reaction between sulphide and hypochlorite and for the catalysed reaction between sulphide and hydrogen peroxide, but did not mention the 620-nm band. At the present time it is not possible to assign the observed emission bands to any particular excited species, though the participation of sulphur in the formation of such an intermediate compound is most probable. This assumption is supported by the fact that besides O_2, S_2 and SO_2 emissions, an SO chemiluminescence with bands in the red region is observed during photolysis of H_2S/O_3 or H_2S/NO_2 mixtures in argon matrices.[12]

The sensitized reaction

In our previous communication[4] we mentioned that the addition of a fluorescent dye can increase the intensity of the emitted light quite dramatically. In spite of its low fluorescence efficiency[13] Methylene Blue in particular yields remarkable amplification factors. A further investigation of this effect showed that all types of Methylene Blue and related thiazine compounds (Azur B, Azur C and Thionine) employed were heavily contaminated by their decomposition products[14,15] (Fig. 10). It became clear that these products play an important role in the sensitization process, though an assignment of the luminescence to individual sensitizer compounds is not yet possible. The most favourable sensitizer solution (Azur B) was found empirically (Fig. 11).

The presence of the sensitizer necessitates some changes in the experimental parameters from those for the non-sensitized reaction between sulphide and hypobromite. Owing to partial oxidation of the sensitizer a distinct increase in the blank signal is observed. Therefore the hypobromite concentration must not exceed $5 \times 10^{-6} M$, so that the amplification factor can be kept as high as possible. The thiazine dyes are deprotonated in alkaline medium ($pK = 12.0$ for Azur B[16]). As a consequence the pH at which maximum light emission is achieved is shifted towards lower values in the presence of the sensitizer. The pH is therefore adjusted to 9.5–10 for the sensitized reaction.

Working ranges and statistical evaluation

Because the sulphide to hypobromite ratio has a significant influence on the emitted light intensity (*cf.* Fig. 7) a linear relationship between sulphide concentration and measured signal over a wide range cannot be expected. In practice, S-shaped calibration graphs are obtained (Fig. 12). Changes in the experimental parameters, especially the use of a new sensitizer sol-

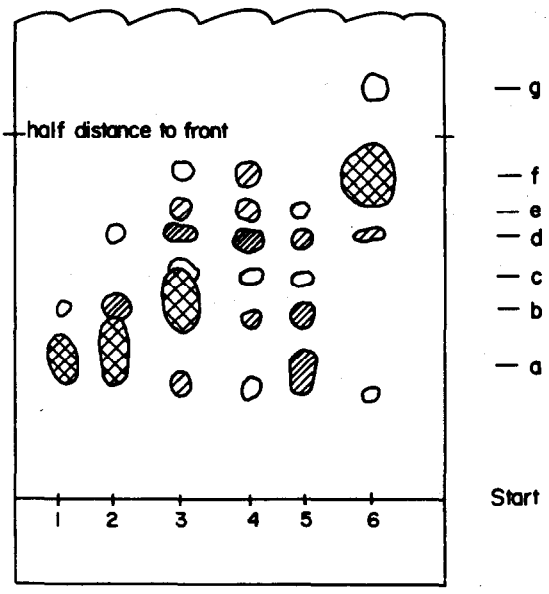


Fig. 10. Thin-layer chromatograms of Methylene Blue and other thiazine dyes. Stationary phase: silica gel; mobile phase: glacial acetic acid + methanol = 2 + 8 v/v. The hatching qualitatively indicates the spot intensities. 1: Methylene Blue, Merck No. 1283, "new" batch; 2: Methylene Blue, Merck No. 1283, "old" batch; 3: Azur B, Merck No. 2910; 4: Azur A, Fluka No. 11665; 5: Azur II (mixture of Methylene Blue and Azur B), Fluka No. 11670; 6: thionine, Chroma No. 11635. Assignment of the spots:[14] a, Methylene Blue; b, Azur B; c, sym. dimethylthionine; d, Azur A; e, Azur C (Methylene Violet?); f, thionine; g, thionol (thiolonine?).

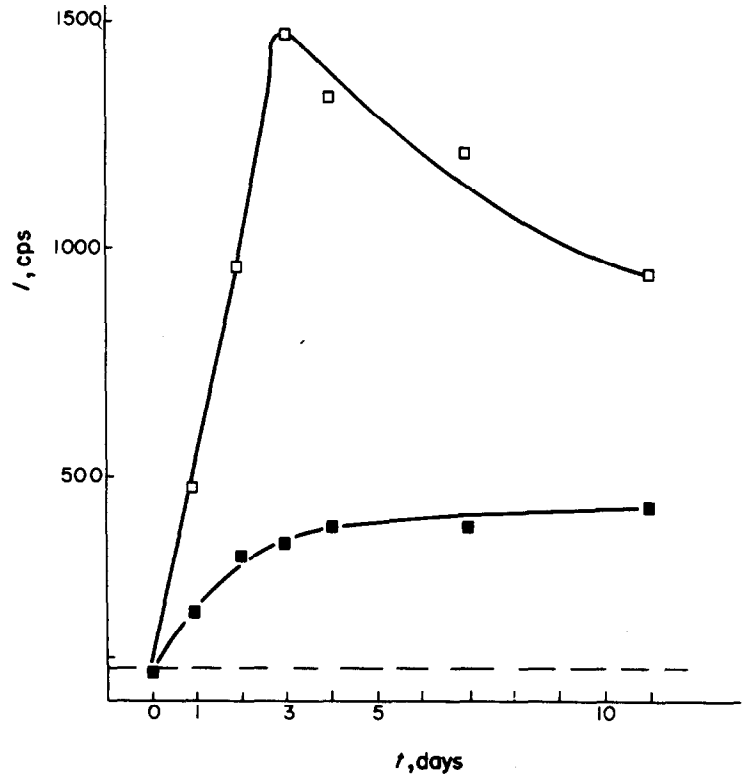


Fig. 11. Activity of Azur B sensitizer solutions ($5 \times 10^{-5}M$ in $10^{-3}M$ carbonate buffer) as a function of time. Measurements made at concentrations of $2 \times 10^{-6}M$ sulphide and $5 \times 10^{-6}M$ hypobromite. Sensitizer solutions stored in the dark (■) and in diffuse daylight (□).

ution, may lead to a distinct shift of the calibration curve. Therefore it is always necessary for standards to be run along with the samples during each series of measurements.

For the sensitized reaction two working ranges were investigated statistically (Tables 1 and 2). The standard range II (Fig. 12), shows satisfactory reproducibility. In the sensitive range I (Fig. 12), a lower hypobromite concentration has to be employed. Here difficulties due to the interaction of the sample with the tubing material become apparent. The sulphide detection limit for range I is $5 \times 10^{-8}M$. At sulphide concentrations above $10^{-6}M$ the non-sensitized reaction can also be used. The corresponding statistical data are presented in Table 3.

The measurements can be evaluated either graphically or by calculation. For this purpose a polynomial of the type

$$y = a + bx + cx^2$$

(second order linear regression), may be derived from the standard signals by means of a least-squares procedure.[17]

The data given in Tables 1–3 were obtained by injecting sample volumes of 1 ml. The time-constant of the counting system at 1 sec counting time is so low that a steady signal is obtained with this sample volume.

Interferences

The interfering compounds investigated and their effects are listed in Table 4. All these substances cause the hypobromite to be partially reduced, so that the optimum hypobromite/sulphide ratio needed for the luminescence reaction (see Fig. 7) cannot be maintained. The deficits caused by mercaptans are remarkably high. Concentrations of non-reactive salts (*e.g.*, KCl, KBr, Na_2SO_4) greater than about $10^{-2}M$ are able to quench the luminescence. No interference was observed which gave rise to positive errors.

The lowering of the signal caused by the presence of sulphite can be partially avoided by addition of formaldehyde,[5] as can be seen from Table 4. Contamination of the analyte by heavy metal ions (*e.g.*, Zn^{2+}, Co^{2+}, Fe^{2+}, Pb^{2+}) will lead to the formation of insoluble metal sulphides which do not yield a chemiluminescence signal. In this case masking of the metal cations with EDTA (up to about $10^{-4}M$ is advisable (see Table 4).

Sample preparation by microdistillation and subsequent chemiluminescence detection

The microdistillation technique was developed for the determination of traces of hydrogen sulphide in ambient air. Because this trace gas is highly sensitive to oxidation, sorption onto surfaces loaded with silver

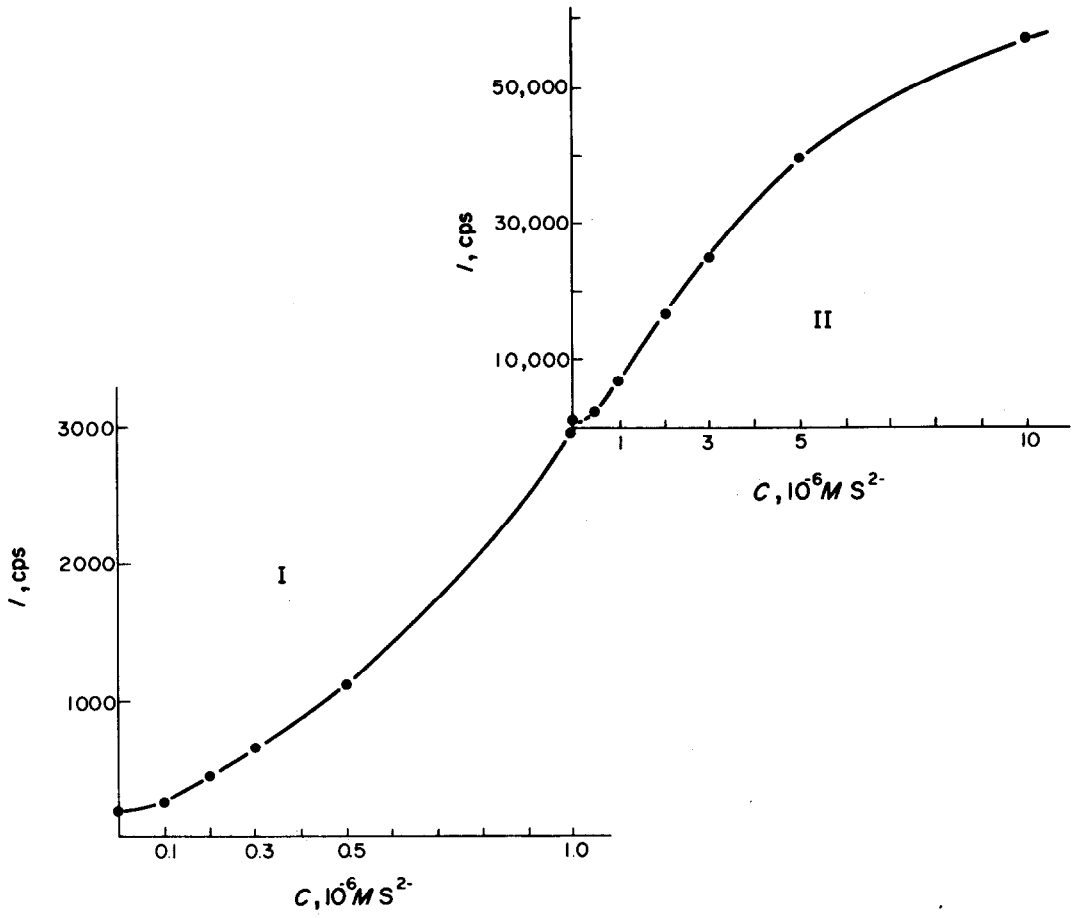


Fig. 12. Calibration curves for working ranges I (0.1–1 × $10^{-6}M$ sulphide) and II (0.05–1 × $10^{-5}M$ sulphide). Regression line for working range I: $I = 156 + 1109 \times 10^{6}C + 1708 \times 10^{12}C^2$. Regression line for working range II: $I = -3341 + 11056 \times 10^{6}C - 499 \times 10^{12}C^2$. $[I]$ = cps; $[C] = M$.

Table 1. Standard deviations for sulphide in range I

c_{taken}, $10^{-6}M$	0.1	0.2	0.3	0.5	1.0
$\bar{c}_{found}$, $10^{-6}M$ (mean of 10 values)	0.085	0.20	0.27	0.54	0.96
s, $10^{-6}M$	0.008	0.02	0.01_4	0.05	0.02

ions is used for sampling,[10,18–20] and also separates SO_2 from H_2S.[18,21] The Ag_2S samples so obtained can be prepared for analysis either by dissolution in a large excess of cyanide[10,19] or by reduction of the silver ions with an acidic tin(II) solution.[18] The latter procedure has the advantage that the hydrogen sulphide produced can be separated from the matrix by distillation. Employing such a technique, Buck and Gies[18] were able to separate and detect as little as 1 μg of sulphide. We have succeeded in reducing this limit by optimizing the distillation apparatus, diminishing the hydrochloric acid concentration of the reduction reagent and keeping the carrier-gas flow-rate low (about 50 ml/min). Separation of the H_2S from the impregnated filter helps to avoid some of the interferences just mentioned. Sulphites, if present, would yield a positive error because of their complete conversion into H_2S by an acidic tin(II) solution.[18] Fortunately, however, trapping the H_2S as silver sulphide separates it from any SO_2 in the air. Sulphates are not reduced by the reagent used, during the distillation time of 12 min.

The filters were impregnated according to a procedure recommended by Jaeschke.[10] Glass fibre filters were chosen because of their resistance towards the

Table 2. Standard deviations for sulphide in range II

c_{taken}, $10^{-6}M$	0.5	1.0	2.0	3.0	5.0	10.0
$\bar{c}_{found}$, $10^{-6}M$ (mean of 10 values)	0.54	0.93	1.93	2.89	4.97	9.58
s, $10^{-6}M$	0.021	0.035	0.08	0.05	0.14	0.60

Table 3. Standard deviations for sulphide in range III (non-sensitized reaction)

c_{taken}, $10^{-6}M$	1.0	2.0	3.0	5.0	7.0	10.0
$\bar{c}_{found}$, $10^{-6}M$ (mean of 10 values)	1.30	2.00	2.79	4.94	7.19	9.83
s, $10^{-6}M$	0.02_4	0.08	0.07	0.37	0.56	0.35

Table 4. Results of interference studies

Interfering compound \ Concentration, M	5×10^{-7}	1×10^{-6}	5×10^{-6}	1×10^{-5}	5×10^{-5}	1×10^{-4}	5×10^{-4}	1×10^{-3}
	Interference							
SO_2	0	0	−31%	−37%	−76%	−83%	S	S
		(0)	(0)	(0)	(−41%)	(−61%)	(S)	(S)
Formaldehyde	0	0	0	0	0	−22%	S	S
SO_2 + formaldehyde	0	0	0	0	0	−34%	S	S
$Na_2S_2O_3$	0	0	−30%	−45%	S	S	S	S
NH_4SCN	0	0	−20%	−25%	S	S	S	S
KNO_2	0	0	0	0	−17%	−25%	S	S
CH_3CH_2SH	−55%	S	S	S	S	S	S	S
EDTA	0	0	0	0	0	0	S	S
							(−41%)	(S)

S = strong negative interference, up to complete quenching of the reaction.
0 = no interference.
( ) = refers to non-sensitized reaction.

Table 5. Recovery, R, for H_2S separation by microdistillation (means of 6 determinations, with standard deviations)

S^{2-} nmole per sample \ Reagent Sample	5 ml of 1M hydrochloric acid 1 ml of sulphide standard solution† R, %	5 ml of reduction reagent 1 ml of sulphide standard solution† R, %	7 ml of reduction reagent impregnated filter* R, %
1.0	90 ± 10	69 ± 12	84 ± 16
2.0	93 ± 5	80 ± 3	79 ± 10
3.0	93 ± 4	99 ± 4	78 ± 8
5.0	91 ± 6	89 ± 5	74 ± 2

* Values corrected for filter blank.
† Liquid samples transferred to still through tube d (Fig. 5).

strongly acidic tin(II) solution. The filters had to be pretreated with this reduction reagent in order to keep the blank values small.

In Table 5 the efficiencies obtained in the microdistillation procedure are listed for four different sample amounts. The separation of H_2S from filters is compared with its separation from pure sulphide solutions [with hydrochloride acid and with acidic tin(II) solution]. The highest yields (92%) are achieved by separating H_2S from a solution acidified with hydrochloric acid (second column of Table 5). The use of tin(II) causes a decrease in efficiency to about 80% regardless of whether the sample is a solution or an impregnated filter (third and fourth columns). Taking into account the filter blank, a detection limit of 0.7 nmole (22 ng) of sulphur per filter was calculated for the overall procedure using the sensitized chemiluminescence reaction.

The distillation procedure in combination with chemiluminescence detection should be suitable not only for the determination of traces of sulphide but likewise for the determination of traces of total sulphur (including sulphate) after reduction to H_2S.[22–24]

Acknowledgement—The financial support of this investigation by the Minister of Science and Research for the State Nordrhein-Westfalen is gratefully acknowledged.

REFERENCES

1. U. Isacsson and G. Wettermark, *Anal. Chim. Acta*, 1974, **68**, 339.
2. D. B. Paul, *Talanta*, 1978, **25**, 377.
3. J. H. Glover, *Analyst*, 1975, **100**, 449.
4. D. Klockow and J. Teckentrup, *Talanta*, 1976, **23**, 889.
5. J. L. Burguera and A. Townshend, *ibid.*, 1980, **27**, 309.
6. J. L. Burguera, A. Townshend and S. Greenfield, *Anal. Chim. Acta*, 1980, **114**, 209.
7. S. Stieg and T. A. Nieman, *Anal. Chem.*, 1978, **50**, 401.
8. E. Bishop, *Mikrochim. Acta*, 1960, 803.
9. R. W. Eldridge and R. P. Buck, *Anal. Chem.*, 1965, **37**, 1242.

10. W. Jaeschke and H. J. Claude, *Staub-Reinh. Luft*, 1978, **38**, 355.
11. *Gmelin Handbuch der anorganischen Chemie*, System-Nr. 6, Weinheim, 1927, p. 260; Erg. Bd. Teil B-II, Weinheim, 1969, p. 392; System-Nr. 7, Berlin, 1931, p. 298; System-Nr. 8, Berlin, 1933, p. 451.
12. D. E. Tevault and R. Smardzewski, *J. Chem. Phys.*, 1978, **69**, 3182.
13. Landolt-Börnstein, *Zahlenwerte und Funktionen aus Naturwissenschaften und Technik*; Neue Serie, Gruppe II, Bd. 3: *Luminescenz organischer Substanzen*, Berlin-Heidelberg, 1976, p. 86.
14. K. W. Loach, *J. Chromatog.*, 1971, **60**, 119.
15. W. W. Dean, G. J. Lubrano, G. H. Heinsohn and M. Stastny, *ibid.*, 1976, **124**, 287.
16. J. Faure and J. Joussot-Dubien, *J. Chim. Phys.*, 1966, **63**, 621.
17. N. R. Draper and H. Smith, *Applied Regression Analysis*, New York, 1966.
18. M. Buck and H. Gies, *Staub-Reinh. Luft*, 1966, **26**, 379.
19. D. F. S. Natusch, H. B. Klonis, H. D. Axelrod, R. J. Teck and J. P. Lodge, Jr., *Anal. Chem.* 1972, **44**, 2067.
20. D. F. S. Natusch, J. R. Sewell and R. L. Tanner, *ibid.*, 1974, **46**, 410.
21. D. F. Adams, W. L. Bamesberger and T. J. Robertson, *J. Air. Poll. Contr. Assoc.*, 1968, **18**, 145.
22. C. M. Johnson and H. Nishita, *Anal. Chem.*, 1952, **24**, 737.
23. H. Silva, *Anal. Lett.*, 1977, **10**, 985.
24. A. Watson, E. Grallath, G. Kaiser and G. Tölg, *Anal. Chim. Acta*, 1978, **100**, 413.
25. J. Růžička and E. H. Hansen, *ibid.*, 1980, **114**, 19.
26. R. C. Weast (ed.), *Handbook of Chemistry and Physics*, CRC Press, Cleveland, Ohio, 1974, D-130.
27. F. A. Cotton and G. Wilkinson, *Anorganische Chemie*, Weinheim, 1975, p. 504.

Talanta, Vol. 28, pp. 665 to 668, 1981
Printed in Great Britain

0039-9140/81/090665-04$02.00/0
Pergamon Press Ltd

INDIRECT METHOD FOR DETERMINING SILICON AND PHOSPHORUS, AND ANALYSIS OF CUBAN LATERITES

GEORGINA L. PINA
Havana University, Cuba

and

T. I. TIKHOMIROVA and E. N. DOROKHOVA
Department of Analytical Chemistry, Moscow State University, Moscow, USSR

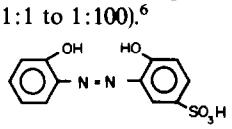
(*Received* 2 *May* 1980. *Revised* 24 *January* 1981. *Accepted* 3 *March* 1981)

Summary—A method has been developed for determining silicon and phosphorus in minerals with high iron content, the method being based on the formation, extraction and stripping of molybdenum heteropoly acids and determination of molybdenum after decomposition of the complexes in the aqueous phase from the stripping.

In the analysis of minerals low in phosphorus and high in silicon, the bulk of the silicon is separated as the hydrated dioxide by treating the sample with mineral acid after an alkaline fusion. Some of the silicon, however, in amount similar to that of the phosphorus, remains in solution. If the silicon content of the mineral is low (<2%), the hydrated silica may not be separated, and it is then necessary to determine a small quantity of phosphorus and a comparatively large amount of silicon in the presence of other ions. In the case of Cuban laterites, these ions are usually Fe(III), Al(III), Ni(II), Cr(III) and Co(II) in amounts at least as large as that of the phosphorus present. Molybdenum heteropoly acids, used for determining Si and P, are formed at a certain ratio between molybdate and mineral acid in the solution. A convenient method for displaying the combined influence of the concentrations of Mo(VI) and of acid is the use of stability diagrams.[1,2]

To enhance the sensitivity, the heteropoly acid can be extracted and then stripped into aqueous medium, where the molybdenum is determined. The extraction methods have been reviewed.[3,4] As the Mo:P molar ratio in the heteropoly acid is 12, this gives a large improvement in sensitivity.

We have already shown that the reaction of molybdenum(VI) with "Chromite Violet K"[5] can be used successfully in this way for determination of phosphorus and silicon over a wide range of concentration ratios (P:Si from 1:1 to 1:100).[6]



Chromite Violet K

EXPERIMENTAL

Reagents

Standard solutions of sodium silicate, $10^{-3}M$, and sodium dihydrogen phosphate, $10^{-2}M$, were prepared by dilution of stock solutions containing 1 mg of silica per ml and 1 mg of phosphorus per ml respectively. The $0.1M$ molybdate solution was prepared by dissolving 30.9 g of ammonium paramolybdate tetrahydrate in 250 ml of water. Other solutions were made from $NiCl_2.6H_2O$, (167 g/l.), $Al_2(SO_4)_3.18H_2O$ (48 g/l.), $Fe_2(SO_4)_3.9H_2O$ (5.6 g/l. in $0.05M$ sulphuric acid), and Chromite Violet K (0.1%). All solutions were stored in polyethylene vessels.

Procedures

Optimization of conditions. The influence of acidity and molybdenum(VI) concentration was investigated by diluting 5 ml of the sodium silicate solution or 0.5 ml of the sodium dihydrogen phosphate solution to about 15 ml in a 25-ml standard flask, with water, adding enough of one of the foreign salt solutions to give a 1–100 molar ratio of foreign element to silicon or phosphorus, then adding various amounts of sulphuric acid and ammonium molybdate, diluting to the mark, measuring the pH and then (after an interval of 15 min) the absorbance at 400 nm, in 1-cm cells against a reagent blank (containing all components except silicate or phosphate). At low acidity an Fe:P ratio of 5 gave a turbid solution, so the effect of Fe(III) had to be studied at higher acidity. Stability diagrams (Fig. 2) were plotted from the curves thus obtained (Fig. 1), as described in the literature.[1,2]

Extraction. The extraction properties were investigated by transferring 10 ml of the heteropoly acid solution (prepared as above) into a separating funnel and extracting silicomolybdic acid (SMA) by adding 5 ml of $5M$ sulphuric acid and 5 ml of isobutanol, and phosphomolybdic acid (PMA) by adding 2 ml of $6M$ sulphuric acid and 5 ml of ethyl acetate, stirring for 3 min and separating the organic layer. The extract was then washed twice with $0.8M$ sulphuric acid, and stripped with 25 ml of $1M$ sodium hydroxide. An aliquot of this solution was placed in a 25-ml standard flask and adjusted to pH 7 with dilute nitric acid, then treated with 1.3 ml of $0.5M$ nitric acid and 2.5 ml of 0.1% dye solution and diluted to the mark with water. The absorbance was measured at 570 nm in a 1-cm cell against water.

Dissolution of sample

A 1-g sample, accurately weighed, is placed in a 250-ml conical flask, 20 ml of *aqua regia* are added, the flask is heated until the bulk of the sample has dissolved, and the

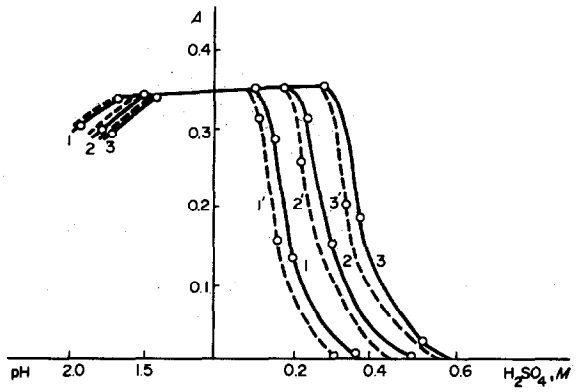


Fig. 1. The dependence of the absorbance of SMA on the sulphuric acid and molybdate concentrations: C_{Mo}: 1, 0.024*M*; 2, 0.060*M*; 3, 0.084*M*. 1', 2', 3'—the same as 1, 2, 3 but in the presence of Fe(III); SMA:Fe(III) = 1:5.

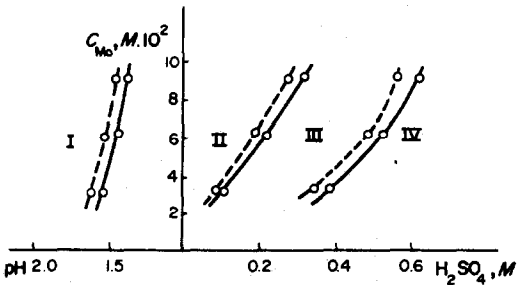


Fig. 2. The stability diagram for SMA: O——O Fe(III) absent; × --- × Fe(III) present.

solution is then evaporated to dryness; 1 ml of concentrated sulphuric and 50 ml of water are added, the mixture is heated to remove nitrogen oxides, and the undissolved residue (mainly silicic acid) is filtered off, the filtrate being collected in a 100-ml standard flask. Samples low in silicon (<2%) are totally dissolved. When the silicon content is high, some phosphorus can precipitate jointly with the silicic acid. In that case, the bulk of the silicon is determined gravimetrically, the precipitate being ignited and weighed, then treated with a mixture of hydrofluoric acid and sulphuric acid in the usual way, ignited and reweighed. The residue is fused with ammonium pyrosulphate, the cooled mass is dissolved in water and filtered, and the filtrate is added to the first filtrate and the mixture diluted with water to the mark.

Phosphorus determination. An aliquot of the solution is taken in a 50-ml separating funnel, and 2 ml of 2% ammonium paramolybdate solution, 1 ml of 5*M* sulphuric acid and water to give approximately 25 ml are added. After 10 min, another 1 ml of 5*M* sulphuric acid and about 5 ml of water are added, and the mixture is shaken with 5 ml of ethyl acetate for 3 min. The aqueous phase is discarded. The organic phase is washed twice with 0.8*M* sulphuric acid to eliminate excess of molybdate. The PMA is decomposed and the molybdate stripped by stirring the organic phase with 25 ml of 1*M* sodium hydroxide. The molybdenum content is determined as described above in the section on extraction. The phosphorus content is calculated from the stoichiometry of the complex (P:Mo = 1:12).

Silicon determination. An aliquot of the sample solution is placed in a 50-ml separating funnel, 1 ml of 2% ammonium paramolybdate solution and 0.5 ml of 5*M* sulphuric acid are added, and water to dilute to about 20 ml. After 10 min, another 5.5 ml of 5*M* sulphuric acid and about 5 ml of water are added and the mixture is diluted with water to about 25 ml. The SMA is extracted by shaking the solution with 5 ml of isobutanol for 3 min. The rest of the procedure is the same as for phosphorus.

RESULTS AND DISCUSSION

The stability diagram in Fig. 1 shows that as the molybdate concentration is increased, the acidity range for maximal absorbance is both broadened and shifted towards higher acidity. Figure 2 is derived from Fig. 1 and shows the acidity/molybdate fields for

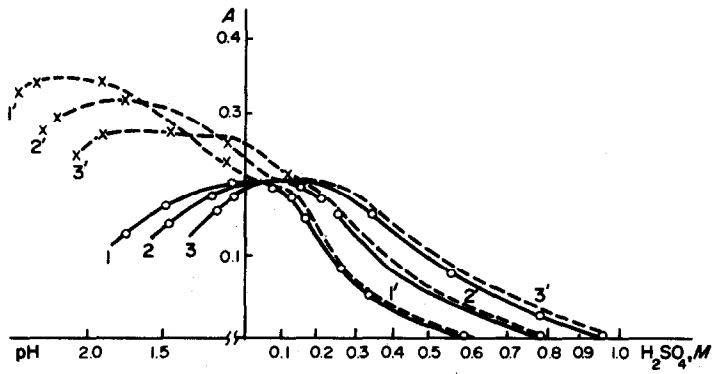


Fig. 3. The dependence of the absorbance of PMA on the sulphuric acid and molybdate concentrations: C_{Mo} and symbols as for Fig. 1.

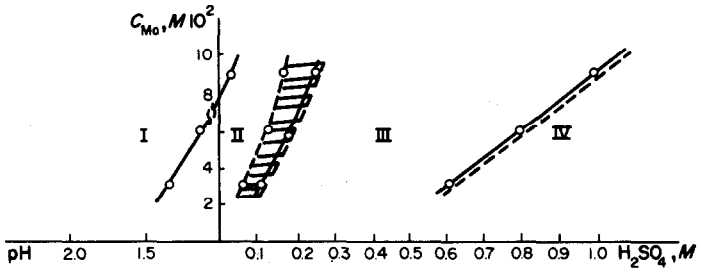


Fig. 4. The stability diagram for PMA: O——O Fe(III) absent; ---- Fe(III) present.

partial formation of the heteropoly acid (I and III), complete formation (II) and non-formation (IV).

Analysis of the stability diagrams shows that of the foreign ions tested, only iron(III) has a significant effect, shifting the regions of partial or complete heteropoly acid formation towards higher pH values. The shift increases with concentration of iron(III). The absorbance is increased by the presence of iron(III), especially when the sulphuric acid concentration is less than 0.1M (Fig. 3), and also the region for complete formation of PMA diminishes sharply (shaded area in Fig. 4). This is due to the formation of a mixed molybdenum–iron–phosphorus complex, which is stable over a wide pH range.[7] It follows that the PMA should be formed at a strictly defined ratio of molybdenum(VI) and sulphuric acid concentrations, found from the stability diagram. Failure to conform to these conditions leads to positive errors in the determination of phosphorus in the presence of iron(III) without extraction and to negative errors in an extraction determination (since the extraction of the mixed complex is poorer than that of PMA). Such errors have been reported in the literature.[8,9] In the light of these conclusions, silicon and phosphorus were determined in artificial mixtures (Table 1) under conditions selected from the diagrams, and a method was worked out for determining silicon and phosphorus in Cuban laterites on the basis of the investigation described above and previous work.[4]

Cuban laterites have a wide range of iron(III) content (0.1–50%), and the usual technique of decomposition by fusion with sodium and potassium carbon-

Table 1. Determination of silicon and phosphorus in synthetic solutions (P:Al:Ni:Co:Cr:Fe = 1:1:1:1:1:5, n = 5)

	Taken, $\mu g/ml$	P:Si	Conditions	Found average, $\mu g/ml$	Std. devn., $\mu g/ml$
P	0.118	1:1	0.4M H_2SO_4 ethyl acetate	0.121	0.004
Si	3.36	1:1	0.4M H_2SO_4 ethyl acetate	3.37	0.11
P	0.116	1:100	0.4M H_2SO_4 ethyl acetate	0.109	0.006
Si	3.36	1:1	1.2M H_2SO_4 isobutanol	3.33	0.13

Table 2. Determinations of silicon and phosphorus in Cuban laterites (6 determinations)

No.	Phosphorus found, 10^{-3}%	Average, 10^{-3}%	Std. dev., 10^{-3}%	SiO_2 in filtrate, % ± std. devn.	Total* SiO_2, %
1	2.1 1.9 2.3	2.1	0.2	2.65	2.65
2	2.1 1.6 1.8	1.8	0.3	1.15 ± 0.01	31.05
3	2.3 2.0 2.5	2.3	0.3	0.43 ± 0.003	15.41
4	2.1 1.6	2.0	0.4	0.43 ± 0.006	17.88

* The sum from the gravimetric determination (if done) and the analysis of the filtrate.

Table 3. Estimation of the accuracy of the method

Element	Initial amount,		Amount added,		Total amount,		Mean found,*	
	$10^{-3}\%$	mg	$10^{-3}\%$	mg	$10^{-3}\%$	mg	$10^{-3}\%$	mg
P	9.3		9.2		18.5		18.4	
	8.9		8.5		17.4		16.2	
	9.8		10.1		19.6		18.7	
	3.8		3.8		7.6		7.7	
	4.8		4.8		9.6		9.5 (n = 6)	
	3.2		3.2		6.4		6.4 (n = 6)	
Si		0.430		0.680		1.110		1.090
		1.151		1.148		2.299		2.285

* Average of two results except where indicated.

ates fails to provide satisfactory results. The minerals can, however, be dissolved by fusion with acid fluxes (potassium bisulphate or pyrosulphate) or treatment with *aqua regia.*

The molybdenum can be determined with Chromite Violet K as described, or the thiocyanate photometric method or atomic-absorption. The detection limit is about the same for all three methods, 5 μg/ml. The atomic-absorption method is applicable only over a relatively narrow range, however.

The method has been used to analyse some Cuban laterites (Fe 30–50%, Al 1–10%, Ni 1–2%, Cr 1–2.5%, Co 0.01–0.15%, Si 1–15%, P 10^{-3}–10^{-2}%); the results are given in Table 2. The accuracy of the method was tested by the standard additions method and the results are given in Table 3.

If the silicon content of the sample is not very high (less than 2–2.5%) it is not necessary to separate the hydrated silica (*e.g.*, sample 1 in Table 2). If the silicon content is high, about 0.2–1 mg of silicon remains in the filtrate after separation of the hydrated silica.

REFERENCES

1. L. Duval, *Chim. Anal. Paris*, 1963, **45**, 237.
2. E. N. Dorokhova and O. G. Cherkasova, *Zh. Neorgan. Khim.*, 1975, **20**, 2782.
3. E. N. Dorokhova and I. P. Alimarin, *Usp. Khim.*, 1979, **48**, 930.
4. S. J. Simon and D. F. Boltz, *Anal. Chem.*, 1975, **47**, 1758.
5. N. V. Arslanova, A. S. Myasoedova and F. P. Sudakov, *Zh. Analit. Khim.*, 1971, **26**, 947.
6. G. L. Pina and T. I. Tikhomirova, *ibid.*, 1978, **33**, 2377.
7. E. N. Dorokhova, Z. F. Shakhova and L. A. Sazanova, *ibid.*, 1966, **21**, 884.
8. P. Pakalns, *Anal. Chim. Acta*, 1968, **40**, 1.
9. Yu. F. Shkaravskii, L. Ya. Kulik and V. V. Chernogorenko, *Zavodsk. Lab.*, 1976, **42**, 141.

Talanta, Vol. 28, pp. 669 to 674, 1981
Printed in Great Britain. All rights reserved

0039-9140/81/090669-06$02.00/0
Copyright © 1981 Pergamon Press Ltd

ION-EXCHANGER COLORIMETRY—VII

MICRODETERMINATION OF IRON(II) AND IRON(III) IN NATURAL WATER

SATORU NIGO, KAZUHISA YOSHIMURA and TOSHIKAZU TARUTANI

Department of Chemistry, Faculty of Science, Kyushu University 33, Hakozaki, Higashiku, Fukuoka, 812 Japan

(*Received* 15 *July* 1980. *Revised* 24 *February* 1981. *Accepted* 2 *March* 1981)

Summary—A trace method for iron, based on ion-exchanger colorimetry, has been developed. 1,10-Phenanthroline is used as the colour reagent for iron(II) and citrate as the masking reagent for iron(III). Total iron can be determined after reduction of iron(III) to iron(II) with hydroxylamine. It is possible to determine iron at μg/l.-levels in different oxidation states in natural waters.

Iron occurs in two oxidation states in nature, and spectrophotometric determination of iron in different oxidation states in water has been investigated by several workers.[1–4] For the determination of iron at μg/l.-levels in natural waters, an appropriate preconcentration process is usually required.[5] This process is time-consuming and the proportion of iron(II) and iron(III) may be altered by atmospheric oxygen in the course of analysis.

A new spectrophotometric method, ion-exchanger colorimetry, based on the direct measurement of the resin phase absorbance after the sorption of coloured sample complex species, has been reported.[6–11] In this paper, it is used for determination of traces of iron, with 1,10-phenanthroline as colour reagent.

EXPERIMENTAL

Reagents

All chemicals used were of analytical grade and demineralized water was used.

Standard iron(III) stock solution (1000 ppm). Prepared by dissolving 4.32 g of ferric alum in 10 ml of concentrated hydrochloric acid and diluting to 500 ml with water.

Standard iron(II) stock solution (1000 ppm). Prepared by dissolving 3.51 g of ferrous ammonium sulphate hexahydrate in 2 ml of concentrated hydrochloric acid and diluting to 500 ml with water. The solution was standardized by EDTA titration.[4]

1,10-Phenanthroline solution (0.2%). The reagent (2 g) was dissolved in 1 litre of hot water, and the solution was cooled.

Dowex 50W-X2 (100–200 mesh) or Dowex 50W-X4 (200–400 mesh) (hydrogen form). Conditioned, air-dried, and stored in a polyethylene container.

Procedure for the determination of iron

For the determination of total iron in a 200-ml water sample (containing 1–50 μg of total iron), 5 ml of 10% hydroxylamine hydrochloride solution, 10 ml of 25% diammonium hydrogen citrate solution, 5 ml of 0.2% 1,10-phenanthroline solution and 0.50 g of Dowex 50W-X2 resin were added. The mixture was stirred for 30 min, the coloured resin was collected and the resin slurry transferred to a 1-mm quartz cell. The absorbances at 514 and 630 or 700 nm were measured.

For the determination of iron(II) in a 200-ml water sample [containing 1–50 μg of iron(II)], the same procedure was used but without the addition of hydroxylamine hydrochloride, and the system was shielded from light throughout. The absorbances of the coloured resin should be measured within 6 hr.

For the determination of lower levels of iron in water, a 1-litre water sample (containing 1–50 μg of iron) was used. The reagents described above were added in 5 times the amount, with the exception of the resin. After the solution has been stirred with 0.50 g of Dowex 50W-X4 resin (200–400 mesh) for 30 min, the absorbance of the resin phase was measured as described above.

When natural waters were sampled, 10 ml of concentrated hydrochloric acid per l. of sample solution were immediately added. The samples were filtered if necessary. For the determination of total iron, it was found important to add 5*M* ammonia solution dropwise after addition of the hydroxylamine solution and to adjust the pH to about 2, because the reduction of iron(III) by hydroxylamine is fairly slow at pH 1. When the amount of iron(II) is determined, 5*M* ammonia solution should be added dropwise to the solution after the addition of citrate buffer solution, to neutralize the hydrochloric acid present. In the absence of the buffer, local hydrolysis of iron by the addition of ammonia solution may arise and the colour development be suppressed.

Absorbance measurements

A Hitachi recording spectrophotometer (Model EPS-2U) was used, with a perforated metal plate (of absorbance 1.0) set in the reference beam to balance the light intensities. The absorbances at 514 and 700 nm were read from the chart.

The net absorbance at 514 nm of the complex species sorbed on the resin, $A_{RC(514)}$, is obtained from the following equations:

$$A_{RC(514)} = A_{(514)} - A_{(700)} - A_R^* \quad \text{(for sample)}$$

$$A_R^* = A_{(514)} - A_{(700)} \quad \text{(for blank)}$$

where A represents the overall absorbance at the wavelength indicated and A_R^* is the difference between the resin background absorbances at 514 and 700 nm. A_R^* should be determined separately for total iron and for iron(II) determinations.

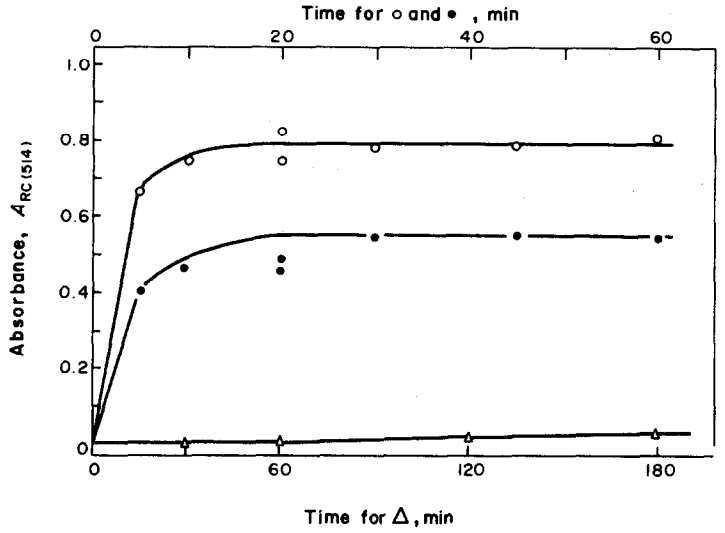


Fig. 1. Time-dependence of colour development. Solution 200 ml (pH 5.0); ○—0.15 ppm Fe(III), procedure for total iron; ●—0.10 ppm Fe(II), △—0.50 ppm Fe(III), procedure for Fe(II). Resin, Dowex 50W-X2 (100–200 mesh, H^+ form), 0.50 g.

Alternatively, the absorbance measurements could be made with air as reference, with a Hirama single-beam spectrophotometer, Model 6B, which can measure absorbance in the range 0–4. The absorbances were measured at 514 and 630 nm in this case.

RESULTS AND DISCUSSION

Only cation-exchange resins sorb the iron(II)–1,10-phenanthroline complex, $Fe(phen)_3^{2+}$, and the absorption spectrum is the same as that of an aqueous solution.[6] The absorbances at the absorption maximum (514 nm) and in a range where only the resin absorbs light (630 or 700 nm) are used.

Applicability of a single-beam spectrophotometer

A single-beam spectrophotometer was found suitable for the present work. Measurements can be carried out in the absorbance range 1.5–2.5 and at least one cheap single-beam spectrophotometer is available for covering this absorbance range. It is easy to transport, so absorbances can be measured at the sampling point in this field. The detector of our single-beam instrument has to be changed over from an Sb–Cs photo-tube to an Ag–Cs one at 630 nm, so the absorbance of the resin was measured at 630 nm instead of 700 nm, in order to simplify the operation.

Optimization of conditions

Stirring time. The effect of stirring time on colour development was investigated. Iron(III) and iron(II) gave similar results (Fig. 1) and the rate of equilibration was not influenced by the rate of reduction of iron(III) to iron(II). The colour development was almost complete within 30 min, 60 min being required for complete development. A stirring time of 30 min was chosen to keep the analysis time reasonably short.

For the determination of iron(II) in the presence of iron(III), it is necessary to suppress the photoreduction of the iron(III)–1,10-phenanthroline complex.[12] As shown in Fig. 1, 100 μg of iron(III) in a 200-ml water sample gave practically no colour development within 60 min, if the solution was shielded from light. The determination of iron in different oxidation states should be performed as soon after sampling as possible.

For the 1-litre sample system, a longer time was required to reach equilibrium. The use of finer resin beads (200–400 mesh) reduces the equilibration time, however, a stirring time of 30 min used can still be used (although complete equilibrium is not reached).

1,10-Phenanthroline concentration. An amount of reagent greater than that required by stoichiometry, (Fe:phen = 1:3) is needed for complete colour development. In order to minimize the influence of foreign ions, the 1,10-phenanthroline should be in excess, and therefore 2.5 ml of 0.2% 1,10-phenanthroline solution was added for 100 ml of water sample.

Citrate concentration. Diammonium hydrogen citrate was used both as masking agent for iron(III) and as buffer. The addition of more than 20 ml of 5% diammonium hydrogen citrate solution makes it possible to maintain the pH of the solution at 5.0 and to suppress the colour due to the coexisting iron(III) in the determination of iron(II) (Fig. 2). For the determination of iron in different oxidation states, 5 ml of 25% diammonium hydrogen citrate solution per 100-ml water sample proved adequate. The absorbance increased slightly with increasing citrate concentration, owing to the iron impurity in the reagent. The

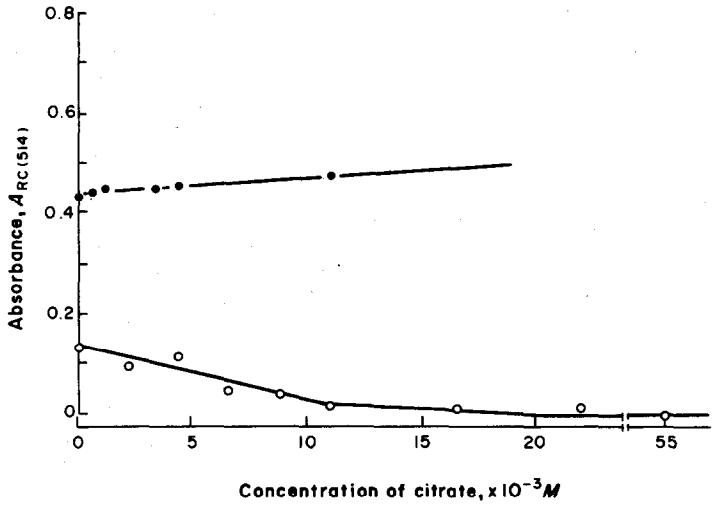


Fig. 2. Effect of citrate concentration on colour development (data obtained with the recording spectrophotometer). Solution 200 ml (pH 5.0), ●—0.10 ppm Fe(III), procedure for total iron; ○—0.50 ppm Fe(III), procedure for Fe(II). Resin, Dowex 50W-X2 (100–200 mesh, H^+ form), 0.50 g. Stirring time 30 min.

background absorbance, A_R^*, should therefore be separately measured for the determination of total iron and of iron(II).

Hydroxylamine concentration. Constant absorbance was obtained with hydroxylamine concentrations in the range 0.002–0.1*M*. For the reduction of iron(III), 5 ml of 10% hydroxylamine hydrochloride solution were employed.

Order of addition of reagents. The order in which the reagents are added is immaterial, except for the hydroxylamine; the absorbance is lower if it is added later in the procedure. To keep the same order as in the procedure for iron(II), hydroxylamine was added first in the procedure for total iron. As iron(III) should be masked by citrate before colour development, it is best to add the citrate buffer before the 1,10-phenanthroline.

Temperature. Constant absorbance was obtained at 20–30°. Below 20° the absorbance decreased, because of the lower rate of sorption of the sample species on the resin. Above 30° the colour reaction is faster and colour development may be complete within 30 min (*i.e.*, the absorbance will be higher). A separate calibration curve should be prepared for use with sample temperatures above 30°.

Calibration

The calibration curves are reasonably linear and may be expressed by the equations:

$$A_{RC(514)} = (4.7 \times 10^{-3})C$$

for 200-ml samples, and

$$A_{RC(514)} = (2.0 \times 10^{-2})C$$

for 1-litre samples in the linear ranges, where C is the concentration of iron in the sample solution, in μg/l. Both iron(II) and total iron can be determined with the same calibration curve, prepared by the procedure for total iron. The sensitivity for 1-litre samples is about 4 times that for 200-ml samples.

Precision and sensitivity

The precision was measured with 200-ml samples, the determination being repeated 10 times. For 0.2-ppm iron solutions, the relative standard deviation was 4.6% with the procedure for total iron. The difference between the background absorbances, A_R^*, for the two procedures is caused by iron in the reagents (Table 1). A_R^* should be determined separately for the two procedures. The relative detection limit,

Table 1. Detection limits

Sample volume, *ml*	Procedure*	*n*	A_R^*†	Detection limit, *μg/l.*
200	A	10	0.059 ± 0.007	6.0
200	B	10	0.049 ± 0.006	5.1
1000	A	6	0.186 ± 0.015	3.0
1000	B	5	0.096 ± 0.005	0.9

*A: Procedure for total iron; B: procedure for iron(II).
†$A_R^* = A_{(514)} - A_{(630)}$ (for blank).

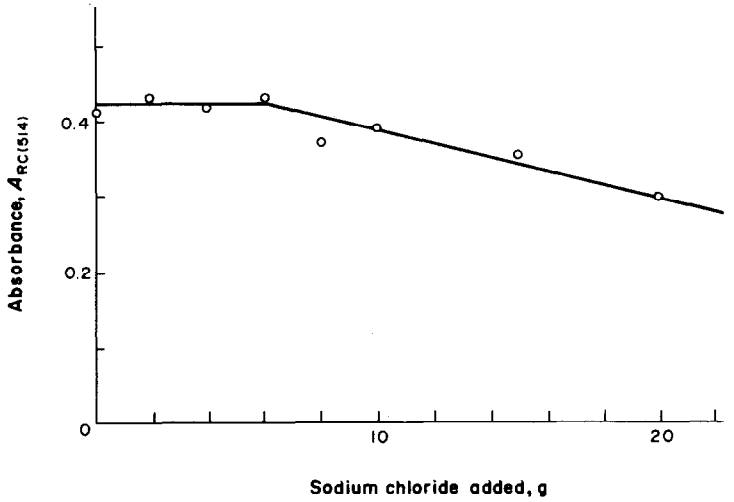


Fig. 3. Effect of background electrolyte (data obtained with the recording spectrophotometer; procedure for total iron). Solution 200 ml (pH 5.0), 0.10 ppm Fe(III). Resin, Dowex 50W-X2 (100–200 mesh, H^+ form), 0.50 g. Stirring time 30 min.

defined as the concentration that produces an absorbance equal to twice the magnitude of the fluctuation in the background absorbance, A_R^*, is also shown in Table 1.

Effect of the concentration of background electrolytes

As shown in Fig. 3, the absorbance decreased as the concentration of sodium chloride increased. The distribution ratio of iron may decrease as the result of competition between sodium ions and iron species. The absorbance was constant at the saline concentration found in sea-water. If the sample solution has a higher saline concentration, it is preferable to use a calibration curve prepared with solutions at the same saline concentration as the sample solution, or to use the standard addition method.

Table 2. Effect of foreign ions on the determination of iron†

Ion	Concentration, *ppm*	A_{RC}	Relative error, %
Fe^{2+}	0.1	0.299	—
		0.338*	—
K^+	100	0.296	−1
Mg^{2+}	100	0.291	−3
Ca^{2+}	100	0.287	−4
Mn^{2+}	100	0.285	−5
Co^{2+}	10	0.285	−5
	100	0.034	−89
Ni^{2+}	10	0.307	+3
	100	0.242	−19
Cu^{2+}	0.01	0.339*	+0.3
	0.05	0.100*	−67
Zn^{2+}	10	0.327	+9
	100	0.096	−68
NO_3^-	100	0.290	−3
ClO_4^-	100	0.287	−4
PO_4^{3-}	100	0.291	−3

* Temperature and amount of resin are different from the others.

† Sample solution 200 ml, 0.1-ppm Fe(III); resin Dowex 50W-X2-H^+ (100–200 mesh), 0.50 g; data obtained with the recording spectrophotometer.

Effect of foreign ions

Table 2 summarizes the effects of foreign ions. The foreign ions tested, except copper, cobalt and zinc did not cause more than 2% error when present at 100 times the concentration of iron, and several caused little interference even when present in 1000-fold ratio to iron. Even when its concentration was only equal to that of iron, copper interfered because of the contribution of its phenanthroline complex to the background absorbance A_R^*. It could not be masked by reagents such as EDTA, but the presence of copper at a concentration one-tenth that of iron did not interfere. The amount of copper found in natural waters is generally much smaller than that of iron. Therefore, the present method may be directly applied to natural water samples. In order to obtain higher accuracy, it is recommended to use the standard addition method.

Table 3 shows that the recovery of iron(III) and iron(II) is satisfactory. The relative error is fairly small.

Application to natural waters

Iron in natural waters may be present as aqua-ions, hydrolysed colloidal iron, complexes with inorganic or organic ligands, and particular matter. For the aqua-ions, the following rate equation has been reported for the oxidation of iron(II) by air at pH >4:

$$-\frac{d[Fe(II)]}{dt} = k[Fe(II)][O_2][OH^-]^2.$$

This equation shows that the rate of oxidation decreases with decrease in pH. In the low pH range

Table 3. Recovery of iron*

Fe(II) added, μg	Fe(III) added, μg	Fe(II) found, μg	Fe(III) found, μg
0.0	19.9	0.0	—
9.9	10.0	10.0	9.5
19.7	99.7	20.1	—
19.7	0.0	19.1	—

* Sample volume 200 ml; temperature 22°.

(pH < 4) the rate of oxidation is independent of pH and only 5% of iron(II) is oxidized in 150 days at pH 2.[13] It is necessary to add hydrochloric acid immediately after sampling, to prevent oxidation of iron(II) in the sample. Mononuclear hydroxo-complexes of iron(III) are inert and may not give the phenanthroline colour rapidly. Adding acid to the sample is also effective for protonation of the hydrolysed iron species. Once converted into aqua-ions, the iron readily produces the colour reaction. Natural organic matter (such as humic acids) and inorganic ligands may be present and form complexes with iron, but the stabilities of these complexes are not high. These complexes, hydroxo-complexes, and part of the colloidal iron can be converted into aqua-ions by the addition of hydrochloric acid.

Figure 4 shows the effect of standing time on colour development after hydrochloric acid has been added to a solution containing colloidal iron. After sodium carbonate solution had been added to a 200 ml of 0.05-ppm Fe(III) solution and the pH adjusted to about 7, 2 ml of concentrated hydrochloric acid added and the mixture was allowed to stand. Formation of the aqua-ions was fairly slow and complete colour development required at least 15 min. By immediate filtration after the addition of hydrochloric acid, the contribution of colloidal iron and also of iron adsorbed on and/or present in particulate matter to the analytical value may be minimized. This procedure will make it possible to determine the concentration of "soluble" iron in different oxidation states in natural waters. If two samples are immediately acidified and one is left to stand for at least 30 min before filtration, whereas the other is filtered immediately, the total iron can be determined from the first sample, and the difference between the two iron results will indicate the amount of "bound" and "particulate" iron.

The method was applied to the determination of iron in hot spring water from Ijiri Spar, Fukuoka. The results of analyses by the standard addition method were 12 μg/l. for iron(III) and 7 μg/l. for iron(II).

REFERENCES

1. A. E. Harvey, Jr., J. A. Smart and E. S. Aims, *Anal. Chem.*, 1955, **27**, 26.
2. H. Tamura, K. Goto, T. Yostuyanagi and M. Nagayama, *Talanta*, 1974, **21**, 314.
3. S. I. Heaney and W. Davison, *Limnol. Oceanog.*, 1977, **22**, 753.
4. Y. Okura, *Bunseki Kagaku*, 1978, **27**, 477.
5. R. B. Willis and D. Sangster, *Anal. Chem.*, 1976, **48**, 59.
6. K. Yoshimura, H. Waki and S. Ohashi, *Talanta*, 1976, **23**, 449.
7. K. Yoshimura and S. Ohashi, *ibid.*, 1978, **25**, 103.

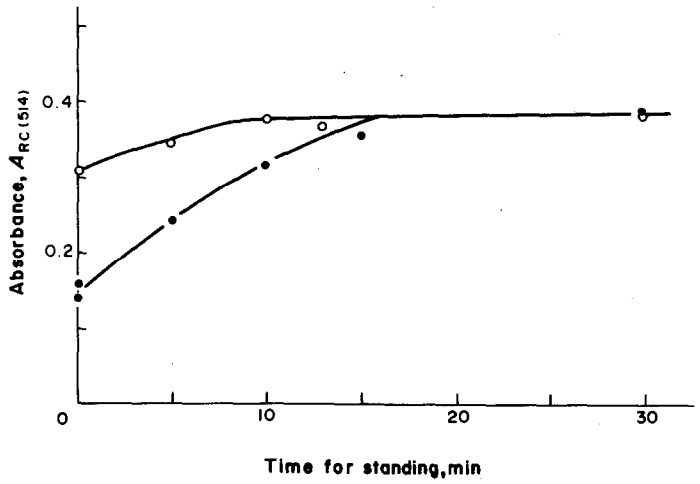


Fig. 4. Effect of standing time on colour development after the addition of hydrochloric acid (procedure for total iron). Solution 200 ml, 0.05 ppm Fe(III). Initial pH: ○—7, ●—9. Resin, Dowex 50W-X2 (100–200 mesh, H^+ form), 0.50 g. Stirring time 30 min.

8. K. Yoshimura, H. Waki and S. Ohashi, *ibid.*, 1978, **25**, 579.
9. Y. Toshimitsu, K. Yoshimura and S. Ohashi, *ibid.*, 1979, **26**, 273.
10. K. Yoshimura and S. Ohashi, *Mem. Fac. Sci., Kyushu Univ., Ser. C*, 1978, **11**, 181.
11. K. Yoshimura, Y. Toshimitsu and S. Ohashi, *Talanta*, 1980, **27**, 693.
12. G. M. Malik and G. S. Laurence, *Inorg. Chim. Acta*, 1978, **28**, L 149.
13. W. Stumm and J. Morgan, *Aquatic Chemistry*, Wiley-Interscience, New York, 1970.

Talanta, Vol. 28, pp. 675 to 680, 1981
Printed in Great Britain. All rights reserved

0039-9140/81/090675-06$02.00/0
Copyright © 1981 Pergamon Press Ltd

IDENTIFICATION ET DOSAGE DES SELS BILIAIRES ET DE LEURS DERIVES CONJUGUES EN CHROMATOGRAPHIE LIQUIDE

A. BAILLET-GUFFROY, D. BAYLOCQ, P. RAFIDISON et F. PELLERIN

U.E.R. de Chimie Thérapeutique, Université Paris-Sud, Laboratoire de Chimie Analytique, Centre de Recherches Pharmaceutiques, 1, Rue J.B. Clément, 92290 Chatenay-Malabry, France

(*Reçu le* 27 *janvier* 1981. *Accepté le* 27 *fevrier* 1981)

Résumé—La détection et le dosage des acides biliaires et de leurs dérivés glyco- et tauro-conjugués sont réalisés par chromatographie liquide à polarité de phases inversée, directe ou après formation de paires d'ions. Les conditions opératoires des deux procédés sont décrites et une interprétation du temps de rétention en fonction de la structure est présentée. Les procédés sont appliqués, après extraction, aux milieux biologiques.

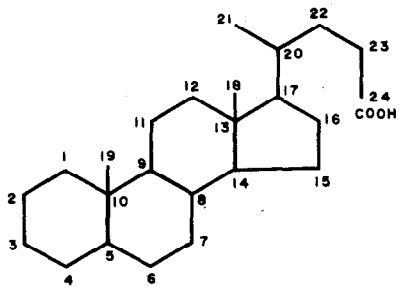
La séparation et le dosage des sels biliaires sous leurs différentes formes présentent un grand intéret en biologie et en clinique. La connaissance de leur métabolisme, les variations pathologiques de leurs taux lors d'une atteinte hépatique conduisent à approfondir leur étude chimique et à perfectionner les méthodes de séparation et de dosage utiles au clinicien pour une meilleure appréciation des fonctions hépatiques.

Les acides biliaires sont des composés stéroïdiques se rattachant au noyau de l'acide 5 β-cholanique (Tableau 1). On distingue classiquement dans les milieux biologiques, deux groupes d'acides biliaires. Le premier comprend les acides synthétisés par le foie à partir du cholestérol:

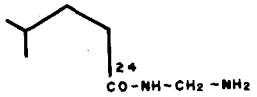
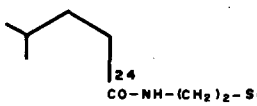
—acide cholique ou acide 3 α, 7 α, 12 α-trihydroxy 5 β-cholanique,
—acide chenodesoxycholique ou acide 3 α, 7 α-dihydroxy 5 β-cholanique.

Le deuxième groupe est constitué par les composés résultant de la deshydroxylation des acides primaires par la flore intestinale:
—acide desoxycholique ou acide 3 α, 12 α-dihydroxy 5 β-cholanique, dérivant de l'acide cholique.

Tableau 1



acide 5 β cholanique

Acide cholique	: 3α, 7α, 12α-trihydroxy 5β-cholanique
Acide desoxycholique	: 3α, 12α-dihydroxy 5β-cholanique
Acide chenodesoxycholique	: 3α, 7α-dihydroxy 5β-cholanique
Acide ursodesoxycholique	: 3α, 7β-dihydroxy 5β-cholanique
Acide lithocholique	: 3α-hydroxy 5β-cholanique
Acide hyodesoxycholique	: 3α,6α-dihydroxy 5β-cholanique
Dérivés glyco-conjugués	
Dérivés tauro-conjugués	

—acide lithocholique ou acide 3 α-hydroxy 5 β-cholanique, dérivant de l'acide chenodesoxycholique.

L'acide ursodesoxycholique est le 7 β epimère de l'acide chenodesoxycholique.

Dans le foie, les acides biliaires sont conjugués avec deux amino-acides, le glycine et la taurine, par formation d'une liaison amide entre la fonction acide carboxylique de l'acide biliaire et la fonction amine de l'amino-acide. Cette réaction se développe dans le foie qui les élimine par la bile sous cette forme.

Les méthodes classiques d'analyse des sels biliaires font intervenir la chromatographie sur couche mince et la chromatographie en phase gazeuse. Elles nécessitent des opérations préliminaires d'extraction et de purification des échantillons précédent une hydrolyse enzymatique, qui transforment les dérivés conjugués en acides libres. Ceci exclut la possibilité de déterminer les teneurs en dérivés conjugués, le taux de conjugaison et le rapport dérivés glyco-conjugués/tauro-conjugués. Ces méthodes impliquent également une dérivatisation préalable des acides en esters méthyliques.

Les opérations nécessaires d'extraction, d'hydrolyse et d'estérification nuisent à la précision des procédés utilisés: elles autorisent une identification spécifique mais les résultats quantitatifs n'ont qu'une valeur approximative et leur dispersion ne permet pas d'apprécier avec une rigueur suffisante les variations normales et pathologiques.

La chromatographie en phase liquide apporte des améliorations sur le plan technique, la précision des résultats et le nombre d'informations utilisables en clinique. Elle a fait l'objet de quelques recherches dans ce domaine, notamment références 1–3. Une étude antérieure[4] a permis de préciser les modalités d'application et de présenter quelques résultats cliniques encourageants pour la poursuite de l'étude.[5]

Le présent mémoire propose deux systèmes d'analyse rapide permettant la séparation directe par chromatographie en phase liquide des acides biliaires et de leurs dérivés sans hydrolyse préalable ainsi que l'étude de leur comportement et plus particulièrement des acides ursodesoxycholique et chenodesoxycholique en fonction de leur structure et de leurs propriétés spectrales et physicochimiques. L'intérêt du procédé est mis en évidence par la description de quelques résultats obtenus sur des sérums sanguins normaux et pathologiques chez des sujets atteints d'hépatites.

PARTIE EXPERIMENTALE

Appareillage

Pompe "Chromatem" équipée d'une vanne à injection munie d'une boucle de 20 μl.

Colonne remplie d'une phase Lichrosorb RP 18 (5 μm, Merck), longueur 15 cm, diamètre 6,35 mm.

Microcolonne de silice greffée en C_{18} (Seppak, Waters).

Système de détection: spectrophotomètre Waters à longueur d'onde variable (200 à 660 nm): lecture effectuée à 201 nm.

Réactifs et échantillons

Solvants purs pour analyse (S.D.S.) distillés, passés sur filtre Millipore puis conservés dans des flacons de verre.

Echantillons témoins de sels de sodium des acides biliaires libres, tauro-conjugués, glyco-conjugués et sulfonés (Calbiochem, Eurobio).

Analyse chromatographique

Solvant I. Méthanol/solution aqueuse de phosphate disodique ($3.10^{-2}M$)/acide perchlorique (Prolabo, 70%, RP Normapur) (76:24:0,02 v/v).

Solvant II. Méthanol/eau/hydroxyde de tétrabutylammonium $5.10^{-3}M$ (75:25:0,8 v/v) additionné d'acide phosphorique (Prolabo, 85%) pour obtenir un pH de 2,8 à 2,9 vérifié au pH mètre.

Ces deux solvants sont filtrés sur Millipore, puis dégazés à la cuve à ultra-sons pendant 20 min. Le débit de ces deux phases mobiles est de 1,2 cm^3/min et la pression de l'ordre de 200 psi. La longueur d'onde du spectrophotomètre est réglée à 201 nm dans la méthode directe et 205 nm dans la méthode avec formation de paires d'ions.

Préparation des échantillons—mode opératoire

Prélever 1 ml de sérum à analyser et le traiter par passages successifs, sur microcolonne de silice greffée en C_{18}, d'eau bidistillée pure puis de 4 mélanges eau–méthanol dans des proportions croissantes en méthanol de 0% à 50%, pour aboutir à une extraction finale par du méthanol pur. Le rendement, déterminé sur des sérums normaux surchargés en acides biliaires, varie de 95% à 100% selon les acides.

Evaporer les filtrats à siccité sous courant d'azote dans un "thermostat à sec" à 80°. Reprendre le résidu par 50 ou 100 μl d'eau bidistillée. Injecter dans la colonne 20 μl de cette solution, par un système de vanne à boucle.

Préparer des solutions aqueuses témoins de sels biliaires à des concentrations comprises entre 10 et 100 μg/ml. Injecter 20 μl de chaque solution.

RESULTATS OBTENUS—DISCUSSION

Optimisation du coefficient d'éxtinction spécifique

Une étude d'optimisation a été effectuée pour améliorer la sensibilité de la détection des acides biliaires par absorption dans l'ultraviolet indépendamment de la séparation chromatographique. La méthode retenue pour cette étude est la méthode Simplex[6–8] présentée par Pesez.

Le facteur à optimiser est le coefficient d'extinction spécifique en lumière ultraviolette, de chaque acide biliaire.

Le mélange méthanol/eau qui sert de solvant de base a un pourcentage fixé à 76% en méthanol et 24% en eau. Les paramètres variables sont la longueur d'onde de lecture, le pH de la solution et la concentration en phosphate monopotassique.

Les pas sont fixés à: $\lambda = 1$ nm, 2 unités pH, $C = 4.10^{-2}M$. Le simplex de départ est le suivant:

Essai	λ nm	pH	$C_{KH_2PO_4}$, M
1	201	2,5	10^{-2}
2	202	2,5	10^{-2}
3	201,5	4,23	10^{-2}
4	201,5	3,06	$4,26.10^{-2}$

Le pH de la solution est ajusté par addition d'acide phosphorique ou d'acide perchlorique. Le coefficient d'extinction spécifique des acides biliaires ne varie pas de façon significative lorsque le solvant est acidifié par l'un ou l'autre de ces acides.

Après étude de plusieurs simplex, nous avons observé des réponses maximales pour trois essais:

λ, *nm*	201	200,6	201,4
pH	3,05	4,04	5,0
$C_{KH_2PO_4}$, $10^{-2}M$	1,0	3,1	4,6

Les valeurs des coefficients d'extinction spécifique sont identiques quelque soit la phase mobile: pH acide à faible concentration en phosphate monopotassique ou pH alcalin avec une concentration en phosphate monopotassique plus élevée.

Des essais chromatographiques effectués avec les trois types de solvant montre que le solvant intermédiaire est le plus favorable.

Séparation des acides libres et conjugués

Le chromatogramme des solutions témoins indique qu'une séparation très efficace des dérivés tauro-conjugués, glyco-conjugués, sulfatés et libres est obtenue (figures 1 et 2).

La méthode permet de déceler des traces d'acides biliaires ou de leurs dérivés conjugués de l'ordre de 1 ng par μl de solution injectée dans l'appareil. Dans le cas de solutions trés diluées, et selon les conditions opératoires retenues, la concentration est proportionnelle à la surface des pics pour des teneurs comprises entre 10 ng et 100 ng par μl de solution injectée (figures 3 et 4).

L'ordre de sortie des différentes acides, sur le chromatogramme, dépend de leur polarité; pour chacun

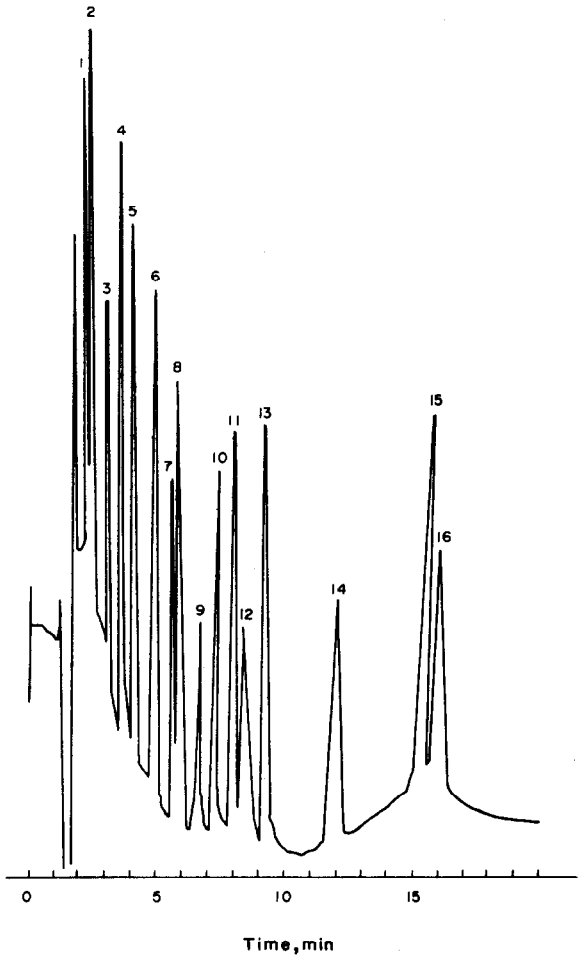


Fig. 1. Chromatogramme d'échantillons standards d'acides tauro-conjugués, glyco-conjugués et libres. Phase mobile: Méthanol/phosphate disodique en solution aqueuse $3.10^{-2}M$/acide perchlorique à 70% (76/224, pH 4). Débit: 1,2 ml/min; détection par spectrophotométrie à 201 nm. Pics: 1 = TUDC; 2 = TC; 3 = GUDC; 4 = TCDC; 5 = TDC; 6 = GC; 7 = KETO; 8 = UDC; 9 = HYO; 10 = TLC; 11 = GCDC; 12 = C; 13 = GDC; 14 = DC; 15 = GLC; 16 = CDC; 17 = LC.

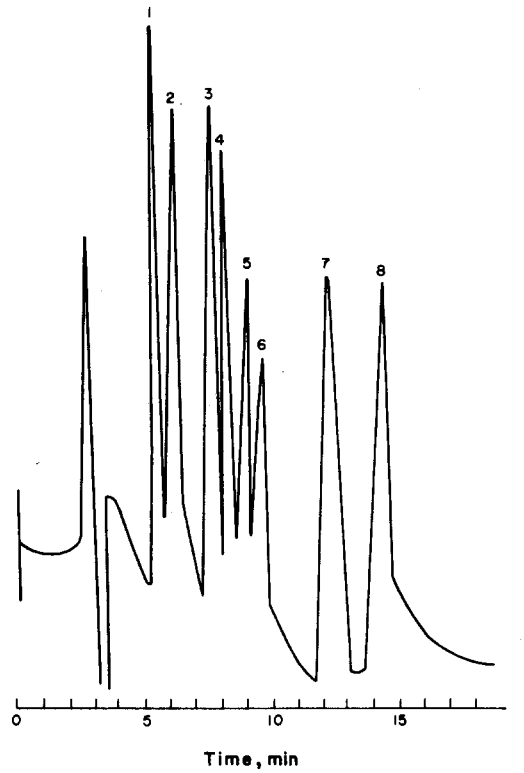


Fig. 2. Chromatogramme d'échantillons standards d'acides tauro-conjugués et glyco-conjugués par formation de paires d'ions. Phase mobile: Méthanol/eau/phosphate de tétrabutylammonium (75/25, TBA $5.10^{-3}M$) pH = 2,85 par addition d'H_3PO_4. Débit: 1,5 ml/min; détection par spectrophotométrie à 210 nm. Pics: 1 = TC; 2 = GC; 3 = TCDC; 4 = GCDC; 5 = TDC; 6 = GDC; 7 = TLC; 8 = GLC.

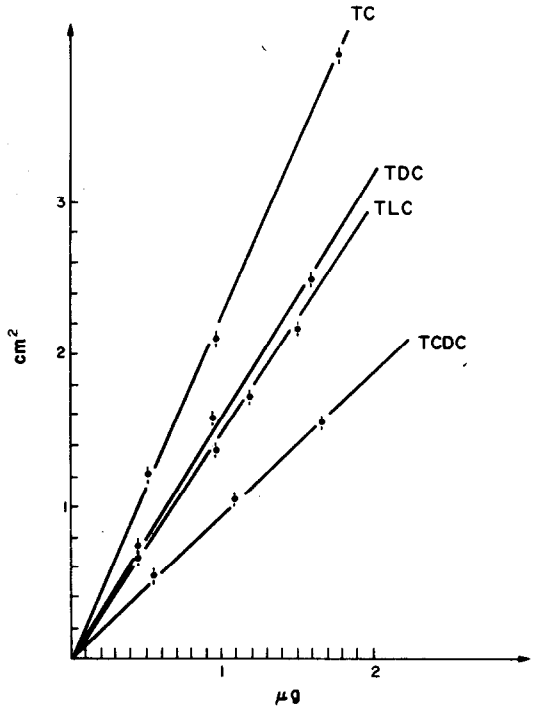


Fig. 3. Dérivés tauro-conjugués: surface du pic en fonction de la quantité injectée.

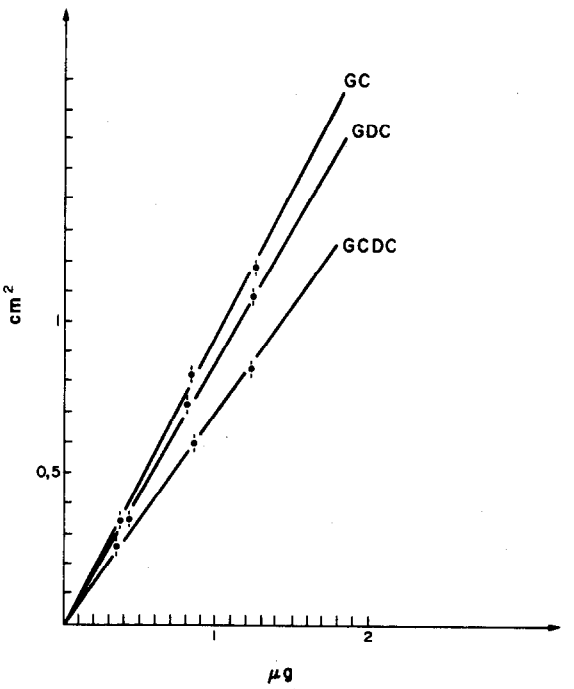


Fig. 4. Dérivés glyco-conjugués: surface du pic en fonction de la quantité injectée.

des acides biliaires, le dérivé tauro-conjugué est élué le premier, suivi du glyco-conjugué puis de l'acide libre. Ceci est en accord avec les valeurs des pK_a en solution aqueuse à 20°;[9] les acides conjugués à la taurine se comportent comme des acides forts avec des pK_a voisins de 1,9. Les pK_a des acides conjugués à la glycine sont de l'ordre de 3,8 à 4,7. Les acides libres, acides faibles dont les pK_a sont compris entre 5 et 6,5 sont donc totalement sous forme moléculaire peu polaire. Au sein des acides tauro- et glyco-conjugués, le composé trihydroxylé est élué le premier puis les dérivés dihydroxylés et enfin le monohydroxylé. Cet ordre d'élution n'est pas suivi par les acides libres, il est le suivant: OH 3 α, 7 β; OH 3 α, 6 α; OH 3 α, 7 α, 12 α; OH 3 α, 12 α; OH 3 α, 7 α; OH 3 α.

La méthode fondée sur la formation de paires d'ions conduit à des résultats différents.

Par suite de la formation d'une paire d'ions entre la fonction acide carboxylique ou sulfonique de l'acide biliaire ou de ses dérivés, et l'hydroxyde de tétrabutylammonium, l'ordre de sortie des composés est seulement lié au nombre de fonctions hydroxylées, successivement TC, GC, TCDC, GCDC, TDC, GDC, TLC, et GLC.

Le cas des acides ursodesoxycholique et chenodesoxycholique mérite une attention particulière. Leur temps de rétention ne paraît pas uniquement lié à leur pK_a. Le temps de rétention de l'acide chenodesoxycholique chromatographié selon la technique directe correspond à celui des acides libres. En revanche, le temps de rétention de son épimère, l'acide ursodesoxycholique, est beaucoup plus faible. Il est en effet élué en même temps que les dérivés glyco-conjugués. Le même phénomène est également observé avec les dérivés tauro- et glyco-conjugués de ces deux acides. L'explication se trouve dans la configuration spatiale des hydroxyles en C_7 située en α pour l'ensemble des acides alors qu'elle se situe en β pour l'acide ursodesoxycholique.

L'interprétation des spectres RMN du proton,[10] du carbone 13, et de spectroscopie infrarouge fait apparaître l'interaction du proton situé sur le carbone C 4 et le carbone C 7. L'encombrement stérique est ainsi moins marqué pour l'acide ursodesoxycholique, sa polarité est plus forte que celle de son épimère et son temps de rétention est plus court en chromatographie liquide à polarité de phases inversée.

Les facteurs de capacité pour chaque groupe de dérivés sont calculés et s'échelonnent pour la méthode directe de 0,60 à 12 (Tableau 2) et pour la méthode d'analyse par formation de paire d'ions de 1,14 à 6,50 (Tableau 3).

La séparation difficile entre les sels conjugués des acides chenodesoxycholique et desoxycholique par chromatographie en phase gazeuse ou par d'autres méthodes classiques d'analyse, est ici réalisable. La résolution des acides taurodesoxycholique et taurochenodesoxycholique est égal à 1,17. La séparation est donc satisfaisante et autorise l'appréciation quantitative de la teneur par mesure de la surface des pics.

Application aux milieux biologiques

Le procédé a été appliqué à l'analyse des sérums normaux et pathologiques.

Dans un premier temps, la reproductibilité de la

Tableau 2. Facteurs de capacité des divers sels biliaires dans la technique directe

		K'
TLC $3SO_4$	Acide taurolithocolique 3 sulfate	0,60
TUDC	Tauroursodesoxycholate de sodium	0,69
TC	Taurocholate de sodium	0,84
GUDC	Glycoursodesoxycholate de sodium	1,30
TCDC	Taurochenodesoxycholate de sodium	1,69
TDC	Taurodesoxycholate de sodium	1,74
GLC $3SO_4$	Acide glycolithocholique 3 sulfate	2,04
GC	Glycocholate de sodium	2,78
KETO	Acide 3α hydroxy 12 keto 9-11 cholénique	3,23
UDC	Acide ursodesoxycholique	3,38
HYO	Acide hyodesoxycholique	4,15
TLC	Taurolithocholate de sodium	4,69
LC $3SO_4$	Acide lithocholique 3 sulfate	5,00
GCDC	Glycochenodesoxycholate de sodium	5,30
C	Cholate de sodium	5,53
GDC	Glycodesoxycholate de sodium	6,15
DC	Desoxycholate de sodium	8,38
GLC	Glycolithocholate de sodium	11,30
CDC	Chenodesoxycholate de sodium	11,46
LC	Lithocholate de sodium	27,15

Tableau 3. Facteurs de capacité des sels biliaires dans la technique par formation de paires d'ions

		K'
TC	Taurocholate de sodium	1,04
GC	Glycocholate de sodium	1,27
TCDC	Taurochenodesoxycholate de sodium	1,81
GCDC	Glycochenodesoxycholate de sodium	1,96
TDC	Taurodesoxycholate de sodium	2,23
GDC	Glycodesoxycholate de sodium	2,54
TLC	Taurolithocholate de sodium	3,5
GLC	Glycolithocholate de sodium	4,39

technique appliquée à des sérums sanguins a été étudiée en ajoutant à des sérums normaux, des quantités connues d'acides libres et conjugués et en procédant à l'extraction dans les conditions de la méthode proposée.

La dispersion expérimentale des résultats dépend de la nature des dérivés et conditionne leur interprétation sur le plan clinique; plusieurs prélèvements sont effectués sur le même échantillon.[11] Dans le cas des acides tauro- et glyco-conjugués, la dispersion des résultats demeure toujours inférieure à 3% et autorise l'interprétation de leur taux pour l'étude des maladies hépatobiliaires. Dans le cas des acides biliaires libres, la dispersion des résultats peut atteindre 15%, en raison des coefficients d'extinction faibles et des facteurs de capacité importants. Les résultats ne sont pas quantitativement exploitables mais présentent seulement un intérêt qualitatif; en effet, la présence d'un ou de plusieurs de ces acides libres est caractéristique de certaines affections hépatiques. Ainsi, la présence d'acide chenodesoxycholique est constatée dans les sérums de sujets atteints de cirrhose, et les acides hyodesoxycholique et cholique dans les sérums de sujets atteints de cholestase par obstruction néoplasique de la voie biliaire principale.

Les chromatogrammes d'un sérum normal et d'un sérum pathologique (malade présentant une cholestase lithiasique) reproduits à titre indicatif montrent que les sels biliaires présents dans un sérum normal sont peu nombreux (TC, TCDC, GC, GCDC, GDC) et à des taux très faibles (0,03 à 0,4 mg/l. selon les dérivés), mais dans les cholestases lithiasiques, au contraire, la concentration en sels biliaires est beaucoup plus grande (1 à 5,5 mg/l. selon les dérivés) et le nombre de sels biliaires présents augmente: TC, TCDC, GUDC (traces), TCDC, TDC, GC, UDC (traces), TLC, GCDC et GDC.

Une étude systématique a été effectuée sur les sérums de quatre groupes de malades atteints d'hépatite aigue virale, de cirrhose, de cholestase néoplasique et de cholestase lithiasique.[5] L étude statistique de chacun de ces groupes a permis de dresser le profil chromatographique de chaque maladie en évaluant la variation des taux d'acides libres et conjugués comparativement à des sérums normaux.

Conclusion

La séparation et le dosage des acides biliaires et de leurs dérivés glyco- et tauro-conjugués sont facilement réalisables en chromatographie liquide. Le procédé

est applicable à leur séparation qualitative et leur dosage dans les milieux biologiques, tel que le sérum sanguin.

Les résultats obtenus font apparaître le rapport entre leur présence, leur taux sanguin et divers types d'affections hépatobiliaires. Les premiers résultats de l'étude en cours montrent sur le plan clinique, l'intérêt de l'application du procédé à l'étude des affections hépatobiliaires.

LITTERATURE

1. N. A. Parris, *J. Chromatog.* 1977, **133**, 273.
2. S. Okuyama, *Chem. Lett.*, 1976, 679.
3. S. Okuyama, N. Kokubun, S. Higashidate, D. Uemura et Y. Hirata, *ibid.*, 1979, 1443.
4. D. Baylocq, A. Guffroy, F. Pellerin et J. P. Ferrier, *Compt. Rend.*, 1978, **286C**, 71.
5. T. Dupont, D. Baylocq, A. Guffroy, G. Champault, M. Beaugrand, Y. Hecht et J. P. Ferrier, *Gastro. Enterol. Clin. Biol.*, 1979, **3**, 349.
6. D. L. Massart et R. Smits, *Anal. Chem.* 1974, **46**, 283.
7. J. A. Nelder et R. Mead, *Computer J.* 1965, **7**, 308.
8. W. Spendley, G. R. Hext et F. M. Himsworth, *Technometrics*, 1962, **4**, 441.
9. P. P. Nair et D. Kritschevsky, *The Bile Acids*, Vol. 1, Chap. 8. Plenum Press, New York, 1971.
10. P. K. Bhattacharya and Y. G. Bankawala, *Anal. Chem.*, 1978, **50**, 1462.
11. A. Baillet-Guffroy, *Thèse Doc. Pharmacie* (à paraître).

Summary—Detection and determination of bile acids and their glycine- and taurine-conjugated derivatives are realized by reversed-phase liquid chromatography either directly or after ion-pair formation. Operating conditions and the relation between capacity factors and structure are investigated. The determination of bile acids extracted from biological samples is possible by these techniques.

Talanta, Vol. 28, pp. 681 to 684, 1981
Printed in Great Britain. All rights reserved

0039-9140/81/090681-04$02.00/0
Copyright © 1981 Pergamon Press Ltd

COMPARISON OF DRY AND WET ASHING PROCEDURES FOR CADMIUM AND IRON DETERMINATION IN BIOLOGICAL MATERIAL BY ATOMIC-ABSORPTION SPECTROPHOTOMETRY*

MAJA BLANUŠA and DJURDJA BREŠKI
Institute for Medical Research and Occupational Health, Zagreb, Yugoslavia

(*Received* 13 *November* 1980. *Accepted* 15 *January* 1981)

Summary—A possible loss of cadmium and iron from the sample during dry ashing of the kidney, liver or carcase was examined by the radioactive isotope labelling technique. Cadmium-115 m or iron-59 was administered to rats 4–7 days before the rats were killed and samples collected. Dry ashing in different types of dishes and wet digestion with nitric acid were compared. There was no loss of cadmium or iron by volatilization during dry ashing at 600° or 450° respectively, but a significant amount of iron was bound on glass or porcelain crucibles. Storage of ashed and dissolved samples (in 10% nitric acid) did not show any change of cadmium or iron concentration up to 9 days.

In toxicity studies, most determinations of cadmium in the liver and kidney are performed after wet digestion of the samples.[1–4] Sometimes it is more convenient to apply dry ashing because of its simplicity and the possibility of handling large samples with the addition of little or no reagent. It is generally considered that dry ashing causes a loss of cadmium at temperatures over 500°.[5] Internal labelling with radioactive isotopes to test for loss of cadmium during ashing showed that some marine organisms lose cadmium even on drying at temperatures up to 90°.[6] Other marine organisms, however, were ashed at up to 500° without any loss.[7] It is therefore considered that biological material should be thoroughly tested before the dry ashing method is applied in the determination of cadmium.

Iron is a less volatile element which is not lost during ashing at up to 500°. However, it has been reported to be lost from some biological materials dry ashed at temperatures as low as 400–500°.[8]

It seems therefore that volatile compounds might be formed in some living organisms, and losses of both cadmium and iron may occur. Before applying the dry ashing method for the determination of both elements in the same samples of the kidney, liver and carcase of rats, we estimated the recovery by the internal radioactive isotope labelling technique. The dry ashing method was compared with wet ashing by labelling the living animals with cadmium-115 m and iron-59. In order to detect external contamination, accuracy tests were performed on standard reference material.

* This work was partially reported at the VIth Meeting of Chemists of Croatia, Zagreb, 1979.

EXPERIMENTAL

Labelling with radioactive isotopes

About 1 μCi of iron-59 (as ferric chloride, Amersham, England) was given to 6-week-old rats orally. Thirty-six animals were killed 4 days after administration of the isotopes and their organs were dissected. The wet weight of the kidney and liver samples was about 0.5 and 2.5 g respectively. The samples were divided into two groups. One group of 18 samples was placed in 25-ml borosilicate glass beakers for dry ashing. Another group of 18 samples was first measured in plastic tubes for gamma-radioactivity and then transferred to 75-ml tubes for wet ashing.

Cadmium-115m (15 μCi, almost carrier free, in chloride form, Amersham, England) was given intraperitoneally to 4-month-old rats. Seven days later, 12 animals were killed and the kidneys and liver were dissected for ashing. The wet weight of the kidney and liver samples was 2.3 and 11.5 g respectively. The samples were placed in porcelain crucibles for dry ashing (6 samples) and into Erlenmeyer flasks (6 samples) for wet ashing. Some carcases of 120 g wet weight were also dry ashed.

Ashing procedures

The cadmium-115m labelled samples were wet ashed with distilled 67% nitric acid. The kidneys were placed in 50-ml Erlenmeyer flasks and the livers in 100-ml flaskes, with small funnels in their necks for refluxing. The acid was first added in amounts of about 1 ml per gram of wet weight of tissue. The flasks were heated on a hot-plate (maximum temperature 200°) until the acid had evaporated, and the addition of acid and evaporation was repeated until a white residue was obtained. For tissues of 10 g wet weight, the addition of acid was repeated 5 or 6 times, and the ashing took up to 6 days. The wet ashing procedure for iron-59 labelled samples was performed in the Tecator Digestion System 40 (Höganäs, Sweden). The system is equipped with 40 glass tubes of 75 ml volume each, suitable for small samples of biological material, of wet weight up to 3 g. The temperature programme was 4 hr at 50°, 4 hr at 120°, 1 hr at 130°, 1 hr at 140°, 1 hr at 150°, 1 hr at 155°, 1 hr at 160°, 1 hr at 170° and 10 hr at

232°.[9] The cycle was repeated after further addition of concentrated nitric acid, until a white residue was obtained.

Dry ashing was performed in containers made of different materials. The cadmium-115m labelled samples were ashed in porcelain crucibles of different sizes, depending on the quantity of sample. The iron-59 labelled samples were ashed in 25-ml glass beakers (Boral, Pula, Yugoslavia). The samples were first dried at 105° and then placed in a muffle furnace. The temperature was carefully raised to 300° during 24 hr. This stage of ashing is critical, because fast increase of the temperature might cause ignition of the sample and induce some losses. The next day the temperature was set to 450° or 600° and the samples were ashed overnight. To obtain a white residue a few ml of 67% nitric acid were added and the solutions were evaporated to dryness on a hot-plate; this was repeated if necessary. The samples were finally transferred to the furnace to ash at 450° or 600° for several hours.

Counting procedure

The samples collected for wet ashing were measured for the gamma-radioactivity of iron-59 in an automatic well-type scintillation counter (Nuclear Chicago). After wet ashing, the residues were disssolved with 1 ml of 67% nitric acid, quantitatively transferred with hot water to 10-ml standard flasks and diluted to the mark. All 18 samples were stored in glass (9 samples) or polythene tubes (9 samples). The first aliquot of 1 ml was counted immediately after preparation. The recovery of iron-59 in the ashing was calculated in relation to the counts obtained before ashing.

One-ml aliquots were taken 1, 2, 3, 5 and 7 days after transfer of the solutions to the storage tubes, and counted to determine any loss by adsorption (calculated on the basis of the first counting after ashing). The samples labelled with iron-59 were counted in the gamma scintillation counter, and the samples labelled with cadmium-115m were counted in the beta liquid-scintillation counter (Packard Instruments, Model 3375) in aqueous solution (Cherenkov effect).

All the samples collected for dry ashing and labelled with iron-59, or the samples labelled with cadmium-115m for dry and wet ashing, were measured in the whole-body scintillation counter (Tobor, Nuclear Chicago) three times: before drying at 105°, during ashing at 450° or 600°, and after ashing and the last addition of nitric acid.

Although the different efficiencies due to different geometry conditions (before and after ashing) were corrected by comparing the samples with adequate standards, there were still some recoveries higher than 100%. The radioactivity counting was performed with a relative standard deviation of less than 3%.

AAS measuring procedure

The samples of NBS bovine liver (National Bureau of Standards, reference material No. 1577) used for testing the accuracy were wet ashed or dry ashed in the same way as the labelled samples of the kidney and liver. Five parallel samples for each ashing procedure and each type of dish were weighed (0.3 g) after drying at 105°. Dry ashing was performed in two different types of dish, porcelain crucibles and glass Erlenmeyer flasks. After ashing, the samples were dissolved and transferred to 10-ml standard flasks as described, to make 10% nitric acid solution. Iron was estimated by flame atomic-absorption spectrophotometry[10] (Varian, Model 375), and cadmium by flameless AAS in a graphite-tube atomizer (CRA-90). The temperature programme was drying at 140° for 35 sec, ashing at 400° for 25 sec and atomizing at 1800° for 2 sec. The ramp rate was 600°/sec. The argon flow-rate was about 6 l./min.

RESULTS AND DISCUSSION

Iron-59

From the experiment with iron-59 labelling it is evident (Table 1) that there is no loss of iron during dry ashing at 450°, but a significant quantity of radioactivity was retained on the surface of glass vials after the quantitative transfer of the sample. This finding is in accordance with a similar experiment by Koirtyohann and Hopkins[11] on blood samples. There was no radioactivity retained on glass tubes after the wet ashing of the liver or kidney. No adsorption or loss of iron-59 was observed after storage of the solution in polythene or glass tubes for up to 7 days after ashing and transfer of the sample (Table 2).

The flame AAS method for determination of the stable isotope of iron was tested by the standard-addition method[12] with the kidney and liver sample. The working curve for iron was linear between 1 and 4

Table 2. Recovery (%) of iron-59 after storage of the acidified sample solutions in different types of tubes

Days of storing	Type of tube*	Kidney	Liver
1	P	99.2 ± 5.4	98.0 ± 2.7
	G	99.2 ± 4.2	97.8 ± 3.6
2	P	106.1 ± 10.5	99.2 ± 3.3
	G	98.4 ± 6.3	98.9 ± 3.9
3	P	103.6 ± 5.7	102.9 ± 2.4
	G	100.7 ± 5.4	99.3 ± 2.7
5	P	105.9 ± 11.4	104.3 ± 3.6
	G	103.5 ± 4.8	101.4 ± 6.9
7	P	103.2 ± 8.7	104.2 ± 2.7
	G	104.1 ± 2.7	100.6 ± 4.2

Results are expressed as arithmetic mean of 9 samples in each group ± standard deviation.

* P = polythene tubes; G = glass tubes.

Table 1. Recovery (%) of iron-59 after wet and dry ashing (at 450°) of the kidney and liver

	No. of samples	Dry ashing: After 1st addition of nitric acid	Dry ashing: After 2nd addition of nitric acid	Dry ashing: Remaining activity on glass vials	Wet ashing
Kidney	16	105.3 ± 4.8	103.6 ± 3.5	5.7 ± 1.6	97.2 ± 7.9
Liver	18	105.3 ± 2.3	107.5 ± 2.6	2.8 ± 0.9	100.4 ± 10.3

Results are expressed as per cent radioactivity from measurements obtained before ashing and are presented as arithmetic mean ± standard deviation.

Table 3. AAS determination of cadmium and iron in NBS bovine liver standard reference material (No. 1577)

Element	NBS value, *ppm*	No. of estimates	Found, *ppm*	Recovery, %
Cd	0.27 ± 0.04	8	0.32 ± 0.04*	118
		5	0.27 ± 0.01†	99
		5	0.28 ± 0.05§	106
Fe	270 ± 20	5	243 ± 6*	90
		5	143 ± 28†	53
		5	140 ± 19§	52

* Wet ashing.
† Dry ashing in porcelain crucibles.
§ Dry ashing in glass.
Results are expressed as arithmetic mean ± standard deviation.

μg/ml. For the determination of iron in NBS bovine liver sample (Table 3) a single addition of standard was used for this linear part of the curve. Very low recoveries were obtained (about 50%) when samples were dry ashed in glass or porcelain dishes at 450°. These recoveries were much lower than those obtained with iron-59. The reason might be the small quantity of bovine liver powder (0.3 g) taken for ashing, compared to the 2.5 g of the liver labelled with iron-59, and a high retention of the iron on glass or porcelain.

Cadmium-115m

The recovery of cadmium-115m after dry ashing of the kidney, liver and carcase at 450° (Table 4) showed there was practically no loss of cadmium. No

Table 4. Recovery (%) of cadmium-115m after wet and dry ashing of the kidney and liver

	Dry ashing			
	Ashing temperature, °C	Recovery after ashing	Remaining activity on porcelain dishes, %	Wet ashing*
Kidney	450	97.2 ± 4.6	2.2 ± 2.9	(4) 93.3 ± 4.5
	600	(5) 106.7 ± 3.5	3.7 ± 1.6	
Liver	450	95.2 ± 0.7	0.2 ± 0.2	
	600	101.1 ± 3.9	1.9 ± 0.6	(5) 93.5 ± 3.3
Carcase	450	(8) 94.0 ± 5.9	—	—

Results are expressed as arithematic mean ± standard deviation.
* Number of samples was 6 or as stated in parentheses.

Table 5. Recovery (%) of cadmium-115m after storage of the acidified sample solutions in different types of tubes

Storage, *hr*	Type of tube	Kidney	Liver	Carcase
5	P	(4) 93.6 ± 5.0†	(4) 100.1 ± 1.8†	(8) 100.0 ± 1.7†
	G	(9) 99.2 ± 1.6†	(9) 97.9 ± 2.6†	(8) 99.6 ± 1.3†
12	P	100.4 ± 1.9	100.6 ± 1.2	100.5 ± 1.8
	G	100.3 ± 1.1	100.7 ± 1.7	100.2 ± 0.6
24	P	97.2 ± 4.8	100.9 ± 1.3	97.5 ± 1.5
	G	99.2 ± 0.7	99.2 ± 1.5	99.0 ± 0.7
48	P	98.4 ± 2.7	98.3 ± 1.2	100.6 ± 1.8
	G	99.8 ± 2.8	99.3 ± 2.1	100.4 ± 1.3
72	P	96.2 ± 2.0	—	99.8 ± 1.9
	G	97.4 ± 3.5	98.9 ± 2.3	99.1 ± 1.2
216	P	—	—	—
	G	95.1 ± 2.4	97.8 ± 3.9	—

Results are expressed as arithmetic mean ± standard deviation.
* P = polythene tubes; G = glass tubes.
† Number of samples in parentheses.

radioactivity remained on the porcelain dishes either. The complete recovery of cadmium at 600° might be due to the presence of traces of sulphate or phosphate (but these were not tested for).

The storage of the solutions prepared with 10% nitric acid caused no adsorption of radioactive cadmium on the walls of the tubes (Table 5) in up to 3 (polythene) or 9 days (glass). This finding could be useful when samples prepared after ashing are stored before determination of this trace element.

The standard-addition method was tested by carbon rod AAS determination of stable cadmium in the kidney and liver. Linearity was found for cadmium between 1 and 3 μg/l. Accuracy testing on NBS bovine liver standard (Table 3) showed no loss of cadmium after dry or wet ashing. The somewhat higher result from wet ashing was found not to be statistically significantly different from the NBS value (*t*-test). All results were corrected for the reagent blank.

Conclusions

Cadmium can be determined in the kidney, liver or carcase after dry ashing of samples at a temperature as high as 600°. There is no volatility loss and no loss on crucibles or glass.

During ashing at 450° significant quantities of iron are bound to porcelain or glass and cannot be washed off when the sample is transferred to the flask. Therefore cadmium and iron can be estimated in the same sample of the kidney and liver only if the sample is wet digested.

No adsorption of iron or cadmium was observed in up to 9 days of storage of the acidified solutions of the ashed samples.

REFERENCES

1. Y. Itokawa, T. Abe, R. Tabei and S. Tanaka, *Arch. Environ. Health*, 1974, **28,** 149.
2. M. Takashima, K. Nishino and Y. Itokawa, *Toxicol. Appl. Pharmacol.*, 1978, **45,** 591.
3. Y. Itokawa, K. Nishino, M. Takashima, T. Nakata, H. Kaito, E. Okamoto, K. Daijo and J. Kawamura, *Environ. Res.*, 1978, **15,** 206.
4. H. Massie and V. R. Aiello, *Mech. Ageing Dev.*, 1979, **11,** 219.
5. T. T. Gorsuch, *Analyst*, 1959, **84,** 135.
6. H. O. Fourie and M. Peisach, *ibid.*, 1977, **102,** 193.
7. J. G. van Raphorst, A. W. van Weers and H. M. Haremaker, *Z. Anal. Chem.*, 1978, **293,** 401.
8. R. Bock, *A Handbook of Decomposition Methods in Analytical Chemistry*, p. 140. International Textbook Co., Glasgow, 1979.
9. A. Frank, *Z. Anal. Chem.*, 1976, **279,** 101.
10. Analytical Methods Committee, *Analyst*, 1978, **103,** 643.
11. S. R. Koirtyohann and C. A. Hopkins, *ibid.*, 1976, **101,** 870.
12. I. Rubeška and B. Moldan, *Atomic Absorption Spectrophotometry*, p. 95. CRC Press, Cleveland, 1971.

Talanta, Vol. 28, pp. 685 to 687, 1981
Printed in Great Britain

0039-9140/81/090685-03$02.00/0
Pergamon Press Ltd

SHORT COMMUNICATIONS

QUALITATIVE AND QUANTITATIVE ANALYSIS OF URACIL ANTICANCER DRUGS

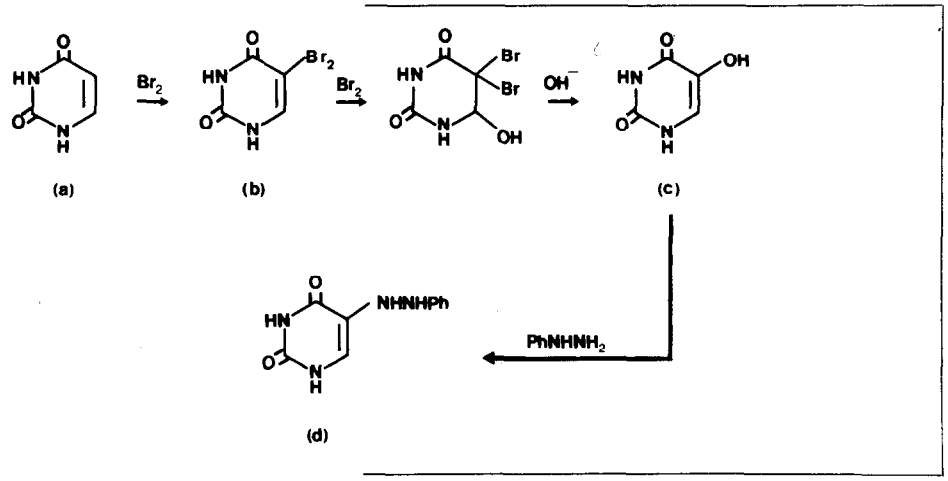
SONIA T. HASSIB

Pharmaceutical Chemistry Department, Faculty of Pharmacy, Cairo University, Cairo, Egypt

(*Received* 23 *January* 1980. *Revised* 4 *August* 1980. *Accepted* 11 *March* 1981)

Summary—Two uracil anticancer drugs can be selectively identified and estimated by means of two colour reactions. 5-Fluorouracil is treated with bromine water in borax medium, and then with 2,4-dinitrophenylhydrazine in acidic medium to give an orange-red precipitate which produces a distinctly violet solution when treated with potassium hydroxide solution. Uracil mustard, containing alkylating groups, is heated with α-picoline in aqueous solution. The quaternary salt thus produced is condensed in alkaline medium with sodium 1,2-naphthoquinone-4-sulphonate, giving a pink colour. The possibility of using these colour tests for the determinations of these anticancer drugs in pure and dosage forms has been studied.

Cytosine and uracil can be identified[1] by oxidation with bromine in aqueous solution and subsequent addition of an excess of barium hydroxide solution. A purple colour develops because of formation of the barium salt of isodialuric acid. Lavene[2] has shown that when uracil (*a*) or 5-bromouracil (*b*) is treated with bromine, followed by phenylhydrazine, a hydrazino compound (*d*) is obtained. It is also produced from isobarbituric acid (*c*) and phenylhydrazine without previous treatment with bromine. Treated directly with phenylhydrazine, 5-bromouracil fails to give compound (*d*). The USP[3] describes a qualitative test in which the colour of bromine water is discharged by a 1% fluorouracil solution in water. In the present work it was found that the product of this reaction, in solution, does not give a precipitate with 2,4-dinitrophenylhydrazine (DNPH) unless the reaction with bromine is carried out in a borax medium. The DNPH derivative gives a characteristic violet colour (λ_{max} 550–560 nm) with aqueous potassium hydroxide. This test can be used for the estimation of fluorouracil in pure form and in ampoules. Uracil mustard, although containing a uracil ring, gives negative results when treated similarly. It is detected and determined through the nitrogen mustard group by a colour reaction based on Feigl's test for heterocyclic nitrogen bases.[4] The uracil mustard is heated with an aqueous solution of α-picoline to form a pyridinium salt which is condensed with sodium 1,2-naphthoquinone-4-sulphonate (SNS) in the presence of alcoholic potassium hydroxide to give a red colour (λ_{max} 530 nm).



EXPERIMENTAL

Materials

All chemicals and reagents used were of pharmaceutical grade and solvents of spectroscopic grade. Pure 5-fluorouracil and ampoules of Lot No. 29221, nominally containing

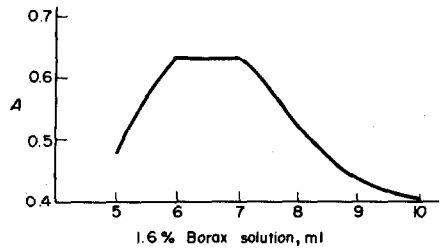


Fig. 1. Effect of volume of 1.6% borax solution in fluorouracil determination.

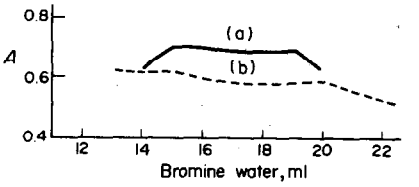


Fig. 3. Effect of volume of bromine water (0.2% v/v bromine) in fluorouracil determination. Reaction time (*a*) 20 sec, (*b*) 10 min.

250 mg of fluorouracil, were supplied by Hoffmann La-Roche, Basle, Switzerland. Pure uracil mustard and capsules of Lot No. 848, nominally containing 1 mg of uracil mustard, were supplied by Upjohn Co., Kalamazoo, Michigan, USA.

Procedure

Determination of 5-fluorouracil. An aqueous solution containing 8–11 mg of fluorouracil is treated with 6.5 ml of 1.6% borax solution, followed by 17–19 ml of 0.2% v/v bromine water. After 20 sec (effectively the mixing time) 2 ml of 2*M* sulphuric acid are added and excess of bromine is removed by dropwise addition of sodium arsenite solution. The mixture is diluted to volume in a 50-ml standard flask with water. A portion containing 40–130 μg of fluorouracil is treated with 1 ml of DNPH solution (0.1 g in 100 ml of 1*M* sulphuric acid). After 75 min 5 ml of 1*M* potassium hydroxide are added and the solution is diluted to 25 ml in a standard flask with water. The absorbance is measured at 560 nm against a blank. The amount of fluorouracil present is obtained from a calibration curve.

For fluorouracil in ampoules the contents of 4 ampoules are transferred to a 1-litre standard flask and diluted to volume with water, and 10 ml of this solution are treated as described above.

Determination of uracil mustard. Uracil mustard (10–22 mg) is heated with 1.25 ml of 4% v/v α-picoline solution in water at 85–90° for 45 min, then the mixture is cooled and transferred to a 100-ml standard flask and diluted to volume with water. An aliquot containing 50–250 μg of uracil mustard is treated with 0.75 ml of 0.1% SNS solution and 8 ml of ethanol (98%), and diluted to 10 ml with water in a standard flask. The absorbance is measured after 20 min, at 530 nm against a blank. The amount of uracil mustard present is obtained from a calibration curve prepared by using the procedure.

For uracil mustard in capsules, the contents of 20 capsules are thoroughly mixed. A portion of the mixed powder containing 2–3 mg of uracil mustard is extracted with 40 ml of acetone. The residue left after evaporation of the acetone is treated as above, the volume being made up to 25 ml after the quaternization.

RESULTS AND DISCUSSION

In the determination of fluorouracil, maximum absorbance is reached with 6–7 ml of 1.6% borax solution (Fig. 1). In the reaction with bromine, the reaction time is rather critical, the final absorbance decreasing with increasing reaction time. There is a choice between using a rather short reaction time (20–60 sec) and obtaining higher sensitivity, or sacrificing some sensitivity in exchange for a less critical reaction time (*e.g.*, 15 min, see Fig. 2).

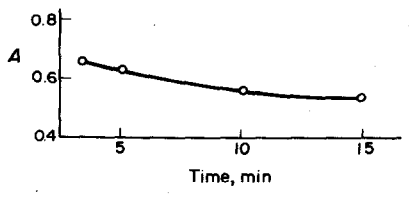
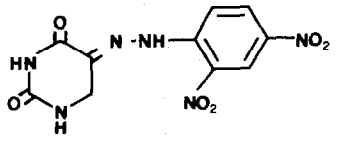


Fig. 2. Effect of oxidation time in fluorouracil determination.

The optimum amount of bromine water is 17–19 ml irrespective of the reaction time (Fig. 3). The reaction is stopped at the proper time by addition of 1*M* sulphuric acid. In the second step, a reaction time of 60–90 min with DNPH gives maximal final absorbance. Constant results are obtained with 0.75–1.5 ml of 0.1% DNPH solution in 1*M* sulphuric acid. The colour obtained on addition of the alkali is stable for at least 1 hr and shows maximum absorbance at 550–560 nm.

Replicate determinations (5 at each of 6 concentrations ranging from 2.5 to 5.0 μg/ml) gave a linear calibration graph passing through the origin and having a slope of 0.170_5 ml/μg, with a standard deviation of 0.003_3 ml/μg. In recovery experiments with 18, 24 and 30 μg of fluorouracil added to a fixed amount (100 μg) of the compound, the recoveries of the spikes were 18, 24 and 29 μg respectively. Analysis by non-aqueous titration[3] gave a relative standard deviation of 1%.

A sample of the DNPH derivative was crystallized from n-butanol, and gave an orange red crystalline powder (m.p. > 350°). It was identified as the isobarbituric acid derivative (*e*) by infrared spectroscopy [bands at 1500 and 1600 cm^{-1}, phenyl ring (no peak at 1580 cm^{-1}, so no conjugation); 1325 and 1560 cm^{-1}, nitro group; 1695 cm^{-1}, 2-carbonyl group of a uracil ring, and >C=N group; 1138, 1190, 1250 and 990 cm^{-1}, 1,2,4-trisubstitution in the phenyl ring; 3400 cm^{-1}, >NH group].



(e)

In the determination of uracil mustard, the optimum temperature for quaternization is 85–100°, and

the heating time 30–60 min. The absorbance obtained depends on the α-picoline concentration, so this reagent must be carefully prepared and measured. The colour obtained with SNS is stable for 100 min and the absorbance is recorded after 20 min. The volume of 0.1% SNS solution used can be varied from 0.5 to 2 ml without affecting the results. The colour obtained has its absorption maximum at 530 nm and obeys Beer's law in the range 5–25 μg/ml. The calibration graph is linear and passes through the origin, its slope being 0.0319 ml/μg, standard deviation 0.0007 ml/μg. Analysis by the 8-hydroxyquinoline method[5] gave a relative standard deviation of 2%.

However, when the method was applied to the Upjohn uracil mustard capsules, only a 72–74% recovery was obtained, and in agreement with this, recoveries of 73–77% were obtained by the standard-additions method. As the contents of the capsules are a trade secret it was not possible to identify the cause of the discrepancy by simple trial and error tests on binary mixtures of uracil mustard with each of the other components in turn. An attempt was made to identify the additives, but only negative results were obtained, the absence of sugars, polyols and methylcellulose being established. All that can be said is that the standard-additions method (a known amount of pure uracil mustard added to the acetone extract) should be used whenever capsules are to be analysed, and an appropriate recovery correction factor should be applied.

Uracil mustard seems to be the only one of five alkylating anticancer drugs tested which can be identified and determined by this method. Myelobromol, elobromol and melphalan could not be quaternized under the conditions used, and zitostop is poorly quaternized by aqueous α-picoline, giving an unstable colour in aqueous alcoholic solution (λ_{max} 535 nm).

Acknowledgements—The author expresses her thanks to Hoffman La-Roche, Basle, and the Upjohn Co., Kalamazoo, for supplying the fluorouracil and uracil mustard.

REFERENCES

1. H. L. Wheeler and T. B. Johnson, *J. Biol. Chem.*, 1907, **3**, 183.
2. P. A. Lavene, *ibid.*, 1925, **63**, 653.
3. *U.S. Pharmacopeia*, XVIII, 1970.
4. F. Feigl and V. Anger, *Spot Tests in Organic Analysis*, 7th Ed., pp. 379–381. Elsevier, Amsterdam, 1966.
5. *The National Formulary*, XIV, p. 756. American Pharmaceutical Association, 1975.

Talanta, Vol. 28, pp. 688 to 690, 1981
Printed in Great Britain. All rights reserved

0039-9140/81/090688-03$02.00/0
Copyright © 1981 Pergamon Press Ltd

THE SYNTHESIS AND REAGENT PROPERTIES OF MAGNESIUM TETRAKIS(4-tert.BUTYLPHENYL)BORATE

G. E. PACEY*
Department of Chemistry, Miami University, Oxford, Ohio 45056, U.S.A.
and
C. E. MOORE
Department of Chemistry, Loyola University Chicago, Illinois 60626, U.S.A.

(*Received* 26 *January* 1981. *Accepted* 9 *March* 1981)

Summary—Magnesium tetrakis(4-tert.butylphenyl)borate, $Mg(BAr_4)_2$, has been synthesized and screened for its properties as an analytical reagent. Although rather more selective than tetraphenylborate, the compound surprisingly precipitates sodium and proves a good gravimetric reagent for its determination. Quaternary ammonium and trialkylamine ions are precipitated only slowly (in contrast to the rapid precipitation with tetraphenylborate). The new compound exhibits better resistance to proton-initiated decomposition and to free radical attack than the other known tetra-arylborates. The presence of the parent peak, $NaBAr_4^+$, in the mass spectrum of the sodium salt is further proof of the remarkable stability. The other tetra-arylborates do not produce parent peaks in the mass spectra of their precipitates.

The synthesis and evaluation of the analytical behaviour of a variety of substituted phenylborates have been reported.[1–6] The substituents that have shown the most stabilizing influence have been the electron-withdrawing groups (F, Cl, CF_3). It has been shown that as the stability toward proton attack in aqueous solutions decreases, the instability due to a presumed free-radical decomposition pathway increases.[7] Our research on the synthesis of tetra-arylborates[8,9] continues in the search for more selective and stable reagents.

It was thought that the substitution of tert. butyl groups in the *para*-positions of the benzene ring would lead to an interesting compound, because of the large anion size and the steric effects. The first attempts to prepare a tetrakis(4-tert.butylphenyl)borate were unsuccessful because of side-product formation. The compound was finally successfully prepared and found to show unusual and interesting analytical behaviour.

EXPERIMENTAL

Synthesis of sodium tetrakis(4-tert.butylphenyl)borate

The synthesis of tetrakis(4-tert.butylphenyl)borate is similar to that of tetra-arylborates reported earlier, but with one important variation. The *in situ* synthesis could not be used. It was found that if the magnesium and sodium fluoroborate were combined in the usual *in situ* process, a dimer (4,4'-ditert.butylbiphenyl) resulted regardless of any other variations in the synthesis.

The synthesis of tetrakis(4-tert.butylphenyl)borate required a 3-necked reaction flask fitted with a condenser, constant-pressure addition funnel, and inlet tube for nitrogen. The entire apparatus was flame dried with a stream of nitrogen passing through. After the system had cooled, 250 ml of specially prepared tetrahydrofuran (THF) (Aldrich) were placed in the flask along with a magnetic stirring bar and 10 g (0.42 mole) of dried magnesium turnings. In the dropping funnel were placed 50 ml of THF, 10 ml (0.12 mole) of dibromoethane and 21 ml (0.12 mole) of 4-bromotert.butylbenzene. The reaction was started by adding 5 ml of this mixture from the dropping funnel. Dropwise addition was continued for 4 hr.

Sodium fluoroborate, 3.2 g (0.03 mole), which had been dried at 110° for at least 1 hr, was then added to the flask and the reaction was continued for a further 5 hr. At the end the reaction mixture was greyish-black with a large amount of insoluble material. The unreacted magnesium was extensively coated.

The reaction mixture was poured into 200 ml of ice-water and stirred with approximately 1 g of sodium carbonate; 200 ml of ether were added and the mixture was stirred, then the ether–THF layer was separated. The aqueous layer was saturated with sodium chloride and extracted with three 100-ml portions of ether. The ether layers were combined and poured into 600 ml of slightly alkaline water. The water–ether mixture was heated, with stirring, to remove the ether and THF. The yellow lumps of product in the water layer were filtered off and dissolved in acetone. The acetone solution was filtered through "Celite" and poured into 700 ml of water. A white precipitate was produced [m.p. > 300; analysis gave C 85.4%, H 9.2%; $(C_{10}H_{13})_4BNa$ requires C 84.8%, H 9.19%].

Usually we have used the sodium salt to study the analytical properties of new tetra-arylborates. The sodium salt of this tetra-arylborate had such low solubility, however, that it was necessary to use the soluble magnesium salt instead. The preparation of the magnesium salt is similar to that used previously.[3] An ether solution of the pure sodium salt (0.1 mole) was shaken with 500 ml of 4*M* ammonia solution, the ether layer was separated and the ether evaporated to yield the ammonium salt. Conversion was practically complete as shown by integration of the phenyl and ammonium NMR peaks. The ammonium salt was refluxed in anhydrous methanol with magnesium methox-

* Address all enquiries to this author.

Table 1. Comparison of precipitation patterns of tetrakis(4-tert.butylphenyl)borate (TBPB) and tetraphenylborate (TPB) (X indicates precipitation)

	TPB	TBPB		TPB	TBPB
Li^+	—	—	Tl^+	X	X
Na^+	—	X	Ag^+	X	X
K^+	X	X	NH_4^+	X	X
Rb^+	X	X	Hg_2^{2+}	X	X
Cs^+	X	X	R_3NH^+	X	slow X
Cu^{2+}	X	X	R_4N^+	X	slow X
Ni^{2+}	X	—	Co^{2+}	X	—
Cd^{2+}	X	—	Mn^{2+}	X	—

ide. When all the ammonia had been eliminated, then methanol was removed and the salt was dissolved in ether. The solution was filtered and the ether evaporated, and the solid was dried under vacuum at 80° (m.p. > 300°; analysis gave C 84.0%, H 1.13%; $[(C_{10}H_{13})_4B]_2Mg$ requires C 84.7%, H 1.17%).

Analytical tests

Qualitative tests were carried out with a 1% solution of the magnesium salt; approximately 1 ml of the reagent was added to 1 ml of 0.1*M* solution of the test ion. The sensitivity for sodium ion was determined by mixing 2 ml of 0.03*M* reagent solution with 2 ml of test solution, the concentration of which was progressively reduced. The solubility of sodium tetrakis(4-tert.butylphenyl)borate was determined by the flame-emission determination of the sodium concentration in a saturated solution of the tetra-arylborate kept at 25° for 48 hr.

For quantitative work the general directions given by Gloss[10] were followed. A 2% solution of the reagent was made in triply distilled water, and any insoluble material was filtered off. The sodium solution was diluted to about 50 ml and heated to 70° and the reagent was added dropwise from a burette. The precipitate was allowed to stand at room temperature for 1 hr and was then collected on a porosity-4 sintered-glass crucible, washed with three 5-ml portions of cold triply distilled water, and dried at 110° for 90 min, cooled in a desiccator and weighed.

RESULTS AND DISCUSSION

Table 1 summarizes the results and compares them with those for tetraphenylborate. The most noteworthy reaction is the precipitation of the sodium salt. This is the first tetra-arylborate to give an insoluble sodium salt. Of additional interest is the observation that the precipitates form slowly with protonated trimethylamine and tetra-alkylammonium ions in general, but rapidly with ammonium ions. This observation leads us to speculate that the steric hindrance introduced by the tert.butyl substituent slows down the rate of precipitation for these ions. It may be possible to increase the size of the tert.alkyl groups to the point that steric effects begin to exclude the larger alkali metal ions, leading to a more selective reagent, especially in view of the fact that the sensitivity of the present reagent for caesium was poorer than that for sodium. The sensitivity data (Table 2) show that the new tetra-arylborate has possibilities as a gravimetric reagent for sodium, since a slight precipitate was seen immediately with a 0.02-mg/ml sodium solution. It does not, however, show a definite selectivity for sodium relative to potassium.

Table 2. Sensitivity* of TBPB for alkali metal ions

	Alkali metal taken (mg/ml)					
Ion	2	0.2	0.1	0.05	0.02	0.01
Na^+	HI	HI	HI	MI	SI	—
K^+	HI	HI	HI	SI	TS	—
Rb^+	HI	HI	HI	SI	TS	—
Cs^+	HI	HI	HI	SI	—	—

* HI = heavy precipitation immediately; MI = medium precipitation immediately; TI = trace precipitation immediately; SI = slight precipitation immediately; TS = trace precipitation slowly.

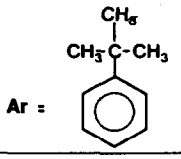
Table 3. Results for sodium precipitation by magnesium tetrakis(4-tert.butylphenyl)borate

Na taken, *mg*	Na found, *mg*	Recovery, %
230	228.1	99.1
230	228.5	99.3
230	227.6	98.8
115	112.8	98.1
115	113.2	98.4
115	112.5	97.8
69	67.0	97.1
69	67.3	97.5
69	66.7	96.7

The solubility values obtained correspond to a sodium tetrakis(4-tert.butylphenyl)borate saturation concentration of 4.68×10^{-2} g/l or $8.26 \times 10^{-5}M$ at 25°. These values indicate that gravimetric determination of sodium with this reagent is a possibility. Table 3 lists the gravimetric results obtained. The recovery of sodium was calculated from the theoretical gravimetric conversion factor 0.04057. Apart from the sodium precipitation, the stability of this compound is its most interesting characteristic. The stability of the magnesium salt was examined by methods previously used.[7] The results obtained indicate a resistance to both acid decomposition in aqueous solutions and

Table 4. Selected mass spectral data for sodium TBPB[11]

m/e	Relative abundance	Identification
410	3.9	BAr_3^+
418	1.4	$Ar_2(C_6H_4)_2^+$ or $NaBAr_2[C_6H_4C(CH_3)_2]^+$
433	4.3	$NaBAr_3^+$
513	1.1	$BAr_2[C_6H_4C(CH_3)_2]_2^+$ or $BAr_3[C_6H_4C(CH_3)]^+$
528	0.4	$BAr_3[C_6H_4C(CH_3)_2]^+$
543	0.7	BAr_4^+
566	1.8	$NaBAr_4^+$



decomposition by free radical pathways. No decomposition was observed within 48 hr. The tetrakis(4-tert.butylphenyl)borate seems to be the most stable tetra-arylborate synthesized to date. Further evidence of the stability of this compound was provided by its mass spectrum. All tetra-arylborates previously studied have produced mass spectra in which the highest *m/e* corresponded to $MBAr_3$ (where M is the metal and Ar is the aryl group.[11] This new compound produces several peaks beyond that for $MBAr_3^+$, including one for the parent $MBAr_4^+$ (Table 4).

Acknowledgements—The authors would like to thank Dr. G. Marks and Dr. J. Huston for running the mass spectra.

REFERENCES

1. F. P. Cassaretto, J. J. McLafferty and C. E. Moore, *Anal. Chim. Acta*, 1965, **32**, 376.
2. C. E. Moore, F. P. Cassaretto, H. Posvic and J. J. McLafferty, *ibid.*, 1966, **35**, 1.
3. J. T. Vandeberg, C. E. Moore and F. P. Cassaretto, *ibid.*, 1969, **44**, 175.
4. M. Meisters, C. E. Moore and F. P. Cassaretto, *ibid.*, 1969, **44**, 287.
5. F. Jarzembowski, F. P. Cassaretto, H. Posvic and C. E. Moore, *ibid.*, 1974, **73**, 404.
6. G. E. Pacey, *ibid.*, in press.
7. M. Meisters, J. T. Vandeberg, F. P. Cassaretto, H. Posvic and C. E. Moore, *ibid.*, 1970, **49**, 481.
8. S. Chao and C. E. Moore, *ibid.*, 1978, **100**, 457.
9. G. E. Pacey and C. E. Moore, *ibid.*, 1979, **105**, 353.
10. G. H. Gloss, *Chemist-Analyst*, 1953, **42**, 50.
11. G. Marks, *Doctoral Dissertation*, Loyola University of Chicago, 1980.

Talanta, Vol. 28, pp. 691 to 693, 1981
Printed in Great Britain. All rights reserved

0039-9140/81/090691-03$02.00/0
Copyright © 1981 Pergamon Press Ltd

INDIRECT DETERMINATION OF SOME ALIPHATIC SECONDARY AMINES BY CATALYTIC THERMOMETRIC TITRATION

NOBUTOSHI KIBA, YO SUZUKI and MOTOHISA FURUSAWA

Department of Chemistry, Faculty of Engineering, Yamanashi University, Takeda 4-3-11, Kofu-shi, 400, Japan

(*Received* 18 *November* 1980, *Accepted* 21 *February* 1981)

Summary—The determination of some secondary aliphatic amines by catalytic titration is described. The amines can be determined in the range 0.1–5 μmole with relative errors of about 3%.

The reaction of amines with carbon disulphide in the presence of metal ions has been used as the basis for determination of aliphatic secondary amines.[1–5] The copper or nickel complex of the dialkyldithiocarbamate is extracted into a suitable organic solvent and the concentration of the amine is determined directly from the absorbance of the complex or indirectly from the amount of metal ion remaining in the aqueous phase. Primary amines react to form the corresponding metal monoalkyldithiocarbamates which are extractable into organic solvents, but, in practice, the formation and extraction are not quantitative. Interference from primary amines can be avoided by reaction with 2-ethylhexaldehyde[6] or salicylaldehyde[7] to yield the imines.

Catalytic titration procedures are suitable for the determination of inhibitors.[8] For example, silver in relatively concentrated mineral acid solution can be determined by iodide titration, with the iodide–catalysed Ce(IV)–As(III) reaction to indicate the end-point.[9–18] In the present work, silver dialkyldithiocarbamate formed in the amine reaction is separated from the reaction medium by extraction into chloroform, and the silver is stripped with 4*M* nitric acid and determined by catalytic titration. The reaction with 2-ethylhexaldehyde is employed for removal of primary amines.

EXPERIMENTAL

Apparatus

A thermometric titrator with recorder (TOA Electric) was used; it has been described before.[19] The titration cell was a 30-ml Dewar flask.

Reagents

Buffered silver solution. Ammonium acetate (300 g) and silver nitrate (6.8 g) dissolved in 1 litre of water.

Ce(IV) solution (*ca.* 0.2*M*). Cerium(IV) sulphate (80 g) dissolved in 100 ml of sulphuric acid and diluted to 1 litre with water.

As(III) solution (*ca.* 0.1*M*). Arsenic trioxide (10 g) dissolved in 500 ml of 2*M* sodium hydroxide, neutralized with 2*M* sulphuric acid and diluted to 1 litre with water.

Ammonia solution (1%). Ammonia solution (s.g. 0.90, 10 ml) diluted to 1 litre with water.

Potassium iodide solution. Stock solution (0.05*M*) prepared from potassium iodide dried *in vacuo* at 40° for 24 hr, and standardized against primary standard silver nitrate solution. Diluted daily as required.

Silver nitrate solution, 0.002*M*. Prepared by dissolving 0.1773 g of silver nitrate in 40 ml of (1 + 1) nitric acid and making up to 1 litre with water. Diluted as required just before measurement.

Silver diethyldithiocarbamate (*AgDDTC*) *solution*, 0.002*M*, *in chloroform.* The commercial salt (Dojin Laboratories) was dissolved in chloroform and the solution used in making all calibration curves. The silver content was checked, after stripping with nitric acid, by titrating with standard iodide solution. The solution was stable for at least a month on storage in the dark.

Secondary amine solutions. Standard solutions of diethylamine, di-n-propylamine, di-n-butylamine, *N*-ethylpropylamine and *N*-ethylbutylamine prepared by dissolving the freshly distilled amines in isopropyl alcohol.

All chemicals used were of reagent grade.

Procedure

One ml of the sample solution in isopropyl alcohol, containing 0.1–5 μmole of secondary amine and not more than 1 mmole of primary amines was transferred to a 50-ml separatory funnel. One ml of 2-ethylhexaldehyde was added and allowed to react at room temperature (20°) for 20 min. Then, 2 ml of 1% ammonia solution and 0.1 ml of carbon disulphide were added. The contents were mixed and the funnel was placed in a water-bath at 30° for 15 min, and occasionally swirled. Then 1 ml of buffered silver solution and 5 ml of chloroform were added. The mixture was shaken vigorously for 5 min in as dim a light as possible. The phases were allowed to separate. The chloroform layer was filtered through a sintered glass disk (porosity 4) under suction and transferred to another 50-ml separatory funnel. The aqueous phase was shaken with a second 5-ml portion of chloroform and the two extracts were combined. The extract was washed with three 20-ml portions of 1% ammonia solution, then stripped with exactly 15 ml of 4*M* nitric acid (vigorous shaking for 10 min). The two phases were allowed to separate completely. From the upper phase 10.0 ml were pipetted into the titration cell. Ce(IV) solution (5 ml) and As(III) solution (2 ml) were added to the titration cell and the solution was titrated with the appropriate standard iodide solution, depending on the silver content. The end-point of the titration was determined graphically from the intersection of straight line

Table 1. Determination of secondary amines

Compound	Taken, μmole	Found, μmole	Recovery, %	C.V. (n = 5), %
Diethylamine	0.185	0.180	97.3	3.9
	0.605	0.598	98.8	3.3
Dipropylamine	1.28	1.27	99.2	2.9
Dibutylamine	0.824	0.834	101.2	3.1
Ethylpropylamine	3.37	3.36	99.7	2.4
Ethylbutylamine	4.65	4.65	100.0	2.1

extrapolations before and after the equivalence point. The results were corrected for the blank.

Calibration graphs were prepared by taking aliquots of the standard solution of AgDDTC, stripping the silver with 4M nitric acid and titrating as described. Calibration curves to give the number of μmoles of silver in the fraction titrated (10.0 ml) were prepared in two ranges (0.05–0.5 and 0.5–5 μmole of AgDDTC), with two iodide standard solutions (10^{-3} and $10^{-2}M$ respectively).

RESULTS AND DISCUSSION

Table 1 summarizes the recovery data for five secondary amines. A linear response in the range 0.1–5 μmole was obtained so a single calibration is enough. Several mixtures of these amines with each other or with primary and tertiary amines were analysed (Tables 2 and 3). However, several other amines failed to react quantitatively, under a variety of conditions. The recoveries (%) for the determination of 1.0 μmole of amines were as follows: di-n-pentylamine (95), di-n-hexylamine (92), di-n-octylamine (91), di(2-ethylhexyl)amine (88), di-isobutylamine (11), di-isopropylamine (7), diethanolamine (65), di-(β-cyanoethyl)amine (53), 2,2′-diaminodiethylamine (72), dicyclohexylamine (2), morpholine (30), pyrrolidine (25), piperazine (41), histamine (22), dibenzylamine (3), N-methylaniline (2), N-ethylaniline (2), N-n-butylaniline (1).

Optimization of conditions

Titration of silver. The influence of the concentrations of Ce(IV) and As(III), the acidity of the titrand, concentration of titrant, and titration speed was studied. The optimal conditions were: Ce(IV) solution 5 ml; As(III) solution 2 ml; acidity of titrand not more than 5M nitric acid; concentration of titrant $10^{-3}M$ for 0.05–0.5 μmole of silver and $10^{-2}M$ for 0.5–5 μmole; total volume below 20 ml; titration speed 1 ml/15 min. Under these conditions 0.05–5 μmole of silver could be determined with an error within 1%. At higher concentrations of nitric acid, the titration curves displayed a gentle rise at the end-point and sharp end-points could not be obtained.

Stripping of silver into nitric acid. Various concentrations of nitric acid were tested. When 10 ml of chloroform solution of AgDDTC were shaken with 15

Table 2. Determination of mixtures of secondary amines

		Taken, μmole	Total taken, μmole	Total found, μmole	Recovery, %	C.V. (n = 5), %
Mixture 1:	diethylamine	1.20	2.48	2.50	100.8	±1.8
	+					
	dipropylamine	1.28				
Mixture 2:	diethylamine	1.20	2.84	2.85	100.4	±2.3
	+					
	dibutylamine	1.64				
Mixture 3:	dipropylamine	2.56	4.20	4.19	99.8	±2.1
	+					
	dibutylamine	1.64				

Table 3. Determination of secondary amines in mixtures of primary, secondary and tertiary amines

		Taken, μmole	Secondary amine, μmole	Recovery, %	C.V. (n = 5), %
Mixture 1:	ethylamine	550			
	diethylamine	1.20	1.18	98.3	±3.0
	triethylamine	200			
Mixture 2:	butylamine	840			
	dibutylamine	1.64	1.62	98.8	±3.0
	tributylamine	1000			

ml of nitric acid, 31, 77, 96, 100 and 100% of the silver was stripped with 1.0, 2.0, 3.0, 3.5 and 4.0*M* nitric acid respectively. With more concentrated acid the stripping was also complete. A nitric acid concentration of 4*M* was chosen.

Washing of chloroform phase

When the AgDDTC is extracted into chloroform in the procedure, the vigorous shaking causes dispersion of aqueous droplets containing the buffered silver solution into the chloroform. Washing the chloroform phase with distilled water gives high recoveries, indicating that the dispersed aqueous silver solution is not removed from the chloroform phase. The washing efficiencies of 1%, 2% and 10% ammonia solution were studied. The most satisfactory results were obtained by washing with three 20-ml portions of 1% ammonia solution. Further washing or the use of more concentrated ammonia solution results in low recoveries, indicating that some AgDDTC is lost from the chloroform phase.

Reaction temperature. At 20° all the secondary aliphatic amines studied took 40 min to react quantitatively. Longer reaction times caused low recoveries. At 30°, the reaction was complete in 10 min. Reaction for 30 min at this temperature yielded low results because of decomposition of the dialkyldithiocarbamate. At higher temperatures quantitative recoveries were not obtained, whatever the reaction time. A reaction time of 15 min and reaction temperature of 30° were chosen.

Amount of carbon disulphide. On account of its volatility, a sufficient amount of carbon disulphide must be present in the reaction medium. Recoveries were found to be quantitative with 0.05–0.2 ml (1–4 mmole) of carbon disulphide. An amount of 0.1 ml was chosen.

Interferences

Ethyl alcohol produced silver ethylxanthate under the reaction conditions but there was no interference, because the xanthate was not extracted into chloroform. Aldehydes, *e.g.*, 2-ethylhexaldehyde, underwent Tollen's reaction, so the shaking time had to be kept short to minimize contact of the sample solution with the buffered silver solution. Any silver metal produced was removed in the filtration. The method is not subject to interference from substances that reduce silver ion to silver metal or form insoluble silver salts.

REFERENCES

1. D. H. Karweik and C. H. Meyers, *Anal. Chem.*, 1979, **51**, 319.
2. T. Mitsui and Y. Fujimura, *Nippon Kagaku Kaishi*, 1974, 1908.
3. P. J. Oles and S. Siggia, *Anal. Chem.*, 1973, **45**, 2150.
4. G. R. Umbreit, *ibid.*, 1961, **33**, 1572.
5. E. L. Stanley, N. Baum and J. L. Gove, *ibid.*, 1951, **23**, 1779.
6. F. E. Critchfield and J. B. Johnson, *ibid.*, 1956, **28**, 430.
7. E. P. Przybylowicz and L. B. Rogers, *Anal. Chim. Acta*, 1958, **18**, 596.
8. H. Weisz, *Angew. Chem. Int. Ed. Eng.*, 1976, **15**, 150; H. Huler and G. Werner, *Z. Chem., Leipzig*, 1976, **16**, 304; H. P. Hadjiioannou, *Rev. Anal. Chem.*, 1976, **3**, 82; N. Kiba, M. Furusawa and T. Takeuchi, *Kagaku no Ryoiki*, 1977, **31**, 14.
9. J. Bognár and S. Sárosi, *Mikrochim. Acta*, 1963, 1072.
10. H. Weisz and U. Muschelknautz, *Z. Anal. Chem.*, 1966, **215**, 17.
11. H. Weisz and D. Klockow, *ibid.*, 1969, **232**, 321.
12. H. Weisz, T. Kiss and D. Klockow, *ibid.*, 1969, **247**, 248.
13. T. Kiss, *ibid.*, 1970, **252**, 12.
14. K. C. Burton and H. M. N. H. Irving, *Anal. Chim. Acta*, 1970, **52**, 441.
15. H. Weisz and H. Ludwig, *ibid.*, 1972, **60**, 385.
16. T. P. Hadjiioannou, E. A. Piperaki and D. S. Papastathopoulos, *ibid.*, 1974, **68**, 447.
17. F. F. Gaal and L. Bjelica, *Chem. Anal. Warsaw*, 1976, **21**, 227.
18. F. F. Gaal and B. F. Abramovic, *Talanta*, 1980, **27**, 733.
19. N. Kiba and T. Takeuchi, *ibid.*, 1973, **20**, 875.

Talanta, Vol. 28, pp. 694 to 696. 1981
Printed in Great Britain. All rights reserved

0039-9140/81/090694-03$02.00/0
Copyright © 1981 Pergamon Press Ltd

DETERMINATION OF CYANIDE BY AN INDIRECT SPECTROPHOTOMETRIC METHOD, USING 5-Br-PADAP

WEI FU-SHENG, LIU YU-QIN, YIN FANG and SHEN NAI-KUI
Department of Chemistry, China University of Science and Technology, Hefei, China

(*Received* 30 *October* 1980. *Accepted* 9 *February* 1981)

Summary—Complexation of Ni^{2+} with cyanide inhibits its colour reaction with 5-Br-PADAP and this reaction is used in the spectrophotometric determination of cyanide at the μg level. Cyanide in industrial waste waters is determined after an initial transfer as hydrogen cyanide from the sample into sodium hydroxide solution with a stream of air.

The methods for the photometric determination of cyanide with pyridine–diphenylamine,[1] pyridine–pyrazolone,[2] pyridine–barbituric acid[3] and isonicotinic acid–pyrazolone[4] are widely known. They have good selectivity and high sensitivity, but possess some drawbacks. Diphenylamine is a carcinogen and the pyridine methods require strictly controlled experimental conditions to maintain good reproducibility. Recent indirect methods for determining cyanides include the application of the Ag–phen–BPR system.[5–7]

In the spectrophotometric determination of Zn^{2+}, Mn^{2+} and Ni^{2+} with 2-(5-Br-pyridylazo)-5-diethylaminophenol(5-Br-PADAP),[8–10] we noticed that the development of colour (with Ni^{2+}, Co^{2+}, Zn^{2+} or Cu^{2+}) in alkaline solution is suppressed by cyanide. This paper reports that the suppression of the reaction of 5-Br-PADAP with Ni^{2+} can be used to determine the concentration of cyanide. The free and complexed cyanide in industrial waste water can be protonated and vaporized and then determined.

EXPERIMENTAL

Apparatus and reagents

The spectrophotometer used was a Zeiss Specord UV–VIS double-beam recording instrument.

Standard potassium cyanide solution. Dissolve 1.00 g of analytical reagent grade potassium cyanide in demineralized water and make up to 1 litre. Standardize with 0.01*M* silver nitrate. Dilute 100-fold to give a final concentration of 10.0 μg/ml to provide a working standard solution.

Standard nickel chloride solution. Dissolve 0.1000 g of pure nickel in dilute hydrochloric acid and make up to 100 ml with demineralized water. Dilute an aliquot to give a final nickel concentration of 10.0 μg/ml in the working standard solution.

Buffer solution, pH 8. A 5% solution of sodium tetraborate adjusted to pH 8 with dilute hydrochloric acid.

5-Br-PADAP. Dissolved in ethanol to give a 0.02% solution.

Procedure

To a 25-ml standard flask add 2 ml of buffer solution (pH 8), an appropriate volume of the test solution, containing <15 μg of cyanide, 1 ml of standard nickel chloride solution (10.0 μg of nickel) and 8 ml of ethanol, and mix. Add 2 ml of 0.02% 5-Br-PADAP solution and make up to volume with demineralized water. After 30 min, measure the absorbance at 560 nm against a reference blank solution which contains neither cyanide nor nickel.

Separation of cyanide by vaporization

Place the cyanide-containing sample (<15 μg of CN^-) in 50 ml of distilled water in a 100-ml flask and acidify with 25% tartaric acid solution to Methyl Orange (pH 3). With a stream of air (1.2 l./min) transfer the hydrogen cyanide produced into an absorption flask containing 10 ml of 0.1*N* sodium hydroxide. After 1 hr determine the cyanide recovered, by use of the procedure given.

RESULTS AND DISCUSSION

Mechanism of the indirect determination of cyanide

The absorption spectra of Ni^{2+}–5-Br-PADAP and Ni^{2+}–5-Br-PADAP–CN^- are shown in Fig. 1. The profiles are similar, but the intensity of absorption is reduced in the presence of cyanide, showing that the colour reaction of the nickel is suppressed. The cyanide presumably forms the tetracyanonickelate complex anion, and the effect of cyanide is linearly related to the amount of cyanide added, until the cyanide:nickel molar ratio reaches 4 (Fig. 2).

Effect of temperature

The formation of the cyanonickelate complex is almost instantaneous and is unaffected by temperature. Provided that the 5-Br-PADAP is added within 1 hr, the final absorbance is independent of the time of addition.

Higher temperatures cause the colour of the Ni^{2+}–5-Br-PADAP complex to develop more rapidly, while lower temperatures give a slower rate of development. The development of colour is complete in 20 min at room temperature (25°). In the presence of cyanide the absorbance of the coloured solution is stable for 1 hr and then increases slightly; in its absence the solution is stable over a longer period.

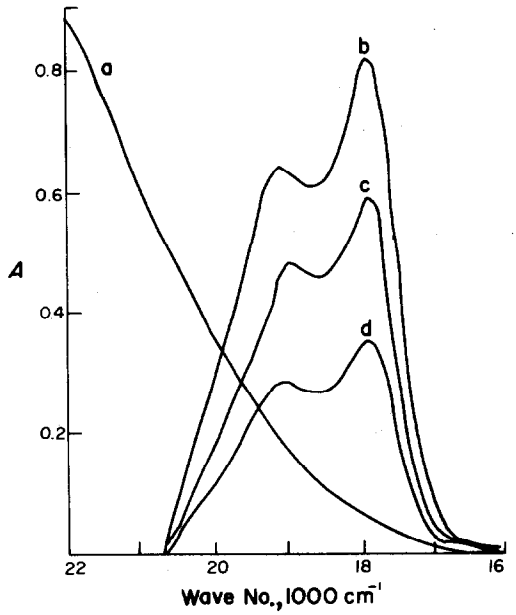


Fig. 1. Absorption spectra; a, 0.0008% 5-Br-PADAP in ethanol; b, 0.0008% 5-Br-PADAP + 10 μg of Ni^{2+} against 0.0008% 5 Br-PADAP in ethanol; c, 0.0008% 5-Br-PADAP + 10 μg of Ni^{2+} + 5 μg of CN^- against 0.0008% 5-Br-PADAP in ethanol; d, 0.0008% 5-Br-PADAP + 10 μg of Ni^{2+} + 10 μg of CN^- against 0.0008% 5-Br-PADAP in ethanol.

The effect of pH

The absorbance for a fixed amount of cyanide was determined by the general procedure at various pH values. For pH 6–6.5, sodium acetate was used as buffer, for pH 7–10, sodium borate was used. Constant absorbance was obtained at pH 6.5–9. Therefore a pH value of 8 is selected for the analytical procedure.

Effect of foreign ions

The reduction in absorbance at 560 nm is directly proportional to the amount of cyanide, in the range 0.5–15.0 μg.

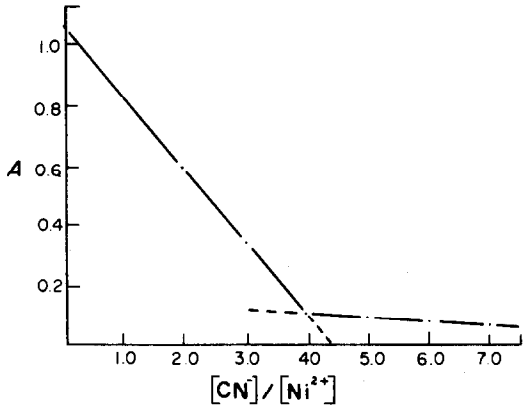


Fig. 2. Effect of cyanide on the Ni^{2+}–5-Br-PADAP complex.

One mg of any of the ions Na^+, K^+, NH_4^+, Cl^-, NO_3^-, Br^-, I^-, SCN^-, SO_4^{2-}, $B_4O_7^{2-}$ and SO_3^{2-} will not interfere in the determination of 10 μg of cyanide. Sulphide is the only interfering ion, but it can be precipitated with lead acetate solution and the cyanide vaporized and collected for subsequent determination. Heavy-metal ions (which produce intensely coloured complexes with 5-Br-PADAP) also remain in the solution.

Vaporization of cyanide

The vaporization of cyanide from various complexes has been reported.[11] With the present method the recovery from the cyanide complexes of zinc or cadmium is nearly 100%, but the recovery from the complexes of Cu^{2+}, Co^{2+}, Ni^{2+}, Hg^{2+} and Ag^+ is only 60, 11, 40, 20 and 54%, respectively. Results of experiments on the recovery of cyanide are summarized in Table 1. Hydrocyanic acid was volatilized

Table 1. Recovery of cyanide

Taken, μg	Found, μg							
100	97.6	100	94.0	102	94.5	95.0	95.0	98.5
75	67.8	75	67.5	67.5	70.9	66.8	66.8	69.0
15	12.6	12.6	12.6	12.9	13.7	12.4	12.5	12.2

Table 2. Analysis of waste waters

Sample	Concentration of CN^-			
	No. of determinations	Average, *ppm*	Standard deviation, *ppm*	Coefficient of variation, %
1	8	13.2	0.36	3
2	8	8.8	0.45	5
3	6	5.0	0.45	9
4	3	0.0	—	—

from a potassium cyanide solution and trapped in 0.1*M* sodium hydroxide. The trapped cyanide was then determined as described.

Determination of cyanide in waste water

For determination of cyanide in industrial waste water the pH is adjusted to 12 with sodium hydroxide solution. A 10–50 ml aliquot is made up to 50 ml with distilled water and the cyanide separated and determined as described previously.

The results for four samples are given in Table 2. Samples 1 and 2 are waste water from a nitrogenous fertilizer plant, sample 3 is from an electroplating workshop and sample 4 is tap water. The recovery of added cyanide is in the range 92–101%.

Sensitivity

The limit of detection of cyanide by the present method is 0.02 μg/ml and this compares favourably with the sensitivities claimed for previous methods, *i.e.*, 0.02 μg/ml with pyrazolone,[2] 0.01 μg/ml with barbituric acid[3] and 0.04 μg/ml with Ag–phen–BPR.[6]

REFERENCES

1. W. N. Aldridge, *Analyst*, 1944, **69**, 262.
2. *Standard Methods for the Examination of Water and Waste Water*. 13th Ed., p. 207 C, American Public Health Association, American Water Works Association and Water Pollution Control Federation, 1971.
3. G. V. L. N. Murty and T. S. Viswanhan, *Anal. Chim. Acta*, 1961, **25**, 293.
4. K. Ishii, T. Iwamato and K. Yamanishi, *Bunseki Kagaku*, 1973, **22**, 448.
5. R. M. Dagnall and T. S. West, *Talanta*, 1964, **11**, 1627.
6. R. M. Dagnall, M. T. El-Ghamry and T. S. West, *ibid.*, 1968, **15**, 107.
7. Huang Jun-hui and Lin Zhi-qing, *J. Univ. Chungshan*, 1978, **3**, 88.
8. Wei Fu-sheng and Zhu Yu-rui, *J. China Univ. Sci. Technol.*, 1979, **9**(2), 41.
9. Wei Fu-sheng, Qu Pei-hua and Zhu Yu-rui, *Fenxi Huaxue*, in the press.
10. Wei Fu-sheng, Qu Pei-hua, Shen Naikui and Yin Fang, *Talanta*, 1981, **28**, 189.
11. M. Chibo and M. Kuroda, *Guide-Book of Analysis of Environmental Pollution*, Vol. 5 (Japanese), p. 63, Kyovitsu Publishing House, 1972.

Talanta, Vol. 28, pp. 697 to 699, 1981
Printed in Great Britain

039-9140/81/090697-03$02.00/0
Pergamon Press Ltd

PHOTOMETRIC DETERMINATION OF NITRITE

W. A. BASHIR and S. FLAMERZ

Departments of Chemistry, College of Science and College of Education,
Mosul University, Mosul, Iraq

(*Received* 8 *May* 1980. *Revised* 25 *December* 1980. *Accepted January* 1981)

Summary—A new sensitive colour reaction for nitrite determination is presented. The method is based on the reaction of nitrite with *p*-aminobenzoic acid to form a diazonium ion, which is coupled with 8-hydroxyquinoline, in alkaline medium, to form a reddish-orange water-soluble azo dye. Diazotization and coupling are very fast and control of temperature is unnecessary. Moreover, the colour is stable and its intensity is in direct proportion to nitrite concentration over a wide range.

Because of the role of nitrite ion as a precursor in the formation of *N*-nitrosamines, many of which have been shown to be potent carcinogens,[1,2] and in view of the increasing interest in the quality of natural and sewage waters, a sensitive, rapid and simple procedure for the microdetermination of nitrite seems desirable. Consequently, we propose the following method.

EXPERIMENTAL

Reagents

All reagents used were of analytical grade.

Standard nitrite solution (1000 μg/ml). Dissolve 1.499 g of sodium nitrite in distilled water and dilute to 1000 ml. Add a pellet of sodium hydroxide to prevent liberation of nitrous acid, and 1 ml of spectroscopic-grade chloroform to inhibit bacterial growth.[3] Dilute this solution for use in construction of the calibration curve.

p-Aminobenzoic acid solution, 0.2%. Dissolve 0.2 g of *p*-aminobenzoic acid in 0.116*M* hydrochloric acid and dilute to 100 ml with the same acid.

8-Hydroxyquinoline solution, 0.05%. Dissolve 0.05 g of oxine in distilled water containing 0.45 g of sodium hydroxide and dilute to 100 ml with distilled water.

Procedure

To a series of 10-ml standard flasks, containing from 1 to 15 μg of nitrite in 1 ml of solution, add 1 ml of 0.2% *p*-aminobenzoic acid solution and 1 ml of the 0.05% 8-hydroxyquinoline solution, and make up to the mark with distilled water; the colour develops immediately and is stable for >48 hr. Measure the absorbance at 499 nm against a reagent blank prepared in the same manner but containing no nitrite, in 1-cm cuvettes. A straight line passing through the origin should be obtained. The apparent molar absorptivity (referred to nitrite) in the region of least photometric error was found to be 3.2×10^4 $l.mole^{-1}.cm^{-1}$.

RESULTS AND DISCUSSION

For the following experiments, 10 μg of nitrite were taken and the final volumes were 10 ml. Under the conditions of the preliminary investigations and of the prescribed procedure, the coloured azo dye showed maximum absorption at 499 nm. This wavelength, at which the blank shows zero absorbance, was adopted in all subsequent experiments.

Choice of compound to be diazotized

Many primary aromatic amines, including orthanilic acid, *o*-aminophenetole, *p*-aminophenetole, *o*-nitroaniline, *p*-aminosalicyclic acid and *p*-aminobenzoic acid were tested. Of these, only *p*-aminobenzoic acid gave satisfactory results. Moreover, it is easily soluble in mineral acids, giving a colourless solution, is easily diazotized, and gives a water-soluble azo dye under the conditions of the determination, thus eliminating the need for an extraction, a time-consuming procedure.

Effect of reagent concentrations

The effect of *p*-aminobenzoic acid concentration on the colour intensity was studied by using the prescribed procedure and adding to a series of nitrite solutions 1 ml of 0.04–0.3% solutions of the acid in 0.104*M* hydrochloric acid. The results showed 0.2% *p*-aminobenzoic acid solution to be optimum. Higher concentrations caused a slight decrease in the absorbance, which might be attributed to self-coupling of the acid as follows:

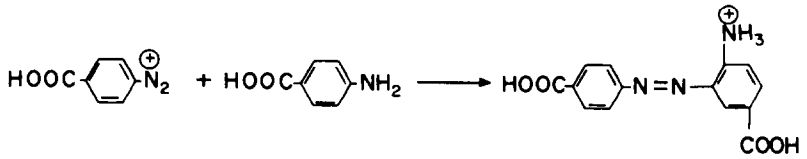


Table 1. Accuracy and precision of method

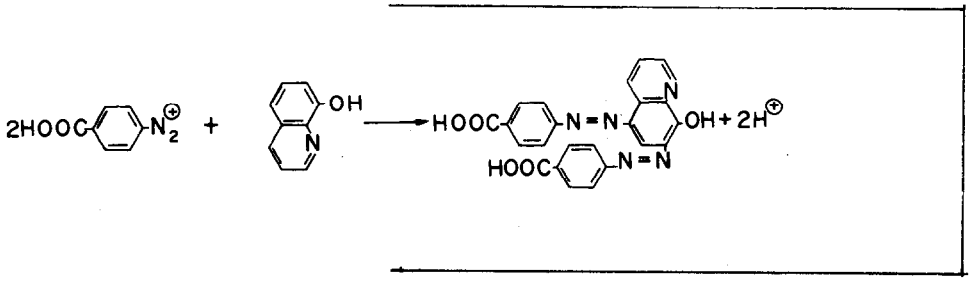
Amount of nitrite taken, μg	1.00	7.00	15.00
Accuracy, %*	+5	+0.2	−0.3
Precision, %†	3.2	0.4	0.5

* Relative error of mean value.
† Relative standard deviation.

Similar experiments were carried out, in which the hydrochloric acid concentration was varied over the range 0.0348–0.174*M*, and 0.116*M* hydrochloric acid was found to give maximum colour intensity. Higher acid concentrations changed the colour of the dye to yellow, which decreased the sensitivity of the method. Other mineral acids were tested and found unsatisfactory.

Choice of coupling agent

Coupling agents tested were tiron, resorcinol, α-naphthol, β-naphthol and 8-hydroxyquinoline. 8-Hydroxyquinoline gave the most useful results and was further studied. To each of a series of nitrite solutions, 1 ml of 0.05–0.25% 8-hydroxyquinoline solution in 0.4% sodium hydroxide was added. The 0.05% solution showed the most effective result; a smaller volume decreased the absorbance, by multiple coupling:[4]



Sodium hydroxide was used to dissolve the 8-hydroxyquinoline, as it is only sparing soluble in water. Organic solvents in which the compound is soluble interfered in the reaction. For example, *N*,*N*-dimethylformamide slowed down the reaction and caused a decrease in the absorbance. The optimum concentration of sodium hydroxide in the reagent was found by another set of experiments in which 0.05 g of 8-hydroxyquinoline was dissolved in 100 ml of 0.1–0.5% sodium hydroxide solution. A 0.45% solution gave the best results. The selected volume of this second composite reagent was 1 ml.

Colour stability

Under the optimized conditions, the reddish-orange colour of the azo dye develops instantaneously and remains stable for 50 hr, after which there is gradual fading.

Table 2. Effect of diverse ions on the determination of (1 ppm) nitrite

Interferent	Permissible concentration, *ppm**
Ammonia	60
Bicarbonate	120
Carbonate	65
Chloride	3120
Cyanide	120
Nitrate	145
Sulphate	1010
Sulphide	2
Sulphite	25
Calcium	35
Cadmium	10
Cobalt(II)	6
Copper(II)	15
Iron(III)	5
Magnesium	20
Mercury(II)	35
Lead(II)	60
Phenol	150
Tin(II)	8
Tin(IV)	10

* Amount of diverse ion causing an error of less than 2% in the determination.

Accuracy and precision of the method

Under the optimized conditions, the accuracy and precision (five replicates) of the method were checked. Table 1 shows the results. The method seems to be reliable.

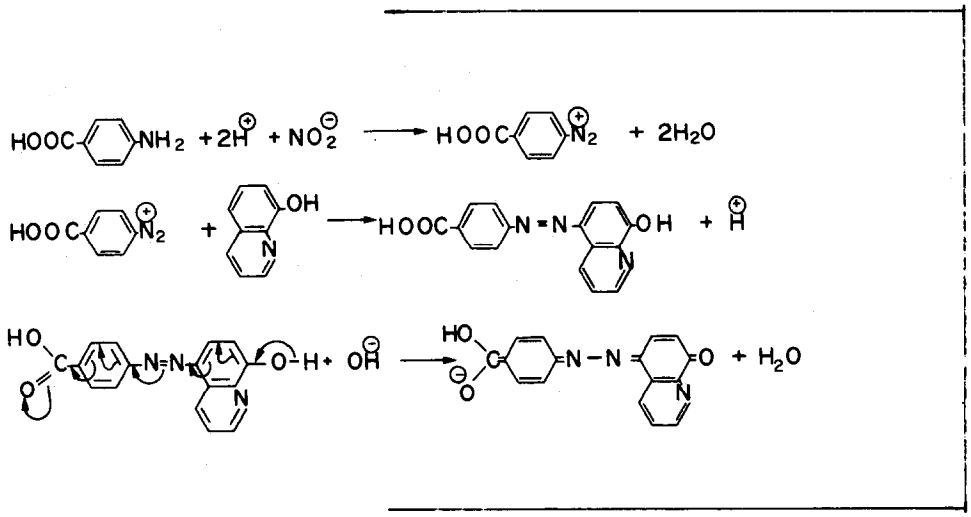
Interferences

In order to assess the possible analytical applications of this new method, the effect of foreign ions that often accompany nitrite was examined by carrying out determinations of 10 μg of nitrite in the presence of each of these ions, in a final volume of 10 ml. The results are summarized in Table 2.

The method seems to be more tolerant towards anions (with the exception of sulphide) than cations, and this is not unexpected because 8-hydroxyquinoline and azo dyes are commonly used chromogens for metal ions. However, an ion-exchange procedure may remove the seriously interfering ions.

Proposed reaction mechanism

The suggested reaction sequence is:



The method is superior to most modifications of the Griess method, owing to its simplicity, rapidity and the avoidance of an extraction step. It compares favourably with another 8-hydroxyquinoline method.[5]

REFERENCES

1. W. Lijinsky and S. S. Epstein, *Nature*, 1970, **225**, 21.
2. I. A. Wolff and A. E. Wasserman, *Science*, 1972, **177**, 15.
3. R. B. Lew, *Analyst*, 1977, **102**, 477.
4. L. R. Whitlock, S. Siggia and J. E. Smola, *Anal. Chem.* 1972, **44**, 534.
5. J. Nair and V. K. Gupta, *Anal. Chim. Acta*, 1979, **111**, 313.

Talanta, Vol. 28, pp. 701 to 704, 1981
Printed in Great Britain

0039-9140/81/090701-04$02.00/0
Pergamon Press Ltd 1981

ANNOTATIONS

ANALYTICAL TECHNIQUES FOR CORROSION STUDIES ON NOBLE METALS

A. VARMA

Laboratory for Research on the Structure of Matter, University of Pennsylvania, Philadelphia, PA 19104, U.S.A.

(*Received* 6 *October* 1980. *Revised* 15 *January* 1981. *Accepted* 9 *March* 1981)

Summary—The suitability of various analytical methods for studying the corrosion of gold, silver and palladium in various electrolytes has been investigated. The methods included potentiometry with ion-selective electrodes, polarography and atomic-absorption spectrophotometry. All three methods are useful for monitoring low corrosion rates by solution analysis but each has its limitations. Concentrations in the ng/ml range can be measured routinely with errors of 10% or less.

Rates of corrosion in aqueous solutions are usually calculated from weight losses determined from immersion tests. Although this method is widely applicable, it is not suitable for the determination of very low corrosion rates (*e.g.*, <0.001 in./yr) since weighing errors become significant. The noble metals corrode at very low rates in many environments. In addition, their high exchange-current densities preclude the use of linear polarization techniques which are capable of detecting ultra-low corrosion rates.[1] Thus, the corrosion rates of noble metals are best determined by solution analyses.

The aim of this investigation was to determine the suitability of different analytical techniques for studying the corrosion of gold, silver and palladium in various electrolytes. Copper was included for comparison purposes.

A variety of analytical techniques such as conventional and pulse polarography, anodic stripping voltammetry, atomic-absorption spectrophotometry, and ion-selective electrodes have been used with varying degrees of success to determine low concentrations of copper, silver, gold and palladium. Copper,[2–4] silver,[2,5,6] gold,[7,8] and palladium[7,9,10] have been measured in purified solutions and polluted environmental samples by anodic stripping voltammetry and pulse polarography. Ion-selective electrodes have been used for determination of silver at low levels[11,12] and of copper.[13,14] Atomic-absorption spectrophotometry has been used to determine these noble metals in microgram quantities.[15–18] The theory and techniques of stripping voltammetry, atomic-absorption spectrophotometry and ion-selective electrodes are well known but these techniques have rarely been applied in corrosion studies. Examples are a polarographic study of corrosion inhibitors,[19] and use of a differential polarographic method for corrosion measurements on Cu–Ni alloys in a flow system.[20]

In our study, four methods were chosen for examination: ion-selective electrodes (ISEs); differential pulse polarography (DPP); differential pulse anodic stripping (DPAS), which combines the best features of anodic stripping voltammetry and differential pulse voltammetry; and atomic-absorption spectrophotometry (AAS). These methods are the most suitable for measuring low corrosion rates quantitatively.

EXPERIMENTAL

A Corning pH-meter and an Orion model 94-29 copper ISE and an Orion model 94-16 silver sulphide ISE were used with an SCE for potentiometric studies. The electrodes were calibrated daily.

The supporting electrolytes used in the DPP and DPAS were purified by controlled potential electrolysis at −1.0 V *vs.* SCE, with a mercury cathode. The process was accelerated by continuous stirring and the solution was deaerated by passage of nitrogen that had been passed through a vanadous chloride solution (ammonium metavanadate in hydrochloric acid, reduced with amalgamated zinc). To reduce airborne contamination, the gas was also passed through a column containing the supporting electrolyte. A Princeton Applied Research model 174 Polarographic Analyzer equipped with a model 172 mercury-drop timer and with an X–Y recorder was used for all measurements. The covered polarographic cell (50-ml capacity), had a top which carried an anode, cathode, reference electrode salt bridge and an outgassing tube. It was left filled with pure 6*M* nitric acid for an hour before experimentation and rinsed thoroughly with distilled water before use.

A hanging mercury-drop electrode (HMDE), a platinum coil electrode, and a carbon-paste electrode (CPE) were used for the polarographic studies. The HMDE was filled with trebly distilled mercury and a fresh drop (3.3 mm^2 surface area) was used for each determination. The platinum coil electrode was cleaned with chromic acid, then ultrasonically cleaned in detergent solution and rinsed in

doubly distilled water before each measurement. The CPE (Princeton Applied Research, Dr. Monien type, EA267) had a surface area of 50 mm^2, which was renewed before each test by extruding some paste and wiping the surface in small circles on filter paper or fine-grained paper.

Atomic-absorption analyses were performed with a Perkin–Elmer model 306 spectrophotometer. A multielement hollow-cathode lamp was used for the copper and silver determinations, and single-element lamps were used for palladium and gold.

Corrosion tests were conducted by immersing metal specimens in 900 ml of air-saturated electrolyte maintained thermostatically at 30°. The electrolytes used (environmental equivalents in brackets) were 0.9% sodium chloride solution (body salinity), 3% sodium chloride solution (seawater) and 5% sodium bisulphite solution (sulphur dioxide in the environment). The specimens were ground with No. 600 emery, mounted on a Stern–Malcrides electrode holder,[21] cleaned ultrasonically in detergent solution, rinsed with doubly distilled water and dried before introduction into the test electrolyte.

Calibration solutions were prepared daily by serial dilution (with doubly distilled water) of commercially available spectroscopic grade standard solutions or stock solutions prepared in the laboratory from reagent grade copper ($CuCl_2$, $CuSO_4$), gold ($HAuCl_2$), silver ($AgNO_3$), and palladium ($PdCl_2$) compounds. Concentrations were checked periodically.

Procedures

Potentiometry. The SCE was connected to a glass test cell by a salt bridge containing supporting electrolyte. The temperature was kept at 30 ± 0.01° and the solution was stirred with a Teflon-covered magnetic stirring bar. The ISE was immersed in the test solution and the potential difference was measured after a time interval selected to ensure less than ±0.1 mV drift.

Calibration graphs were constructed by plotting potential difference *vs.* concentration on semilog graph paper. The ISEs were calibrated in various electrolyte solutions and the electrode surface was wiped with a soft tissue after each experiment. Concentrations were determined from the calibration curves, the potential difference measurements being made directly in the corrosion cell during the test period.

At the end of the corrosion test, the standard addition method was used to find the total concentration, together with titration of silver with chloride and of copper with EDTA.

Polarography. DPP was used to measure palladium (irreversible species) in pyridine–hydrochloric acid medium. Various other supporting electrolytes were tried with no success.

DPAS was studied extensively for determination of gold in 0.1*M* hydrochloric acid medium at the carbon-paste electrode (CPE), of silver in 0.1*M* nitric acid/0.9% sodium chloride medium at the CPE and in 0.2*M* sulphuric acid at two identical platinum electrodes, and of copper in sulphuric acid, doubly distilled water and 0.9% sodium chloride solution at the CPE and HMDE. Calibration graphs were obtained using standard solutions of the respective metals.

A known amount of the solution was taken in the polarographic cell and deaerated for 5 min. Instrument parameters were adjusted to give maximum reproducibility and sensitivity for the metal concerned. The deposition was done at a controlled potential more negative than the reduction potentials of all the species to be determined. Deposition time was usually 75–135 sec, followed by the anodic potential scan. The current peak (i_p) occurs at a potential (E_p) characteristic of the metal ion, and is a quantitative measure of its concentration. The standard addition method was used.

Atomic-absorption measurements. Calibration graphs were prepared by plotting absorbance *vs.* concentration of standard solutions of the respective metals. Sample concentrations were determined either by direct comparison with standard solutions or by linear interpolation on the calibration graphs, 12–15 readings being taken for each sample. Corrosion test solutions were analysed by AAS only after completion of the experiment, to avoid solution loss.

Table 1. Corrosion test data

Metal	Corrosion media	Exposure, *hr*	Metal concentration, *μg/ml*	
			ISE	AAS
Palladium	3*M* HCl	360	NA	1
	3% NaCl	504	NA	ND
Gold	3*M* HCl	504	NA	ND
	3% NaCl	504	NA	ND
Silver	0.1*M* HNO_3	308	ND	ND
	10^{-3}*M* HCl	458	ND	0.003
	10^{-2}*M* HCl	748	NA	0.005
	3*M* HCl	462	0.03 at 142 hr	1.3
	3% NaCl	360	0.15	0.14
		910	16.5	16.1
	0.9% NaCl	500	0.008	0.0064
		964	0.15	0.15
Copper	0.9% NaCl	663	1.78	1.32
	3% NaCl	404	1.23	0.25
	5% alk. Na_2S	548	NA	0.32
	5% Na_2SO_3	568	280	not used
		663	228	not used
		740	210	208

NA—not applicable.
ND—not detectable.

Table 2. Comparison of analytical methods for 0.9% sodium chloride medium

Metal	Differential pulse anodic stripping			Atomic-absorption spectrophotometry		
	Determined, *ng/ml*	Std. devn.* *ng/ml*	Error, %	Determined, *ng/ml*	Std. devn.* *ng/ml*	Error, %
Copper	2	±0.1	5	2	±0.7	35
Silver	0.8	±0.03	5	80	±20	25
Gold	30	±1.2	4	60	±16	27
Palladium	1000	±10	1	100	±19	19

* Ten replicates.

RESULTS AND DISCUSSION

Ion-selective electrodes

ISE measurements were found to be accurate and very sensitive. Factors such as electrode temperature, drift and noise limit the precision. With frequent calibration the measurements were reproducible to ±1–2%. Temperature effects were eliminated by keeping the sample and standard solutions at the same temperature. Electrode response was more rapid when going from dilute to concentrated and constantly stirred solutions.

Copper- and silver-selective electrodes work better in certain pH ranges for direct measurements, namely pH 3–7 for copper and 2–9 for silver. Sulphide interferes with both electrodes and silver interferes with the copper ISE.

The corrosion test results are reported in Table 1 and compared with those obtained by AAS. Generally the agreement is good. The apparent decrease in concentration with time observed for copper exposed to 5% sodium bisulphite solution is probably due to the presence of cuprous ion, which is not detected by the copper ISE.

Polarographic studies

Silver at the 0.8 ng/ml concentration level was determined in 0.9% sodium chloride solution at the CPE. Results were the same when no supporting electrolyte was added. The CPE was very successful for determination of gold in 0.1*M* hydrochloric acid. Palladium was estimated only at the μg/ml level in pyridine–hydrochloric acid medium at the HMDE by differential pulse polarography. Copper was studied in sulphuric acid, water and sodium chloride solution at the HMDE and CPE. Best results were obtained in 0.9% sodium chloride medium at the HMDE.

At very low concentrations, where a linear calibration could not be obtained, the deposition step was increased to 5 min and the concentration was measured by the standard addition method.

The main interference in polarographic analysis is from substances which are reduced at potentials close to or more positive than that of the element studied. This interference does not exist for the metals studied here since the difference in their half-wave potentials is more than 100 mV. Electrode stability, instrument stability and loss of analyte to the vessel are the limitations of the DPAS technique; however, shorter deposition time and quick analyses limit the errors from these sources. Since the signal-processing circuitry of the pulse mode permits the use of higher instrument gains, the sensitivities may be further improved. The great advantage of this technique is its ability to determine a substance in the presence of a very large amount of another substance.

Atomic-absorption measurements

Interference in AAS occurs mainly as the result of chemical effects (interelement compound formation in the flame), background absorption and spectral overlap.[22] These errors can be minimized by various means (addition of releasing agents, background correction, choice of analytical line). The presence of sodium chloride (from corrosion test solutions) caused burner problems, and it is best to clean the burner after its exposure to such solutions. Comparative data for gold, silver, palladium and copper determination by AAS and DPAS are shown in Table 2, giving the lower limits found determinable.

Potentiometry with ion-selective electrodes, polarography and atomic-absorption are useful methods for measuring trace amounts of noble metal ions in solution. The ISE and DPAS techniques are generally more sensitive than AAS. Although there is limited availability of ISEs, they offer the unique advantage of continuous monitoring. DPAS is very rapid but the optimization of the procedure (*e.g.*, choice of supporting electrolyte) may be tedious. AAS methods are simple and rapid but consume sample solution, which complicates periodic monitoring of concentration. The method used must be matched to the element to be determined, in terms of sensitivity and precision (Table 2).

Acknowledgement—The author thanks Norbert D. Greene, University of Connecticut, Storrs for suggesting this work.

REFERENCES

1. D. A. Jones and N. D. Greene, *Corrosion*, 1966, **22**, 198.
2. A. R. Nisbet and A. J. Bard, *J. Electroanal. Chem.*, 1963, **6**, 332.
3. G. W. Tindall and S. Bruckenstein, *Anal. Chem.*, 1968, **40**, 1051, 1402.

4. G. Reusmann and J. Westphalen, *Z. Anal. Chem.*, 1973, **264**, 165.
5. S. P. Perone and H. E. Stapelfeldt, *Anal. Chem.*, 1966, **38**, 796.
6. D. C. Johnson and R. E. Allen, *Talanta*, 1973, **20**, 305.
7. G. M. Schmid and G. W. Bolger, *Clin. Chem.*, 1973, **19**, 1002.
8. S. H. Cadle and S. Bruckenstein, *Anal. Chem.*, 1974, **46**, 16.
9. E. P. Parry and K. B. Oldham, *ibid.*, 1968, **40**, 1031.
10. T. D. Gornostaeva and V. A. Pronin, *Zh. Analit. Khim.*, 1973, **28**, 1973; *Chem. Abstr.*, 1973, **79**, 11431s.
11. G. A. Rechnitz, *Chem. Eng. News*, 1967, **45**, No. 25, 146.
12. D. C. Müller, P. W. West and R. M. Müller, *Anal. Chem.*, 1969, **41**, 2038.
13. M. S. Frant, *Plating*, 1971, 686.
14. M. J. Smith and S. E. Manahan, *Anal. Chem.*, 1973, **45**, 836.
15. F. M. Tindall, *At. Abs. Newsl.*, 1965, **4**, 339.
16. S. P. Perone and J. R. Birk, *Anal. Chem.*, 1965, **37**, 9.
17. N. Fishkova, *Zavodsk. Lab.*, 1970, **36**, 1461.
18. G. Pannetier and P. Tiffoli, *Bull. Soc. Chim. France*, 1971, **10**, 3775.
19. A. Bresle, *Kemian Teollisyus*, 1967, **24**, 508; *Chem. Abstr.*, 1968, **68**, R74504t.
20. B. D. Cahan and R. Haynes, *J. Electroanal. Chem., Interfacial Electrochem.* 1969, **22**, 339.
21. M. Stern and A. C. Makrides, *J. Electrochem. Soc.*, 1960, **107**, 782.
22. E. E. Pickett and S. R. Koirtyohann, *Anal. Chem.*, 1969, **41**, No. 28A.

Talanta, Vol. 28, pp. 705 to 708, 1981
Printed in Great Britain. All rights reserved

0039-9140/81/090705-04$02.00/0
Copyright © 1981 Pergamon Press Ltd

STUDY OF THE BEHAVIOUR OF VARIOUS PHENOLIC COMPOUNDS IN THE 4-AMINOANTIPYRINE AND ULTRAVIOLET-RATIO SPECTROPHOTOMETRIC METHODS WITHOUT AND WITH DISTILLATION

JOHN FARINO*, GEORGE NORWITZ, WALTER J. BOYKO
and PETER N. KELIHER†
Chemistry Department, Villanova University, Villanova, Pa. 19085, U.S.A.

(*Received* 6 *February* 1981. *Accepted* 27 *February* 1981)

Summary—It is customary in industrial analysis in the determination of phenols by the 4-aminoantipyrine (4-AAP) and ultraviolet-ratio spectrophotometric methods to report the total of phenolic compounds as phenol. A study was therefore made of the behaviour of 36 representative phenolic compounds in the 4-AAP and UV-ratio methods, with and without distillation, to ascertain the apparent recoveries relative to that for phenol. The Fisher phenol analyser was used for the UV-ratio method, which depends upon the bathochromic shift (from about 270 to about 290 nm) usually obtained when the solution of the phenol is made alkaline. The apparent recoveries by the 4-AAP method both with and without distillation varied from 0 to 100%. The apparent recoveries by the UV-ratio method without distillation varied from 0 to 148%, and those with distillation varied from 0 to 110%. Sixteen of the compounds tested without distillation gave less than 10% recovery by the 4-AAP method and eleven gave less than 10% recovery by the UV-ratio method. The results after distillation indicated that several of the compounds did not distil completely.

The aminoantipyrine (4-AAP) and ultraviolet-ratio (UV-ratio) spectrophotometric methods are frequently used for the determination of phenols. The 4-AAP method depends on the purplish-red colour obtained on reacting 4-AAP with the phenol in the presence of potassium hexacyanoferrate(III).[1–21] The UV-ratio or difference method depends upon the bathochromic shift obtained when a solution of a phenol is made alkaline.[7,15,20,22–30] It is customary in using these methods in industrial analysis to report the total phenol content as phenol; however, many phenols do not react with 4-AAP or give the bathochromic shift shown by phenol. The type of group in the *para*-position of a phenol markedly affects the 4-AAP reaction.[1,2,5,12,13,17,18] The colours obtained on reacting substituted phenols with 4-AAP may have a different wavelength of maximum absorption than the colour of the phenol product. The UV-ratio method is less susceptible to structural differences, but phenolic compounds that do not give approximately the same bathochromic shift as phenol will give low results.[27,28] In the determination of phenolic compounds in water and wastes, it is customary to distil the phenolic compounds before the actual analysis. It is usually assumed that the distillation is quantitative but this has not been studied.

We have investigated the behaviour of various phenolic compounds in the 4-AAP and UV-ratio methods with and without distillation. The analytical procedures used were essentially those already described.[20]

EXPERIMENTAL

Apparatus and reagents

A Bausch and Lomb Spectronic 20 colorimeter (1-cm cell), a Hewlett-Packard model 8450A recording spectrophotometer (1-cm cell) and a Fisher phenol analyzer (5-cm cell) were used. The last instrument monitors the bathochromic shift of phenols by use of two hollow-cathode lamps, modulated in a time ratio mode.[20,27,29] One of the lamps ("pH sensitive") is a platinum lamp (291.5 nm), while the other ("pH insensitive") is a chromium lamp (360 nm).

The distillation apparatus consisted of a 1-litre round-bottomed flask and a Graham condenser (with jacket 40 cm in length and an outer 24/40 joint at top) joined by a connecting tube (Fisher No. 15-323D) with thermometer opening sealed off by a 10/30 ground-glass stopper. The flask was heated by an electric mantle.

Distilled water and reagent grade chemicals were used. All solutions were stored in glass. Phosphoric acid (1 + 9) was dispensed with 4-oz dropping bottles that gave drops of about 0.08 ml. Sodium hydroxide solution (20%) was dispensed with a medicine dropper about 14 cm long that was inserted into a narrow-mouthed bottle about 10 cm high (to prevent attack on the plastic top or bulb). Phenol solution No. 1 (1 ml = 1.00 mg of phenol) was prepared by dissolving 1.000 g of phenol in water and diluting to 1 litre in a standard flask. Phenol solution No. 2 (1 ml = 0.10 mg of phenol) was prepared fresh daily by diluting phenol solution No. 1 tenfold. 4-AAP solution (2%) and potassium hexacyanoferrate(III) solution (8%) were both prepared fresh weekly.

Preparation of calibration curves

4-AAP method. Portions of phenol solution No. 2 (0.00, 1.00, 2.00, 3.00, 4.00, 5.00 ml) were transferred to 125-ml Erlenmeyer flasks (marked at 100 ml). The volumes were

* Present address: Chemistry Department, Georgia Institute of Technology, Atlanta, Ga. 30332, U.S.A.
† To whom correspondence should be addressed.

brought up to 100 ml, 2.0 ml of ammonium chloride solution (5%) were added, and the solutions were adjusted to pH 10.0 ± 0.2 with ammonia solution (1 + 1) (pH-meter). Then, 2.0 ml of 4-AAP solution (2%) and 2.0 ml of potassium hexacyanoferrate(III) solution were added, the solutions were mixed, and after 15 min the absorbances were measured at 510 nm against distilled water. The absorbance of the blank was deducted and the absorbances were plotted against mg of phenol (per 100 ml).

UV-ratio method. Portions of phenol solution No. 2 (0.00, 1.00, 3.00, 5.00, 6.00, 7.00 ml) were transferred to 100-ml standard flasks and the solutions were diluted to the mark. A portion of the solution was transferred to the cell, 1 drop of phosphoric acid (1 + 9) was added with mixing, and the instrument was set to 0% absorption. Two drops of sodium hydroxide solution (20%) were added with mixing and the per cent absorption was read (normal sensitivity). The cell and stoppers were washed thoroughly with running hot tap water and the next sample was analysed. The per cent absorption was converted into absorbance by using appropriate tables, the absorbance of the blank was deducted, and the absorbances were plotted against mg of phenol (per 100 ml).

Procedures

Stock solutions of the phenols were prepared by dissolving 0.04 g of the compounds, weighed to 0.1 mg, in ethyl alcohol and diluting to 100 ml in standard flasks with ethyl alcohol. For the methods without distillation, 1.00-ml aliquots were analysed as described for the calibration. For the methods with distillation, a 4.00-ml aliquot was added to a 1-litre round-bottomed flask (marked at 550 ml) containing about 500 ml of water. Several drops of Methyl Orange indicator were added and the solution was made just pink with phosphoric acid (1 + 9). The volume was brought up to 550 ml and 500 ml were distilled into a 500-ml Erlenmeyer flask (marked at 500 ml). Then, 100 ml of the distillate were used for the 4-AAP method and another portion was transferred to the cell and the phenol determined as described for the UV-ratio method.

The blanks for both methods had an absorbance of about 0.015. For the results not to be meaningless when the recoveries were very low, the results were recorded as 0% whenever the absorbance reading was 0.02 or less.

Ultraviolet spectra

Spectra were run for several representative phenolic compounds (without distillation) with the recording spectrophotometer. For this study, aliquots of the solutions of the phenolic compounds were treated with 5 drops of phosphoric acid (1 + 9) or 5 drops of sodium hydroxide

Table 1. Recoveries of phenols by the 4-AAP and UV-ratio methods without and with distillation

Compound	Recovery, %			
	4-AAP		UV-ratio	
	Without distillation	With distillation	Without distillation	With distillation
Phenol	100	100	100	100
Hydroquinone	7.0	3.0	0.0	0.0
Resorcinol	26	0.0	126	2.9
Pyrogallol	53	17	0.0	10
m-Chlorophenol	63	45	102	94
o-Chlorophenol	77	73	130	110
p-Chlorophenol	67	67	70	67
2,4-Dichlorophenol	30	29	42	40
2,4,6-Trichlorophenol	0.0	3.0	15	3.0
m-Bromophenol	44	39	80	77
o-Bromophenol	47	53	80	77
p-Bromophenol	39	33	44	48
2,4-Dibromophenol	19	15	12	18
o-Cresol	67	73	117	110
p-Cresol	0.0	0.0	100	100
2,4-Xylenol	0.0	0.0	97	97
4,6-Dibromo-*o*-cresol	36	32	40	35
4-Chloro-2-methylphenol	49	48	83	82
4-Chloro-3,5-dimethylphenol	24	21	71	65
p-Tert.amylphenol	2.4	0.0	76	67
p-Methoxyphenol	50	21	9.5	8.8
o-Aminophenol	0.0	0.0	0.0	0.0
p-Aminophenol	0.0	0.0	38	4.0
2,4-Diaminophenol	2.4	0.0	0.0	0.0
o-Nitrophenol	0.0	0.0	10	17
m-Nitrophenol	0.0	0.0	49	3.0
2,4-Dinitrophenol	0.0	0.0	0.0	0.0
Picric acid	28	0.0	148	19
1-Naphthol	37	20	0.0	0.0
2-Naphthol	2.4	0.0	7.3	6.0
1-Amino-2-naphthol.HCl	2.4	0.0	80	6.1
5-Amino-1-naphthol.HCl	0.0	0.0	0.0	3.1
1,4-Naphthalenediol	0.0	0.0	121	82
8-Hydroxyquinoline	40	23	0.0	0.0
Salicylic acid	0.0	0.0	2.3	0.0
4,4′-Isopropylidine diphenol	49	0.0	102	3.0

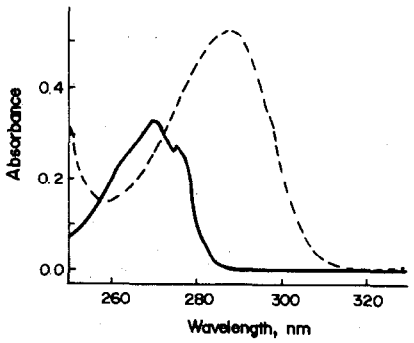


Fig. 1. Spectrum of phenol (2.0 mg/100 ml). The curve for acidic solution is indicated by ——; the curve for basic solution by ---.

solution (20%), the volumes brought up to 100 ml in standards flasks, and the spectra run.

RESULTS AND DISCUSSION

The recoveries obtained for both methods (Table 1) were very diverse. The recoveries in the 4-AAP method without distillation varied from 0% (11 compounds) to 100% (phenol). The recoveries in the 4-AAP method with distillation varied from 0% (17 compounds) to 100% (phenol). The recoveries in the UV-ratio method without distillation varied from 0% (8 compounds) to 148% (picric acid). The recoveries in the UV-ratio method with distillation varied from 0% (7 compounds) to 110% (*o*-cresol and *o*-chlorophenol). Sixteen compounds gave less than 10% recovery with the 4-AAP method without distillation. Eleven gave less than 10% recovery with the UV-ratio method without distillation. In many cases it was difficult to judge the extent to which the compounds distilled, but the results seem to indicate that resorcinol, pyrogallol, *m*-nitrophenol, picric acid, 1-amino-2-naphthol, and 4-isopropylidine diphenol were less than 50% distilled. *p*-Chlorophenol condensed in the condenser but was driven over by shutting off the water after half of the distillate had been collected.

The colours produced in the 4-AAP method were purplish red or red (indicating maximum absorption at about 500 nm), except for 2-naphthol, which gave a faint green. None of the colours was as intense as that from phenol (taken as 100% for reference, without distillation); the next highest was *o*-chlorophenol (77% without distillation). It has been pointed out that when the *para*-position of a phenol is occupied by a hydroxyl, halogen, carboxyl, methoxy, or sulphonic group there is a reaction with 4-AAP, but when it

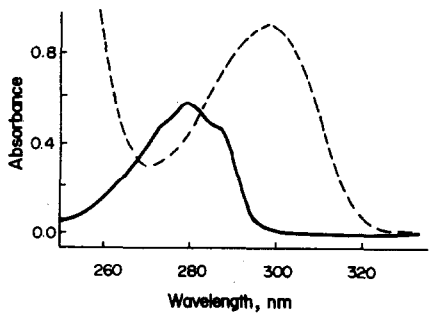


Fig. 2. Spectrum of *p*-chlorophenol (0.50 mg/100 ml).

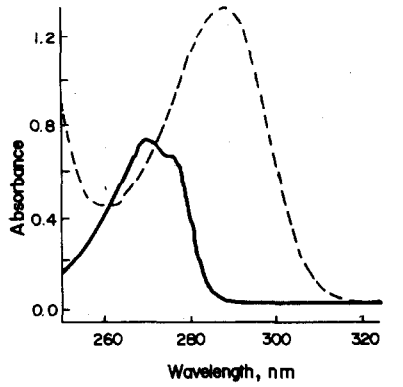


Fig. 3. Spectrum of *o*-cresol (0.50 mg/100 ml).

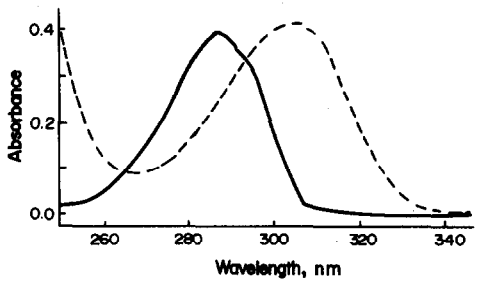


Fig. 4. Spectrum of *p*-methoxyphenol (2.0 mg/100 ml).

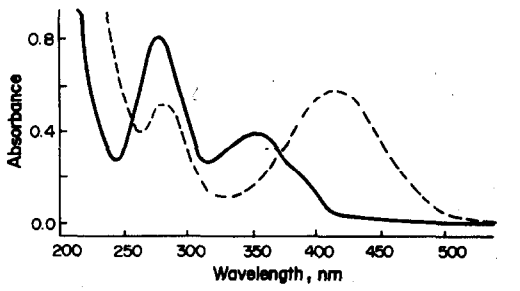


Fig. 5. Spectrum of *o*-nitrophenol (0.20 mg/100 ml).

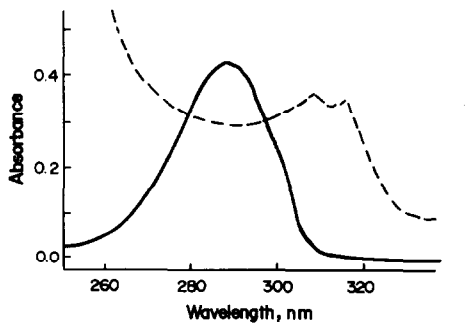


Fig. 6. Spectrum of hydroquinone (2.0 mg/100 ml).

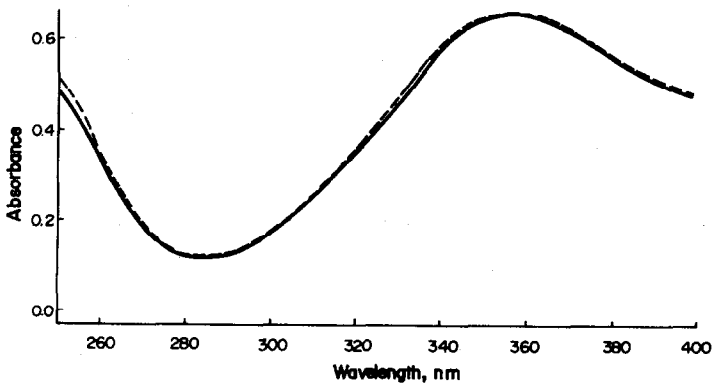


Fig. 7. Spectrum of *p*-aminophenol (2.0 mg/100 ml).

is occupied by an alkyl, nitro, nitroso, benzoyl, or aldehyde group there is no reaction.[1,2,5,12,13,17,18] However, it must be emphasized that these observations were for the most part qualitative and may be misleading.

The spectra obtained for phenol and six representative phenolic compounds are shown in Figs. 1–7 and can be characterized into two groups. The first group (*p*-chlorophenol, *o*-cresol, and *p*-methoxyphenol) (Figs. 2–4) give spectra that are very similar to that of phenol, insofar as the bathochromic shift is concerned. The second group (*o*-nitrophenol, hydroquinone, and *o*-aminophenol) (Figs. 5–7) give spectra very dissimilar to that of phenol, with regard to the bathochromic shift. It is obvious from the spectra why the first group gives reasonably accurate results by the UV-ratio method, while the second group does not. *o*-Nitrophenol and other nitrophenols give yellow solutions and therefore show marked absorption in the visible region (Fig. 5). The compounds of the first group are much more frequently encountered in real samples for water analysis than the second group, being likely to result from oxidation of the phenol or reaction of the phenol with the chlorine or hypochlorite that the water often contains.

Acknowledgements—We thank the Hewlett-Packard Co. for the loan of the Model 8450A spectrophotometer and Jay Levine of the company for useful discussion. This paper was presented at the 6th Federation of Analytical Chemistry and Spectroscopy Societies (FACSS) meeting, Philadelphia, Pennsylvania, September 20, 1979.

REFERENCES

1. E. Emerson, *J. Org. Chem.*, 1938, **3**, 153.
2. *Idem, ibid.*, 1943, **8**, 417.
3. S. Gottlieb and P. B. Marsh, *Anal. Chem.*, 1946, **18**, 16.
4. J. A. Shaw, *ibid.*, 1951, **23**, 1788.
5. M. B. Ettinger, C. C. Ruchhoft and R. I. Lishka, *ibid.*, 1951, **23**, 1783.
6. M. Dennis, *Sewage Ind. Wastes*, 1951, **23**, 1516.
7. E. F. Mohler, Jr. and L. N. Jacob, *Anal. Chem.*, 1957, **29**, 1369.
8. R. J. Lacoste, S. H. Venable and J. C. Stone, *ibid.*, 1959, **31**, 1246.
9. G. E. Gordon, *ibid.*, 1960, **32**, 1325.
10. F. W. Ochynski, *Analyst*, 1960, **85**, 278.
11. S. D. Faust and O. M. Aly, *J. Am. Water Works Assoc.*, 1962, **54**, 235.
12. S. D. Faust and E. W. Mikulewicz, *Water Res.*, 1967, **1**, 405, 509.
13. S. D. Faust and F. G. Lorentz, *Proc. 11th Ontario Industrial Waste Conference*, June 1964, pp. 173–201.
14. P. D. Goulden, P. Brooksbank and M. B. Day, *Anal. Chem.*, 1973, **45**, 2430.
15. B. K. Afghan, P. E. Belliveau, R. H. Larose and J. F. Ryan, *Anal. Chim. Acta*, 1974, **71**, 355.
16. M. E. Gales, Jr. and R. L. Booth, *J. Am. Water Works Assoc.*, 1976, **68**, 540.
17. American Public Health Association, *Standard Methods for the Examination of Water and Waste Water*, 13th Ed., pp. 501–10, Washington, 1971.
18. American Society for Testing and Materials, *ASTM Designation* D-1723, *Standard Methods of Test for Phenolic Compounds in Water*, Philadelphia, Pa., 1979.
19. U.S. Environment Protection Agency, *Methods for Chemical Analysis of Water and Wastes*, STORET Method No. 32730, Cincinnati, Ohio, 1974.
20. G. Norwitz, J. Farino and P. N. Keliher, *Anal. Chem.*, 1979, **51**, 1632.
21. G. Norwitz and P. N. Keliher, *Anal. Chim. Acta*, 1980, **119**, 99.
22. M. J. Murray, *Anal. Chem.*, 1949, **21**, 941.
23. L. J. Schmauch and H. M. Grubb, *ibid.*, 1954, **26**, 308.
24. C. F. Smullin and F. P. Wetterau, *ibid.*, 1955, **27**, 1836.
25. A. S. Wexler, *ibid.*, 1963, **35**, 1936.
26. J. M. Martin, Jr., C. D. Orr, C. D. Kincannon and J. L. Bishop, *J. Water Pollut. Control Fed.*, 1967, **39**, 21.
27. J. E. Fountaine, P. B. Joshipura, P. N. Keliher and J. D. Johnson, *Anal. Chem.*, 1974, **46**, 62.
28. L. S. Smith, *U.S. Environmental Protection Agency, Environmental and Monitoring Support Laboratory, Report* EPA-600/4-76-048, Evaluation of Instrument for the Determination of Phenol in Water, Cincinnati, Ohio, Sept. 1976.
29. *Fisher Scientific Co. Bull.* No. 441/7-028-10, *Fisher Phenol Analyzer.*
30. J. A. Williamson, *Rapid Determination of Phenol Content of Water*, paper presented at International Water Resources Assoc. Seminar on Water Resources Instrumentation, Chicago, Ill., June 1974.

Talanta, Vol. 28, pp. 709 to 716, 1981
Printed in Great Britain. All rights reserved

0039-9140/81/100709-08$02.00/0
Copyright © 1981 Pergamon Press Ltd 1981

ABSORPTION ET FLUORESCENCE D'ALCALOIDES QUATERNAIRES DERIVES DE LA QUINOLEINE: APPLICATIONS ANALYTIQUES

M. MONTAGU* et P. LEVILLAIN

Laboratoire de Chimie Analytique, Faculté de Pharmacie, 37032 Tours Cedex, France

et

M. RIDEAU et J. C. CHÉNIEUX

Laboratoire de Biologie Végétale, Faculté de Pharmacie, 37032 Tours Cedex, France

(*Reçu le* 4 *mars* 1980. *Révisé le* 10 *février* 1981. *Accepté le* 7 *avril* 1981)

Résumé—Les propriétés d'absorption et de fluorescence d'une série de six alcaloïdes dihydrofuroquinoléiques et dihydropyrannoquinoléiques extraits de plantes de la famille des Rutacées sont décrites et reliées à leur structure. Ces propriétés sont ensuite appliquées au dosage dans les milieux biologiques (extraits de tissus végétaux et de cultures cellulaires) de deux d'entre eux: le platydesminium et le balfourodinium, présents dans *Choisya ternata*.

Les alcaloïdes dihydrofuroquinoléiques et dihydropyrannoquinoléiques présents chez certaines espèces de la famille des Rutacées possèdent des propriétés biologiques intéressantes.[1–5] Nous étudions les conditions optimales de production *in vitro* de deux d'entre eux par des cultures de tissus de *Choisya ternata* H.B.K. La faible teneur de ces alcaloïdes dans les cellules végétales et leurs milieux de culture nous a conduits à rechercher une technique de dosage sensible, aucune méthode n'ayant encore été proposée pour ce type d'alcaloïde.

Les propriétés classiques d'absorption dans l'ultraviolet et de fluorescence des dérivés quinoléiques nous ont amenés à étudier dans ce domaine une série de six alcaloïdes.

PARTIE EXPERIMENTALE

Appareillage

Les mesures en absorption ont été effectuées à l'aide d'un spectrophotomètre "Duospac" Jobin et Yvon.

Les spectres de fluorescence ont été obtenus en utilisant un spectrofluorimètre J.Y.3 Jobin et Yvon, équipé d'un photomultiplicateur R212, avec les conditions d'utilisation suivantes: largeur de fente 10 nm; facteur d'amplification 10 à 300. Aucune correction n'a été effectuée pour compenser les variations de l'intensité de la lampe, la transmission des monochromateurs ou la sensibilité du récepteur en fonction de la longueur d'onde.

Echantillons

Les différents échantillons étudiés ont été obtenus par extraction, chromatographie et purification.[1] La formule des produits étudiés figure dans le Tableau 1.

Solutions

Les études ont été effectuées sur des solutions de concentrations exactement connues, voisines de $2.10^{-5}M$ en absorption et de $10^{-6}M$ en fluorescence.

Pour étudier l'influence des conditions opératoires en fluorescence, différents types de milieux ont été utilisés:

—solutions tampons de pH compris entre 2,5 et 11 (tampons acétate, phosphate, carbonate).[6]
—solutions salines 0,1*M* (voir Tableau 3).
—solvants organiques (voir Tableau 4).

Tous les produits utilisés sont purs, pour analyses.

Le dosage dans les milieux biologiques nécessite les solvants et réactifs suivants.

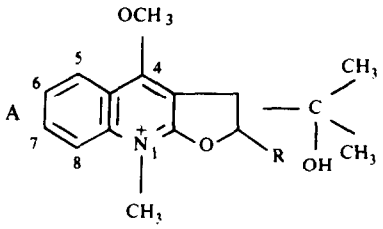
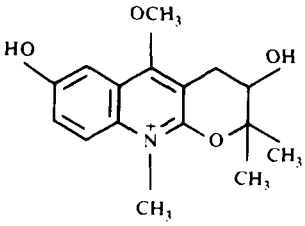
—Méthanol P.A.
—Tampon pH 6: mélange de 87,7 ml d'une solution de phosphate monopotassique (KH_2PO_4) *M*/15 et de 12,3 ml d'une solution de phosphate disodique ($Na_2HPO_4 \cdot 2H_2O$) *M*/15.
—Bleu de bromothymol $3.10^{-4}M$ tamponné à pH 6.
—Plaques de gel de silice (Merck G60, 20 × 20 cm).
—Solvant de migration: acétate d'éthyle–acide formique–eau (10:1:1 v/v).
—Solvant d'élution: méthanol–acide formique (4:1 v/v).

Procédé de dosage du platydesminium et du balfourodinium dans les cultures de Choisya ternata *H.B.K.*

L'échantillon de 25 mg de matériel végétal lyophilisé et broyé est extrait par macération et agitation pendant 1 hr dans 5 ml de méthanol. Après centrifugation, une partie aliquote de l'extrait méthanolique est évaporée à 50° sous courant d'air et le résidu sec est repris par 3 ml d'une solution aqueuse de bleu de bromothymol tamponnée à pH 6. Les complexes formés entre les alcaloïdes et le colorant sont extraits par du dichlorométhane (2 × 1 ml). Le solvant est évaporé et le résidu repris par exactement 50 µl de méthanol. Des dépôts correspondant à 25 µl sont effectués sur une plaque de gel de silice et on chromatographie à front perdu pendant 8 hr dans un mélange acétate d'éthyle–acide formique–eau distillée (10:1:1 v/v). La zone correspondante au balfourodinium est repérée sous ultraviolet (254 nm). Le rapport des R_f du platydesminium (P) et du balfourodinium (B) $R_{f_P}/R_{f_B} \sim 0{,}7$ permet de repérer la zone du platydesminium. Les zones correspondantes sont découpées et l'on élue par macération et agitation (30 mn) dans 5 ml de solvant d'élution (méthanol–acide formique 4:1 v/v). Après centrifugation, on mesure la fluorescence à 343 nm (platydesminium) et à 439 nm (balfourodinium) en excitant à 307 nm. On défalque des mesures précédentes l'émission de l'éluat d'une zone équivalente de gel de silice prélevée dans les mêmes conditions.

* Auteur à qui on doit addresser la correspondance.

Tableau 1. Propriétés spectrales des alcaloïdes

Nom	Substituants	R	Absorption λ_{max}, *nm* (ϵ_M, $l \cdot mole^{-1} \cdot cm^{-1}$)	Fluorescence exc./em., *nm* (~épaulement)	Intensités pour $C = 10^{-6} M$
Platydesminium perchlorate			216 (3,1·10⁴) 236 (3,35·10⁴) 294 (1,06·10⁴) ~317	237/345 307/345	10 41
Balfourodinium chlorure	B — $-OCH_3$ (8)	*idem*	214 (2,53·10⁴) 253 (3,1·10⁴) 301 (6,8·10³) ~320	257/448 310/448	45 38
Ptelefolonium picrate	C — $-OCH_3$ (6) $-OCH_3$ (8)	$-C(CH_3)=CH_2$	217 (3,5·10⁴) 257,5 (5,4·10⁴) 306 (1,02·10⁴) 347 (9,6·10³)	259/464 306/464 345/464 ~506	28 14 16
Isoptelefolonium perchlorate	D — $-OCH_3$ (7) $-OCH_3$ (8)	*idem*	223,5 (3,05·10⁴) 259,5 (4,66·10⁴) 323 (1,22·10⁴)	324/479 324/509	7 7
Ribalinium perchlorate	E — $-OH$ (6)	$-C(CH_3)_2OH$	220 (3,15·10⁴) 245,5 (2,44·10⁴) ~290 298,6 (9,2·10³) 331,5 (6,0·10³)	295/515 342/515	6 8
Rutalinium perchlorate	F		213 (2,96·10⁴) 248 (3,0·10⁴) ~294 304 (9,5·10³) 347 (6,3·10³)	304/518 344/518	5 7
Quinine dans H_2SO_4 0,1*N*			210 (2,93·10⁴) 251 (2,84·10⁴) 317 (4,3·10³) 350 (5,0·10³)	253/450 352/450 ~490	36 79

RESULTATS ET DISCUSSION

Structure et propriétés spectrales

Les propriétés caractéristiques en absorption et en fluorescence obtenues pour les six alcaloïdes étudiés en solution aqueuse sont rassemblées dans le Tableau 1. Bien que la nature des sels soit différente, nous pouvons tout de même envisager une discussion sur la fluorescence et l'absorption de ces alcaloïdes. En effet nous montrons plus loin que, si les anions peuvent perturber la fluorescence de ces composés, ils ne le font qu'à fortes concentrations. Or cette étude est ici effectuée sur les sels purs et donc en présence de faibles concentrations d'anions*. L'étude des spectres ultraviolets montre, comme l'avaient signalé différents auteurs ayant travaillé sur ce type d'alcaloïdes,[7–11] la présence de quatre bandes dans les zones 315–340, 290–305, 235–255 nm et vers 220 nm. En comparant les résultats obtenus pour le platydesminium d'une part, la quinoléine et l'ion quinoléinium d'autre part (Tableau 2), on peut attribuer les trois premières bandes respectivement aux transitions électroniques ^1L_b (315–340 nm), ^1L_a (290–305 nm) et ^1B_b (235–255 nm).[12] Pour la quinoléine en effet, l'attribution est effectuée sans ambiguïté par comparaison avec le

* Seul l'ion picrate absorbant à 347 nm fausse les mesures d'absorption et de fluorescence, mais comparé au picrate de ptéléfolonium, le chlorure de ptéléfolonium[7] absorbe à 214, 255, 292–301, 335–347 nm ce qui ne change pas la discussion ultérieure.

Tableau 2. Maximums d'absorption (*nm*) et absorptivités molaires correspondant aux différentes transitions

	$^1B_b \leftarrow {}^1A$ λ, *nm* (ϵ, $l \cdot mole^{-1} \cdot cm^{-1}$)	$^1L_a \leftarrow {}^1A$ λ, *nm* (ϵ, $l \cdot mole^{-1} \cdot cm^{-1}$)	$^1L_b \leftarrow {}^1A$ λ, *nm* (ϵ, $l \cdot mole^{-1} \cdot cm^{-1}$)
Naphtalène	220 ($1{,}33 \cdot 10^5$)	289 ($9{,}3 \cdot 10^3$)	312 (280)
Quinoléïne	225 ($3{,}5 \cdot 10^4$)	278 ($3{,}5 \cdot 10^3$)	300–315 ($3{,}0 \cdot 10^3$)
Quinoléinium	235 ($3{,}5 \cdot 10^4$)		315 ($7{,}0 \cdot 10^3$)
Platydesminium	236 ($3{,}35 \cdot 10^4$)	294 ($1{,}06 \cdot 10^4$)	317 (épaulement)

naphtalène (composé isoélectronique π) et le passage à l'ion quinoléinium entraîne classiquement un effet bathochrome et hyperchrome général particulièrement marqué pour la transition ^1L_a polarisée transversalement au plan de la molécule. Contrairement à ce qui est admis généralement, la présence chez ces alcaloïdes d'un groupement méthyle fixé sur l'azote produit un effet moins important que celle d'un proton puisque, pour le platydesminium, la transition ^1L_b apparaît comme un épaulement de la bande ^1L_a alors que ces deux bandes sont confondues pour l'ion quinoléinium (Tableau 2).

Normalement, la présence du cycle furanne en 2,3 du cycle quinoléique doit entraîner un déplacement bathochrome par rapport à l'ion quinoléinium: or il n'est rien (Tableau 2). Sans doute cet effet se trouve-t-il compensé par la présence du groupement méthoxy en 4 qui produit un effet hypsochrome dans le cas des hétérocycles azotés.[13] Par contre un effet bathochrome de la bande ^1L_b apparaît lorsque le noyau pyranne remplace le noyau furanne (E et F), effet déjà observé par Szendrei.[14]

L'introduction d'autres substituants dans la molécule intervient classiquement (Tableau 1):

—par leur nature: le groupement phénol entraîne un effet bathochrome plus marqué sur la bande ^1L_b que sur la bande ^1L_a alors que le groupement méthoxy a un effet inverse. Ceci est confirmé pour d'autres composés de la même série comme le ptéléatinium (OH en 8) et le balfourodinium (OCH_3 en 8),[5] mais non vérifié par la comparaison du ribalinium (OH en 6) et du méthylribalinium (OCH_3 en 6) dont les spectres sont identiques.[15]

—par leur position: les substituants en 1, 4, 5, 8 influent sur la position de la bande ^1L_a polarisée transversalement alors qu'en 2, 3, 6, 7 ils agissent surtout sur les bandes ^1B_b et ^1L_b polarisées selon le grand axe de la molécule.[16]

—en cas de polysubstitution, il faut noter l'influence additive des différents substituants: l'effet bathochrome augmente avec leur nombre. Toutefois leur influence se trouve modifiée par la position relative des différents groupements: les substitutions en 7,8 donnent un effet plus net qu'en 6,8 (C et D, Tableau 1). Bien qu'une étude systématique soit difficile dans ce cas, étant donné le petit nombre de composés isolés, il semble que ce soit surtout la nature du groupement qui intervienne.

La bande à 220 nm peut être attribuée à la transition ^1C_b. Cette transition, dans une molécule parfaitement symétrique, est normalement interdite car non polarisée. Toutefois la dissymétrie dans la structure de nos alcaloïdes leve cette interdiction.

En ce qui concerne la fluorescence, il faut d'abord noter l'intensité de phénomène. On sait en effet que, pour les composés aromatiques, le rendement de fluorescence augmente généralement avec le nombre de cycles conjugués accolés. L'inertie plus marquée de la molécule évite ainsi la dissipation de son énergie par collision. De plus, pour ces alcaloïdes, la structure quaternaire implique le blocage du doublet d'électrons de l'azote et empêche ainsi le couplage interne entre état singulet et état triplet qu'on observe généralement chez les hétérocycles azotés tertiaires et qui favorise la phosphorescence aux dépens de la fluorescence. Enfin, la présence de groupements phénol ou méthoxy sur les cycles aromatiques augmente généralement l'intensité de la réponse. Compte tenu de ces influences, ces alcaloïdes se révèlent très fluorescents. Toutefois il est délicat de comparer les intensités d'émission de ces alcaloïdes entre eux. Cette comparaison n'est valable que pour les alcaloïdes présentant des longueurs d'onde d'excitation et d'émission suffisamment voisines (composés E et F, B et quinine). Pour les autres, les résultats doivent être corrigés en fonction des caractèristiques de l'appareil: spectre de la lampe, courbe de réponse du détecteur.

En ce qui concerne la position des maximums d'excitation, on constate qu'elle suit d'assez près la variation des positions des bandes d'absorption ^1L_b et ^1B_b. Les différences que l'on rencontre entre absorption et excitation s'expliquent par l'absence de correction pour l'intensité de la lumière d'excitation et pour la sensibilité de l'appareil en fonction de la longueur d'onde.

Quant à la position du maximum d'émission, on peut noter l'influence très nette des groupements phénoliques, dont la présence entraîne une émission dans la région supérieure à 500 nm (E, F, Tableau 1), alors que les composés renfermant des groupements méthoxy émettent en dessous de cette limite pour la plupart (B, C, D, Tableau 1).

APPLICATION AU DOSAGE D'ALCALOÏDES

Lors de cette étude, nous nous sommes limités à deux alcaloïdes (platydesminium et balfourodinium) que nous avons pu isoler en quantités suffisantes à partir de feuilles de *Choisya ternata.*

Tableau 3. Influence des anions (solutions $10^{-1}M$) sur la fluorescence des alcaloïdes (solutions $10^{-6}M$)

Anions	Platydesminium perchlorate, *unités % à 307/345*	Balfourodinium chlorure, *unités % à 310/448*
Eau	100	100
Acétate de sodium	102	104
Acide borique	103	101
Citrate de sodium	89	114
Halogénures		
Fluorure de sodium	101	101
Chlorure de potassium	63	101
Bromure de potassium	12,5	10
Iodure de potassium	10	2
Hydrogénocarbonate de sodium	100	100
Hydrogénophtalate de potassium	20	35
Nitrate de sodium	10	46
Perchlorate de sodium	104	101
Phosphate monopotassique	104	100
Sulfate de sodium	107	102

Influence des conditions expérimentales

Influence du pH. En dessous de pH 9, il n'existe pas d'influence de l'acidité sur l'intensité de l'absorption comme de la fluorescence (Fig. 1). Toutefois pour cette dernière, les résultats varient avec la nature de l'acide, ce qui laisse supposer une influence de la nature des anions.

Au dessus de pH 9, les alcaloïdes sont dégradés en quinolone-2,[10] ce qui entraîne une modification du spectre avec diminution de l'absorption aux longueurs d'onde usuelles et disparition de la fluorescence.

Influence des anions. Parmi les ions étudiés (Tableau 3), constituants les plus courants des milieux tampons et de cultures cellulaires, on peut noter que les halogénures, les nitrates et les phtalates ont un pouvoir inhibiteur fort. Cependant les résultats du Tableau 3 ont été obtenus pour des concentrations en sels importantes ($10^{-1}M$). La figure 2 montre que l'effet inhibiteur diminue en fonction du rapport des concentrations molaires [anion]/[alcaloïde] et s'annule pour un rapport de 100 environ.

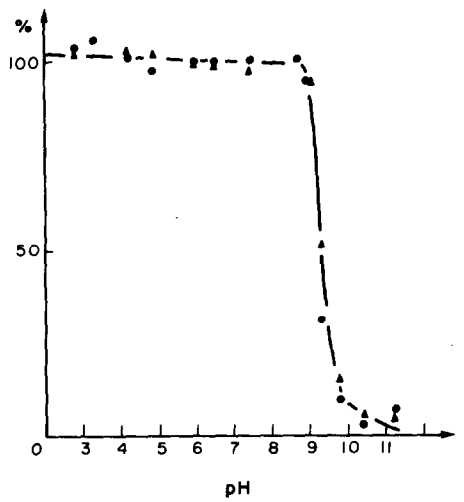


Fig. 1. Effet du pH sur la fluorescence (intensité relative) ● platydesminium, ▲ balfourodinium.

L'importance de l'inhibition est sensiblement proportionnelle à la stabilité des paires d'ions que les anions peuvent former avec des composés chargés positivement. Toutefois cette possibilité d'interaction n'est pas suffisante pour rendre compte de l'inhibition car les perchlorates, connus pour former des paires d'ions particulièrement stables, ne modifient pas la fluorescence; l'anion fixé doit donc en outre faciliter la dissipation non radiative de l'énergie (par exemple couplage singulet-triplet dans le cas des halogénures).

Influence des solvants. Nous avons comparé l'influence des différents solvants sur les propriétés spectrales de nos alcaloïdes (Tableau 4), leur solubilité très faible dans la plupart des milieux en a forcément limité le nombre étudié.

Vers 310 nm, les spectres d'absorption et ceux d'excitation ne dépendent pratiquement pas de la nature du solvant, qui peut toutefois modifier les seconds aux plus courtes longueurs d'onde par suite de son absorption propre. Par contre, l'intensité de fluorescence, et dans le cas du balfourodinium, la longueur d'onde du maximum d'émission (λ_{em}) varient avec le milieu. On distingue en fait trois types de solvants: les solvants chlorés (λ_{em} 431 nm), les alcools et l'acide acétique (λ_{em} 437–439 nm) et l'eau (λ_{em} 448 nm).

Les chiffres du Tableau 4 montrent que l'eau, qui est le solvant le plus polaire et qui présente par ailleurs la meilleure facilité d'emploi, convient très bien aux dosages fluorimétriques.

Application au dosage des alcaloïdes en solution aqueuse

Nous avons ensuite précisé sur des solutions aqueuses les conditions optimales de dosage de ces deux alcaloïdes en absorption et en fluorescence.

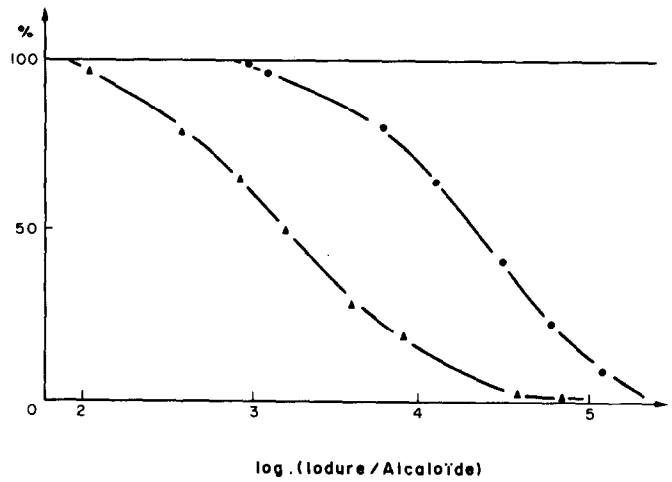


Fig. 2. Inhibition de la fluorescence par les iodures. Intensité de fluorescence: ● du platydesminium, ▲ du balfourodinium, en fonction de log ([iodure]/[alcaloïde]).

Linéarité, détectabilité, sensibilité. La méthode de régression linéaire a permis de déterminer ces trois paramètres:

—en absorbance: pour le platydesminium, en cuve de 1 cm, nous obtenons la droite reliant l'absorbance A et la concentration molaire C: $A = 3{,}35 \cdot 10^4 C$ à 236 nm avec un coefficient de corrélation $r = 0{,}9998$ pour des concentrations de $2{,}10^{-6}$ à $4{,}10^{-5} M$, et pour le balfourodinium, $A = 3{,}10 \cdot 10^4 C$ à 253 nm $r = 1$ pour des concentrations de 3.10^{-6} à $3{,}10^{-5} M$. Les limites de détection pour les deux alcaloïdes peuvent être abaissées par l'utilisation d'un trajet optique supérieur à 1 cm.

—en fluorescence: pour le platydesminium, l'émission à 345 nm avec une excitation à 307 nm est linéaire pour des concentrations comprises entre 10^{-7} et $2{,}10^{-5} M$ avec $r = 0{,}9980$, et pour le balfourodinium, l'émission à 448 nm avec une excitation à 310 nm est linéaire pour des concentrations comprises entre $3{,}10^{-8}$ et $3{,}10^{-5} M$ avec $r = 0{,}9998$. Dans les deux cas, la droite passe par l'origine des coordonnées.

Reproductibilité. Pour définir l'erreur relative en différents points de la droite, nous avons effectué une série de neuf mesures sur chacune des solutions étudiées (Tableau 5). Ces valeurs confirment que la dispersion est plus grande pour les faibles concentrations de platydesminium que de balfourodinium, ce qui explique la différence dans les limites inférieures de détection. A l'état de traces, le balfourodinium, moins polaire, est peut-être moins adsorbé sur le verre que le platydesminium.

Etalonnage, rendement de fluorescence. Le problème de l'étalonnage en vue de dosages répétés est assez délicat à résoudre. En effet, il est très difficile de se procurer des étalons, étant donné la faible teneur en alcaloïdes dans les plantes et la longueur de la méthode d'extraction et de purification. Aussi avons-nous cherché à résoudre cette difficulté. En absorption il est toujours possible d'utiliser les absorptivités molaires indiquées précédemment.

En fluorescence, la réponse obtenue dépend directement de l'appareillage. C'est pourquoi nous avons déterminé le rendement de fluorescence, ce qui permet de rendre compte de l'intensité de fluorescence des deux alcaloïdes, en levant le caractère arbitraire des unités de mesure. Ce rendement de fluorescence ϕ, rapport du nombre de quanta émis sur le nombre de quanta absorbés, peut être obtenu par comparaison à un composé de référence dont le rendement de fluor-

Tableau 4. Action des solvants sur la fluorescence des alcaloïdes $10^{-6} M$

Solvants	Platydesminium		Balfourodinium	
	Exc./Em.	Unités %	Exc./Em.	Unités %
1 Eau	307/345	100	310/448	100
2 Méthanol	307/343	70	309/439	107
3 Ethanol	307/343	70	309/439	114
4 Acide acétique	307/343	90	309/439	140
5 Propanol-1	308/343	67	309/439	114
6 Butanol-1	308/343	58	308/437	104
7 Dichlorométhane	308/344	46	310/431	50
8 Chloroforme	308/344	53	310/431	60

Tableau 5. Etude de la reproductibilité

	Concentrations, M	Coefficient de variation, %
Platydesminium	$7{,}95 \cdot 10^{-6}$	0,4
	$1{,}60 \cdot 10^{-6}$	1,3
	$3{,}20 \cdot 10^{-7}$	3,3
	$6{,}35 \cdot 10^{-8}$	9,1
Balfourodinium	$1{,}30 \cdot 10^{-5}$	0,7
	$2{,}60 \cdot 10^{-6}$	0,3
	$5{,}20 \cdot 10^{-7}$	0,7
	$1{,}05 \cdot 10^{-7}$	0,4

escence est connu et les conditions d'excitation et de réemission suffisamment voisines pour que la réponse de l'appareil soit sensiblement la même pour le produit à étudier x et le composé de référence R.[17] C'est le cas ici de la quinine en solution dans l'acide sulfurique 0,1N [maximum d'excitation (λ_{ex}) 352 nm, λ_{em} 450 nm, rendement de fluorescence $\phi_R = 0{,}55$]. On mesure donc les absorbances A_R et A_x des produits à 310 nm et les intensités de fluorescence F_R et F_x aux λ_{em} de chacun d'eux avec une même λ_{ex} (310 nm). On a alors:

$$\frac{F_x}{F_R} = \frac{\phi_x A_x}{\phi_R A_R}.$$

Ainsi calculé, le rendement de fluorescence est, pour le balfourodinium, $\phi = 0{,}430$.

Pour le platydesminium, la valeur ϕ ainsi calculée est de 0,310 mais doit être corrigée pour tenir compte de la différence de sensibilité du photomultiplicateur aux λ_{em} de la quinine (450 nm) et du platydesminium (345 nm). Pour le photomultiplicateur (R212) de l'appareil utilisé, ce rapport des sensibilités $I_{450\,nm}/I_{345\,nm}$ est de $\simeq 0{,}75$, d'où le rendement du platydesminium $\phi = 0{,}230$.

Inversement, à partir des rendements de fluorescence ainsi calculés, on peut déterminer la concentration des solutions en étalonnant avec la quinine en milieu sulfurique, sachant que les absorptions molaires à 310 nm sont respectivement de $6{,}90 \cdot 10^3$ et de $5{,}50 \cdot 10^3$ l·mole^{-1}·cm^{-1} pour le platydesminium et pour le balfourodinium.

Application à des milieux biologiques

Nous avons cherché à appliquer ces méthodes au dosage des alcaloïdes contenus dans différents milieux biologiques: extraits de feuilles, tiges, racines et cultures cellulaires de diverses Rutacées. Les prises d'essai disponibles importantes pour les organes végétaux sont forcément très limitées dans le cas des cultures de tissus (quelques dizaines de mg) et renferment une teneur en alcaloïdes variant de 2 à 200 ppm. C'est pourquoi nous avons utilisé de préférence la fluorescence qui confère aux dosages une plus grande sensibilité. La difficulté réside dans l'absence de spécificité, étant donné le grand nombre de produits présents (constituants des cellules végétales ou apportés par le milieu de culture) absorbants dans l'ultraviolet, fluorescents ou inhibiteurs de la fluorescence des alcaloïdes dihydrofuroquinoléiques. La méthode de dosage suppose donc une séparation initiale. La technique a été mise au point avec une souche de tissus de *Choisya ternata* isolée en 1972, ainsi qu'avec des suspensions cellulaires en dérivant. Ces tissus produisent *in vitro* un peu de balfourodinium et surtout du platydesminium.[18]

Discussion et justification de la méthode

La séparation des alcaloïdes comprend 3 étapes.

Extraction des milieux végétaux. Nous avons choisi le méthanol pour extraire les alcaloïdes des tissus végétaux pour 2 raisons.

—L'extrait devant être concentré pour le dépôt chromatographique, la volatilité de ce solvant facilite l'opération.

—Cette extraction élimine la majorité des composés non polaires, les protéines par dénaturation et les sels minéraux. Par contre un grand nombre de composés polaires sont entraînés avec les alcaloïdes: sucres, chlorophylles, acides organiques... composés qui gênent le dépôt chromatographique obligeant donc à les éliminer, ce qui est effectué à l'étape suivante.

Extraction des alcaloïdes sous forme de complexe moléculaire dans un solvant peu polaire. La formation, avec le bleu de bromothymol (BBT), d'un complexe moléculaire non polaire permet son extraction par le dichlorométhane. Par contre les autres composés polaires sont peu extractibles et ainsi en grande partie éliminés. L'extrait obtenu peut être facilement soumis à la séparation chromatographique. Toutefois le dichlorométhane étant très volatil, le dépôt quantitatif de la solution n'est pas possible. C'est pourquoi le résidu sec est repris par le méthanol.

Chromatographie sur couche mince et élution des alcaloïdes. La chromatographie sur gel de silice permet de séparer les alcaloïdes quaternaires d'autres produits fluorescents également présents (chlorophylles, alcaloïdes tertiaires, vitamines introduites dans le milieu). Dans le méthanol et dans le solvant de migration, les complexes moléculaires sont dissociés: le bleu de bromothymol migre donc avec un R_f élevé et les alcaloïdes migrent aux mêmes R_f que

Tableau 6. Reproductibilité du dosage sur le matériel végétal

Fluorescence Excitation/Emission, *nm*	Moyennes des mesures	Ecart type	Coefficient de variation, %
307/343	154	5,5	3,6
307/439	47	1,5	3,1

s'ils n'avaient pas été complexés, le rapport des R_f des alcaloïdes et du bleu de bromothymol (BBT) étant pour le platydesminium $R_{f_P}/R_{f_{BBT}} \simeq 0{,}14$ et pour le balfourodinium $R_{f_B}/R_{f_{BBT}} \simeq 0{,}20$. De par leur structure, les alcaloïdes sont fortement adsorbés. Il en résulte une durée de migration assez longue et une difficulté lors de l'élution: cette dernière doit être effectuée avec un solvant très polaire.

Rendements des différentes étapes. Rendement d'extraction: la figure 3 montre l'influence du pH sur la formation du complexe balfourodinium–BBT. Cette détermination a été effectuée en spectrophotométrie après extraction par le dichlorométhane. Le complexe se forme donc entre pH 4 et 8. Les échantillons dont nous disposons présentant des degrés de pureté différents, il est difficile d'effectuer des rendements d'extraction. C'est pourquoi nous avons tourné la difficulté en comparant les résultats de chromatographies effectuées sur un même échantillon avec ou sans extraction par le bleu de bromothymol. Pour le platydesminium, l'intensité moyenne de fluorescence sans extraction est de 20,5 unités, alors qu'après extraction elle est de 21,1 avec un coefficient de variation de 3%. Pour le balfourodinium, elle est de 70,6 unités sans extraction et de 72,9 unités après extraction avec le même coefficient de variation. On peut donc considérer que ces chiffres sont identiques et donc que le rendement de l'extraction est pratiquement de 100%.

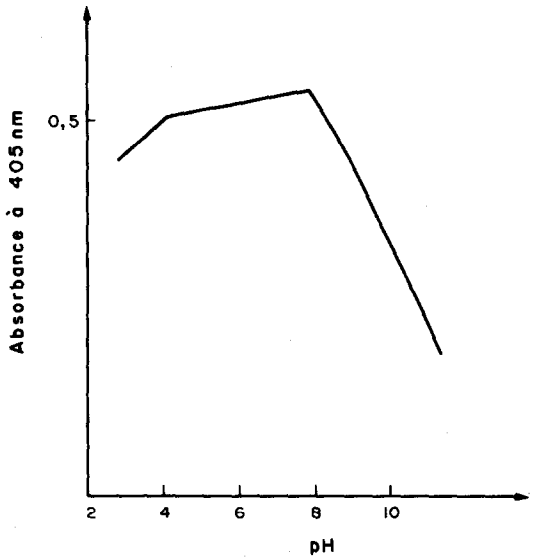


Fig. 3. Influence du pH sur l'extraction du complexe balfourodinium–bleu de bromothymol.

Rendement de la chromatographie: les alcaloïdes étant fortement adsorbés donc susceptibles d'être dénaturés, nous avons vérifié que nous n'avions pas de perte lors de la séparation. En raison de la pureté insuffisante de nos échantillons, nous avons comparé les résultats d'expériences réalisées avec une ou deux migrations, le chiffre obtenu pour la première servant de référence. Pour le balfourodinium, nous avons obtenu 95,6% de rendement et pour le platydesminium 95,5%, pour 4 essais avec un coefficient de variation de 2%.

Rendement d'élution: l'élution des alcaloïdes à partir de la plaque est difficile par suite de leur adsorption. La plupart des solvants essayés donnent un mauvais rendement. Le mélange méthanol–acide formique, qui possède une force éluante très élevée, s'est révélé excellent puisque le rendement moyen d'élution effectué sur 8 essais est égal à 99,5% avec un coefficient de variation de 1% pour les deux alcaloïdes.

Reproductibilité du dosage sur le matériel biologique

Un dosage effectué sur 7 échantillons de 25 mg d'une même poudre de cellules végétales lyophilisées a donné les résultats suivants (Tableau 6).

Essais de surcharge. Une poudre végétale est soumise au dosage, seule et avec des surcharges en platydesminium et en balfourodinium. Les résultats des surcharges sont comparés à la somme des résultats obtenus sur la poudre seule et sur les alcaloïdes purs qui, eux, ne subissent que la chromatographie. Les résultats moyens de 4 essais sont réunis dans le Tableau 7 et montrent la bonne valeur de la méthode.

En conclusion, ces 3 purifications successives permettent:

—d'éliminer toutes les impuretés gênantes puisque les spectres d'absorption et de fluorescence sont similaires à ceux des substances pures,

—de retrouver au minimum 95% des alcaloïdes présents initialement.

En outre la différence des longueurs d'onde d'émission du balfourodinium et du platydesminium permet de les doser sur le même éluat.

CONCLUSION

L'étude systématique des propriétés spectrales de cette série d'alcaloïdes nous a permis d'établir des relations entre la structure, l'absorption et la fluorescence. En particulier nous montrons l'influence de la nature des substituants, hydroxyle ou méthoxy, et de leur position en 1, 4, 5, 8 ou en 2, 3, 6, 7 du noyau

Tableau 7. Essais de surcharge

	Moyennes des mesures		Ecart type	Coefficient de variation, %
	307/344	307/439		
Poudre végétale	65,4 (a)		3,6	5,5
Platydesminium (P)	62,7 (b)		2,9	4,6
Poudre végétale + P	127		5,8	4,5
Valeur calculée (a + b)	128,1			
Poudre végétale		25,9 (c)	0,7	2,7
Balfourodinium (B)		25 (d)	1	4
Poudre végétale + B		51,9	1,2	2
Valeur calculée (c + d)		50,9		

quinoléique, sur le déplacement bathochrome des bandes d'absorption ^1B_b, ^1L_a et ^1L_b. En fluorescence, le spectre d'excitation suit d'assez près les bandes d'absorption ^1B_b et ^1L_b et subit donc les mêmes règles tandis que le maximum d'émission dépend surtout de la nature des substituants. L'influence du pH, de la nature et de la concentration des anions présents en solution et de divers solvants ont permis de préciser les conditions opératoires pour un rendement maximum de fluorescence. Enfin nous avons pu proposer une méthode de dosage par fluorimétrie qui, comparée au dosage par spectrophotométrie, présente une sensibilité 20 à 100 fois plus grande, capable de détecter une quantité d'alcaloïdes de 20 ng/ml, et une sélectivité permettant de doser deux alcaloïdes après extraction d'un matériel végétal.

LITTERATURE

1. M. Rideau, C. Verchere, P. Hibon, J. C. Chénieux, P. Maupas et C. Viel, *Phytochem.*, 1979, **18**, 155.
2. R. Garestier et M. Rideau, *Compt. Rend.*, 1972, **274D**, 3541.
3. *Idem, ibid.*, 1972, **274D**, 2651.
4. J. Reisch, K. Szendrei, E. Minker et I. Novák, *Pharmazie*, 1969, **24**, 699.
5. L. A. Mitscher, M. S. Bathala, G. W. Clark et J. L. Beal, *Lloydia*, 1975, **38**, 109.
6. R. C. Weast, *Handbook of Chemistry and Physics*, 50th Ed., D102. Chemical Rubber Co., Cleveland, 1969.
7. J. Reisch, Y. M. Mirhom, J. Korosi, K. Szendrei et I. Novák, *Phytochem.*, 1973, **12**, 2552.
8. D. R. Boyd et M. F. Grundon, *J. Chem. Soc., C*, 1970, 556.
9. J. R. Price, *Aust. J. Chem.*, 1959, **12**, 458.
10. H. Rapoport et K. G. Holden, *J. Am. Chem. Soc.*, 1959, **81**, 3738.
11. K. Szendrei, E. Minker, M. Koltai, J. Reisch, I. Novák et G. Buzás, *Pharmazie*, 1968, **23**, 519.
12. J. R. Platt, *J. Chem. Phys.*, 1950, **18**, 1168.
13. H. C. Brown et X. R. Mihm, *J. Am. Chem. Soc.*, 1955, **77**, 1723.
14. K. Szendrei, J. Reisch, I. Novák, L. Simon, Zs. Rózsa, E. Minker et M. Koltai, *Herba Hung.*, 1971, **10**, 131.
15. R. A. Corral et O. O. Orazi, *Tetrahedron*, 1965, **21**, 909.
16. S. B. Knight, R. H. Wallick et J. Bowen, *J. Am. Chem. Soc.*, 1954, **76**, 3780.
17. C. A. Parker et W. T. Rees, *Analyst*, 1960, **85**, 587.
18. J. C. Chénieux, M. Rideau et M. Gerard, *Bull. Soc. Bot. Fr.*, 1977, **124**, 265.

Summary—The absorption and fluorescence properties of six furoquinoline or pyranoquinoline alkaloids extracted from Rutaceae plants are described. These properties are related to the molecular structure and used for the fluorometric determination of two of them (platydesminium and balfourodinium) in *Choisya ternata* cell cultures and original plant extracts.

Talanta, Vol. 28, pp. 717 to 723, 1981
Printed in Great Britain. All rights reserved

0039-9140/81/100717-07$02.00/0
Copyright © 1981 Pergamon Press Ltd 1981

SOME ASPECTS OF ROOM-TEMPERATURE PHOSPHORESCENCE IN LIQUID SOLUTIONS

J. J. DONKERBROEK, J. J. ELZAS, C. GOOIJER*, R. W. FREI and N. H. VELTHORST

Department of General and Analytical Chemistry of the Free University, de Boelelaan 1083, 1081 HV Amsterdam, The Netherlands

(*Received* 22 *January* 1981. *Accepted* 7 *April* 1981)

Summary—Experimental requirements for room-temperature phosphorescence measurements in liquids (RTPL) are discussed. Phosphorescence quantum yields and triplet lifetimes of some brominated naphthalenes and halogenated biphenyls at 77 K in 2-methyltetrahydrofuran and at room temperature in hexane are reported and compared. Surprisingly the naphthalenes show only little loss in quantum yields in going from 77 K to room temperature. Sensitized phosphorescence is discussed as a means of expanding the analytical potential of RTPL. Results with a model system of benzophenone as a donor (analyte) and 1,4-dibromonaphthalene as an acceptor are presented.

Until recently the application of phosphorescence in analytical chemistry was limited to rigid systems,[1–3] *i.e.*, glasses at liquid-nitrogen temperature or analytes adsorbed on solid substrates.[4–9] Rigidity is required to suppress the diffusion of different kinds of triplet quenchers, such as molecular oxygen, and to restrict the internal motions of the molecule.

Whereas at 77 K the low diffusion rate of quenchers is caused by the high viscosity of the solution, in the adsorbed state it is ascribed to chemical bonds formed between the analyte and the solid substrate.[4] Schulman and Parker[5] have stated that these chemical bonds are perturbed by moisture, leading to larger admission of molecular oxygen.

The phosphorescence intensity of adsorbed analytes can be increased by adding heavy-atom salts such as sodium iodide,[6,7] and silver, thallium or lead salts.[8] By use of a suitable combination of substrate and heavy-atom species, detection limits in the picogram level can be reached.[9]

It is generally accepted that in liquid solutions, where factors suppressing the diffusion of triplet quenchers are commonly absent, phosphorescence intensities are too low to be used for analytical purposes. Several background studies in this field have been published during the last 20 years.[10–13] The highest emission intensities at room temperature are reported by Almgren[11] for biacetyl ($2.24 \times 10^{-3}M$) in benzene with a phosphorescence quantum yield of 0.08, and by Parker and Joyce[12] for acetophenone ($1.5 \times 10^{-3}M$) in perfluoromethylcyclohexane with a quantum yield of 0.0581. Turro *et al.*[13] showed that in acetonitrile, a solvent widely used in liquid chromatography, a phosphorescence emission could be achieved for 1,4-dibromonaphthalene; they estimated the quantum yield to be of the order of 10^{-3}. Recently, it has been shown that in micellar solutions strong phosphorescence signals can be obtained.[14]

The present paper deals with room-temperature phosphorescence in liquid solutions (RTPL), without the use of micelles. The purpose is to advance understanding of RTPL and eventually to apply it to the detection of organic species in dynamic systems, such as liquid chromatographs (LC) and autoanalysers. Phosphorescence data for some model systems such as halogenated naphthalenes and biphenyls are presented and furthermore some results on phenothiazines are reported. In addition the importance of quenching processes and intramolecular deactivation pathways is studied. It will be shown that the substituted naphthalenes are especially interesting since in principle they are appropriate acceptor molecules in sensitized phosphorescence experiments.

THEORETICAL ASPECTS

For solutions of low concentration, where photochemical reactions such as dimerizations can be neglected, the phosphorescence quantum yield Φ_p is given by

$$\Phi_p = \theta_{isc} \frac{k_p}{k_p + k_{np} + \sum_Q k_Q[Q]} = \theta_{isc} k_p \tau_p \quad (1)$$

where θ_{isc} is the quantum yield of triplet formation, k_p and k_{np} are the rate constants (sec^{-1}) of the phospheresence process and of the intramolecular radiationless deactivation of the triplet state, respectively; $\sum_Q k_Q[Q]$ gives the rate for deactivation by bimolecular quenching; k_Q is the rate constant ($l.mole^{-1}.sec^{-1}$) and [Q] the concentration (mole/l.) of a quencher; τ_p

* To whom correspondence is to be addressed.

is the triplet lifetime (sec). If the quenching processes are diffusion-controlled, k_Q can be written as[15]

$$k_Q = \frac{8RT}{3000\eta} \tag{2}$$

where η denotes the viscosity of the liquid in poise (*i.e.*, $g.cm^{-1}.sec^{-1}$) and R and T are the molar gas constant ($erg.deg^{-1}.mole^{-1}$) and absolute temperature.

In rigid solutions at 77 K, k_Q becomes zero, so equation (1) is simplified to

$$\Phi_p = \theta_{isc} \frac{k_p}{k_p + k_{np}}. \tag{3}$$

In liquid solutions at room temperature, at which k_Q will be of the order of 10^9–10^{10} $l.mole^{-1}.sec^{-1}$, $\sum_Q k_Q[Q]$ will be the dominant term. To make this term as small as possible the solvent has to be purified carefully and the dissolved molecular oxygen removed as completely as possible.

For naphthalenes at 77 K, according to Kellogg and Bennett,[16] $\theta_{isc} = 1 - \Phi_f$, in which Φ_f denotes the fluorescence quantum yield. For bromonaphthalenes this results in $\theta_{isc} = 1.00$, since Φ_f approaches zero. We assume that the same holds at room temperature, in view of the low value of Φ_f. Furthermore, for bromobiphenyls θ_{isc} is also taken as 1.00.

Finally, it should be realized that the intramolecular rate constants k_p and k_{np} are temperature-dependent and that they are both increased by heavy-atom substitution.

EXPERIMENTAL

Apparatus

The luminescence spectra were recorded on an M.P.F.-44 fluorescence spectrophotometer (Perkin–Elmer), provided with 2 Hamamatsu photomultiplier tubes, type R777-01 HA, a phosphorescence attachment (Hitachi, Tokio) and a differential corrected-spectra unit (DCSU-2). By means of the last piece of apparatus, the spectra are readily corrected for the wavelength dependence of the detector, the emission monochromator and the lamp intensity. The spectra were recorded on a BD-8 XT recorder (Kipp, Delft, Holland). As a light-source a 150-W xenon lamp was used. During the scanning of the spectra the chopper was removed from the phosphoroscope.

Measurements at 77 K were performed in a (210–250 rpm) spinning quartz or Midwall glass NMR tube, type 507 PP.[1,2] The room-temperature experiments were done in a sample cell as described in Fig. 1, allowing efficient oxygen removal and protection of the solution for several hours from re-entrance of oxygen. The cuvette was placed in the sample compartment of the phosphoroscope according to the construction given in Fig. 1c.

The triplet lifetimes were measured with a rotating steel can as a chopper, with an inner diameter of 20.0 mm for fixing the square cuvette. For measuring lifetimes longer than 1.5 msec a two-sector chopper (two 60° slots diametrically opposed) was employed and for shorter lifetimes a six-sector chopper (six uniformly spaced 20° slots). The phosphorescence decay curves were displayed on a PM 3200 oscilloscope (Philips, Eindhoven, Holland) and a time averaging computer (Varian, Florham Park, N.J., U.S.A.), triggered by a metal detector, type 9918-28 (Pulsotronic Gummersbach, G.F.R.).

During the RTPL experiments the purity of the solutions was controlled by determining the triplet lifetime of 2-bromonaphthalene ($10^{-4}M$) in hexane. If the value was lower than 2.5 msec the purity was considered insufficient.

The quartz and glass apparatus was stored in chromic acid to guarantee thorough cleaning. Before use, it was carefully rinsed with distilled demineralized water, 100% Extran®, distilled demineralized water and 100% ethanol successively. With these precautions, phosphorescence signals of constant intensity and lifetime could be obtained.

Absorption spectra were recorded on a Beckman Acta CIII spectrophotometer.

Oxygen removal

Ultrapure nitrogen, necessary to remove oxygen from the solutions, was obtained by passing commercially available nitrogen containing about 5 ppm of oxygen through a column filled with pyrophoric copper catalyst BASF R3-11 and kept at a constant temperature of 100°. The purified gas, with an oxygen content less than 0.2 ppm, was led through a trap filled with the solvent used for the sample (see also Fig. 1). Before measurements were started, the solvent in the trap was deoxygenated for 15 min and the solution for 5 min. During the measurements a constant flow of nitrogen was maintained, thus preventing re-entrance of oxygen into the sample. In this way the phosphorescence signals obtained were kept constant over a period of more than an hour.

Determination of quantum yields

The phosphorescence quantum yields were determined by the indirect method, with 9,10-diphenylanthracene (DPA) as a standard. DPA has a fluorescence quantum yield (Φ_f) of 1.00 both in plastic media[17] and solutions,[18] independent of temperature.

By definition, $\Phi_p(X)$, the phosphorescence quantum yield of X, is related to $\Phi_f(DPA)$ by

$$\Phi_p(X) = \Phi_f(DPA) \frac{N_p^X}{N_f^{DPA}} \frac{N_{abs}^{DPA}}{N_{abs}^X} \tag{4}$$

where N_p^X and N_f^{DPA} are the numbers of photons detected in the emission from the solutions of X and DPA, respectively, while N_{abs}^X and N_{abs}^{DPA} are the numbers of photons absorbed. The ratio N_p^X/N_f^{DPA} was set equal to the ratio of the areas under the corresponding corrected emission spectra transferred to a linear wavenumber scale. Rhodamine B was used as a quantum counter to correct for fluctuations of the excitation light.

N_{abs}^X is related to $A(X)$, the absorbance of X, by

$$N_{abs}^X = N_{ex}^X(1 - 10^{-A(X)}) \tag{5}$$

where N_{ex}^X is the number of photons emitted by the light source at the excitation wavelength of X. A similar equation applies for N_{abs}^{DPA}. In our experimental set-up a correction is made for the wavelength dependence of the lamp, so that $N_{ex}^X = N_{ex}^{DPA}$. Therefore, in our case $\Phi_p(X)$ can be written as[19]

$$\Phi_p(X) = \frac{N_p^X}{N_f^{DPA}} \left(\frac{1 - 10^{-A(DPA)}}{1 - 10^{-A(X)}} \right) \tag{6}$$

The absorbances $A(X)$ and $A(DPA)$ are determined in the usual way; if necessary a correction for differences in the cell geometries is applied.

Chemicals

2-Methyltetrahydrofuran (Merck) was dried over sodium and vacuum distilled. Hexane p.a. (Baker) and ethanol

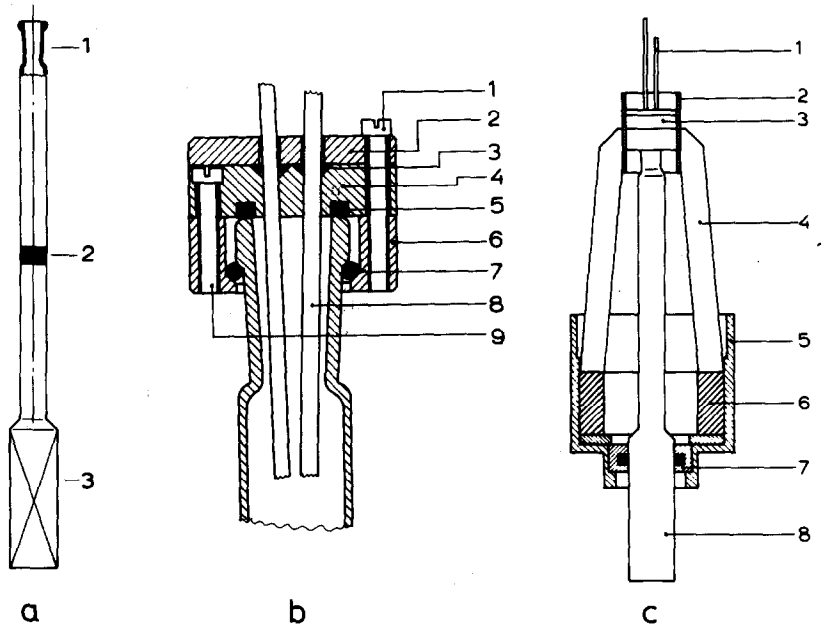


Fig. 1. Sample cell for RTPL measurements (a), with the construction for closing the cell (b), and the construction for fixing the cell in the spectrometer (c). (a): (1) ground-glass joint B 7½; (2) quartz–glass transition; (3) 1-cm cuvette type QS 221 (Hellma, The Hague, Holland). (b): (1) and (9) stainless-steel (SS) screws to connect the different segments; (2) SS upper segment to seat the Buna 002 O-rings (3) around the capillaries; (4) Delrin middle segment; (5) Buna 011 O-ring; (6) SS base segment; (7) Buna 012 O-ring; (8) one of the two SS capillaries, diameter 1/16 × 1.1 in. (c): (1) one of the two capillaries; (2) metal ring for keeping the sample cell in vertical position; (3) closure of the sample cell as depicted in (b); (4) plastic strip for connecting ring (2) with the plastic ring (6); (5) Dewar holder of the phosphoroscope; (7) Delrin ring with Buna 114 O-ring; (8) cuvette.

100%, p.a. (Merck) were doubly distilled before use. 1-Bromonaphthalene (Merck) was doubly vacuum-distilled. 1,4-Dibromonaphthalene (Eastman) 2-bromonaphthalene (Aldrich) and 4,4'-dibromobiphenyl (Fluka) were recrystallized at least twice from ethanol and the first two were also sublimed twice. 2-Bromobiphenyl was synthesized and purified according to Gomberg and Bachman.[20] 4-Bromobiphenyl (Chemical Procurement Laboratories, New York) and thio-, sulpho- and mesoridazine (Sandoz AG, Basel, Switzerland) were used without further purification.

RESULTS AND DISCUSSION

In this study, attention is focused on the model systems of bromonaphthalenes and halogen-substituted biphenyls. The former represent the class of non-flexible molecules, the latter the molecules with a more flexible structure.

Non-flexible molecules

The phosphorescence data for three bromosubstituted naphthalenes in hexane are presented in Table 1. As an example the total emission spectrum (both corrected and uncorrected) of 2-bromonaphthalene is depicted in Fig. 2.

The most interesting feature of Table 1 is that the values of Φ_p are so high at room temperature, ranging from 10 to 20% (at 77 K they range from 25 to 40%). Apparently, the rate of emission at 295 K can compete successfully with the radiationless deactivation process with rate constant $k_{nr}(295) = k_{np}(295) + \sum_Q k_Q[Q]$.

This is obvious from analysis of the rate constants summarized in Table 2, which have been calculated from the Φ_p and τ_p values by means of equation (1). The increase in the radiationless decay is partially compensated by the increase in k_p on going from 77 K to 295 K. For example, for 1,4-dibromonaphthalene (1,4-Br_2N) k_p increases by a factor of almost 2.

Unfortunately it is not possible to calculate k_{np} and $\sum_Q k_Q[Q]$ separately. If it is assumed that the temperature dependences of k_p and k_{np} are similar, it is calculated that $\sum_Q k_Q[Q]$ ranges from 200 to 400 sec^{-1}. Substitution of $k_Q = 10^{10}\,1.mole^{-1}.sec^{-1}$ reveals that [Q] is of the order of 10^{-7}–$10^{-8}M$. It is suspected that the estimate given for $\sum_Q k_Q[Q]$ applies quite generally for hexane solutions at room temperature, both for flexible and non-flexible molecules, provided that the experimental conditions (such as the purity of the sample) are similar and the quenching processes are diffusion-controlled.

On the basis of what has just been said, two basic conditions can be formulated for the occurrence of RTPL of non-flexible molecules:

(*i*) Φ_p at 77 K must be larger than 10%,

(*ii*) k_p at 77 K must be at least 10 sec^{-1}.

Table 1. Phosphorescence data for naphthalene (N), 1-bromonaphthalene (1-BrN), 2-bromonaphthalene (2-BrN) and 1,4-dibromonaphthalene (1,4-Br_2N) in 2-methyltetrahydrofuran at 77 K and in hexane at room temperature (295 K)

	77 K		295 K		
	Φ_p	τ_p, *msec*	Φ_p	τ_p, *msec*	Φ_p (295)/Φ_p (77)
N	0.03	2.1×10^3			
1-BrN	0.27	15.0	0.10	1.9	0.37
2-BrN	0.38	16.8	0.14	2.8	0.37
1,4-Br_2N	0.27	5.3	0.18	1.7	0.69

If these conditions are fulfilled, Φ_p at room temperature is expected to be larger than 0.04, provided that $\sum_Q k_Q[Q]$ is $300\,sec^{-1}$.

For 1,4-Br_2N these conditions are also fulfilled when other purified liquids are used as solvents. For instance, in acetonitrile,[13] dichloromethane, ethanol and methanol it exhibits an appreciable phosphorescence. Methanol–water and acetonitrile–water mixtures can also be used. Even in mixtures with a water content of 50%, which are used in liquid chromatography, no appreciable loss in intensity was observed.

Flexible molecules

The phosphorescence data for the substituted biphenyls studied are assembled in Table 3; Fig. 3 shows the total emission of 4,4′-dichlorobiphenyl (4,4′-Cl_2B) in hexane at room temperature. For these systems the reduction in Φ_p on going from 77 K to room temperature is distinctly larger than for the naphthalenes (see Table 1). This difference is most probably due to the influence of temperature on k_{np}, which is more pronounced for the biphenyls.

For example, analysis of the data for 4,4′-dibromobiphenyl (4,4′-Br_2B) at 77 K on the basis of equation (3) reveals $k_p = k_{np} = 40\ sec^{-1}$. From the data at room temperature it follows that $k_p = 100\ sec^{-1}$ and $k_{nr} = 1100\,sec^{-1}$, so that by substitution of $\sum_Q k_Q[Q] = 300\,sec^{-1}$, k_{np} is estimated as $800\,sec^{-1}$. This implies that k_{np} increases by a factor of about 20.

Two features of Table 3 deserve further comment. First, the phosphorescence of 2-bromobiphenyl at room temperature is too weak to be detected. The position of the substituent probably gives rise to a very large value of k_{np} (295) as a result of steric hindrance. Secondly, it should be noted that both at 77 K and 295 K Φ_p for 4,4′-Cl_2B is larger than that for 4,4′-Br_2B, though the heavy-atom effect of the bromo-substitution is expected to be the larger. Apparently, in biphenyl molecules, on going from 4,4′-Cl_2B to 4,4′-Br_2B, k_{np} is more increased than k_p by the heavy-atom effect.

The results above clearly show that for flexible molecules RTPL will seldom be interesting from an analytical point of view. Generally, k_{np} (295) is too large to make this method successful. This conclusion is illustrated by the results for three phenothiazines. The

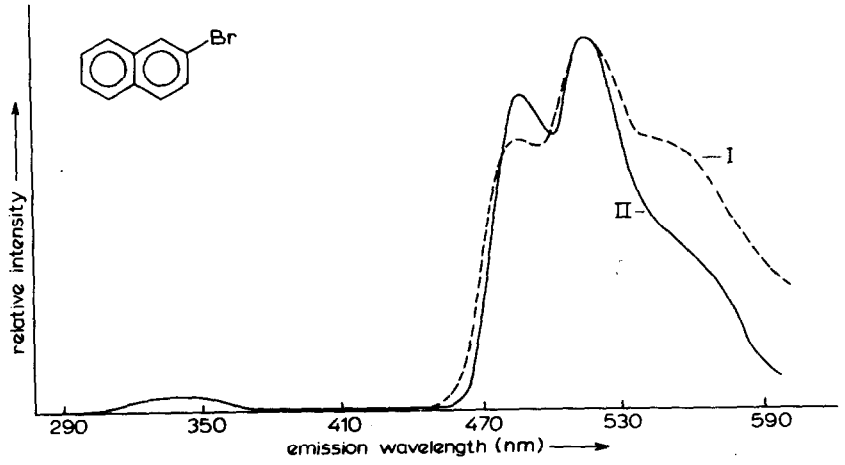


Fig. 2. Total emission spectrum of 2-bromonaphthalene ($10^{-4}M$) in hexane at room temperature, corrected (I) and uncorrected (II). Excitation wavelength 265 nm, band-widths 5 nm (excitation) and 10 nm (emission).

Table 2. Triplet deactivation rate constants (sec^{-1})

	$k_p(77)$	$k_{np}(77)$	$k_p(295)$	$k_{nr}(295) = k_{np}(295) + \sum_Q k_Q[Q]$
N	0.028	0.44		
1-BrN	18	49	53	473
2-BrN	23	37	50	307
1,4-Br_2N	51	140	106	482

ridazines investigated (thio-, meso-, and sulphoridazine) show triplet lifetimes of around 60 msec at 77 K with easily detectable intensities, but no RTPL could be observed.

Sensitized phosphorescence at room temperature

The data discussed in the previous sections demonstrate that it is possible to obtain RTPL spectra for some selected compounds under strictly defined conditions. Hence RTPL is not a common phenomenon, or easily utilized for analytical purposes. Benzophenone, for example, with a phosphorescence yield of 1.0 and a triplet lifetime of around 7 msec at 77 K, does not exhibit RTPL in hexane. Turro[21] reported a Φ_p value of only 9.1×10^{-3} in water, and Parker and Joyce[12] a Φ_p of 0.097 for a solution in perfluoromethylcyclohexane. Chemical reactions with the solvent[22] can further shorten the triplet lifetime by several orders of magnitude.

In view of all this it was decided to resort to sensitized phosphorescence as a means of overcoming these difficulties and to develop a widely applicable RTPL procedure with good analytical potential. Sensitized phosphorescence involves a non-phosphorescing donor (the analyte), which transfers its triplet energy to a suitable acceptor, thus generating an acceptor triplet with a high probability of emission at room temperature. The rate of energy transfer is proportional to the acceptor concentration, hence permitting a degree of flexibility in choosing optimal conditions. Generally such an acceptor has to satisfy the following conditions: (1) its quantum efficiency for RTPL should be high in the solvent system of interest; (2) its triplet energy E_T^A should be lower than the corresponding energy E_T^D of the donor to ensure an efficient diffusion-controlled transfer (if $E_T^D - E_T^A$ is larger than 5 kcal/mole, the reverse transfer reaction is negligible[23]); (3) its molar absorptivity has to be low in the excitation region of the donor.

The different decay processes of the donor and acceptor are shown in Fig. 4. Obviously the efficiency of the energy transfer process, Φ_{DA}, depends on the triplet lifetime of the donor in the absence of the acceptor, τ_0^D, and the rate of the transfer reaction. The transfer rate is equal to $k_t[A]$ where k_t is the bimolecular rate constant of transfer ($l.mole^{-1}.sec^{-1}$), and [A] the concentration of acceptor molecules (mole/l.).

If energy transfer plays a role, the lifetime of D is shortened from τ_0^D to τ^D where

$$\tau^D = \frac{1}{k_t[A] + 1/(\tau_0^D)} \tag{7}$$

and in that case θ_{DA} is given by

$$\theta_{DA} = \frac{k_t[A]}{k_t[A] + 1/(\tau_0^D)}. \tag{8}$$

From equation (8) it follows that 50% of the donor triplets will generate an acceptor triplet if

$$1/(\tau_0^D) = k_t[A]. \tag{9}$$

Equation (9) does not seriously restrict the potential of the sensitized RTPL method. In fact, this condition will be fulfilled quite generally. For a diffusion-controlled reaction, k_t is of the order of 10^{10} $l.mole^{-1}.sec^{-1}$. Substituting $[A] = 10^{-3}M$ into equation (9) gives $\tau_0^D = 10^{-7}$ sec. This implies that even for molecules with the very short triplet lifetime of 0.1 μsec, detection by sensitized RTPL will be possible, at any rate in principle.

As an example we have studied the sensitized RTPL of benzophenone in hexane, with 1,4-dibromonaphthalene as acceptor. For this donor–acceptor pair the difference in triplet energies, which can be estimated from the 77 K phosphorescence spectra, is 11.6 kcal/mole. Therefore, the energy-transfer reaction will be diffusion-controlled. The τ_0^D-value of benzophenone in hexane at room temperature is not known. However, as has been shown by Bäckström

Table 3. Phosphorescence data for biphenyl (B), 4,4′-dibromobiphenyl (4,4′-Br_2B), 4,4′-dichlorobiphenyl (4,4′-Cl_2B), 4,4′-difluorobiphenyl (4,4′-F_2B), 2-bromobiphenyl (2-BrB) and 4-bromobiphenyl (4-BrB) at 77 K in 2-methyltetrahydrofuran and at 295 K in hexane

	77 K		295 K		
	Φ_p	τ_p, *msec*	Φ_p	τ_p, *msec*	$\Phi_p(295)/\Phi_p(77)$
B	0.27				
4,4′-Br_2B	0.49	12.5	0.08	0.86	0.16
4,4′-Cl_2B	0.79		0.12	1.7	0.15
4,4′-F_2B	0.49		0.05	0.85	0.10
2-BrB	0.15		0		—
4-BrB	0.65	22.5	0.012		0.02

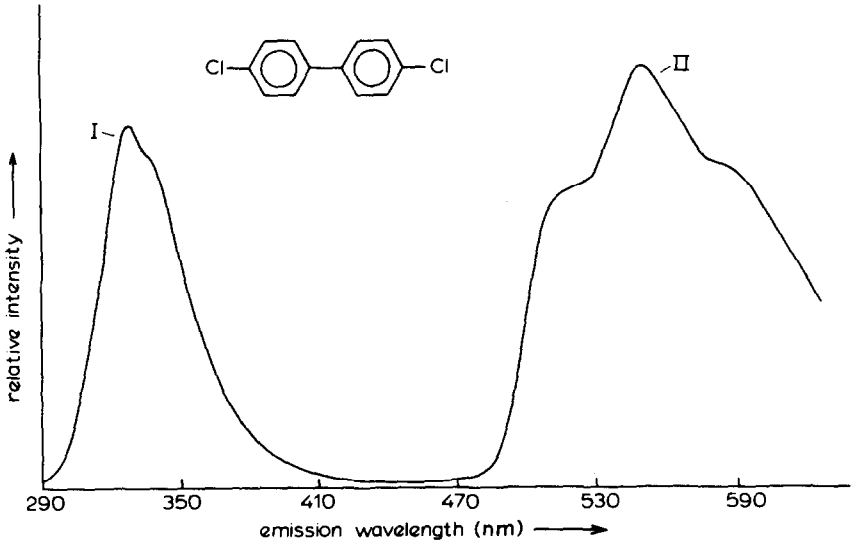


Fig. 3. Corrected total emission spectra (I: fluorescence; II: phosphorescence) of 4,4'-dichlorobiphenyl ($10^{-4}M$) in hexane at room temperature. Excitation wavelength 281 nm; band-widths 5 nm (excitation) and 10 nm (emission).

and Sandros,[24] it is possible to estimate τ_0^D from sensitized phosphorescence experiments. Following this method and substituting $k_t = 10^{10}$ l.mole^{-1}.sec^{-1}, we have found that $\tau_0^D = 6 \times 10^{-7}$ sec. This value is in line with the experimental result that direct RTPL of benzophenone in hexane is not detectable ($\Phi_p < 10^{-4}$).

In Fig. 5 the excitation spectrum of $10^{-3}M$ benzophenone and $3 \times 10^{-4}M$ 1,4-Br_2N in hexane at 293 K is shown, the phosphorescence signal of the acceptor being monitored at 550 nm. From equation (9) it follows that under these conditions $\theta_{DA} = 2/3$. It is obvious that in the excitation range at wavelengths longer than 340 nm, sensitized RTPL is observed.

The sensitivity of RTPL

As observed above, the high phosphorescence quantum yield of 1,4-dibromonaphthalene in hexane at room temperature (see Table 1) implies that it is of analytical interest to determine its limit of detection when direct RTPL is used. We have found a linear relationship between the emission intensity and the concentration over at least two decades (excitation wavelength 300 nm, molar absorptivity 5×10^3 l.mole^{-1}.cm^{-1}, emission wavelength 550 nm). The limit of detection, based on a signal-to-noise ratio of 3, was estimated as $5.4 \times 10^{-9}M$; the straight line has a regression coefficient of 0.999 and an $F_{1,3}$ distribution of 1051.

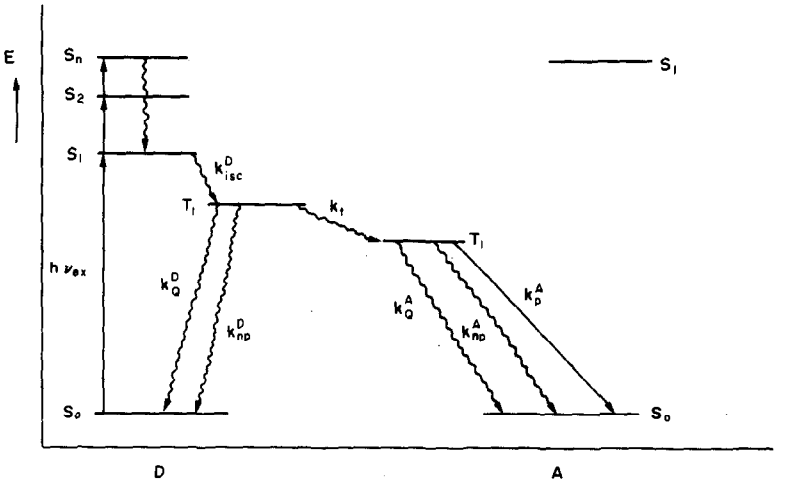


Fig. 4. Energy diagrams for the donor (D) and the acceptor (A) for a model system in sensitized phosphorescence. The rate constants k_p, k_{np} and k_Q are defined in the text; k^D_{isc} is the intramolecular rate constant of intersystem crossing of the donor, k_t the bimolecular rate constant of triplet–triplet energy transfer.

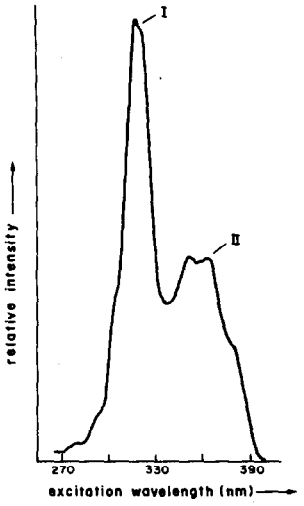


Fig. 5. Uncorrected phosphorescence excitation spectrum of a mixture of benzophenone ($10^{-3}M$) and 1,4-dibromonaphthalene ($3 \times 10^{-4}M$) in hexane at room temperature. I and II correspond to the maxima in the excitation spectra of the acceptor and the donor. Emission wavelength 550 nm (corresponding to the phosphorescence maximum of 1,4-dibromonaphthalene); band-widths 4 nm (excitation) and 6 nm (emission).

We have also determined the limit of detection for benzophenone in hexane at room temperature by sensitized RTPL of 1,4-Br_2N. The resulting calibration curve gives a regression coefficient of 0.992 and an $F_{1,3}$ distribution of 194, implying a significance of linearity >99.5%. The limit of detection of benzophenone is $4 \times 10^{-7}M$.

This value is obviously less favourable than the limit of detection for 1,4-Br_2N. However, the difference is mainly due to the difference in molar absorptivities at the excitation wavelengths, *viz.* 5×10^3 $l.mole^{-1}.cm^{-1}$ for 1,4-Br_2N at 300 nm and 10^2 $l.mole^{-1}.cm^{-1}$ for benzophenone at 360 nm. Unfortunately a better choice for the excitation wavelength of benzophenone is not possible, since excitation of 1,4-Br_2N has to be avoided.

CONCLUSIONS

From this study we conclude that direct RTPL with intensities high enough to be of analytical interest is a rather rare phenomenon. Quantum yields higher than 10% have been observed only for rigid aromatic molecules substituted with heavy atoms such as bromine. In less rigid aromatics, such as biphenyls, the loss in quantum yield in going from 77 K to room temperature conditions is already appreciable.

The use of sensitized phosphorescence offers a viable alternative, as has been shown with the donor–acceptor pair benzophenone and 1,4-dibromonaphthalene. However, this acceptor does not meet all the criteria for a universally applicable acceptor, its major drawback being the high absorption in regions where most potential donors absorb. Consequently, further research is being done on other potential acceptor systems with the goal of eventually applying them in analytical technology.

Acknowledgements—Our collaborators in the electronic and instrumental workshop are thanked for their valuable assistance in the development of the instrumentation.

REFERENCES

1. H. C. Hollifield and J. D. Winefordner, *Anal. Chem.*, 1968, **40**, 1759.
2. R. J. Lukasiewics, J. J. Mousa and J. D. Winefordner, *ibid.*, 1972, **44**, 1339.
3. P. A. St. John and J. D. Winefordner, *ibid.*, 1976, **39**, 500.
4. R. M. A. von Wandruszka and R. J. Hurtubise, *ibid.*, 1977, **49**, 2164.
5. E. M. Schulman and R. T. Parker, *J. Phys. Chem.*, 1977, **81**, 20, 1932.
6. M. L. Meyers and P. G. Seybold, *Anal. Chem.*, 1979, **51**, 1609.
7. T. Vo-Dinh, E. Lue Yen and J. D. Winefordner, *ibid.*, 1976, **48**, 1186.
8. E. Lue Yen Bower and J. D. Winefordner, *Anal. Chim. Acta*, 1978, **102**, 1.
9. T. Vo-Dinh and J. R. Hooyman, *Anal. Chem.*, 1979, **51**, 1915.
10. H. L. J. Bäckström and K. Sandros, *Acta Chem. Scand.*, 1958, **12**, 823.
11. M. Almgren, *Photochem. Photobiol.*, 1967, 829.
12. C. A. Parker and T. A. Joyce, *Trans. Faraday Soc.*, 1969, **65**, 2823.
13. N. J. Turro, L. Kou-Chang, C. Ming-Fea and P. Lee, *Photochem. Photobiol.*, 1978, **27**, 523.
14. L. J. C. Love, M. Skrilec and J. G. Habarta, *Anal. Chem.*, 1980, **52**, 754.
15. P. Debye, *Trans. Electrochem. Soc.*, 1942, **82**, 256.
16. R. E. Kellogg and R. G. Bennet, *J. Chem. Phys.*, 1964, **41**, 3042.
17. W. H. Melhuish, *J. Opt. Soc. Am.*, 1964, **54**, 183.
18. E. J. Bowen and J. Sahu, *J. Phys. Chem.*, 1959, **63**, 4.
19. J. G. Calvert and J. N. Pitts, *Photochemistry*, p. 800. Wiley, New York, 1966.
20. M. Gomberg and W. E. Bachman, *J. Am. Chem. Soc.*, 1924, **46**, 2329.
21. N. J. Turro, *Mol. Photochem.*, 1972, **4**, 213.
22. J. M. Bonnier and P. Jardon, *J. Chim. Phys.*, 1972, **68**, 432.
23. N. J. Turro, *Modern Molecular Photochemistry*, Chapter 9, Benjamin/Cummings, California, 1978.
24. H. L. J. Bäckström and K. Sandros, *Acta Chem. Scand.*, 1960, **14**, 48.

Talanta, Vol. 28, pp. 725 to 729, 1981
Printed in Great Britain. All rights reserved

0039-9140/81/100725-05$02.00/0
Copyright © 1981 Pergamon Press Ltd 1981

DEGRADATION OF AROMATIC COMPOUNDS IN GROUND-WATER, AND METHODS OF SAMPLE PRESERVATION

I. OGAWA, G. A. JUNK* and H. J. SVEC

Ames Laboratory† and Department of Chemistry, Iowa State University, Ames, IA 50011, U.S.A.

(*Received* 4 *March* 1981. *Accepted* 7 *April* 1981)

Summary—The degradation of acenaphthylene, acenaphthene, 2-methylnaphthalene, 2-methylindene, 3-methylindene and indene in water solutions was studied. These compounds at the 25–150 μg/l. level were almost totally degraded at ambient temperature within three days. The microbial population responsible for the degradation occurs naturally in ground-water taken from an aquifer in Ames, Iowa, which is contaminated with coal-tar products. These unidentified micro-organisms adapt readily to other waters when used as an inoculant for the degradation of aromatic compounds. The preservation of water to prevent such degradation was also investigated. Filtration through a 0.45-μm filter was found the most effective procedure for preserving the hydrocarbons in these waters.

The microbial degradation of the aliphatic hydrocarbon content of crude oil and petroleum products has been well documented.[1–3] The degradation of another class of compounds, the polycyclic aromatic hydrocarbons (PAH), is currently of high interest due to the carcinogenicity of some of them, and their occurrence and stability in the environment. Recently, the decay of PAH in oil-contaminated streams and sediments,[4] in controlled marine enclosures[5] and in ground-water[6] has been reported. There are also reports of micro-organisms, originating from marine and terrestrial samples, which utilize PAH as their sole source of carbon.[7–13]

Our investigations of ground-water contaminated with PAH by leaching of residues from an abandoned coal-tar pit[14,15] have led to the regular monitoring of water from contaminated wells. During the course of this monitoring programme some problems with losses of components were encountered. The reports of microbial degradation of organic compounds[1–13] prompted further study of these losses and of procedures for the prevention of such degradation. These investigations comprise the subject matter of this report.

EXPERIMENTAL

Analytical procedure

Most of the ground-water samples were pumped from a contaminated well (well 5) which was 50 m deep and located about 500 m from the site used more than 40 years ago for the disposal of coal-tar residues. The water samples (originally at 17°) were stored at ambient temperature in tightly capped amber vessels to control photolytic effects and to prevent losses by volatilization. Some samples were also stored in loosely capped containers to check for aeration effects. Before use, all vessels were washed with detergent, dilute hydrochloric acid, distilled water, acetone and freshly distilled methanol and autoclaved at 120° for 20 min.

Microbial degradation of six aromatic compounds present at the highest concentrations in the well water was measured. The organic components were isolated by solvent extraction, then separated and determined by gas chromatography, with flame ionization detection.

Chemicals

Analytical-reagent grade methanol and diethyl ether were distilled before use. The other organic chemicals were used without further purification.

Spiking solutions

Solutions for spiking water samples were prepared by dissolving 0.05 g of the appropriate organic compound in 5 ml of methanol or acetone. Aliquots of this concentrated solution were added to 4-l. water samples. For some degradation experiments at high concentration, aliquots of saturated solutions in methanol were added to 4-l. water samples.

Filtration

Water samples were filtered through a 0.45-μm silver membrane (Selas Flotronics, Huntington Valley, Pa.) under nitrogen pressure and through 0.45-μm acetate filters (Millipore) under suction at the water pump.

Solvent extraction

Two different solvent extraction procedures were used. Extraction method I was a conventional solvent extraction procedure in which 20 ml of pentane or other organic solvent were shaken with 200 ml of water in a separatory funnel. After phase separation, the organic solvent was removed and the volume reduced to 1 ml by microdistillation with a three-ball Snyder column. When necessary, for detection purposes, this volume was further reduced to 0.1 ml by free evaporation. Extraction method II was used for most of the analyses reported here. In this method, 850-ml water samples were extracted with 2.5 ml of pentane by use of apparatus and a procedure described in a separate

* Author to whom correspondence should be addressed.

† Operated for the U.S. Department of Energy by Iowa State University under contract No. W-7405-Eng-82. This research was supported by the Assistant Secretary for Environment, Office of Health & Environmental Research, WPAS-HA-02-04-03. It was also supported in part by EPA and NSF contracts, IAG-D5-E681 and CHE77-22691, respectively.

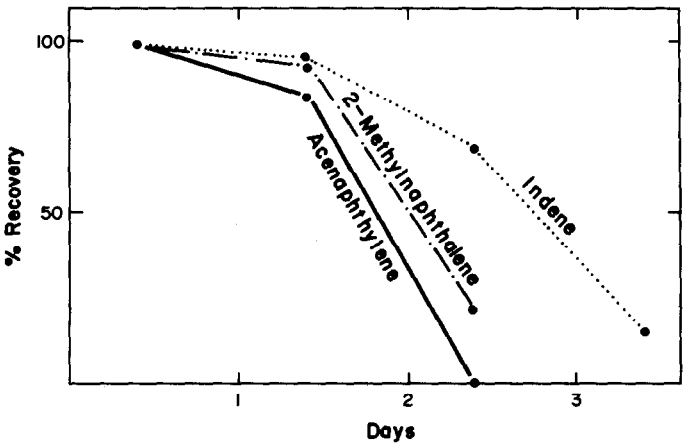


Fig. 1. Degradation of indene, 2-methylnaphthalene and acenaphthylene originally present in water from well 5 at 110, 130 and 150 μg/l., respectively.

report.[16] The small amount of organic solvent used in this method allows direct analysis of the separated organic phase without the need for concentration by microdistillation.

Gas chromatography

A Perkin-Elmer model 3920B instrument was used to separate the components present in the solvent extracts. Quantitation was based on peak heights, with naphthalene or tricosane as internal standards. A 2–4 μl. aliquot was injected into a 3 m × 6 mm O.D. glass column packed with 10% Carbowax 20*M* on 80–100 mesh Supelcoport, held at 50° for 2 min and then heated at 16°/min to 200° and held there for 8 min. To separate some of the higher molecular weight compounds, 10% OV-17 on 80–100 mesh Supelcoport was used.

Micro-organism counts

A spread plate technique[17] with trypticase soy agar was used for measuring the number of organisms present in the water samples.

RESULTS AND DISCUSSION

Degradation

Degradation of all six aromatic compounds present in the contaminated water from well 5 was nearly complete within three days as shown by the decay curves plotted in Figs. 1 and 2. The decay rates were in the order acenaphthylene > acenaphthene > 2-methylnaphthalene > 2-methylindene > 3-methylindene > indene. For acenaphthylene and all other cases where the degradation is complete, the time of completion is indeterminate, so the connecting line from zero to the previous point is indicative but not definitive. All data points in these figures are the average of three measurements, and these had relative deviations of less than 10%. Slight variations in the degradation of these compounds may be due to differences in the number of effective micro-organisms and their adaptability and growth. These factors were not investigated.

Two other wells located in the general vicinity of well 5 contained a total of 1–24 μg/l. of the six compounds. Water taken from these wells showed a similar loss of the major aromatic components.

Water from well 5 was also aged at room temperature and monitored for three days before spiking with

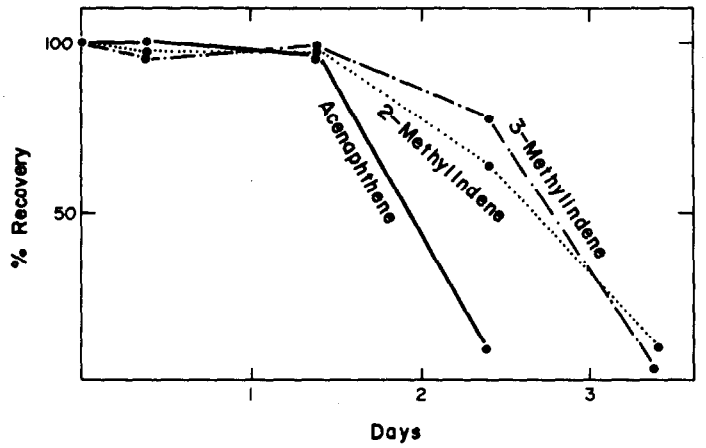


Fig. 2. Degradation of 3-methylindene, 2-methylindene and acenaphthene originally present in water from well 5 at 45, 60 and 25 μg/l., respectively.

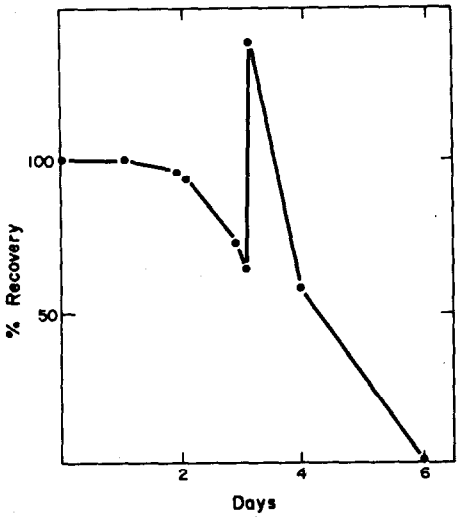


Fig. 3. Degradation of acenaphthylene originally present at 135 μg/l. in water from well 5 and spiked with an additional amount of pure compound on the third day to produce a water solution containing 175 μg/l.

pure acenaphthylene to produce a final concentration of 175 μg/l. on the third day. The subsequent degradation of the acenaphthylene in this spiked solution proceeded as expected. These data are plotted in Fig. 3, which shows an immediate decay without an additional time lag after spiking. When acenaphthylene at the solubility limit of 3 mg/l. was added to water from well 5, the degradation again occurred as expected. The degradation of large amounts of acenaphthylene averaged 137 μg/l. per day.

Other model aromatic compounds were also added to water taken from well 5. When naphthalene was added at 100 μg/l. it was degraded in less than 8 days. When pure acenaphthene, phenanthrene and fluoranthene were added at the 150-μg/l. level, they were all degraded within 36 days. Pyrene at this concentration was only 56% degraded in the same time period. The result with pyrene agrees with the expected increase in the stability of PAH as the number of rings increases.

Water from a private well fed by the same aquifer, but remote from the contamination source, was spiked with pure acenaphthylene at the 80-μg/l. level and inoculated with 12 ml of water from well 5 which had been aged at room temperature for 18 days. The added acenaphthylene was degraded within 9 days. In a control sample from the same private well but without the inoculant, no degradation of acenaphthylene was observed. Degradation also occurred when water freshly distilled from alkaline permanganate was spiked with acenaphthylene at 100 μg/l. and inoculated with aged water from well 5. Again, no degradation occurred in the control distilled water which was not inoculated. The micro-organisms responsible for the degradation of these compounds apparently are present only in the water from well 5, but can accommodate readily to other waters.

Water from the private well was also spiked with acenaphthylene at 190 μg/l. and inoculated with anaerobic and aerobic bacteria from a local sewage plant in an attempt to locate a more convenient source of organisms which might be effective for the degradation of the aromatic compounds. No loss in acenaphthylene occurred even after 20 days.

The cell mass collected by filtration of unspiked water with a 0.45-μm filter increased from 2 mg/l. on the first day to more than 20 mg/l. after 20 days. There was also an increase in the micro-organism count from 10^2 to 10^4 cells/ml of water. These data are plotted in Fig. 4, and show that the increase in cell population was coincident with the decreases in the amounts of the six major aromatic compounds present in the water. This correlation and the increase in cell mass described above suggest that microbiological activity was responsible for the degradation.

The cells and the 0.45-μm filter were subjected to exhaustive solvent extraction with dichloromethane and diethyl ether and to ultrasonic treatment in dichloromethane. The cell mass was also ruptured by refluxing with methanolic potassium hydroxide subsequently extracted with dichloromethane. No test compounds were found in any of these extracts. These observations indicate that adsorption on or within the cells was not the cause of the observed decrease in the aromatic component level in the water.

Sample preservation

The decrease with time in the amount of extractable organic compounds in water from wells contaminated with PAH led to an investigation of methods of preserving the organic material in these and similar water samples. The general methods of preservation reported in the literature involve the addition of heavy metal salts such as mercuric chloride,[18,19] cooling,[17–20] disinfection, heat sterilization,[24] and a combination of filtration, chilling and contact with silver.[25] All these methods were tested with the exception of sterilization by heat.

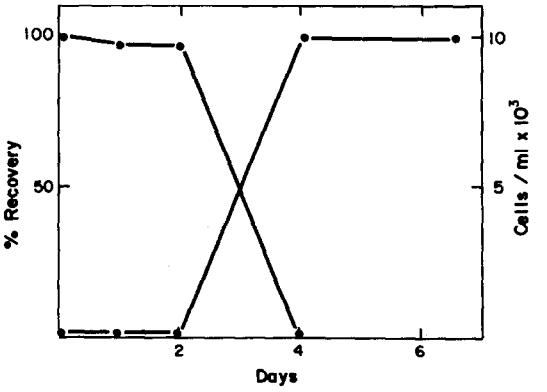


Fig. 4. Decrease of the six major aromatic contaminants in water from well 5, and increase in bacterial cell counts with time.

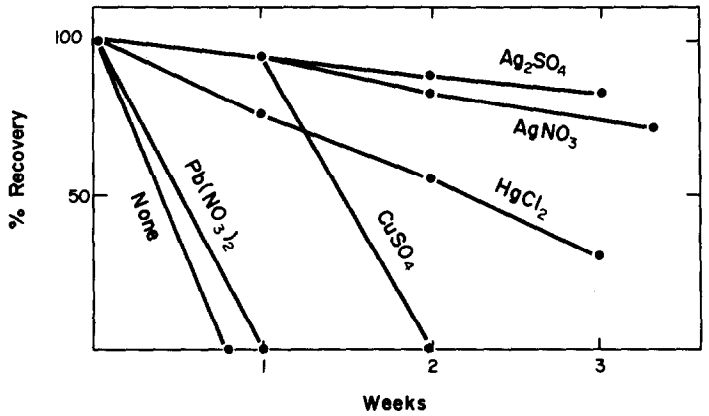


Fig. 5. Degradation of acenaphthylene in 1-litre samples of well 5 water stored at room temperature and preserved with various heavy metal salts.

The effect of using heavy metal salts for preservation of the extractable organic compounds is illustrated in Fig. 5, where the data for the preservative action of five different salts are plotted. Van Steenderen[26] noted that addition of silver sulphate, coupled with cooling to 4°, was the best method for preserving sewage effluents for organic carbon analysis. In agreement with this finding, silver salts were the most effective for preserving the well-water samples at ambient temperature. Although copper sulphate has been reported to be effective in controlling the growth of algae and moulds in water,[27] it was capable of preserving water samples from well 5 for only about one week.

Chilling the water was effective only for short-term storage. Degradation of the major components was almost complete after 12 days of storage at 4°. The organic components could not be preserved by disinfecting with 1 ml of 1*N* sodium hypochlorite per litre of water. The degradation was not monitored continuously but was complete within 18 days.

In contrast to these generally ineffective methods of sample preservation, water filtered through a 0.45-μm silver membrane filter contained 95% of the original amount of the organic components even after 36 days at ambient temperature. If microbiological activity was the cause of loss of aromatic components, the removal of the micro-organisms by filtration should be one of the better methods of sample preservation. The data reported here confirm this expectation. When a sample cannot be filtered, the addition of silver salts is the next best preservation technique. Storage at 4° is a borderline method when used alone, but it is desirable to use it in conjunction with all the other methods as an extra precaution if convenient.

CONCLUSIONS

The observed decrease in the amount of coal-tar products such as acenaphthylene, acenaphthene, 2-methylnaphthalene, 3-methylindene, 2-methylindene and indene in selected ground-water samples stored over a period of time has implications for the analysis of trace organic material, the preservation of water samples, and the removal of aromatic compounds from waste water by micro-organisms.

Although spikes of phenanthrene, fluoranthene and pyrene were also degraded in the stored samples, further study is required to ascertain the ultimate fate of these and other high molecular-weight compounds.

Further work is also required to identify the metabolites produced by the organisms and to characterize the microbial populations in the ground-water. The organisms responsible presumably require oxygen and/or nitrogen to be effective, because no evidence of degradation within the aquifer has been obtained. This speculation requires further investigation.

The ineffectiveness of the aerobic and anaerobic organisms from other sources for the degradation of PAH is noteworthy.

The results of these sample preservation studies are compatible with the notion of microbial degradation. This suggests that filtration to remove the responsible organisms may be the most effective, if not the most convenient, method of preserving water samples to be analysed for organic constituents.

Acknowledgements—The authors gratefully acknowledge Jim McDonald of the City of Ames and John Richard for the sources of well water and Layne Johnson, Peter A. Pattee, Paul A. Hartman, and John G. Holt for helpful suggestions concerning the general topic of microbiology.

REFERENCES

1. E. Beerstecher Jr., *Petroleum Microbiology*, p. 174. Elsevier, Houston, 1954.
2. J. B. Davis, *Petroleum Microbiology*, p. 499. Elsevier, Amsterdam, 1967.
3. J. A. Byron and S. Beastall, in *Microbiology*, P. Hepple (ed.), p. 73. Applied Science Publishers, London, 1971.
4. S. E. Herbes and L. R. Schwall *Appl. Environ. Microbiol.*, 1978, **35**, 306.

5. R. F. Lee, W. S. Gardner, J. W. Anderson, J. W. Baylock and J. Barwell-Clarke, *Environ. Sci. Technol.*, 1978, **12**, 832.
6. T. Kappeler and K. Wuhrmann, *Water Res.*, 1978, **12**, 327.
7. D. T. Gibson, in *Proceedings of the Third International Biodegradation Symposium, Kingston, RI*, 17–23 *August* 1975, J. M. Sharpley and A. M. Kaplan (eds.), p. 57. Applied Science Publishers, London, 1976.
8. T. Yoshida and H. Kojima, *Chemosphere*, 1978, 7, 497.
9. V. Treccani, *Z. Allg. Mikrobiol.*, 1965, **5**, 332.
10. M. H. Rogoff and I. Wender, *Oxidation of Aromatic Compounds by Bacteria*, Bulletin 602, Bureau of Mines, Pittsburgh, 1962.
11. N. L. Karrick, in *Nature and Fate of Petroleum*, D. C. Malins (ed.), Vol. 1, p. 265. Academic Press, New York, 1977.
12. C. E. Zobell, in *Proceedings of the Joint Conference on Prevention and Control of Oil Spills*, p. 317. American Petroleum Institute and Federal Water Pollution Control Administration, New York, 1969.
13. R. Bartha and R. M. Atlas, *Adv. Appl. Microbiol.*, 1977, **22**, 225.
14. A. K. Burnham, G. V. Calder, J. S. Fritz, G. A. Junk, H. J. Svec and R. Willis, *Anal. Chem.* 1972, **44**, 139.
15. A. K. Burnham, G. V. Calder, J. S. Fritz, G. A. Junk, H. J. Svec and R. Vick, *J. Am. Water Works Assoc.*, 1973, **65**, 722.
16. Unpublished results, this laboratory, 1978.
17. *Standard Methods for the Examination of Water and Wastewater*, 14th Edn, p. 142. American Public Health Association, American Water Works Association and Water Pollution Control Federation, New York, 1975.
18. C. McAuliffe, *Chem. Geol.*, 1969, **4**, 225.
19. L. J. Ottendorfer, *Proc. Anal. Div. Chem. Soc.*, 1978, **15**, 52.
20. G. A. Jungclaus, V. Lopez-Avila and R. A. Hites, *Environ. Sci. Technol.*, 1978, **12**, 88.
21. H. S. Hertz, W. E. May, S. A. Wise and S. N. Chesler, *Anal. Chem.*, 1978, **50**, 428A.
22. K. Grasshoff, in *Methods of Seawater Analysis*, p. 215. Verlag Chimie, Weinheim, 1976.
23. H. Gundernatsch, *Wasser, Luft Betr.*, 1977, **21**, 598.
24. R. C. Hoehn, *J. Am. Water Works Assoc.*, 1976, **69**, 302.
25. R. L. Malcolm and J. A. Leenheer, *Proc. Inst. Environ. Sci. Technol.*, 1973, 336.
26. R. A. Van Steenderen, *Water S.A.*, 1976, **2**, 156.
27. J. M. Pelczar Jr. and R. D. Reid, *Microbiology*, p. 411. McGraw-Hill, New York, 1972.

Talanta, Vol. 28, pp. 731 to 735, 1981
Printed in Great Britain. All rights reserved

0039-9140/81/100731-05$02.00/0
Copyright © 1981 Pergamon Press Ltd 1981

DETERMINATION OF MANGANESE(II) BY A CHEMILUMINESCENCE REACTION

J. L. BURGUERA*
Chemistry Department, Birmingham University, P.O. Box 363, Birmingham, England
and
ALAN TOWNSHEND†
Chemistry Department, University of Hull, Hull, England

(*Received* 19 *January* 1981. *Accepted* 16 *March* 1981)

Summary—Manganese(II) ($\geq$1.5 ng/ml) is determined by measuring either of the two emission peaks given by alkaline oxidation of luminol. Several other metal ions, which enhance both emission peaks, are masked by cyanide ions.

Many trace metals, including manganese, have been determined by their catalysis of chemiluminescence reactions.[1,2] Luminol has been used to generate the luminescence in most procedures. For manganese, complexing agents (activators) are added to increase the sensitivity (presumably by stabilizing intermediate oxidation states). Thus, Kalinichenko determined 0.05–5 ng of manganese, using luminol and a citrate–1,10-phenanthroline mixture.[3,4] The procedure was also applied to the determination of ng-amounts of 1,10-phenanthroline and similar compounds.[5] Many other transition metals interfered. Dubovenko and Tovmasyan[6] determined 0.1–1 μg/ml of manganese in a similar system, using triethylamine as activator, but with photographic rather than photoelectric detection. Seitz and Hercules[7] obtained a detection limit of $10^{-8}M$ manganese for this system, and used ion-exchange to remove interferences.

Lucigenin can be used in place of luminol. Photographic detection enables manganese at the 1–3 μg/ml level to be determined, but, again, many metal ions interfere.[8,9] Babko *et al.*[10,11] determined 0.1–10 μg of manganese by oxidation to permanganate with peroxodisulphate and reaction of the permanganate with siloxene to produce chemiluminescence.

We have re-investigated the determination of manganese(II) by its catalytic effect on the luminol–hydrogen peroxide system, in the absence of an activator. In particular, means were sought to mask interferences. During the investigation it was discovered that, whereas addition of luminol to a mixture of oxidant, pH 10 carbonate buffer and manganese produced a single pulse of emission, addition of the manganese to a luminol–oxidant–buffer mixture led to two sequential emissions. This phenomenon has been investigated in some detail.

* Present address: Dpto. de Quimica, Facultad de Ciencias, Universidad de Los Andes, Merida, Venezuela.

† To whom requests for reprints should be addressed.

EXPERIMENTAL

Apparatus

The instrumentation and experimental technique were as described previously.[12]

Reagents

All reagents were laboratory reagent grade, unless otherwise stated. The water used was twice distilled from an all-glass apparatus.

Stock manganese(II) solutions (200 μg/ml) were prepared daily by dissolving 0.104 g of $Mn(NO_3)_2.6H_2O$ in 100 ml of water.

Stock luminol solution ($2 \times 10^{-2}M$) was prepared by dissolving 0.886 g of luminol in 250 ml of 0.1*M* sodium carbonate (or borate or phosphate) buffer. Working solutions were prepared daily from this stock solution by appropriate dilution with the buffer solution chosen.

Hydrogen peroxide ($3–3 \times 10^{-4}M$) was prepared by appropriate dilution of 100-volume hydrogen peroxide with water.

Procedure for chemiluminescence measurements

The manganese solution (0.5 ml) was injected into the mixed luminol–buffer–hydrogen peroxide solution (1 ml) and the emission intensity at 425 nm (except for the variable wavelength experiments) was recorded for 50 sec.

Recommended procedure for determination of manganese

To the sample solution, add sodium cyanide solution to give a concentration of 0.01*M*. For calibration, prepare a series of manganese solutions of appropriate concentrations within the range 0.01–40 μg/ml by dilution of the stock solution. Mix together exactly 0.5 ml of 0.10*M* hydrogen peroxide and 0.5 ml of $4 \times 10^{-3}M$ luminol in 0.10*M* carbonate buffer, pH 10. Inject into this solution, in the luminometer, 0.5 ml of the unknown or standard manganese solution, and measure the emission intensity as described above.

RESULTS

In all experiments the manganese was added last to the reaction mixture. In all instances, a two-peaked emission response was achieved. Multiple responses have previously been obtained for luminol chemiluminescence,[13,14] including systems involving

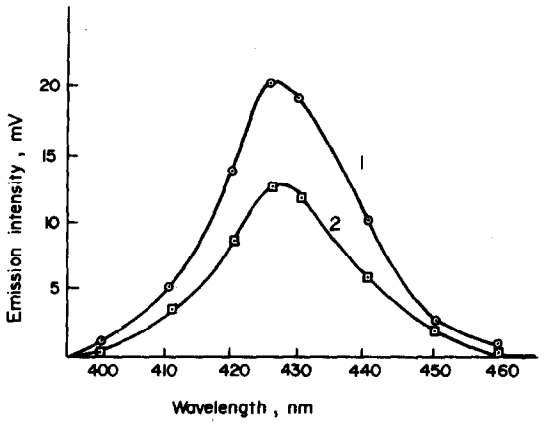


Fig. 1. Spectra of the two chemiluminescence emission peaks given by the luminol–Mn(II)–H_2O_2 system. (1) First peak; (2) second peak. Luminol $4.0 \times 10^{-3}M$, H_2O_2 0.1*M*, Mn(II) 10 ppm, pH 10.0, carbonate buffer.

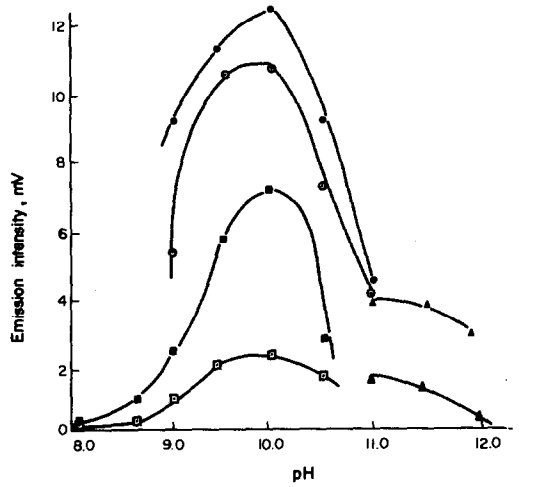


Fig. 2. Effect of pH on the chemiluminescence intensities for the luminol oxidation by H_2O_2 catalysed by 5 ppm of Mn(II). (⊙) First peak; (●) second peak (0.1*M* carbonate buffer); (⊡) first peak; (■) second peak (0.1*M* borate buffer); (△) first peak; (▲) second peak (0.1*M* phosphate buffer). H_2O_2 0.1*M*, luminol $4 \times 10^{-3}M$.

manganese.[15] White and Bursey[13] found that the single emitting species (λ_{max} = 424 nm) obtained by uncatalysed oxidation of luminol in water, changed in aqueous dimethyl sulphoxide solutions to two emitters, the second having a maximum intensity at 485 nm. Bersis and Nikokavouras[15] found that several emission peaks appeared in sequence for manganese-catalysed luminol oxidation as the pH of the solution was gradually decreased. These were attributed to different compounds present in the sample of luminol, which were isolated chromatographically. Neither of these systems, however, gave rise to multipeak emission *vs.* time plots. Neufeld *et al.*[14] found a two-peaked emission *vs.* time plot in the haemoglobin-catalysed oxidation of luminol, but did not carry out any further investigations.

In order to establish whether different emitters were responsible for the two peaks in the present system, the emission spectra were measured for both. This was done by measuring the heights of both peaks produced by a constant amount of manganese and other reagents, at various wavelengths, in a series of experiments. Both spectra (Fig. 1) were identical in shape, having a single peak at 425 nm. The spectra are very similar to those reported previously for luminol oxidation,[13,16] and are attributed to the 3-aminophthalate ion.[13] Thus the same emitter is responsible for both emission peaks.

The effect of pH (8.0–12.0) on the intensity of both peaks was investigated. Chemiluminescence was produced only in an alkaline environment. The pH-dependence showed the same profile for both peaks (Fig. 2). Greatest intensity was observed at pH 10; the carbonate buffer gave a greater intensity than a borate buffer at this pH, and was therefore selected for further study. The first peak always occurred at 4 sec, independent of pH. but the delay before the second peak increased as the pH decreased (Fig. 3).

The intensity of both peaks was strongly dependent on the hydrogen peroxide concentration (Fig. 4), maximum intensities being achieved for both peaks at a hydrogen peroxide concentration of 0.1*M* in the

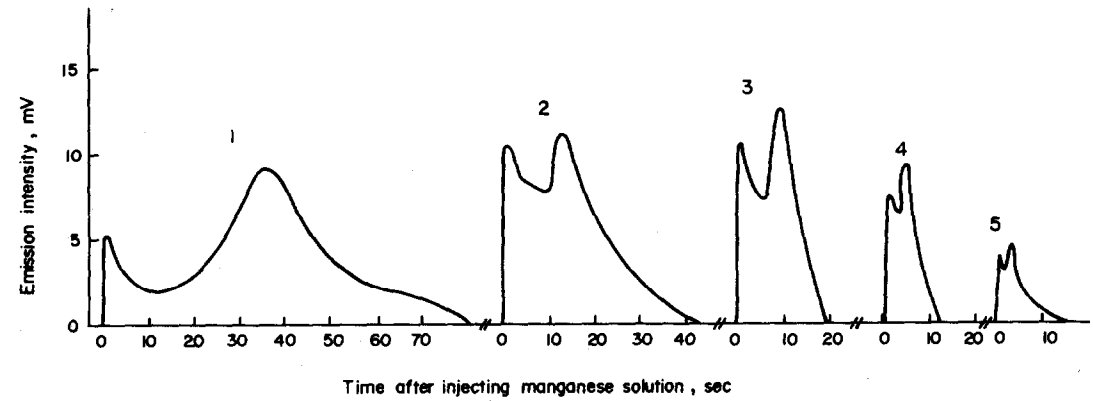


Fig. 3. Emission *vs.* time responses at pH (1) 9.0, (2) 9.5, (3) 10.0, (4) 10.5, (5) 11.0: 0.1*M* carbonate buffer, 0.1*M* H_2O_2, 5 ppm Mn(II).

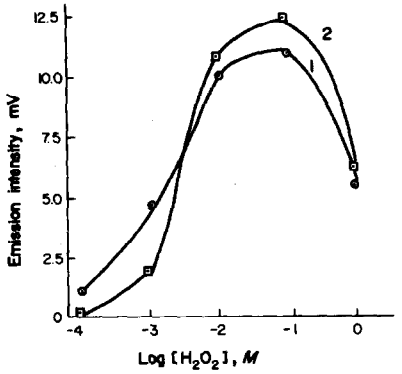


Fig. 4. Effect of hydrogen peroxide concentration on the chemiluminescence emission intensities. (●) First peak; (⊙) second peak: pH 10.0 carbonate buffer, other conditions as for Fig. 2.

solution added. The time of appearance of the second peak depended on the hydrogen peroxide concentration, broader, delayed, less intense peaks being obtained at lower concentrations. The first peak always appeared at 4 sec.

The effect of luminol concentration on the heights of the two peaks is shown in Fig. 5. Both emissions were most intense at *ca.* $4 \times 10^{-3}M$ luminol concentration in the solution added. Again, the first peak always occurred at 4 sec, whereas the second occurred with increasing rapidity as the luminol concentration increased.

On the basis of these experiments, the recommended conditions for manganese were established. Calibration graphs were obtained for both peaks (Fig. 6). The log–log plots were linear from 0.01 to 10 μg/ml manganese concentration with slopes of *ca.* 0.4 in both instances. The limiting effect on the intensity at high manganese concentrations may be the effect of the brown precipitate, probably manganese(IV) oxide, produced under these conditions. The first peak occurred at 4 sec, irrespective of the manganese concentration, but the second was increasingly delayed as the manganese concentration was decreased (Fig. 7). The blank emission (obtained by injecting 0.5 ml of water) gave a signal of 0.3 mV, as compared to 0.8 and 1.0 mV for the first and second peaks for 1.5-ng/ml manganese (0.75 ng of Mn). The

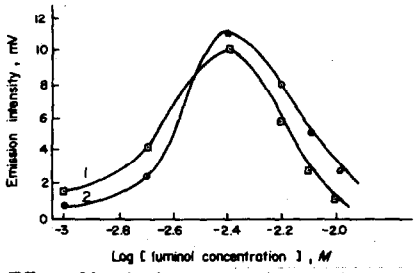


Fig. 5. Effect of luminol concentration on the chemiluminescence emission intensities. (1) First peak; (2) second peak: $0.1M$ H_2O_2, other conditions as for Fig. 4.

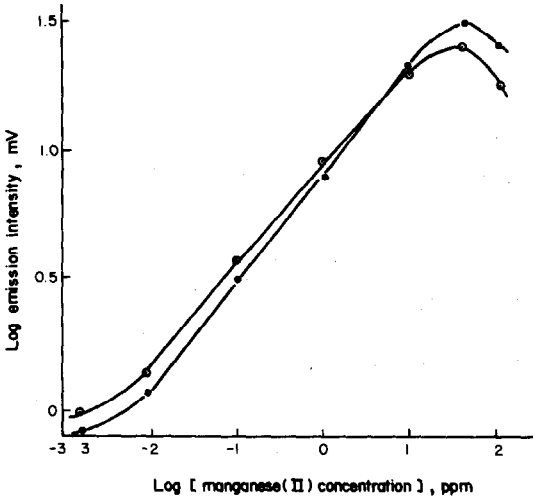


Fig. 6. Effect of manganese(II) concentration on maximum emission intensities. (●) First peak; (⊙) second peak: pH 10.0 carbonate buffer, other conditions as for Fig. 2.

coefficients of variation for 7 measurements of 5-μg/ml manganese were 6 and 7.5% for the first and second peaks, respectively.

Interferences

Most transition metal ions catalyse the luminol reaction, and their interference in the determination of manganese has been noted. This effect was confirmed in the present study, both peaks being enhanced by the presence of Co(II), Cu(II), Hg(II), Ni(II), Fe(II) and Cr(III). Figure 8 shows their effect on the second peak. Their effect on the first peak is very similar, except that the positions of nickel and mercury are exchanged. Cyanide ($0.01M$), however, was found to mask completely the effects of Hg(II), Ni(II), Fe(II) and Co(II), and almost completely mask Cu(II), provided the pH was ≥ 6.5 (Table 1). Manganese was scarcely affected at pH 4.5–10, and $0.01M$ cyanide could be used for masking at pH 10. However, $0.1M$ cyanide at pH 10 has a 14 and 20% depressive effect on the first and second manganese peaks, respectively.

DISCUSSION

As the emitting species is the same for both peaks, the two peaks must arise from two oxidation processes involving luminol and the catalyst. As the catalytic effects are probably the results of one-electron transfers involving the metal ion and hydrogen peroxide, the sequential involvement of manganese(III) and manganese(IV) is a likely explanation of the two peaks. The other common catalysts for the reaction (iron, copper, cobalt, *etc.*) are unable to participate in two such catalytic cycles, and thus give rise to only one peak.

The reaction is capable of giving a rapid (2 min per sample) and selective determination of traces of

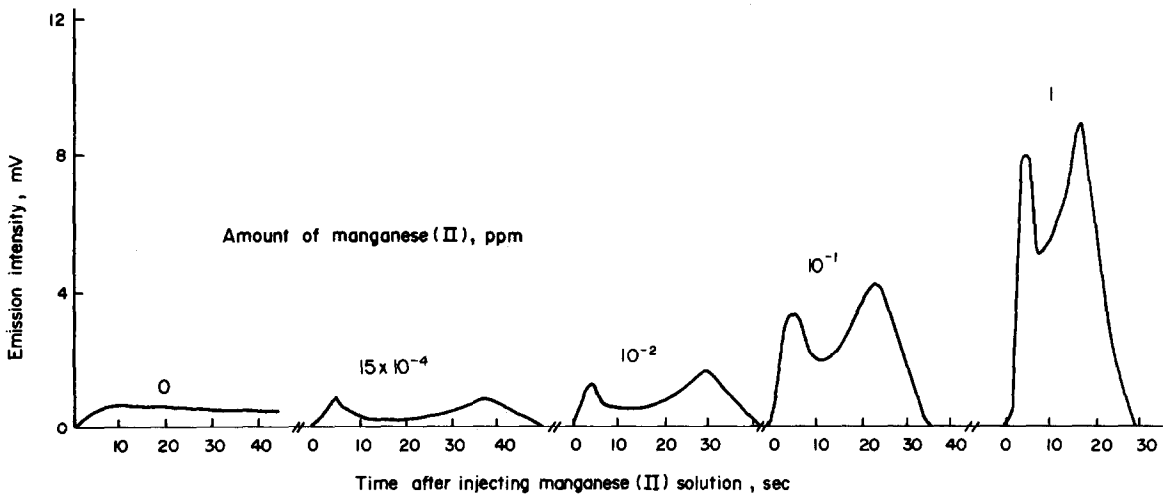


Fig. 7. Emission *vs.* time responses for various amounts of manganese(II) in the luminol–H_2O_2 system. Conditions as for Fig. 6.

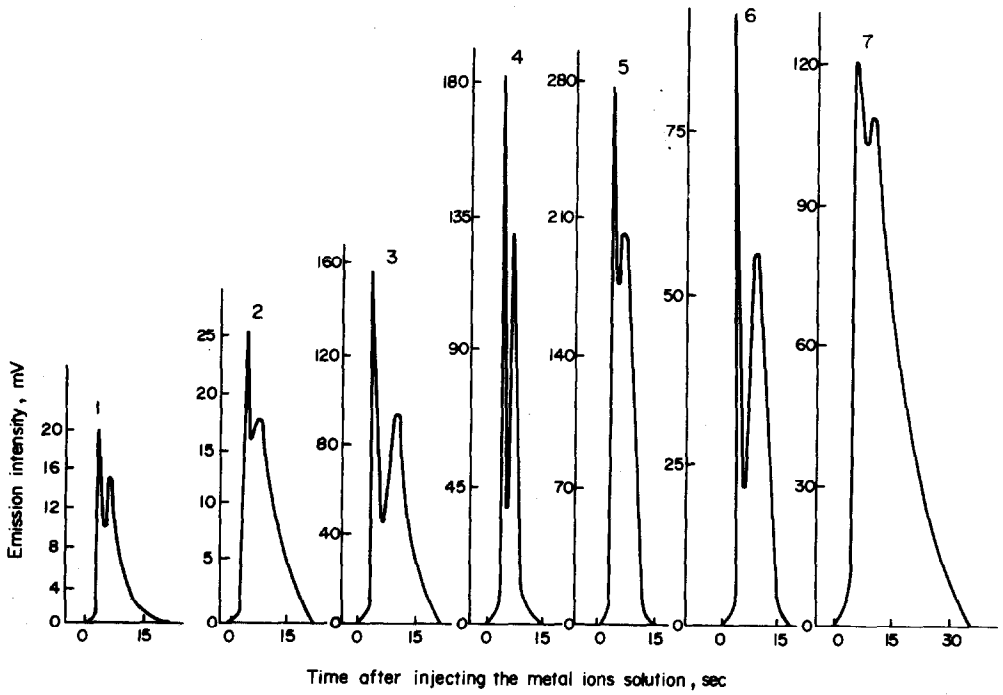


Fig. 8. Chemiluminescence emission intensities of the luminol–H_2O_2–manganese(II) system in the presence of interfering metal ions. (1) Without interferent; (2) Cr(III); (3) Hg(II); (4) Cu(II); (5) Co(II); (6) Fe(II); (7) Ni(II). Mn(II), 10 ppm, interferent 12.5 ppm, pH 10.0, carbonate buffer, other conditions as for Fig. 2.

Table 1. Effect of pH on the masking action of cyanide on peaks I and II in the Mn(II)–luminol–H_2O_2 system*

	Masking effect, % pH											
	4.5		5.0		5.5		6.0		6.5		7.0	
Interferent	I	II	I	II	I	II	I	II	I	II	I	II
Hg(II)	51	58	70	74	76	77	80	85	100	100	100	100
Ni(II)	32	20	53	44	65	65	82	86	100	100	100	100
Fe(II)	3	1	7	1	22	20	64	59	100	100	100	100
Co(II)	1	3	1	3	5	10	43	45	100	100	100	100
Cu(II)	2	1	6	3	17	16	51	60	56	87	90	92
Mn(II)	1	1	3	3	3	3	3	3	3	3	2	2

* Mn(II) 15 ppm, interferent 37.5 ppm in the test solution, 0.01M cyanide, $4 \times 10^{-3}M$ luminol.

manganese, even without an added activator, in a static system. Undoubtedly, by use of an activator such as 1,10-phenanthroline, and the use of an appropriate flow system,[17] greater sensitivity and precision could be attained.

Acknowledgement—J L Burguera thanks FONINVES from Venezuela for a research studentship.

REFERENCES

1. U. Isacsson and C. Wettermark, *Anal. Chim. Acta*, 1976, **83**, 277.
2. D. B. Paul, *Talanta*, 1978, **25**, 377.
3. I. E. Kalinichenko, *Ukr. Khim. Zh.*, 1969, **35**, 755.
4. *Idem*, *Russ. Pat.* 252, 712, Sept. 22, 1969.
5. A. T. Pilipenko, E. I. Kalinichenko and E. Ya. Matveeva, *Zh. Analit. Khim.*, 1977, **32**, 2014.
6. L. I. Dubovenko and A. P. Tovmasyan, *Ukr. Khim. Zh.*, 1971, **37**, 943.
7. W. R. Seitz and D. M. Hercules, *Intern. J. Env. Anal. Chem.* 1973, **2**, 273.
8. L. I. Dubovenko and A. P. Tovmasyan, *Zh. Analit. Khim.*, 1970, **25**, 940.
9. *Idem*, *Arm. Khim. Zh.*, 1970, **23**, 690.
10. A. K. Babko, L. I. Dubovenko and L. S. Mikhailova, *Sov. Prog. Chem.*, 1966, **32**, 471.
11. *Idem*, *Ukr. Khim. Zh.*, 1966, **32**, 614.
12. J. L. Burguera and A. Townshend, *Talanta*, 1979, **26**, 795.
13. E. H. White and M. M. Bursey, *J. Am. Chem. Soc.*, 1964, **86**, 941.
14. H. A. Neufeld, C. J. Conklin and R. D. Towner, *Anal. Biochem.*, 1965, **12**, 303.
15. D. S. Bersis and J. Nikokavouras, *Nature*, 1968, **217**, 451.
16. E. H. White and D. F. Roswell, *Acc. Chem. Res.*, 1970, **3**, 54.
17. J. L. Burguera, A. Townshend and S. Greenfield, *Anal. Chim. Acta*, 1980, **114**, 209.

Talanta, Vol. 28, pp. 737 to 744, 1981
Printed in Great Britain. All rights reserved

0039-9140/81/100737-08$02.00/0
Copyright © 1981 Pergamon Press Ltd 1981

DETERMINATION OF RUTHENIUM AND TIN ON ELECTROCHEMICAL ANODES BY ENERGY-DISPERSIVE X-RAY FLUORESCENCE*

W. R. BRAMSTEDT, K. L. HARDEE, B. R. JOHNSON and D. E. HARRINGTON
Diamond Shamrock Corporation, P.O. Box 348, Painesville, OH 44077, U.S.A.

(*Received* 5 *January* 1981. *Accepted* 13 *March* 1981)

Summary—"Dimensionally Stable Anodes" (DSA)® have gained wide acceptance in electrochemical production of chlorine and caustic soda. The DSAs are usually composed of electrocatalytic layers of precious and non-precious metal oxides produced by thermal decomposition of salts on a valve-metal substrate (*e.g.*, titanium). They have long lifetimes (some years) in commercial service, and accelerated aging is used in testing them. In these tests the cell potential is stable for most of the anode life. Failure of an anode is characterized by a rapid increase in potential to beyond the point of practical operation of the cell. Non-destructive X-ray techniques have been utilized to investigate the mechanism involved. It has been established that the precious metal content has been reduced by 50–60% when the anodes fail. Although present DSA coatings are more than adequate for commercial applications, there is continuing interest in improving them. The materials for DSA formulation include the precious metals iridium, ruthenium and rhodium, the non-precious metals tin, antimony and manganese, and the valve metals titanium and tantalum.

Catalytically active electrochemical anodes have greatly improved the energy efficiency of caustic soda–chlorine production and have found applications in other areas of industrial electrocatalysis. These types of anodes have greatly reduced voltage requirements for cell operation, giving a large saving in electrical power. A secondary economy is realized in the longer cell life and reduced maintenance costs. To understand the functioning of these anodes, it is essential to be able to analyse the coatings quantitatively for the catalytic metals.

The most salient feature of these electrochemical anodes is the precious-metal catalytic coating. New developments in electrode coating technology are centred around partial replacement of the precious metals with cheaper base metals. The most common type of dimensionally stable anode is coated with ruthenium oxide and called a "DSA"®. The preparation and morphology of this anode have been reported.[1]

Evaluation, characterization and future developments are, in part, dependent upon accurate determination of each metal in the coating. We have developed methods for removing the catalyst coating from the substrate and determining the individual elements by atomic-absorption spectroscopy.[2,3] While this approach was useful, there were major disadvantages. Since the method was totally destructive, it was not applicable to quality control or field studies. The method was also very time-consuming, because of the alkaline fusion needed for each sample preparation. Therefore, it was necessary to develop analytical approaches that would meet a number of requirements to be of maximum utility. These requirements are that the method should (1) be non-destructive; (2) be adaptable to large samples; (3) be fast and reasonably accurate; (4) require no sample preparation; (5) require minimal personnel training. X-Ray spectrometry (XRS) methods which meet most of these criteria have been reported by a number of investigators. We have previously reported the advantages of using portable X-ray fluorescence equipment for the non-destructive analysis of DSAs for ruthenium.[4] However, with the addition of tin to the catalyst, the analytical methods needed to be refined.[5] The major drawback of using portable equipment is the lack of resolution in distinguishing different elemental constituents of the catalyst.

There are a number of trade-offs involved in establishing any method for the determination of the metals in these catalysts. Classical X-ray fluorescence measurements for measuring film and coating thicknesses have been summarized and meet many of the requirements.[6] However, most of the methods reported dealt with small objects that could be brought to an analytical laboratory and would fit into a conventional wavelength-dispersive X-ray spectrometer. Most work reported on thin-film techniques employing the conventional crystal spectrometers was concerned with the analysis of very small objects.[7–10]

The coated structures to be analysed were large compared to the sample holders available for conventional XRF equipment. To eliminate sample cutting, we had to use either larger sample holders or more

* This paper was, in part, presented at the Pittsburgh Conference, 1977.

® Registered trademark of Diamond Shamrock Corporation.

adaptable X-ray equipment to take advantage of the non-destructive nature of energy-dispersive X-ray fluorescence (EDXRF). One alternative was to use radioisotopes for excitation, as suggested for measuring coating thicknesses.[11,12] Radioisotope sources provided the flexibility necessary to measure large structures. These sources can be used with portable units[13] or specially designed equipment.[14]

A major problem encountered in using a portable radioisotopic excitation unit with a gas proportional detector was the lack of resolution. It was not possible to obtain good precision and accuracy for ruthenium and tin by using a single-channel mode of operation. When the balance filters were employed for coating-thickness measurements,[15] each sample had to be counted through both filters and counting times had to be increased to offset the loss of precision caused by signal attenuation. Therefore, we investigated multichannel analysis as an alternative. This proved very beneficial with the portable X-ray unit and essential with our source-excited fluorescence analyser (SEFA).

After we had decided X-ray fluorescence was the best choice for solving the analytical problems, we had to decide which calibration procedure should be used. A number of techniques have been suggested.[16] Microscopy methods were discarded because of the irregular "mud-cracked" texture of the catalyst surface.[1] Weight-gain values obtained during preparation were reasonable approximations, but required a detailed knowledge of the oxide content of the substrate and of the solid solutions which formed the catalytic layer. The best calibration procedure was chemical analysis by atomic-absorption spectroscopy. By dissolving the catalytic layer off the substrate by alkaline fusions and using atomic-absorption spectrometric analysis, we were able to establish standards for the X-ray method.[2,3]

Summarizing the possible approaches, we have atomic-absorption spectroscopy, which is destructive and very time-consuming; portable X-ray spectroscopy with radioisotope excitation and single-channel operation; portable X-ray equipment with radioisotope excitation and a multichannel analyser; finally, to gain even more resolution, X-ray analysis using radioisotopic excitation, a lithium-drifted silicon detector and a multichannel analyser. There are advantages and disadvantages to each of these techniques, and the technique must be selected to meet the needs of the particular analysis.

EXPERIMENTAL

Apparatus

For this study we used a portable EDXRF unit (Panametrics, Waltham, Mass.) equipped with a model 4000 probe containing a 10-mCi americium-241 source. The radiation detector probe (LND, Oceanside, Cal.) contained a 2 × 2 in. gas proportional counter filled at 1 atm pressure (with 3–5% carbon dioxide as quenching gas). **Warning**—a "pencil" beam of X-ray leakage from this unit was detected during normal sample-changing procedures.

The second type of X-ray unit available was an Ortec source-excited fluorescence analyser (SEFA) with an Si(Li) detector. Modifications of this unit have been described.[19] The main feature of this spectrometer was that it contained a lithium-drifted silicon detector for high-resolution work. Two multichannel analysers were used with the various pieces of X-ray equipment. They were manufactured by Ortec, Oakridge, and were models 6200 and 6230.

Data-processing was done with a dedicated PDP 11/05 computer equipped with dual floppy disks. Communication was through a Texas Instruments Silent 700 terminal. Various subroutines were available (through Ortec Oracle programming) for saving spectra, stripping background spectra, *etc.* Off-line data-processing could be done with a remote computer terminal connected to a PDP/15, PDP 11/70 or VAX.[17]

RESULTS AND DISCUSSION

With the multichannel analyser systems, it is possible to resolve the ruthenium and tin peaks. The spectra obtained from the portable unit on the multichannel analyser outputs are shown in Fig. 1. In the spectra obtained from this unit on the 6200 multichannel analyser the ruthenium and tin are separated, but each of the peaks is a combination of $K\alpha$ and $K\beta$ lines. In the top spectrum labelled Beer DSA Anode, the ruthenium $K\alpha$ and $K\beta$ lines are contained in the large central peak. The small peak to the left appears in all three spectra and is associated with the background. In the second spectrum, labelled CX DSA, the small peak to the right is the combination of the tin $K\alpha$ and $K\beta$ lines. In the third spectrum, labelled EX DSA, the ruthenium is at a lower concentration than the tin.

In spectra obtained from the lithium-drifted silicon detector and the 6230 multichannel analyser, we see a clear resolution of the ruthenium and tin $K\alpha$ and $K\beta$ peaks, as shown in Fig. 2. With the portable units, the resolution is not complete, but there is sufficient separation to establish appropriate regions of interest for each of the quantitative determinations. Though there are a number of possible sources for background radiation, all were minimized by closely matching calibration standards with the type of samples to be measured.

Representative calibration graphs for ruthenium and tin were established with each of our units. Each type of formulation required from 4 to 8 calibration points. To prepare these calibration standards, matched pairs were analysed by X-ray fluorescence and one sample of each pair was analysed by atomic-absorption spectroscopy. These samples covered the concentration range of interest. Typical calibration curves obtained from three types of formulations with the portable unit are shown in Fig. 3. As we can see from this figure, there appears to be an interelement effect between ruthenium and tin. The lowest slope is obtained when no tin is present. As we increase the amount of tin the slope of the line increases, as well as the total number of counts. One procedure to verify

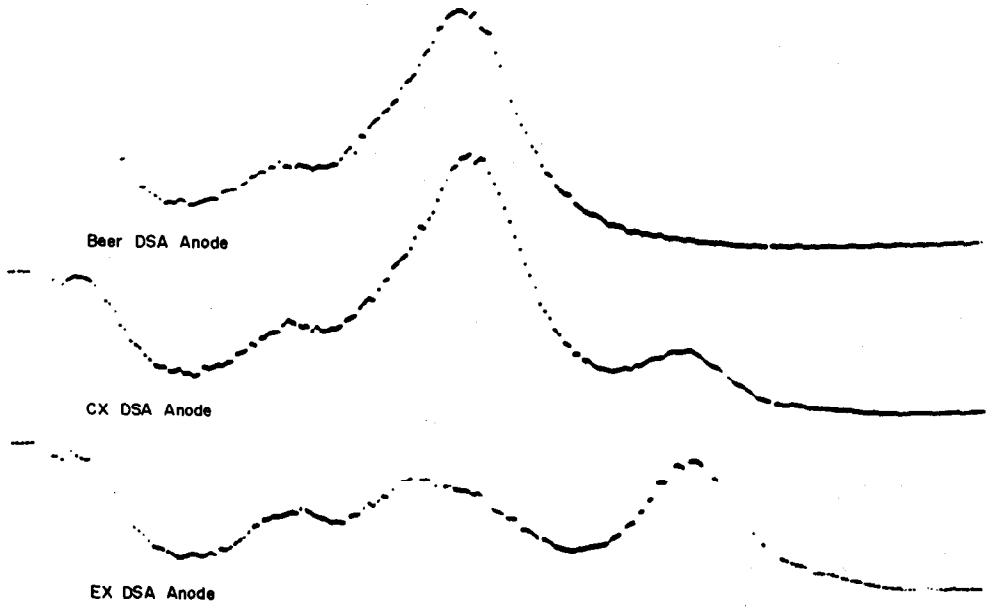
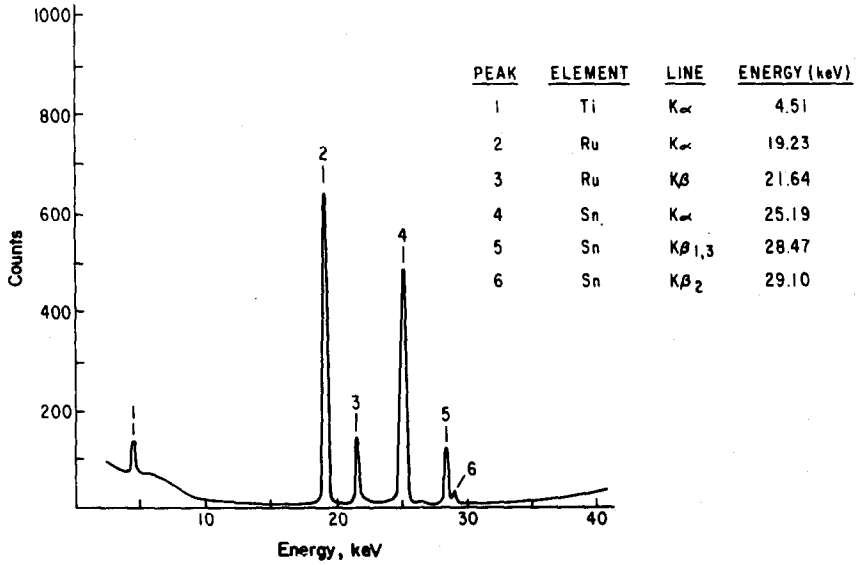


Fig. 1. The X-ray spectra obtained with the Panametrics portable X-ray unit/multichannel analyser system. The ruthenium and tin peaks are resolved, but the $K\alpha$ and $K\beta$ peaks are not.

that this was a true interelement effect was to calibrate for these three types of formulation on one instrument and alter the isotopic excitation source.

Our SEFA unit was equipped with changeable sources. We had americium-241, cadmium-109, and iron-55 sources available. We ran all three types of anodes on this instrument. Since cadmium-109 does not excite the tin K lines, the values for all three formulations fall on the same calibration line as shown in Fig. 4. The effect of tin on the ruthenium calibration curve when the americium source is used is thus presumably due to further excitation of ruthenium by the K radiation of tin. Statistical evaluations of the calibration plots obtained from the various units are given in Table 1.

To evaluate the counting times needed to achieve a specified level of precision, similar samples were counted on both instruments. As expected, and seen in Table 2, the precision is dependent on the total number of counts, which is a function of both the surface density and the counting time. At very low concentrations, it is necessary to count for more than 40 sec to achieve a coefficient of variation of 0.7% for ruthenium. As the surface density increases, it is possible to shorten the counting time but still obtain a higher level of confidence for ruthenium, as shown by



PEAK	ELEMENT	LINE	ENERGY (keV)
1	Ti	K_α	4.51
2	Ru	K_α	19.23
3	Ru	$K\beta$	21.64
4	Sn	K_α	25.19
5	Sn	$K\beta_{1,3}$	28.47
6	Sn	$K\beta_2$	29.10

Fig. 2. The X-ray spectra obtained with the source-excited fluorescence analyser (SEFA). The $K\alpha$ and $K\beta$ peaks for ruthenium and tin are resolved.

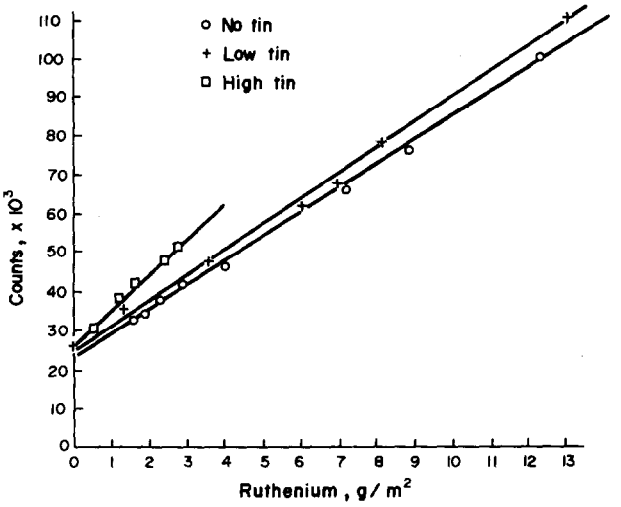


Fig. 3. Ruthenium calibration lines are affected by the tin concentration when the americium-241 excitation source is used.

a 0.5% coefficient of variation when the coating density is over 13 g/m^2.

Precision data obtained with the SEFA unit are given in Table 3. In general, samples must be counted for longer times on the SEFA unit to obtain precision levels comparable to those obtained with the portable unit. Note that the coefficients of variation are nearly identical for the first and fourth entries of Table 3, even though the first entry has more than twice the average total intensity of the fourth. Background corrections are not needed because the peak:background ratio is greater than 10:1.[18] The theoretical standard deviation (σ) of a single determination is closely approximated by the square root of the total number of counts ($\sqrt{N}$).[19] We would expect that the conditions which produce the largest total count would also give the lowest coefficient of variation, provided, of course, other sources of error are minimized. We investigated the apparent conflict in Table 3 by analysing the data from ten sets of 10 replicate counting periods (trials 5–14).

Trials 5–14 give coefficients of variation ranging from 1.0 to 1.5% for the means of the individual sets of 10 results each, calculated from $100\sqrt{\Sigma(\bar{N} - N)^2/N}\sqrt{9}$, values ranging from 1.1_9 to 1.2_4% for each individual result (calculated from $100\sqrt{N}/N$), and a grand overall coefficient of variation

Table 1. Statistical evaluation of calibration by regression analysis

Element	Multiple R^2	Multiple F	Technique
Ru	0.996	985	MCA-Portable Unit
Sn	0.998	1687	MCA-Portable Unit
Ru	0.986	290	SCA-Balanced Filter
Sn	0.990	393	SCA-Balanced Filter
Ru	0.998	880	SEFA
Sn	0.997	612	SEFA

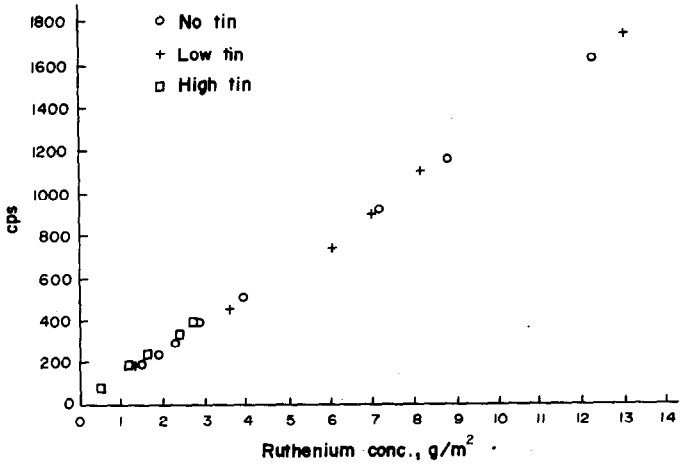


Fig. 4. The interference of tin in the ruthenium calibration can be minimized by using cadmium-109 as the excitation source.

Table 2. Precision of Panametrics analysis

Element	Coating density, g/m^2	Counting time, *sec*	Average total intensity	Coefficient of variation, %
Sn	1.05	10	1044	3.3
	1.05	20	2083	2.1
	1.05	40	4162	1.9
	1.05	80	8591	1.3
	9.78	10	3228	2.6
	9.78	20	6397	1.2
Ru	1.36	10	3006	1.5
	1.36	20	5976	1.6
	1.36	40	11970	0.7
	1.36	80	25320	0.7
	13.04	10	11240	1.1
	13.04	20	22540	0.5

Table 3. Precision of SEFA analysis (ruthenium, 7.22 g/m^2)

Trial	Counting time, *sec*	Average total intensity	Coefficient of variation, %	Source
1	20	10805	1.5	^{109}Cd
2	20	1138	3.1	^{241}Am
3	40	2280	2.0	^{241}Am
4	80	4538	1.5	^{241}Am
5	20	6732	1.1	^{109}Cd
6	20	6744	1.2	^{109}Cd
7	20	6750	1.4	^{109}Cd
8	20	6781	1.3	^{109}Cd
9	20	6754	1.3	^{109}Cd
10	20	6771	1.5	^{109}Cd
11	20	6752	1.0	^{109}Cd
12	20	6844	1.5	^{109}Cd
13	20	6809	1.3	^{109}Cd
14	20	6760	1.5	^{109}Cd
5–14 (Composite)	20	6770	1.4	^{109}Cd

of $1.3_5\%$ for all 100 results (calculated from $100\sqrt{\Sigma(\bar{N}-N)^2}/\bar{N}\sqrt{99}$). The *F*-test indicated no statistically significant difference between these three sets of results, and for calculating the counting time needed for a particular analysis it is perfectly satisfactory to calculate the coefficient of variation from $100\sqrt{N}/N$ $(=100/\sqrt{N})$ instead of running a set of replicates.

Trials 5–14 and trial 1 in Table 3 were run under the same conditions, but separated in time by over 10 months. The large decrease in average total intensity (37% less for 5–14) is due to decay of the ^{109}Cd source. This is a drawback with our SEFA system. To avoid use of large normalization factors, calibration curves must be run frequently when the ^{109}Cd source is used (^{109}Cd half-life = 450 days). Since the half-life of ^{241}Am is 458 years, a similar problem does not arise with it.

To evaluate the overall accuracy of the method, a number of factors have to be taken into account. First, the accuracy of the atomic-absorption measurement for establishing standards is critical in the calibration of the X-ray method. As shown in Table 4, the average relative recovery for ruthenium was 96%. In the experimental evaluation of the recovery there will be errors from the initial X-ray readings on two

Table 4. Accuracy of Panametrics

Element	Sample	XRF, g/m^2	AAS, g/m^2	100 × AAS/XRF, %
Ru	1	4.14	4.11	99
	2	3.98	3.78	95
	3	5.10	4.78	93
	4	7.06	6.28	89
	5	7.91	7.73	98
	6	9.73	10.11	104
	Average			96
Sn	1	2.27	2.14	95
	2	2.51	2.47	98
	3	3.28	3.01	92
	4	4.79	4.50	94
	5	5.18	4.78	93
	6	6.57	6.12	93
	Average			94

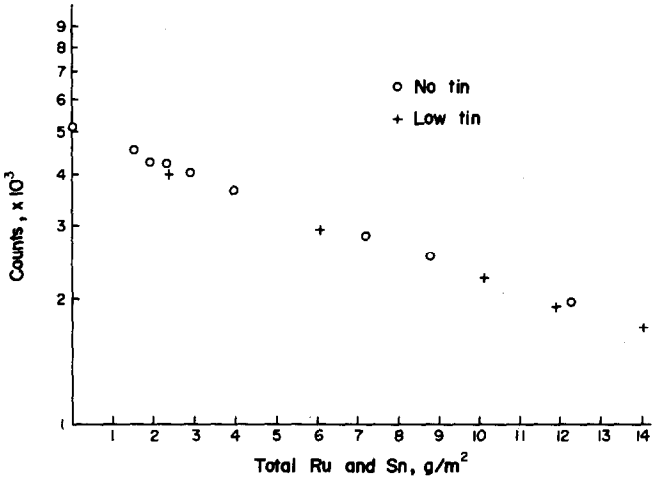


Fig. 5. The substrate attenuation technique allows the determination of total heavy-metal content of the anode coating. While the method cannot distinguish individual components, it is very sensitive for determining low-level coating weights.

matched sets, the atomic-absorption error in analysing one of these matched pairs, error in the analysis of an unknown by the X-ray technique, and in the final analysis by atomic-absorption to prove that the answer was correct. The same procedure was applied for tin and the average recovery was found to be 94%.

One method of evaluating coating thickness is by the substrate attenuation procedure.[20] As the amount of coating is increased, the titanium substrate XRF signal is reduced. By monitoring the total titanium counts as a function of the total ruthenium and tin in the coating, we can create a calibration equation. Data obtained with the portable unit are shown in Fig. 5. This technique measures the total coating thickness but does not give the ratio of precious metal to base metal. One advantage of using this technique is that small variations in formulation do not affect the final result. Minor changes in base or precious metal content can be made without drastically changing the calibration standards. The precision of the substrate attentuation method is shown in Table 5. The coefficient of variation of this technique is better than that of the technique for direct measurement and the technique is very sensitive for low coating levels.

Application of non-destructive analysis

A major application of X-ray analysis is the elucidation of anode failure mechanisms. The development of this analytical technique allowed the design and evaluation of two electrochemical experiments. In the first, 56 coated sheet anodes were examined before and after testing in the 150-g/l. sulphuric acid accelerated life-test unit. The X-ray fluorescence technique allowed the determination of ruthenium on the anodes that were tested in the electrochemical cells. The various anodes were prepared under different conditions, such as baking time. The mean amount of ruthenium retained on an anode was 42%, standard deviation 10%.

In the second, X-ray analysis was used to monitor coating loss periodically during an accelerated life-test. Since the analysis was non-destructive, the entire anode structure (the anode and conductive stems) could be removed from the cell and assayed. This allowed elemental concentration losses to be compared with electrochemical parameters such as single electrode potential (SEP) measurements, corrected for solution resistance. To characterize the coating loss with respect to anode failure, experiments were performed to monitor the coating with SEP measurements and XRS as a function of time on line (TOL) in the life-test unit. Two titanium sheets were coated in the normal manner. EDXRF values were obtained for tin and ruthenium separately. By use of a current-interruption technique, SEP values were measured from the current density in 150-g/l. sulphuric acid at 50° and in 300-g/l. sodium chloride solution (pH 1) at 75°. The anodes were then placed in the life-test cells

Table 5. Precision of Panametrics analysis (substrate attenuation)

Coating density, g/m^2	Counting time, *sec*	Average total intensity	Coefficient of variation, %
2.41	10	1.87×10^5	0.31
2.41	20	3.74×10^5	0.28
2.41	40	7.48×10^5	0.14
22.82	10	0.63×10^5	0.46
22.82	20	1.27×10^5	0.29

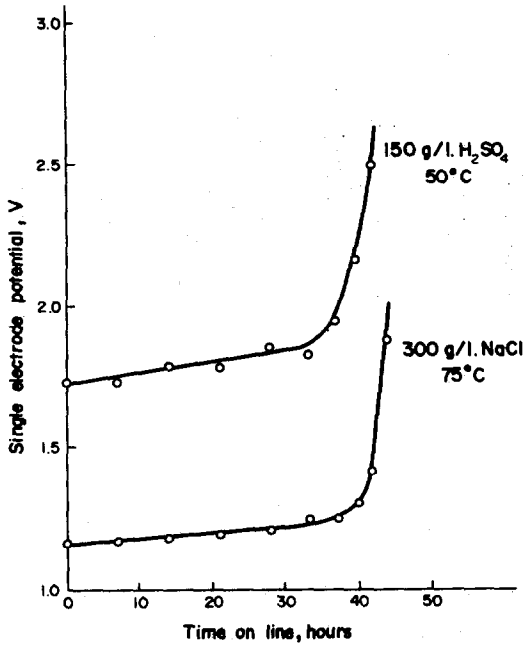


Fig. 6. Single electrode potentials *vs.* time on line for DSA anode during accelerated life-test.

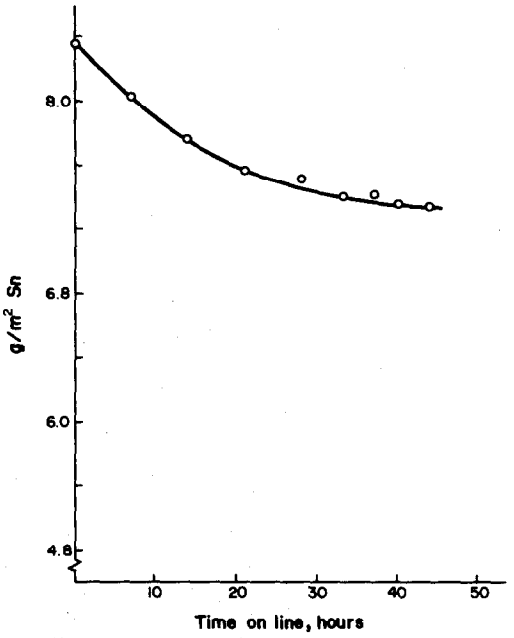


Fig. 8. Tin loss *vs.* time on line for DSA anode during accelerated life-test. The X-ray analysis indicated the per cent loss of tin was much lower than that of ruthenium.

at a current density of 0.75 A/cm^2. After 7 hr or a 0.2-V rise in cell potential (whichever came first) the anodes were removed from the cell and the EDXRF and SEP measurements were repeated. The cycle was repeated until failure of the anode (cell voltage over 8 V).

Figure 6 gives the plot of single electrode potentials *vs.* TOL in both electrolytes for a current density of 0.75 A/cm^2. The potentials have a gradual rise for about 35 hr and then climb very rapidly.

The EDXRF data are consistent with the observed electrochemical data, as shown in Figs. 7 and 8. Figure 7 shows that the coating density of ruthenium drops steadily over the first 20 hr, but then levels off and becomes virtually constant between 30 and 40 hr. This region coincides with the changes in the electrocatalytic activity. The tin coating density shows similar behaviour (Fig. 8) but the relative decrease is smaller. Table 6 shows the rate of loss of the coating elements. The results indicate that coating loss is due to chemical and/or electrochemical causes, rather than mechanical abrasion, assuming the coating is uniform, since ruthenium is preferentially lost.

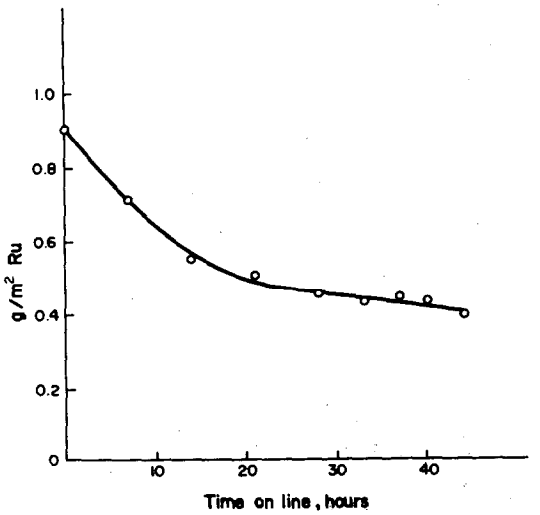


Fig. 7. Ruthenium loss *vs.* time on line for DSA anode during accelerated life-test. The non-destructive X-ray methods allowed determination of actual losses throughout the life-test.

The selective loss of ruthenium is consistent with an electrochemical mechanism of anode failure. Under the oxygen evolution conditions of the acid electrolysis, the anode potential (*ca.* 1.6–1.7 V *vs.* SCE, initially) is in excess of the potential reported for further oxidation of the ruthenium(IV) to higher oxidation states.[21] These states of ruthenium are generally unstable and would thus promote the dissolution of ruthenium from the coating. By contrast, the tin in the coating is already fully oxidized, being in the +4 oxidation state, and thus would be immune to further

Table 6. Retention of coating versus time on line

Time, *hr*	Sn, %	Ru, %
7	96	88
14	97	62
21	93	61
28	95	54
33	89	56
37	92	52
40	92	51
42	91	50

oxidation under the operating conditions of the anode. Since ruthenium is the electrocatalytic component of the coating, its continued loss eventually results in the failure of the anode.

The reason for the failure occurring when 50% of the ruthenium remains in the coating is still unclear. The remaining ruthenium is apparently not catalytically active.

Conclusions

While we have shown that the precision and accuracy of the X-ray techniques can reach a satisfactory level, there are a number of trade-offs that have to be evaluated. The first is the analysis time. Once calibration standards have been prepared, a series of 30 samples can be analysed in an hour by X-ray procedures. The problem with the SEFA technique is that it must be done in a "clean" laboratory and the equipment is very expensive. The least expensive procedure is to use a portable X-ray method in the single-channel mode, if the element or elements of interest can be discriminated. In the case of the portable unit, the sensitivity is good and the procedure can be applied quickly and anywhere, including quality-control areas and field tests.

When the portable units are used in conjunction with the multichannel analyser, the analysis time is reduced and it is probably the best method. The substrate attenuation method is very quick with the portable units, but is non-specific as to which elements it measures. Atomic-absorption spectroscopy, which is our reference method, is totally destructive and definitely the slowest. The same 30 samples would require 3–4 days by AAS methods.

The disadvantages of the portable unit–MCA system, in comparison with the SEFA with lithium-drifted silicon detector, are lack of resolution and sensitivity, the need for frequent standardization, and the fact that the energy of the peaks is not calibrated. The advantages of using the portable unit in conjunction with multichannel analysers, compared with classical wavelength techniques, are that they are totally non-destructive, large structures can be examined without cutting, ruthenium and tin can be determined simultaneously, and trained technicians are not needed. It is usually possible to train someone in 2–3 days to conduct these determinations.

The advantages of portable units over the SEFA system are that they can be used in the field, are much more cost-effective and can be purchased for $6000–8000 as compared to $12,000–20,000 for the SEFA system. Also, the movable head allows analysis of any object in any direction.

We have demonstrated that a number of X-ray techniques can be used to analyse for ruthenium and tin in electrochemical anodes. Each technique has its own advantages and these should be taken into account in the light of the information required to solve specific problems.

Acknowledgements—The authors would like to acknowledge the assistance of Dr. D. L. Lewis for the preparation of samples, and of W. O. Butler, C. L. Tang, J. M. Sutherland and D. L. Kalynchuk in evaluating the X-ray fluorescence procedures.

REFERENCES

1. K. J. O'Leary and T. J. Navin, *Chlorine Bicentennial Symposium*, pp. 174–186. The Electrochemistry Society, 1974.
2. D. E. Harrington and W. R. Bramstedt, *Talanta*, 1975, **22**, 411.
3. *Idem*, *At. Absorpt. Newsl.*, 1975, **14**, 36.
4. W. R. Bramstedt, D. F. DeCraene and D. E. Harrington, *Appl. Spectrosc.*, 1976, **30**, 456.
5. W. R. Bramstedt, D. L. Lewis and D. E. Harrington, Pittsburgh Conference, Cleveland, 1977, Preprint No. 79.
6. H. A. Liebhafsky and P. D. Zemany, *Anal. Chem.*, 1956, **28**, 455.
7. T. N. Rhodin, *ibid.*, 1955, **27**, 1857.
8. R. H. Zimmerman, *Metal Finishing*, 1961, **59**, 67.
9. E. P. Bertin and R. J. Longobucco, *Anal. Chem.*, 1962, **34**, 804.
10. E. P. Bertin, *ibid.*, 1964, **36**, 826.
11. P. D. Zemany, *Rev. Sci. Instr.*, 1959, **30**, 292.
12. G. B. Cook, C. E. Mellish and J. A. Payne, *Anal. Chem.*, 1960, **32**, 590.
13. J. R. Rhodes, *Am. Soc. Testing Materials Spec. Tech. Publ.*, STP 485, 243, 1971.
14. D. E. Harrington, W. O. Butler, S. L. Douglass and W. R. Bramstedt, *Spectrochim. Acta*, 1978, **33B**, 835.
15. F. A. Achey and E. J. Serfase, *J. Electrochem. Soc.*, 1958, **105**, 204.
16. N. Spielberg and G. Abowitz, *Anal. Chem.*, 1966, **38**, 200.
17. D. E. Harrington and W. R. Bramstedt, *Am. Lab.*, 1975, **7**, No. 9, 15.
18. R. Jenkins and J. L. DeVries, *Practical X-Ray Spectrometry*, 2nd Ed., p. 99. Springer-Verlag, New York, 1970.
19. *Idem*, *op. cit.*, pp. 94–96.
20. E. P. Bertin, *Principles and Practice of X-Ray Spectrometric Analysis*, 2nd Ed., pp. 811–814. Plenum Press, New York, 1975.
21. A. J. Bard, (ed.), *Encyclopedia of Electrochemistry of the Elements*, Vol. VI., pp. 277–298. Dekker, New York, 1976.

Talanta, Vol. 28, pp. 745 to 752, 1981
Printed in Great Britain. All rights reserved

0039-9140/81/100745-08$02.00/0
Copyright © 1981 Pergamon Press Ltd 1981

THE APPLICATION OF AN ARGON/NITROGEN INDUCTIVELY-COUPLED PLASMA TO THE ANALYSIS OF ORGANIC SOLUTIONS

J. A. C. BROEKAERT, F. LEIS and K. LAQUA

Institut für Spektrochemie und angewandte Spektroskopie, Postfach 778,
D-4600 Dortmund 1, Federal Republic of Germany

(*Received* 13 *January* 1981. *Accepted* 12 *March* 1981)

Summary—A 4-kW argon/nitrogen inductively-coupled plasma (ICP) is used for multielement trace determinations in organic solutions. After optimization of the pneumatic nebulizer and ICP parameters, trace determinations at sub-μg/ml concentrations with relative standard deviations of 1% are possible. The first application described is the determination of a series of metals (Cd, Cu, Fe, Mn, Zn) after their isolation from the sample matrix by extraction of the ammonium pyrrolidinedithiocarbamate complexes into methyl isobutyl ketone. Alkali and alkaline-earth metal salts at 50-g/l. concentrations do not affect the method, which can be applied to trace determinations in industrial waste waters having high salt contents. The second application is the multielement analysis of oils. The samples are diluted 1:10 with xylene, and the detection limits for Al, Cu, Fe, Mg, Mn, Si and Zn are in the sub-μg/g range. The superior detection power of spectrographic ICP methods in comparison with photoelectric techniques using a monochromator and a polychromator is discussed. Oils of different viscosities can be analysed with use of the same calibration graphs. From experiments with a computer-controlled polychromator with background measurement facilities, it is concluded that the accuracy is improved if background measurements are made at wavelengths near the analytical lines, for each sample independently.

The application of inductively-coupled plasma atomic-emission spectroscopy (ICP–AES) to multielement determinations in aqueous solutions has been described in numerous publications, and has recently been reviewed, *e.g.*, by Boumans.[1] In the same review it was shown that ICP–AES is also suitable for determinations in organic media. Fassel *et al.*[2] and Merryfield and Loyd[3] have used a low-power argon ICP for the analysis of lubricating oils. A high-power argon/nitrogen ICP has been used for the analysis of oils by Greenfield *et al.*,[4] and Ohls has reported routine applications to oil analysis.[5] However, detailed studies on the optimization and power of detection of the argon/nitrogen ICP for analysis of organic solutions have not yet been reported. The aim of the present work is to optimize the operational parameters of the nebulizer and the ICP, study the power of detection, and illustrate the analytical capabilities of the method by two industrially important applications, the analysis of waste water with high salt content, and the multielement trace analysis of oils.

EXPERIMENTAL

ICP equipment

A free-running r.f.-generator was used for powering the argon/nitrogen ICP. The output of the generator was stabilized by using the r.f. stray field in the vicinity of the coil as reference signal.[6] With this system a 10-sec integration of the Ar I 420.1-nm line intensity had a relative standard deviation of 0.2%. With power stabilization, any common organic solvent [acetone, methyl isobutyl ketone (MIBK), chloroform, xylene, carbon tetrachloride, *etc.*] can be introduced into the ICP without influencing the discharge stability or the power dissipation in the system.

The analytical line intensities were measured both photographically and photoelectrically. A 3.5-m Ebert spectrograph was used for photographic survey analyses. Photoelectric measurements were done with a microcomputer-controlled 0.9-m Czerny–Turner monochromator and a computer-controlled 1-m vacuum spectrometer which will be described elsewhere. An observation zone of 4 × 4 mm area located centrally above the plasma coil was selected at the intermediate image so that the aperture of the spectral apparatus was fully illuminated. Detailed instrumental parameters and operating conditions are listed in Table 1.

RESULTS AND DISCUSSION

Optimization of the ICP for analysis of organic solutions

When organic solvents such as MIBK or xylene are introduced into the ICP, the form of the discharge differs from that obtained with aqueous solutions and is shown schematically in Fig. 1. Normally the most favourable observation zone in the ICP is situated relatively low in the plasma, *e.g.*, immediately above the burner edge, as can be understood from consideration of the analyte particle distribution. However, in the case of organic solutions, a luminous cone is formed in the lower zones of the discharge. This is due to band emission by molecular ions and radicals arising from thermal cracking of the solvent molecules. In this case the lower zones of the ICP are not suitable for analytical measurements because the band emission enhances the spectral background,

Table 1. ICP equipment

ICP	
r.f. Generator	FS-10 (Kontron–Linn) maximal output power 10 kW, frequency 27.12 MHz
Torch	As described by Greenfield *et al.*[7]
Nebulization	Pneumatic concentric glass nebulizer (Meinhard Ass.)[8] Nebulization chamber as described by Scott *et al.*[9]
Spectral aparatus	
Illumination	Three-lens system, selection of a 4 × 4 mm observation zone at the intermediate image[10,11]
Spectrograph	3.5-m Ebert grating spectrograph (RSV); grating constant a = 1/1180 mm, dimensions 100 × 100 mm; entrance slit-width 30 μm
Monochromator	0.9-m microcomputer-controlled Czerny–Turner monochromator; grating constant a = 1/2400 mm, 90 × 90 mm; entrance slit-width 12 μm; exit slit-width 15 μm; sequential measurement of line and background intensities with the aid of a quartz refractor plate in front of the exit slit.[12] Microcomputer Intel 80/20. Photomultiplier EMI 9789 QB.
Polychromator	1-m Paschen–Runge vacuum spectrometer (Baird Spectrovac 1000) with computer-controlled displacement of the entrance slit; grating constant a = 1/1440 mm, width 50 mm, height 30 mm; entrance slit-width 25 μm, exit slit-width 80 μm (24 lines can be measured simultaneously and can be selected from 130 slits etched in steel masks placed on the Rowland circle); 173–385 nm 2nd order; 346–767 nm 1st order; photomultipliers 1 P 28, R 166, 1 P 21; computer Modcomp II.

leading to both decreased power of detection and poor analytical precision. This problem can be overcome by using a relatively low aerosol carrier-gas flow, which limits the height of the luminous cone. Indeed, at low aerosol carrier-gas flows the residence

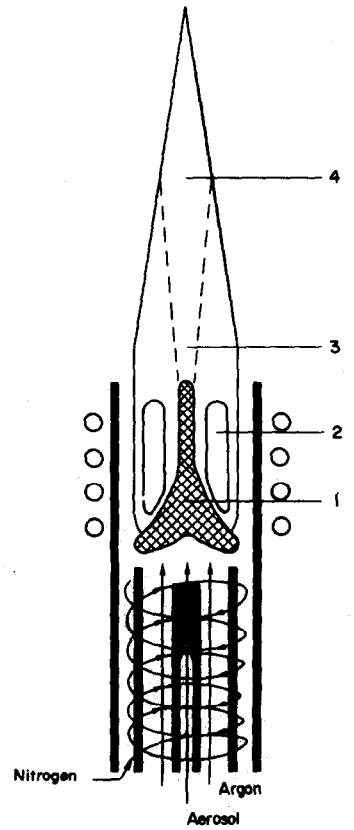


Fig. 1. Form of the argon/nitrogen ICP discharge with introduction of organic solutions. Torch as described by Greenfield *et al.*[7] (1) Heating zone; (2) induction regions; (3) analytical zone; (4) tail plume (nomenclature in compliance with Koirtyohann *et al.*[13]

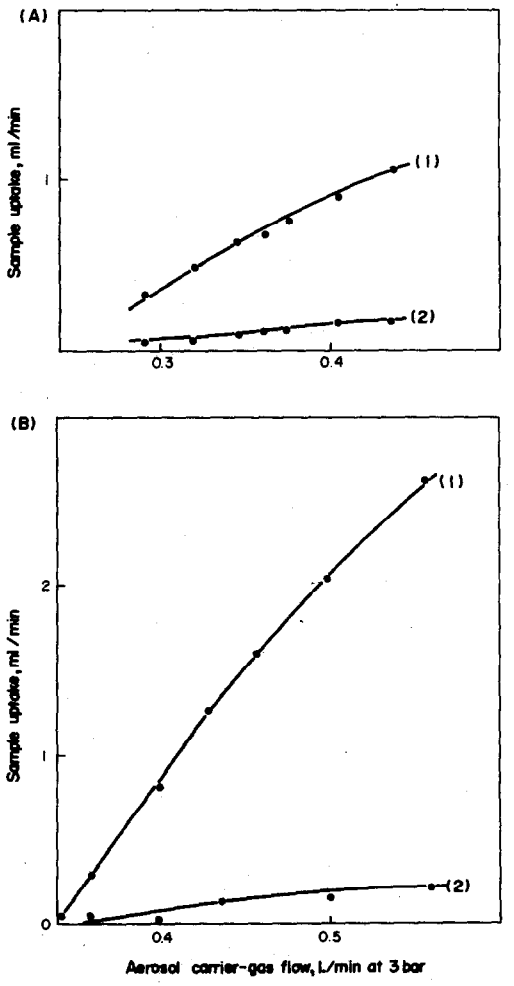


Fig. 2. Characteristics of a concentric glass nebulizer for MIBK (A) and water (B). Nebulizer Meinhard Ass., Type B II; carrier-gas argon; (1) sample uptake rate; (2) sample uptake in the ICP, defined as the difference between the sample uptake rate and the sample waste at the exit of the nebulization chamber.

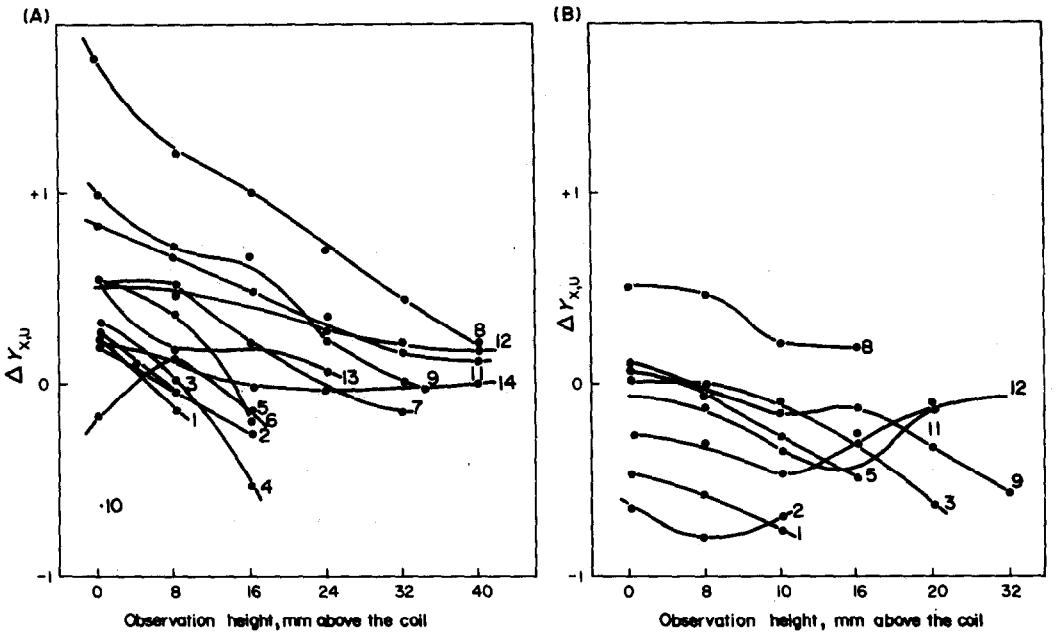


Fig. 3. Logarithmic line-to-background intensity ratios ($\Delta Y_{x,u}$) for a series of lines at different observation heights in an argon/nitrogen ICP. Sample 1 μg/ml of different metals in water (A) or as APDTC-complexes in MIBK (B); power level 4 kW; spectrographic measurement; (1) Cd II 226.5 nm; (2) Co II 228.6 nm; (3) Cd I 228.8 nm; (4) Ba II 230.4 nm; (5) Fe II 238.2 nm; (6) Co II 238.9 nm; (7) B I 249.8 nm; (8) Mn II 257.6 nm; (9) Fe II 259.9 nm; (10) Pb I 283.3 nm; (11) Cr II 283.6 nm; (12) Cr II 284.3 nm; (13) Cr II 285.0 nm; (14) Cr II 285.6 nm.

time of the aerosol particles in the lower part of the aerosol introduction channel (0–10 mm above the tip of the aerosol injector tube) is high (some msec) and the gas temperature in this channel is also high.[14] Consequently, total atomization of the solvent is already accomplished in the low plasma zones inside the r.f.-coil and an observation zone immediately above the burner edge can be selected. With organic solutions the nebulizer can be operated at comparatively low carrier-gas flow because high-pressure pneumatic nebulizers generally have a higher efficiency for organic solvents than for aqueous solutions.[15] With a Meinhard nebulizer, at a carrier-gas flow of 0.35 l./min at 3 bars pressure the transfer of MIBK solution into the ICP is considerably greater than that of an aqueous solution (Fig. 2).

Measurements of line-to-background intensity ratios for a series of lines and different observation heights (Fig. 3) confirm that generally the highest power of detection is obtained by observation at 0–4 mm above the quartz wall of the burner. For a few lines a higher observation zone must be selected, and generally the line-to-background intensity ratios are lower for organic solutions than for aqueous solutions. Both facts result from the overall higher intensity of the spectral background, which arises partly from band emission but is probably also partly due to higher intensities of stray light. When an argon/nitrogen ICP is used for the analysis of either aqueous or organic solutions, the line-to-background intensity ratios vary by less than about 10% over the power range of 3–5 kW, and are practically constant over the range 4–4.5 kW (Fig. 4). A power level of 4 kW was selected as optimum and used in all further experiments.

The optimized ICP working conditions are summarized in Table 2. At the gas flows mentioned, there was no carbon deposition at the burner tip. Under these conditions and with power stabilization (Fig. 5), a relative standard deviation of 1% was obtained for

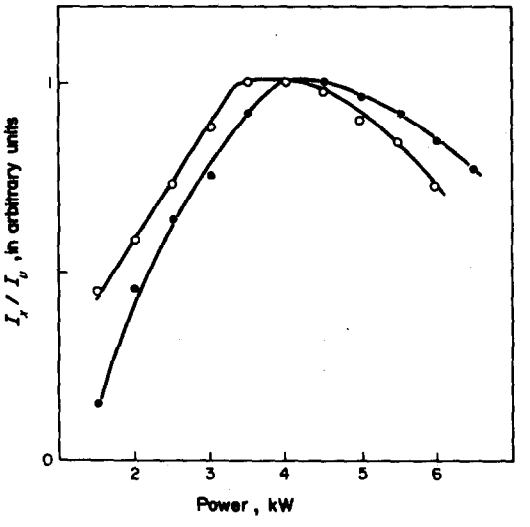


Fig. 4. Optimization of the operation power of the argon/nitrogen ICP. Sample Fe 1 μg/ml in 0.05*M* HCl (○) and as APDTC-complex dissolved in MIBK (●); observation height 2–4 mm above the coil; photoelectric measurements; line Fe II 259.9 nm; integration time 10 sec (alternating integration of line and background intensities).

Table 2. Optimized ICP working conditions for the analysis of organic solutions

Power	4 kW
Gas flows	Outer gas flow: nitrogen 25 l./min intermediate gas flow: argon 6 l./min aerosol carrier-gas flow: argon 0.4 l./min
Sample uptake rate	1 ml/min (free sample aspiration)
Observation height	4–8 mm above the coil
Exposure time	1 min (photoplates: Kodak SA 1)
Integration time	3–5 sec

analysis of an oil sample containing 10 μg of iron per g (after 1:10 dilution with xylene).

Determination of metals after MIBK extraction of their APDTC complexes

This extraction technique (with ammonium pyrrolidinedithiocarbamate and methyl isobutyl ketone) is widely used in flame atomic-absorption spectroscopy (FAAS).[16] It allows the isolation of metals from solution samples with complex composition, *e.g.* from waste water samples with high concentrations of alkalis or detergents, and may also allow preconcentration of the trace elements to be determined. Because of the selectivity of the detection method, but especially because of the quantitative complexation and high extraction efficiency for a large number of metals (Cd, Co, Cu, Fe, Mn, Pb, ...) this extraction technique is very suitable for combination with a multielement analysis technique such as ICP–AES.

The extraction system is similar to that given by Koch and Koch-Dedic.[17] A 50-ml portion of sample solution in a 250-ml separating funnel is adjusted to pH 3 with 0.1% nitric acid or ammonia, mixed with 10 ml of freshly prepared 5% solution of APDTC, and extracted with two 40-ml portions of MIBK. The organic phases are combined and diluted to 100 ml with MIBK.

First, the detection limits for a series of metals extracted as their APDTC complexes into MIBK were determined spectrographically. The detection limits are defined according to Kaiser and Specker,[18] by the equation

$$c_L = c_U 3\sqrt{2} s_r(I_U) \qquad (1)$$

For spectrographic measurements, the background equivalent concentration c_U is calculated by simple proportion from the measured density S_X of the analytical line obtained for a 1-μg/ml standard solution and S_U, the density for the spectral background near the line. The relative standard deviation of the background intensity, $s_r(I_U)$, is calculated from the standard deviation of the densities for the spectral background, $s(S_U)$, as described earlier.[11]

The values in Table 3 show that sub-mg/l. concentrations of a series of metals can be determined after their separation from the sample matrix.

Next, the possibilities of using the extraction ICP technique for the analysis of waste water samples were investigated. Industrial waste waters often contain large amounts of alkali and alkaline-earth metal compounds, which may cause blockage of the pneumatic nebulizer.[19] It was found that such compounds do not affect the extraction ICP method. The results in Table 4 show that the results obtained when high

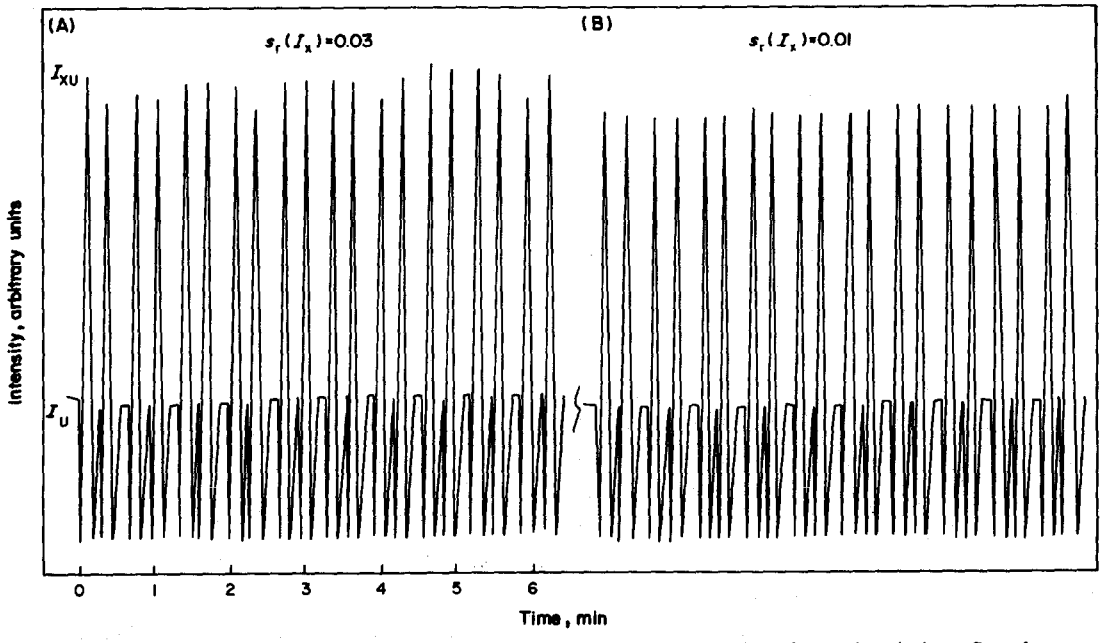


Fig. 5. Operation stability of an argon/nitrogen ICP applied to the analysis of organic solutions. Sample C 114 oil containing 10 μg/g Fe, diluted 1:10 with xylene; power level 4 kW; photoelectric measurements; line Fe II 259.9 nm; integration time 10 sec (alternating integration of line and background intensities); (A) without power stabilization; (B) with power stabilization.

Table 3. Detection limits for metals in solution by the extraction ICP technique (photographic measurements)

Element/line, *nm*		c_L, *mg/l.*
Cd I	228.8	0.08
Co II	238.9	0.06
Mn II	257.6	0.01
Fe II	259.9	0.02
Cr II	283.6	0.06
Cu I	324.8	0.1

concentrations of alkali and alkaline-earth metals are present fall within the concentration range defined by the expected value plus or minus twice the standard deviation for the determination in the absence of the foreign metals (the measured relative standard deviation ranged up to 8%, but there was a bias of +3% and +7% for the means of the copper and iron results, respectively). The method was then applied to a waste water from the plating industry (total inorganic salt content 1.02 g/l.). The sample was decomposed with nitric acid.[19] Calibration was done with a standard addition technique. The results of the extraction ICP technique agree well with those of the ICP injection method described earlier[19] (Table 5). With the extraction ICP technique, however, samples with alkali or alkaline-earth metal salt concentrations of up to 50 g/l. can still be analysed without any matrix effects. The relative standard deviations obtained with the extraction ICP method ranged from 4 to 8% (6 variates). The method is suitable for quantitative multielement characterization of waste waters of varying and complex composition.

Analysis of lubricating oils

Detection limits for a series of metals in oils were determined and the influence of the spectral apparatus was examined. The analysis of different types of oils by use of the same calibration data, and the significance of background-correction methods for the linearity of the calibration curves were investigated.

Table 4. The determination of metals in solutions containing high concentrations of sodium or calcium salts, by the extraction ICP technique (sequential photoelectric measurements)

Samples	Cu, *mg/l.*	Fe, *mg/l.*	Mn, *mg/l.*
Cu, Fe, Mn each 0.5 mg/l. and NaCl 25 g/l. (2 determinations)	0.52	0.47	0.49
	0.53	0.52	0.48
Cu, Fe, Mn each 0.5 mg/l. and $NaNO_3$ 35 g/l. (2 determinations)	0.53	0.48	0.52
	0.47	0.46	0.52
Cu, Fe, Mn each 0.5 mg/l. and $Ca(NO_3)_2$ 55 g/l. (2 determinations)	0.48	0.50	0.53
	0.46	0.52	0.52
Cu, Fe, Mn each 0.5 mg/l. without sodium or calcium salts in solution (6 determinations)	0.51	0.54	0.48
	0.49	0.56	0.55
	0.51	0.55	0.56
	0.53	0.53	0.47
	0.50	0.51	0.48
	0.54	0.51	0.46

Table 5. Application of the extraction ICP technique to the analysis of a plating waste-water sample (sequential photoelectric measurements)

Element	Concentration,* *mg/l.*	
	Extraction ICP technique	ICP injection technique[19]
Cadmium	0.28	0.35
Copper	1.54	1.6
Iron	0.62	0.74
Zinc	11.4	9.5

* Relative standard deviations (6 determinations) were 4–8% for the extraction ICP system and 4–7% for the injection technique.

For analysis the oil samples were diluted tenfold with xylene, and the solutions were nebulized with a conventional pneumatic nebulizer giving free sample aspiration.

Detection limits. The detection limits were in the sub-μg/g concentration range (Table 6), whether de-

Table 6. Detection limits c_L and background equivalent concentrations c_U for a series of metals in oils, samples were metal cyclohexylbutyrates dissolved in C 144 oil: dilution 1:10 with xylene (concentration in μg/g)

Element/line, *nm*		Spectrographic		Photoelectric			
				sequential		simultaneous	
		c_U	c_L	c_U	c_L	c_U	c_L
Zn I	213.8	—	—	0.8	0.04	3.8	0.2
Si I	251.6	1.0	0.1	4.1	0.2	8.0	0.3
Mn II	257.6	0.6	0.04	2.0	0.08	—	—
Fe II	259.9	0.8	0.07	—	—	5.4	0.23
Mg II	279.6	0.08	0.008	0.6	0.03	1.0	0.04
Pb I	283.3	7.9	0.3	8.2	0.3	2.2	0.9
Al I	309.3	2.0	0.07	2.1	0.09	—	—
Cu I	324.8	0.6	0.03	2.2	0.09	4.2	0.2

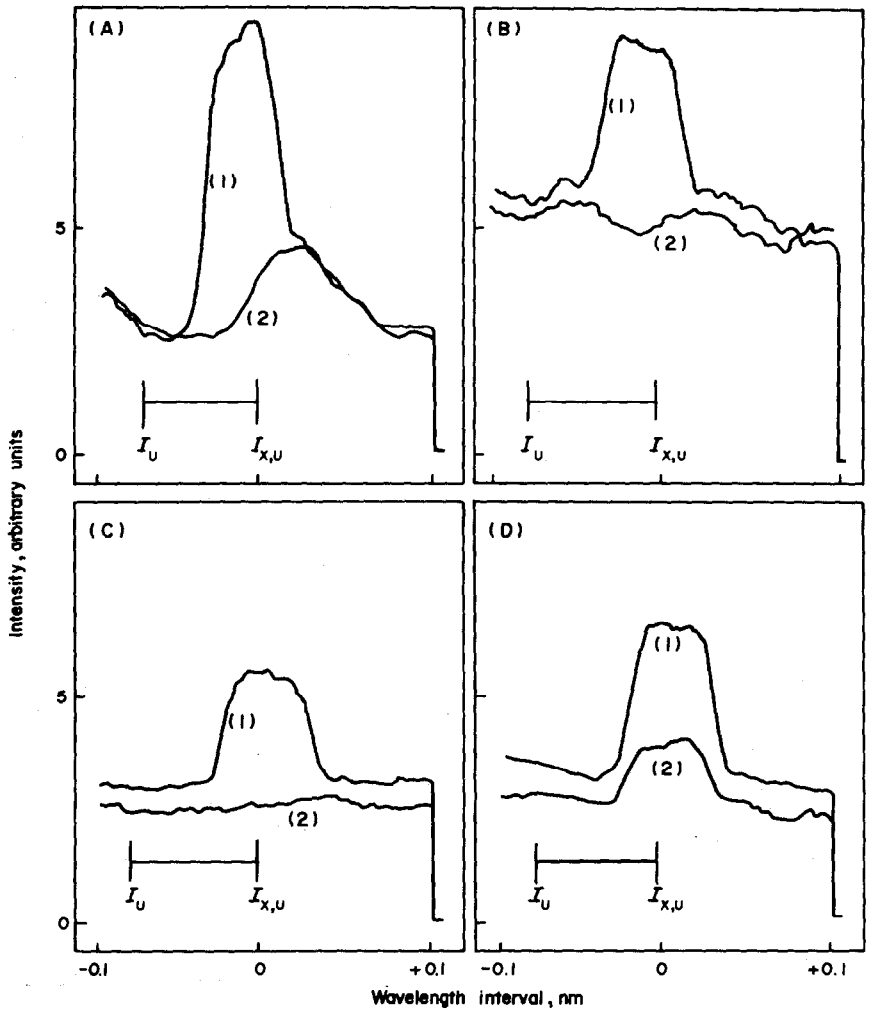


Fig. 6. Wavelength scans by computer-controlled displacement of the entrance slit of the spectrometer. Sample Conostan C 21 in light oil, diluted 1:10 with xylene; argon/nitrogen ICP operated at 4 kW; Baird 1000 vacuum spectrometer; lines (A) Zn I 213.9 nm, (B) Fe II 259.9 nm, (C) Al I 308.2 nm, (D) Si I 288.2 nm; (1) standard sample with $c_{Zn,Fe} = 100\ \mu g/g$ and $c_{Al,Si} = 40\ \mu g/g$; (2) light oil blank sample.

termined photoelectrically or spectrographically, but the photoelectric values, especially in the case of the polychromator, were considerably higher than the spectrographic values. This is partly due to the fact that the analytical and background signals are recorded sequentially in the photoelectric measurements, but simultaneously in the spectrographic work, but the lower practical resolution of the photoelectric technique is also of major importance.

The significance of the parameters of the spectral apparatus for the power of detection are described by Laqua *et al.*[20] and reflected in the equation

$$c_U = c_{U,\infty} \frac{\sqrt{1 + \hat{s}_e^2 + \hat{R}^2}}{\hat{R}} \qquad (2)$$

where $c_{U,\infty}$ is the background equivalent concentration at the spectrally resolved line width, $\hat{s}_e = s_e/s_0$ is the reduced entrance slit-width, s_0 being the diffraction slit-width, given by

$$s_0 = \lambda f/W \qquad (3)$$

λ being the wavelength of the analytical line, f the focal length of the spectral apparatus and W the beam-width at the grating; s_e is the entrance slit-width and $\hat{R} = R_0/R_L$ is the reduced resolving power, calculated from R_0 (the theoretical resolving power of the spectral apparatus) and $R_L = \lambda/\Delta\lambda_L$ (the line-

Table 7. Influence of background correction on the calibration (range 3.9–62.5 $\mu g/g$). Conostan standard oil C 21, dilution 1:10 with xylene; simultaneous photoelectric measurements

Element/line *nm*		Std. devn. from regression line, $s(\log I)$	
		Dynamic background correction	Blank subtraction
Mg II	279.6	0.029	0.031
Si I	288.2	0.13	0.11
Mn II	293.3	0.037	0.039
Al I	308.2	0.054	0.073

Table 8. The analysis of oils of different viscosities with the aid of ICP-AES [metal cyclohexylbutyrates in C 114 (η = 1.13–1.19 cSt at 50°C) and C 144 (η = 1.30–1.65 cSt at 50°C); sequential photoelectric measurements]

Element (x)	C 144 calibration function $\log c_X = c'_U + \eta \log I_X$	Std. devn. from line, $s(\log I)$	C 114 concentration, $\mu g/g$	Result $c_x \pm s(c_x)$, $\mu g/g$
Copper	$\log c = -1.488 + 0.945 \log I$	0.048	10	10.9 ± 0.7
Manganese	$\log c = -1.470 + 0.932 \log I$	0.045	10	9.6 ± 0.6
Silicon	$\log c = -3.968 + 1.215 \log I$	0.081	4	4.6 ± 1.0
Zinc	$\log c = -1.059 + 0.905 \log I$	0.060	10	8.6 ± 0.5

$s(\log I)$ is calculated for calibration with six C 144 oil standard samples, and $s(c_X)$ with six replications for the C 114 oil sample.

width resolving power). For physical line-widths of 3 pm, which is a good mean for analytical lines in ICP–AES,[11,21] and λ = 300 nm, $R_L = 10^5$. For the spectrographic technique (s_0 = 10.5 μm; s_e = 30 μm and $R_0 = 1.18 \times 10^5$), $c_U/c_{U,\infty} = 2.7$, denoting that the spectrographic detection limits are higher than the values at spectrally resolved line-widths by only a factor of less than 3. In the case of the monochromator (s_e = 12 μm, s_0 = 3 μm) the practical resolution is $R_z \leqslant 6 \times 10^4$, so $c_U/c_{U,\infty}$ is at least 5.4 and consequently the detection limits must be higher.

Calibration curves. The log concentration *vs.* log intensity calibration graphs were linear over three orders of magnitude of concentration, provided an accurate background correction was made. Many of the calibration lines had slopes close to unity, indicating linear relationship of concentration and line intensity. In this work the background intensities were measured on both sides of the analytical lines for each sample ("dynamic background correction") with the aid of a quartz refractor plate in front of the exit slit of the monochromator[12] or by displacement of the entrance slit of the polychromator. When organic media are introduced into the plasma, band emission leads to a highly structured background (Fig. 6), so a careful choice of the wavelengths for the background measurement is necessary. As seen from the values given in Table 7, dynamic background correction generally gives a better linear fit of the points on the calibration plot than does background correction by subtraction of the signal for a blank sample. Only when considerable blank contributions occur, *e.g.*, in the case of silicon (Fig. 6), does background correction by blank subtraction lead to a more linear fit.

After tenfold dilution with xylene, oils of different viscosity can be analysed with use of the same calibration graphs (Table 8). The analytical errors lie within the plus or minus two standard-deviation range.

This standard deviation, $s(c_x)$, is calculated from the logarithms of the measured intensities and of the concentrations, according to Nalimov.[22]

$$s(c_x) = 2.303\, c_x\, \eta s(\log I) \times \sqrt{\frac{1}{m} + \frac{1}{n}\frac{(\log c_x - \overline{\log c_i})^2}{\Sigma(\log c_i - \overline{\log c_i})^2}} \quad (4)$$

where c_x is the mean for m replicates of the unknown sample, as calculated from the regression equation

$$\log c_x = \eta \log I_X + \log c'_U \quad (5)$$

calculated from the intensities I_i measured for n standards with concentrations c_i. The slope of the calibration curve, η, is approximately 1. The term $\overline{\log c_i}$ is the mean of the log c values of all standard samples and $s(\log I)$ is the standard deviation of the logarithms of the intensities:

$$s(\log I) = \sqrt{\frac{\Sigma(\log I_i - \overline{\log I_i})^2}{n-2}} \quad (6)$$

where $\overline{\log I_i}$ is the logarithm of the mean of the intensities for the standard samples used for calculations with equation (5).

CONCLUSION

ICP–AES is a powerful method for the analysis of organic liquids. A high power of detection and the same analytical precision as in the case of aqueous solutions were obtained with the set-up described. The method is well suited for dealing with industrially important problems such as the analysis of oils and the analysis of complex samples, *e.g.*, waste waters, requiring extraction techniques.

Acknowledgements—The authors thank Mr. H. Grote (Hoesch Hüttenwerke AG, Dortmund) for providing the oil samples. This work was supported by the Ministerium für Wissenschaft und Forschung des Landes Nordrhein-Westfalen and the Bundesministerium für Forschung und Technologie.

REFERENCES

1. P. W. J. M. Boumans, *Z. Anal. Chem.*, 1979, **299**, 337.
2. V. A. Fassel, C. A. Peterson and F. N. Abercrombie, *Anal. Chem.*, 1976, **48**, 516.
3. R. N. Merryfield and R. C. Loyd, *ibid.*, 1979, **51**, 1965.
4. S. Greenfield and P. B. Smith, *Anal. Chim. Acta*, 1972, **59**, 341.
5. K. Ohls, *Compendium* 77/78, Vorträge der 4. DGMK-Fachgruppentagung (5–7 October 1977) in Köln, 194, Industrieverlag v. Hernhausen.
6. G. Dorn, *Automation and Control of the Inductively Coupled Plasma*, paper presented at the International Winter Conference 1980, Developments in Atomic Plasma Spectrochemical Analyses, San Juan, Puerto Rico, 1980.

7. S. Greenfield, I. Ll. Jones and C. T. Berry, *Analyst*, 1964, **89**, 713.
8. J. E. Meinhard, *ICP Inform. Newsl.*, 1976, **2**, 163.
9. R. H. Scott, V. A. Fassel, R. N. Kniseley and D. E. Nixon, *Anal. Chem.*, 1974, **46**, 75.
10. H. Hansen, *Optik*, 1950, **6**, 337.
11. J. A. C. Broekaert, F. Leis and K. Laqua, *Spectrochim. Acta*, 1979, **34B**, 73, 167.
12. N. Nordmeyer, *Z. Anal. Chem.*, 1967, **225**, 247.
13. S. R. Koirtyohann, J. S. Jones and D. A. Yates, *Anal. Chem.*, 1980, **52**, 1966.
14. G. R. Kornblum and L. de Galan, *Spectrochim. Acta*, 1977, **32B**, 71.
15. K. Szivós, L. Pólos and E. Pungor, *ibid.*, 1976, **31B**, 289.
16. B. Welz, *Atom-Absorptions-Spektroskopie*, Verlag Chemie, Weinheim, 1975.
17. O. G. Koch and G. A. Koch-Dedic, *Handbuch der Spurenanalyse*, Springer Verlag, Berlin, 1961.
18. H. Kaiser and H. Specker, *Z. Anal. Chem.*, 1956, **149**, 46.
19. J. A. C. Broekaert and F. Leis, *Anal. Chim. Acta*, 1979, **109**, 73.
20. K. Laqua, W.-D. Hagenah and H. Waechter, *Z. Anal. Chem.*, 1967, **225**, 142.
21. H. G. C. Human and R. H. Scott, *Spectrochim. Acta*, 1976, **31B**, 459.
22. V. V. Nalimov, *The Application of Mathematical Statistics to Chemical Analysis*, Pergamon Press, Oxford, 1963.

Talanta, Vol. 28, pp. 753 to 757, 1981
Printed in Great Britain. All rights reserved

0039-9140/81/100753-05$02.00/0
Copyright © 1981 Pergamon Press Ltd 1981

SIMULTANEOUS DETERMINATION OF KINETIC AND THERMODYNAMIC PARAMETERS FROM FAST-REACTION KINETIC MEASUREMENTS

HAROLD H. TRIMM, HIDETOSHI USHIO and RAMESH C. PATEL
Chemistry Department, Clarkson College of Technology, Potsdam, NY 13676, U.S.A.

(*Received* 22 *October* 1980. *Revised* 6 *February* 1981. *Accepted* 11 *March* 1981)

Summary—A combined stopped-flow temperature-jump apparatus interfaced with a dedicated microcomputer has been used to study the complexation reaction of iron(III) with thiocyanate in aqueous solution. Kinetic rate-constants (k_f = 143 l.mole^{-1}.sec^{-1} from *T*-jump, k_f = 150 l.mole^{-1}.sec^{-1} from stopped flow), equilibrium constants (K = 143 from *T*-jump, K = 150 from stopped flow) and the thermodynamic enthalpy change (ΔH_c = −6.7 kJ/mole) could be independently determined from the simultaneous application of the two techniques.

There have been several studies of the relatively simple ferric thiocyanate complexation reaction, which is well suited as a test system for fast-reaction kinetic studies.[1–6] In general, the determination of kinetic and thermodynamic parameters of a system have been accomplished by separate experiments, because the thermodynamic information contained in the relaxation data was not exploited. This, combined with the slow techniques used in the past for the collection and analysis of data, made such studies both time-consuming and tedious for the investigators.

Nowadays, with the use of fast analogue-to-digital recorders in conjunction with relatively inexpensive microcomputers, it is possible to obtain more information per experiment, achieve greater accuracy, increase the speed, and introduce the convenience of automation into the experimental set-up.

In this work, a combined stopped-flow temperature-jump apparatus[7] was used to study the reaction of iron(III) with thiocyanate. The advantage of this approach is that there are four different methods of determining the thermodynamic parameters of the system. The time-dependent data from the stopped-flow and temperature-jump experiments both yielded independent values for the forward and backward rate-constants of the complexation reaction. The total absorbance changes of each stopped-flow experiment, as well as the amplitudes of the temperature-jump effects, were analysed to obtain the equilibrium constant. In addition, the temperature-jump data could be analysed to determine the thermodynamic enthalpy change for the reaction.

The experimental data were analysed by means of a multiparametric curve-fitting routine in combination with a TRS-80 microcomputer. Individual reaction recordings were treated by an integration technique with a large number (2048) of data points to achieve further reduction of noise.[8] The data obtained were self-consistent, and it was found that enthalpy changes as small as 6.7 kJ/mole could be determined over a temperature range of 2.4° from *T*-jump amplitudes, with use of about 0.200 ml of solution. This approach is ideally suited for the study of biological reactions involving costly compounds, such as enzyme substrate reactions, especially in the combined stopped-flow *T*-jump arrangement in which stationary states can be perturbed. The programs used are applicable to any second-order (or pseudo second-order) reaction.*

EXPERIMENTAL

All solutions were made from reagent-grade chemicals and doubly distilled water. The ferric perchlorate and the sodium perchlorate were purchased from G. Frederick Smith and the potassium thiocyanate and perchloric acid were obtained from J. T. Baker. The chemicals were not further purified.

The concentration of the ferric perchlorate solution was determined spectrophotometrically from a calibration curve obtained with a standard solution of iron(III) (Fisher) combined with the appropriate amount of thiocyanate. The concentration of the potassium thiocyanate solution was determined gravimetrically, and that of perchloric acid by titration with base.

All solutions contained 0.200 mole of perchloric acid and 0.200 mole of sodium perchlorate per litre. The low pH was used to suppress hydrolysis of iron(III).

For the stopped-flow experiments, absorbances were calculated from

$$A = \log(V_w/V_s) \quad (1)$$

where V_w and V_s are the detector output voltages for the solvent, in this case water, and sample solution, respectively.

The temperature-jump measurements were made about 2 min after mixing, to allow time for complete equilibration. The output voltages can be translated into absorbance changes by means of the equation[9]

$$\Delta A = [0.434 \ln(1 + \Delta V/V_s)]/l \quad (2)$$

* Listings of the programs can be obtained from R. C. Patel.

where ΔV is the voltage change and V_s is the voltage output for the sample solution, and l is the path-length.

The voltage–time data from the stopped-flow/temperature-jump instrument were collected by a Biomation 1010 Waveform Recorder which stores 2048 data points with 10-bit resolution in as little as 200 μsec. A multipurpose digital interface built in our laboratory[10] allows a TRS-80 microcomputer to be connected to the recorder. The entire system is controlled by the keyboard of the computer, on command from which the data from the recorder are loaded into its memory in less than 15 sec. The TRS-80 with its 48 kbyte of memory can operate in either Fortran IV or in Basic, carry out data integration and treatment, and print out results on an appropriately modified IBM "Selectric" typewriter.

RESULTS

If the proton concentration is too low, the hydrolysis reaction of ferric ion begins to predominate and the dimer of this species can also appear. Since coupling of these reactions with complex formation of the ferric thiocyanate is expected, the pH of the solution is kept low by the use of 0.200*M* perchloric acid. This both simplifies the kinetics and maintains a constant pH and ionic strength, both of which affect the rate constants of complex formation. No attempt was made to study the reaction at different pH values.

The kinetics of the formation of ferric thiocyanate can be shown to follow the equation:

$$\begin{array}{ccc} \textbf{I} & (K_c = k_{12}/k_{21}) & \textbf{II} \\ Fe^{3+} + SCN^- & \underset{k_{21}}{\overset{k_{12}}{\rightleftharpoons}} & FeSCN^{2+} \\ +H^+ \uparrow\downarrow -H^+(K_{h1}) & & +H^+ \uparrow\downarrow -H^+(K_{h2}) \\ FeOH^{2+} + SCN^- & \underset{k_{34}}{\overset{k_{43}}{\rightleftharpoons}} & Fe(OH)SCN^+ \\ \textbf{IV} & & \textbf{III} \end{array}$$

Under the experimental conditions used in this study, the reaction characterized by the transformation (**I** $\rightleftharpoons$ **(II)** predominates. Since the proton-transfer reactions (**I**) $\rightleftharpoons$ (**IV**), (**II**) $\rightleftharpoons$ (**III**) are very fast,[11] it can be shown that a single rate-equation is obtained for the slower complexation reaction:

$$\frac{dx}{dt} = k_f(C_A^0 - x)(C_B^0 - x) - k_b x \qquad (4)$$

where C_A^0 and C_B^0 are the analytical concentrations of iron(III) and thiocyanate, respectively, x is the concentration of $FeSCN^{2+}$ at any given time, $k_f = (k_{12} + k_{43}K_{h1}/[H^+])$ and $k_b = (k_{21} + k_{34}K_{h2}/[H^+])$. The rate-equation (4) can be rearranged:

$$\frac{dx}{dt} = a + bx + cx^2 \qquad (5)$$

where $a = k_f C_A^0 C_B^0$, $b = -[k_b + k_f(C_A^0 + C_B^0)]$ and $c = k_f$.

Integration of (5) gives:

$$\ln[(2cx + b - q)/(2cx + b + q)] = qt + C_1 \qquad (6)$$

with $q = \sqrt{b^2 - 4ac}$, and since at $t = 0$, $x = 0$, $C_1 = \ln[(b - q)/(b + q)]$.

The final result is:

$$\ln[(2cx + b - q)/(2cx + b + q)] = qt + \ln[(b - q)/(b + q)] \qquad (7)$$

Concentration is related to absorbance and voltage by:

$$x = A/(\epsilon l); \quad A = \log(V_0/V), \quad x = [\log(V_0/V)]/(\epsilon l)$$

where V_0 = voltage reading obtained for the solvent (water) and V = voltage reading obtained for sample solution.

At time infinity:

$$x_\infty = \log(V_0/V_\infty)/(\epsilon l). \qquad (8)$$

Substitution of x and A in (8) removes the need to know ϵ, and

$$x/x_\infty = \log(V_0/V)/\log(V_0/V_\infty). \qquad (9)$$

Solving for x in equation (7) yields the following time-dependent relation:

$$x = \frac{[\{\exp[qt + \ln([b + q]/[b - q])]\}(b + q) - b + q]}{2c(1 - \exp\{qt + \ln[(b + q)/(b - q)]\})} \qquad (10)$$

Since at time infinity

$$dx_\infty/dt = 0 = k_f(C_A^0 - x_\infty)(C_B^0 - x_\infty) - k_b x_\infty \qquad (11)$$

then:

$$x_\infty = -\tfrac{1}{2}\{(k_b/k_f + C_A^0 + C_B^0) - [(k_b/k_f + C_A^0 + C_B^0)^2 - 4C_A^0 C_B^0]^{1/2}\}. \qquad (12)$$

The final stopped-flow equation is given by dividing equation (10) by equation (12):

$$x/x_\infty = \ln(V_0/V)/\ln(V_0/V_\infty) = (10)/(12). \qquad (13)$$

Thus the voltage data from the flow experiment can be analysed by a multiparametric curve-fitting routine[12] to yield both the forward and backward rate-constants, which are the only unknown quantities in equation (13).

An approximate treatment of the flow data can be made by analysing them as a relaxation curve, particularly during the early stages of the reaction, or when a relatively small amount of $FeSCN^{2+}$ is formed. Here the relaxation time, τ, is equal to the pseudo first-order rate-constant $k_f(C_A^0 + C_B^0) + k_b$. The results obtained from this type of treatment can be conveniently shown graphically and give a linear plot for τ *vs.* $(C_A^0 + C_B^0)$. Identical values of k_f and k_b are obtained from such a plot and the numerical treatment based on equation (13).

For the analysis of the flow amplitudes, the mass-balance and equilibrium equations were solved in terms of the final equilibrium concentration, x_∞, of

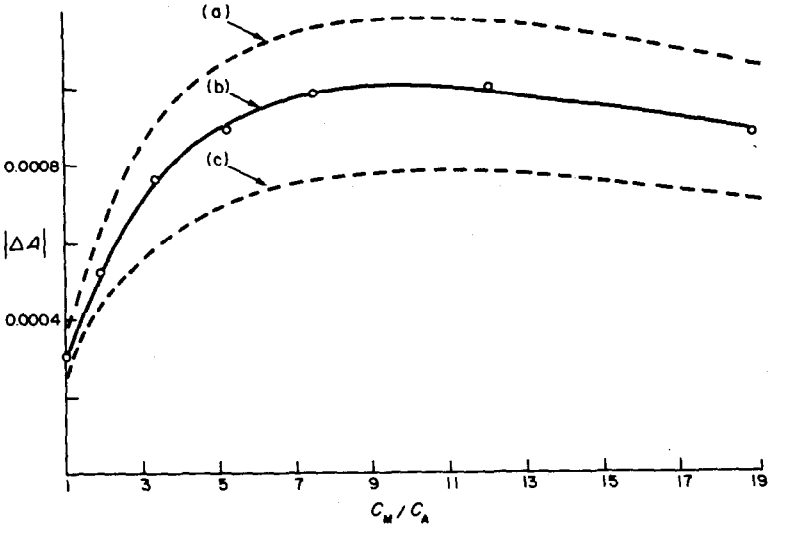


Fig. 1. The absorbance change resulting from T-jump amplitudes of the ferric thiocyanate system, *vs.* the ratio of the analytical concentrations of iron(III) to thiocyanate. The circles represent the experimental values and the solid line, curve (*b*), represents the theoretical curve from equation (19) for the values $\epsilon = 1690$ l.mole^{-1}.cm^{-1}, $\Delta H_c = -6.7$ kJ/mole, $\Delta T = 2.4°$, and $C^0_{SCN} = 0.001M$. Curve (*a*) uses the same values as curve (*b*) but $[H^+] = 0.05M$. Curve (*c*) is the same as curve (*b*) but the value of ΔH_c has been decreased by 25%.

the only species which absorbs at 460 nm. In this case:

$$x_\infty = \tfrac{1}{2}[C^0_A + C^0_B + 1/K - (C^0_A + C^0_B + 1/K - 4C^0_A C^0_B)^{1/2}] \quad (14)$$

Since $A = \epsilon x l$, equation (14) can be used to calculate the value of K from an experimental set of A_∞ values. If the term x^2 is small enough to be neglected, equation (14) can be simplified and rearranged to give:

$$C^0_A C^0_B / A = (C^0_A + C^0_B)/\epsilon l + 1/K\epsilon l \quad (15)$$

A graph of $C^0_A C^0_B / A$ *vs.* $(C^0_A + C^0_B)$ is linear, and the slope divided by the intercept gives the equilibrium constant K; 139 l./mole, the value found for the system investigated, was within a few per cent of the value determined by equation (14).

In the case of the temperature-jump experiments, the relaxation data were first integrated by a method previously described,[8] to reduce noise and increase the signal-to-noise ratio. The integrated data were then analysed by computer, with a multiparametric curve-fitting program, to obtain the relaxation times and the amplitudes.

The rate and equilibrium constants are related to τ by the equation:

$$(1/\tau)^2 = k_f^2[(C^0_A - C^0_B)^2 + 2(C^0_A + C^0_B)/K + 1/K^2] \quad (16)$$

which was also analysed by means of a multiparametric curve-fitting routine in order to determine the values of k_f and K simultaneously.

In terms of equilibrium concentrations, the expression for τ is:

$$\tau^{-1} = k_f(\bar{C}_A + \bar{C}_B) + k_b \quad (17)$$

From the K value determined from (16), $\bar{C}_A$ and $\bar{C}_B$ can be easily calculated and τ^{-1} displayed graphically [plotted *vs.* $(\bar{C}_A + \bar{C}_B)$] according to equation (17).

For small changes in voltage, the change in absorbance can be calculated as:[9]

$$\Delta A = (1/2.303\ \text{l.})\ln(1 + \Delta V/V_0) \quad (18)$$

where ΔV is the voltage change and V_0 is the voltage output for the solution.

A graph showing the change in absorbance as a function of the ratio of the concentration of iron(III) to thiocyanate is shown in Fig. 1. The shape of this curve is very sensitive to those thermodynamic parameters associated with the temperature perturbation and has been used to determine enthalpies, equilibrium constants, and even concentrations of species in solution.

The experimental conditions corresponding to Fig. 1 are such that the equilibrium concentrations of $Fe(OH)SCN^+$ and $FeOH^{2+}$ are negligible.[13] The amplitude expression for the more general binary case can be derived as previously described:[14]

$$\Delta A = \epsilon_{FeSCN^{2+}} \frac{[Fe^{3+}][SCN^-]}{[Fe^{3+}] + 1/K_c + A_{h1}[SCN^-]} \times \{\Delta H_c + (1 - A_{h1})\Delta H_{h1}\} \frac{\Delta T}{RT^2} \quad (19)$$

Table 1. Summary of the kinetic and thermodynamic results for the $FeSCN^{2+}$ system

k_f, $l.mole^{-1}.sec^{-1}$	k_b, sec^{-1}	K, $l.mole^{-1}$	ϵ, $l.mole^{-1}.cm^{-1}$	ΔH_c, $kJ\ mole^{-1}$	Method
143	1.0	143			T-jump curve-fit of equation (16)
		120		−6.7	T-jump curve-fit of equation (19)
150	1.0	150			Stopped-flow curve-fit, equation (13)
		139	1680		Stopped-flow curve-fit of equation (15)
				−6.7	Reference (1)
				−5.0	Reference (5)

$$A_{hl} = \frac{[H^+] + [FeOH^{2+}]}{[H^+] + [FeOH^{2+}] + 1/K_{hl}} \quad (20)$$

K_c, K_{hl}, ΔH_{hl} and ΔH_c are the equilibrium constants and enthalpy changes for the reactions shown in the reaction scheme. ΔT is the magnitude of the temperature jump, 2.4° in the present experiments. The value of $\epsilon_{FeSCN^{2+}}$ was determined to be 1690 l. $mole^{-1}.cm^{-1}$ at 460 nm from the stopped-flow experiments, with identical slit-widths. A two-parameter curve-fit in conjunction with a non-linear least-squares subroutine[12] was used to calculate the values for K_c and ΔH_c in equation (19). The agreement between the calculated and observed absorbance changes is shown in Fig. 1.

At relatively high acidity, the value of A_{hl} [equation (20)] is 1, and equation (19) simplifies to the case of a simple one-step reaction:

$$\Delta A = \epsilon_{FeSCN^{2+}} \frac{[Fe^{3+}][SCN^-]}{[Fe^{3+}] + [SCN^-] + 1/K_c}\left(\frac{\Delta H_c \Delta T}{RT^2}\right). \quad (21)$$

The calculated ΔA-values [curve (*b*) in Fig. 1] are the same in the present series of experiments regardless of whether equation (19) or (21) is used, since $[H^+] = 0.200M$. The dashed curve (*a*), Fig. 1, shows a pronounced effect when $[H^+]$ is lowered, so that it is possible to study the hydrolysis equilibrium if the iron(III)–thiocyanate complexation is used as an indicator reaction. The sensitivity of this method is seen from the small ΔH_c-value of −6.7 kJ/mole determined over the temperature interval of 2.4° with a sample volume of only about 0.2 ml for each experiment. A 25% lower value of ΔH_c results from curve (*c*), Fig. 1, and is clearly outside the error limits of the experimental points.

DISCUSSION

In Table 1 there is a summary of the parameters determined for the ferric thiocyanate complexation reaction, together with the method used. In general, the results agree well with the literature values shown in Table 2, once they have been corrected for the hydrolysis of ferric ion. The data obtained are self-consistent, and small variations from the literature values can be explained by differences in the ionic strength. It should be noted that it was much more accurate to determine the equilibrium constant from either static measurements, stopped-flow, or T-jump amplitudes, than from the ratio of the forward and backward rate-constants. The small value of the backward rate-constant made its independent determination relatively imprecise.

The collection, analysis, and print-out of the results is greatly facilitated by the use of a dedicated microcomputer. Used in conjunction with an automated reagent-delivery system, the entire experiment could be controlled by commands from the keyboard and left to run until the study was complete.

Table 2. Summary of kinetic data for the $FeSCN^{2+}$ system at 25.0°

k_f, $l.mole^{-1}.cm^{-1}$	k_b, sec^{-1}	Ionic strength, M	Method
127	—	0.4	Stopped-flow[1]
150	—	0.5	Pressure-jump[2]
90	1.6	0.5	Stopped-flow[3]
132	—	0.2	Pressure-jump[4]
130	—	0.5	T-jump[5]
97	0.75	1.0	Stopped-flow[6]
143	1.0	0.4	T-jump (this work)
150	1.0	0.4	Stopped-flow (this work)

The advantage of the type of data analysis shown here is that the kinetics are determined by two different methods, stopped-flow and *T*-jump, and the thermodynamic parameters are determined by four different methods, two dynamic and two static. This provides a good check for a proposed mechanism since all four methods must agree if the system is correctly described. This approach will always work for reactions in the stopped-flow time range (about 1 msec) and greater.

Acknowledgement—The authors would like to thank Mr. Mark Sihlanick for his help in the construction of the digital interface. This research was funded in part by NIH grant No. 1 R01 GM24523-01.

REFERENCES

1. J. F. Below, R. E. Connick and C. P. Coppel, *J. Am. Chem. Soc.*, 1965, **80**, 2961.
2. H. Wendt and H. Strehlow, *Z. Elektrochem.*, 1962, **66**, 228.
3. S. Funakaski, S. Adachi and M. Tanaka, *Bull. Chem. Soc. Japan*, 1973, **46**, 479.
4. F. P. Cavasino and M. Eigen, *Ric. Sci., Rend. Sez. A*, 1964, **4**, 509.
5. D. M. Goodall, P. W. Harrison, M. J. Hardy and C. J. Kirk, *J. Chem. Educ.*, 1972, **49**, 675.
6. G. E. Mieling and H. L. Pardue, *Anal. Chem.*, 1978, **50**, 1333.
7. R. C. Patel, *J. Chem. Instr.*, 1976, **7**, 83.
8. U. Strahm, R. C. Patel and E. Matijević, *Talanta*, 1980, **27**, 853.
9. *Idem, J. Phys. Chem.*, 1979, **3**, 1689.
10. M. Sihlanick, R. C. Patel and H. H. Trimm, in preparation.
11. R. S. Sapiesko, R. C. Patel and E. Matijević, *J. Phys. Chem.*, 1977, **81**, 1061.
12. H. H. Trimm and R. C. Patel, *Inorg. Chim. Acta*, 1979, **35**, 15.
13. R. M. Milburn, *J. Am. Chem. Soc.*, 1957, **79**, 537.
14. H. H. Trimm, R. C. Patel and H. Ushio, *J. Chem. Educ.*, 1979, **56**, 762.

Talanta, Vol. 28, pp. 759 to 764, 1981
Printed in Great Britain. All rights reserved

0039-9140/81/100759-06$02.00/0
Copyright © 1981 Pergamon Press Ltd

INVESTIGATIONS ON THE EFFECT OF AQUEOUS ACETONE MEDIUM ON SEPARATION OF METAL IONS ON CHELEX 100 ION-EXCHANGER

KRYSTYNA BRAJTER and IWONA MIAZEK
Department of Chemistry, Warsaw University, Warsaw, Poland

(*Received* 15 *July* 1980. *Revised* 30 *January* 1981. *Accepted* 19 *February* 1981)

Summary—The use of glycine as a complexing agent in acetone–water medium for the separation of metal ions with Chelex 100 chelating resin has been investigated. The affinity of metal ions for Chelex 100 in the presence of glycine in acetone–water and aqueous medium was determined as a function of acidity and it was established that the presence of acetone is an essential factor in production of differentiation in the selectivity and for consequent separation of a number of mixtures of metal ions [Cu(II)–Co(II); Cu(II)–Al(III)–Pb(II); Cu(II)–Ni(II)–Co(II); Cu(II)–Ni(II)–Pb(II)]. The mechanism of the effect of acetone is discussed.

Metal ions cannot always be separated on Chelex 100 chelating ion-exchanger by use of mineral acids, nor are all organic complexing reagents suitable for the purpose. If certain amino-acids, *e.g.*, glycine are present as competing ligands, mixed complexes are formed in the resin phase. If the retention of metal ions takes place by mixed complex formation, the separation of metal ions and their quantitative elution in aqueous medium is impossible. In the present work an attempt is made to deal with this by use of a mixed aqueous–organic medium to shift the equilibria in the competitive complexation reactions.

Aqueous acetone was chosen as the medium and glycine as the competing ligand because it forms transition metal ion complexes of similar stability to the complexes of the same metals with the iminodiacetic groups of the ion-exchanger (Table 1).[1–5] It is also fairly soluble in aqueous acetone.

Glycine in aqueous medium is not useful for ion-exchange chromatography of metal ions,[6–8] but the presence of acetone in the system shifts the equilibria sufficiently to give useful separations.

EXPERIMENTAL

Ion-exchanger

For batch investigations Chelex 100 (hydrogen form), 100–200 mesh, (Bio-Rad Laboratories) was used. The exchange capacity was 3.48 meq/g.

For column studies Dowex A-1 (monosodium form) 50–100 mesh, 3.48 meq/g capacity, was used in columns 10 cm long and 10 mm in diameter.

Standard solutions

These were prepared by dissolving appropriate weights of the sulphates or nitrates of the metals in doubly distilled water. Solutions of Pt(IV) and Pd(II) were prepared from chloroplatinic acid and palladium chloride respectively. The nitrate solutions were standardized by EDTA titration. Glycine and iminodiacetic acid solutions were prepared in doubly distilled water.

Analytical-grade reagents were used throughout.

Determination of metal ions and hydrogen-ion concentration

Electrothermal atomic-absorption spectrophotometry was used, with a Perkin–Elmer model 300 A instrument, HGA-72 graphite furnace, and model 159 recorder, with the methods recommended by Perkin–Elmer. The basic parameters are listed in Table 2.

Table 1. Stability constants of metal-ion complexes with iminodiacetic acid (IDAA) and glycine taken from the literature (references in brackets)

	IDAA		Glycine			Me–IDAA–glycine
Me^{n+}	$\log K_{MeI}^{Me,I}$	$\log\beta_{MeI_2}$	$\log K_{MeL}^{Me,L}$	$\log\beta_{MeL_2}$	$\log\beta_{MeL_3}$	$\log K_{MeIL}^{MeI,L}$
Al^{3+}	8.10[1]	15.07[1]	—	—	—	—
Cd^{2+}	5.35[2]	9.53[2]	6.0[3]	7.9[3]	9.80[3]	3.79[4]
Co^{2+}	6.95[2]	12.29[2]	5.5[3]	9.0[3]	11.3[3]	—
Cu^{2+}	10.55[2]	16.2[2]	8.18[3]	15.2[3]	15.67[3]	5.87[4]
Fe^{2+}	5.8[2]	10.1[2]	—	—	—	—
Ni^{2+}	8.26[2]	14.61[2]	5.66[3]	10.80[3]	14.0[3]	5.02[4]
Pb^{2+}	7.45[3]	—	5.11[3]	7.08[3]	—	—
Pd^{2+}	17.5[5]	26.8[5]	15.25[5]	27.50[5]	—	—
Zn^{2+}	7.03[2]	12.17[2]	4.88[3]	9.01[3]	11.0[3]	4.38[4]

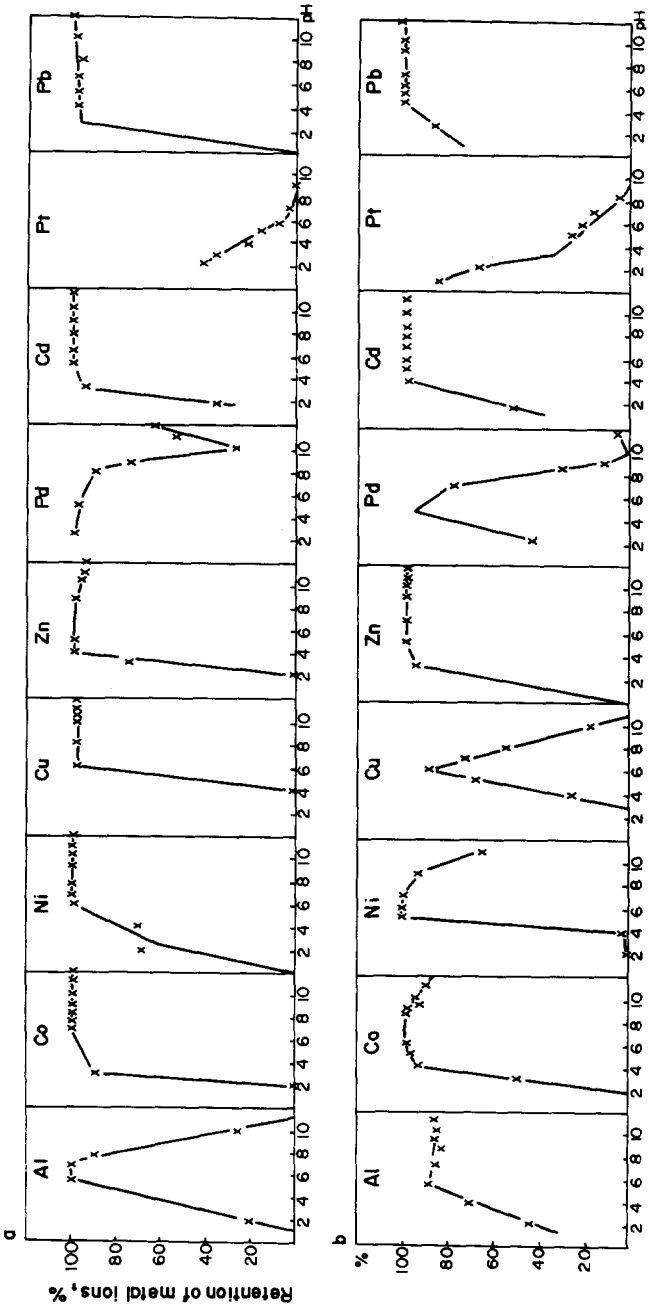


Fig. 1. Retention functions of metal ions on Chelex 100 in presence of glycine (×) and without glycine (○) in (*a*) aqueous medium and (*b*) in aqueous acetone medium.

Table 2. Conditions for AAS determination of the metals

Metal	Wavelength, *nm*	Band-pass, *Å*	Sample volume, *µl*
Cu	223.0	2	10, 20
	217.0	2	10
Ni	346.4	2	10, 20
	341.6	2	10
	232.3	2	10, 20
Cd	326.0	7	10
Co	304.4	2	20
Pb	283.3	7	10, 20
Al	237.9	2	10, 20
Zn	308.0	7	5, 20, 50
Pd	340.4	2	10, 20
Pt	273.4	2	20

The pH of the aqueous acetone solutions was measured with a glass electrode and an SCE as reference. The glass electrode was standardized with aqueous buffers. Standard aqueous solutions of hydrochloric acid and sodium hydroxide[9,10] were used to prepare two series of solutions of different hydrogen-ion concentrations in aqueous and aqueous acetone media. The pH values of both sets of solutions were measured and plotted to give calibration graphs (which were linear) from which the hydrogen-ion concentration corresponding to the measured pH could be obtained. We use the symbol pH for the logarithm of the reciprocal of the calculated hydrogen-ion concentration in the aqueous medium, and pH* for the corresponding quantity in aqueous acetone medium.

Batch studies

The affinity of the metal ions for Chelex 100 in the absence and presence of glycine at a constant molar ratio of the components, was measured as a function of pH, Fig. 1(a). The affinity was defined as the fraction of total added metal ion concentration retained by the ion-exchanger. The affinity for nickel was also studied at constant pH, and varying molar ratio of components. For measurements a constant weight (0.2442 g) of ion-exchanger (hydrogen form) was shaken for 24 hr with 25 ml of a $3.4 \times 10^{-3}M$ metal ion/$6.8 \times 10^{-2}M$ glycine solution adjusted to the desired pH with sodium hydroxide or nitric acid. The concentrations of hydrogen ions and metal ions in the solution were then determined. The experiments were repeated for the 50% aqueous acetone solutions [Fig. 1(b)].

Dynamic studies

A 0.5- or 1-g portion of ion-exchanger (sodium form) was made into a column of length 10 cm and diameter 1.0 cm, and 3 ml of a solution at pH (or pH*) *ca.* 3 containing 1 mg of metal ions were added

Elution curves were obtained by using a fraction-collector and a pump to regulate the flow-rate of the eluent. The metal-ion concentration in successive fractions was determined by atomic-absorption spectroscopy.

RESULTS AND DISCUSSION

Retention of metal ions from aqueous medium was studied for the components in molar ratio Me:Chelex 100:glycine = 1:10:20 as a function of hydrogen-ion concentration. This will be called the retention function.

The retention function for 50% aqueous acetone medium was studied for the same molar ratio of components. In aqueous medium the affinity of the ion-exchanger for the metal ions studied is similar in the presence and absence[11] of glycine, and there is very little difference from ion to ion for most of them. The retention function for Al(III) is affected by OH^- ions, but not by glycine [Fig. 1(a)]. A change in the molar ratio in the system Ni(II):Chelex 100:glycine to 1:10:80 does not change the retention of nickel. Copper is also found to be bound quantitatively by the ion-exchanger at the same molar ratio to glycine. Since (Table 1) stability constants of their glycine complexes are all similar, the other metal ions investigated would be expected to behave similarly in the ion-exchange system. On the other hand, in aqueous acetone medium a differentiation in selectivity of the ion-exchange resin is observed, this being connected with a change in the affinity for Cu(II), Ni(II), Pd(II), and Al(III) with the change in medium (Fig. 1b). The sudden decrease in retention of Cu(II) ions at pH* *ca.* 9 is particularly important for possible separations, because it suggests the feasibility of separating Cu(II) from most of the other metal ions studied, as well as eluting it from the ion-exchange resin. Because of the very high affinity between Cu(II) and the iminodiacetate groups in the ion-exchange resin in aqueous medium it is of considerable practical importance. Moreover, a further decrease in Pd(II) retention is observed, as well as a decrease in the competing effect of hydroxide ions on retention of Al(III) ions. As shown in Fig. 2 an increase in acetone concentration to 69% v/v decreases the retention of Ni(II). Higher acetone concentrations could not be studied, because of a decrease in the solubility of the glycine.

The effect of acetone on the selectivity of Chelex 100 is probably connected with its acid–base properties, as well as its ability to enter into the co-ordination sphere of metal ions. The latter factor is important; for example, dimethylformamide, though having stronger basic properties (on the Gutmann scale), does not enter the metal ion co-ordination sphere,

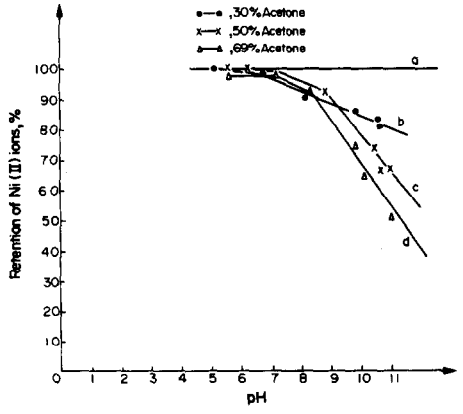


Fig. 2. Retention functions of Ni(II) on Chelex 100 at various acetone concentrations. Molar ratio Me:Chelex 100:glycine = 1:10:20 Acetone, %: (*a*) 0; (*b*) 30; (*c*) 50; (*d*) 69.

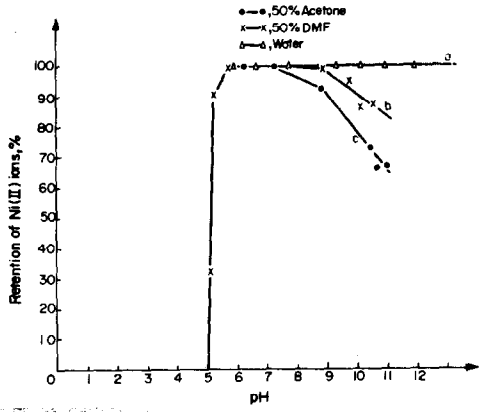


Fig. 3. Effect of DMF on retention of Ni(II) on Chelex 100: (*a*) aqueous medium; (*b*) 50% DMF; (*c*) 50% acetone.

and hence exerts a visibly weaker effect than acetone on retention of metal ions by Chelex 100 (Fig. 3). Our results show that the effect of acetone is mainly evinced in the case of metals which tend to form octahedral complexes [distorted by the Jahn–Teller effect in the case of copper(II)]. This effect may be explained, at least approximately, as follows.

Fridman and Dolgashova[12] have established, by studies on complexes in acetone–water solutions, that increasing the acetone concentration increases the stability of the simple (one-ligand) complexes much more than that of the mixed complexes. Hence when the acetone and glycine concentrations are large enough, there is a shift towards formation of the simple glycine complexes, and their passage into the solution. The effect is presumably connected with displacement of water molecules in the co-ordination sphere of the mixed glycine–metal–Chelex iminodiacetate groups[8] by the more basic acetone. The static studies enabled us to establish the optimum parameters for some quantitative separations, namely Cu(II)–Al(III)–Pb(II), Cu(II)–Co(II), Cu(II)–Ni(II)–Pb(II) and Cu(II)–Ni(II)–Co(II). It was established that the pH* at which Cu(II) ions are not bound by the ion-exchanger under static conditions is the value needed to achieve quantitative elution of copper from the resin, but the greater weight of ion-exchanger used in the column process necessitates changing the excess of competing ligand. However, merely increasing this excess can readily be shown to be insufficient to give the separations if acetone is not also present (*e.g.*, Fig. 4). The importance of the presence of acetone is well illustrated in Fig. 5, showing the effect of several polar organic solvents on the retention of nickel. The method should be particularly useful for analysis of copper alloys. Table 3 and Fig. 6 illustrate this.

The theory of the system will be discussed elsewhere.

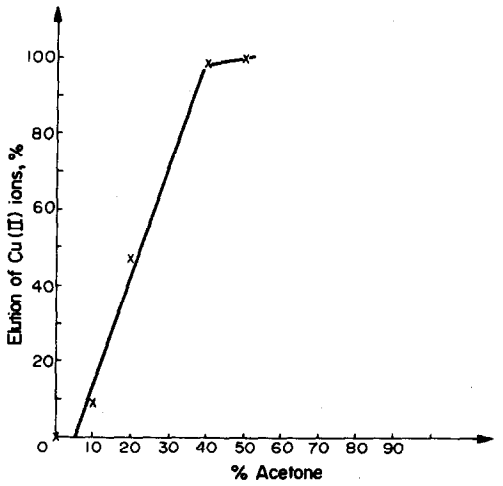


Fig. 4. Elution of Cu(II) from a column containing 0.5 g of Dowex A-1 by means of glycine solutions (pH = 10.5, V = 100 ml) of various acetone content, as a function of the acetone concentration, % v/v; 1 mg of Cu(II) taken, in 1 ml sample volume.

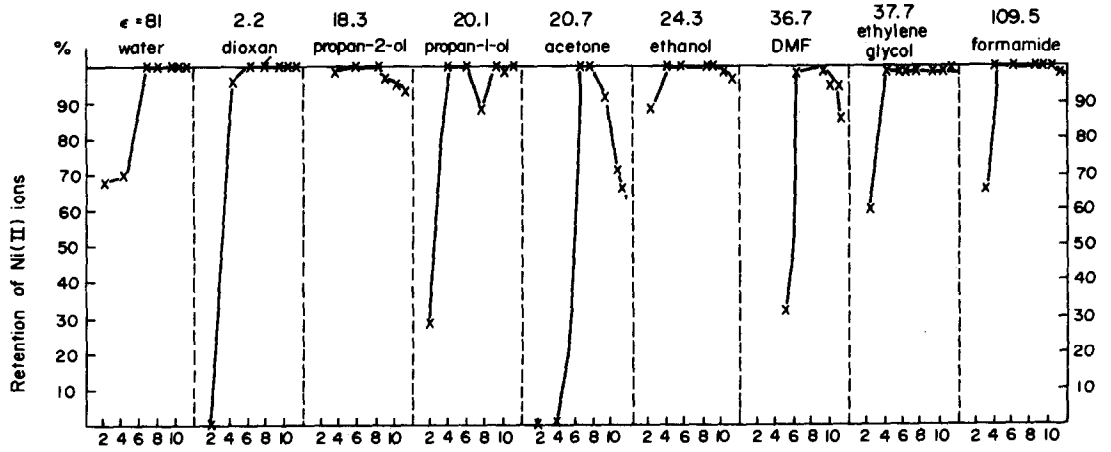


Fig. 5. Effect of different organic-aqueous media (1:1) on Ni(II) retention on Chelex 100 (dioxan 40% v/v).

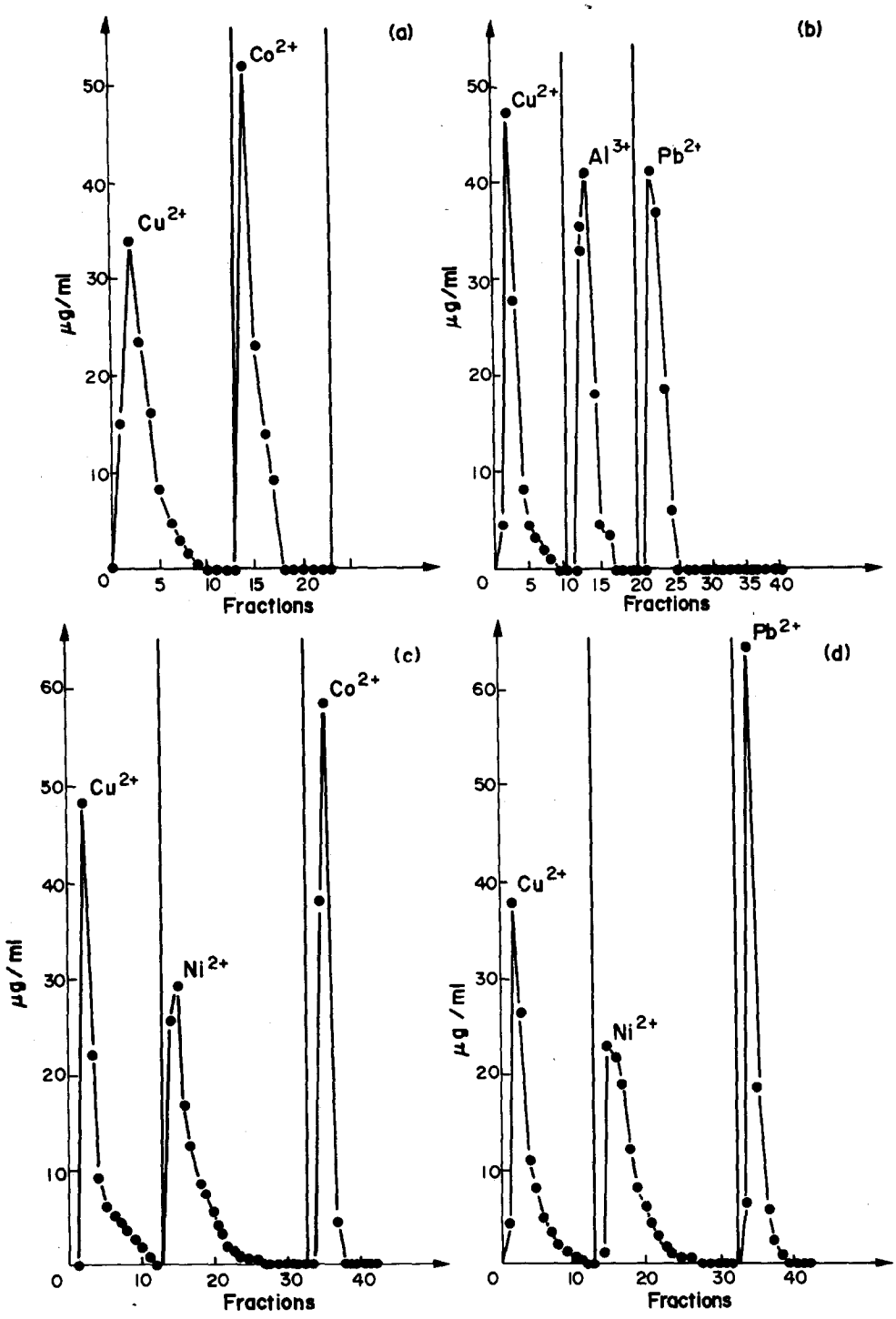


Fig. 6. Elution curves showing the separation of metal ions on Dowex A-1 with the reagents indicated in Table 3 (10-ml fractions).

Table 3. Separation of metal ions on Dowex A-1 columns

	Metal ion	No. of detns.	Eluent	Amount of metal added, *mg*	Amount of metal found, *mg*
Fig. 6(a)	Cu^{2+}	6	0.25*M* glycine (50% acetone), pH = 9.0, *V* = 130 ml	1.00	1.00
	Co^{2+}	6	0.50*M* HNO_3, *V* = 100 ml	1.00	1.00
Fig. 6(b)	Cu^{2+}	6	0.25*M* glycine (50% acetone), pH = 9.0, *V* = 100 ml	1.00	0.99
	Al^{3+}	6	1.00*M* glycine, pH = 11.0, *V* = 100 ml	1.00	1.00
	Pb^{2+}	6	0.20*M* EDTA, pH = 9.0, *V* = 200 ml	1.00	0.98
Fig. 6(c)	Cu^{2+}	6	0.25*M* glycine (50% acetone), pH = 9.0, *V* = 130 ml	1.00	1.00
	Ni^{2+}	6	1.00*M* glycine, pH = 10.5, *V* = 200 ml	1.00	0.98
	Co^{2+}	6	0.50*M* HNO_3, *V* = 100 ml	1.00	1.00
Fig. 6(d)	Cu^{2+}	6	0.25*M* glycine (50% acetone), pH = 9.0, *V* = 130 ml	1.00	1.00
	Ni^{2+}	6	1.00*M* glycine, pH = 10.5, *V* = 200 ml	1.00	0.98
	Pb^{2+}	6	0.50*M* HNO_3, *V* = 100 ml	1.00	0.97

The weight of ion-exchanger was 1.000 g of dry resin in 1,2,6–10 and 0.500 g in 3–5. The flow-rate of eluent was 5.5 ml/min for Cu(II) and Co(II) and 1.2 ml/min for the other metal ions.

REFERENCES

1. A. Liberti and A. Napoli, *J. Inorg. Nucl. Chem.*, 1971, **33**, 89.
2. J. Inczédy, *Analytical Applications of Complex Equilibria*, Horwood, Chichester, 1976.
3. L. G. Sillén and A. E. Martell, *Stability Constants of Metal-Ion Complexes*, Supplement No. 1, Chemical Society, London, 1971.
4. G. Sharma and J. P. Tandon, *Talanta*, 1971, **18**, 1163.
5. G. Anderegg and S. C. Malik, *Helv. Chim. Acta*, 1976, **59**, 1498.
6. H. Friedman and G. Schmuckler, *Israel J. Chem.*, 1963, **1**, 318.
7. G. Schmuckler, *Talanta*, 1963, **10**, 745.
8. H. Loewenschuss and G. Schmuckler, *ibid.*, 1964, **11**, 1399.
9. R. Arnaud, *Bull. Soc. Chim. France*, 1971, 2782.
10. A. P. Kreshkov, L. N. Bykova, Z. G. Blagodatskaya and V. D. Ardashnikova, *Zh. Analit. Khim.*, 1968, **23**, 27.
11. D. E. Leyden and A. L. Underwood, *J. Phys. Chem.*, 1964, **68**, 2093.
12. Ya. Fridman and N. V. Dolgashova, *Zh. Neorgan. Khim.*, 1970, **15**, 395.

Talanta, Vol. 28, pp. 765 to 767, 1981
Printed in Great Britain. All rights reserved

0039-9140/81/100765-03$02.00/0
Copyright © 1981 Pergamon Press Ltd 1981

SHORT COMMUNICATIONS

DETERMINATION OF BROMOPHOS RESIDUES BY FLUOROGENIC LABELLING WITH DANSYL CHLORIDE AND THIN-LAYER CHROMATOGRAPHY

S. TRAORE and J. J. AARON*

Laboratoire de Chimie Physique Organique et d'Analyse Instrumentale,
Département de Chimie, Faculté des Sciences, Université de Dakar, Dakar-Fann (Sénégal)

(*Received* 3 *July* 1980. *Revised* 8 *January* 1981. *Accepted* 18 *March* 1981)

Summary—The use of a highly sensitive and inexpensive method for determination of residues of bromophos (an organophosphate pesticide) in peanut crops, by fluorogenic labelling and thin-layer chromatography (TLC) is described. The bromophos is hydrolysed and the product 4-bromo-2,5-dichlorophenol (BDCP) dansylated with dansyl chloride. The fluorescent dansylated BDCP is separated by TLC and detected fluorimetrically. Linear fluorimetric analytical curves are obtained for bromophos weights ranging between 0.5 and 50 ng. The minimum detectable quantity is estimated to be 0.5 ng. The method can be used to recover as little as 400 ng of bromophos residue from 25 g of peanut seeds.

Bromophos [*O*-(4-bromo-2,5-dichlorophenyl)-*O*,*O*-dimethylphosphorothioate)] is an important aromatic organophosphorus pesticide that is widely used in West Africa to protect peanut and millet crops and storage areas. In spite of its relatively low and short-term toxicity in humans and in warm-blooded animals,[1] its utilization in large amounts makes it worthwhile to devise a technique for determining its residues in crops.

However, very few analytical methods have been proposed for the determination of bromophos.[1,2] Bromometric titration has been recommended for analysis of pesticide formulations containing it, but a gas chromatographic technique using a phosphorus-specific flame-ionization detector is preferred for determining bromophos residues in crops. The limit of determination by gas chromatography (GC) is reported to be 0.01 ppm in crops.[1] A thin-layer chromatography (TLC) enzyme-inhibition technique has also been used.[2]

Until now, fluorimetric methods have not been used for determination of bromophos because it has no native fluorescence, probably because of the presence of the two chlorine atoms and a bromine atom, the effect of which is to increase the probability of intersystem crossing from the excited singlet state to the triplet state, and to quench the fluorescence of the bromophos molecules. One way to overcome this difficulty is to introduce a highly fluorescent moiety into the pesticide molecule. Such an approach, called fluorogenic labelling, was recently developed for some organophosphates pesticides.[3] The reagent used was dansyl chloride (5-dimethylaminonaphthalene-1-sulphonyl chloride) which reacts with phenols to produce the corresponding fluorescent phenolic esters. Quantities as low as 10–25 ng of dansylated pesticide per spot chromatographed have been detected by TLC.[3]

In the present work, we wish to report the application of fluorogenic labelling and TLC to the determination of bromophos residue in peanut crops.

EXPERIMENTAL

Apparatus

A Turner model 111 fluorimeter (Turner, Palo Alto, CA 94303, U.S.A.) equipped with a Camag TLC scanning accessory was used to record the fluorescence intensity directly from the TLC plates, on a Kipp and Zonen recorder. An integrator was used to determine the chromatogram peak areas.

The fluorescent spots on the TLC plates were detected with a Desaga Minuvis mercury lamp (Desaga, Heidelberg, German Federal Republic) and a 254-nm filter.

A Beckman DB-G spectrophotometer was used for identification of the dansyl derivative of the bromophos hydrolysate on the TLC plates.

Reagents

Bromophos (98% pure) was a gift of Rhône-Poulenc, Phyto-Sanitaire, Lyon France. Bromophos powder (2% w/w bromophos) was a gift of the Office National de la Coopération de l'Assistance pour le Développement (ONCAD), Dakar, Sénégal.

Solvents used were reagent-grade methylisobutyl ketone, methylene chloride, acetonitrile and petroleum ether (b.p. 40–65°), and analytical-grade hexane, benzene, propan-2-ol and triethanolamine.

A 0.1% solution of analytical-grade dansyl chloride in methyl isobutyl ketone was used, and the triethanolamine spray was a 1:9 v/v mixture of triethanolamine and propan-2-ol.

* Author to whom all correspondence should be sent.

Dansylation procedure

A 3-ml portion of a 10^{-7}–$10^{-4}M$ solution of bromophos in methylene chloride was placed in a test-tube. The methylene chloride was evaporated at room temperature with a stream of nitrogen. Then, 0.2 ml of 0.5*M* sodium hydroxide was added, and the tube was heated at 80° for 45 min. After the hydrolysis of bromophos, 0.2 ml of 0.1% dansyl chloride solution was added and the mixture was heated for 90 min at 80°. The methyl isobutyl ketone was evaporated with a stream of nitrogen. The tube was cooled to room temperature, and the dansylated product was extracted with 0.2 ml of benzene. The benzene layer was removed by means of a Pasteur pipette and dried with a few granules of anhydrous sodium sulphate.

TLC procedure

The TLC plates were prepared with silica gel 60 (Merck), allowed to dry at 100° in an oven, and stored in the dark. Then, 2, 5, 10 and 20 μl of the benzene solution of the dansylated product were spotted on the plates with a 50-μl syringe. Several solvents such as benzene–hexane (2:1 v/v), acetone–benzene (100:0.4 v/v), benzene and methanol were tested as developing agents (in a fume cupboard). The developed plates were dried, sprayed with triethanolamine solution, dried in an oven, and exposed to a mercury lamp (λ = 254 nm), in order to excite the fluorescence of the spots. The fluorescence intensity was measured by means of the Turner fluorimeter. The zones containing dansylated compounds were scraped from the plates, and extracted with ethanol. The clear supernatant solutions were decanted and analysed spectrophotometrically.

Extraction procedure for bromophos residues

A 1-kg sample of peanut pods and their seeds was treated with 500 mg of 2% w/w bromophos powder and left for a week. The pods were then decorticated, and a 25-g sample of peanut seeds was weighed and ground. The extraction procedure was adapted from that described by Currie.[4] A 25-ml volume of water and, 5 min later, a 100-ml volume of acetonitrile were added to the ground sample and mixed in a blender for 5 min at medium speed. The mixture was filtered and the solid was extracted again in the same way. The combined filtrates were transferred to a 1-litre separatory funnel and rinsed in with four 25-ml portions of 15% methylene chloride solution in petroleum ether (b.p. 40–65). Then 500 ml of 1% sodium chloride solution and 50 ml of 1% sodium carbonate solution (both presaturated with petroleum ether) were added, the mixture was shaken vigorously for 1 min, and the organic phase was collected. After 10 min the aqueous phase was shaken with another 100 ml of methylene chloride solution and the organic extract collected. The combined organic extract was dried with anhydrous sodium sulphate and evaporated to 4 ml, and this was then dansylated as described above.

RESULTS AND DISCUSSION

Dansylation reaction

The bromophos is hydrolysed in the strongly alkaline aqueous solution to the corresponding phenolate which then reacts with dansyl chloride at the interface to form the fluorescent dansylated product which is extracted into the organic phase. To check that the surplus dansyl chloride is hydrolysed with transfer of the hydrolysis product to the aqueous phase, a blank test was performed without bromophos, and the organic phase was analysed by TLC. No significant fluorescent spot was found.

Table 1. Eluents for TLC separation of the dansylated bromophos hydrolysis product

Solvent system	Dansylated product	
	R_f	Elution time, *min*
Benzene–hexane (2:1 v/v)	0.79 ± 0.03	45
Acetone–benzene (100:0.4 v/v)	0.95 ± 0.01	40
Benzene	0.98 ± 0.01	60
Methanol	0.78 ± 0.06	60

Choice of eluent

The R_f values and elution times of the fluorescent product with different eluents are given in Table 1, which shows that benzene–hexane (2:1 v/v) is the most selective and convenient eluent.

Study of the fluorescent spots

Under ultraviolet light (wavelength 254 nm), the dansylated product gives a blue-green fluorescence, with constant intensity for at least 30 min. The absorption spectrum of the dansylated product is given in Fig. 1. The absorption maxima at 280 and 290 nm are attributed to the phenolate moiety, and

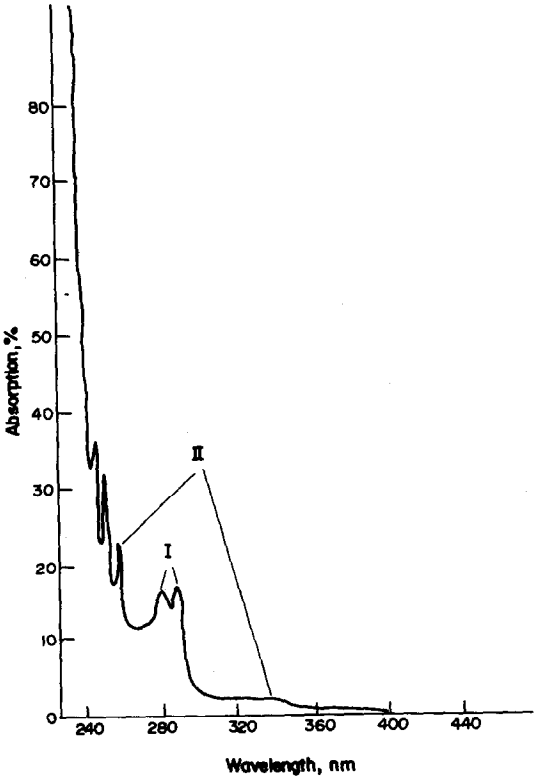


Fig. 1. Absorption spectrum of dansylated bromophos hydrolysis product in hexane ($3 \times 10^{-5}M$; 25°C). I: maxima attributed to the phenolate moiety; II: maxima attributed to the dansyl moiety.

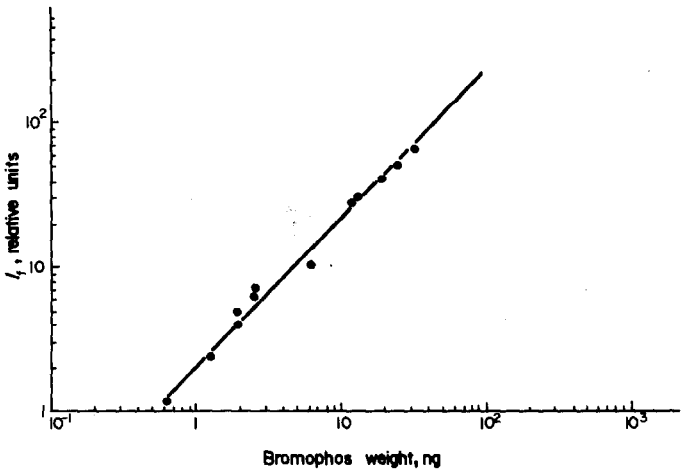


Fig. 2. Fluorimetric calibration curve.

those at 260 and 350 nm to the dansyl part of the molecule, confirming identification of the fluorescent derivative as the dansylated BDCP.

Calibration plot and limits of detection

The logarithm of the integrated fluorescence intensity was found to be a linear function of the logarithm of weight of bromophos taken (over the range 0.5–50 ng). The precision is good, as shown by the regression coefficient of 0.991. The slope value (1.014) is close to unity, indicating good sensitivity (Fig. 2).

The minimum detectable quantity (MDQ), defined as the quantity of compound giving a fluorescence signal equal to two times the fluctuations of the blank and located on the linear portion of the calibration plot, is about 0.5 ng of bromophos, which is particularly low in comparison with the values for other organophosphate pesticides, for which MDQ values of 10–25 ng by TLC, and 5–10 ng by high-pressure liquid chromatography, have been reported.[3] Our MDQ corresponds to a concentration of about 0.09 ppm of bromophos, a value close to the limit of detection of 0.01 ppm found by a gas chromatography technique for bromophos residues.[1]

Determination of bromophos residue in peanut crops

The simulated "residues" sample was treated as described, and 2, 4, 6, 8 and 10 μl volumes of the final extract were subjected to TLC and evaluated by fluorimetry. The values obtained corresponded to 3, 2.5, 2.5, 2.5 and 3 ng/μl in the extract, respectively. In field analysis, the recovery of added bromophos was 95 ± 10%.

Conclusion

This dansylation method is highly sensitive, relatively inexpensive, and reliable for determining bromophos residues in peanut crops. The combination of the selectivity of TLC and the sensitivity of fluorogenic labelling gives analytical results comparable to those obtained by gas chromatography. It is a convenient and simple means of analysis of organophosphate pesticide residues when sophisticated and expensive instrumentation is not available.

REFERENCES

1. R. D. Weeren and D. Eichler, in *Analytical Methods for Pesticides and Plant Growth Regulators*, Vol. X, p. 31, G. Zweig, ed., Academic Press, New York, 1978.
2. H. Ackermann, *J. Chromatog.*, 1968, **36**, 309.
3. J. F. Lawrence, C. Renault and R. W. Frei, *ibid.*, 1976, **121**, 343.
4. R. A. Currie, *J. Assoc. Off. Anal. Chemists*, 1974, **57**, 1056.

Talanta, Vol. 28, pp. 768 to 770, 1981
Printed in Great Britain.

0039-9140/81/100768-03$02.00/0
Pergamon Press Ltd 1981

EXTRACTION AND SEPARATION OF BISMUTH(III)

A. D. LANGADE and V. M. SHINDE
Analytical Laboratory, Department of Chemistry,
Shivaji University, Kolhapur 416004, India

(*Received* 4 *September* 1980. *Revised* 4 *February* 1981. *Accepted* 16 *March* 1981)

Summary—Separation of bismuth from beryllium, lead, iron(III), indium, scandium, lanthanum, antimony(III), zirconium, titanium, thorium, vanadium(V), molybdenum(VI), uranium (VI) and chromium(VI) is achieved by selective extraction of bismuth from 0.1*M* sodium salicylate solution (adjusted to pH 7) into mesityl oxide (MeO). The extracted species is $Bi(HOC_6H_4COO)_3 \cdot 3MeO$. The results are accurate within ± 0.5%, with a standard deviation of 0.8%. The separation and determination of bismuth takes only 15 min.

Bismuth is chiefly employed for the preparation of hard and easily fusible alloys which are useful as safety plugs in boilers, electrical fuses, solders, *etc.* Its determination is therefore important, and for this its separation is necessary. Solvent extraction is excellent for this purpose. This paper describes a new method for separation of bismuth from Be, Pb, Fe, In, Sc, La, Sb, Zr, Ti, Th, V, Cr, Mo and U, by extraction into mesityl oxide from 0.1*M* sodium salicylate solution (pH 7). After scrubbing with 0.5*M* sodium hydroxide it is estimated with thiourea.

Polar solvents such as tributyl phosphate (TBP), methyl isobutyl ketone (MIBK), isoamyl alcohol, isoamyl acetate and diethyl ether[1–4] have been used for extraction of bismuth from iodide or thiocyanate medium. The iodide system requires a longer extraction period.[1] Extraction with TBP or MIBK from thiocyanate medium affords separation of bismuth from Pb, Fe, Co, In, Ga and Zn.[4] High molecular-weight amines[5–8] have also been employed for extraction of bismuth from iodide, thiocyanate, chloride and bromide media but separations from other metals have not been studied. 2-Ethylhexyl dihydrogen phosphate[9,10] has also been used for extraction of bismuth, but the efficiency of separation is only 90%. Extraction of bismuth from nitric acid with sulphoxides as extractants[11] gives separation from Fe, Cu, Ni and Co. The method proposed here describes a systematic study on the extraction and separation of bismuth from a large number of metal ions commonly associated with it.

EXPERIMENTAL

Reagents

Bismuth solution. Prepared by dissolving 1.16 g of bismuth nitrate in 4 ml of nitric acid and diluting to 100 ml with distilled water, standardized[12] and diluted as required.

Mesityl oxide. Doubly distilled (b.p. 125–128°).

Thiourea solution, 12%.

General procedure for extraction

An aqueous solution (25 ml) containing 500 μg of bismuth and 0.4 g of sodium salicylate was adjusted to pH 7 with dilute nitric acid and sodium hydroxide solution and shaken for 30 sec in a 100-ml separatory funnel with 10 ml of mesityl oxide. After separation of the layers, bismuth was removed from the mesityl oxide phase by shaking with two 5-ml portions of 0.5*M* sodium hydroxide, and estimated photometrically in the combined aqueous phase with thiourea,[13] at 470 nm.

Analysis of lead–bismuth and tin–bismuth alloys

Weigh accurately about 0.5 g of the alloy and add 5 ml of water followed by 10 ml of concentrated nitric acid. When the vigorous reaction is over, evaporate on a water-bath to about 5 ml, dilute to 50 ml and filter off the metastannic acid. Dilute the filtrate to 100 ml. Extract bismuth from an aliquot as described in the general procedure.

Analysis of steel and brass

Dissolve 0.5 g of steel or brass as described earlier[14] and make up to standard volume. Extract an aliquot as in the recommended procedure.

RESULTS AND DISCUSSION

Optimum extraction conditions

The extraction of bismuth(III) was studied at various pH values (3–9), sodium salicylate concentrations (0.01–0.1*M*) and mesityl oxide concentrations (30–100% in chloroform as diluent). The extraction curves in Fig. 1 indicate that the extraction of bismuth is effectively quantitative at pH 6.6–7.4 from 0.1*M* sodium salicylate medium with pure mesityl oxide. The degree of extraction was determined by stripping bismuth from the mesityl oxide with 0.5*M* sodium hydroxide and photometric determination with thiourea.[13]

Nature of the extracted species

The usual log–log plots of distribution coefficient *vs.* reactant concentration were made. The slopes for

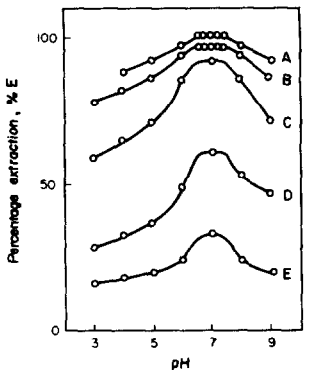


Fig. 1. Extraction behaviour of bismuth salicylate with mesityl oxide as a function of pH and sodium salicylate concentration. Sodium salicylate: A, 0.1*M*; B, 0.075*M*; C, 0.05*M*; D, 0.025*M*; E, 0.01*M*.

the salicylate (fixed pH and [mesityl oxide]) and mesityl oxide graphs (fixed pH and [sodium salicylate]) were both 2.75, suggesting that the bismuth salicylate species extracted is $Bi(HOC_6H_4COO)_3 \cdot 3MeO$, where MeO stands for mesityl oxide.

Period of equilibration

A single extraction for 30 sec with undiluted mesityl oxide is adequate for quantitative extraction of 500 μg of bismuth. Further shaking has no adverse effect on the extraction.

Interferences

Various amounts of foreign ions were added to a fixed amount of bismuth (500 μg) and the general extraction procedure was followed. There was no interference (as shown by less than 1% deviation in bismuth recovery) from 5 mg each of Ba, Sr, Ca, Cu, Pb, Mn, Ni, Zn, Hg, As(III), In(III), Tl(III), Ir(III), Ru(III), Rh(III), Al, Ce(IV), Pt(IV), Zr, Th, Se(IV), Mo(VI), Cr(VI), phosphate, oxalate, thiocyanate, fluoride, sulphate and carbonate; 2.5 mg each of Pd(II), Sb(III), Fe(III), Ga, Cr(III) and V(V); 1 mg each of Be, Sn(II), La, Y, Sc, Ti(IV), Te(IV) and W(VI), and 0.5 mg of Au(III). However, Ag, Cd, Os(VIII), EDTA, tartrate and citrate interfere severely.

Table 1. Degree of extraction of Bi(III) and other metal ions ([sodium salicylate] 0.1*M*, pH 7, 10 ml of mesityl oxide, shaking for 30 sec)

Metal ion	Extraction, %
Bi(III)	100.0
Be(II)	1.0
Pb(II)	1.0
Fe(III)	0.6
In(III)	0.8
Sc(III)	99.2
La(III)	99.2
Sb(III)	1.0
Zr(IV)	99.0
Ti(IV)	1.0
Th(IV)	99.4
V(V)	0.6
Mo(VI)	0.8
U(VI)	99.4
Cr(VI)	0.8

Of the ions studied, Sc, La, U(VI), Th, and Zr are co-extracted quantitatively with the bismuth (Table 1). The first four can be removed by shaking the mesityl oxide extract with two 10-ml portions of 0.01*M* hydrochloric acid, then the bismuth is stripped as already described, and finally zirconium is stripped with 1*M* hydrochloric acid.

Results for some alloys and synthetic mixtures are shown in Tables 2 and 3.

The results are accurate within ±0.5% with a standard deviation of ±0.8%. The total operation for separation and determination of bismuth requires only 15 min. The wide applicability of the method is shown by satisfactory analysis of a variety of synthetic mixtures.

Table 3. Analysis of synthetic mixtures

Composition, *mg*	Bismuth found, *mg*	Relative error, %
Bi, 0.5; Fe, 1.0; Mo 1.0; Cr 1.0; V 1.0	0.49	0.4
Bi, 0.5, Ti, 1.0; Sb, 1.0; Pb, 1.0	0.49	0.4

Table 2. Analysis of standard alloys

Alloy	Composition, %	Bismuth content, *mg*		Relative error, %
		Present	Found	
NBS 33b Cast iron	C, 2.24; Si, 2.0; P, 0.11; S, 0.03; Mn, 0.064; Ni, 2.24; Cr; 0.61; Mo, 0.4; Fe, 91.4 + Bi, 0.50 mg	0.50	0.49	0.4
Brass	Pb, 2.35; Zn, 40.65; Cu, 56.9; Fe, 0.009 + Bi, 0.50 mg	0.50	0.49	0.4
Pb–Bi alloy	Pb + Bi (15.4%)	0.77	0.76	0.5
Sn–Bi alloy	Sn + Bi (25.0%)	0.50	0.50	0.0

Acknowledgements—Thanks are due to CSIR, New Delhi, for awarding a fellowship to one of us (ADL), and also to the University Grants Commission, New Delhi for financing this project.

REFERENCES

1. H. A. Mottola and E. B. Sandell, *Anal. Chim. Acta*, 1961, **24**, 301.
2. E. Jackwerth and H. Specker, *Z. Anal. Chem.* 1960, **177**, 327.
3. K. Takatoshi and N. Akira, *Bunseki Kagaku*, 1975, **24**, 419.
4. C. Rozycki, *Chem. Anal. (Warsaw)*, 1969, **14**, 755.
5. B. Ya. Spivakov, V. I. Lebedev, V. M. Shkinev, N. P. Krivenkova, T. S. Plotnikova, I. P. Kharlamov and Yu. I. Zolotov, *Zh. Analit. Khim.*, 1976, **31**, 757.
6. I. A. Shevchuk, T. N. Simonova, Z. N. Kravtsova, T. I. Pluzhnik and N. I. Gorshkova, *Ukr. Khim. Zh.*, 1975, **41**, 959.
7. G. Nakagawa, *Nippon Kagaku Zasshi*, 1960, **81**, 750.
8. T. Suzuki, *Bunseki Kageku*, 1966, **15**, 666.
9. I. S. Levin, A. A. Shatalova and T. G. Azarenko, *Zh. Analit. Khim.* 1966, **21**, 876.
10. I. S. Levin, Yu. M. Yukhin and I. A. Vorsina, *Izv. Sib. Otdel. Akad. Nauk SSSR, Ser. Khim. Nauk*, 1970, 61.
11. Yu. E. Nikitin, Yu. I. Murinov, N. G. Afzaletdinova and N. Z. Mineeva, *Zh. Analit. Khim.*, 1976, **31**, 181.
12. F. J. Welcher, *The Analytical Uses of Ethylenediamine Tetraacetic Acid*, pp. 180, 209. Van Nostrand, New York, 19.
13. E. B. Sandell, *Colorimetric Determination of Traces of Metals*, 3rd Ed., p. 164. Interscience, New York, 1959.
14. P. S. Patil and V. M. Shinde, *Analyst*, 1978, **103**, 79.

Talanta, Vol. 28, pp. 771 to 773, 1981
Printed in Great Britain. All rights reserved

0039-9140/81/100771-03$02.00/0
Copyright © 1981 Pergamon Press Ltd 1981

DECOMPOSITION OF ORES BY MANGANESE DIOXIDE: ANALYSIS OF CHROME ORE

S. K. MANDAL, S. B. RAO and B. R. SANT
Regional Research Laboratory, Bhubaneswar, India

(*Received* 26 *February* 1980. *Revised* 19 *September* 1980, *Accepted* 13 *March* 1981)

Summary—Pure manganese dioxide, prepared synthetically, has been used for the oxidative decomposition of chrome ores. The usual constituents of the ores, *viz.* Cr_2O_3, FeO, Al_2O_3, MgO, CaO and SiO_2 have been estimated and the results compare favourably with those obtained by standard methods.

In our previous communication[1] we reported on the decomposition of chrome ore by heating with manganese ore or manganese dioxide in sulphuric acid medium, and subsequent determination of chromium. It was then considered worthwhile to study the possibility of applying this decomposition method when other components of chrome ore were to be determined. However, manganese ores and technical grades of manganese dioxide invariably contain iron and other impurities, thus precluding their use for this purpose. It has now been found that if synthetically prepared manganese dioxide is used, all the usual constituents of the ore can be estimated. The present communication describes the determination of chromium, iron, silica, alumina, calcium and magnesium in chrome ores.

EXPERIMENTAL

Reagent

Prepare the manganese dioxide by the method of Selwood *et al.*[2] Make saturated solutions of potassium permanganate in water and of manganous sulphate in sulphuric acid (1 + 4) and filter them through glass-wool plugs. Add the permanganate solution to the manganous sulphate solution slowly with constant stirring, keeping the temperature at about 60° during the reaction (about 30 min). Allow to settle, decant the clear solution and wash the precipitate by decantation a few times with water. Filter off on a Whatman No. 541 filter paper (Buchner funnel) and wash free from permanganate and sulphate. Dry at 110–120°. The purity of the oxide is about 99.98%.

General procedure

Weigh accurately 1 g of finely powdered chrome ore, previously dried at about 110°. Add 2 g of the manganese dioxide and mix thoroughly with a glass rod. Add 50 ml of sulphuric acid (1 + 1) and stir well. Heat the beaker on a hot-plate till white fumes appear. Cool, wash down the inside of the beaker with water and heat the mixture again till the appearance of white fumes, to ensure complete oxidation of Cr(III). Cool, adjust the pH of the solution to about 1 with ammonia solution (1 + 1) and heat on a water-bath till the hydrated manganese oxides have settled completely. Filter the solution through a Whatman No. 40 paper and wash thoroughly with hot water. Transfer the residue from the filter paper into the original beaker with a jet of distilled water and the minimum quantity of hot hydrochloric acid (1 + 1). Wash the filter paper thoroughly with distilled water. Add 1 g of manganese dioxide and 50 ml of sulphuric acid (1 + 1) to the beaker and repeat the decomposition procedure. Filter off on the original paper and wash thoroughly with hot water. Combine the two filtrates in a 500-ml standard flask, make up to the mark and mix. Set aside the residue on the filter paper for the determination of silica.

Chromium. Titrate an aliquot of the solution with 0.1*M* iron(II) ammonium sulphate in presence of barium diphenylaminesulphonate as indicator (1 ml of 0.1*M* $Fe^{2+} \equiv 2.534$ mg of Cr_2O_3).

Separation of chromium from iron, aluminium, magnesium, calcium and manganese.[3] Pass an aliquot of the solution (made 0.5*M* in hydrochloric acid) through a column of Amberlite CG 400 (100–120 mesh), previously conditioned with 0.5*M* hydrochloric acid. Collect the effluent for the determination of iron, aluminium and magnesium.

Separation of iron and aluminium from calcium, magnesium and manganese. To the effluent from the column add 5 g of ammonium chloride and heat just to boiling. Add ammonia solution dropwise from a burette to adjust the pH to about 7.5. Boil the solution for 1–2 min, and filter off at once on a Whatman No. 541 paper. Wash the precipitate thoroughly with hot 2% ammonium chloride solution. Set the filtrate and washings aside. Dissolve the precipitate in a small volume of hot hydrochloric acid (1 + 1), washing the solution into the precipitation beaker, and reprecipitate with ammonia solution as before. Collect the precipitate on a Whatman No. 541 paper and wash with hot 2% ammonium nitrate solution. Combine the filtrates and washings for the determination of magnesium.

Aluminium. Dissolve the mixed hydroxides precipitate with a small volume of hot hydrochloric acid (1 + 1), washing through into the precipitation beaker, add 5 g of sodium hydroxide pellets, and boil for 5 min. Allow the precipitate of hydrous ferric oxide to settle and filter off on a Whatman No. 541 collecting the filtrate in a 400-ml beaker containing 20 ml of hydrochloric acid (1 + 1). Wash the precipitate with hot 1% sodium carbonate solution and then with hot water. Dissolve the precipitate with hot hydrochloric acid and repeat the precipitation, filtration and washing, combining the filtrates and washings. Neutralize the combined filtrate with hydrochloric acid (1 + 1) and then add 4 ml in excess. The volume should now be about 200 ml. Add 4 ml of 50% hydroxylammonium chloride solution and 3 ml of 1% 1,10-phenanthroline solution in acetic acid (1 + 1). Then add 20 ml of 5% oxine solution in acetic acid (1 + 8), followed by 40 ml of 40% ammonium acetate solution, slowly and with stirring. Heat to 70°, digest for 10 min, cool for 30 min, collect the precipitate on a sintered-glass filter crucible (porosity No. 4) and wash with water. Dissolve the complex in warm concentrated hydrochloric acid, collect-

ing the solution in a 250-ml reagent bottle, add 0.5–1 g of potassium bromide and a slight excess of standard bromate solution, dilute considerably with 2*M* hydrochloric acid, then add (after about 5 min) 10 ml of 10% potassium iodide solution and titrate the liberated iodine with standard 0.1*M* sodium thiosulphate, using starch as indicator (1 ml of 0.1*M* $KBrO_3 \equiv 0.4249$ mg of Al_2O_3).

Iron. Dissolve the precipitate of hydrous ferric oxide in the minimum quantity of hot hydrochloric acid (1 + 1), heat the solution to boiling and determine iron(II) by the dichromate titration method, with barium diphenylaminesulphonate as indicator, after the usual stannous chloride–mercuric chloride treatment (1 ml of 0.1*M* $K_2Cr_2O_7 \equiv$ 7.985 mg of Fe_2O_3).

Magnesium. Take the combined filtrates from the ammonia precipitation, slightly acidify with dilute hydrochloric acid and evaporate to about 250 ml. Add 1 ml of concentrated hydrochloric acid and precipitate calcium by adding slowly to the boiling solution 10 ml of hot 4% ammonium oxalate solution, followed by ammonia solution (1 + 10) until the solution is neutral or slightly alkaline. Allow the precipitate to settle for 1 hr. Filter off and wash it two or three times with cold 0.1% ammonium oxalate solution. To the filtrate add 50 ml of concentrated nitric acid and evaporate to dryness on a low-heat hotplate. Only a small residue should remain. Add 2–3 ml of concentrated hydrochloric acid and 20 ml of water, warm the mixture for a few minutes until the solid has dissolved. Add 2 g of hydroxylammonium chloride and 30 ml of buffer solution (dissolve 8 g of ammonium nitrate in 65 ml of water and add 35 ml of ammonia solution, sp. gr. 0.88). Add sufficient Eriochrome Black T indicator to produce a definite red colour, warm to 40° and titrate with standard EDTA solution to a pure blue colour. After the end-point, add 5 g of sodium fluoride and stir for 1 min. Add standard manganous sulphate solution from a burette in 1-ml portions until a permanent red colour is obtained; note the exact volume added. Stir for 1 min and titrate the excess of manganese with EDTA until the colour changes to pure blue (1 ml of 0.05*M* EDTA ≡ 2.016 mg of MgO).

Calcium. Take 100 ml of the original solution in a 500-ml beaker, boil, add 5 g of ammonium oxalate and stir to dissolve it. Add ammonia solution (1 + 10) until the solution is neutral or slightly alkaline. Allow the precipitate to settle for 1 hr, filter off and wash it two or three times with cold 0.1% ammonium oxalate solution. Place the original beaker under the funnel, dissolve the precipitate in the minimum quantity of hot hydrochloric acid (1 + 9) and wash the paper with hot water. Dilute to 100 ml, add 5 ml of 4% ammonium oxalate solution, boil and add ammonia solution dropwise until the solution is just alkaline. Set aside for 1 hr for the precipitate to settle. Filter off on a Whatman No. 540 paper and wash with 0.1% ammonium oxalate solution until free from chloride. Dry the filter paper and precipitate and ignite in a platinum crucible to constant weight. Weigh as CaO.

Silica. Take the filter paper from the original manganese separation and transfer the residue on it into the original beaker with a jet of distilled water. Remove the last traces of black particles by addition of hot hydrochloric acid (1 + 1), and rinse out thoroughly with distilled water. Reserve the filter paper. Heat the solution to dissolve all manganese oxides and add more concentrated hydrochloric acid if necessary. Heat to dryness on a water-bath and then at 105–110° until the acid is completely driven off. Moisten the precipitate with water and evaporate to dryness. Take up with 0.5*M* hydrochloric acid. Leave for 10 min on the water-bath. Filter off on a Whatman No. 540 paper, wash with hydrochloric acid (1 + 100) and finally once or twice with water to remove most of the hydrochloric acid. Place the paper and the precipitate in a weighed crucible together with the original paper, dry and ignite at 1000–1100°, cool and weigh. Moisten with a few drops of water, add a few drops of concentrated sulphuric acid and 5 ml of concentrated hydrofluoric acid and evaporate to dryness. Ignite at 1200° to constant weight. The loss in weight corresponds to silica present. Repetition of the final treatment provides a check on the completeness of the expulsion of silica.

Any silica in solution after the decomposition with manganese dioxide can be estimated spectrophotometrically in an aliquot of the original solution.[4]

RESULTS AND DISCUSSION

Typical results for the analysis of chrome ores with use of manganese dioxide are shown in Table 1.

Chromium, iron and aluminium are determined titrimetrically. Calcium is determined gravimetrically. Magnesium is determined by complexometric titration with EDTA. Since the solution also contains manganese salts, care must be taken in the determination of magnesium. In manganese–magnesium mixtures the sum of both ions is determined by direct EDTA titration. Fluoride demasks magnesium selectively from its EDTA complex, when excess of manganese solution is added.

$$MgY^{2-} + 2F^- + Mn^{2+} = MgF_2 + MnY^{2-}$$

A standard manganese solution is used and the excess back-titrated with EDTA. The amount of standard manganese solution consumed is equivalent to the EDTA liberated from the magnesium complex. Silica is determined by dehydration *etc.*, and a little may pass into solution[5] but we found no sign of this with the samples tested. Any silica passing into solution can be determined spectrophotometrically, or by atomic-absorption spectroscopy.[6]

Chrome ore is generally decomposed by an alkaline or an acidic treatment, but most of the methods are

Table 1. Determination of chromium, iron, silica, alumina, calcium and magnesium in chrome ores

	High grade		Medium grade		Low grade		Grecian (BCS)	
	Present	Found	Present	Found	Present	Found	Present	Found
Cr_2O_3, %	53.5	53.2	35.1	35.0	28.6	29.0	41.5	41.2
Fe (as FeO), %	15.4	15.5	22.2	22.5	36.0	36.3	15.3	15.2
SiO_2, %	4.5	4.6	10.5	10.5	2.4	2.4	4.3	4.2
Al_2O_3, %	11.4	11.5	11.7	11.6	14.4	14.5	19.4	19.6
CaO, %	0.8	0.9	0.9	1.0	1.7	1.8	0.3	0.3
MgO, %	13.0	13.1	9.1	9.0	8.7	8.8	16.4	16.6

rather tedious and proper care needs to be taken for reproducible results. The data in Table 1 show that any type of chrome ore can be analysed by the present method. Further work on the use of manganese dioxide for the decomposition and analysis of other ores is in progress.

Acknowledgements—Grateful thanks are due to the Director, Regional Research Laboratory, Bhubaneswar, India, for permission to publish the paper.

REFERENCES

1. S. K. Mandal, S. B. Rao and B. R. Sant, *Talanta*, 1979, **26**, 135.
2. P. W. Selwood, R. P. Eischens, M. Ellis and K. Wethington, *J. Am. Chem. Soc.*, 1949, **71**, 3039.
3. G. A. H. Roberts, *Talanta*, 1968, **15**, 735.
4. *BS Standard* 1902:1952, Part 2A, British Standards Institution, London, 1964.
5. G. Charlot and D. Bezier, *Quantitative Inorganic Analysis*, p. 562. Methuen, London, 1957.
6. T. S. Harrison, *Handbook of Analytical Control of Iron and Steel Production*, pp. 404, 412. Horwood, Chichester, 1979.

Talanta, Vol. 28, pp. 774 to 776, 1981
Printed in Great Britain. All rights reserved

0039-9140/81/100774-03$02.00/0
Copyright © 1981 Pergamon Press Ltd 1981

DUAL-WAVELENGTH SPECTROPHOTOMETRIC DETERMINATION OF COPPER IN SEA-WATER WITH α,β,γ,δ-TETRAKIS(1-METHYLPYRIDINIUM-4-YL)PORPHINE

HIROTO WATANABE and HIDEKI OHMORI

Department of Applied Chemistry, Muroran Institute of Technology, Mizumoto-cho 27-1, Muroran, Hokkaido, 050 Japan

(*Received* 17 *February* 1981. *Accepted* 13 *March* 1981)

Summary—Copper has been determined by dual-wavelength spectrophotometry with α,β,γ,δ-tetrakis(1-methylpyridinium-4-yl)porphine (TMPyP). The difference in absorbance at the Soret band of the copper complex (423 nm) and that of TMPyP (446 nm) was measured. Copper in a coastal sea-water sample was preconcentrated with a Chelex-100 separation in which L-cysteine was used as eluent. This combination could determine copper at the ng/ml and sub-ng/ml level.

Recently, water-soluble porphyrins have been used as highly sensitive reagents for the determination of trace metals.[1-4] The molar absorptivities of the porphyrins at their Soret bands are (2–6) × 10^5 l. $mole^{-1}$. cm^{-1}, thus making it possible to determine metal ions directly at ng/ml levels.[1] In this study α,β,γ,δ - tetrakis(1 - methylpyridinium - 4 - yl)porphine (TMPyP) was selected for use in the determination of copper in a coastal sea-water sample because it is highly selective for copper, compared with other water-soluble porphyrins.[2] Furthermore, preliminary tests indicated that the absorption spectra of TMPyP and its copper complex were essentially independent of the presence of sodium chloride, up to its concentration in sea-water. The spectra of such water-soluble porphyrins as α,β,γ,δ-tetraphenylporphine trisulphonate,[1] α,β,γ,δ-tetrakis(4-sulphophenyl)porphine,[3] and α,β,γ,δ-tetrakis(carboxyphenyl)porphine[4] are dependent on the concentration of sodium chloride. This is ascribed to association of the porphyrins, as pointed out by other workers.[2,5]

TMPyP was first introduced by Yotsuyanagi *et al.* for the spectrophotometric determination of copper.[2] They found that TMPyP rapidly and selectively forms a very stable complex with copper in a weakly acid medium in the presence of L-cysteine at room temperature. The Soret band of the copper complex (423 nm) seriously overlaps with that of TMPyP (423 nm) in a weakly acid medium. However, the Soret band of TMPyP shifts to 446 nm in 1*M* sulphuric acid solution because of protonation, while that of the complex remains unchanged. The procedure described below is based on these findings reported by Yotsuyanagi *et al.*[2]

In this study a dual-wavelength spectrophotometer was employed.[6,7] This increases the sensitivity of TMPyP for copper, in the same way as for that of Cadion for cadmium.[8]

A Chelex-100 separation was used for preconcentration of copper in sea-water.

EXPERIMENTAL

Reagents

Standard metal-ion solutions were made from high-purity metals or reagents, dissolved in 2*M* hydrochloric acid, then diluted as necessary with distilled demineralized water; the final acid concentration was 0.01*M*. Other reagents were of analytical grade and purified if necessary.

A 1.23 × 10^{-5}*M* TMPyP solution was prepared by dissolving the compound in water.

A buffer solution of pH 5.2 was made by mixing 0.2*M* sodium acetate and 0.2*M* acetic acid, and purified by a co-crystallization method based on the use of 1-(2-pyridylazo)-2-naphthol.[9]

A buffer of pH 9.0 was made by mixing equal volumes of 0.1*M* ammonia solution and 0.1*M* ammonium chloride.

Chelex-100 resin was purified by batch extraction, by washing successively with 6*M* hydrochloric acid and water, converted into sodium form by equilibration with 1*M* sodium chloride, and rinsed with water. The sodium chloride solution was purified by co-crystallization.[9]

A coastal sea-water sample (Muroran) was filtered through a 0.45-μm membrane filter, acidified to pH 1.0 with sulphuric acid, and stored in a polyethylene bottle for more than 24 hr before use.

Recommended procedure

A portion of test solution containing less than 1.3 μg of copper was placed in a 25-ml standard flask, and 4.0 ml of TMPyP solution, 1.0 ml of buffer and 1 ml of 8.25 × 10^{-4}*M* L-cysteine were added in that order. The mixture was allowed to stand for 5 min for full colour development, 2.7 ml of 9*M* sulphuric acid were added, and the mixture was made up to volume with water. The difference in absorbance at 423 nm and 466 nm, $\Delta_{423-446}$, was measured (1-cm cell) with a full-scale range of 0–0.3.

Procedure for preconcentration

For analysis of sea-water samples, the copper was preconcentrated by the Chelex-100 separation introduced by Riley and Taylor,[10] but with L-cysteine as eluent. A sample

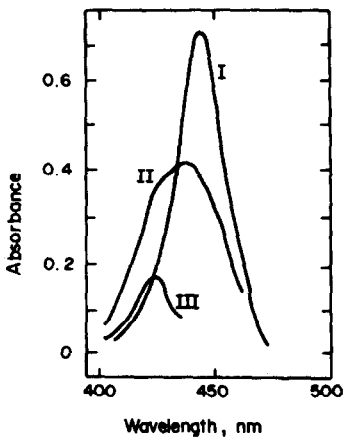


Fig. 1. Absorption spectra of TMPyP and its copper complex. I, TMPyP (ref. water); II, copper complex (ref. water); III, copper complex (ref. reagent blank).

at pH 5.2 was added to a column (1 cm diameter) of 2.4 ml of Chelex-100 resin, at a rate of 0.6 ml/min. Then 20 ml of water and 40 ml of pH-9.0 ammonia buffer were passed through the column successively. The copper was eluted with 20 ml of $1.65 \times 10^{-4}M$ L-cysteine buffered with ammonia to pH 9.0, at a rate of 0.6 ml/min. The effluent was analysed by the recommended procedure (with the L-cysteine omitted). Fresh resin was used for each experiment.

RESULTS AND DISCUSSION

The absorption spectra of TMPyP and its copper complex in $1M$ sulphyric acid are shown in Fig. 1. The Soret band of TMPyP is at 446 nm and that of the complex at 423 nm.

The wavelengths used were chosen so that the difference in absorbance was maximal: 423 and 446 nm. In dual-wavelength spectrophotometry, light of two different wavelengths is passed through the same sample simultaneously and the difference in absorbance is measured. Before the measurement, the optical attenuators of the instrument are adjusted to compensate for the difference in incident radiation intensity at the two wavelengths, a reagent blank, prepared according to the procedure, being used for this purpose. As the mole ratio of copper to TMPyP in the complex is 1:1,[2] the following equation can be written:

$$\Delta_{423-446} = [\mathrm{ML}](\epsilon^{\mathrm{ML}}_{423} + \epsilon^{\mathrm{L}}_{446} + \epsilon^{\mathrm{L}}_{423} - \epsilon^{\mathrm{ML}}_{446}) \quad (1)$$

where ϵ stands for the molar absorptivity of the species indicated by superscript: TMPyP (L) and complex (ML). As the complex is extremely stable, [ML] should be equal to the total concentration of copper, C_M. Equation (1) provides the basis of a linear relation between C_M and $\Delta_{423-446}$. From preliminary experiments $\epsilon^{\mathrm{ML}}_{423}$, $\epsilon^{\mathrm{ML}}_{446}$, $\epsilon^{\mathrm{L}}_{423}$ and $\epsilon^{\mathrm{L}}_{446}$ were estimated to be 2.3×10^5, 6.3×10^4, 7.5×10^4 and 2.95×10^5 $1.\mathrm{mole}^{-1}.\mathrm{cm}^{-1}$, respectively. With these numerical values, the sum of the constant factors in equation (1) becomes 38.7×10^4 $1.\mathrm{mole}^{-1}.\mathrm{cm}^{-1}$, which is very close to the value obtained from the slope of the calibration curve, 36.3×10^4 $1.\mathrm{mole}^{-1}.\mathrm{cm}^{-1}$. This is 1.7 times the apparent molar absorptivity of the original TMPyP method,[2] because the decrease in the absorbance of TMPyP, $[\mathrm{ML}]\epsilon^{\mathrm{L}}_{446}$, is added to the absorbance of the complex, $[\mathrm{ML}]\epsilon^{\mathrm{ML}}_{423}$. Beer's law is obeyed over the range 0.1–1.26 μg of copper. On the basis of the calibration curve the 95% confidence limit for the median (absorbance 0.1500) of nine samples was found to be 0.632 ± 0.026 μg.

Table 1 shows the effect of other elements on the determination of 6.30 μg of copper. These tolerance limits are higher than the amounts of other elements present in 25-ml portions of sea-water, and hence this method would be selective enough for the determination of copper in sea-water.

To ascertain the recovery, we spiked a coastal sea-water sample (20 ml) with 0.600 μg of copper and determined copper by the recommended procedure. The recovery (0.620 μg) was reproducible (coefficient of variation 1.6%). The value was slightly higher than the spike because the sea-water used for the experiment contained approximately 1 μg of copper per litre, as shown below.

The concentration of copper in the sea-water sample is too low to be determined directly (absorbance 0.147 for 0.600 μg of copper). It is thus necessary to preconcentrate the copper. L-Cysteine was used instead of nitric acid as eluent, to avoid the need to evaporate effluents containing nitric acid. An additional advantage is that copper is completely eluted with less than 20 ml of $1.65 \times 10^{-4}M$ L-cysteine, whereas 30 ml of $2M$ nitric acid are required.[10] To prevent lowering of the pH when sea-water samples are added to the column, the Chelex-100 resin is used in the sodium form.

Figure 2 shows the influence of pH of the eluent on the recovery of copper (2.0 μg). The copper sorbed on the resin is quantitatively recovered with eluent at pH 8.3–10. Hence a pH of 9.0 was chosen for the L-cysteine solution. It was separately confirmed that

Table 1. Effect of foreign ions on the determination of 0.630 μg of copper(II)

Foreign ion	Added *mg*	$\Delta_{423-446}$
None		0.1512
Na^+	220	0.1539
K^+	160	0.1515
Ca^{2+}	10	0.1518
Mg^{2+}	10	0.1520
Zn^{2+}	0.1	0.1527
Co^{2+}	0.1	0.1568
Fe^{3+}	0.05	0.1539
Cd^{2+}	0.08	0.1514
Mn^{2+}	0.10	0.1518
Pb^{2+}	0.05	0.1524

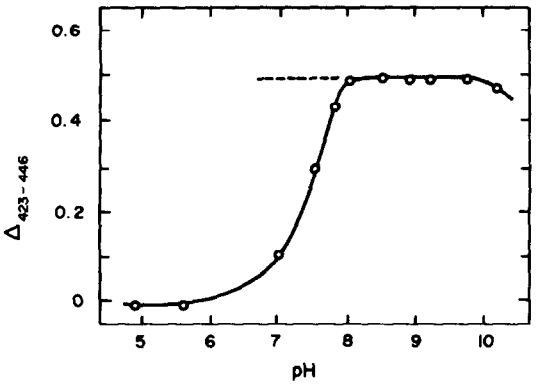


Fig. 2. Effect of pH on the elution of 2.0 μg of copper with 20 ml of $1.65 \times 10^{-4}M$ L-cysteine. The dotted line is the absorbance for the copper determined directly without preconcentration.

18-ml portions of the L-cysteine solution more than suffice for complete recovery.

The modified Chelex-100 separation and analytical procedure were applied to the determination of copper in a coastal sea-water sample. To check the recovery, 200-ml portions of the sample were analysed with and without a 0.60-μg spike of copper. The averages of 5 determinations and the coefficients of variation were 0.957 ng/ml and 1.8% for the unspiked samples and 0.955 ng/ml and 3.2% for the spiked samples. The recovery is satisfactory and 200-ml portions of sample are sufficient for determining copper in the sub-ng/ml range.

Acknowledgements—The authors wish to thank Professor T. Yotsuyanagi of Tohoku University and Dr. S. Igarashi of Hokkaido University for kindly supplying samples of water-soluble porphyrins. They would also like to thank Professor M. Murozumi of their own laboratory and Dr. J. W. McLaren of the National Research Council of Canada for criticizing the manuscript.

REFERENCES

1. J. Itoh, T. Yotsuyanagi and K. Aomura, *Anal. Chim. Acta*, 1975, **74**, 53.
2. T. Yotsuyanagi and J. Itoh, *Kagaku No Ryoiki*, 1977, **31**, 56.
3. H. Ishii and H. Koh, *Nippon Kagaku Kaishi*, 1978, 390.
4. H. Ishii, H. Koh and Y. Okuda, *ibid.*, 1978, 686.
5. R. F. Pasternack, P. R. Huber, P. Boyd, G. Engasser, L. Francesconi, E. Gibbs, D. Fasella, G. C. Venturo and L. D. Hinds, *J. Am. Chem. Soc.*, 1972, **94**, 4511.
6. S. Shibata, M. Furukawa and K. Goto, *Anal. Chim. Acta*, 1969, **46**, 271.
7. S. Shibata, M. Furukawa and T. Honkawa, *ibid.*, 1975, **78**, 487.
8. H. Watanabe and H. Ohmori, *Talanta*, 1979, **26**, 959.
9. M. Y. Vanderstappen and R. E. V. Green, *ibid.*, 1978, **25**, 653.
10. J. P. Riley and D. Taylor, *Anal. Chim. Acta*, 1968, **40**, 479.

Talanta, Vol. 28, pp. 777 to 779, 1981
Printed in Great Britain. All rights reserved

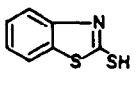
0039-9140/81/100777-03$02.00/0
Copyright © 1981 Pergamon Press Ltd

DETERMINATION OF 2-MERCAPTOBENZOTHIAZOLE, TOLYLTRIAZOLE AND BENZOTRIAZOLE IN COOLANT FORMULATIONS BY LIQUID CHROMATOGRAPHY

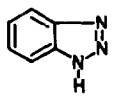
THOMAS M. SCHMITT* and EAD S. MUZHER
Central Research and Development, BASF Wyandotte Corporation, Wyandotte, MI 48192

Summary—An analytical method based on high-performance liquid chromatography is suitable for the determination of corrosion inhibitors in coolant solutions based on ethylene glycol. An isocratic system of methanol/aqueous sodium acetate buffer is used with a Microbondapak C18 column. Recovery is 99+%, with a sensitivity of 0.05% w/w. No sample pretreatment is necessary. Analysis time is 15 min.

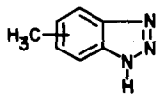
Aqueous heat-exchange fluids universally contain corrosion inhibitors to control the tendency of oxygen/water mixtures to dissolve metals in contact with them. One of the most widely used compounds to protect copper and copper alloys is 2-mercaptobenzothiazole (MBT). This compound, generally used as its water-soluble sodium salt ("NaCap"), is a component of ethylene glycol–water mixtures used as automobile antifreezes, solar collector fluids, and even in the Apollo lunar lander.[1] Tolyltriazole (TTA) and benzotriazole (BTA) are also widely used as inhibitors of the corrosion of copper and certain other metals. The structures are shown below.



2-Mercaptobenzothiazole
(2(3H)-Benzothiazolethione)
CAS 149-30-4



Benzotriazole
(1H-Benzotriazole)
CAS 95-14-7



Tolyltriazole
(Methyl-1H-benzotriazole)
CAS 29385-43-1

MBT first found wide use as a rubber vulcanization accelerator in the 1930s. This is still a very large market. It has also found wide use as a flotation collector in the refining of minerals. Publications have appeared showing its utility as a reagent for determination of nickel and palladium.[2,3] Methods for its determination include ultraviolet spectrophotometry,[4,5] anodic chronopotentiometry,[6] amperometric titration with silver nitrate,[7] titration with copper,[8] and paper chromatography.[9] Unpublished work in our own laboratories shows that MBT can be determined gravimetrically as the silver salt.

The literature is silent on methods for determination of BTA and TTA. In general, these compounds react similarly to MBT. Until development of the liquid chromatographic method, we analysed antifreeze solutions in our laboratory by quantitative precipitation of the silver salt, followed by infrared spectroscopic identification of which compound was present, MBT, TTA or BTA.

Until now, there was no simple specific method for determining any of these three compounds in a coolant of unknown origin. The commercial availability of reverse-phase liquid chromatography columns, which make the separation of many polar compounds an easy matter, led us to investigate a new method for determining coolant corrosion inhibitors. Our investigation centred on the ethylene glycol/water mixtures used as automobile engine coolants.

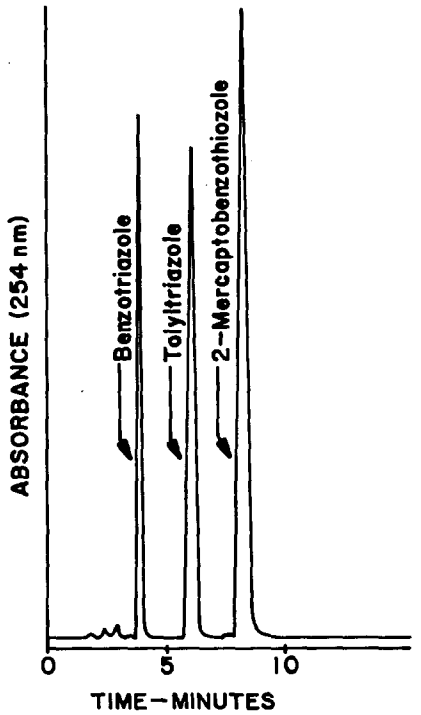


Fig. 1. Representative chromatogram. A commercial automotive antifreeze to which the corrosion inhibitors were added to give 0.2% concentrations.

* To whom correspondence and requests for reprints should be sent.

EXPERIMENTAL

Apparatus

The liquid chromatographic system consisted of a Waters Associates model 6000A pump, U6K injector, Microbondapak C18 column, 300 × 3.9 mm, and model 440 UV detector with 254-nm filter, a Honeywell model AFB strip-chart recorder, and a Hewlett-Packard model 3554A data-processing system. An additional pump and Waters Associates model 660 solvent programmer were connected for ease in periodically rinsing the column with methanol.

Reagents

The methanol (J. T. Baker) and glacial acetic acid (VWR Scientific) were ACS reagent grade; the sodium acetate trihydrate (Fisher) was HPLC grade. Water was from the Wyandotte public water supply, purified by reverse osmosis, ion-exchange, carbon treatment, and filtration, all in a Millipore Milli-Q system. An aqueous 0.08*M* buffer solution was prepared by dissolving 11 g of sodium acetate trihydrate in 1 litre of water, then adding glacial acetic acid dropwise until a pH value of 6.0 was reached. Sodium mercaptobenzothiazole (R. T. Vanderbilt Co., Norwalk, CT 06855), and the sodium salts of benzotriazole and tolyltriazole, (Sherwin-Williams Chemicals, Cleveland, OH 44101), were technical grade 50% aqueous solutions, and were used without further purification.

Chromatographic conditions

The mobile phase was a 40:60 v/v mixture of methanol and aqueous buffer, used at a flow-rate of 1.5 ml/min under isocratic conditions. The column was washed at approximately 4-hr intervals with pure methanol. A 10-min linear gradient programme was used when changing the solvents, to avoid shock to the column owing to differences in temperature and viscosity. Solvents were filtered (0.45 μm filters) and degassed before use. The recorder chart speed was 0.5 cm/min. A representative chromatogram is shown in Fig. 1.

Procedure

Calibration solutions are prepared by weighing out about 10 mg of the sodium salts of MBT, BTA and TTA, dissolving in the mobile phase used and diluting to 100 ml. For samples, a 5-g portion is weighed and diluted to 100 ml with the mobile phase. All standard and sample solutions are filtered (0.45 μm membrane filters) before injection. The volume injected is 5 μl, and the detector sensitivity is set at 0.05 absorbance units full-scale deflection. The concentrations of standards and samples are adjusted, as necessary, so that the peak areas used differ by less than a factor of 2.

RESULTS

Recovery studies were performed by adding calibration solutions to a commercially available ethylene glycol antifreeze formulation. A precision study was made by preparing eight individual dilutions of a

Table 1. Recovery study

	2-Mercaptobenzothiazole			Tolyltriazole			Benzotriazole		
Experiment	Added, *mg*	Recovered, *mg*	Recovery, %	Added, *mg*	Recovered, *mg*	Recovery, %	Added, *mg*	Recovered, *mg*	Recovery %
1	43.24	43.65	100.9	28.09	28.09	100.0	15.9	15.9	100.0
2	32.43	32.42	100.0	21.07	21.09	100.1	11.9	11.9	100.0
3	25.94	25.77	99.3	16.86	16.97	100.7	9.54	9.61	100.7
4	21.62	21.31	98.6	14.05	13.97	99.4	7.95	7.92	99.6
5	10.82	10.05	92.9	7.02	6.99	99.6	3.98	3.98	100.0
6	6.49	5.50	84.7	4.21	4.21	100.0	2.38	2.39	100.4

Table 2. Precision study

Experiment	2-MBT found, *mg*	TTA found, *mg*	BTA found, *mg*
1	27.43	12.92	4.36
	27.36	12.88	4.33
2	27.47	12.97	4.36
	27.51	12.93	4.35
3	27.28	12.84	4.32
	27.37	12.85	4.33
4	27.57	12.91	4.33
	27.63	12.99	4.37
5	27.72	12.97	4.41
	27.74	13.03	4.41
6	27.71	12.96	4.40
	27.59	12.97	4.41
7	27.72	13.00	4.39
	27.96	13.02	4.42
8	27.84	13.03	4.37
	27.89	13.12	4.44
Mean, *mg*	27.61	12.96	4.38
Std. devn., absolute, *mg*	0.20	0.07	0.04
Rel. std. devn., %	0.7	0.6	0.9

single spiked antifreeze solution, and analysing each by duplicate injections. The results of the recovery study are shown in Table 1. Recovery of TTA and BTA was quantitative over the region studied (down to 4.2 mg/5 ml sample = 0.08% and 2.4 mg/5 ml = 0.5%, respectively). MBT recovery dropped off below the 20 mg/5 ml (0.4%) level. This is because the MBT is the last component to be eluted, resulting in a broader peak which is not as accurately integrated. The technique can actually be applied to much lower concentrations than we have shown here, since we found that antifreeze samples can be injected neat, without deterioration of peak shape or resolution being caused by the ethylene glycol. Accurate results can thus be obtained at least down to the 0.004%, 0.002%, and 0.02% levels for TTA, BTA and MBT, respectively.

The results of the precision study are shown in Table 2. They show a relative standard deviation of less than 1% for all three compounds. This is excellent for a chromatographic method, and far superior to the results obtained by the gravimetric procedure which we previously used.

CONCLUSION

A rapid method has been developed for determination of the most common aromatic corrosion inhibitors in automotive coolants. The liquid chromatographic technique is superior to the previous methods in that there is no mutual interference of the three compounds. Sample preparation consists of, at most, a single dilution. We expect the new procedure to find wide application in coolant analysis.

REFERENCES

1. H. D. Bennett, *Anal. Chem.*, 1977, **49**, 322A.
2. E. G. Walliczek, *Talanta*, 1964, **11**, 573.
3. A. K. Majumdar and M. M. Chakrabartty, *Anal. Chim. Acta*, 1959, **20**, 379.
4. M. H. Jones and J. T. Woodcoock, *Can. Met. Quart.*, 1973, **12**, 497.
5. *Idem*, *Anal. Chem.*, 1975, **47**, 11.
6. J. D. Vorhies and J. S. Parsons, *ibid.*, 1959, **31**, 516.
7. D. K. Basu and P. S. Bhattacharyya, *ibid.*, 1976, **48**, 1601.
8. M. Parushev, *Khim. Ind. Sofia*, 1963, **35**, 49; *Anal. Abstr.*, 1965, **12**, 242.
9. M. Stepien and R. Gaczynski, *Chem. Anal. Warsaw*, 1961, **6**, 1045; *Chem. Abstr.*, 1962, **57**, 998i.

Talanta, Vol. 28, pp. 781 to 783, 1981
Printed in Great Britain. All rights reserved

0039-9140/81/100781-03$02.00/0
Copyright © 1981 Pergamon Press Ltd 1981

ANALYTICAL DATA

CALIBRATION OF PLASTIC LABORATORY WARE

MARY R. MASSON
Department of Chemistry, University of Aberdeen, Meston Walk, Old Aberdeen, Scotland

(*Received* 11 *February* 1981. *Accepted* 9 *March* 1981)

Summary—The importance of the calibration of standard laboratory ware is pointed out. Tables for use in calibration of polypropylene and polymethylpentene vessels are presented.

A discrepancy in the concentration of a solution prepared in a 500-ml plastic (polypropylene) standard flask led to the discovery that there was an error of −1.7 ml in the volume of the flask. The results of a subsequent examination of a further thirty plastic flasks—which showed over half to have volume errors outwith the tolerances for Class B glassware—confirm the need for a reminder of the importance of calibration of standard laboratory ware, even when only moderate accuracy is required.

Comparison of values for the coefficient of cubical thermal expansion, γ, derived from literature values for the coefficient of linear expansion for polypropylene[1] and polymethylpentene[2] ($1.8–3.0 \times 10^{-4}$ and 3.5×10^{-4} deg^{-1}) with those for borosilicate and soda glass (1.0×10^{-5} and 2.7×10^{-5} deg^{-1}) made it evident that the Tables for Use in Calibration of Volumetric Glassware[3] would not be applicable. A short table of correction factors for plastics with $\gamma = 2$, 3, 4, 5 and 6×10^{-4} deg^{-1} is given in the British Standard for graduated plastic measuring cylinders,[4] but no indication is given of likely values of γ for particular materials, and extensive interpolation would be required in use.

The glasssware tables[3] are calculated from the equation

$$C = V_{20} - W = V_{20}\left[1 - \frac{\{1 + \gamma(t - 20)\}(\rho_t - \sigma)\Delta}{\Delta - \sigma}\right] \quad (1)$$

where C is the correction to be added to the apparent weight in air of the water contained (or delivered), W, to obtain the volume of the vessel at 20°, V_{20}; σ is the density of air at 20° and 760 mmHg, 0.0011994 g/cm^3; Δ is the density of the weights, 8.0 g/cm^3 (for stainless steel), and ρ_t is the density of water at the temperature t (in °C). Density values for water were calculated from the equation given by Tilton and Taylor,[5] then divided by 1.000028 to convert from g/ml (pre-SI definition) to g/cm^3.

Equation (1) was evaluated for values of γ from 2.0×10^{-4} to 5.5×10^{-4} deg^{-1} in steps of 0.1×10^{-4}, for a nominal volume of 100 ml, and for temperatures from 5 to 40°, to give a calibration table for each value of γ.

A series of calibration weighings of 100-ml polypropylene and polymethylpentene standard flasks was then made, by the procedure recommended for glass flasks,[6] in which the water used to fill the flasks ranged in temperature from 5 to 40°. The volume at 20° was then calculated from each of several calibration tables for γ-values in the region of the literature values. An additional correction of 0.0004 ml/deg was made to compensate for the difference between the temperature of the water and the surrounding air.[7]

For each set of values (over the whole temperature range) obtained from a particular table, the standard deviation of the calculated volumes was evaluated in order to find which table should be chosen. For polypropylene, the optimum table was the one for $\gamma = 3..0 \times 10^{-4}$ deg^{-1}, and for polymethylpentene, the one for $\gamma = 4.3 \times 10^{-4}$ deg^{-1}. In both cases, the standard deviation obtained by use of the best table was approximately the same as the standard deviation for a series of calibrations made at 20.0°, at which temperature the size of the correction factor is independent of γ.

The optimum tables are presented here, in the hope that they may be useful to British readers. Others should use them with caution, since different brands of plastic ware may have differing thermal-expansion properties. If there is any doubt, it would be a useful precaution to work only at 20°.

Both tables refer to vessels of nominal volume 100 ml: corrections for other volumes can be calculated by simple proportion.

It is interesting to note that, although the actual volumes of plastic vessels change with temperature by a much greater amount than do the volumes of glass ones, the weights of water contained vary by rather less. This is illustrated in Table 3.

Table 1. Calibration table for polypropylene [nominal capacity 100 ml; coefficient of thermal expansion 3.0×10^{-4} deg^{-1}; add to weight (g) of distilled water at the temperature of measurement, to obtain volume (ml) at 20°]

Temp.	0.0	0.1	0.2	0.3	0.4	0.5	0.6	0.7	0.8	0.9
5	0.558	0.555	0.553	0.550	0.547	0.544	0.541	0.539	0.536	0.533
6	0.531	0.528	0.525	0.523	0.520	0.517	0.515	0.512	0.510	0.507
7	0.504	0.502	0.499	0.497	0.494	0.492	0.489	0.487	0.485	0.482
8	0.480	0.477	0.475	0.473	0.470	0.468	0.466	0.463	0.461	0.459
9	0.456	0.454	0.452	0.450	0.448	0.445	0.443	0.441	0.439	0.437
10	0.435	0.433	0.430	0.428	0.426	0.424	0.422	0.420	0.418	0.416
11	0.414	0.412	0.410	0.408	0.406	0.404	0.402	0.400	0.399	0.397
12	0.395	0.393	0.391	0.389	0.388	0.386	0.384	0.382	0.380	0.379
13	0.377	0.375	0.373	0.372	0.370	0.368	0.367	0.365	0.363	0.362
14	0.360	0.359	0.357	0.355	0.354	0.352	0.351	0.349	0.348	0.346
15	0.345	0.343	0.342	0.340	0.339	0.337	0.336	0.335	0.333	0.332
16	0.330	0.329	0.328	0.326	0.325	0.324	0.322	0.321	0.320	0.318
17	0.317	0.316	0.315	0.314	0.312	0.311	0.310	0.309	0.308	0.306
18	0.305	0.304	0.303	0.302	0.301	0.300	0.299	0.297	0.296	0.295
19	0.294	0.293	0.292	0.291	0.290	0.289	0.288	0.287	0.286	0.285
20	0.284	0.284	0.283	0.282	0.281	0.280	0.279	0.278	0.277	0.277
21	0.276	0.275	0.274	0.273	0.273	0.272	0.271	0.270	0.269	0.269
22	0.268	0.267	0.267	0.266	0.265	0.265	0.264	0.263	0.263	0.262
23	0.261	0.261	0.260	0.260	0.259	0.258	0.258	0.257	0.257	0.256
24	0.256	0.255	0.255	0.254	0.254	0.253	0.253	0.252	0.252	0.251
25	0.251	0.251	0.250	0.250	0.249	0.249	0.249	0.248	0.248	0.248
26	0.247	0.247	0.247	0.246	0.246	0.246	0.245	0.245	0.245	0.245
27	0.244	0.244	0.244	0.244	0.244	0.243	0.243	0.243	0.243	0.243
28	0.243	0.242	0.242	0.242	0.242	0.242	0.242	0.242	0.242	0.242
29	0.242	0.242	0.242	0.242	0.242	0.242	0.242	0.242	0.242	0.242
30	0.242	0.242	0.242	0.242	0.242	0.242	0.242	0.242	0.242	0.242
31	0.243	0.243	0.243	0.243	0.243	0.243	0.244	0.244	0.244	0.244
32	0.244	0.245	0.245	0.245	0.245	0.246	0.246	0.246	0.246	0.247
33	0.247	0.247	0.248	0.248	0.248	0.249	0.249	0.249	0.250	0.250
34	0.250	0.251	0.251	0.252	0.252	0.252	0.253	0.253	0.254	0.254
35	0.255	0.255	0.256	0.256	0.257	0.257	0.258	0.258	0.259	0.259
36	0.260	0.260	0.261	0.262	0.262	0.263	0.263	0.264	0.265	0.265
37	0.266	0.266	0.267	0.268	0.268	0.269	0.270	0.270	0.271	0.272
38	0.273	0.273	0.274	0.275	0.276	0.276	0.277	0.278	0.279	0.279
39	0.280	0.281	0.282	0.283	0.283	0.284	0.285	0.286	0.287	0.288
40	0.288	0.289	0.290	0.291	0.292	0.293	0.294	0.295	0.296	0.297

Table 2. Calibration table for polymethylpentene [nominal capacity 100 ml; coefficient of thermal expansion 4.3×10^{-4} deg^{-1}; add to weight (g) of distilled water at the temperature of measurement, to obtain volume (ml) at 20°]

Temp.	0.0	0.1	0.2	0.3	0.4	0.5	0.6	0.7	0.8	0.9
5	0.753	0.749	0.745	0.741	0.737	0.732	0.728	0.724	0.720	0.716
6	0.712	0.708	0.704	0.700	0.697	0.693	0.689	0.685	0.681	0.677
7	0.673	0.669	0.666	0.662	0.658	0.654	0.650	0.647	0.643	0.639
8	0.636	0.632	0.628	0.625	0.621	0.617	0.614	0.610	0.606	0.603
9	0.599	0.596	0.592	0.589	0.585	0.582	0.578	0.575	0.571	0.568
10	0.564	0.561	0.558	0.554	0.551	0.548	0.544	0.541	0.538	0.534
11	0.531	0.528	0.524	0.521	0.518	0.515	0.511	0.508	0.505	0.502
12	0.499	0.496	0.492	0.489	0.486	0.483	0.480	0.477	0.474	0.471
13	0.468	0.465	0.462	0.459	0.456	0.453	0.450	0.447	0.444	0.441
14	0.438	0.435	0.432	0.429	0.427	0.424	0.421	0.418	0.415	0.412
15	0.410	0.407	0.404	0.401	0.399	0.396	0.393	0.390	0.388	0.385
16	0.382	0.380	0.377	0.374	0.372	0.369	0.366	0.364	0.361	0.359
17	0.356	0.354	0.351	0.349	0.346	0.344	0.341	0.339	0.336	0.334
18	0.331	0.329	0.326	0.324	0.321	0.319	0.317	0.314	0.312	0.310
19	0.307	0.305	0.303	0.300	0.298	0.296	0.293	0.291	0.289	0.287
20	0.284	0.282	0.280	0.278	0.276	0.273	0.271	0.269	0.267	0.265
21	0.263	0.261	0.259	0.256	0.254	0.252	0.250	0.248	0.246	0.244
22	0.242	0.240	0.238	0.236	0.234	0.232	0.230	0.228	0.226	0.224
23	0.222	0.221	0.219	0.217	0.215	0.213	0.211	0.209	0.207	0.206
24	0.204	0.202	0.200	0.198	0.197	0.195	0.193	0.191	0.190	0.188
25	0.186	0.185	0.183	0.181	0.179	0.178	0.176	0.174	0.173	0.171
26	0.170	0.168	0.166	0.165	0.163	0.162	0.160	0.158	0.157	0.155
27	0.154	0.152	0.151	0.149	0.148	0.146	0.145	0.143	0.142	0.141
28	0.139	0.138	0.136	0.135	0.133	0.132	0.131	0.129	0.128	0.127
29	0.125	0.124	0.123	0.121	0.120	0.119	0.117	0.116	0.115	0.114
30	0.112	0.111	0.110	0.109	0.107	0.106	0.105	0.104	0.103	0.102
31	0.100	0.099	0.098	0.097	0.096	0.095	0.094	0.092	0.091	0.090
32	0.089	0.088	0.087	0.086	0.085	0.084	0.083	0.082	0.081	0.080
33	0.079	0.078	0.077	0.076	0.075	0.074	0.073	0.072	0.071	0.071
34	0.070	0.069	0.068	0.067	0.066	0.065	0.064	0.064	0.063	0.062
35	0.061	0.060	0.059	0.059	0.058	0.057	0.056	0.056	0.055	0.054
36	0.053	0.053	0.052	0.051	0.051	0.050	0.049	0.048	0.048	0.047
37	0.047	0.046	0.045	0.045	0.044	0.043	0.043	0.042	0.042	0.041
38	0.040	0.040	0.039	0.039	0.038	0.038	0.037	0.037	0.036	0.036
39	0.035	0.035	0.034	0.034	0.033	0.033	0.032	0.032	0.032	0.031
40	0.031	0.030	0.030	0.030	0.029	0.029	0.029	0.028	0.028	0.027

Table 3. Effect of temperature on 100-ml vessels

Temperature °C	Borosilicate glass $\gamma = 1.0 \times 10^{-5}$		Soda glass $\gamma = 2.7 \times 10^{-5}$		Polypropylene $\gamma = 3.0 \times 10^{-4}$		Polymethylpentene $\gamma = 4.33 \times 10^{-4}$	
	ΔV	W_r	ΔV	W_r	ΔV	W_r	ΔV	W_r
5	−0.015	1.0016	−0.041	1.0014	−0.45	0.9973	−0.645	0.9953
10	−0.010	1.0014	−0.027	1.0012	−0.30	0.9985	−0.43	0.9972
15	−0.005	1.0008	−0.014	1.0008	−0.15	0.9994	−0.215	0.9987
20	0.0	1.0	0.0	1.0	0.0	1.0	0.0	1.0
25	0.005	0.9989	0.014	0.9990	0.15	1.0003	0.215	1.0001
30	0.010	0.9975	0.027	0.9977	0.30	1.0004	0.43	1.0017
35	0.015	0.9960	0.041	0.9962	0.45	1.0003	0.645	1.0023
40	0.020	0.9942	0.054	0.9945	0.6	1.0000	0.86	1.0026

ΔV = difference in volume from 100.00 ml.
W_r = (weight of water contained)/(weight of water contained at 20°).

REFERENCES

1. G. W. C. Kaye and T. H. Laby, *Tables of Physical and Chemical Constants*, 14th Ed., p. 253. Longmans, London, 1973.
2. *Encyclopedia of Polymer Science and Technology*, Vol. 9, Interscience, New York, 1968.
3. B.S. 1797: 1968.
4. B.S. 5404: Part 2: 1977.
5. L. W. Tilton and J. K. Taylor, *J. Res. Natl. Bur. Stds.*, 1937, **18**, 205.
6. B.S. 1792: 1960.
7. I. M. Kolthoff and P. J. Elving, eds., *Treatise on Analytical Chemistry*, Part 1, Vol. 7, p. 4312. Interscience, New York, 1967.

Talanta, Vol. 28, pp. 785 to 787, 1981
Printed in Great Britain.

0039-9140/81/100785-03$02.00/0
Pergamon Press Ltd 1981

ANNOTATION

DETERMINATION OF COPPER IN ARCHAEOLOGICAL AND CORROSION SAMPLES WITH AN ION-SELECTIVE ELECTRODE

ASHA VARMA

Laboratory for Research on the Structure of Matter, University of Pennsylvania, Philadelphia, PA 19104, U.S.A.

(*Received* 17 *November* 1981. *Revised* 15 *January* 1981. *Accepted* 9 *March* 1981)

Summary—The performances of a copper-selective electrode and atomic-absorption spectrophotometry for the determination of copper at trace and major component levels in archaeological samples and also for corrosion studies have been compared and found similar.

The copper-selective electrode is the most successful of the heavy metal electrodes and its use is widespread.[1–6] It has also been used for potentiometric determination of Al^{3+}, Ca^{2+}, Mg^{2+}, Ni^{2+}, Pb^{2+}, Zn^{2+} and iron[7,8] and for other purposes.[9,10] Its theory, use and properties have been extensively described.[11–14] Its wide applicability suggested its use for determination of copper in archaeological samples and in corrosion studies on copper alloys.

In archaeological analysis the technique selected usually depends on the concentration of the element to be determined, and should preferably be non-destructive, rapid and cheap. If a sample has to be removed from an archaeological specimen it should be as small as possible. The ion-selective electrode (ISE) method meets these requirements. The samples studied in this work were bronze and brass pieces of jewellery and decorative items obtained from excavations in Israel, Egypt and Morocco.

In corrosion studies the rate of corrosion in aqueous solutions is usually determined by monitoring the weight loss of test samples. However, this method is not suitable for the determination of very low corrosion rates (less than 0.001 inch/year). Solution analysis is often the best way to determine very low corrosion rates of metals. Therefore, studies have been conducted by applying the ISE method for *in situ* determination of copper during corrosion of copper alloys in corrosive media such as 0.9% sodium chloride (body fluid salinity), 3.0% sodium chloride (seawater) and 5.0% sodium bisulphite (atmospheric pollution) solutions.

EXPERIMENTAL

Reagents

All the solutions were prepared from "Baker Analyzed" chemicals. Dilutions were made with demineralized water and solutions were stored in polyethylene bottles.

Apparatus

A Corning digital pH-meter model 112 was used with a copper ion-selective electrode (Orion, 94-29) and a saturated calomel electrode (SCE). A Princeton Research K60 cell fitted with a K66 cell top was used as the vessel for ISE analysis. A Jarrell Ash 82-810 atomic-absorption spectrophotometer and Jarrell Ash and Perkin–Elmer single-element hollow-cathode lamps were used for atomic-absorption (AA) determination of copper.

Procedure

The samples from the archaeological specimens were obtained by slicing or drilling at different spots. "Tramp" iron was removed with a magnet. The samples were cleaned ultrasonically, washed thoroughly, dried and weighed. Between 10 and 20 mg were required for the analysis. Sample solutions were prepared by one of the following techniques.[15,16]

(*i*) Dissolution in a small amount of nitric acid or *aqua regia*, followed by heating to remove nitrous fumes, then evaporating to near dryness without caking. Most of the samples from brass and pure copper ornaments were dissolved by this method.

(*ii*) Dissolution in hydrochloric–hydrofluoric acid mixture in a Parr pressure bomb at 110°. It takes 1–2 hr for complete dissolution of samples with high silica content, e.g., clay from the pottery.

The product from the dissolution procedure was cooled and dissolved in demineralized water. If the solution was not clear, a small amount of hydrochloric or nitric acid was added to make the final acid concentration of 2–5%. Sample solutions containing hydrofluoric acid were not allowed to come into contact with glass at any time. Blank solutions were prepared in a similar way. Standard solutions were prepared by serial dilutions of a "Spex" standard copper solution. A 5*M* sodium nitrate solution (2 ml per 100 ml of test solution) was added to adjust the ionic strength of the standard and sample solutions before analysis.

The test solution was taken in the cell and deaerated with argon purified by passage through a column containing the supporting electrolyte (0.1*M* nitric acid or 5*M* sodium nitrate) to reduce airborne contamination. Continuous stirring with a Teflon-coated magnetic bar accelerated the process. A sheet of cork was placed over the magnetic stirrer to avoid heating the cell, which was kept at 30

Table 1. Comparative data for archaeological samples containing Cu as major element

Sample	ISE, %	Std. devn., %	AA, %	Std. devn., %
Arad, Israel	99.8	0.2	99.8	0.2
Yaruba, Africa	99.2	0.2	99.3	0.2
Lixus, Morocco	98.9	0.2	98.9	0.2
Arad, Israel	98.7	0.2	98.6	0.2
Tel Mor, Israel	78.7*	0.4	78.7*	0.5
Ban Chiang, Thailand	72.9	0.5	73.0	0.5
Kom, Israel	68.9	0.5	68.9	0.6
Akko, Israel	66.8†	0.6	66.6	0.6

* Sample contains 12% tin.

† Sample contains 10% iron (and added hydrochloric acid).

± 0.1°. Potentials were measured at 2-min intervals until the drift was less than 0.1 mV.

Calibration curves were prepared with 0.1*M* nitric acid solutions for the archaeological samples and in the appropriate electrolyte solutions for corrosion studies. The ISE was calibrated 2 or 3 times a day, especially after use in the electrolyte solutions. Concentrations were obtained by use of the standard curves, potentiometric titration and the standard-addition method. After each observation, the electrode was rinsed thoroughly with demineralized water and wiped with a soft tissue. The cleaning procedure of Blaedel and Dinwiddie[17] was used after every 10–15 observations and particularly after use in corrosive media.

Copper alloys (10:90 to 90:10 ratio in increment of 10 wt %) with silver and gold were submerged in 100–250 ml of 0.9% sodium chloride, 3.0% sodium chloride and 5.0% sodium bisulphite solutions for 200–400 hr. The solutions were then analysed for copper as for archaeological samples.

Table 2. Copper as trace element in archaeological samples

Sample No.	ISE, %	Std. devn., %	AA, %	Std. devn., %
Taanach, Israel	0.030	0.001	0.030	0.001
Masada, Israel	0.012	0.001	0.015	0.001
Masada, Israel	0.040	0.002	0.042	0.003
Godin, Iran	0.004	0.001	0.005	0.001
Taanach, Israel	0.110	0.001	0.110	0.001
Taanach, Israel	0.008	0.001	0.010	0.001
Taanach, Israel	0.007	0.001	0.010	0.001

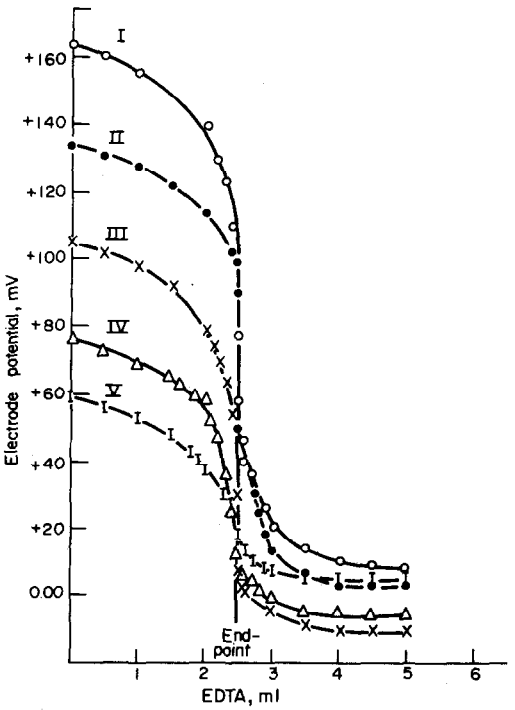


Fig. 2. Potentiometric titration of copper with EDTA, and use of the ISE. I, $10^{-2}M$ EDTA; II, $10^{-3}M$ EDTA; III, $10^{-4}M$ EDTA; IV, $10^{-5}M$ EDTA; V, $10^{-6}M$ EDTA.

Copper was also determined by atomic-absorption for comparison (324.7 nm; spectral band-pass setting number 3, lamp current 7 mA, integration 3 sec, acetylene 12 psig, 3 ft^3/hr, air 45 psig, 10 ft^3/hr).

RESULTS AND DISCUSSION

The archaeological samples containing copper as a major element were analysed successfully by direct potentiometry with the ISE. The high concentration of tin in the sample from Tel Mor, Israel, did not

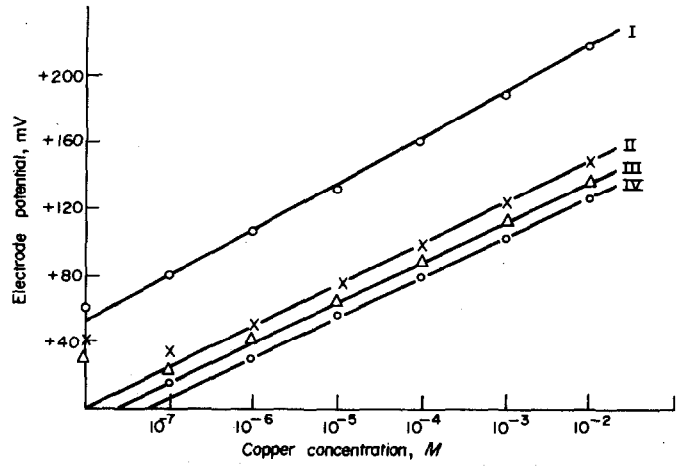


Fig. 1. Calibration graphs for copper by the ISE method: I, ISA medium; II, 0.9% sodium chloride + ISA; III, 3.0% sodium chloride + ISA; IV, 3.0% sodium chloride with no ISA.

Table 3. Comparative evaluation of corrosion study results by ISE and AA methods

Test medium	Copper, μg	
	ISE	AA
0.9% NaCl	0.08	0.07
	0.15	0.15
	1.4	1.4
	2.5	2.4
3.0% NaCl	3.5	3.4
	4.8	4.8
	8.4	8.5
	10.9	10.0
5.0% $NaHSO_3$	12.3	12.3
	15.3	15.3
	19.2	19.2
	26.2	26.1

interfere, but 5–10% of iron did, and iron was therefore removed by the addition of ammonium hydroxide and filtration. The potentiometric and AA results are given in Table 1. The standard addition method was used to determine trace-level copper and the results are reported in Table 2.

In the direct ISE procedure for copper in the corrosion studies, the calibration graphs were linear from $10^{-6}M$ to $10^{-2}M$ copper, the slope and position of the lines being dependent on the background electrolyte. The concavity in the graphs for chloride solutions meant that measurements at levels below about $10^{-6}M$ could be ambiguous (Fig. 1), so this was taken as the lowest observable concentration.

A still more drastic deviation was observed for the 5.0% sodium bisulphite solutions, linearity extending only down to $10^{-5}M$.

ISE was also used for the potentiometric titration of copper with EDTA[18,19] (Fig. 2) and gave more accurate results than the direct method, but was too time-consuming to be used. The standard addition method was used in the corrosion studies. The comparative study of the ISE and AA methods is reported in Table 3.

The results indicate that the ISE method is suitable for major or trace level concentrations of copper in archaeological samples. An advantage is that practically none of the sample solution is consumed in the determination.

For corrosion studies the precision and accuracy of the ISE method seem to be equivalent or superior to those of the AA method.

Acknowledgements—The author is grateful to Robert Maddin, University of Pennsylvania, Philadelphia, for providing the archaeological samples. This investigation was supported in part by the National Science Foundation, Materials Research Laboratory Program, Grant No. DMR-7923647.

REFERENCES

1. J. W. Ross, *Ion Selective Electrodes*, NBS Spec. Publ. No. 314, p. 79, 1969.
2. G. Rechnitz and L. Kenny, *Anal. Lett.*, 1970, **3**, 509.
3. E. H. Hansen, C. G. Lamm and J. Růžička, *Anal. Chim. Acta*, 1972, **59**, 403.
4. G. Johansson and K. Edström, *Talanta*, 1972, **19**, 1623.
5. J. Pick, K. Tóth and E. Pungor, *Anal. Chim. Acta*, 1973, **65**, 240.
6. F. K. Arey, J. W. Chamblee and E. Heckel, *Intern J. Environ. Anal. Chem.*, 1980, **7**, 285.
7. T. M. Florence, *Proc. Royal Austr. Chem. Inst.*, 1970, 261.
8. B. L. Lenz and J. R. Mold, *Tappi*, 1971, **54**, 2051.
9. H. Wada and O. Fernando, *Anal. Chem.*, 1971, **43**, 751.
10. M. Taddia, Z. *Anal. Chem.*, 1979, **296**, 149.
11. P. L. Bailey, *Analysis with Ion Selective Electrodes*, Heydon, London, 1976.
12. P. R. Burton, *Ion-Sel. Electrode Methodol.*, 1979, **1**, 21.
13. G. H. Fricke, *Anal. Chem.*, 1980, **52**, 259R.
14. N. Matsuda, G. Nakagawa, S. Ikeda and K. Ito, *Denki Kagaku Oyobi, Kogyo Butsuri Kogaku*, 1980, **48**, 199.
15. R. Bock, *A Handbook of Decomposition Methods in Analytical Chemistry*, International Textbook Co., London, 1979.
16. P. J. Elving and J. D. Winefordner, *Aracheological Chemistry*, Wiley, New York, 1980.
17. W. J. Blaedel and D. E. Dinwiddie, *Anal. Chem.*, 1975, **47**, 1070.
18. C. N. Reilley and R. W. Schmid, *Anal. Chim.*, 1947, **30**, 947.
19. R. W. Schmid and C. N. Reilley, *J. Am. Chem. Soc.*, 1956, **78**, 5516.

Talanta, Vol. 28, pp. 789 to 797, 1981
Printed in Great Britain. All rights reserved

0039-9140/81/110789-09$02.00/0
Copyright © 1981 Pergamon Press Ltd

FLOW-INJECTION ANALYSIS: A REVIEW OF ITS EARLY HISTORY

KENT K. STEWART

Nutrient Composition Laboratory, Beltsville Human Nutrition Research Center, Human Nutrition, Science and Education Administration, United States Department of Agriculture, Beltsville, Maryland 20705, U.S.A.

(*Received* 22 *April* 1981. *Accepted* 6 *May* 1981)

Summary—A review is given of the development of flow-injection analysis, which seeks to establish the various lines of research which led to the present form of the technique.

Flow-injection analysis may be defined as an automated or semi-automated analytical process consisting of the insertion of sequential discrete sample solutions into an unsegmented continuously flowing liquid stream with subsequent detection of the analyte. It is a relatively new analytical process which shows considerable potential for high-speed precise analysis of discrete samples. Sampling rates of 100 samples per hour with coefficients of variation of less than 1% are usually readily obtained. A number of recent reviews have been written describing the process.[1–5]

In a generalized flow-injection system, a sample is inserted into an unsegmented continuous flowing stream of liquid and the sample then moves with the stream through a detector and to waste. Sometimes the samples are inserted directly into the detector flow-cell. The detector response is registered on a strip-chart recorder. The sample may or may not be mixed with additional reagents, and often there are converging streams in the system. Systems have been described which have relatively low dilution of the original sample; conversely there are flow-injection systems which have considerable dilution of the original sample. Many different detectors have been used. The introduction of each sample may be done manually, or automatically. The term FIA has usually been used to describe the manual injection systems; the term AMFIA has usually been used to describe the automated injection systems.

When a new technique is introduced to the analytical chemistry community, it is usually the case that the process is the sum of many individual concepts developed by different investigators. This has been the case with flow-injection analysis. It is useful to try to document the origins of many of the individual concepts, both to establish the correct historical record and to demonstrate the process by which this new technique was developed. In this review I will present my views on the early history of flow-injection analysis. No attempt has been made to trace the history since 1977, since I believe that the essential critical concepts had been developed by that time.

The seeds for development of flow-injection analysis were present by the end of 1959. The concept of a sample being injected into a continuously flowing steam with continuous recording downstream is inherent in the basic concepts of gas chromatography as developed by James and Martin in 1952.[6] The concept of injecting the sample into the stream with a hypodermic needle was already well established by 1959.[7] The development in 1957 by Skeggs[8] of an automated technique for the analysis of discrete samples by use of segmented continuously flowing streams was a key development in the early history of flow-injection analysis. With this system, Skeggs laid the base for future automation of continuously flowing streams by development of automatic sample measuring, reagent measurement, timing of the reaction, system wash-out, sample segmentation, and sample read-out. A schematic diagram of his system is shown in Fig. 1. The samples were aspirated from their cups by a peristaltic pump into the tubing of the system. The sample volume was determined by the diameter of the pump tubing and the speed of the pump. The amount of sample in the cup was not critical since good practice said that the probe was removed before the level of the sample went below the probe tip. At the end of the sampling period, the probe was moved to a wash vessel for washing to prevent cross-contamination of the samples. The reagents and air-bubbles were continuously fed into the system by peristaltic pumping, the flows again being determined by the diameter of the pump tubings and the speed of the pump: the proportion of sample to reagent was fixed by the initial concentrations of the analyte and reagent and by the ratios of their two flow-rates.

Air-bubbles were used to segment the reaction stream so as to prevent excessive dispersion of the sample by the dispersive forces inherent in the laminar flow of this system. The air-bubbles prevented excessive dilution of the sample and minimized the overlap between sample boluses. The reaction time was determined by the length and bore of the

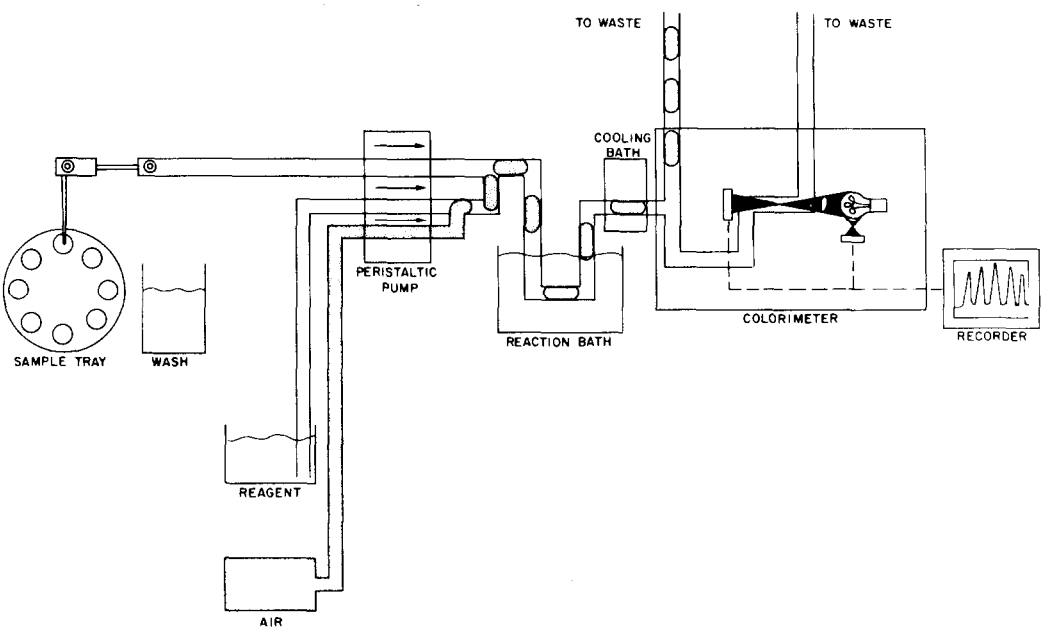


Fig. 1. Schematic diagram of a continuous-flow analyser of the Skeggs type.

reaction tubing and by the flow-rate of the solution. Just before the sample reached the detector, the air-bubbles were removed from the stream and the resulting non-segmented stream passed through a flow-cell in the colorimeter. The response of the detector was recorded and the peak height (in absorbance units) was measured to determine the concentration of the analyte. The system worked well and good precision could be obtained with many analytical systems at sampling rates of 30–50 samples/hour. The development of this system was a monumental advance in the automation of analysis of discrete samples.

In 1958 Spackman, Stein and Moore described the first semiautomated amino-acid analyser.[9] This apparatus, which was the prototype of the modern high-performance liquid chromatographic systems, used a precision positive-displacement pump to move the eluting buffer through the ion-exchange column. As the effluent stream came off the ion-exchange column, it was mixed with ninhydrin reagent (also pumped with a positive-displacement pump) and the reagent and eluent mixture flowed through small-bore tubing (95 ft of 0.7 mm bore Teflon tubing) which was immersed in a boiling water-bath. After emerging from the reaction bath the solution entered capillary tubing which was attached to the bottom of the flow-cell in the colorimeter, and the solution flowed up through the flow-cell and finally to a constant-head waste tube. The output of the colorimeter was automatically recorded on a strip-chart recorder.

The concentrations of the amino-acids were determined by measuring the area under each amino-acid peak on the recorder chart. This was the first case of the use of unsegmented continuously flowing streams for the analysis of discrete samples (*i.e.*, the specific amino-acids as they were eluted from the column). Later, Hamilton[10] used very fine capillary tubing (AWG 32) in his amino-acid analyser (see Table 1 for a conversion table between AWG and mm). The use of small-bore tubing, area measurement and positive-displacement pumps in flow-injection analysis can be traced back to these innovations.

In 1970 Nagy, Feher and Pungor[11] reported on the use of graphite electrodes for the voltammetric measurement of samples injected into continuously flowing streams. This is earliest report I have found of what today would be called flow-injection analysis. These workers injected their samples into an unsegmented continuously flowing stream with a hypoder-

Table 1. Conversion table for tube bore. The internal diameters of the tubing used in flow-injection analysis have been reported in mm, inches, and American Wire Gauges (AWG). It is hoped that this table will aid the reader in coping with these different units

AWG	Internal diameter Inches	mm
18	0.040	1.02
20	0.032	0.81
22	0.025	0.64
24	0.020	0.51
26	0.016	0.40
28	0.013	0.32
30	0.010	0.25
32	0.008	0.20

mic needle, mixed the sample and carrier stream in a small mixer and measured the response downstream with a flow-through electrode. There was no indication of the sampling rate for their system. Although there have been some comments to the contrary, I believe that there is no doubt that this paper described an early version of the technique.

In 1972 there were several papers which provided critical concepts for flow-injection analysis. Bergmeyer and Hagen[12] described what they called a new principle for enzymatic analysis. These workers injected dissolved glucose samples into an unsegmented stream of recirculated oxygenated phosphate buffer and the stream subsequently passed through a small chamber containing bound glucose oxidase and then subsequently past an oxygen electrode. The electrode response was recorded on a strip-chart recorder. Although little information is given in the paper, it would appear that this system would be capable of about 60 analyses per hour with baselines readily obtained between samples. I believe that we should consider this the first use of flow-injection analysis for enzyme analysis.

In the same year, White and Fitzgerald[13] reported on the determination of ascorbic acid by the photobleaching of the ascorbic acid–Methylene Blue complex in a continuously flowing stream. Although the tubing diameter was rather large (6 mm bore) these workers were able to develop conditions in which they could inject discrete 1-ml samples of ascorbic acid solutions at approximately one sample every 1–2 min. Like Bergmeyer and Hagen[12] these workers developed a system by which they could recycle their reagent.

Gerding and his co-workers[14] made a significant contribution in 1972 to the development of AMFIA by devising a sensitive detection system for peptides and proteins in column effluents. These workers developed an unsegmented continuous-flow system, using small-bore tubing (21 m or 0.3 mm bore tubing), very slow delivery syringe pumps (1 ml/hr) and a valving system with two sample loops to transfer samples from the chromatographic effluent stream to the reaction stream while maintaining flow in each stream. The concepts inherent in this sampling system were later incorporated into the AMFIA system developed in our laboratory. From a historical viewpoint one of the most interesting sections of this paper was the discussion of dispersion in small-bore tubing: "Although the chemical principles used in the apparatus described have already been applied in conventional designs of peptide analyzers, a large increase in sensitivity was achieved after study of the properties of liquid flowing in Teflon tubes with a very small inside diameter. It was found that when the inside diameter of the tubing used is very small and very slow pumping syringe pumps were used, no segmentation is necessary." The echoes of this statement are found again and again in later papers on flow-injection analysis.

In 1973 Frantz and Hare[15] described a system for the determination of silica at submicrogram levels by use of an unsegmented continuous-flow system. The reagent was delivered from a pressurized chamber and the reaction coil consisted of 40 ft of 32 AWG Teflon tubing. The sample was injected by inserting a micropipette into the flowing stream of ammonium molybdate reagent. The insertion of the pipette was accomplished by the use of two three-way valves so that the sample-injection system was by-passed while the pipettes were exchanged. A special colorimeter was used; it had been previously described by Hare,[16] and had a flow-cell with an internal diameter of 0.020 in. and path-lengths of 6 or 60 mm. The flow-rates were not given. A schematic diagram of this system is shown in Fig. 2. This system seems to have incorporated into it all the basic concepts inherent to FIA as it is usually described.

In 1974 Feher and Pungor[17] continued their work on the possible uses of the system they first described in 1970. They discussed the general application of their system, including its use for the analysis of electroactive samples in which the solution injected was the analyte and the "streaming solution" was the supporting electrolyte. They also discussed the analysis of non-electroactive samples, which were made either the injected solution or the "streaming solution". The apparatus used was similar to that described in their first paper, except that peristaltic pumps, Hamilton syringes and dropping mercury electrodes were used. Flow-rates of 5–8 ml/min were used. Sample peak-areas were found to be proportional to the amount of the analyte injected into the system. The utility of the system was demonstrated by the determination of calcium and magnesium as electroactive species, and of phenol as a non-electroactive species. The signal responses were a linear function of analyte concentration in each case. The recorder tracings would suggest that about 60 samples/hr could be run with these systems, with a baseline reading between each sample.

In 1974 K. K. Stewart, Beecher and Hare first described the automated analysis of discrete samples with unsegmented continuously flowing streams, in two abstracts of papers presented at national meetings in the United States.[18,19] This apparatus consisted of a segmented sampling system based on the Skeggs's concepts, an unsegmented reaction flow-system based on the system used by Spackman, Stein and Moore,[9] and a sample insertion valve to transfer the sample from the sampling system to the reaction flow-system, based upon the concepts of Gerding *et al.*[14] The system was more fully described in later papers.

By 1975 there was a considerable increase in the reports on flow-injection analysis. Růžička and Hansen published the first in their classic series of papers on flow-injection analysis.[20] In this paper they described their concepts of unsegmented continuous-flow analysers as an adjunct to the segmented continuously flowing systems. Their concepts were illus-

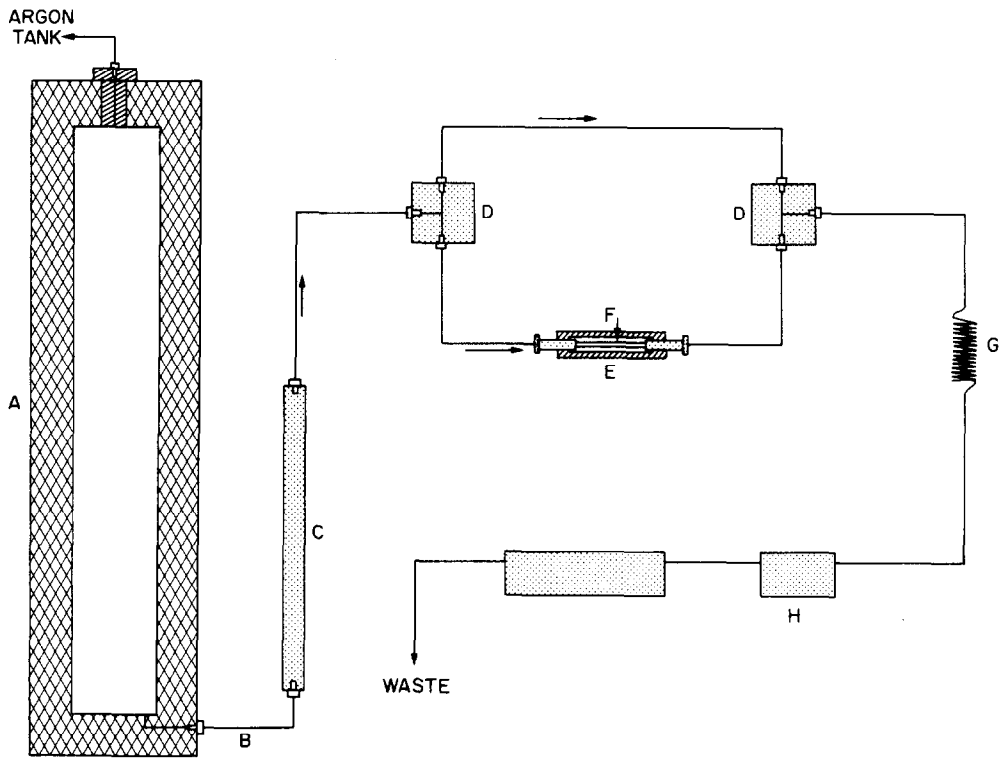


Fig. 2. Schematic diagram of the flow-injection analyser system of Frantz and Hare.[15] (A) Reagent reservoir; (B) 32-gauge Teflon tubing; (C) flowmeter; (D) three-way valve; (E) sample injector; (F) "Voluette" micropipette; (G) 40-ft coil of Teflon tubing; (H) 6-mm colorimetric cell; (I) 60-mm colorimetric cell. Figure reprinted with permission of the Director, Geophysical Laboratory, The Carnegie Institute.

trated by the colorimetric determination of Methyl Orange in a model system, of phosphate by the molybdenum blue method, and of ammonia with an air-gap electrode. Basically their system was similar to that of Frantz and Hare,[16] except that they used peristaltic pumps, larger diameter tubing, and injected the samples with hypodermic needles through the walls of the tubing. High sampling rates (360/hr) and good precision ($\pm 1\%$) were obtained with their manual system. This was the first paper to use the term "flow-injection analysis". In the second paper of this series Růžička and J. W. B. Stewart[21] described their efforts to delineate the important parameters for flow-injection analysis, including such parameters as sample volume, tube diameter, tube length, so that the criteria for the design of the system could be established and the limitations of FIA could be understood. They demonstrated their findings in the development of an improved FIA system for the colorimetric determination of phosphate.

In the same year Beecher, K. K. Stewart and Hare[22] published, in the proceedings of a symposium, the first detailed description of their automated system for the analysis of discrete enzyme samples by use of unsegmented continuously flowing streams. The system was later described elsewhere.[23] A schematic diagram of this system is shown in Fig. 3. This automated flow-injection analysis system used two flowing streams (one for sampling and one for analysis) connected by a sample-insertion valve. Analysis rates of 100 samples/hr were readily obtained with a precision of 1% or better for enzyme analyses. Standard chromtographic fittings and equipment were used in the system. Teflon tubing was used throughout (1/16 in. bore in the sample stream, and AWG 32 in the reaction stream). The enzyme substrate was pumped by air-pressure in this prototype model. The similarity in the concepts described by Beecher, K. K. Stewart, and Hare and those described by Růžička, Hansen and J. W. B. Stewart are striking.

In this same year, Dutt and Mottola[24] described their system for kinetic determinations based on transient redox effects. They used a recirculating reagent system pumped through an absorption cell. The sample aliquot was injected directly into the absorption cell. They were able to do repetitive analyses of injected samples of chromium, vanadium, *etc.* with a reagent-regenerating system, at about 120 samples/hr. Also in 1975, White and Fitzgerald[25] described their continued studies on use of dye-sensitized photochemical analysis in continuously flowing unsegmented streams. In this study they identified and

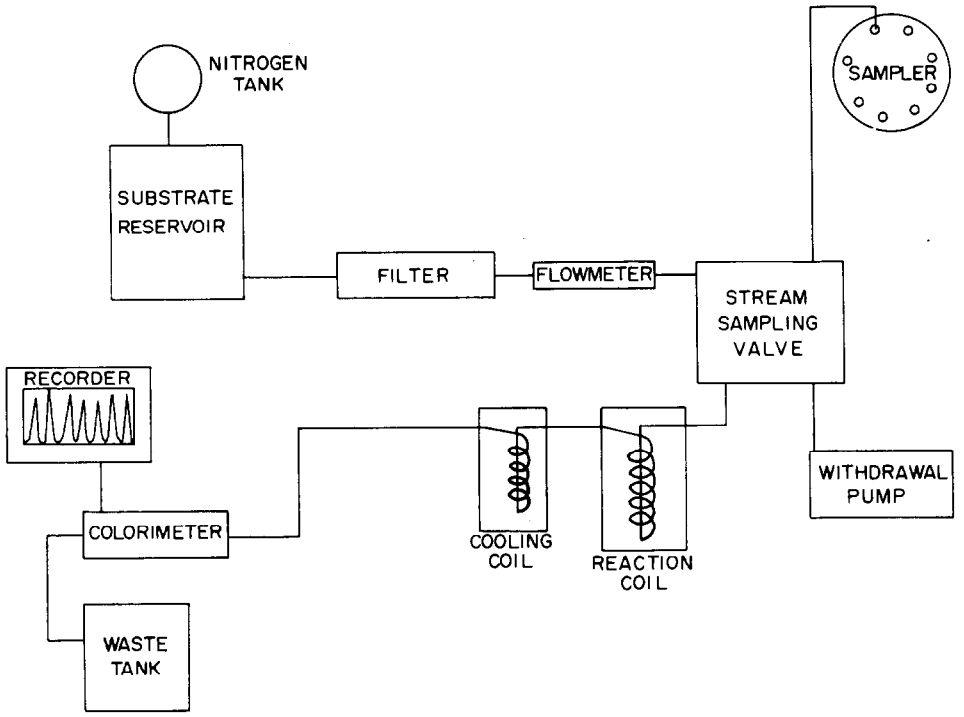


Fig. 3. Schematic diagram of the first automated multiple flow-injection analyser.

characterized the important experimental parameters of their system, using several model substrates. The tubing diameter was 6 mm, which was larger than that usually used in FIA, but little work was reported on the effect of the physical parameters of the tubing system.

In 1976 Dutt *et al.*[26] described the use of their system for equilibrium-based determinations with very fast reactions. Their system appears to have had the potential for doing about 200 analyses/hr of iron(II) with ferrozine. Their detector volume was rather large and flow-rates of 80 ml/hr were needed to obtain these sampling rates.

Růžička and his co-workers published several papers in 1976 on flow-injection analysis. The third paper of this series[27] described their studies on the development of an FIA system for determination of the total nitrogen content of plant digests. They used a flutter valve as an injection valve, for sample introduction a syringe without a needle, the first of several configurations of electrodes in FIA systems, a Lego-block system for manifold construction, and the first of their now standardized flow diagrams. Sampling rates of 110/hr or more were obtained for both manifold systems used, *i.e.*, colorimetric and air-gap electrode, when samples were injected so as to give less than 1% carry-over from the previous sample. No statistically significant differences at the 1% significance level were found between the classical manual distillation and titration system and their two manifold systems.

In the fourth paper of their series[28] they described a stream-splitting system for the colorimetric determination of chloride, based on a iron–thiocyanate system, which covered a wide concentration range. The apparatus was essentially the same as that described in their third paper except for the addition of the stream-splitting system, which used two tubes with different diameters (1.0 and 0.8 mm). The splitter was constructed so that the sample in one of the split streams would clear the colorimeter before the second entered. Sampling rates of 100 samples/hr were obtained with a split-stream system and of up to 300 samples/hr with a single-stream system.

The fifth paper of this series[29] described an ingenious FIA system for the simultaneous determination of both ammonia and phosphate with a single spectrophotometer with two flow-cells and a split-stream manifold. An alkaline hypochlorite and phenol solution was used for the ammonia determination and a molybdate–ascorbic acid system for the phosphate. The keys to the operation of the system were the use of a stream-splitter, a delay coil for the ammonia channel, and two flow-cells in one spectrophotometer. The authors were able to run samples at a rate of 100/hr with this system. In the sixth paper[30] studies on the analysis of blood serum for phosphate and chloride by use of a flow-injection analysis manifold system similar to those used previously were described. A sample-injection valve like those used in liquid chromatography was used. A by-pass coil was placed around the injection valve to limit the pulses in the system that were caused by the movement of the sample valve. Low efficiency (1–4%) dialysers were used in the chloride manifold. Although reasonable

precisions were obtained, there were differences ranging from −15 to +30% between the observed values and the actual concentrations in the samples. When a dilution system was substituted for the dialyser, slightly better agreements were obtained. Sampling rates of 125 samples/hr were reported. Betteridge and Růžička[31] described a means of using flow-injection analysis for the measurement of sample viscosity. They used the decrease in mixing in the sample bolus as a measure of increasing viscosity of water–glycerol mixtures. The samples of water and glycerol were injected into a coloured solvent stream and the decrease in absorbance was measured. The logarithm of the viscosity plotted against the change in absorbance appeared to be linear.

The following year (1977) was an important year for flow-injection analysis. The first patents on the systems were published, South African and South American versions of FIA were presented, and the workers in the field continued to expand the usefulness of flow-injection analysis.

A U.S. patent granted to K. K. Stewart *et al.*[32] described the basic concepts of automated multiple flow-injection analysis. A schematic diagram of the system is shown in Fig. 4. The concepts in this patent may be viewed as a marriage of the continuous-flow apparatus of Skeggs[8] to the post-column reaction-system used in Spackman, Stein and Moore's amino-acid analyser[9] by a stream-sampling valve evolving from that described by Gerding *et al.*[14] Emphasis was placed on the automation of the system, the use of two separate flow-systems (a sampling flow-system and a reaction flow-system) coupled by a stream-sampling valve, the elimination of air-bubbles in the reaction flow-system, the insertion of the sample into a sample solvent which was subsequently mixed with the reagent(s), and numerous details necessary for rapid sampling and good precision. While some discussion of the appropriate pumps for the automated multiple flow-injection analysis was given in the patent, a more detailed description of an acceptable pump was given in a note by K. K. Stewart.[33] This note described the depulsing of positive-displacement pumps. The use of depulsed positive-displacement chromatographic pumps in flow-injection analysis contributes significantly to the precise flow control in systems with back-pressure of up to 500 psi. The potential for operation at these higher back-pressures permits the use of smaller diameter tubing (reducing the dispersion of the sample) and longer tubing (increasing the available reaction time).

A U.S. patent granted to Hansen and Růžička[34] described the injection of discrete samples into continuously flowing carrier streams for subsequent reaction and detection. The system is quite similar to that in their paper published in 1975,[20] and can be described as a combination of the systems described by Nagy *et al.*,[11] Gerding *et al.*,[14] Frantz and Hare,[15] and the hypodermic needle sample-injection used first in gas chromatography.[7] The patent makes several claims about turbulent flow in flow-injection analysis, which have subsequently been questioned and refuted.[35–39]

Růžička and Hansen continued their classic series of papers with a description[40] of a system for the determination of potassium, sodium and nitrate with ion-selective electrodes, for the analysis of soil extracts and blood serum. Using unique flow-cells which could incorporate two ion-selective electrodes and a reference electrode, their system operated at sampling rates of 125 samples/hr with 0.8% relative standard deviation. The dead volume of the electrode was about 10 μl, and the electrode response was excellent, as were the wash-out characteristics of the system. The paper also contains some of the earlier discussions of the theory of flow-injection analysis.

The eighth paper of the series[41] discussed the determination of glucose with glucose dehydrogenase. Both the conventional single-point analysis system and a two-point analysis system were used. The latter

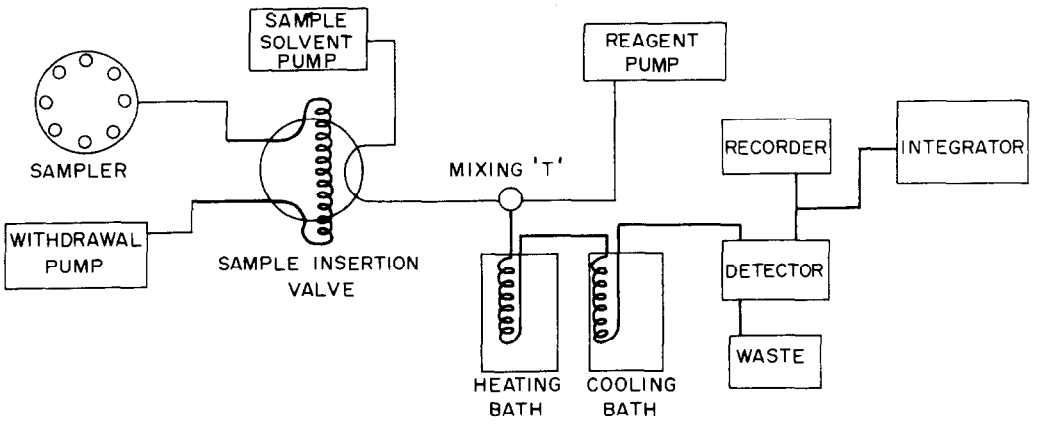


Fig. 4. Schematic diagram of an automated multiple flow-injection analyser.

system is probably the earliest use of flow-injection analysis for kinetic analysis. With single-point determinations using deproteinization and dilution, sampling rates of 120 samples/hr were attained, with in-line dialysis 45 samples/hr, and with the two-point analyser and predilution of samples, 60 samples/hr. There were some differences between the values obtained with each modification.

In the ninth paper,[42] the work of Fleet and Ho[43] on titration of discrete samples in a continuous-flow system was adapted to the titration of discrete samples in flow-injection analysis systems. The key to this work was the use of a fixed titrant concentration and an exponential sample gradient. The sample was inserted into a flowing stream of titrant and then into an exponential mixing chamber. The concentration was measured as the effluent stream left the mixing chamber. The equivalence time was measured as the time during which the signal was above (or below in some applications) a preset level. For the reaction shown in equation (1), the equivalence time is a function of the logarithm of the original sample concentration divided by the titrant concentration [see equation (2)].

This exciting use of flow-injection analysis was demonstrated by the potentiometric titration of calcium with EDTA and the colorimetric titration of hydrochloric acid with sodium hydroxide, with Bromothymol Blue as indicator. Between 20 and 60 samples per hour could be titrated with this system.

$$A + nB \rightleftharpoons AB_n \quad (1)$$

$$t(\text{eq}) = \ln(C_a/nC_b) \quad (2)$$

Using the systems described in their other papers, Hansen *et al.*[44] demonstrated the means of optimizing a flow-injection analysis system for the analysis of environmental samples for nitrate by use of an ion-selective electrode. Particular emphasis was placed on the selection of a mixing buffer to attain the optimal pH for the electrode response and to minimize the effect of interfering ions. An electronic peak-height measurement system was used which gave a digital read-out of the peak height in mV (measured relative to the reference electrode). Chloride and sulphate gave negative trailing peaks in this system. In test runs the sampling rate was 90/hr and the coefficient of variation was 1.6%.

In another applications paper Hansen *et al.*[45] demonstrated the usefulness of their system by describing the determination of nitrate, potassium, phosphate, and ammonia in fertilizer samples. The ammonia and phosphate systems used colorimetric methods, and for potassium and the nitrate ion-selective electrodes were used. Each system employed a separate manifold. Pulsation due to the movement of the sample valve was minimized by the use of a by-pass coil around the sample-injection valve.

Basson[46] described his version of automated flow-injection analysis in 1977. His system used an autosampler and a chromatographic valving system with a peristaltic pump system. High sampling rates (200/hr) were attained with precisions better than 1%. The usefulness of his system was demonstrated by the colorimetric determination of ammonia and phosphate.

Krug *et al.*[47] reported the turbidimetric determination of sulphate in water samples by flow-injection analysis in this same year. They were able to determine sulphate in the range of 40–140 ppm at the rate of 180 samples/hr with a precision of 0.85%; a manual injection system was used. These workers investigated the effects of reagent concentration, reagent flow-rates, and length of mixing coil. The results obtained from the optimized method agreed with those from a standard manual tubidimetric method.

In this same year Dutt and Mottola[48] expanded their 1976 work on the use of ferrozine for the determination of iron(III). By incorporating oxalate into their system they were able to make 45–70 determinations/hr, and regenerate the titrant. When 1,10-phenanthroline was used as the titrant, the use of citrate instead of oxalate was recommended.

These workers also reported the repetitive determination of isonicotinic acid hydrazide with flow-through systems.[49] The method made use of two competitive reactions; the formation of a complex between vanadium and the acid hydrazide, and the destruction of the complex by a reaction with an excess of the vanadium reagent. The rates of these two reactions were adjusted so that a transient peak with height proportional to the analyte level in the sample could be obtained. With this system 360 samples/hr could be done with a coefficient of variation of 1.5%. Wolff and Mottola[50] described a flow-through amperometric three-electrode system (without membranes) for the detection of dissolved oxygen. The lack of a membrane made the system quite sensitive to changes in turbulence, but these workers seem to have solved this problem. The appropriate conditions for optimum operation were investigated. The three-electrode system appeared to be suitable for measurements in both continuously flowing systems and in the monitoring of steady-state systems.

Dutt *et al.*[51] described the determination of iron(III) with a standard thiocyanate system in closed flow-through systems. In an extension of the work described earlier[49] they exploited the adjustment of the reaction rates of two competing reactions to attain a return of the signal to baseline. Both ligand-exchange and redox processes were used. When ligand-exchange was used, sampling rates of up to 350/hr could be obtained; when the redox (iodide) system was used, up to 120 samples/hr could be analysed.

Two papers from Brazil[52,53] were found in the literature search, but I was unable to obtain copies of these papers and cannot comment on them.

Table 2. Source of concepts used in the development of flow-injection analysis

Concept	Year	Authors	Reference
I. Sample injection into continuously flowing stream with continuous recording of signal downstream	1952	James and Martin	6
II. Discrete samples analysed from automated sampler in continuously flowing liquid streams with subsequent colorimetric detection	1957	Skeggs	8
III. Unsegmented continuously flowing streams in small-bore tubing for chemical reaction and subsequent colorimetric detection and automated recording	1958	Spackman *et al.*	9
IV. Use of hypodermic needles for injection into continuously flowing streams for subsequent analysis in gas-liquid chromatography		Before 1959 see ref. 7	
V. Very fine capillary tubing for unsegmented continuously flowing streams	1967	Hamilton	10
VI. Transfer of sample from one continuously flowing stream to another for subsequent analysis	1972	Gerding *et al.*	14
VII. Titrations by continuous-flow analysis using the gradient principle	1974	Fleet and Ho	43

DISCUSSION

A historical review of flow-injection analysis reveals two features of the development of this technique that stand out. The first is that many of the concepts of flow-injection analysis were adopted from other fields (see Table 2 for a chronological listing of the critical concepts that were combined in the development of flow-injection analysis), and that many workers have contributed to its development (see Table 3 for a chronological listing of various concepts as they were incorporated into flow-injection analysis by various authors). The second point is that this technique was one for which the time was ripe. Time and time again

Table 3. Chronological development and modifications of flow-injection systems

Concept	Year	Authors	Reference
I. Hypodermic needle injection of samples into unsegmented continuously flowing streams with subsequent reaction and detection	1970	Nagy *et al.*	11
II. Electrodes used in FIA	1970	Nagy *et al.*	11
III. Pump usage in FIA			
1. Peristaltic	1970	Nagy *et al.*	11
2. Air presssure	1973	Frantz and Hare	15
3. Positive displacement	1977	K. K. Stewart	33
IV. Colorimetry used in FIA	1972	Bergmeyer and Hagen	12
	1972	White and Fitzgerald	13
V. Enzyme analysis with FIA	1972	Bergmeyer and Hagen	12
VI. Use of reagent recirculation in FIA	1972	Bergmeyer and Hagen	12
VII. Use of automated sampler in flow-injection analysis	1974	K. K. Stewart *et al.*	18,19
VIII. Transfer of sample from segmented flowing streams to unsegmented continuously flowing streams for subsequent analysis	1974	K.K. Stewart *et al.*	18,19
IX. Reagent regeneration in FIA	1975	Dutt and Mottola	23
X. Stream-splitting in FIA	1976	Růžička *et al.*	28
XI. Viscosity measurements with FIA	1976	Betteridge and Růžička	31
XII. Use of dialysis in FIA	1976	Hansen and Růžička	30
XIII. Two-point detectors for FIA	1977	Hansen *et al.*	41
XIV. Titrations with FIA	1977	Růžička *et al.*	42
XV. Turbidimetric analysis with FIA	1977	Krug *et al.*	47

I found very similar statements from different authors. It was also common not to find the references to other workers in flow-injection analysis in the first paper of a series, but it was common to find the appropriate references in later papers. When Hansen and Růžička's term "flow-injection analysis" was accepted as a generic term, many of these problems of identification of prior art seemed to diminish and sometimes disappear. Such problems seem to be common in the early history of the development of any new technique.

The acceptance of a new technique requires that a number of requirements be met. The pioneers in the field must publish their new findings and procedures, an adequate theory must be established, commercial instruments must be developed and sold, methods books must be developed, and the advocates of the system must talk and write about the system at every opportunity.

Many of these requirements were well on the way to fulfilment by the end of 1977. The numbers of papers on flow-injection analysis were increasing and new workers were entering the field. Work on the theory had been started. Several manufacturers were considering entering the field, and one (Bifok) had actually demonstrated some prototype instruments, and a number of the early workers were lecturing extensively, especially Růžička and his co-workers. This new technique had successfully survived its birth pains and was well on its way to a lusty childhood. It is the author's hope that he will see it grow into a mature and useful technique in the years to come.

REFERENCES

1. D. Betteridge, *Anal. Chem.*, 1978, **50,** 832A.
2. J. Růžička and E. Hansen, *Chemtech.*, 1979, **9,** 756.
3. *Idem*, National Bureau of Standards Special Publication 519, *Trace Organic Analysis: A New Frontier in Analytical Chemistry*, Proceedings of the 9th Materials Research Symposium, 10–13 April 1978, held at NBS, Gaithersburg, MD, H. S. Hertz and S. N. Chesler, (eds.), p. 501. 1979.
4. *Idem*, *Anal. Chim. Acta*, 1980, **114,** 19.
5. C. B. Ranger, *Anal. Chem.*, 1981, **53,** 20A.
6. A. T. James and A. J. P. Martin, *Analyst*, 1952, **77,** 915; *Biochem. J.*, 1952, **50,** 679.
7. A. I. M. Keulemans, *Gas Chromatography*, 2nd Ed., p. 68. Reinhold, New York, 1959.
8. L. T. Skeggs, *Am. J. Clin. Pathol.*, 1957, **28,** 311.
9. D. H. Spackman, W. H. Stein and S. More, *Anal. Chem.*, 1958, **30,** 1190.
10. P. B. Hamilton, *Methods in Enzymology*, 1967, **19,** 15.
11. G. Nagy, Z. S. Feher and E. Pungor, *Anal. Chim. Acta*, 1970, **52,** 47.
12. H. U. Bermeyer and A. Hagan, *Z. Anal. Chem.*, 1972, **261,** 333.
13. V. R. White and J. M. Fitzgerald, *Anal. Chem.*, 1972, **44,** 1267.
14. J. J. T. Gerding, H. J. M. Kempen, B. J. M. Lamers and M. H. Gerding, *J. Chromatog.*, 1972, **66,** 145.
15. J. D. Frantz and P. E. Hare, *Annual Rept. Director Geophys. Lab.*, 1973, **1630,** 704.
16. P. E. Hare, *ibid.*, 1973, **1630,** 701.
17. Z. S. Feher and E. Pungor, *Anal. Chim. Acta*, 1974, **71,** 425.
18. K. K. Stewart, G. R. Beecher and P. E. Hare, *Fed. Proc.*, 1974, **33,** 1439.
19. G. R. Beecher, K. K. Stewart and P. E. Hare, Abstracts of Symposium on Chemical and Biological Methods for Protein Quality Determination, sponsored by the Agricultural and Food Chemistry Division of the American Chemical Society, paper No. 22, 168th American Chemical Society National Meeting, Atlantic City, NJ, September 1974.
20. J. Růžička and E. H. Hansen, *Anal. Chim. Acta*, 1975, **78,** 145.
21. J. Růžička and J. W. B. Stewart, *ibid.*, 1975, **79,** 79.
22. G. R. Beecher, K. K. Stewart and P. E. Hare, in *Protein Nutritional Quality of Foods and Feeds*, Part 1, p. 411. E. M. Friedman (ed.), Dekker, New York, 1975.
23. K. K. Stewart, G. R. Beecher and P. E. Hare, *Anal. Biochem.*, 1976, **70,** 167.
24. V. V. S. E. Dutt and H. A. Mottola, *Anal. Chem.*, 1975, **47,** 357.
25. V. R. White and J. M. Fitzgerald, *ibid.*, 1975, **47,** 903.
26. V. V. S. E. Dutt, A. E. Hanna and H. A. Mottola, *ibid.*, 1976, **48,** 1207.
27. J. W. B. Stewart, J. Růžička, H. Bergamin Filho and E. A. Zagatto, *Anal. Chim. Acta*, 1976, **81,** 371.
28. J. Růžička, J. W. B. Stewart and E. A. Zagatto. *ibid.*, 1976, **81,** 387.
29. J. W. B. Stewart and J. Růžička, *ibid.*, 1976, **82,** 137.
30. E. H. Hansen and J. Růžička, *ibid.*, 1976, **87,** 353.
31. D. Betteridge and J. Růžička, *Talanta*, 1976, **23,** 409.
32. K. K. Stewart, G. R. Beecher and P. E. Hare, *U.S. Patent*, 4,013,413 (1977).
33. K. K. Stewart, *Anal. Chem.*, 1977, **49,** 2125.
34. E. H. Hansen and J. Růžička, *U.S. Patent* 4,022,575 (1977).
35. M. Margoshes, *Anal. Chem.*, 1977, **49,** 17.
36. J. Růžička, E. H. Hansen, H. Mosbaek and F. J. Krug, *Anal. Chem.*, 1977, **49,** 1858.
37. M. Marsgoshes, *Anal. Chem.*, 1977, **49,** 1861.
38. J. Růžička and E. H. Hansen, *Anal. Chim. Acta*, 1978, **99,** 37.
39. J. T. Vanderslice, K. K. Stewart, A. G. Rosenfeld and D. J. Higgs, *Talanta*, 1981, **28,** 11.
40. J. Růžička, E. H. Hansen and E. A. Zagatto, *Anal. Chim. Acta*, 1977, **88,** 1.
41. E. H. Hansen, J. Růžička and B. Rietz, *ibid.*, 1977, **89,** 241.
42. J. Růžička, E. H. Hansen and H. Mosbaek, *ibid.*, 1977, **92,** 235.
43. B. Fleet and A. Y. W. Ho, *Anal. Chem.*, 1974, **46,** 9.
44. E. H. Hansen, A. K. Ghose and J. Růžička, *Analyst*, 1977, **102,** 705.
45. E. H. Hansen, F. J. Krug, A. K. Ghose and J. Růžička, *Analyst*, 1977, **102,** 714.
46. W. D. Basson, *Lab. Pract.*, 1977, **26,** 541.
47. F. J. Krug, H. Bergamin Filho, E. A. G. Zagatto and S. Storgard-Jorgensen, *Analyst*, 1977, **102,** 503.
48. V. V. S. E. Dutt and H. A. Mottola, *Anal. Chem.*, 1977, **49,** 319.
49. *Idem*, *ibid.*, 1977, **49,** 776.
50. C. H. M. Wolff and H. A. Mottola, *ibid.*, 1977, **49,** 2118.
51. V. V. S. E. Dutt, D. Scheeler and H. A. Mottola, *Anal. Chim. Acta*, 1977, **94,** 289.
52. S. Storgard-Jorgensen, H. Bergamin Filho, E. A. Zagatto, F. J. Krug and S. R. B. Bringel, *Boletim Scientifico*, 1977, *047*.
53. H. Bergamin Filho, F. J. Krug, E. A. Zagatto, H. Fonseca, M. Graner, J. N. Nogueira and A. V. K. O. Annicchino, *ibid.*, 1977, *049*.

Talanta, Vol. 28, pp. 799 to 803, 1981
Printed in Great Britain. All rights reserved

0039-9140/81/110799-05$02.00/0
Copyright © 1981 Pergamon Press Ltd

SPECTROPHOTOMETRIC DETERMINATION OF BERYLLIUM WITH CALCICHROME

HISAHIKO EINAGA*

Institute of Materials Science, University of Tsukuba, Niihari, Ibaraki, 305, Japan

HAJIME ISHII

Chemical Research Institute of Non-Aqueous Solutions, Tohoku University, Sendai, 980, Japan

(*Received* 28 *May* 1980. *Revised* 11 *November* 1980. *Accepted* 5 *May* 1981)

Summary—A method is established for the spectrophotometric determination of small amounts of beryllium as a 1:1 complex with Calcichrome in slightly acidic solution. Beer's law is obeyed over the range 0.05–0.6 ppm Be in the final solution and the apparent molar absorptivity is 9.7×10^3 l.mole^{-1}.cm^{-1} at 625 nm. Up to about 15 μg of beryllium in the final solution can be sensitively and selectively determined with a relative error of less than 2% in the presence of EDTA as masking agent.

Calcichrome was first introduced by Close and West[1] as a reagent specific for calcium under certain conditions; it was also shown[1] that it would react with several other metal ions under different conditions, and the reagent has subsequently been used[2–11] for determination of several metals. This paper is a continuation of these later studies and deals with the determination of beryllium.

EXPERIMENTAL

Reagents

Beryllium solution was prepared from analytical reagent grade beryllium chloride and kept slightly acidic with hydrochloric acid to prevent hydrolysis. It was standardized gravimetrically[12] by precipitation of the hydroxide and ignition at 1000 to the oxide.

Calcichrome was synthesized according to the method of Close and West.[1] The crude product was purified by dissolution in alkali and precipitation with concentrated hydrochloric acid. After repeated purification the product was finally dried over silica gel and solid sodium hydroxide *in vacuo*. It was standardized by converting it into the free acid by cation-exchange and titrating this potentiometrically with sodium hydroxide.

Sodium acetate and acetic acid of analytical reagent grade were used to make 0.2*M* acetate buffer solution (pH 6).

Procedure

To a slightly acidic solution containing 1–15 μg of beryllium, add 6 ml of 0.003*M* Calcichrome, adjust to pH 6 with 0.5 ml of the buffer solution, and finally dilute to volume in a 25-ml standard flask with water. After 40 min, measure the absorbance against a reagent blank at 625 nm and obtain the beryllium content from a calibration curve.

* To whom correspondence and requests for reprints should be addressed.

RESULTS AND DISCUSSION

Spectral characteristics

The absorption spectrum of the complex is shown in Fig. 1 together with that of the ligand. The absorption maxima of the ligand at 422 and 548 nm shift to 410 and 576 nm respectively on formation of the beryllium complex. The second of these shifts is the more suitable for analytical purposes. The difference in absorptivity between the beryllium complex and the free ligand is maximal at 625 nm, which is therefore chosen as the analytical wavelength.

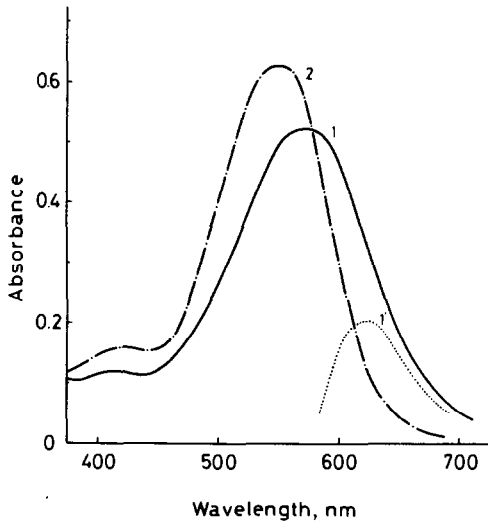


Fig. 1. Absorption spectra of Calcichrome and beryllium(II)–Calcichrome complex. 1, The complex (reference: water); 2, the ligand (reference: water); 1', the complex (reference: the ligand). Beryllium(II) concn. $3.16 \times 10^{-5}M$, Calcichrome concn. $2.32 \times 10^{-5}M$, pH 6.0_5.

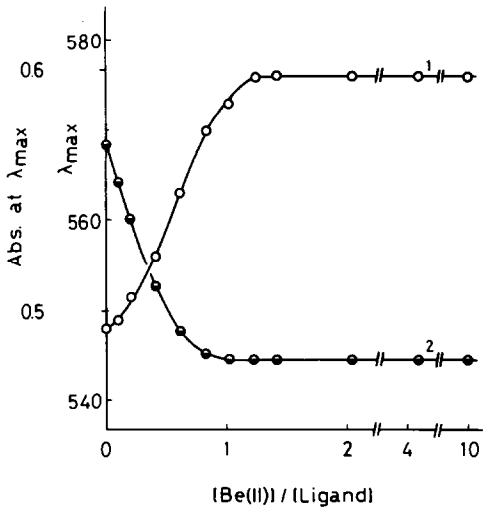


Fig. 2. Relation between wavelength of the absorption maximum (1) or absorbance at the maximum wavelength (2) and metal to ligand ratio. Ligand concn. $2.32 \times 10^{-5} M$, pH 5.9$_0$.

In complex-formation reactions with multidentate ligands, there is the possibility of formation of complexes having different metal to ligand ratios, and of protonated or hydroxo mixed-ligand complexes. When the beryllium:Calcichrome ratio was increased at constant ligand concentration and pH 5.9 it was found that there was a gradual and monotonic shift of λ_{max} (the wavelength of maximum absorption) from that of the ligand (548 nm) to that of the complex (576 nm) and an accompanying monotonic decrease in the absorbance at λ_{max}, but that both changes ceased at metal:ligand ratios greater than about unity (Fig. 2). Only one isosbestic point was found in the spectra, at 574 nm. These findings suggest that only a 1:1 complex is formed under the conditions used. A study of the effect of pH on the absorbance at constant metal:ligand ratio (Fig. 3) showed a similar shift in λ_{max} and decrease in absorbance as the pH was increased, and the spectra showed only one isosbestic point, again at 574 nm. These facts imply that the complex formation begins at pH 3.5 and is quantitative at pH above 5.6, and that with respect to protonated or hydroxo species, only one complex is formed. The optimum pH was selected by measuring the absorbance against the reagent blank (Fig. 4). The absorbance is maximal and constant at pH between 5.7 and 6.7. The decrease in absorbance at pH above 6.7 is due to the increase in absorbance of the ligand caused by deprotonation with increase in pH.

Composition and characteristics of the complex

The metal:ligand ratio was confirmed as 1:1 by the continuous variations and molar-ratio methods.[13]

In the slightly acidic medium recommended for analytical measurements, the beryllium is considered[14, 15] to be present as the partially hydrolysed species $BeOH^+$, Be_2OH^{3+}, $Be_3(OH)_3^{3+}$, *etc.*, together with the aquo-ion Be^{2+}. It is of interest to identify which of these species may be involved in the complexation. First, however, it is necessary to discuss the nature of the ligand. There has been some disagreement since the original report by Close and West[1] that Calcichrome is a *cyclo*-tris-7-(1'-azo-8'-hydroxynaphthalene-3',6'-disulphonic acid), having three hydroxyl groups *peri* and *ortho* to the azo group. Later, but independently, Lukin *et al.*[16] suggested that the ligand Calcion, which is equivalent to Calcichrome as far as its synthesis is concerned, is 1-(1',8'-dihydroxy-3'6'-disulphonaphthyl-7'-azo)-7-(8''-hydroxy-3'',6''-disulphonaphthyl-1''-azo)-8-naphthol-3,6-disulphonic

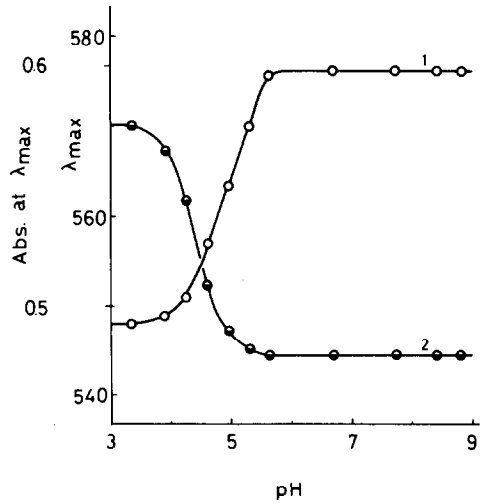


Fig. 3. Relation between wavelength of the absorption maximum (1) or absorbance at the maximum wavelength (2) and pH at equilibrium. Beryllium(II) concn. $3.16 \times 10^{-5} M$, Calcichrome concn. $2.32 \times 10^{-5} M$.

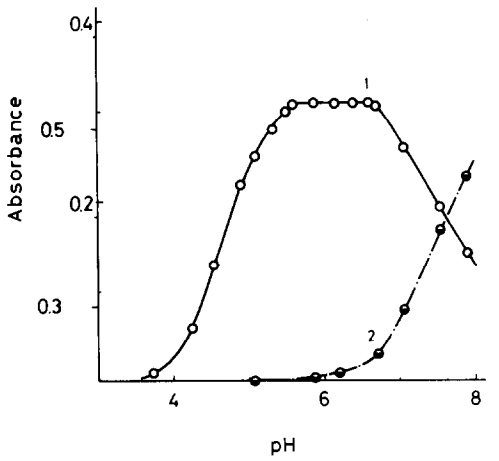


Fig. 4. Relation between absorbance at 625 nm and pH at equilibrium. 1, The complex (reference: the ligand) (right-hand scale); 2, the ligand (reference: water); (left-hand scale); beryllium(II) concn. $3.16 \times 10^{-5} M$, Calcichrome concn. $4.64 \times 10^{-5} M$.

acid and contains three hydroxyl groups *peri* and/or *ortho* to the azo group and another hydroxyl group *peri* to the hydroxyl group of the first category. Then Stead,[17] from proton NMR and elemental analysis studies on the compound prepared under slightly different coupling conditions, suggested that the ligand has neither the Calcichrome nor the Calcion[16] structure but is 1-(8′-hydroxy-3′,6′-disulphonaphthyl-1′-azo)-8-naphthol-3,6-disulphonic acid with two hydroxyl groups *peri* to the azo group. Separately from these studies, Allan *et al.*[18] pointed out, in the course of systematic studies on macrocyclic tris-azo compounds by stepwise synthetic, chromatographic, optical absorption, and proton NMR studies, that H-acid, which is a starting material for the synthesis of Calcichrome, can be diazotized and coupled to give an "aza-[18]-conjugated" macrocyclic compound, with a structure identical to that postulated by Close and West.[1] Our additional studies by potentiometric titration and elemental analysis gave results supporting the deductions by Allan *et al.*[18] We therefore consider that the six sulphonic acid groups of Calcichrome are fully dissociated, and that the resulting anion can be written as H_3cach^{6-} to indicate that three further protons can be dissociated from the hydroxy groups. Further studies on the structure are needed, *e.g.*, by X-ray diffraction and analogous methods, but this is beyond the scope of the present study.

The first two dissociation constants of H_3cach^{6-} have been determined spectrophotometrically, and found to be $pk_{a1} = 7.2$ (at 27°) and $pk_{a2} = 11.5$ (at 23°) in 0.10*M* sodium chloride medium.[2] The value of pk_{a1} was redetermined by the same method at 625 nm and 20° in 0.10*M* sodium perchlorate and found to be $7.1_2 \pm 0.0_5$, and this value is used in the subsequent discussion. The data indicate that the ligand is primarily present as H_3cach^{6-} under the analytical conditions used. The value of pk_{a3} is too high to be determined by spectrophotometry or potentiometry.

The complex-formation equilibrium may then be expressed as

$$Be(OH)_i^{(2-i)+} + H_3cach^{6-} \overset{K_{eq}}{\rightleftharpoons} BeH_ncach^{(7-n)-} + (3-n-i)H^+ + iH_2O$$

$$K_{eq} = [BeH_ncach^{(7-n)-}] \times [H^+]^{(3-n-i)}/[Be(OH)_i^{(2-i)+}][H_3cach^{6-}] \quad (1)$$

If the initial concentration of the metal ion, a, is equal to that of the ligand, equation (1) can be simplified to

$$K_{eq} = x[H^+]^{(3-n-i)}/(a-x)^2 \quad (1')$$

where x is the equilibrium concentration of complex formed. Preliminary studies having revealed that the system obeys Beer's law additively over the wavelength range of interest, it can be deduced that

$$A = \epsilon_L(a-x) + \epsilon_C x \quad (2)$$

$$A_0 = \epsilon_L a \quad (3)$$

where ϵ_L and ϵ_C are the molar absorptivities of the ligand and the complex at a specified wavelength and A and A_0 the absorbances of the solution containing the metal complex and of the solution of the ligand alone, respectively. From equations (1′), (2) and (3), equation (4) can finally be obtained:

$$a/(A-A_0) = 1/(\epsilon_C - \epsilon_L) + [K_w^i/K_{eq}(\epsilon_C - \epsilon_L)]^{\frac{1}{2}} \{[H^+]^{(3-n-i)}/(A-A_0)\}^{\frac{1}{2}} \quad (4)$$

Equation (4) implies that there should be a linear relation between the terms $a/(A-A_0)$ and $\{[H^+]^{(3-n-i)}/(A-A_0)\}^{\frac{1}{2}}$, from which the values of n, i, and K_{eq} can be estimated. A linear relation was experimentally obtained for $(3-n-i) = 1$, so $(n+i)$ should be equal to 2. This condition satisfies the reaction of Be^{2+} with H_3cach^{6-} to form BeH_2cach^{5-}, of $BeOH^+$ to form $BeHcach^{6-}$, and of $Be(OH)_2$ to form $Becach^{7-}$. To deduce the most probable of these three cases, solutions containing equimolar amounts of metal ion and ligand, or the ligand alone, were titrated potentiometrically and it was found that one mole of hydrogen ion was released per mole of complex formed, which implies that the product is BeH_2cach^{5-}. This was further supported by the spectral characteristics shown in Fig. 5, which indicate that the absorption spectrum of the complex is closely related to that of the species H_2cach^{7-}. Hence the reaction of beryllium with Calcichrome may reasonably be expressed as

$$Be^{2+} + H_3cach^{6-} \overset{K_{eq}}{\rightleftharpoons} BeH_2cach^{5-} + H^+$$

$$K_{eq} = [BeH_2cach^{5-}][H^+]/[Be^{2+}][H_3cach^{6-}] \quad (1'')$$

The value obtained from

$$a/(A-A_0) = 1/(\epsilon_C - \epsilon_L) + [1/K_{eq}(\epsilon_C - \epsilon_L)]^{\frac{1}{2}} \{[H^+]/(A-A_0)\}^{\frac{1}{2}} \quad (4')$$

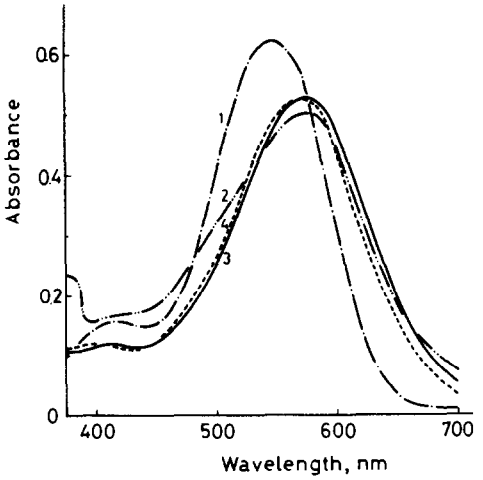


Fig. 5. Absorption spectra of Calcichrome and beryllium(II)–Calcichrome complex. Beryllium(II) concn. $3.16 \times 10^{-5}M$. Calcichrome concn. $2.32 \times 10^{-5}M$. 1, H_3cach^{6-} (pH 6.3_0); 2, H_2cach^{7-} (pH 8.9_5); 3, Be(II) + H_3cach^{6-} (pH 6.0_5); 4, Be(II) + H_2cach^{7-} (pH 8.9_0).

Table 1. Interferences

Ion added*	Be found,† μg	Relative error,† %	Tolerance limit§ (wt. ratio)
Al(III)	14.0(7.24)	96.6(1.6)	4.5
Co(II)	7.49(7.08)	5.2(−0.6)	11.7
Cr(III)	7.08(7.08)	−0.6(−0.6)	11.7
Cu(II)	9.47(7.12)	33.0(0)	200
Fe(III)	9.72(7.22)	36.5(1.4)	5.0
Ni(II)	9.19(7.12)	29.1(0)	200
Ti(IV)	7.71(7.00)	8.3(−1.7)	4.1
V(IV)	15.9(7.02)	123(−1.4)	5.0
Zr(IV)	6.98(7.02)	−2.0(−1.4)	5.0

* Metal ion (50 μg) added as chloride, nitrate, or sulphate; 7.12 μg of beryllium were used each time.

† Results in parentheses were obtained by adding 0.2 ml of 0.01*M* EDTA before the Calcichrome.

§ The limit for 1% relative error, with 0.2 ml of 0.01*M* added before the Calcichrome.

and the experimental data by least-squares treatment is $\log K_{eq} = -0.3_0 \pm 0.05$ for 0.1*M* sodium perchlorate medium at 20 . The stability constant of the complex

$$\beta_{11} = [BeH_2cach^{5-}]/[Be^{2+}][H_2cach^{7-}] \quad (5)$$

was calculated by using the relations

$$k_{a1} = [H^+][H_2cach^{7-}]/[H_3cach^{6-}] \quad (6)$$

$$\log \beta_{11} = \log K_{eq} + pk_{a1} \quad (7)$$

to be $\log \beta_{11} = 6.8_2 \pm 0.1_0$.

Spectrophotometric determination of beryllium(II)

The optimal analytical conditions for determination of beryllium can be summarized as: wavelength 625 nm; pH range 5.7–6.7; ligand:metal ratio > 1.2.

Additional studies were made on the rate of formation and the stability of the complex. The complex forms slowly, about 30 min being necessary for constant absorbance to be attained. The absorbance then remains constant for at least another 60 min. The apparent molar absorptivity at 625 nm is 9.7×10^3 l. mole^{-1}.cm^{-1}.

Potentially interfering ions were examined and their effect expressed as the relative error caused by 50 μg of foreign ion in the determination of 7 μg of beryllium (Table 1). Several ions interfere seriously, but as is well known,[19] EDTA serves as a selective masking agent for prevention of interferences in the determination of metal ions that form only weak complexes with it, *e.g.*, in the determination of beryllium with Thorin,[20] and this technique was therefore tried here. Preliminary tests (Table 2) showed that EDTA did not affect the determination of beryllium unless it was present in over 4-fold molar ratio to the beryllium. Negative errors are caused by higher ratios because of the side-reaction with the metal ion. The addition of 0.2 ml of 0.01*M* EDTA effectively masked 50 μg of any of interfering ions (Table 2) and the method could be made selective for beryllium in this way.

Table 2. Influence of EDTA on determination of 7.12 μg of beryllium

0.01*M* EDTA added, ml	Be found, μg	Relative error, %
0	7.12	0
0.1	7.12	0
0.3	7.12	0
0.5	6.74	−5.4
1.0	6.07	−14.8
2.0	5.03	−29.3

The method was compared with some of the other spectrophotometric methods for beryllium, *e.g.*, with Beryllon II ($\epsilon = 1.2 \times 10^4$ at 630 nm), Beryllon III ($\epsilon = 2.0 \times 10^4$ at 525 nm), Arsenazo I (580 nm and 0–0.5 μg/cm^3), Arsenazo III ($\epsilon = 1.8 \times 10^4$ at 580 nm), 2-methyl-8-hydroxyquinoline ($\epsilon = 3.5 \times 10^3$ at 380 nm), Aluminon (520 nm and 0.05–1 μg/cm^3), Eriochrome Cyanine R ($\epsilon = 1.5 \times 10^4$ at 520 nm), Chrome Blue G ($\epsilon = 3.1 \times 10^4$ at 610 nm), quinizarin-2-sulphonate (575 nm) *etc.*[21] These methods are generally sensitive enough for the determination of small amounts of beryllium but except for the Arsenazo I and Thorin[20] methods are not selective and suffer from various procedural inconveniences. The present method is simple, and selective and sensitive enough to be used for trace amounts for beryllium in some practical samples.

Acknowledgement—One of the authors (H.E.) acknowledges with thanks financial support of this work by the Kazuchika Ohkura Memorial Foundation.

REFERENCES

1. R. A. Close and T. S. West, *Talanta*, 1960, **5**, 221.
2. H. Ishii and H. Einaga, *Bull. Chem. Soc. Japan*, 1966, **39**, 1154.

3. *Idem, ibid.*, 1966, **39**, 1721.
4. *Idem, ibid., Nippon Kagaku Zasshi*, 1966, **87**, 440.
5. *Idem, ibid.*, 1966, **15**, 577.
6. *Idem, ibid.*, 1966, **15**, 821.
7. *Idem, ibid.*, 1966, **15**, 1124.
8. *Idem, Bull. Chem. Soc. Japan*, 1967, **40**, 153.
9. *Idem, Bunseki Kagaku*, 1967, **16**, 322.
10. *Idem, ibid.*, 1967, **16**, 328.
11. *Idem, ibid.*, 1970, **19**, 371.
12. Chemical Society of Japan, *Handbook of Chemistry*, Fundamental Section, 2nd Ed., p. 1518. Maruzen, Tokyo, 1975.
13. H. L. Schläfer, *Komplexbildung in Lösung*, p. 232. Springer, Berlin, 1961.
14. H. Kakihana and L. G. Sillén, *Acta Chem. Scand.*, 1956, **10**, 985.
15. C. F. Baes, Jr. and R. Mesmer, *Hydrolysis of Cations*, p. 88, Wiley, New York, 1976.
16. A. M. Lukin, K. A. Smirnova and B. Zavarikhina, *Zh. Analit. Khim.*, 1963, **18**, 444.
17. C. V. Stead, *J. Chem. Soc. (C)*, 1970, 693.
18. Z. J. Allan, J. Podstata and J. Jarkovsky, *Collection Czech. Chem. Commun*, 1969, **34**, 282.
19. R. Přibil, *Analytical Applications of EDTA and Related Compounds*, Pergamon Press, Oxford, 1972.
20. H. Einaga and H. Ishii, *Anal. Chim. Acta*, 1971, **54**, 113.
21. See, *e.g.*,
E. B. Sandell, *Colorimetric Determination of Traces of Metals*, 3rd Ed., p. 313, Wiley-Interscience, New York, 1953; I. M. Kolthoff and P. J. Elving (eds.), *Treatise on Analytical Chemistry*, Part II, Vol. 6, p. 44, Wiley-Interscience, New York, 1964; D. F. Boltz and M. G. Mellon, *Anal. Chem.*, 1970, **42**, 152R; 1972, **44**, 300R; 1974, **46**, 227R; 1976, **48**, 216R; J. A. Howell and L. G. Hargis, *Anal. Chem.*, 1978, **50**, 243R; Chemical Society of Japan, *Handbook of Chemistry*, Fundamental Section, 2nd Ed., p. 1532, Maruzen, Tokyo, 1975; Z. Marczenko, *Spectrophotometric Determination of Elements*, p 142, Horwood, Chichester, 1976.

Talanta, Vol. 28, pp. 805 to 808. 1981
Printed in Great Britain. All rights reserved

0039-9140/81/110805-04$02.00/0
Copyright © 1981 Pergamon Press Ltd

STUDIES ON SPECTROPHOTOMETRIC METHODS OF THALLIUM DETERMINATION

ZBIGNIEW GREGOROWICZ and JERZY CIBA

Department of Analytical and General Chemistry,
Silesian Polytechnical University, PL 44-101 Gliwice, Poland

BARBARA KOWALCZYK

Department of General and Analytical Chemistry, Pedagogical University, PL-42-200 Częstochowa, Poland

(*Received* 10 *July* 1980. *Revised* 17 *April* 1981. *Accepted* 5 *May* 1981)

Summary—Eight sensitive methods of spectrophotometric determination of thallium have been studied and compared experimentally. The comparative criteria were: molar absorptivity, colour contrast of the basic reaction, working concentration interval and practical determination limit for thallium, precision of the method (the standard deviation), and selectivity. According to these criteria the best methods of extraction–spectrophotometric determination of thallium are those using Brilliant Green, Crystal Violet, Methyl Violet and Rhodamine B. The sensitivity depends very much on the oxidant used for conversion of Tl(I) into Tl(III). The oxidants suitable for each of the recommended methods are discussed.

In the last 10 years more than 150 methods of spectrophotometric determination of thallium, with the use of about 60 reagents, have been described. This large literature makes it difficult to choose the method giving the best results, the more so as the criteria used for evaluation of the various methods may be different. On account of this, we decided to compare experimentally 8 selected methods of spectrophotometric determination of thallium (from 8 papers by various authors) and to choose from them the most sensitive, giving accurate and reproducible results.

In choosing the methods we were guided primarily by the sensitivity and accordingly chose the papers in which the authors reported the highest values of molar absorptivity. These methods were then tested for reproducibility *etc.*

In the methods thus selected the following basic dyes were used as spectrophotometric reagents: Brilliant Green, Crystal Violet, Methyl Violet, Rhodamine B, Methylene Green, Methylene Blue and Methyl Green. The first four are often used for spectrophotometric determination of thallium, whereas the other three have been used only twice.[1,2]

The evaluation of spectrophotometric methods and reagents has been discussed by Koźlicka,[3] Sommer *et al.*,[4] Ackermann *et al.*[5] and Kirkbright.[6] Following their recommendations, we chose as the criteria of performance the sensitivity (molar absorptivity), colour contrast of the reaction, working concentration range, practical determination limit, precision (standard deviation) and selectivity. It is impossible to compare the methods directly from the original papers, because the reagents used in the development may not have been of identical purity.

The mechanism of the spectrophotometric determination of thallium with basic dyes is the formation of an ion-association complex between the cationic dye and anionic thallium complexes with halides, followed by extraction with organic solvents. The thallium(III) is obtained by oxidation of thallium(I). Initially we used the oxidants recommended by the original authors, but later we sometimes changed the oxidants to see the effect on the results.

All the methods were evaluated in the same way: first we obtained the calibration data and then treated them by linear regression to find the molar absorptivity, and the standard deviations of the slope and intercept.

Selectivity was tested in terms of the effect of K^+, Na^+, Al^{3+}, Zn^{2+}, Ca^{2+}, Mg^{2+}, Mn^{2+}, Sn^{2+}, Hg^{2+}, Fe^{3+}, Sb^{3+}, Pb^{2+}, Bi^{3+}, Cd^{2+}, Co^{2+}, Ni^{2+} (50 mg each), NO_3^-, SO_4^{2-} (1000-fold ratio to Tl, added as the acids), citrate and EDTA (1000-fold ratio to Tl). The influence of a mixture of 0.5 mg of each of these ions that did not interfere was also examined.

Calibration graphs were prepared according to Sommer *et al.*[4] The absorbance was measured against a reagent blank.

EXPERIMENTAL

Reagents

Brilliant Green, Methyl Violet, Rhodamine B, Methylene Blue (POCh, Gliwice, Poland), Crystal Violet, Methyl Green (Merck, Darmstadt), Methylene Green (Gurr, London), thallium(I) nitrate (International Enzymes Ltd., England). The dyes were purified as proposed by Fogg *et al.* The data are given in Table 1.

Standard thallium(I) solution, 1 mg/ml. $TlNO_3$ (1.303 g) was dissolved in water containing 2 ml of concentrated

Table 1. Purity of the dyestuffs

Reagent	Content of active dye, % commercial	purified	Moisture, % commercial	purified	Content of inert salt, % commercial	purified
Brilliant Green	74.0	92.8	4.22	4.45	1.22	0.34
Crystal Violet	77.0	92.6	5.13	5.33	0.38	0.36
Methyl Violet	71.5	90.8	3.51	5.28	0.94	0.52
Rhodamine B	62.2	92.5	16.74	4.18	0.95	0.78

* Identified as sodium sulphate.

nitric acid and diluted to 1 litre with water. Working standards were prepared by dilution of this solution.

Doubly distilled water and analytical-grade reagents were used.

Brilliant Green

Fogg *et al.*[7] published an extractive spectrophotometric method for determining microgram amount of thallium with Brilliant Green, in which they achieved high sensitivity (molar absorptivity $\epsilon = 1.03 \times 10^5$ l.mole^{-1}.cm^{-1}). The ion-association complex of $TlBr_4^-$ with the reagent cation is extracted with toluene, from 4*M* hydrochloric acid. Ceric sulphate is used as oxidant, oxidation time 1 min.

Determination of thallium performed by us by this method confirmed the authors' results.[7]

We made six independent absorbance measurements for six different concentrations of thallium and calculated the parameters of the least-squares line (Table 2, No. 1).

All the methods examined were evaluated in the same way, *i.e.*, by plotting the calibration curve and drawing conclusions concerning sensitivity, range, selectivity, precision and so on. The number of absorbance measurements for each experimental point on the calibration curve was always six.

The next stage, for further evaluation of the sensitivity of the Brilliant Green method, was to see how changing the oxidant or extraction solvent would affect the molar absorptivity. The systems tried were Brilliant Green–$Ce(SO_4)_2$–benzene and Brilliant Green–H_2O_2–toluene. Hydrogen peroxide was chosen because it had been successfully used as an oxidant for Tl(I) in another method.[8] It was found that λ_{max} (640 nm) did not change with change of solvent.

The calibration curves for these two systems and their regression analysis gave good results (Table 2, Nos. 2 and 3).

All three systems had similar sensitivity and precision. The working range for thallium and the practical limit of determination were identical in all three cases, being 0.2–2.0 and 0.2 μg/ml, respectively.

The selectivity investigation showed that Sn(II), Hg(II), Sb(III), Fe(III), NO_3^- and citrate interfere. The mixture of non-interfering ions (p. 805) also caused deviation from the expected values, the error being about +25% with peroxide as oxidant, and about −13% with cerium(IV) as oxidant.

It is an advantage of this method that the free dye is not extracted by the organic solvents used.

Crystal Violet

Spectrophotometric determination of thallium with Crystal Violet was done according to Chainani *et al.*[9] who described the determination of thallium in zinc and zinc-base alloys. In their method thallium was extracted as an ion-pair of its bromo-complex and Crystal Violet into isopropyl ether and the absorbance was measured at 595 nm. In this way they obtained the high molar absorptivity of 1.02×10^5 l.mole^{-1}.cm^{-1}, and considered that the system should be 0.05*M* in hydrobromic acid and contain 0.002% Crystal Violet.

Our procedure differed from theirs only in the method of forming the $TlBr_4^-$. Chainini *et al.* used a mixture of hydrobromic acid and bromine because of the need for simultaneous dissolution of the metallic zinc (the excess of bromine was removed by heating). In our work, we started from a standard thallium(I) solution and used a more convenient means of formation of the bromo-complex with bromine water and potassium bromide. The excess of bromine was removed with sulphosalicylic acid.[10]

The absorbances obtained in this way for the various concentrations of thallium were about 40% lower than those in the literature.[9]

Thus it appears that this method is not the most sensitive for spectrophotometric determination of thallium.

Table 2. The linear regression of the calibration plots (36 measurements)

No.	Reagent—oxidant—solvent	ϵ*	q†	s_{xy}§	s_k‡
1	Brilliant Green—$Ce(SO_4)_2$—toluene	9.81	−0.007	0.008	0.002
2	Brilliant Green—$Ce(SO_4)_2$—benzene	9.69	0.002	0.008	0.002
3	Brilliant Green—H_2O_2—toluene	9.81	−0.001	0.006	0.001
4	Crystal Violet—Br_2—benzene	8.03	0.003	0.008	0.001
5	Crystal Violet—H_2O_2—benzene	8.09	−0.002	0.011	0.002
6	Methyl Violet—H_2O_2—toluene	6.26	−0.029	0.009	0.001
7	Methyl Violet—H_2O_2—benzene	6.83	−0.021	0.012	0.002
8	Rhodamine B—Br_2—benzene	8.38	0.000	0.009	0.001
9	Rhodamine B—$NaNO_2$—benzene	7.16	0.003	0.008	0.002

* Molar absorptivity, 10^4 *l.mole*$^{-1}$.*cm*$^{-1}$.

† From the regression equation $y = kx + q$ where y = absorbance, k = regression coefficient (ϵ), x = thallium concentration (mole/l.), q = constant.

§ Standard deviation for spread of points round regression line.

‡ Standard deviation of k.

However, it could be useful when selectivity is more important than sensitivity. Chainani *et al.*[9] gave evidence that only Cu and Pb interfered, when present in high amounts.

The next method chosen for determination of thallium with Crystal Violet was Patrovský's.[10] The ion-pair was extracted with benzene from 2*M* hydrochloric acid and bromine water was used as the oxidizing agent for Tl(I). Our calibration curve for this method was satisfactory and confirmed the results from the literature.[10]

The regression analysis indicated that this is a sensitive and precise method for spectrophotometric determination of thallium (Table 2, No. 4).

Taking this method as a model, we then investigated the influence of different oxidants.

We tried ceric sulphate, sodium nitrite and hydrogen peroxide as oxidants, leaving the other conditions unchanged. The excess of the first oxidant was removed with hydroxylammonium chloride or sulphide, and the excess of the second with a saturated solution of urea. The third oxidant decomposed itself.

We found that only the reaction with peroxide (in 0.6*M* hydrochloric acid) was successful (Table 2, No. 5). The other two oxidants decreased the reaction sensitivity by about 30% and produced a considerable spread of results.

This suggests that the sensitivity of spectrophotometric determination of thallium depends on the oxidant used. Of the four oxidants tested only hydrogen peroxide and bromine water gave high sensitivity and precision in the method with Crystal Violet.

In these two systems (Nos. 4 and 5 in Table 2) the working range for thallium and the practical determination limit were 0.4–2.4 and 0.4 μg/ml, respectively.

The investigation of selectivity showed that Sn(II), Sb(III), NO_3^- and citrate interfere. Moreover, when hydrogen peroxide is used as the oxidant for Tl(I), Fe(III) also interferes. A mixture of non-interfering agents gives no error.

Like Brilliant Green, Crystal Violet is also not extracted into the organic solvent.

Methyl Violet

Spectrophotometric determination of thallium with Methyl Violet is also sensitive. In this method we find reports of molar absorptivities of 5.6×10^4 for the benzene extract[1,11] and 6.4×10^4 for the toluene extract.[12]

Thallium was determined with Methyl Violet according to Vashilova and Khomutova,[8] who oxidized Tl(I) with hydrogen peroxide in 0.18–0.20*M* hydrochloric acid and extracted the coloured complex into toluene.

We obtained satisfactory results in this way (Table 2, No. 6).

Contrary to the literature data,[1,11,12] we found that extraction with benzene instead of toluene increased the sensitivity of the method. The calibration curve obtained with benzene as extractant gave good results, and λ_{max} remained the same as with toluene (605 nm). The regression analysis of this calibration curve is shown in Table 2, No. 7.

The working ranges are 0.4–2.8 μg/ml (for benzene) and 0.4–3.2 μg/ml (for toluene). The practical limit of determination is 0.4 μg/ml with both solvents.

The selectivity investigation showed that Sb(III), Hg(II), Fe(III), NO_3^- and citrate interfere. A mixture of non-interfering agents causes no error.

Methyl Violet is also not soluble in the solvents used.

Rhodamine B

Spectrophotometric determination of thallium with Rhodamine B is also a sensitive method. Marczenko's procedure[13] was used. A bromine solution in 2*M* hydrochloric acid is used as the oxidant and benzene or a mixture of benzene and carbon tetrachloride (2:1) as the extractant.

The molar absorptivities for use of the two solvents are 8.7×10^4 and 9.7×10^4 l.mole^{-1}.cm^{-1} respectively.[13]

In the present work we obtained good results with benzene (Table 2, No. 8).

Marczenko's procedure was then modified. The excess of bromine was removed by addition of sulphosalicylic acid solution until the colour disappeared,[10] which is better than prolonged heating to remove the bromine and can be recommended for removal of the bromine excess.

Replacing bromine with sodium nitrite[14] in this procedure also gives good sensitivity and precision (Table 2, No. 9).

Extraction with the 2:1 mixture of benzene and carbon tetrachloride instead of benzene did not give the expected[13] increase in sensitivity. In our work, benzene gave the better results.

Our investigation confirmed that Rhodamine B is a useful reagent for extraction-spectrophotometric determination of thallium.

The working range and practical limit of determination are 0.2–2.4 and 0.2 μg/ml, respectively, with bromine as oxidant and 0.4–2.8 and 0.4 μg/ml, respectively, with sodium nitrite as oxidant.

The selectivity investigation showed that Sn(II), Sb(III), Fe(III), Hg(II) and NO_3^- interfere. The mixture of non-interfering ions (p. 805) caused a positive error of about 15% when bromine water was used and 40% when nitrite was used.

Rhodamine B was not extracted by the solvents used.

Methylene Green and Methylene Blue

Tarayan *et al.*[1,2] reported a very sensitive extractive spectrophotometric determination of thallium with Methylene Green and Methylene Blue. Molar absorptivities of 8.14×10^4 and 1.14×10^5 l.mole^{-1}.cm^{-1} respectively were obtained with these reagents.[1,2]

We repeated the determination according to these authors and got rather different results. The complex with Methylene Green was formed and extracted with trichloroethylene, but the absorbance measurements showed a large spread and low sensitivity. The reaction did not proceed quantitatively.

The complex with Methylene Blue could not be extracted either with trichloroethylene or other solvents, *e.g.*, benzene, toluene, carbon tetrachloride. It was extracted only with chloroform, but together with the excess of dye.

The absorbance maximum for both complexes was the same, 650 nm.

We stopped further investigation of this method because of the lack of colour contrast between the complex and excess of reagent, and both reagents appear useless for spectrophotometric determination of thallium.

Methyl Green

Determination of thallium with Methyl Green was also described by Tarayan *et al.*[2] They again obtained a high molar absorptivity (1.02×10^5 l.mole^{-1}.cm^{-1}) with this reagent (for extraction into benzene).

In our investigation we could not get such good results. Thallium reacted with the dye, but not quantitatively and we observed a spread of the absorbance measurements and low sensitivity. The method with Methyl Green also appears useless for spectrophotometric determination of thallium.

CONCLUSIONS

From among the eight sensitive methods studied, the most successful were the methods with Brilliant

Green, Crystal Violet, Methyl Violet and Rhodamine B. They are well known in the literature and often applied in analysis for thallium.

Our investigation showed that the sensitivity of spectrophotometric determination of thallium also depends on the oxidant used for the Tl(I). The oxidizing agents suitable for the recommended methods are ceric sulphate or hydrogen peroxide for the Brilliant Green method, bromine water or hydrogen peroxide for the Crystal Violet method, hydrogen peroxide with Methyl Violet, and bromine water or sodium nitrite with Rhodamine B.

The regression analysis showed the high molar absorptivities and good precision of the recommended methods. The intercepts were all close to zero, and always negative when hydrogen peroxide was used as the oxidant. The selectivity of the methods was almost identical, the interfering ions being Sn(II), Sb(III), Hg(II), Fe(III), NO_3^- and citrate.

REFERENCES

1. V. M. Tarayan, E. N. Ovsepyan and V. Zh. Artsruni, *Zavodsk. Lab.*, 1969, **35**, 1435.
2. *Idem*, *Dokl. Akad. Nauk Arm. SSR*, 1968, **47**, 27.
3. M. Koźlicka, *Chem. Anal. Warsaw*, 1970, **15**, 683.
4. L. Sommer, M. Langová and V. Kuban, *Scripta Fac. Sci. Natur. UJEP-Brno, Chemica* 1, 1978, **8**, 13.
5. G. Ackermann, J. Kothe and S. Koch, *ibid.*, 1978, **8**, 1.
6. G. F. Kirkbright, *Talanta*, 1966, **13**, 1.
7. A. G. Fogg, C. Burgess and D. T. Burns, *Analyst*, 1973, **98**, 347.
8. N. I. Vashilova and T. V. Khomutova, *Zh. Analit. Khim.*, 1969, **24**, 999.
9. P. A. Chainani, P. Murugaiyan and Ch. Venkateswarlu, *Anal. Chim. Acta*, 1971, **57**, 67.
10. V. Patrovský, *Chem. Listy*, 1963, **57**, 961.
11. I. M. Korenman, *Analiticheskaya Khimia Talliya*, Izdat. Akad. Nauk SSSR, Moscow, 1960.
12. A. G. Fogg, C. Burgess and D. T. Burns, *Talanta*, 1969, **18**, 1175.
13. Z. Marczenko, *Spectrophotometric Determination of Elements*, Horwood, Chichester, 1976.
14. J. Czerniec, Z. Gregorowicz and B. Niźnik, *Zesz. Nauk. Pol. Sl., Inż. Sanit.*, 1976, **19**, 13.

Talanta, Vol. 28, pp. 809 to 815, 1981
Printed in Great Britain. All rights reserved

0039-9140/81/110809-07$02.00/0
Copyright © 1981 Pergamon Press Ltd

STABILITY CONSTANTS FOR THE COMPLEXES OF TRANSITION-METAL IONS WITH FULVIC AND HUMIC ACIDS IN SEDIMENTS MEASURED BY GEL FILTRATION

SHIZUKO HIRATA

Government Industrial Research Institute, Chugoku, Agency of Industrial Science and Technology, Kure-shi 737-01, Japan

(*Received* 28 *April* 1980. *Revised* 24 *December* 1980. *Accepted* 4 *May* 1981)

Summary—The molecular-weight distributions of fulvic and humic acids in sediments and their complexes with metal ions (Cu^{2+}, Zn^{2+}, Mn^{2+}) were investigated by gel filtration. In all cases, metal complexes were found in the fulvic and humic acids. In the complexes the metals were bound to the high molecular-weight fulvic and humic polymers. By use of gel filtration, stability constants for the complexes of copper, zinc and manganese with fulvic acids have been measured. Scatchard plots indicate the presence of two classes of binding site with stability constants of 2.3×10^7 and 1.4×10^6 for copper, 2.1×10^6 and 6.6×10^4 for zinc and 1.8×10^5 and 7.3×10^3 for manganese, respectively.

Until recently, environmental studies and water quality standards have been concerned with the total concentration of particular trace metals in the aquatic environment. It is now realized that to understand ecological phenomena, knowledge of the total metal concentration alone is not sufficient, and it is necessary to understand the distribution and ecological implications of trace metals, and the chemical speciation of the metal. The stabilities of metal–organic complexes in natural aquatic environments are greater than those of the corresponding inorganic metal complexes and affect their availability to biota, their transport and their accumulation in sediments.

However, there is little quantitative information available about the nature and stability of the complexes formed,[1] because of the low concentration of the organic matter or the relatively high concentration of major cationic species, and particularly because of the chemical complexity of the organic compounds known as fulvic and humic acids. Most of the data have been obtained for fulvic and humic acids in soils and natural waters by use of potentiometric titration,[2,3] equilibrium dialysis,[4] ion-exchange,[5] ion-selective electrodes[6–9] or anodic stripping voltammetry methods.[10–12] Use of such methods requires (1) assumption of the metal binding stoichiometry, (2) a restricted range of pH (1.5–6.0), and (3) unrealistically high metal concentrations.

It is important to know the average molecular weight of the fulvic and humic acids used and gel filtration[13] provides a method of measuring molecular weight distributions of macromolecules and recovering the samples. The dynamic equilibration technique of gel chromatography has been proposed[14] for estimation of the stability constants of metal complexes of biochemical macromolecules, and applied to copper–deoxyribonucleic acid,[15–17] manganese–nucleotide[18] and zinc–plasma.[19]

The Seto Inland Sea (Japan), surrounded by industrial areas,[13] is a strip of inland sea with three exits and poor exchange with the ocean waters. For the past ten years there have been "red tides" in the Seto Inland Sea from spring to autumn, *e.g.*, in Harima Sound. As a result, many fish died and the inshore fishery suffered damage. Our Environmental Chemistry Division laboratory, belonging to the Ministry of International Trade and Industry (MITI), is engaged in investigating the ecological aspects of the Seto Inland Sea and preventing pollution, particularly in connection with the red tide. Accordingly, we have investigated the relation between metals and organic matter (fulvic and humic acids) in the sediments in the Seto Inland Sea.

We have chosen three sediment samples. The Hiro Bay sediment is assumed to be polluted with a pulp mill effluent, but the Osaka and Beppu Bay sediments are ordinary coastal sediments. In this paper we describe the complexation behaviour of certain metal ions (Cu^{2+}, Zn^{2+}, Mn^{2+}, Fe^{2+}) and the stability constants of some metals with the fulvic acids on the basis of the molecular weight distributions of the fulvic and humic acids, obtained by use of gel filtration.

EXPERIMENTAL

Reagents

All solutions were prepared from analytical reagent grade chemicals and demineralized water, and stored in polyethylene bottles.

Eluent for fulvic acids. Prepare 0.01*M* ammonium carbonate solution[20] in 0.1*M* sodium chloride to avoid a Donnan effect.[21]

Table 1. Location of samples

	Location		Depth, *m*
Hiro Bay*	34°13′N	133°37′E	4
Osaka Bay	34°39′N	135°21′E	10
Beppu Bay	33°15′N	131°33′E	70

* Containing a pulp-mill effluent.

Eluent for humic acids. Prepare 0.01*M* sodium hydroxide solution[22] in 0.1*M* sodium chloride.

Sephadex gel. Treat the Sephadex gel with a large excess of deaerated eluent and let it swell overnight. Decant the eluent and entrained "fines" before packing the column.

TRIS buffer.[13] Dissolve 0.58 g of sodium chloride in 800 ml of redistilled water, add 1.21 g of TRIS and titrate to pH 8.0 with 0.5*M* hydrochloric acid. Add the required amount of the metal ion being investigated (use a standard solution of the chloride) and dilute to 1 litre with redistilled water. This solution is 0.01*M* in both sodium chloride and TRIS.

Sephadex G-15. Treat the Sephadex gel with TRIS buffer containing the required concentration of free metal ion.

Fulvic and humic acids. Samples of fulvic and humic acids were extracted according to the methods in the previous paper[22] from the sediments of Hiro, Osaka and Beppu Bays with 0.5*M* sodium hydroxide. Fulvic acid was separated from humic acid by centrifugation (3000 rpm, 15 min) and concentrated at 65° in a vacuum rotary evaporator. The humic acid was redissolved in a small amount of 0.5*M* sodium hydroxide.

Fulvic acids. To remove inorganic contamination, the fulvic acids were sorbed at pH 2.0 on Amberlite XAD-2 resin and eluted with 1:1 methanol–2*M* ammonia mixture,[23] then the eluate was evaporated to dryness at 35° (rotary evaporator). The residue was weighed and dissolved in TRIS buffer. Its average molecular weight was found to be 3400 ± 250 for the fulvic acid of Hiro Bay sediment, 3200 ± 250 for Osaka Bay, and 3500 ± 250 for Beppu Bay, by gel filtration. Blue dextran 2000, vitamin B_{12} and glucose were used as the calibration standards for the molecular weight distribution. Higher molecular-weight fractions in the fulvic acids were concentrated by means of Amberlite XAD-2 resin. Sampling locations are shown in Table 1.

Apparatus

The apparatus used to measure the stability constants is shown diagrammatically in Fig. 1. Column (A) contains 120–130 ml of swollen Sephadex gel in a 62-cm length of 1.6-cm bore chemical pipeline (Amicon Co.). TRIS buffer is led into the column from the polyethylene reservoir (B) through a capillary from a 3-way stopcock (C), the third arm of which is connected to the glass reservoir (D) containing the buffered fulvic acid solution. Eluate flows at 40 ml/hr from the column and is monitored with an ultraviolet spectrophotometer (E) to give a record (F) and finally collected in the fraction collector (G).

Procedure

Molecular weight distributions of fulvic and humic acids. The elution of these acids from Sephadex gel with distilled water varies as the sample concentration of the acid changes.[24] In these experiments a constant amount of sample was placed on the Sephadex gels.

Place 0.5-ml samples of the humic acid solution (organic carbon *ca.* 22.1 mg/ml) on the top of Sephadex G-25 and G-50 columns (both 1.2 × 45 cm), and G-75, G-100 and G-200 columns (all 1.2 × 90 cm) and elute with 0.01*M* sodium hydroxide in 0.1*M* sodium chloride. Place 2.0-ml samples of the fulvic acid solution (organic carbon *ca.* 9.50 mg/ml) on the top of Sephadex G-10, G-15, G-25 and G-50 columns (all 1.2 × 45 cm) and elute with 0.01*M* ammonium carbonate in 0.1*M* sodium chloride. Using an automatic fraction collector, collect 30–45 4.0-ml fractions. Monitor the absorbance of the eluate at 210–360 nm and then determine the concentration of the metal ion concerned in each fraction by atomic-absorption spectrophotometry. Estimate the concentrations of organic matter and metal ions eluted at an effluent volume equal to the void volume of each column, the molecular weight distributions of the fulvic and humic acids, and the distributions of the metal ions.

Stability constants of fulvic acid with metal ions. Weigh out 30–60 mg of the fulvic acid sample into a 10-ml standard flask, dissolve it and make up to volume with metal–TRIS buffer and allow to equilibrate at room temperature. Place 0.2 ml of this solution in reservoir D, and pass it into the gel column, previously equilibrated by passage of 800 ml of the metal–TRIS buffer. Rinse the reservoir with 2 ml of this buffer, passing the washings into the column. Elute with metal–buffer solution from reservoir B. Monitor the absorbance of the eluate at 254 nm.

Use a fraction collector to collect 60–80 3.75-ml fractions. Analyse these for the metal ion by atomic-absorption spectrophotometry.

Distribution coefficients

The values of K_d are calculated from

$$V_e = V_o + K_d V_i \qquad (1)$$

where V_e, V_o and V_i are the elution volume, void volume and inner volume, respectively. For the calculation of V_e, the elution volume of Blue dextran 2000, which is excluded from the gel phase, is used as V_o.

Calculation of stability constants

The stability constants of the metal-fulvic acid complexes were calculated as described by Mantoura and Riley.[13]

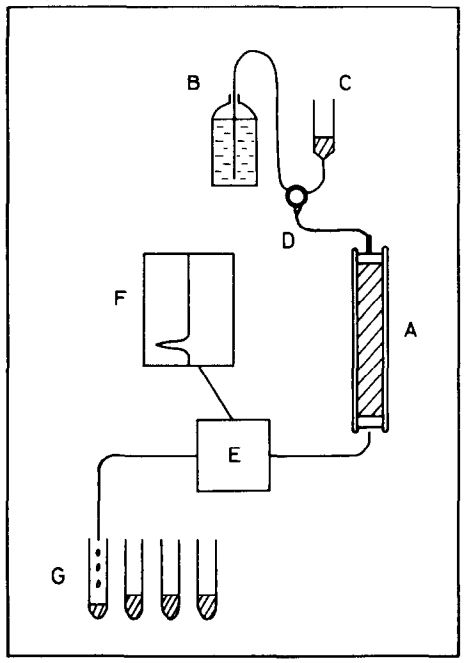


Fig. 1. Diagrammatic representation of the gel-filtration apparatus for the determination of stability constants. (A) Gel column, (B) pH–pM buffer reservoir, (C) sample reservoir, (D) 3-way stopcock, (E) spectrophotometer, (F) recorder, (G) fraction collector.

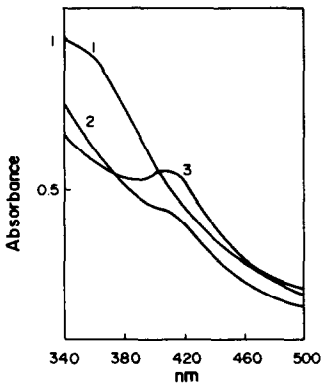


Fig. 2. Visible-region spectra of the humic acids in sediments. 1, Hiro Bay; 2, Osaka Bay; 3, Beppu Bay.

For the reaction

$$n\mathrm{Me} + \mathrm{FA} \rightleftharpoons \mathrm{Me}_n\mathrm{FA}$$

the equilibrium constant can be written as

$$K_n = \frac{[\mathrm{M_b}/n]}{[\mathrm{M_f}]^n([\mathrm{M_{FA}}] - [\mathrm{M_b}/n])} \quad (4)$$

in which $[\mathrm{M_b}]$ is the number of moles of metal bound, $[\mathrm{M_f}]$ the number of moles of free metal, and $[\mathrm{M_{FA}}]$ the number of moles of fulvic acid taken. These results can be treated[13] by the method of Scatchard[25] in which it is assumed that

$$\frac{\tilde{\nu}}{[\mathrm{M_f}]} = K_i(n_i - \tilde{\nu}) \quad (5)$$

where $\tilde{\nu} = [\mathrm{M_b}]/[\mathrm{M_{FA}}]$, K_i is the stability constant of the metal–fulvic acid complex, and n_i is the number of metal binding sites per molecule of fulvic acid. The subscript $i = 1, 2, \ldots$ denotes the type of metal binding site on the fulvic acid molecules. The value of $\tilde{\nu}$ is obtained from a series of runs carried out over a range of free metal concentrations, and $\tilde{\nu}/[\mathrm{M_f}]$ is plotted against $\tilde{\nu}$. It is clear from the Scatchard equation that the slopes of the two branches line give the $-K_i$ values and that the intercepts (of the extrapolations) on the $\tilde{\nu}$ axis correspond to the n_i values. However, it should be noted that use of the information obtainable from Scatchard plots is of very limited use in interpretation.[5]

RESULTS

Molecular-weight distributions of fulvic and humic acids

The visible-region spectra of the humic acids isolated from the coastal sediments are shown in Fig. 2. Characteristic absorption at 410 nm, which may be due to a plankton pigment,[26] was found in the humic acids of the Osaka and Beppu Bay sediments, that for the latter (which was collected at a depth of 70 m) being the more prominent.

However, this characteristic absorption was not found in the humic acid of the Hiro Bay sediment (from near a pulp mill), which was different from usual marine sediment and contained 10.6% of organic carbon. The contents of organic carbon, iron, manganese, zinc and copper in the sediments, *etc.* are shown in Table 2.

The metals extractable with 0.5*M* sodium hydroxide may be inorganic compounds, such as hydroxides, oxides, carbonates and sulphates, or bound to organic matter. For the three sediment samples, the elements extracted with 0.5*M* sodium hydroxide were in the ranges 45.1–75.5% organic carbon, 0.37–8.39% iron, 0.04–6.95% manganese, 2.95–19.3% zinc and 37.8–54.1% copper, all relative to the total amount of these elements in the sediments. Consequently, iron, manganese and zinc may be present mainly in inorganic forms in the sediments with small portions as organic forms, whereas a considerable portion of the copper may be bound to organic matter. The metals extracted with 0.5*M* sodium hydroxide were mainly

Table 2. Elemental composition of the sediments and their fractions, extracted from the sediment of Hiro Bay

Sample	Elements	Sediment, *ppm*	Humic substance,* %	Fulvic acid,† %	Humic acid,§ %
Hiro Bay	Org-C	10.6×10^4	75.5	36.4	63.6
	Fe	1.45×10^4	8.4	75.5	24.5
	Mn	341	7.0	84.4	15.6
	Zn	214	19.3	87.0	13.0
	Cu	74	54.1	20.0	80.0
Osaka Bay	Org-C	3.26×10^4	45.1	93.7	6.3
	Fe	2.07×10^4	0.53	95.5	4.5
	Mn	454	0.15	98.1	1.9
	Zn	745	3.71	98.3	1.7
	Cu	127	37.8	90.5	9.5
Beppu Bay	Org-C	2.98×10^4	50.8	88.8	11.2
	Fe	1.80×10^4	0.37	98.9	1.1
	Mn	306	0.04	96.6	3.4
	Zn	118	2.95	94.1	5.9
	Cu	24	48.6	70.2	29.8

* 100 × content in humic substance/content in sediment.
† 100 × content in fulvic acid/content in humic substance.
§ 100 × content in humic acid/content in humic substance.

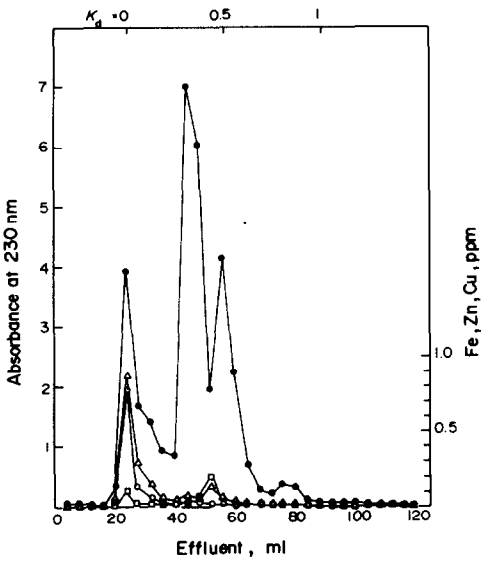


Fig. 3. Fractionation of the fulvic acid from Osaka Bay sediment on Sephadex G-15.
●: Absorbance, ○: Fe, □: Zn, △: Cu
Eluent: 0.1M NaCl + 0.01M NH_4HCO_3. Column: 1.2 × 45 cm K_d: distribution coefficient.

contained in the fulvic acid fractions (not the humic acid fractions) except for copper in the Hiro Bay sample. The elution of fulvic acid from Sephadex G-15 is shown in Fig. 3 as a typical example. Similar results were obtained for the other sediments. The amounts of fulvic and humic acids and metals eluted at the void volume decreased as the gel particle size was increased. In the Osaka Bay sediment, copper was combined strongly with the fulvic acid, and the iron and zinc less strongly. The same trend was observed for binding to the humic acid (Cu > Fe > Zn). The results are shown in Tables 3 and 4.

Stability constants of fulvic acids with metal ions

The use of the method can be illustrated by the complexation of copper by the Beppu Bay fulvic acids (Fig. 4). The amount of complexed copper found from the area of the peak was within 4% of that computed from the area of the trough. The data obtained with the Beppu Bay fulvic acid and a range of copper concentrations ($[M_f] = 2.1 \times 10^{-8}$–$2.1 \times 10^{-6} M$) are shown in a Scatchard plot in Fig. 5.

The two linear portions are attributed to the presence of two different types of binding sites in the fulvic acid polymer. Analysis of the graph shows the presence of an average (per fulvic acid molecule) of 0.4 sites of the more strongly binding ligand (log $K_1 = 7.2$), and 1.1 sites of the weaker ligand (log $K_2 = 6.0$). The technique was also used to study the interaction of zinc and manganese with fulvic acids.

DISCUSSION

It has been reported that the fulvic acids insoluble in tetrahydrofuran, fulvic acids soluble in a tetrahydrofuran–ether mixture, and brown humic acids, all extracted from a podzol soil, have molecular weight ranges of (4–40) × 10^3 (2–4) × 10^3 and (5–>100) × 10^3 respectively,[27,28] and 55% of the humic acid extracted from forest soil has a molecular-weight range up to 5 × 10^3, and 45% in the range (5–10) × 10^3.[29] Molecular weights of organic matter from forest soil do not exceed 10^4. A comparison with Posner's data[30] indicates that over 55% of the humic acid extracted from soil has molecular weight $< 10^4$, whereas about 30–54% of the coastal humic acids reported in this paper, and 25–40% of humic acids of marine origin,[31] lie in that range. However, the molecular-weight distributions of the fulvic and humic acids in our three samples are lower than those of

Table 3. Molecular weight ranges and metal distribution of fulvic acid fractions extracted from sediments with various Sephadex gels

Sample	Molecular weight ranges of the gels used	Fraction in each molecular weight range, % Organic matter*	Fe	Zn	Cu
Hiro Bay	700 and less	70.1	78.2	61.1	60.7
	700–1.5 × 10^3	3.8	0.0	0.0	0.0
	1.5 × 10^3–5 × 10^3	10.0	8.8	8.5	20.1
	5 × 10^3–10^4	14.9	12.5	21.5	19.2
	10^4–5 × 10^4	1.2	0.5	8.9	0.0
	5 × 10^4–10^5	No exclusion		No exclusion	
Osaka Bay	700 and less	75.8	53.1	38.2	17.0
	700–1.5 × 10^3	6.2	0.0	0.0	9.1
	1.5 × 10^3–5 × 10^3	6.9	27.5	34.9	65.5
	5 × 10^3–10^4	11.1	19.4	26.9	8.4
	10^4–5 × 10^4	No exclusion		No exclusion	
Beppu Bay	700 and less	61.3	57.0	18.4	24.6
	700–1.5 × 10^3	6.4	3.7	44.3	11.4
	1.5 × 10^3–5 × 10^3	20.1	20.4	0.0	40.1
	5 × 10^3–10^4	7.2	15.2	22.4	11.2
	10^4–5 × 10^4	3.0	3.7	14.9	12.7
	5 × 10^4–10^5	No exclusion		No exclusion	

* Determined from the absorbance at 230 nm.

Table 4. Molecular weight ranges and metal distributions of humic acid fraction extracted from sediments with various grades of Sephadex gels

Sample	Molecular weight ranges of the gels used	Fraction in each molecular weight range, % Organic matter*	Fe	Zn	Cu
Hiro Bay	0–10^3	17.3	2.3	1.5	13.0
	5×10^3–10^4	12.5	14.3	34.6	17.0
	10^4–5×10^4	48.3	45.1	30.2	47.0
	5×10^4–10^5	2.8	5.5	15.3	7.3
	10^5–2×10^5	9.8	7.6	0.0	8.9
	$>2 \times 10^5$	9.3	25.2	18.4	6.7
Osaka Bay	0–10^3	21.1	15.2	17.5	16.5
	5×10^3–10^4	32.4	27.8	27.2	39.8
	10^4–5×10^4	14.7	0.1	14.4	9.3
	5×10^4–10^5	4.8	20.5	9.9	7.5
	10^5–2×10^5	7.3	7.5	2.2	5.1
	$>2 \times 10^5$	19.7	28.9	28.8	21.8
Beppu Bay	0–10^3	24.8	5.8	13.1	15.3
	5×10^3–10^4	27.4	8.2	20.6	21.0
	10^4–5×10^4	15.1	21.0	7.4	11.3
	5×10^4–10^5	1.7	28.4	17.2	17.6
	10^5–2×10^5	0.0	0.0	0.0	1.2
	$>2 \times 10^5$	31.0	36.6	41.7	33.6

* Determined from the absorbance at 230 nm.

marine origin,[31,32] which were from marine sediments deeper than those dealt with here, and may have higher molecular weight ranges owing to reactions of marine organisms.

The weight-average molecular weight of lignin sulphonate, which is a major component of pulp mill effluent, is reported[33] to be 3.6×10^4. It is of interest that 48.3% of the humic acid, 45.1% of the iron, 30.2% of the zinc and 47.0% of the copper in the total Hiro Bay humic acid were found in the fraction with molecular weight $(1$–$5) \times 10^4$.

The following conclusions may be drawn.

(1) Fulvic acid generally has a narrower molecular weight distribution ($\leqslant 10^4$) than humic acid ($\leqslant 2 \times 10^5$). Iron, zinc and copper are preferentially complexed to fulvic and humic acids having high molecular weights.

(2) As the proportion of organic matter derived from marine organisms increases, the humic acid shows higher molecular weights. The Beppu Bay humic acid had the highest molecular weight.

(3) The amounts of metals contained in the fulvic and humic acids differ according to the environment.

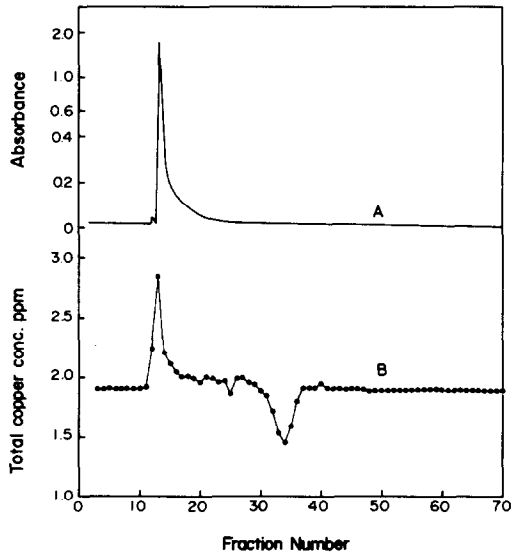


Fig. 4. Gel-filtration chromatograms for the interaction of *ca.* 2.0 μg/ml copper with 0.692 mg of the Beppu Bay fulvic acid at pH 8.0 and $\mu = 0.01$. The absorbance (curve A) and total copper content of the eluate (curve B) were measured for each 3.75-ml fraction.

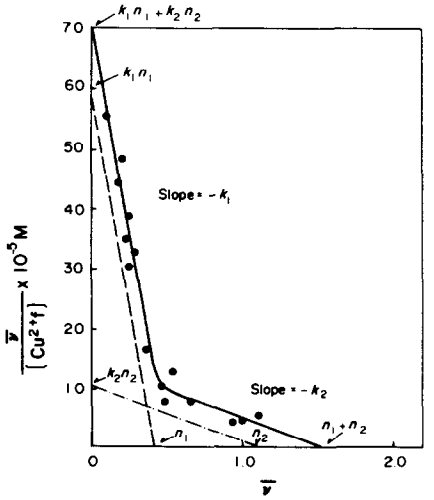


Fig. 5. Scatchard plot for the binding of copper(II) by the fulvic acids of Beppu Bay sediment at pH 8.0 and $\mu = 0.01$. The linear components of the curves are the resolved contributions from the "strong" sites (– – –) and the "weak" sites (— · — · —).

Table 5. Stability constants at 20°C and binding stoichiometries for copper(II), zinc(II) and manganese(II) with sedimentary fulvic acids

Metal	Sample	i*	n_i†	log K_i
Cu(II)	Hiro Bay	1	0.3	7.55
		2	0.8	6.27
		0	1.0	7.02
	Osaka Bay	1	0.3	7.43
		2	2.2	5.64
		0	2.5	6.57
	Beppu Bay	1	0.4	7.24
		2	1.6	5.72
		0	2.0	6.59
Zn(II)	Hiro Bay	1	0.2	6.40
		2	1.2	4.75
		0	1.4	5.60
	Osaka Bay	1	0.2	6.14
		2	0.8	4.81
		0	1.0	5.57
	Beppu Bay	1	0.3	6.36
		2	0.8	4.86
		0	1.1	5.80
Mn(II)	Hiro Bay	1	0.2	5.38
		2	1.1	3.96
		0	1.3	4.64
	Osaka Bay	1	0.3	5.30
		2	1.0	3.93
		0	1.3	4.68
	Beppu Bay	1	0.4	5.22
		2	1.3	3.80
		0	1.6	4.62

* i denotes the type of binding site; $i = 0$ denotes the overall binding.

† n_i signifies the average number of type i sites per molecule of fulvic acid.

The abundance in fulvic and humic acids was Fe > Cu > Zn ≫ Mn for the Hiro Bay sediment polluted with a pulp-mill effluent and Cu > Fe > Zn ≫ Mn for the usual coastal sediments of Osaka Bay.

The reproducibility was assessed with four identical runs (each in duplicate) on the Beppu Bay fulvic acid at pH 8.0. The average K_n value was 4.4×10^6 with a relative standard deviation of 8.5%.

It is impossible to measure quantitatively the stability constant for the iron complexes with fulvic acids by the proposed method, because of adsorption of the fulvic acids on the gel equilibrated with TRIS buffer containing iron.

It is noteworthy that the intrinsic stability constants K_1 and K_2 for any metal with sedimentary fulvic acids did not vary significantly from one sample to another (Table 5). The constants were in the order Cu > Zn > Mn. The number of binding sites n_1 and n_2 per molecule of the same sample of fulvic acid were similar for zinc and manganese, and not much different for copper. The binding sites of type 1 are probably phenolic and carboxylic groups, and those of type 2 the carbonyl and amino groups, which are known to be the metal-complexing sites in fulvic acids,[3,34–37]

Usually fulvic acids contain 100–900 meq of carboxylate per 100 g and humic acids contain 150–500 meq per 100 g.[34,38–44] The fulvic acids with molecular weights 700–10^4 contain 150–300 meq of carboxylate per 100 g.[44] The fulvic acids of molecular weight 3400 used in this experiment should therefore contain about 300 meq of carboxylate per 100 g. On average these fulvic acids have 1.4 binding sites per molecule for copper, zinc and manganese. This can be approximated to two carboxylate groups per molecule, corresponding to about 60 meq per 100 g, which implies that only about a fifth of the carboxylate groups are in an orientation and position suitable for binding metals.

From the values shown in Table 5, it is arbitrarily considered that a bivalent metal ion can be held in five ways: (1) as a 4:1 (ligand:metal) chelate complex, or as a 2:1 complex with only half the binding sites occupied, or a 1:1 complex with a quarter of the binding sites used ($n_i = 0.25$); (2) as a 2:1 chelate complex holding fulvic acid two molecules together as a chain ($n_i = 0.50$); (3) as a 1:1 complex or a complex at the end of the chain ($n_i = 1.0$); (4) as a 1:2 complex ($n_i = 2.0$); (5) as a $1:n$ ($n > 2$) complex ($n_i > 2.0$). These are arranged in order of decreasing stability. The values obtained for numbers of binding sites may be number averages from co-existence of more than one type of complex.

Acknowledgements—The author thanks Y. Yamamoto, Department of Chemistry, Faculty of Science, Hiroshima University and N. Yoza, Department of Chemistry, Faculty of Science, Kyushu University, for their valuable suggestions.

REFERENCES

1. A. Siegel in S. F. Faust and J. V. Hunter (eds.), *Organic Compounds in Aquatic Environments*, Dekker, New York, 1971.
2. M. Schnitzer and S. U. Khan, *Humic Substances in the Environment*, Dekker, New York, 1972.
3. F. J. Stevenson, *Soil Sci.*, 1977, **123**, 10.
4. R. D. Guy and C. L. Chakrabarti, *Can. J. Chem.*, 1976, **54**, 2600.
5. J. Buffle, F. J. Creater and W. Heardi, *Anal. Chem.*, 1977, **49**, 216.
6. W. T. Bresnahan, C. L. Grant and J. H. Weber, *ibid.*, 1978, **50**, 1678.
7. M. J. Stiff, *Water Res.*, 1971, **5**, 585.
8. J. Gardner, *ibid.*, 1974, **8**, 23.
9. V. Cheam, *Can. J. Soil Sci.*, 1973, **53**, 377.
10. R. Ernst, H. E. Allen and K. H. Mancy, *Water Res.*, 1975, **9**, 969.
11. P. L. Brezonik, P. A. Brauner and W. Stumm, *ibid.*, 1976, **10**, 605.
12. T. A. Oshea and K. H. Mancy, *Anal. Chem.*, 1976, **48**, 1603.
13. R. F. C. Mantoura and J. P. Riley, *Anal. Chim. Acta*, 1975, **78**, 193.
14. J. P. Hummel and W. J. Dreyer, *Biochem. Biophys. Acta*, 1962, **63**, 530.
15. S. E. Bryan and E. Freidan, *Biochemistry*, 1967, **6**, 2728.
16. P. A. Price, *J. Biol. Chem.*, 1972, **247**, 2895.

17. E. Breslow and A. W. Girotti, *ibid.*, 1970, **245,** 1527.
18. R. F. Colman, *Anal. Biochem.*, 1972, **46,** 358.
19. F. A. Suso and H. M. Edwards, Jr., *Proc. Soc. Exp. Biol. Med.*, 1791, **138,** 157.
20. D. H. Stuermer and G. R. Harvey, *Nature*, 1974, **250,** 480.
21. N. Yoza, T. Ogata and S. Ohashi, *J. Chromatog.*, 1972, **52,** 329.
22. S. Hirata, *Nippon Kagaku Kaishi*, 1979, 1316.
23. R. F. C. Mantoura and J. P. Riley, *Anal. Chim. Acta*, 1975, **76,** 97.
24. R. S. Swift and A. M. Posner, *J. Soil Sci.*, 1971, **22,** 237.
25. G. Scatchard, *Ann. N.Y. Acad. Sci.*, 1949, **51,** 660.
26. S. Schwartz, M. H. Berg, I. Bossenmaier and H. Dinsmore, *Methods Biochem. Anal.*, 1961, **8,** 229.
27. N. C. Mehta, P. Dubach and H. Deuel, *Z. Pflanzenernähr. Dung. Bodenkund.*, 1963, **102,** 128.
28. P. Dubach, N. C. Mehta, T. Jacob, F. Martin and N. Roulet, *Geochim. Cosmochim. Acta*, 1964, **28,** 1567.
29. A. Prakash and M. A. Rashid, *Limnol. Oceanog.*, 1968, **13,** 598.
30. A. M. Posner, *Nature*, 1963, **198,** 1161.
31. M. A. Rashid and L. H. King, *Geochim. Cosmochim. Acta*, 1969, **33,** 147.
32. R. Ishiwatari, *Geochem. J.*, 1971, **5,** 121.
33. M. Koyama, *Nippon Kagaku Kaishi*, 1977, 25.
34. J. H. Weber and S. A. Wilson, *Water Res.*, 1975, **9,** 1097.
35. S. A. Wilson and J. H. Weber, *Chem. Geol.*, 1977, **19,** 285.
36. A. Albert, *Biochem. J.*, 1950, **47,** 531.
37. M. J. Stiffe, *Water Res.*, 1971, **5,** 585.
38. M. Schnitzer and E. Vendette, *Can. J. Soil. Sci.*, 1975, **55,** 93.
39. M. Schnitzer and J. G. Desjardins, *ibid.*, 1969, **49,** 151.
40. W. Flaig, *Adv. Org. Geochem.*, 1971, p. 49, Pergamon Press, Oxford, 1972.
41. Y. Saito and S. Hayano, *J. Oceanog. Soc. Japan*, 1980, **36,** 59.
42. C. Steelink, *J. Chem. Educ.*, 1977, **54,** 599.
43. M. A. Rashid and L. H. King, *Geochim. Cosmochim. Acta*, 1970, **34,** 193.
44. M. A. Rashid, *Soil Sci.*, 1971, **111,** 298.

Talanta, Vol. 28, pp. 817 to 823, 1981
Printed in Great Britain

0039-9140/81/110817-07$02.00/0
Pergamon Press Ltd

SYSTEMATIC ANALYSIS FOR COMMON CATIONS BY SOLID-STATE SPOT-TESTS

M. QURESHI, ALI. MOHAMMAD and G. GANGA RAJU

Chemistry Section, Z. H. College of Engineering & Technology,
Aligarh Muslim University, Aligarh-202001, India

(*Received* 16 *April* 1980, *Revised* 9 *April* 1981. *Accepted* 27 *April* 1981)

Summary—Solid-state capillary spot-tests for 17 cations with 16 organic and inorganic reagents have been examined. A comparative study of the colour reactions in solution has also been made. Some new reactions are described. The reactions studied have been systematized.

Capillary solid-state spot-tests have certain advantages over the usual spot-tests in solutions, in which only the colour formed is indicative. In the solid-state tests the colour at the junction, the length of the boundary and the direction of movement of the boundary can all be observed and interpreted. Thus two substances giving the same colour with a reagent can be distinguished on the basis of the direction of boundary movement if they move in opposite directions. The utility of these tests has therefore been explored in organic analysis,[1,2] but no effort has been made to explore their use in inorganic analysis. Another advantage of these solid-state spot-tests is that no separation of interfering metal ions is required. Since only capillaries are used, this method is very simple. The procedure is based on classifying the cations into groups according to the colours produced by particular reagents, and then applying the capillary method to each group.

EXPERIMENTAL

Reagents

All the reagents used were of BDH analytical or laboratory reagent grade. The powders used were of 50–100 mesh size.

Solid-state detection

A little of the solid test material was mixed in an ignition tube with a few mg of the reagent. The colours developed at room temperature and on heating to a higher temperature (70–80) were recorded. The limits of identification were determined by starting with known volumes of standard solutions of the compounds concerned, evaporating to dryness and mixing the solid residue with the reagent. The limit of identification is in the range of 5–100 μg for all the metal ions tested.

Solid-state detection in capillaries

A capillary (3 mm bore) was partly filled with the reagent by continuous tapping and then the solid test material was introduced at the open end. The colour of the product at the junction and the direction of movement of the coloured boundary were recorded. The limits of identification were determined by starting with various synthetic mixtures of the solid test material with potassium nitrate as diluent.

DISCUSSION

A survey of the results shows that in a number of cases the colours obtained in solution are different from those obtained in the solid state.

Potassium chromate can be used for the specific detection of Hg_2^{2+} and As^{3+} in the solid state. As^{3+} and Mg^{2+} do not give any colour in solution but do in the solid-state reaction. As^{3+} can be differentiated from As^{5+} by the solid-state test. Mn^{2+} gives a red colour followed by a black colour in the solid state and the coloured boundary moves towards the Mn^{2+}. Ag^+ also gives a black colour in the solid state but does not give any boundary movement, thus this property can be used to distinguish between Mn^{2+} and Ag^+. As Ag^+ gives a red precipitate in solution it appears that in the solid state either the species formed is different from the one formed in solution or there is a particle-size effect on the colour perceived. Mixtures of Cd^{2+} and Sn^{2+}, Cd^{2+} and Cr^{3+}, Cr^{3+} and Mg^{2+}, Cr^{3+} and Zn^{2+}, Bi^{3+} and Zn^{2+}, Bi^{3+} and Mg^{2+}, all give an orange colour at the junction but can be distinguished on the basis of the movement of the coloured boundary. As_2O_3 gives the green colour in the solid-state reaction only very slowly (15 days) but sodium arsenite reacts in only 30 min at 80°.

With 8-hydroxyquinoline Bi^{3+} and Cu^{2+} both give black products in the solid state while in solution Bi^{3+} gives a yellow precipitate and Cu^{2+} gives a brown precipitate. The solid-state test can be applied for the detection of Bi^{3+} and Cu^{2+} in the presence of those metal ions which give colour reactions with oxine, except Hg_2^{2+}, Fe^{2+} and Sb^{3+}, whereas it is not possible in solution state. Fe^{2+} can be distinguished from Bi^{3+} and Cu^{2+} on the basis of the direction of the movement of the coloured boundary. Of all the metal ions which give yellow products with oxine, only Sn^{2+} gives a coloured boundary which moves towards the reagent, leading to selective detection of Sn^{2+}.

Cr^{3+} and Ni^{2+} react with potassium iodide in the solid state to give brown and black colours respectively. Such coloured products are unstable in solution

Table 1

	Potassium chromate					8-Hydroxyquinoline					Potassium iodide					Acridine				
Cation	T	CJ	DM	CsC	CsH	T	CJ	DM	CsC	CsH	T	CJ	DM	CsC	CsH	T	CJ	DM	CsC	CsH
Hg_2^{2+}	40	R	TR	R↓	R↓	50	R	TR	O↓	O↓	50	R, Bk	NM	Br↓	Br↓	50	Y, R	TR	Y↓	Y
Ag^+	70	Bk	NM	R↓	R↓	—	—	—	—	—	60	Gy	NM	LY↓	LY↓	—	—	—	—	—
Pb^{2+}	—	—	—	—	—	70	Y	NM	Y↓	Y	60	LY	NM	Y↓	Y↓	—	—	—	—	—
Bi^{3+}	40	O, Br	TR	Y↓	Y↓	60	Bk	TR	Y↓	Y↓	45	DBr	TR	Br↓	Br↓	60	Y	NM	Y↓	Y↓
Cu^{2+}	—	—	—	—	—	60	Bk	TR	Br↓	Br↓	45	Br	TR	Br↓	Br↓	—	—	—	—	—
Cd^{2+}	50	O	NM	Y↓	Y↓	60	Y	NM	Y↓	Y↓	—	—	—	—	—	60	Y	NM	Y↓	Y
As^{3+}	30	G	TR	NC	NC	—	—	—	—	—	—	—	—	—	—	—	—	—	—	—
Sb^{3+}	—	—	—	—	—	60	G	TR	G↓	G↓	—	—	—	—	—	60	Y	NM	Y↓	Y
Sn^{2+}	40	O	TR	Br↓	Br↓	50	Y	TR	Y↓	Y↓	30	O	NM	O↓	O↓	60	Y	NM	Y↓	Y↓
Mn^{2+}	25	Bk	TM	Bc↓	Bc↓	—	—	—	—	—	—	—	—	—	—	60	Y	NM	Y↓	Y
Fe^{2+}	—	—	—	—	—	70	Bk	TM	Bk↓	Bk↓	—	—	—	—	—	—	—	—	—	—
Cr^{3+}	80	O	TR	LBr↓	LBr↓	—	—	—	—	—	45	Br	TR	NC	NC	—	—	—	—	—
Ni^{2+}	—	—	—	—	—	—	—	—	—	—	60	Bc	TM	NC	NC	—	—	—	—	—
Zn^{2+}	70	O	NM	Y↓	Y↓	70	Y	NM	Y↓	Y↓	—	—	—	—	—	—	—	—	—	—
Mg^{2+}	50	O	NM	NC	NC	60	Y	NM	Y↓	Y↓	—	—	—	—	—	60	R, Br	NM	Y↓	Y

T = temperature (C)
CJ = colour at junction (solid state)
DM = direction of boundary movement
CsC = colour in cold solution (↓ = precipitate)
CsH = colour in hot solution (↓ = precipitate)
TM = towards test material
TR = towards reagent
NM = no movement

NC = no colour
L = light
D = dark
Bk = black
Bl = blue
Br = brown
G = green

Gy = grey
O = orange
P = pink
R = red
V = violet
W = white
Y = yellow

Table 2

	Dithio-oxamide					Oxalic acid					1,10-Phenanthroline					Dimethylglyoxime				
Cation	T	CJ	DM	CsC	CsH	T	CJ	DM	CsC	CsH	T	CJ	DM	CsC	CsH	T	CJ	DM	CsC	CsH
Hg_2^{2+}	—	—	—	—	—	60	LP	NM	W↓	W↓	—	—	—	—	—	—	—	—	—	—
Ag^+	60	Bk	NM	Bk↓	Bk↓	—	—	—	—	—	—	—	—	—	—	—	—	—	—	—
Sn^{2+}	50	Bk	TR	LBr↓	LBr↓	—	—	—	—	—	—	—	—	—	—	—	—	—	—	—
Fe^{2+}	—	—	—	—	—	90	G	NM	Y↓	Y↓	60	P	NM	P	P	—	—	—	—	—
Co^{2+}	60	Br	NM	NC	NC	—	—	—	—	—	—	—	—	—	—	—	—	—	—	—
Ni^{2+}	60	Bl	NM	Bk↓	Bk↓	—	—	—	—		—					80	P	TM	P↓	P↓

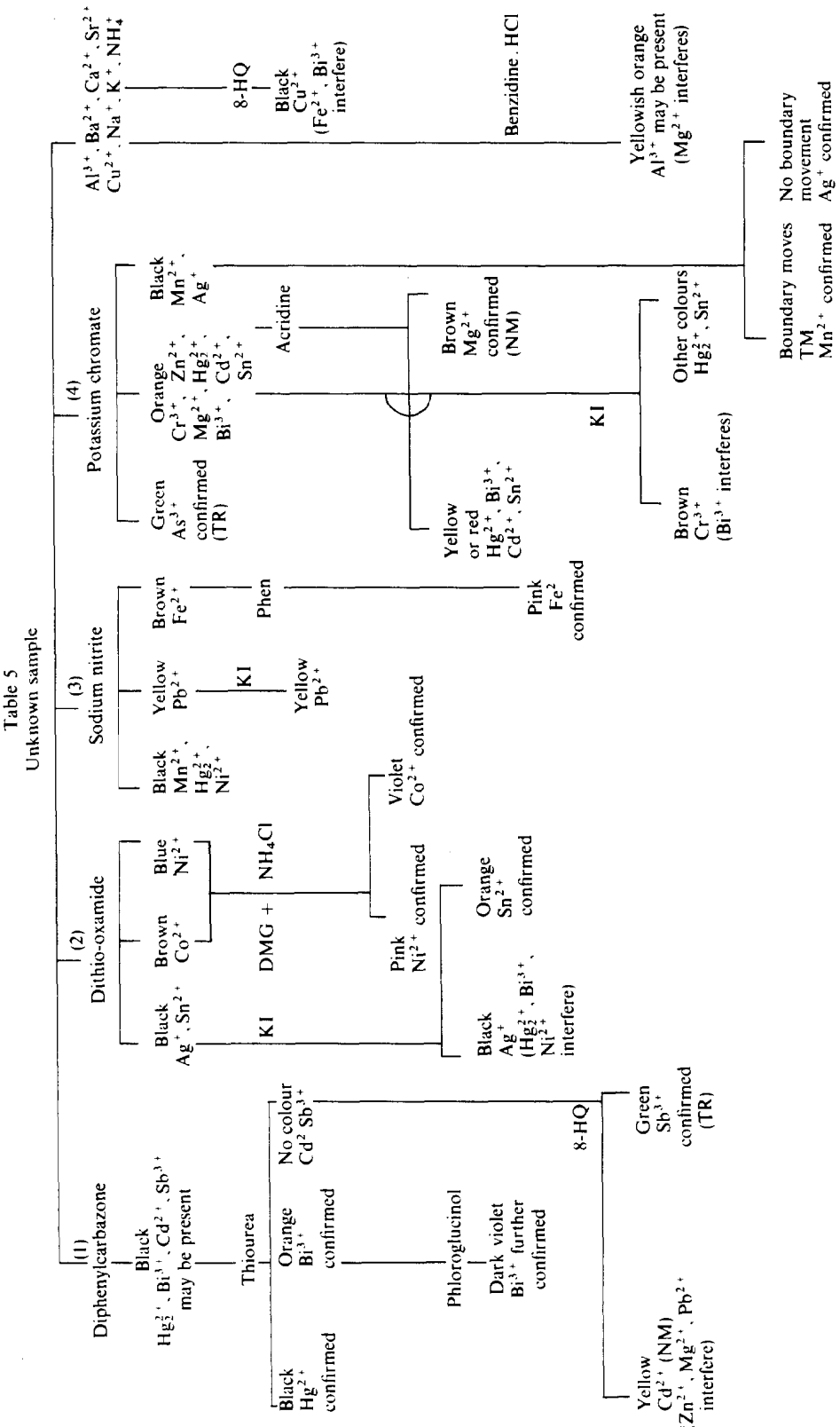
Table 3

Cation	Sodium nitrite					4-Dimethylaminobenzylidine-rhodanine					Resorcinol					Benzidine hydrochloride				
	T	CJ	DM	CsC	CsH	T	CJ	DM	CsC	CsH	T	CJ	DM	CsC	CsH	T	CJ	DM	CsC	CsH
Hg_2^{2+}	60	Bk	NM	Bk↓	Bk↓	60	Bk	NM	DBr↓	DBr↓	60	V	TR	W↓	LY↓	70	Br, Bk	NM	W↓	W↓
Ag^{+}	—	—	—	—	—	60	Bk	NM	Bk↓	Bk↓	60	Br	NM	NC	NC	—	—	—	—	—
Pb^{2+}	60	Y	NM	Y	Y	—	—	—	—	—	—	—	—	—	—	—	—	—	—	—
Bi^{3+}	—	—	—	—	—	40	Y	NM	P↓	P↓	60	V	TR	W↓	W↓	60	Br, Bk	NM	Bl↓	Bl↓
As^{3+}	—	—	—	—	—	—	—	—	—	—	60	Br	TR	W↓	W↓	—	—	—	—	—
Sb^{3+}	—	—	—	—	—	60	R	TR	NC	NC	—	—	—	—	—	—	—	—	—	—
Sn^{2+}	—	—	—	—	—	50	Y	NM	Br↓	Br↓	50	Br	TR	NC	NC	—	—	—	—	—
Mn^{2+}	50	Bk	NM	NC	NC	—	—	—	—	—	—	—	—	—	—	—	—	—	—	—
Fe^{2+}	60	Br	NM	NC	Br↓	—	—	—	—	—	—	—	—	—	—	—	—	—	—	—
Al^{3+}	—	—	—	—	—	—	—	—	—	—	—	—	—	—	—	60	LO	NM	NC	NC
Ni^{2+}	70	Bk	NM	NC	NC	—	—	—	—	—	—	—	—	—	—	—	—	—	—	—
Mg^{2+}	—	—	—	—	—	—	—	—	—	—	—	—	—	—	—	60	LO	NM	W↓	W↓

Table 4

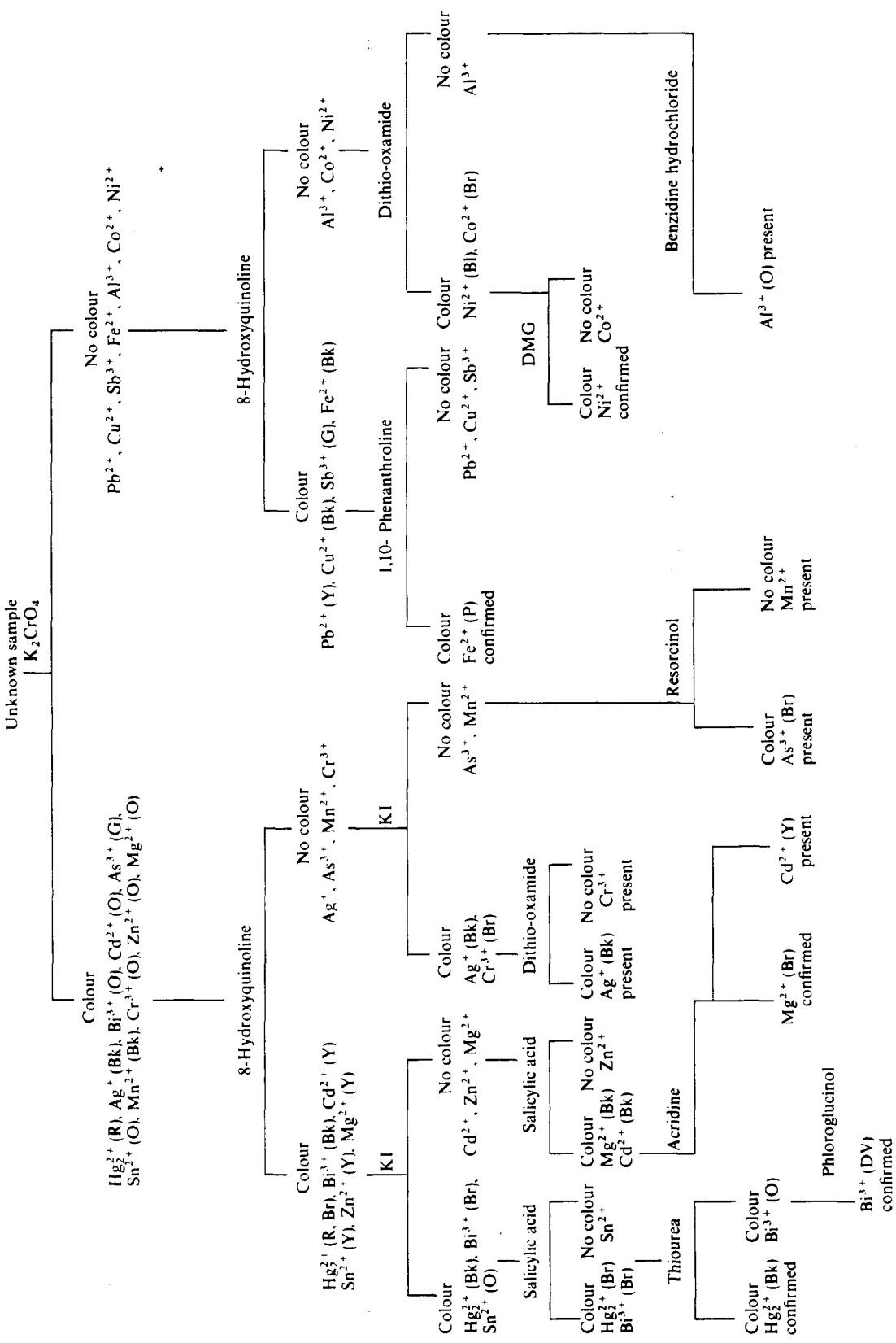
Cation	Salicylic acid					Diphenylcarbazone					Thiourea					Phloroglucinol				
	T	CJ	DM	CsC	CsH	T	CJ	DM	CsC	CsH	T	CJ	DM	CsC	CsH	T	CJ	DM	CsO	CsH
Hg_2^{2+}	60	Br	TR	W↓	W	60	Bk	TM	DBl↓	DBl↓	50	Bk	NM	Bk↓	Bk↓	—	—	—	—	—
Bi^{3+}	60	Br	TR	NC	NC	30	Bk	TR	NC	NC	50	O	TR	O	Br↓	60	DV	TR	LY↓	LY↓
Cd^{2+}	60	Bk	NM	NC	NC	60	Bk	TR	NC	NC	—	—	—	—	—	—	—	—	—	—
Sb^{3+}	—	—	—	—	—	60	Bk	TR	NC	NC	—	—	—	—	—	—	—	—	—	—
Mg^{2+}	60	Bk	NM	W↓	W	—	—	—	—	—	—	—	—	—	—	—	—	—	—	—

Table 5
Unknown sample



DMG = dimethylglyoxime
8-HQ = 8-hydroxyquinoline
Phen = 1,10-phenanthroline

Table 6


Unknown sample
K2CrO4
Colour
Hg2 2+ (R), Ag+ (Bk), Bi3+ (O), Cd2+ (O), As3+ (G), Sn2+ (O), Mn2+ (Bk), Cr3+ (O), Zn2+ (O), Mg2+ (O)
No colour
Pb2+, Cu2+, Sb3+, Fe2+, Al3+, Co2+, Ni2+
8-Hydroxyquinoline
Colour
Hg2 2+ (R, Br), Bi3+ (Bk), Cd2+ (Y) Sn2+ (Y), Zn2+ (Y), Mg2+ (Y)
No colour
Ag+, As3+, Mn2+, Cr3+
8-Hydroxyquinoline
Colour
Pb2+ (Y), Cu2+ (Bk), Sb3+ (G), Fe2+ (Bk)
No colour
Al3+, Co2+, Ni2+
Dithio-oxamide
KI
KI
1,10- Phenanthroline
Colour
Hg2 2+ (Bk), Bi3+ (Br), Sn2+ (O)
No colour
Cd2+, Zn2+, Mg2+
Colour
Ag+ (Bk), Cr3+ (Br)
No colour
As3+, Mn2+
Colour
Fe2+ (P) confirmed
No colour
Pb2+, Cu2+, Sb3+
Colour
Ni2+ (Bl), Co2+ (Br)
No colour
Al3+
DMG
Salicylic acid
Salicylic acid
Dithio-oxamide
Colour
Hg2 2+ (Br) Bi3+ (Br)
No colour
Sn2+
Colour
Mg2+ (Bk) Cd2+ (Bk)
No colour
Zn2+
Colour
Ag+ (Bk) present
No colour
Cr3+ present
Colour
Ni2+ confirmed
No colour
Co2+
Resorcinol
Benzidine hydrochloride
Thiourea
Acridine
Colour
As3+ (Br) present
No colour
Mn2+ present
Al3+ (O) present
Colour
Hg2 2+ (Bk) confirmed
Colour
Bi3+ (O)
Mg2+ (Br) confirmed
Cd2+ (Y) present
Phloroglucinol
Bi3+ (DV) confirmed

and hence no colour is then obtained. Ag^+ (black) can be distinguished from Pb^{2+} (light yellow) in the solid state, whereas in solutions both give yellow colours. Hg_2^{2+} can be distinguished from Bi^{3+} and Cu^{2+}, as Hg_2^{2+} gives a red-black and Bi^{3+} and Cu^{2+} a brown colour in the solid state. All give brown colours in solution. Ag^+ and Ni^{2+} give a black colour in the solid state and can be distinguished since the boundary moves towards the metal only in the case of Ni^{2+}. Similarly Hg_2^{2+} and Ni^{2+} can be distinguished on the basis of the direction of boundary movement.

Acridine gives a red colour with Hg_2^{2+} and a reddish brown with Mg^{2+} in the solid state, but both give a yellow precipitate in solution.

None of the metal ions which give colour products with acridine give any boundary movement except Hg_2^{2+}, which may thus be specifically detected.

Co^{2+} gives a colour with dithio-oxamide in the solid state but not in solution. The coloured products with Sn^{2+} and Ni^{2+} are also different in the solid state from those formed in the solutions. The coloured boundary moves only in the case of Sn^{2+}. Thus the test can be used for the specific detection of Sn^{2+}.

Oxalic acid gives light pink and green colours with Hg_2^{2+} and Fe^{2+} respectively which can be used for selective detection of both.

1,10-Phenanthroline can be used for the specific detection of Fe^{2+} in the solid state, by its characteristic pink colour.

Dimethylglyoxime gives a pink colour only with Ni^{2+} in the solid state and there is no colour with Fe^{2+}, Co^{2+}, Cu^{2+} and Cr^{3+}, which interfere in the detection of Ni^{2+} in solution.[3] Thus this solid-state test can be used for the specific detection of Ni^{2+}. If ammonium chloride is added along with the dimethylglyoxime, Ni^{2+} gives the pink colour, Co^{2+} gives a blue colour, and a mixture of the two gives a violet colour.

Sodium nitrite can be used for the specific detection of Pb^{2+} by the characteristic yellow colour given. The colours of Hg_2^{2+} and Fe^{2+} in the solid state are light pink and green respectively, whereas they give white and yellow precipitates in solution. The test can be used for the specific detection of Fe^{2+} and Hg_2^{2+}. Mn^{2+} and Ni^{2+} do not give any colour in the solid state with sodium nitrite.

4-Dimethylaminobenzylidinerhodanine gives a red product with Sb^{3+} in the solid state, which is not obtained in solution. Bi^{3+} and Sn^{2+} both give yellow products in the solid state but in solution give pink and brown precipitates respectively.

With resorcinol, all the reactions in the solid state differ from those in solution, as given in Table 3.

Benzidine hydrochloride gives new coloured products with Hg_2^{2+}, Bi^{3+}, Al^{3+} and Mg^{2+} in the solid state. In solution Bi^{3+} gives a blue precipitate, Hg_2^{2+} and Mg^{2+} give a white precipitate and Al^{3+} gives no colour.

Hg_2^{2+} gives red, brown and black products with salicylic acid in the solid state, depending on the reaction temperature. In solution it gives a white precipitate which dissolves on heating to give a colourless solution. This shows that the intermediate products of Hg_2^{2+} with salicylic acid are stable in the solid state only under certain experimental conditions. There is no colour given by Bi^{3+} or Cd^{2+} with salicylic acid in solution, but in the solid state these metal ions give brown and black products respectively.

There is no reaction between diphenylcarbazone and Bi^{3+}, Cd^{2+} and Sb^{3+} in solution, all three give

Table 7. Solid state reactions of cations with some general reagents

Cation	1	2	3	4	5	6	7	8	9	10	11	12	13	14	15	16
Hg_2^{2+}	–	–	–	+	+	–	+	+	+	+	+	+	+	+	+	+
Ag^+	–	–	–	–	–	+	–	–	–	+	+	–	–	+	–	+
Pb^{2+}	–	–	–	–	–	–	–	–	–	–	–	+	–	+	+	–
Bi^{3+}	+	–	–	–	+	–	+	+	+	+	+	–	+	+	+	+
Cu^{2+}	–	–	–	–	–	–	–	–	–	–	–	–	–	+	+	–
Cd^{2+}	–	–	–	–	–	–	+	+	–	–	–	–	+	–	+	+
As^{3+}	–	–	–	–	–	–	–	–	–	+	–	–	–	–	–	+
Sb^{3+}	–	–	–	–	–	–	+	–	–	–	+	–	+	–	+	–
Sn^{2+}	–	–	–	–	–	+	–	–	–	+	+	–	+	+	+	+
Mn^{2+}	–	–	–	–	–	–	–	–	–	–	–	+	+	–	–	+
Fe^{2+}	–	+	–	+	–	–	–	–	–	–	–	+	–	–	+	–
Cr^{3+}	–	–	–	–	–	–	–	–	–	–	–	–	–	+	–	+
Al^{3+}	–	–	–	–	–	–	–	–	+	–	–	–	–	–	–	–
Co^{2+}	–	–	–	–	–	+	–	–	–	–	–	–	–	–	–	–
Ni^{2+}	–	–	+	–	–	+	–	–	–	–	–	+	–	+	–	–
Zn^{2+}	–	–	–	–	–	–	–	–	–	–	–	–	–	–	+	+
Mg^{2+}	–	–	–	–	–	–	–	+	+	–	–	–	+	–	+	+

(1) Phloroglucinol
(2) 1,10-Phenanthroline
(3) Dimethylglyoxime
(4) Oxalic Acid
(5) Thiourea
(6) Dithio-oxamide
(7) Diphenylcarbazone
(8) Salicylic acid
(9) Benzidine hydrochloride
(10) Resorcinol
(11) *p*-Dimethylaminobenzylidinerhodanine
(12) Sodium nitrite
(13) Acridine
(14) Potassium iodide
(15) 8-Hydroxyquinoline
(16) Potassium chromate

black products in the solid state. The movement of the coloured boundary of the Hg_2^{2+} product is opposite to that for Bi^{3+}, Cd^{2+} or Sb^{3+}.

Thiourea gives black and orange colours with Hg_2^{2+} and Bi^{3+} respectively in either the solid state or in solution. Thus the test can be used for the specific detection of Hg_2^{2+} and Bi^{3+}.

Phloroglucinol gives a dark violet colour only with Bi^{3+} amongst the metal ions tested, and this can be used for specific detection. In solution Bi^{3+} yields a yellow precipitate.

The tests described above can be used in inorganic analysis. An effort has been made to design a systematic approach, as given in Tables 5–7. Table 5 can be used for systematic analysis of a mixture containing numerous cations, excluding Ba^{2+}, Ca^{2+}, Sr^{2+}, Na^+, K^+ and NH_4^+. A preliminary orientation is obtained by performing the solid-state tests with four reagents: diphenylcarbozone, dithio-oxamide, sodium nitrite and potassium chromate. Confirmatory tests are then performed with thiourea, oxine, dimethylglyoxime and potassium iodide. As far as we are aware this is the first attempt at the systematic solid-state analysis for inorganic ions.

If a single salt is to be analysed the procedure given in Table 6 may be followed.

Another approach to systematic analysis is given in Table 7. NH_4^+, K^+, Na^+, Ca^{2+}, Sr^{2+} and Ba^{2+} do not give any colour and cannot be tested for by this procedure. The chemistry of the new reactions described is being studied, and will be presented in subsequent publications.

Acknowledgement—The authors thank the Department of Science and Technology (India) for financial assistance.

REFERENCES

1. M. Qureshi, H. S. Rathore and A. Mohammad, *Talanta*, 1976, **23**, 874.
2. M. N. Akhtar, H. S. Rathore and M. Qureshi, *ibid.*, 1978, **25**, 235.
3. F. Feigl, *Spot Tests in Inorganic Analysis*, 6th Ed., Elsevier, Amsterdam, 1972

Talanta, Vol. 28, pp. 825 to 831, 1981
Printed in Great Britain

0039-9140/81/110825-07$02.00/0
Pergamon Press Ltd

SPECTROPHOTOMETRIC DETERMINATION OF BORON IN IRON AND STEEL WITH CURCUMIN AFTER SEPARATION BY 2-ETHYL-1,3-HEXANEDIOL–CHLOROFORM EXTRACTION

ELSIE M. DONALDSON

Mineral Sciences Laboratories, Canada Centre for Mineral and Energy Technology, Energy, Mines and Resources Canada, Ottawa, Canada

(*Received* 23 *March* 1981. *Accepted* 27 *April* 1981)

Summary—A simple and reliable method for determining ~0.0001% or more of total boron in iron and low- and high-alloy steels is described. After the sample is decomposed at <70° in the presence of hydrogen peroxide and potassium hydrogen fluoride, the insoluble material is filtered off and ultimately fused with sodium carbonate. The cooled melt is dissolved in dilute hydrochloric acid and the solution is combined with the main solution. Fluoride is subsequently complexed with zirconium and boron is separated from iron and other elements by extraction as borate from 1*M* sulphuric acid medium into chloroform containing 2-ethyl-1,3-hexanediol. Boron, in a 1-ml portion of the extract, is ultimately determined spectrophotometrically at 550 nm in an ethanol medium, after formation of the curcumin rosocyanin complex in a glacial acetic acid–concentrated sulphuric acid medium. Acid-soluble and acid-insoluble boron can also be determined. Common ions, including large amounts of manganese, chromium, vanadium, titanium, molybdenum, tungsten, niobium and tantalum do not interfere.

The determination of small amounts of boron in iron and steel has been a long-standing analytical problem in the CANMET chemical laboratory. A reasonably simple and reliable method for determining ~0.0001% or more of total boron in both low- and high-alloy steels was required for routine use in the Metals and Alloys section.

The most widely used method for determining boron in steel is probably that based on spectrophotometric measurement of the Methylene Blue–fluoroborate complex after its extraction into dichloroethane.[1–5] Other spectrophotometric methods involve the direct determination of boron in an acidic solution of the sample with 1-hydroxy-4-(*p*-toluidino)-anthraquinone (HPTA) without prior separation of the iron,[6] and with curcumin after separation of boron by distillation as methyl borate.[7,8] A recent indirect atomic-absorption method, which has been reported to be very sensitive, is based on the determination of cadmium in the organic phase after separation of boron by distillation followed by extraction into nitrobenzene as the tris(1,10-phenanthroline)cadmium tetrafluoroborate ion-association complex.[9] In a more recent method, boron is separated by pyrohydrolysis and subsequently determined by inductively-coupled argon-plasma spectroscopy.[10] This method,[10] an earlier method involving pyrohydrolysis and a constant-current coulometric finish,[11] and distillation methods were not considered suitable for routine use because they require special apparatus. Methods involving spectrophotometric reagents such as HPTA,[6] other hydroxyanthraquinones (quinalizarin, purpurin and carminic acid) and 1,1′-dianthrimide,[12,13] are not too practical because they require a fairly concentrated sulphuric acid medium for complex formation. In preliminary work, the indirect atomic-absorption finish was investigated and ultimately abandoned because of the toxic and noxious nature of nitrobenzene. The Methylene Blue method was also investigated and abandoned because of the poor reproducibility, the high reagent blank and the critical conditions of acidity and fluoride concentration required for complex formation. Two other spectrophotometric methods for determining boron in steel involve the direct formation of the curcumin rosocyanin complex in a small volume of an acid solution of the sample in the presence of iron and other matrix elements.[14,15] These methods appear to yield reasonable results but one of them is not applicable to high-alloy steels.[14] In the other, titanium interferes, about 3 hr are required for complex formation, and oxidizing agents, which also interfere, cannot be used to decompose carbides during the decomposition step.[15] Recently, Mair and Day[16] determined boron in fertilizers by extracting borate from an acid medium into chloroform containing 2-ethyl-1,3-hexanediol. This was followed by the direct determination of boron with curcumin in a small portion of the extract or after the evaporation of chloroform from a suitable portion. Grotheer[17] applied this method to the determination of boric acid in boron powder. Because of the simplicity and selectivity of this extraction procedure[18] and the high sensitivity of curcumin, it was considered that, with suitable modifications,

Crown Copyrights Reserved.

Mair and Day's method could be advantageously applied to the determination of boron in steel.

This paper describes the determination of total boron or both acid-soluble and acid-insoluble boron in iron and low- and high-alloy steels. After decomposition of the sample at a low temperature in the presence of hydrogen peroxide and potassium hydrogen fluoride, the free fluoride is complexed with zirconium and boron is separated from iron and other matrix elements by extraction as borate from 1*M* sulphuric acid medium into chloroform containing 2-ethyl-1,3-hexanediol. Boron is determined spectrophotometrically with curcumin in a 1-ml portion of the extract by essentially the method reported by Hayes and Metcalfe.[19] This involves the formation of the curcumin rosocyanin complex in a mixture of glacial acetic acid and concentrated sulphuric acid and the subsequent destruction of the excess of protonated curcumin by dilution of the solution with ethanol. The proposed method is simple, sensitive, specific and moderately rapid and it requires no special apparatus other than that used for the decomposition stop.

EXPERIMENTAL

Apparatus

The apparatus for sample decomposition consisted of Nalgene 125-ml narrow-mouth linear (high-density) polyethylene bottles fitted with air condensers made by inserting a 1-ml Nalgene pipette (inner diameter 2 mm), with its tip cut off, into a hole in a suitable size neoprene stopper so that about a 40-mm length of the pipette extended below the stopper.

Funnels for filtering the extracts were made from broken 20- or 25-ml pipettes by cutting the bulb in half.

Polypropylene separatory funnels, 125-ml pear-shape type, marked at 50 and 75 ml were used.

Graduated Nalgene pipettes were used for adding all the reagents except the curcumin solution. An automatic 500-µl pipette with disposable plastic tips was used for adding concentrated sulphuric acid.

Reagents

Standard boron solution, 100 µg/ml. Dissolve 0.5715 g of pure boric acid in about 100 ml of water contained in a 250-ml plastic or Teflon beaker. Transfer the solution to a 1-litre standard flask, dilute to volume with water, mix thoroughly and transfer the solution to a 1-litre plastic bottle. Prepare a 5-µg/ml solution by diluting 10 ml of this stock solution to 200 ml with water (Note 1).

Curcumin, 0.375% solution. Transfer 0.750 g of pure reagent to a dry 250-ml Teflon beaker, add about 150 ml of glacial acetic acid and warm gently until the curcumin has dissolved. Transfer the solution to a dry 200-ml standard flask and dilute to volume with glacial acetic acid (Note 1). This solution is stable for at least one month.

Zirconium sulphate, 20% solution. Dissolve 100 g of zirconyl sulphate trihydrate ($ZrOSO_4.H_2SO_4.3H_2O$) in about 400 ml of water containing 10 ml of 50% sulphuric acid and dilute to 500 ml with water. Store in a plastic bottle.

Potassium hydrogen fluoride, 25% solution. Store in a plastic bottle.

2-Ethyl-1,3-hexanediol. A 10% v/v solution in chloroform. Dilute 50 ml of the reagent to 500 ml with chloroform in a dry glass bottle marked at 500 ml.

Sodium carbonate, 25% solution. Store in a plastic bottle.

Sulphuric acid, 50% v/v.

Hydrogen peroxide, 30%.

Procedures

Calibration curve. Add 8 ml of 50% sulphuric acid to each of seven 125-ml polypropylene separatory funnels; then, from a burette, add to the last six funnels 1, 2, 3, 4, 6 and 8 ml, respectively, of standard 5-µg/ml boron solution. The first funnel contains the blank. Dilute each solution to the 75-ml mark with water, add 10 ml of 10% ethylhexanediol solution, stopper tightly and shake for 2 min. Allow several min for the layers to separate, then filter the chloroform extract through a wad of cotton-wool into a dry 25-ml standard flask (Note 2). Extract the solution once more in a similar manner with 10 ml of ethylhexanediol–chloroform solution, then extract it for 1 min with 3 ml of the chloroform solution. Combine these extracts with the first one, wash the funnel containing the cotton-wool with about 2 ml of ethylhexanediol solution and dilute the extract to volume with the same solution. Transfer two 1-ml aliquots (Notes 3 and 4) of the blank and each of the resulting extracts to dry 25-ml standard flasks (Note 2), add 1 ml of 0.375% curcumin solution (Note 3) and mix thoroughly. Using the automatic pipette, add 0.5 ml of concentrated sulphuric acid to each flask, mix and cover the flasks with a piece of tissue. Allow the solutions to stand for 30 min, then dilute to volume with ethanol and mix thoroughly. Measure the absorbance of each of the resulting solutions at 550 nm against water as the reference solution, using 10-mm cells. Correct the absorbance value obtained for each boron–curcumin solution by subtracting that obtained for the blank (Note 5). Plot µg of boron *vs.* absorbance (Note 6).

Total boron. Transfer up to 0.5 g of sample containing up to 40 µg of boron to a 125-ml Nalgene bottle (Note 7) and add 10 ml of water. Rapidly, in succession and without mixing (Note 8), add 8 ml of 50% sulphuric acid (Note 9), 3 ml of 30% hydrogen peroxide and 2 ml of 25% potassium hydrogen fluoride solution and immediately cap the bottle tightly with an air condenser. Place the bottle in a water-bath maintained at 60–70° for ~2 hr, then cool it to room temperature, open the cap and wash down the inside of the air condenser with a small amount of water. Add about a quarter of a Whatman filter pulp tablet, swirl the bottle to macerate the paper, then, using a plastic funnel, filter the solution (Whatman 11 cm No. 40 paper) into a 125-ml polypropylene separatory funnel. Transfer the residue as quantitatively as possible to the filter paper (Note 10) and wash the paper and residue twice with small portions of water. Add 10 ml of 20% zirconium sulphate solution to the filtrate and stopper the funnel. Carry a blank through the whole procedure.

Transfer the paper containing the residue to a 30-ml platinum crucible, add 4 ml of 25% sodium carbonate solution, then place the crucible in a muffle furnace and dry the paper and evaporate the solution to dryness at a low temperature. Burn off the paper at 500–600°, then ignite at ~900°. Cool the crucible, add ~10 ml of water, then cover it with a plastic or Teflon cover and add 2 ml of concentrated hydrochloric acid. When the melt has dissolved (Note 11), transfer the solution to the separatory funnel containing the filtrate. Wash the crucible several times with small portions of water, dilute the resulting solution to the 75-ml mark with water and proceed with the extraction of borate and the subsequent determination of boron as described above.

Acid-soluble boron. After decomposition of the sample and filtration of the solution to remove the acid-insoluble material as described above (Note 12), add 10 ml of 20% zirconium sulphate solution to the filtrate, dilute to the 75-ml mark with water and proceed with the extraction and determination of boron as described above.

Acid-insoluble boron. After treatment of the insoluble material as described above, transfer the solution of the melt to a 125-ml polypropylene separatory funnel and wash the crucible thoroughly with water. Add 5 ml each of

20% zirconium sulphate solution (Note 13) and 50% sulphuric acid, dilute the solution to the 50-ml mark with water, then proceed with the extraction and subsequent determination of boron.

Notes

1. If a Nalgene standard flask is not available, transfer the solution to a plastic bottle to avoid contamination from boron in glass.
2. Standard flasks and funnels used for the extract, and flasks ultimately used for complex formation, should be washed thoroughly with methanol after use, followed by distilled water, and should be kept in a drying oven until needed. When being cooled (just before use) they should be kept covered with a piece of tissue to prevent contamination from boron contained in the dust in the laboratory.
3. Use a 1-ml glass pipette and wash it with methanol after use.
4. Because of the ease with which the resulting solutions can become contaminated with dust in the laboratory, it is recommended that two aliquots of each extract should be taken for complex formation and that the mean of the two results should be used to plot the calibration curve. Sample extracts should be analysed in a similar manner.
5. In this work, the absorbance of the blank varied from ~0.10 to 0.13 (measured against water as the reference solution).
6. For ease of reference when analysing samples, plot the amount of boron added before the extraction step—not that contained in 1 ml of the ethylhexanediol extract.
7. To avoid contamination, the Nalgene bottle and all pipettes used for adding reagents should be thoroughly washed with distilled water just before use.
8. The solution should not be mixed until the initial reaction has subsided or some may be lost through the air condenser.
9. For stainless steel, add 3 ml of concentrated hydrochloric acid at this point.
10. A plastic squeeze-type wash-bottle with the tip pointed outward and upward is useful for washing any remaining residue down the inside of the Nalgene bottle while it is held over the filter funnel.
11. Any iron oxide present can be ignored. It does not interfere with the extraction of boron.
12. If only the acid-soluble boron content of the sample is required, filtration of the solution is not necessary unless a large amount of residue is present. A small amount will not interfere with the subsequent extraction because it floats on top of the chloroform phase.
13. Zirconium solution is required to complex any fluoride ion that may have remained on the filter paper during the filtration of the residue.

RESULTS

Spectrophotometric determination of boron with curcumin

Low and erratic results were obtained for boron in initial tests in which Mair and Day's method,[16] which involves formation of the boron–curcumin complex in the presence of 1 ml of glacial acetic acid and 0.3 ml of concentrated sulphuric acid, was applied to 1-ml portions of 10% 2-ethyl-1,3-hexanediol (EHD)–chloroform extracts of the borate–EHD complex. In these tests, as recommended by Mair and Day, the solutions were allowed to stand for 15 min after the addition of sulphuric acid to complete the complex formation. However, to increase the range of the proposed method, the final solutions were diluted to 25 ml with ethanol instead of 50 ml. Subsequent work showed that at least 25 min is required for complete complex formation and that the use of 0.4–0.5 ml of concentrated sulphuric acid for a final volume of 25 ml, as recommended by Hayes and Metcalfe,[19] yields more reproducible results. Further work showed that the use of ~2 ml or more of the EHD–chloroform extract for complex formation, after the removal of chloroform by evaporation, yields low results. EHD, which boils at ~130°, is not removed and interferes in the determination of boron. Consequently, a 1-ml aliquot of the extract was chosen for complex formation. In the proposed method, any interference from the EHD (0.1 ml) contained in 1 ml of the sample extract is compensated for by using 1-ml portions of EHD extracts of known amounts of boron to prepare the calibration curve. Beer's law is obeyed for up to at least 2 μg of boron. The absorbance of the red complex remains constant for at least 6 hr and the apparent molar absorptivity is 1.65×10^4 l.mole^{-1}.mm^{-1} at 550 nm, the wavelength of maximum absorption. This is slightly higher than some values calculated from previous work[14,15,20] *viz.* 1.46, 1.43 and 1.39×10^4 l.mole^{-1}.mm^{-1}, respectively, and slightly lower than values reported by other investigators[16,19,21] *viz.* 1.96, 1.80 and 1.80×10^4 l.mole^{-1}.mm^{-1}, respectively.

Separation of boron by extraction of the borate–EHD complex

Mair and Day[16] extracted the borate–EHD complex into chloroform from 2*M* hydrochloric acid medium. However, Agazzi[18] found that up to at least 0.4 mg of boron can be quantitatively extracted into chloroform containing 2–10% EHD in a single extraction from up to at least 6*M* sulphuric acid when the volume ratio of the aqueous to the organic phase is 2:1. Because the decomposition of iron and steel before the ultimate determination of boron usually involves the use of sulphuric acid, this medium was chosen for the extraction step in the present work. Tests showed that up to at least 50 μg of boron as borate can be quantitatively extracted from 75 ml of 1*M* sulphuric acid in three successive extractions with two 10-ml portions and one 3-ml portion of chloroform containing 10% EHD. The extraction of larger amounts was not investigated because iron and steel do not usually contain more than about 0.02% of boron. The extracts are stable for at least 2 weeks and can be kept in glass standard flasks.

Effect of diverse ions

Agazzi[18] found that the separation of boron by chloroform extraction of the boric acid–EHD complex from acid media is highly selective and that up to at least 100 mg of tin(IV), strontium, calcium, barium, magnesium, chromium(III), zinc, iron(III), cobalt, copper(II), nickel, lead, aluminium, bismuth,

Table 1. Recovery of boron from synthetic iron and stainless steel samples

Sample	B present, %*	B found, %
NBS-55e Open-hearth iron	0.0002_0	0.0002_4
	0.0010_0	0.0010_0
	0.0020_0	0.0019_8
	0.0040_0	0.0039_5
	0.0080_0	0.0079_3
	0.0200	0.019_8
NBS-101f 18 Chromium–10 nickel steel (0.9 Si)	0.0012_7	0.0014_4
	0.0022_7	0.0023_3
	0.0052_7	0.0053_0

* Value includes the boron added and soluble boron found by the proposed method, *viz.* none found for 55e, and 0.0002_6 and 0.0002_7% found for 101f.

vanadium(V) and phosphorus as phosphate will not interfere in the extraction of boron or be co-extracted to any significant extent. He found that up to at least 3*M* nitric acid or 2*M* hydrochloric acid also will not interfere and that only manganese, titanium, molybdenum and tungsten are significantly co-extracted. Fluoride interferes because it reacts with boron to form the fluoroborate ion, which is not extracted as an EHD complex. In the proposed method, interference from potassium hydrogen fluoride, which is used in the decomposition step in conjunction with hydrogen peroxide to destroy carbides, is eliminated by complexing it with zirconium before the extraction step.[18] In the presence of 3 ml of 30% hydrogen peroxide, up to at least 50 mg each of manganese(II), titanium(IV), molybdenum(VI), tungsten(VI), niobium and tantalum will not interfere in the extraction of boron or be co-extracted. Presumably, these elements are complexed with either hydrogen peroxide or fluoride during the extraction step.

Decomposition of iron and steel

Several previous investigators[2,5] have reported that boron nitride is decomposed with an acid fluoride such as ammonium hydrogen fluoride and that, in the presence of hydrogen peroxide which decomposes carbides,[14] total boron is obtained. Consequently, in preliminary tests in which the chloroform–EHD extraction step and the curcumin finish were applied to synthetic steel samples, hydrogen peroxide and a similar acid fluoride, potassium hydrogen fluoride (available in a purer form), were used in the decomposition step. In these tests, known amounts of boron were added to suitable amounts (0.2 or 0.5 g) of boron-free[5] National Bureau of Standards (NBS) iron 55e and the samples were subsequently decomposed with sulphuric acid at 60–70° as described in the proposed method to avoid loss of boron by volatilization. The results of these tests (Table 1) show that complete recovery of the added boron was obtained. However, erratic results were obtained in similar tests with synthetic stainless-steel samples in which *aqua regia* was used in the decomposition step. This was attributed to the presence of free chlorine, which probably co-extracts into chloroform and subsequently oxidizes the curcumin. Complete recovery of the added boron was obtained for stainless steel (Table 1) when hydrochloric acid was added during the decomposition step. However, when the sulphuric acid–hydrogen peroxide–potassium hydrogen fluoride method of decomposition was applied to seven NBS and British Chemical Standards (BCS) certified reference iron and steel samples, the results obtained for six of these samples (compare acid-soluble boron in Table 2) were in reasonably good agreement with the certified values, but those obtained for NBS 151 boron steel were considerably lower (0.0018–0.0020%) than the certified value even after 24 hr were allowed for the dissolution process (the result then being 0.0019%). NBS has reported that for this sample from 20 to 35% of the boron appears to be acid-insoluble, depending on the type of decomposition used. This information and the results above suggest that the use of an acid fluoride compound during the decomposition step does not yield total boron. Although the previously recommended methods of decomposition[2,5] involve the use of both hydrofluoric acid and ammonium hydrogen fluoride, tests carried out on NBS 151 with both of these reagents and with a mixture of hydrofluoric acid and potassium hydrogen fluoride also yielded low results (0.0017 and 0.0019%, respectively).

In subsequent tests, three separate portions of NBS 151 were decomposed as described in the proposed method but in the absence of a fluoride compound and the insoluble material was filtered off and ultimately fused with sodium carbonate.[1,14,15] Both acid-soluble and acid-insoluble boron were subsequently determined as described in the proposed method. In these tests, the mean values obtained for soluble and insoluble boron were 0.0016_1 and 0.0011_7%, respectively, and the calculated mean value for total boron (0.0028%) was in excellent agreement with the certified value. The results of these tests show conclusively that very little (if any) of the insoluble boron in this particular sample is decomposed by treatment with ammonium or potassium hydrogen fluoride or with mixtures of these reagents and hydrofluoric acid.

During these tests, it was observed that a mixture of potassium hydrogen fluoride and hydrogen peroxide is more effective in decomposing carbides than hydrogen peroxide alone. Consequently, these reagents, in conjunction with sulphuric acid—and hydrochloric acid, if required—were chosen for sample decomposition in the present work and acid-insoluble material was ultimately fused with sodium carbonate to recover insoluble boron.

Applications

To test the reliability of the proposed method, it was applied to the analysis of the NBS and BCS iron and steel samples mentioned previously. In these tests, both acid-soluble and acid-insoluble boron were de-

Table 2. Determination of boron in NBS and BCS iron and steel

Sample	Nominal composition, %	Certified B value and range, %	B found, %		
			Acid-soluble	Acid-insoluble	Soluble + insoluble
NBS-3 White iron	2.3 C, 0.4 Mn, 1.0 Si	0.0007 (0.0005–0.0008)*	0.0011_5	NF†	0.0012
			0.0010_3	NF†	0.0010
			0.0010_4	NF†	0.0010
NBS-151 Boron steel	0.6 C, 1.0 Cr, 0.2 Mo	0.0027‡	0.0017_8	0.0010_1	0.0028
			0.0018_7	0.0007_5	0.0026
			0.0018_9	0.0007_1	0.0026
BCS-273 Mild steel	0.2 Cu, 0.3 W	0.002_5 (0.0015–0.0030)	0.0023_3	0.0001_8	0.0025
			0.0022_4	0.0000_8	0.0023
			0.0021_1	0.0001_6	0.0023
BCS-327 Mild steel	0.2 Mn, 0.2 Cu	0.003 (0.0025–0.0040)	0.0033_2	NF†	0.0033
			0.0033_9	0.0001_4	0.0035
			0.0034_3	0.0000_3	0.0035
BCS-328 Mild steel	0.4 Mn, 0.2 V, 0.2 Co	0.004 (0.0035–0.0050)	0.0044_5	0.0002_9	0.0047
			0.0043_0	0.0004_0	0.0047
			0.0044_0	0.0003_8	0.0048
BCS-329 Mild steel		0.008 (0.0070–0.0080)	0.0078_5	0.0010_3	0.0089
			0.0076_9	0.0014_3	0.0091
			0.0081_3	0.0011_2	0.0093
BCS-330 Mild steel	0.5 Mn	0.007 (0.0070–0.0080)	0.0081_1	0.0000_4	0.0082
			0.0081_6	0.0000_8	0.0082
			0.0081_2	0.0001_8	0.0083

* Certified value based on the 2 results shown in brackets.
† NF means none found.
‡ NBS provisional result.

termined. The results of these analyses, which are the means of the results obtained for two 1-ml portions of each EHD extract, are given in Table 2. All the results shown are for individual samples.

Precision

The precision for total boron at about the 0.001 and 0.009% levels was tested by analysing six samples each of an NBS iron and a BCS steel. The results of these tests, which are the means of the results obtained for two 1-ml portions of each extract, are given in Table 3.

Table 3. Determination of total boron in iron and steel

Sample	Total B found, %	Sample	Total B found, %
NBS-3 White iron	0.0010_3	BCS-329 Mild steel	0.0091_9
	0.0010_1		0.0092_8
	0.0009_5		0.0092_8
	0.0009_9		0.0090_1
	0.0009_7		0.0090_0
	0.0010_3		0.0090_1
Mean	0.00100		0.00913
Standard deviation	0.000033		0.000137
Relative standard deviation, %	3.3		1.5

DISCUSSION

Table 2 shows that the results obtained for total boron (soluble + insoluble) in the NBS and BCS iron and steel samples are, in some instances, slightly higher than, but still in good agreement with, the certified values. The results also show that NBS 151 and BCS 329 contain a significant amount of acid-insoluble boron. The NBS white iron and most of the remaining BCS steel samples contain little or no acid-insoluble boron. Table 3 shows that the precision of the results for total boron at the 0.001 and 0.009% levels is reasonably good. The relative standard deviation is comparable with or better than that reported by other investigators.[1,4–6,11,15]

Table 4 shows that the mean result obtained for NBS 151, which contains ~0.001% acid-insoluble boron, is in excellent agreement with the results obtained by previous investigators who used spectrophotometric methods after fusion of the insoluble material with sodium carbonate[1,10,15] or pyrohydrolysis methods.[10,11] Except for BCS 329, which also contains ~0.001% acid-insoluble boron, the mean results obtained for the remaining BCS samples, which were found to contain essentially all or mostly all acid-soluble boron, are in reasonably good agreement with those obtained by other investigators who

Table 4. Comparison of results for total boron in NBS and BCS steels

Sample	Certified B value, %	Mean% B*										
		Reference 1	Reference 2†	Reference 4†	Reference 5†	Reference 6	Reference 10	Reference 11	Reference 14	Reference 15	This work
NBS-151	0.0027	0.0027	—	—	—	—	0.0029‡ 0.0027§ 0.0027#	0.0027	—	0.0024	0.0027
BCS-273	0.0025	—	0.0024	—	0.0023	0.0025	—	—	0.0020	0.0026	0.0024
BCS-327	0.003	—	—	—	0.0038	0.0031	—	—	0.0021	—	0.0034
BCS-328	0.004	—	—	0.0037	0.0044	0.0041	—	—	0.0037	—	0.0047
BCS-329	0.008	—	—	0.0079	0.0065	0.0082	—	—	0.0077	—	0.0091
BCS-330	0.007	—	—	0.0070	0.0071	0.0072	—	—	0.0064	—	0.0082

* Boron was determined spectrophotometrically with Methylene Blue in references 1, 2, 4 and 5, with HPTA in reference 6 and with curcumin in references 14 and 15.
† Insoluble boron was not recovered in the insoluble material.
‡ Pyrohydrolysis with an argon-plasma spectroscopic finish.
§ Pyrohydrolysis with a spectrophotometric carminic acid finish.
# Spectrophotometric carminic acid finish after decomposition with acids and recovery of boron in the insoluble material.

used methods that yield total boron[6,14,15] or are believed to yield total boron.[2,4,5] The mean result obtained for BCS 329 is higher than the certified value and higher than those reported previously. However, the mean acid-soluble boron content (0.0079%) of this sample (Table 2) is in excellent agreement with the certified value. No reference has been found in which the acid-insoluble boron content of this reference material or of any of the other BCS steel samples has been reported.

Although preliminary work showed that acid-insoluble boron is not decomposed completely by treatment with ammonium hydrogen fluoride and hydrofluoric acid as reported previously,[2,5] several additional tests were carried out with both NBS 151 and BCS 329 to determine how much of the insoluble boron is actually brought into solution by this treatment. In these tests, 2.5 g of each steel were decomposed according to the proposed method, with five times the recommended volumes of water, 50% sulphuric acid, hydrogen peroxide and potassium hydrogen fluoride solution. The insoluble material was filtered off and washed thoroughly with water to remove soluble boron compounds, and each paper was transferred to a 125-ml Nalgene bottle and macerated thoroughly with a glass rod. The filtrates containing the acid-soluble boron were discarded. Slightly more than the recommended[2,5] volumes of ammonium hydrogen fluoride solution, hydrofluoric acid and hydrogen peroxide were added to each bottle and the bottles were capped with an air condenser and heated at 60–70° for 4 hr. The resulting solutions were filtered into 100-ml Nalgene standard flasks and each paper was again washed thoroughly with water to remove soluble boron compounds. Each of the filter papers containing the remaining insoluble material was treated with sodium carbonate solution and the residue was ultimately ignited and fused as described in the proposed method. Analysis of each filtrate and fused residue showed that for NBS 151 the filtrate contained 0.0003_4% and the residue contained 0.0007_1% of boron. For BCS 329, the filtrate contained 0.0002_2% and the residue contained 0.0010_9% of boron. These results show that only 32 and 17% respectively of the acid-insoluble boron in these materials—presumably present as nitride and probably carbide—was decomposed by the ammonium hydrogen fluoride–hydrofluoric acid treatment. Consequently, it is emphasized that, after decomposition of iron and steel with acids at a low temperature, a reliable result for total boron can only be obtained if the insoluble boron in the insoluble material is decomposed and recovered. To avoid possible error resulting from the presence of small amounts of insoluble boron, it is recommended that the filtration–fusion step should be performed even if no insoluble material can be seen after the acid-decomposition step. A small amount of insoluble material dispersed throughout the sample solution is not readily visible, particularly in an opaque Nalgene bottle.

The proposed method is suitable for samples containing ~0.0001% or more of boron. The EHD extraction step, in conjunction with zirconium as a complexing agent for fluoride, separates boron from titanium, fluoride and oxidizing agents such as hydrogen peroxide and nitrate, which interfere during complex formation with curcumin.[15,16,19,21] It also separates boron from niobium, which interferes in the Methylene Blue method.[3] An added advantage of this method over several previous spectrophotometric methods involving the use of curcumin[14,15] is that the complex is formed in a non-aqueous medium instead of in the presence of water, which interferes if more than ~0.25 ml is present. Other advantages over methods involving the use of Methylene Blue are the simplicity and reproducibility, the much lower reagent blank and the less critical conditions required for complex formation. Both acid-soluble and acid-insoluble boron can readily be determined by the proposed method. This is advantageous because both forms are often requested in iron and steel analysis because of their metallurgical effects. The time required to determine acid-soluble boron in six samples is 4 or 5 hr. About 8 hr are required to determine total boron.

REFERENCES

1. L. Pasztor, J. D. Bode and Q. Fernando, *Anal. Chem.*, 1960, **32**, 277.
2. R. Rosotte, *Chim. Anal. (Paris)*, 1962, **44**, 208.
3. D. Blazejak-Ditges, *Z. Anal. Chem.*, 1969, **247**, 20.
4. F. Vernon and J. M. Williams, *Anal. Chim. Acta*, 1970, **51**, 533.
5. O. P. Bhargava and W. G. Hines, *Talanta*, 1970, **17**, 61.
6. D. Bell and K. McArthur, *Analyst*, 1968, **93**, 298.
7. *Annual Book of ASTM Standards, Chemical Analysis of Metals: Sampling and Analysis of Metal Bearing Ores*, Part 12, p. 29. American Society for Testing and Materials, Philadelphia, 1979.
8. British Steel Corporation, *Methods of Chemical Analysis of Iron and Steel*, pp. 29–31. Sheffield, 1974.
9. Y. Hayashi, S. Matsushita, T. Kumamaru and Y. Yamamoto, *Talanta*, 1973, **20**, 414.
10. R. M. Hamner and L. A. De'Aeth, *ibid.*, 1980, **27**, 535.
11. T. Yoshimori, T. Miwa and T. Takeuchi, *ibid.*, 1964, **11**, 993.
12. I. M. Kolthoff and P. J. Elving, *Treatise on Analytical Chemistry*, Part II, Vol. 10, pp. 27–29, 33. Interscience, New York, 1978.
13. Reference 8, pp. 25–27.
14. T. S. Harrison and W. D. Cobb, *Analyst*, 1966, **91**, 576.
15. A. Tolk, W. A. Tap and W. A. Lingerak, *Talanta*, 1969, **16**, 111.
16. J. W. Mair, Jr. and H. G. Day, *Anal. Chem.*, 1972, **44**, 2015.
17. E. W. Grotheer, *ibid.*, 1979, **51**, 2402.
18. E. J. Agazzi, *ibid.*, 1967, **39**, 233.
19. M. R. Hayes and J. Metcalfe, *Analyst*, 1962, **87**, 956.
20. R. R. Grinstead and S. Snider, *ibid.*, 1967, **92**, 532.
21. G. S. Spicer and J. D. H. Strickland, *Anal. Chim. Acta*, 1958, **18**, 231.

Talanta, Vol. 28, pp. 833 to 837, 1981
Printed in Great Britain. All rights reserved

0039-9140/81/110833-05$02.00/0
Copyright © 1981 Pergamon Press Ltd

KINETIC FLUORIMETRIC DETERMINATION OF TRACES OF VANADIUM(V) BY MEANS OF A CATALYSED AUTOXIDATION PROCESS

F. GARCIA SANCHEZ, A. NAVAS and M. SANTIAGO

Department of Analytical Chemistry, Faculty of Sciences, University of Malaga, Spain

F. GRASES

Department of Analytical Chemistry, Faculty of Sciences, University of Palma de Mallorca, Spain

(*Received* 2 *September* 1980. *Revised* 10 *April* 1981. *Accepted* 24 *April* 1981)

Summary—A kinetic method for determination of traces of vanadium(V) (0.04–0.5 ppm) is described. It is based on the catalytic action of vanadate in the autoxidation of sodium 4,8-diamino-1,5-dihydroxyanthraquinone-2,6-disulphonate, giving rise to kinetic curves characterized by an induction period before the appearance of a product exhibiting an intense red fluorescence in acidic solution. This product has been investigated and the experimental variables and interferences have been studied.

Few methods have been described for the fluorimetric determination of vanadium(V),[1–4] and only one of these[4] is based on kinetic measurements.

In the present work the reaction of sodium 4,8-diamino-1,5-dihydroxyanthraquinone-2,6-disulphonate[5] with vanadium(V) is studied. It is found that the reagent is transformed into a highly fluorescent pink product by the action of dissolved oxygen in acidic medium. This reaction is slow and takes about two months to reach completion, but in the presence of certain cations [Au(III), Fe(III), V(V), Sn(II), Mn(II), Ce(IV)] it is accelerated and completed in about 30 min. In an inert atmosphere, the reaction occurs to only a very small extent.

Generally, the principal advantage of the initial-rate kinetic method over non-kinetic methods lies in its greater speed and specificity, which are achieved because the measurements are made so early in the reaction that there is probably not enough time for the effects of perturbing agents to be noticeable. In the present work, when the vanadium(V):reagent molar ratio is less then unity, the appearance of the fluorescence is preceded by an induction period, the length of which is proportional to the catalyst concentration. This means that as well as the three traditional kinetic methods (initial-rate, fixed-time, fixed-concentration), the induction-period method[6] may also be employed, which improves the selectivity since measurements are made before the fluorescent product is formed, so the action of possible quenching agents is avoided.

Most of the analytical methods based on the induction period are catalytic in nature and grouped under the classification of "Landolt reactions".[7] Up till now, no kinetic fluorimetric method based on the induction period has been described in the literature.

EXPERIMENTAL

Reagents and solutions

Solutions of sodium 4,8-diamino-1,5-dihydroxyanthraquinone-2,6-disulphonate (0.01*M*) and of vanadium(V) (0.001*M*) were prepared (the latter from ammonium vanadate, and gravimetrically standardized). The working solutions were prepared by dilution of these stock solutions. Doubly distilled and demineralized water, and analytical grade reagents were used.

Apparatus and measurement conditions

All fluorimetric measurements were performed on a Perkin–Elmer fluorescence spectrophotometer, model MPF-43A, equipped with an Osram XBO 150-W xenon lamp, excitation and emission grating monochromators, 1 × 1 cm quartz cells, an R-508 photomultiplier and a Perkin–Elmer 023 recorder. A Rhodamine B standard ($1 \times 10^{-7}M$) gave a reading of 60 units with the following parameters: $\lambda_{ex} = 480$ nm, $\lambda_{em} = 570$ nm, excitation and emission slits 5 nm, sensitivity 10 coarse and 7 fine, and temperature 25°. The fluorescence intensity *vs.* time curves were recorded at a chart-speed of 2 cm/min. A Perkin–Elmer RMU-GA mass spectrometer and model 577 infrared spectrophotometer were also used.

Procedure

In a 25-ml standard flask place 5 ml of $1 \times 10^{-4}M$ reagent, 5 ml of 2*M* hydrochloric acid and enough demineralized water necessary to make up a final volume of 25 ml, together with the volume of sample solution needed to give a vanadium(V) concentration between 0.04 and 0.50 ppm in the mixture. Record intensity of the emitted fluorescence as function of time, starting the recording 60 sec after addition of the sample, working at 28°, $\lambda_{ex} = 524$ nm, $\lambda_{em} = 582$ nm.

Isolation of the reaction product

Dissolve 5 g of sodium 4,8-diamino-1,5-dihydroxyanthraquinone-2,6-disulphonate in water, acidify the solution with 2*M* hydrochloric acid and add 3 ml of 30% hydrogen

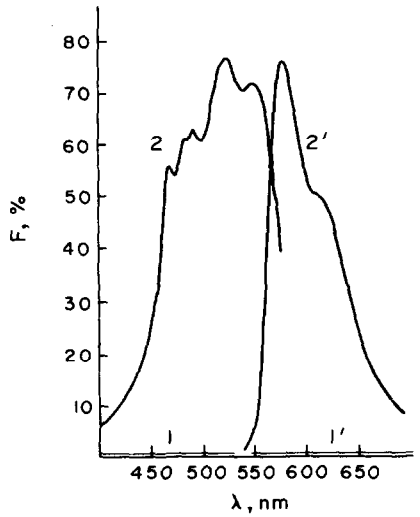


Fig. 1. Uncorrected excitation (1,2) and emission (1', 2') spectra in presence (2, 2') and absence (1, 1') of 0.3 ppm V(V): [reagent] = $2 \times 10^{-5}M$. [HCl] = $0.4M$. Sensitivity: 0.1 coarse, 7 fine (λ_{ex} = 524 nm, λ_{em} = 582 nm).

peroxide. Heat the mixture thus prepared until the blue colour of the initial solution changes to red. Allow to cool and collect the dark red precipitate that appears. Recrystallize from ethanol.

RESULTS AND DISCUSSION

Effect of the reaction variables

The excitation and emission spectra of the reagent and the product of reaction with vanadium(V) are shown in Fig. 1. In the absence of the vanadium, there is no fluorescence from the reagent solution.

The system was optimized by altering each variable in turn, the others being kept fixed. For the induction-period method, the optimal reagent concentrations were taken as those that did not affect the length of the induction period.

For the other methods (initial rate, fixed time, fixed concentration), the optimum concentrations were taken as those giving minimal relative standard deviation for the initial rate measurements under conditions in which the reaction order with respect to the variable concerned was zero or as close to it as possible.

The length of the induction period (Fig. 2) was evaluated from the intercept (on the x axis) by extrapolation of the linear section of the reaction curve. The initial reaction rate is also determined from the tangent.

The influence of acidity on the initial rate and induction period is presented in Fig. 3. The optimum

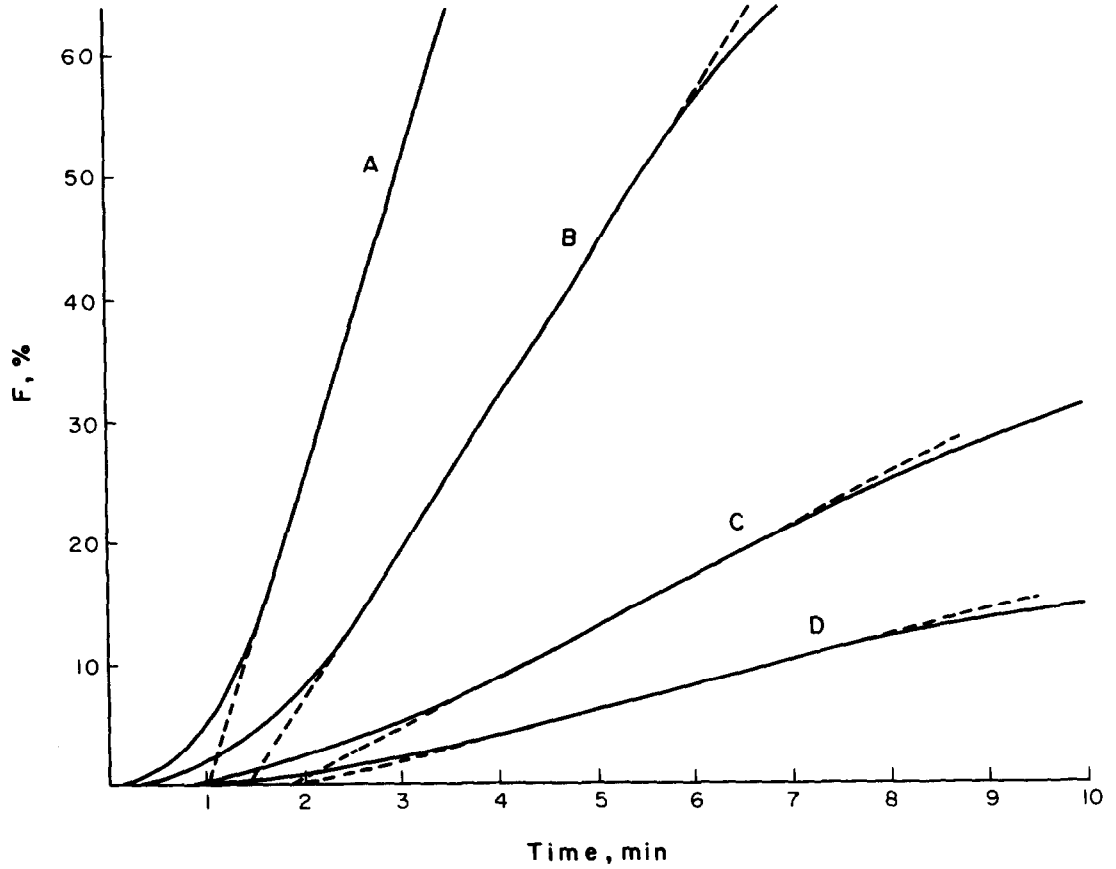


Fig. 2. Curves for fluorescence intensity vs. time for various catalyst concentrations (ppm). A, 0.4; B, 0.2; C, 0.1; D, 0.08; [reagent] = $2 \times 10^{-5}M$, [HCl] = $0.4M$. Sensitivity: 3 coarse, 2 fine. (λ_{ex} = 524 nm, λ_{em} = 582 nm).

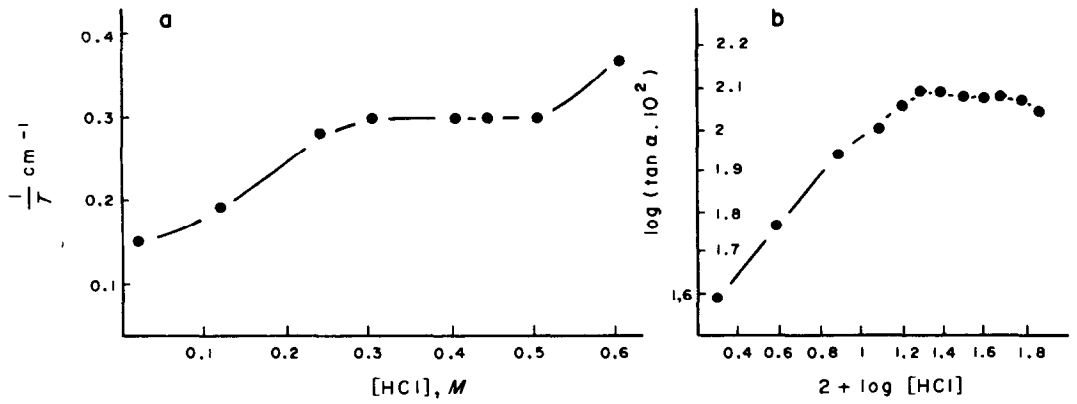


Fig. 3. Influence of the acidity on the induction period (*a*) and the initial rate (*b*); [reagent] = $2 \times 10^{-5}M$, [V(V)] = $2 \times 10^{-6}M$ (*a*), [V(V)] = $2 \times 10^{-4}M$ (*b*). Sensitivity: 3 coarse, 2 fine. (λ_{ex} = 524 nm, λ_{em} = 582 nm).

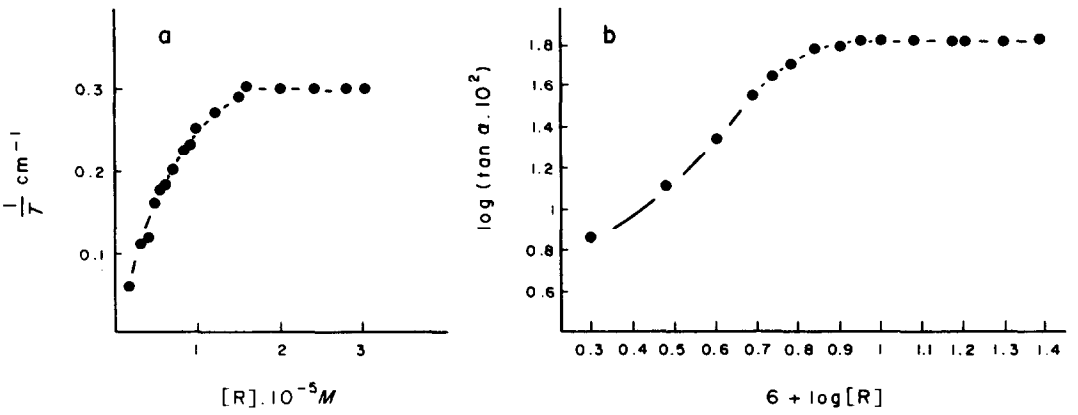


Fig. 4. Influence of the reagent concentration on the induction period (*a*), and the initial rate (*b*) [V(V)] = $2 \times 10^{-6}M$, [HCl] = 0.4*M*. Sensitivity: 3 coarse, 2 fine. (λ_{ex} = 524 nm, λ_{em} = 582 nm).

is 0.4*M* hydrochloric acid for all four methods studied.

The effect of reagent concentration is presented in Fig. 4, from which an optimum concentration of $2 \times 10^{-5}M$ is deduced.

The kinetic data (reaction order and velocity coefficient) resulting from the corresponding logarithmic plots (Figs. 3b and 4b) are collected in Table 1.

Characteristics of the analytical methods

The fluorescence–time curves, obtained with the optimum conditions and excitation and emission wavelengths (λ_{ex}524 nm, λ_{em} = 582 nm), for different amounts of vanadium(V), were analysed by the four kinetic methods; the results are shown in Table 2, which shows that the induction-period method gives the highest sensitivity and precision.

The selectivity of the methods was assayed by studying the effect of foreign ions on the reaction rate and induction period. It was found that fewest interferences arose when the induction-period method was used, with which only Fe(III), Fe(II), Ce(IV) and I^- interfere at concentrations similar to that of the vanadium(V), Table 3.

Of the four methods, the induction-period method is best, giving the highest sensitivity and precision and least number of interferences, and this is therefore recommended.

Table 1. Kinetic data

$v_0 = 3.85[H^+]^1$	for $[H^+] < 0.06M$
$v_0 = 1.17[H^+]^0$	for $0.06M < [H^+] < 0.6M$
$v_0 = 10^{10}[R]^2$	for $[R] < 6 \times 10^{-6}M$
$v_0 = 0.66[R]^0$	for $6 \times 10^{-6}M < [R] < 2.4 \times 10^{-5}M$
$v_0 = 10^{10}[V^{5+}]^2$	for $0.04M < [V^{5+}] < 0.1M$
$v_0 = 1.74 \times 10^7[V^{5+}]^{1/2}$	for $0.1M < [V^{5+}] < 0.5M$

Table 2. Characteristics of the kinetic methods

Methods	Range of applicability, *ppm*	Taken, *ng/ml*	Found($\bar{x}$), *ng/ml*	*n*	*S*, *ng/ml*	*W*,%	*G*,%
Induction period	0.04–0.5	100	103	10	4.8	4.7	3.3
Fixed time	0.08–0.5	200	208	8	7.5	3.6	3.0
Fixed concentration	0.08–0.5	300	291	10	11.9	4.1	2.9
Initial rate	0.04–0.5	300	312	10	22.9	7.4	5.3

$\bar{x}$ = mean value; n = number of determinations; S = standard deviation; W = coefficient of variation: G = relative error ($= 100\,tS/\bar{x}\sqrt{n}$, where t is Student's t for 95% confidence).

Nature of the reaction and the product obtained

The reaction of vanadium(V) with sodium 4,8-diamino-1,5-dihydroxyanthraquinone-2,6-disulphonate has been studied to determine the nature of the reaction and the product formed, with the following results.

(*a*) The reagent can be transformed into the fluorescent product by the action of dissolved oxygen. This reaction is slow and takes approximately two months to reach completion.

(*b*) The reagent is rapidly transformed into the fluorescent product by strong oxidants such as potassium bromate or hydrogen peroxide.

(*c*) The reaction of the reagent with vanadium(V) takes place to a much greater extent in presence of dissolved oxygen than in an inert atmosphere.

(*d*) In presence of cations such as manganese(II) and tin(II), the reagent gives products identical to that resulting from its reaction with vanadium(V).

It may be deduced that vanadium(V) catalyses the

Table 3. Influence of some foreign ions on the determination of micro amounts of vanadium(V) by the induction-period method; $C_{V(V)} = 100$ ng/ml

Ion	C_{Ion}/C_V*	$1/T$, cm^{-1}	C_{Ion}/C_V†
—	—	0.30	—
Li^+	50	0.30	100 (D 0.05)
Na^+	100	0.31	200 (D 0.03)
K^+	20	0.30	50 (A 0.02)
Hg^+	100	0.31	200 (D 0.02)
Cu^{2+}	100	0.30	500 (A 0.02)
Hg^{2+}	100	0.30	200 (D 0.04)
Co^{2+}	100	0.30	200 (A 0.02)
Ni^{2+}	100	0.30	—
Zn^{2+}	100	0.31	100 (D 0.01)
Cd^{2+}	20	0.30	50 (D 0.01)
Pd^{2+}	20	0.30	50 (A 0.03)
Mn^{2+}	20	0.31	100 (D 0.03)
Sn^{2+}	100	0.30	—
Fe^{2+}	0.1	0.28	0.5 (A 0.02)
UO_2^{2+}	100	0.30	200 (A 0.02)
As^{3+}	50	0.31	100 (D 0.07)
Cr^{3+}	50	0.30	100 (A 0.02)
Fe^{3+}	0.1	0.29	150 (D 0.47)
La^{3+}	100	0.31	100 (D 0.01)
Ti^{4+}	100	0.30	200 (A 0.02)
Th^{4+}	20	0.31	50 (A 0.07), 100 (D 0.03)
Ce^{4+}	0.5	0.28	1 (D 0.04
Mo^{6+}	100	0.31	100 (D 0.01)
PO_4^{3-}	50	0.28	100 (D 0.03)
$C_2O_4^{2-}$	100	0.31	100 (D 0.01)
F^-	20	0.30	50 (A 0.03), 100 (D 0.03)
Cl^-	200	0.31	200 (D 0.01)
Br^-	50	0.30	100 (A 0.02)
I^-	0.5	0.31	0.5 (D 0.01)
EDTA	50	0.30	100 (A 0.02)
Citrate	20	0.30	50 (A 0.02)

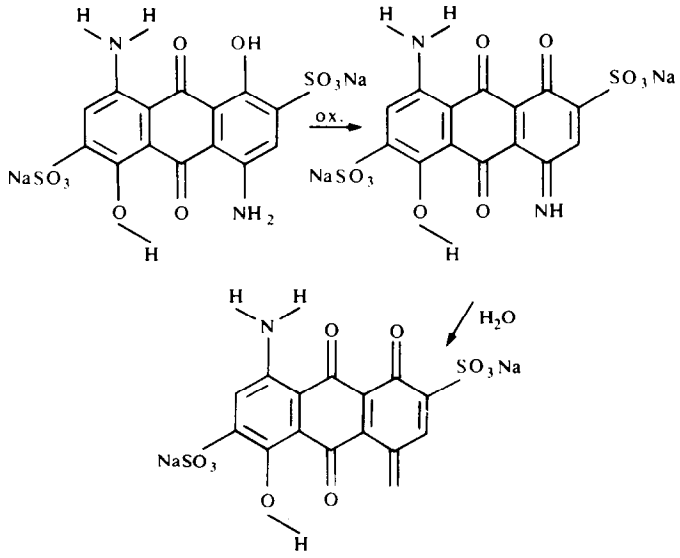
* Concentration ratios which do not interfere.

† Concentration ratios which increase (A) or diminish (D) the induction period by the amount ($1/T$, cm^{-1}) shown in brackets.

aerial oxidation of sodium 4,8-diamino-1,5-dihydroxyanthraquinone-2,6-disulphonate to an oxidation product which is shown by infrared analysis to contain carbonyl groups in a highly conjugated system similar to that of the initial reagent, together with –OH and $-NH_2$ groupings (band at 3000–3800 cm^{-1}) and sulphonic groups (band at 1025 cm^{-1}).

The elemental analysis showed that the carbon content was the same as that of the parent reagent, but the nitrogen content had been halved. The mass spectrum of the isolated product showed that it was a salt and that many of the principal peaks obtained for the parent reagent were also present, indicating that both products would have similar structures and probably identical skeletons.

The literature shows that the oxidation of aromatic amines possessing *ortho* or *para* amino or hydroxy groups leads to the corresponding *o*- or *p*-quinones[8–10] in a manner that involves intermediate formation of an imine.[11] From the experimental and literature data it seems clear that the oxidation proceeds according to the following scheme.



REFERENCES

1. V. Rao and G. Rao, *Z. Anal. Chim.*, 1958, **161**, 406.
2. K. J. Koh and D. E. Ryan, *Anal. Chim. Acta*, 1971, **57**, 295.
3. M. Roman, F. Garcia Sanchez and A. Gomez Hens, *Inf. Quim. Anal.*, 1974, **28**, 191.
4. F. Salinas, F. Garcia Sanchez, F. Grases and C. Genestar, *Anal. Lett.*, 1980, **13**, 473.
5. A. Navas and F. Garcia Sanchez, *An. Quim.*, 1979, **75**, 505.
6. K. B. Yatsimirskii, *Kinetic Methods of Analysis*, Pergamon Press, Oxford, 1966.
7. G. Svehla, *Analyst*, 1969, **94**, 513.
8. J. March, *Advanced Organic Chemistry: Reactions, Mechanism and Structure*, McGraw-Hill, New York, 1968.
9. L. F. Fieser and M. Fieser, *Quimica Organica Superior*, Vol. 2, Grijalbo, Barcelona, 1966.
10. K. L. Rinehart Jr., *Oxidacion y reduccion de compuestos organicos*, Alhambra, Madrid, 1977.
11. I. Krausz and A. Endröi-Havas, *Proc. S.A.C. Conference Nottingham*, 1965, p. 568.

Talanta, Vol. 28, pp. 839 to 842. 1981
Printed in Great Britain. All rights reserved

0039-9140/81/110839-04$02.00/0
Copyright © 1981 Pergamon Press Ltd

DETERMINATION OF TRACE METALS BY ANODIC-STRIPPING VOLTAMMETRY WITH A NEW KIND OF MERCURY ELECTRODE: THE LONG-LASTING SESSILE-DROP ELECTRODE

ROMANO ANDRUZZI and ANTONIO TRAZZA

Istituto di Chimica, Facoltà di Ingegneria, Università degli Studi di Roma and Centro di Elettrochimica e Chimica-Fisica delle Interfasi, C.N.R., Via del Castro Laurenziano, 7-00161 Roma, Italy

(*Received* 27 *February* 1981, *Accepted* 21 *April* 1981)

Summary—A new kind of semi-stationary mercury drop electrode is described, which can be used for the determination of trace metals in natural waters by differential-pulse anodic-stripping voltammetry. Results are reported for the determination of zinc in potassium chloride and in samples of sea-water. The reproducibility of the electrode and of the results obtained with it for zinc at the $10^{-8}M$ level are very satisfactory.

Electroanalytical techniques have been employed in recent years to determine trace metals by direct measurement in a variety of samples (*e.g.*, natural waters, industrial effluents and organic liquids), mainly because it has been found that some heavy metals (such as cadmium, lead and mercury) are toxic even at very low concentrations. Up to now, the technique which has yielded the best results is certainly anodic-stripping voltammetry, by which a metal is cathodically deposited on an electrode and anodically removed under controlled conditions.[1,2] The characteristics of the working electrode, as well as the experimental conditions during the electrolysis, are the main factors affecting the sensitivity of the method. Mercury-film electrodes[2–5] and Kemula's hanging-drop mercury electrode[2,5,6] have been employed, but all these electrodes give poor reproducibility (usually about 5%) even though allowing a detection limit lower than $10^{-9}M$. Moreover, the manipulation is quite tedious and requires great care, especially with mercury-film electrodes, while the synchronization is somewhat difficult with hanging-drop electrodes. Ordinary capillary electrodes with a long drop-time (60–80 sec) have also been employed for the determination of some heavy metals (zinc, cadmium and lead) in natural waters either by linear anodic-stripping voltammetry[7–10] or by differential-pulse anodic-stripping voltammetry.[11] Nevertheless, with such electrodes the electrolysis time must be quite short (30–40 sec) while the voltage range cannot be larger than 500 mV at a scan-rate of 20 mV/sec.

We propose a new kind of semi-stationary mercury electrode: the long-lasting sessile-drop electrode (llsdme) which allows a longer electrolysis time with more vigorous stirring, a longer rest time to obtain a quiescent solution, a larger potential range at slower scan-rates and lastly, a higher current response.

The llsdme was originally employed by one of us for the thin-layer reduction of oxygen.[12] It was obtained by drawing out one end of an ordinary polarographic capillary in the flame and then bending it up in the form of a hook (Fig. 1). Such capillaries, connected to a mercury reservoir (h = 90 cm) and immersed in $0.1M$ potassium chloride (stirred at 800 rpm) showed a drop-time of 2–6 min, in closed circuit (−1.30 V). Therefore with an llsdme the electrolysis time may be of the same order of magnitude (90–240 sec) as is usually employed with thin-film mercury electrodes or with hanging-drop electrodes. Moreover the voltage range may exceed 1.0 V at a scan-rate of 10 mV/sec.

To evaluate the possible analytical applications of the llsdme we have determined zinc both in a simple purified electrolyte ($0.1M$ potassium chloride in doubly-distilled water) and in sea-water samples, by differential-pulse anodic-stripping voltammetry. The results obtained so far and reported in this note show that the detection limit can be lower than $5 \times 10^{-10}M$ while the reproducibility can be better than 2%.

EXPERIMENTAL

Chemicals

Potassium chloride (Merck, GR) and nitric acid, 65% (Merck, suprapur) were used, as received, as supporting electrolyte and for preparing cleaning solutions respectively. The cadmium, lead and zinc standard solutions were prepared by diluting standard solutions of their nitrates (Fluka). The water used in preparation of the reagent solutions and for cleaning was demineralized, distilled from permanganate and then redistilled in a quartz apparatus. Mercury (Merck, GR) was carefully scrubbed with nitric acid (12% v/v) solution then with distilled water. Lastly it was distilled twice under reduced pressure. Argon (99.99% pure) was used to deoxygenate the solutions under examination.

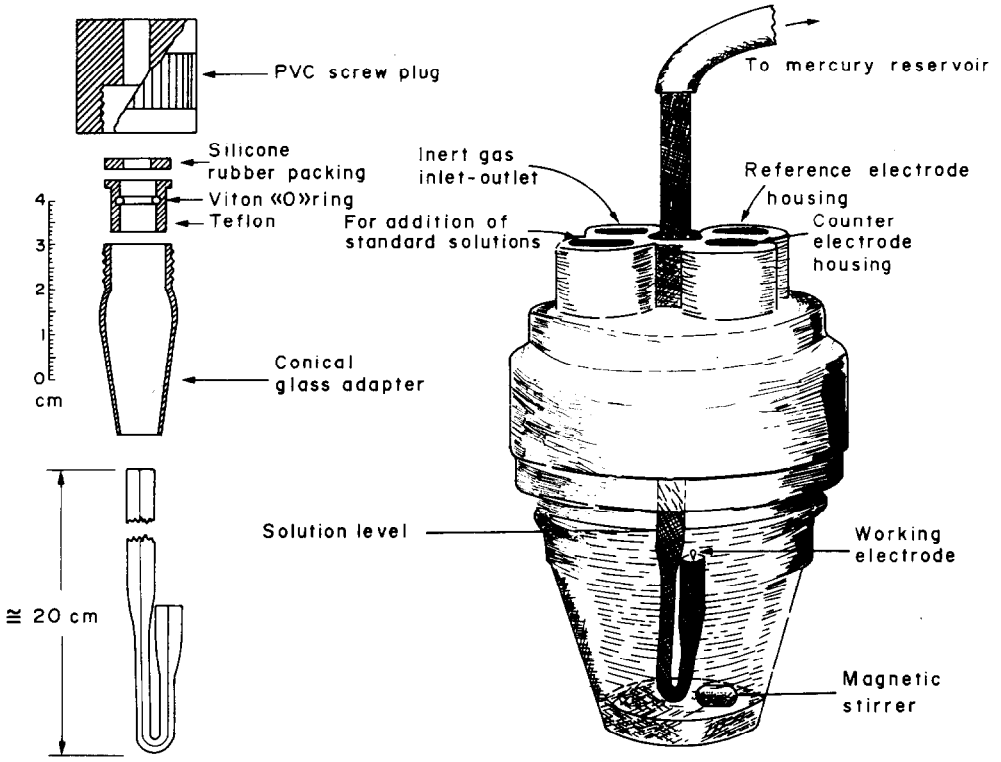


Fig. 1. Electrolysis cell with long-lasting sessile-drop mercury electrode in place (at the right) and details of the electrode (at the left).

Apparatus and procedures

The measurements were carried out by means of a multipolarograph (Amel 471) and a timer (Amel 452/T) in the following sequence: at the first appearance of the mercury drop the timer was switched on manually; the solution (60 ml) was stirred while the drop was polarized at −1.30 V; after 180 sec the timer stopped the stirring; then, after a period of 12 sec (to obtain a quiescent solution around the electrode), the anodic sweep started automatically and the voltamperogram was recorded; at the end of the sweep the drop was manually dislodged by a top on the upper part of the capillary. A new drop then began to appear and the sequence could be repeated. All the measurements were performed at 24°C in a normal polarographic cell (Fig. 1) (Amel 494) with an SCE (Ingold) and a platinum ring (Ingold) as reference and counter-electrode respectively. An Ilsdme, made from a Sargent (6–12 sec) polarographic capillary, with a drop-time of 6 min, was used as working electrode. The test solution (60 ml) was stirred at 800 rpm by a Teflon-covered iron rod (15 mm length, 7.5 mm diameter) and a magnetic stirrer (Amel 291/LF). The standard solutions were added from automatic microlitre pipettes (Gilson). The sea-water samples were collected and stored in polyethylene bottles.

RESULTS AND DISCUSSION

Figure 2 shows a sequence of anodic-stripping voltamperograms for the determination of zinc in 0.1*M* potassium chloride. The curves were recorded with three consecutive drops over a voltage sweep range of 0.50 V at 20 mV/sec after an electrolysis time of 180 sec at −1.30 V (stirring at 800 rpm) followed by

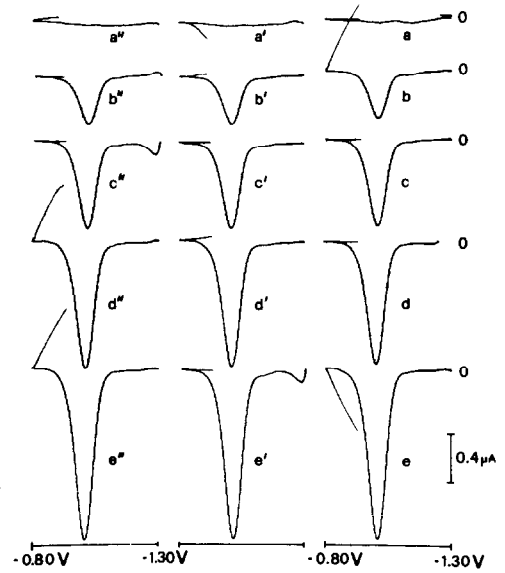


Fig. 2. Anodic-stripping voltamperograms of zinc in a potassium chloride solution. (a) Potassium chloride solution, 0.1*M*, 60 ml, rest time = 192 sec, without stirring and without electrolysis; (b) solution as in (a), electrolysis potential = −1.30 V, electrolysis time = 180 sec with stirring at 800 rpm, rest time = 12 sec; (c–e) as (b) after addition of 100 μl (c), 200 μl (d) and 300 μl (e) of $1.53 \times 10^{-5}M$ standard zinc solution. Voltamperograms a'–e' and a''–e'' were recorded with the second and third consecutive mercury drops after each addition. Pulse interval = 0.25 sec; pulse amplitude = 50 mV; sweep rate = 20 mV/sec; mercury head = 94 cm; temperature = 24°.

a rest time of 12 sec. From curves b, b′ and b″ it is evident that the zinc peak ($E_p = -1.01$ V) is well defined and its height (i_p) exhibits a satisfactory reproducibility (better than 1%) for the three consecutive drops. This is a remarkable result, especially taking into account that each single drop had been dislodged manually at the end of the sweep. Moreover, it is important to note that the mercury used is practically zinc-free. In fact, the three voltamperograms a, a′ and a″ recorded for solutions that had not been pre-electrolysed, but had waited 192 sec for growth of the drop, did not show any peak.

Each increment of the i_p value (curves c–e in Fig. 2) corresponds to consecutive additions of the same amount of a standard zinc solution. In the range $2.8–7.7 \times 10^{-8}M$ i_p is proportional to the zinc concentration (Table 1); in the i_p–concentration plot the intercept on the ordinate corresponds to the zinc content in the original potassium chloride solution. From these data the concentration of zinc in the 0.1*M* potassium chloride was calculated to be $2.86 \times 10^{-8}M$, and three replicate determinations solutions showed a reproducibility better than 2%.

Figure 3 shows the sequence for the determination of zinc in a sea-water sample collected in the Tyrrenian sea about 400 m off the mouth of the harbour-canal of Castiglione della Pescaia (Grosseto, Italy). The voltamperograms reproduced were recorded as before for three consecutive drops (a–d, a′–d′ and a″–d″ respectively) over a voltage sweep range of 0.50 V at 10 mV/sec after an electrolysis time of 180 sec at −1.30 V (stirring at 800 rpm) followed by a rest time of 12 sec.

The zinc peak is well defined (curves a, a′ and a″) and increases (curves b–d, b′–d′ and b″–d″) on addition of known amounts of standard zinc solution. The reproducibility is again very good. In the zinc concentration range $1.3–3.0 \times 10^{-7}M$ there is a linear relationship between peak current and zinc concentration (Table 2); from the i_p–concentration plot the concentration of zinc in the sea-water was evaluated as $1.3–10^{-7}M$.

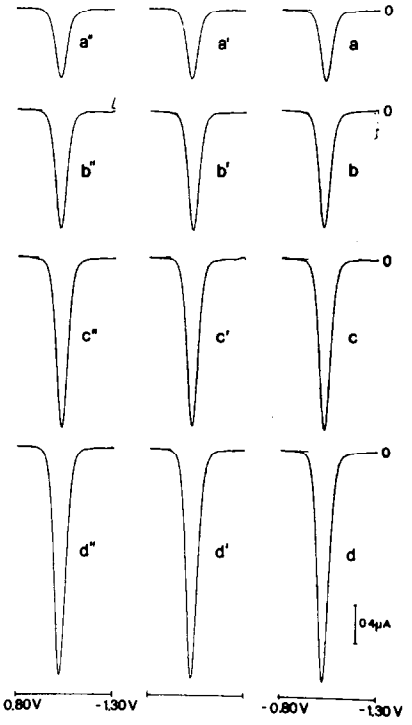


Fig. 3. Anodic-stripping voltamperograms of zinc in a sea-water sample. (a) Sea-water, 60 ml electrolysis potential = −1.30 V, electrolysis time = 180 sec with stirring at 800 rpm, rest time = 12 sec; (b–d) as (a) after addition of 100 μl (b), 200 μl (c), and 300 μl (d) of $6.12 \times 10^{-5}M$ standard zinc solution. Voltamperograms a′–d′ and a″–d″ were recorded with the second and third consecutive mercury drops after each addition. Pulse interval = 0.25 sec; pulse amplitude = 50 mV; sweep rate = 10 mV/sec; mercury head = 87 cm; temperature = 24°.

Finally Fig. 4 shows some anodic-stripping voltammograms for a second sea-water sample collected in the same area, but just at the mouth of the harbour. The experimental conditions were the same as before except for the voltage sweep range (1.0 V) and the use of two different scan rates (10 mV/sec for curves a, a′ and a″; 20 mV/sec for curves b, b′ and b″). In every

Table 1. Correlation between peak currents and concentration of zinc in 0.1*M* KCl*

[Zn], μg/l.	i_p, μA	i'_p, μA	i''_p, μA
1.87†	0.36	0.36	0.36
1.66§	0.68	0.69	0.69
3.32§	1.01	1.01	1.02
4.98§	1.36	1.36	1.36

* The anodic voltamperograms and the experimental conditions are reported in Fig. 2.

† Concentration of zinc in the original sample.

§ Concentration of zinc added.

Table 2. Correlation between peak currents and concentration of zinc in a sea-water sample*

[Zn], μg/l.	i_p, μA	i'_p, μA	i''_p, μA
8.51†	0.70	0.69	0.69
6.66§	1.23	1.23	1.23
13.29§	1.80	1.79	1.81
19.91§	2.43	2.42	2.41

* The anodic voltamperograms and the experimental conditions are reported in Fig. 3.

† Concentration of zinc in the original sample.

§ Concentration of zinc added.

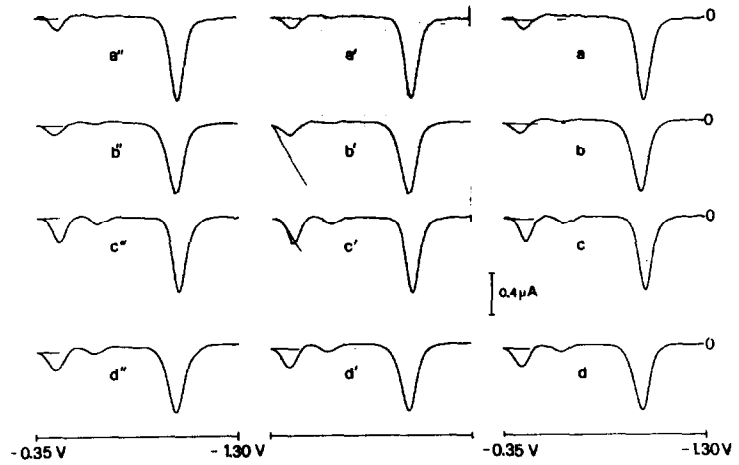


Fig. 4. Anodic-stripping voltamperograms for another sea-water sample. (a) Conditions as for (a) in Fig. 3. (b) as (a) but with sweep rate = 20 mV/sec (c) as (a) after addition of 40 μl of $7.1 \times 10^{-6} M$ standard cadmium and 80 μl of $3.86 \times 10^{-6} M$ standard lead solutions (d) as (c) but with sweep rate = 10 mV/sec. Voltamperograms a'–d' and a''–d'' were recorded with the second and third consecutive mercury drops after each addition. Pulse interval = 0.25 sec; pulse amplitude = 50 mV; mercury head = 87 cm; temperature = 24°.

case the voltamperograms show two peaks ($E_p = -1.02$ V and $E_p = -0.45$ V, curve a) corresponding to oxidation of zinc and lead respectively. On addition of known amounts of standard cadmium and lead solutions, the zinc peak is practically unchanged, the lead peak increases and the cadmium peak ($E_p = -0.65$ V) appears (curves c, c' and c'' or curves d, d' and d''). The concentration of the lead in the sea-water sample was evaluated as $3.85 \times 10^{-9} M$ while the concentration of the cadmium was certainly less than $4.7 \times 10^{-9} M$, which corresponds to the lowest cadmium concentration in the standard addition series.

CONCLUSIONS

The experimental results reported so far, as well as those obtained with five other electrodes of the same kind, suggest that the long-lasting sessile-drop mercury electrode may be employed for the determination of trace metals by the differential-pulse anodic-stripping voltammetry. It is important to note that under the experimental recording conditions for our voltamperograms (5 μA full scale) a detection limit of $2.5 \times 10^{-9} M$ was reached for lead in a sea-water sample. Moreover the reproducibility (better than 2%) was obtained with only a semi-automated sequence (the drop was manually dislodged at the end of each sweep) and a normal electrolytic cell. We think that the determination may be improved to a limit of detection of about $5 \times 10^{-10} M$ and a reproducibility better than 1%.

Work is in progress in our laboratory to improve the factors which can affect the sensitivity of the method, namely: (1) achievement of an automated and well synchronized sequence (mechanical dislodging of the drop, followed by commencement of electrolysis at a precisely controlled time in the life of the drop); (2) constancy and control of the magnetic and/or mechanical stirring; (3) optimized geometry of the different components in the cell, which is to be made of quartz or Teflon; (4) improved sensitivity in the current recording equipment (< 1 μA full scale); (5) study of possible interference effects due to the formation of intermetallic compounds on or in the mercury drop.

Later, this new kind of electrode will be tested for oscillopolarography and for d.c. polarography, mainly in aprotic media where the base-electrolyte discharge may occur at very negative potentials at which the performance of the usual capillaries is no longer reliable.

REFERENCES

1. E. Barendrecht, *Stripping Voltammetry*, in *Electroanalytical Chemistry*, A. J. Bard (Ed.), Vol. 2, Dekker, New York, 1969.
2. H. W. Nürnberg, P. Valenta, L. Mart, B. Raspor and L. Sipos, *Z. Anal. Chem.*, 1976, **282**, 357.
3. T. M. Florence, *J. Electronal. Chem.*, 1970, **26**, 293; 1970, **27**, 273; 1972, **35**, 237.
4. W. J. Blaedel and J. Wang, *Anal. Chem.*, 1979, **51**, 1724.
5. Z. Stojek and Z. Kublik, *J. Electroanal. Chem.*, 1979, **105**, 247.
6. R. Salim and B. G. Cooksey, *ibid.*, 1979, **105**, 127.
7. G. Macchi, *ibid.*, 1965, **9**, 290.
8. R. A. Osteryoung and E. P. Parry, *ibid.*, 1965, **9**, 299.
9. B. Raspor, P. Valenta, H. W. Nürnberg and M. Branica, *Thalassia Jugoslavica*, 1977, **13**, 79.
10. P. Chamard and G. Macchi, *Ann. Chim., Rome*, 1978, **68**, 1.
11. L. Grifone and G. Macchi, *ibid.*, 1978, **68**, 227.
12. P. Silvestroni, R. Andruzzi and F. Rallo, *Electrochim. Metal. Milan*, 1968, **3**, 281.

Talanta. Vol. 28. pp. 843 to 848. 1981
Printed in Great Britain. All rights reserved

0039-9140 81 110843-06$02.00 0
Copyright © 1981 Pergamon Press Ltd

LE *cis*-α,β-DINITROSTILBENE: UN NOUVEAU REACTIF POUR LE DOSAGE COLORIMETRIQUE DES AMINES PRIMAIRES ET SECONDAIRES, DES AMINOACIDES ET DES THIOLS

P. DUBOIS, P. LEVILLAIN et C. VIEL
Faculté de Pharmacie, 2bis boulevard Tonnellé, 37032 Tours Cédex, France

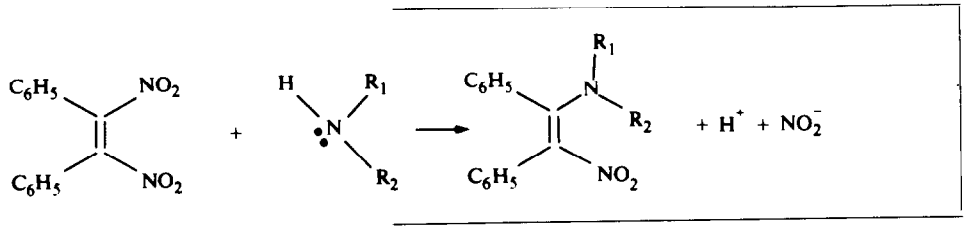
(*Reçu le* 3 *octobre* 1980. *Révisé le* 16 *février* 1981. *Accepté le* 7 *avril* 1981)

Résumé—Le *cis*-α,β-dinitrostilbène réagit avec les amines primaires et secondaires, les aminoacides et les thiols en développant une coloration permettant un dosage spectrophotométrique très sensible de ces composés. L'étude des conditions opératoires conduit à proposer plusieurs méthodes pour doser préférentiellement ces différentes classes d'agents nucléophiles.

Le *cis*-α,β-dinitrostilbène (DNS) réagit facilement avec certains composés nucléophiles[1,2] pour former le dérivé monosubstitué correspondant dont le maximum d'absorption diffère nettement de celui des produits de départ. Nous avons donc pensé que le DNS pouvait constituer un nouveau réactif permettant le dosage colorimétrique de composés aminés et de thiols.[3,4]

Nature des composés réagissant avec le DNS

La réaction de substitution d'un groupement nitré du DNS est le résultat d'une attaque nucléophile sur un carbone vinylique avec départ d'une molécule de HNO_2 selon:



(1) Elle n'est donc possible que pour les composés possédant au moins un hydrogène mobile, notamment les amines primaires et secondaires ainsi que les thiols.

(2) Les coefficients d'extinction molaire vrais obtenus pour les monoamines étant sensiblement du même ordre de grandeur, la variation, lors du dosage, de l'absorbance par mole de composé présent ("coefficient d'extinction moléculaire apparent" Δ_ε) traduit la réactivité de la molécule dans les conditions expérimentales. On constate ainsi que cette réactivité dépend du caractère nucleophile, donc de la densité électronique sur l'azote ou le soufre et varie, en première approximation, parallèlement au pK_a de l'amine. Par exemple, pour les amines aliphatiques, la coloration obtenue pour l'éthanolamine ($pk_a = 9{,}5$*) est plus faible que celle de l'éthylamine ($pk_a = 10{,}7$) (Tableau 1). Généralement, les amines aromatiques (aniline: $pk_a = 4{,}6$; *p*-toluidine: pk_a 5,1) réagissent moins fortement que les amines aliphatiques (Tableau 1). La réactivité devient nulle avec l'*o*-nitroaniline ($pk_a = 0{,}25$), la diphénylamine ($pk_a = 0{,}8$) ou la *N*-phényl-β-naphtylamine (pk_a de l'ordre de 0,3†).

(3) L'encombrement stérique constitue une gêne à la réaction comme on peut le constater pour la série des propylamines et des butylamines et pour le diméthyl-2,4 amino-3 pentane (Tableau 1). De même, les amines secondaires réagissent moins facilement que les amines primaires correspondantes, quoiqu'elles soient plus basiques (diéthylamine: $pk_a = 11{,}05$; pipéridine: $pk_a = 11{,}15$; pyrrolidine: $pk_a = 11{,}25$; *N*-méthylaniline: $pk_a = 4{,}85$) (Tableau 1). Les réactions les plus nettes sont obtenues avec les composés possédant le groupement réactif en bout de chaîne.

(4) La présence d'une fonction acide ou alcool dans la molécule aminée entraîne une diminution de la réactivité avec le DNS comme le montrent la série allant de l'α-alanine à l'acide ω-aminocaproïque (Tableau 5), et l'éthanolamine comparée à l'éthylamine (Tableau 1).

* Les valeurs de pk_a reportées ici représentent la moyenne de plusieurs valeurs concordantes citées dans l'ouvrage de Perrin.[5]

† Valeur approchée de pk_a calculée à partir de celles obtenues pour la β-naphtylamine (4,1), l'aniline (4,6), et la diphénylamine (0,8).[5]

Tableau 1. Résultats obtenus selon la technique no 1

Amines	$\Delta\varepsilon$ $l \cdot mole^{-1} \cdot cm^{-1}$	Limites de dosage, M	Amines	$\Delta\varepsilon$ $l \cdot mole^{-1} \cdot cm^{-1}$	Limites de dosage, M
Méthylamine	$1{,}00 \cdot 10^4$	$2 \cdot 10^{-5}$–$2 \cdot 10^{-4}$	Ethanolamine	$7{,}4 \cdot 10^3$	$4 \cdot 10^{-5}$–$8 \cdot 10^{-4}$
Éthylamine	$1{,}08 \cdot 10^4$	$1{,}5 \cdot 10^{-5}$–$1{,}5 \cdot 10^{-4}$	Heptaminol	$5{,}8 \cdot 10^3$	$4 \cdot 10^{-5}$–$8 \cdot 10^{-4}$
Propylamine	$1{,}08 \cdot 10^4$	$1{,}5 \cdot 10^{-5}$–$1{,}5 \cdot 10^{-4}$	Diéthylamine	$5{,}2 \cdot 10^3$	$4 \cdot 10^{-5}$–$8 \cdot 10^{-4}$
Isopropylamine	$7{,}0 \cdot 10^3$	$4 \cdot 10^{-5}$–$8 \cdot 10^{-4}$	Dipropylamine	$4{,}2 \cdot 10^3$	$5 \cdot 10^{-5}$–$9 \cdot 10^{-4}$
n-Butylamine	$1{,}16 \cdot 10^4$	$1{,}5 \cdot 10^{-5}$–$1{,}5 \cdot 10^{-4}$	Pipéridine	$8{,}7 \cdot 10^3$	$3 \cdot 10^{-5}$–$3 \cdot 10^{-4}$
Isobutylamine	$5{,}0 \cdot 10^3$	$4 \cdot 10^{-5}$–$8 \cdot 10^{-4}$	Pyrrolidine	$1.05 \cdot 10^4$	$1{,}5 \cdot 10^{-5}$–$1{,}5 \cdot 10^{-4}$
Tertbutylamine	0	—	Aniline	$2{,}0 \cdot 10^3$	10^{-4}–$9 \cdot 10^{-4}$
Diméthyl-2-4 amino-3 pentane	0	—	*p*-Toluidine	$4{,}6 \cdot 10^3$	$5 \cdot 10^{-5}$–$9 \cdot 10^{-4}$
			Benzidine	$8{,}2 \cdot 10^3$	$2 \cdot 10^{-5}$–$2 \cdot 10^{-4}$
Benzylamine	$1{,}08 \cdot 10^4$	$1{,}5 \cdot 10^{-5}$–$1{,}5 \cdot 10^{-4}$	*N*-méthylaniline	0	—
Diamino 1-3-propane	$1{,}94 \cdot 10^4$	$1 \cdot 10^{-5}$–$8 \cdot 10^{-5}$			

(5) Par contre les diamines présentent une intensité d'absorption sensiblement double de celle des monoamines correspondantes (par exemple, diaminopropane et benzidine, Tableau 1), ce qui prouve que les deux fonctions amine réagissent simultanément.

Choix des conditions opératoires

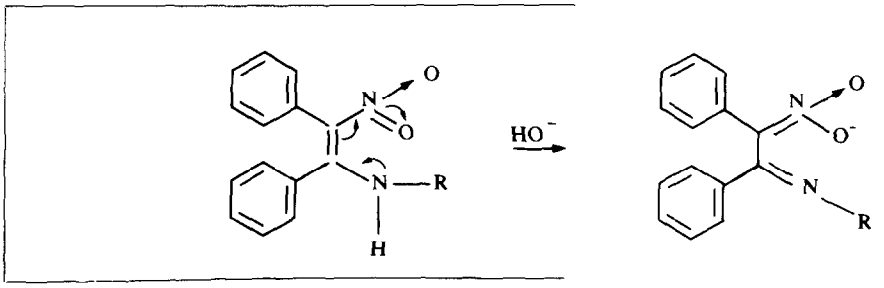
Solubilité. Le DNS et les dérivés de monosubstitution avec les amines et les thiols possèdent une solubilité assez proche qui ne permet pas de les séparer par extraction. Cette solubilité est très faible dans l'eau et l'heptane, faible dans l'éther, l'acétate d'éthyle, le toluène et l'alcool amylique, moyenne dans l'éthanol et le méthanol. Elle devient bonne dans le dioxanne, le tétrahydrofuranne, l'acétone, et forte dans le chloroforme, le diméthylsulfoxyde, le diméthylformamide et la pyridine. Toutefois, dans ces deux derniers solvants, une altération partielle du réactif survient.

Par contre les dérivés des amines dont la chaîne carbonée porte un groupement fonctionnel ionisé au pH de réaction (carboxylate, sulfonate...), sont très fortement solubles dans les milieux mixtes eau–méthanol. C'est ainsi que les dérivés des aminoacides ne sont pas extraits par le chloroforme en milieu alcalin.

Longueur d'onde de lecture. Le maximum d'absorption des composés formés est fortement influencé par l'environnement du groupement nucléophile (Tableau 2).

Le DNS dont le coefficient d'extinction présente un maximum à 330 nm, interfère encore notablement dans la région d'absorption du dérivé énaminonitré. Toutefois, dans les milieux basiques, le réactif se dégrade, ce qui diminue les possibilités d'interférence au-delà de 300 nm.

Cette importance du pH se retrouve pour les dérivés des amines primaires (y compris les acides aminés): on observe un net effet hypsochrome lorsqu'on augmente la basicité d'un milieu mixte méthanol–tampon aqueux (Fig. 1): le maximum se déplace alors vers 300 nm. On peut émettre l'hypothèse que l'effet observé serait du à la possibilité pour les nitroénamines primaire et secondaires de conduire à la formation d'un acide nitronique en milieu alcalin, ce qui est exclu pour les dérivés tertiaires:



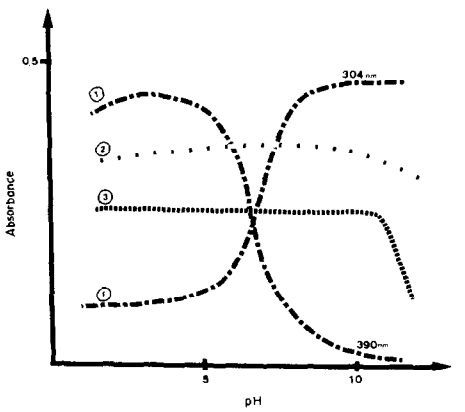


Fig. 1. Influence de la basicité d'un milieu mixte méthanol–tampon aqueux sur les spectres de (1) *cis*-α-nitro β-anilino stilbène; *cis*-α,β-dinitro stilbène (2) *cis*-α-nitro β-méthylanilino stilbène (3).

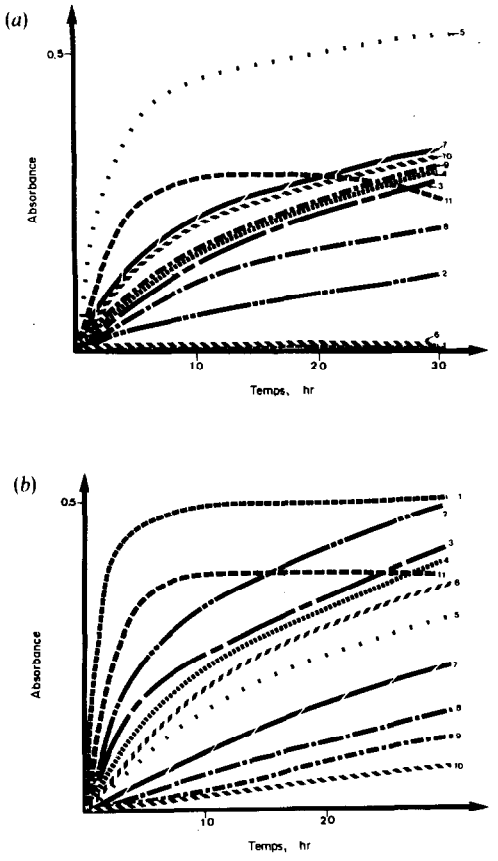


Fig. 2. (*a*) Vitesses de réaction de la benzylamine et du DNS à 20° (concentration équimolaire en réactants) en fonction des solvants: 1, dioxanne–eau (1:4 v/v); 2, méthanol; 3, éthanol; 4, propanol; 5, dioxanne; 6, alcool benzylique; 7, acétate d'éthyle; 8, dichlorométhane; 9, éther; 10, toluène; 11, acétonitrile. (*b*) Vitesses de réaction de la *p*-toluidine et du DNS à 20° (concentration équimolaire en réactants) en fonction des solvants.

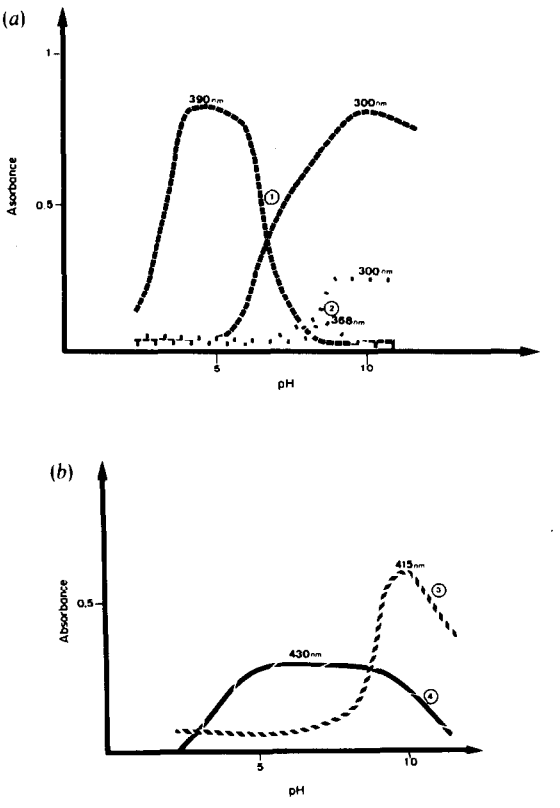


Fig. 3. (*a*) Réactivité des amines primaires en milieu mixte méthanol tampon aqueux (1:1 v/v). Le pH est celui de la phase aqueuse. (1) *p*-Toluidine; (2) benzylamine. (*b*) Réactivité des amines secondaires dans un milieu mixte méthanol–tampon aqueux (1:1 v/v). Le pH est celui de la phase aqueuse. (3) Pipéridine; (4) *N*-méthylaniline.

Influence du solvant. La nature du solvant influence fortement la vitesse de réaction mais de manière différente pour les amines aliphatiques et aromatiques.

Nous avons donc étudié le comportement de deux amines isomères: *p*-toluidine et benzylamine, dans onze solvants. Nous avons écarté ceux pouvant réagir avec les amines (aldéhydes, cétones) ou avec le DNS (diméthylformamide, pyridine).

Les courbes des Figs. 2a et 2b représentent l'absorbance de solutions $5 \cdot 10^{-5} M$, après contact pendant 30 hr à la température du laboratoire avec une solution équimolaire de DNS.

Pour la *p*-toluidine, la vitesse est faible dans les solvants aprotiques. Par contre elle augmente avec la polarité du milieu pour les solvants hydroxylés. C'est donc dans les mélanges avec l'eau qu'on obtient la vitesse de réaction la plus rapide. (L'emploi d'eau seule étant impossible par suite de l'insolubilité du DNS.)

Pour la benzylamine, la réaction s'effectue généralement plus vite dans les solvants aprotiques que pour les arylamines. Par contre, dans les solvants hydroxylés, l'augmentation de polarité entraîne une diminution très nette de la vitesse. Sans doute la basicité supérieure des amines aliphatiques permet-elle la création d'une liaison hydrogène avec le solvant ce qui réduit l'attaque nucléophile.

On voit que, selon la classe de l'amine, il est nécessaire de choisir un solvant différent pour obtenir l'absorbance la plus élevée. Toutefois le dioxanne fournit la sensibilité moyenne la plus favorable pour l'ensemble des amines.

Pour les thiols, la réaction n'est praticable que dans les solvants hydroxylés (mélange eau-méthanol).

Influence du pH. Pour vérifier l'influence du pH sur la réaction, nous avons utilisé des milieux méthanol–tampon aqueux (1:1 v/v), le pH indiqué étant celui de la phase aqueuse et non du mélange.

Le rendement dépend fortement de l'acidité (Fig. 3): la réaction étant du type nucléophile, elle se trouve supprimée par la fixation d'un proton sur le doublet de l'azote.

La limitation vers les pH inférieurs est donc fonction du pk_a des amines. Les arylamines réagissent

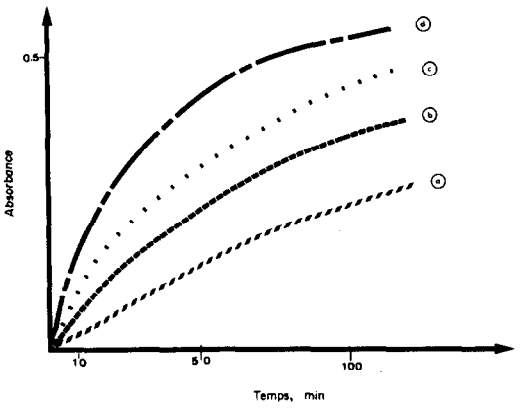


Fig. 4. Influence de la concentration en DNS sur la réactivité de la benzylamine à concentration initiale constante (20°). Concentrations identiques en réactants (*a*); concentrations en DNS double (*b*), triple (*c*), quadruple (*d*), à celle de l'amine.

encore vers pH 4 à 5, alors que les amines aliphatiques ne le font que pour des pH supérieurs à 8. Il est donc possible de doser de manière spécifique les amines aromatiques en présence d'amines aliphatiques en opérant en milieu tamponné à pH 4. De même, le dosage des acides aminés n'est possible qu'à un pH supérieur à leur point isoélectrique.

Pour les thiols l'absorbance maximale est obtenue à pH supérieur à 10.

En milieu alcalin, la limitation résulte de la dénaturation du DNS qui devient importante au-delà de pH 11 et supprime toute réaction.

Concentration en réactif. D'après la figure 4, on voit qu'une augmentation de concentration en réactif facilite l'éxécution de la réaction.

Toutefois cette augmentation se trouve limitée par suite de l'absorption propre du DNS aux longueurs d'onde de lecture. C'est pourquoi nous avons limité sa teneur dans le milieu réactionnel à:

—$3{,}4 \cdot 10^{-4} M$ dans le dioxanne pour les lectures s'effectuant à 368 nm (amines aliphatiques primaires).
—$10^{-3} M$ dans le dioxanne pour les lectures s'effectuant à 410 nm (amines aliphatiques secondaires).
—$5 \cdot 10^{-4} M$ dans les mélanges eau–méthanol (amines aromatiques, thiols).

Dans ces conditions, l'absorbance du témoin des réactifs ne dépasse pas 0,9.

Température et durée de chauffage. De même, une augmentation de température accélère la réaction (Fig. 5). Elle est toutefois susceptible d'entraîner une évaporation du solvant.

C'est pourquoi nous préférons opérer à froid dans le mélange méthanol–eau, où la vitesse est suffisamment rapide pour que la réaction soit quasiment totale en 30 min à la température du laboratoire avec les amines aromatiques, les amines secondaires cycliques et les thiols.

Par contre, en solution dans le dioxanne la réaction n'est pas terminée en 120 min à 20°, même en présence d'un grand excès de réactif. Comme la température d'ébullition de ce solvant est élevée (t_{eb} = 101°), nous opérons en tube bouché, au bain-marie à l'ébullition où la réaction est presque complète en 15 min.

Stabilité du réactif et du composé coloré formé. Lorsque la réaction est effectuée à la lumière, on constate que l'absorbance finale est inférieure à celle obtenue à à l'obscurité. D'après les courbes 3 et 5 (Fig. 2a, 2b), on peut exclure l'hypothèse de la dégradation du composé coloré formé dans les milieux utilisés pour le dosage. Il semble donc qu'on puisse admettre comme seule hypothèse une isomérisation du DNS *cis* en dérivé *trans*,[6] ce dernier ne réagissant pas comme nous l'avons vérifié, avec les amines dans les conditions opératoires que nous avons définies. Il est donc nécessaire d'opérer à l'obscurité pour obtenir un rendement maximum.

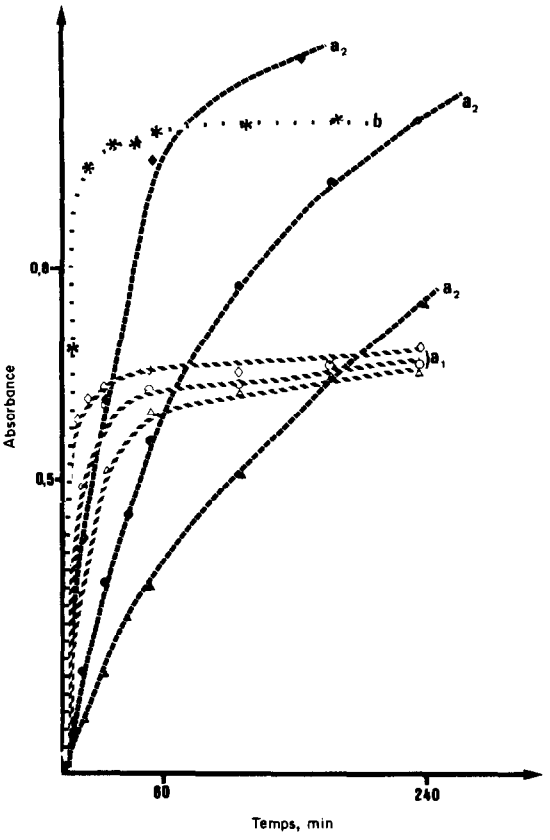


Fig. 5. Influence de la température sur la vitesse de réaction dans le dioxanne (△ 19°, ○ 48°, ◇ 80°) de: (a_1) benzylamine ($5{,}6 \cdot 10^{-5} M$); (a_2) *p*-toluidine ($9 \cdot 10^{-5} M$) (la concentration en DNS est de $3{,}4 \cdot 10^{-4} M$); vitesse de réaction de la *p*-toluidine ($8 \cdot 10^{-5} M$) dans le mélange mixte méthanol–eau (1:1 v/v) à 19° (*b*) (la concentration en DNS est de $5 \cdot 10^{-4} M$).

Tableau 2. Longueur d'onde du maximum d'absorption des composés colorés, *nm*

	Thiol	Amine					
		Aliphatique primaire	β, γ ou ω Carboxylique	α-Carboxylique	Aromatique primaire	Aliphatique secondaire	Aromatique secondaire
λ_{max}	355–360	368	370	375*	390	410–415	420–435

* Proline 410.

Techniques de dosage

Du fait de la variation considérable de réactivité des différents types d'agents nucléophiles nous proposons plusieurs types de technique.

La première est la plus générale et peut être utilisée avec toutes les amines primaires et secondaires réagissant avec le DNS. Les autres améliorent la sensibilité de la réaction (technique no 2 pour les amines aliphatiques secondaires) et sont plus sélectives (techniques no 3 pour les amines aromatiques, no 4 pour les amines solubles dans l'eau et no 5 pour les thiols).

PARTIE EXPERIMENTALE

(1) *Technique générale pour les amines*

Réactif. Solution de *cis*-α,β-dinitrostilbène à 0,180 g/l, dans le dioxanne.

Mode opératoire. Dans un tube bouchant hermétiquement, introduire 1 ml de réactif et 1 ml de solution d'amine dans le dioxanne, dont la concentration est comprise entre les limites du dosage (Tableau 1). Porter 15 min au bain-marie à ébullition, puis refroidir dans un bain d'eau, en opérant à l'obscurité. Préparer de la même manière un blanc des réactif et une gamme d'étalonnage.

Effectuer la lecture à la longueur d'onde du maximum d'absorption (Tableau 2).

Résultats. La linéarité et la reproductibilité de la technique sont excellentes dans les limites du dosage indiquées dans le tableau 1; le coefficient de corrélation de la droite d'étalonnage, déterminé pour 11 des amines figurant dans ce tableau, est compris entre 0,993 et 1,000.

Le coefficient d'extinction moléculaire apparent, Δ_ϵ, est calculé d'après la pente de la droite d'étalonnage statistique. Il ne correspond pas exactement au coefficient d'extinction moléculaire vrai car la réaction consomme du DNS dont la concentration dans le tube de dosage est inférieure à celle du témoin. Or ce DNS présente une légère absorption aux longueurs d'onde de lecture.

La valeur de Δ_ϵ traduit la sensibilité de la méthode qui est très bonne (Δ_ϵ voisin de 10^4) pour les amines aliphatiques primaires non encombrées et un peu plus faible pour les amines secondaires aliphatiques et les amines aromatiques.

(2) *Technique applicable aux amines secondaires*

La lecture s'effectuant à 410–415 nm, il est possible d'utiliser une solution plus concentrée de réactif (solution dans le dioxanne à 0,540 g/l) ce qui augmente la sensibilité comme on peut le voir dans le tableau 3. Le protocole opératoire est le même que pour la technique précédente.

(3) *Technique applicable aux amines aromatiques*

En opérant en milieu mixte méthanol–solution aqueuse de pH 4, il est possible de doser les amines aromatiques de manière spécifique et en augmentant la sensibilité du dosage.

Réactifs, Solution de DNS à 0,405 g/l dans le méthanol. Solution aqueuse tamponnée à pH 4: mélanger 61,45 ml de solution 0,1*M* d'acide citrique et 38,55 ml de solution 0,2*M* de Na_2HPO_4.

Mode opératoire. Dans un tube introduire 2 ml de réactif colorant (DNS), 1 ml de solution d'amine dans le méthanol, à une concentration comprise dans les limites du dosage (Tableau 4) et 3 ml de solution tampon. Laisser en contact 30 min à la température du laboratoire et à l'obscurité. Effectuer la lecture à 390 nm (amine aromatique primaire) ou 435 nm (amine aromatique secondaire) contre un blanc des réactifs préparé dans les mêmes conditions.

Résultats. La sensibilité se trouve fortement augmentée (Tableau 4), alors que le coefficient de corrélation reste pratiquement égal à 1.

En outre la technique permet d'effectuer le dosage des amines aromatiques de manière sélective en présence d'une quantité 100 fois supérieure d'amines aliphatiques.

(4) *Technique applicable aux aminoacides*

Cette technique utilise la très bonne solubilité des dérivés des aminoacides dans les milieux mixtes eau–alcool pour opérer en présence d'un excès de DNS qui est ensuite extrait en milieu organique. La réaction s'effectue en milieu tamponné de pH supérieur au point isoélectrique des acides aminés (pour l'acide aspartique on peut augmenter la sensibilité en opérant à pH 10,2).

Réactifs. Solution à 0,810 g/l de DNS dans le méthanol. Solution aqueuse tamponnée à pH 9,2: mélanger 23,0 ml d'une solution 0,2*M* de $NaHCO_3$ et 2,0 ml d'une solution 0,2*M* de $NaHCO_3$. Compléter à 100 ml avec de l'eau distillée.

Mode opératoire. Dans un tube introduire 4 ml de réactif colorant (DNS), 2 ml de solution aqueuse d'acide aminé de concentration comprise dans les limites du dosage (Tableau 5), et 2 ml de solution tampon.

Tableau 3. Résultats obtenus selon la technique no 2

Amines	Δ_ϵ, $l \cdot mole^{-1} \cdot cm^{-1}$	Limites de dosage, *M*
Dipropylamine	$7{,}1 \cdot 10^3$	$3 \cdot 10^{-5}$–$2 \cdot 10^{-4}$
Diéthylamine	$8{,}8 \cdot 10^3$	$2 \cdot 10^{-5}$–$2 \cdot 10^{-4}$
Pipéridine	$9{,}2 \cdot 10^3$	$2 \cdot 10^{-5}$–$2 \cdot 10^{-4}$
Pyrrolidine	$1{,}05 \cdot 10^4$	$1{,}5 \cdot 10^{-5}$–$1{,}5 \cdot 10^{-5}$

Tableau 4. Résultats obtenus selon la technique no 3

Amines	Δ_ϵ, $l \cdot mole^{-1} \cdot cm^{-1}$	Limites de dosage, *M*
Aniline	$1{,}36 \cdot 10^4$	$4 \cdot 10^{-5}$–$3{,}5 \cdot 10^{-4}$
p-Toluidine	$1{,}23 \cdot 10^4$	$4 \cdot 10^{-5}$–$3{,}5 \cdot 10^{-4}$
Benzidine	$2{,}51 \cdot 10^4$	$2 \cdot 10^{-5}$–$2 \cdot 10^{-4}$
N-Méthylaniline	$7{,}0 \cdot 10^3$	$8 \cdot 10^{-5}$–$7 \cdot 10^{-4}$

Tableau 5. Résultats obtenus selon la technique no 4

Aminoacides	λ_{max}, nm	Δ_ε, $l \cdot mole^{-1} \cdot cm^{-1}$	Limites de dosage, M
Taurine	370	$3{,}6 \cdot 10^3$	$2{,}5 \cdot 10^{-4}$–$2 \cdot 10^{-3}$
Glycine	375	$1{,}60 \cdot 10^4$	$5 \cdot 10^{-5}$–$6 \cdot 10^{-4}$
Sérine	375	$7{,}5 \cdot 10^3$	10^{-4}–10^{-3}
Cystéine	375	$1{,}30 \cdot 10^4$	$8 \cdot 10^{-5}$–$6 \cdot 10^{-4}$
Leucine	375	$1{,}01 \cdot 10^4$	10^{-4}–$8 \cdot 10^{-4}$
Isoleucine	375	$1{,}23 \cdot 10^4$	$8 \cdot 10^{-5}$–$6 \cdot 10^{-4}$
Phénylalanine	375	$1{,}26 \cdot 10^4$	$8 \cdot 10^{-5}$–$6 \cdot 10^{-4}$
Tyrosine	375	$1{,}31 \cdot 10^4$	$5 \cdot 10^{-5}$–$6 \cdot 10^{-4}$
Tryptophanne	375	$1{,}44 \cdot 10^4$	$5 \cdot 10^{-5}$–$6 \cdot 10^{-4}$
Proline	410	$1{,}10 \cdot 10^4$	$8 \cdot 10^{-5}$–$7 \cdot 10^{-4}$
Acide aspartique	375	$4{,}2 \cdot 10^3$	$2 \cdot 10^{-4}$–$1{,}5 \cdot 10^{-3}$
Acide glutamique	375	$7{,}7 \cdot 10^3$	10^{-4}–10^{-3}
Lysine	375	$1{,}76 \cdot 10^4$	$5 \cdot 10^{-5}$–$6 \cdot 10^{-4}$
Arginine	375	$4{,}5 \cdot 10^3$	$2 \cdot 10^{-4}$–$1{,}5 \cdot 10^{-3}$
Histidine	375	$1{,}15 \cdot 10^4$	$8 \cdot 10^{-5}$–$7 \cdot 10^{-4}$
α-Alanine	375	$1{,}00 \cdot 10^4$	$8 \cdot 10^{-5}$–$8 \cdot 10^{-4}$
β-Alanine	370	$8{,}0 \cdot 10^3$	10^{-4}–10^{-3}
Acide γ-aminobutyrique	370	$8{,}5 \cdot 10^3$	10^{-4}–$9 \cdot 10^{-4}$
Acide ω-aminocaproïque	370	$9{,}3 \cdot 10^3$	10^{-4}–$7 \cdot 10^{-4}$

Tableau 6. Résultats obtenus selon la technique no 5

Thiols	λ_{max}, nm	Δ_ε, $l \cdot mole^{-1} \cdot cm^{-1}$	Limites de dosage, M
Éthanethiol	360	$6{,}6 \cdot 10^3$	$8 \cdot 10^{-5}$–$5 \cdot 10^{-4}$
Propanethiol	360	$5{,}2 \cdot 10^3$	$8 \cdot 10^{-5}$–$6 \cdot 10^{-4}$
Benzylthiol	360	$7{,}5 \cdot 10^3$	$6 \cdot 10^{-5}$–$5 \cdot 10^{-4}$
Benzènethiol	350	$7{,}7 \cdot 10^3$	$6 \cdot 10^{-5}$–$6 \cdot 10^{-4}$
Méthyl-4-benzènethiol	355	$6{,}3 \cdot 10^3$	$8 \cdot 10^{-5}$–$6 \cdot 10^{-4}$

Laisser en contact 30 min à la température du laboratoire et à l'obscurité puis extraire par 3 ml de chloroforme.

Effectuer la lecture de la phase aqueuse à 370–375 nm (pour la proline, à 410 nm), contre un blanc des réactifs préparé dans les mêmes conditions.

Résultats. Le tableau 5 présente les résultats obtenus qui montrent la très bonne sensibilité de la méthode.

Technique applicable aux thiols

La réaction du DNS avec les thiols ne se produit qu'en milieu fortement polaire (mélange eau–méthanol) et fortement alcalin. Toutefois le dérivé formé précipite du milieu réactionnel. Aussi est-il nécessaire de l'extraire avec un solvant organique.

Réactifs. Solution de DNS à 0,810 g/l dans le méthanol. Solution aqueuse tamponnée à pH 10,6: mélanger 21,3 ml d'une solution 0,2*M* de Na_2CO_3 et 3,8 ml d'une solution 0,2*M* de $NaHCO_3$. Compléter à 100 ml avec de l'eau distillée.

Mode opératoire. Dans un tube introduire 1 ml de réactif colorant (DNS), 1 ml de solution de thiol dans le méthanol, à une concentration comprise dans les limites du dosage (Tableau 6) et 2 ml de solution tampon.

Laisser en contact 30 min à la température du laboratoire et à l'obscurité puis extraire par 4 ml de chloroforme.

Effectuer la lecture de la phase chloroformique à 350–360 nm contre un blanc des réactifs préparé dans les mêmes conditions.

Résultats. Ils sont rassemblés dans le tableau 6.

CONCLUSION

Le DNS permet de doser les composés nucléophiles (amines, thiols) avec d'excellents résultats tant sur le plan de la sensibilité que sur celui de la linéarité et de la reproductibilité. Une sélection judicieuse des conditions opératoires permet d'adapter la méthode au dosage de différentes classes de ces composés et, pour certaines d'entre elles d'obtenir une bonne spécificité.

LITTERATURE

1. J. C. Doré et C. Viel, *Compt. Rend.*, 1973, **276C**, 1675.
2. *Idem, Eur. J. Med. Chem.*, 1974, **9**, 673.
3. P. Dubois, P. Levillain et C. Viel, *Compt. Rend.*, 1979, **288C**, 311.
4. *Idem, ibid.*, 1980, **290C**, 21.
5. D. D. Perrin, *Dissociation Constants of Organic Bases in Aqueous Solutions*, Butterworths, London, 1965.
6. C. Bellec, D. Bertin, R. Colau, S. Deswarte, P. Maitte et C. Viel, *J. Heterocyclic Chem.*, 1979, **16**, 1611.

Talanta. Vol. 28. pp. 849 to 852. 1981
Printed in Great Britain. All rights reserved

0039-9140/81/110849-04$02.00/0
Copyright © 1981 Pergamon Press Ltd

DETERMINATION OF ISONIAZID IN DRUGS

KRISHNA K. VERMA and ANIL K. GUPTA
Department of Chemistry, University of Jabalpur, Jabalpur 482001, India

(*Received* 31 *December* 1980. *Accepted* 7 *April* 1981)

Summary—A titrimetric method is described for the determination of isoniazid in pharmaceutical preparations. Samples are treated with an excess of iodine monochloride, and the iodine produced is titrated with iodine trichloride to an Andrews end-point. *p*-Aminosalicylic acid undergoes only nuclear iodination and does not interfere. Mixtures of isoniazid with vitamin C or methionine are analysed by first titrating both compounds by the Andrews method and then determining either vitamin C alone by titration with iodine monochloride or methionine by a second Andrews titration after destruction of isoniazid with nitrous acid. In both cases, isoniazid is obtained by difference. A mixture of isoniazid, methionine and vitamin C can also be analysed.

The extensive use of isoniazid (isonicotinic acid hydrazide) in the treatment of tuberculosis has created a need for selective and sensitive analytical procedures for its determination.

Alkaline iodine,[1] ammoniacal silver nitrate[2,3] and chloramine-T[4] have been used as general oxidants to determine isoniazid but reducing sugars used in dispensing forms interfere and should be removed. Direct titration with a bromine reagent[5–8] avoids this error, but cannot be applied to pharmaceutical preparations that also contain sodium *p*-aminosalicylate (PAS) or vitamin C. The PAS undergoes nuclear substitution with bromine,[9] and vitamin C is even more reducing than isoniazid and reacts with every known oxidizing agent.[10] Suitable modifications for dealing with such mixtures have been reported, involving thin-layer chromatographic separation of isoniazid and PAS followed by their densitometric analysis,[11] or measurement of nitrogen, which is only yielded by isoniazid on reaction with *N*-bromosuccinimide,[12] or differential non-aqueous perchloric acid titration of isoniazid after acetylation[13] (since the basicity of the acetylated amino group of PAS is lowered).[14]

A rapid and precise titrimetric method is described here for the selective determination of isoniazid in the presence of PAS. A hydrochloric acid solution of the drug is reacted with iodine monochloride and the iodine formed (in amount equivalent to the isoniazid) is titrated with iodine trichloride to an Andrews end-point. PAS undergoes only nuclear substitution and does not interfere. Methionine and vitamin C, however, if also present, are also titrated. Two additional methods are reported for the analysis of their mixtures with isoniazid. Vitamin C is titrated with iodine monochloride in the presence of potassium iodide, and isoniazid does not interfere. The sum of the two compounds is determined by Andrews titration and the difference of two analyses gives the isoniazid. Mixtures of isoniazid with methionine are analysed by first determining the sum of both compounds by Andrews titration, then treating the mixture with nitrous acid to destroy isoniazid and titrating methionine alone by Andrews titration, the isoniazid being obtained by difference.

EXPERIMENTAL

Reagents

Solutions of iodine trichloride[15] (0.025*M*) *and iodine monochloride*[16] (0.05 and 0.02*M*). Prepared in dilute hydrochloric acid and standardized iodometrically.[16]

Procedures

Determination of isoniazid in the presence of PAS. Take a known number of tablets, grind to a fine powder and stir with 25 ml of water for 10 min. Add 5 ml of concentrated hydrochloric acid, 25 ml of water and again stir for 10 min. Filter (Whatman No. 42 paper), wash with water and make up the filtrate and washings to a known volume. In the case of syrups, dilute a measured portion to known volume with water.

Take a known volume (5–20 ml) of sample solution in a 250-ml flask fitted with a ground-glass stopper, dilute to 30 ml with water and add 10 ml of carbon tetrachloride, 20 ml of 5*M* hydrochloric acid and 20 ml of 0.05*M* iodine monochloride. Stopper the flask, shake it for 1 min and titrate the liberated iodine with 0.025*M* iodine trichloride until the solution becomes pale brown. Stopper the flask and shake well. Continue the addition of titrant in small portions, shaking vigorously after each addition, until the organic layer loses the last trace of violet colour of iodine and becomes essentially colourless. End-point detection is easier if the stoppered flask is inverted after shaking so that the carbon tetrachloride settles in the neck of the flask.

$$\text{Isoniazid (mg)} = 68.55MV$$

where V is the volume used (in ml) of iodine trichloride of molarity M.

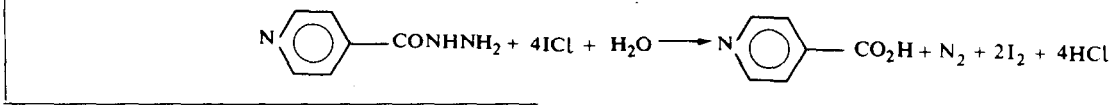
Analysis of mixtures of isoniazid with vitamin C. Take 10 ml of sample solution and determine both compounds by the Andrews titration (V' ml of M' iodine trichloride) described above. Determine vitamin C alone as below and calculate the isoniazid by difference.

Table 1. Determination of isoniazid in the presence of PAS

Isoniazid taken, *mg*	PAS added, *mg*	Isoniazid found* NBS titration, *mg*	Isoniazid found* ICl_3 titration, *mg*	Coefficient of variation, %
2.89	—	2.87	2.91	0.4
3.60	—	3.58	3.62	0.5
5.63	—	5.68	5.68	—
4.17	10	—	4.20	0.6
7.80	20	—	7.85	0.8
8.59	—	8.52	8.64	—
9.69	50	—	9.64	0.8
11.22	70	—	11.12	1.0
13.71	—	13.65	13.80	0.6
15.20	80	—	15.16	1.0
8.71	100	—	8.67	1.0

* Average of eight replicates.

reducing properties of its acid hydrazide group which reacts with iodine monochloride:



Take 10 ml of sample solution in a 150-ml conical flask, mix with 20 ml of water, 0.2 g of potassium iodide, 1 ml of 0.5% starch and titrate with 0.02*M* iodine monochloride (molarity *M*″, volume *V*″ ml) to the appearance of a blue colour.

$$\text{Vitamin C (mg)} = 176.1M''V''$$
$$\text{Isoniazid (mg)} = 68.55\,(M'V' - M''V'')$$

Analysis of mixtures of isoniazid with methionine. Titrate 10 ml of sample solution by the Andrews method to determine the total of the two compounds (*v* ml of iodine trichloride of molarity *M*). Estimate methionine alone as follows.

To 10 ml of sample solution in a 250-ml flask (with ground-glass stopper), add 5 ml of 2% sodium nitrite solution, 25 ml of water and 5 ml of 0.1*M* hydrochloric acid and keep for 5 min. Add about 1 g of urea and let stand for 5 min. Add 5 ml of carbon tetrachloride, 10 ml of 0.05*M* iodine monochloride, 20 ml of 5*M* hydrochloric acid, shake vigorously and titrate the liberated iodine with the same titrant to the Andrews end-point (*v*′ ml). Calculate the isoniazid by difference.

$$\text{Methionine (mg)} = 149.2Mv'$$
$$\text{Isoniazid (mg)} = 68.55M(v - v')$$

Analysis of mixtures of isoniazid, methionine and vitamin C. Titrate the vitamin C and methionine in separate 10-ml portions of sample solution as already described, and the sum of all three components by Andrews titration, and calculate as above.

RESULTS AND DISCUSSION

Results for the determination of isoniazid in pure solutions and various mixtures are given in Tables 1–4. The *N*-bromosuccinimide method[17] was used for comparison, except when PAS was present since it then gives excessively high values for isoniazid.

The determination of isoniazid is based on the

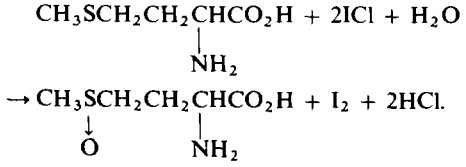
The iodine monochloride added need not be measured provided there is sufficient excess to complete the oxidation. The iodine liberated is titrated with iodine trichloride under Andrews conditions:

$$2I_2 + 2ICl_3 \rightarrow 6ICl$$

PAS undergoes nuclear iodination, giving 3,5-diiodo-4-aminosalicylic acid. Since no iodine is liberated, the determination of isoniazid is not vitiated. The iodinated-PAS precipitates during the reaction and may obscure the Andrews end-point, but increasing the volume of carbon tetrachloride to 20–25 ml (and a little practice) will eliminate this difficulty.

The 1,2-enediol group of vitamin C undergoes a 2-electron change when titrated directly with iodine monochloride or by the Andrews method, dehydroascorbic acid being the reaction product in both cases. In the presence of excess of potassium iodide isoniazid is not attacked by iodine monochloride but vitamin C reacts. This allows the determination of vitamin C in the presence of isoniazid.

Methionine contains a sulphide group which is oxidized to sulphoxide by Andrews titration:



Methionine is determined in the presence of isoniazid after quantitative destruction of the latter by reaction with nitrous acid. Isonicotinyl azide is formed initially:[18]

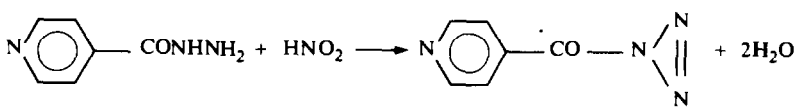


Table 2. Analysis of mixtures of isoniazid with vitamin C or methionine

Taken, *mg*		Found, *mg* (coefficient of variation, %)			
I	II	I		II	
Isoniazid	Vitamin C				
1.59	16.16	1.63	(1.1)	16.23	(0.8)
3.60	13.85	3.54	(1.0)	13.73	(0.3)
4.45	11.54	4.40	(0.5)	11.69	(0.6)
5.28	9.23	5.21	(0.5)	9.31	(0.6)
6.10	4.62	6.13	(0.6)	4.67	(0.5)
Isoniazid	Methionine				
1.39	14.53	1.37	(1.5)	14.56	(0.6)
2.79	10.90	2.78	(1.2)	11.08	(0.8)
3.49	9.08	3.46	(1.0)	9.04	(0.6)
4.19	7.27	4.16	(1.2)	7.23	(0.4)
5.59	3.63	5.62	(0.9)	3.59	(0.5)

* Average of six replicates.

Table 3. Analysis of mixtures of isoniazid, vitamin C and methionine

Taken, *mg*			Found, *mg**		
I	II	III	I	II	III
Isoniazid	Vitamin C	Methionine			
1.80	13.85	3.64	1.79	13.79	3.65
3.69	11.54	7.17	3.65	11.50	7.11
4.73	9.23	9.08	4.69	9.21	9.10
5.68	4.62	10.90	5.62	4.58	10.79

* Average of six replicates; coefficient of variation 0.9–1.8% for isoniazid, 0.4–0.8% for vitamin C and 0.5–0.7% for methionine determination.

Table 4. Determination of isoniazid in drugs

Drug*	Isoniazid, *mg*, per tablet or 5 ml of syrup		
	Manufacturer's specification	Found, *mg*† by titration with ICl_3 (CV, %)	NBS
Isokin 100	100	99.2 (0.5)	98.4
Isokin 300* (*i*)	300	299.0 (0.6)	299.9
Isokin-T Forte (*ii*)	300	326.9 (0.5)	333.7
Uni-Thiben Vf (*iii*)	75	77.7 (0.6)	79.4
Thiocent (*iv*)	150	157.9 (0.5)	159.8
Inapas (*v*)	25	26.2 (1.0)	—
Siozid (*vi*)	280	264.7 (0.8)	260.9

* The excipients were (*i*) vitamin B_6 (10 mg); (*ii*) thiacetazone (150 mg); (*iii*) thiamine hydrochloride (1 mg), thiacetazone (37.5 mg), riboflavin (1 mg), niacin (10 mg), cholesterol USP (150 IU), coloured with tetrazine; (*iv*) thiacetazone (75 mg), thiamine mononitrate (2 mg), pyridoxine hydrochloride (5 mg), riboflavin (2 mg), nicotinamide (10 mg); (*v*) sodium *p*-aminosalicylate (850 mg); (*vi*) cetylpyridinium chloride (1.313 mg), terpin hydrate (13.13 mg), sodium citrate (0.21 mg), citric acid (13.13 mg), vitamin B_6 (0.876 mg) and vitamin C (4.375 mg).

† Average of six replicates; CV, coefficient of variation; NBS, *N*-bromosuccinimide.

Dehydroascorbic acid is formed on reaction of ascorbic acid with nitrous acid.[19] The sulphide group of methionine retains its reducing properties and can be determined. The surplus nitrous acid should be decomposed with urea, otherwise variable results are obtained.

Large amounts of glucose, maltose, lactose and sucrose do not interfere. Other substances which do not interfere are mentioned in Table 4.

REFERENCES

1. M. Balka, D. Bode and H. J. Rhodes, *J. Pharm. Sci.*, 1974, **63**, 1303.
2. R. Soliman and S. A. Belal, *J. Drug Res.*, 1974, **6**, 7.
3. *Idem, Pharmazie*, 1974, **29**, 204.
4. V. R. Nair and C. G. R. Nair, *Anal. Chim. Acta*, 1971, **57**, 429.
5. C. G. R. Nair and L. Kumari, *Indian J. Chem.*, 1976, **14A**, 115.
6. M. K. Abramo, *Farmatsiya*, 1975, **24**, 80.
7. T. Urbányi and R. Winchurch, *J. Assoc. Off. Anal. Chem.*, 1973, **56**, 1464.
8. L. S. Bark and P. Prachuabpaibul, *Anal. Chim. Acta*, 1976, **87**, 505.
9. D. C. Garratt, *The Quantitative Analysis of Drugs*, p. 561. Chapman & Hall, London, 1964.
10. A. Berka, J. Vulterin and J. Zýka, *Newer Redox Titrants*, p. 161, Pergamon Press, Oxford, 1965.
11. L. P. Pavlyuchenkova, *Farmatsiya*, 1976, **25**, 73.
12. M. Sarwar, M. Yaqub, I. Naeem and A. A. Kazi, *Z. Anal. Chem.*, 1977, **285**, 269.
13. E. Kuhni, M. Jacob and H. Grossglauser, *Pharm. Acta Helv.*, 1954, **29**, 233.
14. M. B. Devani and C. J. Shishoo, *J. Pharm. Sci.*, 1970, **59**, 90, 92.
15. Y. A. Fialkov and F. E. Kagan, *Ukrain. Khim. Zh.*, 1952, **18**, 55.
16. Ref. 10, p. 56.
17. M. Z. Barakat and M. Shaker, *Analyst*, 1964, **89**, 216.
18. N. L. Allinger, M. P. Cava, D. C. DeJongh, C. R. Johnson, N. A. Lebel and C. L. Stevens, *Organic Chemistry*, p. 610. Worth, New York, 1974.
19. J. A. Synnott, I. Unger and G. Strunz, *Naturwissenschaften*, 1975, **62**, 138.

Talanta, Vol. 28, pp. 853 to 854, 1981
Printed in Great Britain. All rights reserved

0039-9140/81/110853-02502.00/0
Copyright © 1981 Pergamon Press Ltd

SHORT COMMUNICATIONS

INDIRECT SPECTROPHOTOMETRIC DETERMINATION OF SULPHIDE WITH THE TERNARY COMPLEX SYSTEM Ag(I)–phen–BPR

WEI FU-SHENG, ZHU YU-REI, YIN FANG and SHEN NAI-KUI

Department of Chemistry, China University of Science and Technology, Hefei, Anhui, China

(*Received* 1 *December* 1980. *Accepted* 22 *April* 1981)

Summary—Trace amounts of sulphide can be determined from its effect on the ternary complex system of Ag^+, Bromopyrogallol Red (BPR), and 1,10-phenanthroline (phen). Sulphide in the range 5–120 ng/ml causes a decrease in absorption, that is a linear function of the concentration. Common metal ions such as Na^+, K^+, Ca^{2+}, Mg^{2+}, Al^{3+}, Mn^{2+} and anions such as F^-, Cl^-, NO_3^-, SO_4^{2-}, CO_3^{2-}, and PO_4^{3-} at the 4 μg/ml level or more do not interfere, but I^- or CN^- must be absent.

The ternary complex system Ag(I)–phen–BPR and its application to the spectrophotometric determination of silver, and to indirect determination of cyanide were first reported by Dagnall and West.[1–3] This colour system is very sensitive, but must be applied rapidly because it is easy for a blue precipitate to appear. We have tried using gelatine (0.5% water aqueous solution) as protective agent and found that it stabilizes the coloured complex for over 10 hr. We have also found that traces of sulphide can suppress the colour reaction. On the basis of this effect, we have worked out an indirect method for spectrophotometric determination of sulphide. This paper reports the optimal conditions for this determination. It is more sensitive than the Methylene Blue method[4] and the mercury chloranilate,[5] copper diethyldithiocarbamate[6] and copper thiothenoyltrifluoroacetane indirect methods. The general procedure is simple and the reproducibility good. It is satisfactory for determination of soluble sulphide in domestic sewage.

EXPERIMENTAL

Reagents

Standard silver solution. Prepare a 2.5-mg/ml stock solution and standardize it with sodium chloride. Protect it from sunlight and dilute to 25 μg/ml as working standard.

Standard sulphide solution 1.0 mg/ml. Use $Na_2S.9H_2O$ of general-reagent grade, and standardize.[8] Protect it from air and just before use dilute to 5.0 μg/ml as working standard.

Bromopyrogallol Red (BPR) solution, 0.025%. Dissolve 25.0 mg of BPR in 100 ml of 1% ammonium acetate. Use a freshly prepared solution.

1,10-Phenanthroline solution, 0.2% in alcohol.

Gelatine solution, 0.5% in water.

General procedure

To a 25-ml standard flask, add 1 ml of 20% ammonium acetate solution, 1 ml of 0.1*M* EDTA, 0.5 ml of gelatine solution, 0.5 ml of 1,10-phenanthroline solution, test solution containing up to 3.0 μg of sulphide and 25 μg of silver(I), mix and add 1.0 ml of BPR solution and make up to volume with water. Mix well. After 10 min measure the absorbance in a 1-cm cell at 640 nm against a reference blank containing all the reactants except silver(I) and sulphide.

Determination of soluble sulphide in domestic sewage

To 100 ml of sample add 1 ml of 0.333*M* potassium alum and 1 ml of 1*N* sodium hydroxide to remove suspended organic material and heavy metals. Mix well. Let stand awhile to settle. Pipette 1–15 ml of the supernatant liquid into a 25-ml standard flask, and then apply the general procedure. Recovery of a spike of sulphide added to the supernatant liquid is 93–103%, and the coefficient of variation for the determination is 4.5% (0.68 ppm of sulphide, 11 variates).

RESULTS AND DISCUSSION

The mechanism of the indirect determination of sulphide

The composition of the blue ternary complex was found to be $[Ag(phen)_2]_2$ BPR by Dagnall and West.[1] If a soluble sulphide is added to the system insoluble silver sulphide is formed; the concentration of free silver decreases and so does the colour of the solution. Figure 1 shows that the absorption spectrum of the Ag^+–phen–BPR–S^{2-} mixture is similar to that of Ag^+–phen–BPR, and λ_{max} of both spectra is at the same wavelength. A mole-ratio plot shows that the reacting ratio of silver(I) to sulphide in this system is 2:1.

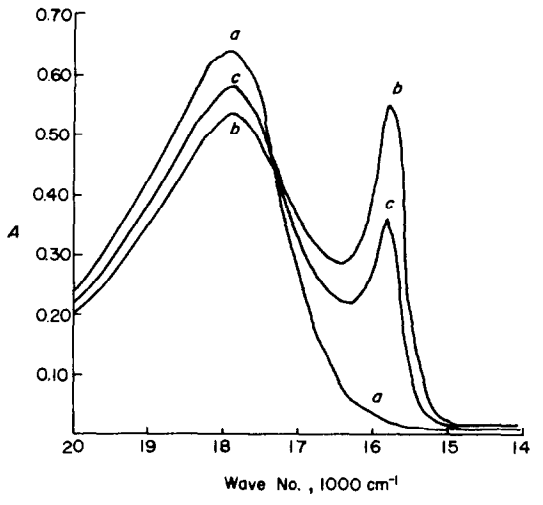


Fig. 1. Absorption spectra: (*a*) 0.001% BPR vs. water; (*b*) BPR as (*a*), plus 25 μg or Ag^+; (*c*) BPR and Ag^+ as (*b*), plus 1.30 μg of S^{2-}.

The molar absorptivity of the ternary complex is 5.1×10^4 l.mole^{-1}.cm^{-1} at 635 nm,[1] so the effective molar "desorptivity" of sulphide in this reaction is -1.02×10^5 l.mole^{-1}.cm^{-1}.

Selection of protective colloid and the order of addition

Since the blue colour formed by silver(I) with phen–BPR is unstable, Triton X-100, starch and gelatine were tried as protective colloids, and gelatine proved the best. With Triton X-100 a precipitate appears within 30 min, and a 1% starch solution stabilizes the colour for only about 2 hr, whereas with 0.5% gelatine solution the colour development is complete within 5 min and the absorbance remains constant for 12 hr.

The order of addition of reagents should be that given in the general procedure, especially the addition of sulphide. If the sulphide is added last, the system takes longer to reach equilibrium.

Calibration and interferences

The calibration graph shows a linear decrease in the absorbance of a fixed amount of ternary complex as the sulphide concentration is increased up to 3.0 μg/25 ml.

There was no interference from ammonium acetate (600 mg); EDTA (50 mg); Li^+, Na^+, K^+, Zn^{2+}, Cl^-, F^-, NO_3^-, SO_4^{2-} (each 1.0 mg); Be^{2+}, Mg^{2+}, Ca^{2+}, Sr^{2+}, Ba^{2+}, Al^{3+}, As^{3+}, Cr^{3+}, Mn^{2+}, Co_3^{2-}, SO_3^{2-}, PO_4^{3-} (each 100 μg); Fe^{3+}, Pb^{2+}, Cd^{2+}, SCN^-, $S_2O_3^{2-}$ (each 10 μg) in determination of 2.5 μg of sulphide. Cyanide and iodide cannot be tolerated at all.

REFERENCES

1. R. M. Dagnall and T. S. West, *Talanta*, 1964, **11**, 1533.
2. *Idem, ibid.*, 1964, **11**, 1627.
3. R. M. Dagnall, M. T. El-Ghamry and T. S. West, *ibid.*, 1968, **15**, 107.
4. Z. Marczenko, *Spectrophotometric Determination of Elements*, p. 506. Horwood, Chichester, 1976.
5. R. E. Humphrey and W. Hinze, *Anal. Chem.*, 1971, **43**, 1100.
6. T. Nakamura, *Bunseki Kagaku*, 1973, **33**, 691.
7. D. M. Degudii and K. A. Kitamura, *ibid.*, 1978, **27**, 527.
8. *Standard Methods for the Examination of Water and Waste Water*, 14th Ed., American Public Health Association, American Water Works Association and Water Pollution Control Federation, 1976.

Talanta, Vol. 28, pp. 855 to 856, 1981
Printed in Great Britain

0039-9140/81/110855-02$02.00/0
Pergamon Press Ltd

ANODIC POLAROGRAPHIC DETERMINATION OF FLUCLOXACILLIN

J. A. SQUELLA, M. M. SILVA and LUIS J. NUÑEZ-VERGARA

Department of Chemical Pharmacology and Physical Chemistry, Faculty of Chemical and Pharmacological Sciences, P.O. Box 233, Santiago, Chile

(*Received* 23 *January* 1981. *Accepted* 25 *April* 1981)

Summary—The hydrolysis of flucloxacillin at pH 4.9 yields a degradation product which is polarographically oxidizable. This derivative has not been identified, but would seem to contain a thiol group. It gives a diffusion-controlled anodic polarographic wave with a half-wave potential at −0.24 V *vs.* SCE. The method developed has been applied to the analysis of flucloxacillin capsules, and a recovery of 99% has been obtained.

In previous papers[1–3] we have reported polarographic methods for penicillins and cephalosporins containing an α-amino group in the side-chain. These methods were based on the electroactivity of degradation products formed by acidic hydrolysis, an approach which has proved applicable to all penicillins and cephalosporins containing an α-amino group in the chain. Flucloxacillin is an isoxazolyl penicillin active against Gram-positive cocci, including penicillin-resistant staphylococci. In man, flucloxacillin taken orally produces total and free serum levels higher than those obtained with other isoxazolyl penicillins.[4]

Spectrophotometric methods[5,6] for the estimation of flucloxacillin have been described elsewhere, but no polarographic assay has yet been developed for it. In this report we propose a polarographic method, and describe the hydrolysis conditions, the effect of pH on the half-wave potential, and the analytical data for the quantitative determination in dosage forms.

EXPERIMENTAL

Flucloxacillin (100% chromatographically pure, 99.8% activity) was obtained from Beecham Research Laboratories, London. All other chemicals were analytical grade.

A Tacussel polarograph was operated in the d.c. mode, but with short, controlled drop-time by being coupled with an EPL-2 recorder equipped with Tipol plug-in, GCMS pulse generator for hammer control and an MPO-3 hammer. A Tacussel CPRA cell was kept at 25° by a flow of water from a thermostatically controlled bath, and was used with a dropping mercury electrode, platinum-wire counter-electrode, and saturated calomel reference electrode.

Operating conditions

The imposed drop-time was 1 sec, the scan-rate 10 mV/sec over the range from 400 mV to −50 mV *vs.* SCE, and the current sensitivity 15 μA full-scale deflection. The capillary characteristics were $m^{2/3}t^{1/6} = 2.678\ mg^{2/3}.sec^{1/6}$.

Solutions for polarography were deoxygenated with nitrogen which had previously been passed through a vanadium(II) scrubber solution. The hydrolysed flucloxacillin solutions contained the equivalent of 3.0 mg of pure drug per ml ($6.3 \times 10^{-3}M$). The effect of pH on the d.c. polarographic curves was studied by using test solutions individually prepared with buffer solutions of the required pH: citric acid–phosphate McIlvaine buffer was used for pH 4–8 and glycine–sodium hydroxide Sørensen buffer for pH 9–11.

Calibration curve. Solutions containing between 1.0 and 5.0 mg of flucloxacillin were diluted to 10 ml with McIlvaine buffer at pH 4.9. For the recovery test, samples containing 3.0 mg of flucloxacillin plus excipients (starch, mannitol, magnesium stearate) were diluted to 10 ml with McIlvaine buffer at pH 4.9. All samples were hydrolysed by heating at 90° for 180 min in a constant-temperature bath.

RESULTS AND DISCUSSION

To obtain a polarographically useful response for flucloxacillin we studied the hydrolysis conditions needed to produce the maximum amount of electroactive degradation product. Figure 1 shows the rate of formation at two temperatures. The hydrolysis conditions selected were: pH 4.9 in McIlvaine buffer, with heating at 90° for 180 min.

The electroactive degradation product exhibits an anodic polarographic wave at −0.24 V *vs.* SCE. The wave is well-defined and is taken to be diffusion-controlled, since the limiting current (μA) is proportional to the square root of the height of the mercury column (corrected for back pressure), the straight line fitting the equation

$$i_d = 6.83H_{corr}^{1/2} - 1.33$$

(correlation coefficient for 10 values: 0.995, for H between 40 and 60 cm).

The variation in the half-wave potential with the height of the mercury column, which might be appreciable if adsorption phenomena affected the characteristics of the wave,[7] was found to be negligible. The calibration plot was linear for 10^{-4}–$10^{-2}M$ of flucloxacillin, its equation being $i_d = 1.16C - 0.012$ where i_d is in μA and C in mg/ml.

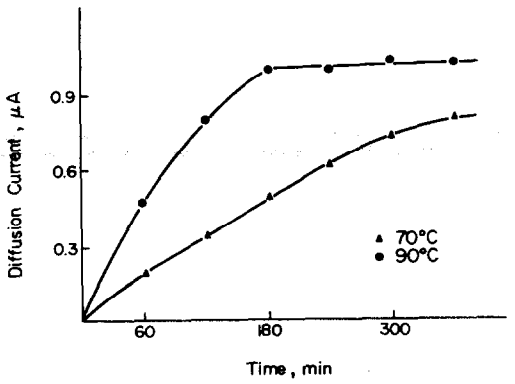


Fig. 1. Rate of formation of the electroactive product from flucloxacillin at different temperatures in McIlvaine buffer (pH 4.9).

The pH-dependence of the half-wave potential for $6.3 \times 10^{-3}M$ flucloxacillin was studied in the pH range 6–10 (Fig. 2). Between pH 6 and 7.5 a linear dependence is observed, suggesting that protons are involved in the electrode reaction mechanism; for the alkaline range, pH 7.5–10, the half-wave potential is constant. This behaviour strongly indicates that the electroactive group is a thiol group, such as those of glutathione and cysteine.[8,9] This assumption was confirmed by chemically blocking the thiol group with *p*-hydroxymercuribenzoate (Fig. 3).

Analysis of Bactopen capsules (Saval laboratories, Santiago, Chile, nominal content 250 mg) gave a mean content of 245 mg and standard deviation of 4 mg (6 samples).

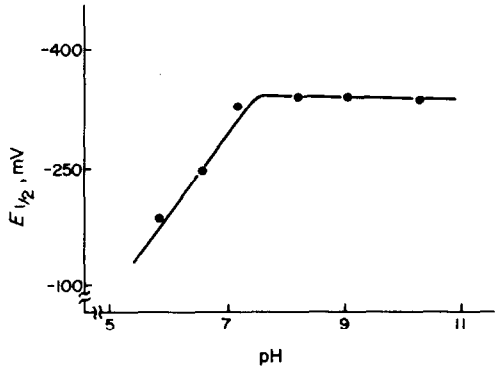


Fig. 2. Half-wave potential for flucloxacillin *vs.* SCE as a function of pH.

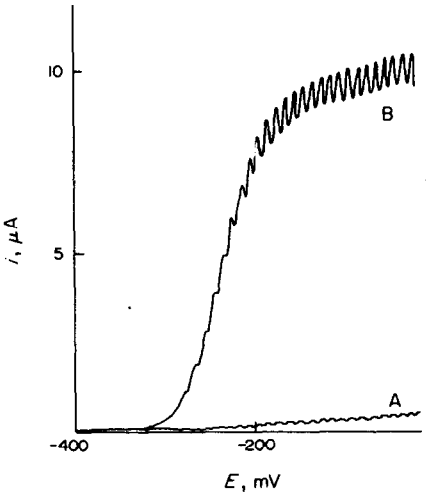


Fig. 3. Effect of *p*-hydroxymercuribenzoate on the polarographic behaviour of flucloxacillin. (A) Typical polarogram of flucloxacillin in presence of *p*-hydroxymercuribenzoate. (B) Typical polarogram of flucloxacillin.

A major advantage of the method is its selectivity, which makes prior separation from the excipients unnecessary. Preparation of the samples is easy and the reproducibility is good, though the hydrolysis time of 180 min limits its application in routine analysis. This method can also be used for degradation studies.

Acknowledgements—The support of the Servicio de Desarrollo Científico, Creación Artística y de Cooperación Internacional is gratefully acknowledged (Q!O 55-803). Thanks are due to Professor Renato V. González for his helpful suggestions.

REFERENCES

1. L. J. Nuñez-Vergara, J. A. Squella and E. M. Gonzalez, *J. Assoc. Offic. Anal. Chem.*, 1979, **62**, 556.
2. J. A. Squella and L. J. Nuñez-Vergara, *Talanta*, 1979, **26**, 1039.
3. L. J. Nuñez-Vergara, J. A. Squella and M. M. Silva, *Farmaco, Pavia*, 1980, **35**, 409.
4. R. Sutherland, E. A. P. Croydon and G. N. Rolinson, *Brit. Med. J.*, 1970, **4**, 455.
5. T. Yasuda and S. Shimada, *J. Antibiot.*, 1971, **24**, 290.
6. H. Bundgaard and K. Ilver, J. *Pharm. Pharmacol.*, 1972, **24**, 790.
7. J. Kuta, *Collection Czech. Chem. Commun.*, 1951, **16**, 1.
8. I. M. Kolthoff and C. Barnum, *J. Am. Chem. Soc.*, 1940, **62**, 3061.
9. W. Stricks and I. M. Kolthoff, *ibid.*, 1952, **74**, 4646.

Talanta, Vol. 28, pp. 857 to 859, 1981
Printed in Great Britain. All rights reserved

0039-9140/81/110857-03$02.00/0
Copyright © 1981 Pergamon Press Ltd

HYDROPHOBIC INDICATORS FOR TWO-PHASE TITRATIONS AND THEIR APPLICATION TO THE DETERMINATION OF SILVER AND PENTACHLOROPHENOL

M. TSUBOUCHI

Laboratory of Chemistry, Kochi Medical School, Oko, Nankoku, Kochi 781-51, Japan

and

N. YAMASAKI, H. MITSUSHIO and K. MATSUOKA

The Research Laboratory of Hydrothermal Chemistry, Kochi University, Akebono, Kochi, Japan

(*Received* 13 *February* 1981. *Accepted* 7 *April* 1981)

Summary—The hydrophobic dyes tetrabromophenolphthalein ethyl ester and 2,6-dichlorophenolindophenol are proposed as visual indicators for two-phase titrations. The aqueous phase is colourless throughout the titration and these indicators make it possible to detect the end-point of the titration by the colour of one or the other phase. The indicators allow the two-phase titration of the silver(I)–1,10-phenanthroline complex with tetraphenylborate and of pentachlorophenol with tetraphenylphosphonium chloride.

Two-phase titrations (ion-pair extraction titrations) employing indicators for visual end-point detection are already well established for the analysis of synthetic detergents,[1–5] and the theory has been elucidated.[6,7] End-point detection can, however, be a problem in two-phase titration methods, because of colour reflection between the phases and differences between the shades or hues of the colour in the two phases. These problems occur because the colour change at the end-point occurs on transfer of the indicator dye from one phase to the other; sometimes the end-point is taken as the point where the colour intensity is judged to be the same in the two phases. Two-phase titration has therefore been applied only to the determination of large ionic surfactants.

The dyes used as indicators in two-phase titrations to date have been hydrophilic. In this paper, the hydrophobic dyes tetrabromophenolphthalein ethyl ester (TBPE) and 2,6-dichlorophenolindophenol (DIP) are suggested as replacements for hydrophilic dyes in two-phase titrations. This makes it possible to detect the end-point in a single phase: the colour changes occur in one phase without transfer of the indicator from one phase to the other. As a result, this type of indicator provides a sharp end-point and allows two-phase titration to be used for ions other than ionic surfactants.

EXPERIMENTAL

Reagents

The potassium salt of TBPE and sodium salt of DIP were dissolved in ethanol to make a 0.1 and a 0.2% solution respectively. Weighed amounts of sodium tetraphenylborate (dried at 80°) and tetraphenylphosphonium chloride (dried at 110°) were dissolved in water. Silver nitrate and recrystallized pentachlorophenol (m.p. 188–189°) were dissolved in water and 0.01*M* sodium hydroxide respectively. Phosphate buffer solution was prepared by adjusting 0.4*M* disodium hydrogen phosphate to the desired pH with 5*M* sulphuric acid (pH-meter). 1,10-Phenanthroline was dissolved in 0.1*N* sulphuric acid.

Titration procedures

Silver. A 1–10 ml sample of silver solution (0.002*M*), 5 ml of 1,10-phenanthroline solution (0.01*M*), 5 ml of phosphate buffer solution (pH 6.5), 2 or 3 drops of TBPE solution, and 10 ml of 1,2-dichloroethane are placed in a 300-ml Erlenmeyer flask. The mixture is titrated with 0.002*M* tetraphenylborate with intermittent shaking to ensure equilibrium between the organic solvent and the aqueous phase. The initial mixture yields a solution with a colourless aqueous layer and a sky-blue 1,2-dichloroethane phase. As the solution is titrated, with thorough shaking after each addition of titrant, the 1,2-dichloroethane solution begins to turn green. On addition of excess of titrant (1 drop), the 1,2-dichloroethane phase changes to yellow, indicating the end-point of the titration.

Pentachlorophenol. A 1–10 ml sample of pentachlorophenol solution (0.005*M*), 5 ml of phosphate buffer solution (pH 6.0), 2 or 3 drops of DIP solution, and 10 ml of nitroethane are placed in a 300-ml Erlenmeyer flask. The mixture is titrated with 0.01*M* tetraphenylphosphonium chloride as for the titration of silver. A colour change from pinkish-red to blue in the organic phase indicates the end-point.

The upper aqueous layer remains colourless throughout the titration, because the indicators are not soluble in it.

RESULTS AND DISCUSSION

Reaction in the titration

The end-points of the titrations are described by the following equations.

$$[\underset{\text{blue}}{Ag(Phen)_2^+.TBPE^-}]_o + [TPB]_a^- + H^+ \rightarrow [\underset{\text{yellow}}{H\text{-}TBPE}]_o + [\underset{\text{colourless}}{Ag(Phen)_2^+.TPB^-}]_o$$

$$[TPP]_a^+ + [\underset{\text{red}}{H\text{-}DIP}]_o \rightarrow [\underset{\text{blue}}{TPP^+.DIP^-}]_o + H^+$$

where Phen is 1,10-phenanthroline, TPB is tetraphenylborate, TPP is tetraphenylphosphonium, o is the organic phase, and a is the aqueous phase. In the absence of TPB, a proton from a hydroxyl group in undissociated TBPE (yellow, $\lambda_{max} = 410$ nm in 1,2-dichloroethane) is easily replaced by $Ag(Phen)_2^+$ to form an ion-pair $Ag(Phen)_2^+.TBPE^-$ in which the indicator is in the dissociated form (blue, $\lambda_{max} = 610$ nm in 1,2-dichloroethane). As the solution is titrated, the $[Ag(Phen)_2^+.TPB^-]$ complex is formed in the organic layer. A proton from a hydroxyl group in undissociated DIP (red, $\lambda_{max} = 520$ nm in nitroethane) is similarly replaced by excess of TPP to form an ion-pair $TPP^+.DIP^-$ in which the indicator is in the dissociated form (blue, $\lambda_{max} = 640$ nm in nitroethane). As the indicators are in the organic phase throughout the titration, the colour changes at the end-points are clearly detected.

Titration conditions

Larger amounts of buffer solution have no influence on the titrations, but amounts of less than 2 ml cause problems with pH-control. Results are consistent when the pH of the aqueous phase is in the range 4.5–7.5 for the titration of silver, and 5.5–7.0 for pentachlorophenol. Various water-immiscible solvents have been tested: nitrobenzene, methyl isobutyl ketone, butyl acetate, isoamyl alcohol, 1,2-dichloroethane, nitroethane, chloroform, toluene, benzene, carbon tetrachloride, chlorobenzene, and n-hexane. Of these, 1,2-dichloroethane and nitroethane are the best solvents for the titrations with TBPE and DIP indicators respectively. Variation in the initial volume of the aqueous layer (10–25 ml) and of the organic layer (7–15 ml) has no influence on the ease of determination of the end-points. The titrants and indicators used are stable for a month.

Table 1. Effect of concentration of tetraphenylborate

Tetraphenylborate, *M*	Ag taken, *M*	Ag found, *M*
2×10^{-3}	2.40×10^{-3}	2.42×10^{-3}
1×10^{-3}	1.20×10^{-3}	1.21×10^{-3}
5×10^{-4}	6.00×10^{-4}	6.12×10^{-4}
2×10^{-4}	2.40×10^{-4}	2.50×10^{-4}

Titration of silver

The results for titration of silver at different concentrations, shown in Table 1, indicate the high sensitivity of the two-phase titration compared with precipitation titration with 0.1*M* halide solution. The relative error is 1–2% when 5 ml of $10^{-3}M$ silver are titrated according to the proposed procedure.

Interferences

The effect of various salts on the titration of 5 ml of 0.002*M* silver and 0.005*M* pentachlorophenol was examined and the results are given in Table 2. The colour change at the end-point is clearly detected even in the presence of precipitates such as barium

Table 2. Effect of other salts (2 ml of salt solution added)

Added as	Concentration, *M*	Titration, *ml*	
		Ag(I)	Pentachlorophenol
none		5.05	2.55
KI	0.0002	4.95	2.55
	0.01	0.0	2.65
KSCN	0.01	4.75	2.60
	0.05	4.40	2.75
NaCN	0.0002	4.80	2.55
	0.01	0.0	2.55
NH_4Br	0.05	5.05	2.55
$NaHCO_3$	0.05	5.00	2.60
KIO_3	0.05	5.05	2.55
$KBrO_3$	0.05	5.05	2.55
$KClO_3$	0.02	5.00	2.65
$NaClO_4$	0.001	5.05	2.70
	0.01	5.05	4.50
$Mg(CH_3COO)_2$	0.05	5.05	2.50
$Ca(NO_3)_2$	0.05	5.05	2.55
$BaCl_2$	0.02	5.05	2.55
$Pb(NO_3)_2$	0.05	5.05	2.50
$AlNH_4(SO_4)_2$	0.02	5.05	2.55
Na_2HAsO_4	0.05	5.05	2.50
Na_2WO_4	0.05	5.10	2.55
Na_2MoO_4	0.02	5.05	2.55
$Na_3(PMo_{12}O_{40})$	0.02	5.10	2.55
$Na_3(WMo_{12}O_{40})$	0.02	5.05	2.55
2,4-Dichlorophenol	0.02	5.05	2.60

sulphate. Metal ions that react with 1,10-phenanthroline give positive errors in the titration of silver(I) when they are present at even the 10^{-4} *M* level. The interference of cadmium, manganese(II) and zinc can be eliminated with EDTA, however. Molybdate, tungstate and their heteropoly acids formed with phosphate do not interfere in the pentachlorophenol titration, though they have been reported[8] as being extracted with tetraphenylphosphonium salts. It is reasonable to suppose that the [TPP^+.pentachlorophenol$^-$] and [TPP^+.DIP^-] ion-pair complexes are more stable than the TPP^+–molybdate, –tungstate, and –heteropoly acid complexes.

Application of the titration

The method was applied to the determination of pentachlorophenol in a herbicide. The result was 83.2% pentachlorophenol by the proposed method, and 81.7% by the official titrimetric method with hydrochloric acid and sodium hydroxide solution.[9] The proposed hydrophobic indicator should have wide application. For instance, the TBPE indicator could be applied to the titration of not only the copper(I)-pyridine complex but also cationic and anionic surfactants, providing a sharp reversible colour change at the equivalence point and reducing the likelihood of error in accurately locating the end-point visually. Perchlorate could be titrated in the same manner as pentachlorophenol.

REFERENCES

1. S. R. Epton, *Nature*, 1947, **160**, 795.
2. D. Hummel, *Identification and Analysis of Surface-Active Agents*, Vol. 1, Interscience, New York, 1962.
3. J. T. Cross, *Analyst*, 1965, **90**, 315.
4. P. J. Cooper and P. W. Hammond, *Analyst*, 1967, **92**, 180.
5. L. K. Wang and P. J. Panzardi, *Anal. Chem.*, 1975, **47**, 1472.
6. K. Behrends, *Z. Anal. Chem.* 1970, **250**, 241.
7. M. A. Leonard, in G. Svehla, ed., *Comprehensive Analytical Chemistry*, Vol. VIII, pp. 377–80. Elsevier, Amsterdam, 1977.
8. R. Ripan and C. Calu, *Talanta*, 1967, **14**, 887.
9. *Japanese Industrial Standard*, K 1552, 1958.

Talanta, Vol. 28, pp. 860 to 862, 1981
Printed in Great Britain. All rights reserved

0039-9140/81/110860-03$02.00/0
Copyright © 1981 Pergamon Press Ltd

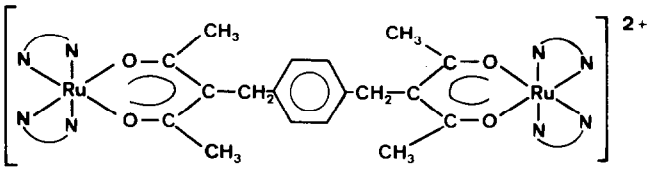
THE USE OF POROUS GLASS BEADS IN THE SEPARATION AND PURIFICATION OF RUTHENIUM COMPLEXES WITH LARGE ORGANIC LIGANDS

NITA A. LEWIS
Department of Chemistry, University of New Brunswick, Fredericton, New Brunswick, Canada

(*Received* 31 *December* 1981. *Accepted* 17 *March* 1981)

Summary—For complexes of highly-charged transition metal cations with large organic ligands, the use of glass beads as a chromatographic support allows the ready isolation of analytically pure samples of species which tend to decompose readily on more traditional supports. The method has been used in the purification of binuclear ruthenium complexes which are usually contaminated with a small amount of the monomer, and in the purification of ferrocene–ruthenium complexes which are difficult to separate from polymeric ferrocene residues.

Binuclear ruthenium complexes have been used extensively to study intervalence electron-transfer reactions since they are substitutionally inert in both oxidation states (II) and (III).[1] One of the major problems encountered in working with these materials is that it is often difficult to purify them by traditional methods. Complexes such as **I** contain large organic ligands and are usually rather insoluble in aqueous media, so ion-exchange procedures are not feasible.

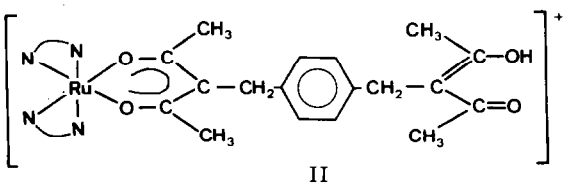


I

N N = 2,2'-bipyridyl

In these cases, traditional chromatographic methods involving silica or alumina supports are sometimes useful, even though the complexes may be rather highly charged (3+, 4+ or 5+ ions).[2] Frequently, however, it is not possible to use these procedures because the supports are too highly activated and catalyse the decomposition of the metal complex. Deterioration may occur rapidly on the column even though the complex may be quite stable otherwise.

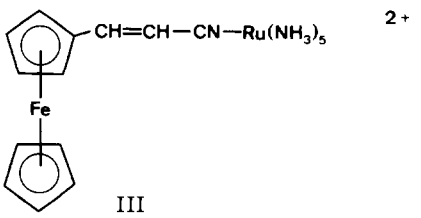
A typical contaminant of the binuclear ruthenium complex **I** is the corresponding uninuclear complex **II**.



II

This may often be separated from the binuclear species by repeated recrystallization but the technique is time-consuming and wasteful of the expensive ruthenium. We have developed a technique employing glass beads which may be used to purify highly-charged organic-soluble ruthenium complexes which decompose on more traditional supports.

The method is a rather general one. We have used it to purify ferrocene–ruthenium complexes, such as **III**.[3]



III

In the case of **III**, the contaminants remain on the glass beads, allowing the heteronuclear complex to pass through.

EXPERIMENTAL

Chemicals

The glass beads were purchased from Sigma Chemical Company (Controlled Pore Glass, PG-240-200). For comparison, a chemically modified support (Glyceryl Glass, Controlled Pore, GG-240-200) was also obtained from Sigma. Solvents used were Omnisolv grade, glass-distilled, from MCB Chemicals. Solvents were deaerated, when necessary, with high-purity argon obtained from Union Carbide Canada Ltd.

Column preparation

The glass column used (17 mm bore, 330 mm long) had a fritted glass disk and a Teflon stopcock at one end. The column was filled with chloroform and the glass beads were poured into it while the liquid was allowed to drain out slowly. More chloroform and glass beads were added as needed, until the column was filled to within 5 cm of the top. This particular packing procedure was found to give the best results. The chloroform was drained to within 1 cm above the top of the beads before the sample was added.

Purification of binuclear ruthenium complexes

Since the complexes containing 2,2'-bipyridyl ligands were light-sensitive, the column was protected from room light as much as possible. The crude material containing both uninuclear and binuclear complexes (see infrared spectrum, (KBr pellets, Beckman IR-12, Fig. 1) was dissolved in chloroform or a minimum of acetone if dissolution in chloroform was difficult. The solution was added to the column, care being taken not to disturb the glass beads, until 4–5 cm of the packing material had been saturated. Elution with a 10% acetone/90% chloroform mixture moved the uninuclear complex but not the binuclear complex. The uninuclear complex was eluted and then concentrated on a rotary evaporator in the dark, yielding purple crystals.



Fig. 1. Infrared spectrum of the mixture.



Fig. 2. Infrared spectra of the complexes after separation (above, binuclear species; below, uninuclear species).

The binuclear complex was eluted with 50% acetone/50% chloroform, and was concentrated in a similar manner, also yielding pure purple crystals (as judged from the absorption spectrum—the compound decomposed too rapidly for analysis with the facilities available).

The infrared spectrum of the binuclear complex (Fig. 2, upper spectrum) shows that no free carbonyl group is present whereas that of the uninuclear species (Fig. 2, lower spectrum), shows a band at 1705 cm^{-1} (free carbonyl), as expected.

Purification of ferrocene–ruthenium complexes

The contaminants in these preparations are apparently small polymeric ferrocene moieties which are difficult to separate from the desired ferrocene–ruthenium species. The crude product from the preparation was dissolved in ace-

tone and placed on a column of glass beads. The desired ferrocene–ruthenium complex slowly passed through the column, leaving the polymeric impurities behind. Since these complexes are air-sensitive, it was necessary to carry out all operations in an argon-flushed glove-bag and to use argon-deaerated solvents. Analytically pure materials were obtained.[3]

Cleaning the glass beads

The procedure usually recommended is to wash the glass beads in nitric acid. However, this may be a dangerous procedure, since two explosions have occurred in our laboratories when this method was used. These violent reactions are presumably due to trace organic matter which was still present on the beads after drying. We have found that washing the beads first with acetone, drying, and then washing them with concentrated hydrochloric acid is safe and works well. The beads may be slightly yellow after this treatment but this does not affect their performance. If desired, the beads may be thoroughly cleaned, first with concentrated hydrochloric acid, then with nitric acid, which leaves them completely white.

RESULTS AND DISCUSSION

The use of glass beads allows the purification of sensitive metal species which tend to decompose on other supports. The mechanism of separation is probably a combination of fractionation based on the sizes of the components in the mixture and of electrostatic attraction between the negatively-charged glass beads and the positively-charged metal complexes. This postulate is based on two observations: first, the use of the glyceryl controlled-pore glass beads did not work, because the negative charge of the glass was masked by the chemical modification, and secondly the method does not work for the separation of anions, which do not appear to have any affinity for this support.

Only halogenated solvents and acetone appear to be suitable eluents, although this may be a peculiarity of the systems studied so far. The use of alcohols, dimethylsulphoxide, dimethylformamide and acetonitrile resulted in permanent adherence of the complexes to the glass beads. The metal species could be removed only by destruction after the use of any of these solvents.

This chromatographic procedure may be widely applicable in the purification of metal species. Its advantages are that it is fast and inexpensive, since there is apparently no limit to the number of times that the glass beads may be reused.

Acknowledgements—The author is grateful to Dr. H. Taube of Stanford University for his hospitality from 1977 to 1979, when she was an NRC post-doctoral fellow in his laboratories. It was during this time that the present work was initiated. Gratitude is also extended to the Natural Sciences and Engineering Research Council of Canada for a grant in aid of this research.

REFERENCES

1. H. Taube, *Ann. N.Y. Acad. Sci.*, 1978, **313**, 481.
2. B. P. Sullivan and T. J. Meyer, *Inorg. Chem.*, 1980, **19**, 752.
3. N. Dowling, P. M. Henry, N. A. Lewis and H. Taube, *Inorg. Chem.*, in the press.

Talanta, Vol. 28, pp. 863 to 865, 1981
Printed in Great Britain. All rights reserved

0039-9140/81/110863-03$02.00/0
Copyright © 1981 Pergamon Press Ltd

ANALYTICAL DATA

SYNTHESIS AND CHROMOGENIC PROPERTIES OF SOME HYDRAZONES OF 3-ISOQUINOLYL-, 2-QUINOLYL- AND 2-PYRROLE-CARBALDEHYDES

ALFRED A. SCHILT

Department of Chemistry, Northern Illinois University, DeKalb, Illinois 60115, U.S.A.

and

FRANCIS H. CASE

Department of Chemistry, Temple University, Philadelphia, Pennsylvania 19122, U.S.A.

(*Received* 18 *February* 1981. *Accepted* 18 *March* 1981)

Summary—Preparation of some new hydrazones is described together with results of spectrophotometric studies of their chromogenic reactions with some first-row transition metal(II) ions. Several of the new compounds show promise as highly sensitive metallochromic reagents.

Some outstanding reagents for trace metal determinations have been found among the *N*-heterocyclic hydrazones,[1–6] encouraging us to explore this class of compounds further,[7–10] this time focusing on hydrazones of 3-isoquinolyl-, 2-quinolyl- and 2-pyrrole-carbaldehydes. We report here their syntheses and chromogenic properties in reactions with some first-row transition metal(II) ions.

EXPERIMENTAL

Synthesis of hydrazones

Equal molar amounts of (0.01 mole) of aldehyde and hydrazine[10] were dissolved together in 15 ml of ethanol and heated under reflux for 15 min. After evaporation of the ethanol, the residue was crystallized from the solvent indicated in Table 1. Melting points and results of elemental analysis are also given in Table 1.

Chromogenic studies

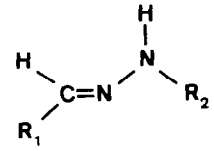
The pH range over which colour formation occurred, wavelengths of maximum absorbance, molar absorptivities, and conformance to Beer's law were determined for the metal(II) chelates by using procedures already described.[7–10] In preparing standard solutions for spectrophotometric examination, the amounts added and order of addition to 25-ml standard flasks were as follows: a weighed amount of standard metal(II) ion solution, 2 ml of 0.010*M* hydrazone (in ethanol), 10 ml of pH 9 buffer, and sufficient ethanol to dilute to volume. The pH 9 buffer was a 1*M* solution of boric acid to which sufficient sodium hydroxide was added to give the desired pH. The chloroform solutions of the complexes were obtained by extracting known aqueous solutions, prepared as described above but without addition of ethanol, with two 10-ml portions of chloroform and, after combining the two extracts, diluting to a total volume of 25.0 ml with chloroform.

RESULTS AND DISCUSSION

With the exception of **VI**, the hydrazones of 2-pyrrole-carbaldehyde proved unsatisfactory or unattractive as metallochromic reagents. Hydrazones **I** and **V** are highly susceptible to aerial oxidation in solution at pH 5–11, forming intensely coloured products within a few minutes on exposure to oxygen. Copper and cobalt were found to catalyse the rate of colour formation and oxidation. Thus **I** and **V** are unsatisfactory as chromogenic reagents for metal ions; however, they might be profitably explored as reagents for the colorimetric determination of dissolved oxygen or other oxidants. Hydrazones **II**, **III** and **IV** formed coloured complexes with only copper(II) and cobalt(II) (see data in Table 2), but these proved to be weak complexes as evidenced by their failure to follow Beer's law in the absence of a large excess of free ligand. Hydrazone **VI** affords high sensitivity for the detection of either copper or cobalt, and both chelates are stable and follow Beer's law. Simultaneous determination of copper and cobalt with **VI**, however, appears to be impractical owing to the close similarities in their spectra.

The hydrazones of the three quinolinecarbaldehydes (**VII–IX**) formed intensely coloured chelates with Mn(II), Fe(II), Co(II), Ni(II), Cu(II) and Zn(II) in aqueous solutions of pH 3–11 (see Table 3). Cadmium(II) and mercury(II) also formed coloured complexes (yellow in each case) but were not studied quantitatively. The molar absorptivities of these chelates compare favourably in magnitude with those of previously reported hydrazones found to have out-

Table 1. Synthesis and analysis of hydrazones



Compound	R_1	R_2	m.p., °C	Crystn. solvent	Formula	Analysis Calculated, % C	H	N	Found, % C	H	N
I	2-Pyrrolyl*	Phenyl	144	C_6H_6							
II	2-Pyrrolyl	2-Pyridyl	175	C_6H_6	$C_{10}C_{10}N_4$	64.50	5.41	30.09	64.7	5.26	29.6
III	2-Pyrrolyl	Pyrazinyl	227	CH_3OH	$C_9H_9N_5$	57.74	4.85	37.41	57.8	4.87	37.5
IV	2-Pyrrolyl	2-Pyrimidinyl	139 dec.	CH_3OH	$C_9H_{11}N_5O$†	52.68	5.40	34.13	53.0	5.38	33.6
V	2-Pyrrolyl	2-Thiazolyl	195	CH_3OH–H_2O	$C_8H_8N_4S$	50.00	4.20	29.15	49.9	4.25	29.0
VI	2-Pyrrolyl	2-Quinolyl	148	C_6H_6	$C_{14}H_{12}N_4$	71.17	5.12	23.71	71.2	5.13	23.4
VII	3-Isoquinolyl	Pyrazinyl	230	C_2H_5OH	$C_{14}H_{11}N_5$	67.46	4.45	28.09	67.2	4.37	27.8
VIII	3-Isoquinolyl	2-Pyridyl	194	C_2H_5OH	$C_{15}H_{12}N_4$	72.56	4.87	22.57	72.5	4.83	22.3
IX	2-Quinolyl	Pyrazinyl	235	Methyl cellosolve	$C_{14}H_{11}N_5$	67.46	4.45	28.09	67.0	4.46	28.0

* Reference 11.
† Hydrate.

Table 2. Absorption properties of metal chelates of hydrazones of 2-pyrrole-carbaldehyde in aqueous ethanol, pH 9

Ligand	Copper(II) Colour	λ, nm	ϵ, $l.mole^{-1}.cm^{-1}$	Cobalt(II) Colour	λ, nm	ϵ, $l.mole^{-1}.cm^{-1}$
I	*	—	—	*	—	—
II	Gold	420	1.71×10^4	Gold	460	1.90×10^4
III	Gold	460	1.43×10^4	Orange	460†	1.90×10^4
IV	Yellow	400†	1.30×10^4†	Yellow	400†	1.90×10^4†
V	‡	—	—	‡	—	—
VI	Gold	500†	9.40×10^3†	Orange	500	1.67×10^4

* Orange colour produced slowly by aerial oxidation of ligand catalysed by base, copper or cobalt.

† Not a maximum but at side of band just before reagent blank becomes appreciable.

‡ Blue-green colour produced by aerial oxidation of ligand, catalysed by base, copper or cobalt.

Table 3. Absorption properties of metal chelates of hydrazones of 2-quinoline-carbaldehyde in aqueous ethanol and in chloroform extracts from pH 9 aqueous solutions

Metal ion	Solvent	Ligand VII Colour	VII λ, nm	VII $\epsilon \times 10^{-3}$*	Ligand VIII Colour	VIII λ, nm	VIII $\epsilon \times 10^{-3}$*	IX Colour	IX λ, nm	IX $\epsilon \times 10^{-3}$*
Mn(II)	EtOH	Gold	464	50	Yellow	444	14.4	Orange	506	27.7
	$CHCl_3$	Gold	487	†	Yellow	463	†	Magenta	519	†
Fe(II)	EtOH	Orange	425	38	Orange	419	37	Brown	443	25.0
			528	7.4		508	9.4		518	16.8
			571	8.9		538	8.7		628	5.8
	$CHCl_3$	Brown	403	70	Gold	440	69	Orange	460	25
			453	38		570	11.6		535	21
			580	9.5						
Co(II)	EtOH	Gold	469	34	Yellow	456	44	Orange	493	30
	$CHCl_3$	Gold	483	32	Yellow	471	41	Magenta	519	30
Ni(II)	EtOH	Yellow	457	54	Yellow	440	72	Orange	505	51
	$CHCl_3$	Yellow	483	60	Yellow	456	69	Magenta	527	55
Cu(II)	EtOH	Gold	458	58	Yellow	442	63	Orange	494	52
	$CHCl_3$	Yellow	481	68	Yellow	465	68	Red	513	56
Zn(II)	EtOH	Yellow	456	59	Yellow	439	71	Orange	504	57
	$CHCl_3$	Yellow	—	†	Yellow	469	†	Red	520	†

* $l.mole^{-1}.cm^{-1}$.

† Recovery of metal incomplete after three extractions with excess of ligand added each time.

standing sensitivity as chromogenic reagents.[1-6] The metal chelates of **VII–IX** follow Beer's law and, with the exception of the Mn(II) and Zn(II) chelates, can be readily and quantitatively extracted into chloroform, allowing separation and concentration of the metal chelates for enhanced detection and measurement. A particular advantage is notable in the case of extraction of the iron(II) chelates of **VII** and **VIII**; here, the molar absorptivities are almost twice those for aqueous ethanol solutions. We conclude that **VII** and **VIII** merit serious consideration as chromogenic reagents for trace metal determinations, especially for iron. Compound **VII** appears particularly promising, judging from the spectra of its chelates, as a possible reagent for simultaneous determination of cobalt and nickel, or of manganese and cobalt, or of iron and any one of the other metal ions tested here.

REFERENCES

1. S. P. Singhal and D. E. Ryan, *Anal. Chim. Acta*, 1967, **37**, 91.
2. V. Zatka, J. Abraham, J. Holzbecher and D. E. Ryan, *ibid.*, 1971, **54**, 65.
3. B. K. Afghan and D. E. Ryan, *ibid.*, 1968, **41**, 167.
4. R. E. Jensen, N. C. Bergman and R. J. Helvig, *Anal. Chem.*, 1968, **40**, 624.
5. G. S. Vasilikiotis, T. Kouimtzis, C. Apostolopoulou and A. Voulgaropoulos, *Anal. Chim. Acta*, 1974, **70**, 319.
6. R. B. Singh, P. Jain, B. S. Garg and R. P. Singh, *Analyst*, 1979, **104**, 1188.
7. A. A. Schilt, J. F. Wu and F. H. Case, *Talanta*, 1975, **22**, 915.
8. A. A. Schilt, P. C. Quinn and C. L. Johnson, *ibid.*, 1979, **26**, 373.
9. A. A. Schilt, N. Mohamed and F. H. case, *ibid.*, 1979, **26**, 85.
10. A. A. Schilt and F. H. Case, *ibid.*, 1980, **27**, 55.
11. E. Bamberger and G. Djierdjian, *Ber.*, 1980, **33**, 536.

Talanta, Vol. 28, pp. 867 to 869, 1981
Printed in Great BritainPergamon Press Ltd

0039-9140/81/110867-03$02.00/0

ANNOTATION

EVIDENCE OF COMPETITIVE MECHANISMS DURING OXIDATION OF $CS_2N_3^-$ BY PERMANGANATE ION IN ALKALINE SOLUTION

EDUARDO F. DE A. NEVES

Instituto de Química, Universidade de São Paulo, Caixa Postal 20780, São Paulo, SP, Brasil

W. L. POLITO, V. L. MORAES and D. W. FRANCO

Instituto de Física e Química de São Carlos, Universidade de São Paulo, Caixa Postal 369, São Carlos, SP, Brasil

(*Received* 24 *September* 1980, *Revised* 30 *March* 1981. *Accepted* 21 *April* 1981)

Summary—The oxidation of the 1,2,3,4-thiatriazole-5-thiolate ion, $CS_2N_3^-$, by permanganate ions in alkaline medium has been investigated over a wide range of oxidant concentrations. With a moderate excess of permanganate ion a 17-electron reaction takes place, yielding sulphate, nitrogen and carbon dioxide. With a high permanganate concentration the pseudohalide undergoes a 26-electron reaction yielding sulphate, carbon dioxide and nitrite as final products. These two different stoichiometries arise from the existence of competitive mechanisms and the ratio $C_{MnO_4^-}/C_{CS_2N_3^-}$ will determine the course of the reaction.

Despite its relevance the chemistry of the 1,2,3,4-thiatriazole ring system is still not well understood.[1-3] The redox chemistry of this type of compound is a theme currently under investigation in our laboratory. In particular our attention has been focused on the first member of this series, the 1,2,3,4-thiatriazole-5-thiol molecule and its salts. The acid HCS_2N_3 has quite a rich chemistry since, besides the typical properties of the 1,2,3,4-thiatriazole ring system, it also exhibits pseudohalide chemical behaviour.[4,5]

Recently we have reported[6,7] some of our results for the oxidation of $CS_2N_3^-$ by several oxidizing agents and have concluded that potassium permanganate in alkaline medium is the most efficient. Since under these conditions the $CS_2N_3^-$ is quantitatively oxidized, this reaction has been proposed for the analytical determination of the thiatriazolethiolate[7] and of carbon disulphide.[8]

This communication reports evidence for competitive mechanisms occurring during the oxidation of 1,2,3,4-tiatriazole-5-thiolate by potassium permanganate.

EXPERIMENTAL

Reagents

All reagents were of analytical grade. Doubly distilled water was used throughout. The $NaCS_2N_3$ was prepared, stored and standardized as described previously.[9] The potassium permanganate solution was standardized in acid medium against oxalate.[10]

Apparatus

All potentiometric titrations were done with a Corning pH-meter model 12. A 10-μA polarizing current was applied to the platinum electrodes in the titration cell.

Standardization of $TlClO_4$ solutions

About 3 g of sodium hydroxide were dissolved in 10 ml of distilled water, and 10–30 ml of standardized potassium permanganate solution and 1 g of solid barium chloride were added. The platinum electrodes were placed in the solution and the permanganate was titrated with thallium(I) perchlorate.[7]

Determination of $CS_2N_3^-$

Known volumes of $NaCS_2N_3$ solution (1–40 ml) were added, with stirring, to an alkaline solution containing potassium permanganate (in a calculated excess of the required amount). The sodium hydroxide concentration was kept in the 2–3*M* range in all experiments, as recommended.[10] After standing for 70 min in the dark at room temperature (23–29°), the excess of permanganate was back-titrated with thallium(I) perchlorate as described above.

Ferrous sulphate and sulphuric acid test

After the complete oxidation of $CS_2N_3^-$ by permanganate, as described above, the excess of oxidant was reduced with thallium(I) solution and the barium manganate formed was separated by filtration. The remaining solution was cooled, carefully acidified with dilute sulphuric acid, and then filtered again to remove the barium sulphate formed. The characteristic colour[11] of $FeNO.SO_4$ appeared after the careful addition of ferrous sulphate to the filtrate.

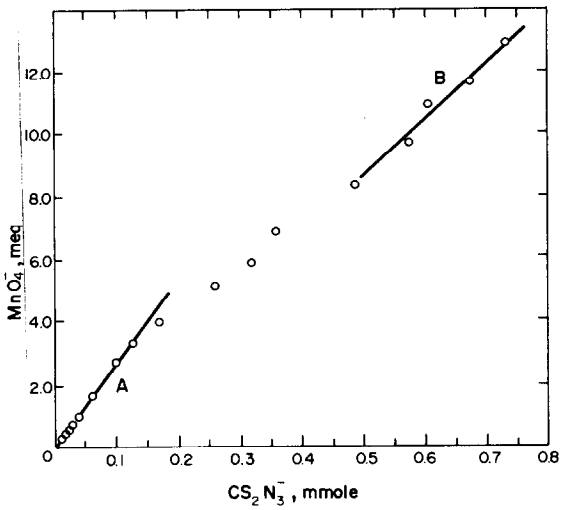


Fig. 1. MnO_4^- consumption by $CS_2N_3^-$. (A) $C_{MnO_4^-}/C_{CS_2N_3^-} > 200$; (B) $C_{MnO_4^-}/C_{CS_2N_3^-} < 100$.

Nitrite determination

Nitrite was determined as ammonia by the Kjeldahl method after reduction with Devarda's alloy. After the oxidation and removal of excess of oxidant, the barium manganate was filtered off, the filtrate being collected in a 250-ml distillation flask. The filtrate was cooled, Devarda's alloy added (twice the required amount), and the ammonia was distilled, collected and titrated. The system was standardized with known amounts of sodium nitrite.

RESULTS AND DISCUSSION

In the course of experiments dealing with the $MnO_4^-/CS_2N_3^-$ reaction in alkaline medium with a large excess of oxidant, we were unable to detect evolution of nitrogen.[7] On the other hand, with the same solution (after suitable treatment) we were able to obtain the characteristic[11] $FeNO.SO_4$ colour. We therefore made a detailed investigation of the system.

Potassium permanganate, in a wide range of concentrations, was used for oxidation of $NaCS_2N_3$ solutions and, as shown in Fig. 1, two straight lines were obtained for the relation between equivalents of permanganate used and amount of $NaCS_2N_3$ taken, the slope depending on the molar concentration ratio $C_{MnO_4^-}/C_{CS_2N_3^-}$. When the ratio is about 20 ($C_{MnO_4^-} = 0.16$–$0.14M$ and $C_{CS_2N_3^-} = 5.4 \times 10^{-3} - 7.0 \times 10^{-3} M$), the slope is 17, consistent with the 17-electron reaction:[7]

$$22OH^- + CS_2N_3^- + 17MnO_4^- \rightarrow 17MnO_4^{2-} + CO_3^{2-} + 2SO_4^{2-} + 11H_2O + {}^3\!/_2 N_2$$

However, when the ratio is >100 ($C_{MnO_4^-} = 0.30$–$0.24M$ and $C_{CS_2N_3^-} = 3.4 \times 10^{-4} - 2.4 \times 10^{-3} M$), the slope is 26, defining another stoichiometry. If the excess of potassium permanganate in such solutions is determined iodimetrically in acid medium, the equivalent weight of $CS_2N_3^-$ is found to be $\frac{1}{32}$ of its formula weight, in accordance with

$$CS_2N_3^- + 32MnO_4^- + 40OH^- \rightarrow 32MnO_4^- + CO_3^{2-} + 2SO_4^{2-} + 3NO_3^- + 20H_2O$$

It is well known that nitrite is not attacked[12] by permanganate in alkaline medium but is easily oxidized to nitrate by the same reagent in acid solution. Thus, the difference of 6 electrons between the basic and stoichiometries in basic and acidic media can be explained as due to nitrite being oxidized to nitrate. However, the procedure involving initial oxidation in alkaline medium and back-titration in acidic medium is not recommended for analytical purposes, because the change from the 1-electron to the 5-electron reduction of permanganate makes the consumption of reductant in the back-titration unduly large. The concentration of nitrite in the reaction product has been determined by the Kjeldahl procedure, giving results in agreement with the reaction:

$$CS_2N_3^- + 26MnO_4^- \rightarrow 26MnO_4^{2-} + CO_3^{2-} + 3NO_2^- + 2SO_4^{2-} + 17H_2O$$

The determination of the carbonate and sulphate produced, performed as described previously,[7] provided additional evidence for the reaction.

These two different stoichiometries arise from the existence of competitive mechanisms and the excess of permanganate used will decide the course of the reaction. When the permanganate concentration lies in the range 0.1–0.2M and the $C_{MnO_4^-}/C_{CS_2N_3^-}$ ratio is 50–80 both nitrite and nitrogen are found in the products, providing experimental support for this assumption. This also indicates the existence of other centres than the sulphur atom suitable for oxidant attack in the 1,2,3,4-thiatriazole ring, as has been suggested before.[6] Considering the complexity of the system involved, the stoichiometric oxidation would be better expressed as:

$$CS_2N_3^- + (17 + 3y)MnO_4^- + (22 + 4y)OH^- \rightarrow (17 + 3y)MnO_4^{2-} + CO_3^{2-} + 2SO_4^{2-} + (1.5\text{–}0.5y)N_2 + yNO_2^- + (11 + 2y)H_2O$$

where y can take values from 0 to 3.

Figure 2 shows the different stoichiometries, as a function of the permanganate concentration, illustrating these comments.

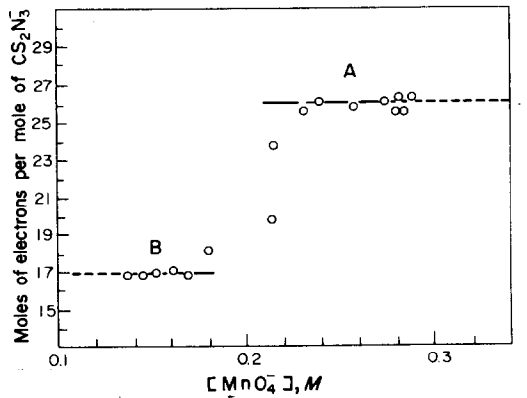


Fig. 2. Number of moles of electrons used per mole of $CS_2N_3^-$ as a function of MnO_4^- concentration; (A) $C_{MnO_4^-}/C_{CS_2N_3^-} > 200$; (B) $C_{MnO_4^-}/C_{CS_2N_3^-} < 100$.

However, in spite of the different stoichiometries possible, the procedure described earlier[7] is still adequate for determination of $CS_2N_3^-$ and CS_2 under well defined experimental conditions. The results obtained when the ratio $C_{MnO_4^-}/C_{CS_2N_3^-}$ is around 20 are reproducible within 0.8%. With the higher ratios ($C_{MnO_4^-}/C_{CS_2N_3^-} > 200$) the error is better than 2%.

We suggest that these reactions could be useful in the analytical determination of organic disulphides, the 1,2,3,4-thiatriazole ring system and mercaptans.

Acknowledgements—We are pleased to acknowledge financial support from FAPESP and CNPq, and to thank Dr. G. O. Chierice and Dr. M. Ferrante for helpful suggestions.

REFERENCES

1. K. A. Jensen and C. Pedersen, *Adv. Heterocyclic Chem.*, 1964, **3**, 263 and references therein.
2. K. Pilgram and F. Goren, *J. Heterocyclic Chem.*, 1971, **8**, 899.
3. A. Holm, K. Schaumburg, N. Dahlberg, C. Christophersen and J. P. Snyder, *J. Org. Chem.*, 1974, **40**, 431.
4. A. W. Browne and R. S. Hamburg, *J. Am. Chem. Soc.*, 1976, **48**, 2313.
5. M. L. Lappertand and H. Pyszora, *Adv. Inorg. Chem. Radiochem.*, 1966, **9**, 133.
6. E. A. Neves and D. W. Franco, *Talanta*, 1979, **26**, 81.
7. E. A. Neves, W. L. Polito, T. Tamura and D. W. Franco, *Anal. Lett.*, 1979, **12**, 741.
8. E. A. Neves, D. W. Franco and P. F. Romanelli, *Anal. Chim. Acta*, 1977, **92**, 393.
9. E. A. Neves and D. W. Franco, *J. Inorg. Nucl. Chem.*, 1974, **36**, 3851.
10. A. Berka, J. Vulterin and J. Zýka, *Newer Redox Titrants*, Pergamon Press, London, 1965.
11. F. Feigl, *Spot Tests in Inorganic Analysis*, 5th Ed., p. 326. Elsevier, Amsterdam, 1962.
12. I. M. Kolthoff and R. Belcher, *Volumetric Analysis*, Vol. III, Interscience, New York, 1957.

Talanta, Vol. 28, pp. 871 to 887, 1981
Printed in Great Britain

0039-9140/81/120871-17$02.00/0
Pergamon Press Ltd

TALANTA REVIEW*

INTERPRETATION OF ANALYTICAL CHEMICAL INFORMATION BY PATTERN RECOGNITION METHODS—A SURVEY

LARS KRYGER
Department of Chemistry, Aarhus University, Langelandsgade 140, 8000 Aarhus C, Denmark

(*Received* 23 *April* 1981. *Accepted* 11 *June* 1981)

Summary—Since the late sixties, pattern recognition techniques have been used by analytical chemists to facilitate the interpretation of multivariate analytical information. Most research within the field has focused on adapting pattern recognition methods to chemical data. This has been necessary since chemical data are often complicated by the fact that distributions are unknown. Through the first decade of chemical pattern recognition, promising results have been obtained even though the data sets studied have frequently been rather small for statistical analysis. The past few years have shown that an increasing number of analytical chemists are interested in the sheer utility of pattern recognition. This can be taken as a valid sign of a useful approach. The present communication surveys this development. Those methods which have proved most useful for analytical chemical data are described in some detail, and applications within the various fields of analytical chemistry are reviewed.

Progress within the field of analytical chemistry has always been closely related to the development of other branches of science: it is important for the analytical chemist to be aware of new discoveries and developments within other fields of chemistry as well as within physics, electronics, engineering, statistics, *etc.* Often, however, methods developed for other branches of science cannot be directly applied to analytical chemical problems. This is, for example, the case with pattern recognition techniques of interpreting multivariate data: only rarely do experimental chemical data constitute the ideal base for studies involving statistical reasoning, such as the pattern recognition approach: in general, only limited knowledge about distributions is available, and because of the time and costs involved in acquiring further information, chemical pattern recognition has so far to a large extent been an art of doing statistics on a small number of samples. Since the late sixties, when the first reports of chemical pattern recognition were published, most research within the field has been on basic studies dealing with the problem of adapting pattern recognition methods to chemical data, and only during the past 4–5 years have a few reports from pure users of the methods been published. The high ratio of the number of basic research reports to the number of application reports is reflected in the priority given to topics in the present review: all but the final section is devoted to a discussion of the basic concepts and methods of pattern recognition, as they have been developed for analytical chemical data.

The final section of the review is devoted to selected applications. The applications summarized there have mostly been used for testing the procedures reviewed in the earlier sections of this communication, but the few papers completely devoted to applications are also reviewed.

A number of textbooks on chemical pattern recognition have been published.[1–5] Other books on pattern recognition methods, which do not specifically deal with chemical problems, are highly recommended for the chemist who wants to enter this field of research,[6–10] and there are several reviews of progress within the field.[11–14]

During the past few decades, the development of analytical chemistry has been characterized by a considerable interaction with other branches of science and with numerous fields within society, where the demand for reliable and fast analytical methods has been rapidly increasing. To comply with the demand for solutions to analytical problems of high complexity, a wealth of instrumental techniques has been developed and the digital computer has been introduced to assist in data acquisition and interpretation. By exploiting automated techniques, the analyst is often able to compile large amounts of information about the chemical system under study, with little effort. This is fortunate, since often analytical problems cannot be solved by a few simple measurements, and the answer may be buried in large amounts of information originating from, for example, feature-rich spectra or from several instrumental techniques. The analytical chemist must therefore devote much of his time to the difficult process of extracting from the experimental data the information relevant to the sol-

* For reprints of this review see Publisher's announcement near end of the issue.

ution of the problem, making multiple comparisons of samples with standards, *etc.*

Pattern recognition techniques may assist the analyst in this process. In its chemical applications, pattern recognition attempts to find or predict properties of samples (atoms, molecules or complex samples) which may not be directly observable by a simple chemical measurement, but which are believed to be related to the chemical composition and/or behaviour of the samples through some unknown relationship. Numerous properties of chemical systems may, although perhaps not directly measurable, be of considerable interest. The term "property" might for example refer to smell,[15] reactivity or carcenogenicity[3] of samples, which, as yet, cannot be predicted by a single chemical measurement, but which are likely to be related to the combined chemical evidence which can be extracted from a sample. The geographical origin of an oil-spill might in this context also be referred to as a property and information about the origin of the spill may, in an unknown and possibly complex manner, be buried in the chemical composition of the spill, which can be determined only by multiple chemical measurements.

The chemist who wants to predict some property of a sample usually uses previous experience with other samples in order to come up with an "educated guess".[16] If the sample considered is in some way similar to a subset of the known samples characterized by a common property, then he might predict that the unknown will have the same property. Whether his prediction turns out to be correct, of course, depends partly on whether the information he used for prediction was relevant and sufficient, and partly on whether irrelevant information was misleading him.

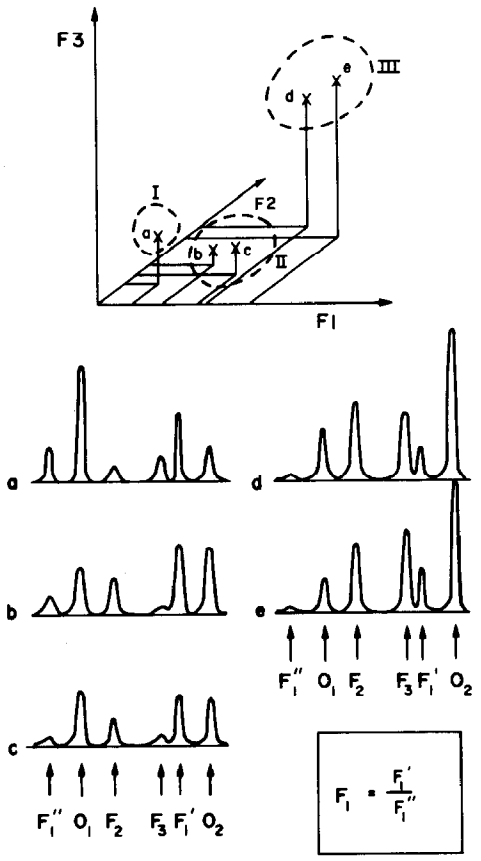


Fig. 1. Three-dimensional representation of five chromatograms. Feature 1 is the ratio of heights of two peaks. Features O_1 and O_2 are not used.

THE PATTERN RECOGNITION APPROACH

Patterns, features, clusters, classes

The pattern recognition approach to the interpretation of multivariate chemical information exploits a multidimensional mapping of the data. In this way, the concepts *distance* and *similarity* can be defined in a concise manner and comparisons of objects exhibiting "similar" behaviour can be carried out conveniently by digital computer. If a sample, out of a set of N samples, is characterized by a total of n measurements made on that sample, and if the same measurements are made on all samples, then the total amount of information available may be represented as N vectors in an n-dimensional space. We shall call this space the *pattern space* and each of the vectors will be referred to as a *pattern*. By the term "*feature*" or "*descriptor*" we shall understand any of the n quantities represented by the n axes of the pattern space. A feature may be a single piece of information (measurement) on the sample or some combined information (*e.g.*, the ratio between two peak amplitudes or areas).

Figure 1 shows schematically a three-dimensional representation of five chromatograms. Four of the chromatographic peaks are for some reason believed to contain the sought-for information about a property of the samples. While the peaks at F2 and F3 are believed to represent useful information directly, the ratio of the heights of the peaks F1′ and F1″ is assumed, for some chemical reason, to be a better descriptor of the property than the raw data are. The remaining peaks at O1 and O2 are not included: the peak at O1 may for example be believed to contain information which is not related to the property considered, and the peak at O2 to be so strongly correlated to the peak at F2 that the information is sufficiently well represented by F2 alone.

By inspection of the three-dimensional representation of the data, the eye is able to distinguish three or two groupings of patterns: either I, II and III, or I + II joined together and III. Such groupings are referred to as *clusters*. Whether, in this example, two or three clusters are formed depends, of course, on the rules used to identify a cluster. This will be discussed later. If we assume that the samples which produced the chromatograms of Fig. 1 belong chemically to two subsets, a + b + c and d + e, each of which is characterized by some common property of the members

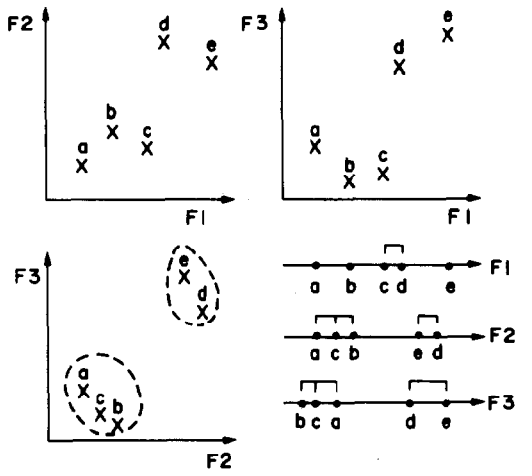


Fig. 2. Two- and one-dimensional representations of data given in Fig. 1.

(*e.g.*, geographical origin), we shall refer to each such subset as a *class*.

The formation of a cluster may reflect that the samples share some common property, *i.e.*, constitute a class. However, that a cluster does not necessarily represent a class and, *vice versa*, that a class cannot always be isolated as a distinct cluster, can be seen in Fig. 2. Here the one-dimensional plots F2 and F3 give good agreement between clusters and classes, but the F1-plot rather suggests one cluster (c + d), which is not representative of any class, and three *outliers*, a, b and e. Going to the two-dimensional plots, it appears that augmenting F3 and in particular F2 with F1 does not produce distinct clusters such as is the case when F2 and F3 are used together. Although the feature F1 by itself does not suggest that two classes exist, its effect in three-dimensional space is weakened by F2 and F3 such that indicative clusters are obtained (Fig. 1): to achieve clustering of patterns according to classes, it is necessary that sufficient relevant information is included, *i.e.*, a sufficient number of relevant features are used. On the other hand, irrelevant features may obscure the existence of classes if they are added to the patterns.

Supervised and unsupervised learning

There are two basically different approaches to the interpretation of chemical data by pattern recognition: *supervised* and *unsupervised learning*.

The supervised learning methods (Fig. 3) assume that a set of patterns of known classifications, a so-called *known set*, is available. The goal is to apply some classification rule to predict the classes to which the members of the set of unknowns, called the *unknown set*, belong. The development of classification rules is often referred to as *training*. During training, two subsets of the known set—the *training set* and the *prediction set*—are selected. Classification rules are then developed on the basis of these two sets, by using the known classifications of the training set to predict the classifications of the prediction set. The classification rules may then be evaluated and possibly improved according to their performance. When satisfactory classification rules are obtained, these rules can then be used to predict the classes of the patterns in the unknown set.

The unsupervised learning methods do not assume any training set. Here the goal is to find clusters of patterns in the n-dimensional space,[10] which may either reflect meaningful classes of known significance or indicate the existence of unknown but possibly meaningful relations between samples.

Distances and similarity

Since classification is based on measures of closeness, pattern recognition techniques use concise definitions of distance and similarity of patterns. The simplest, and most frequently used, measure of distance is the Euclidean distance: in an n-dimensional space, the distance between the two patterns

$$X_i = (x_{i1}, \ldots, x_{in})$$

$$X_j = (x_{j1}, \ldots, x_{jn})$$

is given by

$$d_{ij} = \left[\sum_{k=1}^{n} (x_{ik} - x_{jk})^2 \right]^{1/2}$$

but even the more general Mahalanobis expression:

$$d_{ij} = \left[\sum_{k=1}^{n} (x_{ik} - x_{jk})^p \right]^{1/p},$$

where p is an integer, is occasionally used.[1] Other types of measures of distance can also be defined.[1]

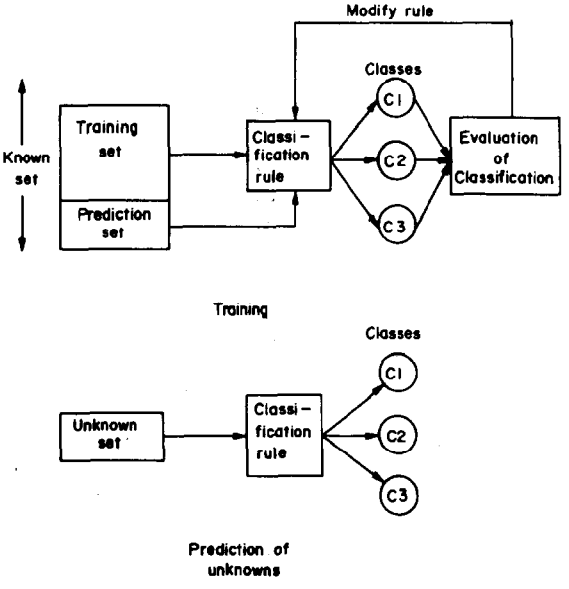


Fig. 3. Training and prediction. The supervised learning approach.

Recently, distance measures, which take data-uncertainty into account, have been proposed: the measurement error is here propagated through the calculations and the distance defined may hence weight the features according to measurement size and uncertainty. Methods using such distance measures do not tacitly assume that the variance due to analytical error is small compared to the variance of the samples.[17] Significant results are likely to emerge from applications of such distance measures to classification problems.

Given the distance d_{ij} between two patterns, a measure of *similarity* can be defined

$$S_{ij} = 1 - d_{ij}/d_{max}$$

where d_{max} is the largest interpattern distance in the data. In this manner identical patterns have $S_{ij} = 1$ and the patterns separated by the maximum distance have $S_{ij} = 0$. This definition of similarity is used in most unsupervised learning.

Data analysis by pattern recognition methods

Although, functionally, pattern recognition methods may be divided into supervised and non-supervised methods, a combination of the two approaches appears to be useful.[16] Unsupervised techniques may, at an early stage of data analysis, assist the chemist in getting an overall idea of the data structure,[18] and methods from factor analysis and principal-component analysis have proved useful for reduction of the dimensions of the data. These techniques attempt to retain as much variance as possible in the data set while reducing the dimensions.[19] Numerous reports on the application of factor analysis and principal-component analysis to chemical data are currently appearing and a separate field of research is developing. A detailed discussion of this field is outside the scope of the present paper, but the application of principal-component analysis to the modelling of clusters[20] will be discussed in some detail later.

Pattern recognition analysis mostly involves several steps and iterations. Figure 4 shows a modular breakdown of the analysis into a typical sequence of operations. Most of the modules of Fig. 4 will be treated as a separate topic in the following discussion.

THE DATA

Data sources

Although pattern recognition techniques are intended to give the chemist an insight into data of high dimensionality, a careful planning of the data-acquisition process is necessary. Chemical "know-how" and intuition are invaluable in the process of deciding which measurements should be made on the samples and which features of these measurements are most likely to contain class-information. It is interesting to notice that, although it is a well established practice in analytical chemistry to draw conclusions based on the combination of data from more than one instrumental technique and even though pattern recognition is well suited for interpreting such *multi-source data*, relatively few workers have exploited this possibility. In an early pattern recognition study on the behaviour of the oxides of 68 elements, the power of multi-source information was demonstrated. Clustering, according to the acidic, basic or amphoteric character of the oxides, could be obtained by using six multi-source features taken from the literature.[16] Also the combination of mass spectra with infrared spectra has proved fruitful.[21] More recently, concatenated infrared and Raman spectra have proved more successful than the corresponding single-source data for classification of compounds as alcohols, esters, ethers, ketones or compounds containing non-aromatic double bonds.[22] A rapidly expanding field within chemical pattern recognition is concerned with elucidating relations between structure and chemical behaviour. The data are here often obtained from the literature[23–25] and could be considered multi-source data. A considerable number of workers in the field of chemical pattern recognition have so far, for data analysis, used data obtained by other workers for other purposes. There are, however, clear signs that the pattern recognition field is approaching the

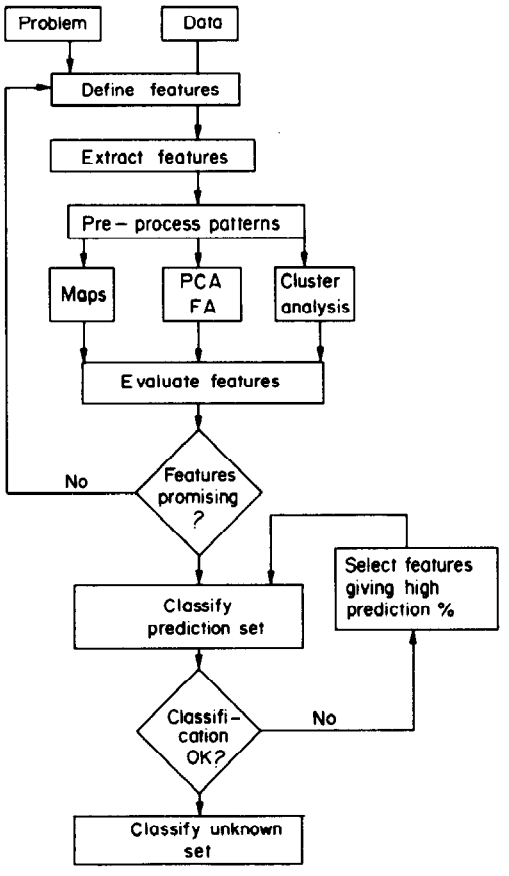


Fig. 4. Typical sequence of operations in pattern recognition. (PCA/FA: principal-components and factor analysis).

mature state,[11] and chemists will probably in the near future be able to spend time on data analysis as well as performing further experiments as suggested by the outcome of the data analysis. This iterative and time-consuming process is likely to provide the chemist with increased insight into complex chemical systems.[26]

Number of patterns, data dimensionality

The importance of a large ratio of the number of patterns to the data dimensionality can hardly be overestimated. A small ratio may lead to completely meaningless separations of data. By the *dimensionality* of the data, we mean the number of orthogonal dimensions spanned by the data.[27] This number, which is computed by eigen analysis of the data, is not necessarily equal to the number of measurements (features) used in the analysis. For a two-class problem, the ratio of number of patterns to dimensionality should exceed three and preferably be about ten.[16]

Since the prediction success-rate is likely to be better for classes containing the greatest number of samples, it is important to acquire approximately equal amounts of data for each class.[28,29]

Theoretical data

When accurate theoretical models of chemical systems are available, it is advantageous to generate by computer a large synthetic data base, which can be used to study the effect of selecting various sets of features. This principle has been used, for example, in a study of overlapping voltammetric peaks.[30] In such cases special consideration must be given to noise, which inevitably exists in real data.

Missing data

The data used for pattern recognition analysis may be incomplete, for several reasons, such as a measurement being impossible to make or yielding an ill-defined value. Data compiled from the literature are almost invariably incomplete. This makes the simple distance calculations impossible. However, with the SIMCA method,[31] provision is made for taking incomplete patterns into account.

FEATURE DEFINITION, SELECTION AND EXTRACTION, PREPROCESSING OF DATA

Feature definition and extraction

In the initial stage of pattern recognition analysis, the chemist must consider carefully which features are likely to contain relevant class information. The experienced chemist will usually have an idea of which type of information should be considered, and which information should be eliminated. The data may contain information of which the classification is already known but irrelevant to the chemist. For example, in voltammetric data, the position and amplitude of peaks may be predominant features containing qualitative and quantitative chemical information. If, however, the object of analysis is to detect overlapping double peaks, such chemical information should be eliminated and features related to peak shape considered.[30,32,33] In many types of spectral analysis, useful features can be extracted directly from peak positions, amplitudes and areas, but here also features related to peak shapes and long-range structure of peak bands may be important for classification. To extract such features, both Fourier and Hadamard transforms have been used.[5] Definite advantages arise from representing the data in the Fourier or Hadamard domain: several features in direct space may, in favourable cases, contribute to a few coefficients/elements in the transforms. On the other hand, unwanted features/elements may also contribute, and the chemical significance of the features, which might turn out to be important for classification, can be difficult to visualize.

Fourier-transformed data

The application of Fourier-transformed chemical data for pattern recognition is reported by a number of workers. With the fast Fourier transform (FFT), feature extraction can be rapidly done on a digital computer. For the FFT to represent a finite record of analytical information accurately, it is a necessary condition that the data record is zero-valued at the terminal data points. Data which do not have this property may, however, be transformed by a rotation/translation operation before the FFT is executed.[30] The basic idea of using Fourier coefficients as features in pattern recognition is to retain *some* information and discard some from *all* parts of direct space. If, for example, it is thought that the low-frequency content of the data represents almost pure analytical information, while the noise contributes mainly at high frequencies, the high frequencies may then be filtered out digitally.

Whether the FFT approach to feature definition is successful depends on the type of data investigated. *A priori*, it could be expected that a limited selection of Fourier coefficients would be better for describing a spectrum with rather few features and wide peaks (such as an NMR spectrum) than a detailed spectrum with numerous narrow peaks (such as a mass spectrum). This is not necessarily the case,[34–36] but there is evidence that voltammetric curves, which are mostly characterized by one or a few wide maxima, are better described by features in the Fourier domain when classification according to peak shapes is attempted.[26,30,32,33,37]

Hadamard-transformed data

The Hadamard transform—also sometimes called the binary Fourier representation transform[38] because of its similarities with the Fourier transform—has been used to extract information from spectra[5,34,38,39] and electrochemical data.[40,41] The Hadamard transform can be based on the discrete Walsh functions: cal(n,t) and sal(n,t) which resemble

infinitely clipped $\cos(n\pi t)$ and $\sin(n\pi t)$, *i.e.*, they assume only the values -1 and $+1$ and have the same number of zero crossings as the trigonometric functions used in Fourier analysis. The Hadamard transform Y of any discrete spectrum X is computed by the equation

$$Y = \frac{1}{k}|H(n)|X$$

where k $(= 2^n)$ is the length of the column vectors X and Y and n is a positive integer. $H(n)$ is the Hadamard matrix of order n, which for example may be computed by the recursive formula

$$\{H(n+1)\} = \left\{\begin{array}{c|c} H(n) & H(n) \\ \hline H(n) & -H(n) \end{array}\right\} \text{ and } \{H(0)\} = \{1\}$$

i.e.,

$$\{H(1)\} = \begin{Bmatrix} 1 & 1 \\ 1 & -1 \end{Bmatrix}, \{H(2)\} = \begin{Bmatrix} 1 & 1 & 1 & 1 \\ 1 & -1 & 1 & -1 \\ 1 & 1 & -1 & -1 \\ 1 & -1 & -1 & 1 \end{Bmatrix}, \text{ etc.}$$

The rows of the matrix are sometimes ordered according to the number of zero crossings, *i.e.*, they generate Walsh functions of increasing order.

The Hadamard transform, especially the fast Hadamard transform, is well suited for digital computer applications both with respect to speed and storage requirements.[38] The feasibility of representing electrochemical data accurately, even after high data-compression by using the Hadamard transform, has been demonstrated.[40,41] Whether features extracted by means of the Hadamard transform are useful for classification depends on the problem and the available data and is still a matter of dispute.[36] However, in a pattern recognition study on mass spectra of hydrocarbons, it was shown that the prediction performance was less sensitive to reductions in the number of features when Hadamard features rather than intensity features were used.[38]

Feature selection during preprocessing

Once a set of features has been defined, extracted and possibly scaled, it may be useful to examine the known data set, one dimension at a time, by drawing histograms of the features.[42] Tendencies of groupings into meaningful clusters may indicate whether a particular feature should be used. To reduce the number of features, it is also common practice to compute a matrix of feature correlations within the data set.[43] From a highly correlated set of features, one may then be selected to represent the set. To assist this selection process, a dendrogram of feature correlations (see "Cluster analysis") may be useful.[43,44]

When a training set of data is given, *i.e.*, the classes are known in advance, some further feature selection may be carried out during preprocessing: a criterion which may be used to evaluate the importance and hence the weight of a feature, is its relative importance in effecting a separation of known classes. The *variance weight* of a feature, which is the ratio of the interclass variance of two classes to the intraclass variance of the classes, and the *Fisher weight* of a feature, which is the ratio of the square of the difference in the two class means to the sum of the intraclass variances, may be used for such purposes.[16,43] Also the McCabe U-statistic, which gives a measure of cluster tightness *vs.* cluster distance for a given set of features, has proved useful in preliminary feature selection.[45] A feature-selection technique, which generates orthogonal features based on their importance to classification and partly retains the relation of the features to the original measurements, has been reported.[15,46] The technique facilitates interpretation of features which eventually turn out useful for classification.

Scaling of data

Since the features used for pattern recognition often represent a variety of measurements with different units and ranges, the features with the largest absolute values are likely to dominate in the classification process if raw data are used. To avoid this, *autoscaling* is frequently used.[16] The N patterns are then scaled so that they each have a zero mean and unit variance; hence, if x_{ik} denotes the kth feature of the ith pattern, then the corresponding autoscaled component x'_{ik} is

$$x'_{ik} = (x_{ik} - \bar{x}_k)/\sigma_k$$

with

$$\bar{x}_k = \frac{1}{N}\sum_{i=1}^{N} x_{ik} \quad \text{and} \quad \sigma_k^2 = \sum_{i=1}^{N}(x_{ik} - \bar{x}_k)^2$$

Other scaling methods such as *range scaling*, *mean subtraction*, *variance normalization* and *mean normalization* have been reported.[43] Knowledge of measurement uncertainty can also be exploited in the scaling of measurements.[43]

Although autoscaling of data is widely used, it is advisable to evaluate critically the effect of the procedure before applying it. If the data for some reason can be divided into *a priori* known classes, some of which are irrelevant, the data should be "type autoscaled"[42] for each of the irrelevant classes, *i.e.*, the data are pulled out of the distribution, autoscaled separately and subsequently returned to the distribution.

REPRESENTATIONS OF n-DIMENSIONAL SPACE

A number of techniques have been developed to assist the human mind in recognizing data structures such as clusters in n-dimensional space. Such methods attempt to represent the information in a manner which is familiar to the human senses, with the constraint that the inevitable distortion of the data structure should be kept low. Most techniques exploit the fact that the human eye is a skilled pattern recognizer in 2- and 3-dimensional space, but the human ear and

its ability to recognize complex acoustic signals have recently been exploited.[47]

Eigenvector projection

Useful information about the pattern distribution in n-dimensional space can be obtained from projections onto two-dimensional space. A commonly used projection, the *eigenvector projection*[4,48,49] uses for projection the plane spanned by the two eigenvectors of the data corresponding to the two largest eigenvalues.

The eigenvectors and eigenvalues are obtained by the Karhunen–Loewe transform, which operates on the data covariance matrix C, composed of the elements

$$C_{kl} = \sum_{i=1}^{N} (X_{ik} - \bar{X}_k)(X_{il} - \bar{X}_l)$$

where N is the number of patterns in the data.

The eigenvectors $\mathbf{v}_k$ and eigenvalues λ_k for $k = 1, n$ are determined by solving

$$\mathbf{C}\mathbf{v}_k = \lambda_k \mathbf{v}_k$$

The projection is linear since the co-ordinates of the two-dimensional plot are linear combinations of all the co-ordinates in n-dimensional space. Moreover, among linear projections, the eigenvector projection retains the maximum amount of variance in the data. Despite this, the eigenvector projection does not necessarily provide the optimum projection for classification. This is indicated in Fig. 5, which schematically shows two data classes I and II and the eigenvectors $\mathbf{v}_1$, $\mathbf{v}_2$ and $\mathbf{v}_3$. Clearly, the eigenvector projection on the $\mathbf{v}_1\,\mathbf{v}_2$ plane here will result in a complete overlap of the two classes, while a projection on the plane spanned by the vectors $\mathbf{v}_2$ and $\mathbf{v}_3$, which correspond to the two smallest eigenvalues, will result in complete class separation.

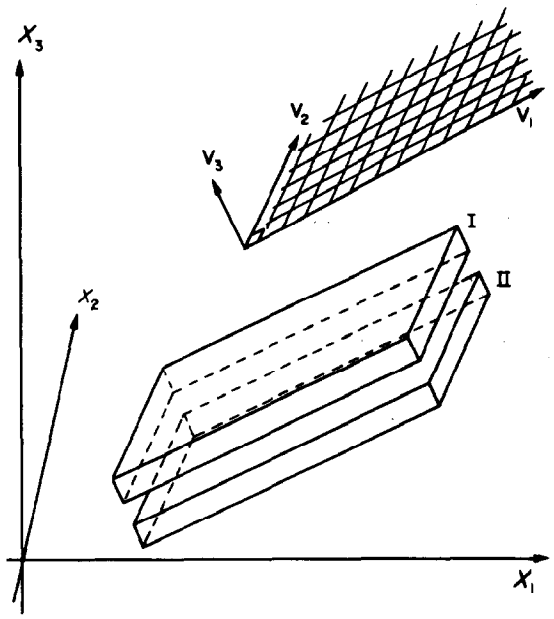


Fig. 5. Eigenvectors $\mathbf{v}_1$, $\mathbf{v}_2$, $\mathbf{v}_3$ of the combined classes I and II. An eigenvector projection of the data is obtained by projecting the data onto the plane spanned by the vectors $\mathbf{v}_1$ and $\mathbf{v}_2$, which correspond to the two largest eigenvalues.

Several recent papers report the application of the eigenvector projection.[15,18,24,25,50–53]

Non-linear maps

Mapping of data from high-dimensional space to a space of low dimension mostly results in distortion of the data structure. To minimize such distortion, the technique known as *non-linear mapping* (NLM) attempts to conserve interpoint distances.[4,6,7,16,48] First, all distances d_{ij}^* between any pair of patterns i and j in n-dimensional space are computed. Secondly, initial values of the pattern co-ordinates in the two-dimensional map are assumed, for example by using the co-ordinates from a simple projection or an eigenvector projection. Now all interpattern distances d_{ij} in the map can be computed, and the object of the procedure is then to minimize an error function $E(\delta)$:

$$E(\delta) = \sum_{i<j} (d_{ij}^* - d_{ij})^2/(d_{ij}^*)^\delta$$

The denominator is a weighting factor, and the value used for δ determines whether small distances or large distances should be preserved better (or equally well, if $\delta = 2$).

$E(\delta)$ is a non-linear function of the $2N$ unknown co-ordinates of the two-dimensional map, and can be minimized by various techniques such as the method of steepest descent, or the conjugate gradient method. Recent applications of non-linear mapping have been reported.[18,26,54,55]

Representation-space transformation

It has been argued that a serious shortcoming of display methods such as the eigenvector projection and the non-linear maps previously discussed is that they treat the data as a set,[56] *i.e.*, whenever patterns are added to or withdrawn from the distribution, a revised calculation is necessary. Moreover, the revised computation may give new co-ordinates for each pattern. To remedy this, a *representation-space transformation* has been proposed.[56] This transformation uses three reference-information pairs in pattern space, and the object of the transform is for any pattern to preserve its proximity relationships to each reference-information pair, and hence make the transform of a pattern independent of other patterns. The usefulness of this transform has recently been reported, but limitations in its ability to preserve data structure have also been indicated.[57]

Other display methods

Other types of visual display methods have been proposed. For example, to simplify the visual recognition of patterns relating structures of tetrachlorodibenzo-*p*-dioxin isomers with photodecomposition

data, a set of graphic symbols for the isomers has been developed.[58]

An interesting method, which as yet has not been used in chemical data analysis, transforms high-dimensional data into two-dimensional pictures of items which are familiar to human recognition, *e.g.*, faces.[7,59] Each feature in *n*-space is represented as a characteristic feature of a face, *e.g.*, the size of the eyes and the length of the nose. With modern computer graphics, such techniques may become important, in particular if the development of the methods is accompanied by an investigation of which features of real human faces are important for recognition.

Audible representation of multivariate data

The characteristics of acoustic signals—pitch, loudness, damping, direction, duration/repetition and rest periods—may be used to represent multidimensional patterns.[47] The pitch may, for instance, because of its large dynamic range of perception by humans, represent as many as nine dimensions. In fact, by controlling the characteristics mentioned above, it is possible to synthesize a signal which represents about twenty dimensions. A human operator can then be trained by listening to one class of data at a time. The technique has been tested with various operators on a set of archaeological data[60] and high classification accuracies have been obtained. It is amusing to observe that while a number of workers have used pattern recognition to analyse and identify music, an almost reversed procedure is valuable for chemists. Combined efforts are likely to give interesting results.

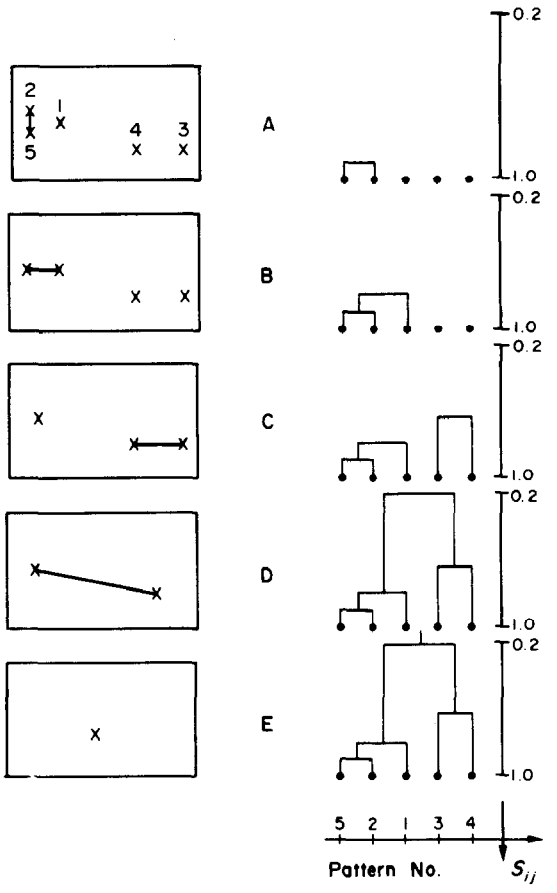


Fig. 6. Hierarchical clustering of patterns with the corresponding dendrogram.

CLUSTER ANALYSIS

Cluster analysis provides for unsupervised learning a useful means of detecting the existence of groups of similar objects in high-dimensional space.[10,18,42,54,61–66] The aim of cluster analysis is to divide the data into subsets (clusters) such that the similarity of the objects within any subset is greater than their similarity to members of other subsets.

The method most commonly used in cluster analysis of chemical data is the so-called hierarchical clustering method "hier".[16] First, the similarities of any pair of patterns are computed and saved in a matrix. Next, this matrix is searched for its maximum value. This identifies the two patterns of highest similarity. These patterns are now replaced by one pattern at their centre of gravity. Subsequently, a new similarity matrix is computed based on this reduced data set, and so forth, until all patterns eventually have been joined in one cluster. Various criteria can be used for halting the process: (*a*) the number of clusters can be preselected by the operator, (*b*) a threshold similarity level can be defined, and (*c*) a maximum can be preselected for the rate of change of similarity level necessary to obtain the next cluster.

Figure 6 illustrates hierarchical clustering applied to five patterns (Fig. 6, A); the bars between pairs of patterns indicate which patterns are to be joined in the next cycle. The right-hand part of Fig. 6 shows the construction of the corresponding *dendrogram*. The dendrogram joins patterns by a connection having a height which reflects the similarity S_{ij}. Visual inspection of the figure clearly shows two main clusters. This shows up in the "similarity jump" in going from C to D.

Cluster analysis is frequently used for preliminary feature selection: a feature-similarity measure may, for example, be defined by means of the feature correlation coefficient and a dendrogram of feature correlations may give an idea of which features may be left out.

The problems dealt with in cluster analysis have analogies in *operational research* and may be approached accordingly.[65,67] Cluster formation may, for example, be thought of as equivalent to siting distribution-centres so that transportation costs are minimized. While, for the siting problem, the number of distribution-centres may be known in advance, the number of clusters in cluster analysis is mostly unknown. A criterion which may be used to determine the number of significant clusters (p) is that the elements of any cluster must be definitively separated from all other elements.[65] The objects shown in Fig.

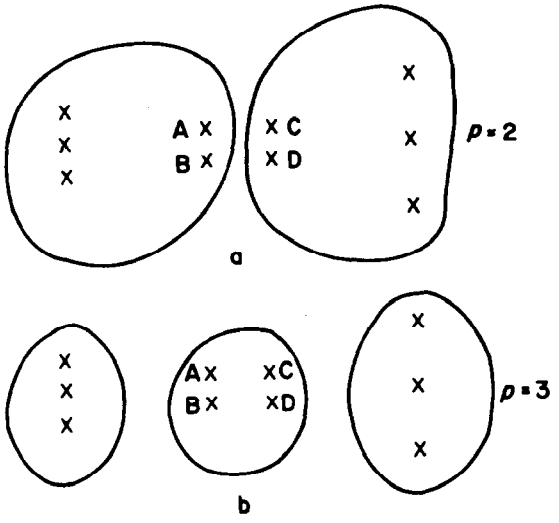


Fig. 7. Insignificant ($p = 2$) and significant clustering ($p = 3$).

7a can be seen intuitively to fall in three clusters. If initially the number of clusters is chosen as $p = 2$, the objects A and B fall in one cluster, while C and D fall in another. If $p = 3$ is used, A, B, C and D leave their original clusters and join with members of another cluster (Fig. 7b). The $p = 2$ solution is hence considered insignificant.

The methods and terminology used in cluster analysis are also related to the field of graph theory:[61] various types of *trees*, *e.g.*, the minimal-spanning tree, have been used for unsupervised learning on chemical data.[18,43,61,64] A minimal-spanning tree is created by connecting patterns in n-dimensional space such that the sum of the interconnecting lines is minimal. Clusters are "pruned" from the tree by breaking lines with lengths greater than the average distance multiplied by some preselected factor, provided such breaking does not isolate a single pattern as a cluster.

The creation of trees may be very demanding with respect to computer memory size and computer time: for example, for a large data base containing 1000 patterns, a 1000 × 1000/2 matrix is necessary to hold the interpattern distances. Recently, an algorithm has been proposed for the creation of trees in such situations.[64] This algorithm adds one pattern at a time to the tree and assigns to all branching vertices the average value of all underlying patterns. The introduction of a new pattern requires at any branching point the calculation of only three distances. The tree obtained by this method depends somewhat on the sequence in which the patterns are presented to the algorithm.

SUPERVISED LEARNING, CLASSIFICATION

The goal of supervised learning techniques is to develop classification rules which accurately predict the classification of unknown patterns, and are based on the availability of a training set.[4,16,49] To some extent, the clustering techniques and mapping methods previously discussed can be used for classification, but the rules of supervised learning methods assign patterns unambiguously (and, it is hoped, correctly) to known classes. The process of improving classification rules on the basis of their prediction performance is referred to as training.

Classification procedures can be characterized as either *parametric* or *non-parametric*.

Parametric methods

The parametric methods assume that probability density functions of the features are known or can be estimated.[16] In such cases, the Bayes theorem from classical statistics can be used to derive a *discriminant function*, *i.e.*, a function the value of which can be used for class assignment.[45] For a p-class problem, the discriminant function for the jth class is the product $d_j = P(\bar{X}/j)\,P(j)$, for j from 1 to p, where $P(\bar{X}/j)$ is the *class conditional probability* for class j and $P(j)$ the *a priori probability* of the occurrence of class j. The *a priori* probability may for example, if the p classes of the training set are of similar size, be taken as $\overline{1}/p$. $P(\bar{X}/j)$ might be taken as the multivariate normal distribution, computed from the mean vector and the covariance matrix of class j. To classify a pattern X, d_j for that pattern is then computed for all classes, and the class which yields the maximum value is then selected. Bayes discriminant functions have recently been used successfully to classify crude oils on the basis of GLC-data.[45]

If reasonable assumptions about the probability density functions can be made, it is possible to estimate the probability of correct classification, or the classification risk.[68] Unfortunately, such assumptions mostly cannot be made, *e.g.*, because only a limited data set is available for the analysis. Hence non-parametric methods have been used in the majority of studies reported.

Non-parametric methods

When no reasonable assumptions about probability densities can be made, classification is in general done by using measures of nearness to patterns of known classes. There are a number of approaches.

Classification by nearness of centre of gravity. The nearness of an unknown pattern to a class can be defined as its distance from the average value of all known patterns belonging to that class, *i.e.*, the centre of gravity of the class. This approach has been useful for the interpretation of steroid mass spectra,[69] for example.

The k *nearest neighbour rule.* The k nearest neighbour classification rule (kNN) assigns to any pattern the class determined by the majority vote of the k nearest patterns, where k is a small odd integer. This rule has had a remarkable success for many classification problems.[18,26,32,37,42,51,52,55,61,66,70–73] Figure 8(I) suggests a reason for this. Here patterns of

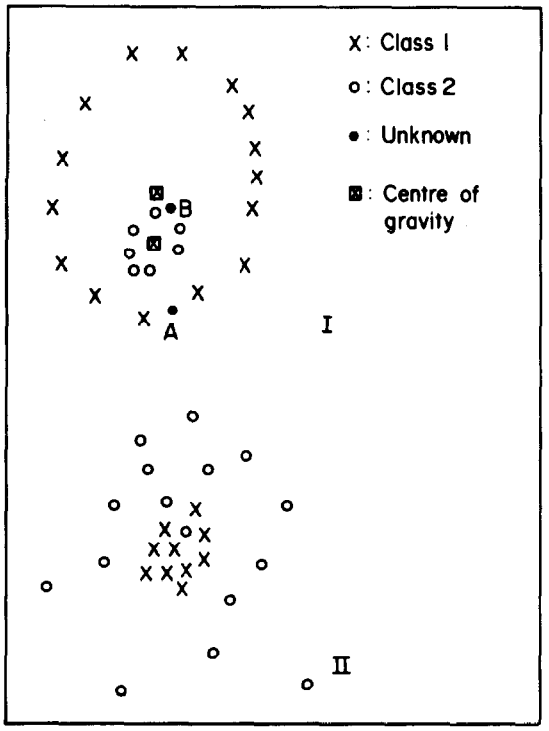


Fig. 8. I, Data structure for which classification according to the k nearest neighbour rule is adequate. II, An asymmetric case.

the training set fall within two clusters: one ring-shaped cluster of class 1 patterns surrounding a cluster of all class 2 patterns. It is reasonable to believe that pattern A belongs to class 1 while B belongs to class 2, *i.e.*, as predicted by the kNN-rule, but if nearness to the centre of gravity is employed as a classification criterion, the opposite classification would result. Furthermore, any attempt to separate classes by a hyperplane (see below) will fail for this data structure. The data structure shown in Fig. 8(II)—an *asymmetric* case,[74] where one tight cluster of samples sharing a common property is surrounded by the diffuse class of samples not having that property—may still, in favourable cases, be treated adequately by the kNN-rule.

The choice of the best value of the number k of voting committee neighbours has been discussed.[6,68] For a data set of limited size, $k = 1$ is a reasonable choice, but in the case of overlapping classes, $k = 3$ or possibly $k = 5$ may improve the prediction performance.

The kNN method is a multiclass method and its implementation is easy. Unfortunately, the computation time involved is large, since for each pattern in the prediction-set all distances to the training-set patterns should be computed. A pattern which is completely surrounded by other patterns of similar class contains little information about the region where classes come close together. Such patterns may be removed from the training set by a *condensation procedure* and a smaller training set with similar performance be defined.[9,30]

Decision surface classification. Classification of patterns may be accomplished by locating surfaces in n-dimensional space such that patterns of one class are separated from those of another class by these *decision surfaces.* Numerous papers deal with this approach to pattern recognition. In particular, the possibility of positioning linear (flat) decision surfaces in pattern space has interested many workers. The approach most commonly used is shown in Fig. 9. Here two classes of 2-dimensional patterns, in the plane PS, should be separated by a hyperplane, the dimension of which is 1 less than the dimension of the pattern space (in this case a line). To simplify the procedure, the pattern space is augmented with an extra orthogonal dimension A, such that the pattern space is now the hyperplane (F1, F2, d): d is mostly defined as unity. The plane HP can be moved around the only fixed point 0, and the position of the plane and hence the line L can be unambiguously described in terms of a vector **W**, the *weight vector*, normal to HP. For any direction of **W**, the position of a given pattern P with respect to HP and hence the line L can be computed from the scalar (or dot) product of **W** and the pattern vector **P**:

$$\mathbf{W}\cdot\mathbf{P} = |\mathbf{W}||\mathbf{P}|\cos\theta$$

The sign of this scalar product determines the side of HP and L on which P is located. Once the plane has

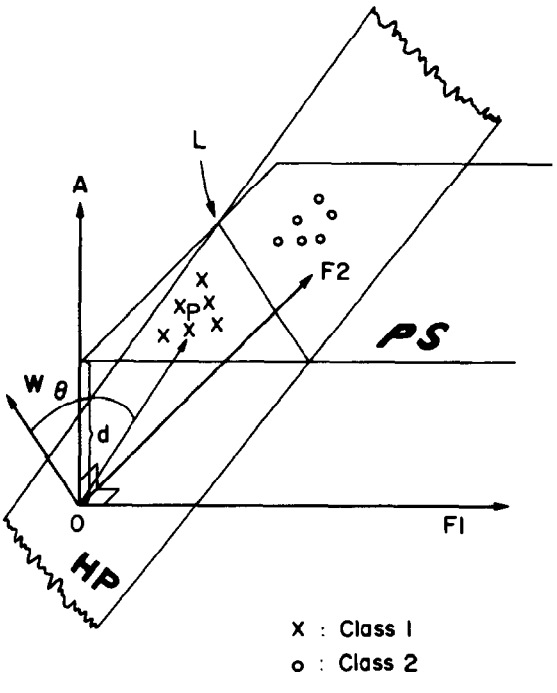


Fig. 9. Linear 2-dimensional decision surface, HP, separating classes in the 2-dimensional pattern space PS. **W**: weight vector. L: one-dimensional decision surface. A: extra dimension added to ensure that HP passes through the origin, 0.

been located, the classification of new patterns requires very little arithmetic: computation of the sign of the product is sufficient for prediction. Such algorithms, which take as input a pattern vector and a weight vector and outputs a binary result, +1 or −1, are often referred to as threshold logic units (TLUs).

The classification problem can now be stated as the problem of determining the weight vector such that the two classes are separated by L. An iterative procedure, the *linear learning machine* (*LLM*), can be used for this purpose:[4,5,8] first, the initial value for the weight vector is arbitrarily chosen. All patterns in the training are subsequently presented to the TLU, which in turn, from the sign of the scalar product, suggests the class of the pattern considered. If this classification is correct, the procedure goes on to the next pattern. If, however, the pattern is misclassified, the hyperplane is moved so that the pattern is classified correctly, *i.e.*, situated on the opposite side of the plane. This *error correction feed-back* amounts to computing a new weight vector $\mathbf{W}'$ such that $\mathbf{W}' = \mathbf{W} + C\mathbf{X}_i$, where $\mathbf{X}_i$ is the vector for the misclassified pattern. The constant C is usually $C = -2\mathbf{W}\cdot\mathbf{X}_i/\mathbf{X}_i\cdot\mathbf{X}_i$.

It can be shown that this procedure, when repeated, will find a discriminating plane *if one exists*. Applications of the linear learning machine are currently being reported.[22,66,75,76]

The chemical/physical significance of a separating hyperplane is strongly dependent on the ratio of the number of training-set patterns to the dimensionality of the data.[27–29] A low ratio and noisy irrelevant features may lead to perfect but meaningless separation.

In *multiple discriminant function analysis*, several TLUs are used to constitute a voting committee. The classification result then depends on the decision of each individual TLU and the rules set for the committee decision: simple majority, unanimous (which may result in no decision), *etc.*[77]

For data structures such as those shown in Fig. 8, for example, no separating hyperplane exists. In such cases, a stepwise linear discriminating function may be used.[78] Linear learning machines have also been implemented by *analogue circuitry* and feed-back mechanisms.[79]

It is the experience of most workers within the field of chemical pattern recognition that linear separability of classes is the exception. A number of papers describe methods of finding optimum hyperplanes which misclassify the fewest patterns. *Simplex* techniques, operating in *response space* can be used to find the optimum response, *i.e.*, to determine the weight vector associated with the optimum hyperplane. This is done by successively replacing the worst weight vector (out of a preselected set of d + 1 weight vectors where d is the pattern-space dimension) by its reflected image with respect to the centroid of the remaining weight vectors.[80–83] An optimum decision

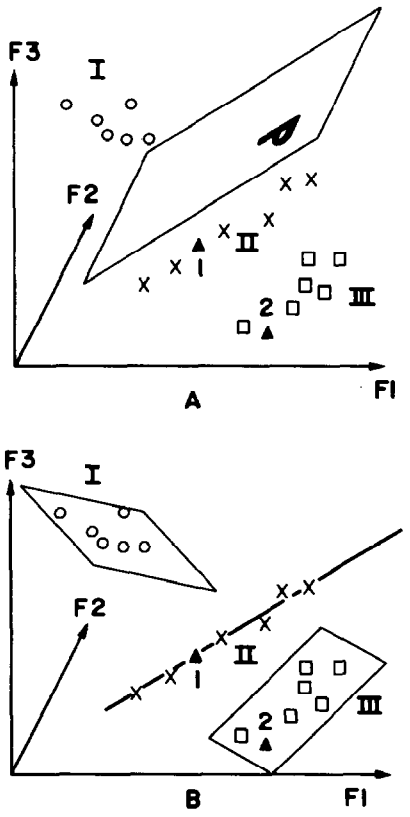


Fig. 10. Classification of unknown patterns. (A) Discriminant function approach. (B) Individual class modelling.

hyperplane may also be obtained by linear regression analysis.[52,84]

Individual class modelling: the SIMCA approach. The decision surface approach is applicable to problems where any unknown pattern should be assigned to one out of a *known* number of different classes. Assumptions about the number of classes must be made with great caution, since errors here may result in misleading classification. This is illustrated in Fig. 10A. Here the data available for training belong to the two classes I and II. A discriminant function could for example be the plane P. If the unknown pattern, 1, is presented to the decision algorithm, a sensible classification (II) would result. The same classification would be given to the unknown pattern, 2, although this pattern is more likely to belong to a third class (III), which was unfortunately not represented in the training set.

The SIMCA method[20,23–25,31,51,52,85–89] associates with any known class an individual mathematical model, such that an unknown pattern can be compared with each class model to check whether it falls within the "normal" interval for that class, or whether it is more likely to belong to some other distribution, *i.e.*, is an "*outlier*" with respect to known classes.

The mathematical model used by SIMCA to describe the qth of L classes containing N n-dimensional

patterns, is a principal-component model:

$$y_{ik}^{q} = \alpha_i^q + \sum_{a=1}^{A_q} \beta_{ia}^q O_{ak}^q + \epsilon_{ik}^q;$$

$$k = 1, N; i = 1, n; q = 1, L$$

where the parameters α and β describe the systematic part of the data (the signal) and the residuals ϵ describe modelling and measurement errors.

An important feature of the SIMCA method is its ability to handle classes of unequal dimensionalities: in the example of Fig. 10, the classes I and III are close to a planar distribution, while class II can be safely described by only one dimension (Fig. 10B). The initial step in the SIMCA method, "cross-validation",[20,87] aims at determining the dimensionality of each known class by fitting the model to various class subsets and studying, as a function of A_q, how well the model describes the remaining patterns. Clearly, if, in Fig. 10, the linearity of cluster II has been discovered, the pattern 2 would immediately be characterized as an outlier rather than a member of cluster II.

Once the dimensionality of a class is established, the parameters of the model are established by methods such as eigenvector decomposition or by the "NIPALS" algorithm,[90] a modification of which has the advantage that it is capable of handling data matrices which are incomplete owing to missing observations. The analysis yields an estimate of a limiting residual variance of the class. Unknown patterns can then be classified by fitting them into the various class models. If a pattern falls within a given range defined by the model plus or minus the standard deviation, this suggests the classification.

Binary decision trees. Computerized library search has frequently been successfully used for the classification of unknowns. Unfortunately, as libraries grow, such methods turn out to be rather demanding with respect to computer resources. A combination with the statistical techniques of pattern recognition may, however, increase the efficiency of library search methods.

A useful aid in the matching procedure and means of estimating the likelihood of the existence of certain properties of unknowns is the structuring of the data file according to the rules referred to as a *decision tree*.[91,92]

Figure 11 illustrates the creation of a decision tree based on the twelve schematic patterns a–l, with 4 binary-coded features f1–f4. By some method, the importance of the features for classification has been ranked as f3 > f1 > f2 > f4. The patterns are now sequentially presented to a binary classification algorithm operating on f3, and the patterns are passed on along two branches (a, g, i, j, k, l) and (b, c, d, e, f, h) to subsequent decisions at the next level. For each branch, the fractions of class 1 and class 2 patterns on that branch are given with the class-1 fraction above the horizontal line and the class-2 fraction below it. Normally, trees are considerably more complex than Fig. 11 suggests. At each terminal node of the tree, the ratio of class-1 patterns to class-2 patterns reaching that node is given. This number, combined with the *a priori* probability of the classes, gives an indication of how to classify an unknown which reaches that node.

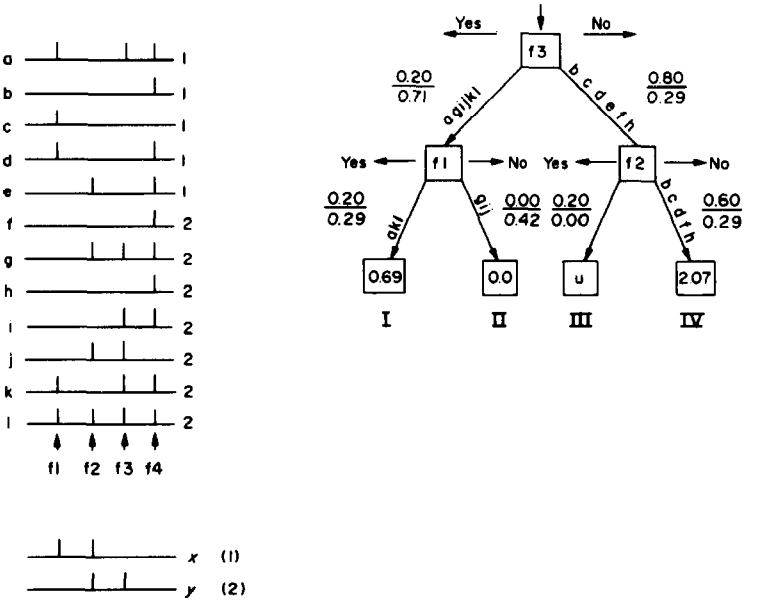


Fig. 11. Binary decision tree for classification of x and y. Patterns a–l comprise the training set. The importance of features is ranked f3 > f1 > f2 > f4. u: undefined fraction.

FEATURE SELECTION

We have already discussed techniques of feature selection. These methods were based on the statistical distributions of the classes within the training set. Once features have been selected and classification algorithms have been tested, there are additional means of reducing the dimension of the pattern space. These methods exploit the information obtained during classification, and generally attempt to reduce the number of features while preserving predictive ability.

The weight-sign feature-selection method may be used in conjunction with applications of the linear learning machine:[93] initially two weight vectors are chosen, with different co-ordinates, and subsequently trained. After convergence has been achieved, the trained weight-vectors are compared. Those components which have opposite signs are regarded as non-intrinsic (*i.e.*, they do not contribute to linear separability) and are discarded. The feature selection is repeated until no more non-intrinsic features are found. When in binary-coded patterns more than one feature is eliminated by this method, special care should be taken to avoid the feature elimination resulting in a contradiction, where two patterns of opposite class merge into one.[94]

For data with linearly separable classes, the *variance feature selection* method is also applicable.[95] This method exploits knowledge of the components of several individually trained weight-vectors, the philosophy being that components which exhibit a large variation across the set of trained weight-vectors are the least important.

Unfortunately, the above-mentioned methods are only applicable in the case of linear separability of classes. When the linear learning machine is not appropriate, and, for example, the kNN classification-rule is used, there is no simple method of exploiting the classification results for feature-ranking. Here an interactive computerized method has proved adequate.[70] First, all patterns are classified, by use of only one feature at a time. Next, subsets of the potentially best features are retained for multidimensional analysis. The operator may interact with the method, for example by selecting subsets on the basis of histogram displays for the individual features.

A feature-weighting method for kNN-analysis, which is also appropriate for feature selection, was recently reported.[71] Here a smooth error function is developed and for each pattern an error term is accumulated during prediction. This accumulated error is closely related to the classification accuracy. A gradient analysis is subsequently carried out to find those feature weights which produce the minimum classification error.

EVALUATION OF CLASSIFICATION PERFORMANCE

Before a classification rule can be used for prediction about unknown samples, its performance on the known training set must be tested. The test may be carried out, for example, by the *leave one out* method,[68] where one pattern at a time is removed from the training set and classified by the remaining patterns.

The classification performance should be evaluated and stated for each class separately,[13] since a pooled performance measure may be strongly misleading. This is obvious if a training set comprising two classes, I containing 98% of all patterns and II containing only 2% of the patterns, is considered. A classification rule which blindly assigns any pattern to class I will for this case have a high overall classification performance, but the performance evaluated separately on class II immediately suggests that some other classification rule should be developed.

In principle, the efficiency of classification methods can be assessed by comparing percentages of correct classification. However, the results of such comparisons are often strongly dependent on the nature of the data. Moreover, when small data sets are studied (which is very often the case), the significance of the percentages cannot be estimated. That is why, in the present review, such comparisons have been deliberately omitted.

Besides evaluation of the classification performance, it is important for the chemist to evaluate the *usefulness* of the pattern recognition analysis. A classification rule with relatively low performance may still assist the chemist in selecting, among a large number of samples, subsets for further experimental investigations. On the other hand, the chemist should not be guided solely by a high prediction performance, unless he has had a close look at those few patterns which were misclassified by the algorithm—such patterns might in unfortunate cases turn out to be those where human judgement also goes wrong, in which case the pattern recognition analysis is of little use.[96] In general, when estimating the significance of classification performance, the chemist should be extremely careful and critically evaluate the relations between the classes and features used.[97]

SELECTED APPLICATIONS

Spectrometry

A very large proportion of the published work on chemical pattern recognition is concerned with the interpretation of complex spectral information.

Mass spectra. These are often complicated by the large number of *m/e* peaks. Pattern recognition methods have been used to search for the most important features in mass spectra and to predict molecular structures and substructures,[38,55,69,78,81,83,84,95,98–103] and comparisons of the pattern recognition approach with other interpretive systems been made.[72,104] The application of combined GC/MS-data[55,105] and combination with library search of structured files[92] is likely to result in methods of great utility for the practising analyst.

NMR spectra. Carbon-13 NMR spectra have been used for pattern recognition identification of functional groups.[34,39,68,77,85,106] A study of dithiocarbamate compounds, where carbon-13 NMR data were concatenated with infrared spectroscopic data, provides a good illustration of the potential power of multisource methods.[18]

Infrared spectra. Functional-group identification by pattern recognition analysis of infrared spectra has been reported by a number of workers.[73,91,107–111] The combination of infrared and Raman spectra has produced improved classification results.[22]

X-Ray spectra, atomic absorption/emission, neutron activation. Pattern recognition applied to (trace) elemental data obtained from X-ray spectra,[60,112] atomic-absorption and emission spectrometry[62,63] and neutron-activation analysis[50,51,113,114] has been successfully used to classify complex mixtures. The (trace) elemental composition of samples is frequently of interest in archaeological research,[60,113–115] environmental investigations[51] and forensic analysis.[50,63] Atomic-emission data have been used to determine the trace elemental distribution in wines. However, pattern recognition analysis showed that the elements did not contribute significantly to the gustatory qualities of the wines.[116,117]

Other spectra. Carbon Auger spectra have been analysed and used for chemical characterization.[118] Atomic spectral transitions have been classified according to configuration.[119,120] Antibacterial "spectra" of biologically active compounds have also been studied (a "spectrum" here is a measure of the activity of the compound against a reference set of bacteria).[54]

Chromatography

Several papers report the interpretation of retention data by pattern recognition.[121–125] Interesting studies on beverages have been published. Pattern recognition applied to GLC-data can be used to detect counterfeit whisky,[52] and the result of a subjective sensory evaluation of wines compares well with the findings from principal-components analysis of GLC data.[116] A GLC-study on monofunctional compounds showed that structural information could be obtained from retention data by pattern recognition methods.[66] The identification of oil samples by means of their chromatograms has also been reported.[45,126]

Electrochemistry

Electroanalytical methods are generally characterized by high sensitivity, but the selectivity is often poor. A number of pattern recognition studies show, however, that even severely overlapping voltammetric peaks may be detected when curve shape features are used.[30,32,33,127,128] Quantitative determinations of interfering heavy metals in solution were obtained by anodic-stripping voltammetry and staircase polarography and subsequent application of the linear learning machine.[75,79]

Classification of electroactive organic compounds[26] and characterization of heterogeneous kinetic parameters from voltammetric data[37] have been reported. The results suggest that the possibilities of qualitative electroanalysis should be further investigated.

Pattern recognition studies on chemical activity

This field of research attempts to predict chemical activity from structural features and physical/chemical parameters.

The stability of complex hydrides has been related to ligand size-parameters and to parameters such as covalent radii and ionization potentials of atoms.[23–25]

Several workers have studied the dependence of biological activity such as carcinogenicity and drug activity on structure.[3,15,54,61,74,129,130]

The cost and tedium of screening procedures where a large number of compounds are to be tested for some property can undoubtedly be significantly reduced if knowledge of such structure–activity relationships is properly exploited.

Other applications

Although a "pattern" of typical fields of application of chemical pattern recognition is rather well defined by now, new promising ways of exploiting the methods are still being found.

Prediction of long-term behaviour. When evaluating the potential practical applications of a chemical system, the chemist is frequently interested in the long-term behaviour of the system. A recent pattern recognition study has shown that the long-term behaviour of spacecraft cells can be correlated to observations made during a short period of time when the cells were charged.[42] In almost any situation, a reliable prediction of future behaviour is an invaluable piece of information; hence this branch of chemical pattern recognition is likely to develop further in the near future.

Selection of analytical techniques. The selection of the optimum instrumental technique for solving a given analytical problem is a multivariate problem of high dimensionality. Several features—accuracy, analysis time, price, concentration range, sample matrix, *etc.*—should influence the decision. A recent paper shows that pattern recognition is a possible way of reaching a conclusion.[76]

This study used, as the training set, patterns composed of experimental conditions and measures of analytical performance, taken from the literature. Classes were associated with the choice of instrument. For certain analytical problems, it was possible (by using a linear decision surface) to predict with good accuracy the instrumental method to choose.

CONCLUDING COMMENTS

Several very impressive results have been published

during the first decade of chemical pattern recognition. Naturally, these results have been obtained mainly by chemists engaged in developing the techniques. However, as pointed out in a recent review,[11] the field is now approaching the mature state: complete program packages are now available for the analytical chemist who is basically interested in the applications. At present, it seems very likely that pattern recognition will eventually become a well established approach to the analysis of multivariate chemical information. Innovations such as individual class modelling, the incorporation and propagation of analytical error, and applications to quantitative analysis will undoubtedly have a strong impact on the development in the near future. An accurate prediction of the utility and future success of chemical pattern recognition cannot, however, be made until more users have had a chance to become acquainted with the methods. In the present phase, the educational aspects therefore seem crucial. Pattern recognition, like any other new method, runs the risk of being rejected if users have been informed of the advantages of the technique but not of the limitations. In particular, the attention of anybody practising pattern recognition should be directed to the fact that the approach is of statistical nature. Misinterpretation of results and frustration are likely to occur if small, non-representative data sets are used. Because of the time and cost involved in acquiring chemical data, there has been an understandable tendency to apply pattern recognition analysis to small sets of data—probably sometimes too small. Another pitfall appears to be the beauty of the linear learning machine algorithm which easily misleads users into trusting blindly in the linear separability of their data.

The rapid development of instrumental analytical techniques and the steadily decreasing prices of computers will undoubtedly affect the development of chemical pattern recognition. Generally, in the years to come, chemical data will be easier to acquire and the data shortage problem may be diminished. The application of a number of accurate pattern recognition methods has previously been restricted to small data sets because the available computers were either too slow or could not hold the necessary data matrices. The availability of fast and cheap processors and storage devices will make analysis of even large volumes of data feasible without turning to approximate algorithms.

In conclusion, we shall re-emphasize what has previously been pointed out by several workers: like any other numerical/statistical method, pattern recognition cannot be expected to produce any useful answers unless relevant questions are asked about quality data. There is really no substitute for the experimental skill and chemical background knowledge of the chemist. It is therefore of crucial importance that chemists, even in the future when access to chemical data will be facilitated through data banks and computer networks, should critically evaluate the data quality and, preferably, not lose contact with laboratory work.

Acknowledgements—The author wishes to thank Lisbeth Heilesen for typing this manuscript and Arne Lindahl for preparing the illustrations.

REFERENCES

1. B. R. Kowalski (ed.), *Chemometrics: Theory and Application*, ACS Symposium Series 52, American Chemical Society, Washington D.C., 1977.
2. P. C. Jurs and T. L. Isenhour, *Chemical Applications of Pattern Recognition*, Wiley, New York, 1975.
3. A. J. Stuper, W. E. Brugger and P. C. Jurs, *Computer Assisted Studies of Chemical Structure and Biological Function*, Wiley, New York, 1979.
4. C. E. Klopfenstein and C. L. Wilkins (eds.), *Computers in Chemical and Biochemical Research*, Vol. 2, Academic Press, New York, 1974.
5. P. R. Griffiths (ed.), *Transform Techniques in Chemistry*, Plenum Press, New York, 1978.
6. R. O. Duda and P. E. Hart, *Pattern Recognition and Scene Analysis*, Wiley, New York, 1973.
7. Yi-tzuu Chien, *Interactive Pattern Recognition*, Dekker, New York, 1978.
8. N. J. Nilsson, *Learning Machines*, McGraw-Hill, New York, 1965.
9. K. Fukunaga, *Introduction to Statistical Pattern Recognition*, Academic Press, New York, 1972.
10. B. Everitt, *Cluster Analysis*, Halsted Press, New York, 1974.
11. B. R. Kowalski, *Anal. Chem.*, 1980, **52**, 112R.
12. D. L. Massart and Y. Michotte, *Bull. Soc. Chim. France*, 1979, I-293.
13. K. Varmuza, *Anal. Chim. Acta*, 1980, **122**, 227.
14. P. S. Shoenfeld and J. R. DeVoe, *Anal. Chem.*, 1976, **48**, 403R.
15. J. R. McGill and B. R. Kowalski, *ibid.*, 1977, **49**, 596.
16. B. R. Kowalski and C. F. Bender, *J. Am. Chem. Soc.*, 1972, **94**, 5632.
17. D. L. Duewer, B. R. Kowalski and J. L. Fasching, *Anal. Chem.*, 1976, **48**, 2002.
18. F. W. Pijpers, H. L. M. Van Gaal and J. G. M. Van der Linden, *Anal. Chim. Acta*, 1979, **112**, 199.
19. E. R. Malinowski, *Abstract Factor Analysis—A Theory of Error and its Application to Analytical Chemistry*, in Reference 1, p. 53.
20. S. Wold, *Pattern Recognition*, 1976, **8**, 127.
21. P. C. Jurs, B. R. Kowalski, T. L. Isenhour and C. N. Reilly, *Anal. Chem.*, 1969, **41**, 1949.
22. J. M. Comerford, P. G. Anderson, W. H. Snyder and H. S. Kimmel, *Spectrochim. Acta*, 1977, **33A**, 651.
23. O. Štrouf and S. Wold, *Acta Chem. Scand.*, 1977, **A31**, 391.
24. S. Wold and O. Štrouf, *ibid.*, 1979, **A33**, 521.
25. *Idem*, *ibid.*, 1979, **A33**, 463.
26. D. R. Burgard and S. P. Perone, *Anal. Chem.*, 1978, **50**, 1366.
27. G. L. Ritter and H. B. Woodruff, *ibid.*, 1977, **49**, 2116.
28. C. P. Weisel and J. L. Fasching, *ibid.*, 1977, **49**, 2114.
29. N. A. B. Gray, *ibid.*, 1976, **48**, 2265.
30. Q. V. Thomas and S. P. Perone, *ibid.*, 1977, **49**, 1369.
31. S. Wold and M. Sjöström, *SIMCA: A Method for Analyzing Chemical Data in Terms of Similarity and Analogy*, in Reference 1, p. 243.
32. R. A. DePalma and S. P. Perone, *Anal. Chem.*, 1979, **51**, 825.
33. Q. V. Thomas, R. A. DePalma and S. P. Perone, *ibid.*, 1977, **49**, 1376.

34. T. R. Brunner, C. L. Wilkins, R. C. Williams and P. J. McCombie, *ibid.*, 1975, **47**, 662.
35. P. C. Jurs, *ibid.*, 1971, **43**, 1812.
36. C. L. Wilkins and P. C. Jurs, *Fourier and Hadamard Transforms in Pattern Recognition*, in Reference 5, p. 307.
37. R. A. DePalma and S. P. Perone, *Anal. Chem.*, 1979, **51**, 829.
38. B. R. Kowalski and C. F. Bender, *ibid.*, 1973, **45**, 2234.
39. T. R. Brunner, R. C. Williams, C. L. Wilkins and P. J. McCombie, *ibid.*, 1974, **46**, 1798.
40. M. Ichise, H. Yamagishi and T. Kojima, *J. Electroanal. Chem.*, 1978, **94**, 187.
41. M. Ichise, H. Yamagishi, H. Oishi and T. Kojima, *ibid.*, 1980, **108**, 213.
42. W. A. Byers and S. P. Perone, *J. Electrochem. Soc.*, 1979, **126**, 720.
43. A. M. Harper, D. L. Duewer, B. R. Kowalski and J. L. Fasching, *ARTHUR and Experimental Data Analysis: The Heuristic Use of a Polyalgorithm*, in Reference 1, p. 14.
44. P. D. Gaarenstroom, S. P. Perone and J. L. Moyers, *Environ. Sci. Technol.*, 1977, **11**, 796.
45. H. A. Clark and P. C. Jurs, *Anal. Chem.*, 1979, **51**, 616.
46. B. R. Kowalski and C. F. Bender, *Pattern Recognition*, 1976, **8**, 1.
47. E. S. Yeung, *Anal. Chem.*, 1980, **52**, 1120.
48. B. R. Kowalski and C. F. Bender, *J. Am. Chem. Soc.*, 1973, **95**, 686.
49. B. R. Kowalski, *Anal. Chem.*, 1975, **47**, 1152A.
50. D. L. Duewer and B. R. Kowalski, *ibid.*, 1975, **47**, 526.
51. D. L. Duewer, B. R. Kowalski and T. F. Schatzki, *ibid.*, 1975, **47**, 1573.
52. B. E. H. Saxberg, D. L. Duewer, J. L. Booker and B. R. Kowalski, *Anal. Chim. Acta*, 1978, **103**, 201.
53. J. W. Sammon, Jr., A. H. Proctor and D. F. Roberts, *Pattern Recognition*, 1971, **3**, 37.
54. Y. Takahashi, Y. Miyashita, H. Abe, S. Sasaki, Y. Yotsui and M. Sano, *Anal. Chim. Acta*, 1980, **122**, 241.
55. J. N. Ziemer, S. P. Perone, R. M. Caprioli and W. E. Seifert, *Anal. Chem.*, 1979, **51**, 1732.
56. Chi-Hsiung Lin and Hwa-Fu Chen, *ibid.*, 1977, **49**, 1357.
57. H. Drack, *ibid.*, 1978, **50**, 2147.
58. T. J. Nestrick, L. L. Lamparski and D. I. Townsend, *ibid.*, 1980, **52**, 1865.
59. H. Chernoff, *J. Am. Stat. Assoc.*, 1973, **58**, 361.
60. B. R. Kowalski, T. F. Schatzki and F. H. Stross, *Anal. Chem.*, 1972, **44**, 2176.
61. K. C. Chu, *ibid.*, 1974, **46**, 1181.
62. J. Webb, W. Niedermeier, J. H. Griggs, K. A. Kirk, M. E. Turner and T. N. James, *Anal. Chim. Acta*, 1976, **81**, 143.
63. P. J. Simon, B. C. Giessen and T. R. Copeland, *Anal. Chem.*, 1977, **14**, 2285.
64. J. Zupan, *Anal. Chim. Acta*, 1980, **122**, 337.
65. D. L. Massart, L. Kaufman and D. Coomans, *ibid.*, 1980, **122**, 347.
66. J. F. K. Huber and G. Reich, *ibid.*, 1980, **122**, 139.
67. D. L. Massart and L. Kaufman, *Anal. Chem.*, 1975, **47**, 1244A.
68. B. R. Kowalski and C. F. Bender, *ibid.*, 1972, **44**, 1405.
69. H. Rotter and K. Varmuza, *Anal. Chim. Acta*, 1977, **95**, 25.
70. M. A. Pichler and S. P. Perone, *Anal. Chem.*, 1974, **46**, 1790.
71. W. A. Byers and S. P. Perone, *ibid.*, 1980, **52**, 2173.
72. S. R. Lowry, T. L. Isenhour, J. B. Justice, Jr., F. W. McLafferty, H. E. Dayringer and R. Venkataraghavan, *ibid.*, 1977, **49**, 1720.
73. H. B. Woodruff and M. E. Munk, *Anal. Chim. Acta*, 1977, **95**, 13.
74. W. J. Dunn III and S. Wold, *J. Med. Chem.*, 1980, **23**, 595.
75. M. Bos and G. Jasink, *Anal. Chim. Acta*, 1978, **103**, 151.
76. B. G. M. Vandeginste, *Anal. Lett.*, 1977, **10**, 661.
77. C. L. Wilkins and T. L. Isenhour, *Anal. Chem.*, 1975, **47**, 1849.
78. N. M. Frew, L. E. Wangen and T. L. Isenhour, *Pattern Recognition*, 1971, **3**, 281.
79. M. Ichise, H. Yamagishi and T. Kojima, *J. Electroanal. Chem.*, 1980, **113**, 41.
80. G. L. Ritter, S. R. Lowry, C. L. Wilkins and T. L. Isenhour, *Anal. Chem.*, 1975, **47**, 1951.
81. T. Fai Lam, C. L. Wilkins, T. R. Brunner, L. J. Soltzberg and S. L. Kaberline, *ibid.*, 1976, **48**, 1768.
82. G. F. Brissey, R. B. Spencer and C. L. Wilkins, *ibid.*, 1979, **51**, 2295.
83. S. L. Kaberline and C. L. Wilkins, *Anal. Chim. Acta*, 1978, **103**, 417.
84. H. Rotter and K. Varmuza, *ibid.*, 1978, **103**, 61.
85. M. Sjöström and U. Edlund, *J. Magn. Resonance*, 1977, **25**, 285.
86. C. Albano, W. Dunn III, U. Edlund, E. Johansson, B. Nordén, M. Sjöström and S. Wold, *Anal. Chim. Acta*, 1978, **103**, 429.
87. S. Wold, *Technometrics*, 1978, **20**, 397.
88. S. Wold and K. Andersson, *J. Chromatog.*, 1973, **80**, 43.
89. S. Wold and M. Sjöström, *Linear Free Energy Relationships as Tools for Investigating Chemical Similarity—Theory and Practice*, in *Correlation Analysis in Chemistry*, N. B. Chapman and J. Shorter (eds.), p. 1. Plenum Press, New York, 1978.
90. H. Wold, in *Festschrift for Jerzy Neyman*, F. N. David (ed.), Wiley, New York, 1966.
91. M. Penca, J. Zupan and D. Hadži, *Anal. Chim. Acta*, 1977, **95**, 3.
92. W. S. Meisel, M. Jolley, S. R. Heller and G. W. A. Milne, *ibid.*, 1979, **112**, 407.
93. P. C. Jurs, *Anal. Chem.*, 1970, **42**, 1633.
94. Y. Miyashita, H. Abe, S. Sasaki and K. Yuta, *ibid.*, 1978, **50**, 1580.
95. G. S. Zander, A. J. Stuper and P. C. Jurs, *ibid.*, 1975, **47**, 1085.
96. J. T. Clerc, *Chimia*, 1974, **28**, 191.
97. J. T. Clerc, P. Nägeli and J. Seibl, *ibid.*, 1973, **27**, 639.
98. H. Abe and P. C. Jurs, *Anal. Chem.*, 1975, **47**, 1829.
99. D. W. Fausett and J. H. Weber, *ibid.*, 1978, **50**, 722.
100. P. C. Jurs, *Appl. Spectrosc.*, 1971, **25**, 483.
101. J. Vink, W. Heerma, J. P. Kamerling and J. F. G. Vliegenthart, *Org. Mass Spectrom.*, 1974, **9**, 536.
102. D. R. Burgard, S. P. Perone and J. L. Wiebers, *Biochemistry*, 1977, **16**, 1051.
103. L. Pietrantonio and P. C. Jurs, *Pattern Recognition*, 1972, **4**, 391.
104. F. W. McLafferty, *Anal. Chem.*, 1977, **49**, 1441.
105. K. Varmuza, *Monatsh. Chem.*, 1976, **107**, 43.
106. C. L. Wilkins, R. C. Williams, T. R. Brunner and P. J. McCombie, *J. Am. Chem. Soc.*, 1974, **96**, 4182.
107. B. R. Kowalski, P. C. Jurs, T. L. Isenhour and C. N. Reiley, *Anal. Chem.*, 1969, **41**, 1945.
108. D. R. Preuss and P. C. Jurs, *ibid.*, 1974, **46**, 520.
109. R. W. Liddell III and P. C. Jurs, *ibid.*, 1974, **46**, 2126.
110. H. B. Woodruff, S. R. Lowry, G. L. Ritter and T. L. Isenhour, *ibid.*, 1975, **47**, 2027.
111. J. S Mattson, C. S. Mattson, M. J. Spencer and F. W. Spencer, *ibid.*, 1977, **49**, 500.
112. W. Wegscheider and D. E. Leyden, *Advances in X-Ray Analysis*, 1979, **22**, 357.
113. J. R. McGill and B. R. Kowalski, *Appl. Spectrosc.*, 1977, **31**, 87.
114. M. De Bruun, P. J. M. Korthoven, C. C. Bakels and F. C. A. Groen, *Archaeometry*, 1972, **14**, 55.

115. G. J. Boulle and M. Peisach, *J. Radioanal. Chem.*, 1979, **50,** 205.
116. Wing-On Kwan and B. R. Kowalski, *Anal. Chim. Acta*, 1980, **122,** 215.
117. Wing-On Kwan, B. R. Kowalski and R. K. Skogerboe, *J. Agric. Food Chem.*, 1979, **27,** 1321.
118. S. W. Gaarenstroom, *J. Vac. Sci. Technol.*, 1979, **16,** 600.
119. K. L. Peterson and M. L. Parsons, *Phys. Rev. A*, 1978, **17,** 261.
120. K. L. Peterson, D. L. Anderson and M. L. Parsons, *ibid.*, 1978, **17,** 270.
121. E. Küllik, M. Kaljurand and M. Koel, *J. Chromatog.*, 1976, **126,** 249.
122. *Idem, ibid.*, 1975, **112,** 297.
123. G. Blomquist, E. Johansson, B. Söderström and S. Wold, *ibid.*, 1979, **173,** 19.
124. M. L. McConnell, G. Rhodes, U. Watson and M. Novotny, *ibid.*, 1979, **162,** 495.
125. A. Zlatkis, Kwan Young Lee, C. F. Poole and G. Holzer, *ibid.*, 1979, **163,** 125.
126. I. Lysyj and P. R. Newton, *Anal. Chem.*, 1972, **44,** 2385.
127. L. B. Sybrandt and S. P. Perone, *ibid.*, 1971, **43,** 382.
128. *Idem, ibid.*, 1972, **44,** 2331.
129. A. J. Stuper, W. E. Brugger and P. C. Jurs, *A Computer System for Structure-Activity Studies Using Chemical Structure Information Handling and Pattern Recognition Techniques*, in Reference 1, p. 165.
130. B. Nordén, U. Edlund and S. Wold, *Acta. Chem. Scand.*, 1978, **B32,** 602.

Talanta, Vol. 28, pp. 889 to 900, 1981
Printed in Great Britain. All rights reserved

0039-9140/81/120889-12$02.00/0
Copyright © 1981 Pergamon Press Ltd

SPECTROPHOTOMETRIC STUDY OF THE REACTION OF ZIRCONIUM WITH CHROME AZUROL S AND FLUORIDE

HISAHIKO EINAGA*
Institute of Materials Science, University of Tsukuba, Niihari, Ibaraki, 305, Japan

IWAJI IWASAKI
Faculty of Science, Toho University, Narashino, Chiba, 275, Japan

(*Received* 7 *May* 1980. *Revised* 11 *November* 1980. *Accepted* 22 *May* 1981)

Summary—A relatively simple and convenient procedure for the determination of small amounts of fluoride has been established. It is based on the decrease in absorbance when fluoride is added to a solution of the zirconium–Chrome Azurol S complex. Microgram amounts of fluoride can be determined with an error of better than about 2%. Some practical applications are presented.

Many methods for the spectrophotometric determination of fluoride have been based on reaction of fluoride with coloured metal chelate complexes,[1] producing either a mixed-ligand ternary complex or replacement of the ligand by fluoride to give a colourless metal–fluoride complex and the free ligand (with a colour different from that of the metal–ligand complex). The reaction of cerium(III) or lanthanum (III) with [3-*N*,*N*-di(carboxymethyl)aminomethyl]-1,2-dihydroxyanthraquinone (Alizarin Fluorine Blue) and fluoride[2–4] is of the first type, the fluoride entering the co-ordination sphere of the lanthanide ion. All the other methods fall into the second category. These include the zirconium–Eriochrome Cyanine R–fluoride, thorium–Alizarin–fluoride systems, *etc.*, and are indirect spectrophotometric methods. All suffer interference from metal ions, and drawbacks such as instability of colour, complexity of procedure, lack of reproducibility, *etc.* These difficulties may be attributed in part to intrinsic instability of the metal chelates used and in part to a lack of fundamental studies on the reaction systems to establish optimum conditions.

The present study aimed to establish a simple but convenient spectrophotometric method for the determination of fluoride by using its reaction with a metal chelate. The zirconium–Chrome Azurol S–fluoride system was chosen because it is a typical example of such a reaction and has not been systematically studied for analytical application.

EXPERIMENTAL

Reagents

Standard zirconium solution was prepared from analytical-reagent grade zirconium oxychloride, and kept slightly acidic with hydrochloric acid to prevent hydrolysis. It was standardized by a back-titration procedure with EDTA and copper(II), and PAN as indicator.[5]

Standard fluoride solution was prepared from sodium fluoride (analytical-reagent grade) recrystallized twice from water.

Chrome Azurol S (Dojindo Lab., Kumamoto and Tokyo Kasei Kogyo Ltd., Tokyo) was purified by repeated recrystallization from hydrochloric acid. The purity was checked by paper chromatography with acetic acid–ethanol–water (6:3:1 v/v). Both purified reagents behaved similarly and their aqueous solutions were used.

All other reagents were of analytical-reagent grade.

Apparatus

Absorption spectra were recorded with a Hitachi model EPS-3T spectrophotometer and absorbances at specified wavelengths were measured with a Hitachi model 139 spectrophotometer and a Japan Spectroscopic Co. model UVIDEC-320, at room temperature (20 ± 2°) with matched 1-cm quartz cells. A Horiba model F-5 pH-meter with glass and saturated calomel electrodes was used, and calibrated with 0.05 *M* buffers: oxalate (pH 1.68), phthalate (pH 4.00), and phosphate (pH 6.86). The standard values given in brackets all refer to 20°.[6] The standards for free hydrogen-ion concentration, $-\log[H^+] = 2.00$, were 0.0900 *M* sodium chloride/0.01 *M* hydrochloric acid for determination of the ligand protonation constants, and 0.390 *M* sodium chloride/0.0100 *M* hydrochloric acid for determination of the complex stability constants.

Recommended procedure

To a solution containing less than about 15 μg of fluoride, add 0.50 ml of 1.00 m*M* zirconium and 2.0 ml of 0.73 m*M* Chrome Azurol S, adjust to about pH 1.1 with 2*M* hydrochloric acid, and dilute to 25.0 ml with water. Measure the absorbance at 555 nm against a reagent blank after about 30 min, and calculate the fluoride content from the working curve obtained by similar treatment of fluoride standards.

RESULTS AND DISCUSSION

Purification of Chrome Azurol S

Chrome Azurol S (3,3′-dimethyl-5,5′-dicarboxy-4-hydroxyfuchsone-2″,6″-dichloro-3″-sulphonic acid, H_4chas) is formally a tetrabasic acid but can be con-

* To whom reprint requests should be sent.

sidered to behave as a pentabasic acid (H_5chas^+) in aqueous solution. It is prepared by the condensation reaction of 2,6-dichloro-3-sulphobenzaldehyde and *o*-cresotic acid but it usually contains some by-products which also form complexes with metal ions, *e.g.*, uranium(VI).[7] Langmyhr and Klausen[8] purified the commercial product by precipitation of the free acid with hydrochloric acid. Sommer and Kuban[9] obtained an 87.4–89.2% pure product by this procedure. Later, Malanik and Malát[7] tested a product purified in this way and claimed it contained both Chrome Azurol S and a "non-sulphonated" Chrome Azurol S (since one product isolated in the paper chromatography did not contain sulphur). In the present study a solution of the commercial product in water at about pH 5 was filtered and made about 6*M* in hydrochloric acid, then the precipitate was collected, dissolved in water, and the filtration/acidification step applied. The reprecipitation procedure was repeated several times, the final precipitate was washed with 6*M* hydrochloric acid and finally with ethanol, and the purified product was dried over silica gel and solid sodium hydroxide to constant weight. The dried product was assayed by potentiometric titration, and paper chromatography with acetic acid–ethanol–water (6:3:1 v/v). Some minor components were detected on the chromatograms of the unpurified reagents but only one spot (R_f 0.92) for the purified material. The final product had a Chrome Azurol S content of about 81%, corresponding to a heptahydrate.

A similar procedure was used by Baldwin and Stranks[10] who purified the commercial product by extraction with ethanol, precipitation with sulphuric acid, extraction with ether, and then repeated precipitation from acetone with benzene. The purity was checked by spectroscopy, paper chromatography and elemental analysis.

Acid–base and spectral characteristics of Chrome Azurol S

Figure 1 shows the absorption spectra of the various protonated forms of the reagent and Fig. 2 the dependence of absorbance at 500 or 590 nm on pH. The protonation equilibria of Chrome Azurol S are given in Fig. 3, from which it may be seen that there may be strong intramolecular hydrogen bonding between the phenolic group or the quinonoid oxygen atom and the adjacent carboxyl groups in the species H_3chas^-, H_2chas^{2-} and $Hchas^{3-}$ but not in the species $chas^{4-}$ and H_4chas. These structural differences may account for the similarity in shape of spectra 2, 3 and 4, and of 1 and 5.

The protonation constants, expressed as

$$k_{a1} = [Hchas^{3-}]/[H^+][chas^{4-}]$$

$$k_{a2} = [H_2chas^{2-}]/[H^+][Hchas^{3-}]$$

$$k_{a3} = [H_3chas^-]/[H^+][H_2chas^{2-}]$$

were determined spectrophotometrically at 20° and constant ionic medium (0.1*M* NaCl) (*cf.* Fig. 2), and are summarized in Table 1. The fourth protonation constant

$$k_{a4} = [H_4chas]/[H^+][H_3chas^{3-}]$$

was determined spectrophotometrically at 540 nm at the same temperature and in constant ionic medium [3*M* (H, Na)Cl]. No reliable data could be obtained

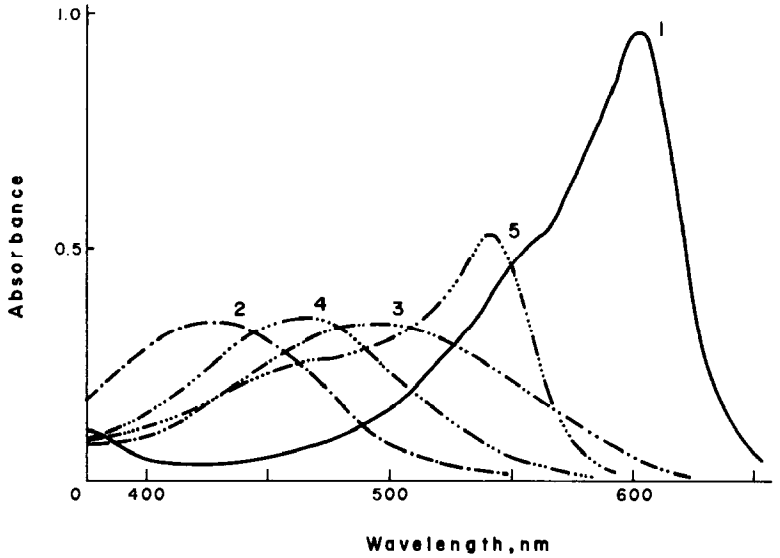


Fig. 1. Absorption spectra of Chrome Azurol S. 1, $chas^{4-}$ ($-\log[H^+] = 13.1_6$); 2, $Hchas^{3-}$ (9.1_8); 3, H_2chas^{2-}(3.7_0); 4, H_3chas^-(1.0_2); 5, H_4chas(-0.72). Ligand concn. = 2.92×10^{-5} *M*. Reference H_2O.

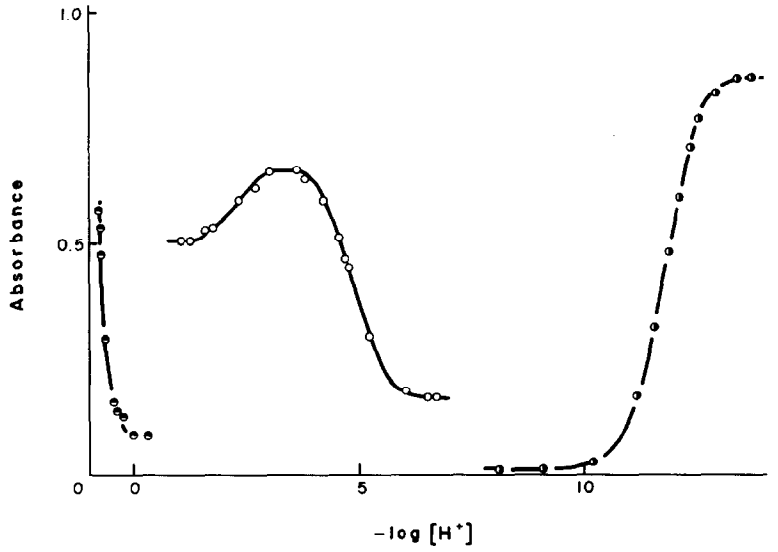


Fig. 2. Relation between absorbance of Chrome Azurol S and acidity. Ligand concn. 1, 2.92×10^{-5} *M*; 2, 5.84×10^{-5} *M*; 3, 2.92×10^{-5} *M*. Wavelength, 1, 540 nm; 2, 500 nm; 3, 590 nm. Ionic medium, 1, >3 *M* (Na, H) Cl; 2 and 3, 0.1 *M* NaCl. Reference H_2O.

even under these conditions, but log k_{a4} seems unlikely to exceed −0.5.

These protonation constants may be compared with those of 5-sulphosalicyclic acid, in which the carboxyl group (log k_{a2} = 2.52) is *ortho* to the hydroxyl group (log k_{a1} = 11.40) and the sulphonate group (log k_{a3} = −0.75, μ = 1.0, 25°)[11] is at a position where no interaction can occur with these groups; hence by analogy, for Chrome Azurol S log k_{a1} may be assigned to protonation at the 4-position (hydroxyl group), log k_{a2} to the 5′-position (carboxyl group), and log k_{a3} to the 5-position (carboxyl group). The fourth protonation constant log k_{a4} may be assigned to either the 3″-position (sulphonate group) or the 4″-position (quinonoid oxygen group) but no definite choice can be made from the data (*cf.* Fig. 3).

Formation of zirconium–Chrome Azurol S complexes

Formation of a complex between zirconium and Chrome Azurol S has been studied spectrophotometrically[15–17] but no consistent results have yet been obtained and even the composition of the complexes

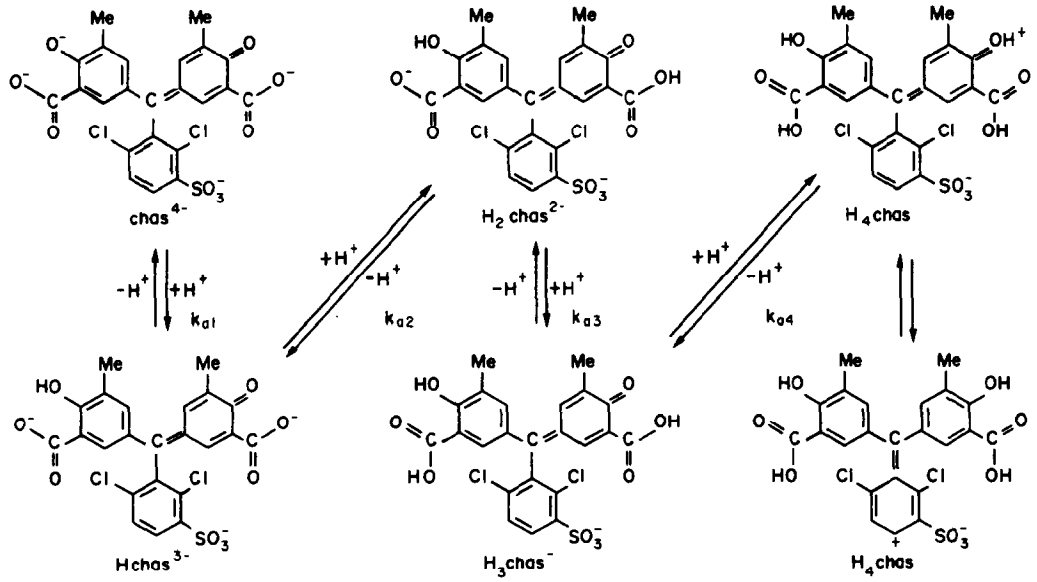


Fig. 3. Probable protonation scheme of Chrome Azurol S anion.

Table 1. Acid–base and spectral characteristics of Chrome Azurol S

Species	$chas^{4-}$	$Hchas^{3-}$	H_2chas^{2-}	H_3chas^-	H_4chas	H_5chas^+	Ref.
Colour	bluish-violet	yellow	red	orange	pink	—	
	598	427	492	463	542	—	8
	598	429	499	469	541, 399	545, 399	9
	600	430	480	464	—	544	10
λ_{max}, *nm*	590	430	500	480	—	540	12
	600	430	500	470	—	—	13
	595	430	490	470	530	—	14
	602	427	494	464	542	—	present study
$\log \epsilon_{max}$	4.74(600 nm)	—	4.17(500 nm)	—	4.74(540 nm)	—	9
	4.52	4.07	4.07	4.08	4.26	—	present study
	11.81	4.71	2.25	<0	—		8
	11.79 ± 0.02	4.88 ± 0.02	2.37 ± 0.01	$-4.8(H_0)$	—		9
	11.75 ± 0.05	4.88 ± 0.05	2.25 ± 0.10	−1.2 ± 0.4	—		10
$\log k_{ai}$	11.47	4.86	2.45	<0	—		12
	12.21	4.92	2.28	—	—		13
	12.4	4.7	3.2	—	—		14
	11.85 ± 0.05	5.05 ± 0.03	2.24 ± 0.02	—	—		15
	$11.8_2 \pm 0.1_0$	$4.8_2 \pm 0.1_0$	$2.2_0 \pm 0.1_0$	< −0.5	—		present study

Note: Experimental conditions: 0.1*M* Cl^-, 20°, purified (8); no spec., purified (9); 0.1*M* $NaClO_4$, 25°, purified (10); no. spec., not purified (12); 0.1*M* Cl^-, 20°, not purified (13); no spec., not purified (14); —, 30°, not purified (15); 0.10*M* (Na, H)Cl, 20° (present study).

is undetermined, probably because of lack of purity of the ligand samples used. Biswas *et al.*[16] found that a single 1:1 complex is formed in the pH range 1.5–5.5 and estimated log $K = 4.9 \pm 0.1$ by Job's method. Later, Horiuchi and Nishida[17] concluded that at pH 1–4 a 2:5 (M:L) complex was formed, its absorption maximum (λ_{max}) being at 555 nm ($\epsilon_{max} = 4.76 \times 10^4$ l.mole^{-1}·cm^{-1}), at pH 2–6 a 1:1 complex with λ_{max} at 595 nm, and at pH > 6 a 1:2 complex with λ_{max} at 555. Gupta and Munshi[15] reported that two complexes were formed, one (1:1) in 0.5*M* hydrochloric acid (λ_{max} at 490 nm) and the other (1:2) in 0.1*M* hydrochloric acid (λ_{max} at 550 nm) and stated that polynuclear complexes cannot be formed in this system. They proposed the reactions

$$Zr^{4+} + H_3chas^- \overset{K}{\rightleftharpoons} [ZrHchas]^+ + 2H^+ \qquad (\log K = 3.49)$$

$$Zr^{4+} + 2H_3chas^- \overset{K'}{\rightleftharpoons} [Zr(Hchas)_2]^{2-} + 4H^+ \qquad (\log K' = 6.60)$$

These authors all paid little or no attention to the purity of the ligand used. In the present work purified Chrome Azurol S was used in a spectrophotometric study. Figure 4 shows three representative absorption spectra for the complexation system at different acidities. It is apparent that there are at least two complexes; one (complex **I**, λ_{max} 555 nm) is formed at pH 2 and the other (complex **II**, λ_{max} 605 nm) at pH > 3. Complex **I** is stable with time but complex **II** is not, because of hydrolysis of zirconium, the colour fading by about 4% per hr.

Figure 5 shows the absorption spectra of complex **II** at constant total ligand concentration and different metal:ligand ratios at pH 4.7, and Fig. 6 shows the dependence of the maximum absorbance and λ_{max} on the metal:ligand ratio under the same experimental conditions as for Fig. 4. The spectrum changed gradually from that of the ligand itself (λ_{max} = 460 nm) as the metal:ligand ratio increased, to that of the complex (overall λ_{max} = 560 nm, shoulder at about 600 nm and corresponding to λ_{max} for the complex). At the same time the maximum absorbance changed regularly as the ratio increased, with an inflection point at a ratio of 1:1. Since the spectral characteristics of complex **II** resemble those of $chas^{4-}$ more than $Hchas^{3-}$ or H_2chas^{2-}, complex **II** is probably Zrchas. Figure 7 shows that when the metal:ligand ratio is very low a different complex is formed.

Figure 8 shows that complex **I** is formed even at pH < 0.7 and that maximum absorbance is attained at pH 1.1–1.5. Formation of complex **I** is maximal at pH 1.4. The rate of formation of complex **I** is rather slow, about 30 min being necessary to reach maximum absorbance. Once formed, complex **I** is stable, with no change in absorbance for a further 60 min after the absorbance reaches its maximum. Figure 9 shows the spectra for increasing zirconium concentration and constant pH and concentration of ligand. There are two isosbestic points, at 382 and 500 nm, and as the metal:ligand ratio increases the absorption spectrum changes from that of the ligand to that of the complex except when the metal:ligand ratio is

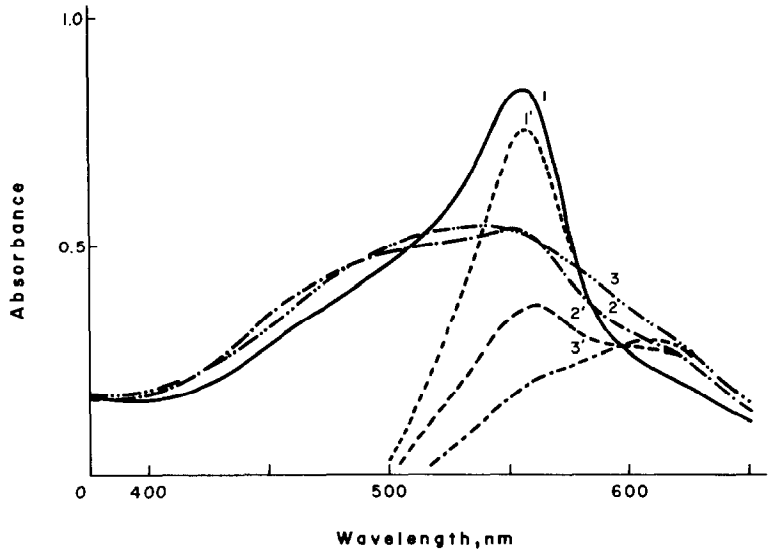


Fig. 4. Absorption spectra of zirconium–Chrome Azurol S complexes. 1 and 1', pH 1.3_8; 2 and 2', pH 2.1_2; 3 and 3', pH 4.4_0. Reference 1–3 H_2O; 1'–3' free ligand. Metal ion concn. 2.00×10^{-5} *M*. Ligand concn. 5.26×10^{-5} *M*.

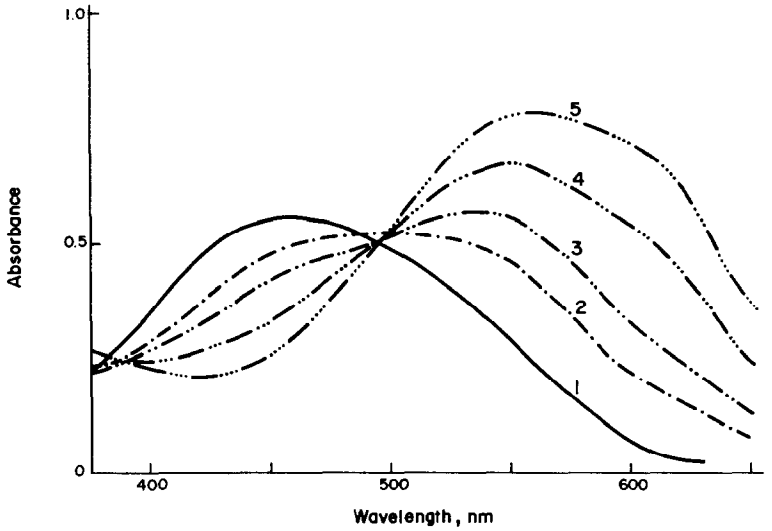


Fig. 5. Absorption spectra of zirconium–Chrome Azurol S system at constant concentration of the ligand. Metal ion/ligand ratio: 1, 0; 2, 0.17; 3, 0.34; 4, 0.68; 5, 1.20. Reference H_2O. Ligand concn. 5.84×10^{-5} *M*; pH 4.7.

very small, in which case there is deviation from Beer's law (Fig. 9). Figure 10 shows that the metal:ligand ratio in complex **I** is 1:2. The deviation from linearity at very low molar fraction of zirconium (Fig. 10) may be attributed to the formation of another complex as already discussed in connection with Fig. 7.

Under conditions where complex **I** is predominantly formed, zirconium may be present as the aquo-ion, Zr^{4+}*, or as partially hydrolysed species, such as $Zr(OH)_3^+$, $[Zr_q(OH)_p]^{(2q-p)+}$, *etc.*,[18] and Chrome Azurol S in the form of H_3chas^-. As for the question of polymeric zirconium species, to a first approximation these may be regarded as at least partly dissociated into mononuclear hydrolysed species of $Zr(OH)_i^{(4-i)+}$ which can react with the ligand anion. Hence the complex formation equilibrium of complex **I** may be expressed as

$$Zr(OH)_i^{(4-i)+} + 2H_3chas^- \overset{k_{eq}}{\rightleftharpoons} Zr(H_nchas)_2^{(2n-4)+} + (6-2n-i)H^+ + iH_2O \quad (I)$$

The equilibrium constant is given by

$$K_{eq} = [Zr(H_nchas)_2^{(2n-4)+}] \times [H^+]^{(6-2n-i)}/[Zr(OH)_i^{(4-i)+}][H_3chas^-]^2 \quad (1)$$

* Water molecules co-ordinated to the metal ion are omitted for simplicity.

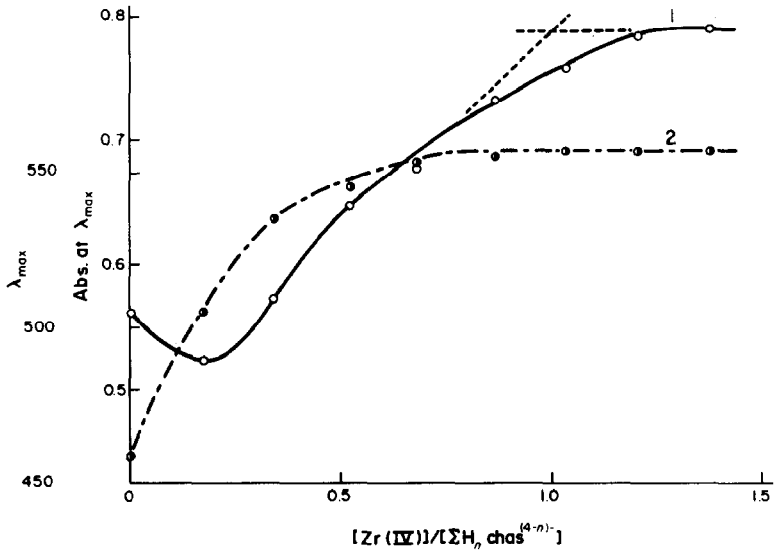


Fig. 6. Relation between metal:ligand mole ratio and wavelength of maximum absorbance, or absorbance maximum. 1, λ_{max}; 2, absorbance at λ_{max}. Ligand concn. 5.84×10^{-5} *M*; pH 4.7. Reference H_2O.

The total concentrations of zirconium, C_M, and ligand, C_L, are

$$C_M = [Zr(OH)_i^{(4-i)+}] + [Zr(H_n chas)_2^{(2n-4)+}] \quad (2)$$

$$C_L = [H_3 chas^-] + 2[Zr(H_n chas)_2^{(2n-4)+}] \quad (3)$$

Also,

$$E = \epsilon_C[Zr(H_n chas)_2^{(2n-4)+}] + \epsilon_L[H_3 chas^-] \quad (4)$$

$$E_L = \epsilon_L C_L \quad (5)$$

$$E_C = \epsilon_C C_M \quad (6)$$

where E is the absorbance of the solution containing both metal complex and the ligand, E_C that for *complete* complexation of all the metal, E_L that for no complexation at all, ϵ_C the molar absorptivity of the complex and ϵ_L that of $H_3 chas^-$. If the experimental conditions are chosen so that C_L/C_M is 2, and complexation is virtually complete, equations (7)–(9) can easily be derived from equations (2)–(6):

$$[Zr(H_n chas)_2^{(2n-4)+}] = (E - E_L)/(\epsilon_C - 2\epsilon_L) \quad (7)$$

$$[Zr(OH)_i^{(4-i)+}] = (E_C - E)/(\epsilon_C - 2\epsilon_L) \quad (8)$$

$$[H_3 chas^-] = 2(E_C - E)/(\epsilon_C - 2\epsilon_L) \quad (9)$$

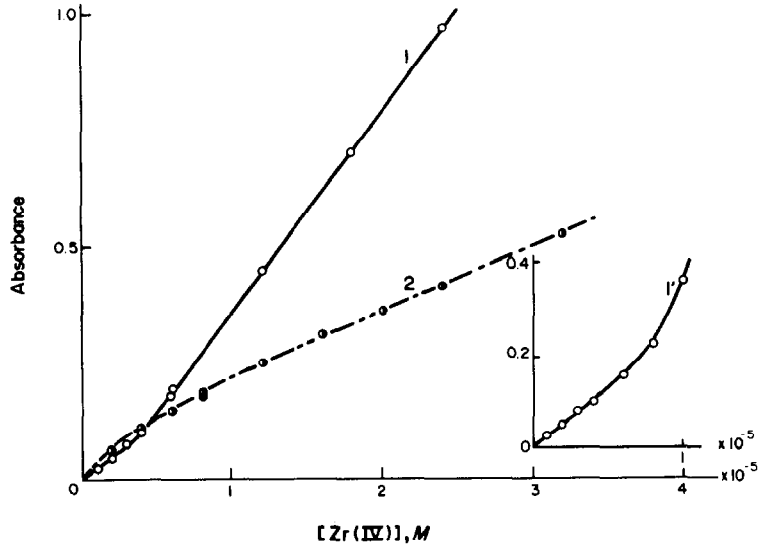


Fig. 7. Concentration of zirconium *vs.* absorbance of the complex. Ligand concn. 1, 5.84×10^{-5} *M*; 1' and 2, 1.17×10^{-4} *M*; wavelength, 1 and 1', 555 nm; 2, 605 nm; pH, 1 and 1', 1.3; 2, 4.7. Reference free ligand.

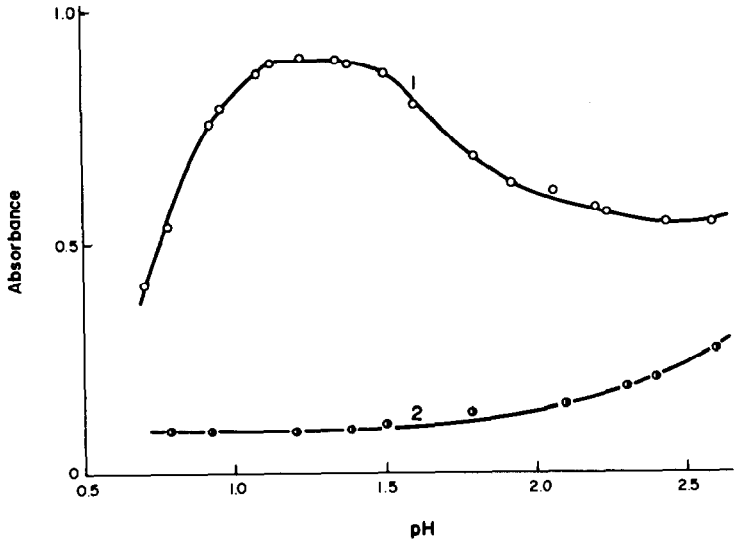


Fig. 8. Absorbance at 555 nm *vs.* pH at equilibrium. Metal concn. 1, 2.00×10^{-5} *M*; 2, 0. Ligand concn. 1 and 2, 5.84×10^{-5} *M*. Reference H_2O.

Finally, equation (10) can be derived from (1), (7), (8), and (9) with suitable rewriting:

$$\log(E - E_L) - 3\log(E_C - E)$$
$$= \log 4K_{eq}(\epsilon_C - 2\epsilon_L)^{-2} - (6 - 2n - i)\log[H^+] \quad (10)$$

There should be a linear relation between the left-hand side of equation (10) and $-\log[H^+]$, with a slope of $(6 - 2n - i)$. Such a relation was found experimentally, with a slope of 5. Hence $2n + l = 1$ and the values of n and i are taken as 0 and 1, respectively. Hence equilibrium (I) may be expressed as

$$Zr(OH)^{3+} + 2H_3chas^- \overset{K_{eq}}{\rightleftharpoons} Zr(chas)_2^{4-} + 5H^+ + H_2O \quad (I')$$

The value of $\log K_{eq}$ (5.8 ± 0.1) obtained in this way was for constant ionic strength (0.4*M* NaCl, 20°). The molar absorptivity of complex I at 555 nm was

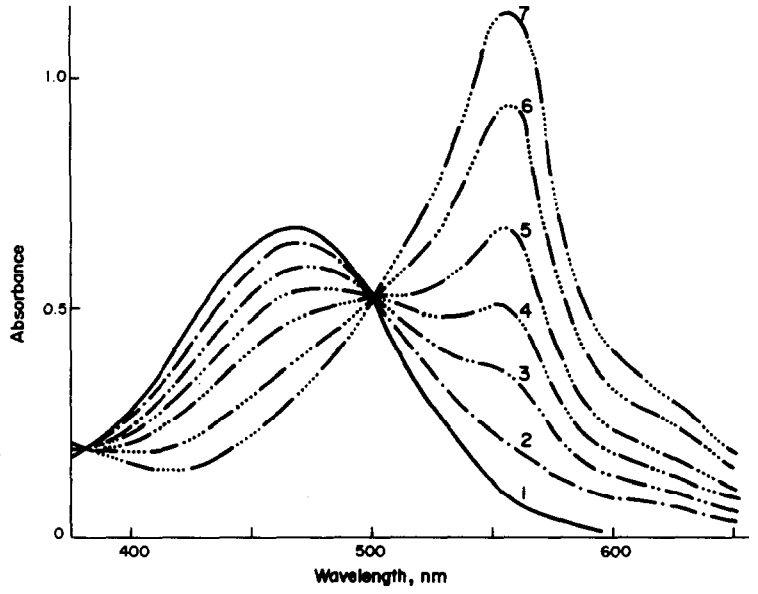


Fig. 9. Absorption spectra of zirconium–Chrome Azurol S system at constant concentration of the ligand. Metal ion:ligand ratio, 1, 0; 2, 0.068; 3, 0.14; 4, 0.21; 5, 0.27; 6, 0.41; 7, 1.40. Reference H_2O. Ligand concn. 5.84×10^{-5} *M*; pH 1.3_0.

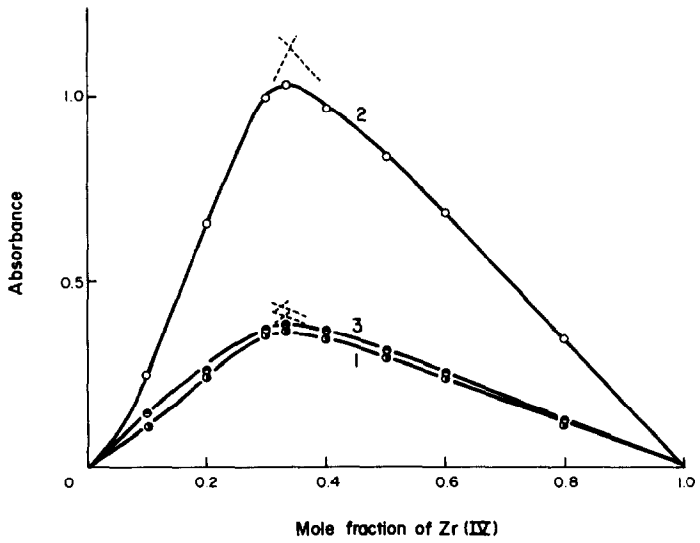


Fig. 10. Method of continuous variation. Wavelength 1, 520 nm; 2, 555 nm; 3, 590 nm. [Metal ion] + [Ligand] = 8.76×10^{-5} M; pH 1.3_0. Reference, total ligand added.

3.76×10^4 l.mole^{-1}·cm^{-1}. The stability constant of **I** is defined by

$$Zr^{4+} + 2chas^{4-} \overset{\beta_2}{\rightleftharpoons} Zr(chas)_2^{4-}$$

$$\beta_2 = [Zr(chas)_2^{4-}]/[Zr^{4+}]\,[chas^{4-}]^2 \qquad (11)$$

can be obtained from K_{eq}, the protonation constants of the ligand (k_{a1}, k_{a2} and k_{a3}), the ionic product of water (K_w), and the hydrolysis constant of Zr^{4+} (K_{OH}), defined by

$$K_{OH} = [Zr(OH)^{3+}]/[Zr^{4+}][OH^-], \qquad (12)$$

the equation being

$$\log \beta_2 = \log K_{eq} + \log k_{a1}^2 k_{a2}^2 k_{a3}^2 + \log K_w + \log K_{OH} \qquad (13)$$

The value of $\log K_w$ was estimated[19] to be -13.7 and that of $\log K_{OH}$ to be[20] 13.8 ($\mu = 4$). The values of k_{a1}, k_{a2}, k_{a3}, and K_{OH} used were corrected for the estimated change in the activity coefficients. The value of $\log \beta_2$ was finally calculated to be 43.7 ± 0.3.

It is worth considering the probable structure of complex **I**. The molecular structure implies that the ligand is bidentate. Taking $n = 0$ and $i = 1$ in reaction (I) implies that the complex is $Zr(chas)_2^{4-}$, but

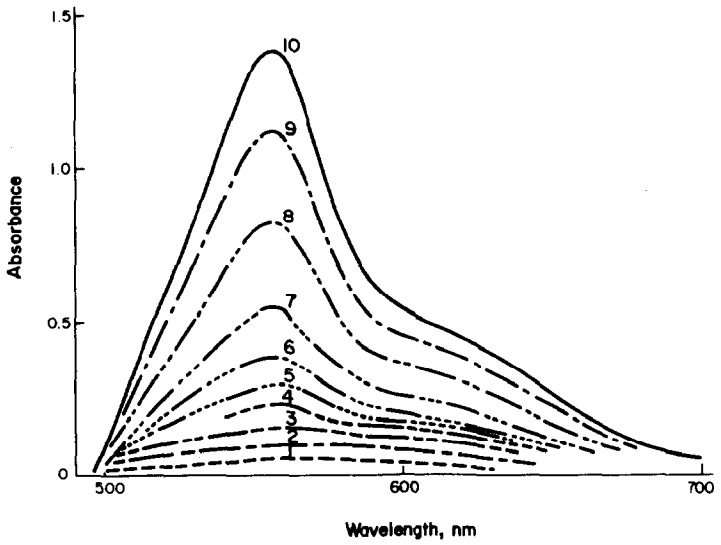


Fig. 11. Absorption spectra at various metal to ligand ratios. Metal ion:ligand ratio: 1, 0.017; 2, 0.034; 3, 0.051; 4, 0.068; 5, 0.086; 6, 0.103; 7, 0.137; 8, 0.205; 9, 0.274; 10, 0.342. Ligand concn. 1.17×10^{-4} M; pH 1.3_0. Reference, free ligand.

Table 2. Spectral characteristics of zirconium–Chrome Azurol S complexes

	Complex I	Complex II	Complex III
λ_{max}, nm	555	560 and 600 (shoulder)	620 (shoulder)
ϵ_{max}	3.76×10^4	—	—
Stable formation region	<pH 2	>pH 3	<pH 2
Metal to ligand ratio	1:2	1:1	1:3(?)

there could be further hydrolysis of the zirconium, with proton-transfer to the ligand, to give $Zr(OH)_2(Hchas)_2^{4-}$, of the iron(III) complex reported by Langmyhr *et al.*[8]

As it had been found [Figs. 9 (shoulder at about 620 nm) and 10] that another type of complex (**III**) may be formed in acidic solution at very high ligand:metal ion concentration ratios, this was investigated spectrophotometrically. Figure 11 shows distinct changes in the spectral characteristics with respect to the metal:ligand ratio. Although no reaction conditions could be found for predominant presence of complex **III**, it may reasonably be deduced that it is a 1:3 Zr:chas complex, by taking into consideration the composition and formation range of complex **I** and also the co-ordination number of zirconium(IV) and co-ordination sites of the ligand. No further studies were made on complex **III**, however, because it has no potential application. The spectral characteristics of complexes **I**, **II**, and **III** are summarized in Table 2.

Reaction of complex I with fluoride

As zirconium(IV) has co-ordination number 8 in solution, some water molecules will be residually co-ordinated to the metal ion in complex **I** and may be more easily replaced than the co-ordinated Chrome Azurol S by fluoride, to form a mixed-ligand complex, which may in turn exhibit different spectral characteristics from the complex **I**, just like the cerium(III) or lanthanum(III) complex of Alizarin Fluorine Blue when complexed with fluoride. This was first checked by spectral measurements of zirconium/Chrome Azurol S/fluoride mixtures. Figure 12 shows the effect of fluoride on the absorption spectrum of complex **I**. The spectrum changes regularly with increasing fluoride concentration, to the limiting absorption spectrum of Chrome Azurol S. This implies that the fluoride either displaces water from the zirconium co-ordination sphere and simultaneously shifts the electronic state of the co-ordinated Chrome Azurol S to that of the free reagent, or it displaces the Chrome Azurol S to form zirconium fluoride species and free Chrome Azurol S. To explore this further, the effect of the Chrome Azurol S/zirconium(IV) molar ratio on the absorbance at λ_{max} for complex **I** was examined in the presence and absence of fluoride. Figure 13 shows clearly that in the absence of fluoride a 2:1 ligand:metal complex is formed, which is consistent with the results in the preceding section. The decrease in absorbance with larger excess of ligand might be due to formation of complex **III**, as pointed out above. The presence of fluoride causes a significant change, how-

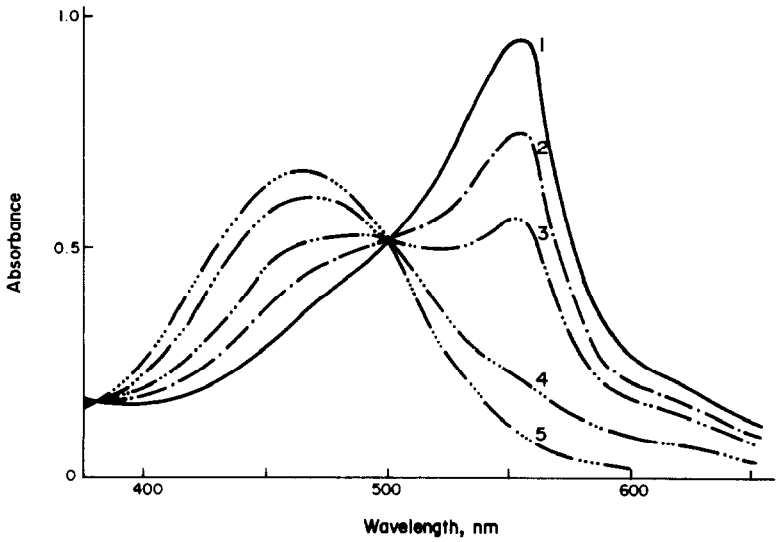


Fig. 12. Absorption spectra of the zirconium–Chrome Azurol S–fluoride system.
Zirconium concn., 1–4, 2.00×10^{-5} *M*; 5, 0. Chrome Azurol S concn., 5.26×10^{-5} *M*; fluoride concn., 1, 0; 2, 1.05×10^{-5} *M*; 3, 2.10×10^{-5} *M*; 4, 4.20×10^{-5} *M*; 5, 0. Reference H_2O.

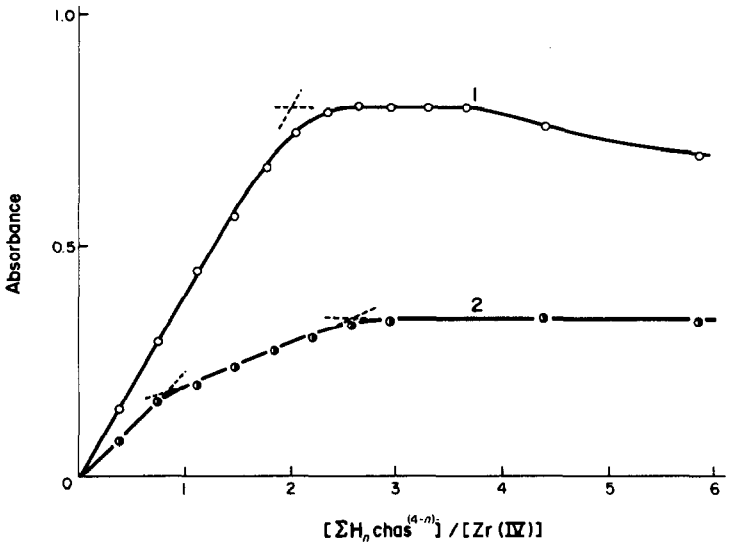


Fig. 13. Absorbance at 555 nm at various mole ratios of Chrome Azurol S to zirconium. Zirconium concn., 2.00×10^{-5} *M*; fluoride concn., 1, 0; 2, 2.10×10^{-5} *M*; pH 1.3_0. Reference total ligand added.

ever. There are two break points, at ligand:metal ratios of about 0.8 and 2.5, and even a very large excess of Chrome Azurol S had no further effect. The complex formed in the presence of fluoride is therefore presumably a mixed-ligand complex containing both Chrome Azurol S and fluoride, and the fractional ratio suggests that a polynuclear complex is formed. This deduction may be supported by the results shown in Fig. 14, showing the pH-region for maximum formation of complex I in the presence of fluoride. This region shifts to higher pH with increased concentration of fluoride. Moreover, the presence of fluoride evidently stabilizes the complex at higher pH values (*cf.* curves 1 and 3 at pH ~ 2), which implies that both Chrome Azurol S and fluoride are present in the complex. The difference in absorbance between solutions with and without fluoride present is constant and maximal at pH 1.0_5–1.1_0.

It can hence be deduced that the fluoride reacts with complex I to form a mixed-ligand complex of zirconium(IV) with both Chrome Azurol S and fluoride, the composition (and reaction scheme) of which may depend on the ratio of the fluoride and Chrome Azurol S concentrations. Of course, there may also be formation of zirconium(IV)–fluoride complexes and free Chrome Azurol S, especially with increasing fluoride:Chrome Azurol S ratio. It is worthwhile discussing this system further. It is known[21] that zirco-

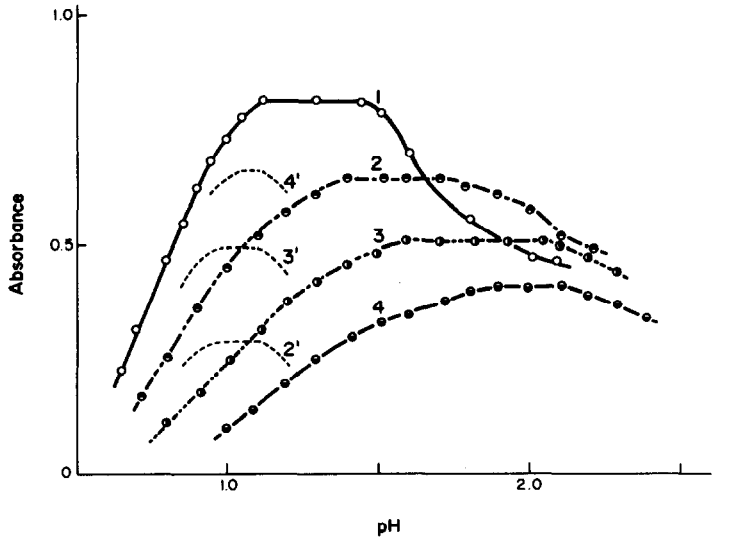


Fig. 14. Absorbance at 555 nm at various pH values in the zirconium–Chrome Azurol S–fluoride system. Zirconium concn., 2.00×10^{-5} *M*; Chrome Azurol S concn., 5.84×10^{-5} *M*; fluoride concn., 1, 0; 2, 1.05×10^{-5} *M*; 3, 2.10×10^{-5} *M*; 4, 3.15×10^{-5} *M*. Reference, 1–4, free ligand: 2', difference between 1 and 2; 3', difference between 1 and 3; 4', difference between 1 and 4.

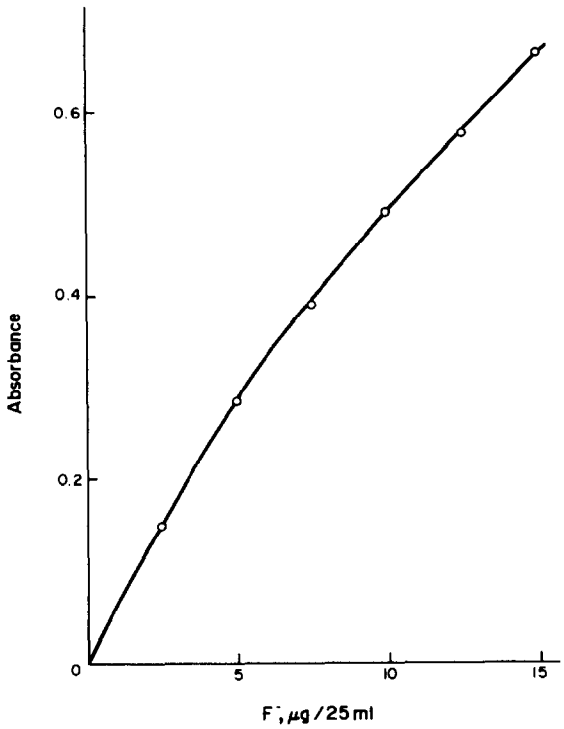


Fig. 15. Absorbance decrease at 555 nm for various fluoride concentrations. Zirconium concn., 2.00×10^{-5} *M*; Chrome Azurol S concn., 5.84×10^{-5} *M*; pH 1.1_0. Measured against reagent mixture with no fluoride present.

nium in aged solutions is polymerized and does not react with *e.g.*, Xylenol Orange unless ions such as fluoride, sulphate or phosphate are present. The hydrolytic behaviour of zirconium has been reviewed by Kragten and Parczewski,[22] who concluded that hydrolysed zirconium(IV) species such as $[Zr_4(OH)_8]^{8+}$, $[Zr_3(OH)_4]^{8+}$, $[Zr_3(OH)_5]^{7+}$ may be present in acidic solution. If this is valid, equilibrium (I) can be interpreted along these lines. Of these hydrolysed species, $[Zr_4(OH)_8]^{8+}$ could give tion product of $[Zr_4(OH)_4(chas)_8]^{20-}$ (or $[Zr_4O_2(chas)_8]^{20-}$), both of which satisfy our experimental results and hence the principle of equilibrium (I). Kragten and Parczewski[22] also point out that a water molecule present as an oxolation bridge is less reactive, although it may be susceptible to attack by fluoride. From these facts we suggest the following plausible reaction scheme: fluoride at low concentration forms a mixed-ligand complex with a polynuclear zirconium(IV)–Chrome Azurol S complex but at higher concentration will displace the co-ordinated Chrome Azurol S anions, which are more reactive than the oxolation-bridge water molecules, to form zirconium(IV)–fluoride complexes and free Chrome Azurol S.

Figure 15 shows the decrease in absorbance as the fluoride concentration increases. The deviation from linearity presumably reflects the complexity of the reaction scheme, but does not invalidate the system for analytical purposes.

Application to determination of fluoride

As no new spectral band(s) could be found for the product of the reaction of complex I with fluoride (in contrast to the case of the rare-earth complexes of Alizarin Fluorine Blue), it was decided to use for analytical purposes the decrease in absorbance at λ_{max} of complex I caused by fluoride. The optimum conditions deduced from the study are therefore as follows: absorbance measurement at 555 nm; pH 1.0_5–1.1_0; molar ratio of Chrome Azurol S to zirconium 2.9–3.6.

Further study of the stability of the mixed-ligand system revealed that the absorbance increased on standing, becoming constant after 30 min and giving no change in absorbance for a further 60 min.

The recommended procedure described in the experimental section was then established. A typical working curve is given in Fig. 15. The lower detection limit for fluoride is 0.1 μg/ml (absorbance 0.005).

The interference studies are summarized in Table 3. Aluminium, thorium and titanium(IV) cause negative errors, and sulphate and phosphate give positive errors. Aluminium and titanium(IV) do not form complexes with Chrome Azurol S, but thorium does under the recommended conditions, so the first two interfere by reacting with fluoride, and the third by its reaction with Chrome Azurol S and/or fluoride. Inter-

Table 3. Influence of foreign ions on determination of 10.0 μg of fluoride

Ions and salts	Molar concn. ratio to fluoride	F⁻ found, μg	Relative error, %
Al(III)	7.0	8.40	−16
Ca(II)	4.7	10.08	0.8
Cd(II)	1.7	9.86	−1.4
Co(II)	3.2	9.90	−1.0
Cr(III)	3.7	9.86	−1.4
Cu(II)	3.0	10.22	2.2
Fe(III)	3.4	9.86	−1.4
Mg(II)	7.8	10.22	2.2
Ni(II)	3.2	10.08	0.8
Pb(II)	0.92	9.94	−0.6
Th(IV)	0.16	8.50	−15.0
	0.82	5.32	−46.8
Ti(IV)	4.0	10.22	2.2
V(V)	3.7	10.12	1.2
Zn(II)	2.9	10.04	0.4
Br^-	2.4	9.90	−1.0
I^-	19	10.08	0.8
PO_4^{3-}	0.095	10.16	1.6
	0.48	11.51	15.0
KNO_3	950	10.00	0
$NaClO_4$	„	9.94	−0.6
KCl	„	9.86	−1.4
NH_4NO_3	„	10.08	0.8
CH_3COONa	„	10.08	0.8
Na_2SO_4	0.95	9.94	−0.6
	9.5	10.61	6.1
	95	14.0	40

Table 4. Analytical results for some ceramic materials

	Sample taken, g	F^- found, μg	F^- content, %
Concrete	3.022	0.75	0.025
	2.895	0.72	0.025
	2.923	0.71	0.024
	3.186	0.74	0.023
By-product gypsum	1.023	2.15	0.21
	0.965	2.22	0.23
	0.891	1.78	0.20

ference by sulphate and phosphate is probably due to reaction with complex I (*cf.* Cabello-Tomas and West[21]). The tolerance limits are 100 μg for aluminium, thorium, and titanium(IV), 50 μg for sulphate, and 5 μg for phosphate, for an error of ±1%.

The reproducibility for 1.0 and 10.0 μg of fluoride (10 replicates) was found to be ±2.2 and ±1.4%, respectively. The procedure is therefore applicable to trace analysis for fluoride.

The procedure established was applied to small amounts of fluoride in ceramic materials. The fluoride was first separated by the Willard and Winter steam-distillation procedure,[23] modified[24] for application to ceramic materials. The improved procedure[24] consists of a double steam-distillation, first from perchloric–sulphuric acid mixture at 135 ± 5° and then from perchloric acid at 125°. The recovery is 95–103% for 200 μg of fluoride.[24] Analytical results are given in Table 4.

Comparison with other analytical methods

The best spectrophotometric method for the determination of fluoride is generally considered to be that with the cerium(III)– or lanthanum(III)–Alizarin Fluorine Blue system,[2-4] so its comparison with the present method will suffice to evaluate the latter. The working curve of the Alizarin Fluorine Blue (AFB) method (5–30 μg of fluoride)[3] covers nearly the same concentration range as the present method (0.2–15 μg of fluoride), but the AFB method gives a product that is rather unstable and suffers from more interferences. Hence the zirconium(IV)–Chrome Azurol S method may be considered more practical for the determination of fluoride. Preliminary separation of the fluoride is considered advisable, however.

Acknowledgements—The authors thank Dr. R. A. Chalmers, University of Aberdeen, for his kind criticism, advice, and discussion on the content and especially on the reaction scheme, and one of them (H.E.) also thanks the Kazuchika Ohkura Memorial Foundation for financial support of this work.

REFERENCES

1. F. D. Snell and C. T. Snell, *Colorimetric Methods of Analysis*, Vol. II, 3rd Ed., p. 743; F. D. Snell, C. T. Snell and C. A. Snell, *op. cit.*, Vol. IIA, p. 632; Van Nostrand, New York, 1957; 1959.
D. F. Boltz (ed.), *Colorimetric Determination of Nonmetals*, 1st Ed., p. 238. Wiley-Interscience, New York, 1958.
I. M. Kolthoff and P. J. Elving (eds.), *Treatise on Analytical Chemistry*, Part II, Vol. 7, p. 207. Wiley-Interscience, New York, 1961.
D. F. Boltz and M. G. Mellon, *Anal. Chem.*, 1970, **42**, 152R; 1972, **44**, 300R; 1974, **46**, 227R; 1976, **48**, 216R.
J. A. Howell and L. G. Hargis, *ibid.*, 1978, **50**, 243R.
2. R. Belcher, M. A. Leonard and T. S. West, *J. Chem. Soc.*, 1959, 3577.
3. M. A. Leonard and T. S. West, *ibid.*, 1960, 4477.
4. M. A. Leonard and G. F. Murray, *Analyst*, 1974, **99**, 645.
5. S. Wakamatsu, *Bunseki Kagaku*, 1958, **7**, 578; K. Ueno, *Kireito Tekitei Ho*, p. 324. Nankodo, Tokyo, 1960.
6. Chem. Soc. Japan, *Handbook of Chemistry*, Fundamental Ed., p. 1213. Maruzen, Tokyo, 1975.
7. V. Malanik and M. Malát, *Anal. Chim. Acta*, 1975, **76**, 464.
8. F. L. Langmyhr and K. S. Klausen, *ibid.*, 1963, **29**, 149.
9. L. Sommer and V. Kuban, *Collection Czech. Chem. Commun.*, 1967, **32**, 4355.
10. W. G. Baldwin and D. R. Stranks, *Aust. J. Chem.*, 1968, **21**, 603.
11. A. E. Martell and R. M. Smith (eds.), *Critical Stability Constants*, Vol. 3, p. 190. Plenum Press, New York, 1977.
12. M. Malát, *Anal. Chim. Acta*, 1961, **25**, 289.
13. L. P. Adamovich, O. V. Morgul-Meshkova and B. V. Yutsis, *Zh. Analit. Khim.*, 1962, **17**, 678.
14. I. S. Mustafin, A. N. Ivanof and N. F. Lisenko, *ibid.*, 1965, **20**, 17.
15. G. P. Gupta and K. N. Munshi, *J. Indian Chem. Soc.*, 1975, **52**, 936.
16. S. D. Biswas, R. L. Seth and A. K. Dey, *Talanta*, 1965, **12**, 119.
17. Y. Horiuchi and H. Nishida, *Bunseki Kagaku*, 1967, **16**, 20.
18. C. F. Baes, Jr. and R. E. Mesmer, *The Hydrolysis of Cations*, p. 152. Wiley, New York, 1976.
19. L. G. Sillén and A. E. Martell, *Stability Constants of Metal-Ion Complexes*, Spec. Publn. No. 17, p. 139; No. 25, p. 14. Chem. Soc., London, 1964; 1971.
20. A. Ringbom, *Complexation Reactions in Analytical Chemistry*, p. 298. Wiley-Interscience, New York, 1963.
21. M. L. Cabello-Tomas and T. S. West, *Talanta*, 1969, **16**, 781.
22. J. Kragten and A. Parczewski, *ibid.* 1981, **28**, 149.
23. H. H. Willard and O. B. Winter, *Ind. Eng. Chem., Anal. Ed.*, 1933, **5**, 7.
24. H. Ishii, H. Einaga and M. Numata, *Onoda Res. Rept.*, 1964, No. 2, 1.

Talanta. Vol. 28. pp. 901 to 907. 1981
Printed in Great Britain. All rights reserved

0039-9140/81/120901-07$02.00/0
Copyright © 1981 Pergamon Press Ltd

FACTORIAL ANALYSIS OF MATRIX EFFECTS IN ICP–OES AND AAS

DETERMINATION OF Ta AND Ni IN Au

J. KRAGTEN

Natuurkundig Laboratorium der Universiteit van Amsterdam, Valckenierstraat 65, 1018 XE Amsterdam, The Netherlands

A. PARCZEWSKI

Department of Analytical Chemistry, Jagiellonian University, Kraków, Poland

(*Received* 9 *February* 1981. *Accepted* 22 *May* 1981)

Summary—In measuring systems in which the signal is linearly related both to the component of interest and to matrix components, 2^n factorial analysis is a convenient tool for applying matrix corrections. In general, the linearity condition is satisfactorily fulfilled if the matrix influences are not very large, but generally the signal is not linearly related to the analyte concentration. k^n ($k > 2$) factorial analysis can then be applied, but it needs extensive calibration to determine all the regression coefficients. When the non-linearity is not too large (as in atomic-absorption spectrophotometry), a more convenient method is to use the calibration curve or the instrumental curve-correction facility to obtain a linearized variable to which 2^n factorial analysis is then applied. It is shown that the systematic deviation introduced often remains negligible if only the upper part of the calibration curves is used.

The matrix components present frequently influence the results of a determination, in particular in atomic-absorption spectroscopy (AAS) and inductively-coupled plasma–optical emission spectroscopy (ICP–OES). The elimination of such interference effects is an important current problem in analytical chemistry. In many cases these effects can be eliminated by using standards which have the same matrix as the samples to be analysed. This matrix-matching procedure requires a separate set of standards for each sample when we deal with varying amounts of the matrix or when the matrix composition changes. In the latter case the standard-addition method can be successfully used for elimination of matrix effects, but this method has some drawbacks. First, the method presupposes that the measured signal will be zero if the element to be determined is not present, and this may not be true. Secondly, it must be certain that the addition of standard does not alter the matrix composition of the sample solution (acidity, *etc.*). Thirdly, the method is time-consuming when many samples have to be analysed, as at least twice as many measurements are needed. Finally the extrapolation implicit in the method decreases the precision unless sufficient points are obtained.

When the amount of matrix varies or the matrix composition changes in a known way, other correction procedures should be applied. A methodology for elimination of matrix effects, based on the theory of design of experiments,[1,2] has recently been developed[3] and applied successfully to spectrophotometric methods,[4,5] flame emission and absorption spectrometry,[6–8] and potentiometry.[9] Similar statistical approaches have been proposed by other authors[10–12] for dealing with interference effects in atomic-absorption spectrophotometry.

In this paper the application of the theory of design of experiments to the determination of tantalum in gold by ICP–OES, and to the determination of nickel in gold by AAS, will be treated in terms of 2^n factorial analysis. Factorial analysis is simple and convenient when the signal S is a linear function of the concentration of the component to be determined (tantalum in our case) and also the relation between S and the concentrations of the matrix component(s) (gold in our case) is approximately linear. It will be shown that even when the signal–concentration function is non-linear (as for nickel with flame-AAS), quite nice results can be obtained with 2^n factorial analysis if the influence of the matrix can be approximated by a linear function. In that case the calibration curve is used to transform the absorbance into a "concentration" signal which is supposed to be linearly related to the real concentration. The point now is that the matrix transforms the original calibration curve in the same way as its linearized forms. If the original calibration curve is not too strongly curved, the errors introduced by this process remain below the 1% level, which is acceptable for most practical cases. When the AAS instrument used has a built-in curve-correction facility, the concentration display can be taken as the signal.

THEORY

The following equation can be adopted for the relationship between the measured signal S and the concentrations c_i of the sample components:[2]

$$S = \sum_{i=0}^{n} b_i c_i + \sum_{\substack{i,j=1 \\ (i \leq j)}}^{n} \sum^{n} b_{ij} c_i c_j + \cdots \qquad (1)$$

in which, by definition, $c_0 = 1$. As usual, the suffix 1 refers to the component to be determined. The other suffixes refer to the other components in the sample solution; n denotes the number of components under consideration. Equation (1) will be satisfactory if sufficient terms are taken into consideration. In principle the regression coefficients b can be found from measurements of standards. The more terms there are to be introduced, however, the more standards will be needed. The errors in S propagate into errors in the coefficients b. This will restrict us to use of only those coefficients which are significant. For not too complicated systems even a restriction to linear and quadratic terms may be satisfactory. The tantalum–gold system considered here can be regarded as linear in the first instance. Equation (1) then transforms into

$$S = b_0 + b_1c_1 + b_2c_2 + b_{12}c_1c_2$$
$$= (b_0 + b_2c_2) + (b_1 + b_{12}c_2)c_1 \qquad (2)$$

in which the suffix 1 refers to tantalum and 2 to gold. The term $(b_0 + b_2c_2)$ accounts for the shift of the calibration line, which is linearly dependent on the gold concentration (c_2). The term $(b_1 + b_{12}.c_2)$ is similarly related to the change in slope of the calibration line.

For an efficient determination of the coefficients b in equation (2) the concentration scale is made dimensionless by introducing "coded" concentrations defined as

$$x_1 = \frac{c_1 - c_1^{(0)}}{\Delta c_1}, \quad x_2 = \frac{c_2 - c_2^{(0)}}{\Delta c_2}. \qquad (3)$$

The meaning of $c_i^{(0)}$ and Δc_i is explained in Fig. 1; Δc_i is half the total span on the concentration scale, $c_i^{(0)}$ corresponds to the centre of this span. If we deal with linear systems, two coded concentrations of each variable will be sufficient for a description of the system. These are chosen according to a specific scheme (2^2 factorial in our case); each of the numbered points in Fig. 1 corresponds to a distinct composition of the standard solution. The higher concentration level of a component is "coded" by $x = +1$, the lower level by $x = -1$ and the centre of the concentration range by $x = 0$. Transformation of equation (2) into coded concentrations leads to:

$$S = B_0 + B_1x_1 + B_2x_2 + B_{12}x_1x_2 \qquad (4)$$

At least 4 S-values have to be measured for the determination of the four unknown B-values. In Table 1 the coded concentrations are related to the measured signals according to the 2^2 factorial of Fig. 1. Solution 5 corresponds to the centre of the factorial.

Because of the orthogonality of the applied design (Table 1) and because of the simple values of the coded variables x_i, very simple relations arise between the values of S and the regression coefficients B:

$$B_0 = \sum_{i=1}^{4} S_i/4;$$

$$B_1 = \sum_{i=1}^{4} S_ix_{1i}/4 = (S_1 + S_2 - S_3 - S_4)/4;$$

$$B_2 = \sum_{i=1}^{4} S_ix_{2i}/4 = (S_1 - S_2 - S_3 + S_4)/4;$$

$$B_{12} = \sum_{i=1}^{4} S_ix_{1i}x_{2i}/4 = (S_1 - S_2 + S_3 - S_4)/4 \qquad (5)$$

where i gives the number of the standard solution concerned.

From correlation of these equations with Table 1 it is obvious that the values of B are found by taking the internal product of column S with one of the three "x" columns. This feature makes the calculations conveniently practicable.

From the errors of the signal S_i the error in B can be calculated. From the variance $\sigma_B^2 = \sigma_S^2/N$, in which $N = k^n$ and σ_S^2 is the signal variance, the Student's variable $t = B/\sigma_B$ can be found. By means of Student's test the significance of each coefficient B can be established. Finally the regression coefficients b of equation (2) can be found through equation (3). The foregoing will be illustrated first by application to the determination of tantalum in gold, an alloy of interest in physical research.

Table 1. Compositions of standard solutions corresponding to a 2^2 factorial (in coded concentrations)

No. of standard solution	x_1	x_2	x_1x_2	S
1	1	1	1	S_1
2	1	−1	−1	S_2
3	−1	−1	1	S_3
4	−1	1	−1	S_4
5	0	0	0	S_5

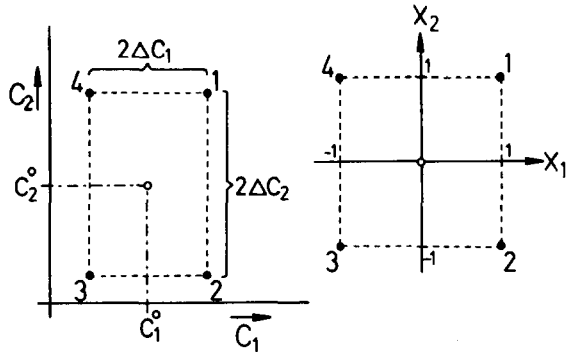


Fig. 1. Schematic representation of the connection between real and coded concentrations in a 2^2 factorial. Each of the numbered points corresponds to a distinct standard solution. The sequence of numbering is maintained throughout the paper.

Determination of tantalum in gold by ICP–OES

The determination of tantalum by colorimetry is laborious, time-consuming, inaccurate and often unre-

liable. The strong tendency to hydrolysis makes it difficult to get tantalum into solution in reproducible form under the conditions wanted for colorimetry. Its strong affinity for oxygen also causes low sensitivity in atomic-absorption spectroscopy, even with N_2O–C_2H_2 flames. Carbide formation excludes the application of graphite-furnace AAS.

Inductively-coupled plasma–optical emission spectroscopy (ICP–OES) combines high temperature with an inert atmosphere. It has been noted as promising because of its high sensitivity, favourable sample consumption, speed of analysis and matrix insensitivity. It seems the best technique for tantalum nowadays. We have investigated the possible interference of gold and the accuracy with which tantalum can be determined in a relatively small sample (100–500 mg of alloy containing 0.002–0.03% Ta). The solutions were prepared by dissolution of tantalum, gold and their alloy in a mixture of hydrofluoric, nitric and hydrochloric acids, and the excess of hydrofluoric acid was expelled by repeated evaporation with concentrated hydrochloric acid. The final solutions were made about 1*M* in hydrochloric acid by dilution with acid of that concentration.

The sample solutions were analysed with a Jarrel-Ash Plasma Atom Comp ICP Spectrophotometer. The samples were nebulized with argon, the feed gas for the plasma. The plasma torch was powered by a 2-kW 27-MHz power supply. With an auxiliary monochromator the 240.06-nm emission line was selected. It is the most sensitive line, with a published detection limit of 0.03 μg/ml for tantalum in aqueous solution, and a linear working range from 0.150 to 3000 μg/ml. The output of the photomultiplier tube was recorded as a photon count.

Linearity, noise, drift and detection limit were tested with standard tantalum solutions covering the range 0–15 μg/ml. Two series of standard solutions were prepared, one without gold and the other with 8 mg/ml. Statistical evaluation of both series of measurements on solutions containing exactly 0, 1, 2.5, 5, 10 and 15 μg of tantalum per ml showed that the linearity of both series was better than 1% for measurements performed within a time span of 15 min, but that both series gave significantly differing lines (Fig. 2):

$$S = 183.45C_{Ta} + 954 \qquad (6a)$$

$$S = 180.80C_{Ta} + 1085 \qquad (6b)$$

(in counts per 10 sec). The equations refer to the series with (6b) and without (6a) gold. The least-squares fit leading to equations (6a) and (6b) was performed with equal weighting factors for the individual points, as there was no reason to assume that the standard deviation σ_S differed for the different tantalum and gold concentrations. From the error-square sum the standard deviation of the individually measured points about the regression lines could be estimated as $\sigma_S = 9$ counts/10 sec in both cases. (The correlation

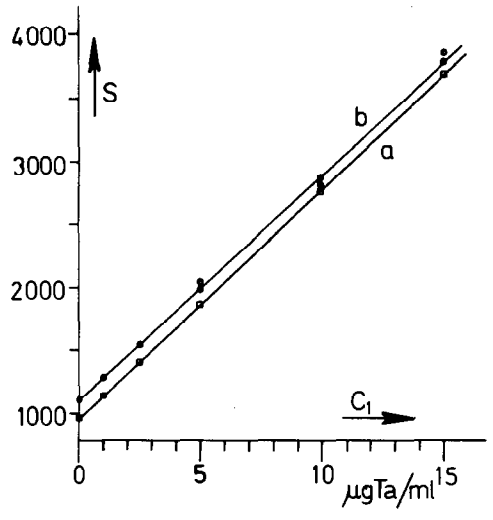


Fig. 2. Calibration graphs for tantalum. The line (a) corresponds to standard solutions without another metal; the line (b) corresponds to standards containing 8 mg of gold per ml. The points indicate experimental results.

coefficients of the regression analysis were 0.99990 and 0.99999 respectively). For $\sigma_S = 9$ the detection limit for tantalum would be 0.05 μg/ml; 0.04 μg/ml was found experimentally.

The sensitivity decreased by about 7% over a 2-hr working period. It is easy to correct for this drift by regular calibration. Equations (6a) and (6b) were derived from results obtained within a time span of 15 min.

Comparing equations (6a) and (6b), it is obvious that the straight lines are shifted and rotated with respect to each other. Considering this in terms of the factorial analysis, the following table can be written analogously to Table 1 in the theory section. By substituting the S_i values and their standard deviations from Table 2 in the equations (5) the *B*-values and their respective standard deviations are obtained ($B_0 = 2385 \pm 5$; $B_1 = 1363 \pm 5$; $B_2 = 56 \pm 5$; $B_{12} = -10 \pm 5$); all the *B*-values are significant (at the 0.1 level).

From Table 2 and equation (3) it follows that $x_1 = (c_1 - 7.5)/7.5$ and $x_2 = (c_2 - 4)/4$. Substitution in equation (4) leads to

$$c_1 = 7.5\left\{\frac{S - B_0 - B_2(c_2/4 - 1)}{B_1 + B_{12}(c_2/4 - 1)} + 1\right\} \qquad (7)$$

Ten gold samples with low tantalum content and different mass were measured during the time span for which the *B*-values given above are valid. Samples 1–8 were diluted to 100 ml, samples 9 and 10 to 50 ml. The results are given in Table 3. The error in *S* was found from the mean of four samples. Application of the law of propagation of errors to equation (7) and insertion of the standard deviations of *S*, the *B*-values and x_i led to the errors in the tantalum results indicated in column "eq. (7)". The last two columns

Table 2. 2^2 factorial applied in the determination of tantalum

No.	c_1 (Ta), *μg/ml*	c_2 (Au), *mg/ml*	x_1 (Ta)	x_2 (Au)	S,* *counts*	σ_s,* *counts*
1	15.0	8.0	1	1	3797	9
2	15.0	0	1	−1	3705	9
3	0	0	−1	−1	954	9
4	0	8.0	−1	1	1085	9

(Note the different units for c_1 and c_2)
* Per 10 sec.

Table 3. Results for determination of tantalum

No.	Mass of sample, *mg*	S*, *counts*/10 *sec*	Ta,% = 0.1 c_1/c_2 eq. (7)	eq. (6a)	eq. (6b)
1	153.4	1746	0.273 ± 4	0.281	0.238
2	145.6	1087	0.040 ± 3	0.050	0.008
3	151.2	1605	0.226 ± 3	0.235	0.190
4	149.6	1454	0.173 ± 3	0.182	0.136
5	182.9	1192	0.062 ± 3	0.071	0.032
6	185.6	1064	0.023 ± 3	0.032	(<0)
7	190.0	1681	0.200 ± 3	0.209	0.174
8	197.0	1760	0.215 ± 3	0.223	0.189
9	208.4	1454	0.057 ± 2	0.065	0.049
10	308.2	1531	0.042 ± 2	0.051	0.040

* σ_s = 9 counts/10 sec.

correspond to results found by neglecting the presence of gold (equation 6a) or by overcompensating for its presence by using equation (6b). Comparison of the results shows that the differences are significant.

Tantalum–gold alloys are used by physicists for measurement of the electrical rest-resistance at liquid-helium temperature. The original nominal tantalum concentrations led to fairly scattered points in a plot of R *vs.* c_1; with the data from equation (7) a perfectly linear relationship was found between rest-resistance and tantalum content.

Several other series of samples were analysed. Each series of ten was sandwiched between standards in order to correct for drift.

It should be noted that the nebulization was controlled by a pumping device. Thus the dependence of S on the gold concentration was not due to variations in fluid supply caused by change in density, surface tension, viscosity, *etc.* Its real origin was not investigated further.

2^n factorial analysis of linearized systems

In atomic-absorption spectrophotometry most calibration graphs are non-linear. Consequently terms of higher order in c_1 have to be added to equation (2) for a proper fit of the graph to the measured points. A problem is that power series are not very suitable for curve-fitting in AAS: many terms are usually needed for an acceptable fit. If, in addition, the matrix influence has to be accounted for, complicated equations will arise, with many regression coefficients B to be estimated by calibration. Correcting for matrix influence purely by calculation is therefore less suitable.

The curvature problem has been attacked by many manufacturers of AAS instruments. It has resulted in the newer instruments having built-in microprocessor facilities for curve-correction. The underlying mathematics is mostly based on series functions other than power series, with a minimum number of constants to be found. The software works remarkably well when applied to pure solutions, provided that recalibration is performed regularly. The error in the concentrations displayed does not differ from that in the values read from calibration curves.

Taking either the read-out value from the instrument or the value from the calibration curve as the signal, we get a variable which is supposed to be linearly related to the real concentration c_1 in the case of pure metal solutions. Actually, we deal here with a sort of linearization and the question arises immediately whether the linearized output can be used for a correction of matrix influence by 2^n factorial analysis in the same way as for tantalum. The answer will be given below by making an analysis of the systematic error occurring when the procedure is applied to a model chosen to simulate practical cases in flame AAS.

Let us suppose that a specific calibration curve for a metal can be approximated by

$$S = 0.040c_1 - 0.001c_1^2 \qquad (8)$$

and that this equation holds for c_1 values in the range 0–10 ppm (line "a", Fig. 3). It is reasonable to expect in the first instance that only first-order effects will

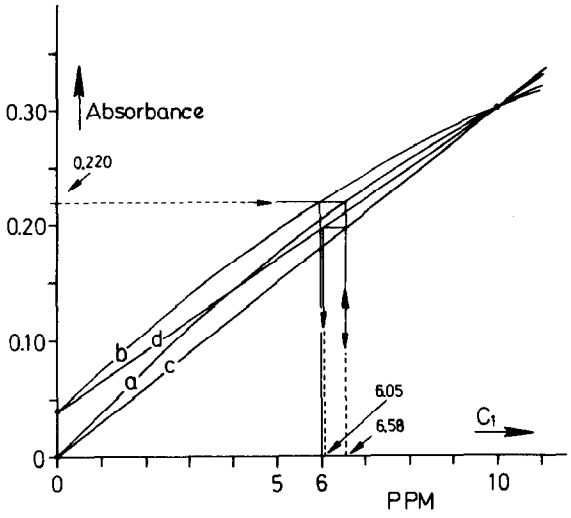


Fig. 3. Model AAS calibration graph, closely resembling a practical case. For line (a) a parabolic shape has been selected. Line (b) is also parabolic and simulates the influence of the matrix. Lines (c) and (d) are the straight lines attributed to the concentration readings; their position is determined by the outermost values of the concentration range. The other lines refer to the example in the text, where the horizontal distance between the curved lines is estimated from the distance between the straight lines.

occur when a matrix species is present in the solution; hence the shift and rotation of the curved calibration line will depend linearly on the matrix concentration. Suppose that a second metal is present at a concentration of 2 mg/ml and that we may estimate the new curve ("b" in Fig. 3) by

$$S = 0.04 + 0.036c_1 - 0.001c_1^2 \qquad (9)$$

It must be noted that in this model both the curvature and the influence of the matrix are rather exaggerated in comparison with the experimental results for determination of nickel in gold by flame-AAS.

Suppose that the instrument is calibrated and the result is in perfect agreement with equation (8). Then the instrument cannot distinguish whether the matrix is present or not. Thus if a sample containing 6.00 ppm nickel in the presence of 2000 ppm of gold is nebulized, the absorbance will be 0.220 according to equation (9) but the display will be 6.58 ppm according to equation (8) (Fig. 3).

To this displayed value a new signal S' is attributed, which is proportional to the displayed concentration:

$$S' = 0.030c_1 \qquad (10)$$

In fact this equation is chosen so that its straight line ("c" in Fig. 3) goes through the points $c_1 = 0$ and $c_1 = 10$ ppm from equation (8). Similarly a straight line ("d" in Fig. 3) can be drawn through the outermost points of equation (9), which leads to

$$S' = 0.04 + 0.026c_1 \qquad (11)$$

This second line [equation (11)] originates from the first one [equation (10)] by a shift and a rotation equal to the displacements of the original lines corresponding to the equations (9) and (8). If we now correct the previously found value 6.58 ppm by the difference between the straight lines of equations (10) and (11), we get $6.58 \times 0.030 = S = 0.04 + 0.26c_1$ from which we find $c_1 = 6.05$ ppm (Fig. 3), an acceptable value in view of the usual accuracy of AAS. In Fig. 4 the real deviation and its approximation from equations (10) and (11) are represented for other concentration displays. It can be concluded that for this model any differences can be neglected in the upper part of the concentration range (5–10 ppm). In practical AAS we always deal with situations similar to this model, but in most practical cases the curvature of the calibration lines is much less than in the model. Thus the correction procedure will usually lead to even better values. The shape of a real calibration curve may deviate from the example given, in that higher-order terms may contribute to equation (2), but in general the difference between shifted and rotated calibration lines can be estimated satisfactorily by the difference between the two straight lines through the outermost points of the concentration range, if we restrict ourselves to the upper part of this range (which is almost always the case, as in practice it is felt common sense to do this for reasons of accuracy).

The advantage of the procedure is that it can be applied even to systems with a calibration line for which no adequate mathematical approximation can

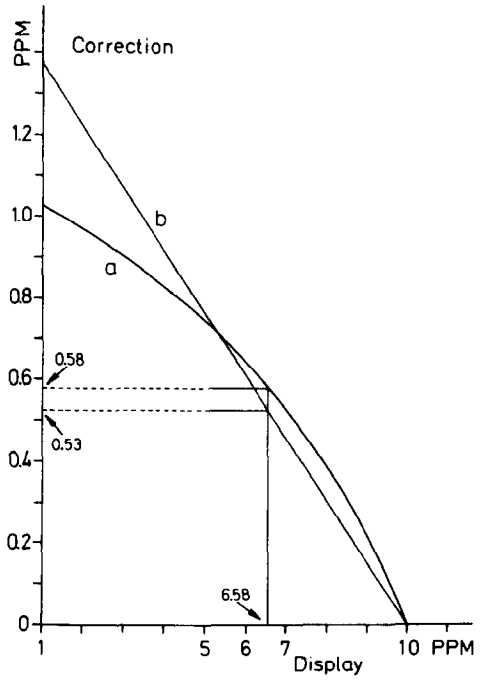


Fig. 4. A comparison of the real deviation between the curved calibration lines (line a) and the correction applied when 2^3 factorial analysis is performed (line b). The figure is related to the model used for Fig. 3.

Table 4. 2^2 factorial applied in determination of nickel

No.	c_1 (Ni), *μg/ml*	c_2 (Au), *mg/ml*	x_1 (Ni)	x_2 (Au)	S'*, *absorbance*
1	9.72	1.5	1	1	0.330_4
2	9.72	0	1	−1	0.348_3
3	0	0	−1	−1	0
4	0	1.5	−1	1	0.009

* Averages calculated on the basis of 24 measurements.
$x_1 = (c_1 - 4.86)/4.86$ and $x_2 = (c_2 - 0.75)/0.75$.

be made; the 2^n factorial analysis is applied to the straight line through the extreme points and the estimated corrections are applied to the real curve. If the matrix effect is not too large, its influence on the calibration line can be approximated by a linear function. As this is generally the case, the procedure is widely applicable.

Let us now consider the practical case of nickel in a gold matrix. Samples with masses between 150 and 450 mg, and containing 0.4–1.0% nickel were dissolved in *aqua regia*. The separate nickel and gold solutions needed for standardization were similarly prepared. The final acidity was 1*M* hydrochloric acid.

The Perkin–Elmer 560 AA spectrophotometer was calibrated with four nickel solutions (without gold) to adjust the curve-correction facility.

Table 4 gives the calibration results (with and without gold present), used for the factorial analysis, together with the coded concentrations.

The *B*-coefficients of equation (4) follow from Table 4 by means of (5):

$$S' = 0.1719 + 0.1674x_1 - 0.0022x_2 - 0.0067x_1x_2 \quad (12)$$

Substitution of x_1 and x_2 then leads to

$$c_1 = 4.86\left\{\frac{S' - B_0 - B_2(1.33c_2 - 1)}{B_1 + B_{12}(1.33c_2 - 1)} + 1\right\} \quad (13)$$

The value of S' to be substituted in equation (13) is found by multiplying the displayed concentrations by the factor 0.03583 [=0.3483/9.72, the slope of the straight line "c" (Table 4)]. With this value of S', equation (13), and the *B*-values of (12), the results for some alloys have been obtained and are given in Table 5.

Samples 1–5 had a volume of 137.5 ml, 6, 7, 9 and 10 a volume of 250 ml, and sample 8 was 500 ml in volume.

The results in the last column were checked by photometric titration. The agreement was within 0.5%. The corrected results have been used by physicists as a support for their rest-resistance measurements at liquid-helium temperature. It turned out that the relative deviations from the straight-line relationship were all less than 2%. This is remarkable, first because the correction for the matrix effect was also applied to nickel concentrations outside the calibration range (samples 5 and 9) and secondly because the correction was carried out for matrix concentrations exceeding 1.5 mg/ml (samples 2, 3, 4, 5 and 9). In general this kind of extrapolation should be made with caution.

DISCUSSION AND CONCLUSION

In the foregoing the instrument display of the Perkin–Elmer 560 atomic-absorption spectrophotometer played a dominant role. Such a facility is not essential, however. With a calibration curve obtained in the absence of a matrix and with S values for the outermost concentrations of the analyte, obtained with a maximum of matrix present, an identical procedure can be followed. The calibration curve replaces the function of the curve-correction facility.

Table 5. Results of determination of Ni in Ni–Au alloys

No.	Displayed concentration, *ppm*	Mass of sample, *mg*	Concn. of Au, *mg/ml*	Ni, % (=0.1 c_1/c_2) uncorrected results	corrected results
1	6.07	191.4	1.392	0.43_6	0.45_2
2	6.97	224.0	1.629	0.42_8	0.44_9
3	7.04	232.6	1.692	0.41_6	0.43_7
4	8.21	268.3	1.951	0.42_1	0.44_9
5	10.95	358.5	2.607	0.42_0	0.46_6
6	8.21	278.0	1.112	0.73_8	0.76_5
7	8.99	312.2	1.249	0.72_0	0.75_1
8	6.58	445.4	0.891	0.73_9	0.75_6
9	11.19	382.7	1.531	0.73_1	0.77_5
10	6.31	216.3	0.865	0.72_9	0.74_6

The method of matrix-correction is simple and economical as long as we deal with linearity, which implies that we may apply equation (2). Slight curvature with respect to the component to be assayed can be corrected by a linearization as elucidated in this paper. With respect to the matrix, it is advisable to determine the outermost S values for intermediate matrix concentrations as well, in order to check whether the shift and rotation of the calibration curve can really be regarded as linear. If higher-order terms have to be added, the first terms will be related to the shift and rotation prior to changes in curvature; thus we may expect $b_{22}c_2^2$ and $b_{122}c_1c_2^2$. In this case k^2 factorial ($k > 2$) or a rotatable design[1,2] will have to be applied for the determination of the b-coefficients. The method of matrix-correction can also be applied to multicomponent systems ($n > 2$). If linearity holds, 2^n factorial analysis can be applied, but for non-linear situations the more elaborate k^n factorial will be necessary and this procedure is generally time-consuming. In practice, however, satisfactory results are achieved in most cases by choosing linear systems or linearizing the system as indicated before for the component to be assayed and approximating the matrix influence as linear. The method has been applied for various metals in different matrices and the results checked against those obtained by photometric complex-formation titrations. In those cases where the AAS calibration curve was not heavily influenced, the system of 2^n factorial analysis always gave answers within 1 or 2% of the real value.

Acknowledgement—We are indebted to Mr. Hans Balke for his contribution in performing the ICP–OES measurements.

REFERENCES

1. W. C. Cochran and G. M. Cox, *Experimental Design*, Wiley, New York, 1950.
2. D. L. Massart, A. Dijkstra and L. Kaufman, *Evaluation and Optimization of Laboratory Methods and Analytical Procedures*, Elsevier, Amsterdam, 1978.
3. A. Parczewski and A. Rokosz, *Chem. Anal. (Warsaw)*, 1978, **32**, 225.
4. A. Madej, A. Parczewski, A. Rokosz and R. Stępak, *ibid.*, 1978, **23**, 231.
5. M. Meus, A. Parczewski, M. Plesińska and A. Rokosz, *ibid.*, 1978, **23**, 925.
6. A. Parczewski and P. Kościelniak, *Z. Anal. Chem.*, 1979, **297**, 148.
7. P. Kościelniak, A. Parczewski and S. Walas, *ibid.*, 1979, **297**, 156.
8. P. Kościelniak, S. Walas and A. Parczewski, *ibid.*, 1980, **302**, 402.
9. A. Parczewski and A. Madej, *Chem. Anal. Warsaw*, submitted for publication.
10. P. Volke, *Silikattechnik*, 1976, **27**, 130.
11. W. Wegscheider, G. Knapp and H. Spitzy, *Z. Anal. Chem.*, 1977, **283**, 9.
12. T. C. Woodis, Jr., G. B. Hunter and F. J. Johnson, *Anal. Chim. Acta* 1977, **90**, 127.

Talanta, Vol. 28, pp. 909 to 913, 1981
Printed in Great Britain. All rights reserved

0039-9140/81/120909-05$02.00/0
Copyright © 1981 Pergamon Press Ltd

DETERMINATION OF ZINC IN SEA-WATER BY ANODIC STRIPPING VOLTAMMETRY

SERGIO DE JESUS ALEVATO and ANGELA DE LUCA REBELLO

Departamento de Química, Pontifícia Universidade Católica do Rio de Janeiro, Rio de Janeiro, Brazil

(*Received* 15 *December* 1980. *Accepted* 14 *May* 1981)

Summary—The horizontal distribution of zinc in surface waters from Guanabara Bay has been studied by use of optimized voltammetric techniques and ultraclean working procedures. The non-linearity observed between the peak current for zinc and the electrolysis time, as well as the appearance of a peak at −1.16 V, are discussed. The values found for total zinc in the samples range between 0.3 and 22 μg/l.

Literature values for zinc concentrations in uncontaminated sea-water range from 0.03 to 10 μg/l.[1] More recent analyses of surface waters from the Pacific Ocean,[2] however, have revealed concentrations as low as 0.006 μg/l., emphasizing the importance of applying ultraclean techniques to both the sampling and the analytical stages. In this context voltammetric methods of analysis present the great advantages of high sensitivity for zinc and of not requiring any pretreatment, and anodic stripping voltammetry has frequently been used for the determination of zinc in natural waters.

This paper reports a study of the zinc levels in samples of sea-water containing high levels of organic compounds, with differential pulse anodic stripping voltammetry (DPASV) used to determine the zinc. The sea-water samples were collected at several stations in the Guanabara bay, as shown in Fig. 1. This bay is surrounded by the city of Rio de Janeiro and receives large loads of industrial and domestic waste delivered by numerous rivers and channels. Several factories and docks located around the ridges are also partly responsible for the severely polluted character of the bay, contributing mainly organic materials such as oil, surfactants, litter and bacteria.

In spite of this situation, environmental studies have only recently been begun in this area and data are not available in the literature. There is a preliminary report[3] on pollutants, including zinc, in which data are given for concentrations of this metal in the waters of some rivers belonging to the bay's hydrographic basin. The values reported ranged from 50 to 320 μg/l.

EXPERIMENTAL

Sampling

Conventional polyethylene bottles (500 or 1000 ml) were used after being carefully cleaned and treated according to the instructions of Patterson and Settle,[4] and Moody and Lindstrom.[5] After being cleaned, the bottles were always kept full of dilute nitric acid and stored inside double polyethylene bags up to the moment of sampling. All the cleaning operations were performed with Merck *p.a.* reagents. Samples were collected by boat from different parts of the bay. During rinsing and filling of the bottles with sea-water the boat was rowed into the wind, and the sample was always collected ahead of the boat and in the direction of movement, at about 30 cm below the water line. The bottles were handled throughout with polyethylene gloves and immediately placed inside new polyethylene bags. At least two samples were collected at each station.

Tests for adsorption of zinc on the bottle walls showed that after storage for 5 days at the natural pH the samples had lost 48–58% of the zinc by adsorption on the walls or dead organisms. The samples were therefore acidified to about pH 2 while still in the sampling bottles, either when collected or in the laboratory 24 hr before analysis. The heating at 65 for 24 hr, as advised by Patterson[6] in the case of lead, did not result in additional desorption of zinc, but decreased the analytical sensitivity by about 30%. The acidification to pH 2 also proved sufficient to release all zinc from particulate matter or complexed forms in the solution.

Reagents and instrumentation

All chemicals added to the samples were Merck Suprapur quality. The water used for washing was doubly demineralized and distilled, giving a zinc content of 0.07–0.11 μg/l.

A PAR 174 A polarograph and a PAR 9333 hanging mercury dropping electrode were used. A PAR K 77 saturated calomel electrode and a platinum wire (0.9 mm diameter) were used as reference and auxiliary electrode, respectively. Stirring was provided by a Teflon-coated bar and a magnetic stirrer.

The nitrogen for deaerating the solutions was purified by passage through an "Oxisorb" tube and then through demineralized water. Before reaching the electrolytic cell the gas was passed through a tube with glass rings to hold back water droplets and any impurities. A PAR K 60 Pyrex electrolytic cell was used once no further significant differences in zinc concentration had been found for samples at pH 4.9 analysed in this cell, conditioned as follows (along with the stirring bar, electrodes, salt bridge and nitrogen bubbler) before each analysis. The electrodes and bubbler unit (mounted in the cell top) were washed several times with jets of dilute nitric acid (Merck *p.a.*) while nitrogen flowed through the bubbler. Doubly demineralized water and a few drops of nitric acid (Merck *p.a.*) were transferred to the cell and stirred. The stirring was

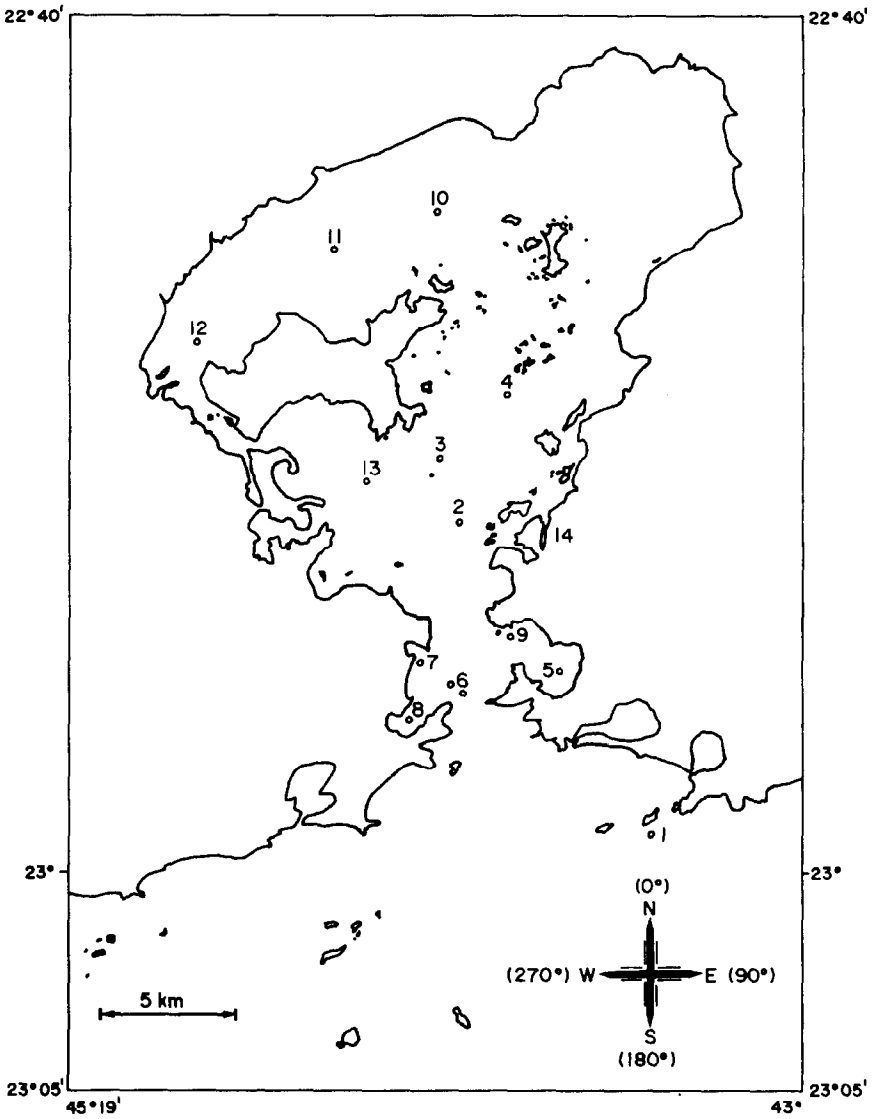


Fig. 1. Sampling stations in Guanabara bay.

stopped, the cell emptied and the procedure repeated several times before the cell top was mounted on the cell.

The assembled cell was then washed several times with doubly demineralized and distilled water and finally with the sample to be analysed. Only then was the sample (15 g) weighed into the cell followed by 50 ± 1 mg of sodium acetate crystals (Merck Suprapur).

The HMDE capillaries were cleaned by aspirating through them 50 ml of nitric acid (1 + 3) (Merck *p.a.*) to which 1% v/v of hydrofluoric acid was added for every third cleaning cycle. The excess of acid was then removed with warm doubly demineralized water before the capillaries were dried (110° for 40 min), siliconed (Desicote, Beckmann) and filled with mercury. Siliconing was done by aspirating the reagent through the capillary, then heating at 240° under vacuum for 15 min.

The mercury used was Merck 4403 (stated zinc concentration 5×10^{-5}%) further purified by washing with nitric acid (1 + 9).

To prevent adsorption of zinc on the walls of the sampling bottles, the samples had to be acidified to about pH 2. However, at this pH the resolution of the zinc voltammetric peak is poor at the low concentration levels encountered. The peak current was known[7] to increase by a factor of 5 if the pH was increased from 2 to 5. Hence a working pH of 4.9 ± 0.1 (sodium acetate buffer) was chosen.

Since the relationship between peak-current and deposition time for zinc under these conditions was found to be non-linear, the same deposition time should be used throughout.

The possibility of adsorption of zinc on the cell walls at pH 4.9 was checked; if a sample was analysed at pH 2, then adjusted to pH 4.9, left in the cell for 15 hr, and then analysed again, the zinc concentration apparently decreased by 6%.

The degree of liberation of zinc from particulate matter and organic complexes by acidification to pH 2 was established by comparing the results with those obtained for aliquots of the same sample that had been evaporated to dryness and redissolved in doubly demineralized and distilled water acidified with hydrochloric acid (Merck Suprapur). The differences for three samples containing 1.21, 1.45 and 22.1 μg of zinc per litre was less than one standard deviation.

The blank for the evaporation and redissolution procedure ranged between 0.085 and 0.130 μg/l.

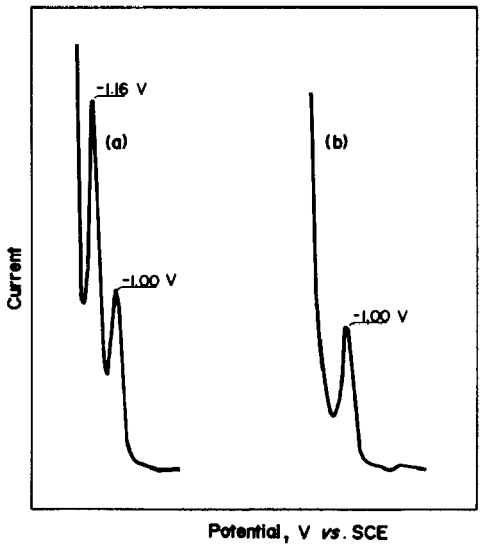


Fig. 2. Zinc-peak resolution related to the electrodeposition potential for sea-water samples analysed by DPASV with the HMDE. (*a*) $E_d = -1.35$ V (*vs.* SCE), (*b*) $E_d = -1.25$ V (*vs.* SCE). Scan-rate 5 mV/sec; electrodeposition time 150 sec; pulse amplitude 50 mV; pulse repetition time 0.5 sec.

DISCUSSION

Electrochemical parameters

The conditions for the electrochemical determination were studied in order to improve the sensitivity and reproducibility. The dependence of the peak-current (i_p) on the scan-rate (v), modulation amplitude (h_p) and pulse repetition time (r_p) was studied for sea-water at pH 4.9. The duration of current sampling was fixed at 16.67 msec.

When the scan-rate was set at 5 mV/sec and the pulse repetition time at 0.5 sec, the peak-height was found to increase as the modulation amplitude was increased, but with a scan-rate of 10 mV/sec a slight decrease in peak-height resulted for an increase in modulation amplitude. For various scan-rates the dependence was found to fit a function of the form $i_p = a(h_p)^{1.14}$ with a correlation coefficient of 0.998–1.000. In accordance with this the maximum i_p was found at an h_p of 100 mV but the peaks were wider, resulting in poorer resolution.

The variation in peak-width at half peak-height ($b_{\frac{1}{2}}$) with modulation amplitude was not in good agreement with expectation for a reversible 2-electron process.[8,9] This seems to confirm the observations of Dillard *et al.*[10] on the sharp increase in $b_{\frac{1}{2}}$ for quasi-reversible electron-transfer reactions. Recently Musani *et al.*[11] also observed an increase in $b_{\frac{1}{2}}$ for zinc in solutions containing organic substances.

With a scan-rate of 5 mV/sec and modulation amplitude of 50 mV, the best resolution and peak-height were found for a pulse repetition time of 0.5 sec.

The experiments above were performed with an electrolysis time of 3 min and stirring at 780 rpm, followed by 30 sec at rest and deposition at a potential of -1.25 V *vs.* SCE. The use of a salt bridge to connect the auxiliary electrode to the test solution did not cause any noticeable variation in i_p, E_p or $b_{\frac{1}{2}}$ over a range of different electrodeposition times.

Tests to establish the best electrolytic deposition potential (E_p) suggested an optimum value of -1.25 V. At smaller values the peak-current also decreased, and for values between -1.35 and -1.25 V a new stripping peak was observed at -1.16 V for several of the samples analysed. This peak, as can be seen in Fig. 2, interfered seriously in the zinc determination. The fact that the peak at -1.16 V could be eliminated by irradiating the sample with ultraviolet light in the presence of hydrogen peroxide indicated the organic character of the substance responsible. Samples which had been acidified and heated at 65° for 24 hr in the sampling bottles gave the peak at -1.16 V, with high i_p values. The bottles were then tested (with artificial sea-water) as a possible source of the organic substances, but no positive results were found.

According to Meites[12] a sudden change in direction of the anodic wave in cyclic voltammetry is evidence of an adsorption wave. Cyclic voltamperograms were therefore performed with different sea-water samples at pH 5, with deposition times of 150 sec and scanning range from -1.35 to -0.80 V. As seen in Fig. 3, a sudden change in curve shape occurred just between the peak at -1.26 V and the zinc peak at -0.98 V. This behaviour and the tendency of the peak at -1.16 V to decrease with increasing pH and increasing elec-

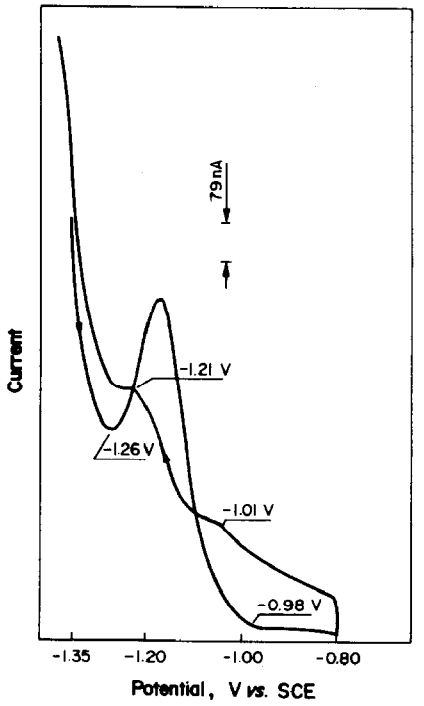


Fig. 3. Cyclic voltammetry of zinc in sea-water from Guanabara Bay with the HMDE. Potential range from -1.35 to -0.80 V; electrodeposition time 150 sec; stirring at 500 rpm.

Table 1. Voltammetric parameters for the determination of zinc in sea-water

Peak potential	-0.997 ± 0.017 V
Deposition potential	-1.25 V
Stirring rate	780 rpm
Mercury drop	1.81 mm^2
Pulse height	50 mV
Pulse repetition time	0.5 sec
Current range	1–10 μA
Scan rate	5 mV/sec
Electrodeposition time	150–600 sec with stirring, 30 sec at rest

trolysis time, leads to the conclusion that the peak must be of tensametric origin. Possibly some organic compounds activated by acid catalysis are responsible for this typically tensametric wave.

The deaeration time required to give the lowest background currrent was found to be about 50 min at moderate nitrogen flow. High flow-rates were tried in order to decrease the bubbling time, but resulted in contamination owing to droplets reaching the cell top and falling back into the test solution. The source of contamination was found to be the rubber sealing ring of the cell top.

Table 1 summarizes the experimental conditions applicable to all the sea-water analyses.

Dependence of peak-height on deposition time

It was observed that the peak-current (i_p) for sea-water samples was not linearly proportional to the electrodeposition time (t_d); this can be seen in Fig. 4.

The fact that test solutions prepared in doubly deionized and distilled water *did* give a linear relation, as shown in Fig. 4a, makes it difficult to attribute the loss of sensitivity at longer deposition times, observed for sea-water, to diffusion of zinc through the mercury capillary or to a shift occurring between the anodic scan and the tail of the dissolution peak of the zinc.

Experiments by d.c. polarography at various pH values with a dropping mercury electrode and on sea-water samples with zinc added to give a concentration

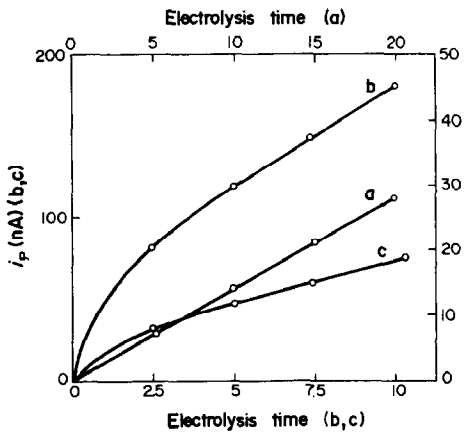


Fig. 4. Relation between zinc peak current and electrodeposition time. (*a*) demineralized and distilled water; (*b*) sea-water plus standard addition; (*c*) sea-water.

Table 2. Diffusion currents for zinc in sea-water at different pH values, with D.M.E. (scan-rate 1 mV/sec, scan range from 0.65 to -1.4 V *vs.* SCE, damping = 30 msec)

Electrolyte pH	Diffusion current, μA
2.1	0.18
4.0	0.20
5.0	0.21
6.5	0.20
8.5	0.05
9.0	—

of 5×10^{-5} *M* showed that at above pH 6.5 the diffusion current of zinc decreased so much that at pH 9 there was no wave at all, owing to the formation of a non-electroactive zinc species. The variation of i_d with pH can be seen from the results in Table 2.

With test solutions initially at pH 4.9 ± 0.1 and a specially constructed antimony electrode (dE/dpH = 52.5 mV/pH from pH 5 to 11) placed beside the capillary of the HMDE, the pH was monitored during the electrolysis and found to increase with electrolysis time: $t_d = 0$, pH = 4.8; $t_d = 5$ min, pH = 8.1. As the conditions arising in the neighbourhood of the dropping electrode during electrolysis may well interfere with the double layer and also with the antimony electrode, these results should be considered as being only qualitative, simply indicating a trend in solution conditions near the electrode. However, it is highly probable that the observed lack of linearity between i_p and t_d is connected with the electrodeposition step, and with the change of pH giving an alkaline environment round the electrode in solutions of high ionic strength and high sodium concentration, where the diffusion constant for zinc is smaller than in pure water.

In order to avoid errors, all sea-water samples were analysed with at least two different electrolysis times. The same conditions were used for the standard addition steps, and no trend was detected either for standards or samples.

The analytical method proved to be reliable, with good linearity between peak-current and zinc concentration, characterized by correlation coefficients larger than 0.9993. No interferences were found when zinc at the 4-μg/l. level in sea-water was determined by DPASV in the presence of Cd^{2+}, Cu^{2+}, Pb^{2+}, Ni^{2+}, Mn^{2+}, Fe^{3+} and Co^{3+} at concentrations up to 3, 16, 6.5, 63, 6.3, 6.5 and 6.5 μg/l. respectively.

Analytical results

The fourteen stations at which samples of sea-water were collected are shown in Fig. 1 and the results obtained for total zinc concentrations are listed in Table 3.

Two stations, BG 12 and BG 14, gave significantly higher values than the average of the other 12 samples and identify the main sources of introduction of metal

Table 3. Zinc determination in sea-water from Guanabara bay

Sampling station	Number of samples	Number of determinations	Zinc concentration, μg/l.	Relative standard deviation, %
1	5	20	0.28	12
2	2	6	1.17	6
3	2	6	1.58	17
4	2	7	1.44	8
5	2	9	0.59	4
6	3	10	1.53	2
7	2	8	1.49	4
8	2	12	1.70	3
9	2	8	0.98	10
10	2	6	1.00	5
11	2	8	2.91	1
12	2	8	22.1	5
13	2	6	2.38	6
14	2	5	8.90	3

into the bay. Those sources are the river S. Joao de Meriti (BG 12) and the factories (canned fish) and docks located at BG 14.

On average the levels of zinc in the bay are lower than those for some other locations reported in the literature.

REFERENCES

1. J. P. Riley and R. Chester, *Introduction to Marine Chemistry*. Academic Press, London, 1971.
2. K. W. Bruland, G. A. Knauer and J. H. Martin, *Nature*, 1978, **271**, 741.
3. FEEMA, Preliminary Report: *Guanabara Basin*, 1979.
4. C. Patterson and D. Settle, in *Accuracy in Trace Analysis*, Proc. 7th Materials Research Symposium, NBS, Washington.
5. J. R. Moody and R. M. Lindstrom, *Anal. Chem.*, 1977, **49**, 2264.
6. C. Patterson, *Marine Chem.*, 1974, **2**, 69.
7. S. R. Arras, *Tese de Mestrado*, Pontificia Universidada Catolica do Rio de Janeiro, 1980.
8. S. R. Arras and S. J. Alevato, *Rev. Metal.* CENIM, 1978, **14**, 149.
9. E. P. Parry and R. A. Osteryoung, *Anal. Chem.*, 1965, **37**, 1634.
10. J. W. Dillard, J. J. O'Dea and R. A. Osteryoung, *ibid.*, 1979, **51**, 115.
11. L. J. Musani, H. W. Nürnberg, P. Valenta, Z. Konrad and M. Branica, *Proc. 5th Intern. Symp. Chem. Mediterranean, Rovinj*, May 1978.
12. L. Meites, *Polarographic Techniques*, 2nd Ed., Interscience, New York, 1965.

Talanta, Vol. 28, pp. 915 to 918, 1981
Printed in Great Britain. All rights reserved

0039-9140/81/120915-04$02.00/0
Copyright © 1981 Pergamon Press Ltd

UNTERSUCHUNGEN ZUR ANWENDUNG TERNÄRER KOMPLEXE IN DER PHOTOMETRIE—II

DIE BESTIMMUNG DES TITANIUM(IV) MIT TIRON IN GEGENWART VON IMINODIESSIGSÄURE, NITRILOTRIESSIGSÄURE BZW. DIETHYLENTRIAMINPENTAESSIGSÄURE

S. KOCH, G. ACKERMANN und V. SCHOLZE

Bergakademie Freiberg, Sektion Chemie, Lehrstuhl für Analytische Chemie, 9200 Freiberg, Deutsche Demokratische Republik

(*Eingegangen am* 12. *Februar* 1981. *Angenommen am* 12. *Mai* 1981)

Zusammenfassung—Zur Bewertung ternärer Komplexe in der Photometrie wurden drei Modell-Systeme, von Titanium(IV) mit Tiron und Iminodiessigsäure bzw. Nitrilotriessigsäure, Diethylentriaminpentaessigsäure, charakterisiert. Neben der Ermittlung der Kennzahlen Arbeitsbereich, Extinktionskoeffizient, Standardabweichung, Variationskoeffizient, Eichfunktion, Nachweisgrenze und Erfassungsgrenze erfolgte auch eine Untersuchung der Störung durch 20 Ionen. Es zeigte sich, daß das Nitrilotriessigsäuresystem gegenüber den anderen Systemen eine höhere Selektivität aufweist.

Im Rahmen systematischer Untersuchungen[1] zur Anwendung ternärer Komplexe in der Photometrie konnte nachgewiesen werden, daß bei dem Tiron-Verfahren[2] zur Bestimmung von Titanium(IV) eine Selektivitätssteigerung eintritt, wenn man bei pH 3,6 in Gegenwart von EDTE (Ethylendiamintetraessigsäure) arbeitet. Unter diesen bedingungen bildet sich ein farbiges ternäres Chelat $[TiO(HY)R]^{5-}$ zwischen Titanium(IV), EDTE, Tiron, und die Störungen durch Bi(III), Cr(III), Cu(II), Fe(III), Mn(II), Mo(VI), Nb(V), Ni(II), U(VI), W(VI) sind geringer, als bei der bekannten Tironmethode unter Bildung von $[TiR_3]^{8-}$.

Die Ursache der Selektivitätserhöhung im ternären System liegt im allgemeinen darin, daß Störionen stabile Chelate mit EDTE bilden, welche mit dem chromophoren Liganden Tiron nicht reagieren. Verantwortlich für die Selektivitätserhöhung sind somit die komplexchemischen Eigenschaften des ternären Systems, welche u.a. vom Zweitligand (EDTE) bestimmt werden. Um in diesem Zusammenhang die Wirkung weiterer Aminopolycarbonsäuren unterschiedlicher Zähnigkeit zu prüfen, wurden Modell-Systeme Titanium(IV) und Tiron mit

—Iminodiessigsäure (IDE, H_2X, $z = 3$) (System 1)
—Nitrilotriessigsäure (NTE, H_3X, $z = 4$) (System 2)
—Diethylentriaminpentaessigsäure (DTPE, H_5X, $z = 8$) (System 3)

analytisch charakterisiert. Auch bei diesen ternären Systemen beobachtet man im stark sauren Milieu goldgelbe bis rote Lösungen, die auf der Bildung von Gemischt-Ligand-Komplexen beruhen.[3]

Titanium(IV), Aminopolycarbonsäuren und Tiron (Brenzcatechin-3,5-disulfonsäure) reagieren in saurem Milieu zu farbigen Lösungen, wobei die Bildung stark pH-abhängig ist. In den entsprechenden Systemen existieren je nach Reaktionsbedingungen verschiedene Komplexindividuen, deren Zusammensetzung von uns[4] nach spektralphotometrischen und elektrophoretischen Messungen mit Hilfe der speziellen Rechenprogramme LITRAFAL[5] aufgeklärt wurde.

Folgende Größen dienen zur Beschreibung der Gleichgewichte:

H_4R (Tiron)
H_nX (Aminopolycarbonsäure)
$p = C_R/C_{Ti} = 100$, $s = C_X/C_{Ti}$ } (Ligandenüberschuß)

System Ti(IV), Tiron, IDE

Nach den Untersuchungen liegt in stark saurer Lösung bei hohen Ligandenüberschüssen mit Iminodiessigsäure ein ternärer Komplex mit dem Komponentenverhältnis Ti:X:R = 1:1:1 vor.

$$TiO(OH)^+ + H_2X + H_2R^{2-} \rightleftharpoons [TiOX(HR)]^{3-} + H_2O + 2H^+ \quad (pH\ 1; s = 1000)$$

$$[TiOX] + H_2R^{2-} \rightleftharpoons [TiOX(HR)]^{3-} + H^+ \quad (pH\ 2; s = 100)$$

Auf Grund der Bildungsbereiche ist das Chelat $[TiOX(HR)]^{3-}$ zur photometrischen Titanbestimmung geeignet (Verfahren 1).

System Ti(IV), Tiron, NTE

In Gegenwart von Nitrilotriessigsäure bildet sich enbenfalls ein 1:1:1-Chelat, wobei zwei Spezies unterschiedlicher Protonisierung existieren.

$$TiO(OH)^+ + H_3X + H_2R^{2-} \rightleftharpoons [TiOX(HR)]^{4-} + H_2O + 3H^+ \quad (pH\ 1.3; s = 10)$$

$$[TiOX(HR)]^{4-} \rightleftharpoons [TiOXR]^{5-} + H^+ \quad (pH\ 3; s = 100)$$

Tabelle 1. Statistische Kennzeichnung von Tiron-Verfahren in Gegenwart von IDE (1), NTE (2) sowie DTPE (3) zur photometrischen Titaniumbestimmung

Kennzahl	Verfahren 1—IDE	Verfahren 2—NTE	Verfahren 3—DTPE
Arbeitsbereich, $\mu g/50$ ml	200–1800	50–800	50–1800
ϵ', $l.mole^{-1}.cm^{-1}$	1293 ± 9	4380 ± 20	1784 ± 1
Standardabweichung, $\mu g/50$ ml	111	60	2
Variationskoeffizient, %	3,10	1,71	0,27
Eichfunktion.*	$E = (0{,}030 \pm 0{,}002)c - (0{,}05 \pm 0{,}03)$	$E = (0{,}091 \pm 0{,}001)c - (0{,}01 \pm 0{,}01)$	$E = (0{,}0366 \pm 0{,}0006)c + (0{,}01 \pm 0{,}01)$
Nachweisgrenze, $\mu g/50$ ml	112	66	19
Erfassungsgrenze, $\mu g/50$ ml	121	73	28

* c = [Ti], μg/50 ml, E = Extinktion.

Das Teilchen $[TiOXR]^{5-}$ ist zur Titanbestimmung (Verfahren 2) anwendbar.

System Ti(IV), Tiron, DTPE

Bei der hochzähnigen Diethylentriaminopentaessigsäure können die Teilchen in Abhängigkeit vom pH-Wert einfach oder auch dreifach protonisiert vorliegen. Das Komponentenverhältnis (Ti:X:R) in diesen ternären Komplexen beträgt erwartungsgemäß auch 1:1:1.

$$TiO(OH)^+ + H_5X + H_2R^{2-} \rightleftharpoons [TiO(H_2X)(HR)]^{4-} + H_2O + 3H^+ \quad (pH\ 1.2;\ s = 10)$$

$$[TiO(H_2X)(HR)]^{4-} \rightleftharpoons [TiO(HX)R]^{6-} + 2H^+ \quad (pH\ 2.5;\ s = 10)$$

Nach den komplexchemischen Eigenschaften dieses Systems eignet sich das ternäre Chelat $[TiO(HX)R]^{6-}$ zur photometrischen Titanbestimmung (Verfahren 3).

EXPERIMENTELLER TEIL

Die Titanium-Stammlösung (Ti 1 mg/ml) wurde wie bereits beschrieben[1] durch Aufschluß von TiO_2 und Lösen in Schwefelsäure erhalten. Sämtliche Chemikalien waren analysenrein. Tiron und Nitrilotriessigsäure (VEB Berlin-Chemie), Iminodiessigsäure und Diethylentriaminpentaessigsäure (Ferak). Zur Herstellung der Aminopolycarbonsäure-Lösungen wurden die Säuren in 2*M* Natriumhydroxid gelöst. Weitere Lösungen, z.B. Puffer, Störionen, sowie die verwendeten Geräte sind der schon angegebenen Arbeit[1] zu entnehmen.

Arbeitsvorschriften

Verfahren 1. Zur schwefelsauren Probelösung gibt man 5 ml 0,1*M* Tiron- und 25 ml 0,2*M* IDE-Lösung. Nach dem Einstellen auf pH 2,5 mit 20%iger Natriumhydroxidlösung fügt man 5 ml Formiat-Puffer-Lösung (1*M*, pH 2,5) hinzu und füllt auf 50 ml auf. Die Proben werden in 1-cm Küvetten nach 90 Minuten bei 455 nm gegen eine Blindprobe gemessen.

Verfahren 2. Zur schwefelsauren Probelösung gibt man 5 ml 0,1*M* Tiron- und 25 ml 0,2 *M* NTE-Lösung. Gleichzeitig mit der NTE werden einige Tropfen 20%iger Natriumhydroxidlösung zugefügt, um ein Ausfallen der NTE zu vermeiden. Nach dem Einstellen auf pH 3,5 mit Natriumhydroxidlösung (vom sauren Bereich her!) fügt man 5 ml Formiat-Puffer-Lösung (1*M*, pH 3,5) hinzu und füllt auf 50 ml auf. Die Proben werden in 1-cm Küvetten nach 70 Minuten bei 455 nm gegen eine Blindprobe gemessen.

Verfahren 3. Zur schwefelsauren Probelösung gibt man 5 ml 0,1*M* Tiron- und 25 ml 0,2*M* DTPE-Lösung. Nach dem Einstellen auf pH 2,5 mit 20%iger Natriumhydroxidlösung fügt man 5 ml Formiat-Puffer-Lösung (1*M*, pH 2,5) hinzu und füllt auf 50 ml auf. Die Proben werden in 1-cm Küvetten nach 60 Minuten bei 440 nm gegen eine Blindprobe gemessen.

ERGEBNISSE

Vergleichende Charakterisierung der Verfahren

Die Bedingungen für die einzelnen Bestimmungsverfahren 1, 2 und 3 wurden aus den komplexchemischen Untersuchungen[4] abgeleitet. Um die erzielten Ergebnisse mit dem Tiron-EDTE-Verfahren (Verfahren EDTE) vergleichen zu können, haben wir die statistische Kennzeichnung der Verfahren und die Untersuchungen zur Selektivität nach den schon beschriebenen Prinzipien[1] durchgeführt. In Tabelle 1 sind die erhaltenen Daten zusammengestellt.

Zur Berechnung der scheinbaren Extinktionskoeffizienten sowie der Standardabweichungen (mit $f = 20$ Freiheitsgraden) dienten Proben mittlerer Titanium-Konzentrationen:

Verfahren 1 (IDE): 1200 μg/50 ml
Verfahren 2 (NTE): 400 μg/50 ml
Verfahren 3 (DPTE): 800 μg/50 ml

Bei der Berechnung der Eichfunktionen (mit $f = 8$ Freiheitsgraden und $P = 0{,}99$) wurde von $y = bx + a$ ausgegangen, da $|a| > 0$. Die zur Kennzeichnung der Verfahren erhaltenen Grenzverhältnisse g (bis maximal $g = 100$) einer Reihe ausgewählter Störionen sind in Tabelle 2 enthalten, wobei die mittleren Titaniumkonzentrationen zu

Verfahren 1 (IDE): 1200 μg/50 ml
Verfahren 2 (NTE): 350 μg/50 ml
Verfahren 3 (DPTE): 800 μg/50 ml

festgelegt wurden. Um eventuelle Störeinflüsse durch Cl^-, NO_3^- und SO_4^{2-} (Stammlösungen!) auszuschließen, haben wir auch die Störungen dieser Ionen

Tabelle 2. Grenzverhältnisse g von Tiron-Verfahren in Gegenwart von IDE (1), NTE (2), DTPE (3) sowie EDTE zur photometrischen Titaniumbestimmung

Störion	Verf. 1	Verf. 2	Verf. 3	Verf. EDTE
Be(II)	0,8	100	1,25	40
Bi(III)	6,4	87	1,25	10
Ce(IV)	0,1	0,1	0,7	4
Co(II)	—	7	7,5	8
Cr(III)	0,2	0,6	5	7
Cu(II)	—	100	97	90
Fe(III)	0,5	0,3	0,5	1,5
In(III)	—	37	20	20
Mg(II)	0,5	100	37	20
Mn(II)	—	48	58	100
Mo(VI)	0,1	0,1	2	8
Nb(V)	→0	5,7	→0	0,1
Ni(II)	—	100	90	100
Sn(II)	—	14	12	16
Ta(V)	→0	0,2	0,2	1
Tl(I)	2,5	100	2,5	20
U(VI)	6	20	15	18
V(V)	1,6	0,6	6	0,2
W(VI)	0,8	45	0,25	4
Zn(II)	0,8	100	20	60
Zr(IV)	0,4	7,4	1	4

untersucht. Zur besseren Übersicht der Selektivitätsverhältnisse sind die g-Werte von Verfahren EDTE[1] mit aufgeführt.

DISKUSSION

Betrachtet man die ermittelten Kennzahlen der Verfahren 1 (Titanium–Tiron–IDE-Chelat), 2 (Titanium–Tiron–NTE-Chelat) und 3 (Titanium–Tiron–DTPE-Chelat), so wird der Einfluß der Aminopolycarbonsäuren (APC) auf die analytischen Eigenschaften der Systeme sichtbar. Die Extinktionskoeffizienten und Eichfunktionen (Tabelle 1) machen deutlich, daß es sich hier um keine sehr empfindlichen Verfahren handelt. Das beruht auf der geringen Wahrscheinlichkeit des Tiron → Ti Elektronenüberganges im ternären Komplex. Des weiteren bilden sich die ternären Cheltate unter den vorliegenden Bedingungen optimal, aber nicht vollständig, wodurch eine ungünstige Beeinflussung der Empfindlichkeit eintritt.

Interessant ist ein Vergleich der Variationskoeffizienten von Verfahren 1, 2 und 3. Mit Hilfe des F-Test ($\bar{P} = 0.99$, $f_1 = f_2 = 20$) läßt sich zeigen, daß signifikante Unterschiede zwischen den Schätzwerten bestehen und somit der Zufallsfehler der Verfahren in der Reihenfolge 1 (IDE) > 2 (NTE) > 3 (DPTE) d.h. mit zunehmender Zähnigkeit (z) der APC abnimmt. Dieser Zusammenhang ist zu erwarten, wenn man davon ausgeht, daß Hydrolyse-Nebenreaktionen des Ti(IV)-Ions durch APC hoher Zähnigkeit auf Grund der Stabilitätsverhältnisse besonders stark unterdrückt werden.

Zur Charakterisierung der Selektivität haben wir die Störungen einiger ausgewählter Kationen untersucht und denen des EDTE-Verfahrens (Verfahren EDTE[1]) gegenübergestellt. Die ermittelten g-Werte (Tabelle 2) geben Aufschluß darüber. Wie man sieht, sind die Verfahren 1 und 3 wenig selektiv. Die Ursache liegt darin, daß für beide Verfahren ein pH-Wert von 2,5 notwendig ist und die maskierende Wirkung der APC auf die Störionen in stark sauren Lösungen wegen der abfallenden scheinbaren Stabilitätskonstanten β' eingeschränkt ist. Verfahren 3 ist dabei gegenüber Verfahren 1 selektiver, weil die Chelate der DTPE ($z = 8$) stabiler als die der IDE ($z = 3$) sind. Auffällig ist in diesem Zusammenhang die geringere Störung durch V(V) bei Verfahren 3 gegenüber den anderen Verfahren.

Bei der Betrachtung der g-Werte von Verfahren 2 und Verfahren EDTE fällt auf, daß eine Reihe von Ionen Be(II), Bi(III), In(III), Mg(II), Nb(V), Tl(I), V(V), W(VI), Zn(II), Zr(IV) bei Verfahren 2 weniger stören als bei Verfahren EDTE obwohl EDTE gegenüber NTE mit den Störionen thermodynamisch stabilere Chelate bildet. Die Ionen Nb(V), W(VI), können die hohe Koordinationszahl von 8 annehmen, so daß sie im EDTE-Chelat ($z = 6$) koordinativ ungesättigt sind und Störreaktionen

$$MeY + R \rightleftharpoons MeYR$$

unter Bildung farbiger Mischkomplexe ablaufen können. Im Falle der NTE ($z = 4$) bilden sich—wie für Nb(V) gezeigt werden konnte[6]—farblose Chelate MeX_2, bei denen alle Koordinationsstellen durch die APC besetzt sind. Eine Anlagerung des chromophoren Liganden Tiron ist somit nicht möglich, was eine große Selektivitätssteigerung für Nb(V) (57-fach) und W(VI) (11-fach) bedeutet.

Die Selektivitätssteigerung für die anderen Ionen kann man nach zwei Gesichtspunkten deuten.

1. Tiron bildet mit einer Reihe von Kationen [Me(II), Me(III), Me(IV),[7]] farblose Chelate, wodurch

eine Erniedrigung der freien Tironkonzentration eintritt. Das System Titanium(IV), EDTE, Tiron reagiert auf Grund der scheinbaren Stabilitätskonstanten[4] [k'(EDTE) < k'(NTE)] gegenüber dem NTE-System stark auf eine Erniedrigung der freien Tironkonzentration.

2. Die Konkurrenzreaktionen der APC-Liganden mit Störionen üben wegen der Stabilitätsverhältnisse MeY/MeX auf das System Titanium(IV), EDTE, Tiron einen besonders großen Einfluß aus.

Die systematischen Untersuchungen an Systemen Titanium(IV), APC, Tiron haben gezeigt, daß die Selektivitätsverhältnisse solcher Verfahren in hohem Maße von der Aminopolycarbonsäure abhängen. Als Ursache für eine Selektivitätserhöhung kommen die veränderten komplexchemischen Eigenschaften des Systems unter Bildung ternärer Komplexe in Betracht. Die Einflußfaktoren können jedoch recht unterschiedlich sein, so daß sichere Voraussagen dazu problematisch sind.

LITERATUR

1. S. Koch, G. Ackermann und G. Winkler, *Talanta*, 1979, **26**, 821.
2. J. H. Yoe und A. R. Armstrong, *Anal. Chem.*, 1947, **19**, 100.
3. S. Koch und G. Ackermann, *Z. Chem.*, 1974, **14**, 103.
4. *Idem*, *Z. Anorg. Allgem. Chem.*, 1981, **473**, 231.
5. S. Koch, P. Weber und G. Ackermann, *Chem. Anal. Warsaw*, 1978, **23**, 563.
6. S. Koch und G. Ackermann, *Z. Chem.*, 1970, **10**, 77.
7. L. Sommer, *Acta Chim. Acad. Sci. Hung.*, 1962, **33**, 23.

Summary—As part of a study to evaluate the use of ternary complexes in photometric methods of analysis, three model systems involving titanium(IV) and tiron plus iminodiacetic acid, nitrilotriacetic acid or diethylenetriaminepenta-acetic acid have been investigated. The methods were compared in terms of working range, molar absorptivity, standard deviation, coefficient of variation, slope of calibration line, limit of detection and limit of determination. The extent of interference from 20 other ions was also examined. The nitrilotriacetic acid system was shown to have better selectivity than the other two.

Talanta, Vol. 28, pp. 919 to 924, 1981
Printed in Great Britain. All rights reserved

0039-9140/81/120919-06$02.00/0
Copyright © 1981 Pergamon Press Ltd

A SOURCE OF ERROR IN THE DETERMINATION OF EQUIVALENCE VOLUMES OF CARBOXYLIC ACIDS FROM POTENTIOMETRIC TITRATIONS

ÅKE OLIN and BO WALLÉN
Department of Analytical Chemistry, University of Uppsala, P.O.B. 531, S-751 21 Uppsala, Sweden

(*Received* 18 *February* 1981. *Revised* 21 *April* 1981. *Accepted* 11 *May* 1981)

Summary—Emf measurements on mixtures of carboxylic acids, HA, and the corresponding bases, A, containing a high and constant salt background, show that the equation $E = E_0 + g\ln h + j_h h$ commonly used in the calculation of equivalence volumes is not strictly followed. Terms linear in [HA] and [A] should be added. The origin of these terms is discussed briefly and their influence on the accuracy of equivalence-volume determinations is evaluated.

A great many methods have been devised for the determination of equivalence volumes from potentiometric acid–base titrations.[1–6] The more recent approaches use non-approximate formulae derived from the appropriate mass-balance and equilibrium expressions. A neutral salt is normally assumed to be present in sufficient amount to keep activity coefficients constant during the titration. Hence these coefficients are not explicitly included in the equations.

The hydrogen-ion concentration is generally measured with a glass electrode. The galvanic cell is best standardized directly on the concentration scale since calibration with pH buffers, *e.g.*, NBS buffers, necessitates introduction of an activity coefficient for H^+ in order to relate the measurements to the concentration scale. With the assumption that the activity coefficients are constant, the emf of the measuring cell, E, can be written

$$E = E_0 + g\ln h + E_j \quad (1)$$

where E_0 is a constant, g is the Nernstian factor RT/F, and h is the hydrogen-ion concentration. E_j represents the liquid-junction potential. If the discussion is restricted to titrations at $-\log h$ values below 10, E_j can be assumed to be caused by hydrogen ions only. E_0 and E_j can be found from measurements on solutions with known hydrogen-ion concentrations, as originally described by Biedermann and Sillén.[7] It is then observed that E_j is a linear function of h, so equation (1) can be written

$$E = E_0 + g\ln h + j_h h \quad (2)$$

The value of j_h is characteristic of the ionic medium. It is assumed to remain unchanged even for mixtures where a small amount of the ionic medium is replaced by other species. In any case, a small inaccuracy in j_h will be negligible if h is $< 10^{-2.5}$.

In order to yield accurate equivalence volumes, the chemical model on which the numerical method is based, as well as the relationship between the measured emf and the hydrogen-ion concentration [equation (2)], must be correct.

EXPERIMENTAL TEST OF THE MODEL FOR CARBOXYLIC ACID-CARBOXYLATE SYSTEMS

The model generally used for monoprotic carboxylic acids has been tested by measurements on carboxylate buffers (HA/A) with the cell

$$\text{Ag, AgCl} \,|\, 1.00M \underset{\text{NaCl}}{|} \text{HA, A in } 1.00M \underset{\text{NaCl}}{|} \text{Glass electrode}$$

For this system the following equations should be valid

$$[\text{HA}]_T = [\text{HA}]^* + [\text{A}]^* = [\text{HA}] + [\text{A}] \quad (3)$$

$$[\text{HA}]^* = [\text{HA}] + h - [\text{OH}] \quad (4)$$

$$\beta = \frac{[\text{HA}]}{h[\text{A}]} \quad (5)$$

where [HA]* and [A]* are the total concentrations of HA and A added to the cell. Equations (2)–(5) yield

$$y = E - g\ln\left(\frac{[\text{HA}]^* + [\text{OH}] - h}{[\text{A}]^* + h - [\text{OH}]}\right)$$

$$- j_h h - E_0 = -g\ln\beta \quad (6)$$

Equation (2) was used to obtain h, for calculation of y. The subsequent treatment will show that this equation is only approximately valid. A small error in h will, however, introduce only a negligible error in y since h is small compared to [HA]* and [A]*, and [OH] can be neglected.

The experiments were carried out as titrations in which increasing amounts of buffer were added to the measuring cell. The buffer solutions were made 1.00*M* in Na^+ by addition of sodium chloride. In each titration the quotient [HA]*/[A]* was kept constant. The experimental result $y = f([\text{HA}]_T)$ at constant [HA]*/[A]* ratios is presented in Fig. 1 for the acetic

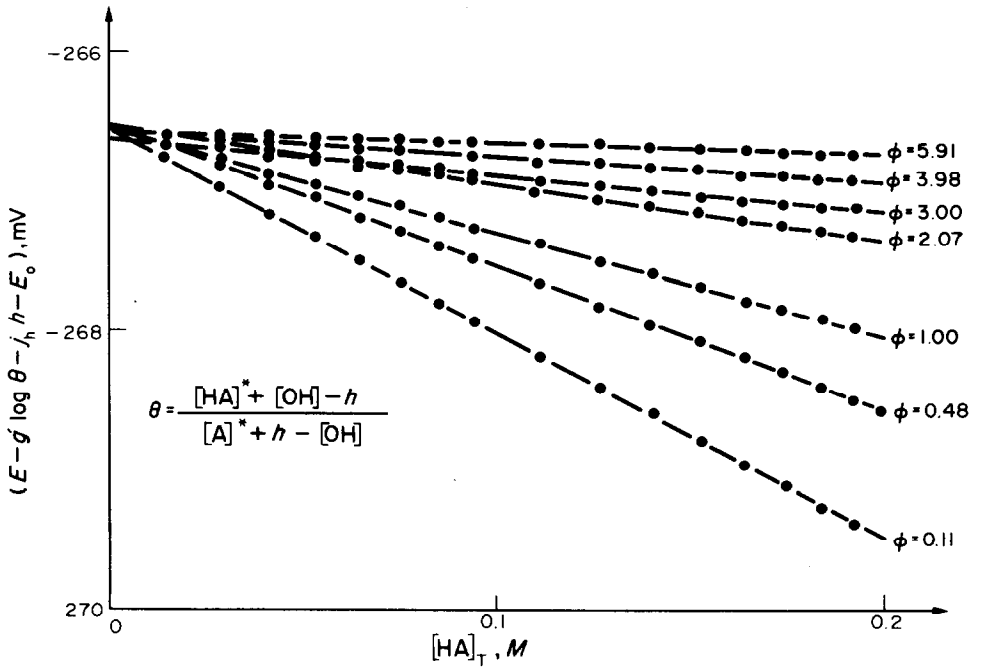


Fig. 1. The experimental values of $E - g'\log\theta - j_h h - E_0$ [see equation (6)] for the acetate system, plotted against $[HA]_T$, at different values of the quotient $\phi = [HA]^*/[A]^*$. In this figure $g' = 59.16$ mV.

acid–acetate system. For all buffers, straight lines were obtained and on extrapolation to $[HA]_T = 0$ had an intercept constant to within 0.1 mV. According to equation (6) the intercept is equal to $-g\ln\beta$.

The non-zero values of the slopes of the lines in Fig. 1 indicate that equations (2)–(5) do not completely describe the acetic acid–acetate system. Correction terms must be included and this is most easily done in equation (2). It is found empirically that these terms are approximately linear in [HA]* and [A]*. Denoting the correction by ϵ and the quotient [HA]*/[A]* by ϕ we have

$$\epsilon = k[HA]_T = k_0[HA]^* + k_1[A]^* \qquad (7)$$

where k is the slope of a line in Fig. 1. Rearrangement of equation (7) yields

$$k(1 + \phi) = k_1 + k_0\phi \qquad (8)$$

Figure 2 shows the plot of $k(1 + \phi)$ as a function of ϕ, from which $k_0 = 1.8$ mV.l.mole^{-1} and $k_1 = -16.5$

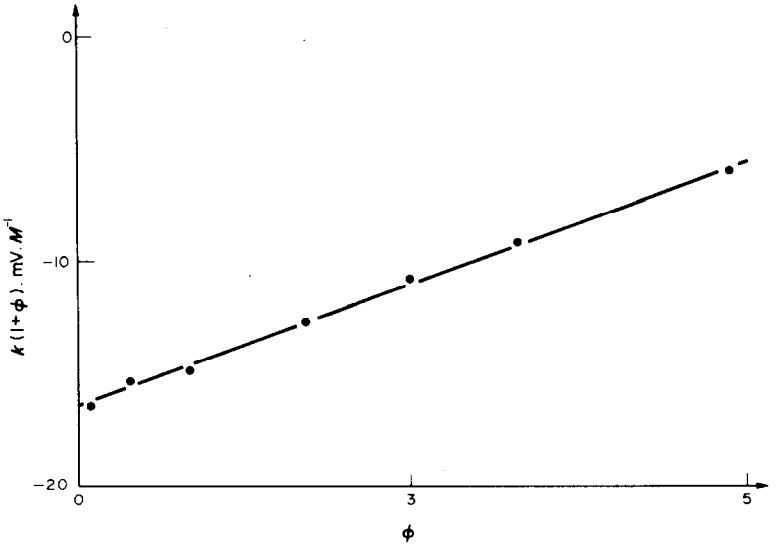


Fig. 2. A plot of $k(1 + \phi)$ as a function of ϕ [see equations (7) and (8)]. The slope yields k_0 and the intercept k_1.

mV.l.mole^{-1} were found. The interpretation of these results has been discussed by Olin and Svanström[8] who concluded that thermodynamic measurements alone cannot distinguish between the contributions to ϵ from liquid-junction potentials, activity-coefficient changes and dimerization. The Henderson equation for liquid-junction potentials and the Guggenheim and Setchenow relations for activity coefficients all predict linear relationships of the type observed. It was also shown[8] that the presence of the dimeric species H_2A_2 and HA_2^- would add linear terms to the right-hand side of equation (6) for small values of the dimerization constants.

p-Hydroxybenzoic acid has also been investigated in detail. In this case $k_0 = -48.8$ mV.l.mole^{-1} and $k_1 = -35.2$ mV.l.mole^{-1}. The coefficients are so large that they cannot be due solely to liquid-junction potentials or activity-coefficient variations. Hence dimerization is strongly indicated. Recently Lajunen *et al.*[9] studied some dihydroxybenzoic acids by emf methods and included dimeric species in the interpretation of their data.

THE INFLUENCE OF ϵ ON EQUIVALENCE VOLUMES

The evaluation of equivalence volumes by numerical methods is based on equations (2)–(5). Hence the accuracy of the methods should be affected if ϵ is neglected. With only one acid present the origin of the correction is immaterial, since what is needed is a valid relationship between the measured emf and the concentration of the components during the titration. When several acids are present, however, it is necessary to know the origin of the correction terms. If they represent a liquid-junction potential they should be applied as a general correction but if they are due to activity-coefficient variations or dimerization they should be applied individually to each system.

The variation of ϵ during the titration of V_0 ml of sample by V ml of strong base with concentration C_{OH} is represented by

$$\frac{\epsilon}{C_{OH}} = \frac{V(k_1 - k_0)}{V + V_0} + \frac{k_0 V_e}{V + V_0} \qquad (9)$$

where V_e is the equivalence volume. This equation presumes that all of the base added reacts with HA to form an equivalent amount of A. This is very nearly true for carboxylic acids. Some of the numerical methods can effectively cope with a constant error in E ("E_0 error"). The variation of ϵ during the titration will then be the main source of error. The total change in ϵ is found by inserting $V = 0$ and $V = V_e$, respectively, in equation (9)

$$\Delta\left(\frac{\epsilon}{C_{OH}}\right) = \frac{V_e}{V_0}\left(\frac{k_1}{V_e V_0^{-1} + 1} - k_0\right) \qquad (10)$$

It is thus the difference between k_0 and k_1 rather than their magnitude that is important.

Titration data, which will be described in the experimental part, have been treated by the Ingman and Still method,[4] Hofstee's method[3] and an iterative least-squares method to obtain the equivalence volume. The influence of ϵ on the error in V_e was very similar for the three methods. Conclusions and results from the following expressions derived from the Ingman and Still equation of the error in V_e due to ϵ can therefore be assumed to be generally valid. This equation can be written

$$V_e - V = \beta V h + (V + V_0)(1 + \beta h)h/C_{OH} = y \qquad (11)$$

since for carboxylic acids terms in [OH] can be neglected before the equivalence point. For correct values of $y = y_0$, equation (11) is represented by a straight line of slope -1 intercepting the V-axis at $V = V_e$ (continuous line in Fig. 3). The presence of ϵ will shift y_0 to $y = y_0 + \Delta y$ and change the slope from its ideal value. The new equivalence volume, Z, is obtained by a linear extrapolation from the point (V, y) (dashed line in Fig. 3). This line has a slope equal to the first derivative of $y = f(V)$. Thus

$$\frac{y_0}{V - V_e} = -1 \quad \text{and} \quad \frac{y}{V - Z} = \frac{dy}{dV} \qquad (12)$$

For small ϵ, y can be written

$$y = y_0 + \left(\frac{\partial y}{\partial \ln h}\right)_V \Delta \ln h \qquad (13)$$

By combining equations (12) and (13) the error in the equivalence volume, $\Delta V_e = Z - V_e$ is found to be

$$-\Delta V_e = (V_e - V)\left[1 + \left(\frac{dy}{dV}\right)^{-1}\right] + \left(\frac{\partial y}{\partial \ln h}\right)_V \left(\frac{dy}{dV}\right)^{-1} \Delta \ln h \qquad (14)$$

The expression for (dy/dV) is quite lengthy and will not be reproduced here. Instead, the derivation of ΔV_e will be simplified by neglecting the last term in equation (11). This is only a minor approximation, as can be seen from Table 1, which contains results from the complete expression for ΔV_e. Then

$$\left(\frac{\partial y}{\partial \ln h}\right)_V = V_e - V \qquad (15)$$

Since

$$E - j_h h = E_0 + g \ln h_0 + \epsilon = E_0 + g \ln h,$$

$\Delta \ln h = \ln h - \ln h_0$ is found to be ϵ/g and y is

$$y = (V_e - V)\left(1 + \frac{\epsilon}{g}\right) \qquad (16)$$

and

$$\frac{dy}{dV} = -1 - \frac{\epsilon}{g} + \left(\frac{V_e - V}{g}\right)\frac{d\epsilon}{dV} \qquad (17)$$

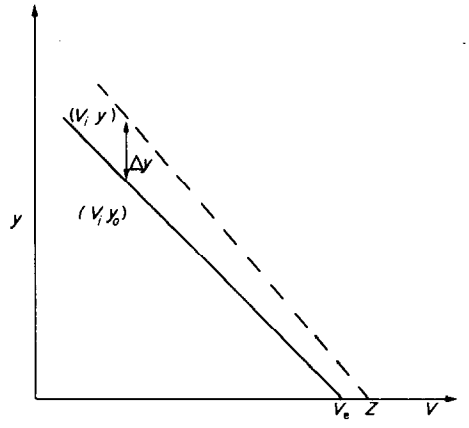


Fig. 3. Plots of $V_e - V = f(V)$ [equation (11)]. The solid line is obtained for correct hydrogen-ion concentrations, h, and the dashed line for incorrect h-values. V_e and Z denote equivalence volumes.

By insertion of equations (15) and (17) in (14), ΔV_e is found to be

$$\Delta V_e = \frac{(V_e - V)^2}{B} \frac{d\epsilon}{dV} \tag{18}$$

where

$$B = g + \epsilon - (V_e - V) \frac{d\epsilon}{dV} \tag{19}$$

Table 1. Example of the influence of ϵ on ΔV_e from a simulated titration (HALTAFALL[10]) of 25 ml of 0.025M monoprotic acid with 0.05M NaOH [log $\beta = 4.5$, $k_0 = -45$ mV.l.mole^{-1} and $k_1 = -30$ mV.l.mole^{-1}; the relative error, $F = 100\ \Delta V_e/V_e$, has been calculated from equations (14), (18) and (21), respectively]

V, ml	F_{14}, %	F_{18}, %	F_{21}, %	$-\epsilon$, mV	$d\epsilon/dV$, mV/ml
2	4.0	2.4	2.2	0.99	0.06
3	2.2	1.8	1.7	0.92	0.06
4	1.5	1.3	1.3	0.87	0.06
5	1.0	1.0	0.9	0.81	0.05
6	0.7	0.7	0.6	0.76	0.05
7	0.5	0.4	0.4	0.71	0.05
8	0.3	0.3	0.3	0.67	0.04
9	0.2	0.2	0.2	0.63	0.04
10	0.1	0.1	0.1	0.59	0.04
11	0	0	0	0.55	0.04
12	0	0	0	0.52	0.03

From equation (9)

$$\frac{d\epsilon}{dV} = C_{OH} \frac{V_0 k_1 - (V_0 + V_e)k_0}{(V + V_0)^2} \tag{20}$$

From equation (18) it is seen that ΔV_e arises from a non-constant ϵ, whereas a constant ϵ does not introduce an error in V_e. In connection with determinations of stability constants of carboxylate complexes the coefficients k_i have been determined for a number of mono-, di-, and triprotic aliphatic and aromatic carboxylic acids. In all cases ϵ could be linearized. Some k_i values (for 1M sodium perchlorate ionic medium) are listed in Table 2. Since ϵ is typically a few millivolts and $|d\epsilon/dV|$ about 0.1–0.05 mV/ml, ΔV_e can be further simplified to

$$\Delta V_e = \frac{(V_e - V)^2}{g} \frac{d\epsilon}{dV} \tag{21}$$

Table 1 contains ΔV_e values for a titration of 25 ml of a 0.025M monoprotic acid with 0.05M sodium hydroxide. Log $\beta = 4.5$, $k_0 = -45$ mV.l.mole^{-1} and $k_1 = -30$ mV.l.mole^{-1} are assumed. ΔV_e has been calculated from equations (14), (18) and (21), respectively. The differences between the estimates are small and the simplified expression from equation (21) is quite satisfactory. ϵ introduces a curvature in the plots used in the graphical methods and systematic trends in the residuals for methods based on least-squares procedures. The error in the equivalence volume will obviously depend on the range of V used and under unfavourable conditions can amount to 1–2%.

EXPERIMENTAL

Apparatus

The titrations were performed in an oil-bath kept at 25 ± 0.1 .

The indicator electrode was an Ingold no. 201 glass electrode. The titrations were done with a time-based automatic titrator,[16] by using a pneumatic system (Autochem Instrument AB, Sweden) delivering stepwise additions (1 ml) of titrant. The potentials were measured with a digital voltmeter (Data Precision 2520) and a voltage follower with a very low input current (10–20 fA), to ±0.01 mV.

Magnetic stirring of the solution was employed and argon was passed through the solution. The gas was purified and humidified by passing it through 10% sodium hydroxide solution, 10% sulphuric acid and finally 1M sodium chloride.

Table 2. Coefficients in the expression $\epsilon = k_0[H_nA] + k_1[H_{n-1}A] + \ldots$ [equation (7)]; the k_i values are given in mV.l.mole^{-1} and the ionic medium is 1M $NaClO_4$

Acid	k_0	k_1	k_2	k_3	Ref.
Maleic	—	−13.5	−9.2		11
1,2,3-Propanetricarboxylic	−0.5	−8.1	−18.8	−33.1	12
Citric	11.6	−6.1	−21.3	−41.7	13
Benzoic	—	−9.5			14
Phthalic	1.3	−25.5	−26.3		14
1,2,4-Benzenetricarboxylic	—	−49.1	−25.2	−31.8	15

Reagents

Unless otherwise stated all chemicals were of analytical-reagent grade. Sodium chloride (the ionic medium) was Merck Suprapur. Hydrochloric acid solutions were prepared from the concentrated acid (Merck) by dilution and standardized with tris(hydroxymethyl)aminomethane. Sodium hydroxide solutions were prepared from 50% sodium hydroxide (EKA Bohus) solution by dilution and standardized with hydrochloric acid. Precautions were taken to exclude carbon dioxide during preparation, storage and titrations. Stock solutions of acetic acid (Merck) were standardized by titration with sodium hydroxide, using phenolphthalein as indicator. *p*-Hydroxybenzoic acid (Fluka AG, puriss.) solutions were prepared from known weights of the recrystallized product.

Procedures

Determination of E_0 *and* j_h. A sample (50.05 ml) of 1.00*M* sodium chloride was titrated with 0.1011*M* hydrochloric acid, 1.00*M* in sodium chloride. Sixteen additions of titrant were made, and the emf was measured after each addition. E_0 and j_h [*cf.* equation (2)] were determined from the linear plot of $E - g\ln h$ *vs.* h.

Determination of strong acid/base as impurity in the ionic medium. A sample (50.05 ml) of 1.00*M* sodium chloride was titrated with 0.009900*M* hydrochloric acid, 1.00*M* in sodium chloride. Ten portions of titrant were added. The equivalence volume was found from a plot of $(V_0 + V)\exp(E/g)$ *vs.* V. A concentration of $3 \times 10^{-6}M$ hydroxide in 1*M* sodium chloride was observed.

Determination of the coefficients in equation (7). A sample (25.03 ml) of 1.00*M* sodium chloride was titrated with the buffer solution. The emf was measured, after each addition of titrant, with a glass electrode. Stable potentials, ±0.01 mV, were obtained within 20 min.

RESULTS

All titrations were performed in a sodium chloride medium at a total sodium-ion concentration of 1.00*M*. Table 3 contains the results from titration of 0.025*M* *p*-hydroxybenzoic acid with sodium hydroxide. The equivalence volume was determined with the aid of a least-squares program similar to that described by Pehrsson *et al.*[6] The program is based on the Ingman and Still equation, which can be written (valid before the equivalence point)

$$V_i = V_e - \beta\left[V_i h_i p + \frac{(V_0 + V_i)h_i^2 p^2}{C_{OH}}\right] - \frac{(V_0 + V_i)h_i p}{C_{OH}} \quad (22)$$

or

$$V_i = V_e - f(V_i, h_i; p) \quad (23)$$

In equations (22) and (23), $i = 1,2 \ldots n$ = the number of titration points, h_i is the hydrogen-ion concentration calculated with a provisional E_0-value, and $p = h_{0_i}/h_i$ (where h_{0_i} represents the correct value of the hydrogen-ion concentration). Linearization about $p = p_0$ yields

$$V_i + f(V_i, h_i; p_0) = V_e - \left(\frac{\partial f}{\partial p}\right)_i \Delta p \quad (24)$$

Table 3a. Titration errors calculated from the expression $E = E_0 + g\ln h + j_h h$ [equation (2)] and the linearized Ingman and Still equation [equation (24)] for evaluation of a titration of 0.025*M* *p*-hydroxybenzoic acid with 0.050*M* NaOH; the theoretical equivalence volume is 12.439 ml; V denotes the titrant volume and V_e the corresponding equivalence volume calculated with the final value of p

V, ml	V_e, ml	Error, %
2	12.483	0.35
3	12.487	0.38
4	12.497	0.46
5	12.505	0.52
6	12.512	0.58
7	12.509	0.56
8	12.507	0.54
9	12.499	0.48
10	12.489	0.40
11	12.476	0.30

V_e (mean) = 12.496 ml.
Error (mean) = 0.46%.

Table 3b. Titration errors obtained by using the relationship $E = E_0 + g\ln h + j_h h + k_0[HA]^* + k_1[A]^*$ and equation (24) for the evaluation of the titration in Table 3a

V, ml	V_e, ml	Error, %
2	12.447	0.06
3	12.434	−0.04
4	12.431	−0.07
5	12.431	−0.06
6	12.435	−0.04
7	12.434	−0.05
8	12.436	−0.03
9	12.437	−0.02
10	12.439	−0.01
11	12.440	0.01

V_e (mean) = 12.435 ml.
Error (mean) = 0.04%.

or

$$y_i = V_e - X_i \Delta p \quad (25)$$

When equations (22), (24) and (25) are combined:

$$y_i = V_i + \beta\left[V_i h_i . p + \frac{(V_0 + V_i)h_i^2 p^2}{C_{OH}}\right] + \frac{(V_0 + V_i)h_i p}{C_{OH}} \quad (26)$$

$$X_i = \left(\frac{\partial f}{\partial p}\right)_i = \beta V_i h_i + \frac{(V_0 + V_i)(2\beta h_i^2 p + h_i)}{C_{OH}} \quad (27)$$

V_e and Δp are then found by linear regression and the calculation is repeated with the new value of p until Δp does not change from cycle to cycle. The result of this calculation is presented in Table 3a. A good fit of the data to equation (23) is found but the value of V_e is in error by about 0.5%. Table 3b gives the results when a correction for ϵ is introduced. A very good fit

Table 4. Titration errors obtained with restricted ranges in V when V_e is evaluated by equations (2) and (24) from a titration of 25 ml of 0.025M *p*-hydroxybenzoic acid with 0.050M NaOH

Range of V/V_e	Error (mean), %
0.15–0.95	0.41
0.30–0.95	0.31
0.40–0.95	0.26
0.47–0.95	0.22
0.55–0.95	0.18
0.60–0.95	0.14
0.75–0.95	0.10

is obtained and V_e has its correct value. Equation (21) suggests that more accurate results will be obtained if the data from the first part of a titration are excluded. This is verified by the results in Table 4.

CONCLUSIONS

The equation for the calculation of the hydrogen-ion concentration in potentiometric titrations of a carboxylic acid, H_nA, in a constant ionic medium should read

$$E = E_0 + \frac{RT}{F} \ln h + j_h + \epsilon$$

when the equivalence volume is determined from data points (E,V) by standard graphical and numerical procedures. ϵ is a linear function, $\epsilon = k_0[H_nA] + k_1[H_{n-1}A] \ldots k_n[A]$, of the concentrations of the species of the acid–base system being titrated. Omission of ϵ will, mainly because of the variation of ϵ during the titration, affect the accuracy of the equivalence volume. Since the coefficients, k_i, are normally not known, the experimental conditions should be chosen so that the influence of ϵ is reduced. Equation (21) and Table 2 can be used for guidance here. By choosing the concentration of the acid to be about 0.01M and/or giving more weight to the data in the later part of the titration the contribution of ϵ to the titration error can be made very small.

REFERENCES

1. G. Gran, *Acta Chem. Scand.*, 1950, **4**, 559.
2. *Idem*, *Analyst*, 1952, **77**, 661.
3. B. H. J. Hofstee, *Science*, 1960, **131**, 39.
4. F. Ingman and E. Still, *Talanta*, 1966, **13**, 1431.
5. A. Johansson, *Analyst*, 1970, **95**, 535.
6. L. Pehrsson, F. Ingman and A. Johansson, *Talanta*, 1976, **23**, 769.
7. G. Biedermann and L. G. Sillén, *Ark. Kemi*, 1953, **5**, 425.
8. Å. Olin and P. Svanström, *Acta Chem. Scand.*, 1978, **A32**, 283.
9. L. H. J. Lajunen, J. Saarinen and S. Parhi, *Talanta*, 1980, **27**, 71.
10. N. Ingri, W. Kakolowicz, L. G. Sillén and B. Warnqvist, ibid., 1967, **14**, 1261 (*Errata*: *Talanta*, 1968, **15**, No. 3, xi).
11. Å. Olin and P. Svanström, *Acta Chem. Scand.*, 1975, **A29**, 849.
12. S. Ajayi, Å. Olin and P. Svanström, *ibid.*, 1979, **A33**, 93.
13. L.-G. Ekström and Å. Olin, *Chem. Scr.*, 1978, **13**, 10.
14. Å. Olin and P. Svanström, *Acta Chem. Scand.*, 1978, **A32**, 435.
15. S. Ajayi, Å. Olin and P. Svanström, *ibid.*, 1979, **A33**, 97.
16. L.-G. Ekström, *Dissertation*, Uppsala University, 1979.

Talanta, Vol. 28, pp. 925 to 929, 1981
Printed in Great Britain. All rights reserved

0039-9140/81/120925-05$02.00/0
Copyright © 1981 Pergamon Press Ltd

DESK-COMPUTER PROGRAM FOR EVALUATION OF COMPLEX EQUILIBRIA FROM SPECTROPHOTOMETRIC DATA

F. GAIZER* and A. PUSKÁS†

Department of Chemistry, College of Food Technology, Hódmezövásárhely, POB 79,* and Gy. Juhász Teacher's Training College,† Szeged, Hungary

(*Received* 17 *March* 1981. *Accepted* 10 *May* 1981)

Summary—The program MINISPEF is designed to run on a desk-computer with 16 kbytes of memory. It can calculate the optimum values of the overall stability constants and molar absorptivities of a maximum of 8 species with compositions $M_qL_pH_r$ (r or q can be zero), or the mixed-ligand complexes formed in the system $MA_N + MB_N$ ($N = 2$, 3 or 4), from spectrophotometric data. The program is based on the authors' program MINIPOT.

We recently published a desk-computer least-squares program MINIPOT which can calculate stability constants from potentiometric and pH-metric data.[1] The central part of that program was constructed as a general procedure for the search for and refinement of parameter values, and it can be used for the evaluation of data originating from any measurements with residuals that can be treated with the same (unit) weights. This criterion is valid for spectrophotometric data.[2] The program MINISPEF described here, which is capable of solving four different types of spectrophotometrically measured equilibria, has been constructed from the central part of MINIPOT, together with a special part and three blocks. The Appendix of this paper includes only the new parts of the program. MINISPEF is based on the program SPEF-3,[3] but in some respects it has been simplified and in other respects made more effective.

THE TYPES OF EQUILIBRIA THAT CAN BE EVALUATED

On the basis of the association (or dissociation) of the hydrogen ion and the species M and L, the following overall stability constant can be defined (charges are omitted for simplicity):

$$qM + pL + rH^+ \rightleftharpoons M_qL_pH_r^+ (\equiv c_j); \qquad \beta = [M_qL_pH_r^+]/[M]^q[L]^p[H^+]^r \quad (1)$$

Since zero values for q or r are allowed, some modifications to achieve shorter running times can be included, so four types of equilibria can be identified.

1. Equilibria involving only the protonation ($+r$) or deprotonation ($-r$) of species L (*i.e.*, only complexes H_rL_p are formed).

2. Equilibria of protonated/deprotonated metal complexes [equation (1)]. These equilibria include those of type 1, if $q = 0$.

3. Equilibria involving metal complexes with compositions M_qL_p, or any association process which can be dealt with mathematically in the same way (*e.g.*, the reaction $HgI_2 + I^-$).

4. Formation of mixed-ligand complex(es) from the parent complexes MA_N and MB_N:

$$qMA_N + pMB_N \rightleftharpoons M_{q+p}A_{Nq}B_{Np} (\equiv c_j) \qquad \beta = [M_{q+p}A_{Nq}B_{Np}]/[MA_N]^q[MB_N]^p \quad (2)$$

In equation (2), $N = 2$, 3 or 4. It can be seen that in this case the parent complexes are treated as the associating species.

In MINISPEF the logarithms of the overall stability constants and the molar absorptivities of all species are treated as unknown parameters, and the values which give the minimum of the non-weighted sum of the squares of the residuals (U) of the measured (A_{meas}) and calculated (A_{calc}) absorbances, reduced to 1-cm path-length, are calculated, together with the probable errors.

$$U = \sum_i (A_{meas,i} - A_{calc,i})^2 = \sum_i \left(A_{meas,i} - \epsilon_M[M] - \epsilon_L[L] - \sum_j \epsilon_j\beta_j[M]^{q_j}[L]^{p_j}[H^+]^{r_j} \right)^2 \quad (3)$$

In equation (3) $\sum_j$ and $\sum_i$ mean summing for all (q, p, r) complex species and experimental points, respectively.

THE PROGRAM

Introductory part

In this part the experimental data are read in first, and prepared for the subsequent calculations, followed by the stoichiometric coefficients of the complexes and the starting values of the parameters with their increments. The quantities to be read in this part of the program are listed in Table 1.

Table 1. Input for the program MINISPEF

Input step	Input quantities or numbers	Comment
I	W, N1, N2, N3, N4, R, X1, X2, M, L	W: Type no.; N1: no. of measured points; N2: no. of parameters; N3: no. of complexes; N4: if = 1, then the percentage distribution of T_M, if = 2, then that of T_L in the complexes is calculated; R: printing instruction for data fed in (if R = 0, then no print); X1, X2: divisors for T_M and T_L, respectively, fed in (to make the input of these quantities more convenient, see, *e.g.*, line 80); M, L: multiplication factors for T_M and T_L, respectively, to produce starting values for [M] and [L] (*e.g.*, = 0.01, if not very strong complexes are formed; see line 850).
II	if W = 1, then: $(V1_i, L_i, E_i)_{N1}$ if W = 2, then: $(V1_i, M_i, L_i, E_i)_{N1}$ if W = 3, then: $(M_i, L_i, E_i)_{N1}$ if W = 4, then: $(M_i, L_i, E_i)_{N1}$	$V1_i$: pH; M_i: T_M; L_i: T_L; E_i: absorbance reduced to 1-cm path-length M_i: T_{MA_N}; L_i: T_{MB_N}; E_i: absorbance
III	$(Q1_i, P1_i, R1_i)_{N3}$	Stoichiometric coefficients of the complexes $M_qL_pH_r$ or mixed-ligand complexes $M_{q+p}A_{N\cdot q}B_{N\cdot p}$
IV	$(P_i, T_i)_{N2}$	$(\log\beta, \text{increment})_{N3}$ $(\epsilon, \text{increment})_{N3}$ ϵ_M, increment, ϵ_L, increment
V	K, V, N, T1	K, V: first and last experimental points to be evaluated; N: step between two consecutive experimental points; T1: = 0 or 1, depending on whether or not there are roots for solution of the mass-balance equations.

Search for and refinement of parameters

This part of the program is identical with lines 260–820 of MINIPOT. However, some small alterations had to be made in it, for three reasons: the LIGOPT procedure is not relevant in these problems; the time-consuming calculation of the distribution of species is not necessary when absorptivities are dealt with; and finally, a check must be made for the improved values of molar absorptivities, and any that become negative must be put equal to zero. The alterations to be carried out are as follows:

1. Replace statement "GOTO 1470" by "V2 = T6" in lines 340, 350 and 380, "V2 = J" in line 480, by "V2 = 1" in line 500 and by "V2 = S1(F1)" in line 710.

2. In lines 380 and 820: in the "ON V1 . . ." statements the numbers 60, 190 and 230 must be changed to 30, 150 and 170, respectively.

3. Insert "STEP N" into statement "FOR J = 1 TO V" in line 630 (this was an error in the program MINIPOT).

4. Insert the following lines into the corresponding places:

```
661 FOR K1 = 1 TO F1: J = S1(K1): IF J < = N3
    THEN 663: F3 = P(J) + G2(K1)
662 IF F3 > 0 THEN 663: G2(K1) = -P(J)
663 NEXT K1
701 IF I6 < 1 THEN 710: FOR K1 = 1 TO F1:
    J = S1(K1)
702 IF J < =N3 THEN 703: IF P(J) > 0 THEN
    703: P(J) = 0
703 NEXT K1
```

Procedures

The EQUSOL procedure executes three tasks: (*i*) it solves the mass-balance equations for each experimental point, using the actual set of overall stability constants; (*ii*) it calculates the absorbances with the set of molar absorbances and concentrations of the free and complex species; and (*iii*) it calculates the residuals and sum of the squares of the residuals.

When the distribution of species is calculated, the measured hydrogen-ion concentrations are taken as known quantities and the task proper is the solution of the T_M and T_L mass-balance equations for [M] and [L], or (in the case of problems of Type 1) the T_L equation for [L]. For solution of the equation, the Newton method is tried first. The values of derivatives necessary to obtain the corrections for the temporary root values are calculated from the concentrations of

the species and their stoichiometric coefficients, *e.g.*, $\partial(T_{L,calc} - T_L)/\partial[L] = 1 + \Sigma p_j c_j/[L]$ *etc.* This results in a very short running time.

The CPXES procedure calculates the concentrations of species, and the PRINT procedure controls the output of the measured and calculated data in various possible formats, depending on the value given for the variable R.

Variables and arrays

In the construction of this program we have tried to keep the same meanings for the variables and arrays of MINIPOT. However, some small changes and new variables had to be introduced.

Variables: M and L: multiplication factors to produce starting values for iteration from T_M and T_L, respectively (see lines 850 and 980); X1 and X2: divisors of T_M and T_L, respectively (see line 80).

Arrays: H: free hydrogen-ion concentration; E: absorbance reduced to 1-cm path-length; M and L: the concentrations of the associating species [equation (1)]; Q1, P1 and R1; stoichiometric coefficients of the species M, L and H^+, respectively, in the individual complexes; V1: the measured pH of the reaction mixture.

Some remarks on the use of the program

1. If the comment lines are omitted, the program will run on a desk-computer with 16 kbyte of memory. The program can treat a maximum of 40 experimental points measured at one wavelength and a maximum of 8 complex species formed. Consequently, the maximum number of parameters is 18, because the last two parameters are always the molar absorbances of the reacting species M and L, in that order. First the log β values, and then the ϵ values must be fed in.

2. The handling of MINISPEF, especially the manner of search for and refinement of parameters, is the same as that of MINIPOT, and therefore is not illustrated and discussed here (the details may be found in our previous paper[1]).

3. MINISPEF allows the simultaneous refinement of a maximum of only four arbitrarily chosen parameters. When log β and ϵ values are refined simultaneously, the serial numbers of the ϵ values must always precede those of the log β values. It has been mentioned that, when molar absorptivities are dealt with, the time-consuming distribution calculation is omitted.

4. For the stoichiometric coefficients of components not present in complexes a value of zero must be fed in.

5. The most often executed statement of the program is the calculation of the individual species in line 1110. When one of the components is not present in the complexes, this statement can be simplified by leaving out the redundant operations. A further, more effective modification is the change of the subscripted variables in this statement for scalars. This intervention necessitates alterations in other parts of the program too, but it is often worth doing.

REFERENCES

1. F. Gaizer and A. Puskás, *Talanta*, 1981, **28**, 565.
2. F. Gaizer, *Coord. Chem. Rev.*, 1979, **27**, 195.
3. F. Gaizer and M. Máté, *Acta Chim. Acad. Sci. Hung.*, 1980, **103**, 355.

APPENDIX

```
0 REM MINISPEF
5 DIM L(40), M(40), E(40), P(18), T(18), A(50), B(50), E1(40), E2(8), E3(10)
10 DIM C(4, 4), C5(4, 4), D(40), G(4, 40), H(40), S1(4), G1(4), G2(4), F(40)
20 DIM C1(8, 40), Q1(8), P1(8), R1(8), V1(40): Z=LOG(10): Z1=1/Z: E5=1E3
30 INPUT W, N1, N2, N3, N4, R, X1, X2, M, L
40 FOR I=1 TO N1: ON W GOTO 50, 70, 90, 90
50 INPUT V1(I), L(I), E(I): H(I)=EXP(-Z*V1(I)): M(I)=1: V2=0
60 L(I)=L(I)/X2: GOTO 100
70 INPUT V1(I), M(I), L(I), E(I): H(I)=EXP(-Z*V1(I))
80 M(I)=M(I)/X1: V2=E5: L(I)=L(I)/X2: GOTO 100
90 INPUT M(I), L(I), E(I): H(I)=1: V1(I)=0: M(I)=M(I)/X1: L(I)=L(I)/X2: V2=E5
100 NEXT I
```

```
110 IF R=0 THEN 150:PRINT TAB(9);"MEASURED DATA. CONCNS. IN MMOL"
120 PRINT :PRINT :PRINT TAB(9);"PH     TOT. M     TOT. L      E":PRINT
130 FOR I=1 TO N1:PRINTUSING 140,I;V1(I);M(I)*V2;L(I)*1000;E(I):NEXT I
140 %###### ###.## ##.###### ##.###### ##.###
150 FOR I=1 TO N3:INPUT B1(I),P1(I),R1(I):NEXT I
160 FOR I=1 TO N2:INPUT P(I),T(I):NEXT I
170 INPUT K,V,N,T1:V2=1

830 REM EQUSOLV
840 FOR I=1 TO N3:E2(I)=EXP(2*P(I)):E3(I)=P(I+N3):NEXT I:E3(N3+1)=P(2*N3+1
850 E3(N3+2)=P(2*N3+2):A=L(1)*L:B=M(1)*M:T1=T1-1:U,S2=0
860 FOR I=K TO V STEP N:IF V2>N3 THEN 950:B1=M(I):A1=L(I)
870 A2=A1*.0011:B2=B1*.0011:T2,S1=0:IF T1>=0 THEN 880:A=A(I):B=B(I)
880 T2=T2+1:IF T2>8 THEN 980:D1,D2=1:D3=0:GOSUB 1090
890 Y1=A3-A1:IF W>1 THEN 900:A=A-Y1/D1:IF A<0 THEN 980:GOTO 930
900 Y2=B3-B1:D4=D3/A:D3=D3/B:D5=D1*D2-D3*D4:IF D5=0 THEN 960
910 A=A+(D3*Y2-D2*Y1)/D5:IF A<0 THEN 980:B=B+(D4*Y1-D1*Y2)/D5
920 IF B<0 THEN 980:IF ABS(Y2)>B2 THEN 880
930 IF ABS(Y1)>A2 THEN 880:IF A>A1 THEN 980
940 A(I)=A:B(I)=B
950 E1(I)=B(I)*E2(N3+1)+A(I)*E3(N3+2)
960 FOR L=1 TO N3:E1(I)=E1(I)+C1(L,I)*E3(L):NEXT L
970 D(I)=E(I)-E1(I):S2=S2+1:U=U+D(I)^2:GOTO 1080
980 T2=9:A=L*L(I):B=M*M(I):IF T1>=0 THEN 990:A=A(I):B=B(I)
990 G1=2:D5=B
1000 G2=2:D6=A
1010 GOSUB 1090:IF ABS(A1-A3)<A2 THEN 1040:IF A1-A3<0 THEN 1060
1020 D6=G2*D6:A=A+D6:GOTO 1010
1030 G2=.5:D6=G2*D6:A=A-D6:GOTO 1010
1040 IF W=1 THEN 940
1050 IF ABS(B1-B3)<B2 THEN 940:IF B1-B2<0 THEN 1070
1060 D5=G1*D5:B=B+D5:GOTO 1000
1070 G1=.5:D5=G1*D5:B=B-D5:GOTO 1000
1080 NEXT I:SELECT PRINT 215(75):RETURN
1090 REM CPXFS
1100 A3=A:B3=B:FOR L=1 TO N3
1110 C1(L,I)=A(I)^R1(L)*B^01(L)*A^P1(L)*E2(L)
```

```
1120 A3=A2+P1(L)*C1(L,I):B3=B2+D1(L)*C1(L,I):IF T2=0 THEN 1150
1130 D1=D1+P1(L)^2*C1(L,I):H:D2=D2+D1(L)^2*C1(L,I):B
1140 D3=D3+P1(L)*D1(L)*C1(L,I)
1150 NEXT L:RETURN



1280 REM PRINT:IF R=0 THEN 1460
1290 PRINT "          O      P      R    LOG BETAS    MOL ABS'S":PRINT :PRINT
1300 FOR I=1 TO N3:PRINTUSING 1310,Q1(I);P1(I);R1(I);P(I);E3(I):NEXT I
1310 %      -##.##-##.##-##.##-##.#####.#### ######.##
1320 PRINT TAB(34);:PRINTUSING 1330,E3(N3+1);E3(N3+2):PRINT
1330 %########.## ######.##
1340 IF R=1 THEN 1420:PRINT TAB(8);"PH     TOT. M     TOT. L     E.MSD   E.CAL     DT
H E":PRINT
1350 FOR I=K TO V STEP N
1360 PRINTUSING 1370,I,V1(I),M(I)*1000,L(I)*1000,E(I),E1(I),D(I)
1370 %###### ###.## ## ###### ##.###### ## ### ## ###-### ###
1380 IF R=2 THEN 1410:X6=100/M(I):IF N4=1 THEN 1390:X6=100/L(I)
1390 FOR L=1 TO N3:PRINTUSING 1400,C1(L,I)*X6;:NEXT L:PRINTUSING 1400,A(I)*X6
1400 % ###.##
1410 NEXT I
1420 PRINTUSING 1430,":";U
1430 %SQUARE OF RESIDUALS#  #.####^^^^
1440 H=SQR(U/(S2-F1-1)):PRINT :PRINTUSING 1450,":";H:PRINT :PRINT :PRINT
1450 %STANDARD DEVIATION #  #.####^^^^
1460 RETURN
```

Talanta, Vol. 28, pp. 931 to 934, 1981
Printed in Great Britain. All rights reserved

0039-9140/81/120931-04$02.00/0
Copyright © 1981 Pergamon Press Ltd

SELECTIVE POTENTIOMETRIC DETERMINATION OF Bi(III) WITH A COATED-WIRE ELECTRODE

P. W. ALEXANDER* and JOSE P. JOSEPH

Department of Analytical Chemistry, University of New South Wales, P.O. Box 1, Kensington, N.S.W., Australia 2033

(*Received* 10 *December* 1980. *Accepted* 6 *May* 1981)

Summary—A bismuth-selective electrode based on the chlorobismuthate(III) salt of Aliquat 336 is described. The electrode gives nearly linear response in the bismuth concentration range 10^{-1}–$10^{-4}M$. The optimum solution conditions for operation of the electrode have been determined together with possible interference effects. The application of the electrode to analysis of samples containing large amounts of other metals is illustrated by the determination of bismuth in pharmaceuticals. The electrode is shown to give results by direct potentiometry and the standard-addition method which differ from atomic-absorption results by not more than 2%.

Coated wire ion-selective electrodes based on anionic halide and pseudohalide complexes have been developed for the determination of a number of metals[1–11] and offer methods for determination of iron,[1] mercury,[2] zinc,[4] and cobalt,[6,11] for example, in a wide range of materials, but are applicable only in the absence of interfering metal complex species of similar type. Despite interference problems, the electrodes have been applied to analysis of metal concentrates and ores either by potentiometric titration[1] or by direct potentiometry.[4] In this study, we report such an electrode for selective determination of bismuth.

The determination of bismuth is of interest in metallurgy, geochemistry, pharmacy, and biology. As a model application, we chose to analyse pharmaceutical formulations containing bismuth, used in the treatment of disorders of the gastrointestinal tract.[12,13] The formulations are commercially available and are produced in a number of different forms, containing bismuth subnitrate or bismuth carbonate.[14,15]

Complexometric titration with EDTA is the method most commonly used for determination of bismuth in pharmaceuticals.[15,16] A complexometric titration method with pyrocatecholsulphonaphthalein as indicator has been reported for the simultaneous determination of bismuth and nitric acid in the manufacture of antidiarrhoeal preparations.[15]

In the present work, the coated-wire electrode method is compared with atomic-absorption analysis of two pharmaceutical preparations containing high and low levels of bismuth. Both direct calibration and the standard-addition method give good agreement with the AAS results.

* To whom correspondence should be addressed.

EXPERIMENTAL

Reagents

Aliquat 336 (A. C. Hatric Pty. Ltd.), polyvinyl chloride (I.C.I.), tetrahydrofuran (Merck) and hexane (May & Baker) were used. All acids were of analytical reagent grade and other chemicals of laboratory-reagent grade.

A stock solution made by dissolving bismuth-sesquioxide in hydrochloric acid to give a bismuth concentration of $0.1M$ in $2.5M$ hydrochloric acid was serially diluted to give standard solutions with bismuth concentrations in the range 10^{-5}–$10^{-2}M$ after addition of appropriate amounts of $10M$ hydrochloric acid to give a fixed acid concentration of either 0.5 or $2.5M$. To vary the total chloride concentration over the range 1–$6M$ in the standards while keeping the hydrochloric acid fixed, lithium chloride was added.

The procedure for preparation of the chlorobismuthate(III) complex with Aliquat 336 was based on that of Cattrall *et al.*[1–6] Bismuth solution ($0.1M$, in $2.5M$ hydrochloric acid, 125 ml) was shaken with 25 ml of $0.05M$ Aliquat 336 in hexane for about half an hour. The organic layer was separated, filtered, and then heated on a water-bath to evaporate the hexane. The light yellow viscous oil obtained was mixed with a 10% (w/v) solution of PVC in tetrahydrofuran so that the Aliquat complex: PVC w/w ratio in the solution was 4:1. The viscous solution obtained was used to coat a copper, silver or platinum wire soldered on to a shielded cable. Each wire was dipped in the solution several times to form a thin membrane film which was allowed to set overnight. The exposed portion of the wire was covered by wrapping cellophane paper tightly around it.

The electrode was conditioned by soaking in $0.1M$ bismuth solution in $2.5M$ hydrochloric acid for 3 hr and then in $2.5M$ hydrochloric acid for about 20 min. The electrode was rinsed with solutions of the same chloride concentration as the test solution. The response of the electrode was studied over the Bi(III) concentration range 10^{-1}–$10^{-5}M$ in solutions with lithium chloride concentrations varying between 0.0 and $3.5M$ at a fixed hydrochloric acid concentration of $2.5M$.

Interference studies

Interference studies were carried out by the method recommended by IUPAC.[17] The concentration of interfering

ion was fixed at $10^{-2}M$ except in the case of severe interference, when a lower concentration was used: the total bismuth concentration was varied between 10^{-1} and $5 \times 10^{-5}M$. The interfering anions were added as sodium or potassium salts and cations as chlorides, nitrates or sulphates. Interference effects were studied at two chloride concentrations, 1.0 and 2.5M.

Analysis of pharmaceuticals

Bismuth subnitrate and "Bismag" [International Home Products (Aust.) Pty. Ltd.] (containing 2.0% bismuth carbonate) were analysed as typical examples, bismuth subnitrate by direct potentiometry and "Bismag" by the standard-addition method. An appropriate weight of sample (as shown in Table 1) was dissolved and the solution made up to 100 ml in 1.5M hydrochloric acid–1.0M sodium chloride to give a final bismuth concentration in the range $1–5 \times 10^{-3}M$ for "Bismag" and $10^{-3}–10^{-2}M$ for bismuth subnitrate. For the standard-addition analysis, the graphical method suggested by Liberti and Mascini[18] was followed. After measurement of the potential of 25 ml of the test solution, four 0.5-ml portions of standard 0.1M bismuth solution were added in succession, the potential being measured after each addition. The standard-addition plot was found to be linear.

For atomic-absorption analysis, calibration plots were prepared from the signals for standard bismuth solutions (covering the range 300–1200 μg/ml in 1% nitric acid medium) aspirated into an air–acetylene flame. The sample solutions were also made up in 1% nitric acid. In the case of "Bismag" powder the standard-addition method was employed.

RESULTS AND DISCUSSION

Response characteristics

Figure 1 shows the response characteristics of the electrode for the bismuth concentration range $10^{-1}–10^{-5}M$ at various chloride concentrations. The response was almost linear over the bismuth range $10^{-1}–10^{-4}M$, with a slope of 36.5 mV/decade. If the electrode responds preferentially to singly-charged $BiCl_4^-$ or doubly-charged $BiCl_5^{2-}$ the slope should be close to 59 or 29.5 mV/decade respectively. The response of 36.5 mV/decade indicates that both species are present and causing a response. The length of the linear portion of the calibration curve was also found to be dependent on the chloride concentration. Figure 1 shows a shorter response range and greater curvature for 6M chloride concentration. This is attributed to the interference effects of chloride itself, as discussed by Cattrall *et al.*[6]

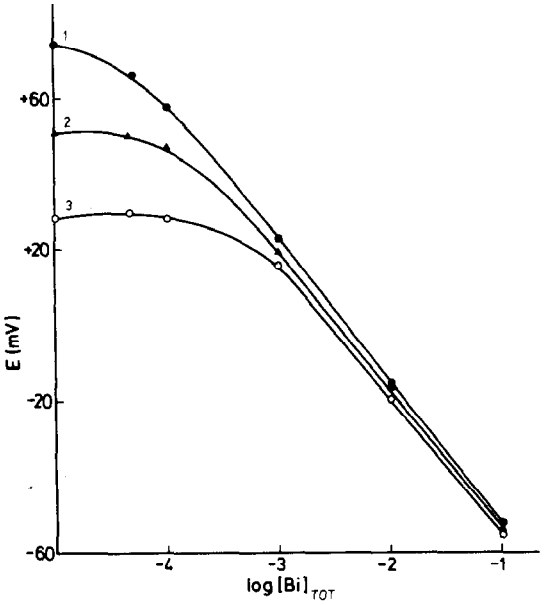


Fig. 1. Effect of chloride concentrations on the response characteristics of the chlorobismuthate(III) electrode. (1) 2.5M Cl^-, (2) 4.0M Cl^-, (3) 6.0M Cl^-.

The response of the electrode was sufficiently rapid to give a stable potential in about 30 sec in stirred solutions, and replicate measurements of the steady-state potentials gave a standard deviation of ± 0.1 mV for $1 \times 10^{-3}M$ bismuth. The reproducibility of the electrode was studied over a period of 45 days. The electrode was stored dry in air and was reconditioned briefly each day by soaking in 0.1M bismuth solution. Even though the absolute potential of the electrode changed, the calibration slope remained the same over this period.

The electrode behaviour, response and lifetime remained the same whether copper, silver or platinum wire was used as support for the membrane.

Interferences

The interference of a number of cations and anions was studied in acid solution. The interference curves given in Fig. 2. show the potentials measured in a series of solutions containing a constant concentration of the interfering ion and increasing concentrations of bismuth. There was no observable change in the potential over the bismuth concentration range $5 \times 10^{-5}–10^{-1}M$ in the presence of $10^{-2}M$ Ba^{2+}, Co^{2+}, Ni^{2+}, Ca^{2+}, Mg^{2+}, Cu^{2+}, Cr^{2+} and Al^{3+}. However, Sn^{4+}, Sb^{3+}, Fe^{3+}, Hg^{2+} and Zn^{2+} showed considerable interference, due to the formation of anionic chloro-complexes of these ions. It was found that the selectivity for bismuth improved considerably at low total chloride concentrations, and shown by the interference curves in Fig. 3. for 1.0M total chloride concentration. Chloride concentrations lower than 1.0M could not be studied, because bismuth oxychloride precipitated.

In the presence of Ag^+ and Pb^{2+} the chloride concentration was reduced by precipitation of the metal chlorides. At low concentration of these ions, *e.g.* $10^{-2}M$, the change in chloride concentration was insufficient to cause any serious change in the potential.

Of the anions tested, nitrate and sulphate showed negligible interference. Iodide and bromide interfered severely owing to the high stability constants of their complexes with Bi(III), and caused interference even at concentrations as low as $1 \times 10^{-3}M$.

A summary of the major interferences from metals is given in Table 1. As discussed above, metals which

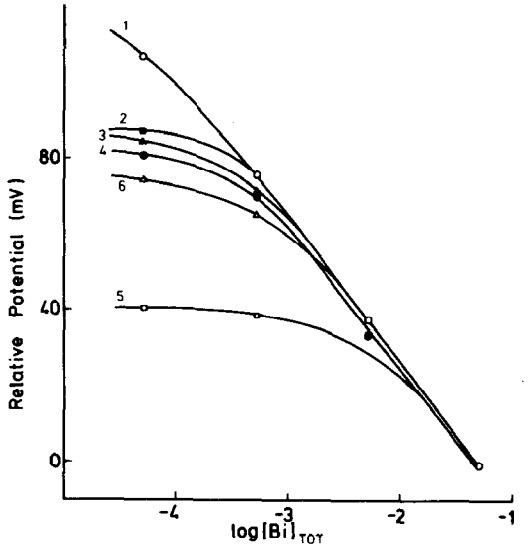


Fig. 2. Interference studies for the chlorobismuthate(III) electrode in 2.5*M* chloride solutions with the following interferences: (1) nil, (2) $1.0 \times 10^{-4}M$ Fe^{3+}, (3) $1.0 \times 10^{-4}M$ Sb^{3+}, (4) $1.0 \times 10^{-4}M$ Hg^{2+}, (5) $1.0 \times 10^{-4}M$ Sn^{4+}, (6) $1.0 \times 10^{-4}M$ Zn^{2+}.

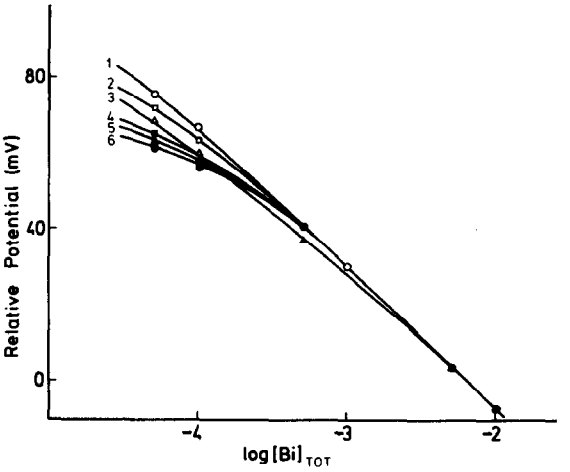


Fig. 3. Interference studies for the chlorobismuthate(III) electrode in 1.0*M* chloride solutions with the following interferences: (1) nil, (2) $1.0 \times 10^{-3}M$ Zn^{2+}, (3) $5.0 \times 10^{-3}M$ Fe^{3+}, (4) $1.0 \times 10^{-3}M$ Sn^{4+}, (5) $1.0 \times 10^{-2}M$ Zn^{2+}, (6) $1.0 \times 10^{-2}M$ Sb^{3+}.

form stable chloro-complexes interfere most seriously. With the exception of Hg(II), none of the metals interferes when present in 1:1 molar ratio to bismuth. At 100-fold molar ratio levels, however, all the interferences are serious, in the order $Hg^{2+} > Sn^{4+} > Fe^{3+} > Sb^{3+} > Zn^{2+}$, because the potential due to the interfering species becomes an appreciable fraction of the total potential.

These interference problems limit the possible applications of the electrode for direct potentiometric determination of bismuth in samples containing large amounts of these ions, and prior separation or masking steps would be required before bismuth could be determined in such samples. Nevertheless, the results indicate that the electrode may have many applications in the analysis of alloys, ores, pharmaceuticals, and biological samples in which the levels of the interferents fall within the limits established in this study.

Analytical applications

As an example, pharmaceutical bismuth formulations were analysed by both direct potentiometry and standard addition. The samples chosen were commercially available formulations labelled "Bismuth Subnitrate" and "Bismag", chosen in order to test the performance of the electrode for determinations of both high and low concentrations of bismuth in samples containing large amounts of other components. Of these two samples, Bismuth Subnitrate is available as a pure bismuth salt,[19] and Bismag is supplied as a formulation of 2% bismuth carbonate with 56% magnesium carbonate and 42% sodium bicarbonate.[19]

Table 1. Interference studies for the tetrachlorobismuthate(III) electrode in 1*M* Cl^- solutions

Interfering ion	Molar ratio to Bi	Conc. of Bi, *M*		Relative error,* %
		Taken	Found	
Zn^{2+} ($1.0 \times 10^{-2}M$)	1	1.0×10^{-2}	1.0×10^{-2}	nil
	10	1.0×10^{-3}	1.0×10^{-3}	nil
	100	1.0×10^{-4}	1.7×10^{-4}	70
Sb^{3+} ($1.0 \times 10^{-2}M$)	1	1.0×10^{-2}	1.0×10^{-2}	nil
	10	1.0×10^{-3}	1.0×10^{-3}	nil
	100	1.0×10^{-4}	1.9×10^{-4}	90
Sn^{4+} ($1.0 \times 10^{-3}M$)	1	1.0×10^{-3}	1.0×10^{-3}	nil
	10	1.0×10^{-4}	1.6×10^{-4}	60
Fe^{3+} ($5.0 \times 10^{-3}M$)	1	5.0×10^{-3}	5.0×10^{-3}	nil
	10	5.0×10^{-4}	6.0×10^{-4}	20
	100	5.0×10^{-5}	8.4×10^{-5}	68
Hg^{2+} ($1.0 \times 10^{-4}M$)	1	1.0×10^{-4}	3.6×10^{-4}	260

* In 2.5*M* Cl^- solution.

Table 2. Determination of bismuth in pharmaceuticals

Sample	No.	Weight of sample, g	Weight of Bi found, g	Bi, % Electrode	Bi, % AAS	Label values*
Direct calibration						
Bismuth	1	0.0623	0.0457	73.3	72.4	
Subnitrate	2	0.0911	0.0660	72.5	72.2	
	3	0.0456	0.0331	72.6	72.1	72.0
	4	0.2310	0.1660	71.8	71.8	
	5	0.1455	0.1040	71.9	72.0	
		Mean values ± s.d.		72.5 ± 0.6	72.1 ± 0.2	
Method of standard addition						
"Bismag"	1	1.8995	0.0301	1.58	1.63	
	2	3.3243	0.0518	1.56	1.62	1.60
	3	2.7484	0.0443	1.61	1.65	
		Mean values ± s.d.		1.59 ± 0.03	1.63 ± 0.02	

* Reference 19.

The results are shown in Table 2, with comparison with atomic-absorption results. The relative standard deviation of replicate determinations of samples containing both high and low conccentrations of bismuth was better than 2%. The mean values agreed with the atomic-absorption analysis within 1% for Bismuth Subnitrate but gave poorer agreement for the Bismag. However, the mean electrode and AAS values both fell within the quality-control limits used by the manufacturer, reported to be 95–105% of the label values,[19] and similar to the ranges reported for other bismuth formulations in the BPC.[14]

The bismuth electrode therefore offers a rapid and convenient method of analysis for bismuth in pharmaceuticals with accuracy agreeing with that of atomic-absorption methods, but replicate analysis is required if it is to be used for quality-control work. Studies of further applications in other areas of analysis are in progress.

Acknowledgement—We thank R. Elliss of International Home Products (Aust.) Pty. Ltd. for supply of some bismuth formulations.

REFERENCES

1. R. W. Cattrall and C. P. Pui, *Anal. Chem.*, 1975, **47**, 93.
2. *Idem, ibid.*, 1976, **48**, 552.
3. *Idem, Anal. Chim. Acta*, 1976, **83**, 355.
4. *Idem, ibid.*, 1976, **87**, 419.
5. *Idem, ibid.*, 1977, **88**, 185.
6. R. W. Cattrall, G. L. Lee and I. C. Hamilton, *ibid.*, 1980, **116**, 391.
7. A. V. Kopytin, A. F. Zhukov, Yu. I. Urusov, L. A. Kopytina and A. V. Gordievskii, *Zh. Analit. Khim.*, 1979, **34**, 465.
8. V. V. Cosofret, *Rev. Roum. Chim.*, 1978, **23**, 1489.
9. V. V. Cosofret, C. Christescu and P. G. Zugravescu, in *Ion Selective Electrodes, Budapest 1977*, E. Pungor and I. Buzás (eds.), p. 325. Akadémia Kiadó, Budapest, 1978.
10. N. K. Evseeva, I. N. Kremenskaya, V. N. Golubev and S. K. Timofeeva, *Zh. Analit. Khim.* 1976, **31**, 822.
11. K. Burger and G. Pethö, *Anal. Chim. Acta*, 1979, **107**, 113.
12. T. R. Wilson, *Post. Grad. Med. J. Suppl.* 1975, **51**, No. 5, 18.
13. AMA Dept. of Drugs, *AMA Drug Evaluations*, 2nd Ed., p. 794. Publishing Sciences Group, Acton, Mass., 1973.
14. *The Pharmaceutical Codex 1973*, pp. 732, 763, 775. Pharmaceutical Press, London.
15. D. E. Hughes and J. Cardone, *Anal. Chem.*, 1980, **52**, 940.
16. H. E. Brookes and C. A. Johnson, *J. Pharm. Pharmacol.*, 1955, **7**, 836.
17. *IUPAC Information Bulletin*, 1978, No. 1, 69.
18. A. Liberti and M. Mascini, *Anal. Chem.*, 1969, **41**, 676.
19. R. Elliss, International Home Products (Aust.) Pty. Ltd., York Rd., Bellambi, Aust. 2518, private communication.

Talanta, Vol. 28, pp. 935 to 938, 1981
Printed in Great Britain. All rights reserved

0039-9140/81/120935-04$02.00/0
Copyright © 1981 Pergamon Press Ltd

ARSENIC SPECIATION BY ION-EXCHANGE SEPARATION AND GRAPHITE-FURNACE ATOMIC-ABSORPTION SPECTROPHOTOMETRY

G. E. PACEY and J. A. FORD
Miami University, Department of Chemistry, Oxford, Ohio 45056, U.S.A.

(*Received* 4 *February* 1981. *Accepted* 6 *May* 1981)

Summary—As(III), As(V), monomethylarsenic acid (MMA) and dimethylarsenic acid (DMA) were determined by graphite-furnace atomic-absorption spectrophotometry after separation of the species by ion-exchange chromatography. The detection limits (ng/ml) were DMA 0.02, MMA 2.0, As(V) 0.4 and total arsenic 4.0. As(III) was determined by difference. This system gave better detection limits and/or shorter analysis times than previously reported systems.

The determination of metal species is essential to the understanding of the toxic and carcinogenic nature of metals found in environmental and biological systems. For example, the measurement of total arsenic content does not indicate the true levels of the individual species. To estimate effectively the hazard involved, the variations in toxicity, transport, and bioavailability, which are dependent on the arsenic chemical species, must be taken into account. It has been shown that arsenic can be found in natural systems as As(III), As(V), monomethylarsenic acid (MMA) and dimethylarsenic acid (DMA).[1–5] Other organic arsenic species have been reported to occur in some manufacturing processes.[6] Analytical methods aimed at differentiating between these species are needed.

As would be expected, a variety of techniques have been used for speciation of arsenic. Gas chromatography[7–10] and spectrophotometry[11–14] have been demonstrated as effective techniques for one or more arsenicals, but neither has been used for mixtures for all four species listed above. Atomic absorption,[1] an obvious choice for determination of metals, has been tried in conjunction with the generation and selective volatilization of arsines, which did resolve the four species,[15] but the possibilities of molecular rearrangement and poor recoveries at low concentrations have raised doubts about this system.[16,17] Separation by thin-layer chromatography followed by graphite-furnace atomic-absorption analysis has also been reported.[18,19]

Some flameless atomic-absorption systems have been reported. One system employed a separation scheme which gave less efficient resolution of species.[19] Woolson[20] published a system combining HPLC with graphite-furnace analysis; the limit of detection was 5 ng.

So far, the most successful detection system has been electrochemical, following separation on ion-exchange columns. Yamamoto[21] and Dietz and Perez[22] observed that DMA has a strong affinity for cation-exchange resins in acid medium. Elten and Geiger[23] used this fact to separate MMA and DMA before determination by differential pulse polarography (DPP). Henry *et al.* reported a method for the determination of As(III) and As(V) and total inorganic arsenic by DPP.[24] Later, Henry and Thorpe[25] reported a complete separation of all four species, using both anion- and cation-exchange columns, and detection with DPP. This separation procedure is superior to all previous systems but suffers from the slowness of the digestions needed to convert the organoarsenicals into As(III). With this in mind, we have modified this separation system for use in conjunction with graphite-furnace atomic-absorption analysis, and have designed an analysis system capable of giving a comparable detection limit without the time delays caused by the digestions.

EXPERIMENTAL

Apparatus

A Perkin–Elmer model 560 atomic-absorption spectrophotometer and HGA-400 graphite-furnace atomizer were used for all the metal determinations. A new hollow-cathode arsenic lamp was used. Purified and dried argon was used as the sweep gas for the HGA-400.

Reagents

High-purity arsenic trioxide was obtained from ROC/RIC (Belleville, N.J.). All other chemicals were those used by Henry and Thorpe.[25] The water was purified with a Barnstead NANO pure system followed by a Barnstead glass double-distillation system. All other chemicals were reagent grade.

Ion-exchange columns

Dowex 50W-X8 and Al-X8 resins (50–100 mesh) were used. Contaminants were removed from the resins by repeated washing alternately with 0.5*M* hydrochloric acid and ammonia solution at a flow-rate of 5–10 ml/min. The

exchange columns were slurry-packed. The cation-exchanger column was 16 cm long (1 cm diameter) and the anion-exchanger column 10 cm long (1 cm diameter). The cation resin was readily regenerated by passage of 1.0*M* hydrochloric acid through the column. It was necessary to convert the anion resin into the acetate form. This was done by passing 300 ml of 0.5*M* ammonia solution through the column, followed by 150 ml of 1.0*M* ammonium acetate at a flow rate of 5–10 ml/min. The column was rinsed with water and then with 0.1*M* acetic acid/ammonium acetate buffer (pH 4.7) until the effluent pH was 4.7. The preparation of the anion column was crucial to the success of the separation since careless preparation caused random errors in the results for the standard solutions. Control of the flow-rate was critical.

Procedure

The separation and determination of the four arsenic species is schematically represented in Fig. 1. The suggestion by Henry and Thorpe[25] of maintaining the pH of a sample between 4 and 10 was adopted. Four equal volumes of sample were used, for determination of total arsenic, DMA, MMA and As(V). As(III) was calculated by difference.

To isolate DMA from the matrix 100 ml of sample were mixed with 1.0 ml of 1.75*M* acetic acid and loaded onto the cation-exchange column at a flow-rate of 5 ml/min, and 70 ml of 0.02*M* acetic acid were passed through the column at a similar flow-rate to ensure complete separation from MMA, As(III) and As(V). Then DMA was stripped by passing 1.0*M* ammonia solution through the column at a flow-rate of 1.0 ml/min. The flow-rate is critical for successful stripping. The fraction of effluent between 40 and 50 ml was analysed.

To isolate MMA 100 ml of sample were mixed with pH 4.7 ammonium acetate/acetic acid buffer (total acetate concentration 0.01*M*) and passed through the anion-exchange column, followed by 50 ml of 0.01*M* buffer of the same pH. The As(III) and DMA were eluted in the first 120 ml of effluent but As(V) remained on the column. The MMA was collected by stripping with 0.5*M* acetate buffer of pH 4.7, the fraction of effluent between 10 and 30 ml being collected and analysed. The As(V) did not begin to elute until 65 ml of the 0.5*M* acetate solution had passed through the column. The next 30 ml were collected and analysed for As(V). Flow-rates of 1.8–2.0 ml/min were required.

As all the MMA was eluted by 40 ml of the 0.5*M* buffer, a 1*M* acetate buffer could then be used to strip the As(V) more compactly, the fraction between 20 and 30 of the 1*M* acetate eluate ml being sufficiently representative of the As(V) sample.

Optimization of graphite-furnace conditions

Table 1 shows the atomization parameters for the atomic-absorption determination of arsenic species. The four species can be determined in an essentially identical manner with the exception of the drying temperature used for MMA and As(V). Because of the high acetate concentration it was found necessary to increase the temperature to prevent sputtering and loss of sample. The stopped-flow gas system gave considerably higher absorbance values, with consistently better precision, than miniflow or high-flow gas-purge systems. The 193.7-nm line was used for all measurements. Deuterium lamp background correction did not affect the quality of the atomic-absorption measurements and was therefore not used.

RESULTS AND DISCUSSION

The system described provides excellent resolution of DMA, MMA, and As(V). The ion-exchange resins also act as a preconcentrator, thus lowering the overall working detection limits.

DMA was retained on the cation-exchange resin in 0.02*M* acetic acid. A break-through volume of greater than 500 ml was observed. By use of large sample volumes and elution with ammonia an initial DMA concentration as low as 0.02 ng/ml could be determined. The DMA detection limit with the graphite-furnace system was 0.01 ng. This is better by a factor of more than 10 than the 0.13-ng detection limit for total arsenic achievable with the HGA-400 system under the same preconcentration conditions. This enhancement is due to the ammonium ion used to elute the DMA from the column. A similar effect has been reported for several alkali and alkaline-earth metal ions, but the ammonium ion was not mentioned.[18] Table 2 shows the efficiency of the system for the determination of low levels of DMA. The recovery is good.

MMA was retained by the anion-exchange resin, with a break-through volume greater than 150 ml. Again a large volume of sample can be used. A sample with an initial MMA concentration of 2.0 ng/ml can be analysed. The absolute detection limit was 0.5 ng. The enhancement found for DMA was not

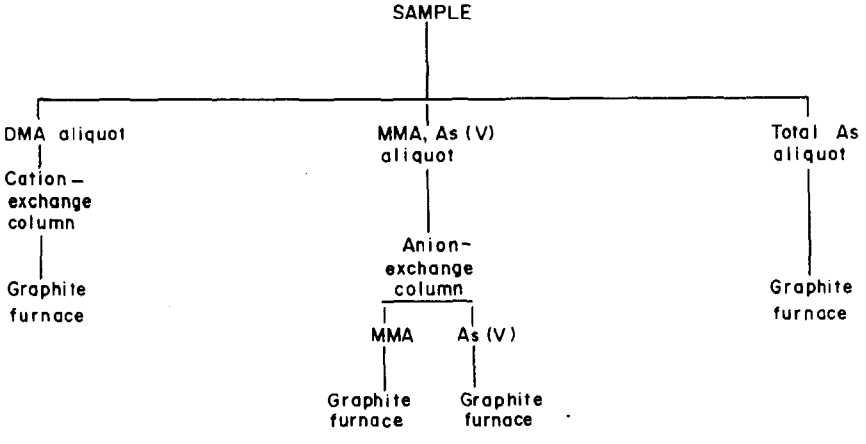


Fig. 1. Flow-chart for the determination of total As, As(V), MMA and DMA.

Table 1. Graphite-furnace parameters for determination of arsenic species (stop-flow mode)

	DMA	MMA	As(V)	Total As
Drying temperature, °C	100	140	140	100
Drying ramp time, *sec*	1	1	1	1
Drying hold time, *sec*	40	40	40	40
Charring temperature, °C	700	700	700	700
Charring ramp time, *sec*	30	30	30	30
Charring hold time, *sec*	15	15	15	15
Atomization temperature, °C	2700	2700	2700	2700
Atomization ramp time, *sec*	0	0	0	0
Atomization hold time, *sec*	5	5	5	5

*50-μl injections into pyrolytically-coated graphite tubes; argon purge at 60 ml/min.

observed for MMA. Table 3 shows the efficiency of the system for MMA determination; again there is good recovery.

Since both As(V) and MMA were retained by the anion-exchange column, it was possible to separate them during the elution. The minimum concentration of As(V) in a sample that could be detected was 0.4 ng/ml and the absolute amount of As(V) detectable in the furnace was 0.2 ng. The As(V) was easily retained and recovered with similar efficiency to that for DMA and MMA.

The detection limit for total arsenic concentration was 4.0 ng/ml, which is more than adequate in view of the concentrations in the EPA reference material and the fly-ash slurry sample of Henry and Thorpe.[25]

At no time was there any evidence that the system allowed any interconversion of species. Therefore, the determination of As(III) by difference was legitimate. Tables 4 and 5 show the recovery of As(V) and As(III). The concentrations used were 30–80 ng/ml since the naturally occurring range is at that level. The recovery of As(V) is slightly lower than that of either MMA or DMA, because of the strong affinity of As(V) for the anionic resin. The resin usually retains a small but fairly constant amount of As(V) regardless of the pH and ionic strength. The As(III) was calculated by difference. The higher recovery for this species may be due to impurities in the DMA and MMA and/or the small inherent negative error in the As(V) determination.

This system gave detection limits lower than those of the differential pulse method, with the added advantage that the time-consuming digestion process was no longer needed. Variations in the actual detection limits will obviously occur with different graphite furnace systems.

The ionic state of each species has not been clearly identified. Dietz and Perez[22] pointed out that the separation of all four species on a cation-exchange column was *not* due to an ion-exchange mechanism, and explained the separation behaviour as due to ion-exclusion chromatography.

Essentially, it was concluded that at the pH-values used with the cation-exchange column As(V) species were behaving as ionized solutes and were excluded from the resin. The non-ionized nature of the As(III) species meant that some penetration of the resin would occur but not to the same extent as for MMA or DMA. The pK_a values of 3.6 and 6.2 for MMA and DMA respectively fall between those for arsenic and arsenious acids. DMA is strongly bound to a cation-exchange column, probably as $(CH_3)_2AsO_2HNH_4^+$ in our case. The MMA is strongly held by the anion-exchange column, probably as a $(CH_3)AsO_3^-$ species.

Table 2. Recovery of DMA on Dowex 50W-X8

Taken, *ng/ml*	Found, *ng/ml*	Recovery, %
0.080	0.076	95
0.080	0.080	100
0.050	0.052	104
0.050	0.050	100
0.050	0.054	108
0.050	0.046	96
0.030	0.033	110
0.030	0.030	100
0.030	0.031	103
0.030	0.029	96

Mean 101%; standard deviation 5%.

Table 3. Recovery of MMA on Dowex Al-X8

Taken, *ng/ml*	Found, *ng/ml*	Recovery, %
7.2	7.1	99
7.2	7.2	100
6.0	5.9	98
6.0	5.9	98
6.0	6.2	103
5.0	5.2	104
4.0	3.8	95
4.0	4.1	103
4.0	4.2	105

Mean 101%; standard deviation 3%.

Table 4. Recovery of As(V) on Dowex Al-X8

Taken, *ng/ml*	Found, *ng/ml*	Recovery, %
80	76	95
80	81	101
50	51	102
50	50	100
50	48	96
50	46	92
30	30	100
30	31	103
30	29	97
30	28	93

Mean 98%; standard deviation 4%.

Table 5. Recovery of As(III) by difference

Taken, *ng/ml*	Found, *ng/ml*	Recovery, %
80	79	99
80	82	103
50	52	104
50	50	100
50	54	108
50	48	96
30	32	107
30	30	100
30	31	103
30	28	93

Mean 101%; standard deviation 5%.

The stronger retention of As(V) as an $AsO_4H_2^-$ species would be consistent with the previously described systems of Dietz and Perez[22] or Henry and Thorpe.[25]

Acknowledgement—Funding for the purchase of the graphite furnace was provided by NSF 69A Grant No. NSF-CDP-8001911.

REFERENCES

1. R. S. Braman and C. C. Foreback, *Science*, 1973, **182**, 1247.
2. F. Challenger, *Chem. Rev.*, 1945, **36**, 315.
3. B. C. McBride and R. S. Wolfe, *Biochemistry*, 1971, **10**, 4312.
4. D. W. VonEndt, P. C. Kearny and D. D. Kaufman, *J. Agric. Food Chem.*, 1968, **16**, 17.
5. E. A. Woolson and P. C. Kearny, *Environ. Sci. Technol.*, 1973, **7**, 47.
6. G. G. Ricci, L. S. Shepard, N. Hester and G. Glovos, Paper delivered at 2nd Chemical Congress of the North American Continent, Las Vegas, 1980.
7. A. W. Fickett, E. H. Daughtrey and P. Mushak, *Anal. Chim. Acta*, 1975, **79**, 93.
8. J. D. Lodmell, *Ph.D. Thesis*, University of Tennessee, Knoxville, Tenn., 1973.
9. L. D. Johnson, K. O. Gerhart and W. A. Auc, *Sci. Total Environ.*, 1972, **1**, 108.
10. C. J. Soderquist, D. G. Crosby and J. B. Bowers, *Anal. Chem.*, 1974, **46**, 155.
11. S. A. Peoples, J. Lakso and T. Lais, *Proc. West. Pharmacol. Soc.*, 1971, **14**, 178.
12. M. G. Haywood and J. P. Riley, *Anal. Chim. Acta*, 1976, **85**, 219.
13. T. Kamada, *Talanta*, 1976, **23**, 835.
14. S. S. Sandhu, *Analyst*, 1976, **101**, 856.
15. Y. Talmi and D. T. Bosik, *Anal. Chem.*, 1975, **47**, 2145.
16. J. E. Portman and J. P. Riley, *Anal. Chim. Acta*, 1964, **31**, 509.
17. M. B. Casvalho and D. M. Hercules, *Anal. Chem.*, 1978, **50**, 2030.
18. Y. O. Danard, O. Matano and S. Goto, *Bunseki Kagaku*, 1979, **28**, 517.
19. R. R. Stanforth, *Env. Sci. Tech.*, 1979, **12**, 1491.
20. E. A. Woolson and N. Aharowsow, *J. Assoc. Off. Anal. Chem.*, 1980, **63**, 523.
21. M. Yamamoto, *Soil Sci. Soc. Am. Proc.*, 1975, **39**, 859.
22. E. A. Dietz and M. E. Perez, *Anal. Chem.*, 1976, **48**, 1088.
23. R. K. Elton and W. E. Geiger, Jr., *ibid.*, 1978, **50**, 712.
24. F. T. Henry, T. O. Kirch and T. M. Thorpe, *Anal. Chem.*, 1979, **51**, 215.
25. F. T. Henry and T. M. Thorpe, *Anal. Chem.*, 1980, **52**, 80.

Talanta, Vol. 28, pp. 939 to 943, 1981
Printed in Great Britain

0039-9140/81/120939-05$02.00/0
Pergamon Press Ltd

ETUDE DES ECARTS A LA LINEARITE DE LA METHODE LINEAIRE DE DOSAGE PAR TITRIMETRIE THERMOMETRIQUE—I

COURBURES DUES A LA VARIATION DE CAPACITE CALORIFIQUE ET AUX FUITES THERMIQUES

A. M. BERNARD

Laboratoire de Cristallographie et Chimie du Solide, L.A. 251, Laboratoire de Chimie Minérale B, ISMRA, Université de Caen, 14032 Caen Cedex, France

J. L. BURGOT

Laboratoire de Chimie Analytique, U.E.R. du Médicament, Faculté de Médecine et Pharmacie, Rennes-Villejean, 2, avenue du Professeur Léon Bernard, 35043 Rennes Cedex, France

(*Reçu le* 15 *Septembre* 1980. *Revisé le* 30 *janvier* 1981. *Accepté le* 24 *avril* 1981)

Résumé—La variation de capacité calorifique et les fuites thermiques qui accompagnent un dosage thermométrique font que le thermogramme, même dans le cas d'une réaction très rapide et irréversible, n'est pas formé de segments de droite, mais sensiblement d'une hyperbole. Ces écarts à la linéarité, gênants pour l'interprétation et pour l'exploitation des thermogrammes peuvent être calculés pour toute fraction titrée. La relation obtenue fait intervenir un paramètre que nous appelons variation de capacité apparente au point équivalent et qui prend en compte les deux causes d'écart à la linéarité. Cette relation est confrontée avec l'expérience.

L'un des principaux avantages de la titrimétrie thermométrique, en tant que technique analytique et d'étude des réactions, est d'être en principe une méthode linéaire. Il est donc utile de pouvoir identifier l'origine des écarts à la linéarité que peuvent présenter les différentes portions du thermogramme, d'en prévoir la valeur numérique et d'indiquer l'influence qu'ils ont sur la forme réelle du thermogramme afin d'éventuellement les minimiser et plus généralement de pouvoir évaluer leur impact sur les résultats espérés.

Parmi les nombreuses équations de base de la titrimétrie thermométrique[1-10] (pour une comparaison de ces équations et une discussion de leur portée, consulter références 11,12), celle de Barthel *et al.*[1] légèrement simplifiée, traduit la période de titrage par l'expression:

$$T - T_0 = \frac{1}{C(t)[1 + \frac{1}{2}\chi t]} \times \left[\int_0^t W_R(t)\,dt - \Delta H_r b v'_0 t + W_0 t \right] \quad (1)$$

Les notations utilisées sont celles des références 1 et 11. On voit que pour la période de titrage les trois causes d'écart à la linéarité du thermogramme sont:

—la capacité calorifique variable, $C(t)$;
—"l'adiabaticité" qui se traduit par le paramètre χ (ou module de transfert);
—éventuellement la puissance thermique chimique $W_R(t)$ lorsqu'elle dépend du temps.

De ces trois causes, c'est évidemment la dernière qui intéresse le plus l'analyste ou le physicochimiste. La puissance $W_R(t)$ peut, en effet, évoluer avec le temps pour différentes raisons: équilibre de la réaction de dosage, cinétique particulière de cette dernière, superposition de plusieurs réactions. Mais avant de pouvoir les étudier, il convient de pouvoir s'affranchir, ou tout au moins de rationaliser les écarts inhérents à la variation de capacité calorifique et aux fuites thermiques. C'est l'objet de ce travail. (Remarquons qu'il peut exister d'autres causes d'écarts à la linéarité liés, non plus à la mise en oeuvre du dosage, mais à la propagation de l'information: non-linéarité de réponse des thermistances[6] et du pont de Wheatstone.[6,13,14] Ils ne se manifestent que pour des grandes variations ΔT, ce qui est très rarement le cas sauf en milieu non-aqueux.[15] Aussi ils ne sont pas considérés plus avant.)

C'est un fait d'expérience que dans certaines conditions expérimentales, une réaction de dosage unique, immédiate et complète peut se traduire sur le thermogramme par une courbe qui s'écarte nettement d'un segment de droite. La figure 1 qui est le thermogramme enregistré lors du dosage d'une solution d'acide chlorhydrique par une solution d'hydroxyde de sodium pour un temps de dosage long (517 sec), en est l'illustration (elle montre aussi que la période de

dilution qui correspond à l'addition d'un excès de solution titrante peut s'incurver également pour les mêmes raisons). Du fait que dans ce cas, l'effet thermique d'origine chimique dissipé au temps t peut s'expliciter comme suit[1,2] (ΔH_R est la variation d'enthalpie molaire accompagnant la réaction de dosage)

$$\int_0^t W_R(t)\,dt = -\Delta H_R b v'_0 t \qquad (2)$$

il est manifeste, d'après l'équation (1), que ce sont la variation de capacité calorifique et les fuites thermiques qui sont seules responsables des écarts à la linéarité. Nous nous placerons toujours pour cette étude, puisque là n'est pas le problème, dans le cas où la relation (2) est vérifiée.

Assez curieusement, si toutes les publications originales et traités généraux qui concernent la théorie et la mise en oeuvre de dosages thermométriques (voir par exemple, références 1,9,13) stipulent clairement que d'une part la variation de capacité calorifique doit être la plus faible possible et que d'autre part la réaction doit avoir lieu dans une enceinte aussi adiabatique que possible, aucun ne mentionne une approche quantitative de l'influence de ces deux facteurs sur la linéarité. Carr[6] a toutefois abordé le problème, de l'influence de ces deux paramètres sur l'exactitude de ces dosages en utilisant le procédé de la tangente initiale[10] pour déterminer le point équivalent. Ce problème nous semble relativement mineur, puisque nous voyons (Fig. 1) que même si la période réactionnelle et la période de dilution se traduisent par des portions de courbe, le point équivalent exact se perçoit aisément du fait de la discontinuité de la variation de la pente, conséquence de l'annulation brutale de la puissance W_R.

En revanche, il nous semble qu'il est plus intéressant de pouvoir calculer *a priori*, en fonction de la variation de capacité calorifique et de "l'adiabaticité" du calorimètre, pour quelles fractions titrées les portions du thermogramme représentant les périodes réactionnelle et de dilution, s'écartent sensiblement d'une droite.

Nous établissons ici de telles formules de prévision et nous tentons de les vérifier expérimentalement. Mais ce double travail, théorique et expérimental, nous amène d'abord à étudier mathématiquement les courbes enregistrées et à proposer un paramètre a, permettant de chiffrer ces deux types d'effets.

PARTIE EXPERIMENTALE

Appareillage

L'appareillage comporte une burette automatique à débit constant, un calorimètre adiabatique, un agitateur, une thermistance, un pont de Wheatstone, un dispositif d'amplification et un enregistreur. Le calorimètre et le dispositif d'amenée de la solution titrante sont immergés dans un bain thermostaté.

La burette automatique est une burette "Tacussel", à commande électronique du type "électroburex" à fonctionnement autonome. La précision sur le volume déterminé, en fonction de la vitesse d'addition, est déterminée par pesée. Pour des vitesses d'addition égales ou supérieures à 1 ml/min, elle se situe vers 0,4%.

Le calorimètre est façonné suivant le modèle de Christensen, Izatt et Coll.[16] Sa contenance est de 104 ml. Empli de 100 ml d'une solution d'acide chlorhydrique à $10^{-2}M$, la capacité calorifique est de 436 J/deg; soit 18 J/deg pour le calorimètre proprement dit, le module d'échange est $\chi = 1{,}74 \cdot 10^{-4}$ sec^{-1}. Son temps d'équilibrage est de 2 à 3 min.

Le bain où est immergé le calorimètre et où circule la solution titrante est un bain "huberunistat" thermostaté au 0,01°.

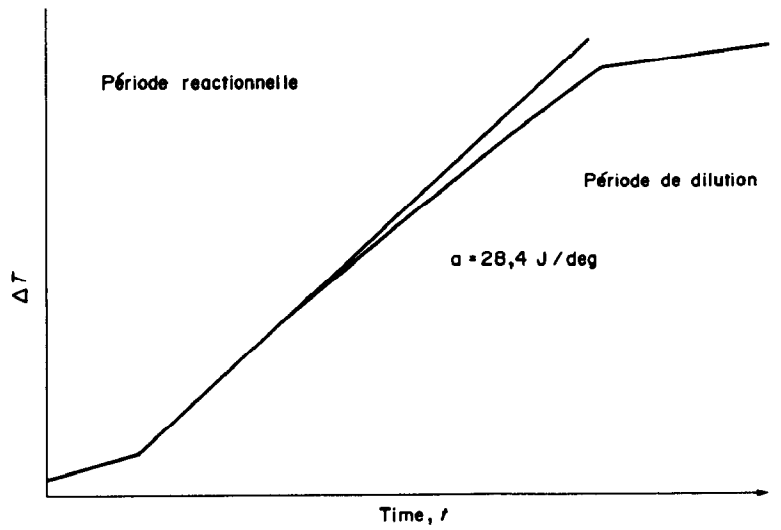


Fig. 1. Thermogramme expérimental obtenu lors du dosage d'une solution d'acide chlorhydrique à $10^{-2}M$ par une solution d'hydroxyde de sodium à $2M$: durée du dosages 515 sec.

L'agitation se fait par le manchon central du calorimètre par une petite hélice entraînée par le système "Tacussel controvit" permettant d'avoir une puissance d'agitation reproductible.

La thermistance utilisée est une VECO ("Victory engineering corporation") 31 A 6.

Le pont de Wheatstone est le même que celui utilisé dans un travail précédent,[17] mais les résistances R_2 et R_4 sont inversées, ceci pour obtenir un gain de sensibilité.[6]

Le dispositif d'amplification est le même.

L'enregistreur est un appareil "Tacussel E.P.L.I.B." équipé d'un tiroir T.V. 11 G.D. dont la gamme s'étend de 1,25 à 2,5 V.

Un dispositif capacitif en T est intercalé entre l'amplificateur et l'enregistreur pour filtrer les parasites.

Avec ce montage, pour la sensibilité maximale de l'enregistreur 64 mm de déviation (verticale) de la plume de l'enregistreur correspondent théoriquement à 10^{-3} K. Enfin, la valeur de l'index enthalpimétrique (ESI)[9] pour une précision de 1,82% est $(E.S.I.)_{1,82\%} = 55{,}76$ J/l.

Réactifs

Les solutions d'acide chlorhydrique sont préparées par dilution de solutions étalon avec de l'eau distillée. Les solutions d'hydroxyde de sodium sont préparées extemporanément par pesée et dilution et sont titrées soit par pH-mètrie soit par titrimétrie thermométrique.

Technique

Elle est décrite dans le mémoire précédent.[17]

PARTIE THEORIQUE

Etudes des thermogrammes

Le plus souvent l'addition de solution titrante s'effectue à l'aide d'une burette automatique. L'expression de la capacité calorifique, en fonction du temps s'écrit

$$C(t) = C_0 + C_B v'_0 t$$

où C_0 est la capacité calorifique au temps $t = 0$ et C_B la capacité calorifique par unité de volume de la solution titrante.

En tenant compte de cette dernière expression et de la relation (2), l'équation (1) s'écrit

$$\Delta T = \frac{[-(\Delta H_R + \Delta H_v)bv'_0 + W_0]t}{C_B v'_0 t + \frac{1}{2}\chi t C_0 + \frac{1}{2}\chi C_B v'_0 t^2 + C_0} \qquad (3)$$

Les valeurs numériques, même très défavorables, montrent que l'on peut négliger au dénominateur le terme en t^2 qui est toujours beaucoup plus faible que les trois autres (*cf.* réf. 11).

Si nous faisons intervenir dans l'équation (3) les fractions titrées telles que $f = t/t^*$ où t^* est le temps nécessaire pour atteindre le point équivalent, nous avons

$$\Delta T = \frac{[-(\Delta H_R + \Delta H_v)bv'_0 + W_0]t^* f}{(C_B v'_0 t^* + \frac{1}{2}\chi t^* C_0)f + C_0}$$

Posons

$$[-(\Delta H_R + \Delta H_v)bv'_0 + W_0]t^* = Q^*$$

et

$$C_B v'_0 t^* + \tfrac{1}{2}t^*\chi C_0 = a$$

(Q^* est la somme de tous les effets thermiques développés durant la période réactionnelle).

Soit:

$$\Delta T = \frac{Q^* f}{af + C_0}. \qquad (4)$$

Dans le cadre d'hypothèses défini ci-dessus, la période réactionnelle ($0 < f < 1$) se traduit, sur le thermogramme par une portion d'une branche d'hyperbole équilatère. Quant à la période de dilution, il est aisé de démontrer qu'elle se traduit également par une portion d'une branche d'hyperbole équilatère d'équation

$$\Delta T = \frac{Q'^* f}{af + C_0} + \frac{Q^* - Q'^*}{C_0 + a} \quad \text{pour} \quad (f \geqslant 1)$$

où $Q'^* = -\Delta H_v bv'_0 t^* + W_0 t^*$ est la somme des effets thermiques autres que celui d'origine chimique dissipés jusqu'au point équivalent.

On voit l'importance du paramètre composite a. En prenant une valeur non nulle, c'est lui qui conditionne les écarts à la linéarité.

Il est donc bien indiqué pour traduire globalement les effets de variation de capacité calorifique et d'adiabaticité que nous étudions. Nous proposons de l'appeler *variation de capacité calorifique apparente au point équivalent théorique*. Il s'exprime en J/deg. A titre d'exemple la figure 1 est un enregistrement pour $a = 28{,}4$ J/deg.

Formules de prévision

L'hypothèse de travail que nous adoptons est que l'écart à la linéarité est perçu par l'observateur lorsque la courbe enregistrée est à une certaine distance Z de la tangente initiale tracée sur le même diagramme (Fig. 2). Rappelons que celle-ci figure ce que serait la période réactionnelle si a était nul. La valeur de Z est

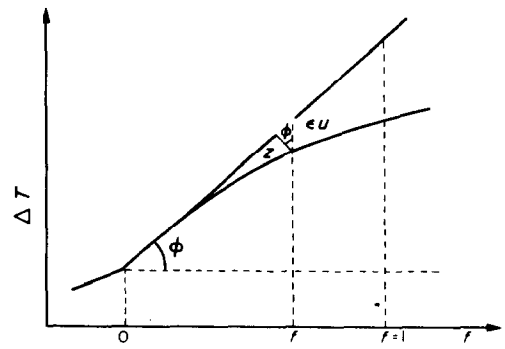


Fig. 2. Justification géométrique de l'équation découlant de l'hypothèse de travail.

purement arbitraire et peut être différente d'un observateur à l'autre et même d'une expérience à l'autre.

Pour une fraction titrée f (Fig. 2) la différence de température entre les cas où a est nul et non nul est

$$\epsilon(k) = \left[\frac{1}{C_0} - \frac{1}{C_0 + af}\right] Q^* f.$$

Si la sensibilité est telle que 1 K donne lieu à une déviation de u cm, la différence de température enregistrée (en cm) pour la fraction titrée est ϵu. L'hypothèse de travail se traduit donc par la relation

$$\epsilon u \cos \phi \geq Z \tag{5}$$

Or (Fig. 2)

$$\phi = \operatorname{arctg}\left(\frac{Q^* u}{C_0 t^* v}\right)$$

étant entendu que $f = 1{,}00$ correspond à t^* sec, soit vt^* cm, v étant le facteur d'élongation suivant l'axe des temps (1 sec correspond à v cm). Le remplacement de ϵ et ϕ par leur expression conduit à la relation cherchée du type

$$f = \frac{A + \sqrt{A^2 + \dfrac{4C_0 A}{a}}}{2} \tag{6}$$

où

$$A = \frac{ZC_0}{uQ^* \cos\left(\operatorname{arctg} \dfrac{Q^* u}{C_0 t^* v}\right)}.$$

Etant données les valeurs numériques utilisées couramment et l'ordre de grandeur de Z (0,03 cm: voir résultats) on a

$$f \approx \frac{1}{2}\sqrt{\frac{4C_0 A}{a}}.$$

Soit:

$$f \approx C_0 \sqrt{\frac{Z}{aQ^* u \cos\left(\operatorname{arctg} \dfrac{Q^* u}{C_0 t^* v}\right)}}. \tag{7}$$

Une autre formule littéralement différente mais mathématiquement équivalente peut être proposée (*cf.* réf. 11).

Cette formule montre que la fraction titrée pour laquelle se manifeste, d'une façon sensible, l'écart à la linéarité varie avec l'inverse de la racine carrée de la variation de capacité calorifique apparente. Elle est d'autre part, d'autant plus importante que:

—la capacité calorifique initiale est plus élevée;
—la vitesse de déroulement du papier v est petite;
—les facteurs u et Q^* sont petits. Il est d'ailleurs intuitif que plus la sensibilité est faible (u petit), moins l'écart à la linéarité se manifestera vite. Il est non moins intuitif que plus les effets thermiques sont faibles et notamment l'enthalpie réactionnelle, moins vite la différence de température minimale, permettant l'appréciation de l'écart Z sera atteinte.

Nous retrouvons dans cette formule la présence du paramètre a, les parts respectives de la variation réelle de capacité calorifique et des fuites thermiques étant précisées par la valeur du temps t^*.

Nous aboutirions à des formules du même type pour la période de dilution. Nous ne les mentionnons pas ici, car elles présentent moins d'intérêt du fait qu'il n'y a plus d'effet chimique à se développer.

VERIFICATION EXPERIMENTALE

Nous adoptons le processus de vérification suivant.

(*A*) Dans un premier temps nous effectuons un grand nombre de dosages de solutions aqueuses d'acide chlorhydrique par des solutions aqueuses d'hydroxyde de sodium, dans des conditions expérimentales variées qui se traduisent par des valeurs diverses du paramètre a. Ces conditions peuvent résulter de différentes concentrations initiales d'acide à doser, vitesses d'addition ou de volumes de solutions à doser variables.

Ces conditions expérimentales diverses peuvent aussi résulter de la simple variation des facteurs d'élongation u et v.

Nous déterminons pour chaque groupe de conditions bien définies, la fraction titrée pour laquelle la courbe s'écarte de la droite idéale correspondante (tangente initiale). Là intervient malheureusement une part d'imprécision importante inhérente à l'observateur, qui a du mal à garder objectivement les mêmes critères d'écart d'une expérience à l'autre. C'est pourquoi nous estimons les fractions titrées d'après les moyennes $\bar{f}$ de 6 à 8 mesures, établies dans des conditions identiques. Etant donné le très grand nombre de paramètres qui peuvent varier, nous vérifions simplement, à partir des valeurs $\bar{f}$ trouvées expérimentalement, que l'application des formules théoriques ci-dessus conduit toujours à une même valeur de Z.

(*B*) Dans un deuxième temps, à partir de cette valeur de Z, nous nous efforçons de prévoir les fractions titrées pour lesquelles il y aura début d'écart à la linéarité, à l'aide des formules théoriques. Nous confrontons ces calculs *a priori* avec l'expérience.

Les résultats de la première série de mesures sont consignés dans le tableau 1. Ce tableau appelle quelques commentaires.

(1) La colonne intitulée C_A^0 regroupe les différentes concentrations initiales (mole/l.) d'acide à doser. Ce sont elles qui fixent l'effet thermique réactionnel. Pour déterminer la somme des effets thermiques Q^*, nous négligeons la chaleur de dilution[18] de l'hydroxyde de sodium ($\Delta H_v = -293$ J/mole). De plus nous adoptons pour la puissance d'agitation la valeur $W_0 = 31{,}3 \cdot 10^{-3}$ J/sec déterminée expérimentalement.

(2) La première colonne intitulée Z groupe les valeurs de Z calculées à l'aide de la formule non simplifiée (6), la deuxième colonne intitulée Z regroupant celles calculées d'après la formule simplifiée (7).

La valeur moyenne de Z ainsi calculée est 0,0340 cm. Nous notons que les valeurs de Z sont proches. Nous notons aussi que l'utilisation de la formule simplifiée (7) est justifiée.

Tableua 1. Calcul de Z à partir des fractions titrées $\bar{f}$ déterminées expérimentalement

a, J/deg	C_A^0, M	u, cm/deg	v, cm/sec	t, sec	$\bar{f}$	C_0, J/deg	Z, cm	Z, cm
7,40	0,0119	64	0,025	129,6	0,65	436,0	0,018	0,018
14,30	0,05	16	0,05	120,9	0,49	415,1	0,044	0,044
15,79	0,05	16	0,025	162,4	0,46	415,1	0,029	0,030
16,99	0,05	16	0,025	195,5	0,39	415,1	0,024	0,025
18,80	0,05	16	0,025	245,7	0,43	415,1	0,045	0,046
27,42	0,0246	32	0,0125	588,0	0,35	436,0	0,041	0,042
28,61	0,05	16	0,0125	517,3	0,28	415,1	0,029	0,029

Dans une deuxième série de déterminations, nous voulons calculer, *a priori*, à partir de quelles fractions titrées les courbes qui représentent la période réactionnelle s'écartent de la linéarité. Nous choisissons le titrage de 100 ml d'acide chlorhydrique à 0,01M. La chaleur de dilution est négligeable et $W_0 = 31{,}3 \cdot 10^{-3}$ J/sec. Le temps de dosage t^* est fixé par le débit de la burette à 320,3 sec, ce qui entraîne une valeur de 14,3 J/deg pour le paramètre a. La sensibilité et la vitesse de déroulement du papier sont telles que $u = 64$ cm/deg et $v = 0{,}025$ cm/sec. La capacité initiale est de 436 J/deg.

L'application des formules (6) et (7) conduit à la valeur $f = 0{,}41$. L'expérience répétée sept fois conduit à la valeur expérimentale $f = 0{,}48$.

Ces résultats expérimentaux sont satisfaisants, surtout eu égard à la difficulté de garder constamment le même critère d'écart à la linéarité.

REFERENCES

1. J. Barthel, *Thermometric Titrations*, Wiley, New York, 1975.
2. J. Barthel, F. Becker et N. G. Schmahl, *Z. Phys. Chem. Frankfurt*, 1961, **29**, 58.
3. F. Becker, J. Barthel, N. G. Schmahl, G. Lange et H. M. Luschow, *ibid.*, 1963, **37**, 33.
4. F. Becker, J. Barthel, N. G. Schmahl et H. M. Luschow, *ibid.*, 1963, **37**, 52.
5. J. J. Christensen, R. M. Izatt, L. D. Hansen et J. A. Partridge, *J. Phys. Chem.*, 1966, **70**, 2003.
6. P. W. Carr, *CRC Crit. Rev. Anal. Chem.*, 1972, **3**, 491.
7. P. Papoff, G. Torsi et P. G. Zambonin, *Gazz. Chim. Ital.*, 1965, **95**, 1031.
8. G. O. Piloyan et Y. V. Dolinina, *Talanta*, 1974, **21**, 975.
9. J. Jordan, dans I. M. Kolthoff et P. J. Elving, *Treatise on Analytical Chemistry*, Part I, Vol. 8, p. 5175. Interscience, New York, 1968.
10. H. J. Keily et D. N. Hume, *Anal. Chem.*, 1956, **28**, 1294.
11. J. L. Burgot, *Thèse*, Rennes, 1980.
12. A. M. Bernard et J. L. Burgot, sous presse.
13. H. J. V. Tyrrell et A. F. Beezer, *Thermometric Titrimetry*, Chapman & Hall, London, 1968.
14. J. Lumbiarres, C. Mongay et V. Cerda, *Analusis*, 1980, **8**, 62.
15. W. L. Everson, *Anal. Chem.*, 1967, **39**, 1894.
16. J. J. Christensen, R. M. Izatt et L. D. Hansen, *Rev. Sci. Instr.*, 1965, **36**, 779.
17. J. L. Burgot, *Talanta*, 1978, **25**, 339.
18. J. M. Sturtevant, *J. Am. Chem. Soc.*, 1940, **62**, 3265.

Summary—The variation in heat capacity and the thermal shifts which accompany a thermometric determination make the thermogram, even in the case of a very rapid and irreversible reaction, hyperbolic instead of formed of straight segments. These departures from linearity, which are inconvenient in the interpretation and exploitation of the thermograms, can be calculated as a function of the degree of titration. The relation obtained introduces a parameter which the authors call the apparent change of capacity at the equivalence point, and which takes into account the two causes of deviation from linearity. This relationship is confirmed experimentally.

Talanta. Vol. 28, pp. 945 to 949. 1981
Printed in Great Britain

0039-9140/81/120945-05$02.00/0
Pergamon Press Ltd

ETUDE DES ECARTS A LA LINEARITE DE LA METHODE LINEAIRE DE DOSAGE PAR TITRIMETRIE THERMOMETRIQUE—II

COURBURES DES THERMOGRAMMES ET ERREUR SUR L'APPRECIATION DU POINT EQUIVALENT LORSQUE LA REACTION DE DOSAGE EST EQUILIBREE

A. M. BERNARD

Laboratoire de Cristallographie et Chimie du Solide, L.A. 251, Laboratoire de Chimie Minérale B, ISMRA, Université de Caen, 14032 Caen Cedex, France

J. L. BURGOT

Laboratoire de Chimie Analytique, U.E.R. du Médicament, Faculté de Médecine et Pharmacie, Rennes-Villejean, 2, avenue du Professeur Léon Bernard, 35043 Rennes Cedex, France

(*Reçu le* 15 *Septembre* 1980. *Revisé le* 30 *janvier* 1981. *Accepté le* 24 *avril* 1981)

Résumé—La reversibilité de la réaction de dosage est le plus souvent la cause d'écarts à la linéarité des thermogrammes traduisant un dosage thermométrique. La détermination du point équivalent par le procédé des tangentes est de ce fait entachée d'une erreur systématique. Les auteurs proposent une relation qui relie quantitativement cette erreur à la constante d'équilibre. Cette relation, vérifiée expérimentalement, est déduite de l'étude mathématique des thermogrammes et semble susceptible d'être généralisée à d'autres dosages linéaires.

Nous nous intéressons ici au cas où la seule cause d'écart à la linéarité que peut présenter un thermogramme enregistré lors d'un dosage thermométrique est dû à la reversibilité de la réaction de dosage (voir mémoire précédent[1]). Ce cas s'exprime par une puissance thermique dépendante du temps. D'une façon plus restrictive nous nous bornons au cas où la réaction de titrage est du type

$$A + B \overset{K}{\rightleftharpoons} AB \qquad (1)$$

Tyrrell[2] puis Carr[3] ont montré que tout comme pour les autres méthodes de dosage linéaire[4,5] c'est le facteur β, produit de la constante d'équilibre K et de la concentration initiale C_A^0 du composé à doser ($\beta = KC_A^0$), qui conditionne dans ce cas les formes du thermogramme. Charlot et Gauguin[4] d'une part, Rosenthal[5] d'autre part, ont montré, pour le cas général des dosages linéaires, que, pourvu que le facteur β soit suffisamment grand, le point de concours des tangentes initiale et finale à la courbe enregistrée figure le point équivalent stoechiométrique. Par contre si β est trop petit, le point de concours des tangentes initiale et finale est un point erroné. Ceci se retrouve dans le cas de la titrimétrie thermométrique comme le montre la considération des enthalpogrammes réduits selon Tyrrell[2] (Fig. 1).

On voit que pour $\beta > 10^2$ le point de concours des tangentes initiale et finale a lieu pour $f = 1$. Cette valeur limite de β de 10^2 est tirée de l'expression de la tangente initiale, donnée par Tyrrell[2]

$$\left(\frac{d\xi}{df}\right)_{f=0} = \frac{1}{1 + 1/\beta},$$

($\beta \neq \infty$). (ξ = "chaleur réduite").

Pour que le point de concours ait bien lieu pour $f = 1$, il faut que la pente de cette tangente initiale soit quasiment identique à celle de la droite représentant la période réactionnelle lorsque la réaction est totale. Dans le cas des enthalpogrammes réduits, cette pente théorique est:

$$\left(\frac{d\xi}{df}\right)_{f=0} = 1 \quad \text{pour} \quad \beta = \infty.$$

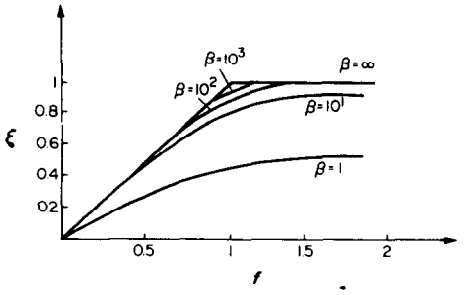


Fig. 1. Enthalpogrammes réduits: influence du paramètre β sur la forme des enthalpogrammes réduits (ξ fonction de f) (d'après Tyrrell[2]).

Il faut donc que $1/\beta$ soit bien inférieur à 1. Tyrrell avance pour β les valeurs de 10^2 et mieux 10^3.

En toute rigueur, on voit qu'à partir du moment où β n'est pas infini, la tangente initiale ne figure pas exactement la période réactionnelle d'un dosage irréversible. Il en résulte une erreur sur la détermination du point équivalent. A notre avis la notion "d'arrondi d'équilibre" est donc inséparable de celle d'erreur, d'ailleurs ici systématique.

Dans ce travail, nous allons relier quantitativement l'erreur systématique que l'on peut attendre sur la détermination du point équivalent lorsque la réaction de dosage est réversible, au paramètre β. Puis nous présenterons un certain nombre de données expérimentales qui la confirment. Mais auparavant il est nécessaire d'effectuer une étude mathématique sommaire des thermogrammes dans le cas où β a une valeur finie.

PARTIE EXPERIMENTALE

Appareillage et technique

Ils sont décrits dans les mémoires précédents.[1,6,7]

Réactifs

Les solutions d'hydroxyde de sodium sont préparées extemporanément par pesée et dilution et sont titrées soit par pH-mètrie soit par titrimétrie thermométrique.

La pureté du chlorhydrate d'éphédrine est vérifiée par son point de fusion, $T_f = 216°$. Les solutions sont préparées extemporanément par pesée et dilution.

PARTIE THEORIQUE

Etude mathématique des thermogrammes

Avec les hypothèses fixées ci-dessus, c'est-à-dire en supposant que l'écart à la linéarité n'a pour seule cause que la réversibilité de la réaction de dosage, autrement dit que la variation de capacité calorifique (ou de volume réactionnel) est négligeable, ainsi que les fuites thermiques, l'effet thermique développé à tout instant t est

$$q = -[AB]_t V \Delta H_{AB} + W_0 t - \frac{\Delta H_v V C_A^0 t}{t^*} \qquad (2)$$

avec les notations de la référence 1, soit en faisant intervenir la fraction titrée f

$$q = -[AB]_f V \Delta H_{AB} + W_0 f t^* - \frac{\Delta H_v V C_A^0 f t^*}{t^*} \qquad (3)$$

où $[AB]_f$ est la concentration de AB pour la fraction titrée f correspondant au temps t. Or Tyrrell[2] a montré que

$$[AB]_f = \left\{\frac{(1 + f + 1/\beta) - \sqrt{(1 + f + 1/\beta)^2 - 4f}}{2}\right\} C_A^0. \qquad (4)$$

La relation (4) n'est qu'une conséquence de la loi d'action de masse, en supposant toutefois le volume réactionnel constant et en confondant activités et concentrations. En remplaçant dans la relation (3) q par le produit de la variation de température ΔT et de la capacité calorifique par hypothèse constante C_0, et $[AB]_f$ par l'expression donnée par la relation (4), on aboutit après réarrangement et regroupement, puis enfin par remplacement de f par t/t^* à l'équation (5)

$$\Delta T^2 - (Q^* + Q'^*)\frac{1}{C_0 t^*}\Delta T t + \frac{Q^* Q'^*}{C_0^2 t^{*2}} t^2 + (1/\beta + 1)\left(\frac{Q'^* - Q^*}{C_0}\right)\Delta T - \left(Q^* + \frac{Q'^*}{\beta}\right)\left(\frac{Q'^* - Q^*}{C_0^2 t}\right) t = 0 \qquad (5)$$

où Q^* est la somme de tous les effets thermiques dissipés au point stoechiométrique

$$Q^* = -C_A^0 V \Delta H_{AB} - \Delta H_v V C_A^0 + W_0 t^*$$

et où $Q'^* = -\Delta H_v V C_A^0 + W_0 t^*$ est la somme, au même point, de tous les effets autres que ceux d'origine chimique.

La période de titrage se traduira donc sur le thermogramme réel, qui est un inregistrement de ΔT en fonction du temps t aux facteurs d'élongation près, par une conique du type

$$Ax^2 + Bxy + Cy^2 + Dx + Ey = 0$$

Il est aisé de vérifier que c'est une hyperbole, et puisque le temps ne peut qu'être supérieur ou égal à zéro, ce sera une portion de branche d'hyperbole. La forme de l'hyperbole dépend des valeurs numériques Q^*, Q'^*, C_0, t^* et du paramètre β. Ce dernier, tous les autres étant fixés, définit une famille d'hyperboles lorsqu'il varie.

Les différents paramètres de l'hyperbole, centre, asymptotes, foyers, directrices et excentricité sont déterminables dans le système de coordonnées naturel ΔT, t par le procédé usuel de réduction des coniques (voir par exemple Bouasse[8]). De l'étude de leurs variations avec le facteur β, il ressort que tous ces paramètres se définissent par une fonction compliquée de β, exceptée l'excentricité qui est indépendante de β. Nous signalons simplement que l'hyperbole admet pour asymptotes, les droites

$$\Delta T = \frac{Q'^* t}{C_0 t^*} + \frac{1}{C_0}(Q^* - Q'^*) \qquad (6)$$

$$\Delta T = \frac{Q^* t}{C_0 t^*} + \frac{1}{C_0}\left(\frac{Q^* - Q'^*}{\beta}\right).$$

Fait intéressant, la première de ces droites est la droite de dilution lorsque la réaction de dosage est totale. Elle est indépendante de β.

Relation entre l'erreur systématique et le paramètre β

Nous représentons en Fig. 2 un thermogramme où le "temps est exprimé en fraction titrée". Imaginons une sécante OY qui passe par l'origine $f = 0$, $\Delta T = 0$ et qui coupe l'hyperbole de la période réactionnelle et

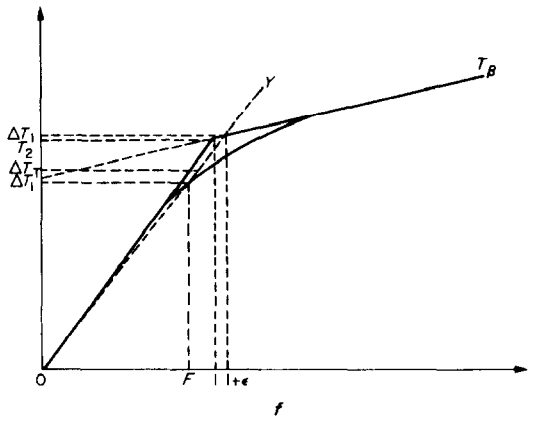


Fig. 2. Représentation géométrique du problème de la détermination de l'erreur lorsqu'il y a "courbure d'équilibre".

la droite de dilution aux points d'abscisses f et $f' = 1 + \epsilon$. Lorsque $f = 0$, cette sécante n'est autre que la tangente. Il s'agit de trouver une relation entre ϵ et β.

De l'équation de la droite de dilution théorique (6), exprimée en fractions titrées, on déduit la variation de température ΔT_1 correspondant à fraction titrée $1 + \epsilon$, d'où l'équation de la sécante qui passe par ce point et l'origine $f = 0$, $\Delta T = 0$, soit

$$\Delta T = \frac{\frac{Q^*}{C_0}(1 + \epsilon) + \frac{1}{C_0}(Q^* - Q'^*)}{1 + \epsilon} f \qquad (7)$$

Le remplacement de ΔT donné par cette relation, dans l'équation générale de l'hyperbole (5), exprimée en fractions titrées, conduit aux deux racines

$$f = 0$$

$$f = -\frac{1 + \epsilon}{\epsilon\beta} + 1 + \epsilon. \qquad (8)$$

La première est évidente par hypothèse. La deuxième est la relation cherchée. Elle a pour conséquence immédiate que pour une erreur ϵ sur la détermination du point équivalent, fixée *a priori*, il existe une valeur limite de β pour laquelle on peut encore tracer la tangente, la sécante devenant tangente lorsque la deuxième racine est aussi égale à zéro, soit

$$\beta_{\text{lim}} = \frac{1}{\epsilon}.$$

Si β est inférieur à $1/\epsilon$, il n'est plus possible de déterminer le point équivalent, même avec une erreur ϵ, exprimée en fractions titrées. En particulier si ϵ tend vers zéro, dosage absolument exact, il faut que β tende vers l'infini. Si on fait β égal à l'infini dans la relation (8) il n'y a aucune impossibilité d'annuler ϵ. Nous retrouvons là la condition de Tyrrell et les deux théories apparaissent comme complémentaires.

Discussion de la relation (8)

Dans cette formule, nous ne voyons apparaître aucun paramètre inhérent à la titrimétrie thermométrique. Elle n'est en fait que la conséquence logique d'une part de la linéarité de résponse de la méthode de titrage, et d'autre part de la loi d'action de masse. Elle nous semble donc, *a priori*, applicable à toutes les méthodes titrimétriques linéaires invoquant une relation équilibrée, tout au moins sous une forme très proche.

Il convient de signaler qu'en sa défaveur, cette formule est établie avec l'hypothèse que la tangente finale, c'est-à-dire la droite de dilution ou l'asymptote de l'hyperbole, est toujours traçable sans erreur. Ceci est en principe toujours possible si l'on continue à ajouter le "réactif" suffisamment longtemps suivant la valeur de β, après le point équivalent. On peut en effet supposer qu'alors la courbe et son asymptote sont confondues. Il faudra donc tracer cette tangente sur un intervalle de fraction titrée d'autant plus élève que β sera petit. Mais le choix d'une fraction titrée trop élevée risque de faire intervenir des erreurs dues aux courbures liées aux effets de capacité calorifique et de "l'adiabaticité" que l'on ne peut plus supposer négligeables pour un temps de dosage long.[1] Essayons de préciser, en fonction de β, l'erreur commise en supposant que, à partir d'une certaine fraction titrée, la droite de dilution théorique ne diffère pas de la courbe enregistrée. Pour ce faire, nous allons supposer maintenant que la tangente initiale représente exactement la période réactionnelle.

Supposons que la droite de dilution que nous adoptons soit définie par les deux points f_1, ΔT_1 et f_2, ΔT_2 (Fig. 3). La fraction titrée f_2 est imposée par les effets de capacité calorifique et de "l'adiabaticité". Les ordonnées ΔT_1 et ΔT_2 sont données par application de la relation (2) exprimée en fractions titrées et en accroissements de température. On en déduit l'équation de la pseudodroite de dilution qui coupe la tangente initiale représentant la période réactionnelle lorsque la réaction de dosage est totale, d'équation $T = fQ^*/C_0$ pour

$$f = \frac{\frac{[AB]_1}{C_A^0} f_2 - \frac{[AB]_2}{C_A^0} f_1}{(f_2 - f_1) - \left\{\frac{[AB]_2}{C_A^0} - \frac{[AB]_1}{C_A^0}\right\}} \qquad (9)$$

c'est-à-dire pour une erreur

$$\epsilon = (f - 1)100\%.$$

Cette formule d'apparence lourde, est en fait facile à manier car les quantités $[AB]/C_A^0$ sont tabulées une fois pour toutes en fonction de β.[5] Par exemple pour $\beta = 100$, si l'on choisit l'intervalle 1,9–2,0, l'erreur est de 2%; l'intervalle 2,5–3,0, l'erreur est de 1,1%.

Bien sûr l'erreur diminue lorsque β augmente. Il est important de noter qu'elle est opposée à celle due au tracé plus ou moins exact en fonction de β, de la tangente initiale.

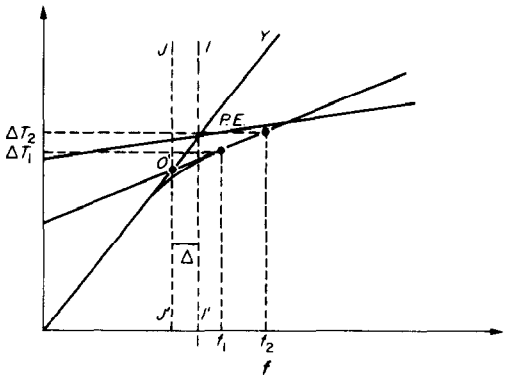


Fig. 3. Calcul de l'erreur commise en confondant la droite de dilution théorique avec la droite passant par les points f_1, ΔT_1 et f_2, ΔT_2.

Tableau 1. Fractions titrées moyennes, en fonction de β, pour lesquelles la tangente quitte la courbe ($\bar{f}_0$) et pour lesquelles les sécantes qui correspondent à 10, 20 et 40% d'erreur coupent la courbe ($\bar{f}_{10}$, $\bar{f}_{20}$ et $\bar{f}_{40}$)

β	$\bar{f}_0$	$\bar{f}_{10}$	$\bar{f}_{20}$	$\bar{f}_{40}$
398	0,23	0,97	1,15	1,36
358	0,16	0,925	1,14	1,37
318	0,14	0,89	1,13	1,38
289	0,08	0,92	1,14	1,38
268	0,07	0,95	1,15	1,39

VERIFICATION EXPERIMENTALE

Il s'agit de la vérification expérimentale de la relation (8). Le principe consiste à apprécier, sur les thermogrammes, pour différentes valeurs de β, les fractions titrées à partir desquelles la courbe quitte la tangente et en même temps les fractions titrées pour lesquelles la sécante OY, correspondant à une erreur imposée, coupe la courbe enregistrée.

La réaction suivie est celle de la neutralisation du chlorhydrate d'éphédrine, de pK_A bien connu,[9] par une solution d'hydroxyde de sodium. La réaction de titrage est

$$BH^+ + OH^- \rightleftharpoons B + H_2O$$

$$\frac{[B]}{[BH^+][OH^-]} = K = \frac{K_A}{K_W}.$$

On fait varier $\beta = K C_A^0$ en changeant la concentration initiale.

Connaissant le titre des solutions d'hydroxyde de sodium et du chlorhydrate d'éphédrine, le débit de la burette et la vitesse du papier enregistreur, on connaît l'abscisse du point équivalent, c'est-à-dire son lieu géométrique qui est la droite II' d'abscisse $f = 1$ (Fig. 3). Attendre qu'un gros excès de réactif soit ajouté pour tracer la droite de dilution pour minimiser l'erreur due à son tracé, présente l'inconvénient de faire apparaître des courbures inhérentes aux effets de capacité calorifique et de "l'adiabaticité" imparfaite, comme le laisse prévoir l'application des formules mentionnées dans le mémoire précédent.[1] Aussi pour déterminer l'ordonnée du point équivalent, tout en évitant ces erreurs, nous utilisons la construction graphique suivante. Nous traçons une pseudodroite de dilution par les points du thermogramme de fractions titrées 1,8 et 2,0 pour lesquels les effets ci-dessus sont négligeables. Eu égard à l'utilisation de cette "fausse" droite de dilution nous commettons une erreur Δ que l'on calcule en appliquant la relation (9) puisque nous connaissons f_1, f_2 et β. Nous traçons alors la parallèle JJ' à II' d'abscisse $1 - \Delta$. L'utilisation de JJ' avec la pseudodroite de dilution détermine un faux point équivalent O'. Par contre, l'intersection P.E. de OO' avec II' détermine le vrai point équivalent. La vraie droite est alors facile à tracer. Pratiquement nous nous appuyons sur le point du thermogramme de fraction titrée égal à 2 et sur le point équivalent. En effet pour les β utilisés, [AB] est très peu différent de C_A^0 à partir de $f = 2$.

Pour les différents β donnés, nous cherchons jusqu'à quelle fraction titrée, nous pouvons tracer la tangente. Nous utilisons une règle plate transparente que nous plaçons comme tangente initiale, et nous cherchons:

—pour quelle fraction titrée la courbe enregistrée "passe" sous la règle;
—pour quelles fractions titrées, les sécantes OY correspondant à 10, 20 et 40% d'erreur coupent la courbe.

Pour chaque valeur de β on répète 9 fois la mesure.

Résultats

Le tableau 1 regroupe les résultats obtenus. Ce tableau appelle les commentaires suivants.

(1) La relation $f = 1 - 300/\beta$ convient très bien pour déterminer à quelle fraction titrée, la tangente quitte la courbe. Elle implique une erreur systématique moyenne de 0,33%.

(2) Malheureusement il est impossible de trouver expérimentalement une telle relation lorsque nous traçons les sécantes. Ceci provient du fait que la variation de β n'entraîne pas de variation de $\bar{f}_i$ appréciable. Par exemple, quel que soit β, la sécante tracée de telle sorte que l'erreur soit de 20% coupe la courbe sensiblement toujours pour la même fraction titrée $f \approx 1{,}14$. Ceci provient de la forme même de la courbe.

(3) Pour chaque β et pour une erreur donnée, on peut calculer ϵ d'après les données du tableau 2. Par exemple pour 40% d'erreur et $\beta = 398$ on a la relation

$$1.36 = -\left(\frac{1+\epsilon}{\epsilon}\right)\frac{1}{398} + 1 + \epsilon$$

d'où on tire $\epsilon = 0{,}37$.

Le tableau 2 regroupe les valeurs calculées de ϵ. L'accord avec la valeur théorique imposée (respectivement 0,4, 0,2 et 0,1) est d'autant meilleur qu'elle est

Tableau 2. Valeurs de ϵ calculées d'après la relation (8) et les données du tableau 1

β	40% ou 0,4	20% ou 0,2	10% ou 0,1
398	0.37	0,17	0,04
358	0,38	0,16	0,03
318	0,39	0,16	0,02
289	0,39	0,17	0,05
268	0,40	0,17	0,04

plus grande. Ce qui n'est pas surprenant. Car lorsqu'on fait de telles déterminations graphiques, se surajoutent d'autres erreurs que celles dues à la réversibilité, lecture par exemple. Plus l'erreur imposée est grande moins les autres erreurs interfèrent, et plus l'accord avec la théorie est bon.

Ces résultats expérimentaux confirment notre théorie.

REFERENCES

1. M. A. Bernard et J. L. Burgot, *Talanta*, 1981, **28**, 939.
2. H. J. V. Tyrrell, *ibid.*, 1967, **14**, 843.
3. P. W. Carr, *CRC Crit. Rev. Anal. Chem.*, 1972, **3**, 491.
4. G. Charlot et R. Gauguin, *Les méthodes d'analyse des réactions en solution*, Masson, Paris, 1951.
5. D. Rosenthal, G. L. Jones, Jr. et R. Megargle, *Anal. Chim. Acta*, 1971, **53**, 141.
6. J. L. Burgot, *Talanta*, 1978, **25**, 339.
7. M. A. Bernard et J. L. Burgot, *Anal. Chem.*, 1979, **51**, 2122.
8. H. Bouasse, *Cours de mathématiques générales*, Delagrave, Paris 1920.
9. R. J. Raffa, M. J. Stern et L. Malspeis, *Anal. Chem.*, 1968, **40**, 70.

Summary—The reversibility of the determination reaction is the most frequent cause of deviations from linearity of thermometric titration curves. Because of this, determination of the equivalence point by the tangent method is associated with a systematic error. The authors propose a relationship which connects this error quantitatively with the equilibrium constant. The relation, verified experimentally, is deduced from a mathematical study of the thermograms and could probably be generalized to apply to other linear methods of determination.

Talanta. Vol. 28. pp. 951 to 954. 1981
Printed in Great Britain

0039-9140/81/120951-04$02.00/0
Pergamon Press Ltd

SHORT COMMUNICATIONS

POTENTIOMETRIC DETERMINATION OF HYDROGEN PEROXIDE WITH PERMANGANATE IN PRESENCE OF FLUORIDE, WITH IRON AS A CATALYST: APPLICATION TO THE TITANIUM–FLUORIDE–PEROXIDE MIXED COMPLEX

L. POLO DIEZ, J. HERNANDEZ MENDEZ and M. J. ALMENDRAL PARRA
Department of Analytical Chemistry, Faculty of Chemistry, University of Salamanca, Spain

(*Received* 6 *November* 1980 *Revised* 30 *April* 1981. *Accepted* 12 *May* 1981)

Summary—A potentiometric permanganate titration has been developed for the determination of hydrogen peroxide in the presence of fluoride, as well as of the peroxide content in the titanium–fluoride–peroxide mixed complex. It is based on the stabilization of manganese(III) with an excess of fluoride in a moderately acidic medium (pH close to 3) and on the use of iron(III) as catalyst. Errors are less than 0.5%.

Several titrimetric methods are available for determination of hydrogen peroxide or the peroxide content of compounds, at macro-levels, those with cerium(IV) or permanganate being the most suitable.[1] In the cerium(IV) methods, the presence of fluoride seems to lead to low results,[2] but there is no information about its effect on the permanganate methods, although several permangate titrations in fluoride medium have been developed.[3–9]

In this paper, a potentiometric method is proposed for the determination of hydrogen peroxide with permanganate in the presence of the fluoride, the permanganate being reduced to manganese(III) stabilized as the fluoride complex. The method is applied to the determination of peroxide in the titanium–fluoride–peroxide mixed complex.

EXPERIMENTAL

Reagents

Potassium permanganate solutions, about 0.1*N*, *i.e.*, 0.02*M*, were standardized against sodium oxalate. Hydrogen peroxide solutions, about 0.1*N*, were standardized against the permanganate. Other solutions included 1*M* and 0.1*M* sulphuric acid, 1.5*M* sodium fluoride, and 0.010*M* copper sulphate, chromic sulphate, ammonium metavanadate and ferric sulphate.

Sample

Solid $(NH_4)_3TiO_2F_5$ was prepared by adding an excess of hydrogen peroxide and ammonium fluoride to a titanium(IV) sulphate solution, which was kept cold and neutralized with an ammonia solution to pH 7.

Apparatus

A Metrohm E-510 potentiometer was used to measure the potentials between a platinum wire indicator electrode and a saturated calomel electrode.

Procedure

Weigh accurately about 0.1–0.5 g of the titanium–fluoride–peroxide complex (or use an equivalent amount of a solution containing this compound or hydrogen peroxide), dissolve it in a small volume of distilled water, and add 10 g of sodium fluoride. Add sufficient 1*M* sulphuric acid to give a pH close to 3 (Methyl Orange as indicator), and enough Fe(III) solution to give a final concentration of about $10^{-4}M$. Titrate potentiometrically with the permanganate solution.

RESULTS AND DISCUSSION

Preliminary results

When the classic permanganate titration in acidic medium was used to determine the peroxide content in the complex, low but reproducible results were obtained.

This error was attributed to partial stabilization of manganese as the manganese(III) fluoride complex, which was confirmed by the pink colour observed before the characteristic permanganate colour appeared. This fluoride interference cannot be avoided by heating in an acidic medium, as this brings about decomposition of the peroxide group.

To overcome this problem the permanganate titration was done in the presence of an excess of fluoride. The best conditions were determined by titrating hydrogen peroxide solutions. The characteristic pink colour of the manganese(III)–fluoride complex necessitated the use of a physical method for the determination of the end-point, the potentiometric method with a platinum wire as the indicator electrode being the most suitable.

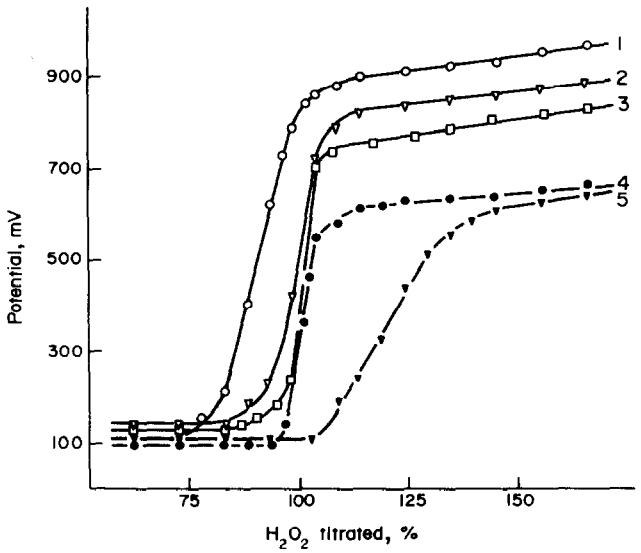


Fig. 1. Effect of pH on the potentiometric curves. H_2O_2: 1.012 meq; NaF: 1.0*M*; Fe(III): $10^{-4}M$; $KMnO_4$: 0.0265*M*. pH values are those specified on the curves.

Potentiometric titration

The reaction between permanganate and hydrogen peroxide in the presence of an excess of fluoride at about pH 3 is very slow, especially near the equivalence point. Moreover, the electrode potential also stabilizes slowly. However, in the presence of copper, vanadium or iron salts, the chemical reaction occurs quickly, as shown by the instantaneous decolorization of permanganate, and the electrode potential stabilizes rapidly. Iron salts produced the best results and were therefore used as the catalyst. According to the literature, iron(III)–peroxide species must be involved in the mechanism of the catalysed chemical reaction.[10]

The potentiometric titration curves obtained in the presence of iron(III) were well defined, making determination of the end-point easy. A single titration took about 10 min, normal for this kind of titration. The potentials obtained with excess of permanganate indicated that the electrode probably responded to a mixed potential.

Effect of pH. Titration curves obtained in the presence of $10^{-4}M$ iron(III) at different pH values are shown in Fig. 1. The change in potential around the equivalence point decreases when the pH is increased, and above pH 4 manganese dioxide is formed. The apparent final oxidation states of manganese (assuming a quantitative reaction between permanganate and hydrogen peroxide) calculated from the titration curves of Fig. 1 are shown in Table 1.

These results lead to the conclusion that permanganate is not reduced stoichiometrically to manganese(II) even at pH 1. On the other hand, at pH values close to 3, it is reduced quantitatively to manganese(III).

Taking into account that under these conditions the MnF_4^- complex must predominate in solution, the following reaction presumably occurs

$$MnO_4^- + 2H_2O_2 + 4F^- + 4H^+ \rightarrow MnF_4^- + 2O_2 + 4H_2O$$

As is clear from the table, at pH values either lower or higher than 3, other reactions occur simultaneously with the formation of manganese(II) or (IV) respectively.

The adjustment of pH to about 3 is easy owing to the presence of the HF/F^- buffer; some Methyl Orange indicator is added, followed by sufficient 1*M* sulphuric acid to turn the colour red. A pH-meter is not needed and a glass electrode should not be used in such a fluoride medium anyway.

Effect of the iron(III) concentration. Concentrations of Fe(III) in the range 5×10^{-5}–$10^{-4}M$ are suitable to make both the chemical and electrochemical reac-

Table 1. Apparent final oxidation state of manganese and titration error, assuming the $MnO_4^- \rightarrow$ Mn(III) half-reaction at different pH values

pH	1.0	2.0	3.0	4.0	5.0
Apparent final oxidation states of Mn	2.51	2.96	2.99	3.04	3.77
Titration error assuming the half-reaction $MnO_4^- \rightarrow$ Mn(III)	−11.0	−1.1	−0.31	+1.0	+20.3

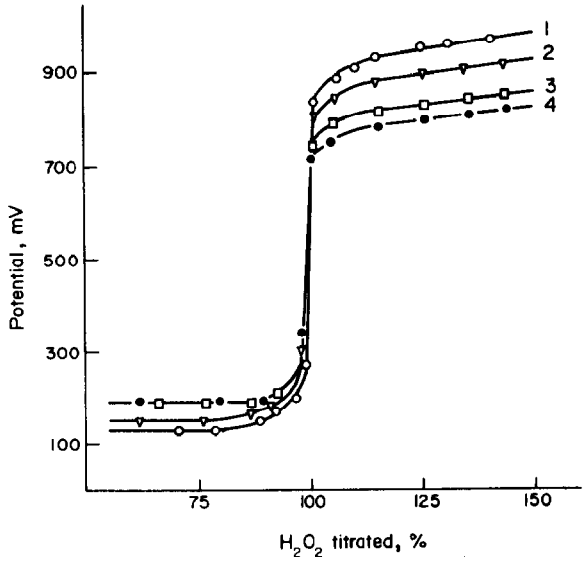


Fig. 2. Effect of the NaF concentration on the potentiometric titration curves. H_2O_2: 0.949 meq: Fe(III): $10^{-4}M$; pH: 3.0: $KMnO_4$: 0.0211M. NaF concentration (M); (1) 0.6: (2) 0.8: (3) 1.2 (4) 1.4.

tions fast enough. However, as the titration times increased significantly for concentrations lower than $5 \times 10^{-5}M$, $10^{-4}M$ was taken as the optimum concentration.

Effect of sodium fluoride concentration. Titration curves obtained at different sodium fluoride concentrations are shown in Fig. 2. The change of potential around the equivalence point decreases slightly for increasing concentrations of sodium fluoride. However, the potential of the $MnO_4^-/Mn(III)$ system should increase with the sodium fluoride concentration. The cause of the effect observed is obscure, but may be due to the effect of fluoride on the titanium complex as a whole. In other words, the increase in fluoride concentration will increase the concentration of the mixed complex and decrease the concentration of free peroxide in equilibrium with it, hence increasing the potential of the oxygen/mixed-ligand complex couple, and accounting for the higher potentials before the end-point. The lower potentials after the end-point could be due to a mixed-potential electrode response.

Effect of temperature. Titration curves obtained at different temperatures are shown in Fig. 3. At room temperatures in the range 15–25° no significant differences are observed in the shape of the titration curves. However, at temperatures higher than about 30°, changes in the titration curves are clear, and low results are obtained. This is probably due to disproportionation of hydrogen peroxide at these temperatures.

Reproducibility and accuracy. When the recommended procedure was applied to ten replicates containing 1.012 meq of hydrogen peroxide, a standard deviation of 0.005 meq was obtained, with a coefficient of variation of 0.5%. The relative error of the mean was −0.25%. The calculated Student's t-value was 2.18, which indicates a significant difference between the experimental mean and the true value. This small error may arise from decomposition of the sample, or the possible mixed potential of the electrode in presence of excess of permanganate might shift the inflexion point of the curve, used as the end-point, to slightly before the equivalence point.

Determination of the peroxide content in the $(NH_4)_3TiO_2F_5$ complex

The proposed procedure was applied to the determination of the peroxide content of the titanium–fluoride–peroxide mixed complex. The contents of Ti, NH_4^+, and F^- had been determined previously and the following stoichiometric composition found: $Ti{:}5F{:}3NH_4^+$, which fits the formula $(NH_4)_3TiO_2F_5$. With this stoichiometry, the theoretical content of

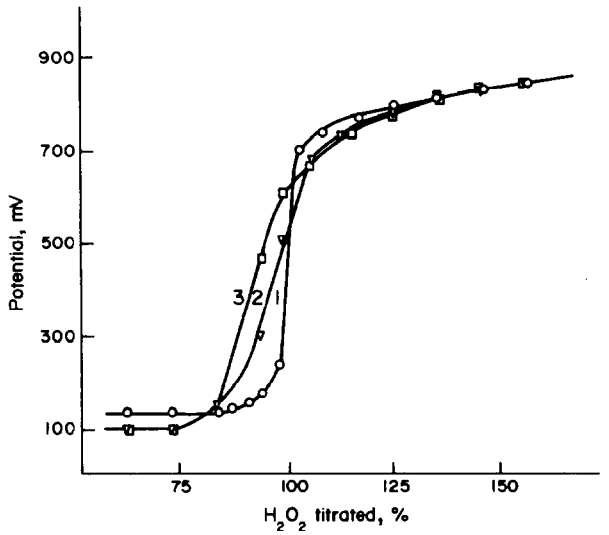


Fig. 3. Effect of temperature on the potentiometric titration curves. H_2O_2: 1.012 meq; Fe(III): $10^{-4}M$; NaF: 1.0M; pH = 3.0 $KMnO_4$: 0.0265M. Temperature; (1): 22°; (2): 30°; (3): 35°.

peroxide in the complex would be 13.98%. The experimental value (mean of five determinations) was 13.94% with a standard deviation of 0.4% for 0.3-g samples.

REFERENCES

1. J. A. Connor and E. A. V. Ebsworth, *Advances in Inorganic Chemistry and Radiochemistry*, 1964, **6**, 280.
2. I. Lange and A. Petzold, *Z. Anal. Chem.*, 1956, **150**, 24.
3. I. M. Issa, M. H. Hamdy and A. S. Misbah, *Microchem. J.*, 1972, **17**, 480.
4. I. M. Issa, R. M. Issa, M. A. Khattab and M. R. Mahmond, *Indian J. Chem.*, 1975, **13**, 942.
5. A. M. Hammam and I. M. Issa, *Mikrochim. Acta*, 1976 **I**, 573.
6. I. M. Issa, M. A. Ghandour and A. M. Hammam, *J. Indian Chem. Soc.*, 1974, **51**, 872.
7. I. M. Issa, K. A. Idriss and M. M. Ghoneim, *Talanta*, 1976, **23**, 249.
8. I. M. Issa and M. M. Ghoneim, *Talanta*, 1973, **20**, 517.
9. K. A. Idriss, A. M. Hammam, M. M. Seleim and Z. R. El-Komi, *Talanta*, 1980, **27**, 561.
10. T. J. Lewis, D. H. Richards and D. A. Salter, *J. Chem. Soc.*, 1963, 2434.

Talanta, Vol. 28, pp. 955 to 956, 1981
Printed in Great Britain. All rights reserved

0039-9140/81/120955-02$02.00/0
Copyright © 1981 Pergamon Press Ltd

TITRIMETRIC MICRODETERMINATION OF CHLORAL HYDRATE BY AMPLIFICATION REACTIONS

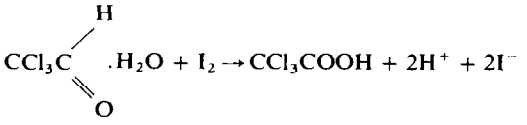
D. AMIN and M. S. AL-AJELY

Department of Chemistry, College of Science, Mosul University, Mosul, Iraq

(*Received* 31 *March* 1981. *Accepted* 24 *April* 1981)

Summary—A simple titrimetric method for estimation of 0.1–5 mg of chloral hydrate is presented. It depends on oxidation of an alkaline solution of chloral hydrate with a chloroform solution of iodine, removal of excess of iodine, oxidation of the resulting iodide with bromine, and iodometric titration of the iodate produced, giving 6-fold amplification. Alternatively, the iodide formed is oxidized with periodate, masking of the excess of periodate with molybdate at pH 3, and iodometric titration of the iodate, giving 24-fold amplification. The coefficient of variation does not usually exceed 2% for above 1 mg of chloral hydrate but increases to 3.8% at the 0.1-mg level.

Iodine,[1] bromine,[2] potassium dichromate[3] and acidic potassium permanganate[4] have been utilized for the quantitative oxidation of chloral hydrate. Kolthoff[1] proposed iodometric determination, based on oxidation with excess of iodine in sodium carbonate medium, and back-titration of the excess of iodine with thiosulphate,



Schwicker[2] found that the reaction is faster in ammonium borate medium. A titrimetric determination of as little as 40 mg of chloral hydrate has been reported, based on its oxidation with alkaline permanganate[5] in the presence of barium ions. These methods are not sensitive and require a large sample.

In order to develop a cheap, reliable and sensitive method we have investigated the use of oxidation of the chloral hydrate with iodine and oxidation of the resulting iodide in the Leipert procedure,[6] or by periodate.[7]

$$I^- + 3IO_4^- \rightarrow 4IO_3^-$$

The excess of periodate is masked with molybdate[8] and the iodate formed is reacted with iodide to give 24-fold amplification.

EXPERIMENTAL

Reagents

All reagents used were of analytical grade and doubly distilled water was always used.

Chloral hydrate solutions. Aqueous solutions of concentrations 0.1 and 1.0 mg/ml were used.

Sodium thiosulphate solutions, 0.02 and 0.04N. Standardized against potassium iodate solutions of similar normality.

Iodine solution. Prepared weekly by dissolving about 0.3 g of pure iodine in 250 ml of pure dry chloroform, and stored in an amber bottle.

Ammonium borate solution, 1N (170 ml of 10% ammonia solution and 20 g of boric acid per litre).

Potassium periodate solution, 0.015M. Made by dissolving 1.75 g of the salt in 500 ml of water and adding 3 ml of saturated borax solution, and stored in a dark glass bottle.[7] Prepared fresh as required.

Ammonium molybdate solution, 25%. Freshly prepared.

Acetate buffer solution, pH 3. Made from 40 ml of 0.2*M* sodium acetate and 110 ml of glacial acetic acid.

Solutions of potassium iodide (10%, prepared daily), formic acid (80%), sulphuric acid (2*N*), and bromine (saturated) were also prepared.

Procedure

In a 50-ml separating funnel, mix 10 ml of iodine solution, 5 ml of ammonium borate solution and a portion of sample solution containing 0.1–5 mg of chloral hydrate. Dilute the aqueous layer to about 10 ml with water. Stopper the funnel and allow the reaction mixture to stand for 25 min. Acidify the solution with 3 ml of 2*N* sulphuric acid, shake the mixture for 1 min, leave it for 1 min, and separate the organic layer. Remove the last traces of iodine from the aqueous layer by extraction with three 10-ml portions of chloroform. Transfer the aqueous phase (containing iodide) quantitatively to a 100-ml conical flask, then treat by one of the following methods. Run a blank determination.

6-Fold amplification. To the iodide solution, add 5 ml of bromine and stir for 3 min. Destroy the excess of bromine by dropwise addition of formic acid, add 5 ml of 2*N* sulphuric acid and 5 ml of 10% iodide solution, and titrate the liberated iodine with 0.02*N* thiosulphate, using starch as indicator.

1 ml of 0.02*N* thiosulphate ≡ 0.2757 mg of chloral hydrate.

24-Fold amplification. To the iodide solution, add 10 ml of periodate solution. Stopper and allow the reaction mixture to stand for 10 min at room temperature, then place the flask in a boiling water-bath for 30 min for complete oxidation. Cool, add 10 ml of ammonium molybdate solution and 5 ml of pH-3 acetate buffer. Add 10 ml of 10% iodide solution and then titrate the liberated iodine with 0.04*N* thiosulphate in the usual manner.

1 ml of 0.04*N* thiosulphate ≡ 0.1379 mg of chloral hydrate.

Table 1. Microdetermination of chloral hydrate by the 6-fold amplification method

Chloral hydrate, μg			
Taken	Found*	Recovery, %	Coefficient of variation, %
500	490	97.9	3.5
700	693	99.0	
1000	989	98.8	1.9
3000	2945	98.1	
5000	4936	98.7	1.3

* Mean of 5 determinations.

Table 2. Microdetermination of chloral hydrate by the 24-fold amplification method

Chloral hydrate, μg			
Taken	Found*	Recovery, %	Coefficient of variation, %
100	98.5	98.5	3.8
200	197	98.7	
500	497	99.4	
700	696	99.3	
1000	998	99.8	1.0
3000	2977	99.2	
5000	4952	99.0	1.1

* Mean of 5 determinations.

RESULTS AND DISCUSSION

The conventional method for assay of chloral hydrate is the iodometric[1] method, which involves oxidation with excess of aqueous iodine solution and back-titration with thiosulphate.

This method has hitherto been applied for macro assay only, yet is still the most popular procedure despite the other titrimetric methods[2–5] available. This motivated us to search for new methods for the determination of micro amounts of chloral hydrate with use of the iodine–starch end-point. An obvious approach was the application of amplification reactions.

The alkaline sample solution of chloral hydrate is quantitatively oxidized when treated with iodine. The iodide formed can be dealt with by the Leipert amplification procedure,[6] after extraction of the excess of iodine with chloroform. In this way, one mole of chloral hydrate is equivalent to 12 iodine atoms, instead of the 2 in the normal reaction, so the amplification is 6-fold.

Preliminary studies confirmed that chloral hydrate decomposes to chloroform if the order of addition is altered,[1] and that the amount of alkali (ammonium borate) added must be carefully controlled;[2] 5 ml of 1*N* ammonium borate gave satisfactory results. Larger amounts of borate solution gave rise to high results because of the formation of hypoiodite. The second factor is the amount of iodine solution; 10 ml of 0.12% solution was found essential for rapid and quantitative oxidation of up to 5 mg of chloral hydrate. Larger excess of iodine should be avoided in order to decrease the number of extractions necessary, since these increase the risk of mechanical loss of aqueous phase, causing low results. Any iodine left in suspension in the aqueous phase would cause high results, so must be removed by washing the aqueous phase with chloroform.

The working procedure finally developed was applied successfully to the determination of 0.5–5 mg amounts of chloral hydrate by the 6-fold amplification method. Sample weights outside this range gave insufficiently accurate results, however. For less than 0.5 mg of chloral hydrate, the inconsistent errors (about ±4%) obtained may be attributed to mechanical losses in the extraction, separation and transfer processes. On the other hand, the low results obtained (about 3.5%) for amounts larger than 5 mg of chloral hydrate are most probably due to volatilization of some of the iodine produced in the amplification reaction. The coefficients of variation for the 6-fold amplification method were 3.5, 1.9 and 1.3% for 0.5, 1.0 and and 5 mg of chloral hydrate, respectively (5 replicates).

For the 24-fold amplification, the resulting iodide was oxidized with periodate in borate buffer at pH 7 as recommended by Belcher *et al.*,[7] who described the determination of 10–200 μg of iodide. It was found that up to 5 mg of iodide can be oxidized quantitatively with 10 ml of 0.015*M* periodate. The unused periodate is masked by molybdate[8] at pH 3–3.5; 10 ml of 25% molybdate solution did not affect the final determination. The coefficients of variation were 3.8, 1.0 and 1.1% for 0.1, 1.0, and 5 mg of chloral hydrate, respectively (5 replicates).

Metals which form insoluble compounds with iodide or reduce iodine to iodide, are expected to interfere. Both methods are satisfactory, but the 6-fold method seems simpler and less time-consuming than the 24-fold method.

REFERENCES

1. I. M. Kolthoff and R. Belcher, *Volumetric Analysis*, Vol. III, p. 376. Interscience, New York, 1957.
2. A. Schwicker, *Z. Anal. Chem.*, 1937, **110**, 161.
3. O. N. Karpov, *Inst. Geokhim. i. Analit. Khim.*, 1963, **13**, 132.
4. J. H. Van der Meulen, *Chem. Weekblad*, 1949, **45**, 91.
5. S. P. Chouksey and R. M. Verma, *J. Indian Chem. Soc.*, 1978, **55**, 88.
6. T. Leipert, *Mikrochemie, Pregl Festschrift*, 1929, 266; *Mikrochim. Acta*, 1938, **3**, 73, 147.
7. R. Belcher, J. W. Hamya and A. Townshend, *Anal. Chim. Acta*, 1970, **49**, 570.
8. D. Burnel, *Compt. Rend.*, 1965, **261**, 1982.

Talanta, Vol. 28, pp. 957 to 959, 1981
Printed in Great Britain. All rights reserved

0039-9140/81/120957-03$02.00/0
Copyright © 1981 Pergamon Press Ltd

PREPARATION AND PROPERTIES OF A NEW CHELATING RESIN CONTAINING 2-NITROSO-1-NAPHTHOL

J. P. GHOSH, J. PRAMANICK and H. R. DAS
Department of Chemistry, Presidency College, Calcutta 700073, India

(*Received* 9 *January* 1981. *Accepted* 16 *May* 1981)

Summary—A new chelating ion-exchange resin based on a macroreticular polystyrene–divinyl benzene copolymer and containing 2-nitroso-1-naphthol as the functional species has been synthesized. It is highly stable in acidic and alkaline solutions. Its sorption characteristics for V(V), Cr(III), Mn(II), Fe(III), Co(II), Ni(II), Cu(II), Zn(II), Hg(II), Pd(II) and U(VI) have been investigated over the pH range 1.0–7.0 and the exchange-capacities have been found to be generally higher than those of a similar resin containing 1-nitroso-2-naphthol.

The preparation and properties of a chelating resin containing 1-nitroso-2-naphthol have been reported.[1] Because of its similar properties to 1-nitroso-2-naphthol, 2-nitroso-1-naphthol has now been incorporated in a resin matrix and its properties examined.

EXPERIMENTAL

Resin synthesis

The resin was made in the same way as the 1-nitroso-2-naphthol resin[1,2] except for the complexing agent, of course, and reduction of the alcohol-extraction period to 24 hr.

Resin characterization

The water regain, nitrogen and amino-group content, exchange capacity, equilibration rate, and the exchange characteristics of certain ions were determined as for the 1-nitroso-2-naphthol resin.[1]

For column operations, a glass tube (8 mm bore) was packed with a 22-cm column of fully swollen resin-beads (5 g of air-dried resin, swollen in water for 24 hr).

Separations

Palladium(II) and platinum(IV). This was done in two ways. In method 1, the sample (containing $PdCl_2$ and H_2PtCl_6), adjusted to pH 4.5 with hydrochloric acid and sodium acetate solution, was passed at 1.5 ml/min through the resin column (previously equilibrated with pH 4.5 buffer). The column was thoroughly washed with pH 4.5 buffer and the sorbed palladium(II) eluted with 10 bed-volumes of concentrated hydrochloric acid (flow-rate 1.5 ml/min).

In method 2, the sample was added to the column in 1*M* hydrochloric acid medium, the platinum was washed through with the same acid, and palladium was eluted as for method 1.

Palladium(II) from silver and lead. The sample (containing the nitrates of the metals) was made 2*M* in nitric acid. The column was washed with 2*M* nitric acid till free from chloride and the sample was passed through it at 1.5 ml/min. After thorough washing of the column with 2*M* nitric acid, the sorbed palladium(II) was eluted as before.

Uranium(VI) and vanadium(V). The separation was done at pH 6.0 (sodium acetate and hydrochloric acid), flow-rate 1 ml/min. The selectively sorbed uranium(VI) was eluted with 10 bed-volumes of 0.5*M* sodium carbonate at 1 ml/min flow-rate.

RESULTS AND DISCUSSION

Resin synthesis and characteristics

The nitrogen contents of the nitro- and amino-polystyrene and of the 2-nitroso-1-naphthol chelating resin were 10.6, 12.2 and 9.9% respectively, and the amino-nitrogen content of the amino-polystyrene was 5% (from estimation of amino-groups). These results show that (*a*) the amination step is 41% efficient, (*b*) there is 74% conversion of amino-groups into azo-groups, (*c*) there should be 1.34 mmole of ligand nitrogen per g of dry chelating resin.

The exchange-capacities for various metal ions are shown in Fig. 1, and are high for palladium(II), copper(II), mercury(II) and uranium(VI), so the resin may be useful for separation of these metal ions from others. The capacities are higher than for the 1-nitroso-2-naphthol resin.[1]

The water-regain was 0.43, compared with 0.53 for the 1-nitroso-2-naphthol resin.

The times required for 50% uptake of palladium(II), copper(II), cobalt(II) and uranium(VI) by the resin were 45, 45, 50 and 90 min respectively, slightly less than the corresponding times for the 1-nitroso-2-naphthol resin (50, 45, 60 and 120 min respectively).

Separations

For the separation of palladium(II) from platinum(IV), in procedure 1 advantage is taken of the fact that at pH 4.5 no platinum(IV) is sorbed and complete separation is possible. In method 2, however, traces of platinum(IV) are sorbed along with palladium(II), so separation is not always quite complete, though it is satisfactory. Separation in 1*M* hydrochloric acid medium is useful for several reasons. First, the resin shows high capacity for palladium in

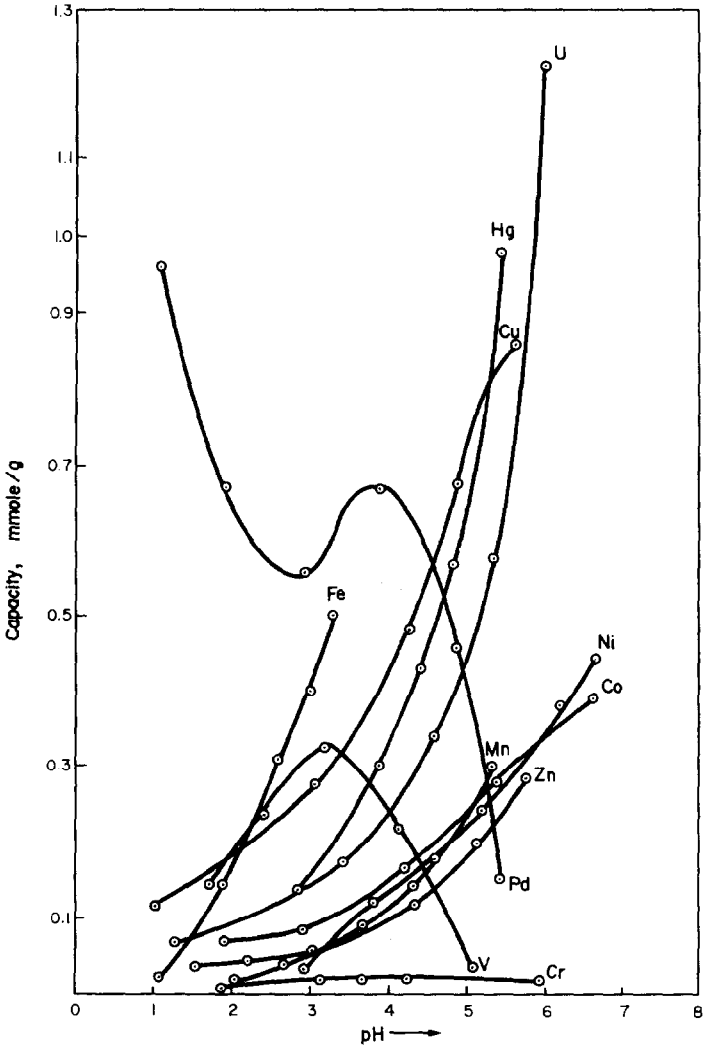


Fig. 1. Total exchange-capacity of the 2-nitroso-1-naphthol resin for different metal ions as a function of pH.

this medium. Secondly, in this medium palladium can be separated from a number of base metals. Thirdly, the traces of platinum(IV) in the eluted palladium may be removed by separation at pH 4.5, if necessary. Table 1 shows the results.

The separation of palladium(II) from silver and lead (Table 1) is based on the fact that only the palladium is sorbed from 2*M* nitric acid medium.

Vanadium(V) is not sorbed at pH > 5.5, and so can be separated from uranium(VI). Between 0.5 and

Table 1. Separation of Pd(II) from Pt(IV) and from Ag(I) and Pb(II)

Separation medium	Taken, *mg*				Found, *mg*			
	Pd(II)	Pt(IV)	Ag(I)	Pb(II)	Pd(II)	Pt(IV)	Ag(I)	Pb(II)
pH 4.5 acetate buffer	1.20	1.00			1.20	1.00		
	1.20	20.0	—	—	1.18	20.0	—	—
	0.10	1.00			0.10	1.01		
	4.80	0.50			4.78	0.48		
1*M* HCl	1.20	5.00			1.19	4.90		
	1.20	20.0	—	—	1.20	19.7	—	—
	0.10	5.00			0.10	4.88		
2*M* HNO_3	6.00		50.0	50.0	6.00		49.9	50.0
	1.20	—	20.0	20.0	1.19	—	19.9	19.9
	0.10		10.0	10.0	0.10		10.0	9.96

5.0 mg of uranium(VI) can be completely separated from up to 50 times as much vanadium(V).

The procedures and results for the separation of palladium(II) and uranium(VI) from various base metal ions, such as Cr(III), Mn(II), Fe(III), Co(II), Ni(II), Cu(II), Zn(II), Cd(II), Hg(II) and Al(III) are more or less the same as those with the 1-nitroso-2-naphthol resin.[1]

CONCLUSION

The 2-nitroso-1-naphthol chelating ion-exchange resin is very suitable for separation of palladium(II) and uranium(VI) from various metal ions, and superior to the 1-nitroso-2-naphthol resin. It could be used for concentration of uranium(VI) from sea-water. Its uranium(VI) capacity is quite high compared with that of other chelating resins studied.[3–5] No significant change in nitrogen-content and exchange-capacity of the resin is caused by prolonged immersion of resin in concentrated hydrochloric acid, 1–6*M* sulphuric acid, 1–5*M* nitric acid or 1–5*M* sodium hydroxide, and the exchange-capacity is little affected by repeated use of the resin.

Acknowledgements—We are thankful to Dr. N. R. Sengupta of the Geological Survey of India, Calcutta for help with AAS analyses. One of us (J.P.G.) thanks the University Grants Commission, New Delhi, for a fellowship under the U.G.C. Faculty Improvement Programme for college teachers.

REFERENCES

1. J. P. Ghosh and H. R. Das, *Talanta*, 1981, **28**, 274.
2. R. V. Davies, J. Kennedy, E. S. Lane and J. L. Willans, *J. Appl. Chem.*, 1959, **9**, 368.
3. H. Eccles and F. Vernon, *Anal. Chim. Acta*, 1973, **63**, 403.
4. A. Sugii and N. Ogawa, *Talanta*, 1979, **26**, 970.
5. H. Eccles and F. Vernon, *Anal. Chim. Acta*, 1973, **66**, 231.

Talanta, Vol. 28, pp. 960 to 962, 1981
Printed in Great Britain

0039-9140/81/120960-03$02.00/0
Pergamon Press Ltd

NON-AQUEOUS CERIMETRIC DETERMINATION OF PHENYLHYDRAZIDES

BALBIR CHAND VERMA and RAJNISH KUMAR SOOD

Department of Chemistry, Himachal Pradesh University, Simla-171005, India

(*Received* 2 *September* 1980. *Revised* 3 *April* 1981. *Accepted* 27 *April* 1981)

Summary—A non-aqueous oxidimetric method is described for the determination of some carboxylic acid phenylhydrazides with ammonium hexanitratocerate(IV) in acetonitrile. The end-points have been detected visually with chemical indicators (diphenylamine, diphenylbenzidine, Methyl Red, Malachite Green, Janus Green, Gentian Violet) and potentiometrically. The compounds are smoothly, rapidly and quantitatively oxidized with a two-electron change per hydrazino group. The method is simple, accurate, reliable and widely applicable.

Hydrazines are very reactive and frequently used in propellants and as intermediates in the manufacture of pharmaceuticals. Acid hydrazides find considerable use in chemotherapy. The determination of hydrazines is therefore of great interest and scope. The compounds are both oxidizable and reducible and most methods for their analysis are based on this.

Although the hydrazino group is readily oxidized, the reaction is quantitative only under properly controlled conditions. The group has been reported to be oxidized to different reaction products, depending on the experimental conditions and nature of the oxidant. Most of the methods use aqueous media and only limited efforts have been made to use redox methods in non-aqueous media. Hladky and Ruza[1] have described the use of lead(IV) chloride (in dimethylformamide) for the indirect determination of phenylhydrazine and 2,4-dinitrophenylhydrazine in dimethylformamide medium, the excess of oxidant being titrated with titanium(III) chloride in the same medium. The potentiometric determination of some hydrazines with bromine cyanide in acetic acid–acetic anhydride medium has been described by Paul *et al.*[2]

This communication reports the use of ammonium hexanitratocerate(IV) as an oxidant for the direct visual and potentiometric titration of carboxylic acid phenylhydrazides in acetonitrile medium. The compounds are not soluble in water and hence non-aqueous redox methods for their determination are of value. Diphenylamine, diphenylbenzidine, Methyl Red, Malachite Green, Janus Green and Gentian Violet have been found suitable indicators for the titration, giving sharp colour changes at the end-point. Potentiometric titrations can be performed with an antimony or modified calomel electrode as reference electrode and a bright platinum wire as indicator electrode.

The compounds are smoothly, rapidly and quantitatively oxidized with a two-electron change per hydrazino group.

EXPERIMENTAL

Apparatus

Potentiometric titrations were performed with a Toshniwal CLO6A potentiometer, with a bright platinum wire as indicator electrode and an antimony or modified calomel (saturated methanolic potassium chloride solution instead of aqueous) electrode as reference.

Reagents

Acetonitrile. Distilled twice from phosphorus pentoxide (5 g/l.).

Ammonium hexanitratocerate(IV) in acetonitrile, 0.04 M. Prepared by dissolving a little more than the calculated amount of dried analytical grade oxidant in acetonitrile and standardized by titration with ferrous ammonium sulphate in presence of dilute sulphuric acid, with ferroin as indicator. The solution was stored in a coloured glass-stoppered bottle.

Carboxylic acid phenylhydrazides. Prepared by the method of Stempel and Schaffel[3] and purified by repeated crystallization until their melting points corresponded to those of analytically pure samples as reported in the literature. Phenylhydrazides, $C_6H_5NHNHCOR$, were prepared from monocarboxylic acids (formic, acetic, propionic, isobutyric and benzoic); bisphenylhydrazides, $[C_6H_5NHNHCO—(CH_2)_n—]_2$ were obtained from dicarboxylic acids (succinic, adipic and sebacic).

Indicator solutions, all in acetonitrile. Diphenylamine, Methyl Red, Malachite Green, Janus Green and Gentian Violet were prepared as 0.1% solutions. Diphenylbenzidine was used as 0.05% solution.

Procedure

Aliquots of acetonitrile solutions of phenylhydrazides and acetic acid solutions of bisphenylhydrazides were transferred to dry titration vessels. The volume of each solution was made up to 30–40 ml with acetonitrile, and indicator solution (2 drops) was added. Each solution was

Table 1. Colour changes (including intermediate colours) observed for various indicators at the end-point

Indicator	Colour changes
Diphenylamine	Colourless → yellow → light blue
Diphenylbenzidine	Colourless → yellowish red → yellow → blue
Methyl Red	Red → rose red → yellow
Malachite Green	Light blue → bluish green → dirty green → reddish yellow
Janus Green	Blue → dirty blue → bluish black → dirty green
Gentian Violet	Violet → deep red

titrated at room temperature (~25) with standard ammonium hexanitratocerate solution (in acetonitrile) from a microburette provided with a guard-tube to protect the titrant from atmospheric moisture. The colour-changes at the end-points are given in Table 1.

The solutions were magnetically stirred during potentiometric titrations. A sharp jump in potential was observed at the end-point in each titration.

The results are recorded in Table 2. Since the choice of reference electrode did not affect the results of the potentiometric titrations, for brevity only one set of results is recorded in Table 2.

RESULTS AND DISCUSSION

The use of non-aqueous solvents for analytical redox reactions has received scant attention, compared to use for acid–base titrimetry. The removal of the last traces of water, so essential in the acid–base work, is not at all necessary in the redox titrimetry, which is a considerable advantage. It is the limited number of solvents having high dielectric constants in addition to resistance to oxidation or reduction that has been the barrier to greater developments in this area. Acetonitrile, however, meets these requirements satisfactorily and has proved quite promising as a solvent, especially with stronger oxidants such as ammonium hexanitratocerate(IV).[4] Verma and Kumar have used the oxidant in acetonitrile for the determination of thioureas,[5,6] xanthates[6] and organotrithiocarbonates.[7] Its use is now extended to the determination of phenylhydrazides in acetonitrile. The oxidation proceeds rapidly and smoothly, and chemical indicators can be used. Again for brevity, only the results with diphenylamine as indicator are shown in Table 2. In the potentiometric titrations (with either reference electrode) the potentials become stable immediately on addition of each increment of oxidant. A sharp jump in potential of 210–400 mV per 0.05 ml of 0.04*M* oxidant solution is observed at the equivalence point when the modified calomel electrode is used, and 160–310 mV per 0.05 ml with the antimony reference electrode. The potentials at the inflection points are 440–770 mV (modified calomel) and 390–630 mV (antimony). The results recorded in Table 2 show that the overall standard deviations calculated from the pooled data for all the visual and potentiometric (modified calomel electrode) titrations are 0.030 and 0.024 mg respectively for 4-mg samples and 0.055 and 0.039 mg for 10-mg samples.

The method is based on the oxidation of phenylhydrazides with a two-electron change per hydrazino group. The most plausible course of reaction is

$$C_6H_5NHNHCOR \rightarrow C_6H_5N{=}NCOR + 2H^+ + 2e$$
$$\downarrow$$
$$C_6H_5COR + N_2$$

The effervescent evolution of a gas is observed during the titrations. That phenylhydrazides can be oxidized to diazonium compounds is already known.[8] More-

Table 2. Titrations of phenylhydrazides with ammonium hexanitratocerate(IV) in acetonitrile

Sample	Amount found*, *mg*				Amount found†, *mg*			
	Visual method		Potentiometric method		Visual method		Potentiometric method	
β-Carboxylic acid phenylhydrazides, $C_6H_5NHNHCOR$								
Carboxylic acid								
Formic	4.03	(0.028)	4.01	(0.022)	10.06	(0.051)	10.05	(0.033)
Acetic	3.98	(0.038)	4.00	(0.028)	10.04	(0.046)	10.01	(0.037)
Propionic	4.03	(0.033)	3.99	(0.029)	9.97	(0.062)	9.98	(0.041)
Isobutyric	4.02	(0.025)	3.99	(0.020)	10.05	(0.051)	9.98	(0.035)
Benzoic acid	4.00	(0.028)	4.00	(0.022)	9.95	(0.051)	10.02	(0.040)
β-Dicarboxylic acid bisphenylhydrazides, $[C_6H_5NHNHCO{-}(CH_2)_n{-}]_2$								
Dicarboxylic acid								
Succinic	3.97	(0.031)	4.01	(0.026)	10.04	(0.056)	10.02	(0.041)
Adipic	4.04	(0.028)	3.98	(0.021)	10.07	(0.061)	10.03	(0.039)
Sebacic	3.96	(0.030)	4.02	(0.024)	9.94	(0.059)	9.96	(0.042)

* Amount taken, 4 mg; mean of 10 results, standard deviation in brackets.

† Amount taken, 10 mg; mean of 10 results, standard deviation in brackets.

over, many di-imides (I) have been prepared by the oxidation of hydrazides.[8]

$$R^1CONHNHCOR^2 \rightarrow R^1CON{=}NCOR^2 + 2H^+ + 2e$$

(I)

Organoisothiocyanates, thiocyanates and isocyanates do not cause any interference even when present in up to fivefold ratio to the phenylhydrazide. Urea, thioacetamide, xanthates, dithiocarbamates and amines interfere, however.

REFERENCES

1. Z. Hladky and J. Ruza, *Chem. Zvesti*, 1969, **23**, 336.
2. R. C. Paul, R. K. Chauhan and R. Parkash, *Talanta*, 1974, **21**, 663.
3. G. H. Stempel and G. S. Schaffel, *J. Am. Chem. Soc.*, 1942, **64**, 470.
4. B. Kratochvil, *Rec. Chem. Prog.*, 1966, **27**, 260.
5. B. C. Verma and S. Kumar, *Talanta*, 1973, **20**, 916.
6. *Idem, ibid.*, 1976, **23**, 241.
7. *Idem, J. Indian Chem. Soc.*, 1976, **53**, 1015.
8. Z. Zabisky, *The Chemistry of Amides*, p. 566. Wiley-Interscience, New York, 1970.

Talanta, Vol. 28, pp. 963 to 965. 1981
Printed in Great Britain

0039-9140/81/120963-03$02.00/0
Pergamon Press Ltd

SEQUENTIAL TITRATION OF IRON(II), ANTIMONY(III) AND ARSENIC(III) IN BINARY OR TERNARY MIXTURE

K. SRIRAMAM, B. S. R. SARMA, N. RAMABRAHMA SASTRY and A. R. K. VARA PRASAD

Department of Chemistry, Nagarjuna University, Nagarjunanagar, 522 510 (A.P.), India

(*Received* 25 *November* 1980. *Accepted* 26 *April* 1981)

Summary—A simple titrimetric procedure for the determination of iron(II), antimony(III) and arsenic(III) in a mixture, with cerium(IV) sulphate as titrant, is proposed. The end-points can all be detected with ferroin or potentiometrically. Phosphoric acid medium is used for titration of the iron(II), then acetic acid medium for the titration of antimony(III), and finally the arsenic(III) is titrated in presence of iodine as catalyst. The procedure utilizes a single portion of test solution; it can be adopted for the analysis of binary mixtures.

Titrimetric procedures for the determination of arsenic(III) and antimony(III) with cerium(IV) sulphate are sparse. Gopala Rao and co-workers[1–5] have investigated these titrimetric reactions and found iodine a suitable catalyst for use with a variety of indicators. Their observations on ferroin are especially interesting. They find that the difficulty in the Willard and Young[6] procedure for titration of arsenic(III) is due to the presence of hydrochloric acid, but that its effect can be offset to some extent by addition of acetic acid.[2] Willard and Young[7] reported the use of ferroin in the cerimetric titration of antimony(III) at elevated temperature, but later workers[8,9] found it very unsatisfactory. Gopala Rao and Viswanath[4] explain the difficulty as due to the formation of an insoluble ferroin–hexachloroantimonate(V) ion-pair, but report that the titration is satisfactory in 50% v/v acetic acid medium. They have developed a sequential titration of antimony(III) and arsenic(III) in mixtures, but the second titration needs to be done slowly or in hot solution (50); these authors have not attempted such titrations of other binary combinations with ferroin as indicator, although similar work was undertaken with diphenylamine-type indicators.[3]

Here we report the sequential titration of iron(II), antimony(III) and arsenic(III) in binary or ternary mixture, with cerium(IV) sulphate, using potentiometry or ferroin as indicator. We have improved the procedure proposed by Gopala Rao and Viswanath[4] and identified the cause of difficulty in it.

EXPERIMENTAL

Reagents

Iron(II) sulphate solution, 0.05*M*. Prepared by dissolving the requisite amount of Mohr's salt in 0.5*M* sulphuric acid, and standardized with pure potassium dichromate.

Antimony(III) chloride solution, 0.025*M*. Prepared by dissolving the requisite amount of antimony(III) chloride in 3*M* hydrochloric acid and standardized with potassium bromate.[10]

Arsenic(III) solution, 0.025*M*. Prepared by dissolving the requisite amount of pure arsenious oxide in 0.6*M* sodium hydroxide solution, and making 0.15*N* in sulphuric acid when diluted to volume.

Cerium(IV) sulphate solution in 0.5M sulphuric acid, 0.05*M*. Prepared from cerium oxide and standardized with arsenious oxide.[11]

Catalyst mixture. Prepared by mixing 20.8 ml of 0.1*M* potassium iodide and 4.16 ml of 0.1*M* potassium iodate and diluting to 250 ml with water.

Ferroin, 0.01*M*.

Apparatus

For the potentiometric titration a bright platinum-rod indicator electrode was used; a U-tube with porous end-plates and filled with 1*M* sulphuric acid served as connecting bridge between the half-cells; the reference electrode was a platinum rod dipped in 1*M* sulphuric acid saturated with quinhydrone.[12] Magnetic stirring was used throughout.

Procedures

Iron(II) and antimony(III). In the titration of iron(II) and antimony(III) in 0.5–1.0*M* sulphuric acid medium with cerium(IV) sulphate (and ferroin as indicator) the colour does not change at the true end-point for iron(II), and the formation of the ferroin–hexachloroantimonate(V) precipitate will not indicate the end-point satisfactorily as it is not sharply defined. Gopala Rao and Viswanath observed[4] that the sum of iron(II) and antimony(III) can be titrated in 50% acetic acid medium but did not attempt a sequential titration. However, in the presence of 5 ml of 85% phosphoric acid per 50 ml of titration mixture, the colour change takes place sharply at the end-point for iron(II). The colour changes from red to pale blue, stable for about 20 sec, then reverts to red, but a red precipitate of the ferroin compound soon appears. On the addition of acetic acid the precipitate dissolves, and the solution is orange red. On further titration the colour change occurs at the end-point for antimony if the titration mixture is 0.5–1.0*M* in chloride (added after the first end-point, if necessary).

The titrand, containing 14–28 mg each of iron(II) and antimony(III) is treated with enough 5*M* sulphuric acid to make the solution 1–2*M* in sulphuric acid when diluted to 40 ml, followed by 4–5 ml of 85% phosphoric acid, and

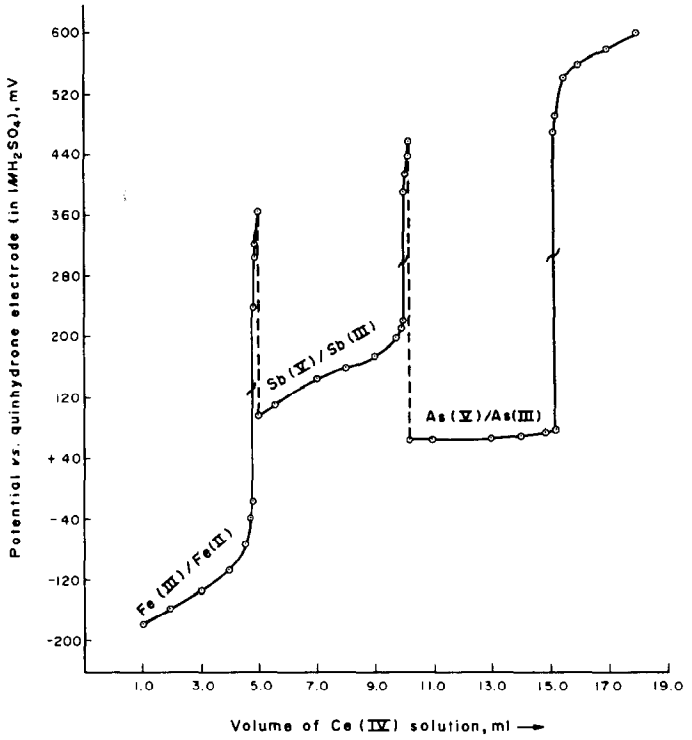


Fig. 1. Sequential potentiometric titration of iron(II), antimony(III) and arsenic(III) in ternary mixture, with cerium(IV) sulphate solution (5.0 ml each of ~0.05*M* iron(II), ~0.025*M* antimony(III) and ~0.025*M* arsenic(III), treated as described in the text, but without addition of indicator and titrated with 0.05*M* cerium(IV) sulphate).

0.1 ml of ferroin solution is added. The solution is titrated with 0.05*M* cerium(IV) sulphate. After the iron(II) end-point, enough glacial acetic acid and 6*M* hydrochloric acid are added to make the medium 40–50% v/v acetic acid and 0.5–1.0*M* hydrochloric acid, and the titration is continued.

Iron(II) and arsenic(III). The Gopala Rao procedure[2] for arsenic(III) in 0.5–1.0*M* sulphuric acid, with iodine as catalyst, can be extended to the sequential titration of iron(II) and arsenic(III). Titration without the catalyst present gives the iron(II) end-point; further titration after addition of the catalyst gives the arsenic(III) end-point. If chloride is present in the titration mixture (up to a maximum concentration of 1*M*), the arsenic(III) can be titrated in a medium to which 20–25% v/v of acetic acid has been added. The presence of 2–3 ml of 85% phosphoric acid per 50 ml of titration mixture does not affect the results.

The titrand containing 14–28 mg of iron(II) and 9–18 mg of arsenic(III) is treated with enough 5*M* sulphuric acid to give a concentration of 0.5–1.0*M* at the iron(II) end-point, the solution is diluted to 50 ml and 0.1 ml of ferroin solution is added. The solution is titrated with 0.05*M* cerium(IV) sulphate solution till pale blue [iron(II) end-point]. Then glacial acetic acid is added to give 20–25% v/v concentration, followed by 0.2 ml of iodide-iodate catalyst mixture. The colour of ferroin reappears in the solution. The titration is continued to the second end-point.

However, when phosphoric acid is present in the titration mixture, the overall sulphuric acid concentration during the titration of arsenic(III) should not fall below 0.5*M*.

Antimony(III) and arsenic(III). The difficulty in the sequential titration procedure of Gopala Rao and Viswanath[4] is traced to the presence of the large excess of acetic acid [50% v/v in the second titration instead of the 10–30% used by them in the simple titration of arsenic(III)]. If the titration mixture at this stage is diluted with water to provide 20–25% acetic acid medium, there is no need to heat the solution or titrate slowly near the end-point. The presence of phosphoric acid has no adverse effect.

The titrand containing antimony(III) and arsenic(III) is adjusted with 10*M* sulphuric acid to be 1–2*M* in sulphuric acid after addition of 25–30 ml of glacial acetic acid and dilution to 60 ml, and 0.1 ml of ferroin solution is added as indicator. The solution is titrated with 0.05*M* cerium(IV) sulphate until the colour of ferroin is discharged (antimony end-point). Then the solution is diluted with water to decrease the acetic acid concentration to 20–25%, 0.2 ml of iodide–iodate catalyst is added, and titration is continued until the restored ferroin colour is discharged (arsenic end-point).

Iron(II), antimony(III) and arsenic(III). Titrate the iron and antimony as already described, then dilute with water to reduce the acetic acid concentration to 20–25%, adjust the sulphuric acid concentration to 0.5–1.0*M* with 5*M* sulphuric acid, add 0.2 ml of iodide–iodate catalyst and titrate the arsenic.

The end-points can all be detected potentiometrically (Fig. 1), but the method is of only academic interest, as long waits of 10–15 min are needed in the region of the antimony(III) end-point to obtain steady potentials, though potential equilibration with the iron and arsenic systems seems to be fairly rapid. The analytical results by both the visual and potentiometric methods are accurate within 0.5%.

RESULTS AND DISCUSSION

The simple procedure proposed for the determination of iron(II), antimony(III) and arsenic(III) in bi-

nary or ternary mixture is useful in that the whole analysis is completed with a single portion of test solution. The titrations of iron(II) and antimony(III) are sharply differentiated by the presence of phosphoric acid. Since iron(II) will reduce antimony(V) in presence of phosphoric acid,[13] any antimony(III) oxidized by local excess of cerium(IV) during the titration will be reduced again by iron(II). The addition of acetic acid leads to dissolution of the ferroin–hexachloroantimonate(V) compound in the titration of antimony(III). Gopala Rao and Viswanath claim that the acetic acid prevents the formation of the $SbCl_6^-$ which binds ferroin to produce an unreactive form. However, our studies have revealed that in the absence of iodine as catalyst, ferriin is not reduced by antimony(III) either in dilute sulphuric acid or in combined dilute sulphuric acid and acetic acid media, unless a certain amount of chloride is present. Thus since the effect of chloride in producing $SbCl_6^-$ is counteracted by the acetic acid, the involvement of free chloride in the mechanism of reduction of ferriin (a substitution-inert complex) by antimony(III) in this reaction medium is very interesting. The iodine-catalysed reaction of ferriin and arsenic(III) is not much affected by the presence of 10–30% v/v acetic acid in the titration medium, but is retarded by larger concentrations. Accordingly after the titration of antimony(III) in 50% v/v acetic acid medium, the solution is suitably diluted to lower the acetic acid content to 20–25%. Enough sulphuric acid must be present to prevent formation of insoluble cerium phosphates.

Acknowledgement—NRBS and ARKVP gratefully acknowledge financial assistance from CSIR, New Delhi.

REFERENCES

1. G. Muralikrishna and G. G. Rao, *Anal. Chim. Acta*, 1973, **65**, 231.
2. G. G. Rao, M. Gandikota and S. G. Viswanath, *ibid.*, 1976, **87**, 511.
3. G. G. Rao, S. G. Viswanath and M. Gandikota, *ibid.*, 1975, **79**, 273.
4. G. G. Rao and S. G. Viswanath, *ibid.*, 1977, **92**, 163.
5. *Idem*, *Talanta*, 1977, **24**, 323.
6. H. H. Willard and P. Young, *J. Am. Chem. Soc.*, 1933, **55**, 3260.
7. *Idem*, *ibid.*, 1933, **55**, 3268.
8. R. Přibil, *Chem. Listy*, 1945, **39**, 19.
9. E. H. Swift, *Introduction to Quantitative Analysis*, Prentice-Hall, New York, 1950.
10. A. I. Vogel, *Text Book of Quantitative Inorganic Analysis*, 4th Ed., p. 386. Longmans, London, 1973.
11. K. Gleu, *Z. Anal. Chem.*, 1933, **95**, 305.
12. F. Hovorka and W. C. Dearing, *J. Am. Chem. Soc.*, 1935, **57**, 446.
13. L. S. A. Dikshitulu and K. V. Raju, *J. Indian Chem. Soc.*, 1978, **55**, 346.

Talanta, Vol. 28, pp. 967 to 972, 1981
Printed in Great Britain. All rights reserved

0039-9140/81/120967-06$02.00/0
Copyright © 1981 Pergamon Press Ltd

ANNOTATIONS

DETERMINATION OF ULTRAMICRO AMOUNTS OF SELENIUM BY GAS CHROMATOGRAPHY WITH ELECTRON-CAPTURE DETECTION

KYOJI TÔEI* and YASUAKI SHIMOISHI

Department of Chemistry, Faculty of Science, Okayama University, 3-1-1 Tsushima-naka, Okayama-shi 700, Japan

(*Received* 24 *November* 1980. *Accepted* 17 *May* 1981)

Summary—Formation of piazselenols by the reaction of Se(IV) with 1,2-diaminobenzene and its derivatives, followed by solvent extraction and gas chromatography with electron-capture detection, provides the most sensitive means of determining selenium. By suitable chemical manipulation, the method can be used for Se(-II), Se(0), Se(IV) and Se(VI). Applications to a wide variety of samples are reviewed.

The chemical properties of selenium closely resemble those of sulphur, and its oxidation numbers are usually −II, 0, IV and VI. Selenium is widely distributed in the earth's crust with an average content of about 0.1 ppm.

The physiological effect of selenium on animals has been studied to some extent, although its effect on plants is not well known. Selenium is an essential micronutrient for animals[1] but excess causes toxicosis; on the other hand, selenium deficiency syndromes are known. Recently selenium has been reported to be an antidote for mercury, cadmium, arsenic and other elements.[2,3]

A minute amount of selenium in pure metals greatly affects their electrical properties, thus necessitating its exact determination, especially in the electronics industry.

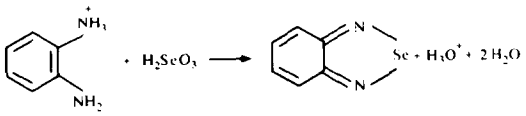
The oxidation state of selenium in the environment, particularly in the hydrosphere, is not known in detail, and the circulation of selenium is an important problem in geochemistry.

With this background, the determination of micro amounts of selenium becomes increasingly important. The present paper describes a very sensitive gas chromatographic method using electron-capture detection of piazselenols, and its application to biological materials, pure metals and natural waters. The oxidation states are also discussed.

Determination of selenium

Hoste[4] proposed determination of low concentrations of selenium by formation of a piazselenol with 3,3′-diaminobenzidine. This colorimetric method was later improved to some extent by Cheng[5] by extracting the piazselenol with toluene, and one of us further developed[6] the method by use of 1,2-diaminobenzene (*i.e.*, half of the 3,3′-diaminobenzidine molecule). 1,2-Diaminobenzene derivatives react specifically with selenium(IV) without being affected by coexisting substances, including other oxidation states (−II, 0 and VI) of selenium itself. Thus the method can be widely applied in various fields.[7]

The reaction between selenious acid and 1,2-diaminobenzene proceeds quantitatively at $1.0 < pH < 2.5$ to form the piazselenol. This pH range and the pK_a values of the acid and base, illustrated in Fig. 1, suggest that undissociated selenious acid and the singly protonated diamine are involved in the reaction, according to the equation:



The piazselenol can be quantitatively separated from the excess of reagent by extraction with toluene.

The piazselenol is thermally stable and volatile.

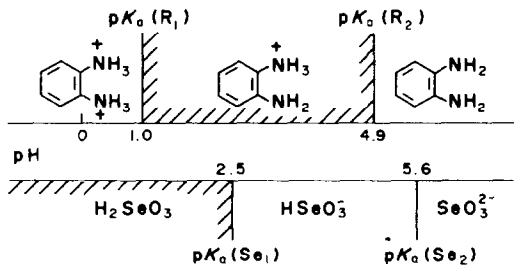


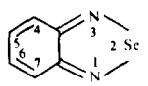
Fig. 1. The state of 1,2-diaminobenzene and selenious acid with change in pH (p*K*a values are the acid dissociation constants).

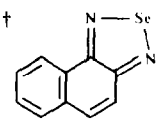
* To whom requests for reprints should be sent.

Table 1. Properties of piazselenol derivatives

Piazselenol*	M.p., °C	Kováts retention index (180°C)	Relative sensitivity	Distribution ratio (pH = 0)
PIS	73–74	1307	1.0	172
5-Me-PIS	72–73	1421	1.4	379
5-Et-PIS	73–73.5	1515	1.2	4.01×10^3
5-MeO-PIS	109–110	1541	1.7	297
5-ETO-PIS	102	1611	1.6	1.66×10^3
5-Cl-PIS	121	1454	17	1.41×10^3
5-Br-PIS	135	1547	30	2.58×10^3
5-NO_2-PIS	222–223	1653	128	250
5,6-diCl-PIS	163–164	1632	102	N.B.
4,6-diBr-PIS	217–218	1812	363	N.B.
4,7-diBr-PIS	273	1864	172	N.B.
4,Br-6-NO_2-PIS	221–222	1908	255	946
5,6-B-PIS†	129	1800		N.B.

N.B. = Not back-extracted.

* 

† 

This allows its detection by gas chromatography with high selectivity, because of the double fractionation achieved by extraction and chromatography. Moreover, use of the highly sensitive electron-capture detector (ECD) permits the determination of ultramicro amounts of selenium.

1,2-Diaminobenzene derivatives[8]

Introduction of an electron-withdrawing group into the 1,2-diaminobenzene nucleus substantially lowers its pK_a value, thus allowing the piazselenol reaction to proceed over a wider acidity range. For example, 1,2-diamino-3,5-dibromobenzene reacts quantitatively with selenious acid in 0.01–6*M* hydrochloric acid. Moreover, piazselenol derivatives bearing halogen or nitro groups have been found to give significantly greater sensitivity in detection by the ECD, as shown in Table 1, which lists the characteristics of a large number of such derivatives.

Extractability of piazselenols into toluene

Although the piazselenols can be extracted quantitatively at any pH, a low pH (usually below 1) is preferred, to avoid co-extracting the excess of reagent. The distribution coefficients for piazselenols between toluene and hydrochloric acid have been determined by shaking 1 or 0.5 ml of toluene (containing a known amount of piazselenol) with 200 ml of 1*M* hydrochloric acid previously saturated with toluene, separating the phases, measuring the peak height in the gas chromatogram for the piazselenol remaining in the toluene phase, and comparing it with that for the initial toluene solution. The distribution ratios calculated from the peak heights are shown in Table 1. It should be noted that the disubstituted halogen derivatives are not back-extracted at all.

Sensitivity of the ECD for piazselenols

The thirteen piazselenols synthesized were examined for their sensitivity of detection with the ECD, and the values relative to the sensitivity for the parent piazselenol are given in Table 1.

4,6-Dibromopiazselenol showed the highest sensitivity as well as the highest extractability, suggesting that 1,2-diamino-3,5-dibromobenzene is the best of these reagents, especially for extracting traces of selenium from water. 1,2-Diamino-4-nitrobenzene was found to have the highest sensitivity among the commercially available reagents.

APPLICATIONS

On the basis of the results above, the following general determination procedure has been recommended. The sample, organic or inorganic, is decomposed by heating with a suitable mineral acid (see below) to bring it into aqueous solution, and all the selenium except for Se(VI) is thereby converted into the quadrivalent state. When nitric acid or its mixture with another acid is used, the residual oxides of nitrogen should be decomposed by heating with urea solution. The aqueous solution is first washed with toluene to remove toluene-soluble substances, then mixed with a solution of 1,2-diamino-4-nitro- or 1,2-diamino-3,5-dibromobenzene. The piazselenol formed is extracted into 1 ml of toluene. The organic layer is washed with acid (then with base if necessary) to remove impurities. A fraction of the toluene extract (2–5 μl) is injected into an ECD gas chromatograph and the selenium content is calculated from the peak height for the piazselenol.

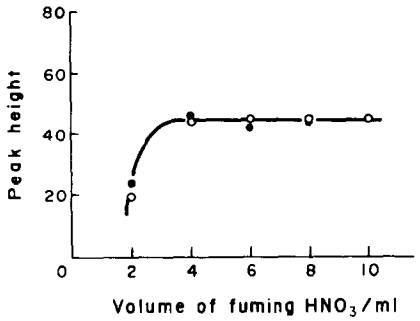


Fig. 2. Effect of the volume of fuming nitric acid: ○, 0.045 μg of selenium(0) on filter paper; ●, 0.045 μg of selenium(0) + 0.2 g of stem of wheat (selenium content below 0.005 μg/g). (By permission of the Chemical Society of Japan.)

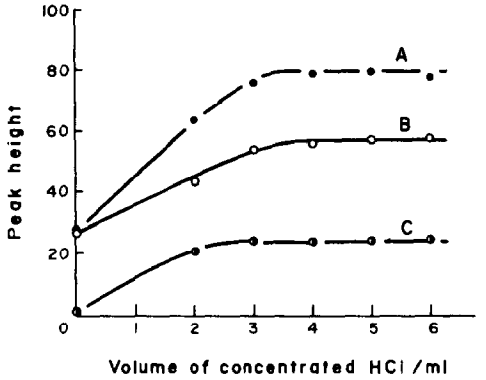


Fig. 3. Effect of the volume of concentrated hydrochloric acid: A, 0.5 g of dried skim milk + 0.02 μg of selenium(VI); B, 0.5 g of dried skim milk; C, 0.020 μg of selenium(VI). (By permission of the Royal Society of Chemistry.)

Selenium in plants[9]

Digestion of plant tissues. Because selenium is volatile, care has to be taken to prevent its loss when the sample is decomposed. The wet-digestion method with fuming nitric acid is recommended. In recovery experiments, pieces of filter paper (0.2 g), each impregnated with carbon disulphide containing 0.045 μg of elemental selenium and dried, were digested with various amounts of fuming nitric acid; at the same time another series of 0.2-g impregnated pieces of the paper was digested along with 0.2-g pieces of wheat-stem containing no selenium. The selenium contents determined by the recommended 1,2-diamino-4-nitrobenzene procedure indicated that more than 4 ml of fuming nitric acid would be required to digest completely the filter paper and the stem of wheat (see Fig. 2). The selenium(0) was all recovered as Se(IV), showing that Se(IV) was not further oxidized to Se(VI) under these conditions. If Se(VI) is present in the digestion liquid, it can be quantitatively reduced to Se(IV) by heating with hydrochloric acid. However, Se(VI) has not been detected in the plant tissues so far investigated (rice, wheat, cabbage and Chinese cabbage grown in selenium-containing soil). Typical results indicating uptake of selenium by plants are listed in Table 2.

Selenium in animal materials[10,11]

Digestion of samples. The sample is heated with concentrated nitric acid on a sand-bath for 2 hr, usually in a 100-ml conical flask. Then the general procedure is used for determination of Se(−II, 0, and IV) in an aliquot. Total selenium is then determined in a second aliquot that has been heated with concentrated hydrochloric acid at 100° for 10 min to reduce Se(VI). The Se(VI) is found by difference. That reduction of Se(VI) to Se(IV) by heating with concentrated hydrochloric acid is quantitative was confirmed by heating three kinds of sample [dried skimmed milk plus Se(VI) (A), dried skimmed milk (B), and Se(VI) (C)], first with concentrated nitric acid, then with various volumes of concentrated hydrochloric acid, and determining the total selenium. The results are illustrated in Fig. 3. The peak heights were the same when the volume of concentrated hydrochloric acid used was in excess of 4 ml. The difference in the peak height between A and B was always equal to that of C, although before the reduction that for C was ident-

Table 2. Selenium content of plant materials

Sample		Selenium content in soil,* μg/g	Selenium content in plant, μg/g
Cabbage	Foliage	none	< 0.005
Chinese cabbage	Foliage	none	0.006
Wheat	Stem	none	< 0.005
		10	0.54
		20	2.7
		50	3.4
		100	4.4
Rice plant	Mixture†	none	0.067
	Stem	20	11
		50	21
		100	22

* Added as SeO_2.
† A mixture of foliage and stem.

Table 3. Selenium content of milk

Material	Sample, *ml*	Selenium(VI),* *μg/ml*	Total selenium,† *μg/ml*	Selenium(VI), %
Milk (human)	2.0	0.003	0.010 ± 0.0004	30
Milk (human)	1.0		0.083 ± 0.004	
Nilk (human)	1.0	0.011	0.039 ± 0.004	28
Raw milk	1.0	0.012	0.021 ± 0.002	57
Raw milk	1.0	0.017	0.027 ± 0.002	63
Raw milk	1.0	0.014	0.022 ± 0.002	64
Bottled milk	1.0	0.009	0.019 ± 0.002	47
Processed milk	1.0	0.012	0.033 ± 0.004	36
Condensed milk	0.50	0.058	0.089 ± 0.004	65

* Results are the means of two determinations.
† Results are the means of five determinations.
(Reprinted by permission of the Royal Society of Chemistry.)

ical with that for the blank. These facts clearly indicated that Se(VI) was quantitatively reduced to Se(IV) with more than 4 ml of concentrated hydrochloric acid, but concentrated nitric acid caused no reduction under the conditions employed.

Selenium(VI) and total selenium in milk, milk

Table 4. Selenium content of milk products and albumin

Material	Sample, *g*	Selenium(VI),* *μg/g*	Total selenium,† *μg/g*	Selenium(VI), %
Dried skim milk	0.5	0.058	0.101 ± 0.002	57
Milk powder (baby food)	0.2–0.4	0.064	0.227 ± 0.017	28
Instant cream powder	0.1–0.2	N.D.	0.235 ± 0.010	0
Cheese	0.1	0.008	0.050 ± 0.002	16
Cheese	0.1	0.034	0.087 ± 0.008	39
Albumin, human (fraction V)	0.05–0.1	0.348	0.477 ± 0.021	73
Albumin, egg	0.05	0.437	0.585 ± 0.024	75
Albumin, egg crystalline	0.04	0.684	0.864 ± 0.037	79
Albumin, bovine (fraction V)	0.2	0.106	0.226 ± 0.007	47
L-Cystine	0.05	N.D.	0.587 ± 0.026	0
L-Methionine	0.5	0.010	0.010 ± 0.001	100
NBS Bovine liver (SRM 1577)		0.30 ± 0.07†	1.24 ± 0.04	24
(total Se 1.1 ± 0.1 μg/g)		0.31 ± 0.11†§	1.22 ± 0.04§	25

* Results are the means of two determinations.
† Results are the means of five determinations.
§ With 1,2-diamino-3,5-dibromobenzene.
N.D. denotes not detected.
(Reprinted by permission of the Royal Society of Chemistry.)

Table 5. Determination of total selenium and selenium(VI) in blood and plasma

Clinical diagnosis	Whole blood		Erythrocytes		Plasma	
	Se, *ng/ml*	Se(VI), *ng/ml*	Se, *ng/ml*	Se(VI), *ng/ml*	Se, *ng/ml*	Se(VI), *ng/ml*
Normal	205	94	316	163	119	34
Newborn	194	117	313	203	84	38
Liver cancer	163	69	294	140	109	39
Liver cirrhosis	158	60	236	112	112	26
Liver cancer + liver cirrhosis	165	74	264	146	99	24
Rheumatic arthritis	197	80	324	152	117	36
Anaemia	179	85	347	208	107	32

products and albumin, and in NBS bovine liver, have been determined with 1,2-diamino-4-nitrobenzene (and in bovine liver also with 1,2-diamino-3,5-dibromobenzene); typical results are given in Tables 3 and 4. To investigate possible links with cancer, the selenium contents of blood and plasma were determined with 1,2-diamino-3,5-dibromobenzene (Table 5).

Determination of selenium in pure metals[12–15]

Selenium in metals is usually present as the element or as selenide. Therefore the sample should be dissolved in *aqua regia* or other suitable mixed acid, to oxidize selenium to the quadrivalent state. Then the selenium(IV) can be determined directly by ECD gas chromatography (ECD–GC) with 1,2-diamino-4-nitrobenzene as reagent, since the complexation reaction is so specific that other metal ions cause no interference.

Tellurium usually contains a trace amount of elemental selenium because of the close resemblance of their properties. It can be dissolved in dilute *aqua regia*.

In pure copper, selenium exists as copper selenide, which is often distributed heterogeneously. Thus the sample should be finely cut into segments and mixed well, then more than 1 g is dissolved in a mixture (1:1:1) of nitric, hydrochloric and perchloric acids, followed by the determination of Se(IV) as before. Tölg *et al.*[16] have reported a similar determination of selenium in pure copper by ECD–GC after decomposing the sample by a dry method, but our wet decomposition method appears to be less troublesome for preparing the sample solution.

Arsenic and arsenious acid can be analysed for selenium by decomposing the sample with a mixture (4:1) of fuming nitric and phosphoric acids on a water-bath and subjecting the Se(IV) solution to the ECD–GC procedure. Use of other acids causes volatilization of some selenium along with arsenic compounds. Phosphoric acid often contains a micro amount of selenium(VI), but this is not reduced to Se(IV) and does not affect the determination.

Various types of steel contain a relatively large amount of selenium (about 0.1%). This can be determined by heating a sample (100 mg, dissolved in dilute *aqua regia*) with a mixture (1:1) of perchloric and phosphoric acid on a sand-bath, and complexing the resulting Se(IV) with 1,2-diamino-4-chlorobenzene and applying gas chromatography with thermal conductivity detection. The use of phosphoric acid effectively avoids the interference of iron(III) in the selenium determination.

Determination of ultramicro amounts of selenium in natural waters[17–19]

The selenium cycle and the oxidation state of the element in the hydrosphere are attractive problems in geochemistry and biology. For example, it has been found recently that the amount of selenium in the environment is inversely proportional to the incidence of cancer.[20]

The quantity of selenium in natural waters is so small that even the fluorimetric or neutron-activation methods often necessitate preconcentration. However, the ECD–GC method using 1,2-diamino-3,5-dibromobenzene as reagent allows the detection of selenium levels as low as 2 ng/l., without preconcentration.

Selenium in various oxidation states has been determined successfully by this method by analysing three sample solutions (500 or 300 ml each), the first with no further treatment [analysis for Se(IV)], the second after treatment with bromine water [for the sum of Se(−II, 0, and IV)], and the third after heating with bromine–bromide redox buffer solution (for total Se). Selenium(−II and 0) and Se(VI) can be readily calculated by simple deduction. Total selenium values for river water were found to vary widely (16–230 ng/l.), whereas those for sea-water were fairly constant at 50–70 ng/l., with Se(VI) predominating.

Conclusion

1,2-Diaminobenzene derivatives react quantitatively with selenium(IV), but not with selenium(−II, 0, and VI), in acidic solutions to form the piazselenols. The oxidation state of selenium can therefore be determined by successively converting selenium(−II, 0, and VI) into the quadrivalent state by suitable oxidation and reduction reactions. The best reagent found so far for the selenium(IV) determination by ECD gas chromatography is 1,2-diamino-3,5-dibromobenzene, while 1,2-diamino-4-nitrobenzene is the most effective of the commercially available reagents. The use of these reagents makes possible the accurate determination of micro amounts of selenium. Since the piazselenols produced are effectively separated from co-existing substances first by extraction with toluene and then by gas chromatography, the method is highly specific and sensitive. The procedure is also simple and rapid, requiring no special skill.

REFERENCES

1. J. N. Thompson and M. L. Scott, *J. Nutr.*, 1969, **97**, 335.
2. J. C. H. Hill, *ibid.*, 1974, **104**, 593.
3. I. S. Palmer and C. W. Bonhorst, *J. Agr. Food Chem.*, 1957, **5**, 928.
4. J. Hoste, *Anal. Chim. Acta*, 1948, **2**, 402.
5. K. L. Cheng, *Anal. Chem.*, 1956, **28**, 1738.
6. H. Ariyoshi, M. Kiniwa and K. Tôei, *Talanta*, 1960, **5**, 112.
7. R. A. Zingaro and W. C. Cooper, *Selenium*, p. 627. Van Nostrand Reinhold, New York, 1974.
8. Y. Shimoishi, *J. Chromatog.*, 1977, **136**, 85.
9. *Idem*, *Bull. Chem. Soc. Japan*, 1974, **47**, 997.
10. *Idem*, *Analyst*, 1976, **101**, 298.
11. K. Kurahashi, S. Inoue, S. Yonekura, Y. Shimoishi and K. Tôei, *ibid.*, 1980, **105**, 690.
12. Y. Shimoishi, *Bull. Chem. Soc. Japan*, 1971, **44**, 3370.

13. *Idem, ibid.*, 1975, **48**, 2797.
14. M. Akiba, Y. Shimoishi and K. Tôei, *Analyst*, 1976, **101**, 644.
15. *Idem, ibid.*, 1975, **100**, 648.
16. A. Meyer, E. Grallath, G. Kaiser and G. Tölg, *Z. Anal. Chem.*, 1976, **281**, 201.
17. Y. Shimoishi, *Anal. Chim. Acta*, 1973, **64**, 465.
18. Y. Shimoishi and K. Tôei, *ibid.*, 1978, **100**, 65.
19. H. Uchida, Y. Shimoishi and K. Tôei, *Environ. Sci. Technol.*, 1980, **14**, 541.
20. R. J. Shamberger and C. E. Willis, *Crit. Rev. Clin. Lab. Sci.*, 1971, **2**, 211.

Talanta, Vol. 28, pp. 973 to 976, 1981
Printed in Great Britain. All rights reserved

0039-9140/81/120973-04$02.00/0
Copyright © 1981 Pergamon Press Ltd

INTRAMOLECULAR HYDROGEN-BONDING IN BETA ADRENERGIC BLOCKING AGENTS

MICHELE LAXER*, A. C. CAPOMACCHIA† and G. E. HARDEE

Department of Pharmaceutics, School of Pharmacy,
University of Georgia, Athens, Georgia 30602, U.S.A.

(*Received* 2 *February* 1981. *Accepted* 29 *April* 1981)

Summary—The acid dissociation constants for nine beta-adrenergic blocking agents have been determined. Their unusually low pK_a values are explained as being due to the formation of an intramolecular hydrogen bond, between the terminal amino group and the β-hydroxyl group on the alkanolamine side-chain which is common to this class of drugs.

Beta-adrenergic blocking agents, as a class of drugs, possess one common structural feature, an alkanolamine side-chain which terminates with a secondary amino group. The acid dissociation constants (pK_a) reported for this group range in value from 9.2 to 9.80.[1-3] The range and magnitude of these values are noteworthy for two reasons. First, the pK_a values are at least one unit lower than those for secondary amines. The terminal amino groups on these agents are sterically unencumbered, so their comparatively low pK_a values indicate that some inter- or intramolecular physical interaction may be occurring that affects their acid–base chemistry. Secondly, the range of pK_a values is remarkable since, if true, it may indicate subtle differences in these physical interactions, from one agent to another. This last point is important in regard to the conformation of these agents at their receptor sites.

EXPERIMENTAL

Solutions of the following ten compounds (as their hydrochlorides) were prepared, each at a concentration of $5.00 \times 10^{-3}M$ in $5.00 \times 10^{-3}M$ hydrochloric acid: 1, pronethalol, 2-[(isopropylamino)methyl]-1-(2-naphthylethanol; 2, propranolol, 1-(isopropylamino)-3-(1-naphthyloxy)-2-propanol; 3, metoprolol, 1-[4-(2-methoxyethyl)phenoxyl]-3-(isopropylamino)-2-propanol; 4, practolol, *N*-([2-hydroxy-3-[(isopropylamino)propoxy]phenyl)acetamide; 5, pindolol, 1-(1H-indol-4-yloxy)-3-(isopropylamino)-2-propanol; 6, oxprenolol, 1-(isopropylamino)-3-[2-(2-propenyloxy) phenoxy]-2-propanol; 7, nadolol, 1-(tert-butylamino)-3-(1-oxy-,5,6,7,8-tetrahydro-,6,7-dihydroxynaphthalene)-2-propanol; 8, timolol, S-1-(tertbutylamino)-3-[(4-morpholino-1,2,5-thiadiazol-3-yl)oxy]-2-propanol; 9, sotalol, *N*-(4-[1-hydroxy-2-(isopropyl amino)ethyl]phenyl)methanesulphonamide; 10, di-n-butylamine. Compounds 1–9 were gifts from their respective manufacturers, while 10 was obtained commercially. Each solution (10 ml) was titrated with $2.00 \times 10^{-1}M$ potassium hydroxide. An equal volume of $5.00 \times 10^{-3}M$ hydrochloric acid was similarly treated and used as the blank. All titrations were done at least in triplicate and monitored potentiometrically with a Corning model 12 pH-meter, with a silver–silver chloride/glass combination pH-electrode by the method of Parke and Davis,[4] which requires that the blank titration curve be subtracted point-by-point from that for the drug. The procedure, for compounds 1, 2, 7 and 10, was twice repeated, with addition of sufficient urea to make the solutions first $8M$ in urea and again with the solutions $16M$ in urea, an equal volume of urea solution, at each concentration, being used as a blank. The results are presented in Table 1. The effect of urea on electrode response was negligible during the time required to complete the acid–base reaction, and in the pH region 8.0–11.3. In this region, solutions of a carbonate buffer system ($\mu = 0.005$)[5] showed no change in pH when the urea concentration was made either 8 or $16M$. Moreover, solutions made with various amounts of our stock hydrochloric acid and potassium hydroxide solution at pH values in this interval also showed no pH change when made $16M$ in urea concentration. Below pH 8.0, the addition of urea to give a $16M$ concentration in a phosphate buffer system ($\mu = 0.005$)[5] raised the apparent pH by 0.1 at pH 7.0, 0.2 at pH 6.0, 0.3 at pH 5.0 and 0.4 at pH 4.0. This did not affect our pK_a determinations.

Corrected fluorescence excitation and emission spectra were generated on a Perkin–Elmer MPF-44A spectrofluorimeter employing an *X–Y* recorder, 1-cm quartz cells and a 150-W xenon lamp. The spectra were corrected for the wavelength response of the light-source, photomultiplier tube and optical system, by means of a microprocessor programmed to perform a correction every 0.2 nm over the wavelength region from 200 to 600 nm. Electronic absorption spectra were taken in 1-cm silica cells on a Cary 119 spectrophotometer.

Fluorometric acid–base studies were conducted with quinine and WR 148,946 [α-dibutylaminomethyl-2,6-bis-(trifluoromethylphenyl)-4-pyridinemethanol]. Solutions (*ca.* $1 \times 10^{-6}M$) of these two agents were prepared in the phosphate and carbonate buffer-system media[5] ($\mu = 0.005$) at various pH values ranging from 7 to 11.3. A second set of solutions was prepared, identical to the first, but with a urea concentration of $16M$; the urea did not interfere with the fluorescence measurements.

All spectral and potentiometric measurements were conducted at room temperature, maintained at 24 ± 2°.

* NSF/SSTP Participant.
† To whom correspondence should be addressed.

RESULTS AND DISCUSSION

We report the acid dissociation constants for the adrenergic beta-blockers pronethalol, pindolol, nadolol and timolol in Table 1. The constants for propranolol, metoprolol, practolol, oxyprenolol and sotalol were also determined so that a comparison could be made with their published values.[1-3] The mean pK_a value for all nine compounds is 9.48 ± 0.06 (mean ± standard deviation); the mean for the five reported values is 9.5 ± 0.3.

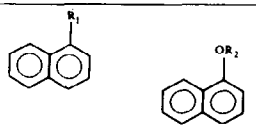
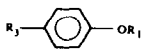
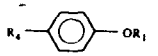
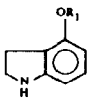
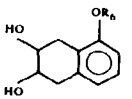
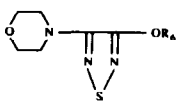
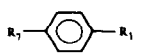
The mean pK_a value we report, for all nine agents, is less than that for a secondary or tertiary amine by more than one unit. For example, diethylamine, dipropylamine, dibutylamine and tripropylamine have pK_a values of 10.98, 10.97, 10.80 (Table 1) and 10.64, respectively.[5,6] The unusually low pK_a values of the beta-blockers could have several causes. Aggregation was ruled out as a cause since the absorption and fluorescence excitation and emission spectra of these agents did not change on thousandfold dilution of the reaction solution. It appears that the lone-pair electrons on the terminal amino group are involved, since this group is less basic than either a secondary or tertiary amine. For this reason, hydrogen-bonding between lone-pair electrons on the hydroxyl-oxygen atom and a positively-polarized hydrogen atom on the protonated amino group was also ruled out. Since the pK_a values for these agents are, for practical purposes, the same, the type or size of the aromatic substituent is apparently not a factor in decreasing the amino-group basicity. With these arguments in mind, the only plausible explanation remaining seems to be formation of a hydrogen bond, in the neutral species, between the lone-pair electrons on the amino-group nitrogen atom and the hydroxyl-group hydrogen atom.

A similar explanation has been used to account for the anomalously low basicity observed for the antimalarials quinine and WR 148,946.[6,7] The pK_a values of their exocyclic amino groups were found to be 8.43 and 8.30 respectively. The lowness of these values, relative to a secondary amine, was attributed to two factors: (1) the alkanolamine or quinuclidine side-chain forms a hydrogen-bonded pseudo-oxazole ring system in the neutral species; (2) the pseudo-oxazole ring system interacts electronically with the aromatic nucleus by rotating into plane with the aromatic core, thus facilitating electron donation to the latter. This diminishes the electron density on the exocyclic amino group and accounts for its relatively low basicity. In the light of these studies, it appears that the lower basicity of the beta-adrenergic blockers, relative to a secondary amine, may be due solely to hydrogen-bond formation. This point is supported by our results which show that the absorption and fluorescence excitation and emission spectra of these agents demonstrate no change as the solution acidity is decreased (in the pH range 2.30–11). This means that the hydrogen-bonded side chain does not interact with the aromatic core to the extent that it does in quinine and WR 148,946. Moreover, since the pK_a values for these agents are more than one unit greater than those for quinine or WR 148,946, the hydrogen bond so formed must be weaker than that in the two antimalarials.

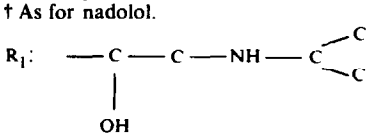
To demonstrate the presence of the intramolecular hydrogen bond in the nine agents studied, we employed a technique commonly used to disrupt hydrogen bonds in aqueous solutions of macromolecules.[8] Addition of urea to solutions of proteins has been shown to cause many proteins to dissociate into separate chains. This has been attributed to disruption of the hydrogen bonds holding the peptide chains together. Compounds 1, 2, 7 and 10 were re-examined in 8*M* and 16*M* urea media. As the urea concentration was increased, the apparent pK_a value of these agents also increased (Table 1). In the most concentrated urea solutions, the pK_a values obtained for these four compounds were very near those obtained for the control compound, di-n-butylamine, in both aqueous and urea solution (Table 1). The results appear to support the explanation offered earlier that the neutral species of these agents form an intramolecular hydrogen bond which is disrupted by urea. Moreover, to the best of our knowledge, this is the first time urea has been used to demonstrate the presence of hydrogen-bonding in an *in vitro* aqueous chemical system.

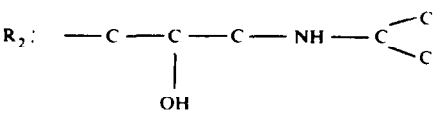
To test further the idea that urea can disrupt intramolecular hydrogen bonds between lone-pair electrons on an uncharged secondary amino group, and a hydroxyl-group hydrogen atom two carbon atoms distant from it, we examined the fluorescence spectra of quinine and WR 148,946, in aqueous and 16*M* urea solution. As mentioned earlier, we have already shown that the neutral species derived from these two compounds have their uncharged amino groups engaged in this type of hydrogen bonding.[5,6] In the pH interval from 7 to 11, the fluorescence from the singly-charged quinine cation is quenched. The mid-point of quenching coincides with the ground-state pK_a value for conversion of the quinine cation into its conjugate base. The reported value[6] is 8.34. However, the mid-point of quenching for the same photolytic process, in the presence of urea (16*M*), is at pH 8.8. This value is 0.44 pH unit more basic than that obtained for quinine in urea-free solution. Moreover, it is essentially the same as that reported for quinidine, pK_a 8.79.[6] In the latter compound, the neutral species is sterically prohibited from engaging in the same type of intramolecular hydrogen bond found in the neutral species of its optical isomer, quinine.[6] This result indicates that urea is disrupting the hydrogen bond present in neutral quinine. The most convincing evidence that this type of bonding exists in these uncharged aminoalkanol systems is the shift, to shorter wavelengths, of the fluorescence excitation and emission spectra of the neutral species derived from WR 148,946, upon going from purely aqueous urea

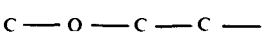
Table 1

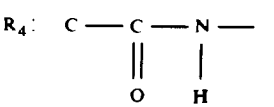
Compound	pK_a, mean ± standard deviation				
	Literature values	(ref)	This work	This work (8*M* urea)	This work (16*M* urea)
1. Pronethalol 	—		9.53 ± 0.04	9.80 ± 0.08	10.70 ± 0.10
2. Propranolol	9.45	(2)	9.42 ± 0.05	9.88 ± 0.07	10.85 ± 0.09
3. Metoprolol 	9.78	(1)	9.53 ± 0.07	*	*
4. Practolol 	9.4	(2)	9.44 ± 0.05	*	*
5. Pindolol 	—		9.46 ± 0.06	*	*
6. Oxprenolol 	9.2	(1)	9.40 ± 0.07	*	*
7. Nadolol 	—		9.50 ± 0.04	9.91 ± 0.08	10.95 ± 0.11
8. Timolol 	—		5.95 ± 0.06 9.40 ± 0.05	†	†
9. Sotalol 	8.30 9.80	(3)	8.30 ± 0.10 9.55 ± 0.11	*	*
10. Di-n-butylamine 	10.8	(4)	10.80 ± 0.03	10.80 ± 0.05	10.80 ± 0.07

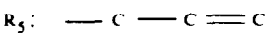
* As for pronethalol.
† As for nadolol.

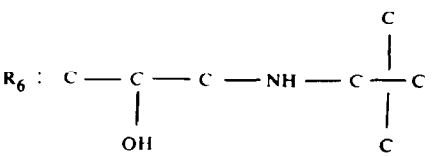
R_1: 

R_2: 

R_3: 

R_4: 

R_5: 

R_6: 

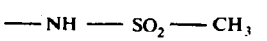
R_7: 

Table 2. Fluorescence excitation and emission spectral features of the singly charged and neutral species of WR 148,946 in aqueous and aqueous urea solution

	Excitation wavelength, *nm*		Emission wavelength, *nm*
	^1L_b	^1L_a	
Singly-charged cation (pH 3)	296*	238*	348*
	286		
Neutral species (pH 12)	305	246*	478*
	290*		
Species generated in urea medium (16*M*, pH 12)	296*	240*	350*
	286		

* Denotes maxima.

solutions. In 16*M* urea medium at pH 12, its excitation and emission spectra resemble those of the singly-charged cation, not the neutral species (Table 2). Clearly, the urea has disrupted the pseudo-oxazole ring system formed by intramolecular hydrogen-bonding, and thereby decreased the intramolecular charge-transfer from it to the aromatic ring system, in both the ground and lowest excited singlet states. Experiments were also conducted to determine the ground and excited state acid dissociation constants for conversion of the singly-charged cation into its conjugate base in 16*M* urea medium. The absorption and fluorescence excitation spectral band overlap was too severe to allow an accurate measurement of the pK_a in urea medium, but the excited-state constant, pK_a^*, was determined as 9, some 4 units more basic than the value calculated for purely aqueous medium (pK_a^* 5).[7] This result, like that for quinine, indicates that urea also disrupts the hydrogen bond in neutral WR 148,946.

A final point to be made is that these drugs all have virtually the same pK_a value. This means that at physiological pH (7.4) they exist as singly-charged cations, and all have the same solution conformation of the alkanolamine side-chain, and most likely the same conformation at the receptor site.

REFERENCES

1. C. Applegren, K. O. Borg, R. Elofsson and K. A. Johansson, *Acta. Pharm. Suec.*, 1974, **11**, 325.
2. C. M. Kaye, D. G. Robinson and P. Turner, *Brit. J. Pharmacol.*, 1973, **49**, 155.
3. E. R. Garrett and K. Schnelle, *J. Pharm. Sci.*, 1971, **60**, 833.
4. T. V. Parke and W. W. Davis, *Anal. Chem.*, 1954, **26**, 642.
5. K. Diem and C. Lentner (eds.), *Documenta Geigy, Scientific Tables*, 7th Ed., pp. 280–293. Ciba-Geigy, Basel, Switzerland, 1970.
6. S. G. Schulman, R. M. Threatte, A. C. Capomacchia and W. L. Paul, *J. Pharm. Sci.*, 1974, **63**, 876.
7. O. J. Bouwsma, J. T. Stewart and A. C. Capomacchia, *ibid.*, 1978, **67**, 1224.
8. R. W. McGilvery, *Biochemistry, a Functional Approach*, p. 147. Saunders, Philadelphia, 1970.

Talanta, Vol. 28, p. 977, 1981
Printed in Great Britain

0039-9140/81/120977-01$02.00/0
Pergamon Press Ltd

LETTER TO THE EDITOR

ON THE ANALYTICAL METHOD OF CALCULATING THE DERIVATIVES OF EQUILIBRIUM CONCENTRATIONS

Sir,

We have read in your journal an article on new analytical expressions for the derivatives of the species concentrations with respect to the equilibrium constants.[1] We would like to draw your attention to the fact that we have for a long time been using these and many other similar derivatives, written in a simple, compact matrix form, for calculating both the generalized buffer properties and the derivatives of the minimized function when determining the equilibrium constants from experimental data.[2-9]

Department of Chemistry,
A.M. Gorky Kharkov State University,
Kharkov, USSR

A.A. Bugaevsky
L.E. Nikishina

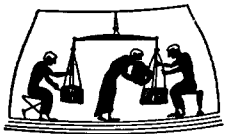
8 July 1981

REFERENCES

1. I. Nagypal, I. Páka and L. Zékány, Talanta, 1978, 25, 549.
2. A.A. Bugaevsky and B.A. Dunai, Zh. Analit. Khim., 1971, 26, 205.
3. Idem, ibid., 1972, 27, 225.
4. A.A. Bugaevsky, L.E. Rudnaya and T.P. Mukhina, ibid., 1972, 27, 1675.
5. T.P. Mukhina, A.A. Bugaevsky and L.E. Rudnaya, ibid., 1972, 27, 1680.
6. L.E. Rudnaya and A.A. Bugaevsky, Dokl. Akad. Nauk Ukrainian SSR, 1975, 344.
7. A.A. Bugaevsky and L.E. Rudnaya, Zh. Neorgan. Khim., 1976, 21, 2827.
8. Matematicheskie voprosy issledovaniya khimicheskikh ravnovecii, Izdat. Tomsk University, Tomsk, 1978.
9. A.A. Bugaevsky and L.E. Nikishina, Zh. Neorgan. Khim., 1980, 25, 2854.

Talanta

The International Journal of Pure and Applied Analytical Chemistry



The illustration of a Greek balance from one of the Hope Vases is reproduced here by kind permission of Cambridge University Press

Editor-in-Chief

DR R.A.CHALMERS, Department of Chemistry, University of Aberdeen, Old Aberdeen, Scotland.

Assistant Editors

PROFESSOR D.BETTERIDGE, University College, Swansea, Wales
DR J.R.MAJER, University of Birmingham, England
DR I.L.MARR, University of Aberdeen, Scotland

Computing Editor

DR MARY R.MASSON, University of Aberdeen, Scotland

Regional Editors

PROFESSOR I.P.ALIMARIN, Vernadsky Institute of Geochemistry and Analytical Chemistry, U.S.S.R. Academy of Sciences, Vorobievskoe Shosse 47a, Moscow V-334, U.S.S.R.
PROFESSOR E.BLASIUS, Institut für Analytische Chemie und Radiochemie der Universität des Saarlandes, D-6600 Saarbrücken 15, Bundesrepublik Deutschland
MR H.J.FRANCIS JR, Pennwalt Corporation, 900 First Avenue, King of Prussia, Pennsylvania 19406, U.S.A.
PROFESSOR J.S.FRITZ, Department of Chemistry, Iowa State University, Ames, Iowa 50010, U.S.A.
PROFESSOR T.FUJINAGA, Department of Chemistry, Faculty of Science, University of Kyoto Sakyo-ku, Kyoto, Japan
DR M.PESEZ, Roussel-Uclaf, 102 et 111 route de Noisy, F–93, Romainville (Seine), France
PROFESSOR E.PUNGOR, Institute for General and Analytical Chemistry, Technical University, Gellért tér 4, 1502 Budapest XI, Hungary

Consulting Editor

DR M.WILLIAMS, Oxford, England

Editorial Board

Chairman: PROFESSOR R.BELCHER, *representing Advisory Board*
DR R.A.CHALMERS, *Editor-in-Chief* — DR J.R.MAJER, *Assistant Editor*
DR M.WILLIAMS, *Consulting Editor* — MR H.J.FRANCIS JR, *representing Regional Editors*
DR I.L.MARR, *Assistant Editor* — MR G.F.RICHARDS, *Managing Director, Pergamon Press Ltd*
PROFESSOR D.BETTERIDGE, *Assistant Editor*

Annual Subscription Rates (1981) $250.00—For libraries, government laboratories, research establishments, manufacturing houses and other multiple-reader institutions. Price includes postage and insurance. $20—For *bona fide* students, who place their orders with the publisher together with a note from their professor or tutor certifying their status. Published monthly—1 volume per annum.

Specially Reduced Rates to Individuals

In the interests of maximizing the dissemination of the research results published in this important international journal we have established a three-tier price structure. Any individual, whose institution takes out a library subscription, may purchase a second or additional subscription for personal use at a much reduced rate of U.S. $55.00 per annum. Subscription enquiries from customers in North America should be sent to: Pergamon Press Inc., Maxwell House, Fairview Park, Elmsford, NY 10523, U.S.A. and for the remainder of the World to: Pergamon Press Ltd, Headington Hill Hall, Oxford OX3 0BW, England. Payments must be made in advance.

Microform Subscriptions and Back Issues

Back issues of all previously published volumes are available in the regular editions and on microfilm and microfiche. Current subscriptions are available on microfiche simultaneously with the paper edition and on microfilm on completion of the annual index at the end of the subscription year.

Publishing Office. Pergamon Press Ltd, Hennock Road, Marsh Barton, Exeter, Devon, EX2 8RP, England (*Tel.* Exeter (0392) 51558; *Telex* 42749).

Advertising Offices. *American Continent:* Pergamon Press Inc., Maxwell House, Fairview Park, Elmsford, New York 10523, U.S.A *Rest of the World:* Pergamon Press Ltd, Headington Hill Hall, Oxford OX3 0BW, England (*Tel.* Oxford 64881).

Copyright © 1981 Pergamon Press Ltd

It is a condition of publication that manuscripts submitted to this journal have not been published and will not be simultaneously submitted or published elsewhere. By submitting a manuscript, the authors agree that the copyright for their article is transferred to the publisher if and when the article is accepted for publication. However, assignment of copyright is not required from authors who work for organizations which do not permit such assignment. The copyright covers the exclusive rights to reproduce and distribute the article, including reprints, photographic reproductions, microform or any other reproductions of similar nature and translations. No part of this publication may be reproduced, stored in a retrieval system or transmitted in any form or by any means. electronic, electrostatic, magnetic tape, mechanical, photocopying, recording or otherwise, without permission in writing from the copyright holder.

U.S. Copyright Law applicable to users in the U.S.A.
The Article Fee Code on the first page of an article in this journal indicates the copyright owner's consent that, in the U.S.A., copies may be made for personal or internal use provided the stated fee for copying, beyond that permitted by Section 107 or 108 of the United States Copyright Law, is paid. The appropriate remittance should be forwarded with a copy of the first page of the article to the Copyright Clearance Center Inc., 21 Congress Street, Salem, MA 01970. If a code does not appear copies of the article may be made without charge, provided permission is obtained from the publisher. The copyright owner's consent does not extend to copying for general distribution, for promotion, for creating new works or for resale. Specific written permission must be obtained from the publisher for such copying.
In case of doubt please contact your nearest Pergamon office.

Talanta, Vol. 28, p. i, 1981
Pergamon Press Ltd. Printed in Great Britain

PAPERS RECEIVED

Synthesis and metallochromic properties of some hydrazones of 2-, 3-, and 8-hydrazinoquinoline: A. A. SCHILT, M. R. DI TUSA and FRANCIS H. CASE. (2 August 1981)

Oxidation of micro or trace amounts of bromide to bromate by peroxodisulphate before their iodometric determination by titration or spectrophotometry: ULLA LUNDSTRÖM. (15 September 1981)

Calibration and quality control in routine chemical analysis: DOUGLAS G. MITCHELL and JOHN S. GARDEN. (16 September 1981)

Spectrophotometric determination of uranium(VI) with 2-(3,5-dibromo-2-pyridylazo)-5-diethylaminophenol in the presence of anionic surfactant: SHUI-CHIEH HUNG, CHANG-LING QU and SHUI-SHENG WU. (16 September 1981)

Spectrophotofluorimetric determination of terbium, europium and samarium with pivaloyltrifluoroacetone and tri-n-octylphosphine oxide in micellar solution of nona-oxyethylene dodecyl ether: TOMITSUGU TAKETATSU. (17 September 1981)

What is selectivity; can it be expressed quantitatively? J. INCZÉDY. (17 September 1981)

Complexometric determination of mercury(II) with 4-amino-5-mercapto-3-propyl-1,2,4-triazole as replacing reagent: H. R. A. GADIYAR, R. V. GADAG and M. T. GAJENDRAGAD. (21 September 1981)

Thiol as spectrophotometric reagent for vanadium(V) determination in aqueous medium: S. P. BAG, A. K. CHAKRABARTI and J. P. GOSWAMI. (21 September 1981)

Determination of indium in aluminium alloys by atomic-absorption spectroscopy and flame photometry: J. L. BERNAL, MA. J. DEL NOZAL, L. DEBAN and A. J. ALLER. (21 September 1981)

Selective extraction of metal ions associated with humic acids: J. SLAVEK, J. WOLD and W. F. PICKERING. (22 September 1981)

Co-precipitation study and spectrophotometric determination of traces of iron, copper, zinc, aluminium and bismuth in lead- and tin-base solders and white-metal bearing alloys: ZHENPU WANG and K. L. CHENG. (14 September 1981)

Diagrams for complete representation of binary mononuclear complex systems: I. NAGYPÁL and M. T. BECK. (23 September 1981)

Hydrazine sulphide—a titrant in amperometric analysis: G. S. DESHMUKH and S. N. JOSHI. (24 September 1981)

Talanta, Vol. 28, p. I, 1981
Pergamon Press Ltd. Printed in Great Britain

PHARMACIA PRIZE

The Pharmacia Prize for the years 1979 and 1980, for the paper published in *Talanta* that was judged to be the best contributed from an industrial laboratory, has been awarded to J. E. KESSLER, S. M. VINCENT and J. E. RILEY, JR., Bell Laboratories, Murray Hill, New Jersey, U.S.A., for their paper "A Micro Co-precipitation Technique for Use in X-Ray Fluorescence Analysis" (*Talanta*, 1979, **26**, 21).

TAL. 28/11 A

However, in spite of the different stoichiometries possible, the procedure described earlier[7] is still adequate for determination of $CS_2N_3^-$ and CS_2 under well defined experimental conditions. The results obtained when the ratio $C_{MnO_4^-}/C_{CS_2N_3^-}$ is around 20 are reproducible within 0.8%. With the higher ratios ($C_{MnO_4^-}/C_{CS_2N_3^-} > 200$) the error is better than 2%.

We suggest that these reactions could be useful in the analytical determination of organic disulphides, the 1,2,3,4-thiatriazole ring system and mercaptans.

Acknowledgements—We are pleased to acknowledge financial support from FAPESP and CNPq, and to thank Dr. G. O. Chierice and Dr. M. Ferrante for helpful suggestions.

REFERENCES

1. K. A. Jensen and C. Pedersen, *Adv. Heterocyclic Chem.*, 1964, **3**, 263 and references therein.
2. K. Pilgram and F. Goren, *J. Heterocyclic Chem.*, 1971, **8**, 899.
3. A. Holm, K. Schaumburg, N. Dahlberg, C. Christophersen and J. P. Snyder, *J. Org. Chem.*, 1974, **40**, 431.
4. A. W. Browne and R. S. Hamburg, *J. Am. Chem. Soc.*, 1976, **48**, 2313.
5. M. L. Lappertand and H. Pyszora, *Adv. Inorg. Chem. Radiochem.*, 1966, **9**, 133.
6. E. A. Neves and D. W. Franco, *Talanta*, 1979, **26**, 81.
7. E. A. Neves, W. L. Polito, T. Tamura and D. W. Franco, *Anal. Lett.*, 1979, **12**, 741.
8. E. A. Neves, D. W. Franco and P. F. Romanelli, *Anal. Chim. Acta*, 1977, **92**, 393.
9. E. A. Neves and D. W. Franco, *J. Inorg. Nucl. Chem.*, 1974, **36**, 3851.
10. A. Berka, J. Vulterin and J. Zýka, *Newer Redox Titrants*, Pergamon Press, London, 1965.
11. F. Feigl, *Spot Tests in Inorganic Analysis*, 5th Ed., p. 326. Elsevier, Amsterdam, 1962.
12. I. M. Kolthoff and R. Belcher, *Volumetric Analysis*, Vol. III, Interscience, New York, 1957.

Talanta, Vol. 28, p. i, 1981
Pergamon Press Ltd. Printed in Great Britain

PAPERS RECEIVED

Colorimetric determination of *p*-aminophenol in the presence of paracetamol with 3-cyano-*N*-methoxypyridinium perchlorate: M. A. KORANY, D. HEBER and J. SCHNEKENBURGER. (6 July 1981)
Fluorimetric determination of aluminium: G. VASILIKIOTIS, A. VOULGAROPOULOS and C. APOSTOLOPOULOU. (8 July 1981)
Studies on metal–metal sulphide electrodes—Part I: Application of arsenic–arsenic sulphide, antimony–antimony sulphide and molybdenum–molybdenum sulphide electrodes in the determination of sulphide ion: PUSHPA SHARMA and MUKHTAR SINGH. (8 July 1981)
Analytical properties of 5,5′-methylenedisalicylhydroxamic acid (MEDSHA): L. F. CAPITAN-VALLVEY, F. SALINAS and D. GAZQUEZ. (8 July 1981)
Polarographic determination of Pd(II) by use of catalytic H-waves: G. MOHAMED RAFI and AGNES PAUL. (14 July 1981)
An internal-monitor method for determination of arsenic, antimony and copper in germanium by neutron-activation analysis: SHUENN-GANG CHEN and HUI-TUH TSAI. (14 July 1981)
Optical emission spectroscopy with a microwave-induced plasma in a sealed microtube: DAVID W. HOLMAN and THOMAS J. VICKERS. (17 February 1981)
***o*-Iodosobenzoate as an oxidimetric titrant:** KRISHNA K. VERMA and ANIL K. GUPTA. (17 July 1981)
Behaviour of membrane graphite electrodes in potentiometric titfations of reducing substances with bromine in acetic acid: T. J. PASTOR, M. M. PASTOR, Ž. SIMONIVIĆ and É. SZEPESVÁRY. (17 July 1981)
Fast pH calculations in aqueous solution chemistry: MARIE-NOËLLE PONS, JEAN-LOUIS GREFFE and JACQUES BORDET. (17 July 1981)
Trace metal analysis by anodic-stripping voltammetry: Effect of surface-active substances: PAUL SAGBERG and WALTER LUND. (20 July 1981)
Application of Xylenol Orange to the separation of metal ions on macroreticular anion-exchange resin Amberlyst A-26: KRYSTYNA BRAJTER and EWA OLBRYCH-ŚLESZYŃSKA. (23 July 1981)
A chelate-forming resin bearing mercapto and azo groups and its application to the recovery of mercury(II) ion: MORIO NAKAYAMA, MASAHIKO CHIKUMA, HISASHI TANAKA and TOMOO TANAKA. (23 July 1981)
Spectrophotometric studies of vanadium(V) chelates with *N*-hydroxy-*N*-phenyl-*N′*-*o*-chlorophenyl-*p*-toluamidine hydrochloride and salicylaldehyde: HEMLATA MOHABEY, PRAMOD KUMAR SHARMA and RAJENDRA KUMAR MISHRA. (23 July 1981)
Extractive spectrophotometric determination of molybdenum as a mixed thiocyanate–2-acetylpyridinethiosemicarbazone: H. SANKE GOWDA, K. N. THIMMAIAH and K. KRISHNA MURTHY. (23 July 1981)
Potentiometric and titrimetric determination of some reductants with bromamine-B: H. SANKE GOWDA and H. NOOR AHMED KHAN. (23 July 1981)
Separation and preconcentration of the trace amounts of several metals in magnesium metal and nitrate, with activated carbon as a collector: MASARU KIMURA and SADAKO EGAWA. (23 July 1981)
Microdetection of some mercaptans with sodium amminepentacyanoferrate(II) on ion-exchange resin grains: V. GRDINIĆ and M. JAKŠEVAC-MIKŠA. (23 July 1981)
Simple and inexpensive microcomputer controllable stepping motor and drive circuit: D. F. MARINO and J. D. INGLE, JR. (3 August 1981)
Extraction of palladium thiocyanate with polyurethane foam: SARGON J. AL-BAZI and ARTHUR CHOW. (3 August 1981)
Determination of neptunium by redox titration: A. G. GODBOLE and S. K. PATIL. (3 August 1981)
Analytical properties of 2,2′-bis(di-2-pyridinyl-methylene)thiocarbohydrazone: J. R. BONILLA ABASCAL, A. GARCIA DE TORRES and J. M. CANO PAVON. (3 August 1981)
The evaluation of NMR spectroscopy for the quantitative characterization of urea–formaldehyde resins: R. TAYLOR, R. J. PRAGNELL, J. V. MCLAREN and C. E. SNAPE. (3 August 1981)
The effect of heat in the determination of phosphorus by wet digestion: S. A. THOMAS and I. F. ANDENYANG. (4 August 1981)

Talanta, Vol. 28, p. I, 1981
Pergamon Press Ltd. Printed in Great Britain

LOUIS GORDON MEMORIAL AWARD



Presentation of the Louis Gordon Memorial Award for 1979 to Professor Hassan (right) by Professor Rechnitz

Talanta, Vol. 28, p. i, 1981
Pergamon Press Ltd. Printed in Great Britain

PAPERS RECEIVED

Colorimetric determination of cobalt and copper as ternary amine–thiocyanate complexes: F. VERNON, I. IKPOKU and S. B. SALAMA. (8 June 1981)
Alizarin-9-imine as indicator in acetonitrile and in pyridine: M. BLANCO and J. BARBOSA. (8 June 1981)
Screening analysis for lead in whole blood and urine by the Delves cup method: New strategy for sample organization: E. GONZALEZ-FERNANDEZ and M. P. GONZALEZ MORENO. (8 June 1981)
Selective extractive separation of zinc, cadmium and lead from iodide media with mesityl oxide: T. PRASADA RAO and T. A. RAMAKRISHNA. (8 June 1981)
Spectrophotometric determination of ruthenium by ternary complex formation: S. JAYA and T. V. RAMAKRISHNA. (8 June 1981)
Zur Anwendung der Hochdruck-Flüssigkeits-Chromatographie in der anorganischen Analytik—VI: Reversed-phase-Chromatographie von PAN-Chelaten: G. SCHWEDT and R. BUDDE. (9 June 1981)
An internal-standard method for the determination of hafnium in zirconium oxide and zircaloy by neutron-activation analysis: TONG-CHUIN PUNG. (9 June 1981)
Determination of Ag, Cd, Pb, Zn and Pd in sea-water by thermal-ionization isotope-dilution mass spectrometry: K. J. R. ROSMAN, J. R. DE LAETER and A. CHEGWIDDEN. (10 June 1981)
Spectrophotometric determination of copper separated by means of solvent extraction with di-n-hexyl sulphide: YASUMASA SHIGETOMI and TAKASHI TAMASHIGE. (10 June 1981)
Fluorometric determination of hydrazine and ammonia separately or in mixtures: NEIL D. DANIELSON and CHRISTINE M. CONROY. (16 June 1981)
Use of 4-sulpho-2-aminobenzenethiol as analytical reagent for vanadium: ANIL K. CHAKRABARTI. (16 June 1981)
Automated square-wave anodic-stripping voltammetry with a flow-through cell and matrix exchange: E. B. BUCHANAN, JR. and D. D. SOLETA. (16 June 1981)
Nature of amine extraction from H_2SO_4-haloacid mixture: Studies on Fe(III): A. HAGGAG, W. SANAD and N. TADROS. (17 June 1981)
Determination of arsenite, arsenate and monomethylarsonic acid in aqueous samples by gas chromatography of their 2,3-mercaptopropanol complexes: SYOZO FUKUI, TERUHISA HIRAYAMA, MOTOSHI NOHARA and YOSHIHIKO SAKAGAMI. (19 June 1981)
Instruments in Analysis—Critical Reviews: Diffuse reflectance spectroscopy in the infrared: HANS MAULHARDT and DIETMAR KUNATH. (5 June 1981)
A new reagent for the determination of copper(II): 2-(α-pyridyl)-thioquinaldinamide: ANIL K. CHAKRABARTI. (23 June 1981)
The solvent extraction of Cu(II), Ni(II) and Co(II) with benzyl mono(2-quinolyl)hydrazone: SELMAN A. BERGER. (23 June 1981)
Fluorimetric reaction-rate methods of inorganic analysis—A review: M. VALCARCEL and F. GRASES. (24 June 1918)
Anion-exchange initiation of new reactions: Detection and spectrophotometric determination of aliphatic amines with 2,4-dinitrophenylhydrazine: MOHSIN QURESHI, S. ASHFAQ NABI, I. A. KHAN and PUSHKIN M. QURESHI. (25 June 1981)
Drying conditions for potassium dichromate: TAKAYOSHI YOSHIMORI and KENJI KAMIJOH. (26 June 1981)
Concentration of trace metals from sea-water by complexation with 8-hydroxyquinoline and adsorption on C_{18}-bonded silica gel: R. E. STURGEON, S. S. BERMAN and S. N. WILLIE. (29 June 1981)
Complexes of copper(II) with diaminoglyoxime, stoichiometry and formation constants: J. LOSADA and S. VICENTE-PEREZ. (29 June 1981)
Determination of thallium content, at sub-trace level, in rocks and minerals by coupling differential pulse anodic-stripping voltammetry with suitable enrichment methods: GILBERTO CALDERONI and TOMMASO FERRI. (30 June 1981)
Determination of cobalt by pyrogallol chemiluminescence: ROBERT J. MILLER and J. D. INGLE, JR. (30 June 1981)
Chemical-ionization mass spectrometry for several nitrosamines: YIN FANG, DING JIAHUA and LIU SHILI. (30 June 1981)
The use of glass electrodes for the determination of formation constants—Part I: A definitive method for calibration: PETER M. MAY, DAVID R. WILLIAMS, PETER W. LINDER and RALPH G. TORRINGTON. (2 July 1981)
Ultraviolet spectrophotometric determination of methyl pentynol carbamate as its mercuric acetate complex: M. RIZK, M. I. WALASH and A. EL-BRASHY. (3 July 1981)

Talanta, Vol. 28, p. i, 1981
Pergamon Press Ltd. Printed in Great Britain

PAPERS RECEIVED

Evaluation of sulphuric acid treatment as clean-up step for the estimation of BHC and DDT in fatty and non-fatty foods: PARM PAL SINGH and RAM PARKASH CHAWLA. (5 May 1981)
Photochemical analysis studies—III. A fluorimetric and ultraviolet spectrophotometric study of the photolysis of chloroquine on silica gel thin-layers and its analytical application: JEAN-JACQUES AARON and JOËLLE FIDANZA. (5 May 1981)
Spectrophotometric determination of osmium with 1,5-diphenylcarbazide: S. JAYA and T. V. RAMAKRISHNA. (5 May 1981)
Titrimetric microdetermination of some aldoses by amplification reactions: D. AMIN and K. Y. SALEEM. (6 May 1981)
Evaluation of differential-pulse anodic-stripping voltammetry at a stationary mercury film electrode with stirred solution: JOSEPH WANG. (6 May 1981)
Analytical properties of 2-acetyl pyridine thiosemicarbazone: SUREKHA DEVI. (6 May 1981)
Tetramethylthiuram monosulphide as an analytical reagent for palladium and osmium: S. Q. R. ILYAS and A. P. JOSHI. (6 May 1981)
Spectrophotometric determination of methylphenobarbitone by using orthogonal polynomials: ABDEL-AZIZ M. WAHBI, SAIED BELAL, HASSAN ABDINE and MONO BEDAIR. (6 May 1981)
The cation chelation mechanism of metal-ion sorption by polyurethanes: R. F. HAMON, A. S. KHAN and A. CHOW. (7 May 1981)
Adsorption of the silver ion on soda glass—I: R. W. HAYES, M. W. WHARMBY, R. W. C. BROADBANK and K. W. MORCOM. (11 May 1981)
Analytical properties of 5-(2-thiophen)methylene-2-thiobarbituric acid: M. GUZMAN CHOZAS and F. J. BAUTISTA PALOMA. (11 May 1981)
Spectrophotometric determination of silver with 2-(3,6-dibromo-2-pyridylazo)-5-diethylaminophenol in the presence of anionic surfactant: SHUI-CHIEH HUNG, CHANG-LING QU and SHUI-SHENG WU. (11 May 1981)
TITFIT, a comprehensive basic program for numerical treatment of potentiometric data, using analytical derivatives and automatically optimized subroutines with the Newton–Gauss–Marquardt algorithm: ANDREAS A. D. ZUBERBÜHLER and THOMAS A. KADEN. (12 May 1981)
Flow-injection analysis of aromatic sulphonyl haloamines: D. J. LEGGETT, N. H. CHEN and D. S. MAHADEVAPPA. (12 May 1981)
Interactions between Ag(I) and insoluble cobalticyanides of bivalent cations: ALESSANDRO DE ROBERTIS, ATHOS BELLOMO and DOMENICO DE MARCO. (12 May 1981)
A comparative study of the application of the method of least-squares in the potentiometric determination of protonation constants: M. CELIA GARCIA, G. RAMIS and C. MONGAY. (13 May 1981)
Spectrophotometric determination of aluminium by using chlorophosphonazo I: ZHU YINGQUAN, ZHANG LIN AND LI JUNYI. (14 May 1981)
Ultraviolet spectrophotometric determination of iron(III) with methylethylenediaminetetra-acetic acid (MEDTA): J. M. FERNANDEZ SOLIS, A. ALVAREZ DEVESA and F. BERMEJO MARTINEZ. (15 May 1981)
Preparation and analytical properties of a chelating resin containing the phenylalanine group: ATSUSHI SUGII, NAOTAKE OGAWA, IWAO KATAYAMA and TOSHIHIDE HIDA. (21 May 1981)
Analytical study of mono- and dihydroxymethylthiourea. Spectrophotometric determination of osmium: E. CASASSAS, G. RAURET and R. RUBIO. (25 May 1981)
The accurate determination of bismuth in lead concentrates and other non-ferrous materials by AAS after separation and preconcentration of the bismuth with mercaptoacetic acid: D. J. HOWELL and B. R. DOHNT. (25 May 1981)
PMR assay of natural products in pharmaceuticals—VI. Theophylline and aminophylline in pharmaceutical formulations: M. M. A. HASSAN, I. A. EL-MESHAL, T. I. KHALIFA and E. A. ABOUTABL. (25 May 1981)
Determination of thiosemicarbazones by reaction with ω-bromoacetophenone: JYOTI TALEGAONKAR, SUMAN MUKHIJA and K. S. BOPARAI. (26 May 1981)
Haematoxylin and haematein as photometric reagents for metals: JOSE VALERO (26 MAY 1981)
Application of personal microcomputers in the analytical laboratory—I. Potentiometric analysis: SAM BEN-YAAKOV, R. RAVIV, H. GUTERMAN, A. DAYAN and BOAZ LAZAR. (27 May 1981)
Hydroxide complexes of lanthanides—IV. Ytterbium(III) in perchlorate medium: J. KRAGTEN and L. G. DECNOP-WEEVER. (27 May 1981)
Représentation des équilibres d'échange d'ions pour les complexes fer–fluorures: F. AULAS, A. P. LAMAZE, D. REIGNIER, M. RUMEAU and B. TYBURCE. (1 June 1981)
Kinetic fluorimetric determination of nanogram amounts of manganese, based on its catalytic effect on the oxidation of 2-hydroxybenzaldehyde thiosemicarbazone by hydrogen peroxide: A. MORENO, M. SILVA, D. PEREZ-BENDITO and M. VALCARCEL. (2 June 1981)
Iron(III) as activator for the catalytic–fluorimetric microdetermination of V(V): A. NAVAS, M. SANTIAGO, F. GRASES, J. J. LASERNA and F. GARCIA SANCHEZ. (2 June 1981)
Solvent extraction separation of tungsten as α-benzoin oximate from sulphide ores: V. S. SASTRI. (2 June 1981)
Ion-exchanger colorimetry—VIII: Microdetermination of copper in natural waters: KAZUHISA YOSHIMURA, SATORU NIGO and TOSHIKAZU TARUTANI. (2 June 1981)
Development of an apparatus with high resolution for inductively-coupled argon-plasma emission derivative spectrometry and its application to the determination of hafnium in high-purity zirconium oxides: HAJIME ISHII and KATSUHIKO SATOH. (5 June 1981)
The speciation of trace elements in waters: T. M. FLORENCE. (5 June 1981)

Talanta, Vol. 28, p. I, 1981
Pergamon Press Ltd. Printed in Great Britain

TALANTA MEDAL

PROFESSOR JAROSLAV RŮŽIČKA

The Publisher and Editorial Board of *Talanta* take pleasure in announcing that, with the approval of the Advisory Board, the Ninth Award of the Talanta Medal has been made to **Professor Jaroslav Růžička** of the Department of Chemistry, Technical University of Denmark.

Jaromir Růžička was born and educated in Prague. He graduated from Charles University with an M.Sc. for his work on polarography in acetic acid (non-aqueous) medium, and was awarded a prize by Professor Heyrovský.

Further research at the Technical University of Prague resulted in a Ph.D. for a thesis on substoichiometry in isotope dilution and activation analysis. Together with J. Starý he received a Czech State Prize in Science for this work, which was the first of his major pieces of original research. Like those to follow, it had the characteristics of being simple, practical and based on original clear thinking. His papers on the topic are clear, and its strengths and limitations are made evident.

In 1971, after various experiments in which he sought to extend into electrochemistry the solvent extraction principles developed for substoichiometry, he developed the "Selectrode", which greatly extended the range and ease of application of ion-selective electrodes.

In 1975 he published his first paper on flow-injection analysis, the automatic analysis technique in which the sample is injected into a continuously flowing stream of reagent, providing an exceptionally high sampling rate, and thus of great use in clinical analysis *etc.* This work stemmed from his earlier work on the automation of the substoichiometric technique, in 1965–66. He has since greatly developed and extended the technique, and assisted in its commercial exploitation.

These three major developments have been made without the benefit of a large research institution: he has either worked on his own or with just a few colleagues. His lectures and enthusiasm for analytical chemistry have enhanced the standing of the subject, and this has been recognized by the establishment of a Chair of Analytical Chemistry at the Technical University of Denmark, to which he has been appointed.

LOUIS GORDON MEMORIAL AWARD

The Publisher and Editorial Board of *Talanta* have pleasure in announcing that the Louis Gordon Memorial Award for the paper judged to be the best written of those published in *Talanta* in 1980 is made to **Richard Markuszewski** and **Harvey Diehl,** for their paper "The infrared spectra and structures of the three solid forms of fluorescein and related compounds" (*Talanta*, 1980, **27**, 937).

Talanta, Vol. 28, p. I, 1981
Pergamon Press Ltd. Printed in Great Britain

TALANTA MEDAL

PROFESSOR JAROSLAV RŮŽIČKA

The Publisher and Editorial Board of *Talanta* take pleasure in announcing that, with the approval of the Advisory Board, the Ninth Award of the Talanta Medal has been made to **Professor Jaroslav Růžička** of the Department of Chemistry, Technical University of Denmark.

Jaromir Růžička was born and educated in Prague. He graduated from Charles University with an M.Sc. for his work on polarography in acetic acid (non-aqueous) medium, and was awarded a prize by Professor Heyrovský.

Further research at the Technical University of Prague resulted in a Ph.D. for a thesis on substoichiometry in isotope dilution and activation analysis. Together with J. Starý he received a Czech State Prize in Science for this work, which was the first of his major pieces of original research. Like those to follow, it had the characteristics of being simple, practical and based on original clear thinking. His papers on the topic are clear, and its strengths and limitations are made evident.

In 1971, after various experiments in which he sought to extend into electrochemistry the solvent extraction principles developed for substoichiometry, he developed the "Selectrode", which greatly extended the range and ease of application of ion-selective electrodes.

In 1975 he published his first paper on flow-injection analysis, the automatic analysis technique in which the sample is injected into a continuously flowing stream of reagent, providing an exceptionally high sampling rate, and thus of great use in clinical analysis *etc.* This work stemmed from his earlier work on the automation of the substoichiometric technique, in 1965–66. He has since greatly developed and extended the technique, and assisted in its commercial exploitation.

These three major developments have been made without the benefit of a large research institution: he has either worked on his own or with just a few colleagues. His lectures and enthusiasm for analytical chemistry have enhanced the standing of the subject, and this has been recognized by the establishment of a Chair of Analytical Chemistry at the Technical University of Denmark, to which he has been appointed.

LOUIS GORDON MEMORIAL AWARD

The Publisher and Editorial Board of *Talanta* have pleasure in announcing that the Louis Gordon Memorial Award for the paper judged to be the best written of those published in *Talanta* in 1980 is made to **Richard Markuszewski** and **Harvey Diehl,** for their paper "The infrared spectra and structures of the three solid forms of fluorescein and related compounds" (*Talanta*, 1980, **27**, 937).

Talanta. Vol. 28. p. i. 1981
Pergamon Press Ltd. Printed in Great Britain

PAPERS RECEIVED

Spectrophotometric determination of 2-amino-3H-phenoxazin-3-one as a colouring matter in *o*-aminophenol: N. R. AYYANGAR, S. R. BHIDE and K. V. SRINIVASAN. (7 April 1981)
Determination of total arsenic with a zinc column arsine generator: W. A. MAHER. (7 April 1981)
Performance characteristics of glassy carbon and mercury film electrodes for reductive LCEC: KARL BRATIN and PETER T. KISSINGER. (1 April 1981)
Electrochemical study of the copper–sulphite system: CHEN-FENG KAO and TSAI-TEH LAI. (9 April 1981)
Faisabilité d'un système d'absorption atomique utilisant un laser à colorant: A. P. GAMOT, G. VERGOTEN and G. FLEURY. (9 April 1981)
Radiotracer studies on ion-selective electrode membranes containing metal complexes of a nonylphenoxypoly(ethyleneoxy)ethanol in poly(vinyl chloride)matrices: B. DOYLE, G. J. MOODY and J. D. R. THOMAS (13 April 1981)
Flameless atomic-absorption studies of copper, cadmium, magnesium and beryllium, with a wire-loop atomizer: J. V. CHAUVIN, D. G. DAVIS and L. G. HARGIS. (10 March 1981)
A study of the stability of alkaline earth complexes with fluoride and chloride ions at various temperatures, by potentiometry with ion-selective electrodes: VLADIMÍR MAJER and KAREL ŠTULÍK. (13 April 1981)
Ionization constants and fluorescence excitation and emission spectra of the isomeric benzo[*a*]pyrene phenols: A. C. CAPOMACCHIA, V. KUMAR and C. BRAZZEL. (30 March 1981)
Spectrophotometric determination of iron and reducing agents with PPTS, a new water-soluble ferroin-type chromogen of superior sensitivity: ALFRED A. SCHILT and MICHAEL R. DI TUSA. (30 March 1981)
4,4′-Diaminotriphenylmethyl cation as a reagent and cyclohexanone as an absorbent for sulphur dioxide determination: JACK L. LAMBERT, MICHAEL J. CHEJLAVA, MOHAMMED H. BEYAD and JOSEPH V. PAUKSTELIS. (30 March 1981)
Spectrophotometric determination of yttrium and cerium subgroup rare earths with a new, sensitive reagent: Chlorophosphonazo-*p*-NO_2: JIAO-MAI PAN, CHUNG-GIN HSU, CHAO-SHENG HU and XI-PING JIA. (16 April 1981)
***N*-Phenyl-*N*′-acetylthiourea: A specific reagent in the photometric determination of ruthenium:** S. C. SHOME and P. K. HALDAR. (16 April 1981)
Determination of some dithiocarbamates by catalytic thermometric titration: NOBUTOSHI KIBA, YASUO SAWADA and MOTOHISA FURUSAWA. (16 April 1981)
Atomic-absorption determination of beryllium previously extracted into MIBK from NH_4SCN medium with trioctylamine: J. AZNAREZ, J. R. CASTILLO, M. A. BELARRA and M. DOMINGUEZ. (21 April 1981)
Polarographic study of As(III)–tri(propan-2-ol)amine reaction: MAMDOUH S. MASOUD and MOHYI EL-DIN M. EL-ESSAWI. (21 April 1981)
Flow-injection analysis: A review of its early history: KENT K. STEWART. (22 April 1981)
Effect of washing on the time stability of extracts: Copper(II)/APCD/IBMK system in strongly acidic media: TAKEO TAKADA. (22 April 1981)
Determination of the fatty acid composition of soybean oil by high-performance liquid chromatography: BRUNO JASELSKIS, NICHOLAS L. STEMM and WILLIAM D. JOHNSTON. (30 March 1981)
Interpretation of analytical chemical information by pattern recognition methods: A survey: LARS KRYGER. (23 April 1981)
Electrothermal atomic-absorption determination of vanadium: MAHMOOD M. BARBOOTI and FADHIL JASIM. (24 April 1981)
Determination of strontium in aluminium alloys by atomic-absorption and flame-emission spectrophotometry: A. JAVIER ALLER FERNANDEZ. (24 April 1981)
Titrimetric determination of chloramine-T by amplification reactions: D. AMIN and W. A. BASHIR. (27 April 1981)
Spectrophotometric determination of triamcinolone acetonide: S. M. KHANNA and S. K. BANERJEE. (27 April 1981)
The total emulation of the Intel 8080 instruction set on a mainframe computer: D. J. LEGGETT. (27 April 1981)
Spectrophotometric determination of some metal ions with metol and hydrogen peroxide: C. S. PRAKASA SASTRY, K. V. S. S. MURTY and B. S. REDDY. (29 April 1981)

Talanta, Vol. 28, p. I, 1981
Pergamon Press Ltd. Printed in Great Britain

EDITORIAL

From time to time editorials are written on the subject of preparation of manuscripts submitted for publication, and on the time that elapses between receipt of a paper and its eventual publication. Very often a great deal of delay can be caused by poor preparation of the original manuscript, especially with regard to the drawing of figures and the typing of references. If figures are badly drawn or the lettering on them is untidy, it is necessary to have them redrawn and relettered, and this not only takes time in the drawing office, but may also lead to error if the draughtsman concerned is unable to decipher or interpret the original correctly. With a set of good quality stencils, a drawing board and a T-square, or alternatively a good typewriter with a carbon film ribbon, lettering should be no problem. Likewise a set of French curves or a flexible ruler should enable the author to produce acceptably smooth curved lines on graphs, *etc.* The size of letters and thickness of line to use will depend on the size of the drawing and the degree of reduction to be used. Measurement of the lettering on a published figure of good quality, in relation to the scale of the figure, should give a good idea of the letter size to use, and the thickness of the stencilled letter will indicate the line thickness needed for the drawing itself.

There is no excuse whatever for carelessness in listing references, since no skill is needed to copy character by character from the original. A conscientious editor may check not only the "suspicious" references, but the whole lot, and this can take a great deal of time, especially in the case of a review paper, and if some of the references are found to be non-existent or to have nothing whatever to do with the paper, the editor will either try to find the correct references to save delay in producing the paper, or be obliged to write to ask the author to do the job. In either case his faith in the scientific work in the paper is bound to be somewhat reduced, and he can scarcely be blamed if he feels annoyed at having to waste time that could be more rewardingly employed. The editor's duty is to protect the reader from false information, and at the same time to protect the author from having his carelessness made public for all to see, but he is entitled to expect authors not to give him occasion to perform this duty. He is also entitled to expect authors to prepare their references in the style used by *his* journal and not that of another journal. It is in the author's own interests to do this anyway, since a referee may well suspect that a paper has been already rejected by the journal that uses the reference style employed by the author! It is also important that references should be checked against the original journal whenever possible—the abstracting journals are not always correct in the details given. Furthermore, the abstracting journals (with the honourable exception of *Zeitschrift für Analytische Chemie*) omit any accents on authors' names, which is discourteous as well as inaccurate.

We therefore urge all authors, whether contributing to this or another journal, to act in their own best interests by taking proper care in preparing their manuscript. The editor will deal with any linguistic problems, and some editors will do their best to make sure the chemistry is correct as well, but responsibility for the figures and references lies primarily with the author(s).

Talanta, Vol. 28. p. i. 1981
Pergamon Press Ltd. Printed in Great Britain

PAPERS RECEIVED

Determination of scandium by precipitation of its cinnamate from homogeneous solution: L. A. AL-KHIAT, S. A. RAHIM and ALAN TOWNSHEND. (9 March 1981)

Determination of trace copper, manganese and silver in a micro amount of steel by atomic-absorption spectrometry using direct atomization of solid sample in a graphite-cup cuvette: KICHINOSUKE HIROKAWA and KUNIO TAKADA. (9 March 1981)

Bacterial electrode for L-arginine: S. R. GROBLER, N. BASSON and C. W. VAN WYK. (10 March 1981)

New method for the determination of uranium(IV), uranium(VI) and total uranium in solutions obtained during leaching of phosphate ores by hydrochloric acid: L. A. GUIRGUIS and MARGUERITE A. WASSEF. (10 March 1981)

The possibility and accuracy of pH-metric equilibrium studies at very high ligand to metal concentration ratio: I. FÁBIÁN and I. NAGYPÁL. (11 March 1981)

Sorption of uranium and thorium on hydrous tin oxide—I: Aqueous HNO_3 medium: N. Z. MISAK and I. M. EL-NAGGAR. (13 March 1981)

Sorption of uranium and thorium on hydrous tin oxide—II: HNO_3–mixed solvent media: N. Z. MISAK, H. N. SALAMA and I. M. EL-NAGGAR. (13 March 1981)

Thermodynamic proton dissociation constants of anilic acids: C. L. SHARMA and R. S. ARYA. (16 March 1981)

Investigation of a novel solid-phase chemiluminescent analytical system, incorporating photographic detection, for the measurement of glucose: T. J. N. CARTER, T. P. WHITEHEAD and L. J. KRICKA. (16 March 1981)

Degradation of aromatic compounds in ground-water and methods of sample preservation: I. OGAWA, G. A. JUNK and H. J. SVEC. (4 March 1981)

Desk-computer program for evaluation of complex equilibria from spectrophotometric data: F. GAIZER and A. PUSKÁS. (17 March 1981)

Le *Z*-α,β-dinitrostilbène: Un nouveau réactif pour le dosage colorimétrique des amines primaires et secondaires, des amino-acides et des thiols: P. DUBOIS, P. LEVILLAIN and C. VIEL. (3 October 1980)

Benzyl 2-pyridyl ketone 2-pyridylhydrazone as reagent for the fluorimetric determination of zinc at ng/ml levels: F. GARCIA-SANCHEZ, A. NAVAS and J. J. LASERNA. (17 March 1981)

Spectrophotometric determination of micro amounts of sodium alkylbenzene sulphonate with 1-(4-*N*-methylpyridinium-azo)4-(4-*N*,*N*-diethylaminophenylazo)naphthalene iodide: KEIRO HIGUCHI, YASUAKI SHIMOISHI, HARUO MIYATA and KYOJI TÔEI. (18 March 1981)

Quantitative study of the reaction between quinones and iron(II) in strong phosphoric acid medium: N. KRISHNA MURTY and PERI M. DAKSHINA MURTY. (18 March 1981)

Spectrophotometric determination of cobalt in steel after its separation from other metal ions by ion-exchange chromatography: ABDUL MAJEED and E. K. BALLANTYNE. (19 March 1981)

Spectrophotometric determination of boron in iron and steel with curcumin after separation by 2-ethyl-1,3-hexanediol–chloroform extraction: ELSIE M. DONALDSON. (23 March 1981)

Analysis of drugs by microcalorimetry: Isothermal power-conduction calorimetry and thermometric titrimetry: B. Z. CHOWDHRY, A. E. BEEZER and E. J. GREENHOW. (23 March 1981)

A potentiometric study of the stability of isothiocyanic acid: E. A. NEVES, L. ANGNES, G. O. CHIERICE and L. H. MAZO. (23 March 1981)

The cupric ion selective electrode?: HANS STÜNZI. (23 March 1981)

Redox titrations using chlorobromamine-T as a new oxidant in non-aqueous media: K. D. MAHILAMONY and P. INDRASENAN. (23 March 1981)

Voltammetric determination of diffusion coefficients of organic compounds in non-aqueous medium with the tubular graphite electrode: L. R. SHARMA, A. K. MANCHANDA, G. SINGH and RANJIT S. VERMA. (25 March 1981)

Titrimetric microdetermination of chloral hydrate by amplification reactions: D. AMIN and M. S. AL-AJELY. (31 March 1981)

Solute–solvent interaction: A basis for mechanistic interpretation of the behaviour of ferroin indicator in redox titrations of antimony(III): K. SRIRAMAM, B. S. R. SARMA, N. RAMABRAHMA SASTRY and A. R. K. VARA PRASAD. (31 March 1981)

Analytical applications of photochemical reduction of Azur B by EDTA: Iodide determination: T. PEREZ-RUIZ, C. MARTINEZ-LOZANO and J. OCHOTORENA. (31 March 1981)

Spectrophotometric determination of trace amounts of iron(III) in fluoride by extraction of the mixed-ligand complex iron–fluoride–purpurin: M. ROMAN CEBA, A. ARREBOLA RAMIREZ and J. J. BERZAS NEVADO. (1 April 1981)

Microscopic processes of dissociation of some tyrosine derivatives: TAMÁS KISS and BÉLA TÓTH. (1 April 1981)

A method of determination of molybdenum by extraction of its thiocyanate into ethyl methyl ketone: USHA MADAN and L. R. KAKKAR. (1 April 1981)

Spectrophotometric determination of trace amounts of selenium with 4,5,6-triaminopyrimidine: MARIO E. BODINI and OMAR ALZAMORA E. (1 April 1981)

Silanization of stainless-steel frits for use in trace metal analysis by high-performance liquid chromatography: YOUNG-TZUNG SHIH and PETER W. CARR. (3 April 1981)

Talanta, Vol. 28, p. I, 1981
Printed in Great Britain

Pergamon Press Ltd

TALANTA ADVISORY BOARD



DR. J. D. INGLE, JR. was born in 1946 in Chicago, Illinois, U.S.A., and obtained a B.S. (high honours and departmental distinction) in chemistry at the University of Illinois, Urbana in 1968 and a Ph.D. in analytical chemistry at Michigan State University in 1971. During his tenure at Michigan State University, he was awarded an NSF traineeship, an NSF fellowship, and an American Chemical Society Analytical Division Fellowship. Since 1972, he has been an analytical chemistry faculty member at Oregon State University and is presently an associate professor. He is a member of Phi Kappa Phi, the American Chemical Society, and the Society for Applied Spectroscopy. His main areas of research are atomic and molecular spectrochemical trace analysis, kinetics and mechanisms of analytical reactions, environmental and clinical chemistry, chemical speciation techniques, flow-injection analysis, automation with microcomputers, development of specific detectors for HPLC, fluorescence and chemiluminescence techniques, multichannel detectors, signal-to-noise ratio theory, and multiple component analysis. In these areas, he has published a book chapter and over 50 articles and has presented over 40 papers at conferences or other universities. He is at present co-authoring a graduate textbook on analytical optical spectroscopy.

Talanta, Vol. 28, p. i, 1981
Printed in Great Britain

Pergamon Press Ltd

PAPERS RECEIVED

The application of an argon/nitrogen inductively-coupled plasma to the analysis of organic solutions: J. A. C. BROEKAERT, F. LEIS and K. LAQUA. (13 January 1981)
Titrimetric determination of uranium(IV) in sulphuric and phosphoric acid media with potassium dichromate, with ferroin as indicator: U. MURALI KRISHNA and G. GOPALA RAO. (13 January 1981)
Extractive photometric determination of palladium and platinum with *o*-mercaptoacetoacetanilide: ARABINDA K. DAS and JYOTIRMOY DAS. (14 January 1981)
Studies on the use of acetothioacetanilide as a gravimetric reagent for palladium, platinum and rhodium: TARASANKAR PAL and JYOTIRMOY DAS. (14 January 1981)
Determination of manganese(II) by a chemiluminescent reaction: J. L. BURGUERA and ALAN TOWNSHEND. (19 January 1981)
Potassium-selective electrode with solid internal contact: M. TROJANOWICZ, Z. AUGUSTOWSKA, W. MATUSZEWSKI, G. MORACZEWSKA and A. HULANICKI. (20 January 1981)
Studies of chelating resins—I: General equation for the calculation of the protonation constants of chelating resins: Ö. SZABADKA. (21 January 1981)
Studies of chelating resins—II: Determination of the protonation constants of a chelating resin containing iminodiacetic acid active groups: Ö. SZABADKA. (21 January 1981)
Determination of W-mercaptobenzothiazole, tolyltriazole and benzotriazole in coolant formulations by liquid chromatography: THOMAS M. SCHMITT and EAD S. MUZHER. (22 January 1981)
Some aspects of room-temperature phosphorescence in liquid solutions: J. J. DONKERBROEK, J. J. ELZAS, C. GOOIJER, R. W. FREI and N. H. VELTHORST. (22 January 1981)
Determination of ruthenium and tin on electrochemical anodes by energy dispersive X-ray fluorescence: W. R. BRAMSTEDT, K. L. HARDEE, B. R. JOHNSON and D. E. HARRINGTON. (5 January 1981)
Anodic polarography of flucloxacillin: J. A. SQUELLA, M. M. SILVA and LUTS J. NUÑEZ-VERGARA. (23 January 1981)
The synthesis and reagent properties of magnesium tetrakis (4-tert.butylphenyl)borate: G. E. PACEY and C. E. MOORE. (26 January 1981)
Equilibria and complex formation of nickel(II) halides: MAMDOUH S. MASOUD and N. E. KHALIL. (27 January 1981)
Determination of scandium by precipitation with sebacic acid: WANDA BRZYSKA and RENATA KURPIEL. (27 January 1981)
Investigation and analytical application of the sulphide–hypobromite chemiluminescence reaction: J. TECKENTRUP and D. KLOCKOW. (30 January 1981)
Identification et dosage des sels biliaires et de leurs dérivés conjugués en chromatographie liquide: A. BAILLET-GUFFROY, D. BAYLOCQ, P. RAFIDISON and F. PELLERIN. (27 January 1981)
La titrimétrie thermométrique: Méthode linéaire de dosage—Etude des écarts à la linéarité—I: Courbures dues à la variation de capacité calorifique et aux fuites thermiques: A. M. BERNARD and J. L. BURGOT. (15 September 1981)
La titrimétire thermométrique: Méthode linéaire de dosage—Etude des écarts à la linéarité—II: Courbures des thermogrammes et erreur sur l'appréciation du point équivalent lorsque la réaction de dosage est équilibrée: A. M. BERNARD and J. L. BURGOT. (15 September 1981)

Talanta, Vol. 28, p. i
Pergamon Press Ltd 1981. Printed in Great Britain

PAPERS RECEIVED

Use of added random noise to improve bit-resolution in digital signal averaging: R. M. BELCHAMBER and GARY HORLICK. (5 December 1980)
Data-logging system based on the Intel 8748 single-chip microprocessor: R. M. BELCHAMBER and GARY HORLICK. (5 December 1980)
Determination of the extraction constant of mixed-ligand complexes: T. ROMAN GALAN, A. ARREBOLA RAMIREZ and M. ROMAN CEBA. (8 December 1980)
Determination of aluminium in iron, steel and ferrous and non-ferrous alloys by atomic-absorption spectrophotometry after a mercury cathode separation and extraction of the aluminium acetylacetone complex: ELSIE M. DONALDSON. (10 December 1980)
Direct potentiometric determination of bismuth(III) with a coated-wire electrode: P. W. ALEXANDER and JOSE P. JOSEPH. (10 December 1980)
Spectrophotometric determination of molybdenum(VI) as molybdenum blue: G. SOMIDEVAMMA, V. HANUMANTHA RAO and N. V. S. RAJU. (11 December 1980)
Simultaneous extractive photometric determination of cobalt, nickel and copper: C. K. BHASKARE and R. G. PAWASHE. (12 December 1980)
The liquid–liquid extraction of nickel(II) and cobalt(II) with chlorendic acid: SELMAN A. BERGER. (15 December 1980)
On the anodic stripping voltammetric analysis of zinc in waters from Guanabara Bay, Brazil: SERGIO DE JESUS ALEVATO and ANGELA DE LUCA REBELLO. (15 December 1980)
Determination of iron in soils and ores with 2,6-dihydroxymethyl-4-chlorophenol: CHEN ZITAO, TIAN LIQING and WU GUOQIANG. (19 November 1980)
The extractive spectrophotometric determination of molybdenum as a thiocyanato mixed complex with pyridylbenzamide: K. S. PATEL and R. K. MISHRA. (16 December 1980)
Indirect spectrophotometric determination of sulphide by applying the ternary complex system Ag(I)–phen–BPR: WEI FU-SHENG, ZHU YU-REI, YIN FANG and SHEN NAI-KUI. (1 December 1980)
The determination of selenium by atomic-absorption spectrophotometry—A review: M. VERLINDEN, H. DEELSTRA and E. ADRIAENSSENS. (22 December 1980)
Determination of copper in archaeological and corrosion samples by using an ion-selective electrode: ASHA VARMA. (17 November 1980)
Preparation and properties of a new chelating resin containing the *o*-hydroxyaldoxime group: S. BHATTACHARYYA and H. R. DAS. (31 December 1980)
The use of glass beads in the separation and purification of ruthenium complexes having large organic ligands: NITA A. LEWIS. (31 December 1980)
The X-ray fluorescence determination of cobalt on polyurethane foam: A. CHOW, G. T. YAMASHITA and R. F. HAMON. (31 December 1980)
Determination of isoniazid in drugs: KRISHNA K. VERMA and ANIL K. GUPTA. (31 December 1981)
Spectrophotometric determination of molybdenum with isonicotinic acid in presence of resacetophenone oxime: K. P. REDDY and S. BRAHMAJI RAO. (31 December 1980)
Ion-exchange in mixed solvents: Adsorption behaviour of metal ions on a strong base anion-exchange resin in aqueous ammonium thiocyanate–organic solvent: JAVED AKHTER, UMA SRIVASTAVA, HARI HAR MISRA, ANIMESH K. GHOSE and ARUN K. DEY. (31 December 1980)
Barium oxalate as a solid selective reagent for the absorption of sulphur trioxide: R. BELCHER and S. J. MORRIS. (7 January 1981)
Gas chromatographic separation of dichloroaniline isomers on new liquid phases: AOI ONO. (7 January 1981)
Studies on the colour reactions of multicomponent complexes—V: Rare earth–chromazurol-S–2,2′-bipyridyl–tetradecylpyridinium chloride system: CI YUN-XIANG and YANG MING-MIN. (7 January 1981)
Preparation and properties of a new chelating resin containing 2-nitroso-1-naphthol: J. P. GHOSH, J. PRAMANICK and H. R. DAS. (8 January 1981)
Dosage par spectrographie d'émission, de traces d'oxygène à l'aide d'une source à impulsion: C. TRICHE, G. PITET and M. R. DORIGNAC. (3 July 1980)
Complexes de dérivés alloxanniques—I: Complexes du fer(II) avec l'acide violurique et l'acide thio-2 violurique: NASEEM DELANNOY, JEAN-MARIE DEGORRE, ALBERT DELANNOY, JACQUES NICOLE and JEAN HENNION. (9 May 1980)

Talanta, Vol. 28, p. i
Pergamon Press Ltd 1981. Printed in Great Britain

0039-9140/81/0201-000i$02.00/0

PAPERS RECEIVED

Differential-pulse anodic voltammetric determination of phosphate, silicate, arsenate and germanate as ϱ-heteropolymolybdates at a stationary glassy-carbon electrode: A. G. FOGG and N. K. BSEBSU (6 November 1980)
Chelating behaviour of Pyrocatechol Violet with micelle-forming cationic surfactant: C. R. VEKHANDE and K. N. MUNSHI. (7 November 1980)
High molecular-weight amines as an extractant for rhenium(VII): S. D. SHETE and V. M. SHINDE. (7 November 1980)
Some reduction and oxidation reactions of sulphonazo III: V. MICHAYLOVA and N. KOULEVA. (10 November 1980)
A systematic approach for estimation of titration errors in acid–base titrations by use of logarithmic diagrams: ÅKE OLIN and BO WALLÉN. (11 November 1980)
Continuous spectrophotometric determination of copper, nickel and zinc in copper-base alloys by flow-injection method of analysis: ROKURO KURODA and TADASHI MOCHIZUKI. (12 November 1980)
Substituent effects on the stability of iron(III), cobalt(II), nickel(II) and copper(II) azo cresol complexes: MAMDOUH S. MASOUD and E. A. KHALIL. (12 November 1980)
Comparison of dry and wet ashing procedures for cadmium and iron determination in biological material by atomic-absorption spectrophotometry: MAJA BLANUŠA and DJURDJA BREŠKI. (13 November 1980)
Oxalic acid as a complexing agent for iron(III) in the titration of iron(II) with sodium vanadate, using visual and potentiometric end-points: G. GOPALA RAO and B. V. S. R. MURTY. (14 November 1980)
Potentiometric titration of small amounts of iron(III) with ascorbic acid in the presence of 1,10-phenanthroline: G. GOPALA RAO and G. SITARAMA SASTRY. (14 November 1980)
Indirect determination of aliphatic secondary amines by catalytic thermometric titration: NOBUTOSHI KIBA, YO SUZUKI and MOTOHISA FURUSAWA. (18 November 1980)
Function for CO_2 evolution in multiparametric refinement of potentiometric data: MICHEL WOZNIAK and GUY NOWOGROCKI. (19 November 1980)
Column extraction chromatography of non-volatile platinum metals: S. PRZESZLAKOWSKI and A. FLIEGER. (21 November 1980)
Gas-chromatographic separation of dimethylphenols on various new liquid phases: AOI ONO. (24 November 1980)
Determination of ultramicro amounts of selenium by gas chromatography with electron-capture detection: KYOJI TÔEI and YASUAKI SHIMOISHI. (24 November 1980)
Protonation thermodynamics of thiovioluric acid: B. R. SINGH and R. GHOSH. (24 November 1980)
Hydrodynamic modulation voltammetry: JOSEPH WANG. (3 November 1980)
Analytical techniques for corrosion studies of noble metals: A. VARMA. (6 October 1980)
An application of silaned glass beads to the preconcentration and spectrophotometric determination of traces of phosphorus with molybdate: SHIGERU TAGUCHI, KATSUMI GOTO and HIROTO WATANABE. (25 November 1980)
Sequential titration of iron(II), antimony(III) and arsenic(III) in binary or ternary mixture: K. SRIRAMAM, B. S. R. SARMA, N. RAMABRAHMA SASTRY and A. R. K. VARA PRASAD. (25 November 1980)
Catalytic influence of Cl^-, Br^-, I^- and SCN^- on the cyclic voltammetric behaviour of Sb(III): H. VERPLAETSE, P. KIEKENS, E. TEMMERMAN and F. VERBEEK. (26 November 1980)
Determination of sulphur functions with iodoso compounds: ASHUTOSH SRIVASTAVA. (26 November 1980)
Determination of cyanide by an indirect spectrophotometric method, using 5-Br-PADAP: F. S. WEI, Y. Q. LIU, F. YIN and N. K. SHEN. (30 October 1980)
Spectrophotometric determination of Ni(II), Pd(II), Pt(II), Pd(IV) and Pt(IV): E. M. KHAIRY, A. F. SHOUKRY and J. AHMAD. (27 November 1980)
Effect of non-ionic surfactants on the electrocapillary maxima and a.c. polarographic curves—a comparative study: WAHID U. MALIK, RAJEEV JAIN and M. J. JOSEPH. (27 November 1980)
Combined assay and determination of bioactivity of polyene antibiotics by flow nephelometry: ANTHONY E. BEEZER and BABUR Z. CHOWDHRY. (27 November 1980)
A compound of iron(II), phenylbiguanide and cyanide: J. MARTINEZ CALATAYUD, F. BOSCH REIG and M. C. GARCIA ALVAREZ-COQUE. (28 November 1980)
Iodamine-B as an oxidimetric titrant in aqueous medium: RANGASWAMY and H. S. YATHIRAJAN. (2 December 1980)
Microdetermination of arsenic(V) in organic compounds by indirect amplification: Application to analysis of pharmaceuticals: S. W. BISHARA, S. T. SULAIMAN and S. BAHJAT. (3 October 1980)
Spectrophotometric study on the reactions of iron(II) and iron(III) with Bromopyrogallol Red and hexadecyltrimethylammonium bromide: XI-WEN HE and DONALD P. POE. (4 December 1980)

Talanta, Vol. 28, p. i
Pergamon Press Ltd 1981. Printed in Great Britain

PAPERS RECEIVED

Quantitative spectrophotometric determination of aliphatic amines by the ninhydrin method: LUCIANO FORLANI, FIORELLA GEMMATI and MAURO MARIOTTI. (13 October 1980)
Effects of some complex-forming ligands on the potential of antimony pH-sensors: STANISŁAW GŁAB, GUNNAR EDWALL, PER-ARNE JÖNGREN and FOLKE INGMAN. (13 October 1980)
Microprocessor-controlled system for automatic acquisition of kinetic data of gas uptake under constant pressure: HARALD GAMPP. (14 October 1980)
The determination of lead in mosses by means of its catalytic effect on the persulphate oxidation of Pyrogallol Red: R. G. ANDERSON and B. C. BROWN. (15 October 1980)
Ion-pair extraction and fluorometric determination of potassium with 18-crown-6 and eosin: A. SANZ-MEDEL, D. BLANCO GOMIS and J. R. GARCIA ALVAREZ. (20 October 1980)
Determination of novocaine from pharmaceutical preparations with novocaine-selective membrane electrodes: D. NEGOIU, M. S. IONESCU and V. V. COŞOFREŢ. (20 October 1980)
Pneumatoamperometric determination of sub-ppm amounts of ruthenate and osmate: PREMYSL BERAN, K. S. CHUNG and STANLEY BRUCKENSTEIN. (22 September 1980)
Etude électrochimique des sels de nitryle en milieu aprotonique: JEAN-CLAUDE FISCHER, ABDELHATEF BOUGHRIET and MICHEL WARTEL. (3 July 1980)
Simultaneous determination of kinetic and thermodynamic parameters from fast reaction kinetic measurements: HAROLD H. TRIMM, HIDETOSHI USHIO and RAMESH C. PATEL. (22 October 1980)
Determination of magnesium by precipitation of magnesium ammonium phosphate from homogeneous solution: M. S. BABU and P. N. RAO. (23 October 1980)
A contribution to Golay's equation for open tubular (capillary) columns for gas chromatography: J. M. TAKÁCS. (23 October 1980)
Simultaneous extraction spectrophotometric determination of niobium and tantalum: C. P. SAVARIAR and K. SOBHANA. –23 October 1980)
Non-explosive pyrolysis—A novel method for the determination of metals in metal perchlorate complexes of organic ligands: M. R. GOPALAKRISHNAN NAIR, M. J. KURIAN and C. P. PRABHAKARAN. (28 October 1980)
Potentiometric and visual end-point detection in determination of potassium with cobaltinitrite: N. KRISHNA MURTHY, A. V. SURYANARAYANA and N. V. SRINIVASA RAO. (28 October 1980)
Influence of some matrix elements on atomization of cobalt in graphite-furnace atomic-absorption spectrometry: A. HULANICKI, R. KARWOWSKA and J. SOWINSKI. (28 October 1980)
On determination of overall stability constants of the complexes formed in metal–ligand systems (Cadmium–formate system): M. I. TASKAEVA and M. H. MIHAILOV. (30 October 1980)
The separation and determination of fatty acids by use of radiogas-liquid chromatography and isotopic dilution analysis: D. A. BEARDSLEY. (3 November 1980)
Thermodynamics of ionic association in aqueous copper acetate solutions, by the spectrophotometric method: MOSTAFA M. EMARA, AHMAD O. BAGHLAF, SOLIMAN N. BASAHEL and YAHYA M. AL-SANUSI. (3 November 1980)
Potentiometric determination of hydrogen peroxide with permanganate in presence of fluoride and iron as a catalyst: Application to the titanium–fluoride–peroxide mixed complex. L. POLO DÍEZ, J. HERNÁNDEZ MÉNDEZ and M. J. ALMENDRAL PARRA. (6 November 1980)
Potentiometric titration of arsenic(III) with potassium dichromate: G. GOPALA RAO and B. SAROJINI. (6 November 1980)
Photometric titration of vanadium(IV) with chromium(VI): G. GOPALA RAO and G. SAVITRI. (6 November 1980)

Talanta, Vol. 28, pp. i to ii, 1981
Printed in Great Britain

Pergamon Press Ltd

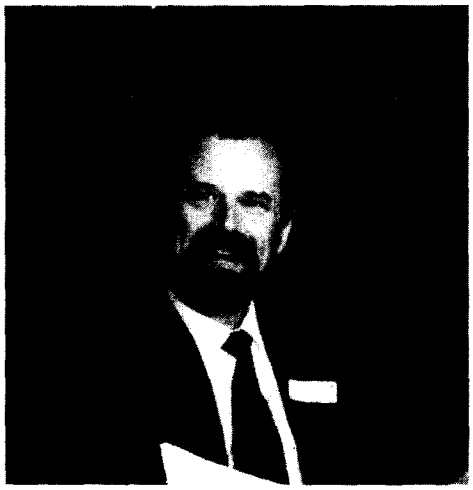
PAPERS RECEIVED

Determination of thallium(III) and vanadium(IV) in a mixture: S. A. CHIMATADAR and J. R. RAJU. (2 February 1981)
Complexometric titration of copper(II) with EDTA, using 5-alkoxy-2-nitrosophenols as indicators: N. F. MODY, K. F. MODY and C. M. DESAI. (2 February 1981)
Organic complexing agents in atomic-absorption spectrometry—a review: J. KOMÁREK and L. SOMMER. (3 February 1981)
Analysis of a potentiometric evaluation method based on the measurement of bound reagent concentration: K. BURGER, L. DOMOKOS, G. PETHŐ and E. PUNGOR. (3 February 1981)
Application of high-performance liquid chromatography and a voltammetric detector to the analysis of 3,4-dihydroxyphenylalanine metabolites: T. ISHIMITSU and S. HIROSE. (4 February 1981)
Arsenic speciation by ion-exchange separation and graphite-furnace atomic-absorption detection: G. E. PACEY and J. A. FORD. (4 February 1981)
Spectrophotometric method for determination of rifamycin: A. K. SHAH, Y. K. AGRAWAL and S. K. BANERJEE. (6 February 1981)
Electrochemical study of the *N,N,N',N'*-1,2-propylenediaminetetra-acetate–bismuth(III) complexes: L. HERNANDEZ, J. ROSAS and S. VICENTE. (9 February 1981)
Factorial analysis of matrix effects in ICP/AES and AAS: The determination of Ta and Ni in Au: J. KRAGTEN and A. PARCZEWSKI. (9 February 1981)
Beta adrenergic blocking agents: Ionization constants reveal intramolecular hydrogen bonding: MICHELE LAXER and A. C. CAPOMACCHIA. (2 February 1981)
Acid–base properties of kojic acid and its co-ordinating behaviour towards platinum(IV): MAMDOUH S. MASOUD and A. A. ABDALLAH. (10 February 1981)
Calibration of plastic laboratory ware: MARY R. MASSON. (11 February 1981)
Untersuchungen zur Anwendung ternärer Komplexe in der Photometrie–II: Die Bestimmung des Titanium(IV) mit Tiron in Gegenwart von Iminodiessigsäure, Nitrilotriessigsäure bzw. Diethylentriaminpentaessigsäure: S. KOCH, G. ACKERMANN and V. SCHOLZE. (12 February 1981)
Hydrophobic indicators for two-phase titration and their application to the determination of silver(I) and pentachlorophenol: M. TSUBOUCHI, N. YAMASAKI, H. MITSUSHIO and K. MATSUOKA. (13 February 1981)
Dual-wavelength spectrophotometric determination of copper in sea-water with $\alpha,\beta,\gamma,\delta$-tetrakis(1-methylpyridinium-4-yl)porphine: HIROTO WATANABE and HIDEKI OHMORI. (17 February 1981)
A note on the determination of equivalence volumes of carboxylic acids from potentiometric titrations by numerical methods: ÅKE OLIN and BO WALLÉN. (18 February 1981)
Polarographic behaviour of pyridine-2-aldehyde guanylhydrazone: M. ROMAN CEBA, A. SANCHEZ MISIEGO, J. J. BERZAS NEVADO and A. ESPINOSA MANSILLA. (19 February 1981)
Cathodic wave of paludrine hydrochloride: F. VICENTE and F. TOMAS. (19 February 1981)
Selection of a suitable counter-cation in the solvent extraction of anionic chelates and spectrophotometric determination of micro amounts of cobalt with 2-nitroso-1-naphthol-4-sulphonic acid and tetrabutylammonium ion: SHOJI MOTOMIZU and KYOJI TÔEI. (20 February 1981)
Study of the behaviour of various phenolic compounds in the 4-aminoantipyrine and ultraviolet-ratio spectrophotometric methods with and without distillation: JOHN FARINO, GEORGE NORWITZ, WALTER J. BOYKO and PETER N. KELIHER. (6 February 1981)
The disodium salt of 1,10-phenanthroline-4,7-diphenyl-*p*-disulphonic acid as an analytical reagent: Study of precipitation reactions: A. CABRERA MARTIN, R. GALLEGO ANDREU and S. RUBIO BARROSO. (23 February 1981)
The disodium salt of 1,10-phenanthroline-4,7-diphenyl-*p*-disulphonic acid as an analytical reagent: A spectrophotometric study of the complexes formed: A. CABRERA MARTIN, R. GALLEGO ANDREU and S. RUBIO BARROSO. (23 February 1981)
Synthesis and analytical properties of di(2-pyridyl)-*N,N'*-di(8-quinolyl)methylenediamine: R. ESCOBAR, J. M. CANO-PAVON, J. BELLANATO, E. GALVEZ and F. PINO. (24 February 1981)
Determination of traces of tellurium in heat-resisting alloys by graphite-furnace atomic-absorption spectrometry after co-precipitation with arsenic: OSAMU KUJIRAI. (24 February 1981)
Spectrophotometric studies of the reactions of pentacyanoferrate(II) complexes with two bis-quaternary pyridinium aldoximes: N. BURGER and V. KARAS-GAŠPAREC. (25 February 1981)
The determination of traces of metals by anodic-stripping voltammetry with a new kind of mercury electrode: The long-lasting sessile-drop electrode: ROMANO ANDRUZZI and ANTONIO TRAZZA. (27 February 1981)
Complexes of cobalt(II) and nickel(II) with 1,2-dimethylethane-1,2-dione dihydrazone and their infrared and electronic spectra: H. C. RAI. (2 March 1981)
A TLC–enzymatic method for on the spot detection and determination of fenitrothion in water: S. UDAYA BHASKAR. (2 March 1981)
Separation of trace elements in solid samples by formation of volatile inorganic compounds (volatilization and gas chromatography): K. BÄCHMANN. (2 March 1981)
Synthesis and chromogenic properties of some hydrazones of isoquinolyl-3-, quinolyl-2- and pyrrol-2-aldehyde: ALFRED A. SCHILT and FRANCIS H. CASE. (18 February 1981)
Extraction–spectrophotometric determination of non-ionic surfactants in water: KYOJI TÔEI, SHOJI MOTOMIZU and TÔRU UMANO. (3 March 1981)
Spectrophotometric determination of platinum with iodide and Rhodamine B: J. R. MUDAKAVI and T. V. RAMAKRISHNA. (3 March 1981)
Extraction of uranium(IV) from phosphoric acid solutions with 1-phenyl-3-methyl-4-benzoylpyrazolone-5 (PMBP): F. TALAVERA CORONEL, ST. MAREVA and N. JORDANOV. (3 March 1981)

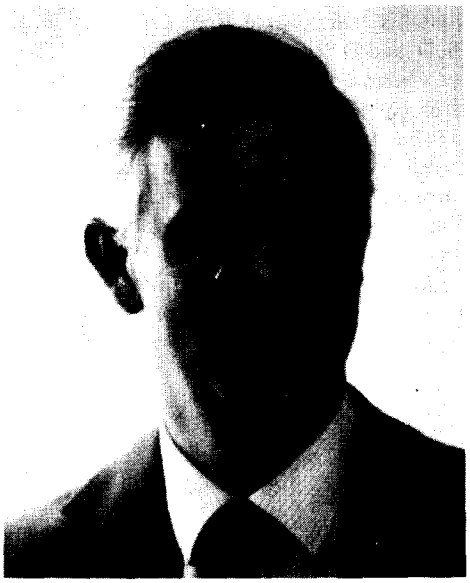
Talanta, Vol. 28, pp. I to II
Pergamon Press Ltd 1981. Printed in Great Britain

0039-9140/81/0201-0001$02.00/0

TALANTA ADVISORY BOARD

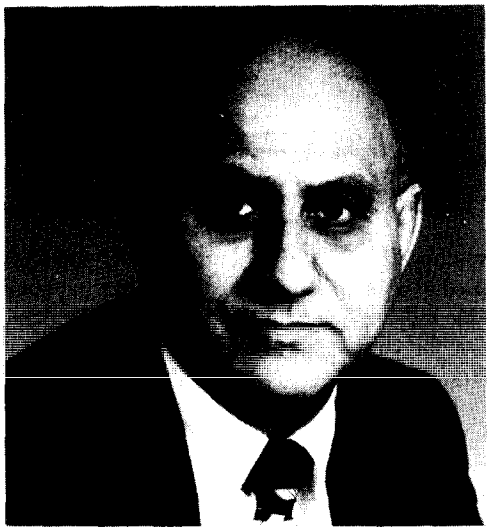


PROFESSOR DIETER KLOCKOW was born on 16 November 1934 in Landsberg/Warthe, Brandenburg Province (now part of Poland) and graduated as a Diplom-Chemiker in 1961 in the University of Freiburg, and took his doctoral degree (Dr. rer. nat.) at the same university in 1965. He spent the next 11 years there, first as Research Assistant and Research Fellow of the German Research Society, then as lecturer, and since 1976 has been Professor of Analytical Chemistry at the University of Dortmund. In 1973 he gained an Award from the Division of Analytical Chemistry of the German Chemical Society. His research interests are in radiochemical separations and methods of analysis, catalytic kinetic methods, gas chromatography of organic acids and inorganic anions, application of chemiluminescence reactions, and analytical chemistry of trace compounds in the atmosphere. He has published about 50 papers in these fields.



DR. OLAV H. J. CHRISTIE was born on 22 December 1930 in Hamar, Norway as the son of the lawyer W. F. K. Christie and his wife Eleanor E. R. Christie (née Kiaer). After finishing musical studies and public appearances as a concert pianist as a teenager, Dr. Christie studied chemistry and geology at several universities in Scandinavia and on the continent before graduating at the University of Oslo as a geologist and mineralogist in

1959. He obtained the degree of Dr. philos. in 1964 and became full-time professor of geology in 1968. Dr. Christie was active at the University of Oslo, Norway, from 1956 to 1979, the last 12 years as head of the laboratory for mass spectrometry. He is now head of the laboratory for quantitative organic mass spectrometry at the Rogaland Regional College, Stavanger, Norway. He is married to Helene Borgen, chief editor in the publishing company Informasjonsforlaget. Dr. Christie has worked in the field of geochemistry since 1967. He has organized a round-robin study on three geological reference materials and has made several contributions to the analysis and geochemistry of the lanthanide elements. He has been interested in multivariate statistics and the extraction of information from data, and was secretary of the Chemometric Society 1977–1979. He was chairman of the Division of Analytical Chemistry of the Norwegian Chemical Society, 1970–1979, and is the Norwegian delegate to the Division of Analytical Chemistry of IUPAC, and the Working Party of Analytical Chemistry of the Federation of European Chemical Societies. Dr. Christie has organized several conferences and was President of the 8th International Mass Spectrometry Conference, 1979. He has published some 200 articles.



CHUNI LAL CHAKRABARTI received his B.Sc. degree from Calcutta University, the M.Sc. degree from the University of Birmingham and Ph.D. and D.Sc. degrees from the Queen's University of Belfast. He has been on the faculty of Carleton University, Canada, since 1965 and is a professor of chemistry. He has been a Consultant to Exxon Production Research Company, U.S.A., and a United Nations Expert at the National Atomic Energy Commission, Argentina. He has given plenary and invited lectures at international conferences and has done advisory and consultancy work in many parts of the world. Dr. Chakrabarti's research interests are in analytical chemistry and environmental chemistry, with special emphasis on the development of analytical atomic spectroscopy, trace and ultratrace analysis, and metal–organic interactions in the aquatic environment. He is the author of about 100 research papers and reports. He is Editor-in-Chief of *Progress in Analytical Atomic Spectroscopy*, Associate Editor of *Canadian Journal of Spectroscopy*, and a member of the Editorial Boards of *Spectrochimica Acta (Part B)*, and *Annual Reports on Analytical Atomic Spectroscopy*. He is a Fellow of the Royal Society of Chemistry, Fellow of the Chemical Institute of Canada, and a member of the American Chemical Society. He is the 4th recipient of the Gerhard Herzberg Award of the Spectroscopy Society of Canada—the award was given in 1977 in recognition of his outstanding contributions to the science of spectroscopy.

Talanta, Vol. 28, pp. I–IV
Pergamon Press Ltd 1981. Printed in Great Britain

TALANTA ADVISORY BOARD

The Editorial Board and the Publisher of *Talanta* take pleasure in welcoming the following new members of the Advisory Board of the journal.

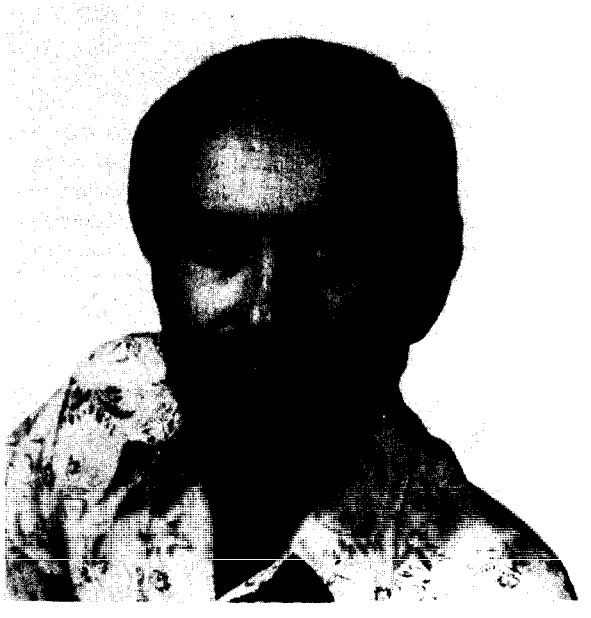
P. W. CARR
C. L. CHAKRABARTI
G. D. CHRISTIAN
O. H. J. CHRISTIE
G. M. HIEFTJE
J. D. INGLE JR
G. F. KIRKBRIGHT
D. KLOCKOW
SHU-CHUAN LIANG
J. F. TYSON

They also wish to record their sincere thanks for the help given by

H. FREISER
D. M. HERCULES
H. V. MALMSTADT
L. MEITES
S. P. PERONE
O. SONGINA
G. SVEHLA
A. TOWNSHEND

who retire from the Advisory Board.

Biographical notes on some of the new members appear below; the remainder will follow in subsequent issues.

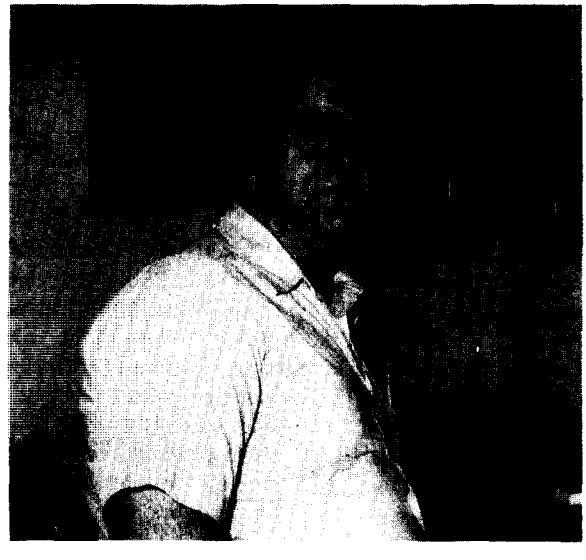


GARY M. HIEFTJE is Professor of Chemistry at Indiana University. He received his AB degree from Hope College in 1964, after working several years at Miles Laboratories in Zeeland, Michigan. From 1964 to 1965, he served as a research assistant in physical chemistry at the Illinois State Geological Survey. He earned his Ph.D. degree in 1969 from the University of Illinois under the direction of H. V. Malmstadt. In the same year, he was appointed assistant professor of chemistry at Indiana University and was promoted to associate professor in September 1973 and to full professor in July 1977. His research interests include the investigation of basic mechanisms in atomic emission, absorption, and fluorescence spectrometric analysis, and the development of atomic methods of analysis. He is also interested in the on-line computer control of chemical instrumentation and experiments, the use of time-resolved luminescence processes for analysis, the application of information theory to analytical chemistry, and the use of stochastic processes to extract basic and kinetic chemical information. He is a member of the American Chemical Society, the Society for Applied Spectroscopy, the Optical Society of America, Sigma Xi, and Phi Mu Alpha. He was co-chairman of the 1979 Analytical Summer Symposium on Lasers in Analytical Chemistry and currently serves on the editorial boards of *Spectrochimica Acta, Part B*, and *Analytica Chimica Acta* and on the instrumentation advisory panel of *Analytical Chemistry*.

TAL. 28/1 -A

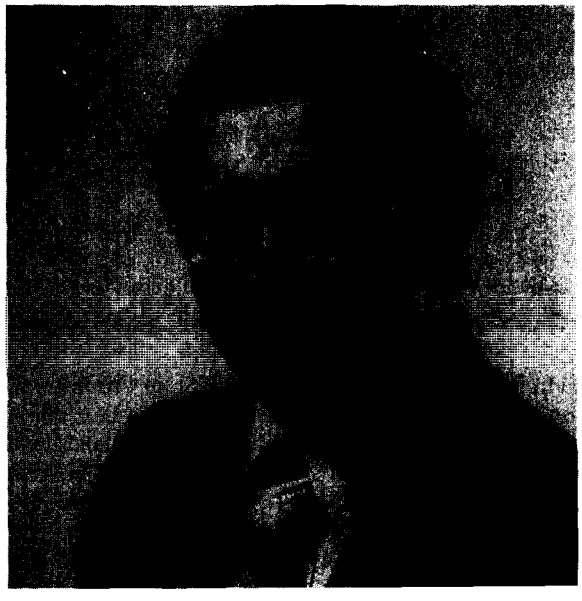


GORDON FRANK KIRKBRIGHT has been appointed to the new Chair in Analytical Sciences at the University of Manchester Institute of Science and Technology, and is to be the first Head of the newly created Department of Instrumentation and Analytical Science. Professor Kirkbright obtained his B.Sc. and in 1962 a Ph.D. in Analytical Chemistry at the University of Birmingham. After post-doctoral research in the USA at the height of the "brain-drain", he was induced to return to Europe, by means of a DSIR/NATO Fellowship, spent first at the Technische Hochschule, Vienna, and then in the Department of Chemistry at Imperial College. He joined the staff at Imperial College in 1964 and progressed to the position of Reader in Analytical Atomic Spectroscopy. He was awarded his D.Sc. by the University of London in 1971 and the first Silver Medal of the Society for Analytical Chemistry in 1974 for contributions to atomic and molecular spectroscopy. From 1977 he was Reader in Analytical Chemistry at Imperial College and led a large research group concerned with the development of novel spectroscopic techniques, including radio-frequency plasma emission spectroscopy and optoacoustic spectroscopy. He was a founder Director and Company Chairman of EDT Research and still takes an active interest in its affairs. Professor Kirkbright is at present a member of the Council of the Chemical Society Analytical Division and past Chairman of the Atomic Spectroscopy Group of the Division. He is currently serving as an Associate Member of Commission V(III) of IUPAC and is a member of the IAEA Advisory Group on Trace Elements in Biological Materials.

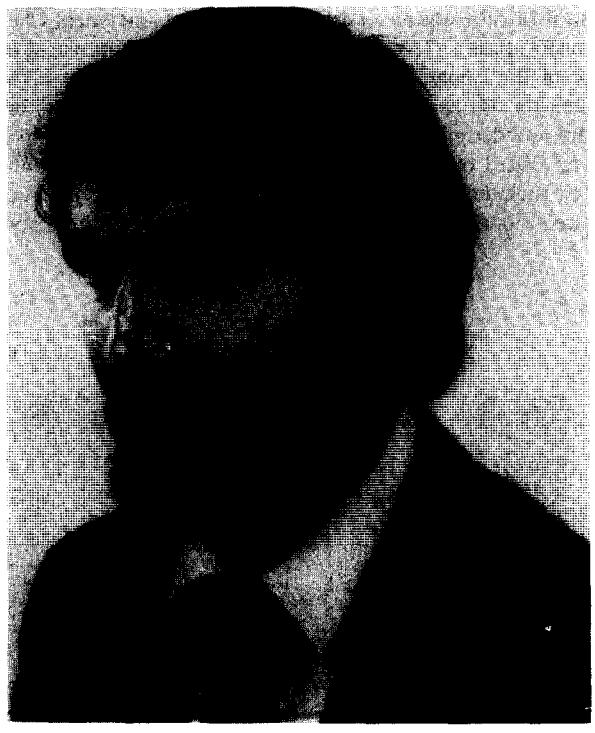


PETER W. CARR received his Bachelor of Science degree in Chemistry from the Polytechnic Institute of Brooklyn in 1965 and completed Ph.D. studies in Analytical Chemistry at the Pennsylvania State University in 1969. During 1968 and 1969 he was a postdoctoral research associate at the Stanford Medical School. Starting

in September of 1969 and until 1975 he was an Assistant Professor of Analytical Chemistry at the University of Georgia in Athens and from 1975 until 1977 was Associate Professor of Analytical Chemistry there. Since 1977 he has been on the faculty of the Chemistry Department of the University of Minnesota as an Associate Professor of Analytical Chemistry. He has been the past president of Symposium on the Analytical Chemistry of Pollutants, Inc., and was a founder and the first president of the Minnesota Chromatography Forum. Until 1980 he was on the Editorial Board of *Analytical Chemistry*. To date he has published 65 papers in various areas of analytical chemistry, including thermoanalytical chemistry, electroanalytical chemistry and chromatography, and has co-authored a book in the area of immobilized enzymes in analytical chemistry.



GARY D. CHRISTIAN obtained his B.S. from the University of Oregon, and his M.S. and Ph.D. degrees from the University of Maryland. He has held several professional posts, starting as a research analyst at the Walter Reed Army Institute of Research from 1961 to 1967, the last two years on leave of absence from the Institute and working as Assistant Professor at the University of Maryland. This was followed by three years as Assistant Professor and two years as Associate Professor at the University of Kentucky, and since 1972 he has been Professor of Chemistry at the University of Washington. He has also enjoyed visiting professorships at Brussels and Geneva. His research interests are in atomic and fluorescence spectroscopy, electroanalytical and clinical chemistry, environmental analysis, flow analysis, and chromatography and detectors. He is a member of the American Chemical Society, the Society for Applied Spectroscopy and the Spectroscopy Society of Canada, and a Fellow of the American Institute for Chemists. He is a member of the Editorial Boards of *Analytical Letters*, *Canadian Journal of Spectroscopy*, and *Biomedical, Chemical and Environmental Instrumentation*, and has served on the Instrumentation Panel of *Analytical Chemistry*. He is author or co-author of three books, and over 140 research publications or review articles.



JULIAN F. TYSON graduated from Aberdeen University with a B.Sc. in Chemistry in 1971. Following a period at Imperial College of Science and Technology, London University as a research student and research assistant with Professor T. S. West, he obtained the Diploma of Imperial College and the degree of Ph.D. (in Analytical Chemistry) in 1975. After a short spell as research assistant at Aberdeen University, Dr. Tyson was appointed Lecturer in Analytical Chemistry at the University of Technology, Loughborough in 1976. He is a Member of the Royal Society of Chemistry and is the Honorary Secretary of the Analytical Division's Education and Training Group and the Honorary Treasurer of its Midlands Region. He is also a member of the Midlands Association for Qualitative Analysis. His main research interests are concerned with developments and applications of atomic absorption and emission spectrometry, gas-phase Auger electron spectrometry and spectroelectrochemistry. He is also concerned with teaching methods and academic staff training. Outside the world of analytical chemistry he enjoys a certain reputation with a sword in his hand, being a Commonwealth silver-medallist and current Scottish National Champion.

SUBJECT INDEX

Acids, Determination, coulometric 81
—, carboxylic, Errors in determination 919
Acid–base titration, Correction for CO_2 evolution 575
———, Curves 565
Aerosols, Preconcentration on liquid electrode 43
Aldoximes, *N*-heterocyclic, Determination, spectrophotometric 323
Alkaline earth metals, Complexes with *o*-cresolphthalexone 127
Alkaloids, Determination, fluorimetric 709
Aluminium, Determination, by AAS 461
Amines, primary and secondary, Determination, spectrophotometric 843
—, secondary aliphatic, Determination, catalytic 691
Amino-acids, Determination, spectrophotometric 843
Aminocarboxylic acids, Complexes with methylmercury(II) 137
Amplification reaction, for determination of chloral hydrate 955
Analytical information, Interpretation by pattern recognition 871
Anorexigenic drugs, Raman spectroscopy of 95
Antibiotics, Determination of bioactivity 647
Antimony(III), Determination in mixtures with Fe(II) and As(III) 963
—, —voltammetric 431
—, Titration of 257
Aromatic compounds, Degradation in ground water 725
Arsenate, Determination by ASV 473
Arsenic, Determination by FAAS 935
Arsenic(III), Determination in mixtures with Fe(II) and Sb(III) 963
β-Aryl-α-mercaptopropenoic acids, Determination, thermometric 341
Ascorbic acid, Determination, titrimetric 332
Ashing, dry and wet, of biological material 681
Atomic-absorption spectrometry (AAS), Comparison to Pt-loop method 334
———, Determination of Al 461
———, —of Cd 681
———, —of Cu 441, 785
———, —of Fe 681
———, —of Ni 901
———, —of nitrates 89
———, —of P 469
———, —of Se 169, 637
———, —of Ta 901
———, —of Te 585
———, flameless (FAAS), Determination of As 935
———, —, —of Ba 353
———, —, —of Ca 177
———, —, —of Hg 271
———, —, —of Mo 359
———, —, —of Sr 177
———, —, —of Y and rare-earth elements 31
———, —, Effect of matrix elements on determination of Co 455
Atomization, electrothermal, of Ca and Sr 177
Autoprotolysis constants, by coulometric titration 183

Barium, Determination, by FAAS 353
Benzo[*a*]pyrene and benzo[*k*]fluoranthene, Determination, fluorimetric 607
Benzotriazole, Determination by HPLC 777
Beryllium, Determination, spectrophotometric 799
Beta-adrenergic blocking agents, Dissociation constants 973
Bile acids, Determination by HPLC 675
Bioactivity, of polyene antibiotics 647
Bismuth(III), Determination, potentiometric 931
—, Extraction of 768
Bit resolution, Improvement in digital signal averaging 547
Boron, Determination, spectrophotometric 817
Bromophos residues, Determination by TLC 765
γ-Butyrolactones, amido-substituted, Hydrolysis of 329

Cadmium, Chelates with 2-thiopicolinamide 69
—, Determination by AAS 681
Cadmium(II), Cyanoacetato complexes of 199
—, Stability constants of chloro complexes 237
Calcium, Atomization, electrothermal 177
—sulphate, Determination, thermogravimetric 265
Calibration, of plastic laboratory ware 781
Carbon, Determination of traces in Mo and W 19
—dioxide, Correction for 575
Cations, common, Spot-tests for 817
Chemiluminescence, Determination of Mn(II) 731
—, of sulphide–hypobromite reaction 653
Chloral hydrate, Determination, titrimetric 955
Chromatography, cation-exchange, Separation of Zn and Pb 207
—, column, of Pt metals 557
—, —, Separation of Ru complexes 857
—, gas (GLC), Determination of dimethylarsinic acid 402
—, —, —of Se 967
—, —, Separation of nitroxylenes 268
—, gel permeation (GPC), of transition metal complexes 809
—, high-pressure liquid (HPLC), Determination of bile acids 675
—, ———, —of thiazoles and triazoles 777
—, ———, Dropping-mercury detector for 251
—, ———, Silanized frits for trace metal analysis 411
—, radio-GLC, Determination of fatty acids 405
—, thin-layer (TLC), of bromophos residues 765
—, ——, of thioureas 115
Chromium, Determination, reductometric 55
Cobalt, Atomization in FAAS 455
—, Determination by XRF 437
Cobalt(II), Cyanoacetato complexes of 199
—, Ion-exchange separation 337
—, Preconcentration of 123
Complex equilibria, from spectrophotometric data 925
—forming ligands, Effect on antimony pH sensors 301
Computer program, for acid–base titrations 565
——, for complex equilibria 925
Copper, Determination by AAS 441
—, —by flow-injection analysis 389
—, —by ion-selective electrode and AAS 785
—, —, spectrophotometric 774
Copper(II), Cyanoacetato complexes of 199
Corrosion, of noble metals 701
$CS_2N_3^-$ ion, Oxidation by permanganate 867
Cyanide, Determination, spectrophotometric 694
—, Preconcentration from water 255
—, Replacement in hexacyanoferrate(II) 591

Data-acquisition capabilities, of microcomputers 519
—logging system, Microprocessor-based 543
Diagrams, Logarithmic, as aid in complexometric titrations 241
Dibenzothiazyl disulphide, Titration, amperometric 262
Digital signal averaging, Improvement of bit resolution 547
Dimethylarsinic acid, Determination by GLC 402
Dispersion, Laminar, in flow-injection analysis 11
Dissociation constants, of beta-adrenergic blocking agents 973
Drugs, Uracil anticancer, Determination, spectrophotometric 685

Electrode, antimony, as pH sensor 301
—, coated-wire, for Bi(III) 931
—, dropping-mercury, as detector for HPLC 251
—, glassy carbon, for ASV 473
—, ——, oxidation of Sn(II) 192
—, ion-selective, for Cu 785
—, liquid, for aerosol preconcentration 43
—, rotating-disc, for nitrogen dioxide 319
—, selective, for novocaine 377
—, —, for sulpha drugs 383
—, sessile-drop mercury, for ASV 839
Environmental pollution, Determination of Hg 610
Ephedrine hydrochloride, Assay by NMR 187
Equilibrium concentrations, Calculation of derivatives 977
Errors, in potentiometric titrations 919

Extraction, of Bi(III) . . . 768
—, of lanthanide complexes . . . 195
—, of S compounds with tributyltin hydroxide . . . 173
—, of Sn . . . 157
—spectrophotometry, of B . . . 825
——, of Os . . . 62
——, of Si and P . . . 665
——, of trace elements . . . 49

Fast-reaction kinetic measurements . . . 753
Fatty acids, Determination by isotope dilution and radio-GLC . . . 405
Flotation, method for Pd . . . 561
—photometry, Determination of Si . . . 7
Flow-injection analysis, Dropping-mercury detector for . . . 251
———, Laminar dispersion . . . 11
———, Review . . . 789
Flow nephelometry, Determination of bioactivity of antibiotics . . . 647
Flucloxacillin, Determination, polarographic . . . 855
Fluorescence, of *N*-heterocyclics . . . 145
Fluoride, Determination, spectrophotometric . . . 889
Formation constants, of alkaline-earth complexes with *o*-cresolphthalexone . . . 127

Gas uptake data, Automatic acquisition of . . . 535
Germanate, Determination by ASV . . . 473
Glass beads, for separation of Ru complexes . . . 857
——, silaned, for determination of P . . . 613

Haloperidol, Electrochemical behaviour . . . 313
Hexacyanoferrate(II), Replacement of cyanide . . . 591
Hydrogen peroxide, Determination, potentiometric . . . 951

Iodide, Determination with iodide . . . 415
Ion-exchange, Separation of Co(II) and Ni(II) . . . 337
——, Speciation of As . . . 935
——colorimetry, for Fe(II) and Fe(III) . . . 669
—exchanger, Chelex 100, for metal ions . . . 759
Iron, Determination by AAS . . . 681
—, —, spectrophotometric . . . 603
Iron(II), Complexes with violuric and 2-thiovioluric acids . . . 451
—, Determination in mixtures with Sb(III) and As(III) . . . 963
Iron(II) and (III), Determination, spectrophotometric . . . 669
———, Reactions with Bromopyrogallol Red . . . 419
Iron(III), Complexes with 1-hydroxy-7-sulpho-2-naphthoic acid . . . 277
—, Determination, kinetic . . . 753
Isoniazid, Determination, in drugs . . . 849
—, —, spectrophotometric . . . 477
Isotope dilution analysis, of fatty acids . . . 405
———, of Sn . . . 73

Kerosene, Adulteration of fuels, by two-phase titration . . . 281
Ketocarboxylic acids, Complexes with methylmercury(II) . . . 137

Laboratory ware, plastic, Calibration of . . . 781
Lanthanides, Extraction of complexes . . . 195
Lead, Determination by ASV . . . 65
—, —, catalytic . . . 365
Lead(II), Cyanoacetato complexes of . . . 199
—and zinc, Separation from other elements . . . 207
Louis Gordon Memorial Award . . . No. 8, I; No. 10, I

Manganese, Determination, reductometric . . . 55
Manganese(II), Determination, by chemiluminescence . . . 731
Matrix, Alloys, Determination of Al . . . 461
—, Aluminium alloys, Determination of P . . . 469
—, Archaeological materials, Determination of Cu . . . 785
—, Biological materials, Determination of Cd and Fe . . . 681
—, Biopolymer preparations, Determination of water . . . 161
—, Brine, Determination of Ba . . . 353
—, Caustic soda solutions, Determination of Ba . . . 353
—, Cement, Determination of Ca sulphates . . . 265
—, Chrome ores, Decomposition of . . . 771
—, Coolants, Determination of thiazoles and triazoles . . . 777
—, Copper, Determination of Te . . . 585

—, —alloys, Determination of Cu, Ni and Zn . . . 389
—, —ores, Decomposition of . . . 121
—, Drugs, Determination of isoniazid . . . 849
—, Gasoline and diesel fuel, Adulteration with kerosene . . . 281
—, Geological materials, Determination of Se . . . 169
—, Gold, Determination of Ta and Ni . . . 901
—, Igneous rocks, Determination of Pb . . . 65
—, Iron and steel, Determination of Al . . . 461
—, ——, —of B . . . 817
—, Laterites, Determination of Si and P . . . 665
—, Lubricating oils, Determination of Cu . . . 441
—, Lead, Determination of Te . . . 585
—, Milk, Determination of Zn . . . 399
—, Molybdenum, Determination of C, N, and O . . . 19
—, Mosses, Determination of Pb . . . 365
—, Nickel refinery slimes, Analysis of . . . 25
—, Pharmaceutical preparations, Determination of novocaine . . . 377
—, ——, Titration of acids . . . 81
—, Plant materials, Determination of Cu . . . 441
—, Polyurethane foam, Determination of Co . . . 437
—, Selenium, Determination of Te . . . 585
—, Soils, Determination of Cu . . . 441
—, Steels, Determination of Mn, Cr and V . . . 55
—, Surfactants, Determination of sulphate . . . 221
—, Tablets, Assay of ephedrine hydrochloride . . . 187
—, Tungsten, Determination of C, N, and O . . . 19
—, Water, Determination of Cu . . . 441
—, —, Preconcentration of cyanide . . . 255
—, —, Recovery of phenolic compounds . . . 215
—, —, ground, Degradation of aromatic compounds . . . 725
—, —, natural, Determination of Co(II) . . . 123
—, —, —, —of Fe(II) and Fe(III) . . . 669
—, —, sea, Determination of Cu . . . 774
—, —, —, Determination of Zn . . . 909
—, —, —, Stability of Cd(II) complexes . . . 237
—effects, Factorial analysis of . . . 901
2-Mercaptobenzothiazole, Determination by HPLC . . . 777
Mercury, Determination by FAAS . . . 271
—, —, kinetic . . . 610
Metal ions, Separation on Chelex 100 . . . 759
——, Sorption on resins . . . 551
——, bivalent, Complexes with Xylenol Orange and Methylthymol Blue . . . 623
—perchlorate complexes, Decomposition of . . . 395
Methylmercury(II), Complexes with keto- and aminocarboxylic acids . . . 137
Microcomputers, Data-acquisition capabilities . . . 519
—, for control of gas uptake data . . . 535
—, for reaction rate ratemeter . . . 539
Microprocessors, and peripheral devices . . . 503
—, Data-logging system . . . 543
—, Introduction to . . . 487
—, Macroapplications of . . . No. 7B, V
Molybdenum, Determination by FAAS . . . 359

Nickel, Chelates with 2-thiopicolinamide . . . 69
—, Cyanoacetato complexes of . . . 199
—, Determination by AAS and plasma emission spectroscopy . . . 901
—, —by flow-injection analysis . . . 389
Nickel(II), Determination, spectrophotometric . . . 189
—, Ion-exchange separation . . . 337
Niobium(V), Determination, spectrophotometric . . . 59
Nitrates, Determination, by AAS, photometry and polarography . . . 89
—, —, conductometric . . . 349
Nitrile salts, Reduction of . . . 233
Nitrite, Determination, spectrophotometric . . . 697
Nitrocompounds, aromatic, Detection of . . . 485
Nitrogen, Determination of traces in Mo and W . . . 19
—dioxide, Determination by rotating-disc electrode . . . 319
—heterocyclics, Phosphorescence and fluorescence of . . . 145
p-Nitrosodiphenylamine, Replacement of cyanide in hexacyanoferrate(II) . . . 591
Nitroxylene isomers, Separation by GLC . . . 268
Noble metals, Corrosion studies . . . 701
Novocaine, Determination with selective electrode . . . 377

Oil spills, Fluorescence spectra of . . . 1
Organic solutions, Analysis by inductively-coupled plasma . . . 745
Osmium, Determination, spectrophotometric . . . 62
Oxygen, Determination of traces in Mo and W . . . 19
—, —, spectrographic . . . 447

Palladium, Determination, complexometric . . . 327
—, —, spectrophotometric . . . 561
Pattern recognition methods, Interpretation of analytical information . . . 871
Pentachlorophenol, Determination by two-phase titration . . . 857
Peripheral devices and microprocessors . . . 503
Pharmacia Prize . . . No. 11, I
Phenols, Determination, kinetic . . . 408
—, —, spectrophotometric . . . 705
—, Recovery from water . . . 215
Phenylhydrazines, Determination, oxidimetric . . . 960
Phosalone insecticide, Determination, kinetic . . . 481
Phosphate, Determination by ASV . . . 473
Phosphorescence, of nitrogen heterocyclics . . . 145
—, Room-temperature, in solutions . . . 717
Phosphorimetry, in organic analysis (Review) . . . 201
—, Reduction of background . . . 119
Phosphorus, Determination by AAS . . . 469
—, —, spectrophotometric . . . 613, 665
Photomultiplier tubes, Read-out systems for . . . 527
Plasma, high-frequency, in analysis . . . 629
—, inductively-coupled, for analysis of organic solutions . . . 745
Platinum metals, Chromatography of . . . 557
Polarography, Determination of flucloxacillin . . . 855
—, of nitrates . . . 89
Polysulphide, Extraction with tributyltin hydroxide . . . 173
Potassium, Determination, fluorimetric . . . 425
Preconcentration, of aerosols . . . 43
—, of Cu for AAS determination . . . 441
—, of P on silaned glass beads . . . 613
—, of solutions . . . 37
Precipitates, Investigation by ESCA . . . 619
Protonation constants, of *o*-cresolphthalexone . . . 127

Rare-earth β-diketonates, Thermal properties of . . . 295
——elements, Determination by FAAS . . . 31
Reaction rate ratemeter, Microcomputer-based . . . 539
Read-out systems, for photomultiplier tubes . . . 527
Reagent, 4-Aminoantipyrine, for phenols . . . 705
—, Antipyrine, Complexes with lanthanides . . . 195
—, Barium oxalate, for SO_3 . . . 599
—, Benzohydroxamic acid, for Mn, Cr and V . . . 55
—, 2-(5-Bromo-2-pyridylazo)-5-diethylaminophenol, for Ni(II) . . . 189
—, Bromopyrogallol Red, for Fe(II) and Fe(III) . . . 419
—, 5-Br-PADAP, for cyanide . . . 694
—, Calcichrome, for Be . . . 799
—, Cerium(IV) sulphate, for V(IV) . . . 287
—, Chloramine-T, for xylenes . . . 259
—, bis[2-(5-Chloro-2-pyridylazo)-5-diethylaminophenolato]cobalt(III), for surfactants . . . 616
—, Chromopyrazole II, for Si . . . 7
—, 18-Crown-6, for K . . . 425
—, Curcumin, for B . . . 817
—, Dansyl chloride, for bromophos residues . . . 765
—, *N,N*-Diethylaniline, for aromatic nitro-compounds . . . 485
—, *cis*-α,β-Dinitrostilbene, for amines, amino-acids and thiols . . . 843
—, Eosin, for K . . . 425
—, Ferricyanide, for ascorbic acid . . . 332
—, Fulvic and humic acids, for transition metals . . . 809
—, Hexamethylphosphoramide, for extraction of Os . . . 62
—, Hydrazones, *N*-heterocyclic, for transition metals . . . 857
—, 1-Hydroxy-4-sulpho-2-naphthoic acid, for Fe . . . 603
—, 1-Hydroxy-7-sulpho-2-naphthoic acid, for Fe . . . 277
—, Hypobromite, for sulphide . . . 653
—, Iodamine-B, as oxidimetric titrant . . . 418
—, Iodate, for iodide . . . 415
—, Magnesium tetrakis (4-tert. butylphenyl)borate, for Na . . . 688
—, Manganese dioxide, for decomposition of ores . . . 121, 771
—, Mercuric chloride, for thiols . . . 397

—, α,β,γ,δ-tetrakis(1-Methylpyridinium-4-yl)porphine, for Cu . . . 774
—, Methylthymol Blue, Metal complexes of . . . 623
—, Metol, for isoniazid . . . 477
—, 1-Nitroso-2-naphthol, for Co(II) . . . 123
—, Pentacyanoferrate(II), for *N*-heterocyclic aldoximes . . . 323
—, Perchlorate, Complexes with lanthanides . . . 195
—, Permanganate, for hydrogen peroxide . . . 951
—, —, for $CS_2N_3^-$ ion . . . 867
—, 1-Phenyl-3-methyl-4-benzoylpyrazol-5-one, for trace elements . . . 49
—, bis(4-Phenyl-3-thiosemicarbazone) of 1,3-cyclohexanedione and derivatives, analytical properties 131
—, Potassium dichromate, for Sb(III) . . . 257
—, Pyridine-2-aldehyde guanylhydrazone, analytical properties . . . 134
—, Rhodamine 6G, Complex with pentabromopalladate(II) . . . 561
—, Salicylidenamino-2-thiophenol, for Sn . . . 73
—, *p*-Sulphobenzeneazo-4-(2,3-dihydroxy-5-chloropyridine), for Nb(V) . . . 59
—, Thiocyanate, for Fe(III) . . . 753
—, 2-Thiopicolinamide, for Ni, Zn and Cd . . . 69
—, 2-Thiovioluric acid, for Fe(II) . . . 451
—, Tiron, for Ti(V) . . . 915
—, —, for trace metals . . . 345
—, Tributyltin hydroxide, for cyanide . . . 255
—, ——, for sulphide, polysulphide, thiocarbonate and S . . . 173
—, Violuric acid, for Fe(II) . . . 451
—, Xylenol Orange, Metal complexes of . . . 623
—, Zirconium–Chrome Azurol S complex, for fluoride . . . 889
Resin, chelating, with 1-nitroso-2-naphthol groups . . . 274
—, —, with 2-nitroso-1-naphthol groups . . . 957
—, poly(vinylpyridine), Metal sorption on . . . 551
Review, Determination of Se by AAS and FAAS . . . 637
—, Flow injection analysis . . . 789
—, Phosphorimetry in organic analysis . . . 201
Riboflavin, Determination, spectrofluorimetric . . . 225
Ruthenium, Determination by XRF . . . 737
—complexes, Separation of . . . 857

Selenium, Determination by AAS . . . 169
—, —by AAS and FAAS (Review) . . . 637
—, —by GLC . . . 967
Silicate, Determination by ASV . . . 473
Silicon, Determination, spectrophotometric . . . 7, 665
Silver, Determination by two-phase titration . . . 857
Solutions, Preconcentration by instrumental method . . . 37
Spectra, fluorescence, Vector model for . . . 1
Spectrography, Determination of oxygen traces . . . 447
Spectroscopy, dye-laser, of uranyl ion . . . 107
—, ESCA, Investigation of precipitates . . . 619
—, fluorescence, of benzo[*a*]pyrene and benzo[*k*]fluoranthene . . . 607
—, —, of quinoline alkaloids . . . 709
—, —, of thiamine and riboflavin . . . 225
—, nuclear-magnetic resonance (NMR), of ephedrine hydrochloride . . . 187
—, plasma emission, Determination of Ta and Ni . . . 901
—, Raman, of anorexigenic drugs . . . 95
—, ultraviolet, of γ-butyrolactones . . . 329
—, X-ray fluorescence (XRF), Determination of Co . . . 437
—, ———, —of Ru and Sn . . . 737
Spot tests, for common cations . . . 817
Stability constants, of Cd(II) chloro complexes . . . 237
——, of cyanoacetato complexes of metals . . . 199
——, of transition metal complexes . . . 809
Stainless-steel frits, for trace metal analysis by HPLC . . . 411
Strontium, Atomization, electrothermal . . . 177
Sulpha drugs, Determination with selective electrode . . . 383
Sulphate, Determination, nephelometric . . . 221
Sulphide, Chemiluminescence of reaction with hypobromite . . . 653
—, Determination, spectrophotometric . . . 853
—, —, titrimetric . . . 601
—, Extraction with tributyltin hydroxide . . . 173
Sulphur, Extraction with tributyltin hydroxide . . . 173
Sulphur trioxide, Absorption of . . . 599
Surfactants, Determination, spectrophotometric . . . 616

Talanta Advisory Board . . . No. 1, I; No. 2, I; No. 4, I
—Medal . . . No. 8, I

—Review, Interpretation of analytical information . . . 871
Tantalum, Determination by AAS and plasma emission spectroscopy . . . 901
Tellurium, Determination by AAS . . . 585
Thallium, Determination, spectrophotometric . . . 805
Thermogravimetry, of Ca sulphates in cement . . . 265
Thiamin, Determination, spectrofluorimetric . . . 225
Thiocarbamyl sulphenamides, Titration, amperometric . . . 262
Thiocarbonates, Extraction with tributyltin hydroxide . . . 173
Thiols, Determination, spectrophotometric . . . 843
—, —, titrimetric . . . 397
Thiosulphate, Determination by hydrogenation . . . 173
Thioureas, Determination, thermometric . . . 115
—, Separation by TLC . . . 115
Thiuram disulphide, Titration, amperometric . . . 262
Tin, Determination, by isotope dilution analysis . . . 73
—, —, by XRF . . . 737
—, Extraction of . . . 157
Tin(II), Oxidation of . . . 192
Titanium(V), Determination, spectrophotometric . . . 915
Titration, acid–base, Computer programme for . . . 565
—, ——, Correction for CO_2 evolution . . . 575
—, amperometric, of thiocarbamyl sulphenamides, thiuram disulphides and dibenzothiazyl disulphide . . . 262
—, catalytic thermometric, of amines . . . 691
—, cerimetric, of phenylhydrazines . . . 960
—, complexometric, of metal–ligand complexes . . . 241
—, —, of Pd . . . 327
—, conductometric, of nitrate . . . 349
—, coulometric, Determination of autoprotolysis constants . . . 183
—, —, of acidic compounds . . . 81
—, Karl Fischer, of water . . . 161
—, photometric, of Zr . . . 149
—, pH-stat, of γ-butyrolactones . . . 329
—, potentiometric, Errors in . . . 919
—, —, of Bi(III) . . . 931
—, —, of hydrogen peroxide . . . 951
—, —, of nitrates . . . 89
—, redox, with chlorbromamine-T . . . 627
—, reductometric, of Mn, Cr and V . . . 55
—, sequential, of Fe(II), Sb(III) and As(III) . . . 963
—, thermometric, Departure from linearity . . . 939
—, —, of β-aryl-α-mercaptopropenoic acids . . . 341
—, —, Reversibility of reactions . . . 945
—, two-phase, of Ag and pentachlorophenol . . . 857
—, ——, of kerosene . . . 281
Tolyltriazole, Determination by HPLC . . . 777
Trace metals, Determination by ASV . . . 839
——, —by HPLC . . . 411
——, —, spectrophotometric . . . 49
Transition metals, Complexes with fulvic and humic acids . . . 809
——, Determination, spectrophotometric . . . 857

Uranyl ion, Determination, by dye-laser spectroscopy . . . 107

Vanadium, Determination, reductometric . . . 55
Vanadium(IV), Titration with Ce(IV) sulphate . . . 287
Vanadium(V), Determination of traces, kinetic . . . 833
Vector model, for fluorescence spectra . . . 1
Voltammetry, hydrodynamic modulation . . . 369
—, anodic stripping (ASV), Determination of Pb . . . 65
—, ——, —of phosphate, silicate, arsenate and germanate . . . 473
—, ——, —of trace metals . . . 839
—, ——, —of Zn . . . 909
—, cyclic, of Sb(III) . . . 431

Water, Determination by Karl Fischer titration . . . 161

Xylenes, Determination with chloramine-T . . . 259

Yttrium, Determination by FAAS . . . 31

Zinc, Chelates with 2-thiopicolinamide 69
—, Determination by ASV 909
—, —by flow-injection analysis 389
—, —, spectrophotometric 399
Zinc(II), Cyanoacetato complexes of 199
—and lead, Separation from other elements 207
Zirconium, Determination, spectrophotometric 149

Printed in Great Britain by A. Wheaton & Co. Ltd., Exeter

Talanta, Vol. 28, p. ii, 1981
Pergamon Press Ltd. Printed in Great Britain

NOTICE

SYMPOSIUM ON AUTOMATED ANALYSIS

10/11 September 1981, Stirling, Scotland

This 2-day symposium, organized jointly by the Scottish Region and the Automatic Methods Group of the Analytical Division of the Royal Society of Chemistry, and the Microcomputer and Microprocessor Group of the RSC, will be held on the 10th and 11th of September 1981, at the Pathfoot Conference Centre of the University of Stirling. The symposium will include lectures on the influence of microprocessors and microcomputers on automation, current and prospective developments in hardware, interfacing microcomputers to analytical equipment and main-frame computers, data-handling and network analysis, microcomputer assisted HPLC method development using linear and simplex optimization, the handling of analytical records, and computer graphics applied to spectroscopy and chromatography. Speakers will include Professor D. Betteridge, Dr. J. C. Berridge, Dr. A. Carrick, Dr. A. S. McLelland, Dr. D. A. Newton, Dr. R. M. Smith, Dr. P. B. Stockwell and Dr. R. L. Tranter.

One afternoon will be devoted entirely to a Workshop and Practical Demonstration session featuring the application of microcomputers to such techniques as: method development, flow-injection analysis, HPLC, infra-red spectroscopy, mass spectrometry, graphics, data acquisition and transmission and interfacing. There will also be a small exhibition of instrumentation relevant to the theme of the Symposium.

For golfing enthusiasts and Symposium will be followed, on the Friday evening, by a golf tournament at Gleneagles (sponsored by the Technicon Instrument Co. Ltd.), to be followed by a Tournament dinner at the Dormie House Restaurant at which the winner will be presented with the Technicon Trophy.

The registration fee is £30 (£10 for students) and full accommodation at the University (room for 2 nights and all meals, including the Conference Dinner and Reception) is £42. Accommodation until the Saturday morning can be arranged.

For further information and registration forms please contact Dr. C. J. Jackson, HSE Laboratories, 403 Edgware Road, London NW2 6LN. Tel: 01-450 8911, ext. 227.

Talanta, Vol. 28, p. ii, 1981
Pergamon Press Ltd. Printed in Great Britain

PUBLICATIONS RECEIVED

Analytical Chemistry Symposia Series Vol. 2: Electroanalysis in Hygiene, Environmental, Clinical and Pharmaceutical Chemistry: W. FRANKLIN SMYTH (ed.), Elsevier, Amsterdam, 1980. Pp. 473. US$70.75.

Good books on electroanalytical chemistry have been a rarity for some while. The position with respect to ion-selective electrodes has been redressed somewhat by the appearance of good books by Peter Bailey and Karl Cammann. On the modern polarographic side the new book by Bond was very welcome and covers the descriptive and theoretical aspects well. On modern polarographic applications W. Franklin Smyth, the editor of the present book, has already edited the best book to date (Academic Press, 1979).

The present volume contains thirty-nine papers presented at the very successful conference held at Chelsea College in 1979, essentially covering the development and application of ion-selective electrodes and modern polarography. The articles are uniformly good but it would be impossible to mention them all here. Suffice it to say that anyone contemplating work on ISEs or modern polarography should study this volume carefully.

In the clinical section Simon writes on ISE exchangers for Na^+, K^+, Ca^{2+}, H_3O^+ and Cl^-, Svehla gives a rare discussion of errors in potentiometry and Scott discusses determination of ions in a segmented-flow system. Kell gives an excellent paper on the use of ISEs in flow-injection work, although more recent papers should now be consulted too. Palacek and Nürnberg/Valenta discuss applications of polarography to the study of damage to large molecules such as nucleic acids. Chayen gives an interesting article on the polarographic investigation of redox balance in clinical systems, and Weitzman's enthusiastic use of polarography with enzyme systems comes over in his article.

In the hygiene section Bergman discusses gas monitors and Jagner gives an application of potentiometric stripping analysis.

In the pharmaceutical section Patriarche's general article is notable for its description of recent applications of coulometric titrations in pharmaceutical systems. Jacobsen's description of the effect of surfactants is important, but could usefully have been supported by some graphs. Stripping voltammetry of drugs is described by W. F. Smyth and Davidson. Brooks gives an important general article on the polarographic determination of trace levels of drugs in body fluids. Burmicz, Brunt *et al.* and Ivaska and Smyth produce some novel ideas in their articles on voltammetric detectors.

The environmental section starts with a lengthy article of the usual high quality by Nürnberg. Van Leeuwen has an interesting article on the problems of determining metals in the presence of adsorbing surfactants, and illustrates the advantages of normal pulse polarography. Davídek discussed the determination of pesticides in food. Janet Osteryoung, M. Smyth and Samuelson determine environmental poisons and carcinogens.

A. G. FOGG

Standards in Absorption Spectrometry: UV SPECTROMETRY GROUP, C. BURGESS and A. KNOWLES (eds.), Chapman & Hall, London, 1981. Pp. 142 + xii. £9.50.

This small but extremely useful volume discusses several important topics in absorption spectrometry, and covers much more than the title initially suggests. There is a general introduction to UV–visible spectrometry, followed by detailed consideration of cell and instrument design, liquid and solid absorbance standards, stray light and its measurement, and wavelength calibration. Recommendations are made on cell-handling techniques and tests of cell performance, and on standardization procedures for use in non-specialized laboratories. All users of UV–visible spectrometers should read this book and heed its recommendations: a copy should be on the shelf in every laboratory. It would be very useful if instrument manufacturers were to supply a copy of the book with every new instrument—it would probably be more useful than the typical instrument operating manual.

MARY MASSON

Inorganic Reaction Chemistry, Vol. 1, Systematic Chemical Separation: D. T. BURNS, A. TOWNSHEND and A. G. CATCHPOLE, Horwood, Chichester, 1980. Pp. 248. £18.50, library edition; £6.95 student edition.

To a first-year university student, this book was quite a revelation. Most of the chemistry described is not even mentioned in the present-day school syllabus, and I found it most interesting. The book is very readable; remarkable, considering the level of the subject being dealt with. The basic theory is well explained and the historical section is short enough not to be boring and lively enough to encourage possible deeper study. The instructions for the practical work are detailed and should pose no problems, though a high degree of precision is required. The diagrams, however, are not nearly up to the standard of the rest of the book.

DONALD TAYLOR

Talanta, Vol. 28, p. ii, 1981
Pergamon Press Ltd. Printed in Great Britain

PUBLICATIONS RECEIVED

Analytical Chemistry Symposia Series Vol. 2: Electroanalysis in Hygiene, Environmental, Clinical and Pharmaceutical Chemistry: W. FRANKLIN SMYTH (ed.), Elsevier, Amsterdam, 1980. Pp. 473. US$70.75.

Good books on electroanalytical chemistry have been a rarity for some while. The position with respect to ion-selective electrodes has been redressed somewhat by the appearance of good books by Peter Bailey and Karl Cammann. On the modern polarographic side the new book by Bond was very welcome and covers the descriptive and theoretical aspects well. On modern polarographic applications W. Franklin Smyth, the editor of the present book, has already edited the best book to date (Academic Press, 1979).

The present volume contains thirty-nine papers presented at the very successful conference held at Chelsea College in 1979, essentially covering the development and application of ion-selective electrodes and modern polarography. The articles are uniformly good but it would be impossible to mention them all here. Suffice it to say that anyone contemplating work on ISEs or modern polarography should study this volume carefully.

In the clinical section Simon writes on ISE exchangers for Na^+, K^+, Ca^{2+}, H_3O^+ and Cl^-, Svehla gives a rare discussion of errors in potentiometry and Scott discusses determination of ions in a segmented-flow system. Kell gives an excellent paper on the use of ISEs in flow-injection work, although more recent papers should now be consulted too. Palacek and Nürnberg/Valenta discuss applications of polarography to the study of damage to large molecules such as nucleic acids. Chayen gives an interesting article on the polarographic investigation of redox balance in clinical systems, and Weitzman's enthusiastic use of polarography with enzyme systems comes over in his article.

In the hygiene section Bergman discusses gas monitors and Jagner gives an application of potentiometric stripping analysis.

In the pharmaceutical section Patriarche's general article is notable for its description of recent applications of coulometric titrations in pharmaceutical systems. Jacobsen's description of the effect of surfactants is important, but could usefully have been supported by some graphs. Stripping voltammetry of drugs is described by W. F. Smyth and Davidson. Brooks gives an important general article on the polarographic determination of trace levels of drugs in body fluids. Burmicz, Brunt *et al.* and Ivaska and Smyth produce some novel ideas in their articles on voltammetric detectors.

The environmental section starts with a lengthy article of the usual high quality by Nürnberg. Van Leeuwen has an interesting article on the problems of determining metals in the presence of adsorbing surfactants, and illustrates the advantages of normal pulse polarography. Davídek discussed the determination of pesticides in food. Janet Osteryoung, M. Smyth and Samuelson determine environmental poisons and carcinogens.

A. G. FOGG

Standards in Absorption Spectrometry: UV SPECTROMETRY GROUP, C. BURGESS and A. KNOWLES (eds.), Chapman & Hall, London, 1981. Pp. 142 + xii. £9.50.

This small but extremely useful volume discusses several important topics in absorption spectrometry, and covers much more than the title initially suggests. There is a general introduction to UV–visible spectrometry, followed by detailed consideration of cell and instrument design, liquid and solid absorbance standards, stray light and its measurement, and wavelength calibration. Recommendations are made on cell-handling techniques and tests of cell performance, and on standardization procedures for use in non-specialized laboratories. All users of UV–visible spectrometers should read this book and heed its recommendations: a copy should be on the shelf in every laboratory. It would be very useful if instrument manufacturers were to supply a copy of the book with every new instrument—it would probably be more useful than the typical instrument operating manual.

MARY MASSON

Inorganic Reaction Chemistry, Vol. 1, Systematic Chemical Separation: D. T. BURNS, A. TOWNSHEND and A. G. CATCHPOLE, Horwood, Chichester, 1980. Pp. 248. £18.50, library edition; £6.95 student edition.

To a first-year university student, this book was quite a revelation. Most of the chemistry described is not even mentioned in the present-day school syllabus, and I found it most interesting. The book is very readable; remarkable, considering the level of the subject being dealt with. The basic theory is well explained and the historical section is short enough not to be boring and lively enough to encourage possible deeper study. The instructions for the practical work are detailed and should pose no problems, though a high degree of precision is required. The diagrams, however, are not nearly up to the standard of the rest of the book.

DONALD TAYLOR

Talanta, Vol. 28, p. ii, 1981
Pergamon Press Ltd. Printed in Great Britain

PUBLICATIONS RECEIVED

Analytical Chemistry Symposia Series Vol. 2: Electroanalysis in Hygiene, Environmental, Clinical and Pharmaceutical Chemistry: W. FRANKLIN SMYTH (ed.), Elsevier, Amsterdam, 1980. Pp. 473. US$70.75.

Good books on electroanalytical chemistry have been a rarity for some while. The position with respect to ion-selective electrodes has been redressed somewhat by the appearance of good books by Peter Bailey and Karl Cammann. On the modern polarographic side the new book by Bond was very welcome and covers the descriptive and theoretical aspects well. On modern polarographic applications W. Franklin Smyth, the editor of the present book, has already edited the best book to date (Academic Press, 1979).

The present volume contains thirty-nine papers presented at the very successful conference held at Chelsea College in 1979, essentially covering the development and application of ion-selective electrodes and modern polarography. The articles are uniformly good but it would be impossible to mention them all here. Suffice it to say that anyone contemplating work on ISEs or modern polarography should study this volume carefully.

In the clinical section Simon writes on ISE exchangers for Na^+, K^+, Ca^{2+}, H_3O^+ and Cl^-, Svehla gives a rare discussion of errors in potentiometry and Scott discusses determination of ions in a segmented-flow system. Kell gives an excellent paper on the use of ISEs in flow-injection work, although more recent papers should now be consulted too. Palacek and Nürnberg/Valenta discuss applications of polarography to the study of damage to large molecules such as nucleic acids. Chayen gives an interesting article on the polarographic investigation of redox balance in clinical systems, and Weitzman's enthusiastic use of polarography with enzyme systems comes over in his article.

In the hygiene section Bergman discusses gas monitors and Jagner gives an application of potentiometric stripping analysis.

In the pharmaceutical section Patriarche's general article is notable for its description of recent applications of coulometric titrations in pharmaceutical systems. Jacobsen's description of the effect of surfactants is important, but could usefully have been supported by some graphs. Stripping voltammetry of drugs is described by W. F. Smyth and Davidson. Brooks gives an important general article on the polarographic determination of trace levels of drugs in body fluids. Burmicz, Brunt *et al.* and Ivaska and Smyth produce some novel ideas in their articles on voltammetric detectors.

The environmental section starts with a lengthy article of the usual high quality by Nürnberg. Van Leeuwen has an interesting article on the problems of determining metals in the presence of adsorbing surfactants, and illustrates the advantages of normal pulse polarography. Davídek discussed the determination of pesticides in food. Janet Osteryoung, M. Smyth and Samuelson determine environmental poisons and carcinogens.

A. G. FOGG

Standards in Absorption Spectrometry: UV SPECTROMETRY GROUP, C. BURGESS and A. KNOWLES (eds.), Chapman & Hall, London, 1981. Pp. 142 + xii. £9.50.

This small but extremely useful volume discusses several important topics in absorption spectrometry, and covers much more than the title initially suggests. There is a general introduction to UV–visible spectrometry, followed by detailed consideration of cell and instrument design, liquid and solid absorbance standards, stray light and its measurement, and wavelength calibration. Recommendations are made on cell-handling techniques and tests of cell performance, and on standardization procedures for use in non-specialized laboratories. All users of UV–visible spectrometers should read this book and heed its recommendations: a copy should be on the shelf in every laboratory. It would be very useful if instrument manufacturers were to supply a copy of the book with every new instrument—it would probably be more useful than the typical instrument operating manual.

MARY MASSON

Inorganic Reaction Chemistry, Vol. 1, Systematic Chemical Separation: D. T. BURNS, A. TOWNSHEND and A. G. CATCHPOLE, Horwood, Chichester, 1980. Pp. 248. £18.50, library edition; £6.95 student edition.

To a first-year university student, this book was quite a revelation. Most of the chemistry described is not even mentioned in the present-day school syllabus, and I found it most interesting. The book is very readable; remarkable, considering the level of the subject being dealt with. The basic theory is well explained and the historical section is short enough not to be boring and lively enough to encourage possible deeper study. The instructions for the practical work are detailed and should pose no problems, though a high degree of precision is required. The diagrams, however, are not nearly up to the standard of the rest of the book.

DONALD TAYLOR

Talanta, Vol. 28, p. ii, 1981
Printed in Great Britain

Pergamon Press Ltd

ERRATA

In the Harvey Diehl Honour Issue (1980, No. 11B), on page 1013, the name of one of the authors was accidentally omitted. It is Sherman Chao (Institute of Gas Technology, Chicago, Illinois 60616).

In the paper by F. W. E. Strelow and T. N. Vander Walt, *Talanta*, 1979, **26**, 537, on page 538, left-hand column, the 9th line from the foot of the column should read:

"In 25-ml standard flasks were placed 4.0 ml of a standard solution"

and in the 8th line from the foot of the same column a comma is needed after 'uranium(VI)' to read:

"...containing 40 μg of uranium(VI), 2.5 ml of...".

Talanta, Vol. 28, p. iii, 1981
Pergamon Press Ltd. Printed in Great Britain

PUBLICATIONS RECEIVED

Factor Analysis in Chemistry: E. R. MALINOWSKI and D. G. HOWERY, Wiley-Interscience, New York, 1980. Pp. ix + 251. £19.35.

A most readable account of the theory, practice and applications of factor analysis in chemistry is given in the monograph. Although detailed study of the mathematical chapters would be necessary for thorough understanding, of the subject, the qualitative discussion also provided allows the less mathematically inclined to gain insight into the potential of factor analysis. Detailed practical instructions are given on "how to do" factor analysis, along with references to the computer programs available to aid in the work. The later chapters are devoted to discussions of what has been achieved by means of factor analysis in a wide range of applications. In analytical chemistry, the topics covered include the testing of the performance of instruments, comparison of methods, and corrections for medium effects.

MARY MASSON

Quantitative Analysis of Organic Mixtures, Part One: General Principles: T. S. MA and R. E. LANG, Wiley-Interscience, New York, 1979. Pp. xvii + 366. £21.25.

This well-referenced text contains a wealth of information on the problems of analysing organic mixtures and on the ways in which these problems can be overcome. Methods of sampling and sample preparation in very varied circumstances are discussed, and method selection is discussed with reference to official standardized *vs.* other methods, and chemical *vs.* instrumental methods. There is detailed discussion of the determination of several components of a mixture without separation, by methods including differential titrimetry, differential reaction rates, polarography, mass spectrometry, absorption spectrophotometry, and other spectral techniques. Determinations involving separations are then discussed. After consideration of the various methods of separation available, including gas chromatography, liquid chromatography, ion-exchange chromatography, paper and thin-layer chromatography, electrophoresis, extraction and distillation, there is more detailed information presented about the separation of acidic, basic and neutral substances.

MARY MASSON

Information Theory as Applied to Chemical Analysis: K. ECKSCHLAGER and V. ŠTĚPÁNEK, Wiley-Interscience, New York, 1979. Pp. xv + 186. £16.20.

Before reading this book, I was unconvinced of the usefulness of information theory in analytical chemistry, and it did little to persuade me otherwise. The topics covered include an introduction and chapters on analysis as a process of obtaining information, basic concepts of probability theory, information theory, some methods of statistical inference, and evaluation and optimization of analytical results and methods. The authors state in their preface that they tried to make the monograph self-contained with respect to theory, and that the mathematical chapters require only knowledge of calculus and combinatorial counting techniques. This suggested to me that I should be well able to follow the mathematics, but instead I found the abstract and symbolic presentation and the highly condensed format extremely difficult to understand (and typographical errors probably did not help). The later, more applied, parts of the book are also presented in very abstract form, and offer little help to the previously uninitiated. In this sense, the book is not at all like Eckschlager's previous book on Errors, Measurement and Results in Chemical Analysis, which is full of practical illustrations and which is easy to read and understand. The book could have been improved by better editing of the English translation, and by elimination of the typographical errors (*e.g.*, p. xi, precision instead of decision; p. 18, supposition instead of superposition; p. 154, elude for elute; p. 159—what are dissolvents?).

MARY MASSON

Talanta, Vol. 28, p. iii, 1981
Pergamon Press Ltd. Printed in Great Britain

PUBLICATIONS RECEIVED

Factor Analysis in Chemistry: E. R. MALINOWSKI and D. G. HOWERY, Wiley-Interscience, New York, 1980. Pp. ix + 251. £19.35.

A most readable account of the theory, practice and applications of factor analysis in chemistry is given in the monograph. Although detailed study of the mathematical chapters would be necessary for thorough understanding, of the subject, the qualitative discussion also provided allows the less mathematically inclined to gain insight into the potential of factor analysis. Detailed practical instructions are given on "how to do" factor analysis, along with references to the computer programs available to aid in the work. The later chapters are devoted to discussions of what has been achieved by means of factor analysis in a wide range of applications. In analytical chemistry, the topics covered include the testing of the performance of instruments, comparison of methods, and corrections for medium effects.

MARY MASSON

Quantitative Analysis of Organic Mixtures, Part One: General Principles: T. S. MA and R. E. LANG, Wiley-Interscience, New York, 1979. Pp. xvii + 366. £21.25.

This well-referenced text contains a wealth of information on the problems of analysing organic mixtures and on the ways in which these problems can be overcome. Methods of sampling and sample preparation in very varied circumstances are discussed, and method selection is discussed with reference to official standardized *vs.* other methods, and chemical *vs.* instrumental methods. There is detailed discussion of the determination of several components of a mixture without separation, by methods including differential titrimetry, differential reaction rates, polarography, mass spectrometry, absorption spectrophotometry, and other spectral techniques. Determinations involving separations are then discussed. After consideration of the various methods of separation available, including gas chromatography, liquid chromatography, ion-exchange chromatography, paper and thin-layer chromatography, electrophoresis, extraction and distillation, there is more detailed information presented about the separation of acidic, basic and neutral substances.

MARY MASSON

Information Theory as Applied to Chemical Analysis: K. ECKSCHLAGER and V. ŠTĚPÁNEK, Wiley-Interscience, New York, 1979. Pp. xv + 186. £16.20.

Before reading this book, I was unconvinced of the usefulness of information theory in analytical chemistry, and it did little to persuade me otherwise. The topics covered include an introduction and chapters on analysis as a process of obtaining information, basic concepts of probability theory, information theory, some methods of statistical inference, and evaluation and optimization of analytical results and methods. The authors state in their preface that they tried to make the monograph self-contained with respect to theory, and that the mathematical chapters require only knowledge of calculus and combinatorial counting techniques. This suggested to me that I should be well able to follow the mathematics, but instead I found the abstract and symbolic presentation and the highly condensed format extremely difficult to understand (and typographical errors probably did not help). The later, more applied, parts of the book are also presented in very abstract form, and offer little help to the previously uninitiated. In this sense, the book is not at all like Eckschlager's previous book on Errors, Measurement and Results in Chemical Analysis, which is full of practical illustrations and which is easy to read and understand. The book could have been improved by better editing of the English translation, and by elimination of the typographical errors (*e.g.*, p. xi, precision instead of decision; p. 18, supposition instead of superposition; p. 154, elude for elute; p. 159—what are dissolvents?).

MARY MASSON

Talanta, Vol. 28, p. iii, 1981
Pergamon Press Ltd. Printed in Great Britain

PUBLICATIONS RECEIVED

Factor Analysis in Chemistry: E. R. MALINOWSKI and D. G. HOWERY, Wiley-Interscience, New York, 1980. Pp. ix + 251. £19.35.

A most readable account of the theory, practice and applications of factor analysis in chemistry is given in the monograph. Although detailed study of the mathematical chapters would be necessary for thorough understanding, of the subject, the qualitative discussion also provided allows the less mathematically inclined to gain insight into the potential of factor analysis. Detailed practical instructions are given on "how to do" factor analysis, along with references to the computer programs available to aid in the work. The later chapters are devoted to discussions of what has been achieved by means of factor analysis in a wide range of applications. In analytical chemistry, the topics covered include the testing of the performance of instruments, comparison of methods, and corrections for medium effects.

MARY MASSON

Quantitative Analysis of Organic Mixtures, Part One: General Principles: T. S. MA and R. E. LANG, Wiley-Interscience, New York, 1979. Pp. xvii + 366. £21.25.

This well-referenced text contains a wealth of information on the problems of analysing organic mixtures and on the ways in which these problems can be overcome. Methods of sampling and sample preparation in very varied circumstances are discussed, and method selection is discussed with reference to official standardized *vs.* other methods, and chemical *vs.* instrumental methods. There is detailed discussion of the determination of several components of a mixture without separation, by methods including differential titrimetry, differential reaction rates, polarography, mass spectrometry, absorption spectrophotometry, and other spectral techniques. Determinations involving separations are then discussed. After consideration of the various methods of separation available, including gas chromatography, liquid chromatography, ion-exchange chromatography, paper and thin-layer chromatography, electrophoresis, extraction and distillation, there is more detailed information presented about the separation of acidic, basic and neutral substances.

MARY MASSON

Information Theory as Applied to Chemical Analysis: K. ECKSCHLAGER and V. ŠTĚPÁNEK, Wiley-Interscience, New York, 1979. Pp. xv + 186. £16.20.

Before reading this book, I was unconvinced of the usefulness of information theory in analytical chemistry, and it did little to persuade me otherwise. The topics covered include an introduction and chapters on analysis as a process of obtaining information, basic concepts of probability theory, information theory, some methods of statistical inference, and evaluation and optimization of analytical results and methods. The authors state in their preface that they tried to make the monograph self-contained with respect to theory, and that the mathematical chapters require only knowledge of calculus and combinatorial counting techniques. This suggested to me that I should be well able to follow the mathematics, but instead I found the abstract and symbolic presentation and the highly condensed format extremely difficult to understand (and typographical errors probably did not help). The later, more applied, parts of the book are also presented in very abstract form, and offer little help to the previously uninitiated. In this sense, the book is not at all like Eckschlager's previous book on Errors, Measurement and Results in Chemical Analysis, which is full of practical illustrations and which is easy to read and understand. The book could have been improved by better editing of the English translation, and by elimination of the typographical errors (*e.g.*, p. xi, precision instead of decision; p. 18, supposition instead of superposition; p. 154, elude for elute; p. 159—what are dissolvents?).

MARY MASSON

Talanta. Vol. 28. pp. iii to iv. 1981
Pergamon Press Ltd. Printed in Great Britain

PUBLICATIONS RECEIVED

Petroleum in the Marine Environment: Advances in Chemistry Series, No. 185: L. PETRAKIS and F. T. WEISS (eds.), American Chemical Society, Washington, 1980. Pp. x + 371. $42.00.

The analytical chemist faced with this topic immediately has three main problems: what to analyse samples for, how to do the analyses, and then how to interpret the results. The sixteen chapters in this book (presented as papers at a meeting in Miami in 1978) go a long way towards providing answers to all of these problems. The review papers emphasize the difficulty in deciding whether hydrocarbon contamination in biological samples is of direct natural origin (oil seepage, coal), from dumping or spillage of crude or fuel oils, or of biogenic origin. A number of chapters discuss the combined use of several techniques to analyse samples for hydrocarbons, showing that GC/MS, HPLC, purging and trapping with GC all have an important role to play. Some of the chapters are more concerned with the results themselves for various types of samples: these figures could be of use to other workers in forming the basis of comparisons. This book scores well on several grounds: it is well written, it contains much fascinating information on the background to the problem (at least one author takes the trouble to explain why phytane and pristane are so interesting), it supplies many details on experimental approaches, and provides a good data base for comparisons. Recommended.

IAIN L. MARR

Analytical Techniques in Environmental Chemistry: J. ALBAIGES (ed.). Pergamon Press, Oxford, 1980. Pp. xii + 646. £43.00.

This book includes 60 papers presented at an international congress in Barcelona in 1978, and presents a fairly detailed picture of research activity in the field at that time. The introductory review (Brassell and Eglinton) deals with the problem of sources of organic compounds in natural waters and how analytical techniques may help in environmental investigations. Rather over half the papers are concerned with determining organic compounds, the remainder with various toxic elements including the heavy metals. Most are concerned with aquatic samples. There is a wealth of data from individual investigations which will be of interest to other workers engaged in similar studies at other locations. In a field where publications are scattered through so many journals, this one large collection could prove a useful introduction to the literature.

IAIN L. MARR

Immobilized Enzymes in Analytical and Clinical Chemistry: P. W. CARR and L. D. BOWERS, Wiley-Interscience, New York, 1980. Pp. 460. £24.

The authors' declared intention is to introduce the subject of immobilized enzymes to analysts. This calls for two qualities (*i*) a good balance between expounding the elements of the subject and giving the most up-to-date review possible, (*ii*) composing the text so that the inexpert can find their way easily round the book for cross-reference. This work succeeds on both counts.

The basics are covered in 150 pages, immobilization techniques in 40, theory and practice of enzyme electrodes in 120 and finally some 50 pages each on the fundamentals of flow-system kinetics, transfer processes in enzyme reactors, and applications of immobilized enzymes in such systems. Extensive tables present useful surveys of analytical applications of electrode and reactor systems with critical comments. The literature has been covered well into 1980.

DEREK MIDGLEY

Mass Spectrometry, Part B: CHARLES MERRITT, JR. and CHARLES N. MCEWEN, Dekker, New York, 1980. pp. 416. SFr. 105.

This, the second part of Volume 3 in the practical spectroscopy series ably maintains the excellent standard achieved by its predecessor and the aims of the series in general. It is a particularly notable feature that the relevance to practical mass spectroscopists of newer techniques is emphasized by reference to a wide range of actual examples in which the reader can see exactly how the results have been obtained and what advantages are apparent compared with more conventional methods. Too often, practising spectroscopists and analysts dismiss newer methods because the theoretical accounts are rendered impenetrable by obscure terminology and lack of obvious application. The approach in this book, with the lucid and careful explanations which take the trouble to define and explain the numerous initial letter technical words and abbreviations (an all too frequent hazard in mass spectrometry), provides a powerful incentive for both the experienced practitioner and newcomer alike to overcome the initial barriers and actually put these methods to use.

Talanta. Vol. 28. pp. iii to iv. 1981
Pergamon Press Ltd. Printed in Great Britain

PUBLICATIONS RECEIVED

Petroleum in the Marine Environment: Advances in Chemistry Series, No. 185: L. PETRAKIS and F. T. WEISS (eds.), American Chemical Society, Washington, 1980. Pp. x + 371. $42.00.

The analytical chemist faced with this topic immediately has three main problems: what to analyse samples for, how to do the analyses, and then how to interpret the results. The sixteen chapters in this book (presented as papers at a meeting in Miami in 1978) go a long way towards providing answers to all of these problems. The review papers emphasize the difficulty in deciding whether hydrocarbon contamination in biological samples is of direct natural origin (oil seepage, coal), from dumping or spillage of crude or fuel oils, or of biogenic origin. A number of chapters discuss the combined use of several techniques to analyse samples for hydrocarbons, showing that GC/MS, HPLC, purging and trapping with GC all have an important role to play. Some of the chapters are more concerned with the results themselves for various types of samples: these figures could be of use to other workers in forming the basis of comparisons. This book scores well on several grounds: it is well written, it contains much fascinating information on the background to the problem (at least one author takes the trouble to explain why phytane and pristane are so interesting), it supplies many details on experimental approaches, and provides a good data base for comparisons. Recommended.

IAIN L. MARR

Analytical Techniques in Environmental Chemistry: J. ALBAIGES (ed.). Pergamon Press, Oxford, 1980. Pp. xii + 646. £43.00.

This book includes 60 papers presented at an international congress in Barcelona in 1978, and presents a fairly detailed picture of research activity in the field at that time. The introductory review (Brassell and Eglinton) deals with the problem of sources of organic compounds in natural waters and how analytical techniques may help in environmental investigations. Rather over half the papers are concerned with determining organic compounds, the remainder with various toxic elements including the heavy metals. Most are concerned with aquatic samples. There is a wealth of data from individual investigations which will be of interest to other workers engaged in similar studies at other locations. In a field where publications are scattered through so many journals, this one large collection could prove a useful introduction to the literature.

IAIN L. MARR

Immobilized Enzymes in Analytical and Clinical Chemistry: P. W. CARR and L. D. BOWERS, Wiley-Interscience, New York, 1980. Pp. 460. £24.

The authors' declared intention is to introduce the subject of immobilized enzymes to analysts. This calls for two qualities (*i*) a good balance between expounding the elements of the subject and giving the most up-to-date review possible, (*ii*) composing the text so that the inexpert can find their way easily round the book for cross-reference. This work succeeds on both counts.

The basics are covered in 150 pages, immobilization techniques in 40, theory and practice of enzyme electrodes in 120 and finally some 50 pages each on the fundamentals of flow-system kinetics, transfer processes in enzyme reactors, and applications of immobilized enzymes in such systems. Extensive tables present useful surveys of analytical applications of electrode and reactor systems with critical comments. The literature has been covered well into 1980.

DEREK MIDGLEY

Mass Spectrometry, Part B: CHARLES MERRITT, JR. and CHARLES N. MCEWEN, Dekker, New York, 1980. pp. 416. SFr. 105.

This, the second part of Volume 3 in the practical spectroscopy series ably maintains the excellent standard achieved by its predecessor and the aims of the series in general. It is a particularly notable feature that the relevance to practical mass spectroscopists of newer techniques is emphasized by reference to a wide range of actual examples in which the reader can see exactly how the results have been obtained and what advantages are apparent compared with more conventional methods. Too often, practising spectroscopists and analysts dismiss newer methods because the theoretical accounts are rendered impenetrable by obscure terminology and lack of obvious application. The approach in this book, with the lucid and careful explanations which take the trouble to define and explain the numerous initial letter technical words and abbreviations (an all too frequent hazard in mass spectrometry), provides a powerful incentive for both the experienced practitioner and newcomer alike to overcome the initial barriers and actually put these methods to use.

Talanta. Vol. 28, pp. iii to iv. 1981
Pergamon Press Ltd. Printed in Great Britain

PUBLICATIONS RECEIVED

Petroleum in the Marine Environment: Advances in Chemistry Series, No. 185: L. PETRAKIS and F. T: WEISS (eds.), American Chemical Society, Washington, 1980. Pp. x + 371. $42.00.

The analytical chemist faced with this topic immediately has three main problems: what to analyse samples for, how to do the analyses, and then how to interpret the results. The sixteen chapters in this book (presented as papers at a meeting in Miami in 1978) go a long way towards providing answers to all of these problems. The review papers emphasize the difficulty in deciding whether hydrocarbon contamination in biological samples is of direct natural origin (oil seepage, coal), from dumping or spillage of crude or fuel oils, or of biogenic origin. A number of chapters discuss the combined use of several techniques to analyse samples for hydrocarbons, showing that GC/MS, HPLC, purging and trapping with GC all have an important role to play. Some of the chapters are more concerned with the results themselves for various types of samples: these figures could be of use to other workers in forming the basis of comparisons. This book scores well on several grounds: it is well written, it contains much fascinating information on the background to the problem (at least one author takes the trouble to explain why phytane and pristane are so interesting), it supplies many details on experimental approaches, and provides a good data base for comparisons. Recommended.

IAIN L. MARR

Analytical Techniques in Environmental Chemistry: J. ALBAIGES (ed.). Pergamon Press, Oxford, 1980. Pp. xii + 646. £43.00.

This book includes 60 papers presented at an international congress in Barcelona in 1978, and presents a fairly detailed picture of research activity in the field at that time. The introductory review (Brassell and Eglinton) deals with the problem of sources of organic compounds in natural waters and how analytical techniques may help in environmental investigations. Rather over half the papers are concerned with determining organic compounds, the remainder with various toxic elements including the heavy metals. Most are concerned with aquatic samples. There is a wealth of data from individual investigations which will be of interest to other workers engaged in similar studies at other locations. In a field where publications are scattered through so many journals, this one large collection could prove a useful introduction to the literature.

IAIN L. MARR

Immobilized Enzymes in Analytical and Clinical Chemistry: P. W. CARR and L. D. BOWERS, Wiley-Interscience, New York, 1980. Pp. 460. £24.

The authors' declared intention is to introduce the subject of immobilized enzymes to analysts. This calls for two qualities (*i*) a good balance between expounding the elements of the subject and giving the most up-to-date review possible, (*ii*) composing the text so that the inexpert can find their way easily round the book for cross-reference. This work succeeds on both counts.

The basics are covered in 150 pages, immobilization techniques in 40, theory and practice of enzyme electrodes in 120 and finally some 50 pages each on the fundamentals of flow-system kinetics, transfer processes in enzyme reactors, and applications of immobilized enzymes in such systems. Extensive tables present useful surveys of analytical applications of electrode and reactor systems with critical comments. The literature has been covered well into 1980.

DEREK MIDGLEY

Mass Spectrometry, Part B: CHARLES MERRITT, JR. and CHARLES N. MCEWEN, Dekker, New York, 1980. pp. 416. SFr. 105.

This, the second part of Volume 3 in the practical spectroscopy series ably maintains the excellent standard achieved by its predecessor and the aims of the series in general. It is a particularly notable feature that the relevance to practical mass spectroscopists of newer techniques is emphasized by reference to a wide range of actual examples in which the reader can see exactly how the results have been obtained and what advantages are apparent compared with more conventional methods. Too often, practising spectroscopists and analysts dismiss newer methods because the theoretical accounts are rendered impenetrable by obscure terminology and lack of obvious application. The approach in this book, with the lucid and careful explanations which take the trouble to define and explain the numerous initial letter technical words and abbreviations (an all too frequent hazard in mass spectrometry), provides a powerful incentive for both the experienced practitioner and newcomer alike to overcome the initial barriers and actually put these methods to use.

Talanta, Vol. 28, pp. iii to iv, 1981
Pergamon Press Ltd. Printed in Great Britain

NOTICES

SECOND INTERNATIONAL WORKSHOP ON TRACE ELEMENT ANALYTICAL CHEMISTRY IN MEDICINE AND BIOLOGY

Neuherberg/Munich, Federal Republic of Germany

21–23 April 1982

This workshop will have the same form as the first one, which is intended to guarantee a free and effective exchange of views between the analytical specialists on the one hand and the biomedical specialists (the users of the analytical data) on the other. It is hoped that the workshop will lead to a productive scientific dialogue between these two groups in regard to the biomedical applications of trace-element analytical research. The international and multidisciplinary character of the workshop should provide a good working forum for all interested in this subject area. The workshop will be repeated at intervals of two years. The aim at each meeting is to bring together, at one table, experts in the analysis and biomedical significance of trace elements. The topics to be covered will be varied from one meeting to the next. The second workshop will have "Essential, Toxic and Analytical Aspects of Trace Elements" as its general theme.

The workshop will consist of a series of invited papers on specific problem areas each followed by an extended discussion period in which all participants will be invited to take part. Short contributed papers (oral or poster presentation) are also solicited for the workshop.

Scope

I. Nutritional requirements as function of age
II. Metabolic (absorption, transfer, transport, storage, mobilization, excretion) and biochemical (metalloprotein, enzymes, hormones) effects
III. Subclinical and chronic effects
IV. Diagnosis of trace element supply
V. Analytical requirements and potentialities (sampling, storage, pretreatment, determination, evaluation, quality control)

Call for papers

Abstracts of papers intended as contributions to the discussions at the workshop must be submitted in English, in three copies, to the Organizing Committee by

30 November, 1981

The abstracts must be typed in double spacing and should not exceed one typewritten page in length. The abstract will be subjected to refereeing for acceptance of the paper and for the "Conference Abstracts". Authors of accepted papers will be asked to submit the full manuscripts in English during the conference (latest) for publication in the Conference Proceedings by W. de Gruyter Publ. Comp. The preliminary application form should be sent to the organizers by 30 July, 1981.

All correspondence concerning the workshop should be addressed to:

Dr. P. Schramel
Gesellschaft fuer Strahlen- und Umweltforschung
Institut fuer Angewandte Physik
Physikalisch-Technische Abteilung
Ingolstaedter Landstrasse 1
D-8042 Neuherberg
Federal Republic of Germany

1982 WINTER CONFERENCE ON PLASMA SPECTROCHEMISTRY

Orlando, Florida

4–9 January 1982

The 1982 Winter Conference on Plasma Spectrochemistry, sponsored by the *ICP Information Newsletter* in cooperation with the Society for Applied Spectroscopy (Florida section) and the American Chemical Society (Tampa section of the Analytical Chemistry Division), will feature developments in atomic plasma spectrochemical analysis by inductively coupled plasma (ICP), DC plasma (DCP), and microwave plasma (MIP) excitation sources. The meeting will convene on Monday, January 4 through Saturday, January 9, 1982 at the Orlando Hyatt Hotel in Kissimmee, Florida, adjacent to Walt Disney World.

Talanta, Vol. 28, p. iii
Pergamon Press Ltd 1981. Printed in Great Britain

PUBLICATIONS RECEIVED

Modern Organic Elemental Analysis: T. S. MA and ROBERT C. RITTNER, Dekker, New York, 1979. Pp. 536. S.Fr. 100.

This book sets out to provide full information on the analysis of small quantities (mg) of material and as such performs a useful function in the microanalytical world. Each chapter is devoted to either the determination of a single element or closely related groups. A format is followed which first of all discusses in general the analytical aspects of that particular element or elements and then goes on to review current methods including the most recent developments. The very useful experimental data for the methods are then dealt with, which should enable most people who are familiar with general analytical procedures to appreciate the possibilities of, and indeed to carry out, the various methods discussed.

Also included are a chapter on ultramicro analysis and one on trace analysis, both of which can be regarded as an extension of microanalysis. The appendix for nitrogen determination refers to macro quantities (g) but this is required by the U.S. Pharmacopeia.

Each chapter is completed by a comprehensive and up to date list of references. The book is well laid out, adequately illustrated and indexed with both author and subject headings.

It should find a useful place in the library of practising analysts in both large and small laboratories and teachers in academic institutions should find it a great help for both theoretical and practical instruction.

DORIS BUTTERWORTH

Dynamics, Exposure and Hazard Assessment of Toxic Chemicals: RIZWANUL HAQUE (Ed.), Ann Arbor Science Publishers Inc., Ann Arbor, 1980. Pp. viii + 496. £18.50.

The significance of being able to predict the behaviour and ultimate fate of organic chemical substances released into the environment has become apparent in recent years and the appearance of a book dealing with such matters is, therefore, timely. The volume under consideration contains the contributions made at a symposium sponsored by the Division of Environmental Chemistry of the American Chemical Society and held in Florida during September 1979. In spite of the title, the subject matter is confined to organic substances. In all, the book contains 31 contributions. The first 7 provide information about such local matters as national laws, agencies concerned with the environment and the funding of projects and they will be of limited interest to those living outside the United States. The remaining contributions (from p. 47) deal primarily with scientific aspects of transport and "fate" studies on organic substances. The extent of partitioning and lifetime of chemicals in air, water and soils, and potential bio-accumulation in biota are discussed. Roles played, for example, by photochemical, oxidative, hydrolytic and biodegradative processes are considered.

The treatment of each topic is variable; some provide good background summaries of previous work as well as recent contributions by the authors and are well-documented, but others are indifferently provided with references, and one scientific paper even has none at all [strangely, it is entitled Environmental Testing of Toxic Substances (Ch. 30)]. It is more difficult to select praiseworthy contributions but those entitled "Assessing the Photochemistry of Organic Pollutants in Aquatic Environments" (Ch. 9) and "Toxicological Dynamics" (Ch. 27) appealed most to the reviewer. The book is very well produced, reasonably priced and contains much of interest to analysts and analytical chemists concerned with its wide-ranging subject matter.

S. J. LYLE

Radioelement Analysis, Progress and Problems: W. S. LYON (Ed.), Ann Arbor Science Publishers Inc., Ann Arbor, 1980. Pp. xii + 424. £16.50.

This book provides a record of the Proceedings of the Twenty Third Conference on Analytical Chemistry in Energy Technology held in October, 1979 at the Oak Ridge National Laboratory. The "proceedings" consisted of a plenary lecture and 45 other contributions. The Three Mile Island accident had occurred in late March of that year and the plenary lecture by R. E. Brookbank gives an interesting account of the role played by analytical chemists in post-accident monitoring of the building complex and surroundings. Other contributions (numbers in parenthesis) are grouped under the headings, Radiochemical Separations and Measurements (6), Radiochemical Determinations and Measurements (7), Gamma Spectrometry and Activation Analysis (7), Environmental Analysis (9), On Line Monitoring and Facilities (8), Mass Spectrometry (4) and Quality Assurance and Standards (4). A short index is provided.

As is inevitable in a collection of contributions of this kind, the quality is variable and regrettably all too large a proportion is poorly documented or entirely without references to background literature; the latter is inexcusable in a well-developed field such as that under consideration. Nevertheless, much material of interest, particularly to those associated with environmental monitoring, is to be found among the contributed papers and this reasonably priced and adequately produced account of the Conference Proceedings is worthy of a place in the radioanalytical chemist's library.

S. J. LYLE

Liquid Chromatography of Polymers and Related Materials II. (Chromatographic Science Series, Volume 13): JACK CAZES and XAVIER DELAMORE (Eds.) Dekker, New York, 1980. Pp. 272. S.Fr. 80.

This volume comprises a selection of papers presented at the Fourth International Liquid Chromatography Symposium held in October 1979. All thirteen contributions examine some aspect of gel permeation chromatography (GPC). Two of the papers deal with the mechanism of GPC and the remainder with practical aspects which range from the determination of average molecular weights of synthetic polymers to the characterization of branched polymers, nitrocelluloses and asphalts.

G. G. CAMERON

Talanta, Vol. 28, pp. iii to iv.
Pergamon Press Ltd 1981. Printed in Great Britain

PUBLICATIONS RECEIVED

Experiments in Environmental Chemistry—A Laboratory Manual: P. D. VOWLES and D. W. CONNELL, Pergamon, Oxford, 1980. Pp. vii + 102. US $9.95 (flexicover version).

This stimulating little book by two Australian authors gives full details, plus a lot of useful additional background information, for 14 laboratory or field experiments dealing with topics such as biochemical processes in aquatic systems, toxic substances in the environment, food additives and contaminants, chemical defence mechanisms in insects, and natural and man-made factors influencing the water quality in streams/estuaries. The experiments are suitable for fairly advanced students only and require the availability of a considerable range of laboratory instrumentation—dissolved-oxygen meters, gas chromatographs with thermal-conductivity, flame-ionization and electron-capture detectors, atomic-absorption spectrometers, non-dispersive gas analysers, gas- and liquid-sampling devices *etc.* Some of the experiments could not be carried out directly in European countries, *e.g.*, in the chemical ecology experiment based on the determination of cardiac glycosides "samples of monarch butterfly larvae and the milk weed plant may be collected during warmer periods of the year in North and South America, Australia, and South East Asia." This, however, should not be taken as a criticism of the book although it may be a disappointment or frustration to some of its purchasers; others attracted by the ambitious nature of the experiments and projects described can use them as models for biological systems and species more readily obtainable in their particular geographical locality.

Some of the bibliography cited is not too readily available and some of it is too directly concerned with American or Australian phenomena to be of general interest, *e.g.*, "Water Pollution—Causes and Effects in Australia." Although a lot more care could have been taken at the proof-reading stage, this book deserves success; perhaps its authors will feel encouraged to produce an enlarged edition that will set out to be more international in its appeal.

D. M. W. ANDERSON

Electrophoresis—A Survey of Techniques and Applications—Part A: **Techniques:** Z. DEYL, F. EVERAERTS, Z. PRUSIK and P. J. SVENDSEN (eds.), Elsevier, Amsterdam, 1980. Pp. xv + 390. US $83.00, Dfl. 170.00.

This is the first part of Volume 18 of the now well-established Elsevier Journal of Chromatography Library; Part B, devoted to applications, will appear subsequently. For this volume, Dr. Deyl assembled a team of 11 contributors based in Czechoslovakia, Denmark, the Netherlands, Poland, Sweden and the U.S.A., the result is a text worthy of international recognition.

Although this volume concentrates on presenting the mathematical and physicochemical theory underlying electromigration techniques, together with experimental details and descriptions of instrumentation *etc.*, sufficient examples of typical separations are given as illustrative examples to make this volume reasonably self-contained without jeopardizing the objectives envisaged for Part B. The mathematical treatment is restricted to fundamental essentials.

For this type of book it seems desirable to use the space available here to give prospective purchasers an indication of the wide extent of the topics covered. The chapters deal with theory and classification of electromigration processes; evaluation of the results of electrophoretic separations; molecular size and shape in electrophoresis; zone electrophoresis; gel-type techniques; quantitative immunoelectrophoresis; moving boundary electrophoresis in narrow-bore tubes; isoelectric focusing; analytical isotachophoresis; continuous flow-through electrophoresis; preparative electrophoresis in gels and in columns; preparative isoelectric focusing and isotachophoresis, including operations on the micro scale. There is a comprehensive subject index. Only two of these chapters cite references to original literature published in 1978 or 1979; the majority of chapters cite nothing more recent than 1976 or 1977. Perhaps this is a reflection on the length of time taken to produce this book (possibly translations into English of several chapters were necessary) or perhaps it is the case that the rate of progress of developments in electromigration techniques started to decrease markedly in the early seventies. Whatever the reason, we have here a substantial and authoritative text that covers the field well up to around 1975.

D. M. W. ANDERSON

Additive Migration from Plastics into Food: T. R. COMPTON, Pergamon, Oxford, 1979. Pp. xi + 234. US $47.00.

The topic covered by this book will be of concern to many practising analysts, who will welcome this compilation of information from a variety of sources, not all readily available in the usual journals. Similarly, the résumé of the legal aspects as applied in the United States and the Common Market countries will be helpful to producers and sales departments. But there is one question an author must ask himself when starting to write such a book: how much detail should be included from the literature consulted? I am inclined to the view that too much has been included here, possibly at the risk of obscuring the more important points rather than clarifying them. While it is a good idea to include standard test methods and perhaps specifications for special apparatus needed for those tests, I do not feel that one needs to include large amounts of experimental detail from papers describing experimental studies, except occasionally to illustrate some point of principle. I am frequently left wondering how much is the work or the opinions of this author, and how much that of the original researchers, as indications of references are rather sparse. There are a few slips which might have been

Talanta, Vol. 28, pp. iii to iv.
Pergamon Press Ltd 1981. Printed in Great Britain

PUBLICATIONS RECEIVED

Experiments in Environmental Chemistry—A Laboratory Manual: P. D. VOWLES and D. W. CONNELL, Pergamon, Oxford, 1980. Pp. vii + 102. US $9.95 (flexicover version).

This stimulating little book by two Australian authors gives full details, plus a lot of useful additional background information, for 14 laboratory or field experiments dealing with topics such as biochemical processes in aquatic systems, toxic substances in the environment, food additives and contaminants, chemical defence mechanisms in insects, and natural and man-made factors influencing the water quality in streams/estuaries. The experiments are suitable for fairly advanced students only and require the availability of a considerable range of laboratory instrumentation—dissolved-oxygen meters, gas chromatographs with thermal-conductivity, flame-ionization and electron-capture detectors, atomic-absorption spectrometers, non-dispersive gas analysers, gas- and liquid-sampling devices *etc.* Some of the experiments could not be carried out directly in European countries, *e.g.*, in the chemical ecology experiment based on the determination of cardiac glycosides "samples of monarch butterfly larvae and the milk weed plant may be collected during warmer periods of the year in North and South America, Australia, and South East Asia." This, however, should not be taken as a criticism of the book although it may be a disappointment or frustration to some of its purchasers; others attracted by the ambitious nature of the experiments and projects described can use them as models for biological systems and species more readily obtainable in their particular geographical locality.

Some of the bibliography cited is not too readily available and some of it is too directly concerned with American or Australian phenomena to be of general interest, *e.g.*, "Water Pollution—Causes and Effects in Australia." Although a lot more care could have been taken at the proof-reading stage, this book deserves success; perhaps its authors will feel encouraged to produce an enlarged edition that will set out to be more international in its appeal.

D. M. W. ANDERSON

Electrophoresis—A Survey of Techniques and Applications—Part A: **Techniques:** Z. DEYL, F. EVERAERTS, Z. PRUSIK and P. J. SVENDSEN (eds.), Elsevier, Amsterdam, 1980. Pp. xv + 390. US $83.00, Dfl. 170.00.

This is the first part of Volume 18 of the now well-established Elsevier Journal of Chromatography Library; Part B, devoted to applications, will appear subsequently. For this volume, Dr. Deyl assembled a team of 11 contributors based in Czechoslovakia, Denmark, the Netherlands, Poland, Sweden and the U.S.A., the result is a text worthy of international recognition.

Although this volume concentrates on presenting the mathematical and physicochemical theory underlying electromigration techniques, together with experimental details and descriptions of instrumentation *etc.*, sufficient examples of typical separations are given as illustrative examples to make this volume reasonably self-contained without jeopardizing the objectives envisaged for Part B. The mathematical treatment is restricted to fundamental essentials.

For this type of book it seems desirable to use the space available here to give prospective purchasers an indication of the wide extent of the topics covered. The chapters deal with theory and classification of electromigration processes; evaluation of the results of electrophoretic separations; molecular size and shape in electrophoresis; zone electrophoresis; gel-type techniques; quantitative immunoelectrophoresis; moving boundary electrophoresis in narrow-bore tubes; isoelectric focusing; analytical isotachophoresis; continuous flow-through electrophoresis; preparative electrophoresis in gels and in columns; preparative isoelectric focusing and isotachophoresis, including operations on the micro scale. There is a comprehensive subject index. Only two of these chapters cite references to original literature published in 1978 or 1979; the majority of chapters cite nothing more recent than 1976 or 1977. Perhaps this is a reflection on the length of time taken to produce this book (possibly translations into English of several chapters were necessary) or perhaps it is the case that the rate of progress of developments in electromigration techniques started to decrease markedly in the early seventies. Whatever the reason, we have here a substantial and authoritative text that covers the field well up to around 1975.

D. M. W. ANDERSON

Additive Migration from Plastics into Food: T. R. COMPTON, Pergamon, Oxford, 1979. Pp. xi + 234. US $47.00.

The topic covered by this book will be of concern to many practising analysts, who will welcome this compilation of information from a variety of sources, not all readily available in the usual journals. Similarly, the résumé of the legal aspects as applied in the United States and the Common Market countries will be helpful to producers and sales departments. But there is one question an author must ask himself when starting to write such a book: how much detail should be included from the literature consulted? I am inclined to the view that too much has been included here, possibly at the risk of obscuring the more important points rather than clarifying them. While it is a good idea to include standard test methods and perhaps specifications for special apparatus needed for those tests, I do not feel that one needs to include large amounts of experimental detail from papers describing experimental studies, except occasionally to illustrate some point of principle. I am frequently left wondering how much is the work or the opinions of this author, and how much that of the original researchers, as indications of references are rather sparse. There are a few slips which might have been

Talanta, Vol. 28, pp. iii to iv, 1981
Pergamon Press Ltd. Printed in Great Britain

NOTICES

THE 1982 PITTSBURGH CONFERENCE & EXPOSITION ON ANALYTICAL CHEMISTRY & APPLIED SPECTROSCOPY

Date: Technical Program 8–12 March, 1982
Exposition 8–11 March, 1982
Special Short Course 12–13 March, 1982
(Infrared Interpretation)

Place: Atlantic City Convention Hall,
Atlantic City, New Jersey, USA

Registration Fee:		
	Advance	$20.00
	On-site	35.00
	Student	10.00
	Exposition only	10.00
	Spouses	10.00

Program Information:

Technical Sessions:	90	
Papers:	850	(760 Contributed)
Invited Symposia	17	(Agenda below)

Exposition Information:

Companies:	500
Booths:	1350

For more information on any aspect of the Pittsburgh Conference & Exposition. Please write: The Pittsburgh Conference, 437 Donald Road, Pittsburgh, PA 15235, USA

Invited Symposia Schedule

Analytical Chemists as Inventors & Problem Solvers
Preparation and Analysis of Derivatives in Chromatography
Process Analysers
Computerized Methods in GC-MS Analysis
State-of-the-Art of the Hyphenated Techniques
Advances in the State-of-the-Art of Liquid Chromatography
New Developments and Applications of Energy-Dispersive X-Ray Fluorescence
Dal Nogare Award Symposium
Electroanalytical Methods & Materials on the Horizon
Surface Analysis—An Important Interface
New Directions in Molecular Luminescence
Advances in Thin-Layer Chromatography
Industrial Hygiene Monitoring of Chemical Hazards
Analysis of Metal–Organic and Metal–Polymer Interfaces
Advanced Techniques and Standards in Environmental Measurements
Coblentz Awards Symposium

Special Short Course

THE USE OF GROUP FREQUENCIES IN INFRARED INTERPRETATION

Cosponsored by the Society for Analytical Chemists of Pittsburgh (SACP) and the Spectroscopy Society of Pittsburgh (SSP) in conjunction with the 1982 Pittsburgh Conference.

Dates: 12–13 March, 1982

Location: Atlantic City Convention Hall

Fee: $125.00 (includes course materials, Friday Lunch and dinner)

Instructors: Professor Dana W. Mayo, Bowdoin College
Professor Foil A. Miller, University of Pittsburgh

Course Description: This will be a basic course on infrared spectral interpretation using group frequency. A third of the time will be devoted to individual work with problem spectra. The course is intended to be an introduction to the subject or a refresher. The goal will be to convey the fundamentals of approaching an unknown spectrum.

PARTICIPATION IS RESTRICTED TO REGISTERED CONFEREES.

MICROCHEMICAL WORKSHOP—1982

The Department of Continuing Education of the Pennsylvania State University will conduct, on 6–8 July 1982 at the University Park Campus, a Microchemical Workshop on the general theme of "Titrimetry". The technical programme will consist of a number of intensive lectures and lecture demonstrations presented by recognized scientists from the United States and from abroad. By utilization of the housing, food service and meeting and recreational facilities of the University, expenses will be minimal.

For more information contact:

Technical programme: Howard J. Francis, Jr.
The Pennwalt Corporation
900 First Avenue
King of Prussia, PA 19406, U.S.A.

Registration and housing: Ronald Avillion
The Pennsylvania State University
J. Orvis Keller Building
University Park, PA 16802, U.S.A.

Talanta. Vol. 28. pp. iii to iv. 1981
Pergamon Press Ltd. Printed in Great Britain

PUBLICATIONS RECEIVED

Petroleum in the Marine Environment: Advances in Chemistry Series, No. 185: L. PETRAKIS and F. T. WEISS (eds.), American Chemical Society, Washington, 1980. Pp. x + 371. $42.00.

The analytical chemist faced with this topic immediately has three main problems: what to analyse samples for, how to do the analyses, and then how to interpret the results. The sixteen chapters in this book (presented as papers at a meeting in Miami in 1978) go a long way towards providing answers to all of these problems. The review papers emphasize the difficulty in deciding whether hydrocarbon contamination in biological samples is of direct natural origin (oil seepage, coal), from dumping or spillage of crude or fuel oils, or of biogenic origin. A number of chapters discuss the combined use of several techniques to analyse samples for hydrocarbons, showing that GC/MS, HPLC, purging and trapping with GC all have an important role to play. Some of the chapters are more concerned with the results themselves for various types of samples: these figures could be of use to other workers in forming the basis of comparisons. This book scores well on several grounds: it is well written, it contains much fascinating information on the background to the problem (at least one author takes the trouble to explain why phytane and pristane are so interesting), it supplies many details on experimental approaches, and provides a good data base for comparisons. Recommended.

IAIN L. MARR

Analytical Techniques in Environmental Chemistry: J. ALBAIGES (ed.). Pergamon Press, Oxford, 1980. Pp. xii + 646. £43.00.

This book includes 60 papers presented at an international congress in Barcelona in 1978, and presents a fairly detailed picture of research activity in the field at that time. The introductory review (Brassell and Eglinton) deals with the problem of sources of organic compounds in natural waters and how analytical techniques may help in environmental investigations. Rather over half the papers are concerned with determining organic compounds, the remainder with various toxic elements including the heavy metals. Most are concerned with aquatic samples. There is a wealth of data from individual investigations which will be of interest to other workers engaged in similar studies at other locations. In a field where publications are scattered through so many journals, this one large collection could prove a useful introduction to the literature.

IAIN L. MARR

Immobilized Enzymes in Analytical and Clinical Chemistry: P. W. CARR and L. D. BOWERS, Wiley-Interscience, New York, 1980. Pp. 460. £24.

The authors' declared intention is to introduce the subject of immobilized enzymes to analysts. This calls for two qualities (*i*) a good balance between expounding the elements of the subject and giving the most up-to-date review possible, (*ii*) composing the text so that the inexpert can find their way easily round the book for cross-reference. This work succeeds on both counts.

The basics are covered in 150 pages, immobilization techniques in 40, theory and practice of enzyme electrodes in 120 and finally some 50 pages each on the fundamentals of flow-system kinetics, transfer processes in enzyme reactors, and applications of immobilized enzymes in such systems. Extensive tables present useful surveys of analytical applications of electrode and reactor systems with critical comments. The literature has been covered well into 1980.

DEREK MIDGLEY

Mass Spectrometry, Part B: CHARLES MERRITT, JR. and CHARLES N. MCEWEN, Dekker, New York, 1980. pp. 416. SFr. 105.

This, the second part of Volume 3 in the practical spectroscopy series ably maintains the excellent standard achieved by its predecessor and the aims of the series in general. It is a particularly notable feature that the relevance to practical mass spectroscopists of newer techniques is emphasized by reference to a wide range of actual examples in which the reader can see exactly how the results have been obtained and what advantages are apparent compared with more conventional methods. Too often, practising spectroscopists and analysts dismiss newer methods because the theoretical accounts are rendered impenetrable by obscure terminology and lack of obvious application. The approach in this book, with the lucid and careful explanations which take the trouble to define and explain the numerous initial letter technical words and abbreviations (an all too frequent hazard in mass spectrometry), provides a powerful incentive for both the experienced practitioner and newcomer alike to overcome the initial barriers and actually put these methods to use.

The chapter on negative-ion chemical-ionization mass spectrometry is an excellent and timely contribution along these lines. Although chemical derivatization is scarcely a new technique, there are, of course, newer reagents which can offer substantial advantages and the review which covers both these and longer established derivatives is a most valuable compilation. Also of general interest is the review of collisional activation in the production of secondary mass spectra. The section devoted to the use of mass spectrometry in the study of drug metabolism will be of particular value to pharmacologists and those in related areas.

Altogether a well balanced and stimulating volume.

D. G. WILLIAMSON

Talanta, Vol. 28, pp. iii to iv, 1981
Pergamon Press Ltd. Printed in Great Britain

WORKING PARTY ON ANALYTICAL CHEMISTRY (WPAC) FEDERATION OF EUROPEAN CHEMICAL SOCIETIES (FECS)

EUROPEAN ANALYTICAL COLUMN 4

In 1980 the Bulgarian Chemical Society joined the WPAC. On behalf of the official representative (Professor Bliznakov), Professor Jordanov took part at the 11th meeting of the WPAC. By January 1981, 27 national societies of 21 European countries are represented by 31 members in the WPAC. Among the FECS member societies, only the Pancyprian Union of Chemists and the Turkish Chemical Society are not represented in the WPAC.

The 11th meeting of the WPAC was held in Graz, on the occasion of the 8th International Microchemical Symposium (August 1980). The following items were discussed.

1. Euroanalysis IV, 23–8 August 1981, Helsinki (25th event of the FECS). This conference will be organized as a broad spectrum conference as before. The second circular announces 4 plenary lectures [Dyrssen—Gothenburg (S), Egan—London (UK), Hadži—Ljubljana (YU) and Ramendik—Moscow (SU)], 9 keynote lectures, 2 special oral sessions (I, Analytical Chemistry, the Analyst and Society; II, Mass Spectrometry in Inorganic Analysis) and a special poster session on Symbolism in Analytical Chemistry. By now there are over 1300 preliminary registrations, from 44 countries and more than 600 preregistered papers.

2. FECS Lecture 1981. The Advisory Board has granted to the WPAC the FECS lecture 1981 on the occasion of the major event of the FECS, the Euroanalysis IV conference. It will be given by Professor Bengt Samuelsson of Karolinska Institutet, Stockholm and will deal with prostaglandins and thromboxanes.

3. The FECHEM conference on Education in Analytical Chemistry in a Changing World (21st event of the FECS) was held in Vienna, 9–11 April 1980. At this conference, under the chairmanship of Professor H. Malissa (Vienna, Austria) 7 plenary lectures and the following questions were discussed in detail:

1. Objectives of teaching Analytical Chemistry
2. Chemometrics and information theory
3. Teaching of problem solving
4. Textbooks of Analytical Chemistry
5. Computers in Analytical Chemistry
6. Definition of Analytical Chemistry

The plenary lectures of this FECHEM conference and a summary of the results of the discussion are published in a special issue of *Z. Anal. Chem.* The results of this conference together with those of the Round Table discussion during Euroanalysis III (*Z. Anal. Chem.*, 1979, **297**, 4), will be the basis for the next FECHEM conference on Education in Analytical Chemistry which is being planned in connection with Euroanalysis V (1984) in Krakow.

4. FECHEM conferences II and III on "Computer-Based Analytical Chemistry—COBAC", 1982 and 1984. It was decided to continue the successful COBAC conferences, started 24–28 September 1979 in Portorož.

COBAC II will be organized as a FECHEM conference on 28/29 April 1982 in connection with Analytica 1982 in Munich, by the Fachgruppe Analytische Chemie of the GdCh (conference chairman E. Fahr, Mainz).

COBAC III is planned to be held as a special session of Euroanalysis V, 1984, in Krakow.

5. Euroanalysis V, 1984, Krakow, Poland. The conference will be held in the new conference centre in Krakow, ready in 1981, and will again be a broad spectrum conference, including special sessions.

6. Joint venture WPAC/IUPAC. A written report on the application of symbolics in Analytical Chemistry, prepared by V. Simeonov, Sofia, was distributed to all WPAC members for consideration and further action. This group is organizing the special poster session on "Symbolism in Analytical Chemistry" at Euroanalysis IV. An oral introduction to the posters will be presented by H. Malissa and V. Simeonov in the form of a keynote lecture. Inquiries should be addressed to Professor Malissa, TU Vienna, A1060 Vienna, Getreidemarket 9.

7. Feasibility of Standard Reference Materials. A written report on "Sources of Reference Materials" was prepared by R. Belcher and distributed to all WPAC members as a basis for further discussion at the 12th WPAC meeting in Helsinki.

8. Nomination for the election of the Chairman of WPAC for the period 1981–84. Two nominations were submitted to the secretariat:

Professor Pungor, nominated at the 11th WPAC meeting by the GdCh (Professor Fresenius);

Professor West, nominated by the French Societies in the WPAC (Professor Guiochon, letter of 6th November 1980).

Both candidates have agreed to be nominated.

9. Next (12th) meeting of the WPAC. The Finnish Chemical Society has invited WPAC to hold its 12th meeting in Helsinki in connection with Euroanalysis IV, preferably on Sunday, 23 August 1981, but possibly on the day before.

Talanta, Vol. 28, pp. iii to iv, 1981
Pergamon Press Ltd. Printed in Great Britain

NOTICES

SECOND INTERNATIONAL WORKSHOP ON TRACE ELEMENT ANALYTICAL CHEMISTRY IN MEDICINE AND BIOLOGY

Neuherberg/Munich, Federal Republic of Germany

21–23 April 1982

This workshop will have the same form as the first one, which is intended to guarantee a free and effective exchange of views between the analytical specialists on the one hand and the biomedical specialists (the users of the analytical data) on the other. It is hoped that the workshop will lead to a productive scientific dialogue between these two groups in regard to the biomedical applications of trace-element analytical research. The international and multidisciplinary character of the workshop should provide a good working forum for all interested in this subject area. The workshop will be repeated at intervals of two years. The aim at each meeting is to bring together, at one table, experts in the analysis and biomedical significance of trace elements. The topics to be covered will be varied from one meeting to the next. The second workshop will have "Essential, Toxic and Analytical Aspects of Trace Elements" as its general theme.

The workshop will consist of a series of invited papers on specific problem areas each followed by an extended discussion period in which all participants will be invited to take part. Short contributed papers (oral or poster presentation) are also solicited for the workshop.

Scope

I. Nutritional requirements as function of age
II. Metabolic (absorption, transfer, transport, storage, mobilization, excretion) and biochemical (metalloprotein, enzymes, hormones) effects
III. Subclinical and chronic effects
IV. Diagnosis of trace element supply
V. Analytical requirements and potentialities (sampling, storage, pretreatment, determination, evaluation, quality control)

Call for papers

Abstracts of papers intended as contributions to the discussions at the workshop must be submitted in English, in three copies, to the Organizing Committee by

30 November, 1981

The abstracts must be typed in double spacing and should not exceed one typewritten page in length. The abstract will be subjected to refereeing for acceptance of the paper and for the "Conference Abstracts". Authors of accepted papers will be asked to submit the full manuscripts in English during the conference (latest) for publication in the Conference Proceedings by W. de Gruyter Publ. Comp. The preliminary application form should be sent to the organizers by 30 July, 1981.

All correspondence concerning the workshop should be addressed to:

Dr. P. Schramel
Gesellschaft fuer Strahlen- und Umweltforschung
Institut fuer Angewandte Physik
Physikalisch-Technische Abteilung
Ingolstaedter Landstrasse 1
D-8042 Neuherberg
Federal Republic of Germany

1982 WINTER CONFERENCE ON PLASMA SPECTROCHEMISTRY

Orlando, Florida

4–9 January 1982

The 1982 Winter Conference on Plasma Spectrochemistry, sponsored by the *ICP Information Newsletter* in cooperation with the Society for Applied Spectroscopy (Florida section) and the American Chemical Society (Tampa section of the Analytical Chemistry Division), will feature developments in atomic plasma spectrochemical analysis by inductively coupled plasma (ICP), DC plasma (DCP), and microwave plasma (MIP) excitation sources. The meeting will convene on Monday, January 4 through Saturday, January 9, 1982 at the Orlando Hyatt Hotel in Kissimmee, Florida, adjacent to Walt Disney World.

Program and Objectives

The rapid growth in popularity of ICP, DCP, and MIP excitation sources and the need to discuss recent developments of these sources in spectrochemical analysis has stimulated the organization of this meeting. The conference will bring together international scientists experienced in applications, theory, and instrumental developments in an informal setting to examine recent progress.

Papers describing applications, fundamentals, and instrumental developments with atomic plasmas (ICP, DCP, MIP) will be presented in lecture and poster sessions. General and special symposia organized and chaired by internationally recognized experts will include the following topics: (1) accuracy, precision, and optimization in plasmas; (2) applications to air, biologicals, chemicals, coal, food, metals, ores, plants, petroleum, soils, rocks, wastes, and water; (3) EPA plasma methods; (4) new instrumentation; (5) plasma detectors for chromatography; (6) plasma interferences and mechanisms; and (7) sample introduction methods. Roundtable discussion sessions will encourage an indepth evaluation of these topics.

Call for papers

Papers describing original work with atomic plasma applications, fundamentals, and instrument developments are solicited. Title and 50-word abstracts are due July 1, 1981, and full abstracts are due October 1, 1981.

Information from:

Dr. Ramon M. Barnes,
Department of Chemistry, GRC Towers
University of Massachusetts
Amherst, MA 01003

determination of sodium azide when the introductory paragraph states that its use is forbidden in almost all countries, because "even small errors in its use could lead to fatal consequences".

The chapter on additives is as chilling as any of the 19th century texts on adulteration, but it, and those on acidity, alcohols, esters, carbonyl and phenolic compounds and others are full of valuable information and analytical expertise.

D. BETTERIDGE

Advances in Chromatography, Vol. 18: J. CALVIN GIDDINGS, ELI GRUSHKA, JACK CAZES, and PHYLLIS R. BROWN (eds.), Dekker, New York, 1980. Pp. 312. SFr. 88.

In this, the eighteenth volume of the series, the editors have maintained their usual high standards. There are general articles on ion-pair chromatography and ligand-exchange chromatography for the resolution of racemates, and discussions of the application of LC to the characterization of long-chain fatty acids, free nucleotides in biological fluids and combination GC–MS for the analysis of marijuana cannabinoids and their metabolites. The range and the depth of treatment makes the series daunting for the general reader, but essential for the library.

D. BETTERIDGE

Talanta, Vol. 28, pp. iii to iv
Pergamon Press Ltd 1981. Printed in Great Britain

0039-9140/81/0201-oiii$02.00/0

PUBLICATIONS RECEIVED

Aquametry, Part III, **The Karl Fischer Reagent:** JOHN MITCHELL, JR. and DONALD MILTON SMITH, 2nd Ed., Wiley, New York, 1980. pp. xv + 851. £41.00.

It is a significant tribute to the ingenuity and inquiring minds of analytical chemists, and to the ubiquity of water, that the 32 years that have elapsed since the first edition of Mitchell and Smith's classic "Aquametry" have witnessed such an enormous amount of work on the development and application of one method—the Karl Fischer titration—that the section of the book dealing with it is now considerably larger than the whole original book. Here is everything the reader is likely to want to know about the reaction, presented in sufficient detail for it seldom to be necessary to resort to the original literature, which is perhaps as well in view of the number of papers published in the less easily accessible literature. The index also covers the major headings in Parts I and II, and thus provides a handy reference to the whole work, as well as a detailed listing for Part III. A minor criticism is the use of alphabetical listing of references by first author's name, so that finding the references to a particular topic involves a good deal of to-ing and fro-ing between text and reference list. Use of consecutive numbering in the text would have obviated this. The authors are to be congratulated on the completion of what must have been a monumental task of searching and abstracting the literature, which is covered up to late 1979.

R. A. CHALMERS

Handbook of Chemical Microscopy, Vol. II, **Chemical Methods and Inorganic Qualitative Analysis:** EMILE MONNIN CHAMOT and CLYDE WALTER MASON, 2nd Ed., Wiley, New York, 1980. pp. xi + 438. £14.75.

As far as can be seen, this is a reprint of the original second edition first published in 1940, together with any updating done in previous reprintings (the reference book list includes a book published in 1944). The 1929 version of the Periodic Table is still included. The book itself was a classic of its day, of course, and is certainly cheap by modern standards. Earlier reviews (*e.g.*, *Analyst*, 1941, **66**, 85) should still be valid.

R. A. CHALMERS

Handbook of Analytical Control of Iron and Steel Production: T. S. HARRISON, Horwood, Chichester, 197 pp. £37.50.

This remarkable handbook is a worthwhile addition to the Ellis Horwood series of books on Analytical Chemistry, and there is no doubt that a copy should find its way into all steelworks laboratories. Analysis in a modern, integrated iron and steel works must not only provide rapid instrumental methods for quality control and established chemical methods for the preparation of standards but also a wide range of techniques and procedures for the analysis of raw materials, by-products, waste waters and fuels. Dr. Harrison is probably the first author to attempt to bring all these requirements into a single, comprehensive text and the result is a very useful guide to the procedures in widespread use today.

The treatment is divided into three parts, the first dealing with the principles of the methods of sampling, and analysis including chemical, physico-chemical and physical methods. In the second part, procedures are given, in sufficient detail for laboratory use, for the determination of 30 elements in iron and steel. A useful chapter has been contributed to J. D. Hobson on the determination of gases in steel, and succeeding shorter chapters cover procedures for the analysis of ferro-alloys, oxide materials such as iron ore, iron-ore sinter and slags, and refractory materials and other important miscellaneous materials such as welding rods and fluxes, manganese ores and non-ferrous alloys. Part 3 details procedures used for the analysis of fuels and coke-oven by-products, waters and effluents and lubricants.

In the first part, the information given is sufficient for a basic but not detailed understanding of the techniques of interest and many references are cited which will lead the interested reader to the most relevant literature. The procedures for the analysis of iron and steel given in Part 2 are principally the established chemical methods but a separate section has been included on atomic-absorption spectrometric methods. The treatment is similar in the other applications chapters. The reviewer was disappointed not to find more detailed information on procedures for emission spectrometry and X-ray fluorescence. Thus, in the section on direct-reading spectrometers, sets of conditions are quoted for a particular instrument from a specific steelworks operating manual, but the important aspects of calibration, standardization and interferences are not discussed. A section on the composition and form of standard reference materials would also be a useful addition to the book, as would a more comprehensive treatment of the role that computers can fulfil in the steelworks laboratory. Apart from these minor points, however, the author must be congratulated on the monumental task that he has undertaken and completed successfully. This book is likely to remain the steel chemist's main standby in the 1980s.

J. M. OTTAWAY

Treatise on Analytical Chemistry, Part I, Vols. 1 and 2: I. M. KOLTHOFF and PHILIP J. ELVING (eds.), 2nd Ed., Wiley-Interscience, New York, 1978 (Vol. 1), 1980 (Vol. 2). Volume 1, pp. xxviii + 881; £42.75. Volume 2, pp. xxv + 815; £39.60.

The extraordinary development of analytical chemistry and its techniques during the last two decades is strikingly witnessed by the need to produce a complete revision of the "Treatise" and by the fact that doing so for Volume 1 of Part I has roughly doubled the number of pages needed. Part of the increase, of course, is due to development of new techniques, but advances have been made in all fields, and this is reflected in the changes in the treatment of the older

techniques. Owners of the first edition will therefore find that they need these two volumes if they are to keep up to date with the rapid changes in analytical chemistry. Although the editors modestly claim that the work is not an extensive textbook, it contains far more basic information than almost any general textbook, and in places rivals some of the monographs. This is not surprising, perhaps, when it is remembered that a great many of the contributors have written monographs on their specialties. Certainly for rapid orientation in a given field, this work is the first place to look. The numerous tables of data and graphical presentations of information also save a lot of time in literature searching. Against this may be set the minor inconvenience of alphabetical listing of the references, and there is a regrettable omission of accents on the names of authors from countries where the orthography demands accents for correctness of pronunciation. This cavalier treatment, whatever the reason for it, is not really excusable. Presumably with the growth of computer storage of information and mechanised retrieval it will become even more widespread. This new edition should be in every library serving analytical chemists.

R. A. CHALMERS

Talanta, Vol. 28, pp. iii to iv.
Pergamon Press Ltd 1981. Printed in Great Britain

PUBLICATIONS RECEIVED

Experiments in Environmental Chemistry—A Laboratory Manual: P. D. VOWLES and D. W. CONNELL, Pergamon, Oxford, 1980. Pp. vii + 102. US $9.95 (flexicover version).

This stimulating little book by two Australian authors gives full details, plus a lot of useful additional background information, for 14 laboratory or field experiments dealing with topics such as biochemical processes in aquatic systems, toxic substances in the environment, food additives and contaminants, chemical defence mechanisms in insects, and natural and man-made factors influencing the water quality in streams/estuaries. The experiments are suitable for fairly advanced students only and require the availability of a considerable range of laboratory instrumentation—dissolved-oxygen meters, gas chromatographs with thermal-conductivity, flame-ionization and electron-capture detectors, atomic-absorption spectrometers, non-dispersive gas analysers, gas- and liquid-sampling devices *etc.* Some of the experiments could not be carried out directly in European countries, *e.g.*, in the chemical ecology experiment based on the determination of cardiac glycosides "samples of monarch butterfly larvae and the milk weed plant may be collected during warmer periods of the year in North and South America, Australia, and South East Asia." This, however, should not be taken as a criticism of the book although it may be a disappointment or frustration to some of its purchasers; others attracted by the ambitious nature of the experiments and projects described can use them as models for biological systems and species more readily obtainable in their particular geographical locality.

Some of the bibliography cited is not too readily available and some of it is too directly concerned with American or Australian phenomena to be of general interest, *e.g.*, "Water Pollution—Causes and Effects in Australia." Although a lot more care could have been taken at the proof-reading stage, this book deserves success; perhaps its authors will feel encouraged to produce an enlarged edition that will set out to be more international in its appeal.

D. M. W. ANDERSON

Electrophoresis—A Survey of Techniques and Applications—Part A: **Techniques:** Z. DEYL, F. EVERAERTS, Z. PRUSIK and P. J. SVENDSEN (eds.), Elsevier, Amsterdam, 1980. Pp. xv + 390. US $83.00, Dfl. 170.00.

This is the first part of Volume 18 of the now well-established Elsevier Journal of Chromatography Library; Part B, devoted to applications, will appear subsequently. For this volume, Dr. Deyl assembled a team of 11 contributors based in Czechoslovakia, Denmark, the Netherlands, Poland, Sweden and the U.S.A., the result is a text worthy of international recognition.

Although this volume concentrates on presenting the mathematical and physicochemical theory underlying electromigration techniques, together with experimental details and descriptions of instrumentation *etc.*, sufficient examples of typical separations are given as illustrative examples to make this volume reasonably self-contained without jeopardizing the objectives envisaged for Part B. The mathematical treatment is restricted to fundamental essentials.

For this type of book it seems desirable to use the space available here to give prospective purchasers an indication of the wide extent of the topics covered. The chapters deal with theory and classification of electromigration processes; evaluation of the results of electrophoretic separations; molecular size and shape in electrophoresis; zone electrophoresis; gel-type techniques; quantitative immunoelectrophoresis; moving boundary electrophoresis in narrow-bore tubes; isoelectric focusing; analytical isotachophoresis; continuous flow-through electrophoresis; preparative electrophoresis in gels and in columns; preparative isoelectric focusing and isotachophoresis, including operations on the micro scale. There is a comprehensive subject index. Only two of these chapters cite references to original literature published in 1978 or 1979; the majority of chapters cite nothing more recent than 1976 or 1977. Perhaps this is a reflection on the length of time taken to produce this book (possibly translations into English of several chapters were necessary) or perhaps it is the case that the rate of progress of developments in electromigration techniques started to decrease markedly in the early seventies. Whatever the reason, we have here a substantial and authoritative text that covers the field well up to around 1975.

D. M. W. ANDERSON

Additive Migration from Plastics into Food: T. R. COMPTON, Pergamon, Oxford, 1979. Pp. xi + 234. US $47.00.

The topic covered by this book will be of concern to many practising analysts, who will welcome this compilation of information from a variety of sources, not all readily available in the usual journals. Similarly, the résumé of the legal aspects as applied in the United States and the Common Market countries will be helpful to producers and sales departments. But there is one question an author must ask himself when starting to write such a book: how much detail should be included from the literature consulted? I am inclined to the view that too much has been included here, possibly at the risk of obscuring the more important points rather than clarifying them. While it is a good idea to include standard test methods and perhaps specifications for special apparatus needed for those tests, I do not feel that one needs to include large amounts of experimental detail from papers describing experimental studies, except occasionally to illustrate some point of principle. I am frequently left wondering how much is the work or the opinions of this author, and how much that of the original researchers, as indications of references are rather sparse. There are a few slips which might have been

picked up with more careful proofing, such as "anthraquinones" on p. 17 where I think "anthocyanines" is intended, and the apparent contradiction between text and figure legend on pp. 78/78. Still, there is much useful material here, and I am sure it will be helpful to analysts facing such problems in food packaging.

IAIN L. MARR

Guide to Good Programming Practice: B. L. MEEK and P. M. HEATH (eds.), Horwood, Chichester, 1980. Pp. 181. Boards £10.50, Paperback £3.95.

Most computer-language courses concentrate mainly on language features and predigested programming exercises, and they usually say very little about what constitutes good programming practice. This little book should do much to rectify the problems caused by this situation. It is aimed to help both the "professional" and "amateur" to become a serious and competent programmer. The topics covered include: choice of language; language standards; structured programming; error prevention; testing and debugging; special problems; program documentation; other people's programs. The authors are to be congratulated on a most readable and useful book. I would recommend that any "amateur" programmers among the *Talanta* readership should buy (or at least, borrow) and read a copy. Many of the programs submitted to *Talanta* would greatly benefit if their authors were to follow the advice given.

MARY MASSON

LIST OF CONTENTS

JANUARY

Talanta Advisory Board I

Timothy J. Killeen, DeLyle Eastwood and Martha Schulz Hendrick 1 Oil-matching by using a simple vector model for fluorescence spectra

P. G. Kaz'min, E. N. Dorokhova and I. P. Alimarin 7 Flotation–photometric determination of silicon in the form of chromopyrazole II molybdosilicate

Joseph T. Vanderslice, Kent K. Stewart, A. Gregory Rosenfeld and Darla J. Higgs 11 Laminar dispersion in flow-injection analysis

C. Vandecasteele, K. Strijckmans, Ch. Engelmann and H. M. Ortner 19 Determination of traces of carbon, nitrogen and oxygen in molybdenum and tungsten

R. S. Young 25 The analysis of nickel refinery slimes and residues

J. G. Sen Gupta 31 Determination of yttrium and rare-earth elements in rocks by graphite-furnace atomic-absorption spectrometry

P. A. Michalik and R. Stephens 37 An instrumental method of solution preconcentration

P. A. Michalik and R. Stephens 43 Aerosol preconcentration on a liquid electrode

M. Y. Mirza and F. I. Nwabue 49 1-Phenyl-3-methyl-4-benzoylpyrazol-5-one as a group-extraction reagent for spectrophotometric determination of trace elements

Short Communications

M. K. Ahmed and C. Subbarao 55 Benzohydroxamic acid as a reductometric titrant: determination of manganese, chromium and vanadium in steels

Yogendu Sharma 59 *p*-Sulphobenzeneazo-4-(2,3-dihydroxy-5-chloropyridine) as a reagent for spectrophotometric determination of niobium(V)

Bijoli Kanti Pal, Rajendra Prasad Chowdhury and B. K. Mitra 62 Liquid–liquid extraction of osmium thiocyanate with hexamethylphosphoramide and direct spectrophotometric determination in the organic phase

G. Calderoni 65 Determination of lead in igneous rocks by differential pulse anodic stripping voltammetry at an HMDE

Analytical Data

M. Molina, C. Melios and N. Barelli 69 Solution studies on chelates of nickel, zinc and cadmium with 2-thiopicolinanilide

Papers Received i

Publications Received iii

FEBRUARY

Talanta Advisory Board I

Hisanori Imura and Nobuo Suzuki 73 Substoichiometric isotope dilution analysis for tin with salicylideneamino-2-thiophenol complexation in non-aqueous medium. Application to the analysis of coal fly-ash

M. H. Livertoux et J. Bessière	81	Titrage coulométrique de composés acides d'interet pharmaceutique en milieu dimethylsulfoxyde
Saad S. M. Hassan	89	New atomic-absorption spectrometric, potentiometric and polarographic methods for the determination of nitrates
A. P. Gamot, G. Vergoten et G. Fleury	95	Etude par spectroscopie Raman de quelques anorexigènes—I. Anorexigènes *N*-substitués
G. A. Kenney-Wallace, J. P. Wilson, J. F. Farrell and B. K. Gupta	107	Direct determination of uranyl ion by nanosecond dye-laser spectroscopy
Short Communications		
Nobutoshi Kiba, Toshiyuki Suto and Motohisa Furusawa	115	Enthalpimetry with catalytic reactions—II. Determination of thioureas by the iodine–azide reaction after thin-layer chromatographic separation
J. L. Ward, E. LueYen-Bower and J. D. Winefordner	119	The use of rinsing and heating of filter paper in an attempt to reduce phosphorescence background at room temperature
S. K. Mandal, S. B. Rao and B. R. Sant	121	Decomposition of ores by manganese dioxide. Analysis of copper ores and concentrates
Kikuo Terada and Kazumitsu Nakamura	123	Preconcentration of cobalt(II) in natural waters with 1-nitroso-2-naphthol supported on silica gel
Analytical Data		
F. Gaizer, M. Máté and J. Lázár	127	Spectrophotometric determination of the protonation constants of *o*-cresolphthalexone and the formation constants of its alkaline-earth metal complexes
J. Rodriquez, A. Garcia de Torres and J. M. Cano-Pavon	131	Analytical properties of the bis(4-phenyl-3-thiosemicarbazone) of 1,3-cyclohexanedione and its 2-methyl and 5,5′-dimethyl derivatives
M. Roman Ceba, J. J. Berzas Nevado and A. Espinosa Mansilla	134	Analytical properties of pyridine-2-aldehyde guanylhydrazone
Papers Received	i	
Publications Received	iii	
Notes for Authors	v	

MARCH

Mohammad Jawaid and Folke Ingman	137	Potentiometric studies on the complex formation between methylmercury(II) and some keto- and amino-carboxylic acids
Robert J. Hurtubise	145	Room-temperature phosphorescence and fluorescence of nitrogen heterocyclics adsorbed on silica gel chromatoplates
J. Kragten and A. Parczewski	149	Photometric complex-formation titration of submicromolar amounts of zirconium
V. S. K. Lo and A. Chow	157	Extraction of tin by the use of polyurethane foam
F. B. Sherman and Yu. I. Khurgin	161	Aquametric submicro determination of water content of biopolymer preparations and its application in deriving hydration isotherms
G. Paolo Sighinolfi and Carlo Gorgoni	169	Atomic-absorption spectrochemical analysis for ultratrace elements in geological materials by hydride-forming techniques: selenium
Mieczysław Wroński	173	Determination of sulphide, polysulphide, thiocarbonates and sulphur by extraction with tributyltin hydroxide, and of thiosulphate by hydrogenation
Masami Suzuki and Kiyohisa Ohta	177	Electrothermal atomization of calcium and strontium in a molybdenum micro-tube

Short Communications

Stanisław Głab and Adam Hulanicki 183 Autoprotolysis constants by coulometric titration

M. M. A. Hassan, M. Uppal Zubair and J. S. Mossa 187 NMR assay of ephedrine hydrochloride in tablets

Wei Fu-sheng, Qu Pei-hua, Shen Nai-kui and Yin Fang 189 Sensitive spectrophotometric determination of nickel(II) with 2-(5-bromo-2-pyridylazo)-5-diethylaminophenol

P. Kiekens, H. Verplaetse and E. Temmerman 192 Electrochemical study of the oxidation of tin(II) at glassy carbon electrodes

M. V. Krishna Murthy and D. Satyanarayana 195 Solvent extraction studies on the mixed ligand complexes of lanthanides with antipyrine and perchlorate

Analytical Data

T. Matusinović and I. Filipović 199 Potentiometric determination of stability constants of cyanoacetato complexes of cobalt(II), nickel(II), copper(II), zinc(II), cadmium(II) and lead(II)

Papers Received i

Publications Received iii

Notice iv

APRIL

Talanta Advisory Board I

J. L. Ward, G. L. Walden and J. D. Winefordner 201 A review of recent uses of phosphorimetry for organic analysis

A. H. Victor and F. W. E. Strelow 207 Selective and quantitative separation of zinc and lead from other elements by cation-exchange chromatography in hydrohalic acid–acetone solutions

B. M. Petronio, A. Laganá and M. V. Russo 215 Some applications of ligand-exchange—I. Recovery of phenolic compounds from water

S. M. F. Tavernier and R. Gijbels 221 Determination of sulphate content of anionic surfactants: sodium di-2-ethylhexyl sulphosuccinate

Mary Andrieu Ryan and J. D. Ingle, Jr. 225 Application of an intensified diode array system to diagnosis of matrix effects and the rapid sequential determination of thiamine and riboflavin with fluorescence detection

Jean-Claude Fischer, Abdelhatef Boughriet et Michel Wartel 233 Etude électrochimique des sels de nitryle en milieu aprotonique

Maria de Lurdes S. Simoes, Maria Cândida T. A. Vaz and J. J. R. Fraústo da Silva 237 Stability constants of chloro-complexes of cadmium(II) in sea-water medium

Sten Johansson 241 Logarithmic diagrams as an aid in complexometric titrations where 1:2 or 2:1 as well as 1:1 metal–ligand complexes are regarded as principal species

Short Communications

Samuel J. Lyle and M. Idris Saleh 251 Observations on a dropping-mercury electrochemical detector for flow-injection analysis and HPLC

Mieczysław Wroński 255 Preconcentration of cyanide from water by extraction with tributyltin hydroxide

K. Sriramam, B. S. R. Sarma, A. R. K. Vara Prasad and P. Ravindranath 257 A new and rapid titration of antimony(III) with potassium dichromate, with iron(II) as inductor

S. M. Mayanna and K. V. Uma 259 Estimation of xylenes with chloramine-T

Dipak K. Basu, Basudam Adhikari, Dhananjay Pal and Ajit K. Chaudhuri 262 Determination of thiocarbamyl sulphenamides, thiuram disulphides and dibenzothiazyl disulphide by amperometric titration

T. B. Smallwood and C. D. Wall 265 The quantitative determination of hydrated calcium sulphates in cement by use of self-generating atmosphere thermogravimetry

Aoi Ono 268 Separation behaviour of nitroxylene isomers on polyols and polyethers in gas–liquid chromatography

Zs. Wittmann 271 Determination of mercury by atomic-absorption spectrophotometry

J. P. Ghosh and H. R. Das 274 Preparation and properties of a new chelating resin containing 1-nitroso-2-naphthol as the functional group

Analytical Data

Lauri H. J. Lajunen, Eero Aitta and Seppo Parhi 277 Complex formation equilibria between 1-hydroxy-7-sulpho-2-naphthoic or 1-hydroxy-4,7-disulpho-2-naphthoic acid and iron(III) in 0.1*M* $NaClO_4$ medium

Papers Received i

Errata ii

MAY

S. K. Suri, K. Prasad, J. C. Ahluwalia and D. W. Rogers 281 Application of phase-titrations for estimation of adulteration of gasoline and high-speed diesel with kerosene

K. Sriramam, B. S. R. Sarma, B. Syama Sundar and N. Ramabrahma Sastry 287 Titration of vanadium(IV) with cerium(IV) sulphate, with ferroin as indicator, in aqueous acetone as facile reaction medium. An analytical and mechanistic study

Taitiro Fujinaga, Tooru Kuwamoto, Kenji Sugiura and Shigekazu Ichiki 295 Fundamental investigation of thermal properties of rare-earth β-diketonates

Stanislaw Glab, Gunnar Edwall, Per-Arne Jöngren and Folke Ingman 301 Effects of some complex-forming ligands on the potential of antimony pH-sensors

J.-C. Vire, M. Fischer, G. J. Patriarche and G. D. Christian 313 Electrochemical behaviour of some neuroleptics: Haloperidol and its derivatives

Short Communications

Noriko Shinozuka and Shigeo Hayano 319 Rotating-disc electrode determination of nitrogen dioxide concentrated in *N*,*N*-dimethylformamide

Nicoletta Burger and Vinka Karas-Gašparec 323 The reactions of pentacyanoferrate(II) ions. Spectrophotometric study, detection and determination of *N*-heterocyclic aldoximes

K. N. Raoot and Sarala Raoot 327 Selective complexometric determination of palladium, with thiourea as masking agent

David M. Rackham, Jiban K. Chakrabarti and Geoffrey L. O. Davies 329 Study of hydrolysis of amido-substituted γ-butyrolactones by pH-stat titration and ultraviolet spectroscopic analyses

N. Rukmini, V. S. N. P. Kavitha and K. Devendra Vijaya 332 Determination of ascorbic acid with ferricyanide

S. Gücer and H. Berndt 334 Basic investigations on background problems in the platinum-loop method in comparison to graphite-furnace and flame atomic-absorption spectrophotometry

H. Akaiwa, H. Kawamoto and K. Ogura 337 Kinetic studies of ion-exchange of cobalt(II) and nickel(II) on a resin loaded with 5-sulpho-8-quinolinol

Analytical Data

A. Izquierdo and J. Carrasco 341 Thermometric titration of β-aryl-α-mercaptopropenoic acids and determination of the stoichiometry of their metal complexes

Annotations

M. Otto, J. Stach, R. Kirmse and G. Werner — 345 The tiron radical as indicator substance in catalytic determination of trace metals

Papers Received — i

Publications Received — iii

JUNE

R. A. Chalmers — I Editorial

Ichiro Hayashida, Mitsuhiko Taga and Hitoshi Yoshida — 349 Conductometric titration of nitrate by formation of the silver–1,10-phenanthroline-nitrate ternary complex

Fadhil Jasim and Mahmood M. Barbooti — 353 Electrothermal atomic-absorption determination of barium in brines and caustic soda solutions

Mahmood M. Barbooti and Fadhil Jasim — 359 Electrothermal atomic-absorption spectrophotometric determination of molybdenum

R. G. Anderson and B. C. Brown — 365 The determination of lead in mosses by means of its catalytic effect on the persulphate oxidation of Pyrogallol Red

Joseph Wang — 369 Hydrodynamic modulation voltammetry

D. Negoiu, M. S. Ionescu and V. V. Coşofreţ — 377 Determination of novocaine in pharmaceutical preparations with novocaine$^+$-selective membrane electrodes

M. Ionescu, P. Cillanu, A. A. Bunaciu and V. V. Coşofreţ — 383 Determination of sulpha-drugs with ion-selective membrane electrodes

Rokuro Kuroda and Tadashi Mochizuki — 389 Continuous spectrophotometric determination of copper, nickel and zinc in copper-base alloys by flow-injection analysis

Short Communications

M. R. Gopalakrishnan Nair, M. J. Kurian and C. P. Prabhakaran — 395 Peaceful pyrolysis—a novel method for the decomposition of metal–perchlorate complexes of organic ligands

K. K. Tiwari and R. M. Verma — 397 Titrimetric determination of certain mercaptans with mercuric chloride

O. S. Chauhan, B. S. Garg, R. P. Singh and Ishwar Singh — 399 A rapid spectrophotometric method for determination of zinc in milk

Syozo Fukui, Teruhisa Hirayama, Motoshi Nohara and Yoshihiko Sakagami — 402 Gas chromatographic determination of dimethylarsinic acid in aqueous samples

D. A. Beardsley — 405 The separation and determination of fatty acids by isotopic dilution and radiogas-liquid chromatography

L. R. Sherman, V. L. Trust and H. Hoang — 408 Kinetic determination of phenols by a fixed-time method

Preliminary Communication

Young-Tzung Shih and Peter W. Carr — 411 Silanization of stainless-steel frits for use in trace metal analysis by high performance liquid chromatography

Letters to the Editor

A. G. Briggs and R. E. Simmons — 415 Temperature effects in the determination of iodide with iodate

Rangaswamy and H. S. Yathirajan — 418 Iodamine-B as an oxidimetric titrant in aqueous medium

Papers Received — i

JULY
Vol. 28, No. 7A

He Xi-Wen and Donald P. Poe	419	Spectrophotometric study on the reactions of iron(II) and iron(III) with Bromopyrogallol Red and hexadecyltrimethylammonium bromide
A. Sanz-Medel, D. Blanco Gomis and J. R. García Alvarez	425	Ion-pair extraction and fluorimetric determination of potassium with 18-crown-6 and eosin
H. Verplaetse, P. Kiekens, E. Temmerman and F. Verbeek	431	Catalytic influence of Cl^-, Br^-, I^- and SCN^- on the cyclic voltammetric behaviour of Sb(III)
A. Chow, G. T. Yamashita and R. F. Hamon	437	X-Ray fluorescence determination of cobalt on polyurethane foam
M. Ejaz, Shamus-Zuha, Wasim Dil, Anis Akhtar and Shamim A. Chaudhri	441	Extraction and preconcentration of copper from water, soils, lubricating oils and plant materials and its subsequent determination by atomic-absorption spectrophotometry
C. Triché, G. Pitet et M. R. Dorignac	447	Dosage par spectrographie d'émission, de traces d'oxygène à l'aide d'une source à impulsion
Naseem Delannoy, Jean-Marie Degorre, Albert Delannoy, Jacques Nicole et Jean Hennion	451	Complexes de dérivés alloxanniques—I. Complexes du fer(II) avec l'acide violurique et l'acide thio-2 violurique
A. Hulanicki, R. Karwowska and J. S. Sowinski	455	Influence of some matrix elements on atomization of cobalt in graphite-furnace atomic-absorption spectrometry
Elsie M. Donaldson	461	Determination of aluminium in iron, steel and ferrous and non-ferrous alloys by atomic-absorption spectrophotometry after a mercury-cathode separation and extraction of the aluminium–acetylacetone complex
Short Communications		
J. L. Bernal, Mª. J. del Nozal, L. Deban and A. J. Aller	469	An indirect method for determining phosphorus in aluminium alloys by atomic-absorption spectrometry
A. G. Fogg, N. K. Beebsu and B. J. Birch	473	Differential-pulse anodic voltammetric determination of phosphate, silicate, arsenate and germanate as β-heteropolymolybdates at a stationary glassy-carbon electrode
P. Siraj, R. Rama Krishna, S. S. N. Murthy, B. S. Reddy and C. S. Prakasa Sastry	477	Spectrophotometric determinations of isoniazid with metol and vanadate, ferricyanide or iron(III)
G. Petrov and D. Bachvarova	481	Kinetic method for microdetermination of the insecticide phosalone
Annotation		
Krishna K. Verma and Sunil K. Dubey	485	Detection of aromatic nitro compounds by means of their π-complexes with *N,N*-diethylaniline
Papers Received	i	
Publications Received	ii	
Notices	iii	

MICROPROCESSORS IN ANALYTICAL CHEMISTRY

Vol. 28, No. 7B

Introduction	V	Microprocessors—Macroapplications
Gary Horlick	487	Introduction to microprocessors
Edward G. Codding	503	Addressing, accessing and interfacing peripheral devices to microprocessors

Eric D. Salin, M. W. Blades and Gary Horlick	519	Laboratory data-acquisition capabilities of microcomputers
M. W. Blades and Gary Horlick	527	Microprocessor-controlled integrating read-out systems for photomultiplier tubes
Harald Gampp	535	A microcomputer-controlled system for automatic acquisition of kinetic data of gas uptake at constant pressure
Mary Andrieu Ryan and J. D. Ingle, Jr.	539	Construction of a microcomputer-based reaction-rate ratemeter
R. M. Belchamber and Gary Horlick	543	Data-logging system based on the Intel 8748 single-chip microprocessor
Short Communication		
R. M. Belchamber and Gary Horlick	547	Use of added random noise to improve bit-resolution in digital signal averaging

AUGUST

Talanta Medal	I	
Louis Gordon Memorial Award	I	
Atsushi Sugii, Naotake Ogawa, Yukikazu Iinuma and Hisashi Yamamura	551	Selective metal sorption on cross-linked poly(vinylpyridine) resins
S. Przeszlakowski and A. Flieger	557	Column extraction chromatography of non-volatile platinum metals
Z. Marczenko and M. Jarosz	561	Flotation–spectrophotometric method for determining palladium by means of the ion-association complex of pentabromopalladate(II) with Rhodamine 6G
F. Gaizer and A. Puskás	565	A desk-computer program for calculation of the parameters of acid–base titration curves and protonation or metal-complex stability constants from potentiometric data
Michel Wozniak and Guy Nowogrocki	575	An arbitrary correction function for CO_2 evolution in acid–base titrations and its use in multiparametric refinement of data
Iwao Tsukahara and Toshimi Yamamoto	585	Determination of tellurium in copper, lead and selenium by atomic-absorption spectrometry after extraction of the trioctylmethylammonium–tellurium bromide complex
Madhu Phull and P. C. Nigam	591	Kinetics and mechanism of mercury(II)-catalysed replacement of cyanide in hexacyanoferrate(II) by *p*-nitrosodiphenylamine
Short Communications		
R. Belcher and S. J. Morris	599	Barium oxalate as a selective solid reagent for the absorption of sulphur trioxide
Nobutoshi Kiba and Motohisa Furusawa	601	Improved method for titrimetric determination of sulphide by the iodine–azide reaction
Lauri H. J. Lajunen and Eero Aitta	603	Spectrophotometric determination of iron with 1-hydroxy-4-sulpho-2-naphthoic acid
A. M. Mohan Rao, R. Rajagopalan and K. G. Vohra	607	A simple method for the determination of benzo[*a*]pyrene and benzo[*k*]fluoranthene in a mixture
Madhu Phull, H. C. Bajaj and P. C. Nigam	610	Trace element determination in environmental pollution: a kinetic method for mercury estimation
Shigeru Taguchi, Katsumi Goto and Hiroto Watanabe	613	An application of silaned glass beads to the preconcentration and spectrophotometric determination of traces of phosphorus with molybdate

Shigeru Taguchi, Issei Kasahara, Yōichi Fukushima and Katsumi Goto — 616 An application of bis[2-(5-chloro-2-pyridylazo)-5-diethylaminophenolato]cobalt(III) chloride to the extraction and spectrophotometric determination of sulphonated and sulphated surfactants

Kichinosuke Hirokawa, Yuetsu Danzaki and Masaoki Oku — 619 ESCA investigation of the surface of mixed precipitates

Annotation

Sadaaki Murakami and Takashi Yoshino — 623 Correlation between the hard and soft character and the visible absorption spectra of Xylenol Orange and Methylthymol Blue complexes with bivalent metal ions

Letter to the Editor

K. D. Mahilamony and P. Indrasenan — 627 Redox titrations using Chlorbromamine-T as a new oxidant in non-aqueous media

Papers Received — i

Notice — ii

iii European Analytical Column 4

SEPTEMBER

P. F. E. van Montfort and J. Agterdenbos — 629 Some fundamental considerations on analytical high-frequency plasmas

M. Verlinden, H. Deelstra and E. Adriaenssens — 637 The determination of selenium by atomic-absorption spectrometry: a review

Anthony E. Beezer and Babur Z. Chowdhry — 647 Combined assay and determination of bioactivity of polyene antibiotics by flow nephelometry

J. Teckentrup and D. Klockow — 653 Investigation and analytical application of the sulphide–hypobromite chemiluminescence reaction

Georgina L. Pina, T. I. Tikhomirova and E. N. Dorokhova — 665 Indirect method for determining silicon and phosphorus, and analysis of Cuban laterites

Satoru Nigo, Kazuhisa Yoshimura and Toshikazu Tarutani — 669 Ion-exchanger colorimetry—VII. Microdetermination of iron(II) and iron(III) in natural water

A. Baillet-Guffroy, D. Baylocq, P. Rafidison et F. Pellerin — 675 Identification et dosage des sels biliaires et de leurs dérivés conjugués en chromatographie liquide

Maja Blanuša and Djurdja Breški — 681 Comparison of dry and wet ashing procedures for cadmium and iron determination in biological material by atomic-absorption spectrophotometry

Short Communications

Sonia T. Hassib — 685 Qualitative and quantitative analysis of uracil anticancer drugs

G. E. Pacey and C. E. Moore — 688 The synthesis and reagent properties of magnesium tetrakis(4-tert.-butylphenyl)borate

Nobutoshi Kiba, Yo Suzuki and Motohisa Furusawa — 691 Indirect determination of some aliphatic secondary amines by catalytic thermometric titration

Wei Fu-Sheng, Liu Yu-qin, Yin Fang and Shen Nai-kui — 694 Determination of cyanide by an indirect spectrophotometric method, using 5-Br-PADAP

W. A. Bashir and S. Flamerz — 697 Photometric determination of nitrite

Annotations

A. Varma — 701 Analytical techniques for corrosion studies on noble metals

John Farino, George Norwitz, Walter J. Boyko and Peter N. Keliher 705 Study of the behaviour of various phenolic compounds in the 4-amino-antipyrine and ultraviolet-ratio spectrophotometric methods without and with distillation

Papers Received i

Publications Received iii

OCTOBER

Louis Gordon Memorial Award 1

M. Montagu, P. Levillain, M. Rideau et J. C. Chénieux 709 Absorption et fluorescence d'alcaloïdes quaternaires dérivés de la quinoléine: applications analytiques

J. J. Donkerbroek, J. J. Elzas, C. Gooijer, R. W. Frei and N. H. Velthorst 717 Some aspects of room-temperature phosphorescence in liquid solutions

I. Ogawa, G. A. Junk and H. J. Svec 725 Degradation of aromatic compounds in ground-water, and methods of sample preservation

J. L. Burguera and Alan Townshend 731 Determination of manganese(II) by a chemiluminescence reaction

W. R. Bramstedt, K. L. Hardee, B. R. Johnson and D. E. Harrington 737 Determination of ruthenium and tin on electrochemical anodes by energy-dispersive X-ray fluorescence

J. A. C. Broekaert, F. Leis and K. Laqua 745 The application of an argon/nitrogen inductively-coupled plasma to the analysis of organic solutions

Harold H. Trimm, Hidetoshi Ushio and Ramesh C. Patel 753 Simultaneous determination of kinetic and thermodynamic parameters from fast-reaction kinetic measurements

Krystyna Brajter and Iwona Miazek 759 Investigations on the effect of aqueous acetone medium on separation of metal ions on Chelex 100 ion-exchanger

Short Communications

S. Traore and J. J. Aaron 765 Determination of bromophos residues by fluorogenic labelling with dansyl chloride and thin-layer chromatography

A. D. Langade and V. M. Shinde 768 Extraction and separation of bismuth(III)

S. K. Mandal, S. B. Rao and B. R. Sant 771 Decomposition of ores by manganese dioxide: analysis of chrome ore

Hiroto Watanabe and Hideki Ohmori 774 Dual-wavelength spectrophotometric determination of copper in sea-water with α,β,γ,δ-tetrakis(1-methylpyridinium-4-yl)porphine

Thomas M. Schmitt and Ead S. Muzher 777 Determination of 2-mercaptobenzothiazole, tolyltriazole and benzotriazole in coolant formulations by liquid chromatography

Analytical Data

Mary R. Masson 781 Calibration of plastic laboratory ware

Annotation

Asha Varma 785 Determination of copper in archaeological and corrosion samples with an ion-selective electrode

Papers Received i

NOVEMBER

The Pharmacia Prize 1

Kent K. Stewart 789 Flow-injection analysis: a review of its early history

Hisahiko Einaga and Hajime Ishii	799	Spectrophotometric determination of beryllium with Calcichrome
Zbigniew Gregorowicz, Jerzy Ciba and Barbara Kowalczyk	805	Studies on spectrophotometric methods of thallium determination
Shizuko Hirata	809	Stability constants for the complexes of transition-metal ions with fulvic and humic acids in sediments measured by gel filtration
M. Qureshi, Ali Mohammad and G. Ganga Raju	817	Systematic analysis for common cations by solid-state spot-tests
Elsie M. Donaldson	825	Spectrophotometric determination of boron in iron and steel with curcumin after separation by 2-ethyl-1,3-hexanediol–chloroform extraction
F. García Sánchez, A. Navas, M. Santiago and F. Grases	833	Kinetic fluorimetric determination of traces of vanadium(V) by means of a catalysed autoxidation process
Romano Andruzzi and Antonio Trazza	839	Determination of trace metals by anodic-stripping voltammetry with a new kind of mercury electrode: the long-lasting sessile-drop electrode
P. Dubois, P. Levillain et C. Viel	843	Le *cis*-α,β-dinitrostilbène: un nouveau réactif pour le dosage colorimetrique des amines primaires et secondaires, des aminoacides et des thiols
Krishna K. Verma and Anil K. Gupta	849	Determination of isoniazid in drugs
Short Communications		
Wei Fu-Sheng, Zhu Yu-Rei, Yin Fang and Shen Nai-Kui	853	Indirect spectrophotometric determination of sulphide with the ternary complex system Ag(I)–phen BPR
J. A. Squella, M. M. Silva and Luis J. Nuñez-Vergara	855	Anodic polarographic determination of flucloxacillin
M. Tsubouchi, N. Yamasaki, H. Mitsushio and K. Matsuoka	857	Hydrophobic indicators for two-phase titrations and their application to the determination of silver and pentachlorophenol
Nita A. Lewis	860	The use of porous glass beads in the separation and purification of ruthenium complexes with large organic ligands
Analytical Data		
Alfred A. Schilt and Francis H. Case	863	Synthesis and chromogenic properties of some hydrazones of 3-isoquinolyl-, 2-quinolyl- and 2-pyrrole-carbaldehydes
Annotation		
Eduardo F. de A. Neves, W. L. Polito, V. L. Moraes and D. W. Franco	867	Evidence of competitive mechanisms during oxidation of $CS_2N_3^-$ by permanganate ion in alkaline solution
Papers Received	i	
Publications Received	iii	
Notice	iv	

DECEMBER

Lars Kryger	871	**Talanta Review:** Interpretation of analytical chemical information by pattern recognition methods—a survey
Hisahiko Einaga and Iwaji Iwasaki	889	Spectrophotometric study of the reaction of zirconium with Chrome Azurol S and fluoride
J. Kragten and A. Parczewski	901	Factorial analysis of matrix effects in ICP–OES and AAS. Determination of Ta and Ni in Au
Sergio de Jesus Alevato and Angela de Luca Rebello	909	Determination of zinc in sea-water by anodic stripping voltammetry

S. Koch, G. Ackermann und V. Scholze	915	Untersuchungen zur Anwendung ternärer Komplexe in der Photometrie—II. Die Bestimmung des Titanium(IV) mit Tiron in Gegenwart von Iminodiessigsäure, Nitrilotriessigsäure bzw. Diethylentriaminpentaessigsäure
Åke Olin and Bo Wallén	919	A source of error in the determination of equivalence volumes of carboxylic acids from potentiometric titrations
F. Gaizer and A. Puskás	925	Desk-computer program for evaluation of complex equilibria from spectrophotometric data
P. W. Alexander and Jose P. Joseph	931	Selective potentiometric determination of Bi(III) with a coated-wire electrode
G. E. Pacey and J. A. Ford	935	Arsenic speciation by ion-exchange separation and graphite-furnace atomic-absorption spectrophotometry
A. M. Bernard et J. L. Burgot	939	Etude des écarts à la linéarité de la méthode linéaire de dosage par titrimétrie thermométrique—I. Courbures dues à la variation de capacité calorifique et aux fuites thermiques
A. M. Bernard et J. L. Burgot	945	Etude des écarts à la linéarité de la méthode linéaire de dosage par titrimétrie thermométrique—II. Courbures des thermogrammes et erreur sur l'appréciation du point équivalent lorsque la réaction de dosage est équilibrée
Short Communications		
L. Polo Diez, J. Hernandez Mendez and M. J. Almendral Parra	951	Potentiometric determination of hydrogen peroxide with permanganate in presence of fluoride, with iron as a catalyst: application to the titanium–fluoride–peroxide mixed complex
D. Amin and M. S. Al-Ajely	955	Titrimetric microdetermination of chloral hydrate by amplification reactions
J. P. Ghosh, J. Pramanick and H. R. Das	957	Preparation and properties of a new chelating resin containing 2-nitroso-1-naphthol
Balbir Chand Verma and Rajnish Kumar Sood	960	Non-aqueous cerimetric determination of phenylhydrazides
K. Sriramam, B. S. R. Sarma, N. Ramabrahma Sastry and A. R. K. Vara Prasad	963	Sequential titration of iron(II), antimony(III) and arsenic(III) in binary or ternary mixture
Annotations		
Kyoji Tôei and Yasuaki Shimoishi	967	Determination of ultramicro amounts of selenium by gas chromatography with electron-capture detection
Michele Laxer, A. C. Capomacchia and G. E. Hardee	973	Intramolecular hydrogen-bonding in beta adrenergic blocking agents
Letter to the Editor		
A. A. Bugaevsky and L. E. Nikishina	977	On the analytical method of calculating the derivatives of equilibrium concentrations
Papers Received	i	
Notice	iii	

Dates: 12–13 March, 1982

Location: Atlantic City Convention Hall

Fee: $125.00 (includes course materials, Friday Lunch and dinner)

Instructors: Professor Dana W. Mayo, Bowdoin College
Professor Foil A. Miller, University of Pittsburgh

Course Description: This will be a basic course on infrared spectral interpretation using group frequency. A third of the time will be devoted to individual work with problem spectra. The course is intended to be an introduction to the subject or a refresher. The goal will be to convey the fundamentals of approaching an unknown spectrum.

PARTICIPATION IS RESTRICTED TO REGISTERED CONFEREES.

MICROCHEMICAL WORKSHOP—1982

The Department of Continuing Education of the Pennsylvania State University will conduct, on 6–8 July 1982 at the University Park Campus, a Microchemical Workshop on the general theme of "Titrimetry". The technical programme will consist of a number of intensive lectures and lecture demonstrations presented by recognized scientists from the United States and from abroad. By utilization of the housing, food service and meeting and recreational facilities of the University, expenses will be minimal.

For more information contact:

Technical programme: Howard J. Francis, Jr.
The Pennwalt Corporation
900 First Avenue
King of Prussia, PA 19406, U.S.A.

Registration and housing: Ronald Avillion
The Pennsylvania State University
J. Orvis Keller Building
University Park, PA 16802, U.S.A.

Talanta, Vol. 28, p. iv, 1981
Pergamon Press Ltd. Printed in Great Britain

NOTICE

INTERNATIONAL SOLVENT EXTRACTION CONFERENCE

Denver, Colorado, U.S.A.
26 August–2 September 1983

SPONSORED BY: AMERICAN INSTITUTE OF CHEMICAL ENGINEERS

For those who have attended previous ISEC meetings, this will be a typical ISEC gathering with a chance to present and exchange the latest in solvent extraction technology and to renew and make friendships with those in the field both at the technical sessions and during our social activities.

ISEC conferences have recently been held on a 3-year cycle—ISEC '80 in Liege, Belgium and ISEC '77 in Toronto, Canada—each attracting some 500 attendees and 150 papers.

For those who have never attended ISEC conferences, 1983 is the time to do so. All phases of solvent extraction and related technologies are included in a broad technical programme interspersed with social interludes.

The American Institute of Chemical Engineers has a concurrent meeting in Denver, August 28–31, 1981. The technical sessions will be open to ISEC registrants.

The subject areas of interest for ISEC '83, for which papers are solicited, are listed below. They are intended to evoke ideas and proposals and are not titles of ultimate sessions.

- Novel Extractants
- Phase Equilibria in Solvent Extraction
- Diluent, Modifier and Solvation Effects
- Physical Chemistry of Extraction
- Characterization of Extracted Complexes
- Analytical Chemistry Utilizing Solvent Extraction
- Solvent Effects in High-Performance Liquid Chromatography (HPLC)
- Interfacial Phenomena in Extraction
- Mass Transfer in Extraction
- Fluid Mechanics in Extractors
- Axial Dispersion in Extractors
- Applications of Extraction:
  - Nuclear
  - Metallurgical
  - Fuels and Chemicals
  - Pharmaceutical
  - Water Pollution Abatement
- New Uses of Extractants
- Liquid Membranes and Related Processes
- Innovations in Extraction Equipment
- Field Performance of Extraction Plants
- Economic Aspects of Solvent Extraction
- Integration of Disciplines Underlying the Field of Solvent Extraction

ISEC '83

NAME .....

ADDRESS .....

.....

.....

Are you interested in presenting a paper? Yes..... No.....

If so, on what topic or in which area?.....

Please complete and return to:

Mr. Don Nowak
ISEC '83
American Institute of Chemical Engineers
345 East 47th Street
New York, NY 10017
USA

determination of sodium azide when the introductory paragraph states that its use is forbidden in almost all countries, because "even small errors in its use could lead to fatal consequences".

The chapter on additives is as chilling as any of the 19th century texts on adulteration, but it, and those on acidity, alcohols, esters, carbonyl and phenolic compounds and others are full of valuable information and analytical expertise.

D. BETTERIDGE

Advances in Chromatography, Vol. 18: J. CALVIN GIDDINGS, ELI GRUSHKA, JACK CAZES, and PHYLLIS R. BROWN (eds.), Dekker, New York, 1980. Pp. 312. SFr. 88.

In this, the eighteenth volume of the series, the editors have maintained their usual high standards. There are general articles on ion-pair chromatography and ligand-exchange chromatography for the resolution of racemates, and discussions of the application of LC to the characterization of long-chain fatty acids, free nucleotides in biological fluids and combination GC–MS for the analysis of marijuana cannabinoids and their metabolites. The range and the depth of treatment makes the series daunting for the general reader, but essential for the library.

D. BETTERIDGE

Talanta, Vol. 28, p. iv
Pergamon Press Ltd 1981. Printed in Great Britain

NOTICE

SECOND INTERNATIONAL CONGRESS ON ANALYTICAL TECHNIQUES IN ENVIRONMENTAL CHEMISTRY

This Congress will be held in Barcelona on 23–25 November 1981 and will be followed by a Workshop on the "Chemistry and Analysis of Hydrocarbons in the Environment" on 26–27 November 1981. The Congress will be concerned with new methodologies and recent advances in analytical instrumentation for the identification of naturally occurring, as well as man-made, environmental chemicals. Persons interested in presenting papers and in receiving further information should write to the Secretariat, Second International Congress on Analytical Techniques in Environmental Chemistry, Expoquimia Plaza de Espana, Barcelona-4, Spain.

picked up with more careful proofing, such as "anthraquinones" on p. 17 where I think "anthocyanines" is intended, and the apparent contradiction between text and figure legend on pp. 78/78. Still, there is much useful material here, and I am sure it will be helpful to analysts facing such problems in food packaging.

IAIN L. MARR

Guide to Good Programming Practice: B. L. MEEK and P. M. HEATH (eds.), Horwood, Chichester, 1980. Pp. 181. Boards £10.50, Paperback £3.95.

Most computer-language courses concentrate mainly on language features and predigested programming exercises, and they usually say very little about what constitutes good programming practice. This little book should do much to rectify the problems caused by this situation. It is aimed to help both the "professional" and "amateur" to become a serious and competent programmer. The topics covered include: choice of language; language standards; structured programming; error prevention; testing and debugging; special problems; program documentation; other people's programs. The authors are to be congratulated on a most readable and useful book. I would recommend that any "amateur" programmers among the *Talanta* readership should buy (or at least, borrow) and read a copy. Many of the programs submitted to *Talanta* would greatly benefit if their authors were to follow the advice given.

MARY MASSON

Talanta, Vol. 28, p. V, 1981
Pergamon Press Ltd. Printed in Great Britain

MICROPROCESSORS—MACROAPPLICATIONS

The microprocessor is now a ubiquitous accessory of new instrumental equipment, but its functional basis remains a mystery to many, indeed probably most, of those who use it. It is for that reason that the Editorial Board of *Talanta* decided to publish two papers on the architecture and function of microprocessor control, partly to explain some of the jargon and mystique to the uninitiated, and partly to show the power of these systems and to indicate how they may best be utilized. The issue is completed with some typical applications in research and development, to show how microprocessors can be built into a particular experiment for a specific purpose.

At the same time, it should be pointed out that microprocessors, like many other modern conveniences, are not a universal answer, and their uncritical use can lead to a lowering of standards and even the introduction of errors larger than those they are intended to eliminate. Almost every new instrument has microprocessor control and often microprocessor calculation and presentation facilities. It is argued that this allows the instrument to be used by relatively unskilled workers, that it avoids errors introduced by manual operation, and that it frees the worker for other tasks. These claims are valid up to a point. Most instruments would work just as satisfactorily if operated manually (and presumably would cost less). The calculation facilities frequently construct a calibration function by polynomial equation fitting to the experimental data points obtained for standards, but may not always have the ability to detect "rogue" data points arising from faulty preparation of the standards, though the latest models warn the operator if an incorrect *single* reference solution is used. Also, it is only too evident from published work that the number of standards run for calibration purposes is steadily diminishing, and polynomials are being fitted to four or even three data points. An "old-fashioned" analyst would run ten standards as a matter of routine and not be happy unless the results gave a smooth curve or a straight line, and would find the reason for any departure from it. Nowdays it seems that seeing a data print-out is believing it must be true, without bothering to check the validity of the belief.

Microprocessors are excellent tools if used intelligently and for the purpose of doing quickly and precisely what the human operator can do only very slowly and with less precision, but if used inappropriately or without proper knowledge of the function and capabilities are about as useful as a chisel is as a screwdriver.

It is hoped that this issue will stimulate readers to take a thoroughly intelligent interest in any microprocessor-control they are using, and to assess its performance in exactly the same way as they would that of a balance, a pipette, or any other analytical instrument.

AUTHOR INDEX

Aaron J. J., 765
Ackermann G., 915
Adhikari B., 262
Agterdenbos J., 629
Ahluwalia J. C., 281
Ahmed M. K., 55
Aitta E., 277, 603
Akaiwa H., 337
Akhtar A., 441
Al-Ajely M. S., 955
Alevato S. de J., 909
Alexander P. W., 931
Alimarin I. P., 7
Aller A. J., 469
Alvarez J. R. G., 425
Amin D., 955
Anderson R. G., 365
Andruzzi R., 839

Bachvarova D., 481
Baillet-Guffroy A., 675
Bajaj H. C., 610
Barbooti M. M., 353, 359
Barelli N., 69
Bashir W. A., 697
Basu D. K., 262
Baylocq D., 675
Beardsley D. A., 405
Beezer A. E., 647
Belchamber R. M., 543, 547
Belcher R., 599
Bernal J. L., 469
Bernard A. M., 939, 945
Berndt H., 334
Bessière J., 81
Birch B. J., 473
Blades M. W., 519, 527
Blanuša M., 681
Boughriet A., 233
Boyko W. J., 705
Brajter K., 759
Bramstedt W. R., 737
Breški D., 681
Briggs A. G., 415
Broekaert J. A. C., 745
Brown B. C., 365
Bsebsu N. K., 473
Bugaevsky A. A., 977
Bunaciu A. A., 383
Burger N., 323
Burgot J. L., 939, 945
Burguera J. L., 731

Calderoni G., 65
Cano-Pavon J. M., 131
Capomacchia A. C., 973
Carr P. W., 411
Carrasco J., 341
Case F. H., 863
Ceba M. R., 134
Chakrabarti J. K., 329
Chaudri S. A., 441
Chaudhuri A. K., 262
Chauhan O. S., 399
Chénieux J. C., 709
Chow A., 157, 437
Chowdhry B. Z., 647
Chowdhury R. P., 62
Christian G. D., 313
Ciba J., 805
Cilianu S., 383
Codding E. G., 503
Coşofreţ V. V., 377, 383

Danzaki Y., 619
Das H. R., 274, 957
Davies G. L. O., 329
Deban L., 469
Deelstra H., 637
Degorre J.-M., 451
Delannoy A., 451
Delannoy N., 451
Diez L. P., 951
Dil W., 441
Donaldson E. M., 461, 825
Donkerbroek J. J., 717
Dorignac M. R., 447
Dorokhova E. N., 7, 665
Dubey S. K., 485
Dubois P., 843

Eastwood D., 1
Edwall G., 301
Einaga H., 799, 889
Ejaz M., 441
Elzas J. J., 717
Engelmann Ch., 19

Fang Y., 189, 694, 853
Farino J., 705
Farrell J. F., 107
Filipović I., 199
Fischer J.-C., 233
Fischer M., 313
Flamerz S., 697
Fleury G., 95
Flieger A., 557
Fogg A. G., 473
Ford J. A., 935
Franco D. W., 867
Fraústo da Silva J. J. R., 237
Frei R. W., 717
Fujinaga T., 295
Fukui S., 402
Fukushima Y., 616
Furusawa M., 115, 601, 691
Fu-Sheng W., 189, 694, 853

Gaizer F., 127, 565, 925
Gamot A. P., 95
Gampp H., 535
Garg B. S., 399
Ghosh J. P., 274, 957
Gijbels R., 221
Glab S., 183, 301
Gomis D. B., 425
Gooijer C., 717
Gorgoni C., 169
Goto K., 613, 616
Grases F., 833
Gregorowicz Z., 805
Gücer S., 334
Gupta A. K., 849
Gupta B. K., 107
Gupta J. G. S., 31

Hamon R. F., 437
Hardee G. E., 973
Hardee K. L., 737
Harrington D. E., 737
Hassan M. M. A., 187
Hassan S. S. M., 89
Hassib S. T., 685
Hayano S., 319
Hayashida I., 349
Hendrick M. S., 1
Hennion J., 451
Higgs D. J., 11
Hirata S., 809
Hirayama T., 402
Hirokawa K., 619
Hoang H., 408
Horlick G., 487, 519, 527, 543, 547
Hulanicki A., 183, 455
Hurtubise R. J., 145

Ichiki S., 295
Iinuma Y., 551
Imura H., 73
Indrasenan P., 627
Ingle J. D. Jr., 225, 539
Ingman F., 137, 301
Ionescu M. S., 377, 383

Ishii H., 799
Iwasaki I., 889
Izquierdo A., 341

Jarosz M., 561
Jasim F., 353, 359
Jawaid M., 137
Johansson S., 241
Johnson B. R., 737
Jöngren P.-A., 301
Joseph J. P., 931
Junk G. A., 725

Karas-Gašparec V., 323
Karwowska R., 455
Kasahara I., 616
Kavitha V. S. N. P., 332
Kawamoto H., 337
Kaz'min P. G., 7
Keliher P. N., 705
Kenney-Wallace G. A., 107
Khurgin Yu. I., 161
Kiba N., 115, 601, 691
Kiekens P., 192, 431
Killeen T. J., 1
Kirmse R., 345
Klockow D., 653
Koch S., 915
Kowalczyk B., 805
Kragten J., 149, 901
Krishna R. R., 477
Kryger L., 871
Kurian M. J., 395
Kuroda R., 389
Kuwamoto T., 295

Laganá A., 215
Lajunen L. H. J., 277, 603
Langade A. D., 768
Laqua K., 745
Laxer M., 973
Lázár J., 127
Leis F., 745
Levillain P., 709, 843
Lewis N. A., 860
Livertoux M. H., 81
Lo V. S. K., 157
LueYen-Bower E., 119
Lyle S. J., 251

Mahilamony K. D., 627
Mandal S. K., 121, 771
Mansilla A. E., 134
Marczenko Z., 561
Masson M. R., 781
Máté M., 127
Matsuoka K., 857
Matusinović T., 199
Mayanna S. M., 259
Melios C., 69
Mendez J. H., 951
Miazek I., 759
Michalik P. A., 37, 43
Mirza M. Y., 49
Mitra B. K., 62
Mitsushio H., 857
Mochizuki T., 389
Mohammad A., 817
Molina M., 69
Montagu M., 709
Montfort P. F. E. van, 629
Moore C. E., 688
Moraes V. L., 867
Morris S. J., 599
Mossa J. S., 187
Murakami S., 623
Murthy M. V. K., 195
Murthy S. S. N., 477
Muzher E. S., 777

Nai-kui S., 189, 694, 853
Nair M. R. G., 395
Nakamura K., 123
Navas A., 833
Negoiu D., 377
Nevado J. J. B., 134
Neves E. F. de A., 867
Nicole J., 451
Nigam P. C., 591, 610
Nigo S., 669
Nikishina L. E., 977
Nohara M., 402
Norwitz G., 705
Nowogrocki G., 575
Nozal Mª. J. del, 469
Nuñez-Vergara L. J., 855
Nwabue F. I., 49

Ogawa I., 725
Ogawa N., 551
Ogura K., 337
Ohmori H., 774
Ohta K., 177
Oku M., 619
Olin Å., 919
Ono A., 268
Ortner H. M., 19
Otto M., 345

Pacey G. E., 688, 935
Pal B. K., 62
Pal D., 262
Parczewski A., 149, 901
Parhi S., 277
Parra M. J. A., 951
Patel R. C., 753
Patriarche G. J., 313
Pei-hua Q., 189
Pellerin F., 675
Petronio B. M., 215
Petrov G., 481
Phull M., 591, 610
Pina G. L., 665
Pitet G., 447
Poe D. P., 419
Polito W. L., 867
Prabhakaran C. P., 395
Pramanick J., 957
Prasad A. R. K. V., 257, 963
Prasad K., 281
Przeszlakowski S., 557
Puskás A., 565, 925

Qureshi M., 817

Rackham D. M., 329
Rafidison P., 675
Rajagopalan R., 607
Raju G. G., 817
Rangaswamy, 418
Rao A. M. M., 607
Rao S. B., 121, 771
Raoot K. N., 327
Raoot S., 327
Ravindranath P., 257
Rebello A. de L., 909
Reddy B. S., 477
Rideau M., 709
Rodriguez J., 131
Rogers D. W., 281
Rosenfeld A. G., 11
Rukmini N., 332
Russo M. V., 215
Ryan M. A., 225, 539

Sakagami Y., 402
Saleh M. I., 251
Salin E. D., 519
Sanchez F. G., 833
Sant B. R., 121, 771
Santiago M., 833
Sanz-Medel A., 425
Sarma B. S. R., 257, 287, 963
Sastry C. S. P., 477
Sastry N. R., 287, 963
Satyanarayana D., 195
Schilt A. A., 863
Schmitt T. M., 777
Scholze V., 915
Shamus-Zuha, 441
Sharma Y., 59
Sherman F. B., 161
Sherman L. R., 408
Shih Y.-T., 411
Shimoishi Y., 967
Shinde V. M., 768
Shinozuka N., 319
Sighinolfi G. P., 169
Silva M. M., 855
Simmons R. E., 415
Simoes M. de L. S., 237
Singh I., 399
Singh R. P., 399
Siraj P., 477
Smallwood T. B., 265
Sood R. K., 960
Sowinski J. S., 455
Squella J. A., 855
Sriramam K., 257, 287, 963
Stach J., 345
Stephens R., 37, 43
Stewart K. K., 11, 789
Strelow F. W. E., 207
Strijckmans K., 19
Subbarao C., 55
Sugii A., 551
Sugiura K., 295
Sundar B. S., 287
Suri S. K., 281
Suto T., 115
Suzuki M., 177
Suzuki N., 73
Suzuki Y., 691
Svec H. J., 725

Taga M., 349
Taguchi S., 613, 616
Tarutani T., 669
Tavernier S. M. F., 221
Teckentrup J., 653
Temmerman E., 192, 431
Terada K., 123
Tikhomirova T. I., 665
Tiwari K. K., 397
Tôei K., 967
Torres A. G. de, 131
Townshend A., 731
Traore S., 765

Trazza A., 839
Triché C., 447
Trimm H. H., 753
Trust V. L., 408
Tsubouchi M., 857
Tsukahara I., 585

Uma K. V., 259
Ushio H., 753

Vandecasteele C., 19
Vanderslice J. T., 11
Varma A., 701, 785
Vaz M. C. T. A., 237
Velthorst N. H., 717
Verbeek F., 431
Vergoten G., 95
Verlinden M., 637
Verma B. C., 960
Verma K. K., 485, 849
Verma R. M., 397
Verplaetse H., 192, 431
Victor A. H., 207
Viel C., 843
Vijaya K. D., 332
Vire J.-C., 313
Vohra K. G., 607

Walden G. L., 201
Wall C. D., 265
Wallen B., 919
Wang J., 369
Ward J. L., 119, 201
Wartel M., 233
Watanabe H., 613, 774
Werner G., 345
Wilson J. P., 107
Winefordner J. D., 119, 201
Wittmann Zs., 271
Wozniak M., 575
Wroński M., 173, 255

Xi-Wen H., 419

Yamamoto T., 585
Yamamura H., 551
Yamasaki N., 857
Yamashita G. T., 437
Yathirajan H. S., 418
Yoshida H., 349
Yoshimura K., 669
Yoshino T., 623
Young R. S., 25
Yu-qin L., 694
Yu-Rei Z., 853

Zubair M. U., 187

Printed in Great Britain by A. Wheaton & Ltd. Exeter